

# Posters and Exhibits

104<sup>th</sup> Scientific Assembly and Annual Meeting November 25–30 | McCormick Place, Chicago





# AI002-EB

A Deep Learning Framework for Radiotherapy Delivery in Thoracic Oncology

All Day Room: AI Community, Learning Center

#### **Participants**

Zaid A. Siddiqui, MD, Royal Oak, MI (Presenter) Nothing to Disclose

# **GENERAL INFORMATION**

Meet the Author: The authors of this poster will be available in person to discuss their project during these times: Sunday, November 25 - 12:30-1:30 pm Monday, November 26 - 12:15-1:15 pm

# **POSTER DESCRIPTION**

This presentation provides an overview of deep learning techniques that can assist various aspects of the radiation therapy planning process. The success of deep learning methods for normal tissue segmentation and their potential use in clinical target volumes are reviewed. Techniques to generate synthetic CT scans are also discussed as are their potential uses for MR-based planning or rapid adaptive plans from daily imaging. Finally, we look at the potential applications of deep learning in dose calculation/optimization and in accelerating development of personalized radiotherapy plans.



# AI003-EB

Ultra Low Dose PET/MRI Imaging of Crohn's Disease Using a Novel Deep Learning Reconstruction Method

All Day Room: AI Community, Learning Center

## Participants

Christian Park, DO, Madison, WI (Presenter) Nothing to Disclose

Meet the Author: The authors of this poster will be available in person to discuss their project during these times: Sunday, November 25 - 12:30-1:30 pm



# AI004-EB

Development and Visual Assessment of a Deep Learning System for Automated Tuberculosis Screening Using Chest Radiographs

All Day Room: AI Community, Learning Center

# Participants

Tae Kyung Kim, Baltimore, MD (Presenter) Nothing to Disclose

Meet the Author: The authors of this poster will be available in person to discuss their project during these times Monday, November 26 - 12:15-12:45 pm



# AI006-EB

Radiomic Modeling to Predict Risk of Vertebral Compression Fracture After Stereotactic Body Radiation Therapy for Spinal Metastases

All Day Room: AI Community, Learning Center

# Participants

Chengcheng Gui, Baltimore, MD (Presenter) Nothing to Disclose

Meet the Author: The authors of this poster will be available in person to discuss their project during these times Tuesday, November 27 12:15-12:45 pm



# AI007-EB

Artificial Intelligence-Assisted Automated Detection and Outcome Prediction of Subarachnoid Hemorrhage: Techniques and Educational Approaches

All Day Room: AI Community, Learning Center

# Participants

Weimeng Ding, Montreal, QC (*Presenter*) Nothing to Disclose Jack W. Luo, Montreal, QC (*Abstract Co-Author*) Nothing to Disclose Josep L. Dolz, MD, Terrassa, Spain (*NON-Presenter*) Nothing to Disclose Ismail Ben Ayed, London, ON (*NON-Presenter*) Research, General Electric Company Jaron Chong, MD, Montreal, QC (*Abstract Co-Author*) Nothing to Disclose

Meet the Author: The authors of this poster will be available in person to discuss their project during these times: Tuesday November 27 12:45-1:15pm



# AI008-EB

Machine Learning to Predict Risk of Upgrade and Recurrence of Ductal Carcinoma In Situ

All Day Room: AI Community, Learning Center

# Participants

Manisha Bahl, MD,MPH, Boston, MA (*Presenter*) Nothing to Disclose Regina Barzilay, PhD, Cambridge, MA (*Abstract Co-Author*) Nothing to Disclose Constance D. Lehman, MD,PhD, Boston, MA (*Abstract Co-Author*) Research Grant, General Electric Company; Medical Advisory Board, General Electric Company

Meet the Author: The authors of this poster will be available in person to discuss their project during these times: Sunday, November 25 - 12:30-1:00 pm



# AI009-EB

Machine Learning-based Virtual Metastasis Biopsy as an Early Predictor of Tumor Progression and Resistance Mutation Acquisition in Colon Cancer Patients

All Day Room: AI Community, Learning Center

# Participants

Dania Daye, MD, PhD, Philadelphia, PA (Presenter) Nothing to Disclose

Azadeh Tabari, Boston, MA (Abstract Co-Author) Nothing to Disclose

Katherine P. Andriole, PhD, Dedham, MA (*Abstract Co-Author*) Research Grant, NVIDIA Corporation; Research Grant, General Electric Company; Research Grant, Nuance Communications, Inc; Advisory Board, McKinsey & Company, Inc Michael S. Gee, MD, PhD, Boston, MA (*Abstract Co-Author*) Nothing to Disclose

Meet the Author: The authors of this poster will be available in person to discuss their project during these times: Monday, November 26 - 12:45-1:15 pm



# AI010-EB

Utilization of Deep Learning on CT Angiogram to Aid in the Detection of Emergent Large Vessel Occlusion

All Day Room: AI Community, Learning Center

#### **Participants**

Anthony D. Yao, Providence, RI (*Presenter*) Nothing to Disclose Matthew T. Stib, MD, Providence, RI (*Abstract Co-Author*) Nothing to Disclose Sumera S. Subzwari, Providence, RI (*Abstract Co-Author*) Nothing to Disclose Amy Wang, Madison, WI (*NON-Presenter*) Luke Zhu, Providence, RI (*Abstract Co-Author*) Nothing to Disclose Jerrold L. Boxerman, MD, PhD, Providence, RI (*Abstract Co-Author*) Nothing to Disclose Grayson L. Baird, PhD, Providence, RI (*Abstract Co-Author*) Nothing to Disclose Ugur Cetintemel, Providence, RI (*Abstract Co-Author*) Nothing to Disclose Ryan A. McTaggart, MD, Barrington, RI (*Abstract Co-Author*) Nothing to Disclose

Meet the Author: The authors of this poster will be available in person to discuss their project during these times: Sunday November 25 1:00-1:30 pm



## AI011-EB

Segmentation and Quantitative Assessment of Prognostic Features in Type B Aortic Dissection Using Machine Learning

All Day Room: AI Community, Learning Center

# Participants

Lewis D. Hahn, MD, Stanford, CA (*Presenter*) Nothing to Disclose Gabriel Mistelbauer, Magdeburg, Germany (*Abstract Co-Author*) Nothing to Disclose Kai Higashigaito, MD, Stanford, CA (*Abstract Co-Author*) Nothing to Disclose Martin J. Willemink, MD,PhD, Menlo Park, CA (*Abstract Co-Author*) Speakers Bureau, Koninklijke Philips NV; Research Grant, Koninklijke Philips NV

Anna M. Sailer, MD, PhD, West Hollywood, CA (Abstract Co-Author) Nothing to Disclose

Michael Muelly, MD, Mountain View, CA (Abstract Co-Author) Employee, Google LLC; Partner, ClariPACS LLC

Michael Fischbein, Stanford, CA (Abstract Co-Author) Nothing to Disclose

Dominik Fleischmann, MD, Stanford, CA (Abstract Co-Author) Research Grant, Siemens AG

Meet the Author: The authors of this poster will be available in person to discuss their project during these times: Wednesday November 28 12:45-1:15pm



# AI012-EB

Automated Liver Biometry and Fat Quantification in Non-alcoholic Fatty Liver Disease with Convolutional Neural Networks

All Day Room: AI Community, Learning Center

# Participants

Kang Wang, MD, PhD, San Diego, CA (Presenter) Nothing to Disclose

Meet the Author: The authors of this poster will be available in person to discuss their project during these times: Thursday November 29 12:45-1:15pm



# AI013-EB

A Deep Learning Approach for Identifying Imaging Biomarkers and Outcome Modeling in Chronic Obstructive Pulmonary Disease

All Day Room: AI Community, Learning Center

# Participants

Tara A. Retson, MD, PhD, San Diego, CA (Presenter) Nothing to Disclose

Meet the Author: The authors of this poster will be available in person to discuss their project during these times: Wednesday November 28 12:15-12:45pm



# AI014-EB

Deep Learning for Radiological Image Quality Improvement: Impact on the Accuracy of Diagnosis and Organ Segmentation

All Day Room: AI Community, Learning Center

# Participants

Leonid Chepelev, MD, PhD, Ottawa, ON (Presenter) Nothing to Disclose

Meet the Author: The authors of this poster will be available in person to discuss their project during these times: Sunday November 25 1:00-1:30pm



## AI015-EB

Combining Genomic and Clinical/Dosimetric Variables to Predict Radiation Toxicity in Localized Prostate Cancer Patients Via Computational Genomics and Machine Learning

All Day Room: AI Community, Learning Center

# Participants

John Kang, MD, PhD, Rochester, NY (Presenter) Nothing to Disclose

Robert Strawderman, DSc, Rochester, NY (Abstract Co-Author) Nothing to Disclose

Russell Schwartz, PhD, Pittsburgh, PA (*Abstract Co-Author*) Research Grant, University of Pittsburgh Medical Center Enterprises (UPMC-E)

Issam El Naqa, PHD, Ann Arbor, MI (*Abstract Co-Author*) Scientific Advisory Board, Endectra, LLC Thomas Mariani, PhD, Rochester, NY (*Abstract Co-Author*) Nothing to Disclose Sarah L. Kerns, PhD, MPH, New York, NY (*Abstract Co-Author*) Nothing to Disclose

Meet the Author: The authors of this poster will be available in person to discuss their project during these times: Thursday November 29 12:15-12:45pm

#### **Poster Information**

Prostate cancer is the most common non-cutaneous cancer and third most deadly cancer in men in the United States. External beam radiotherapy is an effective treatment, but doses are set to limit the population-level incidence of significant toxicity to <5-10% of patients. Currently, there are no validated tools to predict an individual's risk of toxicity and patients are generally treated uniformly. In this project, we will apply machine learning and hypothesis testing to genomic, clinical and dosimetric data from randomized trials to create a predictor of an individual's toxicity. This tool will provide men with upfront information about their personal risk of toxicity to prostate radiotherapy in order to better inform their treatment decision making.



# AI016-EB

Detection of Obstructive and Restrictive Lung Disease on Chest Radiography Using Machine Learning and Integrated Pulmonary Function Data

All Day Room: AI Community, Learning Center

# Participants

Jessica Chan, MD, Salt Lake City, UT (*Presenter*) Nothing to Disclose Ricardo Bigolin Lanfredi, MS,BS, Salt Lake City, UT (*Abstract Co-Author*) Nothing to Disclose Tolga Tasdizen, PhD, Salt Lake City, UT (*Abstract Co-Author*) Nothing to Disclose Tao Li, MS, Salt Lake City, UT (*Abstract Co-Author*) Intern, Koninklijke Philips NV Vivek Srikumar, PhD, Salt Lake City, UT (*Abstract Co-Author*) Nothing to Disclose Clement Vachet, MBA,MS, Salt Lake City, UT (*Abstract Co-Author*) Nothing to Disclose Joyce D. Schroeder, MD, Boulder, CO (*Abstract Co-Author*) Nothing to Disclose

Meet the Author: The authors of this poster will be available in person to discuss their project during these times: Monday November 26 12:45-1:15pm



# AI001-SUA

# **Introduction to Deep Learning**

Sunday, Nov. 25 8:30AM - 10:00AM Room: AI Community, Learning Center

# **Title and Abstract**

Introduction to Deep Learning This class will focus on basic concepts of convolutional neural networks (CNNs), and walk the attendee through a working example. A popular training example is the MNIST data set which consists of hand-written digits. This course will use a data set we created, that we call 'MedNIST' and consists of 1000 images each from 5 different categories: Chest X-ray, hand X-ray, Head CT, Chest CT, Abdomen CT, and Breast MRI. The task is to identify the image type. This will be used to train attendees on the basic principles and some pitfalls in training a CNN. The attendee will have the best experience if they are familiar with Python programming.



# AI001-SUB

# Data Science: Normalization, Annotation, Validation

Sunday, Nov. 25 10:30AM - 12:00PM Room: AI Community, Learning Center

# Title and Abstract

Data Science: Normalization, Annotation, Validation This session will focus on preparation of the image and non-image data in order to obtain the best results from your deep learning system. It will include a discussion of different options for representing the data, how to normalize the data, particularly image data, the various options for image annotation and the benefits of each option. We will also discuss the 'after training' aspects of deep learning including validation and testing to ensure that the results are robust and reliable.



# AI001-SUC

# **Introduction to Deep Learning**

Sunday, Nov. 25 12:30PM - 2:00PM Room: AI Community, Learning Center

# **Title and Abstract**

Introduction to Deep Learning This class will focus on basic concepts of convolutional neural networks (CNNs), and walk the attendee through a working example. A popular training example is the MNIST data set which consists of hand-written digits. This course will use a data set we created, that we call 'MedNIST' and consists of 1000 images each from 5 different categories: Chest X-ray, hand X-ray, Head CT, Chest CT, Abdomen CT, and Breast MRI. The task is to identify the image type. This will be used to train attendees on the basic principles and some pitfalls in training a CNN. The attendee will have the best experience if they are familiar with Python programming.



## AI023-EC-SUA

Real Time Detection and Labeling of Image Objects: YOLO (You Only Look Once), A Case Study (with Pitfalls) in Training and Running a Deep Network to Detect and Label Objects

Sunday, Nov. 25 12:30PM - 1:00PM Room: AI Community, Learning Center Custom Application Computer Demonstration

**FDA** Discussions may include off-label uses.

#### Participants

David W. Piraino, MD, Cleveland, OH (*Presenter*) Medical Advisory Board, Agfa-Gevaert Group; Medical Advisory Board, Siemens AG; Medical Advisory Board, Nuance Communications, Inc

Michael J. Ciancibello, Cleveland, OH (*Abstract Co-Author*) Nothing to Disclose James R. Wetzel, BS, Beachwood, OH (*Abstract Co-Author*) Nothing to Disclose Lindsey Marrero, BS, MS, Beachwood, OH (*Abstract Co-Author*) Nothing to Disclose Roseann Spitznagel, Beachwood, OH (*Abstract Co-Author*) Nothing to Disclose

## CONCLUSION

Open sources deep neural networks can be used detect, localize, and categories abnormalities on medical images in real time.

## FIGURE

http://abstract.rsna.org/uploads/2018/18007883/18007883\_jvlz.jpg

#### Background

Many machine learning models have been developed and trained using the Darknet (https://pjreddie.com/darknet/) deep learning framework to detect, localize, and classify objects in non-medical images from ImageNet (http://image-net.org/). Darknet was developed to provide fast execution of deep learning networks in C. The YOLO (You Only Look Once) object detection system utilizes a convolutional neural network to identify image segments, but unlike other models, is also able to detect and classify images in real time. To apply this technology to radiology, the NIH chest images dataset, available on Kaggle (https://www.kaggle.com/nih-chest-xrays/data), is used in this demonstration for training and test sets.

# **Evaluation**

The NIH dataset, containing around 110,000 chest radiographs, was utilized to train the YOLO convolutional neural network using NVIDIA GeForce GTX Class GPUs. This demonstration will show the steps in developing a machine learning model, which includes data cleansing, data enhancement, training, testing, and attack testing (See Figure using images from NIH dataset). This results in a medical class model which can be used to discover positive findings within medical images, such as atelectasis, cardiomegaly, effusion, infiltration, mass, nodule, pneumonia, and pneumothorax. To create this model, the image bounding boxes from the NIH images are converted to the YOLO format. The model is then retrained with the chest x-ray training set using both the YOLOv2 and YOLOv3 convolutional neural networks and subsequently tested using the test set. A portion of the demonstration will include real time retraining of the model.

#### Discussion

Our computer exhibit will show the steps in developing a convolutional neural network for detection, localization, and categorization of objects/abnormalities on chest x-rays from the NIH data set in real time using the Darknet/YOLO object detection system.



## AI152-ED-SUA2

Deep Learning-Based Texture Classification for Similar CT Image Retrieval

Sunday, Nov. 25 12:30PM - 1:00PM Room: AI Community, Learning Center Station #2

**FDA** Discussions may include off-label uses.

#### Participants

Hiroaki Takebe, Kawasaki, Japan (*Presenter*) Research collaboration, Fujitsu Limited Yasutaka Moriwaki, Kawasaki, Japan (*Abstract Co-Author*) Research collaboration, Fujitsu Limited Takayuki Baba, Kawasaki, Japan (*Abstract Co-Author*) Research collaboration, Fujitsu Limited Hiroaki Terada, MD, Hiroshima, Japan (*Abstract Co-Author*) Nothing to Disclose Toru Higaki, PhD, Hiroshima, Japan (*Abstract Co-Author*) Nothing to Disclose Kazuo Awai, MD, Hiroshima, Japan (*Abstract Co-Author*) Nothing to Disclose Kazuo Awai, MD, Hiroshima, Japan (*Abstract Co-Author*) Research Grant, Canon Medical Systems Corporation; Research Grant, Hitachi, Ltd; Research Grant, Fujitsu Limited; Research Grant, Bayer AG; Research Grant, DAIICHI SANKYO Group; Research Grant, Eisai Co, Ltd; Medical Advisory Board, General Electric Company; ; Akio Ozawa, BS, Chiba, Japan (*Abstract Co-Author*) Researcher, Fujitsu Limited Yasuharu Ogino, Tokyo, Japan (*Abstract Co-Author*) Researcher, Fujitsu Limited Machiko Nakagawa, Tokyo, Japan (*Abstract Co-Author*) Director, Fujitsu Limited Kenji Kitayama, Tokyo, Japan (*Abstract Co-Author*) Director, Fujitsu Limited Nobuhiro Miyazaki, Kawasaki, Japan (*Abstract Co-Author*) Researcher, Fujitsu Limited

#### For information about this presentation, contact:

takebe.hiroaki@jp.fujitsu.com

#### CONCLUSION

We will be able to retrieve morphologically similar case more accurately by using DCNN for classification of texture and may provide diagnostically helpful information.

#### FIGURE

http://abstract.rsna.org/uploads/2018/18015959/18015959\_5zkd.jpg

#### Background

When radiologists encounter a difficult case to diagnose, retrieval of morphologically similar cases in which final diagnosis is established may provide clinically useful information. We proposed a novel method which can retrieve morphologically similar cases based on lesion natures and their 3-dimensional (3D) distribution. As an initial trial, we developed a 3D-similar CT image retrieval method for diffuse lung disease (DLD).

#### **Evaluation**

In our method, we divided a slice image into blocks and classified texture of each blocks as normal or one of several kinds of lesions, and we represented the quantity of each lesion as histograms along a body based on the 3D model and calculated the similarity between cases by matching these histograms. With this method, the precision of retrieval of similar cases depends heavily upon the precision of texture classification. Then, we evaluated precisions of classification methods that use support vector machine (SVM) and deep convolutional neural network (DCNN) for 4 kinds of lesions, ground glass opacity (GGO), consolidation, honeycomb and emphysema in 63 patients with DLDs. These patients were split into training (55 patients) and test (8 patients). As a result, block images were about 21000 for training and about 3500 for test. Two board-certified radiologists consensually determined nature of DLDs and we regarded the results as the gold standard of lesions' nature. For SVM, image features of local binary pattern (LBP) were extracted from block images. For DCNN, block images were used as inputs of VGG16 network and pre-training was not used. The result showed that VGG16 achieved the precision 94.6%, on the other hand the precision of SVM was 74.2%.

## Discussion

The experimental result showed that DCNN proved to be a powerful tool for classifying texture of DLD patients' CT images. We expect that the precision of DCNN will be much better according to increase of data for training.



# AI200-SD-SUA1

Effect of Inter-Observer Variability on Deep Learning in Chest X-Rays

Sunday, Nov. 25 12:30PM - 1:00PM Room: AI Community, Learning Center Station #1

FDA Discussions may include off-label uses.

#### Participants

Harald Ittrich, MD, Hamburg, Germany (*Presenter*) Nothing to Disclose Ivo Matteo Baltruschat, Hamburg, Germany (*Abstract Co-Author*) Nothing to Disclose Leonhard A. Steinmeister, MD, Hamburg, Germany (*Abstract Co-Author*) Nothing to Disclose Michael Grass, PhD, Hamburg, Germany (*Abstract Co-Author*) Employee, Koninklijke Philips NV Axel Saalbach, PHD, Aachen, Germany (*Abstract Co-Author*) Employee, Koninklijke Philips NV Tobias Knopp, DIPLENG, Hamburg, Germany (*Abstract Co-Author*) Nothing to Disclose Gerhard B. Adam, MD, Hamburg, Germany (*Abstract Co-Author*) Nothing to Disclose Hannes Nickisch, Hamburg, Germany (*Abstract Co-Author*) Nothing to Disclose

## For information about this presentation, contact:

ittrich@uke.de

# PURPOSE

Inter-observer variability is a well-known problem for the development of Deep Learning techniques in chest X-rays, especially for diseases with variable characteristics, where binary annotations vary widely between the individual readers. The aim was to investigate the effect of reader-dependent estimation during the annotation processes for Deep Convolutional Neural Networks (DCNN).

## **METHOD AND MATERIALS**

Two expert radiologists annotated the Indiana dataset, which contains 3125 frontal and lateral conventional chest X-rays, in a multi-label setup with eight representative classes of abnormalities (including pleural effusion, infiltrate, congestion, atelectasis, pneumothorax, cardiomegaly, masses and foreign objects). Inter-observer variability (IOV) for all classes were calculated. We trained a ResNet-50 DCNN (with pre-training on ChestXRay14) using each radiologist's annotation: ExpertNet-1 and ExpertNet-2. In contrast to a binary annotation, the trained DCNNs generate continuous value prediction for each abnormality. For our evaluation, we used a 10 times re-sampling scheme. Within each split, we divided the data into 70% training and 30% testing. To evaluate the similarity of the obtained networks, we computed the Spearman's pairwise rank correlation coefficient between the predictions.

# RESULTS

The highest IOV were at congestion and cardiomegaly with  $13.6\% \pm 0.57\%$  and  $10.61\% \pm 0.67\%$ . Despite the differences in the annotation, the network predictions are highly correlated. We estimated rank correlation coefficients of  $0.95\pm0.01$  and  $0.80\pm0.03$  for cardiomegaly and congestion, respectively. By selecting the best threshold for the classification, we reduced the annotation variability from  $13.6\% \pm 0.57\%$  to  $3.81\% \pm 0.49\%$  and from  $10.61\% \pm 0.67\%$  to  $8.36\% \pm 0.78\%$  for congestion and cardiomegaly, respectively.

#### CONCLUSION

We investigated the effect of inter-observer variability on DCNNs. Even though the assignment of (artificial) binary labels by the two readers led to different datasets, our experiments showed a very high rank correlation between the predictions of ExpertNet-1 and ExpertNet-2.

## **CLINICAL RELEVANCE/APPLICATION**

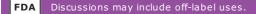
Generating a consensus ground truth of multiple expert annotation can be time-consuming, but is imperative when developing a CAD-System based on DCNNs.



## BR008-EB-SUA

# Where is the Lesion? Mammographic-Sonographic and Breast MR Imaging Correlation

Sunday, Nov. 25 12:30PM - 1:00PM Room: BR Community, Learning Center Hardcopy Backboard



#### **Participants**

Jin Hee Moon, MD, Seoul, Korea, Republic Of (*Abstract Co-Author*) Nothing to Disclose Young Joo Won, Seoul, Korea, Republic Of (*Presenter*) Nothing to Disclose Ji-Young Hwang, Seoul, Korea, Republic Of (*Abstract Co-Author*) Nothing to Disclose Ji Young Woo, Seoul, Korea, Republic Of (*Abstract Co-Author*) Nothing to Disclose

#### For information about this presentation, contact:

geenie-m@hanmail.net

# **TEACHING POINTS**

Breast has very different position according to imaging modality. Lesion detection and accurate correlation in multimodality breast imaging is very important for preventing false or delayed diagnosis. We will provide process for correlation of lesions in mammography, ultrasound and breast MRI and show pearls and pitfalls through illustrations and sample cases.

#### **TABLE OF CONTENTS/OUTLINE**

1. Introduction 2. Basic concept of triangulation 3. Mammographic-sonographic correlation 4. Sonographic-MRI correlation 5. Targeted or second look sonography technique 6. MRI imaging navigated sonography system 7. Summary



# BR013-EB-SUA

Beware of the Rare: A Pictorial Review of Unusual Breast Lesions

Sunday, Nov. 25 12:30PM - 1:00PM Room: BR Community, Learning Center Hardcopy Backboard

#### **Participants**

Denny Lara Nunez, MD, Mexico City, Mexico (*Presenter*) Nothing to Disclose Fernando Candanedo Gonzalez, Mexico City, Mexico (*Abstract Co-Author*) Nothing to Disclose Monica Chapa, MD, Mexico, Mexico (*Abstract Co-Author*) Nothing to Disclose Mariana Licano, MD, Mexico City, Mexico (*Abstract Co-Author*) Nothing to Disclose Antonio Hernandez Villegas, MD, Mexico City, Mexico (*Abstract Co-Author*) Nothing to Disclose Nancy Margarita Gutierrez Castaneda, MD, Cuautla, Mexico (*Abstract Co-Author*) Nothing to Disclose

# For information about this presentation, contact:

dennylaran5@gmail.com

# **TEACHING POINTS**

1. Recognize and familiarize with breast lesions that are not seen routinely on mammographic practice. 2. Identify mutlimodality imaging characteristics of benign and malignant unusual breast lesions. 3. Describe the histopathologic characteristics of rare tumors involving the breast and make correlation with imaging findings for an accurate diagnosis and management.

# TABLE OF CONTENTS/OUTLINE

1. Introduction - General features of breast cancer - Epidemiology 2. A brief review including: - Epidemiology - General features -Clinical presentation - Multimodality imaging characteristics - Histopathologic analysis of the following lesions will be presented: -Sarcoma (angiosarcoma and fusocellular) - Primary neuroendocrine tumor - Lymphoma - Metastases from extramammary malignancies - Fibroadenolipoma - Phyllodes benign tumor, among others 3. Conclusions.



#### BR165-ED-SUA5

Hematopoietic and Connective Tissue Diseases of the Breast

Sunday, Nov. 25 12:30PM - 1:00PM Room: BR Community, Learning Center Station #5

#### Awards Cum Laude

# Participants

Katerina Konstantinoff, MD, Saint Louis, MO (*Presenter*) Nothing to Disclose Shani Aharon, BS, Worcester, MA (*Abstract Co-Author*) Nothing to Disclose Christine O. Menias, MD, Chicago, IL (*Abstract Co-Author*) Nothing to Disclose

Catherine M. Appleton, MD, Saint Louis, MO (Abstract Co-Author) Scientific Advisory Board, Hologic, Inc Royalties, Oxford University Press

Michelle V. Lee, MD, Saint Louis, MO (Abstract Co-Author) Nothing to Disclose

#### **TEACHING POINTS**

Various hematologic and connective tissue diseases that arise from dysfunction of hematopoietic stem cells can present in the breast as primary disease or as a site of systemic involvement, and are important entities to keep in the differential diagnosis in breast imaging. 1. Review the imaging appearance of hematopoietic and connective tissue diseases that involve the breast 2. Review the typical presentation and workup of a patient presenting with suspected hematopoietic or connective tissue disease of the breast 3. Review the differential diagnosis of a patient with hematopoietic disease of the breast

# TABLE OF CONTENTS/OUTLINE

A) Appearance of hematopoietic and connective tissue diseases of the breast in different imaging modalities Mammography US PET/CT MR B) Discussion of hematopoietic and connective tissue diseases of the breast and differential diagnosis of a suspected hematopoietic lesion of the breast with case examples Benign conditions - Amyloidosis, Rosai-Dorfman, scleroderma, dermatomyositis, diabetic mastopathy Malignant lesions - Lymphoma, leukemia, myeloid sarcoma, carcinoma C) Presentation and workup of a patient with a hematopoietic disease of the breast Symptomatic - palpable lump, skin thickening Asymptomatic - abnormality such as lesion or lymphadenopathy on imaging

#### **Honored Educators**

Presenters or authors on this event have been recognized as RSNA Honored Educators for participating in multiple qualifying educational activities. Honored Educators are invested in furthering the profession of radiology by delivering high-quality educational content in their field of study. Learn how you can become an honored educator by visiting the website at: https://www.rsna.org/Honored-Educator-Award/ Christine O. Menias, MD - 2013 Honored EducatorChristine O. Menias, MD - 2014 Honored EducatorChristine O. Menias, MD - 2015 Honored EducatorChristine O. Menias, MD - 2016 Honored EducatorChristine O. Menias, MD - 2018 Honored Educator



## BR166-ED-SUA6

Ouch, That Hurts! Breast Trauma: What the Radiologist Needs to Know

Sunday, Nov. 25 12:30PM - 1:00PM Room: BR Community, Learning Center Station #6

#### **Participants**

Alyssa R. Goldbach, DO, Philadelphia, PA (*Presenter*) Nothing to Disclose Sana Hava, DO, Philadelphia, PA (*Abstract Co-Author*) Nothing to Disclose Shqiponja Hajdinaj, DO, Philadelphia, PA (*Abstract Co-Author*) Nothing to Disclose Suzanne A. Pascarella, MD, Cherry Hill, NJ (*Abstract Co-Author*) Nothing to Disclose Dina F. Caroline, MD, Elkins Park, PA (*Abstract Co-Author*) Nothing to Disclose

# For information about this presentation, contact:

alyssa.goldbach@tuhs.temple.edu

## **TEACHING POINTS**

Breast Trauma is a common and often underreported entity. Accidental injury to the female breast can cause symptoms and signs which may mimic carcinoma, including skin changes and palpable lumps. Breast trauma can also be painful or disfiguring. We will reinforce the imaging features of breast trauma including a review of mechanism of injury when applicable and discuss appropriate follow-up recommendations.

## **TABLE OF CONTENTS/OUTLINE**

The primary goals are to provide a thorough review of imaging findings of breast trauma from our patient database. This will be achieved by: Illustrating the variety of imaging features of traumatic breast lesions. Describing the appropriate management recommendations for traumatic breast lesions. Providing a thorough review of traumatic breast pathologies with practical tips for aiding in diagnosis. Pathologies include gunshot wound, hematoma, hematoma complicated by abscess, seat belt injury, laceration, and pseudoaneurysm. Pathologic correlation from our patient database will be provided when available. It is important for the radiologist to recognize the imaging features of traumatic breast injuries as they can create confusion for both the patient and the clinician. The radiologist is a critical member of the multidisciplinary team working to make the diagnosis and direct patient management.



## BR167-ED-SUA7

# **Inflammatory Processes of the Breast a Pictorial Review**

Sunday, Nov. 25 12:30PM - 1:00PM Room: BR Community, Learning Center Station #7

#### **Participants**

Maria Soledad Nocetti, MD, Vicente Lopez, Argentina (*Abstract Co-Author*) Nothing to Disclose Lucia I. Beccar Varela, MD, Vicente Lopez, Argentina (*Abstract Co-Author*) Nothing to Disclose Elizabeth Quiroga, Vicente Lopez, Argentina (*Abstract Co-Author*) Nothing to Disclose Veronica E. Grondona, MD, Capital Federal, Argentina (*Abstract Co-Author*) Nothing to Disclose Vanina Kuznicki, Vicente Lopez, Argentina (*Abstract Co-Author*) Nothing to Disclose Flavia B. Sarquis, MD, Vicente Lopez, Argentina (*Presenter*) Nothing to Disclose

# For information about this presentation, contact:

lu.beccar.varela@gmail.com

# **TEACHING POINTS**

• Review the clinical, radiographic and histologic features of commonly encountered inflammatory and reactive breast lesions. • Learn a diagnostic algorithm when examining women with mastitis, to distinguish between cancer-related and non cancer-related breast inflammation, since their clinical presentation can be misleading.

#### **TABLE OF CONTENTS/OUTLINE**

Mastitis is the inflammation of breast tissue. It always manifests clinically by three cardinal signs of inflammation, which are redness, heat and pain. From a pathophysiological point of view, mastitis reflects a variety of underlying etiologies. It can be due to non-infectious inflammation, infection (generally of bacterial origin) but can also be caused by inflammation resulting from malignant tumor growth. These processes include fat necrosis, mammary duct ectasia, granulomatous lobular mastitis, diabetic mastopathy, abscess and inflammatory cáncer. The radiologist must be familiar with the radiological signs of breast inflammation, and malignacy must be recognized and diagnosed without fail. Full use of breast imaging techniques is therefore crucial to ensure diagnosis, and subsequently to provide the patient with the most efficient treatment.



## BR168-ED-SUA8

# Testing the Waters: Multimodality Imaging Evaluation of Peri-Implant Effusions

Sunday, Nov. 25 12:30PM - 1:00PM Room: BR Community, Learning Center Station #8

# Awards Magna Cum Laude

#### Participants

Merissa Harris, MD, Dallas, TX (*Presenter*) Nothing to Disclose Emily E. Knippa, MD, Durham, NC (*Abstract Co-Author*) Nothing to Disclose Nicholas Haddock, MD, Dallas, TX (*Abstract Co-Author*) Nothing to Disclose Sumeet Teotia, MD, Dallas, TX (*Abstract Co-Author*) Nothing to Disclose Sunati Sahoo, MD, Dallas, TX (*Abstract Co-Author*) Nothing to Disclose W. Phil Evans III, MD, Dallas, TX (*Abstract Co-Author*) Scientific Advisory Board, VuCOMP, Inc Stephen J. Seiler, MD, Dallas, TX (*Abstract Co-Author*) Nothing to Disclose

# For information about this presentation, contact:

merissa.harris@phhs.org

#### **TEACHING POINTS**

There are a few, but significant, differences in the differential diagnosis of immediate/early vs. delayed peri-implant effusions. Breast Implant Associated-Anaplastic Large Cell Lymphoma (BIA-ALCL) can be associated with either saline or silicone implants and is most frequently seen with textured implant surfaces. When performing an aspiration of a delayed peri-implant effusion, fluid should be sent for culture and cytologic analysis. Cytology should include Wright Giemsa staining as well as immunohistochemistry testing for cluster of differentiation (CD) and anaplastic lymphoma kinase (ALK) markers.

#### **TABLE OF CONTENTS/OUTLINE**

Multimodality appearance of a peri-implant effusion: Mammography Ultrasound Magnetic Resonance Imaging Effusion Mimics Early effusion differential considerations: Seroma Hematoma Infection Delayed effusion differential considerations: Non-specific inflammation Infection Malignant effusion (due to breast cancer) Malignant effusion (due to lymphoma): BIA-ALCL BIA-ALCL: Background Medical device report statistics Diagnostic evaluation Management considerations Procedural Considerations: Tips for performing an ultrasound-guided aspiration



#### BR204-ED-SUA10

# Round Malignancies: A Pictorial Review with Radiologic-Pathologic Correlation

Sunday, Nov. 25 12:30PM - 1:00PM Room: BR Community, Learning Center Station #10

# Participants

Janice Y. Jeon, MD, Washington, DC (Presenter) Nothing to Disclose

#### For information about this presentation, contact:

janice.l.jeon@gunet.georgetown.edu

#### **TEACHING POINTS**

Breast malignancies encompass a host of heterogeneous tumors with a range of appearances on multimodality imaging. The updated BI-RADS lexicon predicts risk of malignancy based on various descriptors including shape and margins. While oval masses confer benignity, round masses warrant evaluation to exclude malignancy. Invasive ductal carcinoma (IDC) is the most common invasive cancer. While most radiologists are familiar with the classic appearance of poorly-differentiated (grade III) irregular IDC, decreased familiarity with the less common round, non-aggressive appearing well-differentiated (grade I) IDC may lead to misinterpretation and misdiagnosis. Other cancers often presenting as round masses are the well-differentiated IDC subtypes which include mucinous, medullary, metaplastic & papillary categories. The aforementioned entities will be presented via pictorial review with pathology correlation. This exhibit aims to increase awareness of the spectrum of round circumscribed malignancies for which cancer should not be excluded from the differential considerations.

## **TABLE OF CONTENTS/OUTLINE**

1. Introduction/Background 2. Multimodality (2D FFDM, 3D Tomo, US & MRI) Pictorial Review with Pathology Correlation & Management A) Invasive Ductal Carcinoma - NOS B) Medullary C) Mucinous D) Metaplastic E) Papillary 3. Take-home Points & Pearls/Pitfalls



# BR220-SD-SUA1

## Breast Density Classification and Follow-Up Decision Support System Using Deep Convolutional Models

Sunday, Nov. 25 12:30PM - 1:00PM Room: BR Community, Learning Center Station #1

#### **Participants**

Sun Young Park, San Diego, CA (*Presenter*) Nothing to Disclose Dustin Sargent, PhD, San Diego, CA (*Abstract Co-Author*) Nothing to Disclose Yoel Shoshan, Haifa, Israel (*Abstract Co-Author*) Employee, IBM Corporation David Richmond, Newton, MA (*Abstract Co-Author*) Senior Data Scientist, IBM Watson Health Ella Barkan, Haifa, Israel (*Abstract Co-Author*) Nothing to Disclose Simona Rabinovici-Cohen, Haifa, Israel (*Abstract Co-Author*) Employee, IBM Corporation Marwan Sati, PhD, Mississauga, ON (*Abstract Co-Author*) Employee, IBM Corporation

#### For information about this presentation, contact:

sypark@us.ibm.com

#### PURPOSE

This paper presents two new deep learning models that achieve objective breast density classification with high accuracy. The models are integrated into a system that automates BI-RADS breast density reporting and aids in making additional screening recommendations for normal patients.

#### METHOD AND MATERIALS

We have trained two deep learning models that provide objective, accurate, and repeatable breast density classification to address the issue of inter-physician variability. Our first deep learning model, used for automated BI-RADS breast density reporting, was trained using four breast density labels (A-almost entirely fatty, B-scattered fibroglandular density, C-heterogeneously dense, Dextremely dense). Our second model was trained to distinguish between the 'scattered density' and 'heterogeneously dense' classes to aid in diagnostic follow-up decisions according to ACR guidelines. That is, the second model is a two-class classifier, combining labels A and B, and labels C and D, into single classes. The two models were combined to produce an optimal follow-up decision. The networks were trained on a large dataset with pre-processing and data augmentation. Performance was evaluated with fivefold cross validation, and ROC analysis was performed.

#### RESULTS

Our models were trained on 6528 MG studies (26112 images) acquired between 2004 and 2016, each with four standard views (L-CC, R-CC, L-MLO, and R-MLO). The age range of the patients was 24-93 years, with an (A, B, C, D) distribution of (24%, 52%, 20%, 4%). The breast densities in the clinical reports were used as ground truth. Our two-class model achieves training and test AUCs of (0.98, 0.96), and our four-class model achieves per-class training and test AUCs of (0.98, 0.96), (0.92, 0.88), (0.92, 0.93), and (0.97, 0.96). These initial results outperform existing breast density classification algorithms.

## CONCLUSION

We report highly accurate breast density classification using deep learning models trained and evaluated on a large dataset of MG studies with a wide distribution of patient demographics. We are continuing this work with a multi-site clinical study and a comparison with inter-physician variance.

#### **CLINICAL RELEVANCE/APPLICATION**

We present a diagnostic aid system for automated classification and reporting of BI-RADS density. Breast density assessment is recommended by the ACR for proper assessment of breast cancer risk.



# BR221-SD-SUA2

Accuracy of the Nodal Staging in Breast Carcinoma Using 18F-FDG-PET/MRI, Comparison with Pathological Findings

Sunday, Nov. 25 12:30PM - 1:00PM Room: BR Community, Learning Center Station #2

# Participants

Eva Ferdova, MD, Plzen, Czech Republic (*Abstract Co-Author*) Nothing to Disclose Jiri Ferda, MD, PhD, Plzen, Czech Republic (*Presenter*) Nothing to Disclose Jan Baxa, MD, PhD, Plzen, Czech Republic (*Abstract Co-Author*) Nothing to Disclose Ilona Zednikova, Plzen, Czech Republic (*Abstract Co-Author*) Nothing to Disclose Ondrej Hes, MD, PhD, Plzen, Czech Republic (*Abstract Co-Author*) Nothing to Disclose

## For information about this presentation, contact:

ferda@fnplzen.cz

# PURPOSE

to evaluate the sensitivity, specificity, positive and negative predictive value of 18F-PET/MRI in the nodal staging of the breast carcinoma.

# METHOD AND MATERIALS

53 women (age 23-72) underwent the nodal staging of the breast carcinoma using 18F-FDG PET/MRI and all of them underwent surgery within two weeks with resection of the suspected lymph nodes including/or sentinel lymph node labeled by the99mTc-nannocolloid application. The examination was performed after intravenous application of 2.5 MBq/kg of 18F-FDG. PET/MRI examination consist of targeted breast imaging in prone position using dedicated 4-channel breast coil including the dynamic Gd-enhanced study after application of gadobutrol in the dose of 0.1 mmol/kg. The finding of PET/MRI was compared with the histological evaluation of the resected lymph nodes.

## RESULTS

In 31 women, the nodal status was N0, in 17 N1, in 2 N2 and in 3 N3 respectively. Using the histological evaluations, there were following findings: 20 true positive, 2 false negative, 22 true negative, 1 false positive lymph node staging. The sensitivity reached 0.91, specificity 0.97, positive predictive value 0.95, and negative predictive value 0.94, respectively.

#### CONCLUSION

Targeted 18F-FDG-PET/MRI in breast carcinoma enables the valuable assessment of nodal metastatic involvement with high sensitivity and specificity

# **CLINICAL RELEVANCE/APPLICATION**

To evaluate the sensitivity, specificity, positive and negative predictive value of 18F-PET/MRI in the nodal staging of the breast carcinoma



# BR222-SD-SUA3

Automated Volumetric Breast Density Estimation: A Comparison with Radiologists' Qualitative Classification

Sunday, Nov. 25 12:30PM - 1:00PM Room: BR Community, Learning Center Station #3

## Participants

Yuan Tian, Beijing, China (*Presenter*) Nothing to Disclose Jing Li, MD, PhD, Beijing, China (*Abstract Co-Author*) Nothing to Disclose Erni Li, MD, Beijing, China (*Abstract Co-Author*) Nothing to Disclose Zhang Renzhi, MD, Beijing, China (*Abstract Co-Author*) Nothing to Disclose Ning Guo, Beijing, China (*Abstract Co-Author*) Nothing to Disclose Shunan Che, MD, Beijing, China (*Abstract Co-Author*) Nothing to Disclose Chenglu Ke, Beijing, China (*Abstract Co-Author*) Nothing to Disclose Xiaohong R. Yang, Rockville, MD (*Abstract Co-Author*) Nothing to Disclose Gretchen Gierach, Bethesda, MD (*Abstract Co-Author*) Nothing to Disclose

#### For information about this presentation, contact:

tianyuanlaura@hotmail.com

# PURPOSE

The purpose of our study was to assess the agreement of automated volumetric mammographic breast density with the radiologists' classification by using the BI-RADS density category (5th edition), and to analyze the clinical-radiologic factors that may influence the discordance between the two density measurements.

#### **METHOD AND MATERIALS**

A total of 7971 full-field digital mammograms with standard views were retrospectively analyzed. Breast density measurements evaluated by radiologists according to BI-RADS category (5th edition) and by an automated volumetric breast density method (VBDM) which was used to measure VBD (% breast density) and VDG (density grade) were compared. A weighted kappa value was calculated to assess the degree of agreement among the visual and volumetric assessments of the density category and each subject was classified into an concordance or discordance group. A number of clinical-radiologic factors including age, history of breast surgery, indication for mammography, volumes of fibroglandular tissue or total breast and the percentage breast density were compared between the two groups.

#### RESULTS

The agreement between breast density evaluations by radiologists and VDG was fair (kappa = 0.346) when using the four-grade scale (A/B/C/D), and moderate (k value = 0.597) when using the two-grade scale (A-B/C-D). VBD showed a significant positive correlation with visual assessment by radiologist (Spearman's p=0.691, p < 0.01), but the distribution of density category was statistically significantly different among visual and volumetric measurements (p < 0.001). Category D was more frequently assigned by VBDM (43.9%) than by the radiologists (17.1%). Discordant subjects were more likely to be younger (p < 0.001), had undergone mammography for diagnostic purposes (p = 0.024), and have higher volumetric breast density (p < 0.001) compared with concordant subjects.

# CONCLUSION

More mammograms were classified as dense breast tissue using VBDM, as compared with visual assessments according to the BI-RADS fifth edition. And age, indication for mammography, and volumetric breast density may contribute to the differences between assessments by radiologists and by VBDM.

## **CLINICAL RELEVANCE/APPLICATION**

Considering the significant positive correlation between VBD and radiologists' classification, the automated method may be used in the future to evaluate the quantitative breast density data.



# BR223-SD-SUA4

# The Many Faces of Contrast Enhancing Benign Breast Lesions in Digital Mammography

Sunday, Nov. 25 12:30PM - 1:00PM Room: BR Community, Learning Center Station #4

## Participants

Eleni Gioutlaki, MD, Athens, Greece (*Presenter*) Nothing to Disclose Christos Tzimas, MD, Athens, Greece (*Abstract Co-Author*) Nothing to Disclose Christina Gkali, MD, Athens, Greece (*Abstract Co-Author*) Nothing to Disclose Sophia Papaioannou, Athens, Greece (*Abstract Co-Author*) Nothing to Disclose Eleni Feida, Athens, Greece (*Abstract Co-Author*) Nothing to Disclose Athanasios N. Chalazonitis, MD, MPH, Athens, Greece (*Abstract Co-Author*) Nothing to Disclose

#### PURPOSE

CEDM is a quite new breast imaging method commercially available for clinical use. The aim of this study was to compare the degree and type of enhancement of benign lesions with pathology results.

# **METHOD AND MATERIALS**

Evaluation of CEDM examination is based on enhancement intensity of the lesion according to a qualitative scale categorized in 4steps as follows:Type -1(negative enhancement),Type 0(no enhancement),Type 1(low enhancement),Type 2(intense enhancement).Type 0 and type -1 findings were considered to be probably benign, and type 1 and type 2 findings were considered to be probably malignant.Within 5 years,1979 females 28 to 85 years, with suspicious finding(s) in DM,U/S,MR,underwent CEDM.29 of these females had bilateral findings,so 2008 lesions were in total examined.

# RESULTS

Of the 2008 breast lesions in 1979 patients in this study, lesions 1363(67,8%)were benign. Among benign lesions, 23,2% presented as enhancement on CEDM. More specific, 317 out of 1363, had low or moderate enhancement on

CEDM(type1:171/317,type2:146/317).Also 978 benign lesions,had no enhancement on CEDM(type-1:74/978,type0:904/978).Moreover,68 cases were non-mass like lesions which were benign.Histopathologically,the 171 benign lesions with type 1 enhancement were:87 sclerosing adenosis,63 fibroadenomas,5 postoperative scar,3 ductal ectasia,1 paget disease,2 intramammary lymph node,5 inflammation,5 no specific findings.Concerning,the 146 lesions with type 2 enhancement,histological proof of benign was:64 sclerosing adenosis,63 fibroadenomas,3 intramammary lymph node,4 ductal ectasia,2 inflammation,2 abscess,8 no specific findings.According to our findings,the specificity of the method is76,7%.

# CONCLUSION

Fibroadenomas, and sclerosing adenosis, were more frequently characterized by moderate or medium enhancements on CEDM. It is very important to recognize the morphological features (as seen in DM) and hemodynamic patterns (as seen in CEDM) of benign lesions of the breast, in order to eliminate number of false positive enhancing lesions.

#### **CLINICAL RELEVANCE/APPLICATION**

The capability of CEDM is to depict tumor angiogenesis in breast cancer and have demonstrated contrast uptake in most malignant lesions independent of size as small as 1mm.Hence,CEDM may improve clinical decision making in breast cancer diagnosis.Breast biopsies in lesions which had type 0 or 1 enhancement(according to our recommendation)can be avoided,because these lesions are very likely to be benign.



## CA162-ED-SUA6

# A Primer on Echocardiography and Cardiac Angiography for the Cardiothoracic Radiologist

Sunday, Nov. 25 12:30PM - 1:00PM Room: CA Community, Learning Center Station #6

#### **Participants**

Kevin R. Kalisz, MD, Cleveland, OH (*Presenter*) Nothing to Disclose Robert C. Gilkeson, MD, Cleveland, OH (*Abstract Co-Author*) Research Consultant, Riverain Technologies, LLC; Research support, Koninklijke Philips NV; Research support, Siemens AG; Research support, General Electric Company Kianoush Ansari-Gilani, MD, Cleveland, OH (*Abstract Co-Author*) Nothing to Disclose

## For information about this presentation, contact:

k-kalisz@fsm.northwestern.edu

# **TEACHING POINTS**

The purpose of this exhibit is to: - Review the basic acquisition techniques, relevant anatomy, and views obtained at routine echocardiography and coronary angiography examinations - Illustrate different pathologies at echocardiography and angiography with cross-sectional cardiac imaging correlation - Evaluate the advantages and limitations of traditional cardiac imaging modalities compared to more advanced cross-sectional techniques

# TABLE OF CONTENTS/OUTLINE

1. Introduction 2. Overview of echocardiography (transthoracic and transesophageal) and coronary angiography Acquisition principles and techniques Standard views with illustration of relevant anatomy (with CTA and MRI correlation) 3. Examples of pathologies evaluated at traditional cardiac imaging modalities, each with cardiac CT and/or MRI correlation Echocardiography: Cardiomyopathies Valvular heart disease Cardiac masses and mass-like entities Pericardial disease Cardiac shunts Coronary angiography: Acquired coronary disease Aberrant coronary anatomy 4. Strengths and weaknesses of traditional and advanced imaging modalities in the assessment of the above pathologies



# CA163-ED-SUA7

# Cut the Mustard: A Pictorial Review of Post-Surgical Anatomy in the Repair of Conotruncal Abnormalities

Sunday, Nov. 25 12:30PM - 1:00PM Room: CA Community, Learning Center Station #7

#### **Participants**

Mary F. Hall, DO, Rochester, NY (*Abstract Co-Author*) Nothing to Disclose Katherine A. Kaproth-Joslin, MD, PhD, Rochester, NY (*Abstract Co-Author*) Nothing to Disclose Alexander Croake, MD, Rochester, NY (*Abstract Co-Author*) Nothing to Disclose Trinh T. Nguyen, DO, Rochester, NY (*Presenter*) Nothing to Disclose

# For information about this presentation, contact:

mary\_hall@urmc.rochester.edu

## **TEACHING POINTS**

1. The surgical repair of common conotruncal abnormalities is complex from both physiologic and imaging perspectives, requiring intimate knowledge of the goals of procedures. 2. Over the years, surgical techniques have been retooled, so as to improve upon common complications with classic surgical approaches. Many of these are radiologically evident. 3. As technique improves, so do patient outcomes, and a new population of patients who survived once-fatal congential abnormalities is emerging. 4. The radiologist must adapt to these changes, and find novel, safe, and effective ways to screen for and monitor such patients. The arsenal of cardiac MRI and CT are invaluable tools for such a task.

# TABLE OF CONTENTS/OUTLINE

1. Review historic and current surgical techniques in the treatment of common congenital conotruncal abnormalities. 2. Provide an image-rich spectrum of the expected postsurgical anatomy, as seen via cardiac MRI. 3. Review the appearance of common complications encountered with these procedures. 4. Demonstrate interpretive pitfalls. 5. Discuss future applications of cardiac MRI in pre and post surgical patients in this population.



## CA165-ED-SUA8

# **CAD-RADS™: Pushing the Limits**

Sunday, Nov. 25 12:30PM - 1:00PM Room: CA Community, Learning Center Station #8

## Awards Certificate of Merit Identified for RadioGraphics

#### **Participants**

Arzu Canan, Dallas, TX (*Abstract Co-Author*) Nothing to Disclose Praveen Ranganath, MD, Dallas, TX (*Abstract Co-Author*) Nothing to Disclose Harold Goerne, MD, Zapopan, Mexico (*Abstract Co-Author*) Nothing to Disclose Suhny Abbara, MD, Dallas, TX (*Abstract Co-Author*) Royalties, Reed Elsevier; Institutional research agreement, Koninklijke Philips NV; Institutional research agreement, Siemens AG Luis A. Landeras, MD, Chicago, IL (*Abstract Co-Author*) Nothing to Disclose Prabhakar Rajiah, MD, FRCR, Dallas, TX (*Presenter*) Nothing to Disclose

## For information about this presentation, contact:

radpr73@Gmail.com

# **TEACHING POINTS**

1. To review the CAD-RADS system 2. To illustrate the CT findings of different categories and modifiers of CAD-RADS 3. To illustrate common clinical situations with ambiguities in classification and management of findings

## TABLE OF CONTENTS/OUTLINE

1. Introduction 2. Background 3. Overview of CAD-RADS with illustrations - Categories- 0, 1, 2,3,4A, 4B, 5, N - Modifiers- S (Stent); G (Graft); V(Vulnerability); N (non-diagnostic) 4. Challenging situations with case illustrations a) Minimal/mild stenosis with non-diagnostic segments -Category N, not modifier N b) High grade stenosis in small vessels- CAD-RADs only for vessels > 1.5 mm c) High-risk anatomy considered into grading (2 vessels/left main with severe stenosis- 4B not 4A) d) LAD & LCX stenosis- 3-vessel equivalent in cath, but 2-vessel in CAD-RADS e) 2 high-risk plaque features in different coronary arteries - Not V f) Coronary artery bypass grafts- Grade/G g) Coronary artery bypass grafts- Stenosis in bypassed vessels is not classified h) Coronary artery stents-If non-evaluable N/S i) Coronary artery stents- If severe in-stent stenosis/occlusion- Grade 5/S j) Coronary artery anomalies k) Non-coronary cardiac or extra-cardiac findings I) Functional information- CT-FFR, CT-perfusion

#### **Honored Educators**

Presenters or authors on this event have been recognized as RSNA Honored Educators for participating in multiple qualifying educational activities. Honored Educators are invested in furthering the profession of radiology by delivering high-quality educational content in their field of study. Learn how you can become an honored educator by visiting the website at: https://www.rsna.org/Honored-Educator-Award/ Prabhakar Rajiah, MD, FRCR - 2014 Honored EducatorSuhny Abbara, MD - 2014 Honored EducatorSuhny Abbara, MD - 2017 Honored Educator



# CA200-SD-SUA1

Clinical and CT Angiographic Characteristics of Coronary Lesions that Later Progressed to Chronic Total Occlusion

Sunday, Nov. 25 12:30PM - 1:00PM Room: CA Community, Learning Center Station #1

**FDA** Discussions may include off-label uses.

#### Participants

Hee Jeong Park, MD, Seongnam, Korea, Republic Of (*Presenter*) Nothing to Disclose Eun Ju Chun, MD, PhD, Seongnam-Si, Korea, Republic Of (*Abstract Co-Author*) Nothing to Disclose Jeehoon Kang, Seongnam-si, Korea, Republic Of (*Abstract Co-Author*) Nothing to Disclose Jeong A Kim, MD, Goyangsi, Korea, Republic Of (*Abstract Co-Author*) Nothing to Disclose Jin Young Yoo, MD, Cheongju, Korea, Republic Of (*Abstract Co-Author*) Nothing to Disclose Young seok Cho, Seongnam, Korea, Republic Of (*Abstract Co-Author*) Nothing to Disclose

#### For information about this presentation, contact:

sadade31@daum.net

# PURPOSE

Since percutaneous coronary intervention (PCI) for chronic total occlusions (CTOs) is still challenging, estimating lesions that later progressed to CTOs are helpful. Thus, we aimed to investigate the clinical and coronary CT angiography (CCTA) characteristics that later progressed to CTO.

# **METHOD AND MATERIALS**

From 2006 to 2015 invasive coronary angiography (ICA) database, we retrospectively enrolled patients with at least 1 vessel disease with a severe stenosis (> 70% in luminal stenosis) confirmed by ICA who underwent prior CCTA more than 12 months before ICA. We reviewed medical chart for patient-level risk factors and analyzed CCTA findings (stenosis degree, lesion length, density, remodeling index and napkin-ring sign) for lesion-level risk factors. Adverse plaque characteristics (APCs) were defined as positive remodeling with >1.1 remodeling index, low attenuation with < 30 HU and napkin ring sign.

#### RESULTS

In a total of 216 patients (159 males, 65.8±10.2 years), 32 patients had a CTO lesion in ICA (CTO group) and 184 patients had stenosis with >70% without CTO (non-CTO group). There was no statistical difference of patient-level risk factor including age, sex and traditional clinical risk factors between CTO and non-CTO group. Comparing the lesion-level risk factors, CTO group had the higher ratio of severe stenosis (CTO vs. non-CTO group, 43.8% vs. 24.5%) and length with >2cm (31.2% vs. 12.5%), and more APCs (40.6% vs. 3.8%) (all p<0.05). In CTO groups, we compared lesion that later CTO (n=32) and the most-stenotic non-CTO lesion, later CTO lesion had longer plaque (15.4±10.8mm vs. 8.9±7.7mm), more stenotic diameter (1.02±0.74mm vs. 2.32±0.92mm), less calcified plaques (3.1% vs. 34.4%) and more APCs (83.3% vs. 43.8%) (all p<0.05).

#### CONCLUSION

Although no differences of patient-level risk factors between CTO and non-CTO groups, the lesion that later CTO had distinctive CCTA findings compared to lesions which did not progress to CTO.

# **CLINICAL RELEVANCE/APPLICATION**

From this retrospective analysis, CCTA might be helpful to predict CTOs in the case of the lesion with severe stenosis, long length with > 2 cm, and adverse plaque characteristics.



# CA201-SD-SUA2

# Prognostic Value of Normal Coronary Diagnosed Using Coronary CT on Long Time Follow up of 10 Years

Sunday, Nov. 25 12:30PM - 1:00PM Room: CA Community, Learning Center Station #2

### Participants

Satoru Shindo, RT, Kasugai, Japan (*Presenter*) Nothing to Disclose Masashi Hayakawa, Kasugai, Japan (*Abstract Co-Author*) Nothing to Disclose Ryosuke Kametani, MD,PhD, Kasugai, Japan (*Abstract Co-Author*) Nothing to Disclose Takayuki Suzuki, Kasugai, Japan (*Abstract Co-Author*) Nothing to Disclose Miyuki Ando, Kasugai-City, Japan (*Abstract Co-Author*) Nothing to Disclose Hidekazu Aoyama, Nagoya, AP (*Abstract Co-Author*) Nothing to Disclose

### PURPOSE

Long-term follow-up of coronary angiography (CCTA) is important. Cardiac events of normal coronary artery patients are expected to be rare. In CCTA, it is possible to identify a small amount of plaque even if it is positive remodeling. So we conducted a prognostic survey of patients diagnosed with normal coronary artery at CCTA 10 years ago.

#### **METHOD AND MATERIALS**

The subjects were 1474 consecutive patients who underwent CCTA from May 2007 to April 2008. Among them, 218 patients with normal coronary artery who can evaluate the coronary artery and do not recognize a small amount of plaque were followed. The CT device is Aquilion 64, coronary artery analysis was performed using Ziostation 2 with Slab MIP method.

#### RESULTS

The average age of 218 people is 60.51±12.25 years old, and 107 (49.1%) men. The survival rate of the patients who was able to follow up for 10 years was 88.07% (192 people), there was no coronary artery disease as a cause of the patient who died.

### CONCLUSION

Patients diagnosed with 'truly' normal coronary arteries by CCTA may have zero coronary events for 10 years.

### **CLINICAL RELEVANCE/APPLICATION**

Patients diagnosed with 'truly' normal coronary artery by CCTA at our hospital had zero coronary events for 10 years.



# CA202-SD-SUA3

Development and Validation of Generalized Linear Regression Models to Predict Vessel Enhancement on Coronary CT Angiography Scans

Sunday, Nov. 25 12:30PM - 1:00PM Room: CA Community, Learning Center Station #3

# Participants

Takanori Masuda, Hiroshima, Japan (*Presenter*) Nothing to Disclose Takeshi Nakaura, MD, Kumamoto, Japan (*Abstract Co-Author*) Nothing to Disclose Yoshinori Funama, PhD, Kumamoto, Japan (*Abstract Co-Author*) Nothing to Disclose Tomoyasu Sato, Hiroshima, Japan (*Abstract Co-Author*) Nothing to Disclose Yukie Kobayashi, Hiroshima, Japan (*Abstract Co-Author*) Nothing to Disclose Kazuo Awai, MD, Hiroshima, Japan (*Abstract Co-Author*) Nothing to Disclose Kazuo Awai, MD, Hiroshima, Japan (*Abstract Co-Author*) Research Grant, Canon Medical Systems Corporation; Research Grant, Hitachi, Ltd; Research Grant, Fujitsu Limited; Research Grant, Bayer AG; Research Grant, DAIICHI SANKYO Group; Research Grant, Eisai Co, Ltd; Medical Advisory Board, General Electric Company; ; Yoriaki Matsumoto, Hiroshima, Japan (*Abstract Co-Author*) Nothing to Disclose

#### For information about this presentation, contact:

takanorimasuda@yahoo.co.jp

#### PURPOSE

If contrast medium (CM) dose is adjusted based on the body size, or using contrast enhancement elicited by a test bolus, in some patients we observed poor or extremely high contrast enhancement. We investigated whether the generalized linear regression models (GLMs) using various patient characteristics and time density curve (TDC) factors of the test bolus facilitates the accurate prediction of contrast enhancement on coronary computed tomography angiography (c-CTA) images.

# METHOD AND MATERIALS

This prospective study received institutional review board approval; prior written informed consent to participate was obtained from all patients. We enrolled 222 patients who had undergone c-CTA under a total body weight (TBW)-tailored-, iodinated contrast medium (CM) protocol. We performed univariate and multivariate regression analysis to evaluate the effect of the patient age, sex, TBW, cardiac output (CO), and the peak time, and to compare contrast enhancement of the ascending aorta per gram of iodine (HU/gI) on test- and c-CTA scans ( $\Delta$ HU/gI). We developed GLMs to predict  $\Delta$ HU/gI at c-CTA. The GLMs using independent variables were validated with leave-one-out cross-validation using the correlation coefficient and Bland-Altman analysis.

#### RESULTS

Univariate linear regression analysis showed that all factors except the peak time on the test scan had a significant effect on  $\Delta$ HU/gI on c-CTA scans. However, by multivariate analysis, only TBW and  $\Delta$ HU/gI on the test scan maintained their independent predictive value (p < 0.01). By validation analysis, the GLM showed the highest correlation coefficient with the predictive values (r = 0.75), followed by  $\Delta$ HU/gI on the test scan (r = 0.69) and TBW (r = 0.63). It also revealed the lowest Bland-Altman limit of agreement with GLM (mean difference -0.0 HU/gI ± 5.0, 95% limit of agreement, -10.1 to 10.1 HU/gI), followed by  $\Delta$ HU/gI at c-CTA (-0.0 HU/gI ± 5.9, -11.9 to 11.9 HU/gI) and TBW (1.1 HU/gI ± 6.1, -11.1 to 13.3 HU/gI).

#### CONCLUSION

The patient TBW and  $\Delta$ HU/gI on the test scan significantly affected contrast enhancement of the ascending aorta on c-CTA images.

# **CLINICAL RELEVANCE/APPLICATION**

The combined use of clinical information and test scan results is a useful methods of predicting aortic enhancement.



# CA203-SD-SUA4

Prevalence and Clinical Sequalae of Non-Ischemic Myocardial Enhancement Detected on Delayed Enhancement Cardiac CT

Sunday, Nov. 25 12:30PM - 1:00PM Room: CA Community, Learning Center Station #4

# Participants

Ahmed H. Heussein, MD,MSc, Tsu, Japan (*Presenter*) Nothing to Disclose Kakuya Kitagawa, MD, PhD, Tsu, Japan (*Abstract Co-Author*) Nothing to Disclose Yoshitaka Goto, MD, Tsu, Japan (*Abstract Co-Author*) Nothing to Disclose Masafumi Takafuji, Tsu, Japan (*Abstract Co-Author*) Nothing to Disclose Satoshi Nakamura, MD, Tsu, Japan (*Abstract Co-Author*) Nothing to Disclose Hajime Sakuma, MD, Tsu, Japan (*Abstract Co-Author*) Nothing to Disclose Group; Research Grant, FUJIFILM Holdings Corporation; Research Grant, Siemens AG; Research Grant, Nihon Medi-Physics Co, Ltd; Speakers Bureau, Bayer AG

#### For information about this presentation, contact:

ahmed.hamdy@kasralainy.edu.eg

### PURPOSE

Myocardial fibrosis can be evaluated by using delayed enhancement CT (DE-CT) obtained following coronary CT angiography (CCTA). The purpose of this study is to investigate the prevalence of non-ischemic pattern of DE detected by DE-CT in patients referred for CCTA and the clinical sequelae following detection of non-ischemic DE.

### METHOD AND MATERIALS

Between January 2015 and January 2018, cardiac CT including acquisition of both CCTA and DE-CT was performed in 955 patients at our institution. DE-CT was evaluated by consensus of cardiovascular radiologists, and when detected, presence of non-ischemic DE (not confined to vascular distribution and/or not involving subendocardium) was notified to the referring physician through a radiology report. Clinical sequelae following detection and reporting of non-ischemic DE was gathered through a review of hospital records.

## RESULTS

Myocardial DE was detected in 286 of 955 subjects (29.9%) with non-ischemic DE in 53 subjects (5.5%). Of patients with nonischemic DE, 68% (36 of 53) were referred to cardiac CT for investigation of suspected coronary artery disease and the remaining 32% were referred for structural evaluation such as pre-radiofrequency ablation assessment in atrial fibrillation (n=6) and adult congenital heart disease (n=4). The most common etiology for the non-ischemic DE was HCM (n=17) followed by hypertensive heart disease (n=12), pulmonary hypertension (n=6) and dilated cardiomyopathy (n=5). Reporting of non-ischemic DE triggered further investigation using cardiac MRI (n=8), myocardial biopsy (n=4), and other tests. Late gadolinium enhancement MRI confirmed the presence of DE in all the patients referred for cardiac MRI after DE-CT and excellent agreement was found for presence or absence of non-ischemic fibrosis in segment-based analysis (kappa=0.829, p<0.001).

# CONCLUSION

Non-ischemic myocardial enhancement is frequently encountered on delayed enhancement cardiac CT and might necessitate further clinical workup in a significant fraction of the newly discovered cases.

# **CLINICAL RELEVANCE/APPLICATION**

Acquisition of delayed enhancement images on cardiac CT might be recommended as it might unveil unsuspected non-ischemic cardiomyopathy/fibrosis.



# CA204-SD-SUA5

Machine Learning Based CT-FFR Integrating With Quantitative Myocardial Mass Subtended By Coronary Stenosis Outperforms Plaque Features for Predicting Hemodynamical Significance of Lesions

Sunday, Nov. 25 12:30PM - 1:00PM Room: CA Community, Learning Center Station #5

#### Participants

Mengmeng Yu, MA, Shanghai, China (*Presenter*) Nothing to Disclose Jiayin Zhang, MD, Shanghai, China (*Abstract Co-Author*) Nothing to Disclose

For information about this presentation, contact:

radiologistmoon@163.com

# PURPOSE

To study the diagnostic performance of the ratio of subtended myocardial mass to the minimal lumen diameter (MLD) at coronary computed tomographic angiography (CCTA) and machine learning based CT-FFR for differentiating functionally significant from insignificant lesions, with reference to fractional flow reserve (FFR).

#### **METHOD AND MATERIALS**

Patients who underwent both coronary CTA and FFR measurement at invasive coronary angiography (ICA) within 2 weeks were retrospectively included in our study. CT-FFR, subtended myocardial mass (V sub), percentage of V sub, V ratio/MLD, along with other parameters, including minimal luminal area (MLA), MLD, lesion length (LL), diameter stenosis, area stenosis, plaque burden, and remodeling index, low attenuation plaque, napkin-ring sign, spotty calcification of lesions were recorded. Lesions with FFR <= 0.8 were considered to be functionally significant.

#### RESULTS

One hundred and seventy-two patients with 196 lesions were ultimately included for analysis. The LL, diameter stenosis, area stenosis, plaque burden, V sub, V ratio and V ratio/MLD were all significantly longer or larger in the group of FFR <= 0.8 (p < 0.001 for all), while smaller MLA, MLD and CT-FFR value were also noted (p < 0.001 for all). There were no significant differences between the hemodynamic significant subgroup and insignificant subgroup with respect to the risky plaque features. The area under the curve (AUC) of V ratio/MLD was comparable to that of CT-FFR (AUC=0.84 vs 0.88; p=0.28) and was significantly better than other parameters and for diagnosing functionally significant stenosis. For vessels with CT-FFR values below 0.70, 0.70 to 0.79, 0.80 to 0.89, and above 0.89, diagnostic accuracy of CT-FFR was 92.6%(25/27), 61.8%(34/55), 83.9%(47/56), 94.8%(55/58), respectively. For lesions with CT-FFR values ranging from 0.70 to 0.79, the accuracy could be improved to 80.0% (44/55) if these lesions were evaluated with Vratio/ MLD instead of CT-FFR.

# CONCLUSION

The "grey-zone" lesions, which have CT-FFR values ranging from 0.7 to 0.8, showed lower diagnostic performance. A stepwise approach, reserving Vratio/ MLD for "grey-zone" lesions instead of CT-FFR, can improve diagnostic accuracy.

# **CLINICAL RELEVANCE/APPLICATION**

integrating ML based CT-FFR and V ratio/MLD allowed the most accurate discrimination between flow-limiting and non flow-limiting coronary lesions.



### CH237-ED-SUA5

# **Tracheal Abnormalities on CT: A Pictorial Review**

Sunday, Nov. 25 12:30PM - 1:00PM Room: CH Community, Learning Center Station #5

#### **Participants**

Felipe Aluja, MD, Bogota, Colombia (*Presenter*) Nothing to Disclose Fernando R. Gutierrez, MD, Saint Louis, MO (*Abstract Co-Author*) Spouse, Stockholder, UnitedHealth Group Sanjeev Bhalla, MD, Saint Louis, MO (*Abstract Co-Author*) Nothing to Disclose Santiago E. Rossi, MD, Buenos Aires City, Argentina (*Abstract Co-Author*) Advisory Board, Boehringer Ingelheim GmbH; Speaker, Boehringer Ingelheim GmbH; Royalties, Springer Nature

# For information about this presentation, contact:

#### macario171@gmail.com

### **TEACHING POINTS**

'To recognize the different types of congenital and acquired tracheal abnormalities, their clinical characteristics and epidemiology.' Describe the imaging findings associated with the different tracheal abnormalities. 'Review the key elements in regard to the imaging diagnosis of the individual tracheal abnormalities, the findings on computed tomography and the key element for differential diagnosis 'Propose an approach to the differential diagnosis of the tracheal abnormalities

# TABLE OF CONTENTS/OUTLINE

Introduction General aspects of the tracheal abnormalities Shared clinical and imaging characteristics Individual approach to the tracheal abnormalities o Increased diameter: - Mounier Kuhn Syndrome - Tracheal diverticulum o Decreased diameter: - Focal: - Granulomatosis with poliangiitis (subglottic) - Sarcoidosis - Tracheal stenosis - Infection (subglottic) - Diffuse: - Tracheomalacia - Saber-Sheath trachea - Relapsing polychondritis - Tracheobronchopathy - Amyloidosis - Tracheobronhitis with ulcerative colitis - Tracheobronchopatia osteochondroplastica Approach to the differential diagnosis of tracheal abnormalities Conclusion

#### **Honored Educators**

Presenters or authors on this event have been recognized as RSNA Honored Educators for participating in multiple qualifying educational activities. Honored Educators are invested in furthering the profession of radiology by delivering high-quality educational content in their field of study. Learn how you can become an honored educator by visiting the website at: https://www.rsna.org/Honored-Educator-Award/ Sanjeev Bhalla, MD - 2014 Honored EducatorSanjeev Bhalla, MD - 2016 Honored EducatorSanjeev Bhalla, MD - 2017 Honored EducatorSanjeev Bhalla, MD - 2018 Honored EducatorSantiago E. Rossi, MD - 2015 Honored Educator



# CH238-ED-SUA6

# Hybrid (CT and MR) 3D Printing Models in Chest Tumors: How I Do It Step-By-Step

Sunday, Nov. 25 12:30PM - 1:00PM Room: CH Community, Learning Center Station #6

# Awards Certificate of Merit

# Participants

Jordi Broncano, MD, Cordoba, Spain (*Presenter*) Nothing to Disclose Antonio Alvarez-Kindelan, Cordoba, Spain (*Abstract Co-Author*) Nothing to Disclose Javier Alarcon Rodriguez, MD, Madrid, Spain (*Abstract Co-Author*) Nothing to Disclose Maria Luisa Sanchez-Alegre, MD, Madrid, Spain (*Abstract Co-Author*) Nothing to Disclose Carlos Simon-Adiego, Madrid, Spain (*Abstract Co-Author*) Nothing to Disclose Javier Sanchez, MD, PhD, Madrid, Spain (*Abstract Co-Author*) Nothing to Disclose Javier Sanchez, MD, PhD, Madrid, Spain (*Abstract Co-Author*) Nothing to Disclose Antonio Luna, MD, PhD, Jaen, Spain (*Abstract Co-Author*) Consultant, Bracco Group; Speaker, General Electric Company; Speaker, Canon Medical Systems Corporation; Royalties, Springer Nature

#### For information about this presentation, contact:

j.broncano.c@htime.org

# **TEACHING POINTS**

1. To review the principles of 3D printing, technical aspects, materials and printing procedures, segmentation tools and fusion algorithms for 3D segmentation in thoracic neoplasms. 2. To detail, in a cased - based approach, the steps necessary to do a pre - surgical 3D printing model combining magnetic resonance and computed tomography datasets. 3. To show our initial clinical results in the application of hybrid 3D printing prospectively for surgical planning of lung cancer and impact on the procedure.

### TABLE OF CONTENTS/OUTLINE

During the exhibit, the following learning points will be discussed and illustrated with real cases and pre-surgical models. The initial results of our clinical essay about the application of hybrid 3D printing in lung cancer will also be available: 1. 3D printing: definition and basic concepts 2. Current background in 3D pre - surgical 3D printing in chest neoplasms 3. CT acquisition and post - processing 4. MR acquisition and post - processing 5. Rigid and non-rigid algorithms for hybrid imaging 6. Mesh archive post-processing: Improving the printing 7. Practical cases database with surgical correlation 8. Clinical and surgical potential impact: Our results 9. Conclusion

### **Honored Educators**

Presenters or authors on this event have been recognized as RSNA Honored Educators for participating in multiple qualifying educational activities. Honored Educators are invested in furthering the profession of radiology by delivering high-quality educational content in their field of study. Learn how you can become an honored educator by visiting the website at: https://www.rsna.org/Honored-Educator-Award/ Antonio Luna, MD - 2018 Honored Educator



# CH256-SD-SUA1

Utility of Ultra High-Resolution CT in Quantitative Evaluation of Airway in Chronic Obstructive Pulmonary Disease (COPD) Using a QIBA Phantom

Sunday, Nov. 25 12:30PM - 1:00PM Room: CH Community, Learning Center Station #1

# Participants

Hidetake Yabuuchi, MD, Fukuoka, Japan (*Presenter*) Nothing to Disclose Takeshi Kamitani, MD, Fukuoka, Japan (*Abstract Co-Author*) Nothing to Disclose Masatoshi Kondo, Fukuoka, Japan (*Abstract Co-Author*) Nothing to Disclose Koji Sagiyama, MD, Fukuoka, Japan (*Abstract Co-Author*) Nothing to Disclose Yuzo Yamasaki, MD, Fukuoka, Japan (*Abstract Co-Author*) Nothing to Disclose Hiroshi Honda, MD, Fukuoka, Japan (*Abstract Co-Author*) Nothing to Disclose Takuya Hino, MD, Fukuoka, Japan (*Abstract Co-Author*) Nothing to Disclose

#### For information about this presentation, contact:

h-yabu@med.kyushu-u.ac.jp

# PURPOSE

Quantitative CT analysis of COPD patients has an important role in the classification of the subtype of COPD, assessing the disease severity and longitudinal changes, and therapeutic responses. Especially, airway analysis is essential for patients with small airway diseases; however, it is predisposed to the effect of image quality including special resolution and noise, and intra- and interobserver variability. Ultra high-resolution CT (UHRCT) with a small detector size of 0.25mm in 3-dimension has recently developed, and is available for a clinical use. Thus, the purpose of our study was to evaluate the utility of UHRCT in the quantitative evaluation of simulated chronic obstructive pulmonary disease (COPD) lesions using a phantom.

# METHOD AND MATERIALS

CT images of a COPD-simulated phantom (COPD Gene 2 Phantom) were obtained by a 320-detector raw CT using 3 types of detector size (normal, NR,  $0.5 \times 0.5 \times 0.5$ mm; high-resolution, HR,  $0.25 \times 0.25 \times 0.5$ mm; super-high-resolution, SHR,  $0.25 \times 0.25 \times 0.25$ mm). One emphysema lesion (CT value, -935HU) and 8 types of non-emphysematous lesions (bronchial wall, 0.4-1.5mm) were analyzed using a commercially available work station. We compared relative errors of wall thickness (WT) and wall area percent (WA%) among three modes (NR, HR, and SHR) using a multi-group comparison. A corrected P-value (0.167) was considered as statistically significant.

### RESULTS

There was no significant difference in the measurement of CT value among three modes. Relative error in the measurement of WT (1.82 - 40.0%) and WA% (0.21 - 23.9%) at SHR were significantly smaller than those at NR (WT, 6.53 - 150%; WA%, 0.79 - 67.6%). There was significantly smaller in relative errors in the measurement of WT and WA% at SHR (3-7%, 6-9%) compared with those of HR (5-15.8%, 6-14.2%) in only diagonally-arranged bronchus.

#### CONCLUSION

UHRCT seems to increase the accuracy in the quantitative airway wall analysis for non-emphysematous COPD lesions, especially in diagonally-running bronchus.

#### **CLINICAL RELEVANCE/APPLICATION**

Accurate airway wall analysis using UHRCT might lead to early detection or appropriate management of small airway diseases with accurate grading of disease severity.



# CH257-SD-SUA2

Electromagnetic Navigational Bronchoscopy (ENB) as an Emerging Diagnostic Tool: The Role of MDCT and the Relevance of the "CT Bronchus Sign"

Sunday, Nov. 25 12:30PM - 1:00PM Room: CH Community, Learning Center Station #2

# Participants

Rupert Berkeley, MBBS, BSc, London, United Kingdom (*Presenter*) Nothing to Disclose Dilan Patel, BSC,MBBS, London, United Kingdom (*Abstract Co-Author*) Nothing to Disclose Kelvin Lau, London, United Kingdom (*Abstract Co-Author*) Consultant, Medtronic plc; Grant, Koninklijke Philips NV; Stephen M. Ellis, MBBCh, FRCR, London, United Kingdom (*Abstract Co-Author*) Nothing to Disclose Emma K. Cheasty, MBChB, London, United Kingdom (*Abstract Co-Author*) Nothing to Disclose Zelena Aziz, London, United Kingdom (*Abstract Co-Author*) Nothing to Disclose Henrietta Wilson, London, AE (*Abstract Co-Author*) Nothing to Disclose Anu Balan, MBBS, MRCP, Cambridge, United Kingdom (*Abstract Co-Author*) Nothing to Disclose

#### For information about this presentation, contact:

Rupert.berkeley@bartshealth.nhs.uk

#### PURPOSE

Elucidate the role of the radiologist's report in planning CT for ENB and highlight the "CT bronchus sign" in predicting positive diagnostic samples.

#### **METHOD AND MATERIALS**

Retrospective analysis of 100 patients who underwent non-contrast CT prior to ENB over a 2 year period at a large tertiary centre for thoracic surgery. Data was acquired pertaining to site and appearance of the pulmonary lesion(s) of concern, presence/absence of an adjacent airway (CT bronchus sign), proximity to the nearest airway of those lesions without an adjacent bronchus and any change in size of the lesion(s) compared with the most recent cross sectional imaging. We assessed the adequacy of the histological sample and the rate of post-procedural chest radiography and complications.

#### RESULTS

100 patients who underwent planning CT studies for ENB were identified (46 male; 54 female; mean age 67.7; range 34 - 86). Of 104 target lesions (mean size 2.7 cm; range 0.6 -10.7 cm) the CT bronchus sign was positive in 82.7 %. Lesions without an adjacent airway were on average 13 mm from the adjacent airway (range 6 mm - 23 mm). 80.0 % of lesions were solid, the remainder subsolid, cavitating or atelectatic lobe. Compared with the most recent previous CT 4.8 % of lesions had decreased in size. In one case the lesion had resolved. 98 % of patients underwent ENB without additional intra-procedural imaging. 88 tissue and cytological samples were obtained, of which 88.6 % were diagnostically adequate. 44.9% had malignant histology, with 51.3 % benign and 3.8 % indeterminate. 93.3 % of lesions with a positive CT bronchus sign resulted in a diagnostically adequate sample, compared with 61.5 % of lesions without an adjacent airway. 97.0% of patients had a post-procedural chest radiograph. Postprocedural pneumothoraces occurred in 8.4 %.

# CONCLUSION

ENB is an emerging diagnostic tool with the potential to sample peripheral lesions with increased accuracy and lower complication rate. Our institutional experience is that 93.3 % of lesions with a positive 'CT bronchus sign' resulted in diagnostic samples. The role of the radiologist in aiding the pre-procedural work up is in identifying the 'CT bronchus sign' as well as any significant change in the lesion that might alter management.

# **CLINICAL RELEVANCE/APPLICATION**

This review provides the radiologist with a toolkit for reporting pre-procedural CT for ENB to aid the bronchoscopist in acquiring a positive diagnosis.



# CH258-SD-SUA3

# EGFR Exon19 and Exon21 Mutations Prediction by CT-Based Radiomics Features in Lung Adenocarcinom

Sunday, Nov. 25 12:30PM - 1:00PM Room: CH Community, Learning Center Station #3

#### **Participants**

Lin Tian, Wuhan, China (*Abstract Co-Author*) Employee, Ruijia Technology, Inc Rong Yuan, PhD, Shenzhen, China (*Abstract Co-Author*) Nothing to Disclose Qiguang Cheng, MD, Wuhan, China (*Abstract Co-Author*) Nothing to Disclose Quan Chen, Wuhan, China (*Presenter*) Nothing to Disclose

# For information about this presentation, contact:

lintian.usc@gmail.com

# PURPOSE

In this study, we try to identify a set of computed tomography(CT)-based radiomic features to predict epidermal growth factor receptor(EGFR) mutation status between EGFR exon 19 deletion(Ex19) and EGFR exon 21 L858R mutation (Ex21) in an Asian cohort of patients with lung adenocarcinoma.

# METHOD AND MATERIALS

This study investigated 130 patients with lung adenocarcinoma harboring Ex19 (n=56) and Ex21 (n=74). Total of 2300 radiomic features are extracted from original and filtered (Exponential, Laplacian of Gaussia, Logarithm, Gabor, Wavelet) 1.5mm CT images with annotation by two radiologists and one oncologist. These features are divided into four classes, including histogram, volumetric, morphologic, texture features. To identify the set of features which gives the best prediction on EGFR mutation status out of 2300 features, we used Random Forest (RF) algorithm to extract the importance of features and run backward elimination feature selection on the ordered feature list based on the importance. To generalize the result, ensemble technique is used to identify the final feature set. The capability to classify Ex19 and Ex21 of the selected feature set is evaluated by Lasso, Ridge, RF, SVC and KNN models.

### RESULTS

Seven features are selected as the set to predict EGFR mutation. It has reached best classification result (AUC 0.743±0.061) on KNN model and reached results of AUC 0.715, 0.736, 0.702, 0.710 respectively from Lasso, Random Forest, Ridge, SVC models with standard deviation 0.121, 0.061, 0.091, 0.110.

# CONCLUSION

We selected a set of radiomics features to predict EGFR mutation type. All of the features are from Wavelet and Gabor filtered image. It has shown the potential connection between EGFR mutation type and high-order deep features in CT image.

# CLINICAL RELEVANCE/APPLICATION

Various methods can be used to detect EGFR mutations, which are generally costly. This study reveals the possible non-invasive and convenient analysis to EGFR mutations in addition to clinical predictors.



## CH259-SD-SUA4

# Using Deep Learning to Predict Emphysema in Early Lung Cancer Screening Low-Dose CT Scan

Sunday, Nov. 25 12:30PM - 1:00PM Room: CH Community, Learning Center Station #4

#### **Participants**

John H. Lee, PhD, Chicago, IL (Presenter) Nothing to Disclose

Artit C. Jirapatnakul, PhD, New York, NY (Abstract Co-Author) Nothing to Disclose

Rowena Yip, MPH, New York, NY (Abstract Co-Author) Nothing to Disclose

Claudia I. Henschke, MD, PhD, New York, NY (Abstract Co-Author) Nothing to Disclose

David F. Yankelevitz, MD, New York, NY (Abstract Co-Author) Royalties, General Electric Company; Stockholder, Accumetra; Advisory Board, GRAIL

Maryellen L. Giger, PhD, Chicago, IL (*Abstract Co-Author*) Stockholder, Hologic, Inc; Shareholder, Quantitative Insights, Inc; Shareholder, QView Medical, Inc; Co-founder, Quantitative Insights, Inc; Royalties, Hologic, Inc; Royalties, General Electric Company; Royalties, MEDIAN Technologies; Royalties, Riverain Technologies, LLC; Royalties, Mitsubishi Corporation; Royalties, Canon Medical Systems Corporation

#### For information about this presentation, contact:

jhl33@uchicago.edu

#### PURPOSE

The patients who are recommended for annual lung cancer screening are at a higher risk for other cardiopulmonary diseases. Therefore, it would be beneficial to use the low-dose CT scans (LDCT) to identify other conditions. This work aims to demonstrate the feasibility of using deep learning method to identify findings, specifically emphysema.

#### **METHOD AND MATERIALS**

The dataset consists of 860 cases of LDCT scans from a lung screening program. Emphysema was identified on each scan as none, mild, moderate, or severe. To evaluate the effect of potential labeling error caused by per case rating system, three different approaches were taken: 1) using the entire lung region, 2) using only the top 50% of the lung since emphysema due to smoking tends to affect the upper lobes more than the lower lobes, and 3) using only the bottom 50% of the lung as a control. Deep learning consisted of feature extraction using a pre-trained VGG-19 network followed by a support vector machine binary classifier that predicted the presence of emphysema (none vs. moderate and severe). The predictions were first performed on a per slice basis and averaged to acquire per case prediction. The area under the receiver operating characteristic curve (AUC) was used to evaluate the performance.

#### RESULTS

Per slice prediction for the entire lung region, the top 50%, and the bottom 50% produced an AUC of 0.76 (SE: 0.01), 0.77 (0.01), and 0.74 (0.01), respectively. Per case prediction produced an AUC of 0.84 (0.03), 0.83 (0.03), and 0.80 (0.03). The higher AUCs for per case prediction demonstrates that aggregating the predictions on slices help reduce the effect of labeling errors. The AUCs for the bottom 50% are lower, but still on par, which is likely due to the fact emphysema does not completely spare the bottom lobes.

# CONCLUSION

We have demonstrated the potential of transfer learning to predict the presence of emphysema on LDCT scans. Fine-tuning work is currently on-going, and given the high performance already achieved with transfer learning, fine-tuning is likely to achieve even higher performance.

### **CLINICAL RELEVANCE/APPLICATION**

LDCT provides an opportunity to identify other pathologies that may otherwise go undiagnosed. Having a suite of algorithms that automatically searches for multiple incidental findings has the potential to increase efficiency and prevent missing important findings.



### ER158-ED-SUA5

# Pelvic Emergencies: The Role of MR Imaging in the Emergency Department

Sunday, Nov. 25 12:30PM - 1:00PM Room: ER Community, Learning Center Station #5

FDA

Discussions may include off-label uses.

#### Awards

**Identified for RadioGraphics** 

#### Participants

Gayatri Joshi, MD, Columbia, MO (*Presenter*) Nothing to Disclose Mohammad Elsayed, MD, Atlanta, GA (*Abstract Co-Author*) Nothing to Disclose Carrie N. Hoff, MD, Ann Arbor, MI (*Abstract Co-Author*) Nothing to Disclose Christine O. Menias, MD, Chicago, IL (*Abstract Co-Author*) Nothing to Disclose

# For information about this presentation, contact:

gayatri.joshi.md@gmail.com

#### **TEACHING POINTS**

Pelvic pain is a commonly presenting symptom in the Emergency Department (ED) and while ultrasound (US) or computed tomography (CT) are often the initial imaging exam, magnetic resonance (MR) imaging plays a vital role for specific populations (such as the pregnant patient) and in clinical scenarios in which diagnosis relies on the greater sensitivity provided by MR imaging. After reviewing this exhibit, learners should be able to: 1. Understand the role of MR imaging in the emergent setting 2. Proficiently recognize emergent pelvic disorders by MR imaging 3. Utilize best practices for diagnosing pelvic emergencies in the ED, including those of infectious, inflammatory, ischemic, obstructive, traumatic, & neoplastic etiologies

# TABLE OF CONTENTS/OUTLINE

This exhibit will: 1. Systematically illustrate the clinical and imaging features of pelvic emergencies that may present in the ED, particularly those of the MSK, vascular, GI & GU body systems. The spectrum of pelvic emergencies discussed in this exhibit will include those of infectious, inflammatory, ischemic, obstructive, traumatic, & neoplastic etiologies 2. Discuss best imaging practices of the acute pelvis in the ED, with pearls & pitfalls for optimizing efficient accurate diagnosis 3. Briefly address relevant management as applicable to the Radiologist to aid in expedient, appropriate management

#### **Honored Educators**

Presenters or authors on this event have been recognized as RSNA Honored Educators for participating in multiple qualifying educational activities. Honored Educators are invested in furthering the profession of radiology by delivering high-quality educational content in their field of study. Learn how you can become an honored educator by visiting the website at: https://www.rsna.org/Honored-Educator-Award/ Christine O. Menias, MD - 2013 Honored EducatorChristine O. Menias, MD - 2014 Honored EducatorChristine O. Menias, MD - 2015 Honored EducatorChristine O. Menias, MD - 2016 Honored EducatorChristine O. Menias, MD - 2018 Honored Educator



# ER201-SD-SUA2

# Utility of Ultrasound After a Negative CT in the Emergency Department - Does It Add Anything?

Sunday, Nov. 25 12:30PM - 1:00PM Room: ER Community, Learning Center Station #2

#### Participants

Varun Chowdhary, MD, BS, Staten Island, NY (*Presenter*) Nothing to Disclose Morris Hayim, MD, Franklin Square, NY (*Abstract Co-Author*) Nothing to Disclose Jonathan N. Stern, MD, Staten Island, NY (*Abstract Co-Author*) Nothing to Disclose

# For information about this presentation, contact:

jonathan.n.stern@gmail.com

### PURPOSE

The purpose of this study is to demonstrate the utility, or lack thereof, of an ultrasound performed within 24 hours after a negative CT abdomen and pelvis in the Emergency Department. Our secondary endpoint is length of stay in the Emergency Department and whether this time is affected by the additional testing.

# **METHOD AND MATERIALS**

We reviewed the imaging reports of 335 patients, over the course of 3 years in our Emergency Department, who had an ultrasound within 24 hours after a negative CT. A negative CT was defined as any CT that was either completely normal or did not have any acute findings. We then subdivided the patient population by location of pain, type of ultrasound, and whether the US showed any acute findings. We also evaluated length of stay in the Emergency Department, using 74 control matched patients with negative CT scans but no subsequent ultrasounds within 24 hours. We compared the duration of time spent in the Emergency Department between the two sets of patients.

#### RESULTS

From the 335 patients reviewed, only 8 patients had an acute finding on subsequent ultrasound (2%). Four of these were seen on abdominal ultrasound and 4 were seen on pelvic ultrasound (none of which were ovarian torsion). When stratified by type of ultrasound, the negative predictive value of a negative CT was 97% for abdominal ultrasound and 98% for pelvic ultrasound. The most common incidental findings on ultrasound not reported on CT were hemorrhagic cysts less than 2.5 cm (21 out of 42 incidental findings). Additionally, we found that the length of stay for patients who received both a CT and US was 119 minutes longer than those patients who received only a CT and was statistically significant (p < 0.001).

# CONCLUSION

From the results of this study, we can conclude that the additional US performed within 24 hours after a negative CT abdomen and pelvis only rarely supplies diagnostic information that changes management in the acute setting. Performing an additional US significantly increases the length of stay in the Emergency Department.

# **CLINICAL RELEVANCE/APPLICATION**

In a patient with a negative CT abdomen and pelvis in the Emergency Department, further evaluation with ultrasound within 24 hours rarely changes managment and may be unnecessary.



# ER202-SD-SUA3

Utility of Whole Survey Spine MRI in Blunt Trauma Patients Sustaining Single Level or Contiguous Spinal Fractures

Sunday, Nov. 25 12:30PM - 1:00PM Room: ER Community, Learning Center Station #3

# Participants

Aleksandr Rozenberg, MD, Philadelphia, PA (*Presenter*) Nothing to Disclose Kofi-Buaku Atsina, MD, Philadelphia, PA (*Abstract Co-Author*) Nothing to Disclose Santosh K. Selvarajan, MD, Philadelphia, PA (*Abstract Co-Author*) Nothing to Disclose

### PURPOSE

To determine the utility of obtaining whole-spine survey MRI after a full-spine CT diagnoses single level or contiguous fractures.

# METHOD AND MATERIALS

A retrospective search from 2015 to 2017 was performed using an institutional PACS database for consecutive patients who sustained spinal fractures from blunt injury. Only patients who received full-spine CT followed by whole-spine MRI were included in the study. All cases had sagittal T2-weighted imaging of the entire spine with additional T1 and T2-weighted axial imaging covering the known injury. Reports from the full-spine CTs were compared to the reports of the whole-spine MRI to determine if additional bony injury was identified on subsequent MRI. Patients with metastatic disease or neurological symptoms that were not explained by the affected level(s) found on CT were excluded from the study. Electronic medical records were reviewed to document the patient's age, sex, and mechanism of injury. All patients had both the CT and MRI interpretations performed by fellowship trained attending neuro-radiologists.

## RESULTS

A total of 158 patients met the inclusion criteria, with an average age of  $59.5 \pm 20.6$  years. 27 patients (17%) had a whole-spine MRI that demonstrated an additional bony injury. 92.5% of the additional injuries were characterized as osseous contusions or vertebral body compression fractures without significant loss of height. The distance between the original injury diagnosed on CT and the additional injury on MR ranged from 1 to 13 vertebrae. 44.4% of the additional injuries occurred within 1 to 4 vertebrae levels of the primary injury and 29.6% occurred within 5 to 8 vertebrae levels of the primary injury.

# CONCLUSION

A 17% rate of additional injury was identified on whole-spine survey MRI after full-spine CT diagnosed single level or contiguous fractures, most which were within 8 vertebrae levels of the original injury. The results suggest that if patients sustain single level or contiguous fractures, a targeted regional MRI is adequate for evaluation of the extent of injury.

# **CLINICAL RELEVANCE/APPLICATION**

Since most additional injuries identified on the survey MRI were minor and within 8 vertebrae levels of the primary site of injury, a targeted regional MRI may be adequate for evaluation of single level or contiguous spinal fractures.



# ER203-SD-SUA4

# The Impact of Socioeconomic Status on CT-Imaging and Management of Acute Appendicitis

Sunday, Nov. 25 12:30PM - 1:00PM Room: ER Community, Learning Center Station #4

#### Awards Student Travel Stipend Award

# Participants

Diana Dinh, MD, Boston, MA (Presenter) Nothing to Disclose Matthew Hartman, BS, Boston, MA (Abstract Co-Author) Nothing to Disclose Nicholas Wilson, MD , Boston, MA (Abstract Co-Author) Nothing to Disclose Nemil Shah, MD, Boston, MA (Abstract Co-Author) Nothing to Disclose Douglas Barnes, MS, Charlestown, MA (Abstract Co-Author) Nothing to Disclose Curtis Hon, Boston, MA (Abstract Co-Author) Nothing to Disclose Neha Khemani, Boston, MA (Abstract Co-Author) Nothing to Disclose Hyunjoong Kim, Boston, MA (Abstract Co-Author) Nothing to Disclose Claire Lis, BS, Boston, MA (Abstract Co-Author) Nothing to Disclose Stephen J. Raulli, BS, MS, Lexington, MA (Abstract Co-Author) Nothing to Disclose Christina A. Snyder, MS, BS, Boston, MA (Abstract Co-Author) Nothing to Disclose Brian Williams, BS, Boston, MA (Abstract Co-Author) Nothing to Disclose Alexandra Gero, MPH, Boston, MA (Abstract Co-Author) Nothing to Disclose Mustafa Qureshi, Boston, MA (Abstract Co-Author) Nothing to Disclose Heidi Wing, Boston, MA (Abstract Co-Author) Nothing to Disclose Tracey Dechert, MD, Boston, MA (Abstract Co-Author) Nothing to Disclose Stephan W. Anderson, MD, Cambridge, MA (Abstract Co-Author) Nothing to Disclose Christina A. LeBedis, MD, Boston, MA (Abstract Co-Author) Nothing to Disclose

#### PURPOSE

To assess the impact of socioeconomic status on CT findings and the management of acute appendicitis.

#### **METHOD AND MATERIALS**

Informed consent was waived for this IRB-approved, HIPAA compliant, retrospective study of 18-64 year old patients with acute appendicitis at our institution by MDCT from 1/1/2006-12/31/2016 (n=1886). Insurance, race/ethnicity, primary language, and education level were obtained from the electronic medical record. Multivariate linear regression was performed to determine crude and adjusted parameter estimates for length of stay. For each metric, the estimates generated from linear regression are interpreted as difference in length of stay associated with one unit change in each covariate. Logistic regression models were run and crude and adjusted odds ratio (OR) were calculated for each categorical outcome. A P value of less than 0.05 was considered statistically significant for all analyses. Statistical computations were performed on SAS 9.3 system (SAS Institute, Cary, NC).

### RESULTS

Free care/Medicaid/Medicare subjects had 0.4 days increase in length of stay as compared to private insurance (p=0.039). Free care/Medicaid/Medicare subjects were also found to have increase odds of surgical site infection or re-operation (OR=1.93, 95% CI= 1.03-3.63, p=0.041), as compared to private insurance patients. Hispanics were associated with lower odds of complicated CT findings (OR=0.55, 95% CI=0.335-0.898, p=0.017), and both Hispanic and Blacks had lower odds of perforation, abscess, or gangrene by intraoperative report (OR=0.67, 95% CI=0.47-0.97, p=0.035; OR=0.68, 95% CI=0.48-0.97, p=0.033, respectively), as compared to Whites. There were no statistically significant differences in CT findings, length of stay, or post-operative complication by primary language or education level.

#### CONCLUSION

Acute appendicitis is a common emergent illness presenting across the socioeconomic spectrum. Free care, Medicaid and Medicare patients have increased length of stay and increased odds of post-operative complication. Hispanics show lower odds of complicated CT findings on initial presentation. Hispanics and Blacks have lower odds of having complicated intraoperative findings.

# **CLINICAL RELEVANCE/APPLICATION**

Further investigation on the impact of socioeconomic status within radiology and the potential for radiologists to join the fight in combating health disparity are necessary to eliminate health inequality.

#### **Honored Educators**

Presenters or authors on this event have been recognized as RSNA Honored Educators for participating in multiple qualifying educational activities. Honored Educators are invested in furthering the profession of radiology by delivering high-quality educational content in their field of study. Learn how you can become an honored educator by visiting the website at: https://www.rsna.org/Honored-Educator-Award/ Stephan W. Anderson, MD - 2018 Honored Educator



### GI008-EB-SUA

A Pictorial Review of Xanthogranulomatous Inflammation of Various Organs in the Abdomen and Pelvis

Sunday, Nov. 25 12:30PM - 1:00PM Room: GI Community, Learning Center Hardcopy Backboard

FDA Discussions may include off-label uses.

#### **Participants**

Dal Mo Yang, Seoul, Korea, Republic Of (*Presenter*) Nothing to Disclose Hyun Cheol Kim, Seoul, Korea, Republic Of (*Abstract Co-Author*) Nothing to Disclose Sang Won Kim, MD, Seoul, Korea, Republic Of (*Abstract Co-Author*) Nothing to Disclose Jung Min Lee, MD, Seoul, Korea, Republic Of (*Abstract Co-Author*) Nothing to Disclose

#### For information about this presentation, contact:

dmy2988@daum.net

# **TEACHING POINTS**

To illustrate the imaging findings of the xanthogranulomatous inflammation of various organs in the abdomen and pelvis.

# TABLE OF CONTENTS/OUTLINE

Xanthogranulomatous inflammations are rare aggressive inflammatory conditions that can be caused by infection, inflammation, histiocytic process. The pathologic features of xanthogranulomatous inflammation are abundant lipid-laden macrophages or histiocytes. Xanthogranulomatous inflammations are usually seen in cholecystitis and pyelonephritis. But they have been reported involving the various organs in the abdomen and pelvis. A variety of imaging features were identified in xanthogranulomatous inflammation of various organs in the abdomen and pelvis. The xanthogranulomatous inflammation of various organs in the abdomen and pelvis. The xanthogranulomatous inflammation of various organs in the abdomen and pelvis. Xanthogranulomatous pyelonephritis, xanthogranulomatous peritonitis, xanthogranulomatous appendicitis, xanthogranulomatous inflammation of urachal cyst, xanthogranulomatous prostatitis and xanthogranulomatous salpingitis.



# GI276-ED-SUA7

# **MR Defecography and Beyond!**

Sunday, Nov. 25 12:30PM - 1:00PM Room: GI Community, Learning Center Station #7

#### **Participants**

Alexandra Roudenko, MD, New York, NY (*Presenter*) Nothing to Disclose Sara Lewis, MD, New York, NY (*Abstract Co-Author*) Nothing to Disclose Alexander C. Kagen, MD, New York, NY (*Abstract Co-Author*) Officer, Nines Inc Ally Rosen, MD, New York, NY (*Abstract Co-Author*) Nothing to Disclose Amita Kamath, MD, MPH, New York, NY (*Abstract Co-Author*) Nothing to Disclose

# For information about this presentation, contact:

sasha.roudenko@gmail.com

#### **TEACHING POINTS**

1. MR defecography (MRD) is increasingly becoming the diagnostic modality for both men and women in characterization of pelvic floor pathology, with a rising role for problem solving in patients with prior bowel surgery or atypical presentations. 2. MRD is easily implemented on 1.5 T MRI platforms with advantages over traditional methods of fluoroscopic defecography and cystography. 3. MRD often guides treatment and surgical planning, however, the use of standardized protocols and reporting templates are critical to minimize subjectivity, and provide standardized communication with referring clinicians. 4. Patients can have multi-compartment pathologic findings on MRD as well as incidental clinically insignificant and significant findings, which can complicate management.

### **TABLE OF CONTENTS/OUTLINE**

1. Review MR defecography (MRD) technique 2. Suggest systematic approach for evaluating pelvic floor cases on MRD a. What constitutes failed or incomplete MRD? b. Valsalva or no? 3. Review pathologic findings at MRD of each compartment a. Anterior b. Middle c. Posterior 4. Reporting of common, atypical, and challenging pelvic floor disorders (PFD) in both men and women a. Pelvic floor dyssynergy b. Anal spasm c. J pouch descent 5. Benign incidental findings a. Fibroids b. Ovarian cysts 6. Malignant incidental findings a. Endometrial cancer b. Rectal cancer



# GI277-ED-SUA8

The Role of Contrast Enhanced Ultrasound (CEUS) in the Assessment of Inflammatory Activity in Crohn's Disease

Sunday, Nov. 25 12:30PM - 1:00PM Room: GI Community, Learning Center Station #8

# Participants

Stephanie A. Nguyen, MD, Calgary, AB (*Presenter*) Nothing to Disclose Alexandra Medellin, MD, Calgary, AB (*Abstract Co-Author*) Nothing to Disclose Christine Merrill, Calgary, AB (*Abstract Co-Author*) Nothing to Disclose Alina Makoyeva, MD, Calgary, AB (*Abstract Co-Author*) Nothing to Disclose Stephanie R. Wilson, MD, Calgary, AB (*Abstract Co-Author*) Equipment support, Koninklijke Philips NV; Equipment support, Siemens AG; Equipment support, Samsung Electronics Co, Ltd; Research support, Koninklijke Philips NV; Research support, Lantheus Medical Imaging, Inc; Speaker, Samsung Electronics Co, Ltd

#### For information about this presentation, contact:

stephanie.wilson@ahs.ca

# **TEACHING POINTS**

CEUS is a valuable adjunct to greyscale and color Doppler for determination of disease activity in those with Crohn's disease Transmural enhancement of the bowel wall and a comb sign, reflective of neoangiogenesis, comprise the subjective features of activity shown on CEUS Generation of a time intensity curve with measurement of the peak enhancement (PE), the area under the curve (AUC) and the time to peak (TTP) comprise the most valuable objective parameters for disease activity determination and response to therapy CEUS effectively resolves indeterminate greyscale bowel assessment in those with thick bowel wall on baseline and no corresponding signal on color Doppler by accurately showing the degree of mural vascularity CEUS and point shear wave elastography (pSWE) are effective biomarkers for predicting the nature of strictures by distinguishing inflammatory from chronic disease

# TABLE OF CONTENTS/OUTLINE

Crohn's disease activity assessment. Why CEUS? Applications of CEUS in CD: inflammatory activity assessment, response to therapy, resolution of indeterminate cases and characterization of strictures Time intensity curve (TIC) creation, analysis, interpretation and reporting for IBD activity assessment Additional applications of CEUS in Crohn's disease Challenges and future directions



# GI278-ED-SUA9

# Bile out of the Bag: Imaging of Biliary Fistulas

Sunday, Nov. 25 12:30PM - 1:00PM Room: GI Community, Learning Center Station #9

## Awards Certificate of Merit

# Participants

Jordan LeGout, MD, Jacksonville, FL (*Presenter*) Nothing to Disclose Vanessa Lewis, MD, Mission Hills, KS (*Abstract Co-Author*) Nothing to Disclose Jacob Lewis, MD, Jacksonville, FL (*Abstract Co-Author*) Nothing to Disclose Lauren F. Alexander, MD, Jacksonville, FL (*Abstract Co-Author*) Spouse, Stockholder, Abbott Laboratories; Spouse, Stockholder, AbbVie Inc; Spouse, Stockholder, General Electric Company Andrew Bowman, MD, PhD, Jacksonville, FL (*Abstract Co-Author*) Nothing to Disclose Candice W. Bolan, MD, Jacksonville, FL (*Abstract Co-Author*) Nothing to Disclose

# For information about this presentation, contact:

LeGout.Jordan@mayo.edu

# **TEACHING POINTS**

1. To review the causes, types, and imaging appearance of biliary fistulas 2. Review appearance on different imaging modalities and provide tips and case examples for modality selection 3. Review associated complications and treatments

### **TABLE OF CONTENTS/OUTLINE**

1. Introduction Incidence/demographics Causes 2. Imaging Appearance with Case Based Examples Ultrasound CT MRI Problem solving methods: Eovist MRI, HIDA, cholangiography, sinogram 3. Complications/Associations Gallstone ileus Abscess Space Contamination (i.e. pleura, peritoneum) 4. Treatment 5. Summary



# GI279-ED-SUA10

# Clinical Implementation of Dual-Energy CT for Bowel Disease: It's Time to Embrace the Change

Sunday, Nov. 25 12:30PM - 1:00PM Room: GI Community, Learning Center Station #10

### Awards Certificate of Merit

# Participants

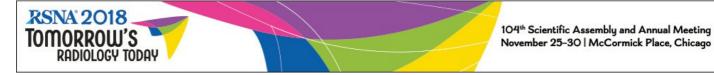
Narumi Taguchi, Kumamoto, Japan (*Presenter*) Nothing to Disclose Seitaro Oda, MD, Kumamoto, Japan (*Abstract Co-Author*) Nothing to Disclose Masanori Imuta, MD, Kumamoto, Japan (*Abstract Co-Author*) Nothing to Disclose Yasuhiro Yokota, Kumamoto, Japan (*Abstract Co-Author*) Nothing to Disclose Takeshi Nakaura, MD, Kumamoto, Japan (*Abstract Co-Author*) Nothing to Disclose Daisuke Utsunomiya, MD, Kumamoto, Japan (*Abstract Co-Author*) Nothing to Disclose Yasunori Nagayama, MD, Kumamoto, Japan (*Abstract Co-Author*) Nothing to Disclose Yoshinori Funama, PhD, Kumamoto, Japan (*Abstract Co-Author*) Nothing to Disclose Tadatoshi Tsuchigame, MD, Kumamoto, Japan (*Abstract Co-Author*) Nothing to Disclose Yasuyuki Yamashita, MD, Kumamoto, Japan (*Abstract Co-Author*) Nothing to Disclose

# **TEACHING POINTS**

1.Dual-energy CT allows the differentiation of materials on the basis of their energy-related attenuation characteristics and to generate dedicated spectral images including virtual monochromatic and material composition images. 2.Using advanced dual-energy imaging a more precise diagnosis can be obtained, and might hold promising potential as an imaging biomarker, risk-stratification, monitoring of disease progression and therapy, and outcome prediction. 3.The clinical utility of dual-energy CT for bowel disease are discussed through this presentation. 4.Familiarity with the capabilities of dual-energy CT can help radiologists to improve their diagnostic performance.

# **TABLE OF CONTENTS/OUTLINE**

1. What we can do with dual-energy CT -Virtual monochromatic imaging -Virtual non-contrast enhanced imaging -Iodine density map -Effective atomic number 2. Application for gastrointestinal tumors -Tumor detection -Assessment of the malignant potential, tumor differentiation grades, and genetic status -Assessment of lymph node metastases -Evaluating response to treatment 3. Application for CT enterography -Identifying active inflammation and fibrosis in Crohn's disease 4. Application for CT colonography -Electronic cleansing in fecal-tagging 5. Application for gastrointestinal emergencies -Small bowel ischemia -Gastrointestinal bleeding 6. Future directions



# GI280-ED-SUA6

Gastrointestinal Adverse Effects Related to Cancer Immunotherapy and Targeted Therapy: A New Challenge in Advanced Oncology

Sunday, Nov. 25 12:30PM - 1:00PM Room: GI Community, Learning Center Station #6

#### Awards Certificate of Merit

#### **Participants**

Natalia B. Gomes, Sao Paulo, Brazil (*Presenter*) Nothing to Disclose Douglas J. Racy, MD, Sao Paulo, Brazil (*Abstract Co-Author*) Nothing to Disclose Bruna B. Libanio, MD, Sao Paulo, Brazil (*Abstract Co-Author*) Nothing to Disclose Barbara P. Matos, MD, Sao Paulo, Brazil (*Abstract Co-Author*) Nothing to Disclose Marilia P. Ferreira, MD, Sao Paulo, Brazil (*Abstract Co-Author*) Nothing to Disclose Jose d. Fernandes SR, Sao Paulo, Brazil (*Abstract Co-Author*) Nothing to Disclose Graziela C. Oliveira, MD, Sao Paulo, Brazil (*Abstract Co-Author*) Nothing to Disclose Carolina P. Abud, MD, Sao Paulo, Brazil (*Abstract Co-Author*) Nothing to Disclose Kamila S. Albuquerque, Sao Paulo, Brazil (*Abstract Co-Author*) Nothing to Disclose

For information about this presentation, contact:

nataliaborgesnunes@gmail.com

# **TEACHING POINTS**

A new approach for cataloging adverse effects from cancer immunotherapy and targeted therapy has been proposed in a new conceptual framework that incorporates molecular mechanisms and associated clinical outcomes. It allows radiologists to more effectively recognize adverse effects and differentiate them from tumor progression, and can therefore more effectively guide oncologists in the management of adverse effects and treatment decisions.

#### TABLE OF CONTENTS/OUTLINE

This exposition addresses radiographic feature of adverse effects focuses on molecular mechanisms and illustrates with images of classic examples. Adverse effects were classified into four categories: (a) Category 1, On-target adverse effects associated with treatment response (Ipilimumab and Pembrolizumab - Colitis; Nivolumab - Sarcoidlike lymphadenopathy); (b) Category 2, On-target adverse effects without associated treatment response (Bevacizumab - Enteritis, Proctitis, Pneumatosis intestinalis, Mesenteric emphysema, Anastomotic Dehiscence, Bowel perforation; Imatinib - Splenic Rupture, Pancreatitis); (c) Category 3, Off-target adverse effects (Ipilimumab and Nivolumab - Fluid retention; Trastuzumab - Steatosis); and (d) Category 4, Tumor necrosis-related adverse effects (Imatinib - Intratumoral Hemorrhage; Sunitinib - Hemoperitoneum).



### GI289-ED-SUA11

Bowel/Mesenteric Vascular Lesions: Multi-Modality Imaging Evaluation

### Participants

Ayman H. Gaballah, MD, FRCR, Columbia, MO (Abstract Co-Author) Nothing to Disclose Aws S. Hamid, MD, Columbia, MO (Presenter) Nothing to Disclose Amr S. Abdelaziz, MD, Birmingham, AL (Abstract Co-Author) Nothing to Disclose Christine O. Menias, MD, Chicago, IL (Abstract Co-Author) Nothing to Disclose Akram M. Shaaban, MBBCh, Salt Lake City, UT (Abstract Co-Author) Contributor, Reed Elsevier; Author, Reed Elsevier Peter S. Liu, MD, Solon, OH (Abstract Co-Author) Nothing to Disclose Khaled M. Elsayes, MD, Ann Arbor, MI (Abstract Co-Author) Nothing to Disclose

#### **TEACHING POINTS**

1- Review etiology of bowel/mesenteric vascular lesions 2- Describe multimodality imaging appearances of bowel/mesenteric vascular lesions 3- Discuss complications and management options of the bowel/mesenteric vascular lesions

#### **TABLE OF CONTENTS/OUTLINE**

TABLE OF CONTENTS/OUTLINE 1- Introduction 2- Etiology of bowel/mesenteric vascular lesions 3- Multimodality imaging findings and case presentation: a. Angiodysplasias b. Arteriovenous malformations (AVMs) and fistulas (AVFs) c. Aorto-enteric fistula d. Mesenteric arterial thrombosis and aneurysms e. Mesenteric venous thrombosis f. Mesenteric vascular injury g. Venous angiomas h. Bowel varices i. Bowel hemangioma j. Active gastro-intestinal bleeding k. Bowel intramural/mesenteric hematomas 4- Complications and management 5- Impact of imaging findings on management 6- Summary & Conclusion

#### Honored Educators

Presenters or authors on this event have been recognized as RSNA Honored Educators for participating in multiple qualifying educational activities. Honored Educators are invested in furthering the profession of radiology by delivering high-guality educational content in their field of study. Learn how you can become an honored educator by visiting the website at: https://www.rsna.org/Honored-Educator-Award/ Christine O. Menias, MD - 2013 Honored EducatorChristine O. Menias, MD - 2014 Honored EducatorChristine O. Menias, MD - 2015 Honored EducatorChristine O. Menias, MD - 2016 Honored EducatorChristine O. Menias, MD - 2017 Honored EducatorChristine O. Menias, MD - 2018 Honored EducatorAkram M. Shaaban, MBBCh - 2015 Honored EducatorAkram M. Shaaban, MBBCh - 2016 Honored EducatorAkram M. Shaaban, MBBCh - 2017 Honored EducatorAkram M. Shaaban, MBBCh - 2018 Honored EducatorKhaled M. Elsayes, MD - 2014 Honored EducatorKhaled M. Elsayes, MD - 2017 Honored EducatorKhaled M. Elsayes, MD - 2018 Honored Educator



# GI290-ED-SUA12

### 3D Printing Applications for Abdominal and Genitourinary Imaging: Anatomic Models and Beyond

Sunday, Nov. 25 12:30PM - 1:00PM Room: GI Community, Learning Center Station #12

FDA Discussions may include off-label uses.

#### Participants

David H. Ballard, MD, Ballwin, MO (*Presenter*) Nothing to Disclose Nicole Wake, PhD, New York, NY (*Abstract Co-Author*) In-kind support, Stratasys, Ltd Beth A. Ripley, MD, PhD, Seattle, WA (*Abstract Co-Author*) Nothing to Disclose Leonid Chepelev, MD, PhD, Ottawa, ON (*Abstract Co-Author*) Nothing to Disclose Waleed M. Althobaity, MD, Ottawa, ON (*Abstract Co-Author*) Nothing to Disclose Uday Jammalamadaka, St Louis, MO (*Abstract Co-Author*) Nothing to Disclose Karthik Tappa, St Louis, MO (*Abstract Co-Author*) Nothing to Disclose Muhammad Naeem, MBBS, Saint Louis, MO (*Abstract Co-Author*) Nothing to Disclose Joseph E. Ippolito, MD, PhD, Saint Louis, MO (*Abstract Co-Author*) Nothing to Disclose Frank J. Rybicki III, MD, PhD, Ottawa, ON (*Abstract Co-Author*) Medical Director, Imagia Cybernetics Inc Adnan M. Sheikh, MD, Ottawa, ON (*Abstract Co-Author*) Nothing to Disclose

#### For information about this presentation, contact:

davidballard@wustl.edu

#### **TEACHING POINTS**

Understand the workflow of 3D printing abdominal, gastrointestinal, and genitourinary anatomic models for preoperative planning Recognize the potential of 3D printing molds for pathologic sectioning Identify relevant 3D printed abdominopelvic prosthetics and implants Summarize the current status of bioprinting and bioactive printing

# TABLE OF CONTENTS/OUTLINE

Brief overview of 3D printing process from image acquisition to model fabrication Optimizing imaging protocols, image reconstructions to facilitate the 3D segmentation process. Preparation of the model, including sterilization techniques for surgical guides and implants Case based illustration of different 3D printed anatomic models for abdominal, gastrointestinal, and genitourinary applications Overview, examples, and how-to guide of creating molds for pathologic sectioning from cross-sectional imaging, using prostate MRI and multiphase CT as examples Prosthetics and implants for body applications - present scope of practice and potential applications Bioprinting and bioactive printing in body implications, including fabricating tissue and the future potential for transplantation

# **Honored Educators**

Presenters or authors on this event have been recognized as RSNA Honored Educators for participating in multiple qualifying educational activities. Honored Educators are invested in furthering the profession of radiology by delivering high-quality educational content in their field of study. Learn how you can become an honored educator by visiting the website at: https://www.rsna.org/Honored-Educator-Award/ Frank J. Rybicki III, MD, PhD - 2016 Honored Educator



### GI291-ED-SUA2

# Pitfalls in the Diagnosis of Hepatocellular Carcinoma: User Errors in Applying LI-RADS v 2017

Sunday, Nov. 25 12:30PM - 1:00PM Room: GI Community, Learning Center Station #2

#### Awards Certificate of Merit

# Participants

Khaled M. Elsayes, MD, Ann Arbor, MI (Presenter) Nothing to Disclose

Alessandro Furlan, MD, Pittsburgh, PA (*Abstract Co-Author*) Book contract, Reed Elsevier; Research Grant, General Electric Company; Consultant, General Electric Company

Victoria Chernyak, MD, MS, Bronx, NY (Abstract Co-Author) Nothing to Disclose

Kathryn J. Fowler, MD, San Diego, CA (Abstract Co-Author) Nothing to Disclose

An Tang, MD, Montreal, QC (Abstract Co-Author) Research Consultant, Imagia Cybernetics Inc; Speaker, Siemens AG; Speaker, Eli Lilly and Company

Mustafa R. Bashir, MD, Cary, NC (*Abstract Co-Author*) Research Grant, Siemens AG; Research Grant, General Electric Company; Research Grant, NGM Biopharmaceuticals, Inc; Research Grant, TaiwanJ Pharmaceuticals Co, Ltd; Research Grant, Madrigal Pharmaceuticals, Inc; Research Consultant, RadMD

Mohab Elmohr, MD, Houston, TX (Abstract Co-Author) Nothing to Disclose

Ania Z. Kielar, MD, Shanty Bay, ON (Abstract Co-Author) Research Grant, General Electric Company

Elizabeth M. Hecht, MD, New York, NY (Abstract Co-Author) Nothing to Disclose

Claude B. Sirlin, MD, San Diego, CA (*Abstract Co-Author*) Research Grant, Gilead Sciences, Inc; Research Grant, General Electric Company; Research Grant, Siemens AG; Research Grant, Bayer AG; Research Grant, ACR Innovation; Research Grant, Koninklijke Philips NV; Research Grant, Celgene Corporation; Consultant, General Electric Company; Consultant, Bayer AG; Consultant, Boehringer Ingelheim GmbH; Consultant, AMRA AB; Consultant, Fulcrum Therapeutics; Consultant, IBM Corporation; Consultant, Exact Sciences Corporation; Advisory Board, AMRA AB; Advisory Board, Guerbet SA; Advisory Board, VirtualScopics, Inc; Speakers Bureau, General Electric Company; Author, Medscape, LLC; Author, Resoundant, Inc; Lab service agreement, Gilead Sciences, Inc; Lab service agreement, ICON plc; Lab service agreement, Intercept Pharmaceuticals, Inc; Lab service agreement, Shire plc; Lab service agreement, Takeda Pharmaceutical Company Limited; Lab service agreement, sanofi-aventis Group; Lab service agreement, Johnson & Johnson; Lab service agreement, NuSirt Biopharma, Inc; Contract, Epigenomics; Contract, Arterys Inc

### For information about this presentation, contact:

kmelsayes@mdanderson.org

### **TEACHING POINTS**

1) Review updated guidelines for LI-RADS v2017 2) Illustrate common and uncommon pitfalls that could result from erroneous application of LI-RADS 3) Describe scenarios where LI-RADS is not used in the appropriate patient population 4) Review examples where LI-RADS terminology is used incorrectly 5) Provide instances of incorrect assumptions about LI-RADS requirements

### TABLE OF CONTENTS/OUTLINE

1) Overview of LI-RADS history and version 2017 2) Potential errors resulting from using LI-RADS in an improper patient population. This includes providing LI-RADS categories in conditions that are not included in the target population. 3) Misdiagnoses resulting from lack of knowledge of technical guidelines. An example includes misinterpreting an area of hypointensity on the hepatobiliary phase (pseudo-washout) as true "washout" (which is a major feature for diagnosing HCC using LI-RADS). Incorrect assumptions about LI-RADS requirements. For example -The assumption that 'washout' requires arterial phase hyperenhancement (APHE) - Assuming that tumor in a vein requires APHE and washout - Misinterpreting arterial enhancement in an observation that is of high signal intensity on T1 weighted images. 5) Misinterpreting bland thrombus as tumor in vein (TIV) 6) Summary of key teaching points

#### **Honored Educators**

Presenters or authors on this event have been recognized as RSNA Honored Educators for participating in multiple qualifying educational activities. Honored Educators are invested in furthering the profession of radiology by delivering high-quality educational content in their field of study. Learn how you can become an honored educator by visiting the website at: https://www.rsna.org/Honored-Educator-Award/ Khaled M. Elsayes, MD - 2014 Honored EducatorKhaled M. Elsayes, MD - 2017 Honored EducatorKhaled M. Elsayes, MD - 2018 Honored EducatorAnia Z. Kielar, MD - 2017 Honored Educator



# GI328-SD-SUA1

Assessment of Diagnostic Imaging Quality of Hepatocellular Carcinoma from Non-Teaching Community Hospitals and Tertiary Referral Center

Sunday, Nov. 25 12:30PM - 1:00PM Room: GI Community, Learning Center Station #1

# Awards

# Student Travel Stipend Award

#### **Participants**

Andrew Chan, MD, Toronto, ON (*Presenter*) Nothing to Disclose Madeleine Sertic, MBBCh, Toronto, ON (*Abstract Co-Author*) Nothing to Disclose Jennifer Sammon, MBBCh, Toronto, ON (*Abstract Co-Author*) Nothing to Disclose Tae Kyoung Kim, MD, PhD, Toronto, ON (*Abstract Co-Author*) Nothing to Disclose Hyun-Jung Jang, MD, Toronto, ON (*Abstract Co-Author*) Nothing to Disclose Luis S. Guimaraes, MD, Toronto, ON (*Abstract Co-Author*) Nothing to Disclose Martin E. O'Malley, MD, Toronto, ON (*Abstract Co-Author*) Nothing to Disclose Korosh Khalili, MD, Toronto, ON (*Abstract Co-Author*) Nothing to Disclose

# For information about this presentation, contact:

AndrewJ.Chan@mail.utoronto.ca

# PURPOSE

To assess guideline compliance & quality of diagnostic imaging of hepatocellular carcinoma (HCC) within community hospitals (CH) and tertiary referral center (TRC) in a moderately high incidence region.

# METHOD AND MATERIALS

All phases/sequences of Initial diagnostic workup CT or MRI scans of a prospective cohort of 155 patients (95 CH, 60 TRC) with HCC in a 6 month period were recorded to assess LIRAD guideline compliance. 120 of the scans were qualitatively rated by 2 independent blinded radiologists for arterial timing (scale 1-3), overall image quality (scale 1-5), noise (1-5) and blur (1-5). CT scans (52 CH, 53 TRC) were quantitatively assessed using ROI HU attenuation of the dominant HCC pre & post contrast. Standard deviation (SD) of background liver was used as measure of noise. MRI quantitative analysis was not performed due to small TRC sample (n=7).

### RESULTS

All 105 CTs had arterial and venous phases. 43/52 (83%) CH & 52/53 (98%) TRC CTs had a precontrast phase (p=0.004). 32/52 (62%) CH & 53/53 (100%) TRC CTs had a delayed phase (p <0.0001). All 50 MRIs had 4 contrast phases. 29/43 (67%) CH & 7/7 TRC MRIs had DWI sequence (p=0.2). Overall image quality (mean rating 3.28 CH vs 3.85 TRC, p = 0.002) and noise (mean 2.39 C vs 2.97 TRC, p=0006) but not blur were rated significantly better for TRC. Arterial phase timing was correct for 14/66 (21%) CH and 28/39 (72%) TRC scans (p < 0.0001). Quantitative assessment of CTs showed lower mean arterial phase rise in CH than in TRC (31.9 vs 65.4 HU p<0.0001) but also lower noise (SD 13.0 vs 16.1 HU p=0.0006).

#### CONCLUSION

Community hospital HCC diagnostic scans significantly lag in critical quality parameters of arterial phase timing, overall image quality, perceived noise and inclusion of CT delayed phase when compared to a tertiary referral center.

# **CLINICAL RELEVANCE/APPLICATION**

Key aspects of HCC imaging technique have not penetrated community practice despite a decade of standard guidelines. Translational interventions directed at above deficiencies are required.



# GI329-SD-SUA3

Quantitative Assessment of Hepatic Iron Deposition by Dual-Energy Computed Tomography: Correlation with MRI Measurements

Sunday, Nov. 25 12:30PM - 1:00PM Room: GI Community, Learning Center Station #3

# Participants

Yueheng Tang, Beijing, China (*Presenter*) Nothing to Disclose Nan Hong, MD, Beijing, China (*Abstract Co-Author*) Nothing to Disclose Zhuo Liu, Beijing, China (*Abstract Co-Author*) Nothing to Disclose Jianying Li, Beijing, China (*Abstract Co-Author*) Employee, General Electric Company

# PURPOSE

To investigate the feasibility of quantitative diagnosis of liver iron deposition using dual-energy computed tomography (DECT) by assessing the correlation between DECT measurements and MRI relaxation measurements .

#### **METHOD AND MATERIALS**

31 patients with hematological diseases underwent abdominal DECT and MRI scanning. DECT projections were used to generate monochromatic image sets to calculate hepatic attenuation difference between 80keV and 140keV ( $\Delta$ H), and effective atomic number (Eff-Z), and iron-based images to calculate iron concentration. The MRI scanning included IDEALIQ R2\* and proton density fat fraction (PDFF) sequences. The correlations between DECT measurements and MRI measurements were analyzed.

#### RESULTS

Among the 31 patients, R2\* averaged  $314\pm253 \text{ s}-1$  (range: 34-959 s-1); PDFF averaged  $5.4\pm3.3\%$  (range: 1.8-14.0%); these values were not significantly correlated (0.278, P=0.130). The average CT values of 80keV and 140keV images were  $64.85\pm9.66$ HU, (range: 37.40-84.41HU),  $56.73\pm8.36$ HU (range: 30.63-73.22HU), respectively. The average measurements with DECT in liver were  $8.12\pm2.88$ HU (range: 0.65-16.25HU) for  $\Delta$ H;  $3.75\pm1.31$ mg/ml (range: 0.31-7.44mg/ml) for iron concentration; and  $7.94\pm0.13$  (range: 7.58-8.29) for Effective-Z. There were high linear positive correlations between DECT iron concentration and effective-Z (correlation coefficient 0.999, p<0.001) and between iron concentration and  $\Delta$ H (correlation coefficient 0.986, p<0.001). Comparing the DECT measurements values with the R2\*of MRI, there was a high linear positive correlation between DECT iron concentration value,  $\Delta$ H, Effective-Z, and R2\* values, the correlation coefficients were 0.827 (P<0.001), 0.831 (P<0.001) and 0.790 (P<0.001). There was a positive correlation between the CT values of the 80keV and 140keV monochromatic images and the R2\* values, the correlation coefficients were 0.631 (P<0.001) and 0.443 (P<0.05). The measured values of DECT had no correlation with PDFF.

# CONCLUSION

The liver iron concentration measurement in DECT and R2\* values in MRI showed a high linear positive correlation, suggesting that DECT has a good value on quantitative diagnosis of liver iron deposition.

#### **CLINICAL RELEVANCE/APPLICATION**

The liver iron concentration measurements in DECT and R2\* showed a high linear correlation, suggesting DECT can provide an cheap alternative on quantitative diagnosis of liver iron deposition.



## GI330-SD-SUA4

PET/CT-Based Radiomics Signature for the Preoperative Prediction of Vascular Invasion in Gastric Cancer

Sunday, Nov. 25 12:30PM - 1:00PM Room: GI Community, Learning Center Station #4

# Participants

Lijing Fan, BS , Zhengzhou, China (Presenter) Nothing to Disclose

# PURPOSE

To develop and validate PET/CT-based radiomics signature for the preoperative prediction of vascular invasion in gastric cancer.

### METHOD AND MATERIALS

A total of 93 surgical confirmed GC patients (65 males, 28 females; mean age: 57.32±12.13 years, range: 24-83 years) who underwent PET-CT scans were retrospectively enrolled and split into a primary cohort (n=60) and validation cohort (n=33). Radiomics features were extracted from the CT and PT images of each patient. A radiomics signature was then constructed with the least absolute shrinkage and selection operator algorithm in the training set. Nomogram performance was assessed in the training set and validated in the validation set. Finally, eceiver operator characteristics (ROC) analysis was performed with the combined training and validation set to estimate the clinical usefulness of the nomogram. A nomogram for risk factors of vascular invasion which incorporated clinical factors,SUV max, histological grade radiomics signature and was developed and its performance was measured using sensitivity and specificity.

# RESULTS

A total of 36 radiomics features showed significant differences between different vascular invasion status. A radiomics signature was constructed based on three features, including two wavelet-based features and one LBP-based feature. The model showed good discrimination both in primary cohort and validation cohort, with AUC of 0.776 (95% CI, 0.693-0.859) and 0.769 (95% CI, 0.689-0.851). The sensitivity and specificity of radiomics signature in the training set were 0.750 and 0.778 respectively to predicte vascular invasion in gastric cancer.

### CONCLUSION

The presented PET-CT based shows favorable predictive accuracy for in patients with gsatric cancer.

#### **CLINICAL RELEVANCE/APPLICATION**

PET/CT-based radiomics nomogram provide more information to predict vascular invasion in gastric cancer.



# GI332-SD-SUA5

# Deep Learning Based Radiomics and Its Usage in Prediction for Metastatic Colorectal Cancer

Sunday, Nov. 25 12:30PM - 1:00PM Room: GI Community, Learning Center Station #5

#### **Participants**

Dominik Noerenberg, MD, Munich, Germany (Presenter) Nothing to Disclose

Thomas Huber, MD, Munich, Germany (*Abstract Co-Author*) Consultant, BrainLAB AG; Consultant, Smart Reporting GmbH Stefan Maurus, MD, Munich, Germany (*Abstract Co-Author*) Nothing to Disclose

Philipp M. Kazmierczak, MD, Munich, Germany (Abstract Co-Author) Nothing to Disclose

Nils Jager, Munich, Germany (Abstract Co-Author) Nothing to Disclose

Alexander Katzmann, Forchheim, Germany (Abstract Co-Author) Consultant, Siemens AG

Jan Moltz, Bremen, Germany (Abstract Co-Author) Nothing to Disclose

Jens Ricke, MD, PhD, Munich, Germany (*Abstract Co-Author*) Research Grant, Sirtex Medical Ltd Research Grant, Bayer AG Volker Heinemann, MD, Munich, Germany (*Abstract Co-Author*) Research funded, Merck KGaA Research funded, F. Hoffmann-La Roche Ltd Research funded, Amgen Inc Research funded, sanofi-aventis Group Advisory Board, Merck KGaA Advisory Board, F. Hoffmann-La Roche Ltd Advisory Board, Amgen Inc Advisory Board, sanofi-aventis Group

Julian Holch, Munich, Germany (Abstract Co-Author) Advisory Board, F. Hoffmann-La Roche Ltd; Speaker, F. Hoffmann-La Roche Ltd; Travel support, Novartis AG

# For information about this presentation, contact:

Dominik.Noerenberg@med.uni-muenchen.de

### PURPOSE

To compare machine learning techniques for predicting tumor growth and one-year overall survival in patients with metastatic colorectal cancer.

### **METHOD AND MATERIALS**

We employed deep convolutional sparse autoencoders (DCAE) to extract deep features from 218 (tumor growth) / 131 (survival) liver metastases in 104 / 78 computed tomography images with contrast of 55 / 33 colorectal cancer patients under first-line therapy after semiautomatic tumor segmentations of colorectal cancer liver metastases and trained a deep convolutional neural network (DCNN) to predict tumor growth and short-term survivors.

#### RESULTS

The classifiers using the deep learning algorithm performed with the highest AUC for tumor growth and one-year-survival ( $0.784 \pm 0.049/0.710 \pm 0.065$ ) with significantly superior  $\Box$ -coefficient over prediction based on RECIST diameters of liver metastases or Radiomics (tumor growth:  $0.400 \pm 0.086$  vs. 0.273/0.294, p<0.05; survival:  $0.449 \pm 0.105$  vs. 0.321/0.180, p<0.05).

### CONCLUSION

This study demonstrates a deep learning model for predicting tumor growth and one-year overall survival in metastatic colorectal cancer patients using semiautomatic tumor segmentations of liver metastases derived from contrast-enhanced CT images.

#### **CLINICAL RELEVANCE/APPLICATION**

Early identification of tumor progression and detection of predictive parameters using machine learning in metastatic colorectal cancer patients may have implications for outcome improvements in the future.



# GU200-SD-SUA1

# Routine versus Structured Expert-Read Pelvic MRI in the Diagnosis & Staging of Endometriosis

Sunday, Nov. 25 12:30PM - 1:00PM Room: GU/UR Community, Learning Center Station #1

### **Participants**

Adrian M. Jaramillo-Cardoso, MD, Boston, MA (*Presenter*) Nothing to Disclose Anuradha S. Shenoy-Bhangle, MD, Boston, MA (*Abstract Co-Author*) Nothing to Disclose Alejandro Garces-Descovich, MD, Boston, MA (*Abstract Co-Author*) Nothing to Disclose Kevin Beker, MD, Boston, MA (*Abstract Co-Author*) Nothing to Disclose Ozum Tuncyurek, MD, Boston, MA (*Abstract Co-Author*) Nothing to Disclose Koenraad J. Mortele, MD, Boston, MA (*Abstract Co-Author*) Nothing to Disclose

# For information about this presentation, contact:

ajaramil@bidmc.harvard.edu

# PURPOSE

To assess the sensitivity for routine pelvic MRI (R-MRI) versus expert-read pelvic MRI (E-MRI) for the diagnosis & staging of endometriosis at a tertiary care academic center.

# METHOD AND MATERIALS

A retrospective review of patients with surgically staged & pathologically confirmed pelvic endometriosis who underwent pelvic MRI was performed. The E-MRI (two expert radiologists, E1-MRI and E2-MRI, detailed structured reporting template) was compared to both R-MRI and surgical/pathological staging for sensitivity. Pelvic compartments were categorized as anterior (AC), middle (MC), posterior (PC), adnexal (AX), and other (OC).

#### RESULTS

24 women (mean age 38.3 years; range: 22-52) met inclusion criteria. Of those, 10 (41.7%) had a suspected diagnosis of endometriosis. Overall sensitivity of R-MRI was 45% (33/68 involved compartments) compared to 78% (53/68) with E1-MRI (p= <0.001) and 91% (61/67) for E2-MRI (p=<0.001). Based on specific location of disease, R-MRI and E1-MRI/E2-MRI detected the following: AC involvement: R-RMI in 20% (2/10) vs. E1-MRI 90% (9/10) (p=0.01) and E2-MRI 100% (p=0.03); MC: R-MRI 40% (2/5) vs. E1-MRI 60% (3/5) (p>0.5) and E2-MRI 100% (5/5)(p=0.03); PC: R-MRI 33% (6/18) vs. E1-MRI 83% (15/18) (p=0.003) and E2-MRI 100% (18/18) (p=0.001); AX: R-MRI 81% (18/22) vs. E1-MRI 86% (19/22) (p>0.5) and E2-MRI 95% (21/22)(p=>0.5); and OC in 38% (5/13) vs. E1-MRI 46% (6/13) (p>0.5) and E2-MRI 53% (p>0.5). E-MRI missed 2/4 cases of appendicular involvement and 2/2 cases of ureteral involvement. R-MRI sensitivity relied heavily on AX involvement, whereas E-MRI showed additional sites of disease, mainly in the AC or PC, in 50% (12/24) of patients. Interobserver agreement between expert readers was overall good but varied by compartments (PC: 66.7%; MC: 33.3%; AC: 66.7%; AX: 79.2%; OC: 62.5%).

### CONCLUSION

Even at a tertiary care academic center, E-MRI is significantly more sensitive than R-MRI to diagnose endometriosis, detecting other lesions than adnexal endometriomas, and can therefore be of assistance in surgical planning and patient counseling. -

# **CLINICAL RELEVANCE/APPLICATION**

Even at a tertiary care academic center, E-MRI is significantly more sensitive than R-MRI to diagnose endometriosis, detecting other lesions than adnexal endometriomas, and can therefore be of assistance in surgical planning and patient counseling. -



# GU202-SD-SUA3

Radiomics Features of Multiparametric MRI for Pre-Treatment Prediction of Bone Metastases in Prostate Cancer

Sunday, Nov. 25 12:30PM - 1:00PM Room: GU/UR Community, Learning Center Station #3

# Participants

Yueren Wang, Shenyang, China (*Presenter*) Nothing to Disclose Bing Yu, MD, Shenyang, China (*Abstract Co-Author*) Nothing to Disclose Qiyong Guo, MD, Shenyang, China (*Abstract Co-Author*) Nothing to Disclose

#### For information about this presentation, contact:

cmuwangyueren@163.com

# PURPOSE

To identify radiomics features of multiparametric MRI for pre-treatment prediction of bone metastases in patients with prostate cancer (PCa).

#### METHOD AND MATERIALS

One-hundred and thirty-seven patients with clinicopathologically confirmed PCa were enrolled, and the data was gathered from January 2015 to March 2018. A total of 490 radiomics features were extracted from T2-weighted (T2-w) and dynamic contrastenhanced T1-weighted (DCET1-w) MRI.Linear regression, ridge regression and logistic regression model was applied to select features and develop the predicting model for bone metastases.The performance of the radiomics features were explored with the respect to the receiver operating characteristics(ROC) curve.Correlations between Gleason score and MRI features were also assessed.

### RESULTS

The radiomics signatures, which consisted of 9 selected features, were significantly associated with bone metastases (P<0.01). The relevant features were Haralick features T2-w correlation, T2-w difference entropy,DCET1-w information measure correlation,Neighbor Intensity Difference feature T2-w compexity,along with geometrical features (tumor volume, ,mean breadth,density,orientation,and tumor area). The radiomics features derived from T2-w showed better prognostic performance than features derived from DCET1-w and Gleason Score for pre-treatment prediction of bone metastases in PCa.As for the prognostic performance of the T2-w radiomics feature,DCET1-w radiomics feature and Gleason Score in bone metastases, the AUC was 0.82, 0.7894 and 0.8113.T2-w and DCET1-w radiomics features were significantly correlated with Gleason score (P < 0.01).

#### CONCLUSION

Multiparametric MRI-based radiomics signature was significant predictor for bone metastases in PCa. These results provide an illustrative example of precision medicine and may affect treatment strategies.

# **CLINICAL RELEVANCE/APPLICATION**

Multiparametric MRI-based radiomics signature was significant predictor for bone metastases in PCa. These results provide an illustrative example of precision medicine and may affect treatment strategies.



# GU203-SD-SUA4

# Normal Magnetic Resonance Imaging Characteristics of the Prostate: Young versus Old

Sunday, Nov. 25 12:30PM - 1:00PM Room: GU/UR Community, Learning Center Station #4

#### **Participants**

Marva D. Shemesh, MD, Petah Tikva, Israel (*Abstract Co-Author*) Nothing to Disclose Shlomit R. Tamir, MD, Toronto, ON (*Abstract Co-Author*) Nothing to Disclose David Margel, MD, Petah Tikva, Israel (*Abstract Co-Author*) Nothing to Disclose Ofer Benjaminov, MD, Petah Tiqva, Israel (*Abstract Co-Author*) Nothing to Disclose Yael Rapson, MD, Petah Tikva, Israel (*Presenter*) Nothing to Disclose

For information about this presentation, contact:

marva.dahan@gmail.com

## PURPOSE

To evaluate imaging features of the prostate in young patients (pts) as compared to older pts, without suspicious or known cancer.

### **METHOD AND MATERIALS**

Asymptomatic pts with normal PSA levels were scanned as part of a screening program for BRCA carriers. Multiparametric magnetic resonance imaging (MRI) was performed in a 3 Tesla machine with no endorectal coil. Random and targeted biopsies were performed in pts who consented. MRIs were retrospectively evaluated by two radiologists with 15 and 3 years of experience for overall dimensions, peripheral zone (PZ) signal on T2 weighted Images (T2WI) (homogenous hyper-intensity, wedge shaped hypo-intensities, patchy hypo-intensities or diffuse hypo-intensity), and transition zone (TZ) texture on T2WI (homogenous, heterogeneous, nodular). Readers were blinded to PSA levels and results of biopsies if performed. A third radiologist used dedicated software to measure PZ and TZ volumes and ADC values of PZ and TZ.

### RESULTS

98 scans were preformed between March 2014 and July 2016. 4 pts with proven cancer, 1 with PIN and 1 post TURP were excluded. 92 pts were finally included, 38 in the younger age group (40-49 y/o), and 54 in the older age group (50-69 y/o). As expected, the older pts had higher PSA levels (2.01 vs 0.91 ng/ml, p=0.002), larger overall size (36.4 vs 21.4 ml, p=0.000), and larger transition zones (20.7 vs 9.6 ml, p=0.000), (mean values, older vs younger age groups, respectively). PZ homogenous hyperintensity and wedge shaped hypo-intensities were more common in the older pts whereas patchy hypointensities and diffuse hypointensity were more common the younger pts. This difference was significant by both readers, with a kappa of 0.749 (data shown in Table 1). TZ texture showed no statistically significant difference between the age groups. ADC values were lower in young pts, both in PZ and TZ, unequal distribution was seen using the Mann Whitney U test (Table 2).

#### CONCLUSION

PZ and TZ ADC values are lower in younger vs older pts. Since DWI image is the main factor determining the PIRADS score in the PZ and contributes to scoring in the TZ, this scoring system should be validated specifically in the younger population.

#### **CLINICAL RELEVANCE/APPLICATION**

PZ and TZ ADC values are lower in younger vs older pts, possibly influencing PIRADS scoring in the young population.



# GU204-SD-SUA5

MRI Evaluation of Vulvar Cancer in Fresh Radical Local Excision Specimens for Cancer Localization and Prediction of the Surgical Tumor-free Margins

Sunday, Nov. 25 12:30PM - 1:00PM Room: GU/UR Community, Learning Center Station #5

# Participants

Jan Heidkamp, Nijmegen, Netherlands (*Presenter*) Nothing to Disclose Petra Zusterzeel, Nijmegen, Netherlands (*Abstract Co-Author*) Nothing to Disclose Ilse Van Engen - Van Grunsven, Nijmegen, Netherlands (*Abstract Co-Author*) Nothing to Disclose Christiaan G. Overduin, MSc, Nijmegen, Netherlands (*Abstract Co-Author*) Nothing to Disclose Andor Veltien, Nijmegen, Netherlands (*Abstract Co-Author*) Nothing to Disclose Arie Maat, Nijmegen, Netherlands (*Abstract Co-Author*) Nothing to Disclose Maroeska M. Rovers, PhD, Nijmegen, Netherlands (*Abstract Co-Author*) Nothing to Disclose Jurgen J. Futterer, MD, PhD, Nijmegen, Netherlands (*Abstract Co-Author*) Research Grant, Siemens AG

#### PURPOSE

In the surgical treatement of vulvar squamous-cell carcinoma (VSCC) tumour free margins of >=8 mm are considered adequate. The purpose of this study was to investigate the feasibility of ex vivo MRI in localizing VSCC and assess the surgical tumor-free margins in fresh radical local excision (RLE) specimens to guide the surgeon during surgical resections.

### **METHOD AND MATERIALS**

Nine patients with biopsy-proven VSCC and scheduled for RLE were prospectively included. Intact fresh specimens were scanned using a 7T preclinical MR-scanner. Whole-mount H&E-stained slides were obtained every 3 mm and correlated with ex vivo MRI. A pathologist annotated VSCC and minimal tumor-free margins (3-, 9 o'clock, basal) on the digitalized histological slides. Both an observer with knowledge of histology (the non-blinded annotation) and a radiologist blinded to histology (the blinded annotation) performed annotation of the same features on ex vivo MRI. Linear correlation and agreement (Bland-Altman analysis) of the ex vivo MRI measurements with histology were assessed. Diagnostic performance for VSCC localization and identification of margins <8 mm were expressed in PPV and NPV.

#### RESULTS

In 153 matched ex vivo MRI slices, the observer correctly identified 79/91 margins as <8 mm (PPV, 87%) and 110/124 margins as >=8 mm (NPV, 89%). The radiologist correctly annotated absence of VSCC in 73/81 (NPV, 90%) and presence in 65/72 (PPV, 90%) slices. Sixty-four of 90 margins were correctly identified as <8 mm (PPV, 71%) and 83/102 margins as >=8 mm (NPV, 81%). Both non-blinded annotations were linearly correlated and demonstrated good agreement with histology. Compared to the non-blinded annotation, the linear correlation between ex vivo MRI and histology was less strong and the Bland-Altman 95% limits of agreement were wider in the blinded annotation.

### CONCLUSION

Accurate localization of VSCC and measurements of the surgical tumour free margins in fresh WLE specimens using ex vivo MRI is technically feasible. The high NPV and PPV for localization of VSCC and identification of margins <8 mm demonstrate clinical applicability of the technique.

# **CLINICAL RELEVANCE/APPLICATION**

Perioperative information on the margin status of RLE specimens provided by ex vivo MRI could assist the surgeon in achieving adequate surgical margins and prevent subsequent secondary treatment.



# HP120-ED-SUA4

Quality Measure Development, Implementation, and Future Needs: A Primer

Sunday, Nov. 25 12:30PM - 1:00PM Room: HP Community, Learning Center Station #4

# Awards Certificate of Merit

#### Participants

Jason N. Itri, MD, PhD, Winston-Salem, NC (*Presenter*) Nothing to Disclose Jennifer C. Broder, MD, Burlington, MA (*Abstract Co-Author*) Nothing to Disclose Kesav Raghavan, MD, San Francisco, CA (*Abstract Co-Author*) Nothing to Disclose Samir B. Patel, MD, Mishawaka, IN (*Abstract Co-Author*) Nothing to Disclose Judy Burleson, Reston, VA (*Abstract Co-Author*) Nothing to Disclose Samantha Tierney, MPH, Chicago, IL (*Abstract Co-Author*) Nothing to Disclose Diedra D. Gray, MPH, Chicago, IL (*Abstract Co-Author*) Nothing to Disclose Scott Macdonald, MD, Sacramento, CA (*Abstract Co-Author*) Nothing to Disclose David J. Seidenwurm, MD, Carmichael, CA (*Abstract Co-Author*) Shareholder, Sutter Medical Group ; Shareholder, RASMG Medical Group ; Director, RASMG Medical Group; Expert Witness, Medical Legal Rafel Tappouni, MBBCh, FRCPC, Winston Salem, NC (*Abstract Co-Author*) Nothing to Disclose

## For information about this presentation, contact:

drjitri@gmail.com

#### **TEACHING POINTS**

The purpose of this exhibit is to: 1. Describe the key components of developing and implementing quality measures using examples: o Targeting high-priority aspects of care o Environmental scan and gap analysis o Evidence to support measures o Measure testing: feasibility, reliability, validity, and unintended consequences o Attribution and risk adjustment for outcome measures o Requirements for CMS and NQF endorsement 2. Discuss needs for new quality measures: o Process measures reflecting diagnostic accuracy o Outcome measures including patient reported outcomes o Cross-cutting measures o Data capture, interoperability, and electronic Clinical Quality Measures o CMS process for evaluating measures and transparency 3. Explain how reporting quality measures impacts reimbursement in the current system: o MIPS and non-MIPS measures o Methods to report data: claims, registries, QCDR, and EHR

# TABLE OF CONTENTS/OUTLINE

1. Background and importance of measure development 2. Quality measure development cycle 3. Measure testing 4. Collaboration with organizations 5. Endorsement and implementation 6. Challenges and future needs for better quality measures 7. Reporting quality measures and reimbursement



### HP200-SD-SUA1

The Diagnostic Performance of Contrast Enhanced Ultrasound Liver Imaging Reporting and Data System (CEUS LI-RADS) for Hepatocellular Carcinoma (HCC)

Sunday, Nov. 25 12:30PM - 1:00PM Room: HP Community, Learning Center Station #1

FDA Discussions may include off-label uses.

#### **Participants**

Jiawu Li, Chengdu, China (*Presenter*) Nothing to Disclose Yan Luo, MD, Chengdu, China (*Abstract Co-Author*) Nothing to Disclose

#### For information about this presentation, contact:

lijiawu-cool@163.com

### PURPOSE

To explore the diagnostic performance of contrast enhanced ultrasound Liver Imaging Reporting and Data System (CEUS LI-RADS) for hepatocellular carcinoma (HCC) .

# METHOD AND MATERIALS

Between January 2013 and December 2015, 1580 patients with high risk factor for hepatocellular carcinoma who underwent liver contrast-enhanced ultrasound were included in this institutional ethics committee-approved retrospective study. Reference diagnostic standard was pathology or at least 2 of the three contrast-enhanced imaging modalities (CEUS, CECT, or CEMRI) as well as followed up at least 6 months. A LI-RADS category was retrospectively assigned to nodules on CEUS. The diagnostic accuracy of CEUS LI-RADS for HCC was described by sensitivity, specificity, and positive and negative predictive values.

#### RESULTS

According to reference diagnostic standard, 1580 patients were as follows: 1006 hepatocellular carcinomas (HCCs), 206 other malignancies except for HCC, and 368 benign lesions. Three (2%) of 181 LI-RADS category 1 lesions, none (0%) of 8 category 2 lesions, 16 (18%) of 88 category 3 lesions, 82 (64%) of 129 category 4 lesions, 724 (90%) of 806 category 5 lesions, 181 (49%) of 368 category M lesions were HCCs. Four category 1 lesion were metastases, 1 category 2 lesion was metastasis, 8 category 3 lesion were metastases, 1 category 2 lesions were metastases, 1 category 3 lesion was hepatic lymphoma, 3 category 4 lesions were metastases, and 40 category 5 lesions were other malignancies except for HCC. 174 (96%) of 181 category 1, 7 (88%) of 8 category 2 lesions, 63 (72%) of 88 category 3 lesions, 44 (34%) of 129 category 4 lesions, 42 (5%) of 806 category 5 lesions, and 38 (10%) of 368 category M lesions were benign. If category 3,4,5 as HCC, category 1,2 as non-HCC, the sensitivity, specificity , PPV, NPV and accuracy CEUS LI-RADS for HCC were 99.64%,48.42%,80.35%,98.41% and 83.17%, respectively. If exclude LR-3, category 4,5 as HCC, category 1,2 as non-HCC, the sensitivity, specificity, specificity, specificity, PPV, NPV and accuracy CEUS LI-RADS for HCC in the population with high risk factor of HCC were 99.63%,59.05%,86.20%,98.41% and 88.26%, respectively.

## CONCLUSION

CEUS LI-RADS had a good diagnostic performance for HCC . In addition, a relevant proportion of lesions categorized as LI-RADS category M were HCCs, for these patients, further biopsy maybe needed to definitive diagnosis.

# **CLINICAL RELEVANCE/APPLICATION**

CEUS LI-RADS had a good diagnostic performance for HCC



# HP201-SD-SUA2

Reporting Bias: Association of Diagnostic Accuracy Estimates in Radiology Conference Abstracts with Full-Text Publication

Sunday, Nov. 25 12:30PM - 1:00PM Room: HP Community, Learning Center Station #2

#### Awards Student Travel Stipend Award

#### **Participants**

Lindsay A. Cherpak, MD, Ottawa, ON (*Presenter*) Nothing to Disclose Daniel Korevaar, Netherlands, Netherlands (*Abstract Co-Author*) Nothing to Disclose Trevor McGrath, MD, Ottawa, ON (*Abstract Co-Author*) Nothing to Disclose Wilfred Dang, MD, Ottawa, ON (*Abstract Co-Author*) Nothing to Disclose Daniel Walker, MD, Ottawa, ON (*Abstract Co-Author*) Nothing to Disclose Jean-Paul Salameh, BSC, Ottawa, ON (*Abstract Co-Author*) Nothing to Disclose Anahita Dehmoobad Sharifabadi, BSC, Ottawa, ON (*Abstract Co-Author*) Nothing to Disclose Matthew D. McInnes, MD, PhD, Ottawa, ON (*Abstract Co-Author*) Nothing to Disclose

### PURPOSE

To evaluate the extent to which imaging diagnostic accuracy studies presented as conference abstracts reached full-text (FT) publication, and to assess associations between reported accuracy estimates and FT publication at 5 years after abstract submission.

#### **METHOD AND MATERIALS**

Diagnostic accuracy abstracts presented at the Radiological Society of North America (RSNA) meeting in 2011-2012 were evaluated. Specificity (Sp) and sensitivity (Sn) from the abstracts were used to calculate Youden's index (YI=Sn+Sp-1). To identify FT publications within 5 years after abstract submission search of databases and follow up with authors were done. Cox regression analysis was used to assess for associations between accuracy estimates (logit-transformed) and FT publication.

# RESULTS

A FT publication was identified for 287/405 (71%) included abstracts. Median YI for abstracts with associated FT publication and without FT at 5 years were 0.80 (interquartile range (IQR) 0.66-0.90) and 0.77 (IQR 0.57-0.88) respectively. No association between reported YI, Sn or Sp with publication status at 5 years post abstract submission was observed (hazard ratio (HR) 1.06, 95% CI 0.99-1.14, p = 0.076; HR 1.04, 95% CI 0.99-1.10, p = 0.134; HR 1.05, 95% CI 1.00-1.11, p = 0.072).

# CONCLUSION

Imaging diagnostic accuracy abstracts with higher reported accuracy estimates were not associated with increased likelihood to be reported in a FT publication; this is in keeping with results of related studies in other medical subspecialties.

### **CLINICAL RELEVANCE/APPLICATION**

Reporting bias regarding abstract publication in imaging research does not appear to be impacted by diagnostic accuracy. As such, extensive search of unpublished literature for imaging systematic reviews may not be indicated.



# HP202-SD-SUA3

Implementation of the Korean Clinical Imaging Guidelines: A Mobile App-Based Decision Support System

Sunday, Nov. 25 12:30PM - 1:00PM Room: HP Community, Learning Center Station #3

### **FDA** Discussions may include off-label uses.

#### **Participants**

Eun Ju Ha, Suwon, Korea, Republic Of (*Presenter*) Nothing to Disclose Jung Hwan Baek, Seoul, Korea, Republic Of (*Abstract Co-Author*) Consultant, STARmed; Consultant, RF Medical Hwan Seok Yong, MD, PhD, Seoul, Korea, Republic Of (*Abstract Co-Author*) Nothing to Disclose Seung Eun Jung, MD, Seoul, Korea, Republic Of (*Abstract Co-Author*) Nothing to Disclose

#### PURPOSE

Korean clinical imaging guidelines (K-CIGs) have been developed to establish the nationally recognized guidelines for an appropriate utilization of imaging modalities since 2015. This study was designed to describe a mobile app-based clinical decision support system (CDSS) for implementation of the K-CIGs and to assess the future developmental direction.

#### **METHOD AND MATERIALS**

K-CIGs were implemented as a web application (http://cdss.or.kr/). Web-view-based mobile app can be downloaded from the Google Play Store. The app contains 25 database of knowledge including 10 subspecialties with 53 recommendations, developed in 2015-2016 by the Korean Society of Radiology (KSR). An email survey of 17 questions on K-CIGs implementation and a mobile appbased CDSS was sent to 66 members of the guideline working group (43 expert members of the KSR and Korean Academy of Oral and Maxillofacial Radiology) and the consultant group (23 clinical experts of a related medical society) to assess the future developmental direction.

# RESULTS

Detailed information on the recommendation level, evidence level and radiation dose of each K-CIGs can be found in the home and side menu. Grades of recommendation are from the most reliable grade A to not recommended grade C, and grade I which means no recommendation. For evidence levels, from the most reliable grade I to the poorest evidence level IV are listed. The radiation dose is divided into 5 categories according to the relative level. Regarding the survey, of 66 members, 32 members finished the survey and responded (response rate of 45%). Twenty-four (70%) of the 32 respondents were the working group and eight of the 32 respondents were the consulting group. Most of respondents (93.8%) were agreed to the necessity of developing K-CIGs and their implementation.

# CONCLUSION

This is the first mobile app-based CDSS for implementation of K-CIGs in Korea. It will be helpful to assist the physicians for an appropriate utilization of imaging modalities.

### **CLINICAL RELEVANCE/APPLICATION**

This is the first mobile app-based CDSS in Korea for implementation of K-CIGs.



# IN007-EC-SUA

Applying Virtual and Augmented Reality to Radiology and Medicine

Sunday, Nov. 25 12:30PM - 1:00PM Room: IN Community, Learning Center Custom Application Computer Demonstration

#### **Participants**

Justin Sutherland, PhD, Ottawa, ON (*Presenter*) Nothing to Disclose Frank J. Rybicki III, MD, PhD, Ottawa, ON (*Abstract Co-Author*) Medical Director, Imagia Cybernetics Inc Leonid Chepelev, MD, PhD, Ottawa, ON (*Abstract Co-Author*) Nothing to Disclose Dimitris Mitsouras, PhD, Boston, MA (*Abstract Co-Author*) Research Grant, Canon Medical Systems Corporation; Daniel La Russa, PhD, Ottawa, ON (*Abstract Co-Author*) Nothing to Disclose

# For information about this presentation, contact:

#### jussutherland@toh.ca

### **TEACHING POINTS**

By combining a 'hands-on' immersive virtual reality experience and standard slides-based narrative, the learner will be able to: 1. Classify experiences as virtual reality (VR) or augmented reality (AR) and list the components of modern VR/AR technologies; 2. Define medical applications of VR/AR for diverse user groups and describe its role in the patient intervention process based on concrete hands-on case-studies; 3. Describe the methods (hardware and software) of visualizing medical images and models in VR/AR using a comprehensive conceptual framework; 4. Describe key considerations for placing VR/AR visualization tools into a radiology-based workflow.

### TABLE OF CONTENTS/OUTLINE

A. Definitions of virtual reality (VR) and augmented reality (AR) and their respective components. B. Modern VR/AR technologies: 1. mobile vs tethered; 2. development platforms; 3. physical and technical limits. C. Clinical applications of VR and AR classification by degree of patient involvement: 1. Training; 2. Surgical planning and guidance; 4. Interpretation assistance; 5. Patient-based VR/AR therapies D. VR visualization of medical images and 3D models: 1. Visualization of segmented images; 2. Visualization of unsegmented images; 3. Manipulation of data in VR/AR; 4. VR/AR 'virtual presence' collaboration tools.

#### **Honored Educators**

Presenters or authors on this event have been recognized as RSNA Honored Educators for participating in multiple qualifying educational activities. Honored Educators are invested in furthering the profession of radiology by delivering high-quality educational content in their field of study. Learn how you can become an honored educator by visiting the website at: https://www.rsna.org/Honored-Educator-Award/ Frank J. Rybicki III, MD, PhD - 2016 Honored Educator



### IN009-EC-SUA

# Improving Radiology Report Quality by Moving a Patient Forward Along a Clinical Spectrum

Sunday, Nov. 25 12:30PM - 1:00PM Room: IN Community, Learning Center Custom Application Computer Demonstration

#### **Participants**

David J. Vining, MD, Houston, TX (*Presenter*) Royalties, Bracco Group; CEO, VisionSR; Stockholder, VisionSR Andreea Pitici, Houston, TX (*Abstract Co-Author*) Employee, Computer Patrisoft SAC Cristian Popovici, Houston, TX (*Abstract Co-Author*) Employee, Patrisoft Outsourcing Adrian Prisacariu, Houston, TX (*Abstract Co-Author*) Employee, Patrisoft Outsourcing Mark Kontak, Houston, TX (*Abstract Co-Author*) Consultant, VisionSR, Inc

## For information about this presentation, contact:

dvining@mdanderson.org

#### CONCLUSION

Radiology reports produced using a structured reporting system that prompts radiologists to include essential information and performs compliance checks can be used to improve report quality and move a patient forward along a clinical spectrum.

#### Background

A method for assessing radiology report quality is based on whether the report advances a patient forward along a clinical spectrum: does the report (1) describe essential findings, (2) provide a differential diagnosis, (3) derive a definitive diagnosis, and (4) follow an established diagnosis consistently until resolution? We have incorporated these principles into the development of a structured reporting system that provides radiologists with visual prompts and compliance checks during image interpretation so that they may incorporate missing elements and link historical data in timelines to improve report quality.

#### **Evaluation**

We developed a structured reporting system that captures key images and verbal descriptions, tags images with metadata referenced to an ontology using NLP, and presents a multimedia report with related findings displayed in timelines. The ontology comprises hierarchies of anatomy and pathology terms that progress from generic observations to definitive diagnoses. Nondescript observations trigger the presentation of differential diagnoses and other salient features as a reminder to the radiologist to include these elements. When a definitive diagnosis is established by correlation with pathology or other information, that data can be included in the timelines to inform the radiologist during subsequent image interpretation. Timeline displays of graphed images and metrics prompt the radiologist to record consistent data during subsequent exams to achieve accurate disease assessment.

### Discussion

Several radiology quality metrics have been proposed for use in pay-for-performance initiatives; however, the assessment of radiology report quality remains a holy grail. The determination of whether a report advances a patient forward along a clinical spectrum has been proposed as a quality measure, and we have incorporated this concept into a structured reporting system that enables radiologists to generate high quality information.



## IN140-ED-SUA1

## Lessons Learned About Diagnostic Radiology Reporting from Practicing Interventional Radiology

Sunday, Nov. 25 12:30PM - 1:00PM Room: IN Community, Learning Center Station #1

#### **Participants**

Andrew J. Gunn, MD, Birmingham, AL (*Presenter*) Nothing to Disclose James A. McFarland, MD, Birmingham, AL (*Abstract Co-Author*) Nothing to Disclose Sabeen Dhand, MD, Chicago, IL (*Abstract Co-Author*) Nothing to Disclose Nathan W. Ertel, MD, Hoover, AL (*Abstract Co-Author*) Nothing to Disclose Ahmed K. Abdel Aal, MD, PhD, Birmingham, AL (*Abstract Co-Author*) Consultant, Abbott Laboratories; Consultant, Baxter International Inc; Consultant, C. R. Bard, Inc; Consultant, Boston Scientific Corporation; Consultant, W. L. Gore & Associates, Inc; Consultant, Sirtex Medical Ltd Michael Devane, MD, Simpsonville, SC (*Abstract Co-Author*) Nothing to Disclose

### For information about this presentation, contact:

agunn@uabmc.edu

#### **TEACHING POINTS**

1. As both consumers and producers of radiology reports, interventional radiologists (IR) bring a unique prospective and experience regarding reporting practices. 2. Effective radiology reports are generated with the patient's clinical history, presentation, and condition in mind while focusing on answering the clinical question.

### TABLE OF CONTENTS/OUTLINE

1. Introduction 2. Perception of radiology reporting by referring physicians, including the concept of referring physician feedback as a mechanism for quality improvement 3. Brief review of radiologist-led efforts to improve reporting practices 4. Pictorial review using images and reports from our IR practices that highlight common problems a. Report does not answer the clinical question (Figure 1) b. Report fails to mention details critical to a planned procedure or diagnosis (Figure 2) c. Report has an unstructured format, making it difficult to extract information d. Report has ambiguous and/or hard to understand terms (Figure 3) e. Report contains clinically irrelevant measurements (Figure 4) f. Report contains an exhaustive list of differential diagnoses g. Report has emergent or urgent findings that are not communicated to the referring team h. Report doesn't conform to established guidelines (Figure 5) 5. Summary and conclusions



### MI002-EB-SUA

## Personalizing Immune-Oncology Therapies by Imaging Guided Adaptive Strategies

Sunday, Nov. 25 12:30PM - 1:00PM Room: MI Community, Learning Center Hardcopy Backboard

#### **Participants**

Laurent Dercle, MD, New York, NY (*Presenter*) Nothing to Disclose Fatima-Zohra Mokrane, MD, Toulouse, France (*Abstract Co-Author*) Nothing to Disclose Samy Ammari, Villejuif, France (*Abstract Co-Author*) Nothing to Disclose Ahmed Mekki, Villejuif, France (*Abstract Co-Author*) Nothing to Disclose Romain-David Seban, Villejuif, France (*Abstract Co-Author*) Nothing to Disclose Randy Yeh, MD, New York, NY (*Abstract Co-Author*) Nothing to Disclose Mathieu Sinigaglia, Paris, France (*Abstract Co-Author*) Nothing to Disclose Binsheng Zhao, DSc, New York, NY (*Abstract Co-Author*) Nothing to Disclose Binsheng Zhao, DSc, New York, NY (*Abstract Co-Author*) License agreement, Varian Medical Systems, Inc; Royalties, Varian Medical Systems, Inc; License agreement, Keosys SAS; License agreement, Hinacom Software and Technology, Ltd; Aurelien Marabelle, Villejuif, France (*Abstract Co-Author*) Nothing to Disclose Lawrence H. Schwartz, MD, New York, NY (*Abstract Co-Author*) Committee member, Celgene Corporation Committee member, Novartis AG Committee member, ICON plc Committee member, BioClinica, Inc

## For information about this presentation, contact:

laurent.dercle@gmail.com

#### **TEACHING POINTS**

The purpose of this exhibit is:1. To explain why immune checkpoint inhibitors are becoming the standard of care in many cancer types.2. To review key elements that are expected to improve the monitoring of immunotherapeutic efficacy at the patient and clinical trial level.3. To discuss new patterns of response and progression, as well as immune related adverse events.4. To explain the utility of imaging modalities in solid tumors, brain tumors and lymphomas.

## TABLE OF CONTENTS/OUTLINE

I. PHYSIOPATHOLOGY: 1. The paradigm shift of immune oncology.II. NEW PATTERNS OF RESPONSE: 1. Hyperprogression, 2. Delayed efficacy, 3. Pseudoprogression, 4. Abscopal effect, 5. Indeterminate response. III. TOXICITY / IMMUNE RELATED ADVERSE EVENTS: 1. Frequency, 2. Sites, 3. ManagementIV. SPECIFIC RESPONSE EVALUATION CRITERIA: 1. Solid tumors (irRECIST, irRC), 2. Brain tumors (iRANO), 3. Lymphoma (LYRIC). V. IMAGING METABOLOMICS: 1. Cellular density, 2. Glucose metabolism, 3. Amino acid metabolism, 4. Membrane proliferation, 5. Growth hormones.VI. IMAGING ANGIOGENESIS, HYPOXIA: 1. Association with drug delivery, 2. Surrogate of hypoxia, 3. Surrogate of vascularity. VII. IMAGING IMMUNE ENVIRONMENT: 1. Radiolabeled ICM, 2. Detecting CD8 and immune environment. 3. TSPO. VIII. ARTIFICIAL INTELLIGENCE AND BIG DATAIX. PERSPECTIVES



## MI200-SD-SUA1

Noninvasive Early Detection and Dynamic Mapping of Liver Fibrosis and Cancer Heterogeneity by Collagen-Targeted Protein MRI Contrast Agent

Sunday, Nov. 25 12:30PM - 1:00PM Room: MI Community, Learning Center Station #1

# Participants

Jenny Yang, Atlanta, GA (*Presenter*) Nothing to Disclose Mani Salarian, Atlanta, GA (*Abstract Co-Author*) Nothing to Disclose Jingjuan Qiao, Atlanta, GA (*Abstract Co-Author*) Nothing to Disclose Pardeep K. Mittal, MD, Atlanta, GA (*Abstract Co-Author*) Nothing to Disclose

### PURPOSE

Early diagnosis and noninvasive detection of liver fibrosis and its heterogeneity remain as major unmet medical needs for stopping further progression toward severe clinical consequences.

## METHOD AND MATERIALS

We have developed a collagen type I targeting protein-based contrast agent (ProCA32.collagen1) (Kd of 1.4 mM). ProCA32.collagen1 possesses high relaxivities (r1 and r2 are 68 and 100 mM-1·s-1 at 1.4 T and 42.6  $\pm$  1.0 and 217  $\pm$  2.4 mM-1s-1 at 7T) per particle with a T1-T2 dual mode action.

#### RESULTS

ProCA32.collagen1 is able to differentiate M15 uveal melanoma metastasized to the liver with nodular pattern from infiltrative with 14-fold increase in contrast to noise ratio (CNR) which has not been achieved using clinical contrast agent. Distinguishing different patterns of uveal melanoma has significant clinical implications in terms of choosing the most effective treatment.

#### CONCLUSION

Based on MRI correlation with histology analysis, ProCA32.collagen1 is capable of detecting tumors as small as 0.250 mm 2 which is much smaller than not only the current detection limit of 10-20 mm but also tumors previously detected by ProCA32-P40. We have further shown that the addition of targeting moiety do not reduce its strong metal binding affinity to Gd3+ and 1011-fold higher selectivity towards Gd3+ over Zn2+ than Eovist.

## **CLINICAL RELEVANCE/APPLICATION**

The development of collagen targeting contrast agent is expected to have a broad applications in detection and staging of liver metastasis from various types of cancer and probing heterogeneous microenvironment changes upon disease progression and treatment.

### **Honored Educators**

Presenters or authors on this event have been recognized as RSNA Honored Educators for participating in multiple qualifying educational activities. Honored Educators are invested in furthering the profession of radiology by delivering high-quality educational content in their field of study. Learn how you can become an honored educator by visiting the website at: https://www.rsna.org/Honored-Educator-Award/ Pardeep K. Mittal, MD - 2016 Honored EducatorPardeep K. Mittal, MD - 2018 Honored Educator



## MI202-SD-SUA3

Multimodal Perfusion Study in an Experimental Ex Vivo Pig Kidney Phantom Using Digital Subtraction Angiography, Magnetic Resonance Imaging, and Magnetic Particle Imaging

Sunday, Nov. 25 12:30PM - 1:00PM Room: MI Community, Learning Center Station #3

# Participants

Michael G. Kaul, Hamburg, Germany (*Presenter*) Nothing to Disclose Isabel Molwitz, Berlin, Germany (*Abstract Co-Author*) Nothing to Disclose Caroline Jung, Hamburg, Germany (*Abstract Co-Author*) Nothing to Disclose Johannes M. Salamon, MD, Hamburg, Germany (*Abstract Co-Author*) Nothing to Disclose Tobias Knopp, DIPLENG, Hamburg, Germany (*Abstract Co-Author*) Nothing to Disclose Gerhard B. Adam, MD, Hamburg, Germany (*Abstract Co-Author*) Nothing to Disclose Harald Ittrich, MD, Hamburg, Germany (*Abstract Co-Author*) Nothing to Disclose

### PURPOSE

We established an experimental setup in ex vivo pig kidneys mimicking in vivo applications and their work flow for digital subtraction angiography (DSA), magnetic resonance imaging (MRI), and Magnetic particle imaging (MPI). MPI is a new imaging modality providing a high temporal resolution scanning magnetic particle distributions in 3D.

#### **METHOD AND MATERIALS**

Kidneys of sacrificed pigs were perfused with heparin and saline. The main blood vessels and the ureter were connected to tubes allowing in and out flow of fluids. Flow through the vessels was later on generated by a perfusion pump. To minimize dislocations, kidneys were placed on a couch compatible with DSA, MRI, and MPI. Measurements were performed in a clinical DSA (Allura, Philips), a preclinical high field MRI scanner (7T ClinScan, Bruker) and preclinical MPI scanner (Bruker/Philips). With each modality a dynamic sequence was performed and a dedicated tracer / contrast agent [DSA (Imeron 300, Bracco), MRI (Ominscan, Ge Healthcare) and MPI (Resovist, Bayer-Schering)] standardized injected by a pump. In MRI, we performed as well Intravoxel Incoherent Motion (IVIM) analysis with and without flow to prove perfusion.

### RESULTS

It was feasible to detect in and out flowing contrast agents/tracer and to produce angiograms with all three systems. MPI provided with 21.5ms per 3D volume the highest temporal resolution but with a voxel size of 3x3x1.5mm<sup>3</sup> the lowest spatial resolution. Nevertheless, this was sufficient enough to image the major vessels. Quality of the data was also sufficient to produce time of arrival maps of the inflowing tracer. As flow can be steered, in MRI, we reduced the flow rate to 2.5mL/min to study the inflow with a 3D sequence with 0.7x0.7x1mm<sup>3</sup> within 2.1s. IVIM perfusion experiments were feasible as well. DSA provides the highest resolution but only as 2D projections.

## CONCLUSION

In the ex vivo kidney phantom is possible to study some of the basic aspects of multimodal perfusion imaging and their analysis techniques. In detail, we studied and proved the feasibility of MPI as new imaging technique for perfusion imaging of kidneys.

## **CLINICAL RELEVANCE/APPLICATION**

Although until now only preclinical MPI systems exist it is a clear vision to build a clinical system for human applications. Its first application will be probably be vessel imaging and will feature dynamic 3D imaging without ionizing radiation.



#### MI203-SD-SUA4

Chemical Exchange Saturation Transfer Imaging for Brain Tumors

Sunday, Nov. 25 12:30PM - 1:00PM Room: MI Community, Learning Center Station #4

#### Participants

Yuki Matsumoto, MS, Tokushima City, Japan (*Presenter*) Nothing to Disclose Masafumi Harada, MD, PhD, Tokushima, Japan (*Abstract Co-Author*) Nothing to Disclose Yuki Kanazawa, PhD, Tokushima, Japan (*Abstract Co-Author*) Nothing to Disclose Maki Ohtomo, Tokushima-shi, Japan (*Abstract Co-Author*) Nothing to Disclose Mitsuharu Miyoshi, Hino, Japan (*Abstract Co-Author*) Employee, General Electric Company

## For information about this presentation, contact:

lakaisbmtyk@gmail.com

## PURPOSE

The purpose of our study is to investigate the relationship among several brain tumors using several estimated parameters derived from chemical exchange saturation transfer (CEST) imaging.

# METHOD AND MATERIALS

This study was approved by the local institution review board. CEST imaging was performed on patients with glioblastoma (n = 5), diffuse large B-cell lymphoma (n = 3), diffuse astrocytoma (n = 3), or oligodendroglioma (n = 2). All imaging data were acquired on a 3.0-T MR system (Discovery 750, GE Healthcare, Waukesha, WI, USA). The imaging parameters for CEST images were as follows: echo time, 20.4 ms; repetition time, 3000 ms; bandwidth, 3906 Hz/pixel; field of view, 22 cm; matrix size, 128 × 128; slice thickness, 5 mm; mean *B*1, 2  $\mu$ T; off set frequency equivalent to ±7 ppm per 32 steps. An axial MR image with the brain tumor was acquired. After acquiring imaging data, amide proton transfer (APT), magnetization transfer (MT), pH, S0, and *T2/T*1 were calculated. Then, regions of interest (ROIs) were placed on the tumor and normal-appearing white matter (NAWM) regions in each patient. A comparative analysis was conducted to determine whether there were differences among each of the brain tumors and the NAWM. For the calculated images, a *P* < 0.05 was considered statistically significant.

#### RESULTS

In all brain tumor patients, the mean APT, S0, and T2/T1 values were significantly higher in the tumor area than in the NAWM region (P < 0.001), and the mean MT value was significantly lower in the tumor area than in the NAWM region (P < 0.001). In the glioblastoma, diffuse astrocytoma, and oligodendroglioma patients, the mean pH value was significantly lower in the tumor area than in the NAWM region (glioblastoma and diffuse astrocytoma, P < 0.001; oligodendroglioma, P < 0.05).

## CONCLUSION

CEST images might help to identify unique information concerning various brain tumors in the future.

# **CLINICAL RELEVANCE/APPLICATION**

CEST images might help to identify unique information concerning various brain tumors and is recommended when identifying the type of tumor.



### MK342-ED-SUA6

# Dual-Energy X-ray Absorptiometry (DXA): Beyond Filling in the Numbers

Sunday, Nov. 25 12:30PM - 1:00PM Room: MI Community, Learning Center Station #6

#### **Participants**

Reza Hayeri, MD, Cleveland, OH (*Abstract Co-Author*) Nothing to Disclose Ali Gholamrezanezhad, MD, Glendale, CA (*Abstract Co-Author*) Nothing to Disclose Christian Pedersen, MD, Darby, PA (*Presenter*) Nothing to Disclose

## **TEACHING POINTS**

To summarize indications and contraindications of DXA To highlight image acquisition protocol and quality control To review current guidelines and proper image interpretation and terminology To discuss the pitfalls and artifacts of DXA in the evaluation of BMD

## TABLE OF CONTENTS/OUTLINE

Introduction Bone structure and metabolism. Definitions and terminology based on recent guidelines. Data and image acquisition (proper patient positioning and placement of regions of interest). Quality control and Artifacts. Proper Interpretation through multiple exmples and case studies. Whole-body composition techniques. Pitfalls. Take home points



## MK346-SD-SUA1

The Echogenic Appearance of the Diabetic Deltoid Muscle on Shoulder Ultrasound: Is This Simply from Adipose Tissue Infiltration, Can This Appearance Predict Type 2 Diabetes and be Used to Detect Pre-Diabetes?

Sunday, Nov. 25 12:30PM - 1:00PM Room: MK Community, Learning Center Station #1

# Participants

Paul Williams, MD, Detroit, MI (*Presenter*) Nothing to Disclose
Kelli A. Rosen, DO, Detroit, MI (*Abstract Co-Author*) Nothing to Disclose
Jessica K. Kim, BS, DO, Detroit, MI (*Abstract Co-Author*) Nothing to Disclose
Paul J. Spicer, MD, Lexington, KY (*Abstract Co-Author*) Nothing to Disclose
Marnix T. van Holsbeeck, MD, Detroit, MI (*Abstract Co-Author*) Minor stockholder, Koninklijke Philips NV; Minor stockholder, General
Electric Company; Stockholder, MedEd3D; Grant, Siemens AG; Grant, General Electric Company;
Steven B. Soliman, DO, Detroit, MI (*Abstract Co-Author*) Nothing to Disclose

#### For information about this presentation, contact:

paulwi@rad.hfh.edu

### PURPOSE

To evaluate the association of an echogenic deltoid muscle seen in type 2 diabetics during shoulder ultrasound versus the deltoid muscle appearance in non-diabetic obese patients and for any corresponding associations.

## **METHOD AND MATERIALS**

The study included 137 shoulder ultrasounds from type 2 diabetics, including 13 pre-diabetics, confirmed by hemoglobin A1c levels and medications. It also included 49 ultrasounds from non-diabetic obese patients based on body mass index (BMI). Images of the deltoid muscle were blindly reviewed by 3 musculoskeletal radiologists as to whether the appearance was normal, suspected diabetic or definite diabetic. These results along with the patient's age, sex, race, hemoglobin A1c level, BMI, and the use of insulin were analyzed.

## RESULTS

A consensus diagnosis of 'definite diabetic' by 3 musculoskeletal radiologists based on an echogenic appearing deltoid muscle on ultrasound was a powerful predictor of diabetic status. The positive predictive value for the accurate designation of 'definite diabetic' was 89% (70 of 79 diabetic patients). An echogenic deltoid muscle was also a powerful predictor of pre-diabetes. Of 13 pre-diabetic ultrasounds reviewed, 13 were assigned either 'suspected diabetic' (3 of 13, 23%) or 'definite diabetic' (10 of 13, 77%) (P= 0.062). Obesity alone cannot solely explain the appearance of an echogenic deltoid muscle in diabetics. Non-obese diabetics were diagnosed 'definite diabetic' with 30% sensitivity (11 of 37 non-obese diabetics). Diabetic patients with a higher BMI, were more often diagnosed 'definite diabetic'. Of 137 diabetic ultrasounds reviewed, 31(22.6%) were designated 'normal' (BMI 30.9  $\pm$  7.3), 36 (26.2%) designated 'suspected diabetic' (BMI 32.6  $\pm$  6.9), and 70 (51.2%) designated 'definite diabetic' (BMI 37.5  $\pm$  8).

### CONCLUSION

The ultrasound appearance of an echogenic deltoid muscle is a strong predictor of type 2 diabetes and seems to be due to more than just adipose infiltration. It could be related to impaired insulin-stimulated intramuscular glycogen synthesis or issues with collagen synthesis. We also conclude that this appearance may be used to detect pre-diabetes.

#### **CLINICAL RELEVANCE/APPLICATION**

Ultrasound of the type 2 diabetic deltoid muscle demonstrates increased echogenicity which is likely secondary to insulin resistance and may be used as a noninvasive means to detect pre-diabetes.



## MK347-SD-SUA2

Sonoelastography of the Supraspinatus and Infraspinatus Tendons in Patients with Adhesive Capsulitis of Shoulder

Sunday, Nov. 25 12:30PM - 1:00PM Room: MK Community, Learning Center Station #2

# Participants

Seong Jong Yun, Seoul, Korea, Republic Of (*Presenter*) Nothing to Disclose Wook Jin, Seoul, Korea, Republic Of (*Abstract Co-Author*) Nothing to Disclose So Young Park, Seoul, Korea, Republic Of (*Abstract Co-Author*) Nothing to Disclose Ga Ram Kang, Seoul, Korea, Republic Of (*Abstract Co-Author*) Nothing to Disclose Ji Seon Park, MD, PhD, Seoul, Korea, Republic Of (*Abstract Co-Author*) Nothing to Disclose Yeo Jin Kim, Seoul, Korea, Republic Of (*Abstract Co-Author*) Nothing to Disclose Kyung Nam Ryu, MD, PhD, Seoul, Korea, Republic Of (*Abstract Co-Author*) Nothing to Disclose

#### For information about this presentation, contact:

jinooki@daum.net

### PURPOSE

The main aim of our study was to evaluate the elasticity of the supraspinatus tendon (SST) and infraspinatus tendon (IST) in healthy individuals and patients with clinical findings suggestive of adhesive capsulitis of shoulder (ACS). The second aim was to compared diagnostic performance between two sonoelastography (SE) methods (shear wave vs. strain).

### **METHOD AND MATERIALS**

The institutional review board approved this single-institution prospective study, which was performed between November 1, 2017, and March 21, 2018. Shear-wave and strain SE were used to evaluate elasticity of the SST and IST in healthy individuals (12 men and six women,  $52.6 \pm 10.5$  years) and those with clinical findings suggestive of ACS (six men and 14 women,  $53.5 \pm 7.9$  years). SE was performed in the coronal oblique plane under sitting and neutral shoulder position. Velocity and stiffness of the SST and IST on shear wave SE, and strain ratio (subcutaneous fat/tendon) on strain SE were measured in random order using specific region-of-interest. Statistically, Mann Whitney U-test, receiver operating characteristic (ROC) curve, and DeLong's tests were used.

### RESULTS

On shear wave SE, SST and IST in ACS patients showed significantly higher mean, minimum, and maximum velocities, and higher mean, minimum, and maximum stiffness than those in the healthy individuals (all p<0.001). On strain SE, SST and IST in ACS patients showed significantly higher strain ratio than those in the healthy individuals (all p<0.001). Among these significant parameters, IST-strain ratio had the highest diagnostic performance (area under the ROC curve [AUC], 0.990; sensitivity, 95.7%, specificity, 100%). Also, IST-mean velocity and stiffness (AUC, 0.985; sensitivity, 92.0%, specificity, 100%), SST-strain ratio (AUC, 0.983; sensitivity, 95.7%, specificity, 100%), SST-mean velocity (AUC, 0.979; sensitivity, 88.0%, specificity, 100%), and SST-mean stiffness (AUC, 0.977; sensitivity, 84.0%, specificity, 100%) had excellent diagnostic performance. There was no difference of the AUC (p=0.36-1.0), sensitivity (p=0.39-1.0), and specificity (p=1.0) between shear wave and strain SE examinations.

#### CONCLUSION

Real-time shear wave and strain SE showed the stiffer SST and IST in the ACS with excellent diagnostic performance

### **CLINICAL RELEVANCE/APPLICATION**

The use of SE may be helpful in patients with clinically suspected ACS in diagnosis and follow-up, especially with emphasis on quantitative evaluation.



## MK348-SD-SUA3

### Bony and Muscular Differences in Temporomandibular Joint Disorders on MRI

Sunday, Nov. 25 12:30PM - 1:00PM Room: MK Community, Learning Center Station #3

#### **Participants**

Jennifer Padwal, La Jolla, CA (*Presenter*) Nothing to Disclose Palanan Siriwanarangsun, MD, Bankok, Thailand (*Abstract Co-Author*) Nothing to Disclose Sheronda Statum, San Diego, CA (*Abstract Co-Author*) Nothing to Disclose Mitsue Miyazaki, PhD, La Jolla, CA (*Abstract Co-Author*) Nothing to Disclose Shantanu Sinha, PhD, San Diego, CA (*Abstract Co-Author*) Nothing to Disclose Won C. Bae, PhD, La Jolla, CA (*Abstract Co-Author*) Nothing to Disclose Christine B. Chung, MD, La Jolla, CA (*Abstract Co-Author*) Nothing to Disclose

#### For information about this presentation, contact:

jpadwal@ucsd.edu

#### PURPOSE

Temporomandibular joint disorders (TMD) pose a significant healthcare problem. Unlike the temporomandibular joint (TMJ) disc, the bony and muscular changes in TMD have not been well-defined. This study characterizes various bony and muscular magnetic resonance imaging (MRI) measurements in a small cohort of control and TMD patients.

#### **METHOD AND MATERIALS**

Healthy volunteers (1 M, 2 F, 28-34 yo) and patients with TMD (3 F, 22-51 yo) were imaged at 3-T with: 3D CUBE sequence (sagittal, TR=1466 ms, TE=36 ms, FOV=160 mm, matrix=320, slice=0.5 mm) to visualize bone and muscle; and spin echo multi echo T2 map sequence (coronal, TR=1325 ms, 16 TEs=10 to 160 ms) to measure muscle T2 values. On each person, using CUBE data, measurements of the mandibular condyle length (CL), angle (CA), volume (CV) and cap angle (CAPA) were obtained along with socket depth (SOCD). In addition, on axial-reformatted CUBE data, bilateral masseter (M), medial pterygoid (MP), and lateral pterygoid (LP) muscle volumes were obtained by segmentation of individual muscle. Using T2 map data, T2 values of bilateral M, LP, and MP muscles were measured. Measurements were compared between normal vs TMD, and left vs right sides (for asymmetry in TMD) using a 2-way repeated measures ANOVA.

#### RESULTS

Bony measurements, including CL, CA, CV, CAPA, and SOCD, were similar between both normal and pathological or left and right sides, with CV (259 vs 316, p=0.081) and CAPA (141 vs 146, p=0.087) demonstrating differences between left and right sides that trended toward significance. Muscle volume for M, MP, and LP were similar between left/right sides and were slightly larger for pathological compared to normal sides. T2 values were smaller for pathological compared to normal M (36.7 vs 35.3 ms, p=0.283) but were otherwise similar.

## CONCLUSION

This study demonstrated differences in bony measurements on MR between pathological and normal sides, suggesting a bony adaptation in TMD. The role of bony and muscular changes in TMD will be elucidated in future studies to evaluate whether such changes are caused by or a result of TMD pathology.

#### **CLINICAL RELEVANCE/APPLICATION**

This study demonstrated differences in bony measurements on MRI between pathological and normal sides, suggesting a bony adaptation in TMD. The role of bony and muscular changes in TMD will be elucidated in future studies to evaluate whether such changes are caused by or a result of TMD pathology.



### MK349-SD-SUA4

Imaging Can Finally Be Used to Decide on Therapy of Cartilaginous Tumors in Long Bones: Resection or Curettage

Sunday, Nov. 25 12:30PM - 1:00PM Room: MK Community, Learning Center Station #4

# Participants

David Hanff, MD, Amsterdam, Netherlands (*Presenter*) Nothing to Disclose Veroniek M. Van Praag, Leiden, Netherlands (*Abstract Co-Author*) Nothing to Disclose Kirsten Van Langevelde, MD, Leiden, Netherlands (*Abstract Co-Author*) Nothing to Disclose Carla S. Van Rijswijk, MD, Leiden, Netherlands (*Abstract Co-Author*) Nothing to Disclose Herman Kroon, Leiden, Netherlands (*Abstract Co-Author*) Nothing to Disclose Michiel van de Sande, MD, Leiden, Netherlands (*Abstract Co-Author*) Nothing to Disclose H J. Bloem, Leiden, Netherlands (*Abstract Co-Author*) Nothing to Disclose

### For information about this presentation, contact:

d.hanff@erasmusmc.nl

# PURPOSE

To determine which radiographic and magnetic resonance imaging (MRI) features differentiate CS2 from an ACT/CS1 in long bones.

#### **METHOD AND MATERIALS**

In this retrospective study we reviewed 82 patients treated at our institution for an ACT/CS1 (58 patients) or CS2 (24 patients) in the long bones. Four observers separately reviewed radiographs and MRI using a fixed set of 19 parameters, and a subjective radiologic diagnosis. Parameters were compared with a reference standard consisting of a, non-imaging dependent, histopathological diagnosis of resected specimens using univariate, multivariate logistic regression analysis. Inter-observer variability (IOV) was calculated (Fleiss kappa).

### RESULTS

Diagnosis (ACT/CS1 or CS2) of the four reviewers matched ultimate histologic diagnosis in 93% (304/328 observations for 82 patients), with an interrater agreement of 91.1%. In multivariate analysis the radiographic <50% chondroid matrix (OR 0.227; p=0.054, 95%CI 0.050-1.025, IOV 81.9%) showed a positive trend for CS2. For MRI prognostic factors were soft tissue mass (OR 0.070; p<0.001, 95%CI 0.024-0.200; IOV 89.2%), reactive soft tissue edema (OR 0.183; p<0.001, 95%CI 0.061-0.551; IOV 90.7%), peri-tumoral intraosseous edema (OR 0.157; p=0.016, 95%CI 0.035-0.710; IOV 92.1%), dynamic enhancement (IOV 62.2%) for 3-6 sec. (OR 0.141; p=0.015, 95%CI 0.029-0.687) and <=3sec (OR 0.566; p=0.374, 95% 0.161-0.1987); expansion of the medullary canal (OR 0.187; p=0.001, 95%CI 0.069-0.504; IOV 78.9%), and cortical thickening (OR 0.142; p=0.005, 95%CI 0.033-0.616; IOV 94.3%)(see table 1). R2 was 0.777, indicating a good level of prediction.

## CONCLUSION

With an accuracy of 93% and high inter-rater reliability we were able to differentiate CS grade 2 from ACT. Most useful parameters are chondroid matrix, soft tissue mass, reactive soft tissue edema, peri-tumoral intraosseous edema, dynamic enhancement, expansion of the medullary canal and cortical thickening.

#### **CLINICAL RELEVANCE/APPLICATION**

Pre-operative radiologic assessment can reliably differentiate between a CS2 and ACT/CS1 and is therefore essential in determining a multidisciplinary and optimal treatment for the patient.



## MK350-SD-SUA5

### MR Anatomical-Histological Correlation of the Adductor Longus-Rectus Abdomins-Pubic Ligament Complex

Sunday, Nov. 25 12:30PM - 1:00PM Room: MK Community, Learning Center Station #5

#### **Participants**

Michel O. De Maeseneer, MD, PhD, Jette, Belgium (*Presenter*) Nothing to Disclose Ramses Forsyth, MD, MBA, Jette, Belgium (*Abstract Co-Author*) Nothing to Disclose Steven Provyn, Brussels, Belgium (*Abstract Co-Author*) Nothing to Disclose Johan de Mey, MD, PhD, Jette, Belgium (*Abstract Co-Author*) Nothing to Disclose Filip De Ridder, Jette, Belgium (*Abstract Co-Author*) Nothing to Disclose Maryam Shahabpour, MD, Brussels, Belgium (*Abstract Co-Author*) Nothing to Disclose

## For information about this presentation, contact:

Michel.demaeseneer@uzbrussel.be

## PURPOSE

The anatomy of the AL, rectus abdominus, pyramidalis insertions is still not completely understood. Recent investigations in the pyramidalis and adductor insertions have shed new light on this anatomy. Our purpose was to correlate high resolution MR imaging with cadaveric and en bloc histologic slicing to elucidate the anatomy of the adductor insertions.

#### **METHOD AND MATERIALS**

3T high resolution MR images in the three planes were correlated with crysosections and 'en bloc' histological sections of the pubic symphysis. Histological slices after decalcification were stained with HES.Findings were interpreted by consensus of a senior MSK radiologist, pathologist and anatomist.

#### RESULTS

Findings The AL is the main tendon inserting on the pubic rami. It inserts in a triangular fashion very strongly anchoring tendon into bone. Its tendon fibers gradually transform in ligament fibers and these ligament fibers form cross connections with the contralateral AL tendon, an additional element of reinforcement. The pubic ligament is made of true strong ligament fibers and no cartilage or fibrocartilage nodule is present. Cartilage does line the joint surface at the symphyseal joint. The posterior aponeurosis of the rectus abdominis forms a 2 cm wide and 2 mm thick band that inserts directly onto the superior aspect of the pubic ligament. Connections of the piramidalis or when absent rectus abdominus continue laterally over the adductor longus but are actually quite delicate and surprisingly less thick and strong than has been typically believed. The other adductor tendons show muscular insertions on the pubic rami. The gracilis inserts on the adductor brevis muscle.

## CONCLUSION

The anatomy-histology at the pubic symphysis is complex. The AL stongly anchors into the bone as 'tendinoligamentous fibers' but also has cross connections with the contralateral side.

## **CLINICAL RELEVANCE/APPLICATION**

Pubic tendon and ligament is extemely important in high level athletes and injuries can be career ending. The anatomy of the tendon insertions is not well understood. This is related to the historical fact that this area is difiifcult to analyse in embalmed cadavers. Our MR correlations with fresh specimens, and histology shed new light on this anatomy.



#### MS180-ED-SUA1

Scleroderma (Systemic Sclerosis): Radiologic Manifestations

Sunday, Nov. 25 12:30PM - 1:00PM Room: MS Community, Learning Center Station #1

#### **Participants**

Joanie M. Garratt, MD, Brookfield, MA (*Presenter*) Nothing to Disclose Brian D. Midkiff, MD, MPH, Worcester, MA (*Abstract Co-Author*) Nothing to Disclose Nooshin Najmi, MD, Encino, CA (*Abstract Co-Author*) Nothing to Disclose

For information about this presentation, contact:

joaniegarratt@gmail.com

### **TEACHING POINTS**

Scleroderma, also known as systemic sclerosis, is a multi-system autoimmune connective tissue disorder that affects many separate structures. The disease is characterized by widespread deposition of collagen and other extracellular matrix proteins. Although a rare disease, scleroderma in its more aggravated forms has been described as "one of the most terrible of all human ills." The objective of this exhibit is to provide a multi-organ system review of the imaging findings of scleroderma manifestations utilizing different modalities.

# TABLE OF CONTENTS/OUTLINE

\* Introduction\* Objectives\* Epidemiology and Pathophysiology\* Manifestations - Musculoskeletal: subcutaneous/periarticular calcification, acroosteolysis, joint space narrowing, erosions, osseous resorption, soft tissue atrophy - Pulmonary/Cardiovascular: interstitial lung disease, bronchiectasis, aspiration pneumonitis, pulmonary cysts, pulmonary arterial hypertension - Gastrointestinal: esophageal dilation, esophagitis, esophageal stricture, delayed esophageal/gastric emptying, small bowel luminal dilatation and hidebound bowel sign, pseudosacculations, pneumatosis intestinalis - Hepatobiliary: primary biliary cholangitis - Renal: malignant hypertension, renal insufficiency\* Summary\* References



### NM002-EB-SUA

The Renaissance of Thallium SPECT in Neuro-Oncology: A Pictorial Review of Radiation Necrosis versus Tumour Recurrence

Sunday, Nov. 25 12:30PM - 1:00PM Room: NM Community, Learning Center Hardcopy Backboard

# Participants

Laura Preston, BMBCh, FRCR, Glasgow, United Kingdom (*Presenter*) Nothing to Disclose Alice Nicol, PhD, MSc, Glasgow, United Kingdom (*Abstract Co-Author*) Nothing to Disclose Ravi V. Jampana, MBBS, MRCP, Glasgow, United Kingdom (*Abstract Co-Author*) Nothing to Disclose Celestine Santosh, BMBCh, FRCR, Glasgow, United Kingdom (*Abstract Co-Author*) Nothing to Disclose Natasha E. Fullerton, MD, PhD, Glasgow, United Kingdom (*Abstract Co-Author*) Nothing to Disclose

# For information about this presentation, contact:

laura.preston4@nhs.net;natasha.fullerton@nhs.net

### **TEACHING POINTS**

Differentiation between radiation necrosis and tumour is an increasing challenge in neuro-oncology imaging due to a greater variety of treatment options and longer patient survival. There is large overlap in appearances on CT/MRI with no reliable imaging finding to enable confident discrimination. Thallium-201 SPECT has shown potential as a tool to help solve this dilemma. Whilst its use for tumour grading has decreased in our institution over the last 10 years, its emerging role in radionecrosis has resulted in a resurgence in its use. The aims of this exhibit are: 1) To review the MRI features of radionecrosis in a variety of scenarios and to illustrate the challenge in differentiation from tumour progression/recurrence. 2) To illustrate the use of thallium-SPECT in differentiating radionecrosis from tumour, using experience from our institution.

### **TABLE OF CONTENTS/OUTLINE**

Overview of thallium SPECT. •Technical aspects (including fusion) •Variety of uses in neuro-oncology <u>Aetiology/ clinical features of radionecrosis</u>. <u>Pictorial review</u>. •Cases to illustrate the shortfalls of structural imaging for radionecrosis versus tumour, and the complementary use of thallium SPECT. <u>Sensitivity and specificity of Thallium-SPECT for distinguishing radionecrosis from tumour</u> •Experience from our institution versus wider literature.



### NM200-SD-SUA1

## Evaluation of a Fast Protocol for Staging Patients with Bronchial Cancer Using PET/MRI

Sunday, Nov. 25 12:30PM - 1:00PM Room: NM Community, Learning Center Station #1

#### **Participants**

Ole Martin, Duesseldorf, Germany (Presenter) Nothing to Disclose

Julian Kirchner, Dusseldorf, Germany (Abstract Co-Author) Nothing to Disclose

Ken Herrmann, Essen, Germany (*Abstract Co-Author*) Co-founder, SurgicEye GmbH; Stockholder, SurgicEye GmbH; Consultant, Sofie Biosciences; Consultant, Ipsen SA; Consultant, Siemens AG; Research Grant, Advanced Accelerator Applications SA; Research Grant, Ipsen SA

Lale Úmutlu, MD, Essen, Germany (*Abstract Co-Author*) Consultant, Bayer AG Gerald Antoch, MD, Duesseldorf, Germany (*Abstract Co-Author*) Nothing to Disclose Philipp Heusch, MD, Duesseldorf, Germany (*Abstract Co-Author*) Nothing to Disclose

#### For information about this presentation, contact:

Ole.Martin@med.uni-duesseldorf.de

### PURPOSE

To evaluate the applicability of a fast MR-protocol for whole-body staging of bronchial carcinoma patients using an integrated PET/MR system.

# METHOD AND MATERIALS

In this prospective study, 52 patients (16 female, 36 male, mean age 63.9±8.7y) underwent clinically indicated PET/CT and subsequent PET/MRI. For PET/MRI imaging, a fast whole-body MR-protocol was implemented. MRI and PET/MRI datasets were analyzed to identify malignant manifestations. The accuracy for the identification of malignant manifestations was calculated and the tumor stage for each examination was determined using the actual TNM classification from UICC 8 (union international contre le cancer). Radiation doses derived from administered tracer activities and CT protocol parameters were estimated and the mean scan duration of PET/CT and PET/MRI imaging were determined. In 26 patients, all available histopathological samples as well as results of follow-up imaging were used for reference standard. In the other cases, the results of PET/CT imaging used for reference standard.

## RESULTS

Active malignant lesions were present in 47/52 examinations. Both MRI and PET/MRI have a 100% accuracy to correctly identify the extent of the primary (T-stage). In nodal staging, PET/MRI revealed higher values of diagnostic accuracy than MRI alone (93.5% for PET/MRI, 83.9% for MRI, p<0.05). However, the results did not differ significantly. In identification of metastases, PET/MRI showed higher diagnostic accuracy than MRI alone (90.3% for PET/MRI vs. 77.4% for MRI, p<0.05). In TNM classification, PET/MRI enabled higher values of correct stage than MRI (86.9% for PET/MRI vs. 64.5% for MRI, p<0.05). The values of correct stage did not differ significantly between PET/CT and PET/MRI (93.5% for PET/CT vs. 86.9% for PET/MRI). Average scan duration of whole-body PET/CT and PET/MRI examinations were 17.5±2.3 min and 29.4±3.9 min, respectively. Estimated mean effective-dose for PET/CT scans were 61.3% higher than for PET/MRI.

## CONCLUSION

Using 18F-FDG PET data in addition to whole-body MRI leads to a more accurate evaluation of patients with bronchial cancer. With regard to patient comfort related to scan duration and reduced radiation exposure, fast PET/MRI may serve as a powerful alternative to PET/CT for a diagnostic workup of bronchial cancer patients.

### **CLINICAL RELEVANCE/APPLICATION**

In staging lung cancer patients, whole body PET/MRI may serve as a powerful alternative to PET/CT



### NM201-SD-SUA2

Value of Quantitative Parameters and Metabolic Heterogeneity of 18F-FDG PET/CT to Predict Prognosis in Patients with Primary Oropharyngeal Carcinoma

Sunday, Nov. 25 12:30PM - 1:00PM Room: NM Community, Learning Center Station #2

**FDA** Discussions may include off-label uses.

#### Participants

Keiichiro Tahara, Fukuoka, Japan (*Presenter*) Nothing to Disclose Shingo Baba, Fukuoka, Japan (*Abstract Co-Author*) Nothing to Disclose Takuro Isoda, Fukuoka, Japan (*Abstract Co-Author*) Nothing to Disclose Yoshiyuki Kitamura, Fukuoka, Japan (*Abstract Co-Author*) Nothing to Disclose Ryo Somehara, Fukuoka, Japan (*Abstract Co-Author*) Nothing to Disclose Masayuki Sasaki, Fukuoka, Japan (*Abstract Co-Author*) Nothing to Disclose Hiroshi Honda, MD, Fukuoka, Japan (*Abstract Co-Author*) Nothing to Disclose

#### For information about this presentation, contact:

md104061@yahoo.co.jp

#### PURPOSE

The aim of this study was to evaluate the impact of quantitative FDG PET/CT imaging parameters and intratumoral metabolic heterogeneity for predicting patient outcomes in primary oropharyngeal cancer.

### METHOD AND MATERIALS

We retrospectively investigated 30 patients with oropharyngeal carcinoma with ipsilateral LN metastasis. SUVmax and metabolic tumor volume (MTV) and Total lesion glycolysis (TLG) were measured for the primary tumors and metastatic lymph nodes. Primary tumor intratumoral metabolic heterogeneity was calculated as the CV (coefficient of variation) of FDG uptake and the area under a cumulative SUV volume histograms curve (AUC-CSH). The median follow-up time was 35.4 months (range, 3-120 months). Each parameters were compared between the good prognosis group and the poor prognosis group.

#### RESULTS

Of the 30 patients included, 8 patients relapsed and 7 deceased during the study period. No significant difference was seen in SUVmax and MTV between two groups. TLG of primary tumor was significantly higher in poor prognosis group compared with good prognosis group (334±86 vs 199±53). Week correlation was observed between AUC-CSH indexes and prognosis but no statistically significant difference was found.As for lymph node metastasis, TLG of poor prognosis group was significantly higher than those of poor prognosis group (264±86 vs 135±53). In addition, CV of FDG uptake in lymph nodes was significantly higher in poor prognosis group (0.51±0.11 vs 0.41±0.10).

### CONCLUSION

In addition to TLG, metabolic heterogeneity of Lymph node metastasis was a prognostic factor for the patients with oropharyngeal cancer. The combined predictive effect of metabolic tumor burden, and heterogeneity provided prognostic survival information in these patients.

# **CLINICAL RELEVANCE/APPLICATION**

Metabolic heterogeneity of Lymph node metastasis was a prognostic factor for the patients with oropharyngeal cancer.



## NM202-SD-SUA3

## Role of Tri-PET in Managing Indolent Lymphomas

Sunday, Nov. 25 12:30PM - 1:00PM Room: NM Community, Learning Center Station #3

### Participants

Shanker Raja, MD, Bellaire, TX (Presenter) Nothing to Disclose Musab M. Ahmed, MBBS, Riyadh, Saudi Arabia (Abstract Co-Author) Nothing to Disclose Shahid Iqbal, MBBS, MRCP, Riyadh, Saudi Arabia (Abstract Co-Author) Nothing to Disclose Sharad P. George, MD, Dhahran, Saudi Arabia (Abstract Co-Author) Nothing to Disclose Syed Z. Zaidi, MD, Riyadh, Saudi Arabia (Abstract Co-Author) Nothing to Disclose Belal M. Albtoosh, BSN, Riyadh, Saudi Arabia (Abstract Co-Author) Nothing to Disclose Atta M. Gill, MD, Riyadh, Saudi Arabia (Abstract Co-Author) Nothing to Disclose Ahmad A. Butt, MD, Riyadh, Saudi Arabia (Abstract Co-Author) Nothing to Disclose Nawal F. AlShehry, MD, Riyadh, Saudi Arabia (Abstract Co-Author) Nothing to Disclose

### PURPOSE

Indolent lymphomas (ind-LYM) are a subset of B-cell lymphomas, characterized by slow growth, protracted, and a tendency to reoccur. The management of ind-LYM is varied and evolving. Reliable tools for prognostication and treatment strategies are limited. We explored the utility of FDG tri-PET (baseline (BAS), interim/6 months (INT), and end of therapy/1 yr (EOT)), in managing ind-LYM.

### METHOD AND MATERIALS

Retrospective analysis of all pts. diagnosed as ind-LYM and having undergone tri-PET from 2015 to current (no 40; male=2,female=13, mean age at diagnosis= 59.68 ± 14.5. All PET scans were obtained per accepted protocols. SUVmax Deauville scores (DS) were obtained from five target lesions, the average (cSUV & cDS) were computed for each pt. to obtain composite scores. Statistical analyses were performed with the cSUV and cDS. The following statistics were performed (T-test, mean delta change (DELch) between each time point (BS, INT, EOT), for both cSUV (cSUV-DELch and cDC(cDC-DELch.

### RESULTS

The types of ind-LYM types were CLL/SLL and Follicular, 17 and 15 respectively, 3 each of mantle cell and marginal zone lymphoma , and 1 each MALT and lymphoplasmocytic lymphoma. The data were analyzed for two arms of the study i.e treatment (chemotherapy arm (CHEMO-22/40)arm, and Rituximab+observation arm (OBSER-18/40). At BAS, pts. on CHEMO had significantly higher cSUV and cDC compared to those who received Rituximab only (cSUV: 6.99 vs. 4.32 p-value 0.0124) (cDC: 4.37 vs 3.71 pvalue 0.0075), respectively. Although there was a DELch in the cSUV and cDC in both arms from INT to EOT, both treatment arms showed no significant difference in the cSUV and cDC (p-value: 0.754 and 0.572, respectively). A 2-tailed t-test was for DELch of cSUV BAS to INT after removal of an outlier was statistically significant p-value 0.05; while it was not significant for BAS to EOT (0.98) nor for any of the cDC-DELch..

### CONCLUSION

The higher cSUV/cDC at BAS for the treatment arm may be due to disease profile/ selection bias; at EOT no difference in both estimates were noted. Both arms showed similar trends in DELch from BS-INT-EOT. Our findings suggest that SUV and DC at BAS may be independent criteria for treatment selection in ind-LYM.

## **CLINICAL RELEVANCE/APPLICATION**

Our findings on tri-PET suggest that metabolic profiles are helpful in selection of treatment strategies at baseline. composite SUVmax is is potentially a good prognosticator.



## NR327-ED-SUA7

Pharyngoesophagram and Videofluoroscopic Evaluation of Oropharyngeal Swallow: The First Step in the Study of Dysphagia

Sunday, Nov. 25 12:30PM - 1:00PM Room: NR Community, Learning Center Station #7

## Participants

Javier Azpeitia Arman, MD, Madrid, Spain (*Presenter*) Nothing to Disclose Rosa M. Lorente-Ramos, MD, PhD, Madrid, Spain (*Abstract Co-Author*) Nothing to Disclose Gloria Liano Esteso, Madrid, Spain (*Abstract Co-Author*) Nothing to Disclose Jose Maria Lopez-Arcas Calleja, Madrid, Spain (*Abstract Co-Author*) Nothing to Disclose Miguel Grande, MD, Madrid, Spain (*Abstract Co-Author*) Nothing to Disclose Pedro Torres Rubio, MD, Madrid, Spain (*Abstract Co-Author*) Nothing to Disclose

#### For information about this presentation, contact:

fjavier.azpeitia@salud.madrid.org

#### **TEACHING POINTS**

- To understand the utility of pharyngoesophagogram and videofluoroscopic evaluation of oropharyngeal swallowing in the study of dysphagia. -To review the study protocols. -To describe normal anatomy and normal imaging appearances of pharynx, esophagus and gastric cardia. -To illustrate appearances of various entities causing dysphagia. CT correlates will also be shown for comparison.

#### **TABLE OF CONTENTS/OUTLINE**

Contrast upper gastrointestinal studies remain a basic skill for radiologists in evaluation of dysphagia We present: - Study protocols of pharyngoesophagram and videofluoroscopic evaluation of oropharyngeal swallow. -Normal anatomy of the oropharynx, esophagus and gastric cardia with imaging correlation in contrast studies. - Imaging findings: 1. Motility disorders. A. Oropharynx: bolus transport from oral cavity, laryngeal vestibular penetration, pharynx residue, transglottic aspiration. B. Esophageal motility. 2. Intrinsic causes. A. Oropharynx: cricopharyngeal bar (prominent cricopharyngeal muscle), Killian-Jamieson diverticulum, web. B. Esophagus and gastric cardia: Esophageal fibrotic strictures, Zenker's diverticulum, squamous cell carcinoma, achalasia (primary and secondary). 3. Extrinsic compression: osteophytes, thyroid gland, lymphadenopathy. 4. Surgery: laryngectomy.



## NR329-ED-SUA9

A Case-based Approach to Understanding Cerebral Proliferative Angiopathy, A Distinct Entity from Classical Brain AVM

Sunday, Nov. 25 12:30PM - 1:00PM Room: NR Community, Learning Center Station #9

### Participants

Camila F. Silveira, MD, Sao Paulo, Brazil (*Presenter*) Nothing to Disclose Bruno S. Inada, MD, Sao Paulo, Brazil (*Abstract Co-Author*) Nothing to Disclose Lazaro F. Amaral, MD, Sao Paulo, Brazil (*Abstract Co-Author*) Nothing to Disclose Leonardo F. Freitas, MD, Sao Paulo, Brazil (*Abstract Co-Author*) Nothing to Disclose Victor R. Marussi, MD, Campinas, Brazil (*Abstract Co-Author*) Nothing to Disclose Anderson Benine Belezia, MD, Sorocaba, Brazil (*Abstract Co-Author*) Nothing to Disclose Samir S. Omar, MD, Sao Paulo, Brazil (*Abstract Co-Author*) Nothing to Disclose Aylla K. Alves Simao, MD, Goiania, Brazil (*Abstract Co-Author*) Nothing to Disclose Micaela M. Mota, MD, Sao Paulo, Brazil (*Abstract Co-Author*) Nothing to Disclose Livia P. Souza, MD, Sao Paulo, Brazil (*Abstract Co-Author*) Nothing to Disclose Marcelo R. Natal, MD, Brasilia, Brazil (*Abstract Co-Author*) Nothing to Disclose Ayrton R. Massaro, Sao Paulo, Brazil (*Abstract Co-Author*) Nothing to Disclose Ticiane Vilas Boas, MD, Assis, Brazil (*Abstract Co-Author*) Nothing to Disclose Ronie L. Piske, PhD, Sao Paulo, Brazil (*Abstract Co-Author*) Nothing to Disclose Christiane M. Campos, MD,MD, Sao Paulo, Brazil (*Abstract Co-Author*) Nothing to Disclose

For information about this presentation, contact:

camisilveira.f@gmail.com

### **TEACHING POINTS**

Diffuse proliferative cerebral angiopathy are composed of multiple small arterial feeders and draining veins with normal brain parenchyma seen intermingled between the abnormal vessels. Therefore it is a distinct entity from classical cerebral arteriovenous malformations (AVM), in terms of epidemiology, clinical presentation, angiographic and histopathological features, natural history and management considerations.

### TABLE OF CONTENTS/OUTLINE

This exposition addresses radiographic features of cerebral proliferative angiopathy, which helps to discern it from classical brain arteriovenous malformations, their typicall and atypicall locations and different clinical presentations. Characteristic features include multiple nondominant arterial feeders, the transdural supply, relatively small draining veins, normal brain intermingled the nidus, the large size and the presence of capillary angioectasia. Unlike classical AVM, these entity contain normal cerebral tissue in-between the abnormal vessels, therefore it is important to recognize this diagnosis in order to avoid aggressive surgery or intervention, preventing permanent damage to the normal intermingled brain parenchyma.



### NR330-ED-SUA10

Eyes Are the Windows to the... CNS When Anterior Visual Pathway Involvement Reflect the Diagnosis of CNS Disorders: Reviewing Patterns and Differential Diagnosis

Sunday, Nov. 25 12:30PM - 1:00PM Room: NR Community, Learning Center Station #10

#### Awards Certificate of Merit

#### **Participants**

Ana Paula A. Fonseca, MD, Sao Paulo, Brazil (*Presenter*) Nothing to Disclose Igor G. Padilha, MD, Sao Paulo, Brazil (*Abstract Co-Author*) Nothing to Disclose Ana Luiza M. Pettengill, MD, Sao Paulo, Brazil (*Abstract Co-Author*) Nothing to Disclose Marcos Rosa Junior, PhD, Vitoria, Brazil (*Abstract Co-Author*) Nothing to Disclose Felipe T. Pacheco, MD, Sao Paulo, Brazil (*Abstract Co-Author*) Nothing to Disclose Renato H. Nunes, Sao Paulo, Brazil (*Abstract Co-Author*) Nothing to Disclose Antonio C. Maia Jr, Sao Paulo, Brazil (*Abstract Co-Author*) Nothing to Disclose Antonio J. da Rocha, MD, PhD, Sao Paulo, Brazil (*Abstract Co-Author*) Nothing to Disclose Moises Oliveira, Sao Paulo, Brazil (*Abstract Co-Author*) Nothing to Disclose

## For information about this presentation, contact:

anapaf.fonseca@gmail.com

## **TEACHING POINTS**

The purposes of this exhibit are: - Review and illustrate the anatomical aspects of anterior visual pathway (AVP), composed of the chiasm, optic nerves and retina. - Describe the main patterns of AVP involvement that reflect CNS disorders (not restricted to AVP), based on clinical aspects and mainly on imaging patterns, highlighting key points to differential diagnosis approach. - Determine an algorithm for the systematic evaluation of differential diagnosis, including inflammatory, metabolic, infectious, neoplastic, toxic and vascular diseases, emphasizing the main clinical features and imaging red flags.

### TABLE OF CONTENTS/OUTLINE

Anatomy of anterior visual pathway - Chiasm - Optic Nerve - Retina - Imaging patterns of involvement of anterior visual pathway
 Laterality, symmetry, extension, contrast enhancement and volume. - Differential diagnosis based on a pictorial review using
 representative cases from our institutional database - Inflammatory - Metabolic diseases - Toxic disorders - Infections - Neoplasms
 Degenerative diseases - Phacomatosis - Vascular - Diagnostic Algorithm - Final remarks



## NR362-SD-SUA1

Small High-Signal Lesion Posterior to the Intracranial Vertebral Artery Incidentally Identified by 3D FLAIR: Analysis of the Relationship to the Spinal Accessory Nerve by 3D Balanced Fast Field Echo MR Imaging

Sunday, Nov. 25 12:30PM - 1:00PM Room: NR Community, Learning Center Station #1

### Participants

Ryota Kogue, MD, Tsu, Japan (*Presenter*) Nothing to Disclose Masayuki Maeda, MD, Tsu, Japan (*Abstract Co-Author*) Nothing to Disclose Maki Umino, MD, Tsu, Japan (*Abstract Co-Author*) Nothing to Disclose Kazuhiro Tsuchiya, MD, Kawagoe, Japan (*Abstract Co-Author*) Nothing to Disclose Hajime Sakuma, MD, Tsu, Japan (*Abstract Co-Author*) Research Grant, Fuji Pharma Co, Ltd; Research Grant, DAIICHI SANKYO Group; Research Grant, FUJIFILM Holdings Corporation; Research Grant, Siemens AG; Research Grant, Nihon Medi-Physics Co, Ltd; Speakers Bureau, Bayer AG

#### For information about this presentation, contact:

r-kogue@clin.medic.mie-u.ac.jp

### PURPOSE

A small, benign, high-signal lesion (HSL) posterior to the intracranial vertebral artery (VA) at the foramen magnum is an emerging new entity incidentally revealed by 3D FLAIR. The pathology is unclear. This incidentally diagnosed benign lesion reportedly has a prevalence of 3.4% on 3T 3D FLAIR and appears to be associated with the ipsilateral spinal accessory nerve (SAN). However, the relationship between an HSL and the SAN is insufficiently delineated by 3D FLAIR. We aimed to elucidate this relationship by using a 3D balanced fast field echo (3D bFFE) MR imaging at 3T.

#### **METHOD AND MATERIALS**

From July 2017 to March 2018, 76 patients (38 males, 38 females; mean age  $55.2 \pm 22.4$  years; age range, 7-86 years) with 86 HSLs were studied by 3D FLAIR and 3D bFFE (3T Ingenia, Philips). The mean size of the HSLs was  $3.6 \pm 1.5$  mm. The dataset of each 3D FLAIR and 3D bFFE was reformatted in the axial and coronal planes with a section thickness of 0.6 mm. HSL contact with the ipsilateral SAN was evaluated by using 3D FLAIR and 3D bFFE. Differentiation between an HSL and the SAN was evaluated by 3D FLAIR and 3D bFFE.

#### RESULTS

All HSLs had contact with the ipsilateral SAN on both 3D FLAIR and 3D bFFE. Signal intensity was higher for all HSLs than for SAN on 3D bFFE, which clearly differentiated between the two in contrast to 3D FLAIR. The SAN was typically surrounded by an HSL using 3D bFFE.

#### CONCLUSION

The 3D bFFE MR imaging clearly distinguished between an HSL and the SAN and showed that the HSL typically surrounded the SAN, which may be characteristic of this entity.

## **CLINICAL RELEVANCE/APPLICATION**

An HSL posterior to the VA was shown to surround the SAN by using 3D bFFE. This characteristic of a benign entity may help prevent unnecessary examinations and interventions.



## NR363-SD-SUA2

Evaluation of Intravoxel Incoherent Motion in Pituitary Adenoma Using Turbo Spin-Echo Diffusion-Weighted Imaging: Comparison with Pathological Microvascular Areamicrovascular Perfusion Assessment of Pituitary Adenomas: A Feasibility Study Using Tu

Sunday, Nov. 25 12:30PM - 1:00PM Room: NR Community, Learning Center Station #2

#### **Participants**

Kiyohisa Kamimura, MD, PhD, Kagoshima, Japan (*Presenter*) Nothing to Disclose Masanori Nakajo, MD, Kagoshima, Japan (*Abstract Co-Author*) Nothing to Disclose Tomohide Yoneyama, Kagoshima, Japan (*Abstract Co-Author*) Nothing to Disclose Shingo Fujio, MD,PhD, Kagoshima, Japan (*Abstract Co-Author*) Nothing to Disclose Takashi Iwanaga, Kagoshima, Japan (*Abstract Co-Author*) Nothing to Disclose Takashi Yoshiura, MD, PhD, Kagoshima, Japan (*Abstract Co-Author*) Nothing to Disclose Yuta Akamine, Tokyo, Japan (*Abstract Co-Author*) Employee, Koninklijke Philips NV Yoshihiko Fukukura, MD, PhD, Kagoshima, Japan (*Abstract Co-Author*) Nothing to Disclose

#### PURPOSE

There is no established imaging method to evaluate vascularity of pituitary lesions. The purpose of this study was to evaluate the feasibility of microvascular perfusion assessment of pituitary adenomas using turbo spin-echo-based intravoxel incoherent motion (TSE-IVIM) imaging.

# METHOD AND MATERIALS

We examined 51 consecutive patients with pituitary adenoma (mean age,  $55.8 \pm 14.3$  years; range, 28-82 years; size range 0.1-17.0 mm3) including 35 non-functioning, 7 GH-secreting, 4 PRL-secreting, 3 TSH-secreting, 2 ACTH-secreting tumors. Eight were microadenomas. Thirty-two patients with normal pituitary gland (mean age,  $43.7 \pm 21.6$  years; range, 12-86 years) were also examined. TSE-IVIM imaging was performed with 13 different b values (0-1,000 s/mm2) on a 3T imager. The diffusion coefficient, D, the perfusion fraction, f, and the pseudo diffusion coefficient, D\* in each adenoma and the normal pituitary gland were obtained. We also evaluated the pathological microvessel area (MVA) of each adenoma. The MVA was defined as the percentage of CD34 immunopositive microvessel area relative to the total area. The correlation between the MVA and the f of the adenoma was analyzed using Pearson's correlation coefficient. The IVIM parameters in the adenoma were compared with those in the normal pituitary gland using Student t-test.

## RESULTS

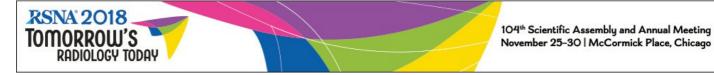
The MVA of adenomas ranged from 1.48 to 11.60%. There was a significant positive correlation between MVA and f in all 51 adenomas (r = 0.451, P = 0.0009) as well as in non-functioning adenomas (n = 35, r = 0.634, P < 0.0001). The mean D (x10-3 mm2/s) in adenomas was  $0.723 \pm 0.253$ , which was significantly lower than that in the normal pituitary gland ( $0.862 \pm 0.128$ ; P < 0.0001). The mean f (%) in adenomas was  $10.74 \pm 4.51$ , which was significantly lower than that in the pituitary gland ( $13.26 \pm 4.32$ , P = 0.025). No significant difference was found in the mean D\*.

## CONCLUSION

Microvascular perfusion assessment of pituitary adenomas based on TSE-IVIM is feasible. This technique may help evaluate vascularity of pituitary and other skull base lesions. Compared to normal pituitary gland, pituitary adenoma was characterized by lower D, ADC and f.

## **CLINICAL RELEVANCE/APPLICATION**

TSE-based IVIM imaging is a viable imaging technique for assessment of vascularity in pituitary adenoma and other skull base lesions.



## NR364-SD-SUA3

Deteriorated Functional and Structural Brain Networks in Diabetic Kidney Disease: A Graph Theory-Based Magnetic Resonance Imaging Study

Sunday, Nov. 25 12:30PM - 1:00PM Room: NR Community, Learning Center Station #3

# Participants

Yun Fei Wang, Nanjing, China (*Presenter*) Nothing to Disclose Rong Feng Qi, MD, Nanjing, China (*Abstract Co-Author*) Nothing to Disclose Qiang Xu, Nanjing, China (*Abstract Co-Author*) Nothing to Disclose Guang Ming Lu, MD, PhD, Nanjing, China (*Abstract Co-Author*) Nothing to Disclose Long Jiang Zhang, MD, PhD, Nanjing, China (*Abstract Co-Author*) Nothing to Disclose

## For information about this presentation, contact:

fmriwangyf@126.com

# PURPOSE

To investigate the topological organization of functional and structural brain networks in diabetic kidney disease (DKD) and its potential clinical relevance.

## METHOD AND MATERIALS

The local institutional review board approved this prospective study, and written informed consent was obtained from each participant. 202 subjects (62 DKD patients, 60 diabetes mellitus [DM] patients, and 80 age-, sex- and education level-matched healthy controls) underwent laboratory examination, neuropsychological test and magnetic resonance imaging (MRI). Large-scale functional and structural brain networks were constructed and graph theoretical network analyses were performed. The effect of renal function on brain functional and structural networks in DKD patients was further evaluated. Correlations were performed between network properties and neuropsychological scores and clinical variables.

### RESULTS

Progressing deteriorated global and local network topology organizations (especially for functional network) were observed for DKD patients compared with control subjects (all p < 0.05, Bonferroni-corrected), with intermediate values for the patients with DM. DKD patients showed normal functional-structural coupling compared with controls while DM patients manifested functional-structural decoupling (p < 0.05, Bonferroni-corrected). Impaired kidney function markedly affected functional and structural network organization in DKD patients (all p < 0.05). Renal toxins (Blood urea nitrogen) correlated with global and local efficiency in the structural networks (r=-0.551, p < 0.001; r=-0.476, p < 0.001; respectively). Global and local efficiency in the structural networks and normalized characteristic path length in the functional networks were associated with information processing speed and/or psychomotor speed.

## CONCLUSION

This study demonstrates that DKD patients showed enhanced functional and structural brain network disruption compared with DM patients, which correlated with kidney function, renal toxins, and cognitive performance.

# **CLINICAL RELEVANCE/APPLICATION**

The results of this study provide an implicative neural basis for the alterations of brain networks in DKD patients and highlight the role of the kidney-brain axis in neurocognitive dysfunction. This will help target and measure the effectiveness of early interventions designed to attenuate adverse brain damage in T2DM patients.



### NR365-SD-SUA4

The Association among Quantitative Contrast Enhanced Ultrasonography Features, TI-RADS Score and BRAF V600E Mutation in Papillary Thyroid Cancer

Sunday, Nov. 25 12:30PM - 1:00PM Room: NR Community, Learning Center Station #4

**FDA** Discussions may include off-label uses.

#### Participants

Luzeng Chen, Beijing, China (*Presenter*) Nothing to Disclose Lei Chen, Beijing, China (*Abstract Co-Author*) Nothing to Disclose Jinghua Liu, Beijing, China (*Abstract Co-Author*) Nothing to Disclose Xun Kong, Beijing, China (*Abstract Co-Author*) Nothing to Disclose Bin Wang, Beijing, China (*Abstract Co-Author*) Nothing to Disclose

#### For information about this presentation, contact:

chenluzeng@bjmu.edu.cn

#### PURPOSE

The objective of this study was to analyze the association among thyroid imaging reporting and data system, quantitative parameters of contrast enhanced ultrasonography and BRAF V600E mutation in papillary thyroid cancer

## METHOD AND MATERIALS

From November 2016 to June 2017, 83 patients who had undergone thyroid CEUS and BRAF mutation analysis for PTC were enrolled in our study. The patients were divided into 2 groups by mutation status. Gender, age, pathologic result, thyroid imaging reporting and data system score and quantitative CEUS parameter were compared between two groups.

#### RESULTS

There were 66 patients in BRAF V600E positive group and 17 patients in BRAF V600E negative group. The age of the patients  $(47.7\pm11.1 \text{ years})$  in BRAF V600E group were older than that  $(40.1\pm10.3 \text{ years})$  in negative group (p=0.006). Gender, vessel invasion, capsular invasion, lymph node metastasis, multiple or single lesion, TI-RADS score were not associated with the mutation status. Begin enhancing time (BET)  $(17.3\pm5.1 \text{ s})$  and time to peak (TTP)  $(26.4\pm7.1 \text{ s})$  of lesion in BRAF V600E positive group were longer than BET  $(14.2\pm4.0 \text{ s})$  and TTP  $(22.4\pm5.7 \text{ s})$  in BRAF V600E negative group. Basic intensity, peak intensity, enhancement extent, rise time, slope of enhancement were not associated with the mutation status.

### CONCLUSION

There is association between quantitative features of CEUS and the status of BRAF mutation. The quantitative features of CEUS may aid to obtain the status of BRAF V600E mutation in PTC patient before invasive procedure.

### **CLINICAL RELEVANCE/APPLICATION**

The quantitative features of CEUS may aid to obtain the status of BRAF V600E mutation in PTC patient before invasive procedure.



## NR366-SD-SUA5

Automated Brain Volumetry of Neuromyelitis Optica Spectrum Disorders: Inter-scanner Variability in White Matter Hyperintensities Segmentations and Volumetric Differences Compared with Multiple Sclerosis

Sunday, Nov. 25 12:30PM - 1:00PM Room: NR Community, Learning Center Station #5

# Participants

Chunjie Guo, Changchun, China (*Presenter*) Nothing to Disclose Yishan Luo, Hong Kong, Hong Kong (*Abstract Co-Author*) Nothing to Disclose Shi L. Lin, Hong Kong, Hong Kong (*Abstract Co-Author*) Director, BrainNow Medical Technology Limited Leongtim Wong, Hong Kong, Hong Kong (*Abstract Co-Author*) Nothing to Disclose Huimao Zhang, Changchun, China (*Abstract Co-Author*) Nothing to Disclose

# For information about this presentation, contact:

guochunjie@hotmail.com

## PURPOSE

To verify AccuBrain is a robust software for white matter lesions (WMLs) and brain volumetric segmentation in neuromyelitis optica spectrum disorders (NMOSD), and to distinguish NMOSD from multiple sclerosis (MS) in neuroimaging.

## METHOD AND MATERIALS

30 NMOSD and 30 MS patients well matched on age and gender from 3D images protocol at the same scanner were recruited in the first study on evaluating brain volumetric and WML differences. In addition, 6 of the NMOSD subjects agreed to enroll in a prospective study on inter-scanner variability and were scanned at 5 different scanners within 24 hours. 2D FLAIR images were obtained from all the sites, while one 3T scanner was also used to acquire 3D T1W and FLAIR images Two automated segmentation software, AccuBrain and lesion segmentation tool (LST) toolbox for SPM were used in WMLs segmentation to assess inter-scanner repeatability. To evaluate the volumetric and WML differences between NMOSD and MS, AccuBrain was used to perform automated segmentation and quantification of WML volumes, regional brain volumes and atrophy. Coefficient of variation (CV) was calculated to assess the effect of scanners on the variability in lesion segmentation, and two-sample t test was used to evaluate the differences of each regional volumetric measure between NMOSD and MS.

### RESULTS

The mean inter-scanner CV of WML volume is  $14.6\% \pm 8.4\%$  when using AccuBrain, which is smaller compared to that of  $23.6\% \pm 11.2\%$  when using LST. In the brain volumetric analysis from 3D T1WI, although NMOSD and MS generally presented similar brain atrophy pattern, we found that they differ significantly in the thalamus-proper, lateral ventricle and third ventricle. In the WML analysis from 3D FLAIR images, significant volume difference was found between NMOSD and MS in white matter hyperintensities, which can be illustrated in the WML prevalence maps from the voxel-based lesion-symptom mapping (VLSM) analysis, with MS group having more WMLs situated over the posterior horns of the lateral ventricles.

### CONCLUSION

AccuBrain is a robust software for calculating WMLs in NMOSD patients in multicenter and longitudinal studies. In addition, NMOSD differs from MS not only in brain atrophy pattern, but also in WML volume and location, and AccuBrain is a suitable software for analysis.

#### **CLINICAL RELEVANCE/APPLICATION**

AccuBrain is a robust software for calculating WMLs and brain volumetric segmentation in NMOSD and MS patients.



### NR367-SD-SUA6

### Alzheimer's Disease Screening Using Structural MRI Biomarker Quantification

Sunday, Nov. 25 12:30PM - 1:00PM Room: NR Community, Learning Center Station #6

FDA Discussions may include off-label uses.

#### Participants

Hong Xiang Yao SR, PhD, Beijing, China (*Presenter*) Nothing to Disclose Yishan Luo, Hong Kong, Hong Kong (*Abstract Co-Author*) Nothing to Disclose Lin Shi, Shatin, Hong Kong (*Abstract Co-Author*) Nothing to Disclose Ningyu An, MD, PhD, Beijing, China (*Abstract Co-Author*) Nothing to Disclose Xi Zhang, Beijing, China (*Abstract Co-Author*) Nothing to Disclose

#### For information about this presentation, contact:

yaohx301@163.com

#### PURPOSE

To identify and validate of structural MRI biomarkers for diagnosing Alzheimer's disease (AD) from normal subjects (NC) and mild cognitive impairment (MCI), T1W-MRIs were collected from different subjects.

## **METHOD AND MATERIALS**

79 AD subjects ( $70.84 \pm 9.31$  years, MMSE 17.66  $\pm 5.65$ ), 98 MCI subjects ( $70.56 \pm 7.94$  years, MMSE 26.66  $\pm 2.28$ ) and 117 NC subjects ( $68.34 \pm 9.71$  years, MMSE 29.11  $\pm 3.71$ ). The three groups are matched with age and gender. MMSE is significant different between different groups (p<0.001). All the MRIs were processed using AccuBrain, an automatic brain segmentation and quantification tool. AccuBrain analyzes T1WI-MRIs and provides volumetric measures (ICV normalized relative volume) of many brain structures. In particular, it produces a lobe atrophy index using the regional ratio of cerebrospinal fluid to whiter matter and gray matter. Independent t test with FDR correction was performed to investigate the volumetric difference in the pre-defined regions. Furthermore, the combination of the volumetric measures were used as features for classification between AD and NC, AD and MCI, MCI and NC group using linear SVM model. The classification accuracy (ACC) and area under the curve (AUC) were measured in the 10-fold cross-validations.

### RESULTS

Comparing AD and NC group, there are significant volumetric difference in brain parenchyma, hippocampus, amygdala, ventricular system, lateral ventricle, thalamus, caudate, putamen, accumbens-area, frontal lobe atrophy, occipital lobe atrophy, temporal lobe atrophy, parietal lobe atrophy, cingulate lobe atrophy, insular lobe atrophy. AD and MCI group have similar pattern as AD and NC group, with significant volumetric difference in all above mentioned regions except for caudate and putamen. Comparing MCI and NC group, there are no significant difference in all the compared regions. Pearson correlation test shows that MMSE is significant positive correlated (p<0.001) with brain parenchyma (r=0.46), amygdala (r=0.43), hippocampus (r=0.27), thalamus (r=0.22), accumbens-area (r=0.22) and putamen (0.13). and significant negative correlated (p<0.001) with temporal lobe atrophy (r=0.4), etc..

## CONCLUSION

AD and MCI shows similar brain atrophy pattern with different degrees.

## **CLINICAL RELEVANCE/APPLICATION**

Using the identified MRI biomarkers, the classification accuracy is high in discriminating AD from NC, which can serve as a useful tool for AD screening in clinical practice.



### OB170-ED-SUA2

The Fetus Unzipped: Understanding Anterior Body Wall Defects

Sunday, Nov. 25 12:30PM - 1:00PM Room: OB Community, Learning Center Station #2

#### Awards Cum Laude

### Participants

Dominik Prosser, MD, Portland, OR (*Presenter*) Nothing to Disclose Alexei Ku, MD, Portland, OR (*Abstract Co-Author*) Nothing to Disclose Roya Sohaey, MD, Portland, OR (*Abstract Co-Author*) Nothing to Disclose Karen Y. Oh, MD, Portland, OR (*Abstract Co-Author*) Nothing to Disclose

## **TEACHING POINTS**

Objectives for this educational exhibit include: Understanding the etiology of various anterior body wall defects Learning imaging clues for accurate diagnosis Review the clinical implications for outcomes after birth

# TABLE OF CONTENTS/OUTLINE

Outline: Embryology of the body wall Review key imaging findings of body wall defects (including ectopic cordis/Pentalogy of Cantrell), gastroschisis, omphalocele, OEIS, bladder exstrophy, and limb body wall) Postnatal correlation with prenatal imaging findings



## OB176-ED-SUA1

## Multimodality Spectrum of Imaging Findings in Ovary Torsion: Radiological-Pathological Correlation

Sunday, Nov. 25 12:30PM - 1:00PM Room: OB Community, Learning Center Station #1

#### Participants

Agustina Urtasun, MD, Quilmes, Argentina (*Presenter*) Nothing to Disclose Mercedes M. Riveros, MD, Buenos Aires, Argentina (*Abstract Co-Author*) Nothing to Disclose Pamela I. Causa Andrieu, MD, La Plata, Argentina (*Abstract Co-Author*) Nothing to Disclose Anastasia Karakachoff, MD, Ciudad Autonoma de Buenos Aires, Argentina (*Abstract Co-Author*) Nothing to Disclose Mara L. Gomez, MD, CABA, Argentina (*Abstract Co-Author*) Nothing to Disclose Maria N. Napoli, MD, Capital Federal, Argentina (*Abstract Co-Author*) Nothing to Disclose Mariano Uzal, CABA, Argentina (*Abstract Co-Author*) Nothing to Disclose Alejandra Wernicke, Buenos Aires, Argentina (*Abstract Co-Author*) Nothing to Disclose Carolina R. Chacon, MD, Capital Federal, Argentina (*Abstract Co-Author*) Nothing to Disclose

#### For information about this presentation, contact:

mercedes.riveros@hospitalitaliano.org.ar

### **TEACHING POINTS**

A normal ovary on US doesn't exclude the clinical diagnosis. Superior/ medialized, enlarged, and edematous ovary and/or Fallopian Tube with twisting sign. Gadolinium: vital from necrotic parenchyma. With / without associated lesions.

## TABLE OF CONTENTS/OUTLINE

<u>Purposes:</u> To highlight the most important characteristics. To describe the most common findings in US/CT/MRI. To describe the different lesions associated with radiologic - pathologic correlation. <u>Methods/Materials</u>: Institutional Research Ethics Committee approval. Retrospective, observational, descriptive. 100 female patients with pathological diagnosis with at least one institutional US/CT/MRI from 01/30/2010 to 12/31/2017. (1) One of the critical emergencies. High index of clinical and radiological suspicion. Subintrant or partial torsion can present with a normal ovary. (2) Medialized / superior and enlarged ovary with edematous stroma: echogenic/ hyperintense on T2 / complex adnexal mass on CT. Displaced peripheral follicles. Twisted vascular pedicle: Whirlpool sign on Doppler and T2 / post-gadolinium T1. Distended and/or thickened Fallopian tube: echogenic / hyperintense on T2. Associated free fluid and fat tissue stranding. (3) Follicular cyst. Mature cystic teratoma. Fibrothecoma. Ovarian abscess. Ovarian endometrioid adenocarcinoma.



### PD171-ED-SUA6

## Pediatric Vasculitis: Multimodality Imaging Review

Sunday, Nov. 25 12:30PM - 1:00PM Room: PD Community, Learning Center Station #6

FDA Discussions may include off-label uses.

## Awards

## **Certificate of Merit**

#### Participants

Evan J. Zucker, MD, Stanford, CA (*Presenter*) Nothing to Disclose Frandics P. Chan, MD, PhD, San Francisco, CA (*Abstract Co-Author*) Nothing to Disclose Shreyas S. Vasanawala, MD, PhD, Palo Alto, CA (*Abstract Co-Author*) Research collaboration, General Electric Company Consultant, Arterys Inc Research Grant, Bayer AG Beverley M. Newman, MD, MBBCh, Stanford, CA (*Abstract Co-Author*) Nothing to Disclose Richard A. Barth, MD, Stanford, CA (*Abstract Co-Author*) Nothing to Disclose

### For information about this presentation, contact:

zucker@post.harvard.edu

## **TEACHING POINTS**

1. To review the classification and unique clinical features of pediatric vasculitis. 2. To illustrate the broad spectrum of pediatric vasculitis using multiple imaging modalities. 3. To emphasize the central role of imaging for diagnosis, monitoring, and management, focusing on CT and MRI.

## TABLE OF CONTENTS/OUTLINE

The pediatric vasculitides are a unique and elusive class of disorders characterized by blood vessel wall inflammation. While rare, their protean symptoms affecting multiple organ systems often evade clinical diagnosis, thus solidifying a role for imaging in recognition, monitoring, and management. The use of multiple complementary imaging modalities in assessing pediatric vasculitis is discussed, focusing on CT and MRI. Using multimodality case examples, the broad spectrum of pediatric vasculitis in different stages of chronicity is illustrated, including Takayasu arteritis, Kawasaki disease, Henoch-Schönlein purpura, Churg-Strauss syndrome, Wegener's, polyarteritis nodosa, Behçet disease, secondary causes, and potential mimics. For each disorder, key clinical features, imaging findings, and management considerations are discussed. In summary, imaging is central to the evaluation of pediatric vasculitis, helping to facilitate precise diagnosis and tailored treatment.



## PD173-ED-SUA8

Use of Intravenous Gadolinium Based Hepatocyte Specific Contrast Agents (HSCA) for Contrast Enhanced Liver MRI in Pediatric Patients - What the Radiologist Needs to Know

Sunday, Nov. 25 12:30PM - 1:00PM Room: PD Community, Learning Center Station #8

**FDA** Discussions may include off-label uses.

#### Awards Certificate of Merit

### Participants

Rama S. Ayyala, MD, Providence, RI (*Presenter*) Nothing to Disclose Sudha A. Anupindi, MD, Philadelphia, PA (*Abstract Co-Author*) Nothing to Disclose Michael J. Callahan, MD, Boston, MA (*Abstract Co-Author*) Nothing to Disclose

## For information about this presentation, contact:

rayyala@gmail.com

# **TEACHING POINTS**

The purpose of this exhibit is to: Review the use of HSCA in pediatric patients Highlight hepaticobiliary pathologies that can be evaluated with HSCA in pediatric patients Report the current practices of members of the Society for Pediatric Radiology (SPR) regarding the use of HSCA in pediatric patients

# TABLE OF CONTENTS/OUTLINE

Introduction Review of HSCA used in Pediatric Patients: Gadoxetate disodium (Eovist) and Gadobentate dimeglumine (Multihance) Indications for use of HSCA in pediatric patients, with imaging examples: Hepatic indications and biliary indications Review of data of Society for Pediatric Radiology (SPR) membership practices in use of HSCA in pediatric patients Conclusion



## PD200-SD-SUA1

Diagnostic Performance of Computed Tomography to Differentiate Kawasaki Disease from Other Causes of Febrile Cervical Lymphadenopathy

Sunday, Nov. 25 12:30PM - 1:00PM Room: PD Community, Learning Center Station #1

# Participants

Hiroyuki Maki, Nagoya, Japan (*Presenter*) Nothing to Disclose Yasuteru Shimamura, Nagoya, Japan (*Abstract Co-Author*) Nothing to Disclose Yumi Maki, Kitanagoya, Japan (*Abstract Co-Author*) Nothing to Disclose Yoshiyuki Ozawa, MD, PhD, Nagoya, Japan (*Abstract Co-Author*) Nothing to Disclose Yuta Shibamoto, MD, PhD, Nagoya, Japan (*Abstract Co-Author*) Nothing to Disclose

# PURPOSE

In 9-23% of patients with Kawasaki disease (KD), fever and cervical lymphadenopathy may be the most notable initial clinical findings, prompting a clinical diagnosis of bacterial cervical lymphadenitis and administration of antibiotics. These patients have a risk for delay in definitive treatment for KD. In such cases, contrast-enhanced computed tomography (CECT) of the neck is performed to investigate resistance to antibiotics. The purpose of the present study was to retrospectively evaluate CECT findings of KD and to develop a diagnostic score for KD.

### **METHOD AND MATERIALS**

Two blinded radiologists, independently and then in consensus, retrospectively evaluated CECT images of 130 patients who had febrile cervical lymphadenopathy. In total, 37 patients with KD (14 male; age range, 8-145 months, mean age, 60 months) and 93 with non-KD (30 male; age range, 10-152 months, mean age, 74 months) were included. The following imaging features were assessed: the presence or absence of retropharyngeal edema, nasopharyngeal wall swelling, posterior cervical space edema, levels I through V and retropharyngeal lymphadenopathy, and focal low attenuation in lymph nodes (LL). The margins of LL, CT attenuation of trapezius muscles (CTL/M) were also documented. These CT features were compared between KD and non-KD, and receiver operating characteristic (ROC) curve analysis was performed to identify predictive features for differentiation of KD from non-KD.

#### RESULTS

The presence of retropharyngeal edema, nasopharyngeal wall swelling, posterior cervical space edema, retropharyngeal lymphadenopathy, level II lymphadenopathy, the absence of well-defined LL,  $CTL/M \leq 0.7$ , and level VB lymphadenopathy were more common with KD (P < 0.001, < 0.001, < 0.001, 0.029, 0.006, 0.007, < 0.001, and 0.002, respectively). When at least six of these eight CT findings were observed in combination, sensitivity, specificity, and the area under the ROC curve were 86.5%, 85.0%, and 0.912, respectively.

#### CONCLUSION

The presence of six of the eight CT findings commonly seen in KD provided excellent accuracy for the differentiation of KD and non-KD.

#### **CLINICAL RELEVANCE/APPLICATION**

CECT is more sensitive than ultrasonography for the detection of deep neck lesions; CECT may be useful to differentiate KD from non-KD.



### PD201-SD-SUA2

The Developmental Change of Glutamate Concentration in Postnatal Normal Rat Brain Using in Vivo Glucest Technique

Sunday, Nov. 25 12:30PM - 1:00PM Room: PD Community, Learning Center Station #2

**FDA** Discussions may include off-label uses.

#### Participants

Wooyul Paik, MD, Gangneung-si, Korea, Republic Of (*Presenter*) Nothing to Disclose Ho Sung Kim, Seoul, Korea, Republic Of (*Abstract Co-Author*) Nothing to Disclose Dong-Cheol Woo, PhD, Seoul, Korea, Republic Of (*Abstract Co-Author*) Nothing to Disclose

#### PURPOSE

Chemical exchange saturation transfer (CEST) is a novel enhanced molecular imaging technique that indirectly monitors neurochemicals in millimolar (mM) concentrations. The concentration of glutamate changes during the brain's developmental period, and the CEST imaging technique is useful for measuring glutamate in the brain on the basis of the exchangeable protons in the amine group. The purpose of this study was to measure in vivo changes in glutamate level in five different regions of the developing healthy rat brain using the glutamate CEST (GluCEST) technique in a longitudinal study design.

#### **METHOD AND MATERIALS**

MRI scans of six rats, including GluCEST, T2 mapping, and diffusion-weighted sequences, were acquired on a 7.0-T 160 mm small animal imaging system, every week, for 2 months from birth. Glutamate levels in five different regions (cerebral cortex, hippocampus, thalamus, basal ganglia, and amygdala) of the developmental rat brain were measured using GluCEST. The weekly values of T2, ADC, and GluCEST from the five different brain regions were compared with t-tests and Pearson's correlation analyses. These correlations were performed for three periods: all 8 weeks, the first to the fifth week, and the fifth to the eighth week.

### RESULTS

An increase in GluCEST values was observed in the five different brain regions during the first 5 postnatal weeks. After the fifth postnatal week, the levels of glutamate in the five brain regions varied. As postnatal weeks went by, T2 and ADC values decreased. Negative correlations between glutamate concentrations and T2 or ADC values were found (p<0.0001).

#### CONCLUSION

In rat brain, the fifth postnatal week is a possible time point for neurochemical developmental maturation, with the trends of glutamate concentration increase and T2 and ADC decrease, which are influenced by myelination and neuronal change, plateauing.

#### **CLINICAL RELEVANCE/APPLICATION**

The result of this study provides reference glutamate change during the first eight weeks of normal developmental rat brain, using glutamate Chemical Exchange Saturation Transfer(CEST) technique, include the week of glutamate peak level during the postnatal period. For studies on the concentration of glutamate in animal brain disease models, this result could be novel comparable reference value of glutamate with the concentration from the animal disease models in the early postnatal period.



## PD202-SD-SUA3

Age Prediction Using Resting-State Functional Connectivity Characteristics in Typically Developing Infants

Sunday, Nov. 25 12:30PM - 1:00PM Room: PD Community, Learning Center Station #3

#### **Participants**

Bin Jing, Chapel Hill, NC (*Presenter*) Nothing to Disclose Han Zhang, Chapel Hill, NC (*Abstract Co-Author*) Nothing to Disclose Weili Lin, PhD, Chapel Hill, NC (*Abstract Co-Author*) Nothing to Disclose Dinggang Shen, Chapel Hill, NC (*Abstract Co-Author*) Nothing to Disclose The UNC/UMN BCP Consortium, Chapel Hill, NC (*Abstract Co-Author*) Nothing to Disclose

### PURPOSE

Early brain development during the first years of life represents one of most critical time period for healthy brain development. In this study, we aimed to use functional connectivity (FC) characteristics and machine learning to predict the age of infants between 0 to 24 months old.

## METHOD AND MATERIALS

All images were acquired by a large-scale longitudinal multimodality neonate/infant brain imaging database. 64 infants (28F/38M, 0-24 months) with a total of 197 longitudinal scans were included. The resting-state fMRI data were obtained using a multi-band EPI sequence with a high spatial (2×2×2mm3) and temporal resolution (TR: 0.8s). The data were preprocessed using the following steps: deleting the first 10 time points, realignment, registration to an EPI template in MNI space, regressing out the linear trend, head motion parameters from Friston-24 model, and mean cerebrospinal fluid and white matter signals by CompCor, scrubbing excessive micro-headmotion (FD>0.5mm) volumes with linear interpolation, and temporal filtering (0.01-0.1Hz). A 268-parcellation atlas was used to construct whole brain FC matrix. Pearson correlation analysis was adopted to select the age-related FC features (P<0.001 and |r value|>0.3) based on the training data. Different features (positive, negative correlations and their combinations) were respectively input into a support vector regression to train the age prediction model. Finally, leave-one-out cross-validation and permutation test were used to evaluate the effectiveness of the model.

#### RESULTS

Among the three models, the model using combined features obtained the best accuracy compared to the others using only positive or negative correlational features. A mean absolute error (MAE) of 75.3 days and an r value (between predicted age and real age) of 0.841 were achieved. The informative features lied in all eight brain functional networks. The permutation test demonstrated that the accuracy of the prediction model was not by chance (P<0.001). In addition, male infants had a better prediction accuracy (MAE=71.1 days) than that in females (MAE=77.6 days).

## CONCLUSION

Age prediction with a reasonable accuracy could be achieved with the current model. Further refinements are ongoing to improve the age prediction accuracy.

## **CLINICAL RELEVANCE/APPLICATION**

fMRI could non-invasively detect the function of human brain and act as a common screening tool for infants.



## PD203-SD-SUA4

Contrast-enhanced MRI Facilitates Monitoring of Feto-placental Unit Development in a Pregnant Mouse Model

Sunday, Nov. 25 12:30PM - 1:00PM Room: PD Community, Learning Center Station #4

#### Participants

Andrew A. Badachhape, PhD, Houston, TX (*Presenter*) Nothing to Disclose Ketan B. Ghaghada, PhD, Houston, TX (*Abstract Co-Author*) Research Consultant, Alzeca Biosciences, LLC Igor Stupin, Houston, TX (*Abstract Co-Author*) Nothing to Disclose Mayank Srivastava, PhD, Houston, TX (*Abstract Co-Author*) Nothing to Disclose Laxman Devkota, PhD, Houston, TX (*Abstract Co-Author*) Nothing to Disclose Verghese George, MBBS, Houston, TX (*Abstract Co-Author*) Nothing to Disclose Eric Tanifum, PhD, Houston, TX (*Abstract Co-Author*) Nothing to Disclose Eric Tanifum, PhD, Houston, TX (*Abstract Co-Author*) Stockholder, Alzeca Biosciences, LLC Stockholder, Sensulin, LLC Stockholder, Abbott Laboratories Stockholder, Johnson & Johnson

#### For information about this presentation, contact:

badachhape@bcm.edu

#### PURPOSE

Non-invasive, longitudinal monitoring of feto-placental development can play an important role in the pre-clinical study of placental pathologies. In this work, we investigated high-resolution contrast-enhanced T1-weighted (CE-T1w) MR imaging for monitoring the development of feto-placental units during gestation; non-contrast T2-weighted (T2w) MRI was used for comparison.

#### **METHOD AND MATERIALS**

In vivo studies were performed in pregnant C57BL/6 mice at five time points during the second half of gestation (e10.5, e12.5, e14.5, e16.5, and e18.5 days). MR imaging was performed on a 1T permanent magnet scanner. At each time point, pre-contrast and post-contrast images were acquired using a T1w gradient-recalled echo (GRE) sequence and a T2w fast-spin echo (FSE) sequence. Post-contrast images were acquired following intravenous administration of liposomal-Gd (0.1 mmol Gd/kg). Contrast-to-noise ratio (CNR) was determined to quantify the visibility of feto-placental units during the course of gestation. Placentae and amniotic fluid compartments were individually segmented near-autonomously using ITK-SNAP to determine their volumes at all time points.

#### RESULTS

Placentae and amniotic fluid compartments were visible in T2w images at all time points; however, margin conspicuity was poor. CE-T1w images demonstrated 6x higher CNR and clear visualization of placental margins compared to non-contrast T2w images. Placental volume increased from 39±17 mm3 on day e10.5 to 109±39 mm3 on day e16.5. There was little change in placental volumes between days e16.5 and e18.5. Amniotic fluid compartment volume increased from 12±10 mm3 at day e10.5 to 1254±460 mm3 at day e18.5. Longitudinal imaging also facilitated the observation of feto-placental units that were identified at day e10.5 but ceased to develop during gestation.

## CONCLUSION

Contrast-enhanced T1w-MRI provided higher CNR between placental and amniotic fluid compartment compared to non-contrast T2w-MRI. As a result, near-automated segmentation of placental and amniotic fluid compartments was feasible to monitor their development throughout gestation.

#### **CLINICAL RELEVANCE/APPLICATION**

Contrast-enhanced MRI facilitates near-automated segmentation of feto-placental units using standard image processing tools. Longitudinal imaging using a liposomal-Gd contrast agent that does not cross the placental barrier during pregnancy may enable better characterization of placental pathology and fetal viability.



## PD204-SD-SUA5

### Initial Experience with Hyperpolarized Carbon-13 Metabolic MRI of Pediatric Patients with Brain Tumors

Sunday, Nov. 25 12:30PM - 1:00PM Room: PD Community, Learning Center Station #5

#### **Participants**

Ilwoo Park, PhD, Gwangju, Korea, Republic Of (*Presenter*) Nothing to Disclose Byung Hyun Baek, Gwangju, Korea, Republic Of (*Abstract Co-Author*) Nothing to Disclose Robert A. Bok, MD,PhD, San Francisco, CA (*Abstract Co-Author*) Nothing to Disclose James B. Slater, PhD, PharmD, San Francisco, CA (*Abstract Co-Author*) Nothing to Disclose Peder E. Larson, PhD, San Francisco, CA (*Abstract Co-Author*) Research Grant, General Electric Company Daniel B. Vigneron, PhD, San Francisco, CA (*Abstract Co-Author*) Research Grant, General Electric Company; Janine M. Lupo, PhD, San Francisco, CA (*Abstract Co-Author*) Research Grant, General Electric Company; Janine M. Lupo, PhD, San Francisco, CA (*Abstract Co-Author*) Grant, General Electric Company Duan Xu, PhD, San Francisco, CA (*Abstract Co-Author*) Nothing to Disclose Sabine Mueller, MD,PhD, San Francisco, CA (*Abstract Co-Author*) Nothing to Disclose Jeremy W. Gordon, PhD, San francisco, CA (*Abstract Co-Author*) Nothing to Disclose Hsin Yu Chen, PhD, San Francisco, CA (*Abstract Co-Author*) Nothing to Disclose

#### For information about this presentation, contact:

ipark@jnu.ac.kr

### PURPOSE

To assess the safety and feasibility of hyperpolarized (HP) 13C metabolic MRI with 13C1-pyruvate for evaluating real-time metabolism in pediatric patients with brain tumor.

#### **METHOD AND MATERIALS**

All experiments were performed using a whole-body 3T MR scanner with 13C clamshell transmit/bilateral 8-channel receive coils. A mixture of GMP 13C1-pyruvic acid and trityl radical was polarized using a SpinLabTM system. The polarized pyruvate solution underwent QC testing to measure the pH, temperature, polarization, sterilization filter integrity, and the concentrations of pyruvate and residual electron paramagnetic agent. Following pharmacist approval, 0.34 (n=3) or 0.43 mL/kg (n=1) pyruvate solution (~250mM) followed by 20mL saline flush was administered at a rate of 5 mL/s. Dynamic 2D 13C spectroscopic imaging data were acquired starting at 5s from the end of injection from a 20 mm thick slice.

#### RESULTS

No adverse effects were observed: All patients tolerated the pyruvate injection well and no adverse effects were observed. Hyperpolarized 13C MRI detected metabolic processes in pediatric human brain: Figure 1 shows an example data. The spatial and temporal evolution of pyruvate and lactate signal was observed throughout the brain. The pyruvate appeared in multiple regions, with the maximum pyruvate near the superficial middle cerebral vein appearing immediately after the start of data acquisition. Maximum lactate signal was observed ~6s from the start of data acquisition and appeared throughout normal-appearing brain. Bicarbonate as well as pyruvate and lactate with high SNR were detected: Figure 2 shows maps of integrated pyruvate, lactate and bicarbonate SNR, which demonstrated excellent detection of brain 13C metabolites. The 13C 8-channel bilateral receive arrays enabled the acquisition of 13C signals across the brain, but with significantly lower SNR in central regions, which was worsened by the reduced signal in the ventricles. The maximum SNR of pyruvate, lactate, and bicarbonate were 791, 105 and 54, respectively.

## CONCLUSION

This study focused on the novel application of hyperpolarized 13C metabolic MRI to pediatric brain tumor patients and have demonstrated initial safety and feasibility of using HP 13C1-pyruvate for assessing in vivo metabolism from pediatric patients with brain tumors.

### **CLINICAL RELEVANCE/APPLICATION**

This imaging strategy holds promise as a noninvasive measure of disease activity in brain diseases.



## PH007-EB-SUA

Utilizing the Exposure Index to Calculate Patient Specific Radiation Doses from Projection Radiography Images

Sunday, Nov. 25 12:30PM - 1:00PM Room: PH Community, Learning Center Hardcopy Backboard

## Participants

Daniel J. Sandoval, PHD, Albuquerque, NM (Presenter) Nothing to Disclose

### CONCLUSION

The algorithm developed in this work uses formulas for calculating entrance and exit dose utilizing a new dose correction factor. The dose correction factor is based on the exposure index and average grayscale from radiographic images specific to the subject and shows improved accuracy of traditional calculation methods for entrance and exit dose calculations.

#### Background

Due to an increase in regulatory scrutiny and medical facility accreditation requirements to monitor patient radiation dose from diagnostic imaging procedures, there is a growing necessity to determine and record accurate patient radiation dose from diagnostic medical imaging procedures. Current methods of patient dosimetry in diagnostic imaging are both extremely difficult and time consuming, require large computing resources (such as Monte Carlo computations), or lack accuracy due to using data based on homogenous materials and "standard-man sized" anthropomorphic models.

#### **Evaluation**

This project provides an algorithm that calculates a more accurate dose using patient-specific projection radiographic images. The algorithm includes measurements acquired during routine physics testing of the x-ray unit, data from two-view radiographic images, and accounts for patient specific and body habitus. Measurements using optically stimulated luminescent dosimeters, physics measurements, and Monte Carlo simulations were used to test and develop the algorithm. This new algorithm uses the mean image grayscale value over the region of interest and the reported Exposure Index to create a correction factor to correct patient dose calculations. The final product is an algorithm for calculating patient specific dose from chest radiographs that is more accurate with less associated uncertainty than current traditional dose calculation methods.

#### Discussion

The algorithm was tested using standard and modified anthropomorphic phantoms. Entrance doses calculated with this algorithm are within 6% of measured doses for anthropomorphic phantom. Traditional calculation method ranged from 2%-104%. Total deposited doses were within 17% of measured doses for anthropomorphic phantom whereas traditional calculation method ranged from 13.5% to 113% difference.



## PH119-ED-SUA6

Technical Optimization of Contrast Enhanced Sequences in Central Nervous System: Making the Most for Every Single Gadolinium Drop

Sunday, Nov. 25 12:30PM - 1:00PM Room: PH Community, Learning Center Station #6

#### Awards Cum Laude

#### Cum Lauue

## Participants

Teodoro M. Noguerol, MD, Jaen, Spain (*Presenter*) Nothing to Disclose Sara Canovas, MD, Cadiz, Spain (*Abstract Co-Author*) Nothing to Disclose Eugenia Aumente, MD, Cordoba, Spain (*Abstract Co-Author*) Nothing to Disclose Lidia Alcala, MD, Jaen, Spain (*Abstract Co-Author*) Nothing to Disclose Jordi Broncano, MD, Cordoba, Spain (*Abstract Co-Author*) Nothing to Disclose Antonio Luna, MD,PhD, Jaen, Spain (*Abstract Co-Author*) Nothing to Disclose Antonio Luna, Spain (*Abstract Co-Author*) Consultant, Bracco Group; Speaker, General Electric Company; Speaker, Canon Medical Systems Corporation; Royalties, Springer Nature

### For information about this presentation, contact:

t.martin.f@htime.org

## **TEACHING POINTS**

1. Review the current situation with Gadolinium Based Contrast Agents (GBCA) and the need to optimize their use in Central Nervous System (CNS). 2. Describe the physical basis and technical adjustments of MRI for GBCA visualization in CNS. 3. Review the different types of sequences that can help to optimize the use of GBCA in CNS from classical MRI approaches to latest advanced techniques.

## TABLE OF CONTENTS/OUTLINE

 Introduction 2. Why is necessary to optimize the use of GBCA in CNS? a. Update of FDA and EMA recommendations. b. Strategies for GBCA optimization 3. GBCA and CNS. a. When do CNS lesions enhance? b. Why is there a change in MRI signal intensity? c. GBCA properties. d. Technical adjustments (Flip Angle, type of magnet, delay time after GBCA administration and MRI).
 Type of sequences with GBCA a. 2D vs. 3D T1 sequences. b. Magnetization transfer contrast c. FLAIR d. Fat Suppresion techniques e. T1 and T2\* perfusion studies f. New approaches: Black Blood and Susceptibility Weighted Imaging (SWI) 5. Conclusions and take home messages

## **Honored Educators**

Presenters or authors on this event have been recognized as RSNA Honored Educators for participating in multiple qualifying educational activities. Honored Educators are invested in furthering the profession of radiology by delivering high-quality educational content in their field of study. Learn how you can become an honored educator by visiting the website at: https://www.rsna.org/Honored-Educator-Award/ Antonio Luna, MD - 2018 Honored Educator



## PH200-SD-SUA1

MRI Projection Mapping for Conserving Surgery of Breast Cancer in the Operation Room: A Feasibility Study

Sunday, Nov. 25 12:30PM - 1:00PM Room: PH Community, Learning Center Station #1

**FDA** Discussions may include off-label uses.

#### Participants

Maki Amano, MD, Tokyo, Japan (*Presenter*) Nothing to Disclose Toshiaki Kitabatake, MD, Tokyo, Japan (*Abstract Co-Author*) Nothing to Disclose Otoichi Nakata, Ebina, Japan (*Abstract Co-Author*) Employee, Ricoh Co, Ltd Reiko Inaba, RT, Tokyo, Japan (*Abstract Co-Author*) Nothing to Disclose Kazuyuki Ito, RT, Tokyo, Japan (*Abstract Co-Author*) Nothing to Disclose Chie Kurokawa, PhD, Tokyo, Japan (*Abstract Co-Author*) Nothing to Disclose Yutaka Ozaki, MD, PhD, Tokyo, Japan (*Abstract Co-Author*) Nothing to Disclose Kuniaki Kojima, MD, Tokyo, Japan (*Abstract Co-Author*) Nothing to Disclose Ryohei Kuwatsuru, MD, Tokyo, Japan (*Abstract Co-Author*) Nothing to Disclose

## CONCLUSION

The developed MRI projection mapping is feasible for defining the extent of breast cancer and allows its conserving surgery.

#### Background

Accurate definition of the extent of the breast cancer is inevitable for its conserving surgery. Physical palpitation or US is used for identifying the lesion with referring breast magnetic resonance imaging (MRI) in the current operation rooms (OR). However, it is often difficult to define the intraductal extent or tumor margin using US. Breast MRI is useful for detecting the tumor extent, but it is usually performed in the prone position which differs from that of the patients under the surgery. Thus, we have added breast MRI in the supine position, installed its data to a developed MRI projection mapping system (prototype) in OR, and assessed its feasibility.

#### **Evaluation**

We have developed a projection mapping system equipped with projector-camera system for projecting MR images to a breast with curved surface. We performed breast MRI studies in the supine position in 4 patients with palpable invasive breast cancer (mean age, 62.8 years), who were indicated to conserving surgery based on the prone breast MRI. A 1.5T scanner (GE) was used, and dynamic fat-suppressed 3D gradient-echo imaging was performed both in the prone and supine positions. Skin markers were placed on the patients' chest wall in the latter scanning. We have installed MIP (maximum projection mapping) images of the supine 3D imaging data to the MRI projection mapping system, and highlighted the tumor extent before the surgery. We compared the tumor extent detected by the MRI projection mapping and that shown by US during surgery or pathologic specimen. The present study demonstrated that the discrepancy of the tumor extent identified using MRI projection mapping, US, and pathology was 5mm or less in all patients. The surgical margin was negative for the tumor.

#### Discussion

MRI projection mapping identified the tumor extent accurately in this study. Therefore, this system can be applied to the breast cancer with intraductal invasion or difficult to be detected by US. The MRI projection mapping may eliminate the labor of repositioning MRI images in the 'surgeons' brains' in OR.



## PH201-SD-SUA2

Reduction of Metal Artifacts During Digital Tomosynthesis Reconstruction from Projection-Based Material Decomposition for Arthroplasty: A Phantom Study

Sunday, Nov. 25 12:30PM - 1:00PM Room: PH Community, Learning Center Station #2

## Participants

Tsutomu Gomi, PhD, Sagamihara, Japan (*Presenter*) Nothing to Disclose Masami Goto, Kanagawa, Japan (*Abstract Co-Author*) Nothing to Disclose Hidetake Hara, RT, Sagamihara-shi, Japan (*Abstract Co-Author*) Nothing to Disclose Yusuke Watanabe, MSc, Sagamihara, Japan (*Abstract Co-Author*) Nothing to Disclose Kazuaki Suwa, Koshigaya, Japan (*Abstract Co-Author*) Nothing to Disclose

## For information about this presentation, contact:

gomi@kitasato-u.ac.jp

## PURPOSE

This study aims to develop a novel dual-energy (DE) material decomposition reconstruction (DE-MD) algorithm using the projection data for reducing metal artifacts during digital tomosynthesis (DT) in arthroplasty.

## METHOD AND MATERIALS

A novel DE-MD algorithm, which is based on a three-material decomposition method and material-specific decomposition projection data, that utilizes weighted hybrid reconstructed images [maximum likelihood expectation maximization (MLEM) and shift-and-add] is implemented to reduce the metal artifacts. Pulsed X-ray exposures with rapid switching between low and high energies (70 and 140 kV, respectively) are used to perform DE-DT imaging. The images were compared using conventional filtered back projection (FBP), MLEM, simultaneous algebraic reconstruction technique total variation (SART-TV), DE virtual monochromatic (DE-VM) processing, and metal artifact reduction (MAR)-processing algorithms. Reductions in low- and high-frequency metal artifacts were compared using an artifact index (AI) and statistical Gumbel distribution model of the largest variations, respectively. The artifact spread functions (ASFs) for the in-focus and focus planes during out-of-plane were evaluated using a prosthesis phantom.

## RESULTS

The overall performance of the novel DE-MD algorithm was adequately effective in terms of the AI, and the resulting images yielded good results regardless of the type of metal that was used in the prosthetic phantom. Good noise artifact elimination was also achieved, particularly at greater distances from metal objects (DE-MD  $0.013 \pm 0.002$ , DE-VM  $0.019 \pm 0.003$ , MLEM-MAR  $0.019 \pm 0.003$ , FBP-MAR  $0.033 \pm 0.006$ , SART-TV-MAR  $0.020 \pm 0.002$ ). Furthermore, the DE-MD algorithm represented the minimum in the largest variations of statistical Gumbel distribution model (DE-MD  $0.0011 \pm 1.47e-05$ , DE-VM  $0.0016 \pm 2.81e-05$ , MLEM-MAR  $0.0021 \pm 4.79e-05$ , FBP-MAR  $0.0036 \pm 2.61e-04$ , SART-TV-MAR  $0.0027 \pm 4.68e-05$ ). Regarding the ASF analysis, the novel DE-MD algorithm yielded a relatively superior metal artifact reduction as compared with that obtained using conventional reconstruction algorithms both with and without MAR processing.

#### CONCLUSION

The DE-MD DT algorithm was particularly useful for reducing the high-frequency metal artifacts.

### **CLINICAL RELEVANCE/APPLICATION**

The imaging quality of DE-MD DT can facilitate arthroplasty-related diagnoses.



## PH202-SD-SUA3

## Detection of Calcification in the Breast Using Ultrasound Tomography: A Feasibility Study

Sunday, Nov. 25 12:30PM - 1:00PM Room: PH Community, Learning Center Station #3

### Participants

Bilal Malik, PhD,MS, Novato, CA (*Presenter*) Employee, QT Ultrasound Labs James Wiskin, PhD, Novato, CA (*Abstract Co-Author*) Employee, QT Ultrasound Labs Alyson Terry, Novato, CA (*Abstract Co-Author*) Consultant, QT Ultrasound, LLC Mark W. Lenox, PhD, Novato, CA (*Abstract Co-Author*) Employee, QT Ultrasound Labs Rajni Natesan, MD, MBA, Houston, TX (*Abstract Co-Author*) Officer, QT Ultrasound Labs John C. Klock, MD, Novato, CA (*Abstract Co-Author*) Employee, QT Ultrasound, LLC;

#### PURPOSE

The detection of microcalcifications is important for the early diagnosis of breast cancer. The extent to which ultrasound tomography (UST) may be helpful in breast calcification detection is not known. In this study, we explore the utility of ultrasound tomography (UST) in the detection of breast calcification.

#### **METHOD AND MATERIALS**

Six 3% gel agar phantoms were fabricated with embedded synthetic calcium particles ranging in size from 0.1 mm to 3 mm. Three cadaver breasts containing calcification were then identified. Imaging of the phantoms and cadaver breasts was performed using both full 3-dimensional inverse scattering UST and x-ray mammography (XRM) on a Senographe Essential unit (GE, New York, NY) and the corresponding contrast to noise ratios (CNR) were calculated as a function of calcium particle size. Resulting UST and XRM images for both the phantoms and cadaver breasts were compared. Algorithms to improve detection and isolation of calcifications in cadaver breasts using UST were investigated and utilized based on (1) image thresholding and (2) connected-components removal.

## RESULTS

In all instances, both UST imaging and XRM demonstrated visualization of calcium, both synthetic and biologic. Results from imaging of phantoms show that UST images exhibit 23% higher CNR in detection of calcium particles equal and greater than 500  $\mu$ m, in comparison to XRM. For particles below 500  $\mu$ m size, UST images exhibit 76% higher CNR. Using algorithms of image thresholding followed by connected-components removal, detection of calcification in cadaver breasts using UST was significantly improved.

## CONCLUSION

Ultrasound tomography is capable of detecting multiple sizes of calcium in the breast. The multimodality comparison in phantoms shows that UST exhibits superior CNR in comparison to XRM. In addition, image processing algorithms can be used to improve visualization of calcifications in cadaver breast tissue. Further work is needed to understand the utility of UST for calcium detection in vivo.

### **CLINICAL RELEVANCE/APPLICATION**

Calcium detection is critical for the early diagnosis of breast cancer. It is important to understand if other imaging modalities aside from mammography may assist in calcium detection.



## PH203-SD-SUA4

## Dose of CT Protocols Acquired in Clinical Routine Using a Dual-Layer Detector CT Scanner

Sunday, Nov. 25 12:30PM - 1:00PM Room: PH Community, Learning Center Station #4

### Participants

Fasco van Ommen, MSc, Utrecht, Netherlands (*Presenter*) Nothing to Disclose Hugo W. de Jong, PhD, Utrecht, Netherlands (*Abstract Co-Author*) Nothing to Disclose Tim Leiner, MD, PhD, Utrecht, Netherlands (*Abstract Co-Author*) Speakers Bureau, Koninklijke Philips NV Research Grant, Bayer AG Jan Willem Dankbaar, MD, PhD, Utrecht, Netherlands (*Abstract Co-Author*) Nothing to Disclose Edwin Bennink, PhD, Utrecht, Netherlands (*Abstract Co-Author*) Nothing to Disclose Arnold Schilham, PhD, Utrecht, Netherlands (*Abstract Co-Author*) Nothing to Disclose

## For information about this presentation, contact:

f.vanommen@umcutrecht.nl

## PURPOSE

Dual energy CT is a highly valuable modality because it provides additional diagnostic information compared to conventional CT scanning. The purpose of this study was to assess the feasibility of dose-neutral dual-energy acquisitions in daily clinical practice in every patient using dual-layer spectral CT (DLCT; IQon spectral CT, Philips Healthcare).

#### **METHOD AND MATERIALS**

Dose-length-product (DLP) data for consecutive examinations over a six-month period acquired with DLCT were collected and compared to consecutive examinations performed on an otherwise technically equivalent single-layer detector CT scanner (SLCT; Brilliance iCT, Philips healthcare). Imaging protocols were optimized for diagnostic image quality for each system prior to data collection. Dose reports of CT protocols that were scanned at least 50 times on both systems were collected. After exclusion of statistical outliers, protocols were evaluated with regard to reported dose levels.

#### RESULTS

In total, 4536 dose reports for DLCT and 5783 reports for SLCT were collected. All DLCT examinations were acquired at 120 kVp, enabling spectral analysis. With SLCT, 79% of examinations were acquired at 120 kVp, and 21% at 100/80 kVp. Protocols for 15 indications were scanned more than 50 times on both scanners. For 7 protocols there was no significant difference between the two scanners (P > 0.05), whereas 7 protocols were acquired with higher mean dose levels at SLCT compared to the DLCT (P < 0.03), with a maximum difference of 40%. For 2 protocols this could be mainly contributed to a difference in temporal sampling of the perfusion acquisition. In the 5 remaining protocols differences were mainly due to the use of automatic exposure control. For one protocol, the DLCT dose was significantly higher (11%) (P < 0.005) compared to the SLCT, which was due to higher exposures in the bolus tracker for the CTA acquisition.

### CONCLUSION

Dual-layer spectral CT using a 120 kVp tube potential in every patient can be used in daily clinical practice without increasing radiation dose when compared to a conventional single-layer detector CT.

### **CLINICAL RELEVANCE/APPLICATION**

A dual-layer detector spectral CT provides additional information, but this does not come at the cost of additional dose compared to a conventional single-layer detector CT scanner.



## QI001-EB-SUA

Taking Musculoskeletal Radiography to the Next Level - A Quality Assurance and Improvement Initiative with a Multimethodology and Multidisciplinary Approach

Sunday, Nov. 25 12:30PM - 1:00PM Room: QR Community, Learning Center Hardcopy Backboard

## Participants

Janni Jensen, MSc, BSc, Odense C, Denmark (*Presenter*) Nothing to Disclose Trine Torfing, MD, Odense C, Denmark (*Abstract Co-Author*) Nothing to Disclose Lene Tarp, Odense, Denmark (*Abstract Co-Author*) Nothing to Disclose

#### For information about this presentation, contact:

janni.jensen@rsyd.dk

## PURPOSE

In emergency radiology, fractures are the most common type of overlooked injury with improper positioning being one of the key reasons. A distal radius fracture is a common injury where even small changes in degrees or mm's can alter the treatment from conservative to surgery or vice versa. Changes in forearm rotation during acquisition of x-rays can alter the measured value of ulnar variance; and radiographically measured volar tilt increase with supination and decrease with pronation of the forearm. Missed and misdiagnosis of any sort can potentially result in delayed treatment and/or unfavorable outcome for the patient. The overall purpose of this quality improvement initiative is to improve quality of care, ultimately benefiting the patients. Beginning with wrist x-rays and the intention of including further anatomical regions when the method has proven to work.

#### METHODS

By recognizing musculoskeletal radiography as a specialty with continuous focus on education, quality improvement and assurance we strive to facilitate that all radiographers working with musculoskeletal x-rays are dedicated and specialized within this field. Various cross-disciplinary and multi-methodological approaches are applied involving all musculoskeletal radiographers and head of musculoskeletal radiology. Initiatives applied: • Introduction of advanced practice where radiographers report musculoskeletal examinations and are responsible for quality assurance and improvement • Regular short educational sessions for radiographers on correlation between positioning and pathology are given in the department by reporting radiographers • Morning conferences presenting yesterday's x-rays are held by a radiologist • A free app with department guidelines on positioning of musculoskeletal xrays is developed to make guidelines easily accessible; going from paper to interactive tool (in English and Danish) • Radiographers are offered a two-day workshop on positioning of musculoskeletal x-rays held by a musculoskeletal radiologist, a reporting radiographer and an orthopedic surgeon • Radiographers are offered one-hour individual sessions with a reporting radiographer reviewing their own x-rays discussing positioning and pathology with a focus on the correlation between positioning and diagnostic accuracy • A PhD on positioning of musculoskeletal x-rays • X-ray of the month is presented highlighting all the criteria All above mentioned points are repeated at various intervals. Outcome: Audits, based on department guidelines of positioning of musculoskeletal x-rays, are performed regularly by three alternating radiographers serving both an educational purpose by performing the audit and a quality assessment purpose when quantifying the results. Each audit contains 5 questions. Each question has 3 possible answers, yes (1 point), almost (0.5 points) and no (0 points). The questions focus on deviation of the wrist (radial/ulnar), supination of forearm (dorsal/volar tilt as assessed by the scaphopisocapitate alignment) and if wrist and elbow is at shoulder height which makes the radius and the ulna parallel. The 15 most recent sets of wrist x-rays are included in the audits.

#### RESULTS

A quality score consisting of 5 indicators was calculated (0; 0.5 and 1) points per indicator depending on fulfilment, maximum 75 points. The quality score increased from 47 points at baseline to 62 points at 6th audit. See figure 1 for results.

#### CONCLUSION

The continuous focus and education on positioning and quality of wrist x-rays showed a marked improvement from baseline to 6th audit, (p=0.002), with an image quality score of 47 points (baseline) and 62 points (6th audit). The audit with quality indicators not only provides a quantitative measurement of quality but also identifies suboptimal areas which allows for a targeted systematic approach on quality improvement. As an example, the first audit showed that volar rotation of the forearm was a frequent occurrence. We consequently adjusted the educational sessions with additional focus on forearm rotation, potential diagnostic implications, how to identify forearm rotation in the x-ray and how to adjust accordingly. This approach, using the plan-do-study-act model, allows for immediate identification of areas in need of improvement, alteration of initiatives with focus on area in need of improvement followed by an assessment of the impact of the change in the very next audit.



### QI003-EB-SUA

Design and Impact of a Musculoskeletal (MSK) Image-Guided Procedure Curriculum for Radiology Residents

Sunday, Nov. 25 12:30PM - 1:00PM Room: QR Community, Learning Center Hardcopy Backboard

#### **Participants**

Samarth Gola, MD, Richmond, VA (*Presenter*) Nothing to Disclose Peter J. Haar, MD, PhD, Richmond, VA (*Abstract Co-Author*) Nothing to Disclose Kevin B. Hoover, MD, PhD, Richmond, VA (*Abstract Co-Author*) Nothing to Disclose Josephina A. Vossen, MD, PhD, Richmond, VA (*Abstract Co-Author*) Nothing to Disclose

#### For information about this presentation, contact:

samarth.gola@vcuhealth.org

## PURPOSE

This study aims to develop an MSK image-guided procedure curriculum for radiology residents and study its impact on various performance metrics: fluoroscopy time, overall procedure time, technical competency, and patient satisfaction.

#### METHODS

A two year prospective study at our institution involved the design and implementation of a MSK procedure-guided curriculum for residents. Year one was defined as the pre-education group and year two was defined as the post-education group. The curriculum consisted of a day one tutorial and a supplemental online training module. The day one tutorial was created specifically for joint injections. A physician assistant from the MSK section reviewed the tutorial with the resident in person on their first day of the rotation in the fluoroscopy suite where the resident was able to become oriented with the equipment. The resident observed shoulder and hip injections for the first several days on service before becoming the primary operator. A supplemental online training module was made available to the resident during the first week of the rotation. This module reemphasized the material discussed during the day one tutorial and that which would have reasonably been experienced during observation of the first few joint injections on service. Residents were encouraged to review this material before each procedure. Fluoroscopic joint injection was performed under the supervision of the physician assistant and/or attending. The procedures primarily included shoulder and hip fluoroscopically-guided aspiration and joint injection either for pain relief or prior to MR/CT arthrography. The four performance metrics recorded were fluoroscopy time, total procedure time, technical competency, and patient satisfaction. These were recorded by a radiology technologist or physician assistant after each procedure and were sent to our statistician after each week. Fluoroscopy time and total procedure time were recorded in seconds. Data on resident technical competency was defined as the level of attending assistance during the procedure: no assistance, provided verbal guidance to resident, provided physical guidance to resident (e.g., redirected the needle for the resident), or finished the procedure. Additional data collected included the level of training and rotation number (e.g., resident's first, second, third, etc. MSK rotation). A four question electronic patient satisfaction survey was given to each patient before leaving the radiology department. Questions included pre- and post-procedure pain rating (on a scale of 1 to 10) and overall procedure satisfaction (on a scale of 1 to 5). Patients were also asked to identify the most painful portion of the procedure. Performance metrics of attendings were included to serve as an internal control for the study, as they did not undergo the additional training.

#### RESULTS

Over the study period, 317 resident-operated MSK procedures were conducted (196 pre-curriculum, 121 post-curriculum). Significance level was set at a = 0.05. There was a significant difference in fluoroscopy time between the two groups (32.2s pre-, 26.3s post-). The overall rate of attending assistance decreased but did not achieve statistical significance (13% pre-, 9% post-). There was no significant difference in overall procedure time (21min pre-, 20min post-) or average reduction in patient discomfort (2.6 pre- vs 2.7 post-). The level of patient satisfaction for both groups remained 4/5 ('satisfied'). The most painful portion of the procedure for patients in both groups was 'manipulating the needle during guidance'. There was no difference in the proportion of patients who experience pain (69% pre-, 64% post-). Since fluoroscopy time was the only statistically significant metric between pre- and post-training residents, a subgroup analysis was performed to potentially uncover additional trends. Significant fluoroscopy time decreases were achieved in residents who were on their second or third rotation, in the R3 class, or performing a hip procedure. Statistically significant differences were not achieved for residents on their fourth or fifth rotation, in the R1, R2, or R4 class, or performing a shoulder procedure. Of note, there were insufficient data points for residents on their first rotation or those performing knee or wrist procedures to include in this analysis.

#### CONCLUSION

Overall, our results demonstrate successful implementation of an MSK interventional curriculum (consisting of an in-person day one tutorial and a supplemental electronic training module) with improved resident performance metrics; specifically, greater technical competence and lower fluoroscopy usage. Furthermore, the data suggests that implementing this training on earlier MSK rotations may provide greater benefit than waiting until a resident's later or final rotation(s).



### QI021-EB-SUA

## Minimizing Patient Delays in Radiology Optimizing On - Time Starts for CT Procedures

Sunday, Nov. 25 12:30PM - 1:00PM Room: QR Community, Learning Center Hardcopy Backboard

#### Awards Identified for RadioGraphics

### **Participants**

Susan Reich, Atlanta, GA (*Abstract Co-Author*) Nothing to Disclose Gail Walls, PhD, Atlanta, GA (*Abstract Co-Author*) Nothing to Disclose Sadhna Nandwana, MD, Atlanta, GA (*Presenter*) Nothing to Disclose

## PURPOSE

The majority of first case interventional computed tomography (CT) guided procedures in the radiology department do not start on time resulting in significant patient wait times which affect susequent scheduled cases of the day. The goal was to identify root causes, implement test of change and evaluate for sustained improvement of delays in the first procedural case of the day

## **METHODS**

Team of key stakeholders assembled and process maps created. Retrospective analysis of start times of first case CT guided procedures between September 8, 2016 thru Janurary 17, 2017 was obtained. Prospective baseline data was obtained via direct observations from the time of patient check in to actural start time in the procedural room over one month. Root cause analysis (RCA) was performed and test of change was implemented. Post implementation data collection via direct observations and data warehouse mining to evaluate for change in number of on time starts and delay times over subsequent 14 week period.

### RESULTS

Retrospecitve analysis of 43 cases demonstrated an 88% delayed start time with an average delay of approximately 71 minutes. Tests of change were developed from17 direct observations and RCA. Tests of change included standardizing pre-procedural process, instituting morning huddle with procedural team, specific time allotments and role assignment for each part of the process map. Bimonthly meetings conducted to provide ongoing feedback. Post implementation data showed 40% improvement of exams starting on time and mean delayed start time decreased fro 71 to 24 minutes after 14 week period.

#### CONCLUSION

Siginificant decrease in patient delays and increased on time starts in the Radiology procedural area can be achieved with an engaged team approach and accountability. Defined standard work and a common direction, every team member was a problem solver at his or her own level.



## QI023-EB-SUA

Improving Breast Imaging and Intervention's Staff Efficiency During an Upright Stereo Biopsy Procedure

Sunday, Nov. 25 12:30PM - 1:00PM Room: QR Community, Learning Center Hardcopy Backboard

### **Participants**

Bryana Johnson, Rochester, MN (*Presenter*) Nothing to Disclose Linda M. Chida, BS, RT, Rochester, MN (*Abstract Co-Author*) Nothing to Disclose Katie Holst, Rochester, MN (*Abstract Co-Author*) Nothing to Disclose Angela Majerus, BA, Rochester, MN (*Abstract Co-Author*) Nothing to Disclose Rebecca Kinnetz, Rochester, MN (*Abstract Co-Author*) Nothing to Disclose Marilyn J. Morton, DO, Rochester, MN (*Abstract Co-Author*) Nothing to Disclose Deb Crossfield, Rochester, MN (*Abstract Co-Author*) Nothing to Disclose

#### For information about this presentation, contact:

Johnson.Bryana@mayo.edu

## PURPOSE

Background: In 2013, Breast Imaging and Intervention's (BII) stereo practice received new upright stereo equipment. Procedures were staffed with two technologists in the room because it felt more safe and comfortable to them in the event that they would need to respond to a patient experiencing a vasovagal reaction while the radiologist was out of the procedure room checking the specimen radiograph. However, in 2016 BII's frontline staff identified the need to reevaluate the upright stereo procedure process because the staffing model was creating double work, downtime, and protential safety risks (e.g., communication hand-off errors). Objective: Decrease the total time BII Stereo Technologists are involved with an upright stereo biopsy procedure from an average of 165 minutes to an average of less than or equal to 125 minutes by July 9th, 2017, while maintaining a 52% radiologist satisfaction score.

## METHODS

A multidisciplinary team developed a current state swim lane diagram to illustrate the duties performed during the procedure by role. Next, the team obtained manual procedural timings for the duration that the Stereo Technologists were dedicating to the upright stereo procedures from 3/31/2017 to 4/18/2017. On average, it was found that the Stereo Technologists were dedicating 165 minutes of total technologists time per upright stereo procedure. After the swim lane was completed, the team analyzed each step with the entire Stereo Technologist group in an effort to investigate areas of improvement opportunities. Staff identified that they were performing several non-value added activities such as double work, waiting and incorrectly assuming ownership of duties. It was also found that the Stereo Technologists were lacking self-confidence during the procedure due to minimal education/training on equipment operation for the procedural support assistants, limited practice nurses, and radiologists. This analysis confirmed that an opportunity to reduce the total technologist time dedicated to upright stereo procedures existed. A baseline survey of the BII Radiologists provided feedback regarding how satisfied they were with the current state upright stereo procedure workflow. The data showed that they were satisfied with the current state workflow 52% of the time. The team decided that they would not want to alter this workflow in a way that would decrease the BII Radiologists' level of satisfaction. Therefore, the BII Radiologist satisfaction score became the counterbalance measure for this project. In order to achieve the target condition of creating a safe environment for our patients while eliminating the non-value added work experience by staff in the upright stereo procedural room, the team tested various Plan-Do-Study-Act (PDSA) cycles to determine whether these changes had a positive impact on the project goal. These PDSA cycles included: 1) Akrus biopsy chair education provided to alled health staff, 2) Healthcare technology management improvement resulting in faster image transfer of specimen radiograph from source to procedure room monitor, 3) Removal of one Stereo Technologist from the upright stereo procedure, and 4) Compression release education for radiologists.

#### RESULTS

After successfully testing and implementing these changes, the group conducted post procedural timings (5/8/2017 to 6/9/2017) to record time durations the Stereo Techonologists were dedicating to the upright stereo procedures. Post implementation, an average of 117 minutes of total technologist time is being utilized to perform an upright stereo procedure. Thus, an average savings of 48 minutes of total technologist time per procedure was achieved. The group is pleased to report that the target goal was not only achieved, but surpassed. The goal strived for 125 minutes and resulted with an average of 117 minutes. Due to this project, the BII Department was able to redistribute \$84,087.19, a monitory value composed of wages and benefits paid, to other areas within the practice. Furthermore, for the counterbalance measure, post implementation data was gathered via the radiologists' survey which resulted in a BII Radiologist satisfaction score of 92%; a 40% increase from the baseline of 52%.

### CONCLUSION

To date, one Stereo Technologist is staffed in each upright stereo procedure. The team continues to measure total technologist time on a quarterly basis and these timings continue to support the project's initial findings. Zero pateint safety incidents have been reported due to these changes. The strategies implemented have created a safe patient environment while eliminating the double work and waiting experienced by the Stereo Technologist during an upright stereo procedure. The team learned that communication amongst each stakeholder is vital when providing an unparalleled patient experience, and having more staff in the room does not always equate to better quality patient care.



## QI100-ED-SUA1

## **Improving MRI Inpatient Access**

Sunday, Nov. 25 12:30PM - 1:00PM Room: QR Community, Learning Center Station #1

# Awards

**Quality Improvement Reports Award Identified for RadioGraphics** 

### Participants

Nancy L. Pritchard, ARRT, Aurora, CO (Presenter) Nothing to Disclose Julia Drose, BA, Aurora, CO (Abstract Co-Author) Nothing to Disclose Denise Snuttjer, RT, MBA, Aurora, CO (Abstract Co-Author) Nothing to Disclose Nancy Cheung, MPH, Aurora, CO (Abstract Co-Author) Nothing to Disclose Christi Janzen, Aurora, CO (Abstract Co-Author) Nothing to Disclose James P. Borgstede, MD, Colorado Springs, CO (Abstract Co-Author) Nothing to Disclose

## PURPOSE

Purpose: To improve MRI access for inpatients (exam order to begin) by: 1. Identifying reasons for current exam delays, 2. Scheduling all inpatient exams. Desired Outcomes: 1. Improved patient and provider satisfaction, 2. Accelerate treatment, 3. Reduce length of stay, 4. Improve MRI efficiency/ equipment utilization.

### METHODS

Methods: Baseline data was collected on the average turn-around-time (TAT) for inpatient MRI exams from the time the exam was ordered to when the exam was begun in the MRI Department. Three two week trials were then undertaken using various methods to provide a scheduled exam time for all inpatient MRI exams ordered. Trial 1 involved all MRI Technologists responsible for scheduling inpatient exams. Trial 2 involved only Lead MRI Technologists scheduling inpatient exams. Trial 3 assigned a specific Technologist per shift/per day to schedule all inpatient exams. Reasons for patient delays were also collected. Once data was reviewed and reasons for delays identified and catagorized, Radiology staff met with key nursing and Transport staff to identiy methods for decreasing or eliminating delays, and providing on-going education to new RN staff.

## **RESULTS**

Results: Baseline Data: Average TAT in minutes from exam order to begin: 751 minutes Average TAT after Trial 1: 626 minutes. Average TAT after Trial 2: 670 minutes. Average TAT after Trial 3: 420 minutes. Overall improvement in TAT from baseline was 44.1% Reasons for delay in completing MRI exams catagoriezed into: Transport Delay, RN Related Delay, Patient Complication, Bumped for STAT patient, Other. Meeting with key MRI, RN and Transport staff resulted in identifying timely and accurate completion of MRI screening form, and RN understanding of importance of screening form and correct patient prep for MRI exams, as the two primary areas of focus. PDCA projects were undertaken to move screening process from RNs to MRI staff and to develop a written guideline for RNs that explained importance of MRI paitent prep, screening and safety. MRI staff completing screening form with inpatients resulted in an average TAT of 410 minutes, which was a 54% improvement from baseline data. RN guide to MRI was reviewed and desiminated to all inpatient floors. TATs were reviewed 5 months after begining initial project and showed a 55% improvement, confirming sustainability.

## CONCLUSION

Conclusions: 1. Scheduling all inpaitent MRI exams resulted in marked and sustainable improvement in TAT, which in turn results in: - Improved Patient Satisfaction - Improved Referring Provider Satisfaction - Increased efficiency and equipment utilization in the MRI Department 2. Working with key hosptial staff (RNs, Transport) involved in inpatient care helped identify reasons for patient delayed to MRI and lead to understanding and implementing long-term solutions for improving exams TAT. 3. Assigning MRI staff to oversee inpatient screening process improved timeliness and accuracy of screeing form, which resulted in increased patient safety in the MRI enviornment 4. Working with key hospital staff to develop educational guides for MRI safety and patient prepensured ongoing education of new RN staff, which should contirubute to sustainability of TAT improvement and patient safety



## QI102-ED-SUA2

Decreasing Duplicative Imaging: Clinical Decision Support Intervention to Reduce Unnecessary Abdominal Ultrasound Following Abdominal CT

Sunday, Nov. 25 12:30PM - 1:00PM Room: QR Community, Learning Center Station #2

### Participants

Nebiyu Adenaw, MD, Baltimore, MD (*Abstract Co-Author*) Nothing to Disclose Karen M. Horton, MD, Baltimore, MD (*Abstract Co-Author*) Nothing to Disclose Pamela T. Johnson, MD, Baltimore, MD (*Presenter*) Consultant, Oliver Wyman

#### For information about this presentation, contact:

PamelaJohnson@jhmi.edu

### PURPOSE

Duplicative imaging contributes to unnecessary health care expenditure. This initiative was designed to reduce inpatient and emergency department abdominal ultrasound exams in patients who had undergone abdominal CT within 72 hours prior to the US order being placed. The diagnostic information in question is often already available on the abdominal CT scan. The most common scenario for this is inpatient acute kidney injury, which is usually due to causes other than renal obstruction, but renal ultrasound is reflexively ordered by house staff and faculty.

#### **METHODS**

Baseline review of reports on 100 inpatients in 2015-2016 imaged for AKI with renal ultrasound (US) revealed absence of hydronephrosis in 89% (89/100). Additional imaging utilization review over a 2 month period in 2017 identified 50 patients imaged with renal US within 10 days after abdominal CT, with a mean time interval of 2.4 days between the US and CT. A best practice advisory (BPA) was created in the electronic medical record (EMR) to advise against routine use of abdominal ultrasound in adult inpatients and emergency department patients who had undergone an abdominal CT within the preceeding 72 hours. Using Diagnosis Group Identifiers, patients with transplants and oncology patients were excluded; many of these patients are unable to receive intravenous contrast enhanced CT, and as such noncontrast CT provides limited information. Two separate BPAs were designed, depending whether the CT result was pending or finalized. Acceptable acknowledgement reasons to proceed with the order were made available with the BPA: Radiologist recommended ultrasound Transplant patient Evaluate gallbladder Evaluate vasculature because CT was noncontrast Paracentesis mark Relevant intervention in the interval (nephrostomy tube, drain placement) Discussed with radiologist Other: comments The frequency of BPA firing and the subsequent ordering behavior were evaluated after integration of the BPA into the EMR in December 2017. Additionally, for all patients whose ultrasounds were canceled in January and February 2018, chart review was conducted to confirm that patient care quality and safety were not compromised by omitting the ultrasound.

## RESULTS

In 1st two months of 2018, a total of 204 inpatient and ED abdominal US orders were placed in patients with a preceding abdominal CT. Following the BPA, 12% (31/204) of the US orders were canceled. The frequency of acknowledgement reasons to override the BPA was as follows: Evaluate gallbladder (N=80) Other & free text comments (N=53) Discussed with radiologist (N=28) Evaluate vasculature because CT was noncontrast (N=5) Relevant intervention in the interval (N=4) Paracentesis mark (N=2) Transplant patient (N=1) Radiologist recommended ultrasound (N=0) Review of free text comments revealed 16 ultrasound exams for AKI that could have potentially been avoided, reflecting a need for better education and prompting modification of the BPA to emphasize that AKI was a primary area of overuse. Two exams targeted the biliary tree, precipitating a change of acknowledgement reason from 'evaluate gallbladder' to 'evaluate gallbladder or biliary tree'. Chart review confirmed that the canceled US exams would not have contributed value to patients' care.

## CONCLUSION

Abdominal CT provides more diagnostic information than abdominal ultrasound in many cases, with exceptions detailed above. As such, inpatient and emergency department abdominal ultrasound may be obviated by a recently performed abdominal CT scan, particularly when ordering renal ultrasound in the setting of hospital acquired AKI. Implementing a smart BPA to avoid an unnecessary abdominal ultrasound in a patient with a recently performed abdominal CT can safely reduce wasteful practice and decrease patients' total cost of care.

### **Honored Educators**

Presenters or authors on this event have been recognized as RSNA Honored Educators for participating in multiple qualifying educational activities. Honored Educators are invested in furthering the profession of radiology by delivering high-quality educational content in their field of study. Learn how you can become an honored educator by visiting the website at: https://www.rsna.org/Honored-Educator-Award/ Pamela T. Johnson, MD - 2016 Honored Educator



## QI104-ED-SUA3

## Targeting the Top 5 On-Call Resident Misses with Focused Lecture Series: A Pilot Study

Sunday, Nov. 25 12:30PM - 1:00PM Room: QR Community, Learning Center Station #3

### Participants

Junjian Huang, MD, Philadelphia, PA (*Abstract Co-Author*) Nothing to Disclose Dayna Levin, MD, Philadelphia, PA (*Abstract Co-Author*) Nothing to Disclose Jonathan Masur, MD, Philadelphia, PA (*Abstract Co-Author*) Nothing to Disclose Alexander Boikov, MD, Philadelphia, PA (*Abstract Co-Author*) Nothing to Disclose Hima Prabhakar, MD, Philadelphia, PA (*Presenter*) Nothing to Disclose

## For information about this presentation, contact:

hima.prabhakar@uphs.upenn.edu

### PURPOSE

Evaluate whether a focused lecture series of the most commonly missed on call diagnoses can reduce resident on call misses in those areas.

## METHODS

CAPRICORN, a computerized natural language processing system for tracking changes to on call resident reports, allows for attending over read categorization. Misses are categorized as major changes if the finding results in significant alteration in patient management. Utilizing this software, resident major changes were reviewed from 7/2015-2/2016. Missed diagnoses were further categorized by topic and ranked based on frequency. A targeted lecture series was then created to review the top 5 most commonly missed diagnoses. Following this, resident on call major changes were reassessed from 3/2017-10/2017 to determine if there were changes in the frequency of resident misses.

## RESULTS

During the initial study period, there were 148 major misses out of 12730 on call cases (1.16%). The most commonly missed diagnoses were: pneumonia (20 cases), upper extremity fracture (16), pulmonary embolism (8), colitis/abdominal abscess (6), and stroke (4). These diagnoses accounted for 36% of major misses. Following targeted lecture series, there were 94 major misses out of 16712 on call cases (0.56%). Of the diagnoses covered by the lecture series, the missed cases were as follows: pneumonia (6 cases), upper extremity fracture (6), pulmonary embolism (3), colitis/abdominal abscess (7), and stroke (6). These diagnoses accounted for 30% of total major miss cases.

### CONCLUSION

There was a decrease in the number and proportion of missed diagnoses of the topics covered by the targeted lecture (54 vs. 28; 0.42% vs. 0.17%) with certain diagnoses experiencing major benefit from the lecture series. Our results brings about an interesting question as diagnoses made by radiograph (pneumonia, upper extremity fractures) experienced greater improvement than those made by cross sectional imaging. We postulate that didactic lectures may not be the best way to improve accuracy of these complex imaging diagnoses and more interactive case-based education to address these topics may better improve resident on call accuracy of these complex diagnoses.



### QI106-ED-SUA4

## Simulation Modeling: Radiology Analytics New Partner

Sunday, Nov. 25 12:30PM - 1:00PM Room: QR Community, Learning Center Station #4

### Participants

Michael M. Zimmer, PhD, Greenville, NC (*Presenter*) Nothing to Disclose Sandra Sackrison, DSc,ARRT, Greenville, NC (*Abstract Co-Author*) Nothing to Disclose

For information about this presentation, contact:

michael.zimmer@vidanthealth.com

#### PURPOSE

At an academic medical center operating nearly 1000 beds, leadership was faced with addressing the demands of radiology services, particularly Magnetic Resonance Imaging (MRI) and Vascular Interventional Radiology (VIR) for a growing inpatient and outpatient population. With millions of dollars of potential investments, hospital operations needed clear understanding of the capacity and utilization of their MRI and VIR services. This would indicate if operational efficiencies could be made to improve capacity and throughput in MRI processes or consider installing additional equipment to meet department needs. There were expectations for volume increases in interventional radiology and neurosurgery services that would present new future challenges. Without clear analytics of the operation, investment decisions became uncertain. Furthermore, Leadership found it difficult to move forward with previous strategic plans due to variable expectations and outcomes.

#### **METHODS**

A dedicate process improvement team utilized the Lean Six Sigma method and its DMAIC (define, measure, analyze, improve and control) approach to deploy discrete event simulation modeling supported with in-depth analytics. The DMAIC approach provided a structured framework to execute process improvement measures. Additionally, SIMIO simulation modeling was leveraged to create replications of processes for MRI and VIR operations. Supporting data analytics were developed from intensive data collection efforts that consisted of analyzing EHR (Epic) reports, collecting unit time logs, and performing onsite observations. A year's worth of patient data and unit data were used to detail daily volumes, procedure types, procedure duration, acuity, appointment scheduling, cancelations, patient needs (sedation, ventilation, contrast, monitored, etc.), transportation delays, and staff schedules. Detailed process maps were designed to outline staff responsibilities, how long each step should take, and what requirements were needed for each step. The incorporation of these components heightened the SIMIO models for a realistic representation of the current environment.

#### RESULTS

MRI operations experienced throughput difficulties with daily backlogs averaging 5 patients per day (the range was as low as 0 to higher than 12) amidst stretched staffing resulting in an average of a 74% utilization rate on the 3 MRIs. Unknown metrics on capacity and utilization to determine best equipment upgrades and unit expansion were seen within VIR's growing service. There was unclear data around the extent of frequency along with a lack of standard performance metrics for the available VIR equipment, which consisted of 3 single-plane and 1 bi-plane system, as well as the use of a CAT Scan (CT). This is important to note, due to the reoccurring redundancies of emergency stroke and neuro cases utilizing the only bi-plane system available. After the process improvement work, simulation models produced new alternatives in MRI operations to resolve backlogs and maximize staffing resources. A resulting simulation scenario showed that adjustments in operating hours and staff resources would produce an increased throughput with a more practical staff utilization. Effective use of MRI times needed to be balanced without long periods of inactivity with feasible efficiencies. The hours captured for an additional 3 FTEs showed increased capacity by over 1500 patients per year with the current MRIs, and an average utilization to 75%. In VIR, clarity in operations was provided to outline each equipment's utilization: the 3 single-planes operating at 30%, the bi-plane at 20% and CT making up 18% utilization of IR procedures. Additionally, the modeling work indicated that the Physicians and IR Techs were operating at a high level of 65% utilization rate. When matched with equipment utilization, the ability to increase capacity with additional staff to perform more procedures within a single shift is realized. Furthermore, this highlighted the significance of CT usage within VIR operations.

### CONCLUSION

The process improvement work with simulation modeling and leveraging analytics had profound effects on strategic planning by Leadership. Simulation modeling has the ability to run many 'what if' scenarios in a risk free environment; thereby, avoiding time consuming and costly pilot trials that may not be executed well for the reliable outcomes needed. The MRI results validated the return-on-investment (ROI) for FTE hiring with a cost avoidance of nearly \$4 million on an MRI purchase and infrastructure construction. Radiology Leadership is able to collaborate with VIR Physician group on future equipment upgrades and unit expansion based on validated data and aligned processes. More importantly, the work established the need and benefit to create defined procedure room metrics and best practices. A cadence has been set to continuously review and evaluate the progress of the recommended solutions.



### RO106-ED-SUA3

Response Assessment in Neuro-Oncology (RANO) Criteria for Gliomas: Practical Topics Using Conventional and Advanced Imaging Techniques

Sunday, Nov. 25 12:30PM - 1:00PM Room: RO Community, Learning Center Station #3

### Awards Identified for RadioGraphics

#### Participants

Diego J. Oliveira, MD, Uberlandia, Brazil (*Presenter*) Nothing to Disclose Ana Patricia F. Vieira SR, MD, Sao Paulo, Brazil (*Abstract Co-Author*) Nothing to Disclose Luis F. Godoy, MD, Sao Paulo, Brazil (*Abstract Co-Author*) Nothing to Disclose Lucas N. Silva, MD, Sao Paulo, Brazil (*Abstract Co-Author*) Nothing to Disclose Hae W. Lee, MD, PhD, Sao Paulo, Brazil (*Abstract Co-Author*) Nothing to Disclose Maria Martin, MD, PhD, Sao Paulo, Brazil (*Abstract Co-Author*) Nothing to Disclose Daniel Delgado, Sao Paulo, Brazil (*Abstract Co-Author*) Nothing to Disclose Marcos F. Docema, MD, Sao Paulo, Brazil (*Abstract Co-Author*) Nothing to Disclose Claudia D. Leite, MD, PhD, Sao Paulo, Brazil (*Abstract Co-Author*) Nothing to Disclose Giovanni G. Cerri, MD, PhD, Sao Paulo, Brazil (*Abstract Co-Author*) Nothing to Disclose

## For information about this presentation, contact:

diegojoseleao@yahoo.com.br

### **TEACHING POINTS**

1. To review the imaging findings associated with pseudoprogression, tumor progression, radionecrosis and pseudoresponse according to Response Assessment in Neuro-Oncology (RANO) criteria for high-grade and low-grade gliomas 2. To discuss the differential diagnosis among such entities and correlate with the findings on advanced techniques such as perfusion and spectroscopy

### TABLE OF CONTENTS/OUTLINE

Brief historic of the RANO criteria development and recent modifications Definition of measurable disease, non-measurable disease, and target lesions Discussion of treatment options for brain tumors and relevant imaging findings associated with them Practical evaluation of brain tumors through RANO criteria This presentation will stress: - The importance of post-operative imaging in the first 48 hours and the concept of maximal safe resection - Tumor response (complete or parcial) - Tumor progression -Pseudoprogression - Pseudoresponse after bevacizumab (anti-VEGF agent) Sample cases and differential diagnosis Summary



### RO201-SD-SUA2

**Atypical Response Patterns in Patients Treated with Nivolumab** 

Sunday, Nov. 25 12:30PM - 1:00PM Room: RO Community, Learning Center Station #2

# Awards

## Student Travel Stipend Award

### Participants

Richard Thomas, MBBS, MD, Boston, MA (*Presenter*) Nothing to Disclose Bhanusupriya Somarouthu, MD, Boston, MA (*Abstract Co-Author*) Nothing to Disclose Francesco Alessandrino, MD, Boston, MA (*Abstract Co-Author*) Nothing to Disclose Vikram Kurra, MD, Cambridge, MA (*Abstract Co-Author*) Nothing to Disclose Atul B. Shinagare, MD, Boston, MA (*Abstract Co-Author*) Advisory Board, Arog Pharmaceuticals, Inc; Research Grant, GTx, Inc

## PURPOSE

To assess the frequency of various patterns of response and incidence of atypical response patterns in patients treated with antiprogrammed death (PD) 1 antibody Nivolumab, across different cancer types and treatment regimens

## METHOD AND MATERIALS

This IRB-approved, HIPAA-compliant retrospective study included 254 patients treated with Nivolumab alone or in combination, identified by review of electronic radiology database, from January 2013 through August 2017. The cancer type, start and end dates of treatment and the therapeutic agents were noted. The tumor response was prospectively assessed starting with the baseline scan, using RECIST1.1 (total 5 target lesions, up to 2 per organ). The median treatment duration was 5.2 months (IQR 2.7-12.8). A total of 166 patients (65%) showing clinical benefit to treatment (defined as stable disease, partial response or complete response) were identified. Among these, four patterns of response were noted: Pattern 1 - patients with decrease or <20% increase in sum of longest diameters (SLD) without any atypical changes, Pattern 2 - patients with 10-19% increase in SLD with subsequent return below baseline, Pattern 3 - patients with >=20% increase in SLD with subsequent return below baseline (pseudoprogression), and Pattern 4 - development of new lesions with decrease in SLD lasting through at least two consecutive scans. Patterns 2, 3 and 4 were defined as atypical response patterns.

## RESULTS

Of 166 patients with clinical benefit, 33 (20%) showed atypical response patterns - 15 (9%) with Pattern 2, 2 (1%) with pattern 3 and 16 (10%) with Pattern 4. The frequency of atypical response patterns was highest in patients treated with Nivolumab and Ipilimumab combination (25/91, 27%) followed by Nivolumab alone (6/46, 13%) and least with Nivolumab and another chemotherapeutic agent (2/29, 7%); p=0.02. The frequency of atypical response was highest among patients with melanoma (14/45, 31%) followed by non-small cell lung carcinoma (7/29, 24%) and genitourinary carcinomas (7/30, 23%)

## CONCLUSION

One in five patients treated with Nivolumab demonstrate atypical response patterns. It is important for the radiologists to be aware of these confusing response patterns to avoid errors in response assessment

## **CLINICAL RELEVANCE/APPLICATION**

Radiologists must be aware of the atypical response patterns that can be seen in patients on immunotherapy, to avoid making an erroneous diagnosis of progressive disease

## **Honored Educators**

Presenters or authors on this event have been recognized as RSNA Honored Educators for participating in multiple qualifying educational activities. Honored Educators are invested in furthering the profession of radiology by delivering high-quality educational content in their field of study. Learn how you can become an honored educator by visiting the website at: https://www.rsna.org/Honored-Educator-Award/ Atul B. Shinagare, MD - 2017 Honored Educator



### UR175-ED-SUA6

An Illustrated Guide to Genitourinary Surgical Procedures for Radiologists

Sunday, Nov. 25 12:30PM - 1:00PM Room: GU/UR Community, Learning Center Station #6

#### **Participants**

Anjuli R. Cherukuri, MD, Madison, WI (*Presenter*) Nothing to Disclose Akshya Gupta, MD, Madison, WI (*Abstract Co-Author*) Nothing to Disclose Jonathan K. Vincent, MD, Boston, MA (*Abstract Co-Author*) Nothing to Disclose Robert D'Agostino, MD, Burlington, VT (*Abstract Co-Author*) Nothing to Disclose Lori Mankowski Gettle, MD, Madison, WI (*Abstract Co-Author*) Nothing to Disclose

## For information about this presentation, contact:

archerukuri@gmail.com

#### **TEACHING POINTS**

Review common and uncommon genitourinary surgical procedural details. Review the normal postoperative appearance with original illustrations. Review complications and how to best image them.

## TABLE OF CONTENTS/OUTLINE

Genitourinary procedures will be reviewed, including indications, original illustrations, brief procedural details, optimal imaging techniques, normal postoperative appearances, and complications. Procedure types reviewed: Renal & ureteral procedures including renal transplant, nephrectomies, nephroureterectomy, pyeloplasty, Boari flap, and psoas hitch. Bladder & urinary diversions including augmentation cystoplasty, Mitrofanoff & Monti vesicostomy procedures, cutaneous ureterostomy, ureterosigmoidostomy, ileal conduit, Indiana pouch, neobladder urinary diversion, and Kock pouch. Prostate & penile procedures including prostatectomy, TURP, vasectomy, urethroplasty, penile implant, and artificial urinary sphincter.



## UR177-ED-SUA7

## Pitfalls in the Interpretation of Adrenal Imaging

Sunday, Nov. 25 12:30PM - 1:00PM Room: GU/UR Community, Learning Center Station #7

### Awards Cum Laude Identified for RadioGraphics

#### Participants

Gurinder Nandra, FRCR, MBChB, London, United Kingdom (*Presenter*) Nothing to Disclose Oliver Duxbury, MBBCh, FRCR, London, United Kingdom (*Abstract Co-Author*) Nothing to Disclose Jaymin H. Patel, MBBS, FRCR, London, United Kingdom (*Abstract Co-Author*) Nothing to Disclose Nirav Patel, MBBS, FRCR, Southampton, United Kingdom (*Abstract Co-Author*) Nothing to Disclose Ioannis Vlahos, MRCP, FRCR, London, United Kingdom (*Abstract Co-Author*) Research Consultant, Siemens AG Research Consultant, General Electric Company

## **TEACHING POINTS**

Overview potential pitfalls in adrenal CT and MRI imaging assessment. Indicate clinical, morphological and chronological features that affect interpretation and further imaging.

## TABLE OF CONTENTS/OUTLINE

A case-based exhibit of potentially misinterpreted cases with referenced teaching points. To include: Evaluation of hyperdense adrenal nodules on post contrast CT MRI or CT washout for hyperdense adrenal nodules on noncontrast CT? Borderline values at CT/MRI Chemical shift pitfalls (calcification, windows, criteria) Misuse of calculated CT washout Size/heterogeneity of lesions Impact of peak enhancement values (e.g. pheochromocytoma) Impact of size on malignancy pre-test probability Discrepant absolute/relative washout values CT washout unusual lesions: adrenal cysts, hematomas, infection Technical pitfalls (ROIs, incorrect/variable kVp) Endocrine disease Solitary adrenal nodule versus bilateral hyperplasia leading to adrenalectomy Assessment criteria for Conn's Syndrome, Cushing's, AIMAH, etc Correlation and lack of correlation with MIBG imaging or venous sampling Unusual lesions, para-adrenal pathology/pseudolesions Including hemangiomas, sarcomas, gastroinstestinal diverticula, Gastrointestinal stromal tumors Collision lesions

### **Honored Educators**

Presenters or authors on this event have been recognized as RSNA Honored Educators for participating in multiple qualifying educational activities. Honored Educators are invested in furthering the profession of radiology by delivering high-quality educational content in their field of study. Learn how you can become an honored educator by visiting the website at: https://www.rsna.org/Honored-Educator-Award/ Ioannis Vlahos, MRCP,FRCR - 2015 Honored Educator



### UR194-ED-SUA8

## Sarcomatoid Renal Cell Carcinoma: Multimodality Radiologic Evaluation and Clinical Significance

Sunday, Nov. 25 12:30PM - 1:00PM Room: GU/UR Community, Learning Center Station #8

#### **Participants**

James H. Wang, MD, Tampa, FL (*Presenter*) Nothing to Disclose Cyrillo R. Araujo, MD, Tampa, FL (*Abstract Co-Author*) Nothing to Disclose Daniel K. Jeong, MD, Madison, WI (*Abstract Co-Author*) Nothing to Disclose

For information about this presentation, contact:

jameswang@health.usf.edu

### **TEACHING POINTS**

The purpose of this educational exhibit is: 1. Define sarcomatoid involvement in renal cell carcinoma and review its clinical significance in early diagnosis. 2. Summarize multimodality characteristic imaging features of sRCC (both qualitative/quantitative techniques and respective confidence levels).

### TABLE OF CONTENTS/OUTLINE

1. What is sarcomatoid involvement in renal cell carcinoma (sRCC)? 2. Clinical significance of diagnosing sRCC. 3. Diagnostic challenges (histologically and radiologically). 4. Characteristic features on CT and MRI. 5. Advanced quantitative imaging techniques to aide diagnosis. 6. How confident can we be in diagnosing sRCC radiologically? 7. IRB approved retrospective review of 93 sRCC and over 500 clear cell RCC (ccRCC) subjects yielded cases for this presentation. 8. Future research directions/opportunities and implications.



### VI006-EB-SUA

Case-Based Pictorial Review of Vascular Plug-Assisted Retrograde Transvenous Obliteration (PARTO) for Bleeding Gastric Varices: A Feasible Alternative to BRTO?

Sunday, Nov. 25 12:30PM - 1:00PM Room: VI Community, Learning Center Hardcopy Backboard

## Participants

Irfan Masood, MD, Galveston, TX (*Presenter*) Nothing to Disclose Arya Bagherpour, Galveston, TX (*Abstract Co-Author*) Nothing to Disclose Arsalan Saleem, MD, Galveston, TX (*Abstract Co-Author*) Nothing to Disclose Gunvir Gill, Galveston, TX (*Abstract Co-Author*) Nothing to Disclose Alper H. Duran, MD, Houston, TX (*Abstract Co-Author*) Nothing to Disclose Manoj K. Kathuria, MBBS, MD, Galveston, TX (*Abstract Co-Author*) Nothing to Disclose

#### For information about this presentation, contact:

irmasood@utmb.edu

### **TEACHING POINTS**

To review the indications and contraindications of vascular plug-assisted retrograde transvenous obliteration (PARTO) procedure. To discuss the PARTO procedure and its difference from conventional balloon-occluded retrograde transvenous obliteration (BRTO). To learn the role of percutaneous techniques in the managment of bleeding gastric varices. To discuss case-based anatomic and hemodynamic factors that affect the success rate of PARTO.

### **TABLE OF CONTENTS/OUTLINE**

Introduction to PARTO Comparison of PARTO with Conventional BRTO: - Procedural Advantages Inherent to PARTO - Duration of procedure and post-procedural patient care and monitoring. - Choice of embolizing agents and thier potential complications; Gelfoam in PARTO and sclerosing agents in BRTO - Risk of re-canalization of gastrorenal shunt and re-bleeding. - Hemodynamic changes in the portal system (portal hypertension, esophgeal bleeding, ascites, and encephalopathy). Summary



## VI151-ED-SUA7

How to Treat Angiographically Occult Hepatocellular Carcinoma with Ultraselective Conventional Transarterial Chemoembolization?

Sunday, Nov. 25 12:30PM - 1:00PM Room: VI Community, Learning Center Station #7

## Participants

Shiro Miyayama, Fukui, Japan (*Presenter*) Nothing to Disclose Masashi Yamashiro, MD, Fukui, Japan (*Abstract Co-Author*) Nothing to Disclose Natsuki Sugimori, Fukui, Japan (*Abstract Co-Author*) Nothing to Disclose Rie Ikeda, Fukui, Japan (*Abstract Co-Author*) Nothing to Disclose Naoko Sakuragawa, Fukui, Japan (*Abstract Co-Author*) Nothing to Disclose Kotaro Okimura, Fukui, Japan (*Abstract Co-Author*) Nothing to Disclose

#### For information about this presentation, contact:

s-miyayama@fukui.saiseikai.or.jp

### **TEACHING POINTS**

Conventional transarterial chemoembolization (cTACE) is one of the effective therapeutic options for inoperable hepatocellular carcinoma (HCC), and it is generally more effective for small HCC lesions. However, angiography frequently cannot demonstrate small HCC lesions because of reduced hypervascularity; therefore, it is important to know how to identify and treat such tumors during the procedure. Cone-beam computed tomography (CBCT) during hepatic arteriography (CBCTHA) can depict angiographically occult HCCs, either alone or in combination with CBCT during arterial portography. Three-dimensional (3D) vessel-tracking software using CBCTHA data can also identify tumor-feeding branches and a microcatheter with a tip of smaller than 2-F can be advanced into a tiny tumor-feeder. Thus, advancement of image guidance system and microcatheter-guidewire technology has enabled superselective cTACE at the most distal portion of the subsubsegmental hepatic artery (ultraselective cTACE) for angiographically occult HCCs.

## TABLE OF CONTENTS/OUTLINE

1) How to perform CBCT during the procedure; 2) how to use 3D vessel-tracking softwre; 3) how to select tiny tumor-feeding branches; 4) how to perform ultraselective cTACE; 5) therapeutic effects of ultraselective cTACE on angiographically occult HCCs.



## VI152-ED-SUA8

Ablative Treatment in Renal Tumors: Complications and How to Avoid Them

Sunday, Nov. 25 12:30PM - 1:00PM Room: VI Community, Learning Center Station #8

#### **Participants**

Yasmina Lamprecht, MBBS, Santander, Spain (*Presenter*) Nothing to Disclose Pedro Lastra Garcia-Baron, MD, Santander, Spain (*Abstract Co-Author*) Nothing to Disclose Alejandro Fernandez Florez, MD, Santander, Spain (*Abstract Co-Author*) Nothing to Disclose Elena Marin-Diez, MD, Santander, Spain (*Abstract Co-Author*) Nothing to Disclose Enrique Montes, MD, Santander, Spain (*Abstract Co-Author*) Nothing to Disclose Victor Fernandez-Lobo, Santander, Spain (*Abstract Co-Author*) Nothing to Disclose Ana Belen Barba Arce, MD, Santander, Spain (*Abstract Co-Author*) Nothing to Disclose Eduardo Herrera, Santander, Spain (*Abstract Co-Author*) Nothing to Disclose Francisco Pozo Pinon, Santander, Spain (*Abstract Co-Author*) Nothing to Disclose Javier Azcona Saenz, Santander, Spain (*Abstract Co-Author*) Nothing to Disclose Carmen Gonzalez-Carrero Sixto, Santander, Spain (*Abstract Co-Author*) Nothing to Disclose Adrian Cardin Pereda, Santander, Spain (*Abstract Co-Author*) Nothing to Disclose

## For information about this presentation, contact:

yasmina.lamprecht@gmail.com

#### **TEACHING POINTS**

To revise the different ablative techniques available. To discuss which tumor characteristics may be important for ablative treatment. To revise the most important complications that may occur by using alternative treatments in kidney tumors. To review which is the best treatment guidance available. To make a straightforward algorithm that allows us, depending on the different renal tumor features, to suspect what type of postablation complications are more prone to occur and how to avoid them.

## TABLE OF CONTENTS/OUTLINE

Different techniques available: Radiofrequency ablation. Microwave ablation. Cryoablation. Different renal tumor characteristics: Diameter. Proximity to adjacent structures. Renal location. Endophytic or exophytic location. Guidance: Ultrasound. Computed tomography. Both. Complications: Hemorrhage. Fistulae or stenosis of the urinary tract. Organ burn. Skin burn. Persistent lumbar pain. Tumor spread. Pneumothorax. How to avoid them: Previous embolization. Transhepatic approach. Pneumo/hydrodisplacement. Preablation a-receptor blockade.



### VI200-SD-SUA1

Significant Importance of Novel Direct Eye Dosimeter and Protective Lead Devices for Complying with ICRP Recommended Limit for the Eye Lens in Transarterial Chemoembolization for HCC

Sunday, Nov. 25 12:30PM - 1:00PM Room: VI Community, Learning Center Station #1

**FDA** Discussions may include off-label uses.

#### **Participants**

Masakazu Hirakawa, MD, Beppu, Japan (*Presenter*) Nothing to Disclose Yoshiki Asayama, MD, Fukuoka, Japan (*Abstract Co-Author*) Nothing to Disclose Kousei Ishigami, MD, Fukuoka City, Japan (*Abstract Co-Author*) Nothing to Disclose Yasuhiro Ushijima, MD, Fukuoka, Japan (*Abstract Co-Author*) Nothing to Disclose Akihiro Nishie, MD, Fukuoka, Japan (*Abstract Co-Author*) Nothing to Disclose Hiroshi Honda, MD, Fukuoka, Japan (*Abstract Co-Author*) Nothing to Disclose

### For information about this presentation, contact:

mahira@radiol.med.kyushu-u.ac.jp

### PURPOSE

This study aimed to evaluate the occupational eye doses estimated using novel direct eye dosimeter (DOSIRIS, 3mm dose equivalent, Hp(3)) during transarterial chemoembolization (TACE) for HCC and to investigate possible number of TACE procedures/y within current dose limit of 20 mSv/y.

## METHOD AND MATERIALS

The measurements of eye doses [Hp(3)]were carried out for 3 Interventional radiologists (IR) (IR1 operator with lead glass and ceiling mounted lead glass screen, IR2 operator without lead glass and with ceiling mounted lead glass screen, IR3 operator without lead glass and ceiling mounted lead glass screen) performing 132 TACE procedures using DOSIRIS. For protective lead devices, wraparound type lead glass eye wear (0.07mmPb) and ceiling mounted lead glass screen are used. To measure the occupational eye dose, DOSIRIS was stuck just lateral to the left eye under lead glass and without lead glass. We calculated the eye dose per TACE procedures and possible number of TACE procedures/ y within current dose limit of 20 mSv/y for each operators.

## RESULTS

The mean fluoroscopy time, air kerma and dose area product/TACE were 38.2min, 1.45Gy and 200587mGy·cm2, respectively. The eye dose per TACE procedure for 1,2, and 3 operator were 34.8, 72.2, and 240 $\mu$ Sv, respectively. The eye dose of IR1 with protective lead devices was significantly lower than IR without protective lead devices (IR3). Possible number of TACE procedures /y within ICRP recommended dose limit of 20 mSv/y for 1, 2, and 3 operator were 574, 277, and 83, respectively.

### CONCLUSION

The eye dose limit of 20mSv/y may be exceeded in IR operators who do not use protective lead glasses and ceiling mounted lead glass screen. For complying with ICRP recommendation, protective lead devices and correct evaluation of the eye dose using direct eye dosimeter (Hp(3)) under protective lead glasses might be needed.

## **CLINICAL RELEVANCE/APPLICATION**

To minimize the radiation-induced risk at the eye lenses during interventional radiological procedures, the routine use of DOSIRIS and protective lead devices might be necessary, additionally, appropriate training on this issue is highly recommended.



## VI201-SD-SUA2

Citation Analysis of Interventional Radiology Articles: General Radiology Journals vs. a Dedicated Interventional Radiology Journal

Sunday, Nov. 25 12:30PM - 1:00PM Room: VI Community, Learning Center Station #2

#### Awards Student Travel Stipend Award

#### Participants

Yannie S. Li, BS, Memphis, TN (*Presenter*) Nothing to Disclose Harris L. Cohen, MD, Memphis, TN (*Abstract Co-Author*) Nothing to Disclose Christopher Cunningham, Memphis, TN (*Abstract Co-Author*) Nothing to Disclose Coleman Breland, Memphis, TN (*Abstract Co-Author*) Nothing to Disclose Dustin Sattler, BS, Memphis, TN (*Abstract Co-Author*) Nothing to Disclose Asim F. Choudhri, MD, Memphis, TN (*Abstract Co-Author*) Nothing to Disclose

## For information about this presentation, contact:

yannie.s.li@gmail.com

## PURPOSE

Interventional radiology (IR) research may be published in either general radiology journals (GRJs) or a dedicated subspecialty journal. Knowledge of citation statistics is important to authors seeking to optimize the impact of published articles. The purpose of this study was to evaluate and compare the citation statistics of IR articles published in four general radiology journals versus those in a dedicated subspecialty journal. We hypothesized that IR articles published in GRJs would have different citation profiles than those published in a subspecialty journal.

## METHOD AND MATERIALS

Article information was collected from SCOPUS. All articles published in 2008-2012 were considered. All articles from the dedicated IR journal, *Journal of Vascular and Interventional Radiology (JVIR)*, from 2008-2012 were included. The four selected GRJs were *Radiology, American Journal of Roentgenology (AJR)*, *Radiographics*, and *European Radiology*. GRJ articles containing 'interventional' in the title or keywords were selected. The average number of citations (ANC) per article was calculated by dividing the number of citations by the number of articles. The social media presence of articles was evaluated by Altmetric score (Altmetric.com).

## RESULTS

2140 IR articles were published in selected journals from 2008-2012; 537 in GRJs and 1603 in *JVIR*. IR articles in the four GRJs received a statistically significantly higher average number of citations (ANC) per article, with an ANC of 29.2 or GRJ and 15.4 for *JVIR* (p=0.0016). IR articles published in *Radiology* had the highest ANC (48.4). All GRJs had a higher ANC than *JVIR*. Altmetric scores were higher in GRJs than *JVIR* (p=0.012). Across all journals, Altmetric scores had a correlation with ANC (R2=0.27).

### CONCLUSION

IR articles published in general radiology journals obtain more citations and social media exposure than those published in *JVIR*, suggesting that interventional researchers seeking to maximize manuscript impact should consider publishing in a GRJ. Our analysis also revealed a weak correlation between an article's social media presence and citations, suggesting that sharing an article on social media may possibly result in more citations.

## CLINICAL RELEVANCE/APPLICATION

Clinical research in IR may reach a broader audience and have a greater impact when published in a general radiology journal.

## **Honored Educators**

Presenters or authors on this event have been recognized as RSNA Honored Educators for participating in multiple qualifying educational activities. Honored Educators are invested in furthering the profession of radiology by delivering high-quality educational content in their field of study. Learn how you can become an honored educator by visiting the website at: https://www.rsna.org/Honored-Educator-Award/ Asim F. Choudhri, MD - 2016 Honored EducatorHarris L. Cohen, MD - 2016 Honored Educator



### VI202-SD-SUA3

## The ALARA Principle in CT Guided Intervention

Sunday, Nov. 25 12:30PM - 1:00PM Room: VI Community, Learning Center Station #3

## **Participants**

Dinesh Brand, BSC, MBBS, Marden, Australia (Presenter) Nothing to Disclose Roger P. Davies, MBBS, Collinswood, Australia (Abstract Co-Author) Nothing to Disclose

#### PURPOSE

Precise needle placement for spinal intervention gives a lower complication rate and better efficacy. For CT intervention the lowest radiation dose is a primary consideration, with accurate needle placement and verification of position before injection.

## **METHOD AND MATERIALS**

A retrospective clinical audit of 200 consecutive patients presenting for therapeutic spinal intervention by two proceduralists was analyzed, including spinal level (lumbar vs cervical), guidance and approach (epidural and facet joint). The technique used sequential single sectored acquisitions of 0.23 or 0.3 seconds. A minimum of 2 and a median of 4 slice acquisitions with 0.5mm to 2mm reconstructions was used to determine needle position in the target space. Z axis needle position was determined by examination of adjacent axial reconstructions in each static acquisition. Contrast was always injected to determine successful positioning.

### RESULTS

A 89- 95 percent reduction of radiation dose was achieved, compared to recent literature, using sequential thin slice multi-level simultaneous axial acquisitions and sectored scans to reduce effective mAs. Partial sector scanning and increased rotational speed significantly contributed to reduced dose without compromising successful needle placement in the target space. There was a significant DLP difference between the 16 and 160 slice scanners. Lumbar needle placement required a higher DLP than cervical intervention. The minimum DLP for cervical needle placement was 0.8 mGy.cm and for lumbar placement 0.9 mGy.cm. The median values were 3.0 and 4.8 mGy.cm respectively. For 160 slice acquisitions, the mean values for cervical and lumbar placement were 2.55 and 4.24 mGy.cm.

## CONCLUSION

Guidance by sequential acquisition of thin slice grouped axial scans with high rotation speed and partial sector reconstruction has greatly reduced radiation dose compared to published data using pulsed or continuous CT fluoroscopy. Needle conspicuity is inversely related to slice thickness and scan acquisition time; image noise does not increase to obscure needle tip identification as slice thickness reduces.

## **CLINICAL RELEVANCE/APPLICATION**

Radiation dose reduction during interventional procedures is a key performance indicator to improve patient and referring clinician acceptance without compromising procedural performance and safety.



## VI203-SD-SUA4

## Injection System and Navigation of Magnetic Microbeads Using MRI Gradients

Sunday, Nov. 25 12:30PM - 1:00PM Room: VI Community, Learning Center Station #4

## Awards

## Student Travel Stipend Award

#### Participants

Francois Michaud, BSC, Montreal, QC (*Presenter*) Nothing to Disclose Ning Li, Montreal, QC (*Abstract Co-Author*) Nothing to Disclose Rosalie Plantefeve, PhD, Montreal, QC (*Abstract Co-Author*) Nothing to Disclose Zeynab Nosrati, BSC, Vancouver, BC (*Abstract Co-Author*) Nothing to Disclose Charles Tremblay, BSC, Montreal, QC (*Abstract Co-Author*) Nothing to Disclose Pierre Perreault, MD, Montreal, QC (*Abstract Co-Author*) Consultant, Abbott Laboratories Urs O. Hafeli, PhD, Vancouver, BC (*Abstract Co-Author*) Nothing to Disclose Samuel Kadoury, Montreal, QC (*Abstract Co-Author*) Nothing to Disclose An Tang, MD, Montreal, QC (*Abstract Co-Author*) Nothing to Disclose Samuel Kadoury, Montreal, QC (*Abstract Co-Author*) Nothing to Disclose Samuel Kadoury, Montreal, QC (*Abstract Co-Author*) Nothing to Disclose Gilles P. Soulez, MD, Montreal, QC (*Abstract Co-Author*) Nothing to Disclose Gilles P. Soulez, MD, Montreal, QC (*Abstract Co-Author*) Speaker, Bracco Group Speaker, Siemens AG Research Grant, Siemens AG Research Grant, Bracco Group Research Grant, Cook Group Incorporated Research Grant, Object Research Systems Inc

For information about this presentation, contact:

f.michaud@umontreal.ca

#### PURPOSE

To demonstrate the in vitro efficacy of an injection system used in conjunction with MRI gradients for magnetic resonance navigation (MRN) in a phantom simulating arterial embolization.

#### **METHOD AND MATERIALS**

A computer-controlled injector was developed to aggregate and inject 200 µm magnetic microparticles. Following the injection of the microparticle aggregates in a Y-shaped arterial phantom positioned at the isocenter of a clinical MRI, a 20 mT/m gradient was applied toward the left or the right of the phantom. Simultaneously, saline was infused through the injection catheter at a constant flow rate of 0.2 mL/s and peripherally at a pulsatile flow averaging 0.4 mL/s with a frequency of 1 Hz and an amplitude of 0.4 mL. The main branch was positioned at 0°, 45° or 90° with respect to the main magnetic field and, for each position, 40 aggregates were steered (20 in each outlet direction). Aggregate size and integrity were measured downstream using an MRI-compatible optical camera. A T1-weighted spin echo sequence was acquired to assess distribution of aggregates. Steering efficiency was determined visually by measuring the fraction of aggregates steered in the same direction as the gradient.

#### RESULTS

The injection system allowed the formation of aggregates composed of 20 to 60 particles, with an uncertainty of 6 particles, corresponding to lengths varying from 1.6 to 3.2 mm. Individual aggregates were MRI-visible due to susceptibility artifacts. Overall, 82% of aggregates remained intact distal to the bifurcation. The steering efficiencies obtained for aggregates of 20 microparticles injected by this method were 100% for all angles and gradient directions.

## CONCLUSION

This study demonstrates that our injection system allows controllable and reproducible microparticle aggregate injections and can be used efficiently to accomplish MRN in vitro in physiologically realistic conditions using the native imaging gradient coils. It shows that both imaging and navigation can be performed reliably with a clinical MRI scanner. Next steps are to design an integrated imaging-navigation sequence to trigger gradient activation and to assess embolization level, followed by in vivo translation.

### **CLINICAL RELEVANCE/APPLICATION**

We propose a new concept for endovascular treatment of hepatocellular carcinoma using MRN for selective and targeted embolization of magnetic drug-eluting beads through an intra-arterial port.

#### **Honored Educators**

Presenters or authors on this event have been recognized as RSNA Honored Educators for participating in multiple qualifying educational activities. Honored Educators are invested in furthering the profession of radiology by delivering high-quality educational content in their field of study. Learn how you can become an honored educator by visiting the website at: https://www.rsna.org/Honored-Educator-Award/ An Tang, MD - 2018 Honored Educator



## VI204-SD-SUA5

No Inferiority of Tonbridge Thrombectomy Device for Acute Thrombus Retrial Compared with Solitaire Device: An Experimental Evaluation Study

Sunday, Nov. 25 12:30PM - 1:00PM Room: VI Community, Learning Center Station #5

## Participants

Yueqi Zhu, MD, Shanghai, China (*Presenter*) Nothing to Disclose Yingsheng Cheng, MD, Shanghai, China (*Abstract Co-Author*) Nothing to Disclose

### PURPOSE

Mechanical thrombectomy (MT) has been widely accepted as a safe and effective treatment for acute ischemic stroke (AIS). Development of stent retriever devices has been intensively developed over the past two decades. In this study, we compared the effectiveness and safety of a new thrombectomy device with Solitaire FR for the treatment of AIS models.

## METHOD AND MATERIALS

Mechanical performance of stent retrievers was tested in vitro. Thrombin-induced thrombus was pre-injected into the right distal external carotidmaxillary artery in 18 dogs to create an acute thrombus occlusion model, and these animals were divided into a Tonbridge group (n=9, with Tonbridge stent Tonbridge Medical Technology) and a Solitaire group as control (n=9, with Solitaire stent, ev3 Neurovascular). Final flow restoration, side branches, recanalization time, distal vessel embolism, and devicerelated complications were recorded and compared. A post-procedure angiogram was obtained at 30 and 90 days after thrombectomy. Device manipulationrelated damage to the arterial walls was evaluated histologically.

#### RESULTS

In vitro test showed that lower maximum friction within the microcatheter and slight increase in radial force was noticed for the Tonbridge (0.763 vs. 0.784 of Solitaire and 0.035 N /mm vs 0.031 N /mm of Solitaire, P>0.05). Eighteen and 16 retriever attempts were done in the Tonbridge (mean 2.0 attempts) and the Solitaire (mean 1.8 attempts) groups (P=0.74). The Tonbridge device led to good flow restoration in all nine (100%) models compared with eight (88.9%) in the Solitaire group (P=0.30). Side branches' influence (P=0.39), distal thromboembolism (P=0.60), and device-related complications (P=1.00) found no difference between the two groups. The rates of disruption of the internal elastic lamina (IEL) were 8.3% (2/24) and 4.2% (1/24) of the specimens, respectively (P=0.683). TICI 2b/3 flow of the right CCA were similar between the two groups at 1 (6/6 vs 6/6) and 3 months (6/6 vs 6/6) follow-up (P>0.05).

## CONCLUSION

Our preliminary study indicated this new device was technically feasible and effective to be used in thrombectomy for the treatment of acute thrombus occlusion in canine models

## **CLINICAL RELEVANCE/APPLICATION**

The Tonbridge is safe and leads to similar chances of recanalization rate in vivo as compared with Solitaire device, thus it can further be applied for the treatment of acute ischemia stroke.



## VI205-SD-SUA6

## Does RFA Treatment Induce Neoplastic Changes in Benign Thyroid Nodules: A Preliminary Study

Sunday, Nov. 25 12:30PM - 1:00PM Room: VI Community, Learning Center Station #6



## Participants

Su Min Ha, MD, Seoul, Korea, Republic Of (*Presenter*) Nothing to Disclose Jun Young Shin, Seoul, Korea, Republic Of (*Abstract Co-Author*) Nothing to Disclose Jung Hwan Baek, Seoul, Korea, Republic Of (*Abstract Co-Author*) Consultant, STARmed; Consultant, RF Medical Dong Eun Song, Seoul, Korea, Republic Of (*Abstract Co-Author*) Nothing to Disclose Sae Rom Chung, MD, Seoul, Korea, Republic Of (*Abstract Co-Author*) Nothing to Disclose Young Jun Choi, MD, Seoul, Korea, Republic Of (*Abstract Co-Author*) Nothing to Disclose Jeong Hyun Lee, MD, PhD, Seoul, Korea, Republic Of (*Abstract Co-Author*) Nothing to Disclose

## PURPOSE

Radiofrequency ablation (RFA) is being accepted as the treatment of choice in cases of symptomatic thyroid nodules instead of surgery. To our knowledge, no data is yet available on whether RFA promotes neoplastic transformation of the undertreated peripheral portion of the benign nodules. Our study was designed to evaluate the clinical feasibility of RFA treatment of benign thyroid nodules along with cytomorphological alteration, and any malignant changes through biopsy.

## METHOD AND MATERIALS

The data were retrospectively collected between April 2008 and June 2013 and core needle biopsy (CNB) was performed on 16 benign thyroid nodules previously treated using RFA. The parameters of the patients were compared, between the time of enrollment and the last follow-up examination, using linear mixed model statistical analysis.

## RESULTS

No atypical cells or neoplastic transformation were detected in the undertreated peripheral portion of treated benign nodules on the CNB specimen. RFA altered neither the thyroid capsule nor the thyroid tissue adjacent to the treated area. On histopathological examinations, we observed 81.2% acellular hyalinization, which was the most common finding. After a mean follow-up period of over 5 years, the mean volume of thyroid nodule had decreased to  $6.4\pm4.2$  ml, with a reduction rate of  $81.3\pm5.8\%$  (p < 0.0001).

## CONCLUSION

RFA is a technically feasible treatment method for benign thyroid nodules, with no carcinogenic effect or tissue damage of the normal thyroid tissue adjacent to the RFA-treated zone.

## **CLINICAL RELEVANCE/APPLICATION**

This preliminary study demonstrated that by CNB of treated thyroid nodules, RFA is effective in treating benign thyroid nodules without any carcinogenic effect, and no tissue damage in the normal thyroid tissue adjacent to the RFA treated zone, thus not interfering with future surgery.



## AI025-EB-SUB

## Deep Learning for Discovery of Latent Information in Contrast Free Cardiac CT Images

Sunday, Nov. 25 1:00PM - 1:30PM Room: AI Community, Learning Center Hardcopy Backboard

### Participants

Daniele Della Latta, Massa, Italy (*Presenter*) Nothing to Disclose Gianmarco Santini, Massa, Italy (*Abstract Co-Author*) Nothing to Disclose Nicola Martini, PhD, Massa, Italy (*Abstract Co-Author*) Nothing to Disclose Lorena Maria Zumbo, Massa, Italy (*Abstract Co-Author*) Nothing to Disclose Gabriele Valvano, MSc, Massa, Italy (*Abstract Co-Author*) Nothing to Disclose Andrea Ripoli, PhD, Massa, Italy (*Abstract Co-Author*) Nothing to Disclose Francesco Avogliero, MD, Massa, Italy (*Abstract Co-Author*) Nothing to Disclose Giuli Jamagidze, Massa, Italy (*Abstract Co-Author*) Nothing to Disclose Dante Chiappino, Massa, Italy (*Abstract Co-Author*) Nothing to Disclose

#### For information about this presentation, contact:

dellalatta@ftgm.it

#### CONCLUSION

By exploiting the ability of the DCNN to mimic the human visual system and to regenerate the imagery and memory retrieval operations, we propose a novel approach to synthesize contrast enhanced CTimages, starting from contrast free CT thoracic scans. The obtained synthetic CT images allow the quantification of shapes and volumes of the cardiac chambers.

## FIGURE

http://abstract.rsna.org/uploads/2018/18015453/18015453\_tx5p.jpg

#### Background

In the European population, the 20% of the CT scans cover the thoracic region. Due to the lack of contrast in the cardiac area, the information about the cardiovascular system remains latent. From the clinical side, it would be important to define the morphology of the cardiac chambers, identifying patients affected by cardiopathies or valvular pathologies. Recently developed Deep Convolutional Neural Networks (DCNN) architectures have achieved breakthrough performance in image processing. Aim of this work is to develop a DCNN able to create contrast enhanced images, starting from contrast free ones.

## **Evaluation**

The study was conducted using both contrast free calcium scoring (CS) and coronary angiography (CTA) CT scans acquired on 200 consecutive patients, during the same cardiac telediastolic phase. By applying rigid registration on CTA and using the CS images as references respiratory motion misalignments were removed. A deconvolutional architecture was chosen for DCNN. Patient's volumes were splitted in 120 cases to train the model, 10 cases for its validation and 70 for the evaluation of its performance. To guarantee a higher generalization power, in the prediction phase data augmentation was used applying random rotation with a max angle of 25 degrees on all the couple of CS and CTA slices provided to the network. The quality of synthesized cardiac image was assessed with Normalized Mutual Information index (NMI) and Peak Signal to Noise Ratio index (PSNR).

#### Discussion

After 960 training epochs, the model was able to generate synthetic CTA images with a good similarity and contrast dynamics compared to the true CTA images ( $NMI=0.95\pm0.04$ ,  $PSNR=53.40\pm1.54$ ). The high quality of generated images allowed a simple extraction of the left cardiac chambers and the quantification of their volumes.



## AI201-SD-SUB1

## Automated Foreign Object Detection in Chest X-Ray Images Based on Deep Learning

Sunday, Nov. 25 1:00PM - 1:30PM Room: AI Community, Learning Center Station #1

### Participants

Chao Huang, PhD, Boston, MA (*Presenter*) Nothing to Disclose Sehyo Yune, MD, MPH, Boston, MA (*Abstract Co-Author*) Nothing to Disclose Myeongchan Kim, MD, Boston, MA (*Abstract Co-Author*) Nothing to Disclose Hyunkwang Lee, Boston, MA (*Abstract Co-Author*) Nothing to Disclose Synho Do, PhD, Boston, MA (*Abstract Co-Author*) Nothing to Disclose

## For information about this presentation, contact:

chuang35@mgh.harvard.edu

### PURPOSE

Chest X-ray (CXR) is the most commonly utilized imaging modality. In the hospital setting, various foreign objects such as endotracheal tubes or central venous catheters can be seen in CXR. The presence of foreign objects, if not carefully addressed, could impede CXR interpretation but is hard to detect and segment due to the wide variety of size and shape. Here we intend to develop an algorithm that automatically detects and localizes various foreign objects seen in CXR to recognize malposition and rapidly triage CXR.

### **METHOD AND MATERIALS**

We collected 2,400 PA-view CXR images and the associated radiology reports from our institutional database. The images that have foreign objects annotated in the corresponding radiology reports were labelled as positive (1,200 images) and all other images are labelled as negative (1,200 images). A convolutional neural network (CNN) was built, which inputs a CXR image and outputs the probability of foreign object existence along with a heatmap localizing the areas of the image most indicative of foreign objects. We randomly selected 80%, 10%, and 10% of the images for training, validation, and testing, respectively. To avoid overfitting and improve generalization, data augmentation is applied to the images in training dataset with affine transformations (translation, scaling, and rotation).

## RESULTS

Althought there were various foreign objects observed in CXR images (catheters, tubes, ECG cables, pacemakers etc.) and we only labeled the images positive and negative, the CNN achieved 99.5% accuracy on separating CXR images without any of these objects from those that has foreign objects. In positive cases, all types of foreign objects were accurately localized using class activation mapping.

## CONCLUSION

We developed a CNN-based algorithm that can accurately detect and localize various foreign objects in CXR images without manual annotation and segmentation.

#### **CLINICAL RELEVANCE/APPLICATION**

Detecting numerous types of foreign objects without manual segmentation will expedite development of high-performance automated interpretation system for CXR.



### BR170-ED-SUB6

Imaging of Free Liquid Silicone Injections in the Transgender Breast

Sunday, Nov. 25 1:00PM - 1:30PM Room: BR Community, Learning Center Station #6

#### **Participants**

Emily B. Sonnenblick, MD, New York, NY (*Presenter*) Nothing to Disclose Karen A. Lee, MD, New York, NY (*Abstract Co-Author*) Nothing to Disclose Shabnam Jaffer, MD, New York, NY (*Abstract Co-Author*) Nothing to Disclose Zil Goldstein, MA, New York, NY (*Abstract Co-Author*) Nothing to Disclose Nishi Talati, MD, New York, NY (*Abstract Co-Author*) Nothing to Disclose Laurie R. Margolies, MD, New York, NY (*Abstract Co-Author*) Research Consultant, FUJIFILM Holdings Corporation Susan Boolbol, MD, New York, NY (*Abstract Co-Author*) Nothing to Disclose Jess Ting, MD, New York, NY (*Abstract Co-Author*) Nothing to Disclose

#### For information about this presentation, contact:

emily.sonnenblick@mountsinai.org

#### **TEACHING POINTS**

1. Review considerations in breast imaging unique to transgender patients on hormone treatment (HT). 2. Free liquid silicone (FLS) injections, while not always symptomatic, may cause pain, palpable masses and disfigurement prompting some patients to seek medical care. 3. FLS breast injections present a challenge in the setting of diagnostic imaging or cancer screening. 4. Specific patterns and distribution of FLS seen with mammography, ultrasound and MRI correlate with surgical pathology and histology.

#### **TABLE OF CONTENTS/OUTLINE**

1. Background • Prevalence, guidelines for transgender care • Expected radiographic and histology correlates of HT for transgender individuals • Historical review of liquid silicone • Radiographic aspects and complications of FLS used for breast augmentation 2. Premastectomy evaluation • Role of pre-op imaging/screening for cancer with consideration of trans population breast cancer risk • Distribution of silicone: superficial location, pectoralis involvement • Fibrotic masses masquerading as cancer • Diffuse silicone granulomas 3. Diagnostic evaluation • Palpable silicone granulomas • Bloody nipple discharge • Post-op peri-prosthetic collection • Free silicone on CT • Post-op residual silicone 4. Silicone may migrate, make calcified granulomas and fibrotic masses, obscure normal tissue, complicating diagnosis of malignancy.



### BR171-ED-SUB67

## Breast Implants for Residents Test Your Knowledge in Common and Uncommon Findings

Sunday, Nov. 25 1:00PM - 1:30PM Room: BR Community, Learning Center Station #7

#### **Participants**

Lucia I. Beccar Varela, MD, Vicente Lopez, Argentina (*Abstract Co-Author*) Nothing to Disclose Maria Soledad Nocetti, MD, Vicente Lopez, Argentina (*Abstract Co-Author*) Nothing to Disclose Veronica E. Grondona, MD, Capital Federal, Argentina (*Abstract Co-Author*) Nothing to Disclose Elizabeth Quiroga, Vicente Lopez, Argentina (*Abstract Co-Author*) Nothing to Disclose Flavia B. Sarquis, MD, Vicente Lopez, Argentina (*Presenter*) Nothing to Disclose

## For information about this presentation, contact:

lu.beccar.varela@gmail.com

#### **TEACHING POINTS**

• Learn through pictures and diagrams to recognize different types of breast implants, including saline, double lumen and silicone gel. • Utilizing clinical cases, analyze the multimodality imaging appearances of common and uncommon complications, including mammographic, ultrasonographic and MRI findings.

## TABLE OF CONTENTS/OUTLINE

An increasing number of patients have breast implants for cosmetic augmentation of the breast, reconstruction after mastectomy or correction of congenital malformations. Any radiologist who interprets breast imaging studies should be familiar with the normal and abnormal findings of common implants. Clinical diagnosis of implant rupture is difficult and the aim of imaging is to provide essential information about tissue and prothesis integrity and detect breast diseases unrelated to implants, such as breast cancer. This work is a resident primer on successfully recognizing common and uncommon findings related to breast implants, learning specific strengths and weaknesses of each imaging technique, to make the correct choice for each individual patient.



### BR172-ED-SUB8

## Law and Order: Staying aBREAST of Medicolegal Issues in Mammography

Sunday, Nov. 25 1:00PM - 1:30PM Room: BR Community, Learning Center Station #8

#### **Participants**

Michael S. Morrow, DO, Worcester, MA (*Abstract Co-Author*) Nothing to Disclose Gopal R. Vijayaraghavan, MD, MPH, Shrewsbury, MA (*Presenter*) Nothing to Disclose Suma C. Kannabiran, MD, Boston, MA (*Abstract Co-Author*) Nothing to Disclose David E. March, MD, Springfield, MA (*Abstract Co-Author*) Nothing to Disclose

## **TEACHING POINTS**

Review current malpractice trends in Radiology with an emphasis on breast imaging. Highlight pitfalls in mammography that commonly lead to false negatives. Present best practices/policies regarding disclosing error to patients.

## TABLE OF CONTENTS/OUTLINE

Review of recent general trends in medical malpractice across specialties Detail malpractice as it relates to breast imaging Highlight types of errors in mammography interpretation Present common pitfalls in mammography leading to false negatives Introduce best practices in mitigating errors in an effort to minimize litigation



## BR173-ED-SUB9

Breast Elastography: How Does It Help? Interactive Case Review Including Helpful Tips for Incorporating Elastography in Your Practice

Sunday, Nov. 25 1:00PM - 1:30PM Room: BR Community, Learning Center Station #9

## Participants

Ana DiPrete, BA, Providence, RI (*Presenter*) Nothing to Disclose Robert C. Ward, MD, Providence, RI (*Abstract Co-Author*) Nothing to Disclose Elizabeth Lazarus, MD, Barrington, RI (*Abstract Co-Author*) Nothing to Disclose

#### For information about this presentation, contact:

ana\_diprete@brown.edu

## **TEACHING POINTS**

-Breast elastography utilizes static and dynamic ultrasound techniques to provide information about the "stiffness" of a lesion.-As malignant lesions tend to be stiffer than benign lesions, qualitative and quantitative assessments are used to score lesions as soft, intermediate or hard.-Adding elastographic qualities to BI-RADs features improves diagnostic accuracy and aids decision-making regarding clinical management (i.e. biopsies), especially with BIRADs category 3 and 4a lesions.-Our objective is to provide an engaging case-based imaging approach with questions and answers to discuss basic principles of elastography, commonly applied techniques, and the elastographic appearance of benign and malignant lesions to emphasize the implications of adding elastography to the diagnostic evaluation of breast disease.

## **TABLE OF CONTENTS/OUTLINE**

Users will be faced with diagnostic scenarios and management questions regarding the following areas:1. Comparing strain and shear wave elastography techniques2. Illustrating how elastographic features of benign and malignant breast disease differ3. Highlighting the clinical application of elastography and how it improves diagnostic accuracy of breast ultrasound 4. Reviewing the literature of breast elastography with a focus on how it supplements screening and diagnostic grey scale breast ultrasound



## BR174-ED-SUB10

New Findings on Breast MRI with Benign or Probably Benign Characteristics: Evaluation, Differential, and Management Dilemmas

Sunday, Nov. 25 1:00PM - 1:30PM Room: BR Community, Learning Center Station #10

## Participants

Sonia P. Sahu, MD, Boston, MA (*Abstract Co-Author*) Nothing to Disclose Sona A. Chikarmane, MD, Boston, MA (*Abstract Co-Author*) Nothing to Disclose Emily Mungovan, BA, Boston, MA (*Abstract Co-Author*) Nothing to Disclose Catherine S. Giess, MD, Wellesley, MA (*Abstract Co-Author*) Nothing to Disclose Mirelys Barrios, MD, Boston, MA (*Presenter*) Nothing to Disclose

## For information about this presentation, contact:

schikarmane@bwh.harvard.edu

## **TEACHING POINTS**

1. To understand the criteria for BIRADS 2 and BIRADS 3 lesions on screening breast MRI. 2. To recognize imaging features that may be new on screening MRI but support a benign or probably benign assessment. 3. To avoid pitfalls in assessing new MRI findings as benign or probably benign and become familiar with imaging features that should prompt immediate biopsy.

#### TABLE OF CONTENTS/OUTLINE

1. Provide a brief overview of the qualifying features for BIRADS 2 and BIRADS 3 lesions on MRI. 2. Demonstrate a rich pictorial review of new lesions and imaging features found on screening MRI that are consistent with a BIRADS 2 or 3 assessment including fat necrosis, asymmetric and diffuse background parenchymal enhancement, and enhancing foci. 3. Present teaching points to help guide management of new benign and probably benign findings on screening MRI. 4. Discuss pitfalls in assessing new MRI findings as benign or probably benign and review imaging features that should prompt immediate biopsy.

#### **Honored Educators**

Presenters or authors on this event have been recognized as RSNA Honored Educators for participating in multiple qualifying educational activities. Honored Educators are invested in furthering the profession of radiology by delivering high-quality educational content in their field of study. Learn how you can become an honored educator by visiting the website at: https://www.rsna.org/Honored-Educator-Award/ Catherine S. Giess, MD - 2015 Honored EducatorCatherine S. Giess, MD - 2017 Honored Educator



### BR175-ED-SUB11

## Imaging Findings Following Image Guided Cryoablation Of Breast Cancer: A New Normal

Sunday, Nov. 25 1:00PM - 1:30PM Room: BR Community, Learning Center Station #10

## Participants

Kenneth R. Tomkovich, MD, Freehold, NJ (Presenter) Consultant, Scion Medical Technologies, LLC;

#### For information about this presentation, contact:

ktomkovich@princetonradiology.com

### **TEACHING POINTS**

The purpose of this exhibit is:1. To introduce the concept of cryoablation as a primary treatment for certain types of breast cancers without the need for surgical excision2. To demonstrate the techniques utilized in the ICE 3 trial for successful treatment of low grade breast cancers with ultrasound guided cryoablation 3. To illustrate different imaging findings as a "new normal" in patients who have undergone cryoablation as a primary treatment for breast cancer including:Mammographic findings post cryoablation Ultrasound findings post cryoablation MRI findings post cryoablation 4. To discuss imaging findings that led to post cryoablation biopsies and why they can be observed if encountered in the future to avoid unnecessary biopsies

## TABLE OF CONTENTS/OUTLINE

Cryoablation as a primary treatment for certain types of breast cancersTechniques of ultrasound guided breast cancer cryoablation Brief description of the ICE 3 trialReview of imaging findings post cryoablation: the "new normal"- Mammography - Ultrasound - MRI-Biopsy examples Future implications and summary



## BR224-SD-SUB1

Evaluation of Gd-Deposits in Healthy Women Participating in High Risk Screening Program for Early Breast Cancer Detection

Sunday, Nov. 25 1:00PM - 1:30PM Room: BR Community, Learning Center Station #1

## Participants

Barbara Bennani-Baiti, MD, Wien, Austria (*Presenter*) Nothing to Disclose Barbara Krug, Cologne, Germany (*Abstract Co-Author*) Nothing to Disclose Daniel Giese, Koln, Germany (*Abstract Co-Author*) Nothing to Disclose Kilian Weiss, PhD, Hamburg, Germany (*Abstract Co-Author*) Employee, Koninklijke Philips NV Thomas H. Helbich, MD, Vienna, Austria (*Abstract Co-Author*) Research Grant, Medicor, Inc Research Grant, Siemens AG Research Grant, C. R. Bard, Inc Pascal A. Baltzer, MD, Vienna, Austria (*Abstract Co-Author*) Nothing to Disclose

### PURPOSE

To determine whether patients at high risk to develop breast cancer, that undergo contrast enhanced breast MRI at regular intervals for early breast cancer detection, exhibit brain signal alterations in the dentate nucleus and globus pallidus.

## METHOD AND MATERIALS

In this IRB-approved, dual centre randomized, prospective study 73 healthy women with no history of cancer or neurological disease that had received at least 6 doses of macrocyclic Gadolinium based contrast agents in the course of a national high risk screening program for the early detection of breast cancer were included. Patients underwent 3T/1.5T MRI of the brain, with a dedicated head coil, including T1 mapping and mpRAGE sequences. T1 times and T1 signal intensities were measured for dentate nucleus (ND), pons, globus pallidus (GP), and crus posterior of the capsula interna (CP) bilaterally, employing Horos software. Ratios of GP to CP as well as ND to pons were calculated for respective signal intensities and further statistical analyses were carried out with SPSS and Medcalc including multivariate regression analysis.

## RESULTS

There were 73 participants (median age 46 +/- 9 years) that had received an average of 9 cumulative dosages of Gd based macrocyclic contrast agents (median 8, SD 3, range 6 - 23). Spearman's rank correlation coefficient analysis revealed a mild correlation between age and number of dosages (R 0.31, p < 0.01) but no statistically significant correlations were found for signal intensity ratios or T1 times in relation to age or number of dosages. T1 times displayed no significant differences between the analysed brain structures (Fig.1.). ANOVA testing reveiled an adjusted R2 of -0.026 and -0.004 for the number of cumulative dosages predicting T1 times and signal intensity ratios, respectively, confirming that the number of previous dosages did not affect T1 signal in globus pallidus or nucleaus dentatus.

### CONCLUSION

Neither nucleus dentatus nor globus pallidus display altered T1 signals after high cumulative dosages of macrocyclic Gd-based contrast agents in healthy women.

### **CLINICAL RELEVANCE/APPLICATION**

Breast MRI being the most sensitive method for breast cancer detection crucially relies on Gd-based contrast agents. These findings show that the currently employed macrocyclic Gd-based contrast agents do not result in Gd-deposits in the brain of healthy women participating in a high risk screening program for early breast cancer detection.



# BR225-SD-SUB2

Radiomics Analysis with Contrast-Enhanced Dual-Energy Mammography for the Differentiation of Hormone Receptor Status and Tumor Invasiveness in Breast Cancer Patients

Sunday, Nov. 25 1:00PM - 1:30PM Room: BR Community, Learning Center Station #2

# Participants

maria adele marino, MD, New York,, NY (*Presenter*) Nothing to Disclose Doris Leithner, MD, New York, NY (*Abstract Co-Author*) Nothing to Disclose Katja Pinker-Domenig, MD, Vienna, Austria (*Abstract Co-Author*) Nothing to Disclose Janice S. Sung, MD, New York, NY (*Abstract Co-Author*) Research Grant, Hologic, Inc Elizabeth A. Morris, MD, New York, NY (*Abstract Co-Author*) Nothing to Disclose Maxine S. Jochelson, MD, New York, NY (*Abstract Co-Author*) Nothing to Disclose

#### For information about this presentation, contact:

marinom@mskcc.org

### PURPOSE

To investigate the potential of radiomics analysis of contrast-enhanced dual-energy mammography (CEDM) for differentiation of breast cancer invasiveness and hormonal status.

#### **METHOD AND MATERIALS**

In this IRB-approved retrospective data analysis, 53 patients with proven breast cancers were included and underwent pretreatment CEDM. There were 58 lesions in 53 patients: 6 non-invasive (ductal carcinoma in situ) and 52 invasive breast cancers. Among the invasive cancers, 39 were hormone-receptor positive (HR+) and 12 hormone-receptor negative (HR-) Radiomics analysis was performed using MaZda software (Technical University of Lodz, Poland). Lesions were manually segmented and radiomic features were derived from the first-order histogram (HIS): co-occurrence matrix (COM), run-length matrix (RLM), absolute gradient (GRA), autoregressive model (ARM), the discrete Haar wavelet transform (WAV), as well as lesion geometry (GEO). Fisher, probability of error and average correlation (POE+ACC), and mutual information (MI) coefficients were used for feature selection. Linear discriminant analysis followed by k-nearest neighbor classification (with leave-one-out cross-validation) was used for pairwise texture-based separation of subtypes/hormonal status. Radiomics parameters were correlated with tumor histology (invasive vs non-invasive) and hormonal status (HR+ vs HR-).

#### RESULTS

Texture analysis yielded the following accuracies for differentiation between invasive/non-invasive breast cancers: 86.2% (based on COM and WAV features/MI), 84.4% (based on COM, WAV, and RLM features/POE+ACC), and 82.8% (mainly through COM+WAV/Fisher). For differentiation between HR+ and HR\_ cancers, diagnostic accuracy was as follows: 76.4% (based on COM features/MI), 72.5% (based on COM+HIS+WAV features/POE+ACC), and 66.6% (mainly through COM features/Fisher).

## CONCLUSION

Data indicate that radiomics analysis with CEDM might be able to differentiate between non-invasive and invasive breast cancer and hormone receptor status.

# **CLINICAL RELEVANCE/APPLICATION**

Radiomics analysis with CEDM might provide additional imaging biomarkers for the non-invasive characterization of breast cancer and thus has the potential to guide treatment decisions.



# BR226-SD-SUB3

Patient, Provider, and Facility Characteristics Associated with Observed Variations in Breast Cancer Screening Outcomes: Findings from A Learning Health System

Sunday, Nov. 25 1:00PM - 1:30PM Room: BR Community, Learning Center Station #3

## Participants

Nila H. Alsheik, MD, Madison, WI (*Abstract Co-Author*) Nothing to Disclose Firas Dabbous, Park Ridge, IL (*Abstract Co-Author*) Nothing to Disclose Zhaohui Su, PhD, Boston, MA (*Abstract Co-Author*) Employee, OM1 Gregory Donadio, Park Ridge, IL (*Abstract Co-Author*) Employee, OM1 Richard Gliklich, MD, Cambridge, MA (*Abstract Co-Author*) Employee, OM1 Scott Pohlman, MSc, BEng, Cambridge, MA (*Abstract Co-Author*) Employee, Hologic, Inc Kathleen Troeger, Marlborough, MA (*Abstract Co-Author*) Employee, Hologic, Inc Vandana Menon, MD,PhD, Cambridge, MA (*Abstract Co-Author*) Employee, OM1 Emily F. Conant, MD, Philadelphia, PA (*Presenter*) Grant, Hologic, Inc; Consultant, Hologic, Inc; Grant, iCAD, Inc; Consultant, iCAD, Inc; Speaker, iiCME

# For information about this presentation, contact:

nila.alsheik@advocatehealth.com

#### PURPOSE

To examine data from a learning health system to identify patient, provider, and imaging facility characteristics associated with optimal screening outcomes.

#### **METHOD AND MATERIALS**

A big data platform was used to integrate EMR, RIS, and tumor registry data to create a learning health system. The analysis included 411,355 screens, performed 2015 to 2017, from 64 imaging facilities across three large healthcare organizations. The imaging facilities were stratified into quartiles of increasing recall rates (RR) (Quartile 1 (Q1) range=6.78-8.37%, Q2=8.84-9.98%, Q3=10.09-10.81%, Q4=10.88-21.00%) and by digital breast tomosynthesis (DBT) conversion (75-100% DBT, 50-75% DBT, 25-50% DBT, 0-25% DBT). Patient, provider and site characteristics, PPV1, biopsy (BX) rate and cancer detection (CDR) were evaluated overall and stratified by modality.

### RESULTS

There were no consistent trends in distribution of age, ethnicity or breast density across quartiles but facilities in the lower recall quartiles had more Caucasian patients and were predominantly DBT. Facilities with higher DBT conversion had lower RR than hybrid or predominantly 2D digital mammography (DM) sites (75-100% DBT: 8.87%, 50-75% DBT: 10.72%, 25-50% DBT:11.39%, 0-25%: 10.11%, p value for trend <0.001). Screening outcomes varied between quartiles. PPV1 decreased from 6.0% in Q1 to 3.3% in Q4; BX rate and CDR were lowest in Q1 (1.0%, 4.0), Q2 had the highest BX rate and CDR (1.7%, 4.7) and Q4 had a high BX rate and low CDR (1.7%, 4.2). DBT had higher PPV1, and higher CDR, in Q1 (6.7% vs 3.3%; 4.4 vs 2.6), Q2 (6.1% vs 3.6%; 5.5 vs 3.5) and Q3 (5.1% vs 3.8%; 5.3 vs 3.8) compared to DM, but not in Q4 (3.2% vs 3.3%; 4.2 vs 4.2).

#### CONCLUSION

Recall rates were influenced by race and DBT conversion. Across quartiles, DBT had lower RR and higher PPV1 and CDR, except in Q4. Facilities that were predominantly DBT had consistently lower RR than hybrid DBT/DM sites. These data demonstrate that DBT offers a more efficient screening option and increasing DBT utilization is associated with improved outcomes. There is an optimal balance between RR, BX rate and CDR and, as RR increased above 9.18%, there were increased BX but no significant gains in either PPV1 or CDR.

## **CLINICAL RELEVANCE/APPLICATION**

Digital Breast Tomosynthesis in hybrid sites, and sites with higher conversion to DBT, have better screening outcomes than 2D Digital Mammography, across all strata of age, race and breast density.



# BR227-SD-SUB4

Breast Imaging (Contrast Enhanced Spectral Mammography)

Sunday, Nov. 25 1:00PM - 1:30PM Room: BR Community, Learning Center Station #4

#### Participants

Norran H. Said, MD, FRCR, Cairo, Egypt (*Presenter*) Nothing to Disclose Ashraf Selim, MD, Cairo, Egypt (*Abstract Co-Author*) Nothing to Disclose

For information about this presentation, contact:

norranhussein@yahoo.com

#### PURPOSE

To identify the typical CEDM imaging characteristics and morphological enhancement patterns of different breast cancer pathological subtypes.

### **METHOD AND MATERIALS**

From Jan 2016 to Jan 2018, 147 patients with pathology proved breast cancer who had undergone CEDM were retrospectively reviewed. Imaging findings were recorded and divided into mass, non mass enhancement & focus. Morphological enhancement criteria for mass and non mass enhancement were interpreted as follows; mass enhancement was described by shape (round, oval, irregular), margin (circumscribed, noncircumscribed : irregular / spiculated), and uptake pattern (rim, homogenous, heterogenous). Non mass enhancement was described by uptake pattern (homogenous, heterogenous, clumped, clustered ring) and distribution (focal, linear, segmental, regional, multiple regions, diffuse). All descriptors were correlated with pathology including subtypes; Triple negative (TN), Estrogen receptor (ER) positive, Human epidermal growth factor receptor 2 (Her 2) positive.

### RESULTS

Out of the 147 cases, there were 24 (16.3%) TN, 90 (61.2%) ER positive and 33 (22.4%) Her 2 positive. Enhancement patterns according to subtype were as follows; TN cases demonstrated 79.2% mass and 20.8% non mass enhancement. ER positive cases included 72.2% mass, 22.2% non mass enhancement and 5.6% foci. Her 2 positive included 45.5% mass, 48.5% non mass enhancement and 6.1% foci. TN tumors demonstrated 68.4% rim enhancement with 73.3% circumscribed margins, and 68.4% round shape. ER positive demonstrated 78.5% heterogenous enhancement , 63% spiculated margins, and 91% irregular shape. Her 2 positive demonstrated 53.3% heterogenous enhancement with spiculated margins, and 100% irregular shape. P value was found significant (p<0.001). There were no significant differences on the non mass enhancement descriptors and foci.

# CONCLUSION

Our findings conclude that the rim enhancement feature on CEDM, along with circumscribed margins and round shape, are significant morphological descriptors for TN cancers compared to other subtypes. No significant difference was detected in non mass and focus uptake patterns.

## **CLINICAL RELEVANCE/APPLICATION**

Application of contrast enhancement characteristics of masses by CEDM, allow detailed estimation of pathological subtypes with radiological-pathological correlation.



## BR228-SD-SUB5

## **Does Tomosynthesis Work For Everyone?**

Sunday, Nov. 25 1:00PM - 1:30PM Room: BR Community, Learning Center Station #5

# Participants

Ethan O. Cohen, MD, Houston, TX (*Presenter*) Spouse, Consultant, Medtronic plc; Spouse, Consultant, Novo Nordisk AS; Spouse, Consultant, Eli Lilly and Company; Spouse, Consultant, AstraZeneca PLC Rachel E. Perry, MD, Birmingham, AL (*Abstract Co-Author*) Nothing to Disclose Ashmitha Srinivasan, MD, Houston, TX (*Abstract Co-Author*) Nothing to Disclose Hilda H. Tso, DO, Houston, TX (*Abstract Co-Author*) Nothing to Disclose Kanchan Phalak, MD, Houston, TX (*Abstract Co-Author*) Nothing to Disclose Michele D. Lesslie, DO, Bellaire, TX (*Abstract Co-Author*) Nothing to Disclose Karen E. Gerlach, MD, Houston, TX (*Abstract Co-Author*) Nothing to Disclose Jessica W. Leung, MD, Houston, TX (*Abstract Co-Author*) Nothing to Disclose Jessica W. Leung, MD, Houston, TX (*Abstract Co-Author*) Nothing to Disclose

#### For information about this presentation, contact:

# ecohen@mdanderson.org

## PURPOSE

To compare the performance of full-field digital screening mammograms (FFDM) with and without digital breast tomosynthesis (DBT) in women with and without breast implants.

#### **METHOD AND MATERIALS**

An IRB-approved, HIPAA-compliant retrospective review was performed of 103,070 consecutive screening mammograms obtained from February 2011 through June 2014. Recall rates (RRs), cancer detection rates (CDRs), and positive predictive values for recall (PPV1s) were analyzed.

### RESULTS

The following data compare FFDM and FFDM-DBT: 67,331 FFDM and 28,835 FFDM-DBT from women *without* implants yielded RRs of 8.0% and 6.3%, respectively (p<0.00001); CDRs of 4.1 and 5.0 per 1000 exams, respectively (p=0.07); and PPV1s of 5.1% and 8.0%, respectively (p<0.0001). 4325 FFDM and 2579 FFDM-DBT from women *with* implants yielded RRs of 5.2% and 4.1%, respectively (p=0.040); CDRs of 1.8 and 2.7 per 1000 exams, respectively (p=0.46); and PPV1s of 3.6% and 6.7%, respectively (p=0.25). The same data is also used to evaluate the effect of implants on screening: 67,331 FFDM *without* implants and 4325 FFDM *with* implants yielded RRs of 8.0% and 5.2%, respectively (p<0.00001); CDRs of 4.1 and 1.8 per 1000 exams, respectively (p<0.00001); and PPV1s of 5.1% and 3.6%, respectively (p=0.30). 28,835 FFDM-DBT *without* implants and 2579 FFDM-DBT *with* implants yielded RRs of 6.3 and 4.1, respectively (p<0.00001); CDRs of 5.0 and 2.7, respectively (p=0.11); and PPV1s of 8.0 and 6.7, respectively (p=0.63).

# CONCLUSION

Tomosynthesis improves the performance of digital screening mammography, while the presence of implants reduces its performance. Specifically, tomosynthesis improved RRs, CDRs, and PPV1s for all women (*with* and *without* implants), though statistically significant differences were seen only for RRs in women *without* implants, RRs in women *with* implants, and PPV1s for women *without* implants. Implants were associated with decreased RRs, worse CDRs, and worse PPV1s for all screening exams (FFDM and FFDM-DBT), but statistically significant differences were seen only for RRs for all screening exams and CDR for FFDM. Further study with larger populations is warranted.

# **CLINICAL RELEVANCE/APPLICATION**

The benefit of tomosynthesis has been incompletely studied in screening mammography patients with implants. This research suggests that tomosynthesis is useful for screening women *with* implants in addition to those *without* implants.



# CA161-ED-SUB7

Cardiac MR in Pulmonary Hypertension: From Magnet to Bedside

Sunday, Nov. 25 1:00PM - 1:30PM Room: CA Community, Learning Center Station #7

### Awards Certificate of Merit Identified for RadioGraphics

#### **Participants**

Jordi Broncano, MD, Cordoba, Spain (*Presenter*) Nothing to Disclose Antonio Luna, MD,PhD, Jaen, Spain (*Abstract Co-Author*) Consultant, Bracco Group; Speaker, General Electric Company; Speaker, Canon Medical Systems Corporation; Royalties, Springer Nature Fernando R. Gutierrez, MD, Saint Louis, MO (*Abstract Co-Author*) Spouse, Stockholder, UnitedHealth Group Eric E. Williamson, MD, Rochester, MN (*Abstract Co-Author*) Nothing to Disclose Daniel Vargas, MD, Aurora, CO (*Abstract Co-Author*) Nothing to Disclose Majesh Makan, MD, St. Louis, MO (*Abstract Co-Author*) Nothing to Disclose Sanjeev Bhalla, MD, Saint Louis, MO (*Abstract Co-Author*) Nothing to Disclose

# For information about this presentation, contact:

j.broncano.c@htime.org

# **TEACHING POINTS**

1. To analyze the value of cardiac imaging in patients with pulmonary hypertension with emphasis on physiopathology and prognosis. 2. To discuss the importance of different cardiac MR based parameters in PH attending on its acquisition, dedicated analysis and potential pitfalls. Correlation with echocardiography will also be applied.

## TABLE OF CONTENTS/OUTLINE

1. Introduction 2. Pulmonary hypertension (PH): definition and classification 3. Cardiac remodeling in PH 4. Biomarkers in cardiac imaging: definition and clinical implications 5. Rationale of CMR protocol in PH 6. Cardiac findings in PH 6.1. Black blood sequences in PH 6.2. Cine SSFP in PH: more than just volumes and function 6.3. Phase contrast imaging and 4D flow: More than velocity 6.4. First pass perfusion imaging in PH: value in prognosis 7. Impact of multiparametric CMR in PH 8. Conclusion

#### **Honored Educators**

Presenters or authors on this event have been recognized as RSNA Honored Educators for participating in multiple qualifying educational activities. Honored Educators are invested in furthering the profession of radiology by delivering high-quality educational content in their field of study. Learn how you can become an honored educator by visiting the website at: https://www.rsna.org/Honored-Educator-Award/ Antonio Luna, MD - 2018 Honored EducatorDaniel Vargas, MD - 2017 Honored EducatorSanjeev Bhalla, MD - 2014 Honored EducatorSanjeev Bhalla, MD - 2018 Honored EducatorSanjeev Bhalla, MD - 2018 Honored Educator



# CA167-ED-SUB8

# Cardiovascular Imaging in Pregnancy - An Update on Current Practice

Sunday, Nov. 25 1:00PM - 1:30PM Room: CA Community, Learning Center Station #8

### Participants

Kamlesh J. Jobanputra, MD, Dallas, TX (*Abstract Co-Author*) Nothing to Disclose Verghese George, MBBS, Houston, TX (*Abstract Co-Author*) Nothing to Disclose Kevin R. Kalisz, MD, Cleveland, OH (*Abstract Co-Author*) Nothing to Disclose Asha Kandathil, MD, Dallas, TX (*Abstract Co-Author*) Nothing to Disclose Abhishek Chaturvedi, MD, Rochester, NY (*Abstract Co-Author*) Nothing to Disclose Prabhakar Rajiah, MD, FRCR, Dallas, TX (*Presenter*) Nothing to Disclose

# For information about this presentation, contact:

radpr73@gmail.com

# **TEACHING POINTS**

1. To review the physiological changes that occur during pregnancy 2. To review the cardiovascular complications that occur during pregnancy/peripartum period 3. To discuss the role of imaging in evaluation of cardiovascular complications during pregnancy 4. To develop an approach on imaging pregnant patients safely

# TABLE OF CONTENTS/OUTLINE

1. Introduction 2. Physiological cardiovascular changes in pregnancy - Increased blood volume - Increased cardiac output -Decreased BP - Pro-inflammatory 3. Role of Imaging in pregnancy 4. Imaging modalities- X-ray, CT, MRI, nuclear, echo, ultrasound, angio 5. Complications related to pregnancy (Discussion, illustration of imaging findings with case examples) - Pulmonary embolism -Amniotic fluid embolism - Post-partum cardiomyopathy - Spontaneous coronary artery dissection - Pulmonary hypertension -Hypertension 6. Exacerbation of pre-existing diseases during pregnancy (Illustration with case examples) - Inherited aortic diseases - Adult congenital heart disease - Hereditary hemorrhagic telangiectasia - Acquired valvular disorders 7. Cardiovascular changes due to abdominal disease 8. Issues related to imaging in pregnancy - CT- Radiation, contrast agents - MRI- Gadolinium 9. Appropriateness criteria for imaging in pregnancy

# **Honored Educators**

Presenters or authors on this event have been recognized as RSNA Honored Educators for participating in multiple qualifying educational activities. Honored Educators are invested in furthering the profession of radiology by delivering high-quality educational content in their field of study. Learn how you can become an honored educator by visiting the website at: https://www.rsna.org/Honored-Educator-Award/ Prabhakar Rajiah, MD, FRCR - 2014 Honored Educator



# CA205-SD-SUB1

Native True T1 Mapping for Non-Contrast Assessment of Myocardial Fibrosis in Patients with Cardiomyopathy: Correlation with Late Gadolinium Enhancement MRI

Sunday, Nov. 25 1:00PM - 1:30PM Room: CA Community, Learning Center Station #1

# Participants

Amarino C. Oliveira JR, MD, Rio de Janeiro, Brazil (*Abstract Co-Author*) Nothing to Disclose Thomas M. Doring, PhD, Rio De Janeiro, Brazil (*Abstract Co-Author*) Employee, General Electric Company Carlos E. Rochitte, MD,PhD, Sao Paulo, Brazil (*Presenter*) Nothing to Disclose Marcela B. Ianes, Rio de Janeiro, Brazil (*Abstract Co-Author*) Nothing to Disclose Denise M. Moreira, MD, PhD, Rio de Janeiro, Brazil (*Abstract Co-Author*) Nothing to Disclose Eduardo Figueiredo, Sao Paulo, Brazil (*Abstract Co-Author*) Employee, General Electric Company Juliana Serafim, MD, Rio de Janeiro, Brazil (*Abstract Co-Author*) Nothing to Disclose

#### For information about this presentation, contact:

amarinojunior@gmail.com

# PURPOSE

The purpose of this study was to reinvestigate native T1 mapping with SmarT1 in the non-contrast assessment of diffuse myocardial fibrosis in patients with cardiomyopathy by comparing it to Late Gadolinium Enhanced cardiac MRI. SmarT1 directly measures true T1, increasing accuracy when compared to other methods, crucial to become an objective quantitative biomarker in different clinical settings.

# **METHOD AND MATERIALS**

90 patients underwent routine CMR at 3T to investigate CMP including SmarT1 (saturation method using adaptive recovery times for cardiac T1 mapping) sequence. Left ventricular ejection fraction (LVEF), left ventricular diastolic volume (LVDVol), left atrium volume (LAVol) and late gadolinium enhancement (LGE) indicators a) diffuse evident (CE) and b) not evident (nCE) were obtained. Native T1 relaxation times were extracted by placing ROIs on the T1 maps within the myocardium (T1nat,myo) and blood by an experienced Radiologist (20y). Statistical Analysis (Normality Kolmogorov Smirnov, Pearson Correlation coefficient; Mann Whitney median dif in native T1 CE and nCE groups) was done using Minitab, considering p<0.05 as statistical significant.

# RESULTS

Native T1 of myocardium in patients without LGE (T1nat, median, nCE = 1477ms) are lower than native T1 in patients with CE in any other segment of the heart (T1nat, median, CE=1500ms), (male group: p=0.0496, T1nat, median, nCE=1468ms, T1nat, median, CE=1500). Increase in native T1 reflects the higher content of fibrosis due to expansion of the extracellular/interstitial volume in patients with cardiomyopathy. T1nat, myo showed a positive correlation with LVDVol (r=0.291,p=0.005), increasing in its strength with exclusion of hypertrophic cardiomyopathy (low cavity volume) patients (r=0.366, p=0.002).

### CONCLUSION

Native true T1 mapping of the myocardium using SmartT1 can detect tissue alterations and functional abnormalities without measuring contrast dynamics. Higher native T1 reflects higher content of fibrosis and/or expansion of the extracelular volume.

# **CLINICAL RELEVANCE/APPLICATION**

Patients with severe renal impairment precluding gadolinium contrast injection may benefit of native T1 mapping. Accurate T1 estimation is crucial to establish itself as an objective biomarker for different clinical settings.



# CA206-SD-SUB2

The Effect on Left Ventricular Diastolic Function 12 Month After Renal Denervation: An Evaluation Based on Cardiac Magnetic Resonance Imaging

Sunday, Nov. 25 1:00PM - 1:30PM Room: CA Community, Learning Center Station #2

# Participants

Malte L. Warncke, MD, Hamburg, Germany (*Presenter*) Nothing to Disclose Andreas Koops, MD, Hamburg, Germany (*Abstract Co-Author*) Nothing to Disclose Gunnar K. Lund, MD, Hamburg, Germany (*Abstract Co-Author*) Nothing to Disclose Fabian Brunner, Hamburg, Germany (*Abstract Co-Author*) Nothing to Disclose Richard A. Coulden, MD, Edmonton, AB (*Abstract Co-Author*) Nothing to Disclose Lennart Well, MD, Hamburg, Germany (*Abstract Co-Author*) Nothing to Disclose Karsten Sydow, Hamburg, Germany (*Abstract Co-Author*) Nothing to Disclose Jitka Starekova, Hamburg, Germany (*Abstract Co-Author*) Nothing to Disclose Johannes Neumann, Hamburg, Germany (*Abstract Co-Author*) Nothing to Disclose Roland Fischer Sr, DiplPhys, Hamburg, Germany (*Abstract Co-Author*) Nothing to Disclose Berhard B. Adam, MD, Hamburg, Germany (*Abstract Co-Author*) Nothing to Disclose Enver G. Tahir, MD, Hamburg, Germany (*Abstract Co-Author*) Nothing to Disclose

## For information about this presentation, contact:

m.warncke@uke.de

# PURPOSE

Catheter-based renal denervation (RDN) has been investigated as a potential treatment for patients suffering from resistant arterial hypertension. It has been demonstrated that RND decreases ventricular hypertrophy (LVH) and improves diastolic left ventricular (LV) function on a short-term follow-up. We investigated the prolonged long-term effect (12 months) of RDN on diastolic function by cardiac magnetic resonance (CMR).

# **METHOD AND MATERIALS**

Fifteen patients with resistant arterial hypertension were examined by CMR before and twelve months after RDN. Clinical visits at the same time points included 24-hour ambulant blood pressure monitoring (ABPM). Functional and structural LV parameters were analyzed. Based on volume-time-curve analyses diastolic LV function was analyzed by calculation of early diastolic (EPFR), atrial peak filling rates (APFR) and EPFR/APFR ratio, which is the equivalent of the echocardiographic E/A ratio. CMR data were analyzed by two independent observers using Cardiovascular Imaging Solutions Ltd. (CVIS) CMRtools. Data are given as the mean of both observers. Statistical analysis was performed using GraphPad Prism 5 and Microsoft Excel.

# RESULTS

Twelve months after RDN systolic ABPM showed a moderate decrease (152.0 mmHg vs. 148.0 mmHg, p=0.076), but did not reach significance. Indexed left ventricular mass (LVMM) decreased from 80.7  $\pm$ 21.2 g/m2 to 74.6  $\pm$ 20.7 g/m2 (p<0.05). This effect was associated with an increase in EPFR (r=-0.528; p<0.05) and with a tendency of APFR reduction (r=0.468; p=0.079). The EPFR/APFR ratio increased significantly over one year (0.89  $\pm$  0.37 vs. 1.05  $\pm$  0.49; p<0.05), indicating improvement of LV diastolic function.

# CONCLUSION

We investigated the sustained effect of RDN on the diastolic function of the left ventricle 12 months after the procedure by CMR. Diastolic LV function was improved 12 months post-RDN and was associated with the significant decrease of LV mass.

# **CLINICAL RELEVANCE/APPLICATION**

Our study indicates that patients may benefit from RDN due to a potential improvement of diastolic function facilitated by LV mass reduction.



# CA207-SD-SUB3

Relationship between Texture Features of Myocardial Late Gadolinium Enhancement and Ventricular Tachyarrhythmias in Hypertrophic Cardiomyopathy

Sunday, Nov. 25 1:00PM - 1:30PM Room: CA Community, Learning Center Station #3

**FDA** Discussions may include off-label uses.

### Participants

Yasuo Amano, MD, Tokyo, Japan (*Presenter*) Nothing to Disclose Fumi Yanagisawa, Tokyo, Japan (*Abstract Co-Author*) Nothing to Disclose Yasuyuki Suzuki, Tokyo, Japan (*Abstract Co-Author*) Nothing to Disclose Naoya Matsumoto, MD, Tokyo, Japan (*Abstract Co-Author*) Nothing to Disclose

#### For information about this presentation, contact:

yas-amano@nifty.com

#### PURPOSE

Hypertrophic cardiomyopathy (HCM) often shows myocardial late gadolinium enhancement (LGE) on magnetic resonance imaging (MRI). Thus, only the presence of LGE does not stratify the risks for serious arrhythmias associated with HCM. Texture analysis may provide new quantitative information about LGE which can induce ventricular tachyarrhythmias, including ventricular fibrillation and ventricular tachycardia. The aim of this study was to evaluate the relationship between texture features of myocardial LGE and ventricular tachyarrhythmias in HCM.

## **METHOD AND MATERIALS**

Twenty-three patients with HCM were enrolled. LGE MRI was performed using a 3-dimensional inversion-recovery T1-weighted segmented gradient echo sequence 10 minutes after 0.1 mmol/kg gadolinium injection. Texture analysis was performed for 43 myocardial LGE areas using an open-access software (MaZda, Technical University of Lodz, Institute of Electronics, Poland). The relationship between the texture features of LGE (i.e., variance, skewness, kurtosis, and entropy of LGE signal intensity) and ventricular tachyarrhythmias were evaluated in the 23 patients with HCM.

#### RESULTS

Sixteen (69.6%) of the 23 HCM patients had myocardial LGE. Six patients (26.1%) had history of ventricular tachyarrhythmias, all of whom showed LGE. Among 4 texture features of the LGE, entropy was significantly lower in HCM patients with ventricular tachyarrhythmias (14969.9  $\pm$  9107.6) than those without (25565.2  $\pm$  1408.5; p = 0.0058). A receiver-operating characteristic analysis gave the threshold of 19624 with the area under the curve of 0.72 for identification of HCM patients with ventricular tachyarrhythmias.

#### CONCLUSION

Patients with HCM and history of ventricular tachyaarrhythmias had myocardial LGE of lower entropy, indicating microscopically less random fibrosis of the myocardium. The texture analysis provides the quantitative information about LGE related to ventricular tachyarrhythmias associated with HCM.

# **CLINICAL RELEVANCE/APPLICATION**

Texture analysis is a quantitative method to identify myocardial late gadolinium enhancement which is related to ventricular tachyarrhythmias in patients with hypertrophic cardiomyopathy.



# CA209-SD-SUB5

**Progression of Coronary Artery Calcification in Primary Chronic Glomerulo-Nephritis After Renal Transplantation** 

Sunday, Nov. 25 1:00PM - 1:15PM Room: CA Community, Learning Center Station #5

# Participants

Changqing Yin, Zhenjiang, China (*Presenter*) Nothing to Disclose Dongqing Wang, Zhenjiang, China (*Abstract Co-Author*) Nothing to Disclose Haitao Zhu, Zhenjiang, China (*Abstract Co-Author*) Nothing to Disclose Lirong Zhang, MD, zhenjiang, China (*Abstract Co-Author*) Nothing to Disclose Shao Xun, Zhenjiang, China (*Abstract Co-Author*) Nothing to Disclose

## For information about this presentation, contact:

ev1lhell@126.com

# PURPOSE

The aim was to determine the effect of renal transplantation on the progression of CAC in common primary chronic glomerulonephritis.

# METHOD AND MATERIALS

Renal transplantation (RT) and dialysis patients with primary chronic glomerulonephritis(IgA, MembranousNephropathy(MN),MesangialProliferativeNephritis(MPN),MembranoproliferativeGlomerulonephritis(MPGN), Focal Segmental Glomerulosclerosis(FGSG), Podocyte Disease(PD)) were enrolled in this study. CAC and serum parameters at baseline and 1 year follow-up were measured. These associations were analyzed by multiple logistic regression.

## RESULTS

The study included 108 RT patients (n=20,18,15,19,18,18,respectively) and 125 dialysis patients (n=22,19,20,21,23,20,respectively) as control groups. The baseline evaluations showed a very high prevalence of CAC in all groups, which was positively correlated with LDL(p=0.001) and CRP (p=0.03). The follow-up evaluations showed a significantly slower progression of calcification after RT, expect MPN, MPGN and PD In MN the decrease was the most pronounced. In all groups, baseline score, calcium and phosphorus had a strong correlation with the progression of CAC (P=0.001, 0.004, 0.03, respectively).

# CONCLUSION

In this study, CAC is high prevalent in all group, and was correlated with LDL and CRP. There was a significantly slower progression of CAC after RT, expect in MPN, MPGN and PD, however in MN was the most pronounced. Baseline score, calcium and phosphorus were correlated with the progression.

# **CLINICAL RELEVANCE/APPLICATION**

Through pathology, there is different attention to CAC in patients with different degrees of renal transplantation and we can reduce the number of follow-up visits of patients with slow calcification progression.



# CH239-ED-SUB5

Radiologic Patterns of Immune Checkpoint Inhibitor-Associated Pneumonitis and Management According to 2018 ASCO Guidelines: A Primer for the Radiologist

Sunday, Nov. 25 1:00PM - 1:30PM Room: CH Community, Learning Center Station #5

#### Awards Certificate of Merit Identified for RadioGraphics

### **Participants**

Kevin R. Kalisz, MD, Cleveland, OH (*Presenter*) Nothing to Disclose Nikhil H. Ramaiya, MD, Jamaica Plain, MA (*Abstract Co-Author*) Nothing to Disclose Amit Gupta, MD, Cleveland, OH (*Abstract Co-Author*) Nothing to Disclose

# **TEACHING POINTS**

The purpose of this exhibit is to: - Review the indications and mechanism of action of immune checkpoint inhibitors as well as pathophysiology of lung toxicity - Describe the imaging patterns of immune checkpoint inhibitor-associated pneumonitis and related clinical classification schemes - Understand the management of immune-related adverse events and the role of the radiologist in the treatment course of these complex patients

# TABLE OF CONTENTS/OUTLINE

1. Introduction 2. Review of commonly used immune checkpoint inhibitors as well as their current indications and mechanisms of action 3. Incidence and pathophysiology of immune checkpoint inhibitor-associated lung injury and adverse reactions 4. Illustration of the basic imaging patterns of immune checkpoint inhibitor-associated pneumonitis with case examples: - Acute interstitial pneumonia (AIP)/acute respiratory distress syndrome (ARDS) - Bronchiolitis - Cryptogenic organizing pneumonia (COP) - Hypersensitivity pneumonitis (HP) - Non-specific interstitial pneumonia (NSIP) - Radiation recall pneumonitis 5. Clinical classification scheme for pulmonary immune-related adverse events 6. Treatment strategies and follow-up for immunotherapy-related pneumonitis with review of 2018 American Society of Clinical Oncology guidelines

#### **Honored Educators**

Presenters or authors on this event have been recognized as RSNA Honored Educators for participating in multiple qualifying educational activities. Honored Educators are invested in furthering the profession of radiology by delivering high-quality educational content in their field of study. Learn how you can become an honored educator by visiting the website at: https://www.rsna.org/Honored-Educator-Award/ Nikhil H. Ramaiya, MD - 2017 Honored Educator



# CH260-SD-SUB1

ECG-Gated Ultra High Resolution CT (UHRCT) in the Lower Lung Field

Sunday, Nov. 25 1:00PM - 1:30PM Room: CH Community, Learning Center Station #1

#### **Participants**

Hiroshi Moriya, MD, Fukushima, Japan (*Presenter*) Advisory, Ziosoft Inc; Research Grant, Canon Medical Systems Corporation; ; Shun Muramatsu, RT, Fukushima, Japan (*Abstract Co-Author*) Nothing to Disclose Yuka Nakajou I, Fukushima, Japan (*Abstract Co-Author*) Nothing to Disclose Kouji Hashimoto I, Fukushima, Japan (*Abstract Co-Author*) Nothing to Disclose Hiroshi Chiba I, Fukushima, Japan (*Abstract Co-Author*) Nothing to Disclose Masahiro Suzuki, Chuo-Ku, Japan (*Abstract Co-Author*) Nothing to Disclose Motoharu Hakozaki, Fukushima, Japan (*Abstract Co-Author*) Nothing to Disclose Shinsuke Tsukagoshi, PhD, Otawara, Japan (*Abstract Co-Author*) Employee, Canon Medical Systems Corporation Takashi Tanaka, MENG, Nasushiobara, Japan (*Abstract Co-Author*) Employee, Canon Medical Systems Corporation Daisuke Suto, Tokyo, Japan (*Abstract Co-Author*) Employee, Amin Co Ltd

#### For information about this presentation, contact:

hrshmoriya@gmail.com

## **TEACHING POINTS**

Background: Ultra high resolution CT(UHRCT) allows for visualization of fine detail and easier interpretation of routine clinical images. However, motion artifact caused by heartbeat degrades image quality. The purpose of this presentation is to discuss the utility of electrocardiography (ECG)-gated UHRCT for assessing the lung CT imaging.

### **TABLE OF CONTENTS/OUTLINE**

Material/Methods: Thirty two cases with abnormal shadow in lower lung field were examined using UHRCT. The scanning parameters were as below. Whole lung UHRCT: SHR mode, helical scan, 0.25mm slice thickness. ECGgated UHRCT: SHR mode, volume scan (40mm), 0.25mm slice thickness. Motion artifact of target lesion, image noise, and clinical advantages were evaluated. Results: Motion artifacts had occured in 84% cases of UHRCT. Some artifacts were seen in rt.S3,S5, lt.S3,S4,S5,and S8, and severe artifact were seen in 53% of target lesion. And, 90% of severe artifacts were reduced by ECG gating. However, image noise was increased in ECG gated UHRCT. Conclusions: ECG-gated CT reduced the motion artifacts and might be useful for UHRCT imaging, especially in region near the heart.

# PDF UPLOAD

http://abstract.rsna.org/uploads/2018/18013794/18013794\_3wad.pdf



# CH261-SD-SUB2

# Superiority of Artificial Intelligence over Radiologists in Detecting Pulmonary Nodules

Sunday, Nov. 25 1:00PM - 1:30PM Room: CH Community, Learning Center Station #2

### **Participants**

Maarten A. Van de Weijer, MD,MSc, Alkmaar, Netherlands (*Presenter*) Nothing to Disclose Paul R. Algra, MD, PhD, Alkmaar, Netherlands (*Abstract Co-Author*) Nothing to Disclose Cornelis F. Van Dijke, MD,PhD, Rotterdam, Netherlands (*Abstract Co-Author*) Nothing to Disclose Edwin J. van Beek, MD, PhD, Edinburgh, United Kingdom (*Abstract Co-Author*) Research support, Siemens AG; Research support, General Electric Company; Advisory Board, Aidence nv; Advisory Board, ImBio, LLC; Consultant, Holoxica Ltd; Founder, QCTIS UK, Ltd; Director, QCTIS UK, Ltd; Spouse, Director, QCTIS UK, Ltd; ; ;

# For information about this presentation, contact:

maj.weijervande@NWZ.nl

# PURPOSE

The aim of this study is to evaluate a new Artificial Intelligence algorithm using different thresholds for detection of lung nodules.

# METHOD AND MATERIALS

For the detection of lung nodules we used a new artificial intelligence (AI) derived imaging algorithm (Deep learning VeyeChest version 1.0, Aidence, Amsterdam, NL), using a detection threshold of either 0.35 or 0.80. A total of 106 and 77 CT chest (with/without contrast) were examined. Two thoracic radiologists with more than 20 years' experience independently reported the number of nodules, their location and the aspect of each nodule (solid, partly solid or pure ground glass). The reference standard was established by consensus of the two radiologists. In case of discrepancies, a third radiologist re-examined the CT scans and established the 'true' nature of the lesions.

#### RESULTS

A total of 278 and 211 nodules with a diameter >=3 mm were identified at threshold 0.35 and 0.8 respectively. A total of 246/187 solid, 26/18 partly solid and 6/6 pure ground glass nodules were found at threshold 0.35/0.8 respectively. The sensitivity of the AI algorithm was 0.91/0.75 at detection thresholds 0.35/0.8, respectively, while this was 0.69/0.76 and 0.68/0.77 for the individual radiologists (p<0.01). After review by the third radiologist, 87/50 and 88/48 false negative nodules were found for the two radiologists at detection threshold 0.35 and 0.8, respectively. AI detected 24/52 nodules at threshold 0.35/0.8 that were missed by radiologists. The average number of false positive nodules per scan was 1.45 and 0.52 at the detection threshold 0.35 and 0.8, respectively. Most false positives were due to concomitant findings, such as fibrosis, atelectasis or infection (132 and 27 false positives at detection thresholds 0.35 and 0.8, respectively).

### CONCLUSION

The AI system outperformed experienced chest radiologists for the detection of lung nodules and performed equivalent to the radiologists at its highest threshold settings at the costs of a limited number of false positives.

#### **CLINICAL RELEVANCE/APPLICATION**

Artificial intelligence is superior in the detection of pulmonary nodules and by embracing artificial intelligence radiologists can become increasingly more accurate in their interpretations.



# CH262-SD-SUB3

Validation of IPF Prediction Model Using Quantum Particle Swarm Optimization Hybridized Random Forest

Sunday, Nov. 25 1:00PM - 1:30PM Room: CH Community, Learning Center Station #3

### **Participants**

Yu Shi, Los Angeles, CA (*Presenter*) Nothing to Disclose Jonathan G. Goldin, MBChB, PhD, Los Angeles, CA (*Abstract Co-Author*) Nothing to Disclose Weng Kee Wong, Los Angeles, CA (*Abstract Co-Author*) Nothing to Disclose Joshua Lai, Los Angeles, CA (*Abstract Co-Author*) Nothing to Disclose Matthew S. Brown, PhD, Los Angeles, CA (*Abstract Co-Author*) Nothing to Disclose Hyung J. Kim, PhD, Los Angeles, CA (*Abstract Co-Author*) Research Consultant, MedQIA Imaging Core Laboratory

### PURPOSE

Idiopathic Pulmonary Fibrosis (IPF) is a fatal lung disease with unpredictable progression status at the time of diagnosis. High resolution computed tomography (HRCT) images have shown to be useful for building a predictive model for IPF. Based on a previously proposed methodology using quantum particle swarm optimization (QPSO) for selecting HRCT features, we validate the algorithm with a larger data set of 172 IPF patients.

### **METHOD AND MATERIALS**

We collect anonymized longitudinal serial volumetric HRCT scans from IPF. Radiologists visually contoured regions of interest (ROI) and annotated lung morphology types into progression or non-progression, at the previous visits before the changes occurred. 191 texture features were extracted from the grid sampled voxels of baseline ROIs. Using the QPSO hybridized random forest algorithm, we calibrated the algorithm on a data set of 99 patients (577 ROIs) using 5-fold cross validation and tested the algorithm on a separate test set of 73 patients (414 ROIs).

## RESULTS

The algorithm yields a parsimonious model with 23 features (12% features selected) and achieves 70.8% sensitivity, 70.1% specificity and 70.4% accuracy at ROI level on the cross-validation set, and 68.2% sensitivity, 65.4% specificity and 66.6% accuracy on the independent test set. Compared to other state-of-the-art algorithms, our approach selects a smaller feature subset, has higher prediction accuracy and achieves more balanced classification.

# CONCLUSION

We validated the previously proposed QPSO hybridized random forest algorithm with a much larger set and showed that the algorithm stably achieves superior prediction performance. This work is also first time showing the possibility to demonstrate the progression by voxel-by-voxel level at a single time-point HRCT scan to predict disease status of future 6 months or 1 year follow-up. The algorithm has great potentials on offering IPF patients timely treatments.

## **CLINICAL RELEVANCE/APPLICATION**

Idiopathic pulmonary fibrosis exhibits a heterogeneous natural history. We build and validate a predictive model to anticipate disease courses and help clinicians make timely decisions.



# CH263-SD-SUB4

# Detection and Phenotyping of Emphysema Using a New Machine Learning Method

Sunday, Nov. 25 1:00PM - 1:30PM Room: CH Community, Learning Center Station #4

#### Participants

Martine J. Remy-Jardin, MD, PhD, Lille, France (*Presenter*) Research Grant, Siemens AG Rainer Kaergel, Forchheim, Germany (*Abstract Co-Author*) Employee, Siemens AG Michael Suehling, PhD, Forchheim, Germany (*Abstract Co-Author*) Employee, Siemens AG Jean-Baptiste Faivre, MD, Lille, France (*Abstract Co-Author*) Nothing to Disclose Thomas G. Flohr, PhD, Forchheim, Germany (*Abstract Co-Author*) Employee, Siemens AG Jacques Remy, MD, Mouvaux, France (*Abstract Co-Author*) Research Consultant, Siemens AG

## For information about this presentation, contact:

martine.remy@chru-lille.fr

# PURPOSE

Emphysema is commonly visually detected but this approach suffers from slight to moderate inter-observer reproducibility that can be compensated by quantitative CT (>6% of pixels of less than -950 HU [LAA 950]). Visual assessment remains important to describe the patterns of lung destruction. We describe the development and validation of a novel machine learning method to detect and phenotype emphysema.

## **METHOD AND MATERIALS**

We used HRCT scans of 981 patients with ground truth labels established by consensus between two radiologists. In the first step, image features that describe the lung parenchyma, airways and vessels were extracted fully automatically for all scans, including 605 normal and 376 emphysematous. Together with the ground truth labels for the presence of various forms of emphysema (i.e. centrilobular [CLE], paraseptal [PSE], panlobular [PLE]), those features were used as the input of a subsequent machine learning step. For each type of emphysema, this procedure yields a discriminator between "this type is present" and "this type is absent", thus enabling emphysema phenotyping. K-fold cross-validation of the machine learning step with all patients was used to validate that the system could correctly deduce the different forms of the disease for previously unseen cases. This prediction was compared to the known ground-truth annotations. The results of this comparison were accumulated over all cases to yield the final evaluation results.

#### RESULTS

The system predictions regarding the presence of emphysema for unseen patients were found to be significantly superior to those applying a threshold of 6% to the LAA 950 value (p < 0.0001; sensitivity: 0.84 (CI: 0.80-0.87) vs 0.43 (CI: 0.38-0.48)); specificity : 0.84 (CI: 0.81-0.87) vs 0.86 (CI: 0.83-0.88)). The performance of the tested system for emphysema phenotyping was as follows: (a) CLE : se : 0.81 (CI: 0.76-0.85); sp : 0.85 (CI : 0.82-0.88); (b) PSE : se : 0.79 (CI : 0.74-0.84); sp : 0.84 (CI : 0.81-0.86); (c) PLE: se : 0.82 (CI : 0.73-0.91); sp : 0.92 (CI : 0.90-0.94).

### CONCLUSION

The performance of our method for detecting and phenotyping emphysema is promising.

## **CLINICAL RELEVANCE/APPLICATION**

Identification of emphysema and description of the predominant morphologic features are important steps in the personalized approach of COPD patients. The tested method could objectively contribute to this approach.



### ER159-ED-SUB4

Penile Emergencies: A Comprehensive Multi-Modality Imaging Review

Sunday, Nov. 25 1:00PM - 1:30PM Room: ER Community, Learning Center Station #4

#### Awards Certificate of Merit Identified for RadioGraphics

#### **Participants**

Gayatri Joshi, MD, Columbia, MO (*Presenter*) Nothing to Disclose Alexander Castilho, MD, Atlanta, GA (*Abstract Co-Author*) Nothing to Disclose Carrie N. Hoff, MD, Ann Arbor, MI (*Abstract Co-Author*) Nothing to Disclose Christine O. Menias, MD, Chicago, IL (*Abstract Co-Author*) Nothing to Disclose Cary L. Siegel, MD, Saint Louis, MO (*Abstract Co-Author*) Nothing to Disclose

## For information about this presentation, contact:

gayatri.joshi.md@gmail.com

## **TEACHING POINTS**

Penile emergencies can pose a diagnostic dilemma given their relatively uncommon presentation in the Emergency Department (ED). However, missed or delayed diagnosis can result in significant morbidity or even mortality. Knowledge of the spectrum of penile emergencies that can present in the ED, the optimal imaging work-up for each clinical entity, and the appropriate next step in management is essential for optimizing patient outcomes. After reviewing this exhibit, learners should be able to: 1. Recognize normal anatomy of the penis by each imaging modality, including US, MRI, CT, and fluoroscopy 2. Proficiently identify and discriminate between types of penile emergencies based on clinical & imaging features 3. Utilize best practices for diagnosing penile emergencies including those of infectious, inflammatory, ischemic, traumatic, & neoplastic etiologies

## **TABLE OF CONTENTS/OUTLINE**

This exhibit will: 1. Review the normal anatomy of the penis 2. Systematically illustrate the clinical & imaging features of penile emergencies that may present in the ED, including those of infectious, inflammatory, ischemic, traumatic, and neoplastic causes 3. Discuss best practices for imaging of the penis, with pearls and pitfalls, for optimizing efficient accurate diagnosis 4. Address relevant management as applicable to the Radiologist to appropriately direct management

## **Honored Educators**

Presenters or authors on this event have been recognized as RSNA Honored Educators for participating in multiple qualifying educational activities. Honored Educators are invested in furthering the profession of radiology by delivering high-quality educational content in their field of study. Learn how you can become an honored educator by visiting the website at: https://www.rsna.org/Honored-Educator-Award/ Christine O. Menias, MD - 2013 Honored EducatorChristine O. Menias, MD - 2014 Honored EducatorChristine O. Menias, MD - 2015 Honored EducatorChristine O. Menias, MD - 2016 Honored EducatorChristine O. Menias, MD - 2018 Honored Educator



# ER204-SD-SUB1

The Feasibility of Point-Of-Care Ankle Ultrasound Examination in Patients with Recurrent Ankle Sprain and Chronic Ankle Instability: Comparison with Magnetic Resonance Imaging

Sunday, Nov. 25 1:00PM - 1:30PM Room: ER Community, Learning Center Station #1

# Participants

Yeji Shin, Seoul, Korea, Republic Of (*Presenter*) Nothing to Disclose Seong Jong Yun, Seoul, Korea, Republic Of (*Abstract Co-Author*) Nothing to Disclose Sun Hwa Lee, Seoul, Korea, Republic Of (*Abstract Co-Author*) Nothing to Disclose

#### For information about this presentation, contact:

zoomknight@naver.com

# PURPOSE

To evaluate the feasibility of point-of-care ankle ultrasound compared with magnetic resonance imaging (MRI) for diagnosing major ligaments and Achilles tendon injuries in patients with recurrent ankle sprain and chronic instability, and to evaluate inter-observer reliability between a musculoskeletal radiology fellow and an emergency physician.

## **METHOD AND MATERIALS**

A prospective cross-sectional study was conducted in an emergency department. Patients with recurrent ankle sprain and chronic instability were recruited. A musculoskeletal radiology fellow and a trained board-certified emergency physician independently evaluated the anterior talofibular ligament (ATFL), calcaneofibular ligament (CFL), distal anterior tibiofibular ligament (ATiFL), deltoid ligament, and Achilles tendon using point-of-care ankle ultrasound. Findings were classified normal, partial tear, and complete tear. The final radiology reports of the ankle MRI, interpreted by a senior musculoskeletal radiologist, were considered the reference standard. We calculated diagnostic values for point-of-care ankle ultrasound for both reviewers and compared them using DeLong's test. Intra-class correlation coefficients (ICCs) were calculated for agreement between each reviewer and the reference standard, and between the two reviewers.

# RESULTS

Eighty-five patients were enrolled. Point-of-care ankle ultrasound showed acceptable sensitivity (96.4-100%), specificity (95.0-100%), and accuracy (96.5-100%); these performance markers did not differ significantly between reviewers. Agreement between each reviewer and the reference standard was excellent (musculoskeletal radiology fellow, ICC=0.930-1.000; emergency physician, ICC=0.846-1.000), as was inter-observer agreement (ICC=0.873-1.000).

#### CONCLUSION

Point-of-care ankle ultrasound is as precise as MRI for detecting major ankle ligament and Achilles tendon injuries

# **CLINICAL RELEVANCE/APPLICATION**

Point-of-care ankle ultrasound could be used for immediate diagnosis and further pre-operative imaging in patients with recurrent ankle sprain and chronic instability. Moreover, it may reduce the time from ED admission to operation, and may save costs.



## ER205-SD-SUB2

Role of 24/7 Emergency Radiology, On-site Staff Radiologist Coverage at a Level 1 Trauma Center, In Reducing the Turn Around Time (TAT) for Acute Brain Computed Tomography Scanning

Sunday, Nov. 25 1:00PM - 1:30PM Room: ER Community, Learning Center Station #2

### Participants

Sabeena Jalal, MBBS, MSc, Vancouver, BC (*Presenter*) Nothing to Disclose Savvas Nicolaou, MD, Vancouver, BC (*Abstract Co-Author*) Institutional research agreement, Siemens AG

## PURPOSE

Medical imaging has been evolving with immense speed leading to development of advanced imaging equipment such as MDCT. MDCT brain scans have several indications. Two of the most important being an acute life threatening bleed and an acute stroke. This study explores the impact of a 24/7 on site, staff radiologist coverage, on reducing the turn around time for CT for the brain.

## METHOD AND MATERIALS

Data was extracted from the HIS, for all consecutive patients presenting to VGH requiring CT brain for a pre 24/7 period, which was 30th march till 30th september 2013 and a post 24/7 period from 30th september 2014 till 30th march 2015. We looked at two TATs. TAT1 was defined as time difference between the time when an exam was completed and when the staff radiologist transcribed the exam; TAT2 was described as the time when the exam report was transcribed and when staff radiologist finalized the report.

### RESULTS

Total of 6366 CT's met the inclusion criterion of this study. The median(IQR=75th-25th) for TAT1 and 2 were calculated. TAT1 for the pre 24/7 group was 578 min(2122), whereas for post 24/7, it was 54 min(132). TAT2 for pre24/7 was 1577 min(3316) and post 24/7 it decreased to 121 min(778). Using wilcoxon rank sum test, we noted that TAT1 was significantly decreased post 24/7 when compared with pre 24/7 among male patients (p value =0.0001) and in females (p value = 0.0001). Analysis showed TAT2 was also significantly lower post 24/7, in both the male(p value = 0.0001) and female patients (p value = 0.0001). Binary logistic regression analysis was run to identify the significant changes pre and post 24/7: LR Chi2 = 2379.04, p value = 0.0001 and pseudo R2 = 0.27. The odds for having a significantly low TAT, post 24/7 with an on site staff radiologist coverage are 3.46 times higher (95% CI: 2.96-4.55; p value =0.0001), as compared with pre 24/7, with no on site, staff radiologist coverage.

## CONCLUSION

24/7 on site staff ER radiologist coverage has a significant impact on reducing both TATs for CT brain scans. This initial analysis allows for further evidence-based approaches in evaluating the impact of such innovations on patient care, policies and cost of care.

#### **CLINICAL RELEVANCE/APPLICATION**

There is a dearth of research data from the 24/7 on site staff radiologist coverage, level 1 trauma centers, regarding the impact on radiology report TATs. This study provides an evidence base supporting significantly reduced TATs for CT brain.



# ER206-SD-SUB3

Doctors Knowledge of Doses and Risks of Radiological Procedures Performed in Emergency Department

Sunday, Nov. 25 1:00PM - 1:30PM Room: ER Community, Learning Center Station #3

# Participants

Rashid Barnawi, MBBS, Jeddah, Saudi Arabia (Presenter) Nothing to Disclose

For information about this presentation, contact:

rashid.ae@windowslive.com

#### PURPOSE

With the growing use of diagnostic imaging in emergency medicine practice, comes the concern about their risks. This study assesses the knowledge of radiation exposure doses and risks among doctors working in emergency department.

# METHOD AND MATERIALS

A questionnaire was distributed to doctors from different specialties and different levels of training working in emergency departments of 8 hospitals. We asked participants to answer questions about possible risks associated with radiation and to estimate radiation doses in different imaging modalities. Chi-squared test, an Independent t-test and One-Way ANOVA test were used for analytical purposes.

#### RESULTS

A total of 171 doctors completed the questionnaires. 109 were residents, 40 were specialists, and 21 were consultants. 20% had formal training on radiation protection. The overall correct dose-estimation rate was 20.8%. Overall dose-underestimation and overestimation rates were 28.6% and 10%, respectively, and 40.6% answered 'I don't know'. Consultants estimated doses more correctly than specialists and residents (p = .007), and emergency physicians answered more correctly than doctors from other specialties (p = 0.05). Those who had formal training did not have significant higher rate of correct answers (p = .065). For the four questions assessing knowledge of risks, overall correct answer rates were not satisfactory. Consultants were more knowledgeable about radiation lifetime risk of cancer than residents and specialists (p = .05), while specialists were more knowledgeable about the risk of imaging on fetus (p = 0.05). There was no difference between them in answering the remaining 2 questions. Doctors with formal training on radiation protection were more knowledgeable about radiation lifetime risk of cancer (p = .028) and risk of imaging on fetus (p = .024). They were more likely to notify patients about the risks (p = .03). There was no difference between them and those without formal training in selection of imaging modalities for pregnant patients (p = .297)

## CONCLUSION

Emergency department doctors had poor knowledge of radiation doses received by their patients and the associated risks. This issue warrants attention considering the increasing use of the radiological investigations.

# **CLINICAL RELEVANCE/APPLICATION**

Emergency doctors' poor knowledge of radiation doses and risks might lead to excessive imaging requests which will risk patients' health.



# GI275-ED-SUB6

# An Illustrated Guide to Gastrointestinal Surgical Procedures for Radiologists

Sunday, Nov. 25 1:00PM - 1:30PM Room: GI Community, Learning Center Station #6

# Awards Certificate of Merit

# Participants

Anjuli R. Cherukuri, MD, Madison, WI (*Presenter*) Nothing to Disclose Akshya Gupta, MD, Madison, WI (*Abstract Co-Author*) Nothing to Disclose Jonathan K. Vincent, MD, Boston, MA (*Abstract Co-Author*) Nothing to Disclose Robert D'Agostino, MD, Burlington, VT (*Abstract Co-Author*) Nothing to Disclose Lori Mankowski Gettle, MD, Madison, WI (*Abstract Co-Author*) Nothing to Disclose

# For information about this presentation, contact:

archerukuri@gmail.com

## **TEACHING POINTS**

Review common and uncommon gastrointestinal surgical procedural details. Review the normal postoperative appearance with original illustrations. Review complications and how to best image them.

# **TABLE OF CONTENTS/OUTLINE**

Gastrointestinal procedures will be reviewed, including indications, original illustrations, brief procedural details, optimal imaging techniques, normal postoperative appearances, and complications. Procedure types reviewed: Hepatopancreaticobiliary procedures including liver and pancreas transplants, Kasai, partial hepatectomies, Whipple, cholecystectomy, cystgastrostomy, partial pancreatectomies, and Puestow and Frey procedures. Upper GI procedures including esophagectomies with reconstructive options, peroral endoscopic myotomy, Nissen and other fundoplications, and Billroth I & II procedures. Colonic procedures including low anterior resection, abdominoperineal resection, partial colectomies, J pouch, Hartmann pouch, Kock pouch, appendectomy, and cecostomy. Bariatric procedures including roux-en-y gastric bypass, sleeve gastrectomy, gastric band, duodenal switch, and jejunal-ileal bypass.



# GI281-ED-SUB7

Biliary Tract Lesions: Cholangio MRI with Hepatobiliary Contrast Study

Sunday, Nov. 25 1:00PM - 1:30PM Room: GI Community, Learning Center Station #7

#### **Participants**

Maria İsabel Puig Povedano, Hospitalet de LLobregat, Spain (*Abstract Co-Author*) Nothing to Disclose Anna Guell Bara, MD, LHospitalet de Llobregat, Spain (*Presenter*) Nothing to Disclose Eva M. Merino Serra, MD, Hospitalet de Llobregat, Spain (*Abstract Co-Author*) Nothing to Disclose Laura Martinez Carnicero, MD, LHospitalet de LLobregat, Spain (*Abstract Co-Author*) Nothing to Disclose Sandra Ruiz, MD, PhD, Barcelona, Spain (*Abstract Co-Author*) Nothing to Disclose Eugenia De Lama, MD, Barcelona, Spain (*Abstract Co-Author*) Nothing to Disclose Jaume Torras Torra, L'Hospitalet de Llobregat, Spain (*Abstract Co-Author*) Nothing to Disclose Maria Pardo Antunez, LHospitalet de Llobregat, Spain (*Abstract Co-Author*) Nothing to Disclose Diego E. Nova Vaca, MD, LHospitalet de Llobregat, Spain (*Abstract Co-Author*) Nothing to Disclose Eduardo Andia Navarro, MD, L'Hospitalet De Llobregat, Spain (*Abstract Co-Author*) Nothing to Disclose

#### For information about this presentation, contact:

ipuig@bellvitgehospital.cat

# **TEACHING POINTS**

Biliary tract injuries become more prevalent with the increase in number and indications of laparoscopic procedures, major liver resections in surgical oncology and the implementation of liver transplant in treatment of tumors or end-stage liver diseases. The radiologist is expected to be familiar with this disease, usually by suspicion of bilomas in US or CT and now with the biliary tract study by CholangioMRI using hepatospecific biliary contrast. We show our experience with this technique as a referral hospital in hepatobiliary surgery and liver transplant. We review standard and with hepatospecific biliary contrast CholangioMRI images and its influence in patient management.

# TABLE OF CONTENTS/OUTLINE

CholangioMRI depicts anatomic bile duct variants and is a noninvasive technique that allows evaluating bile duct morphology proximal and distal to the injury. Hepatospecific contrast improves sensitivity especially localizing the site of bile leaks. We review and show examples of the different types of Strasberg classification, injuries related to major surgery and in transplant recipients (early leaks, anastomotic or preanastomotic stenosis, bilioenteric anastomosis disorders). Other applications and examples can be used to differentiate lesions with biliary origin, (Caroli, bilomas) from others (cysts, fasciola infestation...).



# GI282-ED-SUB8

Optimal Evaluation of Pancreatic Duct and Ductal Anomalies by Secretin Enhanced Magnetic Cholangiopancreatography

Sunday, Nov. 25 1:00PM - 1:30PM Room: GI Community, Learning Center Station #8

# Participants

Steven S. Chua, MD, PhD, Houston, TX (*Presenter*) Nothing to Disclose Rajesh Thampy, MBBS, Pearland, TX (*Abstract Co-Author*) Nothing to Disclose Chakradhar R. Thupili, MD, Beachwood, OH (*Abstract Co-Author*) Nothing to Disclose Verghese George, MBBS, Houston, TX (*Abstract Co-Author*) Nothing to Disclose Roger Jordan Jr, MD, Houston, TX (*Abstract Co-Author*) Nothing to Disclose Venkateswar R. Surabhi, MD, Houston, TX (*Abstract Co-Author*) Nothing to Disclose

### For information about this presentation, contact:

Steven.S.Chua@uth.tmc.edu

## **TEACHING POINTS**

1. Secretin enhanced magnetic resonance cholangiopancreatography (sMRCP) is a powerful noninvasive method that can increase the sensitivity for assessment of the pancreatic duct and ductal abnormalities by distension of the pancreatic ductal system.2. sMRCP can help clarify ductal connections with cystic neoplasms, evaluate pancreatic ductal disruptions in patients with pseudocyst and better characterize the pancreatic duct in chronic pancreatitis.3. sMRCP can be used as a noninvasive method to estimate pancreatic exocrine function, especially in patients with recurrent pancreatitis.4. sMRCP can also evaluate for sphincter of Oddi dysfunction.

## TABLE OF CONTENTS/OUTLINE

\* Discuss anatomy of normal and variant pancreatic ductal development. \* Understand the etiologies of chronic pancreatitis.\* Describe the methodology of MRCP and sMRCP\* Detail the indications for sMRCP \* Characterize chronic pancreatitis.\* Elucidate pancreatic ductal abnormalities.\* Investigate disconnected duct syndrome.\* Differentiate pancreatic cystic neoplasms.\* Assess pancreatic exocrine function.\* Detail pitfalls and conclusion.



### GI283-ED-SUB9

It's a Wrap - Fundoplications: Normal Anatomy and Complications

Sunday, Nov. 25 1:00PM - 1:30PM Room: GI Community, Learning Center Station #9

#### **Participants**

Jose Graterol, MS, Providence, RI (*Presenter*) Nothing to Disclose Rupan Sanyal, MD, Birmingham, AL (*Abstract Co-Author*) Nothing to Disclose Jason A. Pietryga, MD, Riverside, RI (*Abstract Co-Author*) Nothing to Disclose

# For information about this presentation, contact:

jgraterol@lifespan.org

## **TEACHING POINTS**

The purpose of this exhibit is to discuss gastric fundoplications in order for the learner to be able to identify and recognize the normal anatomy of gastric fundoplications, successful fundoplications, and differentiate between potential post surgical complications.

# TABLE OF CONTENTS/OUTLINE

Normal Anatomy Fundoplication Complications - Hinder Type I - Hinder Type II - Hinder Type III - Hinder Type IV - Tight Wrap Summary and Take Away Points



## GI284-ED-SUB10

The Use of Oral and Intravenous Contrast During the Ultrasound Assessment of Crohn's Disease

Sunday, Nov. 25 1:00PM - 1:30PM Room: GI Community, Learning Center Station #10

# FDA Discussions may include off-label uses.

#### Participants

Gurinder Nandra, FRCR, MBChB, London, United Kingdom (*Presenter*) Nothing to Disclose Oliver Duxbury, MBBCh, FRCR, London, United Kingdom (*Abstract Co-Author*) Nothing to Disclose Jaymin H. Patel, MBBS, FRCR, London, United Kingdom (*Abstract Co-Author*) Nothing to Disclose James M. Pilcher, MBBS, London, United Kingdom (*Abstract Co-Author*) Nothing to Disclose

#### **TEACHING POINTS**

Indications, technique and image optimization for using oral contrast and/or intravenous contrast during the ultrasound (US) assessment of Crohn's disease. US evaluation of Crohn's disease enhanced through the administration of intravenous and/or oral contrast.

### **TABLE OF CONTENTS/OUTLINE**

The selective application of oral contrast agents during standard small bowel US provides real-time, functional evaluation of Crohn's disease. Furthermore, there is an emerging interest in the applications of microbubble US contrast agents to assess tissue enhancement kinetics in Crohn's disease. We present a case-based exhibit highlighting the utilization of both contrast techniques in the US assessment of Crohns disease. To include: Intravenous contrast: Indications, technique and image optimization Patterns of enhancement Qualitative vs quantitative evaluation of activity and treatment response Assessment of complications e.g. phlegmon vs abscess, stenotic disease Intravenous contrast vs standard measurements of vascularity e.g color Doppler, advanced dynamic flow, superb microvascular imaging Oral contrast: Indications, technique and image optimisation Functional evaluation of strictures Subtle/early disease detection Use in conjunction with examination without oral contrast



## GI285-ED-SUB11

Schematic Staging of Rectum Neoplasm with MRI Image

Sunday, Nov. 25 1:00PM - 1:30PM Room: GI Community, Learning Center Station #11

# **Participants**

Daniel D. Padron, MD, Burgos, Spain (Presenter) Nothing to Disclose

For information about this presentation, contact:

ddpadron@yahoo.com

## **TEACHING POINTS**

The rectal cancer may be staged with accuracy through MRI if the technic and parameter are optimized and the reader is familiar with the technical limitations. Both circumferential resection margin and the presence of intravascular invasion are no part of the TNM stage, but must be within the radiological report because of these depend the therapeutic approach.

### **TABLE OF CONTENTS/OUTLINE**

The management of patients with rectal cancer has evolved with n important reduction of the local recurrence rate. The role of imaging techniques, specifically MRI, has become increasingly important in the preoperative assessment and control tracking of rectal tumors. Radiologists are finding that their presence is necessary more and more at multidisciplinary meetings for making decision about the treatment of these tumors and therefore they must have a growing role in the therapeutic issues.



# GI333-SD-SUB1

Abdominal Fast Advanced Spin Echo Diffusion-Weighted Imaging at High B Value: Phantom and Clinical Studies

Sunday, Nov. 25 1:00PM - 1:30PM Room: GI Community, Learning Center Station #1

# Participants

Takeshi Yoshikawa, MD, Kobe, Japan (*Presenter*) Research Grant, Canon Medical Systems Corporation Katsusuke Kyotani, RT,MSc, Kobe, Japan (*Abstract Co-Author*) Nothing to Disclose Yoshiharu Ohno, MD, PhD, Kobe, Japan (*Abstract Co-Author*) Research Grant, Canon Medical Systems Corporation; Research Grant, Koninklijke Philips NV; Research Grant, Bayer AG; Research Grant, DAIICHI SANKYO Group; Research Grant, Fuji Pharma Co, Ltd; Research Grant, Guerbet SA; Yoshimori Kassai, MS, Otawara, Japan (*Abstract Co-Author*) Employee, Canon Medical Systems Corporation Masao Yui, Otawara, Japan (*Abstract Co-Author*) Employee, Canon Medical Systems Corporation Daisuke Takenaka, MD, Akashi, Japan (*Abstract Co-Author*) Nothing to Disclose Shinichiro Seki, Kobe, Japan (*Abstract Co-Author*) Research Grant, Canon Medical Systems Corporation

Ryuji Shimada, Kobe, Japan (Abstract Co-Author) Nothing to Disclose

Yuji Kishida, MD, PhD, Kobe, Japan (Abstract Co-Author) Nothing to Disclose

## PURPOSE

To assess fast advanced spin echo (FASE)-diffusion-weighted imaging with high b value in evaluation of abdominal diseases

# METHOD AND MATERIALS

8 bottled phantoms with polyethylene glycol diluted with distilled water (concentrations of 10 to 150 mM), water, and fat were scanned with SE-EPI-DWI (b=0,1000) and FASE-DWI (0,1000). Apparent diffusion coefficients (ADC) were calculated and compared. 109 patients (68 men and 41 women, mean: 67.9 years), who were suspected to have hepato-biliary-pancreatic malignancy and underwent 3T-MRI, were enrolled. FSE-T2WI, EPI-DWI, and FASE-DWI were obtained. Amount of abdominal gas and ascites on images were recorded for each patient. AP and RL abdominal diameters were measured for each sequence and correlations were assessed among all sequences. Image quality and severity of image distortion were assessed on EPI-DWI and FASE-DWI and compared. Regression analyses were done to estimate factors for low image quality and severe distortion. Malignant lesion (n=57) detection for each patient and conspicuity for each lesion were assessed on EPI-DWI and FASE-DWI and compared. ADCs in malignant lesion and background were measured and compared. Relative ADC differences (rADC = (lesion-background) / (lesion+background)) were calculated and compared.

# RESULTS

There was no significant difference in phantom ADCs between EPI-DWI and FASE-DWI. Correlation coefficient was the highest between T2WI and FASE-DWI in both diameters and was lowest in AP direction with EPI-DWI. Image quality was significantly better on FASE-DWI (p=0.026) and distortion was significantly severer on EPI-DWI (<0.0001). For EPI-DWI, Sex and gas were significant factors for quality (0.017, <0.0001), and sex and gas were for distortion (0.002, <0.0001). For FASE-DWI, sex and gas were significant factors for quality (0.012, 0.011) and gas was a significant factor for distortion (0.007). There was no significant difference in lesion detection and conspicuity. Lesion ADC was significantly lower than background only on FASE-DWI. Malignant lesion rADC was significantly higher on FASE-DWI (0.009) than EPI-DWI, especially in HCC cases with cirrhosis or chronic hepatitis (0.002) probably due to smaller iron deposition effect.

# CONCLUSION

FASE-DWI can improve image quality and decrease image distortion and iron deposition effect.

#### **CLINICAL RELEVANCE/APPLICATION**

FASE-DWI can improve image quality and decrease image distortion and iron deposition effect.



# GI334-SD-SUB2

CT Texture Analysis for the Prediction of KRAS Mutation Status in Colorectal Cancer via a Machine Learning Approach

Sunday, Nov. 25 1:00PM - 1:30PM Room: GI Community, Learning Center Station #2

# Participants

Narumi Taguchi, Kumamoto, Japan (*Presenter*) Nothing to Disclose Seitaro Oda, MD, Kumamoto, Japan (*Abstract Co-Author*) Nothing to Disclose Takeshi Nakaura, MD, Kumamoto, Japan (*Abstract Co-Author*) Nothing to Disclose Masanori Imuta, MD, Kumamoto, Japan (*Abstract Co-Author*) Nothing to Disclose Yuji Miyamoto, Kumamoto, Japan (*Abstract Co-Author*) Nothing to Disclose Hideo Baba, Kumamoto, Japan (*Abstract Co-Author*) Nothing to Disclose Satoru Shinriki, Kumamoto, Japan (*Abstract Co-Author*) Nothing to Disclose Yasuhiro Yokota, Kumamoto, Japan (*Abstract Co-Author*) Nothing to Disclose Tadatoshi Tsuchigame, MD, Kumamoto, Japan (*Abstract Co-Author*) Nothing to Disclose Yasuyuki Yamashita, MD, Kumamoto, Japan (*Abstract Co-Author*) Consultant, DAIICHI SANKYO Group

## PURPOSE

The purpose of this study was to investigate whether CT texture analysis with machine learning can predict KRAS mutation status in colorectal cancer.

# METHOD AND MATERIALS

This retrospective study consisted of 40 patients with pathologically confirmed colorectal cancer. Patients underwent KRAS mutation tests, contrast-enhancement CT, and 18F-FDG PET before treatment. Of the 40 patients, 20 had mutated KRAS genes and 20 had wild-type KRAS genes. Fourteen CT texture parameters of primary tumors were extracted from portal venous phase CT images. The maximum standard uptake values (SUVmax) in 18F-FDG PET were also recorded. A prediction models were developed using a univariate logistic regression for each CT texture parameter and SUVmax, and using a machine learning method (multivariate support vector machine) for the CT texture parameters. The area under the receiver operating characteristic curve (AUC) of these models was calculated via 5-fold cross validation. In addition, the performance of the machine learning method with the CT texture parameters was compared with that of SUVmax.

### RESULTS

In univariate analysis, the AUC of each CT texture parameter ranges from 0.4 to 0.6, and that of SUVmax was 0.58. The multivariate support vector machine accounting for CT texture parameters improved the AUC to 0.82 indicating higher prediction performance than SUVmax.

## CONCLUSION

With machine learning method, the use of CT texture analysis was superior to SUVmax for prediction of KRAS mutation status in colorectal cancer.

# **CLINICAL RELEVANCE/APPLICATION**

CT texture analysis with machine learning may be useful for prediction of KRAS mutation status in colorectal cancer, and thus helpful to determine therapeutic strategies.



# GI335-SD-SUB3

Estimation of Extracellular Volume Fraction with Routine Multiphasic Pancreas CT for Predicting Overall Survival in Patients with Metastatic Pancreatic Adenocarcinoma After Chemotherapy

Sunday, Nov. 25 1:00PM - 1:30PM Room: GI Community, Learning Center Station #3

# Participants

Yoshihiko Fukukura, MD, PhD, Kagoshima, Japan (*Presenter*) Nothing to Disclose Yuichi Kumagae, Kagoshima, Japan (*Abstract Co-Author*) Nothing to Disclose Hiroto Hakamada, Kagoshima, Japan (*Abstract Co-Author*) Nothing to Disclose Hiroaki Nagano, MD, Kaogoshima, Japan (*Abstract Co-Author*) Nothing to Disclose Shinya Nakamura, Kagoshima, Japan (*Abstract Co-Author*) Nothing to Disclose Takashi Yoshiura, MD, PhD, Kagoshima, Japan (*Abstract Co-Author*) Nothing to Disclose

#### For information about this presentation, contact:

yoshihiko2002jp@yahoo.co.jp

### PURPOSE

Extracellular volume (ECV) fraction denotes a theoretical space which consists of the intravascular and extravascular extracellular spaces. However, no attempts have been made to apply the ECV fraction to oncologic assessment. Therefore, the purpose of this study was to determine whether ECV with routine multiphasic pancreas CT can predict outcomes for patients with metastatic pancreatic adenocarcinoma treated with chemotherapy.

## **METHOD AND MATERIALS**

One hundred thirty patients (78 men and 52 women; mean age, 68.0 years; age range, 41-86 years) with histologically confirmed metastatic pancreatic adenocarcinoma underwent multiphasic pancreas CT and chemotherapy. Regions of interest were placed as large as possible within the pancreatic adenocarcinoma and the aorta on unenhanced and equilibrium phase enhanced CT. ECV fraction of the tumor was calculated using the following formula: ECV= (1 - Hct) x [Etumor]/ [Eaorta], Where Etumor and Eaorta are absolute enhancements of the tumor and aorta 3-min after contrast administration. The effect on survival of variables including age, sex, tumor location, tumor size, TNM stage, carbohydrate antigen19-9, carcinoembryonic antigen, and tumor ECV fraction were analyzed in univariate analysis using the log-rank test. Variables were analyzed in multivariate analyses using the Cox proportional hazards regression model for variables.

### RESULTS

Median survival for the entire patient population was 10 months. The difference in overall survival between groups divided by median ECV fraction was significant (P = 0.005). Median survival time for patients with contrast enhancement >=0.27 was 11.4 months, compared to 9.1 months in patients with contrast enhancement <0.27. On multivariate analysis, only tumor ECV fraction of <0.27 showed an independent association with poor patient survival (Hazard ratio = 0.62, 95% confidence interval = 0.42-0.93, P = 0.020).

### CONCLUSION

ECV fraction obtained in the equilibrium phase of pancreas CT was an independent prognostic factor in patients with metastatic pancreatic adenocarcinomas after chemotherapy.

## **CLINICAL RELEVANCE/APPLICATION**

Estimation of ECV fraction with routine multiphasic pancreas CT may have the potential to predict overall survival in patients with metastatic pancreatic adenocarcinomas after chemotherapy.



# GI336-SD-SUB4

Development of a Radiomics Nomogram to Predict Microvascular Invasion in Patients with Hepatocellular Carcinoma

Sunday, Nov. 25 1:00PM - 1:30PM Room: GI Community, Learning Center Station #4

# Participants

Xiangpan Meng, BMBS,DMD, Nanjing, China (*Presenter*) Nothing to Disclose Shenghong Ju, MD, PhD, Nanjing, China (*Abstract Co-Author*) Nothing to Disclose

For information about this presentation, contact:

mengxp0711@163.com

# PURPOSE

To develop and validate a radiomics nomogram to predict the presence of microvascular invasion (MVI) in patients with hepatocellular carcinoma (HCC) preoperatively.

## **METHOD AND MATERIALS**

We enrolled 139 patients (training set: n = 75; validation set: n = 42; external-validation set: n = 22) with complete portal venousphase computed tomography imaging(CT) in this retrospective two-centre study. A total of 160 quantitative imaging features were extracted from portal venous-phase CT images. LASSO regression analysis was used to perform variable selection, regularization and radiomic signature building. Logistic regression was used to look for combined predictors of MVI. Radiomic signature and other selected predictors were incorporated to construct the nomogram. Concordance index (C-index) were used to evaluate the performance of the radiomic signature and the nomogram in the training, validation and external-validation sets.

### RESULTS

Six radiomic features were selected to construct radiomic signature distinguishing microvascular invasion based on the LASSO regression model. The radiomic signature yielded C-index of 0.722(95% confidence interval, 0.608-0.835), 0.748(95% confidence interval, 0.574-0.922) and 0.791(95% confidence interval, 0.597-0.985)for the training, validation and external-validation sets, respectively. The nomogram combing AFP and the radiomic signature show good performance in the training, validation and external-validation and external-validation and 0.846 respectively).

# CONCLUSION

The radiomics nomogram presented in this study could make useful preoperative predictions of MVI status in patients with HCC. Our model could be conveniently applied in clinical practice to tailor the best individualized therapeutic strategy for HCC patients.

# **CLINICAL RELEVANCE/APPLICATION**

This machine-learning model for MVI-predicting could help tailor best individualized therapeutic strategy for HCC patients.



# GI337-SD-SUB5

# Development of a CT Enterography Severity Score for Small Bowel Crohn's Disease

Sunday, Nov. 25 1:00PM - 1:30PM Room: GI Community, Learning Center Station #5

### **Participants**

Eric C. Ehman, MD, Rochester, MN (*Presenter*) Nothing to Disclose Shannon P. Sheedy, MD, Rochester, MN (*Abstract Co-Author*) Nothing to Disclose John M. Barlow, MD, Rochester, MN (*Abstract Co-Author*) Nothing to Disclose David Bruining, MD, Rochester, MN (*Abstract Co-Author*) Research Grant, Given Imaging Ltd Consultant, Bracco Group Rickey E. Carter, PhD, Jacksonville, FL (*Abstract Co-Author*) Nothing to Disclose Joel G. Fletcher, MD, Rochester, MN (*Abstract Co-Author*) Grant, Siemens AG; Consultant, Medtronic plc; ; Yong Lee, Rochester, MN (*Abstract Co-Author*) Nothing to Disclose Jeff L. Fidler, MD, Rochester, MN (*Abstract Co-Author*) Nothing to Disclose Cynthia H. McCollough, PhD, Rochester, MN (*Abstract Co-Author*) Nothing to Disclose

#### For information about this presentation, contact:

fletcher.joel@mayo.edu

### PURPOSE

CT and MR enterography (CTE, MRE) are used to objectively measure small bowel Crohn's enteric inflammation. After developing potential CT inflammation severity scores using a variety of statistical modeling strategies, we examined interobserver agreement for the observations, measurements and models.

#### **METHOD AND MATERIALS**

Patients with biopsy-proven Crohn's disease with both CTE and MRE performed within 30 days were identified. MaRIA scores and length of terminal ileum (TI) inflammatory involvement were calculated for MRE. Two GI radiologists examined CTE images for ulceration, mural edema, comb sign, perienteric stranding and fistulae involving the distal 10 cm of TI, measuring wall thickness and attenuation. Recorded variables were applied to an EMBARK visual score, and used to generate predictions using developed statistical models (random forest regression, multiple linear regression, and elasticnet models). Observer agreement was assessed using intraclass correlation coefficients (ICC) or kappa, and accuracy of the fitted models was assessed by comparison with MaRIA values using the R-square (R2).

#### RESULTS

By MRE, 27/43 (63%) patients had evidence of active TI inflammation (mean MaRIA score 17±12; mean inflamed length 13±11 cm). By CT, length of involvement, mean attenuation, and mean wall thickness had ICC's of 0.91, 0.63, and 0.60. Binary visual identification of perienteric stranding, stratification, and ulcers had kappas of 0.51, 0.62, and 0.32. ICC's for EMBARK visual score, and calculated random forest, multiple linear regression, and elasticnet models were 0.67, 0.65, 0.71, and 0.65. R2 values for for EMBARK visual score, random forest, multiple linear regression, and elasticnet models were 0.47, 0.54, 0.50, and 0.46.

### CONCLUSION

There was high reliability for quantitative and qualitative measures of CT severity except for identification of ulceration, with nearperfect agreement for length of disease. Validity of the fitted models was similar between visual and quantitative scores, with scores negatively affected by agreement on ulceration. Automated identification of ulceration of reader training may consequently improve CT severity score validity.

### **CLINICAL RELEVANCE/APPLICATION**

A validated CT severity score would allow for description of Crohn's inflammation severity in patients unable to undergo MRE in addition to measurements of disease length, thereby improving understanding of disease progression or remission.



# GU205-SD-SUB1

Accelerating MR Imaging Three-Dimensional T2-Weighted Turbo Spin-Echo Imaging Using Compressed Sensing of Female Pelvis: Prospective Intraindividual Comparison with Conventional Three-Dimensional T2-Weighted Turbo Spin-Echo Imaging

Sunday, Nov. 25 1:00PM - 1:30PM Room: GU/UR Community, Learning Center Station #1

#### Participants

Tomohiro Namimoto, MD, Kumamoto, Japan (*Presenter*) Nothing to Disclose Masataka Nakagawa, Kumamoto, Japan (*Abstract Co-Author*) Nothing to Disclose Kie Shimizu, Kumamoto, Japan (*Abstract Co-Author*) Nothing to Disclose Seitaro Oda, MD, Kumamoto, Japan (*Abstract Co-Author*) Nothing to Disclose Takeshi Nakaura, MD, Kumamoto, Japan (*Abstract Co-Author*) Nothing to Disclose Yasuyuki Yamashita, MD, Kumamoto, Japan (*Abstract Co-Author*) Consultant, DAIICHI SANKYO Group

## PURPOSE

To evaluate the impact of three-dimensional (3D) volume isotrophic T2-weighted turbo spin-echo acquisition (VISTA) with compressed sensing (CS) of female pelvis on image quality as compared with conventional 3D VISTA.

## **METHOD AND MATERIALS**

Thirty-four patients underwent 3.0T MR imaging for gynecological disease with CS-VISTA and conventional-VISTA. The acquisition time with each protocol was recorded. Two radiologists independently rated in random order on a 4-point scale (1: poor - 4: excellent) for overall image quality, conspicuity of the zonal anatomy of the uterus and ovary, and presence of artifacts (Wilcoxon signed rank test). Signal-to noise ratios (SNRs) were measured for the myometrium, iliacus muscle and bladder fluid (student's t-test). Relative contrast ratio (CR) was calculated for the iliacus muscle to myometrium, bladder fluid and tumor (student's t-test).

### RESULTS

The acquisition time of 130.5 sec for CS-VISTA was significantly shorter (48.6 %) than that of 268.5 sec for conventional-VISTA (P < 0.01). The overall image quality ( $3.4 \pm 0.63$ ,  $3.4 \pm 0.64$ ), conspicuity of the zonal anatomy for uterus ( $3.3 \pm 0.76$ ,  $3.4 \pm 0.75$ ) and ovary ( $3.6 \pm 0.53$ ,  $3.5 \pm 0.59$ ), and presence of artifacts ( $3.5 \pm 0.65$ ,  $3.4 \pm 0.68$ ) were comparable between CS-VISTA and conventional-VISTA, respectively. There was no significant difference in SNR (myometrium: 16.7, 15.9; iliacus muscle: 11.9, 12.1; bladder fluid 63.4, 64.6) between CS-VISTA and conventional-VISTA, respectively. There was no significant difference in CR (uterus: 1.98, 1.92; bladder fluid: 8.64, 8.35; tumor: 4.92, 3.85) between CS-VISTA and conventional-VISTA, respectively.

#### CONCLUSION

The 3D T2-weighted CS-VISTA of the female pelvis provided comparable image quality with conventional VISTA in half of the acquisition time.

### **CLINICAL RELEVANCE/APPLICATION**

The 3D T2-weighted compressed sensing-VISTA of the female pelvis provided comparable image quality with conventional VISTA in half of the acquisition time of 130 sec.



# GU206-SD-SUB2

Diagnosis of Transition Zone Prostate Cancer (TZ PCa): Logistic Regression and Machine Learning Models of Quantitative ADC, Shape and Texture Features Improves Accuracy Compared to Subjective Evaluation with PI-RADSv2

Sunday, Nov. 25 1:00PM - 1:30PM Room: GU/UR Community, Learning Center Station #2

#### **Participants**

Mark Z. Wu, MD,MSc, Ottawa, ON (*Abstract Co-Author*) Nothing to Disclose Satheesh Krishna, MD, Ottawa, ON (*Abstract Co-Author*) Nothing to Disclose Rebecca Thornhill, PhD, Ottawa, ON (*Abstract Co-Author*) Nothing to Disclose Matthew D. McInnes, MD, PhD, Ottawa, ON (*Abstract Co-Author*) Nothing to Disclose Trevor A. Flood, MD, FRCPC, Ottawa, ON (*Abstract Co-Author*) Nothing to Disclose Nicola Schieda, MD, Ottawa, ON (*Presenter*) Nothing to Disclose

#### For information about this presentation, contact:

#### nschieda@toh.on.ca

### PURPOSE

This study compares quantitative ADC, texture and shape analysis using logistic regression and machine learning models to subjective analysis by PI-RADSv2 for diagnosis of TZ PCa.

# **METHOD AND MATERIALS**

With IRB approval, 44 TZ PCa (identified from 3T-mp-MRI-radical prostatectomy (RP) maps and targeted mp-MRI-TRUS Fusion biopsy) were compared to 61 consecutive BPH nodules (26 glandular/35 stromal). Two blinded radiologists assessed each lesion using PI-RADSv2. A third radiologist segmented lesions for quantitative ADC (Mean-ADC, 10th-centile-ADC), T2W shape and texture analysis. Logistic regression modeling and support vector machine (SVM) learning models were compared to PI-RADSv2 using ROC analysis.

#### RESULTS

Subjective analysis by PI-RADSv2 yielded sensitivity/specificity/area under ROC curve (AUC) of: 76.4%/91.5%/0.842 and 67.9%/94.2%/0.796 (K=0.48). Accuracy was reduced in <=15mm lesions: 68.7%/84.3%/0.743 and 61.7%/81.6%/0.694. Mean-ADC, 10th-centile, circularity and texture (Kurtosis, Entropy, RNLU) features differed between groups (p<0.0001); however, at multi-variate analysis only circularity (p=0.005) and 10th-centile-ADC (p<0.001) were significant. Sub-group analyses of TZ PCa versus stromal BPH and only <=15 mm lesions did not alter outcomes. Logistic regression and SVM models were highly accurate (sensitivity/specificity/AUC): 93.2%/95.1%/0.987 and 95.3%/95.2%/0.953. Quantitative model accuracies were unchanged in TZ PCa versus stromal BPH (AUC=0.977) and <=15 lesions (AUC=0.990), p>0.05 and better than subjective analysis (p<0.001).

#### CONCLUSION

Subjective analysis using PI-RADSv2 is accurate to diagnose TZ PCa; however, accuracy is reduced in small lesions. In this study, logistic regression and machine based models incorporating quantitative ADC, T2W shape and texture features were highly accurate for diagnosis and outperformed subjective analysis particularly for smaller lesions.

# **CLINICAL RELEVANCE/APPLICATION**

Quantitative analysis of ADC, T2W shape and texture features improves diagnosis of transition zone prostate cancers compared to analysis by PI-RADS version 2 and may be particularly valuable for small <=15 mm observations. These radiomic features could be studied in larger datasets of TZ abnormalities with artificial neural networks to enable computer aided diagnosis of cancer.



## GU207-SD-SUB3

# Management Impact of Direct MRI-Guided Prostate Biopsy

Sunday, Nov. 25 1:00PM - 1:30PM Room: GU/UR Community, Learning Center Station #3

#### Awards Student Travel Stipend Award

### **Participants**

Nicholas P. Meermeier, Portland, OR (*Presenter*) Nothing to Disclose Bryan R. Foster, MD, Portland, OR (*Abstract Co-Author*) Nothing to Disclose Jen-Jane Liu, Portland, OR (*Abstract Co-Author*) Nothing to Disclose Christopher Amling, Portland, OR (*Abstract Co-Author*) Nothing to Disclose Fergus V. Coakley, MD, Portland, OR (*Abstract Co-Author*) Founder, OmnEcoil Instruments, Inc ; Shareholder, OmnEcoil Instruments, Inc

## For information about this presentation, contact:

coakleyf@ohsu.edu

### PURPOSE

To investigate the management impact of direct MRI-guided prostate biopsy in clinical practice.

## **METHOD AND MATERIALS**

We retrospectively identified 127 patients with unknown (n = 98) or untreated Gleason score 6 (n = 29) prostate cancer who underwent direct MRI-guided biopsy of the prostate at our institution between August 2013 and January 2018 after an initial multiparametric endorectal MRI demonstrated one or more high value targets (scores of 4 or 5 on PiRADS version 2). All available medical and imaging records were reviewed to determine pertinent clinical details, biopsy findings, and post-biopsy management.

## RESULTS

The mean patient age was 68 years (range, 48 to 82) and the mean serum prostate specific antigen level was 9.2 ng/mL (range, 2.2 to 53.9). MRI-guided biopsy was positive in 93 of 127 patients (73%), with 84 of these 93 (90%) patients being diagnosed with Gleason score 7 or higher prostate cancer. When stratified by clinical scenario, the positive biopsy rate was 66% (57/86) for patients with one or more prior negative transrectal ultrasound guided biopsies, 83% (10/12) for biopsy naïve patients, and 90% (26/29) for patients on active surveillance. Overall, 90 of 127 patients (71%) received a new (n = 67) or upgraded (n = 23) diagnosis of prostate cancer, and 57 of these 90 (63%) proceeded to treatment by prostatectomy, radiation, or androgen deprivation therapy.

# CONCLUSION

Our results suggest that direct MRI-guided biopsy is associated with high rates of significant prostate cancer detection and subsequent definitive treatment across common clinical scenarios and should be considered as an important diagnostic tool in appropriate patient care settings.

# **CLINICAL RELEVANCE/APPLICATION**

Our findings that direct MRI-guided biopsy of the prostate in appropriately selected patients results in high rates of detection of clinically significant cancer and of progression to definitive treatment provides a strong and practical evidence basis for the utilization of this complex diagnostic procedure in clinical practice.

# **Honored Educators**

Presenters or authors on this event have been recognized as RSNA Honored Educators for participating in multiple qualifying educational activities. Honored Educators are invested in furthering the profession of radiology by delivering high-quality educational content in their field of study. Learn how you can become an honored educator by visiting the website at: https://www.rsna.org/Honored-Educator-Award/ Bryan R. Foster, MD - 2018 Honored Educator



# GU208-SD-SUB4

Histogram Analysis of Apparent Diffusion Coefficients for Predicting Pelvic Lymph Node Metastasis in Patients with Uterine Cervical Cancer

Sunday, Nov. 25 1:00PM - 1:30PM Room: GU/UR Community, Learning Center Station #4

# Participants

Jiyeong Lee, MD, Seoul, Korea, Republic Of (*Presenter*) Nothing to Disclose Chan Kyo Kim, MD, PhD, Seoul, Korea, Republic Of (*Abstract Co-Author*) Nothing to Disclose Jae-Hun Kim, PhD, Seoul, Korea, Republic Of (*Abstract Co-Author*) Nothing to Disclose Sung Yoon Park, Seoul, Korea, Republic Of (*Abstract Co-Author*) Nothing to Disclose Jung Jae Park, Daejeon, Korea, Republic Of (*Abstract Co-Author*) Nothing to Disclose

## For information about this presentation, contact:

chankyokim@skku.edu

# PURPOSE

Preoperative prediction of lymph node (LN) metastasis in uterine cervical cancer remains a challenge. We aimed to investigate the value of apparent diffusion coefficient (ADC) histogram analysis in predicting pelvic LN metastasis in patients with uterine cervical cancer undergoing surgery.

#### **METHOD AND MATERIALS**

Our retrospective study included 162 cervical cancer patients (mean age, 47.7 years; range, 26-81 years) who received radical abdominal hysterectomy with pelvic LN dissection. All enrolled patients underwent routine pelvic 3T-MRI including diffusion-weighted imaging. The ADC histogram for the tumor was generated using in-house software and several histogram parameters were obtained. For predicting pelvic LN metastasis, clinical parameters (age, FIGO stage, tumor antigen [TA]-4, and histologic type) and imaging parameters (tumor size, maximal and short diameter of LN, MRI T-stage, and ADC histogram parameters) were evaluated using logistic regression analysis.

# RESULTS

At histopathological findings, pelvic LN metastasis occurred in 50 patients (30.9%). In patients with LN metastasis, all ADC histogram parameters were significantly different from those without LN metastasis (all p < 0.05), except maximum, skewness, uniformity and entropy. At receiver operating characteristic (ROC) curve analysis, the area under the ROC curve of the 97.5th ADC percentile (ADC97.5) was 0.782, which was the greatest among other imaging and clinical variables. At univariate analysis, maximal and short diameters of LN, MRI T-stage, TA-4, tumor size and ADC97.5 were significantly associated with pelvic LN metastasis. However, the ADC97.5 was the only independent predictor of pelvic LN metastasis (odd ratio, 0.995; p < 0.001) (Table 1).

# CONCLUSION

As an imaging marker, the ADC97.5 from histogram analysis appears to be useful for the prediction of pelvic LN metastasis in patients with uterine cervical cancer undergoing surgery.

#### **CLINICAL RELEVANCE/APPLICATION**

Preoperative ADC histogram analysis may be a useful tool to predict pelvic lymph node metastasis in patients with uterine cervical cancer, which may be helpful for clinical decision-making.



# GU209-SD-SUB5

Image Quality and Diagnostic Accuracy of Complex-Averaged High B-Value Images in Diffusion-Weighted MRI of Prostate Cancer

Sunday, Nov. 25 1:00PM - 1:30PM Room: GU/UR Community, Learning Center Station #5

## Participants

Hamed Kordbacheh, MD, Boston, MA (*Presenter*) Nothing to Disclose Ravi T. Seethamraju, PhD, Charlestown, MA (*Abstract Co-Author*) Employee, Siemens AG Stockholder, Siemens AG Elisabeth Weiland, Erlangen, Germany (*Abstract Co-Author*) Employee, Siemens AG Marcel D. Nickel, Erlangen, Germany (*Abstract Co-Author*) Employee, Siemens AG Vinit Baliyan, MBBS, MD, Boston, MA (*Abstract Co-Author*) Nothing to Disclose Thitinan Chulroek, MD, Bangkok, Thailand (*Abstract Co-Author*) Nothing to Disclose Martina Cecconi, Cagliari, Italy (*Abstract Co-Author*) Nothing to Disclose Mukesh G. Harisinghani, MD, Boston, MA (*Abstract Co-Author*) Nothing to Disclose

#### For information about this presentation, contact:

hkordbacheh@mgh.harvard.edu

#### PURPOSE

To evaluate image quality and diagnostic accuracy of complex averaging on acquired and calculated high b-value (aHBV & cHBV) images in diffusion MRI of prostate cancer.

### **METHOD AND MATERIALS**

Eighty-four patients underwent multiparametric prostate MRI (mp-MRI) at 3 Tesla without endorectal coil. Three sets of b-values for DWI were acquired with two separate non-product DWI sequences, one with (b=50/900 s/mm2) and the other one with (2000 s/mm2). cHBV (b=2000 s/mm2) was derived from the lower DWI sequence (b= 50, 900 s/mm2) using a mono-exponential model. Complex-averaged data-sets were generated for the aHBV and cHBV images and ADC maps, calculated from the two lower bvalues. Image quality (IQ), level of confidence (LOC), lesion detection, PIRADS score and ADC calculation were performed by two blinded experienced abdominal radiologists (8 and 10 years of experience) using aHBV and cHBV image datasets for both complexaveraged and conventional magnitude-averaged data-sets read in separate reading sessions at 3-week interval. For lesions with histological confirmation (n=42; in 35 patients) the correlation between PIRADS and Gleason scores was performed for each dataset. The comparisons were made using Wilcoxon test.

#### RESULTS

The aHBV sequence accounted for approximately 25% of the total mp-MRI scan time (6 min 30 sec  $\pm 1$  min 16 secs of 28 min 31 sec  $\pm 4$  min 26 sec). Complex-averaging calculated from the two lower b-values, did not have a significant impact on the ADC values of the lesions for both readers (p=0.08 & 0.18). The IQ and LOC of the cHBV were not significantly different than aHBV images for both observer. Complex-averaging improved IQ of the aHBV images and cHBV for both readers. Complex-averaging improved LOC of the aHBV and cHBV for reader A but only for aHBV for reader B. The accuracy of complex averaged cHBV for detection the clinically significant lesion (Gleason score >=7) was higher but not statistically significant compared to conventional magnitude averaged aHBV (79.55% vs. 70.45%, p= 0.317).

# CONCLUSION

The complex-averaging provides better IQ and LOC for DW images in prostate cancer without significant impact on ADC values calculated from two lower b-values.

# **CLINICAL RELEVANCE/APPLICATION**

The complex-averaging cHBV may increase the accuracy for detection the prostate lesion compared to conventional magnitude averaged aHBV and may help in reducing the imaging time for prostate MRI.



# HP007-EB-SUB

Practice-Building for the Modern Interventional Radiologist Using Traditional, Electronic, and Social Media

Sunday, Nov. 25 1:00PM - 1:30PM Room: HP Community, Learning Center Hardcopy Backboard

#### **Participants**

Andrew J. Gunn, MD, Birmingham, AL (*Presenter*) Nothing to Disclose Joel M. Raborn, MD, Birmingham, AL (*Abstract Co-Author*) Nothing to Disclose Aliaksei Salei, MD, Birmingham, AL (*Abstract Co-Author*) Nothing to Disclose Rachel F. Oser, MD, Birmingham, AL (*Abstract Co-Author*) Nothing to Disclose Rakesh K. Varma, MD, Birmingham, AL (*Abstract Co-Author*) Nothing to Disclose Edgar S. Underwood, MD, Birmingham, AL (*Abstract Co-Author*) Nothing to Disclose Nathan W. Ertel, MD, Hoover, AL (*Abstract Co-Author*) Nothing to Disclose Souheil Saddekni, MD, Birmingham, AL (*Abstract Co-Author*) Nothing to Disclose Souheil Saddekni, MD, Birmingham, AL (*Abstract Co-Author*) Nothing to Disclose International Inc; Consultant, C. R. Bard, Inc; Consultant, Boston Scientific Corporation; Consultant, W. L. Gore & Associates, Inc; Consultant, Sirtex Medical Ltd

## For information about this presentation, contact:

agunn@uabmc.edu

# TEACHING POINTS

1. Interventional radiology (IR) increasingly needs to market their services to both referring physicians and patients. 2. Multiple strategies can be employed that will maximize results. 3. Practice-building efforts can help solidify positive relationships with patients, referring physicians, and the hospital or hospital system.

# TABLE OF CONTENTS/OUTLINE

1. Introduction, including the necessity for a proactive approach to practice-building in IR 2. Practice-building strategies from our institution a. Opportunities utilizing traditional media i. Patient information brochures about specific IR procedures ii. Referring physician brochures about specific IR procedures (Figure 1) iii. Videos featuring patient experiences (Figure 2) iv. Utilize local media outlets (Figure 2) b. Opportunities utilizing social media i. Overview of social media platforms ii. Our institutional experience and guidelines (Figure 3) iii. Engaging, interactive internet presence iv. Podcast creation (Figure 4) c. Opportunities for referring physician engagement i. Physician education through speaking engagements ii. Dedicated IR clinic for ease of referral iii. Create working groups with other physicians around a specific disease or problem (Figure 5) d. Overcoming obstacles 3. Summary and conclusions



## HP203-SD-SUB1

Comparison of Total Gadolinium Retention in Human Bone Tissue After Injection of Gadoterate Meglumine versus Gadodiamide in Patients with Normal Renal Function

Sunday, Nov. 25 1:00PM - 1:30PM Room: HP Community, Learning Center Station #1

## Participants

Takaki Maeda, MD, Kobe, Japan (*Presenter*) Institutional research collaboration, Guerbet SA Hitomi Hara, MD, PhD, Kobe, Japan (*Abstract Co-Author*) Nothing to Disclose Toshihiro Akisue, MD, PhD, Kobe, Japan (*Abstract Co-Author*) Nothing to Disclose Ryosuke Kuroda, Kobe, Japan (*Abstract Co-Author*) Nothing to Disclose Masahiko Fujii, MD, Kobe, Japan (*Abstract Co-Author*) Nothing to Disclose Takamichi Murakami, MD, PhD, Osakasayama, Japan (*Abstract Co-Author*) Nothing to Disclose

### PURPOSE

The purpose of this study was to determine the total gadolinium (Gd) retention in human bone tissue after administration of the Gdbased contrast agents (GBCAs) gadoterate meglumine (macrocyclic) or gadodiamide (linear).

### **METHOD AND MATERIALS**

Twenty-two patients (M/F ratio: 18/4, mean age: 22 years) scheduled for surgical bone or soft tissue tumor resection, underwent preoperative contrast-enhanced MRI with randomly selected gadoterate meglumine (Magnescope, Guerbet) or gadodiamide (Omniscan, GE Healthcare) at a standard single clinical dose. Bone tumor was resected within 7-14 days after MRI. Margins of resected tissue, which comprised normal bone tissue, were selected and analyzed for Gd concentration using Inductively Coupled Plasma Mass Spectroscopy (ICP-MS). The two groups were compared with the Fisher permutation test. All statistical analyses were conducted in the R software environment for computing.

## RESULTS

One specimen did not conform to the protocol and was excluded from the analysis. In one other patient, the amount of bone sample was too small to obtain a reliable measurement. The remaining assessable cases included 2 groups of 10 patients with administration of a macrocyclic or linear GBCA. A Gd concentration was measured in all patients who received gadodiamide. However, in the gadoterate meglumine group, 6 of 10 patients showed lower Gd concentration than lower limit of quantification of ICP-MS. The value of lower limit of quantification was used as substitution for these 6 cases. The mean ( $\pm$  SD) concentration of Gd in bone tissue was higher in the gadodiamide group (6.6 $\pm$  6.8 nmol/g) than in the gadoterate meglumine group (0.6  $\pm$  0.6 nmol/g), *P* = 0.02.

## CONCLUSION

Total Gd retention in normal bone tissue was found to be significantly lower with a macrocyclic GBCA compared with a linear GBCA in patients with normal renal function. The mean concentration of Gd was 9.86 times higher with gadodiamide than with gadoterate meglumine.

## **CLINICAL RELEVANCE/APPLICATION**

When using GBCAs, using a macrocyclic contrast agent showed significantly less Gd retention in bone than linear GBCA.



## HP204-SD-SUB2

Lung Cancer Screening Engagement Through Breast Imaging: Population-Based Cross-Sectional Survey Results from the National Health Interview Survey

Sunday, Nov. 25 1:00PM - 1:30PM Room: HP Community, Learning Center Station #2

#### Awards Student Travel Stipend Award

#### Participants

Diego Lopez, Boston, MA (*Presenter*) Nothing to Disclose Efren J. Flores, MD, Boston, MA (*Abstract Co-Author*) Nothing to Disclose Randy C. Miles, MD, Chicago, IL (*Abstract Co-Author*) Nothing to Disclose Jo-Anne O. Shepard, MD, Boston, MA (*Abstract Co-Author*) Nothing to Disclose Constance D. Lehman, MD,PhD, Boston, MA (*Abstract Co-Author*) Research Grant, General Electric Company; Medical Advisory Board, General Electric Company Gary X. Wang, MD, PhD, Boston, MA (*Abstract Co-Author*) Nothing to Disclose Anand K. Narayan, MD,PhD, Boston, MA (*Abstract Co-Author*) Nothing to Disclose

# For information about this presentation, contact:

diego\_lopez@hms.harvard.edu

### PURPOSE

Lung cancer is the leading cause of cancer-related mortality in the US. Lung cancer screening with low dose chest CT (LCS), performed in radiology departments, reduces lung cancer mortality. Millions of women present to radiology departments annually for mammography screening, representing an ideal opportunity for radiologists to identify potentially eligible women who can benefit from LCS enrollment and tobacco cessation efforts. Using a federal nationally representative cross-sectional survey, our purpose was to estimate the prevalence of individuals undergoing mammography screening who are eligible for 1) LCS and 2) tobacco cessation counseling.

#### **METHOD AND MATERIALS**

Retrospective analysis of the 2015 National Health Interview Survey (NHIS), a nationally representative federal cross-sectional survey was conducted. Women aged 55-74 without histories of lung or breast cancer were included. The primary outcome of interest was the proportion of survey participants who were eligible for LCS among participants self-reporting mammography screening within the last two years. The secondary outcomes included prevalence of current smoking (and consequently eligibility for smoking cessation counseling) among patients undergoing mammography screening, and self-reported LCS participation rate among the same patient population. Population covariates such as insurance status, income, education and self-reported demographics, including race/ethnicity, were also collected.

#### RESULTS

5,436 women were included. Of 68.55% of women who reported screening mammography within the last 2 years, 7.63% were eligible for LCS based on pack-year history (representing an estimated 1.74 million women nationwide). Of these women, 92.54% (representing an estimated 1.61 million women nationwide) did not receive LCS. Among those eligible for LCS, 57.33% reported screening mammography within the last 2 years. Of women reporting screening mammography within 2 years, 9.93% reported current smoking and would benefit from tobacco cessation counseling.

### CONCLUSION

A large number of women participating in mammography screening are eligible for LCS or tobacco cessation counseling and are not receiving these services.

#### **CLINICAL RELEVANCE/APPLICATION**

Radiology practices have an opportunity to engage in targeted population health initiatives by leveraging mammography appointments to increase LCS participation and provide smoking cessation counseling among eligible patients.



## HP205-SD-SUB3

Process Simulation and Economic Assessment of a Brain CT to Improve the Patient Journey and Cost Efficiency

Sunday, Nov. 25 1:00PM - 1:30PM Room: HP Community, Learning Center Station #3

## Participants

Nicolai Gossmann, Erlangen, Germany (*Abstract Co-Author*) Employee, Siemens AG Roland Reickersdorfer, Erlangen, Germany (*Abstract Co-Author*) Employee, Siemens AG Arthur Dubowicz, Erlangen, Germany (*Presenter*) Employee, Siemens AG Florian Meier, 90763, Germany (*Abstract Co-Author*) Nothing to Disclose Oliver Schoeffski, MPH, Nuremberg, Germany (*Abstract Co-Author*) Nothing to Disclose Soeren Eichhorst, MD, Erlangen, Germany (*Abstract Co-Author*) Employee, Siemens AG

#### For information about this presentation, contact:

nicolai.gossmann@siemens-healthineers.com

## PURPOSE

To explore process improvement potentials and assess their operational and economic impact on hospital workflows, both process analysis and simulation modeling was applied to patient pathways undergoing a computed tomography (CT) of the brain without contrast enhancement.

#### **METHOD AND MATERIALS**

A discrete event simulation (DES) was developed to analyze the process of a non-contrast enhanced brain CT including patients' pathways using Bizagi BPMN Modeler. Initially, a Business Process Management Notation (BPMN) model was created to visualize the workflow from exam requested to finalized report. Next, this model was parameterized with data from a time-and-motion study in a large maximum-care hospital in Germany comprising 228 patient arrivals over a four-weeks period. Thereafter, multiple scenarios were systematically defined covering various baseline modifications to explore improvement potentials along the workflow. Subsequently, the operational and economic impact of each scenario was simulated to quantify the highest saving potentials using DES.

## RESULTS

In the baseline model total process time accounts for 71.4 min including waiting times [min: 31.1 min, max: 272.8 min]. While administrative activities add up to 12.5% of total time, the average reporting time is 19.7 min (27.6%) including approval and finalization. The remaining share of 59.9% accounted for exam conduct including preparation and after-care. Corresponding staff process costs amount for 39.8 Euro. Main improvement potentials were identified in the fields of patient order-entry, consent, exam, reporting and discharge. Using DES, the highest saving potential was identified in patient order-entry, leading up to 26.5% less staff process cost per patient in an optimal case.

## CONCLUSION

The simulation model is validated for exploring, quantifying, and evaluating operational as well as economic impacts of process improvement measures. This opens up new opportunities when optimizing dynamic, multidirectional and high complex processes in healthcare. Following this approach, specific measures within medical workflows as well as corresponding effects on departmental dynamics can be prototyped and vetted in a digital environment prior to actual implementation.

## **CLINICAL RELEVANCE/APPLICATION**

Simulation modeling enables decision makers to make well-informed decisions and, thus, to optimally allocate their efforts and resources when improving quality of care and reducing costs.



## IN010-EB-SUB

Code2Vec: A Novel, Vector Space Model Representation of Radiology CPT Codes

Sunday, Nov. 25 1:00PM - 1:30PM Room: IN Community, Learning Center Hardcopy Backboard

## Participants

Aditya Sidapara, Phoenix, AZ (*Presenter*) Nothing to Disclose

Jeffry S. Kriegshauser, MD, Phoenix, AZ (Abstract Co-Author) Research support, General Electric Company

Sailen G. Naidu, MD, Phoenix, AZ (Abstract Co-Author) Nothing to Disclose

Grace Knuttinen, MD, PhD, Scottsdale, AZ (*Abstract Co-Author*) Speakers Bureau, Abbott Laboratories; Consultant, Abbott Laboratories

Sadeer Alzubaidi, MD, Birmingham, MI (*Abstract Co-Author*) Nothing to Disclose Amy K. Hara, MD, Scottsdale, AZ (*Abstract Co-Author*) License agreement, General Electric Company Rahmi Oklu, MD,PhD, Phoenix, AZ (*Abstract Co-Author*) Nothing to Disclose

### CONCLUSION

Accurate modeling of Radiology CPT codes in the field of natural language processing enables researchers to perform large-scale data mining operations on electronic health records, giving us an unparalleled quantitative insight on previously qualitative resources. Additionally, models generated by Code2Vec can potentially be used to perform quality assurance on medical coding operations, reducing compliance costs and caseloads among billing departments.

### FIGURE

http://abstract.rsna.org/uploads/2018/18017920/18017920\_lwi5.jpg

#### Background

Complex medical procedures are often an amalgamation of different sub procedures, which are identified and reimbursed by care providers through medical coding. Medical codes, which are unique identifiers for different procedures, play an important role in healthcare analysis, as they help us understand costs associated with care. While codes are technically and strictly defined, the identification is manual and human error prone.

#### **Evaluation**

In this study, we introduce a vector space model for representing Current Procedural Terminology (CPT) codes. Based on the wordvector projection algorithm word2vec, our model combines word-vectors trained on a dataset of over ten thousand deindentified dictations (acquired from the Radiology Department) with CPT code descriptions to create medical code-vectors. We analyze the generated medical code vectors with Principal Component Analysis to gain quantitative insight into the relative frequency of procedures.

#### Discussion

Our analysis uncovered many medical code-vector clusters, indicating that the word-frequencies of the original dataset translated into the code-vectors. The cosine similarity values, which measures document similarity, is consistently above .99 ( $-1 \le x \le 1$ ) for p-significance values ranging from .01 to .1. This is important as the relationships between code-vectors are valid and can be quantitatively scored for significance and relevance.

### **Honored Educators**

Presenters or authors on this event have been recognized as RSNA Honored Educators for participating in multiple qualifying educational activities. Honored Educators are invested in furthering the profession of radiology by delivering high-quality educational content in their field of study. Learn how you can become an honored educator by visiting the website at: https://www.rsna.org/Honored-Educator-Award/ Amy K. Hara, MD - 2015 Honored EducatorAmy K. Hara, MD - 2017 Honored Educator



## IN013-EB-SUB

Data-Driven Capacity Assessment of Nursing Bay Resources Shared Among Multiple Radiology Modalities

Sunday, Nov. 25 1:00PM - 1:30PM Room: IN Community, Learning Center Hardcopy Backboard

### Participants

Petro Kostandy, MD, Rochester, MN (*Presenter*) Nothing to Disclose Miao Bai, PhD, Rochester, MN (*Abstract Co-Author*) Nothing to Disclose Kayse T. Maass, PhD, Rochester, MN (*Abstract Co-Author*) Nothing to Disclose Santiago Romero Brufau, MD, Rochester, MN (*Abstract Co-Author*) Nothing to Disclose Stacy R. Schultz, MA, Rochester, MN (*Abstract Co-Author*) Nothing to Disclose Mustafa Sir, PhD, Rochester, MN (*Abstract Co-Author*) Nothing to Disclose Kalyan S. Pasupathy, PhD, Rochester, MN (*Abstract Co-Author*) Nothing to Disclose Brian J. Bartholmai, MD, Rochester, MN (*Abstract Co-Author*) License agreement, ImBio, LLC; Scientific Advisor, ImBio, LLC; Scientific Advisor, Bristol-Myers Squibb Company

#### For information about this presentation, contact:

kostandy.petro@mayo.edu

### CONCLUSION

One of the benefits of the wealth of data being gathered about radiology processes is that it allows validation of hypotheses and concerns that influence strategic planning. We describe our experience with evaluating our current nursing bay utilization and modeling the expected utilization following an anticipated practice change.

## FIGURE

http://abstract.rsna.org/uploads/2018/18011223/18011223\_mwi3.jpg

### Background

Data-driven decision making is integral to modern radiology practice management. We formed a multidisciplinary team of radiology subject matter experts, informaticists, and scientists with expertise in data science and systems engineering to aggregate, validate and use data to make informed practice changes for our complex hospital-based radiology practice. This Radiology Clinical Engineering Laboratory (RADCELL) team was leveraged to predict the outcomes of practice changes, model future states based on current data and determine potential bottlenecks in departmental workflows. Our practice planned to relocate CT and ultrasound exam rooms to be physically closer to the other radiology modalities, thereby adding additional demand for shared nursing bay resources. Feedback elicited from the staff surfaced a concern about not having enough bays to accommodate the added volume.

## Evaluation

We collected and merged data from multiple hospital data systems in order to link bay usage to individual patient encounters. We subsequently calculated total bay occupancy by time of day, which we aggregated over a period of months into occupancy distributions. The mean, 95th percentile, and maximum occupancy levels were established by time of day, using 1-minute time bins.

#### Discussion

We were able to validate our staff's concerns regarding instances of insufficient capacity by taking into account bay usage constraints that had been in place (some bays being limited to pediatric patients, for example). By relaxing some of those constraints, we were able to show that we could operate well within our existing capacity. We then proceeded to calculate our projected bay occupancy rates following the anticipated practice change with reduced restrictions on bay usage, and ultimately determined that we would be operating within our capacity at least 95% of the time.



## IN141-ED-SUB1

Blockchain Technology: Principles and Applications in Radiology

Sunday, Nov. 25 1:00PM - 1:30PM Room: IN Community, Learning Center Station #1

## Awards Certificate of Merit

Participants Morgan P. McBee, MD, Charleston, SC (*Presenter*) Nothing to Disclose

## **TEACHING POINTS**

The purpose of this exhibit is to: 1. Provide an overview of blockchain technology and its underlying principles 2. Briefly discuss history of blockchain 3. Discuss applications and potential benefits of blockchain technology relevant to radiology 4. Discuss limitations of blockchain

### TABLE OF CONTENTS/OUTLINE

1. History of blockchain 2. Blockchain principles a. Data provenance b. Distributed/decentralized network c. Security via publicprivate key cryptography d. Robustness/fault tolerance e. Public vs. private blockchains 3. Applications a. Outside of healthcare b. Healthcare i. Radiology ii. Medical records 4. Limitations



## IN142-ED-SUB2

# 3D Printing for Liver Surgery Planning: A Step by Step Guide

Sunday, Nov. 25 1:00PM - 1:30PM Room: IN Community, Learning Center Station #2

### **Participants**

Lidia Alcala, MD, Jaen, Spain (*Presenter*) Nothing to Disclose Felix Paulano-Godino, PhD, Jaen, Spain (*Abstract Co-Author*) Nothing to Disclose Rocio Cumbreras Casas, Jaen, Spain (*Abstract Co-Author*) Nothing to Disclose Marta Lopez Leon, DIPLPHYS, Cordoba, Spain (*Abstract Co-Author*) Nothing to Disclose Pedro Lopez Cillero, MD,PhD, Cordoba, Spain (*Abstract Co-Author*) Nothing to Disclose Antonio Luna, MD,PhD, Jaen, Spain (*Abstract Co-Author*) Consultant, Bracco Group; Speaker, General Electric Company; Speaker, Canon Medical Systems Corporation; Royalties, Springer Nature Teodoro M. Noguerol, MD, Jaen, Spain (*Abstract Co-Author*) Nothing to Disclose

### For information about this presentation, contact:

l.alcala.o@htime.org

#### **TEACHING POINTS**

1. Describe the main steps for printing 3D liver models using CT-MRI fusion 2. Analyze the clinical indications as well as the main benefits of integrating 3D printing into a liver surgery procedure. 3. Illustrate with sample cases the impact of 3D printing in the field of liver surgery.

## TABLE OF CONTENTS/OUTLINE

1. Introduction 2. 3D printing based on CT-MRI fusion a. Image acquisition b. CT-MRI fusion c. Segmentation of anatomical structures and findings d. 3D modelling and printing 3. Indications and benefits of 3D printing for liver surgery planning a. In which cases is the use of 3D printing beneficial? b. What does 3D printing based surgery provide with respect to a conventional procedure? c. Potential applications 4. Success stories a. Problematic cases and influence of 3D printing on treatment selection and outcomes 5. Conclusions

### **Honored Educators**

Presenters or authors on this event have been recognized as RSNA Honored Educators for participating in multiple qualifying educational activities. Honored Educators are invested in furthering the profession of radiology by delivering high-quality educational content in their field of study. Learn how you can become an honored educator by visiting the website at: https://www.rsna.org/Honored-Educator-Award/ Antonio Luna, MD - 2018 Honored Educator



## MI116-ED-SUB5

Hybrid Multiparametric 3 Tesla PET/MRI in Pelvic Malignancies: From Protocol Design to Clinical Application

Sunday, Nov. 25 1:00PM - 1:30PM Room: MI Community, Learning Center Station #5

## Awards Certificate of Merit

#### Participants

Ming Yang, MD, Scottsdale, AZ (*Presenter*) Nothing to Disclose Yuxiang Zhou, PhD, Phoenix, AZ (*Abstract Co-Author*) Nothing to Disclose Nitin Mishra, MD,MBBS, Phoenix, AZ (*Abstract Co-Author*) Nothing to Disclose Jonathan B. Ashman, MD,PhD, Scottsdale, AZ (*Abstract Co-Author*) Nothing to Disclose Kristina A. Butler, MD,MS, Scottsdale, AZ (*Abstract Co-Author*) Nothing to Disclose Akira Kawashima, MD, PhD, Scottsdale, AZ (*Abstract Co-Author*) Nothing to Disclose Kelly T. Smith, MD, Phoenix, AZ (*Abstract Co-Author*) Nothing to Disclose Ba D. Nguyen, MD, Scottsdale, AZ (*Abstract Co-Author*) Nothing to Disclose Christine O. Menias, MD, Chicago, IL (*Abstract Co-Author*) Nothing to Disclose Michael C. Roarke, MD, Scottsdale, AZ (*Abstract Co-Author*) Nothing to Disclose

# For information about this presentation, contact:

yang.ming@mayo.edu

# **TEACHING POINTS**

PET/MR is a powerful imaging tool with combined molecular imaging information of PET and outstanding soft tissue resolution of MR. Pelvic malignancies are suitable for PET/MRI as pelvic organs are less influenced by respiration motion artifact. In this current exhibit, we will: 1. Review the NCCN imaging guidelines on TNM staging of pelvic malignances, including colorectal cancer, ovarian/uterine/cervical cancers, and prostate cancer. 2. Introduce an established 'one-stop-shop' PET/MR imaging protocol and discuss the design of multi-specialties interpretation workflow. 3. Demonstrate the performance of PET/MR in pelvic malignancies. 4. Discuss the potential diagnostic pitfall of PET/MR. 5.Explore the future clinical application of pelvic PET/MR.

## TABLE OF CONTENTS/OUTLINE

1. NCCN imaging guidelines on pelvic malignancies. 2. PET/MR imaging protocol and interpretation workflow on a hybrid 3T PET/MR system. 3. Tailored multiparametric pelvic PET/MR protocols. 4. PET/MR case illustration on anorectal cancer, gynecological cancer and biochemically recurrent prostate cancer. 5. Diagnostic pitfall of pelvic PET/MR. 6. Introduction of potential clinical applications: dynamic C11-choline PET/MR, assessment of radiation induced bone marrow toxicity, etc.

#### **Honored Educators**

Presenters or authors on this event have been recognized as RSNA Honored Educators for participating in multiple qualifying educational activities. Honored Educators are invested in furthering the profession of radiology by delivering high-quality educational content in their field of study. Learn how you can become an honored educator by visiting the website at: https://www.rsna.org/Honored-Educator-Award/ Christine O. Menias, MD - 2013 Honored EducatorChristine O. Menias, MD - 2014 Honored EducatorChristine O. Menias, MD - 2015 Honored EducatorChristine O. Menias, MD - 2016 Honored EducatorChristine O. Menias, MD - 2018 Honored Educator



## MI204-SD-SUB1

Radiolabeled Monoclonal Antibody BC8: Differences in Biodistribution and Dosimetry Among Hematologic Malignancies

Sunday, Nov. 25 1:00PM - 1:30PM Room: MI Community, Learning Center Station #1

FDA Discussions may include off-label uses.

### Participants

Manuela C. Matesan, MD, PhD, Seattle, WA (*Presenter*) Nothing to Disclose Darrell Fisher, Richland, WA (*Abstract Co-Author*) Nothing to Disclose Roger Wong, PhD, Seattle, WA (*Abstract Co-Author*) Nothing to Disclose Oliver Press, Seattle, WA (*Abstract Co-Author*) Nothing to Disclose John Pagel, Seattle, WA (*Abstract Co-Author*) Nothing to Disclose Brenda Sandmaier, Seattle, WA (*Abstract Co-Author*) Nothing to Disclose Ryan Cassaday, Seattle, WA (*Abstract Co-Author*) Nothing to Disclose Damian Green, Seattle, WA (*Abstract Co-Author*) Nothing to Disclose William Bensinger, Seattle, WA (*Abstract Co-Author*) Nothing to Disclose Ajay K. Gopal, MD, Seattle, WA (*Abstract Co-Author*) Nothing to Disclose Joseph G. Rajendran, MBBS, Seattle, WA (*Abstract Co-Author*) Nothing to Disclose

For information about this presentation, contact:

mmatesan@uw.edu

# PURPOSE

We reviewed differences in biodistribution and dosimetry among hematologic malignancies on 111In-DOTA-anti-CD45 (BC8) imaging and bone marrow (BM) biopsy measurements.

## **METHOD AND MATERIALS**

Whole-body images were obtained immediately post-infusion of 111In-DOTA-BC8 (176-406 MBq) and then daily for three days using a Philips BrightviewXCT camera in 52 patients with malignancies (lymphoma, multiple myeloma, acute myelogenous leukemia and myelodysplastic syndrome). Median age was 55 (range:26-76). Regions of interest were drawn for spleen, liver, kidneys, testicles (in males) and two marrow sites (acetabulum and sacrum) using anterior and posterior planar images. Correction for attenuation and background was made using a standard and organ volumes. BM biopsy was obtained 14-24 hours post-infusion, adjusting for weight, and counting standard to calculate percent injected dose. Time-activity curves for major organs were integrated and absorbed doses calculated using MIRDS methods.

## RESULTS

Initial uptake(IU) of 111In-labeled-BC8 in the liver averaged  $32\% \pm 8.4\%$  of administered activity (52 patients) clearing monoexponentially with a biological half-time (CHT) of  $293 \pm 157$  hours (33 patients) or to infinity (19 patients). Spleen IU averaged  $22\% \pm 12\%$  and a CHT of  $271 \pm 185$  hours (36 patients) or longer (6 patients); kidney IU was  $2.4\% \pm 2.0\%$  and CHT of  $243 \pm 144$ hours (27 patients) or longer (9 patients); red marrow IU was  $23\% \pm 11\%$  and CHT of  $215 \pm 107$  hours (43 patients) or longer (5 patients). Whole-body retention half-times averaged  $198 \pm 75$  hours. Splenic uptake was higher in leukemia/MDS group when compared to lymphoma group (p<= 0.05) and multiple myeloma group (p<= 0.1). No significant differences between the three groups for liver IU. Extrapolating In111-DOTA-BC8 data, estimated average radiation absorbed doses per unit radioactivity were: marrow  $12.8 \pm 7$  cGy/mCi, liver  $29.7 \pm 8.95$  cGy/mCi, spleen 111.  $3 \pm 52.8$  cGy/mCi, total body  $2.02 \pm 0.53$  cGy/mCi, osteogenic cells 7.77  $\pm 5.4$  cGy/mCi, and kidneys  $6.4 \pm 5.5$  cGy/mCi.

#### CONCLUSION

111In-DOTA-BC8 was retained longer in liver, spleen, kidneys, and red marrow, with the highest doses being estimated for spleen and liver. Higher splenic uptake was observed for leukemia/MDS group when compared to lymphoma and multiple myeloma groups.

## **CLINICAL RELEVANCE/APPLICATION**

For 90Y- DOTA-BC8 therapy, pre-therapy scan can predicts biodistribution of 90Y- DOTA-BC8 and the dose-limiting organ.



## MI205-SD-SUB2

Ex-vivo Monitoring of Hyperpolarized [1-<sup>13</sup>C] Pyruvate Metabolism in Human Breast Cancer Xenograft Tumor Slices

Sunday, Nov. 25 1:00PM - 1:30PM Room: MI Community, Learning Center Station #2

## Participants

Adina Y. Adler Levy, MD, Jerusalem, Israel (*Abstract Co-Author*) Nothing to Disclose Atara Nardi-Schreiber, Jerusalem, Israel (*Abstract Co-Author*) Nothing to Disclose Talia Harris, Jerusalem, Israel (*Abstract Co-Author*) Nothing to Disclose Siva Ranjan Uppala, Jerusalem, Israel (*Abstract Co-Author*) Nothing to Disclose Gal Sapir, Jerusalem, Israel (*Abstract Co-Author*) Nothing to Disclose Ayelet Gamliel, Jerusalem, Israel (*Abstract Co-Author*) Nothing to Disclose Assad Azar, Jerusalem, Israel (*Abstract Co-Author*) Nothing to Disclose Nahum Goldberg, Jerusalem, Israel (*Abstract Co-Author*) Nothing to Disclose Jacob Sosna, MD, Jerusalem, Israel (*Abstract Co-Author*) Nothing to Disclose Svetlana Gourovich, BSC, Jerusalem, Israel (*Abstract Co-Author*) Nothing to Disclose John M. Gomori, MD, Jerusalem, Israel (*Abstract Co-Author*) Nothing to Disclose

### For information about this presentation, contact:

ayal@hadassah.org.il

## PURPOSE

In this study we aimed to assess the feasibility of visualizing and quantifying pyruvate metabolism in isolated viable xenograft breast tumor tissue using hyperpolarized [1-13C]pyruvate

## **METHOD AND MATERIALS**

Five hundred µm slices were produced from MCF-7 breast cancer xenograft tumors (*ca.* 0.7-1 cm3) grown in immunosuppressed mice. The slices were kept in an NMR tube in a 5.8 T NMR spectrometer, preserving their vitality using a continuous, oxygenated, temperature-controlled perfusion system. ATP levels were monitored by 31P-NMR and confirmed the viability of the tissue. Hyperpolarized [1-13C]pyruvate was injected to the NMR tube containing the slices and metabolism was monitored by 13C NMR. Conversion of hyperpolarized [1-13C]pyruvate to [1-13C]lactate informed on the activity of Lactate Dehydrogenase (LDH). Dissolution dynamic nuclear polarization (dDNP) was performed using a commercial dDNP system. Determination of the T1 of the hyperpolarized sites and the reaction rates were performed using a previously developed kinetic model (Allouche-Arnon, NMR Biomed 2014).

### RESULTS

Observed ATP levels showed consistent tissue viability throughout the course of each experiment for *ca.* 8 h. Hyperpolarized [1-13C]lactate production was observed in all of the hyperpolarized [1-13C]pyruvate injections. The rate of lactate production in the perfused slices of MCF-7 tumors was found to be  $1.65 \pm 0.07 \times 10-4$  1/s (3 injections performed on two different samples, on 2 different experimental days, each sample was composed of 3 tumors obtained from 3 different mice). The average T1 values for [1-13C]pyruvate and [1-13C]lactate were found to be  $59 \pm 8$  s and  $20 \pm 2$  s, respectively.

## CONCLUSION

Maintaining tissue vitality of MCF-7 xenograft tumor slices ex-vivo for several hours within an NMR spectrometer is feasible. Observing real time tumor metabolism in a hyperpolarized state and quantifying it with a radiation-free metabolic tracer is feasible. This system can provide the means to assess, ex-vivo, metabolic rates exclusive to a tissue of interest and represents an important milestone in translational research using hyperpolarized substrates.

### **CLINICAL RELEVANCE/APPLICATION**

Functional specific tumor metabolic information can be derived ex-vivo, potentially aiding patient tailored treatment decision making, as well as characterizing tumor tissues.

#### **Honored Educators**

Presenters or authors on this event have been recognized as RSNA Honored Educators for participating in multiple qualifying educational activities. Honored Educators are invested in furthering the profession of radiology by delivering high-quality educational content in their field of study. Learn how you can become an honored educator by visiting the website at: https://www.rsna.org/Honored-Educator-Award/ Jacob Sosna, MD - 2012 Honored Educator



## MI206-SD-SUB3

DWI with FASE Sequence at a 3T System vs. DWIs with EPI Sequence at 1.5T and 3T Systems vs. FDG-PET/CT: Quantitative Capability for Differentiating Malignant from Benign Solitary Pulmonary Nodules

Sunday, Nov. 25 1:00PM - 1:30PM Room: MI Community, Learning Center Station #3

## Participants

Yoshiharu Ohno, MD, PhD, Kobe, Japan (*Presenter*) Research Grant, Canon Medical Systems Corporation; Research Grant, Koninklijke Philips NV; Research Grant, Bayer AG; Research Grant, DAIICHI SANKYO Group; Research Grant, Fuji Pharma Co, Ltd; Research Grant, Guerbet SA;

Masao Yui, Otawara, Japan (Abstract Co-Author) Employee, Canon Medical Systems Corporation

Ho Yun Lee, MD, Seoul, Korea, Republic Of (Abstract Co-Author) Nothing to Disclose

Yuji Kishida, MD,PhD, Kobe, Japan (Abstract Co-Author) Nothing to Disclose

Shinichiro Seki, Kobe, Japan (Abstract Co-Author) Research Grant, Canon Medical Systems Corporation

Takeshi Yoshikawa, MD, Kobe, Japan (Abstract Co-Author) Research Grant, Canon Medical Systems Corporation

Hisanobu Koyama, MD, PhD, Osaka, Japan (Abstract Co-Author) Nothing to Disclose

Katsusuke Kyotani, RT, MSc, Kobe, Japan (Abstract Co-Author) Nothing to Disclose

- Yoshimori Kassai, MS, Otawara, Japan (Abstract Co-Author) Employee, Canon Medical Systems Corporation
- Takamichi Murakami, MD, PhD, Osakasayama, Japan (Abstract Co-Author) Nothing to Disclose

## For information about this presentation, contact:

yosirad@kobe-u.ac.jp

## PURPOSE

To directly and prospectively compare the quantitative capability for diagnosis of solitary pulmonary nodules (SPNs) among diffusion-weighted imagings (DWIs) with fast advanced spin-echo (FASE) and echo planar imaging (EPI) sequences at a 3T system, DWI with EPI sequence at a 1.5T system and FDG-PET/CT.

## METHOD AND MATERIALS

97 consecutive patients (52 men and 35 women; mean age 70 year old) with 129 SPNs underwent DWIs with FASE and/ or EPI sequences at 3T and 1.5T systems, FDG-PET/CT, and pathological and/or follow-up examinations. According to final diagnoses, all SPNs were divided into malignant (n=87) and benign (n=42) SPNs. In each lesion, apparent diffusion coefficients (ADCs) from all DWIs (ADC3TFASE, ADC3TEPI and ADC1.5TEPI) and SUVmax were assessed by ROI measurements. To compare all indexes between two groups, Student's t-test was performed. Then, ROC analyses were performed to compare diagnostic performance among all indexes. Finally, sensitivity, specificity and accuracy were compared among all methods by McNemar's test.

### RESULTS

There were significant difference of all indexes between two SPN groups (p<0.0001). ROC analyses showed area under the curve (Az) of ADC3TFASE (Az=0.90) was significantly larger than that of others (ADC1.5TEPI: Az=0.85, p=0.02; ADC3TEPI: Az=0.83, p=0.01; SUVmax (Az=0.76, p=0.003). Accuracy (AC) of ADC3TFASE (90.7 [117/129] %) was significantly higher than that of others (ADC1.5TEPI: 84.4 [109/129] %, p=0.008; ADC3TEPI: 82.9 [107/129] %, p=0.002; SUVmax: 75.2 [97/129] %, p<0.0001). In addition, accuracy of each ADC with EPI was significantly higher than that of SUVmax (ADC1.5TEPI: p=0.008, ADC3TEPI: p=0.002). Specificity of ADC3TFASE (90.5 [38/42] %) was also significantly higher than that of ADC1.5TEPI (76.2 [32/42] %, p=0.03) and ADC3TEPI (71.4 [30/42] %, p=0.008). Moreover, sensitivity of ADC3TFASE (90.8 [79/87] %) was significantly higher than that of SUVmax (SE: 73.6 [64/87] %, p<0.0001).

## CONCLUSION

DWI with FASE sequence has a better potential for quantitative diagnosis of SPNs than DWIs with EPI sequence at 1.5T and 3T systems and FDG-PET/CT. FASE sequence would be better to be applied for DWI at 3T system to improve diagnostic performance of SPNs.

## **CLINICAL RELEVANCE/APPLICATION**

FASE sequence would be better to be applied for DWI at 3T system to improve diagnostic performance of SPNs.



### MK343-ED-SUB6

## Soft Tissue Calcification - An Interactive Pictorial Quiz

Sunday, Nov. 25 1:00PM - 1:30PM Room: MK Community, Learning Center Station #6

### Awards Certificate of Merit

### **Participants**

Nikola Tomanovic, MBBS, Brighton, United Kingdom (*Presenter*) Nothing to Disclose Thomas Puttick I, MBBS, Reading, United Kingdom (*Abstract Co-Author*) Nothing to Disclose James S. Kho, MBBCh, Brighton, United Kingdom (*Abstract Co-Author*) Nothing to Disclose Ahmed Daghir, MRCP, FRCR, Oxford, United Kingdom (*Abstract Co-Author*) Nothing to Disclose David Yu, MBBS, Nottingham, United Kingdom (*Abstract Co-Author*) Nothing to Disclose

### For information about this presentation, contact:

nikola.tomanovic@bsuh.nhs.uk

## **TEACHING POINTS**

Soft tissue calcifications may be an unspecific local response or present as a symptom of a complex underlying disease. As such, they are commonly seen but often misinterpreted, leading to delayed diagnosis or unnecessary overinvestigation. We present a pictorial quiz composed of a wide range of well selected cases, of varying complexity, collected from a university teaching hospital and aim to:- Demonstrate important, interesting and unusual imaging appearances.- Discuss key learning points, further imaging and differential diagnostic considerations, including imaging pitfalls.- Help participants create a robust systematic approach to reporting similar cases, in order to optimise their diagnostic accuracy and streamline patient pathways.

## TABLE OF CONTENTS/OUTLINE

Amongst many others our cases include: Peri-articular Calcifications including: Chondrocalcinosis (gout, pseudogout, CPPD & hyperparathyroidism) Tumoral calcinosis (primary & secondary) Synovial Osteochondromatosis Calcific TendinopathySystemic SclerosisSynovial SarcomaNon-articular Ossification including:Neurogenic Heterotopic Ossification after CVA Fibrodysplasia Ossificans ProgressivaSecondary to Renal Failure Calcinosis Universalis Vascular Calcifications inc. Chronic Venous Insufficiency Trauma related calcification, inc. Myositis Ossificans



## MK351-SD-SUB1

## Rapidly Progressive Osteoarthropathy of the Hip: A Study of 1471 Patients After Steroid Injection

Sunday, Nov. 25 1:00PM - 1:30PM Room: MK Community, Learning Center Station #1

#### **Participants**

Andrew Wong, MD,MS, Sacramento, CA (*Presenter*) Nothing to Disclose Lawrence Yao, MD, Bethesda, MD (*Abstract Co-Author*) Nothing to Disclose John P. Meehan, MD, Sacramento, CA (*Abstract Co-Author*) Nothing to Disclose Lorenzo Nardo, MD, sacrameto, CA (*Abstract Co-Author*) Nothing to Disclose Joel S. Newman, MD, Boston, MA (*Abstract Co-Author*) Consultant, Pfizer Inc Robert D. Boutin, MD, Davis, CA (*Abstract Co-Author*) Nothing to Disclose

#### For information about this presentation, contact:

aluwong@ucdavis.edu

## PURPOSE

Rapidly progressive osteoarthropathy of the hip (RPOH) is defined by progressive joint space narrowing (JSN) of > 2 mm or > 50% within 1 year. Our aims were to assess the incidence of RPOH after steroid injection, and to investigate the association of RPOH with possible risk factors including: (1) more concentrated anesthetic/steroid mixtures, (2) low bone mineral density, and (3) greater pain reduction after injection.

### **METHOD AND MATERIALS**

After institutional review board approval, a retrospective search of our imaging database was performed, identifying 1471 patients who underwent a fluoroscopically-guided hip injection with triamcinolone acetonide (Kenalog) over a 10-year period ending March 1, 2017. Patients were eligible if they had radiographs at baseline and at least 1 year after injection. Patient demographics, hip DXA results, intra-articular injection data, and patient reported pain scores were gathered from patient records. Pre-injection and follow-up radiographs were systematically assessed for: JSN, femoral head deformity, osteophytes, acetabular/femoral cystic changes, femoral head ascension, and subchondral sclerosis. These radiographic parameters were used to grade osteoarthritis of the hip according to Croft criteria. Statistical analysis included Pearson's chi-square, Mann Whitney and T-tests, with significance defined as p<0.05.

## RESULTS

106 of 1471 injected subjects (7.2%) met the criteria for RPOH. A control group of 229 subjects was randomly selected from injected subjects without RPOH. Compared to controls, patients with RPOH were significantly older (p=0.005), had narrower joint spaces at baseline (p<0.001), and higher Croft scores (p=0.007). Patients who developed RPOH did not differ from controls in sex, BMI, hip DXA T-score, injected steroid dose, injected anesthetic concentration, or post injection pain improvement.

#### CONCLUSION

In our experience approximately 7% of patients undergoing steroid hip injection developed RPOH. More severe osteoarthritis, greater joint space narrowing, and patient age may be risk factors for development of RPOH after intra-articular steroid injection.

### **CLINICAL RELEVANCE/APPLICATION**

RPOA is uncommon, but not rare after hip steroid injection. Obesity, osteoporosis, and a higher injected steroid dose do not appear to increase the risk for RPOH.



## MK352-SD-SUB2

Whole Body MRI for Breast Cancer Staging: The Roles of the Static Field Strength and Gadolinium Contrast Agents in Focus

Sunday, Nov. 25 1:00PM - 1:30PM Room: MK Community, Learning Center Station #2

## Participants

Anne- Kathrin Wagner, Nordhausen, Germany (*Presenter*) Nothing to Disclose Arnhild Kott, MD, Nordhausen, Germany (*Abstract Co-Author*) Nothing to Disclose Claudia Kurrat, MD, Nordhausen, Germany (*Abstract Co-Author*) Nothing to Disclose Joachim Feger, MD, Nordhausen, Germany (*Abstract Co-Author*) Nothing to Disclose Ulf K. Teichgraeber, MD, Jena, Germany (*Abstract Co-Author*) Research Consultant, W. L. Gore & Associates, Inc Research Consultant, Siemens AG Research Consultant, CeloNova BioSciences, Inc Research Consultant, General Electric Company Ansgar Malich, MD, Nordhausen, Germany (*Abstract Co-Author*) Nothing to Disclose Ismini Papageorgiou, PhD,MD, Nordhausen, Germany (*Abstract Co-Author*) Nothing to Disclose

#### For information about this presentation, contact:

ismini.papageorgiou@shk-ndh.de

#### PURPOSE

Whole- body magnetic resonance imaging (WB- MRI) is a powerful diagnostic tool for breast cancer staging, especially for the detection of bone metastasis. However there is a weak level of evidence concersning the role of higher static field strengths and contrast media application. In this study we compare the diagnostic efficacy of WB- MRI in different static field strengths, 1.5T and 3T. Moreover we investigate the necessity for gadolinium contrast agent application for the effective detection of breast cancer bone metastasis.

## METHOD AND MATERIALS

The study was retrospective for 855 patients scanned between 05/2007 and 08/2017. 345 patients were imaged at 1.5T and 510 at 3T static field strength (Philips Achieva or Ingenia) with a T1-w FFE and a STIR or a Dixon at the coronal level. In 431 patients we injected Gadoteridol (ProHance®) 0.1 mmol/kg. Clinical confirmation with skeletal scintigraphy or bioptic confirmation served as the ground truth.

## RESULTS

The sensitivity (SE) and specificity (SPE) for 1.5T was 98.34%/91.24% and the positive predictive value (PPV)/negative predictive value (NPV) was 86.03%/99%. A static field strength of 3T showed a SE/SPE 100%/92.81% and a PPV/NPV of 83.22%/100%. Binary logistic regression with Fisher's exact test revealed no significant difference between 1.5T and 3T WB-MRI (P 0.663, odds ratio 0.839). The SE/SPE of WM-MRI (merged 1.5T and 3T) without enhancement was 98.66% 91.60%, with PPV/NPV 86.54%/99.20%. Upon administration of ProHance, the SE/SPE shifted to 100%/92.83% and the PPV/NPV to 82.70%/100%. Binary logistic regression with Fisher's exact test returned no significant effect for ProHance (P 0.836, odds ratio 0.9).

#### CONCLUSION

WB-MRI is a highly specific and sensitive diagnostic tool for bone metastasis in breast cancer with equal diagnostic efficacy in static field strengths of 1.5T or 3T. Gadolinium can be omitted without affecting the diagnostic accuracy and should be spared only for problem-solving.

## **CLINICAL RELEVANCE/APPLICATION**

WB-MRI is a highly specific and sensitive diagnostic tool for bone metastasis in breast cancer. Gadolinium should be spared only for problem-solving.



## MK353-SD-SUB3

Microflow Imaging Technology of Ultrasound Examination for Diagnosis of Adhesive Capsulitis of the Shoulder

Sunday, Nov. 25 1:00PM - 1:30PM Room: MK Community, Learning Center Station #3

### Participants

Donghyun Kim, MD, Seoul, Korea, Republic Of (*Presenter*) Nothing to Disclose Jee Won Chai, MD, Seoul, Korea, Republic Of (*Abstract Co-Author*) Nothing to Disclose Yoon-Hee Choi, MD,PhD, Seoul, Korea, Republic Of (*Abstract Co-Author*) Nothing to Disclose Jina Park, MD, Seoul, Korea, Republic Of (*Abstract Co-Author*) Nothing to Disclose Seung Woo Cha, MD, Guri, Korea, Republic Of (*Abstract Co-Author*) Nothing to Disclose Joo Hee Lim, Seoul, Korea, Republic Of (*Abstract Co-Author*) Nothing to Disclose

### PURPOSE

The purpose of this study was to investigate whether Superb microvascular imaging (SMI), a new Doppler technique of ultrasonography (USG), correlate with clinical features in patients with adhesive capsulitis.

## METHOD AND MATERIALS

This retrospective study included 34 patients with adhesive capsulitis on only one side shoulder. In USG, we evaluated the blood flow in rotator interval, using SMI and conventional power Doppler imaging (PWI). For quantitative analysis of blood flow, we performed pixel count analysis of blood flow in SMI and PWI. We also evaluated echogenicity in rotator interval, and coracohumeral ligament thickness. These USG findings were correlated with pain intensity (resting, night, motion, worst), range of motion (forward flexion, abduction, external and internal rotation), and duration of symptom in patients of adhesive capsulitis. These USG findings were also measured on the normal shoulder and compared with the affected side.

#### RESULTS

Blood flow in SMI and PWI were associated with range of motion on external rotation (p = 0.003) and forward flexion (p = 0.001), night (p = 0.09) and worst pain intensity (p = 0.007). Wilcox signed ranks test showed the significant higher blood flow in SMI than PWI of adhesive capsulitis (721 vs. 419 pixels, p = 0.001). Blood flow in SMI and PWI of affected shoulder were significantly higher from the normal contralateral shoulder (742 vs. 82, and 459 vs. 23 pixels respectively, p < 0.001). Clinical features were not significant correlated with echogenicity in rotator interval, coracohumeral ligament thickness (p > 0.05).

## CONCLUSION

The blood flow measurement using SMI at rotator interval of adhesive capsulitis was more sensitive test compared to the conventional Doppler technique, and showed significant correlation with ROM and pain intensity. It could be a valuable ultrasonographic finding in the diagnosis of adhesive capsulitis.

## **CLINICAL RELEVANCE/APPLICATION**

The blood flow measurement using SMI at rotator interval of adhesive capsulitis is superior to PWI, could be helpful in diagnosis, and might be used as biomarker for treatment planning or monitoring of adhesive capsulitis.



## MK354-SD-SUB4

## Fat Fraction Variation in Vertebrae: A Potential Biomarker in Evaluation of Bone Marrow Health

Sunday, Nov. 25 1:00PM - 1:30PM Room: MK Community, Learning Center Station #4

#### **Participants**

Huiying Chen, Beijing, China (*Presenter*) Nothing to Disclose Huishu Yuan, Beijing, China (*Abstract Co-Author*) Nothing to Disclose Ning Lang, MD, Beijing, China (*Abstract Co-Author*) Nothing to Disclose

For information about this presentation, contact:

hychen1989@163.com

## PURPOSE

Marrow fat fraction(FF) is considered relevant with bone marrow health. In this study, we tried to figure out the distribution pattern of FF in separate vertebrae body(VB) and evaluate the possible influence factors.

## **METHOD AND MATERIALS**

Ninety-seven healthy volunteers (51females and 46 males, age ranging from 22 to 69 years old) were recruited in this study with written informal consent obtained. All the subjects underwent IDEAL IQ acquisition for L1-L5 vertebras on a 3.0T MR scanner (MR750, GE Healthcare, US). The vertebras were scanned on the axial plane respectively with 3mm slice thickness. The two slices adjacent to the endplates of each VB were removed to avoid volume effect, and the FF of each remaining slice was obtained by drawing a  $20 \times 20$ mm2 region of interest. A biomarker, Fat Fraction Variability Index(FFVI), newly elicited in this study, was computed according to the formula, FFcenter - FFmargin, where FFcenter referred to the FF of the vertebral center, and FFmargin referred to the average FF of two vertebral margins. The univariate analysis of variance was performed with FFVI set as the dependent variable, while the age groups (20-29, 30-39, 40-49, 50-59, and 60-69 years) and VB (L1 to L5) as the independent variables. P <0.05 was considered as statistical significance.

#### RESULTS

Both age and VB affected the dependent variables significantly (P<0.01), however, there was no interaction effect between VB and age. FFVI of L1-L5 VB commonly started with a positive value in 20s and gradually converted to negative values with aging, indicating the FF distribution pattern converted from 'center higher' to 'margin higher' with age growth(Figure.1). Such transformation initially started at L1 and L2, then L4 and L5, and eventually, L3. In addition, FF increasing L5>L1 in the same subjects and FF increasing with aging was also shown in this study.

## CONCLUSION

In lumbar spine, L1 and L2 vertebras demonstrated lower FF level but with more common 'margin higher' FF distribution pattern comparing to other vertebras, which might be related to stress and activities of the vertebras. Considering that compression fracture is also more commonly observed in L1, L2 vertebras, we suggested that FFVI indicate certain skeletal remodeling that affects bone strength.

### **CLINICAL RELEVANCE/APPLICATION**

FFVI may be a promising indicator in assessing prevalent fracture besides the increased average FF of the whole vertebral body.



### MK355-SD-SUB5

Painful Type II Navicular Os: MRI Findings and Classification

Sunday, Nov. 25 1:00PM - 1:30PM Room: MK Community, Learning Center Station #5

#### **Participants**

Jeffrey A. Belair, MD, Philadelphia, PA (*Presenter*) Nothing to Disclose Tarek Hegazi, MBBS, Philadelphia, PA (*Abstract Co-Author*) Nothing to Disclose Adam C. Zoga, MD, Philadelphia, PA (*Abstract Co-Author*) Nothing to Disclose William B. Morrison, MD, Philadelphia, PA (*Abstract Co-Author*) Consultant, AprioMed AB; Patent agreement, AprioMed AB; Consultant, Zimmer Biomet Holdings, Inc; Consultant, Samsung Electronics Co, Ltd; Consultant, Medical Metrics, Inc Johannes B. Roedl, MD, PhD, Philadelphia, PA (*Abstract Co-Author*) Nothing to Disclose Vishal Desai, MD, Philadelphia, PA (*Abstract Co-Author*) Nothing to Disclose

#### For information about this presentation, contact:

jeffrey.belair@jefferson.edu

## PURPOSE

To examine the imaging patterns and severity of osseous stress response at the partially-stable type II navicular os, a cause of medial foot pain.

## **METHOD AND MATERIALS**

From a PACS database of all foot/ankle MRI examinations acquired at our institution over a 5-year period, a report search was performed yielding cases of type II navicular os with bone marrow edema (BME) spanning the synchondrosis. Cases in which there were other potential causes of medial foot pain were excluded from the study. After eliminating confounded cases, 40 lower extremity MRI examinations in 39 subjects were identified with positive findings. Cases were reviewed by 2 MSK radiologists blinded to clinical history, in consensus, graded on an ordinal scale for extent of BME (1 = mild/patchy immediately adjacent to the synchondrosis; 2 = intermediate, within both the os and navicular tuberosity; 3 = extensive, extending to the navicular body). Associated posterior tibial tendon (PTT) pathology was also recorded. Demographics and clinical history (including antecedent trauma and sports activities) were logged, along with duration of symptoms. Baseline MRI incidence rate of type II navicular os was established by performing an age-matched control review of all foot/ankle MRIs performed over the past 5 years.

## RESULTS

Of the subjects, 39/39 (100%) reported medial foot pain. M/F was 11/28 (28%/72%) and mean age was 27.6 years. BME was grade 1 in 17/40 MRIs (43%), grade 2 in 11/40 (28%) and grade 3 in 12/40 (30%). Mean duration of symptoms prior to MRI was 10.2 months (1 day-5 yrs). 20/39 subjects (50%) reported antecedent trauma and 31/39 (77%) reported actively participating in sports. PTT tenosynovitis and tendinosis were present in 92% and 60% of cases, respectively. Age-matched control MRI incidence of type II navicular os was 3.1%.

## CONCLUSION

BME spanning a type II navicular os on MRI highly correlates with medial foot pain, likely accounting for patient symptoms. We hypothesize that in such patients, a history of antecedent trauma or repetitive sports activity likely destabilizes the synchondrosis, causing the os to become symptomatic. Grading degree of BME may be useful to referrers for predicting patient outcomes and making treatment decisions.

# **CLINICAL RELEVANCE/APPLICATION**

BME associated with a type II navicular os strongly correlates with medial foot pain. Accurately grading degree of BME on MRI may be useful to referring clinicians.



## MS181-ED-SUB1

## Quantitative Ultrasound: A Primer for Radiologists

Sunday, Nov. 25 1:00PM - 1:30PM Room: MS Community, Learning Center Station #1

## Participants

Pol Grasland-Mongrain, Montreal, QC (Presenter) Nothing to Disclose

Francois Destrempes, PhD, Montreal, QC (Abstract Co-Author) Nothing to Disclose

Nathalie J. Bureau, MD, MSc, Montreal, QC (Abstract Co-Author) Research Grant, Siemens AG

Isabelle Trop, MD, MPH, Montreal, QC (*Abstract Co-Author*) Nothing to Disclose Gilles P. Soulez, MD, Montreal, QC (*Abstract Co-Author*) Speaker, Bracco Group Speaker, Siemens AG Research Grant, Siemens AG Research Grant, Bracco Group Research Grant, Cook Group Incorporated Research Grant, Object Research Systems Inc

Guy Cloutier, PhD, Montreal, QC (Abstract Co-Author) Nothing to Disclose

An Tang, MD, Montreal, QC (Abstract Co-Author) Research Consultant, Imagia Cybernetics Inc; Speaker, Siemens AG; Speaker, Eli Lilly and Company

### For information about this presentation, contact:

an.tang@umontreal.ca

### **TEACHING POINTS**

(1) To review the key concepts of quantitative ultrasound (QUS), an approach for measurement of tissue properties using ultrasound; (2) To illustrate clinical applications of QUS techniques in different organ systems; and (3) To summarize the diagnostic performance of emerging clinical applications of QUS techniques.

## **TABLE OF CONTENTS/OUTLINE**

-Clinical applications: early disease detection, tissue characterization, classification, and monitoring of treatment response.-Illustration of key concepts of QUS: body waves (compression and shear), wave properties (amplitude, frequency, speed), speckle, and power spectrum.-Examples of QUS techniques: natural pulsation elastography (measurement of strain and shear strain), shear wave elastography, spectral analysis (including measurement of total or local attenuation), statistics of echo envelope (including Khomodyned analysis). - Illustration of emerging QUS clinical applications: characterization of carotid plaque, thyroid nodules, breast lesions, chronic liver disease (liver fat, inflammation, and fibrosis), prostate lesions, and musculoskeletal disease.-Technical assumptions: mathematical and physical models for body waves and tissue. - Future directions: standardization, validation, calibration.

#### Honored Educators

Presenters or authors on this event have been recognized as RSNA Honored Educators for participating in multiple gualifying educational activities. Honored Educators are invested in furthering the profession of radiology by delivering high-quality educational content in their field of study. Learn how you can become an honored educator by visiting the website at: https://www.rsna.org/Honored-Educator-Award/ An Tang, MD - 2018 Honored EducatorIsabelle Trop, MD, MPH - 2014 Honored Educator



## NM141-ED-SUB5

## Oncologic Applications of 18F-Fluorodopa: Current Concepts on a Case-Based Approach

Sunday, Nov. 25 1:00PM - 1:30PM Room: NM Community, Learning Center Station #5

FDA Discussions may include off-label uses

#### **Participants**

Ricardo Martinez Martinez, MD, Mexico City, Mexico (*Presenter*) Nothing to Disclose Belen Rivera Bravo, MD, Mexico City, Mexico (*Abstract Co-Author*) Nothing to Disclose Ailan H. Barrientos-Priego, MD, Mexico, Mexico (*Abstract Co-Author*) Nothing to Disclose Berta Riveros Gilardi, MD, Mexico City, Mexico (*Abstract Co-Author*) Nothing to Disclose Oralia C. Rico Rodriguez, MD, PhD, Mexico City, Mexico (*Abstract Co-Author*) Nothing to Disclose Antonio Hernandez Villegas, MD, Mexico City, Mexico (*Abstract Co-Author*) Nothing to Disclose Jorge Luis Valencia Vazquez, Tlalpan, Mexico (*Abstract Co-Author*) Nothing to Disclose

### For information about this presentation, contact:

rmm\_07@hotmail.com

## **TEACHING POINTS**

To understand the mechanism of 18F-Fluorodopa uptake at molecular level. To review the acquisition protocol for 18F-Fluorodopa PET/CT with an oncological diagnosis purpose. To get acquainted with the normal biodistribution of the 18F-Fluorodopa. To recognize the utility of 18F-Fluorodopa PET/CT in the field of oncology with case examples.

#### **TABLE OF CONTENTS/OUTLINE**

1. 18F-Fluorodopa: Characteristics and Mechanism of Uptake. 2. 18F-Fluorodopa PET/CT: The Acquisition Protocol and Dosimetry for Oncological Diagnosis Purpose. 3. 18F-Fluorodopa: Normal Metabolism and Biodistribution. 4. The Role of 18F-Fluorodopa PET/CT Assessing Certain Types of Solid Malignant Tumors: When to request it?



## NM204-SD-SUB1

Global Analysis of FDG and PiB PET and the Assessment of Joint FDG+PIB Image Analysis of 107 Deceased Dementia Patients in Comparison to Their Autopsy-Verified Diagnoses

Sunday, Nov. 25 1:00PM - 1:30PM Room: NM Community, Learning Center Station #1

FDA Discussions may include off-label uses.

#### **Participants**

Jon J. Camp, PhD, Rochester, MN (*Abstract Co-Author*) Royalties, AnalyzeDirect, Inc Val J. Lowe, MD, Rochester, MN (*Presenter*) Research Grant, General Electric Company; Research Grant, Siemens AG; Research Grant, Eli Lilly and Company; Advisory Board, Merck & Co, Inc Brad Kemp, PhD, Rochester, MN (*Abstract Co-Author*) Nothing to Disclose

#### PURPOSE

Analyze the FDG and PiB pet scans of 107 deceased dementia patients in a population study in comparison to their autopsy-verified findings.

### **METHOD AND MATERIALS**

The PET images are rigidly co-registered to an MRI image of the patient, and the combined images registered affinely to a regional brain atlas. We determined the FDG ratio (FDGr) by normalizing the FDG images by the mean FDG value in the pons and the PiB ratio (PiBr) by normalizing the PiB images by the mean PiB value in the cerebellum, as "global" measures by averaging a (different) set of crucial regions for each tracer. Two additional global measures are also derived from the joint FDG/PiB histogram, the r2 value from a linear regression between the FDG and PiB, and the FDG-Associated PiB Uptake Ratio (FAPUR). Imaging data was compared to pathologic findings of senile change (SC, Braak NFT stage of < 3, with no neuritic plaques), Pathological Aging (PA, Braak NFT stage of < 3, with no more than sparse neuritic plaques), early-onset AD, and AD.

### RESULTS

We found that for FDGr and autopsy the AD group was significantly different (p < 0.0001) from the Pathological Aging (PA, Braak NFT stage of < 3, with no more than sparse neuritic plaques) group. We found that for PiBr the PA group was significantly different (p < 0.001) from both the AD and early-onset AD groups. We found that for the r2 value from a linear regression between the FDG and PiB pixel values the SC group was significantly different (p < 0.0001) from both the AD and early-onset AD groups. For FAPUR we found the PA group was significantly different (p < 0.0001) from the early-onset AD group.

## CONCLUSION

FDG and PiB quantitative measurements can predict neuropathologic findings at autopsy in a population-based, prospective cohort. Joint FDG and PiB histogram evaluation and FAPUR evaluation provide single value assessments that combine the data from the two PET exams into a single measurement that also can predict neuropathologic findings.

## **CLINICAL RELEVANCE/APPLICATION**

Quantified FDG and PiB PET can predict autopsy pathology findings.



## NM205-SD-SUB2

68Ga-Labelled PSMA-11 PET/CT in Prostate Cancer Patients for Primary Staging and Localization of Biochemical Relapse

Sunday, Nov. 25 1:00PM - 1:30PM Room: NM Community, Learning Center Station #2

**FDA** Discussions may include off-label uses.

### Participants

Liene Zemniece, MD, Tukums, Latvia (*Presenter*) Nothing to Disclose Maija Radzina, MD, PhD, Riga, Latvia (*Abstract Co-Author*) Nothing to Disclose Lilita Roznere, Riga, Latvia (*Abstract Co-Author*) Nothing to Disclose Mara Tirane, Riga, Latvia (*Abstract Co-Author*) Nothing to Disclose Egils Vjaters, Riga, Latvia (*Abstract Co-Author*) Nothing to Disclose Vilnis Lietuvietis, Riga, Latvia (*Abstract Co-Author*) Nothing to Disclose Arvis Freimanis, Riga, Latvia (*Abstract Co-Author*) Nothing to Disclose Marika Kalnina, Riga, Latvia (*Abstract Co-Author*) Nothing to Disclose

## PURPOSE

68Gallium-labelled prostate-specific membrane antigen positron emission tomography (68Ga-PSMA PET/CT) is a new diagnostic tool used for primary staging in a patients of prostate cancer (PC), mainly in a high risk disease, as well as to localize a recurrent PC in a biochemical relapse. The goal of this study is to define methods role in a clinical practice and to clarify a relations between prostate specific antigen (PSA) level and results of PET/CT.

## METHOD AND MATERIALS

Total 101 patients with histologically PC cancer underwent 68Ga-PSMA PET/CT. Scanning protocol included body scan 60 min after 68Ga-PSMA injection and, if necessary, the late phase or early phase scan. Maximal standard uptake value (SUVmax) of every lesion was measured. PSA level of each patient < 10 days prior PET/CT was measured. PSA level was compared with PET/CT results.

#### RESULTS

Total 101 PET/CT scans were performed, including 59 patients with biochemical relapse and 25 patients for primary staging. Recurrent spread of disease was diagnosed in 65% cases with 68Ga-PSMA uptake in prostate bed in 26% (n=15/57) cases, in regional lymph nodes (LN) in 37% cases (n=21/57) and distant metastases - 16% (n=9/57). In a primary staging group prior treatment of PC pathological 68Ga-PSMA uptake in prostate were diagnosed in 96% (n=24/25) cases, in additional, regional LN metastases revealed in 8% (n=2/25) and distant PSMA avid metastases revealed in 20% (n=5/20). 75% of all metastatic LN showed no pathological signs seen on CT (no structural changes, no enlargement), but confident high SUVmax value. Methods sensitivity and specificity at PSA level 0,50 ng/ml showed 89% and 71%, but at PSA 0,69 ng/ml reached 87% and 76%, respectively.

## CONCLUSION

68Ga-PSMA PET/CT plays an important role in PC staging and determining the location of recurrent PC in patients with biochemical relapse, it specially, diagnosing small metastatic LN, therefore this method gives clinical impact in patients further therapy planning. PC and its metastasis visualization capabilities with 68Ga-PSMA PET/CT is associated with PSA levels - with PSA above 0,5 ng/ml its reliable diagnostic method.

#### **CLINICAL RELEVANCE/APPLICATION**

Main goals using 68Ga-PSMA PET/CT is to localize a recurrent disease with low PSA values, when the methods clinical impact on a further treatment is crucial. 68Ga-PSMA PET/CT is very useful for primary staging in a high-risk disease, when suspicious of distant lesions is high.



## NM206-SD-SUB3

Acquisition Protocol Optimization for 68ga-PSMA PET/MR Studies Based on Image Quality and Lesion Detectability

Sunday, Nov. 25 1:00PM - 1:30PM Room: NM Community, Learning Center Station #3

## Participants

Taise Vitor, Sao Paulo, Brazil (*Abstract Co-Author*) Nothing to Disclose Karine M. Martins, MS, Sao Paulo, Brazil (*Abstract Co-Author*) Nothing to Disclose Marcelo L. Cunha, MD, Sao Paulo, Brazil (*Abstract Co-Author*) Nothing to Disclose Ronaldo H. Baroni, MD, Sao Paulo, Brazil (*Abstract Co-Author*) Nothing to Disclose Anna Maria Ringheim, MSc, BEng, Sao Paulo, Brazil (*Presenter*) Nothing to Disclose Jairo Wagner, MD, Sao Paulo, Brazil (*Abstract Co-Author*) Nothing to Disclose Guilherme Campos, Sao Paulo, Brazil (*Abstract Co-Author*) Nothing to Disclose

#### For information about this presentation, contact:

taise.vitor@einstein.br

## PURPOSE

68Ga labeled prostate-specific membrane antigen (PSMA) ligand PET/CT and PET/MR are promising modalities in primary staging and biochemical relapse assessment of prostate cancer (PCa) patients. Current acquisition protocols usually recommend whole body and/or pelvic images starting about 60 minutes after radiopharmaceutical administration. Although these late images ensure sufficient time for tracer concentration in the neoplastic tissue, progressive urinary bladder accumulation may impair imaging interpretation. The aim of this study was to determine the optimal imaging time for detection of primary prostate lesions.

## **METHOD AND MATERIALS**

12 patients were studied (mean age 65?±?4 years), with 17 biopsy-proven prostate cancer lesions analyzed. Pelvic images were acquired in list mode for 1 hour, starting immediately after radiopharmaceutical administration (2-4 MBq/kg of 68GaPSMA) in a hybrid PET/MR system. Whole body images were obtained afterwards. List mode data were further grouped into 4 static images (from 0-15, 15-30, 30-45 and 45-60 minutes). These static images were analyzed by 2 experienced nuclear medicine physicians and divergences were solved by consensus.

## RESULTS

The earliest images (0-15 minutes) showed a lower detectability rate (82.4%) compared with the other images starting at 15, 30 and 45 minutes (all showing a detectability rate of 94.1%). As expected, urinary bladder accumulation increased progressively, with moderate or marked activity in all images starting at 30 or 45 minutes. The detection failure in these images occurred due to the interference of urinary activity. The SUVmax value shows a tendency to increase with time, nevertheless, the difference was not significant (p>0,34).

## CONCLUSION

Despite the limitation due to the small number of patients, our study suggests that early PSMA images (15, 30 or 45 minutes) may benefit from less interference from urinary excretion, without impairment of detectability. Earlier images are also more convenient because they maximize radiopharmaceutical usage (reducing radioactive decay losses) and allow a shorter total examination time for the patient. Based on the data of this pilot study, we suggest that 15 minutes might be the ideal delay time for 68Ga PSMA in PET/MR; however, subsequent research is warranted to confirm the best acquisition time.

## **CLINICAL RELEVANCE/APPLICATION**

ACQUISITION PROTOCOL OPTIMIZATION FOR 68Ga-PSMA PET/MR STUDIES



## NM207-SD-SUB4

Global Metabolic Activity of the Rectus Abdominis Muscle with 18F-FDG-PET/CT: Emphysema Patients versus Control Subjects

Sunday, Nov. 25 1:00PM - 1:30PM Room: NM Community, Learning Center Station #4

## Participants

Esha S. Kothekar, MD, Philadelphia, PA (*Presenter*) Nothing to Disclose Abdullah Al-Zaghal, MD, Philadelphia, PA (*Abstract Co-Author*) Nothing to Disclose Pegah Jahangiri, MD, Philadelphia, PA (*Abstract Co-Author*) Nothing to Disclose Kamyar Pournazari, MD,MSc, Philadelphia, PA (*Abstract Co-Author*) Nothing to Disclose Leila S. Arani, MD, Philadelphia, PA (*Abstract Co-Author*) Nothing to Disclose Thomas J. Werner, Philadelphia, PA (*Abstract Co-Author*) Nothing to Disclose Poul Flemming Hoeilund Carlsen, Odense, Denmark (*Abstract Co-Author*) Nothing to Disclose Abass Alavi, MD, Philadelphia, PA (*Abstract Co-Author*) Nothing to Disclose

### For information about this presentation, contact:

esha.kothekar@uphs.upenn.edu

### PURPOSE

Emphysema and chronic bronchitis are main manifestations of chronic obstructive pulmonary disease (COPD). Emphysema is characterized by destruction of alveolar walls and permanent dilation of pulmonary airspaces, resulting in difficulty in the expiration of air. Patients with severe emphysema use respiratory muscles to actively expire air. The purpose of this study was to compare the metabolic activity of the rectus abdominis muscle as measured with 18F-FDG-PET/CT in emphysema patients compared to control subjects.

## **METHOD AND MATERIALS**

In this research study, we included 28 male patients diagnosed with emphysema and a history of heavy smoking (mean (SD) age 66.4±8.0 y, range 51-81), who underwent 18F-FDG-PET/CT imaging for suspected lung cancer, and 35 non-smoker control subjects (mean (SD) age 43.9±13.4 y, range 22-69). The rectus abdominis muscle was identified on fused PET/CT images and regions of interest were manually delineated on the muscle extending from the xiphoid process to the umbilicus using OsiriX MD software (Pixmeo SARL, Bernex, Switzerland). The metabolic activity of the rectus abdominis muscle was quantified using averaged SUVmean. Unpaired t-test was used to assess any difference in the metabolic activity between groups.

#### RESULTS

A statistically significant difference in the uptake of the rectus abdominis muscle was observed between the emphysema patients (average SUVmean= $0.68\pm0.26$ ) and controls (average SUVmean= $0.42\pm0.09$ ), p-value <0.0001.

## CONCLUSION

The rectus abdominis muscle in emphysema patients was observed to have higher metabolic activity than that of healthy controls. This observation is consistent with the known pathophysiology that patients with emphysema use their accessory respiratory muscles excessively to compensate for airway obstruction during the expiratory phase of ventilation. This may be the first actual documentation of hypermetabolism in these muscles.

## **CLINICAL RELEVANCE/APPLICATION**

We believe this methodology will be of great value in determining the efficacy of various therapeutic interventions in this patient population.



## NR331-ED-SUB7

Does this Brain Infection Get Better or Worse? Central Nervous System Immune Reconstitution Inflammatory Syndrome (CNS-IRIS) in Setting of HIV infection

Sunday, Nov. 25 1:00PM - 1:30PM Room: NR Community, Learning Center Station #7

#### Awards Certificate of Merit

#### **Participants**

Dan I. Cohen-Addad, MD, Brooklyn, NY (*Presenter*) Nothing to Disclose Arkadij Grigorian, MD, Brooklyn, NY (*Abstract Co-Author*) Nothing to Disclose Matthew Bobinski, MD, PhD, Sacramento, CA (*Abstract Co-Author*) Nothing to Disclose Vinodkumar Velayudhan, DO, Copiague, NY (*Abstract Co-Author*) Nothing to Disclose

## **TEACHING POINTS**

Review the pathophysiology of IRIS, its clinical and laboratory features. Describe key imaging features seen in IRIS and how they differ with different opportunistic infection. Learn an algorithm integrating imaging, laboratory and clinical finding facilitating the detection of IRIS.

## TABLE OF CONTENTS/OUTLINE

A series of different "pathogen"- IRIS cases will be presented in a quiz format. Classic imaging features of opportunistic infections affecting patients with HIV in pre-HAART era will be reviewed. IRIS cases will be compared to corresponding opportunistic infection (OI) cases without IRIS to highlight key differentiating features. Review of the pathophysiology, prevalence, risk factors, mortality and morbidity of IRIS along with important clinical and laboratory features. General imaging features suggestive of IRIS will be reviewed (Enhancement, increase FLAIR signal, mass effect and restricted diffusion). Specific CNS IRIS features due to specific OI will be reviewed (PML, cryptococcus, CMV, toxomplasmosis, tuberculosis/mycobacterial infection (including extracranial manifestations) and Candida). IRIS not associated with OI, such as HIVE-IRIS and Neuro-IRIS without coinfection is also discussed. Finally, an image-based algorithm is provided to summarize key concepts.



## NR332-ED-SUB8

Stain Your Brain: Neuropathology of Pediatric Brain Tumors

Sunday, Nov. 25 1:00PM - 1:30PM Room: NR Community, Learning Center Station #8

#### **Participants**

Duan Chen, MD, Bronx, NY (*Presenter*) Nothing to Disclose Sharon Gordon, MD, Bronx, NY (*Abstract Co-Author*) Nothing to Disclose Debra Rosenbaum, Jerusalem, Israel (*Abstract Co-Author*) Nothing to Disclose David Ginsburg, MD, Brooklyn, NY (*Abstract Co-Author*) Nothing to Disclose William Gomes, MD, PhD, Katonah, NY (*Abstract Co-Author*) Nothing to Disclose Sara B. Rosenbaum, MD, Bronx, NY (*Abstract Co-Author*) Nothing to Disclose Alex Levitt, MD, New York, NY (*Abstract Co-Author*) Nothing to Disclose Shira Slasky, MD, Tenafly, NJ (*Abstract Co-Author*) Nothing to Disclose Richard Zampolin, MD, Bronx, NY (*Abstract Co-Author*) Nothing to Disclose Judah Burns, MD, Bronx, NY (*Abstract Co-Author*) Nothing to Disclose

#### For information about this presentation, contact:

judahburns@gmail.com

## **TEACHING POINTS**

In the era or radiogenomics, understanding of the histopathologic lexicon is valuable to the clinically savvy radiologist. The purpose of this exhibit is: 1. Describe the various histochemical tools available to the neuropathologist and how these tools lead to diagnosis of specific pediatric brain tumors. 2. Illustrate diagnosis-specific imaging, histopathological and genetic features of CNS tumors in the pediatric population. 3. Elaborate a case-based review of pediatric brain tumors with imaging- pathology correlation.

## TABLE OF CONTENTS/OUTLINE

1. Neuropathology of pediatric brain tumors A. Illustration of the immunohistochemistry stains at the neuropathologist's disposal and selected histological features important to tumor identification and grading, including glial, neuronal, epithelial and proliferation markers. B. Common neuropathology 'buzzwords' such as Rosenthal fibers, sworls, palisades/pseudopalisades, rosettes/pseudorosettes and biphasic growth pattern will be defined. 2. Imaging Genomics in pediatric brain tumors. A. Pediatric-specific molecular/genetic characteristics integrated into the 2016 World Health Organization classification system of CNS tumors B. Review of imaging phenotypes typical of specific genetic tumor subtypes 3. Case-based review of pediatric brain tumors, including radiology-pathology correlation.



### NR333-ED-SUB9

## **DWI Beyond Stroke - Lesion Pattern Approach**

Sunday, Nov. 25 1:00PM - 1:30PM Room: NR Community, Learning Center Station #9

#### **Participants**

Joana R. De Figueiredo, MD, Sao Paulo, Brazil (*Presenter*) Nothing to Disclose Felipe T. Pacheco, MD, Sao Paulo, Brazil (*Abstract Co-Author*) Nothing to Disclose Renato Hoffmann Nunes, MD, Sao Paulo, Brazil (*Abstract Co-Author*) Nothing to Disclose Felipe Scortegagna SR, MD, Sao Paulo, Brazil (*Abstract Co-Author*) Nothing to Disclose Antonio J. da Rocha, MD, PhD, Sao Paulo, Brazil (*Abstract Co-Author*) Nothing to Disclose

## For information about this presentation, contact:

rayanefigueiredop@gmail.com

## **TEACHING POINTS**

The purpose of this exhibit is: 1.To discuss the applications and techniques of diffusion-weighted in magnetic resonance imaging of the brain. 2.To describe a series of cases and reviews the literature on cases of focal lesion on diffusion-weighted imaging to better appreciate the spectrum of disease associated with this neuroimaging finding.

## TABLE OF CONTENTS/OUTLINE

Diffusion-weighted magnetic resonance imaging of the brain: Applications and techniques. Present a series of cases and review the literature on focal and diffuse diffusion-weighted imaging abnormalities, demonstrating the distinct patterns and the broad differential diagnosis in this MR imaging finding. Indicate several strategic factors that should be considered in tailoring the radiologic work-up in order to distinguish between the myriad of nosological entitie.s Current series of focal lesions on DWI: - Transient Global Amnesia - Pyogenic Abscess - Acute necrotizing encephalopathy - Creutzfeldt-Jakob Disease - Autoimmune encephalopathy - Transient splenial lesion - Demyelinating Disease - Mitochondrial disorders - Acute necrotizing encephalopathy - Others Summary



### NR334-ED-SUB10

## Cranial Vault Lesions in Systemic Diseases: Should I Stay or Should I Go (Further)?

Sunday, Nov. 25 1:00PM - 1:30PM Room: NR Community, Learning Center Station #10

### **Participants**

Ana Paula A. Fonseca, MD, Sao Paulo, Brazil (*Presenter*) Nothing to Disclose Gabriel H. Bolsi, MD, Sao Paulo, Brazil (*Abstract Co-Author*) Nothing to Disclose Marcos Rosa Junior, PhD, Vitoria, Brazil (*Abstract Co-Author*) Nothing to Disclose Felipe T. Pacheco, MD, Sao Paulo, Brazil (*Abstract Co-Author*) Nothing to Disclose Renato H. Nunes, Sao Paulo, Brazil (*Abstract Co-Author*) Nothing to Disclose Antonio C. Maia Jr, Sao Paulo, Brazil (*Abstract Co-Author*) Nothing to Disclose Antonio J. da Rocha, MD, PhD, Sao Paulo, Brazil (*Abstract Co-Author*) Nothing to Disclose

#### For information about this presentation, contact:

anapaf.fonseca@gmail.com

# **TEACHING POINTS**

The purposes of this exhibit are: - Review and illustrate the anatomical aspects of cranial vault (CV); - Identify the main systemic disorders which may affect the CV, including endocrinologic, inflammatory, metabolic, infectious, tumor, vascular and hereditary disorders. - Highlight the imaging patterns of CV disorders, demonstrating the main characteristics of the lesion: single or multiple, focal or diffuse, lytic or sclerotic, enhancement, soft tissue invasion and associated findings. - Determine an algorithm for the systematic evaluation of differential diagnosis, emphasizing the main clinical tips and imaging red-flags. - Narrow down a list of hypotheses or even go further and suggest diagnostic possibilities to assist the requesting physician in deciding the best management and assuming the most appropriate therapeutic approach.

## **TABLE OF CONTENTS/OUTLINE**

- Anatomy of the cranial vault; - Patterns of involvement of cranial vault - Single or multiple, focal or diffuse, lytic or sclerotic, enhancement, soft tissue invasion and associated findings. - Differential diagnosis based on a pictorial review using representative cases from our institutional database - Endocrinologic - Inflammatory - Infections - Neoplasms - Vascular - Hereditary disorders -Diagnostic Algorithm - Final remarks



## NR368-SD-SUB1

## **Context-Guided Deep Learning Framework for Skull Stripping**

Sunday, Nov. 25 1:00PM - 1:30PM Room: NR Community, Learning Center Station #1

#### **Participants**

Mingxia Liu, Chapel Hill, NC (*Presenter*) Nothing to Disclose Jun Zhang, Chapel Hill, NC (*Abstract Co-Author*) Nothing to Disclose Chunfeng Lian, Chapel Hill, NC (*Abstract Co-Author*) Nothing to Disclose Dinggang Shen, Chapel Hill, NC (*Abstract Co-Author*) Nothing to Disclose

#### For information about this presentation, contact:

mingxia\_liu@med.unc.edu

### PURPOSE

While several skull stripping algorithms have been successfully applied to brain MRIs, most of them have numerical parameters, i.e., often requiring image-specific parameter tuning to obtain reasonable results. Also, existing methods have rarely used spatial context information (e.g., distance from each voxel to the skull boundary) contained in input images, while such context information plays an important role in performing robust and accurate skull stripping. In this work, we aim to devise a deep learning framework for skull stripping, by establishing a method that requires minimal to no parameter tuning in the application stage.

### **METHOD AND MATERIALS**

There are 359 subjects with MRI from the Calgary-Campinas-359 (CC-359) dataset used in this study. Twelve subjects with manual segmentation are used as test data, and the remaining ones are used as training data. We propose a context-guided deep encoder-decoder network (EDN) for skull stripping, as shown in Fig. 1. In the 1st stage, we model the spatial context of MRI via a distance map using EDN1 (see Fig. 1 top). Here, a distance map denotes a volume of the same size as the input image, with each element indicating the Euclidean distance from a voxel to its nearest skull boundary. In the 2nd stage network, we perform skull stripping using the distance map as guidance (i.e., as the additional input channel along with the original image) via EDN2 (see Fig. 1 bottom).

## RESULTS

In Fig. 2, we compare our method with Advanced Normalization Tools (ANTS), Brain Extraction based on non-local Segmentation Technique (BeaST), Brain Extraction Tool (BET), and Brain Surface Extractor (BSE), by using Dice coefficients to quantitatively measure the overlap between automatic and manual skull stripping results. Fig. 2 suggests that our method achieves better Dice coefficient than the four competing methods. Fig. 3 displays visual segmentation of our method for two subjects, indicating that our method can produce reasonable results compared to manual segmentation. Also, our method requires less than 3 seconds to perform skull stripping for each brain MRI.

## CONCLUSION

Our method is parameter-free in the application stage and performs accurate skull stripping quickly.

#### **CLINICAL RELEVANCE/APPLICATION**

(Dealing with skull stripping for brain MR images) 'Deep-learning-based techniques can quickly generate accurate results of skull stripping and is recommended in the quantitative studies of neuroimages.'



## NR369-SD-SUB2

## Prediction of Parkinson's Disease by Using Deep Learning 3D-Convolutional Neural Networks

Sunday, Nov. 25 1:00PM - 1:30PM Room: NR Community, Learning Center Station #2

#### **Participants**

Silun Wang, MD, PhD, Shenzhen, China (*Presenter*) Nothing to Disclose Sang Na, MS, Shenzhen, China (*Abstract Co-Author*) Nothing to Disclose Wanshun Wei, Shenzhen, China (*Abstract Co-Author*) Nothing to Disclose

## For information about this presentation, contact:

wangsilun@gmail.com

## PURPOSE

Parkinson's disease (PD) is one of the leading degenerative disorder that affects human's motor abilities. It's important to discriminate between healthy ones and patients for accurate diagnosis. In this study, we aimed to predict PD patients with a 3D convolutional neural network (3D-CNN). With deep learning and image preprocessing techniques, we could automatically identify the PD patients from normal ones.

## METHOD AND MATERIALS

Standard T1-weighted 3D MPRAGE MRI scan in the sagittal plane contain 161 PD patients (mean/SD=63.6/7.8 years) and 151 matched healthy controls (mean/SD=71.4/4.8 years) which were obtained from the Alzheimer's Disease Neuroimaging Initiative (ADNI) and Parkinson's Progression Markers Initiative (PPMI) database. All data were preprocessed by SPM12 (UCL, UK) to generate registered, normalized and smoothed images. Then, 80% patients and controls were recruited as training datasets and the others were regarded as testing samples. A 3D 7-layer CNN which contains 3 convolutional layers and 4 fully connected layers were constructed. The input to the network was preprocessed 3D images, and the output was the probability indicating whether it was patient or not.

#### RESULTS

This study showed the model with an accuracy of 97.5%, sensitivity of 98.6%, specificity of 96.5%, positive predictive value of 96.0% and negative predictive value of 98.8% by doing 5-fold validation. In addition, the Receiver Operating Characteristic (ROC) curve of our model showed an AUC value of 0.97. Therefore, the outcomes indicated that our 3D-CNN can accurately predict PD patients from normal ones.

### CONCLUSION

Deep learning models with 3D-CNN can accurately predict PD patients. Our model showed highly sensitivity and negative predictive value and thus appropriate for screening PD patients. Therefore, the current model has potential to be used as diagnostic criteria to investigate the neurodegeneration and associated brain diseases.

### **CLINICAL RELEVANCE/APPLICATION**

the current model has potential to be used as diagnostic criteria to investigate the neurodegeneration and associated brain diseases.



## NR370-SD-SUB3

Usefulness of Dual-Layer Spectral CT in Follow-Up Examinations: Diagnosing Recurrent Lesions of Head and Neck Squamous Cell Carcinomas

Sunday, Nov. 25 1:00PM - 1:30PM Room: NR Community, Learning Center Station #3

## Participants

Koji Takumi, MD,PhD, Boston, MA (*Presenter*) Nothing to Disclose Hiroto Hakamada, Kagoshima, Japan (*Abstract Co-Author*) Nothing to Disclose Hiroaki Nagano, MD, Kaogoshima, Japan (*Abstract Co-Author*) Nothing to Disclose Yoshihiko Fukukura, MD, PhD, Kagoshima, Japan (*Abstract Co-Author*) Nothing to Disclose Edward K. Sung, MD, Boston, MA (*Abstract Co-Author*) Nothing to Disclose Osamu Sakai, MD,PhD, Boston, MA (*Abstract Co-Author*) Consultant, Boston Imaging Core Lab, LLC Takashi Yoshiura, MD, PhD, Kagoshima, Japan (*Abstract Co-Author*) Nothing to Disclose

### PURPOSE

Dual-layer spectral CT (DLSCT) enables the simultaneous acquisition of low- and high-energy data and the dual-energy information is retrospectively available for every scan including follow up examination. The purpose of this study was to evaluate the usefulness of dual energy analyses using DLSCT for diagnosing recurrent lesions of head and neck squamous cell carcinomas (HNSCC).

### **METHOD AND MATERIALS**

The study population consisted of 60 patients with a history of HNSCC (17 patients with recurrent lesions and 43 with benign posttreatment changes). All patients were evaluated using dual energy CT analyses including virtual monochromatic images (VMIs) and iodine concentration (IC) maps. Contrast-to-noise ratio and visual score (lesion conspicuity and lesion boundary delineation) were compared between conventional 120kVp and 40keV VMIs using Wilcoxon signed-rank test. Attenuation value at 120kVp and 40keV images and IC were compared between recurrent lesions and posttreatment changes using Mann-Whitney U test. The receiver-operating characteristic (ROC) analysis was used to assess the ability of the attenuation values and IC to differentiate recurrent lesions from posttreatment changes.

## RESULTS

Contrast-to-noise ratio and visual score (lesion conspicuity and lesion boundary delineation) were significantly higher on 40keV than on conventional 120kVp images (p<0.001, p=0.002, and P<0.001, respectively). Recurrent lesions were significantly higher than posttreatment changes in attenuation value at 120kVp (p<0.001) and at 40 keV images (p<0.001), and IC (p<0.001). The AUCs were 0.859, 0.960, 0.943 for 120kVp image, 40keV image, and IC, respectively.

## CONCLUSION

Dual-energy images using DLSCT, especially 40keV VMIs and IC, may help diagnose recurrent lesions of HNSCC.

#### **CLINICAL RELEVANCE/APPLICATION**

Dual energy analyses using DLSCT can improve diagnostic performance in the recurrent lesions, and may have an impact on the posttreatment surveillance in patient with HNSCC.

### **Honored Educators**

Presenters or authors on this event have been recognized as RSNA Honored Educators for participating in multiple qualifying educational activities. Honored Educators are invested in furthering the profession of radiology by delivering high-quality educational content in their field of study. Learn how you can become an honored educator by visiting the website at: https://www.rsna.org/Honored-Educator-Award/ Osamu Sakai, MD,PhD - 2013 Honored EducatorOsamu Sakai, MD,PhD - 2014 Honored EducatorOsamu Sakai, MD,PhD - 2015 Honored Educator



## NR371-SD-SUB4

**Prospective Multiparametric US Evaluation of Parotid Gland Lesions** 

Sunday, Nov. 25 1:00PM - 1:30PM Room: NR Community, Learning Center Station #4

### Participants

Valeria de Soccio, JD, Rome, Italy (*Abstract Co-Author*) Nothing to Disclose Vito Cantisani, MD, Rome, Italy (*Abstract Co-Author*) Speaker, Canon Medical Systems Corporation; Speaker, Bracco Group; Speaker, Samsung Electronics Co, Ltd; Gregorio Alagna, Rome, Italy (*Abstract Co-Author*) Nothing to Disclose Giuseppe Schillizzi, Roma, Italy (*Abstract Co-Author*) Nothing to Disclose Daniele Fresilli, Roma, Italy (*Presenter*) Nothing to Disclose Giulia de Soccio, Roma, Italy (*Abstract Co-Author*) Nothing to Disclose Valerio Forte, MD, Rome, Italy (*Abstract Co-Author*) Nothing to Disclose Ferdinando D'Ambrosio, Rome, Italy (*Abstract Co-Author*) Nothing to Disclose Carlo Catalano, MD, Rome, Italy (*Abstract Co-Author*) Nothing to Disclose

### PURPOSE

To evaluate the effectiveness of quasistatic ultrasound elastography (USE) in comparison with conventional ultrasound for the characterization of benign and malignant parotid tumors.

## **METHOD AND MATERIALS**

124 consecutive patients with parotid gland tumors, scheduled for surgery, were enrolled. Ultrasound evaluation consisted of Bmode, color-Doppler and USE, conducted with the elasticity contrast index (ECI) technique. For each lesion the echogenicity, margins, vascularization, posterior acoustic enhancement and capsule presence were considered to determine benign or malignant lesions. Histology was considered the gold standard.

## RESULTS

At histology, 126 lesions were benign and 46 were malignant. Sensitivity, specificity, positive predictive value (PPV) and negative predictive value (NPV) were: 69.6, 41.3, 30.2 and 78.8% for echogenicity; 47.8, 96.8, 84.6 and 83.6% for margins; 87.0, 61.9, 45.5 and 92.9% for vascularization; 95.7, 31.7, 33.8 and 95.2% for capsule presence. ECI>3.5 alone was the most accurate parameter (accuracy: 86.0%), with sensitivity of 82.6%, specificity of 87.3%, PPV of 70.4% and NPV of 93.2%. The combination of ECI < 3.5 and vascularization discriminated Warthin tumor with a sensitivity of 83.3%, a specificity of 88.7%, PPV of 74.1%, NPV of 93.2% and an accuracy of 87.0%.

## CONCLUSION

USE with ECI index measurement can help to discriminate preoperatively benign from malignant lesions, with the exception of pleomorphic adenoma which is stiff and it can demonstrate an overlap with malignant tumors. However, worth of note was that pleomorphic adenomas usually are lower vascularized than malignant and warthin tumors. Therefore multiparametric ultrasound evaluation including ECI index USE technique may help to better classify parotid gland lesions.

## **CLINICAL RELEVANCE/APPLICATION**

USE proved to be effective to discriminate salivary gland lesions, with the exception of pleomorphic adenoma. It should be used as part of multiparametric ultrasound pre-operative evaluation.



## NR372-SD-SUB5

Disrupted Hippocampus-Prefrontal Circuitry in Parkinson's Disease Patients with Mild Cognitive Impairment

Sunday, Nov. 25 1:00PM - 1:30PM Room: NR Community, Learning Center Station #5

#### **Participants**

Boyu Chen, Shenyang, China (*Presenter*) Nothing to Disclose Guoguang Fan, PhD, Shenyang, China (*Abstract Co-Author*) Nothing to Disclose

#### For information about this presentation, contact:

cbyzgyk@126.com

### PURPOSE

Cogniive deficit is a common nonmotor manifestation of Parkinson's disease (PD). Evidence implicates abnormalities in the prefrontal cortex and hippocampus in PD patients. However, it is unknown whether hippocampus-prefrontal circuitry abnormalities are associated with cognitive impairment. To investigates the potential disruptions in hippocampus-prefrontal circuitry structural and functional connectivity, as well as their relationship in cognitive deficit in PD.

## **METHOD AND MATERIALS**

Diffusion tensor imaging(DTI) and resting-state functional magnetic resonance imaging (RS-fMRI) data were acquired from 22 PD patients with mild cognitive impairment (PD-MCI) ,19 PD patients with normal cognitive function (PD-NC), and 35 healthy control(HC)participants. FA values of fornix and hippocampus were obtain from DTI.Resting state functional connectivity(RSFC) were performed to assess functional connectivity of Hp-PFC.

## RESULTS

Heterogeneities in Hp-PFC change pattern were observed in PD patients according to different cognitive status, such as fornix structure, orbitofrontal(OFc) and medial prefrontal cortex(MPFC),midcingulate cortex (MCC). (1) PD-MCI and PD-NC showed FA decreased in fornix when compared with HC, while no significant FA change in the fornix between PD-MCI and PD-NC group. (2) PD-NC showed enhanced Hp-FC in OFc and MPFc when compared with HC. However, PD-MCI showed a decrease Hp-FC in the OFc, MPFC, and MCC compared with PD-NC/HC group. (3) Hp-FC strength of OFc and MPFC was positively correlated with the MoCA scores in HC and PD-MCI, while such correlation deficiency in PD-NC. In HC and PD-MCI, fornix FA value and Hp-FC of OFc/MPFc showed a positive correlation, such correlation deficiency in PD-NC yet.

### CONCLUSION

Our findings suggest that alterations in anatomical and functional connectivity of the Hp-PFC neural circuits play an important role in the neuropathophysiology of PD-MCI. Combined DTI and RSFC technologies, we found that the structural damage in fornix and dysfunction in Hp-FC of OFc, MPFC, and MCC are associated with cognitive deficit of PD patients, the functional connection damage were based on anatomical connections damage in PD-MCI. In addition, increased Hp-FC of OFc and MPFc in PD-NC play a compensatory role in cognitive function maintenance.



## NR373-SD-SUB6

Automated Coregistration Improves Diagnostic Accuracy Compared to Conventional Reading in the MRI Follow-Up Assessment of Brain Lesions in Patients with Multiple Sclerosis

Sunday, Nov. 25 1:00PM - 1:30PM Room: NR Community, Learning Center Station #6

## Participants

David Zopfs, Cologne, Germany (*Presenter*) Nothing to Disclose Stefanie Paquet, Cologne, Germany (*Abstract Co-Author*) Nothing to Disclose Kai Roman Laukamp, Cleveland, OH (*Abstract Co-Author*) Nothing to Disclose Christoph Kabbasch, Cologne, Germany (*Abstract Co-Author*) Nothing to Disclose David C. Maintz, MD, Koln, Germany (*Abstract Co-Author*) Nothing to Disclose Jan Borggrefe, Cologne, Germany (*Abstract Co-Author*) Nothing to Disclose

#### PURPOSE

To investigate diagnostic accuracy, interrater agreement and time required to rate axial and sagittal fluid attenuated inversion recovery (FLAIR) sequences in follow-up exams of patients with multiple sclerosis comparing an automated coregistration (AC) reading approach including colored mapping of brain lesions with conventional reading technique (CR).

## **METHOD AND MATERIALS**

We included 70 pairs of consecutive follow-up datasets of 53 patients with multiple sclerosis in this retrospective IRB-approved study. Heterogeneous image datasets of diverse scanners (1.0T/1.5T/3T) and institutions were used. Axial and sagittal FLAIR sequences of the brain were rated by two readers in a conventional reading session and using a FDA approved AC algorithm (LOBI, ISP v.10, Philips, Amsterdam, NL). Brain lesions were assessed for a) progression, b) regression, c) mixed changes or d) stable disease in CR and AC reading. The blinded readings were conducted at intervals of four weeks to avoid a recall bias. Consensus for ground truth was obtained by three radiologists, taking clinical and imaging data from AC and CR into account. The interrater agreement was determined using kappa statistics.

## RESULTS

The data included 75% female patients with a mean age of 40 years ( $\pm$  14 years). Average rating time was reduced from 78 ( $\pm$  36) seconds in CR to 44 ( $\pm$  22) seconds when using the AC approach, which took an average 14 ( $\pm$  1) seconds to start and match the datasets. Interrater agreement improved between both raters (0.52 vs. 0.67) and between both raters and consensus (0.47/0.5 vs. 0.83/0.78) in the AC approach in comparison to CR. In comparison to conventional reading, the diagnostic accuracy increased from 67% to 90% (Reader 1) and 70% to 87% (Reader 2) in the AC reading.

## CONCLUSION

Automated coregistration of brain lesions reduces the required time to evaluate MRI follow-up exams and increases diagnostic accuracy in patients with multiple sclerosis in comparison to conventional reading technique.

## **CLINICAL RELEVANCE/APPLICATION**

MRI follow-up examinations in patients with multiple sclerosis are frequent in daily routine and are often time-consuming and errorprone, especially in patients with pronounced findings. Thus, investigations of automated tools that assist radiological reading are of high clinical interest.



## OB172-ED-SUB1

## **Imaging Spectrum of Vaginal Pathologies**

Sunday, Nov. 25 1:00PM - 1:30PM Room: OB Community, Learning Center Station #1

### **Participants**

Zina J. Ricci, MD, Scarsdale, NY (*Abstract Co-Author*) Nothing to Disclose Sharon Gordon, MD, Bronx, NY (*Abstract Co-Author*) Nothing to Disclose Victoria Chernyak, MD,MS, Bronx, NY (*Abstract Co-Author*) Nothing to Disclose Marjorie W. Stein, MD, New Rochelle, NY (*Abstract Co-Author*) Nothing to Disclose Milana Flusberg, MD, Bronx, NY (*Presenter*) Nothing to Disclose Fernanda S. Mazzariol, MD, Bronxville, NY (*Abstract Co-Author*) Nothing to Disclose Mariya Kobi, MD, New York, NY (*Abstract Co-Author*) Nothing to Disclose

#### For information about this presentation, contact:

zricci@montefiore.org

## **TEACHING POINTS**

1. The spectrum of vaginal diseases seen on US, CT and MRI is vast.2. Most vaginal processes are benign with malignancy relatively rare.3. Certain vaginal pathologies occur in typical locations which can provide a diagnostic clue.4. Knowledge of gynecologic, oncologic or surgical history greatly aids radiologic diagnosis of vaginal disease.

### **TABLE OF CONTENTS/OUTLINE**

I. Vaginitis II. Foreign Body III. Congenital Anomalies• Imperforate hymen • Vaginal septum• Vaginal agenesisIV. Vaginal Cysts• Gartner duct cyst • Epidermal inclusion cyst • Bartholin gland cyst V. Fistulous Disease VI. Vaginal Cuff Disease• Endometriosis• Hematoma• Abscess• DehiscenceVII. Primary Benign Vaginal Mass• Leiomyoma• Prolapsing uterine leiomyoma• Mixed tumor of the vagina• ParagangliomaVIII. Primary Malignant Vaginal Mass• Squamous cell carcinoma• Adenocarcinoma• Sarcoma IX. Secondary Vaginal Malignancy• Lymphatic or hematogenous vaginal metastasis • Recurrent disease X. Local contiguous spread to vagina XI. Miscellaneous• Postoperative edema• Postradiation change



## OB173-ED-SUB2

ACR O-RADS MRI Lexicon and Risk Stratification Scheme

Sunday, Nov. 25 1:00PM - 1:30PM Room: OB Community, Learning Center Station #2

### **Participants**

Caroline Reinhold, MD, MSc, Montreal, QC (*Abstract Co-Author*) Nothing to Disclose Isabelle Thomassin-Naggara, MD, Paris, France (*Abstract Co-Author*) Speakers Bureau, General Electric Company Elizabeth A. Sadowski, MD, Madison, WI (*Presenter*) Nothing to Disclose Evan S. Siegelman, MD, Philadelphia, PA (*Abstract Co-Author*) Nothing to Disclose Katherine E. Maturen, MD, Ann Arbor, MI (*Abstract Co-Author*) Royalties, Reed Elsevier; Royalties, Wolters Kluwer nv; Consultant, Allena Pharmaceuticals, Inc; Andrea G. Rockall, FRCR,MRCP, London, United Kingdom (*Abstract Co-Author*) Speaker, Guerbet SA

Loretta M. Strachowski, MD, San Francisco, CA (*Abstract Co-Author*) Nothing to Disclose Hebert Alberto Vargas, MD, Cambridge, United Kingdom (*Abstract Co-Author*) Nothing to Disclose Rosemarie Forstner, MD, Salzburg, Austria (*Abstract Co-Author*) Nothing to Disclose

## For information about this presentation, contact:

esadowski@uwhealth.org

## **TEACHING POINTS**

Describe all ACR Ovarian Reporting and Data System (O-RADS) MRI lexicon terms, which were agreed on by the ACR O-RADS MRI committee based on evidence in the literature and/or consensus of the expert panel. Familiarize imagers with the ACR O-RADS MRI ratings and risk stratification scheme. Illustrate the ACR O-RADS MRI system using imaging examples.

### TABLE OF CONTENTS/OUTLINE

1. ACR O-RADS MRI lexicon terms and definitions General Definitions: Physiologic structure, lesion, cyst, solid lesion MRI Specific Definitions: Signal Intensity Characteristics Lesion morphology: Unilocular, multilocular, predominantly solid lesion Cyst fluid descriptors: simple, non-simple Solid tissue and non-solid tissue: Solid tissue (solid component that enhances AND has one of the following morphology: Papillary projection, mural nodule, irregular septation, solid portion of a lesion); Non-solid tissue (Normal ovarian stroma, smooth septations, blood clot and debris) Extraovarian descriptors: (Paraovarian cyst, fallopian tube, peritoneal inclusion cyst, peritoneal thickening/nodules, adenopathy 2. Describe the ACR O-RADS MRI risk stratification scheme 3. Example cases to illustrate the O-RADS MRI lexicon and risk stratification system

#### **Honored Educators**

Presenters or authors on this event have been recognized as RSNA Honored Educators for participating in multiple qualifying educational activities. Honored Educators are invested in furthering the profession of radiology by delivering high-quality educational content in their field of study. Learn how you can become an honored educator by visiting the website at: https://www.rsna.org/Honored-Educator-Award/ Caroline Reinhold, MD, MSc - 2013 Honored EducatorCaroline Reinhold, MD, MSc - 2014 Honored EducatorCaroline Reinhold, MD, MSc - 2017 Honored EducatorCaroline Reinhold, MD, MSc - 2013 Honored EducatorCaroline Reinhold, MD, MSc - 2017 Honored Educator



## OB174-ED-SUB3

## Fetal Posterior Fossa Anomalies: Don't Get Left Behind

Sunday, Nov. 25 1:00PM - 1:30PM Room: OB Community, Learning Center Station #3

#### **Participants**

David R. Pettersson, MD, Portland, OR (*Abstract Co-Author*) Nothing to Disclose Jaclyn Thiessen, MD, Portland, OR (*Presenter*) Nothing to Disclose Moses Azubuike, MD, Portland, OR (*Abstract Co-Author*) Nothing to Disclose Neel Patel, MD, Portland, OR (*Abstract Co-Author*) Nothing to Disclose Karen Y. Oh, MD, Portland, OR (*Abstract Co-Author*) Nothing to Disclose Roya Sohaey, MD, Portland, OR (*Abstract Co-Author*) Nothing to Disclose

### **TEACHING POINTS**

1. Develop an approach to the posterior fossa that facilitates the opportunity to detect anomalies of the hindbrain 2. Learn imaging clues for accurate diagnosis in specific scenarios; such as presence of a posterior fossa cyst, cerebellar compression, enlarged cisterna magna, cerebellar and/or vermian dysmorphology 3. Review associated anomalies, clinical implications, and outcomes

## TABLE OF CONTENTS/OUTLINE

Normal ultrasound and MR anatomy of the posterior fossa and hindbrain anatomy throughout gestation, including the anatomy at time of nuchal translucency screening Review key image findings and differential diagnosis for posterior fossa cyst and cyst-like masses Review causes of cerebellar compression and cerebellar/vermis morphology abnormalities and present key findings for accurate diagnosis Post natal correlation with prenatal imaging findings will be presented throughout



### PD174-ED-SUB6

Unravelling the Troublesome Puzzle: A Comprehensive Imaging Review of Pediatric Intracranial Neurovascular Diseases

Sunday, Nov. 25 1:00PM - 1:30PM Room: PD Community, Learning Center Station #6

### Awards Identified for RadioGraphics

#### Participants

Hamid Rajebi, MD, San Antonio, TX (*Presenter*) Nothing to Disclose Bundhit Tantiwongkosi, MD, San Antonio, TX (*Abstract Co-Author*) Nothing to Disclose Laleh Daftaribesheli, MD, San Antonio, TX (*Abstract Co-Author*) Nothing to Disclose Ruchi Tiwari, MD, San Antonio, TX (*Abstract Co-Author*) Nothing to Disclose Aparna R. Yarram, San Antonio, TX (*Abstract Co-Author*) Nothing to Disclose Achint K. Singh, MD, San Antonio, TX (*Abstract Co-Author*) Nothing to Disclose

## For information about this presentation, contact:

rajebi@uthscsa.edu

#### **TEACHING POINTS**

1. Review classification, imaging approach and differential diagnosis of intracranial neurovascular diseases in pediatric patients. 2. Illustrate cases of pediatric intracranial neurovascular diseases in our institution with a brief presentation of epidemiologic, genetic and clinical features. 3. Describe the spectrum of imaging characteristics of each entity with the discussion of hints and pitfalls in proper diagnosis.

# TABLE OF CONTENTS/OUTLINE

Introduction Intracranial Vascular Anatomy Role of different imaging modalities (US, CT, MR, Angiography) Institutional case-based review - Ischemic stroke - Intracranial hemorrhage and cerebral aneurysms - Cerebral venous thrombosis - Cavernoma -Developmental venous anomaly - Arteriovenous malformation - Vein of Galen malformation - Sickle cell disease - Sinus Pericranii -Capillary telangiectasia/Hemorrhagic hereditary telangiectasia - PHACE(S) syndrome - Klippel- Trenaunay syndrome - Moyamoya disease/syndrome Current concepts and updates in the genetics of pediatric neurovascular abnormalities Conclusion

### **Honored Educators**

Presenters or authors on this event have been recognized as RSNA Honored Educators for participating in multiple qualifying educational activities. Honored Educators are invested in furthering the profession of radiology by delivering high-quality educational content in their field of study. Learn how you can become an honored educator by visiting the website at: https://www.rsna.org/Honored-Educator-Award/ Achint K. Singh, MD - 2018 Honored Educator



## PD175-ED-SUB7

Stridor in Children - What the Radiologist Should Know

Sunday, Nov. 25 1:00PM - 1:30PM Room: PD Community, Learning Center Station #7

### Participants

Hiren Panwala, Vellore, India (*Presenter*) Nothing to Disclose Aparna Irodi, MD, FRCR, Vellore, India (*Abstract Co-Author*) Nothing to Disclose Picardo K. Naina, Vellore, India (*Abstract Co-Author*) Nothing to Disclose Sridhar Gibikote, DMRD, Vellore, India (*Abstract Co-Author*) Nothing to Disclose Harsha Vardhan, MD, Vellore, India (*Abstract Co-Author*) Nothing to Disclose Madhavi K. Kandagaddala, Vellore, India (*Abstract Co-Author*) Nothing to Disclose Hariprasad Sudershan, New Delhi, India (*Abstract Co-Author*) Nothing to Disclose Prabhu CS, MBBS, MD, Chennai, India (*Abstract Co-Author*) Nothing to Disclose

#### For information about this presentation, contact:

drhiren1187@gmail.com

### **TEACHING POINTS**

The purpose of this exhibit is to: 1. Review the spectrum of conditions causing stridor in children, in different age groups and presenting acutely or chronically. 2. Illustrative case examples with clinical and imaging pearls of a spectrum of pathologies causing stridor in children. 3. Emphasize the importance of plain radiography, Ultrasound, CT and MRI in evaluation of stridor in children 4. Formulate a clinico-radiological algorithm for evaluation of stridor

# TABLE OF CONTENTS/OUTLINE

\* Classification of the causes of stridor based on age group, duration of the symptoms underlying pathology \* Clinical pearls to help suspect the specific etiology of stridor in children. \* Role of various modalities such as plain radiographs, endoscopy, barium studies, cross section CT and MRI with role of specific protocols \* Large spectrum of illustrative case examples depicting the different causes of stridor and their imaging appearances with imaging pearls \* Flow chart integrating clinical symptoms and imaging features \* Summary and conclusion



## PD205-SD-SUB1

## Stereoscopic Benefits for the Identification of Pulmonary Vein Stenoses with CT Angiograms

Sunday, Nov. 25 1:00PM - 1:30PM Room: PD Community, Learning Center Station #1

#### **Participants**

Jiali Luan, BS, Edmonton, AB (*Presenter*) Nothing to Disclose Brendan E. Morgan, BEng, Edmonton, AB (*Abstract Co-Author*) Nothing to Disclose Ross Cockburn, BSC, Vancouver, AB (*Abstract Co-Author*) Nothing to Disclose Kumaradevan Punithakumar, PhD, Edmonton, AB (*Abstract Co-Author*) Nothing to Disclose Michelle L. Noga, MD, Edmonton, AB (*Abstract Co-Author*) Nothing to Disclose

## For information about this presentation, contact:

jluan1@ualberta.ca

# PURPOSE

This study aims to illustrate the advantage of using stereoscopic 3D volume rendered displays over 2D volume rendered displays for the identification of pulmonary vein stenoses in CT angiograms.

# METHOD AND MATERIALS

23 participants were recruited including: 6 radiologists, 6 radiology trainees, 3 cardiologists, 4 cardiology trainees, 3 cardiac surgeons and 1 cardiac surgery trainee. CT angiograms from 20 pediatric patients were retrospectively selected and cropped to the heart to show the great vessels, creating identical volume rendered 2D (monoscopic) and 3D (stereoscopic) versions of each patient's scan. 3D stereoscopic scans were visualized with 3D glasses. Participants were invited for 2 sessions, at least two weeks apart, to interact with and grade 10 monoscopic and 10 stereoscopic scans per session. They are surveyed to identify stenosed pulmonary veins and we graded them based on the number of missed lesions (type 2 error). The gold standard diagnosis was made by an expert radiologist with access to the CT images, radiology reports and the clinical/surgical diagnosis. In a single session, the participant was shown each patient once, either in 2D or 3D. The scans were also divided based on the complexity, with complex cases having 3 or more lesions. Participants were surveyed after the study to assess their experiences with stereoscopy. The paired Student's t-test, histograms and box plots were used for statistical analysis.

# RESULTS

There were less type 2 errors for the stereoscopic group compared to the monoscopic group (251 vs 272, p=0.13). If we consider complex cases with 3 or more lesions, then stereoscopy performs significantly better in terms of the number of type 2 errors than monoscopy (148 vs 169, p=0.045). Also, 15/23 participants reported subjective benefit with stereoscopy. Stereoscopy was shown to increase the precision of detecting pulmonary vein stenoses as shown by the narrower distribution in both the histogram and box plot. This effect is enhanced if we consider trainee performance.

### CONCLUSION

Stereoscopic volume rendered display is beneficial for the appreciation of CT angiograms with multiple, complex pulmonary vein lesions and enhances consistency among viewers.

# **CLINICAL RELEVANCE/APPLICATION**

Stereoscopic displays may be a valuable tool to enhance the appreciation of complex multi-lesional scans and it may potentially allow trainees to understand more complex cases with less experience.



# PD206-SD-SUB2

Forward Projected Model-Based Iterative Reconstruction Solution for 320-Row CT Angiography Improves Image Quality and Reduces Radiation Exposure in Infants with Complex Congenial Heart Disease

Sunday, Nov. 25 1:00PM - 1:30PM Room: PD Community, Learning Center Station #2

# Participants

Yuzo Yamasaki, MD, Fukuoka, Japan (*Presenter*) Nothing to Disclose Takeshi Kamitani, MD, Fukuoka, Japan (*Abstract Co-Author*) Nothing to Disclose Koji Sagiyama, MD, Fukuoka, Japan (*Abstract Co-Author*) Nothing to Disclose Yuko Matsuura, Fukuoka, Japan (*Abstract Co-Author*) Nothing to Disclose Takuya Hino, MD, Fukuoka, Japan (*Abstract Co-Author*) Nothing to Disclose Hiroshi Honda, MD, Fukuoka, Japan (*Abstract Co-Author*) Nothing to Disclose Soichiro Tsutsui, Fukuoka, Japan (*Abstract Co-Author*) Nothing to Disclose Hidetake Yabuuchi, MD, Fukuoka, Japan (*Abstract Co-Author*) Nothing to Disclose

#### PURPOSE

Multi-detector computed tomography (CT) has been greatly improved and is increasingly used for the diagnosis of congenital heart disease (CHD) in infants. With this increase in use, however, dose exposure has become a major concern in the treatment of pediatric CHD patients undergoing CT angiography (CTA). The forward projected model-based iterative reconstruction solution (FIRST) has recently been proposed to improve image quality in CT. We aimed to investigate the impact of FIRST on 320-row CT angiography (CTA) in infants with complex congenial heart disease (CHD).

# METHOD AND MATERIALS

A total of 60 consecutive infant cases (34 boys and 26 girls, 0-1year and 10 months) with complex CHD who underwent examination by 320-row CT angiography with free-breathing prospective electrocardiogram (ECG) triggered volume target scanning for cardiovascular evaluation from September 2016 to December 2017 were enrolled in the study. In first test, images were reconstructed using filtered back projection (FBP), adaptive iterative dose reduction 3D (AIDR-3D) and FIRST, and the variables were compared among the 3 groups in 20 cases. In second test, the variables were compared between 20 cases scanned with the noise level of standard deviation 20 using AIDR-3D and 20 cases scanned with the noise level of standard deviation 20 using FIRST. CT attenuation and the contrast-to-noise ratio (CNR) of the great vessels and heart chambers were calculated, and 2 reviewers visually evaluated image qualities using a 5-point scale. Total dose length product was recorded for all patients.

# RESULTS

In first test, mean CNR values were 7.7 $\pm$ 2.1 for FBP, 10.5 $\pm$ 2.4 for AIDR-3D, and 13.1 $\pm$ 3.4 for FIRST (p<0.05). The best subjective image qualities in the great vessels and heart chambers were obtained with FIRST. In second test, there were no significant differences between two groups in image qualities. The effective dose for FIRST was significantly lower than that for AIDR-3D (0.6 $\pm$ 0.2 vs 1.1 $\pm$ 0.3 mSv; p<0.001).

# CONCLUSION

The novel knowledge-based FIRST algorithm yields a significantly improved the image quality and reduced radiation exposure with maintaining the image quality in 320-row CTA of infants with complex CHD.

# **CLINICAL RELEVANCE/APPLICATION**

The FIRST algorithm yields a better subjective image quality with low dose radiation exposure. It will contribute to the reduction of radiation expose for patients with congenital heart disease.



# PD209-SD-SUB5

MRI Assessment of Fetuses Referred with Ultrasonographically Suspected Pelvi-Abdominal Cystic Lesions: Is There an Added Value?

Sunday, Nov. 25 1:00PM - 1:30PM Room: PD Community, Learning Center Station #5

# Participants

Sahar Saleem, MD, Cairo, Egypt (*Presenter*) Nothing to Disclose Sara H. Eldessouky III, PhD,MSc, Cairo, Egypt (*Abstract Co-Author*) Nothing to Disclose Hassan Gaafar, Cairo, Egypt (*Abstract Co-Author*) Nothing to Disclose Hossam El Shenoufy, Cairo, Egypt (*Abstract Co-Author*) Nothing to Disclose Walaa Hussien Zedan, Cairo, Egypt (*Abstract Co-Author*) Nothing to Disclose Suzan M. Abdel-Meguid, Cairo, Egypt (*Abstract Co-Author*) Nothing to Disclose

#### For information about this presentation, contact:

saharsaleem1@gmail.com

### PURPOSE

To evaluate the role of prenatal MRI in the assessment of fetuses with sonographically-suspected abdominal and/or pelvic cystic lesions

## **METHOD AND MATERIALS**

After obtaining Institutional Review Board approval, we performed fetal MRI for 43 fetuses at gestational ages ranged from 18 to 36 weeks (average 28.5± 4.7 weeks) referred with sonographically-suspected abdominal and/or pelvic cystic lesions. We assessed the impact of fetal MR imaging findings on prenatal diagnosis. We correlated prenatal US and MRI imaging findings with the definite diagnosis reached by postnatal imaging studies and/or pathology.

#### RESULTS

The outcome measures diagnosed 21 (48.8.1%) cystic lesions originated from urinary tract, 8 (18.6%) ovarian cysts, 3 (6.9%) hepato-biliary cysts, 4 (9.3%) mesenteric cysts, 3 (6.9%) uterovaginal anomalies (hydrocolpos, longitudinal vaginal septum, imperforate hymen, and didelphys), 2 (4.6%) intra-abdominal sacrococcygeal teratomas, 1 (2.3%) cloacal malformation, and 1 (2.3%) encysted ascites as a part of Congenital High Airway Obstructive Syndrome (CHAOS). In correlation with prenatal US findings, fetal MRI correctly changed the US diagnosis of the origin of the abdominal and/or pelvic cystic lesions in 12 (27.9%) fetuses; detected correct additional findings that were not apparent on ultrasonography that significantly influenced their prenatal diagnosis and prognosis in 13 (30.2%); confirmed correct prenatal US diagnosis without additional findings in 16 (37.3%) fetuses; and in 2 (4.6%) cases, both prenatal US and MRI failed to reach the correct diagnosis.

# CONCLUSION

Fetal MRI as an adjunct to sonography can improve assessment of fetuses with suspected abdominal and/or pelvic cystic lesions and can influence pregnancy counseling.

# **CLINICAL RELEVANCE/APPLICATION**

Fetal MRI can be a valuable tool in diagnosis of abdominal and/or pelvic cystic lesions suspected by prenatal US.



### PH008-EB-SUB

Application of Deep Learning Object Detection for CT Scout Localizer-based Clinical Scan Region Planning

Sunday, Nov. 25 1:00PM - 1:30PM Room: PH Community, Learning Center Hardcopy Backboard

### Participants

Dave Chevalier, Waukesha, WI (*Presenter*) Employee, General Electric Company; Spouse, Employee, Childrens Medical Group of Wisconsin

Eric Gros, BS, Waukesha, WI (*Abstract Co-Author*) Nothing to Disclose Jianwei Qiu, Waukesha, WI (*Abstract Co-Author*) Nothing to Disclose

#### CONCLUSION

Results show that a Deep Learning model may provide comparable performance to human operators on the task of scan range planning during patient scan setup. Automated CT scan setup may improve operator consistency and productivity, improve dose utilization and reduce overscan.

#### FIGURE

http://abstract.rsna.org/uploads/2018/18004066/18004066\_dpsg.jpg

### Background

Patient scan setup plays an important role in the diagnostic quality of CT images, but can be a time-consuming and variable task. This study investigates the feasibility of automating the task of scan region selection using Deep Learning techniques to find anatomic regions of interest within a CT scout localizer image. This could potentially improve operator consistency and productivity, improve dose utilization, and reduce overscan.

#### Evaluation

We applied a state-of-the-art object detection Deep Learning model to the task of clinical scan setup. The model's feature extractor was pretrained on ImageNet, then the full model was fine-tuned on a database of 950 scout images with ground truth labels collected from scan regions prescribed as part of routine clinical CT acquisitions. For this study, we limited the anatomy of interest to routine head from Lateral scout images, Chest from AP scout images, and Abdomen-Pelvis from AP scout images. The dataset was separated into training (70%), validation (15%) and test (15%) sets. The model was trained for 50 epochs and 5000 steps per epoch using the Keras TensorFlow framework on Tesla GPUs. The final model for evaluation was selected using minimum validation loss after the fixed number of epochs. The model was evaluated for clinical scan range accuracy compared to human experts using the average DICE score on an independent test set of 212 scout images that were manually annotated by clinical application specialists.

## Discussion

Performance of the Deep Learning model versus human annotated regions by anatomy: Lateral head average DICE score was 95.8% +/- 2.1% std dev (N= 52). AP chest average DICE score was 94.9% +/- 3.5% std dev (N= 94) AP Abd-Pelvis DICE score was 94.8% +/- 3.1% std dev (N= 66)



# PH120-ED-SUB6

How to Optimize Your DTI Acquisition for Spinal Cord Assessment: Physical Basis and Technical Adjustments

Sunday, Nov. 25 1:00PM - 1:30PM Room: PH Community, Learning Center Station #6

### Awards Magna Cum Laude Identified for RadioGraphics

#### **Participants**

Teodoro M. Noguerol, MD, Jaen, Spain (*Presenter*) Nothing to Disclose Rafael Barousse, MD, Buenos Aires, Argentina (*Abstract Co-Author*) Nothing to Disclose Mercedes Vallejo, MD, Seville, Spain (*Abstract Co-Author*) Nothing to Disclose Javier Royuela, Cordoba, Spain (*Abstract Co-Author*) Nothing to Disclose Paula Montesinos de la Vega, Madrid, Spain (*Abstract Co-Author*) Employee, Koninklijke Philips NV Antonio Luna, MD,PhD, Jaen, Spain (*Abstract Co-Author*) Consultant, Bracco Group; Speaker, General Electric Company; Speaker, Canon Medical Systems Corporation; Royalties, Springer Nature

#### For information about this presentation, contact:

t.martin.f@htime.org

# **TEACHING POINTS**

1. Review the physical basis of Diffusion Tensor Imaging (DTI) and their technical adjustment for spinal cord evaluation 2. Explain, from an educational point of view, the biological meaning of parameters derived from DTI studies in spinal cord. 3. Show potential applications of DTI for spinal cord evaluation in different clinical scenarios.

# TABLE OF CONTENTS/OUTLINE

1. Introduction 2. Physical basis of DTI focused in spinal cord evaluation 3. Technical adjustments. a. Sequence design b. Coils selection and patient positioning c. How to identify and avoid potential pitfalls d. 1.5T or 3T magnet? 4. Biological meaning of parameters derived a. Mean Diffusivity b. Fractional Anisotropy c. Axial Diffusivity d. Radial Diffusivity 5. General considerations and Potential applications a. When do I have to perform DTI for spinal cord evaluation? b. Is necessary to integrate DTI in routine protocols? c. Spinal cord fiber tracking techniques. d. Quantitative assessment or fiber tracking? e. Clinical scenarios 6. Conclusions and take home messages

#### **Honored Educators**

Presenters or authors on this event have been recognized as RSNA Honored Educators for participating in multiple qualifying educational activities. Honored Educators are invested in furthering the profession of radiology by delivering high-quality educational content in their field of study. Learn how you can become an honored educator by visiting the website at: https://www.rsna.org/Honored-Educator-Award/ Antonio Luna, MD - 2018 Honored Educator



# PH205-SD-SUB1

Dual-Energy CT, MRI of Rectal Cancer: A Comparison of Diagnostic Performance in Metastatic Lymph Nodes

Sunday, Nov. 25 1:00PM - 1:30PM Room: PH Community, Learning Center Station #1

### Participants

Shao Xun, Zhenjiang, China (*Presenter*) Nothing to Disclose Dongqing Wang, Zhenjiang, China (*Abstract Co-Author*) Nothing to Disclose Lirong Zhang, MD, zhenjiang, China (*Abstract Co-Author*) Nothing to Disclose Haitao Zhu, Zhenjiang, China (*Abstract Co-Author*) Nothing to Disclose Changqing Yin, Zhenjiang, China (*Abstract Co-Author*) Nothing to Disclose

#### PURPOSE

To compare the diagnostic efficiency of dual-energy spectral CT(DECT) and magnetic resonance imaging(MRI) of rectal cancer in metastatic lymph nodes.

# METHOD AND MATERIALS

Forty two histology proven rectal cancer patients underwent DECT and MRI and subsequent surgical resection. The virtual monochromatic images and iodine-based Material decomposition images derived from DECT imaging were interpreted for lymph nodes (LNs) measurement. The short axis diameter and the normalized iodine concentration (nIC) of LNs were measured. A blinded radiologist measured the ADC value in each regional LN after referring to the T2-weighted images and DWI. The diagnostic performance of each method was assessed by receiver-operating characteristic (ROC) curve. The sensitivity, specificity, accuracy, positive predictive value (PPV) and negative predictive value (NPV) were compared using McNemar's test and Fisher's exact test. A Kappa test was used to assess the interobserver agreement.

#### RESULTS

DECT scanning showed statistical difference between metastatic LNs and non-metastatic LNs in the measurements of short axis diameter, nIC value. The mean ADC of the metastatic LNs was significantly lower than that of the non-metastatic LNs. Dual energy CT classified 45 % of the cases correctly compared to a ratio of 41% for MRI.

## CONCLUSION

This study showed statistical difference in both DECT and MRI between metastatic LNs and non-metastatic LNs .DECT is slightly better than that of MRI, but this difference is not statistically significant.

# **CLINICAL RELEVANCE/APPLICATION**

Both MRI and DECT are good for metastatic LNs diagnosing of rectal cancer.



# PH206-SD-SUB2

## Evaluation of Iterative Reconstruction Using 3D-Consolidated Signal Noise to Ratio

Sunday, Nov. 25 1:00PM - 1:30PM Room: PH Community, Learning Center Station #2

#### **Participants**

Mitsunori Goto, MMedSc, RT, Natori, Japan (*Presenter*) Nothing to Disclose Masaaki Taura, BMedSc, RT, Sendai, Japan (*Abstract Co-Author*) Nothing to Disclose Chiaki Tominaga, BSc, Sendai, Japan (*Abstract Co-Author*) Nothing to Disclose Hiroki Azumi, BSc, Sendai, Japan (*Abstract Co-Author*) Nothing to Disclose Kazuhiro Sato, PhD, Sendai, Japan (*Abstract Co-Author*) Nothing to Disclose Noriyasu Homma, PhD, Sendai, Japan (*Abstract Co-Author*) Nothing to Disclose Issei Mori, PhD, Sendai, Japan (*Abstract Co-Author*) Nothing to Disclose

#### PURPOSE

Numerous reports have investigated the image quality of iterative reconstruction (IR) .Most reports based on the noise power spectrum in the axial plane (NPSax) and the modulation transfer function (MTF) have concluded that the image quality of IR was superior to that of filtered back-projection (FBP). However, the slice sensitivity profile (SSP) may be significantly thickened at a low contrast-to-noise ratio (CNR). This SSP difference is often neglected in comparisons and may therefore skewer results. We combine SSP and the longitudinal noise power spectrum (NPSz) with in-plane MTF and NPSax. We test this consolidated method by applying it to the evaluation of Adaptive Iterative Dose Reduction 3D (AIDR-3D).

#### **METHOD AND MATERIALS**

A hypothetical filter H, which equalizes the SSP of FBP to that of AIDR-3D, was determined from SSPs measured at sufficiently low-CNR. Coefficient Kz, which is a noise variance reduction factor attainable by filter H, was obtained from the measured NPSz of FBP. Instead of a simple SNR(f), which is a ratio of axial MTF(f) and the square root of NPSax(f), we defined the z-corrected SNR(f) whereby NPSax(f) is replaced by NPSax(f)/Kz. The appropriate SNR(f) of AIDR-3D is obtained when SSP is corrected to be equivalent to that of FBP. We measured MTF using a tilted-wire method and SSP using a thin plastic sheet, both at sufficiently low-CNR conditions. The NPSax and NPSz were obtained using the three-dimensional Fourier transformation of the noise images. Waterfilled phantoms (18cm diameter) were used for each case and were helically scanned with a pitch of 0.89. The Collimation width and reconstruction slice thickness were both 0.5 mm. Slice interval was 0.1 mm.

#### RESULTS

When based on ordinary SNR(f), AIDR-3D was significantly superior to FBP. However, the z-corrected SNR(f) showed that AIDR-3D was no better than FBP. Conventional in-plane image quality assessment may overvalue IR and hybrid-IR. For fair evaluation, the differences associated with low-contrast SSP and longitudinal NPSz, must be considered.

# CONCLUSION

For correct assessment,z-directional properties must be measured and considered.

#### **CLINICAL RELEVANCE/APPLICATION**

Image quality assessment methods, that are limited to axial plane, tend to overvalue the performance of reconstructionr methods whose z-directional properties are nonlinear (or situation dependent).



## PH207-SD-SUB3

3D Contrast-enhanced Ultrasound and 3D Ultrasound Molecular Imaging for Response Assessment in Models of Triple-negative Breast Cancer

Sunday, Nov. 25 1:00PM - 1:30PM Room: PH Community, Learning Center Station #3

Participants

Man Chen, Shanghai, China (Presenter) Nothing to Disclose

For information about this presentation, contact:

13601803138@126.com

#### PURPOSE

The aim of this study is to explore the value of 3D contrast-enhanced ultrasound and 3D ultrasound molecular imaging (3D USMI) in response assessment of triple-negative breast cancer.

# METHOD AND MATERIALS

Mice with human triple-negative breast cancer xenografts (13 mice) were scanned with clinical ultrasound system and transducer (Toshiba Aplio 500; 14LV7) after injecting nontargeted or VEGFR2-targeted microbubbles respectively. All mice were randomized into two groups (5 in control group and 8 in treatment group). Mice were treated with either adriamycin combined with cetuximab (treatment group) or saline only (control group) on day 1, 3, and 5 respectively and were scanned before each treatment. At day 7, all mice were scanned and then the expression of CD31 and VEGF of tumor were assessed ex vivo. 3D contrast-enhanced ultrasound was performed in all mice and 3D USMI was performed in all mice in control group and 6 mice in treatment group at the same time. The following indexes were recorded: Peak, Time to Peak (TTP), mTT, Slope, Area, Area wash in, Signal Intensity (SI) and their changes during treatment.

### RESULTS

In 3D contrast-enhanced ultrasound, Peak became significantly different between two groups at day 5 (P<0.05) while TTP,Slope,Area,Area wash in became different at day 7 (P<0.05). The difference of  $\Delta$ Area in two groups was significant at day 3 while  $\Delta$ Peak, $\Delta$ TTP and  $\Delta$ (Area wash in) were different at day 5. In 3D USMI, SI became significantly different between two groups from day 3. SI,  $\Delta$ SID3-D1,  $\Delta$ SID5-D1,  $\Delta$ SID7-D1 were strongly related with the expression of VEGF (r>0.600, P<0.05).

# CONCLUSION

3D contrast-enhanced ultrasound can sensitively assess the response to treatment at early stage. 3D USMI can not only reflect the expression of VEGF in tumor, but also monitor the changes of microvascular markers during treatment more early.

### **CLINICAL RELEVANCE/APPLICATION**

3D contrast enhanced-ultrasound and 3D USMI can assess tumor response at early stage and 3D USMI can also monitor the changes of microvascular markers during treatment.



## PH208-SD-SUB4

CNN-Based Image Super-Resolution for CT Slice Thickness Reduction Using Paired CT Scans for Improving Robustness of Computer-Aided Nodule Detection System

Sunday, Nov. 25 1:00PM - 1:30PM Room: PH Community, Learning Center Station #4

#### Participants

Kyu-Hwan Jung, PhD, Seoul, Korea, Republic Of (*Presenter*) Stockholder, VUNO Inc Woong Bae, Seoul, Korea, Republic Of (*Abstract Co-Author*) Nothing to Disclose Seungho Lee, Seoul, Korea, Republic Of (*Abstract Co-Author*) Nothing to Disclose Gwangbeen Park, Seoul, Korea, Republic Of (*Abstract Co-Author*) Nothing to Disclose Hyunho Park, Seoul, Korea, Republic Of (*Abstract Co-Author*) Employee, VUNO Inc Sang Min Lee, MD, Seoul, Korea, Republic Of (*Abstract Co-Author*) Nothing to Disclose

#### For information about this presentation, contact:

khwan.jung@vuno.co

#### PURPOSE

To evaluate the effectiveness of a slice thickness reduction technique in computed tomography(CT) scans using convolutional neural network(CNN)-based super-resolution(SR) network for improving the sensitivity of lung nodule detection in thick section CT scans.

#### **METHOD AND MATERIALS**

We collected 100 sets of CT scans with identical acquisition protocols that were differentiated only by the slice thickness (1mm, 3mm, and 5mm). By employing CNN-based SR network, we trained the model to learn the residuals between synthesized thin section slices and real thin section slices. We used 80 sets of CT scans for training, 5 sets for the validation and the remaining 10 sets were used for quantitative evaluation. We separately collected 100 sets of CT scans (also with 1mm, 3mm, and 5mm slice thickness) with one biopsy-confirmed nodule per scan(46 solid nodules and 54 non-solid nodules, size ranges 6-12mm) to evaluate the effectiveness of the slice thickness reduction techniques for improving the lung nodule detection performance in thick section CT scans. The computer-aided detection(CAD) system used for the evaluation of lung nodule detection performance was internally developed with LUNA16 dataset, which contains 888 CT scans with slice thickness less than 3mm.

#### RESULTS

When slice thickness was reduced from 3mm to 1mm, the peak signal-to-noise ratio(PSNR) and structural similarity index(SSIM) were 30.9624 and 0.8142 respectively; when slice thickness was reduced from 5mm to 1mm PSNR and SSIM were 29.2620 and 0.7439 respectively. In the nodule detection task, all solid and non-solid nodules were detected by the CAD system using 1mm slice thickness scans(100.0% recall). However, 2 solid nodules were missed when using 3mm slice thickness scans (95.7% recall) while their corresponding synthetic 1mm scans improved the recall to 97.8% (1 missed solid nodule). Recall of scans with 5mm slice thickness was 89.1% and 85.2% while their synthetic 1mm scans improved the recall to 100.0% and 96.3% for solid and non-solid nodules respectively.

# CONCLUSION

Our CNN-based SR method generates synthetic thin section slices from thick section slices which improve lung nodule detection performance using CAD.

#### **CLINICAL RELEVANCE/APPLICATION**

Robustness to acquisition protocol is essential for reliable lung CAD systems. Our slice thickness reduction technique may improve the robustness of CAD systems when applied to CT scans with various slice thickness.



# PH209-SD-SUB5

# Vendor-Neutral, DICOM Viewer-Based, Graphical Image Exploration of Clinical Spectral CT Studies

Sunday, Nov. 25 1:00PM - 1:30PM Room: PH Community, Learning Center Station #5

FDA Discussions may include off-label uses.

#### Participants

Matthew A. Lewis, PhD, Dallas, TX (*Presenter*) Research collaboration, CMR Naviscan Corporation; Research collaboration, QT Ultrasound, LLC

Todd C. Soesbe, PhD, Dallas, TX (Abstract Co-Author) Nothing to Disclose

Xinhui Duan, PhD, Dallas, TX (Abstract Co-Author) Nothing to Disclose

Yin Xi, PhD, Dallas, TX (Abstract Co-Author) Nothing to Disclose

Robert E. Lenkinski, PhD, Dallas, TX (Abstract Co-Author) Research Grant, Koninklijke Philips NV Research Consultant, Aspect Imaging

## For information about this presentation, contact:

matthew.lewis@utsouthwestern.edu

### PURPOSE

In clinical spectral CT, the true information content for x-ray attenuation by tissue is at a minimum 2 quantities per voxel. The integration of this additional information into the clinical workflow is extremely challenging.

# METHOD AND MATERIALS

For some tasks, the lower dimensional HU of conventional CT is sufficient, but for spectral CT imaging tasks, the ideal clinical observer will interact with the complete spectral data. Except for effective Z and density pair, all spectral-derived images (VNC,iodine,calcium-removal,fat quant,monoE) are related by linear transformation. To facilitate interaction with the complete spectral CT data, we developed a completely graphical tool that allows the user to create new series and rapidly explore any clinical spectral CT study. Additional scripts were developed for the Spectral CT Toolkbox for pyOsiriX (Blackledge et al, 2016), a rapid development plugin for the popular OsiriX family of DICOM viewers. At the series level, the user interacts with both the conventional CT series and a 2D histogram of PhotoElectric and Compton images (MADplot), low and high kVp, or any two monoenergetic images. By defining localized and linear ROIs on this histogram, new DICOM series can be created for arbitrary 2 and 3 material quantification and differentiation. After calibration, user-created synthetic monoEs are also supported.

#### RESULTS

In vendor-provided, spectral CT analysis packages, generation of custom spectral-derived series is accomplished by manually entering HU to define specific materials. Here the generation of new spectral-derived series is adaptive at the study level. For volume-conserving, 2 material quantification, 2 localized ROIs are specified on the spectral data histogram. For volume-conserving, 3 materials, 3 localized ROIs are user specified. For monoE, material removal, and non-volume conservation, a linear ROI is employed. For longitudinal studies, the same reference ROIs may be used for all subjects, or the analysis can be adapted for each subject.

## CONCLUSION

Reader interaction with conventional CT series and a histogram of underlying spectral CT data facilitates rapid, adaptive exploration of all linear transform-based spectral-derived results.

# **CLINICAL RELEVANCE/APPLICATION**

Integration of the added information inherent to spectral CT is a workflow challenge that may addressed by the reader interfacing with the conventional image and a 2D histogram of underlying spectral CT data.



# QI002-EB-SUB

ICU Radiographs: Appropriate Radiographic Positioning with Timely Recognition of Misplaced Lines, Tubes, and Drains

Sunday, Nov. 25 1:00PM - 1:30PM Room: QR Community, Learning Center Hardcopy Backboard

# Participants

Abhishek Agrawal, MD, Lexington, MA (*Presenter*) Nothing to Disclose Ryan Wolfe, DO, Burlington, MA (*Abstract Co-Author*) Nothing to Disclose Joanne Wozniak, MS, Burlington, MA (*Abstract Co-Author*) Nothing to Disclose Jalil Afnan, MD, Burlington, MA (*Abstract Co-Author*) Nothing to Disclose Christoph Wald, MD, PhD, Burlington, MA (*Abstract Co-Author*) Advisor, Koninklijke Philips NV

#### For information about this presentation, contact:

#### NA

## PURPOSE

Lines, tubes, and drains placement are common hospital procedures, which are routinely performed bedside by clinicians with a varying degree of experience. Like any procedure, there are potential risks, which include improper positioning or misdirection that may not be immediately recognized by beside staff on post-procedural radiographs. The primary bedside clinicians are usually the first to view these radiographs before being sent to the picture archiving and communication system (PACS), and then interpreted by a radiologist. If an incorrectly positioned line, tube, or drain is initially recognized by the bedside clinician, it will allow for earlier intervention and thus, minimize potential resulting complications. <u>EDUCATIONAL GOALS</u>: By completing the educational modules, the clinical participants will be able to identify and differentiate a variety of lines, tubes, and drains on radiographs. Moreover, the participants will have a better understanding of proper positioning of these lines, tubes, and drains and will be able to identify any misplaced or misdirected lines.

#### **METHODS**

Intensive care unit (ICU) clinical staff, medical students, physician assistants, nurse practitioners, residents, and fellows from various departments, viewed sequential patient radiographs and took a pre-test questionnaire asking to identify the position of line, tube, drain and/or their tip location. They then reviewed learning modules, which educated them on the appropriately placed lines, tubes, and drains on radiographs. The lines, tubes and drains were also placed on a mannequin for better anatomical orientation. Additional modules were available for clinicians to review, which included a module on misplaced lines, tubes, and drains, a module to identify foreign bodies and a module demonstrating medical devices on radiographs. Finally, the participants took a post-test questionnaire to assess the effectiveness of the modules and to evaluate improvement in their pre-test scores. A 3-6 month follow up test was conducted on the same set of participants. In addition, short interviews were also conducted to identify areas of improvement and for feedback on the modules.

### RESULTS

Early anecdotal feedback and follow up from the clinical staff suggests improvement in their ability to identify lines, tubes, and drains at bedside post-procedural radiographs as well as an improved ability to recognize improper placement. Based on this positive experience, some of the clinical staff has adopted the modules into their everyday workflow acting as a reference for newly placed lines, tubes, and drains. In addition, few clinical departments are also planning to implement these modules into their resident curriculum and have set aside mandatory resident time to train on these modules.

### CONCLUSION

Educating clinicians on the proper radiographic positioning of commonly placed lines, tubes and drains are important for early intervention and to reduce potential complication when improperly positioned. Although the assessment of positioning is interpreted by the radiologist, the time necessary to upload images to PACS and for the final interpretation, prolongs the detection of potentially misplaced lines, tubes, and drains that could otherwise be recognized early by the bedside clinical staff, minimizing potential complications.



# QI004-EB-SUB

Preventing Radiology Procedural Patient Safety Events by Improving Universal Protocol Through Implementation of a Standardized Time-Out

Sunday, Nov. 25 1:00PM - 1:30PM Room: QR Community, Learning Center Hardcopy Backboard

# Awards

#### Quality Improvement Reports Award Identified for RadioGraphics

#### Participants

James H. Boyum, MD, Rochester, MN (*Presenter*) Nothing to Disclose Anil N. Kurup, MD, Rochester, MN (*Abstract Co-Author*) Research Grant, Galil Medical Ltd; Research Grant, EDDA Technology, Inc; Royalties, Wolters Kluwer nv Ashley Rosier, Rochester, MN (*Abstract Co-Author*) Nothing to Disclose Laura Tibor, MBA, BEng, Rochester, MN (*Abstract Co-Author*) Nothing to Disclose Katie Morgan, RN, Rochester, MN (*Abstract Co-Author*) Nothing to Disclose Amberly Hess, RN, Rochester, MN (*Abstract Co-Author*) Nothing to Disclose Nora J. Harer, Rochester, MN (*Abstract Co-Author*) Nothing to Disclose Carrie Phillips, Rochester, MN (*Abstract Co-Author*) Nothing to Disclose Carrie L. Carlson, RT, Rochester, MN (*Abstract Co-Author*) Nothing to Disclose Mara Turner, Rochester, MN (*Abstract Co-Author*) Nothing to Disclose Sadia Choudhery, MD, Boston, MA (*Abstract Co-Author*) Nothing to Disclose

#### For information about this presentation, contact:

boyum.james@mayo.edu

# PURPOSE

To identify root causes of Universal Protocol (UP) related wrong patient, wrong site, wrong procedure events and implement a solution to prevent future events from occurring in the Radiology procedural practice.

#### METHODS

A multidisciplinary team of Radiology clinical and quality improvement personnel approched this issue with Define-Measure-Analyze-Improve-Control (DMAIC) and A3 problem-solving methodologies. A detailed review of documentation from root cause analyses of three wrong patient, wrong site, wrong procedure events that occurred in our department's procedural practice in 2016 revealed which incorrectly performed elements of the UP process were attributable to each event. Eighty-seven baseline observational audits were conducted during a variety of invasive procedures in different procedural areas within the department to analyze and record how teams were performing UP and to measure noncompliance of the UP elements. A post-audit fish bone diagram identified key gaps in UP performace. A standardized time-out sequence was designed (Fig 1) and included all required time-out elements by The Joint Commission and several 'best practice' elements developed specifically based on findings in the review of root cause analyses. The standardized time-out was tested in an observational audit of 149 radiologic procedures to measure is effect on UP compliance. Each procedural team member involved in the audit was surveyed about the time-out content and sequence and their willingness to adopt the time-out into daily practice. Observational audit data and survey responses were used to make adjustments and create a final standardized version for implementation throughout the procedural practice.

# RESULTS

The root cause analyses revealed key elements attributable to wrong patient, wrong site, and wrong procedure events including verification of the original electronic procedural order, verification of specimen orders, and verification of specimen labels. Compliance of these and other essential elements of UP increased from a baseline average compliance rate of 63% to 91% during testing of the standardized time-out (Fig 2). Ninety percent of survey respondents were willing to adopt the standardized time-out into their daily practice.

### CONCLUSION

UP is essential to avoiding patient safety events in procedural practices as well as the operating room. Increasing complexity of procedures and specimen requests within Radiology creates a unique challenge that may require augmenting the pre-procedural time-out beyond the core requirements set forth by The Joint Commission. Analysis of root cause from wrong patient, wrong site, wrong procedure events in our department identified that most UP errors were avoidable by implementing a standardized time-out. This change showed an increase in compliance with essential elements of UP specific to our procedural practice. Implementation of the standardized time-out across 12 unique procedural practices in our department is in process. Post-implementation auditing will track compliance with the standardized time-out and its relationship to the number of any future wrong patient, wrong site, wrong procedure occurrences.



## QI022-EB-SUB

Implementation of a Two Prong, PACS-based, Continuous Quality Improvement Program into Routine Daily Clinical Operation in the Radiology Department

Sunday, Nov. 25 1:00PM - 1:30PM Room: QR Community, Learning Center Hardcopy Backboard

# Participants

Miranda J. Mares, MS,RT, Albuquerque, NM (*Abstract Co-Author*) Nothing to Disclose Jennifer S. Weaver, MD, Albuquerque, NM (*Presenter*) Nothing to Disclose

For information about this presentation, contact:

jsweaver@salud.unm.edu

### PURPOSE

There are approximately 170 radiology technologists and over 80 radiologists (faculty, fellows, and residents) in our University based Hospital system, which serves as Level 1 Trauma Center, a Children's Hospital, and a Comprehensive Cancer. This large number of technologists and radiologists makes face-to-face communication difficult and often impossible; however, communication and feedback are key when trying to provide the highest level of quality patient care. To increase communication and feedback between radiologists and technologists, we have implemented a two prong, PACS-based, continuous quality improvement process. Radiologists utilize this process to facilitate communication with technologists and to provide educational feedback to the technologists, both when immediate attention is required and when long term education is the goal.

#### **METHODS**

In our system, radiologists and technologists can communicate through a PACS-based portal, decreasing the need for telephone communication. Radiologists have two choices for identifying a quality issue with any imaging study: Immediate QC = Immediate action is required by the technologist in order for radiologist to be able to interpret the study. This often requires repeating images, sending missing images to complete a study, or clarifying provided clinical history. Future Review QC= Radiologist can interpret the study but has identified a potential for technologist education to increase quality of study in the future. When the radiologist places a study into Immediate QC, the technologist is notified, and the study is placed on hold in the PACS. The technologist addresses the quality issue, and the system then notifies the radiologist of the outcome. The radiologist then interprets the study. If the radiologist places a study into Future Review QC, the studies are collected and reviewed on a monthly basis by the modality supervisors. Technologists receive education related to their own QC cases. The Future Review QC studies are also tabulated to identify global issues; these global issues are addressed at monthly staff meetings. The Radiology Quality Manager consolidates the Future Review QC data each quarter, creates a quality scorecard report, and distributes the scorecard report to each section chief radiologist. This scorecard report details the issues identified through Future Review QC for that quarter and summarizes the educational feedback provided to the technologists.

#### RESULTS

To measure the efficiency of the Immediate QC, we did an audit on QC response turnaround times for 2016 and compared with 2017. In the first quarter of 2016, there were many turnaround times exceeding 48 hours, often with no technologist documentation of reason for delay. In the fourth quarter of 2017 turnaround times had greatly decreased, to under an hour in the majority of cases, with technologists consistently documenting reasons for any delay. By utilizing the Future Review QC as an education tool, we have successfully decreased our quality issues. For example, in the General Radiography section, quality issues have decreased by 67% when comparing the first quarter of 2016 to the fourth quarter of 2017. The Quality Manager rounds often with the radiologists to ensure this data represents actual and sustained fixes of these issues, rather than an unintended consequence such as decreased use of the process by the radiologists. The quarterly scorecard report to the radiologists helps our department close the loop on these issues and further increases communication between the radiologists and technologists.

### CONCLUSION

Implementation of a two prong, PACS-based, continuous quality improvement process has facilitated communication between radiologists and technologists, and has expedited the correction of immediate quality issues. This process has become a valuable feedback tool for long-term technologist education resulting in a higher level of patient care through continuously improving imaging quality.



## QI025-EB-SUB

# Improving Accuracy of the On-Call Radiology Worklist

Sunday, Nov. 25 1:00PM - 1:30PM Room: QR Community, Learning Center Hardcopy Backboard

#### **Participants**

Kristin A. Robinson, MD, Phoenix, AZ (*Presenter*) Nothing to Disclose Courtney M. Tomblinson, MD, Nashville, TN (*Abstract Co-Author*) Nothing to Disclose Catherine C. Roberts, MD, Phoenix, AZ (*Abstract Co-Author*) Nothing to Disclose Jonathan A. Flug, MD, MBA, Phoenix, AZ (*Abstract Co-Author*) Nothing to Disclose Clinton V. Wellnitz, MD, Phoenix, AZ (*Abstract Co-Author*) Nothing to Disclose

## For information about this presentation, contact:

Robinson.Kristin2@mayo.edu

#### PURPOSE

Radiographic and cross-sectional examinations on patients admitted to the hospital under observation status during after-hours are not always populated on the diagnostic radiology worklist for the on-call resident or fellow. The algorithm for inclusion of studies on this list is determined by patient demographic data at the time of registration. Currently, the non-populated studies are shuffled to a general imaging list, only some of which will eventually be filtered to the on-call list. This means that the non-populated studies sit for an indeterminate amount of time until the general worklist is manually checked, resulting in delayed patient care. The target goal of this project was to decrease report turnaround time for radiographs performed on patients in observation status by 20% during the study period.

# METHODS

The DMAIC process was used to identify the on-call worklist issue, implement a technological change, and reduce report turnaround time for observation status exams. Electronic health record (EHR), picture archiving and communication system (PACS), and radiology information system (RIS) data from the pre and post observation periods were compiled. The resulting dataset was filtered for radiologic studies performed during Saturday call shifts. Because the primary target measure required alteration of the worklist population algorithm, a potential adverse outcome would be for outpatient studies to inappropriately populate to the on-call list resulting in an unnecessary increase in workload while on call. The technologic error, which automatically populated studies onto the worklist based on a number of factors pertaining to the study (e.g. patient location, admission status, and acuity of the order placed), was fixed by redefining the parameters of the radiographs to be included on the on-call list. The human error was fixed by alerting on-call readers to the inappropriate worklist population and reminding them to periodically check the outpatient list for observation radiographs.

#### RESULTS

The worklist population algorithm was changed to include observation studies which had been erroneously filtered to the outpatient list due to their "outpatient status" (from a financial perspective). Including observation studies on the on-call worklist with Emergency Department and inpatient studies put all exams requiring high priority interpretation on one worklist. Our radiology department's report turnaround time for radiographs performed on patients in observation status was 59.4 minutes in the first quarter of the study period. Our final re-measurement report turnaround time for radiographs performed on patients of observation radiographs over the study time period. The average 23.4 minutes, a 60.6% reduction in report turnaround time of observation radiographs was 21.8 and 35.6 minutes, respectively. Post-implementation of the worklist algorithm change, report turnaround for the emergency and inpatients radiographs were essentially unchanged (25.8 and 34.5 minutes, respectively), confirming that the change to the worklist algorithm did not inadvertently negatively affect report turnaround times for these high priority exams.

#### CONCLUSION

Using the DMAIC process, a critical on-call issue in the radiology department was identified and corrected. Including observation studies on the on-call worklist with Emergency Department and inpatient studies put all exams requiring high priority interpretation on one worklist. This project exemplifies how residents as front line staff are in unique positions to identify critical workflow issues and engage in quality improvement projects.



# QI101-ED-SUB1

Confused About with and Without: Assessment of Medical Providers' Knowledge of Abdominal CT Protocol Appropriateness

Sunday, Nov. 25 1:00PM - 1:30PM Room: QR Community, Learning Center Station #1

# Participants

Alice Yu, MD, Baltimore, MD (*Abstract Co-Author*) Nothing to Disclose Yoshimi Anzai, MD, Salt Lake City, UT (*Abstract Co-Author*) Nothing to Disclose Brandyn D. Lau, MPH, Baltimore, MD (*Abstract Co-Author*) Nothing to Disclose Matthew D. Alvin, MD, MBA, Baltimore, MD (*Abstract Co-Author*) Nothing to Disclose Elliot K. Fishman, MD, Baltimore, MD (*Abstract Co-Author*) Institutional Grant support, Siemens AG; Institutional Grant support, General Electric Company; Co-founder, HipGraphics, Inc Pamela T. Johnson, MD, Baltimore, MD (*Presenter*) Consultant, Oliver Wyman

#### For information about this presentation, contact:

PamelaJohnson@jhmi.edu

# PURPOSE

Abdominal CT is one of the leading contributors to medical radiation exposure, and protocols with more than one acquisition can deliver 2-4 times more radiation than a single acquisition. Furthermore, an abdominal CT protocol that includes unenhanced images followed by IV contrast enhanced acquisition(s) ('CT with and without') is a higher cost exam than either CT with IV contrast or CT without IV contrast. Data published by Guite et al reported that 53% of abdominal CT scans included an unnecessary acquisition, and an unnecessary precontrast acquisition constituted 12% of these unindicated phases [Guite KM, Hinshaw JL, Ranallo FN, Lindstrom MJ, Lee FT Jr. Ionizing radiation in abdominal CT: unindicated multiphase scans are an important source of medically unnecessary exposure. J Am Coll Radiol. 2011; 8:756-61. PMID: 22051457]. Appropriate use of CT with and without IV contrast, also known as 'double scan' is a CMS Outpatient Imaging Efficiency Quality Metric. Nonradiology providers are tasked with selecting from these 3 protocols when ordering an abdominal CT, but traditionally have not received formal education on appropriate indications for abdominal CT with and without IV contrast. The purpose of this study was to evaluate ordering providers' understanding of when to order abdominal CT with and without IV contrast and simultaneously educate them on appropriate practice.

### METHODS

A survey was created to query ordering providers' understanding of the the appropriate abdominal CT protocol for 10 clinical scenarios: suspect appendicitis lymphoma AAA s/p endovascular repair painless gross hematuria painless jaundice adrenal nodule characterization GI bleeding severe pancreatitis refractory pyelonephritis suspect embolic complications of endocarditis Possible responses for each scenario included: CT without oral or IV contrast CT with oral contrast CT with oral and IV contrast CT with IV contrast only CT with and without IV contrast Unsure Correct answers were based on the new ACR Choosing Wisely® recommendation for abdominal CT protocol selection: http://www.choosingwisely.org/clinician-lists/acr-abdominal-ct-with-unenhanced-ct-followed-by-iv-contrast-enhanced-ct/. For some protocols, more than 1 answer was considered correct. Additional questions addressed participants understanding of how abdominal CT with and without contrast is performed and relative exam costs, as well as demographic questions about specialty, level of training and geographic location. After each question, results were immediately available with explanations for questions answered incorrectly and links to relevant ACR Appropriateness Criteria® or Choosing Wisely® resources and/or a JACR article on abdominal CT protocol appropriateness for more information. The IRB of the principle institution acknowledged this as a quality improvement project exempt from approval. The survey was distributed to ordering providers at multiple academic centers in March-April 2018. Performance was correlated with training level and medical specialty.

# RESULTS

101 medical providers participated including: 39 nonradiology residents (16 surgery, 10 emergency medicine, 10 internal medicine and 3 other) 25 radiology residents 22 advanced practice providers (nurse practitioner or physician assistant) 12 nonradiology attendings 3 radiology attendings The average score was 10.61 out of 14 questions correct for radiology respondents and 6.60/14 for nonradiologists (p<0.0001). The mean score for radiology respondents (10.61) was significantly higher than emergency medicine (7.00, p<0.0001), surgery (7.23, p<0.0001) and medicine providers (5.53, p<0.0001). The mean score for medicine respondents was significantly lower than emergency medicine (5.53 vs. 7.00, p=0.02) and surgery (5.53 vs. 7.23, p=0.03) respondents. Nonradiology faculty average score was significantly lower than radiology residents (6.83 vs 10.48, p<0.0001). Advanced practice providers average score was also lower than radiology residents (5.32 vs 10.48, p<0.0001) and nonradiology residents (5.32 vs 6.74, p=0.02).

## CONCLUSION

Nonradiology medical providers at all levels of experience lack understanding about abdominal CT protocol appropriateness. To perform imaging of the highest quality, safety and value, radiologists must be responsible for appropriate protocol selection for each patient, particularly when CT protocols differ in radiation exposure and cost.

#### **Honored Educators**

Presenters or authors on this event have been recognized as RSNA Honored Educators for participating in multiple qualifying educational activities. Honored Educators are invested in furthering the profession of radiology by delivering high-quality educational content in their field of study. Learn how you can become an honored educator by visiting the website at:

https://www.rsna.org/Honored-Educator-Award/ Pamela T. Johnson, MD - 2016 Honored EducatorYoshimi Anzai, MD - 2014 Honored EducatorElliot K. Fishman, MD - 2012 Honored EducatorElliot K. Fishman, MD - 2014 Honored EducatorElliot K. Fishman, MD - 2016 Honored EducatorElliot K. Fishman, MD - 2018 Honored Educator



# QI103-ED-SUB2

Developing a Comprehensive Prostate Imaging Service: Getting It Right & How to Achieve Quality in a Public Sector DGHS (District General Hospital Service) Group of Hospitals

Sunday, Nov. 25 1:00PM - 1:30PM Room: QR Community, Learning Center Station #2

# Participants

Shyamsunder R. Koteyar, MBBS, FRCR, Manchester, United Kingdom (*Presenter*) Nothing to Disclose Jacob Cherian, Manchester, United Kingdom (*Abstract Co-Author*) Nothing to Disclose Arun Jain, Manchester, United Kingdom (*Abstract Co-Author*) Nothing to Disclose

#### For information about this presentation, contact:

shyam.sunder@pat.nhs.uk

# PURPOSE

• There has been global increased awareness and demand for prostate MRI imaging.• There has been rapid development's in prostate imaging with heavy dependence on DWI & ADC sequences • Changes in National policy in UK (NICE guidelines) meant that selected patients have choice of imaging prior to biopsy rather than the other way around.• Imaging can't be performed within 4 weeks of biopsy, as this would lead to errors in interpretation.• Long waiting lists for MRI appointments in NHS hospitals means, it is nearly impossible to meet the national target of 2 weeks waiting pathway.

#### **METHODS**

Methods:Imaging improvements-We are a group of 4 hospitals, with 4 MRI scanners, with 2 different vendors, with varied sequences. A task group of all stake holders (MRI lead radiographer, department manager, uro-radiologist & urologists) was set up with multiple informal & formal meetings.Working with various application specialists, and creating longer appointment slots, we were able to push the machine to its limits & it was possible to change DWI sequences from 800 to DWI 1400. Accurate ADC sequences were computed using at least 3 b values.Scheduling improvements:This was the trickiest part of the developing services, with contradicting demands placed on radiology- of reducing waste (no show) and getting same/next day appointments. After careful analyses of various data, including inpatient demands, and prostate imaging needs, a dedicated 12 slots per week was created in alignment with urology prostate outpatient clinics. A special code for consultant only referrals created to accommodate these patients in the designated slots.After scheduled cut-off time, if no patients were filled in these slots, these were made available for other inpatients; thereby creating zero waste.After a trial of 3 months, the number of slots was reduced to 10 to match the demands.Reporting improvements:Job plans of body imaging reporting radiologists were tweaked to align the scheduled reporting sessions with scan slots, thereby minimizing delay, to make it possible for same/next day reporting.Communication improvement by creating electronic alerts created to further improve turnaround time.Reporting standards improvement achieved by adopting to PIRADS-2 based reporting.

#### RESULTS

Results: Reporting turnaround time-The patient journey from the time of referral to the hospital till diagnosis had a 12 step journey with median time of 30-42 days. By optimizing patient pathway, we have eliminated 6 steps, making it a 6step process, and median turnaround time has been reduced to around 15-20 days. Image quality improvement: Previous MR reporting was confined to staging of prostate cancer, with focus on identifying extra capsular disease. By optimizing imaging, we have been able to identify transition and anterior zone abnormalities, and aid/guide biopsy rather than routine 12 quadrant biopsy. Reporting quality improvement:Rather vague descriptive reports, we have moved on to use of PIRADS-2 based reporting, And as demonstrated on an audit, this has helped us standardize and improve the quality of our reports. As seen from feedback from other tertiary care Centre's, as well as from referrers, we have been able to raise the bar in overall prostate imaging and patient care.Our workload( MRI prostate imaging) has more than doubled in the last 3 years.

# CONCLUSION

Conclusion: Working as a team, we have been able to achieve and develop a high-quality service for MRI prostate imaging, despite constraints of busy public-sector group of Hospitals. Without any extra resources, we have been able to cut down our turnaround time to less than half; thereby complying with national and international standards; this has been achieved despite doubling of work load over last 3 years. Working in tandem with various MR Vendors, we have been able to optimize imagining, which has led to improved cancer detection rate by almost 20 to 30%, particularly in the transition and anterior zone of prostate, and help us aid/guide biopsies.By standardizing our reports by adapting PIRADS-2 for reporting, we have been able to raise the bar in terms of reporting quality.



# QI105-ED-SUB3

Process Improvement: How Can We Reduce Radiation Exposure to the Female Breast During Routine CT Examinations of the Abdomen and Pelvis?

Sunday, Nov. 25 1:00PM - 1:30PM Room: QR Community, Learning Center Station #3

### Participants

Cherisse A. Wada, MD, New York, NY (*Presenter*) Nothing to Disclose Charles Hua, MD,MS, New York, NY (*Abstract Co-Author*) Nothing to Disclose Nolan J. Kagetsu, MD, New York, NY (*Abstract Co-Author*) Spouse, Employee, Pfizer Inc; Spouse, Stockholder, Pfizer Inc

#### PURPOSE

The basis of this project was to determine the number of examinations that included breast tissue on routine CT abdomen and pelvis examinations performed on female patients between the ages of 12-50, for quality improvement purposes. The scan range of a standard CT exam of the abdomen and pelvis extends from the dome of the diaphragm to below the ischial tuberosities. However, this varies by technologist and the lower chest may be included in the examination. This poses a problem, as glandular breast tissue is particularly sensitive to the effects of ionizing radiation. As proponents of ALARA, we must ensure the CT tomogram is properly used to reduce scanning coverage, thereby resulting in CT dose reduction, especially to the radiosensitive breast.

#### METHODS

A retrospective review was performed utilizing PACS (picture archiving and communication systems) search filters to identify 100 routine CT examinations of the abdomen and pelvis in female patients age 12-50 occurring between December 2017 and January 2018. All images were reviewed on PACS workstations and the following data were collected in an Excel spreadsheet: 1) Exam date; 2) Patient age; 3) Breast in field of view? Yes / No; 4) If breast in FOV, was it preventable? Yes / No; 5) Hospital site: A / B; 6) Shift: Day / Evening / Night; 7) Accession number; 8) Indication; 9) DLP, mGy\*cm. The number of examinations that included the breast in the FOV was determined. An exam was not counted if breast collimation could not be performed due to anatomy, such as an elevated diaphragm or pendulous breast tissue. The examinations were then further characterized by hospital site and shift to assess for any differences. An additional 100 examinations utilizing the same search criteria will be reviewed after technologist education to assess for interval change.

#### RESULTS

In our preliminary study of 100 cases, there were 52 exams from Hospital A, and 48 exams from Hospital B. At Hospital A (n = 52), 26 exams (50%) contained the breasts in the FOV.Of these cases,9 were performed during the day (34.6%);11 were performed during the evening (42.3%);6 were performed at night (23%).At Hospital B (n = 48), 39 exams (81%) contained the breasts in the FOV.Of these cases,16 were performed during the day (41%);17 were performed during the evening (43.6%);6 were performed at night (15.4%).

## CONCLUSION

From our preliminary data, it appears that CT technologists overnight did better at collimating breast tissue from the FOV than their counterparts during the day and evening shifts. There are likely other contributing factors which will be queried during our subsequent meeting with the CT Supervisor and technologists, which include and are not limited to: 1) Busier during the day and evening (there are simply more cases);2) The technologist forgot;3) The technologist did not know to collimate the FOV.Technologist are on the frontlines of this dose reduction initiative, and education will be the cornerstone of our intervention. Additionally, feedback regarding the examination will also be crucial, and our institution handles this either by directly calling the technologist who performed the scan, or by filling out a secure online QC form. The benefit of completing the QC form is that it is less disruptive on workflow, and goes to the Supervising Technologist, who discusses the QC issue with all the Technologists during their weekly meeting.



# QI107-ED-SUB4

# Introducing On-Call into Medical Student Radiology Clerkship: Our Experience

Sunday, Nov. 25 1:00PM - 1:30PM Room: QR Community, Learning Center Station #4

### Participants

Janki Patel, Clifton, NJ (*Presenter*) Nothing to Disclose Prapti Y. Shingala, MD, New Brunswick, NJ (*Abstract Co-Author*) Nothing to Disclose Connor Funsch, BS, Piscataway, NJ (*Abstract Co-Author*) Nothing to Disclose Catherine S. King, MD, New Brunswick, NJ (*Abstract Co-Author*) Nothing to Disclose Sarah Pettyjohn, MD, Somerset, NJ (*Abstract Co-Author*) Nothing to Disclose Te-Jung Tsai, MD, New Brunswick, NJ (*Abstract Co-Author*) Nothing to Disclose Rahul Garg, MD, New Brunswick, NJ (*Abstract Co-Author*) Nothing to Disclose Judith K. Amorosa, MD, Somerville, NJ (*Abstract Co-Author*) Nothing to Disclose

### For information about this presentation, contact:

jamorosa@univrad.com

# PURPOSE

This study was conducted to see if on-call experiences provide educational value to medical students in an elective radiology clerkship. Traditionally on-call experiences have been a part of clerkships such as medicine, surgery, ob-gyn, and emergency medicine but are uncommon in radiology despite radiology's role around-the-clock in patient management. We wanted to evaluate the clinical activities students can participate in after usual work hours and assess whether students would be receptive toward an extra time component in an elective clerkship. Ultimately, we wanted medical students, the future physicians, to see the critical importance of radiology in patient management especially after hours.

### METHODS

Medical students were required to take call on two evenings for 2 hours from 5-7 pm as part of the four week diagnostic radiology clerkship. This was a requirement for the course and was 15% of the final grade. Goals and objectives included: observe and help resident with patient information, make phone calls to ED or clinical staff, go to the ED to meet the patient and inquire about clinical presentation, and review images with resident and attending radiologists. The students had a 'passport' with cases they saw (anonymized) which the resident signs and they hand in at the end of the rotation. The medical students were asked to evaluate the usefulness of on-call and their interaction with the resident. They listed their activities, perception of after hours, and provided reasons for and against this on call experience. The evaluations were anonymous. The data was gathered and analyzed.

### RESULTS

129 medical students participated in the study. 89 students submitted one evaluation reflecting on their two call experiences. 40 students submitted two evaluations, one per each call experience. The activities the students were involved in during call included: 18.93% of evaluators saw patients (n =32). 15.38% of evaluators called the primary care physician (n=26). 72.78% of evaluators looked up references (n=123). 15.98% of evaluators accompanied the patient for exam or procedure (n=27). 42.60% of evaluators engaged in other activities (n=72). These other activities included: interpreting imaging, reviewing patient's past medical history and past imaging, generating differential, viewing the resident read, reviewing cases with the resident, identifying anatomy, being part of consulting with primary, discussing patient plan, and overview of imaging modalities. Of the evaluators that selected other, 14.20% interpreted images (n=24), 11.83% reviewed patient's past medical history and past imaging (n=20), 2.37% generated differentials (n=4), 31.43% viewed resident reading (n=11), 16.57% reviewed the case with the resident (n=28), 4.14% identified anatomy (n=7), 1.78 % participated in consulting with primary team (n=3), 1.18% discussed patient plan (n=2), and 1.18% learned overview of imaging modalities (n=2). Approximately 6.0% of evaluators rated the call as not useful, 49.7% said the call experience was somewhat useful, and 44.3% rated the call experience as very useful. Regarding their interaction with the resident, 0% of evaluators were unsatisified, 1.2% of evaluators were unsatisified, 1.8% of evaluators were undecided, 28.0% of evaluators were satisfied, and 69.5% of evaluators were very satisfied.

### CONCLUSION

After hours on-call experience for medical students has been successfully introduced into a Radiology clerkship with satisfactory evaluations. Given the results of this preliminary study, implementing an on-call component in radiology clerkships may be useful for medical students. Our study indicates that medical students had a satisfactory experience with this newly initiated on-call requirement to the radiology clerkship. These results may encourage other radiology programs to incorporate a similar on-call learning experience into their curriculum. Given the results of this study, implementing an on-call component in radiology clerkships may be beneficial to medical student's education. Future studies should seek to gather more information regarding long term evaluation of the on-call experience, types of experiences students have while on call, and the impact on a resident's teaching skills and attitudes. Team learning and the dynamics of being a part of the radiology team may also be explored in future studies. The on-call experience enhances medical education by increasing learning opportunities. It likely conveys to students the integral role radiology plays in patient management around the clock. The experience discredits the long-held impression that radiologists work hours are only from 9 to 5 and provides a first-hand view of what the role of a radiologist entails.



## RO001-EB-SUB

MRI of Malignant Neoplastic Brachial Plexopathy: A Pictorial Review

Sunday, Nov. 25 1:00PM - 1:30PM Room: RO Community, Learning Center Hardcopy Backboard

#### **Participants**

Sandra Ortiz, Mexico City, Mexico (*Presenter*) Nothing to Disclose Adolfo E. Lizardo, MD, Mexico City, Mexico (*Abstract Co-Author*) Nothing to Disclose Diego Reyes, MD, Mexico City, Mexico (*Abstract Co-Author*) Nothing to Disclose Jorge Guerrero Lxtlahuac, MD, Mexico City, Mexico (*Abstract Co-Author*) Nothing to Disclose Juan Armando Reyes Perez, Mexico City, Mexico (*Abstract Co-Author*) Nothing to Disclose

## **TEACHING POINTS**

1. To review the anatomy of the brachial plexus and its correlation with MR. 2. To describe a series of cases that illustrate the most common sources of neoplastic infiltration of the brachial plexus (lymph node metastases and involvement by contiguity). 3. To describe the irradiation-induced brachial plexopathy as an important differential diagnosis to consider.

# TABLE OF CONTENTS/OUTLINE

I. Introduction II. Anatomy III. Neoplastic brachial plexopathy due to lung and breast lymph node metastasic disease. IV. Neoplastic Brachial Plexopathy due to primary extrinsic brachial plexus tumors. V. Irradiation-induced Brachial Plexopathy V. Conclusions



# RO202-SD-SUB1

Pulsed Reduced Dose Rate Re-Irradiation (PRDR) Using Modulated Arc (mARC) IMRT For Recurrent Gliomas: Initial Clinical Outcomes of a Novel Technique

Sunday, Nov. 25 1:00PM - 1:30PM Room: RO Community, Learning Center Station #1

# Participants

Vanica Guignard, Wauwatosa, WI (*Presenter*) Nothing to Disclose Sara Kelm, Wauwatosa, WI (*Abstract Co-Author*) Nothing to Disclose Benjamin Gillingham, Wauwatosa, WI (*Abstract Co-Author*) Nothing to Disclose Selim Y. Firat, MD, Milwaukee, WI (*Abstract Co-Author*) Nothing to Disclose Douglas Prah, PHD, Milwaukee, WI (*Abstract Co-Author*) Nothing to Disclose Christopher J. Schultz, MD, Milwaukee, WI (*Abstract Co-Author*) Medical Advisory Board, Prism Clinical Imaging, Inc Anupriya Dayal, MD, Milwaukee, WI (*Abstract Co-Author*) Nothing to Disclose Jennifer Connelly, Milwaukee, WI (*Abstract Co-Author*) Nothing to Disclose Wade M. Mueller, MD, Milwaukee, WI (*Abstract Co-Author*) Nothing to Disclose Joseph A. Bovi, MD, Milwaukee, WI (*Abstract Co-Author*) Nothing to Disclose Malika L. Siker, MD, Milwaukee, WI (*Abstract Co-Author*) Nothing to Disclose

For information about this presentation, contact:

vguignard@mcw.edu

#### PURPOSE

Limited salvage options exist for patients with recurrent malignant brain tumors after standard treatment. Pulsed reduced dose rate re-irradiation (PRDR) lowers the effective dose rate, potentially decreasing toxicity by allowing for greater sublethal damage repair in normal using a 3DRT technique. We developed a novel technique using PRDR with modulated arc (mARC) IMRT delivery to reduce the amount of normal tissue exposed and will report our initial clinical results using this.

# METHOD AND MATERIALS

We conducted a retrospective review of all brain tumor patients treated with mARC PRDR at our institution. All mARC PRDR plans were generated with Monaco (Elekta Inc) using 1/10 of the total prescription dose. For each treatment fraction a total of 10 identical treatment beams were delivered with a minimum time interval of 3 min between beam initiations. This technique allows for the entire treatment volume to receive exactly 1/10 of the prescription dose every 3 min while limiting the prescription dose rate to less than 0.0667 Gy/min.

### RESULTS

34 patients were treated with mARC PRDR. Primary histology included grades 2 (n=6), 3 (n=10), and 4 (n=15) gliomas. Median dose at initial RT was 60 Gy (range 48-70) at 1.8-2 Gy per fraction. Patients were heavily pre-treated with a mean of 3 prior recurrences (range 1-7) before PRDR. 19 patients had repeat resection at recurrence including 6 just prior to PRDR. Bevacizumab was previously given to 16 patients with 26 receiving bevacizumab while undergoing PRDR (dose 10 mg/kg or 5 mg/kg q2 weeks). All patients had a KPS of 70 or greater. Mean age at PRDR was 53 (range 3-71). Median interval between initial RT and PRDR was 4.75 years (range 0.5-18.3). Median total dose was 54 Gy (range 30-60) at 2 Gy per fraction. At a mean follow-up of 9.3 months (range 0.5-19.3), 6-month OS was 70.5% and 1-year was OS 23.5%. Median time to progression was 6 months with 6-month PFS 47% and 1-year PFS 17.6%. Patients who received concurrent bevacizumab didn't have any improvement in PFS or OS (p>0.1). Five of the 34 patients did not finish treatment due to clinical decline and/or tumor progression.

#### CONCLUSION

This technique appears to be safe, feasible, and well-tolerated for previously-irradiated patients with recurrent gliomas.

#### **CLINICAL RELEVANCE/APPLICATION**

This is the first clinical report of mARC IMRT PRDR for recurrent gliomas and we await long-term clinical data to better define efficacy and toxicity.



## RO203-SD-SUB2

Patterns of Regional Lymph Node Recurrence After Definitive Radiotherapy for Cervical Cancer Patients

Sunday, Nov. 25 1:00PM - 1:30PM Room: RO Community, Learning Center Station #2

#### **Participants**

Shintaro Tsuruoka, Toon, Japan (*Presenter*) Nothing to Disclose Masaaki Kataoka, MD, Matsuyama, Japan (*Abstract Co-Author*) Nothing to Disclose Yasushi Hamamoto, MD, Toon-City, Japan (*Abstract Co-Author*) Nothing to Disclose Noriko Takata, Toon, Japan (*Abstract Co-Author*) Nothing to Disclose Kei Nagasaki, Toon-City, Japan (*Abstract Co-Author*) Nothing to Disclose Teruhito Mochizuki, MD, Toon, Japan (*Abstract Co-Author*) Nothing to Disclose

#### PURPOSE

In this study, we evaluated the pattern of lymph node recurrence after definitive radiotherapy (RT) for cervical cancer patients.

## METHOD AND MATERIALS

From April 2006 to December 2012, 220 patients with cervical cancer were treated with RT in our hospital. Among these patients, 122 patients who were treated with definitive RT (external beam RT and intracavitary brachytherapy) and had more than 12 months follow-up, entered into this retrospective study. RT was delivered to the whole-pelvic field with or without para-aortic lymph node area depending on that involvement status. Total median dose was 50.4 Gy. Intracavitary brachytherapy was performed in median 4 fractions, median 6 Gy per fraction to a typically prescribed point A.

#### RESULTS

The median age was 61 years old (26 to 90). The median follow-up was 60.7 months (5.7 to 123 months). The numbers of patients with FIGO stage IB, II, III, and IV were 23, 54, 43, and 2, respectively. The numbers of patients with cN0 and cM1 were 50 and 13. Three-year OS for FIGO stage IB, II, III, and IV were 86.7%, 75.3%, 74.4%, and 50.0%, respectively. Three-year DFS were 82.4%, 60.6%, 55.8%, and 50.0%, respectively. A total of 45 patients (36.9%) relapsed after definitive treatment: 19 (15.6%) developed local, 23 (18.9%) developed regional, and 15 (12.3%) developed distant metastasis. The median time to recurrence from the treatment was 11.9 months (range, 1.9 to 70.7 months). Among 23 patients of regional recurrence, 12 patients recurred in-field and 18 patients recurred out-field (maginal zone of RT field: 11 (61.1%) patients).

# CONCLUSION

Most regional recurrences after definitive RT for cervical cancer were marginal failure. It may be necessary to consider the radiation field for patients with high recurrence risk.

# **CLINICAL RELEVANCE/APPLICATION**

Most regional recurrences after definitive RT for cervical cancer were marginal zone.



# UR176-ED-SUB6

New and Updated Topics in Targeted Therapies for the Treatment of Advanced and Metastatic Renal Cell Carcinoma: What Radiologists Should Know

Sunday, Nov. 25 1:00PM - 1:30PM Room: GU/UR Community, Learning Center Station #6

#### Awards Certificate of Merit

#### **Participants**

Yoshiko Ueno, MD, PhD, Kobe, Japan (*Presenter*) Nothing to Disclose Satoru Takahashi, MD, PhD, Takatsuki, Japan (*Abstract Co-Author*) Nothing to Disclose Keitaro Sofue, MD, Kobe, Japan (*Abstract Co-Author*) Nothing to Disclose Utaru Tanaka, Kobe, Japan (*Abstract Co-Author*) Nothing to Disclose Tsutomu Tamada, MD, PhD, Kurashiki, Japan (*Abstract Co-Author*) Nothing to Disclose Takamichi Murakami, MD, PhD, Osakasayama, Japan (*Abstract Co-Author*) Nothing to Disclose

## For information about this presentation, contact:

yoshiu0121@gmail.com

# **TEACHING POINTS**

Targeted therapies are currently the standard treatment in patients with advanced and metastatic renal cell carcinoma (RCC). These include vascular endothelial growth factor (VEGF) tyrosine kinase inhibitor (TKI) and the mammalian target of rapamycin (mTOR) inhibitors. Appropriate assessment of treatment response is a key to an optimal treatment strategy. Imaging plays a central role in surveillance and follow-up of advanced and metastatic RCC. The aim of this presentation is: 1) To understand the treatment paradigm of advanced or metastatic RCC 2) To present cases of complications related to VEGF-TKI and mTOR therapy. 3) To review the updated clinical evidence in assessment of treatment response 4) To outline the future research directions using imaging tools

# TABLE OF CONTENTS/OUTLINE

1) Current treatment paradigms 2) Molecular mechanism of targeted therapies a. Signaling molecular pathway b. Classification of the drugs 3) Complications of targeted therapy a. Potential mechanisms of the toxicities b. Radiological images of complications 4) How to assess the treatment response a. Imaging modalities for assessment of treatment response b. RECIST and alternative response criteria 5) Recent clinical trials and new evidence of treatment strategies 6) Future research directions using imaging tools



## UR178-ED-SUB7

MRI Findings of Non-Obstructive Azoospermia: Lesions In and Out of Pelvic Cavity

Sunday, Nov. 25 1:00PM - 1:30PM Room: GU/UR Community, Learning Center Station #7

## Awards Certificate of Merit

## Participants

Jian Guan, MD, Guangzhou, China (*Presenter*) Nothing to Disclose Yang Peng, Guangzhou, China (*Abstract Co-Author*) Nothing to Disclose Huanjun Wang, MD, Guangzhou, China (*Abstract Co-Author*) Nothing to Disclose Jinhua Lin, Guangzhou, China (*Abstract Co-Author*) Nothing to Disclose Yan Guo, MD, Guangzhou, China (*Abstract Co-Author*) Nothing to Disclose

### For information about this presentation, contact:

usefulkey0077@hotmail.com

### **TEACHING POINTS**

1. To be familiar with normal testes on high resolution MRI. 2. To review different causes of non-obstructive azoospermia and their pathophysiology. 3. To be aware of the changes of testes, the abnormalities of central nervous system and adrenal glands as well as past history, which together help to make the correct diagnosis. 4. To introduce the application of functional MRI (such as DWI, MTI and MRS etc) for evaluation of spermatogenesis.

# TABLE OF CONTENTS/OUTLINE

I. MRI findings of normal testes on high resolution MRI by using small surface coil. 2. Different causes of non-obstructive azoospermia and the corresponding pathophysiology. 3. Pelvic, abdominal and intracranial MRI findings of sample cases. 4. Evaluation of spermatogenesis by functional MRI (such as DWI, MTI and MRS etc).



# VI153-ED-SUB7

# **Pelvic Trauma: What to Know**

Sunday, Nov. 25 1:00PM - 1:30PM Room: VI Community, Learning Center Station #7

#### **Participants**

Ambarish Bhat, MD, Wawatosa, WI (*Presenter*) Nothing to Disclose Ryan Davis, MD, Columbia, MO (*Abstract Co-Author*) Nothing to Disclose Sanjit O. Tewari, MD, New York, NY (*Abstract Co-Author*) Nothing to Disclose Nanda Deepa Thimmappa, MD, New York, NY (*Abstract Co-Author*) Nothing to Disclose Talissa A. Altes, MD, Columbia, MO (*Abstract Co-Author*) Speaker, Koninklijke Philips NV; Brian J. Trissell, MD, Columbia, MO (*Abstract Co-Author*) Nothing to Disclose

# For information about this presentation, contact:

Bhatap@health.missouri.edu

# **TEACHING POINTS**

• Review normal anatomy of pelvic vessels on CT and catheter angiography • Identify vascular injuries on CT and catheter angiography • Discuss interventional techniques used to treat acute pelvic hemorrhage • Discuss the WSES protocol for management of pelvic trauma

### **TABLE OF CONTENTS/OUTLINE**

1. Epidemiology, clinical scenarios, and multidisciplinary approach to management of pelvic trauma associated with vascular injury 2. Normal anatomy of pelvic arteries on CT and catheter angiography 3. Imaging appearance of pelvic vascular injuries on CT and angiography 4. Interventional techniques, equipment and materials used to treat acute pelvic hemorrhage 5. Potential complications associated with over and under embolization techniques 6. Conclusions: • Pelvic trauma with vascular injury is a major cause of mortality and morbidity • As a radiologist, it is important to know general vascular distribution of pelvic arteries and to recognize the common vascular injuries on the initial CT • When properly performed, angiography and embolization can stabilize a hemodynamically compromised patient with minimal morbidity



# VI154-ED-SUB8

Cryoablation of Large Tumors: Techniques, Tips, and Risks

Sunday, Nov. 25 1:00PM - 1:30PM Room: VI Community, Learning Center Station #8

FDA Discussions may include off-label uses.

#### Participants

Ahmad Parvinian, MD, Rochester, MN (*Abstract Co-Author*) Nothing to Disclose Jonathan M. Morris, MD, Rochester, MN (*Presenter*) Nothing to Disclose Matthew R. Callstrom, MD,PhD, Rochester, MN (*Abstract Co-Author*) Research Grant, EDDA Technology, Inc; Research Grant, Galil Medical Ltd; Consultant, Medtronic plc; Consultant, Endocare, Inc; Consultant, Johnson & Johnson; Consultant, Thermedical, Inc Grant D. Schmitz, MD, Rochester, MN (*Abstract Co-Author*) Nothing to Disclose John J. Schmitz, MD, Rochester, MN (*Abstract Co-Author*) Nothing to Disclose Adam J. Weisbrod, MD, Rochester, MN (*Abstract Co-Author*) Nothing to Disclose Thomas D. Atwell, MD, Rochester, MN (*Abstract Co-Author*) Nothing to Disclose Patrick W. Eiken, MD, Rochester, MN (*Abstract Co-Author*) Nothing to Disclose Michael R. Moynagh, MD, FFR(RCSI), Dublin 7, Ireland (*Abstract Co-Author*) Nothing to Disclose Anil N. Kurup, MD, Rochester, MN (*Abstract Co-Author*) Research Grant, Galil Medical Ltd; Research Grant, EDDA Technology, Inc; Royalties, Wolters Kluwer nv

#### For information about this presentation, contact:

morris.jonathan@mayo.edu

# **TEACHING POINTS**

Cryoablation of very large tumors require an advanced skill set not needed when treating smaller lesions. This educational exhibit will cover several logistical, technique related, and clinical care points to allow the radiologist to perform these cryoablations safely and learn from our experience of treating 143 lesions with greater than 8 and up to 32 probes. We will discuss preablation planning, intraprocedural techniques, and post procedural patient management. Additionally a review of the procedural, post procedural, and long term risks involving large cryoablations will be covered.

#### **TABLE OF CONTENTS/OUTLINE**

A. Introduction to large tumor cryoablation B. Pre-procedural planning, logistics of opening, stacking, and numbering probes and thermal protection devices C. Pre-procedural visual probe maps D. Line management and order of image guided probe insertion E. Intra-procedural probe management, gas management, protection of critical structures, and ablation techniques used in cases with large number of probes (8-32 probes) F. In-hospital clinical care, renal protection from myogolinuria, and complication prevention/management G. Long term risk and clinical follow up H. Conclusion



#### VI155-ED-SUB9

Contrast-Enhanced Ultrasound for Carotid Artery Plaque: How to Do It

Sunday, Nov. 25 1:00PM - 1:30PM Room: VI Community, Learning Center Station #9

#### **Participants**

Yeo Koon Kim, Seongnam-Si, Korea, Republic Of (*Presenter*) Nothing to Disclose Ji Eun Park, Seongnam, Korea, Republic Of (*Abstract Co-Author*) Nothing to Disclose Hee Jun Bae, Seongnam, Korea, Republic Of (*Abstract Co-Author*) Nothing to Disclose

For information about this presentation, contact:

yeokoon@snubh.org

### **TEACHING POINTS**

1. The readers will learn how to do the carotid contrast-enhanced ultrasound and how to quantify the plaque enhancement. 2. The readers will review the cases of carotid contrast-enhanced ultrasound.

# TABLE OF CONTENTS/OUTLINE

1. Value of contrast-enhanced ultrasound (CEUS) for vascular evaluation 1) Enhancement of lumen: better visualization of plaque surface and ulceration 2) Enhancement of plaque: plaque vulnerability 3) Introduction of an ongoing study to evaluating the prognostic value of plaque enhancement on carotid CEUS in acute stroke patients (NCT03283306) 2. How to do carotid CEUS 1) Preparation: intravenous catheter, informed consent 2) Carotid Doppler ultrasound 3) Injection of ultrasound contrast: twice bolus injections for bilateral carotid arteries 3) Carotid CEUS: lumen and plaque enhancement 4) Quantification of plaque enhancement: quantification with software 3. Review of current status and limitations of carotid CEUS



## VI206-SD-SUB1

Ovarian Function Following Uterine Artery Embolization or Surgery for Symptomatic Uterine Fibroids: A Meta-Analysis

Sunday, Nov. 25 1:00PM - 1:30PM Room: VI Community, Learning Center Station #1

#### Awards Student Travel Stipend Award

#### **Participants**

Vaishali Jadhav, BS, Suwanee, GA (*Presenter*) Nothing to Disclose Gulsedef Arslan, MS, Suwanee, GA (*Abstract Co-Author*) Nothing to Disclose Luis Gutierrez, MS, Suwanee, GA (*Abstract Co-Author*) Nothing to Disclose Matthew Mozzo, MS, Suwanee, GA (*Abstract Co-Author*) Nothing to Disclose Aliu Sanni, MD, Snellville, GA (*Abstract Co-Author*) Nothing to Disclose

# For information about this presentation, contact:

vaishalija@pcom.edu

#### PURPOSE

Uterine artery embolization (UAE) has become a well-recognized minimally invasive treatment alternative to myomectomy (LM) and hysterectomy (Hyst) for symptomatic uterine fibroids. Ovarian failure as a complication of UAE has raised concerns about this treatment modality in young women. The serum Follicular-stimulating hormone (FSH) level is the standard measure of ovarian function and its increased level suggests diminished ovarian reserve. The aim of this study is to compare the ovarian function following these two options of treatment for symptomatic uterine fibroids.

# METHOD AND MATERIALS

A systematic search and review of published research papers were conducted in public database PubMed maintained online by U.S. National Library of Medicine to identify and retrieve relevant studies from January 2004 through March 2014, with the availability of comparative data for ovarian function after UAE or Surgery. The primary outcome analyzed was the post-procedural FSH levels at 6 months. Other outcomes measured were the serum level of Anti-Mullerian Hormone (AMH) and Estradiol. Results are expressed as the standard difference in means with standard deviation. Statistical analysis was done using fixed-effects meta-analysis to compare the mean value of the different groups. (Comprehensive Meta-Analysis Version 3.3.070 software; Biostat Inc., Englewood, NJ).

## RESULTS

Seven out of 168 studies that met the analysis criteria were included in this meta-analysis. Among the seven studies, there were 384 patients with symptomatic uterine fibroids with 214 patients undergoing UAE and 170 patients Surgery (LM/Hysterectomy). Serum FSH (-0.363  $\pm$  0.100, p = 0.000) was significantly higher in the surgical group. Serum AMH level (0.408  $\pm$  0.190, p = 0.032) and Estradiol (0.416  $\pm$  0.143, p = 0.004) were significantly higher in the UAE group of patients.

# CONCLUSION

Ovarian function was reserved better in patients undergoing UAE for symptomatic UF when compared to surgical interventions.

# **CLINICAL RELEVANCE/APPLICATION**

Treatment of symptomatic uterine fibroids with UAE offers the clinical advantage to preserve ovarian function in the childbearing age group of women in contrast to the surgical procedures myomectomy or hysterectomy.



## VI208-SD-SUB3

Effective Dose Management Using Fluoroscopy Save Technique for DSA (Digital Subtraction Angiography)

Sunday, Nov. 25 1:00PM - 1:30PM Room: VI Community, Learning Center Station #3

#### **Participants**

Sanghun Kim, Seoul, Korea, Republic Of (*Presenter*) Nothing to Disclose In Bum Ko, Seoul, Korea, Republic Of (*Abstract Co-Author*) Nothing to Disclose Ahn Miseob, Seoul, Korea, Republic Of (*Abstract Co-Author*) Nothing to Disclose

#### For information about this presentation, contact:

zeroeternal@naver.com

#### PURPOSE

Proper use of the 'fluoroscopy save,' option allows for the DSFS (digital subtraction fluoroscopy save) to be substituted for cases requiring hand injection DSA (digital subtraction angiography) images, upper/lower extremity angiography or pediatrics angiography to ultimately allow efficient control over patients' and operators' radiation dosage

## **METHOD AND MATERIALS**

To best replicate a real clinical situation where a dye is injected into the patient, Phantom and vessel models were used. A polyvinyl chloride tube was curved to represent the vessel, which was placed inside an acryl box (3mm) with an entry and an exit site for the dye. The Phantom was placed above the box to commence the experiment. The device model used was 'Allular X-per FD-20,' with the table height set at 85cm, SID 100, and FD size 48. The lower body x-ray shield was installed at the table and the glass dosimeter was attached at 2 points: surface of the phantom for surface dose and the location of the operator for neighboring dose, with the detector 1cm away. An auto-injector was used to administer 20mL of the dye at 1mL/sec, with the image acquired through both DSA and DSFS.

#### RESULTS

On average, 79.19% of the surface dose was reduced from  $4122.67\mu$ Gy to  $857\mu$ Gy, the neighboring dose from  $117\mu$ Gy to  $23.67\mu$ Gy at 79.75%. Independent t-test was completed through SPSS (version 18; PASW statistics), with the analysis showing significant difference (p<0.001).

# CONCLUSION

Compared to the DSA, DSFS allows image acquisition with 79% reduced radiation dose, and a higher frame rate useful for capturing branching of the vessels. However, the image quality can vary, and thus the method is limited to certain locations in the body as well as the body type; thus the method is useful for parts of the body with thin layers of fat, or specific anatomy such as upper/lower extremities. Furthermore, DSA road map can be used in conjunction with DSFS, further reduction in radiation would be possible without compromise of patients' health.

# **CLINICAL RELEVANCE/APPLICATION**

This method was applied to phrenic artery angiography (which requires many hand injection angiography procedures) and upper/lower extremity procedures (PTA, stent insertion, diagnosis since these images can be acquired even with low dose radiation). The results showed no issues with treatment or clinical outcome of patients, but high BMI patients were excluded for phrenic artery angiography due to low quality images



# VI209-SD-SUB4

Establishing Expected PET/CT Imaging Response Following Radioembolization for Breast Cancer Liver Metastases

Sunday, Nov. 25 1:00PM - 1:30PM Room: VI Community, Learning Center Station #4

# Participants

Ryan W. England, MD, New York, NY (*Presenter*) Nothing to Disclose Christopher C. Riedl, MD, New York, NY (*Abstract Co-Author*) Nothing to Disclose Etay Ziv, MD,PhD, New York, NY (*Abstract Co-Author*) Research Grant, Johnson & Johnson; Research Grant, Cycle for Survival ; Research Grant, Functional Genomics Initiative Constantinos T. Sofocleous, MD, PhD, New York, NY (*Abstract Co-Author*) Consultant, General Electric Company; Consultant, Johnson & Johnson; Consultant Terumo; ; Research Support: BTG, Ethicon J&J; ; ; Lynn A. Brody, MD, New York, NY (*Abstract Co-Author*) Stockholder, Sirtex Medical Ltd Hooman Yarmohammadi, MD, New York, NY (*Abstract Co-Author*) Nothing to Disclose Franz E. Boas, MD,PhD, New York, NY (*Abstract Co-Author*) Co-founder, Claripacs, LLC In-kind support, Bayer AG Investor, Labdoor Investor, Qventus Investor, CloudMedx Investor, Notable Labs Serena Wong, New York, NY (*Abstract Co-Author*) Nothing to Disclose Tiffany A. Traina, MD, New York, NY (*Abstract Co-Author*) Nothing to Disclose Amy R. Deipolyi, MD, PhD, New York, NY (*Abstract Co-Author*) Nothing to Disclose

#### PURPOSE

Transarterial radioembolization (TARE) is an emerging palliative treatment for hepatic tumors due to metastatic breast cancer (MBC). Expected PET/CT imaging outcomes over time following TARE are not well established, and would be helpful to define in order to advise patients and referrers.

### CONCLUSION

In MBC, follow up PET/CT is optimally performed at 8-10 weeks after TARE to detect objective response. A second post-TARE scan 5 months later will demonstrate imaging changes in most patients. These data highlight the value of imaging at 2 and 7 months following TARE. These results may help guide physicians and inform patients of expected outcomes after TARE.

### **CLINICAL RELEVANCE/APPLICATION**

The results of this study aim to provide follow-up imaging guidance for physicians and patients with metastatic breast cancer who have had recent transarterial radioembolization of liver metastases.



# VI210-SD-SUB5

A Multiple Combined Approach (Ablation, Consolidation and Radiotherapy) in the Management of Painful and Osteolytic Metastases of the Spine Only: Experience of a Single Center

Sunday, Nov. 25 1:00PM - 1:30PM Room: VI Community, Learning Center Station #5

# VA

## Participants

Francesco Arrigoni, Coppito, Italy (*Presenter*) Nothing to Disclose Pierpaolo Palumbo, MD, L'Aquila, Italy (*Abstract Co-Author*) Nothing to Disclose Simone Quarchioni, Laquila, Italy (*Abstract Co-Author*) Nothing to Disclose Silvia Mariani, MD, L'Aquila, Italy (*Abstract Co-Author*) Nothing to Disclose Mario Di Staso, L'Aquila, Italy (*Abstract Co-Author*) Nothing to Disclose Luigi Zugaro, L'Aquila, Italy (*Abstract Co-Author*) Nothing to Disclose Antonio Barile, MD, L'Aquila, Italy (*Abstract Co-Author*) Nothing to Disclose Carlo Masciocchi, MD, L'Aquila, Italy (*Abstract Co-Author*) Nothing to Disclose

### For information about this presentation, contact:

arrigoni.francesco@gmail.com

#### PURPOSE

Aim of this study was to evaluate the combined effect of 3 combined therapies in the management of spine metastases: ablation, to destroy the core of the lesion, vertebroplasty, to consolidate the vertebral body weakened by metastases (fracturated or at risk of fracture), and radiotheraphy, to consolidate the therapeutic role of ablation and treat the margins of each lesion.

### METHOD AND MATERIALS

We have prospectively evaluated the outcome of this combined treatment in 8 patients treated for 9 painful lesions that required analgesic therapies. Both vertebral bodies with pathological fractures and vertebral bodies still intact but at risk of fracture were treated. The ablation (RFA or CRYO) and vertebroplasty were performed in a single session with CT guidance; the volume of ablation in all cases covered the lesion completely; the amount of cement injected was little, just to stabilize the vertebral body; the radiotherapy treatment (8 Gy in a single session) was performed no longer than 10 days later.

### RESULTS

Patients were followed up to 6 months with imaging and clinical evaluation. In all the cases we recorded stability of lesions without signs (at the imaging) of relapse of local disease or new fractures. All patients reported regression of symptomatology and interruption of pain medication.

### CONCLUSION

Though limited by a small cohort of patients and short term follow-up studies, the combined approach proved to be quite effective in the management of spinal lesions.

# **CLINICAL RELEVANCE/APPLICATION**

Developments in palliative role of interventional radiology in the spine, a very common location of secondary lesions



# AI001-SUD

# **3D Segmentation of Brain MR**

Sunday, Nov. 25 2:30PM - 4:00PM Room: AI Community, Learning Center

# Title and Abstract

3D Segmentation of Brain MR This session will focus on the use of deep learning methods for segmentation, with particular emphasis on 3D techniques (V-Nets) applied to the challenge of MR brain segmentation. While focused on this particular problem, the concepts should generalize to other organs and image types.



# AI001-MOA

# **Introduction to Deep Learning**

Monday, Nov. 26 8:30AM - 10:00AM Room: AI Community, Learning Center

# **Title and Abstract**

Introduction to Deep Learning This class will focus on basic concepts of convolutional neural networks (CNNs), and walk the attendee through a working example. A popular training example is the MNIST data set which consists of hand-written digits. This course will use a data set we created, that we call 'MedNIST' and consists of 1000 images each from 5 different categories: Chest X-ray, hand X-ray, Head CT, Chest CT, Abdomen CT, and Breast MRI. The task is to identify the image type. This will be used to train attendees on the basic principles and some pitfalls in training a CNN. The attendee will have the best experience if they are familiar with Python programming.



# AI001-MOB

# **Advanced Data Augmentation Using GANs**

Monday, Nov. 26 10:30AM - 12:00PM Room: AI Community, Learning Center

# **Title and Abstract**

Advanced Data Augmentation Using GANs Getting 'large enough' data sets is a problem for most deep learning applications, and this is particularly true in medical imaging. Generative Adversarial Networks (GANs) are a deep learning technology in which a computer is trained to create images that look very 'real' even though they are completely synthetic. This may be one way to address the 'data shortage' problem in medicine.



# AI026-EB-MOA

An Artificial Intelligence-Based System for Triaging of Digital Mammography Exams

Monday, Nov. 26 12:15PM - 12:45PM Room: IN Community, Learning Center Hardcopy Backboard

#### **Participants**

David Richmond, Newton, MA (*Presenter*) Senior Data Scientist, IBM Watson Health Maggie Kusano, Mississauga, ON (*Abstract Co-Author*) Employee, IBM Corporation Guy Amit, PhD, Haifa, Israel (*Abstract Co-Author*) Employee, IBM Corporation Ayelet Akselrod-Ballin, San Jose, CA (*Abstract Co-Author*) Employee, IBM Corporation Efrat Hexter, San Jose, CA (*Abstract Co-Author*) Employee, IBM Corporation Simona Rabinovici-Cohen, Haifa, Israel (*Abstract Co-Author*) Employee, IBM Corporation Yoel Shoshan, Haifa, Israel (*Abstract Co-Author*) Employee, IBM Corporation David Wilson, Cambridge, MA (*Abstract Co-Author*) Employee, IBM Corporation Grant Covell, Cambridge, MA (*Abstract Co-Author*) Employee, IBM Corporation Andjela Azabagic, Brooklyn, NY (*Abstract Co-Author*) Former Employee, IBM Corporation Bill Stoval, Cambridge, MA (*Abstract Co-Author*) Employee, IBM Corporation Marwan Sati, PhD, Mississauga, ON (*Abstract Co-Author*) Employee, IBM Corporation

# For information about this presentation, contact:

david.richmond@ibm.com

# CONCLUSION

A framework for automated processing of medical images within clinical environments has been developed and shown in this early pilot to automatically triage MG studies based on an AI- algorithm.

# FIGURE

http://abstract.rsna.org/uploads/2018/18020191/18020191\_3w6t.jpg

#### Background

Breast screening programs have been established worldwide to facilitate early detection and treatment of breast cancer. However, healthcare quality and affordability initiatives, an aging population, increased data from emerging modalities, and a shortage of radiologists have led to unmanageable throughput, resulting in delayed diagnosis and physician burnout. In this paper we present an AI-based framework for triaging digital screening mammography (MG) exams based on likelihood of cancer.

#### **Evaluation**

A deep learning model was trained to infer a patient's likelihood of abnormality based on her 4-view screening MG exam. The model was integrated in a new platform for automated processing of images within hospital IT and cloud environments. Digital MG studies were de-identified from partner sites and secondary usage rights secured. Normal MGs were defined as screening studies assessed as BI-RADS 1 or 2, confirmed by 4+ years of follow up normal exams. Abnormal MGs were defined as screening studies that were recalled, and led to positive or negative biopsy within 1 year. The system was initially trained on 1192 screening MGs and then tested on a held-out set of 323 screening MGs from a new hospital site, enriched with suspicious cases (165 normal, 158 abnormal). The system achieved a sensitivity of 95% and specificity of 20%. In other words, the system correctly triaged 20% of the BI-RADS 1 and 2 exams as normal. For a cancer prevalence of 0.5%, this corresponds to an NPV of 99.87%. In cross-validation on a set of 1578 MG studies (~700 normal, ~900 abnormal), the system achieved a specificity of 40% at 95% sensitivity, with an ROC AUC of 0.84.

#### Discussion

The system identified a significant portion of normal exams from the worklist, effectively highlighting more complex and challenging cases. We are continuing training with 10,000 screening MGs, and expect that the system will learn to identify more normal studies, further refining the remaining complex cases.



# AI027-EB-MOA

# Abdominal Segmentation for Body Composition Using Deep-Learning U-Net

Monday, Nov. 26 12:15PM - 12:45PM Room: IN Community, Learning Center Hardcopy Backboard

## Participants

Alexander Weston, Rochester, MN (*Presenter*) Nothing to Disclose Panagiotis Korfiatis, PhD, Rochester, MN (*Abstract Co-Author*) Nothing to Disclose Kenneth Philbrick, Rochester, MN (*Abstract Co-Author*) Nothing to Disclose Timothy L. Kline, PhD, Rochester, MN (*Abstract Co-Author*) Nothing to Disclose Naoki Takahashi, MD, Rochester, MN (*Abstract Co-Author*) Nothing to Disclose Bradley J. Erickson, MD, PhD, Rochester, MN (*Abstract Co-Author*) Stockholder, OneMedNet Corporation; Stockholder, VoiceIt Technologies, LLC; Stockholder, FlowSigma;

#### For information about this presentation, contact:

#### weston.alexander@mayo.edu

### CONCLUSION

U-Net is an accurate method of 3D abdominal segmentation based on 2D imaging data. This is important for accurately assessing body composition.

### FIGURE

http://abstract.rsna.org/uploads/2018/18020348/18020348\_7m3i.jpg

#### Background

Body composition (defined as the amount and distribution of fat and muscle present in the body) is a well-known indicator of overall physical health. There are several methods to assess body composition but the most accurate is abdominal CT (or MRI) imaging, which is often already included in the clinical workflow. A limitation to this approach is the need for abdominal segmentation which is time consuming. For this reason, single-slice analysis of body composition is common.

#### **Evaluation**

We trained a deep convolutional neural network (U-Net) on 2430 transverse CT scans at the level of the L3 vertebra. We segmented the abdomen into subcutaneous, muscle, visceral adipose, visceral organ, and bone compartments. Gold-standard segmentation was performed with a semiautomated method with manual correction. On the test set, U-Net had a Dice score of 0.98 on the subcutaneous, 0.96 on muscle, and 0.94 on visceral adipose compartments (compared to the gold-standard). Additionally, the accuracry of our algorithm met or exceeded that of manual segmentation by 2 experts (subcutaneous: 0.98 vs 0.95, muscle: 0.95 vs 0.93, viscera: 0.99 vs 0.99). We evaluated performance of our algorithm on transverse CT scans taken at the level of the L4 vertebra (a different level from our training data) which was not significantly different than accuracy at the L3 level. Finally, we evaluated the performance of our trained U-Net on a secondary dataset of 2369 transverse CT scans taken from subjects with a different underlying condition.

#### Discussion

Our algorithm is an accurate method of assessing body composition. It is generalizable to a different population of subjects. It accurately segments multiple levels of the abdomen despite the fact that it is trained on the L3 level alone. It is therefore capable of 3D segmentation with limited 2D training data. We demonstrate that 3D segmentation to assess body composition is more accurate than the current gold-standard of single-slice segmentation due to the variability in subject anatomy, including shifting GI contents.

# **Honored Educators**

Presenters or authors on this event have been recognized as RSNA Honored Educators for participating in multiple qualifying educational activities. Honored Educators are invested in furthering the profession of radiology by delivering high-quality educational content in their field of study. Learn how you can become an honored educator by visiting the website at: https://www.rsna.org/Honored-Educator-Award/ Naoki Takahashi, MD - 2012 Honored Educator



# AI143-ED-MOA2

Deep Learning Techniques for Automated Segmentation of Diffuse Lung Disease Opacities on CT Images

Monday, Nov. 26 12:15PM - 12:45PM Room: AI Community, Learning Center Station #2

### Participants

Shoji Kido, MD, PhD, Ube, Japan (*Presenter*) Nothing to Disclose Kanako Murakami, Ube, Japan (*Abstract Co-Author*) Nothing to Disclose Noriaki Hashimoto, Ube, Japan (*Abstract Co-Author*) Nothing to Disclose Yasushi Hirano, Ube, Japan (*Abstract Co-Author*) Nothing to Disclose Shingo Mabu, Ube, Japan (*Abstract Co-Author*) Nothing to Disclose Kenji Suzuki, PhD, Chicago, IL (*Abstract Co-Author*) Royalties, General Electric Company; Royalties, Hologic, Inc; Royalties, MEDIAN Technologies; Royalties, Riverain Technologies, LLC; Royalties, Canon Medical Systems Corporation; Royalties, Mitsubishi Corporation; Royalties, AlgoMedica, Inc

### For information about this presentation, contact:

kido.ai@yamaguchi-u.ac.jp

# **TEACHING POINTS**

To segment diffuse lung disease opacities on CT images accurately is important for quantitative pathological evaluation such as radiomics. However, it is difficult to segment pathological lungs correctly by use of conventional algorithms because contours of lungs are blurring by pathological opacities such as consolidation. The state-of-art deep learning techniques can segment lungs with diffuse lung opacities correctly compared with conventional methods. The purpose of this exhibit is: 1. To learn segmentation by use of convolutional neural network (CNN) with a sliding window on a pixel-by-pixel. 2. To learn segmentation by use of fully convolutional neural network (FCN) where the last fully-connected layer of CNN is substituted by another convolution layer with a large 'receptive field'. 3. To learn segmentation by use of U-Net which has ladder networks. U-Net is the state-of-art semantic segmentation algorithm of biological images, and it requires small number of image data. 4. To learn neural network convolution (NNC) which is one of other types of simple structure neural networks. It requires a small number of images and calculation time.

### TABLE OF CONTENTS/OUTLINE

1. Introduction, 2. Segmentation by use of CNN with a sliding window. 3. Segmentation by use of FCN. 4. Segmentation by use of U-Net. 5. Segmentation by use of NNC. 5. Conclusion.



# Automatic Contrast Enhancement Detection on Head CT

Monday, Nov. 26 12:15PM - 12:45PM Room: AI Community, Learning Center Station #1

### Participants

Bernardo Henz, MSc, Porto Alegre, Brazil (*Abstract Co-Author*) Nothing to Disclose Jose E. Venson, MSc, Porto Alegre, Brazil (*Presenter*) Nothing to Disclose Alesson Scapinello, Porto Alegre, Brazil (*Abstract Co-Author*) Nothing to Disclose Daniel Souza, Porto Alegre, Brazil (*Abstract Co-Author*) Nothing to Disclose Cesar C. Cavion, MD, Porto Alegre, Brazil (*Abstract Co-Author*) Nothing to Disclose Felipe C. Kitamura, MD, MSC, Sao Paulo, Brazil (*Abstract Co-Author*) Developer, DASA

# CONCLUSION

Our results showed high accuracy in the detection of contrast on head CT scans. As future work, we are planning validation experiments in a clinical environment

# Background

Intravenous administration of iodinated contrast media has undeniable importance in the evaluation of computed tomography (CT) scans for several clinical indications. The information about contrast administration is usually in the DICOM metadata. However, in teleradiology services, this parameter is frequently not available in a standardized way, being difficult to be automatically populated in the report. Consequently, incorrect contrast information represents 8.73% of report errors in our teleradiology, causing financial and even potentially legal disruptions to diagnostic services. In order to reduce this error rate, we propose a solution to automatically detect contrast enhancement by using convolutional neural networks.

#### **Evaluation**

We selected 500 head CT scans randomly and anonymously, ensuring a balanced distribution between the classes: non-contrastenhanced and contrast-enhanced. Preparing the data: Given that the number of slices of each exam differs, we decided to train a CNN to classify a single image into one of the two classes. Instead of using all slices of an exam, we only take the ones in the range [0.40,0.60] in the z-axis, also cropping the xy-axes to get the sinus rectus. This totalizes more than 10k 192x192 images for training. Strategies used for data augmentation were random rotations, translations, brightness and contrast adjustments, and addition of noise. Our architecture: Our model consists of 6 convolutional and 2 fully-connected layers. After training, our network was able to predict the class of a single image with 93% of accuracy. Exam classification: When classifying an exam, we used a voting scheme to account for the probability of each prediction being correct. In other words, the higher the chance of a prediction being correct, the higher its weight in the voting. By using this scheme, the accuracy of predicting the class of the exam is 98%.

### Discussion

Automatic contrast detection is important to avoid errors in reports and optimize the diagnostic flow.



# AI203-SD-MOA4

Prostate Cancer Lesion Segmentation and Gleason Score Prediction Using Multi-parametric MRI via Deep Residual Neural Network

Monday, Nov. 26 12:15PM - 12:45PM Room: AI Community, Learning Center Station #4

# Participants

Ruiming Cao, Los Angeles, CA (*Presenter*) Nothing to Disclose Sepideh Shakeri, Los Angeles, CA (*Abstract Co-Author*) Nothing to Disclose Xinran Zhong, Los Angeles, CA (*Abstract Co-Author*) Research support, Siemens AG Amirhossein Mohammadian Bajgiran, MD, Los Angeles, CA (*Abstract Co-Author*) Nothing to Disclose Sohrab Afshari Mirak, MD, Los Angeles, CA (*Abstract Co-Author*) Nothing to Disclose David S. Lu, MD, Los Angeles, CA (*Abstract Co-Author*) Nothing to Disclose David S. Lu, MD, Los Angeles, CA (*Abstract Co-Author*) Consultant, Medtronic plc; Speaker, Medtronic plc; Consultant, Johnson & Johnson; Research Grant, Johnson & Johnson; Consultant, Bayer AG; Research Grant, Bayer AG; Speaker, Bayer AG Dieter R. Enzmann, MD, Los Angeles, CA (*Abstract Co-Author*) Nothing to Disclose Steven S. Raman, MD, Santa Monica, CA (*Abstract Co-Author*) Nothing to Disclose Kyunghyun Sung, PhD, Los Angeles, CA (*Abstract Co-Author*) Research support, Siemens AG

#### For information about this presentation, contact:

rcao@mednet.ucla.edu

#### PURPOSE

To automatically contour prostate cancer (PCa) lesion and to predict Gleason score (GS) by training a deep residual neural network (ResNet) from multi-parametric MRI (mp-MRI).

## METHOD AND MATERIALS

In collaboration with Department of Pathology, we utilized GS-labeled whole-mount histopathology after radical prostatectomy to identify and segment PCa lesion on mp-MRI as ground-truth. A total number of 98 pre-operative mp-MRI cases were acquired on 3T MRI systems (Skyra and Prisma, Siemens), and normalized T2-weighted (T2w) imaging, apparent diffusion coefficient (ADC) and transfer constant (Ktrans) were used for training and testing the ResNet. We input each slice of mp-MRI to a fully-supervised ResNet to predict PCa lesion contour and GS. Specifically, we have built a 101-layer ResNet with atrous convolutional filters which help to compensate the misalignment between different imaging sequences. The model was trained using a weighted pixel-wise cross-entropy loss, which optimizes the prediction of both PCa lesion contour and GS. We randomly selected 74 cases consisting a total of 1056 mp-MRI slices as training set and tested the trained ResNet with the remaining 24 cases. For testing, the ResNet had to determine the presence and quantity of lesions on a given slice before segmentation.

### RESULTS

Two experienced abdominal radiologists, with 33 years and 25 years of clinical experience respectively, were asked to independently score the quality of predicted lesion contours from 1 (completely missed) to 5 (sufficiently similar to the ground-truth) based on the ground-truth segmentation for each lesion in testing cases. 77.4% lesion contour predictions received 3 (minimal overlap) or above with 100% inter-rater agreement. Out of those predictions, on average 68.8% received 4 (significant overlap) or above with 79.2% agreement. Of those predictions scored 3 or above, clinically significant lesions (GS3+4 or above) were classified with 81.8% precision and 100% recall.

### CONCLUSION

This study used state-of-the-art ResNet for PCa lesion segmentation and GS prediction. In 24 testing cases, the ResNet had achieved 77.4% success rate in lesion segmentation and 81.8% precision in predicting clinically significant lesion.

### **CLINICAL RELEVANCE/APPLICATION**

This study aims to improve diagnosis of prostate cancer and to further assist clinical decision making for proper treatment.



# AI204-SD-MOA3

# Semi-Automatic RECIST Labeling on CT Scans with Cascaded Convolutional Neural Networks

Monday, Nov. 26 12:15PM - 12:45PM Room: AI Community, Learning Center Station #3

### **Participants**

Youbao Tang, PhD, Bethesda, MD (*Presenter*) Nothing to Disclose Adam P. Harrison, PhD, Bethesda, MD (*Abstract Co-Author*) Nothing to Disclose Mohammad Hadi Bagheri, MD, Bethesda, MD (*Abstract Co-Author*) Nothing to Disclose Jing Xiao, Shenzhen, China (*Abstract Co-Author*) Nothing to Disclose Ronald M. Summers, MD, PhD, Bethesda, MD (*Abstract Co-Author*) Royalties, iCAD, Inc; Royalties, Koninklijke Philips NV; Royalties, ScanMed, LLC; Research support, Ping An Insurance Company of China, Ltd; Researcher, Carestream Health, Inc; Research support, NVIDIA Corporation; ; ; ;

#### For information about this presentation, contact:

youbao.tang@nih.gov

# PURPOSE

Response evaluation criteria in solid tumors (RECIST) is the standard measurement for tumor extent to evaluate treatment responses in cancer patients. Using RECIST annotation faces two main challenges: 1) measuring tumor diameters requires a lot of professional knowledge and is time-consuming. Consequently, it is difficult and expensive to manually annotate large-scale datasets, e.g., those used in large clinical trials or retrospective analyses. 2) RECIST marks are often subjective and prone to inconsistency among different observers. However, consistency is critical in assessing actual lesion growth rates, which directly impacts patient treatment options. To overcome these problems, we propose a cascaded convolutional neural network based method to semi-automatically label RECIST annotations.

## **METHOD AND MATERIALS**

The stacked hourglass networks (SHN) is employed for RECIST estimation, where a relationship constraint loss is introduced to improve the estimation accuracy. Regardless of class, the lesion regions may have large variability in sizes, locations and orientations in different images. To make our method robust to these variations, the lesion region first needs to be normalized before feeding into SHN. The spatial transformer network is used for lesion region normalization, where a localization network is designed for lesion region and transformation parameter prediction. Thus, given a region of interest by a radiologist, our method directly outputs its RECIST annotation. We train our system on a large scale lesion dataset where 32,735 RECIST annotations from 4,459 patients are performed by multiple radiologists over a multi-year period.

## RESULTS

500 lesions from 200 patients have three manual RECIST annotations and are used for test. The mean and standard deviation of inter-reader variation of long diameter are  $3.40\pm5.24$ mm, while those for the variation between our system and the manual annotations are  $2.67\pm3.95$ mm. The results demonstrate that our system performs more stably and with less variability.

### CONCLUSION

Our approach only requires a rough bounding box drawn by a radiologist and produces stable RECIST annotations, suggesting that RECIST can be reliably obtained with reduced labor and time.

### **CLINICAL RELEVANCE/APPLICATION**

If coupled with a reliable lesion localization framework, our approach can be made fully automatic. As such, the proposed system can potentially provide a highly positive impact to clinical workflows.



### BR176-ED-MOA7

Contrast-Enhanced Mammography: Current Applications and Future Direction

Monday, Nov. 26 12:15PM - 12:45PM Room: BR Community, Learning Center Station #7

#### Awards Identified for RadioGraphics

#### **Participants**

Kimeya Ghaderi, MD, Boston, MA (*Presenter*) Nothing to Disclose Jordana Phillips, MD, Boston, MA (*Abstract Co-Author*) Research Grant, General Electric Company; Consultant, General Electric Company Hannah Perry, MD, Boston, MA (*Abstract Co-Author*) Nothing to Disclose Parisa Lotfi, MD, Newton, MA (*Abstract Co-Author*) Nothing to Disclose

Tejas S. Mehta, MD, MPH, Boston, MA (Abstract Co-Author) Nothing to Disclose

### For information about this presentation, contact:

kghaderi@bidmc.harvard.edu

# **TEACHING POINTS**

Contrast-Enhanced Mammography (CEM) employs a dual energy technique to create images that show abnormal morphology and density (similar to conventional mammography) and abnormal enhancement (like MRI). CEM is FDA approved for adjunct use in the diagnostic setting. Diagnostic applications include evaluation of screening callbacks, the symptomatic breast, disease extent in women with known breast cancer, and response to neoadjuvant chemotherapy. Key clinical indication of CEM is as an MRI alterative demonstrating similar sensitivity and positive predictive value. Benefits include reduced patient cost and relative ease of access compared to MRI. Challenges include IV placement, risks associated with contrast in mammography setting, and added time.

### **TABLE OF CONTENTS/OUTLINE**

Background: What is CEM and how are images acquired? FDA approved indications and literature review Screening recall: Architectural distortion, mass, calcifications Follow-up diagnostic imaging Symptomatic breast Evaluation of disease extent Response to neoadjuvant chemotherapy Mammographically occult malignancy Troubleshooting When MRI cannot be performed Supplemental screening Other potential uses: High-risk screening Benefits and Challenges of using CEM for these indications



# BR177-ED-MOA8

Factors Affecting MRI Accuracy in Evaluating of Neoadjuvant Therapy Response in Breast Cancer: A Pictorial Review with Radiopathological Correlation

Monday, Nov. 26 12:15PM - 12:45PM Room: BR Community, Learning Center Station #8

**FDA** Discussions may include off-label uses.

# Awards

**Certificate of Merit** 

# Participants

Gulgun Engin, Istanbul, Turkey (*Presenter*) Nothing to Disclose Semen Onder, MD, ?stanbul, Turkey (*Abstract Co-Author*) Nothing to Disclose Inci Kizildag Yirgin, Istanbul, Turkey (*Abstract Co-Author*) Nothing to Disclose Ekrem Yavuz, MD, ?stanbul, Turkey (*Abstract Co-Author*) Nothing to Disclose

# For information about this presentation, contact:

gengin@istanbul.edu.tr

### **TEACHING POINTS**

To review tumor shrinkage patterns subsequent to NAC To discuss the factors affecting MRI accuracy in evaluating of NAC response To improve the knowledge about the detection accuracy of residual disease after NAC by MRI

# TABLE OF CONTENTS/OUTLINE

Preoperative neoadjuvant chemotheraphy (NAC) is widely performed for patients with locally-advanced breast carcinomas in order to control and downstage the primary breast carcinomas. Breast magnetic resonance imaging (MRI) is the most accurate imaging modality for assessment of tumor response to NAC. However, MRI often over- or underestimate the extent and distribution of residual carcinomas following NAC. The accuracy of MRI in evaluating residual tumor size and extent depends on tumor type, morphology, and biomarker status. Cancers with lobular component, non-mass-like enhancement lesions, HR-positive, and HER2negative cancers had an increased discrepancy between MRI versus pathology tumor size (Figures 1-5). Improved knowledge about the detection accuracy of residual disease after NAC by MRI is crucial to help planning of an optimal surgery to achieve a tumor free margin. This can reduce the re-excision rate and minimize local recurrence. In this pictorial review, the factors affecting MRI accuracy in evaluating of NAC response are analysed and discussed with detailed radiopathological correlation.



# BR178-ED-MOA9

Pitfalls, Tricks, and Tips in the Sonographic Evaluation of Breast. What the Radiology Residents Need to Know?

Monday, Nov. 26 12:15PM - 12:45PM Room: BR Community, Learning Center Station #9

# Participants

Karina Pesce, Capital Federal, Argentina (*Abstract Co-Author*) Nothing to Disclose Maria B. Orruma, MD, Buenos Aires, Argentina (*Abstract Co-Author*) Nothing to Disclose Maria Jose Chico, Buenos Aires, Argentina (*Presenter*) Nothing to Disclose Ana G. Luna, CABA, Argentina (*Abstract Co-Author*) Nothing to Disclose Diana Herbas Galindo, Capital Federal, Argentina (*Abstract Co-Author*) Nothing to Disclose Pamela I. Causa Andrieu, MD, La Plata, Argentina (*Abstract Co-Author*) Nothing to Disclose

#### For information about this presentation, contact:

drakarina.pesce@gmail.com

### **TEACHING POINTS**

1. Review of the anatomy and the factors contributing to the difficulties in the evaluation in the breast ultrasound. 2. Describe common artefacts and image quality issues. Discuss common pitfalls and limitations. 3. Illustrate several examples of the technical artefacts, with helpful suggestions to help optimize images and avoid misinterpretation. 4. Learn tips to optimize images techniques and demonstration of some pitfalls.

## **TABLE OF CONTENTS/OUTLINE**

1. Introduction: We present a review of common pitfalls and troubleshooting. Tips for radiology residents who perform and interpret breast ultrasound. 2. Overview of breast ultrasound protocol 3- Classification of pitfalls A) Anatomical B) Sonography physics C) Instrumentation D) Cross-Correlation with mammographic lesions E) Foreign bodies. 4-Sonography Physics: Artefacts in breast ultrasound a-Gray scale ultrasound b- Artefacts in doppler ultrasound color 5- Tips to optimize imaging techniques, relevant pathologic findings and demonstration of some pitfalls. 6-Conclusions



### BR179-ED-MOA10

# **Breast Imaging STAT: A Pictorial Review of Acute Pathology**

Monday, Nov. 26 12:15PM - 12:45PM Room: BR Community, Learning Center Station #10

#### **Participants**

Rutuparna Sarangi, MD, Boston, MA (*Presenter*) Nothing to Disclose Anna Rives, MD, PhD, Boston, MA (*Abstract Co-Author*) Nothing to Disclose Anastasia F. Barron, DO, Boston, MA (*Abstract Co-Author*) Nothing to Disclose Allyson L. Chesebro, MD, Boston, MA (*Abstract Co-Author*) Nothing to Disclose Kitt Shaffer, MD, PhD, Boston, MA (*Abstract Co-Author*) Nothing to Disclose

# For information about this presentation, contact:

anna.rives@bmc.org

### **TEACHING POINTS**

1. Review the types of acute breast pathology commonly seen in the emergency setting. 2. Describe the imaging features of each entity using case-based examples. 3. Discuss current best practice for management and/or treatment.

# TABLE OF CONTENTS/OUTLINE

1. Review clinical and imaging features of mastitis and breast abscess. a. Puerperal b. Non-puerperal c. Granulomatous mastitis d. Pitfall: inflammatory breast cancer 2. Summarize evidence-based breast abscess management and treatment algorithms for the radiologist, with emphasis on ultrasound-guided drainage. 3. Present imaging manifestations of accidental breast trauma, including hematoma and fat necrosis. Pitfall: breast cancer presenting after trauma. 4. Illustrate acute post-procedural complications following percutaneous breast biopsy and surgery. 5. Describe additional examples of acute breast pathology including Mondor's disease and inflamed epidermal inclusion cyst.



### BR180-ED-MOA11

# **Primary Breast Tuberculosis: Imaging Findings**

Monday, Nov. 26 12:15PM - 12:45PM Room: BR Community, Learning Center Station #11

### Participants

Ali H. Baykan, MD, Adiyaman, Turkey (*Abstract Co-Author*) Nothing to Disclose Ibrahim Inan, MD, Istanbul, Turkey (*Abstract Co-Author*) Nothing to Disclose Hakan S. Sayiner, Adiyaman, Turkey (*Abstract Co-Author*) Nothing to Disclose Ebru Hasbay, Izmir, Turkey (*Abstract Co-Author*) Nothing to Disclose Mustafa Goksu, Adiyaman, Turkey (*Abstract Co-Author*) Nothing to Disclose Safiye Kafadar, Adiyaman, Turkey (*Abstract Co-Author*) Nothing to Disclose Bilge Aydin Turk, Adiyaman, Turkey (*Abstract Co-Author*) Nothing to Disclose Sukru Mehmet Erturk, Adiyaman, Turkey (*Presenter*) Nothing to Disclose

#### For information about this presentation, contact:

drbaykan@gmail.com

### **TEACHING POINTS**

The purpose of this exhibit is: 1. To provide general information about breast tuberculosis in order to raise awareness. 2. To review radiologic findings of breast tuberculosis with some sample cases. 3. To discuss difficulties in the diagnosis of breast tuberculosis and multidisciplinary approach in the management of treatment.

### **TABLE OF CONTENTS/OUTLINE**

1. General information about breast tuberculosis 2. Review of imaging findings with sample cases 3. The role of radiology in the multidisciplinary approach 4.Summary



### BR181-ED-MOA12

## Probably Benign Assessment on Breast MRI: Appropriate and Inappropriate Utilization

Monday, Nov. 26 12:15PM - 12:45PM Room: BR Community, Learning Center Station #12

### Participants

Mirely's Barrios, MD, Boston, MA (*Presenter*) Nothing to Disclose Sona A. Chikarmane, MD, Boston, MA (*Abstract Co-Author*) Nothing to Disclose Emily Mungovan, BA, Boston, MA (*Abstract Co-Author*) Nothing to Disclose Catherine S. Giess, MD, Wellesley, MA (*Abstract Co-Author*) Nothing to Disclose

### For information about this presentation, contact:

schikarmane@bwh.harvard.edu

# **TEACHING POINTS**

ACR BI-RADS Category 3 ('probably benign') should carry <= 2% likelihood of malignancy and was initially defined for a normal risk screening mammography population. The ACR BI-RADS Lexicon states that probably benign lesions should have a very high probability of being benign and many approaches for assessment are intuitive. The objectives of this exhibit are: 1. To review the evolving criteria for findings to be placed in probably benign category on breast MRI, with emphasis on challenges in daily practice. 2. To understand various clinical and patient factors that may affect management and assessment, including high risk patient populations, younger patient population, and baseline studies.

# TABLE OF CONTENTS/OUTLINE

1. To review the published literature on probably benign (BI-RADS 3) lesions on breast MRI. 2. To provide an overview on breast MRI findings currently accepted as probably benign. 3. To present a pictorial review of upgraded BIRADS 3 lesions, benign and malignant, with assessment and management lessons. 4. To review appropriate and inappropriate uses of probably benign category in breast MRI, with emphasis on challenging clinical and patient factors that may affect management.

#### **Honored Educators**

Presenters or authors on this event have been recognized as RSNA Honored Educators for participating in multiple qualifying educational activities. Honored Educators are invested in furthering the profession of radiology by delivering high-quality educational content in their field of study. Learn how you can become an honored educator by visiting the website at: https://www.rsna.org/Honored-Educator-Award/ Catherine S. Giess, MD - 2015 Honored EducatorCatherine S. Giess, MD - 2017 Honored Educator



### BR229-SD-MOA1

Ultrasound Radiomics in the Differentiation Between Benign and Malignant Breast Masses: Comparison Between Conventional Ultrasonography and Shear-Wave Elastography

Monday, Nov. 26 12:15PM - 12:45PM Room: BR Community, Learning Center Station #1

# Participants

Ji Hyun Youk, MD, Seoul, Korea, Republic Of (*Presenter*) Nothing to Disclose Jin Young Kwak, MD, Seoul, Korea, Republic Of (*Abstract Co-Author*) Nothing to Disclose Eun Ju Son, MD, PhD, Seoul, Korea, Republic Of (*Abstract Co-Author*) Nothing to Disclose Jeong-Ah Kim, MD, PhD, Seoul, Korea, Republic Of (*Abstract Co-Author*) Nothing to Disclose

# PURPOSE

To evaluate whether ultrasound radiomics features can differentiate benign and malignant breast mass, compared conventional ultrasonography (US) with shear-wave elastography (SWE).

# METHOD AND MATERIALS

We retrospectively collected 328 pathologically-confirmed breast masses in 296 women who underwent US and SWE before biopsy or surgery from March to November 2014. Their radiomics features were extracted from US and SWE images by texture analysis algorithms in Matlab software. A representative SWE image for measuring elasticity of the index mass was selected for analysis, which had both US and color-coded SWE image displayed in split-screen mode. For a manual lesion segmentation for all masses, an ROI was delineated around the boundary of the index mass on US image from which the same ROI was copied and pasted to SWE image by a dedicated breast radiologist. A total of 730 candidate radiomics features including first order statistics, textural features (GLCM and GLRLM), and wavelet features, were extracted from each image. LASSO regression was used for data dimension reduction and feature selection. Univariate and multivariate logistic regression analysis were performed to identify independent radiomics features of differentiating between benign and malignant masses. The area under the receiver operating characteristic curve (AUC) was calculated.

# RESULTS

Of 328 breast masses, 205(62.5%) were benign and 123(37.5%) were malignant. Following radiomics feature selection, 22 features from US and 6 features from SWE remained. On univariate analysis, all 6 radiomics features from SWE (P<0.0001) and 21 of 22 radiomics features from US (P<0.03) showed significant differences between benign and malignant masses. After multivariate analysis, 3 radiomics features from US and 2 radiomics features from SWE were independently associated with malignant breast masses. The AUC of logistic regression model in differentiating between benign and malignant masses was 0.929 for US and 0.992 for SWE (P<0.001).

# CONCLUSION

Ultrasound radiomics features can differentiate between benign and malignant breast masses with good performance. SWE showed significantly better performance than US.

### **CLINICAL RELEVANCE/APPLICATION**

Quantitative ultrasound radiomics features can be used to diagnose breast cancer with good diagnostic performance and SWE radiomics show superior performance to conventional ultrasonography radiomics.



### BR230-SD-MOA2

Impact of Inflammatory Breast Cancer Heterogeneity for Predicting Survival: Low-Dose Breast CT Texture Analysis

Monday, Nov. 26 12:15PM - 12:45PM Room: BR Community, Learning Center Station #2

# Participants

Myoung-Ae Kwon, Ansan, Korea, Republic Of (*Presenter*) Nothing to Disclose Bo Kyoung Seo, MD, PhD, Ansan, Korea, Republic Of (*Abstract Co-Author*) Research Grant, Canon Medical Systems Corporation; Research Grant, Guerbet SA; Research Grant, Koninklijke Philips NV;

Balaji Ganeshan, PhD, London, United Kingdom (*Abstract Co-Author*) CEO, Feedback plc; Director, Feedback plc; Director, Stone Checker Software Ltd; Director, Prostate Checker Ltd

Eun Kyung Park, MD, PhD, Ansan, Korea, Republic Of (Abstract Co-Author) Nothing to Disclose

Ok Hee Woo, MD, Seoul, Korea, Republic Of (Abstract Co-Author) Nothing to Disclose

Kyu Ran Cho, MD, PhD, Seoul, Korea, Republic Of (Abstract Co-Author) Nothing to Disclose

### For information about this presentation, contact:

kwon4715@gmail.com

### PURPOSE

Inflammatory breast cancer (iBC) is very aggressive and one of the non-measurable lesions in response evaluation criteria in solid tumors, therefore measuring tumor size is inadequate to assess prognosis. The purpose of this study was to investigate the usefulness of low-dose breast CT texture analysis (CTTA) to predict overall survival in patients with iBC.

### **METHOD AND MATERIALS**

This retrospective study was approved by the institutional review board. From 2006 to 2017, fifty-five patients who had iBC and pre-treatment low-dose breast CT were included. CTTA was performed on pre- and post-contrast CT images using a TexRAD research software (TexRAD Ltd, www.texrad.com, Cambridge, UK). CTTA comprised a filtration-histogram technique where the filtration step extracted and enhanced objects of different sizes corresponding to spatial scale filter (0-without filtration; 2mm-fine texture scale; 3-5mm-medium texture scales; 6mm-coarse texture scale) and variation in density followed by quantification of texture using histogram based analysis (mean-M, standard deviation-SD, entropy-E, mean of positive pixels-MPP, skewness-S, and kurtosis-K). Delta texture i.e. difference between post-contrast and pre-contrast texture was also evaluated. The relationship between CT texture features and overall survival was assessed using Kaplan-Meier survival analysis.

#### RESULTS

27/55 patients died within a mean follow-up period of 29.7 (0-100) months. Median survival was 32.0 (95% CI: 3.7-60.3) months. A number of CTTA metrics predicted survival. Higher SD and E without filtration and E across fine to medium texture scales on precontrast CT were significant predictors of poor prognosis (best - E at fine texture scale >=5.55, p=0.003). Lower M and S without filtration and higher M and E across fine to medium texture scales on post-contrast CT were significant predictors of poor prognosis (best - E at fine texture Scale >=5.55, p=0.003). Lower M and S without filtration and higher M and E across fine to medium texture scales on post-contrast CT were significant predictors of poor prognosis (best - E at fine texture scale >=5.91, p=0.0004). Delta texture (Lower E and higher K) without filtration and across fine, medium and coarse texture scales were significant predictors of poor prognosis (best - Delta K at fine texture scale >=0.08, p=0.0002).

# CONCLUSION

Low dose CTTA can be useful to predict survival in patients with iBC.

# **CLINICAL RELEVANCE/APPLICATION**

Filtration histogram based texture analysis increases the utility of low-dose breast CT by reflecting tumor heterogeneity and demonstrates prognostic potential in inflammatory breast cancer.



# BR231-SD-MOA3

# Clinical Impact of Second Opinion Radiology Consultation for Patients with Breast Cancer

Monday, Nov. 26 12:15PM - 12:45PM Room: BR Community, Learning Center Station #3

#### Awards Student Travel Stipend Award

### **Participants**

Debra S. Whorms, MD, Boston, MA (*Presenter*) Nothing to Disclose Catherine S. Giess, MD, Wellesley, MA (*Abstract Co-Author*) Nothing to Disclose Mehra Golshan, MD, Boston, MA (*Abstract Co-Author*) Nothing to Disclose Rachel Freedman, Brookline, MA (*Abstract Co-Author*) Nothing to Disclose Craig A. Bunnell, MD, MPH, Boston, MA (*Abstract Co-Author*) Nothing to Disclose Emily C. Alper, BA, Boston, MA (*Abstract Co-Author*) Nothing to Disclose Katya Losk, Brookline, MA (*Abstract Co-Author*) Nothing to Disclose Ramin Khorasani, MD, Boston, MA (*Abstract Co-Author*) Nothing to Disclose

#### For information about this presentation, contact:

dswhorms@gmail.com

# PURPOSE

Assess the incidence and clinical significance of: interpretation discrepancies when subspecialty consult review of outside imaging is performed at a National Cancer Institute (NCI)-designated tertiary cancer center, for patients with newly diagnosed breast cancer.

### **METHOD AND MATERIALS**

This Institutional Review Board-approved retrospective observational study included patients presenting 7/2016-3/2017 to an NCIdesignated comprehensive cancer center for second opinion after a breast cancer diagnosis. Outside and second-opinion radiology reports of 252 randomly-selected patients were compared by two subspecialty breast radiologists to consensus. A peer review score was assigned using a modification of the American College of Radiology's RADPEER peer review metric: 1-agree; 2-minor discrepancy (unlikely clinically significant); 3-moderate discrepancy (may be clinically significant); 4-major discrepancy (likely clinically significant). Among cases with clinically significant discrepancies, rates of clinical management change (alterations in management including change in follow-up, use of neoadjuvant therapy, and surgical management as a direct result of image review) and detection of additional malignancy were assessed through electronic medical record review.

# RESULTS

A significant difference (RADPEER 3 or 4) in interpretation was seen in 41 cases (16%, 95% Confidence Interval [CI], 11.7%-20.8%). The difference led to additional work-up in 38 cases (15%, 95% CI 10.6%-19.5%) and a change in clinical management in 18 cases (7.1%, 95% CI 4.0%-10.2%), including 15 cases with a change in surgical management (6.0%, 95% CI, 3.0%-8.9%) cases. An additional malignancy or larger area of disease was identified in 12 cases (4.8%, 95% CI, 2.1%-7.4%).

# CONCLUSION

Discrepancy between outside and second-opinion radiologists frequently results in additional work-up for breast cancer patients, changes in treatment plan, and identification of new malignancies.

# **CLINICAL RELEVANCE/APPLICATION**

Formal second opinion imaging consultation in patients with newly diagnosed breast cancer presenting to a multidisciplinary breast oncology program has significant value in identifying additional malignancy and optimizing treatment approach.

# **Honored Educators**

Presenters or authors on this event have been recognized as RSNA Honored Educators for participating in multiple qualifying educational activities. Honored Educators are invested in furthering the profession of radiology by delivering high-quality educational content in their field of study. Learn how you can become an honored educator by visiting the website at: https://www.rsna.org/Honored-Educator-Award/ Catherine S. Giess, MD - 2015 Honored EducatorCatherine S. Giess, MD - 2017 Honored Educator



# BR232-SD-MOA4

Prediction of 21-Gene Recurrence Score in Patients with Estrogen Receptor-positive Early-Stage Breast Cancer Using MRI-based Radiomics Nomogram

Monday, Nov. 26 12:15PM - 12:45PM Room: BR Community, Learning Center Station #4

**FDA** Discussions may include off-label uses.

#### **Participants**

Nam Joo Lee, Seoul, Korea, Republic Of (*Presenter*) Nothing to Disclose Hee Jung Shin, MD, Seoul, Korea, Republic Of (*Abstract Co-Author*) Nothing to Disclose Hwa Jung Kim, Seoul, Korea, Republic Of (*Abstract Co-Author*) Nothing to Disclose Ki Chang Shin, Seoul, Korea, Republic Of (*Abstract Co-Author*) Nothing to Disclose Jong Won Lee, Seoul, Korea, Republic Of (*Abstract Co-Author*) Nothing to Disclose Sae Byul Lee, Seoul, Korea, Republic Of (*Abstract Co-Author*) Nothing to Disclose Eun Young Chae, Seoul, Korea, Republic Of (*Abstract Co-Author*) Nothing to Disclose Woo Jung Choi, MD, Seoul, Korea, Republic Of (*Abstract Co-Author*) Nothing to Disclose Joo Hee Cha, MD, Seoul, Korea, Republic Of (*Abstract Co-Author*) Nothing to Disclose Hak Hee Kim, MD, Seoul, Korea, Republic Of (*Abstract Co-Author*) Nothing to Disclose Ga Young Yoon, MD, Seoul, Korea, Republic Of (*Abstract Co-Author*) Nothing to Disclose

For information about this presentation, contact:

docshin@amc.seoul.kr

# PURPOSE

To develop a breast MRI-based radiomics nomogram including pathologic factors which can predict low-risk recurrence score (RS) on 21-gene RS assay in patients with estrogen receptor-positive early-stage breast cancer (EBC).

## **METHOD AND MATERIALS**

From 2011 to 2017, a total of 547 tumors in 539 patients with EBC who underwent preoperative breast MRI were retrospectively included in this study. Among them, low-risk was 320 (58.5%), intermediate-risk was 180 (32.9%), and high-risk was 47 (8.6%). We extracted 744 quantitative MR radiomic features from computerized three-dimensional segmentations of each tumor generated computer-extracted image phenotypes (CEIP) within the intratumoral regions of early post-contrast T1-weighted images, percent enhancement (PE) map, signal enhancement ratio (SER) map, and T2-weighted images. We divided 547 cases into a training set (n=365) and a validation set (n=182). Elastic net was used for feature selection and radiomics score building. Multivariate logistic regression analysis was used to develop a prediction model, we incorporated the radiomics score and independent pathologic risk factors and build a radiomics nomogram. Internal validation for an independent validation set (n=182) was performed.

### RESULTS

The radiomics score, which consisted of 24 selected CEIPs, was significantly associated with the prediction of recurrence (C-index, 0.769 for training set and 0.745 for validation set). Independent pathologic predictors contained in the nomogram were progesterone receptor status, nuclear grade, histologic grade, extensive intraductal component, lymphovascular invasion, P53, and Ki67 status, and their C-index was 0.858 for training set and 0.774 for validation set. Addition of radiomics score to the pathologic nomogram showed an incremental value of 0.054 and 0.092, respectively. Radiomics nomogram showed good prediction of low-risk RS, with a C-index of 0.912 for training set and 0.866 for validation set.

#### CONCLUSION

This study shows that a radiomics nomogram which incorporates the MRI-based radiomics score and pathologic features, can be used to help the preoperative individualized prediction of low-risk RS in patients with EBC.

#### **CLINICAL RELEVANCE/APPLICATION**

Prediction nomogram using breast MRI-based radiomics score and pathologic predictors can be used to facilitate the preoperative individualized prediction of low-risk RS on 21-gene RS assay in patients with EBC.



# BR233-SD-MOA5

Volumetric versus Area-based Breast Density Assessment: Comparisons using Fully-Automated Quantitative Measurements in a Large Screening Population

Monday, Nov. 26 12:15PM - 12:45PM Room: BR Community, Learning Center Station #5

# Participants

Aimilia Gastounioti, Philadelphia, PA (*Presenter*) Nothing to Disclose Meng-Kang Hsieh, Philadelphia, PA (*Abstract Co-Author*) Nothing to Disclose Lauren Pantalone, BS, Philadelphia, PA (*Abstract Co-Author*) Nothing to Disclose Eric A. Cohen, Philadelphia, PA (*Abstract Co-Author*) Nothing to Disclose Yifan Hu, Philadelphia, PA (*Abstract Co-Author*) Nothing to Disclose Emily F. Conant, MD, Philadelphia, PA (*Abstract Co-Author*) Grant, Hologic, Inc; Consultant, Hologic, Inc; Grant, iCAD, Inc; Consultant, iCAD, Inc; Speaker, iiCME Despina Kontos, PhD, Philadelphia, PA (*Abstract Co-Author*) Nothing to Disclose

#### For information about this presentation, contact:

aimilia.gastounioti@uphs.upenn.edu

#### PURPOSE

Breast density is an important factor affecting the sensitivity of screening mammography due to the masking of tumors within the dense breast tissue, therefore, substantially influencing supplemental screening recommendations for women. We investigate associations between fully-automated quantitative measures of area-based (ABD) and volumetric (VBD) breast density versus categorical (BI-RADS) density assessment and potential implications for supplemental screening.

#### **METHOD AND MATERIALS**

We retrospectively analyzed bilateral digital mammograms (Selenia Dimensions, Hologic Inc.) from an entire one-year screening cohort at our institution (2012-2013; N = 11,107 women). BI-RADS density categories, visually assigned to each study by the reviewing radiologist, were collected from archived screening reports. Fully-automated software (QuantraTM v2.2; Hologic Inc.) was used to extract quantitative measures of ABD, VBD and categorical, BI-RADS-like, density categories. Pair-wise correlation (r) and linear regression were used to investigate the relationship between ABD and VBD measurements, adjusted for age, BMI and race (41% White, 50% Black, 9% Other/Unknown). Analysis of variance (ANOVA) was performed to evaluate ABD and VBD variation by the clinical BI-RADS density categories. Agreement between the radiologist's and the software-assessed density categories was measured via the Cohen's weighted kappa (k).

# RESULTS

VBD (12.5%  $\pm$  6.9%) and ABD (16.5%  $\pm$  16.0%) were strongly correlated (r = 0.95), with VBD being lower than ABD (b = 0.41, 95% CI = [0.40, 0.41]). Both density measures were significantly different across BI-RADS density categories with an increase as BI-RADS density increased (ANOVA, p < 0.001). There was moderate agreement between the radiologists' and the software-assessed breast density categories (k = 0.67, SE = 0.01), on par with reported inter-reader variability between radiologists.

# CONCLUSION

VBD measurements are strongly correlated to ABD estimates in digital mammography; yet, reported breast density is likely to be lower in the volumetric evaluation. The software-generated breast density scores moderately agree with clinical BI-RADS density readings.

# **CLINICAL RELEVANCE/APPLICATION**

Refinement of density thresholds that prompt supplemental screening is likely to be needed for clinical adoption of automated density measures, adjusting also for area-based vs. volumetric evaluation.



# BR234-SD-MOA6

Breast Cancer Risk Assessment at the Time of Screening Mammography: Pathology and BIRADS Outcomes

Monday, Nov. 26 12:15PM - 12:45PM Room: BR Community, Learning Center Station #6

#### Awards Student Travel Stipend Award

#### Participants

Diana Murcia, MD, Burlington, MA (*Presenter*) Nothing to Disclose Megan E. Mcdevitt, Burlington, MA (*Abstract Co-Author*) Nothing to Disclose Maryam Shahrzad, MD, Arlington, MA (*Abstract Co-Author*) Nothing to Disclose Cathleen M. Kim, MD, Burlington, MA (*Abstract Co-Author*) Nothing to Disclose Jeanette Y. Chun, MD, Burlington, MA (*Abstract Co-Author*) Nothing to Disclose Michelle R. McSweeney, DO, Burlington, MA (*Abstract Co-Author*) Nothing to Disclose Meera Sekar, MD, Lexington, MA (*Abstract Co-Author*) Nothing to Disclose Meaghan Mackesy, MD, Burlington, MA (*Abstract Co-Author*) Nothing to Disclose Audrey L. Hartman, MD, MS, Burlington, MA (*Abstract Co-Author*) Nothing to Disclose

# PURPOSE

To evaluate the early experience with breast cancer risk assessment (CRA) in a multicenter breast screening program, utilizing pathology and BIRADS outcomes for patients stratified into high and low risk groups.

# METHOD AND MATERIALS

Patients were offered to complete a commercially available, tablet-based CRA survey at the time of the screening mammogram. The software utilized 3 risk prediction models; BRCAPRO (high risk >=20%), Tyrer-Cuzick v.7 (high risk >=20%), and BRCAMUTATION (high risk >=5%). The patient was identified as high risk (HR) if any of the 3 models predicted high risk. Otherwise, the patient was labeled low risk (LR). A HIPAA compliant and IRB approved retrospective review of all patients offered the survey in a 6 month period was performed. Inclusion criteria: completion of risk prediction survey, BIRADS 0 on screening mammogram, completion of additional imaging (diagnostic mammogram and/or focused ultrasound), resulting in BIRADS 4 or 5, and completion of core biopsy (and surgical biopsy, if indicated). The rate of BIRADS 0, cancer detection rate (CDR), and percentage of invasive cancer were compared for the HR and LR patients, using a chi-square test. CDR and Positive Predictive Value 3 for breast cancer (PPV3) were calculated for both HR and LR groups.

## RESULTS

A total of 10394 patients underwent screening mammogram, of which 88.5% (9200) elected to complete the CRA survey, of which 14% (1293) of patients were HR, and 86% (7897) were LR. The percent of BIRADS 0 at screening was higher for HR than LR (11.2% vs 7.7%, p<0.001). The cancer detection rate (per 1000 patients) was higher for HR than LR (7.8 vs 3.8 p<0.05). The PPV3 was not statistically different (34.5% for HR, 25.2% for LR, P=0.37). The percent of invasive cancers was also not statistically different between the HR and LR patients.

# CONCLUSION

Patients identified as high risk by breast cancer risk assessment at the time of screening mammography had a higher cancer detection rate than low risk patients.

#### **CLINICAL RELEVANCE/APPLICATION**

Breast cancer risk assessment at screening mammogram may provide information towards personalized screening for breast cancer.



### CA164-ED-MOA8

Fontan Circulation in Adults: What a Radiologist Needs To Know

Monday, Nov. 26 12:15PM - 12:45PM Room: CA Community, Learning Center Station #8

# Awards Certificate of Merit

# Participants

Monika Arzanauskaite, MMedSc, Liverpool, United Kingdom (*Presenter*) Nothing to Disclose Evangelia Nyktari, Athens, Greece (*Abstract Co-Author*) Nothing to Disclose Inga Voges, London, United Kingdom (*Abstract Co-Author*) Nothing to Disclose

#### For information about this presentation, contact:

arzanauskaite@gmail.com

### **TEACHING POINTS**

Teaching Points1. To understand the indications for Fontan procedure and types of surgeries2. To review the haemodynamics of Fontan circulation and relevant imaging protocols3. To familiarise with complications on MRI and CT using a case-based approach.

### **TABLE OF CONTENTS/OUTLINE**

Table of contents1. Pre-existing conditions2. Fontan procedure3. Fontan haemodynamics4. Imaging protocols5. Case-based review of imaging findings with a focus on:• satisfactory haemodynamical result• spectrum of complications: ventricular failure, cavity dilatation, Fontan pathway stenosis, shunt formation, specific sites and appearances of thrombus formation, pulmonary arteriovenous malformations, failure of thoracic lymphatic drainage and Fontan hepatopathy.



### CA211-SD-MOA2

Cardiac Magnetic Resonance Reveals Signs of Subclinical Myocardial Disease in Patients with Myotonic Muscular Dystrophy

Monday, Nov. 26 12:15PM - 12:45PM Room: CA Community, Learning Center Station #2

# Participants

Julian A. Luetkens, MD, Bonn, Germany (*Presenter*) Nothing to Disclose Carla Gliem, Bonn, Germany (*Abstract Co-Author*) Nothing to Disclose Daniel Kuetting, MD, Bonn, Germany (*Abstract Co-Author*) Nothing to Disclose Darius Dabir, Bonn, Germany (*Abstract Co-Author*) Nothing to Disclose Frederic Carsten Schmeel, Bonn, Germany (*Abstract Co-Author*) Nothing to Disclose Rami Homsi, Bonn, Germany (*Abstract Co-Author*) Nothing to Disclose Hans H. Schild, MD, Bonn, Germany (*Abstract Co-Author*) Nothing to Disclose Cornelia Kornblum, 53105, Germany (*Abstract Co-Author*) Nothing to Disclose Daniel K. Thomas, MD, PhD, Bonn, Germany (*Abstract Co-Author*) Nothing to Disclose

### For information about this presentation, contact:

julian.luetkens@ukbonn.de

#### PURPOSE

Myotonic muscular dystrophy (DM) is a genetic multisystem disorder characterized by skeletal muscle weakness and myotonia. Cardiac involvement seems to be rare, but patients with DM are at an increased risk for ventricular dysfunction and sudden cardiac death. We aimed to determine the extent of cardiovascular involvement in DM patients by a comprehensive cardiac magnetic resonance (CMR) approach.

# METHOD AND MATERIALS

DM patients (n=12; 6 with type 1 and 6 with type 2) without cardiac symptoms and preserved ejection fraction and age- and gender-matched control subjects (n=24,) underwent CMR. Multiparametric CMR protocol allowed for the determination of late gadolinium enhancement (LGE), visible myocardial edema, T1 relaxation times, T2 relaxation times, extracellular volume (ECV), longitudinal strain and cardiac function.

# RESULTS

When compared with healthy controls, DM patients showed alterations in myocardial tissue composition (native T1 relaxation times:  $1018\pm32 \text{ ms vs. } 953\pm35 \text{ ms; } P<0.001$ ; T2 relaxation times:  $56\pm7\text{ms vs. } 53\pm2\text{ms; } P=0.023$ ; ECV:  $31\pm8\% \text{ vs. } 27\pm5\%$ , P=0.049). No differences in left ventricular ejection fraction were observed ( $59\pm6\% \text{ vs. } 62\pm4\%$ ; P=0.110), but DM patients demonstrated lower average systolic longitudinal values ( $-19\pm4\% \text{ vs. } -22\pm4\%$ ; P=0.036). No alterations in LGE were observed.

### CONCLUSION

Comprehensive CMR revealed a high burden of cardiovascular disease in DM patients without cardiac symptoms. We could demonstrate that DM patients have subtle evidence of impaired myocardial function and also elevated markers of diffuse myocardial fibrosis and injury. Subclinical myocardial disease might be a precursor of cardiac involvement in DM patients.

### **CLINICAL RELEVANCE/APPLICATION**

Comprehensive CMR revealed a high burden of cardiovascular disease in DM patients and might serve as a potential screening parameter for beginning cardiovascular disease in these patients.



# CA212-SD-MOA3

2D/3D CMR-Tissue Tracking in the Assessment of Spontaneous T2DM Rhesus Monkeys with Isolated Diastolic Dysfunction

Monday, Nov. 26 12:15PM - 12:45PM Room: CA Community, Learning Center Station #3

# Participants

Tong Zhu, Chengdu, China (*Presenter*) Nothing to Disclose Wen Zeng, MD, PhD, Chengdu, China (*Abstract Co-Author*) Nothing to Disclose Li Gong, MD,PhD, Chengdu, China (*Abstract Co-Author*) Nothing to Disclose Jie Zheng, PhD, Saint Louis, MO (*Abstract Co-Author*) Nothing to Disclose Fabao Gao, MD, PhD, Chengdu, China (*Abstract Co-Author*) Nothing to Disclose

# For information about this presentation, contact:

13281000839@163.com

# PURPOSE

To investigate the left ventricle dysfunction and myocardial deformation in spontaneous type 2 diabetes mellitus (T2DM) rhesus monkeys with isolated diastolic dysfunction (DD) by 2D/3D CMR-tissue tracking (CMR-TT).

# METHOD AND MATERIALS

Spontaneous T2DM rhesus monkeys with isolated DD (T2DM-DD, n=10) and corresponding non-diabetic healthy animals (ND, n=9) were scanned prospectively for the CMR study. Parameters of myocardial deformation obtained from 2D/3D CMR-TT were compared between the two groups. In addition, all CMR imaging protocols were performed twice (i.e., test and retest scans) in 9 ND animals to assess test-retest reproducibility.

### RESULTS

Compared with ND, T2DM-DD monkeys demonstrated significantly reduced peak systolic circumferential strain (Ecc), peak diastolic circumferential strain rate (CSR), with 2D CMR-TT, and only Ecc with 3D CMR-TT (p<0.05). Test-retest repeatability analysis showed that the ICC of 2D CMR-TT derived Ecc (0.77, p<0.05), CSR (0.86, p<0.05), peak systolic longitudinal strain (Ell) (0.90, p<0.01) and peak diastolic longitudinal strain rate (LSR) (0.87, p<0.01) showed good reproducibility, but only 3D TT-derived Ell (0.77, p<0.05) showed good reproducibility.

# CONCLUSION

Left ventricular systolic and diastolic deformation functions were both impaired in spontaneous T2DM rhesus monkeys with isolated diastolic dysfunction, which were similar to the findings in human T2DM. The 2D CMR-TT derived Ecc and CSR were effective in the evaluation of the myocardial systolic and diastolic functions of early diabetic cardiomyopathy with relatively higher test-retest reproducibility compared with the 3D CMR TT method.

# **CLINICAL RELEVANCE/APPLICATION**

Spontaneous T2DM rhesus monkeys can be used as an effective model, particularly in the investigation and preclinical testing of novel T2DM therapeutic agents, with a high potential for translatability to humans. 2D CMR-TT can be used as an integral part in the one-stop shop of CMR and to evaluate the cardiac function of DCM accessibly.



# CA213-SD-MOA4

Accuracy of RECHARGE Score Derived From Coronary CT Angiography versus Conventional Angiography for the Prediction of Successful Percutaneous Coronary Intervention in Patient with Chronic Total Occlusion

Monday, Nov. 26 12:15PM - 12:45PM Room: CA Community, Learning Center Station #4

# Participants

Rui Wang, Beijing, China (*Presenter*) Nothing to Disclose Yi He, MD, Beijing, China (*Abstract Co-Author*) Nothing to Disclose Lijun Zhang, Beijing, China (*Abstract Co-Author*) Nothing to Disclose Xiantao Song, Beijing, China (*Abstract Co-Author*) Nothing to Disclose

# PURPOSE

To investigate the feasibility and accuracy of coroanry CT angiography (cCTA) versus conventional angiography to predict procedural success and 30-minutes wire crossing in percutaneous coroanry intervention (PCI) for chronic total occlusion (CTO) lesions

# METHOD AND MATERIALS

In this IRB-approved, HIPAA-compliant investigation data of 89 consecutive patients (median 58 years, 79% male) with 99 lesions who underwent cCTA prior conventional angiography (CA) with CTO-PCI were retrospectively analyzed. The RECHARGE score (the sum of the following 6 binary parameters: 1. proximal cap blunt; 2 severe calcification; 3. bending; 4. CTO length > 20mm; 5. diseased distal landing zone; 6. previous bypass graft on CTO vessel) was calculated and compared between cCTA (RECHARGECCTA) and CA (RECHARGECA).

# RESULTS

The procedual success rate of the CTO-PCI procedures was 70.7%, and 60.6% of cases achieved 30-minutes wire crossing. No significant difference was observed between median RECHARGECCTA score (2[IQR1-3]) and median RECHARGECA score (2[IQR1-3]) for procedural success (p=0.084). However, the median RECHARGECCTA score (2[IQR1-3]) was higher than that of the RECHARGECA score (1.5[IQR1-3]) for 30-min wire crossing, p=0.001). The area under the curve (AUC) of the RECHARGECCTA and RECHARGECA score for predicting procedural success showed no statistical significance (0.751 vs. 0.757, p=0.922). The sensitivity, specificity, positive predictive value, negative predictive value of RECHARGECCTA score <=2 for predictive procedural success was 64.25, 79.3%, 88% and 48%, respectively.

# CONCLUSION

Non-invasive cCTA-dervied RECHARGE score performs equally to invasive determination and may help to predict procedural success and within 30-minutes guide wire crossing of CTO-PCI.

# **CLINICAL RELEVANCE/APPLICATION**

CCTA has been demonstrated as an alternative pre-procedural imaging method for CTO-PCI and provided prognostic information beyond angiography alone.



# CA214-SD-MOA5

Compressed SENSE Single-Breath-Hold and Free-Breathing Cine Imaging for Accelerated Clinical Evaluation of Left Ventricle

Monday, Nov. 26 12:15PM - 12:45PM Room: CA Community, Learning Center Station #5

**FDA** Discussions may include off-label uses.

#### **Participants**

Yue Ma, Shenyang, China (*Presenter*) Nothing to Disclose Yang Hou, MD, Shenyang, China (*Abstract Co-Author*) Nothing to Disclose Quanmei Ma, Shenyang, China (*Abstract Co-Author*) Nothing to Disclose

### PURPOSE

To compared the accuracy of CS-SENSE cine CMR with and without breath-hold (BH) and BH standard cine CMR for left ventricular (LV) function assessment.

# **METHOD AND MATERIALS**

Thirty-three healthy volunteers underwent balanced turbo field-echo cine CMR with breath-hold (BTFE-BH; reference standard), single BH CS-SENSE (csBTFE-BH) cine CMR, and free-breathing (FB) CS-SENSE (csBTFE-FB) cine CMR on 3.0T scanner. All images were acquired in stacks of 8 short-axis slices. Image quality was assessed and compared by Wilcoxon matched-pair signed-rank test. Comparison of sequences was made in end-diastolic volumes, end- systolic volumes, stroke volume, ejection fraction, LV end-diastolic (LVED) mass, regional myocardial wall motion, and scan times using paired t-test, linear regression and Bland-Altman analyses.

### RESULTS

All techniques provided acceptable image quality (score >=3) for LV volumetric analysis in all subjects (BTFE-BH [reference]:  $5.00\pm0.00$ ; csBTFE-BH:  $4.03\pm0.17$  [p<0.001]; csBTFE-FB:  $3.76\pm0.44$  [p<0.001]), and all had good agreement on assessment of LV function. However, there was a small but significant underestimation of LVED mass with csBTFE-FB (csBTFE-FB:  $73.63\pm17.31$  g vs. BTFE-BH [reference]:  $75.12\pm18.18$  g, p=0.037). There was strong correlation among all methods for quantitative regional myocardial wall motion. The acquisition times for both csBTFE-BH and csBTFE-FB were significantly shorter than BTFE-BH (BTFE-BH [reference]:  $89.3\pm5.70$  s; csBTFE-BH:  $24.42\pm2.18$  s [p<0.001]; csBTFE-FB:  $22.48\pm1.85$  s [p<0.001]).

#### CONCLUSION

Assessment of LV function with the novel CS-SENSE cine CMR is noninferior to the standard cine CMR irrespective of BH. However, LVED mass is underestimated with csBTFE-FB.

# **CLINICAL RELEVANCE/APPLICATION**

csBTFE cine CMR irrespective of BH commands might be a suitable alternative to standard BH cine CMR for assessment of LV function for CHD patients who cannot tolerate BH. The CS-SENSE technique is time efficient and can potentially improve the clinical utility of CMR.



# CA215-SD-MOA6

Unmodified, Autologous Adipose Tissue Derived Regenerative Cells Improve Cardiac Function, Structure and Revascularization in a Porcine Model of Chronic Myocardial Infarction

Monday, Nov. 26 12:15PM - 12:45PM Room: CA Community, Learning Center Station #6

### Awards

# **Trainee Research Prize - Resident**

# Participants

Alexander Haenel, MD, Luebeck, Germany (*Presenter*) Nothing to Disclose Mohamad Ghosn, PhD, Houston, TX (*Abstract Co-Author*) Nothing to Disclose Dipan J. Shah, MD, Houston, TX (*Abstract Co-Author*) Research Grant, Siemens AG Speaker, Lantheus Medical Imaging, Inc Jody Vykoukal, Houston, TX (*Abstract Co-Author*) Nothing to Disclose Christoph Schmitz, Munich, Germany (*Abstract Co-Author*) Consultant, SciCoTec; Shareholder, InGeneron, Inc Eckhard Alt, MD,PhD, Munich, Germany (*Abstract Co-Author*) Chairman, InGeneron, Inc; Chairman, Isar Klinikum Tahereh Karimi, PhD, New Orleans, LA (*Abstract Co-Author*) Nothing to Disclose Amish Dave, MD, Houston, TX (*Abstract Co-Author*) Nothing to Disclose Miguel Valderrabano, MD, Houston, TX (*Abstract Co-Author*) Nothing to Disclose Alon Azares, Houston, TX (*Abstract Co-Author*) Nothing to Disclose Daryl Schulz, Houston, TX (*Abstract Co-Author*) Nothing to Disclose Albert Raizner, MD, Houston, TX (*Abstract Co-Author*) Nothing to Disclose

# For information about this presentation, contact:

Alexander.Haenel@UKSH.de

#### PURPOSE

Numerous studies have investigated cell-based therapies for acute myocardial infarction (MI), with mixed results. In chronic MI less is known about stem cells and the best delivery route. This study evaluated the effects of unmodified, autologous adipose tissue-derived regenerative cells (UA-ARDCs) in a porcine reperfusion model of chronic MI.

# **METHOD AND MATERIALS**

The left anterior descending (LAD) artery of pigs was occluded for 180 min. Four weeks later, the mean left ventricular ejection fraction (LVEF) was shown to have been reduced to approximately 35%. At that time, 18×106 unmodified, autologous adipose-derived regenerative cells (UA-ADRCs) were delivered into the LAD vein (control: delivery of saline). Myocardial parameters were assessed by cardiac magnetic resonance imaging (CMR) in a blinded manner immediately prior to cell delivery at four weeks after MI induction. Follow-up scans were performed after six weeks (at ten weeks after MI induction).

# RESULTS

Six weeks following UA-ADRCs/saline delivery, the mean LVEF had increased by 18% (p<0.01) after delivery of UA-ADRCs, but was unchanged after delivery of saline. Delivery of UA-ADRCs reduced myocardial fibrosis by 20%, controls exhibited a 22% increase (p<0.002). This is among the best outcome ever reported in studies on porcine animal models of cell-based therapies for MI in which functional and structural outcome was assessed with cardiac magnetic resonance imaging.

### CONCLUSION

In this chronic MI model, the retrograde venous injection of UA-ADRCs is feasible and safe. Treatment significantly improved hemodynamics, myocardial muscle mass and reduced scar as measured by CMR.

# **CLINICAL RELEVANCE/APPLICATION**

The unique combination of the procedure used for isolating UA-ADRCs, the late cell delivery time and the uncommon cell delivery route applied in the present study may open new horizons for cell-based therapies for MI.



# CA216-SD-MOA7

The Correlation Between Coronary Artery Calcification and Biochemical Risk Factors in Non-Dialysis Patients with Chronic Kidney Disease Using 16cm Wide-Detector Computed Tomography

Monday, Nov. 26 12:15PM - 12:45PM Room: CA Community, Learning Center Station #7

# Participants

Changqing Yin, Zhenjiang, China (*Presenter*) Nothing to Disclose Lirong Zhang, MD, zhenjiang, China (*Abstract Co-Author*) Nothing to Disclose Dongqing Wang, Zhenjiang, China (*Abstract Co-Author*) Nothing to Disclose Haitao Zhu, Zhenjiang, China (*Abstract Co-Author*) Nothing to Disclose Shao Xun, Zhenjiang, China (*Abstract Co-Author*) Nothing to Disclose

# For information about this presentation, contact:

ev1lhell@126.com

#### PURPOSE

The aim of this study was to investigate the correlation between the CAC and biochemical risk factors in Chinese non-dialysis patients with CKD.

# METHOD AND MATERIALS

4189 non-dialysis patients with CKD underwent blood biochemical examinations and risk factors including calcium, phosphate, vitamin D3, parathyroid hormone, triglyceride, high- and low-density lipoprotein, total cholesterol, C-reactive protein, creatinine, cystatin C, urate and glomerular filtration rate (eGFR) were collected. Subsequently, CAC severity was determined using a 16-cm detector CT (Revolution, GE Healthcare). The correlation between CAC and these risk factors were analyzed by logistic regression model.

#### CONCLUSION

The reduction of the glomerular filtration rate was not associated with CAC score; low-density lipoprotein and total cholesterol were associated with CAC incidence while and other biochemical risk factors had no correlation with CAC.

# **CLINICAL RELEVANCE/APPLICATION**

Biomarkers derived from blood examinations could potentially assist the prediction of CAC in non-dialysis patients with CKD.



# CH241-ED-MOA6

# Bubbling Over: What Radiologists Should Look for Following a Positive Bubble Study

Monday, Nov. 26 12:15PM - 12:45PM Room: CH Community, Learning Center Station #6

# Awards Certificate of Merit

# Participants

Jennifer A. Febbo, Chicago, IL (*Presenter*) Nothing to Disclose Ramya S. Gaddikeri, MD, Chicago, IL (*Abstract Co-Author*) Nothing to Disclose Haritha Yepuri, MBBS, Vijayawada, India (*Abstract Co-Author*) Nothing to Disclose Palmi N. Shah, MD, Chicago, IL (*Abstract Co-Author*) Nothing to Disclose

# For information about this presentation, contact:

febbo.jennifer@gmail.com

#### **TEACHING POINTS**

Saline contrast echo is performed to evaluate hypoxemia and in paradoxical embolization to look for RT to LT shunting Visualizing saline bubbles in the left heart is a positive study due to RT to LT shunt Presence of bubbles in the left heart chambers <= 3 heartbeats indicates an intracardiac shunt; bubbles after > 3 heartbeats imply intrapulmonary shunt Common causes of RT to LT intracardiac shunts are PFO and ASD Less common causes include other congenital abnormalities RT to LT intrapulmonary shunts include pulmonary AVMs and pulmonary AV anastomosis such as hepatopulmonary syndrome Familiarity with the causes of RT to LT shunt will aid the radiologist to detect it on a preexisting chest CT and also help to protocol a chest CT to detect one

# **TABLE OF CONTENTS/OUTLINE**

Indications and procedure for agitated saline contrast echo Clinical context, pathophysiology and implications of positive study Brief history of the study to better understand the positive interpretation Echo imaging examples and limitations V/Q scan findings Imaging common and uncommon intracardiac, intrapulmonary RT to LT shunts. Eg: pulmonary AVM, hepatopulmonary syndrome, anomalous venous return with anomalous SVC draining into LA, SVC obstruction often with confusing bubble study results CT protocol tips List other causes of intrapulmonary shunting



## CH244-ED-MOA7

Novel Ultra-High-Resolution CT Imaging for Lung Diseases

Monday, Nov. 26 12:15PM - 12:45PM Room: CH Community, Learning Center Station #7

### Participants

Akinor<sup>i</sup> Hata, MD, Suita, Japan (*Presenter*) Nothing to Disclose Masahiro Yanagawa, MD, PhD, Suita, Japan (*Abstract Co-Author*) Nothing to Disclose Osamu Honda, MD, PhD, Suita, Japan (*Abstract Co-Author*) Nothing to Disclose Tomo Miyata, MD, Suita, Japan (*Abstract Co-Author*) Nothing to Disclose Noriko Kikuchi, Suita, Japan (*Abstract Co-Author*) Nothing to Disclose Shinsuke Tsukagoshi, PhD, Otawara, Japan (*Abstract Co-Author*) Employee, Canon Medical Systems Corporation Ayumi Uranishi, Osaka, Japan (*Abstract Co-Author*) Employee, Canon Medical Systems Corporation Noriyuki Tomiyama, MD,PhD, Suita, Japan (*Abstract Co-Author*) Research Grant, Canon Medical Systems Corporation

# **TEACHING POINTS**

Ultra-high-resolution CT (U-HRCT), which has a smaller detector element and X-ray tube focus size, has become commercially available recently. U-HRCT shows improved spatial resolution and has been reported to provide better image quality for lung diseases. The purpose of this exhibit is: 1. To learn the structural and reconstruction features of U-HRCT. 2. To know the image quality of U-HRCT comparing with conventional CT. 3. To understand the clinical usefulness of U-HRCT.

# TABLE OF CONTENTS/OUTLINE

1. Overview of the features of U-HRCT comparing with conventional CT. 2. Comparing U-HRCT image with conventional CT image using cadaveric lungs (emphysema, diffuse panbronchiolitis, diffuse alveolar hemorrhage, usual interstitial pneumonia, and lymphangitic carcinomatosis). 3. Clinical cases (lung cancer, tuberculosis, pneumocysitis pneumonia, interstitial lung diseases, lymphangioleiomyomatosis, and lymphoproliferative diseases) on U-HRCT.



## CH264-SD-MOA1

# Correlation of Sterno-Aortic Distance with FEV1/FVC and FEV1 in Patients with COPD

Monday, Nov. 26 12:15PM - 12:45PM Room: CH Community, Learning Center Station #1

# Participants

Regina Cristina Q. Mangada, MD, Quezon, Philippines (Presenter) Nothing to Disclose

For information about this presentation, contact:

gina.suremed@gmail.com

### PURPOSE

To determine the correlation between sterno-aortic distance with FEV1/FVC and FEV1 in patients with COPD.

# METHOD AND MATERIALS

Eighty-one patients diagnosed with COPD who underwent chest CT scan and PFT within the period of one year were included. Sterno-aortic distance were measured and correlated with PFT results and severity of COPD. Patient's age, gender, height, and weight were recorded. The sterno-aortic distance was obtained thru their CT scan. The sterno-aortic distance was measured from the posterior surface of the sternum to the anterior margin of the aorta at the level of the carina. Two radiologists reviewed the CT scan images independently. These radiologists were blinded to the results of the pulmonary function tests (FEV1/FVC and FEV1). Measurements obtained by these radiologists were analyzed using t-test to check for interobserver variability. These measurements were correlated with the FEV1/FVC and FEV1 of patients who underwent pulmonary function tests results using Pearson correlation. These measurements were correlated with the severity of COPD according to the GOLD criteria.

# RESULTS

Most patients enrolled were males with average age of  $64 \pm 11$ years old. Most of these patients are categorized as mild COPD with 38 % and severe COPD with 38% of the total population. Patients classified as moderate COPD comprise 24 % of the total population. There is significant weak inverse correlation between sterno-aortic distance and PFT results, FEV1 (r = -0.419, p < 0.001) and FEV1/FVC(r = -0.322, p value of 0.003). There is a significant correlation derived between sterno aortic distance and severity of COPD(rho = 0.88, p-value of <0.001).

### CONCLUSION

There is a significant correlation derived between sterno aortic distance and severity of COPD (rho = 0.88, p-value of <0.001).

# **CLINICAL RELEVANCE/APPLICATION**

Sterno-aortic distance is a valuable parameter in the assessment of severity of COPD and is recommended in the initial work up for patients with OCPD.



# CH265-SD-MOA2

Performance of Preoperative N-Staging for Non-Small Cell Lung Cancer Patients: Comparison Among Short Inversion Time Inversion Recovery (STIR), Diffusion-Weighted Imaging (DWI), and FDG-PET/CT in a Multi-Center Study

Monday, Nov. 26 12:15PM - 12:45PM Room: CH Community, Learning Center Station #2

#### Participants

Yuzo Yamasaki, MD, Fukuoka, Japan (Presenter) Nothing to Disclose Hidetake Yabuuchi, MD, Fukuoka, Japan (Abstract Co-Author) Nothing to Disclose Yoshiharu Ohno, MD, PhD, Kobe, Japan (Abstract Co-Author) Research Grant, Canon Medical Systems Corporation; Research Grant, Koninklijke Philips NV; Research Grant, Bayer AG; Research Grant, DAIICHI SANKYO Group; Research Grant, Fuji Pharma Co, Ltd; Research Grant, Guerbet SA; Tae Iwasawa, MD, PhD, Yokohama, Japan (Abstract Co-Author) Research Consultant, Ono Pharmaceutical Co, Ltd; Speaker, Shionogi & Co, Ltd; Speaker, FUJIFILM Holdings Corporation; Speaker, Boehringer Ingelheim GmbH Norinari Honda, MD, Kawagoe, Japan (Abstract Co-Author) Nothing to Disclose Hiroshi Honda, MD, Fukuoka, Japan (Abstract Co-Author) Nothing to Disclose Masayuki Sasaki, Fukuoka, Japan (Abstract Co-Author) Nothing to Disclose Takeshi Kamitani, MD, Fukuoka, Japan (Abstract Co-Author) Nothing to Disclose Shingo Baba, Fukuoka, Japan (Abstract Co-Author) Nothing to Disclose Koji Sagiyama, MD, Fukuoka, Japan (Abstract Co-Author) Nothing to Disclose Yuko Matsuura, Fukuoka, Japan (Abstract Co-Author) Nothing to Disclose Takuya Hino, MD, Fukuoka, Japan (Abstract Co-Author) Nothing to Disclose Soichiro Tsutsui, Fukuoka, Japan (Abstract Co-Author) Nothing to Disclose

#### PURPOSE

The utility of MRI for N-staging in non-small cell lung cancer (NSCLC) has been investigated, and a meta-analysis showed that sensitivity and specificity of STIR and DWI for per-patient were 84% and 91%, and 69% and 93%, respectively. These studies used various MR scanners, pulse sequences and different diagnostic criteria; thus the purpose of our study was to elucidate the utility of STIR and DWI for N-staging in NSCLC patients in comparison with FDG-PET/CT in a multi-center study.

# **METHOD AND MATERIALS**

A total of 125 consecutive NSCLC patients (85 men, 40 women; mean 67.4 years) from 8 hospitals prospectively underwent preoperative STIR, DWI with 1.5-T MR units under a standardized protocol. All patients underwent FDG-PET/CT in the same period. Surgical and pathologic examinations were used as a final diagnosis. To assess the utility of qualitative analysis, two chest radiologists independently analyzed STIR and DWI, and one nuclear medicine radiologist assessed FDG-PET/CT images, respectively. McNemar test was used to compare the diagnostic capabilities for N-staging per-patient, and receiver operating characteristic curve (ROC) analysis was used to compare those per node-area.

#### RESULTS

Pathologic examinations showed that 68% (85/125) patients were negative, and 32% (40/125) had positive lymph node metastasis. For qualitative analysis of N-staging per patient, sensitivity, specificity and accuracy were 59.0-74.4%, 73.3-76.7%, 71.2-73.6% for STIR, 74.4-76.9%, 76.7-83.7%, 76.0-81.6% for DWI, and 74.4%, 67.4%, 71.2% for FDG-PET/CT, respectively. McNemar test showed that there was no significant difference in sensitivity; however, specificity and accuracy of DWI in reader 1 were superior to those of FDG-PET/CT. As for N-staging per node-area, areas under the ROC curve (AUC) were 0.760-0.844 for STIR, 0.787-0.827 for DWI, and 0.789 for FDG-PET/CT, respectively. There was no significant difference in AUC between STIR and FDG-PET/CT, DWI and FDG-PET/CT.

# CONCLUSION

The multi-center study under a standardized protocol and diagnostic criteria using STIR and DWI showed that MRI seems to be useful as well as FDG-PET/CT in N-staging for NSCLC patients.

# **CLINICAL RELEVANCE/APPLICATION**

The standardized protocol and criteria of N-staging using STIR and DWI might benefit patients with non-small cell lung cancer to avoid expensive costs and radiation exposure for FDG-PET/CT.



# CH266-SD-MOA3

# CT Radiomics Model in Predicting Prognosis of Stage I Solid Lung Adenocarcinoma

Monday, Nov. 26 12:15PM - 12:45PM Room: CH Community, Learning Center Station #3

### **Participants**

Huan Chen, Zhuhai, China (*Presenter*) Nothing to Disclose Mingzhu Liang, Zhuhai, China (*Abstract Co-Author*) Nothing to Disclose Xueguo Liu, MD, Zhuhai, China (*Abstract Co-Author*) Nothing to Disclose Xin Li, Shanghai, China (*Abstract Co-Author*) Nothing to Disclose Chuanmiao Xie I, MD,PhD, Guangzhou, China (*Abstract Co-Author*) Nothing to Disclose Lanjun Zhang, Guangdong, China (*Abstract Co-Author*) Nothing to Disclose

# For information about this presentation, contact:

liuxueg@mail.sysu.edu.cn

# PURPOSE

To establish a CT radiomics model and evaluate its accuracy in predicting Disease-Free Survival (DFS) for stage I solid lung adenocarcinoma and compare with the traditional clinical staging.

# METHOD AND MATERIALS

Pathological confirmed stage I solid lung adenocarcinoma after standard video-assisted thoracic surgery lobectomy and mediastinal lymph nodes dissection with DFS data from one institution were enrolled retrospectively. CT images (1-2mm slice thickness, soft kernel reconstruction and 60-70 seconds delay contrast enhancement) were processed using nodule volume segmentation and extraction of radiomics features by a GE algorithm (Analysis-Kinetic Version 1.0.3, GE Company). The training set and testing set ratio is 7:3 .The random forest model of machine learning was used to reduce the dimension of the data and select radiomics signatures that significantly related to prognosis. The confusion matrix and receiver operating characteristic curve (ROC) were used to evaluate the performance of radiomics model in predicting DFS and compare with traditional clinical staging. The Kaplan-Meier survival curve stratified by the risk of recurrence or metastasis of stage I solid lung adenocarcinoma based on the radscore calculated by the COX regression .

### RESULTS

We enrolled 119 cases of stage I solid lung adenocarcinoma(age 22-86years , mean  $60\pm2.2$ ; female 55, male 64; clinical stage Ia 69, Ib 50). The end event was DFS with follow-up time ranging from 3.5 months to 70 months (median 22.5 months). Ten features in 385 radiomics features were significantly associated with DFS. The prognostic performance of radiomcis model of stage I solid lung adenocarcinoma was better than that in the traditional clinical stage (AUC 0.762, vs. 0.599,p<0.05). The survival curve of the radiomics model drawn by Kaplan -Meier method can singnatly distinguish the high-risk and low-risk patients according to Radscore(-1.68) calculated by Cox regression.

### CONCLUSION

This Radiomics model can predict DFS of stage I solid lung adenocarcinoma and better than traditional clinical staging.

# **CLINICAL RELEVANCE/APPLICATION**

Radiomics can be used as a potential biomarker to predict prognosis of early stage solid lung adenocarcinoma patients after surgery .It could guide follow-up police and pre or postoperative adjunctive therapy for some hign risk stage I solid lung adenocarcinma.



# CH267-SD-MOA4

Prediction of Response to Endobronchial Coiling Based on Morphologic Emphysema Characterization of the Lung Lobe to be Treated and the Ipsilateral Non-Treated Lobe as well as on Functional CT-Data: Correlation with Clinical and Pulmonary Function

Monday, Nov. 26 12:15PM - 12:45PM Room: CH Community, Learning Center Station #4

#### Participants

Christopher Kloth, Ulm, Germany (Abstract Co-Author) Nothing to Disclose

Wolfgang M. Thaiss, MD, Tuebingen, Germany (Abstract Co-Author) Nothing to Disclose

Jan Fritz, MD, Baltimore, MD (*Abstract Co-Author*) Research Grant, Siemens AG; Scientific Advisor, Siemens AG; Scientific Advisor, Alexion Pharmaceuticals, Inc; Speaker, Siemens AG

Konstantin Nikolaou, MD, Tuebingen, Germany (Abstract Co-Author) Advisory Panel, Siemens AG; Speakers Bureau, Siemens AG; Speaker Bureau, Bayer AG

Meinrad J. Beer, MD, Ulm, Germany (*Abstract Co-Author*) Nothing to Disclose Juergen Hetzel, Tuebingen, Germany (*Abstract Co-Author*) Nothing to Disclose Marius Horger, MD, Tuebingen, Germany (*Presenter*) Nothing to Disclose

### For information about this presentation, contact:

Christopher.Kloth@uniklinikum-ulm.de

#### PURPOSE

To test if the emphysema type of the targeted lobe, ipsilateral non-targeted lobe, and lobes of the contralateral lung impact outcome of endobronchial lung volume reduction (ELVR) treatment, and to document lobar volume changes in treated and nontreated lung lobes.

### **METHOD AND MATERIALS**

Thirty patients (women =14; median age,  $66.07\pm 6.66$ ; range, 48-78y) underwent chest-CT before and after endobronchial coiling for lung volume reduction (LVR) at our institution between 12/2011 and 03/2016. Forty-five pulmonary lobes were coiled. We classified the treated lobes into homogenous or heterogeneous emphysema phenotype based on the distribution of voxels showing tissue attenuation of less than -950 HU. Clinical response was defined as an increase or consistency in the walking distance (6MWT) 6 months after LVR-therapy. Lung volume changes were compared for treated lobes, ipsilateral lobes, and contralateral lobes. Additionally, pulmonary function tests (PFT), COPD Assessment Test (CAT), and blood gas analysis were performed

#### RESULTS

Responder (19/30, 63.3%) showed a significant improvement of 6 MWT from 281.05 to 335.26 (p=0.001). Non-responder (11/30, 36.7%) showed a decrease in 6MWT from 308.18 to 255.45 (p=0.001). Responders showed a significant reduction in CAT test from 23.23 to 20.73 points (p= 0.038) and pCO2 from 42.94 to 40.31 (p=0.001). In responders, there was a significant volume reduction in treated lobes from 1627.68 mL to 1519.21 mL (p= 0.009). In responders, treated lobes/non-treated ipsilateral lobes were homogenous (n=11/5) and heterogeneous (n=10/28). In responders and non-responders, the emphysema phenotype in treated, ipsilateral non-treated and even contralateral lobes (p=0.250) did not differ and or change significantly before and after therapy. Only the volume of treated lobe in responders changed significantly after coiling.

# CONCLUSION

The emphysema-phenotype in the targeted and non-targeted ipsilateral lobe has no impact on the outcome of endobronchial coiling for LVR and also does not change significantly after treatment, whereas the volume of the treated lobe significantly decreases in responders.

# **CLINICAL RELEVANCE/APPLICATION**

The purpose of our study was to test if the emphysema type of the targeted lobe, ipsilateral non-targeted lobe, and lobes of the contralateral lung impact outcome of ELVR treatment. Furthermore to document lobar volume changes in the different lung lobes.



# CH268-SD-MOA5

Computer-aided Detection of Pulmonary Nodules Can Serve as a First Reader for Lung Cancer Screening Exams When Utilizing Lung-RADs Categorization and Management

Monday, Nov. 26 12:15PM - 12:45PM Room: CH Community, Learning Center Station #5

# Participants

Michelle L. Hershman, MD, Tucson, AZ (*Presenter*) Nothing to Disclose Ryan J. Avery, MD, Tucson, AZ (*Abstract Co-Author*) Nothing to Disclose Diana M. Palacio, MD, Tucson, AZ (*Abstract Co-Author*) Nothing to Disclose Berndt P. Schmit, MD, Tucson, AZ (*Abstract Co-Author*) Nothing to Disclose Matthias Wolff, MD, Erftstadt, Germany (*Abstract Co-Author*) Nothing to Disclose Luca Bogoni, PhD, Malvern, PA (*Abstract Co-Author*) Employee, Siemens AG

#### For information about this presentation, contact:

mlhershman@gmail.com

#### PURPOSE

To assess if nodule detection using CAD for lung cancer screening as an initial reader may correctly determine Lung-RADs categorization with suitable sensitivity and low false-positive rate.

#### **METHOD AND MATERIALS**

A retrospective study of 86 low-dose CT lung screening exams were first assessed using proposed CAD marks by 3 independent readers of variable experience (novice-expert) and then reviewed for any additional nodules. For each finding, readers specified nodule type, diameter and confidence level (1= "not a nodule", 10= "definitively a nodule"). The standard of reference was determined by majority agreement and arbitrated by an expert chest radiologist. The average reader sensitivity, specificity and AUC were calculated with respect to nodule as well as LRAD cutoff scores of 2 and 3. CAD standalone sensitivity and CAD and average reader per case false-positive rates were computed. Standard errors and 95% confidence intervals were derived from 1000 bootstrap samples, which were used to derive p-value comparing CAD alone and CAD plus reader.

# RESULTS

CAD and/or readers identified 505 findings. True nodules (n=119) included findings >=4mm, confidence >=7.5 and were partcalcified, solid or subsolid. Smaller and calcified nodules and lymph nodes were excluded (n=195). Sensitivity of CAD alone was 86% (95% CI, 80-92%) compared to the 3 reader average which was 64% (95% CI 58-69%). False-positives per case for CAD alone was 1.952 (95% CI 1.506-2.446) while the reader average was 0.088 (95% CI 0.052-0.129). Reader average specificity was 96% (95% CI 95-98%) and AUC was 0.799 (95% CI 0.770-0.829) accounting for the 191 false-positives. AUC using LRAD >=2 cutoff demonstrated no significant difference (p=0.80) for CAD alone (0.847, 95% CI 0.795-0.892) compared to CAD plus reader average (0.844, 95% CI 0.796-0.886). Using LRAD >=3 cutoff, AUC also demonstrated no significant difference (p=0.47) for CAD alone (0.821, 95% CI 0.754-0.884) versus CAD plus reader average (0.839, 95% CI 0.778-0.898).

#### CONCLUSION

Using a workflow with CAD as a first reader followed by radiologist review is feasible for determining Lung-RADs categorization and management.

# CLINICAL RELEVANCE/APPLICATION

Computer-aided detection can serve as a first reader for detection of pulmonary nodules on lung cancer screening CT exams, producing improved sensitivity to the human reader with a very low false-positive rate and no significant changes in patient management.



## ER160-ED-MOA5

**Dual Energy CT in Gastrointestinal Bleeding: Pearls and Pitfalls** 

Monday, Nov. 26 12:15PM - 12:45PM Room: ER Community, Learning Center Station #5

## Awards Certificate of Merit

#### Participants

Tugce Agirlar Trabzonlu, MD, Chicago, IL (*Presenter*) Grant, Siemens AG Amirhossein Mozafarykhamseh, MD, Chicago, IL (*Abstract Co-Author*) Grant, Siemens AG Cecil G. Wood III, MD, Chicago, IL (*Abstract Co-Author*) Nothing to Disclose Donald Kim, DO, San Francisco, CA (*Abstract Co-Author*) Nothing to Disclose Jeanne M. Horowitz, MD, Chicago, IL (*Abstract Co-Author*) Nothing to Disclose Vahid Yaghmai, MD, Chicago, IL (*Abstract Co-Author*) Nothing to Disclose

# **TEACHING POINTS**

Teaching Points: 1-To describe dual energy CT image acquisition and post-processing techniques relevant to imaging of gastrointestinal bleeding (GIB) 2-To describe the advantages of dual energy CT compared with CT angiography(CTA) and other standard imaging techniques for the diagnosis of GIB 3-To illustrate dual energy CT findings in GIB 4-To discuss the limitations and pitfalls that may hinder accurate diagnosis of GIB in dual energy CT and how to avoid them

# TABLE OF CONTENTS/OUTLINE

1-Overview of GI bleeding 2-Brief review of the current imaging strategies to evaluate GIB 3-Algorithm for the initial evaluation for upper and lower GIB and the role of MDCT 4-MDCT angiography protocol for GIB 5-Dual energy CT protocol and the application of the post-processing techniques (iodine maps with virtual non-enhanced images, virtual monochromatic imaging) for the detection of GIB 6-Potential advantages of the dual energy CT technique over routine CTA for the diagnosis of GIB 7-Imaging features of GIB with dual energy CT 7.1 Signs of active bleeding 7.2 Evaluating causes of GIB with dual energy CT when there is no sign of active bleeding 7.2.1 Vascular lesions 7.2.2 Infectious and inflammatory processes 7.3.3 Neoplasms 7.3.4 Miscellaneous lesions 8-Pitfallslimitations and challenges in evaluating GIB with dual energy CT and how to avoid them

### **Honored Educators**

Presenters or authors on this event have been recognized as RSNA Honored Educators for participating in multiple qualifying educational activities. Honored Educators are invested in furthering the profession of radiology by delivering high-quality educational content in their field of study. Learn how you can become an honored educator by visiting the website at: https://www.rsna.org/Honored-Educator-Award/ Vahid Yaghmai, MD - 2012 Honored EducatorVahid Yaghmai, MD - 2015 Honored EducatorVahid Yaghmai, MD - 2017 Honored EducatorJeanne M. Horowitz, MD - 2016 Honored Educator



# ER207-SD-MOA1

# Spontaneous Active Bleeding: Which Predictive Factors Influence in the Therapeutic Decision?

Monday, Nov. 26 12:15PM - 12:45PM Room: ER Community, Learning Center Station #1

## Participants

Maria Jesus Garcia Sanchez, MD, Madrid, Spain (*Presenter*) Nothing to Disclose Joaquin P. Moran Marsili SR, MD, Madrid, Spain (*Abstract Co-Author*) Nothing to Disclose Milagros Marti de Gracia, MD, PhD, Madrid, Spain (*Abstract Co-Author*) Nothing to Disclose Aurea Diez Tascon, MD, Madrid, Spain (*Abstract Co-Author*) Nothing to Disclose Alberto Borobia, Madrid, Spain (*Abstract Co-Author*) Nothing to Disclose Alberto Jimenez, MD, Madrid, Spain (*Abstract Co-Author*) Nothing to Disclose Guadalupe Buitrago, MD, Madrid, Spain (*Abstract Co-Author*) Nothing to Disclose Lucia Fernandez Rodriguez, BMBS, Madrid, Spain (*Abstract Co-Author*) Nothing to Disclose Gonzalo Garzon, MD, Madrid, Spain (*Abstract Co-Author*) Nothing to Disclose

#### PURPOSE

To characterize the patients with spontaneous active arterial bleeding diagnosed by angio-CT, and identify potential predictive factors to aid clinitians in the therapeutic decision.

### **METHOD AND MATERIALS**

A retrospective observational analysis of patients with spontaneous active arterial bleeding on angio-CT during 2014-2017 was done. We excluded traumatic, aortic, iatrogenic, digestive and cerebral haemorrhages. Main variable: therapeutic management, (G1) conservative; (G2) angioembolization/surgery. Secondary variables: demographic, clinical (hemodynamic in/stability, coagulopathies, anticoagulant/antiaggregant treatments), laboratory (hematocrit, hemoglobin, lactate, hematic concentrates), radiological (location of the bleeding: peripheral vs. central (visceral/retroperitoneal), extravasation size. Statistical analysis: Chi-square and T-Student test (U-Mann-Whitney in variables that do not follow normal distribution) to identify factors related to therapeutic management. Forward logistic regression including significant factors in the univariate analysis. ROC curve to estimate the value of greater sensitivity and specificity to discriminate the need for invasive treatment in those statistically significant continuous variables. IBM SPSS Statistics V.20 software was used.

### RESULTS

We included 33 patients: 19 men, 14 women. Average age 75 years. G1 = 8 patients, G2 = 25. Stable 24, unstable 9. Peripheric 17, central 16. Anticoagulants 26, antiaggregants 6, coagulopathies 3. There are statistically significant differences among treatment groups for age, extravasation size, hemodynamic stability and location, without finding statistically significant differences for the remaining variables. On multivariate analysis, only the extravasated size remains statistically significant. A ROC curve was constructed with this variable (AUC = 0.872, p = 0.002), concluding that extravasations >= 8.5 mm were managed by angioembolization and / or surgery.

# CONCLUSION

The most important factor significantly influencing the therapeutic management in spontaneous arterial bleeding is radiologic: the size of extravasation identified by CT angiography.

# **CLINICAL RELEVANCE/APPLICATION**

The increasing use of CT angiography allow us to identify arterial bleddings that were not possible to diagnose in the past. Identifying potential predictive factors could help in the therapeutic decision-making in patients with spontaneous arterial bleddings.



### ER208-SD-MOA2

### Point-of-Care Wrist Ultrasonography in Trauma Patients with Ulnar-Sided Pain and Instability

Monday, Nov. 26 12:15PM - 12:45PM Room: ER Community, Learning Center Station #2

### Participants

Seong Jong Yun, Seoul, Korea, Republic Of (*Presenter*) Nothing to Disclose Sun Hwa Lee, Seoul, Korea, Republic Of (*Abstract Co-Author*) Nothing to Disclose

# For information about this presentation, contact:

zoomknight@naver.com

#### PURPOSE

We evaluated the effectiveness of point-of-care wrist ultrasonography compared with 3T-magnetic resonance imaging (MRI) for diagnosing triangular fibrocartilage complex (TFCC) injuries in trauma patients with ulnar-sided pain and instability. Moreover, we assessed the inter-observer variability between a musculoskeletal radiology fellow and an emergency physician.

# METHOD AND MATERIALS

A prospective cross-sectional study was conducted in an emergency department; patients with ulnar-sided sprain and instability were recruited. A musculoskeletal radiology fellow and a trained board-certified emergency physician independently evaluated the TFC, meniscal homologue, volar and dorsal distal radioulnar ligaments, and extensor carpi ulnaris using point-of-care ultrasonography. Findings were classified as normal, partial rupture, or complete rupture. Wrist 3T-MRI was used as the reference standard. We compared the diagnostic values for point-of-care ultrasonography obtained by both reviewers using DeLong's test. Intra-class correlation coefficients (ICCs) were calculated for agreement between each reviewer and the reference standard, and directly between the two reviewers.

#### RESULTS

Sixty-five patients were enrolled. Point-of-care wrist ultrasonography showed acceptable sensitivity (97.2-99.1%), specificity (96.8-97.3%), and accuracy (96.9-97.9%); these diagnostic performance values did not differ significantly between reviewers (p = 0.58-0.98). Agreement between each reviewer and the reference standard was excellent (musculoskeletal radiology fellow, ICC = 0.976; emergency physician, ICC = 0.964), as was the inter-observer agreement (ICC = 0.968).

### CONCLUSION

Point-of-care wrist ultrasonography is as precise as MRI for detecting TFCC injuries.

# **CLINICAL RELEVANCE/APPLICATION**

Point-of-care wrist ultrasonography can be used for immediate diagnosis and further preoperative imaging. Moreover, it may shorten the interval from emergency department admission to surgical intervention while reducing costs.



# GI286-ED-MOA10

Assessment of Treatment Response with LI-RADS on CT/MRI: A Pictorial Review

Monday, Nov. 26 12:15PM - 12:45PM Room: GI Community, Learning Center Station #10

#### **Participants**

Nicolas Voizard, BEng, MD, Montreal, QC (Abstract Co-Author) Nothing to Disclose Milena Cerny, MD, Montreal, QC (Abstract Co-Author) Nothing to Disclose Anis Assad, Montreal, QC (Abstract Co-Author) Nothing to Disclose Damien Olivie, MD, MS, Montreal, QC (Abstract Co-Author) Nothing to Disclose Jean-Sebastien S. Billiard, MD, FRCPC, Montreal, QC (Presenter) Nothing to Disclose Pierre Perreault, MD, Montreal, OC (Abstract Co-Author) Consultant, Abbott Laboratories Richard Kinh Gian Do, MD, PhD, New York, NY (Abstract Co-Author) Consultant, Bayer AG Takeshi Yokoo, MD, PhD, Dallas, TX (Abstract Co-Author) Nothing to Disclose Claude B. Sirlin, MD, San Diego, CA (Abstract Co-Author) Research Grant, Gilead Sciences, Inc; Research Grant, General Electric Company; Research Grant, Siemens AG; Research Grant, Bayer AG; Research Grant, ACR Innovation; Research Grant, Koninklijke Philips NV; Research Grant, Celgene Corporation; Consultant, General Electric Company; Consultant, Bayer AG; Consultant, Boehringer Ingelheim GmbH; Consultant, AMRA AB; Consultant, Fulcrum Therapeutics; Consultant, IBM Corporation; Consultant, Exact Sciences Corporation; Advisory Board, AMRA AB; Advisory Board, Guerbet SA; Advisory Board, VirtualScopics, Inc; Speakers Bureau, General Electric Company; Author, Medscape, LLC; Author, Resoundant, Inc; Lab service agreement, Gilead Sciences, Inc; Lab service agreement, ICON plc; Lab service agreement, Intercept Pharmaceuticals, Inc; Lab service agreement, Shire plc; Lab service agreement, Enanta; Lab service agreement, Virtualscopics, Inc; Lab service agreement, Alexion Pharmaceuticals, Inc; Lab service agreement, Takeda Pharmaceutical Company Limited; Lab service agreement, sanofi-aventis Group; Lab service agreement, Johnson & Johnson; Lab service agreement, NuSirt Biopharma, Inc ; Contract, Epigenomics; Contract, Arterys Inc An Tang, MD, Montreal, QC (Abstract Co-Author) Research Consultant, Imagia Cybernetics Inc; Speaker, Siemens AG; Speaker, Eli Lilly and Company

For information about this presentation, contact:

an.tang@umontreal.ca

# **TEACHING POINTS**

1) Review the Liver Imaging Reporting and Data System (LI-RADS) treatment response assessment algorithm.2) Review locoregional therapies for hepatocellular carcinoma (HCC), treatment concepts and expected posttreatment findings.3) Demonstrate that despite the numerous treatments and variability in posttreatment findings, LI-RADS is a simple and practical way to assess and report treatment response.

# TABLE OF CONTENTS/OUTLINE

1) Introduction: treatment response assessment is critical, yet difficult due to lack of standardization and variable posttreatment imaging.2) LI-RADS treatment response (LR-TR) assessment algorithm: what is it, when to apply it.3) LR-TR categories: nonevaluable, viable, equivocal, nonviable.4) LI-RADS posttreatment reporting requirements and report content. a. Review locoregional treatments and efficacy. b. Review treatment-specific radiologic response for each major locoregional treatments (chemical ablation [ethanol], energy-based ablation [radiofrequency, microwave, cryoablation], transarterial embolization, transarterial chemoembolization (TACE), drug-eluting beads TACE, transarterial radioembolization, stereotactic body radiation therapy) c. Illustrate CT and MRI LR-TR response categories at key time points posttreatment.5) Technical pitfalls and future directions.6) Summary of key teaching points.

# **Honored Educators**

Presenters or authors on this event have been recognized as RSNA Honored Educators for participating in multiple qualifying educational activities. Honored Educators are invested in furthering the profession of radiology by delivering high-quality educational content in their field of study. Learn how you can become an honored educator by visiting the website at: https://www.rsna.org/Honored-Educator-Award/ An Tang, MD - 2018 Honored Educator



### GI287-ED-MOA11

# MRI Quantification of Hepatic Fat, Iron, and Fibrosis: A Practical Guide

Monday, Nov. 26 12:15PM - 12:45PM Room: GI Community, Learning Center Station #11

### Awards Certificate of Merit

### Participants

Julia A. Miranda, MD, Sao Paulo, Brazil (*Presenter*) Nothing to Disclose Regis Otaviano Bezerra, MD, Sao Paulo, Brazil (*Abstract Co-Author*) Nothing to Disclose Rodrigo Azambuja, MD, Sao Paulo, Brazil (*Abstract Co-Author*) Nothing to Disclose Ana I. Oliveira, Sao Paulo, Brazil (*Abstract Co-Author*) Nothing to Disclose Gabriela R. Camerin, MD, Sao Paulo, Brazil (*Abstract Co-Author*) Nothing to Disclose Camila V. Oliveira, MD, Sao Paulo, Brazil (*Abstract Co-Author*) Nothing to Disclose Natally Horvat, MD, Sao Paulo, Brazil (*Abstract Co-Author*) Nothing to Disclose Giovanni G. Cerri, MD, PhD, Sao Paulo, Brazil (*Abstract Co-Author*) Nothing to Disclose

### For information about this presentation, contact:

juazevedomiranda@gmail.com

# **TEACHING POINTS**

•Understand the epidemiology of chronic liver disease; •Understand the current concepts and management of iron and fat hepatic overload and hepatic fibrosis ; •Recognize the qualitative image methods for assess iron, fat and fibrosis on liver; •Know the quantitative methods for assess iron, fat and fibrosis on liver and how to quantify these elements; •Comprehend the liver MRI technique; •Recognize the advantages and disadvantages of these methods; •Be familiar with future directions of MRI in chronic hepatic diseases;

### **TABLE OF CONTENTS/OUTLINE**

A) INTRODUCTION • Hepatic diseases epidemiology B) MANAGEMENT OF IRON OVERLOAD, LIVER FAT AND IRON FIBROSIS • Treatment guidelines and algorithm C) QUALITATIVE IMAGE METHODS FOR ASSESS IRON, FAT AND FIBROSIS ON LIVER • Concepts • Advantages and disadvantages D) QUANTITATIVE METHODS FOR ASSES IRON, FAT AND FIBROSIS ON LIVER • Concepts and protocols • Advantages and disadvantages • How to do it E) FUTURE DIRECTIONS • What's on the horizon for quantification of fibrosis and hepatic metabolic profile (fat and iron)



### GI288-ED-MOA12

**Ischemic Bowel-Steals from Collateral Shunts and Fistulas** 

Monday, Nov. 26 12:15PM - 12:45PM Room: GI Community, Learning Center Station #12

#### **Participants**

Syed Y. Andrabi, MD, Burlington, MA (*Presenter*) Nothing to Disclose Shams I. Iqbal, MD, Burlington, MA (*Abstract Co-Author*) Nothing to Disclose Francis J. Scholz, MD, Burlington, MA (*Abstract Co-Author*) Owner, F Spoon Company

For information about this presentation, contact:

yasir.andrabi@gmail.com

### **TEACHING POINTS**

1.Blood flow diversion by artery-artery collateral SHUNTS or by artery-vein FISTULAS can produce puzzling small&large bowel ischemia and pose diagnostic/treatment challenges 2.Careful study of bowel vessels can show aneurysm or large feeding or draining vessels 3.'Fistula steals' produce acute symptoms with wall thickening. Large systemic to portal shunts may cause portal hypertension/encephalopathy and liver failure 4. 'Compression steals' median arcuate ligament syndrome (MALS) or gradual orifice occlusions, cause progressive chronic pain/GI dysfunction with malabsorption or acutely as aneurysm/dissection

# TABLE OF CONTENTS/OUTLINE

1.GI vascular anatomy and classification of vascular steal: Overview 2.Steals with illustrations from vascular FISTULAS: a.Causes b.Symptomatic patients: clinical, radiographic presentation c.Complication: early and long term d.Management and follow up 3.Steals with illustrations from vascular inflow COMPRESSION/OBSTRUCTION (MALS) a.Varying symptoms from Diaphragm Crus compression on Celiac Axis b.Symptomatic patients may have 1.SMA to Celiac Collaterals through pancreatic arcades 2.Post stenotic Celiac Axis dilatation 3.Contraction or fibrosis of distal SMA from low flow beyond collateral steal 4.High SMA collateral flow associated Aneurysm or Dissection c.Correction of MALS by shunt and balloon dilatation



# GI338-SD-MOA1

Extracellular Volume Fraction with Gd-EOB-DTPA-Enhanced MRI as a Prognostic Factor in Patients with Pancreatic Adenocarcinoma

Monday, Nov. 26 12:15PM - 12:45PM Room: GI Community, Learning Center Station #1

# Participants

Yoshihiko Fukukura, MD, PhD, Kagoshima, Japan (*Presenter*) Nothing to Disclose Yuichi Kumagae, Kagoshima, Japan (*Abstract Co-Author*) Nothing to Disclose Hiroto Hakamada, Kagoshima, Japan (*Abstract Co-Author*) Nothing to Disclose Hiroaki Nagano, MD, Kaogoshima, Japan (*Abstract Co-Author*) Nothing to Disclose Shinya Nakamura, Kagoshima, Japan (*Abstract Co-Author*) Nothing to Disclose Takashi Yoshiura, MD, PhD, Kagoshima, Japan (*Abstract Co-Author*) Nothing to Disclose

### For information about this presentation, contact:

yoshihiko2002jp@yahoo.co.jp

### PURPOSE

Extracellular volume (ECV) fraction denotes a theoretical space which consists of the intravascular and extravascular extracellular spaces. The purpose of this study was to determine whether extracellular volume (ECV) fraction with Gd-EOB-DTPA-enhanced MRI can predict outcomes for patients with pancreatic adenocarcinoma.

#### **METHOD AND MATERIALS**

Seventy-four patients (33 men and 41 women; mean age, 68.6 years; age range, 40-86 years) with histologically confirmed pancreatic adenocarcinoma underwent Gd-EOB-DTPA-enhanced MRI. For T1 mapping, Look-Locker sequences (single slice multiphase imaging using gradient-echo sequence with inversion recovery pulse) were obtained before and 20 min after Gd-EOB-DTPA administration. The image was obtained as only one axial slice at the level of the maximum diameter of tumor. Regions of interest were placed as large as possible within the pancreatic adenocarcinoma and the aorta on T1 maps before and 20 min after Gd-EOB-DTPA administration. ECV fraction of tumor was calculated using the following formula:  $ECV = (1-Hct) \times [R1(tumor 20min) - R1(tumor pre)] / [R1(aorta 20min) - R1(aorta pre)], where R1 = 1/T1; R1(tumor pre) and R1 (tumor 20min) are R1 values of tumor before and 20 min after Gd-EOB-DTPA administration, respectively; R1(aorta pre) and R1(aorta 20min) are R1 values of the aorta before and 20 min after Gd-EOB-DTPA administration, respectively. The effect on survival of variables including age, sex, tumor location, tumor size, TNM stage, treatment, and tumor ECV fraction were analyzed in univariate and multivariate analyses using the Cox proportional hazards regression model.$ 

#### RESULTS

Median survival for the entire patient population was 17.0 months. Increasing tumor ECV fraction (P for trend < 0.001) was associated with a positive effect on overall survival in patients with pancreatic adenocarcinoma. On multivariate analysis, 3 factors showed independent associations with poor patient survival: high TNM stage (P = 0.002), supportive treatment (P = 0.037), and low tumor ECV fraction (P for trend = 0.002) (Figure).

# CONCLUSION

Our study results suggest pancreatic adenocarcinomas with lower ECV fraction on Gd-EOB-DTPA-enhanced MRI is associated with reduced patient survival.

#### **CLINICAL RELEVANCE/APPLICATION**

Pretreatment tumor ECV fraction measured by Gd-EOB-DTPA-enhanced MRI can predict overall survival in patients with pancreatic adenocarcinoma.



# GI339-SD-MOA2

Fat-Suppressed Gadolinium-Enhanced Isotropic High-resolution 3D-GRE-T1WI for Predicting Small Node Metastases in Patients with Rectal Cancer

Monday, Nov. 26 12:15PM - 12:45PM Room: GI Community, Learning Center Station #2

# Participants

Yan Chen, Guangzhou, China (*Presenter*) Nothing to Disclose Xinyue Yang, Guangzhou, China (*Abstract Co-Author*) Nothing to Disclose Ziqiang Wen, Guangzhou, China (*Abstract Co-Author*) Nothing to Disclose Bao Lan Lu, Guangzhou, China (*Abstract Co-Author*) Nothing to Disclose Xiaojuan Xiao, BMedSc, MMedSc, Shenzhen, China (*Abstract Co-Author*) Nothing to Disclose Bingqi Shen, MD, Guangzhou, China (*Abstract Co-Author*) Nothing to Disclose Shen Ping Yu, Guangzhou, China (*Abstract Co-Author*) Nothing to Disclose

#### For information about this presentation, contact:

chenyan\_me@163.com

# PURPOSE

To investigate the application value of fat-suppressed gadolinium-enhanced isotropic high-resolution 3D-GRE-T1WI in regional nodes with different short-axis diameter ranges in rectal cancer, especially in nodes <=5 mm.

### **METHOD AND MATERIALS**

Patients with rectal adenocarcinoma confirmed by postoperative histopathology were included, and all the patients underwent preoperative 3.0 T rectal MRI and total mesorectal excision (TME) within 2 weeks after an MR scan. The harvested nodes from specimens were matched with nodes in the FOV of images for a node-by-node evaluation. The morphological and enhancement characteristics of all the visible nodes in the FOV of images were independently evaluated by two radiologists. The  $\chi^2$  test was used to evaluate differences in morphological and enhancement characteristics between benign and malignant nodes. The enhancement characteristics were further compared between benign and malignant nodes with different short-axis diameter ranges using the  $\chi^2$  test. Kappa statistics were used to describe interobserver agreement.

#### RESULTS

A total of 441 nodes from 70 enrolled patients were included in the evaluation, of which 111 nodes were metastatic. Approximately 85.5% and 95.6% of benign nodes were found to have obvious enhancement and homogeneous or mild-heterogeneous enhancement, respectively, whereas approximately 89.2% and 85.1% of malignant nodes showed moderate or mild enhancement and obvious-heterogeneous or rim-like enhancement, respectively. The AUCs of the enhancement degree for identifying the overall nodal status, nodes <=5 mm and nodes >5mm and <=10 mm were 0.887, 0.859 and 0.766 for radiologist 1 and 0.892, 0.823 and 0.774 for radiologist 2, respectively. The AUCs of enhancement homogeneity were 0.940, 0.928 and 0.864 for radiologist 1 and 0.944, 0.938 and 0.842 for radiologist 2, respectively.

#### CONCLUSION

Enhancement characteristics based on fat-suppressed gadolinium-enhanced isotropic high-resolution 3D-GRE-T1WI were helpful for diagnosing metastatic nodes in rectal cancer and were a reliable indicator for nodes <=5 mm.

### **CLINICAL RELEVANCE/APPLICATION**

Accurate prediction of the regional node status of rectal cancer prior is closely tied to treatment decisions and prognosis. Fatsuppressed gadolinium-enhanced isotropic high-resolution 3D-GRE-T1WI, which maintains higher SNR and higher spatial resolution and can provide MPR images, serves as a promising technique for rectal metastatic node detection.



# GI340-SD-MOA3

Feasibility Study of Generating Virtual Contrast-Enhanced CT Images from Noncontrast Abdomen CT in Patients with Hepatocellular Carcinoma Using Conditional Generative Adversarial Networks

Monday, Nov. 26 12:15PM - 12:45PM Room: GI Community, Learning Center Station #3

### Participants

Jae Seok Bae, MD, Seoul, Korea, Republic Of (*Presenter*) Nothing to Disclose Jung Hoon Kim, MD, Seoul, Korea, Republic Of (*Abstract Co-Author*) Nothing to Disclose Hwiyoung Kim, Seoul, Korea, Republic Of (*Abstract Co-Author*) Nothing to Disclose Joon Koo Han, MD, Seoul, Korea, Republic Of (*Abstract Co-Author*) Nothing to Disclose

### PURPOSE

Feasibility study of generating virtual contrast-enhanced CT images from abdomen non-enhanced CT in patients with hepatocellular carcinoma using conditional generative adversarial networks.

### **METHOD AND MATERIALS**

Using 350 patients with pathologically confirmed HCC who underwent preoperative CT, we divided into the training set (300 patients with 67780 images) and the test set (50 patients with 7144 images). We trained a cGAN to generate virtual CECT images from their corresponding CECT images. A generator convolutional neural network (CNN) was trained to transform NECT images into CECT images, while an adversarial discriminator CNN was simultaneously trained to distinguish the output of the generator CNN from real arterial phase CT images. The result of this discriminator was used as an adversarial loss for the generator. We first used the images of the training set to train a cGAN model for approximately 5 days with 6 TITAN Xp GPUs and the trained model was utilized to generate virtual CECT from NECT images of the test set. To evaluate the sensitivity for detection of hepatic focal lesions, two radiologists evaluated the NECT images of the test set and then re-evaluated the NECT images in conjunction with virtual CECT images generated by cGAN. We also graded the degree of enhancement of major abdominal organs and vessel from no enhancement (0) to perfect enhancement (3).

# RESULTS

Using the NECT images only, 82% (41 of 50) of hypervascular HCCs was detected. With virtual CECT images, additional five lesions were detected to yield 92% (46 of 50) of sensitivity. In terms of degree of enhancement, abdominal aorta showed perfect enhancement in all cases (n=50), kidney and spleen showed perfect (94%, n=47 for both) or moderate (6%, n=3 for both) enhancement, pancreas demonstrated moderate enhancement in all cases (n=50), and the liver showed mild (98%, n=49) or no (2%, n=1) enhancement.

### CONCLUSION

cGAN-based generation of virtual CECT is feasible and is might be helpful for detection of hypervascular hepatic focal lesion.

#### **CLINICAL RELEVANCE/APPLICATION**

cGAN-based generation of virtual CECT may be useful for enhancing abdomen NECT, not only enhancing major abdominal organs and vessel, but also improving detection of hepatic focal lesion.



# GI341-SD-MOA4

Diffusion-Weighted Magnetic Resonance Imaging of Pancreatic Ductal Adenocarcinoma: Correlation with Metastatic Disease Potential and Overall Survival

Monday, Nov. 26 12:15PM - 12:45PM Room: GI Community, Learning Center Station #4

# Participants

Alejandro Garces-Descovich, MD, Boston, MA (*Presenter*) Nothing to Disclose Trevor C. Morrison, MD, Boston, MA (*Abstract Co-Author*) Nothing to Disclose Kevin Beker, MD, Boston, MA (*Abstract Co-Author*) Nothing to Disclose Adrian M. Jaramillo-Cardoso, MD, Boston, MA (*Abstract Co-Author*) Nothing to Disclose Arthur Moser, Boston, MA (*Abstract Co-Author*) Nothing to Disclose Koenraad J. Mortele, MD, Boston, MA (*Abstract Co-Author*) Nothing to Disclose

For information about this presentation, contact:

agarces@bidmc.harvard.edu

### PURPOSE

To analyze the relationship between apparent diffusion coefficient (ADC) of pancreatic ductal adenocarcinoma (PDAC) and the presence or development of metastatic disease, and overall survival (OS).

#### **METHOD AND MATERIALS**

IRB approval with waived informed consent was obtained for this retrospective study. A total of 65 consecutive patients with histopathologically proven, treatment naive PDAC who underwent staging DWI-MRI between January 2012 and December 2014 were evaluated; 17/65 patients were excluded. Outcome data for the remaining 48 patients (24 men; median age, 65.5 years; IQ range, 56 - 77 years) was obtained during a 4-year follow-up period (mean time: 397 days ± 415.1). Overall correlation between the ADC and the presence or development of metastatic disease was assessed using descriptive statistics. Overall survival and mortality analysis was performed using Pearson correlation and Kaplan-Meier curves.

# RESULTS

Of 48 patients, 10 either had either metastatic disease at the time of the staging MRI or went on to develop metastatic disease (n=12). Among the latter, the mean time from staging MRI to metastasis was  $258 \pm 274.1$  days. Metastases were observed in liver (n=19), omentum (n=1), lung and liver (n=1) and bone (n=1). During the follow-up period, the remaining 26 (54 %) patients never developed metastases. Patients with metastatic disease (n=22) had a significantly lower mean pretreatment ADC (1.27 mm2/s) than those without metastases (1.43 mm2/s) (p=0.047). No significant difference between mean ADC of those who had metastatic disease at staging MRI (1.23 mm2/s) compared to those who developed metastasis later (1.31 mm2/s) (p=0.405) was identified. ADC of PDAC had a positive correlation with survival: patients with PDAC that showed lower ADCs (< 1.36 mm2/s) had significantly worse 4-year overall survival rates than patients with PDAC that showed higher ADCs (p=0.036).

### CONCLUSION

Pretreatment ADC values of PDAC are significantly lower in patients who have or will develop metastatic disease and correlate with a worse overall survival.

### **CLINICAL RELEVANCE/APPLICATION**

A MRI biomarker that determines which patients with PDAC have or go on to develop metastatic disease would have a possible impact on clinical management. While further investigation is needed, our results suggest that DWI-MRI can be of value in determining which patients with PDAC will likely develop metastatic disease and will have shorter overall survival.



# GI342-SD-MOA5

Retrospectively Evaluation of Contrast-Enhanced Ultrasound Liver Imaging Reporting and Data System on 2022 Nodules and Proposed Adjustments to Improve the Diagnostic Performance

Monday, Nov. 26 12:15PM - 12:45PM Room: GI Community, Learning Center Station #5

# Participants

Jianhua Zhou, MD, Guangzhou, China (*Presenter*) Nothing to Disclose Wei Zheng, MD, Guangzhou, China (*Abstract Co-Author*) Nothing to Disclose Qing Li, Guangzhou, China (*Abstract Co-Author*) Nothing to Disclose Fei Li, MD, Guangzhou, China (*Abstract Co-Author*) Nothing to Disclose Xuebin Zou, Guangzhou, China (*Abstract Co-Author*) Nothing to Disclose Jianwei Wang, Guangzhou, China (*Abstract Co-Author*) Nothing to Disclose Feng Han, MD,PhD, Guangzhou, China (*Abstract Co-Author*) Nothing to Disclose

#### For information about this presentation, contact:

zhoujh@sysucc.org.cn

# PURPOSE

This study purposed to evaluate the diagnostic performance of Contrast-Enhanced Ultrasound Liver Imaging Reporting and Data System Version 2017 (CEUS LI-RADS v2017) in classifying lesions in patients at risk for hepatocellular carcinoma (HCC).

### **METHOD AND MATERIALS**

A total of 2022 lesions in hepatitis B positive patients were retrospectively analyzed. All lesions were pathologically and/or clinically confirmed on CT/MRI with a minimum of 1-year follow-up. The nodules were analyzed retrospectively and categorized as CEUS LI-RADS categories 1-5 and M (LR-1-5 and -M) according to CEUS LI-RADS v2017.

#### RESULTS

Of 2022 lesions, 128(6.3%) had a LR-1 assessment; 42(2.1%) a LR-2 assessment; 193(9.5%), a LR-3 assessment; 142(7.0%), a LR-4 assessment; 1159(57.3%), a LR-5 assessment; and 358(17.7%), a LR-M assessment based on initial CEUS images. The malignancy rates of LR-1, 2, 3, -4, -5, and -M lesions were 0%, 0%, 17.1%, 88.0%, 99.7%, and 99.2%, respectively; and the HCC rates were 0%, 0%, 14.5%, 82.4%, 98.5%, and 62.8%, respectively. No lesions presented as only marked washout but onset later than 60 seconds. Of 358 LR-M lesions, 42.3% lesions presented as arterial phase hyperenhancement (in whole or in part) with only early washout (within 60 seconds) but no marked washout, of which 92.8% were HCCs, and If these lesions were recategorized as LR-5, the HCC rates of LR-5 and -M were adjusted to 97.9% and 40.8%. After adjustment, for LR-M to classify non-HCC malignancy, the accuracy (from 87.4% to 93.9%, P=0.0292), specificity (from 87.8% to 95.4%, P=0.0151), and positive predicted value (from 36.3% to 58.3%, P<0.001) were significantly increased, while no significantly changed in sensitivity (P=0.527) and negative predicted value (P=0.902).

### CONCLUSION

As LR-M lesions have a high HCC rate, a recommendation of recategorizing nodules with APHE and only early washout as LR-5 would improve diagnostic performance of CEUS LI-RADS v2017.

### **CLINICAL RELEVANCE/APPLICATION**

A suggested revision to the current criteria of LR-M would significantly decrease the HCC rate of LR-M and improve the differential diagnosis of HCC and non-HCC malignancy.



# GI343-SD-MOA6

Radiographic Profiling of Abdominal Immune-Related Adverse Events in Patients with Non-Small Cell Lung Cancer Treated with PD-1 Pathway Inhibitors

Monday, Nov. 26 12:15PM - 12:45PM Room: GI Community, Learning Center Station #6

# Awards

# Student Travel Stipend Award

#### Participants

Francesco Alessandrino, MD, Boston, MA (*Presenter*) Nothing to Disclose

Sonia P. Sahu, MD, Boston, MA (Abstract Co-Author) Nothing to Disclose

Mizuki Nishino, MD, MPH, Newton, MA (*Abstract Co-Author*) Institutional Research Grant, Merck & Co, Inc; Institutional Research Grant, Canon Medical Systems Corporation; Institutional Research Grant, AstraZeneca PLC; Speaker, F. Hoffmann-La Roche Ltd; Consultant, DAIICHI SANKYO Group

Sreeharsha Tirumani, MBBS, MD, Boston, MA (Abstract Co-Author) Nothing to Disclose

Anika E. Adeni, Boston, MA (Abstract Co-Author) Nothing to Disclose

Mark M. Awad, Boston, MA (Abstract Co-Author) Consultant, Novartis AG; Consultant, Nektar Therapeutics; Research funded, Bristol-Myers Squibb Company

Atul B. Shinagare, MD, Boston, MA (Abstract Co-Author) Advisory Board, Arog Pharmaceuticals, Inc; Research Grant, GTx, Inc

#### For information about this presentation, contact:

falessandrino@bwh.harvard.edu

### PURPOSE

Immune-related adverse events (irAEs) have been reported in clinical trial setting but their incidence on imaging remains unknown. The purpose of this study was to investigate the frequency of abdominal irAEs on CT among patients with advanced non-small cell lung cancer (NSCLC) treated with PD-1 inhibitors.

### METHOD AND MATERIALS

In this IRB-approved retrospective study, patients with NSCLC treated with PD-1 inhibitors during 2015-2017 were identified from thoracic oncology database. All included imaging studies were reviewed by a fellowship-trained radiologist blinded to clinical data to identify the following abdominal irAEs: colitis (pancolitis, segmental colitis, enterocolitis), enteritis, hepatitis, biliary toxicity, pancreatitis, nephritis, adrenal and pancreatic atrophy. Likelihood of irAE was scored from 1 (definitely not irAE) to 5 (definitely irAE). Cases with irAE score >=3 were also scored independently by two additional fellowship-trained radiologists. Cases were considered positive if the irAE score was>3 by at least two of the three radiologists.

### RESULTS

Of a total 210 patients identified, 137 patients (62 men, 75 women; median age: 65 years) who had baseline CT and at least one follow-up abdomen/pelvis CT during PD-1 therapy were included. 21 patients (15.3%) had radiologically identified abdominal irAEs. Median interval from PD-1 therapy initiation to irAE development was 3.5 months. A total of 13 patients developed colitis (9 pancolitis, 3 segmental colitis, one enterocolitis), two hepatitis, two biliary toxicity, one adrenalitis, one nephritis, one enteritis and one developed adrenal atrophy. In one case pancolitis on imaging preceded clinical irAE. Imaging resolution of irAEs was observed in 5/21 patients during therapy and in 7/21 cases after treatment. PD-1 therapy was interrupted due to irAE in 5/21 patients, due to disease progression in 3/21 patients, and due to poor performance status in 1/21 patient at the time of irAE.

### CONCLUSION

Abdominal irAEs were detected on CT in 15.3% NSCLC patients treated with PD-1 therapy, with colitis, in the pancolitis form, being the most common irAE.

#### **CLINICAL RELEVANCE/APPLICATION**

Abdominal irAEs associated with PD-1 therapy are frequently detected on abdominal CT. Given the expanding role of immunotherapy, radiologists should be aware of common radiologic presentation of irAEs

# **Honored Educators**

Presenters or authors on this event have been recognized as RSNA Honored Educators for participating in multiple qualifying educational activities. Honored Educators are invested in furthering the profession of radiology by delivering high-quality educational content in their field of study. Learn how you can become an honored educator by visiting the website at: https://www.rsna.org/Honored-Educator-Award/ Sreeharsha Tirumani, MBBS, MD - 2016 Honored EducatorAtul B. Shinagare, MD - 2017 Honored Educator



# GI344-SD-MOA7

The Utility of MR Elastography to Differentiate Nodular Regenerative Hyperplasia from Liver Cirrhosis: A Pilot Feasibility Study

Monday, Nov. 26 12:15PM - 12:45PM Room: GI Community, Learning Center Station #7

#### Awards Student Travel Stipend Award

#### **Participants**

Patrick Navin, MBBCh, MRCPI, Rochester, MN (*Presenter*) Nothing to Disclose Moira Hilscher, MD, Rochester, MN (*Abstract Co-Author*) Nothing to Disclose Taofic Mounajjed, Rochester, MN (*Abstract Co-Author*) Nothing to Disclose Michael Torbenson, Baltimore, MD (*Abstract Co-Author*) Nothing to Disclose Patrick S. Kamath, MD, Rochester, MN (*Abstract Co-Author*) Nothing to Disclose Sudhakar K. Venkatesh, MD, FRCR, Rochester, MN (*Abstract Co-Author*) Nothing to Disclose

# PURPOSE

Nodular regenerative hyperplasia (NRH) is characterized by nodular transformation of the liver with small rgenerative nodules. Portal hypertension and associated complications may develop. Unlike cirrhosis, it is not associated with hepatocellular carcinoma. Differentiating NRH from cirrhosis is therefore important yet difficult on standard imaging. This study aims to assess the utility of MRI and MR Elastography (MRE) in differentiating NRH and cirrhosis

# METHOD AND MATERIALS

Following review of our pathology database, 30 cases were initially identified as NRH. Reexamination by 2 experienced hepatopathologists in consensus revealed 16 definite cases. Eleven patients had both MRI+MRE forming the study group (NRH group). A comparison cohort of age and sex matched patients with biopsy proven cirrhosis was created (Cirrhosis group). Two radiologists blinded to diagnosis evaluated morphological hepatic features (lobe atrophy/hypertrophy, periportal space sign etc), signs of portal hypertension (varices, splenomegaly etc) and overall impression of cirrhosis. Mean liver stiffness (LSM) and spleen stiffness measurements (SSM) were calculated with a ratio obtained (SSM/LSM). Imaging features of NRH and cirrhosis were compared using Chi square analysis. Continous measurements were analyzed using ANOVA. ROC analysis was performed if significant difference was found

# RESULTS

Among MRI morphological features, only periportal space enlargement was significantly more common in the NRH group (n=7 NRH;n=2 cirrhosis, p=0.034). Mean LSM was significantly higher in cirrhosis than NRH group (6.3kPa [range 3.8-8.9] vs 4.4kPa [3.1-6.6], p=0.002) (Fig 1a,b). SSM was not significantly different (7.2kPa [5.3-9.5] vs 7.3kPa [2.2-14.9], p=0.91). SSM/LSM ratio was significantly higher in NRH group (1.7 v 1.2, p=0.046). ROC analysis revealed a cutt-off of mean LSM <4.7kPa had 82% sensitivity, 91% specificity and 86% accuracy to differentiate NRH from cirrhosis. SSM/LSM ratio cut-off > 1.1 had 87.5% sensitivity, 64% specificity and 76% accuracy to differentiate NRH from cirrhosis

### CONCLUSION

MR Elastography may allow greater differentiation of NRH from cirrhosis based on hepatic stiffness and spleen/liver stiffness ratio

### **CLINICAL RELEVANCE/APPLICATION**

Nodular regenerative hyperplasia is difficult to differentiate from cirrhosis clinically and with conventional CT and MRI. MR Elastography may allow increased sensitivity in diagnosis without requiring tissue sampling.

# **Honored Educators**

Presenters or authors on this event have been recognized as RSNA Honored Educators for participating in multiple qualifying educational activities. Honored Educators are invested in furthering the profession of radiology by delivering high-quality educational content in their field of study. Learn how you can become an honored educator by visiting the website at: https://www.rsna.org/Honored-Educator-Award/ Sudhakar K. Venkatesh, MD, FRCR - 2017 Honored Educator



# GI345-SD-MOA8

Preoperative Prediction of Treatment Resistance in Rectal Cancer Patients Treated with Neo-Adjuvant Chemoradiotherapy Using MRI Texture Analysis: A Preliminary Study

Monday, Nov. 26 12:15PM - 12:45PM Room: GI Community, Learning Center Station #8

# Participants

Lan Zhang, PhD, Wuhan, China (*Presenter*) Nothing to Disclose Xin Li, MD,PhD, wuhan, China (*Abstract Co-Author*) Nothing to Disclose Ping Han, MD, Wuhan, China (*Abstract Co-Author*) Nothing to Disclose Yu Zhang, MS, Wuhan, China (*Abstract Co-Author*) Nothing to Disclose Zhengwu Tan, MA, Wuhan, China (*Abstract Co-Author*) Nothing to Disclose Wenliang Fan, BMedSc,PhD, Wuhan, China (*Abstract Co-Author*) Nothing to Disclose

#### For information about this presentation, contact:

zhanglan0211@126.com

### PURPOSE

To investigate the possibility of MRI texture analysis for predicting the treatment resistance in rectal cancer patients treated with neo-adjuvant chemoradiotherapy before operation.

#### **METHOD AND MATERIALS**

52 patients with advanced rectal cancer who received neo-adjuvant chemoradiotherapy were involved. The tumor regression grade(TRG) and down-stage status were evaluated. Patients were scanned while initial diagnosis and 1 week before operation on 3.0T MR scanners using standard rectal protocol(axial and sagittal:T2W STIR, enhanced T1W TSE with fat suppression;DWI). Early arterial phase images and T2W images were exported for analysis. Texture analysis was performed by MaZda version4.6. Regions of interest(ROI) were placed manually without visible necrotic area. Grey-level normalization was performed. 256 texture features were evaluated and exported. Classifications were performed on Weka version3.8 through support vector machine(SVM) classifiers. Diagnostic accuracy of SVM was assessed and 10-folds cross validation was performed.

# RESULTS

31 patients achieved down-stage and 21 patients failed.18 patients achieved TRG0-1 and 14 patients received TRG2-3.There was lower lesion homogeneity and higher lesion entropy in the group failed down-stage and in the group TRG2-3 (P<0.05).The average SVM accuracy of texture features, which related to initial T2W images was 62.9%(AUROC=0.603) for predicting down-stage and 61.5%( AUROC=0.593) for predicting TRG2-3, which related to initial T1 enhanced images was 58.8%( AUROC=0.494) for predicting down-stage and 30.8%( AUROC=0.297) for predicting TRG2-3, which related to T2W images before operation was 82.3%( AUROC=0.841) for predicting down-stage and 70.4%( AUROC=0.709) for predicting TRG2-3, which related to T1 enhanced images before operation was 55.6%( AUROC=0.5) for predicting down-stage and 29.6%( AUROC=0.294) for predicting TRG2-3.

### CONCLUSION

For predicting the treatment resistance, texture analysis based on T2W images has a higher efficiency than that based on T1enhanced images. MR texture analysis can be used to predict the treatment resistance in rectal cancer treated with neo-adjuvant chemoradiotherapy with a potential value.

### **CLINICAL RELEVANCE/APPLICATION**

Neoadjuvant chemoradiotherapy is the standard treatment for advanced rectal cancer, however, there are no prognostic factors for operation timing. The study hopes to seek the potential prediction factors and to construct a clinical prediction model.



# GI346-SD-MOA9

Comparison of Diagnostic Performance of Non-Contrast MRI and Abbreviated MRI in Initially Diagnosed Hepatocellular Carcinoma Patients: A Simulation Study of Surveillance for Hepatocellular Carcinomas

Monday, Nov. 26 12:15PM - 12:45PM Room: GI Community, Learning Center Station #9

# Participants

Sun young Whang, Seoul, Korea, Republic Of (*Presenter*) Nothing to Disclose Joon-Il Choi, Seoul, Korea, Republic Of (*Abstract Co-Author*) Nothing to Disclose Moon Hyung Choi, MD, Seoul, Korea, Republic Of (*Abstract Co-Author*) Nothing to Disclose Young Joon Lee, MD, Seoul, Korea, Republic Of (*Abstract Co-Author*) Nothing to Disclose Sung Eun Rha, MD, Seoul, Korea, Republic Of (*Abstract Co-Author*) Nothing to Disclose

### For information about this presentation, contact:

dumkycji@gmail.com

# PURPOSE

To compare the diagnostic performance of non-contrast MRI and abbreviated MRI using gadoxetic acid for detecting hepatocellular carcinoma (HCC) in initially diagnosed, early stage HCC patients

# METHOD AND MATERIALS

We identified 142 consecutive, initially diagnosed HCC patients within Milan criteria, who performed liver MRI between 2015 and 2016. For the control group, we enrolled 158 consecutive patients without HCC but had risk factors (liver cirrhosis, chronic hepatitis B or C) of HCC, who also performed liver MRI in the same period. Total number of HCCs was 177 and the number of HCCs smaller than 2 cm and 2 cm <= were 92 and 85, respectively. Two radiologists independently reviewed two MRI sets; non-contrast set and abbreviated set. Non-contrast set consists of T2 FSE/ssFSE with fat saturation, T1 in- and out-of-phase image, non-contrast 3D GRE T1 images, DWI (with b-value 500s/mm2) and ADC map. Abbreviated set consists of T2 FSE/ssFSE with fat saturation, 3D GRE T1 images at hepatobiliary phase 20 minutes after gadoxetic acid injection, DWI and ADC map. Both readers recorded the presence, size and location of HCCs.

#### RESULTS

In per-patient analysis, sensitivity of reader 1 of non-contrast and abbreviated set were 90.8% and 89.8%, respectively. Specificity of non-contrast and abbreviated set were 92.7% and 92.3%, respectively. For reader 2, sensitivity of both sets were 87.4% and 87.5%, and specificity were 90.3% and 91.7%, respectively. When comparing two image sets, there was no statistical difference in both readers (p=0.65 and 0.86 for reader 1 and 2, respectively, using MeNemar test). Kappa statistics showed excellent inter-observer agreement (0.86 for non-contrast and 0.84 for abbreviated set). In per-tumor analyses, sensitivity of reader 1 for non-contrast and abbreviated set were 81.9% and 83.1%, respectively. For reader 2, per-tumor sensitivity for both sets were 80.8% and 83.6%, respectively.

### CONCLUSION

Non-contrast and abbreviated MRI using gadoxetic acid showed comparable diagnosing performance for detecting HCCs in early stage HCC patients.

### **CLINICAL RELEVANCE/APPLICATION**

Ultrasonography is not sensitive enough for the surveillance of patients with very high risk of HCCs. Non-contrast MRI is cheaper than abbreviated MRI using gadoxetic acid and can avoid the repeated usage of contrast media which can be accumulated in human brain. Non-contrast liver MRI can be a potential candidate for a surveillance tool of HCC.



# GU210-SD-MOA1

Could Negative Multiparametric MRI of the Prostate Obviate the Need for Biopsy? A Prospective Feasibility Pilot Study

Monday, Nov. 26 12:15PM - 12:45PM Room: GU/UR Community, Learning Center Station #1

# Participants

Milena Spirovski, Novi Sad, Serbia (*Presenter*) Nothing to Disclose Milos Lucic, Sremska Kamenica, Serbia (*Abstract Co-Author*) Nothing to Disclose Milan Popov, Novi Sad, Serbia (*Abstract Co-Author*) Nothing to Disclose Olivera Sveljo, Sremska Kamenica, Serbia (*Abstract Co-Author*) Nothing to Disclose Mladen Bjelan, MD, Sremska Kamenica, Serbia (*Abstract Co-Author*) Nothing to Disclose Katarina Koprivsek, MD,PhD, Sremska Kamenica, Serbia (*Abstract Co-Author*) Nothing to Disclose Dusko Kozic, Sremska Kamenica, Serbia (*Abstract Co-Author*) Nothing to Disclose

#### For information about this presentation, contact:

milena.spirovski@gmail.com

# PURPOSE

To investigate the feasibility of follow up in men with elevated prostate-specific antigen (PSA) level, negative digital rectal exam (DRE) and negative multiparametric MRI (mpMRI).

### **METHOD AND MATERIALS**

Over the period of 13 years, 36 men (age range at the time of the inclusion 45-71 years (mean 64)) with PSA level elevation, negative DRE and negative mpMRI were included in the study. All men were followed up clinically, including PSA and DRE, and with mpMRI. mpMRI examinations included thin slice (3mm) T2 weighted images in three planes, diffusion-weighted images, dynamic postcontrast images in all men and MR spectroscopy in the most.

### RESULTS

Mean follow up was 6.4 years, (range from 16 months to 13 years), mean PSA level during the study was 7.3ng/L (range 1.72-11.29ng/L), mean initial PSA was 8,7ng/L (range 4.3-13.2ng/L). All participants were followed clinically, none of them underwent a single biopsy. After initial negative mpMRI first follow up mpMRI was in 6 months, then one year, and further according to the clinical finding (3-5 follow up mpMRI in total per men). None of the men were diagnosed with prostate cancer; three men died due to cardiovascular disease, two developed other malignancies (one colorectal, other lung cancer).

#### CONCLUSION

In men with increased PSA, negative mpMRI of the prostate can obviate the need for biopsy.

### **CLINICAL RELEVANCE/APPLICATION**

It could be feasible to follow up men with clinically suspected prostate cancer and negative mpMRI safely.



### GU211-SD-MOA2

Impact of Magnetic Resonance Imaging Findings on Management and Clinical Outcome of Morbidly Adherent Placenta

Monday, Nov. 26 12:15PM - 12:45PM Room: GU/UR Community, Learning Center Station #2

# Participants

Mohamed S. Elzawawi, MBBCh,MD, Menoufyia, Egypt (*Presenter*) Nothing to Disclose Hesham A. Ammar, MD, Shebeen Elkom, Egypt (*Abstract Co-Author*) Nothing to Disclose

For information about this presentation, contact:

melzawawi66@yahoo.com

### PURPOSE

To outline the impact of magnetic resonance imaging (MRI)findings on management decision making and clinical outcome in patients with morbidly adherent placenta (MAP).

### **METHOD AND MATERIALS**

The current study included 298 pregnant females (mean age 33.2 years and mean gestational age 32.4 weeks) with placenta previa and suspected MAP diagnosed by color doppler ultrasound referred for prenatal uterine MRI during the period from February 2013 to January2018. Statistical analysis was used to determine the impact of MR findings on surgical decision making and poor clinical outcome including morbidity and morality.

#### RESULTS

Out of the 298 patients, 136(45.6%) had MAP proved by cesarean surgery and pathology. 44(32.4%) were placenta accreta, 54(39.7%) increta and 38(27.9%) percreta. 26(19.1%) had urinary bladder invasion. Statistical analysis showed that MR evidence of bladder invasion was significantly associated with hysterectomy, partial cystectomy, and poor outcome including maternal morbidity, massive blood transfusion, prolonged surgery and hospitalization. 2 cases with bladder invasion (1.5%) died from massive hemorrhage during cesarean hysterectomy.T2 dark bands and peri-uterine serosal hyper-vascularity were significantly associated with massive blood transfusion, prolonged surgery and hospitalization.

### CONCLUSION

MRI findings including urinary bladder invasion, T2 dark bands and per-uterine serosal hyper-vascularity significantly affected the management decision making and clinical outcome of MAP.

# **CLINICAL RELEVANCE/APPLICATION**

MRI findings have significant impact on management decision making and the clinical outcome in patients with MAP.



# GU212-SD-MOA3

Diagnostic Accuracy of Preoperative Tumor Staging in Low-Grade Endometrial Carcinoma with MELF Pattern Invasion

Monday, Nov. 26 12:15PM - 12:45PM Room: GU/UR Community, Learning Center Station #3

# Participants

Ryo Kuwahara, MD, Kyoto, Japan (*Presenter*) Nothing to Disclose Aki Kido, MD, Kyoto, Japan (*Abstract Co-Author*) Nothing to Disclose Ryo Yajima, Kyoto, Japan (*Abstract Co-Author*) Nothing to Disclose Naoko Nishio, Kyoto, Japan (*Abstract Co-Author*) Nothing to Disclose Kyoko K. Nakao, MD, Kyoto, Japan (*Abstract Co-Author*) Nothing to Disclose Yasuhisa Kurata, Kyoto, Japan (*Abstract Co-Author*) Nothing to Disclose Tsukasa Baba, Kyoto, Japan (*Abstract Co-Author*) Nothing to Disclose Sachiko Minamiguchi, Kyoto, Japan (*Abstract Co-Author*) Nothing to Disclose Masaki Mandai, Kyoto, Japan (*Abstract Co-Author*) Nothing to Disclose Kaori Togashi, MD, PhD, Kyoto, Japan (*Abstract Co-Author*) Nothing to Disclose Kaori Togashi, MD, PhD, Kyoto, Japan (*Abstract Co-Author*) Research Grant, Bayer AG; Research Grant, DAIICHI SANKYO Group; Research Grant, Eisai Co, Ltd; Research Grant, FUJIFILM Holdings Corporation; Research Grant, Nihon Medi-Physics Co, Ltd; Research Grant, Canon Medical Systems Corporation

# PURPOSE

To investigate the influence of microcystic, elongated and fragmented (MELF) pattern invasion on preoperative evaluation of lymph node metastasis and myometrial invasion in patients with low-grade endometrial carcinoma.

### **METHOD AND MATERIALS**

The study included 199 consecutive patients with low-grade endometrial carcinoma who underwent preoperative imaging and surgery at our institution from 2005 to 2017. Presence of enlarged lymph nodes was evaluated by using size criteria on contrastenhanced computed tomography (CT). Depth of myometrial invasion was evaluated on T2-weighted imaging (T2WI), Diffusion weighted imaging (DWI) and contrast-enhanced T1-WI (CE-T1). Sensitivity and specificity for lymph node metastasis and deep myometrial invasion were evaluated for MELF group and non-MELF group. The difference of sensitivity between two groups was compared using chi-square and Fisher exact tests. Surgical pathologic findings were used as the reference standard.

### RESULTS

MELF pattern invasion was identified in 44/199 patients (22%). Totally, 168 patients underwent lymph node dissection. Lymph node metastases were observed in 19/40 patients in MELF group and 7/128 patients in non-MELF group. Sensitivity for the detection of lymph node metastasis in MELF group was 15.8% on per-patient basis and 11.9% on per-region basis, which was significantly lower than in non-MELF group (71.4% and 42.9%, p = 0.01 and 0.02, respectively). As for the assessment of the deep myometiral invasion, sensitivities in MELF group versus non-MELF group were as follows; in Reader 1, 43.8% versus 64.7% on T2WI, 40.6% versus 73.5% on DWI, 48.4% versus 63.3% on CE-MRI, in Reader 2, 43.8% versus 61.8%, 53.1% versus 61.8%, 51.6% versus 63.3%. The difference on DWI was significant (p = 0.01) in Reader 1. Intra-reader agreement was good (kappa =0.6-0.65).

# CONCLUSION

In case of low-grade endometrial carcinoma with MELF patter invasion, preoperative staging by CT and MRI have a risk for underestimation.

# **CLINICAL RELEVANCE/APPLICATION**

The knowledge of potential risk of underestimation in preoperative staging by CT and MRI in endometrial carcinoma with MELF pattern invasion may prevent insufficient treatment.



# GU213-SD-MOA4

Value of Revolution CT Perfusion Imaging in Differentiating Adrenal Lipid-Poor Adenoma (ALPA) and Adrenal Metastases (AM)

Monday, Nov. 26 12:15PM - 12:45PM Room: GU/UR Community, Learning Center Station #4

# Participants

Ying Zhao Jr, Dalian, China (*Abstract Co-Author*) Nothing to Disclose Ailian Liu, MD, Dalian, China (*Abstract Co-Author*) Nothing to Disclose Jinghong Liu, MD, PhD, Dalian, China (*Abstract Co-Author*) Nothing to Disclose Yijun Liu, Dalian, China (*Abstract Co-Author*) Nothing to Disclose Xin Fang, Dalian, China (*Abstract Co-Author*) Nothing to Disclose Nan Wang, Dalian, China (*Abstract Co-Author*) Nothing to Disclose Xinying Li, Dalian, China (*Presenter*) Nothing to Disclose

### PURPOSE

To investigate the value of Revolution CT perfusion imaging in differentiating ALPA and AM.

# METHOD AND MATERIALS

Fifteen ALPAs and Ten AM patients were enrolled in this retrospective study, ALPAs were pathologically confirmed, and AM were confirmed by clinical history and follow-up imaging. CT perfusion scan was performed with 16 cm detector, using z-axis coverage mode. The tube voltage and tube current was set according to the patients' BMI. The CTP scanning was initiated 6 s after the injection of contrast, continuous scanning was performed for the anterior 28 s, the data were then collected at 39 s, 43 s, 47 s, 51 s, 63 s, 83 s, 113 s, 153 s, 213 s, 353 s and 593 s, respectively. The arterial, venous and delayed phase enhanced images were obtained at the time of 22 s, 51 s and 153 s. Twenty-six consecutive volume acquisitions were contained and the total perfusion scanning time was 593 s. The size, unenhanced and enhanced CT attenuation numbers and perfusion parameter measurements of tumors were recorded. The above parameters between ALPAs and AM were compared. ROC curves were plotted to analyze diagnostic efficiency. The radiation dose indexes were recorded.

# RESULTS

There was not statistical difference of length, minimum width, unenhanced CT value and enhanced CT values between ALPA and AM (*P* all > 0.05). BF and BV values of ALPA were statistically higher than those of AM ( $66.32 \pm 43.79$  vs.  $36.02 \pm 43.91$  ml/( $100g \cdot min$ ),  $18.33 \pm 5.95$  vs.  $8.04 \pm 6.28$  ml/100g, P = 0.014 and 0.003, respectively), while there was not statistical difference of MTT, TP and PS values between the two tumors (*P* all > 0.05). The area under the ROC curve of BF and BV values were 0.844 and 0.900, and there were a sensitivity of 93.3% and 66.7%, and a specificity of 80% and 100% for differentiating ALPA from AM. The effective radiation dose of adrenal CT plain scan and CTP (including enhanced CT scan) were ( $3.60 \pm 0.75$ ) mSv and ( $19.43 \pm 3.39$ ) mSv, respectively.

# CONCLUSION

Twenty-six phase consecutive CT perfusion scanning protocol can provide high-quality conventional three-phase enhanced images and effective quantitative perfusion data at lower radiation dose. CT perfusion imaging is valuable for differentiating ALPA and AM.

# **CLINICAL RELEVANCE/APPLICATION**

It is difficult to identify ALPA and AM by routine CT examination. However, BF and BV values can be used to identify both of them for higher diagnostic efficacy.



## GU214-SD-MOA5

The Use of Different KV Settings in Dual Energy CT and the Impact on Kidney Stone Detection in Virtual Non-Contrast Reconstructions in the Abdomen

Monday, Nov. 26 12:15PM - 12:45PM Room: GU/UR Community, Learning Center Station #5

# Participants

Mathias Lazar, MD, Vienna, Austria (*Presenter*) Nothing to Disclose Helmut R. Ringl, MD, Vienna, Austria (*Abstract Co-Author*) Nothing to Disclose Anna Ehn, Vienna, Austria (*Abstract Co-Author*) Nothing to Disclose Pascal A. Baltzer, MD, Vienna, Austria (*Abstract Co-Author*) Nothing to Disclose Stephan H. Polanec, MD, Vienna, Austria (*Abstract Co-Author*) Nothing to Disclose Michael Toepker, MD, Vienna, Austria (*Abstract Co-Author*) Nothing to Disclose

### For information about this presentation, contact:

mathias.lazar@meduniwien.ac.at

### PURPOSE

The aim of this phantom based study was to evaluate the impact of different kilovolt (kv) settings and contrast media concentrations for dual energy computed tomography (DE-CT) virtual non-contrast (VNC) reconstructions in urinary stone disease on image quality and on kidney stone detection rate.

#### **METHOD AND MATERIALS**

The research protocol for this study was approved by the Institutional Review Board. A plastic phantom made from a material with an attenuation of approximately 70 Hounsfield units (HU) (Tango Black) simulating normal renal tissue was used. Through 4 open slots in total 16 kidney stones of different sizes and compositions were placed within the renal phantom and a contrast saline solution with increasing attenuation (0, 100 etc. HU) was floated around the stones. Dual Energy Scans with different KV settings were (70kV/140kV; 80kV/140kV; 90kV/140kV; 100kV/140kV) performed using a third generation DE-CT scanner (SOMATOM Definition Force CT, Siemens Health Care, Forchheim, Germany). Two experienced uroradiologists independently rated the images for the presence and absence of stones, luminal contrast and image noise were compared

#### RESULTS

Overall the detection rate of kidney stones in VNC reconstructions was 51.1%. The detection rate of renal calculi with more than 2mm in size was significantly higher compared to renal calculi smaller than 2mm (86.1%; 12.2%; p<.001).Depending on the different kV settings best results were shown at 70kV and 80kV in scans with contrast media attenuation of 600HU or less (100%; 94.2%).Insufficient VNC reconstruction with significantly higher luminal attenuation at the renal pelvis were observed in scans with applied contrast media concentration of equal or more than 900HU.

#### CONCLUSION

Correct kV/HU setting is essential for accurate detection of renal calculi in VNC reconstructions of DE-CT. To improve the dual energy VNC we suggest to use less contrast for the split bolus excretory phase and try to use lower kV for the low tube current.

### **CLINICAL RELEVANCE/APPLICATION**

Dual energy virtual non contrast has the potential to replace the true non contrast scan without losing clinical relevant information and might reduce the overall radiation dose.



# GU215-SD-MOA6

Feasibility Study of Using Virtual On-Contrast Scans in Dual Energy Spectral CT to Replace True Non-Contrast Scans in Diagnosing Renal Cell Carcinoma

Monday, Nov. 26 12:15PM - 12:45PM Room: GU/UR Community, Learning Center Station #6

# Participants

Ma Guangming, MMed, Xianyang City, China (*Presenter*) Nothing to Disclose Haifeng Duan, Xianyang City, China (*Abstract Co-Author*) Nothing to Disclose Chuangbo Yang, MMed, Xianyang City, China (*Abstract Co-Author*) Nothing to Disclose Xirong Zhang, Xianyang, China (*Abstract Co-Author*) Nothing to Disclose Hui Zhong, Xianyang, China (*Abstract Co-Author*) Nothing to Disclose Chenwang Jin, Xi'an, China (*Abstract Co-Author*) Nothing to Disclose

#### PURPOSE

To investigate the clinical value of dual energy spectral CT-generated virtual non-contrast (VNC) images to replace the conventional true non-contrast (TNC) scans in diagnosing renal cell carcinoma.

#### **METHOD AND MATERIALS**

32patients with renal cell carcinoma confirmed by pathology underwent the conventional plain scan, and contrast enhanced spectral CT scans at arterial phase (AP) and venous phase(VP). VNC images at AP and VP were generated on AW4.6 using Gemstone Spectral Imaging (GSI) software and Material Suppressed Iodine technique. CT number, contrast-to-noise ratio (CNR), long and short axis diameters of the lesions were measured from the three image sets and analyzed by ANOVA. Two radiologists subjectively evaluated image quality using 5-pointscore, and lesion signature (hemorrhage, cystic change and fat clearance) using a 3-point score.

### RESULTS

The two physicians had good agreement for image quality assessment (Kappa>0.70) with no difference among the 3 image groups. The lesion signature score was  $2.88\pm0.34$  for VNC(AP) and  $2.84\pm0.37$  for VNC(VP), all above acceptable level. CNR value was  $0.72\pm0.16$  in VNC(AP) and  $0.69\pm0.12$  in VNC(VP), all significantly higher than the  $0.52\pm0.11$  in the normal TNC images (P<0.05). The lesion long and short axis diameters (in mm) were (4.22, 4.48) with TNC, (4.25, 4.48) with VNC(AP) and (4.23, 4.52) with VNC(VP) with no difference. There was statistical difference for the CT number in renal lesion among the 3 image groups ( $30.04\pm4.09HU$ with TNC vs.  $32.69\pm4.07HU$  with VNC(AP) and  $32.56\pm3.52HU$  with VNC(VP), p<0.05). However, the maximum difference between groups was less than 5HU.

### CONCLUSION

Virtual non-contrast images generated from the arterial and portal venous phases in spectral CT imaging provided similar objective measurements (lesion size, CT number and CNR) and subjective evaluation (image quality and lesion sign) as those in the true non-contrast imaging, and may be used to replace the conventional plain scan to reduce scan time and radiation dose.

### **CLINICAL RELEVANCE/APPLICATION**

Virtual non-contrast images generated from in spectral CT imaging may be used to replace the true non-contrast scans in diagnosing renal cell carcinoma for reducing radiation dose.



### HP008-EB-MOA

Mentorship in Radiology: It Doesn't Have to Be All Greek to You

Monday, Nov. 26 12:15PM - 12:45PM Room: HP Community, Learning Center Hardcopy Backboard

#### **Participants**

Elainea N. Smith, MD, Birmingham, AL (*Presenter*) Nothing to Disclose Andrew J. Gunn, MD, Birmingham, AL (*Abstract Co-Author*) Nothing to Disclose Jason C. Hoffmann, MD, Mineola, NY (*Abstract Co-Author*) Speakers Bureau, Merit Medical Systems, Inc; ; Rachel F. Oser, MD, Birmingham, AL (*Abstract Co-Author*) Nothing to Disclose Michael A. Coker, BA, Vestavia, AL (*Abstract Co-Author*) Nothing to Disclose Robert A. Esposito, Birmingham, AL (*Abstract Co-Author*) Nothing to Disclose Anand R. Patel, MD, Birmingham, AL (*Abstract Co-Author*) Nothing to Disclose Benjamin L. Triche, MD, Birmingham, AL (*Abstract Co-Author*) Nothing to Disclose Desiree E. Morgan, MD, Birmingham, AL (*Abstract Co-Author*) Nothing to Disclose Desiree G. Zarzour, MD, Birmingham, AL (*Abstract Co-Author*) Nothing to Disclose

#### For information about this presentation, contact:

agunn@uabmc.edu

### **TEACHING POINTS**

1. Delineate the role of a mentor 2. Review the types of mentors 3. Discuss the fundamentals of establishing a successful mentoring relationship 4. Understand the benefits of mentorship 5. Describe various institutional or organizational approaches to mentorship

### **TABLE OF CONTENTS/OUTLINE**

1. Introduction, including the definition of a mentor, teacher, and role model (Figure 1) 2. Types of mentors (Figure 2) 3. Mentoring takes effort from both the mentor and the mentee (Figures 3 and 4) 4. Approaches to mentoring in radiology a. Societal and organization efforts b. Institutional experience in resident mentoring i. Peer-to-peer mentoring 1. Residents are assigned as a peer mentor to a resident in the class below them ii. Faculty-to-resident mentoring 1. Faculty volunteers to serve as mentors 2. Residents submit their choices for mentors from available faculty 3. Program directors assign mentors after evaluating the residents' choices 4. Financial support available for food, drinks, or coffee in order to facilitate meeting iii. Training materials for mentors and mentees (Figure 5) iv. Program includes local private practice groups to improve the mentoring experience c. Brief review of other institutions' experiences 5. Conclusion



### HP206-SD-MOA1

Comparison of Magnetic Resonance-Guided Focused Ultrasound with Pain Medication for Palliation of Painful Bone Metastases

Monday, Nov. 26 12:15PM - 12:45PM Room: HP Community, Learning Center Station #1

# Participants

Matthew D. Bucknor, MD, San Francisco, CA (*Presenter*) Nothing to Disclose Frandics P. Chan, MD, PhD, San Francisco, CA (*Abstract Co-Author*) Nothing to Disclose Jessica Matuoka, San Francisco, CA (*Abstract Co-Author*) Nothing to Disclose James Kahn, San Francisco, CA (*Abstract Co-Author*) Nothing to Disclose

For information about this presentation, contact:

matthew.bucknor@ucsf.edu

# PURPOSE

To determine if in patients with refractory pain from bone metastases, if palliation with MRgFUS, compared to medication alone, is cost-effective (incremental cost-effectiveness ratio or ICER), for a 24-month time horizon, from a health system perspective.

# METHOD AND MATERIALS

We constructed a Markov state transition model using TreeAgePro®. Probabilities, costs, and effectiveness data were derived from a combination of the available literature, expert opinion, and reimbursement data at two U.S. medical centers performing MRgFUS. In the model, costs and quality adjusted life years (QALYs), discounted at a rate of 3%/year, were accumulated each month over a 24-month time horizon. Willingness-to-pay level was estimated at \$100,000/QALY. Multiple sensitivity analyses were performed.

### RESULTS

In the base case analysis, MRgFUS cost an additional \$8756.23 to accumulate an additional 0.22 QALYs, equal to a \$40150/QALY ICER, making MRgFUS the preferred strategy. 1-way sensitivity analyses showed that the crossover point at which Medication Only would become the preferred strategy was an MRgFUS cost of \$25,711.58. Additional sensitivity analyses performed in which the efficacy of MRgFUS for a second treatment was decreased to 60%, and 40% for a third treatment, compared to the 80% following each of 3 maximum treatments in the base case. With progressively decreasing MRgFUS efficacy, the ICER increased 13.5% to \$45572/QALY (Fig 1). If the percentage of those with persistent pain following a first treatment who elected to repeat MRgFUS increased from 50% to 100%, the ICER increases slightly to \$40240/QALY.

### CONCLUSION

Our base case and sensitivity analyses demonstrated that MRgFUS was a preferred treatment strategy across a wide range of transition state probabilities, costs, and QALYs. Our model was most sensitive to changes in the cost of MRgFUS and QALYs associated with persistent pain or pain relief.

# **CLINICAL RELEVANCE/APPLICATION**

Our model demonstrates that MRgHIFU is cost-effective compared to pain medication alone for palliation of painful bone metastases for patients with medically refractory metastatic bone pain across a broad range of sensitivity analyses.



### HP207-SD-MOA2

Prevalence of Pneumothorax Following Right-Heart Catheterization: Is Routine Post-Procedure Chest Radiography Indicated?

Monday, Nov. 26 12:15PM - 12:45PM Room: HP Community, Learning Center Station #2

#### Awards Student Travel Stipend Award

# Participants

Christopher P. Centonze, MD, Ann Arbor, MI (*Presenter*) Nothing to Disclose Ella A. Kazerooni, MD, Ann Arbor, MI (*Abstract Co-Author*) Nothing to Disclose Matthew S. Davenport, MD, Ann Arbor, MI (*Abstract Co-Author*) Nothing to Disclose

For information about this presentation, contact:

ccentonz@med.umich.edu

### PURPOSE

To determine whether routine post-procedure chest radiography is indicated to exclude pneumothorax following outpatient right heart catheterization and endomyocardial biopsy using an internal jugular vein approach.

# METHOD AND MATERIALS

This HIPAA-compliant retrospective quality improvement cohort study was approved by the institutional review board. All outpatient subjects (n=6,073) who underwent routine post-procedure chest radiography following right heart catheterization and endomyocardial biopsy in one health system from January 1, 2010 to July 1, 2017 were identified by electronic medical record query using current procedural terminology (CPT) codes. The prevalence of pneumothorax was calculated by coded review of chest radiography reports. Pneumothorax size and clinical outcomes were determined. 95% confidence intervals (CI) were calculated.

# RESULTS

Most (99% [99/100 of a random sample]) right-heart catheterizations were performed using an internal jugular vein approach. The prevalence of pneumothorax by post-procedure chest radiography was 0.1% (7/6,073; 95% CI: 0.05-0.24%). Three of the seven pneumothoraces were confirmed within 1 hour to be false positives (i.e., no pneumothorax), resulting in a real pneumothorax rate of 0.06% (4/6,073; 95% CI: 0.00-0.2%). The remaining four pneumothoraces were less than 1 cm. No chest tubes were placed and there was no unexpected prolongation in length of stay.

### CONCLUSION

Pneumothorax following right-heart catheterization utilizing an internal jugular vein approach is rare and usually clinically insignificant. Routine post-procedure chest radiography in this setting is not warranted.

### **CLINICAL RELEVANCE/APPLICATION**

Elimination of routine post-procedure chest radiography will eliminate false positive results, reduce radiation exposure, and reduce costs.

#### **Honored Educators**

Presenters or authors on this event have been recognized as RSNA Honored Educators for participating in multiple qualifying educational activities. Honored Educators are invested in furthering the profession of radiology by delivering high-quality educational content in their field of study. Learn how you can become an honored educator by visiting the website at: https://www.rsna.org/Honored-Educator-Award/ Ella A. Kazerooni, MD - 2014 Honored Educator



### HP208-SD-MOA3

Imaging Criteria Concordance Evaluation in a Multi-Clinical Trial Population: Immune-Related Response Evaluation Criteria in Solid Tumors (irRECIST) and Immune-Related Response Criteria (IrRC) versus Response Evaluation Criteria in Solid Tumors 1

Monday, Nov. 26 12:15PM - 12:45PM Room: HP Community, Learning Center Station #3

FDA

Discussions may include off-label uses.

#### Participants

Anthony Sader, BS, Seattle, WA (*Presenter*) Nothing to Disclose Carolyn L. Wang, MD, Seattle, WA (*Abstract Co-Author*) Nothing to Disclose Ryan O'Malley, MD, Seattle, WA (*Abstract Co-Author*) Nothing to Disclose Danielle Nacamuli, BS, Seattle, WA (*Abstract Co-Author*) Nothing to Disclose Achille Mileto, MD, Seattle, WA (*Abstract Co-Author*) Nothing to Disclose

#### For information about this presentation, contact:

asader@uw.edu

# PURPOSE

To evaluate whether Immune-Related Response Evaluation Criteria in Solid Tumors (irRECIST) and Immune-Related Response Criteria (IrRC) are concordant with Response Evaluation Criteria in Solid Tumors (RECIST 1.1) in clinical trials for patients undergoing immunotherapy.

#### **METHOD AND MATERIALS**

Our single-center, retrospective study was IRB-approved and HIPAA-compliant. Using our commercially available institutional tumor metrics database (Precision Imaging Metrics), we performed a comprehensive search of clinical trials between January 2012-July 2017 and identified all trials that use RECIST 1.1 and irRC criteria or RECIST 1.1 and irRECIST 1.1 across multiple disease groups. Each patient had multiple time points identical for the paired criteria. For each imaging time-point, overall tumor burden and response categories (progressive disease, stable disease, partial response, and complete response) were recorded for both criteria. Concordance of response categories was assessed between different imaging criteria. Confidence intervals calculated using generalized estimating equations with logit link.

#### RESULTS

Our search yielded data for 171 patients (99 men, 72 women; mean age, 61). Subjects were pooled into two categories: irRECIST vs. RECIST1.1 and irRC vs. RECIST1.1. Of the 262 time points in the irRECIST vs. RECIST1.1 group, only 8 (3%) of the responses differed between the two criteria (96.9% concordance, 95% CI [94.0%-98.5%]). In 7/8 discordant responses, the irRECIST response was clinically more favorable (stable disease vs. progressive disease). Of the 144 time points in the irRC vs. RECIST1.1 group, 123 (85%) response assessments were concordant between the two criteria (85.4% concordance, 95% CI [75.9%, 91.6%]). Of the 21 discordant responses, irRC yielded more favorable response in 9 patients (6%), whereas in 12 (8%) RECIST1.1 indicated more favorable response. Discordant case provided with the figure.

# CONCLUSION

Our data show that integration of immune-related imaging response criteria may introduce variability in response evaluation for patients undergoing immunotherapy enrolled in clinical trials. In our analysis, comparing irRC vs. RECIST1.1 assessments yielded the highest discrepancy rates.

### **CLINICAL RELEVANCE/APPLICATION**

Variation in response assessments compared to RECIST 1.1 may be inherent to these novel imaging-based schemes rather than reflecting actual changes in tumor biology or disease course.



### HP209-SD-MOA4

# The Impact of Emerging Technologies on Residency Selection by Medical Students

Monday, Nov. 26 12:15PM - 12:45PM Room: HP Community, Learning Center Station #4

#### **Participants**

Michael K. Atalay, MD, PhD, Providence, RI (*Presenter*) Nothing to Disclose Grayson L. Baird, PhD, Providence, RI (*Abstract Co-Author*) Nothing to Disclose Matthew T. Stib, MD, Providence, RI (*Abstract Co-Author*) Nothing to Disclose Paul George, MD, Providence, RI (*Abstract Co-Author*) Nothing to Disclose John J. Cronan, MD, Providence, RI (*Abstract Co-Author*) Nothing to Disclose

# For information about this presentation, contact:

atalay\_99@yahoo.com

### PURPOSE

Artificial intelligence (AI) and other emerging technologies promise to change the way medicine is practiced. How medical students anticipate these changes may affect their career choices. Our objective was to determine the perceived impact of AI on various specialties by medical students and how this might affect their residency selections.

# **METHOD AND MATERIALS**

We conducted a brief, anonymous survey of all medical students (1st-4th years) at a single medical school. The survey was agnostic to any specialty and was delivered by email from the account of a medical school administrator in November 2017. Survey questions were chiefly designed to interrogate (a) incentives motivating residency selection and career path, (b) the degree of interest in each specialty, (c) the perceived effect that AI will have on future job prospects for each specialty, and (d) those specialties that students would not consider because of concerns levied by emerging technology.

#### RESULTS

A total of 384 medical students (72%; 384/532) participated in the survey. The percentages of respondents who considered each potential motivation 'important' or 'very important' were: (a) Interest in Specialty: 98.9%; (b) Patient Care: 93.2%; (c) Work-Life Balance: 89.9%; (d) Job Security: 73.2%; (e) Job Market: 62.6%; (f) Salary: 56.6%; and (g) Student Debt: 42.5%. The specialties with job prospects felt most likely to be reduced were diagnostic radiology (60.7%), pathology (49.0%), and anesthesiology (44.0%). Of respondents, 164 (42.7%) identified one or more specialties they would NOT consider due to their concern that emerging technology will render them obsolete or less appealing, chief among them diagnostic radiology at 54.9% (90/164), followed by pathology at 18.9% (31/164), anesthesiology and radiation oncology, both at 18.3% (30/164).

# CONCLUSION

Current perceptions of emerging technologies likely affect residency selection for a large proportion of medical students and may independently impact the future of various specialties. Diagnostic radiology, in particular, is squarely in the crosshairs of specialties to avoid.

# **CLINICAL RELEVANCE/APPLICATION**

A large proportion of medical students will reportedly not consider one or more specialties owing to the anticipated impact of emerging technologies.



# HP210-SD-MOA5

# Portable Chest Radiograph Utilization Among Inpatients

Monday, Nov. 26 12:15PM - 12:45PM Room: HP Community, Learning Center Station #5

#### Participants

Sarah I. Kamel, MD, Philadelphia, PA (Presenter) Nothing to Disclose David C. Levin, MD, Philadelphia, PA (Abstract Co-Author) Consultant, HealthHelp, LLC; Board Member, Outpatient Imaging Affiliates, LLC

Laurence Parker, PhD, Philadelphia, PA (Abstract Co-Author) Nothing to Disclose Vijay M. Rao, MD, Philadelphia, PA (Abstract Co-Author) Nothing to Disclose

For information about this presentation, contact:

sarah.kamel@jefferson.edu

#### PURPOSE

According to the March 2018 MedPAC report to Congress, the number of Medicare inpatient discharges declined over the past decade. Daily/screening portable chest x-rays (PCXR) are frequently ordered in the inpatient setting. Recent literature suggests that daily CXR can be eliminated without increasing adverse outcomes, particularly in intensive care patients. Our purpose was to study recent trends of PCXR utilization in inpatients in response to decreasing hospital admissions and stricter guidelines regarding their use.

# METHOD AND MATERIALS

The nationwide Medicare Part B fee-for-service databases for 2003-2016 were used. We selected CPT code 71010 (single view, chest) presuming that most inpatient CXRs are portable. Global and professional-component claims were tabulated to determine volume. Technical-component claims were excluded to avoid double counting. The databases indicate procedure volume for each code from which we calculated utilization rates per 1000 Medicare beneficiaries. Medicare place-of-service codes were used to identify exams performed on inpatients. Data regarding the number of yearly inpatient hospitalizations from 2004-2014 among Medicare beneficiaries was obtained from the Healthcare Cost and Utilization Project database. Because the Medicare Part B databases are complete population counts, sample statistics are not required.

# RESULTS

Among inpatients, the utilization rate of PCXRs fluctuated around 355 per 1000 beneficiaries from 2003-2007, peaked at 371 in 2008 and subsequently declined to 250 in 2016 (-33% from peak). Data regarding inpatient admissions of Medicare beneficiaries shows that they peaked in 2008 at 38.2 million admissions and then declined to 35.3 million by 2014 (-7.5%). The ratio of inpatient PCXR performed per inpatient admission peaked in 2005 at 0.35 and declined to 0.29 by 2014 (-15%).

#### CONCLUSION

In light of data supporting the elimination of routine CXR use among inpatients, it is encouraging that our study demonstrates a 33% drop in inpatient PCXR use. This decline was greater than the decline in inpatient admissions over the past decade, reflected in a falling ratio of PCXR performed per hospital admission.

# **CLINICAL RELEVANCE/APPLICATION**

The use of portable chest x-rays in inpatients is declining more rapidly than the rate of inpatient hospitalizations.



# IN144-ED-MOA1

# Application of Radiomics in Pancreatic Imaging - Current Status and Future Directions

Monday, Nov. 26 12:15PM - 12:45PM Room: IN Community, Learning Center Station # :

FDA Discussions may include off-label uses.

### Awards

# **Certificate of Merit**

#### Participants

Linda C. Chu, MD, Baltimore, MD (*Presenter*) Nothing to Disclose Seyoun Park, Baltimore, MD (*Abstract Co-Author*) Nothing to Disclose Satomi Kawamoto, MD, Laurel, MD (*Abstract Co-Author*) Nothing to Disclose Daniel Fadaei Fouladi, MD, Baltimore, MD (*Abstract Co-Author*) Nothing to Disclose Shahab Shayesteh, MD, Baltimore, MD (*Abstract Co-Author*) Nothing to Disclose Karen M. Horton, MD, Baltimore, MD (*Abstract Co-Author*) Nothing to Disclose Alan Yuille, Baltimore, MD (*Abstract Co-Author*) Nothing to Disclose Elliot K. Fishman, MD, Baltimore, MD (*Abstract Co-Author*) Institutional Grant support, Siemens AG; Institutional Grant support, General Electric Company; Co-founder, HipGraphics, Inc

#### For information about this presentation, contact:

lindachu@jhmi.edu

#### **TEACHING POINTS**

1. Radiomics is the high-throughput extraction of quantitative imaging based on intensity, shape, volume, and textural features. 2. These quantitative imaging features have the potential to provide additional insight in the underlying biological processes. 3. Radiomics features have shown potential benefit in classification and risk stratification of pancreatic cystic neoplasms. 4. Radiomics features have shown promise in predicting survival of patients with pancreatic adenocarcinoma.

### **TABLE OF CONTENTS/OUTLINE**

Review basic principles of radiomics 2. Review application of radiomics in the classification and risk stratification of pancreatic cystic neoplasms: • High grade vs. low grade IPMNs • Different types of pancreatic cystic neoplasms 3. Review application of radiomics features in predicting prognosis of patients with pancreatic adenocarcinoma • Treatment response • Disease-free survival
 Overall survival 4. Technical challenges of radiomics 5. Future directions

### **Honored Educators**

Presenters or authors on this event have been recognized as RSNA Honored Educators for participating in multiple qualifying educational activities. Honored Educators are invested in furthering the profession of radiology by delivering high-quality educational content in their field of study. Learn how you can become an honored educator by visiting the website at: https://www.rsna.org/Honored-Educator-Award/ Elliot K. Fishman, MD - 2012 Honored EducatorElliot K. Fishman, MD - 2014 Honored EducatorElliot K. Fishman, MD - 2016 Honored EducatorElliot K. Fishman, MD - 2018 Honored Educator



# MI117-ED-MOA4

Pancreatic Neuroendocrine Tumors (pNETs) Recognized in New AJCC Staging System 8th Edition: What Radiologists Need to Know

Monday, Nov. 26 12:15PM - 12:45PM Room: MI Community, Learning Center Station #4

#### Awards Certificate of Merit

#### **Participants**

Nicholas Norman, Lexington, KY (*Abstract Co-Author*) Nothing to Disclose Timothy J. Waits, MD, Lexington, KY (*Abstract Co-Author*) Nothing to Disclose Aman Chauhan, Lexington, KY (*Abstract Co-Author*) Nothing to Disclose Lowell Anthony, MD, Lexington, KY (*Abstract Co-Author*) Nothing to Disclose M. Elizabeth Oates, MD, Lexington, KY (*Abstract Co-Author*) Nothing to Disclose Riham H. El Khouli, MD, PhD, Nicholasville, KY (*Presenter*) Nothing to Disclose

# For information about this presentation, contact:

rhel222@uky.edu

# **TEACHING POINTS**

To understand the historical development of the American Joint Committee on Cancer (AJCC) staging systems. To recognize the key differences between the 7th edition of AJCC staging system for pancreatic cancers and the new 8th edition for staging pancreatic neuroendocrine tumors (pNET). To apply the new 2018 AJCC staging system for pNETs in daily practice.

# TABLE OF CONTENTS/OUTLINE

For the first time, the new 8th edition of the AJCC staging system recognizes pNET as a separate tumor entity, and specifies a unique TNM classification staging, one that is different from that applied to exocrine pancreatic cancers. This is an important step forward as well-differentiated pNETs behave differently than exocrine pancreatic cancers. The educational exhibit will follow this outline: 1. Introduction to the AJCC staging system including the history of its development. 2. Rationale behind the necessity to separate staging of the more indolent well-differentiated pNETs from the more aggressive exocrine pancreatic cancers. 3. Case examples illustrating and highlighting the key differences between the 7th edition and the new 8th edition for pNET staging in actual practice. 4. The multimodality imaging approach includes: a. CT b. MRI c. 111In-pentetreotide (OctreoScan) planar, SPECT, SPECT/CT d. 18F-FDG PET/CT e. 68Ga-dotatate (NETSPOT) PET/CT

# **Honored Educators**

Presenters or authors on this event have been recognized as RSNA Honored Educators for participating in multiple qualifying educational activities. Honored Educators are invested in furthering the profession of radiology by delivering high-quality educational content in their field of study. Learn how you can become an honored educator by visiting the website at: https://www.rsna.org/Honored-Educator-Award/ Riham H. El Khouli, MD, PhD - 2012 Honored Educator



### MI208-SD-MOA1

[18F]-Fluoroestradiol PET Imaging of Tumors with Activating Mutations at Tyrosine-537 in Estrogen Receptor Alpha in Breast Cancer

Monday, Nov. 26 12:15PM - 12:45PM Room: MI Community, Learning Center Station #1

**FDA** Discussions may include off-label uses.

# Awards

### **Student Travel Stipend Award**

# Participants

Manoj Kumar, MS, Madison, WI (*Presenter*) Nothing to Disclose Kelley Salem, PhD, Madison, WI (*Abstract Co-Author*) Nothing to Disclose Ciara Michel, Madison, WI (*Abstract Co-Author*) Nothing to Disclose Justin Jeffery, Madison, WI (*Abstract Co-Author*) Nothing to Disclose Yongjun Yan, PhD, Madison, WI (*Abstract Co-Author*) Nothing to Disclose Amy M. Fowler, MD, PhD, Madison, WI (*Abstract Co-Author*) Research support, General Electric Company

### For information about this presentation, contact:

mkumar9@wisc.edu

# PURPOSE

18F-Fluoroestradiol (FES) positron emission tomography (PET) is useful for measuring tumoral estrogen receptor (ER) status, predicting endocrine therapy response, and optimizing antiestrogen doses. Reported mutations in the ER-alpha gene (*ESR1*) are associated with endocrine therapy resistance and reduced progression-free survival. The purpose of this study was to determine if activating *ESR1* mutations at the tyrosine (Y) 537 amino acid residue within the ligand binding domain cause reduced FES binding compared to wild-type (WT)-ER.

#### **METHOD AND MATERIALS**

Stable cell lines were generated using ER-negative MDA-MB-231 breast cancer cells that express either WT-ER, Y537S, or Y537C mutant ER. ER function was measured using an estrogen response element (ERE)-luciferase reporter gene assay and quantitative polymerase chain reaction analysis of expression of ER-regulated endogenous target genes. Saturation binding assays and nonlinear regression were performed to determine the equilibrium dissociation constant (KD) and the total receptor density (Bmax). FES uptake was measured in tumor xenografts grown in female athymic nude mice by microPET/CT imaging using 150 µCi FES injected via tail vein.

# RESULTS

Y537S and Y537C mutations resulted in a 10- and 4-fold increase in ERE reporter gene activity in the absence of estrogen compared to WT-ER, respectively. Constitutive ER activation of two ER target genes in the absence of estrogen had a 6- and 5-fold increase of *PGR* mRNA and a 9- and 4-fold increase of *TFF1* expression in Y537S and Y537C cells compared to WT-ER, respectively. *In vitro* FES binding affinity was decreased in cells expressing Y537S and Y537C mutant ER compared with WT-ER (KD: 0.42±0.21 nM and 0.20±0.13 nM vs 0.075±0.025 nM, respectively). The Bmax values were 421±96 and 113±28 vs 110±11 fmol/mg protein for Y537S and Y537C compared to WT ER, respectively. While FES binding affinity in cells with Y537 mutations was reduced, tumor xenografts had similar FES uptake in mice with Y537S, Y537C, and WT-ER (2.4±0.34, 2.133±0.18, and 2.343±0.12 mean %ID/g, respectively).

# CONCLUSION

While ER mutants have lower binding affinity for FES, tumoral uptake of FES as measured by PET imaging is not significantly impacted.

#### **CLINICAL RELEVANCE/APPLICATION**

Despite lower binding affinity, FES was still able to detect mutant ER in tumor xenografts and likely does not confound the accuracy of FES-PET imaging in metastatic ER+ breast cancer patients.



# MI209-SD-MOA2

# Molecular US Characterization of Metastatic Sentinel Lymph Nodes in Melanoma

Monday, Nov. 26 12:15PM - 12:45PM Room: MI Community, Learning Center Station #2

### **Participants**

Kibo Nam, PhD, Philadelphia, PA (Presenter) Nothing to Disclose

Robert Stapp, DO, Phiadelphia, PA (Abstract Co-Author) Nothing to Disclose

Ji-Bin Liu, MD, Philadelphia, PA (Abstract Co-Author) Nothing to Disclose

Maria Stanczak, MS, Philadelphia, PA (Abstract Co-Author) Nothing to Disclose

Flemming Forsberg, PhD, Philadelphia, PA (*Abstract Co-Author*) Research Grant, Canon Medical Systems Corporation; Research Grant, General Electric Company; Research Grant, Siemens AG; Research Grant, Lantheus Medical Imaging, Inc

Zhou Lin, MD, Shenzhen, China (Abstract Co-Author) Nothing to Disclose

Ziyin Zhu, MD, Beijing, China (Abstract Co-Author) Nothing to Disclose

Charalambos C. Solomides, MD, Philadelphia, PA (Abstract Co-Author) Nothing to Disclose

John R. Eisenbrey, PhD, Philadelphia, PA (*Abstract Co-Author*) Support, General Electric Company Support, Lantheus Medical Imaging, Inc

Andrej Lyshchik, MD, PhD, Philadelphia, PA (*Abstract Co-Author*) Research support, Bracco Group; Advisory Board, Bracco Group; Research support, General Electric Company; Research support, Siemens AG; Research support, Canon Medical Systems Corporation; Speaker, SonoScape Co, Ltd

### For information about this presentation, contact:

Andrej.Lyshchik@jefferson.edu

# PURPOSE

To assess the ability of molecular ultrasound (US) to detect metastatic involvement in the sentinel lymph nodes (SLNs) associated with melanoma.

# METHOD AND MATERIALS

A total of 13 swine (3-7 kg; Sinclair Bio-Resources, Columbia, MO) with naturally occurring melanoma were studied. Contrast enhanced US was performed using an S3000 scanner with a 9L4 probe (Siemens Helathineers, Malvern, PA). Dual-targeted microbubbles were created using a Targestar SA kit (Targeson, San Diego, CA) labeled with both P-selection and aVB3-integrin in a 1:1 ratio. IgG labeled Targestar SA was used as the control contrast agent. The US contrast agent Sonazoid (GE Healthcare, Oslo, Norway) was first injected around the tumor to identify the SLNs. After that dual-targeted or control microbubbles were injected intravenously in random order (30 min apart) to characterize SLNs. Non-SLNs were also imaged as benign controls. All imaged nodes were dissected and histologically examined. The degree of metastatic involvement was calculated as the area of melanin deposition in the lymph node. The intensity of retained targeted US contrast was calculated and compared to results of histological examination of surgically excised lymph nodes using Student t-test and ROC analysis.

# RESULTS

Thirty-five SLNs and 34 non-SLNs were analyzed, with 21 SLNs showing metastatic involvement greater than 5% on histology. All non-SLNs were benign. The mean intensity of dual-targeted bubbles for metastatic nodes was significantly higher than that of benign nodes ( $16.3 \pm 18.3 \text{ AU} \text{ vs.} 3.2 \pm 5.5 \text{ AU}$ ; p<0.001), while control bubbles did not differ between metastatic and benign nodes ( $0.3 \pm 1.1 \text{ AU} \text{ vs.} 0.1 \pm 0.5 \text{ AU}$ ; p=0.15). There was a strong correlation (r=0.64) between the degree of metastatic lymph node involvement and mean intensity from dual-targeted microbubbles. The sensitivity, specificity, and accuracy of molecular US in metastatic SLN characterization were 91%, 67%, and 74%, respectively, with an AUC of 0.85.

#### CONCLUSION

The dual-targeted microbubbles labeled with P-selectin and aVB3-integrin showed the potential to characterize metastatic involvement in SLNs.

# **CLINICAL RELEVANCE/APPLICATION**

It may be possible to noninvasively characterize metastatic involvement in SLNs using molecular US.



# MI210-SD-MOA3

## Lack of Immune Response Following Ultrasound Adenoviral Gene Transfer in a Mouse Cancer Model

Monday, Nov. 26 12:15PM - 12:45PM Room: MI Community, Learning Center Station #3

# Participants

Flavia DeCarlo, PhD, Jackson, MS (*Presenter*) Nothing to Disclose Elliot Varney, BS, Jackson, MS (*Abstract Co-Author*) Nothing to Disclose Bell Brooke, Jackson, MS (*Abstract Co-Author*) Nothing to Disclose Gailen Marshall, MD, Jackson, MS (*Abstract Co-Author*) Nothing to Disclose Pier Paolo Claudio, MD, PhD, Jackson, MS (*Abstract Co-Author*) Nothing to Disclose Candace M. Howard-Claudio, MD, PhD, Philadelphia, PA (*Abstract Co-Author*) Nothing to Disclose

#### For information about this presentation, contact:

pclaudio@olemis.edu

# PURPOSE

Gene transfer to malignant sites using human adenoviruses (hAd) has been limited because of their immunogenic nature. Murine cells often lack some of the receptors needed for hAd infection, which limits translational studies of adenoviral gene transfer techniques. We have developed a gene transfer method, which uses lipid-encapsulated perfluorocarbon microbubbles (MBs) and ultrasound (US) to protect the hAds from the immune system and to deliver them to a site-specific tissue, bypassing the requirement of specific adenoviral receptors.

#### **METHOD AND MATERIALS**

Expression of CAR, Integrins AvB3 and AvB5, transduction efficiency and GFP expression were was measured by flow cytometry and fluorescence microscopy in murine TRAMP-C2 and human DU145 prostate cancer cells. Activation of the innate and acquired immune response was evaluated by ELISA in healthy mice or mice bearing a TRAMP-C2 syngeneic tumor graft following injections of MBs/hAd-GFP complexes in the presence or absence of US. Injection of unprotected Ad-GFP virus was used as positive control.

### RESULTS

We showed in vitro that the transduction rate was increased significantly in both TRAMP-C2 and Du-145 prostate cancer cells when delivering the adenoviral particles by a combination of microbubbles and ultrasound. Lack of activation of the innate and acquired immunity was observed in vivo by quantifying IL-6 and TNF-A cytokines, and by assaying neutralizing IgG antibodies and CTLs activity, following intratumoral and intravenous injections, of MBs-Ad.GFP complexes in the presence or absence of ultrasound compared to the appropriate controls.

## CONCLUSION

Our data provides evidence that the TRAMP-C2 prostate cancer graft model is a suitable system to study in immune competent animals the capacity of lipid-encapsulated perfluorocarbon MBs and US, to shield and deliver hAds to a site-specific diseased tissue bypassing the requirement of specific receptors.

### **CLINICAL RELEVANCE/APPLICATION**

This study brings us a step closer to demonstrate the feasibility of using murine models of cancer to investigate the translation into clinical settings of adenoviral gene therapy mediated by Ultrasound-Targeted Microbubble Destruction.



### MK344-ED-MOA8

A Name to Remember: What is the Eponym of the Fracture?

Monday, Nov. 26 12:15PM - 12:45PM Room: MK Community, Learning Center Station #8

#### **Participants**

Oralia C. Rico Rodriguez, MD, PhD, Mexico City, Mexico (*Presenter*) Nothing to Disclose Alan J. Zavala Vargas, MD, Mexico City, Mexico (*Abstract Co-Author*) Nothing to Disclose Jose Antonio Cienfuegos, Mexico City, Mexico (*Abstract Co-Author*) Nothing to Disclose Pablo A. Montiel Tellez I, MD, Mexico City, Mexico (*Abstract Co-Author*) Nothing to Disclose Dulce A. Sanchez Nava, MD, Mexico City, Mexico (*Abstract Co-Author*) Nothing to Disclose Miguel A. Hernandez Sr, MD, Mexico City, Mexico (*Abstract Co-Author*) Nothing to Disclose Mahatma Isaac Guzman Soto, MD, Chilpacingo de los Bravos, Mexico (*Abstract Co-Author*) Nothing to Disclose Israel Vicente Toledo Coronado, MD , Mexico City, Mexico (*Abstract Co-Author*) Nothing to Disclose Gisela Munoz, MD, Mexico City, Mexico (*Abstract Co-Author*) Nothing to Disclose

#### For information about this presentation, contact:

kriz\_rico@hotmail.com

### **TEACHING POINTS**

The eponyms transmit a lot of information in an abbreviated manner and are present in the daily medical communication, so it is important to know them accurately, since they make it easier for us to learn a lot of concepts in a single name. To make use of the eponyms to transmit and learn information in an abbreviated manner. To review the typical appearance, associated findings, trauma mechanism, differential diagnosis and clinical data of common and not so common fractures. To remember a brief history of the character or situation involved in the eponymous.

# TABLE OF CONTENTS/OUTLINE

The information will be presented in a quiz format. Key images and information will be provided to the reader to answer each question, with subsequent feedback, including differential diagnoses, clinical features, image recommendations and radiological description concepts. The list of cases includes: Bony bankart lesionColles fracture (explaining Smith, Barton, Barton's reverse fracture as differentials diagnosis) Jumper's fracture Pellegrini- Stieda lesionSalter- Harris Classification with some examples. Toodler 's fracture Ueber fracture classification Gamekeeper thumbBennett and Pseudo Bennett's fracture



# MK356-SD-MOA1

Empirical Mathematical Model for Dynamic Contrast-Enhanced MRI in Patients with Rheumatoid Arthritis: A Novel Technique to Monitor the Clinical Disease Activity

Monday, Nov. 26 12:15PM - 12:45PM Room: MK Community, Learning Center Station #1

### Participants

Junko Ochi, MD, Sendai, Japan (*Presenter*) Nothing to Disclose Naoko Mori, MD, PhD, Sendai, Japan (*Abstract Co-Author*) Nothing to Disclose Yu Mori, Sendai, Japan (*Abstract Co-Author*) Nothing to Disclose Shunji Mugikura, MD, PhD, Sendai, Japan (*Abstract Co-Author*) Nothing to Disclose Shin Hitachi, Sendai, Japan (*Abstract Co-Author*) Nothing to Disclose Kei Takase, MD, PhD, Sendai, Japan (*Abstract Co-Author*) Nothing to Disclose

#### PURPOSE

To evaluate whether parameters of empirical mathematical model (EMM) for the dynamic contrast-enhanced MRI (DCE-MRI) correlate with clinical disease activity in patients with rheumatoid arthritis (RA).

### **METHOD AND MATERIALS**

27 consecutive patients with RA underwent an IRB-approved MRI scan including DCE-MRI using a 1.5T system. 20 post-contrast series of DCE-MRI were repeatedly acquired with temporal resolution of 20 seconds per image. ROIs were placed within each lesion where the highest signal increase was observed on DCE-MRI. The kinetic curve obtained from DCE-MRI was analyzed using an empirical mathematical model:  $\Delta S(t) = A^*(1-e-at) *e-Bt$ . Where,  $\Delta S$  is relative enhancement, A is the upper limit of the signal intensity, a (min-1) is the rate of signal increase,  $\beta$  (min-1) is the rate of the signal decrease during washout. The initial slope of the kinetic curve is given by 'A\*a'. Initial area under curve (AUC30) was calculated by integrating the kinetic curve. The time at which the kinetic curve reached peak (Tpeak) can be solved by setting the derivative of  $\Delta S(t)$  equals to zero. Signal enhancement ratio (SER) was defined as the signal intensity change at the first time point ( $\Delta S200$ ) relative to the last time point ( $\Delta S400$ ). The parameters from EMM for DCE-MRI were compared with Disease Activity Score (DAS28)-CRP using Pearson's correlation analysis. After Bonferroni correction of 7 multiple comparisons, the critical value became < 0.0071 (0.05/7).

#### RESULTS

EMM was able to accurately fit the curves of DCE-MRI, with a goodness of fit parameter R2 greater than 0.90 for all cases studied here. Of the parameters of DCE-MRI, A showed the highest correlation with DAS28-CRP (r=0.67; P =0.0001). AUC30 also correlated with DAS28-CRP with a lesser degree (r=0.62; P=0.0005). a,  $\beta$ , A\*a, Tpeak and SER did not correlated with DAS28-CRP (r=0.39; p=0.03, r=0.45; p=0.018, r=0.43; p=0.023, r=-0.37; p=0.21, r=0.50; 0=0.0082, respectively).

#### CONCLUSION

The parameters of the EMM for DCE-MRI were correlated with clinical disease activity in patients with RA. Especially, A or the upper limit of signal intensity showed the highest correlation.

### **CLINICAL RELEVANCE/APPLICATION**

The parameters obtained from EMM analysis for DCE-MRI, especially A or the upper limit of signal intensity showed significant correlation with clinical disease activity in patients with RA.



### MK357-SD-MOA2

# The Comma Sign: Can We Find It on Shoulder MRI?

Monday, Nov. 26 12:15PM - 12:45PM Room: MK Community, Learning Center Station #2

#### Participants

Hye Jung Choo, MD, Busan, Korea, Republic Of (*Presenter*) Nothing to Disclose Sun Joo Lee, MD, Busan, Korea, Republic Of (*Abstract Co-Author*) Nothing to Disclose Sungkwan Kim, Busan, Korea, Republic Of (*Abstract Co-Author*) Nothing to Disclose

# For information about this presentation, contact:

hyejungchoo@gmail.com

### PURPOSE

The comma sign is an important arthroscopic marker of the superolateral corner of the torn subscapularis tendon (SCT) in cases of chronic and retracted SCT tears. However, it has not been evaluated on MRI until now. Thus the aim of this study was to determine accuracy of shoulder MRI in the evaluation of the comma sign.

# **METHOD AND MATERIALS**

Consecutive 37 patients (17 men, 20 women; mean age, 61 years) who underwent the preoperative shoulder MRI and were confirmed full-thickness tear of SCT in arthroscopy were included. The presence of the comma sign, size of SCT tear, presence of fibrotic scarring in SCT, thickness of coracohumeral ligaments (CHL), and presence and characteristics of the posterosuperior rotator cuff (PS cuff) tears (i.e., full-thickness tears or partial-thickness tears; tear size) were evaluated on MRI. Comma sign on MRI was defined as the band-like structure connecting the superolateral corner of torn SCT and the anterior margin of PC cuffs. Fibrotic scarring of SCT was defined as the relatively thin structure at the lateral aspect of SCT where the comma was connected. Tear size of SCT and PS cuff and thickness of CHL were measured on axial, coronal and sagittal planes of MRI, respectively. With arthroscopic results as the reference standards, sensitivity, specificity, and accuracy for the evaluation of the comma sign on MRI was calculated.

#### RESULTS

Arthroscopy showed the comma sign in 30 shoulders and MRI detected the comma sign in 28, resulting in sensitivity of 93%, specificity of 86%, and accuracy of 89%. The tear size of SCT and thickness of CHL were significantly greater in shoulders with the comma sign than in those without the comma sign (p = 0.042 and 0.005, respectively). All 30 shoulders with the comma sign were combined with PS cuff tears. Among them, 29 were full-thickness tears and the size of PS cuffs full-thickness tears was not significantly different between shoulders with and without the comma sign. Fibrotic scarring of SCT was found in 6 shoulders with the comma sign.

### CONCLUSION

Shoulder MRI had a high accuracy to diagnose the comma sign.

### **CLINICAL RELEVANCE/APPLICATION**

Shoulder MRI can be helpful to predict the presence of comma sign before arthroscopy Comma sign can be helpful to differentiate between the retracted tendons and the fibrotic scarring of SCT.



## MK358-SD-MOA3

# Arterial Spin-Labeling MR Imaging of Painful Shoulder Disorders

Monday, Nov. 26 12:15PM - 12:45PM Room: MK Community, Learning Center Station #3

### Participants

Katsumi Nakamura, MD, Kitakyushu, Japan (*Presenter*) Nothing to Disclose Fumihide Arakami, RT, Kitakyushu, Japan (*Abstract Co-Author*) Nothing to Disclose Tomoko Nishi, RT, Kitakyushu, Japan (*Abstract Co-Author*) Nothing to Disclose Kenichi Inoue, RT, Kitakyushu, Japan (*Abstract Co-Author*) Nothing to Disclose Satoshi Masuda, MD, Kitakyushu, Japan (*Abstract Co-Author*) Nothing to Disclose Asaka Aso, Kasuga, Japan (*Abstract Co-Author*) Nothing to Disclose Akiyoshi Yamamoto, RT, Kitakyushu, Japan (*Abstract Co-Author*) Nothing to Disclose Mitsue Miyazaki, PhD, La Jolla, CA (*Abstract Co-Author*) Nothing to Disclose

#### For information about this presentation, contact:

nakamura.katsumi@gmail.com

### PURPOSE

To evaluate the value of arterial spin-labeling (ASL) perfusion MR imaging for the assessment of painful shoulder disorders, especially rotator cuff (RC) tear and adhesive capsulitis.

# METHOD AND MATERIALS

A total of 72 patients (41 men and 31 women [12-86 y.o., mean, 53.6 y.o.]) was involved in this study. The patients were divided into 5 groups; group 1 with no abnormality (n=12); group 2 with degenerative changes or partial tear of RC (n=12); group 3 with full thickness tear of RC (n=32), which subdivided into group 3a, small tear (n=10), 3b, medium (n=6), 3c, large and extensive (n=16); group 4 with adhesive capsulitis (painful stage) (n=12); and group 5 with biceps tendinitis (n=4). All patients underwent the ASL perfusion study as well as routine shoulder MRI examinations using a 1.5-T clinical imager. The acquisition with a 10-mm thick slice was placed longitudinally on the humeral head, including rotator cuff, subacromial bursa, and acromicclavicular joint. A tag IR pulse of a 30-mm thick slice was placed on the subclavian artery. The ASL perfusion was evaluated by three observers regarding the degree of enhancement at the subacromial region using a five-point scoring system; the score 1 has no enhancement and the score 5 is severe enhancement.

#### RESULTS

Group 3, in which joint space communicated with subacromial space, demonstrated significantly higher ASL perfusion score than groups 2 and 1,  $3.41\pm0.90$ ,  $1.33\pm0.47$ ,  $1.42\pm0.49$ , respectively (p<0.01). Larger RC tear tended to show a higher ASL score; however, there was no significant difference between groups 3a, 3b, and 3c. Adhesive capsulitis (painful stage) showed significantly higher ASL score (2.25±0.72) than groups 2 and 1 (p<0.01). Biceps tendinitis also showed enhancement and thickening of rotator interval, which might be resemble to adhesive capsulitis.

## CONCLUSION

Full-thickness tear of RC, symptomatic adhesive capsulitis, and biceps tendinitis showed significant enhancement at the subacromial region, which could reflect increased blood flow due to inflammatory changes around joint. The additional physiological information obtained by ASL perfusion must be valuable for the management of the shoulder disorders.

# **CLINICAL RELEVANCE/APPLICATION**

Non-contrast perfusion using arterial spin labeling MR imaging depicts increased blood flow due to inflammatory response of painful shoulder disorders, and provides useful physiological information for the differential diagnosis.



### MK359-SD-MOA4

Imaging Quantification of Glenoid Bone Loss in Patients with Glenohumeral Instability: A Systematic Review

Monday, Nov. 26 12:15PM - 12:45PM Room: MK Community, Learning Center Station #4

# Participants

William Walter, MD, New York, NY (*Presenter*) Nothing to Disclose Mohammad M. Samim, MD, MRCS, New York, NY (*Abstract Co-Author*) Nothing to Disclose Fred LaPolla, New York, NY (*Abstract Co-Author*) Nothing to Disclose Soterios Gyftopoulos, MD, Scarsdale, NY (*Abstract Co-Author*) Nothing to Disclose

## For information about this presentation, contact:

william.walter@nyumc.org

### PURPOSE

To evaluate the existing evidence on accuracy of imaging techniques to measure glenoid bone loss in patients with glenohumeral instability using a systematic review.

# **METHOD AND MATERIALS**

A comprehensive literature search including 5 medical databases. Inclusion criteria were original research that measured glenoid bone loss on x-ray, CT, or MRI, using prospective or retrospective cohort, case control, cadaveric, or clinical study designs. Studies published in a language other than English were excluded. The Quality Assessment of Diagnostic Accuracy Studies 2 (QUADAS-2) tool aided qualitative assessment of methodology regarding risk of bias and applicability of the analyzed studies. Study results and accuracy were also assessed for possible quantitative analysis.

### RESULTS

Of 1422 abstracts, 73 met inclusion criteria based upon title and abstract text review. Among these, 42 studies were ultimately extracted for analysis and 29 included after full-text review by two independent readers with disagreements resolved in consensus. Study designs included retrospective (n=15) or prospective (n=5) cohort, case control (n=2), or cadaveric (n=7). Glenoid bone loss was measured using several different index tests: radiography (n=5), CT (n=9), 3D-CT (n=16), MRI (n=8), and 3D-MRI (n=6). Measurements were compared to reference standards of CT (n=11), surgery (n=10), or digital photographs (n=6). Risk of bias was low in 14 studies, questionable in 7, and high in 6. All studies had high (17) or questionable (10) applicability to our study purpose. Only 2 studies reported sensitivity and specificity of glenoid bone loss measurements, both comparing CT to arthroscopy, using different thresholds of bone loss. Heterogeneous measurement techniques and statistical methods precluded quantitative meta-analysis assessing accuracy of imaging measurement techniques.

## CONCLUSION

Both CT and MRI appear to accurately measure glenoid bone loss among patients with glenohumeral instability. The current body of literature is heterogeneous with many studies containing significant risk of bias and few studies providing quantitative assessment of imaging techniques for glenoid bone measurements.

### **CLINICAL RELEVANCE/APPLICATION**

Both MRI and CT appear to provide accurate measurements of glenoid bone loss, but heterogeneity of the existing literature precludes rigorous quantitative assessment of measurement techniques.



# MK360-SD-MOA5

Periprosthetic Heating During Metal Artifact Reduction Sequence Magnetic Resonance Imaging of Hip Arthroplasty Implants at 3T

Monday, Nov. 26 12:15PM - 12:45PM Room: MK Community, Learning Center Station #5

**FDA** Discussions may include off-label uses.

#### **Participants**

Iman Khodarahmi, MD, PhD, Baltimore, MD (*Presenter*) Nothing to Disclose Luke W. Bonham, BS, Baltimore, MD (*Abstract Co-Author*) Nothing to Disclose Robert Sterling, Baltimore, MD (*Abstract Co-Author*) Nothing to Disclose John Kirsch, PhD, Charlestown, MA (*Abstract Co-Author*) Nothing to Disclose Sunder S. Rajan, PhD, Silver Spring, MD (*Abstract Co-Author*) Nothing to Disclose Jan Fritz, MD, Baltimore, MD (*Abstract Co-Author*) Research Grant, Siemens AG; Scientific Advisor, Siemens AG; Scientific Advisor, Alexion Pharmaceuticals, Inc; Speaker, Siemens AG

#### For information about this presentation, contact:

ikhodar1@jhmi,edu

### PURPOSE

To quantify periprosthetic heating around total hip arthroplasty implants during Metal Artifact Reduction Sequence (MARS) MRI at 3T.

# **METHOD AND MATERIALS**

A cobalt-chromium-on-polyethylene total hip arthroplasty system was placed in a standard ASTM gel phantom with electrical properties similar to those of the human body. Fiber optic sensors were used to measure the temperature rise at seven points at the implant interface. Clinical MARS MR protocols including high-bandwidth turbo spin echo (HBW-TSE, 28-min), Slice-Encoding-for-Metal-Artifact-Correction (SEMAC, 54-min) TSE, and compressed sensing (CS) SEMAC TSE (34-min) were acquired at 3T including coronal PD, STIR, sagittal PD, sagittal STIR, axial PD, and axial STIR sequences. The clinical sequence (sagittal HBW-TSE PD) with the highest scanner estimated whole-body (WB) specific absorption rate (SAR) value was additionally run continuously for 30-min to assess maximum heating and exclude the effect of preparation pulses that may interleave the clinical sequences. Finally, this sequence was also run for 30 min with non-clinical high energy imaging parameters following disabling of protection limits.

#### RESULTS

Scanner calculated WBSAR values for our experimental setup ranged from 0.6 to 1.3 W/kg with clinical protocols and < 2 W/kg for the non-clinical high energy sequence. The HBW-TSE, SEMAC, and CS-SEMAC protocols resulted in maximum temperature rises of 1.0, 1.6, and 1.2 °C, respectively. The continuous 30-min clinical HBW TSE protocol had a WBSAR of 1.3 W/kg and caused a temperature rise of 1.3 °C. The 30-min non-clinical, high energy sequence caused maximum heating of 1.7 °C.

## CONCLUSION

In our experimental setting, various 3T MARS techniques for MRI of hip arthroplasty implants showed a periprosthetic temperature rise of < 2 °C, which may indicate a low risk of thermal injury when using typical clinical pulse sequences <= 5 min and a WBSAR of < 2 W/kg. Our results provide a baseline for additional research that is required to estimate the actual in-vivo heating, which may be higher due to scanner specific parameters, implant position, and patient-specific local and WBSAR.

### **CLINICAL RELEVANCE/APPLICATION**

In an experimental setting, 3T MARS MRI of hip arthroplasty implants caused only modest periprosthetic temperature rises, which provides baseline data for additional research that is required for extrapolation into patients.



# MK361-SD-MOA6

Asynchronous Quantitative Computed Tomography for Bone Mineral Density Measurement in Two Clinics: A Comparability Study Using Cross-Calibration Phantom

Monday, Nov. 26 12:15PM - 12:45PM Room: MK Community, Learning Center Station #6

### Participants

Alexey Petryaikin, MD,PhD, Moscow, Russia (*Presenter*) Nothing to Disclose Kristina Sergunova, Moscow, Russia (*Abstract Co-Author*) Nothing to Disclose Sergey Morozov, MD,MPH, Moscow, Russia (*Abstract Co-Author*) Clinical Advisory Board, Agfa-Gevaert Group; Clinical Advisory Board, Bayer AG Fedor A. Petriaikin, Moscow, Russia (*Abstract Co-Author*) Nothing to Disclose Anton V. Vladzymyrskyy, MD,PhD, Moscow, Russia (*Abstract Co-Author*) Nothing to Disclose Ekatorina S. Abmad. Moscow, Russia (*Abstract Co-Author*) Nothing to Disclose

Anton V. Vladzymyrskyy, MD,PhD, Moscow, Russia (*Abstract Co-Author*) Nothing to Disclose Ekaterina S. Ahmad, Moscow, Russia (*Abstract Co-Author*) Nothing to Disclose Dmitriy S. Semenov, Moscow, Russia (*Abstract Co-Author*) Nothing to Disclose Ludmila A. Nizovtsova, MD,PhD, Moscow, Russia (*Abstract Co-Author*) Nothing to Disclose

# For information about this presentation, contact:

alexeypetraikin@gmail.com

#### PURPOSE

Our goal was to compare quantitative computed tomography (QCT) for bone mineral density (BMD) measurement in two outpatient clinics with similar populations.

# METHOD AND MATERIALS

QCT results from two outpatient clinics from Sep 2017 to Feb 2018 were analyzed. During this period, 831 women were examined, 420 in clinic A (90.9% aged from 50 to 80 years) and 411 in clinic B (89.8% in the same range). We performed QCT on 64-detector unit with the following parameters: 120 kV, 0.82 pitch, 50-100 mA (depending on the body mass index), kernels FC08 (clinic A) and FC17 (clinic B). Spine (Zsp), femoral neck (Zfn) and total hip (Zth) Z-values were compared using multiple regression analysis. Asynchronous QCT calibration was performed. Comparability of the results between two scanners was evaluated using a cross-calibration phantom (five measurements for 4 different dilutions of K2HPO4 in the range 0-200 mg/cc).

### RESULTS

The data was compared with the UCSF database. Mean BMD values decreased with age. For instance, in clinic A the mean Zsp criteria was -0.43, in clinic B Zsp = -0.77. Similar results were obtained for total hip BMD, in clinic A Zth = -0.69, in the clinic B Zth = -1.42. The average femoral neck BMD values for clinics A and B were Zfn = -0.49 and Zfn = -0.96. Multiple regression analysis had shown that linear regressions of both patient groups differed significantly in their displacement. No significant differences in the slopes of the regressions were found. Phantom studies have shown that BMD values did not depend on CT scanners. The total population per clinic is comparable and amounts to 170 thousand people. Referring physicians were interviewed retrospectively. We found differences in referral justification for QCT. In the clinic A, appointments were less systematic, and the BMD values neared the average population. In the clinic B, mostly high-risk patients with the history of low-energy fractures were assigned to QCT, although the FRAX scale was not used.

# CONCLUSION

In one of the clinics we observed significantly lower QCT-measured BMD values for all regions. Phantom cross-calibration proved comparability of the BMD measurements. Different results in two groups may be attributed to different referral strategies.

# **CLINICAL RELEVANCE/APPLICATION**

When referring a patient to densitometry, general screening principles as well as FRAX tool should be used. This will increase diagnostic yield and decrease unnecessary procedures.



### MK362-SD-MOA7

Structural Abnormalities on Knee MRI Associated with Normal Aging over 6 years: Data from the Osteoarthritis Initiative

Monday, Nov. 26 12:15PM - 12:45PM Room: MK Community, Learning Center Station #7

#### Awards Student Travel Stipend Award

#### **Participants**

Joe Darryl Baal, BS, San Francisco, CA (*Presenter*) Nothing to Disclose Jan Neumann, MD, San Francisco, CA (*Abstract Co-Author*) Nothing to Disclose Julio B. Guimaraes, MD, San Francisco, CA (*Abstract Co-Author*) Nothing to Disclose Gabby B. Joseph, San Francisco, CA (*Abstract Co-Author*) Nothing to Disclose Michael C. Nevitt, PhD, San Francisco, CA (*Abstract Co-Author*) Nothing to Disclose Charles E. McCulloch, San Francisco, CA (*Abstract Co-Author*) Nothing to Disclose Thomas M. Link, MD,PhD, San Francisco, CA (*Abstract Co-Author*) Nothing to Disclose Thomas M. Link, MD,PhD, San Francisco, CA (*Abstract Co-Author*) Research Grant, General Electric Company; Research Consultant, General Electric Company; Research Consultant, InSightec Ltd; Research Grant, InSightec Ltd; Royalties, Springer Nature; Consultant, Springer Nature; Research Consultant, Pfizer Inc; Ursula R. Heilmeier, MD, San Francisco, CA (*Abstract Co-Author*) Nothing to Disclose

For information about this presentation, contact:

joedarryl.baal@ucsf.edu

#### PURPOSE

To describe aging-associated structural knee abnormalities in clinically asymptomatic subjects without risk factors for knee osteoarthritis (OA) using semi-quantitative MRI scoring over a period of six years.

# **METHOD AND MATERIALS**

Sixty-three subjects with no risk factors, clinical symptoms or radiographic evidence of knee OA (Kellgren-Lawrence[KL] grade 0 or 1) at baseline were selected from the Osteoarthritis Initiative (OAI) normal cohort. Subjects that developed KL grade >=2 or experienced maintained knee pain or stiffness (>=2 consecutive follow-up periods) in the follow-up period were excluded. All subjects were serially studied at 2-year intervals with radiographs and 3T MR imaging of the right knee over 6 years. Sagittal and coronal 2D fast spin echo and 3D fat saturated gradient echo sequences were acquired. OA-related knee abnormalities were assessed through the modified whole-organ MR imaging scoring method (WORMS). McNemar's test and paired T-tests were used to compare changes in proportion of patients with WORMS >0 and average WORMS from baseline to the 6-year follow-up period.

#### RESULTS

The proportion of patients with WORMS >0 differed significantly from baseline to the 6-year follow-up for meniscal lesions (p=0.020), cartilage lesions (p=0.005), bone marrow lesions (p=0.020) and subarticular cysts (p=0.005). Change in mean WORMS was significantly different for meniscal lesions (p=0.005), cartilage lesions (p<0.001) and subarticular cysts (p=0.019) (Table 1). Significant differences in the proportion of patients with WORMS >0 were observed in the medial and lateral posterior horns of the menisci (p=0.007, 0.045, respectively), patellar (p<0.001), trochlear (p<0.001), medial femoral (p<0.001) and medial tibia (p=0.045) cartilage compartments.

### CONCLUSION

This study demonstrates that the menisci and cartilage have the highest prevalence of knee abnormalities observed on MRI in asymptomatic subjects without risk factors for OA. Moreover, the regions that are most susceptible to morphologic change over time included the posterior horns of the menisci and the cartilage at the patellar, trochlear and the medial femoro-tibial compartments of the knee.

# **CLINICAL RELEVANCE/APPLICATION**

Our study demonstrates knee abnormalities seen with normal aging of the knee and can help guide the identification of knee MRI findings that are likely not functionally or clinically relevant.



### MS182-ED-MOA1

The Retrocrural Space and Diaphragmatic Crus Revisited: From Azygos Vein Variations to Paraganglioma and Everything in Between

Monday, Nov. 26 12:15PM - 12:45PM Room: MS Community, Learning Center Station #1

# Participants

Tomoya Nishiyama, MD, Tokyo, Japan (*Presenter*) Nothing to Disclose Jay Starkey, MD, Tokyo, Japan (*Abstract Co-Author*) Nothing to Disclose Masaki Matsusako, MD, PhD, Tokyo, Japan (*Abstract Co-Author*) Nothing to Disclose Yasuyuki Kurihara, MD, Tokyo, Japan (*Abstract Co-Author*) Nothing to Disclose

# **TEACHING POINTS**

1. Review the normal and variant anatomy of the retrocrural space and crus of the diaphrpram. 2. Review pathologies of this space, divided into inflammatory, infectious, malignant, vascular, and iatrogenic.

# TABLE OF CONTENTS/OUTLINE

1. Anatomy: - Variations of crus of diaphragm: hypertrophyhypotrophy of diaphragmatic crus, lobulated diaphragmatic crus, diaphragmatic crura with lipoma/fatty degenerative change, unilateral spur formation of vertebral body, aortic /celiac trunk compression due to median arcuate ligament - Variations of azygos/hemiazygos vein: double IVC, azygos continuation associated with (retroaortic) left renal vein, dilated ascending lumber vein associated with left renal vein stenosis, dilated paraesophageal vein/plexus and azygos/hemiazygos vein - Mimicker: Dilated thoracic duct mimicking metastatic lymphadenopathy 2. Pathologies, from benign to malignant - Inflammatory: periaortitis - Infectious: pyogenic spondylitis with abscess - Malignant: lymphoma, metastatic lymphnode, neurilemmoma, paraganglioma, malignant fibrous histiocytoma - Vascular: aortic dissection, median arcuate ligament syndrome, lumbar artery pseudoaneurysm due to blunt trauma - Iatrogenic: cement leakage into paravertebral venous plexus, retrocrural air associated with Hamman syndrome, lymphatic injury/leakage



#### NM142-ED-MOA6

Clinical Pediatric PET/MR Program: A Guide to Successful Implementation

Monday, Nov. 26 12:15PM - 12:45PM Room: NM Community, Learning Center Station #6

#### **Participants**

Sandra Saade-Lemus, MD, Philadelphia, PA (*Abstract Co-Author*) Nothing to Disclose Hansel J. Otero, MD, Philadelphia, PA (*Abstract Co-Author*) Nothing to Disclose Sabah Servaes, MD, Philadelphia, PA (*Abstract Co-Author*) Nothing to Disclose Jeffrey P. Schmall, PhD, Philadelphia, PA (*Abstract Co-Author*) Nothing to Disclose Lisa J. States, MD, Plymouth Mtng, PA (*Presenter*) Nothing to Disclose

### For information about this presentation, contact:

saades@email.chop.edu

### **TEACHING POINTS**

1. To provide a guide for planning and implementation of a pediatric PET/MR program 2. To describe our experience, steps necessary and timeline for designing a PET/MR program including staffing, protocol optimization, clinical implementation and referring physicians outreach 3. To provide practical tips and examples for protocol design, imaging acquisition and interpretation learned over the first year and over 100 cases of our PET/MR program 4. To highlight advantages of PET/MR over PET/CT and Whole Body MRI - After reviewing this exhibit, readers will be able to recognize the necessary steps for providing PET/MR services to children.

# TABLE OF CONTENTS/OUTLINE

1. Why PET/MR? Background 2. Clinical pediatric PET/MR experience at out institution a. PET/MR Whole Body Workflow b. PET/CT vs PET/MR pilot study (N=9) c. Patient sedation (N=30) 3. Clinical Pediatric PET/MR Program a. Phase 1 (Planning): Staffing, protocol design, workflow setup b. Phase 2 (Preclinical): Pilot studies, order sets, billing codes c. Phase 3 (Clinical): Scheduling, image acquisition, interpretation d. Phase 4 (post implementation): Expanded applications, additional staff training 4. Challenges of PET/MR 5. Will PET/MR replace PET/CT? 6. Clinical examples 7. Conclusion



### NM208-SD-MOA1

Is there a Correlation Between Levels of PSA and SUVmax Values in Patients Evaluated with [68Ga]PSMA PET/CT to be Applied in Prostatic Cancer Patient Follow Up and as a Prognosis Factor?

Monday, Nov. 26 12:15PM - 12:45PM Room: NM Community, Learning Center Station #1

# Awards

# Student Travel Stipend Award

#### **Participants**

Erika S. Fajardo, MD, Mexico City, Mexico (*Presenter*) Nothing to Disclose Digna Pachuca Gonzalez, MD, Tlalpan, Mexico (*Abstract Co-Author*) Nothing to Disclose Juan Pablo Chavez-Torres, Mexico City, Mexico (*Abstract Co-Author*) Nothing to Disclose Blanca K. Gonzalez, MD, Mexico City, Mexico (*Abstract Co-Author*) Nothing to Disclose Rodrigo Hernandez Ramirez, Leon, Mexico (*Abstract Co-Author*) Nothing to Disclose Luis Felipe Alva Lopez, MD, Mexico City, Mexico (*Abstract Co-Author*) Nothing to Disclose

### For information about this presentation, contact:

fajardoericka25@gmail.com

# PURPOSE

The purpose of this study was to find out if a correlation exist between levels of PSA and SUVmax values in patients evaluated with [68Ga]PSMA PET/CT with prostate cancer, for the application of new methods in the follow-up of these patients.

#### **METHOD AND MATERIALS**

We evaluated fifty five patients with diagnosis of prostate cancer. These patients were scanned using Ga68-PSMA for either staging or biochemical recurrence. A retrospective, cross-sectional and descriptive study was carried out with the objective of correlating levels of PSA with SUVmax values.

#### RESULTS

55 patients with a known diagnosis of prostatic carcinoma were evaluated using Ga68-PSMAPET Imaging. The patients enrolled between years 2015-2018 were analyzed. The mean age of the study population was 69 years (range 49-84) with a mean prostate-specific antigen (PSA) level of 85.69 ng/ml (range 0.01-3850.90). SUVmax mean found was 12.41 (range 1.9-56.5). The indication for the study was initial staging in 10 patients (18.2%) and to confirm biochemical relapses in 45 (81.8%). The disease sites at the moment of the study was locoregional in 22(40%), distant metastasis 12 (21.8%), and both 21 (38.2%). It seems there is a correlation between PSA/SUVmax values given in our statistical results. Further studies needed. Values of PSA were resume in groups, One (0-5ng/ml), two (5.1-10ng/ml), and three (>10ng/ml), as the same for SUVmax in three groups, one(0-10), two(10-20), three (>20). A correlation was made between PSA groups and SUV groups finding that low values of SUVmax did correlate with low levels of PSA, with 23 patients with PSA in group one, had a SUVMAX between 0-10. We also correlate the PSA groups with the extension of the disease, finding that the PSA group one had only locoregional disease. However, PSA group three had either loco regional as distant disease in this study.

#### CONCLUSION

The [68Ga] PSMA PET / CT has had a boom in the evaluation of biochemical recurrence in prostate cancer, with our results, there may be a correlation of PSA levels with SUVmax values, which could have a prognostic application. No literature specifically mentioning this correlation was found, so studies are needed to support it.

### **CLINICAL RELEVANCE/APPLICATION**

[68Ga] PSMA PET / CT have a high sensitivity and specificity to locate disease sites in prostate cancer, with the use of SUVmax, which being correlated with PSA values have great relevance in the prognosis of the disease.



### NM209-SD-MOA2

18F-Alfatide PET/CT in Assessment of Locoregional Lymph Nodes in Thoracic Esophageal Squamous Cell Cancer: Comparison with 18F-FDG PET/CT

Monday, Nov. 26 12:15PM - 12:45PM Room: NM Community, Learning Center Station #2

**FDA** Discussions may include off-label uses.

#### **Participants**

Yinjun Dong, Jinan, China (*Presenter*) Nothing to Disclose Shuanghu Yuan, PhD, Jinan, China (*Abstract Co-Author*) Nothing to Disclose Yuchun Wei JR, Jinan, China (*Abstract Co-Author*) Nothing to Disclose

### For information about this presentation, contact:

dongyinjun1108@163.com

### PURPOSE

18F-FDG PET/CT has gained acceptance for staging of esophageal cancer. However, FDG is not tumor specific and false-positive results may occur by accumulation of FDG in benign tissue. The tracer RGD might not have these drawbacks. The aim of this study was to investigate the feasibility of novel RGD tracer 18F-Alfatide (18F-ALF-NOTA-PRGD2) PET/CT for the detection of locoregional lymph node (LN) metastases of esophageal squamous cell cancer (ESCC) and to compare 18F-Alfatide PET/CT with 18F-FDG PET/CT

#### **METHOD AND MATERIALS**

62 patients with thoracic ESCC underwent 18F-Alfatide PET/CT (n=29) and 18F-FDG PET/CT (n=33) scans before surgery. The total number of removed LNs and total number of positive LNs (verified by pathologic finding), including their location, were recorded and standard uptake values (SUVs) of the resected LNs were measured on the 18F-Alfatide PET/CT and 18F-FDG PET/CT images, respectively

### RESULTS

52 patients underwent successful surgery, and pathologic examination confirmed nodes positive for metastasis and 99 of 1018 (51/436 for 18F-Alfatide group, 48/582 for 18F-FDG group) excised nodal groups. The sensitivity, specificity, accuracy, positive predictive value (PPV), and negative predictive value (NPV) of 18F-Alfatide were 92.2% (47/51 nodal groups), 89.9% (346/385), 90.1% (393/436), 54.7% (47/86), and 98.9% (346/350), respectively, whereas those of 18F-FDG were 93.8% (45/48), 79.0% (422/534), 80.2% (467/582), 28.7% (45/157), and 99.3% (422/425), respectively. P values were 0.757, <0.001, <0.001, and 0.522, respectively.

#### CONCLUSION

In general, 18F-Alfatide PET/CT improves the specificity, accuracy and PPV than 18F-FDG PET/CT in the assessment of locoregional LNs in thoracic ESCC, and these results could provide an important impact to the field of precision medicine.

### **CLINICAL RELEVANCE/APPLICATION**

18F-Alfatide PET/CT can be used for detecting locoregional LNs in thoracic ESCC and provide an important impact to the field of precision medicine



### NM210-SD-MOA3

Correlation of Simultaneously-Acquired SUV of 18FDG and Apparent Diffusion Coefficient in Soft Tissue and Bone Tumors Using Voxel-By-Voxel Analysis

Monday, Nov. 26 12:15PM - 12:45PM Room: NM Community, Learning Center Station #3

# Participants

Yuji Watanabe, MD, PhD, Kobe, Japan (*Presenter*) Nothing to Disclose Daiki Shinyama, RT, Tokyo, Japan (*Abstract Co-Author*) Nothing to Disclose Sungtak Hong, PhD, Tokyo, Japan (*Abstract Co-Author*) Nothing to Disclose Koji Sagiyama, MD, Fukuoka, Japan (*Abstract Co-Author*) Nothing to Disclose Keisuke Ishimatsu, MD, Fukuoka, Japan (*Abstract Co-Author*) Nothing to Disclose Hiroshi Honda, MD, Fukuoka, Japan (*Abstract Co-Author*) Nothing to Disclose Ryotaro Kamei, MD, Fukuoka, Japan (*Abstract Co-Author*) Nothing to Disclose

#### For information about this presentation, contact:

# yuwata55@gmail.com

# PURPOSE

To evaluate the relationship between simultaneously-acquired SUV of 18FDG and ADC in soft tissue and bone tumors using voxelby-voxel analysis.

### **METHOD AND MATERIALS**

The consecutive 125 patients with tumor of soft tissue and bone were included in this study, and examined with 18FDG-PET/MR hybrid imaging. Diffusion-weighted image (b = 0 and 800) and 18FDG-PET were simultaneously acquired with 3D-T2-weighted TSE images. After image co-registration and reslice of 3D-T2WI and PET image based on ADC map on a workstation (Intellispace Portal 6.0), voxel-based scatter plots of SUV vs ADC and SUV/ADC vs log-ADC were generated for each tumor. Cluster analysis using k-means clustering algorithm was also applied when a tumor consists of multiple components such as liposarcoma, schwannoma and other tumors with large necrotic portions by using our in-house program (MathWorks). Pearson correlation coefficient was compared between SUV vs ADC and SUV/ADC vs log-ADC. The slope of regression line was also compared among malignant, intermediate and benign groups. Statistical analysis was performed with Wilcoxon test, ANOVA and Mann-Whitney test.

### RESULTS

According to the WHO classification 2013, malignancy grades of the 125 tumors were histologically classified into high-grade sarcomas (n=76), intermediate-grade (n=12) and benign tumor (n=37). The relationship between SUV/ADC and log-ADC showed a significant inverse linear correlation (mean r=-0.60, 95%CI: -0.63~-0.57), while that between SUV and ADC showed no significant correlation (mean r=-0.05, 95%CI: -0.10~0.00). All the tumors showed significant higher correlation coefficient for SUV/ADC vs logADC than SUV vs ADC (p<0.001). The slope was much steeper for malignant than benign tumors (p<0.001). In 24 patients with liposarcoma (n=2), myxofibrosarcoma (n=3), schwannoma (n=2), other sarcomas (n=17), cluster analysis demonstrated steep slope of the two clusters showed higher inverse correlation coefficients than that of the whole tumor and represented the tumor grades.

# CONCLUSION

Voxel-by-voxel SUV-ADC analyses could demonstrate significant inverse linear correlation between SUV/ADC and log-ADC, and malignant tumors showed steeper slope of regression line than benign tumors.

# **CLINICAL RELEVANCE/APPLICATION**

The slopes derived from SUV/ADC vs log-ADC scatter plots could be a new quantitative imaging biomarker for the differentiation of malignant and benign soft-tissue and bone tumors.



### NM211-SD-MOA4

Elucidating Mechanisms of Acute Sports Concussion with PET/MRI

Monday, Nov. 26 12:15PM - 12:45PM Room: NM Community, Learning Center Station #4

FDA Discussions may include off-label uses.

#### **Participants**

Paul Vaska, Stony Brook, NY (Presenter) Nothing to Disclose Michael J. Salerno, BS, MBA, Stony Brook, NY (Abstract Co-Author) Nothing to Disclose Kenneth T. Wengler, MS, Stony Brook, NY (Abstract Co-Author) Nothing to Disclose David Ouellette, MS, Stony Brook, NY (Abstract Co-Author) Nothing to Disclose Shouyi Wei, Stony Brook, NY (Abstract Co-Author) Nothing to Disclose Brian Cruickshank, Stony Brook, NY (Abstract Co-Author) Nothing to Disclose David E. Komatsu, PhD, Stony Brook, NY (Abstract Co-Author) Nothing to Disclose Dinko Franceschi, MD, Stony Brook, NY (Abstract Co-Author) Nothing to Disclose Lev Bangiyev, DO, Stony Brook, NY (Abstract Co-Author) Nothing to Disclose Janet Oseni, Stony Brook, NY (Abstract Co-Author) Nothing to Disclose Emmanuel Thomas, Stony Brook, NY (Abstract Co-Author) Nothing to Disclose Sara Yang, Stony Brook, NY (*Abstract Co-Author*) Nothing to Disclose Mark E. Schweitzer, MD, Stony Brook, NY (*Abstract Co-Author*) Consultant, MMI Munich Medical International GmbH; Data Safety Monitoring Board, Histogenics Corporation Kristen Dams-O'Connor, New York, NY (Abstract Co-Author) Nothing to Disclose James M. Paci, MD, Setauket- East Setauket, NY (Abstract Co-Author) Nothing to Disclose Xiang He, PhD, Stony Brook, NY (Abstract Co-Author) Consultant, Endo International plc

### For information about this presentation, contact:

paul.vaska@stonybrook.edu

### PURPOSE

Animal studies have defined a neuropathological cascade following concussion consisting of large and transient disruptions of homeostasis in the acute phase (hours) but this has never been observed in humans. We aim to establish the existence, magnitude, and regional distribution of the most prominent feature of this cascade - a dramatic yet temporary increase in glucose metabolism and related hemodynamic effects.

# METHOD AND MATERIALS

Athletes from a single NCAA Division I university consented to undergo PET/MRI brain imaging in the event of concussion, using a within-subjects (paired) design in which subjects are imaged as soon as possible after injury and again when symptoms have resolved (>3 months later). We also recruited a non-injured control group from the same population. A 20 min PET/MRI scan commenced 40 min after i.v. injection of 3-5 mCi of FDG. MRI included standard structural scans and quantitative measures of cerebral blood flow (CBF), oxygen extraction fraction (OEF), and cerebral metabolic rate of oxygen (CMRO2). Images were registered to standard brain atlas and regions of interest extracted. Clinical data regarding severity of injury and duration of recovery was collected as well.

### RESULTS

Thus far we have completed acute phase scans on 4 subjects within 54 hours of concussion injury and a scan of a control athlete. Clinically, there were no functional or structural abnormalities. We observed that gray matter SUV values in the acute phase were higher than control in all cases except for a subject with extensive history of concussions (including one within the last year). Gray-to-white matter ratios were elevated in all cases. MRI measures demonstrated that acute concussion subjects generally had lower CMRO2, CBF, and OEF in gray matter vs control. Due to the limited number of subjects scanned so far, statistical significance has not yet been established.

#### CONCLUSION

Initial results are consistent with the hypothesis that cortical glucose metabolism is elevated and oxidative metabolism is depressed in the acute phase following sports concussion. Ongoing imaging of study participants will determine the statistical significance and clinical relevance of these findings.

### **CLINICAL RELEVANCE/APPLICATION**

A better understanding of the early pathology of concussion may lead to improved strategies for objective diagnosis and treatment.



### NR016-EB-MOA

Neuroimaging in Autoimmune Limbic Encephalitis: MRI versus PET/CT and Mimickers of Disease

Monday, Nov. 26 12:15PM - 12:45PM Room: NR Community, Learning Center Hardcopy Backboard

#### **Participants**

Solmaz Asnafi, MD, Rochester, MN (*Presenter*) Nothing to Disclose Sean J. Pittock, Rochester, MN (*Abstract Co-Author*) Nothing to Disclose Alfonso S Lopez Chiriboga, Rochester, MN (*Abstract Co-Author*) Nothing to Disclose Eoin Flanagan, Rochester, MN (*Abstract Co-Author*) Nothing to Disclose Christopher H. Hunt, MD, Rochester, MN (*Abstract Co-Author*) Nothing to Disclose

### For information about this presentation, contact:

s.asnafi@gmail.com

#### **TEACHING POINTS**

Autoimmune limbic encephalitis (ALE), characterized by encephalopathy with prominent amnesia and frequent seizures, is increasingly recognized in the context of novel antibody biomarkers. Antibodies targeting NMDA, GABAB, AMPA receptors and extracellular components of the voltage gated potassium channel complex, specifically LGI1 and CASPR2 are the most commonly identified pathogenic antibodies, some of which are associated with neoplasms (paraneoplastic LE) in such patients. Recognition of radiologic features of ALE can assist clinicians in making an early diagnosis, which is important as early treatment is associated with better outcome. For some patients, despite significant encephalopathy, with severe cognitive or behavioral symptoms or seizures, MRI may be normal. Here, we review imaging characteristics of ALE with specific attention to the patterns of metabolism change on brain FDG-PET/CT as well as the features seen on conventional MRI.

#### **TABLE OF CONTENTS/OUTLINE**

1 Overview of the neural antibodies associated with ALE2 Define the clinical spectrum and imaging characteristics of PET/CT in ALE, grouped according to neural antibody3 Discuss potential role of PET in the evaluation of ALE and compare with MRI4 Review literature pertaining to PET and MRI images of patients with LGI1 and CASPR2 autoimmunity5 Illustrate MRI and PET mimickers of ALE



#### NR335-ED-MOA8

# CT Myelos: Dinos or Rhinos? Indications and Pathologies in this Modern MR Era

Monday, Nov. 26 12:15PM - 12:45PM Room: NR Community, Learning Center Station #8

### Awards Identified for RadioGraphics

### Participants

Dhruv Patel, MD, Atlanta, GA (*Presenter*) Nothing to Disclose Brent D. Weinberg, MD, PhD, Atlanta, GA (*Abstract Co-Author*) Nothing to Disclose Jacqueline Junn, MD, Atlanta, GA (*Abstract Co-Author*) Nothing to Disclose Michael J. Hoch, MD, Atlanta, GA (*Abstract Co-Author*) Nothing to Disclose

# For information about this presentation, contact:

dpate31@emory.edu

#### **TEACHING POINTS**

• To review common indications of performing CT myelogram. • To review uncommon indications of performing CT myelogram. • To provide pictorial review of various pathologies seen on CT myelogram including those of nerve roots, meninges, surgical complications and conditions that require interventions.

### **TABLE OF CONTENTS/OUTLINE**

• Current common indications for CT myelogram. • Current uncommon indications for CT myelogram. • CT myelogram findings of various common and rare pathologies: --- Nerve pathologies (e.g. nerve root avulsions) --- Meningeal pathologies (e.g. adhesive arachnoiditis with empty thecal sac sign, arachnoid web with scalpel sign, traumatic lateral meningocele) --- Surgical complications (e.g. duroplural fistula, spinal CSF-venous fistula, CSF leak status post meningocele resection) --- Other pathologies (e.g. disk extrusion within metalic artifact) • Summary



### NR336-ED-MOA9

CT Angiography and CT Perfusion of Brain Tumors with a Reduced Dose of Radiation and Contrast Medium

Monday, Nov. 26 12:15PM - 12:45PM Room: NR Community, Learning Center Station #9

### Participants

Jun Nakane, Kawagoe, Japan (*Presenter*) Nothing to Disclose Kazuhiro Tsuchiya, MD, Kawagoe, Japan (*Abstract Co-Author*) Nothing to Disclose Yoshiharu Kobayashi, Kawagoe, Japan (*Abstract Co-Author*) Nothing to Disclose

### **TEACHING POINTS**

• Consecutive acquisition of CT perfusion and CT angiography can be performed with a reduced contrast dose of 370 mgI/kg per body weight.• Adaptive 4D spiral technique realizes whole brain scan in 1.5 seconds without using a CT scanner with many detector rows such as 320.• 4D noise reduction in postprocessing can decrease the radiation dose because the noise of CT perfusion is reduced by 50%.• By detecting the circulatory dynamics of cerebrovascular vessels on the occasion of CT perfusion, no additional test bolus is required.

# TABLE OF CONTENTS/OUTLINE

• It is necessary to reduce a dose of radiation and contrast medium. As patients with brain tumors often perform MR or CT using a contrast medium many times, it is required to reduce the physical burden due to contrast medium and radiation.• Determination of the dose of contrast medium based on the body weight.• Reduction of radiation dose can be realized by utilizing adaptive 4D spiral technique and 4D noise reduction.• This protocol usually has diagnostic capability equivalent to MR, leading to the finding corresponding to the pathological diagnosis.



### NR337-ED-MOA10

Do Not Get Lost in the Triangle of Guillain-Mollaret: A Pictorial Guide Through the Hypertrophic Olivary Degeneration Flow

Monday, Nov. 26 12:15PM - 12:45PM Room: NR Community, Learning Center Station #10

#### Awards Certificate of Merit

#### **Participants**

Luis Quintana Barriga, MD, Seville, Spain (*Presenter*) Nothing to Disclose Florinda Roldan, Seville, Spain (*Abstract Co-Author*) Nothing to Disclose Rafael F. Ocete Perez, MD, Sevilla, Spain (*Abstract Co-Author*) Nothing to Disclose Fatima Alvarez Janez, MD, Sevilla, Spain (*Abstract Co-Author*) Nothing to Disclose Manuel Avila Macias, Seville, Spain (*Abstract Co-Author*) Nothing to Disclose Pilar Pinero Gonzalez de la Pena, Sevilla, Spain (*Abstract Co-Author*) Nothing to Disclose

### For information about this presentation, contact:

luisquintanaba@gmail.com

### **TEACHING POINTS**

-To know the anatomy of the triangle of Guillain-Mollaret and the physiopathology in the developing hypertrophic olivary degeneration (HOD). -To recognize the clinical presentation HOD. -To describe the MRI imaging findings of HOD and its evolution. - To make an adequate differential diagnosis in order not to misdiagnose other pathologies that should be treated.

# TABLE OF CONTENTS/OUTLINE

- Anatomy of the Dentate-Rubro-Olivary pathway or triangle of Guillain-Mollaret. - Pathophysiology of HOD: ipsilateral, contralateral and bilateral patterns of HOD. - Review imaging findings - Conventional MRI. - Evolution of findings through time: stages of HOD changes according to the time elapsed from injury. - Sample cases and etiologies. - Differential diagnosis. - Conclusions.



### NR374-SD-MOA1

Clinical Value of Vascular Permeability Estimates Using Dynamic Susceptibility Contrast MRI: Improved Diagnostic Performance in Distinguishing Hypervascular Primary CNS Lymphoma from Glioblastoma

Monday, Nov. 26 12:15PM - 12:45PM Room: NR Community, Learning Center Station #1

### Participants

Boeun Lee, MD, Seoul, Korea, Republic Of (*Presenter*) Nothing to Disclose Ji Eun Park, Seoul, Korea, Republic Of (*Abstract Co-Author*) Nothing to Disclose Atle Bjornerud, PhD, Oslo, Norway (*Abstract Co-Author*) Nothing to Disclose Ho Sung Kim, Seoul, Korea, Republic Of (*Abstract Co-Author*) Nothing to Disclose Ji Ye Lee, MD, Bucheon, Korea, Republic Of (*Abstract Co-Author*) Nothing to Disclose

# PURPOSE

A small subset of primary central nervous system lymphomas (PCNSLs) exhibits high cerebral blood volume (CBV), which is indistinguishable from glioblastoma on dynamic susceptibility contrast magnetic resonance imaging (DSC-MRI). Our study aimed to test whether estimates of combined perfusion- and vascular permeability metrics derived from DSC-MRI can improves diagnostic performance in differentiating hypervascular PCNSL from glioblastoma.

# METHOD AND MATERIALS

A total of 119 patients (30 PCNSLs and 89 glioblastomas) exhibited hypervascular foci using the reference method of leakagecorrected CBV (reference normalized CBV, nCBVref). An alternative post-processing method utilized the tissue residue function to calculate vascular permeability (extraction fraction, EF), leakage-corrected CBV (CBVres), cerebral blood flow (CBF), and mean transit time (MTT). Parameters were compared using Mann-Whitney U-tests, and diagnostic performance to distinguish PCNSLs from glioblastoma was calculated using the area-under-the curve from the receiver operating characteristics curve (AUC) and cross-validated with boot-strapping.

### RESULTS

Hypervascular PCNSL showed similar nCBVref and CBVres, compared with glioblastoma (P > .05); however, PCNSL exhibited significantly higher EF (P < .001) and CBF (P = .01), and shorter MTT (P < .001), than glioblastoma. EF showed the highest diagnostic performance (AUC, 0.78; 95% confidence interval 0.69-0.85) for distinguishing hypervascular PCNSL from glioblastoma, with a significantly higher performance than both CBV parameter (AUC, 0.53-0.59, largest P = .02), as well as CBF (AUC, 0.72) and MTT (AUC, 0.71).

### CONCLUSION

Estimation of vascular permeability with DSC-MRI further characterizes hypervascular PCNSL and improves diagnostic performance in terms of glioblastoma differentiation.

#### **CLINICAL RELEVANCE/APPLICATION**

using a novel analysis approach, estimates of combined perfusion and vascular permeability related metrics was obtained from a single DSC-MRI acquisition. Contrast agent extraction fraction derived by this method showed improved diagnostic performance in differentiating hypervascular PCNSL from glioblastoma compared to conventional CBV based analysis. The analysis approach can be achieved with a single dose of gadolinium-based contrast use and can be implemented in a clinical setting.



### NR375-SD-MOA2

### **Resident Call Preparation Website: Preliminary Results**

Monday, Nov. 26 12:15PM - 12:45PM Room: NR Community, Learning Center Station #2

#### Awards Student Travel Stipend Award

#### Participants

Frederick S. Jones, MD, Winston Salem, NC (*Presenter*) Nothing to Disclose Kevin D. Hiatt, MD, Winston-Salem, NC (*Abstract Co-Author*) Nothing to Disclose Valerie George, BA, Winston-Salem, NC (*Abstract Co-Author*) Nothing to Disclose Thomas G. West, MD, Greenville, NC (*Abstract Co-Author*) Nothing to Disclose Carol P. Geer, MD, Winston-Salem, NC (*Abstract Co-Author*) Nothing to Disclose

#### PURPOSE

The purpose of this project was to create a web-based call preparation tool to build core competency among first year residents prior to them interpreting studies without direct attending supervision.

### **METHOD AND MATERIALS**

CT neuroimaging was selected as the first curriculum to develop and pilot and was subdivided into four modules: "traumatic brain," "nontraumatic brain," "spine" and "head and neck." For each module, review articles were referenced to build a list of "must see" diagnoses. Then, both classic and non-classic (either subtle, complex, or ambiguous) cases were collected from our PACS corresponding to each diagnosis. DICOM files were de-identified and then uploaded to a web-based platform designed to simulate the call experience using an open source DICOM viewer. Page templates were arranged such that findings and discussion sections were only visible upon selection to encourage residents to view the images prior to seeing the diagnosis. First year residents electively enrolled and completed the following sequential steps in each module: 1) pre-quiz, 2) review article, 3) "classic" cases, 4) call prep lectures given by neuroradiology faculty, 5) "non-classic" cases, and 6) post-quiz and survey. Usage data, quiz results, and surveys were collected after completion.

#### RESULTS

The curriculum consisted of 217 cases. Ten of the twelve first year residents regularly used the website, with these users spending on average five hours per week on the site. Combined, they completed over 1400 cases. Highlights from the survey results include that 86% of these users used the website as their primary resource for CT neuroimaging call preparation and 80% felt 'a lot more confident' about taking call after the course. Users also scored significantly higher on the post-course quiz in comparison to the pre-course quiz. For example, in the nontraumatic brain module, the average pre-quiz score was 29% versus 73% on the post-quiz.

#### CONCLUSION

Our web-based CT neuroimaging curriculum allows a standardized call preparation that closely simulates the call experience and represents a valuable addition to traditional teaching strategies.

# **CLINICAL RELEVANCE/APPLICATION**

Our call preparation website, which we are currently expanding beyond CT neuroimaging, allows standardized resident education on a platform which closely simulates the call experience and should prove useful for educating future generations of residents.



### NR376-SD-MOA3

Wave-CAIPI Encoding 3D T1-Weighted Magnetization-Prepared Rapid Gradient Echo (MP-RAGE) Brain Imaging: A New Technique for Scan Time Reduction

Monday, Nov. 26 12:15PM - 12:45PM Room: NR Community, Learning Center Station #3

# Participants

Eunjung Lee, Seoul, Korea, Republic Of (*Presenter*) Nothing to Disclose Mi Sun Chung, MD, Seoul, Korea, Republic Of (*Abstract Co-Author*) Nothing to Disclose

### PURPOSE

To investigate the impact of wave-controlled aliasing in parallel imaging (wave-CAIPI) encoding on scan time reduction and image quality for 3D T1-wieghted magnetization-prepared rapid gradient echo (MP-RAGE) acquisition.

### **METHOD AND MATERIALS**

3.0T MRI (Siemens Skyra scanner) studies of the brain were performed in 39 patients with focal brain lesion between November 2017 and January 2018. We acquired three types of 3D isovoxel T1-weighted MP-RAGE images using conventional GRAPPA method with R=2 and wave-CAIPI with R=4(2x2) and R=6(3x2). We compared the image scan time of each MP-RAGE images. And we compared contrast-to-noise ratio (CNR) between gray matter and white matter at the right cerebral coronal radiata and signal-to-noise ratio (SNR) at the right cerebral coronal radiata, pons and cerebellar white matter in each MP-RAGE images. We also evaluated qualitative grading for image quality by blinded test and diagnostic agreement for focal lesion.

# RESULTS

The image scan time was reduced by 67.8% (total scan time=1 min 52 s) in wave-CAIPI R=6(3x2) and 52.8% (2 min 44 s) in wave-CAIPI R=4(2x2), compared with conventional MP-RAGE imaging (5 min 48 s). There was no significant difference in CNR for differentiation of white matter and gray matter at the right cerebral corona radiata and SNR at the right cerebral corona radiata, pons and cerebellar hemisphere. For qualitative analysis, conventional MP-RAGE showed significantly higher grade for image quality, compared to wave-CAIPI R=6(3x2) (4.87±0.34 vs. 3.77±0.58, p < 0.01) and R=4(2x2) (4.87±0.34 vs. 4.08±0.62, p < 0.01). But the diagnosis for focal brain lesion was completely consistent regardless of the image type.

#### CONCLUSION

Wave-CAIPI encoding 3D T1-wieghted MP-RAGE acquisition can reduce scan time effectively without degrading image quality. It can be a promising substitute for the diagnosis of focal brain lesion, employing MP-RAGE for T1-weighted imaging.

## **CLINICAL RELEVANCE/APPLICATION**

(dealing with new MRI sequences for scan time reduction) Wave-CAIPI MP-RAGE can reduce scan time effectively without degrading image quality. This fast sequence is expected to benefit clinical and research applications that routinely employ MP-RAGE for T1-weighted imaging.



### NR378-SD-MOA4

Malignant X Benign: Use of 2D-Shear Wave Sonoelastography for the Risk Stratification of Thyroid Follicular Nodules

Monday, Nov. 26 12:15PM - 12:45PM Room: NR Community, Learning Center Station #4

# Participants

Pedro H. Moraes, MD, Sao Paulo, Brazil (*Presenter*) Nothing to Disclose Maria Cristina Chammas, MD,PhD, Sao Paulo, Brazil (*Abstract Co-Author*) Nothing to Disclose Marcelo V. Schelini, MD, Sao Paulo, Brazil (*Abstract Co-Author*) Nothing to Disclose

#### For information about this presentation, contact:

pedrohenrique.mmoraes@gmail.com

#### PURPOSE

Follicular lesion is found up 30% of FNAB of thyroid nodules. 20% are carcinoma at histology, so 80% are benign. Motivated by unnecessary surgeries performed, we studied nodules with 2D Shear-wave elastography (SWE) ultrasound to distinguish benign from malignant nodules (BETHESDA III and IV) before surgery.

### METHOD AND MATERIALS

Nodules previously submitted to FNAB Bethesda III or IV were included. Scans were performed with GE Logic E9 - SW1 elastogram scale (blue for soft tissues, red for hard). B mode parameters (size, echogenicity, presence of halo / microcalcifications), Doppler and elastography were collected. We identified an elastogram strain pattern of the nodule from 1: high deformity (completely blue) to 4: low strain (completely red). SWE deformation indexes (SWE-index), in kPa, were defined by a ROI including the nodule and other at the pre-thyroid muscle. Mean values of three different SWE-indexes of each nodule was calculated. A deformation ratio (MDR) was calculated dividing the nodule SWE-index by the muscle SWE-index. Patients were submitted to nodule surgical resection with histological analysis.

### RESULTS

42 patients underwent surgical resection of the studied nodule. 20/42 (47.6%) were carcinomas. 17/20 (85%) had elastogram pattern>2. Statistical analysis revealed a significant association between carcinoma and elastogram pattern 3 and 4 (sens:85% spec:90.9% AUC:89.7% p=0.001), with 56.67% higher risk in these groups (95%CI: 8.45-379.79). Nodule SWE-index>33.76 kPa sugested a increased risk for carcinoma (sens90% spec63,6% p=0,002 PPV:69.2% NPV:87.5%). MDR>1.75 was related to carcinoma (sens85% spec81.8% AUC0.894 p=0.0004 95%CI:0.796-0.993). We couldn't find a significant association between b mode and Doppler parameters with carcinoma.

# CONCLUSION

The diagnostic dilemma in front of a thyroid follicular lesion leads to many unnecessarily surgeries. B mode and Doppler parameters aren't able to distinguish carcinoma from other follicular lesions due to their histological similarities. Assuming that increased cellularity and capsular invasion in carcinomas increases its stiffness, we demonstrated that 2D-SWE is useful in predicting risk of malignancy for follicular nodules.

# **CLINICAL RELEVANCE/APPLICATION**

The established parameters of the elastography - nodule SWE-index, elastogram pattern and MDR - helps to drastically reduce the unnecessary surgeries performed in the benign follicular thyroid lesions.



### NR380-SD-MOA6

Noninvasive Prediction of IDH1 and ATRX Mutation in Low-Grade Gliomas Using Multi-Parametric MR Radiomic Features

Monday, Nov. 26 12:15PM - 12:45PM Room: NR Community, Learning Center Station #6

# Participants

Yan Ren, MD, Shanghai, China (*Presenter*) Nothing to Disclose Xi Zhang, Xian, China (*Abstract Co-Author*) Nothing to Disclose Wenting Rui, Shanghai, China (*Abstract Co-Author*) Nothing to Disclose Haopeng Pang, Shanghai, China (*Abstract Co-Author*) Nothing to Disclose Qian Xie, Shanghai, China (*Abstract Co-Author*) Nothing to Disclose Teng Jin, Shanghai, China (*Abstract Co-Author*) Nothing to Disclose Tianming Qiu, Shanghai, China (*Abstract Co-Author*) Nothing to Disclose Hong Chen, Shanghai, China (*Abstract Co-Author*) Nothing to Disclose Junhai Zhang, Shanghai, China (*Abstract Co-Author*) Nothing to Disclose Zhenwei Yao, Shanghai, China (*Abstract Co-Author*) Nothing to Disclose Xiaoyuan Feng, MD, Shanghai, China (*Abstract Co-Author*) Nothing to Disclose

#### For information about this presentation, contact:

renyan\_richard@aliyun.com

### PURPOSE

To explore a radiomic approach based on multi-parametric MR for noninvasively determining molecular status of IDH1+/- and ATRX+/- in patients with LGG.

### METHOD AND MATERIALS

Out of 105 patients with gliomas with a unified 3.0 Tesla MR scan protocol of 3D-ASL, T2FLAIR and DWI, 36 WHO grade II patients with IDH1+/- were enrolled with 19 ATRX+/- and 17 ATRX-/- patients.Two hundred sixty high-throught radiomic features were extracted on each tumor volume of interest from T2FLAIR and the other three parametric maps of ASL-derived cerebral blood flow (CBF), DWI-derived apparent diffusion coefficient (ADC) and exponential ADC (eADC). Optimal feature subsets were selected using the support vector machine with recursive feature elimination algorithm (SVM-RFE), and receiver operating characteristic curve analysis was employed to assess the efficiency for identifying the status of IDH1+/- with ATRX+/-.

#### RESULTS

The constituent ratio of histologic subtypes was significantly different between the status of ATRX+/- and ATRX-/- in patients with IDH1+/- LGG, SVM model for detecting ATRX+/- was established using 6 optimal radiomic features from multi-parametric MR of T2Flair, CBF and ADC selected by SVM-RFE. The predicting accuracy for IDH1+/- with ATRX+/- status was 91.67%, which outperformed any single MR sequence or parametric map alone. In this strategy, T2Flair contributed most greatly to determine the ATRX+/- status with 3 of 6 optimal features, in which, one ranked first in the ranking list.

# CONCLUSION

By using the optimal texture features extracted from multiple MR sequences or parametric maps, a promising strategy was acquired for improving the detecting efficiency of ATRX+/- status in patients with IDH1+/- LGGs. The results suggest radiomic features of T2FLAIR play important roles on the non-invasive identification of IDH1+/- with ATRX+/- status in LGG patients.

#### **CLINICAL RELEVANCE/APPLICATION**

ATRX protein loss status, due to its never being accompanied by 1p/19q co-deletion, is characteristic in identifying diffuse astrocytomas from oligodendrogliomas. Meanwhile, ATRX mutation status was found to correlate with 11 C-methionine uptake and the poor outcomes of patients in LGG with IDH mutation.



### OB169-ED-MOA1

### An Illustrated Guide to Obstetrical & Gynecologic Surgical Procedures for Radiologists

Monday, Nov. 26 12:15PM - 12:45PM Room: OB Community, Learning Center Station #1

### Awards Certificate of Merit Identified for RadioGraphics

### Participants

Anjuli R. Cherukuri, MD, Madison, WI (*Presenter*) Nothing to Disclose Akshya Gupta, MD, Madison, WI (*Abstract Co-Author*) Nothing to Disclose Jessica B. Robbins, MD, Madison, WI (*Abstract Co-Author*) Nothing to Disclose Virginia B. Planz, MD, Winston Salem, NC (*Abstract Co-Author*) Nothing to Disclose Robert D'Agostino, MD, Burlington, VT (*Abstract Co-Author*) Nothing to Disclose Lori Mankowski Gettle, MD, Madison, WI (*Abstract Co-Author*) Nothing to Disclose

### For information about this presentation, contact:

archerukuri@gmail.com

# **TEACHING POINTS**

Review common and uncommon obstetrical and gynecologic surgical procedural details. Review the normal postoperative appearance with original illustrations. Review complications and how to best image them.

### **TABLE OF CONTENTS/OUTLINE**

Obstetrical and gynecologic procedures will be reviewed, including indications, original illustrations, brief procedural details, optimal imaging techniques, normal postoperative appearances, and complications. Procedure types reviewed: Obstetrical procedures including Cesarean section, D&C and D&E, fertility treatments, intrauterine devices, essure device, tubal ligation, tuboplasty, and cervical cerclage. Benign gynecologic procedures including hysterectomy, uterine myomectomy, colporrhaphy, endometrial ablation, and salpingectomy. Gynecologic oncology procedures including radical hysterectomy, salpingoophorectomy, omentectomy & debulking procedures, ovarian transposition, brachytheraphy, trachelectomy, vulvectomy, and pelvic exenteration.



### OB177-ED-MOA2

### Congenital Spine Malformations: Review of Fetal and Postnatal Ultrasound and MRI

Monday, Nov. 26 12:15PM - 12:45PM Room: OB Community, Learning Center Station #2

#### **Participants**

Laura B. Eisenmenger, MD, Salt Lake City, UT (*Abstract Co-Author*) Nothing to Disclose Dorothy J. Shum, MD, San Francisco, CA (*Abstract Co-Author*) Nothing to Disclose Loretta M. Strachowski, MD, San Francisco, CA (*Abstract Co-Author*) Nothing to Disclose Eugene J. Huo, MD, San Francisco, CA (*Presenter*) Nothing to Disclose

### For information about this presentation, contact:

eugene.huo@ucsf.edu

# **TEACHING POINTS**

Review normal spine embryology Review the abnormal embryologic development leading to open and closed spinal dysraphisms Review findings of both open and closed spinal dysraphisms on both ultrasound correlating with imaging findings seen on MRI Emphasize critical findings that differentiate malformations and allow for accurate diagnosis

# TABLE OF CONTENTS/OUTLINE

Normal spine embryology Abnormal embryologic development of the spine Open spinal dysraphisms and Chiari II malformations Myelomeningocele Myelocele (myeloschisis) Closed spinal dysraphisms Associated subcutaneous mass Lipomas with dural defect Lipomyelomeningocele Lipomyelocele (lipomyeloschisis) Terminal myelocystocele Meningocele No subcutaneous mass Dorsal enteric fistula Split cord malformations (diastematomyelia) Intradural Lipoma Filum lipoma Tight filum terminale Persistent terminal ventricle Neuroenteric cysts Caudal regression syndrome Dermal sinus Quiz Summary This exhibit demonstrates the spectrum of fetal sonographic and corresponding MRI findings of congenital neural tube defects. Identification of key imaging features allows for accurate diagnosis leading to appropriate management.



### PD177-ED-MOA6

Adolescent Overhead Athlete: Anatomy, Physiology, and Pathophysiology

Monday, Nov. 26 12:15PM - 12:45PM Room: PD Community, Learning Center Station #6

### Awards Certificate of Merit

#### **Participants**

Jie C. Nguyen, MD,MS, Philadelphia, PA (*Presenter*) Nothing to Disclose Hollis G. Potter, MD, New York, NY (*Abstract Co-Author*) Research support, General Electric Company Institutional research agreement, General Electric Company

### **TEACHING POINTS**

A delicate balance between stability and mobility of the glenohumeral joint in the overhead athlete requires coordinated function of both static/osseous and dynamic/soft tissue stabilizers. In the skeletally mature athlete, failure of the dynamic stabilizers can produce remodeling of the static stabilizers. However, in the skeletally immature athlete, the growth plate is the weaker link, producing a spectrum of findings that can predispose the child to long-term instability and deformity.

### **TABLE OF CONTENTS/OUTLINE**

1) The anatomy of the humerus, scapula, and acromion will be presented, including a review of the timing and appearance of the apophyses and the histoanatomy of the primary physes. 2) The static and dynamic stabilizers of glenohumeral joint will be reviewed, followed by a discussion of the mechanism of injury, highlighting the stereotypical patterns and imaging considerations. 3) A comprehensive review of the various patterns of adaptive remodeling and injury will be reviewed, divided into those that involve the muscular stabilizers (tendinosis, avulsion, tear), labral-capsular complex (labral tear, capsular tears and features of plastic deformation), and chondro-osseous structures (proximal humeral epiphysiolysis, osteochondral lesion, glenoid remodeling/Bennett lesion, acromial apophysiolysis). Treatment algorithms will be discussed.



### PD178-ED-MOA7

# Fetal Cardiac MRI for Structural Congenital Heart Disease

Monday, Nov. 26 12:15PM - 12:45PM Room: PD Community, Learning Center Station #7

#### **Participants**

Su-Zhen Dong, MD,PhD, Shanghai, China (*Presenter*) Nothing to Disclose Dorothy I. Bulas, MD, Washington, DC (*Abstract Co-Author*) Nothing to Disclose Ming Zhu, Shanghai, China (*Abstract Co-Author*) Nothing to Disclose

### For information about this presentation, contact:

dongsuzhen@126.com

### **TEACHING POINTS**

The purpose of this exhibit is: 1. To review the technical considerations of fetal cardiac magnetic resonance imaging 2. To review the imaging appearances of normal heart and great vessels in the second and third trimester by fetal MRI 3. To describe a modified anatomic segmental approach of cardiac structures by fetal MRI 4. To review the appearance of various structural congenital heart anomalies by fetal MRI

# TABLE OF CONTENTS/OUTLINE

Embryology and anatomy of the heart MR technique for fetal cardiac magnetic resonance imaging scanning Standard MR imaging of the normal fetal heart and great vessels Modified anatomic segmental approach of fetal cardiac structures Diagnosis of various structural congenital heart diseases by fetal MRI - Situs anomalies (Situs inversus totalis, Abdominal situs inversus with levocardia, Heterotaxy (right/left isomerism, isolated dextrocardia, etc) - Abnormal cardiac apex and axis - Abnormal ventricular looping -Anomalies of atrioventricular junction and cardiac chambers - Anomalies of ventriculoarterial connections - Anomalies of the aorta and pulmonary artery - Anomalies of the systemic and pulmonary venous connections -Complex congenital heart disease (Tetralogy of Fallot, hypoplastic left heart syndrome, etc)



### PD179-ED-MOA8

### Dentate Nuclei Involvement in Pediatric CNS Conditions: Imaging and Clinicolaboratory Insights

Monday, Nov. 26 12:15PM - 12:45PM Room: PD Community, Learning Center Station #8

### Participants

Hiren Panwala, Vellore, India (*Presenter*) Nothing to Disclose Sniya V. Sudhakar, MBBS, MD, Vellore, India (*Abstract Co-Author*) Nothing to Disclose Vikas K. Yadav, MBBS, MD, Vellore, India (*Abstract Co-Author*) Nothing to Disclose Girish M. Fatterpekar, MBBS, New York, NY (*Abstract Co-Author*) Nothing to Disclose Hariprasad Sudershan, New Delhi, India (*Abstract Co-Author*) Nothing to Disclose Maya Thomas, Vellore, India (*Abstract Co-Author*) Nothing to Disclose Amogh K. Vn, Vellore, India (*Abstract Co-Author*) Nothing to Disclose Sridhar Gibikote, DMRD, Vellore, India (*Abstract Co-Author*) Nothing to Disclose Umar Siddiqi, Vellore, India (*Abstract Co-Author*) Nothing to Disclose

#### For information about this presentation, contact:

drhiren1187@gmail.com

#### **TEACHING POINTS**

1.Review the spectrum of disease conditions causing dentate nuclei abnormality in the pediatric age group 2.Provide a patternbased approach to narrow the differential diagnosis based on the morphological features with/without involvement of other anatomical structures, such as the basal ganglia, thalami, corpus callosum and white matter 3.Emphasize the importance of good clinicolaboratory correlation towards making the correct diagnosis.

### **TABLE OF CONTENTS/OUTLINE**

Illustration of various inheritable and acquired conditions affecting dentate nuclei Pattern-based approach based on signal changes and enhancement characteristics to narrow the differential diagnosis Differential diagnosis based on structures involved: -Predominant dentate nuclei involvement -Dentate nuclei with white matter , basal ganglia with various combination with brainstem and thalami -Dentate nuclei with basal ganglia involvement -Dentate nuclei with calcification -Dentate nuclei with brainstem involvement Importance of clinicolaboratory correlation including evaluation of genetic mutation, enzyme and specific markers pertaining to the suspected disease Flow-chart integrating morphological features with clinicolaboratory correlation to narrow the differential diagnosis Summary and conclusion



### PD210-SD-MOA1

Thoracic Air-Leak Syndrome and Bronchiolitis Obliterans in Pediatric Patients Following Hematopetic Stem Cell Transplantation

Monday, Nov. 26 12:15PM - 12:45PM Room: PD Community, Learning Center Station #1

### Participants

Ekaterina S. Ternovaya, MD, MSc, Moscow, Russia (*Presenter*) Nothing to Disclose Galina V. Tereschenko, Moscow, Russia (*Abstract Co-Author*) Nothing to Disclose

For information about this presentation, contact:

ekaterina.ternovaya@fccho-moscow.ru

### PURPOSE

Chronic pulmonary graft-versus-host disease (cGVHD) remains major complication in patients surviving long-term after allogenic stem cell transplantation (allo-SCT). Bronchiolitis obliterans (BO) is considered as one of manifestation of cGVHD. BO can lead to another not commonly encountred complication of cGVHD - thoracic air-leak syndrome (TALS). Purpose of this study was to establish diagnostic criteria specific to BO and study TALS as it's possible complication.

### METHOD AND MATERIALS

Retrospectively surveyed 21 pediatric patients aged between 1 and 17 years old who received allo-SCT and had radiological and clinical findings consistent with pulmonary cGVHD. Median time between onset of allo-SCT and pulmonary complications was 213 days (interval 635-152 days). All patients have undergone non-enhanced chest computed tomography scan with 16 slice Brightspeed, GE Healthcare. The clinical data was reviewed and none of the patients had iatrogenic TALS that could occur due to transbronchial lung biopsy or mechanical ventilation.

#### RESULTS

The CT findings of BO were mosaic perfusion 13/21 (62%), patchy peribronchial consolidation 3/21 (14%), air trapping 2/21 (9%), diffuse 'ground glass opacities' 4/21 (19%) and 4/21 (19%) demonstrated extra-alveolar air collections. 1/4 patients with airleak syndrome was asymptomatic while the other 3/4 showed clinical symptoms. Their CT findings were consistent with spontaneous pneumothorax 2/21 (9%) and combined pneumomediastinum with pneumothorax and subcutaneous emphysema 2/21 (9%). All patients with thoracic air-leak syndrome did not have other BO-related CT features prior to spontaneous pneumothorax. All patients had follow up chest CT exams. The follow up period ranged from few weeks to months. Most patients with BO had shown clinical improvement and radiological resolution of their pulmonary symptoms. 3 patients have recovered from TALS.

#### CONCLUSION

Extra-alveolar air on CT in posttransplant patients can be manifistation of BO. If not diagnosed early it can lead to potentially lethal outcome. Clinical manifestation of TALS varied from radiological findings alone in asymptomatic patients to severe respiratory insufficiency.

# **CLINICAL RELEVANCE/APPLICATION**

Chest CT should be modality of choice for initial and follow up diagnostic of TALS in post transplant pediatric patients with the suspected BO or proven pulmonary cGVHD with acute onset of dyspnea and/or chest pain.



### PD211-SD-MOA2

### A Comparative Study of Free-Breathing StarVIBE with Conventional VIBE in Fetal Brain T1WI Imaging

Monday, Nov. 26 12:15PM - 12:45PM Room: PD Community, Learning Center Station #2

### FDA Discussions may include off-label uses.

#### Participants

Ming Xing, MMed, MMed, Guiyang, China (*Presenter*) Nothing to Disclose Rongpin Wang, MD, Guiyang, China (*Abstract Co-Author*) Nothing to Disclose

# For information about this presentation, contact:

1959693700@qq.com

### PURPOSE

Conventional T1WI imaging of fetal brain is difficult to obtain high quality images because of the fetal movement and the abdominal breathing movement of the pregnant women. This study is to compare the image quality of free-breathing StarVIBE sequence with conventional volumetric interpolated breath-hold examination (VIBE) sequence and to explore the application value of free-breathing StarVIBE sequence in fetal brain T1WI imaging.

#### RESULTS

The median scan time of the conventional VIBE and StarVIBE sequence is 22s and 195s, respectively. Both SNR and CNR of StarVIBE sequence were significantly higher than those of conventional VIBE sequence (p=0.000). For the image quality scores of anatomical structure of the fetal gray matter, basal ganglia, ventricle, brainstem and cerebellum, the StarVIBE sequence was significantly superior to the conventional VIBE sequence (p=0.000), and image quality scores of the two radiologists were highly consistent, wtih  $\kappa$  value of 0.646, 0.606, 0.67 and 0.758, respectively. Compared with the traditional VIBE sequence, StarVIBE can show the fetal brain structure and lesions more clearly.

### CONCLUSION

The SNR and CNR of StarVIBE sequence is significantly better than those of conventional VIBE sequence, and therefore can replace the conventional VIBE sequence for fetal brain T1WI imaging although more scan time is needed.

#### **METHODS**

This prospective study was approved by the Ethics Committee of Guizhou People's Hospital and written informed consents were obtained from all pregnant women. Eighty-one cases of pregnant women from 20 to 40 gestation weeks were enrolled in this study. Conventional VIBE and free-breathing StarVIBE sequences were performed for the fetuses' brain for T1WI imaging, respectively. The image signal-to-noise ratio (SNR) and contrast to noise ratio(CNR) were measured and calculated blindly by two radiologists. The image quality of the two sequences was evaluated by two radiologists, and the gray matter, basal ganglia, ventricle system and cerebellum were included in the evaluation. Statistical analysis was performed using SPSS version 19.0 software. Student's t test was used for comparising of SNR, CNR and image score between StarVIBE sequence and conventional VIBE sequences. The kapa-tests were used for the consistency check of the image qualities between the two radiologists. P-values<0.05 were considered to be statistically significant.

# PDF UPLOAD

http://abstract.rsna.org/uploads/2018/18016407/18016407\_oqn3.pdf



### PD212-SD-MOA3

# Feasibility of Free-Breathing T1-Weighted 3D Radial VIBE for Fetal MRI

Monday, Nov. 26 12:15PM - 12:45PM Room: PD Community, Learning Center Station #3

### **Participants**

Taotao Sun, MD, Shanghai, China (Presenter) Nothing to Disclose Ling Jiang, Shanghai, China (Abstract Co-Author) Nothing to Disclose Zhaoxia Qian, Shanghai, China (Abstract Co-Author) Nothing to Disclose Zhongshuai Zhang, Shanghai, China (Abstract Co-Author) Nothing to Disclose

### For information about this presentation, contact:

graciass@gmail.com

### PURPOSE

Traditional breath-hold fat-suppressed MR T1-weighted sequences (T1W) may be degraded by motion artifacts from both mother and fetus. The purpose of this study is to evaluate the role of a T1-weighted 3D radial VIBE in multiple sections of the fetus including head and neck, chest and abdomen as compared with standard breath-hold T1W images.

### **METHOD AND MATERIALS**

The study was approved by the hospital Ethics Committee. Thirty one pregnant women with gestation age of 26.3 (20.4-36.3) weeks who underwent fetal MRI were included. All the examinations were performed in a 1.5 T MR scanner (Area, SIEMENS, Erlangen, Germany). Both radial VIBE and conventional T1W sequence were performed. Image quality is evaluated by two radiologists blinded to the acquisition schemes on a five-point scale, with higher score indicating a more optimal examination. Mixed-model analysis of variance and interobserver variability assessment were performed.

#### RESULTS

Images obtained with the radial VIBE sequence have a higher overall image quality score than that of T1W images  $(3.77 \pm 0.76 \text{ vs})$  $3.13 \pm 0.72$ , p = 0.001) and less motion artifact (p = 0.001). Radial VIBE images show better tissue contrast and tissue edge clarity in head and neck region (p<0.001). Fair to good radial VIBE image quality was observed in chest region compared to conventional T1W images (2.97  $\pm$  1.1 vs 2.19  $\pm$  0.90, p = 0.002). The score in abdomen and pelvis region the following parameters are significantly better for the radial-VIBE sequence than that for conventional breath-hold T1W imaging: overall image quality (3.61 ± 1.02 vs 2.77  $\pm$  0.84, p = 0.002), hepatic vessel clarity (p < 0.0001) and intestinal conspicuity (p = 0.04). Streaking artifacts were found only on radial VIBE images.

### CONCLUSION

T1W images acquired by the radial VIBE sequence has a overall better image quality than those obtained by the conventional breath-hold fat-suppressed T1-weighted sequence for fetal MRI.

# **CLINICAL RELEVANCE/APPLICATION**

Traditional breath-hold fat-suppressed MR T1-weighted sequences (T1W) may be degraded by motion artifacts from both mother and fetus. Also breath-hold can be relatively difficult for late trimester pregnancies, twin pregnancies or obese patients. Freebreathing T1-weighted 3D radial VIBE is used in various adult settings. In this study we attempt to evaluate the role of a radial VIBE serie in multiple sections and explore its possible further application.



### PD213-SD-MOA4

# Image Quality and Incidental Findings of Chest MRI in a Large Pediatric Population-Based Study

Monday, Nov. 26 12:15PM - 12:45PM Room: PD Community, Learning Center Station #4

# Awards

### Student Travel Stipend Award

#### Participants

Alice Pittaro, Rotterdam, Netherlands (*Presenter*) Nothing to Disclose Liesbeth Duijts, Rotterdam, Netherlands (*Abstract Co-Author*) Nothing to Disclose Piotr A. Wielopolski, PhD, Rotterdam, Netherlands (*Abstract Co-Author*) Nothing to Disclose Harm A. Tiddens, MD, Rotterdam, Netherlands (*Abstract Co-Author*) Nothing to Disclose Meike W. Vernooij, MD, Rotterdam, Netherlands (*Abstract Co-Author*) Nothing to Disclose Mariette Kemner - Corput van de M.P.C., Rotterdam, Netherlands (*Abstract Co-Author*) Nothing to Disclose Vincent Jaddoe, Rotterdam, Netherlands (*Abstract Co-Author*) Nothing to Disclose Pierluigi Ciet, MD, Rotterdam, Netherlands (*Abstract Co-Author*) Nothing to Disclose

### For information about this presentation, contact:

p.ciet@erasmusmc.nl

#### PURPOSE

To describe image quality (IQ) and incidental findings (IF) of chest MRI in a large pediatric cohort from a population-based prospective multi ethnic study.

### **METHOD AND MATERIALS**

Two end-inspiratory (INSP) and end-expiratory (EXP) breath-old chest MRI scans were performed in 2498 healthy children using a spirometry-gated 3D spoiled gradient echo sequence (TR/TE/FA/voxel-resolution=1.6ms/0.7ms/2°/2mm isotropic) in a 3 Tesla scanner. IQ was assessed using 5-point scale from poor (score 1) to excellent (score 5). IFs were classified in clinically relevant or non clinically relevant. Imaging artifacts included four main categories (motion, wrap, ghosting, low signal-to-noise ratio). Analysis was conducted by two indipendent observers. Descriptive statistic was used to assess IQ, IFs and artifacts. Inter-observer agreement of IQ was assessed with Intra-class Correlation Coefficient (ICC) and Bland-Altman plots. Significant differences between IQ-INSP and IQ-EXP were assessed with Wilcoxon test.

#### RESULTS

47 children were excluded for missing data (i.e. no inspiratory or expiratory scans). Final analysis included 2451 children (median age 9.9 years, range 9.5-11.9). Median IQ was good to excellent 4.5 (Interquartile Range, IQR=4-5). Median IQ-INSP and IQ-EXP was 4.5 (IQR=4-5) for both. Despite deemed excellent, IQ-EXP was significantly lower than IQ-INSP (Z=-8.487, p<0.0001). 1,7% of the cohort subjects had clinically relevant IFs, 45% had non-clinically relevant IFs. Clinically relevant IFs included pulmonary nodules (diameter >10 mm), severe tracheomalacia (collapse>70%), severe trapped-air (>25% lung lobe volume) and congenital abnormalities (i.e. sequester). Non-clinically relevant IFs were: mild trapped-air (23,8%), atelectasis (15,4%) and mild tracheomalacia (4,5%). IQ was mostly affected by motion artifact (31,9%), fat ghosting (7,9%) or both (6,3%). Inter-observer agreement for IQ was good (ICC=0.7, 95% C.I 0.48-0.83).

#### CONCLUSION

Chest MRI is a robust technique for large cohort studies in children. Clinically relevant IFs are rare in children, but a large percentage of the cohort had non-clinically relevant IFs.

### **CLINICAL RELEVANCE/APPLICATION**

Trapped-air, atelectasis and mild tracheomalacia are common non-clinically relevant incidental findings on chest MRI in healthy children.



### PD214-SD-MOA5

Non-Breath Hold Dynamic Contrast Enhanced Abdominal and Thoracic MRI in Pediatric Oncologic Patients Using a GRASP-Sequence at 3T

Monday, Nov. 26 12:15PM - 12:45PM Room: PD Community, Learning Center Station #5

# Participants

Guenther K. Schneider, MD, PhD, Homburg, Germany (*Presenter*) Research Grant, Siemens AG; Speakers Bureau, Siemens AG; Speakers Bureau, Bracco Group; Research Grant, Bracco Group;

Arno Buecker, MD, Homburg, Germany (*Abstract Co-Author*) Consultant, Bracco Group; Speaker, Bracco Group; Consultant, Medtronic plc; Speaker, Medtronic plc; Research Grant, Novartis AG; Research Grant, GlaxoSmithKline plc; Research Grant, Biotest AG; Research Grant, OncoGenex Pharmaceuticals, Inc; Research Grant, Bristol-Myers Squibb Company; Research Grant, Eli Lilly & Company ; Research Grant, Pfizer Inc; Research Grant, F. Hoffmann-La Roche Ltd; Research Grant, sanofi-aventis Group; Research Grant, Merrimack Pharmaceuticals, Inc; Research Grant, Sirtex Medical Ltd; Research Grant, Concordia Healthcare Corp; Research Grant, AbbVie Inc; Research Grant, Takeda Pharmaceutical Company Limited ; Research Grant, Merck & Co, Inc; Research Grant, Affimed NV; Research Grant, Bayer AG; Research Grant, Johnson & Johnson; Research Grant, Seattle Genetics, Inc; Research Grant, Onyx Pharmaceuticals, Inc; Research Grant, Synta Pharmaceuticals Corp; Research Grant, Siemens AG; Research Grant, iSYMED GmbH; Research Grant, Abbott Laboratories; Co-founder, Aachen Resonance GmbH Paul S. Raczeck, MD, Homburg, Germany (*Abstract Co-Author*) Nothing to Disclose

### For information about this presentation, contact:

dr.guenther.schneider@uks.eu

### PURPOSE

One of the few advantages of modern CT scanning over MRI in pediatric abdominal and thoracic imaging is the possibility to perform dynamic CE studies without the need of a breath-hold due to the very fast scanning capabilities of multislice CT. However, new MRI techniques like Golden-Angel Radial Sparce Parallel MRI (GRASP) allow for free-breathing dynamic contrast enhanced volumetric imaging, which can even offer more information as compared with arterial and portalvenous CE CT. The aim of our study was to evaluate GRASP sequences in evaluation of abdominal and thoracic malignancies in pediatric patients.

#### **METHOD AND MATERIALS**

In 26 pediatric patients MRI was performed on a 3T scanner (Siemens,VIDA) with either the use of a dedicated pediatric body coil or a standard abdominal multichannel coil. Patients below 10 years of age were sedated for imaging studies. MR protocol included non breath-hold unenhanced radial T2w images, radial T1w and T1w fs VIBE sequences as well as DWI. During contrast medium administration (0.05 mmol/kg MultiHance,Bracco) a GRASP Sequence with a temporal resolution of 4 - 6 sec and reconstruction of 16 - 26 phases was performed. After CM injection radial VIBE sequences were repeated. In patients with liver lesions another set of radial VIBE sequences was performed in the biliary phase of contrast medium excretion to further characterize lesions. Patient population included hepatoblastoma, neuroblastoma, nephroblastoma, rhabdoid tumor, Hodgkin- and Non-Hodgkin lymphoma, different types of sarcoma, teratoma and abdominal or thoracic metastases of different primary tumors.

# RESULTS

Dynamic non-breath-hold imaging of the abdomen was successful in all cases and even excellent in thoracic imaging depiction of perfusion characteristics of tumors. Characterization of liver lesions based on the typical enhancement characteristics was feasible in all cases and in a similar manner renal and adrenal tumors could be evaluated.

### CONCLUSION

Non-breath-hold dynamic contrast enhanced imaging is feasible in pediatric patients using GRASP sequence and gives detailed information about perfusion characteristics of abdominal and thoracic tumors without radiation exposure.

# **CLINICAL RELEVANCE/APPLICATION**

Non-breath-hold dynamic CE abdominal and thoracic imaging is possible using GRASP sequence. Without radiation exposure or the need for intubation detailed information about perfusion characteristics of tumors can be gained in MRI.



### PH210-SD-MOA1

Medical Student Device Design for Interventional Radiology: Design of a Needle Stabilization Device for CT-Guided Procedures

Monday, Nov. 26 12:15PM - 12:45PM Room: PH Community, Learning Center Station #1

# Awards

# **Student Travel Stipend Award**

#### Participants

Alexander W. Song, BS, Washington, DC (*Presenter*) Nothing to Disclose Olumide Olulade, PhD, Washington, DC (*Abstract Co-Author*) Nothing to Disclose Shannon A. Sullivan, BS, Washington, DC (*Abstract Co-Author*) Nothing to Disclose Hamza Haider, BS, Glen Ellyn, IL (*Abstract Co-Author*) Nothing to Disclose Roger C. Lin, MD, PhD, Silver Spring, MD (*Abstract Co-Author*) Founder, Ultraviolet Interventions, Inc

### For information about this presentation, contact:

#### awsong4@gmail.com

### CONCLUSION

The Stanford Biodesign process is a structured process that can be applied to problems in radiology. In one application, medical students designed a low-cost, lightweight device compatible with various imaging environments that provides stability and accurate guidance of a biopsy needle at multiple angles. Reference 1. Sista et al. Applying a structured innovation process to interventional radiology: a single-center experience. JVIR 2012;23(4):488-94.

#### Background

Innovative medical devices can be developed through the Stanford Biodesign process. CT-guided biopsy is a commonly performed procedure in which tissues are sampled for testing. However, needle stability is a persistent problem without a simple, low-cost, effective solution.

# **Evaluation**

Medical students interested in interventional radiology used the Stanford Biodesign process[1] to address a clinical need. The process consists of observing problematic clinical situations, creating a clinical need statement, evaluating pre-existing solutions, and brainstorming new solutions. We identified a need for needle stabilization during CT-guided biopsies. Biopsy needles are placed using hand-eye coordination, but once released, its position changes with gravity. Existing solutions are complex, bulky, expensive, or non-disposable. Some may interfere with imaging or cannot fix angles of needle entry. Specifications were developed that identified essential requirements of a solution: radiolucent, sterile, disposable, lightweight, able to hold multiple needle sizes at multiple angles, readjustable, usable on hairy skin, and unaffected by body fluids.

#### Discussion

Two needle stabilization devices were designed: 1) A semisolid, gel-like dome placed directly on a patient, and 2) a perforated, plastic dome with channels for needle entry. The gel dome provides needle support from the semisolid material, whereas the plastic dome supports the needle from its rigid shell. Both accommodate a variety of entry angles and readjustment. The semisolid dome uses an adhesive base to attach to skin. The plastic dome can be fixed in place with adhesive tape and has two walls with layer of air that can be suctioned out, creating a vacuum to seal the device to skin.



### PH211-SD-MOA2

Chemical Exchange Saturation Transfer MR Imaging for Mediastinal Masses: Phantom Study and Clinical Cases

Monday, Nov. 26 12:15PM - 12:45PM Room: PH Community, Learning Center Station #2

### Participants

Masahiro Yanagawa, MD, PhD, Suita, Japan (*Presenter*) Nothing to Disclose Hiroyuki Tarewaki, Osaka, Japan (*Abstract Co-Author*) Nothing to Disclose Akinori Hata, MD, Suita, Japan (*Abstract Co-Author*) Nothing to Disclose Tetsuya Wakayama, PhD, Hino, Japan (*Abstract Co-Author*) Employee, General Electric Company Osamu Honda, MD, PhD, Suita, Japan (*Abstract Co-Author*) Nothing to Disclose Noriyuki Tomiyama, MD,PhD, Suita, Japan (*Abstract Co-Author*) Nothing to Disclose Noriko Kikuchi, Suita, Japan (*Abstract Co-Author*) Nothing to Disclose Tomo Miyata, MD, Suita, Japan (*Abstract Co-Author*) Nothing to Disclose Mitsuharu Miyoshi, Hino, Japan (*Abstract Co-Author*) Nothing to Disclose

### PURPOSE

To compare chemical exchange saturation transfer (CEST) effects under various conditions of the respiratory gating (RG) on dynamic phantoms, and to quantify CEST effects of mediastinal masses in a clinical setting.

### **METHOD AND MATERIALS**

In a phantom study, 5 raw eggs were used as materials for the CEST effect. Five volunteers (mean age,25 years) with normal respiratory rates (RR) (mean,15/min;range,11-22/min) were included. First, each egg on the static condition (CO) was scanned on amide proton transfer (APT)-weighted CEST MR imaging using echo planar imaging after a series of magnetization transfer(MT) pulses. Next, each egg on the anterior chest of the volunteers was scanned on CEST MR imaging under various conditions of the RG: C1, voluntary breathing without the RG; C2, voluntary breathing with the RG; C3, slow breathing(half the normal RR) with the RG; and C4, fast breathing(normal RRx2) with the RG. A region of interest(ROI) was placed over the egg white, making it as large as possible to minimize the effects of inhomogeneity. Each z-spectrum within the ROI(offset frequency, 7 to -7ppm) was computationally generated. An MT ratio (MTR) asymmetry at 3.5 ppm (MTRasym[3.5ppm]) was measured as a CEST effect(%): MTRasym[3.5ppm]=MTR[+3.5ppm]-MTR[-3.5ppm]. The mean MTR values at z-spectrum of 5 volunteers were statistically compared among C0-4 using Friedman test followed by post-hoc tests. In a clinical study, 4 solid mediastinal masses(2thymomas, 1thymic carcinoma, 1embryonal carcinoma) and 3 cystic mediastinal masses(thymic cysts) were scanned on CEST MR imaging without the respiratory gating in order to quantify MTRasym[3.5ppm].

# RESULTS

The mean MTR values at z-spectrum had no significant differences among C0-4 (p>0.05). Each mean MTRasym[3.5ppm] was as follows:C0,16%; C1,11.9%; C2,10.9%; C3,11.9%; and C4,11.4%. MTRasym[3.5ppm] of 4 solid mediastinal masses (mean $\pm$ SD) were 9.2% $\pm$ 7.1. Those of 3 cystic mediastinal masses were -24.4% $\pm$ 19.9.

# CONCLUSION

Even under respiration, APT-weighted CEST effects equivalent to those at static condition can be acquired. In a clinical setting, APT-weighted CEST effects of solid mediastinal masses are accurately quantifiable, but those of cystic mediastinal masses are not.

### **CLINICAL RELEVANCE/APPLICATION**

APT-weighted CEST MR imaging under respiration is a potential tool for diagnosing solid mediastinal masses.



### PH212-SD-MOA3

Accuracy of Volume Measurements of Coronary Calcification at CT Using Model-Based Iterative Reconstruction: A Phantom Study

Monday, Nov. 26 12:15PM - 12:45PM Room: PH Community, Learning Center Station #3

# Participants

Toru Higaki, PhD, Hiroshima, Japan (*Presenter*) Nothing to Disclose Fuminari Tatsugami, Hiroshima, Japan (*Abstract Co-Author*) Nothing to Disclose Chikako Fujioka, RT, Hiroshima, Japan (*Abstract Co-Author*) Nothing to Disclose Kazushi Yokomachi, PhD, Hiroshima, Japan (*Abstract Co-Author*) Nothing to Disclose Yuko Nakamura, MD, Hiroshima, Japan (*Abstract Co-Author*) Nothing to Disclose Kazuo Awai, MD, Hiroshima, Japan (*Abstract Co-Author*) Nothing to Disclose Kazuo Awai, MD, Hiroshima, Japan (*Abstract Co-Author*) Research Grant, Canon Medical Systems Corporation; Research Grant, Hitachi, Ltd; Research Grant, Fujitsu Limited; Research Grant, Bayer AG; Research Grant, DAIICHI SANKYO Group; Research Grant, Eisai Co, Ltd; Medical Advisory Board, General Electric Company; ;

#### PURPOSE

The assessment of coronary calcification on CT scans is important for predicting the outcome in patients with coronary artery disease. Recently, a lot of image reconstruction methods have been developed, they have own properties about image quality. The purpose of this study is to assess the accuracy of volumetry for coronary calcification using various image reconstruction method.

#### **METHOD AND MATERIALS**

Our coronary calcification phantom (body diameter 300 x 200 mm) was created with a 3D printer (Fig. 1). Soft tissue consisted of an acrylic material, the area of the cortical bone was filled with plaster. The vessel was an acrylic pipe filled with 2% gelatin (Fig. 2). Lipiodol diluted with poppy oil was used to create the calcification models [200-, 400-, and 600 Hounsfield units (HU), volume 1.0-, 3.0-, and 5.0 mm3, respectively]. They were inserted into the gelatin with a micro-syringe. Scanning was on a 320-row detector CT instrument (Aquilion ONE, Canon Medical Systems Corp., Otawara, Japan). The tube voltage was 120 kV; the tube current was determined as the target noise level of 23 HU. Filtered back projection (FBP), hybrid iterative reconstruction (hIR), and model-based iterative reconstruction (mbIR) were the image reconstruction methods. The calcification volume was measured with the threshold method; the threshold value was 50% of the peak CT number for each model.

#### RESULTS

With the 5.0 mm3 model, the volume on mbIR scans was 4.94-, 4.96-, and 5.29 mm3 at 200-, 400-, and 600 HU, respectively (Fig. 3). Spatial resolution was best on mbIR images, rendering it the most accurate reconstruction method. This was also true for 3.0 mm3 models. With all reconstruction methods the accuracy of volumetry decreased as the concentration of the object decreased. With all reconstruction methods, the measured volume of 1.0 mm3 models were inaccurate, possibly due to the limited physical specifications of CT scanner.

### CONCLUSION

The best reconstruction method for the quantitative assessment of coronary artery calcification was mbIR. However, the accurate assessment of small calcifications remains difficult even on mbIR.

# **CLINICAL RELEVANCE/APPLICATION**

The scoring of coronary artery calcification is most accurate on CT scans with mbIR.



### PH213-SD-MOA4

### Eliminating Susceptibility Induced Hyperintensities in Ultra High Field T1w MPRAGE Brain Images

Monday, Nov. 26 12:15PM - 12:45PM Room: PH Community, Learning Center Station #4

### **Participants**

Ruoyun Ma, Minneapolis, MN (*Presenter*) Nothing to Disclose Thomas R. Henry, MD, Minneapolis, MN (*Abstract Co-Author*) Nothing to Disclose Pierre-Francois Van de Moortele, Minneapolis, MN (*Abstract Co-Author*) Nothing to Disclose

### For information about this presentation, contact:

rma@umn.edu

### PURPOSE

Hyperintensities in inferior brain regions close to air-tissue boundaries are commonly seen in MPRAGE images acquired at ultra high field(UHF), leading to the loss of anatomical information and severe problems in segmentation process(Seiger et al.,2015). These artefacts stem from local frequency offsets exceeding the inversion pulse bandwidth(BW) and could be mitigated by shifting the center frequency of the inversion pulse by 200Hz(Wiggins,2008). However, we found this approach alone to be insufficient at 7T. In this study, this artefact was eliminated by increasing the inversion pulse BW additionally to applying a frequency offset  $\Delta f$ .

### METHOD AND MATERIALS

A standard MPRAGE sequence was modified, allowing user to change the RF frequency and duration(standard:10240us) of the hyperbolic secant inversion pulse. BW was increased by shortening the pulse duration. The modified sequence was tested on 7 subjects on a 7T MRI scanner(Siemens Magnetom,Erlangen,Germany), equipped with a 32 channel head coil(Nova Medical,Wilmington,MA). Gradient echo B0 maps were acquired to assess the frequency variation within the brain. Different combinations of the  $\Delta f$  and BW were applied to test optimal parameters to achieve the complete inversion in all brain areas. The specific absorption rate(SAR) was monitored for all scans.

#### RESULTS

The frequency difference between the inferior frontal area and the center of the brain ranged from 240Hz to 360Hz throughout the recruited subjects. The amount of incomplete inversion was reduced when increasing  $\Delta f$ . However, additional hyperintensities were observed in other brain areas presenting a frequency drift of -240Hz when  $\Delta f$  reached 250Hz without increasing BW. The optimal combination of pulse duration and  $\Delta f$  was determined to be 6144us and 300Hz, resulting in whole brain fully complete inversion. Image quality improvement was particularly pronounced in the inferior frontal and temporal lobes. No difference in image quality was noticed when  $\Delta f$  varied from 240Hz to 360Hz. SAR for all scan sessions was below 40% of the maximum allowed.

### CONCLUSION

Robust elimination of susceptibility induced hyperintensities in UHF MPRAGE images, is demonstrated by shifting the inversion frequency by 300Hz and reducing inversion pulse duration by 20%.

### **CLINICAL RELEVANCE/APPLICATION**

Eliminating signal hyperintensities in UHF T1w MPRAGE images allows for recovering missing anatomical information and avoiding severe brain segmentation errors.



### PH214-SD-MOA5

Potential of a New High Capacity X-Ray Tube to Enable Low-kV Contrast-Enhanced CT Imaging of Large Patients with Improved Image Quality: A Phantom Study

Monday, Nov. 26 12:15PM - 12:45PM Room: PH Community, Learning Center Station #5

### Participants

Justin B. Solomon, PhD, Durham, NC (*Presenter*) License agreement, Sun Nuclear Corporation; License agreement, 12 Sigma Technologies

Dominic Crotty, PhD, Waukesha, WI (Abstract Co-Author) Employee, General Electric Company

Daniele Marin, MD, Durham, NC (Abstract Co-Author) Research support, Siemens AG

Rendon C. Nelson, MD, Durham, NC (*Abstract Co-Author*) Research Consultant, General Electric Company; Research Consultant, Nemoto Kyorindo Co, Ltd; Consultant, VoxelMetrix, LLC; Co-owner, VoxelMetrix, LLC; Advisory Board, Bracco Group; Advisory Board, Guerbet SA; Research Grant, Nemoto Kyorindo Co, Ltd; Speakers Bureau, Bracco Group; Royalties, Wolters Kluwer nv Ehsan Samei, PhD, Durham, NC (*Abstract Co-Author*) Research Grant, General Electric Company; Research Grant, Siemens AG; Advisory Board, medInt Holdings, LLC; License agreement, 12 Sigma Technologies; License agreement, Gammex, Inc

### For information about this presentation, contact:

justin.solomon@duke.edu

#### PURPOSE

To demonstrate the potential of a new high-capacity x-ray tube to image larger patients at low kV with improved image quality for a contrast-enhanced task, compared to a current generation standard capacity tube.

# METHOD AND MATERIALS

A multi-sized phantom (Mercury 4.0, Gammex) was imaged on two iterations (next gen. [NG] high capacity and current gen. [CG] standard capacity tube) of a modern CT scanner (Revolution CT, GE Healthcare), at 70, 80, and 120 kV (CG only) based on a routine 120kV abdomen pelvis protocol. For each image series and phantom size (160 - 355 mm diameter), noise power spectrum, task transfer function (TTF), iodine contrast, and detectability index (d', 5 mm iodinated lesion detection task) were measured using IQ analysis software. Three metrics were calculated for each tube and kV setting: dose efficiency, defined as d'/sqrt(CTDIvol) at a reference size (310 mm); f50%, defined as the 50% TTF spatial frequency; and the maximum size at which the d' at low-kV was greater than or equal to the d' at 120 kV.

### RESULTS

Dose efficiency was estimated at 33, 32, and 21 d'/sqrt(mGy) for 70, 80, and 120 kV, respectively, indicating that low-kV imaging is potentially more dose efficient for detecting 5 mm iodinated lesions. f50% was 0.30, 0.36, 0.38, 0.40, and 0.39 cycles/mm for 70 kV-CG, 80 kV-CG, 120 kV-CG, 70 kV-NG, and 80 kV-NG, respectively, demonstrating comparable image resolution at low-kV in the NG tube compared to CG at 120 kV. Without changing the routine protocol, for the task studied, the higher max output capacity of the NG tube enabled a 16% and 10% increase in the diameter of the largest patient that could be imaged at 70 kV and 80 kV, respectively. Additional IQ improvements for larger patients may be possible using further optimizations to current protocol settings.

### CONCLUSION

The NG tube at low kV achieved superior dose efficiency and detectability at larger phantom sizes compared to the CG tube due to higher mA capacity. Furthermore, the NG tube achieved comparable image resolution to that of today's routine abdomen pelvis protocol.

### **CLINICAL RELEVANCE/APPLICATION**

A new high-capacity x-ray tube stands to overcome limitations of traditional limited capacity tubes, offering the low-kV benefits of increased dose efficiency and improved IQ to a broader population.



### PH215-SD-MOA6

A CT Protocol Management System for Reviewing and Version Tracking of CT Protocols from Multiple CT Vendors

Monday, Nov. 26 12:15PM - 12:45PM Room: PH Community, Learning Center Station #6

### Participants

Jia Wang, PhD, Stanford, CA (*Presenter*) Nothing to Disclose Biying Kong, MS, Stanford, CA (*Abstract Co-Author*) Nothing to Disclose Lior Molvin, Stanford, CA (*Abstract Co-Author*) Speakers Bureau, General Electric Company Fangmingyu Yang, Stanford, CA (*Abstract Co-Author*) Nothing to Disclose Dan Giulvezan, Stanford, CA (*Abstract Co-Author*) Nothing to Disclose Christoph Zorich, Stanford, CA (*Abstract Co-Author*) Nothing to Disclose Dominik Fleischmann, MD, Stanford, CA (*Abstract Co-Author*) Research Grant, Siemens AG

#### For information about this presentation, contact:

wangjia@stanford.edu

# PURPOSE

To develop a CT protocol management system that allows web-based protocol review, protocol version tracking, and compatibility to CT scanners of different vendors and models

#### **METHOD AND MATERIALS**

A CT protocol management system was developed using open source software (Python 3.6.1) to track all CT protocols from overall 16 CT scanners at our institution (8 models from GE HealthCare, 5 models from Siemens, and one model from Canon). CT protocol information is obtained using either data transferring via remote access or manual exporting, depending on the scanner models. On a routine basis or when necessary, CT protocols of all scanners are obtained and fed into the system for version tracking. Any changes of scanning or reconstruction parameters, addition, or deletion of any protocols are recorded and examined. A webpage was created to reflect the latest protocol data of all CT scanners and display the detailed scanning and reconstruction parameters. This system is used in two on-going CT protocol QA projects: 1. An institution-wide protocol review; 2. Monitoring of changes of all protocols on all CT scanners on a monthly basis.

#### RESULTS

The webpage of this system allows user to first select a target CT scanner, then narrow the list of protocols by clinical sections and age groups. Once a protocol is chosen, the scanning and reconstruction parameters are displayed (Fig.1). As an example of the protocol review project, the accuracy of naming, scanning and reconstruction parameters of 93 protocols of a CT scanner (Siemens FORCE) were examined. Corrections and improvement were made during the reviewing process. For version tracking of all 1864 CT protocols on 16 scanners between two recent months, 121 protocols were revised, 23 new protocols added, and 127 protocols deleted. Majority of revisions and deletions happened on two scanners that underwent a recent systematic protocol review.

#### CONCLUSION

A web based CT protocol management system was developed using open source software to assist CT protocol review, and automatically track changes of protocols for CT scanners from multiple vendors.

### **CLINICAL RELEVANCE/APPLICATION**

Quality assurance of CT protocol is critical to ensure satisfactory CT image quality and appropriate radiation dose to patients. The system developed in this work enables convenient CT protocol review and accurate protocol tracking for an institution with CT systems from different vendors.



### PH216-SD-MOA7

Breast Structural Noise Analysis of Narrow- and Wide-angle Tomosynthesis and Masking Risk Assessment for Mass Detection

Monday, Nov. 26 12:15PM - 12:45PM Room: PH Community, Learning Center Station #7

# Awards

### **Student Travel Stipend Award**

#### Participants

Hailiang Huang, MS, Stony Brook, NY (*Presenter*) Research support, Siemens AG
David A. Scaduto, PhD, Stony Brook, NY (*Abstract Co-Author*) Research Grant, Siemens AG
Anastasia Plaunova, MD, Stony Brook, NY (*Abstract Co-Author*) Nothing to Disclose
Kim Rinaldi, RT, Stony Brook, NY (*Abstract Co-Author*) Nothing to Disclose
Andreas Fieselmann, PhD, Erlangen, Germany (*Abstract Co-Author*) Employee, Siemens AG
Axel R. Hebecker, PhD, Forchheim, Germany (*Abstract Co-Author*) Employee, Siemens AG Stockholder, Siemens AG
Thomas Mertelmeier, PHD, Forchheim, Germany (*Abstract Co-Author*) Employee, Siemens AG; Stockholder, Siemens AG
Paul R. Fisher, MD, East Setauket, NY (*Abstract Co-Author*) Research Grant, Siemens AG;
Wei Zhao, PhD, Stony Brook, NY (*Abstract Co-Author*) Nothing to Disclose

### For information about this presentation, contact:

hailiang.huang@stonybrook.edu

### PURPOSE

Previous studies have indicated limited cancer detection rates for digital breast tomosynthesis (DBT) in patients with heterogeneously to extremely dense breasts. Most of these studies have used narrow-angle DBT. Increasing angular range (AR) may potentially improve mass detection in dense breast tissue by reducing breast structural noise and increasing image contrast for large masses. We analyzed and compared breast tissue structural noise using patient images from both wide- and narrow- angle DBT systems. We also analyzed the masking risk of background breast tissue and correlated the results with diagnostic performance for mass detection.

# METHOD AND MATERIALS

Under IRB-approval, DBT images for 11 patients with heterogeneously or extremely dense breasts were acquired using both the narrow-angle (Hologic Selenia Dimensions,  $AR = 15^{\circ}$ ) and the wide-angle (Siemens MAMMOMAT Inspiration,  $AR = 50^{\circ}$ ). Two breast radiologists were presented with both sets of images for each patient and compared lesion conspicuity using a five-point scale (-2: lesion much more conspicuous on narrow-angle DBT, to +2: lesion much more conspicuous on wide-angle DBT). The structural noise power spectra (NPS) were analyzed for both sets of DBT images as a quantitative measure for breast tissue overlap. The volumetric breast density map was computed using our previously developed methodology, and the local masking risk surrounding the lesions was assessed.

### RESULTS

The NPS analysis shows reduced structural noise with increasing AR. The measured clutter exponent ß are  $3.08\pm0.24$  for DBT projections,  $2.81\pm0.22$  for narrow-angle DBT and  $2.39\pm0.25$  for wide-angle DBT. The measured clutter magnitude K for wide-angle DBT is smaller ( $22.6\%\pm1.3\%$ ) than that for narrow-angle DBT using the same reconstruction method. Clinical findings show wide-angle DBT has superior mass conspicuity with a mean score of 1.58 (95% CI: 1.29, 1.79). The improvement in mass conspicuity was similar for lesions with low and high masking risk.

#### CONCLUSION

Wide-angle DBT improves mass conspicuity by reducing breast structural noise. This pilot study indicates a larger clinical trial to compare DBT with different acquisition geometries.

## **CLINICAL RELEVANCE/APPLICATION**

Tomosynthesis with wider angular range may improve mass detection for patients with heterogeneously to extremely dense breasts.



#### PH217-SD-MOA8

### Use of KZ-Space in Multislice MRI for Sub-mm Through-Plane Resolution

Monday, Nov. 26 12:15PM - 12:45PM Room: PH Community, Learning Center Station #8

#### Awards Student Travel Stipend Award

#### Participants

Soudabeh Kargar, MSc, Rochester, MN (*Presenter*) Nothing to Disclose Eric A. Borisch, Rochester, MN (*Abstract Co-Author*) Nothing to Disclose Roger C. Grimm, MS, Rochester, MN (*Abstract Co-Author*) Nothing to Disclose Akira Kawashima, MD, PhD, Scottsdale, AZ (*Abstract Co-Author*) Nothing to Disclose Eric Stinson, PhD, Rochester, MN (*Abstract Co-Author*) Nothing to Disclose Stephen J. Riederer, PhD, Rochester, MN (*Abstract Co-Author*) Nothing to Disclose

#### For information about this presentation, contact:

riederer@mayo.edu

#### PURPOSE

The goal of this work is to reconstruct T2SE images with sub-mm resolution in the slice select direction. This may allow elimination of multi-slice acquisition in other orientations and reduce the overall exam time.

### **METHOD AND MATERIALS**

Previously, iterative methods have been used in the image domain to reconstruct resolution in the slice-select direction. However, in this work we use a new approach in which slices with modest slice-to-slice overlap are juxtaposed and transformed into kZ-space. In the reconstruction process we precisely account for the slice profile due to RF excitation as well as the kZ sampling effects based on slice-to-slice spacing. This is tested on a resolution phantom, an SNR phantom, and in vivo prostate MRI with 3.2 mm slices and slice spacing of 0.8 mm (75% overlap), 1.6 mm (50%), or 3.2 mm (0%). In the reconstruction process, to compensate for the slice profile, the inversion problems due to zero crossing are addressed by Tikhonov regularization. The resolution phantom allows measurement of modulation at specific spatial frequencies (0.152 - 0.5 lp/mm) enabling construction of a modulation transfer function (MTF). In each experiment the reconstructed images are compared with the directly acquired images for reference.

### RESULTS

The results show improved resolution for slice spacings of 0.8 mm (75% overlap) and 1.6 mm (50%) vs. 3.2 mm (0%) for the resolution and prostate phantoms, and in vivo. Adjusting the regularization parameter allows control of the balance between resolution and noise level. Reconstructed images show similar quality with the images that were acquired directly. When 0.8 mm slice spacing is used for sagittal acquisition, the 0.5 lp/mm resolution pattern is clearly visible in the reconstructed axial image. Visualization of this pattern demonstrates sub-mm resolution.

# CONCLUSION

In this work we have demonstrated the newly proposed kZ-space-based technique that provides finer through-plane resolution than the slice thickness and is superior to simple zero padding. This method is particularly applicable to multislice scans in which averaging is used.

### **CLINICAL RELEVANCE/APPLICATION**

2D multi-slice T2SE acquisition is a mainstay of clinical MRI, used in essentially all exams. In this work we overcome the limits of current methods and demonstrate the reconstruction of sub-mm through plane resolution.



### QI005-EB-MOA

# Eliminating Radiology Specimen Labeling Errors Using a 2-Person Check

Monday, Nov. 26 12:15PM - 12:45PM Room: QR Community, Learning Center Hardcopy Backboard

# Awards Quality Improvement Reports Award

Identified for RadioGraphics

# Participants

Michael A. Schwartz, BA,BS, Scottsdale, AZ (*Presenter*) Nothing to Disclose Howard Osborn, RN, Scottsdale, AZ (*Abstract Co-Author*) Nothing to Disclose Jennifer Palmieri, RT, Phoenix, AZ (*Abstract Co-Author*) Nothing to Disclose Bhavika K. Patel, MD, Phoenix, AZ (*Abstract Co-Author*) Speaker, Hologic, Inc Jonathan A. Flug, MD, MBA, Phoenix, AZ (*Abstract Co-Author*) Nothing to Disclose

### For information about this presentation, contact:

Schwartz.Michael@mayo.edu

### PURPOSE

Improper specimen labeling of biopsy samples is a serious problem that may be improved through quality improvement methods. Misidentification of samples can cause substantial harm to patients through diagnostic delays, administration of inappropriate treatments, and can result in a loss of trust in healthcare. Labeling errors of specimens occur at a rate of 1 to 50 per 1000 labels and laboratories with ongoing quality monitors for specimen identification are associated with lower labeling error rates. 2-Step verification has been used effectively to prevent medication errors and can be translated into the practice of radiology specimen labeling.

# METHODS

Quality improvement meetings in the radiology department identified a reduced rate of labeling errors specifically in breast imaging, which utilized a process consisting of a 2-person verification of samples before being sent to pathology. In the fourth guarter of 2017, the radiology department implemented a 2-person verification pause in the specimen collection procedure workflow throughout all care teams obtaining biopsies in the radiology department. The specimen labeling workflow is as follows with the addition at Step 11: Pre-Procedure 1) Verify orders 2) Gather supplies, including generating labels and forms Procedural Room 3) Clean Sweep (staff & room) 4) Prepare for procedure, including setting up specimen containers, labels and requisitions 5) Identify patient - escort/transport to room as needed 6) Pause and review labels and requisition before calling Radiologist 7) Procedural pause when all staff present, to include verification of correct labels 8) Procedure complete/specimen collected 9) Complete labeling process, ensuring requisitions are complete and correct Radiologist signs requisition as appropriate 10) Discharge patient from area 11) Final verification with 2nd staff member 12) Package specimen appropriately and deliver to pathology This study attempts to identify the effectiveness of the 2-person verification on the labeling error rate overall and among care teams. Data on radiology specimen labeling errors were collected from the Radiology department's Statit Scorecard and the Safety Even Report From database from Q1 of 2015 through Q1 of 2018. Information on specimen labeling error rates were determined by looking at the number of errors for all modalities as well as individual areas such as ultrasound, general imaging, CT, and breast imaging. Labeling errors were classified and weighted based on severity using a scale for both patient identification and specimen information as follows respectively: Misidentification, Mismatch, Illegible, and No Label. The number of errors per quarter and severity were assessed from before and after the 2-person verification was implemented in Q4 2017.

#### RESULTS

31 specimen labeling errors were self-reported by the procedural staff over a period of 12 quarters (3 years) resulting in an error rate of 2.6 errors per quarter with an average severity rating of 4.4. Mismatch of specimen labels accounted for 48.4%(15/31) of the labeling errors. The next highest error was for specimens sent without patient ID labels, occurring at a rate of 35.5%(11/31). The ultrasound modality had the most frequent labeling errors detected, occurring in 54.8%(17/31) of the samples studied. Since the intervention was implemented, one mismatch patient identification labeling error occurred in ultrasound in Q1 of 2018, representing a severity rating of 5. Ultrasound had the highest frequency of specimen labeling errors with one occurring even after numerous interventions. Constraints on time and feelings of production pressure may contribute to process deviation, resulting in workflow shortcuts that increase the risk of errors. Mismatching specimen labels as well as samples not containing a patient identification label indicate a need for greater adherence for the 2-person verification process. More time is needed to assess the effectiveness of the modified workflow procedure as Poisson's test was not significant (x=1, $\lambda$ =2.583,P(X<=1)=.271).

# CONCLUSION

Quality improvement analysis as well as refinement of workflow procedures can help reduce labeling error rates and improve reliability of processes. Finding outliers within one's institution can provide an excellent option for identifying best practices and disseminating those practices across service lines. As institutions continue to grow and merge, this will be both a challenge and opportunity for improvement. It is important to work with staff and other stakeholders to come up with innovative solutions that can be effectively implemented in the workplace. Additional interventions such as the application of bar code-based patient identification may be applied to radiology samples, as it has shown effectiveness in other areas of medicine. Understanding process constraints, empowering medical staff, and educating providers on the dangers of labeling errors will benefit patients and improve quality of care.



# QI007-EB-MOA

Targeting the Root Causes of Dissatisfaction with Root Cause Analysis: A Project to Improve the Process Around Patient Safety Events in Radiology

Monday, Nov. 26 12:15PM - 12:45PM Room: QR Community, Learning Center Hardcopy Backboard

# Awards

#### Quality Improvement Reports Award Identified for RadioGraphics

#### Participants

Ashley Rosier, Rochester, MN (*Presenter*) Nothing to Disclose Anil N. Kurup, MD, Rochester, MN (*Abstract Co-Author*) Research Grant, Galil Medical Ltd; Research Grant, EDDA Technology, Inc; Royalties, Wolters Kluwer nv Laura Tibor, MBA, BEng, Rochester, MN (*Abstract Co-Author*) Nothing to Disclose Karl N. Krecke, MD, Rochester, MN (*Abstract Co-Author*) Nothing to Disclose Carrie Phillips, Rochester, MN (*Abstract Co-Author*) Nothing to Disclose

#### For information about this presentation, contact:

rosier.ashley@mayo.edu

#### PURPOSE

Unsolicited feedback from participants and facilitators in Root Cause Analyses (RCA) of patient safety events in Radiology indicated opportunity for improvement in the Department's process. The project's goal was to improve the overall average satisfaction score of RCA participants from 3.9 to >= 4.0 and RCA facilitators from 3.6 to >= 4.0 by the completion of 5 event reviews after implementation. Satisfaction was measured using a 5-point scale where a score of 1 equates to very dissatisfied and 5 equals very satisfied, the project goal of a score >= 4 would equate to satisfied.

### **METHODS**

A multidisciplinary team was formed to measure and investigate feedback. The team utilized Define-Measure-Analyze-Improve-Control (DMAIC) and A3 problem solving methodologies, Plan-Do-Study-Act (PDSA) testing, process mapping, and standard work to develop appropriate solutions to improve satisfaction scores. The team utilized an electronic satisfaction survey to measure overall satisfaction rates and collect additional free-text feedback for baseline analysis and following each PDSA cycle. Survey responses were collected from RCA participants and facilitators. Free-text survey comments were analyzed and sorted by similarity to identify targets for improvement.

### RESULTS

Averaged overall satisfaction scores equaled 3.9 for participants and 3.6 for facilitators with a maximum possible score of 5. Survey comments identified the following root causes for decreased satisfaction scores: 1. Non-standard process and disjointed coordination of event investigation and RCA efforts 2. Imprecise root cause identification process during RCA; inconsistent use of quality tools or methods 3. Lacking frontline staff and stakeholder input during RCA 4. Lack of sustainment and accountability for implementing solutions By the completion of 5 RCAs, the improvement team had reached participant and facilitator satisfaction scores that met or exceeded the target goal of 4. The following solutions were implemented as a result of successful PDSA tests: 1. Future state process map detailing the roles responsible for each process step and associated standard work 2. Radiologist-facilitated RCA process 3. Visual documentation of root causes by facilitators at RCA meetings for immediate confirmation by participants 4. Standard communication for event review and investigation 5. Shortened RCA meetings from 60 to 45 minutes Implementation has been completed and the project has transitioned to control. To date, three control cycles have been completed and have met or exceeded satisfaction scores of 4 out of 5.

#### CONCLUSION

Satisfaction surveys are still distributed after each RCA meeting. Satisfaction scores are averaged and monitored quarterly to ensure compliance with the ongoing goal of scores greater than or equal to 4 out of 5. All free-text comments are also analyzed and reviewed quarterly. Quarterly satisfaction scores (average score/event) have been maintained at goal or above. Free-text comments by the few individuals reporting satisfaction scores below the goal have helped the facilitation team to continuously evaluate our standard work and recognize opportunities for continued improvement.



# QI024-EB-MOA

Will The Real STAT Exam Please Stand Up? Reducing Inappropriately Ordered STAT Imaging Studies

Monday, Nov. 26 12:15PM - 12:45PM Room: QR Community, Learning Center Hardcopy Backboard

#### **Participants**

Samer L. Soussahn, MD, Westlake, OH (*Presenter*) Nothing to Disclose Myroslav Gerasymchuk, MD, Beachwood, OH (*Abstract Co-Author*) Nothing to Disclose Samuel Azeze, MD, Cleveland, OH (*Abstract Co-Author*) Nothing to Disclose Michael Wien, MD, Cleveland, OH (*Abstract Co-Author*) Nothing to Disclose Sheila C. Berlin, MD, Chagrin Falls, OH (*Abstract Co-Author*) Nothing to Disclose

# For information about this presentation, contact:

samer.soussahn@uhhospitals.org

#### PURPOSE

The commonly used term "STAT" is an abbreviation for the Latin word statim - meaning immediate or instant. A lack of consensus regarding the criteria for an immediate imaging exam has resulted in the insidious expansion of STAT orders among radiology departments. Unclear order priorities and lack of guidance for providers has contributed to the overuse of the STAT designation. By developing clearly articulated electronic medical record (EMR) order priorities, we aim to increase the frequency of appropriately ordered STAT exams.

# METHODS

After institutional review board approval, we retrospectively reviewed exams ordered as STAT (both prior to and following order priority enhancements) to determine if they were appropriately ordered. STAT studies were identified as those with the highest-level order designation: 'Level 1 Critical' in the old EMR ordering system and 'Acutely Life/Limb Threatening' in the new EMR ordering system. At the outset of this study, there were many options for imaging exam order priority in the EMR (Figure 1). These options were simplified in the revised EMR order priorities (Figure 2). All STAT CT, US and MRI examinations that were ordered by the emergency department and inpatient services over a three-week period were reviewed. These reviews were performed both prior to and following the EMR order priority modifications four months later. During that time interval, our ordering providers were educated about the EMR changes using digital presentations with group discussion at departmental meetings before the EMR changes went live. We defined appropriate STAT conditions as those that were 'acutely life or limb threatening'. For guidance, we included conditions that 'could lead to death or significant morbidity if not promptly recognized, communicated, and acted upon' as defined by the American College of Radiology Actionable Reporting Work Group. This project also identified the specific type of ordering provider (attending physician, resident physician, and mid-level provider) and their likelihood of ordering STAT studies appropriately. All data were managed in REDCap, a HIPAA-compliant software. Statistical analysis was computed using chi-square and t-test with statistical significance defined as p<0.05.

### RESULTS

After the EMR enhancement, the number of ordered STAT studies was reduced from 583 to 229. The percentage of appropriately ordered studies that warranted a STAT priority increased from 70% to 95% (p<0.0001) (Table 1). The turnaround time (from order placement to available for dictation) for STAT CT studies decreased from 140 minutes to 70 minutes, and for STAT MRI studies the turnaround time decreased from 194 minutes to 60 minutes. The number of STAT orders for ultrasound exams decreased dramatically after the EMR modifications. Since only 10 ultrasound exams were requested as STAT following the EMR changes, these data were not included. Overall, for STAT ordered CT and MRI studies, turnaround time was statistically significant after EMR ordering process modifications at p<0.01. For all three groups of ordering providers, the frequency of appropriately-ordered STAT exams after EMR modification was statistically significant at p<0.0001 for resident physicians and mid-level providers and p<0.01 for attending physicians (Figure 3).

# CONCLUSION

Simplifying the EMR order priority designations coupled with educating ordering provides resulted in a system wide decrease in both turnaround time and volume of STAT imaging studies, as well as an increase in the percentage of appropriately-ordered STAT studies. Regardless of the level of training of the ordering provider, the decrease in inappropriately-ordered STAT examinations was observed across all groups of providers after the EMR changes. This is likely related to the fact that the original EMR ordering system was inherently confusing. For instance, in the old EMR, 'Level 1 Critical' could be interpreted to apply to any exam that was critical to a patient's care - not necessarily an exam required to be performed immediately. Further, there was no disincentive to using 'Level 1 Critical' for any exam desired (but not needed) to be completed as quickly as possible. The enhancement of the EMR imaging ordering system improved our radiology workflow for technologists who now can easily segregate the sickest patients in their order queues. Patients who warrant a medically-necessary immediate imaging study are now easily identified and receive potentially life-saving imaging prior to patients with less acute conditions.



## QI108-ED-MOA1

# Addressing Overutilization of Inpatient Renal US Within 48 Hours of CT/MR Abdomen

Monday, Nov. 26 12:15PM - 12:45PM Room: QR Community, Learning Center Station #1

#### **Participants**

Ravi S. Jayavarapu, MPH, MD, Lexington, KY (*Presenter*) Nothing to Disclose Lindsay Clements, Lexington, KY (*Abstract Co-Author*) Nothing to Disclose Audrey Yates, Lexington, KY (*Abstract Co-Author*) Nothing to Disclose Halemane S. Ganesh, MD, lexington, KY (*Abstract Co-Author*) Nothing to Disclose

# For information about this presentation, contact:

ravi.jayavarapu@uky.edu

## PURPOSE

Performing a renal US within 48 hours of having had an abdominal CT/MRI where the kidneys have been clearly imaged and commented upon in a structured report does not yield additional information or alter management. Imaging overutilization leads to elevated healthcare costs stretching valuable human and capital resources particularly in the inpatient setting. The purpose of this quality improvement project is to reduce the overutilization of inpatient renal US.

### METHODS

Retrospective data analysis for six months (Jul 2016 to Dec 2016) was performed to compare the findings of a renal US within 48 hours of an abdominal CT/MRI. The results were summarized and utilized to implement a referring physician call back program which was instituted for a period of one year (Jan 2017 to Dec 2017). Referring physician call back program included review of prior imaging results by the technologist, referring physician communication with either the US scan being performed or cancelled following evidence based imaging decision support. The results were analyzed by using descriptive statistics, average monthly renal US requests within 48 hours of CT/MR Abdomen, and paired t-test to compare pre and post-intervention of average monthly renal US requests. SAS 9.4 was used for analysis.

#### RESULTS

Retrospective data analysis (n =204) showed the most common clinical indications for request of a renal US with 48 hours of CT/MR Abdomen were acute kidney injury (72%), flank pain (7%), infection (4%), prior CT/MR recommendation (3%), calculi (2%), and others (12%). Comparison of imaging findings between renal US and CT/MR abdomen showed 95.2% of renal US scans yield no additional clinical information that altered patient management, 98.4% scans led to no additional information when prior CT/MRI was normal, and 100% of scans for acute renal failure evaluating for hydro nephrosis were negative. Following implementation of the physician call back program, a total of 74 renal US requests were received (63.7% decrease). Among these for 58% (43) a timely communication with the referring physicians failed to occur, in 42 %( 31) the clinical team was successfully contacted of which 28 (90.3%) exams were cancelled and 3 scans (9.7%) were performed. Paired t-test performed pre (34.0) and post-intervention (6.2), the average monthly renal US requests showed a statistically significant reduction in number (p < 0.05) with an 82% decrease in monthly utilization of renal US among inpatients.

### CONCLUSION

The overutilization of the renal US among inpatients within 48 hours of having had abdominal CT/MR can be reduced through appropriate education combined with institutional policy changes which promotes efficient imaging utilization, streamlined workflow thereby saving valuable human and capital resources in the inpatient setting. Promoting referring physician - radiologist communication and providing evidence-based imaging decisions at point of care are essential for value based care.



## QI110-ED-MOA2

Code Angio: A Lean Multidisciplinary Protocol to Decrease Interventional Radiologist Response Times for Trauma Patients with Acute Vascular Injury

Monday, Nov. 26 12:15PM - 12:45PM Room: QR Community, Learning Center Station #2

# Participants

Gautam Rao, DO, San Antonio, TX (*Abstract Co-Author*) Nothing to Disclose Rajeev Suri, MD, San Antonio, TX (*Presenter*) Nothing to Disclose Brandon C. Lam, BS, San Antonio, TX (*Abstract Co-Author*) Nothing to Disclose John A. Walker, MD, San Antonio, TX (*Abstract Co-Author*) Nothing to Disclose Jorge E. Lopera, MD, San Antonio, TX (*Abstract Co-Author*) Shareholder, Tecnostent SA

### For information about this presentation, contact:

suri@uthscsa.edu

### PURPOSE

There has been a progressive paradigm shift towards non-operative management of vascular injury in trauma patients. This has been associated decreasing need for blood transfusion and similar to better survival compared to surgical treatment. With Interventional Radiologists now actively participating at the forefront of trauma care by providing precise and timely control of bleeding, the rate limiting factor is becoming the time from the decision to intervene to the start of the image guided intervention. Both the American College of Surgeons (ACS) Committee on Trauma, and the UK National Institute for Health and Care Excellence (NICE) have recognized the value of IR and have asserted the need for qualified IR to be available within 30 minutes after the need for an intervention is established. To achieve this 30 minute turnaround time, a multidisciplinary workflow was created at our institution to decrease IR response times for patients with acute vascular injury.

### METHODS

CODE ANGIO is a multidisciplinary lean process protocol/workflow to decrease IR response times for patients with acute vascular injury. 1. Activation of CODE ANGIO: by Trauma Surgery, Emergency Radiology, or Interventional Radiology, following direct communication between these services, based on pre-established guidelines2. Indications for CODE ANGIO: Definite active extravasation on CT scan in hemodynamically borderline stable patient; s hemodynamically unstable patient with suspect vascular injury where non-surgical management is deemed necessary.3. Activation process: Simultaneous activation of multiple teams - IR (faculty/fellow, IR technologist), OR (transport, technician, nurses), Anesthesia and Trauma surgery4. Resuscitation and procedure: Hybrid OR/IR suite with Massive transfusion protocol and resuscitation as needed. Patient prepped for IR access and if need be operative intervention 5. IR role: aim to get arterial access and start the endovascular procedure within 30 minutes of activation of the CODE ANGIO

### RESULTS

CODE ANGIO has replaced the erstwhile practice of workflow happening in series - the Trauma Surgeon calling IR, discussing the pros/cons of intervention, individually contacting the IR team members, and transporting the patient to the IR suite, only after the IR team arrived in-house. This previous practice had several inefficiencies, often with turnaround times (TAT) of 2 hours (or longer) before the interventional procedure would start. Over the last 4 years, CODE ANGIO has progressively decreased our IR TAT to now 30 minutes with improved patient outcomes (decreased need for operative interventions and massive blood transfusions). A monthly review is conducted of all cases to assure appropriate utilization and to assess outcomes of the CODE ANGIO system

### CONCLUSION

CODE ANGIO is a resource intensive lean multidisciplinary response to acutely bleeding patients with trauma, with Interventional Radiologists being the core element in reducing response times to interventions. Further research is needed to see how the CODE ANGIO experience improved patient outcomes in specific trauma categories (solid organ vs pelvic trauma; decreased need for interventions for re-bleeds), and to see if restructuring other IR practices would improve overall outcomes for trauma patients.



## QI112-ED-MOA3

## The Affidea MR Excellence Program: A Comprehensive MRI Optimization and Standardization Project

Monday, Nov. 26 12:15PM - 12:45PM Room: QR Community, Learning Center Station #3

#### **Participants**

Nikolaos Papanikolaou, Budapest, Hungary (*Presenter*) Owner, MRICONS Ltd Peter Szatmari, Budapest, Hungary (*Abstract Co-Author*) Employee, Affidea Rowland O. Illing, BMBCh, FRCR, London, United Kingdom (*Abstract Co-Author*) Officer, Affidea

For information about this presentation, contact:

nickolas.papanikolaou@mricons.eu

## PURPOSE

To harmonize and optimize quality and patient experience across 15 MRI centers in 5 European countries.

### METHODS

The Affidea MR Excellence Project (MREP) was deployed in 5 European Countries (Lithuania, Greece, Poland, Ireland and Portugal) in 15 different sites. A total number of 93 standardized protocols were developed in consensus from a working group of Affidea Medical Counsel comprising 6 Radiologists with more than 10 years of clinical MRI experience. More than 1500 pulse sequences in total were included in the standardized protocols of 14 different models and three main MRI vendors (Siemens, GE and Philips). Initially all participating sites implemented standardized sequence names that were divided into three sets (one of each vendor). Pulse sequences were categorized into i) core, ii) recommended, iii)conditional and iv) optional sequences. Core sequences are the most important to guarantee high diagnostic confidence, recommended are those that are improved versions of core sequences but needs optional software to be purchased, conditional are those that are executed when a specific condition is met and optional are those that can be reimbursed separately. Following to that, each site was connected through a VPN channel to the centralized MREP server located in Budapest and transmitted automatically in the background all MRI exams performed on a daily basis at least for a duration of 1 month. Consequently, a 2 days visit of an MRI Applications Expert was organized and the 5 most common examinations performed on each site were selected for sequence optimization. Following the visit and for a 1-month duration, all exams were transmitted to the MREP server. 2 Radiologists were recruited for each site and ranked the image quality using a 5point grading scale of sequences presented to them in a blind fashion obtained before, during and after the visit. A key performance indicator called SPI (Sequence Performance Index) was calculated taking into account the image guality radiological score, as well as, the scan time, the voxel size and the number of slices for each sequence. Finally, the optimal sequences were selected based on the highest scores of SPIs achieved. An automated report was generated by the MREP server for each site including mean examination time, average daily number of exams, average non-scanning time, average utilization rate, mean compliance and deviation to standardized protocols. Compliance was defined as the percentage of core sequences that were included in the exam as compared to the standardized Affidea protocol, while deviation was the percentage of "alien" sequences that did not fall into any of the four categories. All KPIs were compared before and after the visit to evaluate the impact of the MREP to each site/country.

# RESULTS

Results from all five countries indicated significant improvement both in terms of quality and patient experience. More specifically, in Lithuania, the mean IQ scores were 2.87 (before the visit), 3.28 (during the visit) and 2.91 (after the visit), while the corresponding mean SPI's were 1.44, 1.83 and 1.38, respectively. There was a 6.8% reduction in examination time after the visit, a 7.3% reduction in the non-scanning time, a 10.9% increase in the number of exams, a 1.3% reduction in utilization rate, a 7.3% improvement in the compliance to standardized protocol and a 17.2% improvement in the deviation of the standardized protocol.

## CONCLUSION

MREP has been successfully deployed in very heterogeneous environments in terms of MRI culture, equipment and level of expertise of the local staff. It proved a challenging process that demands active engagement of a very diverse workgroup including Radiologists, Radiographers, Clinical Scientists, Software Engineers and active support of the Affidea local management.



## QI114-ED-MOA4

What Are Our Blind Spots? Using Peer-Learning to Create a Case Archive of Common Diagnostic Errors

Monday, Nov. 26 12:15PM - 12:45PM Room: QR Community, Learning Center Station #4

#### Participants

Karen Cedeno-Kelly, Grand Rapids, MI (*Presenter*) Nothing to Disclose Andrew K. Moriarity, MD, Grand Rapids, MI (*Abstract Co-Author*) Nothing to Disclose

For information about this presentation, contact:

andy.moriarity@gmail.com

#### PURPOSE

Peer learning in radiology promotes continued practice improvement through shared feedback. Radiologists frequently encounter cases in their daily workflow that present opportunities for learning, feedback, and improvement which could benefit not just the original interpreting radiologist but others at the same institution. Recognizing the need to provide the best possible service to our patients and to promote a culture of continuous learning within our department, our quality committee worked to identify these cases and improve peer learning opportunities for our radiologists. Radiology departments are increasingly transitioning from peer review systems to environments that promote peer learning. We discuss the implementation of a successful case archive methodology that is well received by participants and has potential to benefit all individuals in the department.

#### **METHODS**

A "peer learning" case submission module was developed at our institution to identify and archive cases with opportunities for improved interpretation/reporting as well as "great calls" from the daily workflow. Radiologists identify eligible cases during daily reading, multi-disciplinary patient conference participation, requests from referring clinical services, and other available avenues. Submitted cases are categorized by our quality committee on the basis of subspecialty, anatomy, and type of pathology. The archive is used by section heads to review areas of education need in the department and for potential inclusion at monthly peer learning conferences. A searchable version available to all radiologists is undergoing user testing by interested individuals. The conferences are advertised to division members, radiology residents, and visiting trainees in graduate and undergraduate medical education as well as technologists.

## RESULTS

During the first 18 months of the program 260 cases were submitted, of which 244 (94%) were identified as peer learning opportunities and 16 (6%) were "great calls" and there was an overall trend of increasing case submission. Twenty-two (8%) were selected for peer-learning conferences. The 5 most common topics by frequency were fracture 44 (17%), missed diagnosis 32 (12%), missed priors 18 (7%), lesion/mass (7%), and infarct 10 (4%). The greatest volume of cases identified in abdominal imaging 66 (25%), cardiothoracic imaging 63 (24%), and neuroradiology 53 (20%). The peer-learning division conferences have been well received by participants.

## CONCLUSION

The peer learning archive is widely used and indicates that the current areas of greatest educational need are in fracture identification, perception, and comparison with all relevant prior imaging. The system provides learning opportunities to all of our radiologists and should help to monitor future trends in department and division performance.



## RO204-SD-MOA1

Risk Factors of Radionecrosis Subsequent of Stereotactic Radiosurgery in Patients with Brain Metastases

Monday, Nov. 26 12:15PM - 12:45PM Room: RO Community, Learning Center Station #1

#### **Participants**

Qi-Wen Li, Guangzhou, China (*Presenter*) Nothing to Disclose Jiang Hu, Guangzhou, China (*Abstract Co-Author*) Nothing to Disclose Bo Qiu, Guangzhou, China (*Abstract Co-Author*) Nothing to Disclose Yu-Jia Zhu, Guangzhou, China (*Abstract Co-Author*) Nothing to Disclose Fan-Jun Meng, Jieyang, China (*Abstract Co-Author*) Nothing to Disclose Pei-Qiang Cai, Guangzhou, China (*Abstract Co-Author*) Nothing to Disclose Mei-Ling Deng, Guangzhou, China (*Abstract Co-Author*) Nothing to Disclose Chuan-Miao Xie, Guangzhou, China (*Abstract Co-Author*) Nothing to Disclose Hui Liu, Guangzhou, China (*Abstract Co-Author*) Nothing to Disclose

#### For information about this presentation, contact:

liuhui@sysucc.org.cn

#### PURPOSE

The balance between tumor response and subsequent development of radionecrosis following stereotactic radiosurgery (SRS) for brain metastasis is a major dilemma. The purpose of this study is to demonstrate the incidence and risk factors of radionecrosis by investigating serial magnetic resonance imaging (MRI) studies.

#### **METHOD AND MATERIALS**

Eighty-five brain metastases treated with linear accelerator-based SRS in a single fraction were analyzed retrospectively. Serial brains MRIs, performed at an interval of 3-6 months, were reviewed to evaluate the occurrence of radionecrosis. Clinical data was assessed to determine radionecrosis-related symptoms. Univariate and multivariate analyses were performed to reveal the potential risk factors of radionecrosis, including dosimetric data, clinicopathologic characteristics of patients, prior whole brain irradiation and the delivery of chemotherapy and/or targeted therapy.

### RESULTS

Median prescribed dose was 20 (range: 14-24) Gy. After a median radiologic follow-up of 8 months, the two-year cumulative incidences of radiologic and symptomatic radionecrosis were 20.0% and 5.3%. Patients were at higher risk of radiologic radionecrosis if the ratio of in-field maximum point dose (Dmax) to prescribed dose exceeded 1.1 (p=0.033), or the volume of surrounding brain tissue receiving 20 Gy or above (V20) exceeded 1.5 cc (p=0.041). V20 exceeding 1.5 cc tended to be significantly associated with symptomatic radionecrosis (p=0.088).

### CONCLUSION

Limiting the in-field maximum point dose within 110% of the prescribed dose, and ensuring V20 of the normal tissue less than 1.5 cc might be beneficial in reducing the appearance of radiologic brain radionecrosis determined on series MRIs after SRS.

# **CLINICAL RELEVANCE/APPLICATION**

Dose limitations of both the target and normal tissue in brain SRS can reduce the incidence of brain radionecrosis determined on series MRIs.



## RO205-SD-MOA2

Correlating Multi-Parametric Tumor Imaging Kinetics And Circulating Tumor Cells During Radiotherapy In Patients With Head And Neck Cancer: Preliminary Results

Monday, Nov. 26 12:15PM - 12:45PM Room: RO Community, Learning Center Station #2

## Participants

Sweet Ping Ng, MBBS, FRANZCR, Houston, TX (*Presenter*) Nothing to Disclose Carlos Cardenas, MS, Houston, TX (*Abstract Co-Author*) Research Grant, Varian Medical Systems, Inc Houda Bahig, Houston, TX (*Abstract Co-Author*) Nothing to Disclose Jihong Wang, PhD, Houston, TX (*Abstract Co-Author*) Speaker, Elekta AB Salyna Meas, Houston, TX (*Abstract Co-Author*) Nothing to Disclose Vanessa Sarli, Houston, TX (*Abstract Co-Author*) Nothing to Disclose Carolyn Hall, Houston, TX (*Abstract Co-Author*) Nothing to Disclose Yao Ding, PHD, Dallas, TX (*Abstract Co-Author*) Nothing to Disclose Shalin Shah, MD, Bronx, NY (*Abstract Co-Author*) Nothing to Disclose Anthony Lucci, Houston, TX (*Abstract Co-Author*) Nothing to Disclose Abdallah S. Mohamed, MD, MSc, Houston, TX (*Abstract Co-Author*) Nothing to Disclose Clifton D. Fuller, MD,PhD, Houston, TX (*Abstract Co-Author*) Research Consultant, Elekta AB; Research Grant, Elekta AB; Speaker, Elekta AB

#### PURPOSE

To quantify and correlate imaging changes (volume of primary tumor and apparent diffusion coefficient change, ADC) on weekly MRIs with weekly circulating tumor cell (CTC) count changes.

## METHOD AND MATERIALS

Patients with localized mucosal head and neck squamous cell carcinomas undergoing definitive radiotherapy were eligible for enrolment on a prospective observational study. Pre-treatment and weekly in-treatment MRIs were obtained in radiotherapy treatment position. T1-weighted, T2-weighted and DWI sequences were obtained on 1.5T Siemens MRI. ADC maps were generated. Gross tumor volume (GTV) was contoured on T2-weighted MRI. GTV volume and ADC parameters were recorded. Peripheral blood samples were collected pre-radiotherapy and weekly during radiotherapy. CTCs were assessed and quantified using the FDAapproved CellSearch System. Patient, tumor and treatment characteristics were recorded.

## RESULTS

A total of 8 patients completed the study. 2 patients were excluded from the analysis - one with small primary tumor (<5cc) and another who missed an MRI. Hence, 6 patients were eligible for analysis. All patients had squamous cell carcinomas and all received concurrent chemotherapy. Three patients had oropharyngeal, 2 had laryngeal and 1 with nasopharyngeal tumors. Median pre-treatment tumor volume was 17.85cc (range: 9.4 - 33.7cc). Approximately 25% of tumor volume shrinkage happened between week 2 and 3. 5 patients achieved >50% tumor shrinkage by week 3 of treatment. The change in weekly median ADC compared to baseline was -0.3%, 2 %, 2.7%, 6.9%, -0.5%, and 6.6%. No patient had detectable CTC before treatment. After week 1, 1 patient had 2 CTCs. In week 4, 5 patients had detectable CTCs - 4 had 1 CTC and 1 had 2 CTCs. CTC became detectable or increased in week 4 - where the greatest increase in median ADC was noted and the week after greatest GTV shrinkage is seen on MRI.

## CONCLUSION

No correlation between tumor response seen on MRI with circulating tumor cell count during radiotherapy. It appeared that CTC became detectable or increased in week 4 suggesting that tumor cells may be released into the circulation as the tumor microvasculature is affected by the radiation resulting in increased 'leakiness' into the vasculature. Further investigation into the viability of these cells is required.

### **CLINICAL RELEVANCE/APPLICATION**

Although no correlation between imaging kinetics and CTC counts during radiotherapy was noted in this preliminary data, CTC release into the circulation during treatment require further investigation.



### UR179-ED-MOA7

# **Remnant of the Umbilical Vein and Artery in Adults**

Monday, Nov. 26 12:15PM - 12:45PM Room: GU/UR Community, Learning Center Station #7

### Participants

Jun Isogai, MD, Asahi, Japan (*Presenter*) Nothing to Disclose Naoki Harata, Asahi, Japan (*Abstract Co-Author*) Nothing to Disclose Jun Kaneko, Hasuda, Japan (*Abstract Co-Author*) Nothing to Disclose Katsuya Yoshida, MD, Asahi, Japan (*Abstract Co-Author*) Nothing to Disclose

# **TEACHING POINTS**

To demonstrate normal variants and mimics of periumbilical structures To illustrate a wide variety of remnants of the umbilical vein and artery

### **TABLE OF CONTENTS/OUTLINE**

A. Review of anatomical relationship of the ligamentum teres and obliterated umbilical arteries B. A wide spectrum of remnants imaging of the umbilical vein and artery 1) Right-sided ligamentum teres / Left-sided gallbladder causing difficult cholecystectomy and hepatectomy 2) Falciform ligament abscess related to cholangitis or pancreatitis 3) Hemorrhage of the hepatic falciform artery 4) Recanalized paraumbilical vein in Cruveilhier-Baumgarten syndrome (Inferior veins of Sappey) 5) Focal enhancement of the left medial lobe of liver related to SVC obstruction (Superior veins of Sappey) 6) Primary falciform ligament tumor 7) Patent umbilical artery with an anastomosis of the inferior epigastric artery 8) Supravesical hernia via the fascia between the obliterated umbilical artery and urachus



## UR180-ED-MOA8

Multi-Parametric MR, Anterior Fibromuscular Stroma and Prostate Cancer: What Do You Need to Know?

Monday, Nov. 26 12:15PM - 12:45PM Room: GU/UR Community, Learning Center Station #8

## Awards Certificate of Merit

## Participants

Lidia Alcala, MD, Jaen, Spain (*Presenter*) Nothing to Disclose Violeta Catala, Barcelona, Spain (*Abstract Co-Author*) Nothing to Disclose Eloisa Navas Campos, MD, Jerez de la Frontera, Spain (*Abstract Co-Author*) Nothing to Disclose Marcelo Potolicchio, MD, Cadiz, Spain (*Abstract Co-Author*) Nothing to Disclose Xavier Alomar, Barcelona, Spain (*Abstract Co-Author*) Nothing to Disclose Antonio Luna, MD,PhD, Jaen, Spain (*Abstract Co-Author*) Consultant, Bracco Group; Speaker, General Electric Company; Speaker, Canon Medical Systems Corporation; Royalties, Springer Nature

## For information about this presentation, contact:

l.alcala.o@htime.org

# **TEACHING POINTS**

- Review the anatomy and normal appearance on MRI of anterior fibromuscular stroma (AFMS) - Highlight the different presentations of prostate cancer (Pca) of AFMS - identify potential pitfalls of prostate cancer in AFMS The cases are selected from our data base with 70 Pca of the AFMS (histological confirmation with targeted MRI/US fusion biopsy and/or prostatectomy specimens) and 68 normal AFMS (histological confirmation with targeted prostatectomy specimens)

## TABLE OF CONTENTS/OUTLINE

1. Anatomy and normal appearance of AFMS in MRI (schems and histologic correlation). 2. Pca of AFMS - T2-weighted sequences - DWI: ADC, IVIM and kurtosis - DCE-MRI: semiquantitative and pharmakocinetic modelling 3. Role of targeted MRI/US fusion biopsy in the diagnosis of anterior elusive tumors 4. Pitfalls of prostate cancer of AFMS - Hypertrophic AFMS - Focal benign prostatic hyperplasia - Prostatitis 5. Conclusions

#### **Honored Educators**

Presenters or authors on this event have been recognized as RSNA Honored Educators for participating in multiple qualifying educational activities. Honored Educators are invested in furthering the profession of radiology by delivering high-quality educational content in their field of study. Learn how you can become an honored educator by visiting the website at: https://www.rsna.org/Honored-Educator-Award/ Antonio Luna, MD - 2018 Honored Educator



## VI156-ED-MOA8

Beyond the Basics of Prostatic Artery Embolization (PAE): Controversies, Managing Complex Anatomy, and Keys to Successful Practice Building

Monday, Nov. 26 12:15PM - 12:45PM Room: VI Community, Learning Center Station #8

# Participants

Jung H. Yun, Closter, NJ (*Presenter*) Nothing to Disclose
Ragni Jindal, MD, Tucson, AZ (*Abstract Co-Author*) Nothing to Disclose
Siavash Behbahani, MD, Mineola, NY (*Abstract Co-Author*) Nothing to Disclose
Aaron E. Katz, MD, Mineola, NY (*Abstract Co-Author*) Nothing to Disclose
Shivank S. Bhatia, MD, MBBS, Miami, FL (*Abstract Co-Author*) Consultant, Merit Medical Systems, Inc; Speaker, Merit Medical Systems, Inc
Jason C. Hoffmann, MD, Mineola, NY (*Abstract Co-Author*) Speakers Bureau, Merit Medical Systems, Inc; ;
Juan M. Puertas, DO, Mineola, NY (*Abstract Co-Author*) Nothing to Disclose

#### For information about this presentation, contact:

Jason.Hoffmann@nyulangone.org

#### **TEACHING POINTS**

1. The age of the patient population, associated comorbidities, and size and tortuosity of vasculature makes PAE one of the most challenging arterial interventions performed by interventional radiologists.2. After appropriate training and education, careful patient selection and thoughtful program development is essential for building a successful PAE program with the best possible patient outcomes.

### TABLE OF CONTENTS/OUTLINE

Brief review of essential BPH concepts, prostate imaging, and arterial supply of the prostateWhere does PAE fit in the BPH treatment algorithm?-Detailed review of the PAE literature (including a "top 10" list of essential PAE articles)-Comparison of PAE outcomes to other urologic interventions, including TURP, Urolift, and Rezum-Comparing PAE studies to eachother, to determine the best procedural technique-PAE outcomes in patients with urinary retention/indwelling Foley catheters-Is CTA necessary prior to PAE?-Advanced imaging techniques: cone-beam CT, Syngo, and Emboguide (current applications and future directions)Managing complex anatomy and collateralsRole of PAE in prostate cancerTop 10 recommendations for building a successful, collaborative PAE program, including detailed description of PAE program success at two different institutions



### VI158-ED-MOA10

**Optical Coherence Tomography: A Practical Primer for the Radiologist** 

Monday, Nov. 26 12:15PM - 12:45PM Room: VI Community, Learning Center Station #10

FDA Discussions may include off-label uses.

#### **Participants**

Steven Kao, MD, Los Angeles, CA (*Presenter*) Nothing to Disclose Jonathan K. Park, MD, Los Angeles, CA (*Abstract Co-Author*) Nothing to Disclose Osama Elbuluk, MD, Los Angeles, CA (*Abstract Co-Author*) Nothing to Disclose Alice S. Chen, MD, Los Angeles, CA (*Abstract Co-Author*) Nothing to Disclose Hsin-Yi Lee, MD, Los Angeles, CA (*Abstract Co-Author*) Nothing to Disclose Matthew K. Walsworth, MD, MS, Santa Monica, CA (*Abstract Co-Author*) Nothing to Disclose John M. Moriarty, MD, Los Angeles, CA (*Abstract Co-Author*) Speaker, AngioDynamics, Inc Consultant, AngioDynamics, Inc Speaker, Sequent Medical, Inc Consultant, Sequent Medical, Inc Speaker, Argon Medical Devices, Inc Consultant, Argon Medical Devices, Inc

#### **TEACHING POINTS**

1. Explain the development, technology and physics underpinning optical coherence tomography (OCT) 2. Illustrate the technical and logistical issues that may be involved with the use of OCT during procedures 3. Describe the clinical utility of OCT relevant for the interventional radiologist, particularly its use in peripheral and pulmonary arterial vascular disease 4. Describe the existing literature on the clinical use of OCT in peripheral and pulmonary arterial vascular disease

## **TABLE OF CONTENTS/OUTLINE**

A. Provide an overview of the history, technology and physics of OCT B. Explain the technical and logistical issues with the use of OCT C. Review of the imaging findings in normal and abnormal vessels on OCT, in comparison to findings on conventional pulmonary angiography, computed tomography angiography, and intravascular ultrasound D. Review the existing literature E. Case-based format to illustrate the above.



## VI212-SD-MOA1

Intraprocedural FDG Perfusion PET During PET/CT Guided Liver Tumor Ablation for Assessment of the Ablation Margin

Monday, Nov. 26 12:15PM - 12:45PM Room: VI Community, Learning Center Station #1

# Participants

Alan J. Cubre, MD, Boston, MA (*Presenter*) Nothing to Disclose Paul B. Shyn, MD, Boston, MA (*Abstract Co-Author*) Research Grant, Siemens AG Leslie K. Lee, MD, Boston, MA (*Abstract Co-Author*) Nothing to Disclose Hyewon Hyun, MD, Boston, MA (*Abstract Co-Author*) Nothing to Disclose Kemal Tuncali, MD, Boston, MA (*Abstract Co-Author*) Nothing to Disclose Vincent M. Levesque, MA, Boston, MA (*Abstract Co-Author*) Research Consultant, Galil Medical Ltd Tina Kapur, PhD,MSc, Boston, MA (*Abstract Co-Author*) Research Grant, Siemens AG Consultant, Varian Medical Systems, Inc Victor Gerbaudo, PhD, Boston, MA (*Abstract Co-Author*) Nothing to Disclose Stuart G. Silverman, MD, Brookline, MA (*Abstract Co-Author*) Nothing to Disclose

## PURPOSE

To evaluate 18F-fluorodeoxyglucose (FDG) perfusion PET during FDG PET/CT-guided liver tumor ablations for intraprocedural assessment of the ablation margin.

#### **METHOD AND MATERIALS**

21 adult patients underwent FDG PET/CT-guided microwave ablation of 34 FDG-avid liver tumors under general anesthesia. 8 mCi FDG was administered IV preprocedurally for PET/CT targeting and an additional 3 mCi intraprocedurally for perfusion PET immediately after ablation. Perfusion PET was acquired during a 60-second breath-hold. Tumor FDG activity was not dissipated by ablation. Ablation margins appeared as photopenic bands between preprocedurally administered FDG trapped in tumor and perfusion FDG activity in unablated liver. Impact of perfusion PET on intraprocedural decisions was recorded. Ablation margin visibility and the minimum ablation margin were compared between perfusion PET and 24-hour postprocedural contrast-enhanced MRI by two radiologists. Local progression was assessed on follow-up imaging from 1.2 to 32.4 months (mean 7.5).

#### RESULTS

Intraprocedural perfusion PET revealed inadequate ablation margins prompting additional overlapping ablations during 3/21(14%) procedures. Reader 1 judged 26/31(84%) ablation margins fully assessable by intraprocedural perfusion PET and 21/31(68%) by 24-hour post-procedural MRI (p=0.14). Reader 2 judged 23/31(74%) margins fully assessable by intra-procedural perfusion PET and 18/31(58%) by 24-hour postprocedural MRI (p=0.18). Minimum margins measured on Perfusion PET and MRI for each ablation zone differed by 0-7 mm (mean 3.2) for reader 1, and by 0-11 mm (mean 2.5) for reader 2. Local progression occurred in 6/31 (19%) tumors, but in none of the 3 tumors where intraprocedural PET prompted additional ablations.

### CONCLUSION

Intraprocedural FDG perfusion PET immediately following ablation of FDG-avid liver tumors is non-inferior to 24-hour postprocedure MRI for assessing ablation margins yet offers the potential to guide intraprocedural ablation decisions.

# **CLINICAL RELEVANCE/APPLICATION**

18-FDG Perfusion PET/CT during PET/CT guided liver ablations allows assessment of the ablation margin intraprocedurally and may guide intraprocedural overlapping ablations.



## VI213-SD-MOA2

Clinical Impact of Bone Biopsy on Treating Osteomyelitis of the Foot: A Single Tertiary Institution Experience

Monday, Nov. 26 12:15PM - 12:45PM Room: VI Community, Learning Center Station #2

#### **Participants**

Aaditya A. Nagaraj, MD, Houston, TX (*Presenter*) Nothing to Disclose Hassan A. Al-Balas, MBBS, MD, Houston, TX (*Abstract Co-Author*) Nothing to Disclose Zeyad A. Metwalli, MD, Bellaire, TX (*Abstract Co-Author*) Nothing to Disclose David Sada, MD, Houston, TX (*Abstract Co-Author*) Nothing to Disclose

## For information about this presentation, contact:

#### sada@bcm.edu

### PURPOSE

Management of osteomyelitis associated with diabetic foot disease with ulceration can be challenging. Biopsy of the involved bone is frequently requested to guide antibiotic therapy. The aim of this study is to report the impact of percutaneous image-guided bone biopsy on antibiotic therapy and the rate of amputations.

# METHOD AND MATERIALS

An institutional review board approved chart review of patients with lower extremity ulcers who underwent percutaneous imageguided bone biopsy between June 2009 and August 2016 was performed. A total of 98 patients underwent bone biopsy, and 87 patients were included in the study. 11 patients were excluded for incomplete data or ineligibility due to alternate indications for the biopsy, including malignancy or trauma. Procedure indication, pre-procedure imaging, bone specimen pathology and culture results, antibiotic therapy prior to biopsy and changes in the antibiotic regimen after biopsy were recorded. The rate of amputation following bone biopsy procedures was also assessed.

### RESULTS

Of the 87 study patients, 40 patients had positive bone cultures. 65 patients had foot radiographs within one month of the biopsy. Patients with radiographic evidence of osteomyelitis were more likely to have positive biopsy culture (p<0.05) than those without radiographic changes suspicious for osteomyelitis. 18 patients had an MRI within one month of biopsy. 14 patients had positive MRI findings and 2 had equivocal findings. MRI abnormalities were not predictive of positive bone biopsy cultures (p>0.05). 53 patients were on antibiotics prior to the biopsy, which were withheld for variable durations prior to biopsy. Prior antibiotic therapy was not associated with positive bone biopsy culture results. Positive bone biopsy cultures were associated with a change in the antibiotic regimen. Positive bone cultures had no impact on the rate of future amputations.

## CONCLUSION

Bone biopsy of the foot in the setting of suspected osteomyelitis was more likely to be positive in the presence of osseous radiographic changes. Positive bone biopsy cultures were associated with changes to the antibiotic regimen. Positive cultures did not have a significant impact on the rate of future amputation.

### **CLINICAL RELEVANCE/APPLICATION**

Osseous radiographic changes in patients with diabetic foot ulcers are predictive of positive culture on bone biopsy specimens. Positive bone biopsy cultures often yield a change in antibiotic therapy.



## VI214-SD-MOA3

TIPS in Cirrhotic in Patients with Complications of Portal Hypertension: A Single-Centre Preliminary Experience Using a New Controlled-Expansion e-PTFE Covered Stent

Monday, Nov. 26 12:15PM - 12:45PM Room: VI Community, Learning Center Station #3

**FDA** Discussions may include off-label uses.

#### **Participants**

Luigi Maruzzelli, MD, Palermo, Italy (*Presenter*) Nothing to Disclose Roberto Miraglia, MD, Palermo, Italy (*Abstract Co-Author*) Nothing to Disclose Fabio Tuzzolino, Palermo, Italy (*Abstract Co-Author*) Nothing to Disclose Ioannis Petridis, Palermo, Italy (*Abstract Co-Author*) Nothing to Disclose Angelo Luca, MD, Palermo, Italy (*Abstract Co-Author*) Nothing to Disclose

#### For information about this presentation, contact:

rmiraglia@ismett.edu

## PURPOSE

To prospectively evaluate short-term outcome of TIPS creation using the new controlled-expansion e-PTFE covered stent (VCX), in patients with portal hypertension complications.

## METHOD AND MATERIALS

Between 7/2016 and 3/2018, 75 patients received TIPS using VCX. Efficacy and complications rate was evaluated.

### RESULTS

TIPS indications were: refractory ascites (n=45), variceal bleeding (n=22), other (n=8). Mean age 58.1 years ( $\pm$ 11.7), mean followup 5.8 months ( $\pm$ 4.5, range 1-20). 29 patients had partial portal vein thrombosis. In 69 patients TIPS was dilated to 8 mm of diameter reaching the hemodynamic target of a porto systemic pressure gradient (PSG) < 12 mmHg. In 6 patients, not reaching the hemodynamic target the stent was dilated to 10 mm of diameter during the same session. Mean PSG pre-TIPS was 15.7 mmHg ( $\pm$ 4.8), post-TIPS was 6.4 mmHg( $\pm$ 2.6). Overall encephalopathy was registered in 17 patients (22%), grade II-III encephalopaty was observed in 5 patients (6%). Portal vein thrombosis partially/completely resolved in 24 patients (82%). Overall clinical success was achieved in 66/75 (88%) patients (82% in refractory ascites, 95% variceal bleeding, 100% other). TIPS revision with stent dilatation to 10 mm was performed in 7 patients: in 3 patients with ascites persistence, without evidence of stent dysfunction and in 4 patients for stent stenosis. One patient with grade III encephalopaty, with 8 mm stent, underwent stent reduction. 16 patients (21%) died in the follow-up for causes not related to TIPS. 5 patients (6%) underwent liver transplant.

#### CONCLUSION

VCX for TIPS creation is associated with a good clinical short-term outcome with a reasonably low complications rate.

## **CLINICAL RELEVANCE/APPLICATION**

This stent could have an important role in a multi-step dilatation strategy in cirrhotic patients with portal hypertension complications.



### VI215-SD-MOA4

# **Transvaginal Pelvic Interventions: A Road Less Traveled**

Monday, Nov. 26 12:15PM - 12:45PM Room: VI Community, Learning Center Station #4

#### Awards Student Travel Stipend Award

#### Participants

Kirema Garcia-Reyes, MD, San Francisco, CA (*Presenter*) Nothing to Disclose Liina Poder, MD, Mill Valley, CA (*Abstract Co-Author*) Nothing to Disclose Tara A. Morgan, MD, San Francisco, CA (*Abstract Co-Author*) Nothing to Disclose Ruth B. Goldstein, MD, San Francisco, CA (*Abstract Co-Author*) Nothing to Disclose Evan Lehrman, MD, San Francisco, CA (*Abstract Co-Author*) Nothing to Disclose Maureen P. Kohi, MD, San Francisco, CA (*Abstract Co-Author*) Nothing to Disclose Maureen P. Kohi, MD, San Francisco, CA (*Abstract Co-Author*) Research Grant, Boston Scientific Corporation; Consultant, LaForce; Advisory Board, Boston Scientific Corporation; Advisory Board, AbbVie Inc

## For information about this presentation, contact:

kirema.garcia-reyes@ucsf.edU

# PURPOSE

To determine the safety and efficacy of ultrasound-guided transvaginal procedures in female patients with pelvic pathologies.

### **METHOD AND MATERIALS**

A retrospective review of consecutive female patients with pelvic pathologies undergoing ultrasound-guided transvaginal pelvic aspiration, drain placement or biopsy between August 2013 and December 2017 was performed. Patient characteristics, imaging and pathology results, and follow up clinic notes were reviewed. Technical success was defined as the ability to perform an aspiration, collect samples for biopsy, or place a drain. Clinical success was defined as a diagnostic pathology sample from a biopsy or resolution of symptoms related to the indication for aspiration/drain without the need for additional interventions.

#### RESULTS

A total 28 patients were included; median age was 47 (range: 23-77). The most common presenting pelvic pathologies for aspiration/drain placement were tubo-ovarian abscess and pyosalpinx whereas a pelvic mass in the setting of history of current or prior malignancy was the primary indication for biopsy. Of the 28 patients, 13 underwent biopsies, 14 underwent aspirations, and one patient underwent drain placement. The overall technical success rate was 96% (27/28). Of the biopsies, 12/13 (92%) were technically successful and all were diagnostic on pathology. All 14 aspirations were technically successful. Of these 14 patients, two required additional drain placement due to re-accumulation of fluid and one underwent surgical management. The remaining one patient underwent successful drain placement that was removed 12 days later without need for additional intervention. There were no reported complications.

## CONCLUSION

Ultrasound-guided transvaginal procedures are a safe and effective option for the management of pelvic pathologies. This approach may be an alternative to the more frequently utilized transgluteal approach which is often more painful and requires CT guidance with resultant radiation exposure.

## **CLINICAL RELEVANCE/APPLICATION**

A transvaginal approach can be utilized to access pelvic pathologies in women, limiting morbidity and radiation exposure in this patient population when compared to the more frequently utilized CT-guided transgluteal approach.



## VI216-SD-MOA5

# Notions of Pre-Procedural Anxiety in the Realm of Interventional Radiology

Monday, Nov. 26 12:15PM - 12:45PM Room: VI Community, Learning Center Station #5

#### **Participants**

Arif Pendi, MS, Detroit, MI (*Presenter*) Nothing to Disclose David Baron, Los Angeles, CA (*Abstract Co-Author*) Nothing to Disclose Arash Anavim, MD, Orange, CA (*Abstract Co-Author*) Nothing to Disclose Amaan Ali, BS, La Jolla, CA (*Abstract Co-Author*) Nothing to Disclose Arleen Grewal, MS, Elk Grove, CA (*Abstract Co-Author*) Nothing to Disclose Kasim Pendi, Riverside, CA (*Abstract Co-Author*) Nothing to Disclose Ramon Ter-Oganesyan, MD, Los Angeles, CA (*Abstract Co-Author*) Nothing to Disclose

#### For information about this presentation, contact:

arif.i.pendi@gmail.com

## PURPOSE

Pre-procedural Anxiety (PA) is experienced by the majority of patients scheduled to undergo interventional radiological procedures. This study was performed to determine current management practices and professional views of interventional radiologists with regards to managing PA.

#### **METHOD AND MATERIALS**

A cross-sectional study of practicing members of the international organization Society for Interventional Radiology (SIR) was performed. The questionnaire consisted of items to capture attitudes regarding the occurrence, measurement, and management of PA. Survey responses were collected from March to April 2018.

#### RESULTS

A total of 728 responses were obtained from American (n=672, 92.3%) and international (n=56, 7.7%) members of SIR. The vast majority of respondents described PA management as somewhat to very important in the practice setting (n=603, 88.4%) and important for the patient (n=677, 99.1%). PA was also believed to often or sometimes interfere with the delivery of healthcare (n=505, 74.0%). Most respondents discussed PA if raised by the patient (n=575, 95.2%) but did not directly measure it otherwise (n=604, 88.4%). Patient education (n=573, 87.4%), anxiolytic medications (n=492, 75.0%), and fostering therapeutic or empathetic interactions (n=419, 63.9%) were the most preferred methods to reduce PA. Radiologists were held most responsible to manage PA, but responsibility to reduce PA was also allocated to nurses, patients, primary care

#### CONCLUSION

Interventional radiologists understand the importance of PA as well as its clinical relevance in terms of compromising patient care. As a result, radiologists are willing to discuss PA if raised by the patients. Respondents most preferred pre-procedural education, anti-anxiety medication, and therapeutic interactions to manage PA, but responsibility for PA management was believed to be shared among radiologists, patients, family members, and other healthcare providers.

# CLINICAL RELEVANCE/APPLICATION

Pre-procedural anxiety is exhibited by most patients. This study suggests that anxiety management is important to radiologists and the most preferred practices to reduce pre-procedural anxiety include patient education, anxiolytic medications, and empathetic care.



## VI217-SD-MOA6

## Prostate Artery Embolization: How Does Additional Cone-Beam-CT Influence the Procedure

Monday, Nov. 26 12:15PM - 12:45PM Room: VI Community, Learning Center Station #6

### Participants

Rene Aschenbach, MD, Jena, Germany (*Presenter*) Nothing to Disclose Ioannis Diamantis, Jena, Germany (*Abstract Co-Author*) Nothing to Disclose Felix V. Guettler, Jena, Germany (*Abstract Co-Author*) Nothing to Disclose Ulf K. Teichgraeber, MD, Jena, Germany (*Abstract Co-Author*) Research Consultant, W. L. Gore & Associates, Inc Research Consultant, Siemens AG Research Consultant, CeloNova BioSciences, Inc Research Consultant, General Electric Company Tobias Franiel, Jena, Germany (*Abstract Co-Author*) Nothing to Disclose

## For information about this presentation, contact:

rene.aschenbach@med.uni-jena.de

# PURPOSE

To evaluate the influence of additional cone-beam-CT on the radiation dose, the contrast-media amount, the number of series and the fluoroscopy time of prostate artery embolization.

## METHOD AND MATERIALS

42 patients were retrospectively analyzed undergoing bilateral prostate artery embolization. 21 patient receive additional conebeam-CT to evaluate the origins of prostatic arteries, 21 patients didn't. Characteristical imaging parameters like contrast-media amount, number of needed series (projections), dose-area-product in total and overall fluoroscopy time were analyzed and compared.For statistical evaluation the median values were calculated and compared with student 's 2-sided t-test. Statistical significance was determined as 0.05 (95%).

#### RESULTS

All procedures were performed without adverse events. Following results for evaluated parameters for procedure without/with cone-beam-CT: contrast-media amount: 67ml/114ml, p=0.001 statistically significant; number of series: 29/19, p=0.02 statistically significant; dose-area-product: 24180µGy/mSquared / 29933µGy/mSquared, p= 0.2 statistically not significant and overall fluoroscopy time: 18:34 min / 22:00 min, p= 0.3, statistically not significant.

## CONCLUSION

Additional cone-beam-CT can reduce the needed number of projections/series by better identification of the origins of the prostatic arteries. In contrast additional cone-beam-CT causes significant higher contrast-media amount and radiation dose (not significant) as well as higher fluoroscopy times. Therefore the use of cone-beam-Ct should be indicated very strictly. Alternative vascular imaging techniques , e.g. MR-angiography, and sophisticated post processing can be used to determine prostate artery origins prior to embolization and can help to reduce imaging time, radiation exposure and contrast media amount for the patient.

## **CLINICAL RELEVANCE/APPLICATION**

Interventionalist should be aware of the relevant radiation exposure for the patient and the staff in prostate artery embolization. The use of cone-beam-CT should be indicated very strong, because it causes more radiation and contrast-media amount.



## VI218-SD-MOA7

Intrahepatic Cholangiocarcinoma: Treatment Approaches and Survival Trends for Surgically Ineligible Patients

Monday, Nov. 26 12:15PM - 12:45PM Room: VI Community, Learning Center Station #7



# Participants

Johannes Uhlig, Goettingen, Germany (*Presenter*) Nothing to Disclose Cortlandt Sellers, New Haven, CT (*Abstract Co-Author*) Nothing to Disclose Hyun S. Kim, MD, New Haven, CT (*Abstract Co-Author*) Nothing to Disclose

# For information about this presentation, contact:

johannes.uhlig@med.uni-goettingen.de

## PURPOSE

To evaluate current treatment approaches and survival trends among surgically ineligible patients with surgically intrahepatic cholangiocarcinoma (ICC).

## **METHOD AND MATERIALS**

The 2004-2015 National Cancer Database was retrospectively analyzed for histopathologically proven ICC. Interventional oncology (IO) included local tissue destruction and radioembolization. Baseline variables were evaluated as predictors for treatment allocation. Overall survival was analyzed via multivariable Cox models.

## RESULTS

9,655 patients with ICC were included, of which 401 patients received IO (4.1%), 776 patients radiation oncology (RO; 8%), 4,749 patients chemotherapy (49.2%), and 3,729 patients remained untreated. Increased likelihood of treatment via interventional oncology was observed for younger male patients, those with Medicare or private insurance, higher income and education, lower comorbidities and cancer stage, and patients treated at academic centers compared to other treatment approaches (p<0.05).Interventional oncology yielded highest overall survival compared to all other treatment approaches (2-year overall survival rate: IO 41.5%; RO 28.2%; chemotherapy 17.6%; no treatment 7.2%). After multivariable adjustment for potential confounders, a statistically significant survival benefit was observed for interventional oncology versus radiation oncology (HR=0.86, p=0.02), chemotherapy (HR=0.7, p<0.001) and no treatment (HR=0.31, p<0.001). A significant interaction term between treatment year and approach was evident (p<0.01), indicating that treatment effectiveness of IO, RO and chemotherapy increased from 2004-2015.

# CONCLUSION

Treatment allocation for surgically ineligible ICC patients shows marked variation depending on socioeconomic and cancer factors. Interventional oncology demonstrated superior overall survival compared to other non-surgical treatment options. Healthcare access and utilization must be targeted to address outcome discrepancies, potentially providing interventional oncology to a broader patient population.

### **CLINICAL RELEVANCE/APPLICATION**

For surgically ineligible ICC, interventional oncology via local tissue destruction or radioembolization offers superior overall survival compared to radiation oncology, chemotherapy and no treatment.



# AI001-MOC

# **Multi-modal Classification**

Monday, Nov. 26 12:30PM - 2:00PM Room: AI Community, Learning Center

# Title and Abstract

Multi-modal Classification This session will focus on multimodal classification. Classification is the recognition of an image or some portion of an image being of one type or another, such as 'tumor' or 'infection'. Multimodal classification means that there are more than 2 classes. While this is logically simple to understand, it presents some unique challenges that will be discussed.



## AI205-SD-MOB1

Solid Renal Tumor Detection Using Convolutional Neural Networks

Monday, Nov. 26 12:45PM - 1:15PM Room: AI Community, Learning Center Station #1

#### **Participants**

Osvaldo Landi Junior, MD, Sao Paulo, Brazil (*Presenter*) Nothing to Disclose Hanna R. Dalla Pria, MD, Sao Paulo, Brazil (*Abstract Co-Author*) Nothing to Disclose Juliana C. Yoshitani, MD, Sao Paulo, Brazil (*Abstract Co-Author*) Nothing to Disclose Lucas Pereira, Goiania, Brazil (*Abstract Co-Author*) Nothing to Disclose Felipe C. Kitamura, MD, MSC, Sao Paulo, Brazil (*Abstract Co-Author*) Developer, DASA Daisy T. Kase, Sao Paulo, Brazil (*Abstract Co-Author*) Nothing to Disclose Marcelo Arcuri, MD, Sao Paulo, Brazil (*Abstract Co-Author*) Nothing to Disclose Anderson Soares, Goiania, Brazil (*Abstract Co-Author*) Nothing to Disclose Marcio Ricardo T. Garcia, MD, Sao Paulo-SP, Brazil (*Abstract Co-Author*) Nothing to Disclose Nitamar Abdala, MD, PhD, Mogi Das Cruzes, Brazil (*Abstract Co-Author*) Nothing to Disclose

#### For information about this presentation, contact:

osv.landi@gmail.com

### CONCLUSION

The present model proved to be able to differentiate solid renal tumors from normal kidneys with a high accuracy rate. It's refinement and implementation could help to guide patients through healthcare system workflows, aiding in early tumor detection and thus allowing prompt intervention for better clinical outcomes.

#### Background

The wide application of diagnostic imaging methods in recent years has lead to an increasing number of incidental tumors, including kidney tumors. These lesions are often presented as early-stage localized renal malignancies, which has possibly contributed to the reduced mortality and morbidity of renal cancer as a whole due to its early detection. In addition, while the standard care for these patients is excision, nephron sparing surgery has emerged as an oncologically equivalent alternative to radical nephrectomy in most cases of localized renal cell carcinoma, reducing the negative sequelae of traditional surgical interventions, such as chronic kidney disease. In this study, we propose a convolutional neural network (CNN) model to detect solid renal tumors in abdominal computed tomography, with potential to collaborate in early detection and consequent improvement to patient prognosis.

#### **Evaluation**

This retrospective study was approved by our institutional review board, and written informed consent was waived. A total of 73 anonymized abdominal computed tomography studies were selected based on the hospital records. Kidney images were cropped from these studies in axial, coronal and sagittal axis, yielding 951 normal kidney images and 888 solid renal tumor images. This dataset was randomized in the patient level into training (65%), validation (15%) and test (20%) subsets. After preprocessing, an in-house CNN with ice modules was trained from scratch with online data augmentation. Optimization was done with random grid search and regularization.

#### Discussion

In the present study, our model achieved up to 79% accuracy for differentiating normal kidneys from solid renal tumors, with a precision of 91.81%, recall of 59%, f-score of 71.88% and area under the ROC curve of 0.89.



## AI206-SD-MOB2

## Improving Radiology Appointment Wait Time Prediction with Machine Learning

Monday, Nov. 26 12:45PM - 1:15PM Room: AI Community, Learning Center Station #2

#### **Participants**

Steven P. Guitron, MS,BS, Boston, MA (*Presenter*) Nothing to Disclose Darren P. Parke, BA,MA, Boston, MA (*Abstract Co-Author*) Nothing to Disclose Oleg S. Pianykh, Newton Highlands, MA (*Abstract Co-Author*) Nothing to Disclose

### CONCLUSION

We implemented a real-time model that can generate accurate wait time predictions using only common RIS data. Using machine learning with large predictor sets significantly improved the prediction quality. Our approach can be easily replicated at other facilities to provide patients with the most accurate wait time information.

### Background

Radiology patients can be frustrated by the seemingly opaque experience of waiting for their exams as daily wait time patterns can change significantly. Previously, to address this problem at Massachusetts General Hospital, a simple 3-predictor linear regression model was made to display estimated patient wait times. By studying the nonlinearity of historical waits, our goal was to develop a more accurate model that could better capture wait time fluctuations using the power of machine learning (ML).

#### **Evaluation**

Raw data was pulled from the hospital's Radiology Information System (RIS). 52 predictors were automatically generated, including line size, previous wait times, and appointment lengths. A custom ML library was developed, and several models were implemented: least squares regression, elastic net, lasso, generalized linear model, and random forest. After training each, the model with the least error is chosen to predict wait times. To display real time predictions, models are stored in the database with expiration dates. The expired models are retrained, enabling capture of any changes in patient workflow. Performance was optimized to compute predictions in less than 2 sec. Thus, the algorithm was optimized to automatically choose which model to use and when to retrain, completely unsupervised. Additionally, our algorithm provides an interactive display of recent prediction history, where less accurate predictions can be investigated.

#### Discussion

Using our ML-based model, we explained up to 60.4% of out-of-sample variance (improved from 0% with the 3-predictor model). Using a popular CT resource, we improved average prediction error from 30.72 min to 19.83 min. Our best models can predict better than the historical average 74% of the time.



## AI208-SD-MOB3

3D Context Enhanced Region-based Convolutional Neural Network for Universal Lesion Detection in a Large Database of 32,735 Manually Measured Lesions on Body CT

Monday, Nov. 26 12:45PM - 1:15PM Room: AI Community, Learning Center Station #3

#### Participants

Ke Yan, Bethesda, MD (Presenter) Nothing to Disclose

Mohammad Hadi Bagheri, MD, Bethesda, MD (Abstract Co-Author) Nothing to Disclose

Ronald M. Summers, MD, PhD, Bethesda, MD (*Abstract Co-Author*) Royalties, iCAD, Inc; Royalties, Koninklijke Philips NV; Royalties, ScanMed, LLC; Research support, Ping An Insurance Company of China, Ltd; Researcher, Carestream Health, Inc; Research support, NVIDIA Corporation; ; ; ;

### For information about this presentation, contact:

yankethu@foxmail.com

#### PURPOSE

Detecting lesions from CT scans is an important yet challenging problem because non-lesions and lesions can have similar appearance. 3D context is very helpful in such differentiation tasks. However, most existing detection frameworks of convolutional neural networks (CNNs) are designed for 2D images. Methods which use 3D information are either not efficient or memory-consuming. In this paper, we propose 3D context enhanced region-based CNN (3DCE) to incorporate 3D context information efficiently by aggregating feature maps of 2D images. Besides, current lesion detectors can typically find only one kind of lesion. We develop a universal lesion detector that covers all kinds of lesions in one framework.

#### **METHOD AND MATERIALS**

The universal lesion detector relies on the DeepLesion dataset, which was collected by us and contains 32,735 lesions manually annotated on CT scans. It includes a variety of lesions such as lung nodules, liver tumors, adenopathy, bone lesions, etc. The proposed 3DCE is designed based on a 2D region-based fully convolutional network. To incorporate 3D information, we input 3M slices to the network. The central slice contains the ground-truth bounding-box and the other slices provide the 3D context. They are grouped to M 3-channel images. M feature maps are then extracted and concatenated to aggregate 3D information. We combine this fused feature map and the lesion proposals generated by a region proposal network to obtain the final detection results. 3DCE is memory-friendly, easy to train, less prone to overfitting, with the training and inference process both end-to-end (requiring only one run).

### RESULTS

The train/val/test sets of the challenging DeepLesion dataset contain 70%, 15%, 15% of the data split in patient level. On the test set, the sensitivity of 3DCE at 4 false positives per image is 84.37%, compared to 80.32% of the baseline faster RCNN algorithm. Smaller lesions and bone lesions benefit more from 3D information (5% and 8% improvement).

## CONCLUSION

We proposed an algorithm to leverage the 3D context when detecting lesions in volumetric data. It consistently improved the detection accuracy on the DeepLesion dataset.

## **CLINICAL RELEVANCE/APPLICATION**

The proposed algorithm can be applied in all automated lesion detection problems where 3D context is helpful. The universal lesion detector can help radiologists find all types of lesions, which is more useful than single-purpose detectors in practice.



## AI209-SD-MOB4

Recognition of Pediatric Long-Bone Fractures in the Setting of Variable Open Growth Plates by Convolutional Neural Networks

Monday, Nov. 26 12:45PM - 1:15PM Room: AI Community, Learning Center Station #4

## Participants

Zbigniew Starosolski, PhD, Houston, TX (*Presenter*) Stockholder, Alzeca Biosciences, LLC J. H. Kan, MD, Houston, TX (*Abstract Co-Author*) Nothing to Disclose Ananth Annapragada, PhD, Houston, TX (*Abstract Co-Author*) Stockholder, Alzeca Biosciences, LLC Stockholder, Sensulin, LLC Stockholder, Abbott Laboratories Stockholder, Johnson & Johnson

For information about this presentation, contact:

zastaros@texaschildrens.org

## PURPOSE

Convolutional neural networks (CNNs) show promise for radiologic imaging interpretation. Fracture morphology heterogeneity in the setting of skeletal immaturity with variable appearances of physes and apophyses are a challenge for automatic classification. The purpose of this study was to evaluate the effect of CNN architecture on the computer-aided diagnosis (CAD) of long-bone fractures in pediatric patients of age 3 months to 18 years.

#### **METHOD AND MATERIALS**

An IRB approved dataset obtained at a children's hospital from 2015-18 that included 1444 pediatric fractures and 1147 normal radiographs of the appendicular skeleton was used. Fracture locations were recorded in image coordinates for further dataset generation. Radiographs were patched into 512x512 imagesets from the raw DICOM images. Patches were automatically generated in a random fashion along the calculated centerline of the long bone. Training set including 256000 patches with fractures and the same number showing normal bone. The validation set and test set each had 32000 images for each class. Four different CNN architectures were tested: VGG19, U-net and with the utilization of transfer learning Xception and DenseNet.

#### RESULTS

The accuracies of classification for relatively shallow VGG19, U-net (10 and 26 layers respectively) were 50.0% and 52.9% respectively. Transfer learning networks Xception and DenseNet (126 and 201 layers respectively) resulted in 71.3% and 65.8% respectively. The latest CNNs achieved specificity 81.7% and 86.3%, sensitivity 60.9% and 45.3% respectively. The majority of the false negative exams included indistinct fracture lines or were one of the fracture types not well represented in the training set. The false positive exams were all not well represented in the training set and constituted fractures near a joint line of the lower extremity.

### CONCLUSION

The most accurate binomial fracture classification was recorded by well parameterized CNNs using transfer learning. The automated patch approach eliminated image scaling, and allowed localization of the classified fracture within a relatively narrow spatial domain.

#### **CLINICAL RELEVANCE/APPLICATION**

Binomial fracture identification is possible by CNN architecture on CAD of pediatric long bone fractures in the setting of open growth plates and apophyses and is able to distinguish fractures from physius. We expect that with the larger representation of each fracture type accuracy will improve.



## BR182-ED-MOB7

Advances in Radiology Education: Development of Subspecialty Specific Entrustable Professional Activities Using a Double Delphi Technique

Monday, Nov. 26 12:45PM - 1:15PM Room: BR Community, Learning Center Station #7

## Participants

Monica M. Sheth, MD, Lake Success, NY (*Presenter*) Nothing to Disclose Alice Fornari, Manhassett, NY (*Abstract Co-Author*) Nothing to Disclose Ryan W. Woods, MD, MPH, Madison, WI (*Abstract Co-Author*) Nothing to Disclose Katherine A. Klein, MD, Ann Arbor, MI (*Abstract Co-Author*) Nothing to Disclose Priscilla J. Slanetz, MD, MPH, Belmont, MA (*Abstract Co-Author*) Nothing to Disclose Petra J. Lewis, MD, Lebanon, NH (*Abstract Co-Author*) Nothing to Disclose

#### For information about this presentation, contact:

msheth@northwell.edu

### **TEACHING POINTS**

1. EPAs provide practicality to our current means of assessing trainee readiness for clinical practice by representing an essential skill or task performed in daily clinical practice. 2. The developed breast imaging specific EPAs support the General Radiology EPAs published in 2016 while providing a more refined scope of practice specific to the subspecialty. 3. The Delphi technique is a methodologically approved consensus driven process used to synthesize and validate expert opinion when evidence is not available.

## TABLE OF CONTENTS/OUTLINE

\*Introduction: Background; development of EPAs to bridge gap between competency based training and clinical practice by framing competencies into clinical context; 5 Levels of entrustment; Alignment with ACGME competencies, subcompetencies and milestones; extension of general radiology EPAs; Need for subspecialty specific EPAs \*Methods: Development of EPA list; Validation via Double Delphi Technique; Refinement by educational theorists; role of facilitator in entire process \*Outcome: 8 EPAs specific to breast Imaging \*Challenges \*Next Steps: EPA-based online curriculum development and assessments; providing guidance for other subspecialties in radiology to develop their own EPAs



#### BR183-ED-MOB8

Two Faces Breast Cancer: Shooting the Enemy More Than One Time with Biopsy Gun to Unmask It

Monday, Nov. 26 12:45PM - 1:15PM Room: BR Community, Learning Center Station #8

#### Awards Cum Laude

## Participants

Lee Van Diniz, MD, Botucatu, Brazil (*Presenter*) Nothing to Disclose Lucas P. Rodrigues, MD, Botucatu, Brazil (*Abstract Co-Author*) Nothing to Disclose Eduardo C. Pessoa, PhD,MD, Botucatu, Brazil (*Abstract Co-Author*) Nothing to Disclose Julia d. Veloso, Botucatu, Brazil (*Abstract Co-Author*) Nothing to Disclose Guilherme B. Neves, MD, Botucatu, Brazil (*Abstract Co-Author*) Nothing to Disclose Carla P. Pessoa, PhD,MD, Botucatu, Brazil (*Abstract Co-Author*) Nothing to Disclose Joana C. Machado, Botucatu, Brazil (*Abstract Co-Author*) Nothing to Disclose Ana Carolina D. Augusto, MD, Botucatu, Brazil (*Abstract Co-Author*) Nothing to Disclose Seizo Yamashita, Botucatu, Brazil (*Abstract Co-Author*) Nothing to Disclose

# For information about this presentation, contact:

leevandiniz@gmail.com

## **TEACHING POINTS**

Molecular subtypes classification is important to guide treatment, including primary chemotherapy, and developing new therapies. The purposes of this Education Exhibit are: 1. To discuss about molecular subtypes of breast cancer. 2. To demonstrate an association between the molecular subtype and ultrasound images. 3.To discuss some cases that we chose to do the biopsy in more than one location because ultrasound characteristics showed different patterns in the same patient and the histopathology confirmed different results.

### TABLE OF CONTENTS/OUTLINE

1. Introduction. 2. Molecular subtypes of breast cancer. 3. Radiopathological characteristics of molecular subtypes. 4. Show cases that we chose to do the biopsy in more than one location because the image characteristics showed different patterns in the same patient. 5. To discuss about possibility of choosing biopsy in two different locations and whether these radiological changes showed different histopathological characteristics in our cases. 5. To emphasize how the decision in making biopsy in more than one location can alter the patient's prognosis and treatment.



#### BR184-ED-MOB9

## Don't Forget the Breast: Incidental Breast Findings on CT

Monday, Nov. 26 12:45PM - 1:15PM Room: BR Community, Learning Center Station #9

#### **Participants**

Ayushi Singh, DO, New York, NY (*Presenter*) Nothing to Disclose Priyanka Kadaba, MD, New York, NY (*Abstract Co-Author*) Nothing to Disclose Mary M. Salvatore, MD, New York, NY (*Abstract Co-Author*) Nothing to Disclose Richard H. Stern, PHD, Englewood, NJ (*Abstract Co-Author*) Nothing to Disclose Laurie R. Margolies, MD, New York, NY (*Abstract Co-Author*) Research Consultant, FUJIFILM Holdings Corporation

## For information about this presentation, contact:

ayushi.singh@mountsinai.org

#### **TEACHING POINTS**

Evaluation of the breast parenchyma on CT can lead to earlier diagnosis of breast cancer Demonstrate malignant and benign lesions in the breast on CT and which lesions warrant further work-up Demonstrate the appearance of the breast on CT in the postoperative setting Provide guidelines for interpretation of breast lesions on CT on the basis of the breast imaging lexicon

## TABLE OF CONTENTS/OUTLINE

1. Introduction a. Incidence and outcome of breast findings on CT imaging b. Advantages of imaging the breast on CT i. Improved contrast resolution ii. Larger field of view/cross-sectional capability iii. Better lesions located near the chest wall and medially 2. Breast Findings a. Malignant i. Invasive ductal carcinoma ii. Invasive lobular carcinoma iii. Invasive ductal and lobular carcinoma iv. Secondary lymphoma of the Breast v. Inflammatory Carcinoma b. Benign i. Fibroadenoma ii. Benign Calcifications iii. Hamartoma iv. Lactating breast c. Postoperative findings i. Hematoma/Seroma ii. Fibrous Scar 3. Breast Imaging Lexicon for CT a. Rule of Thumb: Always include shape, density, pattern of enhancement and associated findings



#### BR185-ED-MOB10

You Sow What You Reap: Tumoral Needle Tract Seeding After Percutaneous Breast Biopsy

Monday, Nov. 26 12:45PM - 1:15PM Room: BR Community, Learning Center Station #10

## Awards Certificate of Merit

## Participants

Heni D. Skaf, MD, Sao Paulo, Brazil (*Presenter*) Nothing to Disclose Rafael L. Macedo, MD, Sao Paulo, Brazil (*Abstract Co-Author*) Nothing to Disclose Caio D. Pinheiro, MBBS, Sao Paulo, Brazil (*Abstract Co-Author*) Nothing to Disclose Cecilia S. Goldman, MD, Sao Paulo, Brazil (*Abstract Co-Author*) Nothing to Disclose Matheus V. Paulino, MD, Sao Paulo, Brazil (*Abstract Co-Author*) Nothing to Disclose Su J. Kim, Sao Paulo, Brazil (*Abstract Co-Author*) Nothing to Disclose Carlos Shimizu, MD, Sao Paulo, Brazil (*Abstract Co-Author*) Nothing to Disclose Juliana H. Catani, MD, Sao Paulo, Brazil (*Abstract Co-Author*) Nothing to Disclose Tatiana C. Tucunduva, MD, Sao Paulo, Brazil (*Abstract Co-Author*) Nothing to Disclose Vera Christina C. Ferreira, MD, Sao Paulo, Brazil (*Abstract Co-Author*) Nothing to Disclose Erica Endo, MD, Sao Paulo, Brazil (*Abstract Co-Author*) Nothing to Disclose Luciano F. Chala, MD, Sao Paulo, Brazil (*Abstract Co-Author*) Nothing to Disclose Nestor Barros, Sao Paulo, Brazil (*Abstract Co-Author*) Nothing to Disclose

For information about this presentation, contact:

## rafajf85@gmail.com

#### **TEACHING POINTS**

The purposes of this exhibit are: 1- Review our institution's cases of tumoral needle tract seeding after percutaneous breast biopsy. 2- Review the prevalence of tumoral needle tract seeding after percutaneous breast biopsy. 3 - Review which tumors are more susceptible to this complication. 4 - Evaluate the factors that aggravate this phenomenon. 5 - Identify the best ways to prevent this complication.

### TABLE OF CONTENTS/OUTLINE

Review breast tumoral needle tract seeding cases at our radiology department, documented in multiple methods (MRI, ultrasound and mammography).
 Background: epidemiology and clinical aspects of needle tract tumoral seeding after percutaneous biopsy.
 Histopathological and imaging features of the most involved tumors.
 Identify factors that increase the risk of this complication and how to minimize it.



#### BR186-ED-MOB11

# **Increased Unnaturally? What Lies Beneath Markedly Enlarged Breast**

Monday, Nov. 26 12:45PM - 1:15PM Room: BR Community, Learning Center Station #11

#### **Participants**

Sungmin Moon, Gwangju, Korea, Republic Of (*Presenter*) Nothing to Disclose Hyo Soon Lim, MD, Jeollanam-Do, Korea, Republic Of (*Abstract Co-Author*) Nothing to Disclose So Yeon Ki, Gwangju, Korea, Republic Of (*Abstract Co-Author*) Nothing to Disclose

## **TEACHING POINTS**

To aid approach for evaluation of enlarged breast : diffuse breast enlargement or presence of huge mass or other unusual cause of enlarged breast Provide pictorial review of diseases using multimodality image and discuss clinicopathological findings and management To know enlarged breast can be associated with benign as well as malignant condition in peripuberty, adult women and men

# TABLE OF CONTENTS/OUTLINE

1. Normal breast development stage 2. Categorization for evaluation of enlarged breast 3. Case based review of diseases (A) Diffuse breast enlargement Infection - Mastitis Hormonal disturbance - Gynecomastia Other cause - Edema caused by extramammary origin - Edema caused by mammary procedure (B) Neoplasm Benign - Hamartoma - Fibroadenoma - Giant juvenile fibroadenoma - Fibrocystic disease - Benign phyllodes tumor Malignant - Invasive ductal cancer - Inflammatory breast cancer -Malignant phyllodes tumor (C) Extrammamary location of mass: Chest wall - Lipoma - Malignant fibrous histiocytoma 4. Differential diagnosis: mastitis vs. inflammatory breast cancer 5. Conclusion



### BR187-ED-MOB12

# 2018 New Trends! Axillary Ultrasound

Monday, Nov. 26 12:45PM - 1:15PM Room: BR Community, Learning Center Station #12

#### **Participants**

Karina Pesce, Capital Federal, Argentina (*Abstract Co-Author*) Nothing to Disclose Maria Jose Chico, Buenos Aires, Argentina (*Presenter*) Nothing to Disclose Carolina Hadad, Capital Federal, Argentina (*Abstract Co-Author*) Nothing to Disclose Roberto Secco, Capital Federal, Argentina (*Abstract Co-Author*) Nothing to Disclose Griselda Choque Leniz, MEd, MEd, Longchamps, Argentina (*Abstract Co-Author*) Nothing to Disclose

## For information about this presentation, contact:

drakarina.pesce@gmail.com

### **TEACHING POINTS**

1-Analyze the role of axillary ultrasound in the patient with breast cancer 2-Discuss the role of axillary ultrasound in the evaluation of newly diagnosed breast cancer patients given recent changes in the surgical management of the axilla. 3- Emphasize the common sonographic features of axillary metastasis

## TABLE OF CONTENTS/OUTLINE

 Introduction: Axillary staging in the context of breast cancer is a contentious topic. Ultrasound is the most commonly used modality for axillary evaluation given its wide availability. Current debate questions whether there is a benefit to diagnosing metastasis with ultrasound-guided needle biopsy as this may lead to more axillary node dissections in an era of its decreasing role.
 What is the future of axillary ultrasound in the axillary management of breast cancer?
 An updated literature review 4- Future Developments 5-Conclusion



### BR235-SD-MOB1

Does the Tumor Stiffness of Shear Wave Elastography Correlate with Tumor Hypoxia or Fibrosis of Breast Cancer?

Monday, Nov. 26 12:45PM - 1:15PM Room: BR Community, Learning Center Station #1

# Participants

Myoung-Ae Kwon, Ansan, Korea, Republic Of (*Presenter*) Nothing to Disclose Bo Kyoung Seo, MD, PhD, Ansan, Korea, Republic Of (*Abstract Co-Author*) Research Grant, Canon Medical Systems Corporation; Research Grant, Guerbet SA; Research Grant, Koninklijke Philips NV; Eun Kyung Park, MD,PhD, Ansan, Korea, Republic Of (*Abstract Co-Author*) Nothing to Disclose Jaehyung Cha, Seoul, Korea, Republic Of (*Abstract Co-Author*) Nothing to Disclose Ok Hee Woo, MD, Seoul, Korea, Republic Of (*Abstract Co-Author*) Nothing to Disclose Kyu Ran Cho, MD, PhD, Seoul, Korea, Republic Of (*Abstract Co-Author*) Nothing to Disclose Sung Eun Song, MD, Seoul, Korea, Republic Of (*Abstract Co-Author*) Nothing to Disclose

#### For information about this presentation, contact:

kwon4715@gmail.com

### PURPOSE

Hypoxic and stiff microenvironments of breast cancer promote metastasis and resistance to therapy. The purpose of this study was to investigate whether the tumor stiffness parameters of shear wave elastography (SWE) are related with tumor hypoxia or fibrosis in invasive breast cancer.

## METHOD AND MATERIALS

This retrospective study was approved by the institutional review board. From June 2016 to January 2018, eighty-two women with invasive breast cancers who underwent SWE before treatment were enrolled. We used Aplio 500 US equipment (Toshiba Medical Systems Corporation, Japan). On the SWE features, average tumor elasticity (Eaverage) and tumor-to-fat elasticity ratio (Eratio) were extracted. Glucose transporter 1 (GLUT1) for evaluation of tumor hypoxia and Masson's trichrome staining (MT) for fibrosis were used. Immunostaining and automated digital image analysis were performed for assessment of GLUT1 and MT activities. Correlations analysis was performed between SWE parameters (Eaverage and Eratio) and GLUT1 or MT activities using spearman's correlation. Correlations with biomarkers according to molecular subtype, tumor grade, lymph node, hormone receptor, HER2, and Ki67 were compared using t-test, Mann-Whitney test, and Kruskal-Wallis test with Bonferroni correction.

#### RESULTS

SWE parameters including Eaverage (r=0.676) and Eratio (r=0.411) were significantly correlated with GLUT1 activities (P<0.001 for all). On the other hand, SWE parameters were not related with MT activities (P>0.05 for all). Eaverage values were significantly higher in breast cancers with positive lymph node, negative hormone receptor, high Ki67, and high grade (P<0.03 for all). Eratio values were higher in breast cancers with high Ki67 and high grade (P<0.05 for all). Eaverage values were different according to molecular subtypes of breast cancer (P=0.009). Eaverage values were significantly higher in triple negative cancers than those in luminal A cancers (P=0.03).

## CONCLUSION

Tumor stiffness measured by SWE is associated with tumor hypoxia and biomarkers that affect tumor prognosis and it not related to fibrous components.

## **CLINICAL RELEVANCE/APPLICATION**

Tumor stiffness parameters as measured by SWE is significantly correlated with tumor hypoxia and histologic biomarkers and can be used to predict prognosis of invasive breast cancer.



### BR236-SD-MOB2

Therapeutic Nipple Sparing Mastectomy (NSM): Tumor-To-Nipple Distance (TND) on Preoperative MRI as Useful Variable in Surgical Patient Selection and Outcomes

Monday, Nov. 26 12:45PM - 1:15PM Room: BR Community, Learning Center Station #2

## Participants

Jiyon Lee, MD, New York, NY (*Presenter*) Nothing to Disclose Kristin L. Harris, DO, New York, NY (*Abstract Co-Author*) Nothing to Disclose Jordan Frey, MD, New York, NY (*Abstract Co-Author*) Nothing to Disclose Ara Salibian, MD, New York, NY (*Abstract Co-Author*) Nothing to Disclose Mihye Choi, MD, New York, NY (*Abstract Co-Author*) Nothing to Disclose Nolan Karp, MD, New York, NY (*Abstract Co-Author*) Nothing to Disclose Deborah Axelrod, MD, New York, NY (*Abstract Co-Author*) Nothing to Disclose

#### For information about this presentation, contact:

jiyon.lee@nyumc.org

## PURPOSE

Newer surgical oncological nipple-sparing mastectomy (NSM) enables nipple-areola complex (NAC) preservation. Patient selection criteria and oncologic outcomes data are being established. We evaluated tumor-to-nipple distance (TND) on preop MR in NSM patients to help determine cancer recurrence risk factors.

## **METHOD AND MATERIALS**

Retrospective institutional review of 2/2006- 7/2017 yielded 496 therapeutic NSMs in 312 women (mean f/u 48.25 m). Demographics, outcomes, trends, and cancer recurrences were reviewed. TND was measured on available preop MRIs using axial, sagittal, or multiplanar reconstruction images. Univariate analysis identified independent risk factors for cancer recurrence. p-values <0.05 significant.

## RESULTS

Mean patient age was 48.66 yo (23-65 y). 74.2% of NSMs were part of bilateral surgery. Most common were: IDC (52.4%) and DCIS (50.4%); and stage IA (42.5%) and stage 0 (31.3%) disease. Mean tumor size was 1.48 cm. 25.2% of NSMs had multifocal disease, 11.5% had LVI; 59.9% were ER+, 56.3% were PR+, and 42.5% were HER 2-neu +. SLN biopsy performed in 79.8% of cases. Positive subareolar biopsy on 6.4% frozen section and 6.7% permanent biopsy. Per NSM, the rate of local in-breast recurrence was 1.6% (N=8) and regional was 0.6% (N=3). Per patient, rates were 2.6% local, 1.0% regional, and 1.3% (N=4) distant mets. One local recurrence (12.5%) had positive permanent subareolar biopsy treated with NAC resection. Preop MRI in 171 NSMs showed mean TND 4.78 cm. TND did not signif differ between NSMs with and w/o locoregional recurrence (4.62 vs 4.78 cm; p=0.8758). However, NSMs with TND <=1 cm (25.0% vs 2.4%, p=0.0031) and <=2 cm (8.7% vs 2.0%; p=0.0218) were signif associated with locoregional recurrence. In univariate analysis, TND <=1 cm was the only signif risk factor (OR=13.5833, p=0.0385). Age <50 years (p=0.0503) and multifocal disease (p=0.0820), TND <=2 cm (p=0.1052), and positive permanent subareolar biopsy (p=0.1094) trended towards association with higher recurrence risk.

#### CONCLUSION

NSM had locoregional recurrence of 2.0%. TND of  $\leq 1$  cm and  $\leq 2$  cm were significantly associated with recurrence risk. TND  $\leq 1$  cm was significant predictor of locoregional recurrence on univariate analysis.

#### **CLINICAL RELEVANCE/APPLICATION**

NSM is oncologically safe with low locoregional recurrence of 2.0% in appropriately selected patients. TND of <=1 cm and <=2 cm on preoperative MRI can be useful variables in predicting recurrence.



## BR237-SD-MOB3

Determining the Appropriateness of Second Look Targeted Sonography Recommendation Following Detection of Suspicious Non-Mass Enhancement (NME) Detected on Breast Magnetic Resonance Imaging (MRI)

Monday, Nov. 26 12:45PM - 1:15PM Room: BR Community, Learning Center Station #3

## Participants

Jennifer J. Young, MD, MPH, Los Angeles, CA (*Presenter*) Nothing to Disclose Iram Dubin, MD, Los Angeles, CA (*Abstract Co-Author*) Nothing to Disclose Sonya Khan, MD, Los Angeles, CA (*Abstract Co-Author*) Nothing to Disclose Meghan Jardon, MD, Los Angeles, CA (*Abstract Co-Author*) Nothing to Disclose Kara-Lee Pool, MD, Los Angeles, CA (*Abstract Co-Author*) Nothing to Disclose Melissa M. Joines, MD, Santa Monica, CA (*Abstract Co-Author*) Nothing to Disclose

#### For information about this presentation, contact:

mjoines@mednet.ucla.edu

## PURPOSE

There are currently no evidence-based guidelines detailing the appropriateness of recommending targeted sonography versus proceeding directly to MRI-guided biopsy for suspicious non-mass enhancement (NME) detected on breast MRI. The purpose of this study is to determine if characteristics of suspicious NME are associated with detection of appropriate sonographic correlates on second look ultrasound.

#### **METHOD AND MATERIALS**

IRB approved, retrospective review of 4,292 contrast enhanced screening and diagnostic bilateral breast MRI examinations performed on female patients (ranging in age from 20 to 87 years old) at our institution between January 1, 2012 and December 31, 2015 was performed, focusing on the subset of 134 studies in which targeted sonography was recommended and subsequently performed for suspicious NME detected on MRI. Multivariate linear regression analysis (p > 0.05) was employed to analyze patient demographics as well as imaging study findings and characteristics in order to determine the likelihood of identifying an appropriate sonographic correlate on targeted sonography performed for suspicious NME.

#### RESULTS

Sonographic correlates were detected in 26% (35/134) of targeted ultrasounds performed for suspicious NME (all subtypes). Multivariate linear regression analysis demonstrating that suspicious linear NME seen on screening MRI was significantly associated with negative targeted sonography, coefficient -0.0787454 (p = 0.05, CI [-0.1576416, 0.0001507]), while segmentally distributed NME was significantly associated with detection of a sonographic correlate, coefficient 0.6343792 (p < 0.0001, CI [0.5294839, 0.7392745]). NME seen in the same quadrant as an enhancing mass on MRI was also significantly associated with detection of a sonographic correlate, coefficient 0.6343792 (p < 0.0001, CI [0.6914279, 0.889658]).

## CONCLUSION

This study demonstrates that specific characteristics of suspicious NME are differentially associated with detection of sonographic correlates on second look ultrasound, findings that can be further studied to guide appropriateness criteria for targeted sonography after detection of suspicious NME on breast MRI.

### **CLINICAL RELEVANCE/APPLICATION**

Developing appropriateness criteria for targeted sonography for suspicious NME detected on MRI aides patient care by reducing unnecessary second look ultrasound examinations, health care costs, and delay in time to diagnosis.



## BR238-SD-MOB4

Prediction of Neoadjuvant Chemotherapy Response using Radiogenomics of MR Imaging in Breast Cancer: Correlation of Quantitative and Qualitative MR findings with Results of Multi-Gene Classifier

Monday, Nov. 26 12:45PM - 1:15PM Room: BR Community, Learning Center Station #4

# Participants

Yukiko Tokuda, MD,PhD, Suita, Japan (*Presenter*) Nothing to Disclose Kaori Minamitani, MD, Suita, Japan (*Abstract Co-Author*) Nothing to Disclose Masahiro Yanagawa, MD, PhD, Suita, Japan (*Abstract Co-Author*) Nothing to Disclose Yasuto Naoi, MD,PhD, Suita, Japan (*Abstract Co-Author*) Research Grant, Sysmex Corporation; Speaker, Sysmex Corporation Shinzaburo Noguchi, MD,PhD, Suita, Japan (*Abstract Co-Author*) Research funded, Sysmex Corporation Speaker, Sysmex Corporation

Noriyuki Tomiyama, MD, PhD, Suita, Japan (Abstract Co-Author) Research Grant, Canon Medical Systems Corporation

# PURPOSE

To examine the correlation of magnetic resonance imaging (MRI) features with results of multi-gene classifier for predicting neoadjuvant chemotherapy (NAC) response of breast cancer.

## **METHOD AND MATERIALS**

This study included 120 patients with breast cancer who were classified into response (R) group (n=46) and non-response (NR) group (n=74) by using the immune-related 23-gene signature for NAC (IRSN23) for NAC sensitivity prediction. All patients had undergone a dynamic contrast-enhanced breast MRI (DCE-MRI). For quantitative data, the following DCE-MRI features were measured: volume ratio of each fast, medium and slow to whole mass in the initial phase; volume ratio of each washout, plateau and persistent to whole mass in the delayed phase; and both kurtosis and skewness of intensity histogram in whole mass on each phase. Mass size and volume were measured. For qualitative data, two breast radiologists independently interpreted and decided the findings by consensus reading. The value in examining associations with R- and NR-group were analyzed using univariate logistic regression (ULR). Significant parameters identified by the URL analysis were included in the multiple logistic regression (MLR) analysis. Each binary group of quantitative data was designated by a cutoff value decided by receiver-operating characteristic analysis.

#### RESULTS

ULR analysis revealed that volume ratio of slow, medium, washout, persistent, medium-washout, medium-plateau, and slowpersistent volume ratio, volume of the whole mass, skewness in the delayed phase, mass shape, mass margin, and multiple masses were significant indicators to divide into R- and NR- group. MLR analysis revealed that volume ratio of slow in the initial phase>34.4% and medium-washout<=4.5%, and round/oval shape were significant indicators associated with R-group (Odds ratio, 3.76, 4.16, and 4.35; 95% confidence interval, 1.44 to 9.86, 1.78 to 9.76, and 1.72 to 11.03; p=0.007, p=0.001, and 0.002, respectively).

## CONCLUSION

Volume ratio of slow >34.4% in the initial phase and medium-washout <=4.5% to the mass, and round/oval shape were found to be independent indicators associated with R-group.

# **CLINICAL RELEVANCE/APPLICATION**

Both quantitative and qualitative data of dynamic contrast-enhanced breast MRI might contribute to the prediction of neoadjuvant chemotherapy response of breast cancer using multi-gene classifier.



### BR239-SD-MOB5

### Breast Cancer and Breast Imaging Malpractice Litigation: A 10-Year Analysis and Update in Trends

Monday, Nov. 26 12:45PM - 1:15PM Room: BR Community, Learning Center Station #5

#### Awards Student Travel Stipend Award

#### Participants

Katerina Konstantinoff, MD, Saint Louis, MO (*Presenter*) Nothing to Disclose Catherine M. Appleton, MD, Saint Louis, MO (*Abstract Co-Author*) Scientific Advisory Board, Hologic, Inc Royalties, Oxford University Press Alison R. Gegios, MD, St. Louis, MO (*Abstract Co-Author*) Nothing to Disclose

Katie M. Miles, Saint Louis, MO (*Abstract Co-Author*) Nothing to Disclose Dawn Hui, MD, Saint Louis, MO (*Abstract Co-Author*) Nothing to Disclose Michelle V. Lee, MD, Saint Louis, MO (*Abstract Co-Author*) Nothing to Disclose

## For information about this presentation, contact:

konstantinoff@wustl.edu

# PURPOSE

The purpose of this study is to evaluate factors contributing to breast cancer and breast imaging-related medical malpractice cases.

## **METHOD AND MATERIALS**

A retrospective analysis of jury verdict and settlement reports in US state and federal courts on the Westlaw legal database was performed. The database was searched for 'malpractice' and 'breast cancer' related terms from 2005 to 2015. 253 cases were evaluated for factors including outcome, award amount, alleged causes of malpractice, patient demographics, defendant specialities, and other alleged factors claimed in the litigation. Data were summarized using descriptive statistics. Logistic regression was used to evaluate associations between factors and plaintiff award.

#### RESULTS

Median plaintiff age was 46 (IQR 39, 56). In cases that resulted in plaintiff payment, award amount was \$978,858±2,308,598. Delay in diagnosis was cited as a reason for claimed negligence in 82% of cases. Mean length of delay was 17±13 months. Named defendants were radiologists (43%), surgeons (27%), obstetrician/gynecologists (26%), and internal medicine/family practice (15%). Age, defendant type, and cancer stage were not significant predictors of case outcome. Failure to refer to a surgeon was two-fold (OR [95% CI]: 2.44 [1.085, 5.489]) more likely to be resolved with payment. Cases with a delay in diagnosis of >12 months were two-fold (OR [95% CI]: 2.129 [1.086, 4.175]) more likely to be resolved with payment compared to a delay <12 mos. Patients who failed to follow up as recommended were two-fold (OR [95% CI]: 2.31 [1.05, 5.10]) less likely to have their case be resolved with payment.

# CONCLUSION

Plaintiffs involved in breast cancer imaging-related malpractice cases tend to be younger than the median age of diagnosis of breast cancer for US women (62 per NCI Surveillance, Epidemiology and End Results data). Breast cancer-related suits involve physicians from multiple specialties, radiology being the most common. Delay in diagnosis, lack of surgeon referral, and lack of recommended follow-up are related to plaintiff payments and may be areas of professional practice to target to prevent over- and misuse of the medical malpractice system.

### **CLINICAL RELEVANCE/APPLICATION**

Breast cancer imaging-releated medical malpractice remains prevalent and costly for all involved. A better understanding of factors and trends in malpractice litigation can lead to medical malpractice system improvement.



#### BR240-SD-MOB6

**Measurement of Breast Density Using Bioimpedance** 

Monday, Nov. 26 12:45PM - 1:15PM Room: BR Community, Learning Center Station #6

FDA Discussions may include off-label uses.

#### Participants

Susan M. Astley, PhD, Manchester, United Kingdom (Presenter) Nothing to Disclose Elaine Harkness, PhD, Manchester, United Kingdom (Abstract Co-Author) Nothing to Disclose Ryan Halter, Hanover, NH (Abstract Co-Author) Nothing to Disclose Ethan Murphy, Hanover, NH (Abstract Co-Author) Nothing to Disclose Ethan Du-Crow, Manchester, United Kingdom (Abstract Co-Author) Nothing to Disclose Annabel L. Davies, Manchester, United Kingdom (Abstract Co-Author) Nothing to Disclose Josh W. Lindsay, Manchester, United Kingdom (Abstract Co-Author) Nothing to Disclose Katherine Graves, Slough, United Kingdom (Abstract Co-Author) Nothing to Disclose Jessica Ritchie, Manchester, United Kingdom (Abstract Co-Author) Nothing to Disclose Charlotte Day, Manchester, United Kingdom (Abstract Co-Author) Nothing to Disclose Kim Denton, Manchester, United Kingdom (Abstract Co-Author) Nothing to Disclose Sarah Sampson, Manchester, United Kingdom (Abstract Co-Author) Nothing to Disclose Anthony Maxwell, MBChB, FRCR, Manchester, United Kingdom (Abstract Co-Author) Nothing to Disclose Sacha Howell, Manchester, United Kingdom (Abstract Co-Author) Nothing to Disclose Anthony Howell, Manchester, United Kingdom (Abstract Co-Author) Nothing to Disclose D. Gareth Evans, Manchester, United Kingdom (Abstract Co-Author) Nothing to Disclose

## For information about this presentation, contact:

sue.astley@manchester.ac.uk

### PURPOSE

Breast density is associated with both risk of developing breast cancer and the effectiveness of mammography as a screening tool. An accurate and practical measurement method is crucial for personalising screening programmes and assessing the efficacy of preventive interventions. We evaluate the relationship between breast bioimpedance and volumetric breast density measured from mammograms. If mammographic density can be estimated using bioimpedance, this would provide a non-invasive, inexpensive and safe method of assessment.

# METHOD AND MATERIALS

Volumetric breast density (VBD) measured by Volpara from mammograms and bioimpedance measurements using a custom Electrical Impedance (EI) data acquisition device were measured in 211 women commencing a chemoprevention trial. Bioimpedance measurements at 3.2-102.4 kHz were made with the woman reclining at an angle of approximately 30°. Eight paediatric ECG electrodes were placed around and equidistant to the nipple. Bioimpedance was recorded from eight combinations of four electrodes (two delivering current and two measuring potential difference). The bioimpedance recorded from these eight combinations is averaged for each breast and compared to VBD. Data from women with missing VBD or bioimpedance signatures and those with poor electrode contact were excluded from the analysis.

### RESULTS

EI and VBD data were available for 106 women. As expected, VBD is inversely related to bioimpedance; low VBD breasts with a greater adipose content have higher impedance than more glandular breasts. Weighted least squares regression analysis suggests the relationship between EI and VBD is of the form y=AxB, where A=582.926 $\pm$ 6.062  $\Omega$ -1, B=-1.008 $\pm$ 0.0204, and has a Xred2 value of 14.05.

# CONCLUSION

EI has the potential to identify women with high breast density who are at increased risk of cancer or require supplemental screening, and those with low breast density who could potentially be screened less frequently. Further development of the technology is necessary to improve reliability.

## **CLINICAL RELEVANCE/APPLICATION**

A safe, practical and inexpensive method of assessing breast density is needed for personalising screening by risk of cancer and masking, and for assessing the efficacy of preventive interventions.



## CA166-ED-MOB8

Pap in a Snap: All You Need to Know About Papillary Muscles

Monday, Nov. 26 12:45PM - 1:15PM Room: CA Community, Learning Center Station #8

**FDA** Discussions may include off-label uses.

#### **Participants**

Prachi P. Agarwal, MD, Canton, MI (*Presenter*) Nothing to Disclose Sara Saberi, Ann Arbor, MI (*Abstract Co-Author*) Nothing to Disclose Sharlene M. Day, MD, Ann Arbor, MI (*Abstract Co-Author*) Nothing to Disclose Prabhakar Rajiah, MD, FRCR, Dallas, TX (*Abstract Co-Author*) Nothing to Disclose Elizabeth Lee, MD, Ann Arbor, MI (*Abstract Co-Author*) Nothing to Disclose Nicholas S. Burris, MD, San Francisco, CA (*Abstract Co-Author*) Entitled to royalties from liscensure of intellectual property to Imbio LLC Brent Little, MD, Boston, MA (*Abstract Co-Author*) Author, Reed Elsevier; Editor, Reed Elsevier

Kristopher W. Cummings, MD, Phoenix, AZ (*Abstract Co-Author*) Nothing to Disclose

## For information about this presentation, contact:

prachia@med.umich.edu

## **TEACHING POINTS**

1. Understand the anatomy of mitral subvalvular apparatus with emphasis on left ventricular papillary muscles (PM). 2. Recognize the radiologic findings of a wide spectrum of PM abnormalities 3. Develop an understanding of the relation between morphologic abnormalities and hemodynamic consequences

# TABLE OF CONTENTS/OUTLINE

1. Anatomy of mitral sub valvular apparatus 2. Spectrum of anatomic abnormalities and variants: a. Congenital: These include a wide spectrum ranging from variant anatomy to complex lesions such as parachute (single papillary muscle) and parachute like mitral valve. Variant anatomy becomes particularly important in the context of hypertrophic cardiomyopathy. Examples include accessory PM, displaced PM, anomalous direct insertion of PM to the mitral valve leaflet with absent or short chordae tendineae b. Ischemic heart disease/ trauma leading to scarring or rupture of PM c. Mitral valve prolapse and delayed enhancement of PM d. Tumors: Fibroelastoma, metastases e. Pitfalls: PM (especially accessory) can be misinterpreted for intraventricular mass/thrombus, apical insertion can be confused for hypertrophy 3. Functional consequences of papillary muscle abnormalities: a. Mitral valve dysfunction b. Sub aortic obstruction 4. Comprehensive imaging protocols for assessment

## **Honored Educators**

Presenters or authors on this event have been recognized as RSNA Honored Educators for participating in multiple qualifying educational activities. Honored Educators are invested in furthering the profession of radiology by delivering high-quality educational content in their field of study. Learn how you can become an honored educator by visiting the website at: https://www.rsna.org/Honored-Educator-Award/ Prabhakar Rajiah, MD, FRCR - 2014 Honored EducatorBrent Little, MD - 2018 Honored Educator



## CA217-SD-MOB1

A Comprehensive Comparison of Two Accelerated 4D-Flow Sequences in Healthy Volunteers Regarding Acquisition Time, Diagnostic Accuracy, Image Quality, and Importance of Eddy Currents Using the Software "Bloodline"

Monday, Nov. 26 12:45PM - 1:15PM Room: CA Community, Learning Center Station #1

#### Participants

Sebastian Ebel, MD, Leipzig, Germany (Presenter) Nothing to Disclose

#### For information about this presentation, contact:

sebastian.ebel@icloud.com

## PURPOSE

To prove the non-inferiority of a kt-GRAPPA 4D flow sequence compared to a standard GRAPPA sequence in healthy volunteers. In addition to the quantification of flow-parameters, image quality, susceptibility to artifacts, and the importance of eddy current correction (ECC) were assessed.

## METHOD AND MATERIALS

Fourty healthy volunteers (22 females, mean age 41.8±11.8 years) were examined at a 3T scanner. Anatomic and flow datasets of the thoracic aorta were acquired using a 3D-T2w-SPACE- and two accelerated 4D-flow sequences, one with k-t undersampling and one with a standard GRAPPA parallel imaging protocol. Additional 2D-flow measurements were used as the standard reference in the ascending and descending aorta. A new comprehensive, custom-made software tool ("Bloodline") allowed measurements of the flow volume and peak velocity at the exact same location using a standardized segmentation of the anatomical images for all measurements. Quantitative flow analyses were performed with and without ECC. Furthermore, overall image quality (oIQ) and the occurrence of motion artifacts (mIQ) were assessed using a qualitative scale from 0-2 with 2 indicating the best IQ

#### RESULTS

The use of the kt-GRAPPA sequence allowed a mean scan time reduction of 60% and provided significantly less motion artefacts than the standard GRAPPA sequence (mIQ 1.6 $\pm$ 0.6 vs. 0.84 $\pm$ 0.8; p<0.001). Both 4D-flow sequences demonstrated neither significant differences of the mean flow volume in the ascending aorta with 83.54 $\pm$ 25.0 ml/min (GRAPPA), 88.14 $\pm$ 26.2 (kt-GRAPPA) and 87.86 $\pm$ 23.1(2D-flow) nor of the mean peak velocity with 1.2 $\pm$ 0.4m/s or with and without ECC. Nevertheless, the correlation between both 4D-sequences and 2D-flow was better with ECC; the best correlation showed the kt-GRAPPA sequence (R=0.96 vs. 0.90) with good limits of agreement (LOA).

#### CONCLUSION

The significantly faster kt-GRAPPA sequence provided no significant different flow volumes or peak velocities as the standard GRAPPA sequence with less motion artifacts and better correlation to the standard reference; is therefore non-inferior and can be used for future research.

## **CLINICAL RELEVANCE/APPLICATION**

In clinical and scientific settings acceptable acquisition times are crucial, therefore we showed that 4D-flow with kt-GRAPPA is noninferior to standard GRAPPA and can be used for future research and for clinical studies.



## CA218-SD-MOB2

Pulsatile Lung Deformation Derived from Feature Tracking of Cardiac Cine Magnetic Resonance Imaging: Assessment of Systemic Sclerosis Related Pulmonary Fibrosis

Monday, Nov. 26 12:45PM - 1:15PM Room: CA Community, Learning Center Station #2

**FDA** Discussions may include off-label uses.

#### **Participants**

Noriko Kasuga, Tokyo, Japan (*Presenter*) Nothing to Disclose Michinobu Nagao, MD, Tokyo, Japan (*Abstract Co-Author*) Nothing to Disclose Ryoko Ohashi, Tokyo, Japan (*Abstract Co-Author*) Nothing to Disclose Akiko Sakai, MD, PhD, Tokyo, Japan (*Abstract Co-Author*) Nothing to Disclose Risako Nakao, MD, Tokyo, Japan (*Abstract Co-Author*) Nothing to Disclose Eri Watanabe, MD, PhD, Tokyo, Japan (*Abstract Co-Author*) Nothing to Disclose Seiko Shimizu, Chuo-ku, Japan (*Abstract Co-Author*) Nothing to Disclose Shuji Sakai, MD, Shinjuku-Ku, Japan (*Abstract Co-Author*) Nothing to Disclose

### For information about this presentation, contact:

nori.68.asclepius@gmail.com

### PURPOSE

Systematic sclerosis (SSc) is characterized by the progression of fibrosis in the all organs. Pulmonary fibrosis and cardiac involvement are important prognostic factors. The present study proposes a new imaging technique to analyze pulsatile lung deformation using feature tracking of cardiac cine MRI (FT-CMR), and investigates the relation to pulmonary fibrosis and cardiac deterioration in SSc.

# METHOD AND MATERIALS

Data of cardiac MRI for 25 SSc patients with (mean age, 60.6 years, Female 96%) who were suspected cardiac involvement and age-matched 10 healthy controls with a left ventricle ejection fraction (LVEF) > 50% was analyzed. Cardiac cine MR imaging of short-axis left ventricle was performed using a SSFP sequence with 3.0 Tesla. Cine images in which posterior wall of the left ventricle is closest to the left lung and the mostly movement by heart beat were selected. Peripheral zone of the lower lung with a depth of 1 cm from the pleura were set as a region of interest, and the strain in the radial direction to the center of the left lung was calculated using FT-CMR. The maximum absolute value of the strain during a cardiac cycle was defined as lung strain, and was used as an estimate of pulsatile lung deformation. The presence of pulmonary fibrosis was identified by chest high-resolution CT. Comparison of lung strain was analyzed by Mann-Whitney test.

# RESULTS

CT showed pulmonary fibrosis in 14 SSc patients (56%). Lung strain was significantly lower for SSc patients with pulmonary fibrosis (7.2 $\pm$ 5.5%) than those without it and controls. (11.3 $\pm$ 11.1%; 10.5 $\pm$ 7.4%; p50% (6.8 $\pm$ 3.6% vs.9.8 $\pm$ 9.9%).

# CONCLUSION

Development of pulmonary fibrosis in SSc associates with decreasing pulsatile lung deformation regardless of cardiac deterioration. FT-CMR derived lung strain is a new functional technique for assessment of pulmonary fibrosis.

# **CLINICAL RELEVANCE/APPLICATION**

Cardiac cine MRI adding lung strain enables non-invasively both evaluations of cardiac function and pulmonary fibrosis.



# CA219-SD-MOB3

# Effect of Long Term CPAP Usage on Cardiac Parameters Assessed with Cardiac MRI

Monday, Nov. 26 12:45PM - 1:15PM Room: CA Community, Learning Center Station #3

### **Participants**

Wolfgang Wust, MD, Erlangen, Germany (*Presenter*) Speakers Bureau, Siemens AG Rafael Heiss, Erlangen, Germany (*Abstract Co-Author*) Speakers Bureau, Siemens AG Michael Uder, MD, Erlangen, Germany (*Abstract Co-Author*) Speakers Bureau, Bracco Group Speakers Bureau, Siemens AG Speakers Bureau, Bayer AG Research Grant, Siemens AG Matthias S. May, MD, Erlangen, Germany (*Abstract Co-Author*) Speakers Bureau, Siemens AG

# For information about this presentation, contact:

wolfgang.wuest@uk-erlangen.de

### PURPOSE

The obstructive sleep apnoea syndrome (OSAS) is a disorder with a high prevalence and is associated with an elevated cardiovascular risk and increased morbidity and mortality. Common OSAS associated cardiovascular disorders include coronary artery disease, heart failure, hypertension, cardiac arrhythmias and stroke. Continuous positive airway pressure (CPAP) has been demonstrated to improve daytime performance and to reduce cardiovascular effects associated with OSAS. For longitudinal studies and functional analysis cardiac MRI is regarded as the gold standard. Aim of this study was to evaluate the long term effect of CPAP therapy on cardiac functional parameters with cardiac Magnetic Resonance Imaging (cMRI).

### **METHOD AND MATERIALS**

54 patients with OSAS (mean AHI: 31) were prospectively enrolled in this study and cMRI was performed before and after 7 months of CPAP therapy. Data were acquired on a 1.5T MRI and right and left ventricular cardiac morphology and function were analysed. CPAP treatment was considered compliant when used >= 4 h per night. 24-hour blood pressure was measured at baseline and follow up.

# RESULTS

33 patients could be assigned to the compliance group. Left ventricular stroke volume (LV SV) and right ventricular ejection fraction (RV EF) improved significantly with CPAP therapy (LV SV from  $93\pm19$ ml to  $99\pm20$ ml, p=0.02; RV EF from  $50\pm6\%$  to  $52\pm6\%$ , p=0.04). All other cardiac parameters did not change significantly while mean systolic and diastolic blood pressure improved significantly (p<0.01). 21 patients were assigned to the non-compliance group and were considered as a control group; there were no relevant differences in cardiac parameters between baseline and follow up examination in these patients.

# CONCLUSION

CPAP therapy significantly improved LV SV, RV EF, systolic and diastolic blood pressure in OSAS patients.

### **CLINICAL RELEVANCE/APPLICATION**

CPAP therapy has a postive long term effect on the right ventricle.



# CA221-SD-MOB5

Effect of Collateral Circulation on Left Ventricular Myocardial Strain in Patients with Coronary Artery Chronic Total Occlusion by Cardiovascular Magnetic Resonance Feature Tracking

Monday, Nov. 26 12:45PM - 1:15PM Room: CA Community, Learning Center Station #5

## Participants

Chen Hui, Dalian, China (*Abstract Co-Author*) Nothing to Disclose Zhiyong Li, Dalian, China (*Abstract Co-Author*) Nothing to Disclose Ailian Liu, MD, Dalian, China (*Abstract Co-Author*) Nothing to Disclose Qingwei Song, MD, Dalian, China (*Abstract Co-Author*) Nothing to Disclose Shuangchun Ma, Dalian, China (*Presenter*) Nothing to Disclose

# PURPOSE

To study the relation between different levels of collateral circulation to the strain of left ventricular myocardium in the segment of the CTO territory by means of the cardiovascular magnetic resonance feature tracking(CMR-FT) in the patients with coronary artery chronic total occlusion.

### **METHOD AND MATERIALS**

In the patients who underwent CMR during the period of 2015 - 2017 in our hospital, and diagnosed by coronary angiography with chronic total occlusion (CTO), 12 patients (age 44-77 years old, mean age 64.64±9.90 years old, 4 male, 8 female,3LAD,5LCX, 4RCA) were randomly selected as the research objects. Coronary angiography was performed using the standard Judkins technique. The collateral circulation was graded with the Cohen and Rentrop classification with scores of 0 (no collateral flow), 1 (collateral circulation fills only the side branches), 2 (partial filling of the main epicardial coronary vessel) and 3 (complete filling of the epicardial coronary vessel) applied. According to 17 segments to quantitatively evaluate the myocardial strain of two groups by Circle Cardiovascular Imaging 42 software, outline the endocardium and epicardium in the left ventricular short axis, two chamber long axis and four chambe cine image,respectively, then calculate the strain of 17 myocardial segments and got the corresponding bovine eye diagram. Analyze the relation among radial strain(RS), circumferential strain(CS) and longitudinal strain(LS) to the different levels of collateral circulation by SPSS 22.0 software.

### RESULTS

There was significant difference in RS, CS of left ventricular myocardium in the segment of the CTO territory among Rentrop grade 0 and Rentrop grade 1, Rentrop grade 2, Rentrop grade 3 in CTO patients (P = 0.000, 0.000, 0.000, 0.002, 0.000, 0.011, respectively), and there was no difference in the strain among Rentrop grade 1, Rentrop grade 2 and Rentrop grade 3.

### CONCLUSION

The RS and CS of CTO patients without collateral circulation were significantly decreased. CMR-FT can quantitatively evaluate the RS, CS and LS of left ventricular myocardial in the patients with CTO, and provide a new method of noninvasive, accurate and convenient for the objective assessment of left ventricular function in patients with CTO.

#### **CLINICAL RELEVANCE/APPLICATION**

CMR-FT can provide a non-invasive, accurate and easy method for objective evaluation of left ventricular function in patients with myocardial ischemia.



## CA222-SD-MOB6

Usefulness of Strain Imaging During Stress-CMR with Adenosine Infusion for a Combined Perfusion-Contractility Evaluation in Detection of Myocardial Ischaemia and Viability

Monday, Nov. 26 12:45PM - 1:15PM Room: CA Community, Learning Center Station #6

# Participants

Ester Cannizzaro, MD, L'Aquila, Italy (*Presenter*) Nothing to Disclose Pierpaolo Palumbo, MD, L'Aquila, Italy (*Abstract Co-Author*) Nothing to Disclose Camilla De Cataldo, L'Aquila, Italy (*Abstract Co-Author*) Nothing to Disclose Antonella Corridore, L'Aquila, Italy (*Abstract Co-Author*) Nothing to Disclose Silvia Torlone, L'Aquila, Italy (*Abstract Co-Author*) Nothing to Disclose Alessandra di Sibio, L'Aquila, Italy (*Abstract Co-Author*) Nothing to Disclose Ernesto E. Di Cesare, MD, L'Aquila, Italy (*Abstract Co-Author*) Nothing to Disclose Carlo Masciocchi, MD, L'Aquila, Italy (*Abstract Co-Author*) Nothing to Disclose

#### For information about this presentation, contact:

estercannizzaro@hotmail.it

#### PURPOSE

Cardiac Magnetic Resonance Stress Imaging with adenosine is an accurate tool for the detection of perfusion abnormalities. Neverthless, it shows low sensibility in the evaluation of cardiac contractility defects, allowing an exclusively visual assessment of wall movement abnormalities in case of inducible perfusion defects. The aim of our study is the identification of global and segmental deformation abnormalities during perfusional examination with adenosine, through feature tracking analysis

#### **METHOD AND MATERIALS**

CINE-sequences of 30 patients with known CAD performed during and after adenosine infusion were evaluated: 10 patients showed focal reversible defects ("ischemic"group), 10 patients focal irreversible perfusion defects and LGE ("infarcted"group), 10 patients did not show any perfusion abnormalities or LGE (control group). 3D values analysis of global, per planes and segmental (according to AHA classification ) LS and CS were performed. The increase of Strain values between rest and stress during adenosine infusion was calculated

## RESULTS

Statistical analysis showed regular growth of all Longitudinal and Circumferential Strain values during stress in the control group (>10%). In the "ischemic" group with focal defect and in the "infarcted" group with subendocardic defect, there was a significant rise of global and per planes values of LS and CS during stress; however, per segments analysis showed focal alterations of longitudinal deformability (increase <10%)(p<0,05) at the level of segments with perfusion defects identified through dedicated sequences. In addition, a significant modification of CS values was observed in all patients except in case of LGE>50%

## CONCLUSION

In conclusion, Strain analysis showed high capability of identifying myocardial global and segmental deformability alterations in patients with focal subendocardic defects and good residual function of the remaining myocardial portions.

### **CLINICAL RELEVANCE/APPLICATION**

Strain analysis is a reliable analysis applicable in a clinical routine setting thanks to its capability to provide information necessary for clinical decision making, particularly about myocardial contractility, avoiding more stressed evaluation as the dobutamine stress.



# CA223-SD-MOB7

The Correlation Between Kidney Pathological Type and Coronary Artery Calcification in End-Stage Dialysis Patients Using 16cm Wide-Detector CT

Monday, Nov. 26 12:45PM - 1:15PM Room: CA Community, Learning Center Station #7

# Participants

Changqing Yin, Zhenjiang, China (*Presenter*) Nothing to Disclose Dongqing Wang, Zhenjiang, China (*Abstract Co-Author*) Nothing to Disclose Lirong Zhang, MD, zhenjiang, China (*Abstract Co-Author*) Nothing to Disclose Haitao Zhu, Zhenjiang, China (*Abstract Co-Author*) Nothing to Disclose Shao Xun, Zhenjiang, China (*Abstract Co-Author*) Nothing to Disclose

## For information about this presentation, contact:

ev1lhell@126.com

# PURPOSE

The aim of this study was to investigate the associations between kidney pathological type and CAC in end-stage dialysis patients.

# METHOD AND MATERIALS

1125 dialysis patients were enrolled in this study, baseline as well as follow-up CAC were measured (average interval of 2.5 years) by 16cm wide-detector CT (Revolution, GE Healthcare). Biomarkers from blood examinations (Serum calcium, phosphorus, HDL/LDL, PTH) and nephropathy were also measured. These individuals then conducted pathology and pathological categories include IgA, Membranous Nephropathy(MN), Mesangial Proliferative Nephritis(MPN), Membranoproliferative Glomerulonephritis(MPGN), Focal Segmental Glomerulosclerosis(FGSG), Podocyte Disease(PD), Diabetic Nephropathy(DN), Hypertensive Nephropathy(HN), Nephritis of Schonlein-Henoch purpura and Lupus Nephritis(LN). Among 1125 patients, number of patients with various pathological conditions are as follows: IgA(n=183), MN(n=105), MPN(n=93), MPGN(n=88), FSGS(n=95), PD(n=102), DN(n=126), HN(n=92), HPN(n=89), LN(n=83).The associations of nephropathy with CAC was analyzed using multiple logistic regression.

### RESULTS

At baseline, CAC was present in 69% (87 of 126) DN patients, the percentage was higher than that in other types. At follow-ups, the most new-onset CAC developed in 33% (31 of 95) in IgA; MN patients' severity increased from a median CAC score of 38 to 82 in those with baseline CAC was higher than others. In multiple logistic regression, phosphate level(B=4.6; 95% confidence interval [95% CI],1.42 to 9.11; P=0.002) and baseline scores(B=7.0;95%CI,1.8 to 7.5;P=0.003) were associated with CAC progression in all nephropathy;high total PTH (>540pg/ml;B=7.1;95%CI,2.8to11.3;P=0.001)and elevated whole PTH(>450pg/ml;B=6.9;95%CI,2.4to11.4;P=0.003) were the predictors for CAC progression except in MPN, MPGN, PD, HPN, LN.

#### CONCLUSION

In this study, CAC is more prevalent in DN; whereas CAC has a higher incidence in IgA and a faster progression in MN. Phosphate level and baseline scores are associated with CAC progression in all nephropathy. However, high total PTH and elevated whole PTH are the predictors for CAC progression except in MPN, MPGN, PD, HPN, and LN.

# **CLINICAL RELEVANCE/APPLICATION**

Through pathology, different degrees of CAC need different attention.



### CH242-ED-MOB6

# MR Imaging of The Lung Pathology: Why and How?

Monday, Nov. 26 12:45PM - 1:15PM Room: CH Community, Learning Center Station #6

## Awards Certificate of Merit

#### Participants

Tugce Agirlar Trabzonlu, MD, Chicago, IL (*Presenter*) Grant, Siemens AG Amirhossein Mozafarykhamseh, MD, Chicago, IL (*Abstract Co-Author*) Grant, Siemens AG Hatice Savas, MD, Chicago, IL (*Abstract Co-Author*) Nothing to Disclose Pamela J. Lombardi, MD, Chicago, IL (*Abstract Co-Author*) Nothing to Disclose Frank H. Miller, MD, Chicago, IL (*Abstract Co-Author*) Research Grant, Siemens AG Vahid Yaghmai, MD, Chicago, IL (*Abstract Co-Author*) Nothing to Disclose

# **TEACHING POINTS**

CT is commonly used for assessing acute and chronic lung pathologies. Although MRI is emerging as a valuable lung imaging modality to provide diagnostic utility in the evaluation of lung pathologies, it is not routinely used in clinical practice. MRI can provide a combination of valuable anatomical and functional information without the risk of radiation. MRI is widely available and may be an alternative method in evaluation the lung pathologies. The aim of this exhibit is to illustrate lung pathologies on MRI and correlate those findings with CT. Advantages of MRI in diagnosis, follow-up and characterization of lung disease will be discussed.

# TABLE OF CONTENTS/OUTLINE

1. Introduction and technical aspects 2. Advantages of using MRI for evaluating lung pathologies a. No radiation dose b. Better soft-tissue contrast c. Diffusion-weighted imaging 3. MRI findings in evaluating lung pathologies with CT correlations a. Lung nodules and lung masses b. Interstitial lung disease c. Infections d. Vascular diseases e. Chest wall and mediastinal diseases 4. Pitfalls a. Availability b. Cost 5. Role of MRI in diagnostic test algorithms for lung pathologies 6. Protocol and Workflow optimization

### **Honored Educators**

Presenters or authors on this event have been recognized as RSNA Honored Educators for participating in multiple qualifying educational activities. Honored Educators are invested in furthering the profession of radiology by delivering high-quality educational content in their field of study. Learn how you can become an honored educator by visiting the website at: https://www.rsna.org/Honored-Educator-Award/ Vahid Yaghmai, MD - 2012 Honored EducatorVahid Yaghmai, MD - 2015 Honored EducatorFrank H. Miller, MD - 2017 Honored EducatorFrank H. Miller, MD - 2012 Honored EducatorFrank H. Miller, MD - 2014 Honored EducatorFrank H. Miller, MD - 2017 Honored EducatorFrank H. Miller, MD - 2018 Honored Educator



### CH243-ED-MOB7

# Recent Modifications to the TNM Lung Cancer Stage Classification: Wait, What? How Do I Do That?

Monday, Nov. 26 12:45PM - 1:15PM Room: CH Community, Learning Center Station #7

### **Participants**

Jonathan Chahin, MD, Charlottesville, VA (*Presenter*) Nothing to Disclose Alan M. Ropp, MD, Brooklyn, NY (*Abstract Co-Author*) Nothing to Disclose Juliana M. Bueno, MD, Charlottesville, VA (*Abstract Co-Author*) Nothing to Disclose

# For information about this presentation, contact:

jc5eh@virginia.edu

# **TEACHING POINTS**

After reviewing this educational exhibit, the learner will be able to: Identify the key distinguishing features of the 8th edition of the TNM lung cancer stage classification. Identify specific challenging situations that may arise when applying the new T and M descriptors. Apply the new criteria for lung cancer staging in potentially challenging cases with a better understanding of the classification.

# TABLE OF CONTENTS/OUTLINE

Key distinguishing features between the 7th and 8th editions Potential challenges to application in clinical practice: Distance of a lesion from the carina is no longer a T descriptor, but involvement of the carina is. How is carinal involvement defined? Diaphragmatic invasion is now classified as T4. How is diaphragmatic invasion defined? Parietal pleural invasion is defined as T3. How is parietal pleural invasion defined? Mediastinal pleural invasion is no longer a descriptor, although parietal pericardial invasion is considered T4. How is pericardial invasion identified and distinguished? Involvement of the great vessels is considered T4. How is vascular involvement defined? How are multiple synchronous lung cancers staged? How are infiltrative tumors measured?



# CH269-SD-MOB1

Visibility of Intralobular Bronchioles by Ultra-High Resolution CT

Monday, Nov. 26 12:45PM - 1:15PM Room: CH Community, Learning Center Station #1

### **Participants**

Hiroshi Moriya, MD, Fukushima, Japan (*Presenter*) Advisory, Ziosoft Inc; Research Grant, Canon Medical Systems Corporation; ; Masahiro Suzuki, Chuo-Ku, Japan (*Abstract Co-Author*) Nothing to Disclose Kouji Hashimoto I, Fukushima, Japan (*Abstract Co-Author*) Nothing to Disclose Shun Muramatsu, RT, Fukushima, Japan (*Abstract Co-Author*) Nothing to Disclose Hiroshi Chiba I, Fukushima, Japan (*Abstract Co-Author*) Nothing to Disclose Yuka Nakajou I, Fukushima, Japan (*Abstract Co-Author*) Nothing to Disclose Motoharu Hakozaki, Fukushima, Japan (*Abstract Co-Author*) Nothing to Disclose Shinsuke Tsukagoshi, PhD, Otawara, Japan (*Abstract Co-Author*) Employee, Canon Medical Systems Corporation Takashi Tanaka, MENG, Nasushiobara, Japan (*Abstract Co-Author*) Employee, Canon Medical Systems Corporation Daisuke Suto, Tokyo, Japan (*Abstract Co-Author*) Employee, Amin Co Ltd

#### For information about this presentation, contact:

hrshmoriya@gmail.com

### **TEACHING POINTS**

Objective: To assess the spatial resolution on the bronchiole of ultra high resolution CT(UHRCT). To present intralobular bronchioles and intra-acinar bronchioles of extension fixed lung in UHRCT images. To compare UHRCT images with HRCT images.

### **TABLE OF CONTENTS/OUTLINE**

Materials and methods: 1. phantom: We installed the extension fixed lung into the chest phantom (standard type and fat type). Extension fixed pig lung. Chest Phantom N1 LUNGMAN (Kyoto Kagaku). Chest plates for N1 (a set of anterior and posterior plates). 2. CT scanners: UHRCT(Aquilion Precision), HRCT(Aquilion ONE). 3. reconstruction using 512, 1024, and 2048 matrix sizes. 4. evaluated bronchioles: diameter of lumen was 0.4-0.8mm, bronchial wall thickness was 0.1-0.5mm. 5. Observer subjectively scored the images on a 5 point scale (1=worst, 3=middle, 5=best), in terms of image quality of bronchial wall and bronchial lumen, and the invisible images were scored zero point. Results and conclusions: Intralobular bronchioles (Ø 0.8mm) and intra-acinar bronchioles (Ø 0.4mm) were depicted by UHRCT. In chest phantom, intralobular bronchioles were depicted by UHRCT, however, intra-acinar bronchioles and were not depicted by HRCT. In the fat type phantom, the visualization was poor. We expect a futher noise reduction of iterative reconstruction.

## PDF UPLOAD

http://abstract.rsna.org/uploads/2018/18008440/18008440\_m1d5.pdf



# CH270-SD-MOB2

Machine Learning-Based Analysis of MRI Radiomics: Pathological Classification and Clinical Staging Prediction of Thymic Epithelial Tumors

Monday, Nov. 26 12:45PM - 1:15PM Room: CH Community, Learning Center Station #2

# Participants

Gang Xiao, Xian, China (*Presenter*) Nothing to Disclose Wei-Cheng Rong, Xian, China (*Abstract Co-Author*) Nothing to Disclose Zhongqiang Shi, Xi an, China (*Abstract Co-Author*) Nothing to Disclose Yang Yang, Xian, China (*Abstract Co-Author*) Nothing to Disclose Bo Li, Xian, China (*Abstract Co-Author*) Nothing to Disclose Xiao-Cheng Wei, Beijing, China (*Abstract Co-Author*) Nothing to Disclose Wen Wang, Xi'an, China (*Abstract Co-Author*) Nothing to Disclose Yu-Chuan Hu, Xi'an, China (*Abstract Co-Author*) Nothing to Disclose Guang-Bin Cui, MD, Xian, China (*Abstract Co-Author*) Nothing to Disclose

# PURPOSE

To predict the pathological classification and clinical staging of thymic epithelial tumors (TETs) with machine learning-based analysis of MRI radiomics.

#### METHOD AND MATERIALS

Preoperative MRI were retrospectively obtained in 189 TETs patients with confirmed pathological classification and clinical stage. Radiomic features (histogram, texture, form factor, co-occurrence matrix, run-length matrix and size zone matrix) were extracted from T2-weighted and T2-weighted fat-suppressed images. Cases were randomly assigned to either the training or validation cohort, and the patient imbalance were adjusted using synthetic minority oversampling technique (SMOTE). By using support vector machine with recursive feature elimination (SVM-RFE), the optimal feature subsets with the best discriminative performance were selected and used to construct two predictive models for pathological classification and clinical staging, respectively, and the performance of models were assessed.

#### RESULTS

Of the 2088 extracted features, the optimal feature subset including 78 features or 29 features for pathological three classification or clinical binary staging were selected to generate the predictive model. The model used for differentiating low-, high-risk thymoma and thymic carcinoma achieved accuracies of 76% (area under the curve [AUC] = 0.892) in the training cohort and 67% (AUC = 0.747) in the validation cohort, and the model used for differentiating early (stage I, II) from advanced stages (stage III, IV) of TETs achieved accuracies of 93% (area under the curve [AUC] = 0.942) in the training cohort and 83% (AUC = 0.878) in the validation cohort.

### CONCLUSION

Results show that machine learning analysis of MRI radiomic features can facilitate the accurate prediction of pathological classification and clinical staging in TETs.

# **CLINICAL RELEVANCE/APPLICATION**

Our findings indicate that quantitative radiomic analysis is a noninvasive, reliable, and reproducible methodology that may help assess and characterize TETs.



# CH271-SD-MOB3

Assessment of Different Lung Cancer Subtypes: Diagnostic Value of Quantitative Dual-Energy CT Iodine Maps Combined with Morphological CT Features

Monday, Nov. 26 12:45PM - 1:15PM Room: CH Community, Learning Center Station #3

# Participants

Xiao Li Xu, MD, Beijing, China (*Presenter*) Nothing to Disclose Xin Sui, MD, Beijing, China (*Abstract Co-Author*) Nothing to Disclose Yao Huang, Beijing, China (*Abstract Co-Author*) Nothing to Disclose Lan Song, MD, Beijing, China (*Abstract Co-Author*) Nothing to Disclose Zheng Yu Jin, MD, Beijing, China (*Abstract Co-Author*) Nothing to Disclose Wei Song, MD, Beijing, China (*Abstract Co-Author*) Nothing to Disclose

### For information about this presentation, contact:

xxllpositive@163.com

### PURPOSE

To investigate the clinical usefulness of quantitative dual-energy CT (DECT) iodine enhancement metrics combined with morphological CT features in distinguishing lung cancer subtypes.

### **METHOD AND MATERIALS**

Consecutive patients suspected with lung cancer were prospectively enrolled and underwent dual-source DECT prior to biopsy or surgery. Tumor histological subtypes were determined in 110 patients. Two radiologists interpreted CT morphologic features of 110 lesions in a consensual manner. Besides, radiologists contoured lesions and acquired automated computer measurements, including Iodine density and iodine ratio (the ratio of iodine density of lesion to that of artery on the same section). Multinomial logistic regression models were applied to evaluate the accuracy of DECT parameters combined with CT features and CT features alone in discriminating lung cancer subtypes.

# RESULTS

Histology revealed adenocarcinoma in 48, squamous cell carcinoma (SCC) in 36 and small cell lung cancer (SCLC) in 26 patients. In analysis of CT features, tumor diameter, distribution, spiculation, pleural retraction, vascular involvement, confluent mediastinal lymphadenopathy, encasement of mediastinal structures and enhancement heterogeneity showed statistical difference (all Ps<0.05). Iodine density and iodine ratio were statistically different among three lung cancer subtypes (H=16.817,P<0.001; H=20.338, P<0.001). Iodine density of adenocarcinoma and SCC was ( $1.50\pm0.80$ ) mg/ml and ( $1.40\pm0.40$ ) mg/ml, respectively, higher than the ( $1.20\pm0.40$ ) mg/ml for SCLC (Ps<0.01). Iodine ratio of adenocarcinoma and SCC was ( $16.10\pm7.02$ ) % and ( $15.05\pm4.62$ ) %, higher than the ( $11.55\pm3.15$ ) mg/ml for SCLC (Ps<0.01). No significant difference of DECT parameters were observed between adenocarcinoma and SCC. Accuracy of the model based on CT features was 69.1%, accuracy of the model based on CT features combined with DECT parameters was 80.9%.

#### CONCLUSION

Quantitative DECT metrics were different among adenocarcinoma, SCC and SCLC, when combined with morphological CT features for differentiating lung cancer subtypes, higher diagnostic performance can be achieved.

### **CLINICAL RELEVANCE/APPLICATION**

Quantitative iodine-related parameters of dual-energy CT can improve the diagnostic performance of lung cancer subtypes on the basis of CT morphological features and is recommended in the routine evaluation of suspected lung cancers.



# CH272-SD-MOB4

Evaluation of a Virtual Anti-Scatter Grid for Bedside Chest Radiography at Intensive Care Unit: Effects on Image Quality and Radiation Dose

Monday, Nov. 26 12:45PM - 1:15PM Room: CH Community, Learning Center Station #4

# Participants

Ibrahim Yel, Frankfurt, Germany (*Presenter*) Nothing to Disclose Benjamin Kaltenbach, MD, Frankfurt, Germany (*Abstract Co-Author*) Nothing to Disclose Julian L. Wichmann, MD, Frankfurt, Germany (*Abstract Co-Author*) Speaker, General Electric Company; Speaker, Siemens AG Christoph Polkowski, MD, Frankfurt, Germany (*Abstract Co-Author*) Nothing to Disclose Moritz H. Albrecht, MD, Frankfurt am Main, Germany (*Abstract Co-Author*) Speaker, Siemens AG Lukas Lenga, Frankfurt, Germany (*Abstract Co-Author*) Nothing to Disclose Simon S. Martin, MD, Frankfurt, Germany (*Abstract Co-Author*) Nothing to Disclose Thomas J. Vogl, MD, PhD, Frankfurt, Germany (*Abstract Co-Author*) Nothing to Disclose Christian Booz, MD, Frankfurt am Main, Germany (*Abstract Co-Author*) Nothing to Disclose

### For information about this presentation, contact:

DrIbrahimYel@gmail.com

#### PURPOSE

To assess the performance of a post-processed virtual anti-scatter grid (VG) for intensive care unit (ICU) bedside chest radiography compared to a conventional grid (CG).

# **METHOD AND MATERIALS**

127 consecutive ICU patients underwent bedside chest radiography using three different acquisition techniques with the same flatpanel detector: CG (125 kV; 1.4 mAs), VG1 (125 kV; 1.4 mAs) and VG2 (125 kV; 1.0 mAs). Overall image quality, lung parenchyma, soft tissue, thoracic spine, foreign bodies and assessment of pathology were evaluated by four radiologists using a 9-point visibility scale. Dose-area product was noted for each examination.

### RESULTS

Overall image quality was significantly better for VG1/VG2 compared to CG ( $7.3\pm1.1$  /  $7.2\pm0.8$  vs.  $6.7\pm0.8$ ; p<0.001). Soft tissue, thoracic spine, foreign bodies and visibility of pathology were also rated significantly higher for both VG protocols compared to the CG examination (p<0.001), whereas visibility of lung parenchyma was equivalent (p=0.53). Lowest dose-area product was achieved with the VG2 protocol ( $1.1\pm0.2$  mGy\*cm2; p<0.001) while VG1 and CG showed the same dose-area product ( $1.5\pm0.3$  vs.  $1.5\pm0.3$  mGy\*cm2; p=0.54).

# CONCLUSION

Bedside ICU chest radiography using a virtual anti-scatter grid resulted in largely superior image quality and similar or lower radiation exposure.

### **CLINICAL RELEVANCE/APPLICATION**

Virtual anti-scatter grid post-processing may be particularly useful to optimize radiation exposure for ICU patients undergoing frequent follow-up imaging and to improve image quality in often suboptimal contrast conditions.



# CH273-SD-MOB5

Workup of Positive Findings on Baseline Lung Cancer Screening: Implications of the Use of Two Protocols and Methods of Nodule Measurement

Monday, Nov. 26 12:45PM - 1:15PM Room: CH Community, Learning Center Station #5

# Participants

Dorith Shaham, MD, Jerusalem, Israel (*Presenter*) Nothing to Disclose Eliezer Terespolsky, MS, Jerusalem, Israel (*Abstract Co-Author*) Nothing to Disclose

## For information about this presentation, contact:

dshaham@hadassah.org.il

## PURPOSE

Several protocols guide the management of positive findings on low-dose CT screening for lung cancer, in order to minimize unnecessary workup. We aimed to compare the recommendations for workup based on two protocols, I-ELCAP and Lung-RADS, and to investigate the implications of using different methods for measuring of pulmonary nodule size on the rate of positive findings and, consequently, on the rates of additional follow-up exams.

# METHOD AND MATERIALS

The effect of using either I-ELCAP or Lung-RADS protocol on workup recommendations was evaluated by applying each protocol to all 105 available cases which included at least one non-calcified nodule >=5.5 mm in our database of 1233 cases. Two nodule measurement methods were also applied to the eligible cases, and were evaluated independently for each of the two protocols. Comparison between protocols and the methods of measurement were analyzed by the McNamer test.

### RESULTS

The follow-up recommendations according to the I-ELCAP protocol were significantly inconsistent (p < 0.001) with the Lung-RADS recommendations, mostly due to the significantly higher recommendation rate for PET-CT by Lung-RADS (p < 0.001). Measuring of only the maximal diameter of the nodule vs. the average of maximal diameter and width, resulted in a higher rate of recommendations for invasive procedures. These differences weres significant for each of the protocols (Lung-RADS and I-ELCAP) separately (p < 0.001). The difference in the recommendations when rounding up to the next millimeter vs. avoiding rounding up, was significant for both I-ELCAP (p < 0.011) and Lung-RADS (p < 0.018).

# CONCLUSION

Application of the I-ELCAP protocol and a policy that doesn't support rounding up of nodule size may reduce the rate of unnecessary workup and prevent collateral harm. A measurement method that considers only the maximal diameter results in a higher invasive procedure rate.

# **CLINICAL RELEVANCE/APPLICATION**

Use of I-ELCAP protocol and nodule measurement method may reduce unnecessary workup but prospective studies are required to assess any possible delay in lung cancer diagnosis and its consequences.



## ER161-ED-MOB4

# Abdominal Pain After ERCP: What Should We Look For?

Monday, Nov. 26 12:45PM - 1:15PM Room: ER Community, Learning Center Station #4

## Awards Certificate of Merit

#### Participants

Yasmina Lamprecht, MBBS, Santander, Spain (*Presenter*) Nothing to Disclose Raul D. Pellon, MD, Santander, Spain (*Abstract Co-Author*) Nothing to Disclose Juan Crespo Del Pozo, Santander, Spain (*Abstract Co-Author*) Nothing to Disclose Sara Sanchez Bernal, MD, Santander, Spain (*Abstract Co-Author*) Nothing to Disclose Elena Marin-Diez, MD, Santander, Spain (*Abstract Co-Author*) Nothing to Disclose Enrique Montes, MD, Santander, Spain (*Abstract Co-Author*) Nothing to Disclose Victor Fernandez-Lobo, Santander, Spain (*Abstract Co-Author*) Nothing to Disclose Ana Belen Barba Arce, MD, Santander, Spain (*Abstract Co-Author*) Nothing to Disclose Eduardo Herrera, Santander, Spain (*Abstract Co-Author*) Nothing to Disclose Beatriz Garcia Martinez, BDS, Santander, Spain (*Abstract Co-Author*) Nothing to Disclose Faula Gallego Ferrero, MD, Santander, Spain (*Abstract Co-Author*) Nothing to Disclose Francisco J. Gonzalez, MD,CMD, Santander, Spain (*Abstract Co-Author*) Nothing to Disclose

### For information about this presentation, contact:

yasmina.lamprecht@gmail.com

#### **TEACHING POINTS**

• To review the general features of this technique, indications, and contraindications. • To present an overview of the associated risks of the Endoscopic retrograde cholangiopancreatography (ERCP) procedure. • To revise the most common complications and their characteristic imaging findings.

# TABLE OF CONTENTS/OUTLINE

• Introduction. • Specific ERCP complications: o Pancreatitis. o Duodenal perforation. o Duodenal hemorrhage. o Infection. o Stent migration. • Endoscopy-related complications: o Esophageal injury. o Liver injury. o Splenic injury.



# ER211-SD-MOB1

Efficacy of Changing the Pitch in Single CT Scan Regarding the Reduction of the Pulsatile Motion Artifact at the Aortic Root Without Increasing the Image Noise

Monday, Nov. 26 12:45PM - 1:15PM Room: ER Community, Learning Center Station #1

# Participants

Takahiro Yano, RT, Suita, Japan (*Presenter*) Nothing to Disclose Tatsuya Nishii, MD, PhD, Suita, Japan (*Abstract Co-Author*) Nothing to Disclose Akiyuki Kotoku, MD, Kawasaki, Japan (*Abstract Co-Author*) Nothing to Disclose Yasuhiro Nagai, Suita, Japan (*Abstract Co-Author*) Nothing to Disclose Atsushi K. Kono, MD, PhD, Suita, Japan (*Abstract Co-Author*) Nothing to Disclose Susumu Morikawa, Osaka, Japan (*Abstract Co-Author*) Nothing to Disclose Yoshiaki Watanabe, MD, Suita, Osaka, Japan (*Abstract Co-Author*) Nothing to Disclose Yoshiaki Morita, Suita, Japan (*Abstract Co-Author*) Nothing to Disclose Yoshio Hori, Osaka, Japan (*Abstract Co-Author*) Nothing to Disclose Kazuto Harumoto, Suita, Japan (*Abstract Co-Author*) Nothing to Disclose Tetsuya Fukuda, Suita, Japan (*Abstract Co-Author*) Nothing to Disclose

For information about this presentation, contact:

ttsynishii@gmail.com

#### PURPOSE

High pitch CT scan with high rotation speed can reduce the pulsatile motion artifact of the aortic root for the evaluation for the acute aortic disease, however, can worsen the image quality of the abdominal area due to the photon insufficiency. We hypothesized that changing from high-pitch in the chest area to low-pitch in the abdominal area using the variable helical pitch (VHP) scan can balance both temporal resolution and photon flux in a single scan. This study aimed to evaluate the image quality of VHP scan compared with the reference scan.

# METHOD AND MATERIALS

The institutional review board approved this retrospective study of 104 patients who had undergone non-ECG gated, non-enhanced CT with VHP scan ( $80 \times 0.5$  mm detector configuration, 120 kV, 0.35 s rotation speed, 1.388-0.813 pitch). The axial 2mm images of the patients who had the previous reference scan ( $64 \times 0.5$  mm detector configuration, 0.5 s rotation speed, and 0.823 pitch) were evaluated by a board-certified radiologist using the 4-point blurring score (0, not diagnostic due to the motion artifact; 3, excellent) at the aortic root. Further, the maximum distance between the doubled lines of the contour of the aortic root due to the motion artifact was measured. For the image noise analysis, the standard deviation of the region of interest placed at the ascending, descending, and abdominal aorta was measured. We compared the blurring score, distance, and size-specific dose estimates (SSDE) as the radiation metrics of between the two scans. The non-inferiority (the margin fixed to 1 HU) of the noise amount of VHP scan from reference scan was evaluated.

# RESULTS

The total of 96 patients (17 females, median 74 years) was included; the median interval between two scans was 0.98 years. The heart rate was median 65 [IQR 60-74] bpm. VHP scan achieved significantly better blurring score (median 2 to 1) and distance (median 1.9 to 3.8 mm) compared with the reference scan (P<.001 for both). Further, the noise was non-inferior in VHP scan (P<.001), besides reducing the SSDE (median 13.2 to 19.6 mGy, P<.001).

### CONCLUSION

VHP scan achieved less motion artifact at the aortic root due to the high temporal resolution and maintained the image noise compared with the reference scan.

#### **CLINICAL RELEVANCE/APPLICATION**

VHP scan can adapt to a single scan of the routine emergency CT using potential for assessing the ascending aorta with less motion artifact, without increasing the image noise.



## ER212-SD-MOB2

Abdominal Computed Tomography for Acute Appendicitis Is Necessary Even in Patients with an Equivocal Alvarado Score (3-6), in the Emergency Department

Monday, Nov. 26 12:45PM - 1:15PM Room: ER Community, Learning Center Station #2

**FDA** Discussions may include off-label uses.

### Participants

Georgios Masouris, Athens, Greece (*Presenter*) Nothing to Disclose Chrisovalantis Vergadis, Athens, Greece (*Abstract Co-Author*) Nothing to Disclose Christos Chronis, Athens, Greece (*Abstract Co-Author*) Nothing to Disclose Kalliopi Kokkali, Athens, Greece (*Abstract Co-Author*) Nothing to Disclose Konstantinos Revenas, Athens, Greece (*Abstract Co-Author*) Nothing to Disclose Alexandra Zormpala, Vrilissia, Greece (*Abstract Co-Author*) Nothing to Disclose

# PURPOSE

The Alvarado score is a clinical decision rule to suggest which patients presenting to the emergency department (ED) with acute abdominal pain, are at high risk for appendicitis. Patients with an Alvarado score of 7 or higher, are at high risk and should undergo computed tomography (CT) scan to confirm appendicitis. We hypothesised that patients with equivocal Alvarado scores (3-6) might also have a considerable risk for appendicitis and should undergo CT scan as well.

### **METHOD AND MATERIALS**

We performed a prospective observational study of adult patients presented with acute abdominal pain at an academic urban ED, within a period of 36 months. Patient demographics, presenting signs and symptoms were recorded, and the Alvarado score has been calculated for each patient. All patients underwent abdominal CT to rule out appendicitis. A final diagnosis of appendicitis was confirmed by CT, laparotomy, or 7-day follow-up. The sensitivity and specificity were calculated with 95% confidence interval (CI) for a high and equivocal Alvarado scores.

### RESULTS

One hundred ninety-three patients were included for analysis (mean age 41 years [range 17 to 89 years], 46% female patients). Seventy-eight patients (40%) had a final diagnosis of acute appendicitis. Ninety-one patients had an Alvarado score of 7 or higher. Among them, 51 (56%) had appendicitis. The high Alvarado score had a sensitivity and specificity of 65,4% and 65%, respectively. One hundred-two (52.8%) patients had an equivocal Alvarado sore (3-6). Among them, 27 (16.4%) had a final diagnosis of appendicitis. The equivocal Alvarado score had a sensitivity for not having appendicitis of 65,2% and 65,4%, respectively. No patients with Alvarado scores 1-2, were included in the study.

# CONCLUSION

In the equivocal clinical presentation of appendicitis as defined by Alvarado scores of 3 to 6, adjunctive CT is recommended to confirm or rule out the diagnosis in the ED setting.

# **CLINICAL RELEVANCE/APPLICATION**

In the emergency department, patients with equivocal Alvarado scores (3-6) should undergo CT scan, because they have a considerable risk for appendicitis.



# ER213-SD-MOB3

MDCT Evaluation of Acute Lower Gastrointestinal Bleeding (LGIB)

Monday, Nov. 26 12:45PM - 1:15PM Room: ER Community, Learning Center Station #3

## Participants

Vega Garcia Blazquez, Madrid, Spain (*Presenter*) Nothing to Disclose Esther Garcia Casado, Madrid, Spain (*Abstract Co-Author*) Nothing to Disclose Olga M. Sanz de Leon, PhD, Madrid, Spain (*Abstract Co-Author*) Nothing to Disclose Ines Pecharroman, PhD, Madrid, Spain (*Abstract Co-Author*) Nothing to Disclose Inmaculada Mota Goitia, Madrid, Spain (*Abstract Co-Author*) Nothing to Disclose Agustina Vicente Bartulos, MD, Madrid, Spain (*Abstract Co-Author*) Nothing to Disclose

### PURPOSE

To determine the ability of MDCT to identify the source and etiology of acute LGIB. To review several different causes of lower gastrointestinal bleeding (LGIB) and the role of MDCT in diagnosis in the acute setting.

## **METHOD AND MATERIALS**

We reviewed retrospectively 253 patients presenting with acute LGIB between January 2013 to March 2018 and who were referred for MDCT. The protocol included unenhanced and arterial and portal venous phase of contrast enhancement. The diagnosis and identification of the site of bleeding were based on the presence of extravasated contrast material in the bowel lumen. We correlated the MDCT findings with the results of other diagnostic and therapeutic tests performed to the patient (colonoscopy, arteriography and/ or surgery if any).

# RESULTS

MDCT was performed in 253 patients (53% women/47% men) with mean age of 72 years. Arterial phase CT demonstrated intraluminal contrast material extravasation indicating active LGIB in 55 patients (21.7%). Other imaging findings were colitis, vascular malformations, intraluminal clots, wall thickening, bleeding after therapeutic interventions, diverticulosis and others. 33 of the 55 positive MDCT were confirmed by standard of reference (TP) and 22 no (FN). There were 6 FP and 192 TN. Sensitivity was 84.6% and specificity 89.7%

# CONCLUSION

MDCT offers a valuable option as a first line screening modality for patients with active bleeding and hemodynamic instability. It allows accurate identification of etiology and site of bleeding with good sensitivity and specificity, help to obviate an angiographic examination with negative findings and help guide optimal treatment as well as determine the optimal timing to implement these interventions.

# **CLINICAL RELEVANCE/APPLICATION**

MDCT is a useful tool in patients with LGIB and helps the multidisciplinary management and select the appropriate treatment for patients.



### GI292-ED-MOB9

Pancreaticobiliary Maljunction: Tips and Traps for Radiologists

Monday, Nov. 26 12:45PM - 1:15PM Room: GI Community, Learning Center Station #9

#### Awards Identified for RadioGraphics

#### Participants

Ayako Ono, MD, Kyoto, Japan (*Abstract Co-Author*) Nothing to Disclose Shigeki Arizono, MD,PhD, Kyoto, Japan (*Presenter*) Nothing to Disclose Hiroyoshi Isoda, MD, Kyoto, Japan (*Abstract Co-Author*) Nothing to Disclose Kaori Togashi, MD, PhD, Kyoto, Japan (*Abstract Co-Author*) Research Grant, Bayer AG; Research Grant, DAIICHI SANKYO Group; Research Grant, Eisai Co, Ltd; Research Grant, FUJIFILM Holdings Corporation; Research Grant, Nihon Medi-Physics Co, Ltd; Research Grant, Canon Medical Systems Corporation

# **TEACHING POINTS**

Pancreaticobiliary maljunction (PBM) is a congenital malformation, which is known to be associated with biliary duct and gallbladder cancer. Imaging plays an important role in diagnosis and follow-up management of PBM.The purpose of this exhibit is: 1. To review pathophysiology and carcinogenesis of PBM.2. To learn morphological characteristics of PBM.3. To learn how to diagnose both PBM with biliary dilatation (congenital biliary dilatation) and PBM without biliary dilatation.4. To understand the role of CT and MR images in the management and long-term follow up of PBM.

# TABLE OF CONTENTS/OUTLINE

1. Definition and pathophysiology2. Morphological characteristics with an emphasis on clinical and imaging features of PBM with and without biliary dilatation3. Diagnosis: diagnostic criteria and various imaging modalities4. Complications such as biliary tract and gallbladder cancer, acute pancreatitis and gallstone5. Carcinogenesis6. Pearls and pitfalls for diagnosis of PBM and associated cancer7. Management and treatment8. Complications during postoperative follow-up



### GI293-ED-MOB10

# Spleen Elastography and Portal Hypertension: An Overview and the Nitty-Gritties

Monday, Nov. 26 12:45PM - 1:15PM Room: GI Community, Learning Center Station #10

# FDA Discussions may include off-label uses

#### **Participants**

David X. Liu, MD, Philadelphia, PA (*Presenter*) Nothing to Disclose Flavius F. Guglielmo, MD, Philadelphia, PA (*Abstract Co-Author*) Nothing to Disclose Dina Halegoua-De Marzio, MD, Philadelphia, PA (*Abstract Co-Author*) Nothing to Disclose

### For information about this presentation, contact:

David.Liu@jefferson.edu

# **TEACHING POINTS**

Cilinically significant portal hypertension (CSPH) is an important prognostic factor in patient with cirrhosis. Currently, the only method of measuring portal system pressure is the highly invasive hepatic venous pressure gradient (HVPG). Thus, the development and validation of a noninvasive method of measuring the portal pressure can have significant impact on this patient population. The purpose of this exhibit is to highlight the emerging imaging technique of splenic ultrasound elastography (USE) and its role in assessment of portal hypertension. The exhibit will review: 1) The importance of Portal Hypertension and CSPH in clinical practices, 2) The principles of tissue elasticity, 3) The technical aspects of quantitative measurement of splenic stiffness, including how to perform the exam and study limitations 4) The current literature and possible future applications.

#### **TABLE OF CONTENTS/OUTLINE**

Portal Hypertension: a. Clinical importance; b. Current diagnosis of PH and CSPH, and limitations Elastography: a. Concept of elastography imaging; b. Review of different elastography techniques and utilities Spleen Elastography: a. Technical aspects; b. Limitations, troubleshooting; c. Current data behind spleen stiffness and PH/CSPH; d. Importance of splenic USE for radiology and other specialties



### GI294-ED-MOB11

Errare Humanum Est: A Case-Based Review on Errors and Pitfalls in Abdominal CT and How to Avoid Them

Monday, Nov. 26 12:45PM - 1:15PM Room: GI Community, Learning Center Station #11

#### **Participants**

Ulysses S. Torres, MD, PhD, Sao Paulo, Brazil (*Presenter*) Nothing to Disclose Elisa A. Bretas, MD, Sao Paulo, Brazil (*Abstract Co-Author*) Nothing to Disclose Gabriella S. Silva, MD, Sao Paulo, Brazil (*Abstract Co-Author*) Nothing to Disclose Ana Carolina R. Buissa, MD, Sao Paulo, Brazil (*Abstract Co-Author*) Nothing to Disclose Clarissa G. Pancotte, MD, Rio de Janeiro, Brazil (*Abstract Co-Author*) Nothing to Disclose Hanna R. Dalla Pria, MD, Sao Paulo, Brazil (*Abstract Co-Author*) Nothing to Disclose Giuseppe D'ippolito, MD, PhD, Sao Paulo, Brazil (*Abstract Co-Author*) Nothing to Disclose

### **TEACHING POINTS**

Errors in abdominal CT are not uncommon, usually occurring when the radiologist do not see a subtle or obvious finding (perceptual error) or misinterpret it (interpretative error). In addition, pressure or insufficient time for reading, satisfaction of search (leading to interruption of vigilant reading of the whole exam) and inability in having access to pertinent clinical data also play a role in the occurrence of routine errors. These errors may be avoided by adoption of simple strategies such as using checklists, taking enough time to read the studies, making comparison with previous examinations, and using clinical and laboratory data. This case-based review, therefore, aims at analyzing some examples of errors and pitfalls (ranging from the most common to the uncommon ones) in interpretation of CT of the abdomen, also offering clues to avoid them.

# **TABLE OF CONTENTS/OUTLINE**

Introduction: description and classification of the most common types of errors in diagnostic CT imaging of the abdomen. Illustration with several cases, some of which include non-visualization of residual ureteral calculi after placement of ureteric stents, abnormal liver lobulation misinterpreted as exophytic gastric neoplasm, focal hepatic steatosis misinterpreted as liver laceration, bulging papilla misinterpreted as ampullary cancer, etc.



### GI295-ED-MOB12

New Hepatocellular Adenoma Classification System: What the Radiologist Needs to Know

Monday, Nov. 26 12:45PM - 1:15PM Room: GI Community, Learning Center Station #12

#### **Participants**

Justin Tse, MD, Stanford, CA (Presenter) Nothing to Disclose

Bita Naini, Los Angeles, CA (Abstract Co-Author) Nothing to Disclose

David S. Lu, MD, Los Angeles, CA (*Abstract Co-Author*) Consultant, Medtronic plc; Speaker, Medtronic plc; Consultant, Johnson & Johnson; Research Grant, Johnson & Johnson; Consultant, Bayer AG; Research Grant, Bayer AG; Speaker, Bayer AG Steven S. Raman, MD, Santa Monica, CA (*Abstract Co-Author*) Nothing to Disclose

# For information about this presentation, contact:

jrtse@stanford.edu

### **TEACHING POINTS**

1) Understand the new classification schematic for hepatocellular adenoma (HCA) subtypes 2) Appreciate how this new classification affects clinical management 3) Recognize known and unknown MR imaging findings for each HCA subtype 4) Discuss implications for future research

# TABLE OF CONTENTS/OUTLINE

1) Molecular genotype and risk factors of each HCA subtype using both the prior and new classification schematic 2) Potential complications of each HCA subtype and implications for clinical care 3) Known (and unknown) MR imaging findings of each HCA subtype 4) Examples of how genotype determines MR imaging findings 5) Future research directions



# GI347-SD-MOB1

Imaging Features Associated with Failure of Non-Operative Management of Intra-Abdominal Abscesses in Crohn's Disease

Monday, Nov. 26 12:45PM - 1:15PM Room: GI Community, Learning Center Station #1

# Participants

Ryan W. Stidham, MD, Ann Arbor, MI (*Abstract Co-Author*) Consultant, AbbVie Inc; Consultant, Johnson & Johnson; Consultant, Merck & Co, Inc; Advisory Board, AbbVie Inc; Advisory Board, Johnson & Johnson; Advisory Board, Merck & Co, Inc Daniel Perl, Ann Arbor, MI (*Abstract Co-Author*) Nothing to Disclose Shrininvas Bishu, Ann Arbor, MI (*Abstract Co-Author*) Nothing to Disclose Ashish P. Wasnik, MD, Ann Arbor, MI (*Presenter*) Nothing to Disclose

# For information about this presentation, contact:

ashishw@med.umich.edu

# PURPOSE

To determine whether baseline clinical, therapeutic, and image-based abscess and disease features were associated with the avoidance of future surgery in patients with a non-operatively managed intra-abdominal abscess due to Crohn's disease (CD).

# METHOD AND MATERIALS

In this retrospective, IRB approved, HIPAA compliant study, adult patients with CD, hospitalized for an index presentation of an intra-abdominal abscess between 2007-2015 were identified. Inclusion: Abdominal CT or MR imaging within 1 week of hospitalization, non-operative abscess management with intravenous antibiotics with/without percutaneous drainage, and minimum of 2 years follow up. Exclusion: surgical management decision either at the index hospitalization or an agreement to undergo an operation following medical abscess management. Primary outcome was surgical resection of the diseased bowel segment involving the abscess within two years of the index hospitalization. Radiographic features recorded included: Maximum linear abscess dimension, abscess margin, associated enteric fistula. CD activity: bowel wall thickening, mural hyperenhancement, bowel length involved, bowel obstruction (diameter > 3 cm)

# RESULTS

121 patients met selection criteria, with 36.4% of patients avoiding bowel resection for at least 2 years from index imaging. Primary indication for bowel resection was refractory abscess in 59.7% and fibrostenotic obstructive disease in the remaining 40.3%. Abscesses overwhelmingly involved the distal ileum (85.9%). Abscess maximum dimension did not differ between those avoiding vs. undergoing surgery (4.7±3.1cm vs. 4.8±2.8cm, p=0.767) on unadjusted analysis. On multivariable analysis, controlling for demographics, medication use, and percutaneous drainage, abscess size >6cm was associated with a HR 2.47 (95% CL 1.17-5.21). Disease activity features including bowel wall thickness >6mm (HR 3.08, 95% CL 1.20-6.21) and disease length greater than 15cm (HR of 2.67 (95% CL 1.40-6.20) were associated with future bowel resection.

## CONCLUSION

Though majority of patients require bowel resection, abscess size and disease activity features including length and maximum bowel wall thickness can aid in stratifying the likelihood of eventual surgery.

#### **CLINICAL RELEVANCE/APPLICATION**

An understanding of radiographic features associated with the success of non-operative CD-related abscess management can aid in treatment planning at index hospitalization.



# GI348-SD-MOB2

In Vivo Hyperpolarized 13C MR Spectroscopy and Metabolic Kinetics for the Differential Diagnosis of the Stages of Liver Fibrosis

Monday, Nov. 26 12:45PM - 1:15PM Room: GI Community, Learning Center Station #2

# Participants

Sang Soo Shin, MD, Gwangju, Korea, Republic Of (*Presenter*) Nothing to Disclose Chung-Man Moon, Gwangju, Korea, Republic Of (*Abstract Co-Author*) Nothing to Disclose Yong-Yeon Jeong, MD, Chonnam, Korea, Republic Of (*Abstract Co-Author*) Nothing to Disclose

#### For information about this presentation, contact:

kjradsss@dreamwiz.com

# PURPOSE

To investigate the cellular metabolic and kinetic changes at different stages of liver fibrosis for the differential diagnosis of the stages of hepatic fibrosis using hyperpolarized 13C dynamic MR spectroscopy.

### METHOD AND MATERIALS

Mild and severe hepatic fibrosis were induced in C3H/HeN mice (n=10) by injecting thioacetamide (TAA) with 10% ethanol. Other C3H/HeN mice (n=5) were injected with phosphate buffer saline (PBS) (7.4 pH) as normal controls. After intravoxel incoherent motion (IVIM) diffusion-weighted imaging (DWI) with 12 b-values was performed using a free-breathing single-shot echo-planar imaging (EPI) sequence, hyperpolarized 13C dynamic MR spectroscopy and metabolic imaging were performed on the livers of the mice. The differential metabolite ratios, kinetic changes of metabolites, and values of IVIM parameters and ADC among the three groups were analyzed by a one-way analysis of variance (ANOVA) test.

### RESULTS

The ratios of [1-13C] lactate/pyruvate, [1-13C] lactate/total carbon (tC), [1-13C] alanine/pyruvate, and [1-13C] alanine/tC were significantly higher in both the mild and severe fibrosis groups than in the normal control group (P<.05). While the [1-13C] lactate/tC ratios were not significantly different between mild and severe fibrosis groups, the ratios of [1-13C] alanine/pyruvate and [1-13C] alanine/tC were significantly higher in the severe fibrosis group than in the mild fibrosis group (P<.05). Also, averages of VPyr?Lac and VPyr?Ala ( $\mu$ mol/kg/sec) were higher in mild (to the extent of 29.2% and 30.9%, respectively) and severe (to the extent of 55.6% and 122.5%, respectively) fibrosis groups compared with the normal control group. In addition, the levels of [1-13C] alanine and [1-13C] lactate were negatively correlated with D\* values.

#### CONCLUSION

It was possible to differentiate mild from severe fibrosis using the cellular metabolic and kinetic changes with hyperpolarized 13C MRS and metabolic imaging.

# **CLINICAL RELEVANCE/APPLICATION**

Hyperpolarized 13C MR spectroscopy and metabolic kinetics may have a potential for early diagnosis and staging of hepatic fibrosis.



# GI349-SD-MOB3

Intraindividual Comparison of Double Arterial-Phases Using Compressed Sensing Reconstruction with Conventional Single Arterial-Phase for Gadoxetic Acid Liver MR Imaging

Monday, Nov. 26 12:45PM - 1:15PM Room: GI Community, Learning Center Station #3

# Participants

Masataka Nakagawa, Kumamoto, Japan (*Abstract Co-Author*) Nothing to Disclose Tomohiro Namimoto, MD, Kumamoto, Japan (*Presenter*) Nothing to Disclose Takeshi Nakaura, MD, Kumamoto, Japan (*Abstract Co-Author*) Nothing to Disclose Seitaro Oda, MD, Kumamoto, Japan (*Abstract Co-Author*) Nothing to Disclose Daisuke Utsunomiya, MD, Kumamoto, Japan (*Abstract Co-Author*) Nothing to Disclose Yasuyuki Yamashita, MD, Kumamoto, Japan (*Abstract Co-Author*) Nothing to Disclose Yasuyuki Yamashita, MD, Kumamoto, Japan (*Abstract Co-Author*) Nothing to Disclose Mika Kitajima, MD, Kumamoto, Japan (*Abstract Co-Author*) Nothing to Disclose Mika Kitajima, MD, Kumamoto, Japan (*Abstract Co-Author*) Nothing to Disclose Hiroyuki Uetani, Kumamoto, Japan (*Abstract Co-Author*) Nothing to Disclose Narumi Taguchi, Kumamoto, Japan (*Abstract Co-Author*) Nothing to Disclose Machiko Tateishi, Kumamoto, Japan (*Abstract Co-Author*) Nothing to Disclose Taihei Inoue, MD, Kumamoto, Japan (*Abstract Co-Author*) Nothing to Disclose

# PURPOSE

To the impact of double arterial-phases using compressed sensing (CS) reconstruction compared with conventional single arterialphase on gadoxetic acid-enhanced liver dynamic magnetic resonance imaging (MRI).

### **METHOD AND MATERIALS**

Ninety-eight patients who underwent gadoxetic acid-enhanced liver MRI at 3T with both present CS double- and previous conventional single arterial-phase were retrospectively included. CS double arterial-phases and conventional single arterial-phase were obtained with 9.8-sec acquisition time (total time: 21.1 sec), and 16-sec acquisition time, respectively. Signal-to-noise ratios (SNRs) and contrast ratios (CRs) were measured for the liver and erector muscle of the spine. Image quality and degree of artifact and enhancement of the portal vein for all arterial-phases were qualitatively rated on a four-point scale with higher score indicating the more optimal exam.

### RESULTS

SNRs of the liver for 1st-, 2nd- and single arterial-phases were  $21.7\pm7.43$ ,  $20.0\pm5.73$ , and  $18.8\pm6.13$ , respectively. CRs of the liver for 1st-, 2nd- and single arterial-phases were  $0.52\pm0.32$ ,  $0.65\pm0.37$ , and  $0.66\pm0.78$ , respectively. There were no significant differences among all arterial phases. Image quality and degree of artifacts were comparable among all arterial phases. The degree of enhancement of the portal vein at 2nd arterial-phase ( $3.03\pm0.92$ ) was significantly higher than that at 1st- ( $1.76\pm0.83$ ) and single arterial-phase ( $2.38\pm0.81$ ). Of all 98 patients, the number of patients whose best score of double arterial phase was higher than that of conventional arterial phase were 46(46.9%) (Reviewer1) and 33(33.7%) (Reviewer2), respectively. The number of patients with hypervascular lesion was 22. Of the 22 patients, the number of patients with corona like enhancement was 6(27.3%).

#### CONCLUSION

The image quality with CS double arterial-phase was comparable with conventional single-phase on gadoxetic acid liver dynamic MRI.

# **CLINICAL RELEVANCE/APPLICATION**

Double arterial-phase imaging may provide additional information.



# GI350-SD-MOB4

Nationwide, Longitudinal Trends in CT Colonography Usage: Cross Sectional Survey Results from the 2010 and 2015 National Health Interview Survey

Monday, Nov. 26 12:45PM - 1:15PM Room: GI Community, Learning Center Station #4

# Participants

Anand K. Narayan, MD, PhD, Boston, MA (Presenter) Nothing to Disclose

Diego Lopez, Boston, MA (Abstract Co-Author) Nothing to Disclose

Avinash R. Kambadakone, MD, Boston, MA (Abstract Co-Author) Nothing to Disclose

Peter F. Hahn, MD,PhD, Belmont, MA (*Abstract Co-Author*) Stockholder, Abbott Laboratories; Stockholder, Medtronic plc; Stockholder, CVS Caremark Corporation; Stockholder, Kimberly-Clark Corporation; Stockholder, LANDAUER, Inc; Spouse, Stockholder, Medtronic plc; Spouse, Stockholder, Gilead Sciences, Inc; Spouse, Bondholder, Bristol-Myers Squibb Company; Spouse, Bondholder, Johnson & Johnson

Debra A. Gervais, MD, Boston, MA (Abstract Co-Author) Nothing to Disclose

### For information about this presentation, contact:

aknarayan@mgh.harvard.edu

### PURPOSE

Colorectal cancer screening reduces mortality however screening rates have plateaued. Prior studies have found that giving patients choices between different screening tests improves adherence. CT colonography is an emerging minimally invasive screening test that demonstrates high sensitivity for colonic polyps(>1 cm). With increasing health insurance coverage, there are limited national, population-based estimates of CT colonography utilization over time. Our purpose was to estimate longitudinal utilization of CT colonography among eligible participants using nationally representative cross sectional survey data.

# METHOD AND MATERIALS

We used nationally representative cross sectional survey data from 2010 and 2015 National Health Interview Surveys including information about CT colonography usage. 2010 response rate was 77% and 2015 response rate was 80%. Participants between ages 50-75 without histories of colon cancer were included. Logistic regression analyses were used to evaluate longitudinal changes in the proportion of eligible individuals undergoing CT colonography, adjusted for potential confounders and stratified by type of health insurance and age category. Analyses were conducted taking into account complex survey design elements (adjusted weights, strata and sampling units).

# RESULTS

8,965 survey respondents in 2010 and 12,721 survey respondents in 2015 were included. 1.2% reported usage of CT colonography in 2010 and 0.9% reported usage of CT colonography in 2015, a statistically significant decrease (Adjusted OR 0.92, 95% CI 0.86 - 0.99). Optical colonoscopy usage increased from 57.9 to 63.6% (Adjusted OR 1.04, 95% CI 1.02 - 1.06). In our stratified analyses, patients with private health insurance(p = 0.35), patients below 65 (not Medicare eligible)(p = 0.07) and patients who had heard of CT colonography(p = 0.28), did not experience changes in CT colonography usage. Overall awareness of CT colonography decreased from 20.5% to 15.9%, a statistically significant decrease (Adjusted OR 0.94, 95% CI 0.92 - 0.96).

# CONCLUSION

Despite increasing overall usage of optical colonoscopy from 2010 to 2015, CT colonography awareness (~16%) and utilization (~1%) remained low.

# CLINICAL RELEVANCE/APPLICATION

Improved public awareness and coverage expansion to Medicare age populations will promote increased CT colonography utilization and improvements in overall colorectal cancer screening.

# **Honored Educators**

Presenters or authors on this event have been recognized as RSNA Honored Educators for participating in multiple qualifying educational activities. Honored Educators are invested in furthering the profession of radiology by delivering high-quality educational content in their field of study. Learn how you can become an honored educator by visiting the website at: https://www.rsna.org/Honored-Educator-Award/ Debra A. Gervais, MD - 2012 Honored Educator



# GI351-SD-MOB5

Application of Machine Learning to Infer Ultrasound LI-RADS Categories across Multi-Institutional Radiology Reports

Monday, Nov. 26 12:45PM - 1:15PM Room: GI Community, Learning Center Station #5

# Participants

Imon Banerjee, PhD, Stanford, CA (*Abstract Co-Author*) Nothing to Disclose Hailey Choi, MD, San Francisco, CA (*Presenter*) Nothing to Disclose David T. Fetzer, MD, Dallas, TX (*Abstract Co-Author*) Researcher, Koninklijke Philips NV; Consultant, Koninklijke Philips NV; Consultant, Siemens AG; Speakers Bureau, Koninklijke Philips NV; ; Aya Kamaya, MD, Stanford, CA (*Abstract Co-Author*) Nothing to Disclose Hersh Sagreiya, MD, Palo Alto, CA (*Abstract Co-Author*) Nothing to Disclose Daniel L. Rubin, MD, MS, Stanford, CA (*Abstract Co-Author*) Nothing to Disclose Terry S. Desser, MD, Stanford, CA (*Abstract Co-Author*) Nothing to Disclose

#### For information about this presentation, contact:

haileyc@stanford.edu

#### PURPOSE

To generate and validate a scalable computerized approach for large-scale inference of American College of Radiology (ACR) Ultrasound Liver Imaging Reporting and Data System (LI-RADS) categories from multi-institutional radiology report data.

### **METHOD AND MATERIALS**

In this IRB-approved, HIPAA-compliant, multi-institutional retrospective study, radiology reports of hepatocellular carcinoma (HCC) screening and surveillance ultrasound exams from two large academic institutions were collected. The report body text pertaining to the liver was segmented, pre-processed and analyzed with neural word embedding. To infer the final LI-RADS category, we applied an ensemble machine learning method where the text classifier that considered vector representation of the report segment was combined with a decision tree classifier that considered the number of liver lesions and the long axis length of largest lesion extracted from the text as input features. The model was trained using one institution's LI-RADS coded reports as the validation and training set; and was then applied to both institutions' datasets. When assessing the model's performance, the LI-RADS category assigned by the original radiologist was used as ground truth.

### RESULTS

The model was trained and validated on 1744 reports from one institution, where it demonstrated 0.93 precision, 0.88 recall, and average F1 score of 0.90. When tested on 2381 reports from the second institution without retraining, it predicted with 0.89 precision, 0.84 recall, with an average F1 score of 0.85.

### CONCLUSION

A scalable machine learning approach successfully identifies Ultrasound LI-RADS categories based on report body text with high level of precision. In addition to being able to handle large-scale data, the model is also translatable to a second institution despite being trained only on one institution's data.

### **CLINICAL RELEVANCE/APPLICATION**

Our computerized approach for predicting Ultrasound LI-RADS categories is generalizable to large-scale data and translatable to multi-institutional data. Our approach enables large-scale data mining of ultrasound reports, even those without specified LI-RADS categories, and will be helpful in future outcomes research of ACR Ultrasound LI-RADS.

### **Honored Educators**

Presenters or authors on this event have been recognized as RSNA Honored Educators for participating in multiple qualifying educational activities. Honored Educators are invested in furthering the profession of radiology by delivering high-quality educational content in their field of study. Learn how you can become an honored educator by visiting the website at: https://www.rsna.org/Honored-Educator-Award/ Daniel L. Rubin, MD, MS - 2012 Honored EducatorDaniel L. Rubin, MD, MS - 2013 Honored Educator



# GI352-SD-MOB6

# Advanced Hepatic Fibrosis May Limit US Screening For HCC: A Multicenter Study Using ACR US LI-RADS

Monday, Nov. 26 12:45PM - 1:15PM Room: GI Community, Learning Center Station #6

### **Participants**

Hailey Choi, MD, San Francisco, CA (*Presenter*) Nothing to Disclose
Marcelina G. Perez, MD, Menlo Park, CA (*Abstract Co-Author*) Nothing to Disclose
John D. Millet, MD, Ann Arbor, MI (*Abstract Co-Author*) Nothing to Disclose
Tie Liang, PhD, Stanford, CA (*Abstract Co-Author*) Nothing to Disclose
Ashish P. Wasnik, MD, Ann Arbor, MI (*Abstract Co-Author*) Nothing to Disclose
Katherine E. Maturen, MD, Ann Arbor, MI (*Abstract Co-Author*) Royalties, Reed Elsevier; Royalties, Wolters Kluwer nv; Consultant, Allena Pharmaceuticals, Inc;
Aya Kamaya, MD, Stanford, CA (*Abstract Co-Author*) Nothing to Disclose

### For information about this presentation, contact:

haileyc@stanford.edu

### PURPOSE

To evaluate the association between imaging features of advanced liver fibrosis and visualization scores, as specified by American College of Radiology (ACR) Ultrasound Liver Imaging Reporting and Data System (LI-RADS), on hepatocellular carcinoma (HCC) screening and surveillance ultrasound exams.

### **METHOD AND MATERIALS**

In this multi-center retrospective study, HCC survey ultrasound reports containing ultrasound elastography measurements were reviewed. Ultrasound machines from several vendors were used across two large academic institutions. Median shear wave velocity was translated to METAVIR fibrosis scores based on previously published data; subjects were categorized as those with and without advanced fibrosis (METAVIR fibrosis scores 3 and 4). Report data was analyzed for subject age, gender, reason for HCC screening, spleen size, fibrosis scores, and assigned visualization scores. Jonckheere-Terpstra trend and Kendall's tau-b coefficient analyses were performed to assess association.

### RESULTS

Total 714 subjects who underwent ultrasound HCC screening or surveillance with elastography were included. 308 (43%) of subjects had clinically declared cirrhosis; 406 (57%) did not. Majority (75%) of exams were without significant limitations, or visualization score A (VIS-A). 22% had moderate limitations (VIS-B), and 3% were severely limited (VIS-C). Increasing spleen size and patient age were associated with worsening visualization scores (p < 0.001). Suboptimal visualization was also associated with advanced fibrosis scores by elastography (f-3 and f-4) (Kendall's tau-b=0.156, p < 0.001) and clinically declared cirrhosis (Kendall's tau-b=0.433, p < 0.001). There was no association between visualization score and gender.

### CONCLUSION

25% of HCC screening exams were moderately or severely limited using ACR Ultrasound LI-RADS visualization scores. Sonoelastographic diagnosis of advanced fibrosis, clinical cirrhosis, increased patient age, and spleen size were associated with greater diagnostic limitations.

#### **CLINICAL RELEVANCE/APPLICATION**

Although most HCC screening ultrasound exams were diagnostic, clinical cirrhosis and advanced fibrosis by elastography were both associated with moderately or severely limited visualization.

#### **Honored Educators**

Presenters or authors on this event have been recognized as RSNA Honored Educators for participating in multiple qualifying educational activities. Honored Educators are invested in furthering the profession of radiology by delivering high-quality educational content in their field of study. Learn how you can become an honored educator by visiting the website at: https://www.rsna.org/Honored-Educator-Award/ Katherine E. Maturen, MD - 2014 Honored Educator



# GI353-SD-MOB7

Differential Diagnosis Nonhypervascular Pancreatic Neuroendocrine Tumors from Pancreatic Ductal Adenocarcinoma with CT Features and Texture Analysis: Preliminary Study

Monday, Nov. 26 12:45PM - 1:15PM Room: GI Community, Learning Center Station #7

**FDA** Discussions may include off-label uses.

#### **Participants**

Haopeng Yu, Chengdu, China (*Presenter*) Nothing to Disclose Bin Song, MD, Chengdu, China (*Abstract Co-Author*) Nothing to Disclose Zixing Huang, Chengdu, China (*Abstract Co-Author*) Nothing to Disclose Mou Li, Chengdu, China (*Abstract Co-Author*) Nothing to Disclose Xin Li, Shanghai, China (*Abstract Co-Author*) Nothing to Disclose Yuanan Wu, Chengdu, China (*Abstract Co-Author*) Nothing to Disclose

## For information about this presentation, contact:

yhp-cd@outlook.com

### PURPOSE

To determine useful computed tomography (CT) imaging features to differentiate nonhypervascular pancreatic neuroendocrine tumors (PNETs) from pancreatic ductal adenocarcinomas (PDACs).

## **METHOD AND MATERIALS**

Patients with pathologically proven PNETs and PDACs at Sichuan University West China Hospital between January 2010 and May 2017 were included. We compared nonhypervascular PNETs with age-matched controls of PDACs in a 1:2 ratio. The preoperative CT images both in the arterial phase (AP) and the portal vein phase (PVP) were obtained. The images were evaluated by two radiologists independently. Regions of interests (ROIs) drawn by ITK-SNAP software were input into AK software (Artificial Intelligent Kit,GE.) to extract texture features of AP and PVP images. Chi-squared test, the least absolute shrinkage and selection operator (Lasso) and kappa statistics were used to differentiate between PNETs and PDACs. Sensitivities (SEN), specificities (SPE) and area under receiver operating characteristic curve (AUC) were assessed by receiver operating characteristic (ROC) analysis.

## RESULTS

41 nonhypervascular PNETs and 82 PDACs were included. At multivariate analysis, tumor margin (odds ratio, 32.164), tumor location (odds ratio, 33.746), presence of calcification (odds ratio, 9.856), presence of hepatic metastasis (odds ratio, 8.245), Maximum3DDiameter\_PVP (AUC 0.773 SEN 0.793 SPE 0.683) and GLCMEntropy\_AllDirection\_offset7\_SD (AUC 0.645 SEN 0.805 SPE 0.488) were independent significant differentiators of PNETs from PDACs.

### CONCLUSION

Both CT Features and Texture Analysis are useful to distinguish nonhypervascular PNETs from PDACs.

### **CLINICAL RELEVANCE/APPLICATION**

The typical imaging appearance of PNETs has been described as a hypervascular solid mass with relatively intense enhancement on AP. However, nonhypervascular PNETs do not show arterial hyperenhancement and these PNETs may be difficult to differentiate from PDACs. In consideration of the giant disparity on prognosis, patient mortality rate, and resectability rate between PNETs and PDACs, it would be of great clinical value to differentiate PNETs from PDACs with preoperative imaging.



# GI354-SD-MOB8

## CT Radiomics for the Evaluation of Pancreatic Intraductal Papillary Mucinous Neoplasms

Monday, Nov. 26 12:45PM - 1:15PM Room: GI Community, Learning Center Station #8

#### **Participants**

Melissa J. McGettigan, MD, Tampa, FL (*Presenter*) Nothing to Disclose Trevor A. Rose, MD, Tampa, FL (*Abstract Co-Author*) Nothing to Disclose Jennifer B. Permuth, PhD, Tampa, FL (*Abstract Co-Author*) Nothing to Disclose Jung-Wook Choi, MD, PhD, Tampa, FL (*Abstract Co-Author*) Nothing to Disclose Alisha Rathi, MD, Jacksonville, FL (*Abstract Co-Author*) Nothing to Disclose Daniel K. Jeong, MD, Madison, WI (*Abstract Co-Author*) Nothing to Disclose

# For information about this presentation, contact:

Melissa.mcgettigan@moffitt.org

# PURPOSE

To evaluate whole lesion CT radiomic features of IPMNs for predicting malignant histology compared to International Consensus Guidelines 2012 (ICG)

# METHOD AND MATERIALS

Whole lesion manual segmentation was performed on preoperative CTs of 51 IPMN subjects in this retrospective cohort using Healthmyne QIDS (Healthmyne, Madison, WI). 41 relevant radiomic features were extracted from each lesion on each available contrast phase. Univariate analysis was performed for each phase and values were compared between histology groups using logistic regression. Conventional quantitative and qualitative CT measurements were also compared between groups, via univariate logistic regression, Chi Square (categorical) and Mann Whitney U (continuous) variables.

### RESULTS

29 subjects (15 males, age 71±9y) with high grade or invasive tumor histology comprised the malignant cohort, while 22 subjects (11 males, age 70±7y) with low grade histology were included in the benign cohort. 14/41 precontrast, 15/41 arterial, and 17/41 venous phase features differentiated malignant from benign IPMNs (p<0.05). The most significant features for predicting malignancy were textural and included arterial phase histogram entropy (OR(95% CI): 31.6 (2.6-383.0), p=0.007, venous phase histogram entropy 11.2 (1.6-80.3), p=0.016, and arterial phase gray level co-occurrence matrix (GLCM) entropy 2.1 (1.2-3.6), p= 0.007. Of ICG criteria, worrisome features (1 or more) had an AUC 0.74 (0.60-0.88), p= 0.003. High Risk Stigmata (1 or more) AUC 0.75 (0.61-0.90), p=0.002. Multivariable logistic regression model involving ICG and all radiomic features included 3 significant variables: Worrisome features (1 or more); High risk stigmata (1 or more); and arterial phase entropy. AUC 0.923 (0.852-0.995), p<0.001 Model threshold 0.051; sensitivity 0.93; specificity 0.82.

### CONCLUSION

CT radiomic evaluation of IPMNs could play a role in improving predictive capability in diagnosing malignancy. Larger studies would be helpful to determine the significance of our findings and establish whether radiomics can be combined with conventional biomarkers for future clinical diagnosis.

### **CLINICAL RELEVANCE/APPLICATION**

Radiomic quantitaive biomarkers can potentially improve diagnostic accuracy in prediction of IPMN malignant histology when combined with ICG 2012 criteria.



### GU216-SD-MOB1

## Can Subcentimetre Ultrasound Detected Hyperechoic Renal Lesions Be Safely Disregarded?

Monday, Nov. 26 12:45PM - 1:15PM Room: GU/UR Community, Learning Center Station #1

#### Awards Student Travel Stipend Award

#### **Participants**

Tahir Hussain, MBBS, FRCR, Leicester, United Kingdom (*Presenter*) Nothing to Disclose Vincent Lam, MBBS, Leicester, United Kingdom (*Abstract Co-Author*) Nothing to Disclose Arumugam Rajesh, MBBS, Leicester, United Kingdom (*Abstract Co-Author*) Nothing to Disclose James A. Stephenson, MD, FRCR, Leicester, United Kingdom (*Abstract Co-Author*) Nothing to Disclose Mustafa Farhad, MBBCh, Leicester, United Kingdom (*Abstract Co-Author*) Nothing to Disclose Sangoh Lee, MBBS, Leicester, United Kingdom (*Abstract Co-Author*) Nothing to Disclose

### For information about this presentation, contact:

tahir.hussain@uhl-tr.nhs.uk

### PURPOSE

Advances in ultrasound (US) have led to a rise in detection of incidental hyperechoic renal lesions, with many found as subcentimetre lesions in asymptomatic patients. This often results in subsequent imaging characterisation. Lack of consensus on management may result in surveillance with associated patient anxiety, cost and potential radiation for lesions that are likely to be clinically insignificant. The aim of this study is to optimise the follow up strategy by dismissing lesions on baseline ultrasound if the lesion conforms to US criteria of an angiomyolipoma (AML)

# METHOD AND MATERIALS

10-year retrospective review of patients who were found to have incidental hyperechoic renal lesions on US and ascertain the outcome from subsequent imaging, clinical encounters & cancer registrations. Patients were excluded if they had Tuberous Sclerosis, Von-Hippel Lindau or a known cancer.

## RESULTS

1535 patients were identified with 39 exclusions, with a final cohort of 1496. 23 % male & 77 % female. Mean age 57 (range 16-97). 160 had more than one lesion, 87 patients having bilateral lesions. 890 patients had subsequent imaging within 5 years (62.8%) regardless of indication. The average size of all AMLs was 14.9 mm. In the group with lesions less than 10 mm (808), 439 had imaging follow up with an average imaging follow up time of 1.5 years. Mean lesion size in this group was 7 mm, with an average increase of <1 mm on follow up. No lesions were found to be a malignancy on subsequent imaging, with none of these patients having a subsequent renal cancer diagnosis on cancer database search with an interval time period of 3-12 years.

### CONCLUSION

No incidental sub centimetre hyperechoic renal lesion with imaging characteristics of an AML demonstrated significant growth or developed into a malignancy on follow up.

# **CLINICAL RELEVANCE/APPLICATION**

Our retrospective 10-year study supports that sub centimetre asymptomatic AMLs with no concerning features on US can be reliably excluded from further assessment or follow up. Concerning features include lesion heterogeneity, irregular borders, calcification, extension into adjacent fat or structures - these features mandate further evaluation.



# GU217-SD-MOB2

10 Year Survival in Percutaneous CT and US-Guided Radiofrequency Ablation of 135 Pathologically Proven Renal Cell Carcinomas

Monday, Nov. 26 12:45PM - 1:15PM Room: GU/UR Community, Learning Center Station #2

# Participants

Sepideh Shakeri, Los Angeles, CA (*Presenter*) Nothing to Disclose Amirhossein Mohammadian Bajgiran, MD, Los Angeles, CA (*Abstract Co-Author*) Nothing to Disclose Sohrab Afshari Mirak, MD, Los Angeles, CA (*Abstract Co-Author*) Nothing to Disclose Danielle Ponzini, Los Angeles, CA (*Abstract Co-Author*) Nothing to Disclose Allan Pantuck, MD, Los Angeles, CA (*Abstract Co-Author*) Nothing to Disclose Steven S. Raman, MD, Santa Monica, CA (*Abstract Co-Author*) Nothing to Disclose

#### For information about this presentation, contact:

sshakeri@mednet.ucla.edu

### PURPOSE

To assess the long term outcomes of percutaneous US & CT guided Radiofrequency Ablation (RFA) in biopsy-proven renal cell carcinoma (RCC)

### **METHOD AND MATERIALS**

With IRB approval & HIPAA compliance, the study cohort comprised 135 biopsy-proven RCC lesions in 106 patients who underwent RFA from 2004 to 2012. Primary outcomes were assessed by technical success (TS), local tumor progression (LTP), estimated glomerular filtration rate (eGFR) before / after RFA, & complications. Overall survival (OS) & 10-year cancer-specific survival (CSS) rates are presented using the Kaplan-Meier curves. Technical success was evaluated with multiphase contrast enhanced multidetector computed tomography (MDCT) or magnetic resonance (CEMRI) immediately after ablation procedure. Presence LTP was examined with Imaging at 3-month target intervals for the first 2 years & every 6 months thereafter.

### RESULTS

In 106 patients (67.4% men) with 135 biopsy-proven renal lesions the mean age was 68.6 (34-89) years & the mean imaging follow up was 89.8 months (30-120). The median tumor size was 2cm (0.5-8) & median nephrometry score was 8 (4-12). 52.6 %(71/135) of lesions were in right kidney, 27.4% in the upper pole (37/135), 37.8% midpole (51/135) & 34.8% lower pole (37/135). Clear cell (CC) RCC comprised 68.1 %(92/135), and the remainder were papillary 9.6 %(13/135), chromophobe 4.4% (6/135) & epithelial neoplasms 12.6% (17/135). 123/135 lesions were ablated in a single session & 8.9% (12/135) required a second session, of which 11/12 (91.6 %) were CC RCC.The primary, secondary & overall technical success rate were 91.1%, 81.4% & 100% respectively & correlated inversely with lesion size (P=0.000). The local recurrence rate was 6.6 % (9/135) & complication rate was 4.4% (6/135). There were 3 patients with minor complications (hematoma & pain) & 3 with major complications (urinoma, granulomatous mass & retroperitoneal abscess requiring interventions).Overall & RCC specific survival rates (for subset of 87/106 patients) were 58% & 91% for 120 months.

# CONCLUSION

Percutaneous US & CT guided RFA appears a safe and effective treatment for RCC and has a good 10y CSS rate with low complication & recurrence rates

## **CLINICAL RELEVANCE/APPLICATION**

RFA shows a great performance as a non-invasive procedure in RCC treatment with reasonable cancer specific survival rate



# GU218-SD-MOB3

Intraductal Carcinoma of the Prostate (IDC-P): A Newly Described Pattern of Spread That Lowers Apparent Diffusion Coefficient (ADC) Values in Intermediate Risk Prostate Cancers

Monday, Nov. 26 12:45PM - 1:15PM Room: GU/UR Community, Learning Center Station #3

### Participants

Stephen S. Currin, MBBCh, Ottawa, ON (*Abstract Co-Author*) Nothing to Disclose Nicola Schieda, MD, Ottawa, ON (*Presenter*) Nothing to Disclose Satheesh Krishna, MD, Ottawa, ON (*Abstract Co-Author*) Nothing to Disclose Trevor A. Flood, MD, FRCPC, Ottawa, ON (*Abstract Co-Author*) Nothing to Disclose

### For information about this presentation, contact:

nschieda@toh.on.ca

# PURPOSE

IDC-P is a recently recognized pattern of spread of prostate cancer (PCa) where tumor distends/spans the lumen of pre-existing prostatic ducts and acini. Our hypothesis was that tumor within ducts and acini may lower ADC values due to displacement of glandular/ductal secretions which are replaced by tumor cells, making tumors appear more aggressive on mp-MRI. This study assesses ADC values in intermediate risk (Gleason score [GS] 7) acinar PCa with IDC-P compared to GS7 and high risk tumors without IDC-P.

### **METHOD AND MATERIALS**

With IRB approval, we identified 15 consecutive men with GS7 (3+4=7 N=4, 4+3=7 N=11; mean %pattern.4 52± 20%) acinar PCa with >20% IDC-P (mean 46±16%) at radical prostatectomy with pre-operative 3T mp-MRI. Two control groups were studied: 1) GS7 acinar PCa without IDC-P pair-matched for %pattern.4 and 2) GS8 or GS9 PCa without IDC-P. A blinded radiologist measured ADC of tumors and ADC.ratio (ADC.tumor/ADC.normal peripheral zone) and assigned PI-RADSv2 scores. Comparisons were performed using Chi-square and ANOVA.

# RESULTS

There were no differences in patient age, PSA or size of tumors (measured on axial T2W-MRI) between groups (p>0.05). 11/15 patients with GS7 tumors showing IDC-P had extraprostatic extension (EPE) and 6/15 had seminal vesicle invasion (SVI) (versus 12/15 [EPE] and 5/15 [SVI] with GS7 tumors without IDC-P and 12/15 [EPE] and 6/15 [SVI] with GS8/9 tumors, p=0.881 and 0.931). GS7 tumors with IDC-P had lower ADC and ADC.ratio (0.741±0.152 mm2/sec and 0.44±0.07) compared to GS7 tumors without IDC-P not accounted by %pattern.4 (0.888±0.167 mm2/sec and 0.62±0.14; p=0.006 and <0.001) and were similar to GS8/GS9 tumors (0.705±0.141 mm2/sec and 0.44±0.08; p>0.05). GS7 tumors with IDC-P were mostly PI-RADSv2 score 5 (14/15) compared to GS7 tumors without IDC-P (10/15) and GS8/9 tumors (9/15) though the difference was not significant (p=0.092).

### CONCLUSION

Intermediate risk prostate cancers with intraductal component (a pattern of spread where tumor spread fills prostatic ducts/acini) have significantly lower ADC values compared to tumors without this pattern of spread, resembling high risk tumors on diffusion-weighted MRI.

### **CLINICAL RELEVANCE/APPLICATION**

Among intemediate risk prostate cancers diagnosed at biopsy with lower than expected ADC values, intraductal component of tumor may be considered as a potential cause for discordant diffusion weighted imaging and biopsy results.



### GU219-SD-MOB4

Usefulness of Digital Post-processed Kidney Ureter Bladder for Detection of Ureteral Stones: Preliminary Study

Monday, Nov. 26 12:45PM - 1:15PM Room: GU/UR Community, Learning Center Station #4

### **Participants**

Sang Lim Choi, Seoul, Korea, Republic Of (*Presenter*) Nothing to Disclose Sung Bin Park, MD, Seoul, Korea, Republic Of (*Abstract Co-Author*) Nothing to Disclose Semin Chong, MD, Seoul, Korea, Republic Of (*Abstract Co-Author*) Research Consultant, Samsung Electronics Co, Ltd Seungwook Yang, PhD, Suwon, Korea, Republic Of (*Abstract Co-Author*) Employee, Samsung Electronics Co, Ltd Jong Beum Lee, Seoul, Korea, Republic Of (*Abstract Co-Author*) Nothing to Disclose Hyun Jeong Park, Seoul, Korea, Republic Of (*Abstract Co-Author*) Nothing to Disclose Eun Sun Lee, MD, PhD, Seoul, Korea, Republic Of (*Abstract Co-Author*) Nothing to Disclose

#### For information about this presentation, contact:

#### pksungbin@paran.com

#### PURPOSE

In the novel post-processing method proposed in this study, noise estimation, reduction, and whitening were used in the postprocessing. The purpose of this study was to determine diagnostic performance of ureteral stones in the digital post-processed kidney ureter bladder (KUB) images.

# METHOD AND MATERIALS

Thirty consecutive patients who diagnosed with ureteral stones and underwent both digital KUB and computed tomography (CT) KUB were included in this retrospective study. The interval between digital KUB and CT KUB was less than 15 days (mean duration, 3days). These 30 original digital KUB images were performed post procession to improve visibility of ureteral stones as post-processed digital KUB. Thus total of 60 digital KUB images were obtained and ordered randomly to review. The four reviewers (2 staff radiologists and 2 radiology residents) who did not know whether the image was processed or not independently evaluated. The objective parameters were the location and size of ureteral stones. The subjective parameter was the visibility of ureteral stones. The visibility was graded subjectively between 1 and 5, with very subtle as 1 and very obvious as 5. Statistical analysis was performed with ANOVA test to compare to the detection rates and visibility between original and post-processed KUB data set. The paired t-test was performed to correlate of stone size among CTKUB and digital KUB data sets.

#### RESULTS

In all reviews, the grade of visibility was higher in the post-processed KUB (original vs. post-processed, 3.52 vs 3.91, p=0.1536, 3.89 vs. 4.33, p<0.05, 4.47 vs. 4.74, p=0.2871, 2.9 vs. 3.15, p=0.3092). The detection rates showed improved without significant difference between original and post-processed KUB (80% vs. 83.3%, 66.7% vs. 66.7%, 66.7% vs. 66.7%, 70% vs. 76.7%, p>0.05). There was no significant difference of stone size (range: 3.48 - 14.79 mm) among CTKUB and digital KUB data sets (p>0.05).

# CONCLUSION

Digital post-processed KUB images show higher visibility of the ureteral stones and can be improved detection.

### **CLINICAL RELEVANCE/APPLICATION**

In view of its high visibility, digital post-processed KUB image can be an excellent modality to detect ureteral stones and measure the exact size. In other words, it may be diagnosed ureteral stone at least radiation dose in patients with suspicious of stone disease.



# GU220-SD-MOB5

# Comparison of Dual-Energy CT and Subtraction CT for Renal Lesion Detection and Characterization

Monday, Nov. 26 12:45PM - 1:15PM Room: GU/UR Community, Learning Center Station #5

## Participants

Ali Pourvaziri, MD, MPH, boston, MA (*Presenter*) Nothing to Disclose Anushri Parakh, MBBS, MD, Boston, MA (*Abstract Co-Author*) Nothing to Disclose Amirkasra Mojtahed, MD, Boston, MA (*Abstract Co-Author*) Nothing to Disclose Avinash R. Kambadakone, MD, Boston, MA (*Abstract Co-Author*) Nothing to Disclose Dushyant V. Sahani, MD, Boston, MA (*Abstract Co-Author*) Research support, General Electric Company Medical Advisory Board, Allena Pharmaceuticals, Inc

# For information about this presentation, contact:

apourvaziri@mgh.harvard.edu

# PURPOSE

To compare the performance of material-density iodine(MDI) images and subtraction CT(CT-S) on reader confidence and diagnostic accuracy for characterizing renal lesion.

# METHOD AND MATERIALS

In this retrospective clinical study, 111patients (59M, 51F; mean age:72yrs) who underwent dedicated contrast enhanced CT for evaluation of suspected renal mass on rapid KVP switching DECT were included. Scan protocol was: true unenhanced (TUE,120kVp) SECT and nephrographic-phase DECT with similar slice coverage to enable subtraction CT. DECT image reconstructions included quality-check 140 kvp, 65 keV monochromatic (axial, coronal and sagittal reformats), MDI and material-density water. Images were evaluated by 3 blinded abdominal radiologists, with variable experience (2-15 years), independently as four datasets in the following order: (A) MDI only, (B)MDI + axial 65keV + material-density water, (C) CT-S only and (D) CT-S + TUE+ nephrogenic phase CECT (axial, coronal, sagittal). Readers evaluated (a) image quality (4- scale, 1: worst; 4: best) (b) number of lesions and most likely diagnosis and (c) level of confidence. Time to read was recorded for all datasets. Standard of reference was combination of histopathology, clinical data and follow up imaging.

### RESULTS

A total number of 157 lesions (45 enhancing vs 112 non-enhancing; size 25mm±17mm) were evaluated. MDI only images were rated significantly higher for image quality compare to CT-S only (median score 4 vs 3; p,0.050). For all readers, Groups A, B and D had comparable sensitivity (91.3% /92%/ 88.6%) and specificity (86.2%/ 87 %/ 93%), while group C had significantly lower sensitivity (66.23%) but comparable specificity (91.37%). MDI only provided higher level of confidence in 58% lesions compared to CT-S only. Interpretation time for DECT data set only (group B) tends to be faster than conventional renal mass protocol with SECT (group D, TUE +CECT +subtraction) (49s vs 77s/ per exam; p,0.05).

#### CONCLUSION

MDI images are of a higher quality, increases reader confidence for renal lesion detection and characterization and provide a more efficient radiologist workflow, irrespective of readers' experience.

# **CLINICAL RELEVANCE/APPLICATION**

Utilization of rsDECT improves reader confidence for renal lesion characterization, with faster interpretation time and comparable specificity to conventional multi-phase renal mass protocol

### **Honored Educators**

Presenters or authors on this event have been recognized as RSNA Honored Educators for participating in multiple qualifying educational activities. Honored Educators are invested in furthering the profession of radiology by delivering high-quality educational content in their field of study. Learn how you can become an honored educator by visiting the website at: https://www.rsna.org/Honored-Educator-Award/ Dushyant V. Sahani, MD - 2012 Honored EducatorDushyant V. Sahani, MD - 2015 Honored EducatorDushyant V. Sahani, MD - 2016 Honored EducatorDushyant V. Sahani, MD - 2017 Honored Educator



## HP119-ED-MOB6

Translating Research into Reimbursement: Taking New Technology through the CPT Code and RUC Valuation Processes

Monday, Nov. 26 12:45PM - 1:15PM Room: HP Community, Learning Center Station #6

# Participants

Andrew J. Degnan, MD, Philadelphia, PA (*Presenter*) Nothing to Disclose Chul Y. Chung, MD, Pittsburgh, PA (*Abstract Co-Author*) Nothing to Disclose Mark D. Alson, MD, Fresno, CA (*Abstract Co-Author*) Nothing to Disclose Richard Duszak JR, MD, Atlanta, GA (*Abstract Co-Author*) Nothing to Disclose

For information about this presentation, contact:

degnana@email.chop.edu

# **TEACHING POINTS**

List the process by which a new imaging test or procedure goes through the process of being clinically validated to becoming a reimbursable procedure.
 Summarize the roles of the FDA, CPT editorial panel and RUC in translating new procedures to practice.
 Provide examples of recent successes in translating imaging research into novel studies with billable CPT codes and highlight the role that radiologists play in advocating for new procedures.

### **TABLE OF CONTENTS/OUTLINE**

(1) Overview of the process by which an experimental test or procedure becomes a reimbursable clinical service. (2) Translating an experimental imaging study or procedure to approved use. (3) Overview of regulatory processes and FDA's role in approving new imaging technology and procedures. (4) Converting an approved radiology examination into a reportable CPT code. (5) Obtaining reimbursement for CPT codes through the Relative Value Services Update Committee (RUC). (6) Payment issues for novel imaging services. (7) Recent successes in translating radiology research into clinical practice (Fetal MRI, Contrast-enhanced ultrasound, MR Elastography, US Elastography). (8) Future directions for imaging research and technologies. (9) Role of specialty societies and radiologist advocacy in facilitating reimbursement for new beneficial imaging services.



# HP211-SD-MOB1

## Examination of Online Options for Patients Seeking Second Opinions in Radiology

Monday, Nov. 26 12:45PM - 1:00PM Room: HP Community, Learning Center Station #1

### Participants

Aleksandr Rozenberg, MD, Philadelphia, PA (*Presenter*) Nothing to Disclose Jonathan Weinstein, MD, Philadelphia, PA (*Abstract Co-Author*) Nothing to Disclose Sandeep P. Deshmukh, MD, Philadelphia, PA (*Abstract Co-Author*) Nothing to Disclose Christopher G. Roth, MD,MS, Philadelphia, PA (*Abstract Co-Author*) Nothing to Disclose William B. Morrison, MD, Philadelphia, PA (*Abstract Co-Author*) Consultant, AprioMed AB; Patent agreement, AprioMed AB; Consultant, Zimmer Biomet Holdings, Inc; Consultant, Samsung Electronics Co, Ltd; Consultant, Medical Metrics, Inc Adam C. Zoga, MD, Philadelphia, PA (*Abstract Co-Author*) Nothing to Disclose Vijay M. Rao, MD, Philadelphia, PA (*Abstract Co-Author*) Nothing to Disclose

### PURPOSE

Due to the continued globalization of health care, patients seeking second opinions have an array of available choices on the Internet. The aim of this study was to assess the online services that are available to patients exploring second opinions of their own imaging studies.

### **METHOD AND MATERIALS**

An online search was performed to identify radiology services and departments that provide online secondary interpretations of previously performed imaging studies. A public website was identified for each of the included practices. A list of measures were evaluated for each practice, including the patient experience and billing/payment information.

#### RESULTS

A total of 25 practices were included in the analysis, 12 of which were private companies and 13 of which were part of an academic radiology department. A total of 8 of the 25 (32%) only performed secondary reads, without capabilities to perform their own diagnostic imaging. Four of the 25 (16%) allowed the patient to select the interpreting radiologist and 7 of the 25 (28%) provided a phone or video consultation between the patient and radiologist. The average stated time to interpretation is  $2.0 \pm 1.5$  days for private companies and  $7.1 \pm 3.6$  days for academic departments. The average cost per imaging modality is \$90 ± \$60 for radiography, \$166 ± \$35 for ultrasound, \$181 ± \$65 for CT, \$207± \$80 for MRI, \$232 ± \$35 for mammography, and \$267 ± \$103 for PET/CT. The average total cost for a comprehensive consultation was \$629 ± \$244. Only 5 of the 25 (20%) practices did not list pricing on their publicly available website.

## CONCLUSION

A growing number of academic and private radiology practices offer online services to patients seeking second opinions. As radiologists continue to explore telehealth options, opportunities may exist in direct patient service offerings like online-based second opinions. These services are uniquely positioned to provide advanced consultation to patients and help them navigate the modern health care system.

# **CLINICAL RELEVANCE/APPLICATION**

Although the majority of secondary consultations in radiology are initiated by referring clinicians, there is growing demand for patient initiated second opinions. By understanding this developing market, radiologists have an opportunity to directly address patient concerns and ultimately improve the healthcare experience.



### HP212-SD-MOB2

### Outcomes of Radiology Medical Malpractice Lawsuits in Three States, 2008-Present

Monday, Nov. 26 12:45PM - 1:00PM Room: HP Community, Learning Center Station #2

### **Participants**

Frances B. Lazarow, MD, Norfolk, VA (*Presenter*) Nothing to Disclose Jonathan M. Lazarow, BA,MSc, Norfolk, VA (*Abstract Co-Author*) Nothing to Disclose Jake Lallo, BA, Richmond, VA (*Abstract Co-Author*) Nothing to Disclose Sarah C. Shaves, MD, Virginia Beach, VA (*Abstract Co-Author*) Nothing to Disclose

# PURPOSE

Litigation is of significant concern to radiologists. 90% of radiologists will have experienced a malpractice suit by age 65 and radiology is the eighth most likely service to be implicated in a malpractice claim. Anecdotally, fear of litigation sometimes prompts radiologists to recommend additional follow-up studies or offer expansive differential diagnoses in order to minimize their liability. Radiologists are often unfamiliar with litigation and do not understand the progression or potential results of these cases. This study analyzes malpractice lawsuits brought against radiologists in three states from 2008-present, in order to better characterize the volume, resolution, and payout of malpractice claims, as well as the type of error and imaging modality implicated.

### **METHOD AND MATERIALS**

A search for radiology malpractice cases from 2008-present in 3 states (all top 20 population) was performed using LexisAdvance, a subscription database, yielding 274 cases. Any cases where the radiologist was dropped by summary judgment prior to resolution were excluded, as were cases which did not have a reported judgment or award (confidential). Each case summary was analyzed to determine which cases went to trial, the resolution, the type of error (diagnostic error, procedural complication, or communication failure), the imaging modality implicated, and the average plaintiff award.

# RESULTS

44 cases met the above criteria. 20 were settled out of court (45%). 7 of these settlements resulted in payments to the plaintiff (average award \$950,000). Of the cases that went to trial, 11 resulted in a verdict for the plaintiff (46%), with an average award of \$1,564,708 (range: \$0-\$2,650,000). In cases that resulted in payments to the plaintiff, 13 were due to diagnostic error, 1 was a communication failure, and 2 were procedural complications. In cases that resulted in plaintiff payments, CT was the most commonly implicated modality (7 cases).

#### CONCLUSION

A similar number of cases proceeded to trial as were resolved out of court. Settlements resulted in substantially lower payouts to the plaintiff than plaintiff-favorable jury verdicts. In cases that resulted in plaintiff awards, diagnostic error was most common, with CT the most common modality implicated.

# **CLINICAL RELEVANCE/APPLICATION**

Increased awareness of the volume and outcomes of malpractice cases can help radiologists cope with some of the uncertainty that accompanies a lawsuit.



### HP213-SD-MOB3

## Whole-Body MRI Screening of an Asymptomatic Cohort: A Long-Term Follow-Up Study

Monday, Nov. 26 12:45PM - 1:00PM Room: HP Community, Learning Center Station #3

#### **Participants**

Cindy Xue, Hong Kong, Hong Kong (*Presenter*) Nothing to Disclose Victor Ai, Hong Kong, China (*Abstract Co-Author*) Nothing to Disclose Jing Yuan, PhD, Hong Kong, Hong Kong (*Abstract Co-Author*) Nothing to Disclose Oi Lei Wong, PhD, Happy Valley, Hong Kong (*Abstract Co-Author*) Nothing to Disclose Gladys G. Lo, MD, Happy Valley, Hong Kong (*Abstract Co-Author*) Nothing to Disclose

## PURPOSE

To evaluate the usefulness of whole-body MRI (WBMRI) screening in an asymptomatic cohort with respect to long-term clinical outcome.

# METHOD AND MATERIALS

A pilot feasibility study was performed in 2005 on 132 asymptomatic medical doctors (111 male, 21 female; mean age, 56; age range, 38-82) who underwent baseline WBMRI during 2005-2006. 90 of them (74 male, 16 female; mean age, 55.6; age range, 38-82) had 160 subsequent follow-up WBMRI during 2008-2017 (follow up interval, 1-7 years). All scans were performed using 1.5T and 3T MRI scanners covering the brain, neck, thorax, abdomen, pelvis, and spine. Images were evaluated by a group of radiologists with 10+ years experience. Abnormalities detected were categorized as Q1 (requiring immediate or early treatment), Q2 (requiring further evaluation or follow up) and Q3 (requiring no further evaluation or follow up). All lesions including treatment and outcome were retrospectively studied.

#### RESULTS

In the baseline scans, 280 lesions were found, of which 4 (1.4%; 3.8% of cohort) were Q1 lesions (bronchoalveolar cell carcinoma, Hurtle cell tumor of thyroid, retroperitoneal tumor, and renal cell carcinoma; all treated surgically). 51 (18.2%) were Q2 lesions, of which 3 (1.1%; 2.3% of cohort) subsequently had surgery (indeterminate benign renal mass, gallstone, benign prostatic hypertrophy). All treated patients remained well without recurrent disease after 10+ years. In the follow-up scans, 400 lesions were found, of which 3 (0.75%; 1.88% of cohort) were de novo Q1 lesions (lung carcinoma, palatal tumor, and pulmonary TB). 34 Q2 lesions in the baseline were again observed, and a total of 8 Q2 lesions (2%; 5% of cohort) required subsequent treatment (pulmonary embolism, gallstones, diverticulitis, and benign prostatic hypertrophy) in the follow-up study.

### CONCLUSION

WBMRI is effective not only in the detection of Q1 lesions but also in monitoring of Q2 lesions which may require subsequent treatment. It is, therefore, a useful tool for long-term screening and clinical management of the asymptomatic population.

### **CLINICAL RELEVANCE/APPLICATION**

This study provides an insight into the role of long-term screening and clinical management of asymptomatic population using WBMRI.



## HP214-SD-MOB4

Gender Disparity in Editorial Boards of Major Radiological Societies

Monday, Nov. 26 12:45PM - 1:15PM Room: HP Community, Learning Center Station #4

#### Participants

Waleed Abdellatif, MD, Vancouver, BC (*Presenter*) Nothing to Disclose Faisal Khosa, Vancouver, BC (*Abstract Co-Author*) Scholarship, Canadian Association of Radiologists; Scholarship, Vancouver Coastal Health Michael C. Shao, BSC, Vancouver, BC (*Abstract Co-Author*) Nothing to Disclose

For information about this presentation, contact:

#### waleed.abdellatif@vch.ca

#### PURPOSE

To investigate gender differences in editorial boards of the major radiological societies in the world. This study is part of longitudinal multi-faceted investigative inquiry into gender disparity in medical sciences.

## **METHOD AND MATERIALS**

All radiological societies with English publications with impact factor of 1 or more were included: RSNA, CAR, BIR, ASMIRT, ESR and KSR. Websites of those societies were reviewed for editor listings. Each editor was subsequently searched for on Elsevier's SCOPUS, LinkedIn, PubMed and Google Scholar to further extract editor metrics: academic rank, department leadership, subspecialty, h-index, number of publications, number of citations and years since first publication (as an index of active research).

## RESULTS

Skewed male predominance was evident (80.9% males and 19.1% females). Males were the majority overall at all editor ranks, except in associate editor for breast. The publication gap was the widest at lecturer/instructor rank (median "m" = 84 and 10 for males and females respectively) and narrowest at associate professor rank (m= 80 and 75 for males and females respectively).Number of citations was higher for males at all academic ranks except at associate professor rank (males=females) and at assistant professor rank where females had higher number of citations (m=520.5 and 414 for females and males respectively). The h-index was higher for RSNA editors in comparison to other editorial boards. h-index of female editors was lower than male counterparts in all editorial boards.Numbers of years since first publication was higher in males overall (overall median = 22.5 and 18 y for males and females respectively) and this is also true for males across all academic ranks except at associate and assistant professor rank (m= 20, 17 for females and males at associate professor respectively; m= 14.5, 11.5 at assistant professor rank).Leadership positions were higher in males (131; 87.9%) than females (18; 12.1 %). Survival analysis revealed that females have a lower probability to become leaders.

#### CONCLUSION

Gender disparity exits in editorial boards of major radiological societies. Females held significantly less leadership positions with lower probability to become leaders.

#### **CLINICAL RELEVANCE/APPLICATION**

This study serves as evidence-based reference database to evaluate the magnitude of gender disparity in editorial boards and facilitate future investigative initiatives and remedy plans.



## HP215-SD-MOB5

## Multisite Implementation of Integrated Clinical Decision Support at the Simulated Point-of-Order Entry

Monday, Nov. 26 12:45PM - 1:15PM Room: HP Community, Learning Center Station #5

#### **Participants**

Marc H. Willis, MMM,DO, Houston, TX (*Presenter*) Investor, Resonea Karla A. Sepulveda, MD, Houston, TX (*Abstract Co-Author*) Nothing to Disclose Joseph Fotos, Hershey, PA (*Abstract Co-Author*) Nothing to Disclose Pauline Germaine, DO, Camden, NJ (*Abstract Co-Author*) Nothing to Disclose John W. Gilpin, MD, Greenville, SC (*Abstract Co-Author*) Nothing to Disclose Kristopher N. Lewis, MD, Evans, GA (*Abstract Co-Author*) Nothing to Disclose Alana D. Newell, Houston, TX (*Abstract Co-Author*) Nothing to Disclose Marjorie W. Stein, MD, New Rochelle, NY (*Abstract Co-Author*) Nothing to Disclose Christopher M. Straus, MD, Chicago, IL (*Abstract Co-Author*) Nothing to Disclose

#### For information about this presentation, contact:

mwillis@bcm.edu

#### PURPOSE

Based upon the successful pilot of a case-based education portal with integrated clinical decision support (CDS) at the simulated point-of-order at our institution, we expanded our efforts to evaluate if this novel approach is transferable to other institutions.

#### **METHOD AND MATERIALS**

The education portal is built within a content management system and integrated with clinically available CDS, we partnered with eight academic institutions from around the country. A total of 199 students participated in the multi-site between July 2016 and June 2017. Institutional review board approval was obtained. For the purpose of the analysis, only the sites that used all MIII students (Sites A-E) were included in the analysis. First, data were explored descriptively by calculating means and standard deviations for each site. Then, multilevel linear regression was used to investigate the differences in posttest scores across treatment groups, while accounting for site-level variance.

## RESULTS

An initial inspection of the descriptive statistics aggregated across all sites showed that the module groups had an average increase from pre- to posttest, while the control groups did not have any increase. Once variance between sites was taken into consideration, students who participated in the module group had a statistically significant average content knowledge gain of about 4-points as compared to their peers in the comparison group (t(124)=7.261, p<0.001). Additionally, no other predictors in the module group had a statistically significant average content knowledge gas captured on the pretest, the number of days between the tests, the time during the academic year in which they completed the module or the interactions between prior knowledge and group membership or time of the academic year. For the students in the module group, the greatest subject matter gains came in questions related to chest x-rays (22% increase) and adnexal cysts (20.33% increase), while students struggled with the items related to pulmonary embolisms (0.33% increase).

#### CONCLUSION

This novel approach to teaching important components of Health System Science (appropriate utilization, cost, and patient safety) are transferable and scalable.

#### **CLINICAL RELEVANCE/APPLICATION**

As the health care system transitions from volume to value, there is a need to fill traditional gaps in medical education curricula.



## IN145-ED-MOB2

Right Diagnosis, Wrong Patient! A Picture is Worth a Thousand Images: The Value of Photo-Verification Technology

Monday, Nov. 26 12:45PM - 1:15PM Room: IN Community, Learning Center Station #2

FDA Discussions may include off-label uses.

#### **Participants**

Srini Tridandapani, MD,PhD, Decatur, GA (*Presenter*) Co-founder, CameRad Technologies, LLC; Spouse, Co-founder, CameRad Technologies, LLC;

Pamela T. Bhatti, PhD, Atlanta, GA (*Abstract Co-Author*) Co-founder, Camerad Technologies, LLC Richard K. Brown, MD, Ann Arbor, MI (*Abstract Co-Author*) Nothing to Disclose Elizabeth A. Krupinski, PhD, Atlanta, GA (*Abstract Co-Author*) Nothing to Disclose Carson A. Wick, PhD, Atlanta, GA (*Abstract Co-Author*) Employee, CameRad Technologies, LLC; Nabile M. Safdar, MD, Milton, GA (*Abstract Co-Author*) Nothing to Disclose

#### For information about this presentation, contact:

srinit@yahoo.com

#### **TEACHING POINTS**

The incidence of wrong patient errors is non-negiligible and can cause serious patient safety problems. Photographs obtained simultaneously with portable radiographs can help prevent wrong-patient errors. Photographs provide additional clinical context and help with 1) evaluation of lines and tubes, 2) evaluation of soft tissue injury, and 3) confidence in patient positioning.

# TABLE OF CONTENTS/OUTLINE

1. Point-of-Care Photographs: How, What and Why? 2. Benefits of Point-of-Care Photography. 2.1. Examples of Wrong-Patient Error Detection. 2.2. Examples of Providing Clinical Context Through Point-of-Care Photographs. 2.3. Examples of Radiography-Photography Correlations Potentially Leading to Improved Physical Examinations. 3. Discussion of Potential Privacy Issues. 4. Conclusions. 5. References.

### **Honored Educators**

Presenters or authors on this event have been recognized as RSNA Honored Educators for participating in multiple qualifying educational activities. Honored Educators are invested in furthering the profession of radiology by delivering high-quality educational content in their field of study. Learn how you can become an honored educator by visiting the website at: https://www.rsna.org/Honored-Educator-Award/ Elizabeth A. Krupinski, PhD - 2017 Honored Educator



## IN207-SD-MOB1

## Lossless Compression of Segmented 3D Binary Data for Efficient Telemedicine Applications

Monday, Nov. 26 12:45PM - 1:15PM Room: IN Community, Learning Center Station #1

#### **Participants**

Erdogan Aldemir, Izmir, Turkey (*Abstract Co-Author*) Nothing to Disclose Gulay Tohumoglu, Izmir, Turkey (*Abstract Co-Author*) Nothing to Disclose Oguz Dicle, MD, Izmir, Turkey (*Abstract Co-Author*) Nothing to Disclose Alper M. Selver, PhD, Izmir, Turkey (*Presenter*) Nothing to Disclose

#### For information about this presentation, contact:

alper.selver@deu.edu.tr

## CONCLUSION

This study provides a necessary step for extending repeatability and mobility capabilities of 3D medical imaging by developing a DICOM compatible object, which covers visualization parameters together with compressed binary segmented data for efficient transmission in telemedicine applications.

#### Background

In the current state of the DICOM standard, there are no modules that provide the possibilities of parametric representation by 2D Presentation States (2DPR) to 3D imaging. Once the final 3D rendering is obtained, current methods use video/image exporting to save the rendering result. To increase the utility of 3DPR in clinical practice, it is important to attach the available segmentation results, which are in binary form. Moreover, for effective use in telemedicine applications, this binary volumetric data should be compressed in a lossless way. In previous studies, several lossless compression methods were applied to various segmented anatomical organs (aorta, skeleton, skull, liver and kidneys etc.). Unfortunately, the results show the lack of 3D processes for lossless compression. Thus, in this study, the compression ratios of an existing effective method (i.e. Run Length Encoding - RLE) pipeline is improved by offering various scan forms (such as spiral and chevron) which are morphologically coherent with the organs in the binary image.

## Evaluation

A large set of scanning possibilities provide low-entropy sequences for coding. Thereby, the compression performance of the RLE based system is improved. The developed system is applied to 20 segmented liver data sets having 70 to 110 images. Each image is processed by JPEG lossless (JPEG-LS) and lossy versions, RLE based compression scheme with column wise, row wise, zigzag, chevron and spiral scan orders. The result has shown that RLE based technique with spiral order give the best compression performance. The average compression efficiencies by total size is found as 22.25 MB (uncompressed), 3.04 MB (JPEG-LS), 0.52 MB (JPEG), and 0.23 MB (RLE-Spiral).

#### Discussion

Extending RLE based methods with 3D scanning provide a significant compression performance over 95% while the performance of the 2D techniques remains under %90.



### MI118-ED-MOB4

# Carcinoma Tongue: It's Comparative Evaluation on 3T MRI, DWI, PET- CT and PET-MRI Fusion

Monday, Nov. 26 12:45PM - 1:15PM Room: MI Community, Learning Center Station #4

#### **Participants**

Suvinay Saxena, MBBS, Bhopal, India (*Presenter*) Nothing to Disclose Drushi V. Patel, MBBS, MD, Ahmedabad, India (*Abstract Co-Author*) Nothing to Disclose Rajendra N. Solanki, MD, Ahmedabad, India (*Abstract Co-Author*) Nothing to Disclose Hemant T. Patel, MD, Ahmedabad, India (*Abstract Co-Author*) Nothing to Disclose

## For information about this presentation, contact:

suvinaysaxena@gmail.com

# **TEACHING POINTS**

To ascertain the normal radiolgical anatomy of tongue To describe various types of carcinoma tongue and its routes of spread. To compare and assess the diagnostic accuracy of 3T MRI,DWI, PET-CT and PET-MRI fusion imaging.

## TABLE OF CONTENTS/OUTLINE

Radio-anatomy of tongue. Pathophysiology of Carcinoma tongue. Review of imaging findings - MRI, DWI and PET-MRI fusion imaging. Sample cases. Further directions and summary



## MI211-SD-MOB1

In Vivo Imaging of the Tumor Microenvironment Allows for Estimation of Local Invasive and Metastatic Potential

Monday, Nov. 26 12:45PM - 1:15PM Room: MI Community, Learning Center Station #1

# Participants

Anne Helfen, MD, Muenster, Germany (*Presenter*) Nothing to Disclose Nils Grosse Hokamp, MD, Cleveland, OH (*Abstract Co-Author*) Nothing to Disclose Christiane Geyer, Muenster, Germany (*Abstract Co-Author*) Nothing to Disclose Max Masthoff, MD, Muenster, Germany (*Abstract Co-Author*) Nothing to Disclose Walter L. Heindel, MD, Muenster, Germany (*Abstract Co-Author*) Nothing to Disclose Christoph B. Bremer, MD, Muenster, Germany (*Abstract Co-Author*) Nothing to Disclose Thomas Vogl, PhD, Muenster, Germany (*Abstract Co-Author*) Nothing to Disclose Michel Eisenblaetter, MD, Muenster, Germany (*Abstract Co-Author*) Nothing to Disclose

#### PURPOSE

Tumor development and metastasis are dependent on tumor infiltrating immune cells, which form a characteristic inflammatory tumor microenvironment (TME). Activated monocytes secrete the protein heterodimer S100A8/A9, promoting TME formation. Monocyte-dependent proteases facilitate local tumor cell invasion by degradation of the extracellular matrix. We aimed for target-specific in vivo imaging of S100A8 and proteases to provide differentiating biomarkers for local tumor growth and metastatic potential.

## **METHOD AND MATERIALS**

Murine breast cancer cells of the 4T1 model with graduated metastatic potential (4T1: hematogenous metastasis>168FAR: lymphnode metastasis>67NR: no metastasis) were orthotopically implanted into female BALB/c mice. At 4 mm tumor size we intravenously injected the protease-specific probe ProSense 750EX (PerkinElmer, 4T1:n=7,168FAR:n=16,67NR:n=15) and anti-S100A8-Cy5.5 (n=6 each) and performed flurorescence reflectance imaging 0 and 24h after injection. In vivo imaging was correlated with immunohistology and FACS analyses.

## RESULTS

At 24h, S100A8-specific signals in 4T1 were significantly higher (1714.05AU) as compared to 168FAR and 67NR (174.85/167.95AU, p<0.00001), reflecting the capability of hematogenous spread. Protease-specific signals were significantly higher in 4T1 (348.01AU) as compared to 168FAR and 67NR (p<0.00001). Signal intensities in 67NR were significantly lower (129.78AU) than in 168FAR tumors (214.91AU, p<0.00001), reflecting local vessel invasion and tumor cell shedding, although without the capability of forming solid metastases. Histology and FACS supported the in vivo imaging results.

## CONCLUSION

Non-invasive in vivo imaging of S100A8 and monocytic proteases allows for differentiation of the tumors' local invasive and systemic metastatic potential and reflects TME build-up. While proteases augment local tumor cell invasion, solid metastases seem to be dependent on a pro-tumoral TME.

## **CLINICAL RELEVANCE/APPLICATION**

By differentiation of local tumor growth and metastatic potential, S100A8/A9 and monocytic protease-specific in vivo imaging may serve as important non-invasive biomarkes for tumor aggressiveness.



## MI212-SD-MOB2

Imaging of Peptide Functionalized Nanoparticles Using T1 Mapping in Detecting Marginal Infiltration of GBM

Monday, Nov. 26 12:45PM - 1:15PM Room: MI Community, Learning Center Station #2

#### Participants

Yingwei Wu, MD, Shanghai, China (*Presenter*) Nothing to Disclose Guangyu Wu, Shanghai, China (*Abstract Co-Author*) Nothing to Disclose Xiaofeng Tao, Shanghai, China (*Abstract Co-Author*) Nothing to Disclose

For information about this presentation, contact:

WUYW0103@HOTMAIL.COM

## PURPOSE

To apply cMBP peptide functionalized nanoparticles in detecting marginal infiltration with T1 mapping technique.

## **METHOD AND MATERIALS**

cMBP peptide was selected as specific binding ligand to MET receptors. MR-based cMBP peptide functionalized nanoparticles (DENcMBP-Gd) and control NPs (DEN-PEG-Gd) were synthetized. In-vitro DEN-cMBP-Gd with different Gd concentrations (0.1, 0.2, 0.4, and 0.8 mM) were prepared and T1 GBM rodent models were sub-grouped and intravenously administered with DEN-cMBP-Gd, DEN-PEG-Gd and Gd-DTPA, respectively. T1 mapping was acquired pre/post-contrast agent administration. GBM tumor was segmented into central area and marginal area using principal morphologic operation erosion. Image erosion was applied to the origin mask(tumor margin) for each tumor using a disk with a defined pixel radius which was then eroded (disk radius of 5 pixels) to generate the marginal region mask. T1 relaxation time of each part and whole tumor were measured. HE staining and Immunohistological staining were performed to verify tumor margin and cells infiltration.

### RESULTS

The MET targeted NP (DEN-cMBP-Gd) showed excellent binding affinity to MET receptors, with Kd value of 1.316\*1-10 while control NPs did not bind to MET receptors. The T1-weighted phantom demonstrated a good linear correlation between Gd concentration and 1/T1 (r1=9.1mM-1•s-1). In comparison with baseline in-vivo T1 mapping, GBM tumors were enhanced post administration of DEN-cMBP-Gd, the control NP, and the non-specific clinical contrast agent Gd-DTPA.Clinical Gd-GTPA yielded highest percentage of T1 relaxation time decline(57%) of whole tumor among three contrast agents while DEN-cMBP-Gd (decreased by 36%) and DEN-PEG-Gd (decreased by 29%) showed similar decreased level. Although no superiority DEN-cMBP-Gd had in enhancement of whole tumor, it typically enhanced in marginal tumor area, with the normalized T1 relaxation time decreased by 53% in marginal tumor area and 30% for tumor central area(31% in marginal area and 68% in central area for Gd-DTPA,14% marginal area and 43% in central area DEN-PEG-Gd, respectively) ,which was consistent with the evidence shown by MET staining in HE and immuno-histological analysis.

## CONCLUSION

Using T1mapping of DEN-cMBP-Gd would be helpful to detect tumor margin and cells infiltration of GBM

## **CLINICAL RELEVANCE/APPLICATION**

The peptide functionalized NP would be applied as alternative modality for MET receptors imaging



## MI213-SD-MOB3

Diagnostic Utility of 68-Galium-Prostate Specific Membrane Antigen Positron Emission Tomoraphy-Computed Tomography (68-Ga- PSMA PET-CT) in High and Intermediate Risk Prostate Cancer

Monday, Nov. 26 12:45PM - 1:15PM Room: MI Community, Learning Center Station #3

## Participants

Smita Kulkarni, MBBS,MD, Bagalkot, India (*Presenter*) Nothing to Disclose Shanmuga Sundaram P, Cochin, India (*Abstract Co-Author*) Nothing to Disclose Padma Subramanyam, Cochin, India (*Abstract Co-Author*) Nothing to Disclose Chinmay B. Kulkarni, MD,MBBS, Cochin, India (*Abstract Co-Author*) Technical support, Koninklijke Philips NV

#### For information about this presentation, contact:

smitamoodi@gmail.com

## PURPOSE

To assess the diagnostic accuracy of the 68-Ga- PSMA PET-CT in detecting the primary tumor and lymph nodal metastases in patients with high and intermediate risk prostate cancer prior to definitive surgical treatment.

## METHOD AND MATERIALS

We retrospectively analyzed 51 patients (average age  $68.1 \pm 6.8$  years ; range:56-79 years) with biopsy proven intermediate and high risk prostatic cancer (intermediate risk, n=23 and high risk, n = 28) who underwent technically successful whole body 68Ga-PSMA PET-CT scan and subsequently managed by radical prostatectomy and extended pelvic lymph nodal dissection between January 2016 to December 2017. The sensitivity, specificity, Positive Predictive Value (PPV) & Negative Predictive Value (NPV) of 68Ga-PSMA PET-CT in detecting primary tumor and lymph nodal metastases were calculated and analyzed using histopathology as reference.

#### RESULTS

The average PSA value was  $39 \pm 37$  ng /ml and median Gleason's score was 3+4. The sensitivity and the PPV of 68Ga- PSMA PET-CT in detecting the primary tumor was 94 % (CI 83.7-98.7%) and 100 % (CI 94.5 - 96.3%) respectively with accuracy of 94.1%. The average Maximum Standardized Uptake Value (SUV max) of the primary tumor was  $11.3 \pm 7.3$  (range: 4.1-26.3). 68Ga- PSMA PET-CT detected lymph nodal metastases in 19 out of 25 patients with histopathology proven lymphnodal metastases with sensitivity, specificity, PPV,NPV and accuracy of 76%, 96%, 95%,80% and 86.2% respectively. The average size of the lymph nodes was  $1.2 \pm 0.6$  cm (range: 0.6-2.5 cm) and average SUV max of the detected lymph nodes was  $9.8 \pm 8.8$  (range, 4.0 - 34.4).

#### CONCLUSION

68Ga- PSMA PET-CT allows accurate detection of primary tumor as well as lymph nodal metastases in patients with intermediate and high risk prostate cancer prior to definitive surgical treatment.

## **CLINICAL RELEVANCE/APPLICATION**

68Ga- PSMA PET CT allows for accurate detection of primary tumor as well as lymph nodal metastases and cab be one stop technique for evaluating patients with intermediate and high risk prostate cancer prior to definitive surgical treatment.



### MK345-ED-MOB8

Guess Who is Who: Tumor versus Tumor Mimicker-Bone and Soft Tissue Tumor Mimickers

Monday, Nov. 26 12:45PM - 1:15PM Room: MK Community, Learning Center Station #8

#### Participants

Young Kwang Lee, MD, Jeonju, Korea, Republic Of (*Presenter*) Nothing to Disclose Jin Hee You, MD, Jeonju, Korea, Republic Of (*Abstract Co-Author*) Nothing to Disclose Eun Hae Park, Jeonju, Korea, Republic Of (*Abstract Co-Author*) Nothing to Disclose Ji Soo Song, MD, Jeonju, Korea, Republic Of (*Abstract Co-Author*) Nothing to Disclose Eun Jung Choi, MD, PhD, Jeonju, Korea, Republic Of (*Abstract Co-Author*) Nothing to Disclose Gong Yong Jin, MD, PhD, Jeonju, Korea, Republic Of (*Abstract Co-Author*) Nothing to Disclose

## For information about this presentation, contact:

jiml0826@gmail.com

## **TEACHING POINTS**

Most noticeable point in this presentation is that we carefully selected 1:1 matched tumor vs tumor mimicker cases. By solving this 1:1 matched quiz, readers will be able to involve actively. In pages that give answers, we stressed two key points in each mimicking lesion at the top of the page, followed by detail explanation at the below of the page.

## TABLE OF CONTENTS/OUTLINE

1. Soft tissue tumor mimicker : Hematoma / Proliferative myositi / Tumoral calcinosis 2. Bone tumor mimicker : Osteomyelitis / Brodie's abscess / Stress fracutre / BPOP / Periosteal desmoid / Brown tumor / Post procedural site 3. In radiograph : Humeral pseudocyst / Light bulb appearance / Supracondylar process / Radial tuberosity / Herniation Pit / Ward's triangle / Ischiopubic synchondrosis / Dorsal defect of patella / Calcaneal pseudocyst



## MK363-SD-MOB1

Fast MR Imaging of Isotropic Volumetric Ankle: Acceleration of Three-Dimensional Fast Spin Echo Sequence Using Compressed Sensing Combined with Parallel Imaging

Monday, Nov. 26 12:45PM - 1:15PM Room: MK Community, Learning Center Station #1

#### Participants

Jisook Yi, MD, Busan, Korea, Republic Of (*Presenter*) Nothing to Disclose Young Han Lee, MD, Seoul, Korea, Republic Of (*Abstract Co-Author*) Nothing to Disclose Seok Hahn, MD, Busan, Korea, Republic Of (*Abstract Co-Author*) Nothing to Disclose Sungjun Kim, MD, Seoul, Korea, Republic Of (*Abstract Co-Author*) Nothing to Disclose Ho-Taek Song, MD, Seoul, Korea, Republic Of (*Abstract Co-Author*) Nothing to Disclose Jin-Suck Suh, MD, Seoul, Korea, Republic Of (*Abstract Co-Author*) Nothing to Disclose

### PURPOSE

To investigate the feasibility of three-dimensional fast spin echo (3D-FSE) sequence with compressed sensing (CS) combined with parallel imaging (PI) compared to conventional 3D-FSE imaging in evaluating ankle joint pathology.

## **METHOD AND MATERIALS**

Twenty patients underwent ankle MRI including image sets of 2D-FSE sequences, intermediate weighted (IW) 3D-FSE sequence without CS and with CS. Ankle MRI was performed using a 3.0-T magnetic resonance system with a 16-channel GEM Flex-medium flexible coil. Acceleration factors of 2x2 were used for parallel imaging, and 1.5 k-space undersampling factor was used for CS accerelation. The image sets were independently rated by two radiologists for the presence or absence of ankle pathology and interobserver agreements were analyzed. Overall image quality (structural similarity index) and subjective image quality (using a 4-point scale) of IW 3D-FSE sequence without CS and with CS-PI were evaluated. Inter-sequence agreement between IW 3D-FSE sequence without CS and with CS-PI in both readers was evaluated.

#### RESULTS

IW 3D-FSE with CS-PI provided good intersequence and interobserver agreements in evaluating ankle pathology with 33% decreased scan time. Interobserver agreement showed good agreement for anterior talofibular (k=0.773), osteochondral lesion of talus (k=0.763-0.877), and os subfibulare (k=0.615-0.643). Structural similarity index was acceptable (mean, 0.996; range, 0.990-0.997), and there was no statistically significant difference in subjective image quality between two imaging sequences. Intersequence agreement between IW 3D-FSE sequence with and without CS showed nearly perfect for all evaluated structure in both readers.

## CONCLUSION

Compressed sensing accelerated isotropic 3D-FSE ankle MRI provides acceptable diagnostic performance with reduced scan time. Compressed sensing-related artifacts could be minimized with CS reconstruction enhancement, allowing better image quality for evaluation of ankle joint pathology.

## **CLINICAL RELEVANCE/APPLICATION**

Volumetric isotropic 3D-FSE sequence of ankle MRI is potential fast imaging tools with a reduced scan time as well as acceptable diagnostic performance, proper spatial resolution, and soft tissue contrast.



## MK364-SD-MOB2

## Evaluation of CT Fat Quantification Techniques for Assessing the Rotator Cuff Musculature

Monday, Nov. 26 12:45PM - 1:15PM Room: MK Community, Learning Center Station #2

#### **Participants**

Amanda M. Baillargeon, MD, Rochester, MN (*Presenter*) Nothing to Disclose Lifeng Yu, PhD, Chicago, IL (*Abstract Co-Author*) Nothing to Disclose Michael R. Bruesewitz, Rochester, MN (*Abstract Co-Author*) Nothing to Disclose Katrina N. Glazebrook, MBChB, Rochester, MN (*Abstract Co-Author*) Nothing to Disclose

## PURPOSE

To determine the best CT fat quantification technique of the rotator cuff musculature by comparing single energy (SE) and dualenergy (DE) CT fat quantification using Goutallier's grading system as the reference standard.

### **METHOD AND MATERIALS**

With IRB approval, 12 shoulders from 10 patients who underwent clinically indicated, routine shoulder CT using the DECT technique (100/Sn150kV, Force, Siemens Healthcare) were evaluated. Fat fraction was calculated from the DECT data by using basis material decomposition. Region of interest (ROI) were placed on the supraspinatus, infraspinatus, teres minor, subscapularis and teres major muscles in the sagittal plane and deltoid muscle in the axial plane to obtain quantitative measurments of the fat fraction within each ROI (Syngo.Via VB10, Liver VNC application). An ROI was also obtained in the sagittal plane of the subcutaneous fat to be used as an internal standard. Hounsfield units (HU) of each region on the SE 100 kV images and the 70 keV virtual monochromatic images were also recorded and used for fat fraction calculation. Fatty degeneration of the rotator cuff muscles was assessed using Goutallier's system.

#### RESULTS

The fat fraction determined from DECT quantification was highly correlated with the Goutallier score for all muscles evaluated (Pearson product-moment correlation coefficient R=0.93, 95% CI: [0.88, 0.96]). The fat fraction of teres major muscle was  $2.8\% \pm 4.0\%$ , which is close to 0% fat, and the fat fraction of the subcutaneous fat was  $99.5\% \pm 2.6\%$ , which is close to 100% fat, indicating reliable internal standards for using the material decomposition technique. The DE fat fraction correlated better with the Goutallier score than using the HU of DE monochromatic images (R=0.90, 95% CI: [0.84, 0.94]) or from the SE 100 kV images (R=0.89, 95% CI: [0.82, 0.93]).

#### CONCLUSION

Fatty atrophy of the rotator cuff musculature plays a significant role in determining functional outcome after cuff repair. High grades of fatty infiltration are associated with higher rates of repair failure. Our study shows that DECT fat quantification is a reliable technique for assessing rotator cuff muscle atrophy, and that it correlates better with Goutallier score than single energy CT or virtual monochromatic images from DECT using HU.

## **CLINICAL RELEVANCE/APPLICATION**

DECT fat quantification is a reliable technique for assessing rotator cuff muscle atrophy and can be used for preoperative evaluation.



## MK365-SD-MOB3

Automatic Diagnosis Of ACL Tear On X-Ray In Trauma Patients: Achieving "Expert Level" Perception Of Subtle Radiology Findings (Segond Fracture) Using a Sparse Data Set

Monday, Nov. 26 12:45PM - 1:15PM Room: MK Community, Learning Center Station #3

#### Awards Student Travel Stipend Award

#### **Participants**

Charles X. Fang, MD, San Jose, CA (*Presenter*) Nothing to Disclose Joshua J. Reicher, MD, Stanford, CA (*Abstract Co-Author*) Investor, Health Companion, Inc; Consultant, Alphabet Inc Christopher F. Beaulieu, MD, PhD, Stanford, CA (*Abstract Co-Author*) Nothing to Disclose Sandip Biswal, MD, Stanford, CA (*Abstract Co-Author*) Research Grant, General Electric Company; Bao H. Do, MD, Stanford, CA (*Abstract Co-Author*) Nothing to Disclose

## For information about this presentation, contact:

charlesxxfang@gmail.com

#### PURPOSE

Deep convolutional neural networks (CNNs) are an evolving computer vision technique that facilitates rapid, unsupervised learning. Regional CNN focuses on a particular region, increasing the likelihood of identifying subtle findings while reducing training data sample size requirements. We propose to build and validate a 2 part machine that consists of (1): a regional CNN to identify the arcuate region of the knee, and (2): a more granular CNN to detect Segond fracture.

## METHOD AND MATERIALS

235 anonymized frontal knee radiographs without hardware, severe athrosis or deformity were annotated with rectangular regions bounding the arcuate region. 29 separate Segond fracture cases were labeled similarly. Part 1: We trained a deep CNN (single shot multibox/InceptionV2) architecture using Google TensorFlow to identify the arcuate region using 172 normal frontal knee x-rays (63 were held out for test set). Training was performed until classification and localization loss graphs plateaued in TensorBoard. Accuracy for detection and localization were measured. Part 2: We trained a higher parameter deep CNN model (InceptionV3 using transfer learning of the final layer, learning rate 0.01 and 5000 training steps) for further classification of the bounding boxes extracted by phase 1 using 24 frontal knee x-rays with Segond fracture and 129 normal knee x-rays. We created a separate test set of 5 Segond and 15 normal cases.

#### RESULTS

Part 1: Classification and localization loss plateaued at 3797 steps. Detection and localization of the arcuate region was 100% (63/63) accurate. Part 2: Classification of whole knee images as Segond fracture VS no fracture was 100% accurate (5/5 and 15/15 cases, respectively).

## CONCLUSION

We have built a system that achieves expert level perception of a subtle radiological finding (Segond fracture, indicating an ACL tear, consisting less than 0.04% of the entire image) using an extremely sparse set of training data (24 samples).

# **CLINICAL RELEVANCE/APPLICATION**

Regional CNN may address the challenge of big data in radiology machine learning by reducing the size of training sets required to teach AI systems to diagnose subtle and rare pathology with high sensitivity and specificity.



## MK366-SD-MOB4

Precision of Bone Mineral Density Measurements Around Total Ankle Arthroplasty Using Dual Energy X-ray Absorptiometry

Monday, Nov. 26 12:45PM - 1:15PM Room: MK Community, Learning Center Station #4

# Participants

Carmelo Messina, MD, Milan, Italy (*Presenter*) Nothing to Disclose Salvatore Gitto, MD, Milan, Italy (*Abstract Co-Author*) Nothing to Disclose Domenico Albano, Palermo, Italy (*Abstract Co-Author*) Nothing to Disclose Vito Chianca, MD, Napoli, Italy (*Abstract Co-Author*) Nothing to Disclose Angelo Corazza, MD, Genova, Italy (*Abstract Co-Author*) Nothing to Disclose Luca Maria Sconfienza, MD, PhD, Milano, Italy (*Abstract Co-Author*) Travel support, Bracco Group; Travel support, Esaote SpA; Travel support, ABIOGEN PHARMA SpA; Speakers Bureau, Fidia Pharma Group SpA

#### For information about this presentation, contact:

carmelomessina.md@gmail.com

#### PURPOSE

Joint replacement survival is associated with the quality of the surrounding bone. Dual-energy X-ray absorptiometry (DXA) can measure periprosthetic bone mineral density (BMD) with metal removal software. We evaluated short-term reproducibility of the periprosthetic BMD measurements after total ankle arthroplasty (TAA) in 15 patients

#### **METHOD AND MATERIALS**

Each ankle was measured thrice in two projections (frontal and lateral) with DXA (Hologic Discovery W). We evaluated periprosthetic BMD at up to 6 different regions of interest (ROIs) in the two projections, at the level of periprosthetic bone around tibia and talus; an additional ROI was placed in the lateral projection over the calcaneus. Metallic elements were automatically excluded with dedicated software ('metal removal'). Precision is expressed as a coefficient of variation (CV%).

### RESULTS

In the frontal projection, the average precision error was 1,88%, with the lowest value at the tibial side (0,77%) and the highest value at the talus side (4,19%). In the lateral projection, the average precision error was 1,74%, with the lowest CV values at the calcaneus (1,08%) and the highest CV value at the anterior tibial side (3,37%). Both in the frontal and lateral projection the highest variability was found in the nearby of metallic implants (screws, plates).

#### CONCLUSION

As for previous studies at other joint prostheses, our results show that DXA is able to precisely measure small bone mineral changes around TAA, making it possible to eventually monitor bone remodeling around TAA. Further prospective studies are warranted in the future.

# **CLINICAL RELEVANCE/APPLICATION**

Low reproducibility values are mandatory in order to open the use of periprosthetic DXA for monitor bone remodeling around TAA.



## MK367-SD-MOB5

Evaluation of Age-related Changes in the Posterior Cruciate Ligament using T2\* Maps Derived from MR Images with an Ultra-short TE Sequence

Monday, Nov. 26 12:45PM - 1:15PM Room: MK Community, Learning Center Station #5

# Participants

Yoshiko Iwakado, Hiroshima, Japan (Presenter) Nothing to Disclose Yuji Akiyama, Hiroshima, Japan (Abstract Co-Author) Nothing to Disclose Seijyu Hayashi, Hiroshima, Japan (Abstract Co-Author) Nothing to Disclose Masaaki Umeda, Otawara, Japan (Abstract Co-Author) Employee, Canon Medical Systems Corporation Nobuo Adachi, Hiroshima, Japan (Abstract Co-Author) Nothing to Disclose Kazuo Awai, MD, Hiroshima, Japan (Abstract Co-Author) Research Grant, Canon Medical Systems Corporation; Research Grant, Hitachi, Ltd; Research Grant, Fujitsu Limited; Research Grant, Bayer AG; Research Grant, DAIICHI SANKYO Group; Research Grant, Eisai Co, Ltd; Medical Advisory Board, General Electric Company; ; Yasushi Nagata, MD, PhD, Kyoto, Japan (Abstract Co-Author) Nothing to Disclose Kazushi Yokomachi, PhD, Hiroshima, Japan (Abstract Co-Author) Nothing to Disclose Yuji Takahashi, Hiroshima, Japan (Abstract Co-Author) Nothing to Disclose Shogo Kamioka, Hiroshima, Japan (Abstract Co-Author) Nothing to Disclose Akira Nishikori, RT, Hiroshima, Japan (Abstract Co-Author) Nothing to Disclose Takayuki Tamura, Hiroshima, Japan (Abstract Co-Author) Nothing to Disclose Hiroomi Sumida, Hiroshima, Japan (Abstract Co-Author) Nothing to Disclose Ryuji Akita, RT, MS, Hiroshima, Japan (Abstract Co-Author) Nothing to Disclose Rena Usuki, Hiroshima, Japan (Abstract Co-Author) Nothing to Disclose

#### PURPOSE

The generation of T2\* maps from MR images with an ultra-short TE sequence (UTE-MRI) is a novel quantitative MR technique. T2\* maps may allow the evaluation of fast-relaxing tissues such as the posterior cruciate ligament (PCL) whose T2\* is short. They are useful for the in vivo evaluation of degenerative changes in the PCL. We examined the correlation between the patient age and the T2\*value of the PCL on T2\* maps derived from UTE-MRI scans.

### **METHOD AND MATERIALS**

We enrolled 32 healthy volunteers (23 women, 9 men, age range 13-82 years, median 61 years) with asymptomatic knee joints. Scanning was on a 3T instrument (Vantage Titan 3T v3.5, Canon Medical Systems, Otawara, Japan) with the subject in the supine position. The knee joint was firmly fixed and centered in a 16 ch SPEEDER knee coil. The UTE sequence was 3D fast field echo; data were obtained along non-Cartesian trajectories for ultra-short TE. The scan parameters were TR, 9 ms; TE, 0.5-, 0.7-, 2.5-, 3.0-, 5.0 ms; flip angle, 5; field of view, 20 cm; slice thickness, 1 mm. We generated T2\* maps by using a post-processing function of the MRI scanner. Regions of interest were manually placed on the proximal-, middle-, and distal portion of the PCL. The correlation between the age and the T2\* value was investigated with Pearson's correlation coefficient.

## RESULTS

In subjects aged from 10-29 years, 30-59 years, and 60 years or more, the mean T2\*value of the whole PCL was 17.1 (SD 5.2), 41.2 (SD 9.8), and 71.7 (SD 7.2), respectively. There was a positive linear correlation between the age and the T2\*value (r=0.465, p=0.0072). The proximal PCL portion showed the strongest correlation with the age (r=0.512, p=0.0027) followed by the middleand the distal portion (r=0.364, p=0.04 and r=0.276, p=0.126, respectively).

#### CONCLUSION

There was a significant positive correlation between the T2\* value of the proximal portion of the PCL and the subjects' age, suggesting it as the first site of PCL degeneration.

## **CLINICAL RELEVANCE/APPLICATION**

T2\* maps derived from UTE-MRI scans may allow the in vivo evaluation of degenerative changes in tendons and ligaments with very short T2\* values.



## MK368-SD-MOB6

Real-Time Dynamic MRI of Finger Motion: A Feasibility Study

Monday, Nov. 26 12:45PM - 1:15PM Room: MK Community, Learning Center Station #6

#### **Participants**

Marc Garetier, MD, Brest, France (*Presenter*) Nothing to Disclose Bhushan Borotikar, Brest, France (*Abstract Co-Author*) Nothing to Disclose Karim Makki, Brest, FL (*Abstract Co-Author*) Nothing to Disclose Jean Rousset, MD, Brest, France (*Abstract Co-Author*) Nothing to Disclose Francois Rousseau, Brest, France (*Abstract Co-Author*) Nothing to Disclose Douraied Ben Salem, MD, PhD, Brest, France (*Abstract Co-Author*) Nothing to Disclose

#### PURPOSE

To evaluate the feasibility of a real-time sequence using balanced Fast Field Echo (bFFE) sequence to study tendon and bone motion during dynamic MRI of the finger.

## METHOD AND MATERIALS

A real-time bFFE sequence was used to acquire dynamic data in sagittal plane on 10 index finger, without history of injury or inflammatory rheumatism, on 3T MRI scanner (Philips Achieva dStream). Following sequence parameters were used: TR=4.7, TE=2.3, FOV=176X176, FA=45°, pixel=1.09X1.46, acquisition time=18s, slice thickness=4mm, time frames=16. Surface coils were placed on proximal phalanx bone using a custom build fixture. Patients performed two dynamic trials, one using only metacarpophalangeal (MCP) joint, and another using only proximal and distal inter-phalangeal (IP) joint with MCP joint constrained. During each trial, two cycles of flexion-extension of the joint of interest were performed. Flexor tendon and cortical bone contrast with surrounding tissues was determined by measuring the signal-difference-to-noise ratio (dSNR) with a ROI in flexor tendon, subcutaneous fat, cortical bone and bone marrow of proximal phalanx, and background area on each image during motion from hyperextension (E) to full flexion (F). Data were compared with those obtained on a sagittal T2-weighted spin echo sequence of the index finger in extension.

#### RESULTS

The average dSNR of flexor tendon was 278 during MCP motion (E=355, F=206), and 124 during IP motion (E=181, F=134). The average dSNR of cortical bone with subcutaneous fat was 320 during MCP motion (E=369, F=280) and 139 during IP motion (E=152, F=212), and with bone marrow was 418 during MCP motion (E=508, F=334) and 118 during IP motion (E=204, F=90). On sagittal T2-weighted sequence, the average dSNR was 148 for flexor tendon, 149 for cortical bone with subcutaneous fat, and 276 for cortical bone with bone marrow.

## CONCLUSION

Contrast for flexor tendon and cortical bone visualisation was good on real-time bFFE sequence during MCP flexion-extension motion, compared to T2-weighted sequence, but dSNR of these structures decreased in full flexion. Contrast was better for cortical bone than flexor tendon during motion.

## **CLINICAL RELEVANCE/APPLICATION**

Real-time bFFE sequence is a quick and useful sequence for in vivo evaluation of finger joint movement, with good contrast between structures.



### MK369-SD-MOB7

Prospective Comparison Between Radiofrequency Ecographic Multi-Spectrometry (REMS) and Dual Energy X-Ray Absorptiometry (DXA) Osteoporosis Risk Assessment

Monday, Nov. 26 12:45PM - 1:15PM Room: MK Community, Learning Center Station #7

**FDA** Discussions may include off-label uses.

#### Participants

Davide Orlandi, MD, PhD, Genova, Italy (*Presenter*) Nothing to Disclose Pietro Caruso, MD, Genova, Italy (*Abstract Co-Author*) Nothing to Disclose Francesca La Mantia, Palermo, Italy (*Abstract Co-Author*) Nothing to Disclose Pietro Francaviglia, Genova, Italy (*Abstract Co-Author*) Nothing to Disclose Luigi Satragno, MD, Genova, Italy (*Abstract Co-Author*) Nothing to Disclose Enzo Silvestri, MD, Genoa, Italy (*Abstract Co-Author*) Nothing to Disclose

#### For information about this presentation, contact:

my.davideorlandi@gmail.com

### PURPOSE

To assess the clinical effectiveness of an advanced quantitative echographic method for osteoporosis diagnosis on lumbar spine and femoral neck, compared to dual energy x-ray absorptiometry.

## **METHOD AND MATERIALS**

50 female patients (mean age 63 years, range 50 -70 years) underwent both a lumbar spine and femoral DXA (QDR-Discovery W Hologic densitometer, Hologic, Marlborough, US) and an echographic scan of the lumbar spine and proximal femur (Echosound, Ecolight SPA, Lecce, Italy). Both lumbar and femoral bone mineral density (BMD) were calculated in all patients using the two methods and diagnostic agreement between DXA, assumed as the gold standard reference, and the proposed echographic method was assessed by accuracy calculationStatistical analysis of the obtained data were performed using Cohen's k, Pearson correlation coefficient (r), and Bland-Altman analysis.

#### RESULTS

The overall agreement with DXA patient classification was 88.1% for the lumbar spine (k=0,757, p<0.01) and 80,9% for the femoral neck (k=0.698,p<0.01) A significant correlation was found between the US values of BMD and the corresponding DXA-measured ones (r=0.86, p<0.001).

## CONCLUSION

REMS BMD evaluation is comparable to DXA representing a valuable and radiation-free diagnostic imaging technique for osteoporosis detection and follow-up.

## **CLINICAL RELEVANCE/APPLICATION**

Ultrasound-aided BMD assessment is comparable to DXA



### NM003-EB-MOB

# Signs and Artifacts in Amyloid PET Imaging

Monday, Nov. 26 12:45PM - 1:15PM Room: NM Community, Learning Center Hardcopy Backboard

#### Awards Certificate of Merit

## Participants

Tamara Lundeen, MD, Tucson, AZ (*Presenter*) Nothing to Disclose Phillip Kuo, MD,PhD, Tucson, AZ (*Abstract Co-Author*) Author, MD Training at Home; Research Grant, Astellas Group; Consultant, Endocyte, Inc; Consultant, General Electric Company; Education Grant, General Electric Company; Speakers Bureau, Eli Lilly and Company; Consultant, inviCRO, LLC; Consultant, Imaging Endpoints; Consultant, Progenics Pharmaceuticals, Inc Matthew Covington, MD, St. Louis, MO (*Abstract Co-Author*) Nothing to Disclose Naghmehossadat Eshghi, MD, PhD, Tucson, AZ (*Abstract Co-Author*) Nothing to Disclose John Seibyl, MD, New Haven, CT (*Abstract Co-Author*) Researcher, inviCRO, LLC

# **TEACHING POINTS**

1. Discuss the appropriate use criteria for amyloid PET imaging. 2. Explain the algorithmic approach to scan interpretation. 3. Introduce the common amyloid PET imaging signs and artifacts.

# TABLE OF CONTENTS/OUTLINE

Introduction to amyloid PET imaging. -Discuss radiopharmaceutical properties of the three FDA approved PET amyloid agents -Review the current existing appropriate use criteria for amyloid PET imaging - Review manufacture-specific recommendations for amyloid PET interpretation. Present a detailed algorithmic approach to amyloid PET scan interpretation. - Discuss a novel regionbased search pattern to aid with amyloid PET interpretation - Provide examples of normal and abnormal amyloid PET scans. Provide an atlas of regional amyloid PET imaging signs in normal and abnormal brains. - Example amyloid PET scans with MRI correlation of the temporal/occipital, frontal, parietal and striatal regions. Illustrate common imaging artifacts with example images. Conclusion and summary table with the composite atlas of imaging signs.



### NM143-ED-MOB5

## The Many Faces of Parathyroid Adenoma - Approach to Multimodality Imaging in Challenging Cases

Monday, Nov. 26 12:45PM - 1:15PM Room: NM Community, Learning Center Station #5

#### **Participants**

Michael N. Pakdaman, MD, Los Angeles, CA (*Abstract Co-Author*) Nothing to Disclose Peyman Kangavari, MD, Los Angeles, CA (*Presenter*) Nothing to Disclose Catherine Evans, MD, Los Angeles, CA (*Abstract Co-Author*) Nothing to Disclose

## **TEACHING POINTS**

Obtain a diagnostic approach to evaluation of parathyroid lesions, including adenoma, using mutlimodality imaging including nuclear studies with correlation to MRI and CT. Gain insight on special approaches to identification of parathyroid lesions on mare challenging and equivocal cases, including algorithms for next step imaging.

# TABLE OF CONTENTS/OUTLINE

Overview of parathyroid anatomy and physiology as it relates to pathogenesis parathyroid adenoma Review of cross-modality imaging characteristics of Parathyroid Adenoma Correlate imaging characteristics of parathyroid adenoma with disease pathophysiology Imaging modalities to be reviewed include neck CT, neck MRI, PET/CT, US, Nuclear Thyroid Scan, and Nuclear Parathyroid Scan Present approaches to differentiating thyroid versus parathyroid adenoma using these modalities Review of interesting cases from our institution



### NM214-SD-MOB2

### Treatment of Castration-Resistant Prostate Cancer with Radium-223 Dichloride: A Clinical Experience

Monday, Nov. 26 12:45PM - 1:15PM Room: NM Community, Learning Center Station #2

### Participants

Catherine M. Doyle, BS, Tampa, FL (*Presenter*) Nothing to Disclose Matthew Mills, BS, Tampa, FL (*Abstract Co-Author*) Nothing to Disclose Sultan Damgaci, MSc, Tampa, FL (*Abstract Co-Author*) Nothing to Disclose Jingsong Zhang, MD,PhD, Tampa, FL (*Abstract Co-Author*) Nothing to Disclose Mayer Fishman, MD,PhD, Tampa, FL (*Abstract Co-Author*) Nothing to Disclose Ghassan El-Haddad, MD, Tampa, FL (*Abstract Co-Author*) Nothing to Disclose

## For information about this presentation, contact:

catherinedoyle@health.usf.edu

## PURPOSE

The benefits of incorporating Radium-223 dichloride (Ra-223) in the treatment of castration-resistant prostate cancer (CRPC) has not yet been fully delineated in real life setting. Therefore, we evaluated the outcome of patients with CRPC who were treated with Ra-223 in terms of side effects, pain improvement, bone scan response (BSR), overall survival (OS) and progression free survival (PFS).

#### **METHOD AND MATERIALS**

A total of 114 patients with CRPC and bone metastases referred for treatment with Ra-223 between March 2010 and February 2018 were identified for retrospective analysis. Clinical characteristics, treatments, and outcomes were extracted from clinical chart review and radiologic bone scans. Survival rates and survival curves were generated using Kaplan-Meier analysis. Chi-square and independent student t test were used for comparison of categorical variables. Multivariate analysis (MVA) Cox proportional hazard ratios (HR) model was used to assess OS and PFS.

#### RESULTS

Of the 114 patients referred for treatment, 107 received at least one dose of Ra-223, 56 receiving full treatment (6 doses). Median OS was 12.6 months for the entire cohort. In multivariate analysis, improved OS was significantly associated with the following: completion of treatment (p<0.001), baseline PSA<30 ng/mL (0.013), ALP decline after Ra-223 (p=0.003), and no prior chemotherapy (p=0.014). In addition to the previously listed factors, univariate analysis demonstrated significance for baseline alkaline phosphatase (ALP)<200 U/L (p=0.016) and prior use of Sipuleucel-T (p=0.019).

## CONCLUSION

The key factors notable for significant prolongation in OS for patients with CRPC who received Ra-223 may be helpful when deciding which patients would benefit most from this therapy. The potential synergistic effect between cellular immunotherapy and Ra-223 warrant further evaluation in a prospective study.

#### **CLINICAL RELEVANCE/APPLICATION**

Use of Ra-223 for treatment of CRPC has potential to significantly increase OS in patients with certain key pre-treatment factors, including a possible synergistic effect with cellular immunotherapy.



### NM215-SD-MOB3

Comparing F18-Fluorodeoxyglucose Positron Emission Tomography with MRI (F18-FDG PET-MRI), F18-FDG PET-CT and MRI Imaging for Staging and Restaging of Head and Neck Cancer (HNC)

Monday, Nov. 26 12:45PM - 1:15PM Room: NM Community, Learning Center Station #3

## Participants

Hossein Mehdikhani, MD, New York, NY (*Presenter*) Nothing to Disclose Maria Habib, MD, New York, NY (*Abstract Co-Author*) Nothing to Disclose Somali Gavane, MBBS, New York, NY (*Abstract Co-Author*) Nothing to Disclose Brett Miles, MD, New York, NY (*Abstract Co-Author*) Nothing to Disclose Peter M. Som, MD, New York, NY (*Abstract Co-Author*) Nothing to Disclose Lale Kostakoglu, MD, MPH, New York, NY (*Abstract Co-Author*) Research Consultant, F. Hoffmann-La Roche Ltd

#### For information about this presentation, contact:

lale.kostakoglu@mountsinai.org

#### PURPOSE

Our objective was to compare the sensitivity and specificity of F18-FDG PET/MRI (Siemens, Biograph mMR) with F18-FDG PET/CT (Siemens, Biograph mCT) and dedicated MRI for detection of HNC at both staging and restaging.

#### **METHOD AND MATERIALS**

A total of 94 HNC patients, 24 for initial staging and 70 for restaging, underwent sequential whole body PET/CT and integrated PET/MRI of head and neck after a single injection of FDG as well as a dedicated head and neck MRI (79 with and 15 without gadolinium contrast). Using a 5-point scale, all none-lymph node (nLN) and lymph node (LN) lesions were classified into likely benign, probably benign, indeterminate, probably malignant and likely malignant on each modality. The first 2 and the last 3 categories were combined as negative and positive groups for malignancy, respectively. Histopathology or follow-up imaging results were used for final diagnosis of malignant versus benign etiology. Sensitivity and specificity of each modality were calculated. In addition, beam hardening artifacts and the SUVmax of lesions were compared between PET/CT and PET/MRI.

## RESULTS

A total of 223 lesions (104 nLNs and 119 LNs) were evaluated in 94 HNC patients (57 squamous cell carcinoma and 37 other malignancies). Sensitivity and specificity of distinguishing malignant from benign were 89% and 47% for PET/CT, 70% and 82% for MRI and 85% and 84% for PET/MRI, respectively. Beam-hardening and metal artifact was significantly less on PET/MRI compared to PET/CT. There was high correlation of SUVmax between PET/CT and PET/MRI (spearman correlation coefficient 0.96, P<0.001) with systematically higher values on PET/CT by an average of 2.05 units (95% CI 1.63 - 2.47). The optimal SUVmax cutoff to differentiate malignant vs benign lesions were 9.6 for PET/CT and 7.2 for PET/MRI at initial staging. The corresponding value in the follow-up cases was 5.8 for PET/CT and 4 for PET/MRI.

#### CONCLUSION

This study suggest that integrated PET/MRI has the advantage of combining the sensitivity of PET with specificity of MRI and is associated with less beam-hardening artifact compared to PET/CT. However, more studies with larger patient populations are required to prove the accurate clinical utility of PET/MRI.

### **CLINICAL RELEVANCE/APPLICATION**

Integrated PET/MRI is potentially superior to PET/CT and MRI alone and can be considered as a one-stop shopping for staging and restaging of HNC.

#### **Honored Educators**

Presenters or authors on this event have been recognized as RSNA Honored Educators for participating in multiple qualifying educational activities. Honored Educators are invested in furthering the profession of radiology by delivering high-quality educational content in their field of study. Learn how you can become an honored educator by visiting the website at: https://www.rsna.org/Honored-Educator-Award/ Lale Kostakoglu, MD, MPH - 2012 Honored Educator



### NM216-SD-MOB4

Whole-body Staging Concept of Patients with Temporal Lobe Epilepsy Using Hybrid [(18) FDG] - PET/MRI

Monday, Nov. 26 12:45PM - 1:15PM Room: NM Community, Learning Center Station #4

#### **Participants**

Cornelius Deuschl, Essen, Germany (*Presenter*) Nothing to Disclose Theodor Ruber, Bonn, Germany (*Abstract Co-Author*) Nothing to Disclose Leon Ernst, Bonn, Germany (*Abstract Co-Author*) Nothing to Disclose Christoph Moenninghoff, MD, Essen, Germany (*Abstract Co-Author*) Nothing to Disclose Thorsten D. Poeppel, Essen, Germany (*Abstract Co-Author*) Nothing to Disclose Julian Kirchner, Dusseldorf, Germany (*Abstract Co-Author*) Nothing to Disclose Michael Forsting, MD, Essen, Germany (*Abstract Co-Author*) Nothing to Disclose Ken Herrmann, Essen, Germany (*Abstract Co-Author*) Nothing to Disclose Ken Herrmann, Essen, Germany (*Abstract Co-Author*) Nothing to Disclose Ken Herrmann, Essen, Germany (*Abstract Co-Author*) Nothing to Disclose Ken Herrmann, Essen, Germany (*Abstract Co-Author*) Nothing to Disclose Ken Herrmann, Essen, Germany (*Abstract Co-Author*) Nothing to Disclose Ken Herrmann, Essen, Germany (*Abstract Co-Author*) Nothing to Disclose Ken Herrmann, Essen, Germany (*Abstract Co-Author*) Nothing to Disclose Ken Herrmann, Essen, Germany (*Abstract Co-Author*) Nothing to Disclose Ken Herrmann, Essen, Germany (*Abstract Co-Author*) Nothing to Disclose Ken Herrmann, Essen, Germany (*Abstract Co-Author*) Nothing to Disclose Ken Herrmann, Essen, Germany (*Abstract Co-Author*) Nothing to Disclose Ken Herrmann, Essen, Germany (*Abstract Co-Author*) Nothing to Disclose Ken Herrmann, Essen, Germany (*Abstract Co-Author*) Nothing to Disclose Ken Herrmann, Essen, Germany (*Abstract Co-Author*) Nothing to Disclose Ken Herrmann, Essen, Germany (*Abstract Co-Author*) Nothing to Disclose Ken Herrmann, Essen, Germany (*Abstract Co-Author*) Nothing to Disclose Ken Herrmann, Essen, Germany (*Abstract Co-Author*) Nothing to Disclose Ken Herrmann, Essen, Germany (*Abstract Co-Author*) Nothing to Disclose

Christian Elger, Bonn, Germany (*Abstract Co-Author*) Nothing to Disclose Lale Umutlu, MD, Essen, Germany (*Abstract Co-Author*) Consultant, Bayer AG

## For information about this presentation, contact:

Cornelius.deuschl@uk-essen.de

#### PURPOSE

Simultaneous PET/MRI enables morphologic and metabolic imaging with an excellent co-registration in a single examination, rendering this hybrid imaging modality available for an easy and broad clinical application 1. The purpose of this study is to evaluate the diagnostic impact of hybrid 18F-FDG PET/MRI in the diagnostic work up of patients with temporal lobe epilepsy using the simultaneous imaging modality for a cerebral and whole-Body imaging concept.

## **METHOD AND MATERIALS**

Nineteen patients with temporal lobe epilepsy were enrolled in this prospective study (mean age: 39,1 years, range: 19-76 years, 14 female). All patients underwent a dedicated PET/MRI protocol of the brain (T1-MPRAGE, 3D-FLAIR, STIR cor, T2 ax and SWI) and the whole body (T2 ax., DWI, T1 VIBE ax. with and without ce). Image analyses were performed by a radiologist and a nuclear medicine physician in consensus reading for MRI (1), and fused PET/MR datasets (2) for potential epileptogenic lesions of the brain and potential neoplasms in whole-body staging. Diagnostic confidence was evaluated on a modified Likert scale.

## RESULTS

All examinations were obtained successfully without any relevant artifacts. Based on morphologic MR readings, 15 out of the 19 patients were found to show subtle changes of the temporal lobe, whereas PET/MRI showed changes in 17/19 patients in PET/MRI. Whole-Body staging revealed neoplasms in 2 of the 19 patients, that were identified by MRI and PET/MRI (Figure 1). Based on the fused image analysis the diagnostic confidence was rated higher (mean 2.6) when compared to sole morphologic reading (2.3).

# CONCLUSION

This study shows hybrid 18-F-FDG PET/MRI feasible for brain and whole body staging of patients with temporal lobe epilepsy

#### **CLINICAL RELEVANCE/APPLICATION**

Hybrid PET/MRI might have the potential as a valuable imaging tool for the diagnostic work-up for patients with temporal lobe epilepsy. Literatur1. Jadvar H, Colletti PM. Competitive advantage of PET/MRI. Eur J Radiol 2014;83:84-94



## NR005-EC-MOB

CT Imaging of the Lumbar Spine: An Interactive Program on the Differential Diagnosis Beyond Trauma

Monday, Nov. 26 12:45PM - 1:15PM Room: NR Community, Learning Center Custom Application Computer Demonstration

#### **Participants**

Hannah S. Recht, MD, Baltimore, MD (*Abstract Co-Author*) Nothing to Disclose Sara Raminpour, BS, Baltimore, MD (*Abstract Co-Author*) Nothing to Disclose Jan Fritz, MD, Baltimore, MD (*Abstract Co-Author*) Research Grant, Siemens AG; Scientific Advisor, Siemens AG; Scientific Advisor, Alexion Pharmaceuticals, Inc; Speaker, Siemens AG Elliot K. Fishman, MD, Baltimore, MD (*Presenter*) Institutional Grant support, Siemens AG; Institutional Grant support, General Electric Company; Co-founder, HipGraphics, Inc

## For information about this presentation, contact:

#### efishman@jhmi.edu

# **TEACHING POINTS**

the user will test their knowledge on the CT appearance of various pathologies that involves the lumbar spine in a iPad/iPhone application that focuses on individual learning. A series of 50 cases will be presented and upon finishing the program the user will; a. increase their knowledge of the range of pathologies that involve the lumbar spineb. help develop a systematic approach to the analysis of spinal pathologyc. learn the value of computer assisted learning methods that combine a quiz format with case explanations in discussion and text formatsd. help develop a more comprehensive knowledge base of a wide range of pathologies

### TABLE OF CONTENTS/OUTLINE

quiz format is used and 50 individual cases are provided. for each case (see PDF);a. 2 images are provided in the sagittal planeb. the user has the opportunity to think about the case and formulate an answer. c. the user then clicks on the "show answer button" to get the correct answerd. the user can click on "audio discussion" where a 60 second audio discussion of the case is providede. the user can click on "imaging pearls" where a set of 2-8 pearls on the case topic is presentedf. if the user wants they can review the cases in a non-quiz mode and see the answers from the startThe goal of the iPhone/iPad program is to provide a learn at your own place scenario

#### **Honored Educators**

Presenters or authors on this event have been recognized as RSNA Honored Educators for participating in multiple qualifying educational activities. Honored Educators are invested in furthering the profession of radiology by delivering high-quality educational content in their field of study. Learn how you can become an honored educator by visiting the website at: https://www.rsna.org/Honored-Educator-Award/ Elliot K. Fishman, MD - 2012 Honored EducatorElliot K. Fishman, MD - 2014 Honored EducatorElliot K. Fishman, MD - 2016 Honored EducatorElliot K. Fishman, MD - 2018 Honored Educator



## NR338-ED-MOB9

# 3D Ultrasonography of the Larynx: Anatomic Correlation with CT and Direct Endoscopic Visualization

Monday, Nov. 26 12:45PM - 1:15PM Room: NR Community, Learning Center Station #9

#### **Participants**

Susan J. Frank, MD, Bronx, NY (*Presenter*) Nothing to Disclose Terry L. Levin, MD, Mamaroneck, NY (*Abstract Co-Author*) Nothing to Disclose Janet Y. Mei, MD, Bronx, NY (*Abstract Co-Author*) Nothing to Disclose Michael o. Nassar, MD, Bronx, NY (*Abstract Co-Author*) Nothing to Disclose Richard Smith, MD, Bronx, NY (*Abstract Co-Author*) Nothing to Disclose

## For information about this presentation, contact:

sfrank@montefiore.org

### **TEACHING POINTS**

1. Demonstrate the anatomic landmarks of the larynx as visualized by 3D Ultrasonography 2. Correlate 3D ultrasonographic findings with CT and direct endoscopic visualization 3. Assess utility of 3D ultrasonographic oblique view of the vocal cords

# TABLE OF CONTENTS/OUTLINE

Background:Ultrasonography of the airway has not previously been used for upper airway management or to assess for vocal cord dysfunction. Purpose: 1. To present the normal anatomy as well as the 3D sonographic anatomy of the larynx including the glottis. 2.To explore an alternative ultrasound imaging approach for visualizing the vocal cords . Methods: Sonographic imaging with 3 D reconstructions of the larynx will be presented. Evaluation of the vocal cords will be demonstrated using both an oblique approachand a standard axial approach. Benefits of this new approach will be presented.Three dimensional ultrasound imaging findings will be correlated with images from direct endoscopic examination and CT images.



#### NR339-ED-MOB10

## A "Pseudo" Review of Neuroradiology

Monday, Nov. 26 12:45PM - 1:15PM Room: NR Community, Learning Center Station #10

#### **Participants**

Karthik M. Sundaram, MD, PhD, Nashville, TN (Presenter) Nothing to Disclose Cara C. Connolly, MD, Nashville, TN (Abstract Co-Author) Nothing to Disclose Shelby Payne, Nashvile, TN (Abstract Co-Author) Nothing to Disclose Sumit Pruthi, MBBS, Nashville , TN (Abstract Co-Author) Nothing to Disclose

# For information about this presentation, contact:

k.sundaram@vanderbilt.edu

## **TEACHING POINTS**

In medicine, the prefix 'pseudo' is used to indicate an entity that superficially appears like a specific entity but represents something else. Since 'pseudo' can connote coincidence, imitation, or deception, 'pseudo' neuro-radiological entities as described by radiologists can often be confusing to referring providers and patients. We review entities with 'pseudo' as a prefix and further subdivide them into clinical, pathological, and/or radiological entities. We then compare & contrast 'pseudo' radiological entities (including diseases & descriptors) with their non-pseudo correlates, provide imaging pearls & review relevant literature. Our exhibit will serve as a reference for radiologists & providers in regard to this often-confusing terminology.

## **TABLE OF CONTENTS/OUTLINE**

A. Review of medical nomenclature & use of 'pseudo' as a prefix. B. Classification of 'pseudo' entities, as the term pertains to clinical, pathological, & imaging characteristics (slide 2). Example of cases to be reviewed include pseudo-subarachnoid hemorrhage, pseudotumors, and pseudomeningocele. C. Compare & contrast a radiological 'pseudo' entity with the corresponding 'non-pseudo' entity. Imaging pearls & pitfalls and pathology will be included when pertinent. D. Review of the pertinent literature, discussion, and clinical implications will be included.



### NR340-ED-MOB11

## Mind the Black Spots: A Pictorial Review of Cerebral Amyloid Angiopathy-Related Inflammation

Monday, Nov. 26 12:45PM - 1:15PM Room: NR Community, Learning Center Station #11

#### Participants

Luis Quintana Barriga, MD, Seville, Spain (*Presenter*) Nothing to Disclose Rafael F. Ocete Perez, MD, Sevilla, Spain (*Abstract Co-Author*) Nothing to Disclose Angela Fernandez Plaza, Huelva, Spain (*Abstract Co-Author*) Nothing to Disclose Fatima Alvarez Janez, MD, Sevilla, Spain (*Abstract Co-Author*) Nothing to Disclose Florinda Roldan, Seville, Spain (*Abstract Co-Author*) Nothing to Disclose Nieves Gomez-Coronado Suarez de Venegas, Seville, Spain (*Abstract Co-Author*) Nothing to Disclose

## For information about this presentation, contact:

luisquintanaba@gmail.com

## **TEACHING POINTS**

- To know and recognize the clinical presentation of cerebral amyloid angiopathy-related inflammation (CAA-ri). - To describe the CT and MRI imaging findings of CAA-ri. - To make an adequate differential diagnosis in order to provide proper therapy that may improve the clinical outcome.

#### **TABLE OF CONTENTS/OUTLINE**

- Pathophysiology in CAA and CAA-ri. - Histology of CAA-ri. - Clinical symptoms of CAA-ri and diagnostic criteria. - Imaging findings. - CT. - MRI. - Relation between haemorrhagic foci and vasogenic oedema. - Patterns of enhancement. - Differential diagnosis. -Classic form of CAA. - Hypertensive microangiopathy. - Posterior reversible encephalopathy syndome (PRES). - Central nervous system vasculitides. - Haemorrhagic metastases. - Treatment and evolution of imaging findings. - Conclusion.



## NR382-SD-MOB1

## Treatment-Naïve First Episode Depression Diagnosis Based on Brain Functional Network

Monday, Nov. 26 12:45PM - 1:15PM Room: NR Community, Learning Center Station #1

#### Participants

Yanting Zheng, PhD, Guangzhou, China (*Presenter*) Nothing to Disclose Xiaobo Chen, Chapel Hill, NC (*Abstract Co-Author*) Nothing to Disclose Danian Li, Guangzhou, China (*Abstract Co-Author*) Nothing to Disclose Yujie Liu, MD, Guangzhou, China (*Abstract Co-Author*) Nothing to Disclose Xin Tan, Guangzhou, China (*Abstract Co-Author*) Nothing to Disclose Yi Liang, MD, Guangzhou, China (*Abstract Co-Author*) Nothing to Disclose Chunhong Qin, Guangzhou, China (*Abstract Co-Author*) Nothing to Disclose Hui Zeng, Guangzhou, China (*Abstract Co-Author*) Nothing to Disclose Jingxian Chen, Guangzhou, China (*Abstract Co-Author*) Nothing to Disclose Jiarui Liu, Guangzhou, China (*Abstract Co-Author*) Nothing to Disclose Jiarui Liu, Guangzhou, China (*Abstract Co-Author*) Nothing to Disclose Shijun Qiu, MD, Guang-Zhou, China (*Abstract Co-Author*) Nothing to Disclose Shijun Qiu, MD, Guang-Zhou, China (*Abstract Co-Author*) Nothing to Disclose Dinggang Shen, Chapel Hill, NC (*Abstract Co-Author*) Nothing to Disclose

### For information about this presentation, contact:

dgshen@med.unc.edu

## PURPOSE

Recent studies have shown potential value of resting-state functional magnetic resonance imaging (rs-fMRI) for major depression disorder; yet, the rs-fMRI-based individualized diagnosis of treatment-naïve first episode depression (FED) is still challenging. We aim to evaluate the feasibility of computer-aided FED diagnosis based on whole-brain high-order FC networks, and to explore the potential imaging biomarkers for FED.

#### **METHOD AND MATERIALS**

We enrolled, to date, the largest rs-fMRI data of treatment-naïve FED adults (N = 82, 53 females) and healthy volunteers (N = 72, 39 females), matched with age, gender and education. A computer-aided diagnosis framework was utilized to classify the patients from the controls based on the brain functional networks. Instead of merely using traditional 'Low-Order' FC networks (LON) features that characterize the temporal synchronization of the rs-fMRI signals, we also calculated more complex, high-level brain functional associations and modeled High-Order functional Network (HON) for joint FED diagnosis. The HON was calculated by the temporal synchronization among dynamic FC time series. We constructed two classifiers (*CHON* and *CLON*) on the basis of HON and LON respectively, and further integrated them together to enhance classification performance.

### RESULTS

Diagnostic accuracy of CHON was 82.5% compared to 67.5% for CLON. The joint classification was further improved (accuracy = 83.8%). The detected brain regions with diagnostic values mainly mediate higher cognitive functions and encompass the default mode, central executive and salience networks. We also found new biomarkers in the cerebellar vermis and crus II, which reveals potential FED pathological associations with the cerebellum. In addition, several imaging biomarkers were found to be correlated with individual clinical scores.

#### CONCLUSION

Depression diagnosis could be much improved by using features that better capture the higher-level brain functional interactions.

## **CLINICAL RELEVANCE/APPLICATION**

A feasible individual FED diagnosis framework based on comprehensive brain network modeling and machine learning for clinical applications.



### NR383-SD-MOB2

Susceptibility-Weighted Angiography (SWAN) for the Detection of Vessel Wall Calcification and Intramural Hemorrhage/Hematoma in Intracranial Vertebral Arteries

Monday, Nov. 26 12:45PM - 1:15PM Room: NR Community, Learning Center Station #2

# Participants

Hideki Ishimaru, MD, Nagasaki, Japan (*Presenter*) Nothing to Disclose Yohei Ikebe, Nagasaki, Japan (*Abstract Co-Author*) Nothing to Disclose Minoru Morikawa, MD, Nagasaki, Japan (*Abstract Co-Author*) Nothing to Disclose Reiko Ideguchi, Nagasaki, Japan (*Abstract Co-Author*) Nothing to Disclose Masataka Uetani, MD, Nagasaki, Japan (*Abstract Co-Author*) Nothing to Disclose

# PURPOSE

Susceptibility-weighted MR sequences, which enhance the susceptibility of hemorrhage and calcification (CA), have been hardly studied for intracranial vessel wall. We assessed the vessel wall susceptibility (VWS) of intracranial vertebral arteries using susceptibility-weighted angiography (SWAN) in patients with posterior circulation infarction.

## **METHOD AND MATERIALS**

We studied a consecutive 200 patients with acute ischemic stroke in posterior circulation territory. Regarding stroke subtypes based on the modified TOAST criteria, cardioembolism (CE) was the most common, observed in 66 patients (33%), followed by atherothrombosis (AT) in 65 (32.5%), small-artery disease (SAD) in 39 (19.5%), undetermined etiology in 16 (8%), and other determined etiology in 14 (7%). All other determined etiology was vertebral artery dissection (VAD) in this series. As a preliminary validation, arterial luminal signal of vertebral arteries (VA) on SWAN was assessed using TOF-MRA as the reference of standard. VWS on SWAN was retrospectively evaluated and correlated with CT (n=158) and vessel-wall MR imaging (n=43).

## RESULTS

SWAN displayed luminal signal as high in VA of 195 (98%) patients. Sensitivity and specificity of VWS for CA in VA was 74/76 (97%) and 40/82 (48.7%) respectively. In 42 false positives for CA, 14 positives were proved to be due to intramural hematoma and 2 positives to intraplaque hemorrhage, which were T1 hyperintense on vessel wall imaging. Otherwise, there were 8 positives with T1 low/intermediate plaque, 1 positive with no definite plaque, and 17 positives which were not verified on vessel wall imaging. According to stroke subtypes, VWS was observed in 14/14 (100%) of VAD and 51/65 (78%) of AT, which were significantly higher than frequencies of CE (34/66; 52%) and SAD (18/39; 40%) (P < 0.01). VWS in VAD corresponded to intramural hematoma on vessel wall imaging unexceptionally. Meanwhile in the AT group, calcification was the most common cause of VWS (n=32; 62.7%).

## CONCLUSION

SWAN visualized lumens of VA as high signal in most patients and highlighted VWS corresponding to CA, intramural hematoma or intraplaque hemorrhage. Focusing on VWS would help us to estimate stroke subtypes.

## **CLINICAL RELEVANCE/APPLICATION**

SWAN would provide a novel MRI contrast that emphasize calcification, intraplaque hemorrhage, and intramural hematoma.



## NR384-SD-MOB3

Computed Tomographic Angiography and Perfusion Select Patients with Large Vessel Occlusion for Endovascular Treatment

Monday, Nov. 26 12:45PM - 1:15PM Room: NR Community, Learning Center Station #3

### Participants

Francesca Di Giuliano, MD, Roma, Italy (*Presenter*) Nothing to Disclose Eliseo Picchi, Rome, Italy (*Abstract Co-Author*) Nothing to Disclose Silvia Minosse, Roma, Italy (*Abstract Co-Author*) Nothing to Disclose Valentina Ferrazzoli, MD, Rome, Italy (*Abstract Co-Author*) Nothing to Disclose Simone Marziali, MD, Rome, Italy (*Abstract Co-Author*) Nothing to Disclose Francesco G. Garaci, MD, Rome, Italy (*Abstract Co-Author*) Nothing to Disclose Roberto Floris, MD, Rome, Italy (*Abstract Co-Author*) Nothing to Disclose

#### For information about this presentation, contact:

francescadigiuliano@msn.com

#### PURPOSE

CTP and multiphase CTA (mCTA) help patient's selection for endovascular treatment in acute anterior ischemic stroke. Aim of this work was to investigate the ability of perfusion maps and collateral score to predict functional outcome after endovascular thrombectomy.

#### **METHOD AND MATERIALS**

71 patients with M1-middle cerebral artery or tandem occlusion were studied by mCTA and CTP and underwent successfully endovascular thrombectomy. Parametric maps of CBF, CBV and the time-to-maximum of the tissue residue function (Tmax) were generated. Collateral vessels were assessed on mCTA; functional outcome was evaluated by the mRS at 3 months. Wilcoxon ranksum test t was used to compare ischemic core and penumbra volumes in the parametric maps between Good Outcome and Poor Outcome groups. The discriminative ability was determined by receiver operating characteristic (ROC) analysis. The goal of logistic regression analysis was to find the best model to differentiate Good and Poor Outcome by Tmax, CBF, Collaterals

## RESULTS

Ischemic core volumes were significantly higher in Poor Outcome than Good Outcome in all parametric maps. On ROC analysis, the CBF had the best discriminative value for distinguishing between Good Outcome and Poor Outcome (AUC 0.73; sensitivity 64.5%; specificity 74.4%). The logistic regression model might be the most promising for differentiating Good from Poor Outcome, (AUC 0.79, 64.5% sensitivity, 82.1% specificity).

### CONCLUSION

The combined use of CTP and mCTA increase careful selection of patients with acute ischemic stroke who will benefit from endovascular thrombectomy allowing a better clinical outcome.

#### **CLINICAL RELEVANCE/APPLICATION**

In this work we considered a population of 71 Patients with large vessel occlusion acute ischemic stroke that underwent endovascular treatment. We analyzed two imaging techniques, Computer Tomographic Angiography and Computer Tomographic Perfusion performed in the acute phase. Through the evaluation of multiple perfusion maps, our aim was to find which parameter is better related with patients' functional outcome an may help in the therapeutic choice. Considering indeed the role of collateral flow in predicting the response to endovascular therapy we analyzed the contribution of a multiparametric approach in patients' selection



### NR385-SD-MOB4

### Age Related Changes in Topological Properties of Brain Functional Network and Structural Connectivity

Monday, Nov. 26 12:45PM - 1:15PM Room: NR Community, Learning Center Station #4

### Participants

Chandan Shah, Chengdu, China (*Presenter*) Nothing to Disclose Lu Su Sr, PhD, Chengdu, China (*Abstract Co-Author*) Nothing to Disclose

# For information about this presentation, contact:

shah\_chandan@yahoo.com

#### PURPOSE

There are still uncertainties about the true nature of age related changes in topological properties of the brain functional network and its structural connectivity during various developmental stages. In this cross- sectional study, we investigated the effects of age and its relationship with regional nodal properties of the functional brain network and white matter integrity.

## METHOD AND MATERIALS

METHOD: DTI and fMRI data were acquired from 458 healthy Chinese participants ranging from age 8 to 81 years. Tractography was conducted on the DTI data using FSL. Graph Theory analyses were conducted on the functional data yielding topological properties of the functional network using SPM and GRETNA toolbox. Two multiple regressions were performed to investigate the effects of age on nodal topological properties of the functional brain network and white matter integrity.

### RESULTS

RESULT: For the functional studies, we observed that regional nodal characteristics such as node betweenness were decreased while node degree and node efficiency was increased in relation to increasing age. Perversely, we observed that the relationship between nodal topological properties and fasciculus structures were primarily positive for nodal betweenness but negative for nodal degree and nodal efficiency. Decrease in functional nodal betweenness was primarily located in superior frontal lobe, right occipital lobe and the global hubs. These brain regions also had both direct and indirect anatomical relationships with the 14 fiber bundles. A linear age related decreases in the Fractional anisotropy (FA) value was found in the callosum forceps minor.

#### CONCLUSION

CONCLUSION: These results suggests that age related differences were more pronounced in the functional than in structural measure indicating these measures do not have direct one-to-one mapping. Our study also indicates that the fiber bundles with longer fibers exhibited a more pronounced effect on the properties of functional network.

## **CLINICAL RELEVANCE/APPLICATION**

help us to understand the possible mechanisms behind age related neurodegenerative diseases



## NR386-SD-MOB5

Comparison of Morphology and Enhancement Characteristics of Ectopic and Eutopic Parathyroid Adenomas.

Monday, Nov. 26 12:45PM - 1:15PM Room: NR Community, Learning Center Station #5

#### Awards Student Travel Stipend Award

#### **Participants**

Harika Tirumani, MBBS, MD, Little Rock, AR (*Presenter*) Nothing to Disclose Rohan Samant, MD, Little Rock, AR (*Abstract Co-Author*) Nothing to Disclose Raghu H. Ramakrishnaiah, MBBS, FRCR, Little Rock, AR (*Abstract Co-Author*) Nothing to Disclose Jennifer L. McCarty, MD, Houston, TX (*Abstract Co-Author*) Nothing to Disclose Stephen J. Geppert, MD, Little Rock, AR (*Abstract Co-Author*) Nothing to Disclose Rudy L. Van Hemert JR, MD, Little Rock, AR (*Abstract Co-Author*) Nothing to Disclose Edgardo J. Angtuaco, MD, Little Rock, AR (*Abstract Co-Author*) Nothing to Disclose Manoj Kumar, MD, MBBS, Little Rock, AR (*Abstract Co-Author*) Nothing to Disclose

#### For information about this presentation, contact:

htirumani@uams.edu

## PURPOSE

4D-CT is a novel technique for pre-surgical localization of parathyroid adenomas (PA). PA can be eutopic or ectopic. Detection of ectopic PA is crucial for surgical success especially if patient has multigland disease with both eutopic and ectopic PA. Purpose of our study is to determine the differences in morphology and enhancement characteristics between eutopic and ectopicPA which will help in increasing the confidence of radiologist for suggesting high probability.

#### **METHOD AND MATERIALS**

This is an IRB approved retrospective study of 232 patients with surgically proven PA who underwent 4D CT imaging for pre surgical localization of PA between 2014 and 2017. All 4D CT scans were performed with initial noncontrast followed by 30 sec and 90 sec postcontrast images on 64 slice MDCT scanner. Contrast washout ratios (CWR) were calculated by measuring Hounsfield units (HU) of PA on the noncontrast, 30 second post contrast early arterial exam (30A) and on the 90 second post contrast delayed exam (90D). CWR =  $[100 \times (HU \text{ on } 30A - HU \text{ on } 90D)/HU \text{ on } 30A]$ .

## RESULTS

Out of 232 patients, 186 patients - 1 gland, 37 patients - 2 gland, 6 patients - 3 gland and 3 patients - 4 gland adenomas constituting a total of 290 radiologically diagnosed lesions. Out of these, 25 (6M, 17F) PA were in ectopic and 265 (37M, 228F) PA were eutopic. Out of 290 radiologically reported lesions, 242 lesions (21 Ectopic and 221 Eutopic) matched to the adenomas found on surgery and pathology constituting to 242 radiological-surgical-pathology matched lesions. 48 lesions were false positive, which did not correlate with the location on surgical pathology. Morphological characteristics like shape, size, heterogeneity were studied and compared between eutopic and ectopic adenomas. Enhancement characteristics of eutopic and ectopic adenomas were compared and were categorized at 10% washout intervals, for example: 1-10%, 11-20% and so on.

### CONCLUSION

1. 217 out of 265 eutopic adenomas and 20 out of 25 ectopic adenomas demonstrated contrast washout ratios between 31%-80% and did not demonstrate significant difference in washout characteristics. 2. Size and shape of ectopic PA did not show significant influence on washout characteristics. 3. Measurement of contrast enhancement and washout dynamics is limited in lesions with large cystic areas.

#### **CLINICAL RELEVANCE/APPLICATION**

Detection of ectopic PA is crucial for surgical success especially in the setting of multigland disease.



### NR387-SD-MOB6

## T1rho of Malignant Gliomas Can Be a Biomarker of IDH1 and ATRX Immunohistochemical Stainability

Monday, Nov. 26 12:45PM - 1:15PM Room: NR Community, Learning Center Station #6

#### **Participants**

Toshiaki Akashi, MD, Sendai, Japan (*Presenter*) Nothing to Disclose Shiho Sato, Sendai, Japan (*Abstract Co-Author*) Nothing to Disclose Shuko Nomura, Sendai, Japan (*Abstract Co-Author*) Nothing to Disclose Masahiro Kitami, Tokyo, Japan (*Abstract Co-Author*) Nothing to Disclose Makoto Obara, Minato-Ku, Japan (*Abstract Co-Author*) Employee, Koninklijke Philips NV Kei Takase, MD, PhD, Sendai, Japan (*Abstract Co-Author*) Nothing to Disclose

### PURPOSE

Pathological diagnosis of gliomas is based on both morphology and genetical information including immunohistochemical (IHC) stains and FISH 1p/19q codeletion. To predict these genetical biomarkers preoperatively, we examined utility of T1rho MRI.

# METHOD AND MATERIALS

We enrolled 41 malignant gliomas (WHO grade III and IV; 4 anaplastic oligodendrogliomas, 11 anaplastic astrocytomas, and 26 glioblastomas) undergone preoperative T1rho MRI and pathological examination after surgical resection or biopsy. T1rho MRI was acquired by a 3.0 T clinical scanner with Head-32ch coil (Achieva Ingenia CX, Philips Healthcare, The Netherlands). Each signal was read out by fast field echo sequence (TR=4.0ms, TE=1.9ms, flip angle=35°, Slice thickness;7mm, FOV;210mm, matrix;256x256) after the spin lock pulse of 500 Hz for the time of spin lock (TSL=1, 10, 20, and 80ms). T1rho map was obtained by fitting the equation for T1rho; S(TSL) = S(0) \* exp(-TSL / T1rho). ROIs were located in the enhanced solid part of contrast enhancing tumors or solid part if non-enhancing tumors. T1rho (mean, minimum, maximum, and median) of ROIs were examined by t test with respect to individual biomarkers; IHC stainabilities including IDH1, MGMT, p53, and ATRX and FISH 1p/19q codeletion.

### RESULTS

Mean, minimum, maximum, and median T1rho (ms) of IDH1(+) grade IV gliomas and ATRX(-) grade IV gliomas were significantly longer than that of IDH1(-) (146.5 vs 107.8; p=.02, 122.3 vs 92.2; p=.026, 180.5 vs 123; p=.022, 145.7 vs 108; p=.024) and ATRX(+) (158.5 vs 107.8; p=.007, 122.3 vs 92.2; p=.012, 197 vs 123; p=.01, 157.8 vs 108; p=.008) respectively. Max T1rho of IDH1(+) grade III and IV gliomas ware significantly longer than that of IDH1(-) (152.1 vs 118.3; p=.044). Mean and max T1rho of ATRX(-) grade III and IV gliomas were significantly longer than that of ATRX(+) (130.9 vs 105.4; p=.048, 161.2 vs 118.3; p=.024) respectively, while stainability of MGMT and p53 and FISH 1p/19q codeletion did not.

## CONCLUSION

T1rho can be a biomarker of IDH1 and ATRX IHC stainability of malignant gliomas.

### **CLINICAL RELEVANCE/APPLICATION**

Pathological diagnosis of malignant gliomas is based on the mutation of IDH1 and ATRX. T1rho of malignant gliomas can be a biomarker of IDH1 and ATRX immunohistocheical stainability



## NR388-SD-MOB7

Source Space MEG Delta Waves Increase Following Concussion

Monday, Nov. 26 12:45PM - 1:15PM Room: NR Community, Learning Center Station #7

#### **Participants**

Elizabeth M. Davenport, PhD, Dallas, TX (*Presenter*) Nothing to Disclose Jillian Urban, Winston- Salem, NC (*Abstract Co-Author*) Nothing to Disclose Ben Wagner, BS, Dallas, TX (*Abstract Co-Author*) Nothing to Disclose Mark A. Espeland, PHD, Winston-Salem, NC (*Abstract Co-Author*) Nothing to Disclose Alexander K. Powers, MD, Winston Salem, NC (*Abstract Co-Author*) Nothing to Disclose Christopher T. Whitlow, MD, PhD, Winston-Salem, NC (*Abstract Co-Author*) Nothing to Disclose Joel Stitzel, Winston-Salem, NC (*Abstract Co-Author*) Nothing to Disclose Joseph A. Maldjian, MD, Dallas, TX (*Abstract Co-Author*) Consultant, BioClinica, Inc; Consultant, Koninklijke Philips NV

#### For information about this presentation, contact:

elizabeth.davenport@utsouthwestern.edu

#### PURPOSE

The purpose of this study is to determine if delta waves, measured by magnetoencephalography (MEG), increase due to a sports concussion.

# METHOD AND MATERIALS

From a larger study on subconcussive impacts in high school football, five players were diagnosed with a concussion during the season (mean age=16.1). Subjects followed returned-to-play protocols. Eight minutes of eyes-open, resting-state MEG data were acquired for each subject and control using a 275 channel CTF whole-head system. Football players were scanned pre-season, within 36 hours post-concussion, and post-season. Seven age and gender matched non-contact sports athletes (controls) were also recruited (mean age=16.2). Controls received baseline and follow-up scans 4 months later. Using Brainstorm, MEG data were baseline corrected, band-stop filtered (60Hz), down-sampled to 250Hz, and band-pass filtered to 1-100Hz. Eye blinks, and muscle artifacts were removed using independent component analysis. Data was source localized using a minimum norm method. The average whole-brain power of the delta frequency and total power was computed for each scan. The delta frequency power was normalized by the total power. In the concussed football players, pre-season delta power was subtracted from post-concussion delta power. For the control subjects, baseline delta power was subtracted from the 4-month follow-up scan. A t-test was performed to compare the change in delta power of controls to the change in delta power of concussed football players.

#### RESULTS

The change in delta power following concussion was significantly different from controls (p=0.014). In addition to the statistical difference, delta waves visibly increased from pre-season to post-concussion (Figure 1).

## CONCLUSION

We demonstrate that a single concussion can visibly and statistically increase delta frequency power in MEG.

### **CLINICAL RELEVANCE/APPLICATION**

Traditional imaging is typically unremarkable in concussion. This study demonstrates that MEG may be a new and useful diagnostic tool for concussion.



### OB178-ED-MOB1

Technical Considerations and Pathology of Hysterosalpinography: More than Just 'Going with the Flow'

Monday, Nov. 26 12:45PM - 1:15PM Room: OB Community, Learning Center Station #1

#### Participants

Talal Åkhter, MD, Philadelphia, PA (*Presenter*) Nothing to Disclose Sana Hava, DO, Philadelphia, PA (*Abstract Co-Author*) Nothing to Disclose Alyssa R. Goldbach, DO, Philadelphia, PA (*Abstract Co-Author*) Nothing to Disclose Tejas Patel, MD, Philadelphia, PA (*Abstract Co-Author*) Nothing to Disclose Harshad K. Patel, MD, Media, PA (*Abstract Co-Author*) Nothing to Disclose Partha Hota, DO, Philadelphia, PA (*Abstract Co-Author*) Nothing to Disclose

## For information about this presentation, contact:

takht3r@gmail.com

## **TEACHING POINTS**

1.Illustrate normal and abnormal uterine and tubule anatomy on hysterosalpingography (HSG). 2. Describe the HSG technique used at our institution with practical tips for aiding in real-time troubleshooting and diagnosis. 3.Discuss and illustrate a variety of uterine and fallopian tubule pathologies which can be assessed on HSG from our fluoroscopic imaging department.

## TABLE OF CONTENTS/OUTLINE

1. Indications of Hysterosalpinography 2. Normal uterine anatomy 3. Technique 4. Normal study 5. Müllerian abnormalities a. Uterus didelphys b. Unicornuate uterus c. Biconuate uterus d. Septate uterus 6. Intrauterine masses a. endometrial polyp b. submucosal leiomyoma c. cervical mass 7. Other uterine and tubule pathologies a. Asherman Syndrome b. Hydrosalpinx c. Adenomyosis d. Salpingitis isthmica nodosa 8. EssureTM Sterilization Confirmation Test a. Successful EssureTM b. Unsuccessful EssureTM c. Malpositioned EssureTM d. Vascular contrast intravasation 9. Fallopian tube recanalization a. Indications b. Technique c. Outcomes



## OB179-ED-MOB2

## Multimodality Imaging of Ovarian Cystic Lesions: A Primer for Residents

Monday, Nov. 26 12:45PM - 1:15PM Room: OB Community, Learning Center Station #2

#### **Participants**

Amir R. Honarmand, MD, Chicago, IL (*Presenter*) Nothing to Disclose Cristina I. Olivas Chacon, MD, Darby, PA (*Abstract Co-Author*) Nothing to Disclose Olutayo I. Olubiyi, MD, Darby, PA (*Abstract Co-Author*) Nothing to Disclose Christian Pedersen, MD, Darby, PA (*Abstract Co-Author*) Nothing to Disclose Aparna Srinivasa Babu, MD, Darby, PA (*Abstract Co-Author*) Nothing to Disclose

## For information about this presentation, contact:

arhonarmand@yahoo.com

## **TEACHING POINTS**

Ovarian cystic lesions comprise numerous entities with overlapping imaging features. Knowledge of multimodality imaging characteristics of these lesions plays a pivotal role in accurate diagnosis. The goal of this exhibit is to: - Review background, clinical presentation, and non-imaging evaluation of the ovarian cystic lesions- Review modality-based imaging characterization - Offer helpful tips to distinguish lesions with overlapping imaging features - Review latest guidelines regarding post-diagnosis next step strategies, including recommendations for follow up and intervention

## TABLE OF CONTENTS/OUTLINE

-Benign: Functional cyst (follicle/simple/hemorrhagic cysts, corpus luteum), theca lutein cyst, polycystic ovarian disease, ovarian hyperstimulation syndrome, endometrioma, ovarian abscess, dermoid/teratoma, cystadenoma/cystadenofibroma -Malignant: Primary and metastatic -Non-ovarian origin mimics of ovarian cysts: Hydrosalpinx, peritoneal inclusion cyst, appendiceal mucocele, lymphangioma, ectopic pregnancy, etc.- Overview of current Society of Radiologists in Ultrasound (SRU) guidelines for ovarian cystic lesions- Multimodality imaging appearances of various cystic lesions- Tips and pointers for accuate diagnosis- Summary of current follow up guidelines and management options, including the role of interventional radiology



## OB180-ED-MOB3

## Large Fetal Cervicofacial Masses: Diagnosis, Management, and Postnatal Outcome

Monday, Nov. 26 12:45PM - 1:15PM Room: OB Community, Learning Center Station #3

## Awards Certificate of Merit

## Participants

Francoise Rypens, MD, Montreal, QC (*Presenter*) Nothing to Disclose Chantale Lapierre, MD, Montreal, QC (*Abstract Co-Author*) Nothing to Disclose Julie Dery, MD, Montreal, QC (*Abstract Co-Author*) Nothing to Disclose Ramy El-Jalbout, Montreal, QC (*Abstract Co-Author*) Nothing to Disclose Marie-Ange Delrue, MD, Montreal, QC (*Abstract Co-Author*) Nothing to Disclose Sandrine Wavrant, MD, Montreal, QC (*Abstract Co-Author*) Nothing to Disclose Annie Lapointe, MD, Montreal, QC (*Abstract Co-Author*) Nothing to Disclose Josee Dubois, MD, Montreal, QC (*Abstract Co-Author*) Nothing to Disclose

### For information about this presentation, contact:

francoise.rypens.hsj@ssss.gouv.qc.ca

## **TEACHING POINTS**

A multidisciplinary approach is essential to manage complex fetal cervicofacial soft tissue masses (vascular tumors and malformations, teratomas, ...). Specific diagnosis, precise extension, airway patency and therapeutic options are key facts for counselling.

## TABLE OF CONTENTS/OUTLINE

Retrospective review of 30 fetuses and neonates with significant cervicofacial masses observed in a mother-child university hospital (11 teratomas, 10 lymphatic malformations, 4 congenital hemangiomas, 4 upper lip lesions, 1 thyroglossal cyst). The following points will be discussed and illustrated: the difficulty of a precise early diagnosis the differential diagnosis of such masses the impact of diagnosis on fetal and mother management the respective role of US, MRI and CT-scan, for diagnosis, differential diagnosis, extension, evaluation of airways and biomechanical repercussions the follow-up according to the presumptive diagnosis (i.e. extension of teratomas, lymphatic malformations and potential spontaneous regression of congenital hemangiomas) the utility of a multidisciplinary approach to offer the best counselling about management, delivery mode (EXIT, C/S section, or natural delivery), postnatal management (i.e. umbilical artery vascular approach), treatment and prognosis



### PD180-ED-MOB6

# Clinical and CT findings of Tracheal Agenesis: Single Center Experience and Literature Review

Monday, Nov. 26 12:45PM - 1:15PM Room: PD Community, Learning Center Station #6

#### **Participants**

Yeonu Choi, Seoul, Korea, Republic Of (*Presenter*) Nothing to Disclose So Young Yoo, MD, Seoul, Korea, Republic Of (*Abstract Co-Author*) Nothing to Disclose Haewon Kim, Seoul, Korea, Republic Of (*Abstract Co-Author*) Nothing to Disclose

For information about this presentation, contact:

yeounu718.choi@samsung.com

### **TEACHING POINTS**

Trachea agenesis (TA), a lethal congenital airway malformation, is very challenging with its rarity and difficulty in making correct prenatal diagnosis, usually presented with unexpected severe respiratory distress at birth and failed endotracheal intubation. The purpose of this exhibit are: 1. To review normal development of the trachea and esophagus. 2. To know three types of tracheal agnesis and related CT findings. 3. To demonstrate associated clinical findings and clinical outcome.

# TABLE OF CONTENTS/OUTLINE

A. Normal development of trachea and esophagus. -Traditional and recent developmental theories. B. Radiologic findings of tracheal agenesis. - Floyd classification (I, II, III) - Parenchymal change, air leak C. Clinical features of tracheal agenesis. - Prenatal and postnatal findings, associated anomalies and clinical outcome D. Summary



### PD181-ED-MOB7

# **Prenatal Imaging Findings in Anorectal Malformations**

Monday, Nov. 26 12:45PM - 1:15PM Room: PD Community, Learning Center Station #7

#### **Participants**

Lysiane Rohrer, Lausanne, Switzerland (*Presenter*) Nothing to Disclose Yvan Vial, MD, Lausanne, Switzerland (*Abstract Co-Author*) Nothing to Disclose Reto A. Meuli, MD, PhD, Lausanne, Switzerland (*Abstract Co-Author*) Nothing to Disclose Estelle V. Tenisch, MD, Lausanne, Switzerland (*Abstract Co-Author*) Nothing to Disclose Leonor Alamo, MD, Lausanne, Switzerland (*Abstract Co-Author*) Nothing to Disclose

### **TEACHING POINTS**

1. To know the classification of Anorectal Malformations (ARMs) according to the location of the rectal pouch and the associated fistulae, if present. 2. To adequately evaluate the anatomy of the fetal normal anus - the "target sign"- and rectum at prenatal US and MRI studies. 3. To recognize the direct and indirect findings of ARMs and cloaca at prenatal imaging studies.

# TABLE OF CONTENTS/OUTLINE

1. Classification of ARMs. 2. Evaluation of the normal rectum, anus and perineum at prenatal US and MRI exams. Normal anal anatomy: the "target sign" in the posterior perineal triangle. 3. Description and examples of the main imaging findings suggesting ARMs at prenatal US and MRI exams: - Main direct signs: small anus, absent "target sign". - Main indirect signs: rectal distension, high position of the rectal pouch, abnormal meconium echogenicity / intensity, enterolithiasis. 4. Suggesting signs of cloacae: hydrocolpos, multiple pelvic cystic masses, vaginal or uterine duplication; poor bladder / rectal visualisation. 5. Representative examples of low type-, intermediate/high type of ARM and cloacae.



# PD182-ED-MOB8

#### Supratentorial Glioblastoma Multiforme in Children: Conventional and Advanced MRI Features

Monday, Nov. 26 12:45PM - 1:15PM Room: PD Community, Learning Center Station #8

# Awards Certificate of Merit

### Participants

Ady M. Viveros Castano, MD, Barcelona, Spain (*Presenter*) Nothing to Disclose Angel Sanchez-Montanez, MD, Barcelona, Spain (*Abstract Co-Author*) Nothing to Disclose Ignacio Delgado, MD, Barcelona, Spain (*Abstract Co-Author*) Nothing to Disclose Elida Vazquez, MD, Barcelona, Spain (*Abstract Co-Author*) Nothing to Disclose Albert Pons Escoda, Barcelona, Spain (*Abstract Co-Author*) Nothing to Disclose Elena Martinez, Barcelona, Spain (*Abstract Co-Author*) Nothing to Disclose Luis Gros, MD, Barcelona, Spain (*Abstract Co-Author*) Nothing to Disclose Paola Cano, Barcelona, Spain (*Abstract Co-Author*) Nothing to Disclose

#### For information about this presentation, contact:

mildred.viveros@hotmail.com

# **TEACHING POINTS**

The purpose of this exhibit is:1 To review the imaging features and applications of conventional and advanced neuroimaging techniques in a pediatric population diagnosed of supratentorial glioblastoma multiforme (GBM).2 To achieve a systematic analysis of GBM including molecular and biological characteristics and current classification of the World Health Organization (2016).3 To provide the main differences with their adult counterparts from the imaging, genetic and molecular points of view. 4 To develop an imaging-based approach that can be used as a diagnostic algorithm in children with unclassified supratentorial tumor.

#### **TABLE OF CONTENTS/OUTLINE**

1. Introduction2. Clinical presentation3. Radiological findings of typical GBMs3.1 Conventional anatomic and advanced MRI techniques, such as DWI, DTI, functional MRI, perfusion imaging, MRS4. Pathological examination (WHO 2016)4.1 Histological and molecular characteristics 4.1.1 Cellularity/Necrosis 4.1.2 Glioblastoma IDH mutant/IDH wild-type. TERT Promoter/TP53/ATRX mutations, EGFR amplification.5. Discussion6. MR imaging pitfalls7. Useful points to distinguish between GBMs and other supratentorial tumors8. Main differences between location, imaging, genetics and metabolism of adults and children GBM9. References



### PD215-SD-MOB1

# Imaging Findings of Abdominal Compartment Syndrome: Unique Features in Children

Monday, Nov. 26 12:45PM - 1:15PM Room: PD Community, Learning Center Station #1

#### Participants

Bo-Kyung Je, MD, PhD, Ansan, Korea, Republic Of (*Presenter*) Nothing to Disclose Hee Kyung Kim, MD, Cincinnati, OH (*Abstract Co-Author*) Nothing to Disclose Paul Horn, Cincinnati, OH (*Abstract Co-Author*) Nothing to Disclose

# PURPOSE

To identify imaging findings in children with abdominal compartment syndrome (ACS).

# METHOD AND MATERIALS

A total 50 patients under 18 years of age diagnosed with ACS (17 female, 33 male) were included and reviewed for clinical and imaging findings. Clinical findings included the underlying condition, therapeutic approach, and clinical outcome. Twelve preoperative cross sectional images were reviewed for known imaging findings of ACS in adults; increased ratio of anterior-posterior to transverse distance (AT ratio) and bowel wall thickening with enhancement. We also recorded all other abnormal findings. Imaging findings were compared to age matched control who had abdominal distension, but did not have ACS (Fisher exact test).

#### RESULTS

Among 50 children with ACS, 38 children had surgical decompression. The mortality rate was 45% in the surgical decompression group vs 48% without intervention. Ascites (83%) and basal lung atelectasis (70%) were the most common findings followed by abnormal bowel wall enhancement (60%), bowel dilatation (58%), subcutaneous edema (50%), heterogeneous perfusion of liver (50%) and kidney (38%), and bowel wall thickening (33%). As compared to the group without ACS, the incidence of basal lung atelectasis and heterogeneous enhancement of kidney was significantly higher in ACS (P<0.05). However, no statistical difference was seen in other findings or AT ratio (0.81 vs. 0.84, P=0.379).

#### CONCLUSION

Except basal lung atelectasis and compromised renal perfusion, no other imaging findings are specific for ACS in children. Differing from adults with ACS, increased AT ratio proves not specific for ACS.

#### **CLINICAL RELEVANCE/APPLICATION**

In pediatric patients with ACS, imaging interpretation needs to be approached differently from adult.



# PD216-SD-MOB2

Early Prediction of Progression to Severe Post Hemorrhagic Hydrocephalus on Cranial Ultrasound of Premature Newborns

Monday, Nov. 26 12:45PM - 1:15PM Room: PD Community, Learning Center Station #2

# Participants

Pooneh Roshanitabrizi, Washington, DC (*Abstract Co-Author*) Nothing to Disclose Rawad Obeid, MD, Washington, DC (*Abstract Co-Author*) Nothing to Disclose Awais Mansoor, PhD, Washington, DC (*Abstract Co-Author*) Nothing to Disclose Juan Cerrolaza, PhD, Washington, DC (*Abstract Co-Author*) Nothing to Disclose Anna Penn, MD,PhD, Washington, DC (*Abstract Co-Author*) Nothing to Disclose Marius G. Linguraru, DPhil,MS, Washington, DC (*Presenter*) Nothing to Disclose

#### For information about this presentation, contact:

PROSHNANI2@childrensnational.org

### PURPOSE

To investigate the hypothesis that progression to severe post hemorrhagic hydrocephalus (PHH) could be objectively predicted using ventricular morphology phenotypes on the first cranial ultrasound (CUS) where bleeding was noted.

#### **METHOD AND MATERIALS**

We performed a retrospective study of 62 newborns < 29 weeks gestational age (range 23-28) and < 1500 grams birth weight (range 410-1280g) admitted in the first week of life and diagnosed with intraventricular hemorrhage on CUS. 15/62 newborns developed severe PHH and required an intervention to temporize PHH. From the first CUS, a slice in the coronal plane at the level of the foramen of Monro was selected for evaluation. The lateral ventricles were manually segmented. Then automated ventricular morphology phenotypes were extracted from both lateral ventricles to quantify the ventricle shape, including descriptors of global and local shape and asymmetry. The predictive model of severe PHH development was created using a machine learning model with automatically selected optimal set of predictive morphology phenotypes. The machine learning-based predictive model was compared to the logistic regression model based on two manual clinical measurements of ventricular index (VI) and frontal and temporal horn ratio (FTHR) performed on the same CUS.

## RESULTS

The ventricular morphology phenotypes predicted the progression to severe PHH with an average sensitivity, specificity, and accuracy level of 1.00, 0.88, and 0.94, respectively. The machine learning model outperformed (p-value<0.01) the regression model based on clinical measurements only (VI and FTHR), which had sensitivity, specificity, and accuracy of 1.00, 0.54, and 0.77, respectively.

#### CONCLUSION

CUS-based ventricular morphology phenotypes in premature newborns could predict the progression to severe PHH. An automated machine learning model was better predictive of PHH development than clinical manual measurements.

#### **CLINICAL RELEVANCE/APPLICATION**

Early prediction of severe PHH development in premature newborns could potentially improve criteria for diagnosis and offer an opportunity for early interventions to improve outcome.



### PD217-SD-MOB3

# Disease-Specific Dose Estimate (DSDE): Optimization of Radiation Dose for Children with Hepatomegaly

Monday, Nov. 26 12:45PM - 1:15PM Room: PD Community, Learning Center Station #3

### Participants

Rumi Imai, Setagaya, Japan (*Presenter*) Nothing to Disclose Osamu Miyazaki, MD, Setagaya, Japan (*Abstract Co-Author*) Nothing to Disclose Tetsuya Horiuchi, Osaka, Japan (*Abstract Co-Author*) Nothing to Disclose Keisuke Asano, Tokyo, Japan (*Abstract Co-Author*) Nothing to Disclose Naruhito Suzuki, Tokyo, Japan (*Abstract Co-Author*) Nothing to Disclose Shunsuke Nosaka, MD, Tokyo, Japan (*Abstract Co-Author*) Nothing to Disclose

# For information about this presentation, contact:

imai-rm@ncchd.go.jp

# **TEACHING POINTS**

1. A weight-based CT protocol is useful to regulate the radiation dose for pediatric patients. However, inadequate image quality was often encountered in patients with hepatomegaly even though the parameters were correctly selected using a routine weight-based protocol. 2. The present study proposes a new concept of Disease-Specific Dose Estimate (DSDE) for CT in pediatric patients with hepatomegaly using a similar methodology of effective diameter combined with SSDE.

# TABLE OF CONTENTS/OUTLINE

1. A retrospective analysis of effective diameter was obtained for abdominal CT aged less than 10 years (control:n=94, hepatomegaly:n=85) A comparison of effective diameter was carried out between the two groups. 2. In the hepatmegaly group, the effective diameter was statistically larger than that in the control group (p<0.05) even though the body weight was similar. This result suggests the dose setting for hepatomegaly patients could be inadequate. For this reason, a new concept for DSDE needs to be established that includes a conversion factor in order to determine the appropriate dose. 3. The conversion factor for hepatomegaly patients ranged from 1.0 to 2.5. According to the conversion factor, there is no need to change the CTDIvol setting in patients who weigh between 6 and 18 kg, however, if the body weight exceeds 19 kg, the dose setting should be changed.

# PDF UPLOAD

http://abstract.rsna.org/uploads/2018/18011644/18011644\_434g.pdf



### PD218-SD-MOB4

Does 18F-FDG Dose Reduction for PET/MRI Affect Treatment Response Assessment of Lymphomas and Sarcomas?

Monday, Nov. 26 12:45PM - 1:15PM Room: PD Community, Learning Center Station #4

### Participants

Ketan Yerneni, Stanford, CA (*Presenter*) Nothing to Disclose Anne M. Muehe, MD, Stanford, CA (*Abstract Co-Author*) Nothing to Disclose Praveen Gulaka, PhD, Stanford, CA (*Abstract Co-Author*) Nothing to Disclose K. Elizabeth Hawk, MD,PhD, Los Angeles, CA (*Abstract Co-Author*) Nothing to Disclose Ashok Joseph Theruvath, MD, Mainz, CA (*Abstract Co-Author*) Nothing to Disclose Heike E. Daldrup-Link, MD, Palo Alto, CA (*Abstract Co-Author*) Nothing to Disclose

# For information about this presentation, contact:

ketanyerneni@gmail.com

### PURPOSE

18F-FDG is widely used for PET imaging of cancer patients. Integrated PET/MR images can be obtained with reduced 18F-FDG doses compared to PET/CT due to longer PET data acquisition times and highly sensitive PET detectors. The goal of our study was to evaluate the effect of simulated 18F-FDG dose reductions on treatment response assessment of pediatric cancers on PET/MR scans.

#### **METHOD AND MATERIALS**

We retrospectively evaluated eighteen 18F-FDG PET scans of 9 pediatric patients and young adults (13-30 years; mean 21.4  $\pm$  7.1 years) with Ewing sarcoma (n=3), soft tissue sarcomas (n=1) or lymphomas (n=5). At baseline and after induction chemotherapy, the patients underwent an integrated PET/MR scan at 60 minutes after intravenous injection of 18F-FDG at a dose of 3 MBq/kg BW. PET data were acquired for 3:30 minutes per bed position. 18F-FDG dose reduction was simulated by reducing acquisition times per PET bed. These data were then reconstructed at the following doses: 100%, 75%, 50%, 25%, 12.5%, and 6.25%. SUVmax of tumors and SUVmean of liver and mediastinal blood pool were measured at baseline and on follow-up scans. On follow up scans, treatment response assessment of lymphomas, according to the Lugano classification, was compared between <= 50% and >= 50% dose groups using a Chi-squared test.

### RESULTS

At baseline and follow-up scans, SUVmax of all tumors increased with lower dosages while SUVmean of the liver and mediastinal blood pool remained stable. All lymphoma patients were deemed treatment responders in the > 50% dose groups. However, 80% of lymphoma patients were upstaged in the <= 50% dose groups due to a higher Deauville visual score (p = 0.0098). All sarcoma patients showed similar tumor SUVmax values from 100%-25% radiotracer dosage. However, 75% of these patients exhibited increased tumor SUVmax values upon lowering the dosage to <= 12.5%.

### CONCLUSION

18F-FDG dose reduction for PET/MRI below 1.5 MBq/kg for lymphoma and below 0.38 MBq/kg for sarcoma patients leads to incorrect assessment of pediatric cancer patients on follow-up scans.

### **CLINICAL RELEVANCE/APPLICATION**

Reduction of 18F-FDG dose in PET/MRI may affect treatment response assessment of pediatric cancer patients. It is important to adhere to current recommendations of a minimum dose of at least 26 MBq.



# PD219-SD-MOB5

Automatic Computation of Iso-perimetric Ratio as Quantitative Index for Degree of Left Ventricular Trabeculation in Adolescents and Young Adults: Potential Indicator for Left Ventricular Non-Compaction

Monday, Nov. 26 12:45PM - 1:15PM Room: PD Community, Learning Center Station #5

# Participants

Amol Pednekar, PhD, Houston, TX (*Presenter*) Nothing to Disclose Siddharth P. Jadhav, MD, Houston, TX (*Abstract Co-Author*) Nothing to Disclose Cory Noel, Houston, TX (*Abstract Co-Author*) Nothing to Disclose Prakash M. Masand, MD, Houston, TX (*Abstract Co-Author*) Nothing to Disclose

For information about this presentation, contact:

vedamol@gmail.com

# PURPOSE

The purpose of this study is to assess the discriminating power of fractal analysis and perimetric ratio to distinguish between pathologic left ventricular noncompaction (LVNC) and physiologic variant of hyper-trabeculation in bright blood cine balanced steady-state free precession (bSSFP) MR images at end-diastole using an automated analysis tool in a pediatric population.

# METHOD AND MATERIALS

Short-axis stack of end-diastolic balanced SSFP images from 26 (age 15±4.9, range 8-31yrs, 21m) LVNC positive (noncompacted(NC)/compacted(C) length ratio (LR)>2.3 and mass ratio(MR)>35%), 20 (age 16±6.6, range 6-35yrs, 12m) hyper trabeculated (NC/C LR<2.3 and MR>35%), and 18 (age 16±5.5, range 6-28yrs, 12m) LVNC negative (NC/C LR<2.3 and MR<35%, anomalous coronary origins or Kawasaki) patients with normal anatomy, preload and afterload, were analyzed with an automated tool. Manually drawn epicardial contours were used to automatically segment the blood pool and extract endocardial boundaries. Using blood pool edges and endocardial contour fractal dimension (FD) and iso-perimetric ratio (PR) i.e. ratio of blood pool to endocardial contour perimeter, are computed for each slice. Mean of top half - 50 percentile FD (mthFD) and cumulative PR (cPR) were used as geometric markers to quantify degree of hyper-trabeculation. Rays normal to and from epicardial contour are generated to compute Endo-blood/Epi-Endo length ratios. The 95 percentile of length ratios in apical third is used as LR.

### RESULTS

Both NC/C LR and MR increase with degree of trabeculation as a continuous spectrum. Values for both mthFD and cPR were statistically significantly higher (p<0.0001) for LVNC +ve compared to LVNC -ve subjects. However, mthFD values have overlap between LVNC +ve and -ve subjects.Values for mthFD and cPR for patients with MR>35 and LR<2.3 overlap with both LVNC +ve and LVNC -ve subjects.

#### CONCLUSION

This study indicates that automatic computation of cPR can be used for quick assessment of degree of trabeculation. This quantification can serve as potential indication for LVNC which can be assessed further by manual drawings of epi- and endocardial contours to check against established diagnostic criteria

# **CLINICAL RELEVANCE/APPLICATION**

Automatic computation of cumulative iso-perimetric ratio as quantitative index for degree of trabeculation is feasible and can serve as a potential indicator for further evaluation of LVNC.



### PH001-EC-MOB

# Computer-Based Interactive X-Ray Simulation Tools for Radiology and Radiography Education

Monday, Nov. 26 12:45PM - 1:15PM Room: PH Community, Learning Center Custom Application Computer Demonstration

#### **Participants**

Stephen M. Kengyelics, PhD, Leeds, United Kingdom (*Presenter*) Nothing to Disclose Ann Westmoreland, Leeds, United Kingdom (*Abstract Co-Author*) Nothing to Disclose Laura A. Treadgold, PhD, Leeds, United Kingdom (*Abstract Co-Author*) Nothing to Disclose Andrew G. Davies, MSc, Leeds, United Kingdom (*Abstract Co-Author*) Nothing to Disclose

# For information about this presentation, contact:

S.M.Kengyelics@leeds.ac.uk

# **TEACHING POINTS**

The purpose of this exhibit is to: 1. Demonstrate two fully interactive computer-based x-ray simulation tools for radiology and radiography physics and imaging education that can be deployed in the classroom. 2. Guide users through an interactive learning session on either one of the simulators to demonstrate their potential use in the classroom by following specially designed worksheets. 3. Report on the impact of the simulation tools on student experience and learning gain in our institution.

# TABLE OF CONTENTS/OUTLINE

1. User selects computer-based interactive simulation software tool on PC. 2.Two simulators are available (X-ray Calculation Tool & X-ray Imaging Tool) 3. A worksheet guides the user through a specially designed activity to demonstrate the use of the simulators in a classroom environment. 4. Summary information is presented at the end of the worksheet to inform the user of the impact of the simulators on student learning experience in our institution.



### PH009-EB-MOB

Investigation into the Outliers in Body CT Radiation Dose as Determined by a Patient Size Dependent Threshold

Monday, Nov. 26 12:45PM - 1:15PM Room: PH Community, Learning Center Hardcopy Backboard

# Participants

Kerry T. Krugh, PhD, Toledo, OH (*Abstract Co-Author*) Nothing to Disclose Tyler van Well, Toledo, OH (*Presenter*) Nothing to Disclose

#### Background

CT radiation dose monitoring has become standard practice for the radiology department. One aspect of CT dose monitoring involves investigation into 'high-dose' outliers. For body CT that utilizes tube current modulation it is prudent and of more value to use a dose threshold that is a function of patient size in lieu of a fixed value dose threshold. This work discusses the results of our investigation into the dose outliers identified by a novel patient-size dependent dose threshold.

#### **Evaluation**

Previous work at our institution has shown that CTDIvol when plotted as a function of patient water equivalent diameter (Dwed) can be modeled effectively by a modified logistic function. The resultant fit parameters of the logistic function can be adjusted to obtain a dose threshold curve as a function of Dwed. We exported from our dose monitoring software the Dwed and corresponding CTDIvol for our commonly-used body CT protocols over the past year. The data was separated into two groups based upon the tube current modulation settings. Each group was analyzed for outliers using the patient-size dependent dose threshold curve established from the logistic function. Each identified outlier was subsequently investigated to determine the cause of dose deviation.

#### Discussion

Out of a total of 6,439 body CT scans we identified 62 examinations as outliers (0.96%). The results of our investigation: 1) 30.6% of the outliers were found to have entire scans or additional scans performed without the use of tube current modulation; 2) 24.2% of the outliers had a technique factor adjusted by the technologist; 3) 21.0% of the outliers involved inappropriate protocol selection; 4) 9.7% of the outliers had a significant portion of the scan performed outside of the localizer range; 5) in 4.8% of the outliers the patient was found to be significantly off-center; and 6) in 19.4% of the outliers there was no identifiable problem found.

# CONCLUSION

This work demonstrates how a patient-size dependent dose threshold can be utilized to accurately identify CT dose outliers. The investigative results of the outliers can prove beneficial in identifying problems and for quality improvement in CT imaging.

### FIGURE

http://abstract.rsna.org/uploads/2018/18013909/18013909\_g6wo.jpg



### PH121-ED-MOB8

# The 10 Commandments of Artefact Reduction in Cardiac MRI

Monday, Nov. 26 12:45PM - 1:15PM Room: PH Community, Learning Center Station #8

**FDA** Discussions may include off-label uses.

# Awards

Certificate of Merit Identified for RadioGraphics

#### **Participants**

Prashanth Reddy, MBBS, MD, Bangalore, India (*Presenter*) Nothing to Disclose Bharath B. Das, MD, MBBS, Bangalore, India (*Abstract Co-Author*) Nothing to Disclose Sankar Neelakantan, MD, Bangalore, India (*Abstract Co-Author*) Nothing to Disclose Bhavana Nagabhushana Reddy, MBBS, MD, Bangalore, India (*Abstract Co-Author*) Nothing to Disclose Sanjaya Viswamitra, MD, Bengaluru, India (*Abstract Co-Author*) Nothing to Disclose

### For information about this presentation, contact:

prashanth.d@sssihms.org.in

# **TEACHING POINTS**

The heart is a complex dynamic structure which changes shape and position throughout the cardiac cycle. MRI sequences with high temporal and spatial resolution are required to image the heart. Even with a fully functioning MRI scanner small changes in imaging parameters can result in artifacts. The purpose of this article is to:1. Identify the most commonly encountered artifacts and their sources. 2. Discuss methods to reduce or remove these artefacts.

# TABLE OF CONTENTS/OUTLINE

Causes as well as methods to remove or reduce artifacts including aliasing, gradient decay or fall-off, RF zipper, ECG gating mistriggers, flow-related artifacts, susceptibility-induced signal loss, banding of balanced SSFP images, imaged-based parallel imaging reconstruction artifact, k-Space-based parallel imaging artifact and perfusion dark-rim artifact will be discussed.



# PH218-SD-MOB1

The Value of Shear Wave Elastography and Contrast Enhanced Ultrasound for Benign-Malignant Lymph Nodes Differentiation in Rabbits

Monday, Nov. 26 12:45PM - 1:15PM Room: PH Community, Learning Center Station #1

# Participants

Shi Tan, Peking, China (*Presenter*) Nothing to Disclose Li-Ying Miao, Beijing, China (*Abstract Co-Author*) Nothing to Disclose Li Gang Cui, PhD, MD, Beijing, China (*Abstract Co-Author*) Nothing to Disclose Shi-Rong Liu, Beijing, China (*Abstract Co-Author*) Nothing to Disclose Ying Fu, Beijing, China (*Abstract Co-Author*) Nothing to Disclose Chang Liu, Beijing, China (*Abstract Co-Author*) Nothing to Disclose Xiao-Hua Wang, Beijing, China (*Abstract Co-Author*) Nothing to Disclose Lin-Xue Qian, Beijing, China (*Abstract Co-Author*) Nothing to Disclose

#### For information about this presentation, contact:

tanshi@outlook.com

#### PURPOSE

to evaluate the efficacy of shear wave elastography (SWE) in the differential diagnosis of lymphadenopathy.

#### **METHOD AND MATERIALS**

28 New Zealand rabbits were randomly divided into two groups. egg yolk emulsion and VX2 solution were injected into the quadriceps femoris of the rabbit respectively, resulting in reactive hyperplastic and metastatic popliteal lymph node respectively. The largest lymph node was evaluated using both CEUS and SWE. The value of maximum elastic modulus (Emax), mean elastic modulus (Emean), standard deviation of the elastic modulus (ESD) and minimum elastic modulus (Emin) in differentiating benign and malignant lymph nodes were evaluated, and the status of elastography were identified by comparing with the contrast-enhanced ultrasound.

# RESULTS

16 of the 28 lymph nodes were reactive hyperplasia while the other 12 were metastasis. The Emax, Emean and ESD were significantly higher in malignant lesions than in benign ones. The sensitivity of differential diagnosis of the lymph nodes were 83.3%, 91.7%, and 58.3%, the specificity were 75.0%, 81.3%, and 81.3%, respectively. and the accuracy were 78.6%, 85.7%, and 71.4% with thresholds of 13.7kpa, 6.5kpa and 2.3kpa, respectively. There was a statistically difference(P value was 0.006, 0.001, 0.029, respectively). Elastography can accurately differentiate the lymph nodes. Contrast-enhanced ultrasound demonstrated 15 homogeneous enhanced lymph nodes (all reactive hyperplasia) and 13 heterogeneous enhanced lymph nodes (12 metastatic lymph nodes and 1 reactive hyperplasia). The sensitivity, specificity and accuracy of CEUS were 100%, 92.3and 96.4%, respectively, and the contrast enhanced ultrasonic manifestation in diagnosing the benign lymph nodes showed statistical difference (X2 = 31.192, P<0.001). The accuracy of CEUS in differentiating the benign and malignant lymph nodes were higher than that of SWE, but there was no statistical difference in the Emax and Emean (Z value was 1.753 and 1.331, respectively. P value was 0.0795 and 0.1833), which showed similar diagnostic capability between SWE and CEUS.

# CONCLUSION

SWE is an accurate diagnosis method in differentiating malignant and benign LNs, which has a better diagnostic efficiency.

#### **CLINICAL RELEVANCE/APPLICATION**

conventional ultrasonography differentiating malignant and benign lymph nodes remains a diagnostic challenge ,To establish a new technique for evaluation of LN is important to improve the diagnosis level.



### PH219-SD-MOB2

Dynamic ADC Analysis of the Brain in the Supine and Upright Postures

Monday, Nov. 26 12:45PM - 1:15PM Room: PH Community, Learning Center Station #2

**FDA** Discussions may include off-label uses.

#### Participants

Naoki Ohno, PhD, Kanazawa, Japan (*Presenter*) Nothing to Disclose Tosiaki Miyati, PhD, Kanazawa, Japan (*Abstract Co-Author*) Nothing to Disclose Masatomo Uehara, Kanazawa, Japan (*Abstract Co-Author*) Nothing to Disclose Yuki Hiramatsu, BS,RT, Kanazawa, Japan (*Abstract Co-Author*) Nothing to Disclose Riho Okamoto, Kanazawa, Japan (*Abstract Co-Author*) Nothing to Disclose Mitsuhito Mase, MD, Nagoya, Japan (*Abstract Co-Author*) Nothing to Disclose Satoshi Kobayashi, MD, Kanazawa, Japan (*Abstract Co-Author*) Nothing to Disclose Toshifumi Gabata, MD, PhD, Kanazawa, Japan (*Abstract Co-Author*) Nothing to Disclose

# PURPOSE

We have previously demonstrated that the apparent diffusion coefficient (*ADC*) of the brain significantly changed during the cardiac cycle. The dynamic change in *ADC* ( $\Delta ADC$ ) shows the degree of fluctuation of water molecules in the brain and reflects intracranial condition. Although body posture strongly affects intracranial conditions, eg., intracranial pressure (ICP), cerebral hemodynamics, and cerebrospinal fluid flow (CSF) dynamics, the effect of body posture on  $\Delta ADC$  has yet to be confirmed because MRI of the brain is usually constrained to the horizontal supine posture. Therefore, the purpose of this study was to evaluate the  $\Delta ADC$  of the brain in the supine and upright postures using a multi-posture MRI that enables us to perform MRI of the brain at any postures.

#### **METHOD AND MATERIALS**

On a 0.4-T multi-posture MRI, seven healthy volunteers (all males; mean age, 23.9 years; range, 21-28 years) were scanned in the supine and upright postures. ECG-synchronized single-shot diffusion echo-planar imaging (b = 0 and 500 s/mm2) was performed to obtain *ADC* images in each cardiac phase (22-33 cardiac phases). We then determined the maximum change in *ADC* ( $\Delta ADC$ ) during the cardiac cycle in the white matter. Moreover, the transcranial arterial inflow, venous outflow, and CSF flow in both postures were measured using ECG-synchronized phase-contrast cine MRI. We compared these values between the supine and upright postures.

# RESULTS

Compared with the supine posture,  $\Delta ADC$  of the white matter was significantly increased in the upright posture. This result indicates that body posture affects fluctuation of water molecules in the brain. Moreover, venous outflow of the internal jugular veins (IJVs) and CSF stroke volume were significantly decreased in the upright posture due to the decreased ICP. Interestingly, the rate of increase in  $\Delta ADC$  of the brain had a linear relationship with the rate of decrease in venous outflow of the IJVs. Therefore, the increase in  $\Delta ADC$  in the upright posture may be associated with decrease in ICP.

# CONCLUSION

In the upright posture,  $\Delta ADC$  of the brain was increased in association with the decrease in venous outflow of the IJVs. Multiposture MRI facilitates the noninvasive evaluation of the effect of gravity on intracranial conditions.

#### **CLINICAL RELEVANCE/APPLICATION**

Dynamic ADC analysis of the brain in the supine and upright postures facilitates the noninvasive evaluation of the effect of gravity on intracranial conditions.



### PH220-SD-MOB3

Coronary Stent Imaging with Photon Counting CT: Can Dedicated Sharp Convolution Kernels Improve Image Quality?

Monday, Nov. 26 12:45PM - 1:15PM Room: PH Community, Learning Center Station #3

# Participants

Jochen von Spiczak, MD,MSc, Zurich, Switzerland (*Presenter*) Nothing to Disclose Manoj Mannil, Zurich, Switzerland (*Abstract Co-Author*) Nothing to Disclose Benjamin B. Peters, Deurne, Belgium (*Abstract Co-Author*) Nothing to Disclose Tilman Hickethier, MD, Cologne, Germany (*Abstract Co-Author*) Nothing to Disclose Matthias Baer, DiplPhys, Erlangen, Germany (*Abstract Co-Author*) Nothing to Disclose Andre Henning, MENG,MSc, Forchheim, Germany (*Abstract Co-Author*) Employee, Siemens AG Bernhard Schmidt, PhD, Forchheim, Germany (*Abstract Co-Author*) Employee, Siemens AG Thomas G. Flohr, PhD, Forchheim, Germany (*Abstract Co-Author*) Employee, Siemens AG Robert Manka, Zurich, Switzerland (*Abstract Co-Author*) Nothing to Disclose David C. Maintz, MD, Koln, Germany (*Abstract Co-Author*) Nothing to Disclose Hatem Alkadhi, MD, Zurich, Switzerland (*Abstract Co-Author*) Nothing to Disclose

# PURPOSE

To assess whether dedicated sharp convolution kernels for photon counting detector (PCD) CT can improve image quality of coronary stent imaging and whether potential increase in image noise can be reduced by iterative reconstruction (IR).

# METHOD AND MATERIALS

A phantom simulating coronary stenting was prepared including 18 different coronary stents expanded in plastic tubes. Tubes were filled with diluted contrast agent, sealed, and immersed in oil simulating pericardial fat. The phantom was scanned in a 128-slice research dual-source CT equipped with a PCD (100kVp/100mAs). Images were reconstructed using a conventional convolution kernel for stent imaging with filtered back projection (B46) and IR at SAFIRE level 3 (I46-3). For comparison, a dedicated sharp convolution kernel with filtered back projection (D70) and IR at SAFIRE level 3 and 5 (Q70-3/Q70-5) was used. Two readers evaluated image quality (scale 0-3, 3=excellent), in-stent diameter difference, in-stent attenuation difference, mathematically defined image sharpness, and noise. Interreader reliability was calculated. Differences in image quality were evaluated using a Wilcoxon signed-rank test. Differences in in-stent diameter, in-stent attenuation, image sharpness, and noise were tested using a paired sample t-test.

# RESULTS

Interreader reliability was excellent (ICCs=0.952-0.999). Reconstructions using the dedicated sharp convolution kernel yielded significantly better results regarding image quality (B46:  $0.4\pm0.5$  vs. D70:  $2.9\pm0.3$ , p<0.001), in-stent diameter difference ( $1.5\pm0.3$  vs.  $1.0\pm0.3$ mm, p<0.001), and image sharpness ( $728\pm246$  vs.  $2069\pm411$  CT-numbers/voxel, p<0.001). Regarding in-stent attenuation difference, no significant differences were observed ( $151\pm76$  vs.  $158\pm92$  CT-numbers, p=0.627). Noise was significantly higher in all sharp kernel images, but could be reduced applying SAFIRE levels 3 and 5 (B46:16±1, D70:  $111\pm3$ , Q70-3:  $65\pm2$ , Q70-5:  $46\pm2$  CT-numbers, p<0.001 for all comparisons).

#### CONCLUSION

A dedicated sharp convolution kernel for PCD CT imaging of coronary stents yields superior qualitative and quantitative image characteristics compared to conventional reconstruction kernels. Resulting higher noise levels can be reduced using IR.

#### **CLINICAL RELEVANCE/APPLICATION**

Our in-vitro study indicates considerably improved imaging characteristics of PCD technology when used with dedicated sharp convolution kernels for coronary in-stent lumen visualization.



# PH221-SD-MOB4

Development a Software Which Assists Radiologists to Determine Optimal Contrast Material Administration Protocol at CT: Validation Study Using a Computer Simulation

Monday, Nov. 26 12:45PM - 1:15PM Room: PH Community, Learning Center Station #4

# Participants

Toru Higaki, PhD, Hiroshima, Japan (*Presenter*) Nothing to Disclose Yoriaki Matsumoto, Hiroshima, Japan (*Abstract Co-Author*) Nothing to Disclose Takanori Masuda, Hiroshima, Japan (*Abstract Co-Author*) Nothing to Disclose Yuko Nakamura, MD, Hiroshima, Japan (*Abstract Co-Author*) Nothing to Disclose Fuminari Tatsugami, Hiroshima, Japan (*Abstract Co-Author*) Nothing to Disclose Kazuo Awai, MD, Hiroshima, Japan (*Abstract Co-Author*) Nothing to Disclose Kazuo Awai, MD, Hiroshima, Japan (*Abstract Co-Author*) Research Grant, Canon Medical Systems Corporation; Research Grant, Hitachi, Ltd; Research Grant, Fujitsu Limited; Research Grant, Bayer AG; Research Grant, DAIICHI SANKYO Group; Research Grant, Eisai Co, Ltd; Medical Advisory Board, General Electric Company; ;

#### CONCLUSION

Our software may provide a stable contrast enhancement and reduced inter-patient variability at coronary CTA.

#### Background

To determine contrast material (CM) injection protocol at CT, we should take consideration of patient factors such as body size and cardiac function, CM factors such as administration dose and injection duration, scan factors such as timing for scan start, and X-ray tube voltage. Furthermore, we should consider diagnostically optimal CT number of the target organs and time in which optimal CT number is sustained. Thus, it is highly complex to customize CM injection protocol for a specific purpose and each patient. We developed a software which can determine the optimal CM injection protocol accommodating to a specific purpose and each patient based on the whole body circulation model. The purpose of this study was to investigate utility of our software for coronary CT angiography (CTA) in a simulation study.

# **Evaluation**

The operation window of our software is shown in Fig 1: the specific condition is 'Keep the CT value of the ascending aorta at 400 HU or higher for 8 seconds.', and the optimization result is shown in Fig 2. To evaluate validity of our software, we used data of 93 patients (F:42, M:51, 67±11 y.o.) who underwent coronary CTA. CT scan was performed using 64-detector CT and the dose of CM was decided by patient's body weight (BW). The CT value of the aorta in actual CT was 441.0  $\pm$  67.9 HU, and the average of the CM used was 43.1 ml. By using our software, we optimized the CM volume for each patient with a specific condition of 'CT number 400 HU sustained during 8 seconds in the ascending aorta'. BW, body height (BH), and cardiac output (CO) were used for the optimization of CM dose. We also calculated simulated aortic CT value against the optimized CM dose. The simulated CT value of the aorta was 445  $\pm$  8.8 HU, and the average of the CM used was 43.4 ml (Fig 3-4).

### Discussion

The aortic CT value in the actual CT scan varied widely as standard deviation (SD) = 67.9. By using our software, the variation decreased to SD = 8.8 in the simulation. There was no change in mean CT value and average contrast agent volume between actual CT and simulated CT.



### PH222-SD-MOB5

Comparison of Diagonal and Three-Scan Trace Diffusion Modes in Diffusion-Weighted Imaging of Bladder Cancer

Monday, Nov. 26 12:45PM - 1:15PM Room: PH Community, Learning Center Station #5

# Participants

Luguang Chen, Shanghai, China (*Presenter*) Nothing to Disclose Haihu Chen, Shanghai, China (*Abstract Co-Author*) Nothing to Disclose Fang Liu, Shanghai, China (*Abstract Co-Author*) Nothing to Disclose Qingsong Yang, Shanghai, China (*Abstract Co-Author*) Nothing to Disclose Chao Ma, Shanghai, China (*Abstract Co-Author*) Nothing to Disclose Li Wang, Shanghai, China (*Abstract Co-Author*) Nothing to Disclose Jianping Lu, MD, Shanghai, China (*Abstract Co-Author*) Nothing to Disclose

#### For information about this presentation, contact:

chen\_lu\_guang@sina.com

# PURPOSE

To assess whether single-shot echo planar imaging with diagonal diffusion-weighted imaging (d-DWI) can provide better image quality in imaging bladder cancer in comparison with three-scan trace DWI (t-DWI), and to compare quantitative image parameters, derived from d-DWI with those of t-DWI.

### **METHOD AND MATERIALS**

<u>Subjects</u> Nineteen patients with bladder cancer were enrolled in this prospective study, which was approved by the local institutional review board and written informed consent was obtained from each patient. <u>MRI protocols</u> All patients were performed on a 3T MR system using the following examination protocols, axial T1WI, T2WI, two axial DWI with RS-EPI and SS-EPI techniques and contrast enhanced T1WI. <u>Image analysis</u> t-DWI and d-DWI images were evaluated by two independent observers for identification of susceptibility, detectability, motion artifacts and image blurring of the lesions using quantitative 4-point scale. Signal-to-noise ratio (SNR), contrast-to-noise ratio (CNR), signal intensity ratio (SIR) and ADC values of bladder lesions were measured and compared. <u>Statistical analysis</u> Significant differences between t-DWI and d-DWI for visual scores, and quantitative parameters were assessed by using Wilcoxon signed rank tests.

# RESULTS

There were no significant differences between d-DWI and t-DWI techniques in susceptibility, detectability and image blurring and motion artifacts of bladder lesions (all p > 0.05). No significant differences were observed for SNR (72.05±41.32 vs. 97.66±59.36, p = 0.053), CNR (3.33±1.15 vs. 3.63±1.50, p = 0.071), SIR (4.97±1.16 vs. 4.45±1.12, p = 0.647) and ADC (1.287±0.271 vs. 1.209±0.232 ×10-3mm2/s, p = 0.064) values of bladder lesions between t-DWI and d-DWI techniques.

### CONCLUSION

d-DWI demonstrated equivalent image quality and quantitative parameters of bladder cancer compared with t-DWI technique, which showed that d-DWI is a promising method for reducing examination time in bladder cancer without degrade image quality.

#### **CLINICAL RELEVANCE/APPLICATION**

(Dealing with MRI) d-DWI is equal to t-DWI in evaluating image quality and quantitative parameters of bladder cancer and is recommended in the routine examination of bladder cancer.



# PH224-SD-MOB7

Multimodal Anthropomorphic Breast Phantoms for Microwave Imaging (MWI), B-Mode Ultrasound, Mammography, Magnetic Resonance Imaging, and Computed Tomography

Monday, Nov. 26 12:45PM - 1:15PM Room: PH Community, Learning Center Station #7

# Participants

Jacinta Browne, PhD, Dublin 8, Ireland (*Presenter*) Nothing to Disclose Gaia Fiaschetti, Rome, Italy (*Abstract Co-Author*) Nothing to Disclose Antonio Cuccaro, Aversa, Italy (*Abstract Co-Author*) Nothing to Disclose Jorge Tobon, Torino, Italy (*Abstract Co-Author*) Nothing to Disclose Raffaele Solimene, Aversa, Italy (*Abstract Co-Author*) Nothing to Disclose Max Ammann, Dublin, Ireland (*Abstract Co-Author*) Nothing to Disclose Andrew Fagan, Rochester, MN (*Abstract Co-Author*) Nothing to Disclose Sean Cournane, MSc, PhD, Dublin 8, Ireland (*Abstract Co-Author*) Nothing to Disclose Jennie Cooke, MSc, PhD, Dublin, Ireland (*Abstract Co-Author*) Nothing to Disclose Giuseppe Ruvio, Dublin, Ireland (*Abstract Co-Author*) Nothing to Disclose

# PURPOSE

MWI is an emerging technique and suitable anthropomorphic breast phantoms are required for testing and benchmarking different MWI scanning setups and reconstruction algorithms. Furthermore, these phantoms can be used as a reference between this emerging imaging technique and conventional imaging for Radiologists. The aim of this work was to develop a multimodal anthropomorphic breast phantom for MWI, B-mode ultrasound, mammography, MRI and CT. Multimodal anthropomorphic phantoms need to mimic breast tissues in terms of heterogeneity, anatomy, morphology, and mechanical and dielectric characteristics.

# METHOD AND MATERIALS

Five different breast tissue-mimicking materials (TMMs) were developed: skin, subcutaneous fat, fibroglandular tissue, tumour (malignant lesion) and pectoral muscle, to mimic for the heterogeneity of the breast. These novel TMMs were integrated into two realistic anthropomorphic breast phantoms. The dielectric and acoustic properties, together with magnetic resonance relaxation times and X-rays attenuation coefficients, were measured for the assessment of the five TMMs. In particular, the complex permittivity of each TMM was measured across the frequency bandwidth 0.5 - 4 GHz by using an open-ended coaxial probe.

#### RESULTS

A satisfactory match in dielectric properties (for MWI), acoustic properties (for ultrasound), relaxation times (for MRI) and X-rays attenuation coefficients (for mammography and CT) was achieved between real breast tissues and the tissue-mimicking materials integrated in the multimodal anthropomorphic phantoms. Two phantoms were developed with a different inner structure but identical constituent materials. Shape and tissue composition accurately mimicked the structure of a human breast and its interaction with different imaging modalities. Furthermore, the phantoms were non-toxic, inexpensive and easy to manufacture. Clinically-realistic artifact-free images of the anthropomorphic breast phantoms were obtained using the conventional imaging techniques of Mammography, CT, Ultrasound, MRI as well as the emerging technique of MWI.

### CONCLUSION

The anthropomorphic breast phantoms presented in this study can be used as a standard multimodality phantom for the evaluation of MWI of breast lesions against conventional techniques.

# **CLINICAL RELEVANCE/APPLICATION**

This evaluation process is important for ensuring the safety, efficacy and accuracy of the imaging techniques to ensure optimal patient management.



# QI006-EB-MOB

Clean Reading Room Initiative: Impact of Various Interventional Processes

Monday, Nov. 26 12:45PM - 1:15PM Room: QR Community, Learning Center Hardcopy Backboard

#### **Participants**

Ami V. Vakharia, MD, Chapel Hill, NC (*Abstract Co-Author*) Nothing to Disclose Ellie R. Lee, MD, Chapel Hill, NC (*Abstract Co-Author*) Nothing to Disclose Katrina A. McGinty, MD, Chapel Hill, NC (*Abstract Co-Author*) Nothing to Disclose John Campbell, MD, Chapel Hill, NC (*Presenter*) Nothing to Disclose

### For information about this presentation, contact:

vakharia.ami@gmail.com

## PURPOSE

To assess basic hand and workstation hygiene habits of radiologists before and after installation of hand sanitizing and disinfectant wipe facilities within the reading rooms and subsequent educational interventions on environment cleaning.

#### **METHODS**

A prospective study was performed on evaluation of designated workstations used by radiology attendings and residents at a university teaching hospital between March 2017 and April 2018. Beginning in March, 2017, we initiated monitoring of workstation cleaning. Designated workstations were marked in 5 separate sites (phone receiver, phone keypad, mouse, keyboard and microphone) with safety-grade photo luminescent material prior to the start of the workday. At the end of the workday, an ultraviolet black light was used to evaluate whether the workstations showed evidence of cleaning by their user. In September 2017, wall-mounted disinfectant wipe dispensers, hand sanitizer dispensers and glove stations were installed at the entrances of 17 separate reading rooms along with laminated instructional placards but without an educational session. At this time, workstations were again evaluated for evidence of user cleaning. Subsequently, the radiologists were educated on the importance of handwashing and workstation cleanliness. Also, the radiologists received personalized instructions on how to properly clean their workstations and the effectiveness of their efforts over a one-week period. After these interventions were implemented, the designated workstations were evaluated at 1 week post education and then again approximately 1, 3 and 6 months later to assess for changes in behavior.

# RESULTS

Workstations were evaluated for both evidence of cleaning as well as completeness of cleaning (i.e. how many of the 5 marked sites showed evidence of cleaning). Initially, 24 workstations were sampled with 13% of the workstations showing evidence of cleaning. However, cleaning of these stations was incomplete, with only 8% of the sites marked showing evidence of cleaning. Following the installation of the sanitizing stations and prior to educational initiatives, 23 workstations were sampled with 17% of workstations showing evidence of cleaning and 15% of sites sampled showing evidence of cleaning. In October 2017, there was a one week educational initiative regarding workstation hygiene in which 25-33 workstations were sampled daily with 37-58% of workstations showing evidence of cleaning. Workstations were sampled 1 week post educational initiative with 68% of workstations showing evidence of cleaning and 57% of sites sampled showing evidence of cleaning. To assess long term effectiveness of the educational initiative, workstations were sampled at 1, 3 and 6 months post educational initiative with 43-45% of workstations showing persistent evidence of cleaning and 39-43% of sites sampled showing evidence of cleaning and 39-43% of sites sampled showing evidence of cleaning and 39-43% of sites sampled showing evidence of cleaning and 39-43% of sites sampled showing evidence of cleaning and 39-43% of sites sampled showing evidence of cleaning and 39-43% of sites sampled showing evidence of cleaning and 39-43% of sites sampled showing evidence of cleaning and 39-43% of sites sampled showing evidence of cleaning and 39-43% of sites sampled showing evidence of cleaning and 39-43% of sites sampled showing evidence of cleaning and 39-43% of sites sampled showing evidence of cleaning and 39-43% of sites sampled showing evidence of cleaning and 39-43% of sites sampled showing evidence of cleaning and 39-43% of sites sampled showing evidence of cleaning and 39-43% of sites sampled showing evidence of cleaning and 39-43% o

# CONCLUSION

In recent years, there is compelling evidence on the importance of health care professional hand and workstation hygiene in protecting the staff and patients against health-care associated infections. Educating the radiologists on the importance of handwashing and workstation cleanliness behavior and providing easily accessible cleaning supplies in the reading rooms has successfully and sustainably improved radiologists' workstation disinfection and hand hygiene at our institution.



# QI008-EB-MOB

Ensuring MIPS/MACRA Radiation Dose Reduction Compliance: Automated Evaluation of Enterprise Radiology Reports

Monday, Nov. 26 12:45PM - 1:15PM Room: QR Community, Learning Center Hardcopy Backboard

# Participants

Joshua Groeniger, MD, Arlington, VA (*Presenter*) Nothing to Disclose Jill Bruno, DO, Baltimore, MD (*Abstract Co-Author*) Nothing to Disclose Ross W. Filice, MD, Chevy Chase, MD (*Abstract Co-Author*) Co-founder, DexNote, LLC; Research Grant, NVIDIA Corporation; Advisor, BunkerHill Health, Inc

# PURPOSE

Traditionally, physician reimbursements have been rooted in a fee-for-service model which, over time, has garnered a reputation for "volume over value". To mitigate concerns regarding quality of care while simultaneously addressing rising costs, The Medicare Access and CHIP Reauthorization Act (MACRA) was introduced to shift the paradigm towards value-based payments. To receive Medicare Part B payments, medical practices must participate in either the advanced alternative payment model (APM) or the Merit-Based Incentive Payment System (MIPS). The MIPS payment program is a quality-centric fee-for-service reimbursement scheme that dictates future payment rates based on a performance score calculated from 4 categories: Quality, Improvement Activities, Advancing Care Information, and Cost. As part of the process to become MIPS compliant, our enterprise has ensured that dose lowering techniques are in place for patient safety across all CT examinations, and to reflect that, we have implemented enterprise-wide template standardization to document this and ensure MACRA/MIPS compliance. Lack of documentation results in inaccurate reporting which may both cause the patient harm and jeopardize future reimbursement. To address this issue, CT dictations across our enterprise were evaluated for compliance, and all noncompliant individuals were then targeted for individualized intervention in an effort to improve the accuracy of our enterprise-wide reporting.

### METHODS

An indexed database (Solr; Apache) containing all dictated CT reports across 9 facilities in our enterprise was evaluated for total number of compliant and non-compliant dictated reports. This was achieved by creating a search algorithm specific to CT examinations excluding all other modalities, PET and SPECT examinations, and outside administrative reports. Data from January through March, 2018 was used to establish a baseline of non-compliant dictations. This information was made site specific to compare across facilities, and then separated into individual attending dictations. This data was then compared to results after individually targeted intervention to measure the impact on individual and enterprise non-compliance. The intervention, which consisted of a personalized email addressed to noncompliant individuals, was initiated on 3/30/2018. Preintervention data (1/1/2018 through 3/1/2018) was compared to data generated in the initial post intervention phase (4/1/2018 through 4/10/2018) at the enterprise, facility, and individual level. Data points where compared using a two-tailed chi-squared test with Yates correction with p-values to evaluate for statistical significance.

#### RESULTS

A total of 32,776 diagnostic CTs were performed and dictated across 9 sites in our enterprise from January 1st 2018 through April 10th 2018, excluding the month of March (month of intervention). Of those, 31,322 were compliant with this particular MIPS quality performance measure, while 1,454 were not. After the introduction of standardized templates in August 2017 non-compliance gradually decreased without intervention secondary to the adoption of standardized templates but reached a steady state noncompliance rate of 4.7% during our pre-intervention observation period. Preliminary data gathered in the immediate post-intervention phase demonstrated a statistically significant decrease in percent noncompliant reporting across our enterprise (4.7% to 2.9%, p < 0.0001). A significant decrease in noncompliance at our least compliant facility was also observed (8.5% to 2.7%, P < 0.0001). Additionally, there was improvement in overall reporting compliance amongst a group of frequent offenders responsible for more than 40% of all enterprise wide noncompliant reports, with a significant decrease in inaccurate reporting by our least compliant radiologist (66.5% to 13.8%; p < 0.01).

#### CONCLUSION

Through use of an automated process to filter compliant and noncompliant dictated reports, an enterprise wide improvement in dose reduction compliance was achieved after targeted intervention with a series of personalized emails addressed to those with report infractions. In the immediate post intervention phase, compliance rates have already shown statistically significant improvement suggesting the success of the automated system and intervention. Analysis is ongoing, with plans for long term post-intervention data comparisons across all facilities and individuals.



# QI109-ED-MOB1

# **Reliable Projectile Hazard Reduction in MRI**

Monday, Nov. 26 12:45PM - 1:15PM Room: QR Community, Learning Center Station #1

### Participants

Darwin Roth, BSN, Aurora, CO (Presenter) Nothing to Disclose Beth English, BA, Aurora, CO (Abstract Co-Author) Nothing to Disclose Katherine Bushur, BS, ARRT, Aurora, CO (Abstract Co-Author) Nothing to Disclose Jill Chuita, RN,BSN, Aurora, CO (Abstract Co-Author) Nothing to Disclose Robert B. Lentz, MBA, ARRT, Aurora, CO (Abstract Co-Author) Nothing to Disclose Jerrod Milton, BSC, MBA, Aurora, CO (Abstract Co-Author) Nothing to Disclose

# For information about this presentation, contact:

darwin.roth@childrenscolorado.org

# PURPOSE

MRI safety continues to be a topic of ongoing professional interest with various ferromagnetic detection systems (FMDS) employed in accordance with ACR guidelines. Often eluding radiology professionals are cultural elements impeding MRI safety and other notable challenges associated with the implementation of highly reliable measures. Despite decades of heightened awareness and mitigation, tactics such as staff training programs and patient screening are hopeful, but not reliable measures. The inherent risk of undetected or misplaced metal objects causing MRI accidents remains widespread in the industry. Our institution operates seven MRI suites throughout our system with FMDS installed at the entrance into Zone IV at each location. Despite this mitigation measure, potentially harmful incidents involving metal objects have occurred at an unacceptably high rate (n=16/yr). Other important concerns observed include numerous gaps in screening effectiveness and alarm fatigue. Project aims were to reduce FMDS alarm rates on entry to Zone IV from 95% to 5%, and reduce the annual occurrence rate of any harmful incidents by 100%.

### METHODS

In August 2016, a partnership between radiology, performance improvement and patient safety departments was established to address the project aims. Three primary improvement objectives were established (involving place, people and process). A series of nine standardized PDSA testing sessions were completed in the clinical setting and included the use of a pre-screened ferrous-free person who transported a 'control' projectile through the FMDS at separate intervals. The controls consisted of either a 4.5' straight scissors or a 5' curved forceps. Controls were further separated into two groups: 1) exposed, where one control item from each group exposed to magnet field resulting in an elevated magnetic signature of the object, and 2) non-exposed, where one control item from each group was not exposed to magnet field resulting in non-elevated magnetic signature of the object. All controls were deemed a 'projectile hazard', according to the ASTM deflection test. During each PDSA session, samples from each control group were tested in conjunction with incremental adjustment of the sensitivity of the FDMS systems from the lowest to the highest setting. The purpose of these tests was to determine the minimally effective setting necessary in order to reliably detect each control. In conjunction with each concurrent PDSA cycle modifications were made by the manufacturer to each of the FMDS tested to optimize the Fluxgate and Anisotropic Magneto-Resistive (AMR) systems in an attempt to more reliably detect the controls.

#### RESULTS

Testing algorithms revealed significant gaps in effectiveness, and programmatic variables were identified within the expected performance of the FMDS installed. Variables included the physical location of the projectile on the transport person, as well as the horizontal or vertical orientation of the potential hazard while being carried. When set at maximum sensitivity, in numerous instances the FMDS were unable to reliably detect the 'non-exposed' controls due to environmental (far field) interference. With the current settings and modifications made, we discovered there is an approximate twelve-inch gap that exists at the center region of each door passageway where detection of ferrous targets was minimal. In all testing cycles the pre-screener detectors provided by leading FMDS manufacturers were able to detect each control group with 100% reliability. Through our project, 42 new practice changes were implemented, and 68 existing process improvements were achieved. A 78% reduction in alarm rates was achieved, resulting in the alarms having more meaning (Fig.1); a 100% reduction of incidents where hazards entered Zone IV was realized (Fig.2). These reductions were achieved in conjunction with the implementation and customization of the latest FMDS technology and various process improvements.

#### CONCLUSION

Considering the inherent limitations to currently available technology, institutions using these devices may not be able to reliably detect metallic objects classified as projectile hazards due to a given object's relatively low magnetic signature or strength. This phenomenon should be understood by practitioners (false sense of security). Proper risk evaluation and mitigation strategies should also be implemented. Validation of installed systems can, and should be accomplished in order to optimize the level of sensitivity and effectiveness of each FMDS installed in situ. It would appear that in clinical settings where FMDS technology is in use, but does not also incorporate available pre-screener detectors within pre-screening processes, the risk of a ferrous projectile hazard entering Zone IV is elevated. Lastly, application of rigorous process improvement methodologies can yield tremendous practical value in improving safety and reliable processes in this environment.



# QI111-ED-MOB2

Optimization of a Prostate MRI Value Chain to Increase Patient Access and Improve Prostate Cancer Care

Monday, Nov. 26 12:45PM - 1:15PM Room: QR Community, Learning Center Station #2

#### **Participants**

Leslie K. Lee, MD, Boston, MA (Presenter) Nothing to Disclose

William W. Mayo-Smith, MD, Boston, MA (Abstract Co-Author) Nothing to Disclose

Vera Kimbrell, Mendon, MA (Abstract Co-Author) Nothing to Disclose

Stuart Hooton, RT, Boston, MA (Abstract Co-Author) Nothing to Disclose

Aida Faria, Boston, MA (Abstract Co-Author) Nothing to Disclose

Andrew R. Menard, JD, Boston, MA (Abstract Co-Author) Board of Directors, Cary Pharmaceuticals Inc; Stockholder, Cary

Pharmaceuticals Inc; Board of Directors, Millikelvin Technologies, LLC; Stockholder, Millikelvin Technologies, LLC; Stockholder, Handa Pharmaceuticals, LLC

Karen Lemaire, MBA, Waltham, MA (Abstract Co-Author) Nothing to Disclose

Clare M. Tempany-Afdhal, MD, Boston, MA (*Abstract Co-Author*) Research Grant, InSightec Ltd; Research Grant, Gilead Sciences, Inc; Advisory Board, Profound Medical Inc; Spouse, Employee, Spring Bank Pharmaceuticals, Inc; Spouse, Director, Trio Healthcare; Spouse, Consultant, Gilead Sciences, Inc; Spouse, Consultant, Merck & Co, Inc; Spouse, Consultant, Echosens SA; Spouse, Consultant, Shinogi; Spouse, Consultant, Ligand Pharmaceuticals, Inc; Spouse, Stock options, Spring Bank Pharmaceuticals, Inc;

Spouse, Stock options, Allurion; Spouse, Stock options, Trio Healthcare; ;

Ramin Khorasani, MD, Boston, MA (Abstract Co-Author) Nothing to Disclose

Stuart G. Silverman, MD, Brookline, MA (Abstract Co-Author) Nothing to Disclose

Srinivasan Mukundan, MD, PhD, Durham, NC (*Abstract Co-Author*) Institutional research support, Siemens AG; Institutional research support, Canon Medical Systems Corporation; Consultant, Canon Medical Systems Corporation

Giles W. Boland, MD, Boston, MA (Abstract Co-Author) Nothing to Disclose

# For information about this presentation, contact:

llee22@bwh.harvard.edu

### PURPOSE

MRI is a critical tool in the diagnosis and staging of prostate cancer, but its availability can be limited by resource and workflow constraints. We assessed the impact of a multi-faceted Continuous Quality Improvement (CQI) initiative designed to improve patient access to, and availability of, multiparametric prostate MRI (mpMRI).

# METHODS

The CQI initiative was implemented at a tertiary-care academic medical center which performs 70,000 MRI exams annually. The CQI program involved the re-design of multiple elements of the prostate 3T MRI value chain, chiefly: the PI-RADS v2 compliant mpMRI protocol, including a transition from scanning with an endorectal coil to scanning without; and re-structuring of exam/resource scheduling. New process metrics were developed and implemented to inform and support the CQI program. The CQI period, from April 2016 - March 2018, was divided into four consecutive 6-month intervals: 1. In the Observation period (Apr - Sept 2016), baseline mpMRI slots allowed for 3 endorectal coil exams per day, at one MRI scanner on four weekdays; 2. Phase 1 (Oct 2016 -Mar 2017) increased mpMRI slots to 5 per day, at one scanner on four weekdays. A metric for MRI exam access, the number of days to the 3rd - next available exam, was measured starting in March 2017 at the end of Phase 1; 3. Phase 2 (Apr - Sept 2017) increased mpMRI slots to 7 per day, at one scanner on four weekdays, and the acquisition and implementation of a MRI scanning package that allowed for the introduction of a new MRI scanning protocol without an endorectal coil (maintaining PI-RADS v2 compliance); 4. Phase 3 (Oct 2017 - Mar 2018) completed the transition to mpMRI without endorectal coil, allowing for a total of 10 Prostate MRI exams per day, at expanded access to three 3T MRI scanners on weekdays and weekends alike, including evenings. Primary outcome measures were: a. access to (defined as 3rd -next available appointment, measured beginning March 2017) and b. availability of mpMRI (defined as percentage of weekly outpatient MRI operating hours from 0800-2000 hours during which mpMRI was offered). Secondary outcome measures were: c. mpMRI exam volume, d. mean mpMRI in-room exam time, e. mean time spent per day by a radiologist for endorectal coil placement, f. number of mpMRI exams flagged for CQI review. We used statistical process control (SPC) analysis for a. and chi-squared test of proportions for f. outcome measures.

### RESULTS

During the CQI period: a. mpMRI access improved significantly as days to the 3rd-next available appointment decreased from 21 days in March 2017 to <1 day (same day availability) in March 2018 (p<0.0001, SPC); b. mpMRI availability improved in each period: 14% (12/84 hrs) in the Observation period, 24% (20/84 hrs) in Phase 1, 33% (28/84 hrs) in Phase 2, and 100% (84/84 hours) in Phase 3; c. mpMRI volume increased in each period: 357 exams in Observation, 504 in Phase 1, 634 in Phase 2, 653 in Phase 3, an 83% increase overall; d. mpMRI mean in-room exam time decreased overall: 75 minutes in Observation, 83 min in Phase 1, 64 min in Phase 2, 41 min in Phase 3; a 45% overall reduction; e. mean daily time for endorectal coil placement decreased, and was eliminated in Phase 3: 41 minutes in Observation, 68 min in Phase 1, 61 min Phase 2, 0 min in Phase 3; f. the proportion of mpMRI exams submitted for CQI review did not differ significantly (p=0.36): Phase 1, 12 exams for review (2.4% of total); Phase 2, 15 exams for review (2.4%); Phase 3, 23 exams for review (3.5%).

# CONCLUSION

A multi-faceted CQI initiative resulted in improved access to and availability of mpMRI for patients. Optimizing the mpMRI value chain achieved same day availability, nearly doubled mpMRI volume, and maintained exam quality. Patient access to a critical resource in prostate cancer care was thus expanded, an important development given increasing demand for this exam.



# QI113-ED-MOB3

Improving Reporting of Lesion Location by Unifying the Acquisition Angles on Prostate MR in Our Trust - A Quality Improvement Project

Monday, Nov. 26 12:45PM - 1:15PM Room: QR Community, Learning Center Station #3

# Participants

Anu Kamalasanan, MBBS, Dundee, United Kingdom (*Abstract Co-Author*) Nothing to Disclose Magdalena Szewczyk-Bieda, MBBS, Dundee, United Kingdom (*Abstract Co-Author*) Nothing to Disclose Vilte Balcaityte, BSC, MBBS, Dundee, United Kingdom (*Presenter*) Nothing to Disclose

#### For information about this presentation, contact:

vilte.balcaityte1@nhs.net

#### PURPOSE

There is increasing clinical expectation for precise communication on location and local extent of suspicious prostatic lesions detected on MRI to aid targeted biopsy and focal treatment. This in turn brings pressure on reporting radiologists to use standardised reporting with reproducible terminology and template localisation maps. Orientation of prostate gland within pelvis is highly variable and dependant on its size, shape and presence of benign prostatic hyperplasia. There is conflicting evidence in the literature on the preferred angle of acquisition for pelvic sequences, when scanning prostate gland. For example, ESUR guidelines 2012 suggests 'plan to rectum' and consensus of uroradiologists of UK favours 'plan true axial', for ease of planning and uniformity of scanning. We have 5 MRI scanners in 3 different locations within our trust performing prostate imaging on unsupervised lists. No unified acquisition angle planning protocol for prostate MR existed in our institution. Various planning angles of acquisition were used, including 'true axial', 'to rectum', 'to prostate' and other combinations of both. This variation in prostate imaging made precise reporting challenging. The lack of understanding of reasoning behind the expectation and the difficulty in identifying the prostate and lack of confidence among radiographers performing these studies. This quality improvement project was born out of this mix and the main aim was to unify the prostate planning protocol for our trust - with scans planned to prostate chosen as the optimal one (98% target). This protocol, although the most difficult to follow, is ideal for reporting as it allows visualisation of anterior and posterior gland at the same level on axial slices.

### **METHODS**

A retrospective review of all prostate MRI was performed throughout our trust for a period of 2 months to assess variation in current practice and to establish a need for change. T2 axial and sagittal images were reviewed to assess acquisition angles. The scans were then categorised into 6 categories - 'true axial', 'to rectum' and 'to prostate' (which were accepted as satisfactory) and other combinations (such as true axial/to rectum, true axial/to prostate, to rectum/to prostate) which were not deemed acceptable. Training and education workshops for the radiographers were organised at the 3 separate imaging sites on how to identify the prostate in the sagittal sequence with reproducible landmarks. Time for teething issues to be sorted out was allowed and followed by 2 month prospective review of all prostate MRI using same criteria as 1st round.

### RESULTS

1st round: Axial and sagittal images reviewed by 2 registrars. The planning series were divided into defined categories. Although the first 3 were accepted as satisfactory for the purpose of this round the main aim was to unify planning. The data was analysed using excel spreadsheet and simple mathematic equations. Number of scans performed in 2 months = 47 Satisfactory planning = 28 (60%) Planned to prostate = 15 (32%) of total Intervention: Small group tutorials and workshops conducted for the radiographers in our health trust with hands-on workshop with aim to recognise reproducible landmarks and plan 'to prostate'. The landmark was identified as 'v-point' which is the anatomical transition of bladder neck into prostatic urethra (see PDF upload) as agreed by all reporting radiologists. Templates were displayed in each site for reference. Trial period with open access to the registrars taking part in this project was given to iron out teething issues. 2nd round: At the end of 4 months a prospective data gathering for 2 months performed exactly like the 1st round. Total number of scans: 35 Planned to prostate: 34 (97%) Planned to rectum: 1 (3%)

### CONCLUSION

Unification of prostate planning was achieved with 97% planned 'to prostate' at the end of 2nd round of data collection (target met). This resulted in a more confident work force and ease of reporting for the radiologists with more precise communication to clinicians. There are some limitations to this protocol, which were recognised and identified.



# QI115-ED-MOB4

Implementation of TIRADS Ultrasound Reporting in a Pediatric and Adult Practice Group: What We Learned

Monday, Nov. 26 12:45PM - 1:15PM Room: QR Community, Learning Center Station #4

FDA Discussions may include off-label uses.

#### Participants

Kavya Sudanagunta, MD, Lexington, KY (*Presenter*) Nothing to Disclose Kimberly E. Applegate, MD, MS, Lexington, KY (*Abstract Co-Author*) Nothing to Disclose Adrian A. Dawkins, MD, Lexington, KY (*Abstract Co-Author*) Nothing to Disclose Wang Xin, Lexington, KY (*Abstract Co-Author*) Nothing to Disclose Leslie Anaskevich, Lexington, KY (*Abstract Co-Author*) Nothing to Disclose

### PURPOSE

Thyroid nodules are one of the most common finding on ultrasound (US) with a prevalence of 20-69% with at least 80 % of them being benign [ref]. Current practice at our institution does not use a standard lexicon for description of thyroid nodules, nor recommendations for timing of follow up US nor when to biopsy these lesions. Inconsistent reporting of these nodules leads to confusion about recommendations for further management and to unnecessary resource expenditures. The purpose of this study is to standardize the evaluation of thyroid nodules on ultrasound through the implementation of American College of Radiology recommended Thyroid Imaging Reporting and Data System (TIRADS). The specific AIM 1 was to use TIRADS reporting in 90% of children and 75% of adults within the first 6 months after implementation. Specific AIM 2 was to decrease the frequency of inappropriate biopsy by 20% and decrease the frequency of inappropriate follow-up thyroid US by 30%.

### METHODS

The retrospective study comprised of both adults and pediatric patients who underwent sonography for thyroid nodules from Jan 1, 2017 to Dec 31, 2017. The two departmental divisions implemented the TIRADS with some differences, with the pediatric division adopting earlier, mandatory use, and the abdominal division using a more gradual, optional approach (Fig 1). US reports issued by the interpreting radiologists were retrospectively reviewed for nodule description, and presence/clarity of follow-up recommendations, before and after the implementation of TIRADS. Nodules were assigned points for each feature, and the points were totaled to determine the final TIRADS level (TR1-TR5). The recommendations given by the radiologist in the report and which would have been given according to TIRADS level of the nodule, were compared before and after implementation of Intervention. TIRADS Structured reporting began July 2017. All biopsy outcomes were compared to the assigned TIRADS score.

#### RESULTS

A total of 265 adult thyroid ultrasounds, of which 121 were after implementation and 144 baseline, were studied (Fig.2). A total of 27 pediatric thyroid nodule ultrasounds were included in the study, of which 14 baseline and 13 after implementation. Utilization of TIRADS lexicon or template reached up to 81% towards the last month for adult patient reports. Overall pediatric radiologists utilized TIRADS 50% of the time after implementation but the numbers were small. Both biopsy and follow up recommendation rates decreased with use of TIRADS (Fig. 3): The frequency with which pediatric radiologists and adult radiologists provided 'No or Unclear Recommendations' reduced from 21.4% to 15.3% and 19.4% to 14.06% respectively post intervention. Adult inappropriate biopsies-as scored by the TIRADS method were reduced by 50% and inappropriate follow ups by 84% post intervention. In continued interaction amongst the team and the two divisions, there was a sense that the template, after modification was useful. In discussion with two key referring clinicians, they felt it was useful, however, the prepared email survey for all referring providers has yet to be performed.

# CONCLUSION

There was steady increased use in the implementation of TIRADS, with most radiologists gradually opting to use this reporting framework over the measured 6-month period. The data suggest that use of the TIRADS lexicon standard reporting led to more consistent reporting of nodules which reduced the frequency of inappropriate biopsies and follow ups.



# RO207-SD-MOB1

Multiple Metastatic Melanoma: Pretreatment Contrast-Enhanced CT Texture Parameters as Predictive Biomarkers of Survival in Patients treated with Pembrolizumab

Monday, Nov. 26 12:45PM - 1:15PM Room: RO Community, Learning Center Station #1

#### Awards Student Travel Stipend Award

# Participants

Carole Durot, MD, Reims, France (*Presenter*) Nothing to Disclose Sebastien Mule, MD,PhD, Creteil, France (*Abstract Co-Author*) Nothing to Disclose Philippe A. Soyer, MD, PhD, Paris, France (*Abstract Co-Author*) Consultant, Guerbet SA Aude Marchal, Reims, France (*Abstract Co-Author*) Nothing to Disclose Florent Grange, Reims, France (*Abstract Co-Author*) Nothing to Disclose Christine C. Hoeffel, MD, Reims, France (*Abstract Co-Author*) Nothing to Disclose

# PURPOSE

To determine whether texture analysis features on pretreatment contrast-enhanced computed tomography (CT) images can predict progression-free survival (PFS) and overall survival (OS) in patients with multiple metastatic (MM) melanoma treated with Pembrolizumab.

# METHOD AND MATERIALS

This institutional review board-approved retrospective study included 31 patients from one university hospital with MM melanoma treated with Pembrolizumab. Texture analysis of 74 metastatic lesions was performed on CT scanners obtained within one month prior to treatment. Mean grey-level, entropy, kurtosis, skewness, mean of positive pixels and standard deviation values were derived from the pixel distribution histogram before and after spatial filtration at different texture scales, ranging from fine to coarse. Univariate and multivariate Cox regression analysis were performed to identify independent predictors of PFS and OS.

#### RESULTS

Median PFS was 91 days (range 35-968) and median OS was 321 days (range 42-1095). Skewness at medium (hazard ratio HR = 3.82, p = 0.046) and at coarse (HR = 4.25, p = 0.017) texture scales independently predicted OS. No textural feature was identified as an independent predictor of PFS. Intrareader agreement regarding CT texture parameters was excellent for all textures parameters (skewness: ICC = 0.86). Interreader agreement was good for all textures parameters (skewness: ICC = 0.62).

# CONCLUSION

Pretreatment CT texture analysis-derived tumor skewness may act as predictive biomarker of overall survival in patients with advanced MM melanoma treated with Pembrolizumab.

# **CLINICAL RELEVANCE/APPLICATION**

Pretreatment contrast-enhanced CT Texture analysis may allow independent prediction of survival in patients with MM melanoma treated with pembrolizumab and may help to identify patients who are likely to benefit from this therapy.



### RO208-SD-MOB2

The D value of Diffusion Kurtosis Imaging May Early Predict Treatment Response Within 7 Days After Radiotherapy Initiation in Loco-Regionally Advanced Nasopharyngeal Carcinoma

Monday, Nov. 26 12:45PM - 1:15PM Room: RO Community, Learning Center Station #2

# Participants

Qiuyuan Yue, Fuzhou, China (*Presenter*) Nothing to Disclose Yunbin Chen, MD, Fuzhou, China (*Abstract Co-Author*) Nothing to Disclose Dechun Zheng, MS, Fuzhou, China (*Abstract Co-Author*) Nothing to Disclose Ying N. Chen, PhD, Fuzhou, China (*Abstract Co-Author*) Nothing to Disclose

# PURPOSE

To investigate whether the parameters of Diffusion Kurtosis Imaging (DKI) may early predict the treatment response in locoregionally advanced nasopharyngeal carcinoma (NPC) patients who received sequential neoadjuvant chemotherapy (NAC) and radical intensity-modulated radiotherapy (IMRT).

# METHOD AND MATERIALS

52 consecutive, and newly diagnosed advanced NPC patients who received sequential two cycles of platinum-based NAC, following radical IMRT and completed three scheduled MRI scans at baseline (Pre-Tx), after two cycles (42nd days) of NAC (Pre-RT), one week after RT initiation (RT-1w) were enrolled in current study. The absolute change between RT-1w and Pre-Tx, RT-1w and Pre-RT, Pre-RT and Pre-Tx were defined as  $\Delta 1, \Delta 2$  and  $\Delta 3$ . The similar definitions were applied to DKI parameters. Patients were divided into responder group (RG) and non-responder group (NRG) in the third months after completion of RT according to the response evaluation criteria in solid tumors (RECIST 1.1v). Mann-Whitney U test, student's t-test, paired  $\chi 2$  test, univariate and multivariate logistic regression, and receiver operating characterstics (ROC) curves were applied in statistical analysis.

### RESULTS

17 patients achieved completed remission (CR), 26 patients achieved partial remission (PR) and 9 patients remained stable disease (SD). Hence, 43 patients were classified as RG and 9 patients were classified as NRG. Univariate logistic regression analysis showed that D1 (P=0.022), D2 (P=0.025),  $\Delta$ D2 (P=0.008) and Chemotherapy (CT) cycles (P=0.044) were significant predictor and clinical stage was borderline significant predictor (P=0.051) for tumor response when defined RG as the primary endpoint. Next, only  $\Delta$ D2 (Adjusted OR 19.36; P=0.021) and CT cycles (Adjust OR 18.17; P=0.022) were identified as independent predictors in multivariate logistic regression analysis. In addition, when defined CR as the primary endpoint, only  $\Delta$ D2 was identified as the significant predictor (P=0.047).

### CONCLUSION

The absolute change of D value within 7 days after RT initiation and CT cycles may serve as the independent predictors for tumor response in loco-regionally advanced NPC patients who undergo sequential NAC and IMRT.

# **CLINICAL RELEVANCE/APPLICATION**

DKI may help to identify proper candidates to undergo sequetial NAC and IMRT thus provide a reference of tumor radiosensitivity to optimize individual therapeutic strategies.



### RO209-SD-MOB3

A Phase II, Proof-of-Concept Clinical Study of an Oral Mouth Rinse Containing Sandalwood Oil (SAO) for the Prevention of Oral and Oropharyngeal Mucositis Associated with (Chemo-) Radiation Therapy in Head and Neck Cancer Patients

Monday, Nov. 26 12:45PM - 1:15PM Room: RO Community, Learning Center Station #3

FDA Discussions may include off-label uses.

#### Participants

Chul S. Ha, MD, San Antonio, TX (*Presenter*) Investigator, Santalis Pharmaceuticals, Inc Ying Li, MD, San Antonio, TX (*Abstract Co-Author*) Investigator, Santalis Pharmaceuticals, Inc Carol Jenkins, RN,MS, San Antonio, TX (*Abstract Co-Author*) Nothing to Disclose Corey Levenson, PhD, San Antonio, TX (*Abstract Co-Author*) Officer, Santalis Pharmaceuticals

### PURPOSE

Mucositis is one of the most debilitating side effects in patients treated with (chemo-) radiation therapy for head and neck cancer. This study was intended to evaluate the efficacy in alleviating mucositis, safety and tolerability of SAO (0.25% aqueous solution of an anti-inflammatory and anti-microbial essential oil from Santalum album trees).

### **METHOD AND MATERIALS**

Patients to be treated with (chemo-) radiation therapy (>= 60 Gy) for cancers of oral cavity/oropharynx were asked to swish and gargle for 30 seconds, and spit, with 15 ml of the SAO three times a day throughout the radiation therapy. Pain in the oral cavity/oropharynx was measured using the numerical rating pain scale (NRPS) and mucositis was graded using the RTOG scale every week. Our data were compared with historical data in table 2 (incidence of mucositis), figure 1 (mean mucositis grade) and figure 2 (mean oral pain grade) from MD Anderson Cancer Center (MDACC) (doi:10.1016/j.ijrobp.2007.01.053) and table 4 (incidence of mucositis) from Memorial Sloan Kettering Cancer Center (MSKCC) (doi:10.1016/j.ijrobp.2010.10.041).

### RESULTS

Fourteen subjects were enrolled but 6 withdrew (4 of them due to taste/smell of the rinse, 1 due to fatigue, 1 due to perceived ineffectiveness of the rinse). Among the 8 who completed the course of SAO treatment, 6 were treated with chemo-radiation and 2 with radiation only. IMRT was used for everyone. The median dose was 6,996 cGy in 33 fractions. There were no serious adverse events from SAO. The mean RTOG mucositis grades from weeks 3,6 and 9 were 1.125, 2.125 and 1.875. Two of 8 patients experienced mucositis >= 3. The corresponding mean NRPS were 3.700, 4.988 and 3.875.

# CONCLUSION

The incidence of mucositis >= 3 were 70% from MDACC and 22% from MSKCC. Distribution of our mean NRPS and RTOG mucositis data compared favorably against figures 1 and 2 from MDACC. Though SAO was difficult to use due to poor taste/smell, it was otherwise well tolerated and appears to have enough signal to warrant further development as a potential alleviator of mucositis.

### **CLINICAL RELEVANCE/APPLICATION**

This is a proof-of-concept clinical trial for an oral mouth rinse containing Sandalwood Oil for the prevention of mucositis associated with (chemo-) radiation therapy in head and neck cancer patients. We believe our results have generated enough signal to pursue further development of this preparation.



# UR181-ED-MOB7

Multi-Modality Review of Upper Tract Urothelial Carcinoma and Its Mimics

Monday, Nov. 26 12:45PM - 1:15PM Room: GU/UR Community, Learning Center Station #7

# Awards Certificate of Merit

### Participants

Kien Tran, MD, Royal Oak, MI (*Presenter*) Nothing to Disclose Monisha Shetty, MD, Royal Oak, MI (*Abstract Co-Author*) Nothing to Disclose Christine O. Menias, MD, Chicago, IL (*Abstract Co-Author*) Nothing to Disclose Syed Zafar H. Jafri, MD, Royal Oak, MI (*Abstract Co-Author*) Nothing to Disclose

# For information about this presentation, contact:

kien.tran@beaumont.edu

#### **TEACHING POINTS**

1. To review the pathogenesis of upper tract urothelial carcinoma 2. To review characteristic multimodality imaging features of upper tract urothelial carcinoma 3. To discuss staging of upper tract urothelial carcinoma and role of imaging in diagnosis 4. To provide a focused imaging review of common and uncommon mimics of upper tract urothelial carcinoma. Specific case examples will be used to illustrate key features and distinguishing factors that may aid in making the diagnosis.

### TABLE OF CONTENTS/OUTLINE

General Overview of Upper Tract Urothelial Carcinoma Epidemiology Patterns of Tumor Spread and Pathogenesis -Multifocality and recurrence -Synchronous and metachronous tumor development Multimodality Imaging Appearances of Upper Tract Urothelial Carcinoma Staging of Upper Tract Urothelial Carcinoma -TNM Staging Classification -Staging Groups Role of Imaging in Diagnosis and Distinguishing Early-stage and Advance-stage Tumors -Ultrasound -CT -MRI -Pyelography Additional sample cases and mimics - Renal pelvic amyloidosis -Perirenal lymphoma -Subepithelial hemorrhage -Infiltrating renal cell carcinoma -Squamous cell carcinoma of ureter -Ureteral endometriosis -Obstruction/infection -Schwannoma -Metastases -Others Summary and Conclusion

#### **Honored Educators**

Presenters or authors on this event have been recognized as RSNA Honored Educators for participating in multiple qualifying educational activities. Honored Educators are invested in furthering the profession of radiology by delivering high-quality educational content in their field of study. Learn how you can become an honored educator by visiting the website at: https://www.rsna.org/Honored-Educator-Award/ Christine O. Menias, MD - 2013 Honored EducatorChristine O. Menias, MD - 2014 Honored EducatorChristine O. Menias, MD - 2015 Honored EducatorChristine O. Menias, MD - 2016 Honored EducatorChristine O. Menias, MD - 2017 Honored EducatorChristine O. Menias, MD - 2018 Honored Educator



### UR182-ED-MOB8

Testicular Torsion Mimics: A Review of Alternative Testicular Pathologies That Resemble Torsion

Monday, Nov. 26 12:45PM - 1:15PM Room: GU/UR Community, Learning Center Station #8

#### Participants

Allison Forrest, BA, Rochester, NY (*Abstract Co-Author*) Nothing to Disclose Akshaar N. Brahmbhatt, MD, Rochester, NY (*Presenter*) Nothing to Disclose Vikram S. Dogra, MD, Rochester, NY (*Abstract Co-Author*) Editor, Wolters Kluwer nv;

### For information about this presentation, contact:

akshaar\_brahmbhatt@urmc.rochester.edu

### **TEACHING POINTS**

Testicular torsion commonly occurs in younger patients usually under 25. Early and accurate diagnosis is key as testicular compromise can occur within a few hours. Depending on the age of the patient and other factors, orchiectomy rates can be as high as 49.9%. There are important considerations when evaluating imaging related to possible testicular torsion. 1. Radiologists must understand the basic principles of torsion and common sonographic findings. 2. Radiologists should be aware of other etiologies with similar imaging findings that can mimic testicular torsion and the history and nuanced imaging characteristics that can aid in differentiation. Here we will present a brief overview of testicular torsion. Then we will explore several other etiologies that can mimic testicular compromise of the testes, through a series of cases.

#### **TABLE OF CONTENTS/OUTLINE**

-Basics of Torsion and Sonographic Findings and Technical Limitations. -Types of Torsion Mimics Type and imaging review -Extrinsic vascular compression (Hernia, Hydrocele, Hematoma, etc) -Intrinsic vascular abnormality (Vasculitis, Vasoconstriction, Embolism, etc) -Inherent testicular pathology. (Mass, Orchitis, Xanthogranuomatous, Parasitic, etc) -Summary



#### VI007-EB-MOB

Emergency with a Birth Canal Injury Due to Vaginal Delivery? Interventional Radiology Will Save Your Patient - Usefulness of Embolization for Birth Canal Injury in Vaginal Delivery

Monday, Nov. 26 12:45PM - 1:15PM Room: VI Community, Learning Center Hardcopy Backboard

# Participants

Sung-Joon Park, MD, Seoul, Korea, Republic Of (*Presenter*) Nothing to Disclose Tae Seok Seo, MD, PhD, Seoul, Korea, Republic Of (*Abstract Co-Author*) Nothing to Disclose Myung Gyu Song, MD, Seoul, Korea, Republic Of (*Abstract Co-Author*) Nothing to Disclose

# For information about this presentation, contact:

dpcult.md@hanmail.net

# **TEACHING POINTS**

To understand <u>the role of interventional radiologic embolization</u> in active bleeding due to birth canal injury. To understand <u>which</u> <u>vessels are more likely to be associated</u> with birth canal injury. To understand <u>the technical concept</u> of arterial embolization for birth canal injury.

# TABLE OF CONTENTS/OUTLINE

Our exhibit will be divided into 3 sections and presented with illustration and relevant cases regarding <u>usefulness of arterial</u> <u>embolization for birth canal injury in vaginal delivery</u>. 1. Background and anatomy of internal iliac artery associated with birth canal injury Uterine artery Vaginal artery Internal pudendal artery 2. Technical aspect of embolization for birth canal injury Embolic material Steps of procedure 3. Clinical application of embolization for birth canal injury Experience with 12 cases Clinical outcome



### VI159-ED-MOB7

# **Flowing Through Time and Space**

Monday, Nov. 26 12:45PM - 1:15PM Room: VI Community, Learning Center Station #7

### Awards Certificate of Merit

#### Participants

Ece Meram, MD, Madison, WI (Presenter) Nothing to Disclose

Carson Hoffman, Madison, WI (Abstract Co-Author) Nothing to Disclose

Gabe Shaughnessy, PhD, Madison, WI (Abstract Co-Author) Nothing to Disclose

Martin Wagner, PhD, Madison, WI (Abstract Co-Author) Owner, LiteRay Medical LLC

Christopher J. Francois, MD, Madison, WI (*Abstract Co-Author*) Departmental research support, General Electric Company; Michael Speidel, PhD, Madison, WI (*Abstract Co-Author*) Nothing to Disclose

Oliver Wieben, PhD, Madison, WI (Abstract Co-Author) Research support, General Electric Company

Charles M. Strother, MD, Madison, WI (*Abstract Co-Author*) Research Consultant, Siemens AG Research support, Siemens AG License agreement, Siemens AG

Thomas M. Grist, MD, Madison, WI (*Abstract Co-Author*) Institutional research support, General Electric Company; Institutional research support, Bracco Group; Institutional research support, Siemens AG; Institutional research support, Hologic, Inc; Institutional research support, McKesson Corporation; Stockholder, Elucent; Stockholder, HistoSonics, Inc;

Charles A. Mistretta, PhD, Madison, WI (*Abstract Co-Author*) Founder, Mistretta Medical Intellectual Property Licensing Activities; Research, Siemens AG; Co-Founder, LiteRay Medical LLC

Paul F. Laeseke, MD, PhD, Madison, WI (*Abstract Co-Author*) Consultant, NeuWave Medical, Inc; Shareholder, Elucent Medical; Shareholder, HistoSononics; Shareholder, McGinley Orthopaedics

# For information about this presentation, contact:

meram@wisc.edu

### **TEACHING POINTS**

Angiographic imaging modalities have revolutionized the way vascular information can be utilized in the clinical setting. They provide extensive anatomical detail on vasculature, help diagnose vascular disease processes, and even allow prompt interventions such as stenting and embolization. Aside from the vascular anatomy, recent advances also provide information on the hemodynamics within blood vessels including blood flow and velocity. This exhibit aims (1) To review the evolution of angiographic imaging modalities, (2) To discuss hemodynamics and its clinical implications, (3) To illustrate imaging methods that can quantify blood flow, and (4) To highlight the use of flow imaging methods with case examples.

### **TABLE OF CONTENTS/OUTLINE**

A. Evolution of Angiography and Flow Imaging 1. Current and Emerging Angiographic Modalities 2D-Digital Subtraction Angiography (DSA) CT Angiography (CTA) MR Angiography (MRA) 3D-DSA Time-resolved 3D-DSA (4D-DSA) 4D-CTA 2. Hemodynamics and Features of Blood Flow 3. What can be used to quantify flow in the vasculature? Doppler Ultrasonography 4D Flow MRI 4D-DSA Other methods B. Clinical Applications of Flow Imaging Methods Case Examples (Not just pretty pictures!) Practical Points: What to use, when to use? C. Quiz



# VI160-ED-MOB9

This is Glue, Strong Stuff: Non-Vascular Applications of N-butyl-2-cyanoacrylate (NBCA) and Review of Technique

Monday, Nov. 26 12:45PM - 1:15PM Room: VI Community, Learning Center Station #9

**FDA** Discussions may include off-label uses.

### Awards

# **Certificate of Merit**

# Participants

Lisa Rauschert, MD, Providence, RI (*Presenter*) Nothing to Disclose Douglas T. Hidlay JR, MD, Providence, RI (*Abstract Co-Author*) Nothing to Disclose Sun Ho Ahn, MD, Providence, RI (*Abstract Co-Author*) Nothing to Disclose Lauren S. Park, BA, Providence, RI (*Abstract Co-Author*) Nothing to Disclose Matthew E. Pouw, MD, Providence, RI (*Abstract Co-Author*) Nothing to Disclose

# For information about this presentation, contact:

lisa.rauschert@lifespan.org

# **TEACHING POINTS**

Understand the mechanism of action of n-butyl-2-cyanoacrylate (NBCA) glue Review of non-vascular applications of NBCA in the body Review of technique, pearls, and potential complications of NBCA applications

# **TABLE OF CONTENTS/OUTLINE**

1. Background and Mechanism of action of N-butyl-2-cyanoacrylate (NBCA) glue 2. Advantages and disadvantages of NBCA as an embolic medium a. Speed b. Distal Delivery c. Expense 3. Proper technique for NBCA embolization a. Micro-catheter use b. D5 preparation c. Common dilutions of NBCA 4. Review of Nonvascular applications/indications a. Biliary - cutaneous fistula tract embolization b. Urinary leaks - permanent urinary occlusion c. Lymphatic leaks - thoracic duct embolization, post-operative lymphatic leaks 5. Tips and Pearls



### VI219-SD-MOB1

# Clinical Impact of Collateral Circulation in Patients with Median Arcuate Ligament Syndrome

Monday, Nov. 26 12:45PM - 1:15PM Room: VI Community, Learning Center Station #1

#### Participants

Subin Heo, Suwon, Korea, Republic Of (*Abstract Co-Author*) Nothing to Disclose Hye Jin Kim, MD, Suwon, Korea, Republic Of (*Presenter*) Nothing to Disclose Bohyun Kim, MD, Suwon, Korea, Republic Of (*Abstract Co-Author*) Research Grant, Bracco Group Jimi Huh, MD, Suwon, Korea, Republic Of (*Abstract Co-Author*) Nothing to Disclose Jei Hee Lee, MD, Suwon, Korea, Republic Of (*Abstract Co-Author*) Nothing to Disclose Jai Keun Kim, MD, PhD, Suwonsi, Korea, Republic Of (*Abstract Co-Author*) Nothing to Disclose

# For information about this presentation, contact:

hjkotter@gmail.com

# PURPOSE

To analyze the computed tomographic (CT) findings and medical records of patients diagnosed with median arcuate ligament syndrome (MALS), and to evaluate the possible risk factors associated with vascular complications that develop in patients with MALS.

#### **METHOD AND MATERIALS**

This retrospective study was approved by the institutional review board, and the requirement to obtain informed consent was waived. A total of 37 consecutive patients were diagnosed with MALS using both axial and sagittal CT reconstruction imaging at a single institution over a seven year period. Dynamic contrast-enhanced CT data, medical records, and angiography results were reviewed.

#### RESULTS

Thirty-two (86.5%) patients were asymptomatic and incidentally diagnosed with MALS using CT. Seventeen (45.9%) patients exhibited significant arterial collateral circulations and nine (24.3%) were found to have splanchnic artery aneurysms, including one (2.7%) with acute bleeding secondary to aneurysm rupture. Peripancreatic vascular network including pancreaticoduodenal arcades and dorsal pancreatic artery was the most common site for development of both collateral circulations (16/22, 72.7%) and aneurysms (9/16, 56.3%). Splanchnic artery aneurysms were significantly more common in patients with collateral circulations (8/17, 47.1%) compared to those without collateral circulations (1/20, 5%) (P < 0.01). At least one peripancreatic vascular aneurysm was found in five (55.6%) of nine patients with splanchnic artery aneurysms.

# CONCLUSION

Splanchnic artery aneurysms are not uncommon in asymptomatic patients with collateral circulations caused by significant celiac trunk stenosis or obstruction due to median arcuate ligament. Therefore, careful imaging evaluation is necessary in patients with peripancreatic collateral circulations associated with MALS and regular follow-up is recommended for possibility of aneurysm development and rupture. Prophylactic endovascular treatment should be specifically performed in patients with pancreaticoduodenal arcade aneurysms to prevent life-threatening aneurysm rupture regardless of size.

#### **CLINICAL RELEVANCE/APPLICATION**

Our study showed the pancreaticoduodenal arcade aneurysms detected in MALS patients should be prophylactically treated due to the high potential for life-threatening rupture regardless of size.



### VI220-SD-MOB2

Inconclusive Computed Tomography Angiography for Pulmonary Embolism: The Importance of Significative Venous Compression in the Thoracic Outlet

Monday, Nov. 26 12:45PM - 1:15PM Room: VI Community, Learning Center Station #2

# Participants

Andrei S. Albuquerque, MD, Sao Paulo, Brazil (*Presenter*) Nothing to Disclose Andre P. Romualdo, Sao Paulo, Brazil (*Abstract Co-Author*) Nothing to Disclose Cecil W. Carvalho, Sao Paulo, Brazil (*Abstract Co-Author*) Nothing to Disclose Paulo Savoia, MD, Sao Paulo, Brazil (*Abstract Co-Author*) Nothing to Disclose Rafael P. Oliveira, MD, Sao Paulo, Brazil (*Abstract Co-Author*) Nothing to Disclose Ibraim M. Pinto, MD, PhD, Sao Paulo, Brazil (*Abstract Co-Author*) Nothing to Disclose

#### For information about this presentation, contact:

andrei.albuquerque@grupofleury.com.br

#### PURPOSE

The objective of our study is to analyze the presence of significant venous compression in the thoracic outlet as a important cause of poor pulmonary artery opacification in the computed tomography angiography studies for pulmonary embolism (CTAP).

#### **METHOD AND MATERIALS**

We retrospectively analyzed 110 CTAP performed between January 1 and March 31, 2018 at our institution. All the exams were performed with the same protocol of acquisition (bolus tracking in the pulmonary artery, level of detection of 80 UH, delay of 5s and time of scan of 3s, in the caudal - cranial direction), the same type of venous access (18G catheter in the antecubital vein), the same volume and type of contrast (60 ml of 350 mg/ml) and the same rate of infusion (5 ml/s). Measurement of the density in the pulmonary artery of all patients was performed, with values lower than 250 Hounsfield units being considered as poor opacification. Significant venous compression in the thoracic outlet was considered as a luminal reduction greater than 70% of the vessel's transverse area, using as reference the vessel segment without compression.

# RESULTS

25 of the 110 CATP (22.7%) evaluated had poor pulmonary artery opacification. Of these 25 exams, 22 (88%) had significant venous compression in the thoracic outlet. In 10 (45.4%) of these cases, the compression was located in the pre-scalene space, 9 (40.9%) in the costoclavicular space and 3 (13.6%) in the retropectoralis minor space.

### CONCLUSION

Despite the use of a protocol optimized for CTPA, some of the studies present poor opacification of the pulmonary arteries. Significant venous compression in the thoracic outlet seems to play a relevant role in these cases, presumably by reducing the effective flow velocity of the constrat column.

# **CLINICAL RELEVANCE/APPLICATION**

When acquiring an inconclusive CTAP, the radiologist must decide whether to perform the study again. If he chooses to repeat, we recommend to analyze in advance if there is significant venous compression in the thoracic outlet. If there is, possibly the new study will be similar to the first, with poor opacification of the pulmonary arteries. Therefore, considering that significant venous compression is an important cause of poor pulmonary artery opacification, despite an optimized acquisition protocol, we suggest modifying the position of the upper limb with the venous access to a higher position or even beside the body.



# VI221-SD-MOB3

# Radiopaque 3D Printed Phantoms for Simulation and Development of CT-Guided Procedures

Monday, Nov. 26 12:45PM - 1:15PM Room: VI Community, Learning Center Station #3

### Participants

Maximilian Nunninger, MD, Berlin, Germany (*Presenter*) Nothing to Disclose Felix B. Schwarz, Berlin, Germany (*Abstract Co-Author*) Nothing to Disclose Marco Ziegert, Berlin, Germany (*Abstract Co-Author*) Nothing to Disclose Victor Braun, Berlin, Germany (*Abstract Co-Author*) Nothing to Disclose Bernd K. Hamm III, MD, Berlin, Germany (*Abstract Co-Author*) Research Consultant, Canon Medical Systems Corporation; Stockholder, Siemens AG; Stockholder, General Electric Company; Research Grant, Canon Medical Systems Corporation; Research Grant, Koninklijke Philips NV; Research Grant, Siemens AG; Research Grant, General Electric Company; Research Grant, Bayer AG; Research Grant, Guerbet SA; Research Grant, Bracco Group; Research Grant, B. Braun Melsungen AG; Research Grant, KRAUTH medical KG; Research Grant, Boston Scientific Corporation; Equipment support, Elbit Imaging Ltd; Investigator, CMC Contrast AB

Michael Scheel, Berlin, Germany (*Abstract Co-Author*) Nothing to Disclose Paul Jahnke, MD, Berlin, Germany (*Abstract Co-Author*) Nothing to Disclose

# For information about this presentation, contact:

maximilian.nunninger@charite.de

#### PURPOSE

Radiopaque 3D printing can be modified to construct detailed anthropomorphic phantoms of individual patients for CT-guided procedures. The aim was to construct and use such phantoms to develop a novel ultra low dose protocol for CT-guided periradicular infiltration.

#### **METHOD AND MATERIALS**

In a first step, five phantoms were constructed from patient CT data sets using a modified approach of radiopaque 3D printing with aqueous potassium iodide solution (c = 1 g/mL). The CT images were printed on paper, which were stacked in alternation with polyethylene foam sheets, cut to the patient shape and covered with a nontransparent film. In a second step, the phantoms were used to develop an ultra low dose protocol for periradicular infiltration, using only scout imaging for precise planning of needle placement. 50 needle placements were performed with the novel protocol. Dose and number of image acquisitions were compared with a clinical cohort of 70 procedures performed with the conventional protocol.

### RESULTS

The patient phantoms constructed with the modified radiopaque 3D printing technique provided a detailed visualization of the patient anatomy and allowed realistic CT-guided needle navigation. CT-guided periradicular infiltration was feasible with metrics measured on the scout images (needle access point, puncture depth, angulation). Using this technique, the number of acquired single shot images could be reduced by >60% and the overall dose could be reduced by >90% in comparison with the conventional protocol.

# CONCLUSION

Radiopaque 3D printed phantoms allow realistic simulation of CT-guided periradicular infiltration. Training and development of interventional protocols on these phantoms yield potential for procedure optimization and dose reduction.

#### **CLINICAL RELEVANCE/APPLICATION**

Procedure optimization on radiopaque 3D printed patient phantoms can reduce dose and improve patient safety.



### VI222-SD-MOB4

### Endovascular Uterine Artery Embolization in Symptomatic Leiomyomas: A Single Center Experience

Monday, Nov. 26 12:45PM - 1:15PM Room: VI Community, Learning Center Station #4

#### **Participants**

Cristina Alvarez, Ciudad Autonoma de Buenos Aires, Argentina (*Abstract Co-Author*) Nothing to Disclose Carolina Parada Villavicencio, MD, Buenos Aires, Argentina (*Presenter*) Nothing to Disclose Vanessa Munoz, Ciudad Autonoma de Buenos Aires, Argentina (*Abstract Co-Author*) Nothing to Disclose Carlos D. Bleise SR, MD, Capital Federal, Argentina (*Abstract Co-Author*) Nothing to Disclose Javier O. Lundquist, MD, Buenos Aires, Argentina (*Abstract Co-Author*) Nothing to Disclose Nestor Kisilevsky, Ciudad Autonoma de Buenos Aires, Argentina (*Abstract Co-Author*) Nothing to Disclose Pedro Lylyk, MD, Buenos Aires, Argentina (*Abstract Co-Author*) Consultant, Cardiatis SA; Consultant, Stryker Corporation

#### For information about this presentation, contact:

cparada@sagradafamilia.com.ar

#### PURPOSE

To report our experience with uterine artery embolization (UAE) techniques as the endovascular treatment for women with symptomatic uterine leiomyomas.

### METHOD AND MATERIALS

We retrospectively review the clinical charts and imaging records of 196 patients with symptomatic uterine leiomyomas who underwent endovascular treatment with uterine artery embolization between the period of 2011 and 2015. Structural modifications of the uterus and myomas as well as clinical symptoms following the interventional procedures were recorded. Endocavitary ultrasound (US) and magnetic resonance imaging (MRI) were performed previous to surgery and three months after for follow up. A questionnaire for grading of clinical symptoms and patient satisfaction rates was completed by the patients. Complications related to the procedure and successful pregnancy cases post-embolization were also recorded.

#### RESULTS

The average hospitalization time was 26 hours (minimum 14 - maximum 56). Seven patients (3,5 %) were readmitted during the first week after the procedure because of residual pain and transcervical expulsion of myomas. In the 3 months follow up 39% of the patients showed decrease in size and volume of the leiomyomas (p=<0,0001). Metrorrhagia improved in 89,6% of patients and abdominal distension in 70,5%. Patient satisfaction rates were as high as 92%. Only two patients (1,02%) underwent total hysterectomy because of prolonged fever and leukocytosis. Minor complications were seen in 16% of patients. Clinical follow up was satisfactory during the first year after the endovascular treatment. Ten pregnancies were reported during follow up and all ended with the birth of a healthy child.

### CONCLUSION

Uterine artery embolization has proven to be an efficient and safe endovascular procedure for symptomatic uterine leiomyomas and should be kept in mind as and feasible option for treatment of symptomatic patients. The benefits of minimally invasive procedures overcome those from conventional surgery with preservation of the uterus, short times of hospitalization and minor complications.

#### **CLINICAL RELEVANCE/APPLICATION**

Symptomatic uterine leiomyomas entail considerable negative impact on patient's morbidity, quality of live, and childbearing desires. While clinically challenging, there are many treatment options that should be address individually for each patient. Among these, uterine artery embolization has proven to be an efficient and safe procedure.



# VI223-SD-MOB5

Locoregional Treatments for Unresectable Early Stage HCC in Patients with High Risk for Intraprocedural Bleeding: Is Single-Step Combined Therapy Safe and Feasible?

Monday, Nov. 26 12:45PM - 1:15PM Room: VI Community, Learning Center Station #5

# Participants

Francesca Carchesio, MD, Rome, Italy (*Presenter*) Nothing to Disclose Roberto Iezzi, MD, Rome, Italy (*Abstract Co-Author*) Nothing to Disclose Alessandro Posa, MD, Rome, Italy (*Abstract Co-Author*) Nothing to Disclose Giuseppe Veltri, Rome, Italy (*Abstract Co-Author*) Nothing to Disclose Antonio Gasbarrini, Rome, Italy (*Abstract Co-Author*) Nothing to Disclose Riccardo Manfredi, MD, Rome, Italy (*Abstract Co-Author*) Nothing to Disclose

For information about this presentation, contact:

francesca.carchesio@gmail.com

### PURPOSE

To assess the feasibility and safety of a single-step combined therapy with radiofrequency ablation and drug-eluting beads transarterial chemoembolization (RFA+TACE) in patients with hepatocellular carcinoma (HCC) and low platelet count (LPC). The secondary aim was to compare the effectiveness of this approach with that obtained in a matched population with severe coagulopathy treated with drug-eluting beads transarterial chemoembolization (DEB-TACE) alone.

#### **METHOD AND MATERIALS**

143 consecutive cirrhotic patients with single HCC smaller than 8 cm were enrolled (mean diameter: 4.2±1.6cm). Patients were divided in 3 groups based on the platelet count (>150.000/mm3 group A, low risk; 150.000-50.000/mm3 group B, intermediate; <50.000/mm3, group C, high risk). A single-step combined treatment (RFA + DEB-TACE) was always performed. Feasibility and safety of the procedure were evaluated in terms of technical success rate, peri-procedural mortality and morbidity rates, laboratory values variations, blood transfusion needing, and 1-month TC follow up. Control group was composed by 16 matched patients with severe coagulopathy and single HCC smaller than 8 cm in size who underwent DEB-TACE performed by the same operator in a previous period

## RESULTS

Technical success was achieved in all patients. There were no major complications or death, nor need of blood transfusion. There was a significant increase of the minor complications rate in group C after RFA (high risk, 5/21, 23.8%) when compared to both Group A (low risk, 1/46, 2.4%) and Group B (average risk, 2/76, 2.6%), respectively (p<.05), all treated successfully with the subsequent TACE. No significant differences between pre and post-procedural values of PLT count, INR, and Hemoglobin level in all three subgroups of patients. No significant differences were found between subgroups of patients in terms of post-procedural minor complications.

### CONCLUSION

Single-step RFA plus DEB-TACE allows to expand the indication for percutaneous thermal ablation to previously contraindicated cases due to procedural high-risk of bleeding complications improving patient outcome

### **CLINICAL RELEVANCE/APPLICATION**

Single-step RFA plus DEB-TACE allows to expand the indication for percutaneous thermal ablation to previously contraindicated cases due to procedural high-risk of bleeding complications improving patient outcome



## VI224-SD-MOB6

## Cost Efficiency of Lung Biopsy Tract Collagen Solution Injection (BTCI)

Monday, Nov. 26 12:45PM - 1:15PM Room: VI Community, Learning Center Station #6

### Participants

Hakob Kocharyan, MD, Detroit, MI (*Presenter*) Nothing to Disclose Hussein D. Aoun, MD, Dearborn, MI (*Abstract Co-Author*) Reviewer, Galil Medical Ltd Ali Rastegarpour, MD, Detroit, MI (*Abstract Co-Author*) Nothing to Disclose Christopher T. Bailey, DO, Detroit, MI (*Abstract Co-Author*) Nothing to Disclose Kavi S. Raval, DO, Detroit, MI (*Abstract Co-Author*) Nothing to Disclose Kristian Loveridge, DO, Detroit, MI (*Abstract Co-Author*) Nothing to Disclose Osama Intikhab, MD, Detroit, MI (*Abstract Co-Author*) Nothing to Disclose Jeffrey J. Critchfield, MD, Royal Oak, MI (*Abstract Co-Author*) Nothing to Disclose

#### For information about this presentation, contact:

hkochary@dmc.org

## PURPOSE

To assess the cost efficiency of absorbable collagen solution tract injection post lung biopsy.

## METHOD AND MATERIALS

This is a retrospective review of 488 patients who underwent CT-guided lung biopsy between 2014 and 2018 by two experienced interventional radiologists. All patients underwent CT-guided core biopsies utilizing the coaxial technique with 19-G outer Trocar needle and a 20 gauge core biopsy needle. 169 patients underwent post- biopsy tract collagen (Helitiene) solution injection (BTCI) as the needle was withdrawn. This was compared to a control group of 319 patients who underwent the biopsy without collagen agent injection. The primary endpoint of this review was to assess the cost efficacy of BTCI in preventing intervention for pneumothorax. Comparison of the two groups for pneumothorax, pneumothorax requiring intervention and the associated costs was performed. Specifically, Helitine cost, chest tube cost, chest tube placement cost (ie: IR time, CT time), and extended hospital stay cost were evalutated. Statistical analysis to compare the two groups was performed by Chi Square analysis (SPSS package).

## RESULTS

In a total of 488 patients, pneumothorax occurred in 92 patients (18.9%): 73 patients (22.9%) in the control group (N=319), and 19 patients (11.2%) in the BTCI group (N=169) which was statistically significant difference (p=0.002). Nineteen interventions (6%) were required in the control group (10 chest tubes and 9 blood patches), and 1 (0.6%) in the BTCI group (chest tube) which was statistically significant (p<0.001). The average hospital stay per patient who required an intervention was 1 night in the BTCI group and 4.5 nights in the control group. The mean additional time spent by the IR team during intervention for pneumothorax (chest tube or blood patch) was 31.5 minutes. Helitene prevented approximately 5 interventions per 100 patients which is associated with \$11.750 total cost (average hospital stay cost of \$2000/night, an intervention kit of \$300 and ~procedure cost of \$250). The corresponding costs in the BTCI group per patient is approximately \$6550 (\$2000 per hospital stay night, an intervention kit of \$300, ~ procedure cost of \$250 plus \$4000 total cost of helitene per 100 patients is \$4000).

## CONCLUSION

BTCI has a significant cost reduction in the management of lung biopsy.

# **CLINICAL RELEVANCE/APPLICATION**

Routine utilization of BTCI in lung biopsy is associated with significant cost efficiency.



### CA220-SD-MOB4

Non-Ischemic Myocardial Fibrosis: Diagnostic Performance of Delayed Enhancement Cardiac CT in Comparison with Late Gadolinium Enhancement Cardiac MRI

Monday, Nov. 26 1:00PM - 1:15PM Room: CA Community, Learning Center Station #4

# Participants

Ahmed H. Heussein, MD,MSc, Tsu, Japan (*Presenter*) Nothing to Disclose Kakuya Kitagawa, MD, PhD, Tsu, Japan (*Abstract Co-Author*) Nothing to Disclose Yoshitaka Goto, MD, Tsu, Japan (*Abstract Co-Author*) Nothing to Disclose Masafumi Takafuji, Tsu, Japan (*Abstract Co-Author*) Nothing to Disclose Satoshi Nakamura, MD, Tsu, Japan (*Abstract Co-Author*) Nothing to Disclose Hajime Sakuma, MD, Tsu, Japan (*Abstract Co-Author*) Nothing to Disclose Group; Research Grant, FUJIFILM Holdings Corporation; Research Grant, Siemens AG; Research Grant, Nihon Medi-Physics Co, Ltd; Speakers Bureau, Bayer AG

#### For information about this presentation, contact:

ahmed.hamdy@kasralainy.edu.eg

#### PURPOSE

Delayed enhancement CT (DE-CT) obtained following coronary CT angiography (CCTA) can be used to evaluate myocardial fibrosis either visually or through estimation of the extracellular volume fraction (ECV). The purpose of this study is to assess diagnostic performance of DE-CT and CT-derived ECV in comparison to late gadolinium enhancement (LGE)-MRI and MRI-ECV in non-ischemic myocardial fibrosis.

#### **METHOD AND MATERIALS**

Between January 2015 and January 2018, 28 patients with proven non-ischemic cardiomyopathies/myocardial fibrosis who underwent both cardiac MRI with LGE and comprehensive cardiac CT protocol including acquisition of CCTA and DE-CT comprised the final study population. DE-CT was acquired 5 minutes after CCTA using dual-source CT. Diagnostic performance of DE-CT and agreement with LGE-MRI on patient and segment levels (28 patients with 476 segments) were investigated. Similarly, agreement and correlation between CT-ECV and MRI-ECV were studied in a subset of patients with pre- and post-contrast T1 mapping on MRI (17 patients).

### RESULTS

Delayed enhancement CT had a sensitivity and specificity of 100% on patient-based analysis and 85% sensitivity, 98% specificity, 90% PPV, 96% NPV and 95% diagnostic accuracy on segment-based analysis when compared to LGE-MRI for detection of nonischemic myocardial scarring. ROC analysis showed an AUC of 0.908. Agreement with LGE-MRI for detection and localization of myocardial scars was good (kappa=0.836, p<0.001). In the subset of patients with pre- and post-contrast T1 mapping, CT-ECV correlated well with MRI-ECV (r=0.71, p=0.001). Bland-Altman analysis showed a mean difference of 1% with 95% limits of agreement between -4.4 and 6.3%. The average radiation dose of the delayed scans was 2.1 mSv.

#### CONCLUSION

Delayed enhancement cardiac CT is a reliable and accurate method for detection of focal or diffuse non-ischemic myocardial fibrosis.

#### **CLINICAL RELEVANCE/APPLICATION**

Cardiac CT, which is an easier and faster imaging technique than cardiac MRI, can be used confidently to assess focal or diffuse non-ischemic myocardial fibrosis when cardiac MRI is not available or contraindicated, e.g. in patients with implanted cardiac electronic devices.



## AI001-MOD

# **Introduction to Deep Learning**

Monday, Nov. 26 2:30PM - 4:00PM Room: AI Community, Learning Center

# **Title and Abstract**

Introduction to Deep Learning This class will focus on basic concepts of convolutional neural networks (CNNs), and walk the attendee through a working example. A popular training example is the MNIST data set which consists of hand-written digits. This course will use a data set we created, that we call 'MedNIST' and consists of 1000 images each from 5 different categories: Chest X-ray, hand X-ray, Head CT, Chest CT, Abdomen CT, and Breast MRI. The task is to identify the image type. This will be used to train attendees on the basic principles and some pitfalls in training a CNN. The attendee will have the best experience if they are familiar with Python programming.



# AI001-TUA

# **3D Segmentation of Brain MR**

Tuesday, Nov. 27 8:30AM - 10:00AM Room: AI Community, Learning Center

# Title and Abstract

3D Segmentation of Brain MR This session will focus on the use of deep learning methods for segmentation, with particular emphasis on 3D techniques (V-Nets) applied to the challenge of MR brain segmentation. While focused on this particular problem, the concepts should generalize to other organs and image types.



## AI001-TUB

# **Introduction to Deep Learning**

Tuesday, Nov. 27 10:30AM - 12:00PM Room: AI Community, Learning Center

# **Title and Abstract**

Introduction to Deep Learning This class will focus on basic concepts of convolutional neural networks (CNNs), and walk the attendee through a working example. A popular training example is the MNIST data set which consists of hand-written digits. This course will use a data set we created, that we call 'MedNIST' and consists of 1000 images each from 5 different categories: Chest X-ray, hand X-ray, Head CT, Chest CT, Abdomen CT, and Breast MRI. The task is to identify the image type. This will be used to train attendees on the basic principles and some pitfalls in training a CNN. The attendee will have the best experience if they are familiar with Python programming.



### AI212-SD-TUA1

## Transfer-Learning for Imaging-Based Lung Cancer Stratification

Tuesday, Nov. 27 12:15PM - 12:45PM Room: AI Community, Learning Center Station #1

## Awards

## **Student Travel Stipend Award**

#### Participants

Tafadzwa Chaunzwa, BEng, MS, Boston, MA (*Presenter*) Nothing to Disclose Yiwen Xu, PhD, Boston, MA (*Abstract Co-Author*) Nothing to Disclose Raymond H. Mak, MD, Boston, MA (*Abstract Co-Author*) Nothing to Disclose David Christiani, MD, Boston, MA (*Abstract Co-Author*) Nothing to Disclose Michael Lanuti, MD, Boston, MA (*Abstract Co-Author*) Nothing to Disclose Andrea Shafer, MPH, Boston, MA (*Abstract Co-Author*) Nothing to Disclose Nancy Diao, DSc, Boston, MA (*Abstract Co-Author*) Nothing to Disclose Hugo Aerts, PhD, Boston, MA (*Abstract Co-Author*) Stockholder, Sphera Inc

#### For information about this presentation, contact:

tafadzwa.chaunzwa@yale.edu

#### CONCLUSION

Transfer-learning is a viable approach to building powerful deep-learning based tools for image analysis and performing prognostic calculations in early-stage NSCLC. This model can aid clinical decision making in the treatment of lung cancer.

#### Background

In this study we present a deep-learning model that can act as a non-invasive biomarker in early stage Non-Small Cell Lung Cancer (NSCLC). Our model would be able to assign patients to short term or long term survival groups, based on computed tomography (CT) characteristics.

#### **Evaluation**

Pre-treatment CT studies were retrieved for 186 NSCLC surgical Stage-I patients at Massachusetts General Hospital between 2004 and 2010. Median follow-up from time of diagnosis was 1074 days, with 90.3% 2-year survival. To mitigate bias against a low probability event (mortality), data augmentation was performed on the training and validation images (n = 178). A VGG-16 deep neural network pretrained on ImageNet was used, with fine-tuning of the last two convolutional layers, dense layers, and softmax for stratification. Inputs of this model were 50 x 50 mm2 patches. Training was performed on 144 labeled CT scans, matched to one of two groups based on 2 year survival. 34 samples were used for initial cross-validation.

#### Discussion

Our model stratified patients with long term and short term survival in an independent test set of 46 patients (accuracy of 87%, AUC=0.92, p<0.0023). Given the relatively small datasets encountered in this and other clinical studies, optimal results would not have been attained by training a deep-learning model from scratch (AUC=0.89, p<0.0041). By tailoring a powerful solution for other computer vision tasks, we were able to build a robust prognostic model. A multivariate linear model of conventional clinical prognostic factors (age, gender, tumor stage IA/1B, histology, and smoking status) had a significant but lower predictive performance (AUC=0.665).



### AI213-SD-TUA2

Synthetic PET Generator: A Novel Method to Improve Lung Nodule Detection by Combining Outputs from a Pix2pix Conditional Adversarial Network and a Convolutional Neural Network Based Malignancy Probability Estimator

Tuesday, Nov. 27 12:15PM - 12:45PM Room: AI Community, Learning Center Station #2

#### Participants

Vasanthakumar Venugopal, MD, New Delhi, India (*Abstract Co-Author*) Nothing to Disclose Abhijith Chunduru, MENG, Bengaluru, India (*Presenter*) Stockholder, Predible Health Suthirth Vaidya, BEng, MENG, Bengaluru, India (*Abstract Co-Author*) Employee, Predible Health Vidur Mahajan, MBBS, New Delhi, India (*Abstract Co-Author*) Nothing to Disclose Harsh Mahajan, MD, MBBS, New Delhi, India (*Abstract Co-Author*) Nothing to Disclose

### For information about this presentation, contact:

drvasanth@mahajanimaging.com

### CONCLUSION

Synthetic PET images can potentially increase the sensitivity of malignant nodule detection from Lung CT images. Such a modality can be easier for radiologists to understand than naive probability heatmaps. Further research is required to investigate the effect of potential biases and investigate appropriate clinical application.

### Background

Assessment of malignancy of lung nodules on CT scans is a subjective and arduous task for radiologists with low reported accuracy rates, especially for small nodules. We propose a novel method to generate a synthetic PET image of the lung from CT images using Conditional Generative Adversarial Networks (cGAN) that can improve the sensitivity of the radiologist in the detection of malignant lung nodules.

### **Evaluation**

We used a combination of a PET Generator combined with a Malignancy Probability Estimator to generate a synthetic PET image from Lung CT scan. The PET Generator is a conditional adversarial network (pix2pix) trained on slices containing the Lung from 100 PET-CT scans which were acquired on patients suspected or diagnosed with Lung Cancer. The model performed at a mean squared error of 0.08 when compared in SUV units. The malignancy probability estimator is a 20-layer deep residual convolutional neural network trained on a dataset of 1595 scans from the NLST trial. The model performed produced a ROC of 0.89 when tested on 822 patients. The outputs of the PET Generator provides a background for overlaying outputs of the Malignancy Probability Estimator which together produce the synthetic PET image.

#### Discussion

When tested on a dataset of 30 images, the synthetic PET model performed at a mean squared error of 0.08 when compared in SUV units. The malignancy model was independently tested on 350 scans and produced an AUC of 0.89. A dataset of 22 malignant scans is used to benchmark performance of malignancy detection. Using the CT scan alone, three radiologists had sensitivities of 86%, 81% and 72% in detecting malignant studies. Using the synthetic PET as an additional modality, an increased sensitivity of 95% can be obtained. However, it is important to note that the SUV values detected on the nodules were not correlated with the actual SUV values.



### BR009-EB-TUA

### Quantitative MRI Radiomics in Breast Cancer: Tumor Perfusion and Heterogeneity

Tuesday, Nov. 27 12:15PM - 12:45PM Room: BR Community, Learning Center Hardcopy Backboard

**FDA** Discussions may include off-label uses.

#### Participants

Myoung-Ae Kwon, Ansan, Korea, Republic Of (*Presenter*) Nothing to Disclose Bo Kyoung Seo, MD, PhD, Ansan, Korea, Republic Of (*Abstract Co-Author*) Research Grant, Canon Medical Systems Corporation; Research Grant, Guerbet SA; Research Grant, Koninklijke Philips NV; Eun Kyung Park, MD,PhD, Ansan, Korea, Republic Of (*Abstract Co-Author*) Nothing to Disclose Chang Sub Ko, Ansan, Korea, Republic Of (*Abstract Co-Author*) Nothing to Disclose Young Ju Son, Ansan, Korea, Republic Of (*Abstract Co-Author*) Nothing to Disclose Kyu Ran Cho, MD, PhD, Seoul, Korea, Republic Of (*Abstract Co-Author*) Nothing to Disclose Ok Hee Woo, MD, Seoul, Korea, Republic Of (*Abstract Co-Author*) Nothing to Disclose

### For information about this presentation, contact:

kwon4715@gmail.com

#### **TEACHING POINTS**

Radiomics is defined as the use of automated post-processing and analysis of quantitative imaging characteristics that can be extracted from medical images. Quantification of imaging features is important to link the biomarkers with biological processes and clinical endpoints. Magnetic resonance imaging(MRI) is the most sensitive imaging modality in breast cancer and has been used for staging before treatment and assessing the response to the chemotherapy. Perfusion and tumor heterogeneity are related with cancer biological characteristics and prognosis. In this exhibit, we will illustrate how to quantitatively assess tumor perfusion and heterogeneity on breast MRI and correlate radiological imaging parameters with prognostic biomarkers and clinical outcomes. In addition, we will discuss the future potential of radiomics in oncology imaging.

### TABLE OF CONTENTS/OUTLINE

1) Radiomics : Definition : Requirements for quantification of medical images 2) Assessment of tumor perfusion on breast MRI : Imaging technique : Quantitative parameters 3) Assessment of tumor heterogeneity on breast MRI : Texture analysis mechanism : Quantitative parameters 4) Correlation of quantitative parameters of tumor perfusion and heterogeneity with biomarkers and clinical outcomes 5) Future potential of radiomics in oncology imaging



### BR188-ED-TUA7

Missed Breast Cancers: The Unconscious Bias in Breast Imaging

Tuesday, Nov. 27 12:15PM - 12:45PM Room: BR Community, Learning Center Station #7

### Awards Cum Laude Identified for RadioGraphics

#### **Participants**

Leslie Lamb, MD, Boston, MA (*Presenter*) Nothing to Disclose Raman Verma, MD, Ottawa, ON (*Abstract Co-Author*) Nothing to Disclose Jean M. Seely, MD, Ottawa, ON (*Abstract Co-Author*) Nothing to Disclose

### **TEACHING POINTS**

Medical errors are a substantial cause of morbidity and mortality and the third leading cause of death in the United States. Errors resulting in missed breast cancer are the most prevalent condition precipitating medical malpractice lawsuits against all physicians. In breast imaging, missed and interval breast cancers at screening mammography ranges from 1 to 35%. As such, it is important to understand various cognitive processes during mammographic interpretation to improve awareness of unconscious biases and decrease the number of missed breast cancers. It is particularly important to be aware of these biases when encountering the most commonly missed and misinterpreted breast lesions. The purpose of this educational exhibit is to demonstrate various cognitive processes that lead to unconscious biases through a pictorial review of missed breast cancers, and highlight strategies to reduce the rates of these missed cancers.

### **TABLE OF CONTENTS/OUTLINE**

The most commonly missed and misinterpreted lesions will be reviewed (stable, benign appearing and one-view masses, developing asymmetries). These will help illustrate the common unconscious biases with appropriate minimization strategies in breast imaging (anchoring, confirmation, satisfaction of search, hindsight, inattention, satisfaction of report and premature closing).



## BR189-ED-TUA8

Perceptive and Interpretive Pitfalls at Digital Breast Tomosynthesis (DBT) - Lessons from Continued Clinical Practice

Tuesday, Nov. 27 12:15PM - 12:45PM Room: BR Community, Learning Center Station #8

#### Awards Certificate of Merit

#### **Participants**

Sushma Gaddam, MD, New York, NY (*Presenter*) Nothing to Disclose Samantha L. Heller, MD, PhD, New York, NY (*Abstract Co-Author*) Nothing to Disclose Yiming Gao, MD, New York, NY (*Abstract Co-Author*) Nothing to Disclose

### For information about this presentation, contact:

sushma.gaddam@nyumc.org

## **TEACHING POINTS**

Digital breast tomosynthesis (DBT) is rapidly becoming the standard of care in mammographic screening, replacing conventional 2D mammography. DBT technique continues to evolve, with synthetic 2D images (s2D) increasingly substituting for full field 2D mammography, decreasing radiation dose. Because DBT is a relatively new technology, continued learning and improvement of radiologist skills are essential. We will discuss perceptive and interpretive pitfalls of DBT interpretation, illustrate exceptions to the rules in DBT diagnosis, and highlight teaching points via a case-based review.

### **TABLE OF CONTENTS/OUTLINE**

1. Intro: a. 2D vs. DBT/2D vs. DBT/s2D b. Perceptive vs Interpretive errors2. Perceptive errors a. Satisfaction of search b. Localization or triangulation errors on DBT c. Calcifications on synthetic 2D images d. DBT occult cancers e. Extremely dense breast f. Invasive lobular cancers g. Technical issues - patient positioning, motion3. Interpretive errors a. Skin vs. superficial lesions b. One-view-only findings c. Developing asymmetries d. Fat containing lesions e. Architectural distortions f. DBT-only architectural distortions4. Case illustrations - highlight pearls and pitfalls



### BR190-ED-TUA9

## Breast Imaging of Ductal Carcinoma in Situ: Dilemma Between Overtreatment and Underestimation

Tuesday, Nov. 27 12:15PM - 12:45PM Room: BR Community, Learning Center Station #9

#### Participants

Hiroko Satake, MD, Nagoya, Japan (*Presenter*) Nothing to Disclose Satoko Ishigaki, MD, Nagoya, Japan (*Abstract Co-Author*) Nothing to Disclose Shinji Naganawa, MD, Nagoya, Japan (*Abstract Co-Author*) Nothing to Disclose

## **TEACHING POINTS**

Given the uncertainty in determining whether ductal carcinoma in situ (DCIS) is likely to progress, every DCIS is intensively treated as invasive breast cancer. Overdiagnosis and overtreatment may potentially occur, especially for low-grade DCIS. On the other hand, a pathologically positive or a close-to-margin status, due to preoperative underestimation, are risk factors for local DCIS recurrence post-excision. Furthermore, we occasionally encounter preoperatively diagnosed DCIS that is then upgraded to invasive cancer postoperatively. We review the image findings in DCIS and discuss how they can be used to resolve dilemmas between overtreatment and underestimation.

### TABLE OF CONTENTS/OUTLINE

1. Explain the controversies surrounding DCIS diagnosis and treatment. 2. Review the imaging features of DCIS on mammography, ultrasonography, and MRI. 3. Review the usefulness and pitfalls of preoperative MRI for DCIS to estimate tumor extensions. 4. Review the current literature and discuss the capabilities of diagnostic imaging, focusing on the following topics: • Differentiating low-grade from high-grade DCIS • Preoperative predictions concerning occult invasion in DCIS • Identifying imaging risk factors for local DCIS recurrence • Quantitative imaging analysis of DCIS



### BR191-ED-TUA10

## Not Your Mother's Breast Cancer - Imaging and Review of Breast Cancer Under 30 and Other Mimics

Tuesday, Nov. 27 12:15PM - 12:45PM Room: BR Community, Learning Center Station #10

### **Participants**

Vincent G. Champion, MD, Westwood, MA (Presenter) Nothing to Disclose Bonny Lee, MD, MS, brookline, MA (Abstract Co-Author) Nothing to Disclose Eileen Delaney, MD, Worcester, MA (Abstract Co-Author) Nothing to Disclose Amy K. Patel, MD, Boston, MA (Abstract Co-Author) Nothing to Disclose Evguenia J. Karimova, MD, Memphis, TN (Abstract Co-Author) Nothing to Disclose Valerie J. Fein-Zachary, MD, Boston, MA (Abstract Co-Author) Nothing to Disclose Michael D. Fishman, MD, Boston, MA (Abstract Co-Author) Consultant, Zebra Medical Vision Ltd Jordana Phillips, MD, Boston, MA (Abstract Co-Author) Research Grant, General Electric Company; Consultant, General Electric Company

Priscilla J. Slanetz, MD, MPH, Belmont, MA (Abstract Co-Author) Nothing to Disclose

### **TEACHING POINTS**

1. Review the role of imaging in the diagnosis of breast cancer and potential mimics for women under 30 years old. 2. Discuss the unique challenges involved in the diagnosis and management of breast cancer in young patients.

# TABLE OF CONTENTS/OUTLINE

1. Review the current state of breast cancer in young women. 2. Discuss risk factors related to development of breast cancer in young women including socioeconomic status and race 3. Review unique pathologic features encountered in young women with breast cancer as opposed to those in older women. 4. Review imaging protocols used in the diagnosis and management of breast cancer in the young women. 5. Provide examples of mimickers of breast cancer encountered in young women. 6. Discuss management considerations for the adolescent or young adults with breast cancer including risks of surgery, chemotherapy, radiation, and hormonal therapy.



## BR192-ED-TUA11

### The Bright Side of the Post-Surgical Breast: Benign Findings After Breast Manipulation

Tuesday, Nov. 27 12:15PM - 12:45PM Room: BR Community, Learning Center Station #11

#### **Participants**

Pedro Henrique Hasimoto e Souza, MD, Sao Paulo, Brazil (*Presenter*) Nothing to Disclose Juliana H. Catani, MD, Sao Paulo, Brazil (*Abstract Co-Author*) Nothing to Disclose Tatiana C. Tucunduva, MD, Sao Paulo, Brazil (*Abstract Co-Author*) Nothing to Disclose Sofia R. Cartaxo, MD, Sao Paulo, Brazil (*Abstract Co-Author*) Nothing to Disclose Carla C. Caravatto, MD, Sao Paulo, Brazil (*Abstract Co-Author*) Nothing to Disclose Carlos Shimizu, MD, Sao Paulo, Brazil (*Abstract Co-Author*) Nothing to Disclose Nestor Barros, Sao Paulo, Brazil (*Abstract Co-Author*) Nothing to Disclose

#### For information about this presentation, contact:

pedrohenriquehs@hotmail.com

#### **TEACHING POINTS**

Prepare the radiologist to face common and uncommon presentations of manipulation / post-surgical benign changes in breast imaging; Exhibit clinical cases from our radiology department, with various types of manipulation resulting in breast benign imaging findings; Discuss the effects of manipulation on breast cancer detection; Provide management recommendations.

### **TABLE OF CONTENTS/OUTLINE**

- Brief discussion on post-treatment follow-up care in breast cancer; - Risk factors and incidence of recurrence; - Imaging features (mammography, ultrasound and magnetic resonance imaging) of manipulation / post-surgical benign changes in breast imaging: 1. Mastectomy and variants 2. Breast implants Expanders and silicone implants Double prosthesis Implants in transexual patients Intra and extracapsular ruptures Industrial liquid silicone injection 3.Mastopexy Mesh Internal suture 4. Reduction mammoplasty Vertical incision Inferior pedicle 5. Autologous reconstruction Autologous fat grafting Pedicled TRAM flap Dorsal flap 6. Miscellaneous Fat necrosis Subcutaneous emphysema Radiotherapy actinic changes Keloid Tattoo Others



## BR198-ED-TUA12

Luminal B Subtype Breast Cancer: Radiogenomic Correlation

Tuesday, Nov. 27 12:15PM - 12:45PM Room: BR Community, Learning Center Station #12

### **Participants**

Bruna Mannato, MD, Sao Paulo, Brazil (Presenter) Nothing to Disclose Decio Roveda Junior, PhD, PhD, Sao Paulo, Brazil (Abstract Co-Author) Nothing to Disclose Caio Castro, MD, Santo Andre, Brazil (Abstract Co-Author) Nothing to Disclose Mario S. Campos, MD, Sao Paulo, Brazil (Abstract Co-Author) Nothing to Disclose Gustavo M. Badan, MD, PhD, Sao Paulo, Brazil (Abstract Co-Author) Nothing to Disclose

## For information about this presentation, contact:

brunamannato@hotmail.com

### **TEACHING POINTS**

1. The main objective of this pictorial review is to show the most prevalent imaging patterns of that luminal B subtype at mammography (MMG), ultrasound (US) and magnetic resonance (MR). 2. Series of cases of patients diagnosed with invasive breast cancer, between January 2015 and March 2018, classified as luminal B, analyzing the most prevalent features in the different imaging modalities (MMG, US and MR). 3. Recent literature review and comparison with the data found in our service.

### **TABLE OF CONTENTS/OUTLINE**

• Introduction - The traditional clinicopathological model. - New classification Immunohistochemical • Luminal Subtype Breast -Cancer Luminal B x Luminal A • Imaging features - MMG - US - MR • Radiogenomics correlation • Conclusion



## BR241-SD-TUA1

Evaluating the Timeliness of Abnormal Mammography Follow-up Based on Race at an Urban Safety Net Hospitalty

Tuesday, Nov. 27 12:15PM - 12:45PM Room: BR Community, Learning Center Station #1

#### Awards Student Travel Stipend Award

# Participants

Neeta Kannan, MD, San Francisco, CA (*Presenter*) Nothing to Disclose Amie Y. Lee, MD, San Francisco, CA (*Abstract Co-Author*) Nothing to Disclose Kimberly M. Ray, MD, San Francisco, CA (*Abstract Co-Author*) Nothing to Disclose Bonnie N. Joe, MD, PhD, San Francisco, CA (*Abstract Co-Author*) Nothing to Disclose Jessica H. Hayward, MD, San Francisco, CA (*Abstract Co-Author*) Nothing to Disclose

## For information about this presentation, contact:

neeta.kannan@ucsf.edu

#### PURPOSE

To investigate racial and ethnic disparities in timeliness of abnormal mammography follow-up at an urban safety net hospital.

#### **METHOD AND MATERIALS**

All women who underwent screening or diagnostic mammography at our facility between 4/1/2016-4/1/2017 whose examinations received actionable Breast Imaging Reporting and Data System (BI-RADS) assessments 0, 4 or 5 were identified. Self-reported racial or ethnic group was recorded. Median follow-up times from abnormal screening to diagnostic mammogram and abnormal diagnostic mammogram to biopsy were calculated. Normality of time to follow-up values was assessed by the Shapiro-Wilk test. Median values were compared using the Wilcoxon test.

### RESULTS

Seven hundred seventy-eight women were included in the study: 98 (12.6%) Caucasian, 275 (35.3%) Asian, 256 (32.9%) Hispanic, and 100 (12.9%) African-American. Six-hundred sixty-two women were recalled for abnormal screening mammograms of whom 30 were lost to follow-up. The remaining 632 women had median follow-up time for an abnormal screening mammogram as follows: 15 days (95% CI 15.5, 17.5) for all women combined, 14 (10, 22.8) for Caucasian, 15 (10, 22) for Asian, 14 (9, 21.5) for Hispanic, and 15 (12, 28) for African-American women. Of the 280 women with diagnostic mammography BI-RADS assessment of 4 or 5, 13 declined biopsy and 12 were lost to follow-up. The remaining 255 patients underwent biopsy with a median time interval to biopsy in days of 7.4 (95% CI 1.5, 14.5) for all women combined, 7.5 (3.5, 14.5) for Caucasian, 7.6 (2.5, 8.5) for Asian, 5.6 (1.4, 14.6) for Hispanic, and 8.4 (2.4, 14.5) for African-American women. Relative to Caucasian women, there were no significant differences in abnormal screening or diagnostic mammography follow-up intervals for any racial or ethnic group.

#### CONCLUSION

In contrast to previous studies, there were no significant delays in follow-up for abnormal screening and diagnostic mammograms for minority women relative to Caucasian women at the studied urban safety-net hospital. Further research is needed to identify factors that promote timely follow-up in the studied minority patient population.

### **CLINICAL RELEVANCE/APPLICATION**

Delay in follow-up of abnormal mammograms can lead to adverse outcomes. Identifying where disparities occur can help address barriers to care.



## BR242-SD-TUA2

Outcome Analysis of BI-RADS Category 3 Lesions in Young Women Imaged in Tertiary University Versus Safety-Net Hospital Setting: Is There an Impact of Healthcare Disparity?

Tuesday, Nov. 27 12:15PM - 12:45PM Room: BR Community, Learning Center Station #2

## Participants

Jody C. Hayes, MD, Southlake, TX (*Presenter*) Nothing to Disclose Lindsay Compton, MD, Dallas, TX (*Abstract Co-Author*) Researcher, QT Ultrasound, LLC Lena A. Omar, MD, Dallas, TX (*Abstract Co-Author*) Researcher, QT Ultrasound, LLC Kanwal A. Merchant, MD, Dallas, TX (*Abstract Co-Author*) Stockholder, Sensogram Technologies; Spouse, Stockholder, Sensogram Technologies Yin Xi, PhD, Dallas, TX (*Abstract Co-Author*) Nothing to Disclose

Basak E. Dogan, MD, Dallas, TX (*Abstract Co-Author*) Nothing to Disclose

## PURPOSE

To compare the follow up, image-guided biopsy and surgical excision patterns of women <30 with BI-RADS Category 3 lesions in a safety-net hospital and an academic tertiary care center.

## **METHOD AND MATERIALS**

In an IRB approved, HIPAA compliant study, consecutive women younger than 30 years who received sonographic (US) BI-RADS 3 assessment between January 2013 to December 2014 in breast imaging facilities of a safety-net (PMH) and a tertiary university hospital (CUH) provided by the same fellowship-trained breast imaging group were retrospectively reviewed. We compared the patient clinical presentation, imaging findings, lesion size and number, frequency and time interval of follow up, and biopsy and excision status. Statistical analysis including chi-square and Cochran-Mantel-Haenszel (CMH) analysis for overall odds ratios were performed.

## RESULTS

One hundred and ninety-seven lesions in 157 women in PMH and 92 lesions in 70 patients in CUH had US BI-RADS 3 assessment. Median patient age was the same in both groups (25 yrs). In PMH, 178 of 197 (90%) and in CUH 71 of 92 (77%) of lesions were palpable (p=0.2965). Mean lesion size was 1.6 cm (SD±0.8) in PMH, and 1.3 cm (SD±0.6) at CUH (p=0.2338). Patients were less likely to complete all imaging follow up time points in PMH (n=29, 14.7%) compared to those in CUH (n=37, 52.8%) (p<0.05).While the overall biopsy rates were similar (PMH, 23.5%, CUH, 19.1%), a higher rate of initial biopsies was observed in PMH (35 of 50 biopsies,70%) vs CUH (4 of 14, 29%) (p=0.004). The odds of undergoing a biopsy at initial presentation at PMH were significantly higher [OR: 4.783 (95%CI 1.9-11.6)] compared to CUH [OR: 0.485, (95%CI 0.02-10.7)] (p=0.0044). Biopsy was more likely to be prompted by patient preference in PMH (39,70%) compared to CUH (22.2%)(p=0.005). Surgical excision rates were similar (8%PMH vs 5%CUH) between the two groups. No malignancy was identified in either group.

## CONCLUSION

There is a higher probability of incomplete follow up and initial needle biopsy for US BI-RADS Category 3 lesions identified in young women in safety-net setting compared to university setting.

# **CLINICAL RELEVANCE/APPLICATION**

Radiologists should consider disparities between population groups while recommending follow up for probably benign lesions in women under 30, considering the low probability of malignancy in this age group.



### BR243-SD-TUA3

Pre-Treatment Prediction of Pathologic Complete Response to Neoadjuvant Chemotherapy in Node-Positive Breast Cancer Patients: A Breast MRI Radiomics Pilot Study

Tuesday, Nov. 27 12:15PM - 12:45PM Room: BR Community, Learning Center Station #3

## Participants

Karen Drukker, PhD, Chicago, IL (Presenter) Royalties, Hologic, Inc

Christopher Doyle, MD , Chicago, IL (Abstract Co-Author) Nothing to Disclose

Alexandra V. Edwards, Chicago, IL (*Abstract Co-Author*) Research Consultant, QView Medical, Inc; Research Consultant, Quantitative Insights, Inc

John Papaioannou, MSc, Chicago, IL (Abstract Co-Author) Research Consultant, QView Medical, Inc

Maryellen L. Giger, PhD, Chicago, IL (*Abstract Co-Author*) Stockholder, Hologic, Inc; Shareholder, Quantitative Insights, Inc; Shareholder, QView Medical, Inc; Co-founder, Quantitative Insights, Inc; Royalties, Hologic, Inc; Royalties, General Electric Company; Royalties, MEDIAN Technologies; Royalties, Riverain Technologies, LLC; Royalties, Mitsubishi Corporation; Royalties, Canon Medical Systems Corporation

Kirti M. Kulkarni, MD, Chicago, IL (Abstract Co-Author) Nothing to Disclose

#### For information about this presentation, contact:

kdrukker@uchicago.edu

#### PURPOSE

Evaluate the ability of breast MRI radiomics to predict pathologic complete response of tumor and lymph nodes *prior* to neoadjuvant chemotherapy (NAC) treatment in patients with invasive lymph node-positive breast cancer.

#### **METHOD AND MATERIALS**

Sixtyfive patients were included in this retrospective HIPAA compliant IRB approved study. Upon surgery, 15 showed post-NAC complete pathologic response (pathologic TNM stage T0,N0,MX, 'complete-responders') and 50 showed incomplete response to NAC ('incomplete-responders'). Only pre-NAC MRIs underwent computer analysis, initialized by an expert breast radiologist indicating index cancers and metastatic axillary sentinel lymph nodes (LNs) on DCE-MRI (T2 and T1 postcontrast subtraction) images. Subsequent automated analysis included computer segmentation and extraction of 38 radiomic features describing (i) size, (ii) shape, (iii) margin, (iv) kinetic curve, (v) contrast-enhancement texture, and (vi) variance kinetics. For cancers and LNs separately, each radiomic feature was evaluated to determine whether a statistically significant difference between the complete-responders and incomplete-responders was demonstrated (Mann-Whitney U-test). The area under the ROC curve was calculated for the task of distinguishing between the two groups.

#### RESULTS

All radiomic features describing index cancers failed to show a statistically significant difference between complete-responders and incomplete-responders (p>0.05). Four radiomic features describing pre-treatment metastatic LNs demonstrated statistically significant differences between the two groups: effective diameter, sphericity, surface to volume ratio, and most enhancing nodal volume. The most predictive feature was sphericity with area under the ROC curve of 0.75 (standard error 0.07) in the prediction of pathologic response.

# CONCLUSION

Radiomics for breast MRI shows promise in the pre-treatment prediction of pathologic response to neoadjuvant chemotherapy in patients with lymph-node positive invasive breast cancer.

## **CLINICAL RELEVANCE/APPLICATION**

The ability to predict which patients will demonstrate pathologic complete response before initiating neoadjuvant chemotherapy could positively impact patient management by saving the cost of unnecessary chemotherapy and also the mortality and morbidity associated with additional adjunct treatment in cases of incomplete pathologic response such as axillary dissection and radiation therapy.



## BR244-SD-TUA4

Histological Whole-Slide Imaging for Invasive Breast Cancer: A Novel Technique to Obtain Quantitative Parameters Correlating with the Apparent Diffusion Coefficient

Tuesday, Nov. 27 12:15PM - 12:45PM Room: BR Community, Learning Center Station #4

### Participants

Naoko Mori, MD, PhD, Sendai, Japan (*Presenter*) Nothing to Disclose Chihiro Inoue, Sendai, Japan (*Abstract Co-Author*) Nothing to Disclose Shunji Mugikura, MD, PhD, Sendai, Japan (*Abstract Co-Author*) Nothing to Disclose Kei Takase, MD, PhD, Sendai, Japan (*Abstract Co-Author*) Nothing to Disclose

For information about this presentation, contact:

naokomori7127@gmail.com

## PURPOSE

To evaluate whether parameters obtained by quantitative analysis of histological whole-slide imaging (WSI) correlates with the apparent diffusion coefficient (ADC) in diffusion-weighted imaging (DWI) for invasive breast cancer.

### **METHOD AND MATERIALS**

The Institutional Review Board approved this retrospective study and waived the requirement for informed consent. Between September 2015 and July 2016, 46 consecutive patients with 46 invasive breast cancer lesions diagnosed by surgery underwent preoperative breast magnetic resonance imaging (MRI), including DWI (b value: 50, 850s/mm2), followed by mastectomy or lumpectomy without neoadjuvant therapy. Regions of interest (ROIs) covering as much of the tumor volume as possible were placed manually on the maximum cross-section of the tumor on ADC maps, and the mean ADC values of the ROIs were recorded. For histological analyses, the digital data of cytokeratin-immunostained thin-slice sections using the largest cross-sectional area of the tumor were used for WSI. The cytoplasm, interstitium, and nucleus were identified and segmented by their brown, light blue, and purple colors, respectively. The area ratios of cancer cells (the sum of the cytoplasm and nucleus) and interstitial space were calculated by identifying the color of each component for the whole tumor area. For conventional cell counts, we randomly selected five areas at ×200 field and manually counted cancer cells, and then the average counts of five areas were recorded as cell counts. Then, all histological parameters were compared with the ADC using Pearson's correlation coefficient. A value of p < 0.05 was considered statistically significant.

### RESULTS

The area ratios of the interstitial space were significantly positively correlated with the ADC (r=0.53; p=0.0001). The area ratios of cancer cells and conventional cell counts were significantly negatively correlated with the ADC with a lesser degree. (r=-0.36 and -0.32, respectively; p=0.012 and 0.027, respectively).

#### CONCLUSION

There is a significant positive correlation between the ADC value and area of the interstitium, as measured by WSI.

#### **CLINICAL RELEVANCE/APPLICATION**

There is a significant positive correlation between the ADC and the area of the interstitium, as measured by whole-slide imaging (WSI). The ADC reflects the amount of interstitium in breast cancer tissue.



### BR245-SD-TUA5

### Usefulness of CAD (Computer-Aided Detection) System for Screening Automatic Breast Ultrasound

Tuesday, Nov. 27 12:15PM - 12:45PM Room: BR Community, Learning Center Station #5

### Participants

Jeong Min Lee, Seoul, Korea, Republic Of (*Abstract Co-Author*) Nothing to Disclose Bong Joo Kang, Seoul, Korea, Republic Of (*Abstract Co-Author*) Nothing to Disclose Sung Hun Kim, Su Won, Korea, Republic Of (*Abstract Co-Author*) Nothing to Disclose Kim Myeongjong, Suwon, Korea, Republic Of (*Presenter*) Nothing to Disclose

## PURPOSE

To evaluate diagnostic performance of screening automated breast ultrasound using computer aided detection (CAD) system and to analyze the characteristics of CAD marks and the causes of false positive marks.

## **METHOD AND MATERIALS**

A total of 846 women aged 40-49 years who underwent automated breast ultrasound for screening from January 2017 to December 2017 were included. We applied the CAD (QVCADTM) to all of the automated breast ultrasound examinations and evaluated its diagnostic performance. Then, we analyzed the frequency, characteristics, and causes of false positive marks and tried to find out a way to reduce the false positive marks. Furthermore, we analyzed whether adding CAD would shorten the reading time.

### RESULTS

Out of a total of 846 patients, 534 CAD marks were displayed with an average CAD mark per person of  $0.8 \pm 1$  (range 0-6). Through screening automated breast ultrasound, five breast cancers were diagnosed. The sensitivity, specificity, PPV, NPV, and accuracy of CAD were 60.0%, 59.0%, 0.9%, 99.6% and 59.0% for 846 patients, respectively, while those of 534 CAD marks were 60.0%, 48.3%, 0.6%, 99.6%, and 48.4%. Among 531 false positive marks, 459 false marks for pseudolesions were well identified; the most common cause was marginal shadowing (209, 39.1%), then, Cooper's ligament shadowing (143, 26.8%), periareolar shadowing (64, 12%), rib (37, 6.9%), and skin lesion (6, 1.1%). The false marks for pseudolesions appeared in the upper portion rather than mid to inner portion. In the case of a negative study, it was less time-consuming and easier to make a decision.

## CONCLUSION

Adding CAD does not improve accuracy for screening automated breast ultrasound in this study, but adding it helps to reduce reading time nonetheless for negative screening ultrasound.

## **CLINICAL RELEVANCE/APPLICATION**

Using CAD system is helpful to reduce reading time for screening automated breast ultrasound, but does not improve accuracy.



## BR246-SD-TUA6

Analysis of Background Echotexture on Automated Breast Ultrasound: Correlation with Mammographic Density

Tuesday, Nov. 27 12:15PM - 12:45PM Room: BR Community, Learning Center Station #6

## Participants

Eun Jung Choi, MD, PhD, Jeonju, Korea, Republic Of (*Presenter*) Nothing to Disclose Ji Hyun Youk, MD, Seoul, Korea, Republic Of (*Abstract Co-Author*) Nothing to Disclose Bo Ram Kim, Jeonju, Korea, Republic Of (*Abstract Co-Author*) Nothing to Disclose

#### For information about this presentation, contact:

cejcej80@hanmail.net

## PURPOSE

To analyze the background echotexture (BE) on automated breast ultrasound (ABUS) according to BI-RADS and modified BE classification in correlation with mammographic breast density (BD).

#### **METHOD AND MATERIALS**

196 women (age, 31-72 yrs) who underwent ABUS and mammography were included. Their menopausal status, parity, and family history of breast cancer were collected. After independently reviewing all ABUS and mammography images, three radiologists assigned BE as homogeneous-fat, homogeneous-fibroglandular, or heterogeneous based on BI-RADS as well as homogeneous-fat, homogeneous-fibroglandular, or hetergeneous-mild, moderate, and marked based on modified BE classification. BD was classified into category A, B, C, or D based on BI-RADS. The interobserver agreement was measured by kappa statistics ( $\kappa$ ). The association among demographics, BE, and BD was analyzed by Spearman's correlation coefficient ( $\rho$ ) and multiple linear regression.

#### RESULTS

The overall interobserver agreement for BE based on BI-RADS ( $\kappa$ =0.83), modified BE classification ( $\kappa$ =0.66), and BD ( $\kappa$ =0.84) was substantial to nearly perfect. By consensus, 29 homogeneous-fat (14.8%), 144 homogeneous-fibroglandular (73.5%), and 23 heterogeneous (11.7%) were assigned based on BI-RADS, while 41 homogeneous fat (20.9%), 9 homogeneous-fibroglandular (4.6%), or 46 hetergeneous-mild (23.5%), 65 moderate (33.2%), and 35 marked (17.9%) were assigned based on modified BE classification. For BD, 21 category A (10.7%), 79 category B (40.3%), 63 category C (32.1%), and 33 category D (16.8%) were assigned. The result of modified BE classification was positively correlated with BD (P<0.0001; overall,  $\rho$ =0.61; premenopausal,  $\rho$ =0.42; postmenopausal,  $\rho$ =0.57). BE based on BI-RADS was significantly correlated with BD in overall ( $\rho$ =0.2, P=0.005) and postmenopausal women ( $\rho$ =0.3, P=0.006). On multiple linear regression, BD and modified BE classification or parity and BE based on BI-RADS was associated (P<0.0001).

### CONCLUSION

Interobserver agreement of BE based on BI-RADS was nearly perfect, higher than modified BE classification. BE based on BI-RADS and modified BE classification on ABUS had good correlation with BD.

#### **CLINICAL RELEVANCE/APPLICATION**

Automated breast ultrasound would enable the objective analysis of background echotexture throughout the whole breast and its chronological change in correlation with mammographic density.



## CA224-SD-TUA1

Preliminary Evaluation of Main Pulmonary Artery Changes in Chronic Mountain Sickness Patients with Phase Contrast MR Imaging

Tuesday, Nov. 27 12:15PM - 12:45PM Room: CA Community, Learning Center Station #1

FDA Discussions may include off-label uses.

### Participants

Wen Wang, Xining, China (Presenter) Nothing to Disclose

# For information about this presentation, contact:

1570865391@qq.com

# PURPOSE

To investigate the clinical value of measurement of main pulmonary artery(MPA) structure and hemodynamics, and mean pulmonary artery pressure(MPAP) in Chronic Mountain Sickness(CMS) patients with MRI phase contrast method(PC-MRI).

## METHOD AND MATERIALS

22 male adult patients who were diagnosed with CMS and 20 healthy male adult volunteers at the same altitude were recruited from Dec.2016 to Feb.2018. T1WI Turbo Field Echo and 2D/QF sequence of Philips 1.5T magnetic resonance scanner was used for main pulmonary artery(MPA). Then cross-sectional area(CSA), peak velocity(PV), right ventricular stroke volume(RVSV) and regurgitant fraction(RF) were obtained. Meanwhile, relative dilatation degree (RDD) and MPAP were calculated.

### RESULTS

1.Structure data: CSA and RDD of patients were(7.52 $\pm$ 0.71)cm2 and(36.11 $\pm$ 11.27)%;Respectively, CSA and RDD of volunteers were(6.34 $\pm$ 1.12)cm2 and(52.08 $\pm$ 7.54)%; CSA was bigger than that of volunteers(P<0.01);RDD was smaller than that of volunteers(P<0.01).2.Hemodynamics data: PV,RVSV and RF of patients were(72.19 $\pm$ 9.41)cm/s,(64.43 $\pm$ 21.48)ml and(4.31 $\pm$ 0.93)%;PV,RVSV and RF of volunteers were(80.32 $\pm$ 11.15)cm/s,(59.12 $\pm$ 19.34)ml and(1.51 $\pm$ 0.48)%.PV was lower than that of volunteers(P=0.015);RVSV was higher than that of volunteers(P=0.411);RF was bigger than that of volunteers(P=0.004). 3.MPAP(36.71\pm12.36)mmHg was obviously higher than that(15.77 $\pm$ 6.69)mmHg of volunteers(P<0.01).

#### CONCLUSION

The long-term hypobaric and hypoxic environment leads to pulmonary hypertension such as MPA dilatation, decrease of flexibility and PV, and increase of RF and MPAP.

## **CLINICAL RELEVANCE/APPLICATION**

PC-MRI can noninvasively provide accurate information about MPA structure, hemodynamics and pressure, so as to evaluate MPA changes in CMS patients preliminarily.



### CA225-SD-TUA2

### Evaluation of Gravity Effect on Inferior Vena Cava and Abdominal Aortic Flow Using Multi-Posture MRI

Tuesday, Nov. 27 12:15PM - 12:45PM Room: CA Community, Learning Center Station #2

### **Participants**

Yoshisuke Kadoya, MD, Kanazawa, Japan (*Presenter*) Nothing to Disclose Tosiaki Miyati, PhD, Kanazawa, Japan (*Abstract Co-Author*) Nothing to Disclose Naoki Ohno, PhD, Kanazawa, Japan (*Abstract Co-Author*) Nothing to Disclose Satoshi Kobayashi, MD, Kanazawa, Japan (*Abstract Co-Author*) Nothing to Disclose Toshifumi Gabata, MD, PhD, Kanazawa, Japan (*Abstract Co-Author*) Nothing to Disclose

#### PURPOSE

To evaluate the differences of inferior vena cava flow (IVCF) and abdominal aortic flow (AAF) in the supine position (SP) and upright position (UP) of healthy volunteers, using an original magnetic resonance imaging (MRI) system that can obtain images in any posture (multi-posture MRI).

### **METHOD AND MATERIALS**

Caval velocity-mapped images were obtained with ECG-triggered cine phase-contrast technique in the supine and upright positions using multi-posture MRI (N = 12). The mean IVCF and AAF velocities in the region of interest in each cardiac phase were determined. In addition, flow curves in the cardiac cycle were obtained from the IVCF and AAF velocity multiplied by the each cross-sectional area. The following parameters in SP and UP were assessed. The mean IVC velocity (IVC-Vmean), the maximum IVC velocity (IVC-Vmax), the mean IVCF (IVCFmean), the maximum IVCF (IVCFmax), the cross-sectional area of IVC (IVC-CA), the mean AA velocity (AA-Vmean), the maximum AA velocity (AA-Vmax), the mean AAF (AAFmean), the maximum AAF (AAFmax), and the cross-sectional area of AA (AA-CA).

### RESULTS

The IVC-Vmean in UP  $(3.34 \pm 2.29 \text{ cm/s})$  was significantly lower than in SP  $(8.56 \pm 4.46 \text{ cm/s})$ , the IVC-Vmax in UP  $(4.10 \pm 2.25 \text{ cm/s})$  was significantly lower than in SP  $(13.1 \pm 5.09 \text{ cm/s})$ , the IVCFmean in UP  $(345 \pm 229 \text{ mL/min})$  was significantly lower than in SP  $(1453 \pm 461 \text{ mL/min})$ , the IVCFmax in UP  $(433 \pm 278 \text{ mL/min})$  was significantly lower than in SP  $(2453 \pm 926 \text{ mL/min})$ , and the IVC-CA in UP  $(205 \pm 121 \text{ mm2})$  was significantly lower than in SP  $(372 \pm 207 \text{ mm2})$ . The AA-Vmean in UP  $(2.10 \pm 0.79 \text{ cm/s})$  was significantly lower than in SP  $(6.71 \pm 2.30 \text{ cm/s})$ , the AA-Vmax in UP  $(5.22 \pm 2.39 \text{ cm/s})$  was significantly lower than in SP  $(17.9 \pm 6.52 \text{ cm/s})$ , the AAFmean in UP  $(241 \pm 113 \text{ mL/min})$  was significantly lower than in SP  $(699 \pm 306 \text{ mL/min})$ , and the AAFmax in UP  $(572 \pm 303 \text{ mL/min})$  was significantly lower than in SP  $(1823 \pm 630 \text{ mL/min})$ . However, no significant difference was observed between UP and SP in terms of the AA-CA  $(184 \pm 50.1 \text{ mm2})$  and  $175 \pm 43.6 \text{ mm2})$ .

### CONCLUSION

Both IVCF and AAF decrease in the upright position. Multi-posture MRI makes it possible to evaluate the effect of gravity on systemic circulation.

# **CLINICAL RELEVANCE/APPLICATION**

Clarifying the effect of gravity on IVCF and AAF might be valuable for the treatment of heart failure patients.



## CA226-SD-TUA3

MR Black Blood Thrombus Imaging in the Detection of Lower Extremity Vein using Optimized 3D FSE Sequence

Tuesday, Nov. 27 12:15PM - 12:45PM Room: CA Community, Learning Center Station #3

# Participants

Ling Zhang, Beijing, China (*Presenter*) Nothing to Disclose Jie Zhang, Beijing, China (*Abstract Co-Author*) Nothing to Disclose Rui Li, Beijing, China (*Abstract Co-Author*) Nothing to Disclose Shuo Chen, Beijing, China (*Abstract Co-Author*) Nothing to Disclose Chaohong Wang, Shanghai, China (*Abstract Co-Author*) Nothing to Disclose Nanjie Gong, Shanghai, China (*Abstract Co-Author*) Nothing to Disclose Guobin Li, Shanghai, China (*Abstract Co-Author*) Nothing to Disclose Guobin Li, Shanghai, China (*Abstract Co-Author*) Employee, Shanghai United Imaging Healthcare Co, Ltd Ruchen Peng, Beijing, China (*Abstract Co-Author*) Nothing to Disclose

#### For information about this presentation, contact:

zerozhangling@126.com

#### PURPOSE

Accurate detection of lower extremity deep vein thrombosis (LEDVT) and assessment of its stage are crucial for treatment decision-making. Challenges such as long scan time, and limited 3D coverage hampered the routine MR imaging for LEDVT detection. Thrombus imaging using a novel 3D FSE sequence with modulated refocusing flip angles and random k-space undersampling (referred to as MATRIX) has been evaluated in the current study.

#### **METHOD AND MATERIALS**

A total of 11 cases with acute LEDVT detected by ultrasound, with D-dimer> 500 µg/L on admission and clinical manifestation within 15 days, were prospectively enrolled in this study. All patients underwent 3.0T MR scans (uMR 770, United Imaging, Shanghai, China). Both 3D T2-weighted MATRIX and T1-weighted MPRAGE were performed in every examination with an isotropic resolution of 1mm. Seven patients received follow-up scans after one month.The thrombus area and signal intensity were measured on both T1WI and T2WI by two independent observers (Figure 1). The diagnostic agreement of thrombus detection between T2WI and T1WI was conducted using Cohenk test. The agreement between T1WI and T2WI in the measurement of thrombus area was performed by Bland-Altman analysis.

### RESULTS

Thirty segments were included in the study. There was a good agreement between the T1WI and T2WI in the detection of LEDVT ( $\kappa$ =1.000, p=0.000). Bland-Altman chart also showed strong agreement between T1WI and T2WI in the measurement of thrombus area. Among the 7 patients with follow-up scans, thrombi disappeared in 1 patient who underwent a thrombectomy, but were still present in the other 6 patients who underwent anticoagulation therapy only. The size of the thrombus was decreased remarkably on both T1WI and T2WI at the follow-ups. The signal intensity of thrombus decreased in 4 patients while increased in 2 patients on T2WI (Figure 1).

## CONCLUSION

3D isotropic MATRIX imaging provides sufficient coverage of interested regions within 4~5minutes, and its arbitrary multi-planar reconstruction facilitates the visualization and detection of suspected thrombus. This preliminary study shows the results of MATRIX are highly consistent with that of MPRAGE in the detection of LEDVT. Furthermore, the combination of MATRIX and MPRAGE may help to assess the stage of thrombus with great confidence, as reported in an early study using 2D imaging.

# **CLINICAL RELEVANCE/APPLICATION**

Optimized 3D FSE sequence can be used in assessment of LEDVT.



## CA227-SD-TUA4

Cardiac MRI (CMR) Strain Parameters in Determining the Need for Cardiac Re-Interventions in Patients with Repaired Tetralogy of Fallot (TOF)

Tuesday, Nov. 27 12:15PM - 12:45PM Room: CA Community, Learning Center Station #4

### Participants

Jiali Luan, BS, Edmonton, AB (*Presenter*) Nothing to Disclose Edythe Tham, MBBS, Edmonton, AB (*Abstract Co-Author*) Nothing to Disclose Kumaradevan Punithakumar, PhD, Edmonton, AB (*Abstract Co-Author*) Nothing to Disclose Michelle L. Noga, MD, Edmonton, AB (*Abstract Co-Author*) Nothing to Disclose

For information about this presentation, contact:

jluan1@ualberta.ca

## PURPOSE

To estimate the diagnostic value of CMR derived strain in determining repeat invasive cardiac intervention in patients with repaired TOF.

# METHOD AND MATERIALS

65 patients with repaired TOF, aged 1-20 years at time of CMR underwent endocardial strain analysis of the longitudinal 4 chamber, circumferential short axis cine and volumetric function measured by right ventricular ejection fraction (RVEF). Right ventricular (RV) strains were calculated using a semi-automated MRI deformation software developed in-house. The 4 chamber RV endocardial contour was also divided into 6 wall regions (septal-basal, septal-mid wall, septal-apical, lateral-apical, lateral-mid wall and lateral-basal). Patients were divided into those who had CMR between two consecutive cardiac interventions (percutaneous or surgical) within 10 years (n=18) and those who had no re-interventions after 10 years of the complete TOF repair (n=47). Maximum strain was compared between the two groups with the Student's t-test (a=0.05). In addition, receiver operating characteristic (ROC) curves, which quantify the effectiveness of the strain parameters in detecting the need for re-intervention were generated. Optimal threshold values were determined based on the greatest sum of sensitivity and specificity based on the ROC curve.

## RESULTS

Longitudinal global maximum strain was decreased in the re-intervention group compared to the no intervention group and 8 out of 9 segmental strain parameters were significantly decreased in the re-intervention group. Longitudinal global strain showed better diagnostic accuracy than segmental strain parameters for the longitudinal scans. Longitudinal maximum global strains of > -18.10 or circumferential mid-wall strains of >-14.94 were predictive of the need for re-intervention within 10 years with sensitivities of 60-67%, specificities of 85-87% and diagnostic accuracies of 78-83%. Longitudinal global and short axis mid-wall strains perform similarly compared to RVEF in detecting the need for re-intervention.

#### CONCLUSION

Patients with repaired TOF who required re-intervention within a 10 year period show impaired systolic function and contractility. Maximum strain measures perform similarly compared to RVEF in predicting the need for re-intervention.

### **CLINICAL RELEVANCE/APPLICATION**

The use of contractility measures may complement existing criteria to guide decisions regarding re-intervention in patients with repaired TOF.



## CA228-SD-TUA5

Cardiac T1, T2 and T2\* Mapping: Intersegmental, Interregional and Inter-level Reproducibility

Tuesday, Nov. 27 12:15PM - 12:45PM Room: CA Community, Learning Center Station #5

### Participants

Rafael Heiss, Erlangen, Germany (Abstract Co-Author) Speakers Bureau, Siemens AG

Christoph Treutlein, Erlangen, Germany (Presenter) Nothing to Disclose

Marco Wiesmueller, MD, Erlangen, Germany (Abstract Co-Author) Speakers Bureau, Siemens AG

Michael Uder, MD, Erlangen, Germany (Abstract Co-Author) Speakers Bureau, Bracco Group Speakers Bureau, Siemens AG Speakers Bureau, Bayer AG Research Grant, Siemens AG

Wolfgang Wust, MD, Erlangen, Germany (Abstract Co-Author) Speakers Bureau, Siemens AG

Matthias S. May, MD, Erlangen, Germany (Abstract Co-Author) Speakers Bureau, Siemens AG

#### PURPOSE

Evaluation of the intersegmental, interregional and interlevel comparability of T1, T2 and T2\* relaxation times.

### **METHOD AND MATERIALS**

Native cardiac MRIs of 26 healthy subjects (14 w and 12 m, 26  $\pm$  3 years) were performed on a 1.5 T scanner with automated inline motion correction. For each subject, three long (LAX) and three short axes (SAX) were acquired at corresponding slice positions. The evaluation of each segment was performed according to the AHA model by placing a segmental mid myocardial ROI. The corresponding segments of the LAX and SAX were compared in pairs. In addition, the cardiac segments were divided into groups (anterior, anteroseptal, inferior, inferolateral and anterolateral as well as basal, medial, apical and the corresponding interlevel or interregional differences were analyzed.

### RESULTS

In the intersegmental comparison between the corresponding LAX and SAX segments showed a significant difference in 33% in T1, 28% in T2 and 44% in T2\* mapping. In the interregional comparison of the SAX segments a significant difference in 60% of grouped segments in T1, in 63% of grouped segments in T2 and in 93% of grouped segments in T2\* mapping occurred. In the same comparison of LAX segments 80% of grouped segments in T1, 46% of grouped segments in T2, and 87% of grouped segments in T2\* mapping showed a significant difference. In the interlevel comparison of the SAX segments, there was a significant difference in T1 mapping between basal vs. medial (p < 0.01) and for basal vs. apical (p < 0.01), in T2 mapping between basal vs. apical (p < 0.01). In the interlevel comparison of the LAX segments a significant difference in T1 mapping between basal vs. apical (p < 0.01) and for medial vs. apical (p < 0.01) and for medial vs. apical (p < 0.01) and medial vs. apical (p < 0.01) and for medial vs. apical (p < 0.01) and in T2\* mapping between basal vs. medial (p < 0.01) occurred.

### CONCLUSION

T1, T2 und T2\* times can vary between single heart segments in healthy people in dependence of anatomic location and acquired axes.

## **CLINICAL RELEVANCE/APPLICATION**

Analyzing of left ventricular mapping should be done in multiple segments to get accurate results and follow-up examinations should be measured in the identical segment to obtain consistent results.



## CA229-SD-TUA6

## Radiomics of Coronary Artery Calcium in the Framingham Heart Study

Tuesday, Nov. 27 12:15PM - 12:45PM Room: CA Community, Learning Center Station #6

#### Awards **Student Travel Stipend Award**

#### Participants

Parastou Eslami, PhD, Boston, MA (Presenter) Nothing to Disclose Chintan Parmar, Boston, MA (Abstract Co-Author) Nothing to Disclose Borek Foldyna, MD, Boston, MA (Abstract Co-Author) Nothing to Disclose Jan-Erik Scholtz, MD, Boston, MA (Abstract Co-Author) Nothing to Disclose Alexander Ivanov, BS, Boston, MA (Abstract Co-Author) Nothing to Disclose Roman Zeleznik, Boston, MA (Abstract Co-Author) Nothing to Disclose Michael T. Lu, MD, Boston, MA (Abstract Co-Author) Nothing to Disclose Maros Ferencik, MD, Boston, MA (Abstract Co-Author) Nothing to Disclose Vasan Ramachandran, Boston, MA (Abstract Co-Author) Nothing to Disclose Kristin Baltrusaitis, Boston, MA (Abstract Co-Author) Nothing to Disclose Joseph M. Massaro, PhD, Boston, MA (Abstract Co-Author) Nothing to Disclose Ralph D'Agnostino, PhD, Boston, MA (Abstract Co-Author) Nothing to Disclose Christopher J. O'Donnell, MD, MPH, West Roxbury, MA (Abstract Co-Author) Nothing to Disclose Hugo Aerts, PhD, Boston, MA (Abstract Co-Author) Stockholder, Sphera Inc Udo Hoffmann, MD, Boston, MA (Abstract Co-Author) Institutional Research Grant, Kowa Company, Ltd; Institutional Research Grant, Abbott Laboratories; Institutional Research Grant, HeartFlow, Inc; Institutional Research Grant, AstraZeneca PLC

### For information about this presentation, contact:

### peslami1@mgh.harvard.edu

## PURPOSE

To assess whether detailed coronary artery calcium (CAC) characterization based on radiomic feature extraction followed by machine learning improves prediction of cardiovascular (CV) events.

# **METHOD AND MATERIALS**

Participants from the Offspring and third Generation cohorts of the community-based Framingham Heart Study who underwent chest CT between 2002 and 2005 were followed over a median of 9.1 years for cardiovascular events (CV) events (myocardial infarction, stroke, or death). Of those, 624 participants who had excellent image guality and CAC (Agatston score (AS)> 0) were randomly divided into discovery (n=318) and validation cohorts (n=306). CAC was segmented manually using 3DSlicer, and about 2000 radiomic features (based on intensity, shape, and texture of CAC) were extracted using pyRadiomics software. In the derivation cohort, we used an internal minimum redundancy maximum relevancy algorithm (without knowledge of events) to identify the 20 highest ranked features. Finally, a random forest classifier was used to optimize decision trees for prediction for CV events. The weighted predictive probability of events for each of the 20 features was summarized into a radiomic score. The performance of this score was tested independent in the validation cohort.

## RESULTS

The discovery (66.1% men, 58.1±11.1 age) and validation cohorts (61.4% men, 59.3±11.2 age) had similar CV risk profile, median AS, and CV event rates (30/318 =9.7% and 29/306=9.5%, respectively). In adjusted multivariate analysis (for Framingham risk factors and AS), participants in the validation cohort, who had radiomic scores in the mid and upper tertiles had significantly higher risk for events as compared to the lower tertile (mid: HR= 9.3, p=0.03, upper: HR=16.5, p=0.007). The area under the curve (AUC) was higher for AS, radiomic score (RS), and combined AS/RS were 0.73, 0.76 and 0.79; respectively in the overall population. Performance was best in the subgroup with AS <300 (n=250, Figure)

#### CONCLUSION

This proof-of-concept study demonstrates that detailed CAC characterization based on radiomic feature extraction predicts CV events independent of traditional risk factors and AS. Further validation is necessary to determine clinical impact.

## **CLINICAL RELEVANCE/APPLICATION**

Artificial intelligence may identify a prognostically important radiomic signature of CAC.

## **Honored Educators**

Presenters or authors on this event have been recognized as RSNA Honored Educators for participating in multiple qualifying educational activities. Honored Educators are invested in furthering the profession of radiology by delivering high-quality educational content in their field of study. Learn how you can become an honored educator by visiting the website at: https://www.rsna.org/Honored-Educator-Award/ Udo Hoffmann, MD - 2015 Honored Educator



## CA230-SD-TUA7

Cardiac Magnetic Resonance T1 Mapping in Adolescent and Young Adult Survivors of Childhood Cancers

Tuesday, Nov. 27 12:15PM - 12:45PM Room: CA Community, Learning Center Station #7

**FDA** Discussions may include off-label uses.

#### **Participants**

Ming-Yen Ng, MBBS, Toronto, ON (*Presenter*) Nothing to Disclose Xiaowan Tong, Hong Kong, Hong Kong (*Abstract Co-Author*) Nothing to Disclose Vivian Wing-Yi Li, Hong Kong, Hong Kong (*Abstract Co-Author*) Nothing to Disclose Anthony Pak-Yin Liu, Hong Kong, Hong Kong (*Abstract Co-Author*) Nothing to Disclose Edwina Kam-fung So, Hong Kong, Hong Kong (*Abstract Co-Author*) Nothing to Disclose Nathan Leung, Hong Kong, Hong Kong (*Abstract Co-Author*) Nothing to Disclose Wanshu Huang, Hong Kong, Hong Kong (*Abstract Co-Author*) Nothing to Disclose Queenie Chan, PhD, Hong Kong, China (*Abstract Co-Author*) Nothing to Disclose Karin Kar-Huen Ho, Hong Kong, Hong Kong (*Abstract Co-Author*) Nothing to Disclose Jeffrey Ping-Wa Yau, Hong Kong, Hong Kong (*Abstract Co-Author*) Nothing to Disclose Daniel Ka-Leung Cheuk, Hong Kong, Hong Kong (*Abstract Co-Author*) Nothing to Disclose Yiu-Fai Cheung, Hong Kong, Hong Kong (*Abstract Co-Author*) Nothing to Disclose

For information about this presentation, contact:

myng2@hku.hk

## PURPOSE

Limited data based on small T1 mapping studies of childhood cancer survivors, in particular females, treated with anthracyclinebased chemotherapy suggested an increase in left ventricular (LV) fibrosis. We determined using T1 mapping the severity of fibrosis in a relatively large cohort of adolescent and young adult long-term childhood cancer survivors.

#### **METHOD AND MATERIALS**

This is a prospective case-control study of 55 survivors (34 male) aged 25±7 years and 42 age-and gender-matched controls. The patients were studied at 17±7 years after completion of chemotherapy. The mean cumulative anthracycline dose was 229±86 mg/m2. Ventricular volumes, ejection fraction, native myocardial T1 and extracellular volume (ECV) were determined by cardiac magnetic resonance using modified Look-Locker (MOLLI) sequence. Late gadolinium enhancement was also quantified.

## RESULTS

Left ventricular ejection fraction was lower in survivors than controls ( $54\pm5\%$  vs  $56\pm4\%$ , p=0.008). However, there were no statistically significant differences in native T1 ( $1222\pm23$  ms vs  $1226\pm19$  ms, p=0.31) and ECV ( $22.9\pm2.2\%$  vs  $23.8\pm2.4\%$ , p=0.06) between survivors and controls. Quantification of LGE similarly did not demonstrate significant difference between survivors and controls ( $0.92\%\pm1.32\%$  vs.  $0.46\%\pm0.96\%$ , p=0.07). Furthermore, T2 values were similar in both groups ( $57\pm4$  ms vs.  $58\pm6$  ms, p=0.225). While females survivors had higher native T1 ( $1232\pm19$  ms vs  $1219\pm22$  ms, p<0.001) and ECV ( $24.7\pm1.8\%$  vs  $22.1\pm2\%$ , p<0.001) than male survivors, no differences were found when compared with female controls who had native T1 of  $1228\pm19$  ms (p=0.56) and ECV of  $25.1\pm1.8$  (p=0.23). Native T1 but not ECV correlated positively with duration since completion of chemotherapy (r=0.34, p=0.01).

### CONCLUSION

In adolescent and young adult cancer survivors, T1 mapping does not reveal evidence of significant myocardial fibrosis. Intrinsic gender differences in T1 parameters probably account for the observation of increased T1 mapping values in female survivors.

### **CLINICAL RELEVANCE/APPLICATION**

Provides incremental information that the T1 mapping values previously demonstrated in other studies is probably related to gender differences and when compared to normal volunteers, there is no significant difference. Future investigation should focus on longitudinal follow-up and using T1 mapping for risk stratification of patients with heart failure rather than asymptomatic patients.



### CA236-SD-TUA8

### Quantitative Evaluation of Monoexponential High B Value DWI in Cardiac Tumors

Tuesday, Nov. 27 12:15PM - 12:45PM Room: CA Community, Learning Center Station #8

### Participants

Jordi Broncano, MD, Cordoba, Spain (*Presenter*) Nothing to Disclose Fernando Caro Mateo, Cadiz, Spain (*Abstract Co-Author*) Nothing to Disclose Javier Sanchez, MD, PhD, Madrid, Spain (*Abstract Co-Author*) Nothing to Disclose Pilar Caro, MD, Cadiz, Spain (*Abstract Co-Author*) Nothing to Disclose Paula Montesinos de la Vega, Madrid, Spain (*Abstract Co-Author*) Employee, Koninklijke Philips NV Antonio Luna, MD, PhD, Jaen, Spain (*Abstract Co-Author*) Consultant, Bracco Group; Speaker, General Electric Company; Speaker, Canon Medical Systems Corporation; Royalties, Springer Nature

#### For information about this presentation, contact:

j.broncano.c@htime.org

#### PURPOSE

To evaluate the feasibility, reproducibility and diagnostic performance of quantitative analysis of DWI in cardiac tumors

## METHOD AND MATERIALS

18 patients, 6 males and 12 females with mean age and heart rate of 61.06+/-19.79 years-old and 66.5+/-9.17 bpm, respectively. High b value (b=0 and 300 s/mm2) DWI was done with cardiac triggering at end diastole. Manual ROI was placed by two radiologists in the lesion and pectoralis muscle at high b value and ADC map. Absolute and normalized (SIR =SIlesion /SIpectoralis muscle; ADCr=ADClesion/ADCpectoralis muscle) mean and miminum signal intensity (SIb300) and ADC were recorded. U Mann - Whitney tests, ROC curves and intraclass correlation coefficient (CCI) were calculated (=0.05).

#### RESULTS

5 malignant lesions (2 metastasis, lymphoma and 2 sarcoma) and 13 benign lesions (6 mixomas, 2 mitral valve caseous necrosis, 2 pericardial cysts, 1 intracavitary thrombus and 1 hydatid cyst) were observed. Significant differences in mean and minimum SIb300 (153.17 +/- 45.97 vs. 362.02 +/- 104.6 and 58.58 +/- 18.17 vs. 256.41 +/- 89.49; p0.05). Contrarilly to ADC based measures, SI and SIR displayed excellent interobserver reproducibility. ROC curves showed higher area under the curve in SI based measurements (0.82-0.89) compared to ADC based ones (0.57-0.81).

## CONCLUSION

High b value DWI is feasible and reproducible technique for differentiating benign from malignant cardiac tumors. SI based measurements displayed better diagnostic performance compared to ADC based ones with excellent interobserver agreement.

# **CLINICAL RELEVANCE/APPLICATION**

Cardiac DWI allow the characterization of cardiac lesions and masses with great diagnostic performance, high reproducibility and without the use of intravenous contrast.

#### **Honored Educators**

Presenters or authors on this event have been recognized as RSNA Honored Educators for participating in multiple qualifying educational activities. Honored Educators are invested in furthering the profession of radiology by delivering high-quality educational content in their field of study. Learn how you can become an honored educator by visiting the website at: https://www.rsna.org/Honored-Educator-Award/ Antonio Luna, MD - 2018 Honored Educator



### CH245-ED-TUA6

## **Radiomics in Lung Cancer: State of the Art**

Tuesday, Nov. 27 12:15PM - 12:45PM Room: CH Community, Learning Center Station #6

### Awards **Certificate of Merit**

### **Participants**

Alessandra Farchione, MD, Rome, Italy (Presenter) Nothing to Disclose Alessandra Ottavianelli, MD, Rome, Italy (Abstract Co-Author) Nothing to Disclose Jacopo Lenkowicz, Rome, Italy (Abstract Co-Author) Nothing to Disclose Lucio Calandriello, MD, Rome, Italy (Abstract Co-Author) Nothing to Disclose Annemilia del Ciello, MD, Rome, Italy (Abstract Co-Author) Nothing to Disclose Giuseppe Cicchetti, MD, Rome, Italy (Abstract Co-Author) Nothing to Disclose Giuliano Sica, Rome, Italy (Abstract Co-Author) Nothing to Disclose Anna Rita Larici, MD, Rome, Italy (Abstract Co-Author) Nothing to Disclose Riccardo Manfredi, MD, Rome, Italy (Abstract Co-Author) Nothing to Disclose

## For information about this presentation, contact:

alessandra.farchione@gmail.com

### **TEACHING POINTS**

1) To describe the Radiomics process 2) To discuss Radiomics clinical role in lung cancer management

### **TABLE OF CONTENTS/OUTLINE**

Tumour's stage is the prognosticator used in the management of lung cancer, indeed, in addition to the anatomic extend other factors determine prognosis. The interaction between microenvironment and neoplastic cells is responsible of the genetic/phenotypic mutations in neoplastic tissue and of the deriving heterogeneity. Radiomics refers to the extraction of quantitative image features from standard-of-care medical imaging that can be related to underlie phenotype/genotype, to their analysis and modelling in relation to prediction targets. The workflow includes: - Data selection and image acquisition; -Segmentation; - Features extraction; - Model building and validation. Radiomics's field of interest are multiple: - Histopathology correlation; To obtain a "virtual biopsy" by relating imaging analysis with the genetic one - Lesion Characterization; Malignant lesions are characterized by greater heterogeneity and irregular shape.- Prediction of tumour aggressiveness and clinical outcome; heterogeneous tumours tend to be more aggressive and to have be poorer outcomes. Strength and critical points of the process will be described.



## CH246-ED-TUA7

# Imaging After Conventional and Stereotactic Body Radiation Therapy in the Thorax

Tuesday, Nov. 27 12:15PM - 12:45PM Room: CH Community, Learning Center Station #7

## Awards Certificate of Merit

#### Participants

Luke A. Ginocchio, MD, New York, NY (*Presenter*) Nothing to Disclose Lea Azour, MD, New York, NY (*Abstract Co-Author*) Nothing to Disclose Benjamin Cooper, New York, NY (*Abstract Co-Author*) Travel support, Ion Beam Applications SA; Barry Hutchinson, MBBCh, MRCS, Galway, Ireland (*Abstract Co-Author*) Nothing to Disclose William H. Moore, MD, Port Washington, NY (*Abstract Co-Author*) Consultant, Merck & Co, Inc; Consultant, BTG International Ltd; Jane P. Ko, MD, New York, NY (*Abstract Co-Author*) Research collaboration, Siemens AG

### For information about this presentation, contact:

jane.ko@nyumc.org

### **TEACHING POINTS**

Radiation therapy has a major role in adjuvant, neoadjuvant and palliative therapies for lung cancer and includes conventional (CRT) and 3D conformal techniques. Stereotactic body radiation therapy (SBRT) uses a small number of fractions for definitive treatment of early stage lung cancer and metastatic disease. Post-CRT and -SBRT therapy changes manifest with differing appearances of which the radiologist should be aware to avoid pitfalls in interpretation and identify when tumor recurrence exists. The reviewer of this exhibit will have an improved understanding of a) Indications for CRT and SBRT and amenable lesions for these therapies b) the patterns of radiation pneumonitis for CRT and SBRT that can occur to improve understanding of complications and c) complications, including tumor recurrence.

### TABLE OF CONTENTS/OUTLINE

1. RT techniques and indications -CRT -3D techniques -SBRT2. Imaging of the post RT patient: time and technique3. CRT and SBRT complications -Acute and chronic radiation pneumonitis: CRT (conventional pattern) SBRT (masslike consolidation, modified conventional pattern) -Pericarditis/pleuritis4. Complications and tumor recurrence: CT findings -Tumor recurrence -Infection -Rib fracture



## CH274-SD-TUA1

Thin-Section CT May Identify the Cases Meeting the Histological Criteria of Interstitial Pneumonia with Autoimmune Features Among the Population Showing Usual Interstitial Pneumonia Pattern Fibrosis

Tuesday, Nov. 27 12:15PM - 12:45PM Room: CH Community, Learning Center Station #1

## Participants

Ryoko Egashira, MD,PhD, Saga, Japan (*Presenter*) Nothing to Disclose Mikiko Hashisako, Fukuoka, Japan (*Abstract Co-Author*) Nothing to Disclose Hiromitsu Sumikawa, MD, Suita, Japan (*Abstract Co-Author*) Nothing to Disclose Junya Tominaga, PhD, Sendai, Japan (*Abstract Co-Author*) Nothing to Disclose Tomonori Tanaka, MD, Toyama, Japan (*Abstract Co-Author*) Nothing to Disclose Yasuhiko Yamano, Aichi, Japan (*Abstract Co-Author*) Nothing to Disclose Yasuhiro Kondoh, Seto, Japan (*Abstract Co-Author*) Nothing to Disclose Kiminori Fujimoto, MD, PhD, Kurume, Japan (*Abstract Co-Author*) Nothing to Disclose Takeshi Johkoh, MD, PhD, Itami, Japan (*Abstract Co-Author*) Nothing to Disclose Hiroyuki Irie, MD, PhD, Saga, Japan (*Abstract Co-Author*) Nothing to Disclose

# For information about this presentation, contact:

egashira@cc.saga-u.ac.jp

#### PURPOSE

To find thin-section CT (TSCT) findings which correspond to the histological criteria of interstitial pneumonia with autoimmune features (IPAF) among the population showing usual interstitial pneumonia (UIP) pattern fibrosis.

### METHOD AND MATERIALS

This retrospective study included 149 consecutive cases with unknown causes who had undergone surgical lung biopsy and showing UIP pattern fibrosis on histology (M:F=105:44; median age, 65). TSCT images were evaluated for the disease extent, and presence or absence of parenchymal findings considered as the candidates. Histological images were reviewed for the findings sited as IPAF findings. TSCT findings were compared with each histological finding and clinical information using chi-square test/Fisher's test and multivariate logistic regression analyses by stepwise method.

### RESULTS

Histopathological IPAF findings were seen in a total of 34 cases (interstitial lymphoid aggregates with germinal center, 12; diffuse lymphoplasmacytic infiltration, 14; pleuritis, 8; airway disease, 15; vasculopathy, 0). On multivariate analyses, following CT findings were significantly associated with histological features: extent of ground-glass opacification and focal fissure thickening for any of histological criteria (P=0.046 and 0.007, respectively), extent of consolidation, dense reticulation and focal fissure thickening for interstitial lymphoid aggregates with germinal center (P=0.008, 0.022 and 0.245, respectively); subpleural sparing and centrilobular nodules for airway lesion (P=0.008 and 0.024, respectively); subpleural sparing and centrilobular nodules for pleuritis (P=0.0007 and 0.042, respectively). In addition, mosaic attenuation, shaggy thickening of interlobular septa, pulmonary artery enlargement were independent factors for positive serological domain (P=0.003, 0.049 and 0.016 respectively), mosaic attenuation was for IPAF cases (P=0.016).

## CONCLUSION

Several CT findings including centrilobular nodules and extent of ground-glass opacification might be a potential marker of histopathological IPAF features in UIP pattern cases without doing surgical lung biopsy.

### **CLINICAL RELEVANCE/APPLICATION**

TSCT may help identify the cases with IPAF showing UIP pattern which immunosuppressive therapy work well without invasive surgical lung biopsy.



# CH275-SD-TUA2

Performance of Various Machine Learning Methods in CT Texture Analysis to Differentiate Lung Cancer from Benign Nodule with Small Ground-Glass Opacity Nodules

Tuesday, Nov. 27 12:15PM - 12:45PM Room: CH Community, Learning Center Station #2

# Participants

Takeshi Nakaura, MD, Kumamoto, Japan (*Presenter*) Nothing to Disclose Yuji Iyama, MD, Kumamoto, Japan (*Abstract Co-Author*) Nothing to Disclose Kouichi Kawanaka, MD, Kumamoto, Japan (*Abstract Co-Author*) Nothing to Disclose Seitaro Oda, MD, Kumamoto, Japan (*Abstract Co-Author*) Nothing to Disclose Daisuke Utsunomiya, MD, Kumamoto, Japan (*Abstract Co-Author*) Nothing to Disclose Yoshinori Funama, PhD, Kumamoto, Japan (*Abstract Co-Author*) Nothing to Disclose Masafumi Kidoh, Kumamoto, Japan (*Abstract Co-Author*) Nothing to Disclose Yasunori Nagayama, MD, Kumamoto, Japan (*Abstract Co-Author*) Nothing to Disclose Yasunori Nagayama, MD, Kumamoto, Japan (*Abstract Co-Author*) Nothing to Disclose Yasuyuki Yamashita, MD, Kumamoto, Japan (*Abstract Co-Author*) Nothing to Disclose Taihei Inoue, MD, Kumamoto, Japan (*Abstract Co-Author*) Nothing to Disclose Shinichi Tokuyasu, RT,MS, Minato-ku, Japan (*Abstract Co-Author*) Nothing to Disclose

## PURPOSE

To evaluate the performance of various machine learning method based on CT texture analysis to differentiate lung cancer from benign nodule with solitary ground-glass opacity nodules.

## METHOD AND MATERIALS

This retrospective study was approved by the institutional review board. The requirement to obtain informed consent was waived. We included 132 patients who was pointed out small (<3cm) ground-glass opacity nodules with lung CT scan and were diagnosed by the biopsy. Of 132 patients, 59 was diagnosed as benign nodule and 73 was diagnosed as lung cancer. Twelve kinds of the histogram and the texture parameters (minimum normalized signal, mean normalized signal, standard deviation of normalized signal, max normalized signal, skewness, kurtosis, homogeneity, energy, contrast, correlation, entropy, dissimilarity) were assessed for unenhanced CT. A prediction model was developed using various machine learning methods (univariate logistic regression and K-nearest neighbor, Support vector machine, Random forest, multivariate Logistic regression and eXtreme gradient boosting with all features) and the area under the receiver operating characteristic curve of this model was calculated via 5-fold cross validation. In addition, the performance of the machine learning method was compared with the judgments of three board certified radiologists.

### RESULTS

With the univariate logistic regression models, the skewness offered the highest AUC (0.66), followed by mean value (0.65), standard value (0.59), kurtosis (0.58), max value (0.57) and entropy (0.56). With the multivariate models, the eXtreme Gradient Boosting offered the highest AUC (0.73), followed by multivariate Logistic regression (0.70), Random Forest (0.69), Support Vector Machine (0.67) and K-Nearest Neighbor (0.65). The AUC of the eXtreme Gradient Boosting was comparable to that of the two radiologists (0.68 and 0.73, respectively)

#### CONCLUSION

The performance of machine learning was comparable to that of experienced radiologists to differentiate lung cancer from benign nodule with solitary ground-glass opacity nodules, and the diagnostic performance varies by the machine learning algorisms.

## **CLINICAL RELEVANCE/APPLICATION**

We must choose adequate machine learning algorism for datasets to improve the diagnostic performance of machine learning.



## CH276-SD-TUA3

Prognostic Implications of Radiomic Features for EGFR Mutation Status in Patients with Lung Adenocarcinoma

Tuesday, Nov. 27 12:15PM - 12:45PM Room: CH Community, Learning Center Station #3

#### **Participants**

Quan Chen, Wuhan, China (*Presenter*) Nothing to Disclose Rong Yuan, PhD, Shenzhen, China (*Abstract Co-Author*) Nothing to Disclose Shuyue Shi, Wuhan, China (*Abstract Co-Author*) Employee, Ruijia Technology, Inc Qiguang Cheng, MD, Wuhan, China (*Abstract Co-Author*) Nothing to Disclose Ruiguang Zhang, Wuhan, China (*Abstract Co-Author*) Nothing to Disclose

## For information about this presentation, contact:

cq7355023@163.com

### PURPOSE

This study retrospectively evaluated the clinical availability of computed-tomography (CT) based radiomic features to predict EGFR mutation status in patients with lung adenocarcinoma.

# METHOD AND MATERIALS

We analyzed 417 primary lung adenocarcinomas from an unselected Chinese population. 219 quantitative 3D features were extracted from segmented volumes of each tumor, and 59 of these which were considered as independent features were included in theanalysis. Clinical and pathological information were obtained from the institutional database.

## RESULTS

Mutant EGFR was significantly associated with female gender (p=0.0005); never smoker status (p<0.0001), lepidic predominant adenocarcinomas (p=0.017), and low orintermediate pathologic grade (p=0.0002). Statistically significant differences were found in 11 radiomic features between EGFR mutant and wild type groups on univariate analysis. Mutant EGFR status could be predicted by a set of seven radiomic features that fall in three broad groups: CT attenuation energy, tumor main direction and texture defined by wavelets and Laws (AUC 0.740). Multiple logistic regression model showed that adding radiomic features to a clinical model resulted in a significant improvement of predicting power, as the AUC increased from 0.667 to 0.720 (p<0.0001).

# CONCLUSION

CT-based radiomic features of lung adenocarcinomas can capture useful information regarding tumor phenotype, and the model we built can be useful to predict thepresence of EGFR mutations in lung adenocarcinoma in patients when mutational profiling is not available or possible.

## **CLINICAL RELEVANCE/APPLICATION**

Based on the analysis of the histologic features of CT images, the EGFR mutation prediction system for non-small cell lung cancer was established.



## CH277-SD-TUA4

Automatic Segmentation for Pulmonary Pure Ground-Glass Nodules from Follow-Up CT Scans Using Recurrent Convolutional Neural Networks

Tuesday, Nov. 27 12:15PM - 12:45PM Room: CH Community, Learning Center Station #4

## Participants

Linlin Qi, Beijing, China (*Presenter*) Nothing to Disclose Jianwei Wang, MD, Beijing, China (*Abstract Co-Author*) Nothing to Disclose Quanlong Feng, PhD, Beijing, China (*Abstract Co-Author*) Nothing to Disclose Xiuli Li, Beijing, China (*Abstract Co-Author*) Nothing to Disclose Botong Wu, Beijing, China (*Abstract Co-Author*) Nothing to Disclose Ning Wu, MD, Beijing, China (*Abstract Co-Author*) Nothing to Disclose Shichao Feng, Beijing, China (*Abstract Co-Author*) Nothing to Disclose Wei Tang, MD, Beijing, China (*Abstract Co-Author*) Nothing to Disclose Lina Zhou, MD, Beijing, China (*Abstract Co-Author*) Nothing to Disclose

### PURPOSE

To present a recurrent convolutional neural networks for automatic and accurate pure ground-glass nodule (pGGN) segmentation for follow-up CT scans.

#### **METHOD AND MATERIALS**

The test dataset contains 104 pGGNs from 104 patients with 441 follow-up CT scans. As for the method, we present a recurrent convolutional neural networks to segment pGGNs iteratively for automatic segmentation and assisting observation of pGGNs in follow-up CT scans. Specifically, a 3D UNet was utilized as the base segmentation model to generate prior nodule boundaries, while a proposed recurrent neural network with ranking loss was adopted to refine the nodule boundaries based on all previous segmentation results in a recurrent way. The proposed network was first trained with the Lung Image Database Consortium and Image Database Resource Initiative (LIDC-IDRI) dataset with a test Dice coefficient of 83.18% and then fine tuned by a pGGN dataset from our hospital. In addition, several key indicators of the pGGNs were derived automatically from the segmentation results including volume, mass, volume double time (VDT), mass double time (MDT), etc., which can assist doctors in deciding on strategy of follow-up.

#### RESULTS

The present segmentation method was tested on the above test dataset, with a total of 441 pGGNs. Consider each slice as an individual nodule sample, 8091 pGGN slices were included in the test dataset. Experimental results show that 6746 pGGN ROIs were identified and segmented successfully while the false positive rate is 24.51% and the recall is 96.54%. The average F-measure is 0.8473 which shows that our method is reliable for the segmentation of various shapes of pGGNs. Besides, the results also show that our method is robust to the growth of pGGNs. As for the efficiency, it takes only an average time of 0.39s to segment one nodule on a single Titan X pascal GPU.

### CONCLUSION

In this study, we presented a recurrent convolutional neural networks and showed the feasibility of the proposed method on segmenting pure ground-glass nodules from follow-up CT scans.

### **CLINICAL RELEVANCE/APPLICATION**

We present an automatic recurrent convolutional neural networks for pure ground-glass nodule segmentation from follow-up CT scans with reliable and robust performance, which can lighten the reading burden and help compute the VDT and MDT for radiologists.



## CH278-SD-TUA5

STIR Turbo Spin-echo Imaging versus Contrast-Enhanced Thin-Section CT: Capability for Chest Wall Invasion Assessment in Candidates for Surgical Resection due to Non-Small Cell Lung Cancer

Tuesday, Nov. 27 12:15PM - 12:45PM Room: CH Community, Learning Center Station #5

# Participants

Daisuke Takenaka, MD, Akashi, Japan (Presenter) Nothing to Disclose

Yuji Kishida, MD, PhD, Kobe, Japan (Abstract Co-Author) Nothing to Disclose

Shinichiro Seki, Kobe, Japan (Abstract Co-Author) Research Grant, Canon Medical Systems Corporation

Hisanobu Koyama, MD, PhD, Osaka, Japan (Abstract Co-Author) Nothing to Disclose

Takeshi Yoshikawa, MD, Kobe, Japan (*Abstract Co-Author*) Research Grant, Canon Medical Systems Corporation Yoshiharu Ohno, MD, PhD, Kobe, Japan (*Abstract Co-Author*) Research Grant, Canon Medical Systems Corporation; Research Grant, Koninklijke Philips NV; Research Grant, Bayer AG; Research Grant, DAIICHI SANKYO Group; Research Grant, Fuji Pharma Co, Ltd; Research Grant, Guerbet SA;

### For information about this presentation, contact:

daisuket@hp.pref.hyogo.jp

### PURPOSE

To directly and prospectively compare the capability for chest wall invasion assessment between STIR turbo spin-echo (SE) imaging and contrast-enhanced multidetector-row CT (CE-MDCT) in candidates for surgical resection due to non-small cell lung cancer (NSCLC).

## METHOD AND MATERIALS

51 consecutive NSCLC patients who were candidates for surgical treatment underwent CE-MDCT, STIR turbo SE imaging, surgical resection and pathological examination. STIR turbo SE imaging was obtained by using the respiratory-triggered STIR turbo SE imaging (TR=2-4 ms, TEeff=15 ms, TI=150 ms) at a 1.5T whole body scanner in each subject. According to the final pathological diagnosis of chest wall invasion, all patients were divided into two groups as follows: invasion group (n=10) and non-invasion group (n=41). In this study, prevalence of chest wall invasion on CE-MDCT was evaluated by 5-point visual score based on previously published criteria such as 1) contact angle, 2) contact length longer than 3cm, 3) pleural thickening, 4) the obliteration of subpleural fat of chest wall, 5) the obvious infiltrating mass, and 6) rib destruction. On STIR turbo SE imaging, chest wall invasion was assessed by using the contrast ratio (CNR) of signal intensity of abutting chest wall and muscle. To determine difference of each index between invasive and non-invasive groups, Fischer's PLSD or Student's t-test were performed. To determine the feasible threshold values of each index for chest wall invasion evaluation, ROC-based positive test was performed. Finally, diagnostic performance was compared by McNemar's test.

## RESULTS

CNR and visual CT findings except contact angle, pleural thickening and rib destruction had significant difference between two groups (p<0.05). When feasible threshold value applied to each index, specificity (SP: 100 [41/41] %) and accuracy (AC: 94.1 [48/51] %) were significantly higher than those of contact length longer than 3cm (SP: 68.3 [28/41] %, p=0.0002; AC: 70.6 [36/51] %, p= 0.0005).

# CONCLUSION

STIR turbo SE imaging is more useful than CE-MDCT to assess chest wall invasion in candidates for surgical treatment due to NSCLC.

### **CLINICAL RELEVANCE/APPLICATION**

STIR turbo SE imaging is more useful than CE-MDCT to assess chest wall invasion in candidates for surgical treatment due to NSCLC.



### ER162-ED-TUA4

# Added Value of Dual Energy CT in Clinical Routine

Tuesday, Nov. 27 12:15PM - 12:45PM Room: ER Community, Learning Center Station #4

#### Awards Cum Laude

#### Participants

Aaron D. Sodickson, MD, PhD, Boston, MA (*Presenter*) Institutional research agreement, Siemens AG; Speaker, Siemens AG; Speaker, General Electric Company Jeremy R. Wortman, MD, Boston, MA (*Abstract Co-Author*) Nothing to Disclose

Abhishek R. Keraliya, MD, Boston, MA (Abstract Co-Author) Nothing to Disclose

## For information about this presentation, contact:

### asodickson@bwh.harvard.edu

#### **TEACHING POINTS**

Dual Energy CT (DECT) capitalizes on differences in energy-dependent x-ray absorption from two different x-ray energy spectra.
 Novel image types can be created, and routinely incorporated into clinical workflow to interrogate underlying tissue characteristics.
 Multiple DECT applications add value in day to day clinical practice, as demonstrated in this case-based exhibit.

#### **TABLE OF CONTENTS/OUTLINE**

1. Summarize principles of DECT image acquisition and post-processing: Virtual monochromatic; Three-material decomposition; Material characterization 2. Case-based illustration of how DECT adds value: Improved <u>DETECTION</u>: Subdural hematomas; Noncalcified gallstones; Pancreatic necrosis; Solid organ injuries; Bone marrow edema Enhanced <u>CHARACTERIZATION</u>: Enhancing vs non-enhancing; Iodine vs calcium; Calcium vs hemorrhage; Renal stones; Gout <u>EASE OF INTERPRETATION</u>: Metal artifact reduction; Polycystic kidney evaluation <u>PROGNOSTICATION</u>: Pulmonary embolus; Bowel viability <u>PROTOCOL ROBUSTNESS</u>: Characterization of unexpected findings <u>LENGTH OF STAY REDUCTION</u>: Differentiation of intracranial calcification from hemorrhage <u>RADIATION DOSE</u> <u>REDUCTION</u>: Elimination of additional pre- or post-contrast phases <u>REDUCED IMAGING UTILIZATION</u>: Characterization of incidental findings at time of initial detection

#### **Honored Educators**

Presenters or authors on this event have been recognized as RSNA Honored Educators for participating in multiple qualifying educational activities. Honored Educators are invested in furthering the profession of radiology by delivering high-quality educational content in their field of study. Learn how you can become an honored educator by visiting the website at: https://www.rsna.org/Honored-Educator-Award/ Aaron D. Sodickson, MD,PhD - 2014 Honored EducatorAaron D. Sodickson, MD,PhD - 2017 Honored EducatorAaron D. Sodickson, MD,PhD - 2018 Honored EducatorJeremy R. Wortman, MD - 2017 Honored Educator



# ER215-SD-TUA1

# Optic Nerve Sheath Diameter as a Predictor of Acute Infarction in Patients with Acute Vertigo

Tuesday, Nov. 27 12:15PM - 12:45PM Room: ER Community, Learning Center Station #1

### Participants

Eung Koo Yeon, Seoul, Korea, Republic Of (*Presenter*) Nothing to Disclose Seong Jong Yun, Seoul, Korea, Republic Of (*Abstract Co-Author*) Nothing to Disclose Sun Hwa Lee, Seoul, Korea, Republic Of (*Abstract Co-Author*) Nothing to Disclose

For information about this presentation, contact:

zoomknight@naver.com

### PURPOSE

To evaluate the predictive utility of optic nerve sheath diameter (ONSD) for diagnosing acute cerebellar infarction in patients with acute vertigo without computed tomography (CT) abnormalities.

# METHOD AND MATERIALS

We retrospectively enrolled patients with acute vertigo without CT abnormalities who underwent magnetic resonance imaging (MRI) including diffusion-weighted imaging at our emergency department between January 2016 and December 2017. One board-certified radiologist and one board-certified emergency physician independently measured ONSD at 3-mm (ONSD3) and 10-mm (ONSD10) behind the globe in each patient. Final MRI reports with clinical progress notes were used as the reference standard. A multivariate logistic regression analysis, receiver operating characteristic (ROC) curves, and intra-class correlation coefficients (ICCs) were calculated to estimate predictive value.

## RESULTS

Thirty-four patients (16.1%) were diagnosed with acute infarction and 177 patients (83.9%) were diagnosed with peripheral vertigo. Mean ONSD3 (p<0.001) and ONSD 10 (p<0.001) were independent predictive factors for distinguishing acute infarction and peripheral vertigo. ONSD3 (cut-off, 4.22 mm) had 100% (95% CI, 89.7-100.0) sensitivity and 97.7% (95% CI, 95.1-99.6) specificity with area under the ROC curve (AUC) of 0.988 (95% CI, 0.978-1.0), while ONSD10 (cut-off, 3.63 mm) had 100% (95% CI, 89.7-100.0) sensitivity and 87.6% (95% CI, 81.8-92.0) specificity with AUC of 0.976 (95% CI, 0.959-0.997). There were good inter- and intra-observer agreements for both sides of ONSD3 and ONSD10 (ICC range, 0.652-0.773).

### CONCLUSION

ONSD measurement is a feasible predictive marker of acute infarction in patients with acute vertigo without CT abnormalities. In particular, ONSD3 larger than 4.22 mm showed good sensitivity and specificity for predicting infarction.

# **CLINICAL RELEVANCE/APPLICATION**

This information can assist decision-making in ordering brain MRI for the assessment of acute vertigo.



# ER216-SD-TUA2

# Ultrasound Findings of Strangulated Obstruction with Varied Ischemic Degrees

Tuesday, Nov. 27 12:15PM - 12:45PM Room: ER Community, Learning Center Station #2

### **Participants**

Chunwang Huang, MD,PhD, Philadelphia, PA (*Presenter*) Nothing to Disclose Ji-Bin Liu, MD, Philadelphia, PA (*Abstract Co-Author*) Nothing to Disclose Guangxia Wang, Tianjin, China (*Abstract Co-Author*) Nothing to Disclose Shuzhen Cong, Guangzhou, China (*Abstract Co-Author*) Nothing to Disclose

# For information about this presentation, contact:

huangchunwang@126.com

# PURPOSE

To observe ultrasonic findings in strangulated obstruction, and to assess clinical value of ultrasound for evaluation on strangulated obstruction with varied ischemic degrees.

## **METHOD AND MATERIALS**

52 patients were enrolled with a diagnosis of strangulated obstruction and were divided into ischemia and ischemic necrosis. Their ultrasound findings were retrospectively reviewed and explorative statistical analysis were performed by using Pearson chi-square or Fisher's exact chi-square test to compared with the surgical and/or pathologic records.

# RESULTS

There were 27 cases of intestinal ischemia without necrosis, and 25 cases of intestinal ischemia necrosis. Preoperative ultrasonography showed ischemia in 18 cases (18/27, 66.7%) and intestinal ischemic necrosis in 20 cases (20/25, 80.0%). Intestinal ischemia showed the bowel walls were hypoecho and thickened as 'doughnut' (transverse scan) and 'coral' (longitudinal scan) signs, while the 'beads' sign (longitudinal scan) and vein flow spectrum were observed in 8 cases. The echogenicity of peritoneal effusion was homogeneous echoless in 15 patient. Intestinal necrosis showed the structure of bowel wall were indistinct and lacked expansibility. The mucosal layer and the serous layer were separated as 'separation' or 'strip' sign, while CDFI could not detective signals of blood flow in bowel wall. And ascites increasing rapidly in a short time as dense and dotted echoless in 12 cases.

# CONCLUSION

Ultrasound can diagnose and evaluate strangulated obstruction with different extent of intestinal ischemia, and bowel wall of strangulated obstruction at different stages have different findings in ultrasound.

# **CLINICAL RELEVANCE/APPLICATION**

Strangulation obstruction means obstruction accompanied by intestinal wall lumen blood supply obstacles caused by ischemic and necrotic bowel wall change, common cause with internal hernias, volvulus, and intussusception, incarcerated hernia and the mesenteric vascular disease, etc., once the diagnosis of early surgical treatment [1]. Therefore, early diagnosis and assess the presence of ischemic necrosis of bowel wall and degree of pathological changes, choosing the right treatment for clinical early has positive effect, but more difficult preoperative judgment of bowel ischemia.



# ER217-SD-TUA3

Analysis of Imaging Findings of Patients Admitted to the Emergency Department with a Diagnosis of Seizure

Tuesday, Nov. 27 12:15PM - 12:45PM Room: ER Community, Learning Center Station #3

## Participants

Javid Isayev, Ankara, Turkey (*Abstract Co-Author*) Nothing to Disclose Erhan Akpinar, MD, Ankara, Turkey (*Presenter*) Nothing to Disclose Emre Unal, MD, Ankara, Turkey (*Abstract Co-Author*) Nothing to Disclose Mehmet Ruhi Onur, MD, Ankara, Turkey (*Abstract Co-Author*) Nothing to Disclose Bulent Erbil, Ankara, Turkey (*Abstract Co-Author*) Nothing to Disclose

For information about this presentation, contact:

emreunal.rad@gmail.com

# PURPOSE

To analyze the imaging findings of patients admitted to the emergency room following seizures.

### **METHOD AND MATERIALS**

A total of 800 patients (57.3%, male) were included into the study as two groups; those with new-onset of seizures (n=311), and those with previous history of seizure (n=489). Patients with a previous history of epilepsy were further divided into 2 groups, as cases with primary/idopathic or secondary symptomatic epilepsy. Positive findings on CT and MRI were categorized as a new pathology (diagnostic) or as a finding that would change management (prognostic).

## RESULTS

The average age of patients was  $46.7\pm19.7$  years. A significant medical history was present in 40.5% ( 23.8% neoplastic and 16.7% non-neoplastic) of patients with new onset seizures. The neoplasia were localized extracranially in 74% and intracranially in 26%, among these patients experiencing their initial seizures. The most common extracranial neoplasm was primary lung cancer, while glioblastoma was the most common intracranial neoplasm (33.3%), followed by meningioma and low grade glial tumors. Cerebrovascular accident was the most common cause of non-neoplastic disorders (26.5%). Primary epilepsy was more common than secondary epilepsy (57.7% vs. 42.3%) in patients with a previous history of seizure. In patients with secondary epilepsy, neoplasia were more frequently detected as the culprit, compared to non-neoplastic diseases (23.5% vs 18.8%). The incidence of positive imaging findings in secondary epilepsy patients was high in case of neoplasm (p=0.023) and glioblastoma (p=0.030), and low in patients with primary epilepsy (p<0.001). In patients with negative CT and positive MRI findings, seizures were primarily related to vascular ischemia and meningitis/encephalitis. The sensitivity of CT for a positive finding, was higher in neoplasia related new onset of seizures (65-80%) and secondary epilepsies (75-100%), compared to non-neoplastic etiologies in both groups.

#### CONCLUSION

The incidence of positive imaging findings that will guide management, was higher in patients with new onset seizure. The yield of CT was high in patients with new onset seizure, secondary epilepsy, and history of an underlying disease. In case of vascular etiology, MRI should be used as a complementary method to CT.

# **CLINICAL RELEVANCE/APPLICATION**

The diagnostic yield of imaging studies is higher in patients with new onset seizures and secondary symptomatic epilepsy.



# GI298-ED-TUA8

Contrast Enhanced MR Angiography Combined with Dynamic Acquisition in Focal Liver Lesions at 3T: How to Obtain Both of These Techniques with One Dose of Contrast Medium

Tuesday, Nov. 27 12:15PM - 12:45PM Room: GI Community, Learning Center Station #8

# Participants

Bac Nguyen, BSC, Oslo, Norway (*Presenter*) Consultant, Bayer AG Anders H. Tomterstad, Oslo, Norway (*Abstract Co-Author*) Nothing to Disclose Ane J. Krog, BSC,MSc, Oslo, Norway (*Abstract Co-Author*) Nothing to Disclose Andreas Abildgaard, MD, PhD, Oslo, Norway (*Abstract Co-Author*) Nothing to Disclose

### For information about this presentation, contact:

#### og\_23@hotmail.com

# **TEACHING POINTS**

The purpose of this abstract is to highlight the usefulness of performing both Contrast Enhanced MR Angiography (CE-MRA) and dynamic acquisitions of focal liver lesions at 3T with a single dose of contrast medium. In addition, technical aspects of the examination will be highlighted. Based on present knowledge of possible side effects of MR-contrast media containing gadolinium, we need to employ caution and carefully weigh the risks and benefits of contrast administration. CE-MRA (fig.1) and the evaluation of focal liver lesions (fig.2) are typically two different examination approaches, each requiring one dose of contrast medium. We only highlight the specific CE-MRA and dynamic liver part, with the work flow illustrated in (fig.4). Table 1 and 2 gives an overview of chosen sequences. Our approach is to combine both techniques with a single dose of contrast agent. 3T MRI scanners may provide rapid acquisitions whilst obtaining explicit image quality. We believe this approach may be useful in cases where both vessels and dynamic enhancement of focal liver lesions need to be visualised. Not only does this save contrast dosage, but it also saves examination time for the patients.

### **TABLE OF CONTENTS/OUTLINE**

Learning objectivesBackgroundFindings and procedure detailsConclusionReferences



# GI299-ED-TUA9

MDCT as a Pre-Endoscopic Emergent Examination for Acute Lower Gastrointestinal Bleeding: What Information Can MDCT Provide for Treatment?

Tuesday, Nov. 27 12:15PM - 12:45PM Room: GI Community, Learning Center Station #9

### Participants

Eliko Tanaka, MD, Yokohama, Japan (*Presenter*) Nothing to Disclose Nobuyuki Takeyama, MD, Yokohama, Japan (*Abstract Co-Author*) Nothing to Disclose Akio Kotake, MD, Yokohama, Japan (*Abstract Co-Author*) Nothing to Disclose Yuki Tashiro, Yokohama, Japan (*Abstract Co-Author*) Nothing to Disclose Akira Furukawa, MD, PhD, Tokyo, Japan (*Abstract Co-Author*) Nothing to Disclose Toshi Hashimoto, MD, Yokohama, Japan (*Abstract Co-Author*) Nothing to Disclose Kyoko Nagai, MD, Tokyo, Japan (*Abstract Co-Author*) Nothing to Disclose Makiko Ishikawa, MD, Yokohama, Japan (*Abstract Co-Author*) Nothing to Disclose Takaki Hayashi, MD, Yokohama, Japan (*Abstract Co-Author*) Nothing to Disclose

## **TEACHING POINTS**

Lower gastrointestinal bleeding (LGIB) is a commonly encountered symptom in the emergency department. The indications for a radiological assessment of acute LGIB are limited to the current guidelines such as ACG Clinical Guideline or ACR Appropriateness Criteria. However, as CT can be rapidly performed without any bowel preparation, initial CT examination is preferred, particularly in patients who are unlikely to tolerate bowel preparation. The purpose of this exhibition is to demonstrate the usefulness of MDCT as a pre-endoscopic emergent examination for acute LGIB, and it will focus on the following: (1) the current guidelines for LGIB, and the role of imaging on the guidelines; (2) the selection of appropriate image modalities for LGIB; (3) the significance of pre-endoscopic emergent CT as an assessment alternative for LGIB; and (4) the CT findings on the localization of hemorrhage and potential lesions in three-phase CT.

#### **TABLE OF CONTENTS/OUTLINE**

1. Current guidelines for LGIB 2. The role of pre-endoscopic emergent CT as an alternative examination for endoscopy 3. Choice of imaging modalities: MDCT, DSA, and Tc-99m RBC scan 4. The aim and methods of three-phase CT 5. CT findings on the localization of hemorrhage and pitfalls 6. Etiology of potential lesions and their findings on three-phase CT and its pitfalls



## GI300-ED-TUA10

**Cinematic Rendering of Liver Diseases: Preliminary Observations** 

Tuesday, Nov. 27 12:15PM - 12:45PM Room: GI Community, Learning Center Station #10

## FDA Discussions may include off-label uses.

#### **Participants**

Linda C. Chu, MD, Baltimore, MD (*Presenter*) Nothing to Disclose Steven P. Rowe, MD, PhD, Baltimore, MD (*Abstract Co-Author*) Research funded, Progenics Pharmaceuticals, Inc Elliot K. Fishman, MD, Baltimore, MD (*Abstract Co-Author*) Institutional Grant support, Siemens AG; Institutional Grant support, General Electric Company; Co-founder, HipGraphics, Inc

#### For information about this presentation, contact:

lindachu@jhmi.edu

## **TEACHING POINTS**

1. Cinematic rendering (CR) is a new 3D rendering technique that generates photorealistic images based on a new lighting model. 2. The dynamic interactive display has the potential to improve perception of fine anatomic detail (e.g. internal septations, mural nodule) and appreciation of enhancement pattern, which may be helpful in characterization of focal liver masses. 3. CR can increase appreciation of surface nodularity and sequela of portal hypertension in patients with cirrhosis. 4. CR also can provide exquisite vascular maps, which may be helpful for pretreatment planning.

### TABLE OF CONTENTS/OUTLINE

1. Review basic principles of cinematic rendering (CR). 2. Illustrate potential role of CR in the characterization of focal liver masses, with case examples: • Hemangioma • Focal nodular hyperplasia • Hepatocellular carcinoma • Metastatic disease 3. Illustrate potential role of CR in assessment of diffuse liver parenchymal disease (i.e. cirrhosis) and its sequela. 4. Current limitations of CR and future directions.

#### **Honored Educators**

Presenters or authors on this event have been recognized as RSNA Honored Educators for participating in multiple qualifying educational activities. Honored Educators are invested in furthering the profession of radiology by delivering high-quality educational content in their field of study. Learn how you can become an honored educator by visiting the website at: https://www.rsna.org/Honored-Educator-Award/ Elliot K. Fishman, MD - 2012 Honored EducatorElliot K. Fishman, MD - 2014 Honored EducatorElliot K. Fishman, MD - 2016 Honored EducatorElliot K. Fishman, MD - 2018 Honored Educator



## GI301-ED-TUA11

Implementation of MR Elastography: Interpretation, Troubleshooting, and Tips From Three Institutions' Experiences

Tuesday, Nov. 27 12:15PM - 12:45PM Room: GI Community, Learning Center Station #11

# Participants

Karen Tran-Harding, MD, Lexington, KY (*Presenter*) Nothing to Disclose Alvin C. Silva, MD, Scottsdale, AZ (*Abstract Co-Author*) Nothing to Disclose Michael A. Ohliger, MD,PhD, Burlingame, CA (*Abstract Co-Author*) Nothing to Disclose James T. Lee, MD, Lexington, KY (*Abstract Co-Author*) Nothing to Disclose

#### For information about this presentation, contact:

#### jtlee3@uky.edu

# **TEACHING POINTS**

Illustrate and discuss technical issues that arise when obtaining MR elastography images. Suggest steps and tips to improve reliability and reproducibility of the technique based on experiences from three seperate institutions. Illustrate and discuss tips for image interpretation.

## TABLE OF CONTENTS/OUTLINE

Background - Basic principles, literature supporting reliability and reproduciblity Technical Issues at Implementation - Paddle placement Breath Hold Auto sleep function Inability to adjust MRE driver amplitude Driver tubing length MRI Technologist training FOV Selection Interpretation Issues: Assessing Quality of Images What do the different sequences mean? How do I produce stiffness values? How do they correlate with stiffness grade? How do I know when MRE sequence fails? Are we giving accurate results? What about focal lesions?



### GI302-ED-TUA12

# Computer-Aided Detection (CADe) for CT Colonography: Benefits and Pitfalls

Tuesday, Nov. 27 12:15PM - 12:45PM Room: GI Community, Learning Center Station #12

#### **Participants**

Yasuji Ryu, MD, Boston, MA (*Presenter*) Nothing to Disclose Janne J. Nappi, PhD, Boston, MA (*Abstract Co-Author*) Royalties, Hologic, Inc Royalties, MEDIAN Technologies Chinatsu Watari, MD, Boston, MA (*Abstract Co-Author*) Nothing to Disclose Hiroyuki Yoshida, PhD, Boston, MA (*Abstract Co-Author*) Patent holder, Hologic, Inc; Patent holder, MEDIAN Technologies;

# For information about this presentation, contact:

yoshida.hiro@mgh.harvard.edu

# **TEACHING POINTS**

The use of CADe enhances radiologists' performance in CT colonography (CTC). The teaching points of this exhibit are (1) to review recently introduced advanced uses of CADe to detect colorectal lesions in CTC and (2) to review challenging clinical cases that were incorrectly dismissed by readers regardless of the use of CADe under these scenarios.

# TABLE OF CONTENTS/OUTLINE

Introduction: Describe the role of CTC in detecting colorectal lesions; describe the benefits of CADe in interpreting CTC images.
 Laxative-free CTC: Review the benefits and pitfalls of the use of CADe in laxative-free CTC, with representative example cases.
 Colorectal flat lesions: Review the benefits and pitfalls of CADe in the detection of flat lesions in CTC, with representative example cases.
 Single-position CTC reading: Review the benefits and pitfalls of CADe in single-position CTC reading, with representative example cases.



# GI355-SD-TUA1

# **Role of DWI for Evaluation of Pancreas Lesions**

Tuesday, Nov. 27 12:15PM - 12:45PM Room: GI Community, Learning Center Station #1

### Participants

Yoshihiko Fukukura, MD, PhD, Kagoshima, Japan (Presenter) Nothing to Disclose Yuichi Kumagae, Kagoshima, Japan (Abstract Co-Author) Nothing to Disclose Hiroto Hakamada, Kagoshima, Japan (Abstract Co-Author) Nothing to Disclose Hiroaki Nagano, MD, Kaogoshima, Japan (Abstract Co-Author) Nothing to Disclose Masanori Nakajo, MD, Kagoshima, Japan (Abstract Co-Author) Nothing to Disclose Kiyohisa Kamimura, MD, PhD, Kagoshima, Japan (Abstract Co-Author) Nothing to Disclose Takashi Yoshiura, MD, PhD, Kagoshima, Japan (Abstract Co-Author) Nothing to Disclose

## **TEACHING POINTS**

Diffusion-weighted imaging is a promising technique for the evaluation of pancreas lesions, including detection, characterization, monitoring treatment response, and prediction of patient prognosis. The purpose of this exhibit is: 1. To illustrate diffusionweighted imaging findings of pancreas lesions 2. To discuss how to characterize pancreatic lesions on diffusion-weighted imaging 3. To discuss the feasibility of diffusion-weighted imaging for monitoring treatment response, and prediction of patient prognosis in pancreatic adenocarcinoma

# TABLE OF CONTENTS/OUTLINE

1. Review of diffusion-weighted imaging findings and the optimal b-value for delineating pancreatic adenocarcinoma. 2. Highlight key differential diagnostic points of pancreatic lesions on diffusion-weighted imaging. 3. Review of the feasibility of diffusion-weighted imaging for monitoring treatment response, and prediction of patient prognosis in pancreatic adenocarcinoma. 4. Summary: The utility of diffusion-weighted imaging for the detection, characterization, and monitoring treatment response of pancreas lesions is now well accepted but there are a number of limitations.

## PDF UPLOAD

http://abstract.rsna.org/uploads/2018/18010052/18010052\_66g6.pdf



# GI356-SD-TUA2

Utility of Extracellular Volume Fraction Measured from Multiphasic Contrast-Enhanced Computed Tomography for the Estimation of Pancreatic Fibrosis

Tuesday, Nov. 27 12:15PM - 12:45PM Room: GI Community, Learning Center Station #2

# Participants

Keitaro Sofue, MD, Kobe, Japan (*Presenter*) Nothing to Disclose Yoshiko Ueno, MD, PhD, Kobe, Japan (*Abstract Co-Author*) Nothing to Disclose Eisuke Ueshima, Kobe, Japan (*Abstract Co-Author*) Nothing to Disclose Ryuichiro Tani, Kobe, Japan (*Abstract Co-Author*) Nothing to Disclose Koji Maruyama, Kobe, Japan (*Abstract Co-Author*) Nothing to Disclose Takamichi Murakami, MD, PhD, Osakasayama, Japan (*Abstract Co-Author*) Nothing to Disclose Hiroki Horinouchi, Kobe, Japan (*Abstract Co-Author*) Nothing to Disclose Takuya Okada, Kobe, Japan (*Abstract Co-Author*) Nothing to Disclose Masato Yamaguchi, MD, PhD, Kobe, Japan (*Abstract Co-Author*) Nothing to Disclose Koji Sugimoto, MD, Kobe, Japan (*Abstract Co-Author*) Nothing to Disclose

# PURPOSE

Pancreatic fibrosis is associated with increased risk for postoperative pancreatic fistula and pancreatic carcinoma. The purpose of this study was to investigate whether extracellular volume fraction (fECVs) measured from multiphasic contrast-enhanced computed tomography (CE-CT) can be used to estimate pancreatic fibrosis.

## **METHOD AND MATERIALS**

This retrospective study was approved by our institutional review board. A total of 68 patients (37 men, 31 women; mean age, 68 years) underwent multiphasic CE-CT (precontrast, arterial, portal venous and equilibrium phases) and subsequent pancreatectomy with histological confirmation of pancreatic fibrosis. Absolute enhancements (in Hounsfield units) of the pancreatic parenchyma ( $\Delta$  HUPanc) and aorta ( $\Delta$  HUAorta) were measured on between precontrast and equilibrium phase images. The fECV was calculated using the following equation: fECV (%) =  $\Delta$  HUPanc/ $\Delta$  HUAorta × (100 - hematocrit [%]). The fECVs were compared among fibrosis stages by using the Kruskal-Wallis test. Correlation between fECV and histological pancreatic fibrosis stage (F0-F3) was evaluated by using the Spearman correlation coefficient. The Mann-Whitney's U test was used to compare fECVs between patients with advanced fibrosis (F2-F3) and those without (F0-F1). Diagnostic performance of fECV for the prediction of advanced fibrosis was evaluated by using receiver operating characteristic (ROC) curve analysis. Sensitivity and specificity were calculated based on the estimated optimal cutoff values.

# RESULTS

The fECV ranged from 21.4 to 66.2 (mean, 39.1) among the 68 patients. The fECV significantly increased according to the pancreatic fibrosis stage (P<.001) and moderately correlated ( $\rho$ = 0.676, P<.001). The mean fECV in advanced fibrosis (F2-F3) was significantly higher than in no advanced fibrosis (F0-F1) (fECV; 46.6 ± 10.5 vs. 32.6 ± 7.9, P<.001). Area under the ROC curve showed 0.859 for the diagnostic performance of advanced fibrosis, and cutoff value of 34.8 yielded 87.5% sensitivity and 72.2% specificity.

#### CONCLUSION

The fECV measured from multiphasic CE-CT is associated with histological pancreatic fibrosis and can obtain quantitative information for the assessment of pancreatic fibrosis.

#### **CLINICAL RELEVANCE/APPLICATION**

Extracellular volume fraction measured from multiphasic CE-CT proves useful for the estimation of pancreatic fibrosis, which can potentially predict the risk for postoperative pancreatic fistula.



# GI357-SD-TUA3

MRI-based Monitoring of the Patients with Hepatitis C, Who Achieved Sustained Virological Response (SVR) by DAA Treatment

Tuesday, Nov. 27 12:15PM - 12:45PM Room: GI Community, Learning Center Station #3

# Participants

Hisato Kobayashi, Chuo, Japan (*Presenter*) Nothing to Disclose Utaroh Motosugi, MD, Chuo, Japan (*Abstract Co-Author*) Nothing to Disclose Shintaro Ichikawa, MD, PhD, Chuo-Shi, Japan (*Abstract Co-Author*) Nothing to Disclose Nobuyuki Enomoto, MD, PhD, Yamanashi, Japan (*Abstract Co-Author*) Nothing to Disclose Taisuke Inoue, Chuo, Japan (*Abstract Co-Author*) Nothing to Disclose Hiroshi Onishi, MD, Yamanashi, Japan (*Abstract Co-Author*) Nothing to Disclose

For information about this presentation, contact:

hisatok@yamanashi.ac.jp

### PURPOSE

Type C viral hepatitis causes active inflammation and fibrosis, which increases the risk of hepatocellular carcinoma (HCC) development. MR elastography enables to measure liver stiffness, which represents inflammation and fibrosis in the liver. Nodules showing non-hypervascularity and low signal intensity during hepatobiliary phase (NLH nodules) is known as a precursor and a risk of hypervascular HCCs. Intrahepatic inflammation/fibrosis and the reduction of the risk of HCC development are of great interest in the patients who achieved sustained virological response (SVR) by direct acting agent (DAA) treatment. Therefore, the purpose of this study was to monitor liver function tests and MRI findings including liver stiffness measurement by MR elastography (MRE) in patients with hepatitis C who achieved SVR by DAA treatment.

## METHOD AND MATERIALS

Twenty-nine patients with hepatitis C who received oral DAA treatment and achieving SVR were included. Image findings (liver stiffness by MRE, ADC value, number of nodules with non-hypervascular and low signal intensity during hepatobiliary phase (NLH nodules), ascites, and blood test findings (serum albumin, total bilirubin, total cholesterol, AST, ALT, platelet count, PT - INR, AFP) as factors. As for the image findings, two radiologists performed measurements separately. Each factor was compared and examined using Paired t-test or Chi-square test.

## RESULTS

The liver stiffness after SVR was significantly lower than that before treatment (average before treatment,  $4.67 \pm 2.01$  kPa; after SVR,  $3.79 \pm 1.50$  kP; P <0.0001), whereas serum albumin level (P = 0.0036) and platelet count (P = 0.001) were significantly increased. There were no differences in the number of cases with NLH nodule compared with 13 cases before treatment and 12 cases after SVR.

#### CONCLUSION

Oral DAA treatment and removal of the hepatitis C virus would probably improve inflammation and decrease fibrosis in the liver. However, the precursor lesions of hypervascular HCC can stay same.

## **CLINICAL RELEVANCE/APPLICATION**

Improvement of inflammation and fibrosis after DAA treatment can be measured by MR elastography. However, the risk of HCC might not decrease.



## GI358-SD-TUA4

The B-Mode Image-Guided Ultrasound Attenuation Parameter Accurately Detects Hepatic Steatosis in Chronic Liver Disease

Tuesday, Nov. 27 12:15PM - 12:45PM Room: GI Community, Learning Center Station #4

# Participants

Yudai Fujiwara, Morioka, Japan (*Presenter*) Nothing to Disclose Hidekatsu Kuroda, Morioka, Iwate, Japan (*Abstract Co-Author*) Nothing to Disclose Tamami Abe, Morioka, Japan (*Abstract Co-Author*) Nothing to Disclose Yuriko Mikami, Morioka, Japan (*Abstract Co-Author*) Nothing to Disclose Takuma Oguri, Hino, Japan (*Abstract Co-Author*) Nothing to Disclose Sachiyo Noguchi, Hino, Japan (*Abstract Co-Author*) Nothing to Disclose Naohisa Kamiyama, PhD, Otawara, Japan (*Abstract Co-Author*) Nothing to Disclose Yasuhiro Takikawa, Morioka, Japan (*Abstract Co-Author*) Nothing to Disclose

#### PURPOSE

Nonalcoholic fatty liver disease is a main cause of chronic liver disease (CLD) worldwide. However, a quantitative, non-invasive modality for the follow-up of hepatic steatosis has not been established. We investigated the diagnostic performance of ultrasound-guided attenuation parameter (UGAP) and quantification for assessing hepatic steatosis by a liver biopsy (LB). We then compared the findings with controlled attenuation parameter (CAP) and evaluated the usefulness of UGAP based on the course of hepatic steatosis of patients who underwent laparoscopic sleeve gastrectomy (LSG).

# METHOD AND MATERIALS

We prospectively analyzed 163 consecutive CLD patients who underwent UGAP, CAP, and a LB on the same day. UGAP was performed using the LOGIQ E9. We acquired a B-mode image of the liver parenchyma. RF signals corresponding to the images were compensated by the reference signal previously measured from the uniform phantom with known attenuation (0.5 dB/cm/MHz). The attenuation coefficient (AC) was calculated from the signals' decay slope. Steatosis was categorized as S0, <5%; S1, 5%-33%; S2, 34%-66% or S3, >=67%. In addition, we analyzed 11 patients who had been diagnosed with nonalcoholic steatohepatitis with LSG. LB and UGAP were performed intraoperatively and at 6 and 12 months after surgery.

#### RESULTS

The success rate of UGAP and CAP was 100% and 95.5%, respectively. The median AC values in patients with S0 (n = 57), S1 (n = 70), S2 (n = 26) and S3 grade (n = 10) were 0.49, 0.56, 0.66 and 0.72 dB/cm/MHz, respectively, demonstrating a stepwise increase with increasing severity of steatosis (P < 0.0001). A significant correlation between the AC and the percentage steatosis and CAP values was found (P < 0.001). The area under the receiver operating curve of UGAP for identifying >=S1/>=S2/>=S3 was 0.919/0.957/0.960, respectively. The median steatosis and AC values intraoperatively and at 6 and 12 months after surgery were 21.36%, 5.25% and 5.33% and 0.61, 0.47 and 0.49 dB/cm/MHz, respectively, changes that were observed in parallel.

# CONCLUSION

UGAP showed high diagnostic accuracy for detecting hepatic steatosis in patients with CLD, indicating that it can be used to screen for fatty liver and for follow-up observation.

# **CLINICAL RELEVANCE/APPLICATION**

In a prospective, cross-sectional study, we found ultrasound-guided attenuation parameter is indicating that it can be used to screen for fatty liver and for follow-up observation.



# GI359-SD-TUA5

# Exploratory Study of ADC Histogram Metrics in Assessing Ampullary/Pancreatic Malignancy

Tuesday, Nov. 27 12:15PM - 12:45PM Room: GI Community, Learning Center Station #5

#### **Participants**

Myles T. Taffel, MD, New York City, NY (*Presenter*) Nothing to Disclose Lyndon Luk, MD, New York, NY (*Abstract Co-Author*) Nothing to Disclose Justin M. Ream, MD, Ann Arbor, MI (*Abstract Co-Author*) Nothing to Disclose Andrew B. Rosenkrantz, MD, New York, NY (*Abstract Co-Author*) Nothing to Disclose

## For information about this presentation, contact:

myles.taffel@nyumc.org

## PURPOSE

To evaluate the utility of whole-lesion 3D-histogram apparent diffusion coefficient (ADC) metrics in the assessment of ampullary/pancreatic malignancy.

## **METHOD AND MATERIALS**

Forty-two ampullary/pancreatic malignancies (36 adenocarcinoma, 6 neuroendocrine) underwent abdominal MRI with DWI followed by endoscopic ultrasound biopsy or surgical resection. A single radiologist used dedicated post-processing software to place 3Dvolumes-of-interest encompassing the entire masses to derive whole-lesion histogram ADC metrics. Mann-Whitey tests and ROC analyses were used to assess the diagnostic performance of the histogram metrics for determining lesion histology, and among adenocarcinomas, T-stage, N-stage, and grade.

### RESULTS

Whole-lesion ADC histogram metrics demonstrating significant differences between adenocarcinoma and neuroendocrine tumors were mean ADC (1.40 vs. 1.04 x10-3mm2/sec, respectively; p=0.020, AUC = 81%), mean of the bottom 10th percentile (mean0-10) (0.97 vs. 0.50; p<0.001, AUC=88%), and mean of the 10th-25th percentile (mean10-25) (1.16 vs. 0.77, p<0.001, AUC=92%). For the metric with highest AUC for histology (mean10-25), a threshold >0.94 achieved sensitivity of 94% and specificity of 83%. Metrics with significant differences between nodal status No vs. >=N1 were mean ADC (1.69 vs.1.24; p=.004; AUC = 81%), mean0-10 (1.19 vs. 0.71, p=0.012, AUC=82%), and mean10-25 (1.45 vs. 0.96; p=0.002, AUC=82%). For the metric with highest AUC for nodal status (mean10-25), a threshold >0.94 achieved sensitivity of 94% and specificity of 83%. No metric was significantly associated with T stage (all p>0.195) or tumor grade (all p>0.215). Skewness and kurtosis were not significantly different between any groups (all p>0.087).

# CONCLUSION

Volumetric ADC histogram metrics may serve as non-invasive biomarkers in assessing ampullary/pancreatic malignancy. The metric reflecting the bottom quarter of the histogram distribution outperformed the standard mean in determining lesion histology and nodal status, supporting the role of histogram analysis. More advanced methods may be needed for T stage and tumor grade differentiation.

# **CLINICAL RELEVANCE/APPLICATION**

Although these findings require validation in larger studies, histogram diffusion metrics may be helpful in guiding prognosis and treatment selection for ampullary/pancreatic malignancy.



# GI360-SD-TUA6

Automated CT and MR Liver Biometry Using a Generalized Convolutional Neural Network for Liver Segmentation

Tuesday, Nov. 27 12:15PM - 12:45PM Room: GI Community, Learning Center Station #6

# Participants

Kang Wang, MD, PhD, San Diego, CA (Presenter) Nothing to Disclose Adrija Mamidipalli, MD, San Diego, CA (Abstract Co-Author) Nothing to Disclose Tara A. Retson, MD, PhD, San Diego, CA (Abstract Co-Author) Nothing to Disclose Naeim Bahrami, PhD, MSc, San Diego, CA (Abstract Co-Author) Nothing to Disclose Kevin Blansit, MS, BS, La Jolla, CA (Abstract Co-Author) Nothing to Disclose Evan Masutani, La Jolla, CA (Abstract Co-Author) Nothing to Disclose Timoteo I. Delgado, BA, San Diego, CA (Abstract Co-Author) Nothing to Disclose Claude B. Sirlin, MD, San Diego, CA (Abstract Co-Author) Research Grant, Gilead Sciences, Inc; Research Grant, General Electric Company; Research Grant, Siemens AG; Research Grant, Bayer AG; Research Grant, ACR Innovation; Research Grant, Koninklijke Philips NV; Research Grant, Celgene Corporation; Consultant, General Electric Company; Consultant, Bayer AG; Consultant, Boehringer Ingelheim GmbH; Consultant, AMRA AB; Consultant, Fulcrum Therapeutics; Consultant, IBM Corporation; Consultant, Exact Sciences Corporation; Advisory Board, AMRA AB; Advisory Board, Guerbet SA; Advisory Board, VirtualScopics, Inc; Speakers Bureau, General Electric Company; Author, Medscape, LLC; Author, Resoundant, Inc; Lab service agreement, Gilead Sciences, Inc; Lab service agreement, ICON plc; Lab service agreement, Intercept Pharmaceuticals, Inc; Lab service agreement, Shire plc; Lab service agreement, Enanta; Lab service agreement, Virtualscopics, Inc; Lab service agreement, Alexion Pharmaceuticals, Inc; Lab service agreement, Takeda Pharmaceutical Company Limited; Lab service agreement, sanofi-aventis Group; Lab service agreement, Johnson & Johnson; Lab service agreement, NuSirt Biopharma, Inc ; Contract, Epigenomics; Contract, Arterys Inc Albert Hsiao, MD, PhD, La Jolla, CA (Abstract Co-Author) Founder, Arterys, Inc; Consultant, Arterys, Inc; Consultant, Bayer AG;

Research Grant, General Electric Company; For information about this presentation, contact:

kaw016@ucsd.edu

### PURPOSE

Automated liver segmentation have many clinical applications, including liver volumetry or estimation of hepatic proton-density fatfraction (PDFF) for non-alcoholic fatty liver disease. Multiple methods have been explored for liver segmentation, but most have limited generalizability. We aim to develop a convolutional neural network (CNN) for automatic liver segmentation that is robust across imaging techniques and modalities observed in clinical practice.

## **METHOD AND MATERIALS**

In this IRB-approved and HIPPA-compliant study, we retrospectively collected 500 multimodal image datasets including multi-echo non-contrast T2\*-weighted (NC-T2\*w) MR, non-contrast and contrast-enhanced CT, and contrast-enhanced T1-weighted (CE-T1w) MR. We trained a 2D U-Net CNN for liver segmentation in two stages. First, we trained with T2\*w MR image datasets (n=300) with multiple echo times (TEs) to be robust against different signal-weightings. Then, we used transfer learning to generalize our CNN to other imaging modalities (10 CT, 20 T1w-MR). We validated the CNN using image data from 200 patients distinct from the training group. Segmentation accuracy was evaluated by computing Dice score. Utilizing the segmentations, we computed liver volume from CT and CE-T1w MR and estimated hepatic PDFF from multi-echo NC-T2\*w MR. We compared quantitative volumetry and fat fraction estimates between automated and manual segmentation using Pearson correlation and Bland-Altman statistics.

### RESULTS

The Dice score was  $0.92\pm0.02$  for NC-T2\*w MR,  $0.93\pm0.09$  for CT,  $0.95\pm0.02$  for CE-T1w MR. Liver volume between manual and automated segmentation agreed closely for CT (95% limit of agreement (LoA)=[-166 mL, 211 mL]) and CE-T1w MR (LoA=[-131 mL, 161 mL]). Hepatic PDFF between the two segmentations was also agreed closely (LoA=[-0.88%, 1.02%]).

# CONCLUSION

Utilizing transfer learning and limited number of datasets, we showed that it is possible to generalize a CNN to perform liver segmentations on different imaging techniques and modalities. With further refinement and validation, this CNN may have broad applicability for multimodal liver volumetry and hepatic tissue characterization.

# **CLINICAL RELEVANCE/APPLICATION**

A generalized CNN shows promise for accurate automated multimodal quantification of liver volume and hepatic MRI-PDFF computation.



# GI361-SD-TUA7

Differential Subsampling with Cartesian Ordering (DISCO) with Respiratory Triggering versus Conventional Liver Acquisition with Volume Acquisition (LAVA): A Multiple-Reader Preference Study

Tuesday, Nov. 27 12:15PM - 12:45PM Room: GI Community, Learning Center Station #7

## Participants

Brian C. Allen, MD, Durham, NC (*Presenter*) Nothing to Disclose Wendy L. Ehieli, MD, Durham, NC (*Abstract Co-Author*) Nothing to Disclose Benjamin Wildman-Tobriner, MD, Durham, NC (*Abstract Co-Author*) Nothing to Disclose Mohammad Chaudhry, MBBS, Durham, NC (*Abstract Co-Author*) Nothing to Disclose Erol Bozdogan, MD, Sanliurfa, Turkey (*Abstract Co-Author*) Nothing to Disclose Gemini L. Janas, RT, Durham, NC (*Abstract Co-Author*) Nothing to Disclose James S. Ronald, MD, PhD, Durham, NC (*Abstract Co-Author*) Nothing to Disclose Mustafa R. Bashir, MD, Cary, NC (*Abstract Co-Author*) Research Grant, Siemens AG; Research Grant, General Electric Company; Research Grant, NGM Biopharmaceuticals, Inc; Research Grant, TaiwanJ Pharmaceuticals Co, Ltd; Research Grant, Madrigal Pharmaceuticals, Inc; Research Consultant, RadMD

#### For information about this presentation, contact:

brian.allen@duke.edu

#### PURPOSE

To compare respiratory-triggered Differential Subsampling with Cartesian Ordering (rtDISCO) and breath held Liver Acquisition with Volume Acquisition (LAVA) image quality with respect to motion and noise in abdominal MRI.

#### **METHOD AND MATERIALS**

This was an IRB approved, HIPAA compliant prospective study; all patients provided informed consent. Twenty-five inpatient subjects (12 male, 13 female; mean age 58 years  $\pm$  13 years) underwent a clinical abdominal MRI at 1.5T (MR450w, General Electric, Milwaukee, WI). T1-weighted (T1w) imaging of the abdomen was performed with rtDISCO (free breathing) and LAVA (breath held) prior to and following the intravenous administration of gadobenate dimeglumine (Bracco Diagnostics, Princeton, NJ) at 2 mL/sec in the equilibrium phase. Three readers independently scored individual series, presented blinded and in random order for motion and noise from 1 (no degradation) to 5 (highly degraded), and in blinded side-by-side comparisons ranging from -2 (strongly preferred LAVA) to +2 (strongly preferred rtDISCO). Readers then qualitatively assessed for focal liver, adrenal and renal lesions, portal vein patency, gallbladder and pancreatic margins, and common duct and peritoneal thickening. Mixed effects linear models were used to assess reader preferences.

## RESULTS

For individual series assessments, readers rated rtDISCO images as more degraded by motion on both pre- (mean rtDISCO score=2.7, LAVA=1.6; p<0.001) and post-contrast images (rtDISCO=2.4, LAVA=1.8; p<0.001). For side-by-side assessments, readers preferred LAVA images based on motion on both pre- (mean preference=-1.2; p<0.001) and post-contrast images (mean preference=-0.7; p<0.001). There was no significant reader preference for noise. On side-by-side assessment, there was a preference for LAVA for assessment for focal liver lesions and portal vein patency post-contrast (mean preferences<-0.6; both p<0.05); there was no significant preference between sequences for the other 6/8 clinical tasks on post-contrast images or any of the 8 tasks on pre-contrast images.

# CONCLUSION

Readers preferred LAVA compared to rtDISCO with respect to motion but not noise; there was no preference in the majority of tested clinical tasks.

## **CLINICAL RELEVANCE/APPLICATION**

rtDISCO did not reduce motion artifacts in dynamic contrast-enhanced imaging of the abdomen in inpatients. However, clinical task performance was similar between rtDISCO and conventional LAVA.



# GU222-SD-TUA1

PET/CT and PET/MR with 68ga-Psma-11 for the Evaluation of Prostate Cancer Recurrence in Vas Deferens

Tuesday, Nov. 27 12:15PM - 12:45PM Room: GU/UR Community, Learning Center Station #1

### **Participants**

Karine M. Martins, MS, Sao Paulo, Brazil (*Abstract Co-Author*) Nothing to Disclose Taise Vitor, Sao Paulo, Brazil (*Abstract Co-Author*) Nothing to Disclose Guilherme Campos, Sao Paulo, Brazil (*Abstract Co-Author*) Nothing to Disclose Eduardo Kaiser Ururahy Nunes Fonseca, MD, Sao Paulo, Brazil (*Presenter*) Nothing to Disclose Ronaldo H. Baroni, MD, Sao Paulo, Brazil (*Abstract Co-Author*) Nothing to Disclose

## For information about this presentation, contact:

kminaif@uol.com.br

# PURPOSE

To describe the incidence and characteristics of prostate cancer recurrence (PCa) in vas deferens on PET/CT and PET/MR with 68Ga-PSMA-11.

# METHOD AND MATERIALS

We conducted a retrospective study to evaluate all cases of 68Ga-PSMA PET/CT with biochemical recurrence after prostatectomy for PCa in our PACS system, from October 2015 until August 2016 (236 patients). We then searched for all cases with positive radiotracer uptake in the remaining vas deferentes. All positive cases were compared with multiparametric MRI (mpMRI) or 68Ga-PSMA PET/MR to confirm the anatomic correspondence of the vas deferentes, and histological confirmation was obtained if available.

#### RESULTS

Among 236 men with biochemical recurrence after prostatectomy due to PCa, 176 patients (74,6%) had positive findings for recurrence on PET/CT 68Ga-PSMA-11. Of these patients, 5 (2,8%) had radiotracer uptake in the distal (periprostatic) remaining portion of the vas deferens, all of them unilateral. In 3 of these patients (60%), recurrence was detected only in vas deferens, while in 2 (40%) there were other concomitant sites (local or systemic). On mpMRI, all positive cases showed a thickened, asymmetric vas deferens as compared to the contralateral side. One patient also underwent a PET/MR with 68Ga-PSMA-11 and subsequent fusion-biopsy, with histological confirmation of local recurrence in the vas deferens.

# CONCLUSION

Although relatively rare, local recurrence in the vas deferens poses a diagnostic challenge on PET/CT and PET/MR with 68Ga-PSMA. There is a perspective for changes in the surgical technique for radical prostatectomy according to this new knowledge.

# **CLINICAL RELEVANCE/APPLICATION**

Although relatively rare, local recurrence in the vas deferens poses a diagnostic challenge on PET/CT and PET/MR with 68Ga-PSMA. There is a perspective for changes in the surgical technique for radical prostatectomy according to this new knowledge.



# GU223-SD-TUA2

Added Value of MRI Tractography of Periprostatic Nerve Plexus to Conventional t2-WI in Detection of Extra-Capsular Extension of Prostatic Cancer

Tuesday, Nov. 27 12:15PM - 12:45PM Room: GU/UR Community, Learning Center Station #2

# Participants

Matteo Catania, MD, Trieste, Italy (*Presenter*) Nothing to Disclose Adam J. Cybulski, MD, Verona, Italy (*Abstract Co-Author*) Nothing to Disclose Sara Brancato, Verona, Italy (*Abstract Co-Author*) Nothing to Disclose Riccardo Negrelli, MD, Verona, Italy (*Abstract Co-Author*) Nothing to Disclose Enrico Boninsegna, Verona, Italy (*Abstract Co-Author*) Nothing to Disclose Giulia A. Zamboni, MD, Verona, Italy (*Abstract Co-Author*) Nothing to Disclose Roberto Pozzi Mucelli, Verona, Italy (*Abstract Co-Author*) Nothing to Disclose Giancarlo Mansueto, MD, Verona, Italy (*Abstract Co-Author*) Nothing to Disclose

#### For information about this presentation, contact:

matteocatania89@gmail.com

#### PURPOSE

In staging of prostate cancer, it would be valuable to assess the extra-capsular extension (ECE) before surgery for a correct therapeutic planning. The purpose of this study was to evaluate the role of DTI (with fibertracking) and T2-weighted imaging (T2-WI) used together for predicting extra-capsular extension in patients with localized prostate cancer, using radical prostatectomy as the reference standard.

#### **METHOD AND MATERIALS**

46 patients with biopsy-proven diagnosis of prostatic neoplasia performed MRI and underwent radical prostatectomy. Histopathological analysis showed ECE in 20/46 and capsule sparing in 26/46. By means of T2-WI, ECE was evaluated in a qualitative manner, according to PI-RADS v.2(two groups with low and high risk of ECE); sensitivity and specificity were calculated for both group. We performed a quantitative analysis on two tractographic parameters, fractional anisotropy(FA) and apparent diffusion coefficient(ADC), and computed the ratio between the lesion quadrant and its controlateral (L/H ratio). We compared L/H ratios of patients with and without ECE; ROC analyses were performed to determinate ECE cut-off values of tractographic parameters. These cut-off values were used in association with T2-WI to reassess patients and to evaluate if specificity and sensitivity of ECE detection change.

## RESULTS

T2-WI showed a sensitivity of 80% and a specificity of 71% in detection of ECE. Tractography displayed a significant difference in L/H ratio for FA and ADC between patients with and without ECE. The simultaneous use of T2-WI and tractography revealed high sensitivity(100%) on patients with low suspect of ECE(on T2-WI) and high specificity(87%) on patients with high suspect of ECE(on T2-WI).

# CONCLUSION

The morphologic component of T2-weighted imaging and functional aspect of DTI should be interpreted together to more successfully assess the presence of ECE. In particular, in patients without the suspicion on T2-WI, DTI has incremental value to exclude extra-capsular extension, while in patients with the suspicion of ECE on T2-WI, DTI has incremental value to confirm extra-capsular extension.

# **CLINICAL RELEVANCE/APPLICATION**

The morphologic component of T2-weighted imaging and functional aspect of DTI should be interpreted together to more successfully assess the presence of ECE.



# GU224-SD-TUA3

Detection of Prostate Cancer: Abbreviated Biparmetric versus Standard Multiparametric MR Imaging - A Systematic Review and Diagnostic Meta-analysis

Tuesday, Nov. 27 12:15PM - 12:45PM Room: GU/UR Community, Learning Center Station #3

Participants Zhen Kang, Wuhan, China (Presenter) Nothing to Disclose

For information about this presentation, contact:

kangzh07@yeah.net

#### PURPOSE

To systematically evaluate the diagnostic accuracy of abbreviated bpMRI versus standard mpMRI for PCa, using guided biopsy or prostatectomy histopathology as the reference standard.

# METHOD AND MATERIALS

A comprehensive literature search of PUBMED, Web of Science, the Cochrane Library was performed by two researchers independently, as well as the relevant references. Original researches comparing bpMRI with mpMRI in diagnosing PCa were included. The methodological quality was assessed using the Quality Assessment of Diagnostic Accuracy Studies (QUADAS-2) tool. Data necessary to complete 2 × 2 contingency tables were obtained from the included studies. Diagnostic sensitivity, specificity, positive likelihood ratio (LR+), negative likelihood ratio (LR-), diagnostic OR (DOR)value of bpMRI and mpMRI were obtained by Stata 14.

# RESULTS

Ten studies were included, total of 1705 patients and 3419 lesions were analyzed. Sensitivity, specificity, LR+, LR-, DOR of mpMRI in diagnosing PCa were 0.79(95%CI: 0.69-0.87), 0.89(95%CI: 0.70-0.96), 0.89(95%CI: 0.70-0.96), 0.24(95%CI: 0.16-0.35), 29(95%CI: 10-83). The corresponding data for bpMRI were 0.79(95%CI: 0.69-0.87), 0.88(95%CI: 0.73-0.95), 6.4(95%CI: 2.9-14.5), 0.24(95%CI: 0.16-0.35), 27(95%CI: 11-67), respectively. Meta regression showed that there was no statistical difference between bpMRI and mpMRI in diagnosis of PCa, with corresponding area under ROC curve of 0.89 and 0.88 (RDOR=1, 95CI% 0.31-3.24, P=0.9944 > 0.05). Sensitivity analysis was consistent, with AUC of both 0.89 (RDOR=1.05, 95CI% 0.30-3.62, P = 0.9349 > 0.05).

### CONCLUSION

Currently available evidence indicates that bpMRI has basically the same sensitivity and specificity in diagnosis of PCa comparing with mpMRI.

# **CLINICAL RELEVANCE/APPLICATION**

In consideration of the time-consuming of DCE in standard mpMRI, mpMRI could be omitted and replaced by abbreviated bpMRI.



# GU225-SD-TUA4

# Blurring the Lines: Where POP-Q and MR Pelvic Floor Imaging Meet

Tuesday, Nov. 27 12:15PM - 12:45PM Room: GU/UR Community, Learning Center Station #4

# Awards

**Student Travel Stipend Award** 

#### Participants

Nayanatara Swamy, MD, Little Rock, AR (*Presenter*) Nothing to Disclose Gitanjali Bajaj, MD, Little Rock, AR (*Abstract Co-Author*) Nothing to Disclose Kedar Jambhekar, MD, Little Rock, AR (*Abstract Co-Author*) Nothing to Disclose Tarun Pandey, MD, FRCR, Little Rock, AR (*Abstract Co-Author*) Nothing to Disclose Sallie Oliphant, MD, Little Rock, AR (*Abstract Co-Author*) Nothing to Disclose Roopa Ram, MD, Little Rock, AR (*Abstract Co-Author*) Nothing to Disclose

#### For information about this presentation, contact:

nswamy@uams.edu

## PURPOSE

To bridge the gap between radiologists and gynecologists in understanding pelvic organ descent.

### **METHOD AND MATERIALS**

1. Background: POP-Q is described using midline sagittal MR female pelvis images. MR quantification of organ prolapse is elucidated. A tabular summary of relevant similarities and differences is provided. 2. All female patients >18 years of age undergoing dynamic pelvic floor imaging from 1/2013 to 12/2017, who also had pelvic organ prolapse quantification (POP-Q) at our institution's urogynecology clinic were included in our study. Patients who underwent non-dynamic MR pelvis study, who did not undergo POP-Q, in whom MR study and POP-Q were >12 months apart and those who underwent interim surgery between their POP-Q and MR study were excluded from the study.

## RESULTS

Out of 280 female patients who visited the urogynecology clinic for evaluation of pelvic organ prolapse, 68 met the inclusion criteria. Subjects were  $57\pm12$  years with a mean BMI of  $29\pm6$ kg/m<sup>2</sup>. 90% of our patients were Caucasians; 7% African American and 3% Asian or other. The mean time-span between POP-Q and MR was  $2\pm2$ months. POP-Q stage ranged from 0-4 and 82% were post-hysterectomy. We found strong correlation between POP-Q and dynamic MR pelvic floor imaging for anterior compartment prolapse (Pearson's correlation = 0.67 (p-value<0.001), n = 64) and moderate correlation for middle compartment prolapse (0.4 (0.01), n=45) and levator hiatus assessment (0.40 (0.02), n=33). However, there was no significant correlation for posterior compartment prolapse (-0.16 (0.20), n=65) and total vaginal length (0.29 (0.08), n=38). The incongruity in assessment of posterior compartment and total vaginal length may be explained by altered normal vaginal angulation during POP-Q (which is modified by vaginal speculum placement), distention of rectum with gel during MR and the complex interplay between myofacial, sacrococcygeal angulation and neurological factors in pelvic floor kinematics.

# CONCLUSION

Dynamic 3D MR visualization of the pelvis shows good to moderate correlation for anterior and middle compartments with POP-Q. Caution should be used in extrapolating findings to the posterior compartment.

## **CLINICAL RELEVANCE/APPLICATION**

MRI can be used as an adjunct to POP-Q in management of complex cases of pelvic organ prolapse involving the anterior and middle compartments.



# GU226-SD-TUA5

Histopathological to Multiparametric MRI Spatial Mapping of Extended Systematic Sextant and MR/TRUS-Fusion Targeted Biopsy of the Prostate

Tuesday, Nov. 27 12:15PM - 12:45PM Room: GU/UR Community, Learning Center Station #5

# Participants

David Bonekamp, MD, PhD, Heidelberg, Germany (*Presenter*) Speaker, Profound Medical Inc Patrick Schelb, Heidelberg, Germany (*Abstract Co-Author*) Nothing to Disclose Tristan A. Kuder, PhD, Heidelberg, Germany (*Abstract Co-Author*) Co-founder, HQ Imaging GmbH Fenja Deister, Heidelberg, Germany (*Abstract Co-Author*) Nothing to Disclose Markus Hohenfellner, MD, PhD, Heidelberg, Germany (*Abstract Co-Author*) Nothing to Disclose Heinz-Peter W. Schlemmer, MD, Heidelberg, Germany (*Abstract Co-Author*) Nothing to Disclose Jan P. Radtke, Heidelberg, Germany (*Abstract Co-Author*) Nothing to Disclose

#### PURPOSE

MRI has limited ability to detect multifocal disease or the full extent of prostate involvement with clinically significant prostate cancer (csPC, Gleason grade group >= 2). We compare the spatial matching of mpMRI lesions with sextant resolution histopathological mapping by extended targeted and systematic biopsies.

#### **METHOD AND MATERIALS**

A histopathological mapping of csPC was generated by combining prostate and MR lesion segmentations of MR images with matched histopathology from 24-core transperineal systematic and additional targeted biopsies in 224 consecutive patients with suspicion for csPC. Additionally, MR lesion segmentations were dilated by 10 mm to assess the effect of a security margin on lesion coverage. The overlap of histopathological mapping and clinically detected lesions was examined using descriptive statistics.

## RESULTS

460 (34%) of 1344 sextants were MR positive, harboring csPC in 38%, while MR negative sextants harbored csPC in 11%. 268 sextants harbored csPC, of these 174 (65%) were MR positive and 94 (35%) MR negative. Of 82 patients with sPC 79 patients (96%) had a positive MRI. Within MR positive patients with sPC, mpMRI missed the presence of any additional sPC outside the MR lesions in 48 patients (61%). Using a security margin of 10 mm around MR lesions mpMRI missed any sPC outside the MR lesions in 16 patients (20%). Using a hemispheric approach, mpMRI missed any sPC outside the hemisphere indicated by mpMRI in 14 (18%) of patients, while it indicated both hemispheres to be affected in 41 patients (52%) and correctly indicated hemispheric-only disease in 24 patients (30%). MR positive sextants contained 3.5 times more csPC than MR negative sextants.

## CONCLUSION

In 20% of patients correctly diagnosed by MRI there was additional sPC outside the mpMRI mapped prostate tissue. While detection of the presence of csPC is possible with MRI at very high sensitivity based on the presence of an MR index lesion, complete spatial mapping of sPC by mpMRI is limited.

### **CLINICAL RELEVANCE/APPLICATION**

The false negative rate of MRI with regard to additional disease in MRI positive patients is important to recognize and new approaches to improve lesion detection are needed to overcome this limitation.



# GU227-SD-TUA6

Super-Resolution Ultrasound Imaging: In Vivo Demonstration for Characterization of Testicular Lesions

Tuesday, Nov. 27 12:15PM - 12:45PM Room: GU/UR Community, Learning Center Station #6

#### Participants

Kirsten M. Christensen-Jeffries, PhD, London, United Kingdom (Presenter) Nothing to Disclose Dean Y. Huang, FRCR, London, United Kingdom (Abstract Co-Author) Nothing to Disclose Jemma Brown, London, United Kingdom (Abstract Co-Author) Nothing to Disclose Sevan Harput, London, United Kingdom (Abstract Co-Author) Nothing to Disclose Christopher Dunsby, London, United Kingdom (Abstract Co-Author) Nothing to Disclose Mengxing Tang, London, United Kingdom (Abstract Co-Author) Nothing to Disclose Paul S. Sidhu, MRCP, FRCR, London, United Kingdom (Abstract Co-Author) Speaker, Koninklijke Philips NV; Speaker, Bracco Group; Speaker, Hitachi, Ltd; Speaker, Siemens AG; Speaker, Samsung Electronics Co, Ltd; Advisory Board, Samsung Electronics Co, Ltd; Advisory Board, Itreas Ltd Robert J. Eckersley, PhD, London, United Kingdom (Abstract Co-Author) Nothing to Disclose

# For information about this presentation, contact:

kirsten.christensen-jeffries@kcl.ac.uk

### PURPOSE

Microvascular structure and flow is of clinical importance in studying disease processes. The purpose of this study is to aid differentiation of benign (such as Leydig cell tumors) and malignant (such as seminomas or lymphoma) vascular testicular tumors using recently developed ultrasound super-resolution (US-SR), which is able to visualize micro-vascular structures beyond the diffraction limit using US contrast agents.

# **METHOD AND MATERIALS**

US-SR was performed on historical, pre-operative contrast-enhanced ultrasound (CEUS) clinical datasets acquired from benign and malignant intra-testicular lesions using a clinical Acuson S3000 system (Siemens Medical Solutions, Mountain View, CA) at 4 MHz (wavelength  $\lambda$ =380 µm). Firstly, sub-pixel rigid cross-correlation motion correction was performed on B-mode frames. A rolling background subtraction was then applied on CEUS frames, before spatially isolated microbubble signals were extracted and localized. Direction and speed maps were generated by tracking individual bubble trajectories. Furthermore, quantitative measures such as vessel density and tortuosity were made on 5 regions of interest (ROIs) within each lesion, for 6 patients with seminomas and Leydig cell tumors.

# RESULTS

US-SR provided high resolution structural and directional maps of microbubble flow in the vasculature of testicular lesions. Microvascular structures, which cannot be resolved using conventional US, could be visualised in US-SR with an estimated size down to 20  $\mu$ m (equal to  $\lambda$ /19). Our preliminary study of only 6 patients demonstrated vessel densities of 26.6 ± 5.2 vessels/mm<sup>2</sup> for Leydig cell tumors, and  $13.7 \pm 7.9$  vessels/mm<sup>2</sup> for seminomas, and tortuosities of  $1.97 \pm 0.06$  and  $2.04 \pm 0.07$  respectively.

# CONCLUSION

Alongside highly detailed vascular images providing further information in testicular lesions, US-SR provides access to multiple new quantitative morphological and functional parameters for lesion characterisation and differentiation of vascular abnormalities. Further studies are ongoing to ensure results are consistent over a larger patient cohort.

#### **CLINICAL RELEVANCE/APPLICATION**

Structural and functional measures generated by US-SR have potential to improve pre-operative diagnostic confidence for vascular abnormalities to avoid unnecessary surgery.



# HP121-ED-TUA6

Past, Current, and Future About Consultation of Outside Radiology Studies: A Comprehensive Review with Emphasis on Patient's, Referring Physician's, and Radiologist's Perspective

Tuesday, Nov. 27 12:15PM - 12:45PM Room: HP Community, Learning Center Station #6

# Participants

Keita Onoue, MD, Boston, MA (*Presenter*) Nothing to Disclose Nemil Shah, MD, Boston, MA (*Abstract Co-Author*) Nothing to Disclose Nayana R. Somayaji, MBBS, Bengaluru, India (*Abstract Co-Author*) Nothing to Disclose Nagaraj-Setty Holalkere, MD, Boston, MA (*Abstract Co-Author*) Founder and CEO, Imaginglink Inc;

For information about this presentation, contact:

#### nholalkere@gmail.com

# **TEACHING POINTS**

The purpose of this exhibit is to,1) Review the various methods of consultation provided by Radiologists to images or studies acquired at an outside hospital or facility.2) Review of format of images provided via films, discs, storage devices and online cloud service to Radiologists for official reporting versus curb side consultation.3) Pros and Cons of various methods with respect to patient, referring physician and radiologists perspective will be discussed.4) A brief discussion on potential legal liabilities, reimbursement and major concerns related to consultation to outside studies will be discussed.

# TABLE OF CONTENTS/OUTLINE

Background of consultation provided by Radiologists to outside hospital study.Why, When and to whom the consultation needs to be provided.Review of Methods;a) Past Method: Printed/developed filmsb) Current Method: Images on a CD, dvd or storage devices.c) Future method: Transfer of Images to PACS via cloud services such as LifeImagePros and Cons of above methodsTypes of consultations; a) Full official report that gets documented on patient's records.b) Unofficial verbal or curb side opinion.What are the ideal requirements for Patients, Referring Physician and Radiologists?Potential legal liabilities and reimbursement for full report. Summary of major concerns and benefits.



# HP216-SD-TUA1

Are Patient-Centered Outcomes Reported in the Imaging Literature? a Secondary Analysis of the American College of Radiology Appropriateness Criteria

Tuesday, Nov. 27 12:15PM - 12:45PM Room: HP Community, Learning Center Station #1

# Participants

Victoria E. Hardy, MSc, Seattle, WA (*Abstract Co-Author*) Nothing to Disclose Monica Zigman Suchsland, MPH,BS, Seattle, WA (*Abstract Co-Author*) Nothing to Disclose Jeffrey G. Jarvik, MD, Seattle, WA (*Presenter*) Consultant, Wolters Kluwer nv; Co-editor, Springer Nature; Royalties, Springer Nature Rebecca Haines, Reston, VA (*Abstract Co-Author*) Nothing to Disclose Anne Brittain, PhD, Falls Church, VA (*Abstract Co-Author*) Spouse, Employee, General Electric Company David Kurth, Fairfax, VA (*Abstract Co-Author*) Nothing to Disclose James V. Rawson, MD, Boston, MA (*Abstract Co-Author*) Nothing to Disclose

Beth A. Devine, Seattle, WA (*Abstract Co-Author*) Nothing to Disclose Danielle C. Lavallee, Seattle, WA (*Abstract Co-Author*) Nothing to Disclose Annette J. Fitzpatrick, Seattle, WA (*Abstract Co-Author*) Nothing to Disclose Matthew J. Thompson, MD,PhD, Seattle, WA (*Abstract Co-Author*) Nothing to Disclose

# PURPOSE

In 1977 Fineberg proposed a framework for evaluating new imaging tests. Since then evaluation of tests has centered on their comparative accuracy, and inclusion of patient preferences and values in imaging decision making remains elusive. We aimed to identify the patient-centered outcomes (PCOs) included in studies of imaging tests across multiple clinical areas, using a secondary analysis of the American College of Radiology Appropriateness Criteria (AC).

## **METHOD AND MATERIALS**

We systematically reviewed Appropriateness Criteria evidence tables within the following clinical areas: breast, cardiac, gastrointestinal, musculoskeletal, neurologic, urology, vascular, thoracic, and women's health. The search dates of included evidence tables were between 2012 and 2017. We included articles which described original research performed for any reason (screening, surveillance, or staging) on adults and reported PCOs related to the imaging study. PCOs and methods used to measure them were extracted and synthesized using narrative analysis.

# RESULTS

Of the 255 clinical topics listed within the AC, 83 topics consisting of 5,195 articles were screened for eligibility. Of these, 4,815 articles were excluded based on initial review, and total of 292 full text papers were excluded after detailed review of full text. We included 89 articles in the final analysis. The most frequently reported PCOs were radiation exposure (n=37), downstream testing (n=22), complications (n=19), incidental findings (n=11) and patient values and experiences (n=8). Methods for measuring or identifying PCOs included use of standard dosing protocols/formulas, clinical observation, medical record review, and patient reports (e.g. questionnaires).

## CONCLUSION

Although a minority imaging studies do report PCOs, most were derived from clinical measures rather than from soliciting the patient's perspective, and they failed to incorporate a wide range of PCOs. As radiology moves to a more patient centered approach, it will be important to prioritize all outcomes that are relevant to patients, ensure that they are measured, and incorporated into decision making.

#### **CLINICAL RELEVANCE/APPLICATION**

Gaps in patient-centered outcomes research are present in radiology literature, findings from this study highlight a need to measure these outcomes.

#### **Honored Educators**

Presenters or authors on this event have been recognized as RSNA Honored Educators for participating in multiple qualifying educational activities. Honored Educators are invested in furthering the profession of radiology by delivering high-quality educational content in their field of study. Learn how you can become an honored educator by visiting the website at: https://www.rsna.org/Honored-Educator-Award/ Jeffrey G. Jarvik, MD - 2017 Honored EducatorJeffrey G. Jarvik, MD - 2018 Honored EducatorJames V. Rawson, MD - 2017 Honored Educator



### HP217-SD-TUA2

Cost-Effectiveness Analysis of US versus MRI for the Initial Evaluation of Superficial Masses of the Extremities

Tuesday, Nov. 27 12:15PM - 12:45PM Room: HP Community, Learning Center Station #2

### Participants

Brian Y. Chan, MD, Madison, WI (*Presenter*) Nothing to Disclose Andrew B. Ross, MD, MPH, Madison, WI (*Abstract Co-Author*) Nothing to Disclose

#### For information about this presentation, contact:

brian.chan@utah.edu

#### PURPOSE

To determine the most cost-effective imaging strategy for the diagnostic evaluation of superficial soft-tissue masses in the extremities.

### **METHOD AND MATERIALS**

A decision tree was created comparing three imaging strategies for diagnosis of superficial soft-tissue masses in the extremities: US, MRI, and US-selective. An imaging test was considered negative if the mass was diagnosed as benign and considered positive if the mass was interpreted as indeterminate or likely malignant. In the US and MRI arms, positive tests were followed by biopsy. In the US selective arm, a positive test was followed by MRI and then biopsied if the MRI was also positive. Diagnostic test costs (in 2017 US\$) and performance characteristics were obtained from a review of the literature. Outcomes included cost per correct diagnosis, false-positive rate, and false-negative rate. One-way and two-way sensitivity analyses were performed.

## RESULTS

For the base input values the US-selective strategy was dominant with a cost per correct diagnosis of \$514 compared to \$557 and \$1018 for the US and MRI strategies respectively. False-negative rate was lowest for MRI arm at 0.01% compared to 0.04% for the US arm and 0.05% for US-selective arm. One-way sensitivity analyses were performed for the sensitivity of US, sensitivity of MRI, pre-test probability of malignancy cost of ultrasound, and cost of MRI. The US-selective strategy remained dominant with the lowest cost per correct diagnosis in all scenarios. False negative and positive rates varied with varying input values but remained low. Multivariate sensitivity analysis also showed continued dominance of the US-selective strategy when minimizing US sensitivity, maximizing US cost, and minimizing MRI cost.

### CONCLUSION

This analysis suggests that an US-selective strategy is the most cost-effective strategy for the initial evaluation of superficial soft-tissue masses compared to US or MRI alone.

# **CLINICAL RELEVANCE/APPLICATION**

Using US as an initial imaging modality for evaluation of superficial soft-tissue masses followed by MRI when necessary may reduce health care costs without adversely affecting patient outcomes.



## HP218-SD-TUA3

# Nasopharyngeal Carcinoma: Choosing Chest CT or DR as a Baseline Staging Imaging Modality?

Tuesday, Nov. 27 12:15PM - 12:45PM Room: HP Community, Learning Center Station #3

#### **Participants**

Huan Čhen, Zhuhai, China (*Abstract Co-Author*) Nothing to Disclose Mingzhu Liang, Zhuhai, China (*Abstract Co-Author*) Nothing to Disclose Xueguo Liu, MD, Zhuhai, China (*Presenter*) Nothing to Disclose

# For information about this presentation, contact:

liuxueg@mail.sysu.edu.cn

### PURPOSE

The baseline staging imaging modality for nasopharyngeal carcinoma (NPC) patients is chest radiography or digital radiography (DR) from NCCN 2013 and ESMO 2012 guideline. But United Kingdom National Multidisciplinary Guidelines recommend chest CT to all NPC patients. We compare baseline and follow-up thoracic metastasis and lung cancer detection rate differences of chest DR group and CT group of NPC patients in our hospital.

# METHOD AND MATERIALS

The general clinical data, NPC local stage, baseline and follow-up DR(A-P and left lateral view) or chest CT images (Siemens Somatom Sensation 16 and Somatom Definition Flash CT, 120kV, auto-regulated mAs, plain scan, 1-2 mm slice thickness reconstruction) and clinical follow-up results of all NPC patients of our hospital from June 2013 to June 2017 were collected retrospectively. The detection rate differences of thoracic metastasis and lung cancer between baseline DR group and CT group were compared and analyzed.

#### RESULTS

284 NPC cases (local staging I 8, II 25, III 165, IV 86) chosen chest DR and 84 NPC cases (local staging I 2, II 12, III 43, IV 25) chosen chest CT as baseline staging imaging modality. The thoracic metastasis detection rate was 0.7% (2/284) and 7.3% (6/82) in DR group and CT group respectively in baseline staging (P<0.05). In follow-up period, thoracic metastasis were detected in 3.5% (10/282) in DR group with median interval 5.5 months (11 days to 15 months) and 5.3% (4/76) in CT group with median interval 20.5 months (3 months to 27 months) (P<0.05). The primary lung cancer were detected and confirmed in 0% (0/284) in DR and 3.7% (3/82) in CT group respectively in baseline staging, and 0.7% (2/284) in DR group and 0% (0/79) in CT group in follow-up.

# CONCLUSION

Chest CT should be recommended as baseline staging imaging modality for NPC patients, because of its higher thoracic metastasis and lung cancer detection rate and longer thoracic metastasis detection interval in follow-up comparing with choosing chest DR.

# **CLINICAL RELEVANCE/APPLICATION**

We recommand choosing chest CT for all NPC patients as baseline staging imaging modality, not chest DR.



# HP219-SD-TUA4

It Takes a Village: Active Faculty Engagement in Quality Improvement Using a Departmental Quality Improvement Committee

Tuesday, Nov. 27 12:15PM - 12:45PM Room: HP Community, Learning Center Station #4

# Participants

Kerry L. Thomas, MD, Tampa, FL (*Abstract Co-Author*) Nothing to Disclose Daniel K. Jeong, MD, Madison, WI (*Abstract Co-Author*) Nothing to Disclose Sebastian Feuerlein, MD, Tampa, FL (*Abstract Co-Author*) Nothing to Disclose Melissa J. McGettigan, MD, Tampa, FL (*Abstract Co-Author*) Nothing to Disclose Kenneth L. Gage, MD, PhD, Tampa, FL (*Abstract Co-Author*) Nothing to Disclose Nainesh Parikh, MD, New York, NY (*Abstract Co-Author*) Nothing to Disclose Robert A. Gatenby, MD, Tucson, AZ (*Abstract Co-Author*) Nothing to Disclose John A. Arrington, MD, Tampa, FL (*Presenter*) Nothing to Disclose Donald L. Klippenstein, MD, Tampa, FL (*Abstract Co-Author*) Nothing to Disclose

# For information about this presentation, contact:

Kerry.Thomas@moffitt.org

### PURPOSE

As healthcare transitions from volume care to value care, physicians and hospital systems must continually evaluate departmental quality to improve outcomes and patient satisfaction. It is imperative for radiologists to participate in quality improvement to maintain certification. However, departmental quality improvement initiatives and individual physician Patient Quality Initiative (PQI) projects are typically performed independently. As a result, radiology faculty members are often not fully engaged in departmental quality improvement initiatives. Even when asked to participate, radiologists can be reluctant because they often do not receive meaningful recognition for their time-consuming "behind the scenes" efforts. Similarly absence of departmental support for individual faculty PQI projects can render them impossibly difficult. To address this problem, we developed a physician- led departmental quality improvement committee.

### RESULTS

Prior to the creation of the Quality Improvement Committee, individual faculty members were struggling to accomplish improvement efforts on their own. In the year prior to committee implementation, only 4 quality improvement projects were actively pursued or completed by the body imaging department's 13 faculty members. However, over 30 new projects were initiated within a year of the committee's initiation. Implemented projects stemming from the committee include: patient feedback surveys, MRI protocol updates, patient wait time reduction, CT oral contrast water utilization, structured reporting, technologist QA conferences, improved contrast reaction reporting, website improvement and faculty scheduling optimization. The creation of the committee generated several advantages. One advantage was a project management system to identify, track, timeline, and prioritize projects. Second, a fully sanctioned committee brought the advantage of full administrative support increasing buy-in, resources, and enthusiasm for projects. Lastly, by bringing several members together with different areas of expertise, projects could be solved quickly and efficiently often using similar resources and methods by using a multidisciplinary approach. Due to these factors and by increasing the numbers of stakeholders involved, the total number of projects in progress or completed is well over 30. Planned quarterly committee meetings allowed cross-talk to generate an overall improved patient experience. Also, each committee member reports becoming immediately more involved with interdepartmental staff and hospital leadership as a direct result of each improvement project.

## CONCLUSION

Developing a formal quality improvement committee in the radiology department and actively engaging faculty members increased the number of faculty members engaged in patient quality improvement. The strong support and participation by the departmental leadership (chairman, vice chairs and department administrator) was crucial to the success of the committee. The committee facilitated an expeditious ability to complete improvement projects efficiently within the radiology department by developing a tracking system, prioritizing departmental resources, and using a multidisciplinary approach. In less than one year, we have successfully completed several projects and identified new areas for continuous quality improvement. We believe this committee could serve as a model for other radiology groups and hospital practices who are struggling with quality improvement success.

#### **METHODS**

Invitations to join the committee were sent to faculty members who had previously expressed interest in quality improvement initiatives. Additional invitations were sent to the departmental chair and vice chairs, the department administrator, modality supervisors, and the nursing supervisor. At the initial meeting, the committee established multiple subcommittees, each led by a faculty radiologist. These include: CT, MRI, Ultrasound, Nuclear Medicine, Interventional Radiology, Safety and Patient experience. Each subcommittee chair identified at least one project for improving quality and/or the patient experience. The subcommittees worked with other departmental and hospital staff to achieve their aims using a multidisciplinary approach. As projects progressed, committee members reported updates and obstacles to other faculty members for feedback and ideas for moving forward. To avoid additional long meetings, much communication utilized email, updates at already scheduled faculty, and division meetings as well as "water cooler chats" in the reading room.

#### **PDF UPLOAD**

http://abstract.rsna.org/uploads/2018/18008053/18008053\_corx.pdf



# HP220-SD-TUA5

# Quantifying the Radiation Safety Benefits of a New Interventional Radiology Suite

Tuesday, Nov. 27 12:15PM - 12:45PM Room: HP Community, Learning Center Station #5

### Participants

Jung H. Yun, Closter, NJ (*Presenter*) Nothing to Disclose Ezra Margono, Mineola, NY (*Abstract Co-Author*) Nothing to Disclose Fiza Khan, Glen Head, NY (*Abstract Co-Author*) Nothing to Disclose Faraz Khan, MD, Pittsford, NY (*Abstract Co-Author*) Nothing to Disclose Daniel Napolitano, RT, Mineola, NY (*Abstract Co-Author*) Nothing to Disclose Jason C. Hoffmann, MD, Mineola, NY (*Abstract Co-Author*) Speakers Bureau, Merit Medical Systems, Inc; ;

# For information about this presentation, contact:

Jason.Hoffmann@nyulangone.org

# PURPOSE

As higher numbers of more complex angiography and interventions are performed in interventional radiology (IR), radiation safety is a topic of great importance and concern for physicians, patients, and procedural staff. Newer IR suites reportedly have lower-dose imaging, but the literature on this topic is relatively limited. We evaluate the difference in radiation exposure index when performing complex angiography and interventions in a new, state-of-the-art IR suite compared to an older suite.

### **METHOD AND MATERIALS**

A single-institution, IRB-exempt retrospective cohort analysis of complex vascular angiography and intervention procedures performed in a new IR suite (Infinix-I Biplane, Toshiba Medical, installed late 2017) during a 10-week period in 2018. Comparison was then made to a similar cohort of procedures performed in an older IR suite during a 10-week period in 2017 (Axiom Artis Biplane, Siemens Medical, installed late 2008). Cases using cone-beam CT in the new room were excluded, as this technology was not available in the older room and this would substantially impact radiation exposure indices. Data collected included type of procedure, procedure time, and radiation exposure index (dose area product/DAP, uGy.m2). Analysis of results was performed using Microsoft Excel (Microsoft, Redmond, VA), with statistical significance defined as P<.05.

# RESULTS

34 complex angiography procedures were performed in the "new" IR suite during the study period, and then compared to 40 similar procedures were performed in the "older" suite. Procedures included prostatic artery embolization, hepatic embolization, renal embolization, and pelvic and mesenteric angiography and embolization. Mean DAP was 17,605.8 and 41,253.36 in the new and older rooms, respectively (P<.05). Mean procedure time was 74 and 97 minutes in the new and older rooms, respectively (P<.05).

### CONCLUSION

Performing complex vascular interventions in a newer IR suite can lead to more efficient procedures and lower radiation exposure.

# **CLINICAL RELEVANCE/APPLICATION**

Dose reduction techniques, including post-process magnification, have a quantifiable, positive impact of radiation safety during IR procedures.



# IN006-EC-TUA

RadSim: A Single Vendor-Neutral Portal of Real Life Experience to Its Users on All Generic and Specific Aspects of CT Scanning Including Principles of CT Hardware, Scan Parameters, Scanning Protocol, Dual Energy, Image Quality, and Radiation Dose

Tuesday, Nov. 27 12:15PM - 12:45PM Room: IN Community, Learning Center Custom Application Computer Demonstration

#### Participants

Anders Persson, MD, PhD, Linkoping, Sweden (*Presenter*) Nothing to Disclose Nils Dahlstrom, MD, PhD, Linkoping, Sweden (*Abstract Co-Author*) Nothing to Disclose Petr Vorel, MD, Linkoping, Sweden (*Abstract Co-Author*) Nothing to Disclose Angie D. Liu, MD, Linkoping, Sweden (*Abstract Co-Author*) Nothing to Disclose FILIP LANDGREN, MD, Linkoping, Sweden (*Abstract Co-Author*) Nothing to Disclose Alexandr Malusek, PhD, Linkoping, Sweden (*Abstract Co-Author*) Nothing to Disclose

# For information about this presentation, contact:

anders.persson@cmiv.liu.se

#### **TEACHING POINTS**

To present the result from a RSNA Educational Scholar Grant 'RadSim' To increase the understanding of CT scanning parameters To undertake simulation based training exercise To assess radiology personnel on post-simulation knowledge of CT protocols, iterative reconstruction and dual energy CT applications

## **TABLE OF CONTENTS/OUTLINE**

Importance of radiation dose optimization has been stressed due to concerns over radiation-induced carcinogenesis. Since Computed Tomography contributes to the largest portion of radiation from medical imaging, special attention has been given to dose reduction for CT. Prior studies have highlighted lack of understanding of CT technologies, leading to high variability in CT protocols. In radiology, simulation techniques have been mostly assessed in interventional radiology and contrast media safety. We strongly believe that 'RadSim' when presented as a stand-alone computer display at RSNA will provide 'real-life' scanning experience and training opportunity to promote safe and efficient use of current, modern,CT technology. 'RadSim' provide a unique single vendor-neutral consolidated portal of real life experience on all generic and specific aspects of CT scanning including principles of CT hardware, scan parameters, scanning protocol, image quality and radiation dose.



# IN210-SD-TUA1

Improving Computer Aided Classification of Breast Lesions on Mammograms Using Simulated Masses by Generative Adversarial Networks

Tuesday, Nov. 27 12:15PM - 12:45PM Room: IN Community, Learning Center Station #1

# Participants

Chisako Muramatsu, PhD, Gifu, Japan (*Presenter*) Nothing to Disclose Takako Morita, MD, Nagoya, Japan (*Abstract Co-Author*) Nothing to Disclose Mikinao Ooiwa, Nagaya, Japan (*Abstract Co-Author*) Nothing to Disclose Hiroshi Fujita, PhD, Gifu City, Japan (*Abstract Co-Author*) Nothing to Disclose

# CONCLUSION

Simulated data may be useful for training deep neural networks when the training sample size is small. Further investigation is needed for studying effective training methods and creating better simulated samples.

#### Background

Computer aided classification systems using deep learning technique are considered to provide promising results without requiring segmentation of lesions, defining effective features, and tuning the rules. However, for the success of deep learning, generally a large number of training data is required. Data augmentation and transfer learning are some techniques considered useful for improving test results when the number of training cases is small. Another possible way is to increase samples with simulated data generated by a generative adversarial networks (GAN).

### **Evaluation**

In this study, computerized classification of breast masses on mammograms is studied. For evaluating the effect of data augmentation, several schemes are compared: conventional machine learning scheme with use of hand crafted features, convolutional neural network (CNN) pre-trained with natural images and fine-tuned with digital mammography images, CNN pre-trained with digital mammography images and fine-tuned with digital mammography images, CNN trained with digital mammography images with regular data augmentation such as image rotation and contrast adjustment, CNN trained with digital mammography images together with simulated images by GAN, and CNN pre-trained with simulated images by GAN and fine-tuned with digital mammography images. The classification performance of above methods are evaluated using an area under the receiver operating characteristic curve.

### Discussion

In the preliminary investigation, result for the CNN pre-trained with natural images was lower than those for the CNN pre-trained with digitized images and the CNN with data augmentation. The result for the CNN pre-trained with the simulated samples was comparable; however, including them together with the original samples may not be effective. The conventional machine learning method had a relatively high performance because the hand-crafted features were based on the manual contours of the lesions.



# IN211-SD-TUA2

Deep Learning-Enabled Normalization of Reconstruction Kernel-Induced Variability of Emphysema Index in Low-Dose Lung CT

Tuesday, Nov. 27 12:15PM - 12:45PM Room: IN Community, Learning Center Station #2

# Participants

Hyeongmin Jin, Seoul, Korea, Republic Of (*Presenter*) Nothing to Disclose Chang Yong Heo, BS, Seoul, Korea, Republic Of (*Abstract Co-Author*) Nothing to Disclose Jong H. Kim, PhD, Seoul, Korea, Republic Of (*Abstract Co-Author*) Nothing to Disclose

## CONCLUSION

Our study demonstrates the feasibility of deep learning technique for reducing the variability of EI induced by differing CT reconstruction kernels. This deep learning model is promising for improving the reliability of EI assessment for evaluating the longitudinal changes where patient scans may obtained at different scanners and with different reconstruction kernels.

#### Background

Differing CT reconstruction kernels are known to affect the variability of emphysema quantification, and thus remain as a barrier in translating the computer aided quantification techniques into clinical practice. This study presents a deep learning application for the cross conversion of CT images reconstructed with different kernels and evaluates its impact on normalization of the emphysema index (EI) in low-dose chest CT.

#### **Evaluation**

One hundred twenty-six cases of low-dose chest CT exams scanned by 2 CT scanners (LightSpeed 16 and LightSpeed Ultra, GE Healthcare, Waukesha, WI) with 2 reconstruction kernels (STANDARD and BONE) were selected from the lung screening trial database. We trained a deep learning model with fully convolutional network architecture to translate the CT scans with BONE kernel into those with STANDARD kernel. The deep learning system was trained with CT images from one CT scanner and validated on an independent dataset scanned with another CT scanner for inter scanner variability. The EI (RA950) was measured with a software package (ClariPulmo, ClariPI, Seoul, South Korea) and compared among the data sets of BONE, STANDARD, and the converted BONE. The effect of kernel conversion was evaluated with the mean and standard deviation of pair-wise differences in EI.

#### Discussion

Population mean of EI was 11.08±6.07% for BONE kernel, 3.03±3.32% for STANDARD kernel, and 2.69±2.77% for normalized BONE kernel, respectively. The pair-wise absolute difference in EI between standard and sharp kernel datasets decreased from 8.05±3.67% to 0.67±0.79% after kernel normalization.



## IN214-SD-TUA3

Are Patients Using Online Portals to View Radiology Reports?

Tuesday, Nov. 27 12:15PM - 12:45PM Room: IN Community, Learning Center Station #3

#### **Participants**

Andrew J. Gunn, MD, Birmingham, AL (Presenter) Nothing to Disclose

James A. McFarland, MD, Birmingham, AL (Abstract Co-Author) Nothing to Disclose

Kamil Arif, MD, Birmingham, AL (Abstract Co-Author) Nothing to Disclose

Ahmed K. Abdel Aal, MD, PhD, Birmingham, AL (Abstract Co-Author) Consultant, Abbott Laboratories; Consultant, Baxter

International Inc; Consultant, C. R. Bard, Inc; Consultant, Boston Scientific Corporation; Consultant, W. L. Gore & Associates, Inc; Consultant, Sirtex Medical Ltd

Andrew D. Smith, MD,PhD, Birmingham, AL (*Abstract Co-Author*) President and Owner, Radiostics LLC; President and Owner, eRadioMetrics LLC; President and Owner, Liver Nodularity LLC; President and Owner, Color Enhanced Detection LLC; Patent holder Garry Choy, MD, MS, Boston, MA (*Abstract Co-Author*) Nothing to Disclose William M. Parkhurst, MD, Birmingham, AL (*Abstract Co-Author*) Nothing to Disclose

#### For information about this presentation, contact:

agunn@uabmc.edu

### PURPOSE

To understand the traffic generated by the "radiology" tab within a secure, online patient portal.

#### **METHOD AND MATERIALS**

The number of unique logins to our institution's online patient portal from March 2017 through March 2018 were collected. The results were analyzed for the number of times that the "radiology" tab within the portal was accessed and the average amount of time spent within the "radiology" page. The number of interactions with the page once within the "radiology" tab was also collected. As an additional measure of interest in the patient portal, the number of times that the portal was searched for through the medical center's homepage was collected. The terms "portal" and "patient portal" were combined for analysis.

## RESULTS

There were 435,571 unique logins to the patient portal (mean: 33,505 unique users/month; range: 27,637-38,005). There were 83,088 unique views of the "radiology" tab (mean: 6,391 views/month; range: 4,752-8,800 views). Thus, on average, 19.1% of portal users viewed the "radiology" tab during the study period. Users spent an average of 90 seconds within the "radiology" tab (range: 59-121 seconds). The number of unique logins and number of "radiology" tab views on a per month basis are summarized in Figure 1. On average, 75.4% of users interacted with the radiology results page after they entered the "radiology" tab. During the study period, 171,332 search terms were entered into the medical center's homepage. The patient portal was searched for 176 times, representing 0.1% of all search terms.

# CONCLUSION

Online patient portals are utilized frequently by patients although the viewing of radiology reports accounts for a smaller percentage of overall use. Once within the "radiology" tab, patients interact with the page at a high rate even though the interactions do not last for a significant period of time.

### **CLINICAL RELEVANCE/APPLICATION**

Secure, online portals are a convenient way for patients to access their medical information, including radiology reports. Radiologists can use this information to tailor the information found through the portal to maximize patient engagement.



## MI119-ED-TUA5

The ABCs of FACBC: Helpful Hints to Interpret FDA Approved Fluciclovine F-18 PET/CT For Prostate Cancer Recurrence

Tuesday, Nov. 27 12:15PM - 12:45PM Room: MI Community, Learning Center Station #5

#### Awards Cum Laude

#### -----

# Participants

Huyen D. Tran, MD, Philadelphia, PA (*Abstract Co-Author*) Nothing to Disclose Timothy Lu, MD, Philadelphia, PA (*Presenter*) Nothing to Disclose Lee P. Adler, MD, Jenkintown, PA (*Abstract Co-Author*) Research Grant, Merck & Co, Inc; Research Grant, Eli Lilly and Company ; Research Grant, General Electric Company ; Speakers Bureau, Eli Lilly and Company ; Consultant, Eli Lilly and Company ; Research Grant, Blue Earth Diagnostics Ltd

# For information about this presentation, contact:

tranh@einstein.edu

#### **TEACHING POINTS**

1. Identify indications for Fluciclovine F-18 (Axumin, Blue Earth Diagnostics) PET/CT. 2. Recognize normal biodistribution of Fluciclovine F-18. 3. Distinguish abnormal uptake not due to prostate cancer recurrence. 4. Discuss interpretation criteria for Fluciclovine F-18. 5. Review various positive and negative scans, with reading pearls to improve interpretive skills.

### TABLE OF CONTENTS/OUTLINE

Helpful hints to interpret Fluciclovine F-18 PET/CT are presented in a Quiz format with case examples. Topics include: 1. Prostate cancer recurrence, current imaging modalities 2. Efficacy, multi-center trials 3. Indication 4. Acquisition 5. Normal uptake 6. Urethra 7. Bladder (prone, delayed scans) 8. Pre- vs. Post- prostatectomy 9. BPH vs local recurrence 10. Inflammation/infection 11. Other cancers 12. AJCC TNM 8th edition effective 1/1/2018 13. Lymphatic pathways (Lateral, Hypogastric, Anterior, Presacral) 14. Regional true pelvic nodes: N1 (Internal iliac, External iliac) 15. Non-regional (distant) nodes: M1a (Paraaortic, Common iliac, inguinal) 16. Interpretation: Visual criteria 17. Quantitative criteria 18. Sclerotic bone lesions M1b: necessity for correlative imaging



## MI216-SD-TUA2

Prediction of Tumor Biological Characteristics in Different Colorectal Cancer Liver Metastasis Animal Models Using 18F-FDG and 18F-FLT

Tuesday, Nov. 27 12:15PM - 12:45PM Room: MI Community, Learning Center Station #2

### Participants

Huijie Jiang, PhD, MS, Harbin, China (Presenter) Nothing to Disclose

#### For information about this presentation, contact:

jhjemail@163.com

#### PURPOSE

Positron emission tomography (PET) is a noninvasive method to characterize different metabolic activities of tumors, providing information for staging, prognosis, and therapeutic response of patients with cancer. The aim of this study was to evaluate the feasibility of 18F-fludeoxyglucose (18F-FDG) and 3'-deoxy-3'-18F-fluorothymidine (18F-FLT) PET in predicting tumor biological characteristics of colorectal cancer liver metastasis.

#### METHOD AND MATERIALS

The uptake rate of 18F-FDG and 18F-FLT in SW480 and SW620 cells was measured via an in vitro cell uptake assay. The region of interest was drawn over the tumor and liver to calculate the maximum standardized uptake value ratio (tumor/liver) from PET images in liver metastasis model. The correlation between tracer uptake in liver metastases and VEGF, Ki67 and CD44 expression was evaluated by linear regression.

# RESULTS

Compared to SW620 tumor-bearing mice, SW480 tumor-bearing mice presented a shorter survival time and a higher rate of liver metastases. The uptake rate of 18F-FDG in SW480 and SW620 cells was  $6.07\pm1.19\%$  and  $2.82\pm0.15\%$ , respectively (t=4.69, P=0.04); that of 18F-FLT was  $24.81\pm0.45\%$  and  $15.57\pm0.66\%$ , respectively (t=19.99, P<0.001). Micro-PET scan showed that all parameters of FLT were significantly higher in SW480 tumors than those in SW620 tumors. A moderate relationship was detected between metastases in the liver and 18F-FLT uptake in tumors (r=0.73, P=0.0019). 18F-FLT uptake was also positively correlated with the expression of CD44 (r=0.81, P=0.0049).

## CONCLUSION

The uptake of 18F-FLT in metastatic tumor reflects different biological behaviors of colon cancer cells. 18F-FLT can be used to evaluate the metastatic potential of colorectal cancer in nude mice.

### **CLINICAL RELEVANCE/APPLICATION**

The uptake of 18F-FLT in metastatic tumor reflects different biological behaviors of colon cancer cells. 18F-FLT can be used to evaluate the metastatic potential of colorectal cancer in nude mice and is recommended in the initial evaluation of metastatic potential of colorectal cancer.



## MI218-SD-TUA4

# MR Imaging of Zinc Depletion in Prostate Cancer

Tuesday, Nov. 27 12:15PM - 12:45PM Room: MI Community, Learning Center Station #4

#### **Participants**

Yue Yuan, PhD, Baltimore, MD (*Abstract Co-Author*) Nothing to Disclose Chengyan Chu, Baltimore, MD (*Abstract Co-Author*) Nothing to Disclose Zhiliang Wei, Baltimore, MD (*Abstract Co-Author*) Nothing to Disclose Xiaolei Song, Baltimore, MD (*Abstract Co-Author*) Nothing to Disclose Jeff W. Bulte, PhD, Baltimore, MD (*Presenter*) Research Grant, Koninklijke Philips NV; Research Grant, Weinberg Physics, LLC

# For information about this presentation, contact:

jwmbulte@mri.jhu.edu

### PURPOSE

Of all soft tissues, the normal prostate has the highest mobile zinc content, but this level decreases dramatically during malignant transformation. We aimed to use iCEST (ion chemical exchange saturation transfer) 19F MRI as a non-invasive means to probe zinc depletion in prostate cancer.

# **METHOD AND MATERIALS**

For in vitro validation studies, normal (RWPE1), ZIP1 zinc transporter-downregulated (RWPE2), and malignant (DU145 and LNCaP) human prostate cells were incubated with 75 µM ZnSO4 and induced to secrete zinc using glucose stimulation. Following the addition of 2.5 mM TF-BAPTA, 19F-derivative of BAPTA which is a fluorescent dye indicator for zinc, the supernatant was assessed with 1H and 19F iCEST MRI at 17.6 T. For in vivo studies, 1E6 cancer cells were injected into the prostate of 6-8 weeks old immunodeficient NSG mice and allowed to grow for 21 days. Immediately after i.p. injection of 80 µL of 20% w/v D-glucose and injection of 0.15 g/kg bw TF-BAPTA into the anterior prostate through a catheter, iCEST MR images were collected at 17.6T using a modified RARE sequence with a FOV=2.6×2.6 cm, 3 mm slice thickness, and a resolution of 0.8x0.8 mm.

### RESULTS

In vitro, the strongest iCEST signal was observed for glucose-stimulated RWPE1 cells with a normal zinc transporter level. In normal prostate cells with a downregulated ZIP1 zinc transporter (RWPE2), a weaker iCEST signal was observed. No signal could be observed for DU145 and LNCaP prostate cancer cells. In vivo, the strongest iCEST signal was observed for the normal prostate following i.p. glucose stimulation (Fig. 1). Both the normal prostate without glucose stimulation and the two orthotopic tumor models with glucose stimulation showed much weaker iCEST signal.

# CONCLUSION

Using iCEST MRI, differences in glucose-induced zinc secretion between normal and malignant prostate cells can be readily detected, both in vitro and in vivo.

### **CLINICAL RELEVANCE/APPLICATION**

Monitoring the conversion of normal prostate cells into malignant cells using iCEST 19F MRI may be further developed to diagnose prostate cancer in its earliest stages.



# MK370-SD-TUA1

Automatic Femoral Neck Fracture Detection and Classification Utilizing Advanced Deep Learning Techniques

Tuesday, Nov. 27 12:15PM - 12:45PM Room: MK Community, Learning Center Station #1

#### Awards Student Travel Stipend Award

#### Participants

Simukayi Mutasa, MD, New York, NY (*Presenter*) Nothing to Disclose Sowmya L. Varada, MD, Boston, MA (*Abstract Co-Author*) Nothing to Disclose Akshay Goel, MD, New York, NY (*Abstract Co-Author*) Nothing to Disclose Tony T. Wong, MD, New York, NY (*Abstract Co-Author*) Nothing to Disclose Michael J. Rasiej, MD, New York, NY (*Abstract Co-Author*) Nothing to Disclose

#### For information about this presentation, contact:

s.mutasa@columbia.edu

# PURPOSE

To use an algorithm augmented by recent advances in deep learning to accurately diagnose femoral neck fractures.

# METHOD AND MATERIALS

An IRB approved retrospective case-control study of patients with femoral neck fractures was performed. 1063 unique AP hip radiographs without hardware were obtained from 550 patients. Ground truth labels of Garden fracture classification were applied by a fellowship trained MSK radiologist. Group A consisted of 127 Garden I and II fractures, Group B consisted of 610 Garden III and IV fractures and the third group consisted of 326 normals. An initial convolutional neural network (CNN) was trained to localize the femoral neck and produce an 850x850 pixel crop. These crops were used as inputs into a second CNN which predicted the presence of Garden I/II versus III/IV fracture or absence of a fracture. Advanced data augmentation techniques were used to expand the training set including using images produced by a generative adversarial network (GAN). Additionally, the training set was augmented by digitally reconstructed radiographs (DRRs) from affine warped hip CT scans representing 31 patients in the training data set who had a pre operative hip CT for concern of fracture. In all, 6000 total examples, real and generated were available for training. 256x256 pixel images were input into the final network. A baseline deep neural network with a wide-residual architecture and a spatial transformer layer was utilized. Parameters were tuned based on a 20% validation group. A class balanced holdout set of 105 patients was utilized as the testing set with 35 patients of each class.

### RESULTS

Two class prediction of fracture vs no fracture (AUC 0.92): Accuracy 91.4%, sensitivity 0.90, specificity 0.94, PPV 0.97, NPV 0.83. Three class prediction of normal, Garden I/II and Garden III/IV (macro AUC 0.96): Accuracy 86.0%, sensitivity 0.79, specificity 0.94, PPV 0.80, NPV 0.80.

### CONCLUSION

Advanced data augmentation and deep learning techniques can be used for accurate diagnosis of femoral neck fractures with a relatively small data set.

# **CLINICAL RELEVANCE/APPLICATION**

This may improve radiologist workflow and allow for faster patient triage in the emergency setting.



# MK371-SD-TUA2

CT-Guided Percutaneous Cryoablation of Musculoskeletal Lesions: Success and Fail

Tuesday, Nov. 27 12:15PM - 12:45PM Room: MK Community, Learning Center Station #2

### Participants

Maria Jesus Garcia Sanchez, MD, Madrid, Spain (Presenter) Nothing to Disclose Irene Miguelsanz, MD, Tres Cantos, Spain (Abstract Co-Author) Nothing to Disclose Mar Tapia Vine, Madrid, Spain (Abstract Co-Author) Nothing to Disclose Victor M. Muley, Madrid, Spain (Abstract Co-Author) Nothing to Disclose Daniel Bernabeu Taboada, Madrid, Spain (Abstract Co-Author) Nothing to Disclose

#### PURPOSE

-Evaluation of image criteria of favorable response to treatment of musculoskeletal lesions by percutaneous cryoablation. -To identify the basis for treating musculoskeletal lesions with cryoablation and to explain the expected outcomes and how to minimize procedure-related complications.

# **METHOD AND MATERIALS**

Observational retrospective study of heterogeneous sample of patients (n=11, 7 females, 4 males) with musculoskeletal lesions. We analyze of imaging outcomes of 13 CT-guided cryoablations performed in our center since 2016. Histological diagnosis included 4 bones and 9 soft tissue lesions: metastasis (n=2), angioendothelioma (n=1), chondroblastoma (n=1), chondrosarcoma (n=2), deep fibromatosis (n=4), pleomorphic sarcoma (n=1); saphenous neuropathy (n = 1); endometriosis in the abdominal wall (n=1). Cryoablation methods, clinical outcomes, complications and oncological outcomes were analyzed. 17 G and 15 G probes were used.

# RESULTS

The patients' average age was 51 years (17-68). The average length of the procedure was 140 min, and the number of probes was 2.7 (range 1-7). The average size of tumor after 3-6 months changed from 45 mm to 39 mm (0-115) for soft tissue lesions, and from 32,5 mm to 10mm (0-25) for bone lesions. During follow-up, three fibromatosis cases (3m, 9m, 24m), endometriosis (3m), mandibular (9m) and chordoma metastasis (18m) showed favorable response with no evidence of local recurrence. A fibromatosis case was incompletely ablated because nerve involvement with enlargement of the non-ablated component. Chondrosarcoma cases, bone angioendothelioma (6m), and chondroblastoma (6m) have shown initial positive response with local progression afterwards. Saphenous nerve neurolysis got 5 months of absolute pain relieve. Complications included 1st grade skin burns, three transient palsies of adjacent nerves, and intraarticular dissemination of knee chondroblastoma, from a previous pathological fracture.

## CONCLUSION

Percutaneous cryoablation is effective achieving local control for <5 cm lesions and alleviating pain in larger size tumors and could be used as a minimal invasive therapeutic option in selected patients.

#### **CLINICAL RELEVANCE/APPLICATION**

Current advances in the field of cryoablation have improved the capabilities for this technique, and provides a complementary treatment option for many patients with musculoskeletal lesions. According to our results, we propose several indications and practice patterns.



# MK372-SD-TUA3

Proton Density Fat Fraction (PDFF) MR Imaging for Differentiation of Acute Benign and Malignant Vertebral Body Fractures

Tuesday, Nov. 27 12:15PM - 12:45PM Room: MK Community, Learning Center Station #3

## Participants

Frederic Carsten Schmeel, Bonn, Germany (*Abstract Co-Author*) Nothing to Disclose Julian A. Luetkens, MD, Bonn, Germany (*Presenter*) Nothing to Disclose Frank Traeber, Bonn, Germany (*Abstract Co-Author*) Nothing to Disclose Simon J. Enkirch, Bonn, Germany (*Abstract Co-Author*) Nothing to Disclose Andreas Feisst, MD, Bonn, Germany (*Abstract Co-Author*) Nothing to Disclose Christoph H. Endler, MD, Bonn, Germany (*Abstract Co-Author*) Nothing to Disclose Leonard C. Schmeel, Bonn, Germany (*Abstract Co-Author*) Nothing to Disclose Hans H. Schild, MD, Bonn, Germany (*Abstract Co-Author*) Nothing to Disclose Guido M. Kukuk, MD, Bonn, Germany (*Abstract Co-Author*) Nothing to Disclose

### For information about this presentation, contact:

carsten.schmeel@ukb.uni-bonn.de

#### PURPOSE

The aim of this prospective study was to evaluate the diagnostic performance of quantitative proton density fat fraction (PDFF) magnetic resonance imaging (MRI) to differentiate between acute benign and malignant vertebral compression fractures.

#### **METHOD AND MATERIALS**

Fifty-seven consecutive patients with a total of 87 vertebral compression fractures were prospectively enrolled in this institutional review board approved study. All patients underwent routine clinical MRI with an additional six-echo modified Dixon sequence of the spine at a clinical 3.0-Tesla scanner. Intravertebral PDFF and PDFF-ratio (fracture PDFF / normal vertebrae PDFF) for benign and malignant vertebral compression fractures were calculated using region-of-interest (ROI) analysis and compared between both groups. Additional receiver operating characteristic (ROC) and binary logistic regression analyses were performed. All fractures were categorized as benign or malignant according to either direct bone biopsy or 6-month follow-up MRI.

### RESULTS

There were 46 acute benign and 41 malignant vertebral compression fractures. Both PDFF and PDFF-ratio of malignant vertebral compression fractures were significantly lower compared to acute benign VCFs (PDFF,  $3.48\pm3.30\%$  vs.  $23.99\pm11.86\%$  [p<0.001]; PDFF-ratio,  $0.09\pm0.09$  vs.  $0.49\pm0.24$  [p<0.001]). The areas under the ROC-curves were 0.98 for PDFF and 0.97 for PDFFratio, yielding an accuracy of 96% and 95% for the differentiation of acute benign from malignant vertebral compression fractures. On multivariate analysis, intravertebral PDFF remained as the only imaging-based variable to independently differentiate between acute benign and malignant vertebral compression fractures (odds ratio, 0.454; p=0.005).

#### CONCLUSION

Quantitative assessment of PDFF derived from modified Dixon water-fat MRI has high diagnostic accuracy for the differentiation of acute benign and malignant vertebral compression fractures.

### **CLINICAL RELEVANCE/APPLICATION**

Quantitative PDFF MRI provides high diagnostic accuracy for the differentiation of acute osteoporotic and malignant vertebral body fractures and may help to avoid potentially harmful bone biopsies.



# MK373-SD-TUA4

# Non-invasive MRI Biomarkers of Muscle Injury and Recovery for Muscular Dystrophy

Tuesday, Nov. 27 12:15PM - 12:45PM Room: MK Community, Learning Center Station #4

### **Participants**

Joshua Park, BS, Seattle, WA (*Abstract Co-Author*) Nothing to Disclose Guy Odom, PhD, Seattle, WA (*Abstract Co-Author*) Nothing to Disclose Feng Zhang, MD, Seattle, WA (*Abstract Co-Author*) Nothing to Disclose Ravneet Vohra, PhD, Seattle, WA (*Abstract Co-Author*) Nothing to Disclose Daniel S. Hippe, MS, Seattle, WA (*Abstract Co-Author*) Research Grant, Koninklijke Philips NV; Research Grant, General Electric Company; Research Grant, Canon Medical Systems Corporation; Research Grant, Siemens AG Jeffrey Chamberlain, PhD, Seattle, WA (*Abstract Co-Author*) Nothing to Disclose Donghoon Lee, PhD, Seattle, WA (*Presenter*) Nothing to Disclose

## PURPOSE

To monitor temporal changes in skeletal muscle healing following myotoxin-induced injury in dystrophic mice using multi-parametric MRI (mpMRI).

# METHOD AND MATERIALS

We used the *mdx4cv* mouse model of Duchenne muscular dystrophy (DMD) and age-matched wild-type control mice. All mice were injected with 50 µL of 0.125 M myotoxin (BaCl2) to induce local injury in the right tibialis anterior (TA) muscle and 50 µL of saline into the contralateral TA, to serve as a sham control. Five *mdx4cv* mice and age-matched controls were imaged longitudinally beginning on the day of injection with follow-up imaging at: 1, 2, 3, 5, 7, 14, and 21 days post-injection. The remaining 40 *mdx4cv* mice were injected and imaged for a single time point to provide histology for each time point (5 mice per time point). mpMRI was conducted on a 14T MR scanner (Bruker Corp, Billerica, MA) to acquire relaxation times T1 and T2, magnetization transfer ratio (MTR) and diffusion parameters such as apparent diffusion coefficients (ADCs), fractional anisotropy (FA) and diffusion tensor eigenvalues. Values of the MR parameters were measured in three muscle types including TA, gastrocnemius (GA) and soleus (SOL) muscles. Histological quantifications are currently being processed to validate the mpMRI findings.

#### RESULTS

TA muscles showed significant differences in the T2 when comparing the myotoxin-injected leg of the mdx4cv group against the saline control injected leg - the TA showed significant differences for the post-injection, 2 and 3 day post-injection time points (Figure). T1, T2, diffusion parameters and MTR showed the myotoxin-injected mdx4cv muscles returning to similar baseline values of saline-injected muscle by the end of 21 days with the recovery occurring within 7 days. T2 continues to be the most sensitive measure in the mdx4cv mice. MTR has been shown to decrease in the presence of acute injury processes.

# CONCLUSION

The time course change in the mpMRI measurements during the progression of muscle damage and repair shows mpMRI methods can be used to distinguish these processes. Damage appears to be more substantial and recovery is delayed in dystrophic muscle compared to normal muscle.

# **CLINICAL RELEVANCE/APPLICATION**

Similar multi-parametric MRI methods used in this study can be utilized as a noninvasive means of tracking the process of muscle damage and recovery, as well as therapeutic interventions in DMD patients.



# MK374-SD-TUA5

Quantitative Assessment of Power Doppler Signal in the Subchondral Bone Region is an Effective Predictor of Radiographic Progression in the Hand of Rheumatoid Arthritis

Tuesday, Nov. 27 12:15PM - 12:45PM Room: MK Community, Learning Center Station #5

# Participants

Motoshi Fujimori, Sapporo, Japan (*Presenter*) Nothing to Disclose Tamotsu Kamishima, MD, Sapporo, Japan (*Abstract Co-Author*) Nothing to Disclose Akihiro Narita, Sapporo, Japan (*Abstract Co-Author*) Nothing to Disclose Mihoko Henmi, Sapporo, Japan (*Abstract Co-Author*) Nothing to Disclose Masaru Kato, Sapporo, Japan (*Abstract Co-Author*) Nothing to Disclose Kenneth Sutherland, Hokkaido, Japan (*Abstract Co-Author*) Nothing to Disclose Mutsumi Nishida, PhD, Sapporo, Japan (*Abstract Co-Author*) Nothing to Disclose Yuki Tanaka, Sapporo, Japan (*Abstract Co-Author*) Nothing to Disclose Lu Yutong, Sapporo, Japan (*Abstract Co-Author*) Nothing to Disclose Kazuhide Tanimura, Sapporo, Japan (*Abstract Co-Author*) Nothing to Disclose Tatsuya Atsumi, MD, PhD, Sapporo, Japan (*Abstract Co-Author*) Nothing to Disclose

#### For information about this presentation, contact:

moko-925@eis.hokudai.ac.jp

#### PURPOSE

To investigate the predictive value in radiographic progression in terms of the location of power Doppler (PD) signal in the joint using quantitative assessment in patients with rheumatoid arthritis (RA).

## METHOD AND MATERIALS

Twenty-two patients (20 women and 2 men) with RA on disease-modifying anti-rheumatic drugs underwent power Doppler ultrasonography (PDUS) of the bilateral 1-5 metacarpophalangeal joints at baseline. Radiography of the both hands was performed at baseline and at 1 year. PDUS in the joint was evaluated according to the semi-quantitative scoring (0-3) and quantitative measurement, which is the percentage of vascular fiow pixels in the region of interest. PD signal in the subchondral bone region was qualitatively (presence or absence) and quantitatively assessed. For quantitative assessment, the subchondral bone region was manually defined. The interval changes of joint space narrowing and bone erosion on radiographs at 1 year follow up were assessed by the Sharp/van der Heijde method (SvdH). We compared PDUS assessments with SvdH progression using a receiver operating characteristic curve and risk ratio (RR).

#### RESULTS

Quantitative PDUS assessment in the subchondral bone region was a better predictor for SvdH progression (AUC = 0.842, p < 0.01) than semi-quantitative (AUC = 0.754 (p < 0.05) and 0.704 (p = 0.106) for rater1 and 2, respectively) and quantitative PDUS assessment (AUC = 0.817, p < 0.05). RR of SvdH progression for quantitative and qualitative PDUS assessment in the subchondral bone region was 5.40 (p < 0.01), 1.60 (p = 0.204) and 1.71 (p < 0.05) for rater1 and 2.

#### CONCLUSION

Quantitative PDUS assessment in the subchondral bone region may have a stronger predictive value in radiographic progression than conventional PDUS assessment for synovitis or qualitative assessment of PDUS in the subchondral bone region.

#### **CLINICAL RELEVANCE/APPLICATION**

Quantitative PDUS assessment in the subchondral bone region is a simple and rapid technique but can serve as a strong predictor of joint damage progression for RA.



# MK375-SD-TUA6

# Multiple Myeloma: Differentiation of ISS Stage Based on a Diffusion MRI-based Radiomic Signature

Tuesday, Nov. 27 12:15PM - 12:45PM Room: MK Community, Learning Center Station #6

#### **Participants**

Nickolas Papanikolaou, PhD, Lisbon, Portugal (*Presenter*) Owner, MRIcons LTD Vassilis Koutoulidis, MD, Athens, Greece (*Abstract Co-Author*) Nothing to Disclose Joao Santinha, Lisbon, Portugal (*Abstract Co-Author*) Nothing to Disclose Ioanna Klapa, Athens, Greece (*Abstract Co-Author*) Nothing to Disclose Euaggelos Terpos, Athens, Greece (*Abstract Co-Author*) Nothing to Disclose Sofia Fontara, MD, Athens, Greece (*Abstract Co-Author*) Nothing to Disclose Maria Lisitskaya, Lisbon, Portugal (*Abstract Co-Author*) Nothing to Disclose Efstathios Kastritis, Athens, Greece (*Abstract Co-Author*) Nothing to Disclose Meletios-Athanasios Dimopoulos, Athens, Greece (*Abstract Co-Author*) Nothing to Disclose Lia A. Moulopoulos, MD, Athens, Greece (*Abstract Co-Author*) Nothing to Disclose

## For information about this presentation, contact:

nickolas.papanikolaou@research.fchampalimaud.org

## PURPOSE

To develop a Radiomic signature that can differentiate multiple myeloma (MM) patients with different ISS (International Staging System) stage using ADC maps.

## **METHOD AND MATERIALS**

A total number of 1569 Radiomic features were computed from ADC maps of 48 patients with MM ISS 1 (n=17), ISS 2 (n=11) and IIS 3 (n=20). Manual segmentation of the bone marrow of the 5 lumbar vertebral bodies was done on diffusion b0 images. Radiomic features classes comprised first order statistics, shape based, Gray Level Co-occurrence Matrix (glcm), Gray Level Run Length Matrix (glrlm), Gray Level Size Zone Matrix (glszm), Neighboring Gray Tone Difference Matrix (ngtdm) and Gray Level Dependence Matrix (gldm). The later features were extracted from filtered images using exponential, Laplacian of Gaussian and Wavelets. Multivariate modeling comprised of 4 features with the highest rank after maximum relevance minimum redundancy feature selection algorithm was applied. Various machine learning algorithms were evaluated and compared. A 10-fold cross-validation technique with 3 repetitions was used.

#### RESULTS

A naive Bayes classifier using wavelet2.HLL\_firstorder\_Median, wavelet.HHL\_gldm\_DependenceVariance, wavelet.HLL\_ngtdm\_Busyness and wavelet2.LLH\_ngtdm\_Coarseness, provided the highest area under the ROC of 0.95 for the discrimination between ISS 1 and ISS 3 patients. A Linear Discriminant Analysis model comprising wavelet2.HLL\_firstorder\_Mean, wavelet.HHL\_gldm\_DependenceVariance and wavelet.HLL\_ngtdm Strength, provided the highest area under the ROC of 0.95 for the discrimination between ISS 2 and ISS 3 patients. A GLM-NET classifier using wavelet2.LLL\_firstorder\_Minimum, wavelet2.LHL\_firstorder\_Median and wavelet.HHH\_glszm\_GrayLevelNonUniformity provided the highest area under the ROC of 0.85 for the discrimination between ISS 1 and ISS 2 patients.

# CONCLUSION

Radiomic signatures extracted from ADC maps are capable of discriminating myeloma patients with different ISS stage.

### **CLINICAL RELEVANCE/APPLICATION**

Radiomic features extracted from ADC maps are highly correlated with ISS, the most widely used staging system for MM.



# MK376-SD-TUA7

Color-Coded Virtual Non-Calcium Dual-Energy CT for the Detection of Lumbar Disc Herniation in Comparison with Standard Grayscale CT using MR Imaging as Standard of Reference: A Multireader Diagnostic Performance Study

Tuesday, Nov. 27 12:15PM - 12:45PM Room: MK Community, Learning Center Station #7

#### Participants

Christian Booz, MD, Frankfurt am Main, Germany (*Presenter*) Nothing to Disclose Ibrahim Yel, Frankfurt, Germany (*Abstract Co-Author*) Nothing to Disclose Moritz H. Albrecht, MD, Frankfurt am Main, Germany (*Abstract Co-Author*) Speaker, Siemens AG Tatjana Gruber-Rouh, Frankfurt Am Main, Germany (*Abstract Co-Author*) Nothing to Disclose Katrin Eichler, MD, Frankfurt Am Main, Germany (*Abstract Co-Author*) Nothing to Disclose Julian L. Wichmann, MD, Frankfurt, Germany (*Abstract Co-Author*) Speaker, General Electric Company; Speaker, Siemens AG Thomas J. Vogl, MD, PhD, Frankfurt, Germany (*Abstract Co-Author*) Nothing to Disclose Lukas Lenga, Frankfurt, Germany (*Abstract Co-Author*) Nothing to Disclose Simon S. Martin, MD, Frankfurt, Germany (*Abstract Co-Author*) Nothing to Disclose

#### For information about this presentation, contact:

boozchristian@gmail.com

#### PURPOSE

To assess the diagnostic performance of a dual-energy computed tomography (CT) virtual non-calcium (VNCa) technique for the detection of lumbar disc herniation compared to standard CT image reconstruction.

#### **METHOD AND MATERIALS**

This retrospective study was approved by the institutional review board. Data from 243 lumbar intervertebral discs in 41 patients who had undergone clinically indicated third-generation dual-source dual-energy CT and 3-T magnetic resonance (MR) imaging within two weeks between January and December 2017 were analyzed. Six blinded radiologists independently evaluated conventional grayscale dual-energy CT series for the presence and degree of lumbar disc herniation and spinal nerve root affection; after 8 weeks, readers reevaluated all cases using color-coded VNCa reconstructions optimized for analysis of intervertebral discs. Results from MR imaging evaluated by two separate blinded experienced readers (20 and 32 years of experience in musculoskeletal imaging) served as standard of reference. Diagnostic performance was calculated taking into account clustering.

#### RESULTS

A total of 112 herniated lumbar discs were detected on MR imaging. VNCa showed higher overall sensitivity (91.2% vs. 79.7%), specificity (91.7% vs. 84.6%), positive predictive (90.6% vs. 81.8%) and negative predictive values (92.3% vs. 82.7%) for detecting lumbar disc herniation compared to standard CT (all p<0.001). Area under the curve (AUC) analysis showed superior results for VNCa (0.914 vs. 0.821; p<0.001). Inter-reader agreement was excellent for VNCa and substantial for standard CT ( $\kappa$ =0.82 vs.  $\kappa$ =0.67; p<0.001). VNCa also showed higher diagnostic performance for detecting spinal nerve root affection (sensitivity, 92.0% vs. 69.5%; specificity, 98.2% vs. 96.0%; AUC, 0.951 vs. 0.828; all p<0.001). VNCa achieved substantially increased levels regarding diagnostic confidence for detecting lumbar disc herniation and spinal nerve root affection (all p<0.001).

# CONCLUSION

Color-coded dual-energy CT VNCa reconstructions substantially improve the diagnostic accuracy and confidence for the detection of lumbar disc herniation and spinal nerve root affection compared to standard CT.

# **CLINICAL RELEVANCE/APPLICATION**

Detection of lumbar disc herniation and spinal nerve root affection on CT may be substantially improved by using color-coded dualenergy CT VNCa reconstructions, representing a possible alternative to MR imaging in patients with contraindications.



## NM144-ED-TUA6

# The Utility of PET/MR in Head and Neck Cancer

Tuesday, Nov. 27 12:15PM - 12:45PM Room: NM Community, Learning Center Station #6

#### **Participants**

Tetsuro Sekine, MD, PhD, Tokyo, Japan (*Presenter*) Nothing to Disclose Felipe D. Barbosa, MD, Sao Paulo, Brazil (*Abstract Co-Author*) Nothing to Disclose Gaspar Delso, PhD, Cambridge, United Kingdom (*Abstract Co-Author*) Employee, General Electric Company; Edwin E. ter Voert, PhD, Zurich, Switzerland (*Abstract Co-Author*) Nothing to Disclose Patrick Veit-Haibach, MD, Zurich, Switzerland (*Abstract Co-Author*) Research Grant, Bayer AG Resaarch Grant, F. Hoffmann-La Roche Ltd Research Grant, General Electric Company Martin W. Huellner, MD, Zurich, Switzerland (*Abstract Co-Author*) Institutional Grant, General Electric Company

#### For information about this presentation, contact:

#### tetsuro.sekine@gmail.com

#### **TEACHING POINTS**

The combined MRI components on PET/MR system serve detailed anatomy which could impact on the diagnosis of head and neck cancer. The aim of this presentation is to understand the role of PET/MR in the assessment of head and neck cancer by comparing it with PET/CT.

# TABLE OF CONTENTS/OUTLINE

All presentations will be performed as a manner of the comparison of PET/MR with PET/CT. The contents of the presentation are as below. 1. T staging 2. N staging 3. Follow up study 4. Resectability defining findings 5. Perineural spreading 6. Artifact 7. Unknown primary tumor



## NM145-ED-TUA7

# Lymphoscintigraphy in Cutaneous Melanoma: Usual and Unexpected Pathways of Lymphatic drainage

Tuesday, Nov. 27 12:15PM - 12:45PM Room: NM Community, Learning Center Station #7

## Participants

Amit Gupta, MD, Cleveland, OH (*Presenter*) Nothing to Disclose Joseph M. Curcio, DO, Cleveland, OH (*Abstract Co-Author*) Nothing to Disclose Elias Kikano, MD, Cleveland, OH (*Abstract Co-Author*) Nothing to Disclose Maharshi A. Rajdev, MD, Cleveland, OH (*Abstract Co-Author*) Nothing to Disclose Nils Grosse Hokamp, MD, Cleveland, OH (*Abstract Co-Author*) Nothing to Disclose Kai Roman Laukamp, Cleveland, OH (*Abstract Co-Author*) Nothing to Disclose

# For information about this presentation, contact:

amit.gupta@uhhospitals.org

# **TEACHING POINTS**

To Understand the basis behind the procedure, the actual technique and different radiotracers used for this study. To know the usual pathways of lymphatic drainage in different regions of the body. To have understanding of unexpected pathways of lymphatic drainage and additional nodal basins which may be important in treatment planning. To emphasize the complementary role of SPECT imaging and SPECT/CT fusion

# TABLE OF CONTENTS/OUTLINE

- History of Lymphoscintigraphy - Various radionuclides that are commonly used - Technique - Different cutaneous malignancies that are currently being evaluated by lymphoscintigraphy - Examples of usual drainage pathways: Head and Neck Anterior trunk Back Upper extremities Lower extremities - Examples of unusual pathways of lymphatic drainage: Epitrochlear lymph node in upper extremity lesoin Popliteal lymph node drainage in lower extremity lesion Retroperitoneal drainage from a back melanoma



# NM217-SD-TUA1

Radiation Dose Reduction of PET-CT Scans by Adjusting F18-FDG Dose Based On Patient BMI and Modifying Low-Dose CT Protocol

Tuesday, Nov. 27 12:15PM - 12:45PM Room: NM Community, Learning Center Station #1

# Participants

Hasnain Hasham, MD, Kansas City, KS (*Presenter*) Nothing to Disclose Daniel L. Kirkpatrick, MD, Kansas City, KS (*Abstract Co-Author*) Nothing to Disclose Wendell Y. Yap, MD, Shawnee, KS (*Abstract Co-Author*) Nothing to Disclose Carissa Walter, Kansas City, KS (*Abstract Co-Author*) Nothing to Disclose Shelby James Cullom, PhD, Kansas City, KS (*Abstract Co-Author*) Nothing to Disclose Yu Wang, Kansas City, KS (*Abstract Co-Author*) Nothing to Disclose Suzanne L. Hunt, Kansas City, KS (*Abstract Co-Author*) Nothing to Disclose Mark A. Perry, MD, Spring Hill, KS (*Abstract Co-Author*) Nothing to Disclose

#### PURPOSE

To evaluate a BMI-based radiation dose reduction technique for patients undergoing F18-FDG PET-CT scans combining TOF and penalized likelihood reconstruction for noise optimization.

### **METHOD AND MATERIALS**

This retrospective study included 36 patients who underwent PET-CT scans on a GE Discovery MI DR from 1/1/2017-5/1/2017. Quantitative measurements of the mean and maximum SUVs for hepatic, blood pool, and largest lesions were obtained from original and reformatted list-mode data to simulate the administration of different FDG doses, 0.15 mCi and 0.20 mCi per BMI. Two radiologists qualitatively assessed each study independently for diagnostic quality.

## RESULTS

There was a statistically significant decrease in median radiation dose for both 0.15 mCi (-3.26 mSv, p<0.01) and 0.20 mCi (-1.79 mSv, p<0.01) images. Radiologist agreement of baseline and reconstructed exams ranged from 67-81%, suggesting the reconstructed images were of equivalent quality. Metabolic tumor volume was not significantly different between the baseline and dose reduction exams. However, there were varied results when comparing maximum SUV, mean SUV, and total lesion glycolysis (TLG) between studies.

# CONCLUSION

This study demonstrates a decrease in patient radiation dose using a dose reduction model, while maintaining diagnostic image quality. There were statistically significant differences in hepatic and blood pool SUV values when comparing the baseline SUV's to the reconstructed exams. However, the SUV values of the lesions did not significantly change. This should be taken into consideration when using lesion to liver and/or blood pool comparisons, such as Deauville and Lugano scores in lymphoma.

## **CLINICAL RELEVANCE/APPLICATION**

Evaluation of new imaging technology is important to decrease patient radiation dose while maintaining diagnostic quality and quantitative accuracy in PET/CT.



# NM218-SD-TUA2

Controlled Technique of F18 FDG Dose Reduction for Digital Photon Counting PET/CT Using List Mode Data Truncation

Tuesday, Nov. 27 12:15PM - 12:45PM Room: NM Community, Learning Center Station #2

#### Awards Student Travel Stipend Award

#### **Participants**

Patrick Silveira, MS, Burlington, VT (*Presenter*) Nothing to Disclose Janusz K. Kikut, MD, Burlington, VT (*Abstract Co-Author*) Nothing to Disclose Norman V. Sturtevant, MD, Burlington, VT (*Abstract Co-Author*) Nothing to Disclose

#### For information about this presentation, contact:

psilveir@med.uvm.edu

# PURPOSE

Digital Photon Counting (DPC) PET/CT system with silicon photomultiplier detectors is estimated to have double the clinical sensitivity, opening opportunity to lower injected activity. The process of injection-dose selection and time per table position optimization has traditionally been an empiric one. Software solutions on DPC PET platform allow simulating scans with reduced imaging time by truncation of the list mode data. The aim of this study is to evaluate if this solution can be used as a guide in the process of injected activity reduction.

#### **METHOD AND MATERIALS**

48 consecutive F18FDG DPC PET/CT scans were evaluated. All patients were administered 18F-FDG 0.165 mCi/kg per lean body weight. In addition to routine clinical image reconstruction a second reconstruction was performed with simulated decreased time as follows (BMI<20: 27% from 90s to 75s; BMI 20-40: 25% from 120s to 90s; BMI>40: 20% from 150s to 120s). Additional reconstruction and image processing added less than 10 minutes of technologist time. Nuclear Radiology reader with 12 years of experience in PET/CT compared the image quality of the simulated reduced time vs the standard time on a dedicated NM console allowing simultaneous display of both. If the reader determined a difference between the images, the difference was scored 1 to 3 (1- negligible, 2-degraded but acceptable for interpretation, 3- non interpretable).

#### RESULTS

The reader identified 5 out of the 48 cases as showing a difference in quality between the reduced time vs standard time. All 5 cases were rated 1 (negligible) and both images would render the same clinical interpretation. All 5 images images that were noted to be better qualitatively were the standard scan time. The results allowed reduction of the prescribed F18FDG activity by 20% without adjustment to acquisition time per table position.

# CONCLUSION

Qualitative analysis of simulated shorter acquisition scans allows an expedited, informed radiopharmaceutical dose reduction in DPC PET and can be used without an impact on daily workflow. The procedure allows a controlled optimization of radiopharmaceutical dose and acquisition time minimizing the risk of non-diagnostics exams.

# **CLINICAL RELEVANCE/APPLICATION**

Analysis of simulated shorter acquisition scans allows for an informed radiopharmaceutical dose reduction in DPC PET. The process enables one to optimize dose and acquisition time, thus minimizing the risk of non-diagnostics exams.



# NM219-SD-TUA3

Correlation of Immunohistochemical Parameters, Apparent Diffusion Coefficient (ADC) and Standardized Uptake Value (SUV) in Lung Cancer Using Hybrid PET/MRI

Tuesday, Nov. 27 12:15PM - 12:45PM Room: NM Community, Learning Center Station #3

# Participants

Ole Martin, Duesseldorf, Germany (Presenter) Nothing to Disclose

Philipp Heusch, MD, Duesseldorf, Germany (Abstract Co-Author) Nothing to Disclose

Ken Herrmann, Essen, Germany (*Abstract Co-Author*) Co-founder, SurgicEye GmbH; Stockholder, SurgicEye GmbH; Consultant, Sofie Biosciences; Consultant, Ipsen SA; Consultant, Siemens AG; Research Grant, Advanced Accelerator Applications SA; Research Grant, Ipsen SA

Lale Umutlu, MD, Essen, Germany (*Abstract Co-Author*) Consultant, Bayer AG Gerald Antoch, MD, Duesseldorf, Germany (*Abstract Co-Author*) Nothing to Disclose Lino Sawicki, MD, Dusseldorf, Germany (*Abstract Co-Author*) Nothing to Disclose

#### For information about this presentation, contact:

Ole.Martin@med.uni-duesseldorf.de

### PURPOSE

To correlate various prognostically relevant immunohistochemical parameters of primary lung cancer with simultaneously acquired standardized uptake values (SUV) and apparent diffusion coefficient (ADC) derived from hybrid PET/MRI.

### **METHOD AND MATERIALS**

55 consecutive patients with histologically proven lung cancer (mean age 62.5±9.1y) underwent PET/MRI. Diffusion-weighted imaging (DWI, b values: 0,500,1000s/mm<sup>2</sup>) was performed simultaneously with PET acquisition. A region of interest (ROI) encompassing the entire primary tumor was drawn into each patient's PET/MRI images to determine the glucose metabolism represented by maximum and mean SUV and also into ADC maps to assess tumor cellularity represented by mean and minimum ADC values. Histopathological tumor grading was available in 43/55 patients. In 15/55 patients, additional prognostically relevant immunohistochemical markers, i.e. phospho-AKT Ser473 (pAKTS473), extracellular signal-regulated kinase (pERK), phosphatase and tensin homolog (PTEN), and human epidermal growth factor receptor 2 (erbB2) were determined. Pearson's correlation coefficients were calculated to compare SUV and ADC values, while Spearman's were used for the immunohistochemical markers.

### RESULTS

The average SUVmax, SUVmean, ADCmin, and ADCmean in lung cancer primaries was  $12.6\pm5.9$ ,  $7.7\pm4.6$ ,  $569.9\pm96.1$  s/mm<sup>2</sup>, and  $825.8\pm93.2$  s/mm<sup>2</sup>, respectively. We found a significant inverse correlation between the ADCmin and SUVmax (r=-0.58, p<0.001) as well as between the ADCmin and SUVmean (r=-0.44, p<0.001). Tumor grading showed a significant positive correlation with SUVmax and SUVmean (r=0.34 and r=0.31, both p<0.05) and a significant inverse correlation with ADCmin and ADCmean (r=-0.30 and r=-0.40, both p<0.05). In addition, erbB2 showed a significant inverse correlation with SUVmax and SUVmean (r=-0.50 and r=-0.49, both p<0.05). There was no significant correlation with other immunohistochemical markers.

# CONCLUSION

The present data show a correlation between increased glucose-metabolism, cellularity, degree of differentiation as well as erbB2 expression of lung cancer primaries. 18F-FDG-PET and DWI from hybrid PET/MRI may offer complementary information for evaluation of lung cancer aggressiveness in initial staging and treatment response.

# **CLINICAL RELEVANCE/APPLICATION**

SUV in PET/MRI, ADC and tumor grading show a correlation in lung cancer patients leading to complementary information for staging workup



# NM220-SD-TUA4

PET/3-T MRI in Locally Advanced Rectal Cancer: Role of SUV and ADC Volumetric Histograms-Based Analyses in Predicting the Tumor Regression Grade After Preoperative Chemoradiotherapy

Tuesday, Nov. 27 12:15PM - 12:45PM Room: NM Community, Learning Center Station #4

## Participants

Giovanna Orsatti, MD, Padova, Italy (*Presenter*) Nothing to Disclose Filippo Crimi, MD, Padova, Italy (*Abstract Co-Author*) Nothing to Disclose Alessia Varotto, MD, Padova, Italy (*Abstract Co-Author*) Nothing to Disclose Pietro Zucchetta, Padova, Italy (*Abstract Co-Author*) Nothing to Disclose Chiara Giraudo, MD, PhD, Padova, Italy (*Abstract Co-Author*) Nothing to Disclose Michael Weber, Vienna, Austria (*Abstract Co-Author*) Nothing to Disclose Fabio Pomerri, MD, Padua, Italy (*Abstract Co-Author*) Nothing to Disclose

#### For information about this presentation, contact:

giovanna.orsatti@gmail.com

## PURPOSE

To evaluate the relationship among simultaneously acquired SUVs, ADCs, and histopathologic tumor regression grade (TRG) in patients with locally advanced rectal cancer (LARC) by using volumetric histogram analyses.

# METHOD AND MATERIALS

Patients with LARC referring to our local tertiary care center were enrolled in this prospective study and underwent a whole body [18F]-FDG-PET/MR scan (integrated hybrid PET/MR), including DWI, at staging and after preoperative chemoradiotherapy (pCRT). PET images were resliced and resampled according to the ADC maps (i.e., Osirix Software). For each LARC, a region of interest (ROI) was manually drawn on the T2weighted images along the boundaries of the lesion in each slice containing visible mass; each ROI was then copied on the corresponding PET and ADC datasets. Pixel-based SUVs and ADCs were collected from the entire volume of the lesions. Mean, median, skewness, kurtosis of SUVs and ADCs values as well as tumor volume ratio (pre-pCRT volume/post-pCRT volume) were computed. ADCmean and ADCmin as well as SUVmean and SUVmax were also collected from a ROI manually drawn at the level of maximum diameter of each lesion. Pearson correlation coefficient was applied to evaluate the correlation among all the investigated variables and TRG.

# RESULTS

Eleven patients met the inclusion criteria (7M; mean age 64.3 $\pm$ 5.1 years). Five LARC showed a complete regression (TRG 4). A significant negative correlation emerged between TRG and post-pCRT SUVs' kurtosis (r=-0.644; p=0.033), skewness (r=-0.634; p=0.036), mean (r=-0.631; p=0.037), median (r=-0.624; p=0.040) and SD (r=-0.629; p=0.019). The single-ROI-based SUVmax negatively correlated with the TRG (r=-0.637, p=0.035). A positive correlation emerged between volume ratio and TRG (r=0.688, p=0.019). No significant correlation was found between TRG and ADCs, neither pre nor post-pCRT, or between TRG and pre-pCRT SUVs.

# CONCLUSION

Our preliminary results demonstrated that post-pCRT volumetric histogram analyses of SUV values are predictor of response to pCRT. Additional studies on a larger population are necessary to further assess this evidence and the predictive role of volume-based ADCs' in LARC.

## **CLINICAL RELEVANCE/APPLICATION**

SUVs' volumetric histograms-based analyses seem to be a useful tool to predict the response to pCRT, allowing the selection of patients candidate to a wait-and-see approach instead of surgery.



## NM221-SD-TUA5

# The Role of 18F-FDG SPECT/CT in Predicting EGFR Gene Mutation Status in Lung Adenocarcinoma

Tuesday, Nov. 27 12:15PM - 12:45PM Room: NM Community, Learning Center Station #5

### Participants

Zhao Long, MD, Shanghai, China (*Presenter*) Nothing to Disclose Wang Huoqiang, MD, Shanghai, China (*Abstract Co-Author*) Nothing to Disclose

#### For information about this presentation, contact:

egg1961@aliyun.com

### PURPOSE

In most 18F-fluorodoxyglucose positron emission tomography/computed tomography (18F-FDG PET/CT) studies, tumor FDG uptake is generally reported to be decreased in lung cancers with EGFR mutation. In the literatures, 18F-FDG single photon emission computed tomography/computed tomography (18F-FDG SPECT/CT) scan was a powerful and reliable tool for evaluating patients with lung neoplasms, and with which results obtained are in most cases concordant with those obtained with 18F-FDG PET/CT. The purpose of this study is to investigate the predictive value of 18F-FDG SPECT /CT in evaluating EGFR mutation status in primary pulmonary adenocarcinoma (ADA).

# **METHOD AND MATERIALS**

ADAs were retrospectively identified in 276 consecutive patients who underwent 18F-FDG SPECT/CT scan from July 2014 to December 2015. The histopathological results were confirmed by resected, aspirated or biopsied samples. Tumor-to-normal tissue (T/NT) uptake ratios of 18F-FDG were calculated for the primary lesion. We analyzed the association between T/NT value and EGFR mutation status in ADA. Associations between quantitative continuous variables and EGFR mutation status were investigated by using the Mann-Whitney U test.

## RESULTS

EGFR mutations were identified in 152 patients (55.3%). EGFR mutations occurred more frequently in females (p < 0.001), in nonsmokers (p < 0.001), in those with smaller lesions (p < 0.001), and in those with lower T/NT value (p < 0.001). In multivariate analysis, sex, T/NT, and tumor size were significantly associated with EGFR mutation. The receiver operating characteristic (ROC) curve yielded area under the curve (AUC) values of 0.636 (95%CI, 0.568-0.704, p < 0.001) and 0.719 (95%CI, 0.657-0.782, p <0.001) for low T/NT alone and the combination of the three factors, respectively.

## CONCLUSION

We demonstrated that T/NT value of FDG uptake may be helpful in predicting the EGFR mutation status, which is consistent with results of 18F-FDG PET/CT. Especially in China, 18F-FDG SPECT/CT scan is included in the Medicare program, while 18F-FDG PET/CT is not, which enhances the clinical value of 18F-FDG SPECT/CT scan for cost reasons.

## **CLINICAL RELEVANCE/APPLICATION**

For the first time, we demonstrated that EGFR mutations were more frequent in lung adenocarcinomas with lower T/NT value, which is a semi quantitative parameter of FDG uptake in 18F-FDG SPECT/CT scan.



# NR020-EB-TUA

Imaging Findings in Medication-Induced Changes of the Central Nervous System: What Radiologists Should Know

Tuesday, Nov. 27 12:15PM - 12:45PM Room: NR Community, Learning Center Hardcopy Backboard

#### Awards Cum Laude Identified for RadioGraphics

#### **Participants**

Taisuke Harada, Sapporo, Japan (*Presenter*) Nothing to Disclose Kohsuke Kudo, MD, Sapporo, Japan (*Abstract Co-Author*) Nothing to Disclose Noriyuki Fujima, MD, Sapporo, Japan (*Abstract Co-Author*) Nothing to Disclose Hiroyuki Kameda, Sapporo, Japan (*Abstract Co-Author*) Nothing to Disclose Khin Khin Tha, MBBS, PhD, Sapporo, Japan (*Abstract Co-Author*) Nothing to Disclose Yukunori Korogi, MD, PhD, Kitakyushu, Japan (*Abstract Co-Author*) Nothing to Disclose Maki Umino, MD, Tsu, Japan (*Abstract Co-Author*) Nothing to Disclose

# For information about this presentation, contact:

taisuke.harada@med.hokudai.ac.jp

# **TEACHING POINTS**

To review the typical and atypical image findings: State of the Art To summarize the image findings of molecular targeted drugs To explain the category of molecular targeted drugs and these iatrogenic image changes.

## **TABLE OF CONTENTS/OUTLINE**

1. Introduction 1-A. Anti-tumor drugs vs. molecular targeted drugs (MTD) 1-B. Category of MTD 1-C. Naming rules of MTD 2. MTD 2-A. Tyrosine kinase inhibitors: lenvatinib, dasatinib, nilotinib 2-B. Immunomodulating agents: natalizumab, infliximab 2-C. Anti-VEGF inhibitor: bevacizumab 2-D. Immune-checkpoint inhibitors: nivolumab, pembrolizumab, ipilimumab 3. Anti-tumor drugs: temozolomide, gliadel wafer, methotrexate, 5-FU, etc. 4. Others: metronidazole, tacrolimus, phenytoin, ACTH, etc.



# NR342-ED-TUA11

Dental Emergencies: A Practical Guide to Identify Them

Tuesday, Nov. 27 12:15PM - 12:45PM Room: NR Community, Learning Center Station #11

#### Awards Certificate of Merit Identified for RadioGraphics

#### **Participants**

Erica A. Naves, MD, Sao Paulo, Brazil (*Presenter*) Nothing to Disclose Rafael F. Zanello, MD, Sao Paulo, Brazil (*Abstract Co-Author*) Nothing to Disclose Rafael Maffei Loureiro, MD, Sao Paulo, Brazil (*Abstract Co-Author*) Nothing to Disclose Daniel V. Sumi, MD, Sao Paulo, Brazil (*Abstract Co-Author*) Nothing to Disclose Regina L. Gomes, PhD, MD, Sao Paulo, Brazil (*Abstract Co-Author*) Nothing to Disclose Mauro M. Daniel, MD, Sao Paulo, Brazil (*Abstract Co-Author*) Nothing to Disclose Carolina R. Soares, Sao Paulo, Brazil (*Abstract Co-Author*) Nothing to Disclose Rodrigo W. Murakoshi, MD, Sao Paulo, Brazil (*Abstract Co-Author*) Nothing to Disclose Fabio A. Dalpra, MD, Sao Paulo, Brazil (*Abstract Co-Author*) Nothing to Disclose Marcelo D. Lemos, MD, Sao Paulo, Brazil (*Abstract Co-Author*) Nothing to Disclose Hugo Tames, MD, Sao Paulo, Brazil (*Abstract Co-Author*) Nothing to Disclose Luziany C. Araujo, MD, Sao Paulo, Brazil (*Abstract Co-Author*) Nothing to Disclose Eduardo Kaiser Ururahy Nunes Fonseca, MD, Sao Paulo, Brazil (*Abstract Co-Author*) Nothing to Disclose Marcelo B. Funari, MD, Sao Paulo, Brazil (*Abstract Co-Author*) Nothing to Disclose Francisco K. de Araujo, MD, Sao Paulo, Brazil (*Abstract Co-Author*) Nothing to Disclose

# For information about this presentation, contact:

ericaanaves@gmail.com

# **TEACHING POINTS**

- Dental emergencies can have many causes, including infection, trauma and complications of dental procedures. - To illustrate the imaging findings in computed tomography and magnetic resonance imaging of the most common causes of dental emergencies.

# TABLE OF CONTENTS/OUTLINE

Dental pathologies are a challenge for the radiologist who is unfamiliar with them, especially in emergencies. Odontogenic infections arise from the tooth or from adjacent structures, and they can directly spread into adjacent bone and soft tissues, through superficial and deep neck spaces. Imaging plays a key role in identifying the source of infections, the extent of the disease process, and detecting any complications. Dental trauma can be classified into fractures, dislocations and avulsions of the permanent dentition and injuries of the deciduous dentition. Knowledge of the most common imaging findings in cases of dental trauma is important for the appropriate treatment and follow-up, reducing aesthetic problems, avoiding dental loss and related complications. Dental procedures are very common on daily practice. Some complications may require imaging assessment, and the radiologist must be prepared to evaluate haematomas, abscesses, oroantral fistulas, osseous fractures or even nerve lesions.



## NR343-ED-TUA12

# Central Nervous System Parasitic Infections: What Radiologists Should Know

Tuesday, Nov. 27 12:15PM - 12:45PM Room: NR Community, Learning Center Station #12

#### Participants

Lucas L. Resende, MD, Sao Paulo, Brazil (*Presenter*) Nothing to Disclose Sergio Brasil Tufik, MD, Sao Paulo, Brazil (*Abstract Co-Author*) Employee, Alliar Leandro T. Lucato, MD, Sao Paulo, Brazil (*Abstract Co-Author*) Nothing to Disclose Claudia D. Leite, MD, PhD, Sao Paulo, Brazil (*Abstract Co-Author*) Nothing to Disclose

#### For information about this presentation, contact:

lucaslopesresende@hotmail.com

#### **TEACHING POINTS**

Infectious and parasitic diseases are neglected treatable conditions that remain the primary cause of death worldwide. Although parasitic diseases essentially occur in developing countries, there are reports of increasing incidence in developed countries. Global travel, immunosuppression (i.e. HIV infection) have contributed to parasitic infections to become more commonplace. Symptoms of CNS parasitic infection are mild and produce a variety of unspecific signs and symptom. Thus, diagnosis and work up may be challenging. To be familiar with epidemiological characteristics and distinguishing image findings may increase the likelihood of diagnosis and proper treatment. The purpose of this exhibit is: to review the imaging presentation of different types of parasitic CNS infection and to provide keys to recognize then and perform the correct diagnosis and treatment.

## TABLE OF CONTENTS/OUTLINE

 Parenchymal neurocysticercosis stages o Vesicular o Vesicular colloidal o Nodular-Granular o Calcified o SWI o DWI o Perfusion o Spectroscopy
 Ventricular, subarachnoid and cisternae neurocysticercosis o Cystic presentation (racemosa) o Arachnoiditis
 Disseminated neurocysticercosis o Brain o Muscle o Orbits
 Schistosomiasis o Brain o Spine
 Chagas diseases o Brain o Spine
 Echinococcosis
 Toxoplasmosis
 Amebiasis



## NR344-ED-TUA9

Extra-Nodal Extension in Head and Neck Cancer: How Radiologists Can Help Staging and Treatment Planning

Tuesday, Nov. 27 12:15PM - 12:45PM Room: NR Community, Learning Center Station #9

## Awards Magna Cum Laude

#### Participants

Takashi Hiyama, MD, Kashiwa, Japan (*Presenter*) Nothing to Disclose Hirofumi Kuno, MD, PhD, Kashiwa, Japan (*Abstract Co-Author*) Nothing to Disclose Takahiko Nagaki, MD,PhD, Kashiwa-Shi, Japan (*Abstract Co-Author*) Nothing to Disclose Kotaro Sekiya, DDS, PhD, Kashiwa-Shi, Japan (*Abstract Co-Author*) Nothing to Disclose Satoshi Fujii, MD, PhD, Kashiwa, Japan (*Abstract Co-Author*) Nothing to Disclose Ryuichi Hayashi, MD, PhD, Kashiwa, Japan (*Abstract Co-Author*) Nothing to Disclose Tatsushi Kobayashi, MD, Kashiwa, Japan (*Abstract Co-Author*) Nothing to Disclose

# For information about this presentation, contact:

medtak39@gmail.com

# **TEACHING POINTS**

Extra-nodal extension (ENE), a significant prognostic factor in p16 negative head and neck squamous cell carcinoma, is classified as N3b by the American Joint Committee on Cancer (AJCC) 8th edition. Unambiguous evidence of ENE on clinical examination supported by radiographic evidence is required for the disease to be classified as ENE-positive. While most prior radiological studies have focused on diagnostic performance, radiologists must provide more information on ENE for treatment planning and post-treatment assessment. Aims of this exhibit: 1. To review the clinical implication of ENE 2. To describe key imaging features of ENE with clinical and histopathological correlations 3. To discuss evaluation of ENE for clinical staging, treatment planning, and treatment response in multidisciplinary management

# TABLE OF CONTENTS/OUTLINE

1. ENE basics - Clinical and pathological ENE in AJCC, 8th edition - CT and MRI findings - Role of imaging in staging and treatment planning 2. Case illustrations ENE with adjacent structure invasion - Invasion patterns based on location (level system) - Imaging findings for surgical planning with pathologic correlation - Assessment of the post-treatment lymph node with ENE ENE without adjacent structure invasion - Dealing with radiological ENE without physical evidence 3. Summary



## NR347-ED-TUA10

CNS Vasculopathies: Diagnostic Clues on MR Imaging

Tuesday, Nov. 27 12:15PM - 12:45PM Room: NR Community, Learning Center Station #10

FDA Discussions may include off-label uses.

#### **Participants**

Rodrigo Beber De Bem, MD, Rio de Janeiro, Brazil (*Presenter*) Nothing to Disclose Pedro N. Castro, MD, Rio de Janeiro, Brazil (*Abstract Co-Author*) Nothing to Disclose Fernanda M. Pessoa, MD, Rio de Janeiro, Brazil (*Abstract Co-Author*) Nothing to Disclose Luiz Celso H. Da Cruz, MD, Rio de Janeiro, Brazil (*Abstract Co-Author*) Nothing to Disclose Eduardo C. Castro Netto, MD, Rio de Janeiro, Brazil (*Abstract Co-Author*) Nothing to Disclose

#### For information about this presentation, contact:

rodrigodebem@hotmail.com

#### **TEACHING POINTS**

There is a wide overlap between inflammatory and non inflammatory causes of vessel injury in their imaging appearance, and their differentiation has important therapeutic implications. Pulse sequences before and after intravenous gadolinium designed for vascular disorders are classified as "black blood," providing good contrast between the lumen and the arterial wall, being useful for the detection of early arterial wall changes.CADASIL is an important cause of dementia characterised by migraine and cumulative stroke in young patients, and should be distinguish from other causes of white matter lesions, such as multiple sclerosis, progressive multifocal leukoencephalopathy and others.Cerebral amyloid angiopathy is a rare pathology that leads to cognitive dysfunction and is associated with intracerebral hemorrhage in the elderly. Its inflammatory form shows white matter lesions with or without gadolinium enhancement.Thrombotic microangiopathies can be seen with diffuse hemorrhagic lesions and that involves cortex, subcortical and deep white matter to varying degrees.

### **TABLE OF CONTENTS/OUTLINE**

- Approach to analysis inflammatory and non inflammatory causes of vessel injury.- MR typical protocol.- Review of imaging findings:Moyamoya;Primary angiitis;Neuro-Behçet 's;Sistemic lupus erythematosus;Susac;CADASIL;CAA;TMA.



# NR390-SD-TUA1

Deep Learning for Automatic Detection and Segmentation of Acute Epidural and Subdural Hematomas in Head CT

Tuesday, Nov. 27 12:15PM - 12:45PM Room: NR Community, Learning Center Station #1

# Participants

Ian Pan, MA, Providence, RI (*Presenter*) Nothing to Disclose Owen Leary, Providence, RI (*Abstract Co-Author*) Nothing to Disclose Stefan Jung, BSC, Providence, RI (*Abstract Co-Author*) Nothing to Disclose Krishna Nand Keshava Murthy, MSc, New York, NY (*Abstract Co-Author*) Nothing to Disclose Jason W. Allen, MD, PhD, Atlanta, GA (*Abstract Co-Author*) Nothing to Disclose David Wright, MD, Atlanta, GA (*Abstract Co-Author*) Nothing to Disclose Lisa H. Merck, MD, MPH, Providence, RI (*Abstract Co-Author*) Nothing to Disclose Derek Merck, PhD, Providence, RI (*Abstract Co-Author*) Nothing to Disclose

#### For information about this presentation, contact:

ian\_pan@brown.edu

#### PURPOSE

Epidural and subdural hematomas (EDH/SDH) are common lesions associated with traumatic brain injury (TBI). The aim of this study is to leverage deep learning for automatic detection and segmentation of EDH/SDH.

### **METHOD AND MATERIALS**

Our dataset consisted of 882 head CT images collected during a national randomized multicenter clinical trial to study TBI. All imaging was then reviewed centrally by a single board-certified neuroradiologist. Manual hemorrhage segmentations of the largest lesion were produced using a standardized protocol. Studies for this subanalysis were stratified into groups characterized by the largest hemorrhagic lesion: SDH (n=192), EDH (n=46), and normal (n=203). The remaining 441 images were excluded due to absence of segmented EDH/SDH. Image preprocessing steps involved: isotropic resampling, denoising, and brain extraction. Data were split into stratified training (n=350), validation (n=43), and test (n=46) folds. We used the DeepMedic 3D convolutional neural network (CNN) architecture to train a model for automatic segmentation. This 3D CNN was used to obtain candidate segmentations for positive and negative cases. Intensity, shape, and texture features were extracted from the candidate segmentations and their wavelet transforms. A logistic regression model was trained to discriminate between true positive and false positive segmentations based on these features. Segmentation quality and detection ability were evaluated using the Dice similarity coefficient (DSC) and the area under the ROC curve (AUC), respectively.

## RESULTS

For the 25 positive test cases, we achieved a lesion-wise median DSC of 0.712, 95% CI (0.597, 0.782). Automatic segmentations tended to underestimate bleed volume. The median percent difference between the volumes of predicted and manual segmentations was -10.3%, 95% CI: (-21.4%, 1.1%). For detection, we obtained an AUC of 0.914, 95% CI: (0.819, 0.985).

## CONCLUSION

Deep learning tools can be leveraged to both detect and segment EDH/SDH in the setting of small sample size and heterogeneous data. Future work will consider how our models can be used to assess evolution of hemorrhage over time and investigate the generalizability of our approach to other intracranial hemorrhage subtypes.

# **CLINICAL RELEVANCE/APPLICATION**

Automatic detection and segmentation can be useful in helping to identify and characterize the presence, size, and location of EDH/SDH in head CT.



# NR392-SD-TUA2

CTA Findings Predictive of Postoperative Vasospasm in Patients with SAH secondary to Ruptured Intracranial Aneurysm

Tuesday, Nov. 27 12:15PM - 12:45PM Room: NR Community, Learning Center Station #2

# Participants

Charles G. Colip, MD, Seattle, WA (*Presenter*) Nothing to Disclose Sean Wo, MD, Pittsburgh, PA (*Abstract Co-Author*) Nothing to Disclose Daniel S. Hippe, MS, Seattle, WA (*Abstract Co-Author*) Research Grant, Koninklijke Philips NV; Research Grant, General Electric Company; Research Grant, Canon Medical Systems Corporation; Research Grant, Siemens AG Hiroko Watase, Seattle, WA (*Abstract Co-Author*) Nothing to Disclose Alfonso R. Urdaneta-Moncada, MD, Los Angeles, CA (*Abstract Co-Author*) Nothing to Disclose Michael Levitt, MD, Seattle, WA (*Abstract Co-Author*) Research Grant, Koninklijke Philips NV; Research Grant, Medtronic plc; Research Grant, Stryker Corporation; Consultant, Medtronic plc; Consultant, Minnetronix Mahmud Mossa-Basha, MD, Seattle, WA (*Abstract Co-Author*) Nothing to Disclose

# PURPOSE

CTA is integral in the initial workup of patients with subarachnoid hemorrhage (SAH) for characterizing intracranial vascular anatomy and identifying the presence/location of ruptured aneurysm. The purpose of this study is to investigate the utility of CTA findings for predicting vasospasm in patients undergoing surgical or endovascular repair of ruptured intracranial aneurysm.

## **METHOD AND MATERIALS**

IRB-approved retrospective study of 193 aneurysmal SAH patients with CTA head who presented between August 2005 and July 2015. Two neuroradiologists reviewed the CTA for findings of intracranial arterial calcification, arterial undulation, and non-calcified arterial stenosis. Potential clinical factors including treatment type, age, sex, smoking, stimulant use, and modified Fisher score (mFS) were recorded. Associations of clinical factors and CTA findings with development of vasospasm was initially assessed using univariate logistic regression. The LASSO machine learning algorithm was used to develop a multivariate prediction model for vasospasm. Internal validation of the model was performed using the bootstrap with overall performance summarized using the c-statistic.

#### RESULTS

Ninety (47%) of 193 patients developed vasospasm after surgical clipping (n=125), endovascular repair (n=60) or a combination of treatments (n=8). Age (odds ratio [OR] 0.7, p=0.001), current smoking (OR 2.0, p=0.02), mFS (OR 1.3, p=0.03), intracranial calcification (OR 0.5, p=0.004), and non-calcified stenosis (OR 4.2, p=0.04) were significantly associated with vasospasm during univariate analysis. The LASSO selected coiling, age, smoking, mFS, intracranial vascular calcification, vessel undulation, and non-calcified stenosis for the multivariate model. The resulting bootstrap-adjusted c-statistic was 0.70 (p=0.01), which was significantly higher than that of mFS alone for predicting vasospasm (0.58, p=0.01).

## CONCLUSION

These results indicate that lack of arterial calcification and non-calcified arterial stenosis on preintervention CTA may be useful for predicting vasospasm in patients in addition to current prognostic models such as the mFS.

# **CLINICAL RELEVANCE/APPLICATION**

Multivariate models to predict vasospasm after aneurysmal SAH may perform better than current prediction algorithms.



# NR393-SD-TUA3

# Is MRI-based Deep Brain Stimulation (DBS) Programming the New Clinician?

Tuesday, Nov. 27 12:15PM - 12:45PM Room: NR Community, Learning Center Station #3

FDA Discussions may include off-label uses.

#### Awards

#### **Student Travel Stipend Award**

#### Participants

Alexandre Boutet, MD,MSc, Toronto, ON (*Presenter*) Nothing to Disclose Radhika Madhavan, PhD, Bengaluru, India (*Abstract Co-Author*) Nothing to Disclose Suresh E. Joel, PhD, Bengaluru, India (*Abstract Co-Author*) Nothing to Disclose Gavin Elias, Toronto, ON (*Abstract Co-Author*) Nothing to Disclose Alfonso Fasano, MD,PhD, Toronto, ON (*Abstract Co-Author*) Nothing to Disclose Walter Kucharczyk, MD, Toronto, ON (*Abstract Co-Author*) Nothing to Disclose Andres Lozano, MD,PhD, Toronto, ON (*Abstract Co-Author*) Nothing to Disclose

## For information about this presentation, contact:

alexandre.boutet@mail.utoronto.ca

## PURPOSE

Deep brain stimulation (DBS) is a neurosurgical technique that modulates dysregulated brain circuits in motor, psychiatric, and cognitive neurological disorders. It is most commonly used to treat Parkinson's disease (PD), for which it provides striking symptomatic relief. After being surgically inserted into the desired brain target, DBS electrodes generate constant electricity. Empirically-derived programming algorithms, which optimize clinical benefits by gradually titrating the delivered energy, require time-consuming and costly visits for patients and the health care system. An objective measure of clinical response to DBS could result in time and costs benefits. We hypothesized that functional magnetic resonance imaging (fMRI) may be used to quantify response to DBS.

# METHOD AND MATERIALS

3 Tesla fMRI was acquired on 24 PD patients with DBS. We compared the patterns of brain response obtained when the optimal DBS lead contacts (defined a priori clinically) versus non-optimal contacts were turned ON. A discriminative machine-learning model was used to classify the brain response patterns and the model accuracy was tested on unseen data.

#### RESULTS

The clinically optimal contact demonstrated consistent engagement of motor circuitry whereas non-optimal contacts recruited heterogeneous circuits. Using our discriminative model, we were able to predict the optimal contact (as determined by the clinical gold standard) with 76% accuracy based on a single fMRI session.

# CONCLUSION

This study demonstrates that fMRI can objectively measure clinical response to DBS in PD patients and can be used to predict the optimal energy settings. These findings could be used to improve DBS programming by leading the way to autonomous DBS fMRI-based programming, thereby improving DBS patient care and contributing to major cost-savings for the healthcare system.

## **CLINICAL RELEVANCE/APPLICATION**

fMRI can quantify clinical benefits of deep brain stimulation (DBS) in Parkinson's disease patients and could lead the way to autonomous DBS MRI-based programming.



# NR394-SD-TUA4

# The Predictive Value of Lumbar Spine MRI Findings Using the Provocative Discogram

Tuesday, Nov. 27 12:15PM - 12:45PM Room: NR Community, Learning Center Station #4

#### **Participants**

Lydia Chelala, MD, Baltimore, MD (*Presenter*) Nothing to Disclose James W. Reinig, MD, Annapolis, MD (*Abstract Co-Author*) Nothing to Disclose Azar P. Dagher, MD, Baltimore, MD (*Abstract Co-Author*) Nothing to Disclose Greer Waldrop, MD,MSc, Baltimore, MD (*Abstract Co-Author*) Nothing to Disclose Trent Graham, MD, Baltimore, MD (*Abstract Co-Author*) Nothing to Disclose

# For information about this presentation, contact:

adagher@umm.edu

#### PURPOSE

To calculate the positive predictive value (+PV) of factors on lumbar spine MRI for a painful disc using the provocative discogram as the reference standard.

# METHOD AND MATERIALS

Lumbar spine discogram records and pre-discogram MRI's of 736 patients (2457 discs) were retrospectively reviewed in an IRBexempt and HIPAA-compliant protocol. Each level was identified as having High Intensity Zone (HIZ) disc, disc protrusion, disc extrusion, or combination (any herniation type), disc bulge, disc degeneration, and spondylolisthesis. Statistical analysis used a 2 x 2 contingency table of discogram results for each of the categorizations. The p-value, sensitivity, specificity, and +PV were calculated for each factor.

#### RESULTS

An HIZ disc has a +PV of 0.71 (0.65-0.76) for a provocative discogram. A disc protrusion has a +PV of 0.79 (0.73-0.83). A disc extrusion has a +PV of 0.93 (0.79-0.98), a bulge 0.43 (0.37-0.48), a degenerative disc 0.32 (0.28-0.35), and spondylolisthesis has a +PV of 0.67 (0.59-0.73). A herniation of either type (extrusion or protrusion) has a +PV of 0.80 (0.75-0.84).

#### CONCLUSION

Disc herniations and HIZ discs have high predictive value in identifying a pain generator followed by spondylolisthesis. An extruded disc herniation is statistically the most likely to generate pain.

#### **CLINICAL RELEVANCE/APPLICATION**

Lumbar MRI findings have varying efficacy in identifying the level of discogenic back pain, with annular tears and herniations being the most predictive.



# NR395-SD-TUA5

Prediction of IDH-1 Mutation and 1P/19Q Codeletion Status in Diffuse Gliomas Using Magnetic Resonance Textural Analysis

Tuesday, Nov. 27 12:15PM - 12:45PM Room: NR Community, Learning Center Station #5

# Participants

Peter Brown, MBChB, BSc, Leeds, United Kingdom (*Presenter*) Nothing to Disclose Hamed Nejadhamzeeigilani, MBBS, Leeds, United Kingdom (*Abstract Co-Author*) Nothing to Disclose Russell Frood, MBBCh, Leeds, United Kingdom (*Abstract Co-Author*) Nothing to Disclose John Goodden, Leeds, United Kingdom (*Abstract Co-Author*) Nothing to Disclose Paul Chumas, Leeds, United Kingdom (*Abstract Co-Author*) Nothing to Disclose Susan Short, Leeds, United Kingdom (*Abstract Co-Author*) Nothing to Disclose Jeremy A. Macmullen-Price, MBChB, FRCR, Edinburgh, United Kingdom (*Abstract Co-Author*) Nothing to Disclose Stuart Currie, FRCR, MD, Leeds, United Kingdom (*Abstract Co-Author*) Nothing to Disclose

#### For information about this presentation, contact:

stuartcurrie@nhs.net

#### PURPOSE

MR textural analysis (MRTA) enables the quantification of spectral properties of an image and therefore can assist lesion stratification in neuro-imaging. The prognosis of diffuse gliomas and their sensitivity to adjuvant therapy is influenced by their histological phenotype and genotype. Entropy (a measure of a tumours' heterogeneity obtained through MRTA) may categorize the relationship between radiological and genomic features, therefore it may serve as a pre-operative imaging biomarker. The purpose of this study was to determine whether entropy, extracted using first order MRTA of T2-weighted and FLAIR sequences, could be used to differentiate diffuse gliomas according to their genetic and histological subtypes. Specifically, to determine: (1) the diagnostic accuracy of entropy in differentiating IDH-1 mutated from IDH-1 wild type gliomas; (2) the diagnostic accuracy of entropy in differentiate grade II from grade III gliomas.

#### **METHOD AND MATERIALS**

From a surgical database of 371 patients with suspected low-grade glioma, 45 (Male=25, median age 41-years-old) patients were identified that fulfilled the criteria of histological confirmation of diffuse glioma (WHO grade II or III), known tumour genetics, and identical preoperative MR imaging protocol. On preoperative imaging, manual tumour segmentation and automated software was used to calculate the mean entropy values that were compared amongst the genetic subtypes.

### RESULTS

Mean entropy values on T2-weighted imaging were statistically significant between diffuse gliomas with IDH-1 mutation and those with IDH-1 wild type genome and between diffuse gliomas with and those without 1p/19q codeletion. Entropy values using the FLAIR imaging were not statistically significant.

#### CONCLUSION

Tumour entropy extracted using MRTA of T2-weighted imaging is a potential biomarker for IDH-1 mutation and 1p/19q codeletion status in diffuse gliomas.

#### **CLINICAL RELEVANCE/APPLICATION**

Entropy calculated from MRI texture analysis in diffuse gliomas shows potential for the pre-operative identification of IDH-1 mutation and 1p/19q codeletion, which are known genomic markers of prognosis and treatment sensitivity.



# NR396-SD-TUA6

Event-Based Model of Diffusion MRI Shows that sCJD Strains Have Similar Epicenter but Different Lesion Propagation in the Brain

Tuesday, Nov. 27 12:15PM - 12:45PM Room: NR Community, Learning Center Station #6

# Participants

Alberto Bizzi, MD, Milan, Italy (*Abstract Co-Author*) Nothing to Disclose Riccardo Pascuzzo, PhD, Milan, Italy (*Presenter*) Nothing to Disclose Alexandra Young, London, United Kingdom (*Abstract Co-Author*) Nothing to Disclose Janis Blevins, Cleveland, OH (*Abstract Co-Author*) Nothing to Disclose Neil Oxtoby, London, United Kingdom (*Abstract Co-Author*) Nothing to Disclose Sara Garbarino, Sophia Antipolis, France (*Abstract Co-Author*) Nothing to Disclose Gianmarco Castelli, Milano, Italy (*Abstract Co-Author*) Nothing to Disclose Lawrence Schonberger, Atlanta, GA (*Abstract Co-Author*) Nothing to Disclose Pierluigi Gambetti, Cleveland, OH (*Abstract Co-Author*) Nothing to Disclose Brian Appleby, Cleveland, OH (*Abstract Co-Author*) Nothing to Disclose Daniel Alexander, London, United Kingdom (*Abstract Co-Author*) Nothing to Disclose

#### For information about this presentation, contact:

alberto\_bizzi@fastwebnet.it

### PURPOSE

Sporadic Creutzfeldt-Jakob (sCJD) is a very heterogeneous prion disease with five subtypes or strains that have different clinical presentation and survival times. We tested the hypothesis that different subtypes have different path of lesion propagation in the brain. This study aimed at modeling the DWI signal abnormalities spreading in 5 pure strains, in order to determine the epicenter (starting point) and the sequence of propagation of prion lesions in 12 brain regions.

# METHOD AND MATERIALS

We considered a novel data-driven model, the event-based model (EBM), recently introduced to study the evolution of Alzheimer's and Huntington's diseases. The EBM describes the disease progression as a sequence of events, defined as the switching from a normal to an abnormal state for a biomarker of a patient. Considering a set of 12 events related to the appearance of DWI hyperintensity in 12 specific brain regions, the EBM finds the most likely sequence of DWI abnormalities given the observed DWI measurements of the subjects. A neuroradiologist blind to the pathological diagnosis visually scored the DWI of 306 patients with definite autopsy diagnosis of sCJD subtype and 123 patients with rule-out diagnosis of prion disease. An ordinal scale (0-3) was implemented to visually score the images and grade the DWI hyperintensities in 12 brain regions. Patients with 5 sCJD pure subtypes were included: MM/MV1 (n=89), MM/MV2C (n=42), MV2K (n=22), VV1 (n=15) and VV2 (n=49). The EBM sequences were based on cross-sectional data and their longitudinal consistency was validated comparing the stages at follow-ups with the baseline.

## RESULTS

Results showed that the 5 sCJD strains have different sequence of lesion propagation. The anterior cingulate cortex was affected very early in all strains. Then, three propagation trajectories emerged from the orderings: neocortex is affected before striatum in MM/V1 and MM/V2C; striatum is affected before neocortex in VV2 and MV2K; limbic regions are affected before neocortex and striatum in VV1.

#### CONCLUSION

The EBM is a good model to determine DWI signal abnormality propagation in the brain. The 5 main sCJD strains share the epicenter but have a different path of lesion propagation in the brain.

## **CLINICAL RELEVANCE/APPLICATION**

EBM provided for the first time data-driven models of spreading of DWI signal hyperintensities in sCJD subtypes. This result may have an impact on patient management and clinical trials.



# NR397-SD-TUA7

Fast, Robust and Accurate Segmentation of the Complete Cerebral Vasculature in 4D-CTA Using Deep Learning

Tuesday, Nov. 27 12:15PM - 12:45PM Room: NR Community, Learning Center Station #7

# Participants

Midas Meijs, MSc, Nijmegen, Netherlands (*Presenter*) Research funded, Canon Medical Systems Corporation Ajay Patel, MSc, Nijmegen, Netherlands (*Abstract Co-Author*) Research funded, Canon Medical Systems Corporation Sil Van de Leemput, MSc, Nijmegen, Netherlands (*Abstract Co-Author*) Research funded, Canon Medical Systems Corporation Bram Van Ginneken, PhD, Nijmegen, Netherlands (*Abstract Co-Author*) Stockholder, Thirona BV; Co-founder, Thirona BV; Research Grant, Varian Medical Systems, Inc; Research Grant, Canon Medical Systems Corporation

Mathias Prokop, PhD, Nijmegen, Netherlands (*Abstract Co-Author*) Speakers Bureau, Bracco Group; Speakers Bureau, Bayer AG; Research Grant, Canon Medical Systems Corporation; Speakers Bureau, Canon Medical Systems Corporation; Research Grant, Siemens AG; Speakers Bureau, Siemens AG; Departmental spinoff, Thirona; Departmental licence agreement, Varian Medical Systems, Inc; ;

Rashindra Manniesing, PhD, Nijmegen, Netherlands (Abstract Co-Author) Research funded, Canon Medical Systems Corporation

#### For information about this presentation, contact:

midas.meijs@radboudumc.nl

#### PURPOSE

Segmentation of the complete cerebral vasculature in 4D-CTA is important for improved visualization, automated pathology detection and assessment of the collateral flow. We present a deep learning approach to segment the complete cerebral vasculature in 4D-CTA of patients with suspected stroke.

# METHOD AND MATERIALS

In total 162 patients that underwent 4D-CTA for suspicion of stroke were retrospectively included in this study. The scans were acquired on a 320-detector row scanner (Canon Medical Systems Corporation, Japan). Image size was 512x512x320 voxels by 19 time points with isotropic voxel sizes of approximately 0.5 mm. A 3D fully convolutional neural network (CNN), U-Net, was proposed with integration of a spatial feature in the final convolutional layer of the network. The weighted temporal average and variance were derived from the 4D-CTA and used as input for the network. As spatial feature the Euclidean distance from the center of the brain to the skull was used. Training was done on 19 patients with manually annotated data. The remaining 143 patients were used as testing set. Segmentations were visually inspected for completeness and overall quality. Two observers manually annotated three dimensional sub-volumes throughout the brain to include different sized vessels for quantitative evaluation. The Dice similarity coefficient (DSC) and the Mean Contour Distance (MCD) of the segmentations were reported.

# RESULTS

Overall the method was capable of segmenting the complete cerebral vasculature. Smaller distal vessels (e.g. M3) showed similar segmentation results as the larger vessels (e.g. internal carotid artery). The DSC was  $0.91\pm0.08$  and the MCD was  $0.26\pm0.24$  mm which is below voxel spacing. Computation time was less than 90 seconds for processing a full 4D-CTA data set.

## CONCLUSION

A 3D U-Net with spatial features provides fast, robust and accurate segmentations of the full cerebral vasculature in 4D CTA.

## **CLINICAL RELEVANCE/APPLICATION**

The high quality segmentation provided by our method is an important step towards the automated localization and evaluation of vascular pathology in acute stroke patients.



# NR398-SD-TUA8

Machine Learning Based Radiomics for Glial Tumor Classification

Tuesday, Nov. 27 12:15PM - 12:45PM Room: NR Community, Learning Center Station #8

#### Awards Student Travel Stipend Award

#### Participants

Sevcan Turk, MD, izmir, Turkey (*Presenter*) Nothing to Disclose Kaya Oguz, Izm?r, Turkey (*Abstract Co-Author*) Nothing to Disclose Omer Kitis, Izmir, Turkey (*Abstract Co-Author*) Nothing to Disclose Cem Calli, Izmir, Turkey (*Abstract Co-Author*) Nothing to Disclose Cenk Eraslan, MD, Izmir, Turkey (*Abstract Co-Author*) Nothing to Disclose Mehmet N. Orman, Izmir, Turkey (*Abstract Co-Author*) Nothing to Disclose Taner Akalin, Izmir, Turkey (*Abstract Co-Author*) Nothing to Disclose Taskin Yurtseven, Izm?r, Turkey (*Abstract Co-Author*) Nothing to Disclose

# For information about this presentation, contact:

sevcanturk.ege@hotmail.com

#### PURPOSE

The purpose of this study is to classify glial tumors into grade II, III and IV categories noninvasively by application of machine learning to multi-modal MRI features.

### **METHOD AND MATERIALS**

We retrospectively studied 57 glioma patients with pre-postcontrast T1, T2, FLAIR, ADC maps which were acquired 3T MRI. Two radiologists segmented the tumors into enhancing and nonenhancing part, tumor necrosis, cyst and edema using semi-automated segmentation tools. We measured total tumor volume, enhancing and nonenhancing tumor volume, edema volume, tumor necrosis volume and the ratios to the total volume for each image. Training of a support vector machine (SVM) classifier was performed with labeled data designed to answer the question of interest. Specificity, sensitivity, and AUC of the predictions were computed by means of ROC analysis. Differences in continuous measures between groups were assessed by using Kruskall Wallis, with post hoc Dunn correction for multiple comparisons.

#### RESULTS

When we compared the volume ratios between groups there was statistically significant difference between grade IV and grade II-III glial tumors. Edema and tumor necrosis volume ratios for grade IV glial tumors were higher than that of grade II and III. Volumetric ratio analysis could not distinguish grade II and III tumors. However, SVM correctly classified each group with accuracies up to 93%.

#### CONCLUSION

Radiomics and machine learning are emerging techniques that extract unrevealed information from medical images. Application of machine learning methods to MRI features can be used to classify tumors noninvasively and more readily in clinical settings.

# **CLINICAL RELEVANCE/APPLICATION**

The large amount of data produced by MRI limits the use of precise quantitative measurements in the clinical practice. Therefore, automated and reliable machine learning methods are required. Application of machine learning methods to MRI features can be used to classify tumors noninvasively and to predict prognostic information.Our study will be helpful to extract radiomic information from MRI features that are useful for making predictions noninvasively and for making classifications more readily in clinical settings.



# OB181-ED-TUA1

# Female Pelvic Inflammatory Disease: From Simple Salpingitis to Xanthogranulomatous Oophoritis

Tuesday, Nov. 27 12:15PM - 12:45PM Room: OB Community, Learning Center Station #1

## Awards Certificate of Merit

#### **Participants**

Grace G. Zhu, MD, Salt Lake City, UT (*Presenter*) Nothing to Disclose Maryam Rezvani, MD, Salt Lake City, UT (*Abstract Co-Author*) Nothing to Disclose Khaled M. Elsayes, MD, Ann Arbor, MI (*Abstract Co-Author*) Nothing to Disclose Christine O. Menias, MD, Chicago, IL (*Abstract Co-Author*) Nothing to Disclose Ahmed H. Ebada Salem, MBBCh, MSc, Alexandria, Egypt (*Abstract Co-Author*) Nothing to Disclose Akram M. Shaaban, MBBCh, Salt Lake City, UT (*Abstract Co-Author*) Contributor, Reed Elsevier; Author, Reed Elsevier

## For information about this presentation, contact:

akram.shaaban@hsc.utah.edu

### **TEACHING POINTS**

After viewing this exhibit, the reader will be able to: Recognize the imaging features and various presentations of pelvic inflammatory disease (PID). Recognize the imaging features of unusual causes of PID that may mimic ovarian malignancies.

## TABLE OF CONTENTS/OUTLINE

Introduction Caustative organisms Pathophysiology Clinical presentation Imaging Features <u>Typical PID</u> Salpingitis Pyosalpinx Tuboovarian abscess Hydrosalpinx Pyometritis <u>Unusual Presentations</u> Fitz-Hugh-Curtis Syndrome PID due to extension from other pelvic structures Infection of uterine leiomyoma (Pyomyoma) <u>Unusual Infections</u> Tuberculosis Actinomycosis Xanthogranulomatous oophoritis

# **Honored Educators**

Presenters or authors on this event have been recognized as RSNA Honored Educators for participating in multiple qualifying educational activities. Honored Educators are invested in furthering the profession of radiology by delivering high-quality educational content in their field of study. Learn how you can become an honored educator by visiting the website at: https://www.rsna.org/Honored-Educator-Award/ Akram M. Shaaban, MBBCh - 2015 Honored EducatorAkram M. Shaaban, MBBCh - 2016 Honored EducatorAkram M. Shaaban, MBBCh - 2017 Honored EducatorAkram M. Shaaban, MBBCh - 2018 Honored EducatorChristine O. Menias, MD - 2015 Honored EducatorChristine O. Menias, MD - 2013 Honored EducatorChristine O. Menias, MD - 2014 Honored EducatorChristine O. Menias, MD - 2017 Honored EducatorChristine O. Menias, MD - 2017 Honored EducatorChristine O. Menias, MD - 2018 Honored EducatorChristine O. Menias, MD - 2014 Honored EducatorChristine O. Menias, MD - 2018 Honored EducatorChristine O. Menias, MD - 2014 Honored EducatorChristine O. Menias, MD - 2018 Honored EducatorChristine O. Menias, MD - 2017 Honored EducatorChristine O. Menias, MD - 2018 Honored EducatorChristine O. Menias, MD - 2018 Honored EducatorChristine O. Menias, MD - 2017 Honored EducatorChristine O. Menias, MD - 2018 Honored EducatorChristine O. 2017 Honored EducatorChristine O. 2018 Hon



## OB182-ED-TUA2

# **Current Concepts in Imaging of Endometrial Cancer**

Tuesday, Nov. 27 12:15PM - 12:45PM Room: OB Community, Learning Center Station #2

#### **Participants**

Anuradha Rao, Bangalore, India (Presenter) Nothing to Disclose Rutuparna Sarangi, MD, Boston, MA (Abstract Co-Author) Nothing to Disclose Jaimee E. Mannix, MD , Boston, MA (Abstract Co-Author) Nothing to Disclose Nicholas Wilson, MD , Boston, MA (Abstract Co-Author) Nothing to Disclose Pooja Subbarao, Boston, MA (Abstract Co-Author) Nothing to Disclose Diana Dinh, MD, Boston, MA (Abstract Co-Author) Nothing to Disclose Nagaraj-Setty Holalkere, MD, Boston, MA (Abstract Co-Author) Founder and CEO, Imaginglink Inc;

#### For information about this presentation, contact:

nholalkere@gmail.com

# **TEACHING POINTS**

Uterine cancer is the fourth most common cancer in women in USA. Oncologic imaging is an integral part in the care of patients with endometrial cancer. This exhibit focuses on 1) Understanding different imaging modalities available for the diagnosis, staging, treatment planning and management of endometrial cancer. 2) Highlighting the advantages and limitations of each modality with a brief note on the evolving concepts. 3) Educate the viewer in major advancements in imaging and treatment of endometrial cancer which will help better management of the patients with suspected, diagnosed, or previously treated endometrial cancer.

# **TABLE OF CONTENTS/OUTLINE**

1) Brief introduction with incidence, etiology, prognostic factors of endometrial carcinoma. 2) 2009 FIGO staging of endometrial carcinoma 3) Imaging modalities like transvaginal ultrasound, hysterosonography, CT, PET, MRI- their advantages and disadvantages. 4) Introduction to advanced and functional imaging including diffusion weighted MR imaging, PET-MRI and new radio tracers. 5) Brief discussion about novel immuno-therapy and challenges in imaging after this treatment due to new patterns of treatment response and early recognition of autoimmune mediated toxic effects of these new therapies.



# PD183-ED-TUA6

To Improve is to Change, to Be Perfect is to Change Often: A Review of the Many Pediatric Urinary Tract Dilation Classifications Through Ultrasound History

Tuesday, Nov. 27 12:15PM - 12:45PM Room: PD Community, Learning Center Station #6

# Participants

Marcelo S. Takahashi, Sao Paulo, Brazil (*Presenter*) Nothing to Disclose Taisa D. Gasparetto, MD, PhD, Sao Paulo, Brazil (*Abstract Co-Author*) Nothing to Disclose Antonio S. Souza, MD, Sao Jose Rio Preto, Brazil (*Abstract Co-Author*) Nothing to Disclose Giovanna B. Motta, MD, Sao Paulo, Brazil (*Abstract Co-Author*) Nothing to Disclose

# **TEACHING POINTS**

The purpose of this exhibit is: 1) To review the main causes and presentations of urinary tract dilation in the pediatric patients. 2) To discuss the necessity of adequate communication between the radiologist and referring physician to provide the best possible practice for pediatric patients presenting with urinary tract dilation. 3) To review, illustrate and discuss the use and limitations of the many ultrasound urinary tract dilation classifications.

# TABLE OF CONTENTS/OUTLINE

Incidence and main causes of urinary tract dilation in children: - Transient or physiologic - Vesicoureteral reflux - Ureteropelvic junction obstruction - Uretervesical junction obstruction - Megaureter - Posterior urethral valve - Multicystic dysplastic kidney - Duplex system - Ureterocele - Ectopic ureter Outcome of children presenting with urinary tract dilation Importance of adequate ultrasound evaluation and reporting. Classifications: - Descriptive - Antero-posterior renal pelvis diameter - Society for fetal urology consensus - European Society for Pediatric Radiology Task Force - Onen Classification - Multidisciplinary consensus on the classification.



# PD184-ED-TUA7

# **Case Based Approach to Hindbrain Malformations**

Tuesday, Nov. 27 12:15PM - 12:45PM Room: PD Community, Learning Center Station #7

FDA Discussions may include off-label uses

#### **Participants**

Akash Kumar B Y, MBBS, Chennai, India (*Presenter*) Nothing to Disclose Gopinathan K, MBBS, MD, Chennai, India (*Abstract Co-Author*) Nothing to Disclose Reginald Wesley, MBBS, Chennai, India (*Abstract Co-Author*) Nothing to Disclose Devimeenal J, MD, FRCR, Chennai, India (*Abstract Co-Author*) Nothing to Disclose Chirtrarasan P, MBBS, MD, Chennai, India (*Abstract Co-Author*) Nothing to Disclose

#### For information about this presentation, contact:

akashkumarby150@gmail.com

#### **TEACHING POINTS**

To know the embryological development of hindbrain. Classification of these hindbrain malformations. To understand the MRI characteristics of few important cases and distinguishing them from mimics.

## **TABLE OF CONTENTS/OUTLINE**

Embryological development - Pons and medulla develops from Metencephalon and myelencephalon respectively together with cerebellum (hindbrain). Classification I.Malformations secondary to early antero-posterior and dorso-ventral patterning defects, or to misspecification of mid-hindbrain germinal zones II. Malformations associated with later generalized developmental disorders that significantly affect the brainstem III. Localized brain malformations that significantly affect the brainstem IV. Combined hypoplasia and atrophy in putative prenatal onset degenerative disorders. Imaging approach Sample cases- • Pontine tegmental cap dysplasia • Horizontal gaze palsy with progressive sclerosis • Joubert syndrome • Congenital muscular dystrophy • Rhombencephalosynapsis • Lhermitte-Duclos disease • Pontocerebellar hypoplasia



## PD185-ED-TUA8

# When Animals Attack! What the Radiologist Needs to Know About Pediatric Animal Related Injuries

Tuesday, Nov. 27 12:15PM - 12:45PM Room: PD Community, Learning Center Station #8

#### Participants

Yoon-Jin Kim, MD, San Francisco, CA (*Presenter*) Nothing to Disclose Pierre-Alain Cohen, MD, San Francisco, CA (*Abstract Co-Author*) Nothing to Disclose Matthew A. Zapala, MD,PhD, San Francisco, CA (*Abstract Co-Author*) Nothing to Disclose Jesse L. Courtier, MD, San Francisco, CA (*Abstract Co-Author*) Founder, HoloSurg3D, Inc; Consultant, HoloSurg3D, Inc

### For information about this presentation, contact:

yoon-jin.kim@ucsf.edu

## **TEACHING POINTS**

Learn common mechanisms and locations of pediatric animal related injuries Review appropriate imaging modalities in these situations

### TABLE OF CONTENTS/OUTLINE

Overview Children are not only the most common victims of animal-related injuries, but also are more likely to be severely injured. Knowledge of the most common mechanisms and complications of animal-related injuries guides diagnostic evaluation Common mechanisms Most injuries are limited to one body region with the head, face and neck comprising fifty percent of cases. Range from non-penetrating, penetrating, crush and blunt traumatic injuries Case series Summary of complicated skin and soft tissue infections Domesticated pets: injuries from dogs and cats Horse-related injuries: females 10 - 14 years old are the most likely victims. Traumatic brain injuries are common. Role of Imaging Radiographs identify fractures and foreign bodies that increase the risk of infection. Ultrasound and MR assess for complications of skin and soft tissue infections such as an abscess and osteomyelitis. Computed tomography evaluates for bony injuries, especially those to the cranium. For reconstructive planning CT is the imaging modality of choice.



# PD220-SD-TUA1

The Comparison Between Improved T2 SPACE and Other Traditional MRU Sequences in Children with Congenital Urinary Tract Malformation

Tuesday, Nov. 27 12:15PM - 12:45PM Room: PD Community, Learning Center Station #1

# Participants

Yan Dai, Guangzhou, China (*Presenter*) Nothing to Disclose Yingqian Chen, Guangzhou, China (*Abstract Co-Author*) Nothing to Disclose Lang Chen, Guangzhou, China (*Abstract Co-Author*) Nothing to Disclose Miao Fan, MD, PhD, Guangzhou, China (*Abstract Co-Author*) Nothing to Disclose

#### For information about this presentation, contact:

617736918@qq.com

# PURPOSE

Congenital urinary tract malformation is a common disease in children. Early diagnosis and treatment are essential to protect the renal function. The display of urinary tract obstruction in traditional MRU sequences are not very well, which need a new sequence to solve it. The purpose of this study is to compare the image quality and diagnostic capacity of Improved T2 SPACE and Traditional MRU on the disease.

#### **METHOD AND MATERIALS**

For each sequence (including Tradition T2 SPACE, T2 TSE, T2 HASTE and Improved T2 SPACE), the MR images of 10 cases of children with congenital urinary tract malformation were collected, which were examined in our hospital during May 2015 to April 2018, using MAGNETOM Trio Siemens 3.0T MR. The scanning parameters are: Tradition T2 SPACE: TR=2400ms, TE=694ms, flip angle=110; T2 TSE: TR=2000ms, TE=759ms, flip angle=170; T2 HASTE: TR=1280ms, TE=122ms, flip angle=150; Improved T2 SPACE: TR=2400ms, TE=135ms, flip angle=120. Qualitative image analysis was assessed utilizing a five-point-scale with regard to image quality, display of urinary tract obstruction area, renal papilla and ureter wall, urinary system sharpness, background and intestinal tract movement artifacts. Wilcoxon test was used as the statistic method.

# RESULTS

Each group were comparable with respect to age, gender and other baseline parameters. The scanning time of Improved T2 SPACE is significantly shorter than those of T2 TSE and Traditional T2 SPACE. The image quality, display of urinary tract obstruction area and renal papilla in the group of Improved T2 SPACE were better than those in Traditional T2 SPACE and T2 TSE (p<0.05). The display of ureter wall in Improved T2 SPACE was better than those in T2 TSE and T2 HASTE (p<0.05). The background artifacts of Improved T2 SPACE group were less than those of Traditional T2 SPACE and T2 TSE (p<0.05). However, the urinary system sharpness of all groups were similar (p>0.05). The only deficiency of Improved T2 SPACE was the intestinal tract movement artifacts, which was greater than those of T2 HASTE sequence (p<0.05).

## CONCLUSION

The Improved T2 SPACE sequence can reach the better image quality and information display than other sequences with a shorter scanning time.

### **CLINICAL RELEVANCE/APPLICATION**

Proved by our comparative study, the Improved T2 SPACE can display the information needed by the clinic better, which is conducive to the imaging diagnosis and operation.



# PD221-SD-TUA2

# Infants Limb Fractures in Household Accidents: Beyond the Shaken-Baby Syndrome

Tuesday, Nov. 27 12:15PM - 12:45PM Room: PD Community, Learning Center Station #2

### Participants

Annachiara Cavaliere, MD, Este, Italy (*Presenter*) Nothing to Disclose Silvia Karem Janet Flores Quispe, MD, Padua, Italy (*Abstract Co-Author*) Nothing to Disclose Rodica Mardari, Padova, Italy (*Abstract Co-Author*) Nothing to Disclose Mariagiulia Anglani, Padova, Italy (*Abstract Co-Author*) Nothing to Disclose Tiziana Toffolutti, Padova, Italy (*Abstract Co-Author*) Nothing to Disclose Roberto Stramare, MD, Padova, Italy (*Abstract Co-Author*) Nothing to Disclose Chiara Giraudo, MD,PhD, Padova, Italy (*Abstract Co-Author*) Nothing to Disclose

#### For information about this presentation, contact:

annachiara88cavaliere@gmail.com

## PURPOSE

The patterns of cranial and limb skeletal fractures of children and infants victims of abuses are well known. On the contrary, little is known about the traumatic mechanism and the radiological features of limb injuries due to household accidents. Thus, aim of this study is to assess the occurrence and patterns of limb fractures occurring in infants (<12 months) involved in household casualties

### **METHOD AND MATERIALS**

An electronic search (2 years interval) of the database of our tertiary pediatric center for skeletal x-rays was performed. Inclusion criteria were: i) access to the ER of children younger than 12 months; ii) skeletal x-ray examination of the extremities; iii) anamnestic non-accidental (e.g., car accident) and non-abusive traumatic mechanism. Descriptive statistics was applied (i.e., most affected skeletal bone, pattern of fractures, reported mechanism of injury).

#### RESULTS

11715 newborns and infants were admitted to the ER during 2 years, 960 were evaluated for traumatic accidents and 116 underwent an x-ray. 57 patients had a fracture and 19 were extra-cranial. 13 out of the 19 patients meeting the inclusion criteria were female (mean age 7.7±2.2 months). In 8 patients (42%) a fracture of the clavicle occurred and in 7 out of 8, the middle third was involved. In 9 (47%) patients a fracture of the diaphysis of long bones (three of the femur) was diagnosed. The most common pattern was a complete transverse fracture (14 out of 19) with displacement and angulation of the fragments in 40% of the cases. One spiroid fracture of the 16 also occurred. The traumatic mechanisms belonged to three categories: fall from orthostatic position (10%), fall from low heights (e.g., furniture) (55%), miscellaneous (e.g., traumatic injury playing with siblings) (20%).

### CONCLUSION

Even if household accidents rarely cause severe injuries of the extremities, our preliminary results revealed that the trauma dynamics may overlap with the one of children abuse and the mostly involved bone is the clavicle. The radiologists are thus expected to become confident with this evidence, aiming to do not overlook fractures in infants victim of household casualties.

#### **CLINICAL RELEVANCE/APPLICATION**

Household accidents may have traumatic mechanisms partially overlapping with those of child abuse but seem to have skeletal fractures that are quite uncommon in battered children.



# PD223-SD-TUA4

## **Rickets in Vienna Revisited**

Tuesday, Nov. 27 12:15PM - 12:45PM Room: PD Community, Learning Center Station #4

# Participants

David M. Ayoub, MD, Springfield, IL (Presenter) Nothing to Disclose

#### For information about this presentation, contact:

raypoke@mac.com

#### PURPOSE

Wimberger's landmark study on radiology of rickets was based on the observations of institutionalized infants in Vienna, Austria from 1919-1922 following WWI. I sought to reanalyze the original radiographic findings in greater detail.

#### RESULTS

Classical GP fraying was seen in 80% of infants but only sporadically (9% of all GPs). Fraying in slower growing GPs was rare. Indistinctness of the zone of provisional calcification (ZPC) was only seen in 20% of GPs during active stages. On the other hand, mineralization above a distinct ZPC indicating healing was seen in all infants and in 39% of all GPs. During healing, a new ZPC appeared above the original ZPC in all infants (range 2-7 GPs per infant), three times more likely in the lower extremity, particularly the fibula. Perichondrial spurs were observed in all infants (range 3-8 GPs per infant). Subperiosteal new bone was present in 90% of cases, but never during pre-rachitic or healed states. Inward bowing of the fibula developed in 67% of infants and distal tibia varus in 44%. Classical knee region bowing was not observed. Five infants (50%) had at least one subclinical fracture. Generalized osteopenia was uncommon, seen in 30% of infants during active stages, often worsening during the healing process, suggesting that mineral may redistribute as part of the natural recovery process. Cupping of the ends of the ulna was present in each infant. There was evidence of subperiosteal bone resorption in the proximal medial tibia in 22% of infants. The changes of both active and healing rickets commonly occurred asynchronously in time. The disease never involved all bones.

#### CONCLUSION

Rickets presents as a much more diverse range of radiographic changes than widely assumed.

#### **CLINICAL RELEVANCE/APPLICATION**

The awareness of the full spectrum of rickets should include its variable and nonuniform appearance during active and healing stages.



## PD224-SD-TUA5

Specific CT Imaging Characteristics of Congenital Mesoblastic Nephroma and Correlation with Ultrasound and Pathology

Tuesday, Nov. 27 12:15PM - 12:45PM Room: PD Community, Learning Center Station #5

# Participants

Yingqian Chen, Guangzhou, China (*Presenter*) Nothing to Disclose Yan Dai, Guangzhou, China (*Abstract Co-Author*) Nothing to Disclose Lang Chen, Guangzhou, China (*Abstract Co-Author*) Nothing to Disclose Miao Fan, MD, PhD, Guangzhou, China (*Abstract Co-Author*) Nothing to Disclose

For information about this presentation, contact:

chen-yingxi@163.com

# PURPOSE

Congenital mesoblastic nephroma (CMN) is a common solid renal tumor in the neonate, whose prognosis is very optimistic. But CMN can easily be misdiagnosed as the other malignant renal tumors by radiology. However, no studies have described the CT imaging appearance of CNM in detail. The objective of this study is retrospective analyses of the CT characteristics of CMN and their corresponding ultrasound findings and pathology.

#### **METHOD AND MATERIALS**

This retrospective study reviewed the enhanced CT images of the CMNs and other renal tumors in children younger than 1 year old in the past 10 years from our hospital. Two radiologists had noted the CT imaging characteristics of these images. *t*-test and Fisher's exact test were used in the comparison of imaging characteristics between the CMNs and other renal tumors.

#### RESULTS

Compare with other malignant renal tumors, the CMNs tend to appear as smaller round masses without clear coverage or clear boundary with the kidney in CT images (p < 0.01). The intratumor pelvis, as well as the double-layer sign are the specific characteristics of CMNs (p < 0.01). The gender, quality of tumor (solid or solid-cystic), character of enhancement (homogeneous or heterogeneous enhancement), peri-renal hemorrhage, or peripheral lymph node enlargement showed no statistical significance (p > 0.05) between CMNs and other renal tumors. The appearances of CMN with classic components in the CT images are relevant to the pathological findings. The intratumor pelvis is caused by the classic components of CMN growing to encapsulate the pelvis. The double-layer sign in CT image correlates with the specific hypoechoic ring in ultrasound, which is caused by the slow blood flow and delay contrast agent filling in the blood sinus located in the peripheral part of the tumor. The differential diagnosis of CMN should include the other solitary renal tumors like Wilms' tumor, clear-cell sarcoma of the kidney and rhabdoid tumor of the kidney.

## CONCLUSION

The unclear coverage and unclear boundary with the kidney, the intratumor pelvis, and double-layer sign after contrast were specific CT imaging characteristics of CMN.

#### **CLINICAL RELEVANCE/APPLICATION**

These specific CT imaging characteristics can help radiologist to make the correct diagnosis of CMN, in order to choose the correct treatment.



# PH012-EB-TUA

Non-Enhanced and Non-Gated MR Angiography for Peripheral Arteries using Improved Acceleration-Selective Arterial Spin Labelling (iAccASL)

Tuesday, Nov. 27 12:15PM - 12:45PM Room: PH Community, Learning Center Hardcopy Backboard

# Participants

Shuhei Shibukawa, PhD, Isehara, Japan (*Presenter*) Nothing to Disclose Natsuo Konta, Isehara, Japan (*Abstract Co-Author*) Nothing to Disclose Tetsu Niwa, MD, Yokohama, Japan (*Abstract Co-Author*) Nothing to Disclose Makoto Obara, Minato-Ku, Japan (*Abstract Co-Author*) Employee, Koninklijke Philips NV Yuta Akamine, Tokyo, Japan (*Abstract Co-Author*) Employee, Koninklijke Philips NV Takashi Okazaki, Isehara, Japan (*Abstract Co-Author*) Nothing to Disclose Tosiaki Miyati, PhD, Kanazawa, Japan (*Abstract Co-Author*) Nothing to Disclose Yutaka Imai, MD, Tokyo, Japan (*Abstract Co-Author*) Nothing to Disclose

## CONCLUSION

Optimized iAccASL achieved non-enhanced and non-gated MRA for peripheral arteries.

## FIGURE

http://abstract.rsna.org/uploads/2018/18004443/18004443\_1jyh.jpg

#### Background

Most non-enhanced magnetic resonance angiography (MRA) techniques for peripheral artery disease (PAD) require electrocardiographic gating., which leads to a relatively long scan time and vulnerability for arrhythmia. To obtain MRA for PAD without ECG gating, we applied improved acceleration-selective arterial spin labeling (iAccASL) on 3.0T MRI.

## Evaluation

Eight healthy volunteers and one patient were examined on a 3.0T MR system. The iAccASL MRA was created by subtracting the labeling image from the control image (Figure a). We used 3D T1-weighted turbo-field-echo based iAccASL with voxel size,  $0.99 \times 0.97 \times 2.0$  mm; and scan time, 4 min 18 s. To assess the influence of motion sensitization gradients, defined as acceleration encoding (AENC), we compared five AENC values (i.e., 0.5, 1.0, 1.5, 3.0, and 6.0 m/s2). Since suppression of the arterial signal is important on the labeling image, the signals of the peroneal artery (PA) and the gastrocnemius muscle (GM) on each image were measured, and the signal intensity ratio (SIRPA/GM) was calculated. Two radiologists reviewed the arterial depiction and the venous contamination using 5-point scale. These scores on iAccASL MRA with each AENC value were compared using Friedman test and a post-hoc test.

#### Discussion

The SIRPA/GM on labeling image decreased with lower AENC value (Figure b). The arterial depiction was significantly higher with lower AENC value (P < 0.01), but not significantly different between AENC of 0.5 and 1.0 m/s2 on the post-hoc test (P > 0.05) (Figure c). A significantly marked venous contamination was found with AENC of 0.5 m/s2 than those with the other AENC on the post-hoc test (P < 0.001). Representative MRAs with maximum intensity projection (MIP) in a case are shown in Figure d. We assumed that AENC value of 1.0 m/s2 was optimal for non-gated MRA of peripheral arteries. Figure e shows the MIP image using iAccASL with AENC of 1.0 m/s2 in the patient with PAD. The occlusion of the right peroneal artery and the stenosis of the right anterior tibial artery were clearly visualized.



# PH122-ED-TUA4

New Concept of Pathological Diagnosis Support by Micro CT System: How Does CT Technology Change Pathologist's Workflow?

Tuesday, Nov. 27 12:15PM - 12:45PM Room: PH Community, Learning Center Station #4

# Participants

Tomonari Hayakawa, Toyoake, Japan (*Presenter*) Nothing to Disclose Ayumi Yamada, Toyoake, Japan (*Abstract Co-Author*) Nothing to Disclose Atsushi Teramoto, PhD, Toyoake, Japan (*Abstract Co-Author*) Nothing to Disclose Tetsuya Tsukamoto, Toyoake, Japan (*Abstract Co-Author*) Nothing to Disclose Kuniaki Saito, Toyoake, Japan (*Abstract Co-Author*) Nothing to Disclose Hiroshi Fujita, PhD, Gifu City, Japan (*Abstract Co-Author*) Nothing to Disclose

#### **TEACHING POINTS**

In surgical treatment of cancer, pathological diagnosis is performed to analyze resected lesions intraoperatively and postoperatively. Pathological diagnosis is the final diagnosis, and it is important because it is greatly involved in the determination of the subsequent treatment policy. In the examination, the lesion is sliced to prepare a specimen. If the internal structure is imaged in advance, it is possible to more accurately determine the region for analysis. Therefore, we have developed a new device for supporting pathological diagnosis using micro CT system. The purpose of this exhibition is to show whether our developed CT system is effective for pathological diagnosis. The major teaching points of this exhibit are:1. In pathological diagnosis, it is important to know the fine internal structure of the analysis region.2. We can observe the microstructure of organs and support doctors with the developed CT system.3. Volume rendering image of micro CT offers accurate analysis of target region of organ.

## TABLE OF CONTENTS/OUTLINE

1. Importance of determining accurate analysis area in pathological examination2. Explanation about developed CT system - Block diagram and key parts of prototype CT- Organ fixation, scanning procedure and method of reconstruction3. inspection result - Visualization ability of scanned organs



## PH225-SD-TUA1

Deep Learning Approach for Image Denoising in Low-Dose CT

Tuesday, Nov. 27 12:15PM - 12:45PM Room: PH Community, Learning Center Station #1

#### **Participants**

Chul Kyun Ahn, Seoul, Korea, Republic Of (*Presenter*) Nothing to Disclose Hyeongmin Jin, Seoul, Korea, Republic Of (*Abstract Co-Author*) Nothing to Disclose Zepa Yang, PhD, Suwon, Korea, Republic Of (*Abstract Co-Author*) Nothing to Disclose Chang Yong Heo, BS, Seoul, Korea, Republic Of (*Abstract Co-Author*) Nothing to Disclose Jong H. Kim, PhD, Seoul, Korea, Republic Of (*Abstract Co-Author*) Nothing to Disclose

## For information about this presentation, contact:

ahnck@snu.ac.kr

#### CONCLUSION

The deep learning model could reduce image noise substantially while improving visibility of fine pulmonary structures and preserving image texture. The deep learning technique has a potential to reduce the radiation dose and improve the quality in the low-dose CT.

#### Background

Effective elimination of CT noise and improving overall image quality is crucial for reducing radiation exposures in low-dose CT imaging. In this study, we present a deep learning approach for CT denoising which eliminates noise selectively while preserving fine anatomical structures and image texture with multi-scale filter sets sharply tuned to separate noise patterns from noisy CT images.

#### **Evaluation**

2,997 regular-dose chest CT images from 30 patients were used for training of a Convolutional Neural Network (CNN). The CT images were of 140 kVp, 100 mAs, and FBP reconstruction with B60f kernel. In addition, we created simulated low-dose CT images by using a synthetic sinogram-based low-dose simulation technique. We trained the CNN model by feeding the simulated low-dose CT image into its input nodes with the output nodes fed by the CT noise pattern obtained by subtracting the simulated low-dose CT image from the regular dose CT image. Given a new low-dose CT image, the noise image was predicted from the trained CNN, which in turn was subtracted from the new low-dose image to produce a denoised CT image. To evaluate the performance of the trained CNN model, we selected 10 CT cases from independent data set scanned at 120 kVp and 20 mAs. We evaluated the image quality by measuring noise standard deviation and noise power spectrum (NPS) at homogeneous liver region, and with visual scoring of small vessels, bronchial wall, and lung fissure. For comparison, the image quality was assessed on FBP, iDose4, iDose6, and deep learning-denoised FBP.

#### Discussion

Noise standard deviation was 380, 237, 184 and 107 (HU) in FBP, iDose4, iDose6, and deep learning-denoised images. The NPS peak frequency was 6.0 lp/cm in both iDose4 and iDose6 images, and 6.1 lp/cm in both FBP and deep learning-denoised images. The visual scoring made with 4 point scale was 3.0, 3.4, 3.4 and 4.0 in FBP, iDose4, iDose6 and deep learning-denoised images.



# PH226-SD-TUA2

A New 3D Tomographic Image Reconstruction Process: More Than 10-Fold Acceleration and Reduced Artifacts Compared to SART on Same Hardware

Tuesday, Nov. 27 12:15PM - 12:45PM Room: PH Community, Learning Center Station #2

## Participants

Wolfram R. Jarisch, PhD, Potomac, MD (*Presenter*) Nothing to Disclose Peter J. Basser, PhD, Bethesda, MD (*Abstract Co-Author*) Nothing to Disclose

For information about this presentation, contact:

wolfram@cyber-inc.us

## CONCLUSION

The new, highly efficient CT process, implemented in a research laboratory, offers significant advantages over traditional methods: (i) stable convergence; (ii) over 10-fold acceleration; and (iii) resilience to noise. De Man, B., et al., 2005 IEEE Nucl. Sci. Symp. Conf. Rec.

#### Background

Current nonlinear iterative reconstruction (IR) of CT suffers from slow convergence. De Man et al. analyze computation of key techniques used for numerical hill-climbing in IR. From a wider perspective, however, the problem is to minimize a quadratic cost function, often in a 108 dimensional space. Above techniques, however, can only address large eigenvalues in a small sub-space of that cost function. Here we demonstrate an iterated analytic approach (IAA) to avoid this limitation.

#### **Evaluation**

The new approach transforms the nonlinear constrained optimization into a sequence of linear small signal processing steps that use analytic results. Two mechanisms provide the linear scenario: (i) gradual increase of image resolution with linear interpolation of function values; and (ii) repeated application of linear analytic approximations, scaling errors of preceding iterations with derivatives of transformed measurement values, producing optimal update innovations (UI). A third mechanisms evaluates and constrains UI for the next iteration. Voxel counts during iterations form a geometric series making the last iteration(s) the dominant computational effort. Key evaluation criteria of the new method are reconstruction time, final iteration count, and artifacts, relative to existing methods.

#### Discussion

Present nonlinear iterative CT typically starts with a filtered backprojection (FBP). Then data processing is switched to iterative numerical hill-climbing. For this purpose a step relaxation parameter is chosen to insure stable conversion towards an improved solution. In the high dimensional optimization space, however, these one-dimensional steps cope only with large eigenvalues. By contrast, the IAA, using e.g. FBP, operates on all eigenvalues, although not optimally. Nevertheless, since FBP represents a highly error contractive operation, two iterations at the highest resolution yield well converged reconstructions.



# PH227-SD-TUA5

Whole Body Low-Dose CT-Study Combined With Model Based Iterative Reconstruction Algorithm for Follow-Up of Oncologic Patients: Image Quality and Dose Reduction

Tuesday, Nov. 27 12:15PM - 12:45PM Room: PH Community, Learning Center Station #5

#### Participants

Ilaria Salemi, MD, Cinisello Balsamo, Italy (*Presenter*) Nothing to Disclose Davide Ippolito, MD, Monza, Italy (*Abstract Co-Author*) Nothing to Disclose Cammillo R. Talei Franzesi, Milan, Italy (*Abstract Co-Author*) Nothing to Disclose Cecilia Cangiotti, MD, Monza, Italy (*Abstract Co-Author*) Nothing to Disclose Cesare Maino, MD, Milano, Italy (*Abstract Co-Author*) Nothing to Disclose Sandro Sironi, MD, Monza, Italy (*Abstract Co-Author*) Nothing to Disclose

#### PURPOSE

To compare radiation dose and image quality of low-dose CT protocol combined with iterative model-based reconstruction algorithm (IMR) with standard-dose CT approach combined with hybrid-iterative reconstruction algorithm (iDose) for follow-up of oncologic patients.

#### **METHOD AND MATERIALS**

Ninety-four patients with known oncological diseases who underwent, during their clinical follow-up, both low dose CT performed on 256-row scanner (iCT Elite, Philips) with 100 kV and automated mAs modulation (depending on patient weight) and standard-dose CT performed on 256-row scanner (iCT Brilliance, Philips) with 120 kV and automated mAs modulation were enrolled. Images were reconstructed with IMR for the first CT examination and iDose algorithm for the second CT examination. We evaluated density values in liver and spleen and signal-to noise ratio (SNR), along with image noise, dose parameters, sharpness and diagnostic quality with 4-point scale.

#### RESULTS

Noise of images expressed as SD values, measured in liver and spleen, was significantly lower in IMR images (liver 11,42 vs 14,57, p<0,001) whereas SNR was statistically higher (liver 10,68 vs 7,94, p<0,001) compared to iDose reconstruction. Volumetric-Computed-Tomographic-Dose-Index (CTDIvol) and Dose-Length-Product (DLP) were significantly lower in IMR compared to iDose reconstruction (DLP 559,83 vs 959,77 mGy\*cm, p<0,001), with overall dose reduction of 45,72%. 4-point scale qualitative analysis did not reveal any significant differences in terms of diagnostic quality (p=0,04).

#### CONCLUSION

Automatic tube-current modulation combined with IMR algorithm and low kV setting allows dose reduction of 45,72% in whole body CT imaging without loss of diagnostic quality, thus representing a useful diagnostic approach in reducing dose exposure in oncologic patients who undergo several follow-up studies.

# **CLINICAL RELEVANCE/APPLICATION**

In the follow-up of oncologic patients CT has a main role, so lowering doses is desirable. Low-kV CT combined with IMR allows to reduce doses significantly, offering high diagnostic image quality.



## PH228-SD-TUA6

A Study on the Correlation between Body Mass Index (BMI) and 'Four Low' Coronary Artery CT Angiography

Tuesday, Nov. 27 12:15PM - 12:45PM Room: PH Community, Learning Center Station #6

### Participants

Zhijun Hu SR, xi`an, China (*Abstract Co-Author*) Nothing to Disclose Dou Li, Xi'an, China (*Presenter*) Nothing to Disclose Xin Li, Xian, China (*Abstract Co-Author*) Nothing to Disclose Haitao Yu SR, MD, MD, Peking, China (*Abstract Co-Author*) Nothing to Disclose Donghong Wei Sr, Xi'an, China (*Abstract Co-Author*) Nothing to Disclose Qi Wang, Xi'an, China (*Abstract Co-Author*) Nothing to Disclose Zhen Tang Liu, Xi'an, China (*Abstract Co-Author*) Nothing to Disclose Jun Gu SR, Beijing, China (*Abstract Co-Author*) Nothing to Disclose Aiping Ren, Xi'an, China (*Abstract Co-Author*) Nothing to Disclose Jingming Chen, Xi'an, China (*Abstract Co-Author*) Nothing to Disclose

## PURPOSE

To explore the correlation between four low (low kVp, low contrast agent, low flow rate, low radiation dose) coronary artery CT angiography and BMI.

#### **METHOD AND MATERIALS**

60 patients underwent CT (Revolution, GE Healthcare) coronary angiography in our hospital. Tube voltages are: 120 kvp in group A, 100 kvp in group B and 80 kvp in group C with 20 cases in each group. Injection protocols of contrast agent iopamidol (370 mgI/mL) are shown in Table (1). Trigger scan with threshold of 220HU, fixed NI of 26, collimation width of 140mm, Atuo gating ECG mode, Pre -Asir-V fixed 70% and Post-Asir-V of 80%. CT and SD values in aortic root, coronary artery RCA, LAD, LCX, proximal lumen and peripheral adipose tissue were measured. Vascular SNR, CNR and radiation dose (ED) were calculated. Subjective evaluation was conducted by two senior radiologists according to the American Heart Association (AHA) coronary 13 segments in a 4-point scale.

#### RESULTS

Age, heart rate for patients , Aortic root vessels and coronary artery CT, SNR, CNR had no statistically significant difference (P> 0.05). There was no statistically significant difference in subjective evaluation scores between the three groups (P>0.05). Contrast doses among the three groups were: A group ( $63.32\pm10.32$  ml), B group ( $42.12\pm5.31$  ml), and C group ( $22.64\pm2.70$ ). Ml), B contrast dosage was 33.5% less than that of group A, and group C contrast dosage was 64.2% less than group A. Flow rates were: group A( $5.08\pm0.45$  ml/s), group B ( $3.50\pm0.45$  ml/s) and group C ( $1.90\pm0.21$  ml/s). The flow rate of contrast agent in group B was lower than that in group A by 31.2%; the rate of contrast agent in group C was lower than that in group A by 62.6%. Effective radiation dose (ED) in the three groups were: group A ( $3.27\pm1.68$  mSv), B ( $1.62\pm0.73$  msv), and C ( $0.73\pm0.30$  mSv). B had a 50.1% reduction in effective radiation dose compared to group A. Group C had a 77.7% reduction in effective radiation

#### CONCLUSION

Low-kVp, low-contrast agent, low-flow rate, low-dose CCTA coronary imaging is feasible using 16cm wide-detector CT. Image quality is not affected and scanning protocols are closely related to the patient's BMI index.

## **CLINICAL RELEVANCE/APPLICATION**

Low-kVp, low-contrast agent, low-flow rate, low-dose CCTA coronary imaging is feasible using 16cm wide-detector CT. Image quality is not affected and scanning protocols are closely related to the patient's BMI index.



## PH229-SD-TUA8

A Novel Direct-Conversion Detector with Variable Charge Gain

Tuesday, Nov. 27 12:15PM - 12:45PM Room: PH Community, Learning Center Station #8

## FDA Discussions may include off-label uses.

#### Participants

Denny L. Lee, PhD, West Chester, PA (*Presenter*) Research Consultant, Vieworks Co Hyunsuk Jang, BEng, Anyang-Si, Korea, Republic Of (*Abstract Co-Author*) Employee, Vieworks Co; Stockholder, Vieworks Co

#### For information about this presentation, contact:

dlee@directxray.com

#### PURPOSE

By manipulating the electric field in direct conversion material, a novel detector is being developed without using a Thin Film Transistor (TFT) array. Lower noise images can be achieved by eliminating TFT gate switching, and lower lag images can be achieved by minimizing the induced image from counter charge movements. Proportional charge gain from impact ionization can also be achieved by controlling the transfer field during image readout. This new detector can be used for low dose, high resolution and dynamic imaging.

## METHOD AND MATERIALS

Each pixel of this new detector consists of a central charge readout electrode surrounded by a dielectric surface, with an underneath buried electrode. In an array, rows of readout electrodes are connected to charge amplifiers and columns of buried electrodes are connected to push-pull voltage drivers. A direct-conversion material such as selenium (Se) is deposited on this platform together with a top bias electrode. During x-ray, negatively-biased buried electrodes direct holes to the pixel dielectric surface and store the charges above the buried electrode with 100% fill factor. During readout, one column of buried electrodes changes from negative potential to positive potential and re-directs the holes to the respective pixel central readout electrodes. No TFT is required and therefore no gate switching noise is added to the image. Readout electrodes are located at the node point of the charge transfer push-pull potential to minimize readout noise. Impact charge gain can also be achieved by controlling the amplitude of the push-pull potential.

#### RESULTS

Electric field and charge movements of this structure have been simulated, investigated and will be presented. Data have been obtained from prototype samples to verify the charge collection, charge transfer and charge gain of the detector.

# CONCLUSION

Controllable gain of this new structure can compensate for the low charge-generation properties of conventional Se detectors and can enable efficient imaging over the entire range of diagnostic imaging energy. This new structure has avoided many common problems associated with TFT in Se detectors such as electrostatic damage, temperature or impact delamination.

## **CLINICAL RELEVANCE/APPLICATION**

This new detector structure can provide low dose imaging as well as continuous and infinite loop readout for dynamic imaging while maintaining the high-resolution nature of the direct-conversion detector.



## PH230-SD-TUA3

Does Biopsy Influence Effectiveness of Radiomics in the Classification of Benign Lesions and Cancers on Breast MRI?

Tuesday, Nov. 27 12:15PM - 12:45PM Room: PH Community, Learning Center Station #3

# Participants

Yu Ji, MD, Chicago, IL (Presenter) Nothing to Disclose

Heather Whitney, PhD, Wheaton, IL (Abstract Co-Author) Nothing to Disclose

Hui Li, PHD, Chicago, IL (Abstract Co-Author) Nothing to Disclose

Alexandra V. Edwards, Chicago, IL (*Abstract Co-Author*) Research Consultant, QView Medical, Inc; Research Consultant, Quantitative Insights, Inc

John Papaioannou, MSc, Chicago, IL (Abstract Co-Author) Research Consultant, QView Medical, Inc

Karen Drukker, PhD, Chicago, IL (Abstract Co-Author) Royalties, Hologic, Inc

Peifang Liu, MD, PhD, Tianjin, China (Abstract Co-Author) Nothing to Disclose

Maryellen L. Giger, PhD, Chicago, IL (*Abstract Co-Author*) Stockholder, Hologic, Inc; Shareholder, Quantitative Insights, Inc; Shareholder, QView Medical, Inc; Co-founder, Quantitative Insights, Inc; Royalties, Hologic, Inc; Royalties, General Electric Company; Royalties, MEDIAN Technologies; Royalties, Riverain Technologies, LLC; Royalties, Mitsubishi Corporation; Royalties, Canon Medical Systems Corporation

# For information about this presentation, contact:

yuji710@uchicago.edu

#### PURPOSE

To assess robustness of radiomic features extracted from DCE-MR images acquired pre- or post-biopsy for classification of breast lesions as benign or malignant and to compare to previous results for breast lesions imaged at a different center.

# METHOD AND MATERIALS

Dynamic contrast-enhanced magnetic resonance (DCE-MR) images of 602 breast lesions (283 benign lesions and 248 malignant cancers imaged pre-biopsy, 17 benign lesions and 54 malignant cancers imaged post-biopsy) were acquired under HIPAA/IRB compliance. The lesions were segmented automatically using a fuzzy c-means method. Radiomic features describing shape, morphology, kinetics and texture were extracted using previously reported CADx methods. Feature distributions with respect to biopsy condition were compared using the Kolmogorov-Smirnov statistic. For classification of lesions as benign or malignant, areas under the ROC curve (AUC) were determined for each feature using 2000 bootstrap iterations. Median of AUC and confidence interval for difference in AUC were determined for each feature by biopsy condition and compared using correction for multiple comparisons. The results were compared to those in a previous study of 361 cases (92 benign and 30 luminal A pre-biopsy lesions) collected at a different imaging center, wherein all features failed to demonstrate significant difference in median AUC for the classification task.

# RESULTS

Seven features of malignant cancers (irregularity, variance of radial gradient histogram, five texture features) demonstrated significant difference in features compared pre- and post-biopsy, while one feature of benign lesions (irregularity) demonstrated significant difference. All features failed to demonstrate significant difference in median AUC.

# CONCLUSION

Radiomic features extracted from DCE-MR images failed to show significant differences in AUC performance in classifying breast lesions as benign or malignant and may be robust for use in this task. This independent finding validates similar results in classification of breast lesions as benign or luminal A in images acquired at a different medical center.

## **CLINICAL RELEVANCE/APPLICATION**

Classification of breast lesions by extracted radiomic MRI signatures might not be sensitive to biopsy condition.



# PH231-SD-TUA7

# Cone Beam Tomosynthesis (CBT): A New Approach for 3D Surgical Imaging

Tuesday, Nov. 27 12:15PM - 12:45PM Room: PH Community, Learning Center Station #7

#### **Participants**

Lisa Last, MS, BS, Salt Lake City, UT (Presenter) Employee, nView Medical Inc; Research collaboration, NuVasive, Inc Cristian Atria, MBA,MS, Salt Lake City, UT (Abstract Co-Author) Employee, nView Medical Inc Collaboration, NuVasive, Inc Frederic Noo, Salt Lake City, UT (Abstract Co-Author) Research Grant, Siemens AG; Consultant, nView medical;

For information about this presentation, contact:

info@nviewmed.com

### PURPOSE

To assess a novel Cone Beam Tomosynthesis (CBT) 3D surgical imaging modality by assessing Image Quality (IQ) and dose when compared to Cone Beam Computed Tomography (CBCT).

# METHOD AND MATERIALS

The CBT system operates by acquiring fast fluoro acquisitions taken in a circular tomosynthesis geometry and reconstructing a 3D volume providing near real-time 3D images of the surgical scene. Both the CBT and CBCT system have a low dose mode and a high image quality (IQ) mode. Two patient scans were performed on each system using each mode. The high IQ mode in CBT was achieved using a stereotactic acquisition. To assess IQ, an accreditation phantom (Catphan-504, Phantom Laboratory, Salem, NY) was used to quantify image quality metrics, with a focus on metrics relevant to imaging for spinal fusion procedures: geometric accuracy and high-contrast resolution. Standard noise measurements (CNR) over homogenous bony, and soft tissue regions were recorded and two metrics were computed. Uniformity metric was computed as the difference (in Hounsfield Units (HU)) between the center and the edge of an imaged homogenous module. CNR was computed as the ratio of the contrast in a bony area over the noise in the surrounding water area. To assess dose, an anatomic phantom (RANDO®, RSD Phantoms, Long Beach, CA) was outfitted with 24 OSL dosimeters (nanoDotTM, Landauer, Glenwood, IL) placed both on the surface of the lung inside the phantom, and on the skin surface. The absorbed dose was computed by combining the 24 dosimeter readings.

## RESULTS

Initial CBT images have shown to have similar image quality when compared to CBCT. Uniformity (CBT vs CBCT) was 130.0 HU vs 92.6 HU for high IQ and 391.6 HU vs. 178.3 HU in low dose. CNR (CBT vs CBCT) was 11.0 vs 10.7 for high IQ mode. Absorbed Dose was reduced by more than 90% with CBT. (0.60mSv in CBT vs. 10.30mSv in CBCT in the low resolution mode, and 1.20mSv in CBT vs. 15.95mSv in CBCT for high resolution mode).

## CONCLUSION

When looking at high contrast bony anatomy, CBT is comparable to CBCT in terms of Uniformity, CNR, and MFT with considerable less dose to the patient. CBT shows potential to provide near-real time intraoperative 3D imaging for procedures such as spinal fusion.

#### **CLINICAL RELEVANCE/APPLICATION**

Cone Beam Tomosynthesis has potential to reduce dose and increase accuracy as compared to CBCT. CBT also provides an open geometry which has the potential for concurrent 3D imaging during surgery.



# QI009-EB-TUA

TIPS Ultrasound Improvement from a Different Angle: A Web-Based Training Lecture to Provide On-going Education to Ultrasonographers

Tuesday, Nov. 27 12:15PM - 12:45PM Room: QR Community, Learning Center Hardcopy Backboard

# Participants

Adonteng A. Kwakye, MD, Lexington, KY (*Presenter*) Nothing to Disclose Angela Stepp, RT, Lexington, KY (*Abstract Co-Author*) Nothing to Disclose Andres R. Ayoob, MD, Lexington, KY (*Abstract Co-Author*) Nothing to Disclose Halemane S. Ganesh, MD, lexington, KY (*Abstract Co-Author*) Nothing to Disclose Rashmi T. Nair, MD, Lexington, KY (*Abstract Co-Author*) Nothing to Disclose Adrian A. Dawkins, MD, Lexington, KY (*Abstract Co-Author*) Nothing to Disclose James T. Lee, MD, Lexington, KY (*Abstract Co-Author*) Nothing to Disclose Joseph W. Owen, MD, Lexington, KY (*Abstract Co-Author*) Nothing to Disclose

#### PURPOSE

At our institution, there is a high turnover rate for ultrasonographers, which leads to suboptimal quality of complex ultrasound (US) exams. Transjugular intrahepatic portosystemic shunt (TIPS) Doppler US is one of the more challenging exams performed on a routine basis in our department. The purpose of this study was to provide an on-going, readily available, educational opportunity to new or inexperienced ultrasonographers to refresh their understanding of Doppler US so that accurate and properly angle corrected TIPS Doppler US are routinely obtained.

#### METHODS

A web-based lecture (WBL) and quick reference handout were created that reviewed the Doppler equation, the importance of accurate angle correction, and the components of the TIPS Doppler US examination. The accuracy of angle correction for the main portal vein, proximal TIPS, middle TIPS, and distal TIPS were the focus of the lecture and handout. The WBL was made continuously available, and given as an in-person lecture for CE credit. The handout was made available in the ultrasound workroom and provided to attendees of the in-person lecture. The images from TIPS Doppler US studies were retrospectively reviewed 1 year prior to intervention, 3 months prior to intervention, immediately following intervention, and 3 months after intervention. Images were assessed for proper angle correction with the number of discordant angles recorded. The number of times the angle of incidence exceeded 60 degrees was recorded.

# RESULTS

The percentage of discordant angles 1 year prior to availability of the WBL (PreWBL) was 36% (35/96), and immediately after the WBL (PostWBL) was 17% (23/136). Control points 3 months prior to the WBL availability and 3 months after the WBL availability were assessed by the percentage of discordant angles, which were 42% and 22% respectively. The percentage of angles > 60° PreWBL was 20% (19/96) and PostWBL was 17% (23/136). The percentage of discordant angles PostWBL decreased for all measurement locations compared to PreWBL.

# CONCLUSION

Through increased communication and a web-based training lecture available to the ultrasonographers at our institution, there was an improvement in angle correction when performing TIPS Doppler ultrasound. On-going availability of the web-based lecture and handout should ensure high quality TIPS Doppler US on a continuing basis.



# QI011-EB-TUA

The Effects of a National Dissemination Project Aimed at Reducing Radiation Dose for Kidney Stone CT

Tuesday, Nov. 27 12:15PM - 12:45PM Room: QR Community, Learning Center Hardcopy Backboard

#### **Participants**

Melissa M. Shaw, BS, New Haven, CT (*Presenter*) Nothing to Disclose Priyadarshini Karthik, Reston, VA (*Abstract Co-Author*) Nothing to Disclose Debapriya Sengupta, MBBS, MPH, Reston, VA (*Abstract Co-Author*) Nothing to Disclose Judy Burleson, Reston, VA (*Abstract Co-Author*) Nothing to Disclose Mytheryi Chatfield, Reston, VA (*Abstract Co-Author*) Nothing to Disclose Mannudeep K. Kalra, MD, Boston, MA (*Abstract Co-Author*) Research Grant, Siemens AG; Research Grant, Canon Medical Systems Corporation Christopher Moore, MD, New Haven, CT (*Abstract Co-Author*) Consultant, Koninklijke Philips NV

#### For information about this presentation, contact:

melissa.m.shaw@yale.edu

## PURPOSE

Kidney stones will afflict approximately 9% of the population during their lifetime and are responsible for 2 million emergency department visits annually. Patients with renal colic are typically relatively young and prone to have multiple imaging studies per stone episode and throughout their lifetime. Despite 2012 American College of Radiology (ACR) Appropriateness Criteria promoting the use of reduced-radiation dose CT (RDCT) exams for kidney stone evaluation, recent data found a 2015-2016 mean dose length product (DLP) nationwide was 689 mGy\*cm, with less than 8% of renal colic CTs being reduced dose. The DOSE (Dose Optimization for Stone Evaluation) Project aims to promote the increased use of RDCT and reduce dose variability in kidney stone (KS) CT throughout the U.S. We performed a randomized, controlled trial to determine the effect of the DOSE intervention on radiation dose for KS CT.

#### METHODS

DOSE collaborated with the ACR Dose Image Registry (DIR) in Reston Virginia to identify facilities contributing CT for renal colic to their radiation dose registry. We identified exam study descriptors consistent with KS CT. Facilities were eligible for randomization if they contributed 40 or more single phase examinations using a KS CT descriptor. Facilities were randomized 50:50 by the DIR after stratification for demographics. Facilities randomized to intervention were blinded to DOSE staff and were recruited through an email inviting them to participate. Emails were sent to 30 facilities every two weeks with a reminder email to non-responding facilities after all facilities were notified. If a facility was interested, they would respond to DOSE via email or through the DOSE website seeking more information. If email responses were not received individualized phone calls were attempted. Interested facilities were free to choose the intervention components that best suited the facility. Intervention included access to free online educational modules (8.75 CMEs) and individualized consultation. Education modules consisted of 2 modules on the RadIQ platform (http://www.radiq.org/pagesStaticContent/RadIQCourses.aspx) ; the first providing RDCT images to allow users to increase diagnostic proficiency for KS and other significant findings with RDCT images. The second module provided an overview of CT scanner settings and their subsequent effects on dose. DOSE consultation consisted of conference calls to discuss facilities' obstacles for protocol change, provide PQI guidance, and provide an individualized consultation report including recommendations for RDCT protocols specific to facilities' scanner(s). Our statistical analysis sought to compare mean DLP for the baseline year (2015) and intervention year (2017) between control facilities and intervention facilities that were enrolled. Medians and means with 95% confidence intervals were compared using a Student' t test.

# RESULTS

The DIR identified 224 eligible facilities for calendar year 2015. Of these facilities, 108 were randomized to DOSE intervention. Of the 108 intervention facilities, 31 facilities accepted invitation to DOSE intervention. However, given the DIR allows multiple child facilities to be linked to a parent facility, there were two facilities that crossed over from control to intervention. These facilities were removed from the control group and counted towards intervention; resulting in 33 facilities that were intervened on (30% of attempted). Intervention and control facilities had no significant baseline differences in number of KSCT exams (N=50,700 and 54,034 respectively) nor mean DLP (682.87 and 676.41 mGy\*cm). Follow-up DLP for control and participating facilities were 626.76 and 538.44 mGy\*cm. The DLP decreased by 149.2 (95% CI: 5.87-170.76) mGy\*cm in the facilities undergoing intervention (P<0.05). In the control group mean facility DLP declined slightly over the two-year period (64.5 mGy\*cm, 95% CI 22.37-89.24) but this was not a significant change.

#### CONCLUSION

Practice quality improvement projects, facilitated by education and individualized consultation, can lead to significant reductions in radiation exposure. Collaborative efforts such as these can facilitate better adherence to the As Low As Reasonably Achievable (ALARA) principal. Future DOSE direction includes providing intervention to control facilities to further promote its important message. Funding: AHRQ Grant# R18HS023778



# QI116-ED-TUA1

Use of New Proforma for Pre-Procedure Documentation for Ultrasound and Fluoroscopy Guided Musculoskeletal Radiology Interventional Procedures Improves Adherence to ACR/SIR Practice Guidelines - A Quality Improvement Project Based on PDSA Cycle

Tuesday, Nov. 27 12:15PM - 12:45PM Room: QR Community, Learning Center Station #1

#### Participants

Daichi Hayashi, MD,PhD, Stony Brook, NY (*Presenter*) Nothing to Disclose Kwan Y. Chen, MD, Stony Brook, NY (*Abstract Co-Author*) Nothing to Disclose Michael A. Samuel, MD, Centereach, NY (*Abstract Co-Author*) Nothing to Disclose Mingqian Huang, MD, Syosset, NY (*Abstract Co-Author*) Nothing to Disclose Kevin S. Baker, MD, Stony Brook, NY (*Abstract Co-Author*) Nothing to Disclose Elaine S. Gould, MD, Stony Brook, NY (*Abstract Co-Author*) Consultant, Endo International plc

# For information about this presentation, contact:

daichi\_hayashi@hotmail.com

# PURPOSE

The American College of Radiology and Society of Interventional Radiology (ACR/SIR) together published a revised practice parameter for the reporting and archiving of interventional radiology procedures in 2014. According to this document, the preprocedural documentation "provides a baseline record of patient status and documents the indication for the procedure. It should be entered in the chart before the procedure.' We conducted a Fellow-led quality improvement project at our institution to improve adherence to ACR/SIR practice guidelines for preprocedure documentation prior to ultrasound or fluoroscopy guided musculoskeletal (MSK) radiology interventional procedures in the MSK section of our Radiology department.

#### METHODS

Our quality improvement project involved retrospective chart review and received IRB-exemption. ACR/SIR guidelines (revised in 2014) for imaging-guided procedures state preprocedure documentation should include: The plan for each procedure to be performed; Indication for procedure and brief history; Findings of targeted physical examination; Relevant laboratory and other diagnostic findings; Risk stratification, such as the American Society of Anesthesiologists Physical Status Classification; Documentation of informed consent. Based on this guideline, we identified 13 items that are considered pertinent for preprocedure planning to ensure performing the procedure safely by minimizing potential risk to patients. These items included the following: Name of procedure, procedure site, laterality (right or left, if relevant), requesting physician, history and indication, prior imaging (date and findings), physical examination findings, use of anticoagulation medications, allergies, labs (platelet counts and INR with dates), informed consent, ASA status, and plan for the procedure. One point was given to each item documented prior to the procedure, giving max score of 13 per case. First cycle of audit of preprocedure documentation of randomly selected 50 ultrasound or fluoroscopy guided MSK procedures (including steroid/anesthetic injections to joints, bursae and tendon sheaths, cyst aspiration, joint aspiration, arthrogram injection) performed within our Department of Radiology between October 2016 and September 2017, and revealed poor quality of documentation. Discussions were held among MSK radiology fellow, radiology residents and MSK attending radiologists and the main reasons for such poor performance were thought to include lack of awareness regarding ACR/SIR quidelines and a tool to help document required information efficiently and systematically. Therefore, we aimed to improve the quality of preprocedure documentation by creating a proforma for use within our electronic medical record (EMR) system enabling MSK fellows and/or residents to systematically collect and document necessary items. We then implemented the proforma in clinical practice and performed the second cycle of audit for 36 ultrasound or fluoroscopy guided MSK procedures (similar to those listed above) performed between October 2017 and March 2018.

#### RESULTS

Prior to the use of the proforma, the mean score per case was 3 for 50 procedures, giving overall adherence rate of 13.3%. More specifically, none of the cases had preprocedure documentation of history and indication, prior imaging, physical exam findings, anticoagulation medications, allergies, labs (platelet counts and INR), and ASA status. There was incomplete documentation of other items listed above. After the implementation of the proforma, all 13 items were recorded in 34 of 36 cases, and 12 items were recorded in the remaining 2 cases (in which wrong dates of prior imaging were recorded) making the overall adherence rate 99.6%.

#### CONCLUSION

Utilizing the new proforma in EMR has significantly improved quality of preprocedure documentation. This improvement is a result of a completion of Plan-Do-Study-Act cycle as advocated by the American Board of Radiology. Improving quality of pre-procedure documentation and making it almost 100% adherent to available guidelines can improve patient safety by stratifying risks and identifying potentially preventable adverse events.



## QI118-ED-TUA2

# Reducing Radiology Referral Form Inadequacies to Improve Patient Safety and Quality of Care

Tuesday, Nov. 27 12:15PM - 12:45PM Room: QR Community, Learning Center Station #2

#### Participants

Dinesh S. Baviskar, MD, MBBS, Thane - West, India (*Presenter*) Nothing to Disclose Sheetal B, Thane, India (*Abstract Co-Author*) Nothing to Disclose

For information about this presentation, contact:

dr.dineshsb@gmail.com

#### PURPOSE

Radiology request forms / referral forms are essential communication tools for Radiological investigations, however their importance is underestimated. Incomplete radiology request forms are common occurrences impacting the workflow and efficiency of the radiology departments in the hospitals world over. Incomplete request forms can lead to: Increase the risk of performing the wrong tests, Using incorrect protocols of imaging technique, Imaging the wrong patient, Inaccurate interpretation of the tests. The risks to patient safety and potential for delayed treatment, with time wasted and frustration experienced by the radiology staff makes it a significant problem. The tests may be repeated and this can result in avoidable unnecessary radiation exposure and delays in investigating and treating patients. The problem of inaccurately filled radiology request forms is a costly problem both for the organization and the patients. Although radiology department personnel need to pre-check before any investigation to mitigate the risks, it is essential to develop a culture of 'patient centered clinical behavior' to improve patient safety and deliver quality healthcare. As per our initial survey, the inadequacies in the referral form amount to 35 - 40 % of the randomly surveyed Radiology referral forms. Most of these inadequacies are avoidable and preventing them can go a long way to improve the quality of patient care.

#### **METHODS**

Our Aim : To reduce the incidence of the inadequacies in the Radiology referral forms filled by the physicians, to 50% of the current occurrences; within 4 months from the start of the project. We performed 3 PDSA cycles in this project over a period of 4 months. The following metrics were measured for each cycle: 1. Number of radiology referral forms evaluated 2. Incidence of errors (inadequacies) per modality 3. Incidence of Type of error - a. Patient data error - wrong MRN, wrong name, wrong sex. b. Clinical data error - wrong investigation, wrong side / site, absent / wrong previous medical / surgical history c. Other errors - Illegible writing, absent stamp / signature 4. Repeat / recall Rates for Radiology investigations 5. Survey of Radiology Department personnel (technicians, nurses, radiologists) with regards to Radiology Referral forms inadequacies - before and after our intended study. 6. Focus group Meeting - with the referring physicians. Challenges encountered: Acceptance of the goals to be achieved by the 'TEAM' members and sponsors Formulating a mechanism to gather information / data Presenting the data analysis to the stakeholders as an opportunity for improvement rather than a punitive / fault-identifying mechanism. Compliance of the Referring physicians. Sustaining the implementation of the positive outcomes. Overcoming Challenges: Team meetings & brain storming sessions with the team members, staff in Radiology department, out patient clinics and in the hospital departments. Focus group meetings with referring physicians. Sharing of the information and analysis with the higher management for further policy improvements.

#### RESULTS

We evaluated 2000 radiology referral forms in each PDSA cycle. The incidence of errors in these forms decreased by almost 30% at the end of third cycle, as compared to the first cycle. The commonest cause of errors was found to be illegible handwriting of the physician. The recall-retake rate of radiological investigations reduced by 80%. The surveys during each cycle showed increased acceptance of the interventions and increased physician satisfaction. Increased productivity was observed in the radiology department during this period. The patient satisfaction levels also increased.

# CONCLUSION

Improved interdisciplinary and physician-physician communication leads to tremendous improvement in the overall outcome of the diagnostic procedures, which definitely contributes to timely care and better patient outcomes. It also contributes towards improving patient safety by reducing the incidences of unnecessary recall and retake investigations.



## QI120-ED-TUA3

# Impact of a Standardized Reporting Format on the Quality of MRI Reports for Rectal Cancer Staging

Tuesday, Nov. 27 12:15PM - 12:45PM Room: QR Community, Learning Center Station #3

#### Participants

Shivan<sup>i</sup> R. Mahajan, MD, Mumbai, India (*Abstract Co-Author*) Nothing to Disclose Akshay D. Baheti, MD, Mumbai, India (*Presenter*) Nothing to Disclose Suman Kumar, Mumbai, India (*Abstract Co-Author*) Nothing to Disclose Nitin S. Shetty, MBBS, MD, Mumbai, India (*Abstract Co-Author*) Nothing to Disclose Suyash Kulkarni, Mumbai, India (*Abstract Co-Author*) Nothing to Disclose Avanish Saklani, Mumbai, India (*Abstract Co-Author*) Nothing to Disclose Reena Engineer, MD, Mumbai, India (*Abstract Co-Author*) Nothing to Disclose

#### For information about this presentation, contact:

shivani.mahajan@hotmail.com

#### PURPOSE

To assess the impact of using a structured reporting template in MRI reports for the staging of rectal cancer

#### **METHODS**

Standardized rectal cancer MRI reporting template was introduced in the radiology department of a dedicated academic cancer hospital in August 2017. We analyzed 100 MRI reports for rectal cancer staging that were generated from 1.1.2017 to 3.31.2018. These included 50 consecutive free text reports before the implementation of the template, and 50 consecutive standardized template based reports. These were made both by subspecialty oncoradiologists attached to the institute's colorectal tumor board, and also by non-subspecialty oncoradiologists. We assessed the quality of the reports by the number of parameters that were mentioned out of a total of 14 quality measures, which were pre determined in consultation with the institute's colorectal tumor board.

## RESULTS

A total of 87 patients (79% males; mean age: 44 years) with 100 reports were included. Before the implementation of the template, a median of 10 out of 14 items [range 6 to 13; interquartile range (IQR), 8-11 items]were reported. After introduction of the template, a median of 14 out of 14 items were reported(range 12-14; IQR 14-14 items).13 patients had both free text and template reports, and in this subgroup of patients the total parameters mentioned in the reports increased from a median value of 9(range 5-12) to a median value of 13 (range 12-14) The most commonly unreported parameters before the introduction of the template were the T staging (unreported in 42% cases), presence or absence of restricted diffusion in the tumor (39%), involvement of the anterior peritoneal reflection (35%) and presence or absence of extra- mural vascular invasion (25%). These improved to 98-100% reporting after template introduction. After the implementation of the template, the most common unreported para meter was tumoral T2 signal intensity (missed in 4% cases). The number of parameters mentioned increased from a median value of 9 to 14 amongst general oncoradiologists, and from a median value of 10 to14 amongst subspecialty oncoradiologists.

#### CONCLUSION

There was a significant improvement in the completeness of the MRI reports post implementation of the standardized template.



## QI122-ED-TUA4

## Improving Procedures Of Children MRI Under Sedation - Benefits From Quality Control Circle

Tuesday, Nov. 27 12:15PM - 12:45PM Room: QR Community, Learning Center Station #4

#### Participants

Jia Xiaoqian, Xian, China (*Presenter*) Nothing to Disclose Jianxin Guo, Xian, China (*Abstract Co-Author*) Nothing to Disclose Zhe Liu, Xian, China (*Abstract Co-Author*) Nothing to Disclose Miao Li, Xian, China (*Abstract Co-Author*) Nothing to Disclose Xiaoyu Wang, Xi'an, China (*Abstract Co-Author*) Nothing to Disclose Yannan Cheng, BS,BS, Xi'an, China (*Abstract Co-Author*) Nothing to Disclose Xingxing Tao, Xi'an, China (*Abstract Co-Author*) Nothing to Disclose Huifang Zhao, Xi'an, China (*Abstract Co-Author*) Nothing to Disclose Xianjun Li, Xian, China (*Abstract Co-Author*) Nothing to Disclose Chao Jin, Xian, China (*Abstract Co-Author*) Nothing to Disclose Yang Jian, PhD, MD, Xi An, China (*Abstract Co-Author*) Nothing to Disclose

#### For information about this presentation, contact:

363448088@qq.com

# PURPOSE

In children MR imaging, the failure rate of MRI examinations is considerably high in contrast to adult MRI due to motion artifacts even with administration of sedation. Quality control circle (QCC), a participatory management technique first established in Japan in 1962, has been widely used in medical and healthcare fields today aiming to increase the quality of medical service by improving medical workers' awareness of spotting and solving medical problems. In this work, we investigated the feasibility of using QCC to reduce the failure rate of the MR examinations for the sedated children and evaluated the improved workflow through our daily clinical practice. The proposed method of using QCC in children MRI might be also beneficial to other radiologic practice in the quality management and control.

#### **METHODS**

The QCC program was launched based on the QCC theory, and the basic steps of QCC program used in this study include: 1) Formation of the QCC Set up a QCC named Nice Image Circle, with a total of 16 circles members, including imaging doctors, image nurses, imaging technicians, pharmacologists, and registrars. 2) Determination of QCC theme Chose the theme through the Brainstorming theory: to reduce the failure rate of MRI in children requiring sedation. 3)Development of activity plan Made the Gantt chart in order to make plan which was approved by the ethics committee and conducted between October 2016 and May 2017 4) Survey of current situation and setting of target Firstly in the PACS system, the information of the MRI examination of children from October 2016 to January 2017 was investigated and the failure rate was 29.1%. Then, we calculated the target value according to the target calculation formula: the target value=current value- improvement value=current value - (current value × value of focus × ability of circle)=29.1%- (29.1%× 0.78 × 70%)=13.2%. 5) Analysis of the cause of failure First, a fishbone diagram demonstrated all possible reasons for failure rate of MRI in children requiring sedation Then, the focus problem of the failure of MRI in children according to the Pareto principle (insert related reference here), also known as the 80/20 rule, was: poor sedative effect 6) Selecting the principal causes By using the '5,3,1' method (insert related reference here) to score potential causes, three main reasons of the focus problem were selected according to the 80/20 rule (insert related reference here): lack of standard reservation process, lack of sedative assessment tools and irrational order of MR sequence; 7) Countermeasures According to the above situation, and using the Brain-storming theory and the 80/20 rule, the following measures were taken: Constructing a MRI quidance system for children: one to one education for parents, a WeChat platform (Tencent Inc, Shenzhen, China) for communication between reservations and scanning technicians, short-term sleep adjustment Setting up a sedation standard for children MRI: University of Michigan Sedation Scale was used to assess the degree of sedation for children and the score of 2 or 3 points was considered to be met the requirements of the MRI Adjusting the MRI program of children: according to the sequence of sequence noise from small to large 8) Survey after improvement After improvement, we investigated for three months in a row, and the failure rate dropped to 13.6% 9) Statistical methods All data were analyzed by using SPSS 20.0. Measured data were quoted as mean $\pm$ standard deviation and analyzed by Chi-square test. P < 0.05 was considered statistically significant.

#### RESULTS

1)A total of 192 children were investigated, of which the pre and post improvement were 101 and 91, respectively; 2)The failure rate of MRI was reduced from 29.1% to 13.6% (P < 0.05), the target achievement rate was 97.5%

#### CONCLUSION

Quality management tools can effectively reduce the failure rate of MRI examination for children and improve the inspection process and quality. The children MRI optimization process based on scientific management method is standardized, quantified and feasible. It can effectively identify invalid inspections, reduce costs and improve efficiency, and is worthy of promotion.



# RO211-SD-TUA1

Institutional Experience Treating Locally Advanced Non-Melanomatous Cutaneous Malignancies of the Head and Neck with Intensity Modulated Radiation Therapy (IMRT)

Tuesday, Nov. 27 12:15PM - 12:45PM Room: RO Community, Learning Center Station #1

# Participants

Lucas Gilbride, MD, Milwaukee, WI (*Presenter*) Nothing to Disclose Mohamed Abdelhakiem, Milwaukee, WI (*Abstract Co-Author*) Nothing to Disclose Adam D. Currey, MD, Milwaukee, WI (*Abstract Co-Author*) Nothing to Disclose Jared R. Robbins, MD, Milwaukee, WI (*Abstract Co-Author*) Nothing to Disclose

## PURPOSE

Advanced non-melanomatous skin cancers of the head and neck pose a challenge to treating physicians due to complicated and often morbid surgical procedures. Superficial radiation therapies can be difficult to deliver due to irregular body/tumor contours and nearby critical structures. Therefore different forms of intensity modulated radiation therapy (IMRT) may provide an effective and safe treatment modality for these patients.

#### **METHOD AND MATERIALS**

Sixty-seven patients with basal cell carcinoma (n=19) or cutaneous squamous cell carcinoma (n=48) of the head and neck treated between 2004 and 2018 with IMRT at a single institution were retrospectively reviewed. Baseline characteristics of the patients included: age (mean 73.3 yrs), innumocompromised (n=14), recurrent disease (n=31), Stage III/IV (n=44), tumor size (mean 3.9 cm), satellitosis (n=20), poorly differentiated histology (n=24), and PNI (n=20). Surgery was performed prior to IMRT in 25 patients with 12 having positive margins. Chemotherapy was used in 11 patients. Radiation therapy doses ranged from 37.5-70 Gy (mean 57.1 Gy) at 1.8-3.0 Gy/fraction.

## RESULTS

After a median follow up of 32 months there were 20 local failures, 6 regional failures, and 3 distant failures leading to an estimated median recurrence free survival of 50.2 months. The estimated median overall survival was 72.2 months. Almost all patients experienced acute skin toxicity during the course of their treatment but only 5 patients experienced Grade 3 skin toxicity. The most common late toxicities were alopecia (n=38), telangiectasia (n=28), hypopigmentation (n=17), hyperpigmentation (n=5), skin atrophy (n=7), fibrosis (n=4), and skin ulceration (n=5). One patient developed osteoradionecrosis but the tumor had extensive involvement of the external auditory canal. However, no patients demonstrated evidence of brain radionecrosis.

#### CONCLUSION

Locally advanced non-melanomatous cutaneous malignancies of the head and neck pose a unique challenge to treating physicians. IMRT providess a treatment option that affords patients a durable recurrence free survival with acceptable toxicity and reasonable cosmetic outcomes.

## **CLINICAL RELEVANCE/APPLICATION**

This single institution experience demonstrates the effectiveness and safety of treating advanced non-melanomatous malignancies of the head and neck with IMRT.



# RO212-SD-TUA2

A Correlation Study of Epidermal Growth Factor Receptor Gene Mutations, Computed Tomography Image Findings, and Clinical Features Among Patients with Pulmonary Adenocarcinoma

Tuesday, Nov. 27 12:15PM - 12:45PM Room: RO Community, Learning Center Station #2

**FDA** Discussions may include off-label uses.

#### Participants

Tongxin Xu, Shijiazhuang, China (*Presenter*) Nothing to Disclose Gaofeng Shi, MD, Shijiazhuang, China (*Abstract Co-Author*) Nothing to Disclose

#### PURPOSE

To explore the correlation between computed tomography (CT) findings and epidermal growth factor receptor (EGFR) status, and the correlation between clinical features and EGFR mutations.

# METHOD AND MATERIALS

The study cohort included 192 pulmonary adenocarcinoma patients (82 men and 110 women; age range,32-83 years)who underwent tumor resection at No.4 Hospital of Hebei Medical University between January 2015 and October 2015. Of these patients, 108 had symptoms of cough, expectoration, and/orhemoptysis. There were 56 smokers and 136 non-smokers, 46 drinkers and 146 nondrinkers. CT scans were conducted on a dual-source CT (SOMATOM Definition Flash, Siemens Healthcare, Erlangen, Germany) at 120 kV, 110mAs, 0.2-s rotation, 0.6 pitch, and 128×0.6 collimation. CT images were evaluated for the presence of ground glass opacity (GGO), cavitation, marginal spiculation, marginal lobulation, and pleural indentation. GGO proportions and maximum diameters of tumors were measured.

#### RESULTS

EGFR mutationswerefound in 115 patients (59.8%) with a significantly greater mutation rate in females (73.6%; p<0.001). Wildtype EGFR was more commonin smokers(p<0.001). The mutation was more commonin patients without symptoms (p=0.022). The mutation rate in nondrinkers and drinkers was 65.1% and 43.4%, respectively (p=0.009). EGFR mutation occurred more often in patients with atumor diameter of <=30 mm (p=0.003). Mutation was more commonin tumors with pleural indentation (p=0.002). The EGFR mutation rate wasnot correlated with GGO, speculation, lobulation, or cavitation. The mutation of exon19 was more commonin tumors with GGO (p=0.013).

# CONCLUSION

EGFR mutation wasmore prevalent in females without symptoms, who neithersmoked nor drank alcohol. The mutation occurred more frequently in tumors with pleural indentation and a diameter <=30 mm. The mutation rate of exon19 was higher in tumors with GGO.

# **CLINICAL RELEVANCE/APPLICATION**

(dealing with EGFR mutation) "EGFR mutation was more prevalent in females without symptoms, who neither smoked nor drank alcohol. The mutation occurred more frequently in tumors with pleural indentation and a diameter <=30 mm. The mutation rate of exon19 was higher in tumors with GGO. EGFR mutation is recommended in helping to improve patient management in their treatment plan."



# RO213-SD-TUA3

Evaluation of Focal Liver Reaction after Proton Beam Therapy for Liver Metastasis Examined Using Gd-EOB-DTPA Enhanced Hepatic Magnetic Resonance Imaging

Tuesday, Nov. 27 12:15PM - 12:45PM Room: RO Community, Learning Center Station #3

# Participants

Shigeyuki Takamatsu, MD, PhD, Kanazawa, Japan (*Presenter*) Nothing to Disclose Miu Mizuhata, MD, Kanazawa, Japan (*Abstract Co-Author*) Nothing to Disclose Satoshi Shibata, Kanazawa, Japan (*Abstract Co-Author*) Nothing to Disclose Yoshitaka Sato, Fukui, Japan (*Abstract Co-Author*) Nothing to Disclose Sayuri Bou, Fukui, Japan (*Abstract Co-Author*) Nothing to Disclose Hiroyasu Tamamura, Fukui, Japan (*Abstract Co-Author*) Nothing to Disclose Satoshi Kobayashi, MD, Kanazawa, Japan (*Abstract Co-Author*) Nothing to Disclose Tomoyasu Kumano, Ishikawa, Japan (*Abstract Co-Author*) Nothing to Disclose Gabata Toshifumi, Kanazawa, Japan (*Abstract Co-Author*) Nothing to Disclose

#### For information about this presentation, contact:

shigerad@staff.kanazawa-u.ac.jp

#### PURPOSE

Focal liver parenchymal damage in radiotherapy is described as the focal liver reaction (FLR); the threshold doses (TDs) for FLR in the background liver have been analyzed in proton beam therapy (PBT). To develop a safer approach for PBT, both TD and liver volume changes are considered clinically important in predicting the extent of damage before treatment, and subsequently in reducing background liver damage. We investigated appearance time, TDs and volume changes regarding FLR after PBT for normal liver with hepatic metastasis.

### **METHOD AND MATERIALS**

This retrospective analysis of the data was approved by the institutional review board of our institution. Patients who were treated using PBT and were followed up using gadolinium ethoxybenzyl diethylenetriamine pentaacetic acid-enhanced magnetic resonance imaging (Gd-EOB-DTPA MRI) after PBT were enrolled. Eight patients were eligible for analysis (median age, 74 years). The primary lesions were colon cancer (6 cases), cholangiocellular carcinoma (1 case) and pancreas cancer (1 case), total doses of 71.2 (60-83.6) cobalt Gy equivalent (CGE), 17 (8-34) fractions (Fr), and BED10: 109CGE (72-115). MRI was acquired at the end of treatment, and at 1, 2, 3 and 6 months after PBT. We defined the FLR as a clearly depicted hypointense area on the hepatobiliary phase of Gd- EOB-DTPA MRI, and we visually monitored TDs. Based on the TD defined by MRI at 3 months after PBT, we hypothesized the irradiated liver area receiving a dose greater than the TD isodose lines at planning MRI as the destined FLR area (dFLR). The volume of the dFLR was calculated and compared with the FLR volume on follow-up MRI.

# RESULTS

FLR was depicted in all lesions at 3 months after PBT. TDs were expressed as the 2-Gy equivalent dose, 24.4Gy (a/B = 2 Gy), 25.3Gy (a/B = 3 Gy) and 24.2Gy (a/B = 8 Gy). The volume of the dFLR area decreased and the residual liver volume increased, particularly during the initial 3 months.

# CONCLUSION

This study established the FLR dose and volume change for normal liver, which might be useful in the prediction of remnant liver volume for normal liver.

## **CLINICAL RELEVANCE/APPLICATION**

We could investigate the FLR dose and volume change for normal liver, which might be useful in the prediction of remnant liver volume after PBT for normal liver.



# RO214-SD-TUA4

Pulmonary Metastases from Pancreatic Cancer: Frequency of Atypical Radiological Features and Comparison with Pulmonary Metastases from Colorectal Cancer

Tuesday, Nov. 27 12:15PM - 12:45PM Room: RO Community, Learning Center Station #4

## Participants

Ilaria Vicentin, MD, Vicenza, Italy (*Presenter*) Nothing to Disclose Mattia Pecorilla, MD, Milano, Italy (*Abstract Co-Author*) Nothing to Disclose Roberto Ronza, Caserta, Italy (*Abstract Co-Author*) Nothing to Disclose Cristiano Sgrazzutti, Milano, Italy (*Abstract Co-Author*) Nothing to Disclose Claudia Khouri Chalouhi, MD, Settala, Italy (*Abstract Co-Author*) Nothing to Disclose Angelo Vanzulli, MD, Segrate, Italy (*Abstract Co-Author*) Travel support, Bracco Group

#### For information about this presentation, contact:

ilaria.vicentin@libero.it

#### PURPOSE

To compare the frequency of radiological CT features of lung metastases from pancreatic adenocarcinoma (PC) versus those from colorectal cancer (CRC).

#### **METHOD AND MATERIALS**

In this retrospective observational study 2 radiologists independently reviewed CT images of 182 patients with newly detected pulmonary metastases (86 with PC, 96 with CRC) diagnosed between October 2005 and December 2017. Lung lesions were classified into 5 categories on the basis of the radiological aspect: solid nodule with smooth margins, solid nodule with spiculated margins, cavitated nodule, solid nodule with halo sign, ground glass nodule. In case of multiple metastases, the two largest lesions or those with different features were considered. For examinations with disagreement between the 2 radiologists, a consensus review was obtained.

## RESULTS

We evaluated 165 pulmonary metastases from PC and 172 pulmonary metastases from CRC. Among those from PC, 64(38,8%) were solid with smooth margins, 25(15,2%) were solid with spiculated margins, 32(19,4%) were cavitated, 33(19,9%) were solid with halo sign, 11(6,6%) were ground glass. Among those from CRC, 108(62,8%) were solid with smooth margins, 38(22,1%) were solid with spiculated margins, 20(11,6%) were cavitated, 4(2,3%) were solid with halo sign, 2(1,2%) were ground glass.

## CONCLUSION

CT features of pulmonary metastases from PC are very different from those of colorectal origin. In particular, an increased frequency of ground glass components (ground glass nodules and solid nodules with halo sign) emerged in pulmonary metastases from PC compared to those from CRC (26.5% vs 3.5%); in pulmonary metastases from CRC solid nodules with smooth margins were prevalent (62.8% vs 38.8% of pancreatic metastases).

#### **CLINICAL RELEVANCE/APPLICATION**

Pulmonary metastases from Pancreatic Cancer show peculiar radiological features, in particular when considering the ground glass components which are significantly more frequent than in Colorectal metastases.



## UR183-ED-TUA7

Bigger Can Sometimes Mean Better: Assessing Response of Novel Anti-Cancer Drugs in Metastatic Renal Cell Carcinoma

Tuesday, Nov. 27 12:15PM - 12:45PM Room: GU/UR Community, Learning Center Station #7

# Participants

Matthew J. Seager, MBChB, London, United Kingdom (*Presenter*) Nothing to Disclose Pawan Patel, MD, London, United Kingdom (*Abstract Co-Author*) Nothing to Disclose Lisa Pickering, London, United Kingdom (*Abstract Co-Author*) Nothing to Disclose Michael Gonsalves, MBBS, London, United Kingdom (*Abstract Co-Author*) Nothing to Disclose

For information about this presentation, contact:

matthew.seager1@nhs.net

# **TEACHING POINTS**

The purpose of this exhibit is: To review the indications for the use of novel anticancer agents in metastatic renal cell carcinoma (RCC) To review the mechanisms of action of novel anticancer agents used in metastatic RCC To illustrate the problems with traditional methods of radiological response assessment in this setting and review other methods of assessment To illustrate common side effects associated with these drugs

## **TABLE OF CONTENTS/OUTLINE**

1. The common subtypes of RCC and their genetic bases 2. The indications for and mechanisms of actions of: a. The passive immunotherapy agents: the antiangiogenics b. The active immunotherapy agents: nivolumab c. The mechanistic target of rapamycin inhibitors 3. Imaging response assessment - the benefits, problems and example applications: a. Response Evaluation Criteria in Solid Tumours (RECIST) 1.1 b. Choi and Modified Choi Criteria c. Immune RECIST 4. Common side effects of the novel metastatic RCC agents with examples



## UR184-ED-TUA8

Missed Lesions on Prostate 3TmpMRI: What Do We Assigned A PI-RADS Score 2, Which Were High-Grade Tumor on Whole Mount Histopathology

Tuesday, Nov. 27 12:15PM - 12:45PM Room: GU/UR Community, Learning Center Station #8

# Participants

Amirhossein Mohammadian Bajgiran, MD, Los Angeles, CA (*Presenter*) Nothing to Disclose Sepideh Shakeri, Los Angeles, CA (*Abstract Co-Author*) Nothing to Disclose Sohrab Afshari Mirak, MD, Los Angeles, CA (*Abstract Co-Author*) Nothing to Disclose Anthony Sisk, DO, Los Angeles, CA (*Abstract Co-Author*) Nothing to Disclose Ely R. Felker, MD, Los Angeles, CA (*Abstract Co-Author*) Nothing to Disclose David S. Lu, MD, Los Angeles, CA (*Abstract Co-Author*) Nothing to Disclose Johnson; Research Grant, Johnson & Johnson; Consultant, Bayer AG; Research Grant, Bayer AG; Speaker, Bayer AG Steven S. Raman, MD, Santa Monica, CA (*Abstract Co-Author*) Nothing to Disclose

#### For information about this presentation, contact:

ambajgiran@ucla.edu

#### **TEACHING POINTS**

1- Review PI-RADS v2 2-Review of 3T mpMRI imaging findings of missed lesions (e.g. PI-RADSv2 score 2 lesions proven to be highgrade(>= 3+4 Gleason Score ) on histopathology

### TABLE OF CONTENTS/OUTLINE

- Brief explanation of PIRADS V2 Scoring for each clinical sequence (T2-weighted, Diffusion weighted imaging(DWI), Dynamic contrast-enhanced (DCE) imaging) - Scoring method for peripheral lesions - Scoring method for transition zone lesions - Review 3T mp-MR Imaging of missed lesions with PI-RADS v2 2 but Gleason score >= 3+4 (T2 weighted, Diffusion weighted imaging(DWI), Dynamic contrast-enhanced (DCE) imaging, Pathology)



# VI161-ED-TUA9

# Line of Sight: Multi-Modality Techniques for Challenging Tissue Biopsies

Tuesday, Nov. 27 12:15PM - 12:45PM Room: VI Community, Learning Center Station #9

FDA Discussions may include off-label uses.

#### Awards

## **Identified for RadioGraphics**

#### Participants

Mark D. Sugi, MD, Scottsdale, AZ (*Abstract Co-Author*) Nothing to Disclose Jeffry S. Kriegshauser, MD, Phoenix, AZ (*Presenter*) Research support, General Electric Company William G. Eversman, MD, Scottsdale, AZ (*Abstract Co-Author*) Nothing to Disclose Sailen G. Naidu, MD, Phoenix, AZ (*Abstract Co-Author*) Nothing to Disclose Grace Knuttinen, MD, PhD, Scottsdale, AZ (*Abstract Co-Author*) Speakers Bureau, Abbott Laboratories; Consultant, Abbott Laboratories Sadeer Alzubaidi, MD, Birmingham, MI (*Abstract Co-Author*) Nothing to Disclose Christopher Czaplicki, Phoenix, AZ (*Abstract Co-Author*) Nothing to Disclose Rahmi Oklu, MD,PhD, Phoenix, AZ (*Abstract Co-Author*) Nothing to Disclose

#### For information about this presentation, contact:

sugi.mark@mayo.edu

#### **TEACHING POINTS**

1. To illustrate multi-modality strategies for obtaining tissue samples in cases made complex by lesion location, variable enhancement characteristics or other clinical factors. 2. To highlight specific techniques and adjunct pre-sampling procedures that may facilitate targeted tissue biopsy. 3. To recognize, through case-based imaging, opportunities for image-guided procedures that may otherwise have been sent for surgical biopsy.

#### TABLE OF CONTENTS/OUTLINE

Target Lesion Location. Enhancement characteristics. Clinical factors. Techniques Patient position, gantry angle. Ultrasound GPS and contrast-enhanced ultrasound. Hydrodissection. Transosseous approach. Stylet techniques, e.g. blunt and lever. Adjunct procedures, e.g. phrenic nerve block.



# VI162-ED-TUA10

Management of Classic Budd-Chiari Syndrome and Hepatic Vena Cava Budd-Chiari Syndrome (HVC-BCS): A Pictorial Review

Tuesday, Nov. 27 12:15PM - 12:45PM Room: VI Community, Learning Center Station #10

# Participants

Venkatesh Arumugam Murugan, Worcester, MA (*Presenter*) Nothing to Disclose Daniel Burritt, MD, Worcester, MA (*Abstract Co-Author*) Nothing to Disclose Hao Xu, Xuzhou, China (*Abstract Co-Author*) Nothing to Disclose Hai Bin Shi, MD, Nanjing, China (*Abstract Co-Author*) Nothing to Disclose Ducksoo Kim, MD, Boston, MA (*Abstract Co-Author*) Nothing to Disclose Young H. Kim, MD, Worcester, MA (*Abstract Co-Author*) Nothing to Disclose

#### For information about this presentation, contact:

venkatesh.murugan@umassmemorial.org

# **TEACHING POINTS**

1. Classical Budd-Chiari Syndrome (BCS) occurs more commonly in Western populations while Hepatic Vena Cava Budd-Chiari Syndrome (HVC-BCS) is seen predominately in East Asia. 2. The etiology of Classical BCS is attributed to myeloproliferative neoplasms in most cases while most HVC-BCS cases remain idiopathic.3. Classical BCS presents as acute abdominal pain, ascites, and hepatomegaly while HVC-BCS presents more insidiously with chronic abdominal pain and extensive portosystemic varices.4. Treatment of these entities differ as Classical BCS is amenable to medical management or transjugular intrahepatic portosystemic shunt (TIPS) while angioplasty and stenting is more effective in the treatment of HVC-BCS.5. Prognosis post intervention.

## **TABLE OF CONTENTS/OUTLINE**

Pathophysiology of Budd-Chiari syndrome Classic Budd-chiari syndrome vs Hepatic vena cava Budd Chiari syndrome (HVC-BCS) Clinical manifestations of Budd-Chiari syndrome Treatment options for Classic Budd-Chiari syndrome Treatment options for HVC-BCS Summary



# VI163-ED-TUA11

A Novel Approach to Sedation Management for Interventional Radiology Procedures-Utility of Dexmedetomidine

Tuesday, Nov. 27 12:15PM - 12:45PM Room: VI Community, Learning Center Station #11

# Participants

Emiko Chiba, MD, Saitama, Japan (*Presenter*) Nothing to Disclose Kohei Hamamoto, MD, Saitama, Japan (*Abstract Co-Author*) Nothing to Disclose Osamu Tanaka, MD, Saitama, Japan (*Abstract Co-Author*) Nothing to Disclose

## **TEACHING POINTS**

To manage the patient's pain and discomfort during procedure is important in interventional radiology (IR). Dexmedetomidine is a relatively new sedative drug that can be applied for sedation during IR procedures as substitute for general anesthesia. This drug has several advantages compared to other sedative drugs, such as the ease in the ability to control the sedative level and no respiratory depression. The purpose of this exhibit is to describe the efficacy of dexmedetomidine for sedation during IR procedures.

## TABLE OF CONTENTS/OUTLINE

1. The basic pharmacological mechanism and features 2. Application of dexmedetomidine. 3. The preprocedural assessment and periprocedural management 4. The feasibility and efficacy of dexmedetomidine during IR procedures 5. Tips and points for the use of dexmedetomidine



# VI225-SD-TUA1

Tumescence Anesthesia Solution-Assisted Laser Ablation Treatment of Lower Limb Varicose Veins: Effect of Temperature of Tumescence Anesthesia Solution on Intraoperative and Postoperative Pain, Clinical Observations, and Nursing Care

Tuesday, Nov. 27 12:15PM - 12:45PM Room: VI Community, Learning Center Station #1

#### Participants

Zhu Chen, Changsha, China (Presenter) Nothing to Disclose

For information about this presentation, contact:

chenzhu415@csu.edu.cn

# PURPOSE

To investigate the effect of cold and room temperature tumescence anesthesia solution (TAS) on the intraoperative and postoperative pain associated with the treatment of lower limb varicose veins via endovenous laser ablation (EVLA).

## **METHOD AND MATERIALS**

Based on the TAS temperature, 51 patients were divided into two groups: Group A (n=26) received room temperature (24°C) TAS, and group B (n=25) received cold (4°C) TAS.A numerical rating scale (NRS) was used to evaluate pain on the day of surgery and 3 days after the operation, and the data were summarized. Perioperative and intraoperative nursing care and clinical observations were performed following a generalized standard. We conducted a thorough and comprehensive nursing care with regard to preoperative preparation, intraoperative nursing coordination, postoperative handling, perioperative pain assessment, and many other aspects, primarily observing the role that TAS plays in safety and comfort during EVLA and summarizing the precautions during the treatment.

## RESULTS

During the operation, percentages of patients who did not feel significant pain in groups A and B were 30.8% and 64%, respectively. Percentage of patients without pain in group A was lower than that in group B, and this difference was significant (P<0.05). Average NRS scores of patients in the two groups on the day of surgery and on postoperative days 1, 2, and 3 were 4.3 and 2.1, 3.5 and 1.0, 3.0 and 0.8, and 1.6 and 0.3, respectively. Average postoperative NRS scores on the day of surgery and the following three days of group A were higher than those of group B, and these differences were significant (P<0.05). On postoperative day 1, only 30.8% of the patients in group A resumed their daily activities, whereas 68% of those in group B did so. The percentage of patients who resumed their daily activities in group A was significantly smaller than that of group B (P<0.05).

## CONCLUSION

The application of TAS during the treatment of lower limb varicose veins via EVLA improves patient safety and comfort; cold TAS reduces intraoperative and postoperative pain more effectively than room temperature TAS; and the nurses of the ward and the operation room should work with doctors to successfully complete the entire treatment via thorough and comprehensive perioperative nursing.

# **CLINICAL RELEVANCE/APPLICATION**

The use of tumescence anesthesia solution (TAS) allows patients to avoid general anesthesia and alleviates pain.



## VI226-SD-TUA2

The Applications of Time Resolved Imaging of Contrast Kinetics (TRICKS) in the Assessment of the Proximal Venous System of Dialysis Patients

Tuesday, Nov. 27 12:15PM - 12:45PM Room: VI Community, Learning Center Station #2

#### Awards Student Travel Stipend Award

# Participants

Maira Hameed, MA,BMBCh, London, United Kingdom (*Presenter*) Nothing to Disclose Cillian D. McNamara, BMBCh,MSc, London, United Kingdom (*Abstract Co-Author*) Nothing to Disclose Wladyslaw M. Gedroyc, MBBS, MRCP, London, United Kingdom (*Abstract Co-Author*) Nothing to Disclose

#### For information about this presentation, contact:

mhameed@ic.ac.uk

# PURPOSE

The assessment of the proximal venous system is vital in dialysis patients. It has applications in cases with difficult vascular access as well complications in established dialysis patients such as, graft stenosis and thrombotic occlusion. Historically, this has proved to be challenging. Venography is typically inappropriate due to the osmotic load imposed and contrast toxicity. In the case of linear gadolinium-based contrast agents, the risk of nephrogenic systemic fibrosis (NSF) is well documented. We present our novel technique which harnesses first pass time resolved imaging of contrast kinetics (TRICKS); a form of time resolved magnetic resonance angiography (MRA). This enables dynamic, selective, three-dimensional MRA with high temporal and spatial resolution.

## METHOD AND MATERIALS

Peripheral veins were cannulated in both upper limbs. 1ml of a 1 in 9 diluted macrocyclic gadolinium compound were injected intravenously for a first pass study on each side. All studies were performed with a 1.5 T MRI scanner. Patients were scanned head-first, supine with arms positioned alongside the body. TRICKS sequences covering the superior vena cava, brachiocephalic, subclavian and axillary veins bilaterally were acquired.

#### RESULTS

A total of 69 TRICKS studies have been performed in a large renal unit. All studies were diagnostic without reported complications. The applications included, assessment of suspected graft dysfunction, central venous occlusion complicating long term dialysis lines and vascular access planning.

## CONCLUSION

We have utilised TRICKS sequences to successfully image the proximal veins of dialysis patients in a large renal unit. This represent a safe, rapid and readily reproducible tool. It offers improved temporal resolution compared to conventional contrast enhanced MRA, and enables selective venous imaging of a high spatial resolution. Our method involves much lower doses of contrast than conventional MRA only using macrocyclic compounds not associated with NSF. This sequence does not depend on accurate operator timing of contrast bolus delivery.

#### **CLINICAL RELEVANCE/APPLICATION**

Time-resolved imaging of contrast kinetics MRA provides a safe, high resolution, dynamic diagnostic approach in the challenging cohort of dialysis patients. It visualises complex, often bilateral central venous stenosis and therefore allows appropriate decision making in the creation of successful dialysis access.



## VI227-SD-TUA3

# Incidence of Post-Biopsy Arteriovenous Fistula in Native and Transplant Kidneys

Tuesday, Nov. 27 12:15PM - 12:45PM Room: VI Community, Learning Center Station #3

# Awards

# Student Travel Stipend Award

#### Participants

Abhimanyu Aggarwal, MD, Norfolk, VA (*Presenter*) Nothing to Disclose Victor Fong, MD, Norfolk, VA (*Abstract Co-Author*) Nothing to Disclose Harlan L. Vingan, MD, Virginia Beach, VA (*Abstract Co-Author*) Nothing to Disclose

# PURPOSE

The aim of this study was to compare the incidence of arteriovenous fistula (AVF) complication following CT guided biopsy of native versus transplanted kidneys.

#### **METHOD AND MATERIALS**

Retrospective analysis was performed on 278 CT guided biopsies of native and transplant kidneys in adults at a tertiary care teaching hospital from January 1, 2015 to December 31, 2016. Patient inclusion criteria included age between 18 and 90 years old; male or female; and both outpatients and inpatients. Biopsies targeted specifically for renal masses were excluded. All biopsies were performed under CT guidance by a fellowship trained interventional radiologist or diagnostic radiology resident under direct supervision. Medical chart review for each patient to identify biopsy-related complications extended up to 90 days post-procedure.

## RESULTS

Of the 278 biopsies performed during the study period, 111 (40%) were done on native kidneys while 167 (60%) on transplanted kidneys. A total 11 AVFs were identified on post-procedure Doppler renal ultrasound; 1 was in a native kidney versus 10 observed in transplanted kidneys. Therefore the incidence was 0.9% for native kidneys and 6.0% for transplanted kidneys (p=0.03), 95% confidence interval for percent difference (0.2, 9.8). 2 of the transplanted kidney biopsies with AVFs had significant anemia/bleeding which required interventional selective coil embolization of discovered pseudoaneurysm. No further intervention required in the single native kidney post-biopsy AVF case.

## CONCLUSION

This single center, retrospective study shows a statistically significant greater incidence of arteriovenous fistula formation after CT guided biopsy in transplant kidneys compared to native kidneys.

## **CLINICAL RELEVANCE/APPLICATION**

This is the first known study recording arteriovenous fistula formation after CT-guided biopsy by interventional radiologists. Although renal post-biopsy arteriovenous fistula formation is low, the occurrence is greater in transplanted compared to native kidneys. Recognizing this can aid the radiologist and patient for informed consent of potential complications.



# VI228-SD-TUA4

Increased Hepatic Metastatic Growth following Radiofrequency Ablation

Tuesday, Nov. 27 12:15PM - 12:45PM Room: VI Community, Learning Center Station #4

# VA

# Participants

Haixing Liao, PhD, Jerusalem, Israel (Presenter) Nothing to Disclose

Aurelia Markezana, MSc, Jerusalem, Israel (Abstract Co-Author) Nothing to Disclose

Muneeb Ahmed, MD, Boston, MA (*Abstract Co-Author*) Research Grant, General Electric Company; Stockholder, Agile Devices, Inc; Scientific Advisory Board, Agile Devices, Inc

Jianxing He, MD, Guangzhou, China (Abstract Co-Author) Nothing to Disclose

Eithan Galun, MD, PhD, Jerusalem, Israel (Abstract Co-Author) Nothing to Disclose

S. Nahum Goldberg, MD, Ein Kerem, Israel (*Abstract Co-Author*) Consultant, AngioDynamics, Inc; Consultant, Cosman Medical, Inc; Consultant, XACT Robotics;

#### For information about this presentation, contact:

liaohaixing4@gmail.com

# PURPOSE

To elucidate the effect of radiofrequency ablation (RFA) on metastatic growth in the liver.

# METHOD AND MATERIALS

Sixty mice were used in this institutional animal care and use committee-approved study. First, a mouse hepatic metastasis model was established by implanting 2\*105 tumor cells via splenic injection followed by immediate splenectomy. Two mouse colorectal cancer tumor cell lines, CT26 and MC38, were injected into 24 Balb/C and 36 C57B/6 mice, respectively. Next, animals were randomized to receive either standardized RFA or a sham procedure 24hr post-transplantation. Procedures were performed by means of laparotomy that exposed the liver surface for placement of a 21-gauge needle with a 1-cm exposed tip. Energy was titrated to a mean temperature of 70°C±1 for 300sec. Sham procedures consisted of electrode placement without energy application. The whole liver was harvested at 14 days for CT26 and 21 days for MC38 to permit quantification of tumors. Immunohistochemistry was also performed for Ki-67 and CD-34 to measure proliferative indexes and microvascular density, respectively. Data were compared with analysis of variance and two-tailed Student t test.

#### RESULTS

For both tumor lines, RFA of  $3.5\%\pm0.02$  of the mouse liver volume induced an increased tumor load distributed throughout the entire liver in comparison to that of sham procedure (RFA vs Sham:  $68.9\pm25.0$  vs  $21.1\pm14.2$ , P<0.001 for CT26;  $100.6\pm60.7$  vs  $43.0\pm22.4$ , P<0.05 for MC38, respectively). A corresponding significant elevation of Ki-67 positive cells was noted indicating marked increased hepatocyte proliferation (CT26:  $199.3\pm53.3$  vs  $58.0\pm33.0$ ; MC38: $138.4\pm56.2$  vs  $33.2\pm24.3$ ; P<0.0001, both comparisons). Additionally, CD-34 positive staining was likewise elevated following RFA indicating increased neovasculation and angiogenesis (CT26:  $63.2\pm33.4$  vs  $13.8\pm5.1$ ; MC38:  $29.1\pm5.6$  vs  $16.3\pm6.4$ ; P<0.0001, both comparisons).

# CONCLUSION

RFA of the liver increases tumor load, proliferation, and neovasculation of colorectal metastasis in mice, when performed 24hr after splenic tumor injection. Thus, RFA may potentially stimulate metastatic growth of unablated tumor foci at distant sites within the liver.

# **CLINICAL RELEVANCE/APPLICATION**

Development of animal models for studying the unwanted phenomenon of RF-induced tumorigenesis is imperative for both elucidating the responsible cellular pathways and determining how to best neutralize such mechanisms in clinical practice.



## VI229-SD-TUA5

Transarterial Chemoperfusion (TACP) and Transvenous Pulmonary Chemoembolization (TPCE) for the Treatment of Primary Lung Cancer

Tuesday, Nov. 27 12:15PM - 12:45PM Room: VI Community, Learning Center Station #5

# Participants

Thomas J. Vogl, MD, PhD, Frankfurt, Germany (*Presenter*) Nothing to Disclose Ahmed i. Ahmed, MBCHB, Assiut, Egypt (*Abstract Co-Author*) Nothing to Disclose Duaa B. Thabet, Assiut, Egypt (*Abstract Co-Author*) Nothing to Disclose Mostafa A. El-Sharkaway, Assiut, Egypt (*Abstract Co-Author*) Nothing to Disclose Hossam M. Kamel, Assiut, Egypt (*Abstract Co-Author*) Nothing to Disclose Nour-Eldin A. Nour-Eldin, MD,PhD, Frankfurt Am Main, Germany (*Abstract Co-Author*) Nothing to Disclose Nagy N. Naguib, MD, MSc, Frankfurt Am Main, Germany (*Abstract Co-Author*) Nothing to Disclose Afaf A. Hassan, Assiut, Egypt (*Abstract Co-Author*) Nothing to Disclose

#### For information about this presentation, contact:

T.Vogl@em.uni-frankfurt.de

#### PURPOSE

To evaluate tumor response, local tumor control and patient survival after the treatment of primary lung cancer using transpulmonary chemoembolization (TPCE) and transarterial chemoperfusion (TACP) in a palliative intent.

## **METHOD AND MATERIALS**

This retrospective study included 118 patients (mean  $62\pm9.7$  years; 59 females/59 males) who underwent either repetitive TPCE (n=56) or TACP (n=62) between January 2006 and April 2017 for the treatment of unresectable primary lung tumors not responding to systemic chemotherapy or recurrent after curative treatment. The mean number of sessions per patient was  $5.3\pm2.2$ , the median number of nodules was 3 and bilateral lung involvement was 44.9%. The chemotherapeutic agents used were a combination of mitomycin C and Gemcitabine with (n=14) or without cisplatin (n=98). Six patients received other combinations according to their physicians' recommendations. Regional delivery of the chemotherapeutic agents was performed either through selective catheterization of the tumor-supplying pulmonary arteries with subsequent injection of iodized oil and/or microspheres or through non-selective intraaortic chemo-infusion opposite the orifices of the main tumor-supplying arteries. The response was assessed according to the revised RECIST criteria.

#### RESULTS

After evaluation of the tumor response partial response was achieved in 15.3% (=18), stable disease in 65.3% (n=77) and progressive disease in 19.5% (n=23). The estimated mean survival time and time to progression were 14.9 $\pm$ 1.6 and 9.2 $\pm$ 1.3 for the TPCE group and 18.1 $\pm$ 2.1 and 11.1 $\pm$ 1.7 for the TACP group, respectively. There was a non-significant tendency of patients who underwent TACP to attain a longer time to progression and mean survival time compared to the TPCE group.

#### CONCLUSION

TPCE and TACP have the potential to improve local tumor control and to prolong survival in a selected group of patients with limited treatment options.

# **CLINICAL RELEVANCE/APPLICATION**

TACP and TPCE improve local tumor control and prolong survival in primary lung cancer patients.



## VI230-SD-TUA6

Differential Diagnosis of Bland and Neoplastic Portal Vein Thrombosis with Dual Energy Spectral CT

Tuesday, Nov. 27 12:15PM - 12:45PM Room: VI Community, Learning Center Station #6

#### Participants

Jun Zhao, Lanzhou, China (*Presenter*) Nothing to Disclose Junlin Zhou, Lanzhou, China (*Abstract Co-Author*) Nothing to Disclose

For information about this presentation, contact:

396897247@qq.com

#### PURPOSE

To investigate the value of dual energy spectral CT in differential diagnosis of neoplastic and bland portal vein thrombosis.

#### **METHOD AND MATERIALS**

68 cases of portal vein thrombosis (PVT) ,including 33 cases of bland PVT(BPVT) and 35 cases of neoplastic PVT(NPVT) were confirmed by following pathological experiments or diagnosed as having hepatitis B- or C-related cirrhosis, were analyzed retrospectively. All patients underwent dual phase contrast enhanced CT with dual energy spectral mode. For each case, the CT value on monochromatic images of 40~140keV, thrombus iodine concentration(I) and thrombus blood concentration (IB)in the portal venous phase(PVP)were measured, thrombus-aorta iodine concentrations ratio(IT/IA,NICA),and thrombus-PV iodine concentrations ratio(IT/IP,NICP)were calculated and spectrum curve slope was calculated according to the formula: the slope=(CT40keV-CT70keV)/30. Data was compared with independent samples t-test. Sensitivity and specificity of the quantitative parameters were analyzed by receiver operating characteristic curve.

#### RESULTS

The CT40keV, CT70keV, the mean slope, I, IB and NICP of NPVT differed significantly from those of BPVT during PVP (P=0.007, P=0.012, P=0.007, P=0.005, P=0.009, P<0.001, respectively).(Table1).NICA had no statistically significant during PVP (P=0.162). The CT threshold value, slope, I, IB and NICP had high sensitivity and specificity during PVP in differentiating NPVT from BPVT.

## CONCLUSION

Dual energy spectral CT with the quantitative analysis of iodine concentration, the CT value and slope in the PVP may help increase the accuracy of differentiating neoplastic and bland of portal vein thrombosis.

# **CLINICAL RELEVANCE/APPLICATION**

Differentiating the nature of the thrombus is of great clinical significance in determining the therapeutic approach, predicting survival, and assessing candidates for liver transplantation. Dual energy spectral CT may contribute to diagnosis of portal vein thrombosis preoperatively.



# VI231-SD-TUA7

CT Angiography of Entire Aorta with 30ml Contrast Medium Volume at 70kVp: Comparison with a Standard Protocol

Tuesday, Nov. 27 12:15PM - 12:45PM Room: VI Community, Learning Center Station #7

# Participants

Zhefan Song, Xi'an, China (*Presenter*) Nothing to Disclose Jianxin Guo, Xian, China (*Abstract Co-Author*) Nothing to Disclose Jian Yang, MD, PhD, Xian, China (*Abstract Co-Author*) Nothing to Disclose Jingjing Bai, Xian, China (*Abstract Co-Author*) Nothing to Disclose Yannan Cheng, BS,BS, Xi'an, China (*Abstract Co-Author*) Nothing to Disclose Hong Huang, Xi'an, China (*Abstract Co-Author*) Nothing to Disclose

#### PURPOSE

Purpose: To evaluate the feasibility, image quality and radiation dose of using 70 kVp and 30 mL contrast medium (CM) volume for Aortic CT Angiography (ACTA).

# METHOD AND MATERIALS

Methods: Thirty patients (BMI<25kg/m2) undergoing ACTA with clinical justifications were prospectively divided randomly into two groups: group A (n = 15), with conventional 100 kVp, IR with 60% strength (60%ASIR-V) and 65 mL CMand group B (n = 15), with 70 kVp, iterative reconstruction (IR) with80% strength (80%ASIR-V) and 30 mL CM.CT values, noisewere measured in regions of interest at four locations: ascending and descending aorta at the level of the pulmonary trunk, and abdominal aorta at the levels of the coeliac trunk and aortic bifurcation. The objective image qualitywas evaluated by two experienced radiologists using a five-point Likert scale. The CTDIvol and DLP values were recorded from dose report and effective dose was calculated. All measurements between the two groups were statistically compared.

#### RESULTS

Results: There was no significant difference in CT value, noise, SNR of all aortic segments between the two groups. The CNRs of the aortas in four locations in group B were higher than those in group A (P < 0.05). There was no significant difference in subjective image quality of all aortic segments between the two groups. The contrast medium (CM) volume in Group B was reduced by 54% compared with Group A.Effective dose was  $1.45 \pm 0.17$  mSv for group B, which was significantly decreased by 57% than that of group A ( $3.38 \pm 0.65$ mSv).

#### CONCLUSION

Conclusion: ACTA at 70 kVp with higher IR strength provides diagnostic image quality with 57% reduction in radiation dose and 54% reduction in contrast volume compared with standard protocol.

## **CLINICAL RELEVANCE/APPLICATION**

Clinical Relevance/Application: Aortic CT Angiography can be performed at 70 kVp and with IR to maintain image quality while significantly reducing contrast dose and radiation dose.



# VI232-SD-TUA8

02-03 Chemiodyscolysis and 02-03 Retreatment: A Retrospective Outcome Evaluation of Different Multiple-Treatment Sessions in Partially-Responder Patients

Tuesday, Nov. 27 12:15PM - 12:45PM Room: VI Community, Learning Center Station #8

# Participants

Pierpaolo Palumbo, MD, L'Aquila, Italy (*Presenter*) Nothing to Disclose Federico Bruno, MD, L'Aquila, Italy (*Abstract Co-Author*) Nothing to Disclose Simone Quarchioni, Laquila, Italy (*Abstract Co-Author*) Nothing to Disclose Maria Valeria Marcella Micelli, Laquila, Italy (*Abstract Co-Author*) Nothing to Disclose Antonio Izzo, LAquila, Italy (*Abstract Co-Author*) Nothing to Disclose Marco Varrassi, L'Aquila, Italy (*Abstract Co-Author*) Nothing to Disclose Sergio Carducci, L'Aquila, Italy (*Abstract Co-Author*) Nothing to Disclose Francesco Arrigoni, Coppito, Italy (*Abstract Co-Author*) Nothing to Disclose Aldo Victor Giordano, L'Aquila, Italy (*Abstract Co-Author*) Nothing to Disclose Luigi Zugaro, L'Aquila, Italy (*Abstract Co-Author*) Nothing to Disclose

#### For information about this presentation, contact:

palumbopierpaolo89@gmail.com

## PURPOSE

O2-O3 dyscolysis has shown a high efficacy rate in the treatment of disc herniation, with a reported success rate about 70%; furthermore, injection of corticosteroid and local anaesthetic at the periradicular site even more improve the treatment outcome of this procedure. However, the patient treated with O2-O3 therapy, are often patients with insidious low back pain, refractory to the conservative approach, who needs often multiple treatment. But exact definition of protocol for number and timing of treatment session doesn't exist. So, the purpose of this study was to evaluate the outcome of different O2-O3 therapy in the patient with disc-herniation-related low back pain

## METHOD AND MATERIALS

We retrospectively evaluated 526 patients who underwent O2-O3 lumbar dyscolysis in different multiple session. All patients were followed-up by MRI at 1 year, and MRI examinations were compared with the ones performed before the procedure. All procedures had been performed at our institution with standardized CT-guided technique and drug administration

## RESULTS

Our analysis revealed 4 groups: 1.Patients treated with 2 sessions of intradiscal o2-o3 injection associated with periganglionic steroid injection; 2. Patients treated with an intradiscal and periradicular injection and a second periganglionic steroid injection; 3. Patients treated with 3 consecutive intradiscal O2-O3 injections; 4. Patients treated with 1 intradiscal administration associated with 2 subsequent periganglionic steroid injection. Injective treatment was repeated at least one month later from each other. Our comparing-analysis, reveals no statistically significant difference between the 4 groups outcomes (p>0,05), with a mean success rate of 74,1%

#### CONCLUSION

In conclusion, O2-O3 therapy showed similar result even in different protocol

#### **CLINICAL RELEVANCE/APPLICATION**

Considering the possible complication reported in the literature, maybe the 1-intradiscal approach associated with 2 other periganglionic injections could be preferred



# AI001-TUC

# Data Science: Normalization, Annotation, Validation

Tuesday, Nov. 27 12:30PM - 2:00PM Room: AI Community, Learning Center

# Title and Abstract

Data Science: Normalization, Annotation, Validation This session will focus on preparation of the image and non-image data in order to obtain the best results from your deep learning system. It will include a discussion of different options for representing the data, how to normalize the data, particularly image data, the various options for image annotation and the benefits of each option. We will also discuss the 'after training' aspects of deep learning including validation and testing to ensure that the results are robust and reliable.



## AI215-SD-TUB1

Impact of Deep Learning-based CT Denoising on Normal Anatomical Structures in Low Dose Chest CT: FBP vs IRT vs Deep Learning

Tuesday, Nov. 27 12:45PM - 1:15PM Room: AI Community, Learning Center Station #1

# Participants

Semin Chong, MD, Seoul, Korea, Republic Of (*Presenter*) Research Consultant, Samsung Electronics Co, Ltd Jong H. Kim, PhD, Seoul, Korea, Republic Of (*Abstract Co-Author*) Nothing to Disclose Kyungmin Lee, Seoul, Korea, Republic Of (*Abstract Co-Author*) Nothing to Disclose

#### CONCLUSION

DL image denoising is expected to provide the same or better quality than the IRT in the mediastinum and airway. However, IRT also seems to have some limitations now, and it is thought that more software improvement or machine training is needed to apply DL technology to pulmonary parenchyma.

#### Background

The dramatic development of CT image denosing technology enabled to achieve ultra low-dose CT scans. Deep learning (DL) based techniques are applied in image processing algorithms to solve many difficulties in image reconstruction and lead to changes in paradigm. In this study, we propose the possibility of DL method to reduce image noise and compare it with FBP and IRT.

#### **Evaluation**

We evaluated a new CT denoising solution (ClariCT+, ClariPI, Seoul, South Korea) based on a fully convolutional deep learning (DL) model, which was trained by using 11,500 slices of normal patients with two-tissue mode where soft tissue and lung tissue were segmented and were used for training of two separate denoising models. All images (n = 30) were acquired by applying FBP, IRT (i4 and i6, iDose, Philips Healthcare, The Netherlands) and DL (DLmd and DLstr, moderate and strong denosing levels). Mean (HU), SD (HU), and area(mm2) of ROI were measured for mediastinum (aortic arch), right lung, left lung, and airway (trachea) using a fixed size ROI in each image.

#### Discussion

Mean of mediastinum and left lung did not differ statistically between FBP, IRT, and DL. Mean of right lung was significantly different between FBP and DLstr. Mean and SD of airway were not significantly different between DLmd and DLstr. The SD of the mediastinm decreased statistically significantly from FBP to DLstr, but there was no statistically significant difference between i4 and i6, DLmd and DLstr, and DLmd and DLstr for right lung, left lung and airway, respectively. In this study, reducing the image noise applied to the mediastinum was the most ideal and showed anatomical characteristics suitable for the hypothesis. However, some lungs showed instability of the mean HU when DL was applied, and DL as well as IRT were not consistent in SD reduction. One interesting point was that the mean and SD of the trachea were consistent when applying DL.



# AI216-SD-TUB2

Machine Learning for Identifying the Value of Digital Breast Tomosynthesis using Data from a Multicentre Retrospective Study

Tuesday, Nov. 27 12:45PM - 1:15PM Room: AI Community, Learning Center Station #2

# Participants

Ahmed M. Alaa, Los Angeles, CA (*Abstract Co-Author*) Nothing to Disclose Fiona J. Gilbert, MD, Cambridge, United Kingdom (*Presenter*) Research Grant, Hologic, Inc; Research Grant, General Electric Company; Research Grant, GlaxoSmithKline plc; Research Consultant, Alphabet Inc Yuan Huang, Cambridge, United Kingdom (*Abstract Co-Author*) Nothing to Disclose Mihaela van der Schaar, Oxford, United Kingdom (*Abstract Co-Author*) Nothing to Disclose

# CONCLUSION

Machine learning helps to identify subpopulations of women who benefit most from DBT, and can be used to design individualized screening.

## Background

We sought to identify subgroups of women for whom digital breast tomosynthesis (DBT) showed improved diagnostic accuracy for different types of malignant lesions than 2D mammography. The study used multicenter retrospective data from 6,040 women (934 biopsy-confirmed cancers) who underwent both DBT and 2D mammography. An ensemble of 20 state-of-the-art machine learning models was created to predict biopsy outcomes based on radiological classification of 2D and DBT images, Volpara breast composition measures and age. We used this ensemble to assess the diagnostic accuracy of DBT- and 2D-based predictors, to identify subgroups of women for whom DBT is more informative, and to quantify the value of the individual predictors with respect to different types of malignant lesions.

#### **Evaluation**

Accuracy and precision of DBT-based and 2D-based predictive models were evaluated using the area under receiver operating characteristic curve (AUC-ROC) and the area under precision-recall curve (AUC-PR), respectively. At the population level, DBT-based models significantly outperformed 2D-based models in terms of both AUC-ROC ( $0.943 \pm 0.009 \text{ vs } 0.915 \pm 0.018$ ) and AUC-PR ( $0.812 \pm 0.042 \text{ vs } 0.776 \pm 0.051$ ). The gains achieved by DBT-based models were superior in patient groups with fibroglandular volume ranging from 40 cm3 - 80 cm3, and in invasive lobular cancers compared to ductal tumours. The gain from DBT became insignificant for patients >60 years old or with fibroglandular volume exceeding 80 cm3.

#### Discussion

Using state-of-the-art machine learning techniques, we established that DBT mammography is significantly more informative than 2D mammography, especially for patients with moderate fibroglandular breast volume but was not advantageous in those women > 60 years or in those with dense breast volume >80cm3. For both DBT and 2D imaging, our machine learning models lead to higher detection rates and fewer false alarms.



# AI218-SD-TUB3

# Patient Data Adapted Deep Learning for Multi-Label Chest X-Ray Classification

Tuesday, Nov. 27 12:45PM - 1:15PM Room: AI Community, Learning Center Station #3

FDA Discussions may include off-label uses.

#### Participants

Ivo Matteo Baltruschat, Hamburg, Germany (*Presenter*) Nothing to Disclose Hannes Nickisch, Hamburg, Germany (*Abstract Co-Author*) Koninklijke Philips NV Michael Grass, PhD, Hamburg, Germany (*Abstract Co-Author*) Employee, Koninklijke Philips NV Tobias Knopp, DIPLENG, Hamburg, Germany (*Abstract Co-Author*) Nothing to Disclose Axel Saalbach, PHD, Aachen, Germany (*Abstract Co-Author*) Employee, Koninklijke Philips NV

#### For information about this presentation, contact:

i.baltruschat@uke.de

#### PURPOSE

Neural network based chest X-ray image classification can serve multiple purposes in diagnostic radiology. These include the reordering of task lists for the radiologist, the exclusion of pathology up to diagnosis prediction. Most neural networks train pure image data against the multi-label chest X-ray classification. Here, we include additional patient data e.g. patient age and gender as well as the view position in the training. Together with the images, we evaluate the improvement in classification accuracy.

## **METHOD AND MATERIALS**

We used the ChestXray14 dataset with about 112120 images for training of our neural networks and investigated the ResNet-50 architecture in the experiments. Following up on early work in this domain, we considered transfer learning with and without finetuning as well as the training of a dedicated X-ray network. Furthermore, we included a network integrating non-image data (patient age, gender, and acquisition type) in the classification pipeline. In a systematic evaluation using a 5 times re-sampling scheme and a multi-label loss function, we evaluated the performance of the different approaches for pathology classification by ROC statistics. In this context, we observed the best performance for the X-ray specific ResNet-50 integrating non-image data.

#### RESULTS

For our empirical assessment, we evaluated two different setups with varying network schemes and architectures with and without patient data inclusion. For all pathologies, we performed an ROC analysis and computed the area under curve (AUC). The mean AUC increases across all pathologies from  $73.0\pm1.1$  to  $74.8\pm1.1$  ( $\pm1.8$ ) /  $81.7\pm1.0$  to  $82.0\pm0.9$  ( $\pm0.3$ ) for off-the-shelf / fine-tuned networks.

#### CONCLUSION

Neural network based chest X-ray image classification profits from patient data inclusion in contrast to pure image data based multi-label classification. Increased mean AUC results can be achieved for the majority of target pathologies.

# **CLINICAL RELEVANCE/APPLICATION**

Automatic multi-label chest X-ray classification based on neural networks can improve various processes in diagnostic radiology. By combining image and patient data the diagnosis prediction can be improved.



## BR193-ED-TUB8

## Freezing Instead of Excising: Cryoablation for Breast Cancer - How It's Done

Tuesday, Nov. 27 12:45PM - 1:15PM Room: BR Community, Learning Center Station #8

## Awards Magna Cum Laude

# Participants

Linda DeMello, MD, Providence, RI (*Presenter*) Nothing to Disclose Robert C. Ward, MD, Providence, RI (*Abstract Co-Author*) Nothing to Disclose Martha B. Mainiero, MD, Providence, RI (*Abstract Co-Author*) Nothing to Disclose Ana P. Lourenco, MD, Providence, RI (*Abstract Co-Author*) Nothing to Disclose

# For information about this presentation, contact:

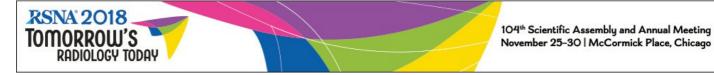
#### ldemello2@lifespan.org

#### **TEACHING POINTS**

1. To illustrate the cryoablation techniques utilized in early stage breast cancer, highlighting the importance of avoiding potential complications and pitfalls. 2. To present a series of cryoablation cases from our breast center, including follow-up imaging. 3. To recognize the role of cryoablation in treating early stage cancers in patients who are not surgical candidates or prefer an alternative treatment to surgery.

# TABLE OF CONTENTS/OUTLINE

1. Introduction to Cryoablation 2. Techniques and Equipment 3. Presentation of at least 5 cases from our breast center a. Each with a different dilemma with regard to clinical context and technique b. Detail potential pitfalls and complications along with strategies to avoid them 4. Patient experience and outcomes 5. Future applications of cryoablation and summary



## BR194-ED-TUB9

Getting Acquainted with the Man(I)y Facets of the Lesser Known Male Breast: Lessons Learned From a 10year Institutional Look-Back

Tuesday, Nov. 27 12:45PM - 1:15PM Room: BR Community, Learning Center Station #9

#### Awards Certificate of Merit

#### **Participants**

Nayanatara Swamy, MD , Little Rock, AR (*Presenter*) Nothing to Disclose Gwendolyn M. Bryant-Smith, MD, Little Rock, AR (*Abstract Co-Author*) Nothing to Disclose

### For information about this presentation, contact:

nswamy@uams.edu

## **TEACHING POINTS**

1. The fundamental anatomical differences between the male and female breast helps us understand the vast difference in epidemiology of male and female breast diseases, including breast cancer. Accordingly, breast imaging guidelines are different in men and women. 2.We used our institutional experience over the past decade to understand our regional male breast epidemiology. a. The most common finding in male diagnostic mammograms is gynecomastia. Hence, familiarity with the wide spectrum of gynecomastia appearances on mammography is crucial. b. Male patients are less likely to return for short term follow-up imaging. A change in our approach to male patients is necessary to improve their compliance.

## **TABLE OF CONTENTS/OUTLINE**

1. Differences between male and female breast: - Anatomical differences. - The transgender breast. - How do male breast diseases differ from female breast diseases? - How does male breast cancer differ from female breast cancer? - Difference in screening guidelines for men and women. - Difference in ACR appropriateness criteria for an indeterminate palpable breast mass in males compared to females. - Is Imaging utilization different in male versus female patients? 2. Our Institutional 10 year results. 3. Lessons learned. 4. Conclusion.



## BR195-ED-TUB10

# The 123's of Breast Cancer Staging

Tuesday, Nov. 27 12:45PM - 1:15PM Room: BR Community, Learning Center Station #10

### **Participants**

Tirth V. Patel, MD, Chapel Hill, NC (Presenter) Nothing to Disclose Marie Vogel, BS, Chapel Hill, NC (Abstract Co-Author) Nothing to Disclose Sheila S. Lee, MD, Durham, NC (Abstract Co-Author) Nothing to Disclose Sheryl G. Jordan, MD, Chapel Hill, NC (Abstract Co-Author) Nothing to Disclose

## For information about this presentation, contact:

tirth.patel@unchealth.unc.edu

# **TEACHING POINTS**

The purposes of this exhibit are to: 1. Educate radiologists on the American Joint Committee on Cancer (AJCC) eighth edition staging manual, the newly published (2018) prognostic stage for breast cancer 2. Review relevant breast and locoregional lymph node anatomy 3. Present breast cancer survival statistics by stage 4. Identify key imaging findings for radiologists to assure accurate breast cancer staging

# **TABLE OF CONTENTS/OUTLINE**

1. Introduction with relevant anatomy and survival statistics on breast cancer 2. Outline the AJCC 8th edition breast cancer staging system and define the TNM (Tumor, Nodes, Metastasis) system 3. Case-based illustration of each breast cancer stage 4. Short video animation teaching tool highlighting key teaching points



### BR196-ED-TUB11

The Future Breast Imager: Understanding the Clinician's Perspective

Tuesday, Nov. 27 12:45PM - 1:15PM Room: BR Community, Learning Center Station #11

## Awards Certificate of Merit

### **Participants**

Hyung Won Choi, MD, Los Angeles, CA (*Presenter*) Nothing to Disclose Irene S. Tsai, MD, Los Angeles, CA (*Abstract Co-Author*) Nothing to Disclose Bo Li, MD, Los Angeles, CA (*Abstract Co-Author*) Nothing to Disclose

## **TEACHING POINTS**

As there is increasing advocacy for a multidisciplinary approach to provide higher quality of patient care, it is becoming more pertinent for the radiologist to have an adequate understanding of current breast cancer treatment. The ideal breast radiologist will be able to identify salient imaging findings that change clinical management. After reviewing this presentation, participants will be familiar with: 1. Indications for surgical, radiation, and systemic treatment of breast cancer 2. Imaging findings that change the surgeon, radiation oncologist, or oncologist's treatment plan.

# TABLE OF CONTENTS/OUTLINE

1. Surgical management A. Indications for mastectomy versus lumpectomy with example cases B. Types of mastectomy: Radical, modified radical, simple, and nipple sparing mastectomy C. Indications for full axillary dissection versus sentinel lymph node biopsy 2. Radiation treatment A. Indications for radiation treatment with example cases B. Types of radiation treatment: Whole breast versus partial breast irradiation 3. Systemic therapy A. Indications for neoadjuvant and adjuvant chemotherapy with example cases B. Different types of systemic therapy - chemotherapy, hormonal blockade, and biologic therapies



### BR197-ED-TUB12

## The Dark Side of the Post-Surgical Breast: Recurrence in Breast Cancer Follow-Up Care

Tuesday, Nov. 27 12:45PM - 1:15PM Room: BR Community, Learning Center Station #12

#### **Participants**

Pedro Henrique Hasimoto e Souza, MD, Sao Paulo, Brazil (*Abstract Co-Author*) Nothing to Disclose Tatiana C. Tucunduva, MD, Sao Paulo, Brazil (*Abstract Co-Author*) Nothing to Disclose Juliana H. Catani, MD, Sao Paulo, Brazil (*Abstract Co-Author*) Nothing to Disclose Barbara H. Bresciani, MD, Sao Paulo, Brazil (*Abstract Co-Author*) Nothing to Disclose Carlos Shimizu, MD, Sao Paulo, Brazil (*Presenter*) Nothing to Disclose Nestor Barros, Sao Paulo, Brazil (*Abstract Co-Author*) Nothing to Disclose

## For information about this presentation, contact:

pedrohenriquehs@hotmail.com

## **TEACHING POINTS**

Prepare the radiologist to face common and uncommon presentations of recurrence in breast imaging; Exhibit clinical cases from our radiology department, with breast malignant imaging findings in the post-surgical follow-up care, showing its pathologic correlation; Discuss the effects of manipulation on breast cancer detection; Provide management recommendations.

## TABLE OF CONTENTS/OUTLINE

Brief discussion on post-treatment follow-up care in breast cancer; Risk factors and incidence of recurrence; Imaging features (mammography, ultrasound, computerized tomography and magnetic resonance imaging) of recurrence in post-treatment breast imaging, with their pathologic correlation; Describe alarming signs that should raise suspicion for malignancy; Review differential diagnosis for recurrent breast cancer; Management recommendations.



# BR247-SD-TUB1

Clinical Usefulness of Digital Breast Tomosynthesis (DBT) and Hybrid 18F-FDG PETMRI (PETMR) for Monitoring Neoadjuvant Chemotherapy (NAC) in Breast Cancer

Tuesday, Nov. 27 12:45PM - 1:15PM Room: BR Community, Learning Center Station #1

# Participants

Nachiko Uchiyama, MD, Tokyo, Japan (*Presenter*) Nothing to Disclose Hiroaki Kurihara, MD, Tokyo, Japan (*Abstract Co-Author*) Nothing to Disclose Takayuki Kinoshita, Tokyo, Japan (*Abstract Co-Author*) Nothing to Disclose Masayuki Yoshida, Tokyo, Japan (*Abstract Co-Author*) Nothing to Disclose Mari Kikuchi, MD, Chuou-ku, Japan (*Abstract Co-Author*) Nothing to Disclose Kyoichi Otsuka, Toyko, Japan (*Abstract Co-Author*) Nothing to Disclose Masahiko Kusumoto, MD, Chuo, Japan (*Abstract Co-Author*) Nothing to Disclose

#### For information about this presentation, contact:

nuchiyam@ncc.go.jp

# PURPOSE

To compare the usefulness of DBT and PETMR for evaluation of loco-regional staging and treatment response of NAC with reference to pathological findings.

### **METHOD AND MATERIALS**

30 invasive breast cancers (IDC: n=27, ILC n=2, and Metaplastic Ca: n=1) among 28 cases with 29 breasts, that NAC was preoperatively underwent, were enrolled. The average age was  $49.71 \pm 11.94$  y. o. Clinical stages were IIA (n=6), IIB (n=9), IIIA (n=4), and IIIC (n=10). MMG+DBT, US, and PETMR were obtained before and after NAC. Regarding PETMR, as whole-body scans was obtained after intravenous injection of 18F-FDG followed by a resting period of 60 min in a spine position as early phase In addition, breast MRI were conducted with a dedicated bilateral 8-channel breast radiofrequency coil in a prone position and contrast enhanced four phases of dynamic studies were obtained. As well as breast MRI, breast PET images as late phase of 80 min. Regarding DBT, the images were acquired by MLO and CC views with the rotation angle of  $\pm$  25° and reconstructed into 2mm thick slice having 1mm overlap with high in-plane resolution of 85µm. NAC response was classified in accordance with RECIST and compared with pathological response in accordance with JBCS.

### RESULTS

Before NAC, PETMR detected primary lesions with CEMR and with PET by 100% (30/30). Regarding LN metastasis, the diagnostic accuracy was 96.6% (28/29) by CEMR and 93.1% (27/29) by PET. Among the pathological response of Grade 0-1a (n=5), MMG+DBT demonstrated as SD (3/5: 60%) and PR (2/5: 40%). PETMR demonstrated as SD (2/5: 40%) and PR (3/5: 60%). Among Grade 1b-2 lesions (n=17), MMG+DBT detected as PR (13/17: 76.5%) and CR (4/17: 23.5%). PETMR demonstrated as PR (14/17: 82.4%) and CR (3/17: 17.6%). Among Grade 3 (n=8), MMG+DBT demonstrated as CR (6/8: 75.0%) and PR (2/8: 25.0%). PETMR demonstrated as CR (4/8: 50%) and PR (4/8: 50%). In addition, we evaluated estimated pathological responses with MMG+DBT and PETMR to compare the actual pathological results.

### CONCLUSION

Concurrent usage of MMG+DBT and PETMR can demonstrate promising results for loco-regional staging prior to NAC and can predict more accurate treatment response after NAC.

# **CLINICAL RELEVANCE/APPLICATION**

Concurrent usage of MMG+DBT and hybrid PETMR are useful among NAC cases of breast cancer, because they can provide detailed analysis by morphological evaluation with DBT, by evaluation of vascularity with dynamic MR, and by metabolic evaluation with PET.



# BR248-SD-TUB2

Changes in the Utilization of the BI-RADS Category 3 Assessment in Recalled Patients Screened with Digital Mammography Before and After the Implementation of Diagnostic Digital Breast Tomosynthesis

Tuesday, Nov. 27 12:45PM - 1:15PM Room: BR Community, Learning Center Station #2

# Participants

Tricia Stepanek, Cleveland, OH (*Presenter*) Nothing to Disclose Niki M. Constantinou, MD, Westlake, OH (*Abstract Co-Author*) Nothing to Disclose Holly N. Marshall, MD, Cleveland, OH (*Abstract Co-Author*) Nothing to Disclose Ramya M. Pham, MD, Solon, OH (*Abstract Co-Author*) Nothing to Disclose Cheryl L. Thompson, Cleveland, OH (*Abstract Co-Author*) Nothing to Disclose Donna M. Plecha, MD, Strongsville, OH (*Abstract Co-Author*) Research Grant, Hologic, Inc

### PURPOSE

To compare the utilization of the Breast Imaging Reporting and Data System (BI-RADS) category 3 assessment in patients recalled from digital mammography (DM) screening before and after the implementation of digital breast tomosynthesis (DBT) in the diagnostic setting.

# METHOD AND MATERIALS

This was an IRB-approved and HIPAA-compliant retrospective review of 22980 DM screening exams. The diagnostic DM cohort was limited to patients screened with DM between January 1, 2010 and August 31, 2011 (n = 11478) who were assigned a category 3 after diagnostic DM work-up without tomosynthesis. The diagnostic DM+DBT cohort was limited to patients screened with DM between January 1, 2014 and June 30, 2015 (n = 11502) who were assigned a category 3 after diagnostic DM+DBT work-up. Diagnostic ultrasound was performed at the discretion of the radiologist in both cohorts. Category 3 lesions were classified as architectural distortion, asymmetry, calcification, mass, and other and followed for a minimum of 2 years.

### RESULTS

The addition of DBT to diagnostic work-up after screening with DM resulted in a 61.9% reduction (22.6 women per 1000) in the utilization of BI-RADS category 3 compared to diagnostic DM work-up alone (3.7% for DM vs. 1.4% for DM+DBT; p < 0.0001). There was a statistically significant change in the distribution of category 3 findings with DM+DBT characterized by an increase in masses (p = 0.0056) and a decrease in calcifications (p = 0.0024). There was no change in category 3 assessment for distortions (p > 0.99), asymmetries (p = 0.073), or other findings (p = 0.58). Diagnostic DM+DBT resulted in a two-fold increase in incidental findings leading to a category 3 compared to DM alone (2.3% for DM vs. 7.0% for DM+DBT; p = 0.0053). The delayed cancer detection rate was 1.4% (10 malignancies in 419 patients) for category 3 lesions diagnosed by DM and 0% (0 malignancies in 160 patients) for category 3 lesions diagnosed by DM+DBT (p = 0.069).

## CONCLUSION

DBT in the diagnostic evaluation of patients recalled from DM screening decreased the number of patients assigned to short-term follow-up by 22.6 women per 1000 (61.9%), despite increased rates of category 3 incidental findings with 0% delayed cancer detection.

# **CLINICAL RELEVANCE/APPLICATION**

The use of DBT for diagnostic work-up at recall from DM screening may reduce the utilization of the BI-RADS category 3 assessment, decreasing the number of women committed to short-term follow-up.



## BR249-SD-TUB3

Management of Atypical Breast Papillomas by US-Guided Vacuum-Assisted Removal: Long-Term Outcomes

Tuesday, Nov. 27 12:45PM - 1:15PM Room: BR Community, Learning Center Station #3

### Participants

Jose Maria Oliver-Goldaracena, Madrid, Spain (*Abstract Co-Author*) Nothing to Disclose Maria Jose Roca Navarro, Madrid, Spain (*Abstract Co-Author*) Nothing to Disclose Vicenta Cordoba Chicote, Madrid, Spain (*Abstract Co-Author*) Nothing to Disclose Diego Garrido Alonso, Madrid, Spain (*Abstract Co-Author*) Nothing to Disclose Agustin Andres Mateo, Madrid, Spain (*Abstract Co-Author*) Nothing to Disclose Cesar Oterino Serrano, MBBS, Madrid, Spain (*Presenter*) Nothing to Disclose Miguel Bello Erias, MD, Madrid, Spain (*Abstract Co-Author*) Nothing to Disclose Alberto Jimenez, MD, Madrid, Spain (*Abstract Co-Author*) Nothing to Disclose Maria Jesus Garcia Sanchez, MD, Madrid, Spain (*Abstract Co-Author*) Nothing to Disclose

#### For information about this presentation, contact:

jmolivergoldaracena@gmail.com

#### PURPOSE

To review long-term outcomes of the percutaneous management of bening breast papillomas with atypia (AP) by US-Guided Vacuum-Assisted Removal (US-VAR).

### **METHOD AND MATERIALS**

In our Institution, probable intraductal papillomas diagnosed with US (benign intraductal mass within a dilated duct or cyst with Color-Doppler signal or correlation on ductography) or papillomas diagnosed at US-CNB of less than 30mm are managed by US-VAR. Between April 2010 and March 2018, 149 probable intraductal papillomas and 62 papillomas (diagnosed at US-CNB :54 Benign papillomas, BP and 8 atypical papillomas, AP) in 188 patients (pts) were removed with US-VAR. Histology showed benign papilloma (BP) in 149 (168pts), atypical papilloma in 12(11pts) and papillary carcinoma in 9 (9pts). Conservative management was decided in the 12 APs (mean size 7mm, range 5-26mm) of 11pts (mean age 61, range 35-68) because of appropiate radiologic-pathologic correlation (pathology report showed atypical hyperplasia without suspected DCIS). Pathologic dischargue was present in 4APs (4pts) with US findings that showed probable intraductal papillomas. The 8 asymptomatic APs(7pts) were previously diagnosed by US-CNB as 4 BPs and 4 APs. The US findings of the 12 APs were classified BIRADS 3 (8), BIRADS 4A (2) and BIRADS 4B (2). All patients underwent US follow-up at 1-2 months, 6-8 months, and 12-14 months after US-VAR and later annual US follow-up. When a residual or recurrent suspicious papilloma was detected at US follow-up, re-excision by US-VAR was performed. Clinical, US follow-up and pathologic outcomes were recorded.

# RESULTS

US follow-up ranged between 84 and 19 months (mean 68 months). No recurrent lesions were detected . None were upgraded to carcinoma at long term US follow-up. Nipple discharge disappeared in all 4 symptomatic patients.

## CONCLUSION

US-VAR allows percutaneous long-term management of atypical papillomas with proper radiologic-pathologic correlation.

### **CLINICAL RELEVANCE/APPLICATION**

US-VAR is appropriate for the long-term percutaneous management of atypical papillomas with proper radiologic-pathologic correlation.



## BR250-SD-TUB4

Longitudinal Investigation of Tumor Heterogeneity in Breast DCE-MRI to Improve Early Response Assessment to Neoadjuvant Chemotherapy for Locally Advanced Breast Cancer: Results From the ACRIN 6657/I-SPY-1 Trial

Tuesday, Nov. 27 12:45PM - 1:15PM Room: BR Community, Learning Center Station #4

#### Participants

Nariman Jahani, Philadelphia, PA (*Presenter*) Nothing to Disclose Eric A. Cohen, Philadelphia, PA (*Abstract Co-Author*) Nothing to Disclose Meng-Kang Hsieh, Philadelphia, PA (*Abstract Co-Author*) Nothing to Disclose Lauren Pantalone, BS, Philadelphia, PA (*Abstract Co-Author*) Nothing to Disclose Susan Weinstein, MD, Philadelphia, PA (*Abstract Co-Author*) Nothing to Disclose Christos Davatzikos, PhD, Philadelphia, PA (*Abstract Co-Author*) Nothing to Disclose Despina Kontos, PhD, Philadelphia, PA (*Abstract Co-Author*) Nothing to Disclose

### For information about this presentation, contact:

nariman.jahani@uphs.upenn.edu

### PURPOSE

Utilizing longitudinal dynamic contrast-enhanced magnetic resonance imaging (DCE-MRI) scans of locally advanced breast cancer under neoadjuvant chemotherapy (NAC), we evaluate voxel-wise spatio-temporal changes in tumor heterogeneity to improve early prediction of pathologic complete response (pCR) and recurrence free survival (RFS).

### **METHOD AND MATERIALS**

We retrospectively analyzed 106 women from a subset of ACRIN 6657/I-SPY TRIAL with complete imaging and prognostic marker data using DCE-MRI scans acquired before and after the first cycle of NAC. Utilizing a robust deformable image registration technique, we identified corresponding voxels between pre- and post-treatment images and extracted two groups of voxel-wise features to quantify longitudinal tumor heterogeneity: 1) voxel-wise tumor deformation including local volume ratio and anisotropic deformation; and 2) parametric response maps of DCE-MRI kinetic variables (signal enhancement ratio, peak enhancement, wash-in/wash-out slope). Using best-subset regression, features were added to a baseline model including established prognostic markers and functional tumor volume to predict pCR and RFS. Multivariate logistic regression and Cox proportional hazard models were used to assess pCR and RFS, respectively. Furthermore, conventional analysis where analogous metrics were averaged over the tumor was conducted to compare to voxel-wise analysis. The performances of models were evaluated with area under curve (AUC) and c-statistics for pCR and RFS analyses, respectively (flowchart in Fig.1).

#### RESULTS

Voxel-wise analysis improved prediction significantly for both pCR and RFS, with AUC=0.85 and c-statistics=0.79, compared to the baseline model with AUC=0.76 and c-statistics=0.69, respectively. The aggregate model indicated similar performance to the baseline model with AUC=0.76 and c-statistics=0.70, respectively.

# CONCLUSION

Our results suggest that quantification of voxel-wise changes after NAC can extract markers revealing spatio-temporal tumor heterogeneity that can significantly improve early tumor response assessment, while conventional aggregate tumor features may not adequately capture such longitudinal changes to add significant new information for prognosis.

## **CLINICAL RELEVANCE/APPLICATION**

Improvement of early treatment assessment using markers based on voxel-wise feature analysis may provide complementary new information to better modify treatment plans and to optimize therapy.



# BR251-SD-TUB5

Development and Validation of a Deep Learning Model For More Accurate and Consistent Assessment of MRI Background Parenchymal Enhancement

Tuesday, Nov. 27 12:45PM - 1:15PM Room: BR Community, Learning Center Station #5

# Participants

Benjamin Wang, MD, Boston, MA (*Abstract Co-Author*) Nothing to Disclose
Tally Portnoi, Cambridge, MA (*Abstract Co-Author*) Nothing to Disclose
Regina Barzilay, PhD, Cambridge, MA (*Abstract Co-Author*) Nothing to Disclose
Brian N. Dontchos, MD, Boston, MA (*Presenter*) Nothing to Disclose
Dorothy A. Sippo, MD, Boston, MA (*Abstract Co-Author*) Research Grant, General Electric Company
Christine E. Edmonds, MD, Boston, MA (*Abstract Co-Author*) Nothing to Disclose
Randy C. Miles, MD, Chicago, IL (*Abstract Co-Author*) Nothing to Disclose
Constance D. Lehman, MD,PhD, Boston, MA (*Abstract Co-Author*) Research Grant, General Electric Company; Medical Advisory
Board, General Electric Company

### For information about this presentation, contact:

### bdontchos@mgh.harvard.edu

#### PURPOSE

Increased MRI background parenchymal enhancement (BPE) is associated with breast cancer risk. However, radiologist BPE assessment is variable. Our goal was to train a deep learning (DL) model to assess breast MRI BPE and to evaluate its performance compared to expert radiologists.

## METHOD AND MATERIALS

After IRB approval, consecutive breast MRI examinations from January 2011 to December 2014 with BPE assessment were identified (n=4683). 3249, 696, and 885 exams were selected for the training, validation, and test data sets, respectively. A single representative maximum intensity projection image from each examination and the radiologist's prospective assessment of BPE were used to train a deep learning classifier (ResNet). From the test data set, a sample of 100 MRI exams were then randomly selected and submitted for blinded review by 5 fellowship trained breast imaging radiologists for binary assessment of BPE (minimal versus non-minimal). We estimated both our DL model agreement and our radiologist readers' agreement with the original radiologist's BPE assessment using percent agreement with Wilson confidence intervals (CI) and with linear-weighted kappa statistics, compared across 5,000 bootstrap samples to assess significance.

### RESULTS

For the subset of 100 reader study exams, DL model agreement with the original radiologist's BPE assessment was 80.0% (95% CI of 71.1, 86.7) for binary assessment. The 5 radiologist readers' agreement with the original radiologist's BPE assessment for the same 100 cases was 69.8% (95% CI 65.4, 73.5) for binary assessment (p=0.02). Compared to the original radiologist's BPE assessment, our DL model showed moderate agreement (K=0.55, 95% CI 0.38-0.74) on this subset compared to weak agreement by the 5 radiologist readers' consensus assessment (K=0.43, 95% CI 0.26-0.61).

### CONCLUSION

A deep learning model can more accurately and reliably assess BPE based on maximal intensity projection images than a human reader.

## **CLINICAL RELEVANCE/APPLICATION**

A deep learning model that accurately and consistently predicts BPE could reduce variability in radiologist BPE assessment and may also serve as a reliable tool for breast cancer risk prediction.



## BR252-SD-TUB6

Diagnosis of Triple Negative Breast Cancer Using Machine Learning Methods of Quantitative Computerized Ultrasound Features

Tuesday, Nov. 27 12:45PM - 1:15PM Room: BR Community, Learning Center Station #6

# Participants

Tong Wu, Philadelphia, PA (*Abstract Co-Author*) Nothing to Disclose Laith R. Sultan, MD, Philadelphia, PA (*Presenter*) Nothing to Disclose Theodore Cary, Philadelphia, PA (*Abstract Co-Author*) Nothing to Disclose Jiawei Tian, Harbin, China (*Abstract Co-Author*) Nothing to Disclose Chandra Sehgal, PhD, Philadelphia, PA (*Abstract Co-Author*) Nothing to Disclose

## For information about this presentation, contact:

lsutlan@pennmedicine.upenn.edu

## PURPOSE

Triple negative (TN) breast cancers are known for aggressive biological characteristics and poor clinical outcomes. In the currentstate-of-the-art much of the technological advances have been aimed at differentiating malignant and benign tumors where all the subtypes are grouped together. In this study, we go beyond this discrimination of the solid breast masses by applying computer methods with ultrasound imaging to differentiate TN and non-triple negative (NTN) subtypes.

#### **METHOD AND MATERIALS**

140 surgically confirmed breast cancer were classified into triple negative (TN) and non-triple negative (NTN) subtypes based on the expression of ER, PR, HER2. Nine quantitative grayscale features describing margin and shape characteristics of the lesion, and three tumor vascularity features describing the magnitude of vascularity were extracted from a manually drawn region of interest on grayscale and color Doppler images. The features that showed difference (P<0.05) were used with logistic regression and leaveone-out cross validation to train and test the differentiation of TN and NTN masses. Diagnostic performance was measured by the area under ROC (AUC) and sensitivity and specificity measured at the Youdons index.

## RESULTS

Twenty-five of the 140 cases were found to be TN. Of the twelve grayscale and Doppler features, eight showed statistical difference (P< 0.002) for the TN and NTN. AUC of the statistically significant GS and Doppler features when used alone was 0.850 and 0.657, respectively. The AUC increased to 0.882 when all the significant GS and CD features were used. The improvement by inclusion of Doppler features was significant (P <0.001). Sensitivity and specificity of combined grayscale and Doppler was 78.26% and 85.47%, respectively. Consideration of patient age in the analysis did not improve discrimination of TN and NTN.

### CONCLUSION

The analysis of breast ultrasound by machine learning can achieve high level of differentiation between the TN and NTN subtypes that is comparable to the diagnostic performance by standard visual assessments of the images.

### **CLINICAL RELEVANCE/APPLICATION**

TN breast cancers are high grade and aggressive with shorter survival time, higher metastasis and recurrence. This study proposes a quantitative sonographic approach for improving the TN diagnosis



### BR253-SD-TUB7

Comparison of Automated Breast Ultrasound (ABUS) QVCAD Standalone Performance on Somo-v and Invenia Cases

Tuesday, Nov. 27 12:45PM - 1:15PM Room: BR Community, Learning Center Station #7

### Participants

Yulei Jiang, PhD, Chicago, IL (*Presenter*) Research Grant, QView Medical, Inc; Research Consultant, QView Medical, Inc; Research Consultant, Quantitative Insights, Inc; Research Consultant, RadOnc eLearning Center, LLC Gene Pennello, PhD, Silver Spring, MD (*Abstract Co-Author*) Nothing to Disclose

#### For information about this presentation, contact:

yjiang@uchicago.edu

# PURPOSE

To evaluate QVCAD standalone performance on somo•v and Invenia cases, and to infer likely effect of QVCAD on Invenia cases from its effect on somo•v cases.

### METHOD AND MATERIALS

Evaluation was made on 164 somo•v (31 with cancer) and 145 Invenia (25 with cancer) cases, all of BI-RADS density C or D. Area under ROC curve (AUC), per-patient sensitivity and specificity, false-positives per volume, and FROC curves were compared. Noninferiority on Invenia vs. somo•v cases was tested with Bonferroni correction at a family-wise a=0.05 level for non-inferiority margins of -0.05 for AUC, -5% for sensitivity, -5% for specificity, and +0.05 for false positives per volume. A previous observer study of somo•v cases evaluated QVCAD effect on reader performance.

#### RESULTS

Somo•v and Invenia results were comparable. AUC was 0.73±0.05 (AUC ± standard error) for somo•v vs. 0.79±0.07 for Invenia. For QVCAD computer marks, sensitivity was 71.0% (22/31) [95% CI: 53.4%, 84.8%] vs. 84.0% (21/25) [65.8%, 94.7%], specificity was 49.6% (66/133) [41.2%, 58.0%] vs. 55.0% (66/120) [46.0%, 63.7%], and false-positive rate was 0.11 (101/891) [0.09, 0.14] per volume vs. 0.15 (107/697) [0.12, 0.19] per volume, respectively. For QVCAD computer-enhanced dark areas, sensitivity was 96.8% (30/31) [85.1%, 99.8%] vs. 100.0% (25/25) [88.7%, 100.0%], specificity was 6.0% (8/133) [2.8%, 11.1%] vs. 7.5% (9/120) [3.7%, 13.3%], and false-positive rate was 0.67 (596/891) [0.60, 0.74] per volume vs. 0.75 (525/697) [0.65, 0.85] per volume, respectively. Non-inferiority tests with Bonferroni correction did not show statistical significance. FROC curves were similar or apparently higher for Invenia than somo•v (Fig.). Previous observer study showed concurrent read of somo•v screening cases with QVCAD reduced reading time and produced non-inferior diagnostic accuracy compared with no QVCAD.

# CONCLUSION

QVCAD standalone performance is comparable on somo•v and Invenia cases. Its benefit for reducing reading time and producing non-inferior reader performance can be expected on Invenia cases.

## **CLINICAL RELEVANCE/APPLICATION**

This study provides a performance benchmark for clinical use of QVCAD on the current Invenia ABUS system and a frame of reference to the results of a previous observer study done on somo•v cases.



# CA168-ED-TUB7

Fluoroscopic Anatomy of the Heart: Comprehensive Understanding with Endocast Imaging and Virtual Dissection Imaging

Tuesday, Nov. 27 12:45PM - 1:15PM Room: CA Community, Learning Center Station #7

# Participants

Shumpei Mori, Kobe, Japan (*Presenter*) Nothing to Disclose Yu Izawa, Kobe, Japan (*Abstract Co-Author*) Nothing to Disclose Shinsuke Shimoyama, MD, Kobe, Japan (*Abstract Co-Author*) Nothing to Disclose Takayoshi Toba, Himeji, Japan (*Abstract Co-Author*) Nothing to Disclose Justin T. Tretter, Cincinnati, OH (*Abstract Co-Author*) Nothing to Disclose Diane Spicer, Valrico, FL (*Abstract Co-Author*) Nothing to Disclose Ken-Ichi Hirata, Kobe, Japan (*Abstract Co-Author*) Nothing to Disclose Robert Anderson, MD, Newcastle, United Kingdom (*Abstract Co-Author*) Nothing to Disclose

#### **TEACHING POINTS**

Since any invasive procedures in a catheter laboratory are performed with fluoroscopic support, correct appreciation of the fluoroscopic cardiac anatomy is the fundamental basis of the procedures. To facilitate such understanding, structural anatomy within the cardiac contour should be visualized from multiple directions. Using computed tomography, several reconstruction techniques can be executed to achieve this, depending on the focus of attention and the structures selected for rendering. Endocast imaging, which extracts several cardiac chambers with enhancement, can demonstrate well the relationship among each chamber. The technique, however, shows only the cavities of the cardiac components without showing walls and septa. Virtual dissection imaging retracts the chambers enhanced in endocast imaging, thus visualizing the walls, septa, and intracardiac structures. Virtual dissection images are of far greater value for interventional cardiologists, because it is these structures that are their main targets. Combination of these methodologies facilitates full appreciation of the fluoroscopic anatomy of the living heart.

### **TABLE OF CONTENTS/OUTLINE**

1. Image acquisition techniques 2. Various reconstruction techniques 3. Representative serial images to show fluoroscopic cardiac anatomy 4. Clinical implications



## CA170-ED-TUB8

# **Tutorial for Myocardial Perfusion CT**

Tuesday, Nov. 27 12:45PM - 1:15PM Room: CA Community, Learning Center Station #8

### **Participants**

Lior Molvin, Stanford, CA (*Presenter*) Speakers Bureau, General Electric Company Aya Kino, MD, Palo Alto, CA (*Abstract Co-Author*) Nothing to Disclose Virginia Hinostroza, Stanford, CA (*Abstract Co-Author*) Nothing to Disclose Ted Iovino, Emeryville, CA (*Abstract Co-Author*) Nothing to Disclose Roberto Rodriguez, Emeryville, CA (*Abstract Co-Author*) Nothing to Disclose Fiona Holtzclaw, Emeryville, CA (*Abstract Co-Author*) Nothing to Disclose Heiko Schmiedeskamp, PhD, Malvern, PA (*Abstract Co-Author*) Employee, Siemens AG Dominik Fleischmann, MD, Stanford, CA (*Abstract Co-Author*) Research Grant, Siemens AG Koen Nieman, MD, PhD, Rotterdam, Netherlands (*Abstract Co-Author*) Nothing to Disclose

#### For information about this presentation, contact:

Imolvin@stanfordhealthcare.org

### **TEACHING POINTS**

• Specificity in detection of hemodynamically significant coronary arteries stenosis on coronary CTAs can be improved when combined with myocardial perfusion

### TABLE OF CONTENTS/OUTLINE

• BACKGROUND Myocardial CT perfusion can identify perfusion defects during vasodilator stress • TECHIICAL REQUIREMENTS Minimal requirements for CT scanner: rotation and detectors Patient monitoring requirements Personnel: cardiologist, radiologist, nursing team and CT technologist Safety requirements: drugs • PROTOCOL TECHNIQUES Patient and image team preparation Scan parameters: tube voltage, radiation dose Patient positioning Stress agen and IV contrast volume and timing Patient monitoring Iterative reconstruction and image processing algorithms Pitfalls, artifacts that can mimic false positive/negative myocardial perfusion • EXAMPLE Benefits and challenges of this protocol in practice Examples of normal/abnormal myocardial perfusion CT • IMPLEMENTATION CHALLENGES Increase awareness and availability of myocardial perfusion CT by the ordering clinicians Provide quick test results for the ordering clinicians • CONCLUSION Myocardial perfusion CT can add additional physiological information of ischemia in patients referred to coronary CTA, increasing specificity to a lower positive predictive value of obstructive lesions detected by coronary CTA



# CA231-SD-TUB1

Influence of Readers' Experience on the Classification Performances of the Deep Neural Network (DNN) for Classifying Myocardial Delayed Enhancement on Cardiac MRI

Tuesday, Nov. 27 12:45PM - 1:15PM Room: CA Community, Learning Center Station #1

# Participants

Yasutoshi Ohta, MD, Yonago, Japan (*Presenter*) Nothing to Disclose Hiroto Yunaga, Yonago, Japan (*Abstract Co-Author*) Nothing to Disclose Atsushi K. Kono, MD, PhD, Suita, Japan (*Abstract Co-Author*) Nothing to Disclose Tatsuya Nishii, MD, PhD, Suita, Japan (*Abstract Co-Author*) Nothing to Disclose Yoshiaki Morita, Suita, Japan (*Abstract Co-Author*) Nothing to Disclose Aiko Takami, Yonago, Japan (*Abstract Co-Author*) Nothing to Disclose Natsuko Mukai, MD, Yonago, Japan (*Abstract Co-Author*) Nothing to Disclose Shinichiro Kitao, Yonago, Japan (*Abstract Co-Author*) Nothing to Disclose Ryoya Ochiai, Yonago, Japan (*Abstract Co-Author*) Nothing to Disclose Kazuhiro Yamamoto, Yonago, Japan (*Abstract Co-Author*) Nothing to Disclose Toshihide Ogawa, MD, Yonago, Japan (*Abstract Co-Author*) Nothing to Disclose

## PURPOSE

To investigate whether readers' experience influences on the classification performances of the deep neural network in recognition of myocardial delayed enhancement (MDE) on cardiac MRI.

# METHOD AND MATERIALS

Four junior readers (JR) with less than 5 years' experience and four senior readers (SR) with greater than 5 years' experience from two separate institutions evaluated 1888 MDE images from consecutive 200 cardiac MRI cases. All readers were blinded to patient information. The 388 test MDE images from another 50 cases for DNN performance evaluation were classified by three senior readers by consensus. MDE patterns were classified into 7 categories (epicardial, focal, midwall, non-diagnostic, none, subendocardial and transmural). GoogLeNet was used for the architecture of DNN in recognizing images. Each reader's labeled dataset was used for training the DNNs. The trained DNNs' image classification performances were evaluated by classifying the test MDE images. The performances of detecting MDE and discriminating ischemic MDE (subendocardial and transmural) from other categories were assessed using receiver operating characteristic (ROC) curves. The MDE category concordances among readers were assessed using Fleiss's Kappa(K).

### RESULTS

The agreement in classification among senior readers (K= 0.51) was stronger than for junior readers (K= 0.243). The mean area under the curves (AUC) of ROC in MDE detection by SR-trained DNNs were higher compared to JR-trained DNNs ( $0.836\pm0.014$  vs.  $0.783\pm0.030$ , p=0.018, respectively). The mean AUCs in discriminating ischemic MDE from other MDE categories by SR-trained DNNs were higher compared to JR-trained DNNs ( $0.884\pm0.012$  vs.  $0.803\pm0.039$ , p=0.007, respectively). The median accuracy for MDE classification for SR-trained DNNs was higher compared to JR-trained DNNs (51.3% vs. 44.0%, p=0.0286, respectively).

# CONCLUSION

The classification performances for MDE by DNN depend on the experience of the observer who created the teacher data.

## **CLINICAL RELEVANCE/APPLICATION**

Labeling of teacher data is necessary for DNN learning, but since the radiologist's experience affects the DNN learning result, it is necessary to pay attention to the quality of the teacher data.



# CA232-SD-TUB2

# Validation of Deep Learning Technique for Quantification of Cardiac Left Ventricle

Tuesday, Nov. 27 12:45PM - 1:15PM Room: CA Community, Learning Center Station #2

### Participants

Wufeng Xue, London, ON (*Presenter*) Nothing to Disclose Gary L. Brahm, BMedSc, MD, London, ON (*Abstract Co-Author*) Nothing to Disclose Stephanie E. Leung, MD, London, ON (*Abstract Co-Author*) Nothing to Disclose Ogla Shmuilovich, London, ON (*Abstract Co-Author*) Nothing to Disclose Shuo Li, PhD, London, ON (*Abstract Co-Author*) Nothing to Disclose

# For information about this presentation, contact:

xwolfs@hotmail.com

## PURPOSE

Accurate quantification of left ventricle is of great significance for reliable clinical cardiac function assessment. This study validates the effectiveness of deep learning techniques for simultaneous quantification of multiple clinical-significant left ventricle (LV) indices from short-axis cardiac MR sequences, and compare it with traditional segmentation methods and non-deep learning estimation methods. The considered indices include six regional wall thicknesses (RWT) of myocardium, three directional cavity dimensions, as well as two areas (areas of LV cavity and myocardium).

## **METHOD AND MATERIALS**

A deep convolution neural network, equipped with recurrent network and multi-task learning is proposed to directly estimate the multiple LV indices from short axis cardiac MR sequences. A dataset of 2D short axis cine MR images of 145 subjects is used to validate the method against manually labeled ground truth following a 5-fold cross validation strategy. The subjects ages from 16 yrs to 97 yrs, with average of 58.9 yrs. The pixel spacings of the MR images range from 0.6836 mm/pixel to 2.0833 mm/pixel, with mode of 1.5625 mm/pixel. Each subject contains 20 frames throughout a cardiac cycle. For each subject, a representative mid-cavity slice is selected in this study.

## RESULTS

The deep learning method achieves average mean absolute error (MAE) of 180 mm2, 2.51 mm, and 1.39 mm for areas, dimensions and RTWs. This clearly outperforms traditional segmentation-based method (274 mm2, 2.65 mm, 3.21mm) and non-deep learning method (242mm2, 2.88mm, 1.85mm). Fore reference, the maximums of these indices in our dataset are 4936 mm2, 81.0 mm, 24.4 mm, respectively.

### CONCLUSION

The deep learning method provides accurate quantification results of multiple significant LV indices for all frames across the whole cardiac cycle, and outperforms traditional segmentation based method and non-deep learning estimation method.

# **CLINICAL RELEVANCE/APPLICATION**

Deep learning method offers a feasible and reliable solution for automatically cardiac function assessment, and has a great potential implementation in clinical practice.



# CA233-SD-TUB3

Impact of Virtual Monoenergetic Image Types on Image Quality of Late Iodine Enhancement with Dual-Layer Spectral CT in Patient with Hypertrophic Cardiomyopathy (HCM)

Tuesday, Nov. 27 12:45PM - 1:15PM Room: CA Community, Learning Center Station #3

# Participants

Koji Sasaki, RT, Sapporo, Japan (Presenter) Nothing to Disclose

Noriko Oyama-Manabe, MD, PhD, Sapporo, Japan (*Abstract Co-Author*) Grant, Canon Medical Systems Corporation Shinichi Tokuyasu, RT,MS, Minato-ku, Japan (*Abstract Co-Author*) Employee, Koninklijke Philips NV Tsutomu Fujita, MD, Sapporo, Japan (*Abstract Co-Author*) Nothing to Disclose

## PURPOSE

Late iodine enhancement (LIE) has been used for evaluation of various cardiomyopathies. The aim of this study was to compare the image quality of LIE using dual-layered detector spectral CT among five type reconstruction algorithm: conventional 120kVp (Conventional image), virtual monoenergetic image (VM) at 70keV, 60keV, 50keV, 40keV.

## **METHOD AND MATERIALS**

Twenty patients (12men, mean age 63 years old) were referred for evaluation of hypertrophic cardiomyopathy. They underwent cardiac LIE CT by electrocardiogram-gated scan. Paired three slices of myocardial basal, mid, apical image were created with five types of reconstruction (conventional, VM 70keV, 60keV, 50keV, 40keV).Each patient was visually evaluated for presence of LIE according to American Heart Association 17-segment model except for the apical segment.Objective image quality measurements such as image noise determined as the standard deviation of the attenuation value, myocardial signal-to-noise ratio (SNR), and if LIE positive, contrast-to-noise ratio between late enhancement and remote myocardial regions (CNR) were also evaluated using 16 regions of interest.

## RESULTS

The median image noises of VM 70keV, 60keV and 50keV were significantly lower than that of conventional image (3.4, 3.7, 4.2 and 4.5, respectively) (p=0.02 for 50keV, p<0.0001 for others), while that of VM 40keV (5.3) was significantly higher than conventional one (p<0.001). The median SNR of VM 70keV, 60keV, 50keV, 40keV (19.1, 19.8, 20.5, and 20.2) were significantly higher than that of conventional image (14.3) (p<0.0001 for all). The median CNR of VM 70keV, 60keV, 50keV, 40keV (4.3, 6.0, 7.9 and 10.9) were significantly higher than conventional one (3.1) (p=0.0012 for 70keV, p<0.0001 for others).

# CONCLUSION

The VM images showed significant noise reduction and increased SNR/CNR compared to conventional ones with spectral CT. The clinical impact of VM is warranted to improve diagnostic ability for LIE in HCM.

## **CLINICAL RELEVANCE/APPLICATION**

The virtual monoenergetic images especially at 50keV showed significant noise reduction and increased SNR/CNR compared to conventional ones for evaluation of late iodine enhancement with spectral CT.



# CA234-SD-TUB4

Utility of Dual-Energy CT for Assessment of Myocardial Fibrosis: Calculation of Extracellular Volume Fraction (ECV) Using Measured Hematocrit versus Virtual Hematocrit

Tuesday, Nov. 27 12:45PM - 1:15PM Room: CA Community, Learning Center Station #4

# Participants

Jamie L. Schroeder, MD, DPhil, Baltimore, MD (*Presenter*) Nothing to Disclose Pallavi Pandey, MD, Baltimore, MD (*Abstract Co-Author*) Nothing to Disclose Ankur Pandey, MD, Baltimore, MD (*Abstract Co-Author*) Nothing to Disclose Matthew Czarny, Baltimore, MD (*Abstract Co-Author*) Nothing to Disclose Rani K. Hasan, MD, Baltimore, MD (*Abstract Co-Author*) Nothing to Disclose Cheng Ting Lin, MD, Baltimore, MD (*Abstract Co-Author*) Nothing to Disclose Ihab R. Kamel, MD, PhD, Baltimore, MD (*Abstract Co-Author*) Nothing to Disclose Elliot K. Fishman, MD, Baltimore, MD (*Abstract Co-Author*) Nesearch Grant, Siemens AG Elliot K. Fishman, MD, Baltimore, MD (*Abstract Co-Author*) Institutional Grant support, Siemens AG; Institutional Grant support, General Electric Company; Co-founder, HipGraphics, Inc Stefan L. Zimmerman, MD, Ellicott City, MD (*Abstract Co-Author*) Project consultant, Siemens Healthcare; Research grant, American Heart Association;

### For information about this presentation, contact:

jschro14@jhmi.edu

#### PURPOSE

Diffuse myocardial fibrosis is a complication associated with various chronic heart diseases, including aortic stenosis. In cardiac CT or MRI, fibrosis is quantified by the fraction of tissue comprised of extracellular volume (ECV), which is equal to the blood plasma fraction (1 - hematocrit) times the ratio of delayed enhancement ( $\Delta$ HU) between myocardium and blood pool. Our purpose was to evaluate two methods for calculation of a virtual hematocrit-derived ECV to simplify quantification of fibrosis, using ECV calculated from actual hematocrit (Hct) measured at time of CT examination as the standard of reference.

## **METHOD AND MATERIALS**

61 patients with aortic stenosis (35M/26F; mean age 81 yrs) undergoing preoperative CT angiography for transcatheter aortic valve replacement (TAVR) underwent dual energy multiphase protocol including non-contrast phase and 10-minute delayed phase imaging. Virtual hematocrit values were calculated from linear regression equations developed from true measured hematocrit vs. either 1) density of blood pool from the non-contrast phase (vHct), or 2) density of blood pool from a virtual non-contrast image derived from the dual energy delayed phase using spectral separation (DEvHCT). The reference ECV was calculated from measured hematocrit and compared to the virtual methods.

### RESULTS

The regression between non-contrast phase blood pool density and measured hematocrit was vHct= $0.75^{*}(HU)+7.6$  (R<sup>2</sup>=0.51). The regression between dual energy virtual-non-contrast blood pool density and measured hematocrit was DEvHct= $0.34^{*}(vHU)+27.6$  (R<sup>2</sup>=0.28). Reference mean ECV was 28.1%, mean ECV measured using vHct was 28.2% and mean ECV measured using DEvHct was 28.1%. Mean bias for ECV using vHct and DEvHct was 0.1% [-2.6% to +2.7% CI] and 0.0% [-3.3% to +3.2% CI], respectively.

# CONCLUSION

Non-contrast blood pool density correlated better with measured Hct than blood pool density obtained from virtual-non-contrast images. However, this did not translate into significant differences in ECV measurements when using either virtual Hct method (vHct or DEvHct). Both virtual methods showed close agreement with the reference standard with no significant bias.

### **CLINICAL RELEVANCE/APPLICATION**

Myocardial fibrosis may be one of several variables that may help predict outcomes after TAVR. This study demonstrates that ECV measurements derived from virtual hematocrit are accurate and may eliminate the need for additional blood tests.

### **Honored Educators**

Presenters or authors on this event have been recognized as RSNA Honored Educators for participating in multiple qualifying educational activities. Honored Educators are invested in furthering the profession of radiology by delivering high-quality educational content in their field of study. Learn how you can become an honored educator by visiting the website at: https://www.rsna.org/Honored-Educator-Award/ Ihab R. Kamel, MD, PhD - 2015 Honored EducatorElliot K. Fishman, MD - 2012 Honored EducatorElliot K. Fishman, MD - 2014 Honored EducatorElliot K. Fishman, MD - 2016 Honored EducatorElliot K. Fishman, MD - 2018 Honored EducatorStefan L. Zimmerman, MD - 2012 Honored EducatorStefan L. Zimmerman, MD - 2015 Honored Educator



## CA235-SD-TUB5

Changes of Left Ventricular Myocardial Strain in Acute ST-Elevation Myocardial Infarction Patients before Left Ventricular Remodeling and Its Relation to Microvascular Obstruction: A CMR Feature Tracking Study

Tuesday, Nov. 27 12:45PM - 1:15PM Room: CA Community, Learning Center Station #5

**FDA** Discussions may include off-label uses.

#### **Participants**

Xiaonan Wang, Shenyang, China (*Presenter*) Nothing to Disclose Yang Hou, MD, Shenyang, China (*Abstract Co-Author*) Nothing to Disclose

#### For information about this presentation, contact:

cmuwxn@163.com

### PURPOSE

To characterize the alteration in quantification of global left ventricular (LV) strain by cardiovascular magnetic resonance(CMR) feature tracking after acute ST-elevation myocardial infarction(STEMI) before LV remodeling, and to explore the relation to microvascular obstruction (MVO).

# METHOD AND MATERIALS

The prospective study enrolled 32 patients with STEMI successfully treated with primary PCI who underwent CMR after 3-5days (baseline) and 4-6 months (follow-up). Cine imaging and late gadolinium enhancement(LGE) was performed at 3.0 T MR. Longitudinal global strains(GLS),circumferential global strains (GCS),global radial strains(GRS) and cardiac volume were measured by CVI 42 software based on cine sequences. MVO was assessed based on LGE sequence. According to the existence of MVO or not, all patients were divided into MVO(+) group and MVO(-) group. Mean values of GLS, GCS and GRS were compared between the two groups of patients using an independent-samples t-test. Means of baseline and follow-up measurements were compared using a paired t-test.

### RESULTS

In this study, none of the patients had LV remodeling, according to the end-systolic volume improvement <=15%. Seventeen patients were classified as MVO(+) and 15 patients as MVO(-).At baseline, there were no significant differences of GRS, GCS and GLS between the two groups (P=0.47,0.64 and 0.71). At follow-up, the GRS and GCS between MVO(+) and MVO(-) still make no significant differences (P=0.06, 0.12), while the GLS mean values of MVO(+) group significantly lower than that of MVO(-) group [(-14.10 $\pm$ 0.51)%vs. (-16.35 $\pm$ 0.75)%, P=0.048]. From baseline to 4-6 follow-up, the GRS, GCS and GLS of the two groups were all increased {MVO(-): [(34.51 $\pm$ 8.52)% vs. (34.65 $\pm$ 9.07)%, P =0.007 ], [(-16.91 $\pm$ 3.14)% vs.( -18.13 $\pm$ 3.64)%, P=0.038 ], [(-15.04 $\pm$ 2.53)%vs. (-16.35 $\pm$ 3.08)%,P=0.010]; MVO(+):[(29.12 $\pm$ 6.84)%vs. (30.61 $\pm$ 5.68)%,P=0.101], [(-14.27 $\pm$ 3.04)%vs.( -16.33 $\pm$ 0.66,)%, P=0.014 )], [(-11.97 $\pm$ 2.21)%vs.(-14.10 $\pm$ 1.98)%, P=0.657 ]}.

### CONCLUSION

For acute STEMI patients without LV remodeling in 4-6 months after PCI, the GRS, GCS and GLS of LV were all increased irrespective of MVO existed or not, and the changes of GLS in group with MVO was more obvious. Which may be the evidence of LV early remodeling.

### **CLINICAL RELEVANCE/APPLICATION**

Feature tracking can assess myocardial systolic function and myocardial damage and is recommended for prognosis assessment following acute STEMI patients.



## CH247-ED-TUB6

## The Surgical 3DCT Anatomy of the Pulmonary Vessels for Lung Cancer: What Radiologists Should Know

Tuesday, Nov. 27 12:45PM - 1:15PM Room: CH Community, Learning Center Station #5

### Participants

Makiko Murota, MD, Kitagun, Japan (*Presenter*) Nothing to Disclose Yuka Yamamoto, MD, PhD, Kagawa, Japan (*Abstract Co-Author*) Nothing to Disclose Katashi Satoh, MD, Takamatsu, Japan (*Abstract Co-Author*) Nothing to Disclose Yoshihiro Nishiyama, MD, Kagawa, Japan (*Abstract Co-Author*) Nothing to Disclose

# **TEACHING POINTS**

Preoperative identification of pulmonary vessels is considered one of the key issues for successful surgical resection of lung cancer. Anatomical variants of pulmonary vessels can cause serious problems such as unexpected bleeding. The purpose of the exhibit is: 1. To describe the types of surgery for lung cancer, and utility of 3D-CT angiography (3D-CTA). 2. To recognize the basic branching patterns of the pulmonary artery (PA) and pulmonary vein (PV), and then to understand the variations of them that are the key point for surgery.

## TABLE OF CONTENTS/OUTLINE

1. Introduction 2. Describe the common types of surgery for lung cancer and anatomical information what are needed for each procedure -wedge resection, segmentectomy, lobectomy, pneumonectomy 3. The 3D-CTA techniques of the PA and PV for preoperative information -traditional CTA images -the separate demonstration 3DCT-PA and 3DCT-PV -visualization in the pulmonary bronchovascular pattern using CTA and 3D-bronchography 4. The basic branching patterns and the important variations for the lung cancer surgery -PA -PV 5. Take home points



# CH248-ED-TUB7

Imaging Follow-Up After Radiofrequency Ablation (RFA) in Patients with Early Stage Non-Small Cell Lung Cancer (NSCLC): An Experience-Based Pictorial Review

Tuesday, Nov. 27 12:45PM - 1:15PM Room: CH Community, Learning Center Station #7

# Participants

Alessandra Ottavianelli, MD, Rome, Italy (*Presenter*) Nothing to Disclose Annemilia del Ciello, MD, Rome, Italy (*Abstract Co-Author*) Nothing to Disclose Alessandra Farchione, MD, Rome, Italy (*Abstract Co-Author*) Nothing to Disclose Lucio Calandriello, MD, Rome, Italy (*Abstract Co-Author*) Nothing to Disclose Giuseppe Cicchetti, MD, Rome, Italy (*Abstract Co-Author*) Nothing to Disclose Francesca Giubbolini, Rome, Italy (*Abstract Co-Author*) Nothing to Disclose Roberto Iezzi, MD, Rome, Italy (*Abstract Co-Author*) Nothing to Disclose Lucia Leccisotti, MD, Rome, Italy (*Abstract Co-Author*) Nothing to Disclose Anna Rita Larici, MD, Rome, Italy (*Abstract Co-Author*) Nothing to Disclose Riccardo Manfredi, MD, Rome, Italy (*Abstract Co-Author*) Nothing to Disclose

#### For information about this presentation, contact:

ottavianellialessandra@gmail.com

#### **TEACHING POINTS**

- To review, according to the time of unset, the most common CT and 18F-FDG PET/CT patterns occurring during follow-up after RFA in patients with NSCLC, through the experience of our center- To describe findings which are not expected after successful RFA and therefore labelled as "red flags" for progression of incompletely ablated tumor or recurrence

## TABLE OF CONTENTS/OUTLINE

Radiological and functional patterns after RFA are classified according to the time of onset. EARLY PHASE ( <=1 week) CT: ground glass opacities (GGO). INTERMEDIATE PHASE ( > 1 week - 2 months) CT: increasing of size, concentric rings of attenuation, peripheral enhancement; 18F-FDG PET/CT: absence of central uptake. LATE PHASE ( >2 months) CT: gradual reduction of lesion size and enhancement; 18F-FDG PET/CT: gradual reduction of uptake. BENIGN ADDITIONAL FIDINGS: cavitation, scar formation, pleural thickening."RED FLAGS" FOR RECURRENCE: CT: increase in volume and enhancement, new satellite nodule, lymphadenopathy; 18F-FDG PET/CT: increase in metabolic activity.



# CH279-SD-TUB1

Quantitative Computed Tomography Phenotypes, Spirometric Parameters, and Clinical Findings in Heavy Smokers

Tuesday, Nov. 27 12:45PM - 1:15PM Room: CH Community, Learning Center Station #1

# Participants

Marcelo C. Barros, MD, Santana do Livramento, Brazil (*Abstract Co-Author*) Nothing to Disclose Bruno Hochhegger, MD, PhD, Porto Alegre, Brazil (*Abstract Co-Author*) Nothing to Disclose Adriano Basso Dias, MD, Porto Alegre, Brazil (*Presenter*) Nothing to Disclose Daniela Cavalet-Blanc, Porto Alegre, Brazil (*Abstract Co-Author*) Nothing to Disclose Guilherme Watte, Porto Alegre, Brazil (*Abstract Co-Author*) Nothing to Disclose Gabriel Sartori Pacini, Porto Alegre, Brazil (*Abstract Co-Author*) Nothing to Disclose Matheus Zanon, Porto Alegre, Brazil (*Abstract Co-Author*) Nothing to Disclose Yana Pallaoro, Porto Alegre, Brazil (*Abstract Co-Author*) Nothing to Disclose Romulo Roxo, Porto Alegre, Brazil (*Abstract Co-Author*) Nothing to Disclose Eryn D. Wilke, Porto Alegre, Brazil (*Abstract Co-Author*) Nothing to Disclose Ana Paula G. Sartori, MD, Porto Alegre, Brazil (*Abstract Co-Author*) Nothing to Disclose Stephan Altmayer, Porto Alegre, Brazil (*Abstract Co-Author*) Nothing to Disclose Jose M. Chatkin, Porto Alegre, Brazil (*Abstract Co-Author*) Nothing to Disclose

### PURPOSE

To evaluate the quantitative computed tomography (QCT) phenotypes, airflow limitations, and exacerbation-like episodes in heavy smokers undergoing a screening for lung cancer.

# METHOD AND MATERIALS

We enrolled 172 smokers with a smoking history >=30 pack-years who underwent pulmonary function tests (PFTs) and CT scan for screening of lung cancer. Patients were classified regarding airflow limitation (VEF1/FVC <0.7) and the presence of emphysema on the QCT. The QCT were analyzed in a specialized software and patients were classified in two disease-predominant phenotypes: emphysemapredominant (EP) and non-emphysema-predominant (NEP). EP was defined as 6% or more pixels with less than -950 Hounsfield units, while NEP shows less than 6% of pixels below this value.

#### RESULTS

Most patients in our sample had air-flow limitation (61%), of those most were male (68.5%) and had a mean smoking history of 77.2  $\pm$ 38.0 packs-year. The group with limitation had more exacerbation-like episodes compared to those without airflow limitation (26.6% vs. 9%, p <0.001) and greater areas of low attenuation on QCT (17.01  $\pm$ 9.96 vs. 4.52  $\pm$ 3.55, p<0.001). Most of our patients were classified in the EP phenotype. The EP group had significant worse pulmonary function (VEF1 60.6  $\pm$ 22.9 vs. 89.7  $\pm$ 15.9, p <0.001), and had more exacerbation episodes (25.8% vs. 8.3%, p <0.001) compared to the NEP group.

## CONCLUSION

Heavy smokers with the EP phenotype on QCT had worse pulmonary function, and more exacerbation-like episodes than those with the NEP phenotype. About 23.8% of those with no airflow limitation on PFTs were classified as EP.

# **CLINICAL RELEVANCE/APPLICATION**

Quantitative computed tomography (QCT) allows objective and noninvasive identification and quantification of emphysema earlier than spirometry, and possibly before the emergence of symptoms. Assessment of airway morphology and other underlying conditions can be used to define the patient's predominant phenotype, which plays an important role in determining outcomes related to exacerbations, antimicrobial therapy, decline in pulmonary function, and mortality.



## CH280-SD-TUB2

Is a Chest CT Alone Sufficient to Determine Progression of Disease in Stage 4 Lung Cancer Clinical Trial Patients?

Tuesday, Nov. 27 12:45PM - 1:15PM Room: CH Community, Learning Center Station #2

**FDA** Discussions may include off-label uses.

#### Participants

Anthony Sader, BS, Seattle, WA (*Presenter*) Nothing to Disclose Renato G. Martins, MD, MPH, Seattle, WA (*Abstract Co-Author*) Nothing to Disclose Ryan O'Malley, MD, Seattle, WA (*Abstract Co-Author*) Nothing to Disclose Achille Mileto, MD, Seattle, WA (*Abstract Co-Author*) Nothing to Disclose Danielle Nacamuli, BS, Seattle, WA (*Abstract Co-Author*) Nothing to Disclose Janet M. Busey, MS, Seattle, WA (*Abstract Co-Author*) Nothing to Disclose Kent M. Koprowicz, Seattle, WA (*Abstract Co-Author*) Nothing to Disclose Kent Spiekerman, PhD, Seattle, WA (*Abstract Co-Author*) Nothing to Disclose Carolyn L. Wang, MD, Seattle, WA (*Abstract Co-Author*) Nothing to Disclose

# For information about this presentation, contact:

asader@uw.edu

### PURPOSE

To determine if a chest CT alone with measurable chest disease is sufficient to determine progression of disease (PD) in stage 4 lung cancer patients on clinical trial as assessed by RECIST 1.1.

# METHOD AND MATERIALS

IRB approved HIPAA compliant retrospective review of treatment response of patients with stage 4 lung cancer on clinical trial assessed by RECIST 1.1 in a tumor metrics database (Precision Imaging Metrics). Only patients with known progression of measurable disease were analyzed for sites of PD classified as chest only progression, outside chest only progression or a combination of chest and outside of chest progression. Further classifications of the sites were grouped as abdomen, brain versus pelvis. An equivalence test of the observed proportion using chest alone with null hypothesis proportion observed proportion using chest and other and equivalence margin of 0.07 was conducted.

#### RESULTS

Of the 328 patients identified, 188 had PD. 116 (61.7%) patients were classified as PD based on the chest, 57 (30.3%) based on chest and other sites, and 15 (7.98%) based only on sites outside the chest. The most common sites of PD other than the chest was the liver, adrenals, and brain. The most common site of chest independent progression was the brain. Altogether, 61.7% of patients could be labelled as PD with only a chest CT, 96.81% would be labelled if an abdomen CT was included, and 99.47% of patients would be labelled if a brain MRI was included. Only 1 case (0.53% of patients) had PD exclusively in the pelvis. The two one-sided tests (TOST) for equivalence yielded an overall p-value of 1, indicating the null hypothesis of non-equivalence of a chest CT alone compared to chest with other should not be rejected.

# CONCLUSION

Although a chest CT alone in this sample of patients with stage 4 lung cancer on clinical trial with measurable disease in the chest can determine PD in 61.7%, it was statistically inferior to chest CT plus abdomen and brain MRI. However CT pelvis only rarely is necessary to establish progression of disease alone and may not be necessary at each follow-up time point.

#### **CLINICAL RELEVANCE/APPLICATION**

Although a chest CT alone is not sufficient to determine PD in stage 4 lung cancer patients on clinical trial, CT pelvis rarely demonstrates PD and may not be necessary at each follow-up time point.



# CH281-SD-TUB3

Predicting Pathological Noninvasiveness in T1 Non-Small Cell Lung Cancer on Chest CT Scan Using Deep Learning Algorithm

Tuesday, Nov. 27 12:45PM - 1:15PM Room: CH Community, Learning Center Station #3

# Participants

Kyongmin S. Beck, MD, Seoul, Korea, Republic Of (*Abstract Co-Author*) Nothing to Disclose Yoon Ho Ko, MD,PhD, Seoul, Korea, Republic Of (*Abstract Co-Author*) Nothing to Disclose Sungsoo Park, Deajeon, Korea, Republic Of (*Abstract Co-Author*) Nothing to Disclose Junghwa Choi, MD, Seoul, Korea, Republic Of (*Presenter*) Nothing to Disclose Sae Jung Na, Seoul, Korea, Republic Of (*Abstract Co-Author*) Nothing to Disclose Ji Hyung Hong, Incheon, Korea, Republic Of (*Abstract Co-Author*) Nothing to Disclose Tae-Jung Kim, MD,PhD, Seoul, Korea, Republic Of (*Abstract Co-Author*) Nothing to Disclose

#### For information about this presentation, contact:

koyoonho@catholic.ac.kr

# PURPOSE

to evaluate the ability of an artificial intelligence (deep learning algorithm) to predict pathological noninvasiveness of T1 non-small cell lung cancer (NSCLC) using computed tomography (CT) images.

### **METHOD AND MATERIALS**

468 preoperative CT images of NSCLC smaller than 3 cm, resected at our institution from 2008 to 2015 were used to train and validate the deep learning algorithm. Noninvasiveness was defined as the absence of nodal involvement, vascular invasion, and lymphatic invasion, and NSCLCs were classified as either noninvasive or invasive according to the pathological reports. A deep 3D convolutional neural network (CNN) was trained using 5-fold cross-validation method. To normalize input data, we rescaled CT image to let one voxel size be represented as (1mm,1mm,1mm). Input cube size was (32mm, 32mm,32mm). Horizontal flip and vertical flip augmentation were applied, and max-pooling and dropout layer were used to avoid overfitting. Receiver operating characteristic (ROC) curves and areas under the curve (AUCs), accuracy, and sensitivity/specificity were used to assess the performance of 3D CNN. We also added tumor size as an external feature to the 3D CNN model and evaluated the performance of the combined model using Xgboost classifier.

### RESULTS

157 out of 486 samples (33.5%) were invasive. A subsample group composed of 10% of the data (32 noninvasive and 16 invasive samples) was retained for the validation set. The 3D CNN showed an AUC of 0.826, 77.08% accuracy, 68.7% sensitivity, and 81.2 % specificity. Adding tumor size to the 3D CNN model showed an AUC of 0.855, 81.25% accuracy, 87.5% sensitivity, and 78.1% specificity.

## CONCLUSION

Artificial intelligence can accurately predict pathological noninvasiveness in T1 size NSCLC on CT images.

# **CLINICAL RELEVANCE/APPLICATION**

Because of the risk of recurrence, lobectomy is indicated even for small lung cancers. If we could accurately predict and classify noninvasive small lung cancers on CT images using deep learning algorithm prior to surgery, a more refined selection of candidates who would benefit from limited resection without increasing the risk of recurrence would be possible.



## CH282-SD-TUB4

Inter-Observer Agreement in the Classification of Perifissural Nodules as Lymphnodes on Chest CT

Tuesday, Nov. 27 12:45PM - 1:15PM Room: CH Community, Learning Center Station #4

#### **Participants**

Juan Carlos Diaz Patino, Santiago, Chile (*Abstract Co-Author*) Nothing to Disclose Claudio Silva, MD, Santiago, Chile (*Abstract Co-Author*) Nothing to Disclose Javier A. Cacho I, MD, Santiago, Chile (*Presenter*) Nothing to Disclose Julia Alegria, MD, Santiago, Chile (*Abstract Co-Author*) Nothing to Disclose Cristobal A. Ramos Sr, MD, Santiago, Chile (*Abstract Co-Author*) Nothing to Disclose

## For information about this presentation, contact:

jcdiaz@alemana.cl

### PURPOSE

Determine inter-observer agreement of chest radiologists classifying perifissural nodules (PFN) as intrapulmonary lymphnodes on chest CT.

# METHOD AND MATERIALS

IRB-approved retrospective study, who approved a waiver on informed consent. All chest CT performed during a four-month period (March through July 2016) were reviewed for incidental pulmonary nodules by a senior chest radiologist who sub-classified them into three categories (typical PFN - likely intrapulmonary lymph node, atypical PFN and non-PFN) by using criteria by de Hoop et al. 120 cases were selected, studies were anonymized and reviewed by three other senior chest radiologists, who classified them using the same criteria, unaware of the patients' history. Inter-observer agreement was analyzed using Cohen's kappa coefficient. 95% CI were calculated and statistical significance was considered at p<0.05.

#### RESULTS

The global agreement measured by Cohen's Kappa was 0.603 (95% CI: 0.560 - 0.661). When categories were regrouped, Kappa value for classifying "typical PFN" compared to the remaining categories ("atypical PFN" and "not PFN") was 0.728 (95% CI: 0.690 - 0.754), in good range of concordance according to Altman et al. When the "not PFN" category was considered (grouping together the remaining categories), Kappa values dropped to 0.530 (95% CI 0.473 - 0.587), moderate concordance according to Altman et al.

### CONCLUSION

Incidental pulmonary nodules are a frequent finding in routine chest CT and are followed according to guidelines. Some of these nodules represent intrapulmonary lymph nodes and should require no follow-up. Our results show that there is good interobserver agreement in the classification of pulmonary nodules as "typical" intrapulmonary lymph nodes. However, classifying as "atypical" lymphnode has a higher degree of variability, which might hinder its widespread use.

## **CLINICAL RELEVANCE/APPLICATION**

The category of intrapulmonary lymph node has been incorporated in some European incidental pulmonary nodule guidelines, and recently mentioned on the Fleischner Society guidelines. To our knowledge, there are no studies analyzing inter-observer agreement in classifying nodules as intrapulmonary lymph nodes. Our results show that there is good interobserver agreement in the classification of pulmonary nodules as typical PFN, therefore highly suggestive of intrapulmonary lymph nodes and amenable to support the incorporation of this category in future guidelines.



## CH283-SD-TUB5

# **T1** Mapping in Thoracic Neoplasms: Initial Experience

Tuesday, Nov. 27 12:45PM - 1:15PM Room: CH Community, Learning Center Station #5

### **Participants**

Jordi Broncano, MD, Cordoba, Spain (*Presenter*) Nothing to Disclose Fernando Caro Mateo, Cadiz, Spain (*Abstract Co-Author*) Nothing to Disclose Javier Sanchez, MD, PhD, Madrid, Spain (*Abstract Co-Author*) Nothing to Disclose Pilar Caro, MD, Cadiz, Spain (*Abstract Co-Author*) Nothing to Disclose Paula Montesinos de la Vega, Madrid, Spain (*Abstract Co-Author*) Employee, Koninklijke Philips NV Antonio Luna, MD, PhD, Jaen, Spain (*Abstract Co-Author*) Consultant, Bracco Group; Speaker, General Electric Company; Speaker, Canon Medical Systems Corporation; Royalties, Springer Nature

#### For information about this presentation, contact:

j.broncano.c@htime.org

#### PURPOSE

To evaluate the feasibility and diagnostic performance of T1 mapping in the evaluation of tumoral and non-neoplastic lesions of the chest.

## METHOD AND MATERIALS

31 patients (36 tumoral and non-neoplastic lesions) were prospectively included. There were 23 males and 8 females, with normal renal function and mean age of  $66.1 \pm 12.41$  years-old. Added to a normal chest MR protocol, a modified look-locker (MOLLI) T1 mapping sequence was included native (5s(3s)3s) and post-contrast (4s(1s)3s(1s)2s) with ECG-gating at end diastole and during one breathold (15 seconds). 0.015 mmol/kg of Gadopentetate of dimeglumine was administered, acquiring post-contrast images after 15 minutes. Two independent blinded radiologist analyze the images placing ROIs at the target lesions, fat tissue, striated muscle and descending aorta. Native and enhanced T1, R1 values, differences in native and post-contrast T1 ( $\Delta$ T1) and R1 ( $\Delta$ R1) values, and partition coefficient ( $\lambda$ ). Independent Student T test ROC analysis and intraclass correlation coefficient were done applying a two-tailed alpha error of 0.05.

#### RESULTS

We analyzed 19 tumoral lesions (lung cancer, metastasis, solitary fibrous tumor of the pleural, malignant pleural mesothelioma and esophageal leiomioma) and 17 benign lesions (post-obstructive neumonitis, atelectasis, hamartomas, lipoma, lymphangioma, necrosis). Significant statistical differences between non tumoral and neoplastic lesions were obtained in T1 post-contrast (1112.76  $\pm$  878.77 vs. 495 $\pm$ 182.37 ms; p< 0.05),  $\Delta$ T1 (666.12 $\pm$ 747.5 vs. 1199.68 $\pm$ 278.5 ms; p< 0.05), R1 post-contrast (1.67 $\pm$ 1.02 vs. 2.33 $\pm$ 0.64 ms; p< 0.05),  $\Delta$ R1 (0.82 $\pm$ 1.17 vs. 1.71 $\pm$ 0.58 ms; p< 0.05) and  $\lambda$  (0.21 $\pm$ 0.74 vs. 0.73 $\pm$ 0.25 ms; p< 0.05). Non-significant differences were obtained on T1 native and post-contrast derived parameters of fat, striated muscle and blood pool. ROC analysis revealed significant higher area under the curve of  $\Delta$ T1 (0.844),  $\lambda$  (0.738),  $\Delta$ R1 (0.726) and T1 post-contrast (0.697).

#### CONCLUSION

T1 mapping of chest lesions is a feasible technique being post-contrast T1 derived parameters and  $\lambda$  the best markers for differentiating tumoral and non-neoplastic lesions.

### **CLINICAL RELEVANCE/APPLICATION**

T1 mapping of chest lesions is a feasible technique being post-contrast T1 derived parameters and  $\lambda$  the best markers for differentiating tumoral and non-neoplastic lesions.

### **Honored Educators**

Presenters or authors on this event have been recognized as RSNA Honored Educators for participating in multiple qualifying educational activities. Honored Educators are invested in furthering the profession of radiology by delivering high-quality educational content in their field of study. Learn how you can become an honored educator by visiting the website at: https://www.rsna.org/Honored-Educator-Award/ Antonio Luna, MD - 2018 Honored Educator



# ER163-ED-TUB5

## Dual Energy CT to The Rescue: How DECT Can Help in The Emergency Department

Tuesday, Nov. 27 12:45PM - 1:15PM Room: ER Community, Learning Center Station #5

### Participants

Amirhossein Mozafarykhamseh, MD, Chicago, IL (*Presenter*) Grant, Siemens AG Tugce Agirlar Trabzonlu, MD, Chicago, IL (*Abstract Co-Author*) Grant, Siemens AG Donald Kim, DO, San Francisco, CA (*Abstract Co-Author*) Nothing to Disclose Jeanne M. Horowitz, MD, Chicago, IL (*Abstract Co-Author*) Nothing to Disclose Paul Nikolaidis, MD, Chicago, IL (*Abstract Co-Author*) Nothing to Disclose Vahid Yaghmai, MD, Chicago, IL (*Abstract Co-Author*) Nothing to Disclose

## **TEACHING POINTS**

Dual-energy CT (DECT) acquires images at two different x-ray energy levels and uses the attenuation differences at these different energy levels for processing data. DECT can provide both anatomic and functional information of different organ systems such as material decomposition, virtual unenhanced images, and artifact reduction. These features can also be used to optimize the workflow by reducing re-scans in an emergency setting where managing the time is of paramount importance. This exhibit reviews the role of DECT in improving the reader confidence and diagnostic accuracy of different study protocols.

## **TABLE OF CONTENTS/OUTLINE**

1. Overview of technical aspects of DECT 2. Clinical applications where DECT can be used to help reduce the additional scans A. Abdominopelvic CT for detection of pancreatitis, appendicitis, diverticulitis, colitis, cholecystitis B. CT abdominal angiography C. CT pulmonary angiography 3. Advantages of DECT in emergency department A. Impact of DECT in reducing additional scans a) Improving contrast enhancement in images with suboptimal acquisition due to technical errors or patient underlying diseases b) Eliminating unenhanced images B. Contrast volume optimization C. Radiation dose reduction D. Contrast dose reduction 4. Pitfalls A. Limited availability B. Technical limitations

## **Honored Educators**

Presenters or authors on this event have been recognized as RSNA Honored Educators for participating in multiple qualifying educational activities. Honored Educators are invested in furthering the profession of radiology by delivering high-quality educational content in their field of study. Learn how you can become an honored educator by visiting the website at: https://www.rsna.org/Honored-Educator-Award/ Vahid Yaghmai, MD - 2012 Honored EducatorVahid Yaghmai, MD - 2015 Honored EducatorPaul Nikolaidis, MD - 2017 Honored EducatorJeanne M. Horowitz, MD - 2016 Honored Educator



# ER218-SD-TUB1

Dual-Energy Head CT Accurately Distinguishes Small Foci of Intracranial Hemorrhage from Calcium: A Quantitative Analysis and Reader Study Validation

Tuesday, Nov. 27 12:45PM - 1:15PM Room: ER Community, Learning Center Station #1

# Participants

Walter F. Wiggins, MD, PhD, Boston, MA (*Presenter*) Nothing to Disclose Christopher A. Potter, MD, Boston, MA (*Abstract Co-Author*) Nothing to Disclose Aaron D. Sodickson, MD,PhD, Boston, MA (*Abstract Co-Author*) Institutional research agreement, Siemens AG; Speaker, Siemens AG; Speaker, General Electric Company

For information about this presentation, contact:

wwiggins@bwh.harvard.edu

# PURPOSE

Diagnostic uncertainty on CT imaging of possible intracranial hemorrhage requires short-interval follow-up imaging, resulting in decreased efficiency in clinical workflows and increased costs. This study quantifies performance of dual-energy CT (DECT) in distinguishing small foci of hemorrhage from calcification in a clinical population.

## METHOD AND MATERIALS

A retrospective review of 465 consecutive dual-source, DECT scans of the head performed in an academic emergency department identified 149 cases with hyperdense intracranial lesions, 43 of which were small lesions classified as indeterminate on initial review of simulated single-energy CT ('mixed') images. A definitive diagnosis of intracranial hemorrhage or calcification was established for each lesion on prior or follow-up imaging. Quantitative analysis was performed on region-of-interest (ROI) data obtained from DECT postprocessing of non-indeterminate lesions to establish thresholds for attenuation values on virtual noncalcium (VNCa) and calcium overlay (CaO) images. Indeterminate lesions were used for validation of thresholds and for a blinded reader study performed by two expert emergency radiologists.

## RESULTS

A receiver operating characteristic (ROC) analysis of DECT ROI data for non-indeterminate lesions established optimal thresholds of 45 +/- 3.18 HU (mean +/- SEM) for VNCa and 10 +/- 2.13 HU for CaO images, with diagnostic accuracy of 88% and 94%, respectively, on indeterminate lesions. A logistic regression (LR) model incorporating both DECT values resulted in 98% accuracy. DECT increased inter-reader agreement to 1.00 (from 0.64 on mixed images) and accuracy for both readers to 100% (from 86 and 93% on mixed images). Diagnostic confidence was also increased, resulting in similar performance to the LR model on ROC analysis. Importantly, use of ROI threshold values did not significantly change diagnostic confidence or accuracy over qualitative assessment of DECT images.

### CONCLUSION

Qualitative assessment of DECT images affords very high diagnostic performance in the differentiation of small foci of intracranial hemorrhage from calcium, independent of the use of threshold attenuation values for ROI data obtained from DECT postprocessing.

## **CLINICAL RELEVANCE/APPLICATION**

DECT provides accurate, confident distinction between small foci of intracranial hemorrhage and calcification, potentially reducing follow-up imaging and improving clinical workflows.

#### **Honored Educators**

Presenters or authors on this event have been recognized as RSNA Honored Educators for participating in multiple qualifying educational activities. Honored Educators are invested in furthering the profession of radiology by delivering high-quality educational content in their field of study. Learn how you can become an honored educator by visiting the website at: https://www.rsna.org/Honored-Educator-Award/ Aaron D. Sodickson, MD,PhD - 2014 Honored EducatorAaron D. Sodickson, MD,PhD - 2017 Honored EducatorAaron D. Sodickson, MD,PhD - 2018 Honored Educator



# ER219-SD-TUB2

Diagnostic Performance and Essential Imaging Pulse Sequences of MRI for Acute Abdominal Pain by Gastrointestinal Disorders

Tuesday, Nov. 27 12:45PM - 1:15PM Room: ER Community, Learning Center Station #2

# Participants

Akitoshi Inoue, MD, PhD, Higashioumi-city, Japan (*Presenter*) Nothing to Disclose Akira Furukawa, MD, PhD, Tokyo, Japan (*Abstract Co-Author*) Nothing to Disclose Kai Takaki, MD, Otsu, Japan (*Abstract Co-Author*) Nothing to Disclose Norihisa Nitta, MD, Kyoto, Japan (*Abstract Co-Author*) Nothing to Disclose Shinichi Ota, MD, PhD, Otsu, Japan (*Abstract Co-Author*) Nothing to Disclose Shigetaka Sato, MD, Otsu, Japan (*Abstract Co-Author*) Nothing to Disclose Kiyoshi Murata, MD, Otsu, Japan (*Abstract Co-Author*) Nothing to Disclose

### PURPOSE

The aim of this study is to disclose diagnostic performance of abdominal MRI in acute abdomen caused by gastrointestinal disorders and investigate important imaging pulse sequence for correct diagnosis.

## **METHOD AND MATERIALS**

Among consecutive 93 patients with acute abdominal pain who underwent MRI, 14 cases with urogenital cases were excluded and 79 patients with gastrointestinal disorders were enrolled in this study. After the acquisition of localizer images, axial and coronal imaging with T2-weighted image (T2WI), fat-suppression T2WI (FS-T2WI), True-FISP sequence, and axial imaging with T1-weighted image (T1WI) and diffusion-weighted image (DWI) (b=50, 1000) were obtained (Table.1). MR images were reviewed by two abdominal radiologists. In addition to make imaging diagnosis, presence of bowel thickening, bowel dilatation, mass, bowel wall defect, fat stranding, and difference of signal intensity on DWI between suspected sites and normal bowel were evaluated by using 5-point score. CT, endoscopic or surgical findings and/ or clinical follow up were used as the reference standard for calculating sensitivity, specificity, positive predict value (PPV), negative predict value (NPV), and accuracy of MR diagnosis. The scores were evaluated using Wilcoxon signed-rank test on T2WI, FS-T2WI, T1WI, and True-FISP with Bonferroni correction: p values of <0.0083 and on DWI: p value of <0.05 were considered statistically significant.

### RESULTS

Specific diagnoses were obtained in 63 patients including 35 cases with acute appendicitis (Table. 2) and conditions of acute abdominal pain were excluded in 16 patients. Diagnostic sensitivity, specificity, PPV, NPV, and accuracy of MRI of reader 1 and 2 are shown in Table. 3. Depiction of wall thickening in acute appendicitis was more sensitive on T2WI and FS-T2WI than T1WI and identification of fat stranding around lesion was most sensitive T2WI and FS-T2WI. The score on DWI was high in cases with acute appendicitis (Table.4).

## CONCLUSION

MRI is an effective modality in the diagnosis of acute abdomen and T2WI, FS-T2WI, and DWI were essential imaging sequences for correct diagnosis.

# **CLINICAL RELEVANCE/APPLICATION**

MRI provides high diagnostic performance in acute abdomen. It is free from radiation exposure and does not require intravascular contrast administration to diagnose acute abdomen, which is helpful for pediatric and pregnant patients and patients who are contraindicated in use of contrast media.



## ER220-SD-TUB3

## Whole Brain CT-Perfusion in the Emergency Room: Its Utility Beyond Acute Stroke

Tuesday, Nov. 27 12:45PM - 1:15PM Room: ER Community, Learning Center Station #3

### Participants

Esther Garcia Casado, Madrid, Spain (*Presenter*) Nothing to Disclose Alfonso Lopez-Frias Lopez-Jurado, MD, Madrid, Spain (*Abstract Co-Author*) Nothing to Disclose Jose M. Blanc Molina, MD, Madrid, Spain (*Abstract Co-Author*) Nothing to Disclose Pablo Marazuela Garcia, MD, Madrid, Spain (*Abstract Co-Author*) Nothing to Disclose Beatriz Alba Perez, MD, Madrid, Spain (*Abstract Co-Author*) Nothing to Disclose Agustina Vicente Bartulos, MD, Madrid, Spain (*Abstract Co-Author*) Nothing to Disclose

### PURPOSE

The aim of this study is to show the perfusion maps and review the perfusion patterns observed in neurological entities that can mimic acute stroke clinically in emergency settings.

# METHOD AND MATERIALS

We identified patients who presented at our hospital between January 2016 to March 2018 with suspected acute stroke and underwent examination thorough a 'stroke protocol' including noncontrast brain CT, whole brain CT perfusion (WB-PCT) and CT angiography. We reviewed the cases in which the radiologic findings showed signs that may relate to neurologic conditions different from acute stroke. All examinations were performed using 320 detector row CT. Color-coded maps of cerebral blood flow (CBF), cerebral blood volume (CBV), mean transit time (MTT), time to peak (TTP) and Delay were calculated automatically and then evaluated. We correlated the perfusion findings with patient symptoms and with the results of other diagnostic tests performed to the patient that gave the final diagnosis.

## RESULTS

A total of 1441 WB-PCT studies where revised, 120 (8%) revealed either unspecific findings or signs suggestive of pathologies different from acute stroke. We found several entities to be clinical 'mimics' of acute stroke, each of them revealing patterns in the CT-perfusion color maps according to their specific pathophysiology and perfusion dynamics: epileptic crisis, encephalitis, migraine aura, reversible cerebral vasoconstriction syndrome, aggressive primary cerebral tumors and metastases, arterio-venous malformations, and a rare case of Moya Moya disease.

### CONCLUSION

WB-PCT in emergency settings has its utility further than only the diagnosis of acute stroke. Though it is primarily used for ischemic stroke, WB-PCT parameters are altered in many other pathologic conditions that may cause focal neurologic symptoms. Recognizing lesions that cross arterial territory boundaries, selectively affect gray matter and alter perfusion parameters are helpful in distinguishing ischemic stroke from other disease entities.

## **CLINICAL RELEVANCE/APPLICATION**

Until now, the use of CT-Perfusion studies was limited to ruling out acute stroke. With our research we aim to expand the spectrum of neurologic conditions that can be analyzed with this technique. CT-perfusion has a huge potential in characterizing cerebral blood dynamics and we must learn how to take the most out of it in order to make better and more accurate diagnosis.



# ER221-SD-TUB4

Novel Post Processing CT Technique of "Rib Flattening and Spine Straightening": An Aid in Accelerated and Efficient Detection of Fractures!- Single Institute Experience

Tuesday, Nov. 27 12:45PM - 1:15PM Room: ER Community, Learning Center Station #4

### Participants

Surendra KI, DMRD, Bangalore, India (*Abstract Co-Author*) Nothing to Disclose Praveen P. Wali, MBBS, DMRD, Bangalore, India (*Abstract Co-Author*) Nothing to Disclose Paramita Hota, MBBS,MD, Bangalore, India (*Presenter*) Nothing to Disclose Harsha C. Chadaga, MBBS, Tamilnadu, India (*Abstract Co-Author*) Nothing to Disclose Rekha B P, DMRD,MBBS, Bangalore, India (*Abstract Co-Author*) Nothing to Disclose Sriram Patwari, MBBS, MD, Bangalore, India (*Abstract Co-Author*) Nothing to Disclose Salman R. Khan, MBBS, Thane, India (*Abstract Co-Author*) Nothing to Disclose Naajia Perothayil, MBBS, Thrissur, India (*Abstract Co-Author*) Nothing to Disclose Renu Jadiya, Bangalore, India (*Abstract Co-Author*) Nothing to Disclose Anoop P. Mangalappilly, MBBS, Bangalore, India (*Abstract Co-Author*) Nothing to Disclose

#### For information about this presentation, contact:

drsurendrakl@gmail.com

#### PURPOSE

To compare the diagnostic performance of 'Conventional multiplanar ' and 'Post processing software enabled rib flattened and spine straightened' images (aka In-plane images)' in terms of ability to detect the fractures in shorter duration and yet be accurate.

#### **METHOD AND MATERIALS**

Study type:Retrospective observational study. Sample size:CT data of 75 patients with suspected chest trauma during june 2017 to feb 2018. Methodology:Evaluation of the CT images was done by an experienced radiologist. First, as a screening method, each study was evaluated for 30 sec (to simulate clinical practice) to decide if at least a single fracture was present (per patient analysis). Afterwards, evaluation was continued as a diagnostic method to identify all the fractures without time limit (per bone analysis). Both steps were performed with conventional and post processing in-plane approaches with a gap of 50 - 60 days to avoid recall bias. Evaluation time and total number of fractures were documented. Sensitivities, specificities, positive/negative predictive values were calculated. Findings of conventional method were considered as reference standard.

### RESULTS

43 of 75 patients had at least one rib fracture. 178 of 1800 ribs were fractured.Reduction in the time taken to analyse per rib using in plane method was 39 % (18.3 sec vs 11.2 sec for conventional and in-plane methods respectively). Sensitivity, specificity, positive/negative predictive values were 79/100/100/78 %, respectively, for screening conventional reading whereas 95.3/65.6/78.8/91.3 %, respectively, for screening and 95.5/96.7/76.5/99.4 %, respectively, for diagnostic in-plane reading of ribs.Reduction in the time taken to analyse thoracic vertebral bodies in a patient using in plane method was 71 %. Sensitivity, specificity, positive/negative predictive values were 100/99.6/90.6/100 %, respectively, for diagnostic in-plane reading of vertebral bodies.

# CONCLUSION

Post processing in-plane reading is an advanced method that converts the complex 3D structures like ribs and vertebrae into easy to analyse flattened 2D images. In-plane evulation reduces the review time with accuracy similar to that of conventional method.

## **CLINICAL RELEVANCE/APPLICATION**

In-plane reading potentially reduces the turnaround time, eases the rib counting and helps in reducing the errors in identifying fractures, thereby enabling faster and efficient patient care.



## GI304-ED-TUB8

An Image-Driven Review of the Fluoroscopic Swallow Evaluation

Tuesday, Nov. 27 12:45PM - 1:15PM Room: GI Community, Learning Center Station #8

#### **Participants**

Evan Allgood, MD, Los Angeles, CA (*Presenter*) Nothing to Disclose Barbara M. Kadell, MD, Los Angeles, CA (*Abstract Co-Author*) Nothing to Disclose Michael L. Douek, MD, MBA, Los Angeles, CA (*Abstract Co-Author*) Nothing to Disclose Steven S. Raman, MD, Santa Monica, CA (*Abstract Co-Author*) Nothing to Disclose

# For information about this presentation, contact:

evan.allgood@gmail.com

# **TEACHING POINTS**

Though its prevelance in some applications has diminished over the years, fluoroscopy is still the test of choice to dynamically evaluate pharyngeal and esophageal structure and function. This exhibit aims to review fluoroscopic depiction of normal anatomy of the pharynx and esophagus, as well as anatomic variants and common diagnoses.

# TABLE OF CONTENTS/OUTLINE

This image driven review will be given in an open-ended quiz format. Explanations of the quiz questions will address relevant pearls and pitfalls as they pertain to the images presented. The questions will relate to images of the following: Laryngeal squamous cell carcinoma, pre and post treatment, with depiction of pseudodiverticulum Duplicated esophagus Achalasia Scleroderma Epiphrenic diverticulum Zenker's diverticulum Esophageal webs Foreign body Extrinsic mass Stricture, post-esophageal atresia repair Stricture, caustic ingestion Stricture, radiation Leak Normal anatomy and swallow function Normal variants



## GI305-ED-TUB9

Ultrasound of Bowel in Acute (Non-IBD Related) Emergencies

Tuesday, Nov. 27 12:45PM - 1:15PM Room: GI Community, Learning Center Station #9

## Participants

Mana Modares, Toronto, ON (*Presenter*) Nothing to Disclose Hournaz Ghandehari, MD, Toronto, ON (*Abstract Co-Author*) Nothing to Disclose

For information about this presentation, contact:

mana.modares@mail.utoronto.ca

### **TEACHING POINTS**

The purpose of this exhibit is to: 1. Review the technical requirements, patient preparation, and process of examination to ensure an optimized study 2. Review sonographic differentiation of bowel from adjacent structures, and normal from abnormal bowel 3. Demonstrate ultrasound characteristics of acutely inflamed bowel and differentiation from neoplastic processes 4. Demonstrate and review sonographic findings in acute inflammatory bowel pathologies (excluding inflammatory bowel disease) 5. Emphasize usefulness of ultrasound in assessment of the acute bowel given its relatively high sensitivity and specificity (70-96% and 80-97% respectively), low cost, and lack of radiation exposure

# TABLE OF CONTENTS/OUTLINE

1- Review of sonographic technique for assessment of bowel 2- Ultrasound criteria for differentiating normal and abnormal bowel 3-Sample cases illustrating sonographic characteristics of non-IBD bowel emergencies with CT correlate: - Acute appendicitis (uncomplicated, perforated with collection, appendiceal mucocele) - Acute right sided diverticulitis - Acute sigmoid diverticulitis -Acute pancolitis - Acute epiploic appendagitis - Acute bowel intussusception 4- Future directions and summary



### GI306-ED-TUB10

The Pelvic Mass: Safe Approaches to CT Guided Biopsy

Tuesday, Nov. 27 12:45PM - 1:15PM Room: GI Community, Learning Center Station #10

### Participants

Bindu Kaul, MBBS, Scarsdale, NY (*Presenter*) Nothing to Disclose David Erlichman, MD, Bronx, NY (*Abstract Co-Author*) Nothing to Disclose Karen E. Sperling, MD, New Rochelle, NY (*Abstract Co-Author*) Nothing to Disclose Mariya Kobi, MD, New York, NY (*Abstract Co-Author*) Nothing to Disclose Zina J. Ricci, MD, Scarsdale, NY (*Abstract Co-Author*) Nothing to Disclose

## **TEACHING POINTS**

1. Determining the appropriate clinical indication for biopsy avoids placing the patient at unnecessary risk.2. Careful review of diagnostic imaging is critical to select biopsy site, plan patient positioning and choose the best approach.3. Checking pre-procedure coagulation profile, platelet count and medication history will identify patients at higher risk of bleeding.4. Proper administration of local anesthesia and moderate sedation improves patient comfort, decreases procedure time and may increase diagnostic yield.5. Approach selection should consider patient comfort, provide easy accessibility to the mass, and carry low risk of injury to adjacent vital structures.

## TABLE OF CONTENTS/OUTLINE

1. Relevant pelvic anatomy to ensure the safest percutaneous access will be reviewed. 2. Fine needle aspiration and core biopsy techniques (coaxial method and tandem needle technique) will be reviewed.3. Biopsy approaches (anterior transabdominal, anterolateral transabdominal, transgluteal, transosseus, and uncommonly through bowel) will be demonstrated with case illustrations and safety tips.4. Techniques including placement of localizing grid, patient positioning, needle selection, local anesthesia, moderate conscious sedation, saline administration to displace bowel, use of hemostatic agents and angling the CT gantry will be reviewed.



## GI307-ED-TUB11

From Path to Pearls - Linking the Pathophysiology of Celiac Disease to Diagnostic Imaging Findings on CT and MRI

Tuesday, Nov. 27 12:45PM - 1:15PM Room: GI Community, Learning Center Station #11

# Participants

Michael N. Pakdaman, MD, Los Angeles, CA (*Abstract Co-Author*) Nothing to Disclose Peyman Kangavari, MD, Los Angeles, CA (*Abstract Co-Author*) Nothing to Disclose Catherine Evans, MD, Los Angeles, CA (*Presenter*) Nothing to Disclose

### **TEACHING POINTS**

Understand the general pathophysiology and histopathology of Celiac disease and the relationship between the disease process and imaging findings. Imaging evaluation of Celiac Disease remains a challenge, however many direct and indirect imaging findings on CT and MRI can be used to assist the referring physician in diagnosis.

# TABLE OF CONTENTS/OUTLINE

Describe the challenges in initially identifying Celiac disease on imaging Emphasize the importance of understanding Celiac Disease pathophysiology in aiding imaging assessment Identify common imaging findings that may point to diagnosis of Celiac Disease. Celiac Disease Pathophysiology and Histopathology as it relates to malabsorption, inflammation, and delayed transit. Common barium fluoroscopic findings in celiac disease, including flocculation, diluation of contrast, and reversal of jejunization pattern. Common CT and MRI findings in Celiac Disease Concomitant pathology in patients with Celiac Disease, and associated imaging findings Putting it all together - case conceptualization in challenging cases.



## GI308-ED-TUB12

## Imaging Appearances of Focal Hepatic Lesions with Ferumoxytol-Enhanced MRI

Tuesday, Nov. 27 12:45PM - 1:15PM Room: GI Community, Learning Center Station #12

**FDA** Discussions may include off-label uses.

#### **Participants**

Puja Shahrouki, Los Angeles, CA (*Abstract Co-Author*) Nothing to Disclose
Steven S. Raman, MD, Santa Monica, CA (*Abstract Co-Author*) Nothing to Disclose
Ely R. Felker, MD, Los Angeles, CA (*Abstract Co-Author*) Nothing to Disclose
Woo Kyoung Jeong, MD, Seoul, Korea, Republic Of (*Abstract Co-Author*) Nothing to Disclose
David S. Lu, MD, Los Angeles, CA (*Abstract Co-Author*) Consultant, Medtronic plc; Speaker, Medtronic plc; Consultant, Johnson & Johnson; Research Grant, Johnson & Johnson; Consultant, Bayer AG; Research Grant, Bayer AG; Speaker, Bayer AG
J. Paul Finn, MD, Los Angeles, CA (*Presenter*) Speakers Bureau, Bayer AG; Scientific Advisory Board, AMAG Pharmaceuticals, Inc

## For information about this presentation, contact:

pfinn@mednet.ucla.edu

# **TEACHING POINTS**

Illustrate the normal contrast-enhancement of liver on T1 and T2-weighted ferumoxytol-enhanced MRI (FE-MRI). Review the imaging appearances of benign and malignant focal hepatic lesions in FE-MRI.

# TABLE OF CONTENTS/OUTLINE

Normal contrast-enhancement of FE-MRI in solid abdominal organs a. Liver b. Spleen c. Kidneys d. Pancreas Imaging appearances of benign focal hepatic lesions on FE-MRI a. Cyst b. Hemangioma Imaging appearances of malignant focal hepatic lesions on FE-MRI a. Hepatocellular carcinoma b. Metastasis



# GI362-SD-TUB1

Texture Features Analysis to Predict Overall Survival and Overall Response Rate in Patients Treated with FOLFIRINOX for Pancreatic Cancer

Tuesday, Nov. 27 12:45PM - 1:15PM Room: GI Community, Learning Center Station #1

# Participants

Regis Otaviano Bezerra, MD, Sao Paulo, Brazil (*Presenter*) Nothing to Disclose Felipe R. Ferreira, Sao Paulo, Brazil (*Abstract Co-Author*) Nothing to Disclose Aley Talans, MD, Sao Paulo, Brazil (*Abstract Co-Author*) Nothing to Disclose Debora Z. Recchimuzzi, MD, Sao Paulo, Brazil (*Abstract Co-Author*) Nothing to Disclose Raisa Karla d. Bispo, MD, Sao Paulo, Brazil (*Abstract Co-Author*) Nothing to Disclose Frederico Costa, Sao Paulo, Brazil (*Abstract Co-Author*) Nothing to Disclose Marcio Ricardo T. Garcia, MD, Sao Paulo, Brazil (*Abstract Co-Author*) Nothing to Disclose Manoel S. Rocha, MD, PhD, Sao Paulo, Brazil (*Abstract Co-Author*) Nothing to Disclose Giovanni G. Cerri, MD, PhD, Sao Paulo, Brazil (*Abstract Co-Author*) Nothing to Disclose

### For information about this presentation, contact:

### regisfranca@gmail.com

### PURPOSE

To assess whether CT-derived texture features predict overall survival (OS) and overall response rate (ORR) in patients receiving FOLFIRINOX chemotherapy for inoperable pancreatic ductal adenocarcinoma (PDAC)

### METHOD AND MATERIALS

We analyzed CT texture features from 52 patients with histologically confirmed PDAC at initial staging. All patients were metastatic/advanced tumors and received FOLFIRINOX as the first-line chemotherapy. A ROI was drawn by a radiologist blinded to patient outcome on the slice with the largest portion of the pancreatic lesion on the portal phase using IBEX. Nineteen features derived from grey level co-occurrence matrices (GLCM) were calculated: Auto Correlation/Cluster Prominence/Cluster Shade/Cluster Tendency/Contrast/Correlation/ Difference Entropy/Dissimilarity/Energy/Entropy/Homogeneity/InformationMeasureCorr/ InverseDiffMomentNorm/InverseVariance/MaxProbability/SumAverage/SumEntropy/ SumVariance and Variance. Receiver operating characteristics (ROC) analysis, Cox regression and Kaplan-Meier tests were used to assess association of texture features with OS and ORR assessed by RECIST criteria and defined as partial or complete response

#### RESULTS

Mean age was 59 years(39-72 years), 44 % women. The median overall survival was 14.9 months(95%CI, 2.1- 24 months). Inverse difference normalized (AUC0.71, 95%CI 0.54 -0.87, P<0,02), homogeneity (AUC 0.70, 95%CI 0.52-0.86 P<0,03) and correlation (AUC0.75, 95%CI 0.59-0.90, P<0,007) were associated with OS. Cluster Prominence (AUC0.77, 95%CI 0.62-0.9, P<0,002), Cluster Tendency (AUC0.75, 95%CI 0.60-0.89, P<0,003), Entropy (AUC0.74, 95%CI 0.60-0.89, P<0,004) and Variance (AUC0.75, 95%CI 0.60-0.89, P<0,004) were associated with ORR. On the other hand, Inverse Variance was associated with progressive disease (AUC0.73, 95%CI0.59-0.88, P<0,01). The other textural features were not associated with OS/ORR

### CONCLUSION

CT-derived texture features of Inverse difference normalized, homogeneity and correlation are prognostic factors of OS for patients with PADC treated with FOLFIRINOX. Cluster Prominence, Cluster Tendency, Entropy and Variance are promising prognostic imaging biomarkers for ORR, while Inverse Variance is associated with progressive disease

## **CLINICAL RELEVANCE/APPLICATION**

CT-derived texture features have potential to be a non-invasive and cost-effective prognostic biomarker in PADC patients treated with FOLFIRINOX, with great impact on clinical decision making.



# GI363-SD-TUB2

Diagnostic Performance of Diffusion-Weighted Imaging for Differentiating Benign and Malignant Gallbladder Lesions: A Systematic Review and Meta-Analysis

Tuesday, Nov. 27 12:45PM - 1:15PM Room: GI Community, Learning Center Station #2

# Participants

Myung-Won You, MD, Seoul, Korea, Republic Of (*Presenter*) Nothing to Disclose Seong Jong Yun, Seoul, Korea, Republic Of (*Abstract Co-Author*) Nothing to Disclose Seong Jin Park, MD, PhD, Seoul, Korea, Republic Of (*Abstract Co-Author*) Nothing to Disclose Jung Min Lee, MD, Seoul, Korea, Republic Of (*Abstract Co-Author*) Nothing to Disclose Hyun Cheol Kim, Seoul, Korea, Republic Of (*Abstract Co-Author*) Nothing to Disclose Dal Mo Yang, Seoul, Korea, Republic Of (*Abstract Co-Author*) Nothing to Disclose

### For information about this presentation, contact:

zoomknight@naver.com

### PURPOSE

Although diffusion-weighted imaging (DWI) has been characterized as an alternative imaging modality for gallbladder (GB) lesions, it has not been routinely used in clinical practice because of relatively low signal-to-noise ratio. The aim of our meta-analysis was to assess the diagnostic performance of DWI for differentiating benign and malignant GB lesions.

# **METHOD AND MATERIALS**

PubMed and EMBASE were searched following the Preferred Reporting Items for Systematic Reviews and Meta-Analyses of Diagnostic Test Accuracy guidelines. Bivariate modeling and hierarchical summary receiver operating characteristic (HSROC) modeling were performed to compare the overall diagnostic performance of DWI. Subgroup analyses were performed for qualitative and quantitative assessment of the DWI. Meta-regression analyses were performed according to the characteristics of the patients, study, and magnetic resonance imaging.

### RESULTS

Eight studies (including 557 patients) were included. The DWI exhibited a pooled sensitivity of 91%, a pooled specificity of 87%, and HSROC of 0.95. In subgroup analyses, qualitative assessment (sensitivity, 90%; specificity, 87%; HSROC, 0.94) was more accurate than quantitative assessment (sensitivity, 82%; specificity, 86 %; HSROC, 0.88). On meta-regression analysis, studies that used 3.0-T field strength and thinner slices (<=5 mm) reported a significantly higher sensitivity (p<=0.02) than those using only 1.5-T field strength and thicker slices (>5 mm).

# CONCLUSION

DWI can discriminate malignant from benign GB lesions with excellent diagnostic performance in both qualitative and quantitative assessments. To enhance the diagnostic ability of DWI, images obtained with thinner slices (<=5 mm) with 3-T field strength and qualitative assessment are recommended.

#### **CLINICAL RELEVANCE/APPLICATION**

Qualitative assessment of DWI is useful and applicable to patients with GB lesions without the support of the quantitative assessment.



# GI365-SD-TUB4

3D MR Elastography of the Pancreas as a Novel Approach in Detecting Chronic Pancreatitis in Children and Young Adolescents

Tuesday, Nov. 27 12:45PM - 1:15PM Room: GI Community, Learning Center Station #4

# Participants

Suraj D. Serai, PhD, Philadelphia, PA (Presenter) Nothing to Disclose

Andrew T. Trout, MD, Cincinnati, OH (*Abstract Co-Author*) Author, Reed Elsevier; Research Grant, Siemens AG; Research Grant, Canon America Medical Systems Corporation; Board Member, Joint Review Committee on Educational Programs in Nuclear Medicine Technology; Travel support, Koninklijke Philips NV; Consultant, Guerbet SA

Maisam Abu-El-Haija, MD, Cincinnati, OH (Abstract Co-Author) Nothing to Disclose

# PURPOSE

Pancreatic disease, including chronic pancreatitis is being increasingly recognized in the pediatric population. Early diagnosis of chronic pancreatitis and exocrine insufficiency remains elusive. Non-invasive, imaging-based diagnostic techniques are of particular interest in the pediatric population and early data suggest differences in pancreatic stiffness, measured by MR elastography (MRE), can be observed in both acute and chronic disease. Due to its location, size, shape, and the impact of geometric boundary conditions, pancreatic MRE requires a 3D analysis of wave field data. Our objectives were to explore the use of 3D MRE of the pancreas in pediatric subjects with no known history of pancreatic disease ('healthy controls') and in pediatric patients with suspected pancreatic disease.

# METHOD AND MATERIALS

Under IRB approval, 50 healthy controls (age matched pediatric volunteers with no known history of pancreatic disease) and 40 patients with suspected pancreatic disease underwent 3D MRE was on a 1.5T MR scanner (HDx, GE Healthcare, WI, USA) using an 8-channel phased array torso coil. A soft passive driver positioned in the sub-xyphoid region was utilized and a motion encoding frequence of 40 Hz was used. Guided by a matched T2W image, regions of interest (ROI) were drawn on the elastogram images to encompass as much of the pancreatic parenchyma as possible excluding the boundary and peripancreatic tissues. Mean pancreatic stiffness values were recorded for each patient and comparisons were made between groups.

#### RESULTS

For healthy controls, mean age was 10.9 years  $\pm$  2.7 (23/50 males) and mean pancreas stiffness was 1.7kPa  $\pm$  0.2. For patients with suspected pancreatic disease, mean patient age was 15.4 years  $\pm$  5.1 (22/40 males) and mean pancreas stiffness was 0.91kPa  $\pm$  0.1 (Figure 1). Pancreas stiffness was significantly lower in patients with suspected pancreatic disease as compared to healthy controls (p<0.0001).

# CONCLUSION

3D MRE of the pancreas was successfully performed on both healthy controls and pediatric patients with suspected pancreatic disease. Significantly lower stiffness values were observed in patients with pancreatitis as compared to healthy controls.

### **CLINICAL RELEVANCE/APPLICATION**

3D MRE of the pancreas offers a novel approach for detecting pancreatic disease based on changes in tissue mechanical properties.



# GI366-SD-TUB5

Assessment of Immediate Response to Irreversible Electroporation in Normal Liver Using Intravenous Dynamic Contrast Enhancement in a Rabbit Model

Tuesday, Nov. 27 12:45PM - 1:15PM Room: GI Community, Learning Center Station #5

#### Awards Student Travel Stipend Award

#### **Participants**

Junjie Shangguan, Chicago, IL (*Presenter*) Nothing to Disclose Liang Pan, Chicago, IL (*Abstract Co-Author*) Nothing to Disclose Matteo Figini, Chicago, IL (*Abstract Co-Author*) Nothing to Disclose Chong Sun, Chicago, IL (*Abstract Co-Author*) Nothing to Disclose Bin Wang, MD, Chicago, IL (*Abstract Co-Author*) Nothing to Disclose Quanhong Ma, Chicago, IL (*Abstract Co-Author*) Nothing to Disclose Yuri Velichko, PhD, Chicago, IL (*Abstract Co-Author*) Nothing to Disclose Jia Yang, PhD, Chicago, IL (*Abstract Co-Author*) Nothing to Disclose Zhuoli Zhang, MD,PhD, Chicago, IL (*Abstract Co-Author*) Nothing to Disclose Vahid Yaghmai, MD, Chicago, IL (*Abstract Co-Author*) Nothing to Disclose

# For information about this presentation, contact:

junjie.shangguan@northwestern.edu

#### PURPOSE

Irreversible electroporation (IRE) delivers high voltages to cause tissue death in the irreversibly ablated zone surrounded by a reversibly ablated zone. Dynamic contrast enhanced MRI (DCE-MRI) allows measurement of vascular blood flow and blood vessel permeability in vivo; diffusion weight imaging (DWI) allows measurement of tissue microstructure. In this study, we hope to demonstrate that DCE-MRI and DWI allows visualization of IRE ablation margins and differentiation of IRE zones to provide an accurate prediction of the ablated tissue region in normal liver tissue.

### **METHOD AND MATERIALS**

All experiments were approved by institutional animal care and use committee. 6 healthy rabbits underwent IRE ablation and baseline and post-IRE imaging. DCE-MRI was performed by injection of  $8\mu$ L/g Gd-DTPA solution. All images (T1w, T2w, DWI, and DCE-MRI) were acquired using a Tx/Rx knee coil in a 3.0-T clinical MR scanner. IRE involved 8 pulses at 2000 V and 100 µs/pulse to the liver using 0.4 mm diameter 2 Needle Array Tips and a BTX Electroporator. The apparent diffusion coefficient (ADC) map was computed from DWI images using Matlab. Area Under Curve (AUC) was calculated from the time of contrast arrival in DCE-MRI images using JIM7. All statistical analyses were performed in Excel.

#### RESULTS

IRE lesions were hyperintense in T1-FLASH and T2 images. ADC was decreased after IRE ablation compared with baseline due to inclusion of necrotic regions in the ROI, which were indistinguishable from reversible IRE zone (P < 0.05). Time intensity curves of DCE-MRI images showed 2 distinct regions in the IRE lesion with different response to contrast arrival (P < 0.05). AUC curves showed that the outer reversible ablation zone retained some tissue perfusion immediately after IRE while there was minimal tissue perfusion in the irreversible ablation zone.

# CONCLUSION

We have shown that DWI and DCE-MRI allows visualization of IRE margins after IRE. While DWI did not distinguish between different zones of ablation, DCE-MRI allowed differentiation of zones of ablation as well as evaluation of tissue perfusion after IRE. We will further confirm the imaging results with histology of the ablated area to determine blood vessel damage.

# **CLINICAL RELEVANCE/APPLICATION**

DCE-MRI may allow early evaluation of IRE ablation tissue margins and IRE ablation zones, thus potentially allowing early prediction of response to IRE in an HCC.

#### **Honored Educators**

Presenters or authors on this event have been recognized as RSNA Honored Educators for participating in multiple qualifying educational activities. Honored Educators are invested in furthering the profession of radiology by delivering high-quality educational content in their field of study. Learn how you can become an honored educator by visiting the website at: https://www.rsna.org/Honored-Educator-Award/ Vahid Yaghmai, MD - 2012 Honored EducatorVahid Yaghmai, MD - 2015 Honored Educator



# GI367-SD-TUB6

Predicting Transplant-Free Survival in Primary Sclerosing Cholangitis using Novel Liver and Spleen Volumetric Measurements

Tuesday, Nov. 27 12:45PM - 1:15PM Room: GI Community, Learning Center Station #6

# Participants

Pegah Khoshpouri, MD, Baltimore, MD (*Presenter*) Nothing to Disclose Sanaz Ameli, MD, Baltimore, MD (*Abstract Co-Author*) Nothing to Disclose Bharath Ambale Venkatesh, PhD, Baltimore, MD (*Abstract Co-Author*) Nothing to Disclose Mounes Aliyari Ghasabeh, MD, Baltimore, MD (*Abstract Co-Author*) Nothing to Disclose Angela Jacob, Baltimore, MD (*Abstract Co-Author*) Nothing to Disclose Ankur Pandey, MD, Baltimore, MD (*Abstract Co-Author*) Nothing to Disclose Manijeh Zarghampour, MD, Baltimore, MD (*Abstract Co-Author*) Nothing to Disclose Yan Luo, MD, Wuhan, China (*Abstract Co-Author*) Nothing to Disclose Pallavi Pandey, MD, Baltimore, MD (*Abstract Co-Author*) Nothing to Disclose Farnaz Najmi Varzaneh, MD, Baltimore, MD (*Abstract Co-Author*) Nothing to Disclose Ihab R. Kamel, MD, PhD, Baltimore, MD (*Abstract Co-Author*) Nothing to Disclose

For information about this presentation, contact:

### pkhoshp1@jhmi.edu

#### PURPOSE

To create a predictive model of PSC severity and indication for liver transplant based on novel measurement of total and segmental liver volume and total spleen volume.

# METHOD AND MATERIALS

This HIPAA-compliant single center study included 166 PSC patients with imaging studies (MR/CT) and laboratory data between 1/2003 and 12/2017. Total liver (T), right and left lobes (R, L), caudate (C) and spleen (S) volumes were measured. MELD and Mayo scores were calculated using clinical data (INR, creatinine and total bilirubin to calculate MELD, and total bilirubin, serum albumin, AST, age, and variceal bleeding history for Mayo score calculation). Correlations between volume measurements, MELD and Mayo scores were performed. Cox regression was used to assess the predictive ability of radiologic (volumetric) variables to predict transplant-free survival over a mean follow-up period of 18 months (median=7 months, maximum=136 months).

#### RESULTS

The mean age of the population was  $46\pm17$  years, 42% were women. MELD and Mayo scores correlated with the volumes of total liver (r=0.23, r=0.16, respectively), left lobe (r=0.33, r=0.35, respectively), caudate (r=0.36, r=0.36, respectively) and spleen (r=0.34, r=0.40, respectively) (all p<0.05). MELD (HR: 1.18, CI: 1.14-1.22) and Mayo (HR: 1.98, CI: 1.7-2.3) scores as well as the volumes of total liver (HR: 1.6, CI: 1.14-2.27), left lobe (HR: 2.4, CI: 1.6-3.6), caudate (HR: 23.7, CI: 7.1-78.5) and spleen (HR: 1.5, CI: 1.3-1.7) were all predictive of the transplant-free survival. Caudate to total liver volume ratio (C/T) was also predictive of outcome (HR: 164, CI: 17-1565) and this association was independent of MELD or Mayo scores (p<0.05 after adjustment). Including C/T in the models with MELD and Mayo scores, increased the chi-squared value from 85.4 to 89.5 (p<0.05) and from 83.6 to 86.7 (p=0.07), respectively.

### CONCLUSION

In this single institution large cohort, the caudate to total liver volume ratio was the best quantifiable imaging biomarker to predict transplant-free survival in patients with PSC.

### **CLINICAL RELEVANCE/APPLICATION**

Imaging added a significant prediction value to the identification of patients at a higher risk of having severe PSC.

### **Honored Educators**

Presenters or authors on this event have been recognized as RSNA Honored Educators for participating in multiple qualifying educational activities. Honored Educators are invested in furthering the profession of radiology by delivering high-quality educational content in their field of study. Learn how you can become an honored educator by visiting the website at: https://www.rsna.org/Honored-Educator-Award/ Ihab R. Kamel, MD, PhD - 2015 Honored Educator



# GI368-SD-TUB7

Tumor Recurrence versus Post-Surgical Fibrosis: Differentiation in Patients Resected for Pancreatic Adenocarcinoma

Tuesday, Nov. 27 12:45PM - 1:15PM Room: GI Community, Learning Center Station #7

# Participants

Andrea Mazzaro, MD, Verona, Italy (*Presenter*) Nothing to Disclose Giulia A. Zamboni, MD, Verona, Italy (*Abstract Co-Author*) Nothing to Disclose Matteo Catania, MD, Trieste, Italy (*Abstract Co-Author*) Nothing to Disclose Fabio Lombardo, MD, Verona, Italy (*Abstract Co-Author*) Nothing to Disclose Marco Chincarini, MD, Verona, Italy (*Abstract Co-Author*) Nothing to Disclose Giancarlo Mansueto, MD, Verona, Italy (*Abstract Co-Author*) Nothing to Disclose

### For information about this presentation, contact:

andrea.mazzaro1558@gmail.com

### PURPOSE

To compare the CT features of post-operative fibrosis and tumor recurrence in patients with resected adenocarcinoma of the pancreas.

### **METHOD AND MATERIALS**

We selected 80 consecutive patients with resected pancreatic adenocarcinoma that had an early detection of solid hypodense tissue in the surgical bed at the after-surgery follow-up CT and with further follow-up CTs performed. Two readers in consensus analyzed the images measuring the solid tissue dimensions and measuring its attenuation by drawing a ROI in the late-arterial and venous phase. The density increase between the two phases (HUven-HUart) and ratio of enhancement (HUven-HUart/HUart) were calculated. The presence of metastases, pathological lymph-nodes and peritoneal carcinomatosis was noted. Statistical analysis included t-test, Fisher's and chi-square test.

### RESULTS

Among the 80 patients, the further follow-up CTs revealed for 38 patients the development of local tumor recurrence and 42 patients with post-surgical scar tissue which remained stable for size and imaging features. The longest diameter of tumor recurrence at the first CT was significantly larger than for fibrosis  $(30.4\pm2.8 \text{ mm vs } 21.7\pm1.3 \text{ mm}; p=0,0049)$ . Mean difference of density between venous and arterial phase was  $19.9\pm6.5$  HU for patients with fibrotic tissue and  $9.7\pm0.5$  HU for patients with neoplastic recurrence (p<0,0001). The enhancement ratio was +62.5% for the fibrosis and +22.8% for the recurrence (p<0,0001). No statistically significant difference was observed between the two groups for the presence of metastases, pathologically enlarged lymph-nodes or peritoneal carcinomatosis.

#### CONCLUSION

Tumor recurrence appeared to be larger and with poorer progressive enhancement than post-surgical fibrosis. Local recurrence appears to have no correlation with the presence of metastases, pathological lymph-nodes and peritoneal carcinomatosis.

# **CLINICAL RELEVANCE/APPLICATION**

Assessment of dimensions and enhancemet features of solid tissue found in the surgical bed in patients resected for pancreatic adenocarcinoma can be an effective instrument in the detection of local recurrence and a help in the post-operative treatment strategy.



# GU228-SD-TUB1

Integration of Patient and Tumor Metabolic Imaging to Predict Outcomes in Cervical Cancer Patients Using CT-Based Visceral Fat Measurements and FDG-PET

Tuesday, Nov. 27 12:45PM - 1:15PM Room: GU/UR Community, Learning Center Station #1

### Participants

Jonathan H. Stein, MD, Saint Louis, MO (*Presenter*) Nothing to Disclose John M. Floberg, MD, PhD, St. Louis, MO (*Abstract Co-Author*) Nothing to Disclose Julie K. Schwarz, MD, PhD, Saint Louis, MO (*Abstract Co-Author*) Nothing to Disclose Joseph E. Ippolito, MD, PhD, Saint Louis, MO (*Abstract Co-Author*) Nothing to Disclose

### For information about this presentation, contact:

jhstein@wustl.edu

# PURPOSE

Recent studies have shown that enhanced glucose uptake in cervical tumors measured with FDG-PET inversely correlates with overall survival (OS). However, the metabolism of the patient may also play a role. We recently identified that visceral obesity in cancer patients predicts poor outcomes, specifically in women. We sought to determine if increased visceral fat and FDG tumor uptake (i) independently predicted poor outcomes in women with cervical cancer and (ii) could synergize to better predict outcomes.

### **METHOD AND MATERIALS**

We performed an analysis of 77 patients with cervical cancer from the Siteman Cancer Center who received PET/CT scans at initial diagnosis. Using published methods, abdominal body fat was segmented and multiple fat metrics were obtained, including the subcutaneous fat area, visceral fat area, total fat area, and the normalized relative visceral fat area (rVFA). These metrics were compared to BMI. FDG uptake metrics, including the standardized uptake value (SUV), total lesion glycolysis (TLG) and metabolic tumor volume (MTV) of the primary tumor and lymph nodes were also obtained. Biomarker optimization analyses were conducted to identify imaging metric thresholds that maximally stratified the patients.

# RESULTS

Patients with an rVFA of >36.24% had significantly decreased OS (median OS = 565 days) compared to those patients with rVFA <36.24% (undefined OS, p=0.001). No other fat metric significantly stratified patients. Women with MTV of >118.6 mL had significantly decreased OS (median OS = 320 days) compared to those with a lesser MTV (undefined OS, p=0.0009). We were unable to identify any significant correlations between visceral fat and FDG uptake metrics. Because of this, we developed a stratification system combining rVFA and MTV. We identified that women with high rVFA (>36.24%) and high MTV (>118.6 mL) had the lowest OS (median OS = 141 days). Women with either a high rVFA or a high MTV had a median OS of 610 days. Women with low rVFA and low MTV did the best, with an undefined OS (p<0.0001).

### CONCLUSION

Metabolic markers of patient metabolism using visceral obesity can be combined with metabolic markers of tumor glucose metabolism to predict outcomes in cervical cancer patients.

### **CLINICAL RELEVANCE/APPLICATION**

Fat quantification, in combination with metabolic tumor markers, can help determine prognosis in cervical cancer patients.



# GU229-SD-TUB2

MR Imaging Evaluation for the Risk of Pelvic Organ Prolapse (POP): Focus on the Pelvic Floor (PF) Configuration and Aging

Tuesday, Nov. 27 12:45PM - 1:15PM Room: GU/UR Community, Learning Center Station #2

# Participants

Itsuko Okuda, MD, Minato-Ku, Japan (*Presenter*) Nothing to Disclose Naoki Yoshioka, Tokyo, Japan (*Abstract Co-Author*) Nothing to Disclose Keiichi Akita, MD, PhD, Tokyo, Japan (*Abstract Co-Author*) Nothing to Disclose Masahiro Irimoto, MD, Kunitachi, Japan (*Abstract Co-Author*) Nothing to Disclose Shigeru Nawano, MD, Tokyo, Japan (*Abstract Co-Author*) Nothing to Disclose Hiroaki Ohta, MD,PhD, Tokyo, Japan (*Abstract Co-Author*) Nothing to Disclose

### For information about this presentation, contact:

okudai812@yahoo.co.jp

### PURPOSE

In a super-aging society, the patients suffering from pelvic organs prolapse (POP) are increasing and many women are becoming more concerned about it. The pelvic floor (PF) fragility, attributable to aging, is regarded as one of the factors of POP, and the PF drops with aging. However, the changing process of the PF descensus is not fully known. So, we evaluated the PF configuration using MRI and assessed association to aging.

### **METHOD AND MATERIALS**

Our studies were approved by the institutional review board. The pelvic MR images from the medical checkup were used, and 74 healthy women from 20 to 91 years (49.8 ± 49.5 years) were enrolled. On coronal T2 weighted images, configurations of the levator ani (LA) muscles which were the biggest and main muscle of the PF were evaluated. Two observers assessed those images cooperatively. Configuration changes caused by the PF descensus was classified into four types; Gullwing (G), Shallow V (S-V), Deep V (D-V) and Wine glass (W). These types were then used to analyze the relationship to age.

#### RESULTS

The LA muscles of all subjects were recognized clearly. Based on the age of the women, the configuration of the LA muscles transition from G type (13 subjects,  $25.7 \pm 13.4$  years) to S-V type (27 subjects,  $40.9 \pm 24.0$  years), then to D-V type (20 subjects,  $59.9 \pm 15.6$  years) and finally to W type (14 subjects,  $75.1 \pm 19.1$  years). There was a significant difference between the mean age of the 4 types of the LA muscle configurations. In addition, the relationship between LA configuration changes caused by the PF descensus and age had a strong correlation.

#### CONCLUSION

On coronal T2 weighted images, the LA muscle configurations can be identified and grouped easily. It was observed that changes caused by age-related PF descensus, can help to predict the onset of POP.

#### **CLINICAL RELEVANCE/APPLICATION**

Coronal T2 weighted images are a useful tool to evaluate the degree of the PF descensus, and this examination is recommended for detecting the warning signs of POP.



# November 25-30 | McCormick Place, Chicago

# GU230-SD-TUB3

# Body Mass Index is a Regulating Factor for CT Attenuation of Adrenal Adenoma

Tuesday, Nov. 27 12:45PM - 1:15PM Room: GU/UR Community, Learning Center Station #3

# **Participants**

Akihiro Nishie, MD, Fukuoka, Japan (Presenter) Nothing to Disclose Yoshiki Asayama, MD, Fukuoka, Japan (Abstract Co-Author) Nothing to Disclose Kousei Ishigami, MD, Fukuoka City, Japan (Abstract Co-Author) Nothing to Disclose Yasuhiro Ushijima, MD, Fukuoka, Japan (Abstract Co-Author) Nothing to Disclose Daisuke Kakihara, Fukuoka, Japan (Abstract Co-Author) Nothing to Disclose Hiroshi Honda, MD, Fukuoka, Japan (Abstract Co-Author) Nothing to Disclose Tomohiro Nakayama, MD, PhD, Tokyo, Japan (Abstract Co-Author) Nothing to Disclose Nobuhiro Fujita, MD, PhD, Fukuoka, Japan (Abstract Co-Author) Nothing to Disclose Koichiro Morita, Fukuoka, Japan (Abstract Co-Author) Nothing to Disclose Keisuke Ishimatsu, MD, Fukuoka, Japan (Abstract Co-Author) Nothing to Disclose Seiichiro Takao, Fukuoka, Japan (Abstract Co-Author) Nothing to Disclose Masaaki Sugimoto, Fukuoka, Japan (Abstract Co-Author) Nothing to Disclose Tomoyuki Hida, Boston, MA (Abstract Co-Author) Research Grant, Konica Minolta, Inc

# PURPOSE

We encountered a case of adrenal adenoma (AA) that showed increased CT attenuation after bariatric surgery. We hypothesized that systemic lipid metabolism could affect CT attenuation of AA. The purpose of our study was to elucidate the lipid metabolismrelated factors regulating CT attenuation in AA.

# **METHOD AND MATERIALS**

Thirty-six patients (11 male, 25 female, mean age of 52 years) with surgically proven AA were enrolled. AA was present on the right in 13 patients and on the left in 23 patients. The mean size of AA was 2.2 cm (range: 1.2 to 4.2 cm). CT attenuation of AA and the liver was measured on unenhanced CT. Pathologically, the clear cell ratio (CCR) constituting each AÁ was qualitatively assessed. Clinical data including body mass index (BMI), HbA1c, TG, T-Chol, cortisol in blood and plasma aldosterone were also obtained. Multiple linear regression analysis was performed to evaluate the factors regulating CT attenuation of AA among these radiological and clinicopathological factors.

# RESULTS

The result was shown in Figure. There was a significant correlation between CT attenuation of AA and CCR, BMI and cortisol in blood (p<0.05). The t value of BMI was the highest among the three factors.

# CONCLUSION

CT attenuation of AA can be affected by the lipid metabolism-related factors such as BMI and cortisol in blood, except for CCR.

# **CLINICAL RELEVANCE/APPLICATION**

(dealing with CT diagnosis of AA) Although CT attenuation on unenhanced CT is usually used for diagnosis of AA, the compensation of this value with BMI and cortisol in blood may improve the diagnostic performance of unenhanced CT.



# GU231-SD-TUB4

Comparison between Conventional Cystourethrography and MRI with Voiding MR-Cystourethrography in the Evaluation of Male Urethral Strictures

Tuesday, Nov. 27 12:45PM - 1:15PM Room: GU/UR Community, Learning Center Station #4

# Participants

Marco Di Girolamo, MD, Rome, Italy (*Presenter*) Nothing to Disclose Francesco Carbonetti, MD, Rome-Roma, Italy (*Abstract Co-Author*) Nothing to Disclose Valentina Caturano, Roma, Italy (*Abstract Co-Author*) Nothing to Disclose Ines Casazza, Rome, Italy (*Abstract Co-Author*) Nothing to Disclose Salvatore Sansalone, Rome, Italy (*Abstract Co-Author*) Nothing to Disclose Andrea Laghi, MD, Rome, Italy (*Abstract Co-Author*) Nothing to Disclose

#### For information about this presentation, contact:

digirolamomarco@hotmail.com

#### PURPOSE

To evaluate the accuracy of conventional retrograde and voiding cystourethrography and MRI together with voiding MRcystourethrography in the evaluation of male urethral strictures.

#### **METHOD AND MATERIALS**

We evaluated 39 male patients with urethral strictures diagnosed with urine flow velocity recording and conventional retrograde and voiding cystourethrography. All these patients underwent MRI and voiding MR-cystourethrography using a 1.5T superconductive magnet. The patients had urine-filled bladders and high-resolution sagittal TSE T2-weighted scans were performed (TR:6250ms; TE:90ms;sl.thick.:3mm; acq.time:3'38'). Voiding MR-cystourethrography was performed with T1-weighted spoiled 3D gradient-echo acquisitions on sagittal plane (TR:12ms; TE:2,7ms; flip-angle:40°; sl.thickness: 2mm; acq.time:12s) after the filling of bladder lumen with contrast-material-enhanced urine obtainded by the i.v administration 20 mg of furosemide followed by ¾ of the normal dose of a paramagnetic contrast agent (Magnevist, Bayer Pharma, Germany). After micturition high-resolution coronal TSE T2-weighted scans were performed at the level of the stenosis. Two radiologists in consensus evaluated the morphology and length of the urethral stenosis with the two modalities and with MRI the entity and the site of spongio-fibrosis was assessed.

# RESULTS

6 patients were not able to perform voiding MR-cystourethrography. In 33 patients evaluated with two imaging modalities 42 urethral strictures were detected. The measurement of the stenosis length was equal or superior with voiding MR cystourethrography and the analysis of 3D sagittal scans allowed a better evaluation of the morphology of the urethral strictures in comparison with conventional cystourethrography. 32 strictures with Spongio-fibrosis were found (76%). The site of spongio-fibrosis was always assessed with MRI (dorsal, ventral, dorsal and ventral and circular fibrosis).

# CONCLUSION

MRI with voiding MR-cystourethrography shows the morphology and the length of the urethral strictures better than conventional cystourethrography and allows the detection and site of spongio-fibrosis, avoiding radiation exposure to the gonads and urinary catheterization.

# **CLINICAL RELEVANCE/APPLICATION**

MRI could be proposed as all-in-one technique for the evaluation of urethral stenosis, allowing their detection and length assessment and determining the presence and site of spongiofibrosis.



# GU232-SD-TUB5

# Displaying Normal Ovaries on Dual-Energy CT by Optimizing Image Reconstructions

Tuesday, Nov. 27 12:45PM - 1:15PM Room: GU/UR Community, Learning Center Station #5

### **Participants**

Haijiao Li, MD, Beijing, China (*Presenter*) Nothing to Disclose Kun Cao, MD, Beijing, China (*Abstract Co-Author*) Nothing to Disclose Rong Long, Beijing, China (*Abstract Co-Author*) Nothing to Disclose Yingshi Sun, Beijing, China (*Abstract Co-Author*) Nothing to Disclose

### For information about this presentation, contact:

lihaijiao126@126.com

# PURPOSE

To evaluate the possibility for improving the display of normal ovaries on dual-energy CT, by using different sets of monochromatic images and different degree of adaptive statistical iterative reconstruction(ASIR).

### **METHOD AND MATERIALS**

Female patients who came for pelvic CT because of non-gynecologic diseases were prospectively recruited to be scanned on a dual-energy equipment. Original data of images acquired at portal venous phase after administration of contrast medium were collected for reconstruction of imaging sets as follows: 5 sets of spectral monochromatic images with different KeVs (from 40 to 120 KeV with 20 KeV intervals), and 4 sets with different ASIR levels (from 40% to 70% with 10% intervals). All images were evaluated both objectively and subjectively in term of ovary display. Contrast-to-noise ratios (CNR) and signal-to-noise ratios (SNR) were obtained as objective assessments. Image qualities were scored by two radiologists separately using a 5-point scale as subjective evaluation. Differences among various sets of images were compared using t-test and non-parametric tests.

### RESULTS

36 patients diagnosed with non-remarkable ovaries on CT were enrolled. No significant differences of CNR were observed among images reconstructed with 40%-70% ASIR, but those with 70% and 60% ASIR showed better subjective score than 50% and 40% ASIR( $3.86\pm0.35\&3.83\pm0.38$  v.s.  $3.39\pm0.55\&2.89\pm0.47$ , all P<0.001). The comparison of different KeVs showed that the ovary CNR and SNR scores were decreasing with increasing of KeVs, while the subjective score of 80 KeV( $3.83\pm0.38$ ) and 60 KeV ( $3.81\pm0.47$ ) were higher than that of others(all P<0.001).

# CONCLUSION

For better display of normal ovaries on CT, imaging reconstructions on dual-energy using monochromatic 60 to 80 KeV is better, while using 60% to 70% ASIR are acceptable, especially considering the possibility of low radiation dose.

# **CLINICAL RELEVANCE/APPLICATION**

Due to the limited efficiency of CT for normal ovary display, large amount of patients were subject to additional examinations because of suspicious ovarian lesions on CT. So the improvement of ovary imaging quality on CT is in demand.



# GU233-SD-TUB6

Variables That Predict a Better Performance of MR/TRUS Fusion-Guided Biopsy over Routine Sextant Biopsy of the Prostate in a Clinical Cohort

Tuesday, Nov. 27 12:45PM - 1:15PM Room: GU/UR Community, Learning Center Station #6

### Participants

Leonardo K. Bittencourt, MD, PhD, Rio De Janeiro, Brazil (*Presenter*) Nothing to Disclose Caio L. Leidersnaider Sr, MD, Rio de Janeiro, Brazil (*Abstract Co-Author*) Nothing to Disclose Andrei S. Purysko, MD, Cleveland, OH (*Abstract Co-Author*) Nothing to Disclose Anke Bergmann, Rio De Janeiro, Brazil (*Abstract Co-Author*) Nothing to Disclose Andrea L. Monnerat, MD,MSc, Niteroi, Brazil (*Abstract Co-Author*) Nothing to Disclose

#### For information about this presentation, contact:

lkayat@gmail.com

# PURPOSE

To determine imaging and clinical variables that predict a better performance of MR-TRUS fusion-guided biopsy of the prostate over a conventional sextant-based approach.

# METHOD AND MATERIALS

171 patients were included in this IRB approved study. MR/TRUS fusion-guided biopsies were directed to lesions indicated by mpMRI (1.4±0.7 targets), followed by 14-core set of sextant biopsies in the same procedure. Reference-standard was combined histopathology of the procedure. Cases were classified as 'Targeted better' when ISUP group and/or % of core involvement were higher on MR-TRUS set, and 'Targeted only' when only MR/TRUS cores were positive for PCa. Variables such as PSA level/density, prior biopsies, number of targets, location, size and PI-RADS scores were tested as predictors for 'Targeted better' and 'Targeted only' groups. Fisher's exact test was used for comparing categorical variables and Mann-Whitney test for continuous variables. Each variable was tested through simple logistic regression, and variables showing statistical significance were further adjusted in a multiple logistic regression model. Statistical significance was indicated by p<0.05.

# RESULTS

139/171 patients (81.2%) were positive for PCa. MR/TRUS fusion detected 128/139 (92%), whereas standard biopsy detected 106/139 (76.2%). 99/171 patients (58%) were classified as 'Targeted better', and 33/171 patients (19%) were 'Targeted Only'. PI-RADS score >=4 was the only significant predictor for 'Targeted better' group (p<0.00001), with AUC=0.77, and OR=33.8. On the prediction of 'Targeted only' lesions, PI-RADS scores >=4 (p<0.019, AUC=0.68, OR=5.9) and an anteriorly located lesion (p<0.001, OR=4.5) were the only significant variables among the parameters that were tested.

# CONCLUSION

PI-RADS scores were the only significant predictor and a very strong indicator for a better performance of MR-TRUS fusion-guided biopsies over the standard sextant-based approach, whereas PI-RADS scores and an anteriorly located lesion were strong predictors for the detection of PCa only on the MR-TRUS fusion-guided set.

### **CLINICAL RELEVANCE/APPLICATION**

Patients with PI-RADS 4 or 5 lesions on mpMRI would benefit from MR/TRUS fusion biopsies, which provide higher cancer detection rates and more accurate assessment of aggressiveness, with fewer cores than the standard sextant based approach.

#### **Honored Educators**

Presenters or authors on this event have been recognized as RSNA Honored Educators for participating in multiple qualifying educational activities. Honored Educators are invested in furthering the profession of radiology by delivering high-quality educational content in their field of study. Learn how you can become an honored educator by visiting the website at: https://www.rsna.org/Honored-Educator-Award/ Andrei S. Purysko, MD - 2017 Honored Educator



# HP122-ED-TUB6

# 'Imaging' the Current State of Patient Experience and Imagining the Future State

Tuesday, Nov. 27 12:45PM - 1:15PM Room: HP Community, Learning Center Station #6

# Awards Certificate of Merit

#### Participants

Ruhani Doda Khera, MD, Boston, MA (*Presenter*) Nothing to Disclose Kristen L. Dean, Boston, MA (*Abstract Co-Author*) Nothing to Disclose Philip Jones, Boston, MA (*Abstract Co-Author*) Nothing to Disclose David A. Rosman, MD, Boston, MA (*Abstract Co-Author*) Nothing to Disclose Sanjay Saini, MD, Boston, MA (*Abstract Co-Author*) Nothing to Disclose

### For information about this presentation, contact:

rdodakhera@mgh.harvard.edu

# **TEACHING POINTS**

The purpose of this exhibit is: 1. To review and summarize the entire patient journey process for MRI, CT, Ultrasound, Breast Imaging, and X-Ray, and acknowledge that patient experience is substantially more complex and varied than moments spent during imaging. 2. To identify best practices and work together to develop site specific implementation plans. 3. To discuss the future design of imaging experience and prepare for it.

### **TABLE OF CONTENTS/OUTLINE**

1. Patient Experience Program Overview 2. Project Scope and Timeline 3. Discovery Phase 4. Design Pillars for Patient and Employee Satisfaction • Personal connection with every patient • Loyalty to each other and to patients • Empowerment to provide caring and responsive service • Commitment to training and individual staff development • Operation as an integrated ecosystem • Innovation 5. Patient Journey Mapping • Diagnostic Customer Experience Maps for MRI, CT, USG, Mammography and X-Ray 6. Patient Findings and Perspective 7. Opportunities Based on Patient Journey • Lack of Information • Unnecessary Emotional Tensions • Inconsistent Connections • Gaps in Imaging Experience • Private not always Perceived as Private 8. Recommendations - Enhance, Optimize, Innovate • Integrate Earlier • Front Desk as Hosts • CT Prep Suite • Strong Closing • Make Private Private 9. Future Design of Imaging Experience and Preparedness



### HP222-SD-TUB2

Patients Who Underwent Percutaneous Liver RFA for Malignancy Did Better When Admitted to Racially Diverse Hospitals

Tuesday, Nov. 27 12:45PM - 1:15PM Room: HP Community, Learning Center Station #2

### Participants

Yuzhou Liu, MBBS, New York, NY (Presenter) Nothing to Disclose

For information about this presentation, contact:

liuyuzhou2200@gmail.com

#### PURPOSE

It is known that racial disparity drives unfavorable outcomes. We aim to explore the relationship between hospital inpatient racial diversity and outcomes including major complications, mortality and cost for patients who electively received percutaneous liver RFA.

### **METHOD AND MATERIALS**

Using Nationwide Inpatient Sample database from 2005 to 2015, hospital inpatient racial diversity was defined as the percentage of non-Caucasian patients discharged from each hospital. Racially diverse hospitals are hospitals which have over 50% of discharges being non-Caucasian. Logistic regression was performed to determine the association between hospital racial diversity and RFA outcomes.

### RESULTS

There were 1265 discharges across 549 hospitals. The patient population was on average 42% minority. Caucasian patients had more iatrogenic pneumothorax (OR 1.80, 95% CI 1.01-3.22). However, when treated at hospitals with racial diversity, no outcome difference between Caucasian and non-Caucasian population was observed. Regardless of race, patients treated at hospital with higher non-Caucasian discharge percentage did better in terms of complication rate including iatrogenic pneumothorax (OR 0.09, 95% CI 0.02-0.35) and liver failure (OR 0.13, 95% CI 0.02-0.84). No difference in term of mortality and cost was observed.

#### CONCLUSION

Patients who underwent percutaneous liver RFA for malignancy had less complications when admitted to racially diverse hospitals though the mortality and cost did not differ. Failure to detect further difference might be due to limited patients number in our study.

### **CLINICAL RELEVANCE/APPLICATION**

Radially diverse hospitals might have better experience managing patients of different ethnic background and this could even be reflected on outcomes of interventional radiology procedures.



# HP223-SD-TUB3

Comprehensive Assessment of Fat Depots Using Multilayer Segmentation Techniques and Its Correlation with Anthropometric Measures on Computed Tomography Images

Tuesday, Nov. 27 12:45PM - 1:15PM Room: HP Community, Learning Center Station #3

# Participants

Cristiane A. Tuma Santos, MD, Jackson, MS (*Presenter*) Nothing to Disclose Edward Florez, PhD, Jackson, MS (*Abstract Co-Author*) Nothing to Disclose Elliot Varney, BS, Jackson, MS (*Abstract Co-Author*) Nothing to Disclose David Caballero, Jackson, MS (*Abstract Co-Author*) Nothing to Disclose William Flowers, Jackson, MS (*Abstract Co-Author*) Nothing to Disclose Lauren Dyess, Jackson, MS (*Abstract Co-Author*) Nothing to Disclose Charlene Claudio, Jackson, MS (*Abstract Co-Author*) Nothing to Disclose Seth Lirette, MS, Jackson, MS (*Abstract Co-Author*) Nothing to Disclose Kevin A. Zand, MD, Jackson, MS (*Abstract Co-Author*) Nothing to Disclose Luciano D. Villarinho, MD, Madison, MS (*Abstract Co-Author*) Nothing to Disclose Candace M. Howard-Claudio, MD, PhD, Philadelphia, PA (*Abstract Co-Author*) Nothing to Disclose

### For information about this presentation, contact:

chowardclaudio@umc.edu

#### PURPOSE

To assess the correlation between body weight, abdominal visceral and superficial adipose volumes, waist circumference, and sagittal abdominal diameter measured on CT images in a high risk population.

### METHOD AND MATERIALS

For this HIPPA-compliant, IRB approved retrospective observational study, non-enhanced CT images of the upper and lower abdomen were analyzed in a cross section of 150 African Americans. Patient age, gender and weight were gathered. Waist circumference (WCx) and sagittal abdominal diameter (SAD) were measured using the Digital Imaging and Communications in Medicine (DICOM) viewer through specific tools from Osirix MD v 9.0.2. Abdominal adiposity was subdivided into three distinct anatomic components. Visceral adipose tissue (VAT) was measured as the intraabdominal fat deposited around and within organs. Superficial adipose tissue (SAT), defined as the subcutaneous anatomic region, was subdivided into superficial (sSAT) and deep components (dSAT) by the superficial fascia. Fat volumes were obtained using multi-layer segmentation techniques using sliceOmatic v5.0 (Tomovision, Canada). Twenty four consecutive 2.5mm slices centered at the L4-L5 intervertebral space were measured. Volumes for each fat compartment (cm3) were segmented and correlated with SAD and WCx. SAD (cm) was measured in the slice centered at L4-L5 intervertebral disk, at the top of iliac crest. WCx (cm) was measured on the last slice from cranial to caudal not showing the iliac bone.

#### RESULTS

Both anthropometric measures (SAD and WCx) showed positive correlation with weight and volume of adipose tissue. SAD correlated more strongly with visceral adipose tissue than with other fat compartments (r=0.47). The strongest correlation was found between WCx and SAT (r=0.55). Please refer to the attached linear regression plots.

### CONCLUSION

SAD and WCx are inexpensive and readily obtained anthropometric measures that correlated with visceral and superficial adipose tissue, respectively. Anthropometric measures derived from CT measures may be easily incorporated in the assessment of cardiovascular risks.

#### **CLINICAL RELEVANCE/APPLICATION**

Anthropometric measures derived from CT images can be readily obtained. SAD correlates with visceral adiposity and consequently, may predict cardiovascular risk.



# HP224-SD-TUB4

Sonographer as a Source of Variability for Swear Wave Elastography: Separating Patient and Sonographer Variability Using Complete Block Design

Tuesday, Nov. 27 12:45PM - 1:15PM Room: HP Community, Learning Center Station #4

### Participants

Grayson L. Baird, PhD, Providence, RI (*Presenter*) Nothing to Disclose Alyssa S. Berube, Providence, RI (*Abstract Co-Author*) Nothing to Disclose Wendy J. Smith, RT, Providence, RI (*Abstract Co-Author*) Nothing to Disclose Michael D. Beland, MD, Providence, RI (*Abstract Co-Author*) Research Grant, Canon Medical Systems Corporation; Consultant, General Electric Company

# PURPOSE

Shear Wave elastography (SWE) is a non-invasive method of estimating liver fibrosis in patients with suspected liver disease. Variations in the elastic properties of soft tissue are measured by evaluating tissue behavior when a mechanical stress is applied. Quality assurance checks revealed that SWE values were systematically higher and more variable for some sonographers compared with others. These differences could be caused by differences between patients, SWE machines/probes, sonographers, or a combination thereof. The present study aims to determine the source of these differences.

#### **METHOD AND MATERIALS**

Complete balanced block design was conducted where 6 healthy liver subjects were scanned by the same 6 sonographers at the same time using the same machine. As recommended by the manufacturer, 12 SWE measurements were obtained from the right lobe of the liver; this was done for each subject by each sonographer. Generalized mixed modeling with sandwich estimation, where observations were nested within patients, was used to evaluate SWE differences between sonographers using SAS/GLIMMIX.

### RESULTS

Because the same healthy subjects were scanned at the same time using the same machine by all sonographers, median SWE values obtained between sonographers should be almost identical. Nonetheless, statistically significant differences were observed between sonographers such that one sonographer's median SWE value was as low as 4.9 while another's was as high as 5.5 (which also passes a clinical threshold), p<.001. Variability was also different between sonographers, where some sonographers SWE values were more variable than others, p<.01.

### CONCLUSION

These results highlight the need to standardize scanning protocols to reduce systematic differences and variability in SWE values between sonographers; these results may also justify a second scanning of patients who border clinical thresholds. Given that healthy liver volunteers, as a group, passed a clinical threshold, and if the variability inherent between sonographers cannot be controlled for in practice, then the reliability of clinical thresholds is placed into question.

### **CLINICAL RELEVANCE/APPLICATION**

Liver shear wave elastography is subject to variability between sonographers. Caution should be used in interpreting shear wave values, particularly when relying on strict thresholds for determining treatment.



### HP225-SD-TUB5

Gun Violence and Image Utilization at a Level-one Trauma Center

Tuesday, Nov. 27 12:45PM - 1:15PM Room: HP Community, Learning Center Station #5

#### Awards Student Travel Stipend Award

#### Participants

Ankit V. Gandhi, MD, Philadelphia, PA (*Presenter*) Nothing to Disclose Kimberly Klinger, MD, MS, Philadelphia, PA (*Abstract Co-Author*) Nothing to Disclose Lauren A. Brown, MD, Philadelphia, PA (*Abstract Co-Author*) Nothing to Disclose Corbin L. Pomeranz, MD, Philadelphia, PA (*Abstract Co-Author*) Nothing to Disclose Adam C. Zoga, MD, Philadelphia, PA (*Abstract Co-Author*) Nothing to Disclose William B. Morrison, MD, Philadelphia, PA (*Abstract Co-Author*) Consultant, AprioMed AB; Patent agreement, AprioMed AB; Consultant, Zimmer Biomet Holdings, Inc; Consultant, Samsung Electronics Co, Ltd; Consultant, Medical Metrics, Inc

# For information about this presentation, contact:

gandhi.v.ankit@gmail.com

# PURPOSE

National health databases lack substantial information related to gun violence. Sites of initial evaluation and management of gunshot injuries, such as level one trauma centers and their radiology departments, are in a position to investigate this issue. The goal of our study is to assess the demographics, injury patterns, and image utilization in patients with acute and remote gunshot injuries at our institution.

# METHOD AND MATERIALS

A retrospective analysis was performed by searching a database from a single institution for gunshot wound (GSW)-related imaging exams from January 2016 to April 2018. Exams with keywords 'gunshot wound', 'GSW', 'bullet', 'shrapnel', 'buckshot', and 'pellet' were included. Studies without an acute or remote history of GSW and without evidence of retained bullet shrapnel were excluded. Data was classified into subcategories of acute and remote gun-related injury. Information regarding radiologic exam modality, injury location, patient age and sex were recorded.

#### RESULTS

The average patient age for the acute gunshot injury category is 31 (SD 13). Men account for 93% of acute and 89% of remote GSW injuries. Most common modalities used, regardless of injury chronicity, are radiographs (acute N=257, remote N=941) and computed tomography (acute N=146, remote N=407). A total of 432 imaging studies were performed for acute GSW-related trauma on 120 patients, yielding approximately 4 studies per patient. A total of 1437 studies performed on 840 patients show sequelae of remote gunshot injury with the majority demonstrating retained bullets/shrapnel. The most common site of injury is the musculoskeletal system (N=579), followed by the chest (N=577) and the abdomen (N=374).

# CONCLUSION

Healthcare cost, morbidity, and mortality related to gun violence can only be assessed after a firm understanding of demographics, injury patterns, and image utilization is attained. By characterizing these fundamental aspects of gunshot injuries, our study contributes to defining gun violence as a public health issue. Data collection is ongoing and future plans include collaborating with regional trauma centers, categorizing injuries using ICD-10 codes to analyze imaging costs, and determining patient outcome.

#### **CLINICAL RELEVANCE/APPLICATION**

Gun violence imaging analysis can elucidate associated medical cost and limitations in advanced imaging due to the presence of retained shrapnel.



### IN147-ED-TUB3

Computational Fluid Dynamics in Practice: An Illustrated 'How-To' with Examples from CT Fractional Flow Reserve, Endothelial Shear Stress, Abdominal Aortic Aneurysms, and Congenital Heart Disease

Tuesday, Nov. 27 12:45PM - 1:15PM Room: IN Community, Learning Center Station #3

# Participants

Anji Tang, Boston, MA (*Presenter*) Nothing to Disclose Andreas Giannopoulos, MD, Zurich, Switzerland (*Abstract Co-Author*) Nothing to Disclose Dimitris Mitsouras, PhD, Boston, MA (*Abstract Co-Author*) Research Grant, Canon Medical Systems Corporation;

### For information about this presentation, contact:

dmitsouras@alum.mit.edu

# **TEACHING POINTS**

1. CFD is increasingly used in patient care. 2. CFD requires "boundary conditions" (BCs) for which to solve the equations of blood motion. These are the arterial lumen, blood properties (viscosity, density), and driving forces, eg flow or pressure at inlets/outlets of the simulated domain. 3. CTA, MRI, and invasive angiography with or without US or optical coherence tomography provides the arterial lumen BC. 4. Fixed (Newtonian) or flow-dependent viscosity (non-Newtonian) blood models can be used for the blood model. The quantity of interest (eg, endothelial shear stress, CT-FFR) often dictates the choice.5. Estimating patient-specific inlet/outlet BCs are key to successful clinical applications. Methods to select them will be reviewed, including coupling to distal vascular beds such as myocardial microvascular beds for CT-FFR.

### **TABLE OF CONTENTS/OUTLINE**

1. Angiography & Black blood Imaging techniques and segmentation tools.2. Blood models. 3. Estimating flow BCs (Murray law, physiology, venc MR, etc) and coupling to distal vascular beds.4. CFD tools: meshing and solver.5. Post-CFD tools: visualizing and measuring the value of interest.6. Examples: coronary CT-FFR, coronary endothelial shear stress, anomalous origin coronary flow, abdominal aneurysm growth, Norwood procedure.



### IN148-ED-TUB4

Designing and Performing State-of-the-Art Virtual Clinical Trials: Everything You Wanted to Know About VCTs but Dared Not Ask

Tuesday, Nov. 27 12:45PM - 1:15PM Room: IN Community, Learning Center Station #4

# Participants

Bruno Barufaldi, PhD, Philadelphia, PA (*Presenter*) Nothing to Disclose Predrag R. Bakic, PhD, Philadelphia, PA (*Abstract Co-Author*) Research collaboration, Barco nv; Research collaboration, Hologic, Inc; Andrew D. Maidment, PhD, Philadelphia, PA (*Abstract Co-Author*) Research support, Hologic, Inc; Research support, Barco nv; Research support, Analogic Corporation; Spouse, Employee, Real-Time Tomography, LLC; Spouse, Stockholder, Real-Time Tomography, LLC; Scientific Advisory Board, Real-Time Tomography, LLC; Ali N. Avanaki, PhD, Beaverton, OR (*Abstract Co-Author*) Employee, Barco nv Kathryn S. Espig, MSc, Beaverton, OR (*Abstract Co-Author*) Employee, Barco nv Albert Xthona, BS, Beaverton, OR (*Abstract Co-Author*) Employee, Barco nv Susan Weinstein, MD, Philadelphia, PA (*Abstract Co-Author*) Nothing to Disclose Tom Kimpe, Kortrijk, Belgium (*Abstract Co-Author*) Employee, Barco nv

#### For information about this presentation, contact:

predrag.bakic@uphs.upenn.edu

#### **TEACHING POINTS**

1. To understand the concept of and motivations for performing Virtual Clinical Trials (VCTs) 2. To illustrate the procedure of designing a VCT 3. To review examples of recent VCT applications and results 4. To identify open questions and future directions

#### TABLE OF CONTENTS/OUTLINE

 Motivation for VCTs: Limitations of clinical imaging trials: Cost, time, risk; Limited variety of clinical data; Lack of ground truth; Availability of fast processing and accurate simulation.
 Flow-chart of VCT pipeline: Anatomy and lesion simulation; Lesion insertion; Deformation and positioning; Image acquisition, processing, reconstruction; Display and post-processing simulation; Model observers; Statistical analysis.
 Control of VCTs and need for standardization: XML schema and VCTX format; VCT database; VCT standard.
 Illustrative examples of recent VCTs: Detectability of lesions in DM and DBT; Customization of novel imaging systems.
 Future work on resolving current challenges: Designing populations; Need for fast simulation; Extension to other organs and scales.



# IN217-SD-TUB1

### Evaluating the Completeness of a Radiology Glossary for the Vocabulary of Breast Imaging Reports

Tuesday, Nov. 27 12:45PM - 1:15PM Room: IN Community, Learning Center Station #1

### Participants

Jennifer Levy, MD, Philadelphia, PA (Presenter) Nothing to Disclose

Emily F. Conant, MD, Philadelphia, PA (*Abstract Co-Author*) Grant, Hologic, Inc; Consultant, Hologic, Inc; Grant, iCAD, Inc; Consultant, iCAD, Inc; Speaker, iiCME

Charles E. Kahn JR, MD, Philadelphia, PA (Abstract Co-Author) Nothing to Disclose

# CONCLUSION

The PORTER glossary provides excellent coverage of the vocabulary of breast imaging reports. The glossary could be used to annotate reports to improve patient understanding, and thereby might improve breast imaging outcomes.

### Background

Successful communication of radiology results to patients improves follow-up after abnormal breast imaging exams. However, radiology reports often contain words that are foreign to the average patient. The PORTER (Patient-Oriented Radiology Reporter) glossary was developed as a tool to annotate radiology reports so that patients can better understand their content. The completeness of the glossary for the terms appearing in breast imaging reports has not yet been studied.

#### **Evaluation**

The PORTER glossary contained 4,320 concepts with their lexical variants for a total of 13,614 terms. A random sample of 1,000 breast imaging reports (including screening and diagnostic mammograms, ultrasounds, and MRIs) was divided into 10 cohorts of 100 reports each. Each cohort was reviewed in sequence to identify terms not in the glossary, which then were added and potentially matched in subsequent cohorts. Using this "iterative refinement" approach, 283 new terms were identified from the first 500 reports and 83 new terms from the last 500 reports. Cohorts 1-5 contained a mean ( $\pm$  standard deviation) of 474  $\pm$  58 matched terms and 57  $\pm$  17 new terms. Cohorts 6-10 contained 548  $\pm$  69 matched terms and 17  $\pm$  8 new terms. The mean number of new terms in cohorts 1-5 versus cohorts 6-10 was statistically significant using the Student t-test (p=.002).

#### Discussion

After iterative refinement, the PORTER glossary included 98% (647/657) of terms encountered in the final cohort of breast imaging reports. A resource to improve patients' understanding of their results would be especially beneficial because breast imaging outcomes rely heavily on patient adherence to follow-up.

### **Honored Educators**

Presenters or authors on this event have been recognized as RSNA Honored Educators for participating in multiple qualifying educational activities. Honored Educators are invested in furthering the profession of radiology by delivering high-quality educational content in their field of study. Learn how you can become an honored educator by visiting the website at: https://www.rsna.org/Honored-Educator-Award/ Charles E. Kahn JR, MD - 2012 Honored EducatorCharles E. Kahn JR, MD - 2018 Honored Educator



# IN219-SD-TUB2

Radiologist Adoption of an Innovative Radiology Reporting Technique: The Inclusion of Active Hyperlinks to Key Image Findings in the PACS

Tuesday, Nov. 27 12:45PM - 1:15PM Room: IN Community, Learning Center Station #2

### Participants

Cree M. Gaskin, MD, Charlottesville, VA (*Presenter*) Author with royalties, Oxford University Press; Author with royalties, Thieme Medical Publishers, Inc; Research Grant, Carestream Health, Inc; Steven Beesley, MD, Charlottesville, VA (*Abstract Co-Author*) Nothing to Disclose James Patrie, MS, Charlottesville, VA (*Abstract Co-Author*) Nothing to Disclose

#### For information about this presentation, contact:

cree@virginia.edu

# PURPOSE

To determine adoption rates by radiologists of a new reporting enhancement - the inclusion in radiology reports of active hyperlinks to key image findings archived in the PACS

# METHOD AND MATERIALS

HIPAA compliant, retrospective study of 559,841 diagnostic reports over 20 months. Our practice uses a reporting application (Vue Reporting, Carestream Health) that supports the creation of active hyperlinks. Dictated text describing key findings can be highlighted and quickly linked to annotated images stored in the PACS, where they are available to report consumers, including care providers. Brief training of radiology residents occurred at months 3 & 16 after implementation. Data on use was collected, including: modality, presence of hyperlinks, subspecialty of radiologists, and role [resident (r), fellow (f), attending (a)] of the initial report creator. The most recent 6-month period represented established reporting habits (see Fig).

### RESULTS

6-month average percentages of reports containing hyperlinks to imaging findings by modality & role: CT [r=28%, f=17%, a=24%](Fig); MRI [r=26%, f=9%, a=5%]; PET-CT [r=54%, f=48%, a=21%]; Nuc Med [r=1%, f=2%, a=0%]; Xray [r<1%, f<1%, a<1%]; US [r=2%, f=0%, a<1%]. 6-month average percentages of CT and MRI reports with hyperlinks to imaging findings by subspecialty: CT [body=30%, chest=57%, MSK=6%, peds=27%, cardiovasc=6%, neuro=6%]; MRI [body=40%, chest=36%, MSK=6%, peds=18%, cardiovasc=0%, neuro=7%]. Residents' reports were more likely to contain hyperlinks than those created by faculty and fellows (p<0.001).

# CONCLUSION

Once enabled, radiologists commonly elect to insert active hyperlinks connecting report text to images themselves, suggesting that users find such a tool to be beneficial, and that it likely increases the value of radiology reports. There is variability in 1) adoption by subspecialty, and 2) application by modality. Residents with training were more likely to adopt this reporting technique than faculty and fellows who did not receive training.

### **CLINICAL RELEVANCE/APPLICATION**

Sustained common use of this innovative reporting enhancement indicates perceived value by our radiologists and functional readiness for adoption by others.



# MI219-SD-TUB1

MR Imaging Radiomics of NSCLC Brain Metastases: A Potential Targetable Imaging Biomarker for EGFR Status

Tuesday, Nov. 27 12:45PM - 1:15PM Room: MI Community, Learning Center Station #1

FDA Discussions may include off-label uses.

#### Participants

Abhishek Mahajan, MBBS, MD, Mumbai, India (*Presenter*) Nothing to Disclose Abhijeet B. Ghaytidak JR, MD, Mumbai, India (*Abstract Co-Author*) Nothing to Disclose Devendra Goyal, MBBS, Mumbai, India (*Abstract Co-Author*) Nothing to Disclose Sujeet Agarwal, MBBS, Mumbai, India (*Abstract Co-Author*) Nothing to Disclose Kumar Prabhash, Mumbai, India (*Abstract Co-Author*) Nothing to Disclose Vanita Noronha, Mumbai, India (*Abstract Co-Author*) Nothing to Disclose Amit Joshi, MBBS, MD, Mumbai, India (*Abstract Co-Author*) Nothing to Disclose Vijay M. Patil, Mumbai, India (*Abstract Co-Author*) Nothing to Disclose

### For information about this presentation, contact:

drabhishek.mahajan@yahoo.in

### PURPOSE

The purpose of the study was to study MRI imaging biomarkers of brain metastases NSCLC and their correlation with molecular subtyping (EFGR status). To correlate these imaging features with response to therapy and clinical outcomes.

### **METHOD AND MATERIALS**

We analyzed clinical data on 75 patients who were tested for EGFR mutation and underwent brain MR imaging at diagnosis. Multiparametric MRI was performed in all cases. The associations between EGFR mutation status and clinical features, specifically age, sex, smoking, TNM stage, and imaging variables, as well as brain metastasis, were analyzed using logistic regression analysis. Clinical factors known to be associated with EGFR mutation status in NSCLC patients and staging factors of TNM were included in the logistic regression multivariate analysis.

#### RESULTS

38 EGFR positive and 37 EGFR negative cases. EGFR positive showed early and wide spread development of brain metastasis (within 6 months after 1st presentation) (p- 0.00). Statistically significant difference (p- 0.00) was observed in border/ margins on T2W imaging, fuzzy and infiltrative borders in EGFR positive while well defined in EGFR negative. Lesions in EGFR wild group showed focal restriction on DW images (p-0.001). In EGFR wild cases showed good response to WBRT (p< 0.00). Incidence of recurrent metastatic disease, meningeal involvement was significantly higher in EGFR positive (p- 0.00, 0.04). On multivariate analysis, statistically significant association was found between T2 border, number, restricted diffusion, meningeal positivity and TTP (p < 0.05).

# CONCLUSION

EGFR positive brain metastases have characteristic MR imaging features that can be potential non-invasive diagnostic, predictive and prognostic imaging biomarkers. These MR based Radiogenomic imaging biomarkers have potential role in personalized therapy of EGFR positive brain metastasis in NSCLC.

### **CLINICAL RELEVANCE/APPLICATION**

Brain is a common site of metastases with EGFR mutated lung cancer. Oral targeted therapies have broadened the treatment options in the advanced setting with the potential for periods of long term response. Literature on MR imaging metrics or feature analysis of NSCLC brain metastasis as a biomarker for predicting EGFR mutation is limited and less investigated.



# MI220-SD-TUB2

Synthesis and Evaluation of a 68Ga-DOTA Labelled Peptidomimetic Inhibitor of Matriptase for PET Imaging

Tuesday, Nov. 27 12:45PM - 1:15PM Room: MI Community, Learning Center Station #2

#### Awards Student Travel Stipend Award

#### Participants

Daniel Kwon, MSc, Vancouver, BC (*Presenter*) Nothing to Disclose Julie Rousseau, PhD, Vancouver, BC (*Abstract Co-Author*) Nothing to Disclose Zhengxing Zhang, PhD, Vancouver, BC (*Abstract Co-Author*) Nothing to Disclose Jianghong An, PhD, Vancouver, BC (*Abstract Co-Author*) Nothing to Disclose Helen Merkens, BSC, Vancouver, BC (*Abstract Co-Author*) Nothing to Disclose Nadine Colpo, Vancouver, BC (*Abstract Co-Author*) Nothing to Disclose Chengcheng Zhang, Vancouver, BC (*Abstract Co-Author*) Nothing to Disclose Steven J. Jones, PhD, Vancouver, BC (*Abstract Co-Author*) Nothing to Disclose Kuo-Shyan Lin, Vancouver, BC (*Abstract Co-Author*) Nothing to Disclose Francois Benard, MD, Vancouver, BC (*Abstract Co-Author*) Nothing to Disclose

For information about this presentation, contact:

dkwon@bccrc.ca

# PURPOSE

Matriptase, an epithelial type II membrane-type serine protease, plays a key role in activating several proteases implicated in metastasis, and is overexpressed in a number of human epithelial cancers, including breast, prostate, pancreatic, ovarian and colorectal cancers. In this study, we modified a previously existing peptidomimetic inhibitor of matriptase by appending a DOTA-chelator group at the N-terminus of the sequence and evaluated them *in vitro* and *in vivo* in tumour-bearing mice.

#### **METHOD AND MATERIALS**

The peptidomimetic inhibitor was synthesized as outlined in the literature. The cold standard was prepared by reacting the DOTAconjugated inhibitor with GaCl3. 3D *in silico* docking studies predicted the DOTA-conjugated inhibitor would fit in the binding pocket without significant loss of binding affinity, which was confirmed by a fluorescence-based enzymatic assay. The tracer was prepared via microwaving the DOTA-conjugated inhibitor with 68GaCl3 in HEPES buffer. Imaging and biodistribution studies were performed in HT29-bearing immunocompromised mice.

# RESULTS

The Ga-DOTA-conjugated peptidomimetic matriptase inhibitor was determined to have an IC50 value of 2.6 nM. Biodistribution and imaging studies determined that the tracer was excreted renally. The decay-corrected radiochemical yield of the tracer synthesis was  $18\pm8\%$  n = 3, with a radiochemical purity of >97%. The HT-29 xenografts showed uptake of 0.42 and 0.36 percentage injected dose per gram (%ID/g) at 30 minutes and 1 hour post-injection, respectively. PET imaging of a HT-29 bearing immunocompromised mice at 1 hour post-injection enabled visualization of the tumour with modest contrast. Crucially, at 30 minutes post-injection, urine analysis via HPLC showed most of the tracer had been metabolized and excreted renally. Co-injection of phosphoramidon did not significantly improve tumour uptake or prevent metabolization of the tracer.

#### CONCLUSION

We have identified a nanomolar-binding inhibitor of matriptase that does not lose binding affinity with conjugation to Ga-DOTA. Further studies are needed to determine the nature of the metabolite to enable rational structural modification of the peptidomimetic inhibitor to further improve tumour uptake of the tracer.

### **CLINICAL RELEVANCE/APPLICATION**

The successful development of PET imaging agents targeting matriptase will enhance the detection of invasive and aggressive epithelial cancers, improving patient outcomes.



# MI221-SD-TUB3

Solitary Pulmonary Nodules: Comparison of Differentiation Capability Among Actual Diffusion-Weighted Imaging and Computed Diffusion-Weighted Imaging at Different b Values and FDG-PET/CT

Tuesday, Nov. 27 12:45PM - 1:15PM Room: MI Community, Learning Center Station #3

# Participants

Yuji Kishida, MD, PhD, Kobe, Japan (Presenter) Nothing to Disclose

Yoshiharu Ohno, MD, PhD, Kobe, Japan (*Abstract Co-Author*) Research Grant, Canon Medical Systems Corporation; Research Grant, Koninklijke Philips NV; Research Grant, Bayer AG; Research Grant, DAIICHI SANKYO Group; Research Grant, Fuji Pharma Co, Ltd; Research Grant, Guerbet SA;

Masao Yui, Otawara, Japan (*Abstract Co-Author*) Employee, Canon Medical Systems Corporation Yoshimori Kassai, MS, Otawara, Japan (*Abstract Co-Author*) Employee, Canon Medical Systems Corporation Shinichiro Seki, Kobe, Japan (*Abstract Co-Author*) Research Grant, Canon Medical Systems Corporation Takeshi Yoshikawa, MD, Kobe, Japan (*Abstract Co-Author*) Research Grant, Canon Medical Systems Corporation Katsusuke Kyotani, RT,MSc, Kobe, Japan (*Abstract Co-Author*) Nothing to Disclose Takamichi Murakami, MD, PhD, Osakasayama, Japan (*Abstract Co-Author*) Nothing to Disclose

#### For information about this presentation, contact:

yjk121@med.kobe-u.ac.jp

#### PURPOSE

To directly compare the capability for differentiating malignant from benign pulmonary nodules among actual and computed diffusion-weighted image (aDWI and cDWI) and FDG-PET/CT.

#### **METHOD AND MATERIALS**

Sixty-five consecutive patients (44 men and 21 women; mean age, 69.5±8.7 years) with 85 pulmonary nodules prospectively underwent DWIs at 3T MR system, integrated PET/CT, pathological, microbacterial and follow-up examinations. All DWIs were obtained by using fast advanced spin-echo (FASE) sequence with b values at 0 (aDWIb=0) and 1000s/mm2 (aDWIb=1000). cDWIs were generated at b value as 600 (cDWIb=600), 800 (cDWIb=800) and 1500 (cDWIb=1500) s/mm2 by commercially available software from aDWIb=0 and aDWIb=1000. According to results of pathological and follow-up examinations, all nodules were divided into malignant (n=48) and benign (n=37) nodule groups. Then, contrast ratio (CR) between nodule and thoracic muscles on each DWI and SUVmax were evaluated by ROI measurement. To compare all indexes between two groups, Student's t-test was performed. Then, differentiation capability was compared by ROC analysis among all methods. Finally, sensitivity, specificity and accuracy were compared among each other by McNemar's test.

### RESULTS

There were significant difference of all indexes between two groups (p<0.05). Area under the curve (AUC) of cDWIb=600 (AUC=0.92) was significantly larger than that of SUVmax (AUC=0.82, p=0.02). Sensitivity (SE) and accuracy (AC) of aDWIb=1000 (SE: 79.2 [38/48] %, AC: 83.5 [71/85] %) and all cDWIs except cDWIb=1500 (SE: 85.4 [41/48] % - 93.8 [45/48] %, AC: 85.9 [73/85] % - 90.6 [77/85] %) were significantly higher than those of PET/CT (SE: 60.4 [29/48] %, p<0.05; AC: 75.3 [64/85] %, p<0.05). Sensitivity (93.8 %) and accuracy (90.6 %) of cDWIb=600 were significantly higher than those of aDWIb=1000 (SE: p=0.0002, AC: p=0.0009).

### CONCLUSION

Computed and actual DWIs have a better potential for differentiating malignant from benign pulmonary nodules than FDG-PET/CT. In addition, computed DWI would be better to be generated at b value as 600s/mm2 for improving diagnostic performance of DWI in routine clinical practice.

### **CLINICAL RELEVANCE/APPLICATION**

Computed DWI is considered at least as useful as actual DWI for differentiation of malignant from benign pulmonary nodules, when compared with FDG-PET/CT. In addition, computed DWI would be better to be generated at b value as 600s/mm2.



### MI222-SD-TUB4

Comparison Of 68 GA PSMA And Whole Body Diffusion Weighted MR Imaging In Staging Of High Risk Prostate Cancer

Tuesday, Nov. 27 12:45PM - 1:15PM Room: MI Community, Learning Center Station #4

# Participants

Murali K. Logudoss, MBBS, MD, Chennai, India (*Presenter*) Nothing to Disclose Jayaraj Govindaraj, MD, MBBS, Chennai, India (*Abstract Co-Author*) Nothing to Disclose Amarnath Chellathurai, MD, FRCR, Chennai, India (*Abstract Co-Author*) Nothing to Disclose Amritha Asokan, MBBS, Chennai, India (*Abstract Co-Author*) Nothing to Disclose Vijay Karthik Jagan, MBBS, Coimbatore, India (*Abstract Co-Author*) Nothing to Disclose

### For information about this presentation, contact:

drlmkmdrd@gmail.com

### PURPOSE

Multiparametric MRI has evolved as the gold standard for local staging of Prostate cancer. However for the nodal and metastases staging in high risk prostate cancer several modalities including contrast enhanced CT, MRI, Bone scan, PET CT based tracers like 11C choline, 18 F Choline and 18 FDG are being used. But all of them have poor sensitivity and specificity. However recently 68 GA PSMA seems to be very promising for the diagnosis of nodal and visceral metastases. The purpose of the study is to compare the sensitivity and specificity of 68 GA PSMA and Whole body Diffusion Weighted MR imaging in staging of high risk prostate cancer.

### **METHOD AND MATERIALS**

The study design was a prospective observational study. 68 patients who have been recently diagnosed with high-risk prostrate cancer were included in the study. Inclusion criteria included biopsy proven prostate cancer with PSA more than 20ng/ml and Gleason score more than 7. After obtaining informed consent all the patients underwent 68 GA PSMA and whole body diffusion weighted imaging within 1week duration. Two radiologists read both modalities independently and the results were compared for staging of nodal and distant metastases.

#### RESULTS

The mean age of the patients included in the study was 63 years (Range 41-78 yrs) and the mean PSA value was 15 ng/ml. The median Gleason score was 8. Regional nodal metastases were detected by 68 GA PSMA in 48 patients and by DWI in 45 patients. Non-regional nodal metastases were detected in 18 patients by 68GA PSMA and in 17 patients in DWI. Skeletal metastases were detected in 24 patients by both 68GA PSMA and whole body DWI. Both 68GA PSMA and whole body DWI detected hepatic metastasis in one patient. Additionally 68GA PSMA detected pulmonary metastasis in one patient, which was missed by DWI. Statistically it was found that the efficacy of Whole body Diffusion Weighted Imaging was almost equal to that of 68GA PSMA (p<0.05).

### CONCLUSION

Whole Body Diffusion Weighted Imaging has sensitivity and specificity almost equal to 68GA PSMA in the detection of nodal and distant metastases in high risk prostate cancer and can be used with Multiparametric imaging of the prostate for complete TNM staging of prostate cancers.

### **CLINICAL RELEVANCE/APPLICATION**

Multiparametric MRI with Wholebody Diffusion Weighted Imaging can be used as an alternative for the local and metastatic staging of high risk prostate cancer instead of 68 GA PSMA.



### MI223-SD-TUB5

68Ga-RM2 PET/MRI Detection of Recurrent Prostate Cancer in Patients with Negative Conventional Imaging

Tuesday, Nov. 27 12:45PM - 1:15PM Room: MI Community, Learning Center Station #5

### Participants

Lucia Baratto, Stanford, CA (*Presenter*) Nothing to Disclose Caitlyn Harrison, MD, Stanford, CA (*Abstract Co-Author*) Nothing to Disclose Guido A. Davidzon, MD, Stanford, CA (*Abstract Co-Author*) Nothing to Disclose Thomas Yohannan, MD, Chicago, IL (*Abstract Co-Author*) Nothing to Disclose Andrei Iagaru, MD, Emerald Hills, CA (*Abstract Co-Author*) Research Grant, General Electric Company

### For information about this presentation, contact:

lbaratto@stanford.edu

### PURPOSE

Gastrin-releasing peptide receptors (GRPRs), are highly overexpressed in many cancers, including prostate cancer (PCa). Different GRPRs analogs have been radiolabeled and used for imaging diagnosis, staging, evaluation of biochemical recurrence, and assessment of metastatic disease in PCa patients. 68Ga-RM2 is a synthetic bombesin receptor antagonist that targets GRPr. Here we present data from the use of 68Ga-RM2 in patients with biochemical recurrence (BCR) of PCa and negative conventional imaging (CI).

# METHOD AND MATERIALS

We enrolled 65 men with BCR PCa, 59-83 year-old (mean $\pm$ standard deviation (SD): 69.2 $\pm$ 5.7). Imaging started at 41-89 minutes (mean $\pm$ SD: 53.6 $\pm$ 11.4) after injection of 127.5-149.7 MBq (mean $\pm$ SD: 141.6 $\pm$ 4.4) of 68Ga-RM2 using a time-of-flight (TOF)-enabled simultaneous positron emission tomography (PET) / magnetic resonance imaging (MRI) scanner. T1-weighted (T1w), T2-weighted (T2w) and diffusion-weighted images (DWI) were acquired.

#### RESULTS

All patients had rising prostate specific antigen (PSA) (range: 0.2-119.0 ng/mL; mean±SD:  $7.7\pm16.8$ ) and negative CI (CT or MRI, and 99mTc MDP bone scan) prior to enrollment. The observed 68Ga-RM2 PET detection rate was 67.7%. 68Ga-RM2 PET identified recurrent PCa in 44 of the 65 participants, while the simultaneous MRI scan identified findings compatible with recurrent PCa in 20 of the 65 patients. PSA velocity (PSAv) values were  $0.32\pm0.59$  ng/ml/year (range: 0.04-1.9) in patients with negative PET scans and  $2.51\pm2.16$  ng/ml/year (range: 0.13-8.68) in patients with positive PET scans (P: 0.006).

### CONCLUSION

The high uptake in multiple areas compatible with cancer lesions suggests that 68Ga-RM2 is a promising PET radiopharmaceutical for localization of disease in patients with BCR PCa and negative CI.

# **CLINICAL RELEVANCE/APPLICATION**

68Ga-RM2 is a promising tracer for assessment of GRPr expression in patients with BCR PCa.



# MK377-SD-TUB1

Predictor of Short-Term Poor Prognosis Following Percutaneous Vertebroplasty in Postmenopausal Women of Different Ages with Osteoporotic Related Vertebral Compression Fractures

Tuesday, Nov. 27 12:45PM - 1:15PM Room: MK Community, Learning Center Station #1

# Participants

Jia-Ying Zhou, Nanjing, China (*Presenter*) Nothing to Disclose Yuan-Cheng Wang, Nanjing, China (*Abstract Co-Author*) Nothing to Disclose Shenghong Ju, MD, PhD, Nanjing, China (*Abstract Co-Author*) Nothing to Disclose

### For information about this presentation, contact:

zjyseucm@163.com

# PURPOSE

To determine the predictors of short-term poor prognosis after following percutaneous vertebroplasty (PVP) in postmenopausal women of different ages with osteoporotic-related vertebral compression fractures (OVCFs)

### METHOD AND MATERIALS

Human studies were compliant with HIPAA and approved by the institutional review board. The study included postmenopausal women with OVCFs who underwent their first PVP between January 2012 and December 2016 in our department using unenhanced CT scans. They were divided into two groups, postmenopausal women less than 65y, and older than 75y. Short-term poor prognosis is defined as the cement leakage or new adjacent vertebral fractures in three months after PVP. The CT images were reconstructed with post-processing program. We assessed and recorded all the potential risk predictors of short-term poor prognosis. The inter-observer agreement on CT images was also compared. Univariate and multivariate analysis were used to identify the independent risk factors. The nomogram was then respectively created based on the identified independent risk factors.

# RESULTS

A total of 232 postmenopausal women and 295 vertebrae were included. Short-term poor prognosis was respectively observed in 9 (17.3%) of younger group and in 70 (38,8%) of older group. Older aged (P=0.010), larger BMI (p<0.001), greater fracture severity (P = 0.016) were the independent risk factors for short-term poor prognosis in younger group. Greater fracture severity (p=0.009), cortical disruption of the endplate (P < 0.0001), thicker cortex (P = 0.010), and higher computed tomography (CT) values (P = 0.050) were the independent risk factors for short-term poor prognosis in older group.

### CONCLUSION

In postmenopausal women less than 65y, older age, BMI, greater fracture severity are the independent risk predictors of short-term poor prognosis. However, greater fracture severity, cortical thickness, cortical disruption of the endplate and higher CT values are adverse factors in postmenopausal women older than 65y. The novel nomograms accurately predict short-term poor prognosis. These predictors in different ages may potentially improve therapeutic effect of PVP.

#### **CLINICAL RELEVANCE/APPLICATION**

This study may potentially avoid risk factors to improve therapeutic effect of PVP in postmenopausal women of different age.



### MK378-SD-TUB2

Quantitative Assessment of Skin Stiffness Using Ultrasound Shear Wave Elastography in Systemic Sclerosis

Tuesday, Nov. 27 12:45PM - 1:15PM Room: MK Community, Learning Center Station #2

### Participants

Xi Xiang, Chengdu, China (*Presenter*) Nothing to Disclose Yujia Yang, Chengdu, China (*Abstract Co-Author*) Nothing to Disclose Liyun Wang, MD,PhD, Chengdu, China (*Abstract Co-Author*) Nothing to Disclose Yuanjiao Tang, Chengdu, China (*Abstract Co-Author*) Nothing to Disclose Li Qiu, Chengdu, China (*Abstract Co-Author*) Nothing to Disclose

# For information about this presentation, contact:

wsqiuli@126.com

### PURPOSE

To investigate the performance of ultrasound shear-wave elastography (US-SWE) in the assessment of skin (the dermis) stiffness in patients with systemic sclerosis (SSc).

# METHOD AND MATERIALS

The thickness and elastic modulus of the skin were measured using US-SWE at 6 sites in 60 SSc patients and 60 healthy volunteers, i.e. the bilateral middle fingers and forearms, and the anterior chest and abdomen. In order to evaluate clinical scores, the measurements were also extended to 17 skin sites in 30 patients. The diagnostic performance of US-SWE in the differentiation of SSc from healthy skin was determined by receiver operating characteristic (ROC) curve analysis and the reliability of the measurement was evaluated by intra- and inter-class correlation coefficients (ICC). The results of US-SWE were compared to the modified Rodnan total skin score (mRTSS).

### RESULTS

The elastic modulus values were significantly higher in SSc patients than in controls, with or without normalization by skin thickness. ROC analysis revealed normalized US-SWE cutoff values with a very high accuracy for right and left fingers (AUC=0.974, 0.949), followed by left forearm (0.841), anterior abdomen (0.797), right forearm (0.772) and anterior chest (0.726). A good reliability of US-SWE measurements was obtained for all the examined sites with ICC of 0.845-0.996 for intra-observer and 0.824-0.985 for inter-observer. Total scores of skin involvement determined at 17 sites (mRTSS) correlated with skin stiffness (r=0.832) and thickness: (r=0.736).

### CONCLUSION

US-SWE is a quantitative method with high specificity, sensitivity and reliability in the detection of SSc involvement. This noninvasive, real-time and operator-independent imaging technique could be an ideal tool for the assessment of SSc disease.

# **CLINICAL RELEVANCE/APPLICATION**

The use of shear wave elastography in systemic sclerosis can provide quantitative assessment of skin stiffness changes, which ishopeful to become an objective approach for monitoring disease progression.



# MK379-SD-TUB3

Determination of Musculoskeletal Magnetic Resonance Imaging Protocol between Routine Protocol and Radiologist-Tailored Protocol Using Deep-learning Convolutional Neural Networks

Tuesday, Nov. 27 12:45PM - 1:15PM Room: MK Community, Learning Center Station #3

# Participants

Jin Kyem Kim, Seoul, Korea, Republic Of (*Presenter*) Nothing to Disclose Yoon Ah Do, Seoul, Korea, Republic Of (*Abstract Co-Author*) Nothing to Disclose Young Han Lee, MD, Seoul, Korea, Republic Of (*Abstract Co-Author*) Nothing to Disclose Hwiyoung Kim, Seoul, Korea, Republic Of (*Abstract Co-Author*) Nothing to Disclose Sungjun Kim, MD, Seoul, Korea, Republic Of (*Abstract Co-Author*) Nothing to Disclose

# PURPOSE

To evaluate the accuracy of a convolutional neural networks (CNN) classifier for determining MRI protocols between routine protocol and radiologist-tailored dedicated protocol according to the purpose of examination.

# METHOD AND MATERIALS

We collected 11,116 musculoskeletal MRI examinations and corresponding data from the hospital information system (HIS), and we preprocessed the text data by radiologists. Text data were used as a input of a CNN classifier, which consisted of patient age, gender, scan region, contrast media or not, referring department, and patient's history or scan purpose for clinical information. All exams were classified to routine joint imaging protocol, routine tumor imaging protocol, and dedicated imaging protocol. Preprocessed data of all exams were divided to training set and data set with 9:1 ratio. Dedicated imaging protocol, and radiologist-tailored MRI scan, and was defined as MRI scan with radiologists, patient-specific dedicated MRI protocol, and radiologist-designed MRI scan. The deep neural networks with Word-Embedding were performed with neural network algorithms of supervised text categorization. Each class label contained short sentences and each token was converted to an embedded vector given by a pre-trained word-embedding model (Word2Vec model of Google news vectors). The accuracies were evaluated by comparing the results with radiologist-confirmed protocols. Receiver operating characteristic curves and areas under the curve(AUCs) were used to assess the performance.

# RESULTS

The optimal cut-off values for protocol discrimination between routine protocols and tumor protocols was 0.4476 with a sensitivity of 85.3%, a specificity of 94.8%, and an area under curve (AUC) of 0.923. The cut-off values for high sensitivity was 0.2747 with a sensitivity of 90.4% and a specificity of 83.4%. The overall accuracy was 93.9% for the ConvNet model.

### CONCLUSION

Deep-learning-based convolutional neural networks can discriminate the routine protocol and radiologist-tailored protocols, and it can be utilized to screen the MR exams with routine imaging protocols. It can improve the work efficiency of the radiologists, by reducing working burden of MRI scan protocoling.

### **CLINICAL RELEVANCE/APPLICATION**

The CNN discrimination can be applied to protocolling MRI exams between routine protocol and radiologist-tailored dedicated protocol, and it can improve the work efficiency of the radiologists.



# MK380-SD-TUB4

Deep Learning for Detection of Hip, Knee, and Shoulder Arthroplasty Dislocations and "Transfer Learning" to Native Joint Dislocations

Tuesday, Nov. 27 12:45PM - 1:15PM Room: MK Community, Learning Center Station #4

#### Awards

### **Trainee Research Prize - Resident**

#### Participants

Tae Kyung Kim, Baltimore, MD (*Presenter*) Nothing to Disclose Paul H. Yi, MD, Baltimore, MD (*Abstract Co-Author*) Nothing to Disclose Jinchi Wei, Baltimore, MD (*Abstract Co-Author*) Nothing to Disclose Yotam Barnoy, Baltimore, MD (*Abstract Co-Author*) Nothing to Disclose Tae Soo Kim, Baltimore, MD (*Abstract Co-Author*) Nothing to Disclose Gregory D. Hager, PhD, MSc, Baltimore, MD (*Abstract Co-Author*) Co-founder, Clear Guide Medical LLC CEO, Clear Guide Medical LLC Haris I. Sair, MD, Baltimore, MD (*Abstract Co-Author*) Nothing to Disclose Cheng Ting Lin, MD, Baltimore, MD (*Abstract Co-Author*) Nothing to Disclose Ferdinand K. Hui, MD, Richmond, VA (*Abstract Co-Author*) Nothing to Disclose Stockholder, Blockade Medical Inc Jan Fritz, MD, Baltimore, MD (*Abstract Co-Author*) Research Grant, Siemens AG; Scientific Advisor, Siemens AG; Scientific Advisor, Alexion Pharmaceuticals, Inc; Speaker, Siemens AG

# For information about this presentation, contact:

#### pyi10@jhmi.edu

#### PURPOSE

The purpose of this study was to develop and compare the performance of deep convolutional neural networks (DCNNs) for detection of dislocations of 1) total hip arthroplasty (THA), 2) total knee arthroplasty (TKA), and reverse total shoulder arthroplasty (RTSA). A secondary purpose was to test the ability of these DCNNs for detection of native joint dislocations of the hip, knee, and shoulder ("transfer learning").

# **METHOD AND MATERIALS**

We obtained 100 de-identified radiographs (XRs) [50 dislocations, 50 no dislocation] each of the pelvis (AP), knee (lateral), and shoulder (AP) with a THA, TKA, or RTSA, respectively. Groundtruth was determined by 2 musculoskeletal radiologists and a 2nd-year radiology resident with 2 years of orthopaedic training. Each XR dataset was divided into training (70%), validation (10%), and test (20%) datasets. We augmented the training & validation datasets 22x using random rotations, flips, cropping, and non-rigid deformation. We then trained and validated the ResNet-18 DCNN (pretrained on ImageNet) 3 times (once for each joint) using these images to detect presence or absence of a dislocation. Each DCNN was tested on separate sets of 100 XRs containing 50 located and 50 dislocated analogous native joints. Receiver operating characteristic (ROC) curves with area under the curve (AUC) were used to evaluate the DCNNs; AUCs were statistically compared between DCNNs.

### RESULTS

Our DCNNs trained for detection of dislocations of THA, TKA, and RTSA achieved AUCs of 0.95, 0.98, and 0.91, respectively (p>0.2, all). In evaluation of "transfer learning," our DCNNs has mixed results, with the TKA DCNN achieving AUC of 0.79 compared to 0.62 for THA (p=0.016) and 0.46 for RTSA (p<0.0001).

### CONCLUSION

DCNNs trained on small datasets augmented 22x using standard processing techniques are able to accurately detect dislocations of THA, TKA and RTSA, which may help expedite diagnosis and care of these emergencies. We have demonstrated "transfer learning" of DCNNs trained on images of THA and TKA towards the native hip and knee, respectively; the RTSA DCNN was unable to consistently detect native shoulder dislocations, possibly owing to more subtle appearances of shoulder dislocations.

### **CLINICAL RELEVANCE/APPLICATION**

DCNNs are able to accurately identify dislocations of THA, TKA and RTSA, which may help expedite diagnosis and care of these orthopaedic emergencies.



### MK382-SD-TUB6

Classification of Median Nerve Swelling Pattern in Patients with Carpal Tunnel Syndrome and its Clinical Significance

Tuesday, Nov. 27 12:45PM - 1:15PM Room: MK Community, Learning Center Station #6

**FDA** Discussions may include off-label uses.

#### **Participants**

Dong-Ho Ha, Busan, Korea, Republic Of (*Presenter*) Nothing to Disclose Bo Ra Kim, MD, Busan, Korea, Republic Of (*Abstract Co-Author*) Nothing to Disclose

#### For information about this presentation, contact:

hdhdoc@dau.ac.kr

### PURPOSE

To classify the pattern of median nerve swelling in patients with carpal tunnel syndrome (CTS) and evaluate the clinical significance of distal tunnel measurement.

# METHOD AND MATERIALS

This retrospective study was approved by our IRB. 120 hands of 78 patients with confirmed CTS and 60 hands of 49 control subjects were examined with ultrasonography (US). Cross sectional area (CSA) was measured at the proximal to tunnel (from the level of the distal radius to tunnel inlet), mid portion of carpal tunnel (or most compressed portion within the carpal tunnel), and distal to tunnel (from tunnel outlet to just before the nerve branching). When the CSA was larger than 10 mm2, it was regarded as the presence of the swelling. The pattern of median nerve was divided into four types according to the different location of the swelling.

#### CONCLUSION

Isolated distal median nerve swelling occurred not infrequently, and careful evaluation of distal carpal tunnel will increase the diagnostic value of ultrasound in patients with CTS.

### **CLINICAL RELEVANCE/APPLICATION**

Even though there are some problems with technical issues, anatomical definition of carpal tunnel outlet, etc., measurement of CSA of distal median nerve can increase the sensitivity of US diagnosis.



# MK383-SD-TUB7

# Acoustic Radiation Force Impulse (ARFI) Imaging of Myositis: An Added Value?

Tuesday, Nov. 27 12:45PM - 1:15PM Room: MK Community, Learning Center Station #7

#### Participants

Manuel M. Kolb, MD, Tuebingen, Germany (*Presenter*) Nothing to Disclose Michael Esser, MD, Tuebingen, Germany (*Abstract Co-Author*) Nothing to Disclose Mustafa Kurucay, Tuebingen, Germany (*Abstract Co-Author*) Nothing to Disclose Christer Ruff, MD, Tuebingen, Germany (*Abstract Co-Author*) Nothing to Disclose Johannes B. Hofmann, Tuebingen, Germany (*Abstract Co-Author*) Nothing to Disclose Marius Horger, MD, Tuebingen, Germany (*Abstract Co-Author*) Nothing to Disclose

# For information about this presentation, contact:

manuel.kolb@med.uni-tuebingen.de

# PURPOSE

To evaluate the information gained by non invasive acoustic radiation force Impulse (ARFI) imaging in patients suspected for myositis in comparison to controls, MRI and invasive biopsy.

# METHOD AND MATERIALS

In this prospective study, we enrolled consecutive patients suspected for myositis that underwent MRI and targeted biopsy from April 2017 until March 2018 and also 20 controls who were clinically inconspicuous. Biopsy was used as a gold standard of reference in symptomatic patients. We evaluated the muscular regions presumed to be involved based on symptoms using MRI and ARFI, the latter being applied in the transversal orientation of the muscle fibers. ARFI was performed after 20 minutes of rest. Three representative ROIs were set in involved muscular regions registering their mean shear wave velocity (SWV) values in m/s. Distribution of SWVs was classified homogeneous vs. heterogeneous by two radiologists with 26 and 4 years of experience in consensus. Creatine kinase (CK) values over 170 U/I and lactate dehydrogenase (LDH) over 250 U/I were considered pathological and were measured the same day as MRI. All controls consisting of healthy test persons underwent the same ARFI imaging protocol. Welch-test for parametric data was used due to unequal variances.

### RESULTS

16 patients ( $45.45\pm16.13$  years; f:9) met inclusion criteria. Mean delay between MRI and SWE was 3.7 days. Pathology distribution based on biopsy was as following: polymyositis (n=9), dermatomyositis (n=6), paraneoplastic myositis (n=1). CK was  $4455\pm9494$  U/I and LDH was  $533\pm283$  U/I. For discerning presence of myositis, MRI was correct in .94. Transversal SWE was correct in .94. In comparison to the healthy controls cohort, mean SWV in transversal orientation was  $3.13\pm1.26$  m/s vs.  $2.68\pm.46$  m/s (p=.21).

### CONCLUSION

ARFI proved equal to MRI for assessment of myositis and could be a potential tool for diagnosis and treatment monitoring in patients with muscular inflammation.

### **CLINICAL RELEVANCE/APPLICATION**

ARFI has a potential role as a cost effective surveillance of treatment in patients suffering from myositis.



# NM146-ED-TUB5

Our First Year with Gallium-68 DOTATATE PET/CT: Lessons Learned Through RAD-PATH Correlation and Potential Pitfalls

Tuesday, Nov. 27 12:45PM - 1:15PM Room: NM Community, Learning Center Station #5

#### Awards Magna Cum Laude

### Participants

Brian L. Bones, MD, Winston-Salem, NC (*Presenter*) Nothing to Disclose Jennifer A. Schroeder, MD, Winston-Salem, NC (*Abstract Co-Author*) Nothing to Disclose Angela Niehaus, MD, Winston Salem, NC (*Abstract Co-Author*) Nothing to Disclose William J. Beuerlein, MD, Winston Salem, NC (*Abstract Co-Author*) Nothing to Disclose Wencheng Li, MD, Winston Salem, NC (*Abstract Co-Author*) Nothing to Disclose Alexei V. Mikhailov, Winston Salem, NC (*Abstract Co-Author*) Nothing to Disclose Kimberly Stogner-Underwood, MD, Winston Salem, NC (*Abstract Co-Author*) Nothing to Disclose Anita J. Thomas, MD, Winston-Salem, NC (*Abstract Co-Author*) Nothing to Disclose Shane C. Masters, MD,PhD, Winston Salem, NC (*Abstract Co-Author*) Nothing to Disclose Jean-Luc C. Urbain, MD,PhD, Lebanon, PA (*Abstract Co-Author*) Software support, General Electric Company Paige Bennett, MD, Winston-Salem, NC (*Abstract Co-Author*) Nothing to Disclose

#### For information about this presentation, contact:

bbones@wakehealth.edu

#### **TEACHING POINTS**

This exhibit provides a clinical overview of Gallium-68 DOTATATE PET/CT. The learner should be able to describe the radiopharmacology of Ga-68 DOTATATE, imaging characteristics for different pathologies and their radiologic-pathologic correlation, and potential pitfalls when interpreting and communicating Ga-68 DOTATATE findings.

### TABLE OF CONTENTS/OUTLINE

1. Radiopharmacy of Ga-68 DOTATATE.2. Normal Biodistribution.3. Radiological-pathological correlation of Ga-68 DOTATATE PET/CT including: Well-differentiated Neuroendocrine (NET), Poorly-differentiated NET of the rectum with comparison of Ga-68 DOTATATE PARTY and F-18 FDG PET/CT, Pheochromocytoma in the setting of Multiple endocrine neoplasia type 2, Paraganglioma, Synchronous Pancreatic NET and Renal Cell Carcinoma.4. Metastatic disease workups without pathology including: Small bowel NET with liver metastasis, metastatic medullary thyroid, metastatic VIPoma, NET of unknown primary with osseous metastatic disease.5. Pitfalls and Incidentals including: Metastatic NET to the liver with incidental meningioma, Breast cancer uptake from somatostatin expression, uptake with osteoclastic activity and osteoarthritis, importance of communicating with referrers the differences between Ga-68 DOTATATE PET/CT and F-18 FDG PET/CT.



# NM222-SD-TUB1

To Evaluate the Unknown Primary Site of Tumour with 68Ga-DOTATOC PET/CT in Patients with Known Metastatic Neuroendocrine Tumor

Tuesday, Nov. 27 12:45PM - 1:15PM Room: NM Community, Learning Center Station #1

# Participants

Sikandar M. Shaikh, DMRD, Hyderabad, India (Presenter) Nothing to Disclose

#### PURPOSE

It is very difficult to evaluate the Localization of the primary site of the unknown primary tumor by various modalities .This is critical for management of patients presenting with neuroendocrine tumor (NET) with metastases.

# METHOD AND MATERIALS

This was the retrospective study which was performed to evaluate the efficacy of 68Ga-DOTATOC PET/CT in patients with diagnosis of or suspected NET with metastases. A subgroup of patients with metastases and unknown primary after initial work-up was analyzed. The 68GaGa-DOTATOC Whole body PET/CT was done .This was evaluated by the SUV max uptake values.The study was considered true positive if the positive primary site has significant uptake and which was confirmed by histology or follow-up imaging. The scan was considered false positive if no primary lesion was found corresponding to 68aGa-DOTATOC positive site. All negative scans for primary tumor were considered false negative. A scan was classified unconfirmed if 68Ga-DOTATOC PET/CT suggested a primary, however, no histology was obtained and imaging follow-up was not confirmatory.

#### RESULTS

Forty patients with known metastatic NET and unknown primary underwent 68Ga-DOTATOC PET/CT. After evaluation and quantification the study was true positive, false positive, false negative and unconfirmed rates for unknown primary tumor were 38%, 7%, 50% and 5% respectively.

#### CONCLUSION

The efficacy of 68Ga-DOTATOC PET/CT is an effective modality in localization of unknown primary in patients with metastatic NET as compared to other modalities including F FDG PET-CT.

### **CLINICAL RELEVANCE/APPLICATION**

Thus 68Ga-DOTATOC PET/CT is an effective modality for evaluation of Neuroendocrine tumours.



# NM223-SD-TUB2

Effects of New Block Sequential Regularized Expectation Maximization (BSREM) Reconstruction Algorithm on SUVmax, MTV, and Changes of SUVmax on FDG PET-CT Before and After Neoadjuvant Chemotherapy in Patients with Esophageal Cancer

Tuesday, Nov. 27 12:45PM - 1:15PM Room: NM Community, Learning Center Station #2

#### Participants

Mitsuaki Tatsumi, MD, PhD, Suita, Japan (*Presenter*) Nothing to Disclose Takashi Kamiya, Suita, Japan (*Abstract Co-Author*) Nothing to Disclose Kayako Isohashi, Suita, Japan (*Abstract Co-Author*) Nothing to Disclose Hiroki Kato, Suita Osaka, Japan (*Abstract Co-Author*) Nothing to Disclose Noriyuki Tomiyama, MD,PhD, Suita, Japan (*Abstract Co-Author*) Research Grant, Canon Medical Systems Corporation Jun Hatazawa, MD, PhD, Osaka, Japan (*Abstract Co-Author*) Nothing to Disclose

#### PURPOSE

BSREM reconstruction algorithm, or so called "Q. Clear", was recently introduced to improve image quality and quantification in PET examinations. The purpose of this study was to evaluate the effects of this new algorithm on SUVmax, metabolic tumor volume (MTV), and changes of SUVmax on FDG PET-CT before and after neoadjuvant chemotherapy (NAC) in patients (pts) with esophageal cancer (EC), comparing the results to those by an ordered subset expectation maximization (OSEM) reconstruction algorithm.

# METHOD AND MATERIALS

FDG PET-CT examinations were performed before and after 2 cycles of NAC in 39 EC pts before surgery. PET images acquired with a GE Discovery 710 scanner were reconstructed using BSREM beta 700 and OSEM (subset 8, iteration 3, and Gaussian filter 4mm; regular setting in our hospital) algorithms. SUVmax and MTV were compared between BSREM and OSEM images in all 39 primary EC lesions before and after NAC. Changes of SUVmax after NAC were also compared. Statistical analysis was performed with a paired t-test and a Spearman's correlation method.

### RESULTS

SUVmax ranged from 3.2 to 40.9 (mean+/-SD: 16.0+/-8.8) and MTV from 1.1 to 149.5 ml (24.8+/-30.0 ml) in OSEM before NAC. MTV in BSREM was significantly lower than that in OSEM (7.1% decrease), while SUVmax was almost the same. A moderate negative correlation was observed between [%increase of SUVmax or MTV with BSREM] and [SUVmax in OSEM] (|Rho|=0.45-0.52) as well as [%increase of SUVmax with BSREM] and [MTV in OSEM] (|Rho|=0.58). After NAC, SUVmax ranged from 2.3 to 22.6 (6.5+/-4.5) and MTV from 0 to 70.2 ml (7.0+/-11.7 ml) in OSEM. SUVmax in BSREM was significantly higher than that in OSEM (3.7% increase), while MTV did not differ. A moderate negative correlation was observed between [%increase of MTV with BSREM] and [SUVmax or MTV in OSEM] (|Rho|=0.35-0.44). Changes of SUVmax after NAC did not differ between BSREM and OSEM (52.9% vs. 53.2%).

### CONCLUSION

This study demonstrated that BSREM decreased MTV and increased SUVmax before and after NAC, respectively, in EC patients. However, changes of SUVmax after NAC did not differ between BSREM and OSEM. Further studies are required to confirm these results in a larger population.

### **CLINICAL RELEVANCE/APPLICATION**

The effect of BSREM on PET was different before and after NAC in EC patients.



### NM224-SD-TUB3

Time Course Change and Reproducibility of 18F-FAZA in the Patient with Head and Neck Squamous Cell Carcinoma

Tuesday, Nov. 27 12:45PM - 1:15PM Room: NM Community, Learning Center Station #3

# Participants

Shingo Baba, Fukuoka, Japan (*Presenter*) Nothing to Disclose Takuro Isoda, Fukuoka, Japan (*Abstract Co-Author*) Nothing to Disclose Yoshiyuki Kitamura, Fukuoka, Japan (*Abstract Co-Author*) Nothing to Disclose Ryo Somehara, Fukuoka, Japan (*Abstract Co-Author*) Nothing to Disclose Keiichiro Tahara, Fukuoka, Japan (*Abstract Co-Author*) Nothing to Disclose Masayuki Sasaki, Fukuoka, Japan (*Abstract Co-Author*) Nothing to Disclose Hiroshi Honda, MD, Fukuoka, Japan (*Abstract Co-Author*) Nothing to Disclose

### PURPOSE

18F- fluoroazomycin arabinoside (18F-FAZA) PET has been recently introduced for noninvasive evaluation of hypoxia. Since its clearance is faster than the conventional hypoxia tracer, the possibility of early phase imaging is expected. However, the time course change and the reproducibility of 18F-FAZA uptake has remained unclarified. We therefore investigated the change of serial two 18F-FAZA PET scans by using quantitative analysis of uptake.

### **METHOD AND MATERIALS**

Nine patients with untreated head and neck cancer underwent serial 18F-FAZA PET/CT scans (18F-FAZA(1) and 18F-FAZA(2)). All images were acquired at 2h and 4 h after intravenous 18F-FAZA injection. The maximum standardized uptake (SUVmax), and tumor-to-muscle ratio (TMR) of 18F-FAZA uptake were statistically compared between the two 18F-FAZA scans by use of intraclass correlation coefficients (ICCs). The hypoxic volume was calculated as the area with a TMR of greater than or equal to 1.25 to assess differences in hypoxic volume between the two 18F-FAZA scans.

# RESULTS

The SUVmax (mean  $\pm$  SD) for 18F-FAZA(1) and 18F-FAZA(2) was 2.14  $\pm$  0.65 and 2.11  $\pm$  0.84, respectively, with the difference between the 2 scans being -2.2%  $\pm$  7.8%. Uptake of the muscle significantly decreased with time (p<0.05). TMRs for 18F-FAZA(1) and 18F-FAZA(2) were 1.35  $\pm$  0.37 and 1.55  $\pm$  0.48, respectively, with a difference of 13.4%  $\pm$  7.4%. The ICCs for SUVmax, and TMR were 0.971, and 0.923, respectively. The hypoxic volume based on TMR was increased with time (0.9  $\pm$  1.3 mL and 2.19  $\pm$  0.67), with ICCs of 0.910.

### CONCLUSION

The values for 18F-FAZA PET uptake in head and neck tumors between the two 18F-FAZA scans were highly reproducible. However, TMRs increase with time because of the washout from the muscle. As the result, defined hypoxic area was increased. Therefore, scan after 4 h cannot be omitted or replaced by 2h scan.

#### **CLINICAL RELEVANCE/APPLICATION**

The values for 18F-FAZA PET uptake in head and neck tumors between the two scans were highly reproducible. But to impriove the TMR, relative long tilme uptake time (4 hrs) after tracer injection is still needed in this tracer.



# NM225-SD-TUB4

Are Staging F-18-FDG PET/MRI Radiomic Features Associated with Metastases in Cancer of the Gastro-Esophageal Junction?

Tuesday, Nov. 27 12:45PM - 1:15PM Room: NM Community, Learning Center Station #4

# Participants

Serena Baiocco, Bologna, Italy (*Abstract Co-Author*) Nothing to Disclose Bert-Ram Sah, MD, London, United Kingdom (*Presenter*) Nothing to Disclose Andrew Mallia, London, United Kingdom (*Abstract Co-Author*) Nothing to Disclose James Stirling, Middlesex, United Kingdom (*Abstract Co-Author*) Nothing to Disclose Sami Jeljeli, BSc, London, United Kingdom (*Abstract Co-Author*) Nothing to Disclose Alessandro Bevilacqua, PhD,MSc, Bologna, Italy (*Abstract Co-Author*) Nothing to Disclose Gary Cook, MD, FRCR, London, United Kingdom (*Abstract Co-Author*) Research support, General Electric Company Research support, Alliance Medical Limited Research support, Siemens AG Research Consultant, Blue Earth Diagnostics Ltd Speakers Bureau, Bayer AG Vicky J. Goh, MBBCh, London, United Kingdom (*Abstract Co-Author*) Research Grant, Siemens AG Speaker, Siemens AG

# PURPOSE

To identify quantitative imaging biomarkers at staging F-18-Fluorodeoxyglucose (FDG)-positron-emission-tomography/magneticresonance-imaging (PET/MRI) for predicting distant metastases in patients with gastro-esophageal junction (GEJ) cancer.

### **METHOD AND MATERIALS**

Following IRB approval and informed consent, 24 patients with histologically proven GEJ cancer were prospectively recruited; 4 patients were excluded for technical reasons. Finally, 19 male and 1 female (68.3±9.1 years) were considered. Patients were injected with 326±28 MBq FDG intravenously. Uptake time was 90 minutes. Two experienced radiologists and nuclear physicians reviewed the images in consensus. Maximum standardized uptake value (SUVmax) and tumor size were analyzed. First-order and second-order statistical texture features were computed on SUV values of the whole tumor volume. *k*-means clustering algorithm was used to assess the correlation of feature-pairs with the presence of distant metastases. Sensitivity (SE), specificity (SP), positive predictive value (PPV), negative predictive value (NPV) and accuracy (ACC) were calculated to quantify the discrimination ability of features.

#### RESULTS

Second-order entropy and maximum probability, linked to texture irregularity and homogeneity respectively, were the best featurepair in discriminating patients with and without metastatic disease (SE=80%, SP=70%, PPV=73%, NPV=78%, ACC=75%). SUVmax (SE=80%, SP=30%, PPV=53%, NPV=60%, ACC=55%) and tumor size (SE=90%, SP=10%, PPV=50%, NPV=50%, ACC=50%) performed worse, particularly for specificity.

#### CONCLUSION

These results confirm the common expectation that greater intra-tumor heterogeneity correlates with metastatic potential. The extraction of advanced quantitative PET imaging features from the primary lesion may help prognostication.

### **CLINICAL RELEVANCE/APPLICATION**

Radiomics may help in improving prognostication at staging.



### NR341-ED-TUB10

It Is Not Always Adenoma: Other Sellar and Parasellar Injuries

Tuesday, Nov. 27 12:45PM - 1:15PM Room: NR Community, Learning Center Station #10

#### **Participants**

Rodrigo Beber De Bem, MD, Rio de Janeiro, Brazil (*Presenter*) Nothing to Disclose Nina Ventura, MD, Rio De Janeiro, Brazil (*Abstract Co-Author*) Nothing to Disclose Fernanda S. Castro, Rio de Janeiro, Brazil (*Abstract Co-Author*) Nothing to Disclose

## For information about this presentation, contact:

rodrigodebem@hotmail.com

### **TEACHING POINTS**

Tumor and tumor-like conditions may involve the sellar and parasellar region and its anatomic localization is essential in the creation of differential diagnosis.Magnetic resonance (MR) imaging is important for complete characterization, including localization, regional extension or invasion, and surveillance after medical or surgical treatment. Computed tomography (CT) is complementary to MR imaging for the depiction of bony changes.Vascular lesions, such as an aneurysm, may involve the sellar region. CT or MR angiography should be performed if suspected.On MR imaging, a sella protocol is necessary. T2 sagittal and coronal as well as pre-and postcontrast T1 sagittal and coronal images with a slice thickness of 2.5 mm are the optimum planes to examine the region.

### **TABLE OF CONTENTS/OUTLINE**

-Approach to analysis of sellar and parasellar processes, for commom/uncommon regional pathologies.-MR typical sellar protocol.-Review of imaging findings:1) Solid Lesions:1.1)Hypothalamic-chiasmatic / tuber cinereum origin:Glioma;Germinoma;Tuber cinereum hamartoma;Langerhans cell histiocytosis.1.2) Lateral structures origin:Aneurysm;Meningioma.1.3) Clivus origin:Chordoma2) Cystic Lesions:Empty sella;Arachnoid Cyst;Rathke Cleft Cyst;Craniopharyngioma.-Summary with the main MRI findings on sellar and parasellar injuries.



## NR345-ED-TUB11

## Lesions of the Pineal Region: A Clinical-Radiological Approach to Differential Diagnosis

Tuesday, Nov. 27 12:45PM - 1:15PM Room: NR Community, Learning Center Station #11

#### **Participants**

Felipe Scortegagna SR, MD, Sao Paulo, Brazil (*Presenter*) Nothing to Disclose Felipe T. Pacheco, MD, Sao Paulo, Brazil (*Abstract Co-Author*) Nothing to Disclose Renato Hoffmann Nunes, MD, Sao Paulo, Brazil (*Abstract Co-Author*) Nothing to Disclose Antonio Carlos M. Maia Jr, Sao Paulo, Brazil (*Abstract Co-Author*) Nothing to Disclose Antonio J. da Rocha, MD, PhD, Sao Paulo, Brazil (*Abstract Co-Author*) Nothing to Disclose

## For information about this presentation, contact:

felipescortegagna@hotmail.com

### **TEACHING POINTS**

To review the normal anatomy of the pineal region, describe the signs and symptoms of pineal region masses, and present the pathologic and imaging features of lesions of the pineal region, including tumors of pineal parenchymal origin, germ cell neoplasms, pineal cyst, and other pineal region masses. Increase knowledge regarding the variety of lesions that occur in the pineal region, their imaging appearances, and their clinical features, helping in narrowing the radiologic differential diagnosis and optimizing patient treatment.

# TABLE OF CONTENTS/OUTLINE

We will be using case material from our neuroradiology and pathology departments to illustrate the imaging findings. We have collected imaging data on several patients with pineal region lesions. The purpose of this exhibit is: 1. To review the normal anatomy of the pineal region, describing signs and symptoms of pineal region masses 2. Present the pathologic and imaging features of lesions of the pineal region, including tumors of pineal parenchymal origin, germ cell neoplasms, pineal cyst, and other pineal region masses, discussing the utility of CT and particularly MRI in narrowing the differential diagnosis



### NR346-ED-TUB12

Old But Gold? The Role of Digital Sialography and Its Correlations with Other Diagnostic Methods in Modern Radiology

Tuesday, Nov. 27 12:45PM - 1:15PM Room: NR Community, Learning Center Station #12

## Participants

Lucas V. Pazinato, MD, Sao Paulo, Brazil (*Presenter*) Nothing to Disclose Sabrina M. Ando, MD, Sao Paulo, Brazil (*Abstract Co-Author*) Nothing to Disclose Felipe A. Bezerra SR, MD, Sao Paulo, Brazil (*Abstract Co-Author*) Nothing to Disclose Andre L. Bordini, MD, Sao Paulo, Brazil (*Abstract Co-Author*) Nothing to Disclose Diego B. Baptista, MD, Sao Paulo, Brazil (*Abstract Co-Author*) Nothing to Disclose Dalton L. Ferreira, Sao Paulo, Brazil (*Abstract Co-Author*) Nothing to Disclose Hernane A. Holzmann, MD, Sao Paulo, Brazil (*Abstract Co-Author*) Nothing to Disclose

# For information about this presentation, contact:

lucasvpazinato@gmail.com

### **TEACHING POINTS**

This exhibit will: 1) Present data from 141 digital sialographies (DS) of 109 patients performed in a single center. 2) Review digital sialography technique and main indications. 3) Discuss normal and pathological DS through cases in which different diagnostic modalities were performed. 4) Show situations in which DS is still useful or when newer methods should be employed.

## TABLE OF CONTENTS/OUTLINE

Digital sialography (DS): - Sialography history. - Main indications. - Advantages, disadvantages and complications. - Salivary glands anatomy. - Imaging technique. Cases from our institution and correlation with ultrasound, computer tomography and magnetic resonance: - DS of normal parotid and submandibular glands. - Chronic sialadenitis. - Sialolithiasis. - Salivary duct stenosis and ectasia. - Salivary glands manifestations of systemic disorders (eg. Sjögren and IgG4 deficiency).



## NR399-SD-TUB1

## Utility of Contrast-Enhanced Ultrasound in Preoperative Evaluation of Primary Hyperparathyroidism

Tuesday, Nov. 27 12:45PM - 1:15PM Room: NR Community, Learning Center Station #1

### Participants

Miguel Bello Erias, MD, Madrid, Spain (*Presenter*) Nothing to Disclose Antonio Santiago Hernando, MD, Madrid, Spain (*Abstract Co-Author*) Nothing to Disclose Paola Parra Ramirez, Madrid, Spain (*Abstract Co-Author*) Nothing to Disclose Dolores Montero Rey, Madrid, Spain (*Abstract Co-Author*) Nothing to Disclose Sonia Agueda Martin, Madrid, Spain (*Abstract Co-Author*) Nothing to Disclose Carmen Martin Hervas, MD, PhD, Madrid, Spain (*Abstract Co-Author*) Nothing to Disclose

### PURPOSE

The aim of this study was to evaluate the utility of contrast-enhanced ultrasound (CEUS) in detection of pathological parathyroid gland in patients with primary hyperparathyroidism in comparison to the 99m-MIBI-SPECT scintigraphy and high-resolution ultrasound (US).

### **METHOD AND MATERIALS**

Between December 2013 and December 2017, 29 consecutive patients (22 female, 7 male) with biochemically confirmed primary hyperparathyroidism, who underwent preoperative imaging with Techenetium 99m-MIBI-SPECT scintigraphy, US, CEUS and subsequent successful parathyroidectomy were reviewed. CEUS was performed by an experienced examiner who was blinded to the result of the scintigraphy and US. The sensitivity of all the imaging tests was analyzed in comparison with the findings of pathological anatomy.

#### RESULTS

17 patients underwent a focused unilateral or minimally invasive parathyroidectomy. On pathologic examinations, 31 abnormal glands were confirmed (two patients had double adenomas). All the glands were adenomatous. CEUS revealed a sensitivity of 62.1% (95% IC 42.3-79.3) for detection of single gland disease in comparison to 74.2 %(95% IC 52.7-87.3) for 99m-MIBI-SPECT scintigraphy and 48.3% (95 IC 29.4-67.6). Moreover, using CEUS, double adenomas could be detected in all 2 cases (sensitivity 100%). However, scintigraphy and ultrasound did not detect any cases of double adenoma. US had two false positives, being actually adenopathies. CEUS could clarify it. No side effects were observed using CEUS.

### CONCLUSION

In our study, CEUS facilitates the detection and diagnosis of double adenomas compared to results of US and MIBI-SPECT scintigraphy. Additionally, CUES is useful in the differentiation between parathyroid adenoma and adenopathy.

## **CLINICAL RELEVANCE/APPLICATION**

CEUS represents a new diagnostic tool for the localization of parathyroid gland adenomas and is able to improve diagnostic accuracy for double adenomas in comparison with other techniques.



# NR400-SD-TUB2

Detection of Local Recurrence in Patients with Head and Neck Squamous Cell Carcinoma Using Voxel-Based Color Maps of Initial and Final Area under the Curve Values Derived From DCE-MRI

Tuesday, Nov. 27 12:45PM - 1:15PM Room: NR Community, Learning Center Station #2

### Participants

Ji Ye Lee, MD, Bucheon, Korea, Republic Of (*Presenter*) Nothing to Disclose Kai-Lun Cheng, MD, Taichung, Taiwan (*Abstract Co-Author*) Nothing to Disclose Jeong Hyun Lee, MD, PhD, Seoul, Korea, Republic Of (*Abstract Co-Author*) Nothing to Disclose Young Jun Choi, MD, Seoul, Korea, Republic Of (*Abstract Co-Author*) Nothing to Disclose Hyo Weon Kim, Seoul, Korea, Republic Of (*Abstract Co-Author*) Nothing to Disclose Sae Rom Chung, MD, Seoul, Korea, Republic Of (*Abstract Co-Author*) Nothing to Disclose Mi Sun Chung, MD, Seoul, Korea, Republic Of (*Abstract Co-Author*) Nothing to Disclose Jung Hwan Baek, Seoul, Korea, Republic Of (*Abstract Co-Author*) Consultant, STARmed; Consultant, RF Medical

#### For information about this presentation, contact:

peachwh@naver.com

#### PURPOSE

Distinguishing recurrent tumor from post-treatment change is a clinically challenging decision using conventional MR imaging in patients with head and neck squamous cell carcinoma (HNSCC). We aimed to evaluate the added value of DCE-MRI voxel-based color mapping for detecting local recurrence of HNSCC.

### **METHOD AND MATERIALS**

We retrospectively enrolled 63 consecutive patients with HNSCC after definitive treatment (surgery, chemoradiation, surgery with radiation) with focal enhancement at the primary site on MRI. Three independent readers assessed color maps of initial 90-s time-signal intensity area under the curve (IAUC90) and final 90-s time-signal intensity area under the curve (FAUC90) derived from DCE-MRI. 'Progressive increment' pattern was designated as post-treatment scar and 'plateau' or 'washout' pattern were considered as recurrence. Diagnostic accuracy was assessed and compared with clinicopathologic diagnosis as a reference standard. Added value of DCE-MRI was assessed by subgroup analysis of 20 inconclusive cases.

### RESULTS

There were 28 patients with local recurrence and 35 with post-treatment scar. DCE-MRI significantly increased the diagnostic performance to detect local recurrence (AUC, 0.51 vs. 0.69-0.75, P < 0.05). Subgroup analysis of 20 inconclusive cases on conventional MRI revealed that the false positive rate (FPR) decreased by 74-80 percentage point without increasing the false negative rate (FNR).

### CONCLUSION

Voxel-based color maps of IAUC90 and FAUC90 derived from DCE-MRI are useful to detect local tumor recurrence in HNSCC patients by decreasing FPR, especially when conventional MRI findings are inconclusive.

# **CLINICAL RELEVANCE/APPLICATION**

Visual assessment of voxel-based color maps from DCE-MRI is feasible for detecting local recurrence, which might be helpful for proper management of patients with HNSCC after definite treatment.



## NR401-SD-TUB3

Amide Proton Transfer Imaging in the Head and Neck: A Feasibility Study for Differentiating Malignant from Benign Lesions

Tuesday, Nov. 27 12:45PM - 1:15PM Room: NR Community, Learning Center Station #3

# Participants

Koji Takumi, MD,PhD, Boston, MA (*Presenter*) Nothing to Disclose Hiroto Hakamada, Kagoshima, Japan (*Abstract Co-Author*) Nothing to Disclose Hiroaki Nagano, MD, Kaogoshima, Japan (*Abstract Co-Author*) Nothing to Disclose Yoshihiko Fukukura, MD, PhD, Kagoshima, Japan (*Abstract Co-Author*) Nothing to Disclose Jochen Keupp, PhD, Hamburg, Germany (*Abstract Co-Author*) Employee, Koninklijke Philips NV Edward K. Sung, MD, Boston, MA (*Abstract Co-Author*) Nothing to Disclose Osamu Sakai, MD,PhD, Boston, MA (*Abstract Co-Author*) Consultant, Boston Imaging Core Lab, LLC Takashi Yoshiura, MD, PhD, Kagoshima, Japan (*Abstract Co-Author*) Nothing to Disclose

#### PURPOSE

Amide proton transfer (APT) imaging is an emerging MR molecular imaging that detects intrinsic proteins and peptides. Despite successful applications in brain tumor imaging, to our knowledge, no reports on APT imaging in the head and neck regions have been made, mainly due to magnetic field inhomogeneity. Our purpose was to evaluate the feasibility of APT for the differentiation of benign and malignant head and neck lesions.

## **METHOD AND MATERIALS**

Our study population consisted of 54 consecutive patients with 37 malignant and 17 benign head and neck lesions. All patients were evaluated on a 3T MRI before treatment. APT imaging data were acquired in a coronal plane using a single-slice turbo-spinecho sequence after localized high-order shimming. The saturation pulse strength was 2 T and the duration was 2 s. Imaging parameters were as follows: field of view, 230 × 230mm2; voxel size, 2×2mm2; slice thickness, 5 mm; TE/TR = 5 ms/6700 ms; echo train length, 128; number of signal averages, 1. The scan time of APT imaging was about 2 minutes. Diffusion-weighted imaging was also performed in the same imaging session. The mean APT-related signal intensity (APTSI) and the mean apparent diffusion coefficient (ADC) within the lesion were compared between the malignant and benign lesions using the Mann-Whitney U test. In addition, performances of APTSI, ADC, and their combination in diagnosing malignant lesions were evaluated using the receiver operating characteristic (ROC) analysis.

# RESULTS

The mean APTSI value in malignant lesions ( $2.41 \pm 0.71\%$ ) was significantly higher than that in benign lesions ( $1.72 \pm 1.13\%$ ) (p=0.003). The mean ADC in malignant lesions ( $0.93 \pm 0.25 \times 10-3 \text{ mm2/s}$ ) was significantly lower than that in benign lesions ( $1.40 \pm 0.63 \times 10-3 \text{ mm2/s}$ ) (p=0.012). The diagnostic accuracies of APTSI (cut-off >1.22%), ADC (<= $1.33 \times 10-3 \text{ mm2/s}$ ), and their combination were 83.3%, 83.3%, and 90.7%, respectively.

# CONCLUSION

Our preliminary results suggested that APT imaging is feasible in the head and neck region, and that it may be useful in differentiating malignant vs. benign lesions especially in combination with ADC.

# **CLINICAL RELEVANCE/APPLICATION**

APT imaging is feasible and has additional usefulness, especially in combination with ADC, for diagnosing the head and neck lesions.

### **Honored Educators**

Presenters or authors on this event have been recognized as RSNA Honored Educators for participating in multiple qualifying educational activities. Honored Educators are invested in furthering the profession of radiology by delivering high-quality educational content in their field of study. Learn how you can become an honored educator by visiting the website at: https://www.rsna.org/Honored-Educator-Award/ Osamu Sakai, MD,PhD - 2013 Honored EducatorOsamu Sakai, MD,PhD - 2014 Honored EducatorOsamu Sakai, MD,PhD - 2015 Honored Educator



## NR402-SD-TUB4

Cervical Spondylotic Myelopathy: Changes of Fractional Anisotropy and Magnetic Resonance Spectroscopy Dependent on Symptoms and Symptom Duration

Tuesday, Nov. 27 12:45PM - 1:15PM Room: NR Community, Learning Center Station #4

# Participants

Robin F. Gohmann, MD, Aachen, Germany (*Presenter*) Nothing to Disclose Christian Blume, Aachen, Germany (*Abstract Co-Author*) Nothing to Disclose Mikhail Zvyagintsev, Aachen, Germany (*Abstract Co-Author*) Nothing to Disclose Verena Mainz, Aachen, Germany (*Abstract Co-Author*) Nothing to Disclose Hans Clusmann, Aachen, Germany (*Abstract Co-Author*) Nothing to Disclose Martin Wiesmann, MD, Munich, Germany (*Abstract Co-Author*) Nothing to Disclose Marc A. Brockmann, MD, Mainz, Germany (*Abstract Co-Author*) Nothing to Disclose Christian A. Mueller, Aachen, Germany (*Abstract Co-Author*) Nothing to Disclose

#### For information about this presentation, contact:

robin.gohmann@gmx.de

#### PURPOSE

Cervical spondylotic myelopathy (CSM) is the most common cause of chronic spinal cord injury - ultimately leading to tetraparesis if left untreated. We assessed diffusibility (fractional anisotropy (FA)) at the level of the medulla oblongata and magnetic resonance spectroscopy (MRS) of the precentral gyrus in patients with CSM in correlation to clinical symptoms and duration.

### **METHOD AND MATERIALS**

Patients with clinical signs of cervical myelopathy and corresponding imaging findings scheduled to undergo neurosurgical cervical decompression were included in our study. Clinical and MRI-examinations (FA and MRS) were performed preoperatively. Healthy age matched controls underwent identical MRI and clinical examinations. Clinical examinations included modified Japanese Orthopedic Association score (mJOA) and neck disability index (NDI). MRI measurements (3.0 T) included FA at the medulla oblongata and MRS of the left and right precentral gyrus. The metabolic profile of the precentral gyrus included: Creatinine (Cr); N-acetyl-aspartame (NAA); myo-Inositol (Ins) and Ins/Cr. Clinical correlation between the patients and controls, as well as subgroup analyses were performed.

### RESULTS

Twenty CSM patients (13 male, mean age  $63.5 \pm 6.6$  years) and 18 healthy volunteers (9 male, mean age  $64.6 \pm 10.5$  years) were included. There was no statistically significant difference between the groups regarding age or sex. The difference of clinical scores between both groups was highly statistically significant (mIOA: p=.001; NDI: p=.009). FA was significantly lower in CSM patients (p=.005). MRS at the precentral gyrus showed significant differences of metabolite concentrations between both groups: in regards to Cr (p=.03) and NAA (p=0.05). Subanalysis of patients showed a significantly higher Ins (p=.02) and Ins/Cr (p=.01) in patients with shorter duration of symptoms (<= 6 months).

# CONCLUSION

Metabolic profile of the precentral gyrus and FA at the medulla oblongata differ significantly in patients and healthy controls. Ins, thought to be a marker of endogenous neuroinflammatory response, is high in the early course of CSM and decreases over time.

# **CLINICAL RELEVANCE/APPLICATION**

As decompressive surgery is the only known effective treatment of CSM and postsurgical results do vary, novel imaging markers can be helpful for selction of surgical candidates. Thus Ins may be an early indicator of relevant disease in CSM.



# NR403-SD-TUB5

Grading Meningiomas Using Mono-Exponential, Bi-Exponential and Stretched Exponential Model-Based Diffusion-Weighted MR Imaging

Tuesday, Nov. 27 12:45PM - 1:15PM Room: NR Community, Learning Center Station #5

# Participants

Lin Lin, MBBS, Fuzhou, China (*Presenter*) Nothing to Disclose Yunjing Xue, MD, Fuzhou, China (*Abstract Co-Author*) Nothing to Disclose Qing Duan, MD, Fuzhou, China (*Abstract Co-Author*) Nothing to Disclose

### For information about this presentation, contact:

#### 84088100@qq.com

# PURPOSE

To prospectively evaluate and compare the potential of various diffusion metrics obtained from mono-exponential model (MEM), biexponential model (BEM) and stretched exponential model (SEM)-based diffusion-weighted imaging (DWI) the grading of meningiomas.

## METHOD AND MATERIALS

Consecutive 93 patients with pathologically confirmed meningiomas received DWI of multiple b values. Apparent diffusion coefficient (ADC), pure molecular diffusion (D), pseudo-diffusion coefficient (D\*), perfusion fraction (f), water molecular diffusion heterogeneity index (a), and distributed diffusion coefficient (DDC) were calculated and compared between low-grade and high-grade meningiomas. Receiver operating characteristic and multivariable stepwise logistic regression were performed to evaluate the diagnostic performance of different parameters.

### RESULTS

The mean and normalized ADC, D, f and DDC values were significantly lower in high-grade meningiomas than those in low-grade meningiomas (all P < .05). The AUCs of D, ADC and DDC was significantly higher than that of f in the differentiation (all P < .05). D was the only variable that could be used to independently differentiate high-grade and low-grade meningiomas (P < .001).

### CONCLUSION

Different models of DWI, including MEM, BEM and SEM, were useful in the differentiation between high-grade and low-grade menigiomas. Moreover, diffusion-related parameters had significantly better diagnostic performances than perfusion-related metrics in the differentiation. In addition, D was the most significant diffusion parameter in grading meningiomas.

### **CLINICAL RELEVANCE/APPLICATION**

Multiple models of DWI enable the grading of meningiomas and is recommended to determine therapeutic strategies and to evaluate the prognosis of meningiomas.



## NR404-SD-TUB6

# Correlation of 99mTc-TRODAT-1 SPECT Imaging Findings and Clinical Staging of Parkinson's Disease

Tuesday, Nov. 27 12:45PM - 1:15PM Room: NR Community, Learning Center Station #6

### **Participants**

Vanshika Gupta, New Delhi, India (*Abstract Co-Author*) Nothing to Disclose Rajeev Ranjan, New Delhi, India (*Abstract Co-Author*) Nothing to Disclose Ritu Verma, New Delhi, India (*Presenter*) Nothing to Disclose Harsh Mahajan, MD, MBBS, New Delhi, India (*Abstract Co-Author*) Nothing to Disclose Vidur Mahajan, MBBS, New Delhi, India (*Abstract Co-Author*) Nothing to Disclose Ethel S. Belho, New Delhi, India (*Abstract Co-Author*) Nothing to Disclose Nikhil Seniaray, New Delhi, India (*Abstract Co-Author*) Nothing to Disclose Ankur Pruthi, New Delhi, India (*Abstract Co-Author*) Nothing to Disclose

### For information about this presentation, contact:

vidur@mahajanimaging.com

### PURPOSE

Parkinson's disease (PD) in a progressive neurodegenerative disorder that results in loss of dopaminergic neurons in the striatum. Its clinical diagnosis relies on the presence of cardinal motor symptoms of bradykinesia, rigidity, resting tremors and postural instability. 99mTc-TRODAT-1 is a sensitive diagnostic test for early detection of PD. We evaluate 99mTc-TRODAT-1 SPECT imaging patterns and assess their correlation with disease severity in clinically diagnosed patients of Parkinson's disease.

### METHOD AND MATERIALS

The study included 241 diagnosed patients of clinically probable PD who underwent 99mTc-TRODAT-1 SPECT scan. Binding ratios (BR) were calculated for each striatum, caudate, and putamen individually, by drawing region of interest (RoI). Occipital cortex was taken for background correction. Correlation of binding ratio with increasing clinical stage was derived.

### RESULTS

Median binding ratio (BR) was the least in the contralateral putamen for all stages of Modified Hoehn and Yahr. A statistically significant negative correlation was found between increasing disease severity and BR in all sub-regions of striatum. Significant decline was noted in the binding ratio of the putamen as compared to caudate. Patients were further clinically categorized into postural-instability gait disorder (PIGD) group, and tremor-dominant PD (TD) group. No significant asymmetry was found between the left and right striatum in patients belonging to PIGD group and in those with bilateral tremors without lateralization. Significant correlation was found between decline in striatal binding on both the sides, even in early stages when patients presented with unilateral symptoms.

## CONCLUSION

99mTc-TRODAT-1 SPECT can successfully detect and assess disease severity of PD.

## **CLINICAL RELEVANCE/APPLICATION**

99mTc-TRODAT-1 SPECT should be used for early detection and assessment disease severity of PD and thereby guide treatment.



## NR405-SD-TUB7

Identification of Autism Spectrum Disorder Using Deep Learning

Tuesday, Nov. 27 12:45PM - 1:15PM Room: NR Community, Learning Center Station #7

### **Participants**

Xiaowu Liu, Shenzhen, China (*Abstract Co-Author*) Nothing to Disclose Sang Na, MS, Shenzhen, China (*Abstract Co-Author*) Nothing to Disclose Wanshun Wei, Shenzhen, China (*Abstract Co-Author*) Nothing to Disclose Qingchen Diao, Shenzhen, China (*Abstract Co-Author*) Nothing to Disclose Silun Wang, MD, PhD, Shenzhen, China (*Presenter*) Nothing to Disclose

## For information about this presentation, contact:

wangsilun@gmail.com

### PURPOSE

Autism Spectrum Disorder(ASD) is associated with a range of phenotypes that vary in severity of social, communicative and sensorimotor deficits. The goal of the present study is to apply deep learning method of 3D-Convolutional Neural Networks(CNN) to identify ASD patients.

## **METHOD AND MATERIALS**

Image data from ABIDEI consortium were applied to training the deep learning model among which 500 were from ASD patients with mean age of  $11.8\pm3.1$  years and 500 were age and sex matched healthy controls(mean age= $12.2\pm3.5$ ). 80% ASD and controls were used as training set and the rest were regarded as validation set. To test our model, 25 ASD patients (mean age= $4.0\pm2.3$ ) and 22 controls (mean age= $8.3\pm3.0$ ) were scanned by a 3D high-resolution T1-weighted MPRAGE (TR/TE/TI=2300ms/3.3ms/900ms) with isotropic resolution of 1mm. All images were segmented into gray matter and white matter by using the SPM12 software package (UCL,UK), and then registered, normalized to MNI space. The deep learning model we used was a two-stage approach (Figure 1). We applied an auto-encoder to learn filters for convolution operations, and then built a 3D 7-layer (5 convolutional layers and 2 fully connected layers) CNN whose convolutional layers used the filters learned from the auto-encoder. The model took the gray matter image as input, and output the probability showing whether it was ASD or not.

### RESULTS

By doing 3-fold cross validation, our current system achieves a mean classification accuracy of 95.0% over validation set with sensitivity of 96.3%, specificity of 93.8%. The model shows a mean classification accuracy of 74.5%, sensitivity of 65.6% and specificity 93.0% on the testing set.

# CONCLUSION

ASD predictions can be accurately generated on raw T1-MRI data, bringing the process closer to giving early diagnosed information on brain health in clinical settings.

## **CLINICAL RELEVANCE/APPLICATION**

Deep learning model using T1-MRI may be conducive to early diagnosis of ASD.



## NR406-SD-TUB8

Prediction of Clinical Outcome of Acoustic Neuromas Treated with Cyberknife Stereotactic Radiosurgery Using a Radiomic Approach: A Preliminary Study

Tuesday, Nov. 27 12:45PM - 1:15PM Room: NR Community, Learning Center Station #8

# Participants

Natascha Claudia D'Amico, MSc, Milan, Italy (*Presenter*) Nothing to Disclose Isa Bossi Zanetti, MD, Milano, Italy (*Abstract Co-Author*) Nothing to Disclose Giovanni Valbusa, Ivrea, Italy (*Abstract Co-Author*) Research Consultant, CDI; Research Consultant, Bracco Group; Paolo Soda, Rome, Italy (*Abstract Co-Author*) Nothing to Disclose Enzo Grossi, Milano, Italy (*Abstract Co-Author*) Nothing to Disclose Rosa Sicilia, Rome, Italy (*Abstract Co-Author*) Nothing to Disclose Ermanno Cordelli, Rome, Italy (*Abstract Co-Author*) Nothing to Disclose Deborah Fazzini, MD, Milan, Italy (*Abstract Co-Author*) Nothing to Disclose Giancarlo Beltramo, Milano, Italy (*Abstract Co-Author*) Nothing to Disclose Giuseppe Scotti, MD, Milano, Italy (*Abstract Co-Author*) Nothing to Disclose Giuseppe Scotti, MD, Milan, Italy (*Abstract Co-Author*) Nothing to Disclose Sergio Papa, MD, Milan, Italy (*Abstract Co-Author*) Nothing to Disclose

## For information about this presentation, contact:

NataschaClaudia.D'Amico@cdi.it

### PURPOSE

The purpose of this study was to predict the clinical outcome of acoustic neuromas treated with Cyberknife stereotactic radiosurgery, analysing Contrast Enhanced (CE) T1 weighted (T1w) brain MR images acquired for the treatment guidance through a Radiomic approach

# METHOD AND MATERIALS

CE T1w MR images of 38 patients presenting an acoustic neuroma treated with CyberKnife in our institution, were considered in this study. At the last available follow-up exam (mean length of follow-up: 52months (range: 10-105 months)) 65,8% patients showed a Volume Reduction (VR), 26.3% a Stable Volume (VS), 7.9% a Volume Increase (VI), which correspond to the three response classes to be predicted. Images were acquired on 1.5T MR scanners with CE T1w axial sequences. Semi-automatic tumour segmentation was carried out on MR images using the 3DSlicer image analysis software program. In total, 1135 shape-based, intensity-based and texture-based features were extracted from the area of interest using the open-software platform IBEX. Radiomic signature was found by performing a pairwise Mann-Whitney feature selection. The skewness of the dataset makes useless traditional learning approaches: we oversampled the training data using the Synthetic Minority Oversampling Technique (SMOTE). A Random Forest (RF), an algorithm not suffering from the course of dimensionality, was trained and tested to predict patient response using the radiomic signature. All the experiments were performed according to a leave-one-out cross-validation approach, and the Area Under the ROC Curve (AUC) was evaluated.

## RESULTS

Feature selection detected 427 discriminant features, composed of semantic data, first- and second-order histograms, shape, gradient-based measures. RF achieved an AUC per class of VR, VS and VI equal to 0.92, 0.93 and 1, respectively.

#### CONCLUSION

The proposed method based on class imbalance learning and pairwise feature selection allowed to build a model offering promising performances in the field of precision medicine in oncology.

## **CLINICAL RELEVANCE/APPLICATION**

This machine learning approach could be instrumental in the early recognition of patients assessed as "non responder" to a Cyberknife treatment, to avoid unnecessary, expensive and stressful therapies



## NR407-SD-TUB9

## Diffusion Tensor and DSC Perfusion Imaging of CNS Lymphoma: A Comparison with Glioblastoma Multiforme

Tuesday, Nov. 27 12:45PM - 1:15PM Room: NR Community, Learning Center Station #9

### **Participants**

Rafael Diwischek, Vienna, Austria (*Presenter*) Nothing to Disclose Sophie Bartsch, Vienna, Austria (*Abstract Co-Author*) Nothing to Disclose Georg Widhalm, MD, Vienna, Austria (*Abstract Co-Author*) Nothing to Disclose Barbara Kiesel, Vienna, Austria (*Abstract Co-Author*) Nothing to Disclose Daniela Prayer, MD, Vienna, Austria (*Abstract Co-Author*) Nothing to Disclose Ammar Mallouhi, MD, Vienna, Austria (*Abstract Co-Author*) Nothing to Disclose

## For information about this presentation, contact:

Ammar.Mallouhi@meduniwien.ac.at

## PURPOSE

The role of MR perfusion is gaining clinical acceptance in the diagnosis of brain tumors while the role of diffusion tensor scalars remain controversial. This study aims to evaluate the presence of a difference in perfusion and diffusion properties between primary CNS Lymphoma (PCNSL) and glioblastoma multiforme (GBM).

#### **METHOD AND MATERIALS**

Seventeen patients with PCNSL and 17 age-and sex-matched patients with GBM who underwent MR perfusion (MRP) and diffusion tensor imaging (DTI) directly before neurosurgical resection or biopsy were retrospectively included. Scalars of perfusion (CBV and CBF) and diffusion (FA, RA, AD, RD, ADC and EADC) were obtained from regions of interest (ROIs) placed within and around the tumor and in normal-appearing white matter. Differences between both tumors were analyzed by using two-sample T-Test to determine significance, and receiver operating characteristic (ROC) curve analyses to estimate areas under the curve (AUC).

#### RESULTS

The contrast-enhancing part of PCNSL showed significant differences in all perfusion and diffusion scalars when compared with those of peritumoral region. On the contrary, all values measured in contrast-enhancing part of GBM did not differ significantly from those of peritumoral region. All scalars of peritumoral region showed significant discrepancy to normal-appearing white matter. While FA and RA showed no significant differences between contrast-enhancing part of PCNSL and GBM, all other scalars differed significantly between both tumors. Furthermore, ROC analyses reviled that AD, RD, ADC and EADC had significant high AUC (0.88, 0.83, 0.85 and 0.87 respectively; p < .0001) for differentiating PCNSL from GBM, while FA and RA showed moderate not significant AUC (0.61 and 0.60 respectively; p > .05) and CBV and CBF showed moderate but significant AUC (0.77 and 0.72 respectively; p < .003).

## CONCLUSION

AD, RD, ADC and EADC can be helpful as much as CBV in differentiating PCNSL from GBM according to detected microstructural differences in tumor and peritumoral regions.

# **CLINICAL RELEVANCE/APPLICATION**

DTI scalars AD, RD, ADC and EADC can be helpful as much as CBV in differentiating PCNSL from GBM.



# OB183-ED-TUB1

# The Elephant in the Womb: Approach to Classifying Uterine Fibroids

Tuesday, Nov. 27 12:45PM - 1:15PM Room: OB Community, Learning Center Station #1

### **Participants**

Ayush<sup>i</sup> Gupta, MD, Baltimore, MD (*Presenter*) Nothing to Disclose Dzmitry Fursevich, MD, Baltimore, MD (*Abstract Co-Author*) Nothing to Disclose My-Linh Nguyen, MD, Baltimore, MD (*Abstract Co-Author*) Nothing to Disclose Katarzyna J. Macura, MD,PhD, Baltimore, MD (*Abstract Co-Author*) Author with royalties, Reed Elsevier; Research Grant, Profound Medical Inc; Research Grant, GlaxoSmithKline plc; Research Grant, Siemens AG

## For information about this presentation, contact:

#### agupta72@jhmi.edu

### **TEACHING POINTS**

After viewing this exhibit, the learner will be able to: Understand the 2011 International Federation of Gynecology and Obstetrics (FIGO) fibroid classification system utilized by clinicians. Precisely classify submucosal, intramural and subserosal fibroids according to FIGO, which is important for clinicians in treatment planning. Learn to incorporate FIGO system into a radiology template with the goal of reducing fibroid mischaracterization and improving communication with referring clinicians.

## TABLE OF CONTENTS/OUTLINE

Basic anatomy and pathophysiology of uterine fibroids Classic radiologic fibroid classification and its pitfalls FIGO fibroid classification used by clinicians MR examples of fibroids classified using FIGO system Sample cases of miscategorized fibroids and fibroid mimics Proposed template and examples of FIGO fibroid reporting Summary

#### **Honored Educators**

Presenters or authors on this event have been recognized as RSNA Honored Educators for participating in multiple qualifying educational activities. Honored Educators are invested in furthering the profession of radiology by delivering high-quality educational content in their field of study. Learn how you can become an honored educator by visiting the website at: https://www.rsna.org/Honored-Educator-Award/ Katarzyna J. Macura, MD, PhD - 2012 Honored EducatorKatarzyna J. Macura, MD, PhD - 2014 Honored Educator



# OB184-ED-TUB2

# Role of CT, MRI, and PET-CT in Staging of Gynecological Malignancies

Tuesday, Nov. 27 12:45PM - 1:15PM Room: OB Community, Learning Center Station #2

### Participants

Junko Takahama, MD, Kashihara, Japan (*Presenter*) Nothing to Disclose Satoshi Yamauchi, Kashihara, Japan (*Abstract Co-Author*) Nothing to Disclose Natsuhiko Saito, Kashihara, Japan (*Abstract Co-Author*) Nothing to Disclose Kiyoyuki Minamiguchi, Kashihara, Japan (*Abstract Co-Author*) Nothing to Disclose Aki Takahashi, MD, Kashihara, Japan (*Abstract Co-Author*) Nothing to Disclose Hiroshi Okada, Kashihara, Japan (*Abstract Co-Author*) Nothing to Disclose Nagaaki Marugami, Kashihara, Japan (*Abstract Co-Author*) Nothing to Disclose Toshiko Hirai, MD, Kashihara, Japan (*Abstract Co-Author*) Nothing to Disclose Kimihiko Kichikawa, MD, Kashihara, Japan (*Abstract Co-Author*) Nothing to Disclose

### For information about this presentation, contact:

jtakaham@naramed-u.ac.jp

### **TEACHING POINTS**

The stage of FIGO system is determined mainly by preoperative vaginal examination in cervical cancer, and by surgical and pathological findings after operation in endometrial and ovarian cancer. The FIGO still suits CT MRI, and PET-CT to the assistant role. The purpose of this presentation is to show the key radiologic findings and clinical knowledge to impact gynecologist for the diagnosis and staging of gynecologic malignancies

# TABLE OF CONTENTS/OUTLINE

Key diagnostic points for gynecologic malignancy will be highlighted in the discussion of each case. The list of cases includes: INTRODUCTION, FIGO STAGING, THE ROLE OF RADIOLOGIC IMAGING FOR FIGO STAGING, INDICATIONS of CT, MRI, PET and Following radiologic images of gynecologic malignancies. Uterine cervical cancer, Uterine endometrial cancer, Ovarian and peritoneal cancer.



### PD186-ED-TUB6

Rethinking ADEM: The Changing Landscape of Neuroinflammatory Disorders

Tuesday, Nov. 27 12:45PM - 1:15PM Room: PD Community, Learning Center Station #6

#### Awards Cum Laude

## Participants

Mika Shapira Rootman, MD, PhD, Toronto, ON (*Abstract Co-Author*) Nothing to Disclose Ann Yeh, MD, Toronto, ON (*Abstract Co-Author*) Nothing to Disclose Helen M. Branson, MBBS, FRCR, Toronto, ON (*Abstract Co-Author*) Nothing to Disclose Manohar M. Shroff, MD, Toronto, ON (*Presenter*) Nothing to Disclose

# For information about this presentation, contact:

mikashap@gmail.com

### **TEACHING POINTS**

1. To define CNS inflammatory disorders and describe the major classifications (demyelinating syndromes, antibody mediated encephalitis, vasculitis, epileptic syndromes, systemic inflammatory disorders with secondary CNS involvement). 2. To describe the major clinical and neuroimaging findings typically associated with the various disorders.

### TABLE OF CONTENTS/OUTLINE

1. Definition of neuroinflammatory disease and major classifications. 2. Diagnostic workup of neuroinflammatory disorders. 3. General considerations, diagnosis and imaging findings of: a. Demyelinating syndromes: i. The monophasic syndromes. ii. Childhood multiple sclerosis. iii. Antibody-mediated demyelinating syndromes (NMOSD, anti MOG) b. Childhood primary CNS angiitis c. Epileptic syndromes (Rasmussen encephalitis). d. Antibody-mediated encephalitis. e. Systemic inflammatory disease with secondary CNS involvement 4. mimics



# PD225-SD-TUB1

Microstructural Changes of Brain White Matter for the Children Patients with Obstructive Sleep Apnea Syndrome Based on Diffusional Kurtosis Imaging Study

Tuesday, Nov. 27 12:45PM - 1:15PM Room: PD Community, Learning Center Station #1

# Participants

Wenfeng Li, Beijing, China (*Abstract Co-Author*) Nothing to Disclose Yue Liu, MD, Beijing, China (*Presenter*) Nothing to Disclose Hongwei Wen, Beijing, China (*Abstract Co-Author*) Nothing to Disclose Hongbin Li, Beijing, China (*Abstract Co-Author*) Nothing to Disclose Yun Peng, MD, Beijing, China (*Abstract Co-Author*) Nothing to Disclose

## For information about this presentation, contact:

#### 1332542019@qq.com

# PURPOSE

We used tract-based spatial statistics (TBSS) to analyze the microstructural changes of white matter in obstructive sleep apnea syndrome (OSAS) and age and gender matched healthy children.

# METHOD AND MATERIALS

1.subject The study includes children with obstructive sleep apnea syndrome examined in our hospital inpatient and outpatient visits for the first time without treatment from August 2016 to February 2017 to scan routine MRI and evaluate polysomnography and cognitive ability test. There were a total of 42 cases including the OSAS group and healthy control group, with 16 males and 19 females, age between 3years -10 years old (mean age: 8 months). 2.MRI protocol All subjects were imaged on a 3-T MRI system( GE Discovery 750),All children are routine scan (T1WI,T2WI,T2-FLAIR,DWI )and DKI scan.

## RESULTS

Cognitive ability tests demonstrated that the developmental quotient of children with OSAS group in different cognitive testing were decreased. Compared to healthy controls, the diffusion parameter fractional anisotropy (FA) were decreased in white matter regions (anterior limb of internal capsule, anterior thalamic radiation, fornix, inferior longitudinal fasciculus and corpus callosum) with coherent fiber arrangement, while the kurtosis parameter kurtosis fractional anisotropy (KFA) were decreased in white matter regions (superior longitudinal fasciculus and posterior corona radiata) with complex fiber arrangement. The two parameters were sensitive to reveal abnormality of white matter in OSAS children. There are multiple abnormal brain lobes in OSAS patients, The KFA values in the right forelimb of internal capsule and the left parietal lobe were positively correlated with lowest oxygen saturation (LSaO2). The values FA, KFA of DKI parameters in the corpus callosum, right posterior coronaries, left post central and left anterior parietal lobes were negatively correlated with SaO2 <90% and hypoventilation index .

### CONCLUSION

The abnormal KFA value is existed in multiple brain lobes in OSAS patients, which showed significantly positive correlations with hypoxia. These may be mechanism of cognitive impairment for OSAS children and provides the scientific imaging manifestations for the research of pathophysiological mechanisms (such as neuronal damage and necrosis).

## **CLINICAL RELEVANCE/APPLICATION**

To explore neurophysiological mechanisms of cognitive impairment in patients with OSAS.



## PD226-SD-TUB2

Improved Method for Estimating Brain Structural Location for Mapping of Magnetoencephalography in Young Children

Tuesday, Nov. 27 12:45PM - 1:15PM Room: PD Community, Learning Center Station #2

# Participants

Norio Hayashi, PhD, Maebashi, Japan (*Presenter*) Nothing to Disclose Miyu Saito, Maebashi, Japan (*Abstract Co-Author*) Nothing to Disclose Tomoko Maruyama, Maebashi, Japan (*Abstract Co-Author*) Nothing to Disclose Yusuke Sato, Midori, Japan (*Abstract Co-Author*) Nothing to Disclose Yuko Yoshimura, Kanazawa, Japan (*Abstract Co-Author*) Nothing to Disclose Mitsuru Kikuchi, Kanazawa, Japan (*Abstract Co-Author*) Nothing to Disclose Yuta Wakayama, Maebashi, Japan (*Abstract Co-Author*) Nothing to Disclose Toshihiro Ogura, PhD, Maebashi, Japan (*Abstract Co-Author*) Nothing to Disclose Akio Ogura, PhD, Maebashi, Japan (*Abstract Co-Author*) Nothing to Disclose Yoshio Minabe, Kanazawa, Japan (*Abstract Co-Author*) Nothing to Disclose

## PURPOSE

Magnetoencephalography (MEG) is a non-invasive procedure with high time resolution, which is very useful to predict the degree of pediatric psychiatric disorders. An anatomical position is obtained by superimposing the MEG data on a magnetic resonance (MR) image; however, in infants, the acquisition of MR image is difficult. In this study, we proposed an improved method for constructing an age-specific head template to allow superimposition of MEG without the MR image.

### **METHOD AND MATERIALS**

Subjects (age range 3-8 years) who had undergone MR imaging (MRI) were included in this study. The brain template was constructed using the following four steps: 1) plotting of head surface points; 2) selection of suitable template data; 3) registration of the template to personalized data; 4) correction of the registration using hearing stimulus used in the MEG examination. Error between the personalized template data and MR images of the subjects were evaluated using distance between the primary auditory cortex (PAC) and functional results of MEG examinations.

#### RESULTS

Distance between the PAC and functional area was  $28.0\pm16.0$  mm by the previous method and  $2.5\pm3.1$  mm by the improved method. Action potential was shown in the PAC when superimposed on the personalized image and the hearing stimulus of MEG examination.

### CONCLUSION

We developed an improved method for constructing a personalized age-specific head template for superimposition of MEG without MRI. Using this method, the MEG data could be accurately superimposed on the brain surface without performing MRI for mapping.

### **CLINICAL RELEVANCE/APPLICATION**

Using this method, the MEG data could be accurately superimposed on the brain surface without performing MRI for mapping.



# PD227-SD-TUB3

Frequency Selective Non-Linear Blending Technique Can Improve Detection of Acute Infarcts on Preenhanced Brain CT in Children

Tuesday, Nov. 27 12:45PM - 1:15PM Room: PD Community, Learning Center Station #3

## Awards

### **Trainee Research Prize - Fellow**

#### Participants

Seunghyun Lee, Seoul, Korea, Republic Of (*Presenter*) Nothing to Disclose Young Hun Choi, MD, Seoul, Korea, Republic Of (*Abstract Co-Author*) Nothing to Disclose Yeon Jin Cho, Seoul, Korea, Republic Of (*Abstract Co-Author*) Nothing to Disclose Jung-Eun Cheon, MD, Seoul, Korea, Republic Of (*Abstract Co-Author*) Nothing to Disclose Woo Sun Kim, MD, Seoul, Korea, Republic Of (*Abstract Co-Author*) Nothing to Disclose In-One Kim, MD, Seoul, Korea, Republic Of (*Abstract Co-Author*) Nothing to Disclose

## PURPOSE

To evaluate whether the frequency selective non-linear blending ("best contrast"/BC) technique can improve the detection of acute infarction on non-enhanced brain CT (NECT) in children.

### **METHOD AND MATERIALS**

From January 2014 to December 2017, 44 children with Moyamoya disease (18 boys and 26 girls; mean age  $8.8 \pm 3.6$  years) underwent NECT followed by diffusion MRI for suspected postoperative ischemic complications. NECT images were post-processed using BC for enhanced delineation of infarction. Subjective detection rates of hypodense infarctions were calculated with original NECT images and processed BC images. Contrast-to-noise ratios (CNRs) between infarcted area and gray matter and between normal cortex and white matter were calculated.

### RESULTS

Twenty-one of 44 children was confirmed with acute infarction through diffusion MRI. Detection rate of infarction was 61.9% (13/21) and 38.1% (8/21) on BC and NECT images, respectively. CNR was improved with BC (BC vs. NECT;  $6.7 \pm 1.8$  vs.  $2.9 \pm 0.8$  for infarcted area, and  $5.6 \pm 1.1$  vs.  $2.8 \pm 0.6$  for the normal gray and white matter, all p < 0.05).

### CONCLUSION

BC technique can improve the detectability of infarction on NECT by improving tissue contrast in children.

### **CLINICAL RELEVANCE/APPLICATION**

Frequency-selective non-linear blending technique improves detection of brain infarction in Moyamoya disease patients and it seems to be particularly valuable for implementation in CT systems not equipped for dual-energy or spectral CT imaging.



# PD228-SD-TUB4

Imaging of the Temporomandibular Joint in Juvenile Idiopathic Arthritis: A Comparison of Quantitative and Semi-Quantitative MRI Scoring

Tuesday, Nov. 27 12:45PM - 1:15PM Room: PD Community, Learning Center Station #4

#### Awards Student Travel Stipend Award

### **Participants**

Grace Mang Yuet Ma, MD, Boston, MA (*Presenter*) Nothing to Disclose Carly Calabrese, Boston, MA (*Abstract Co-Author*) Nothing to Disclose Timothy J. Donohue, MD, Portland, ME (*Abstract Co-Author*) Nothing to Disclose Cory Resnick, MD, Boston, MA (*Abstract Co-Author*) Nothing to Disclose

#### For information about this presentation, contact:

grace.ma@childrens.harvard.edu

### PURPOSE

Contrast-enhanced MRI is the diagnostic standard for temporomandibular joint (TMJ) involvement in juvenile idiopathic arthritis (JIA). MRI assessment is complicated by qualitative reporting, normal background enhancement and lack of standardized protocols. The purpose of this study is to compare a quantitative MRI analysis (enhancement ratio, ER) to a new semi-quantitative system developed by OMERACT (Outcome Measures in Rheumatology and Clinical Trials). ER quantitates degree of synovial enhancement. The OMERACT system accounts for acute inflammation and chronic joint damage.

## METHOD AND MATERIALS

Retrospective study of children (age<=16years) with JIA who had TMJ MRIs with gadolinium at our institution. Each MRI was assessed using both methods by one radiologist. ER was calculated by dividing the average TMJ synovium pixel intensity by the longus capitis muscle pixel intensity. OMERACT scores were determined using an additive scale incorporating inflammatory and damage domains. Randomly selected TMJs were re-measured by the primary and a second reader in a blinded fashion. ER was compared to total OMERACT (T), OMERACT inflammatory domain (I), and OMERACT damage domain (D) scores.

#### RESULTS

50 subjects and 124 TMJs were included. Mean ER was  $2.5\pm0.9$ . Mean OMERACT (T) was  $4.9\pm3.3$ . There was moderate correlation between ER and: OMERACT (T) (r=0.531), OMERACT (I) (r=0.531), and OMERACT (D) (r=0.420). Controlling for age, sex, JIA subtype, and medications, for every 1 unit increase in ER, OMERACT score increased by: 3.11 in total score (p<0.0001), 1.01 in inflammatory domain score (p<0.001), and 0.86 in damage domain score (p<0.0001). Intraclass correlation coefficients for intrarater variability were 0.83 for ER and 0.77 for OMERACT. Inter-rater agreements were 0.96 for ER and 0.35 for OMERACT.

#### CONCLUSION

Quantitative evaluation of TMJ synovial enhancement (ER) and semi-quantitative assessment of TMJ inflammation and damage (OMERACT) in subjects with JIA were moderately correlated. ER is easier to score and has superior intra-and inter-rater agreement but only evaluates inflammation. OMERACT adds insight on chronic changes.

# **CLINICAL RELEVANCE/APPLICATION**

No standard exists for MRI evaluation of TMJ involvement in JIA. Enhancement ratio reliably quantitates inflammation. OMERACT adds insight on chronic joint damage. Scores are moderately correlated.



# PD229-SD-TUB5

Clinical Implication of Hepatic Subcapsular and Capsular Flow in Doppler Ultrasound and Microvascular Imaging after Receiving Kasai Operation

Tuesday, Nov. 27 12:45PM - 1:15PM Room: PD Community, Learning Center Station #5

**FDA** Discussions may include off-label uses.

#### **Participants**

Suji Lee, Seoul, Korea, Republic Of (*Presenter*) Nothing to Disclose Myung-Joon Kim, MD, Seoul, Korea, Republic Of (*Abstract Co-Author*) Nothing to Disclose Mi-Jung Lee, MD, PhD, Seoul, Korea, Republic Of (*Abstract Co-Author*) Nothing to Disclose Haesung Yoon, MD, Seoul, Korea, Republic Of (*Abstract Co-Author*) Nothing to Disclose Hyun Joo Shin, MD, Seoul, Korea, Republic Of (*Abstract Co-Author*) Nothing to Disclose

### For information about this presentation, contact:

sjlee37@yuhs.ac

### PURPOSE

To know the clinical implication of presence of hepatic subcapsular and capsular flows using color Doppler ultrasonography (US) and microvascular imaging (MVI) in children after receiving Kasai operation.

### **METHOD AND MATERIALS**

In this retrospective study, children (<=18 years old) who underwent liver US examinations including color Doppler US and MVI from May to October 2017 were included. From them, children with grossly normal liver on US and no history of liver disease were included in normal group. Children who had Kasai operation due to biliary atresia were included in Kasai group. Presence of hepatic subcapsular and capsular flows on color Doppler US and MVI was compared between normal and Kasai groups using following flow scores; score 0, no subcapsular flow reaching hepatic capsule; score 1, presence of subcapsular flow; score 2, presence of contiguous hepatic capsular flow. Multiple and ordinal logistic regression tests were used to know the correlation between flow scores and age, number of intrahepatic biliary cysts, liver stiffness measured with transient elastography (TE), spleen size in Kasai group.

### RESULTS

Among total 65 children (M:F=27:38, mean 7.6  $\pm$  5.3 years old), 21 children were included in normal group and 44 children were included in Kasai group. In normal group, only one child had score 1 flow using MVI, while others had score 0 flow in both Doppler US and MVI. In Kasai group, 28 children had score 1 flow and 16 children had score 0 flow using Doppler US. Using MVI, 24 children had score 2 flow, 18 children had score 1 flow, and one child had score 0 flow. In logistic regression test, increased liver stiffness was significantly associated with increased flow scores in Doppler US. In addition, increased spleen size was significantly associated with increased flow scores.

## CONCLUSION

Detection of hepatic subcapsular and capsular flows on US could be an additional method for predicting liver fibrosis and splenomegaly after receiving Kasai operation.

### **CLINICAL RELEVANCE/APPLICATION**

Hepatic subcapsular and capsular flows in Doppler US and MVI after Kasai operation can be added for predicting the prognosis.



# PH232-SD-TUB7

Pelvic Diagnostic: Dose Assessment of CT vs. Conventional X-Ray in a Phantom Study considering different CT Protocols including Tin Filtering

Tuesday, Nov. 27 12:45PM - 1:15PM Room: PH Community, Learning Center Station #7

### Participants

Arthur P. Wunderlich, PhD, Ulm, Germany (*Presenter*) Nothing to Disclose Meinrad J. Beer, MD, Ulm, Germany (*Abstract Co-Author*) Nothing to Disclose Carsten Hackenbroch, Ulm, Germany (*Abstract Co-Author*) Nothing to Disclose

#### For information about this presentation, contact:

arthur.wunderlich@uni-ulm.de

## PURPOSE

Diagnosis of pelvic fractures is often performed with conventional x-ray. CT offers additional information at higher x-ray exposure. To evaluate tin filtering, promising dose reduction, and compare dose and diagnostic value (DV) to conventional x-ray exams, seven different CT protocols including tin filtering technology, a conventional x-ray system and a fluoroscopy unit were evaluated for dose and image quality in a phantom study.

### **METHOD AND MATERIALS**

Pelvis of an Alderson-Phantom was scanned with Somatom Force/AS scanners (Siemens, Forchheim, Germany) at 90 or 100 kV and 26 to 300 mAs w/o tin filtering. Conventional x-ray images (AP, inlet, outlet) were acquired with a DRX (Carestream, Atlanta, GA) flat panel detector system, and corresponding projections taken at an Axiom Artis fluoroscopy unit (Siemens, Erlangen, Germany). Effective dose was measured by thermoluminescence dosimetry (TLD) calculating weighted sum of organ doses separated by gender. Diagnostic value (DV) was scored subjectively on a four point likert-scale (best=1, worst=4) independently by two radiologists and two trauma surgeons blinded for protocol settings and dose.

### RESULTS

Effective dose of fluoroscopy was 0.2/0.25 mSv (males/females), for conventional x-ray 0.24/0.25 (m/f) mSv with identical value rating of 1.5 average score. Radiation dose ranged from 0.26/0.46 mSv (m/f) to 1.95/2.9 mSv (m/f) for CT. Low-dose CT (100 kV, 300 mAs with tin filter, Somatom Force) showed good DV (average score 1.1), but 100 kV, 26 mAs performed identically in dose (.26/.46 mSv m/f) and DV (1.1). 100 kV, 26 mAs at the Somatom AS scanner resulted in the same dose, but reduced DV (1.8). For standard protocols, the Force showed best DV of 1 at 0.8/1.2 mSv (m/f) dose (100 kV, 75 mAs), the AS yielded a DV score of 1.1 at 1.2/1.9 mSv (m/f; 100 kV, 146 mAs).

# CONCLUSION

Low-dose CT protocols are able to reduce CT dose substantially with only slightly impaired diagnostic value (DV). Tin filtering proved helpful in our study, but detector technology is probably the key factor to maintain sufficient image quality at reduced mAs. Standard CT protocols seem to be optimized for image quality at the cost of radiation dose. Concerning DV, fluoroscopy and conventional x-ray were both rated worse than CT.

## **CLINICAL RELEVANCE/APPLICATION**

Low-dose CT should be considered in pelvic diagnosis due to diagnostic information. Dose is equal to conventional x-ray for males, slightly higher for females.



## PH233-SD-TUB1

## Using Magnification for Increasing DR Spatial Resolution of Pediatric Extremities

Tuesday, Nov. 27 12:45PM - 1:15PM Room: PH Community, Learning Center Station #1

### **Participants**

Ashley Tao, PhD, Rochester, MN (*Abstract Co-Author*) Nothing to Disclose Kristopher Loewen, Rochester, MN (*Presenter*) Nothing to Disclose Timothy R. Daly, RT, Rochester, MN (*Abstract Co-Author*) Nothing to Disclose Kenneth A. Fetterly, PhD, Rochester, MN (*Abstract Co-Author*) Nothing to Disclose Kristen B. Thomas, MD, Rochester, MN (*Abstract Co-Author*) Nothing to Disclose Beth A. Schueler, PhD, Rochester, MN (*Abstract Co-Author*) Nothing to Disclose Alisa Walz-Flannigan, PhD, Rochester, MN (*Abstract Co-Author*) Nothing to Disclose

#### For information about this presentation, contact:

Walz-Flannigan.Alisa@mayo.edu

# PURPOSE

Diagnostic confidence in pediatric extremity imaging was seen to be limited when imaging with a lower resolution DR detector system despite efforts at improvement through pediatric-specific processing. Geometric magnification can be used to increase the image spatial resolution but is limited by focal spot blurring. The purpose of this work was to evaluate whether magnification imaging could be used to improve pediatric extremity imaging.

### **METHOD AND MATERIALS**

The modulation transfer function (MTF) was measured for several different magnification factors on an X-ray system (focal spot size = 0.6 mm) with a digital detector (pixel size = 0.2 mm). Geometric sharpness was extracted from the MTF as a primary figure of merit for optimization and compared with the theoretical value for each magnification. Magnification increases the projected size of the anatomy and thereby the interaction of the frequency-based image processing with that anatomy in ways that are not readily quantifiable. To evaluate this effect, the results of image processing settings optimized for adult hands were qualitatively evaluated for pediatric extremities with contact and x1.45 magnification imaging.

### RESULTS

Perceived image resolution is impacted by technique, processing and intrinsic system resolution. Attempts to modify technique and processing to improve imaging of pediatric extremities when using a lower resolution detector (0.2 mm pixels) did not yield acceptable results. Geometric sharpness was determined to be optimal at x1.25 magnification. While magnification imaging provided only marginal improvement in intrinsic resolution, clinical images acquired at x1.45 magnification resulted in appreciable improvement to image quality. The benefit of magnification was difficult to perceive for adult hand phantom images at x1.33 magnification.

### CONCLUSION

This work suggests the need for a comprehensive approach to balance optimization of intrinsic image properties with optimization of processed images, specific to the spatial frequency content of the raw image and the selected image processing settings.

### **CLINICAL RELEVANCE/APPLICATION**

Low resolution digital detectors have been found to limit diagnostic quality in pediatric extremity imaging. The use of geometric magnification can qualitatively improve image quality for small pediatric extremities.



## PH234-SD-TUB2

# Application of Multimodal Imaging and Photothermal Therapy in HER-2 Positive Breast Cancer

Tuesday, Nov. 27 12:45PM - 1:15PM Room: PH Community, Learning Center Station #2

## **FDA** Discussions may include off-label uses.

#### **Participants**

Xiaojun Luo, Beijing, China (*Presenter*) Nothing to Disclose Chunwu Zhou, MD, Beijing, China (*Abstract Co-Author*) Nothing to Disclose

## For information about this presentation, contact:

xiaojunluo0228@126.com

### PURPOSE

To create multifunctional super paramagnetic iron oxide nanoparticles (SPIONs) based on anti-HER2 monoclonal antibodytrastuzumab and indocyanine green (ICG). To test whether the nanoparticles (NPs) could target HER-2 receptors on breast cancer cells in vitro and vivo.

## METHOD AND MATERIALS

Fe3O4-trastuzumab-ICG NPs was created. The targeted cell uptake of Fe3O4-trastuzumab-ICG in vitro was identified by TEM. In vivo, MR imaging was conducted on mice engrafted with HER-2 overexpressed SK-BR-3 cells. We observed whether NPs could aggregate in the tumor site by MRI and fluorescent imaging. When the NPs was gathered at the tumor site, the near infrared thermal imaging system was used to monitor the temperature of tumor in the near infrared radiation.

#### RESULTS

The Fe3O4-trastuzumab-ICG NPs was successfully constructed.

#### CONCLUSION

This study revealed that Fe3O4-trastuzumab-ICG NPs had the potential to become a theranostic agent for HER-2 positive breast cancer.

### **CLINICAL RELEVANCE/APPLICATION**

We created multifunctional nanoparticles based on Fe3O4, anti-HER2 monoclonal antibody and ICG to target HER2 positive breast cancer cells in vitro and in vivo. As a result, Fe3O4-trastuzumab have shown great potential to be an excellent theranostic tool for HER2-expression in breast cancer cells.



# PH235-SD-TUB3

Estimating Radiation Dose of Digital Tomosynthesis and in Comparison with Other Chest Examinations for Adult Patients of Wide Ranging Body Sizes

Tuesday, Nov. 27 12:45PM - 1:15PM Room: PH Community, Learning Center Station #3

# Participants

Le Ma, Guangzhou, China (*Presenter*) Nothing to Disclose Genggeng Qin, MD, PhD, Guangzhou, China (*Abstract Co-Author*) Nothing to Disclose Yuxing Cai, Guangzhou, China (*Abstract Co-Author*) Nothing to Disclose Weiguo Chen, Guangzhou, China (*Abstract Co-Author*) Nothing to Disclose

For information about this presentation, contact:

male2@mail2.sysu.edu.cn

# PURPOSE

Digital tomosynthesis (DTS) as a low-dose intervention for chest diagnosis, estimating radiation dose accurately that patients receive is crucial. The purpose of this study is to propose and validate a simple method of calculating radiation dose in DTS. Further investigation is to explore the effect of wide ranging body sizes of adult patients on radiation dose among different chest examinations of digital radiography (DR), dual energy subtraction (DES), digital tomosynthesis (DTS), low-dose CT and CT.

#### **METHOD AND MATERIALS**

In this study, 50 subjects undergoing DTS using VolumeRAD are recruited for field-size correction factor calculation accounting for angle-induced change during projections acquisition. With the correction factor and developed method, dose-area product (DAP) can be estimated. Further comparison with actual DAP is to validate the proposed factor through another 50 subjects. Additional 400 subjects recruited are distributed equally to DR, DES, low-dose CT and CT examinations. A systematic comparison on radiation dose is investigated between DTS and other chest examinations above. And further linear fittings between radiation dose and chest effective diameter are explored.

#### RESULTS

The correction factor of 0.924 for DAP is determined. Small average difference of  $0.28\pm0.21\%$  is found between estimated DAP and actual DAP. Effective dose of DTS is only 6% of low-dose CT and 3% of CT, about twice that of DR and DES examinations, while DES is slightly higher than that of DR. Significant differences are found between each two examinations of DR, DES, DTS, LDCT and CT (P<0.05). After linear fittings between effective doses and chest effective diameter, DTS has the lowest correlation coefficient of 0.56 (P<0.05); highest correlation coefficient is found in DES of 0.69 (P<0.05), while 0.63~0.68 are in DR, LDCT and CT (P<0.05).

# CONCLUSION

The small average difference between estimated DAP and actual DAP suggests the proposed correction factor is available for DAP prediction. No additional work would be needed to sum up all the DAP from 60 projections in DTS. Patient body size has a great impact on radiation dose among different chest examinations. More X-ray photons may be needed to penetrate with the increased chest effective diameter.

### **CLINICAL RELEVANCE/APPLICATION**

The size of a patient should be considered when choosing the best modality for chest examination and DTS is recommended as the lower correlation coefficient.



## PH236-SD-TUB4

Comparison of Two Free-breathing Coronary Computed Tomography Angiography (CCTA) Protocols for Patients with Severe Cardiac Insufficiency

Tuesday, Nov. 27 12:45PM - 1:15PM Room: PH Community, Learning Center Station #4

Participants Zhao Li, Liaocheng, China (*Presenter*) Nothing to Disclose

#### For information about this presentation, contact:

5151674@qq.com

### PURPOSE

CCTA for patients with cardiovascular disorders often fails because the bolus may be completely missed if the delay is not properly chosen. This research compared two free-breathing CCTA protocols for patients with severe cardiac insufficiency (grade III).

### **METHOD AND MATERIALS**

40 patients clinically diagnosed cardiac insufficiency (grade III) were randomly divided into two groups and underwent CCTA on a 256-row CT (Revolution CT, GE Healthcare). For Group A (n=20) test bolus (20mL contrast medium and 20mL saline) was conducted before CCTA. The peak time was used as the delay time for the following CCTA. For Group B (n=20), bolus triggering was used with a trigger threshold of 250HU and a trigger delay of 1.1s. For both groups, contrast agent (370mgI/ml, Iopamidol) injection rate was proportional to the patient weight 0.85ml/kg, and the injection time was 12s. All CCTA exams were completed within one cardiac cycle and patients were breathing normally during the entire process. Image quality was assessed using a 5-point Likert scale (1-nondiagnostic to 5-excellent). CT values of the ascending aorta, image noise and signal-to-noise-ratio (SNR) were measured. The volume of contrast agent usage, trigger time and effective radiation dose (ED) were recorded.

#### RESULTS

Body height, body weight, age and heart rate were not different between the two groups. Group B used additional 20mL contrast medium than Group A due to the test bolus (80ml vs. 60ml, P<0.01). The ED of CCTA was not different between the two groups (A: 2.35mSv, B: 2.25mSv, P=0.848), but the ED of test bolus for Group A (0.42mSv) was greater than bolus tracking for Group B (0.23mSv), P<0.01. Neither the objective image quality measurements nor the subjective image quality ratings were different between the two groups (see details in Figure 1).

### CONCLUSION

The application of free-breathing in combination with high-threshold, rapid-triggering technique significantly reduced total usage of contrast medium and the obtained image quality was comparable with those obtained using test bolus technique.

## **CLINICAL RELEVANCE/APPLICATION**

The high-threshold, rapid-triggering technique can be routinely used for patients with severe cardiac insufficiency.



## PH237-SD-TUB5

Reproducibility Analysis on Computer Aided Abnormality Detection with Convolutional Neural Net in Chest PA X-Ray Images within Short-term Period

Tuesday, Nov. 27 12:45PM - 1:15PM Room: PH Community, Learning Center Station #5

# Participants

Yongwon Cho, Seoul, Korea, Republic Of (*Presenter*) Nothing to Disclose Sang Min Lee, MD, Seoul, Korea, Republic Of (*Abstract Co-Author*) Nothing to Disclose Eunsol Lee, MD, Seoul, Korea, Republic Of (*Abstract Co-Author*) Nothing to Disclose Younghoon Cho, MD, Seoul, Korea, Republic Of (*Abstract Co-Author*) Nothing to Disclose Namkug Kim, PhD, Seoul, Korea, Republic Of (*Abstract Co-Author*) Stockholder, Coreline Soft, Co Ltd Joon Beom Seo, MD, PhD, Seoul, Korea, Republic Of (*Abstract Co-Author*) Nothing to Disclose

### For information about this presentation, contact:

dragon1won@gmial.com

### PURPOSE

To evaluate reproducibility of computer aided abnormality detection with convolutional neural net (CNN) in chest PA X-ray images of same patient acquired within short-term period.

### **METHOD AND MATERIALS**

We proposed new CAD system for detecting five abnormalities in chest X-ray including nodule (N), consolidation (C), interstitial opacity (I), pleural effusion (PE), and pneumothorax (PT). For training and testing, 3722 images were enrolled and 4678 abnormality ROIs were manually drawn. All data were randomly split into 80 percent for training and 20 percent for test. The YOLO v2 of DenseNet201 model was used and the pre-trained model was fine-tuned. For evaluation of reproducibility of computer aided abnormality detection, chest X-ray images (N=121pairs, C=28 pairs, IO=12 pairs, PE=67 pairs, and PT=20 pairs) of same patient scanned within one week were independently acquired. Reproducibility was evaluated in terms for percent positive agreement (PPA) and Chamberlain's percent positive agreement.

## RESULTS

The PPA in reproducibility test set was 89.10%, 88.37%, 100%, 98.41%, and 89.60% for N, C, I, PE, and PT, respectively. The Chamberlain positivity in reproducibility test set was 80.30%, 79.16%, 100%, 96.82%, and 81.25% for N, C, I, PE, and PT, respectively. The consolidation showed the worst reproducibility and the interstitial opacity is the best reproducibility.

### CONCLUSION

CAD with deep learning showed variable reproducibility for detecting abnormality in chest X-ray images. Therefore, For evaluation of CAD performance in later, reproducibility testing will be necessary.

# **CLINICAL RELEVANCE/APPLICATION**

This study showed variable reproducibility of CAD with deep learning. For evaluation of CAD performance in later, reproducibility testing will be necessary.



## PH238-SD-TUB6

## Combined Respiratory and Cardiac 3D Imaging with a Single-Sweep C-Arm Acquisition

Tuesday, Nov. 27 12:45PM - 1:15PM Room: PH Community, Learning Center Station #6

### Participants

Tess Reynolds, PhD, Sydney, Australia (Abstract Co-Author) Nothing to Disclose

Chun-Chien (andy) Shieh, Sydney, Australia (Abstract Co-Author) Nothing to Disclose

Paul J. Keall, PhD, Camperdown, Australia (*Abstract Co-Author*) Research agreement, Koninklijke Philips NV; Research agreement, Varian Medical Systems, Inc; Research agreement, Siemens AG; Research agreement, Ion Beam Applications SA; Founder, Cancer Research Innovations; Partner, Cancer Research Innovations; Founder, Leo Cancer Care Pty Ltd; Stockholder, Leo Cancer Care Pty Ltd; Stockholder, Leo Cancer Care Pty Ltd; Director, SeeTreat Pty Ltd; Stockholder, SeeTreat Pty Ltd; Founder, Opus Medical Pty Ltd; Director, Opus Medical Pty Ltd; Stockholder, Opus Medical Pty Ltd; Spouse, Stockholder, Leo Cancer Care Pty Ltd; Spouse, Stockholder, Respiratory Innovations Pty Ltd

Ricky O'Brien, Everleigh, Australia (Presenter) Stockholder, Opus Medical Pty Ltd

#### For information about this presentation, contact:

tess.reynolds@sydney.edu.au

#### PURPOSE

Adaptive CaRdiac cOne BEAm computed tomography (ACROBEAT) is our novel 3D gated cardiac CBCT imaging protocol. ACROBEAT uses the patient's electrocardiograph (ECG) signal to adapt the gantry velocity and projection acquisition in real-time, enabling personalised imaging in a single-sweep that compensates for cardiac rhythm variations within the interventional suite. Here, we investigate employing the ACROBEAT protocol for combined respiratory and cardiac 3D imaging, potentially eliminating the need to induce apnea in ventilated patients.

## METHOD AND MATERIALS

Simulated in-silico scans using a patient's ECG signal (average heart rate 66 bpm) and breathing trace (average breath length 3.7 seconds) were completed employing our adaptive ACROBEAT protocol with various scan parameters. The resulting dual-gated 3D cardiac images were reconstructed using 40, 100, 130 and 199 projections with even angular spacing from the XCAT software phantom during 60-70% of the cardiac cycle and 10%, 20% and 40% displacement at peak exhale of the breathing cycle. Image metrics of contrast-to-noise ratio and edge response width were used to compare and characterise the quality of the reconstructed images.

### RESULTS

The total scan times ranged from 1 minute through to 5 minutes and were dictated by the number of projections and respiratory displacement bins, heart rate and length of the breathing cycle. The contrast-to-noise ratio increased with the number of projections collected from an average of 7 (40 projections) to 46 (199 projections). The edge response width decreased with increasing number of respiratory displacement bins from an average of 4.5 mm (5 bins) to 2.1 mm (20 bins), indicating sharper more defined images.

## CONCLUSION

For the first time, the potential of adapting image acquisition to changes in the patient's cardiac and respiratory rates was investigated. The ACROBEAT protocol enables the ability to trade desired image quality for total scan time. Further, by customizing the scan parameters, ACROBEAT can be tailored for a variety of different image-guided interventional surgical cardiac procedures.

#### **CLINICAL RELEVANCE/APPLICATION**

Combined respiratory and cardiac 3D imaging with a single-sweep C-arm acquisition can reduce breath hold requirements and imaging dose and time, increasing the accessibility of 3D cardiac imaging.



## PH239-SD-TUB8

Suppression of Longitudinal Aliasing (Windmill) Artifact in MDCT/CBCT: Detector Cell Interlacing vs Focal Spot Flying

Tuesday, Nov. 27 12:45PM - 1:15PM Room: PH Community, Learning Center Station #8

# Participants

Xiangyang Tang, PhD, Atlanta, GA (*Abstract Co-Author*) Research Grant, SINOVISION Technology Co, Ltd Huiqiao Xie, PhD, Atlanta, GA (*Presenter*) Nothing to Disclose

For information about this presentation, contact:

xiangyang.tang@emory.edu

### PURPOSE

Due to insufficient sampling along longitudinal direction, aliasing (windmill) artifacts exist in both MDCT and CBCT (MDCT/CBCT henceforth). Focal spot flying and detector cell interlacing have been the two optional techniques for aliasing (windmill) artifacts suppression. In this study, we investigate the efficacy of the two options in suppressing the aliasing (windmill) artifacts and compare their pros and cons from the perspective of CT architecture and system integration to reach an optimal trade-off over artifacts, spatial resolution and noise.

# METHOD AND MATERIALS

Under the framework of sampling on lattice, the data acquisition in CT with detector cell interlacing and focal spot flying is simulated and analyzed on the reciprocal lattice in the frequency domain. With deliberately designed spherical, tungsten wire and thin foil phantoms, tomographic images are reconstructed using the FDK algorithm to evaluate the efficacy of detector cell interlacing and focal spot flying, respectively, in suppressing aliasing (windmill) artifact and maintaining cross-plane and in-plane spatial resolution. Furthermore, the efficacy in suppressing artifacts and maintaining spatial resolution by combination of the detector cell interlacing and focal spot flying is also thoroughly investigated.

### RESULTS

The preliminary data shows that both detector cell interlacing and focal spot flying can effectively suppress the aliasing (windmill) artifacts in MDCT/CBCT both helical/spiral and axial MDCT/CBCT. It is also found that the former outperforms the latter significantly in artifacts suppression. Moreover, the combination of detector interlacing and focal spot flying can offer even better efficacy in suppressing the aliasing (windmill) artifacts and performance in maintaining the spatial resolution and its uniformity.

### CONCLUSION

As technical options, detector cell interlacing outperforms focal spot flying in suppression of aliasing (windmill) artifacts and maintaining spatial resolution and it uniformity. A combination of the two techniques outperforms each of them individually.

## **CLINICAL RELEVANCE/APPLICATION**

The preliminary results presented in this study provide information for the clinical community to better understand the technical solutions that may be available in state-of-the-art MDCT/CBCT and thus optimize the protocols in their clinical practice.



## QI010-EB-TUB

A Collaborative Approach to Reducing Potential Cross-Contamination in Nuclear Medicine Department Restrooms

Tuesday, Nov. 27 12:45PM - 1:15PM Room: QR Community, Learning Center Hardcopy Backboard

# Participants

Moshe Grossman, MD, Philadelphia, PA (*Presenter*) Nothing to Disclose Sean Maratto, MD, Philadelphia, PA (*Abstract Co-Author*) Nothing to Disclose Tanya Weston, Philadelphia, PA (*Abstract Co-Author*) Nothing to Disclose Karen Rosenspire, MD,PhD, Philadelphia, PA (*Abstract Co-Author*) Nothing to Disclose

#### For information about this presentation, contact:

Moshe.grossman@uphs.upenn.edu

## PURPOSE

Detail how a collaborative interdepartmental approach with a systematic analysis of potential harmful waypoints can lead to successful decrease of radioactivity contamination levels in a Nuclear Medicine practice with the addition of Hands-Free utilities and altered water pressure.

### **METHODS**

We systematically reviewed every waypoint in a patient's journey through the Nuclear Medicine department to attempt to reduce potential sources of radioactive exposure to patients and healthcare workers. After identifying the department restrooms as sources of radioactive contamination, we began collecting data on the extent of cross contamination on commonly contacted surfaces in the departmental restrooms. While bathrooms are not an area under mandated regulation of radioactivity levels, we wanted to take a quality assurance approach to evaluate the extent of contamination and identify solutions under the principles of ALARA. Our first step was designed to provide data to prove that there was significant radioactivity within the restrooms of the nuclear medicine department restrooms due to urinary excretion of nuclear medicine radiotracers. It was felt that a data driven approach would allow the various hospital teams involved in the project to best reduce potential cross contamination. We established a threshold for significant radioactivity using the measurements and critical radioactive thresholds in designated examination rooms and nuclear medicine work rooms (>200 cpm above background). Over the course of a month, we obtained radioactive contamination measurements of commonly contacted surfaces in the nuclear medicine and PET/CT bathrooms from the door handle, light switch, faucet, soap dispenser, floor, flush handle, and toilet seat (using the usual swipe testing technique). With the technical assistance of the hospital engineering department and environmental services department, a remediation plan was made that included the installation of motion sensor based light switch, automatic toilet flusher, automatic soap dispenser, and hands-free sink faucet. Additionally, we added disposable toilet seat covers and decreased the flush pressure of the toilets by approximately 30% in an effort to decrease the splash effect. We re-evaluated for surface radioactive contamination on the same surfaces and assessed for change in contamination levels.

# RESULTS

Prior to the Hands-Free conversion, the number of days of critical radioactive thresholds was determined in each bathroom on the door handle, light switch, faucet, soap dispenser, floor, flush handle, toilet seat and repeated after conversion as shown in the graphs below. While it is difficult to completely resolve surface contamination, there were significant improvements on all surfaces overall. After the conversion, the number of days of critical contamination for each surface decreased by 25-100%.

## CONCLUSION

Including multiple teams on a quality improvement project that involves capital improvements and expenditures within the hospital system can be a challenge. We describe a possible method for improving cooperation from various teams within the hospital system by using a systematic approach to first identify areas of potentially harmful radioactivity within the department and then utilizing data driven quality assurance approach to gain cooperation from hospital administration, environmental services, and hospital engineers. We have demonstrated that eliminating the requirement of hand contact with bathroom surface fomites and decreasing 'splash back' from powerful water flushing that there is a potential to decrease and/or actually eliminate the risk of inadvertent radioactivity transfer in keeping with ALARA.



# QI117-ED-TUB1

## **Reducing Extrinsic Distractions to Radiologists Under Mounting Pressure**

Tuesday, Nov. 27 12:45PM - 1:15PM Room: QR Community, Learning Center Station #1

### **Participants**

Jonathan Dunbar, BMBS, Southampton, United Kingdom (*Presenter*) Nothing to Disclose Peter Jarvis, MBBS, Bournemouth, United Kingdom (*Abstract Co-Author*) Nothing to Disclose Ganesh Vigneswaran, PhD, MBBS, Southampton, United Kingdom (*Abstract Co-Author*) Nothing to Disclose Rania E. Zaher, BMBCh, Southampton, United Kingdom (*Abstract Co-Author*) Nothing to Disclose Richard J. Hughes, MBChB, Southampton, United Kingdom (*Abstract Co-Author*) Nothing to Disclose Howard D. Portess, MBBCh, Southampton, United Kingdom (*Abstract Co-Author*) Nothing to Disclose

## For information about this presentation, contact:

Ganesh.vigneswaran@uhs.nhs.net

# PURPOSE

To reduce the number and duration of phone call interruptions by 50% to radiologists in the general and cardiothoracic radiology reporting rooms over a 6 months period.

### METHODS

Background The radiology reporting room has numerous extrinsic distracters, one of which is a high volume of phone calls. Some of these phone calls could potentially be avoided1-2. Recent studies have shown that interruptions to reporting radiologists increase the incidence of errors3. Reducing the number of inappropriate calls (wrong number) would decrease interruptions and potential reporting/protocol errors and increase productivity, thereby improving patient safety. Method The stakeholders identified included patients, radiologists, radiographers, junior doctors and switchboard. Discussion with a number of stakeholders revealed problems contacting the correct specialty radiologist to discuss and organise scans. Discussion with senior radiologists revealed concerns regarding distractions caused by multiple avoidable phone calls. Driver diagrams were created to identify possible interventions and a PDSA cycle was used for this quality improvement project. We collected baseline and post-intervention data over two 4-hour morning/afternoon periods in the general and cardiothoracic radiology reporting rooms, respectively, over a 6 month period to account for baseline variation over time. Outcome measures included the number and duration of all calls. These were correlated with switchboard call logs. Inappropriate calls were defined as the incorrect number dialled for the subtype of radiologist, for example, calling the abdominal radiologist for a CT chest request. Intervention We used a freely available online hospital phone directory application (induction app) for smart phones. This was updated with correct contact details, then promoted at a grand round to the medical trainees (primary stakeholder).

# RESULTS

(figure 1) Inappropriate calls were of a shorter duration (0.9 mins) compared with appropriate calls (1.4 mins, p=0.02), this was unchanged after intervention. General radiology reporting room: Prior to intervention there were a total number of 78 calls over 2 sessions. 17 calls were inappropriate, which lasted a total duration of 22.4 minutes (average 0.9minutes per call). Following intervention there were 88 total calls (13% increase). However, there were 13 fewer inappropriate calls (76% reduction,  $\chi$ 2= 11.1, p < 0.01). Overall this resulted in a 20.7-minute reduction in inappropriate call duration (92% reduction). Cardiothoracic reporting room: Prior to intervention there were a total number of 34 calls over 2 sessions. 19 calls were inappropriate, which lasted a total duration of 6.5minutes (average duration = 0.5minutes). Following intervention there were 18 total calls (47% reduction). There were 7 fewer inappropriate calls (37% reduction,  $\chi$ 2=0.57, p = 0.45). Overall this resulted in a 1.4 minutes reduction in inappropriate call duration (22% reduction) in appropriate call difference in average call duration, with no significant difference in call duration pre or post intervention for both appropriate and inappropriate calls (p>0.05).

#### CONCLUSION

Introducing and updating the directory of an online Smartphone application is a simple and effective way to reduce interruptions to reporting radiologists. We demonstrated a significant reduction in the number and duration of inappropriate calls to the general radiology reporting room surpassing our aim of a 50% reduction. We saw a reduction in the number of inappropriate calls to the cardiothoracic radiology department; however the relative proportion of inappropriate calls was not significantly reduced. This may be explained by inadequate promotion of the induction app to the cardiothoracic team who do not attend the general medical grand round. We are currently performing our second cycle (April 2018), with a focus on the cardiothoracic department. In this, we will further promote the updated induction app to other stakeholders through the use of posters and electronic correspondence. Our driver diagram also indicated further areas to target to reduce distraction including inappropriate GFR queries from radiologists and reduce reporting error. This simple, yet effective intervention can be also used by other clinical teams to improve multi-disciplinary communication and thus patient safety. References 1. Busby LP, C. J. (2018). Bias in Radiology: The How and Why of Misses and Misinterpretations. Radiographics , 236-247. 2. Schemmel A, L. M. (2016). Radiology Workflow Disruptors: A Detailed Analysis. Journal of the American College of Radiology , 1210-1214. 3. Balint BJ, S. S. (2014). Do telephone call interruptions have an impact on radiology resident diagnostic accuracy? Academic Radiology , 1623-8.



# QI119-ED-TUB2

Hypnosis as an Alternative to Pharmacologic Sedation in MR: An Initial Experience with Claustrophobic Patients

Tuesday, Nov. 27 12:45PM - 1:15PM Room: QR Community, Learning Center Station #2

# Participants

Nicole Ferrera Espinosa, Arogno, Switzerland (*Presenter*) Nothing to Disclose Emanuele Pravata, MD, Rome, Italy (*Abstract Co-Author*) Nothing to Disclose Filippo Del Grande, MD, Lugano, Switzerland (*Abstract Co-Author*) Speaker, Siemens AG; Speaker, Bayer AG; Institutional research collaboration, Siemens AG;

For information about this presentation, contact:

nicole.ferrera@bluewin.ch

# PURPOSE

Claustrophobia during magnetic resonance (MR) is a regular problem in our clinical practice. Although the number of claustrophobic patients is relatively small, such patients generally have a major impact on clinical workflow, requiring pharmacologic sedation by an anesthesiologist during the MR exam. Sedation has potentially undesirable side effects, is relatively expensive and difficult to integrate in the daily workflow. Our aim was to assess the feasibility and impact of medical hypnosis on our daily practice as an alternative to pharmacologic sedation in obtaining diagnostic images in claustrophobic patients undergoing MRI.

#### METHODS

As a quality improvement project no authorization of our local ethical committee was required. Our project started in December 2015 and ended in March 2018. During this period we proposed medical hypnosis to 61 claustrophobic patients undergoing MR. After exam scheduling, every patient was directly contacted by the physician specialized in hypnotherapy who explained the procedure and asked for patient agreement for hypnosis. A preliminary session to experience a trance prior to the MR was then proposed. The day of MR exam the physician induced a hypnotic trance outside the MR room and accompanied the patient during the entire MR exam. We assessed the percentage of success of hypnosis in these patients defined as the percentage of patients having completed the MR exam with diagnostic images (based on the radiologist's report). Furthermore, we assessed the length and the costs of the MR with hypnosis and patient satisfaction after the completion of the procedure.

# RESULTS

We selected 61 patients with claustrophobia who required an MR exam for diagnostic purposes. Out of these patients, 3 refused to participate. Of the remaining 58 patients, 9 (15%) had previously been subjected to an MR with pharmacologic sedation; 27 (46%) were previously unable to complete a close bore MR exam due to claustrophobia; 14 (24%) refused to undergo an MR without sedation; and 9 (15%) had contra-indication to pharmacologic sedation due to the type of MR exam. In total, 52 (90%) patients completed the MR. The image quality was diagnostic in all of these cases (100%). The length of the exam was on average 10 minutes longer than a standard MR, as compared to an average of 20-30 additional minutes for an MR with pharmacologic sedation. Costs were approximately 160-200 USD for hypnosis and 370-410 USD for pharmacologic sedation, respectively. After having completed the MR under hypnosis, we observed notable patient satisfaction and self-empowerment, a feature particularly useful for those suffering from chronic disease.

# CONCLUSION

According to our preliminary experience medical hypnosis is an interesting alternative to pharmacologic sedation in claustrophobic patients undergoing MR. Hypnosis can easily be integrated in the clinical workflow and limit costs compared to pharmacologic sedation. Furthermore, medical hypnosis seems to enhance patients' self-empowerment, a characteristic that is particularly useful in chronic disease. Further scientific studies are needed to assess the validity of hypnosis in selected patients undergoing an MR.



# QI121-ED-TUB3

Streamlined Pancreatic Cyst Evaluation on MRI Abbreviated Protocol (SPaCEMAP) - Reducing Waiting Times in a General Hospital Setting

Tuesday, Nov. 27 12:45PM - 1:15PM Room: QR Community, Learning Center Station #3

## Participants

Gideon Ooi, MBBS, Singapore, Singapore (*Abstract Co-Author*) Nothing to Disclose Colin Tan, MBBS, Singapore, Singapore (*Abstract Co-Author*) Nothing to Disclose Sook Chuei Cheong, MD, Singapore, Singapore (*Abstract Co-Author*) Nothing to Disclose Jeffrey Fong, FRCR, MBBS, Singapore, Singapore (*Presenter*) Nothing to Disclose

For information about this presentation, contact:

gideonooi@gmail.com

## PURPOSE

Pancreatic cysts (PC) are common incidental findings picked up during routine Computed Tomography (CT) or Magnetic Resonance Imaging (MRI) examinations. Many are not characterisable initially and need follow up. In some cases these may turn out to be malignant and early pick-up allows early intervention, improving overall outcomes. Patients often need repeated MRI imaging to assess for interval changes or high risk stigmata. Nonetheless, standard MRI protocols for surveillance in this specific group of patients prove time-consuming and expensive, resulting in prolonged waiting times for MRI appointments for patients with other more urgent problems. We aim to achieve a 50% reduction in MRI scan acquisition time for a patient attending for follow-up of a known pancreatic cystic lesion. The project will be implemented using the Plan-Do-Study-Act cycle within a six-month time frame.

### **METHODS**

The Quality Improvement project was carried out in Changi General Hospital's Radiology Department which houses over 1000 beds caring for a community of 1.4 million people in eastern Singapore. After evaluating the various factors possibly resulting in prolonged waiting times for outpatient MRI appointments, we decided to streamline our MRI scanning protocols for surveillance of known PC (see Figure 1). A qualitative study was performed involving attending body-imaging radiologists regarding their perception on the most important imaging sequences for diagnosis in follow up of known PC. Several abbreviated MRI protocols for such clinical contexts were also obtained during a literature review. We then conducted a pilot study utilising retrospectively obtained scans performed for 30 consecutive patients who presented for PC follow up between January 2015 and July 2017. The scans were prepared into two sets, the first containing the full set of images, and in the second set only images in an abbreviated protocol were present. Two attending radiologists then read the images from the two sets separately and scored the adequacy of images for diagnosis using a self-administered survey form (see Figure 2). They were also asked to rate the effectiveness of specific sequences in diagnosis within this clinical context. Findings from the qualitative survey were analysed using Statistical Package for Social Sciences (SPSS).

## RESULTS

All MRI examinations were performed on the Siemens MAGNETOM Aera (1.5 Tesla) machine. The original full protocol (FP) included coronal T2 HASTE, axial T2 HASTE, axial T2 Fat-saturation (FS), axial T1 in-and-out of phase, axial diffusion-weighted imaging (DWI), pre-contrast axial VIBE, dynamic post-contrast axial VIBE, delayed post-contrast axial VIBE, coronal SPACE 3D (see Figure 3). The short protocol (SP) omitted use of intravenous gadolinium-based contrast agent and consists only of axial T1 in-and-out of phase, coronal T2 HASTE, axial T2 HASTE, axial VIBE, coronal SPACE 3D sequences (see Figure 4). The abbreviated scan protocol omitted contrast-enhanced sequences and reduced overall scan times by 53.6%, from a mean of 17 minutes and 22 seconds to 8 minutes and 3 seconds. Calculated potential cost savings may be up to S\$372 per scan per patient, given the shorter scan time and omission of contrast agent. Using the FP, radiologists rated their confidence in verifying the scan at a mean score of 7.95 out of 9, while their diagnostic confidence averaged 7.67 on the short protocol (SP) with no statistically significant difference (t-test p<0.05). Radiologists deemed that the SP is sufficient in assessment of interval change with a median score of 8 (mean 7.92). The radiologists perceived that, on average, in 89.7% of cases a post-contrast T1 weighted sequence did not add value to the diagnosis in this clinical context, compared with 82.7% for volumetric T2-weighted MRCP sequence and 96.6% for T1 weighted in-and-out of phase sequences. No additional finding was detected in the omitted sequences that could not be detected in the SP.

### CONCLUSION

The pilot study reveals that evaluation of known pancreatic cystic lesions can be adequately performed on a shortened MRI protocol with no statistically difference in the diagnostic confidence it accords radiologists. Benefits of a shortened protocol includes shortened scan times, reduced cost of examination and potentially improved patient safety as we have omitted the use of gadolinium-based contrast agent. We have started the shortened protocol for routine examination in patients with known pancreatic cystic lesions and will continue to monitor the diagnostic accuracy and confidence it accords the reporting radiologists with regular audits.



# QI123-ED-TUB4

Tailoring Reports to Clinicians' Needs: Use of Structured Templates to Categorize Intracranial Metastases Treated with Stereotactic Radiosurgery

Tuesday, Nov. 27 12:45PM - 1:15PM Room: QR Community, Learning Center Station #4

# Participants

John C. Benson, MD, Saint Paul, MN (*Presenter*) Nothing to Disclose Matthew Burgstahler, Collegeville, MN (*Abstract Co-Author*) Nothing to Disclose Lei Zhang, MS, Minneapolis, MN (*Abstract Co-Author*) Nothing to Disclose Matthew Rischall, MD, Minneapolis, MN (*Abstract Co-Author*) Nothing to Disclose

For information about this presentation, contact:

Benso905@umn.edu

## PURPOSE

Stereotactic radiosurgery is a well-tolerated therapy for intracranial metastatic disease due to localized dose, allowing for multiple treatments of new and recurrent disease over time. The number and location of previously treated metastatic lesions often presents a record keeping challenge for the radiologist on follow up MR imaging, especially enhancing lesions that resolve temporarily and then reappear at a later date. Due to the burden of imaging comparison and historical detail required to interpret these examinations, radiology reports may rely on nonspecific descriptive language that does not fully characterize treatment response and address the needs of referring physicians. The purpose of this study was to improve the quality of radiology reports in patients previously treated with stereotactic radiosurgery through increasing lesion characterization by creating and disseminating a structured report template that requires categorization of enhancing lesions into one of three discrete categories: 1) (presumed) new metastases, 2) treated metastases, or 3) indeterminate, may represent increased tumor size versus radiation necrosis.

# METHODS

Following the initiation of the structured template, a retrospective review was completed of examinations of patients with intracranial metastases that underwent radiotherapy: "pre-template" reports completed between 1/1/2017 and 11/10/2017, and "post-template" reports completed between 11/21/2017 and 2/26/2018. Reports were assessed for definitive versus nonspecific descriptions of lesions: "(presumed) new metastases," defined as new enhancing lesions remote from treatment site(s), "treated metastases," defined as stable or decreased size of previously treated lesions, and "indeterminate lesions," defined as enlarged size of previously treated lesions, and "indeterminate lesions," defined as enlarged size of previously treated lesions necrosis. Nonspecific language was subdivided based on the type of lesion(s) it was used to describe: e.g. "stable enhancing foci" was deemed a nonspecific description of "treated metastases" as it neither addressed the presence of malignancy nor the prior treatment, and "increased size of metastasis" was deemed nonspecific as it failed to raise the possibility of radiation necrosis.

#### RESULTS

139 patients were included in the cohort; 88 female (63.3%). 94 patients (67.6%) were imaged prior to the structured template implementation ("pre-template"), and 45 (32.4%) were imaged afterwards ("post-template"). Nonspecific descriptions of were used in 25/94 reports (26.6%) pre-template, and in 8 reports (17.8%) post-template. Of the lesion types, "indeterminate lesions" were inappropriately described most commonly (13/32 reports pre-template (40.6%), and 6/20 reports post-template (30.0%)), followed by "treated metastases" (13/74 reports pre-template (17.6%), and 2/32 reports post-template (6.3%)); no inappropriate descriptions of "new metastases" were noted. Following the dissemination of the structured template, 27/45 of the reports (60.0%) used the template; the rest of the reports were written using semi-standardized or free-prose text. No significant difference was found in the overall number of inappropriate/ambiguous descriptions of intracranial lesions following the initiation of the template (p=0.52). However, of the reports that used the structured template following its initiation, significantly less ambiguous descriptions of lesions was noted (p=0.02).

## CONCLUSION

When utilized, a structured report template results in decreased nonspecific description and improved definitive characterization of intracranial metastatic disease in patients treated with stereotactic radiosurgery. However, no difference was found between overall rate of nonspecific language usage before and after the template initiation, likely related to limited radiologist compliance with template utilization.



# RO216-SD-TUB1

Long-Term Outcome of Low-Dose Rate Brachytherapy with I-125 Seeds as a Monotherapy for High-Risk Prostate Cancer Patients: A Propensity Score-Matched Analysis

Tuesday, Nov. 27 12:45PM - 1:15PM Room: RO Community, Learning Center Station #1

## Participants

Takashi Kawanaka, MD, PhD, Tokushima, Japan (*Presenter*) Nothing to Disclose Akiko Kubo, MD, Tokushima, Japan (*Abstract Co-Author*) Nothing to Disclose Shunsuke Furutani, Tokushima, Japan (*Abstract Co-Author*) Nothing to Disclose Chisato Tonoiso, MD, Tokushima, Japan (*Abstract Co-Author*) Nothing to Disclose Hitoshi Ikushima, MD, Tokushima, Japan (*Abstract Co-Author*) Nothing to Disclose Masafumi Harada, MD, PhD, Tokushima, Japan (*Abstract Co-Author*) Nothing to Disclose

#### PURPOSE

The aims of this study is to report long-term outcome of patients treated with I125 low-dose-rate brachytherapy (LDR-BT) as a monotherapy for high-risk prostate cancer with a minimum five years follow-up after the LDR-BT using a propensity score-matched analysis

### **METHOD AND MATERIALS**

A group of 498 patients with clinically localized prostate cancer treated with I125 LDR-BT between July 2004 and October 2012 at our University Hospital were identified. Of the 498 patients, 223 (44.8%) had low-risk disease, 205(41.2%) had intermediate-risk disease, 70 (14.1%) patients had high-risk disease. Cohorts were categorized according to D'Amico's risk classification, and biochemical outcomes plus overall survival were examined. Biochemical failure was defined as nadir prostate-specific antigen (PSA) level + 2 ng/mL. A propensity score matching analysis (PSM) was performed using a logistic regression for high-risk patients.

### RESULTS

A total of 498 patients met the criteria with a median follow-up of 107 months (range 18-158 months). The median age was 67.5 years (range 49-82) at the time of treatment. The 5- and 10-year biochemical failure-free survival rates were 100 and 98.7% for low-risk group, 95.2 and 93.0% for the intermediate-risk group 84.3 and 81.8% for the high-risk group, respectively. Under the PSM of the 70 high-risk patients, age during 65 to 75 years group has significant superior biochemical failure-free survival rates compare to another age group (93.3 vs. 75.0% at five years, p=0.04). Treatment age, D90, V100, hormonal therapy and count of a high-risk factor were associated with biochemical failure-free survival on univariate analysis in a high-risk group. Additionally treatment age, hormonal therapy and D90 were associated with biochemical failure-free survival in multivariate models.

### CONCLUSION

This study shows that LDR-BT monotherapy has acceptable cancer control even in high-risk prostate cancer patients with proper treatment technic and patient selection under PSM.

# **CLINICAL RELEVANCE/APPLICATION**

LDR-BT monotherapy has acceptable cancer control even in high-risk prostate cancer patients with proper treatment technic and patient selectio.



## RO217-SD-TUB2

The Diagnostic Value of Intravoxel Incoherent Motion Diffusion Weighted Imaging in Different Pathological Types of Cervical Carcinoma in 3.0T MRI

Tuesday, Nov. 27 12:45PM - 1:15PM Room: RO Community, Learning Center Station #2

FDA Discussions may include off-label uses.

### Participants

Dong Jiangning, Hefei, China (Presenter) Nothing to Disclose

# For information about this presentation, contact:

dongjn@163.com

### PURPOSE

To explore the diagnostic value of the parameters of the intaravoxel incoherent motion diffusion-weighted imaging in 3.0T magnetic resonance imaging for different pathological histological types of cervical carcinoma.

### **METHOD AND MATERIALS**

A retrospective analysis of 101 cases of cervical carcinoma confirmed by surgery and pathology in our hospital, including11 cases of cervical adenocarcinoma(Fig A1-A7), 87 cases of cervical squamous cell carcinoma(Fig B1-B7)and 3 cases of cervical small cell carcinoma(Fig C1-C7). Intravoxel incoherent motion diffusion-weighted imaging was performed by using 10b values (b=0,10,20,50,100,200,400,800,1200,2000s/mm2). The Statistical analysis software SPSS 22.0 was used to statistically analyze the differences between different types of cervical cancer. The receiver operating characteristic (ROC) curve was used to evaluate IVIM-DWI related parameters for diagnostic the efficiency of different types of cervical cancer.

### RESULTS

The ADCstand, D, D\* and f values of cervical squamous cell carcinoma were respectively  $0.73\pm0.11$ )×10-3mm2/s, $(0.53\pm0.12)$ ×10-3mm2/s,(10.84,9.60)×10-3mm2/s,(0.31,0.18); The ADCstand, D, D\* and f values of cervical adenocarcinoma were respectively  $(0.92\pm0.26)$ ×10-3mm2/s, $(0.74\pm0.11)$ ×10-3mm2/s,(8.67,7.64)×10-3mm2/s,(0.35,0.13); The ADCstand, D, D\* and f values of cervical small cell carcinoma were respectively  $(0.52\pm0.070)$ ×10-3mm2/s, $(0.41\pm0.084)$ ×10-3mm2/s,(16.13,8.87)×10-3mm2/s, (0.28,0.049), the comparison of the ADCstand and D value was statistically significant (P < 0.05), and the comparison between D\* and f value was not statistically significant (P = 0.185 and 0.209). The cutoff values of ADCstand and D of cervical adenocarcinoma and cervical squamous cell carcinoma was 0.75×10-3mm2/s and 0.66×10-3mm2/s, and the sensitivity, specificity and the area under the curve were 59.8%, 100%, 0.812, 88.5%, 90.9% and 0.929. The cut off values of ADCstand and D for identifying cervical squamous cell carcinoma and cervical small cell carcinoma were respectively 0.61×10-3mm2/s, and 0.49×10-3mm2/s, the sensitivity, specificity and the area under the curve were 90.8%, 100%, 0.962, 65.5%, 100% and 0.807.

## CONCLUSION

The ADCstand, D values of IVIM-DWI related parameters have better diagnostic value for different pathological types of cervical cancer.

## **CLINICAL RELEVANCE/APPLICATION**

It can provide non-invasive and quantitative molecular imaging basis for the individual treatment of cervical cancer.



# RO218-SD-TUB3

Evaluation in Correlation of Magnetic Resonance Diffusion Kurtosis Imaging and AQP Expression in Esophageal Carcinoma

Tuesday, Nov. 27 12:45PM - 1:15PM Room: RO Community, Learning Center Station #3

# Participants

Yanfei Wang, Shijiazhuang, China (*Abstract Co-Author*) Nothing to Disclose Gaofeng Shi, MD, Shijiazhuang, China (*Abstract Co-Author*) Nothing to Disclose Andu Zhang, Shijiazhuang, China (*Abstract Co-Author*) Nothing to Disclose Ruxun Li, Shijiazhuang, China (*Abstract Co-Author*) Nothing to Disclose Li Yang, MD, Shijiazhuang, China (*Abstract Co-Author*) Nothing to Disclose Hui Feng, Shijiazhuang, China (*Abstract Co-Author*) Nothing to Disclose Xiaohui Qi, MD, Shijiazhuang, China (*Abstract Co-Author*) Nothing to Disclose Tongxin Xu, Shijiazhuang, China (*Presenter*) Nothing to Disclose

#### For information about this presentation, contact:

feinier\_1989@sina.com

### PURPOSE

To investigate the expression of AQP expression in mice models with esophageal cancer xenografts before and during radiotherapy and to evaluate whether the AQP levels correlate with magnetic resonance diffusion kurtosis imaging (MR-DKI) values.

### **METHOD AND MATERIALS**

There were 84 Eca-109 nude mice models with esophageal cancer xenogrfts before and during radiotherapy (test group=42; control group=42) used in this study. Seven time points for testing AQP expression and evaluating MR-DKI values selected at 1 day before radiotherapy, and at 1st, 3rd, 5th, 7th, 15th, and 29th days during the radiotherapy. Real-time fluorescence quantitative PCR (RT-PCR) and Western blot were tested the expression of AQP3 levels in the transplanted esophageal carcinoma. The correlation of AQP3 expression and MR-DKI values (using ADC, MK, and MD values) was analyzed and compared.

### RESULTS

AQP3 protein levels showed that there was no significant difference at the 1st day before radiotherapy  $(0.30\pm0.06 \text{ and } 0.30\pm0.06)$ , at the 1st day after radiotherapy  $(0.30\pm0.10 \text{ and } 0.34\pm0.13)$ , and at the 29th day  $(0.26\pm0.02 \text{ and} 0.28\pm0.03)$  after radiotherapy (P=0.868, 0.337, 0.228), between test and control groups. There were statistically significant differences in levels of AQP3 protein at the 3rd  $(0.28\pm0.03 \text{ and } 0.35\pm0.06)$ , 5th  $(0.26\pm0.07 \text{ and } 0.37\pm0.08)$ , 7th  $(0.23\pm0.08 \text{ and } 0.36\pm0.08)$ , and 15th  $(0.24\pm0.03 \text{ and } 0.31\pm0.03)$  days after radiotherapy between the two groups (P<0.05). AQP3 gene expression levels were negatively correlated with the MR-DKI ADC value and MD value whereas were positively correlated with the MR-DKI MK value (all P<0.05).

### CONCLUSION

Esophageal cancer in animal models before radiotherapy and during radiotherapy or during non-radiotherapy showed significantly different in expression of AQP3 levels correlated with MR-DKI values. The MR-DKI imaging values may reflect the tumor sensitivity for radiotherapy and may help to manage patient treatment.

## **CLINICAL RELEVANCE/APPLICATION**

(dealing with MR-DKI) 'Esophageal cancer in animal models before radiotherapy and during radiotherapy or during non-radiotherapy showed significantly different in expression of AQP3 levels correlated with MR-DKI values. The MR-DKI imaging values may reflect the tumor sensitivity for radiotherapy and is recommended in helping to manage patient treatment.'



### RO219-SD-TUB4

Hybrid Regularization in Sliding Organ Motion Correction for Motion-Compensated (MoCo) Cone-Beam CT (CBCT)

Tuesday, Nov. 27 12:45PM - 1:15PM Room: RO Community, Learning Center Station #4

**FDA** Discussions may include off-label uses.

#### **Participants**

Shaohua Zhi, Xian, China (*Abstract Co-Author*) Nothing to Disclose Marc Kachelriess, PhD, Heidelberg, Germany (*Presenter*) Nothing to Disclose Xuanqin Mou, Xian City, China (*Abstract Co-Author*) Nothing to Disclose

### For information about this presentation, contact:

zhishaohua.1203@stu.xjtu.edu.cn

## PURPOSE

To develop an algorithm to suppress the non-physiological motion, due to the discontinuous movements in the proximity of lung borders for motion-compensated (MoCo) cone-beam volumetric images while maintaining features in the static regions.

## METHOD AND MATERIALS

Respiratory motion leads to blurred-artifacts in CBCT scans, which as a result, will influence the accuracy of design of treatment planning in radiation therapy. While the artifact model-based cyclic motion compensation (acMoCo) algorithm [Brehm et al., MedPhys 40(10)] estimates motion vector fields (MVFs) between different respiratory phases, there is still room for reducing the estimation errors especially at the boundaries of sliding organs. The proposed method utilizes the acMoCo results as an initialization to extract motion features by robust principal component analysis (RPCA) and then generates a set of phase-resolved images combined with 3D-FDK reconstruction from the entire projection data as a prior, which incorporates knowledge of static features. The intermediate images are then incorporated into the iterative reconstruction framework to minimize the inconsistency of the corresponding rawdata. We tested the performances of the proposed method on patient data of three radiation therapy patients scanned with the CBCT of a Varian True Beam System.

#### RESULTS

The proposed method proved to be effective to reduce physiologically incorrect motion in the region of ribs and spine in visual evaluation. While spatial resolution is somewhat lower than in the original acMoCo reconstructions the motion patterns appear to be more consistent with the expected patterns.

#### CONCLUSION

The proposed RPCA-guided acMoCo approach successfully suppresses the non-physiological ribs and spine movements in patient data, without relying on segmentation.

## **CLINICAL RELEVANCE/APPLICATION**

A correct estimation of the tumor motion can significantly improve the accuracy of treatment planning in radiation therapy.



## UR185-ED-TUB7

Follow the Stream: Imaging of Urinary Tract Augments, Reconstructions, and Non-Cystectomy Diversions in Adult Patients

Tuesday, Nov. 27 12:45PM - 1:15PM Room: GU/UR Community, Learning Center Station #7

## Participants

Ryan D. Clayton, MD, Richmond, VA (*Presenter*) Nothing to Disclose Laura R. Carucci, MD, Richmond, VA (*Abstract Co-Author*) Nothing to Disclose Lauren Moomjian, MD, Richmond, VA (*Abstract Co-Author*) Nothing to Disclose Georgi Guruli, MD, Richmond, VA (*Abstract Co-Author*) Nothing to Disclose Adam Klausner, Midlothian, VA (*Abstract Co-Author*) Nothing to Disclose

# **TEACHING POINTS**

1) Gain working understanding of surgical procedures, including bladder augments, reconstructions and non-cystectomy diversions. 2) Recognize expected postoperative radiologic appearance of the above procedures 3) Recognize the imaging findings of complications including leaks, fistulas, abscess, mucus formation, stones, and obstruction.

## TABLE OF CONTENTS/OUTLINE

1) Briefly review indications for bladder augments, reconstructions and non-cystectomy urinary diversions. 2) Review the surgical procedures: Augments Reconstructions Non-Cystectomy Diversions 3) Discuss radiologic evaluation and imaging techniques - expected imaging findings 4) Describe the imaging findings of complications: leak, fistula, abscess, mucus formation, stones, obstruction



## UR186-ED-TUB8

## Tomographic Findings and Management in Renal Trauma: An Interactive Approach

Tuesday, Nov. 27 12:45PM - 1:15PM Room: GU/UR Community, Learning Center Station #8

#### **Participants**

Bernardo S. Oliveira, MD, Sao Paulo, Brazil (*Presenter*) Nothing to Disclose Camila C. Tavares, MD, Sao Paulo, Brazil (*Abstract Co-Author*) Nothing to Disclose Guilherme O. Rego, MD, Sao Paulo, Brazil (*Abstract Co-Author*) Nothing to Disclose Marcio V. Nastri, MD, Sao Paulo, Brazil (*Abstract Co-Author*) Nothing to Disclose Shri Krishna Jayanthi, MD, Sao Paulo, Brazil (*Abstract Co-Author*) Nothing to Disclose Natally Horvat, MD, Sao Paulo, Brazil (*Abstract Co-Author*) Nothing to Disclose Julia A. Miranda, MD, Sao Paulo, Brazil (*Abstract Co-Author*) Nothing to Disclose Publio C. Viana, MD, Sao Paulo, Brazil (*Abstract Co-Author*) Nothing to Disclose

### For information about this presentation, contact:

salgado.bernardo@gmail.com

### **TEACHING POINTS**

To review and illustrate tomographic findings after blunt and penetrating renal trauma. To highlight the complications that cannot go unnoticed. To test reader's knowledge about grading system and current management guidelines using a case-based approach.

### **TABLE OF CONTENTS/OUTLINE**

The kidney is the most commonly injured genitourinary organ in the setting of trauma. Some mechanisms raise suspicion of renal injury such as rapid deceleration or a direct blow to the flank, and haematuria is an indicator of urinary tract trauma. Computed tomography is the method of choice for evaluating blunt and penetrating renal injuries in stable patients. Renal trauma can be graduated based on tomographic findings in order to predict the need for intervention and to access prognostic information such as morbidity and mortality. Furthermore, new volume rendering techniques may improve radiological interpretation and help surgical management of complex renal injuries. Therefore, every radiologist must be aware of the possible complications after renal trauma in order to provide a report that fits the appropriate therapy.



### VI164-ED-TUB9

## Radiofrequency Ablation for Thyroid Nodules: Current Evidences and Future Perspectives

Tuesday, Nov. 27 12:45PM - 1:15PM Room: VI Community, Learning Center Station #9

### FDA Discussions may include off-label uses.

#### **Participants**

Eun Ju Ha, Suwon, Korea, Republic Of (*Presenter*) Nothing to Disclose Jung Hwan Baek, Seoul, Korea, Republic Of (*Abstract Co-Author*) Consultant, STARmed; Consultant, RF Medical

## For information about this presentation, contact:

radhej@naver.com

### **TEACHING POINTS**

1. Describe the basic concept of thyroid radiofrequency ablation (RFA) 2. Describe the basic and advanced techniques of thyroid RFA 3. Describe the updated clinical outcomes of thyroid RFA, in terms of benign thyroid nodules and recurrent cancers 4. Describe the possible complications and prevention methods of thyroid RFA

## TABLE OF CONTENTS/OUTLINE

1. Basic priciples of thyroid RFA 1-1. Basic principle of how RFA works 1-2. Indications 2. Basic and advanced techniques of thyroid RFA 2-1. Basic Techniques: moving-shot technique, trans-isthmic approach 2-2. Advanced Techniques: vasuclar ablation techniques for hypervascular tumors hydrodissection technique for recurrent thyroid cancers 3. Updated clinical outcomes of thyroid RFA 3-1. Treatment of benign thyroid nodules 3-2. Treatment of recurrent thyroid cancers 3-3. Others (primary thyroid cancer, parathyroid) 4. Possible complications and prevention methods of thyroid RFA 4-1. Nerve injury and prevention methods 4-2. Vessel injury and prevention methods 4-3. Others (nodule rupture, lidocain tonxicity, pain..) 5. Interesting cases



## VI165-ED-TUB10

Let It Flow: Endovascular Management of Vascular Complications Post-Liver Transplant

Tuesday, Nov. 27 12:45PM - 1:15PM Room: VI Community, Learning Center Station #10

#### **Participants**

Nicholas Voutsinas, MD, New York, NY (Presenter) Nothing to Disclose

Aaron M. Fischman, MD, New York, NY (*Abstract Co-Author*) Advisory Board and Consultant- Terumo Interventional Systems, Embolx Inc.; ; Speakers Bureau - Boston Scientfic, BTG; ; Royalties - Merit Medical; ; Investor - Adient Medical Edward Kim, MD, East Meadow, NY (*Abstract Co-Author*) Consultant, Koninklijke Philips NV Advisory Board, Onyx Pharmaceuticals, Inc Advisory Board, Sterigenics International LLC

Mona B. Ranade, MD, Brookfield, WI (Abstract Co-Author) Nothing to Disclose

Vivian L. Bishay, MD, Philadelphia, PA (Abstract Co-Author) Nothing to Disclose

Francis S. Nowakowski, MD, New York, NY (Abstract Co-Author) Nothing to Disclose

Robert A. Lookstein, MD, New York, NY (*Abstract Co-Author*) Consultant, Boston Scientific Corporation Consultant, Medtronic plc Rahul S. Patel, MD, New York, NY (*Abstract Co-Author*) Consultant, Sirtex Medical Ltd; Research Consultant, Medtronic plc; Consultant, Penumbra, Inc; Consultant, Terumo Corporation

#### For information about this presentation, contact:

nicholas.voutsinas@mountsinai.org

## **TEACHING POINTS**

1. Review normal vascular anatomy of the post-operative liver transplant patient and its multi-modality imaging appearance. 2. Discuss risk factors and clinical manifestations of vascular complications in liver transplant patients 3. Describe various endovascular techniques that can be used to manage and treat vascular complications in the post-liver transplant patients as alternatives to surgery and re-transplantation.

### **TABLE OF CONTENTS/OUTLINE**

1. Introduction a. Incidence and Indications for Liver Transplantation b. Surgical Technique 2. Normal Post-Surgical Vascular Anatomy a. Hepatic Artery b. Hepatic Vein c. Portal Vein 3. Imaging Modalities to Assess Liver Transplant Vascular Anatomy and Anomalies a. Liver Duplex Ultrasound b. CT Angiogram c. MR Angiogram d. Direct Angiography 4. Potential Complications and Endovascular Treatments a. Hepatic Artery • Stenosis->Angioplasty and Stenting • Thrombosis->Thrombectomy and Thrombolysis • Pseudoaneurysm->Coiling • Splenic Steal Syndrome->Embolization b. Portal Vein • Stenosis->Venoplasty and Stenting • Thrombosis->Thrombectomy and Thrombolysis • Recurrent Portal Hypertension->TIPS, Variceal Embolization c. Hepatic Vein • Stenosis->Venoplasty and Stenting • Thrombosis->Thrombectomy and Thrombolysis



## VI175-ED-TUB11

What Should Diagnostic Radiologists Know About Endoscopic Ultrasound-Guided Biliary Intervention?

Tuesday, Nov. 27 12:45PM - 1:15PM Room: VI Community, Learning Center Station #11

#### Awards Certificate of Merit Identified for RadioGraphics

#### **Participants**

Shunsuke Sugawara, Tokyo, Japan (*Presenter*) Nothing to Disclose Yasuaki Arai, Tokyo, Japan (*Abstract Co-Author*) Nothing to Disclose Miyuki Sone, MD, Tokyo, Japan (*Abstract Co-Author*) Speakers Bureau, Nippon Kayaku Co, Ltd; Speakers Bureau, DAIICHI SANKYO Group; Speakers Bureau, Canon Medical Systems Corporation; Masahiko Kusumoto, MD, Chuo, Japan (*Abstract Co-Author*) Nothing to Disclose Susumu Hijioka, Tokyo, Japan (*Abstract Co-Author*) Nothing to Disclose Yasunari Sakamoto, Tokyo, Japan (*Abstract Co-Author*) Nothing to Disclose

## **TEACHING POINTS**

Recently, endoscopic ultrasound (EUS)-guided biliary interventions are developing, and this technique allows extra-anatomical endoscopic biliary drainage and stent placement. The teaching points of current presentation is following. 1. Showing what endoscopists can do with EUS-guided biliary intervention. 2. Demonstrating type of biliary obstruction correlating to indication of EUS-guided biliary intervention. 3. Explaining tips of interpreting images before EUS-guided biliary intervention. 4. Learning what may happen after EUS-guided biliary intervention.

### **TABLE OF CONTENTS/OUTLINE**

1. Introduction A) Representative technique of EUS-guided biliary intervention B) Comparison with percutaneous biliary intervention 2. Type of biliary obstruction and indication of EUS-guided biliary intervention A) Bismuth classification B) Indication and contraindication 3. Evaluation of preoperative images A) Basic knowledge of anatomy and anomaly of biliary tree B) Relationship of gastrointestinal tract and biliary tree C) Pathological findings influencing EUS-guided biliary intervention 4. Assessment of images after EUS-guided biliary intervention A) Position and direction of placed stent B) Condition of intrahepatic bile duct C) Complications related to EUS-guided biliary intervention 5. Case presentations



## VI233-SD-TUB1

The Early Evaluation of Carotid Arterial Elasticity in Patients with Prediabetes Using Pulse Wave Velocity by Ultrafast Imaging

Tuesday, Nov. 27 12:45PM - 1:15PM Room: VI Community, Learning Center Station #1

## Participants

Rui F. Zhang, MD,PhD, Zhengzhou, China (*Presenter*) Nothing to Disclose Guo h. Yan I, MD,MD, Zhengzhou, China (*Abstract Co-Author*) Nothing to Disclose Haiyan Liu, Zhegzhou, China (*Abstract Co-Author*) Nothing to Disclose Li-na Wu, Zhengzhou, China (*Abstract Co-Author*) Nothing to Disclose Guo W. Tao, MD,MMed, Zhengzhou, China (*Abstract Co-Author*) Nothing to Disclose Ling-xiao Yang, Zhengzhou, China (*Abstract Co-Author*) Nothing to Disclose

#### For information about this presentation, contact:

gwt892254594@163.com

## PURPOSE

To evaluate carotid arterial elasticity in patients with prediabetes using pulse wave velocity by ultrafast imaging (UF) .

## METHOD AND MATERIALS

Routine carotid ultrasonography and UF technique were performed in 80 prediabetes and 71 diabetes, which were together called high blood glucose groups, and 68 normal subjects were selected as the controls. Intima media thickness (IMT), end systolic diameter (D) and peak systolic velocity (PSV) were measured by conventional Ultrasound. Carotid arterial PWV was detected by UF technique, including beginning of systolic (BS) and end of systolic (ES).

#### RESULTS

(1) Compared with controls,ES in both prediabetes and diabetes were significantly increased. and the parameter increased significantly through the comparison of diabetes with prediabetes (P < 0.05). (2) ES in high blood glucose groups had a positive relevance with blood glucose level, age and IMT (r = 0.578, 0.300, 0.2680, respectively, all P < 0.05). (3) The optimal ES cutoff values for the detection of prediabetes was 7.22m/s, with 90.0% sensitivity and 63.2% specificity.

## CONCLUSION

UF could be a method to assess carotid arterial elasticity in patients with prediabetes.

## **CLINICAL RELEVANCE/APPLICATION**

UF could be a method to assess carotid arterial elasticity in patients with prediabetes.



## VI235-SD-TUB3

Analyzing the Costs of Mechanical Thrombectomy in Acute Stroke in Our Reference Center over a Population of 390,000 Inhabitants

Tuesday, Nov. 27 12:45PM - 1:15PM Room: VI Community, Learning Center Station #3

**FDA** Discussions may include off-label uses.

#### Participants

Amaya Iturralde Garriz, Vitoria, Spain (*Presenter*) Nothing to Disclose Fernando Lopez Zarraga, Vitoria, Spain (*Abstract Co-Author*) Nothing to Disclose Francisco Javier Maynar Moliner, Vitoria, Spain (*Abstract Co-Author*) Nothing to Disclose Rebeca Bastida Torre, Vitoria, Spain (*Abstract Co-Author*) Nothing to Disclose Eva Pampin Alvarez, Vitoria, Spain (*Abstract Co-Author*) Nothing to Disclose

#### For information about this presentation, contact:

amayaitu@gmail.com

#### PURPOSE

- We retrospectively analyze the direct costs derived from mechanical thrombectomy treatment in 85 patients between March 2015 and September 2017. - We expose the economical savings that represent the performance of mechanical thrombectomy compared to the usual treatment in those patients who, if not treated, would have had a severe stroke outcome.

### **METHOD AND MATERIALS**

Stroke is an increasingly frequent health problem that incurs a greater economic impact, especially in developed countries. Nowadays, more and more patients maintain their quality of life after an acute stroke thanks to mechanical thrombectomy, which is the first therapeutic option in selected patients. We have taken into account the costs of material and professionals who are involved in the treatment of acute ischemic stroke. We have compared that value with the average cost per year and per person that a patient with severe stroke represents, according to the society of Neurology in our country.

#### RESULTS

In our case, we changed the prognosis of 27 patients who, in case of not being treated, would have ended up being socially dependent. This has meant an approximate saving (taking into account the first year post-episode) up to 86,200 euros.

### CONCLUSION

We conclude that already during the first year post-treatment, if we analyze the clinical situation of the patient postthrombectomy vs fibrinolysis (which is the traditional treatment) taking the mRS-score <3 as a reference, endovascular therapy is cost-effective compared to the traditional treatment. It is important to evaluate economic data to justify the investment that is made by the hospital management in the neurointerventional unit, which finally achieves long-term health savings.

### **CLINICAL RELEVANCE/APPLICATION**

Mechanical thrombectomy in acute stroke can change the clinical course of many patients, which come to health resources savings in the long-term. This can be translated into monetary terms for making comparisions with other techniques.



### VI236-SD-TUB4

Common Femoral Vein Lumen Area on MR Venography Changes with Patient Position and Hydration Status

Tuesday, Nov. 27 12:45PM - 1:15PM Room: VI Community, Learning Center Station #4

### Awards

## Student Travel Stipend Award

#### Participants

Ashkan Heshmatzadeh Behzadi, MD, New York, NY (*Presenter*) Nothing to Disclose Weiguo Zhang, MD, New York, NY (*Abstract Co-Author*) Nothing to Disclose Neil M. Khilnani, MD, New York, NY (*Abstract Co-Author*) Nothing to Disclose Amanda H. Bares, New York, NY (*Abstract Co-Author*) Nothing to Disclose Srikanth R. Boddu, MBBS, MRCS, New York, NY (*Abstract Co-Author*) Nothing to Disclose Robert J. Min, MD, New York, NY (*Abstract Co-Author*) Nothing to Disclose Martin R. Prince, MD,PhD, New York, NY (*Abstract Co-Author*) Patent agreement, General Electric Company; Patent agreement, Hitachi, Ltd; Patent agreement, Siemens AG; Patent agreement, Canon Medical Systems Corporation; Patent agreement, Koninklijke Philips NV; Patent agreement, Nemoto Kyorindo Co, Ltd; Patent agreement, Bayer AG; Patent agreement, Lantheus Medical Imaging, Inc; Patent agreement, Bracco Group; Patent agreement, Mallinckrodt plc; Patent agreement, Guerbet SA;

### PURPOSE

To determine the effect of hydration as well as prone, supine and decubitus positioning on the cross sectional area of the common femoral vein (CFV) during MR Venography (MRV).

#### **METHOD AND MATERIALS**

Under institutional review board approval, 8 healthy volunteers underwent non-contrast MRV of the pelvis to measure CFV using 2D steady state free precession (SSFP) in prone, supine and both decubitus positions, and were then instructed to drink 1-2 liters (water + Gatorade®) within 1 hour to restore normal hydration levels. Urine specific gravity was tested again, and the SSFP scanning protocol repeated. MRV from 22 patients imaged both supine and prone were retrospectively reviewed and measurements of CFV areas were compared using student's paired t test. CFV cross-sectional area was measured immediately superior to the common femoral artery bifurcation . These areas were measured by two reviewver manually contouring a region of interest (ROI) around the vein lumen .

## RESULTS

The volunteers' CFV area on MRV increased with prone positioning ( $83 \pm 35 \text{ mm2}$ ) compared to supine positioning ( $59 \pm 21 \text{mm2}$ ) (p=0.02) and further increased with hydration to 123±44 mm2 (p<0.01). With right and left side down decubitus positioning, the CFV area on dehydration increased from,  $29 \pm 17 \text{ mm2}$  in the ante-dependent position to 134 ± 36 mm2 in the dependent position (p<0.0001). MRV on patients also demonstrated an increase in mean CFV luminal area from 103±44 mm2 in supine position to 151±52 mm2 with prone positioning (p<0.0001).Inter observer agreement for MRV measurements of CFV area was excellent, ICC = 0.95. Intra observer agreement was also excellent, ICC = 0.98.

### CONCLUSION

Common femoral vein lumen area on MR venography is affected by position and hydration status. Routine clinical MR venography of the common femoral vein should include both prone and supine positions and dehydration should be avoided.

#### **CLINICAL RELEVANCE/APPLICATION**

These results demonstrate that patients should be encouraged to hydrate before arriving for MR venography to ensure veins are fully distended. In addition, MRI technicians should changepatient position if common femoral vein appear stenotic, providing multiple diagnostic images for the radiologist to fully evaluate if venous disease is actually present and not an artifact of scanning position. The prone and dependent decubitus positons resulted in the largest common femoral vein areas.



## VI237-SD-TUB5

Spectral CT Angiography Demonstration of the Lateral Circumflex Femoral Artery Descending Branch for Anterolateral Thigh Flap: Comparison of Monochromatic and Polychromatic Imaging

Tuesday, Nov. 27 12:45PM - 1:15PM Room: VI Community, Learning Center Station #5

### Participants

Anwei He, Tianjin, China (*Presenter*) Nothing to Disclose Fei Fu, Tianjin, China (*Abstract Co-Author*) Nothing to Disclose Jiyang Zhang, Tianjin, China (*Abstract Co-Author*) Nothing to Disclose Yue Zhang, Tianjin, China (*Abstract Co-Author*) Nothing to Disclose Yeda Wan SR, Tianjin, China (*Abstract Co-Author*) Nothing to Disclose

### For information about this presentation, contact:

heanwei2009@163.com

### PURPOSE

To evaluate the demonstration of spectral CT angiography in depiction of the lateral circumflex femoral artery descending branch for anterolateral thigh flap compared to conventional polychromatic CT.

## METHOD AND MATERIALS

Fifty trauma patients underwent lower extremity artery angiography on a single source dual energy CT (Discovery CT750 HD, GE healthcare). For each patients, both conventional polychromatic (140kVp) images and monochromatic images with energy levels ranging from 40 to 140keV were generated, from which an optimal energy level was selected for obtaining the best signal-noise-ratio (SNR,SNR=CTart/SD)for the lateral circumflex femoral artery descending branch relative to the muscle with a dedicated software (GSI Viewer). The CT value and noise of the lateral circumflex femoral artery descending branch were measured and the SNR was calculated on both polychromatic images and optimal monochromatic images. Two radiologists assessed all images with 5-point scale. Data was compared with student T-test and rank sum test.

#### RESULTS

The monochromatic images at 62 keV (mean 62.12 $\pm$ 1.53) provided the optimal SNR for the lateral circumflex femoral artery descending branch. At this energy level, the artery CT value of monochromatic images and polychromatic images were 526.13 $\pm$ 27.66 and 471.39 $\pm$ 22.87(p<0.05), SD were 25.10 $\pm$ 4.20 and 31.29 $\pm$ 4.01 (p<0.05), SNR were 17.53 $\pm$ 3.67 and 14.08 $\pm$ 3.05 (p<0.05), and the subjective image score for monochromatic images was significantly higher than that of polychromatic images(4.10 $\pm$ 0.70 vs 3.14 $\pm$ 0.65; p<0.05).

## CONCLUSION

Monochromatic images at 62keV by spectral CT provide better image quality than polychromatic images and improve the demonstration of the lateral circumflex femoral artery descending branch for anterolateral thigh flap.

## **CLINICAL RELEVANCE/APPLICATION**

Monochromatic images at 62keV by spectral CT provide better image quality than polychromatic images and improve the demonstration of the lateral circumflex femoral artery descending branch for anterolateral thigh flap.



## VI240-SD-TUB8

## Single-Center Experience of IVC Filter Placement and Retrieval Practice Patterns

Tuesday, Nov. 27 12:45PM - 1:15PM Room: VI Community, Learning Center Station #8

#### **Participants**

Peter Lo, St Louis, MO (*Abstract Co-Author*) Nothing to Disclose Marah Van Diest, BS, Saint Louis, MO (*Abstract Co-Author*) Nothing to Disclose Adam Fang, St Louis, MO (*Presenter*) Nothing to Disclose Keith Pereira, MD, Saint Louis, MO (*Abstract Co-Author*) Nothing to Disclose Louis M. Morel, MD, Omaha, NE (*Abstract Co-Author*) Nothing to Disclose Jerome L. Kao, MD, Knoxville, TN (*Abstract Co-Author*) Nothing to Disclose Sameer D. Gadani, MD, St. Louis, MO (*Abstract Co-Author*) Nothing to Disclose Kirubahara Vaheesan, MD, Chennai, India (*Abstract Co-Author*) Research Grant, Siemens AG; Proctor, Terumo Corporation; Consultant, Terumo Corporation; Proctor, Sirtex Medical Ltd; Speaker Bureau, Sirtex Medical Ltd

### For information about this presentation, contact:

adam.fang@health.slu.edu

### PURPOSE

To compare practice patterns in the placement and retrieval of inferior vena cava filters (IVCF) at a single academic center over four years (2013-2017).

### METHOD AND MATERIALS

Retrospective analysis of 238 patients (136 M,102 F; mean age, 58.6±16.8 y) who underwent IVCF placement and retrieval at a single academic center from 2013-2017. Variables assessed were placement indication, filter type, fluoroscopy time, dwell time, and placement and retrieval differences over time and between services (interventional radiology [IR] or vascular surgery [VS]).

#### RESULTS

We identified 233 IVCF placements and 44 retrievals from 2013-2017. IVCF placement for classic indications increased compared to extended or prophylactic indications (85% in 2013 vs 96% in 2017). There was an increase in the percent of filters retrieved (17% in 2013 vs 30% in 2015) and the percent of filters placed and retrieved by the same service (13% in 2013 vs 28% in 2015). Filter dwell time decreased over the years (p<0.0001). The percent of IVCF placed by IR increased with time (76% in 2013 vs 92% in 2016) and decreased for VS (24% in 2013 vs 8% in 2016). IR preferred placing Bard Denali IVCF (53%) while VS preferred placing Optease IVCF (33%). IR used venograms for IVCF placement more often than VS (84% vs 16%, p<0.0001), while VS used intravascular ultrasound more often than IR (82% vs 18%, p<0.0001). Mean fluoroscopy time (min) was 3.8 [95%CI (2.6,4.9)] for IR IVCF placement and 1.4 [95%CI (1.0,1.8)] for VS IVCF placement (p=0.001). IVCF retrievals paralleled placement trends, with IR rates increasing (8% in 2013 vs 22% in 2016) and VS rates decreasing (27% in 2013 vs 0% in 2016) over time. The percentages of placed filters retrieved were similar between IR and VS. IVCF placed by IR had shorter dwell times compared to those placed by VS (median 503 vs 975 days, p<0.05).

## CONCLUSION

Within four years at a single academic center, changes in IVCF placement and retrieval patterns over time and between services were observed. Increasing contribution of a single service may not only improve patient follow-up and oversight, but may also provide a more consistent patient experience, including the use of similar pre-procedure modalities and filter types.

#### **CLINICAL RELEVANCE/APPLICATION**

Single service placement and retrieval of IVC filters may lead to better patient follow-up and improve patient experience.



## AI001-TUD

# **Multi-modal Classification**

Tuesday, Nov. 27 2:30PM - 4:00PM Room: AI Community, Learning Center

## Title and Abstract

Multi-modal Classification This session will focus on multimodal classification. Classification is the recognition of an image or some portion of an image being of one type or another, such as 'tumor' or 'infection'. Multimodal classification means that there are more than 2 classes. While this is logically simple to understand, it presents some unique challenges that will be discussed.



## AI001-WEA

# Data Science: Normalization, Annotation, Validation

Wednesday, Nov. 28 8:30AM - 10:00AM Room: AI Community, Learning Center

## Title and Abstract

Data Science: Normalization, Annotation, Validation This session will focus on preparation of the image and non-image data in order to obtain the best results from your deep learning system. It will include a discussion of different options for representing the data, how to normalize the data, particularly image data, the various options for image annotation and the benefits of each option. We will also discuss the 'after training' aspects of deep learning including validation and testing to ensure that the results are robust and reliable.



## AI001-WEB

# **Introduction to Deep Learning**

Wednesday, Nov. 28 10:30AM - 12:00PM Room: AI Community, Learning Center

## **Title and Abstract**

Introduction to Deep Learning This class will focus on basic concepts of convolutional neural networks (CNNs), and walk the attendee through a working example. A popular training example is the MNIST data set which consists of hand-written digits. This course will use a data set we created, that we call 'MedNIST' and consists of 1000 images each from 5 different categories: Chest X-ray, hand X-ray, Head CT, Chest CT, Abdomen CT, and Breast MRI. The task is to identify the image type. This will be used to train attendees on the basic principles and some pitfalls in training a CNN. The attendee will have the best experience if they are familiar with Python programming.



## AI146-ED-WEA1

"Virtual" High-Dose Technology: Radiation Dose Reduction in Thin-Slice Chest CT at a Micro-Dose (mD) Level by Means of 3D Deep Neural Network Convolution (NNC)

Wednesday, Nov. 28 12:15PM - 12:45PM Room: AI Community, Learning Center Station #1

## **Participants**

Amin Zarshenas, MSc, Chicago, IL (Presenter) Nothing to Disclose

Yuji Zhao, MSc, Chicago, IL (Abstract Co-Author) Nothing to Disclose

Junchi Liu, MS, Chicago, IL (Abstract Co-Author) Nothing to Disclose

Toru Higaki, PhD, Hiroshima, Japan (*Abstract Co-Author*) Nothing to Disclose Kazuo Awai, MD, Hiroshima, Japan (*Abstract Co-Author*) Research Grant, Canon Medical Systems Corporation; Research Grant,

Hitachi, Ltd; Research Grant, Fujitsu Limited; Research Grant, Bayer AG; Research Grant, DAIICHI SANKYO Group; Research Grant, Eisai Co, Ltd; Medical Advisory Board, General Electric Company; ;

Kenji Suzuki, PhD, Chicago, IL (Abstract Co-Author) Royalties, General Electric Company; Royalties, Hologic, Inc; Royalties, MEDIAN Technologies; Royalties, Riverain Technologies, LLC; Royalties, Canon Medical Systems Corporation; Royalties, Mitsubishi Corporation; Royalties, AlgoMedica, Inc

## For information about this presentation, contact:

mzarshen@hawk.iit.edu

#### **TEACHING POINTS**

1) To understand the radiation dose issue with CT in lung cancer screening. 2) To learn the basic principles of NNC as a deep learning technique to reduce the radiation dose in chest CT. 3) To understand the performance and clinical utility of our radiation dose reduction technology for chest CT.

## **TABLE OF CONTENTS/OUTLINE**

A. Radiation dose issue with CT in lung cancer screening B. Basic principles of NNC for converting micro-dose (mD) to higher-dose (HD) chest CT images to reduce radiation dose C. Radiation dose reduction, pre-clinical study: Anthropomorphic phantom image analysis D. Radiation dose reduction, clinical translation study: Clinical cases image analysis E. Quantitative evaluation: Image quality vs. radiation dose reduction F. Benefits and limitations of NNC for chest CT



### BR199-ED-WEA8

# The Forgotten Male Breast: A Comprehensive Review of Male Breast Disease

Wednesday, Nov. 28 12:15PM - 12:45PM Room: BR Community, Learning Center Station #8

## Awards Certificate of Merit

#### Participants

Cheryce P. Fischer, MD, Santa Monica, CA (*Presenter*) Nothing to Disclose Cecil Patel, MD, Los Angeles, CA (*Abstract Co-Author*) Nothing to Disclose Melissa M. Joines, MD, Santa Monica, CA (*Abstract Co-Author*) Nothing to Disclose Brian L. Dubin, MD, Los Angeles, CA (*Abstract Co-Author*) Nothing to Disclose

## For information about this presentation, contact:

#### cpfischer@mednet.ucla.edu

#### **TEACHING POINTS**

Although males make up a small percentage of our clinical practice, male breast disease is important to recognize and be familiar with. Gynecomastia is the most common disease affecting males. However, there is a wide spectrum of other conditions which can also occur in the male breast. Two major teaching points the learner should accomplish by viewing this exhibit is: 1) To become familiar with the appearance and work up of gynecomastia 2) To become familiar with the numerous other conditions that affect the male breast

# TABLE OF CONTENTS/OUTLINE

This is an educational exhibit demonstrating the spectrum of disease in the male breast. The exhibit will include the following cases seen in the male breast at our institution and will be presented with a brief history and pertinent mammographic and sonographic images. 1. Unilateral gynecomastia 2. Bilateral gynecomastia 3. Pseudogynecomastia 4. Epidermal inclusion cyst 5. Abscess 6. Hematoma 7. Lipoma 8. Hibernoma 9. Intraductal papilloma and ductal carcinoma in situ 10. Papillary carcinoma 11. Metastatic infiltrating ductal carcinoma 12. Infiltrating ductal carcinoma and ductal carcinoma in situ 13. Lymphoma 14. Transgender male to female breast after hormone replacement therapy



### BR200-ED-WEA9

## What the Breast Radiologist Needs to Know About Imaging Transgender Patients

Wednesday, Nov. 28 12:15PM - 12:45PM Room: BR Community, Learning Center Station #9

#### Awards Identified for RadioGraphics

#### Participants

Ujas N. Parikh, MD, New York, NY (*Presenter*) Nothing to Disclose Elizabeth V. Mausner, MD, New York, NY (*Abstract Co-Author*) Nothing to Disclose Chloe M. Chhor, MD, Brooklyn, NY (*Abstract Co-Author*) Nothing to Disclose Yiming Gao, MD, New York, NY (*Abstract Co-Author*) Nothing to Disclose Samantha L. Heller, MD, PhD, New York, NY (*Abstract Co-Author*) Nothing to Disclose

#### For information about this presentation, contact:

ujas.parikh@nyumc.org

### **TEACHING POINTS**

There is increasing awareness of the need for optimal breast imaging approaches for transgender individuals, as well as for evidence-based understanding of transgender breast cancer risk. In this case-based review, we will focus on screening and diagnostic imaging scenarios involving transgender individuals and will also explore what is known about breast cancer risk and breast cancer detection in the transgender population.

### **TABLE OF CONTENTS/OUTLINE**

1. Intro a. Define "transgender" i. Terminology: transgender, transsexual, male-to-female (MtF), female-to-male (FtM)2. Mammographic screeninga. Review of literature/paucity of datab. Screening and risk factors i. Exogenous Hormone use (MtF)ii. Breast densityiii. Residual breast tissue (FtM)iv. Risk associated with natal sexv. High risk mutations and family historyc. Screening and suggested guidelinesi. UCSF Center of Excellence for Transgender Healthii. Fenway Guide3. Diagnostic imaging a. Review of the literatureb. Diagnostic scenarios with attention to pearls and pitfalls i. Hormone related symptoms and imagingii. Altered breast 1. Augmentation/silicone injections (MtF)2. Post-mastectomy (FtM)4. Special considerations and challengesa. Healthcare access and public educationb. Patient and physician awareness



#### BR201-ED-WEA10

## **Unilateral Palpable Male Breast Lump: What Is Underneath!**

Wednesday, Nov. 28 12:15PM - 12:45PM Room: BR Community, Learning Center Station #10

#### **Participants**

Pramod K. Gupta, MD, Plano, TX (*Presenter*) Nothing to Disclose Soume D. Foshee, MD, Dallas, TX (*Abstract Co-Author*) Nothing to Disclose Francisco Garcia-Morales, MD, Plano, TX (*Abstract Co-Author*) Nothing to Disclose

### For information about this presentation, contact:

pramod.gupta@va.gov

### **TEACHING POINTS**

Broad range of lesions from benign to malignant can present in male breast as palpable mass. The purpose of this scientific exhibit is: 1. To describe the imaging findings of various lesions that present as unilateral masses. 2. To help the viewer learn an imaging pattern-based approach to develop a reasonable differential diagnosis and in many cases make the specific diagnosis. 3. To familiarize the viewer with those imaging findings which can be definitely considered benign, require no further work-up and to familiarize from those findings which should be considered sufficiently suspicious or indeterminate to warrant further work-up.

## TABLE OF CONTENTS/OUTLINE

The contents of this exhibit will be organized as follows with short discussions, illustrated examples and images: 1. Male breast anatomy 2. Imaging work-up Algorithm 3. Categories: A. Skin and subcutaneous tissues origin: Sebaceous cyst/epidermal inclusion cyst -Lipoma -Angiolipoma -Hematoma -Fat necrosis -Oil cyst B. Glandular and Stromal elements origin: -Gynecomastia -Pseudogynecomastia -Pseudoangiomatous stromal hyperplasia -Myofibroblastoma -Hemangioma -Mason tumor -Schwanomma -Granular cell tumor -Fibroadenoma -Abscess C. Malignancies: -Invasive ductal carcinoma -Recurrent breast carcinoma -Lymphoma -Angiosarcoma -Metastasis



## BR202-ED-WEA11

Multimodality Imaging of Lobular Neoplasia: Review of Imaging Features and Updates on Controversies in Management

Wednesday, Nov. 28 12:15PM - 12:45PM Room: BR Community, Learning Center Station #11

## Participants

Linda Ratanaprasatporn, MD, Boston , MA (*Presenter*) Nothing to Disclose Lisa Ratanaprasatporn, MD, Boston, MA (*Abstract Co-Author*) Nothing to Disclose Sona A. Chikarmane, MD, Boston, MA (*Abstract Co-Author*) Nothing to Disclose Beth T. Harrison, Boston, MA (*Abstract Co-Author*) Nothing to Disclose Eva C. Gombos, MD, Boston, MA (*Abstract Co-Author*) Nothing to Disclose

## For information about this presentation, contact:

Iratanaprasatporn@partners.org

### **TEACHING POINTS**

Atypical lobular hyperplasia (ALH) and lobular carcinoma in situ (LCIS) are noninvasive proliferations of lobular cells. The term 'lobular neoplasia' (LN) is used to encompass both ALH and LCIS. LN is not an obligate precursor of invasive carcinoma. However, LN is associated with increased risk of developing invasive carcinoma or ductal carcinoma in situ in either breast. Usually incidental findings at core needle biopsy, LN has no reliable imaging features attributable to them. Knowing the most common imaging findings of LN on mammography, ultrasound, and MRI is important to understand if there is imaging-histologic concordance or discordance as this will affect management. The management of incidental ALH and LCIS at core biopsy is controversial and ranges from immediate surgical excision to monitoring with clinical and imaging evaluation.

### **TABLE OF CONTENTS/OUTLINE**

Review the definition of ALH and LCIS and their distinction on histopathology. Describe LN's natural history, its clinical significance, and its associated increased risk of developing invasive cancer and DCIS. Demonstrate the most common imaging findings of LN on mammography, ultrasound, and MRI using a case-based approach. Examine the different strategies and controversies for management of LN including surgical excision, chemoprevention, and monitoring with imaging.



#### BR203-ED-WEA12

### Inserting Colors into the Diagnosis: When Doppler Makes the Difference in Breast Ultrasound

Wednesday, Nov. 28 12:15PM - 12:45PM Room: BR Community, Learning Center Station #12

#### **Participants**

Cecilia S. Goldman, MD, Sao Paulo, Brazil (*Abstract Co-Author*) Nothing to Disclose Juliana H. Catani, MD, Sao Paulo, Brazil (*Presenter*) Nothing to Disclose Nestor Barros, Sao Paulo, Brazil (*Abstract Co-Author*) Nothing to Disclose Pedro Henrique Hasimoto e Souza, MD, Sao Paulo, Brazil (*Abstract Co-Author*) Nothing to Disclose Flavia T. Horigome, MD, Sao Paulo, Brazil (*Abstract Co-Author*) Nothing to Disclose Carlos Shimizu, MD, Sao Paulo, Brazil (*Abstract Co-Author*) Nothing to Disclose Tomie H. Ichihara, MD, Sao Paulo, Brazil (*Abstract Co-Author*) Nothing to Disclose Carla C. Caravatto, MD, Sao Paulo, Brazil (*Abstract Co-Author*) Nothing to Disclose Heni D. Skaf, MD, Sao Paulo, Brazil (*Abstract Co-Author*) Nothing to Disclose Caio D. Pinheiro, MBBS, Sao Paulo, Brazil (*Abstract Co-Author*) Nothing to Disclose Rafael L. Macedo, MD, Sao Paulo, Brazil (*Abstract Co-Author*) Nothing to Disclose

## **TEACHING POINTS**

1- Review types of lesion vascularity and their blood flow characteristics 2-Describe the importance of color Doppler to distinguish solid and cystic lesions, including complicated and complex cysts, as well as assessing vascular lesions.3- Correlate the amount and distribution of blood-flow in breast lesions and their tendency to malignancy.4- Describe how color and pulsed-wave Doppler can influence BIRADS classification as an associated feature, and consequently the patient's management and prognosis.

## TABLE OF CONTENTS/OUTLINE

1. Doppler as an associated feature in the BI-RADS classification2. Imaging aspects of lesion vascularity and its assessment by power/ color Doppler, and pulsed-wave Dopplerinternal and rim-like vascularitynumber of vesselsblood-flow velocityintra-tumoral vessel resistance3. Applicability of color Doppler in the evaluation of breast lesionsCorrelation of blood flow and lesion suspiciousnessCan vascularity evidence in a breast lesion change its BI-RADS category?4. Illustration of vascular breast lesions, including:Cystic lesionsSolid lesionsVascular lesionsNon-mass lesions



## BR254-SD-WEA1

Associations Between Magnetic Resonance Imaging (MRI) Biomarkers and Tumor-Infiltrating Lymphocytes (TILs) in Breast Cancer: Results from a Preliminary Study

Wednesday, Nov. 28 12:15PM - 12:45PM Room: BR Community, Learning Center Station #1

## Participants

Elena Venturini, MD, Milan, Italy (*Presenter*) Nothing to Disclose Marta Maria Panzeri, MD, Milan, Italy (*Abstract Co-Author*) Nothing to Disclose Claudio Losio, MD, Milan, Italy (*Abstract Co-Author*) Nothing to Disclose Silvia Ravelli, MD, Milan, Italy (*Abstract Co-Author*) Nothing to Disclose Francesca Gallivanone, Milan, Italy (*Abstract Co-Author*) Nothing to Disclose Pietro Panizza, Milan, Italy (*Abstract Co-Author*) Speaker, Koninklijke Philips NV; Research Grant, Koninklijke Philips NV

#### For information about this presentation, contact:

venturini.elena@hsr.it

### PURPOSE

TILs reflect the attempt of the host immune system to eradicate malignancies and own an interesting prognostic value in breast cancer. Our purpose is to assess the role of multiparametric breast MRI in the prediction of the presence of TILs.

#### **METHOD AND MATERIALS**

We retrospectively reviewed the examinations of patients who underwent a multiparametric breast MRI from 01/2015 to 04/2017 and fulfill the following inclusion criteria: invasive ductal carcinoma histotype, core needle/VABB performed at our Institute with TILs evaluation, mass-like lesion at breast MRI. MRI protocol included T2, diffusion-weighted imaging (DWI) and dynamic contrastenhanced (DCE) study (1.5T). The immunohistochemical and histologic data were evaluated on core biopsies by experienced pathologists. On T2 presence of intratumoral necrosis, pseudocapsule and perilesional edema was assessed. On subtracted images presence of early peripheral and delayed rim enhancement (DRE) was recorded. DWI, DCE and T2 images were analyzed using OLEA software; tumor VOIs were manually depicted slice by slice avoiding necrosis. The software generated histograms for each VOIs and first order texture parameters were obtained. Univariate and multivariate regression analyses were performed.

#### RESULTS

The study population was composed by 45 women with 47 breast carcinomas (23 G1-G2 24 G3; 19/47 40% HER2- luminal, 23/47 26% HER2+, 16/47 34% triple negative). The presence of TILs was significantly associated to high tumor grade and molecular subtype quale ? (p<0,05). A significant association was found between TILs and DRE (p<0,05). A correlation was found between presence of TILs and lower mean ADC (Apparent Diffusion Coefficient) (p<0,05), higher ADC skewness and kurtosis (p<0,05). Focusing on G3 and TN tumors the association between the presence of TILs and DRE or lower mean ADC remained significant (p<0,05). At multivariate analysis, the variables associated to presence of TILs are tumor grade, DRE and mean ADC (p<0,05).

### CONCLUSION

The results of our exploratory study provide a new insight into the relationships between MRI biomarkers and tumor environment. The presence of TILs seems to be related to lower mean ADC, reflecting an increased cellularity in the tumoral stroma.

#### **CLINICAL RELEVANCE/APPLICATION**

Multiparametric MRI may provide new insights into breast cancer micro-environment suggesting the presence of Tumor-Infiltrating Lymphocytes.



### BR255-SD-WEA2

Patient and Tumor Characteristics to Predict the Benefit of Pre-Operative Breast MRI: Results from a Machine Learning Approach at a High Volume Academic Center

Wednesday, Nov. 28 12:15PM - 12:45PM Room: BR Community, Learning Center Station #2

# Awards

# Student Travel Stipend Award

#### **Participants**

Safia H. Cheeney, MD, Seattle, WA (*Presenter*) Nothing to Disclose

Habib Rahbar, MD, Seattle, WA (Abstract Co-Author) Research Grant, General Electric Company

Daniel S. Hippe, MS, Seattle, WA (*Abstract Co-Author*) Research Grant, Koninklijke Philips NV; Research Grant, General Electric Company; Research Grant, Canon Medical Systems Corporation; Research Grant, Siemens AG

Yifan Wu, MS, Seattle, WA (Abstract Co-Author) Nothing to Disclose

Christoph I. Lee, MD, Mercer Island, WA (*Abstract Co-Author*) Research Grant, General Electric Company; Investigator, General Electric Company

Savannah C. Partridge, PhD, Seattle, WA (Abstract Co-Author) Research Grant, General Electric Company

#### PURPOSE

Pre-operative breast MRI (pMRI) is a powerful tool for identifying additional mammographically occult disease in women newly diagnosed with breast cancer. However, it also prompts many unnecessary biopsies, which are costly and can lead to treatment delays. Surgeons vary in their use of pMRI, often basing their decisions on breast density, age, and tumor type without evidence to support these approaches. We sought to identify patient and tumor characteristics that can predict which patients benefit from pMRI using a machine learning approach.

#### **METHOD AND MATERIALS**

In this IRB-approved retrospective study, we identified all patients who underwent pMRIs (1/2005-2/2015) less than 6 months after a core needle biopsy (CNB) diagnosis of breast cancer from our prospectively populated MRI database linked to pathology outcomes. CNBs that occurred after pMRI were classified by worst outcome (invasive>DCIS>high-risk>benign). Patient and tumor features, including age, density, tumor type, grade, hormone receptor, HER2, and Ki-67 were also extracted from the database. The LASSO machine learning algorithm was used to generate multivariate models using these factors to predict additional, true positive (TP) (DCIS or invasive breast cancer), and false positive (FP) (benign or high-risk pathology) CNBs after pMRI. The resulting models were internally validated using the bootstrap with overall performance summarized using the c-statistic.

### RESULTS

1396 women underwent pMRI during the study period, and 30% underwent a pMRI-prompted CNB (13% TP, 17% FP). While women with dense breasts more often underwent pMRI-prompted CNB (32% vs 26%, p=0.02) with greater FP CNB rates (19% vs 14%, p=0.02), there was no significant difference in TP CNB rate (13% vs 12%, p=0.6). During multivariate analysis, the LASSO selected age, density, and HER2 status for predicting additional CNBs and FP CNBs; however, overall prediction performance was low (c-statistics 0.55 and 0.56, p<0.05). The LASSO did not find any factors with sufficient predictive value to create a model for predicting TP CNBs.

#### CONCLUSION

Our study demonstrates that clinical features, including age, density, and tumor features are weak predictors of who will benefit most from pMRI.

## **CLINICAL RELEVANCE/APPLICATION**

Pre-operative breast MRI is not more or less likely to benefit patients based on patient age, breast density, or tumor characteristics and should not be denied to patients solely on these factors.



### BR256-SD-WEA3

Peritumoral Fat Content Correlates with Histologic Prognostic Factors in Breast Carcinoma: Iterative Decomposition of Water and Fat with Echo Asymmetry and Least-Squares Emission (IDEAL) Study

Wednesday, Nov. 28 12:15PM - 12:45PM Room: BR Community, Learning Center Station #3

## Participants

Sachi Hisanaga, MD, PhD, Fukuoka, Japan (Presenter) Nothing to Disclose Takatoshi Aoki, MD, PhD, Kitakyusyu, Japan (Abstract Co-Author) Nothing to Disclose Shohei Shimajiri, MD, Kitakyushu, Japan (Abstract Co-Author) Nothing to Disclose Masanori Hisaoka, MD, Kitakyushu, Japan (Abstract Co-Author) Nothing to Disclose Toshiyuki Nakayama, Kitakyushu, Japan (Abstract Co-Author) Nothing to Disclose Yukunori Korogi, MD, PhD, Kitakyushu, Japan (Abstract Co-Author) Nothing to Disclose Akitaka Fujisaki, MD, Kitakyushu, Japan (Abstract Co-Author) Nothing to Disclose Chihiro Chihara, MD, Kitakyushu, Japan (Abstract Co-Author) Nothing to Disclose Yoshiko Hayashida, MD, Fukuoka, Japan (Abstract Co-Author) Nothing to Disclose

## PURPOSE

Breast cancer cells express receptors for adipokines secreted by adipocytes, which can affect tumor growth. In vitro and in vivo data indicate that adipocytes are modified by cancer cells to acquire characteristics different from naive adipocytes (cancerassociated adipocytes: CAAs). Histologically, CAAs located around breast cancer display smaller sizes and are less lipid. The purpose of this study is to correlate peritumoral fat content using IDEAL with histologic prognostic factors in breast carcinoma.

### METHOD AND MATERIALS

This study consisted of 100 patients who were diagnosed with invasive carcinoma of breast and underwent breast MRI including IDEAL before surgery. The scan time of IDEAL fat fraction (FF) map imaging was 23 sec. Four regions of interests (ROIs), which are a distance of 5mm from the tumor edge, and 4 ROIs in the mammary fat of the healthy side were set on the FF map. Then average peri-tumoral FF values (FT), average FF values in the healthy side (FH), and peri-tumoral fat ratio (pFTR: defined as FT/FH) were calculated. Histologically, the presence of lymph node metastasis and the MIB-1 index were evaluated by 2 pathologists.

#### RESULTS

FT and pTFR for breast carcinoma with lymph node metastasis (79.27±10.36 and 0.897±0.078) were significantly lower than those without (86.23±4.53 and 0.945±0.032) (p<.001 and p=.005). Spearman rank correlation suggested that the FT correlated with the MIB1 index (r=-340, p=.001).

### CONCLUSION

The peritumoral fat content calculated with IDEAL is associated with the histologic prognostic factors, and may therefore be a useful prognostic biomarker for breast carcinoma.

## **CLINICAL RELEVANCE/APPLICATION**

In vivo IDEAL imaging is simple to perform without extrinsic contrast agent and the quantification of the peritumoral FF using IDEAL may be useful for therapeutic strategy for breast carcinoma.



### BR257-SD-WEA4

Cancer Detection Rate for Stereotactic Biopsies Performed on Initially Categorized BI-RADS 3 Calcifications

Wednesday, Nov. 28 12:15PM - 12:45PM Room: BR Community, Learning Center Station #4

#### Participants

Monica Froicu, MD, Danville, PA (*Presenter*) Nothing to Disclose Katherine Chung, Scranton, PA (*Abstract Co-Author*) Nothing to Disclose Margarita L. Zuley, MD, Pittsburgh, PA (*Abstract Co-Author*) Investigator, Hologic, Inc

For information about this presentation, contact:

mfroicu@geisinger.edu

#### PURPOSE

To determine the malignancy rate and indications for biopsy of calcifications initially categorized as BI-RADS 3 and converted to BI-RADS 4/5 during the ensuing surveillance period.

## METHOD AND MATERIALS

Following IRB approval, our Radiology Information System (RIS) was searched for all BI-RADS 4/5 categorized mammograms performed from January 1, 2013 to July 30, 2016 that underwent stereotactic biopsy and had been classified as BI-RADS 3 for calcifications within the prior 2 years. Data collected included: patient age, prior biopsies, personal/family history of breast cancer, pathogenic mutations, breast density, calcification morphology, extent, distribution and increase in size or change in morphology during surveillance. BI-RADS scores changed from 3 to 4/5 with no change in the grouping were categorized as difference in interpretation.

#### RESULTS

The search identified 162 patients with mean age 55.7 (range 32-81) years. 55% (90/162) were heterogeneously dense, 15% (25/162) had personal history and 17.8% (29/162) had family history of breast cancer, none had pathogenic mutations and 14% (23/162) had prior benign biopsies. The average BI-RADS conversion time was 9.5 months with 41.9 % (69/162) changed at 6 months. Change was due to increasing calcifications in 42.3% (69/162), morphology change 9.8% (16/162), distribution change 2.4% (4/162) or difference in interpretation 16.6% (27/162). Distribution was 78.4% (127/162) grouped, 11.11% (18/162) regional, 10.5% (17/162) linear, 1.2% (2/162) segmental, 0.6% (1/162) diffuse. PPV at biopsy was 11.7 % (19/162) including 13 DCIS and 6 invasive carcinomas. There were 67.2% (109/162) benign and 20.9% (34/162) high risk lesions 2 of which were upgraded to low grade DCIS at surgery.

### CONCLUSION

Calcifications initially classified as BI-RADS 3 that increase in number or change in morphology during surveillance have a significant upgrade rate to malignancy.

## **CLINICAL RELEVANCE/APPLICATION**

BI-RADS 3 lesions that change during surveillance should undergo biopsy.



### BR258-SD-WEA5

Radiologists versus Deep Learning Model Inter-Observer Variability in Mammographic Breast Density Assessment

Wednesday, Nov. 28 12:15PM - 12:45PM Room: BR Community, Learning Center Station #5

## Participants

Brian N. Dontchos, MD, Boston, MA (*Presenter*) Nothing to Disclose Regina Barzilay, PhD, Cambridge, MA (*Abstract Co-Author*) Nothing to Disclose Adam Yala, Cambridge, MA (*Abstract Co-Author*) Nothing to Disclose Tal Schuster, Cambridge, MA (*Abstract Co-Author*) Nothing to Disclose Kyle Swanson, Boston, MA (*Abstract Co-Author*) Nothing to Disclose Manisha Bahl, MD,MPH, Boston, MA (*Abstract Co-Author*) Nothing to Disclose Christine E. Edmonds, MD, Boston, MA (*Abstract Co-Author*) Nothing to Disclose Constance D. Lehman, MD,PhD, Boston, MA (*Abstract Co-Author*) Research Grant, General Electric Company; Medical Advisory Board, General Electric Company

#### For information about this presentation, contact:

#### bdontchos@mgh.harvard.edu

#### PURPOSE

Qualitative breast density assessment by radiologists is highly variable and currently available automated quantitative tools are limited. Our purpose was to evaluate the inter-observer variability amongst radiologists vs our deep learning (DL) model in mammographic breast density assessment.

#### **METHOD AND MATERIALS**

Four expert radiologists independently assessed BI-RADS density on a random subset of 100 screening mammograms, blinded to the original radiologist's assessment. Our DL model (previously reported) was trained and tested using a deep convolutional neural network on 50,071 consecutive digital screening mammograms performed June 2009 to June 2014 to predict the original radiologist's assessment. We estimated both our DL model agreement and our radiologists blinded reader agreement with the original radiologist's density assessment using percent agreement with Wilson confidence intervals (CI) and with linear-weighted kappa statistics, compared across 5,000 bootstrap samples to assess significance.

#### RESULTS

Radiologist agreement with the original assessment was 80.5% (95% CI 76.8, 84.5) for binary assessment (dense vs not dense) and was 66.3% (95% CI 61.5, 70.9) for 4-category density assessment. Our DL model agreement for the same cases was 85.0% (95% CI of 76.7, 90.7) for binary assessment and 71.0% (95% CI of 61.5, 79.0) (p>0.05 for each comparison). Compared to the original density assessment, our DL model showed substantial agreement (K=.61, 95% CI .49-.74) compared to moderate agreement by radiologists (K=.57, 95% CI .50- .63).

#### CONCLUSION

Our DL model can accurately and consistently assess breast density, particularly into clinically relevant dense vs non-dense categories.

### **CLINICAL RELEVANCE/APPLICATION**

Implementation of a deep learning model that accurately and consistently assesses breast density could lead to more precise identification of women who might benefit from supplemental imaging.



### BR259-SD-WEA6

### Convolutional Neural Network Based Breast Cancer Risk Stratification Using a Mammographic Dataset

Wednesday, Nov. 28 12:15PM - 12:45PM Room: BR Community, Learning Center Station #6

### Participants

Simukayi Mutasa, MD, New York, NY (*Presenter*) Nothing to Disclose Peter Chang, MD, San Francisco, CA (*Abstract Co-Author*) Nothing to Disclose Jenika Karcich, MD, New York, NY (*Abstract Co-Author*) Nothing to Disclose Eduardo Pascual Van Sant, BS, New York, NY (*Abstract Co-Author*) Nothing to Disclose Mary Q. Sun, MD, Manhasset, NY (*Abstract Co-Author*) Nothing to Disclose Michael Z. Liu, MS, New York, NY (*Abstract Co-Author*) Nothing to Disclose Sachin Jambawalikar, PhD, New York, NY (*Abstract Co-Author*) Nothing to Disclose Richard S. Ha, MD, New York, NY (*Abstract Co-Author*) Nothing to Disclose

#### For information about this presentation, contact:

s.mutasa@columbia.edu

#### PURPOSE

We propose a novel convolutional neural network (CNN) based pixel-wise breast cancer risk model using a mammographic dataset.

## METHOD AND MATERIALS

An IRB approved retrospective case-control study of 1474 mammographic images was performed in average risk women. First, 210 patients with new incidence of breast cancer were identified. Mammograms from these patients at least two years prior to developing breast cancer were identified and made up the case group [420 bilateral craniocaudal (CC) mammograms]. The control group consisted of 527 patients without breast cancer from the same time period. Prior mammograms from these patients made up the control group [1054 bilateral CC mammograms]. A CNN architecture was designed for pixel-wise breast cancer risk prediction. Briefly, each mammogram was normalized as a map of z-scores and resized to an input image size of 256x256. Then a contracting and expanding fully convolutional CNN architecture was composed entirely of 3x3 convolutions, a total of four strided convolutions instead of pooling layers, and symmetric residual connections. L2 regularization and augmentation methods were implemented to prevent overfitting. Cases were separated into training (80%) and test sets (20%). Fivefold cross validation was performed.

## RESULTS

The average age of patients between the case and the control groups was not statistically different [case: 57.4 years (SD, 10.4) and control: 58.2 years (SD, 10.9), p=0.33]. Mammographic breast density (BD) was significantly higher in the case group [2.39 (SD, 0.7)] than the control group [1.98 (SD, 0.75), p<0.0001]. On multivariate logistic regression analysis, both CNN pixel-wise mammographic risk model and BD were significant independent predictors of breast cancer risk (p < 0.0001). The CNN risk model showed greater predictive potential [OR=4.42 (95% CI, 3.4-5.7] compared to BD [OR =1.67 (95%CI, 1.4 -1.9). The CNN risk model achieved an overall cross validation accuracy of 72% (95%CI, 69.8-74.4%) in predicting patients in the case group.

#### CONCLUSION

A novel pixel-wise CNN architecture can stratify breast cancer risk in mammography, independent of the BD. A larger dataset will likely improve our model.

#### **CLINICAL RELEVANCE/APPLICATION**

Personalized breast cancer risk stratification may be aided by using a novel pixel-wise CNN model. This may have clinical implications in screening guidelines.



### BR260-SD-WEA7

#### The Significance of Asymmetries in Screening Mammograms with Digital Breast Tomosynthesis

Wednesday, Nov. 28 12:15PM - 12:45PM Room: BR Community, Learning Center Station #7

#### Awards Student Travel Stipend Award

#### **Participants**

Yarisma Frometa, MD, New Haven, CT (*Presenter*) Nothing to Disclose Maryam Etesami, MD, New Haven, CT (*Abstract Co-Author*) Nothing to Disclose Liva Andrejeva-Wright, MD, New Haven, CT (*Abstract Co-Author*) Nothing to Disclose Liane E. Philpotts, MD, New Haven, CT (*Abstract Co-Author*) Consultant, Hologic, Inc

## For information about this presentation, contact:

yarisma.frometa@yale.edu

#### PURPOSE

Digital breast tomosynthesis (DBT) can result in significantly decreased recall rate (RR) of screening mammograms. However, asymmetries remain one of the most frequently recalled abnormalities and a major source of false positives. The purpose of this study is to determine the significance and characteristics of asymmetries detected in DBT screening and their diagnostic work up to aid in further reducing false positive findings on DBT.

### **METHOD AND MATERIALS**

In this retrospective Institutional Review Board approved study, we reviewed all DBT screening mammograms performed from 10/1/2014 through 9/30/2016 at our academic center. The number of recalled exams and type of recalled abnormalities were identified. For each recalled asymmetry, imaging characteristics, diagnostic work up, biopsy, and imaging follow up were documented. RR and positive predictive value (PPV1, PPV2, and PPV3) of asymmetries were calculated. The characteristics of true and false positive asymmetries were compared.

#### RESULTS

Of 15620 DBT screening mammograms, 1100 exams were recalled for further evaluation (overall RR=7.04%). 482 asymmetries were recalled in 440 exams (asymmetry RR=3.09%). The false positive rate of recalled asymmetries was 97.93% with only 10 true positive cancers (asymmetry PPV1=2.07%). There was a significant difference in cancer yield of "developing" asymmetries (7%) versus asymmetries not otherwise specified (1.2%) (p=0.002). Focal asymmetries had higher cancer yield (3.3%) compared to asymmetries seen only on one view (1.3%), but the difference was not significant (p=0.19). The majority of true positive asymmetries (9 out of 10) had a suspicious ultrasound correlate at the time of first diagnostic work up and underwent ultrasound guided biopsy yielding invasive carcinoma. Only one case of ductal carcinoma in situ did not have an immediate sonographic correlate.

#### CONCLUSION

Asymmetries recalled on DBT screening have a high false positive rate. Identifying asymmetries with a higher cancer yield such as developing asymmetries may further reduce RR while preserving the cancer detection rate. In addition, our findings suggest that follow up imaging of recalled asymmetries without suspicious ultrasound correlates may not be necessary.

#### **CLINICAL RELEVANCE/APPLICATION**

Given the relatively high RR and low PPV1 of asymmetries on DBT screening, efforts can be made towards reducing recall of benign asymmetries and avoiding unnecessary follow up.



### CA172-ED-WEA8

Left Ventricular Outflow Tract: A Complete Review of Imaging Related Anatomy, Pathology, and Surgical Techniques

Wednesday, Nov. 28 12:15PM - 12:45PM Room: CA Community, Learning Center Station #8

#### Awards Cum Laude Identified for RadioGraphics

#### **Participants**

Cameron Hassani, MD, Los Angeles, CA (*Presenter*) Nothing to Disclose Shumpei Mori, Kobe, Japan (*Abstract Co-Author*) Nothing to Disclose Farhood Saremi, MD, Los Angeles, CA (*Abstract Co-Author*) Nothing to Disclose

### For information about this presentation, contact:

#### ch602nyc@gmail.com

## **TEACHING POINTS**

The purpose of this exhibit is: 1. Review the anatomy of the left ventricular outflow tract (LVOT) 2. Review LVOT appearance on CT, MR and Echocardiography 3. Explore disease processes primarily affecting the LVOT (including imaging manifestations) 4. Discuss planning of transcatheter aortic and mitral valve replacement in the context of the LVOT 5. Review common and uncommon surgical techniques for LVOT repair

## **TABLE OF CONTENTS/OUTLINE**

Anatomy - Development - Normal variability - Dilation - Morphology changes with stenosis Imaging modalities - CT, MR, Echo -Normal appearances (eg. Normal flow acceleration on MRI) Stenosis - Subvalvuar vs valvular stenosis Obstruction - HCM - Systolic anterior motion of the mitral valve - Mitral-septal contact - Tako-tsubo - Hypoplastic left heart syndrome - Williams syndrome Membranes - Congenital assocations (Shone's) Pseudoaneurysm - Endocarditis - Post surgical Masses - Thrombus - Neoplasm -HCM Role in Percutaneous Interventions - Neo-LVOT in Mitral Valve Replacement (TMVR) - Role in transcather aortic valve replacement (TAVR) planning - Pre-procedural LVOT calcium score in transcather aortic valve replacement (TAVR) - Percutaneous transluminal septal myocardial ablation (PTSMA) Repair - Aneurysm resection - Valve replacement - Yasui procedure - Myotomy -Konno procedure (LVOT widening)

#### **Honored Educators**

Presenters or authors on this event have been recognized as RSNA Honored Educators for participating in multiple qualifying educational activities. Honored Educators are invested in furthering the profession of radiology by delivering high-quality educational content in their field of study. Learn how you can become an honored educator by visiting the website at: https://www.rsna.org/Honored-Educator-Award/ Cameron Hassani, MD - 2018 Honored EducatorFarhood Saremi, MD - 2015 Honored Educator



## CA238-SD-WEA1

### The Devil Is In the detail: Prognostic Factors in CT of Chronic Aortic Dissection

Wednesday, Nov. 28 12:15PM - 12:45PM Room: CA Community, Learning Center Station #1

#### **Participants**

Hug Cuellar, Barcelona, Spain (*Abstract Co-Author*) Nothing to Disclose Gemma Burcet Rodriguez, MD, Barcelona, Spain (*Presenter*) Nothing to Disclose Alberto Roque, MD, Barcelona, Spain (*Abstract Co-Author*) Nothing to Disclose Maria Nazarena Pizzi, Barcelona, Spain (*Abstract Co-Author*) Nothing to Disclose Victor S. Pineda, MD, Barcelona, Spain (*Abstract Co-Author*) Nothing to Disclose Filipa Valente, Barcelona, Spain (*Abstract Co-Author*) Nothing to Disclose

#### For information about this presentation, contact:

hcuellar@vhebron.net

## PURPOSE

To determine the performance of classic morphological factors in predicting adverse events in chronic aortic dissection; To describe and validate a new predictive factor based on the relation between the size of the proximal and distal flap tears.

## METHOD AND MATERIALS

72 patients with dissection of the descending thoracic aorta were assessed by CT during the subacute phase and followed clinically and with an annual CT or MRI for a median of 9 years. Previously described morphological factors in the subacute phase (aortic size, false lumen size, proximal tear size, partial lumen thrombosis) were evaluated as predictors of fast dilation and adverse clinical events. A new parameter (tear size dominance) describing the relation between the size of the proximal and distal tears was also tested.

#### RESULTS

A maximum diameter larger than 45 mm in the dissected descending thoracic aorta and tear size dominance greater than  $1 \text{ cm}^2$  were the only independent predictors of rapid dilation and clinical complications (both p <0.01) in our cohort. The combination of both parameters detected a subset of patients with worse clinical evolution and a shorter average time of survival free of complications (7.5 years; p <0.001).

### CONCLUSION

The maximum diameter of the thoracic descending aorta and the relation between the size of the proximal and distal tears measured in CT predicted adverse clinical events during the follow-up of chronic aortic dissection.

### **CLINICAL RELEVANCE/APPLICATION**

CT performed during the subacute phase of dissection of the descending thoracic aorta provides important prognostic factors which may help determine the best treatment options for each patient.



## CA239-SD-WEA2

Pitfall of Preoperative CT Information on Aortic Valvuloplasty - Analysis of Measuring Methods Intended to Comprehend Risk Factors in Image Processing and Improve the Procedure

Wednesday, Nov. 28 12:15PM - 12:45PM Room: CA Community, Learning Center Station #2

## Participants

Toshiya Ito, RT, Sayama, Japan (*Presenter*) Nothing to Disclose Daigo Fujii, RT, Sayama, Japan (*Abstract Co-Author*) Nothing to Disclose Jun Shionoya, RT, sayama city, Japan (*Abstract Co-Author*) Nothing to Disclose Kazuhiko Aramaki, MD, Sayama, Japan (*Abstract Co-Author*) Nothing to Disclose Muneaki Yamada, MD, Sayama, Japan (*Abstract Co-Author*) Nothing to Disclose

## For information about this presentation, contact:

toshiya-itou@saitama-sekishinkai.org

### PURPOSE

In this study, our purposes were to revamp and standardize the measuring and image supply methods of preoperative CT in order to reduce the cases described below: (1) Cases where valve replacement was chosen for patients with aortic regurgitation (AR) as an indication for valvuloplasty (2) Cases where an intraoperative change of surgical methods increased operating time, blood loss, and complications. The goal was improvement in measuring precision in addition to elimination of dependence on years of experience.

## **METHOD AND MATERIALS**

50 patients with AR for whom aortic valvuloplasty was appropriate. (Age 62.2±10.6) We devised a new measuring and image display method based on anatomy and organized it into a manual. The precision of measuring before and after standardization was evaluated by comparing the measured values of CT images with actual intraoperative values. (gH:geometric height, eH:effective height) Examination of gH and eH values obtained from CT images and actual intraoperative values. <u>1) Comparison and statistical analysis of measured values obtained by different measuring methods 2) Examination of influences from scan conditions, heart rates, and cardiac phases for imaging on measurement</u>

## RESULTS

As a result of the analysis of measured values of CT images and actual values, the groups with lower HR showed a higher correlation (HR < 70: R = 0.94, HR 70-90: R = 0.86, HR > 90: R = 0.79). There was a weak positive correlation concerning the influence of cardiac phases for image production(R = 0.32). The variations between examiners improved by an average of 43% through standardization. Among the cases examined in this study, the fall of the valve cusp was able to be reported before surgery in 49 cases because of improved precision in the measurement of eH. Partial bending was visualized in three of the 49 cases.

### CONCLUSION

The standardization established by this study increased the precision of measurement. Also, this measuring method and supplied images compiled into a manual offered secure information without variations between examiners because they required no special imaging or measuring procedures.

## **CLINICAL RELEVANCE/APPLICATION**

Surgeons: Accurate simulations before surgery became performable and enabled precise choices of operative technique. Patients: The increase in the cases to which valvuloplasty was applicable improved the QOL, reduced operating time and blood loss, and decreased complications.



### CA240-SD-WEA3

Low Radiation Dose Cardiac Computed Tomography for Left Atrium and Pulmonary Vein Imaging Using a New <u>Protocol Based on Contrast-to-Noise Ratio</u>

Wednesday, Nov. 28 12:15PM - 12:45PM Room: CA Community, Learning Center Station #3

## Participants

Yoriaki Matsumoto, Hiroshima, Japan (*Presenter*) Nothing to Disclose Yoshinori Funama, PhD, Kumamoto, Japan (*Abstract Co-Author*) Nothing to Disclose Takanori Masuda, Hiroshima, Japan (*Abstract Co-Author*) Nothing to Disclose Yukari Yamashita, Hiroshima, Japan (*Abstract Co-Author*) Nothing to Disclose Naoyuki Imada, Hiroshima, Japan (*Abstract Co-Author*) Nothing to Disclose Kazuo Awai, MD, Hiroshima, Japan (*Abstract Co-Author*) Nothing to Disclose Kazuo Awai, MD, Hiroshima, Japan (*Abstract Co-Author*) Research Grant, Canon Medical Systems Corporation; Research Grant, Hitachi, Ltd; Research Grant, Fujitsu Limited; Research Grant, Bayer AG; Research Grant, DAIICHI SANKYO Group; Research Grant, Eisai Co, Ltd; Medical Advisory Board, General Electric Company; ;

#### For information about this presentation, contact:

yori\_8592\_8592@yahoo.co.jp

#### PURPOSE

In patients receiving catheter ablation (CA) for atrial fibrillation (AF), radiation dose in pre-procedural left atrium computed tomography (LACT) is significantly higher than fluoroscopy during the procedure. Thus, there is a need for reduction of radiation dose of LACT imaging. The purpose of this study was to compare the radiation dose between conventional protocol based on noise and a new protocol based on contrast-to-noise ratio (CNR) in LACT, and to evaluate the registration accuracy of electro-anatomic mapping (EAM) system at CA procedure in patients with AF.

## **METHOD AND MATERIALS**

We divided 100 consecutive patients with AF underwent LACT prior to CA into the two protocols. In protocol A (n = 50), we used a tube voltage of 120 kVp and tube current of 100 to 800 mA. Target image noise level was set at 25 using attenuation based tube current adaptation at the maximal heart diameter technique. In protocol B (n = 50), tube voltage was set at 80 kVp, and the tube current was adjusted so as to obtain CNR equivalent to protocol A. CT number, image noise, CNR of the LA and muscle, and dose length product (DLP) were evaluated for each examination and compared between two protocols. Registration error between LA geometry obtained from EAM and LACT was calculated as the mean distance between EAM points and LACT surface. Procedure duration, fluoroscopy time and air kerma during the CA were compared in the two protocols.

### RESULTS

The mean CT number of LA with protocol B was increased as compared with protocol A ( $618 \pm 97$  HU vs.  $396 \pm 55$ , respectively, p < 0.01). The mean image noise of LA with protocol B was increased as compared with protocol A ( $41 \pm 5$  HU vs.  $26 \pm 1$ , respectively, p < 0.01). Consequently, CNR of LA did not show any significant difference between the two protocols (p = 0.21). The mean DLP of protocol A and B were  $1701 \pm 529$  mGy-cm and  $774 \pm 514$  mGy-cm, respectively (p < 0.01). There was no significant difference in the registration error between protocol A and B at CA (p = 0.12). There were no significant differences in procedure duration, fluoroscopy time and air kerma between protocol A and B (p > 0.05 for all).

## CONCLUSION

CNR based 80-kVp protocol achieves radiation dose reduction for LACT without sacrificing the image quality and accuracy of CA procedure.

## **CLINICAL RELEVANCE/APPLICATION**

LACT with CNR protocol 80-kVp is useful for reducing radiation dose without degrading accuracy of the CA procedure in patients with AF.



### CA241-SD-WEA4

Patients with Atrial Fibrillation Mediated Left Ventricular Systolic Dysfunction Do Not Have Left Ventricular Fibrosis

Wednesday, Nov. 28 12:15PM - 12:45PM Room: CA Community, Learning Center Station #4

## Participants

Suvai Gunasekaran, PhD, Chicago, IL (*Presenter*) Nothing to Disclose Jeremy D. Collins, MD, Chicago, IL (*Abstract Co-Author*) Consultant, Guerbet SA Grant, Siemens AG Grant, C. R. Bard, Inc Rod Passman, Chicago, IL (*Abstract Co-Author*) Nothing to Disclose Bradley Knight, MD, Chicago, IL (*Abstract Co-Author*) Nothing to Disclose James C. Carr, MD, Chicago, IL (*Abstract Co-Author*) Research Grant, Astellas Group; Research support, Siemens AG; Speaker, Siemens AG; Advisory Board, Guerbet SA Daniel Lee, Chicago, IL (*Abstract Co-Author*) Nothing to Disclose Daniel Kim, PhD, Chicago, IL (*Abstract Co-Author*) Nothing to Disclose

## PURPOSE

Atrial fibrillation (AF) is known to be associated with left ventricular (LV) systolic dysfunction (LVD). The incidence and etiology of AF-induced LVD are currently unknown. One plausible mechanism for AF-mediated LVD is ventricular fibrosis; however, the association between AF and LV fibrosis is less established than it is for atrial fibrosis. We hypothesize that AF-induced LVD is not mediated by fibrosis and is thus reversible following restoration of sinus rhythm. To test this, we enrolled patients with AF undergoing pulmonary venous isolation ablation and measured baseline LV fibrosis and LV ejection fraction (EF) changes before and after ablation.

## METHOD AND MATERIALS

AF ablation candidates without LV hypertrophy or ischemic heart/severe valve disease were retrospectively enrolled from 12/16-07/17 if they had undergone Arrhythmia Insensitive Rapid (AIR) T1 mapping during their pre-ablation MRI. Pre and post-contrast T1 maps and hematocrit were used to calculate extracellular volume fraction (ECV), a marker of LV fibrosis. Baseline EF values came from the clinical MRI report, and post-ablation rhythm status and EF values came from EKG, echocardiogram, or MRI reports (23±16 weeks post-ablation). Patients were considered to have LVD if their baseline EF<50%. 61 patients (mean age = 61±11 years, 41 men) were analyzed for baseline ECV and EF, of which 11 and 7 had LVD with and without post ablation EF data, respectively.

#### RESULTS

AIR T1 mapping created high-quality ECV maps. LV ECV was not significantly different (p=0.12) between LVD and normal EF groups. 93% of patients had normal ECV levels (<30%) and the maximum ECV measured was 32% (borderline fibrosis). The change in EF linearly decreased with increasing baseline EF (R2=0.76). For 11 patients with LVD who underwent ablation with follow-up EF measurements, 10 patients maintained sinus rhythm and their EF increased on average by absolute 14%. Two-tailed t-tests assuming equal variance indicate that there is significant ECV difference between patients based on age (<60 vs >=60 years) (p=0.04) but not based on gender (p=0.09) or AF type (paroxysmal vs. persistent) (p=0.49).

## CONCLUSION

Our cohort of patients with AF-induced LVD did not have evidence of myocardial fibrosis. This suggests that patients with AF-induced LVD is reversible.

# CLINICAL RELEVANCE/APPLICATION

Patients with AF-induced LVD are likely to experience improvement in EF following successful AF ablation.



### CA242-SD-WEA5

Diagnostic Value of Global Cardiac Strain in Patients with Myocarditis

Wednesday, Nov. 28 12:15PM - 12:45PM Room: CA Community, Learning Center Station #5

#### **Participants**

Caterina B. Monti, MD, 20100, Italy (*Presenter*) Nothing to Disclose Francesco Secchi, MD,PhD, Milano, Italy (*Abstract Co-Author*) Nothing to Disclose Francesco Carbone, Milan, Italy (*Abstract Co-Author*) Nothing to Disclose Marco Ali, Milan, Italy (*Abstract Co-Author*) Nothing to Disclose Paola M. Cannao, MD, Milano, Italy (*Abstract Co-Author*) Nothing to Disclose Francesco Sardanelli, MD, San Donato Milanese, Italy (*Abstract Co-Author*) Speakers Bureau, Bracco Group; Advisory Board, Bracco Group; Research Grant, Bayer AG; Advisory Board, General Electric Company; Reserach Grant, General Electric Company; Speakers Bureau, Siemens AG; Reserach Grant, Real Imaging Ltd;

### For information about this presentation, contact:

francesco.secchi@grupposandonato.it

#### PURPOSE

To investigate the diagnostic value of myocardial strain obtained by feature-tracking cardiac magnetic resonance (CMR), comparing myocarditis patients to controls.

## METHOD AND MATERIALS

A total of 46 patients with a diagnosis of myocarditis and preserved ejection fraction, who had undergone two enhanced CMR exams one during the acute phase and one at follow-up, were compared to 46 CMR exams from healthy age- and sex-matched controls. Global circumferential strain and global radial strain were calculated for each exam, along with myocardial edema and late gadolinium enhancement percentages, and with left ventricle functional parameters, through manual contouring of the myocardium.

#### RESULTS

Significant differences in global circumferential strain were found for controls (median -20.4, interquartile range (IQR) -23.4- -18.7) versus patients in the acute phase (-18.4, IQR -21.0- -16.1, P=.001) or at follow-up (-19.2, IQR -21.5- -16.1, P=.020). Significant differences in global radial strain were also found for global radial strain in controls (82.4, IQR 62.8-104.9) versus patients in the acute phase (65.8, IQR 52.9-79.5, P=.001), but only borderline significance was found versus follow-up (73.1, IQR 58.7-86.5, P=.066). Correlations were found between global radial and circumferential strain in all groups (acute, R=-0.580 P<.001; follow-up R=-0.399 P=.006; controls R=-0.609 P<.001), and between global circumferential strain and late gadolinium enhancement only in myocarditis patients (acute R=0.035 P=.024, follow-up R=0.307 P=.038).

## CONCLUSION

Cardiac strain could have a role in reducing the need for sequences other than cine in some low-risk acute myocarditis patients where CMR is the main diagnosing technique.

### **CLINICAL RELEVANCE/APPLICATION**

Given the diagnostic performance of the two short-axis strain indices, global circumferential strain and global radial strain, CMRderived strain could potentially have a role in reducing the need of sequences in addition to cine in low-risk myocarditis patients where CMR is the main diagnosing technique.



### CA244-SD-WEA7

Interobserver Agreement of Virtual Transcatheter Heart Valve to Coronary Distance in Aortic Valve-in-Valve Implantation

Wednesday, Nov. 28 12:15PM - 12:45PM Room: CA Community, Learning Center Station #7

## Participants

Lancia L. Guo, MD, Calgary, AB (*Abstract Co-Author*) Nothing to Disclose Jose Gutierrez Chacoff, MD, Santiago, Chile (*Abstract Co-Author*) Nothing to Disclose Anastasia Oikonomou, MD, PhD, Toronto, ON (*Abstract Co-Author*) Nothing to Disclose Harindra Wijeysundera, MD, PhD, Toronto, ON (*Abstract Co-Author*) Nothing to Disclose Laura Jimenez-Juan, MD, Toronto, ON (*Presenter*) Nothing to Disclose

# For information about this presentation, contact:

laura.jimenezjuan@sunnybrook.ca

### PURPOSE

Valve-in-valve (ViV) transcatheter aortic valve replacement (TAVR) has recently emerged as a successful alternative to redo surgery in patients with a failing bioprosthetic aortic valve. Coronary ostial obstruction is a serious complication of ViV TAVR, associated with high mortality. The virtual transcatheter heart valve to coronary (VTC) distance is an important CT measurement that helps in risk stratification for coronary obstruction. We aim to determine the interobserver agreement of VTC measurements in the planning CT for ViV TAVR.

#### **METHOD AND MATERIALS**

Our cohort consisted of 54 patients with failing bioprosthetic valve considered for ViV TAVR. They all had a planning CT-gated angiography prior to the procedure. Two readers measured the VTC distance by placing a virtual cylinder of the diameter of the future transcather valve centered in the basal ring plane of the bioprosthetic valve and then propagated to the level of each coronary ostium. The VTC is calculated as the distance between the edge of the virtual cylinder and the coronary ostium. Risk stratification was performed according to two published classifications in:1)low, intermediate or high risk of coronary obstruction if VTC<3, 3-6 or >6mm respectively and 2)high or low risk if VTC<=4 or >4mm. Agreement was determined by intraclass correlation coefficient (ICC) for continuous variables and by kappa coefficient for categorical variables.

### RESULTS

VTC distance agreement was excellent, especially for the left [ICC (95% CI) left VTC=0.99(0.99-0.99) and right VTC=0.94(0.89-0.96)]. When measurements were stratified in low, intermediate or high risk if VTC<3, 3-6 or >6 mm, there was a fair to good agreement for left and right VTC, with k(95% CI)=0.69(0.52-0.86) and 0.61(0.40-0.81) respectively. When measurements were stratified in high or low risk if VTC<=4 or >4mm, the agreement was good to excellent, with k(95% CI)=0.93(0.79-1.00) and 0.70(0.52-0.88) for left and right VTC respectively.

### CONCLUSION

VTC distance is a highly reproducible measurement performed in the pre-evaluation CT of candidates for ViV TAVR. It is an accurate and essential measure to stratify risk of coronary obstruction. When VTC was categorized in <=4 or >4mm (high or low risk), agreement was good to excellent.

### **CLINICAL RELEVANCE/APPLICATION**

Obtaining an accurate measurement of the VTC distance on the CT prior to ViV TAVR is crucial to stratify risk of coronary obstruction. VTC distance is highly reproducible.



## CH249-ED-WEA7

Pictorial Review of Complications and Growth Patterns in Target Therapy and Immunotherapy: The Challenge of the Oncologist Radiologist in the New Era of Cancer Care

Wednesday, Nov. 28 12:15PM - 12:45PM Room: CH Community, Learning Center Station #7

### Participants

Masao Yamamoto Ramos, MD, Mexico City, Mexico (*Presenter*) Nothing to Disclose Jose L. Villalobos Juarez, MD, 14080, Mexico (*Abstract Co-Author*) Nothing to Disclose Irlanda Pacheco Bravo, MD, PhD, Mexico City, Mexico (*Abstract Co-Author*) Nothing to Disclose Maria I. Sollozo Dupont, PhD,MSc, Mexico City, Mexico (*Abstract Co-Author*) Nothing to Disclose Beatriz Y. Cortes Garcia, MD, Mexico City, Mexico (*Abstract Co-Author*) Nothing to Disclose Jaime Garcia Gomez, MD, Mexico City, Mexico (*Abstract Co-Author*) Nothing to Disclose Elisa Lopez Rodriguez, Mexico City, Mexico (*Abstract Co-Author*) Nothing to Disclose

#### For information about this presentation, contact:

myamamotor@hotmail.com

### **TEACHING POINTS**

The first randomized trials with immunotherapy in lung cancer with anti PDL-1 agents (nivolumab), identified the effect of pseudoprogression that difficults the assessment of the disease-free period and monitoring of response. Currently target therapy and immunotherapy, is used in patients with metastatic and locally advanced disease with progression in first-line chemotherapy and is characterized by unique adverse effects and exceptional growth patterns. This presentation aims to be a guide in the evaluation of the response to treatment according to the criteria i RECIST 2017. Exemplify the adverse reactions characteristic in relation to the different drugs. Analyze the phenomenon of pseudoprogression. Evaluate the CT characteristics of EGFR, ALK and KRAS mutations.

### TABLE OF CONTENTS/OUTLINE

Characteristics by CT in the pattern of pseudoprogression. CT Radiogenomic; characterization of EGFR, ALK and KRAS mutations. Adverse effects in PDL-1 inhibitors: Pneumonitis, colitis and hypophysitis. Adverse effects on CTLA4 antibodies: Colitis, pneumonitis and myocarditis Sarcoid like lymphadepathy. Bleeding in VEGF Take home points



### CH250-ED-WEA8

## Quantitative Computed Tomography Analysis of Diffuse Lung Disease

Wednesday, Nov. 28 12:15PM - 12:45PM Room: CH Community, Learning Center Station #8

#### Awards Identified for RadioGraphics

#### Participants

Alicia Chen, MD, Rochester, MN (*Presenter*) Nothing to Disclose Brian J. Bartholmai, MD, Rochester, MN (*Abstract Co-Author*) License agreement, ImBio, LLC; Scientific Advisor, ImBio, LLC; Scientific Advisor, Bristol-Myers Squibb Company Chi Wan Koo, MD, Rochester, MN (*Abstract Co-Author*) Nothing to Disclose

### For information about this presentation, contact:

#### chen.alicia@mayo.edu

#### **TEACHING POINTS**

1. To review the development and methods of computed tomography(CT) quantitative analysis tools 2. To demonstrate the role of quantitative analysis in the diagnosis and management of diffuse lung disease 3. To explain pitfalls in quantitative analysis interpretation

### **TABLE OF CONTENTS/OUTLINE**

The complexity of diffuse lung diseases and variability of their imaging evaluation reinforces the clinical need for quantitative analysis tools. Computer-Aided Lung Informatics for Pathology Evaluation and Rating (CALIPER), one of the novel image analysis tools for characterizing and quantifying lung parenchymal diseases such as emphysema and interstitial lung diseases on high resolution CT, has been shown to be useful in prognostication and management of diffuse lung diseases. In this exhibit, we will review the development of machine learned texture analysis tools and discuss the application of such quantitative analysis in diagnosis, prognostication, and management of various diffuse lung diseases such as emphysema, interstitial lung disease, and lymphangioleiomyomatosis. Pitfalls of interpretation and potential solutions will be explored, including artifacts secondary to erroneous extraction of non-parenchymal structures and respiratory inconsistency.



## CH284-SD-WEA1

Differences of CT Bone Density, Pulmonary Function, and Bone Mineral Density According to Smoking Status and Amount in Healthy Men

Wednesday, Nov. 28 12:15PM - 12:45PM Room: CH Community, Learning Center Station #1

## Participants

Cherry Kim, MD, Ansan, Korea, Republic Of (*Presenter*) Nothing to Disclose Soriul Kim, Seoul, Korea, Republic Of (*Abstract Co-Author*) Nothing to Disclose Ki Yeol Lee, MD, PhD, Ansan, Korea, Republic Of (*Abstract Co-Author*) Nothing to Disclose Nan Hee Kim, Ansan, Korea, Republic Of (*Abstract Co-Author*) Nothing to Disclose Ji A Seo, Ansan, Korea, Republic Of (*Abstract Co-Author*) Nothing to Disclose Hwan Seok Yong, MD, PhD, Seoul, Korea, Republic Of (*Abstract Co-Author*) Nothing to Disclose Chol Shin, Ansan, Korea, Republic Of (*Abstract Co-Author*) Nothing to Disclose

### PURPOSE

To determine whether CT bone density can show differences in bone quality, and whether there is a difference in pulmonary function test (PFT) according to smoking status and amount, and to examine the correlation between CT bone density (CTBD) and bone mineral density (BMD) in healthy men.

#### **METHOD AND MATERIALS**

This cross-sectional study used data from in the \*\*\* cohort included in the \*\*\* Genome Epidemiology Study. Participants diagnosed with chronic obstructive lung disease (forced expiratory volume in one second [FEV1]/forced vital capacity [FVC]<0.70) were excluded. Finally, a total of 1034 men who underwent chest CT, BMD, PFT were included in this study. The CT attenuation value of T4, T7, T10, and L1 vertebral bodies (VD) was measured in each chest CT to obtain CTBD value. BMD, PFT, and CTBD were compared between smoking status (non-, ex-, and current smokers) and the number of pack-year (PY) of smoking (G1, PY<15; G2, 15<=PY<30; G3, PY>=30). The correlation between BMD and CTBD was also evaluated.

## RESULTS

CTBD of current smokers was significantly lower than non-smokers and ex-smokers ( $203\pm50$  vs.  $194\pm47$  vs.  $193\pm48$  at T4;  $158\pm42$  vs.  $149\pm41$  vs.  $149\pm39$  at L1; all P<0.01). BMD was also significantly lower in current smokers than in non-smokers and ex-smokers ( $1.24\pm0.2$  vs.  $1.23\pm0.2$  vs.  $1.18\pm0.2$ , P=0.005), and there was significantly more osteoporosis patients in current smokers than in non-smokers and ex-smokers (P=0.01). FEV1 and FEV1/FVC of current smokers were significantly lower than those of non-smokers and ex-smokers. According to the number of PY of smoking, G3 of CTBD at all vertebral body levels was significantly lower than G2 and G1 (all P<0.03), although there was no significant difference in BMD between the groups. FEV1 was significantly lower in G3 than G1 and G2 (P<0.001). There were significant correlations between BMD and CTBD in non-, ex-, and current smokers (r, 0.433-0.652, range).

### CONCLUSION

CT bone density were significantly different between smoking status and according to smoking amount. PFT was also significantly different. CT bone density was significantly correlated with BMD.

## **CLINICAL RELEVANCE/APPLICATION**

This study demonstrated the effect of smoking status and amount on bone quality by measuring CT bone density, which may be helpful in detecting BMD in normal subjects.



### CH285-SD-WEA2

### Hepatocellular Metastasis in the Thorax

Wednesday, Nov. 28 12:15PM - 12:45PM Room: CH Community, Learning Center Station #2

#### **Participants**

Shima Tafreshi, Rochester, NY (*Presenter*) Nothing to Disclose Susan K. Hobbs, MD,PhD, Pittsford, NY (*Abstract Co-Author*) Nothing to Disclose Brandon W. Sur, MD, Rochester, NY (*Abstract Co-Author*) Nothing to Disclose

#### For information about this presentation, contact:

Shima\_tafreshi@urmc.rochester.edu

### PURPOSE

This project analyzes the imaging features and time period for metastatic manifestation of Hepatocellular Carcinoma (HCC) in the thorax and correlates the findings with intra-abdominal tumor staging based on CT or MR findings. The goal was to establish followup recommendations for patients with HCC and to estimate the time period of thoracic metastasis to guide thoracic CT re-staging for HCC patients. Assessing time period and patterns for metastasis in the thorax helps reduce unnecessary short-term surveillance scans and helps to provide a guideline for the time line during which intervention to prolong survival could take place.

## **METHOD AND MATERIALS**

A retrospective review of 310 HCC patient using records from October 2010 to August 2014 was conducted. The patient's first Abdomen CT or MRI with signs of HCC was found, and the date and the characteristics of the hepatic nodules were noted. Initial CT or MR imaging study of the abdomen was also reviewed to determine the abdominal extent of the disease. Signs of thoracic metastasis on staging or surveillance chest CT scan were recorded.

#### RESULTS

27 patients had metastasis as lymphadenopahty, bone lesions, and enlarged lung nodules. Initial staging or surveillance CT scans led to detection of extrahepatic metastasis in 8.7% of patients with HCC. The most common thoracic metastasis was pulmonary nodules, 62.9% of those with metastasis. Other patterns of metastasis include lymphadenopathy (44%) and bony metastasis (14.8%). The average time period for thoracic metastasis since the initial diagnosis of HCC was 722 days and the median time for thoracic metastasis since the initial diagnosis of HCC was 335 days.

#### CONCLUSION

Staging and surveillance chest CT for HCC was shown to reliably detect thoracic metastasis given that surveillance imaging helped with metastasis discovery in 8.7 % of patients with HCC. The appropriate time period for subsequent thoracic surveillance should be within 1-2 years of initial diagnosis.

## **CLINICAL RELEVANCE/APPLICATION**

Currently there are no recommendations for imaging surveillance for thoracic HCC metastasis. Given the substantial number of patients developing thoracic metastasis and various metastatic patterns, it is valid to include chest CT studies as a part of followup imaging protocol for HCC. Further analysis of these patients based their intra-abdominal staging and prior treatment will help determine appropriate time interval for surveillance scan.



## CH287-SD-WEA4

Interstitial Lung Abnormalities in Stage IV Non-Small Cell Lung Cancer Patients: A Validation Study for the <u>Association with Poor Clinical Outcome</u>

Wednesday, Nov. 28 12:15PM - 12:45PM Room: CH Community, Learning Center Station #4

## Participants

Tetsuro Araki, MD, PhD, Boston, MA (Presenter) Nothing to Disclose

Suzanne E. Dahlberg, Boston, MA (Abstract Co-Author) Consultant, AstraZeneca PLC

Michael S. Rabin, MD, Boston, MA (Abstract Co-Author) Nothing to Disclose

Hiroto Hatabu, MD, PhD, Boston, MA (*Abstract Co-Author*) Research Grant, Canon Medical Systems Corporation ; Research Grant, Konica Minolta, Inc

Bruce E. Johnson, MD, Boston, MA (*Abstract Co-Author*) Research support, Toshiba Corporation; Research support, Novartis AG; Royalties, EGFR Mutation Testing; Researcher, Dana-Farber Cancer Institute

Mizuki Nishino, MD, MPH, Newton, MA (*Abstract Co-Author*) Institutional Research Grant, Merck & Co, Inc; Institutional Research Grant, Canon Medical Systems Corporation; Institutional Research Grant, AstraZeneca PLC; Speaker, F. Hoffmann-La Roche Ltd; Consultant, DAIICHI SANKYO Group

Tomoyuki Hida, Boston, MA (*Abstract Co-Author*) Research Grant, Konica Minolta, Inc Christine Lydon, Boston, MA (*Abstract Co-Author*) Nothing to Disclose

## For information about this presentation, contact:

mizuki\_nishino@dfci.harvard.edu

### PURPOSE

The presence of interstitial lung abnormalities (ILA) at diagnosis of stage IV non-small cell lung cancer (NSCLC) patients have previously shown to be associated with shorter survival. The present study aimed to validate the association in a larger cohort of treatment-naïve stage IV NSCLC patients.

## METHOD AND MATERIALS

This study included 484 patients (205 males and 279 females, median age: 62) with stage IV NSCLC. ILA was scored on the baseline chest CT scans at diagnosis prior to therapy using 3-point scale (0=no ILA, 1=equivocal for ILA, 2=ILA) using a sequential reading method by 3 readers as published previously. Clinical characteristics and overall survival (OS) were compared in patients with ILA (score 2) vs. those without ILA (score 0 or 1).

### RESULTS

ILA was present (score 2) on baseline CT in 19 of the 484 patients (3.9%, 95%CI: 2.4 - 6.1%). Patients with baseline ILA were older (median age: 69 vs. 62 years, Wilcoxon p=0.0008) and were more commonly male (68.4% (13/19) vs. 41.3% (192/465); Fisher p=0.03) compared to those without ILA. Other variables including race, smoking history, and histology were not significantly associated with baseline ILA. Patients with baseline ILA had significantly shorter overall survival compared to those without (median OS: 9.95 months [95%CI: 5.88-15.5] vs. 16.95 months [95%CI: 14.65-18.7]; Log-rank p=0.002). In multivariable analyses, baseline ILA remained significant as a marker for shorter overall survival (HR=2.09; Cox p=0.004), after adjusting for age (>70 years using the 75th percentile; HR=1.48; Cox p=0.001), male gender (HR= 1.22; Cox p=0.055) and smoking (never vs. current/former smoker; HR=0.79; Cox p=0.051).

## CONCLUSION

The presence of ILA at diagnosis of stage IV NSCLC was significantly associated with shorter survival, validating ILA as an independent marker for poor outcome.

## **CLINICAL RELEVANCE/APPLICATION**

Recognition of ILA on chest CT at diagnosis of stage IV NSCLC is important, because ILA can serve as a marker for shorter survival and may contribute to patient monitoring and management.



## CH288-SD-WEA5

The Value of Clot Volume in Risk Stratification of Acute Pulmonary Embolism Based on a 3-Dimentional Technique

Wednesday, Nov. 28 12:15PM - 12:45PM Room: CH Community, Learning Center Station #5

**FDA** Discussions may include off-label uses.

#### **Participants**

Cong Shen JR, PhD,MD, Xian, China (*Presenter*) Nothing to Disclose Youmin Guo, Xian, China (*Abstract Co-Author*) Nothing to Disclose Nan Yin, Xian, China (*Abstract Co-Author*) Nothing to Disclose Jun Wang, Xian, China (*Abstract Co-Author*) Nothing to Disclose

For information about this presentation, contact:

shencong1002@stu.xjtu.edu.cn

### PURPOSE

To investigate the value of clot volume in risk stratification of acute pulmonary embolism (APE) by a 3-dimentational technique.

## METHOD AND MATERIALS

One hundred and thirty-nine APE patients were enrolled from March 2015 to July 2016 and divided into high-risk, intermediate-risk and light-risk group according to 2014 ESC guideline. The clot volume was measured using an automated program, clot burden was assessed using semi-quantitative scores (Qanadli and Mastora), and signs of right ventricular dysfunction (RVD) were evaluated. Spearman rank coefficient was used to analyze the correlation among clot volume, semi-quantitative scores and signs of RVD. One-way ANOVA and Mann-Whitney U nonparametric test were used to compare the above indexes among three groups. Receptor operation characteristics (ROCs) curve was used to compare the AUC of the above indexes. Uni- and multivariate analyses were used to identify the independent predictors of life-threaten APE.

## RESULTS

Strong positive correlations were noted between clot volume and Qanadli (r=0.831, p<001) and Mastora (r=0.844, p<001), intermediate positive correlations were noted between clot volume and signs of RVD. Clot volume, semi-quantitative scores, signs of RVD showed significantly different in three groups (p<0.05). ROC showed clot volume has the highest AUC area of determination between high risk and intermediate risk (AUC=0.968), and intermediate risk and low risk (AUC=0.971). Only increase in clot volume was independently associated with life-threaten APE in Univariate analysis(OR=1.859,95%CI:1.368-2.527, p<0.001) and in multivariate analysis ( OR=2.379,95%CI:1.216-4.653, p<0.001).

#### CONCLUSION

Clot volume obtained by computerized software is strongly correlated with traditional semi-quantitative CT scores, and is the independent factor of life-threaten APE patients.

## **CLINICAL RELEVANCE/APPLICATION**

Acute pulmonary embolism (APE) is a common disease with high mortality, morbidity and hospitalization, ranking the third cause of death among all cardiovascular diseases. High-risk APE is confirmed to be in the presence of shock or persistent arterial hypotension. Multi-detector computed tomographic pulmonary angiography (CTPA) has been the first-line diagnostic technique in APE patients. However, semi-quantified method has limitations. The value of clot volume obtained by computer-aided detection in predicting the degree of risk of APE is faster, easier and more subjective.



## CH289-SD-WEA6

Deep Learning Reconstruction in Thoracic CT: Comparison of Image Quality with Iterative Reconstruction Methods

Wednesday, Nov. 28 12:15PM - 12:45PM Room: CH Community, Learning Center Station #6

## Participants

Patrik Rogalla, MD, Toronto, ON (*Presenter*) Institutional Research Grant, Canon Medical Systems Corporation Masakazu Matsuura, MS, Vernon Hills, IL (*Abstract Co-Author*) Employee, Canon Medical Systems Corporation Jian Zhou, PhD, Vernon Hills, IL (*Abstract Co-Author*) Principal Scientist, Canon Medical Systems Corporation; Christin Farrell, Toronto, ON (*Abstract Co-Author*) Employee, Canon Medical Systems Corporation Bernice E. Hoppel, PhD, Vernon Hills, IL (*Abstract Co-Author*) Employee, Canon Medical Systems Corporation; Sonja Kandel, MD, Toronto, ON (*Abstract Co-Author*) Nothing to Disclose

### For information about this presentation, contact:

patrik.rogalla@uhn.ca

### PURPOSE

To evaluate whether deep learning reconstruction (DLR) based on convolutional neural network will improve image quality in thoracic CT compared to two clinically established iterative reconstruction methods (IR).

### **METHOD AND MATERIALS**

48 projection datasets from subsequent patients who underwent CT of the chest (120 kV, 50 mA, 0.5 s rotation time, 0.5\*80 detector rows; Canon Aquilion Genesis) were reconstructed in 5 series: hybrid-iterative IR (AIDR) and forward-projection based IR (FIRST), both with body and lung settings, and DLR. All images were reconstructed with 1 mm slice thickness and presented as 5 on 1 (random order, no image annotation) on a 4K monitor. By using forced ranking, 2 readers (23, 10 years on staff) evaluated the series in the categories: (C1) lung, (C2) noise texture lung, (C3) mediastinum, (C4) noise texture mediastinum, (C5) artifacts, and (C6) overall appeal. The readers also graded image quality in C6 on a Likert scale (1=excellent, 10=low quality). Inter-reader agreement was calculated for all categories. Image noise (SD in ROI) was measured within the aorta and in air. All values were statistically analyzed.

#### RESULTS

DLR was unanimously preferred (rank 1) over all other reconstructions by both readers in all patients and in all categories (p<0.001) except for artifacts (C5) where DLR ranked 2nd behind AIDR body. The mean rank of AIDR body/DLR in (C5) for reader 1 and 2 was 2.19/1.70 and 2.25/1.67 respectively, p>0.05. The mean ranking/Likert score in category (C6) for AIDR body, lung, FIRST body, lung and DLR for reader 1 and 2 was 3.85/6.17, 3.29/5.76, 4.81/7.12, 2.13/3.80 and 1.00/1.88, and 3.90/5.25, 2.92/4.25, 5.00/6.88, 2.17/3.31 and 1.00/2.00, respectively, p<0.001. Inter-reader agreement for forced ranking was k=0.90, for the Likert score k=0.78. Noise in the aorta was lowest (12.2 HU) and in air second highest (22.2 HU) on DLR, p<0.01.

## CONCLUSION

Deep learning reconstruction provides superior subjective image quality in thoracic CT for lungs and mediastinum when compared to both clinically established iterative methods. DLR holds promise to eliminate the need for separate reconstructions for lungs and soft tissues.

### **CLINICAL RELEVANCE/APPLICATION**

Deep learning reconstruction carries the potential to become the future standard-of-care reconstruction in thoracic CT.



### ER164-ED-WEA5

Pancreatic Trauma: A Diagnosis Requiring a Multidisciplinary Approach

Wednesday, Nov. 28 12:15PM - 12:45PM Room: ER Community, Learning Center Station #5

#### **Participants**

Claire K. Sandstrom, MD, Seattle, WA (*Presenter*) Royalties, Cambridge University Press; Spouse, Advisory Board, BTG International Ltd;

Bryan Balmadrid, MD, Seattle, WA (*Abstract Co-Author*) Nothing to Disclose Guy E. Johnson, MD, Seattle, WA (*Abstract Co-Author*) Consultant, BTG International Ltd Barclay Stewart, MD,MPH, Seattle, WA (*Abstract Co-Author*) Nothing to Disclose

## For information about this presentation, contact:

#### cks13@uw.edu

#### **TEACHING POINTS**

Pancreatic trauma is accompanied by a high morbidity and mortality and necessitates a multidisciplinary team to treat optimally. In the era of non-operative management and minimally invasive procedures, MDCT, MRI/MRCP, and ERCP are vital diagnostic tools that guide management decisions. Due to potential pitfalls, early diagnosis remains difficult, particularly if the radiologist is not attuned to this important but uncommon diagnosis.

## **TABLE OF CONTENTS/OUTLINE**

With regards to pancreatic trauma, we will explore: Epidemiology Relevant anatomy Injury grading according to AAST Diagnosis of pancreatic injury Physical exam Laboratory findings MDCT diagnosis and pitfalls MRI/MRCP findings Endoscopic findings Indications and strategies for injury management Non-operative Endoscopic Surgical Complications



## ER222-SD-WEA1

Rapid Imaging Protocol of the Bilateral MCA Territories for Thrombectomy in Acute Ischemic Stroke by 80-Row Area Detector CT

Wednesday, Nov. 28 12:15PM - 12:45PM Room: ER Community, Learning Center Station #1

## Participants

Takahisa Mori, Kamakura, Japan (*Presenter*) Nothing to Disclose Yuhei Tanno, Kamakura, Japan (*Abstract Co-Author*) Nothing to Disclose Kazuhiro Yoshioka, Kamakura, Japan (*Abstract Co-Author*) Nothing to Disclose Noriyoshi Nakai, Kamakura, Japan (*Abstract Co-Author*) Nothing to Disclose

#### For information about this presentation, contact:

morit-koc@umin.net

## PURPOSE

The aim of our study was to design the acute stroke protocol of the 80-row area detector CT (80ADCT) scanning with short time of image reconstruction and transfer within acceptable limits of quality loss to provide soon useful information about collateral development in any institutions.

## METHOD AND MATERIALS

Volume scanning (VS) using the 80-row ADCT for 4-Dimentional (4D) CT angiography (CTA) of the bilateral MCA territories was performed with injecting non-ionic contrast medium 40ml at a rate of 4mL/s. Acquisition of the 80ADCT was performed along the MCA. CTA used 1 s single rotation and 1 s intermittent dataset scans acquired at 80kVp. Beginning 8 s after contrast medium injection, 24 intermittent volume scans at 100mA are acquired every other second during the contrast medium arrival. Each volume consisted of 40 images of 1-mm thickness with z-axis coverage of 4-cm. After transferring volumetric data (VD) to a workstation, axial 4D-CTA was generated. Examination time and image quality were evaluated.

### RESULTS

VD was transferred to workstation in about 5 minutes since starting VS and 4D axial images of the CTA were generated in mean 2 minutes. Total time until viewing images on PACS was about 7 minutes. Image quality of 4D axial images was enough in acute stroke setting.

#### CONCLUSION

Our protocol can provide useful information of collateral development by 4D axial images of CTA within 7 minutes in acute stroke setting.

## **CLINICAL RELEVANCE/APPLICATION**

Precise and objective decision of collateral development of the middle cerebral artery territories in acute stroke thrombectomy setting.



## ER223-SD-WEA2

Implementing 24/7 Onsite Cardiac Computed Tomography Angiography (CCTA) in the Emergency Department Impact on Patient Care: Retrospective Analysis of One Center Experience

Wednesday, Nov. 28 12:15PM - 12:45PM Room: ER Community, Learning Center Station #2

## Participants

Rawan Abu Mughli, MD, Vancouver, BC (*Presenter*) Nothing to Disclose Tong Wu, MD, Vancouver, BC (*Abstract Co-Author*) Nothing to Disclose Adam I. Kramer, Vancouver, BC (*Abstract Co-Author*) Nothing to Disclose Nicolas Murray, MD, Vancouver, BC (*Abstract Co-Author*) Nothing to Disclose Ana-Maria Bilawich, MD, Vancouver, BC (*Abstract Co-Author*) Nothing to Disclose John R. Mayo, MD, Vancouver, BC (*Abstract Co-Author*) Speaker, Siemens AG Anto Sedlic, MD, Vancouver, BC (*Abstract Co-Author*) Nothing to Disclose Faisal Khosa, Vancouver, BC (*Abstract Co-Author*) Scholarship, Canadian Association of Radiologists; Scholarship, Vancouver Coastal Health

Savvas Nicolaou, MD, Vancouver, BC (Abstract Co-Author) Institutional research agreement, Siemens AG

### PURPOSE

Acute chest pain is a very common and challenging presentation for emergency departments (ED). Although only a minority are true acute coronary syndrome (ACS), missed ACS carries significant morbidity and mortality and is the largest source of ED malpractice lawsuits. The other concern is that these patients can present any hour of the day. Thus, an onsite 24/7 CCTA programme is required. We evaluated the impact of implementing 24/7 onsite staff radiology coverage for CCTA in our ED on patient care.

### **METHOD AND MATERIALS**

We retrospectively reviewed 250 consecutive cases that underwent CCTA for acute chest pain in our ED over approximately 12 months. Nine were considered non-diagnostic for coronary artery evaluation and were excluded. Sex, age, cardiovascular risk factors(RFs), ECG, troponin, and disposition of groups with different degree of coronary artery stenosis(CAS) found on CCTA were analyzed.

### RESULTS

Patients' age ranged between 26 and 89 ( $\mu$ =55.9,  $\sigma$ =11.3) years. Hypertension in females (p<0.0001) and dyslipidemia in males (p=0.0003) were the most significant RFs for presence of coronary artery atherosclerosis on CCTA. All patients with negative CCTA (n=114, 47%) were discharged from the ED, and those with cardiovascular RFs were offered outpatient cardiology follow up. In the <50% CAS (n=85, 35%) group, only 1 was deemed to be of higher risk and underwent subsequent emergency coronary catheterization (CC), where no significant stenosis was identified. Out of the >50% CAS group (n=42, 17%), 31(13%) underwent subsequent CC, of which 15(6.2%) underwent percutaneous coronary intervention, 6(2.5%) were advised to have coronary artery bypass grafting, and 10(4.1%) were treated medically. Eleven(4.6%) patients did not undergo CC due to an alternative diagnosis, negative EKG and troponin, or findings of stable or distal coronary disease.

## CONCLUSION

Onsite 24/7 CCTA in the ED helped physicians in making diagnoses accurately, discharging patients confidently, and identifying cases that required urgent intervention expeditiously. Out of the low to intermediate risk patients scanned in the ED,17% had >50% stenosis, and half of these (8.7% of 241) underwent urgent catheterization with PCI or advice of CABG.

## **CLINICAL RELEVANCE/APPLICATION**

Introducing 24/7 onsite CCTA into the ED helped triage patients with acute chest pain, and helped identify ACS in low to intermediate risk patients, thus expedited and improved their care.



## ER224-SD-WEA3

Assessment of a Computer Decision Support System (CDSS) for Ordering Cardiac-CT Scan in Patients with Acute Chest Pain Based on Diamond-Forrest Pretest Probability

Wednesday, Nov. 28 12:15PM - 12:45PM Room: ER Community, Learning Center Station #3

## Participants

Olga M. Sanz de Leon, PhD, Madrid, Spain (*Presenter*) Nothing to Disclose Agustina Vicente Bartulos, MD, Madrid, Spain (*Abstract Co-Author*) Nothing to Disclose Jesus Corres Gonzalez SR, Madrid, Spain (*Abstract Co-Author*) Nothing to Disclose Ines Pecharroman de las Heras, MD, Alcala de Henares, Spain (*Abstract Co-Author*) Nothing to Disclose Javier Zamora Romero, Madrid, Spain (*Abstract Co-Author*) Nothing to Disclose Alfonso Muriel Garcia, Madrid, Spain (*Abstract Co-Author*) Nothing to Disclose

#### PURPOSE

To compare the Pre-test probability (PPT) of significant stenosis predicted by Diamond-Forrest scale (DF) with the frequency of findings in Cardiac-CT scans in patients with chest pain in an Emergency Department. To evaluate the adherence to the recommendation of a Computer Decision Support System (CDSS) on the appropriateness of Cardiac-CT scan orders.

## METHOD AND MATERIALS

Prospective study of 162 consecutive patients who underwent urgent cardiac-CT scanning (volumetric MDCT-320 detectors) recruited from March 2016 and March 2018 after implementing a CDSS aimed to aid in the decision of what patients receive imaging. CAD-RADS classification was used to harmonise radiological diagnosis. We considered significant coronary stenosis (SCS) when the reduction of the luminal diameter was  $\geq$ 50% in at least one vessel. Diamond-Forrest algorithm was implemented as a CDSS in the Emergency Department to aid in the selection of patients to undergo or not a CT scan based on their age, sex and chest pain characteristics.

#### RESULTS

60% of patients were male with mean age 57 yr. (SD 11.4). Typical angina was present in 25 (15.4%), atypical angina in 40 (24.6%) and non-anginal pain in 97 (60%). Eleven CT scans were disregarded as inconclusive. Among the 151 scans, none of them had PPT <15% nor >85%, so there was a complete adherence to the CDSS recommendation. PPT ranged between 17%-77%. The vast majority (97%) of patients has PPF within 15-65% range (mean 33.3; SD 12.5) while only 20% had radiological coronary stenosis >50%. The remaining 5 patients had PPT with 66-85% range (mean 71.5; SD 4.3) and 1 of them (20%) showed an SCS>50%. The most affected was anterior descendent artery. The observed frequency of significant stenosis in our series was much lower than the one expected by DF algorithm.

## CONCLUSION

In our ED, clinicians fully adhered to the recommendations of the CDSS thus avoiding inappropriate scans to patients with acute chest pain with PPT <15% or PPT >85%. Estimated PPT with DF model overestimates the frequency of radiological findings.

### **CLINICAL RELEVANCE/APPLICATION**

We need to refine the PPT estimative model to achieve better calibration and discrimination abilities at ED. This will improve the adequacy of ionising imaging diagnostic procedures.



### ER225-SD-WEA4

### Implementation of an Ultra-Low-Dose CT-Protocol for Extremities: Initial Experience with 106 Subjects

Wednesday, Nov. 28 12:15PM - 12:45PM Room: ER Community, Learning Center Station #4

### Participants

Zlatan Alagic, Solna, Sweden (*Presenter*) Nothing to Disclose Robert Bujila, Stockholm, Sweden (*Abstract Co-Author*) Nothing to Disclose Subhash Srivastava, Stockholm, Sweden (*Abstract Co-Author*) Nothing to Disclose Seppo K. Koskinen, MD, PhD, Stockholm, Sweden (*Abstract Co-Author*) Nothing to Disclose

### For information about this presentation, contact:

zlatan.alagic@karolinska.se

### PURPOSE

To assess if ultra-low-dose Computed Tomography (ULD-CT) is a useful clinical alternative to Digital Radiography (DR) in the evaluation of wrist and ankle fractures in the acute phase.

## **METHOD AND MATERIALS**

A ULD-CT protocol (no localizer, single rotation, 16 cm coverage) on a RevolutionTM CT (General Electric Medical Systems, Waukesha, WI, USA) was designed for scanning wrist and ankle fractures. Patients admitted to the emergency department with suspected wrist or ankle fractures were evaluated prospectively. After the standard DR obtained on a Discovery™ XR650 radiography system (General Electric Medical Systems, Waukesha, WI, USA), a ULD-CT was performed. Two readers independently analyzed DR and ULD-CT images, and the results were blinded to the readers. Also, the radiation dose (RD), examination time, as well as the time to preliminary report was compared between DR and CT.

#### RESULTS

In 106 subjects DR and ULD-CT detected 55 and 69 fractures, respectively, corresponding to an odds ratio of 1.7 for ULD-CT vs. DR. In showing the presence of a fracture, the sensitivity of DR was 76.8 %, specificity was 94.6 %, positive predictive value was 96.4 % and negative predictive value was 68.6 %. Furthermore, ULD-CT provided important additional information about soft tissue in 3 cases (2.8 %), non-fracture related findings that explained the patients symptoms in 10 cases (7.4 %), additional fracture-related findings (articular involvement or additional fractures) in 22 cases (15.7 %) and was able to confirm or rule out suspected fractures on DR in 8 cases (5.6 %). The average examination time was shorter for ULD-CT than DR ( $3.5\pm1.4$  vs.  $6.7\pm3.8$  min, p<0.001) as well as the average time to preliminary report ( $22.6\pm13.6$  min for ULD-CT vs.  $35.6\pm33.2$  min for DR, p=0.057). The average estimated effective dose was comparable between ULD-CT and DR ( $0.66\pm0.45 \mu$ Sv vs.  $0.51\pm0.47 \mu$ Sv).

## CONCLUSION

ULD-CT is an excellent alternative to DR for imaging the peripheral skeleton as it provides additional clinically important information at a comparable RD as well as faster examination and reporting times.

## **CLINICAL RELEVANCE/APPLICATION**

Ultra-low-dose Computed Tomography is an excellent alternative to Digital Radiography for imaging the peripheral skeleton in the acute setting as it provides additional clinically important information at a comparable radiation dose as well as faster examination and reporting times.



## GI309-ED-WEA8

How Low Can You Go? Challenges and Updates to MRI of Low Rectal Tumors (ESGAR 2017 Consensus Guidelines)

Wednesday, Nov. 28 12:15PM - 12:45PM Room: GI Community, Learning Center Station #8

## Participants

Brendan LoGiurato, MD, New York, NY (*Presenter*) Nothing to Disclose Iva Petkovska, MD, New York, NY (*Abstract Co-Author*) Nothing to Disclose Viktoriya Paroder, MD, PhD, Bronx, NY (*Abstract Co-Author*) Nothing to Disclose David D. Bates, MD, New York, NY (*Abstract Co-Author*) Nothing to Disclose Marc J. Gollub, MD, New York, NY (*Abstract Co-Author*) Nothing to Disclose Jennifer S. Golia Pernicka, MD, New York, NY (*Abstract Co-Author*) Nothing to Disclose

### For information about this presentation, contact:

brl9069@nyp.org

### **TEACHING POINTS**

Why is low rectal cancer treated differently than middle or high rectal cancer? What are the treatment options and considerations for low rectal cancer? Illustrate the complex anatomy of the rectum and surrounding structures: mesorectal fascia, sphincter complexes, pelvic floor muscles. How does the radiologist alter management of rectal cancer? Describe the MRI features of low rectal cancer and how they affect staging and treatment. What are the latest guidelines and updates to rectal cancer MRI (ESGAR 2017)?

## TABLE OF CONTENTS/OUTLINE

Overview of rectal cancer epidemiology and risk factors. Anatomy of the rectum and definition of low rectal cancer. Staging/treatment of low rectal cancers: NCCN Practice Guidelines (2016) vs. ESMO Clinical Practice Guidelines (2017). Updates to MRI Staging: ESGAR 2016 MRI-guided Management of Rectal Cancer Changes from 2012 guidelines, specifically addressing low rectal tumors. Optimization of MRI protocols and technical limitations. Ways that the radiologist can add value and alter treatment. Cases from our institution of low rectal tumors, for both initial staging and treatment response, involving the pelvic floor, internal and/or external sphincter, and mesorectal fascia. Case-based low rectal tumor staging quiz for interactive learning and feedback.



## GI310-ED-WEA9

**Review of Contrast Enhanced Ultrasound Scanning Errors and Artifacts** 

Wednesday, Nov. 28 12:15PM - 12:45PM Room: GI Community, Learning Center Station #9

## **FDA** Discussions may include off-label uses.

### **Participants**

Richard G. Barr, MD, PhD, Campbell, OH (*Presenter*) Consultant, Siemens AG; Consultant, Koninklijke Philips NV; Research Grant, Siemens AG; Research Grant, SuperSonic Imagine; Speakers Bureau, Koninklijke Philips NV; Research Grant, Bracco Group; Speakers Bureau, Siemens AG; Consultant, Canon Medical Systems Corporation; Research Grant, Esaote SpA; Research Grant, BK Ultrasound; Research Grant, Hitachi, Ltd

Cynthia L. Peterson, MPH, Salem, OH (Abstract Co-Author) Speakers Bureau, Bracco Group

### **TEACHING POINTS**

The purpose of this exhibit is:1. To discuss scanning parameters and how to optimize them for contrast enhanced ultrasound2. Review artifacts seen in contrast enhanced ultrasound and how to recognize and limit them3. Provide answers to frequently asked questions4. With increasing use of CEUS easily avoidable errors and pitfalls are discussed

### TABLE OF CONTENTS/OUTLINE

Review of key scanning parameters and how to optimize themCommon imaging errors caused by suboptimal scanning parametersArtifacts - artifacts that can be corrected by optimizing scanning parameters - artifacts that can not be corrected

#### **Honored Educators**

Presenters or authors on this event have been recognized as RSNA Honored Educators for participating in multiple qualifying educational activities. Honored Educators are invested in furthering the profession of radiology by delivering high-quality educational content in their field of study. Learn how you can become an honored educator by visiting the website at: https://www.rsna.org/Honored-Educator-Award/ Richard G. Barr, MD, PhD - 2017 Honored Educator



### GI311-ED-WEA10

A Resident's Guide to Understanding the New 2017 ACR White Paper for the Management of Incidental Liver Lesions on CT

Wednesday, Nov. 28 12:15PM - 12:45PM Room: GI Community, Learning Center Station #10

## Participants

Matthew Grant, MD, Tacoma, WA (*Abstract Co-Author*) Nothing to Disclose Samuel Douglass, DO, Joint Base Lewis-McChord, WA (*Presenter*) Nothing to Disclose David Tu K. Nguyen, DO, Lakewood, WA (*Abstract Co-Author*) Nothing to Disclose

## **TEACHING POINTS**

1. Review the new ACR White Paper recommendations on the Management of Incidental Liver Lesions on CT. 2. Review the ACR White Paper Algorithm with case based examples. 3. Understand the features of benign and suspicious lesions and when further evaluation is appropriate. 4. Understand the limitations of the ACR recommendations and to which scenarios they do not apply.

## TABLE OF CONTENTS/OUTLINE

I. Introduction a. Nature and scope of the problem b. Define incidentally detected liver lesion c. When to apply the algorithm II. Algorithm with case-based examples a. Basic principles b. Define low and high risk patient factors c. Define benign, suspicious, and flash-filling imaging features d. Review most commonly encountered benign liver lesions e. Case-based examples i. < 1.0 cm 1. Low-risk 2. High-risk ii. 1.0 - 1.5 cm 1. Benign 2. Suspicious 3. "Flash-filling" a. Low risk b. High risk iii. > 1.5 cm 1. Benign 2. Suspicious or "Flash-filling" a. Low risk b. High risk iii. > 1.5 cm 1. Benign 2. Suspicious or "Flash-filling" a. Low risk b. High risk III. Protocol optimization IV. Report considerations V. Summary VI. References



## GI312-ED-WEA11

Timed Barium Swallow in the Assessment of Esophageal Emptying in Patients with Achalasia: How to Do It and What to Look For

Wednesday, Nov. 28 12:15PM - 12:45PM Room: GI Community, Learning Center Station #11

### Participants

Maria Augusta Serrano Cueva, MD, Distrito Federal, Mexico (*Presenter*) Nothing to Disclose Lourdes M. Avila, MD, Mexico, Mexico (*Abstract Co-Author*) Nothing to Disclose

## For information about this presentation, contact:

magusserrano@gmail.com

### **TEACHING POINTS**

The purpose of this exhibit is: To describe the Time Barium Esophagogram (TBE) technique To get acquainted with the proper way to perform the measurements of the height and width of the barium column To learn how to avoid inadequate measurements in difficult scenarios (barium foam interface) To show key points in the interpretation of images for correlation with clinical response to treatment

## TABLE OF CONTENTS/OUTLINE

Normal anatomy Normal esophagogram Time barium swallow technique How to interpret data Pitfalls and how to avoid them



### GI313-ED-WEA12

## LI-RADS v2017: Understanding the "Ancillary Features"

Wednesday, Nov. 28 12:15PM - 12:45PM Room: GI Community, Learning Center Station #12

#### **Participants**

Fernanda G. Velloni, MD, Sao Paulo, Brazil (*Presenter*) Nothing to Disclose Hanna R. Dalla Pria, MD, Sao Paulo, Brazil (*Abstract Co-Author*) Nothing to Disclose Guilherme M. Cunha, MD, Rio de Janeiro, Brazil (*Abstract Co-Author*) Nothing to Disclose Roberto Blasbalg, MD, Sao Paulo, Brazil (*Abstract Co-Author*) Nothing to Disclose

## For information about this presentation, contact:

fernandavelloni@gmail.com

## **TEACHING POINTS**

- To address the computed tomography (CT) and magnetic resonance (MR) imaging features of focal liver lesions in patients at high risk for HCC development;- To highlight the new ancillary features displayed in the 2017 LI-RADS;- To illustrate how the new rules of application of the auxiliary features may favor the diagnosis of HCC, non-HCC malignancy or benignity;

## TABLE OF CONTENTS/OUTLINE

- Brief review of the Liver Imaging Reporting and Data System (LI-RADS);- Outline the LI-RADS ancillary features and explore the new application rules proposed in the 2017 version;- Demonstrate using clinical cases how the ancillary features make the final LI-RADS category more assertive;- Take home messages;



## GI369-SD-WEA1

Accelerating MR Elastography: Comparison of Breath-Held, Free-Breathing, and Compressed Sensing Gradient Recalled Echo MR Elastography for Evaluating Liver Stiffness

Wednesday, Nov. 28 12:15PM - 12:45PM Room: GI Community, Learning Center Station #1

**FDA** Discussions may include off-label uses.

#### **Participants**

Cara E. Morin, MD,PhD, Memphis, TN (*Presenter*) Nothing to Disclose Hui Wang, Louisville, KY (*Abstract Co-Author*) Employee, Koninklijke Philips NV Jean A. Tkach, PhD, Cleveland, OH (*Abstract Co-Author*) Nothing to Disclose Suraj D. Serai, PhD, Philadelphia, PA (*Abstract Co-Author*) Nothing to Disclose Andrew T. Trout, MD, Cincinnati, OH (*Abstract Co-Author*) Author, Reed Elsevier; Research Grant, Siemens AG; Research Grant, Canon America Medical Systems Corporation; Board Member, Joint Review Committee on Educational Programs in Nuclear Medicine Technology; Travel support, Koninklijke Philips NV; Consultant, Guerbet SA Jonathan R. Dillman, MD, Cincinnati, OH (*Abstract Co-Author*) Research Grant, Siemens AG; Research Grant, Guerbet SA; Travel support, Koninklijke Philips NV; Research Grant, Canon Medical Systems Corporation; Research Grant, Bracco Group

### For information about this presentation, contact:

jonathan.dillman@cchmc.org

#### PURPOSE

To compare breath-held, free-breathing, and compressed sensing (CS) two-dimensional (2D) gradient recalled echo (GRE) MR elastography (MRE) techniques for measuring liver stiffness.

## **METHOD AND MATERIALS**

Institutional review board approval was obtained for this HIPAA-compliant study; participant informed consent was obtained. Twenty-five adult volunteers (20 without and 5 with known liver disease) underwent MRE with five different 2D GRE techniques: breath-held, free-breathing, and CS (acceleration factors=1.5, 2, and 3). Four axial images were obtained through the mid liver with each technique, and liver stiffness measurements (kPa) were made by three blinded readers using elastograms with 95% confidence maps. Liver stiffness measurements were expressed as a mean for each technique and compared between techniques using repeated-measures analysis of variance. Absolute agreement between techniques was evaluated for each reader using singlemeasure intra-class correlation coefficients (ICC). Bland-Altman analyses were used to assess bias between techniques, using breath-held MRE as the reference technique.

#### RESULTS

Mean liver stiffness ranged from 1.42 to 5.25 kPa for the population. There was no difference in mean liver stiffness between MRE techniques for readers 1 and 3 (p>0.05); a significant difference was observed for reader 2 (p=0.02, due to higher stiffness measurements using free-breathing MRE). There was excellent absolute agreement between MRE techniques for each reader (all ICCs >0.94). Bias between techniques ranged from -0.102 to 0.089 kPa, -0.119 to 0.121 kPa, and -0.074 to 0.085 kPa for readers 1, 2, and 3, respectively.

### CONCLUSION

Both free-breathing and compressed sensing 2D GRE MRE techniques can yield similar results to conventional breath-held technique with only slight bias. Free-breathing and compressed sensing MRE may be useful in pediatric and adult patients with limited ability to breath-hold.

## **CLINICAL RELEVANCE/APPLICATION**

Free-breathing and compressed sensing MR elastography may be useful in pediatric and adult patients with limited breath-hold capacity.

#### **Honored Educators**

Presenters or authors on this event have been recognized as RSNA Honored Educators for participating in multiple qualifying educational activities. Honored Educators are invested in furthering the profession of radiology by delivering high-quality educational content in their field of study. Learn how you can become an honored educator by visiting the website at: https://www.rsna.org/Honored-Educator-Award/ Jonathan R. Dillman, MD - 2016 Honored Educator



## GI370-SD-WEA2

Evaluation of Iodine Concentration Measurement by Dual Energy CT Scan on Tumor Response for Patients with Advanced Gastric Cancer

Wednesday, Nov. 28 12:15PM - 12:45PM Room: GI Community, Learning Center Station #2

### Participants

Li Yang, MD, Shijiazhuang, China (*Presenter*) Nothing to Disclose Gaofeng Shi, MD, Shijiazhuang, China (*Abstract Co-Author*) Nothing to Disclose Jiangyang Pan, Shijiazhuang, China (*Abstract Co-Author*) Nothing to Disclose

### For information about this presentation, contact:

13582165802@163.com

## PURPOSE

To evaluate iodine concentration (IC) measurement by dual energy CT scan on tumor response for patients with advanced gastric cancer under preoperative neoadjuvant chemotherapy (NAC).

### **METHOD AND MATERIALS**

A total of 30 patients with advanced gastric cancer who had enhanced dual energy CT scan were used in this study. The IC values of primary tumors were measured before and after NAC, and the standardized IC (SIC) values were calculated. The performance in evaluation of tumor response by IC measurement was evaluated by the accuracy, sensitivity, specificity, positive predictive value (PPV), and negative predictive value (NPV). Other methods, including the criteria of T staging, Response Evaluation Criteria in Solid Tumors (RECIST 1.1) criteria, Choi's criteria and Lee SM's volume evaluation criteria, were used in comparison. All imaging measurement response methods were compared with postoperative pathological assessment results.

#### RESULTS

Using a decrease rate of >=26.5% for  $\Delta$ SIC, the accuracy, sensitivity, specificity, PPV, and NPV values were 77%, 68%, 91%, 93% and 63%, respectively. The performance by using the SIC method in evaluation of tumor response was similar to by using Choi's criteria (80%, 95%, 54%, 78% and 86%, respectively), and was superior to using the criteria of T staging (53%, 32%, 91%, 86% and 43%, respectively), RECIST 1.1 criteria (63%,47%, 91%, 90% and 50%, respectively), and Lee SM's volume evaluation criteria (60%,58%, 64%, 73% and 47%, respectively). The consistencies of postoperative pathological assessment results and the iodine measurement and Choi's density measurement were moderate (k=0.541,P<0.05 and k=0.534,P<0.05, respectively), The consistencies of postoperative pathological assessment results and the iodine measurement and Choi's density measurement results and RECIST measurement, the T staging , volume measurement and were poor (k=0.327,P<0.05, k=0.183,P>0.05, and k=0.200,P>0.05, respectively).

## CONCLUSION

Standardized iodine concentration measurement is about equal to Choi's density measurement on tumor chemotherapy response for patients with advanced gastric cancer; however, it is simpler than the Choi's measurement and has the potential to be used in clinical practice.

### **CLINICAL RELEVANCE/APPLICATION**

Standardized iodine concentration measurement has the potential to be used in clinical practice of tumor chemotherapy response for patients with advanced gastric cancer.



## GI371-SD-WEA3

Role of CT Texture Analysis (CTTA) in Differentiating Benign vs Metastatic Lymph Nodes in Patients with Anal Cancer

Wednesday, Nov. 28 12:15PM - 12:45PM Room: GI Community, Learning Center Station #3

## Participants

Hamed Kordbacheh, MD, Boston, MA (*Presenter*) Nothing to Disclose Vinit Baliyan, MBBS, MD, Boston, MA (*Abstract Co-Author*) Nothing to Disclose Thitinan Chulroek, MD, Bangkok, Thailand (*Abstract Co-Author*) Nothing to Disclose Mukesh G. Harisinghani, MD, Boston, MA (*Abstract Co-Author*) Nothing to Disclose

### For information about this presentation, contact:

hkordbacheh@mgh.harvard.edu

## PURPOSE

Inflammatory lymph nodes can be metabolically active and mimic metastatic lymph nodes on staging FDG PET CT studies in patients with anal cancer. The purpose of this study was to evaluate the potential of CTTA in differentiating benign metabolically active lymph nodes from metastatic lymph nodes

## METHOD AND MATERIALS

Consecutive anal cancer patients who were found to have metabolically active suspicious inguinal/pelvic lymph nodes on FDG-PET imaging were retrospectively included. In all patients who underwent a biopsy of the suspicious lymph nodes, CTTA was performed on contrast enhanced CT images that were either acquired concurrently or within 1 month of the PET scan but before the biopsy. CTTA parameters comprised a filtration-histogram technique with different spatial scale filter (SSF) values (0-6). CTTA quantification at each SSF value included histogram-based statistical parameters including mean intensity, standard deviation (SD), entropy, mean of positive pixels (MPP), skewness, and kurtosis. The values between benign and metastatic nodes were compared using Mann-Whitney test. Two-tailed p<0.05 were considered significant.

#### RESULTS

31 patients were included (F/M: 17/14; mean age:  $61.7 \pm 14.8$  years). Total 36 Lymph nodes were biopsied (32 inguinal, 4 pelvic) and 24 were found to be positive while 12 nodes were negative. Malignant lymph nodes had a greater size ( $2.15\pm 1.19$  cm vs.  $1\pm 0.25$  cm) compared to benign lymph nodes. The mean attenuation of the benign and malignant nodes was not different ( $68.02 \pm 19.78$  vs.  $78.95 \pm 10.66$ ). Among the different CTTA metrics entropy showed a significant difference between benign and malignant nodes at all filter values. MPP were significantly different for SSF 0, 2 & 3. Skewness showed a significant difference on SSF 0 & 2. Mean showed a significant difference on SSF 2 & 3. The remaining texture variables were not different between two groups.

### CONCLUSION

CTTA parameters including entropy, MPP, Skewness and mean particularly on smaller filter scales can differentiate metabolically active benign lymph nodes from metastatic ones.

#### **CLINICAL RELEVANCE/APPLICATION**

CTTA parameters can differentiate metabolically active benign lymph nodes from metastatic ones. This may be helpful in enhancing accuracy of FDG PET in staging patients with anal cancer.



## GI372-SD-WEA4

Magnetic Resonance Liver Hepatic Quantification: Hepatic Steatosis Normalization after 6 Months of Sleeve Gastrectomy-Preliminary Results

Wednesday, Nov. 28 12:15PM - 12:45PM Room: GI Community, Learning Center Station #4

## Participants

Adriano Liguori, MD, Natal, Brazil (*Presenter*) Nothing to Disclose Ana Paula Faygh, Natal, Brazil (*Abstract Co-Author*) Nothing to Disclose Galtieri Medeiros, Natal, Brazil (*Abstract Co-Author*) Nothing to Disclose Eudes P. de Godoy, Natal, Brazil (*Abstract Co-Author*) Nothing to Disclose Jacob Szejnfeld, MD, Sao Paulo, Brazil (*Abstract Co-Author*) Nothing to Disclose Suzan M. Goldman, MD, Sao Paulo, Brazil (*Abstract Co-Author*) Nothing to Disclose

### For information about this presentation, contact:

adrianoliguori@gmail.com

## PURPOSE

Quantify ectopic liver fat deposits changes after laparoscopic Sleeve Gastrectomy using MRI and correlate to subcutaneous and visceral fat tissues reduction.

### METHOD AND MATERIALS

From Feb 2017 to Apr 2018 we conducted a prospective cohort study in 11 patients undergoing laparoscopic Sleeve Gastrectomy with hepatic biopsy for obesity treatment. Mean age was 40.1 years (30 - 60). Each patient performed 2 MRI exams (30 days prior and 06 months after surgery). A proton density fat fraction (IDEAL-IQ®) and a T1 volumetric (LAVAflex) were performed to generate a Fat Fraction map and a fat-only volumetric volume. Images were interpreted on OsiriX (v7.0, Pixmeo SARL). Circle ROIs were drawn over the right and left liver lobes on Fat Fraction map. On a single slice at L3-L4 level, subcutaneous and visceral fat areas were calculated using sliceOmatic (v5.0, TomoVision). Statistical analysis were performed using SPSS for Mac (2018 release, IBM). Wilcoxon test was used for comparison between pre- and post-surgery variables and Spearman test for correlation analysis. Data were expressed through median, minimum and maximum values.

#### RESULTS

Median BMI before surgery was 47.3 kg/m2 (39.3 - 50.1) and after 06 months was 35.8 kg/m2 (29.2 - 40.6) (p = 0.003). Median percentage of excess weight loss was 49.1% (31-62.2). Hepatic biopsies were possible in 5 patients. Four had hepatic steatosis grade I (Fat Fraction ranging from 5.6 to 9.3%) and one grade II (Fat Fraction 25.3%). Median right liver lobe Fat Fraction was 8.0% (4.6 - 26.8) preoperatively and 3.0% (2.2 - 11.3) on follow-up (p = 0.003). Median left liver lobe Fat Fraction was 7.2% (4.4 - 25.3) preoperatively and 3.6% (1.9 - 6.8) on follow-up (p = 0.003). Median subcutaneous fat area was 533.9 cm2 (421 - 688.5) preoperatively and 321.3 cm2 (273.7 - 534.5) on follow-up (p = 0.003). Median visceral fat area was 244.3 cm2 (170.1 - 322.7) preoperatively and 151.1 cm2 (94.6 - 193.3) on follow-up (p = 0.003). There were no identifiable correlations between reduction in steatosis and reduction in visceral or subcutaneous fat areas.

### CONCLUSION

Sleeve gastrectomy significantly reduces hepatic steatosis as soon as 06 months following surgery.

#### **CLINICAL RELEVANCE/APPLICATION**

MRI with quantification techniques is reliable to monitor hepatic steatosis reduction and body composition changes after laparoscopic Sleeve gastrectomy. MRI might preclude liver biopsy during Sleeve gastrectomy.



## GI373-SD-WEA5

## Can MR Differentiate Between Low Rectal Cancer and Anal Cancer?

Wednesday, Nov. 28 12:15PM - 12:45PM Room: GI Community, Learning Center Station #5

### Awards Student Travel Stipend Award Student Travel Stipend Award

#### **Participants**

Kamonwon Cattapan, MD, Hatyai, Thailand (*Presenter*) Nothing to Disclose Thitinan Chulroek, MD, Bangkok, Thailand (*Abstract Co-Author*) Nothing to Disclose Hamed Kordbacheh, MD, Boston, MA (*Abstract Co-Author*) Nothing to Disclose Dearada Wangcharoenrung, MD, Boston, MA (*Abstract Co-Author*) Nothing to Disclose Mukesh G. Harisinghani, MD, Boston, MA (*Abstract Co-Author*) Nothing to Disclose

### For information about this presentation, contact:

kamonwon.c@psu.ac.th

#### PURPOSE

To evaluate role of pelvic MRI in differentiating between low rectal cancer and anal cancer using pathological result as gold standard

### METHOD AND MATERIALS

In this IRB approved retrospective study a total of 96 patients with history of low rectal (n=48) or anal cancers (n=48) who underwent pelvic MR imaging before treatment were included. Two radiologists with 3 and 8 year-experiences in reading abdominal MRI reviewed the studies while they were blinded to the clinical history and histopathological result, independently. Distance from anal verge to lower part of the tumor, percentage of the tumor above puborectalis muscle, size of the tumor, T2W signal intensity, sphincter/levator ani muscle invasion, organ invasion, and diagnosis of the studies were recorded. Univariable logistic regression was performed, followed by multivariable logistic regression that included variables selected to determine factors associated with low rectal and anal cancers. The distance from anal verge to the tumor was compared using receiver-operating characteristic (ROC) curve.

### RESULTS

Forty-eight cases were rectal cancer (F/M;18/30), mean age  $60.27\pm14.7$  (22-87), and the remainder 48 were anal cancer (F/M; 34/14), mean age  $61.68\pm11.21$  (42-86). Based on the ROC curves, the cut-off value for the distance from anal verge to the lower part of the tumor was 2.1 cm, with area under the ROC curve of 0.90 (95%CI: 0.83, 0.87). Multivariate logistic regression revealed rectal cancer was highly associated with T2 mixed hyper/hyposignal intensity (odds ratio [OR] 62.95, 95% CI: 4.44, 892.11), a distance cut-off value (OR = 33.12, 95%CI: 5.47, 200.75), and the absence of sphincter invasion (OR 18.12, 95%CI: 1.85, 177.93). Combining these three significant factors, the sensitivity, specificity, positive predictive value, and negative predictive value in diagnosis of low rectal cancer were 97.9, 87.5, 88.7, and 97.7%, respectively, and increased the diagnostic accuracy, from 78.1% (reader 1) and 81.3% (reader 2) to 92.7%.

### CONCLUSION

Combining the distance cut-off value from the anal verge to tumor, T2 mixed hyper/hyposignal intensity, and absence of sphincter invasion, may increase the accuracy in differentiating low rectal from anal cancers.

#### **CLINICAL RELEVANCE/APPLICATION**

The anatomic locations of low rectal and anal cancers are close and often overlap. Using these three MRI findings can increase diagnostic accuracy which benefit for staging and treatment planning.



## GI374-SD-WEA6

## Whole Liver Quantification of Hepatic Steatosis Using Dual-Energy Computed Tomography

Wednesday, Nov. 28 12:15PM - 12:45PM Room: GI Community, Learning Center Station #6

#### **Participants**

Ahmed M. Amer, MD, Birmingham, AL (Presenter) Nothing to Disclose

Samuel J. Galgano, MD, Birmingham, AL (*Abstract Co-Author*) Research support, Blue Earth Diagnostics Ltd Andrew D. Smith, MD,PhD, Birmingham, AL (*Abstract Co-Author*) President and Owner, Radiostics LLC; President and Owner, eRadioMetrics LLC; President and Owner, Liver Nodularity LLC; President and Owner, Color Enhanced Detection LLC; Patent holder Kristin K. Porter, MD,PhD, Baltimore, MD (*Abstract Co-Author*) Nothing to Disclose Desiree E. Morgan, MD, Birmingham, AL (*Abstract Co-Author*) Institutional Research Grant, General Electric Company

### For information about this presentation, contact:

amamer@uabmc.edu

## PURPOSE

To investigate a volumetric whole liver dual-energy computed tomography (DECT) biomarker for hepatic steatosis compared to true unenhanced single energy (SECT).

## METHOD AND MATERIALS

IRB approved HIPAA compliant retrospective search of radiology information system for consecutive adult patients (pts) at risk for hepatic steatosis who had standardized multiphasic abdominal DECT from 4/13/15 through 5/10/17, including true unenhanced SECT and arterial phase DECT acquisitions. A single operator analyzed the DECT images with VCAR software to automatically segment the whole liver and generate 70 keV, virtual unenhanced (VUE), fat density map (FD) images. 2D hepatic ROIs were populated to identical image locations on DECT and SECT images for each subject, avoiding lesions or vessels; 3 ROIs on consecutive slices were averaged to provide a 2D mean value. The 3D volumetric whole liver FD and VUE values were compared to their corresponding 2D mean values and the 2D true unenhanced SECT mean value. Based on SECT measurements, pts were divided into 4 groups: severe (<=25 HU), moderate (26-40 HU), mild (41-55 HU), and no steatosis (>=56HU). Pearson correlation was used to compare continuous variables; Mann-Whitney (Wilcoxon) test was used to compare separation between the groups.

### RESULTS

202 pts (72M, 130F, mean age 59.5) had severe (7%), moderate (35%), mild (50%) and no steatosis (7%). Mean 2D value of FD (mg/mL) increased with higher severity of steatosis (severe=24.1, moderate=16.3, mild=7.32, and no steatosis=3.05; P<0.0001). Pearson correlation between CU values and 2D FD, CU and 3D FD, CU and VUE values were -0.86, -0.83, and 0.88, respectively. There was a difference between overall mean values of 2D FD ROI ( $11.9\pm7.5$  mg/mL) and 3D whole liver values ( $14.5\pm6.6$  mg/mL) (P= <0.0001), and consistent separation between the 4 groups was achieved using mean 3D whole liver FD values (P <0.0001).

### CONCLUSION

DECT whole liver fat density highly correlates with hepatic steatosis based on attenuation on unenhanced SECT scans.

#### **CLINICAL RELEVANCE/APPLICATION**

DECT volumetric whole liver fat density is a quantitative biomarker that correlates highly with hepatic steatosis based on HU, warranting comparison to MR hepatic fat fraction and biopsy.



## GI375-SD-WEA7

Correlation between Changes in Liver and Spleen Volumes and Mayo Risk Score Over Long Term Follow-up in Primary Sclerosing Cholangitis Patients

Wednesday, Nov. 28 12:15PM - 12:45PM Room: GI Community, Learning Center Station #7

## Participants

Pegah Khoshpouri, MD, Baltimore, MD (*Presenter*) Nothing to Disclose Sanaz Ameli, MD, Baltimore, MD (*Abstract Co-Author*) Nothing to Disclose Mounes Aliyari Ghasabeh, MD, Baltimore, MD (*Abstract Co-Author*) Nothing to Disclose Angela Jacob, Baltimore, MD (*Abstract Co-Author*) Nothing to Disclose Ankur Pandey, MD, Baltimore, MD (*Abstract Co-Author*) Nothing to Disclose Pallavi Pandey, MD, Baltimore, MD (*Abstract Co-Author*) Nothing to Disclose Manijeh Zarghampour, MD, Baltimore, MD (*Abstract Co-Author*) Nothing to Disclose Farnaz Najmi Varzaneh, MD, Baltimore, MD (*Abstract Co-Author*) Nothing to Disclose Yan Luo, MD, Wuhan, China (*Abstract Co-Author*) Nothing to Disclose Ihab R. Kamel, MD, PhD, Baltimore, MD (*Abstract Co-Author*) Research Grant, Siemens AG

#### For information about this presentation, contact:

pkhoshp1@jhmi.edu

#### PURPOSE

To determine if changes in liver volumes, both total (T) and lobar (right and left including caudate; R, L, C), spleen (S) volume, and ratios of L and C to total liver volume (L/T, C/T) correlate with changes in Mayo risk score on long term follow-up of PSC patients.

#### METHOD AND MATERIALS

This HIPAA compliant, retrospective single center study included 101 PSC patients with baseline and follow-up imaging studies (MR/CT) with the average of 43 months (range 3-154 months) interval between 2000 and 2017. T, R, L, C, and S were measured using Advantage Workstation (GE) on both imaging studies for each case. Patients were stratified into group 1 and 2 with low (<2) and high (>=2) baseline Mayo score, respectively. Within each group patients were subdivided based on changes in Mayo score over extended follow-up into group A and group B (change in Mayo score <1 and >=1 respectively). To evaluate the differences between baseline and follow-up liver and spleen volumes between group A and B, T test was performed. P value <0.05 was considered statistically significant.

#### RESULTS

Our cohort included 61 males and 40 females with mean age of 42 at baseline and 45 at follow-up, with no significant differences in age between males and females. In group 1, extended follow up showed smaller T and R and larger S in subgroup A, where Mayo score was stable (n=50). However, in subgroup B where Mayo score deteriorated over time (n=36) L, C, S, L/T, and C/T significantly increased and R significantly decreased compared to baseline and no difference in T was seen. There was no significant change in liver and spleen volumes in patients in group 2 (high baseline Mayo score; n=23) in spite of worsening Mayo score over extended follow-up (p=ns).

### CONCLUSION

On long term follow-up of PSC patients with low baseline Mayo score, stable Mayo score correlated with stable left lobe liver and caudate volumes and their ratio to total liver. However, increase in Mayo score correlated with increase in those volumes and also spleen volume. In patients with high baseline Mayo score there was no correlation between changes in Mayo and changes in liver and spleen volume.

### **CLINICAL RELEVANCE/APPLICATION**

Patients with mild PSC at baseline demonstrate significant changes in liver and spleen volumes as the disease progressed and Mayo score increased.

#### **Honored Educators**

Presenters or authors on this event have been recognized as RSNA Honored Educators for participating in multiple qualifying educational activities. Honored Educators are invested in furthering the profession of radiology by delivering high-quality educational content in their field of study. Learn how you can become an honored educator by visiting the website at: https://www.rsna.org/Honored-Educator-Award/ Ihab R. Kamel, MD, PhD - 2015 Honored Educator



## GU234-SD-WEA2

## Magnetic Resonance Imaging in Chylous Leakage of Female Reproductive System

Wednesday, Nov. 28 12:15PM - 12:45PM Room: GU/UR Community, Learning Center Station #2

**FDA** Discussions may include off-label uses.

#### **Participants**

Meng Huo, Beijing, China (*Presenter*) Nothing to Disclose Yunlong Yue, MD, Beijing, China (*Abstract Co-Author*) Nothing to Disclose Zhenchang Wang, MD, PhD, Beijing, China (*Abstract Co-Author*) Nothing to Disclose ChunYan Zhang, Beijing, China (*Abstract Co-Author*) Nothing to Disclose Rengui Wang, MD, Beijing, China (*Abstract Co-Author*) Nothing to Disclose Mengjun Wang, Beijing, China (*Abstract Co-Author*) Nothing to Disclose

#### For information about this presentation, contact:

weimeng0322@163.com

#### PURPOSE

To evaluate the value of magnetic resonance thoracic ductography (MRTD) and magnetic resonance (MR) pelvic scanning in the chylous leakage of female reproductive system.

### **METHOD AND MATERIALS**

A retrospective evaluation of the imaging findings of MRTD and pelvic MR in 7 patients was performed, and compared with direct lymphangiography (DLG) ,lymphoscintigraphy and surgery.

## RESULTS

The rate of thoracic duct visualization in DLG was 71.4% (5/7). The rate of venous angle visualization in lymphoscintigraphy was 71.4% (5/7). The rate of thoracic duct visualization in MRTD was 100% (7/7). Except for 1 case with generally normal findings, the remaining 6 cases showed obstruction of the thoracic duct in MRTD. Among those cases, bilateral drainage was found in 1 case, right thoracic duct was seen in 1 case, multiple tortuous dilated lymphatic channels around the venous angle was detected in 4 cases, and multiple lymphangiomas was seen in 1 case. All of the 7 patients were conducted by surgery. 6 cases were confirmed as obstruction of the thoracic duct. MRTD & pelvic MR found more multiple lymphangiomas lesions and detected 2 cases with bone abnormalities.

## CONCLUSION

MRTD combined with pelvic MR could not only make up the false absence of thoracic duct in DLG and lymphoscintigraphy, but also provided more comprehensive assessment of reproductive system chylous leakage. It should be used as routine examination before operation.

### **CLINICAL RELEVANCE/APPLICATION**

Maybe it's the fist time to use magnetic resonance thoracic ductography (MRTD) in chylous leakage of female reproductive system.



## GU235-SD-WEA3

## Error and Discrepancy: Advantages of Double Reading Protocol in Prostate MRI

Wednesday, Nov. 28 12:15PM - 12:45PM Room: GU/UR Community, Learning Center Station #3

#### **Participants**

Eduardo Alvarez-Hornia, MD, Bilbao, Spain (*Presenter*) Nothing to Disclose Pedro Arguis Gimenez, Bilbao, Spain (*Abstract Co-Author*) Nothing to Disclose Maria Aguilar Muniz, Bilbao, Spain (*Abstract Co-Author*) Nothing to Disclose Gonzalo Solis Polo, Bilbao, Spain (*Abstract Co-Author*) Nothing to Disclose

## For information about this presentation, contact:

eduhornia@gmail.com

### PURPOSE

To describe our work methodology using a Double Reading protocol in the evaluation of all prostate MRI performed in our center. To emphasize the importance of quality control in the radiology reports, avoiding the omission of important findings, misinterpretation of images and mistakes by distraction, minimizing the number of inaccuracies in the reports. To emphasize the importance of a homogeneous language and communication among radiologists to facilitate reading and understanding of the report by the responsible physician.

### **METHOD AND MATERIALS**

We reviewed all prostate MRI reports assessed by Double Reading from January to December 2017. 671 studies were reviewed. 2017 was taken as reference to illustrate the level of agreement and homogeneity achieved with our double reading protocol (which we have applied systematically in a total of 1719 studies in the period 2014-2017) All the studies were performed in a 1.5 Tesla using a surface coil and following our prostate MRI protocol. All the reports were made and reviewed by four expertise radiologists. In our center, prostate MRI report process follows this sequence: First radiologist supervises the study during its execution and makes a report following the PI-RADS-2 guidelines. This report is available for a second radiologist to perform the review. Level of disagreement was assessed using a 5 grade score, based on the clinical impact on patient management.

## RESULTS

91.5% of the reports (614 studies) were approved without changes (Grades 0 and 1), with majority (67.79%) with total agreement (455 cases). In cases with discrepancies (216 reports), majority (73.61%) were Grade 1. 55 cases (8.2%) required reevaluation and discussion of the study. The cases of discrepancy with clinical repercussion (grades 3 and 4) were minority (0.75%), not appreciating any Grade 4 report.

## CONCLUSION

Quality control with double reading: Reduce diagnostic errors and misinformation. It favors a homogeneous, uniform and comprehensible reporting style. Encourages communication between the radiologists themselves and with the requesting doctors and increases their confidence in our report.

### **CLINICAL RELEVANCE/APPLICATION**

Errors and discrepancies in radiological practice are not uncommon and are not always unavoidable. Establishing a double reading system is a valuable tool to minimize the error in the evaluation of prostatic MRI.



### GU236-SD-WEA4

## Clinical Utility of Contrast Enhanced MRI in Diagnosis of Ectopic Pregnancy

Wednesday, Nov. 28 12:15PM - 12:45PM Room: GU/UR Community, Learning Center Station #4

### Participants

Naoko Nishio, Kyoto, Japan (*Presenter*) Nothing to Disclose Aki Kido, MD, Kyoto, Japan (*Abstract Co-Author*) Nothing to Disclose Yasuhisa Kurata, Kyoto, Japan (*Abstract Co-Author*) Nothing to Disclose Manabu Minami, MD, PhD, Yokohama, Japan (*Abstract Co-Author*) Nothing to Disclose Koji Tokunaga, MD, Kyoto, Japan (*Abstract Co-Author*) Nothing to Disclose Maya Honda, Kyoto, Japan (*Abstract Co-Author*) Nothing to Disclose Kyoko K. Nakao, MD, Kyoto, Japan (*Abstract Co-Author*) Nothing to Disclose Kyoko K. Nakao, MD, Kyoto, Japan (*Abstract Co-Author*) Nothing to Disclose Ryo Kuwahara, MD, Kyoto, Japan (*Abstract Co-Author*) Nothing to Disclose Ryo Yajima, Kyoto, Japan (*Abstract Co-Author*) Nothing to Disclose Masaki Mandai, Kyoto, Japan (*Abstract Co-Author*) Nothing to Disclose Kaori Togashi, MD, PhD, Kyoto, Japan (*Abstract Co-Author*) Nothing to Disclose Kaori Togashi, MD, PhD, Kyoto, Japan (*Abstract Co-Author*) Research Grant, Bayer AG; Research Grant, DAIICHI SANKYO Group; Research Grant, Eisai Co, Ltd; Research Grant, FUJIFILM Holdings Corporation; Research Grant, Nihon Medi-Physics Co, Ltd; Research Grant, Canon Medical Systems Corporation

## PURPOSE

To investigate whether contrast enhanced (CE-) MRI improves diagnostic accuracy of ectopic pregnancy compared with noncontrast enhanced (non-CE) MRI.

## METHOD AND MATERIALS

This study enrolled 63 patients with ectopic pregnancy who underwent surgical procedures and were pathologically confirmed for the implantation sites. Two radiologists who were familiar with female gynecologic imaging (expert (Ex) group) and two radiologists who were not (non-Ex group) independently reviewed non-CE MRI and combination of non-CE and CE-MRI with more than 2 weeks interval. Any disagreement was resolved by consensus in each group. Following features were evaluated: extrauterine gestational sac (GS)-like structure (shape, signal intensities on T1WI, T2WI and DWI, presence of "T2 three rings" appearance and T2-distinct low intensity area, presence of tree-like component, degree of contrast enhancement), dilatation of the fallopian tubes, presence of fresh hematoma and bloody ascites. Implantation sites were also determined and compared with operation records. The detection of these imaging findings were compared between non-CE and CE-MRI.

## RESULTS

Ex group correctly diagnosed implantation sites in 58/63(92%) at both non-CE and CE-MRI. In non-Ex group, diagnostic accuracy was improved from 54/63(86%) at non-CE MRI to 58/63(92%) at CE MRI, but the difference was not significant (p=.29). In non-Ex group, confidence level for implantation sites significantly increased after contrast enhancement (p<.01). In comparison between Ex and non-Ex group, confidence level was significantly different at non-CE MRI (p<.01), but not at CE-MRI. As for the comparison between non-CE and CE MRI, dilation of the fallopian tubes was more frequently observed at CE-MRI in non-expert group (p=.004). Also, there was significant difference in signal intensities of GS on T1WI between the first and second evaluation in non-expert group (p<.05). There was not significant difference in every findings in Ex-group.

## CONCLUSION

CE-MRI did not significantly improved diagnostic accuracy of ectopic pregnancy in both Ex and non-Ex groups, though confidence level might improve at CE-MRI in non-Ex group.

### **CLINICAL RELEVANCE/APPLICATION**

In ectopic pregnancy, it is not necessary to add contrast enhanced MRI for determining implantation sites of GS for specialists. This result leads to reduce scan time and risk for the patients.



## GU237-SD-WEA5

Quantitative Analysis of Tumor Morphology in Small (< 4 Cm) Renal Tumors on Computed Tomography: Differentiation of Fat-Invisible Angiomyolipoma from Renal Cell Carcinoma

Wednesday, Nov. 28 12:15PM - 12:45PM Room: GU/UR Community, Learning Center Station #5

## Participants

Hye Seon Kang, MD, Daejeon, Korea, Republic Of (*Presenter*) Nothing to Disclose Jung Jae Park, Daejeon, Korea, Republic Of (*Abstract Co-Author*) Nothing to Disclose In Ho Lee, MD, Daejeon, Korea, Republic Of (*Abstract Co-Author*) Nothing to Disclose

#### PURPOSE

To evaluate the value of quantitative shape factor of small renal tumor on computed tomography (CT) in differentiating fat-invisible angiomyolipoma (AML) from renal cell carcinoma (RCC).

## METHOD AND MATERIALS

In 252 consecutive patients (167 men and 85 women), 257 pathologically confirmed renal tumors (either AML or RCC) which did not include visible fat on pre-contrast CT image were enrolled in this study. An experienced genitourinary radiologist drew region of interest along the tumor margin in all contrast-enhanced axial CT images covering entire tumor by using the image processing software (ImageJ). The tumor perimeter and area were recorded in each axial image and a quantitative shape factor, circularity was calculated as following equation:  $4 \times \pi \times (area / perimeter2)$ . The median circularity (C\_median) was adopted as representative value in each tumor. The C\_median was compared between fat-invisible AML and RCC and the receiver operating characteristics (ROC) curve analysis was done for evaluating diagnostic performance for differentiating AML from RCC. An additional reader (second year resident) independently evaluated the images to assess inter-reader agreement for measurement.

### RESULTS

Of 257 tumors, 26 were AML and 231 were RCC (184 clear cell RCC, 25 papillary RCC, and 22 chromophobe RCC). The mean C\_median of AML was significantly lower than RCC ( $0.86 \pm 0.04 \text{ vs.} 0.93 \pm 0.02$ , P < 0.001). The mean C\_median was not different between subtypes of RCC ( $0.93 \pm 0.02$ ,  $0.92 \pm 0.02$ , and  $0.92 \pm 0.02$  for clear cell, papillary, and chromophobe RCC, respectively, P = 0.21). The area under the ROC curve of C\_median for differentiating fat-invisible AML from RCC was 0.924. The sensitivity and specificity were 90.9 % and 88.5 %, respectively (cut-off of C\_median, 0.90). The inter-reader agreement for evaluating C\_median was excellent (intraclass correlation coefficient, 0.84).

## CONCLUSION

Circularity calculated on CT image is a useful quantitative shape factor of small renal tumor for differentiating fat-invisible AML from RCC.

### **CLINICAL RELEVANCE/APPLICATION**

Radiologic differentiation between fat-invisible AML and RCC is clinically important to avoid unnecessary interventional or surgical manipulation.



## GU238-SD-WEA6

Clinicopathological Characteristics of False-Negative Clinically Significant Prostate Cancers on Multiparametric MRI

Wednesday, Nov. 28 12:15PM - 12:45PM Room: GU/UR Community, Learning Center Station #6

## Participants

Ayumu Kido, Kurashiki, Japan (*Presenter*) Nothing to Disclose Tsutomu Tamada, MD,PhD, Kurashiki, Japan (*Abstract Co-Author*) Nothing to Disclose Naoki Kanomata, Kurashiki, Japan (*Abstract Co-Author*) Nothing to Disclose Hidemitsu Sotozono, MD, Kurashiki, Japan (*Abstract Co-Author*) Nothing to Disclose Takeshi Fukunaga, Kurashiki, Japan (*Abstract Co-Author*) Nothing to Disclose Akihiko Kanki, MD, Kurashiki, Japan (*Abstract Co-Author*) Nothing to Disclose Akira Yamamoto, MD, Kurashiki, Japan (*Abstract Co-Author*) Nothing to Disclose

#### For information about this presentation, contact:

ttamada@med.kawasaki-m.ac.jp

### PURPOSE

To clarify the diagnostic performance of Prostate Imaging and Reporting Data System Version 2 (PI-RADS v2) and the clinicopathological features of false-negative, clinically significant prostate cancer (csPC) on overall multiparametric prostate MRI (mpMRI) assessment.

### **METHOD AND MATERIALS**

A total of 95 prostate cancer patients with 136 csPC (>0.5 cc with Gleason score (GS) =6 or >5 mm with GS >6) undergoing 3-T mpMRI including T2-weighted imaging (T2WI), diffusion-weighted imaging (DWI), and dynamic contrast-enhanced MRI (DCE-MRI) before radical prostatectomy were included. Two radiologists independently assigned each lesion a score of 1 to 5 on T2WI and DWI, positive or negative early enhancement effect (EEE) on DCE-MRI, and overall PI-RADS assessment category according to PI-RADS v2. The mean tumor apparent diffusion coefficient (ADC) was also measured. Clinicopathological findings were compared between detectable tumors and undetectable tumors, using overall mpMRI criteria: if the lesion showed a positive finding on at least one of the three MR sequences (T2WI score >3, DWI score >3, and positive EEE), the lesion was considered a detectable tumor.

### RESULTS

The detection rate of csPS using a cutoff value of category 3 or more on PI-RADS for a positive lesion was 72.1% (98/136 lesions) on lesion-based analysis and 83.2% (79/95 patients) on patient-based analysis. In 38 lesions with a PI-RADS assessment category <3, 4 lesions (all peripheral zone (PZ)), 7 lesions (all transition zone (TZ)), and 14 lesions (PZ in 6 and TZ in 8) showed positive MRI findings for T2WI, DWI, and DCE-MRI, respectively. A total of 17 undetectable lesions (12.6%) on overall mpMRI criteria had lower PSA, PSA density, and D'Amico risk classification and higher tumor ADC than 118 detectable lesions (87.4%; P =0.042 to <0.001). There were no significant differences in age, prostate volume, tumor size, tumor location (PZ or TZ), prostatectomy GS, pathological T stage, and degree of suspected extraprostatic extension (P =0.061 to 0.373).

### CONCLUSION

These observations showed that continued revision of PI-RADS with limited tumor detection ability for csPC is warranted, and the role of DCE-MRI should be reconsidered. Undetectable tumors on mpMRI may be accepted as insignificant PC, because they may be at low risk and have low cellularity.

## **CLINICAL RELEVANCE/APPLICATION**

Further revision of PI-RADS v2 including overall mpMRI criteria will improve the detection of csPC.



## GU239-SD-WEA7

Doppler Assessment of the Fetal Pulmonary Artery as a Predictor of Neonatal Respiratory Distress Syndrome in Diabetic Mothers

Wednesday, Nov. 28 12:15PM - 12:45PM Room: GU/UR Community, Learning Center Station #7

## Participants

Shaktiprada Nayak, MBBS, New Delhi, India (*Presenter*) Nothing to Disclose Mahesh K. Mittal, MBBS, MPH, New Delhi, India (*Abstract Co-Author*) Nothing to Disclose

For information about this presentation, contact:

shak.it07@gmail.com

## PURPOSE

To assess the accuracy of various Doppler parameters as a predictor of neonatal RDS in Diabetic mothers

### **METHOD AND MATERIALS**

1. Study design: Prospective Observational study.2. Study setting:Department of Radiodiagnosis3. Subjects and Inclusion criteria:150 consecutive singleton pregnant female patients between 34-40 weeks of gestation with known history of Gestational Diabetes Mellitus and/or Diabetes Mellitus4. Exclusion criteria:Multiple pregnancyUncertain gestational ageIntrauterine growth retardationCongenital anomaliesAmniotic fluid index less than 10 or more than 20Use of antenatal steroids prior to delivery5. Methodology: INFORMED WRITTEN CONSENT, FULL HISTORY TAKING6. Personal history, Past history, Family history7. Obstetric history8. Menstrual and Contraceptive history9. GENERAL EXAMINATION10. ABDOMINAL EXAMINATION11. INVESTIGATIONS: FBS, 2hPP, Oral Glucose Tolerance Test (75 gms)12. ULTRASOUND: The main pulmonary artery would be followed to the point where it divides into right and left branches by rotating the transducer from the 4 chamber view to the short axis view of the heart. Pulsed and Color Doppler would be used. The fetal pulmonary artery flow waveform (FPAF) measurements would be taken within the proximal portion of the main pulmonary artery.A number of different parameters will be measured from the FPAF waveform.13. Assessment by senior neonatologist

### RESULTS

13 out of 147 neonates developed respiratory distress (8.84%). The mean AT/ET ratio value was higher in those mothers whose neonates developed RDS ( $0.24\pm0.07$ ) compared to those that did not ( $0.18\pm0.04$ ). A cutoff value of 0.22 provided a sensitivity of 61.5% (95% CI 31.6-86.1), specificity of 88% (95% CI 81.3-93), negative predictive value of 95.9% (90.8-98.7) and positive predictive value of 33.3% (15.6-55.3) (p=0.0023).

#### CONCLUSION

We found a moderately high sensitivity (61.5%) for a AT/ET ratio value of 0.2292, the high specificity (88%) and negative predictive value (95.9%) suggests that it is highly useful in excluding normal fetuses. Hence, a AT/ET ratio < 0.2292 can be taken as an indirect marker for maturity of the fetal lungs.

## **CLINICAL RELEVANCE/APPLICATION**

Doppler sonographic assessment of the fetal pulmonary artery is a promising non-invasive, easily performed tool for prediction of the fetal lung maturity.



### HP226-SD-WEA1

## The Role of Post-Mortem CT in Cases of Murder with Corpse Concealment

Wednesday, Nov. 28 12:15PM - 12:45PM Room: HP Community, Learning Center Station #1

### Participants

Amalia Lupi, MD, Padova, Italy (*Presenter*) Nothing to Disclose Sofia Moschi, Padova, Italy (*Abstract Co-Author*) Nothing to Disclose Maria De Matteis, Padova, Italy (*Abstract Co-Author*) Nothing to Disclose Guido Viel, Padova, Italy (*Abstract Co-Author*) Nothing to Disclose Giovanni Cecchetto, Padova, Italy (*Abstract Co-Author*) Nothing to Disclose Diego Miotto, MD, Padova, Italy (*Abstract Co-Author*) Nothing to Disclose Chiara Giraudo, MD, PhD, Padova, Italy (*Abstract Co-Author*) Nothing to Disclose

#### For information about this presentation, contact:

amalialupi88@gmail.com

#### PURPOSE

To analyze the role of post-mortem computed tomography (PMCT) in cases of murder with subsequent corpse concealment.

## METHOD AND MATERIALS

An electronic database search of cases of murder with subsequent corpse concealment investigated by PMCT at our university hospital between 2010 to 2017 was performed. Information about gender and age of the victims, method of concealment, autopsy and PMCT findings were collected for each case.

### RESULTS

Thirteen cases met the inclusion criteria. The victims were seven males and six females (age range 20-72 years). The methods of concealment were: abandonment in an isolated area (n=6) in one case associated with dismemberment of the corpse, immersion (n=3), combustion combined with covering or burial (n=3), and burial (n=1). PMCT turned out to be useful for a preliminary evaluation, especially when the victims were wrapped in materials preventing an immediate visual inspection and/or identification. The PMCT has contributed to the identification of the victim in two cases, allowing the detection of an amputated distal phalanx of the right hand and enabling the comparison between the ante and post-mortem dental characteristics, respectively. In 12 homicides PMCT allowed the recognition of the cause of death (skull-brain trauma in seven cases and hemorragic shock in five cases) and the type of weapon (i.e., blunt object and sharp object in eight and four cases, respectively). In one case the features of the skull fracture at PMCT enabled the identification of the weapon (i.e., hammer). Only in one case of strangulation, PMCT didn't provide any additional information.

### CONCLUSION

Our results suggest that PMCT provides precise and immediate information on bodies altered by concealment and is therefore an essential tool for these forensic investigations.

#### **CLINICAL RELEVANCE/APPLICATION**

PMCT guarantees an accurate assessment, prior to the autospy, of corpses altered by concealment and may lead to the identification of the victim.



## HP227-SD-WEA2

Follow-up of Abdominopelvic Imaging Findings Indeterminate for Malignancy in Hospitalized and Emergency Department Patients: Reporting Imaging Findings Alone is Insufficient

Wednesday, Nov. 28 12:15PM - 12:45PM Room: HP Community, Learning Center Station #2

## Participants

Sophia R. O'Brien, MD, Philadelphia, PA (*Presenter*) Nothing to Disclose Jossie A. Carreras, MS, Philadelphia, PA (*Abstract Co-Author*) Nothing to Disclose Maria A. Bedoya-Velez, MD, Philadelphia, PA (*Abstract Co-Author*) Nothing to Disclose Brian Park, MD, Phildelphia, PA (*Abstract Co-Author*) Nothing to Disclose Darco Lalevic, Philadelphia, PA (*Abstract Co-Author*) Nothing to Disclose Tessa S. Cook, MD, PhD, Philadelphia, PA (*Abstract Co-Author*) Royalties, Osler Institute Hanna M. Zafar, MD, Philadelphia, PA (*Abstract Co-Author*) Nothing to Disclose

#### For information about this presentation, contact:

bedoya3@gmail.com

## PURPOSE

To evaluate the importance of social determinants of health and communication in follow-up of abdominopelvic imaging findings indeterminate for malignancy.

## **METHOD AND MATERIALS**

Our radiology department uses standardized codes to categorize abdominopelvic imaging findings as benign, indeterminate, or suspicious for malignancy on all ultrasound, CT and MRI reports. We assessed ED and inpatients with imaging findings indeterminate for malignancy over 7 randomly selected weeks between October 2015 and January 2017. Patient demographics, social determinants of health and inclusion of the indeterminate finding in the radiology report impression or discharge instructions were gathered from the electronic health record (EHR). Potentially inappropriate follow-up was defined as no completed relevant pathology, imaging, or clinical follow-up within our health system, and no documented rationale for lack of follow-up. Univariate analysis evaluated the association between inappropriate follow-up and included co-variates.

#### RESULTS

Among 176 patients with 194 abdominal imaging findings indeterminate for malignancy, half of patients (88/176, 50%) and imaging findings (95/194, 49%) received potentially inappropriate follow-up; 28% (25/88) of patients had no subsequent health system encounters and 69% (61/88) had no reason for inappropriate follow-up in the EHR. Potentially inappropriate follow-up was higher among patients with no prior health-system visits (p=.001), no known PCP (p=.001), and widowed patients (p=.038). Including the indeterminate finding in the report impression or the need for follow up in the discharge instructions did not correlate with further follow up ((P=.601 and p=.449).

## CONCLUSION

Half of patients with imaging findings indeterminate for malignancy detected during an ED visit or inpatient admission are at risk for inappropriate follow-up. Fragmented patient access to health care correlated with inappropriate follow-up; communication of radiology findings in the report impression or discharge summary did not.

### **CLINICAL RELEVANCE/APPLICATION**

Communication of imaging findings indeterminate for malignancy in radiology reports or directly to vulnerable ED and inpatients is insufficient to ensure appropriate follow-up.



### HP228-SD-WEA3

**Under-Representation of Women on Radiology Editorial Boards** 

Wednesday, Nov. 28 12:15PM - 12:45PM Room: HP Community, Learning Center Station #3

#### **Participants**

Rozita Jalilianhasanpour, MD, Baltimore, MD (*Presenter*) Nothing to Disclose Paniz Charkhchi, MD, Ann Arbor, MI (*Abstract Co-Author*) Nothing to Disclose Mohammadhassan Mirbolouk, Baltimore, MD (*Abstract Co-Author*) Nothing to Disclose David M. Yousem, MD, Baltimore, MD (*Abstract Co-Author*) Royalties, Reed Elsevier; Speaker, American College of Radiology; Employee, Medicolegal Consultation; ; ;

## For information about this presentation, contact:

rjalili1@jhmi.edu

#### PURPOSE

Women in radiology are known to be underrepresented in leadership positions, spanning many supervisory roles in academia. We sought to determine if women are appropriately represented on editorial boards and in editor-in-chief positions in radiology compared with their first authored contributions to the radiology literature.

## METHOD AND MATERIALS

We assessed the first authorship male/female gender ratio of manuscripts published in the 5 high impact American journals in radiology: Radiographics, Human Brain Mapping, American Journal of Neuroradiology and Journal of Magnetic Resonance Imaging, for the years 2002 to 2017. We looked at the gender make-up of the first authors, editorial board members and editors-inchief of these journals for the same years to see if there was a discrepancy.

#### RESULTS

In every year of every journal, women were under-represented on the editorial boards compared to their first-authored manuscript contribution. The percentage of women as first authors ranged from 11.8% to 50% (Mean= $30.3\% \pm 9.8$ ), contrasted with just 5.1% to 29.3% (Mean= $14.2\% \pm 4.9$ ) as editorial board members. The absolute difference between the percentage of women as first authors and editorial board members ranged from 2.3% to 40% (Mean= $16.1\% \pm 9.3$ ) for all journals over all the years. Notably, there was no woman as editor in chief for any of the journals reviewed.

### CONCLUSION

There is a gender gap in the composition of editorial boards in radiology compared to first authored contributions by women. Given the implications of editorial board assignment and editorship of journals on academic advancement, journals may wish to consider strategies that may help narrow the gap.

## **CLINICAL RELEVANCE/APPLICATION**

There is a gender gap between women's contribution to the radiology literature and their representation on editorial boards that should be addressed.



### HP229-SD-WEA4

## **Diagnostic Radiology Has the Most Patient Encounters**

Wednesday, Nov. 28 12:15PM - 12:45PM Room: HP Community, Learning Center Station #4

#### Awards Student Travel Stipend Award

# Participants

Jason P. Davis, MD,BS, Indianapolis, IN (*Presenter*) Nothing to Disclose Richard B. Gunderman, MD, PhD, Indianapolis, IN (*Abstract Co-Author*) Nothing to Disclose

#### PURPOSE

The decision for medical students to select a medical specialty is complex and influenced by many factors. One factor is the quantity of patients each specialty impacts over time. Our goal was to identify and compare the number of patient encounters of physicians in the 13 most commonly encountered specialties by medical students.

#### **METHOD AND MATERIALS**

Patient encounters, as defined and measured by the Center for Medicare and Medicaid Services, are encounters where medical services including treatment, evaluation, or management are provided to patients. Encounters are objectively recorded as notes, procedures, or reports in the Electronic Health Records system. We collected data from a health system with an annual total of 117,245 hospital admissions and 2,629,251 outpatient visits. Encounters were totaled for providers of 13 medical specialties from January 2016 to December 2016. Selection criteria for providers included attending physicians only. The total encounters for the top 30 producing providers were identified and then used to calculate the average number of encounters for each specialty.

### RESULTS

Arrayed in decreasing order, we found the following average number of patient encounters in each medical specialty: diagnostic radiology (17,189), pathology (10,860), emergency medicine (4,588), family medicine (4,108), internal medicine (3,610), pediatrics (2,098), neurology (1,419), interventional radiology (1,399), hospital medicine (1,354), obstetrics and gynecology (1,326), anesthesiology (1,017), general surgery (839), and psychiatry (526).

#### CONCLUSION

Based on these results, there is no other medical specialty that impacts the care of a larger number of patients than diagnostic radiology. This can be explained by the ability of radiologists to efficiently produce a high output of interpretations and reports for many patients in a relatively small amount of time. Although, the number of patients a physician encounters is only one factor in a larger account of the physician's overall impact.

## **CLINICAL RELEVANCE/APPLICATION**

Radiologists who have the opportunity to educate and counsel medical students need to ensure that students are well-informed about the typical numbers of patient encounters in each medical specialty. In this regard, there is no clinical medical specialty that comes close to diagnostic radiology in the number of patients to whose care it enables physicians to contribute.

#### **Honored Educators**

Presenters or authors on this event have been recognized as RSNA Honored Educators for participating in multiple qualifying educational activities. Honored Educators are invested in furthering the profession of radiology by delivering high-quality educational content in their field of study. Learn how you can become an honored educator by visiting the website at: https://www.rsna.org/Honored-Educator-Award/ Richard B. Gunderman, MD, PhD - 2018 Honored Educator



## HP230-SD-WEA5

Citation Bias in Imaging Research: Are Studies with Higher Diagnostic Accuracy Estimates Cited More Often?

Wednesday, Nov. 28 12:15PM - 12:45PM Room: HP Community, Learning Center Station #5

#### Awards Student Travel Stipend Award

#### **Participants**

Robert A. Frank, MD, Ottawa, ON (*Presenter*) Nothing to Disclose Anahita Dehmoobad Sharifabadi, BSC, Ottawa, ON (*Abstract Co-Author*) Nothing to Disclose Jean-Paul Salameh, BSC, Ottawa, ON (*Abstract Co-Author*) Nothing to Disclose Trevor McGrath, MD, Ottawa, ON (*Abstract Co-Author*) Nothing to Disclose Noemie Kraaijpoel, MD, Amsterdam, Netherlands (*Abstract Co-Author*) Nothing to Disclose Wilfred Dang, MD, Ottawa, ON (*Abstract Co-Author*) Nothing to Disclose Nicole Li, Ottawa, ON (*Abstract Co-Author*) Nothing to Disclose Isabelle D. Gauthier, BSC, Ottawa, ON (*Abstract Co-Author*) Nothing to Disclose Mark Z. Wu, MD,MSc, Ottawa, ON (*Abstract Co-Author*) Nothing to Disclose Patrick M. Bossuyt, PhD, Amsterdam, Netherlands (*Abstract Co-Author*) Nothing to Disclose Deborah Levine, MD, Boston, MA (*Abstract Co-Author*) Editor with royalties, Taylor & Francis Group; Editor with royalties, Reed Elsevier;

Matthew D. McInnes, MD, PhD, Ottawa, ON (Abstract Co-Author) Nothing to Disclose

For information about this presentation, contact:

mcinnes.matt@gmail.com

#### PURPOSE

To assess the risk of citation bias in imaging diagnostic accuracy research by evaluating whether studies with higher accuracy estimates are cited more frequently than those with lower accuracy estimates.

### **METHOD AND MATERIALS**

Search of Medline for diagnostic accuracy meta-analyses published in imaging journals from January 2005 to April 2016 was performed. Primary studies from the meta-analyses were screened; those assessing the diagnostic accuracy of an imaging test and reporting sensitivity and specificity were eligible for inclusion. Studies not indexed in Web of Science, duplicates, and inaccessible articles were excluded. Topic (modality and subspecialty), study design, sample size, journal impact factor, publication date, times cited, sensitivity and specificity were extracted for each study. A negative binomial regression analysis was performed to evaluate for association of citation rate (times cited per month since publication) with Youden's index (YI= sensitivity+specificity-1), highest sensitivity, and highest specificity, controlling for the potential confounding effects of modality, subspecialty, impact factor, study design, sample size, and source meta-analysis.

#### RESULTS

There were 1016 primary studies included. We observed a significant positive association between Youden's index and citation rate, with a regression coefficient of 0.33 (p=0.016). The regression coefficients for association of sensitivity and specificity with citation rate were 0.41 (p=0.034) and 0.32 (p=0.15), respectively.

### CONCLUSION

A moderate positive association exists between diagnostic accuracy estimates and citation rates, indicating that citation bias is present in imaging diagnostic accuracy literature.

## **CLINICAL RELEVANCE/APPLICATION**

Preferential citation of studies with higher accuracy estimates may contribute to overestimation of imaging test accuracy in clinical practice, with potential for adverse patient outcomes.



## IN221-SD-WEA2

## Integrating an Ontology of Radiology Differential Diagnosis with RadLex, SNOMED CT, and ICD-10-CM

Wednesday, Nov. 28 12:15PM - 12:45PM Room: IN Community, Learning Center Station #2

#### **Participants**

Ross W. Filice, MD, Chevy Chase, MD (*Abstract Co-Author*) Co-founder, DexNote, LLC; Research Grant, NVIDIA Corporation; Advisor, BunkerHill Health, Inc

Charles E. Kahn JR, MD, Philadelphia, PA (Presenter) Nothing to Disclose

For information about this presentation, contact:

## ckahn@upenn.edu

### CONCLUSION

Mappings from the Radiology Gamuts Ontology to related ontologies create an infrastructure to support automated knowledge discovery, data mining, and diagnostic reasoning in radiology.

#### Background

An ontology offers a human-readable and machine-computable representation of the concepts in a domain and the relationships among them. Mappings between ontologies enable the reuse and interoperability of biomedical knowledge. We sought to map concepts of the Radiology Gamuts Ontology (RGO), an ontology that links diseases and imaging findings, to terms in key vocabularies for clinical radiology: RadLex, the Systematized Nomenclature of Medicine - Clinical Terms (SNOMED CT), and the International Classification of Diseases, version 10, Clinical Modification (ICD-10-CM).

### **Evaluation**

RGO (version 0.7; January 2018) incorporated 16,918 classes of diseases, interventions, and imaging observations linked by 1,782 subsumption (class-subclass) relations and 55,569 causal ('may cause') relations. RGO classes were mapped to RadLex (46,656 classes, version 3.15), SNOMED CT (327,128 classes, version 2016AB), and ICD-10-CM (94,276 classes, version 2016AB) using the National Center for Biomedical Ontology (NCBO) Annotator web service. We identified 1275 exact mappings from RGO to RadLex, 5302 to SNOMED CT, and 941 to ICD-10-CM. RGO terms mapped to one ontology (n=3401), two ontologies (n=1515), or all three ontologies (n=198). For example, 'esophageal web' mapped to ICD-10-CM code Q39.4, RadLex term RID34693, and SNOMED CT term 19216006.

### Discussion

The mapped ontologies provide additional terms to support data mining from textual information in the electronic health record. Integration with RadLex facilitates linking to radiology reference information, such as teaching files and journal articles. SNOMED CT and ICD-10-CM allow one to inform radiological diagnosis with information encoded in patients' electronic health records. The current work builds on efforts to map RGO to the Human Disease Ontology and the Human Phenotype Ontology.

### **Honored Educators**

Presenters or authors on this event have been recognized as RSNA Honored Educators for participating in multiple qualifying educational activities. Honored Educators are invested in furthering the profession of radiology by delivering high-quality educational content in their field of study. Learn how you can become an honored educator by visiting the website at: https://www.rsna.org/Honored-Educator-Award/ Charles E. Kahn JR, MD - 2012 Honored EducatorCharles E. Kahn JR, MD - 2018 Honored Educator



## IN222-SD-WEA3

## Accuracy of Using Google Translate to Convert Radiology Terminology from English to Chinese

Wednesday, Nov. 28 12:15PM - 12:45PM Room: IN Community, Learning Center Station #3

### Participants

David J. Vining, MD, Houston, TX (*Presenter*) Royalties, Bracco Group; CEO, VisionSR; Stockholder, VisionSR Xiaomeng Li, MD, Beijing, China (*Abstract Co-Author*) Nothing to Disclose Andreea Pitici, Houston, TX (*Abstract Co-Author*) Employee, Computer Patrisoft SAC Cristian Popovici, Houston, TX (*Abstract Co-Author*) Employee, Patrisoft Outsourcing Adrian Prisacariu, Houston, TX (*Abstract Co-Author*) Employee, Patrisoft Outsourcing Mark Kontak, Houston, TX (*Abstract Co-Author*) Consultant, VisionSR, Inc

## For information about this presentation, contact:

dvining@mdanderson.org

## CONCLUSION

The use of structured reporting incorporating an ontology offers the potential to automatically translate radiology reports to foreign languages, however, the accuracy of the translations must be verified by native foreign-language speaking radiologists. Corrected translations must be incorporated into ontologies and translation tables for desired results.

#### Background

The use of ontologies in radiology reporting offers the promise of being able to automatically translate radiology reports to foreign languages. Several online translation tools exist but the desired results can be lost in translation, thus requiring careful review and development of more accurate translation tables.

#### **Evaluation**

We developed an ontology containing anatomical terms arranged in hierarchies for each body section (head, neck, chest, abdomen, pelvis, upper extremity, and lower extremity) for use in a structured reporting solution. We translated the list of terminology using a publicly available online tool (https://translate.google.com, Google Translate, Menlo Park, CA) and had the results reviewed by a native-speaking Chinese radiologist working in Beijing with nine years of practice experience to identify inaccuracies and make corrections to the translated terminology.

#### Discussion

A total of 1317 anatomical terms and phrases were processed using Google Translate, and it correctly interpreted 602 (45.7%). Modifications were made by the expert radiologist to 715 (54.3%) terms and phrases that were incorrectly translated, and the revised terminology was incorporated into a translation table used in a structured reporting system that is equipped with an automated translation function. Future directions include consideration for synonymous terms and phrases, evaluation of translation accuracy for pathology, and assessment of other online translation tools.



## IN223-SD-WEA4

## Direct Validation of Quantitative MRI Cerebral Perfusion at Rest, Stress and Ischemia

Wednesday, Nov. 28 12:15PM - 12:45PM Room: IN Community, Learning Center Station #4

### Participants

Niloufar S. Saadat, MD, Chicago, IL (*Presenter*) Nothing to Disclose Yong I. Jeong, Chicago, IL (*Abstract Co-Author*) Nothing to Disclose Timothy J. Carroll, PhD, Chicago, IL (*Abstract Co-Author*) Nothing to Disclose Steven Roth, MD, Chicago, IL (*Abstract Co-Author*) Nothing to Disclose Keigo Kawaji, PhD, Chicago, IL (*Abstract Co-Author*) Consultant, Myocardial Solutions, Inc Gregory A. Christoforidis, MD, Columbus, OH (*Abstract Co-Author*) Nothing to Disclose

## For information about this presentation, contact:

nsaadat@uchicago.edu

## PURPOSE

This study sought to assess the accuracy of a quantitative MRI-based (qMRI) measure of cerebral blood flow (qCBF) against reference stable isotope neutron capture microsphere-based cerebral blood flow quantification in an experimental model during normocapnia, hypercapnia and middle cerebral artery (MCAO)

### **METHOD AND MATERIALS**

Five female, mongrel dogs (20-30 kg) each studied over two days. On day 1, qCBF images acquired during normocapnia (target PaCO2 30-40 mmHg) and hypercapnia (target PaCO2 > 60 mmHg) induced by CO2 gas inhalation (5% CO2/95% O2). On day 2 animals underwent angiographically verified permanent endovascular occlusion of the M1 segment while in a normocapnic state. Anesthesia selected to minimize the influence on cerebrovascular reactivity. Physiologic parameters kept within normal range except for PCO2 for hypercapnia. Microspheres injected at the time of qMRI acquisition to obtain reference-standard CBF values. qMRI acquired on a 3 Tesla unit using a 15-channel receive-only head coil a 'bookend dynamic susceptibility (DSC)' approach, which uses pre- and post-contrast T1 maps bookended to a DSC MRI sequence to calculate parenchymal T1 changes and calibrate the DSC scan for quantitative perfusion in ml/100 g/min. Quantitative T1 maps created using a standard inversion recovery Look-Locker imaging, co-localized to the DSC perfusion scan using a previously reported approach

## RESULTS

MRI correlated strongly with microsphere perfusion (qCBFMRI = 0.93\*qCBFSPHERES + 3.85 ml/100g/min; r2 = 0.96; p < 0.001), for individual CVR (CVRMRI = 1.17\*CVRSPHERES - 0.95 %;CBF/mmHg CO2; r2 = 0.84; p < 0.001), and for post-occlusion CBF (qCBFMRI = 0.80\*qCBFSPHERES + 12.9 ml/100g/min; r2 = 0.82; p = 0.002). Correction for delay and dispersion resulted in a significant improvement in the correlation between MRI and microsphere deposition in the ischemic state (qCBFMRI = 0.97\*qCBFSPHERES + 2.58 ml/100g/min; r2 = 0.96; p < 0.001).

## CONCLUSION

MRI derived values of CBF are strongly correlated with reference value microsphere deposition in normocapnia, hypercapnia, and MCAO ischemic stroke. Correction for delay and dispersion significantly improved the accuracy of this quantification during MCAO, underscoring the importance of this correction under focal ischemic condition

## **CLINICAL RELEVANCE/APPLICATION**

Quantitative CBF by MRI perfusion accurately measures CBF, improving our ability to triage patients with acute ischemic stroke for treatment



### IN224-SD-WEA5

# Comparative Analysis of 3D Printed Materials for Cortical Mastoidectomy Simulation

Wednesday, Nov. 28 12:15PM - 12:45PM Room: IN Community, Learning Center Station #5

#### Awards Student Travel Stipend Award

#### **Participants**

Elias Kikano, MD, Cleveland, OH (*Presenter*) Nothing to Disclose Simone E. Dekker, MD,PhD, Cleveland Heights, OH (*Abstract Co-Author*) Nothing to Disclose Jeanie Sozansky Lujan, MD, Cleveland, OH (*Abstract Co-Author*) Nothing to Disclose Christos Kosmas, MD, Cleveland, OH (*Abstract Co-Author*) Consultant, BioClinica, Inc Sarah Mowry, MD, Cleveland, OH (*Abstract Co-Author*) Nothing to Disclose

#### For information about this presentation, contact:

egk8@case.edu

# PURPOSE

3D printed models of the temporal bone provide the opportunity to practice lateral skull base procedures in the laboratory prior to taking a patient for surgery. This may improve both the trainee learning experience and overall patient outcomes. This study seeks to validate and compare the accuracy of various 3D printing materials to simulate cortical mastoidectomy.

#### **METHOD AND MATERIALS**

A normal computed tomography (CT) scan of the temporal bone was segmented using Materialise Mimics (Leuven, Belgium). Postprocessing of the 3D mesh was completed and the virtual model was verified against the original CT images for anatomical accuracy. The standard model was 3D printed using comparable and consistent settings across multiple 3D printers and materials including Formlabs Form 2 (Tough and Standard White resins), Makerbot Replicator 2X (Red Acrylonitrile Butadiene Styrene), Fortus (White Polycarbonate), and Objet (Yellow Photopolymer). The senior author performed a mastoidectomy on the 6 different models and completed a questionnaire survey with qualitative and quantitative evaluation of the 3D printed models. Additional simulated mastoidectomy procedures by other residents, fellows, and experienced clinicians are in progress.

#### RESULTS

Preliminary results from the senior author demonstrated agreement that the 3D printed bone model accurately recreated the experience of a cortical mastoidectomy. Each of the 3D printed materials had varying degrees of correlation with temporal bone anatomy including tegmen and sigmoid sinus contours, antrum anatomy, and drilling texture. Some materials were limited by the odor and powder formed from contact with drilling tools. The majority of the 3D printed models were felt to be suitable as a simulation to a real patient mastoidectomy.

#### CONCLUSION

Utilization of 3D printed anatomical models in lateral skull base procedures has the potential to generate realistic surgical simulations of normal and pathological cases. Validating and verifying 3D printers and their materials for this purpose is important in order to standardize the techniques, ensure reproducibility, and compare to in vivo procedures.

#### **CLINICAL RELEVANCE/APPLICATION**

This abstract compares various 3D printed materials of temporal bone models to better educate and prepare clinicians for lateral skull base procedures.



### MI224-SD-WEA1

### Inter-Reader and Inter-Criteria Agreement of Three Interpretation Criteria of 68Ga-PSMA PET

Wednesday, Nov. 28 12:15PM - 12:45PM Room: MI Community, Learning Center Station #1

FDA Discussions may include off-label uses.

#### **Participants**

Akira Toriihara, Stanford, CA (*Presenter*) Nothing to Disclose Tomomi Nobashi, MD,PhD, Palo Alto, CA (*Abstract Co-Author*) Nothing to Disclose Lucia Baratto, Stanford, CA (*Abstract Co-Author*) Nothing to Disclose Sonya Y. Park, MD, Seoul, Korea, Republic Of (*Abstract Co-Author*) Nothing to Disclose Negin Hatami, Stanford, CA (*Abstract Co-Author*) Nothing to Disclose Heying Duan, Stanford, CA (*Abstract Co-Author*) Nothing to Disclose Carina Mari Aparici, MD, Palo Alto, CA (*Abstract Co-Author*) Nothing to Disclose Guido A. Davidzon, MD, Stanford, CA (*Abstract Co-Author*) Nothing to Disclose Thomas Yohannan, MD, Chicago, IL (*Abstract Co-Author*) Nothing to Disclose Andrei Iagaru, MD, Emerald Hills, CA (*Abstract Co-Author*) Research Grant, General Electric Company

### PURPOSE

To compare three interpretation criteria of 68Ga-PSMA PET (EANM, PROMISE, and PSMA-RADS) by evaluating inter-reader and inter-criteria agreement.

# METHOD AND MATERIALS

Scans of 78 patients with prostate cancer were evaluated in this retrospective analysis. Our cohort consisted of two groups. Group 1 included 40 patients (mean age,  $70.3\pm7.0$  years old) who underwent 68Ga-PSMA PET/CT due to biochemical recurrence. Group 2 included 38 patients (mean age,  $64.9\pm5.9$  years old) who underwent 68Ga-PSMA PET/MRI for initial staging of biopsy-proven prostate cancer. Two nuclear medicine physicians independently evaluated all 68Ga-PSMA PET/CT or PET/MRI studies according to the three interpretation criteria. K's alpha was calculated to evaluate inter-reader agreement in each criterion, as well as inter-criteria agreement in each reader, based on the following sites: prostate bed after radical prostatectomy or primary tumor, lymph node metastasis, distant metastasis, and final judgement. The degree of agreement according to K's alpha was considered as follows: 0.00-0.20 = slight agreement, 0.21-0.40 = fair agreement, 0.41-0.60 = moderate agreement, 0.61-0.80 = substantial agreement, 0.81-1.00 = almost perfect agreement.

#### RESULTS

In the group 1, all criteria showed moderate to almost perfect inter-reader agreement. The minimum K's alpha of inter-reader agreement was 0.53 in the final judgement of PSMA-RADS. In the group 2, judgement of lymph node metastasis in three criteria and distant metastasis in EANM showed relatively poor agreement (K's alpha <0.40). Inter-criteria agreement in each reader were substantial to almost perfect, except judgement of distant metastasis by one reader in the group 2 (K's alpha = 0.53).

# CONCLUSION

Three criteria can be applied to evaluate 68Ga-PSMA PET/CT in biochemical recurrent cases with good inter-reader agreement. On the other hand, when these criteria are used to evaluate 68Ga-PSMA PET/MRI as an initial staging method, inter-reader disagreement may be problematic particularly in the judgement of status of lymph node metastases. This indicates that further work is needed to address the issue.

### **CLINICAL RELEVANCE/APPLICATION**

Three representative criteria of 68Ga-PSMA PET are applicable to PET/CT in biochemical recurrent cases, while their application to PET/MRI may be limited in terms of inter-reader agreement.



#### MI225-SD-WEA2

#### Prevalence and Characteristics of 68Ga-PSMA-11 Uptake in the Prostatic Central Zone on PET-MR

Wednesday, Nov. 28 12:15PM - 12:45PM Room: MI Community, Learning Center Station #2

#### **Participants**

Munique R. Borges Do Cruz Rios, MD, Sao Paulo, Brazil (*Abstract Co-Author*) Nothing to Disclose Thais Mussi, MD,PhD, Sao Paulo, Brazil (*Presenter*) Nothing to Disclose Cecilia P. Fassbender, MD, Sao Paulo, Brazil (*Abstract Co-Author*) Nothing to Disclose Julio Cesar Oliveira, MD, Sao Paulo, Brazil (*Abstract Co-Author*) Nothing to Disclose Jairo Wagner, MD, Sao Paulo, Brazil (*Abstract Co-Author*) Nothing to Disclose Taise Vitor, Sao Paulo, Brazil (*Abstract Co-Author*) Nothing to Disclose Ronaldo H. Baroni, MD, Sao Paulo, Brazil (*Abstract Co-Author*) Nothing to Disclose Marcelo L. Cunha, MD, Sao Paulo, Brazil (*Abstract Co-Author*) Nothing to Disclose Karine M. Martins, MS, Sao Paulo, Brazil (*Abstract Co-Author*) Nothing to Disclose

#### For information about this presentation, contact:

thaiscaldara@gmail.com

#### PURPOSE

To describe the prevalence and characteristics of 68Ga-PSMA-11 uptake in prostatic central zone in patients submitted to PET/MRI for detection or staging of prostate cancer, and to correlate this uptake with the presence of suspected lesions detected on mpMRI.

# METHOD AND MATERIALS

Retrospective IRB approved study. Seventeen patients underwent 68Ga-PSMA-11 PET/MR scans from March 2016 to March 2017. The 68Ga-PSMA-11 uptake in the central zone of the prostate was measured by an experienced radiologist in this type of study. Patient's epidemiological profile, level of serum PSA, ISUP score of the prostatic biopsies, the correlation between the lesions detected in the MRI scans and, if present, the classification of these lesions according to the PI-RADS V2 were also assessed.

#### RESULTS

Patients were aged between 51 and 83 years (median 65 years). The mean of PSA level was 11 (0.9-26 ng/mL). 76.5% of the patient was PI-RADS score >= 4, 5.8% was PI-RADS score 3 and 11.7% was PI-RADS score 2. 94.1% of patients had undergone previous prostate biopsies. The ISUP grade score was: 25 % ISUP 1, 12.5% ISUP 2, 37.5% ISUP 3, 6.25% ISUP 4 and 6.25 ISUP 5. 12.5% of patients had negative biopsies. 82.3% of the patients underwent 68Ga-PSMA-11 PET/MR for staging and the remaining patients (17.6%) performed the exam for the detection of clinically significant prostatic neoplasms prior to biopsy. Sixteen of the seventeen patients (94.1%) presented a slight symmetrical 68Ga-PSMA-11 uptake in the central zone with a SUV range of 1.6 to 3.2. This uptake was not associated with the presence of clinically significant lesions on the prostate MRI.

#### CONCLUSION

Prostatic central zone usually presents a mild and symmetrical uptake of 68Ga-PSMA-11 on PET/MR, that should be considered physiological. This pattern was not associated with the presence of clinically significant lesions on mpMRI.

### **CLINICAL RELEVANCE/APPLICATION**

This knowledge is fundamental to avoid false-positive results. The correlation of 68Ga-PSMA-11 PET/MRI with the multiparametric MRI of the prostate allows evaluation not only of the prostatic anatomy, as well as the presence of suspicious lesions for clinically significant neoplasms, which is one of the advantages of PET/MR over PET/CT.



### MI228-SD-WEA5

The Imaging and Uptake Properties of 5 nm USPIO Nonspecific MR Contrast Agents in Vitro and In Rats' Liver

Wednesday, Nov. 28 12:15PM - 12:45PM Room: MI Community, Learning Center Station #5

#### **Participants**

Xiaohong Ma Jr, MD, PhD, Beijing, China (*Presenter*) Nothing to Disclose Xinming Zhao, Beijing, China (*Abstract Co-Author*) Nothing to Disclose Han Ouyang, MD, Bejing, China (*Abstract Co-Author*) Nothing to Disclose

#### PURPOSE

To study the imaging and uptake properties of ultra-small superparamagnetic iron oxide (USPIO) with a size of 5 nm as a nonspecific contrast agent for liver and to evaluate its potential for liver cancer imaging.

### METHOD AND MATERIALS

The relationship between the USPIO concentration and T1/T2 relaxation properties were characterized by phantom test to direct the agent dosage for in vivo pharmacokinetic studies in rats' liver. The phantom consists of seven tubes of USPIO water solutions with 7 concentration gradients and 1 tube of pure water as reference. The T1-weighted, T2-weighted, T1-mapping and T2-mapping images were obtained by GE Discovery 750 3.0T MR. The relationship between the image signal intensity and the concentration of USPIO solution was analyzed by the Pearson's correlation coefficient. In addition, the relationships between USPIO concentration and quantitative T1 and T2 value were also investigated. Healthy rats were used for in vivo pharmacokinetic measurements. USPIO solution with concentration of 20µl (1.0mg/kg Fe) was injected into rats through the tail vein. T2-weighted images were scanned before USPIO injection and every 10 min after injection, and the residence time of USPIO in rat's liver was analyzed by the relative enhancement curve of signal intensity compared to the pre-injection signal intensity.

#### RESULTS

T1(ms)-value and T2(ms)-value was negatively correlated with the concentration of the USPIO solution (r = -0.97, r=0.92, respectively). T1-value and T2-value were positively correlated with each other (r = 0.89, p < 0.01). These results convey that, the higher the concentration of USPIO, the smaller the value of the two. In addition, the signal intensity enhancement curve showed that 30 minutes later, the signal restored to the level before USPIO injection.

# CONCLUSION

The 5 nm USPIO could be used as effective liver MRI nonspecific contrast agent. Meanwhile, 5 nm USPIO possess the potential to be served as the carrier for further tumor-targeted probes. The 30-minute residence time of 5 nm USPIO in normal liver implies the potential for background signal suppression of 5 nm-USPIO-based targeting probes in tumor targeted MR imaging.

### **CLINICAL RELEVANCE/APPLICATION**

The 5 nm USPIO might be used as the 5 nm-USPIO-based targeting probes in the specific MR imaging for the liver tumor.



### MK384-SD-WEA1

Diagnostic Outcome of Image-Guided Percutaneous Core Needle Biopsy of Sclerotic Bone Lesions: A Meta-Analysis

Wednesday, Nov. 28 12:15PM - 12:45PM Room: MK Community, Learning Center Station #1

# Participants

Wook Jin, Seoul, Korea, Republic Of (*Presenter*) Nothing to Disclose Seong Jong Yun, Seoul, Korea, Republic Of (*Abstract Co-Author*) Nothing to Disclose Sun Hwa Lee, Seoul, Korea, Republic Of (*Abstract Co-Author*) Nothing to Disclose Ga Ram Kang, Seoul, Korea, Republic Of (*Abstract Co-Author*) Nothing to Disclose

For information about this presentation, contact:

zoomknight@naver.com

### PURPOSE

This meta-analysis aimed to evaluate the diagnostic outcome (diagnostic yield and accuracy) of image-guided percutaneous core needle biopsy (CNB) of sclerotic bone lesions.

### METHOD AND MATERIALS

This meta-analysis followed the guidelines of the Preferred Reporting Items for a Systematic Review and Meta-analysis (PRISMA) statement. A computerized search of the PubMed and EMBASE databases was performed to identify relevant original articles on the use of image-guided percutaneous CNB of sclerotic bone lesions. The pooled proportions of the diagnostic yield and pooled accuracy estimates were assessed using random-effects modeling. We also performed subgroup analyses of the diagnostic yield according to the drill systems (battery-powered vs. manual). Heterogeneity among studies was determined using the inconsistency index (I2). Meta-regression analyses were performed to evaluate the potential sources of heterogeneity.

#### RESULTS

Fifteen eligible studies, involving 969 sclerotic bone lesions for diagnostic yield, and 242 sclerotic bone lesions for diagnostic accuracy, were included. The pooled proportion of the diagnostic yield of image-guided percutaneous CNB of sclerotic bone lesions was 74.3% (95% CI, 61.6-83.9%), and the pooled accuracy estimate for differentiation between benign and malignant lesions was 86.9% (95% CI, 77.3-92.8%). In the subgroup analysis, the pooled proportion of the diagnostic yield of the battery-powered drill system (76.7% [95% CI, 64.0-85.8%]) was higher than that of the manual drill system (65.2% [95% CI, 58.0-71.8%]). In the meta-regression analyses, no variables were significantly different (p=0.12-0.93).

#### CONCLUSION

In conclusion, we determined that image-guided percutaneous CNB of sclerotic bone lesions is an accurate diagnostic technique with good diagnostic yield, particularly when the battery-powered bone biopsy system is used.

# **CLINICAL RELEVANCE/APPLICATION**

The radiologists and orthopedic surgeons can routinely use the image-guided percutaneous CNB to diagnose sclerotic bone lesions without fear of significant non-diagnostic or inaccurate results.



### MK386-SD-WEA3

Efficacy of Hybrid Compressed Sensing in Three-Dimensional Isotropic T2-Weighted Fast Spin-Echo for the Lumbar Spine

Wednesday, Nov. 28 12:15PM - 12:45PM Room: MK Community, Learning Center Station #3

# Participants

Takeshi Nakaura, MD, Kumamoto, Japan (*Presenter*) Nothing to Disclose Yuji Iyama, MD, Kumamoto, Japan (*Abstract Co-Author*) Nothing to Disclose Natsuki Maruyama, MD, Kumamoto, Japan (*Abstract Co-Author*) Nothing to Disclose Seitaro Oda, MD, Kumamoto, Japan (*Abstract Co-Author*) Nothing to Disclose Tomohiro Namimoto, MD, Kumamoto, Japan (*Abstract Co-Author*) Nothing to Disclose Yasuyuki Yamashita, MD, Kumamoto, Japan (*Abstract Co-Author*) Nothing to Disclose Yasuyuki Yamashita, MD, Kumamoto, Japan (*Abstract Co-Author*) Nothing to Disclose Mika Kitajima, MD, Kumamoto, Japan (*Abstract Co-Author*) Nothing to Disclose Mika Kitajima, MD, Kumamoto, Japan (*Abstract Co-Author*) Nothing to Disclose Hiroyuki Uetani, Kumamoto, Japan (*Abstract Co-Author*) Nothing to Disclose Masafumi Kidoh, Kumamoto, Japan (*Abstract Co-Author*) Nothing to Disclose Yasunori Nagayama, MD, Kumamoto, Japan (*Abstract Co-Author*) Nothing to Disclose Masataka Nakagawa, Kumamoto, Japan (*Abstract Co-Author*) Nothing to Disclose

# PURPOSE

This study aims to assess the efficacy of a hybrid compressed sensing (hybrid-CS) technique for three-dimensional isotropic T2-weighted fast spin-echo (3D-T2FSE) magnetic resonance imaging (MRI) of the lumbar spine.

# METHOD AND MATERIALS

In this study, 16 volunteers underwent 3D-T2FSE for the lumbar spine with conventional parallel imaging - SENSitivity Encoding (SENSE) and hybrid-CS at 3T MRI. We recorded the image acquisition time of SENSE (acceleration factor = 2, number of sample averaged = 1) and hybrid-CS (acceleration factor = 8, number of sample averaged = 2) and compared the signal-to-noise-ratio (SNR) of the spine, cerebrospinal fluid (CSF), lumbar disc (disc), epidural fat, and erector spinae muscle and contrast of the spine, CSF, and disc between two sequence images with paired t-test. Furthermore, two board certified radiologists performed the qualitative image analysis assessment of two sequence images with Wilcoxon signed-rank test.

#### RESULTS

The image acquisition time of hybrid-CS (3 min 36 sec) was 46% shorter than that of SENSE (6 min 38 sec). The contrast of CSF (76.3  $\pm$  15.1 vs. 62.9  $\pm$  16.3) and SNR of the spine (6.4  $\pm$  1.4 vs. 5.6  $\pm$  1.3) were significantly higher with hybrid-CS than with SENSE (P < 0.05). Moreover, the SNR of the disc (5.9  $\pm$  2.0 vs. 5.1  $\pm$  1.7) and muscle (2.4  $\pm$  0.4 vs. 2.1  $\pm$  0.3) were significantly higher with SENSE than with hybrid-CS (P < 0.05). No significant differences were observed in the contrast of the spine, disc, and epidural fat and SNR of CSF and fat between hybrid-CS and SENSE. Furthermore, no considerable differences were observed in the quantitative evaluation between hybrid-CS and SENSE.

### CONCLUSION

The hybrid-CS for 3D-T2FSE images for the lumber spine can shorten the image acquisition time without sacrificing the image quality compared with SENSE sequence.

# **CLINICAL RELEVANCE/APPLICATION**

The hybrid-CS is useful to shorten the image acquisition time without sacrificing the image quality for 3D T2WI images compared with SENSE sequence.



### MK387-SD-WEA4

### MRI-Based Radiomic to Assess Lipomatous Soft Tissue Tumors Malignancy: A Pilot Study

Wednesday, Nov. 28 12:15PM - 12:45PM Room: MK Community, Learning Center Station #4

### Participants

Amine BOUHAMAMA, Lyon, France (*Presenter*) Nothing to Disclose Benjamin Leporq, MS, Villeurbanne, France (*Abstract Co-Author*) Nothing to Disclose Fabrice Lame, Lyon, France (*Abstract Co-Author*) Nothing to Disclose Catherine Bihane, Lyon, France (*Abstract Co-Author*) Nothing to Disclose Michael Sdika, Villeurbanne, France (*Abstract Co-Author*) Nothing to Disclose Jean-yves Blay, Lyon, France (*Abstract Co-Author*) Nothing to Disclose Olivier Beuf, PhD, Villeurbanne, France (*Abstract Co-Author*) Nothing to Disclose Frank Pilleul, MD, Lyon, France (*Abstract Co-Author*) Nothing to Disclose

#### For information about this presentation, contact:

amine.bouhamama@lyon.unicancer.fr

#### PURPOSE

The aim of this study was to develop a MRI-based radiomic method to assess lipomatous soft tissue tumors malignancy

### METHOD AND MATERIALS

105 subjects with lipomatous soft tissue tumors with histology and fat-suppressed T1w contrast enhanced MR images available were retrospectively enrolled to constitute the database. According to histology, three groups have been constituted: the benign group including deep lipomas (n = 23), the intermediate group including ALT and WDL (n = 41) and the malignant group including high grade liposarcomas (myxoid, dedifferentiated, and pleomorphic) (n = 41). Radiomic features extraction: Images were automatically loaded on an in-house software developed on Matlab R2017a. First, the tumor was segmented manually by two observers blinded to histology in order to evaluate the inter-observer reproducibility. 87 radiomic features were extracted. They included size, shape, intensity distribution, image domain (based on GCLM, GLRLM, GLSZM and NGTDM matrices) and frequency domain (based on Gabor filtering) textures features. Data mining - A 2 step decisional algorithm was built. In a first step, a multivariate model was used to classify between benign and (intermediate + malignant) groups. If result of test is 'benign' algorithm is stopped. If it is not the case, a second model was used to classify between intermediate and malignant groups.

#### RESULTS

55 radiomic features (63.2%) were found to be reproducible enough. To classify between benign and (intermediate + malignant) groups, the radiome was reduced to 24 features and the 12th order model gave the best performance (AUROC = 0.959 (95% CI: 0.921 - 0.996); sensitivity = 89% (95% CI: 80.2 - 94.9%) and specificity = 95.7% (95% CI: 78.1 - 99.9%). To classify between intermediate and malignant groups, the radiome was reduced to 21 features and the 17th order model gave the best diagnosis performances (AUROC = 0.907 (95% CI: 0.844 - 0.970); sensitivity = 85.4% (95% CI: 70.8 - 94.4%) and specificity = 90.2% (95% CI: 76.9 - 97.3%).

#### CONCLUSION

These results show that the evaluation of lipomatous tumor malignancy is feasible using a routinely used MRI acquisition in clinical practice.

### **CLINICAL RELEVANCE/APPLICATION**

Radiomic features may be useful to determine malignancy of lipomatous tumors. Benign tumors could be operated without previous biopsy or if asymptomatic, being left without medical supervision



### MK388-SD-WEA5

Correlation of Quantitative MRI Measures of Rotator Cuff Muscle Fatty Infiltration to Shoulder Strength and Range of Motion: A Pilot Study of Subjects with Painful Full-Thickness Supraspinatus Tendon Tear and Asymptomatic Controls

Wednesday, Nov. 28 12:15PM - 12:45PM Room: MK Community, Learning Center Station #5

#### **Participants**

Derik L. Davis, MD, Baltimore, MD (*Presenter*) Research Grant, Hitachi, Ltd Ranyah Almardawi, MBBS, MPH, Baltimore, MD (*Abstract Co-Author*) Nothing to Disclose Jiachen Zhuo, PhD, Baltimore, MD (*Abstract Co-Author*) Nothing to Disclose Mohit N. Gilotra, MD, Baltimore, MD (*Abstract Co-Author*) Nothing to Disclose Michael E. Mulligan, MD, Baltimore, MD (*Abstract Co-Author*) Nothing to Disclose Charles S. Resnik, MD, Baltimore, MD (*Abstract Co-Author*) Nothing to Disclose Selwan B. Abdullah, MD, Baltimore, MD (*Abstract Co-Author*) Nothing to Disclose Hussain Al Khalifah, MD, Baltimore, MD (*Abstract Co-Author*) Nothing to Disclose Steven Roys, Baltimore, MD (*Abstract Co-Author*) Nothing to Disclose Steven Roys, Baltimore, MD (*Abstract Co-Author*) Nothing to Disclose Syed A. Hasan, MD, Baltimore, MD (*Abstract Co-Author*) Nothing to Disclose Rao P. Gullapalli, PhD, Baltimore, MD (*Abstract Co-Author*) Nothing to Disclose

For information about this presentation, contact:

ddavis7@umm.edu

### PURPOSE

(1) To determine if supraspinatus muscle fat fraction (FF) by 6-point Dixon MRI correlates with shoulder strength and range of motion (ROM) and (2) whether FF has higher inter-rater reliability compared to Goutallier grade (GG). (3) To determine differences in supraspinatus muscle extramyocellular lipid (EMCL) by MR spectroscopy (MRS) between subjects with painful full-thickness supraspinatus tendon tear (pFT-STT) and asymptomatic controls without full-thickness tear.

### **METHOD AND MATERIALS**

Adults (40 to 85 years) were recruited prospectively over a 1-year period and received one shoulder MRI. Cohorts: pFT-STT (N=15; age,  $62.6 \pm 9.0$  years; 53% male) and control (N=17; age,  $63.0 \pm 10.2$  years; 53% male). Two blinded musculoskeletal radiologists assigned a GG for each supraspinatus muscle on the same oblique sagittal T1-weighted Y-shaped view MR image. Two blinded diagnostic radiology residents calculated supraspinatus FF on each corresponding oblique sagittal Dixon MR image. A blinded MR physicist measured EMCL by MRS. All subjects were tested for shoulder strength (abduction [ABD];adduction external rotation [AdER]) and ROM (forward flexion [Fflex];ABD;AdER). Cohorts were stratified by gender. Descriptive, correlative and reliability analyses were performed.

#### RESULTS

The pFT-STT cohort had higher FF (0.073  $\pm$  0.051 vs 0.033  $\pm$  0.024, p=0.010) and higher GG (0.9  $\pm$  0.7 vs 0.4  $\pm$  0.5, p=0.022) vs controls. Male and female pFT-STT cohorts were weaker and had less ROM vs controls for all categories. For entire study population, FF exhibited strong correlation with strength (ABD: r = -0.454, p=0.013) and ROM (Fflex: r = -0.505, p=0.005; ABD: r = -0.468, p=0.009; AdER: r = -0.416, p=0.022). GG showed weak correlation and no significance for all categories. Inter-rater reliability was higher for FF (ICC: 0.901) vs GG (Kappa: 0.362). The pFT-STT sub-cohort (N=9) had higher EMCL (22.9  $\pm$  17.5 mmol/L vs 7.5  $\pm$  9.2 mmol/L, p=0.131) compared to controls (N=4).

### CONCLUSION

Quantitative MRI Dixon fat fraction of supraspinatus muscle has higher correlation to shoulder strength and ROM, and higher interrater reliability, compared to qualitative MRI Goutallier grade. Supraspinatus EMCL trends higher in pFT-STT compared to controls.

### **CLINICAL RELEVANCE/APPLICATION**

Evaluation of rotator cuff (RC) muscle fatty infiltration (FI) is key for clinical decision making in patients with RC tear. Quantitative MRI techniques offer potential for improved measurement of FI.



### MK389-SD-WEA6

### Contrast Extravasation after Shoulder Arthrography: Is it Avoidable?

Wednesday, Nov. 28 12:15PM - 12:45PM Room: MK Community, Learning Center Station #6

FDA Discussions may include off-label uses.

#### **Participants**

Michel O. De Maeseneer, MD, PhD, Jette, Belgium (*Presenter*) Nothing to Disclose Nico Buls, DSc, PhD, Jette, Belgium (*Abstract Co-Author*) Nothing to Disclose Nicole Pouliart, Jette, Belgium (*Abstract Co-Author*) Nothing to Disclose Freddy Machiels, Brussels, Belgium (*Abstract Co-Author*) Nothing to Disclose Cedric Boulet, Brussels, Belgium (*Abstract Co-Author*) Nothing to Disclose Maryam Shahabpour, MD, Brussels, Belgium (*Abstract Co-Author*) Nothing to Disclose

#### For information about this presentation, contact:

Michel.demaeseneer@uzbrussel.be

#### PURPOSE

Contrast extravasation after standard anterior artrographic puncture of the shoulder is common and negatively affects image quality and interpretation. We hypothezised that strict shoulder immobilisation in the time interval between arthrography puncture and subsequent MR arthrography would limit extravasation.

#### **METHOD AND MATERIALS**

Fifty patients underwent shoulder MR arthrography using a standard shoulder puncture in the anteroinferior quadrant. Ten mL of a mixture of saline contrast, iodine contrast and gadolinium contrast were injected by one of two senior MSK radiologist using a 20 G needle. Half of the patients were immediately immobilized with a sling, and the other half were allowed to move shoulder and arm freely in the time interval before MR. MR arthrography was performed with a 3 T system using standard T1 and PD weighted sequences. No ABER position was performed. The MR images were reviewed and leakage in the axilarry region and subcorocoid region was noted. Extravasation was graded independently by two MSK radiologist. A five point scale was used (1:none; 2: less tan 2 cm; 3: 2-5 cm; 4: 5-10 cm; 5: more than 10 cm). Chi square test was performed for analysis and Conen's kappa was caculated.

#### RESULTS

The mean age of the patients was 47 years (18-77 years). There were 27 men and 23 women. The mean time between puncture and MR was 35 minutes, similar for both groups. Eight (36 %) (reader 1), and 10 (45 %) (reader 2) that were immobilized were graded as 3-5. Seven (32%) (reader 1) and 5 (23%) (reader 2) of the non immobilized patients were graded 3-5. There was no statistically significant difference between both groups. Interobserver agreement was substantial (kappa: 0.64).

#### CONCLUSION

Contrast extravasation after arthrography puncture is common, even in experienced hands. It is unavoidable and negatively affects image quality and interpretation, such as capsular rupture and the J sign. Our hypothesis that extravasation can be avoided by struct immobilisation is false.

### **CLINICAL RELEVANCE/APPLICATION**

Contrast extravasation after arthrography puncture of the shoulder in the time interval before MR is a major and common problem. It negatively affects image quality and limits interpretation of certain signs such as the J sign and capsular rupture. It can not be avoided by strict immobilisation of the shoulder.



### NM226-SD-WEA1

Impact of Different Iterative Metal Artifact Reduction (iMAR) Algorithms on PET/CT Attenuation Correction in Artifacts After Port Implantation

Wednesday, Nov. 28 12:15PM - 12:45PM Room: NM Community, Learning Center Station #1

# Participants

Ole Martin, Duesseldorf, Germany (*Presenter*) Nothing to Disclose Johannes Boos, MD, Dusseldorf, Germany (*Abstract Co-Author*) Nothing to Disclose Christian Buchbender, Duesseldorf, Germany (*Abstract Co-Author*) Nothing to Disclose Gerald Antoch, MD, Duesseldorf, Germany (*Abstract Co-Author*) Nothing to Disclose Christina Antke, Duesseldorf, Germany (*Abstract Co-Author*) Nothing to Disclose Benedikt M. Schaarschmidt, MD, Essen, Germany (*Abstract Co-Author*) Stockholder, Bayer AG; Stockholder, General Electric Company; Stockholder, Siemens AG; Stockholder, Teva Pharmaceutical Industries Ltd

#### For information about this presentation, contact:

Ole.Martin@med.uni-duesseldorf.de

### PURPOSE

To evaluate the impact of iterative metal artifact reduction (iMAR) algorithms on Hounsfield units (HU) and standardized uptake values (SUV) in bright-band artefacts caused by port catheter systems.

### **METHOD AND MATERIALS**

In this prospective study, 30 oncological patients (12 female, 18 male, mean age 59.6±10.5y) with port chambers undergoing clinical indicated PET/CT on a Biograph mCT were included. An additional phantom scan was performed, consisted of a 25-L container containing a standard port catheter system in a solution of 18F-fluorodeoxyglucose (18F-FDG) and water. CT datasets were reconstructed on a dedicated workstation using standard weighted filtered back projection (WFBP) CT and three different iMAR algorithms (algorithm for dental filling (DF), hip and pacemaker (PM)). PET attenuation correction was performed with all four datasets. SUVmean and HU measurements were performed in fat and muscle tissue in the vicinity of the port chamber at the location with the most prominent bright band artifacts. Differences between HU and SUVmean values across all CT and PET-images were investigated using paired t-tests. Bonferroni correction was used to prevent alpha-error accumulation (p<0.008).

#### RESULTS

In comparison to WFBP (fat:  $94.2 \pm 53.9$  HU, muscle:  $197.6 \pm 49.2$  HU) all three iMAR algorithms led to a significant decrease of HU in bright band artifacts. iMAR-DF led to a decrease of 159.2% (fat:  $-51.9 \pm 58.5$  HU, muscle:  $94.5 \pm 55.3$  HU), iMAR-hip of 138.3% (fat:  $-30.3 \pm 58.5$ , muscle:  $70.4 \pm 28.8$ ) and iMAR-PM of 122.3% (fat:  $-21.2 \pm 47.2$  HU, muscle:  $72.5 \pm 25.1$  HU; for all p<0.008). There was no significant effect on SUVmean in bright band artifacts (SUVmean  $0.48\pm0.23$  with WFBP,  $0.43\pm0.21$  with iMAR-DF,  $0.46\pm0.22$  with iMAR-hip and  $0.47\pm0.22$  with iMAR-PM). Similar results were observed for HU and SUVmean measurements in the phantom scan.

### CONCLUSION

Using iMAR-CT images for attenuation correction of PET-datasets led to a significant change of HU values in artifacts caused by port catheter chambers in comparison to WFBP. However, these findings did not translate to significant changes in attenuation correction and consecutive differences in SUV.

### **CLINICAL RELEVANCE/APPLICATION**

iMAR reconstructions in PET/CT improve CT image quality by reducing bright band artifacts but do not influence attenuation correction.



### NM227-SD-WEA2

Essential Information Which Helps to Reduce Negative FDG PET-CT Study in Investigating Large Vessel Vasculitis

Wednesday, Nov. 28 12:15PM - 12:45PM Room: NM Community, Learning Center Station #2

# Participants

Heok Cheow, MBBCh, MSc, Cambridge, United Kingdom (*Presenter*) Nothing to Disclose Badriya Al-Saqri, MD, Cambridge, United Kingdom (*Abstract Co-Author*) Nothing to Disclose Ines D. Harper, MBChB,FRCR, Cambridge, United Kingdom (*Abstract Co-Author*) Nothing to Disclose

#### PURPOSE

In recent year, FDG PET-CT has been advocated as the technique of choice for investigating large vessel vasculitis. The goal of the study is to correlate (1) the use of steroid prior PET-CT study, (2) serum inflammatory markers (CRP & ESR) with the results of PET-CT study in order to reduce the number of negative studies.

#### **METHOD AND MATERIALS**

Patients referred for FDG PET-CT investigation of large vessel vasculitis over two-year period were recruited; serum inflammatory markers (within two weeks window prior to PET-CT study) and the use of steroid were used to compare with the results of the PET-CT.

### RESULTS

In total, 74 patients (30 men, 44 women) were identified. None of the 13 patients with positive PET-CT study was on steroid. Of the 61 PET-CT negative studies, 24 patients were on steroid ranging from 2mg to 60mg. All except one positive PET-CT have high CRP. 28 patients with negative study have normal CRP whereas 30 of them with raised CRP have a negative study. 9 out of 13 patients with high ESR were PET-CT positive. 42 out of 52 patients with normal ESR were PET-CT negative. Combining CRP and ESR results, 9 out of 13 patients with high CRP & ESR were PET-CT positive compared to only 1 with normal inflammatory markers. 10 out of 52 patients with high CRP & ESR were PET-CT negative compared to 27 with normal inflammatory markers.

#### CONCLUSION

From this study, we would not advocate PET-CT study if patients were on steroid or have normal inflammatory markers. On the other hand, raised inflammatory markers do not predict a positive study.

# **CLINICAL RELEVANCE/APPLICATION**

PET-CT should be done prior starting of steroid therapy.



### NM228-SD-WEA3

Comparing TNM Staging Adequacy and Processing Time of Structured Reports versus Fully Segmented and Annotated PET/CT Data of Non-Small Cell Lung Cancer

Wednesday, Nov. 28 12:15PM - 12:45PM Room: NM Community, Learning Center Station #3

# Participants

Raphael Sexauer, Basel, Switzerland (*Abstract Co-Author*) Nothing to Disclose Thomas Weikert, MD, Basel, Switzerland (*Abstract Co-Author*) Nothing to Disclose Kevin Mader, DPhil,MSc, Basel, Switzerland (*Abstract Co-Author*) Employee, 4Quant Ltd; Shareholder, 4Quant Ltd Andreas Wicki, MD, Basel, Switzerland (*Abstract Co-Author*) Nothing to Disclose Bram Stieltjes, MD,PhD, Basel, Switzerland (*Presenter*) Nothing to Disclose Jens Bremerich, MD, Basel, Switzerland (*Abstract Co-Author*) Nothing to Disclose Gregor Sommer, Basel, Switzerland (*Abstract Co-Author*) Nothing to Disclose Alexander Sauter, Basel, Switzerland (*Abstract Co-Author*) Nothing to Disclose

#### For information about this presentation, contact:

raphael.sexauer@usb.ch

#### PURPOSE

Results of PET/CT examinations are usually communicated as text-based reports. These are often unstructured and may be incomplete, possibly causing staging errors. We examined to what extent text-based reports differ from a full 3D-segmentation approach regarding the completeness of TNM information and processing time.

#### **METHOD AND MATERIALS**

TNM information was extracted retrospectively from 395 text-based reports by a dual-board-certified radiologist and nuclear medicine physician. Also the RIS time tracking of the reports was analyzed. The corresponding image data were transferred to a 3D slicer-based software, where 2995 lesions were segmented manually using a set of 41 classification labels (TNM features + location). The time required per lesion was automatically recorded. Information content and processing time of text-based reports and segmentations were compared using descriptive statistics and modelling.

#### RESULTS

The TNM/UICC stage was mentioned explicitly in only 6% (n=22) of the reports, but could be extracted in 78% (n=309) of the cases. In the remaining 22% (n=86), information was incomplete, most frequently affecting T-stage (19%, n=74), followed by N-(6%, n=22) and M-stage (2%, n=9). Full lesion segmentation required less time (median: 12.9 min) than the lowest estimator of the reporting time (dictation: median 18.1, p=.01). Tumor stage (UICC I/II: 5.2min, UICC III/IV: 20.3min, p<.001), lesion size (p<.001) and lesion count (n=1: 4.4min, n=12: 37.2min, p<0.001) correlated significantly with the segmentation time, but not with the dictation time.

#### CONCLUSION

A considerable number of text-based staging reports are lacking important information. A segmentation-based reporting approach tailored to the staging task can improve report quality with manageable efforts in terms of processing time.

#### **CLINICAL RELEVANCE/APPLICATION**

Segmentation-based reporting can improve report quality and avoid erroneous therapy decisions based on incomplete reports. Segmented data may be used for multimedia enhancement and automatization.



#### NM229-SD-WEA4

To Evaluate the Role of FDG PET/CT in Patients with Cutaneous Squamous Cell Carcinoma for Initial Staging

Wednesday, Nov. 28 12:15PM - 12:45PM Room: NM Community, Learning Center Station #4

# Participants

Sikandar M. Shaikh, DMRD, Hyderabad, India (Presenter) Nothing to Disclose

For information about this presentation, contact:

idrsikandar@gmail.com

#### PURPOSE

Cutaneous squamous cell carcinoma (cSCC) comprises of 20-25% of non melanoma skin malignancies. CT and/or MRI is used in evaluating local extent of disease in advanced stages. The role of 2-fludeoxyglucose positron emission tomography/computed tomography (FDG PET/CT) is not clearly defined.

### **METHOD AND MATERIALS**

This was retrospective study which was conducted in patients with cutaneous SCC who presented for a period of two years. Patients who received FDG PET/CT scan at diagnosis for initial staging were evaluated for lesion detection by FDG PET/CT. These images were assessed for abnormal sites of increased uptake as compared to normal adjacent background. All suspicious increased uptake sites of uptake were noted. Standard uptake value (SUV) in primary and secondary sites was measured. Findings were correlated with biopsy/histopathological findings and follow up imaging and clinical data

## RESULTS

Of the 22 patients screened, 13 patients with primary cSCC who had FDG PET/CT scan at diagnosis were evaluated (mean age: 76; range 60-90 years; M:F = 12:1) (pathological stage II; n=5, stage III; n=3 and stage IV; n=5). Primary sites were located in scalp (n=5), eyebrow (n=1), ear (n=1), cheek (n=3), nose (n=1), neck (n=1) and foot (n=1). All patients had positive FDG scan with areas of increased uptake . A total of 26 lesions were detected. All primary lesions (n=14) showed high FDG uptake (SUV 2.3-22.8; mean 11.6). Additional 12 FDG avid lesions were noted in 7 patients (2 cutaneous lesions in arm and cheek in a patient; 1 bone lesion, 1 lung nodule, and 8 nodes). Pathology correlation was available for 22/26 lesions; 20/22 sites were positive for malignancy while 2/22 were benign nodes. 2/20 positive lesions were basal cell carcinoma. Remaining 4/26 FDG positive sites included 3 nodes that were also malignant on follow up. SUV (mean  $\pm$ SD; (range)) was 9.7 $\pm$ 6.8 (2.3-22.8) for malignant lesions (n=20) and 4.5 $\pm$ 1.3 (3.5-5.4) for benign lesions (n=2). Overall sensitivity and accuracy of FDG PET/CT was 100% and 92% respectively. FDG detected four prior unknown secondary lesions and changed management plan in 3 of 13 patients (23%).

### CONCLUSION

Thus FDG PET/CT has significant high sensitivity in detection of lesions in cutaneous SCC. It has potential role in initial staging and management of primary cutaneous SCC.

# **CLINICAL RELEVANCE/APPLICATION**

Thus FDG PETCT is very sensitive modality for evaluation of cutaneous squamous cell carcinoma.



### NM230-SD-WEA5

Implications of Empiric I-131 Activity Administration to Treat Thyroid Cancer in Patients with Abnormal Renal Function

Wednesday, Nov. 28 12:15PM - 12:45PM Room: NM Community, Learning Center Station #5

# Participants

Kenneth Nichols, PhD, New Hyde Park, NY (*Presenter*) Royalties, Syntermed, Inc; Maria B. Tomas, MD, New Hyde Park, NY (*Abstract Co-Author*) Nothing to Disclose Gene G. Tronco, MD, New Hyde Park, NY (*Abstract Co-Author*) Nothing to Disclose Fritzgerald Leveque, New Hyde Park, NY (*Abstract Co-Author*) Nothing to Disclose Kuldeep K. Bhargava, PhD, New Hyde Park, NY (*Abstract Co-Author*) Nothing to Disclose Christopher J. Palestro, MD, New Hyde Park, NY (*Abstract Co-Author*) Nothing to Disclose

#### For information about this presentation, contact:

knichols@northwell.edu

### PURPOSE

Accepted post-surgical treatment of pts with thyroid carcinoma is I-131 ablation. Empiric amounts of I-131 are administered based on the assumption that the administered activity will deliver a dose to blood (D) below 200 cGY. In the setting of renal disease, reduced iodine clearance potentially could result in excessive red bone marrow doses. The objective of this retrospective investigation was to determine the effects of renal disease on the maximum permissible activity (MPA) of I-131 that can be safely administered to pts with thyroid cancer & renal disease.

#### **METHOD AND MATERIALS**

One hundred pts (age =  $59\pm16$  years; 50 female pts; 50 male pts) with thyroid cancer underwent blood sample collection of 4-7 days following ingestion of 1-4 mCi I-131, & whole-body I-131 scanning 48 hrs after administration of I-131. Ninteen of the 100 pts had impaired renal function (IRF), defined as BUN & creatinine values exceeding normal limits. I-131 blood-measurement-only dosimetry was used to compute I-131 MPA. The % of pts for whom D > 200 cGy for administered activity of 100-200 mCi I-131 were tabulated.

### RESULTS

MPA ranged from 106-361 mCi for the 19 patients. None would have received > 200 cGy at an empiric activity of 100 mCi, but 1 pt (5%) would have received 237 cGy at 125 mCi, 6 pts (32%) would have received  $311\pm37$  cGy at 150 mCi & 12 pts (63%) would have received  $277\pm46$  cGy at 200 mCi.

# CONCLUSION

Pts with impaired renal function who are candidates for treatment with 125 mCi or more of I-131 should undergo prior dosimetry to ensure that MPA is not exceeded.

# **CLINICAL RELEVANCE/APPLICATION**

I-131 MPA should be assessed prior to thyroid cancer therapy to avoid excessive radiation dose.



### NR348-ED-WEA10

How the Ocular Ultrasound Helps the Ophthalmologist: Review of the Technique and the Most Frequent Pathologies Seen with Its Use in the Emergency Room

Wednesday, Nov. 28 12:15PM - 12:45PM Room: NR Community, Learning Center Station #10

# Participants

Francisco Pozo Pinon, Santander, Spain (*Presenter*) Nothing to Disclose Alejandro Fernandez Florez, MD, Santander, Spain (*Abstract Co-Author*) Nothing to Disclose Enrique Montes, MD, Santander, Spain (*Abstract Co-Author*) Nothing to Disclose Carmen Gonzalez-Carrero Sixto, Santander, Spain (*Abstract Co-Author*) Nothing to Disclose Yasmina Lamprecht, MBBS, Santander, Spain (*Abstract Co-Author*) Nothing to Disclose Elena Marin-Diez, MD, Santander, Spain (*Abstract Co-Author*) Nothing to Disclose Beatriz Gonzalez Humara, Santander, Spain (*Abstract Co-Author*) Nothing to Disclose Pedro Lastra Garcia-Baron, MD, Santander, Spain (*Abstract Co-Author*) Nothing to Disclose

#### **TEACHING POINTS**

We have reviewed the images of ocular ultrasound from our hospital's archive, taken from urgent and routine studies. Based on these images we will review the principal characteristics of the anatomy of the eye and the orbit visualized with ultrasound. In addition, we want to show the most common pathologies of the eye and the orbit in which the ultrasound can play an important role, either because of its good diagnostic value or because the impossibility performing other studies, such as traumatic pathologies, vitreous pathologies (vitreous hemorrhage, inflammatory processes), posterior wall pathologies (retinal detachment, posterior vitreous detachment and choroid detachment), tumors (melanoma, metastasis), or pathologies of the orbit.

## TABLE OF CONTENTS/OUTLINE

Indications of ocular ultrasound: eyelid problems (severe edema, wound), corneal opacifications, hyphema, hypopyon, myosis, dense cataract, vitreous opacifications (hemorrhage). Anatomic characteristics seen with ultrasound: Cornea. Esclera. Anterior chamber. Iris. Lens. Vitreous chamber. Posterior wall. Most frequent pathologies seen with ultrasound: Traumatic pathologies. Vitreous pathologies. Posterior wall pathologies. Ocular tumors. Pathologies of the orbit (traumatisms or tumors).



#### NR349-ED-WEA11

### Primary CNS Lymphoma: Role of the Radiologist from Diagnosis to Surveillance of the Disease

Wednesday, Nov. 28 12:15PM - 12:45PM Room: NR Community, Learning Center Station #11

#### Participants

Tyler Richards, MD, Cleveland, OH (*Presenter*) Nothing to Disclose Joseph M. Curcio, DO, Cleveland, OH (*Abstract Co-Author*) Nothing to Disclose Chaitra A. Badve, MD, Cleveland, OH (*Abstract Co-Author*) Nothing to Disclose Nikhil H. Ramaiya, MD, Jamaica Plain, MA (*Abstract Co-Author*) Nothing to Disclose

# For information about this presentation, contact:

tyler.richards@uhhospitals.org

# **TEACHING POINTS**

1. Overview of primary CNS lymphoma subtypes and demonstration of their spectrum of imaging findings from presentation to recurrence. 2. Understand how the radiologist can assist the oncologist in evaluation of treatment response and recognition of treatment-related drug toxicities.

# TABLE OF CONTENTS/OUTLINE

Epidemiology, clinical features, immunophenotypes, and prognosis of the subtypes of primary CNS lymphoma (PCNSL) with imaging examples Diffuse Large B-cell Intravascular large B-cell Marginal zone B-cell T-cell Patterns of presentation of PCNSL (including immunocompromised patients) with imaging examples Parenchymal mass Dural-based mass Periventricular enhancing tumor Leptomeningeal carcinomatosis Intravascular lymphomatosis Role of radiologist Diagnosis Imaging examples of features suggestive of PCNSL Role of advanced MR imaging Staging CT chest/abdomen/pelvis with contrast +/- FDG PET LP with CSF cytology and flow cytometry +/- Scrotal US Treatment Response criteria with imaging examples Imaging biomarkers Role of chemotherapy, surgery, radiation, and stem cell transplant Treatment for immunocompromised patients Surveillance Patterns of recurrence Imaging frequency

### **Honored Educators**

Presenters or authors on this event have been recognized as RSNA Honored Educators for participating in multiple qualifying educational activities. Honored Educators are invested in furthering the profession of radiology by delivering high-quality educational content in their field of study. Learn how you can become an honored educator by visiting the website at: https://www.rsna.org/Honored-Educator-Award/ Nikhil H. Ramaiya, MD - 2017 Honored Educator



### NR350-ED-WEA12

A User Guide for Head and Neck Lesions Evaluation with DIXON: Technical Adjustments and Potential Applications

Wednesday, Nov. 28 12:15PM - 12:45PM Room: NR Community, Learning Center Station #12

# Participants

Teodoro M. Noguerol, MD, Jaen, Spain (*Presenter*) Nothing to Disclose Eloisa Santos Armentia, MD, Vigo, Spain (*Abstract Co-Author*) Nothing to Disclose Marta Gomez Cabrera, MD, Cadiz, Spain (*Abstract Co-Author*) Nothing to Disclose Antonio Luna, MD,PhD, Jaen, Spain (*Abstract Co-Author*) Consultant, Bracco Group; Speaker, General Electric Company; Speaker, Canon Medical Systems Corporation; Royalties, Springer Nature

#### For information about this presentation, contact:

t.martin.f@htime.org

# **TEACHING POINTS**

1. Review the physical basis of DIXON sequences focusing on head and neck area. 2. Describe the advantages and disadvantages of DIXON compared to conventional fat suppresion techniques. 3. Review the potential role of DIXON for head and neck lesions evaluation in different clinical scenarios.

#### TABLE OF CONTENTS/OUTLINE

1. Introduction 2. Physical basis of DIXON technique. a. T1 DIXON b. T2 DIXON c. It's possible to quantify? How we do it? 3. DIXON vs. other Fat Suppresion techniques. a. Advantages and disadvantages b. Potential pitfalls of DIXON in head and neck. 4. Clinical scenarios a. Globes and orbits b. Skull base and temporal bone c. Paranasal sinuses d. Salivary glands e. Suprahyoid and infrahyoid lesions f. Other head and neck lesions 5. Conclusions and take home messages

#### **Honored Educators**

Presenters or authors on this event have been recognized as RSNA Honored Educators for participating in multiple qualifying educational activities. Honored Educators are invested in furthering the profession of radiology by delivering high-quality educational content in their field of study. Learn how you can become an honored educator by visiting the website at: https://www.rsna.org/Honored-Educator-Award/ Antonio Luna, MD - 2018 Honored Educator



### NR408-SD-WEA1

Peritumoral Bone Change in Oral Squamous Cell Carcinoma: A Prospective Study Through Radiologic-Pathologic Correlation

Wednesday, Nov. 28 12:15PM - 12:45PM Room: NR Community, Learning Center Station #1

# Participants

Gyu-Dong Jo, Seoul, Korea, Republic Of (*Abstract Co-Author*) Nothing to Disclose Kyung-Hoe Huh, Seoul, Korea, Republic Of (*Presenter*) Nothing to Disclose Jo-Eun Kim, DDS, Seoul, Korea, Republic Of (*Abstract Co-Author*) Nothing to Disclose Min-Suk Heo, Seoul, Korea, Republic Of (*Abstract Co-Author*) Nothing to Disclose Sam-sun Lee, Seoul, Korea, Republic Of (*Abstract Co-Author*) Nothing to Disclose Soon-Chul Choi, Seoul, Korea, Republic Of (*Abstract Co-Author*) Nothing to Disclose Won-Jin Yi, Seoul, Korea, Republic Of (*Abstract Co-Author*) Nothing to Disclose

#### PURPOSE

When oral squamous cell carcinoma (OSCC) invades the jaw bone, abnormal CT attenuation or MR signal intensity (SI) are frequently observed in remaining bone margin, which makes it difficult to determine the extent of tumor invasion. We hypothesized that there is no tumor cell nest in the region of peritumoral bone change. To prove this hypothesis, we evaluated peritumoral bone changes on pre-operative CT, MR, PET-CT images and post-operative cone beam CT images of resected specimen, then compared the radiologic findings with histopathologic findings.

### METHOD AND MATERIALS

Twenty consecutive patients with OSCC in the mandible were enrolled. The degree of sclerosis on pre-operative CT image and SI of underlying bone marrow on pre-operative MR image were analyzed. On pre-operative PET-CT images, the degree of fluorodeoxyglucose(FDG) uptake was assessed. After partial mandibulectomy, histopathologic slides were prepared for three regions of the specimens. Histopathologic findings, such as presence of malignant cell nests, density of peritumoral inflammation, pattern of trabecular bone alteration, peritumoral stroma reaction, were evaluated. The relationships between radiologic and histopathologic findings were evaluated using Pearson's Chi-square test.

### RESULTS

On CT images, sclerosis was observed in 15/20 cases. On MR images, pathologic SI of underlying bone marrow was observed in 13/20 cases. Peritumoral bone change commonly presented high SI on T2-weighted image and enhancement on postcontrast T1-weighted image. However, SI of peritumoral change on MR image was different from that of a main mass. On PET-CT images, hyperuptake was observed in 2/20 cases, which was very rare. According to histopathologic findings, no malignant cell nest but mild inflammation was observed in peritumoral bone change area. Sclerosis on CT images tended to show a higher level of trabecular thickness and a normal trabecular number. Abnormal SI of bone marrow on MR images showed desmoplastic stromal reaction rather than fibromyxoid one.

# CONCLUSION

Peritumoral bone changes are often accompanied by OSCC as sclerosis or pathologic signal change of bone marrow. Those changes should not be considered as bone invasion by OSCC.

# **CLINICAL RELEVANCE/APPLICATION**

Peritumoral bone change adjacent to OSCC makes it difficult to determine the extent of tumor invasion.



### NR409-SD-WEA2

### MRI Quantitative Phantom Study of OMAR/SEMAC Metal Suppression for Spine Instrumentation at 3T

Wednesday, Nov. 28 12:15PM - 12:45PM Room: NR Community, Learning Center Station #2

#### **Participants**

Devon M. Middleton, Philadelphia, PA (*Presenter*) Nothing to Disclose Feroze B. Mohamed, PhD, Philadelphia, PA (*Abstract Co-Author*) Nothing to Disclose Adam E. Flanders, MD, Philadelphia, PA (*Abstract Co-Author*) Nothing to Disclose Laura Krisa, Philadelphia, PA (*Abstract Co-Author*) Nothing to Disclose Kiran S. Talekar, MBBS, MD, Philadelphia, PA (*Abstract Co-Author*) Spouse, Employee, GlaxoSmithKline plc Scott H. Faro, MD, Haddonfield, NJ (*Abstract Co-Author*) Nothing to Disclose

### PURPOSE

Metal instrumentation is a particular confound in MRI in spinal cord injury due to differing configurations and proximity to imaged tissue. Metal suppression sequences can mitigate this using slice encoding for metal artifact correction (SEMAC), but this is an expensive technique with respect to imaging time. This study examines common instrumentation configurations in phantoms to quantify improvement in image quality with SEMAC encoding.

### METHOD AND MATERIALS

The configurations examined were: cervical anterior plate (CA), cervical posterior rods/screws (CP), cervical with plate and rods/screws (CAP), and thoracic with anterior plate with posterior rods and screws (TAP). Phantoms were constructed by implanting plastic spine models with titanium surgical implants by trained neurosurgeons. Models were suspended in a 2% agar gel with a stalk of asparagus as a spinal cord surrogate. Imaging was performed on a 3T Philips Ingenia MR scanner using the OMAR metal suppression sequence which employs view-angle tilting and SEMAC. Sagittal and axial T1 and T2 weighted images were acquired with a conventional high bandwidth turbo-spin-echo sequence and with the OMAR sequence at levels of 9 (weak), 17 (moderate), and 25 (strong) steps of SEMAC encoding. Cord ROIs were defined on the metal suppressed images and cord homogeneity was measured as the percentage of intensity standard deviation with respect to cord mean intensity. Imaging time ranged from 2:20-3:15 min for conventional sequences and 2:54-12:27 for OMAR sequences depending on the amount of SEMAC encoding

#### RESULTS

The OMAR sequence showed clear reduction of metal artifact and provided a clearer view of the cord. Average improvements of 34%, 36%, and 44% were found for weak, moderate and strong suppression respectively for all phantoms. Greater SEMAC encoding provided the greatest benefit for axial images with average improvements of 25%, 29%, and 43%, where sagittal images remained comparable at 42%, 42%, and 46%.

### CONCLUSION

Phantom studies can provide guidance for imaging differing spinal implant configurations. Minimal SEMAC encoding performs similarly to much longer scans in sagittal acquisitions, but additional encoding may be worth the time cost in axial images with greater instrumentation.

### **CLINICAL RELEVANCE/APPLICATION**

Quantitative analysis of image quality in metal suppression sequences for spinal cord can help guide imaging parameters to balance quality and imaging time.



### NR410-SD-WEA3

The Filter Back Projection Revisited: The Sharp Filter Kernel Improve the Visualization of the Adamkiewicz Artery in Low-kV CT Angiography

Wednesday, Nov. 28 12:15PM - 12:45PM Room: NR Community, Learning Center Station #3

# Participants

Tatsuya Nishii, MD, PhD, Suita, Japan (*Presenter*) Nothing to Disclose Akiyuki Kotoku, MD, Kawasaki, Japan (*Abstract Co-Author*) Nothing to Disclose Yoshiro Hori, Osaka, Japan (*Abstract Co-Author*) Nothing to Disclose Yoshiki Higashino, RT, Suita, Japan (*Abstract Co-Author*) Nothing to Disclose Hironori Tanaka, RT, Suita, Japan (*Abstract Co-Author*) Nothing to Disclose Susumu Morikawa, Osaka, Japan (*Abstract Co-Author*) Nothing to Disclose Yoshiaki Watanabe, MD, Suita, Osaka, Japan (*Abstract Co-Author*) Nothing to Disclose Atsushi K. Kono, MD, PhD, Suita, Japan (*Abstract Co-Author*) Nothing to Disclose Yoshiaki Morita, Suita, Japan (*Abstract Co-Author*) Nothing to Disclose Atsushi K. Kono, MD, PhD, Suita, Japan (*Abstract Co-Author*) Nothing to Disclose Kazuto Harumoto, Suita, Japan (*Abstract Co-Author*) Nothing to Disclose Tetsuya Fukuda, Suita, Japan (*Abstract Co-Author*) Nothing to Disclose

For information about this presentation, contact:

ttsynishii@gmail.com

#### PURPOSE

The confidence level for the assessment of the Adamkiewicz artery (AKA) before the aortic repair, still highly depends on the display of the continuity of the AKA from the aorta mainly around the vertebral pedicle in CT angiography (CTA). We hypothesized that the sharp filter kernel can improve this continuity of the vessel structure due to its edge-enhancement and high spatial resolution. This study aimed to compare the subjective and objective image quality for the AKA assessment of the CTA reconstructed with the sharp and smooth filter kernels.

### **METHOD AND MATERIALS**

We retrospectively analyzed 34 patients (12 females, and median 74 years) who had undergone 80-kV CTA to detect the AKA before the aortic repair. We reconstructed the CTA with the sharp (I50f), and the smooth (I31f) filter kernels. Further, we deducted the non-enhanced CT from the CTA with the sharp filter kernel to obtain the bone subtracted CTA using a commercially available workstation. Firstly, we compared the CT number of the anterior spinal artery (ASA) (CTASA), the CNR of the ASA to the spinal cord (CNRASA-Cord) between two filters by the Wilcoxon signed-rank test. Secondly, a board-certified radiologist evaluated the CTAs using the 4-point continuity score (0, undetectable; 1, equivocal; 2, conceivable; and 3, absolute) of the vessel to the aorta. Then, the ratio of the subjects of scored as the absolute continuity (score 3) in each CTA was compared.

# RESULTS

The AKA was identified in 94% subjects. The CTA with the sharp filter kernel showed significantly higher CTASA and CNRASA-Cord than the smooth filter kernel (median CTASA 130.6 from 89.7HU, and median CNRASA-Cord 4.4 from 3.7, P < .001 for both). With the sharp filter kernel, 56% subjects scored to the absolute continuity of AKA, besides only 26% with the smooth filter kernel (P < .01). Further, the bone subtracted CTA showed the absolute continuity in 79% subjects (P < .01, compared with the sharp filter kernel).

### CONCLUSION

The sharp filter kernel significantly improved the image quality in CTA for the AKA assessment. Further, the unification of the sharp filter kernel and the bone subtraction technique showed the best imaging of the continuity of the AKA from the aorta.

### **CLINICAL RELEVANCE/APPLICATION**

The CTA with the sharp filter kernel can generate the high confidence level of the AKA evaluation, and become more efficient for preventing neurologic complications in the aortic repair.



### NR411-SD-WEA4

Initial Clinical Experience of Synthetic MRI as a Routine Neuroimaging Protocol in Daily Practice: A Single-Center Study

Wednesday, Nov. 28 12:15PM - 12:45PM Room: NR Community, Learning Center Station #4

# Participants

Hye Jin Baek, Changwon, Korea, Republic Of (*Abstract Co-Author*) Nothing to Disclose Kyeong Hwa Ryu, MD, Seoul, Korea, Republic Of (*Abstract Co-Author*) Nothing to Disclose Yedaun Lee, MD, Busan, Korea, Republic Of (*Presenter*) Nothing to Disclose Moonjung Hwang, Seoul, Korea, Republic Of (*Abstract Co-Author*) Research support, General Electric Healthcare

#### For information about this presentation, contact:

sartre81@gmail.com

### PURPOSE

We investigated the clinical feasibility of synthetic MRI with a 4-min single scan using a 48-channel head coil as a routine neuroimaging protocol in daily practice by assessing its diagnostic image quality.

### METHOD AND MATERIALS

We retrospectively reviewed the imaging data of 89 patients who underwent routine brain MRI using synthetic MRI acquisition between February 2017 and April 2017. Image quality assessments were performed by two independent readers on synthetic T1 fluid-attenuated inversion recovery (FLAIR), T2-weighted, T2 FLAIR, and phase-sensitive inversion recovery sequences acquired using multiple-dynamic multiple-echo imaging. Interobserver reliability between the two readers was assessed using kappa ( $\kappa$ ) statistics.

### RESULTS

On a 4-point assessment scale, the overall image quality and anatomical delineation provided by synthetic brain MRI were found to be good with scores of more than 3 points for all sequences except for the T2 FLAIR sequence. The synthetic T2 FLAIR sequence provided sufficient image quality but showed more pronounced artifacts, especially the CSF pulsation artifact and linear hyperintensity along the brain surface. Interobserver agreement for evaluating image quality of all synthetic sequences was good to excellent ( $\kappa$ , 0.61-0.99; P < 0.001).

#### CONCLUSION

Synthetic MRI can be acceptable as a routine clinical neuroimaging protocol with a short scan time. It can help design customized and flexible neuroimaging protocols for each institution.

# **CLINICAL RELEVANCE/APPLICATION**

Conventional brain MRI is a time-consuming modality because of the acquisition of multiple sequences with different contrast weightings. In contrast to conventional MRI, synthetic MRI can reduce scan times, thereby increasing its availability for both clinical and research applications. The routine use of synthetic MRI for neuroimaging may have inherent benefits such as reducing scan time, decreasing the need for rescanning owing to motion artifacts, reducing the need for sedation, providing quantitative information, and allowing the acquisition of additional sequences.



### NR412-SD-WEA5

Predicting Hemorrhagic Transformation by 3DpCASL Following Acute Stroke in Patients with Good Collateralization

Wednesday, Nov. 28 12:15PM - 12:45PM Room: NR Community, Learning Center Station #5

### Participants

Yina Lan, Beijing, China (*Presenter*) Nothing to Disclose Jinhao Lyu, Beijing, China (*Abstract Co-Author*) Nothing to Disclose Xiaoxiao Ma, Beijing, China (*Abstract Co-Author*) Nothing to Disclose Xin Lou, MD, PhD, Beijing, China (*Abstract Co-Author*) Nothing to Disclose

### PURPOSE

Previous studies have shown that deficient collateralization may be a potential indicator of hemorrhagic transformation (HT). However, it has recently been discovered that good leptomeningeal collateralization can also lead to HT. The present study aimed to compare the difference in cerebral blood flow (CBF) between HT of cerebral infarction and no HT of cerebral infarction in patients with good collateralization using pseudo continuous arterial spin labeling (pCASL), in order to develop a prognostic index for HT.

#### **METHOD AND MATERIALS**

From January 2016 to February 2017, nineteen patients (11 males and 8 females;  $age=59.5\pm9.9$  years) with unilateral acute cerebral infarction caused by 70%-99% thromboembolic stenosis of middle cerebral artery (MCA) and high perfusion in the infarction area or peripheries of the infarction area by multiple delay 3DpCASL were consecutively enrolled in the retrospective study. Of these patients, 9 had HT of cerebral infarction and 10 had no HT of cerebral infarction. A volumetric MCA territory based on gray matter mask according to a previous study was extracted to measure the mean CBF value of the infarct and contralateral side. Collateral flow was calculated using a previously reported method, and defined as [CBF2.5 s-CBF1.5 s] at lesion side - [CBF2.5 s-CBF1.5 s] at normal side, while antegrade flow was defined as CBF1.5 s at lesion side and late-arriving antegrade flow was defined as [CBF2.5 s-CBF1.5 s] at the normal side. CBF values were compared between patients with and without HT using the student't-test for two independent samples. P<0.05 was considered statistically significant.

### RESULTS

No significant difference was found in collateral flow values between patients with HT and no HT (9.81 vs. 6.26, P>0.05). However, antegrade flow values of HT was significantly lower than no HT on the infarct side (29.43 vs. 39.83, P=0.014). Meanwhile, CBF values of HT were higher than those of no HT in late-arriving antegrade flow (6.68 vs. 1.89, P=0.13).

### CONCLUSION

HT are likely to occur in patients with low antegrade flow and good collateralization. Meanwhile, late-arriving antegrade flow of patients with HT is easy to delay compared with those with no HT.

### **CLINICAL RELEVANCE/APPLICATION**

3DpCASL can quantificationally measure CBF and is recommended to compare the difference in CBF between hemorrhagic transformation of cerebral infarction and no hemorrhagic transformation of cerebral infarction.



### NR413-SD-WEA6

An fMRI Study of Expert Radiologists and Non-Radiologists

Wednesday, Nov. 28 12:15PM - 12:45PM Room: NR Community, Learning Center Station #6

#### **Participants**

David Ouellette, MS, Stony Brook, NY (*Presenter*) Nothing to Disclose Sindhuja Tirumalai Govindarajan, MS, Stony Brook, NY (*Abstract Co-Author*) Nothing to Disclose Eric K. van Staalduinen, DO, Stony Brook, NY (*Abstract Co-Author*) Nothing to Disclose Patricia Stefancin, MSc,BSC, Stony Brook, NY (*Abstract Co-Author*) Nothing to Disclose Dan-Ling Hsu, Stony Brook, NY (*Abstract Co-Author*) Nothing to Disclose Lev Bangiyev, DO, Stony Brook, NY (*Abstract Co-Author*) Nothing to Disclose Annapurneswara R. Chimpiri, MD, Stony Brook, NY (*Abstract Co-Author*) Nothing to Disclose Mark E. Schweitzer, MD, Stony Brook, NY (*Abstract Co-Author*) Consultant, MMI Munich Medical International GmbH; Data Safety Monitoring Board, Histogenics Corporation Zengmin Yan, MS, MD, Stony Brook, NY (*Abstract Co-Author*) Nothing to Disclose Syed H. Hussaini I, DO, Holtsville, NY (*Abstract Co-Author*) Nothing to Disclose

#### PURPOSE

With repeated practice, relevant brain substructures undergo anatomical and functional changes. The goal of our study was to measure functional activity during radiological problem-solving tasks in which participants make diagnostic decisions from medical images.

#### **METHOD AND MATERIALS**

Radiologists (N=6) and non-radiologists (N=11) were studied. The paradigm was: scrambled image (6s), display of medical image with basic patient history as the puzzle (12s), display of three diagnoses for subjects to choose from (6s), and display of the correct answer (3 s). Each subject carried out 4 trials of 20-puzzle blocks (80 puzzles). fMRI results were analyzed with FSL's FEAT toolbox. Brain activation during the initial puzzle phase and multiple choice phase were contrasted with activation from scrambled images. The resulting activation patterns were then contrasted between experts and novices using a fixed-effects model.

### RESULTS

Radiologists showed consistently reduced fMRI activity in the visual circuits (occipital pole and lateral occipital cortex) during 'puzzle' and 'multiple choice' phases when compared with non-radiologists. Since radiology practice is primarily a visual task, experts likely expend less energy analyzing images and reaching diagnostic decisions. During the puzzle phase, experts also had reduced activation in the posterior cingulate gyrus and the supramarginal gyrus. The posterior cingulate gyrus is a central node of the Default Mode network and is associated with dorsal attention network. Lower activity in this region suggests increased external attention during the puzzle phase. This suggests the brain of the expert radiologist devotes more focus to reading medical images than the novice viewer. The supramarginal gyrus is associated with perception, vision, reading, and speech, and also makes up part of the posterior parietal cortex, which is associated with visual attention.

#### CONCLUSION

Radiologists, compared to non-radiologists, showed overall and consistently lower fMRI activity, suggesting they expended less energy in completing the task. This study implicates not just visual circuits but also the posterior cingulate gyrus and the supramarginal gyrus in the acquisition of radiological expertise.

# **CLINICAL RELEVANCE/APPLICATION**

Improving the understanding of the neural correlates underpinning expertise may prove useful in designing individualized training strategies for radiologists.



#### NR414-SD-WEA7

### Deep Learning for Acute Ischemic Stroke on Diffusion-Weighted MR Imaging

Wednesday, Nov. 28 12:15PM - 12:45PM Room: NR Community, Learning Center Station #7

#### **Participants**

Bernardo C. Bizzo, MD, MSc, Boston, MA (*Presenter*) Nothing to Disclose Christopher Bridge, Boston, MA (*Abstract Co-Author*) Nothing to Disclose Stefano Pedemonte, PhD, Boston, MA (*Abstract Co-Author*) Nothing to Disclose Brad Wright, Boston, MA (*Abstract Co-Author*) Nothing to Disclose Renata R. Almeida, MD, Boston, MA (*Abstract Co-Author*) Nothing to Disclose Sean Doyle, Watertown, MA (*Abstract Co-Author*) Nothing to Disclose Mark Walters, Boston, MA (*Abstract Co-Author*) Nothing to Disclose Neil Tenenholtz, PhD, Boston, MA (*Abstract Co-Author*) Nothing to Disclose Adam McCarthy, Boston, MA (*Abstract Co-Author*) Nothing to Disclose Stuart R. Pomerantz, MD, Boston, MA (*Abstract Co-Author*) Nothing to Disclose Stuart R. Pomerantz, MD, Boston, MA (*Abstract Co-Author*) Research Grant, General Electric Company Katherine P. Andriole, PhD, Dedham, MA (*Abstract Co-Author*) Research Grant, NVIDIA Corporation; Research Grant, General Electric Company; Research Grant, Nuance Communications, Inc; Advisory Board, McKinsey & Company, Inc Ramon G. Gonzalez, MD, PhD, Boston, MA (*Abstract Co-Author*) Nothing to Disclose Mark H. Michalski, MD, Boston, MA (*Abstract Co-Author*) Nothing to Disclose

#### For information about this presentation, contact:

bbizzo@mgh.harvard.edu

## PURPOSE

To introduce a semi-supervised, multi-tasking, convolution neural network model trained for classification and segmentation of acute ischemic stroke using a heterogeneous set of weakly labeled and manually segmented diffusion-weighted MR imaging (DWI) and apparent diffusion coefficient (ADC) maps.

### METHOD AND MATERIALS

This is an IRB approved, retrospective study. Radiology reports over a ten-year period (2007-2017) were parsed using keyword pattern matching and a Support Vector Machine report classifier trained on n-gram based features, creating a balanced set of 4096 negative and 4096 positive studies for acute ischemic stroke on DWI and ADC. Initial classification results were manually validated and corrected by a trained radiologist during image review. Stroke cores of 500 studies were manually segmented by two trained radiologists. Images were re-sampled and a normalization algorithm was applied independently to DWI and ADC image intensities. We developed YNet, a semi-supervised multi-tasking deep neural network architecture that enables the combination of both weak labels derived from radiology report classification and manually delineated pixel level training data, and operates on multichannel (DWI and ADC) image data at full resolution. The model was evaluated on a test set containing studies independent of the training set.

### RESULTS

By using end-to-end multi-task learning, the YNet learned to classify acute ischemic stroke from weak labels and to segment from manual lesion delineation, achieving initial classification sensitivity of 0.981, specificity of 0.980, and preliminary segmentation Dice score of 0.623 on the test set.

#### CONCLUSION

We introduced a deep learning architecture that demonstrated high sensitivity and specificity to automatically detect and accurately delineate acute ischemic stroke lesions on DWI and ADC images, utilizing a heterogeneous set of weakly labeled and manually segmented studies.

#### **CLINICAL RELEVANCE/APPLICATION**

Given that many problems in image interpretation require detection and segmentation of lesions, we believe that the approach we explored can have wide applicability in medical image interpretation, enabling machine learning at large scale with less annotation effort. In the future, this method could be extended to account for multiple segmentation and classification labels.



### NR415-SD-WEA8

Artifact Reduction for Spectral Imaging Using a Three-state Projection-based Metal Artifact Reduction Algorithm

Wednesday, Nov. 28 12:15PM - 12:45PM Room: NR Community, Learning Center Station #8

# Awards

# Student Travel Stipend Award

#### **Participants**

Griselda T. Romero Sanchez, MD, Montreal, QC (*Presenter*) Nothing to Disclose Elizabeth Nett, Waukesha, WI (*Abstract Co-Author*) Employee, General Electric Company Reza Forghani, MD,PhD, Cote-saint-Luc, QC (*Abstract Co-Author*) Stockholder, Real-Time Medical, Inc; Founder, 4 Intel Inc; Stockholder, 4 Intel Inc; Consultant, General Electric Company; Speaker, General Electric Company

#### For information about this presentation, contact:

#### grirs@hotmail.com

# PURPOSE

To evaluate the effectiveness of artifact reduction for spectral imaging of the head and neck using a new, three-stage projectionbased metal artifact reduction algorithm.

### **METHOD AND MATERIALS**

Ten patients underwent a CT angiogram of the head and neck or head with a rapid kV-switching CT scanner (Revolution CT, GE Healthcare). Eight patients had dental hardware, one an aneurysm clip, and one an aneurysm coil. Scan-data were reconstructed without (baseline reconstruction) and with GSI MAR (Gemstone Spectral Imaging Metal Artifact Reduction; GE Healthcare), a three-stage, projection-based metal artifact reduction algorithm developed to further improve spectral imaging in the presence of dense metal objects such as dental fillings and hip implants. Subjective analysis and quantitative analysis was performed by placing 157 regions of interest (ROI) on various soft tissues of the neck or intracranially in areas with moderate or severe image degradation on the baseline reconstructions on 65 keV and 70 keV virtual monochromatic images (VMI), typically considered similar to a single energy CT acquisition. Spectral Hounsfield unit attenuation curves were then obtained by measuring CT attenuation (HU) and standard deviation (SD) within the ROIs at different VMI energy levels ranging from 40 to 140 keV, in 5-keV increments, for a total of 21 energy levels per ROI. The effects of dental artifact were quantitatively evaluated by the level of noise within the ROIs, determined based on the standard deviation within the ROI.

#### RESULTS

In this population, there was significant artifact reduction in areas affected by moderate or severe artifact both on subjective and objective, quantitative analysis. Statistically significant, lower noise (SD) measurements were observed at all energies evaluated on GSI MAR compared to baseline reconstructions. On 65 keV VMIs, there was an average of 1.8x or 78% noise (SD) reduction using GSI MAR compared to baseline reconstructions.

# CONCLUSION

The three-stage projection-based metal artifact reduction algorithm developed significantly reduces artifact and increases image quality in a wide range of virtual monochromatic energies.

#### **CLINICAL RELEVANCE/APPLICATION**

This new metal artifact reduction algorithm significantly reduced artifact in the cases studied, enabling assessment of areas that would otherwise be obscured by artifact.



### NR416-SD-WEA9

Evaluation of Accumulation of The Gadolinium-based Contrast Agents on Brain Tissues of Subjects With No Brain Abnormalities Using Quantitative Mapping of Susceptibility and Gray Matter Tissue Volume

Wednesday, Nov. 28 12:15PM - 12:45PM Room: NR Community, Learning Center Station #9

### Participants

Young Hoon An, Seoul, Korea, Republic Of (*Presenter*) Nothing to Disclose Soonchan Park, MD, Seoul, Korea, Republic Of (*Abstract Co-Author*) Nothing to Disclose Chang-Woo Ryu, MD, Seoul, Korea, Republic Of (*Abstract Co-Author*) Nothing to Disclose Geon-Ho Jahng, PhD, Seoul, Korea, Republic Of (*Abstract Co-Author*) Nothing to Disclose Yeji Shin, Seoul, Korea, Republic Of (*Abstract Co-Author*) Nothing to Disclose Na Young Choi, Seoul, Korea, Republic Of (*Abstract Co-Author*) Nothing to Disclose

#### For information about this presentation, contact:

yanayh22@gmail.com

#### PURPOSE

To evaluate the short-term effects of the gadolinium-based contrast agents (GBCAs) on brain tissues of subjects with no brain abnormalities with quantitative mapping of susceptibility and gray matter tissue volume.

#### **METHOD AND MATERIALS**

Twenty-six subjects were included in this study. Four-echo three-dimensional gradient-echo sequence was run to obtain the magnitude and phase images with 0.43 x 0.43 x 2 mm3 spatial resolution three times (before, 8 minute and 13 minutes after the GBCA injection). Furthermore, isotropic-voxel 3D T1-wighted images using the MPRAGE sequence was also acquired to process quantitative susceptibility map and to obtain the gray matter volume twice, before and after the GBCA injection. The MRI images were scanned in the following orders - pre-3DT1, pre-3D GRE, post1-3D GRE, post2-3D GRE, and then post-3DT1. QSM was obtained using the acquired phase images with the STI Suite toolbox. 3DT1-weighted images were segmented into gray matter and white matter using the cat12 toolbox. QSM and the corresponding magnitude images were compared among three different time points (pre, post1 and post2) and gray matter volume was compared between two time points(pre and post) using paired t-test.

#### RESULTS

Region-of-interests (ROIs) were defined at the anterior/posterior cingulate, caudate, cuneus, fusiform gyrus, insula, cerebral tonsil, and Brodmann areas based on the result of the voxel-based analyses. Additional ROIs were defined at the globus pallidus, thalamus, pons, and dentate based on the result of some previous studies. GMV significantly decreased after the GBCA injection for each ROI (p<0.001), except for pons(p>0.05). Signal intensity of the magnitude images were significantly different between pre and post1/post2 for each selected ROI (p<0.001), but were not between post 1 and post 2 (p>0.016). QSM values were not significantly different among the three different time points for each selected ROI (p>0.016).

### CONCLUSION

This study showed that the specific brain tissues had short-term signal intensity changes or tissue volume changes on the specific MR images after the GBCA injection. However, magnetic susceptibility on the brain tissues had no significant changes after the GBCA injection.

# **CLINICAL RELEVANCE/APPLICATION**

The short-term effect of the gadolinium-based contrast agents on normal human brain tissues may give us knowledge for the histophysiologic mechanism of gadolinium deposition in human brain tissues.



### OB185-ED-WEA1

Ultrasound Diagnosis of Fetal Anomalies in the First Trimester

Wednesday, Nov. 28 12:15PM - 12:45PM Room: OB Community, Learning Center Station #1

### Awards Magna Cum Laude

#### **Participants**

Catherine Phillips, MD, Boston, MA (*Presenter*) Nothing to Disclose Carol B. Benson, MD, Boston, MA (*Abstract Co-Author*) Nothing to Disclose

#### **TEACHING POINTS**

1. During the 1st trimester, the fetus undergoes rapid growth & complete organ development, resulting in considerable changes in sonographic appearance. Recognition of these changes permits timely diagnosis of a number of fetal anomalies. 2. By mid to late 1st trimester, important structures of the fetal cranium, brain, heart, face, thorax, abdomen, & extremities can be visualized.3. Anomalies of 1st trimester pregnancy may be subtle. Diagnosis of fetal abnormalities may be facilitated by transvaginal scanning, which provides superior resolution & is particularly helpful in obese patients.4. Up to 50% of major anomalies can be detected on a 10-14 week scan. The most commonly detected anomalies include those involving the GI system, fetal heart, & spine.

# TABLE OF CONTENTS/OUTLINE

1. Normal anatomy of the 1st trimester fetus including a development timeline accompanied by the normal sonographic appearance.2. Review of proper techniques for sonographic evaluation in the 1st trimester, including measurements of crown rump length & nuchal translucency, as well as transvaginal scanning of fetal anatomy.3. Sonographic appearance of early 1st trimester anomalies by category: cranium, brain, face, thorax, abdomen, & extremities.4. Diagnosis of syndromes & aneuploidy, including prune belly, pentalogy of Cantrell, amniotic bands, Trisomies 13, 18, & 21.



### OB186-ED-WEA2

### Double Trouble: Monochorionic Twin Pregnancy and Associated Complications

Wednesday, Nov. 28 12:15PM - 12:45PM Room: OB Community, Learning Center Station #2

#### **Participants**

Lindsay P. Busby, MD, MPH, San Francisco, CA (*Presenter*) Nothing to Disclose Tara A. Morgan, MD, San Francisco, CA (*Abstract Co-Author*) Nothing to Disclose Dorothy J. Shum, MD, San Francisco, CA (*Abstract Co-Author*) Nothing to Disclose

### For information about this presentation, contact:

lindsay.busby@ucsf.edu

#### **TEACHING POINTS**

The purpose of this exhibit is to: explain the embryogenesis of monochornionic twins, identify sonographic findings to determine chorionicity and amnionicity, describe the complications, recognize the indications for magnetic resonance imaging, and discuss treatment options.

# TABLE OF CONTENTS/OUTLINE

Background: Monochorionic twins share a placenta and are subject to an increased risk of complications. Twin-twin transfusion syndrome: A common complication of MoDi pregnancies resulting from arteriovenous anastomoses. Asymmetric blood flow results in a smaller twin with oligohydramnios and a larger twin, 'the recipient', with a larger proportion of blood flow resulting in polyhydramnios. Twin reversed arterial perfusion sequences (TRAP): A rare diagnosis resulting from an abnormal arterial-arterial anastomosis, resulting in a 'pump' and 'acardiac' twin, with near 100% mortality of the acardiac twin. Additional complications: Unequal sharing, twin anemia polycythemia syndrome, and cord entanglement. Summary & Clinical Implications: Monochorionic twin pregnancies are at increased risk of morbidity and mortality, compared to singleton or dichorionic pregnancies. Early identification of chorionicity, amnionicity, and resultant complications, can help improve delivery planning and reduce morbidity and mortality.



#### PD188-ED-WEA6

Characterizing Pediatric Liver Masses and Mimics by MR: A Radiologist's Primer

Wednesday, Nov. 28 12:15PM - 12:45PM Room: PD Community, Learning Center Station #6

### Participants

Allison Forrest, BA, Rochester, NY (*Presenter*) Nothing to Disclose Unni K. Udayasankar, MD, FRCR, Tucson, AZ (*Abstract Co-Author*) Nothing to Disclose Philip J. Katzman, MD, Rochester, NY (*Abstract Co-Author*) Nothing to Disclose Abhishek Chaturvedi, MD, Rochester, NY (*Abstract Co-Author*) Nothing to Disclose Apeksha Chaturvedi, MD, Rochester, NY (*Abstract Co-Author*) Nothing to Disclose

### **TEACHING POINTS**

Liver masses and mimics in children include distinct clinico-pathologic entities, many of which are unique to children (hepatoblastoma, infantile hemangioma, mesenchymal hamartoma, metastatic neuroblastoma). Magnetic resonance imaging is increasingly being used for diagnosis, characterization, and follow-up of pediatric liver masses due to lack of ionizing radiation, excellent soft tissue contrast, dynamic post contrast imaging, and use of hepatocyte-specific contrast media. Signal intensity, diffusivity characteristics, and hepatocyte-specific contrast enhancement patterns on MRI and tracer uptake on PET-MR are useful for accurate detection and non-invasive characterization of benign and malignant pediatric liver lesions.

### **TABLE OF CONTENTS/OUTLINE**

Common pediatric hepatic neoplasms and tumor-like lesions. Overview of morphologic and functional techniques in MRI with discussion of hybrid PET/MRI. Discussion of hepatocyte-specific and blood pool contrast agents and their role in characterizing liver masses. Table of commonly used non-contrast and contrast-enhanced MR sequences for characterization of pediatric liver masses with techniques for optimizing these sequences. Case presentations, including case details, teaching points, key imaging sequences, and pathology slides where relevant.



#### PD189-ED-WEA7

# MRI of the 1st Trimester Pregnancy Fetus and Placenta

### Awards **Certificate of Merit**

### **Participants**

Morgan McLuckey, BS, Indianapolis, IN (Presenter) Nothing to Disclose Rachel L. Leon, MD, PhD, Indianapolis, IN (Abstract Co-Author) Nothing to Disclose Jordan K. Swensson, MD, Indianapolis, IN (Abstract Co-Author) Nothing to Disclose Brandon P. Brown, MD, MA, Indianapolis, IN (Abstract Co-Author) Nothing to Disclose

### For information about this presentation, contact:

brpbrown@iu.edu

#### **TEACHING POINTS**

In this presentation, we describe: 1) MR imaging findings in the normal 1st trimester pregnancy, during the transition from embryo to fetus 2) Normal MR appearance of the gestational sac as it evolves within the endometrial space, including decidual reaction and early placental development 3) Expected appearance of the gravid female uterus during the first weeks of pregnancy, and the changing cervical/fundal relationship as seen on MRI

# **TABLE OF CONTENTS/OUTLINE**

1) Background of recent increase in 1st trimester MR imaging, given the rise of MR imaging for the diagnosis of acute appendicitis, and in the setting of recent population studies confirming no evidence of increased risk to pregnant women 2) Describe rapid changes to gravid uterus during 1st trimester requires awareness of evolving appearances on MRI 3) Demonstrate prominent appearance of liver and cerebral ventricles on MR imaging of later embryo and early fetus 4) Review MRI images showing expansion of gestational sac, decidual reaction at implantation and growth, and development of the placenta.



# PD231-SD-WEA2

# Longitudinal Prediction of Pediatric Diffusion MRI Data using Graph-Based Deep Learning

Wednesday, Nov. 28 12:15PM - 12:45PM Room: PD Community, Learning Center Station #2

#### Participants

Jaeil Kim, PhD, Daegu, Korea, Republic Of (*Presenter*) Nothing to Disclose Yoonmi Hong, PhD, Chapel Hill, NC (*Abstract Co-Author*) Nothing to Disclose Geng Chen, Chapel Hill, NC (*Abstract Co-Author*) Nothing to Disclose Weili Lin, PhD, Chapel Hill, NC (*Abstract Co-Author*) Nothing to Disclose Pew-Thian Yap, PhD, Chapel Hill, NC (*Abstract Co-Author*) Nothing to Disclose Dinggang Shen, Chapel Hill, NC (*Abstract Co-Author*) Nothing to Disclose

### For information about this presentation, contact:

threeyears@gmail.com

# PURPOSE

Diffusion MRI affords great value for studying brain development, owing to its capability in assessing brain microstructure despite on-going myelination. With longitudinal acquisition of pediatric diffusion MRI data, one can chart the temporal evolution of microstructure and white matter connectivity. However, due to subject dropouts and failed scans, it is not always possible to acquire complete longitudinal scans for subjects. In this work, we introduce a graph-based deep learning method to predict missing diffusion MRI data. The relationships between sampling points in spatial domain (x-space) and wave-vector domain (q-space) are considered jointly (x-q space) in a form of graph. We then use a graph convolution neural network (GCNN) to learn the non-linear mapping across longitudinal scans.

### **METHOD AND MATERIALS**

Sampling points in the x-q space are represented as nodes in a graph. The adjacency between a pair of nodes is determined by their spatial distance, angular difference in gradient directions, and difference in diffusion weightings. Convolution is performed in spectral domain using the graph Fourier basis, determined by the Laplacian of the graph. For prediction, we construct a UNet-based GCNN with skip connections from encoder layers to decoder layers. We demonstrate the effectiveness of our method using a dataset of 13 full-term subjects. Diffusion-weighted (DW) images corresponding to 42 gradient directions were acquired using a spin-echo echo planar imaging sequence with TR/TE = 7680/82 ms, resolution =  $2 \times 2 \times 2$  mm<sup>3</sup>, and b = 1000 s/mm<sup>2</sup>.

#### RESULTS

We predict the 3-month DW images from the neonatal DW images. We randomly select 9 subjects for training, 1 for validation, and the remaining 3 for testing. The Mean Absolute Error and Signal-to-Noise Ratio for conventional CNN and GCNN are 0.0610/29.60 and 0.0523/30.63, respectively. We also compare the fractional anisotropy maps, shown in the figure. As illustrated, the proposed GCNN outperforms conventional CNN.

# CONCLUSION

In this work, we introduce a graph convolutional neural network (GCNN) for longitudinal prediction of diffusion MRI data. GCNN allows the relationships between sampling points in the x-q space to be taken into account for prediction and yields better performance than the conventional CNN.

#### **CLINICAL RELEVANCE/APPLICATION**

Charting longitudinal changes of the infant brain provides fundamental insights into brain development and neurodevelopmental disorders.



#### PD232-SD-WEA3

### Pulmonary Metastases of Neuroblastoma - CT Differential Features at the Initial Diagnosis

Wednesday, Nov. 28 12:15PM - 12:45PM Room: PD Community, Learning Center Station #3

# Participants

Ekaterina S. Ternovaya, MD, MSc, Moscow, Russia (Presenter) Nothing to Disclose

### For information about this presentation, contact:

ekaterina.ternovaya@gmail.com

#### PURPOSE

Identification of radiological findings, typical features and incidence rate of pulmonary metastases in pediatric patients with neuroblastoma at the initial diagnosis.

### **METHOD AND MATERIALS**

The retrospective study consisted of the 132 patients with INSS stage IV neuroblastoma that were treated during period from 01.2012 to 12.2016. The imaging data from plain radiogrhapy and computed tomography was analyzed. All patients have undergone plain radiography and chest CT with bolus contrast enhancement ,performed by 16 slice Brightspeed, GE Healthcare, scanner.

#### RESULTS

10/132 (7,6%) patients had pulmonary metastases at the diagnosis. 6/10 (60%) had multiple lesions and 5/10 (50%) had bilateral distribution. In our cohort of patients lesions medium and large in calibre prevailed. Some lesion exceeded 1 cm in diameter. All patients showed different degree of pleural involvement. 5/10 (50%) had involvement of mediastinal lymphatic nodes. 2/10 (20%) had tumor thrombosis of the large and medium vessels from primary site. 2/10 (20%) had nodal lung lesions visible on plain radiograhpy. Only 1/10 (10%) had calcification.

# CONCLUSION

During the studies were formulated diagnostic criteria specific to the pulmonary metastases of neuroblastoma - foci of medium and large calibre, of rounded shape with even, sharp edges, of a homogeneous structure, presence of tumor thrombosis of large and medium calibre blood vessels, absence of calcification or 'halo' sign, even enhacment after contrast agent administration, absence of cavitation during follow-up imaging.

### **CLINICAL RELEVANCE/APPLICATION**

Pulmonary metastases of neuroblastoma are rare and their presence requires differential diagnosis with inflammatory and some nodal lung lesions for correct staging and treatment options. Obtained data can help in differential diagnosis at the initial staging and chest CT with bolus contrast enhancement should be considered as part of initial diagnostic process.



#### PD233-SD-WEA4

# Indigo Mechanical Thrombectomy in Children: An Initial Experience

Wednesday, Nov. 28 12:15PM - 12:45PM Room: PD Community, Learning Center Station #4

#### Awards Student Travel Stipend Award

#### **Participants**

Carlos B. Ortiz, BS, Houston, TX (*Presenter*) Nothing to Disclose Kamlesh U. Kukreja, MD, Bellaire, TX (*Abstract Co-Author*) Nothing to Disclose

#### PURPOSE

Penumbra's indigo device for mechanical thrombectomy has been successful in stroke interventions. However, use of this device in deep venous thrombosis (DVT) for children has been limited due to the large size of the device and unknown feasibility. Another concern has been the significant blood loss during aspiration. We intend to assess technical feasibility, clinical outcomes, and safety from our experiences with the indigo device for treating upper extremity (UE) and lower extremity (LE) DVT in children.

### METHOD AND MATERIALS

Chart review revealed 13 children (14 limbs) underwent indigo catheter mechanical thrombectomy at a tertiary care pediatric hospital from January 2016 to March 2018. Clinical and imaging data was reviewed. No patients were excluded. Among 6 boys and 7 girls (mean age 16.3 years, range 13-18 years), two 6-french indigo catheters and twelve 8-french indigo catheters were used. Venograms obtained during the intervention were graded by clot burden in 7 venous segments before and after mechanical thrombectomy with the following scale: grade 1 (<50% thrombolysis), grade 2 (50-99%), and grade 3 (100%). Technical success was set as greater than 50% thrombolysis.

# RESULTS

There was technical success in 13 of 14 limbs (92.8%). Grade 1 improvement was present in 1 LE limbs (7.1%). Additionally, there was grade 2 improvement in 9 limbs (64.3%) and grade 3 improvement in 4 limbs (28.6%). Catheter directed pharmacotherapy (7 limbs) and balloon angioplasty (12 limbs) were combined with the indigo device to further decrease clot burden. In patients with a preoperative and postoperative hemoglobin check (n=11), there was a significant 48-hour change:  $10.4\pm1.2$  g/dL preoperative to  $8.4\pm1.5$  g/dL postoperative (p<0.01). Two patients required blood transfusions within 48-hours and responded well with no further complications. One transfused patient had a low hemoglobin (8.0 g/dL) prior to the procedure. No deaths or events of acute kidney injury occurred.

#### CONCLUSION

In this limited pediatric population, indigo device for DVT in older children is safe and technically feasible. Further quantification of blood loss in children may increase use of this device, reducing the need for adjuvant infusion therapy to resolve DVT.

# **CLINICAL RELEVANCE/APPLICATION**

Reviewing the use of this device in a pediatric population for treating LE/UE DVT helps physicians in choosing safe and effective methods to perform mechanical thrombectomy.



# PD234-SD-WEA5

Artificial Intelligence in Bone Age Assessment: Evaluation of Diagnostic Accuracy and Efficiency of a Novel Fully Automated Algorithm in Comparison to the Greulich Pyle Atlas Method

Wednesday, Nov. 28 12:15PM - 12:45PM Room: PD Community, Learning Center Station #5

# Participants

Christian Booz, MD, Frankfurt am Main, Germany (*Presenter*) Nothing to Disclose Julian L. Wichmann, MD, Frankfurt, Germany (*Abstract Co-Author*) Speaker, General Electric Company; Speaker, Siemens AG Ibrahim Yel, Frankfurt, Germany (*Abstract Co-Author*) Nothing to Disclose Sabine Boettger, Frankfurt am Main, Germany (*Abstract Co-Author*) Nothing to Disclose Simon S. Martin, MD, Frankfurt, Germany (*Abstract Co-Author*) Nothing to Disclose Boris Bodelle, MD, Frankfurt Am Main, Germany (*Abstract Co-Author*) Nothing to Disclose Moritz H. Albrecht, MD, Frankfurt am Main, Germany (*Abstract Co-Author*) Nothing to Disclose Thomas J. Vogl, MD, PhD, Frankfurt, Germany (*Abstract Co-Author*) Nothing to Disclose Lukas Lenga, Frankfurt, Germany (*Abstract Co-Author*) Nothing to Disclose

#### For information about this presentation, contact:

boozchristian@gmail.com

#### PURPOSE

To evaluate the diagnostic accuracy and clinical efficiency of a novel artificial intelligence (AI) system for bone age (BA) assessment compared with the Greulich Pyle (GP) atlas method.

# METHOD AND MATERIALS

Data from clinically indicated hand and wrist radiographs of 414 pediatric patients (mean chronological age 10.31 years, range 3-17 years) were retrospectively analyzed. Total BA was assessed independently by three blinded radiologists with varying levels of experience using the GP method. In addition, a novel AI system developed for BA assessment automatically calculated total BA. Results of both approaches were compared regarding diagnostic accuracy, methods agreement and time efficiency, while the reference BA was determined by the consensus of two different blinded experienced radiologists (28 and 32 years of experience in pediatric imaging) using the GP method. For statistical analysis, we calculated root mean square deviation (RSMD), mean absolute difference (MAD), Pearson product-moment correlation, Bland-Altman plot and further agreement analyses.

#### RESULTS

Mean total BA assessed by the reference standard was 9.91 years. AI-derived mean total BA was 9.98 years, while mean total BA calculated by the three reviewers was 10.18 years. RSMD and MAD were significantly lower between BA values assessed by the AI system and the reference standard (RSMD 0.18 years, MAD 0.08 years) than between BA values calculated by the three reviewers and the reference standard (RSMD 0.69 years, MAD 0.49 years) (all p<0.001). Statistical analysis demonstrated significantly higher correlation between AI-derived BA and reference BA (r=0.985) than between GP-derived BA assessed by the three reviewers and reference BA (r=0.901) (p<0.001). GP-derived BA values of the three reviewers showed excellent inter-reviewer agreement (Fleiss'  $\kappa$ =0.88). Mean evaluation times were reduced by 86.9% using the AI system compared to reviewer-based BA assessments.

#### CONCLUSION

A novel AI system allows for accurate automated BA assessment using the GP method as standard of reference and may improve clinical efficiency by reducing evaluation times without compromising the diagnostic accuracy.

#### **CLINICAL RELEVANCE/APPLICATION**

BA assessment is currently based on two different main reviewer-based approaches such as the GP method using reference radiographs but may drastically benefit from a novel AI algorithm for automated BA determination.



### PH240-SD-WEA1

Occupational Eye Lens Dose in Endoscopic Retrograde Cholangiopancreatography Using a Dedicated Eye Lens Dosimeter: A Phantom Study

Wednesday, Nov. 28 12:15PM - 12:45PM Room: PH Community, Learning Center Station #1

# Participants

Shinya Imai, MSc, Sakai, Japan (*Presenter*) Nothing to Disclose Hitoshi Satoh, RT, Inashiki-Gun, Japan (*Abstract Co-Author*) Nothing to Disclose Nobuyoshi Tanki, Sakai, Japan (*Abstract Co-Author*) Nothing to Disclose Kazuma Tameike, Fujiidera, Japan (*Abstract Co-Author*) Nothing to Disclose Atsushi Noguchi, Sakai, Japan (*Abstract Co-Author*) Nothing to Disclose Toshizo Katsuda, Sakai, Japan (*Abstract Co-Author*) Nothing to Disclose Tatsuhiro Gotanda, Kurashiki, Japan (*Abstract Co-Author*) Nothing to Disclose Rumi Gotanda, Kurashiki, Japan (*Abstract Co-Author*) Nothing to Disclose Yuji Ogata, Osaka, Japan (*Abstract Co-Author*) Nothing to Disclose

# PURPOSE

The International Commission on Radiological Protection (ICRP) recommended in 2011 that the radiation dose to the eye lens should not exceed 20 mSv averaged over a 5-year period, with no more than 50 mSv per year. The radiography and fluoroscopy system with the X-ray tube over the patient table can produce scattered X-rays around the upper body of the examiner; hence, there is significant concern about the increased exposure to the eye lens of the physician. In order to examine the dose of X-ray radiation that physicians are exposed to during endoscopic retrograde cholangiopancreatography (ERCP), X-ray exposure to the eye was measured in a phantom model with or without radiation-protective devices.

# METHOD AND MATERIALS

X-ray exposure of the eye was measured using novel dedicated direct eye lens dosimeters, which specifically measure 3-mm dose equivalent [Hp(3)]. In our study, a phantom's examination model was used to apply the ERCP procedure. The eye dosimeters were attached inside and outside lead (Pb) glasses that were attached to the human phantom head [Figure 1 (a)]. In addition, the X-ray equipment was covered with radiation-protective curtains to reduce scattered X-rays [Figure 1 (b)]. The duration of radiation was 30 minutes by the X-ray television system.

#### RESULTS

In this study, the radiation dose to the eyes was found to be 3.70 mSv for the left eye and 1.50 mSv for the right eye without the use of radiation protective devices. When radiation protection glasses were attached to the phantom head, the dose of radiation exposure to the eye were 1.80 mSv for the left eye and 1.00 mSv for the right eye. Moreover, when the equipment was covered by radiation-protective curtains, the doses measured were 0.12 mSv for the left eye and undetectable for the right eye. Notably, radiation exposure to the eye was reduced by 78.1% when the Pb glasses were attached and by 96.7% when radiation-protective curtains were in place.

### CONCLUSION

It was shown that the physician's maximum exposure dose of eyes during ERCP procedure was 3.7 mSv. This exposure dose corresponds to 18.5% of the 20 mSv/year proposed by the ICRP. However, when the radiation protection devices were used, the exposure dose was extremely reduced.

### **CLINICAL RELEVANCE/APPLICATION**

(dealing with eye lens dosimeter) 'Eye lens dosimeter can measure personal dose equivalent [Hp(3)] and is recommended for detailed measurements of occupational eye doses in IVR."



### PH241-SD-WEA2

System Performance Comparison of Ultra-High-Resolution Scans Using Two Clinically Available Multi-Detector CT Systems

Wednesday, Nov. 28 12:15PM - 12:45PM Room: PH Community, Learning Center Station #2

# Participants

Hiroki Kawashima, Kanazawa, Japan (*Presenter*) Nothing to Disclose Katsuhiro Ichikawa, PhD, Kanazawa, Japan (*Abstract Co-Author*) Nothing to Disclose Noriaki Akagi, RT, Okayama, Japan (*Abstract Co-Author*) Nothing to Disclose Hiroji Nagata, RT, Kanazawa, Japan (*Abstract Co-Author*) Nothing to Disclose Satoshi Kobayashi, MD, Kanazawa, Japan (*Abstract Co-Author*) Nothing to Disclose

# PURPOSE

To evaluate and compare image qualities of ultra-high-resolution (UHR) scans between a 0.25 mm  $\times$  160 row detector (detector-UHR) CT system and a 0.6 mm  $\times$  32 row detector mode with an in-plane comb filter (comb-UHR) in third-generation dual source CT system.

### **METHOD AND MATERIALS**

A thin metal wire for the measurement of the modulation transfer function (MTF), a 300-mm cylindrical water bath phantom for noise power spectrum (NPS) measurement, and a micro coin for slice sensitivity profiles (SSP) were scanned using the aforementioned detector-UHR (Precision, Cannon medical) and comb-UHR (SOMATOM Force, Siemens healthineer). The focal spot size of both scans was same ( $0.4 \text{ mm} \times 0.5 \text{ mm}$ ); the CTDIvol was set to 10 mGy. Images with nominal thicknesses of 1.0 mm were reconstructed using filtered back projection. The square of system performance (SP2) functions, based on the pre-whitening theorem, were calculated from the MTF and NPS. Furthermore, a rod phantom made of a soft tissue-equivalent material, placed inside the water bath phantom, was scanned and its disk image was visually checked.

#### RESULTS

The 10%/50% MTF values of detector-UHR and comb-UHR were 1.24/0.54 mm-1 and 1.55/1.14 mm-1, respectively. The spatial resolution of comb-UHR was much higher than of detector-UHR for the reconstruction kernels we selected. The SP2 values of comb-UHR were higher than those of detector-UHR over the entire frequency range, and the ratios of these quantities, of comb-UHR to detector UHR, at 0.1 mm-1 and 1.5 mm-1 were 2.15 and 2.25, respectively. The edge of the disk image obtained via comb-UHR was more sharply visualized than that obtained via detector-UHR.

### CONCLUSION

This phantom study assessed potential system performances of two UHR scans, which currently offer the highest spatial resolutions. Our results show that comb-UHR has two-fold better performance than detector-UHR, despite the dose efficiency penalty caused by the attenuation of the comb on the detector surface. However, comb-UHR has limitations of a maximum FOV of 350 mm, half scanning speed, and a minimum slice thickness of 0.6 mm, compared with detector-UHR.

#### **CLINICAL RELEVANCE/APPLICATION**

The UHR scan mode in third-generation dual source CT can provide better image quality with similarly high spatial resolution compared to the latest 0.25-mm detector CT system, or, alternately, similar image quality can be obtained with the dose halved.



## PH242-SD-WEA3

Fast-Frame-Rate Digital X-Ray Tube Based on Carbon-Nanotube Field-Emitters and Its Application to Cone-Beam Breast Computed Tomography for High-Resolution Imaging

Wednesday, Nov. 28 12:15PM - 12:45PM Room: PH Community, Learning Center Station #3

FDA Discussions may include off-label uses.

### **Participants**

Jeong-Woong Lee, BA, Daejeon, Korea, Republic Of (*Presenter*) Nothing to Disclose Yoon-Ho Song, Daejeon, Korea, Republic Of (*Abstract Co-Author*) Nothing to Disclose Jin-Woo Jeong, PhD, Daejeon, Korea, Republic Of (*Abstract Co-Author*) Nothing to Disclose Jun-Tae Kang, MS, Daejeon, Korea, Republic Of (*Abstract Co-Author*) Nothing to Disclose Jae-Woo Kim, PhD, Dae-Jeon, Korea, Republic Of (*Abstract Co-Author*) Nothing to Disclose Sora Park, PhD, Daejeon, Korea, Republic Of (*Abstract Co-Author*) Nothing to Disclose Ki Nam Yun, Daejeon, Korea, Republic Of (*Abstract Co-Author*) Nothing to Disclose Hyojin Jeon, BA, Daejeon, Korea, Republic Of (*Abstract Co-Author*) Nothing to Disclose Eunsol Go, BA, Daejeon, Korea, Republic Of (*Abstract Co-Author*) Nothing to Disclose

# For information about this presentation, contact:

jwlee@etri.re.kr

## PURPOSE

In medical X-ray diagnostic system, motion blur on images can occur from a rotating gantry or moving of patient. To reduce these motion artifacts on image, a fast-frame-rate digital modulation of X-ray radiation should be employed. This fast digital modulation can be easily realized by a field emission X-ray tube. In this work, we fabricated rotating-anode-type digital X-ray tube (RDXT) based on carbon-nanotube field-emitters and set up a prototype gantry system for cone-beam breast computed tomography (CBCT) with the RDXT. We obtained improved resolution images with reduced motion blur artifacts from the gantry system equipped with the RDXT.

#### **METHOD AND MATERIALS**

We fabricated the RDXT as shown in figure 1 (a). After fabrication, electrical seasoning process was conducted for the reproducible X-ray dose for the same operation condition. This RDXT was mounted on the prototype CBCT gantry system (figure 1 (c)) with the flat panel detector (Varex Paxscan4030X). To evaluate motion blur of this system, images of a bunch of zirconia balls were acquired in the rotating gantry whose speed is 3.6 degree/s.

#### RESULTS

The reproducible voltage-current performances of the RDXT are shown in figure 1 (b), which is suitable for the CBCT system. The inset of figure 1 (b) is the response characteristics of the cathode current by the input operating signal for the RDXT. This fast response indicates that the X-ray radiation of the RDXT can be modulated very fast. Figure 1 (d) shows the X-ray images of a bunch of zirconia balls (0.2 mm in diameter) with the variation of X-ray radiation pulse width of 10, 2.5, and 1 ms, respectively, on the rotating gantry. It is clear that the image acquired from short X-ray radiation has the enhanced image quality compared to one with relatively long radiation. Therefore, the fast-frame-rate X-ray modulation can lead to high-resolution image by reducing the motion blur of the image.

## CONCLUSION

The prototype CBCT gantry system with the RDXT was set up and evaluated in this work. The X-ray images obtained from this system with fast modulation of X-ray radiation successfully suppress the motion blur artifacts. We expect that this system could determine microcalcifications of a woman breast more clearly than the one using a conventional slow response X-ray tube.

#### **CLINICAL RELEVANCE/APPLICATION**

The breast CT system with fast-frame-rate digital x-ray tube could determine microcalcifitations of a woman breast.



### PH243-SD-WEA4

# Eye-lens Shielding in Cranial CT: Evaluation of Image Quality and Artifact Frequency

Wednesday, Nov. 28 12:15PM - 12:45PM Room: PH Community, Learning Center Station #4

### **Participants**

Arthur P. Wunderlich, PhD, Ulm, Germany (*Presenter*) Nothing to Disclose Teresa K. Grunke, Ulm, Germany (*Abstract Co-Author*) Nothing to Disclose Meinrad J. Beer, MD, Ulm, Germany (*Abstract Co-Author*) Nothing to Disclose Stefan A. Schmidt, MD, Ulm, Germany (*Abstract Co-Author*) Nothing to Disclose

# For information about this presentation, contact:

arthur.wunderlich@uni-ulm.de

## PURPOSE

The eye lens is one of the most radiosensitive organs of the human body. It's well proven that radiation leads to cataracts. To protect the eye lens from developing radiation induced cataract during head CT examinations, protectors are available. This study aims to evaluate retrospectively how often they are used, check proper positioning, and frequency of artifacts occurring in CT images due to protectors.

# METHOD AND MATERIALS

1426 consecutive routine head CTs acquired between July 1st and October 15th, 2015 have been assessed. Only examinations performed with eye protectors were evaluated. Artifacts in brain and bone, if present, were examined for possible misdiagnosis, e.g. of subarachnoid hemorrhage. In the orbit, artifact size was measured, and correct positioning of the protector with respect to the eye lens was checked out. Finally, artifact frequency was correlated to CT detector row number - 16, 64 and 256 detector rows were studied.

#### RESULTS

Protectors were used in 261/1426 (18.3%) of CT examinations. 28% of the examinations performed with protector showed brain artifacts, with impaired diagnosis in 6% of the cases. Artifacts in the orbit, mainly elevated CT numbers, were observed much more frequently, in 95% of investigations. In 43%, there were no bulbar artifacts, or they were limited to the eye lens. The lens was not properly covered by the protector in 25% of cases. Cranial bones were affected by artifacts in only 2% of investigations. We found a significant correlation of artifact frequency with detector row number. 16 detector rows showed artifacts in 40%, 64 rows in 22%, and 256 rows in 21% of CT scans, P < 0.01.

## CONCLUSION

The currently available protectors do significantly reduce radiation dose of the eye lens. We were able to figure out a large prevalence for artifacts, especially in the orbit. Therefore, for CT diagnosis concerning eye bulb, protectors should be omitted. We see the need to study whether alternative protector materials could be able to ensure diagnostic image quality, namely for eye socket diagnosis, in order to increase frequency of protector usage. Care should be taken when positioning the protector to assure proper radiation protection of the lens.

# **CLINICAL RELEVANCE/APPLICATION**

Care should be taken when positioning eye protectors in CT exams to ensure radiation protection. While a higher number of detector rows helps to reduce artifacts, effort is required to develop new protection concepts.



## PH244-SD-WEA5

Iodine Quantification in Photon-counting CT: Accuracy Based on Dose

Wednesday, Nov. 28 12:15PM - 12:45PM Room: PH Community, Learning Center Station #5

### **Participants**

Jayasai R. Rajagopal, BA, Durham, NC (Presenter) Nothing to Disclose

Pooyan Sahbaee, Malvern, PA (Abstract Co-Author) Employee, Siemens AG

Daniele Marin, MD, Durham, NC (Abstract Co-Author) Research support, Siemens AG

Bradford J. Wood, MD, Bethesda, MD (*Abstract Co-Author*) Researcher, Koninklijke Philips NV; Researcher, Celsion Corporation; Researcher, BTG International Ltd; Researcher, Siemens AG; Researcher, XAct Robotics; Researcher, NVIDIA Corporation; Intellectual property, Koninklijke Philips NV; Intellectual property, BTG International Ltd; Royalties, Invivo Corporation; Royalties, Koninklijke Philips NV; ; ;

Elizabeth C. Jones, MD, Bethesda, MD (Abstract Co-Author) Nothing to Disclose

Ehsan Samei, PhD, Durham, NC (*Abstract Co-Author*) Research Grant, General Electric Company; Research Grant, Siemens AG; Advisory Board, medInt Holdings, LLC; License agreement, 12 Sigma Technologies; License agreement, Gammex, Inc

### For information about this presentation, contact:

jayasai.rajagopal@duke.edu

## PURPOSE

To assess the impact of dose level on iodine quantification in a photon-counting CT system

### **METHOD AND MATERIALS**

A commercial phantom (Gammex Multi Energy CT phantom) with inserts of three different concentrations of iodine (2, 5, 15 mg/ml) was scanned on a prototype photon-counting CT system (Siemens, Germany) at four dose levels (CTDIvol of 4, 8, 16, and 24 mGy) and the Macro imaging mode, a mode designed for material quantification. Images were reconstructed with a quantitative medium-smooth kernel (D30f) with a slice thickness of 3 mm. Virtual monoenergetic images (VMIs) were generated from binned photon-counting images at 50 and 70 keV. Regions of interest were drawn around relevant inserts and accuracy of HU value was calculated as a percent difference between measured and actual expected value (NIST).

# RESULTS

The average percent differences for iodine accuracy across different iodine inserts and dose levels ranged from +/- 0.8% to +/- 11.5%, with a mean value of -3.6%. Increasing dose was shown to have only a minor effect on increasing the accuracy across iodine concentrations. Percent differences were lower for 50 keV when compared to 70 keV VMIs. At 70 keV, the HU accuracy of iodine was consistently underestimated. Percent differences were similar for all three iodine concentrations.

## CONCLUSION

Photon-counting CT showed the value of iodine concentrations had small variations across different doses. Percent difference of HU accuracy increased with keV of virtual monoenergetic images.

### **CLINICAL RELEVANCE/APPLICATION**

Photon-counting can potentially offer a more systematic and reliable assessment of iodine in CT imaging than other CT techniques, largely independent of dose.



## PH245-SD-WEA6

Magnetization Transfer Helps to Evaluate the Curative Effect Before and After Treatment of Diabetic Nephropathy

Wednesday, Nov. 28 12:15PM - 12:45PM Room: PH Community, Learning Center Station #6

# Participants

Jing Chen, Xianyang City, China (*Presenter*) Nothing to Disclose Zhang Xirong, MMed, Xianyang City, China (*Abstract Co-Author*) Nothing to Disclose Qi Yang, Xianyang, China (*Abstract Co-Author*) Nothing to Disclose Chuangbo Yang, MMed, Xianyang City, China (*Abstract Co-Author*) Nothing to Disclose Nan Yu, MD, Xian Yang, China (*Abstract Co-Author*) Nothing to Disclose

# For information about this presentation, contact:

345717558@qq.com

## PURPOSE

To observe the magnetization transfer ratio(MTR) changes of the renal cortex and medulla before and after clinical treatment of diabetic nephropathy patients with magnetization transfer (MT) technique, and to objectively evaluate the clinical curative efficacy of diabetic nephropathy.

#### **METHOD AND MATERIALS**

20 patients with clinically diagnosed diabetic nephropathy who had significant symptomatic relief after hospitalization were enrolled in this study. All the MR imaging were obtained on a 3.0 T MRI (Skyra, Siemens Healthineers) scanner. MT study was conducted using a 3D fast low angle shot(FLASH) sequence, this sequence was run two times; first one without a MT saturation pulse(MToff), second one with a MT(MTon) saturation pulse. For MT imaging postprocessing, MTR =(MToff-MTon)×100/MToff, MTR values were expressed in percentage units. The magnetization transfer rate (MTR) of the renal cortex and medulla was measured on the MT map of each subject using the region of interest method. Multiple regions of interest are drawn and averaged in the medullitary region of the upper kidney, renal hilum, and lower pole. A paired sample t-test was used for statistical analysis.

# RESULTS

The average renal cortical MTR in patients with diabetic nephropathy after treatment  $(736.55\pm75.95)$ % was lower than that before treatment  $(824.15\pm77.45)$ %, and there was a statistically significant difference (P<0.0001)(Figure 1,Table 1). There was no significant difference in the MTR of renal medulla before and after treatment.

## CONCLUSION

For diabetic nephropathy patients, the MTR about renal cortical was slightly lower after clinically treatment than before treatment, to a certain extent, MTR can reflect the changes in renal function.

# **CLINICAL RELEVANCE/APPLICATION**

MT responds to changes in the microstructure of the tissue, more scientific and objective assessment of clinical efficacy of diabetic nephropathy, with potential clinical application value.



# QI013-EB-WEA

Quality Initiative to Improve the Transcription of Clinical Information to the Radiology Information System

Wednesday, Nov. 28 12:15PM - 12:45PM Room: QR Community, Learning Center Hardcopy Backboard

### **Participants**

Michael J. Mills, MD, Southfield, MI (*Abstract Co-Author*) Nothing to Disclose John X. Nguyen, MD, Southfield, MI (*Presenter*) Nothing to Disclose Sumita Joseph, MD, Royal Oak, MI (*Abstract Co-Author*) Nothing to Disclose Ben Himelhoch, MBA, East Lansing, MI (*Abstract Co-Author*) Nothing to Disclose Abdelouahid Souala, BS, East Lansing, MI (*Abstract Co-Author*) Nothing to Disclose Anthony Khashola, BS, East Lansing, MI (*Abstract Co-Author*) Nothing to Disclose Roger L. Gonda JR, MD, Southfield, MI (*Abstract Co-Author*) Nothing to Disclose

### PURPOSE

Accurate study indications clinical histories have been shown to improve interpretive accuracy and efficiency, can potentially affect patient safety, and carry billing implications. Implementation of computerized physician order entry remains incomplete, and in many settings registration clerks play a critical role in choosing which information to transfer from the clinical provider's order to the radiology imaging requisition. When patients present to our institution for outpatient imaging, they provide a registration clerk with an imaging requisition form given to them by the referring physician. The clerk transcribes the imaging requisition form into the radiology information system (RIS) that is used to convey study indications and pertinent patient information being transcribed from the image requisition form to the RIS, grammatical errors in transcription and inadequate clinical history provided by the ordering physician. The errors can lead to compromised patient safety, diminished efficiency for the radiology practice associated with unnecessary loss of time and resources and unprofessional summary reports being sent back to the referring physician. Our initiative seeks to identify areas of deficiency and introduce applicable measures of improvement in the transcription process.

#### **METHODS**

A root-cause analysis was used to determine the possible etiologies for discordance. Phase I of the study utilized retrospective chart review to assess the most common sources of errors. Data from a randomized sample of 500 subjects was gathered from the image requisition and RIS documents within the PACS system. Data from the image requisition and RIS documents was recorded on several different variables and cross-referenced by the data collector to assess for degree and quality of concordance. Following phase I, an intervention was implemented that included an initial team meeting and email, which included all radiology registration clerks, emphasizing attention to accurate transcription. An 8x11 inch poster with the same emphasis was also placed at each work station. A reminder was included as part of the regular mid-month team meeting. Phase II of the study was conducted, with the data collection process mirroring that of phase I. Degree and quality of concordance was assessed. The indication/clinical history listed on the RIS and the indication/clinical order listed on the clinical order were considered concordant if the descriptions matched without omission of any information. The indications were categorized as partially discordant if the RIS indication/clinical history omitted information contained on the clinical order. The indications were considered completely discordant if substantial information was missing from the RIS indication. The RIS indications which were considered concordant or partially discordant were also assessed for quality of concordance. Quality of concordance was categorized as 'highest' if it matched the clinical order verbatim, contained a complete and informative patient history, and was free of grammatical errors. The quality of concordance was categorized as 'high' if it was concordant but contained grammatical errors (incorrect capitalization, non-standard abbreviation, misspellings or misused punctuation). The quality of concordance was categorized as 'low' if the RIS was partially concordant with the clinical order but failed to provide complete or accurate patient history. Also categorized as 'low' were significant grammatical errors and/or omissions that added ambiguity or could easily be misunderstood.

### RESULTS

Phases I and II of the study assessed both the degree and quality of concordance present between the image requisition and the radiology information system (RIS) document. 60% (266) of the phase I subjects' documentation were found to be truly concordant, meaning that the content provided for the indication and clinical history was identical between the image requisition and RIS documents. Phase II demonstrated 81% (374) true concordance - a 21% improvement post-intervention (P<0.001). 34% (121) of the RIS documents from phase I included an inadequate study indication, compared to 15% (68) in phase II (P<0.001). Regarding the quality of concordance, there was a 22% (168 pre-intervention and 265 post-intervention) increase in the number of transcriptions that possessed the highest level of concordance, meaning verbatim transcription free of any grammatical errors (P<0.001).

# CONCLUSION

Educating staff members responsible for transcription of study indication and clinical history, along with a reminder poster placed at each workstation, significantly improved the concordance and quality of the information presented to radiologists on the radiology information system (RIS) document.



# QI015-EB-WEA

Impact of a Same-Day Biopsy Program on Time to Diagnosis for Patients with Suspicious Breast Findings

Wednesday, Nov. 28 12:15PM - 12:45PM Room: QR Community, Learning Center Hardcopy Backboard

### **Participants**

Emily L. Ebert, MD, Boston, MA (*Presenter*) Nothing to Disclose Benjamin Wang, MD, Boston, MA (*Abstract Co-Author*) Nothing to Disclose Brian N. Dontchos, MD, Boston, MA (*Abstract Co-Author*) Nothing to Disclose Constance D. Lehman, MD,PhD, Boston, MA (*Abstract Co-Author*) Research Grant, General Electric Company; Medical Advisory Board, General Electric Company

## For information about this presentation, contact:

eebert@partners.org

### PURPOSE

Numerous studies have shown that there is substantial psychological distress for patients awaiting breast biopsy and subsequent tissue diagnosis following an abnormal breast imaging examination. While improving patient experience is multifactorial, we focused on the opportunity to offer same-day biopsies for patients with suspicious findings on diagnostic imaging. Decreasing the time between diagnostic imaging and biopsy not only enhances the patient experience, but also may be a quality metric for which centers are measured in the future.

### METHODS

Prior to August 2017, same-day biopsies were not routinely offered at our center, with biopsies usually scheduled days or occasionally weeks after diagnostic imaging. Utilizing a multidisciplinary team of expert breast imaging radiologists, breast imaging fellows, nurse practitioners and technologists, an algorithm was created to offer patients the option of a core needle biopsy on the same day of diagnostic evaluation of both abnormal imaging and symptomatic findings. This algorithm was introduced in our clinic over several weeks in August 2017. We measured the time in days of two segments of typical imaging workup scenarios: screening mammogram to a diagnostic exam and diagnostic exam to biopsy. Diagnostic exams included patients with abnormal screening mammograms, patients seen for follow-up of probably benign findings, and patients with symptomatic breast concerns. Only ultrasound and mammographic biopsies were included. For mammographic guided biopsies, a tomosynthesis guided device was utilized for both pre- and post-implementation time periods. Patients with times between screening and diagnostic exams, or diagnostic exam and biopsy greater than 60 days were excluded. The wait times were evaluated during two comparable periods of time: pre-implementation (September 1, 2016 through March 31, 2017) and post-implementation (September 1, 2017 through March 31, 2018). We also compared the percentage of same-day biopsies that were US guided versus mammographic guided. Significance was determined by 2-tailed t-test and Z-score for population proportions.

### RESULTS

There were 668 and 484 biopsies performed during the pre- and post-implementation periods meeting inclusion criteria, respectively. Mean age was similar between the two time periods, 54.6 (pre-implementation) versus 55.5 (post-implementation) (p=0.33). There was a significant decrease in mean time from screening exam to biopsy when comparing pre- and post-implementation time periods (19.6 versus 9.4 days, p<0.005). Additionally, the time between diagnostic exam and biopsy decreased from 9.6 (preimplementation) to 3.6 days (post-implementation) (p<0.005). Time between screening and diagnostic exams also decreased after the implementation (10.0 versus 6.4 days, p<0.005). During the pre-implementation period, 11.4% (76/668) of biopsies were performed on the same day as the biopsy recommendation, versus 50.4% (244/484) during the post-implementation period (p<0.05). This increase in same-day biopsies was true for both US and manmographic guided biopsies: 16.0% of US guided biopsies were performed as same day during pre-implementation compared to 58.4% post-implementation (p<0.05) as well as for stereotactic guided biopsies were performed as same day during pre-implementation compared to 38.4% post-implementation (p<0.05) as well as for compared to 34.6% post-implementation (p<0.05).

### CONCLUSION

Offering same-day biopsies is feasible and reduces patient wait time between diagnostic exams and biopsies.



## QI124-ED-WEA1

### A Peer-Review Tool for X-Ray Technologists to Assess Image Quality in General Radiography

Wednesday, Nov. 28 12:15PM - 12:45PM Room: QR Community, Learning Center Station #1

## Participants

Petar Seslija, MSc, Signal Hill, CA (*Abstract Co-Author*) Nothing to Disclose Annemarie Bymoen, RT, Vancovuer, BC (*Presenter*) Nothing to Disclose Yogesh Thakur, PhD, Vancouver, BC (*Abstract Co-Author*) Nothing to Disclose

### PURPOSE

Peer review of x-ray technologists' image acquisitions in general radiography provides a valuable indicator of clinical performance. It is also an excellent feedback mechanism for staff to identify and correct common issues to continually improve exam quality. Monthly image quality audits providing feedback to technical staff is a mandatory requirement in some jurisdictions, such as ours. Our region encompasses 28 hospitals; contains over 100 DR rooms, conventional rooms, and mobile radiography units; and performs over 1 million general radiography exams per year. In order to meet accreditation standards, a computer-based tool was developed and implemented across our region to facilitate efficient, standardized peer review of general radiography exams.

#### **METHODS**

A peer review tool, which includes a graphical user interface, was developed in Microsoft Excel using the Visual Basic development tools (Figure 1a). The tool allows reviewers to document exam specific details, including hospital name, exam room, performing technologist(s), patient identifiers, exam date, exam, and views acquired. Image quality review for each acquired view of an exam is scored by the reviewer according to 14 criteria: the hanging protocol, side marker visibility, tech initials visibility, positional marker visibility, the presence of foreign objects, presence of image artifacts, appropriate image exposure, presence of image burn, appropriate use of collimation, appropriate use of masking, proper centering, inclusion of the required structures, patient positioning, and whether the view should have been rejected and repeated. Each criterion has a standardized answer set (made available via a drop-down menu) which facilitates a common scoring regime. Many criteria have an additional comment button which allows the reviewer to input more specific, non-standardized feedback, which provides further context (either why an image scored poorly, or why an image scored excellently, providing positive feedback) on the reviewer's scoring. The tool also provides peer review of exam related documentation, including whether the patient requisition was properly documented, whether the correct patient was imaged, technologist's notes were properly documented when required, patient Pb protection was properly used and documented, and if pregnancy status and LMP was determined and documented when appropriate. Finally, the tool facilitates storage and data analysis of all peer reviews performed. Outcomes of reviews can be analyzed and categorized based on specific sites or region-wide data, body part, exams, and view. The computer-based peer review tool was deployed throughout our region, along with an audit protocol specifying the body parts, exams, and number of exams that each site is required to review each month (Figure 1b). Results of the monthly peer review are presented at each sites' general radiography staff meeting providing technologists with feedback to correct commonly identified issues. The monthly audit scheduled is repeated semi-annually to ensure common exams undergo peer review a minimum of twice per year, thus providing on-going education. Audit results from each site are combined to provide an overall representation of the healthcare region's image quality.

#### RESULTS

Initial audit findings identified many equipment related issues, including CR plate scratches and dust affecting image quality, which prompted increased scheduled cleaning and replacement of worn out plates; pressure marks on CR plates due to patients' weight bearing directly on plates, which initiated a project to design and manufacture CR plate protectors for weight-bearing exams; faulty AEC settings; and foreign object artifacts caused by patient gowns and decade-old sponges used for positioning aides, both of which were replaced. These problems were only detected as a result of the sequential review of multiple exams. Regional results of the peer review of image quality for several commonly performed general radiography exams are shown in Figures 1c-f. The results are based on data collected from 2016 to 2017 from a total of over 10,000 peer-reviewed general radiography exams. Results show a significant improvement in the use of leaded positional markers for routine chest, and pelvis/hip exams. It also highlights areas that require improvement, such as use of appropriate collimation for portable chest exams, and use of leaded positional markers for abdomen examinations.

#### CONCLUSION

The development and implementation of a computer-based peer review tool for general radiography exams effectively meets accreditations standards for monthly image quality audits and feedback to technologists. The peer review tool has helped identify and correct many issues affecting image quality, and has increased team work and collaboration between staff. In addition, by using an Excel based tool, our sites are able to perform image quality review in an efficient and standardized manner.



## QI126-ED-WEA2

A Quality Improvement Project on Reducing Inappropriate Imaging Requests by Increasing Awareness of iRefer Guidelines

Wednesday, Nov. 28 12:15PM - 12:45PM Room: QR Community, Learning Center Station #2

## Participants

Meedya Sharifpour, MBChB, MS, Dundee, United Kingdom (*Presenter*) Nothing to Disclose Richard Cooper, FRCR, MBChB, South Shields, United Kingdom (*Abstract Co-Author*) Nothing to Disclose

For information about this presentation, contact:

meedya.sharifpour@nhs.net

# PURPOSE

Acute abdominal radiographs (AXA) accounts for up to 10% of accident and emergency department admissions. AXA is requested for a large number of patients inappropriately. Majority of these investigations are negative or non-specific. Additionally this investigation exposes patients to a relatively high amount of ionising radiation. Majority of inappropriate radiological investigations are requested inappropriately in emergency settings or in primary care, as some requesters are not familiar with the correct imaging technique for every clinical presentation. The royal college of radiologists has developed a guideline known as iRefer guidelines, which is primarily aimed to help referring primary care physicians, clinicians and other healthcare workers to request the most appropriate imaging investigations based on the best available evidence. The purpose of this quality improvement project was to reduce the number of inappropriate AXA requested by the accident and emergency department (A&E) and subsequently reduce inappropriate ionising radiation to the patients. Awareness and education regarding iRefer guidelines was used in order to achieve the purpose of this project.

### METHODS

In order to review the appropriateness of the requested AXA, fifty consecutive AXA that were requested by the accident and emergency department were reviewed. This was carried out in a district general hospital in north east of England. The results were then summarised and presented to the clinicians at the A&E and general surgery department. Information regarding indications of AXA and iRefer guidelines were discussed in clinical meetings and demonstration on how to access and use the iRefer guidelines were carried out. Additionally posters on how to access iRefer guidelines were displayed in the A&E's doctor office. Two months following this period, further fifty consecutive AXA requested by the A&E department were reviewed to see whether there has been any reduction in the number of inappropriate AXA.

### RESULTS

The information that were collected retrospectively included patient's demographics, presenting complaint, abdominal examination findings, whether patients were admitted or discharged and the final diagnosis upon discharge. These information were collected before and after the discussions in the monthly clinical meetings. In the first cycle of this quality improvement project, 25 (50%) of the patients were male and the other half were female. The age of patients having AXA ranged from 21 to 95 with mean age of 77 years. The number of patients who were admitted to hospital following their AXA was 31 (62%) and 19 (38%) were discharged. Abdominal pain was by far the biggest presenting complaint (82%) followed by vomiting (16%). Majority of patients were diagnosed with constipation (18%) followed by urinary tract infection (12%) and non-specific abdominal pain (12%) upon discharge. In total, 37 AXA requests (74%) met the iRefer guidelines and were requested appropriately. In the second cycle of this project following discussion and education of clinicians regarding iRefer guidelines and display of information regarding iRefer guidelines accessibility, the number of AXA that met the iRefer guidelines increased to 84%. The results have been summarised in table 2.

#### CONCLUSION

Educating requesting clinicians regarding iRefer guidelines has demonstrated in a reduction in the number of inappropriate AXA. This has also meant reduction in inappropriate ionising radiation exposure of patients and reduction in inappropriate use of already stretched resources. The different types of imaging techniques available to clinicians for investigation of different conditions has increased. This project has only looked at one imaging modality, it would be appropriate to assume that awareness and education of requesting clinicians regarding such powerful resources will result in reduction in inappropriate number of imaging requests. The Royal College of Physicians has piloted incorporating this tool into requesting software used by primary care physicians and hospitals in order to make accessibility of such resources easier and maximise number of requested that meet the iRefer guidelines.



# QI128-ED-WEA3

Development of the Diagnostic Reference Level for Plain Radiographic Exams: Results of the Nation-Wide Survey in South Korea

Wednesday, Nov. 28 12:15PM - 12:45PM Room: QR Community, Learning Center Station #3

# Participants

Younghoon Cho, MD, Seoul, Korea, Republic Of (*Presenter*) Nothing to Disclose Kyung-Hyun Do, MD, Seoul, Korea, Republic Of (*Abstract Co-Author*) Nothing to Disclose Hong Eo, Seoul, Korea, Republic Of (*Abstract Co-Author*) Nothing to Disclose Kwang Pyo Kim, Suwon, Korea, Republic Of (*Abstract Co-Author*) Nothing to Disclose

For information about this presentation, contact:

dokh@amc.seoul.kr

## PURPOSE

The purpose of this study was to perform nation-wide survey regarding the radiation exposure associated with plain radiographs for various parts of the body, and assess the accumulated data, especially in comparison with previous reports, to establish recommendation diagnostic reference levels (DRLs) of each radiographic exam for adults and children.

### METHODS

Total of 103 hospitals (tertiary referral medical centers, 23; general hospitals, 51; private clinics, 29) in various regions within South Korea with installed x-ray examination machines (total number, 115) were chosen for thorough survey and testing from February 2017 to November 2017. Radiation exposure was measured as entrance surface dose (ESD, mGy) with dedicated phantoms design to represent adults, 10-year (yr) old children, and 5-yr old children. Since neonatal phantom was not available for this survey, kVp and mAs of neonatal x-ray exams were documented in 55 hospitals. Tested fourteen plain radiographic exams were as follow: skull anteroposterior (AP) and lateral (Lat), chest posteroanterior (PA), Lat, and AP, abdomen AP, pelvis AP, cervical spine (C-spine) AP and Lat, thoracic spine (T-spine) AP and Lat, Lumbar spine (L-spine) AP, Lat, and Oblique. Skull, chest, and pelvis exams were tested for children. For neonates, ESD for chest and abdomen AP projection images were obtained. Recommendation DRL was established as the upper quartile (75 percentile) value of the average ESD for each exam. Collected radiation dose data were compared to prior reports and recommendations from the current study were informed and educated.

## RESULTS

Third quartile values (in mGy) of various plain radiographic exams were as follow: skull AP 2.85, skull Lat 2.48, chest PA 0.40, chest Lat 1.26, chest AP 0.90, abdomen AP 3.64, pelvis AP 3.59, c-spine AP 1.65, C-spine Lat 0.74, T-spine AP 3.64, T-spine Lat 7.29, L-spine AP 4.89, L-spine Lat 10.55, L-spine oblique 6.09, 5-yr skull AP 1.02, 5-yr skull Lat 0.92, 5-yr chest PA 0.17, 5-yr chest Lat 0.33, 5-yr chest AP 0.35, 5-yr abdomen AP 0.80, 5-yr pelvis AP 0.88, 10-yr skull AP 1.38, 10-yr skull Lat 1.20, 10-yr chest PA 0.24, 10-yr chest Lat 0.50, 10-yr chest AP 0.47, 10-yr abdomen AP 1.38, 10-yr pelvis AP 1.43. Third quartile values ESD for neonates were 0.14mGy for chest AP and 0.26mGy for abdomen AP projections. Radiation exposure was consistently higher (average 2.1 fold) in computed radiography than digital radiography. In general, tertiary referral medical centers were associated with low radiation exposure and private clinics were associated with higher radiation exposure per exam. Of the 14 DRLs for adult exams, relative improvements compared to previous Korean data (2009~2011) was noted in 7 (50%) exams. When compared to data from other countries, current study's DRLs were generally higher than those of England 2010 guideline and comparable to European 2014 guidelines.

# CONCLUSION

Through nation-wide testing, exam-specific DRLs for plain radiographs were established for both adults and children. Further education, research, and development of radiation-control program based on current DRL, along with the survey itself, would have a beneficial effect on reducing the potential harm of radiation exposure for patients.



# QI130-ED-WEA4

Auditing an ACR-TIRADS Implementation Program - Effect on Reporting and Management of Thyroid Nodules in an Academic Ultrasound Department

Wednesday, Nov. 28 12:15PM - 12:45PM Room: QR Community, Learning Center Station #4

# Participants

Emily Pang, MD, Vancouver, BC (*Abstract Co-Author*) Nothing to Disclose Mohammed M. Bukhari, MBBS, Vancouver, BC (*Presenter*) Nothing to Disclose Alison C. Harris, MBChB, Vancouver, BC (*Abstract Co-Author*) Nothing to Disclose

### PURPOSE

To assess the effect of a program implementing the American College of Radiology Thyroid Imaging Reporting and Data System (TI-RADS) on standardizing report quaity, thyroid nodule management practices, estimated costs and biopsy wait-times in an academic ultrasound department.

# METHODS

The TIRADS implementation process consisted of tech and radiologist education sessions, multidisciplinary consultations with endocrinology and ENT/Surgery, development of a reporting template as well as tech worksheets, and development of a abbreviated scanning protocol and FNA triaging workflow. 100 consecutive patients from Feb 2017 (pre-TIRADS) and Feb 2018 (post-TIRADS implementation) who presented for diagnostic thyroid ultrasound were selected as the audit populations (n=200), with exclusion criteria including known thyroid cancer and requested assessment of a previously biopsied nodule. The reports for both populations were reviewed comparing pre and post TIRADS groups, assessing reports for inclusion of description of various nodule ultrasound features and final management recommendations. For both assessments, estimated costs as a result of the management received date to date of biopsy were also determined in the pre and post TIRADS groups as a secondary outcome measurement. In order to assess if any malignancies would have been missed as a result of the TIRADS implementation, an additional 81 consecutive nodules which had been adequately biopsied prior to TIRADS implementation had TIRADS retrospectively applied by 2 readers, with histopathology and hypothetical management recommendations documented.

## RESULTS

Post TIRADS, overall descriptions of thyroid nodules in reports were more thorough with inclusion of composition, echogenicity, shape, margins, and echogenic foci/calcification descriptions improving from 65%, 31%, 3%, 5%, and 33% in the pre TIRADS reports to 89%, 91%, 82%, 85%, and 87% respectively in the post TIRADS reports, particularly when a reporting template was utilized. Overall adoption of TIRADS was 93%. The distribution of management recommendations pre and post TIRADS was as follows, with recommended FNAs reduced (36% vs 21%), followup ultrasounds (13% vs 41%) and no further followups (23% vs 31%) increased, and fewer reports with no specific recommendations (28% vs 7%). A conservative estimate of the costs to MSP to implement the recommendations pre and post TIRADS were CAD \$5743.06 and \$5595.05 respectively. Average biopsy wait-times improved from 77 to 64 days in the pre and post TIRADS groups respectively. Of the 81 pathologically proven nodules biopsied during the pre TIRADS period, with TIRADS retrospectively applied a total of 52 (64%) would have been biopsied, 12 (15%) would not have required any further followup. The vast majority of nodules positive for malignancy or atypia (n=10) would have been biopsied after TI-RADS implementation, one Bethesda III nodule would have been followed up, and all the nodules which did not require follow-up as per TIRADS were histologically benign.

# CONCLUSION

Post implementation of a program utilizing ACR TI-RADS guidelines to report and manage thyroid nodules, there was a dramatic improvement in report quality. Fewer biopsies and more follow-up ultrasounds were recommended post TIRADS with overall modest cost savings in the assessed population and theoretically no cancers missed. Biopsy wait-times were also improved. Continuation of the audit process to assess if these trends apply long term would be of benefit and is ongoing.



## RO221-SD-WEA1

Treatment Patterns of High Dose Rate (HDR) and Low Dose Rate (LDR) Brachytherapy for Prostate Cancer

Wednesday, Nov. 28 12:15PM - 12:45PM Room: RO Community, Learning Center Station #1

# Participants

William R. Kennedy, MD, Saint Louis, MO (*Presenter*) Nothing to Disclose Benjamin W. Fischer-Valuck, MD, MS, St. Louis, MO (*Abstract Co-Author*) Nothing to Disclose Brian Baumann, St. Louis, MO (*Abstract Co-Author*) Nothing to Disclose Jeff M. Michalski, MD, Saint Louis, MO (*Abstract Co-Author*) Nothing to Disclose Hiram A. Gay, MD, Greenville, NC (*Abstract Co-Author*) Nothing to Disclose

### PURPOSE

HDR and LDR brachytherapy (BT) are both NCCN recommended treatment modalities for localized prostate cancer. The choice of HDR versus LDR is dependent on patient, physician, and hospital preference. The purpose of this registry-based analysis was to investigate patient and clinical characteristics associated with the receipt of HDR or LDR brachytherapy for localized prostate cancer.

#### **METHOD AND MATERIALS**

We queried the National Cancer Database (NCDB) for patients with localized low or intermediate risk prostate cancer (<=cT2c, Gleason score <=7, and/or PSA <20) treated with either HDR or LDR brachytherapy. Descriptive statistics were used to analyze patterns of HDR compared to LDR use. Patient demographics and disease characteristics were correlated with HDR vs LDR using multivariable logistic regression.

## RESULTS

A total of 50,326 patients from 2004-2014 were included (LDR: 37,863 (75.2%) vs. HDR: 12,463 (24.8%)). Median follow-up was 70.3 months and similar in both groups. In 2004, HDR accounted for 27.0% of brachytherapy cases compared to 19.2% in 2014. Using multivariable analysis, variables associated with increased likelihood of receiving HDR included: increasing year of age (OR: 1.01, 95% CI, 1.01-1.01;P=0.007), cT2c disease (OR: 1.25, 1.11-1.41;P<0.0001), treatment at an academic/research center (OR: 2.45, 2.24-2.65; P<0.0001), non-white race (OR: 1.34, 1.27-1.42; P<0.0001), and income >\$63,000 (OR: 1.73, 1.59-1.88; P<0.0001). LDR was more common in the years of 2010-2014 (OR: 0.59, 0.54-0.65; P<0.0001), for patients with Charlson-Deyo comorbidity >0 (OR: 0.89, 0.84-0.95; P=0.001), and for patients receiving hormone therapy (OR: 0.88, 0.83-0.93; P<0.0001). No difference in PSA value or Gleason Score and receipt of HDR vs. LDR was observed. Mean overall survival was 127.0 months for HDR and 125.4 months for LDR.

# CONCLUSION

Despite similar overall survival outcomes, the use of HDR brachytherapy declined over the study period examined. In this cohort, HDR was more common in patients with cT2c disease and hormone therapy was more common in the LDR group.

## **CLINICAL RELEVANCE/APPLICATION**

Our work revealed a decline in HDR brachytherapy for localized prostate cancer and identified important factors influencing use of LDR vs. HDR in the largest comparison of BT modalities to date.



# RO222-SD-WEA2

Effect of the Change in a Reactor Power on the Response of Murine Solid Tumors in Vivo, Referring to that in Intratumor Quiescent Cells and Its Clinical Significance in Boron Neutron Capture Therapy (BNCT)

Wednesday, Nov. 28 12:15PM - 12:45PM Room: RO Community, Learning Center Station #2

# Participants

Shinichiro Masunaga, MD, Osaka, Japan (*Presenter*) Nothing to Disclose Yoshinori Sakurai, Osaka, Japan (*Abstract Co-Author*) Nothing to Disclose Hiroki Tanaka, Osaka, Japan (*Abstract Co-Author*) Nothing to Disclose Takushi Takata, Osaka, Japan (*Abstract Co-Author*) Nothing to Disclose Keizo Tano, PhD, Osaka, Japan (*Abstract Co-Author*) Nothing to Disclose Yu Sanada, Osaka, Japan (*Abstract Co-Author*) Nothing to Disclose Minoru Suzuki, MD, PhD, Sennan, Japan (*Abstract Co-Author*) Nothing to Disclose Akira Maruhashi, Osaka, Japan (*Abstract Co-Author*) Nothing to Disclose Koji Ono, MD, PhD, Osaka, Japan (*Abstract Co-Author*) Nothing to Disclose

# PURPOSE

To examine the effect of the change in a reactor power on the response of solid tumors in vivo, with reference to that in quiescent (Q) tumor cells, and discuss its clinical significance in boron neutron capture therapy (BNCT).

## **METHOD AND MATERIALS**

SCC VII tumor-bearing mice received 5-bromo-2-deoxyuridine (BrdU) continuously to label all intratumor proliferating (P) cells, and were treated with a 10B-carrier, boronophenylalanine-10B (BPA) or sodium mercaptododecaborate-10B (BSH). Right after reactor neutron beam irradiation at a power of 1 or 5 MW with a similar beam spectrum each other at Kyoto University Research Reactor, cells from some tumors were isolated and incubated with a cytokinesis blocker. The responses of BrdU-unlabeled Q and total (= P+Q) tumor cells were assessed based on the frequencies of micronucleation using immunofluorescence staining for BrdU.

# RESULTS

Following reactor neutron irradiation with or without 10B-carrier administration, the reduction in sensitivity caused by a decrease in radiation dose rate due to a decrease in a reactor power was clearly observed in both tumor cells, especially with BPA or in Q tumor cells. The sensitivity difference between total and Q tumor cells was widened in combination with 10B-carrier administration, especially with BPA, and through decreasing a reactor power. The calculated values of compound biological effectiveness (CBE) factors for each 10B-carrier showed a tendency that the values for BPA, in Q cells, and at a power of 5 MW were larger than those for BSH, in total cells, and at a power of 1 MW, respectively.

# CONCLUSION

The observed dose rate effect supported a better advantage of 5 MW as a reactor power than 1 MW. Moreover, 5 MW showed a better advantage than 1 MW in terms of reducing the sensitivity difference between total and Q cells. The rise in a reactor power enlarged the values of CBE factor for both 10B-carriers. In clinics, it takes 5 times longer time at a power of 1 MW than 5 MW to perform one session of BNCT. Patients cannot move their body at the optimum treatment position during BNCT. Thus, 5 MW is more useful and convenient than 1 MW as a reactor power in clinical BNCT.

# **CLINICAL RELEVANCE/APPLICATION**

The higher a reactor power is, the better clinical results are thought to be able to be expected in BNCT.



## UR007-EB-WEA

Computer Assistance in Comparison of Kidney Function Variation Between Pre- and Post-nephrectomy

Wednesday, Nov. 28 12:15PM - 12:45PM Room: GU/UR Community, Learning Center Hardcopy Backboard

**FDA** Discussions may include off-label uses.

### Participants

Chenglong Wang, Nagoya, Japan (*Presenter*) Nothing to Disclose Masahiro Oda, PhD, Nagoya, Japan (*Abstract Co-Author*) Nothing to Disclose Jun Nagayama, Nagoya, Japan (*Abstract Co-Author*) Nothing to Disclose Yasushi Yoshino, Nagoya, Japan (*Abstract Co-Author*) Nothing to Disclose Tokunori Yamamoto, Nagoya, Japan (*Abstract Co-Author*) Nothing to Disclose Kensaku Mori, PhD, Nagoya, Japan (*Abstract Co-Author*) Nothing to Disclose

#### For information about this presentation, contact:

cwang@mori.m.is.nagoya-u.ac.jp

### **TEACHING POINTS**

The purpose of this exhibit is To learn the semi-automated segmentation of renal cortex and renal medulla using CT volume data. To learn the fully-automated and accurate renal artery segmentation method. To demonstrate assistance system for renal vascular dominant region estimation. To show that the cortex and medulla volume ratio in unclamped kidney region increased after nephrectom.

### TABLE OF CONTENTS/OUTLINE

What is partial nephrectomy? How will kidney function change after nephrectomy? What can our assistance system do? Extraction of precise renal arteries using our blood vessel segmentation method. Extraction of renal cortex and medulla using level-set method automatically. Estimation of dominant regions using Voronoi diagram. Statistics of cortex and medulla in dominant regions. Analysis of volume variation between pre- and post-operation. Clinical application A more deep insight into variation of kidney function between pre- and post-operation. Demonstrate our computer-aided system Processes of semi-automated renal artery, renal cortex and medulla segmentation. Computation of dominant regions of renal cortex and medulla. Interactive demonstration of partition results in 3D display and 3D printed model.



## UR187-ED-WEA8

What Radiologists Need to Focus on Renal Imaging for Preventing Pathological Upstaging of Clinical T1 to Pathological T3 Renal Cancer Managed by Partial Nephrectomy

Wednesday, Nov. 28 12:15PM - 12:45PM Room: GU/UR Community, Learning Center Station #8

#### Awards Certificate of Merit

#### **Participants**

Satoru Takahashi, MD, PhD, Takatsuki, Japan (*Presenter*) Nothing to Disclose Yoshiko Ueno, MD, PhD, Kobe, Japan (*Abstract Co-Author*) Nothing to Disclose Noriyuki Negi, RT, Kobe, Japan (*Abstract Co-Author*) Nothing to Disclose Kiyosumi Kagawa, Kobe, Japan (*Abstract Co-Author*) Nothing to Disclose Utaru Tanaka, Kobe, Japan (*Abstract Co-Author*) Nothing to Disclose Takamichi Murakami, MD, PhD, Osakasayama, Japan (*Abstract Co-Author*) Nothing to Disclose

## For information about this presentation, contact:

satorutakahashi1120@gmail.com

# **TEACHING POINTS**

Partial nephrectomy is now a preferred treatment option for most patients with T1 renal tumors. Because pathological upstaging from cT1 to pT3 is related to a negative prognosis, perinephric invasion &/or gross tumor thrombus in the renal vein have attracted radiologists' attention. We radiologists or urologists, even pathologists, have, however, paid little attentions to sinus fat invasion, although considering an anatomic perspective, sinus fat invasion could be greater risk for recurrence after partial nephrectomy. The purpose of this exhibit is:1. To review the current status of Partial nephrectomy2. To understand vital structure/anatomy in the renal sinus for the pre-operative assessment3. To explain CT techniques to visualize the required anatomy in detail4. To demonstrate how to evaluate and report renal CT focusing on partial nephrectomy

### **TABLE OF CONTENTS/OUTLINE**

Partial nephrectomy-indication-surgical technique with robotic or open surgery-oncologic outcomes of pT1 vs. pT3 tumor-pattern of recurrenceCT anatomy in the renal sinus-renal artery & vein-collecting systemCT scanning technique-contrast injection-scan timing-image reconstruction-low energy or dual-energy imagingPost processing-3D CTAImage assessment-renal sinus fat invasion-tumor thrombus in the sinus branch -key phase in dynamic renal CT



# VI166-ED-WEA10

The Essentials of Prostatic Artery Embolization (PAE): A Beginners' Guide and Laying the Foundation for Success

Wednesday, Nov. 28 12:15PM - 12:45PM Room: VI Community, Learning Center Station #10

# Participants

Ragni Jindal, MD, Tucson, AZ (*Presenter*) Nothing to Disclose Jung H. Yun, Closter, NJ (*Abstract Co-Author*) Nothing to Disclose Siavash Behbahani, MD, Mineola, NY (*Abstract Co-Author*) Nothing to Disclose Aaron E. Katz, MD, Mineola, NY (*Abstract Co-Author*) Nothing to Disclose Shivank S. Bhatia, MD, MBBS, Miami, FL (*Abstract Co-Author*) Consultant, Merit Medical Systems, Inc; Speaker, Merit Medical Systems, Inc Jason C. Hoffmann, MD, Mineola, NY (*Abstract Co-Author*) Speakers Bureau, Merit Medical Systems, Inc; ; Juan M. Puertas, DO, Mineola, NY (*Abstract Co-Author*) Nothing to Disclose Jonathan Minkin, Mineola, NY (*Abstract Co-Author*) Nothing to Disclose Mudassir Syed, Mineola, NY (*Abstract Co-Author*) Nothing to Disclose

# For information about this presentation, contact:

Jason.Hoffmann@nyulangone.org

#### **TEACHING POINTS**

1. A thorough understanding of benign prostatic hyperplasia (BPH) pathophysiology and management options is essential before embarking on developing a PAE program.2. While the risks of PAE are low when done with proper technique, major complications can occur and have negative impact on a patient and/or a PAE program.3. Pursuing dedicated PAE training and education is strongly encouraged prior to performing these procedures.

### **TABLE OF CONTENTS/OUTLINE**

BPH (pathophysiology, anatomy, symptoms, and prevalence)Describe key concepts in evaluating BPH, including International Prostate Symptom Score, Sexual Health Inventory for Men Score, ultrasound, role of CTA and MRI, role of prostate biopsy and PSA, and urodynamicsReview treatment options for symptomatic BPH, including medical and procedural management.Describe the history of PAE, including relevant literature review and timeline of use across the world.PAE concepts:-Indications-Review arterial pelvic anatomy-Tools: catheters, microcatheters, particles, coils, adjunctive devices, Foley catheter-Role of the PErFecTED technique-Identifying and managing collateral vasculature-Post embolization syndrome and complications-General post-procedural care end expectations-Outcomes and long-term follow-up-Role of PAE in prostate cancer-Recommendations for building a PAE program



# VI167-ED-WEA11

Vascular Intervention for Aortic Dissection -What Should Radiologists Know When Making a Decision About the Optimal Treatment?

Wednesday, Nov. 28 12:15PM - 12:45PM Room: VI Community, Learning Center Station #11

# Participants

Yoshiaki Watanabe, MD, Suita, Osaka, Japan (*Presenter*) Nothing to Disclose Yoshiro Hori, Osaka, Japan (*Abstract Co-Author*) Nothing to Disclose Akiyuki Kotoku, MD, Kawasaki, Japan (*Abstract Co-Author*) Nothing to Disclose Yoshiaki Morita, Suita, Japan (*Abstract Co-Author*) Nothing to Disclose Hitoshi Matsuda, Suita, Japan (*Abstract Co-Author*) Nothing to Disclose Tetsuya Fukuda, Suita, Japan (*Abstract Co-Author*) Nothing to Disclose Keisuke Kiso, MD, Suita, Japan (*Abstract Co-Author*) Nothing to Disclose Emi Tateishi, Suita, Japan (*Abstract Co-Author*) Nothing to Disclose Tatsuya Nishii, MD, PhD, Suita, Japan (*Abstract Co-Author*) Nothing to Disclose Atsushi K. Kono, MD, PhD, Suita, Japan (*Abstract Co-Author*) Nothing to Disclose

# For information about this presentation, contact:

ds14095@gmail.com

#### **TEACHING POINTS**

Recently, indications of vascular intervention for aortic dissection (AD) have expanded, due to the accumulation of new evidence. Now, stent graft (SG) is becoming the first choice for type B AD. Promoting aortic remodeling is important for the success of SG for AD, and various methods have been devised to realize this. In addition, SG is sometimes not enough for branch-vessel obstructions, so the stenting of branch vessels is sometimes added. To choose between stent-grafting or adding a stent, we must know the type of obstruction. CT plays an important evaluation role, and 4D CT and phase contrast MRI are sometimes useful. From these points, we exhibit an actual IR for AD and representative image findings, which are necessary to decide the optimal treatment. The teaching points of this exhibit are: 1) learning the indication of vascular intervention for AD, and 2) showing various vascular interventions for AD. Then, we can understand the evaluation of the points of the pre and postoperative images.

#### **TABLE OF CONTENTS/OUTLINE**

1.Background of AD 2 The indication of SG for AD 3 Various techniques to promote aorta remodeling 3-1 PETTICOAT Technique 3-2 Candy-Plug Technique 4. Branch-vessel compromise 4-1 Dynamic obstruction 4-2 Static obstruction 4-3 4D CT and phase contrast MRI 5 Complications after vascular interventions



## VI168-ED-WEA12

## Tools for 'Superactive Surveillance' for Local Focal Ablation of Low Grade Prostate Cancer

Wednesday, Nov. 28 12:15PM - 12:45PM Room: VI Community, Learning Center Station #12

FDA Discussions may include off-label uses.

#### **Participants**

Hayet Amalou, MD, Bethesda, MD (Presenter) Nothing to Disclose

Sheng Xu, PhD, Bethesda, MD (Abstract Co-Author) Nothing to Disclose

Peter L. Choyke, MD, Rockville, MD (Abstract Co-Author) Nothing to Disclose

Peter Pinto, Bethesda, MD (Abstract Co-Author) Nothing to Disclose

Baris Turkbey, MD, Bethesda, MD (Abstract Co-Author) Nothing to Disclose

Bradford J. Wood, MD, Bethesda, MD (*Abstract Co-Author*) Researcher, Koninklijke Philips NV; Researcher, Celsion Corporation; Researcher, BTG International Ltd; Researcher, Siemens AG; Researcher, XAct Robotics; Researcher, NVIDIA Corporation; Intellectual property, Koninklijke Philips NV; Intellectual property, BTG International Ltd; Royalties, Invivo Corporation; Royalties, Koninklijke Philips NV; ; ; Tom Sanford, MD, Bethesda, MD (*Abstract Co-Author*) Nothing to Disclose

Victoria L. Anderson, MS, Bethesda, MD (*Abstract Co-Author*) Nothing to Disclose

## For information about this presentation, contact:

bwood@nih.gov

# **TEACHING POINTS**

The shifting landscape in the diagnosis and management of low-grade prostate cancer will be better understood in terms of recent changes in PSA screening recommendations, the role of MRI / PIRADS classifications, the growth of TRUS/MRI fusion biopsy, and the lack of consensus surrounding the management of low-Gleason prostate cancer. Opportunities for radiologists and interventional radiologists to play major roles in the diagnosis and treatment of the patient with Gleason 3 + 3 or 3 + 4 prostate cancer. Better understand the different mechanisms, strengths, risk profiles, workflow, and applications for image guided focal therapy options available for the patient who chooses active surveillance, or 'super-active surveillance' with annual MRI, annual fusion biopsy, and focal local laser ablation for MRI or fusion-visible index lesions.

# TABLE OF CONTENTS/OUTLINE

A. Background of recent changes in guidelines for screening and use of PSA, MRI, and Fusion B. Inclusion criteria for 'active surveillance' C. Brief role of MRI D. Development of TRUS/MRI fusion biopsy E. Comparison of ablative technologies applied to prostate cancer: cryoablation, focal laser ablation, TRUS HIFU, trans-urethral HIFU F. 'Super-active surveillance' technique of focal laser ablation under ultrasound guidance or TRUS/MRI fusion guidance



# VI241-SD-WEA1

MR Lymphography in Patients with Lymphedema: Does Compression Therapy Increase False Negative Cases?

Wednesday, Nov. 28 12:15PM - 12:45PM Room: VI Community, Learning Center Station #1

## Participants

Fabio Panzuto, Pavia, Italy (*Presenter*) Nothing to Disclose Andrea Franconeri, MD, Pavia, Italy (*Abstract Co-Author*) Nothing to Disclose Francesco Ballati, MD, Milano, Italy (*Abstract Co-Author*) Nothing to Disclose Luca Lungarotti, MD, Pavia, Italy (*Abstract Co-Author*) Nothing to Disclose Carlo Asteggiano, Castelnuovo Scrivia, Italy (*Abstract Co-Author*) Nothing to Disclose Maria Vittoria Raciti, MD, Pavia, Italy (*Abstract Co-Author*) Nothing to Disclose Alessia Maggi, MD, Pavia, Italy (*Abstract Co-Author*) Nothing to Disclose Antonella Smedile, MD, Pavia, Italy (*Abstract Co-Author*) Nothing to Disclose Marcello Esposito, Pavia, Italy (*Abstract Co-Author*) Nothing to Disclose Chandra Bortolotto, MD, Pavia, Italy (*Abstract Co-Author*) Nothing to Disclose Harcello Esposito, Pavia, Italy (*Abstract Co-Author*) Nothing to Disclose Chandra Bortolotto, MD, Pavia, Italy (*Abstract Co-Author*) Nothing to Disclose Hatroio Calliada, MD, Pavia, Italy (*Abstract Co-Author*) Nothing to Disclose Hatroio Calliada, MD, Pavia, Italy (*Abstract Co-Author*) Nothing to Disclose Hatroio Calliada, MD, Pavia, Italy (*Abstract Co-Author*) Research Grant, Canon Medical Systems Corporation; Speakers Bureau, Hitachi, Ltd; Speakers Bureau, Shenzhen Mindray Bio-Medical Electronics Co, Ltd

### PURPOSE

In the last few years lymphography MRI assumed a crucial role in diagnosis and follow-up of lymphedema. Therapeutic options of this chronic pathology are both surgical and non-surgicalt. The aim of our study is to evaluate if compression therapies can affect MR sensitivity in lymphedema diagnosis

# METHOD AND MATERIALS

91 patients (15 males, 76 females, age 6-73 years, median 46,4 $\pm$ 15,4 years), clinically diagnosed as idiopathic or secondary lymphedema of the limbs and classified according to International Society of Lymphology Staging System, were retrospectively enrolled. All patients, underwent in our Institute their first MR lymphography without contrast administration. 21(first group) had never been treated for lymphedema before or had stopped any treatment at least one month before the MRI. 70 were treated conservatively at the time of MR lymphography and only 11 of these (second group) had not removed compressive bandages or braces for at least 6 hours before MR examination.

### RESULTS

21 patients of the first group were positive for lymphedema at MR lymphography. In the second group, 8 out of 11 (72.7%) resulted false negative for lymphedema. 7 of them had not removed bandages or braces at the time of MR lymphography, while 1 patient resulted negative despite having removed compression 24 hours before.

## CONCLUSION

Lymphedema conservative treatment is one of the commonest therapeutic strategies, but the lack in removing compressive materials before MR examination significantly reduces the MRI sensitivity (27.3%). Since2017 we asked our patients to remove any kind of compression material at least 6 hours before undergoing MR lymphography, recording a remarkable reduction in false negatives.

# **CLINICAL RELEVANCE/APPLICATION**

Evaluation of Lymphedema



# VI242-SD-WEA2

Assessing Lag Time after CTA in the Diagnosis of Acute Lower Gastrointestinal Bleed on Catheter Angiography: Towards Improving Yield

Wednesday, Nov. 28 12:15PM - 12:45PM Room: VI Community, Learning Center Station #2

#### Awards Student Travel Stipend Award

# Participants

Matthew E. Pouw, MD, Providence, RI (*Presenter*) Nothing to Disclose Joseph W. Albright, MD, Providence, RI (*Abstract Co-Author*) Nothing to Disclose Grayson L. Baird, PhD, Providence, RI (*Abstract Co-Author*) Nothing to Disclose Sun Ho Ahn, MD, Providence, RI (*Abstract Co-Author*) Nothing to Disclose

## For information about this presentation, contact:

matthew\_pouw@brown.edu

## PURPOSE

Acute lower gastrointestinal bleeding (LGIB) is a common and potentially life-threatening problem especially in the older adult population. CT angiography (CTA) is useful in detection of acute LGIB, but diagnostic yield of subsequent catheter angiography (CA) can be poor as bleeding can be intermittent, limiting possible catheter-based therapeutic intervention. We aimed to assess whether lag time (LT) from the detection of a hemorrhagic blush on CTA to the start of subsequent CA was predictive of diagnostic yield of CA when assessing for LGIB.

### **METHOD AND MATERIALS**

We retrospectively reviewed our PACS for all positive CTA studies with subsequent CA examinations performed to assess for gastrointestinal (GI) bleeding from Oct 2012 to Oct 2017. All upper GI bleed studies were excluded. LT was recorded for each instance. Noninitial CA observations were not analyzed to prevent violation of independence. Generalized modeling assuming a binary distribution was used to model the relationship between LT and positive CA examination using the GLIMMIX Procedure within SAS.

### RESULTS

A total of 60 qualifying CA examinations were included from 56 different patients with a maximum observation per patient of 3. The median LT from CTA to CA observed was 225 minutes with a range of 35 to 2900 minutes. A significant inverse relationship between LT and positive CA status was observed in our model (p=0.04) with the odds of detecting active extravasation on CA decreasing by 8% with every 1-hour delay after CTA. Conversely, with every 1-hour delay spared before initiating CA examination, a 9% increase in odds of detecting active extravasation on CA was observed.

## CONCLUSION

The odds of detecting active extravasation on CA after identifying acute LGIB on CTA examination decrease with increased lag time between studies.

## **CLINICAL RELEVANCE/APPLICATION**

Catheter angiography should be pursued as urgently as possible after positive CTA examination to improve yield in detection and possible catheter-based treatment of acute lower gastrointestinal bleed.



# VI243-SD-WEA3

## **CEUS** Monitoring of Intratumoral Microcirculation After Electroporation of Liver Tumors

Wednesday, Nov. 28 12:15PM - 12:45PM Room: VI Community, Learning Center Station #3

# Participants

Luciano Tarantino, MD, Torre Del Greco, Italy (Presenter) Nothing to Disclose

For information about this presentation, contact:

dr.tarantino@libero.it

#### PURPOSE

to assess, with Contrast enhanced Ultrasound (CEUS), the early and late changes in intra- and peri-tumoral microcirculation of Liver Tumors treated with Electroporation, a new non thermal ablation technique.

## **METHOD AND MATERIALS**

We studied with a serial perioperative and post operative CEUS examinations, 12 consecutive patients (10M,2F; 43-85 year, mean: 72 year), with 6 Hepatocellular Carcinoma, 4 Cholangiocarcinoma, 2 single metastasis (1 from colon, 1 from breast carcinoma) treated with Irreversible Electroporation (IRE) (4 cases) or Electrochemotherapy (ECT) (8 cases). Diameter of tumors ranged 3.2 - 7.5 cm (mean:4.3 cm). CEUS examinations were performed using a commercially available US equipment (EPIC-Q7, PHILIPS, USA) after peripheral intravenous injection of 4.8 ml of a second generation US contrast agent (SonoVue , Bracco, Milan, Italy). All patients underwent : 1)Pretreatment CEUS within 24 hours before Electroporation; 2) Intraoperative CEUS at the end of the procedure; 3) Post-treatment CEUS 24 hours after Electroporation; 4) week-one CEUS control ; 5) One-month CEUS control.

# RESULTS

Before treatment, in comparison with liver parenchyma, CEUS showed : a) hyperenhancement in 10 and isoenhancement in 2 cases in arterial phase; isoenhancement in 6 and hypoenhancement in 6 cases in the venous phase; hypoenhancement in the late phase (wash-out) in all cases. After Electroporation CEUS showed :a) a completely avascular treated area (absence of enhancent during all CEUS phases) at the end of procedure, intraoperatively; b) irregular and faint enhancement in the peripheral parts of the treated areas at 24-hours after treatment; c) a well demarcated avascular central area and complete recovery of enhancement of peripheral portions of the treated volume at one-week CEUS; d) shrinkage of the central unenhanced area at one-month CEUS.

# CONCLUSION

CEUS is a useful tool to assess the efficacy of Electroporation in the treatment of liver tumors. Also, CEUS can show the transient hypovascularity followed from "vascular recovery" of the peritumoral normal tissue and the fast progressive shrinkage of the killed tumor mass .

## **CLINICAL RELEVANCE/APPLICATION**

CEUS is non invasive, repeatable, well tolerated examination and reporesent a useful tool to detect changes in vascularity of tumor and peritumoral tissue, as well as the fast progressive shrinkage of the killed tumor mas, after Electroporation of Liver tumors.



# VI245-SD-WEA5

## Mid-Term Result of Thoracic Endovascular Aortic Repair in Octogenarians and Nonagenarians

Wednesday, Nov. 28 12:15PM - 12:45PM Room: VI Community, Learning Center Station #5

## Participants

Takashi Hashimoto, Tsu, Japan (*Presenter*) Nothing to Disclose Noriyuki Kato, Tsu, Japan (*Abstract Co-Author*) Nothing to Disclose Takafumi Ouchi, Tsu, Japan (*Abstract Co-Author*) Nothing to Disclose Ken Nakajima, Tsu, Japan (*Abstract Co-Author*) Nothing to Disclose Takatoshi Higashigawa, MD, Tsu, Japan (*Abstract Co-Author*) Nothing to Disclose Shuji Chino, MD, Matsusaka, Japan (*Abstract Co-Author*) Nothing to Disclose Hajime Sakuma, MD, Tsu, Japan (*Abstract Co-Author*) Nothing to Disclose Group; Research Grant, FUJIFILM Holdings Corporation; Research Grant, Siemens AG; Research Grant, Nihon Medi-Physics Co, Ltd; Speakers Bureau, Bayer AG

## PURPOSE

Thoracic endovascular aortic repair (TEVAR) is expected to benefit old patients with high operative risk. We investigated the outcome of TEVAR in octogenarians and nonagenarians.

# METHOD AND MATERIALS

From May 1997 through December 2017, 638 patients had undergone TEVAR for TAA or AD in our hospitals. We retrospectively reviewed the medical records of 113 patients aged 80 years or older (17.7%) among them.

# RESULTS

There were 78 men and 35 women. The mean age was 83.4±3.1 years (mean±standard deviation). Emergent TEVAR was performed in 28 patients (25.7%). Thirty-day mortality rate and the rate of 30-day mortality plus major adverse events calculated using Japan score were 24.0±22.5% and 40.7%±20.2%, respectively. Mortality rate and the rate of mortality plus morbidity calculated using STS score were 6.6±5.1% and 25.8±13.9%, respectively. Operative mortality rate calculated using euroSCORE was 11.7±10.9%. To preserve aortic arch branches, bypass surgery was added to 1 aortic branch in 6 patients, 2 branches in 11 patients, 3 branches in 1 patient. In 5 patients, chimney technique was used to preserve the left subclavian artery. To preserve a celiac artery, periscope technique was used in 1 patient, and bypass surgery was added in 1 patient. The mean follow-up term was 23.5±21.1 months. Overall survival rate was 96.4% at 1 month, 94.5% at 3 months, 88.1% at 1 year, and 83.7% at 3 years. Cause of early death was aortic rupture in 2 patients, sepsis in 1, and cancer in 1. Aorta-related adverse event free rate was 88.5% at 1 month, 85.6% at 3 months, 81.3% at 1 year, and 71.3% at 3 years. Regarding patients undergoing elective TEVAR, overall survival rate was 98.4% at 1 month and 3 months, 85.3% at 1 year, and 76.7% at 3 years.Excluded 6 patients whose discharge to unknown, 107 patients were analyzed about discharge to home or not. After logistic regression, emergency and combined procedure were the negative predictors of home discharge.

#### CONCLUSION

TEVAR in octogenarians and nonagenarians seems to be acceptable in terms of life prognosis. Emergency and combined procedure were the negative predictors of home discharge.

# **CLINICAL RELEVANCE/APPLICATION**

TEVAR in octogenarians and nonagenarians seems to be acceptable in terms of life prognosis or high operative risk.



# VI246-SD-WEA6

Psoas Muscle Density in Combination with Model of End-Stage Liver Disease Score Can Improve Survival Predictability Following Transjugular Intrahepatic Portosystemic Shunt

Wednesday, Nov. 28 12:15PM - 12:45PM Room: VI Community, Learning Center Station #6

## Participants

Mohamed G. Shoreibah, Birmingham, AL (*Abstract Co-Author*) Nothing to Disclose Khalid H. Mahmoud, MBBS, Birmingham, AL (*Presenter*) Nothing to Disclose Noha A. Aboueldahab, MBBCh, Birmingham, AL (*Abstract Co-Author*) Nothing to Disclose Andrew J. Gunn, MD, Birmingham, AL (*Abstract Co-Author*) Nothing to Disclose Mostafa Massoud, Birmingham, AL (*Abstract Co-Author*) Nothing to Disclose Ahmed K. Abdel Aal, MD, PhD, Birmingham, AL (*Abstract Co-Author*) Consultant, Abbott Laboratories; Consultant, Baxter International Inc; Consultant, C. R. Bard, Inc; Consultant, Boston Scientific Corporation; Consultant, W. L. Gore & Associates, Inc; Consultant, Sirtex Medical Ltd

### For information about this presentation, contact:

akamel@uabmc.edu

### PURPOSE

The aim of this study was to examine the role of pre-TIPS psoas muscle density (PD) measurement in predicting survival when combined with model of end-stage liver disease (MELD) score.

### **METHOD AND MATERIALS**

We retrospectively reviewed the medical records of 287 patients who had TIPS from June 2005 and June 2015. The patients were separated into two groups; group A (n=134) and group B (n=153), who had TIPS for variceal bleed (VB), and Volume overload (VO) respectively. PD was measured in Hounsfield Units (HU) by creating a region of interest on the whole muscle on a non-contrast CT prior to TIPS, and pre-TIPS MELD score was calculated. The primary endpoint was to determine a threshold sensitivity of pre-TIPS PD for assessing mortality in each group and measure its correlation with survival following TIPS. The secondary endpoint was to determine if combining the PD threshold with MELD score can improve survival predictability following TIPS, compared to MELD score alone. The optimal cutoff for the PD threshold was defined as the point with the most significant log-rank test split. Hazard ratios (HR), including 95% confidence intervals, were calculated. Harrell's C-index, an extension of the area under the ROC curve (AUC), were assessed for MELD score alone compared to MELD score and PD thresholds to compare the predictability of the selected variables.

### RESULTS

The study included 175 (62%) males, 253 (88%) Caucasians, age 56 years (SD=9.8). There was no significant difference in the baseline characteristics between the two groups. The average pre-TIPS MELD score of 12.4 (SD=7.5). The threshold of pre-TIPS PD for discriminating survival was 29.42 HU (p=00026). PD below these thresholds was associated with higher risk of mortality. Compared to using MELD alone, adding PD measurement significantly decreased the -2 Log Likelihood of the model (p=0.0022). A higher pre-TIPS PD was associated with lower risk of mortality [HR= 1.64, 95% CI (1.14, 2.35), p=0.0081].

### CONCLUSION

When used in conjunction with MELD score, PD improves overall survival predictability of cirrhotic patients undergoing TIPS. The best survival outcome was reported in patients with PD > 29.42 HU.

## **CLINICAL RELEVANCE/APPLICATION**

(dealing with muscle density measurement to predict mortality after TIPS) 'measuring muscle mass in conjunction with MELD score demonstrate better survival prediction for patients undergoing TIPS procedure.



## VI247-SD-WEA7

# **Carotid Occlusions in the Setting of Acute Stroke**

Wednesday, Nov. 28 12:15PM - 12:45PM Room: VI Community, Learning Center Station #7

### **Participants**

Iqra N. Akhtar, MD, Kansas City, MO (*Abstract Co-Author*) Nothing to Disclose Brett Donegan, MD, Kansas City, MO (*Presenter*) Nothing to Disclose Zain Haq, MD, Kansas City, KS (*Abstract Co-Author*) Nothing to Disclose Jared S. Halpin, MD, Kansas City, MO (*Abstract Co-Author*) Nothing to Disclose William E. Holloway, MD, Mission Hills, KS (*Abstract Co-Author*) Nothing to Disclose Coleman Martin, MD, Kansas City, MO (*Abstract Co-Author*) Nothing to Disclose Naveed Akhtar, MD, Mission Hills, KS (*Abstract Co-Author*) Nothing to Disclose

#### For information about this presentation, contact:

#### nakhtar56@gmail.com

## PURPOSE

Carotid artery occlusion in the setting of acute stroke with concurrent intracranial involvement is a serious and deadly combination, and can prove to be a challenging endeavor when encountered. The stroke is usually more severe due to poor collaterals and successful revascularization is difficult to achieve, resulting in a higher morbidity and mortality. We aim to assess the revascularization rates and clinical outcomes in this subset of patients treated with endovascular therapy.

## **METHOD AND MATERIALS**

An IRB approved retrospective chart review of cases presenting with acute ischemic stroke with carotid occlusions and concurrent intracranial involvement treated with endovascular therapy over a 4-year period was conducted. Of these reviewed cases, 75 patients had carotid occlusions with intracranial involvement. The carotid T occlusions and critical ICA stenosis with intracranial flow were excluded from the study. Based on the CT and catheter angiogram findings, the 75 patients fell into two groups: 1) Group A (n=35): Carotid occlusion with underlying atherosclerotic disease/dissection resulting in occlusion and were treated with angioplasty and stenting followed by thrombus retrieval. 2) Group B (n=40): No underlying pathology was found and ICA was occluded due to a large embolus to the ICA with no anterograde flow in the ICA. This group was treated with thrombus retrieval alone.

#### RESULTS

Our data shows that the presence of a stent in the ICA does not adversely affect the intracranial recanalization rate (91.4% TICI>=2b). There was also no significant increase in hemorrhage rate with revascularization and antiplatelet therapy (2.9%). This finding was especially significant due to the large amount of wake up strokes in our study that were treated with intervention (17.3%). The successful reperfusion rate (TICI >=2b) overall in both groups was 82.7%. In the successfully recanalized group, the mortality was 16% compared to the mortality in the unsuccessfully recanalized group (69.2%).

#### CONCLUSION

Our study results show that it is possible to achieve a high success rate of revascularization and clinical outcomes with an endovascular approach to managing carotid occlusion with intracranial involvement.

### **CLINICAL RELEVANCE/APPLICATION**

Acute carotid occlusions can be successfully recanalized with improvement in stroke severity.



## VI248-SD-WEA8

The Effects of miR-34a on the Function of Human Colon Cancer Cell SW480 and Growth of Subcutaneous Xenograft Tumor

Wednesday, Nov. 28 12:15PM - 12:45PM Room: VI Community, Learning Center Station #8



FDA Discussions may include off-label uses.

## Participants

Chuanzhuo Wang, BMedSc, MMed, Shenyang, China (*Presenter*) Nothing to Disclose Zhao Yu Liu, Shen Yang, China (*Abstract Co-Author*) Nothing to Disclose

## For information about this presentation, contact:

Captainwang1982@163.com

# PURPOSE

To investigate the function of miR-34a on cell proliferation, apoptosis and cell cycle in human colon cancer cell line SW480 and growth of subcutaneous xenograft tumor in nude mice

# METHOD AND MATERIALS

Experiments were divided into 2 groups: miR-34a group(miR-34a over-expression lentivirus were transfected into SW480 cells) and NC group(negative control group,empty vector were transfected into SW480 cells). Analyze the expression of miR-34a in 2 groups and the effects of miR-34a on cell proliferation, apoptosis and cell cycle in human colon cancer cell line SW480. Nude mice were subcutaneously injected by tumor cells to culture subcutaneous xenograft tumor. Tumor volumes were examined every 7 days and construct tumor growth curve. Mice were executed on the 28 days, and the eventual tumor weights were examined. Analyze the effects of miR-34a on xenograft tumors

## RESULTS

The relative expression of miR-34a in miR-34a group was higher than that of NC group(P<0.05). The cell proliferation efficiency of miR-34a group after 2d was lower than that of NC group(P<0.05); The apoptosis rate of miR-34a group was higher than that of NC group(P<0.05); The cell cycle in G2/M phase of miR-34a group was higher than that of NC group(P<0.05). The volumes after 14d and the eventual tumor weights of xenograft tumors in nude mice-miR-34a group were lower than that of mice-NC group(P<0.05)

## CONCLUSION

miR-34a can inhibit proliferation, induce apoptosis and arrest cell cycle of G2/M phase in colon cancer cell line SW480. And also inhibit the growth of subcutaneous xenograft tumor in nude mice

# **CLINICAL RELEVANCE/APPLICATION**

miR-34a is expected to become a molecular target for the treatment of colon cancer



## VI249-SD-WEA9

Risk Assessment of Chronic Kidney Disease Following Thermal Ablation: Comparative Assessment of Radiofrequency, Cryo-and Microwave Ablation for T1a Renal Masses

Wednesday, Nov. 28 12:15PM - 12:45PM Room: VI Community, Learning Center Station #9

# Participants

Wenhui Zhou, BS , Boston, MA (*Abstract Co-Author*) Nothing to Disclose Sanna Herwald, BA, Boston, MA (*Abstract Co-Author*) Nothing to Disclose Ronald S. Arellano, MD, Boston, MA (*Presenter*) Nothing to Disclose

#### For information about this presentation, contact:

wenhui.zhou@tufts.edu

# PURPOSE

To compare the renal function outcome and assess the relative risk of chronic kidney disease (CKD) following radiofrequency ablation (RFA), cryoablation (CA) and microwave ablation (MWA) fo the treatment of T1a renal masses.

### METHOD AND MATERIALS

A retropsective study of 320 patients (mean age 71 yrs, range 22-90 yrs) was performeb between October 2006 and December 2017. Patient baseine and follow-up renal function surrogates including serum creatinine (Cr) and estimate glomerular filtration rate (eGF) were statistically compared. Assessement of peri-and post-procedural complication rates were performed.

# RESULTS

365 T1a biopsy proven RCC measuring 1.2-4.0 cm were treated with computed tomography (CT)-guided MWA (n=40, 11%), RFA (n=291, 80%), or CA (n=34, 9%). At 1-year and last follow-up, there were on significant differences in eGFR change between the three cohorts (p=0,18, 0.09, respectively). The 2-yr freedome from GFR decline below 60 was 99% (RFA), 96% (CA), and 100% (MWA). Among the patients that had pre-exisiting CKD, before ablation, there was no significant post-ablative onset of decline or CKD upstaging among the three groups (p=0.08). Complication rate and treatment response were simlar between the three groups.

# CONCLUSION

CT-guided MWA for RCC has similar nephron preservation profile to RFA and CA.

# **CLINICAL RELEVANCE/APPLICATION**

CT-guided percutaneous MWA has minimal impact or predispostion to chronic kidney disease.



# AI001-WEC

# **Advanced Data Augmentation Using GANs**

Wednesday, Nov. 28 12:30PM - 2:00PM Room: AI Community, Learning Center

# Title and Abstract

Advanced Data Augmentation Using GANs Getting 'large enough' data sets is a problem for most deep learning applications, and this is particularly true in medical imaging. Generative Adversarial Networks (GANs) are a deep learning technology in which a computer is trained to create images that look very 'real' even though they are completely synthetic. This may be one way to address the 'data shortage' problem in medicine.



# AI149-ED-WEB1

Quality Assurance for Crowdsource Annotation of the Chest X-ray 14 Dataset for the RSNA-STR Machine Learning Challenge: How We Did It

Wednesday, Nov. 28 12:45PM - 1:15PM Room: AI Community, Learning Center Station #1

### Awards Certificate of Merit

### Participants

Carol C. Wu, MD, Bellaire, TX (*Presenter*) Author, Reed Elsevier Safwan Halabi, MD, Stanford, CA (*Abstract Co-Author*) Nothing to Disclose Luciano M. Prevedello, MD, MPH, Dublin, OH (*Abstract Co-Author*) Nothing to Disclose Marc D. Kohli, MD, San Francisco, CA (*Abstract Co-Author*) Nothing to Disclose Myrna C. Godoy, MD, PhD, Houston, TX (*Abstract Co-Author*) Research Grant, Siemens AG George L. Shih, MD, MS, New York, NY (*Abstract Co-Author*) Consultant, Image Safely, Inc; Stockholder, Image Safely, Inc; Consultant, MD.ai, Inc; Stockholder, MD.ai, Inc; Ritu R. Gill, MBBS, Boston, MA (*Abstract Co-Author*) Nothing to Disclose Anouk Stein, MD, Paradise Valley, AZ (*Abstract Co-Author*) Consultant, MD.ai, Inc; Stockholder, MD.ai, Inc

### For information about this presentation, contact:

ccwu1@mdanderson.org

# **TEACHING POINTS**

1. Review known inter-observer variabilities in the interpretation and annotation of chest radiographs and the implications for machine learning challenge 2. Describe the processes utilized to improve inter-observer consistency during crowdsource annotation 3. Provide lessons learned and methods to further refine quality assurance for crowdsouce annotation

# TABLE OF CONTENTS/OUTLINE

A. Known inter-observer variability in: 1. clinical interpretation of chest radiograph due to lack of gold standard and variability of perception of overlapping findings 2. crowdsource annotations required for large dataset 3. general versus subspecialty chest radiologists B. Implications of 'noisy' annotation for machine learning C. Methods used to improve inter-observer consistency in annotation: 1. written instructions for annotation tasks 2. practice annotation dataset to detect possible sources of variabilities 3. group conference to formulate concensus for various scenarios D. Adjudication process 1. real-time feedback from subspecialty chest radiologist for difficult cases marked as 'Question' 2. adjudication by subspecialty radiologist of cases with discrepant labels/bounding boxes E. Lessons learned and potential refinements



### BR205-ED-WEB8

## Interval Breast Cancers in the Era of Precision Medicine: A Multimodality Approach

Wednesday, Nov. 28 12:45PM - 1:15PM Room: BR Community, Learning Center Station #8

#### **Participants**

Sarah G. Mizuguchi, MD, Louisville, KY (*Abstract Co-Author*) Nothing to Disclose Lane M. Roland, MD, Louisville, KY (*Abstract Co-Author*) Nothing to Disclose Stacey M. Crawford, MD, Louisville, KY (*Abstract Co-Author*) Nothing to Disclose Elizabeth Riley, MD, Louisville, KY (*Abstract Co-Author*) Nothing to Disclose Mary Ann Sanders, MD, PhD, Louisville, KY (*Abstract Co-Author*) Nothing to Disclose Jason D. Messinger, MD, ST LOUIS, MO (*Presenter*) Nothing to Disclose

## **TEACHING POINTS**

1. Review the definition of interval breast cancers and how they present. 2. Display imaging findings of interval cancers. 3. Discuss how interval breast cancers typically have a worse prognosis. 4. Review receptor sensitivity, with histopathologic correlation, to correlate with prognosis. 5. Review the current trend of precision medicine with medical oncology perspective. 6. Highlight the role of the radiologist in precision medicine for breast cancer.

# TABLE OF CONTENTS/OUTLINE

Interval breast cancer subtypes - true negative, false negative, occult, minimal sign - prognosis of interval cancers vs screen detected - imaging findings Receptor sensitivity and tumor marker - review ER, PR, HER2 - Luminal A, Luminal B, HER2 enriched, and Normal like - Ki-67 - histopathologic correlation Review of precision medicine - history - how receptor sensitivity influences treatment - treatment strategies and outcomes from medical oncology persepctive Case examples to include imaging, histopathology, and treatment with multimodality approach Summary



## BR206-ED-WEB9

A Wolf in Sheep's Clothing: Cancer Masquerading as a Benign-appearing Breast Mass

Wednesday, Nov. 28 12:45PM - 1:15PM Room: BR Community, Learning Center Station #9

## Awards Certificate of Merit

## **Participants**

Lindsey Storer, MD, Los Angeles, CA (*Presenter*) Nothing to Disclose Cheryce P. Fischer, MD, Santa Monica, CA (*Abstract Co-Author*) Nothing to Disclose Stephanie A. Lee-Felker, MD, Los Angeles, CA (*Abstract Co-Author*) Nothing to Disclose Melissa M. Joines, MD, Santa Monica, CA (*Abstract Co-Author*) Nothing to Disclose

# **TEACHING POINTS**

Although most circumscribed breast masses are benign, up to 10-20% of breast malignancies can be relatively circumscribed. Invasive ductal carcinoma, not otherwise specified, is the most common form of breast cancer and most often presents as an irregular mass with spiculated margins; however, less common types can present as round or oval masses with predominately circumscribed margins. After reviewing this presentation, participants will: Expand their differential diagnosis of circumscribed breast masses to include less common types of breast cancer, including mucinous carcinoma, medullary carcinoma, papillary carcinoma, malignant phyllodes tumors, and high grade triple negative intraductal carcinoma, as well as lymphoma and metastases; describe the common and distinct imaging characteristics of these tumors; and integrate radiologic assessment with clinical scenario to provide appropriate BIRADS category and management recommendation.

### **TABLE OF CONTENTS/OUTLINE**

Mutimodality imaging review of the types of breast cancer that more often present as circumscribed masses on 2D and 3D mammography, ultrasound, and MRI with clues that may help favor a specific diagnosis among these entities Epidemiology of these breast cancer subtypes Clinical clues that may aid in diagnosis and review of prognosis Correlation with histologic features



## BR207-ED-WEB10

**Coming Out: Making Your Breast Imaging Center LGBT Friendly** 

Wednesday, Nov. 28 12:45PM - 1:15PM Room: BR Community, Learning Center Station #10

### Awards Certificate of Merit

#### **Participants**

Valerie J. Fein-Zachary, MD, Boston, MA (*Presenter*) Nothing to Disclose Jordana Phillips, MD, Boston, MA (*Abstract Co-Author*) Research Grant, General Electric Company; Consultant, General Electric Company Hannah Perry, MD, Boston, MA (*Abstract Co-Author*) Nothing to Disclose Nancy Littlehale, Boston, MA (*Abstract Co-Author*) Nothing to Disclose Tejas S. Mehta, MD, MPH, Boston, MA (*Abstract Co-Author*) Nothing to Disclose

Vandana M. Dialani, MD, Boston, MA (*Abstract Co-Author*) Nothing to Disclose Michael D. Fishman, MD, Boston, MA (*Abstract Co-Author*) Consultant, Zebra Medical Vision Ltd Evguenia J. Karimova, MD, Memphis, TN (*Abstract Co-Author*) Nothing to Disclose Priscilla J. Slanetz, MD, MPH, Belmont, MA (*Abstract Co-Author*) Nothing to Disclose

### For information about this presentation, contact:

vfeinzac@bidmc.harvard.edu

# **TEACHING POINTS**

1. Diversity and inclusion in healthcare includes respect for and understanding of lesbian, gay, bisexual and transgender (LGBT) people. 2. Improving access to care includes creating a welcoming environment. 3. Improving healthcare outcomes can be achieved as providers increase their knowledge about issues specific to LGBT people and support patients by empowering them. 4. Including lesbian, gay, bisexual and transgender women, and transgender men in breast cancer outcomes research is critical to fill in gaps in medical knowledge.

## **TABLE OF CONTENTS/OUTLINE**

1. Diversity and Inclusion: Understanding Healthcare Disparities in the LGBT population a. Historic discrimination by the medical community b. Factors contributing to health disparities c. Current disparity issues 2. Improving access to care a. Create a welcoming space, with verbal and visual clues of inclusion b. Provide staff education and training about LGBT issues c. Publicize your efforts 3. Improve health outcomes for your LGBT patients a. Understand the unique needs of lesbians, gay women and bisexual patients b. Know appropriate screening examinations and intervals for transgender patients c. Improve patient compliance with recommendations d. Expand knowledge of the LGBT community through increased inclusion in research



## BR208-ED-WEB11

# Anything but Binary: Exploring the Spectrum of Imaging Concerns in the Transgender Patient

Wednesday, Nov. 28 12:45PM - 1:15PM Room: BR Community, Learning Center Station #11

### **Participants**

Christopher McAdams, MD, Atlanta, GA (*Presenter*) Nothing to Disclose Jean M. Kunjummen, DO, Atlanta, GA (*Abstract Co-Author*) Nothing to Disclose Margaret Fleming, MD, Atlanta, GA (*Abstract Co-Author*) Nothing to Disclose

# **TEACHING POINTS**

1. Discuss appropriate terminology and the review the gender spectrum concept 2. Identify pre-imaging considerations for transgender patients with suggestions for application to your practice 3. Highlight unique pathologies and teaching points through case examples

# TABLE OF CONTENTS/OUTLINE

I. Introduction II. Patient-Centered Approach & Terminology (Gender Spectrum, etc.) III. Barrier to Care (Discrimination, Provider Training, Insurance Coverage, Clinic Environment) IV. Current Screening Recommendations V. Case Vignettes (e.g. - Abscess, Ectatic Ducts, Kaposi's Sarcoma, etc.) VI. Conclusions & Future Needs



## BR209-ED-WEB12

A Comprehensive Breast Cancer Risk Management Program Developed in a Radiology Department to Share with Referring Physicians

Wednesday, Nov. 28 12:45PM - 1:15PM Room: BR Community, Learning Center Station #12

# Participants

Richard G. Barr, MD, PhD, Campbell, OH (*Presenter*) Consultant, Siemens AG; Consultant, Koninklijke Philips NV; Research Grant, Siemens AG; Research Grant, SuperSonic Imagine; Speakers Bureau, Koninklijke Philips NV; Research Grant, Bracco Group; Speakers Bureau, Siemens AG; Consultant, Canon Medical Systems Corporation; Research Grant, Esaote SpA; Research Grant, BK Ultrasound; Research Grant, Hitachi, Ltd

# **TEACHING POINTS**

The purpose of this exhibit is: 1. To review the different risk methods and describe their pros and cons 2. To highlight the importance of the involvement of refering physicians for a better patient's empowerment

### TABLE OF CONTENTS/OUTLINE

- Different breast cancer risk scores Breast density and breast cancer risk management The unsuitability of lifetime risk - Breast cancer risk management program development - Evaluation of the referring physicians point of view

# **Honored Educators**

Presenters or authors on this event have been recognized as RSNA Honored Educators for participating in multiple qualifying educational activities. Honored Educators are invested in furthering the profession of radiology by delivering high-quality educational content in their field of study. Learn how you can become an honored educator by visiting the website at: https://www.rsna.org/Honored-Educator-Award/ Richard G. Barr, MD, PhD - 2017 Honored Educator



## BR261-SD-WEB1

# Utility of Targeted Ultrasound for the Evaluation of Palpable Breast Symptoms in Breastfeeding Women

Wednesday, Nov. 28 12:45PM - 1:15PM Room: BR Community, Learning Center Station #1

### Participants

Amie Y. Lee, MD, San Francisco, CA (*Presenter*) Nothing to Disclose Anna Knobel, MD, New York, NY (*Abstract Co-Author*) Nothing to Disclose Kimberly M. Ray, MD, San Francisco, CA (*Abstract Co-Author*) Nothing to Disclose Heather I. Greenwood, MD, San Francisco, CA (*Abstract Co-Author*) Nothing to Disclose Bonnie N. Joe, MD, PhD, San Francisco, CA (*Abstract Co-Author*) Nothing to Disclose Jessica H. Hayward, MD, San Francisco, CA (*Abstract Co-Author*) Nothing to Disclose

## PURPOSE

To determine the accuracy of targeted breast ultrasound as the primary imaging modality for the evaluation of palpable symptoms in breastfeeding women.

# METHOD AND MATERIALS

A retrospective database review identified all breastfeeding women with a palpable symptom evaluated by targeted breast ultrasound over a 15-year period (1/1/2000 - 1/1/2015) at an academic facility. No patients were pregnant at time of imaging. Each palpable site was designated as a case and all analyses were performed at the case level. BI-RADS assessments and lesion characteristics were obtained from review of the radiology reports. Malignant outcomes were determined by pathology results. Benign outcomes were determined by biopsy or >2 years clinical or imaging follow-up. Descriptive statistics and 2x2 contingency table analyses were performed.

### RESULTS

The final study cohort consisted of 139 palpable cases in 119 patients. Mean age was 36, and 24% were at least 40-years-old. Sixty-three (45%) underwent targeted ultrasound alone and 76 (55%) underwent mammography in addition to ultrasound. On ultrasound, 53 had no sonographic correlate (BI-RADS 1), 41 had benign findings (BI-RADS 2), and 3 were probably benign (BI-RADS 3). In the 42 positive ultrasound cases, 39 were suspicious (BI-RADS 4) and 2 were highly suggestive of malignancy (BI-RADS 5). The most common biopsy results were galactocele, lactating adenoma, and lactational change. Frequency of malignancy was 1.4% (n=2), and all malignancies were assessed as BI-RADS 5. Targeted ultrasound had high sensitivity (100%) and NPV (100%), but limited specificity (71%) and low PPV2 (5%). In cases with mammography, 95% had heterogeneously or extremely dense breasts. The addition of mammography yielded no additional cancers, and mammography missed one sonographically identified malignancy. Mammography detected 7 false positive lesions unrelated to the palpable symptom.

### CONCLUSION

Targeted ultrasound detected all malignancies in breastfeeding patients with palpable symptoms. The addition of mammography increased false positives and yielded no additional cancers. Our results suggest that targeted ultrasound alone may be sufficient for evaluation of symptomatic breastfeeding women.

# **CLINICAL RELEVANCE/APPLICATION**

Current literature on breast imaging for symptomatic lactating women is sparse, and practice patterns vary widely. Our results support the use of ultrasound as the primary imaging modality in this setting.



# BR262-SD-WEB2

Ductal Carcinoma in Situ Detected on Ultrasound Only Showed More Favorable Features Than Ductal Carcinoma in Situ Detected on Mammography in Asymptomatic Women with Dense Breasts

Wednesday, Nov. 28 12:45PM - 1:15PM Room: BR Community, Learning Center Station #2

# Participants

Hee Jung Moon, MD, Seoul, Korea, Republic Of (*Presenter*) Nothing to Disclose Eun-Kyung Kim, MD, Seoul, Korea, Republic Of (*Abstract Co-Author*) Nothing to Disclose Min Jung Kim, MD, Seoul, Korea, Republic Of (*Abstract Co-Author*) Nothing to Disclose Jung Hyun Yoon, MD, Seoul, Korea, Republic Of (*Abstract Co-Author*) Nothing to Disclose Vivian Y. Park, MD, Seoul, Korea, Republic Of (*Abstract Co-Author*) Nothing to Disclose

### For information about this presentation, contact:

artemis4u@yuhs.ac

### PURPOSE

To compared the clinical and pathological characteristics of ductal carcinoma in situ detected on mammography and ultrasound (US) in asymptomatic patients with dense breasts.

# METHOD AND MATERIALS

From February 2014 to September 2016, 236 asymptomatic patients with primary pure ductal carcinoma in situ and dense breasts were included. The patients were classified into two groups. The mammography group (n=165) included patients with ductal carcinoma in situ detected on mammography, and the US group (n=71) included patients with ductal carcinoma in situ detected on US only. Clinico-pathological characteristics were compared between the two groups. Subgroup analyses were performed with a cut-off age of 50 years and a cut-off tumor size of 20 mm.

### RESULTS

Tumor size was significantly smaller in the US group ( $11.8\pm9.9 \text{ mm vs. } 17.9\pm13.8 \text{ mm}$ , p<0.001). Younger age, smaller tumor size, low nuclear grade, no comedo necrosis, and progesterone receptor positivity were observed more in the US group (p<0.05). HER2 and Ki67 positivity were observed more in the mammography group (p<0.05). Similar results were found in 168 patients with ductal carcinoma in situ < 20 mm. Regardless of the patient age, smaller tumor size, low nuclear grade, and no comedo necrosis were observed significantly more in the US group.

# CONCLUSION

Ductal carcinoma in situ in the US group showed significantly more low nuclear grade, no comedo necrosis, and hormone receptro positivity, while HER2 and Ki67 positivity were observed significantly more in the mammography group. Ductal carcinoma in situ detected on US only showed more favorable prognostic features than ductal carcinoma in situ detedted on mammography in asymptimatic patients with dense breasts.

# **CLINICAL RELEVANCE/APPLICATION**

Ductal carcinoma in situ detected on US only in asymptomatic patients showed nore favorable prognostic factors than ductal carcinoma in situ detected on mammography.



# BR263-SD-WEB3

Is the Contrast Enhanced Mammography an Alternative to Magnetic Resonance Imaging for the Presurgical Evaluation of Tumor Response in Breast Cancer Patients Treated with Neoadjuvant Chemotherapy?

Wednesday, Nov. 28 12:45PM - 1:15PM Room: BR Community, Learning Center Station #3

# Participants

Angela Iglesias Lopez, MD, A Coruna, Spain (*Presenter*) Nothing to Disclose Joaquin J. Mosquera Oses, MD, La Coruna, Spain (*Abstract Co-Author*) Nothing to Disclose Jose Ramon Varela Romero, MD, La Coruna, Spain (*Abstract Co-Author*) Nothing to Disclose Alberto Bouzon Alejandro, A Coruna, Spain (*Abstract Co-Author*) Nothing to Disclose Andres Vega Chaves, MD,MD, A Coruna, Spain (*Abstract Co-Author*) Nothing to Disclose Diego Dominguez Conde, MD, A Coruna, Spain (*Abstract Co-Author*) Nothing to Disclose

### For information about this presentation, contact:

a-iglesias@hotmail.com

## PURPOSE

The neoadjuvant chemotherapy (NAC) is the standard therapeutic strategy for locally advanced breast cancer, allowing to increase the breast conservation rate and it is increasingly being used for patients with early stage breast cancer. The magnetic resonance imaging (MRI) is the most accurate diagnostic tool for assess the residual invasive disease after NAC. The Contrast Enhanced Mammography (CE2D) is a recent imaging method that allows to show if tumor neovascularization exists in the breast parenchyma. To evaluate the CE2D diagnostic accuracy to assess the residual disease extension of breast cancer patients receiving NAC.

#### **METHOD AND MATERIALS**

A prospective CE2D study was performed in 43 breast cancer patients treated with NAC from March to December 2017. All patients underwent a CE2D and breast MRI after NAC. The residual tumor size determined by both techniques was correlated with the pathological tumor size of the specimen.

### RESULTS

CE2D showed a superior interclass correlation coefficient than MRI (0.9 vs. 0.7). The CE2D sensibility and specificity (83,9% and 83,3% respectively) were high and comparable to the MRI ones (74,2% and 91,6% respectively). Besides, the negative predictive value of the CE2D was higher than the MRI one (66,7% vs. 57,9%) and the positive predictive value was similar (92,9% vs. 95,8%). All these results could lead us to reduce the overall costs of diagnostic tests during the follow-up of breast cancer patients in the neoadjuvant setting. CE2D could even replace pre- and post-treatment MRI studies, particularly for claustrophobic patients.

# CONCLUSION

CE2D can replace MRI for the presurgical assessment of residual tumor size as well as on additional breast lessions visualization in the ipsilateral breast or in the contralateral one, and therefore leading to costs savings and better accessibility.

# **CLINICAL RELEVANCE/APPLICATION**

The CE2D could be an effective alternative to MRI for the residual tumor evaluation after neoadjuvant chemotherapy in breast cancer patients. This technique could significantly save costs and improve patient flows. Furthermore, CE2D has almost no contraindications.



## BR264-SD-WEB4

Microcalcifications of Ductal Carcinoma in Situ of the Breast: Correlation between Breast Imaging and Pathological and Biological Features

Wednesday, Nov. 28 12:45PM - 1:15PM Room: BR Community, Learning Center Station #4

# Participants

Eunji Lee, MD, Seoul, Korea, Republic Of (*Presenter*) Nothing to Disclose Yun Woo Chang, MD, PhD, Seoul, Korea, Republic Of (*Abstract Co-Author*) Nothing to Disclose Jinah Kim, Seoul, Korea, Republic Of (*Abstract Co-Author*) Nothing to Disclose Hwa jin Cha, MD, Seoul, Korea, Republic Of (*Abstract Co-Author*) Nothing to Disclose Jiyoung Hwang, Seoul, Korea, Republic Of (*Abstract Co-Author*) Nothing to Disclose Seong Sook Hong, MD, Seoul, Korea, Republic Of (*Abstract Co-Author*) Nothing to Disclose

### For information about this presentation, contact:

ywchang@schmc.ac.kr

## PURPOSE

To evaluate the correlation between microcalcifications of ductal carcinoma in situ (DCIS) visible in breast imaging and pathological and biological features.

### **METHOD AND MATERIALS**

From December 2003 to December 2016, we retrospectively reviewed the mammography findings of 159 lesions of 155 patients who were diagnosed with pure DCIS, and comparable sonographic images of 150 lesions of 146 patients, according to the Breast Imaging Reporting and Data System (BI-RADS) lexicon. Sonographic findings of microcalcifications were divided into three groups compared with mammographic microcalcifications: G1 (MMG -, US -), G2 (MMG +, US -) and G3 (MMG +, US +). Pathological findings (nuclear grades, comedo necrosis) and biological features (ER positive group, HER2 positive group, triple negative group, Ki-67 index) were compared with mammography and sonographic features. P values less than 0.05 were considered statistically significant.

## RESULTS

Mammographic microcalcifications were observed in 90 out of 159 lesions (56.6%) of DCIS. Presence of microcalcifications on mammography was significantly more common in high nuclear grade (p=0.001) and comedo necrosis (p=0.001). Fine pleomorphic, fine linear or linear branching microcalcifications is the only morphologic feature that is significantly associated with nuclear grade (p=0.004). Presence of microcalcifications on mammography were significantly associated with ER-negative group (p=0.010), HER2-positive group (p=0.025), and increased Ki 67 index (p=0.001) respectively. Lesions with no visible microcalcifications in ultrasound (G1+G2) were 93 out of 150 lesions (62%) and 57 out of 150 lesions (38.0%) showed microcalcifications in ultrasound (G3). Calcification outside of a mass was the most common feature of sonographic microcalcification (36/150, 25.4%). Presence of microcalcifications in the ultrasound were associated with high nuclear grade (p=0.001), comedo necrosis (p=0.001), ER-negative group (p=0.028), HER2-positive group (p=0.028) and high Ki-67 index (p=0.001).

### CONCLUSION

Microcalcifications of DCIS visible on mammography and ultrasound showed statistically significant association with poor pathological and biological features.

## **CLINICAL RELEVANCE/APPLICATION**

When DCIS, precursor of invasive breast cancer, developing to invasive cancer, ER and HER2 status and breast cancer subtype are usually maintained and emphasize the evolution of breast cancer subtype specificity.



## BR265-SD-WEB5

Potential of Deep Learning and Conventional Radiomics in the Task of Distinguishing Between Malignant and Benign Breast Lesions in a Large Clinical MRI Dataset from China

Wednesday, Nov. 28 12:45PM - 1:15PM Room: BR Community, Learning Center Station #5

# Participants

Hui Li, PHD, Chicago, IL (Presenter) Nothing to Disclose

Yu Ji, MD, Chicago, IL (Abstract Co-Author) Nothing to Disclose

Natalia O. Antropova, Chicago, IL (Abstract Co-Author) Nothing to Disclose

John Papaioannou, MSc, Chicago, IL (Abstract Co-Author) Research Consultant, QView Medical, Inc

Alexandra V. Edwards, Chicago, IL (Abstract Co-Author) Research Consultant, QView Medical, Inc; Research Consultant,

Quantitative Insights, Inc

Peifang Liu, MD, PhD, Tianjin, China (Abstract Co-Author) Nothing to Disclose

Maryellen L. Giger, PhD, Chicago, IL (*Abstract Co-Author*) Stockholder, Hologic, Inc; Shareholder, Quantitative Insights, Inc; Shareholder, QView Medical, Inc; Co-founder, Quantitative Insights, Inc; Royalties, Hologic, Inc; Royalties, General Electric Company; Royalties, MEDIAN Technologies; Royalties, Riverain Technologies, LLC; Royalties, Mitsubishi Corporation; Royalties, Canon Medical Systems Corporation

## For information about this presentation, contact:

huili@uchicago.edu

#### PURPOSE

To evaluate the potential of combining deep learning and lesion-based radiomic methods in the task of distinguishing between malignant and benign breast lesions in a large MRI dataset from China.

## **METHOD AND MATERIALS**

Our research involved a HIPAA-compliant, DCE-MRI database of 600 breast cases [average patient ages of the 300 benign and 300 malignant patients were 41.8 and 47.2 years with a standard deviation of 9.5 and 9.6 years, respectively]. MRIs had been obtained using gadodiamide-enhanced T1-weighted spoiled gradient-recalled acquisition in the steady state sequence. A breast radiologist located the lesions on the MRIs as input to our artificial intelligence workflow, which subsequently conducted two analyses. In the first analysis, each lesion was automatically segmented from the surrounding parenchyma, and lesion phenotypes were extracted serving as "lesion-segmented radiomics", including categories of size, shape, morphology, enhancement texture, kinetics, and enhancement-variance kinetics. In the second analysis, transfer learning with a pre-trained deep convolutional neural network (CNN), VGGNet, allowed for the extraction of features derived directly from the MRI data, yielding CNN-based radiomics. Each method was investigated separately and in combination in the task of distinguishing between malignant and benign lesions, with area under the ROC curve (AUC) serving as the figure of merit.

# RESULTS

Both methods yielded promising classification performances with AUC values of 0.88 (se=0.01) and 0.84 (se=0.02) for the lesion-segmented radiomics and the CNN-based radiomics methods, respectively. Combination of the two methods enhanced the performance in malignancy assessment resulting in an AUC value of 0.90 (se=0.01), a statistically significant improvement over the performance of the lesion-segmented radiomics method alone (p=0.0017).

## CONCLUSION

Deep learning and lesion-segmented radiomics methods provide different information to the diagnostic classification task as demonstrated by both yielding high but different performance levels, thus promoting the use as a combined predictor of malignancy.

# **CLINICAL RELEVANCE/APPLICATION**

Our computerized combination of deep learning and segmentation-based radiomics CADx methods has potential to help radiologist improve breast cancer diagnostic accuracy.



## BR266-SD-WEB6

## Performance of Screening Breast MRI According to Different Risk Categories

Wednesday, Nov. 28 12:45PM - 1:15PM Room: BR Community, Learning Center Station #6

## **Participants**

Min Sun Bae, MD, New York, NY (*Presenter*) Nothing to Disclose Janice S. Sung, MD, New York, NY (*Abstract Co-Author*) Research Grant, Hologic, Inc Christopher E. Comstock, MD, New York, NY (*Abstract Co-Author*) Nothing to Disclose Elizabeth A. Morris, MD, New York, NY (*Abstract Co-Author*) Nothing to Disclose

#### For information about this presentation, contact:

minsunb@gmail.com

## PURPOSE

To evaluate screening breast MRI performance according to different risk categories in women at elevated risk of breast cancer

#### **METHOD AND MATERIALS**

This retrospective IRB-approved, HIPPA-compliant study included all screening breast MRI examinations performed between 2010 and 2012 in 5039 women (9208 examinations). Risk category were categorized as follows: (1) known BRCA1 or 2 mutation or untested first degree relative of known BRCA carrier (BRCA), (2) history of chest radiation (CR), (3) high (>=20%) lifetime risk (HLR), (4) personal history of breast cancer (PH), and (5) low (<20%) lifetime risk (LLR). Recall rate (BI-RADS assessment 0, 3, 4, or 5), cancer detection rate (CDR), positive predictive value of biopsies performed (PPV3), sensitivity, and specificity were compared for the risk categories.

## RESULTS

Of the 9208 MRI examinations, there were 5310 (57.7%) in PH, 2442 (26.5%) in HLR, 973 (10.5%) in BRCA, 257 (2.8%) in LLR, and 226 (2.5%) in CR. 138 cancers were diagnosed, 114 at MRI, 19 at mammography, and 5 interval cancers. Recall rate ranged from 8.6% to 15.6% and the highest recall rate was found in the BRCA group (15.6%; 95% CI: 13.4%, 18.1%). The CDR was highest in the BRCA group (19.5/1000), followed by CR (17.7/1000), HLR (14.3/1000), PH (10.2/1000), and LLR (7.8/1000). The PPV3 was highest in the CR group (36.4%; 95% CI: 10.9%, 69.2%) and lowest in the LLR group (16.7%; 95% CI: 2.1%, 48.4%). Overall sensitivity was 84.1% (95% CI: 76.9%, 89.7%) for all cancers and 84.8% (95% CI: 76.2%, 91.3%) for invasive cancers. Sensitivity was lowest in the BRCA group (79.2%; 95% CI: 57.8%, 92.9%) and higher in the PH group (88.7%; 95% CI: 78.1%, 95.3%) and the LLR group (100%). Specificity was highest in the PH group (92.5%; 95% CI: 91.7%, 93.2%) and lowest in the BRCA group (86.1%; 95% CI: 83.7%, 88.2%).

## CONCLUSION

MRI performance differed among women with various risk categories for breast cancer. Recall rate and CDR were highest and sensitivity lowest in the BRCA group. Performance of screening breast MRI in women with PH was similar to that in other high-risk women.

#### **CLINICAL RELEVANCE/APPLICATION**

Screening MRI may be possibly expanded to women at intermediate risk of breast cancer such as a personal history of breast cancer or high-risk lesion.



## BR267-SD-WEB7

Multi-reader Multi-case Virtual Clinical Trial of Lesion Detection in Digital Mammography and Digital Breast Tomosynthesis

Wednesday, Nov. 28 12:45PM - 1:15PM Room: BR Community, Learning Center Station #7

# Participants

Andrew D. Maidment, PhD, Philadelphia, PA (*Presenter*) Research support, Hologic, Inc; Research support, Barco nv; Research support, Analogic Corporation; Spouse, Employee, Real-Time Tomography, LLC; Spouse, Stockholder, Real-Time Tomography, LLC; Scientific Advisory Board, Real-Time Tomography, LLC; Predrag R. Bakic, PhD, Philadelphia, PA (*Abstract Co-Author*) Research collaboration, Barco nv; Research collaboration, Hologic, Inc;

Bruno Barufaldi, PhD, Philadelphia, PA (*Abstract Co-Author*) Nothing to Disclose Ali N. Avanaki, PhD, Beaverton, OR (*Abstract Co-Author*) Employee, Barco nv Kathryn S. Espig, MSc, Beaverton, OR (*Abstract Co-Author*) Employee, Barco nv Albert Xthona, BS, Beaverton, OR (*Abstract Co-Author*) Employee, Barco nv Susan Weinstein, MD, Philadelphia, PA (*Abstract Co-Author*) Nothing to Disclose Tom Kimpe, Kortrijk, Belgium (*Abstract Co-Author*) Employee, Barco nv

# For information about this presentation, contact:

predrag.bakic@uphs.upenn.edu

#### PURPOSE

To compare detectability of lesions between digital mammography (DM) and digital breast tomosynthesis (DBT) in virtual clinical trials (VCTs) using multi-reader multi-case (MRMC) analysis.

## METHOD AND MATERIALS

VCTs were conducted using an open-source VCT pipeline (OpenVCT) with observer modeling software (MeVIC), to assess the detection of masses and microcalcifications in DM and DBT. Twelve breast phantoms were used (simulating 700ml breasts with compressed thickness of 6.33cm) with variations in simulated anatomy. Breast masses were simulated by oblate ellipsoids with various diameter and thickness. Single calcifications were simulated as polycubes with various numbers of 100 µm cubes. A total of 1920 lesions were simulated. A clinical imaging geometry (Selenia Dimensions, Hologic) was simulated; exposure settings were selected to match AEC performance. Mammographic phantom projections were processed and tomosynthesis images reconstructed using commercially available software (Briona, Real-Time Tomography). Lesion detection was modeled by channelized Hotelling observers with 15 Laguerre-Gauss channels and a spread of 22, using independent training and testing sets (each set consisting of 160 ROIs). The detectability of simulated lesions was assessed by the area under the ROC (AUC) using a one-shot MRMC approach, assuming five independently trained observers. Two-sided Students' t-tests were used to test the statistical significance between estimated AUCs.

## RESULTS

For detection of simulated calcifications, we observed AUC of  $0.802\pm0.023$  and  $0.799\pm0.026$ , for DM and DBT, respectively; these AUCs do not differ significantly (p=0.856; 95% CI -0.040, 0.034). For the detection of masses, we observed AUC of  $0.794\pm0.022$  and  $0.900\pm0.017$ , for DM and DBT, respectively, which is statistically significant (p<0.001; 95% CI 0.089, 0.124). Our observations show close agreement with clinical results by Rafferty et al., who obtained AUC difference of 0.025 and 0.096, for calcifications and masses respectively.

## CONCLUSION

VCTs have demonstrated significant improvement in the detection of masses between DM and DBT, while AUCs for simulated microcalcifications did not differ, in close agreement with published clinical results.

# **CLINICAL RELEVANCE/APPLICATION**

We have demonstrated that virtual clinical trials can predict the clinical performance improvements seen with DBT over DM in the detection of breast masses and microcalcifications.



## CA245-SD-WEB1

CT-Derived 3D Strain for Cardiac Resynchronization Therapy in Patients with Congenital Corrected Transposition of the Great Arteries

Wednesday, Nov. 28 12:45PM - 1:15PM Room: CA Community, Learning Center Station #1

# Participants

Michinobu Nagao, MD, Tokyo, Japan (*Presenter*) Nothing to Disclose Kenji Fukushima, Tokyo, Japan (*Abstract Co-Author*) Nothing to Disclose Yuka Matsuo, MD, Shinjuku, Japan (*Abstract Co-Author*) Nothing to Disclose Hiroki Mori, MD, Tokyo, Japan (*Abstract Co-Author*) Nothing to Disclose Yumi Shiina, Tokyo, Japan (*Abstract Co-Author*) Nothing to Disclose Kei Inai, Tokyo, Japan (*Abstract Co-Author*) Nothing to Disclose Yamato Shimomiya, Tokyo, Japan (*Abstract Co-Author*) Nothing to Disclose Kenji Endo, Shinjuku, Japan (*Abstract Co-Author*) Nothing to Disclose Shuji Sakai, MD, Shinjuku-Ku, Japan (*Abstract Co-Author*) Nothing to Disclose

#### For information about this presentation, contact:

nagao.michinobu@twmu.ac.jp

#### PURPOSE

Systemic right ventricle (RV) dysfunction is one of prognostic factors in congenital corrected transposition of the great arteries (ccTGA) and TGA after atrial switch procedure. Contraction of systemic RV is easily deteriorated because the RV has no effective torsion and compensates this weakness keeping cardiac output. If RV dyssynchrony develops, early timing of cardiac resynchronization therapy (CRT) should be considered. We aim to analyze ventricular dyssynchrony and deformation using CT-derived 3D strain algorithm in patients with ccTGA, TGA, and Fontan circulation pre- and post-CRT.

## **METHOD AND MATERIALS**

Multiphase cardiac CT data set with 320-detector scanner for 13 patients (ccTGA, 7; TGA, 3; Fontan circulation, 3) who underwent implant of device for CRT or were scheduled due to refractory heart failure was retrospectively analyzed. Volume of interest (VOI) was drawn on multi-planar reconstruction of the ventricle with strain overlay using 3D-strain algorithm. Time-curves of 3D-strain for 12 VOIs in free walls of systemic and pulmonary ventricles were calculated throughout a cardiac cycle. The maximum value of 3D-strain was defined as a representative value. Dyssynchrony index was defined as the standard deviation of the phase to peak strain for 6 VOIs in systemic ventricles. Comparisons of the parameters was analyzed using Mann-Whitney u-test and paired t-test.

## RESULTS

3D-strain could be obtained from the all sites with implantable device. Dyssynchrony index was significantly lower post-CRT than pre-CRT ( $0.44\pm0.16$  vs.  $0.19\pm0.07$  phase, p<0.05). There was no significant difference in 3D-strain between pre- and post-CRT ( $0.35\pm0.13$  vs.  $0.42\pm0.22$ ). In patients with corrected TGA, 3D-strain was significantly lower for systemic RV than for pulmonary LV ( $0.43\pm0.08$  vs.  $0.62\pm0.19$ , p<0.05). In patients with complete TGA and Fontan circulation, there was no difference in 3D-strain between systemic and pulmonary ventricles ( $0.33\pm0.04$  vs.  $0.26\pm0.16$ ).

# CONCLUSION

CT-derived 3D strain demonstrates that dyssynchrony of systemic ventricle improves post-CRT. In corrected TGA, systolic ventricular deformation impairs dominantly in systemic RV.

# **CLINICAL RELEVANCE/APPLICATION**

CT-derived 3D-strain can assess CRT response and determine treatment strategy in adult congenital heart disease patients even if MRI cannot be performed due to implantable cardiac devices.



## CA246-SD-WEB2

The Effect of Motion Correction Algorithm at Low Energy Level of Virtual Monochromatic Images in Coronary CT Angiography with Fast kVp Switching Dual-Energy CT

Wednesday, Nov. 28 12:45PM - 1:15PM Room: CA Community, Learning Center Station #2

## Participants

Satoshi Inada, Hiroshima, Japan (*Presenter*) Nothing to Disclose Masashi Takahashi, RT, Hiroshima, Japan (*Abstract Co-Author*) Nothing to Disclose Tsuyoshi Kagimoto, Hiroshima, Japan (*Abstract Co-Author*) Nothing to Disclose Tomohiro Murakami, Hiroshima, Japan (*Abstract Co-Author*) Nothing to Disclose Naohiro Yamagami, Hiroshima, Japan (*Abstract Co-Author*) Nothing to Disclose Masahiro Nakano, Hiroshima, Japan (*Abstract Co-Author*) Nothing to Disclose Takafumi Sakai, Hiroshima, Japan (*Abstract Co-Author*) Nothing to Disclose Fang Wang, Yinchuan, China (*Abstract Co-Author*) Nothing to Disclose

#### PURPOSE

The purpose of this study was to investigate the effect of the motion correction algorithm (SnapShot Freeze: SSF; GE Healthcare) at the low energy level of virtual monochromatic images (VMI, 50 keV) in coronary CT angiography with fast kVp switching dualenergy CT (DE-CCTA).

#### **METHOD AND MATERIALS**

Twenty-five patients with heart rate below 65 bpm (42 - 65 bpm) underwent DE-CCTA using ECG-gated axial step-and-shoot scanning mode on a 64-row single-source dual-energy CT (Revolution GSI; GE Healthcare). The scan parameters for CCTA scan were used as follows: tube voltage 80/140 kVp fast switching, rotation time 0.35 s/rot, and tube current was determined to be 375 mA or 600 mA or 640 mA based on patient's BMI. VMIs at 70 keV (with and without SSF), 50 keV (with SSF), and 50 keV (with ASiR 50% and SSF) were reconstructed at the cardiac phases of 60%, 75%, and 90%, respectively. Two radiographers assessed the image quality of the 4 major coronary arteries (right coronary artery: RCA, left main trunk: LMT, left anterior descending artery: LAD, and left circumflex: LCX) by using 5-point scores (5, no motion artifacts; 4, minor artifacts; 3, moderate artifacts; 2, severe artifacts; 1, image not evaluated and vessel structures not differentiable). Average scores on the per-vessel in each cardiac phase were compared among VMIs at 70keV (with and without SSF), 50 keV (with SSF), and 50 keV (with ASiR50% and SSF).

#### RESULTS

In all cardiac phases, average scores with SSF were higher than those without SSF in all vessels: {70 keV (without SSF):  $2.9 \pm 0.8$  at 60%,  $3.8 \pm 0.5$  at 75%,  $2.0 \pm 2.1$  at 90%; 70 keV (with SSF):  $3.3 \pm 0.8$  at 60%,  $4.3 \pm 0.4$  at 75%,  $2.2 \pm 0.6$  at 90%; 50 keV (with SSF):  $3.5 \pm 0.7$  at 60%,  $4.0 \pm 0.3$  at 75%,  $2.5 \pm 0.6$  at 90%; 50 keV with (ASiR 50% and SSF),  $3.6 \pm 0.8$  at 60%,  $4.4 \pm 0.4$  at 75%,  $2.4 \pm 0.6$  at 90%). In addition, average scores of VMI at 50 keV (with ASiR 50% and SSF) were higher as compared with other VMIs.

## CONCLUSION

With the application of motion correction algorithm SSF, motion artifact and image quality of DE-CCTA were greatly improved. Moreover, the use of low keV (50keV) VMI combined with SSF was more effective to control the motion artifact.

# **CLINICAL RELEVANCE/APPLICATION**

Motion correction algorithm (SSF) in coronary CT angiography with fast kVp switching single source dual-energy CT was useful to reduce the motion artifacts and the use of low keV (50keV) VMI was more effective for controlling the motion artifact.



## CA247-SD-WEB3

# Venous Air Embolism in CT Coronary Angiography

Wednesday, Nov. 28 12:45PM - 1:15PM Room: CA Community, Learning Center Station #3

## **Participants**

Alexander W. Davies, BMedSc, MBBS, Melbourne, Australia (*Abstract Co-Author*) Nothing to Disclose Kenneth K. Lau, MBBS, FRANZCR, Melbourne, Australia (*Presenter*) Nothing to Disclose Marcus Crossett, Melbourne, Australia (*Abstract Co-Author*) Nothing to Disclose

#### For information about this presentation, contact:

Alexander.davies@monashhealth.org

## PURPOSE

Venous air embolization (VAE) from incompletely primed peripheral lines is a known risk of any intravenous procedure. Depending on the quantity of air inadvertently introduced, it may potentially result in catastrophic sequelae, including air lock in right ventricular outflow tract or systemic air embolism (SAE) in patients with cardiac septal wall defects that may lead to cerebrovascular event. The risk of VAE in contrast CT coronary angiography (CTCA) that requires intravenous dual contrast and saline injections may be higher than conventional single bolus contrast CT chest imaging (CTC). This was a retrospective study of the prevalence of VAE in CTCA compared to CTC.

#### **METHOD AND MATERIALS**

All consecutive adult CTCAs and CTCs over a 3-month period were included. CTs that had no saline push or contrast were excluded. The CTCAs and CTCs were blindly, randomly and independently read by 2 cardiac CT radiologists. All patients aged over 18 were included in the study. Location and amount of VAE and SAE were assessed. Shunts, including patent foramen ovale (PFO), atrial septal defects (ASD), ventricular septal defects (VSD) and patent ductus arteriosus (PDA) were recorded. Results were compared.

#### RESULTS

There were 418 CTCAs (62% male; mean age: 62 years) and 100 CTC (65% male, mean age: 64 years). PFO, ASD, VSD and PDA were seen in 14.8%, 12.5%, 7.6% and 0.5% of CTCA's respectively. No shunts were indentified in CTC. VAE was seen in 22.5% of all CTCAs (with similar result in patients with shunts). Mean air volume was 1.5 mls. This was significantly higher than CTC which had 1% VAE. No SAE was identified.

## CONCLUSION

The significantly increased incidence of VAE in CTCA compared to CTC is likely related to the use of dual chambered injector with doubling of peripheral lines that may be incompletely primed prior to intravenous injections. It is compounded by the frequent necessity of giving on-table intravenous beta-blocker for heart rate control in CTCA. Cardiac CT departments would need to take extreme care to exclude air in peripheral lines prior to injection as 23.7% of these patients have shunts between right and left heart posing a risk of SAE which may potentially lead to serious sequelae, including CVA.

#### **CLINICAL RELEVANCE/APPLICATION**

Secondary to the dual-bolus injection techniques of conventional cardiac CT, there is a likely appreciable increased risk of VAE, which this study aims to quantify.



## CA248-SD-WEB4

Analysis of the Anatomical Features of Pulmonary Veins on Pre-Procedural Cardiac CT Images Resulting in Incomplete Cryoballoon Ablation for Atrial Fibrillation

Wednesday, Nov. 28 12:45PM - 1:15PM Room: CA Community, Learning Center Station #4

# Participants

Yoriaki Matsumoto, Hiroshima, Japan (*Presenter*) Nothing to Disclose Yoshinori Funama, PhD, Kumamoto, Japan (*Abstract Co-Author*) Nothing to Disclose Takanori Masuda, Hiroshima, Japan (*Abstract Co-Author*) Nothing to Disclose Toru Ishibashi, RT, Hiroshima, Japan (*Abstract Co-Author*) Nothing to Disclose Yukari Yamashita, Hiroshima, Japan (*Abstract Co-Author*) Nothing to Disclose Kazuo Awai, MD, Hiroshima, Japan (*Abstract Co-Author*) Nothing to Disclose Kazuo Awai, MD, Hiroshima, Japan (*Abstract Co-Author*) Research Grant, Canon Medical Systems Corporation; Research Grant, Hitachi, Ltd; Research Grant, Fujitsu Limited; Research Grant, Bayer AG; Research Grant, DAIICHI SANKYO Group; Research Grant, Eisai Co, Ltd; Medical Advisory Board, General Electric Company; ;

#### For information about this presentation, contact:

yori\_8592\_8592@yahoo.co.jp

#### PURPOSE

Cryoballoon (CB) ablation is non-inferior to radiofrequency (RF) ablation for treating paroxysmal atrial fibrillation (pAF). However, some cases require additional touch-up ablation for gaps on the pulmonary vein (PV) isolation line after CB ablation. To investigate the anatomical features related to the success or failure of CB ablation for pAF on pre-procedural cardiac computed tomography (CT) images.

### **METHOD AND MATERIALS**

We retrospectively analyzed pre-procedural cardiac CT images of 100 patients with pAF who had undergone a first CB ablation at our institution between June 2016 and April 2017. Blinded to the outcomes, we measured the angle, short- and long axis length, and the area and ovality of 4 major PV ostials on CT images. Logistic regression analysis was performed to analyze the anatomical features related to the failure (incomplete CB ablation) of PV isolation.

#### RESULTS

We analyzed 400 PVs in 100 patients [aged 64 (27 - 82) years, 59% male]. The rate of incomplete CB ablation was significantly higher for right- than left-sided PVs (p < 0.001). The anatomical feature significantly associated with incomplete CB ablation was the PV angle (adjusted odds ratio = 0.97; 95% confidence interval = 0.96 - 0.98, p < 0.001).

# CONCLUSION

Our findings may help to select the appropriate ablation strategy (CB ablation or conventional RF ablation) to treat patients with pAF. We show that the angle is an anatomical feature significantly related to failed CB ablation.

# **CLINICAL RELEVANCE/APPLICATION**

Anatomical information obtained on pre-procedural cardiac CT scans is useful for selecting CB ablation strategies and for predicting the treatment outcome.



## CA249-SD-WEB5

Automated Cardiac MR Plane Classification Using VGG-19 Convolutional Neural Network: A Deep Learning Study

Wednesday, Nov. 28 12:45PM - 1:15PM Room: CA Community, Learning Center Station #5

# Participants

Naeim Bahrami, PhD, MSc, San Diego, CA (*Presenter*) Nothing to Disclose Kevin Blansit, MS,BS, La Jolla, CA (*Abstract Co-Author*) Nothing to Disclose Tara A. Retson, MD, PhD, San Diego, CA (*Abstract Co-Author*) Nothing to Disclose Kang Wang, MD,PhD, San Diego, CA (*Abstract Co-Author*) Nothing to Disclose Albert Hsiao, MD,PhD, La Jolla, CA (*Abstract Co-Author*) Founder, Arterys, Inc; Consultant, Arterys, Inc; Consultant, Bayer AG; Research Grant, General Electric Company;

## For information about this presentation, contact:

naeim.bahrami@gmail.com

## PURPOSE

Cardiac MRI (cMRI) requires acquisition of multiple oblique imaging planes. Automated recognition of imaging planes may be a necessary component for automating cardiac MRI scan prescription or automating hanging protocols. We therefore developed a convolutional neural network (CNN) to classify cMRI planes. Moreover, we sought to investigate what spatial information the CNN uses to recognize each imaging plane.

## **METHOD AND MATERIALS**

With HIPAA-compliance and IRB waiver of informed consent, we retrospectively collected SSFP images from clinically-performed cMRIs performed at our institution from 2012 to 2017, including 195 short axis (SAX) and 945 long axis (LAX). We trained a pair of VGG-19 deep neural networks to perform classification of images into five classes: SAX, 2-chamber (2-ch), 3-chamber (3-ch), 4-chamber (4-ch), and other. The first VGG-19 network was trained to differentiate short-axis from LAX with a binary crossantropy loss. The second VGG-19 network was trained to differentiate between each of the different long-axis views using a categorical crossantropy loss function. Images from 80% of the patients were used for training, and images from 20% of the patients were used for validation. We apply saliency maps, occlusion tests and Deep Dream to assess in inner layers of the neural network.

## RESULTS

The first network distinguished SAX from LAX with accuracy of 96.1%. The second network was able to classify each of the long axis views with accuracy of 88.8%. Inspection of the saliency maps showed greater attention of the CNN to several cardiac structures when discriminating each of these views, including the endocardial cushion and basal lateral wall for the 4ch and the left ventricular outflow tract for the 3ch.

#### CONCLUSION

We demonstrate the feasibility of convolutional neural networks to accurately classify cardiac imaging planes with high fidelity for use in multiple potential clinical applications. Furthermore, study of the saliency maps of the neural network appear to emphasize characteristic features that discriminate between each of the imaging planes.

#### **CLINICAL RELEVANCE/APPLICATION**

Convolutional neural networks can accurately classify cardiac imaging planes, and may perform this task utilizing different features than human readers. Further exploration of these CNNs may yield new observations about image data.



# CA250-SD-WEB6

Employing Artificial Intelligence to Predict Hematocrit Values from Non-Contrast CT Imaging Data-Towards Fully Automated CT-derived Myocardial Extracellular Volume Fraction Quantification

Wednesday, Nov. 28 12:45PM - 1:15PM Room: CA Community, Learning Center Station #6

# Participants

Maximilian J. Bauer, Charleston, SC (*Presenter*) Nothing to Disclose
Marly van Assen, MSc, Charleston, SC (*Abstract Co-Author*) Nothing to Disclose
Carlo N. De Cecco, MD, PhD, Atlanta, GA (*Abstract Co-Author*) Research Grant, Siemens AG
Marco Scarabello, MD, Milan, Italy (*Abstract Co-Author*) Nothing to Disclose
Parkwood Griffith, Charleston, SC (*Abstract Co-Author*) Nothing to Disclose
U. Joseph Schoepf, MD, Charleston, SC (*Abstract Co-Author*) Research Grant, Astellas Group; Research Grant, Bayer AG; Research Grant, Siemens AG; Research support, Bayer AG; Consultant, Guerbet SA; Consultant, General Electric Company; Consultant, HeartFlow, Inc; Consultant, Bayer AG; Consultant, Siemens AG; ; ;
Akos Varga-Szemes, MD, PhD, Charleston, SC (*Abstract Co-Author*) Nothing to Disclose
Taylor M. Duguay, Charleston, SC (*Abstract Co-Author*) Nothing to Disclose

## For information about this presentation, contact:

schoepf@musc.edu

#### PURPOSE

Imaging approaches for the quantification of the myocardial extracellular volume fraction require the patient's hematocrit as an input variable. We assessed the performance of a machine learning approach to predict hematocrit values from non-contrast CT imaging data, demographic, and clinical information, in comparison to a linear regression model employing HU values alone.

#### **METHOD AND MATERIALS**

A total of 260 patients were retrospectively included who had undergone non-contrast cardiac CT and whose records provided hematocrit values determined from blood sampling within 2 days of the scan. We measured HU values in the ascending aorta and employed a linear regression analysis to model the relationship between the image-derived data and laboratory hematocrit values. Additional information on patient demographics, clinical history, and imaging parameters was gathered for the machine learning approach. A total of 45 features were extracted and used to train a linear Support Vector Machine (SVM) employing k-fold cross validation.

## RESULTS

The model provided by the linear regression approach was Hct [%] =  $0.90 \times HU_blood + 0.19$ . This approach demonstrated a weak relationship between the model and the laboratory hematocrit values (R^2=0.49; p<.001). The machine learning model showed a moderate relationship to the hematocrit values obtained from blood sampling (R^2=0.62; p<.001). Friedman's test indicated that the medians of the laboratory hematocrit values ( $40.1\pm4.7$ ) and the predicted hematocrit values from both models (linear regression:  $39.8\pm3.3$ ; SVM:  $39.7\pm3.4$ ) did not differ significantly (p=.38). Decisively, analysis of the residuals demonstrated an increase in accuracy for the machine learning approach compared to the linear regression model (RMSE\_linReg=3.35 vs. RMSE\_SVM=2.90).

# CONCLUSION

Employment of artificial intelligence (AI) is a promising approach for the calculation of CT-derived hematocrit values. While a regression model is capable of representing the approximately linear relation between HU values and the patient's hematocrit, our machine learning approach profits from additional information resulting in an increased accuracy.

## **CLINICAL RELEVANCE/APPLICATION**

The benefit of AI in deriving hematocrit values from CT datasets is demonstrated. This has various conceivable applications, such as CT-derived myocardial extracellular volume fraction quantification.



# CA251-SD-WEB7

Delayed Enhancement of Papillary Muscles on Cardiac Magnetic Resonance Imaging in Patients with Mitral Regurgitation

Wednesday, Nov. 28 12:45PM - 1:15PM Room: CA Community, Learning Center Station #7

# Participants

Sujin Lim, Seoul, Korea, Republic Of (*Presenter*) Nothing to Disclose Hyun Jung Koo, MD, Seoul, Korea, Republic Of (*Abstract Co-Author*) Nothing to Disclose Dong Hyun Yang, MD, Seoul, Korea, Republic Of (*Abstract Co-Author*) Nothing to Disclose Joon-Won Kang, MD, Seoul, Korea, Republic Of (*Abstract Co-Author*) Nothing to Disclose

#### For information about this presentation, contact:

elfin19@gmail.com

# PURPOSE

To evaluate late gadolinum enhancement of the mitral apparatus on cardiac magnetic resonance imaging (MRI) in patients with mitral regurgitation.

# METHOD AND MATERIALS

Between Jan 2000 and Dec 2017, 131 consecutive patients with mitral regurgitation (38 mitral valve prolapse without concomitant valvular diseases, 7 severe aortic regurgitation, 2 aortic stenosis, 18 severe tricuspid regurgitation, 51 rheumatic mitral disease, 13 functional mitral regurgitation, 2 others) underwent cardiac MRI. Ischemic heart disease, non-ischemic cardiomyopathy such as sarcoidosis or hypertrophic cardiomyopathy, myocarditis, endocarditis and cardiac tumors were excluded. Delayed enhancement images on cardiac MRI, clinical characteristics such as echocardiographic findings and presence of arrhythmia, pacemaker, or implantable cardioverter-defibrillator were reviewed. In 38 patients with pure mitral valve prolapse, we measured the quantitative amount of delayed enhancement of papillary muscles and left ventricular myocardium.

#### RESULTS

In 131 mitral regurgitation patients, papillary muscle enhancement was found in 13 patients (3 pure mitral valve prolapse, 1 severe aortic regurgitation, 2 severe tricuspid regurgitation, 3 rheumatic mitral regurgitation, 1 rheumatic mitral stenosis, 3 functional mitral regurgitation). Among them, 2 (1 pure mitral valve prolapse, 1 severe aortic regurgitation) had bilateral diffuse papillary muscle enhancement and sudden cardiac arrest due to ventricular fibrillation. In 38 mitral valve prolapse patients, 13 showed delayed enhancement (10 had myocardial enhancement, 2 had papillary muscle enhancement, and 1 had both myocardial and papillary muscle enhancement). On echocardiography, grade 4 mitral regurgitation is noted in the 13 patients. Among 3 patients with papillary muscle enhancement, 1 had ventricular arrhythmia.

## CONCLUSION

In patients with mitral regurgitation, delayed enhancement of papillary muscles on cardiac MRI is not uncommon. Even in patients with mitral valve prolapse alone, 34% of the patients showed delayed myocardial or papillary muscle (8%) enhancement.

#### **CLINICAL RELEVANCE/APPLICATION**

Although we could not find the strong relationship between papillary muscle enhancement and occurrence of ventricular arrhythmia, papillary muscle enhancement on cardiac MRI should not be overlooked, considering the incidence of papillary muscle enhancement and ventricular arrhythmia in patients with mitral regurgitation.



## CH251-ED-WEB7

2017 Updates to the Fleischner Society Guidelines for Management of Small Pulmonary Nodules Detected on CT Scans: What the Radiologist Should Know

Wednesday, Nov. 28 12:45PM - 1:15PM Room: CH Community, Learning Center Station #7

**FDA** Discussions may include off-label uses.

#### Participants

Neil Anand, MD, Morristown, NJ (*Presenter*) Nothing to Disclose Jasleen Saini, DO, Jersey City, NJ (*Abstract Co-Author*) Nothing to Disclose Osmani Deochand, MD, Morristown, NJ (*Abstract Co-Author*) Nothing to Disclose Sean K. Calhoun, DO, Long Valley, NJ (*Abstract Co-Author*) Nothing to Disclose

#### For information about this presentation, contact:

neilanandmd@gmail.com

#### **TEACHING POINTS**

The purpose of this exhibit is to make radiologists and clinicians aware of the updates made in the second version (2017) of the Fleischner Society guidelines for management of incidental pulmonary nodules. The orginial paper was initially released in 2005 with a separate guideline for sub-solid nodules issued in 2013. This exhibit aims to highlight the changes made as well as make radiologists aware of the current guidelines.

## **TABLE OF CONTENTS/OUTLINE**

Introduction and History Recommendations for Managing incidentally discovered pulmonary nodules • General recommendations • Recommendations for solid lung nodules & solitary sub-solid nodules Risk factors for Malignancy: General Considerations • Nodule size, morphology, location, multiplicity, & growth rate • Emphysema and Fibrosis • Age, sex, race, & family history • Tobacco & other inhaled carcinogens • Risk estimation and risk models • Invasive diagnostic and therapeutic procedures Additional Considerations • Apical Scarring • Peri-fissural Nodules • Incidentally detected lung nodules on incomplete thoracic CT scans • Partial thoracic CT scans for nodule follow-up Conclusions Advances in Knowledge Implications for Patient Care



## CH252-ED-WEB8

# The IASLC Lung Cancer Staging The New TNM (Eighth Edition): What You Have to Know

Wednesday, Nov. 28 12:45PM - 1:15PM Room: CH Community, Learning Center Station #8

#### **Participants**

Andrea V. Pavani, MD, Sao Paulo, Brazil (*Abstract Co-Author*) Nothing to Disclose Alexandre M. Silva, MD, Sao Paulo, Brazil (*Abstract Co-Author*) Nothing to Disclose Julia Capobianco, MD, Sao Paulo, Brazil (*Abstract Co-Author*) Nothing to Disclose Viviane B. Antunes, MD, MS, Sao Paulo, Brazil (*Presenter*) Nothing to Disclose Gustavo S. Meirelles, MD, PhD, Sao Paulo, Brazil (*Abstract Co-Author*) Partner, Ambra Saude; Stockholder, Fleury SA; Advisory Board, Boehringer Ingelheim GmbH;

## For information about this presentation, contact:

andrea.pavani@grupofleury.com.br

# **TEACHING POINTS**

- Explain the changes in T, N and M in the Eighth Edition.- Pratical Implications of the New TNM.- Show examples of tomographic images in patients with lung cancer and its staging.

# TABLE OF CONTENTS/OUTLINE

- Explain the changes in the new TNM (Eighth Edition).- To show in a practical way the main points of the new TNM.- Show the importance of staging correctly with the new TNM to make the correct treatment and also to predict.- We will be using cases material from our Radiology Department to describe and illustrate the lung cancer staging.- Conclusion and "take home messages".



# CH290-SD-WEB1

Clinical Usefulness of Combined Use of Ultra-High-Resolution CT and Iterative Reconstruction in CT Virtual Bronchoscopy

Wednesday, Nov. 28 12:45PM - 1:15PM Room: CH Community, Learning Center Station #1

## Participants

Takuya Adachi, Tokyo, Japan (*Presenter*) Nothing to Disclose Haruhiko Machida, Tokyo, Japan (*Abstract Co-Author*) Nothing to Disclose Makiko Nishikawa, MD, Tokyo, Japan (*Abstract Co-Author*) Nothing to Disclose Takahiro Arai, Tokyo, Japan (*Abstract Co-Author*) Nothing to Disclose Wataru Yamamura, Tokyo, Japan (*Abstract Co-Author*) Nothing to Disclose Masamichi Koyanagi, Tokyo, Japan (*Abstract Co-Author*) Nothing to Disclose Yuta Shimizu, Mitaka, Japan (*Abstract Co-Author*) Nothing to Disclose Takehiro Nakai, Tokyo, Japan (*Abstract Co-Author*) Nothing to Disclose Toshiya Kariyasu, Tokyo, Japan (*Abstract Co-Author*) Nothing to Disclose Akihito Nakanishi, Tokyo, Japan (*Abstract Co-Author*) Nothing to Disclose Kenichi Yokoyama, MD, Mitaka-Shi, Japan (*Abstract Co-Author*) Nothing to Disclose

## PURPOSE

A state-of-the-art combination of ultra-high-resolution CT (UHRCT) scanner (Aquilion Precision, Canon) with 0.25 mm x 160 slice collimation, 1024-matrix size, and full iterative reconstruction (IR) algorithm (FIRST) can simultaneously improve spatial resolution and reduce noise in CT images. We assessed the clinical usefulness of this combination for CT virtual bronchoscopy (VB).

## **METHOD AND MATERIALS**

We retrospectively enrolled consecutive 21 patients (13 men, mean age:  $68\pm14$  years) who underwent chest CT by UHRCT; reconstructed VB images with the following modes: 1) 512 matrix, 0.5-mm thickness, and hybrid IR (AIDR 3D); 2) 1024 matrix, 0.25mm thickness, and hybrid IR (AIDR 3D enhanced); 3) 1024 matrix, 0.25-mm thickness, and FIRST for each patient. Using a dedicated workstation, two readers by consensus determined the maximal order of recognizable bronchial bifurcation in the segment 1+2 of the left lung and segment 10 of the right lung in those three modes. The two readers independently graded the subjective image quality (IQ) of the airway surface using a 5-point scale (1, poor; 5, excellent). The maximal bifurcation order and IQ grades at the most distal bifurcation recognizable in the three modes for each observer were compared using Kruskal-Wallis test. Interreader agreement of the IQ grades was assessed using  $\kappa$ -statistics.

## RESULTS

Both in the left S1+2 and right S10, the maximal bifurcation order increased from the mode one (8.2±1.3 and 11.5±1.7, respectively) to two (9.3±1.3 and 12.5±1.7) to three (10.2±1.5 and 13.3±1.6) and mean IQ grades improved from the mode one (1.5±0.6 and 1.7±0.5, respectively) to two (2.8±0.5 and 2.8±0.4) to three (3.5±0.5 and 3.4±0.6). For the maximal bifurcation order and IQ grades, significant differences were found between the modes one and three (P<0.05). The IQ grade in the left S1+2 was significantly better with the mode three than the mode two. The inter-reader agreement of the IQ grades was substantial to excellent ( $\kappa$ : 0.77-0.83).

#### CONCLUSION

Combined use of UHRCT and FIRST is useful for improving delineation of more distal bronchial bifurcation on VB images.

## **CLINICAL RELEVANCE/APPLICATION**

Combined use of ultra-high-resolution CT and full iterative reconstruction can offer higher-quality virtual bronchoscopy images, which may improve clinical management for peripheral pulmonary lesions.



# CH291-SD-WEB2

Lung Nodule Detection Performance Using a Deep Convolutional Neural Network Model Using Wide Detector Spectral Ct Monochromatic Imaging? A Preliminary Phantom Study

Wednesday, Nov. 28 12:45PM - 1:15PM Room: CH Community, Learning Center Station #2

# Participants

Li Long, Shenzhen, China (*Presenter*) Nothing to Disclose Lin Meng, Beijing, China (*Abstract Co-Author*) Nothing to Disclose Luo Dehong, Beijing, China (*Abstract Co-Author*) Nothing to Disclose Hua Huang, Shenzhen, China (*Abstract Co-Author*) Nothing to Disclose Wenming Deng, BMedSc, Shenzhen, China (*Abstract Co-Author*) Nothing to Disclose Hai Yan Pan, Shenzhen, China (*Abstract Co-Author*) Nothing to Disclose

#### PURPOSE

To compare the nodule detection capability using artificial intelligent computer-aided detection (CAD) system using wide detector spectral CT monochromatic imaging and to determine the intra-scan variability of volumetric measurements of artificial pulmonary nodules.

## **METHOD AND MATERIALS**

The study adopted chest simulation phantom with 16 homogeneous simulated nodules with different sizes and densities. The scans were conducted by GE 256 MDCT scanner(Revolution CT)using GSI mode . Noise Index was set as 20. Monochromatic image data sets were reconstructed as 40-140kev(10kev interval) named A1~A11 group. Other parameters were the same with detector coverage:80mm, pitch: 0.992, rotation speed: 0.5 s/r, scan slice and interval thickness: 5mm. All the scan images were reconstructed as standard algorithm with thickness of 1.25mm. Nodule detections were automatically performed on an artificial intelligence CAD system using DCNN model . To determine the utility of IR method for improving nodule detection capability, sensitivity and specificity of the CAD system were compared among all scans. The measurements of the nodules were evaluated and compared. Statistical analyses were performed using the intraclass correlation coefficients (ICC)

## RESULTS

Nodules detected by CAD system compared with true nodules and Youden index of eleven groups were shown in the following table. While in the group of A2(50kev), true nodules detected by CAD system was 14.Sensibility, specificity and Youden index were 87.5%,85% and 0.730.Average diameter of nodules were 7.37~10.42mm, average volume of nodules were 0.38~0.71mm3, CT value of nodules were-381.71~-321.58HU, and malignant probabilities of nodules were 61%~85%. Results revealed high intraclass correlation coefficients for measurement (ICCs : 0.980,0.915,0.940,0.995,P<0.05). Lung nodule detection rate and evaluation performance can be maintained well among monochromatic imaging reconstructions.

## CONCLUSION

Lung nodule detection rate and evaluation performance can be maintained well among monochromatic imaging reconstructions. Using wide detector spectral CT monochromatic imaging, lung nodule detection rate, sensibility and specificity performance was found the best by using 50kev.

# **CLINICAL RELEVANCE/APPLICATION**

Monochromatic imaging reconstructions with good results of CAD detection may be an alternative for patient chest CT scan.



## CH292-SD-WEB3

# Evaluation of Deep Bone Suppression Imaging (deepBSI) for Lung Nodule Detection: A Comparative Study

Wednesday, Nov. 28 12:45PM - 1:15PM Room: CH Community, Learning Center Station #3

## **Participants**

Jiefang Wu, Guangzhou, China (*Presenter*) Nothing to Disclose Genggeng Qin, MD, PhD, Guangzhou, China (*Abstract Co-Author*) Nothing to Disclose Zilong He, Guangzhou, China (*Abstract Co-Author*) Nothing to Disclose Weiguo Chen, Guangzhou, China (*Abstract Co-Author*) Nothing to Disclose

# For information about this presentation, contact:

## 1425221889@qq.com

## PURPOSE

The aim of this study is to evaluate a newly developed bone suppression methods (deep bone suppression imaging, deepBSI)for detecting lung nodules, comparing to Digital radiograph(DR), Dual energy substraction(DES), and Digital tomosymthesis(DTS).

## **METHOD AND MATERIALS**

Standard Chest radiographs in 126 Patients with solitary nodules and 29 Patients with multiple nodules were included in the observer study.CT was used as reference standard.A total of 305 lung nodules were detected by CT.The mean diameter of the 305 lung nodules was 13.10mm. Three radiologists and three residents marked suspicious-appearing nodules on the original chest radiographs, deepBSI images, DES images, and DTS images in this study.The evaluation was performed separately for the upper, middle, lower lung field. McNemar's test, weighted kappa, Chi-square test were used for statistical analysis.

#### RESULTS

The sensitivity for DR, deepBSI, DES and DTS was 69.68%, 82.58%, 84.52% and 91.61% respectively, the performance of deepBSI, DES and DTS was significantly better than DR respectively (P < 0.05), there was no statistical difference between deepBSI and DES(P>0.05). The specificity for DR, deepBSI, DES and DTS was 79.70%, 81.20%, 78.95% and 85.71% respectively. When the nodule was located in the lower lung field, there was no statistical difference between DR and DES (P>0.05). When the nodules was located in the upper lung field, comparing to DR, the nodule detection rates of deepBSI, DES and DTS were the highest respectively.

# CONCLUSION

The images of deepBSI,DES,DTS improve radiologists' detection performance for lung nodules respectively,especially for nodules which located in the upper and middle lung field. DTS imaging exhibited greater sensitivity than deepBSI and DES radiography for detecting nodules. The deepBSI program and DES used in this study provided similar detection rates for lung nodules.

# **CLINICAL RELEVANCE/APPLICATION**

The aim of this study was to evaluate the clinical value of the Deep bone suppression imaging (deepBSI)in detecting pulmonary nodules



# CH293-SD-WEB4

Interstitial Lung Involvement in Idiopathic Inflammatory Myopathies: Ultrasound Evaluation of Pleural Irregularities Compared to CT Quantitative and Semi-Quantitative Analysis

Wednesday, Nov. 28 12:45PM - 1:15PM Room: CH Community, Learning Center Station #4

## Participants

Chiara Romei, Pisa, Italy (*Presenter*) Nothing to Disclose Claudia Roncella, Pisa, Italy (*Abstract Co-Author*) Nothing to Disclose Simone Barsotti, Pisa, Italy (*Abstract Co-Author*) Nothing to Disclose Elisa Cioffi, Pisa, Italy (*Abstract Co-Author*) Nothing to Disclose Davide Caramella, MD, Pisa, Italy (*Abstract Co-Author*) Nothing to Disclose Ronald Karwoski, BS, Rochester, MN (*Abstract Co-Author*) License agreement, ImBio, LLC Brian J. Bartholmai, MD, Rochester, MN (*Abstract Co-Author*) License agreement, ImBio, LLC; Scientific Advisor, ImBio, LLC; Scientific Advisor, Bristol-Myers Squibb Company Rossella Neri, Pisa, Italy (*Abstract Co-Author*) Nothing to Disclose Falaschi Fabio, Pisa, Italy (*Abstract Co-Author*) Nothing to Disclose

#### For information about this presentation, contact:

chiara.romei@gmail.com

#### PURPOSE

To compare ultrasound assessment of pleural irregularities and computed tomography (CT) semi-quantitative and quantitative analysis of interstitial lung involvement in idiopathic inflammatory myopathies (IIM).

#### **METHOD AND MATERIALS**

Thirty-seven patients affected by IIM were enrolled and underwent a thoracic ultrasound exam (US). In 53 anterior and posterior bilateral intercostal spaces, we evaluated the US irregularities of the pleural profile. We assigned a score for each space, according to a 3 points scale (0=regular, 1=mild irregularities between 3 mm and 5 mm, 2=irregularities > 5 mm) and summed the score in each space to obtain the total score (PIs). A CT was performed and quantified by a thoracic radiologist using a semi-quantitative score of parenchymal abnormalities (Warrick's score (WS)). In 21 patients a quantitative analysis of interstitial lung involvement was obtained by a volumetric texture and local volumetric histogram feature-based analysis software (CALIPER). Interstitial lung involvement was evaluated as a percent of interstitial lung abnormalities (ILD%): combination of percent of areas of ground glass, reticulation and honeycombing. Analysis of the vascular involvement was obtained as percent of pulmonary vessel volume (PVRS %).

#### RESULTS

Twelve out of 37 patients had a WS=0. In the 25/37 patients who had a positive CT scan a good correlation between PIs and WS was demonstrated (r=0.65; p<0.001). From the analysis of ROC curve, a cut-off of PIs<19 was found, that might be able to identify all patients without CT abnormalities (sensitivity 100%). A high correlation between WS and ILD% (r=0.802; p<0.001), WS and PVRS % (r=0.746; p<0.001), ILD% and PIs (r=0.777; p<0.001) and PVRS% and PIs (r=0.738; p<0.001) was demonstrated.

#### CONCLUSION

The good correlation between PIs and WS may lead to a possible role of US as a first level exam to evaluate lung involvement in IIM patients. The high correlation between WS and ILD% may define the role of CALIPER, as an instrument to quantify lung involvement in IIM patients.

# **CLINICAL RELEVANCE/APPLICATION**

The US evaluation of pleural irregularities is a new promising technique to screen lung involvement in connective tissue interstitial lung disease such as IIM. Automatic software may be useful to evaluate the interstitial lung involvement in a reproducible and easy way.



## CH294-SD-WEB5

# Hemodynamic Status of Main Pulmonary Artery in Pulmonary Hypertension

Wednesday, Nov. 28 12:45PM - 1:15PM Room: CH Community, Learning Center Station #5

## Participants

Lan Wang, Shanghai, China (*Presenter*) Nothing to Disclose Yuan Ren, Shanghai, China (*Abstract Co-Author*) Nothing to Disclose Jingyun Shi, Shanghai, China (*Abstract Co-Author*) Nothing to Disclose Chenwei Li, Shanghai, China (*Abstract Co-Author*) Nothing to Disclose

## For information about this presentation, contact:

lanwanguih@163.com

## PURPOSE

To retrospectively study the morphological and hemodynamic changes of main pulmonary artery (MPA) in patient with pulmonary arterial hypertension (PAH).

## **METHOD AND MATERIALS**

38 patients (21 women; 43.1 years±17.7) who were suspected of having PAH underwent both computed tomography angiography (CTA) and right heart catheterization (RHC).Based on RHC, 31 patients were diagnosed with PAH (mean pulmonary artery pressure [MPAP], >25mmHg) and the remaining 7 subjects were treated as normal controls. Then the PAH patients were divided into three groups by their clinical severity:mild, moderate and severe. A combined CTA and computational fluid dynamics (CFD) approach was used to construct patient-specific pulmonary models and simulate blood flow at steady-state. Hemodynamic parameters, including MPA wall shear stress (MPA-WSS) and velocity (vMPA), were generated in each patient locally. Morphological parameters such as diameter of MPA, left (LPA) and right (RPA) pulmonary artery were also measured. All the parameters will be compared between the PAH cohort and the normal cohort, and evaluated the difference in the three PAH groups. The association between two variables was assessed by a Pearson correlation coefficient (r) and a Wilcoxon ranked-sum test was used to determine if parameter means were significantly different.

## RESULTS

Compared with controls, PAH cohort demonstrated smaller MPA-WSS (0.19 + 0.08 vs 0.54 + 0.23 Pa, P<0.001) and vMPA (6.07 + 1.44 vs 15.57 + 5.5 cm/s, P<0.001). However, PAH patients always had larger diameter in MPA (3.6 + 0.32 vs 2.79 + 0.27 cm, P<0.001), LPA (2.54 + 0.32 vs 2.11 + 0.25 cm, P<0.001) and RPA (2.7 + 0.33 vs 2.27 + 0.35 cm, P<0.001). Additional, MPA-WSS showed a significant negative correlation with MPAP (r = -0.71, P < 0.01), pulmonary vascular resistance (PVR) (r = -0.62, P < 0.01) and MPA diameter (r = -0.65, P < 0.01). Conversely, vMPA had a strong positive correlation with MPA-WSS (r = 0.79, P < 0.01). With the aggravation of PAH, MPA-WSS decreased from 0.24 Pa in mild group to 0.17 in moderate group, then to 0.15 in severe group. However, the correlation was not strong between the MPA and MPA-WSS when we just consider the PAH patients (r = -0.43, r = 0.017).

## CONCLUSION

MPA-WSS and vMPA decreased in PAH patients and significantly associated with MPAP, PVR and the deformation of MPA.

## **CLINICAL RELEVANCE/APPLICATION**

Hemodynamic changes of MPA may play a role in the pathogenesis and progression of PAH.



# CH295-SD-WEB6

Development and Validation of a Deep Learning-Based Automatic Detection Algorithm for Active Pulmonary Tuberculosis on Chest Radiographs

Wednesday, Nov. 28 12:45PM - 1:15PM Room: CH Community, Learning Center Station #6

# Participants

Eui Jin Hwang, Seoul, Korea, Republic Of (*Presenter*) Nothing to Disclose Sunggyun Park, Seoul, Korea, Republic Of (*Abstract Co-Author*) Employee, Lunit Inc Kwang Nam Jin, MD, PhD, Seoul, Korea, Republic Of (*Abstract Co-Author*) Nothing to Disclose Jung Im Kim, MD, Seoul, Korea, Republic Of (*Abstract Co-Author*) Nothing to Disclose So Young Choi, MD, Daejeon, Korea, Republic Of (*Abstract Co-Author*) Nothing to Disclose Jong Hyuk Lee, MD, Seoul, Korea, Republic Of (*Abstract Co-Author*) Nothing to Disclose Jin Mo Goo, MD, PhD, Seoul, Korea, Republic Of (*Abstract Co-Author*) Nothing to Disclose Grant, Lunit Inc Chang Min Park, MD, PhD, Seoul, Korea, Republic Of (*Abstract Co-Author*) Nothing to Disclose

#### For information about this presentation, contact:

#### ken921004@hotmail.com

#### PURPOSE

To develop and validate a deep learning-based automatic detection (DLAD) algorithm for active pulmonary tuberculosis (TB) on chest radiographs (CRs).

# METHOD AND MATERIALS

For the development of DLAD, 54,221 normal CRs and 6,768 CRs with active pulmonary TB were retrospectively collected from a single institution and labeled by 13 board-certified radiologists. DLAD was developed with a 27-layer deep convolutional neural network, and its performance was validated using 6 external validation datasets (4 datasets from 4 institutions and 2 datasets from the US National Library of Medicine). Finally, to compare the performances of DLAD and physicians, an observer performance test was conducted by 15 physicians (5 non-radiology physicians, 5 board-certified radiologists, and 5 thoracic radiologists) using one of the external validation datasets. Diagnostic performance was measured using area under the receiver operating characteristic (ROC) curves for image-wise classification and with area under the alternative free-response ROC curves for lesion-wise localization. Sensitivities and specificities of DLAD were calculated using two cutoffs [high sensitivity (98%) and high specificity (98%)] obtained from the results of in-house validation.

#### RESULTS

DLAD demonstrated an image-wise classification performance of 0.977-1.000 and localization performance of 0.973-1.000 in the 6 external validation datasets. Sensitivities and specificities for image-wise classification were 94.3-100% and 91.1-100% using the high sensitivity cutoff and 84.1-99.0% and 99.1-100% using the high specificity cutoff. DLAD showed significantly higher performance in both classification (0.993 vs. 0.746-0.971 according to physician groups, all Ps <0.05) and localization (0.993 vs. 0.664-0.925 according to physician groups, all Ps <0.05) compared to physicians.

#### CONCLUSION

DLAD showed excellent and consistent performance in the detection of active pulmonary TB on CRs, outperforming physicians.

#### **CLINICAL RELEVANCE/APPLICATION**

DLAD can classify CRs with active pulmonary TB and localize lesions at an expert's level, and thus may play a key role in the diagnosis and screening of active pulmonary TB.



#### ER165-ED-WEB4

# Dual-Energy CT: Added-Value in Trauma

Wednesday, Nov. 28 12:45PM - 1:15PM Room: ER Community, Learning Center Station #4

Awards Certificate of Merit

## Participants

Nicolas Murray, MD, Vancouver, BC (*Presenter*) Nothing to Disclose Erik Venalainen, Vancouver, BC (*Abstract Co-Author*) Nothing to Disclose Savvas Nicolaou, MD, Vancouver, BC (*Abstract Co-Author*) Institutional research agreement, Siemens AG

#### For information about this presentation, contact:

nicolas.murray@vch.ca

#### **TEACHING POINTS**

DECT has an added-value in trauma by identifying critical findings not depicted with standard CT imaging. Useful post-processing applications in trauma are the material-specific imaging including the virtual non-contrast and non-calcium images, iodine maps, bone marrow edema and tendon applications, and the virtual monoenergetic imaging.

#### **TABLE OF CONTENTS/OUTLINE**

Review of DECT physic, DECT applications used in trauma, and presentation of interesting cases. Multidetector CT (MDCT) is the cornerstone investigation in trauma given its availability, rapidity of acquisition, and high sensitivity/specificity in depicting traumatic injuries. DECT has reinforced the utilization of CT in the acute setting, with its added-value. In this review, we will briefly discuss the principle of DECT and some useful applications in the trauma setting such as utilization of the virtual non-contrast and virtual non-calcium images, iodine maps, bone marrow edema and tendon applications, and virtual monoenergetic imaging. We will present interesting cases where DECT has an added-value in identifying critical findings not seen on conventional MDCT imaging. DECT can improve identification of contrast extravasation, traumatic organ and bowel injuries, bone marrow edema and tendon rupture, and is helpful in decreasing artifacts caused by metallic prosthesis and external hardware.



# ER226-SD-WEB1

Utility of 'Whole Brain' CT-Perfusion in Stroke of Less Frequent Territories

Wednesday, Nov. 28 12:45PM - 1:15PM Room: ER Community, Learning Center Station #1

## Participants

Agustina Vicente Bartulos, MD, Madrid, Spain (Presenter) Nothing to Disclose Beatriz Alba Perez, MD, Madrid, Spain (Abstract Co-Author) Nothing to Disclose Pablo Marazuela Garcia, MD, Madrid, Spain (Abstract Co-Author) Nothing to Disclose Jose M. Blanc Molina, MD, Madrid, Spain (Abstract Co-Author) Nothing to Disclose Alfonso Lopez-Frias Lopez-Jurado, MD, Madrid, Spain (Abstract Co-Author) Nothing to Disclose Esther Garcia Casado, Madrid, Spain (Abstract Co-Author) Nothing to Disclose

## PURPOSE

To know the utility of 'whole brain' CT-perfusion in stroke affecting territories different from the middle cerebral artery (MCA), which mainly involve the posterior territory (PT) and the anterior cerebral artery (ACA).

# **METHOD AND MATERIALS**

We reviewed 1,441 Multimodal CT studies (non contrast CT, CT perfusion and angiography CT), performed in patients admitted to the emergency room with suspected 'stroke code', during the period from January-2016 to January-2018. We worked with a CTMD-320 detectors scanner, which performs a volumetric study of 16 cm length, obtaining dynamic images of the whole brain. We collected different variables: sex, age, reason for consultation and findings in CT-multimodal protocol (ASPECTS, time parameters, flow, volume and penumbra, occlusion and vascular collaterality...)

# RESULTS

Within the 1,441 studies reviewed, 723(50%) were normal and 16(2%) were invalid. Of the remaining, 405(57.7%) were strokes of the territory of middle cerebral artery (MCA), 130(18.5%) of other vascular territories, 120(17.1%) anomalous perfusions (stroke simulators) and 47(6.7%) bleeds. In the 130 patients studied, 54% was male. The ASPECTS in non contrast CT brain was >7 in 83%. CT-Perfusion showed an increase in time parameters in more than 90% of cases, with decreased flow and normal volume in 39% and decreased volume in 58% The penumbra was <20% only in 8%, 50-80% in 74% and> 80% in 24%. Vascular occlusion was identified in 85%, being the most frequently isolated vessel the posterior cerebral artery (30%), ACA (15%) and basilar artery (8%). The occlusions were multiple in 35%. Regarding collaterality, more than 50% showed an adequate degree.

# CONCLUSION

'Whole brain' CT-perfusion is very useful to study less common strokes, like posterior territory and ACA, which sometimes are not clinically suspected and would not be included in the images obtained with less detectors scanners. Identifying alterations in perfusion helps us searching for vascular occlusions in the affected territory. Knowing the percentage of retrievable tissue is also useful to choose better which patients could benefit the most with of endovascular therapy.

# **CLINICAL RELEVANCE/APPLICATION**

The information provided by the 'whole brain' CT-perfusion studies is very useful, especially for the evaluation of strokes far from the territory of the MCA and also for patients with equivocal clinical signs, stroke mimics, encephalitis ...



## ER227-SD-WEB2

Cardiac CT in the Emergency Department: Prevalence and Spectrum of Imaging Findings Beyond the Coronary Plaques

Wednesday, Nov. 28 12:45PM - 1:15PM Room: ER Community, Learning Center Station #2

# Participants

Rawan Abu Mughli, MD, Vancouver, BC (*Presenter*) Nothing to Disclose Adam I. Kramer, Vancouver, BC (*Abstract Co-Author*) Nothing to Disclose Tong Wu, MD, Vancouver, BC (*Abstract Co-Author*) Nothing to Disclose Luck J. Louis, MD, Vancouver, BC (*Abstract Co-Author*) Nothing to Disclose Nicolas Murray, MD, Vancouver, BC (*Abstract Co-Author*) Nothing to Disclose Ana-Maria Bilawich, MD, Vancouver, BC (*Abstract Co-Author*) Nothing to Disclose Anto Sedlic, MD, Vancouver, BC (*Abstract Co-Author*) Nothing to Disclose John R. Mayo, MD, Vancouver, BC (*Abstract Co-Author*) Speaker, Siemens AG Savvas Nicolaou, MD, Vancouver, BC (*Abstract Co-Author*) Institutional research agreement, Siemens AG

# PURPOSE

Although the main goal of cardiac computed tomography angiography (CCTA) performed in the emergency department (ED) is to rule out significant coronary artery stenosis, there is a variety of non-plaque related coronary, cardiac, and non-cardiac findings that can account for patients' acute chest pain. Our study aimed to evaluate the prevalence and provide a systemic analysis of different non-plaque related findings encountered in our ED.

## METHOD AND MATERIALS

Two hundred and fifty consecutive CCTA cases performed for acute chest pain in the ED over approximately 12 months were reviewed for the non-plaque coronary, cardiac, and non-cardiac findings that might have accounted for patients' symptoms. We correlated with laboratory tests, subsequent imaging, and clinical notes to confirm the accuracy and significance of those findings.

# RESULTS

The patients' age ranged between 26 and 89. Non-plaque coronary findings were observed in 22(8.8%) patients: 1(0.4%) spontaneous coronary artery dissection, 3(1.2%) anomalous coronary arteries, of which one(0.4%) had a malignant course, 1(0.4%) vasculitis of the coronary arteries, and 17(6.8%) cases of myocardial bridging, of which one(0.4%) was considered clinically significant due to marked compression in systole. Eleven(4.4%) patients had non-coronary cardiac findings: 1(0.4%) Takotsubo cardiomyopathy, 2(0.8%) dilated cardiomyopathy, 1(0.4%) hypertrophic cardiomyopathy, 1(0.4%) endocardial vegetations, 1(0.4%) atrial septal defect, 2(0.8%) pericardial effusions subsequently treated as pericarditis, 1(0.4%) pericardial cyst, and 2(0.8%) ventricular aneurysms. As for non-cardiac findings, 3(1.2%) cardiac computed tomography(CT) scans identified pulmonary embolism, 2(0.8%) identified pneumonia, and 2(0.8%) combined cardiac and chest CT scans identified cholecystitis.

# CONCLUSION

Evaluation of CCTA in the ED goes beyond coronary plaques. Keeping in mind the spectrum of different imaging findings and adopting an anatomic pattern of review can help the radiologist in identifying all potential diagnoses relevant to the presenting complaint and lead to timely appropriate management.

# **CLINICAL RELEVANCE/APPLICATION**

Adopting a systematic approach to analyze CCTA helps to identity numerous non-plaque related findings that may account for, or contribute to patient presentation and affect management.



## ER228-SD-WEB3

Can We Adequately Select Patients with Chest Pain Who Consult in the Emergency Room to Perform Angiography Multidetector CT (MDCT) Coronary?

Wednesday, Nov. 28 12:45PM - 1:15PM Room: ER Community, Learning Center Station #3

## Participants

Jesus Corres Gonzalez SR, Madrid, Spain (*Presenter*) Nothing to Disclose Agustina Vicente Bartulos, MD, Madrid, Spain (*Abstract Co-Author*) Nothing to Disclose Olga M. Sanz de Leon, PhD, Madrid, Spain (*Abstract Co-Author*) Nothing to Disclose Miguel Castillo Orive, Madrid, Spain (*Abstract Co-Author*) Nothing to Disclose Alfonso Muriel Garcia, Madrid, Spain (*Abstract Co-Author*) Nothing to Disclose Javier Zamora Romero, Madrid, Spain (*Abstract Co-Author*) Nothing to Disclose

#### PURPOSE

In patients with suspected ischemic coronary disease (ICD), the MDCT has a high sensitivity and specificity to diagnose coronary lesions with a high NPV (>99%). MDCT-Coronary use is recommended in clinical practice guidelines for cases with low-intermediate pre-test probability (PTP) of ICS. However, is not entirely defined what scale is best for estimating patients' pre-test probability when they arrive at the emergency room with chest pain. The aim of this study was to evaluate the utility of the Diamond-Forrest (DF) clinical scale as a tool to triage patients with chest pain suggestive of ICD for coronary MDCT imaging in an emergency department.

# METHOD AND MATERIALS

A 2-year retrospective study that included 143 patients attending an emergency department with chest pain and suspected ICD who underwent coronary MDCT. The MDCT study was inconclusive in 11 patients due to technical problems and were excluded. A coronary injury was defined as a significant stenosis of 1 or more vessels >50% (SCS >50%).

## RESULTS

Of the 132 patients analysed (89 men, 54 women, mean age 57 years), 20 patients (14%) had typical angina, 44 (31%) atypical angina and 79 (55%) non-anginal pain. 18 patients had PTP <15% for ICD and none showed SCS >50% in the MDCT. Of the 98 patients with PTP between 15-65%, 24 cases (24.5%) showed SCS >50%. Of the 13 patients with PPT between 66-85%, 5 (38.5%) had SCS >50% and the 3 cases with PTP of 85% had SCS>50%. The association between PTP and MDCT findings was statistically significant (Fisher test p < 0.001).

## CONCLUSION

The DF scale is useful to triage MDCT requests in patients with chest pain suggestive of ICD in the emergency department. We suggest performing coronary MDCT to patients with PTP between 15-85%. Patients who have low clinical PTP (<15%) should be managed without MDCT imaging. Those patients with PTP above 85% can undergo a hemodynamic study without requiring MDCT.

## **CLINICAL RELEVANCE/APPLICATION**

This study suggests that the request of MDCT in patients with chest pain who consult in the emergency department suggestive of ischemic heart disease could be performed using DF scale.



## GI303-ED-WEB12

A Distinct Modality: Application of MR Imaging in the Assessment of Anorectal Fistula in Patients with Crohns Disease

Wednesday, Nov. 28 12:45PM - 1:15PM Room: GI Community, Learning Center Station #12

# Participants

Pooja Subbarao, Boston, MA (*Presenter*) Nothing to Disclose Hamed Kordbacheh, MD, Boston, MA (*Abstract Co-Author*) Nothing to Disclose Mukesh G. Harisinghani, MD, Boston, MA (*Abstract Co-Author*) Nothing to Disclose

## For information about this presentation, contact:

poojasubbarao1234@gmail.com

## **TEACHING POINTS**

MRI is becoming the primary modality for detecting and classifying anorectal fistulas in patients with Crohns disease. These fistulas can be classified by more than one classification schemas. The Van Assche Scoring systems is used to assess the complexity and activity within the fistulas. The purpose of this exhibit is to: 1. Highlight the Importance of the Van Assche Scoring System in Evaluating the Complexity and Activity of the Anorectal Fistulas 2. Delineating the Various Elements of the Van Assche Scoring System 3. Exhibiting the Significance of Van Assche Scoring System in a Clinical Setting

#### **TABLE OF CONTENTS/OUTLINE**

1. Classification of perianal Fistula Describe the components of the Van Assche Scoring system Demonstrate the advantage of using this scoring system in clinical practice 2. Evaluation of Perianal Fistula using MR imaging Imaging Anatomy MR utilization in Treatment Response Evaluation and follow up 3. Perils in Imaging Evaluation of Anal Canal



## GI314-ED-WEB7

Liver MR Elastography Technique and Interpretation: Pearls and Pitfalls

Wednesday, Nov. 28 12:45PM - 1:15PM Room: GI Community, Learning Center Station #7

## Awards **Certificate of Merit Identified for RadioGraphics**

#### Participants

Flavius F. Guglielmo, MD, Philadelphia, PA (Presenter) Nothing to Disclose Sudhakar K. Venkatesh, MD, FRCR, Rochester, MN (Abstract Co-Author) Nothing to Disclose Donald G. Mitchell, MD, Philadelphia, PA (Abstract Co-Author) Consultant, CMC Contrast AB

# For information about this presentation, contact:

flavius.guglielmo@jefferson.edu

#### **TEACHING POINTS**

Liver MR Elastography (MRE) is an imaging technique that measures liver stiffness to evaluate for fibrosis or cirrhosis. While liver stiffness values are well established for determining liver fibrosis stages, obtaining accurate liver stiffness measurements requires high quality imaging technique and proper elastogram interpretation. This exhibit will review the proper technique for performing and interpreting liver MRE.

#### **TABLE OF CONTENTS/OUTLINE**

LIVER MRE TECHNIQUE 1. Patient preparation 2. Passive driver placement 3. MRE breathing technique 4. Sequence timing QUALITY CONTROLLING CASES 1. Non-diagnostic scans a. Liver iron overload b. Disconnected connecting tube c. Active driver turned off 2. Low diagnostic quality scans a. Active driver power output too low or high b. Poor shear wave delivery to liver c. Parenchymal causes d. Paramagnetic material interference INTERPRETING ELASTOGRAMS 1. Understanding the magnitude, phase & wave image, the greyscale & color elastogram, & confidence map 2. Liver stiffness measurement a. Areas to include or avoid b. Interpretation pitfalls i. Wave interference ii. Liver dome artifact iii. Recognize & avoid "Hot Spots" CAUSES OF INCREASED LIVER STIFFNESS MIMICKING FIBROSIS/CIRRHOSIS 1. Inflammation 2. Biliary obstruction 3. Infiltrative processes 4. Venous congestion

#### Honored Educators

Presenters or authors on this event have been recognized as RSNA Honored Educators for participating in multiple qualifying educational activities. Honored Educators are invested in furthering the profession of radiology by delivering high-quality educational content in their field of study. Learn how you can become an honored educator by visiting the website at: https://www.rsna.org/Honored-Educator-Award/ Sudhakar K. Venkatesh, MD, FRCR - 2017 Honored Educator



## GI315-ED-WEB8

# Multi-Energy CT of the Intestinal Tract: What the Radiologist Needs to Know

Wednesday, Nov. 28 12:45PM - 1:15PM Room: GI Community, Learning Center Station #8

FDA Discussions may include off-label uses.

# Awards

# Cum Laude

## Participants

Markus M. Obmann, MD, San Francisco, CA (*Presenter*) Nothing to Disclose Zhen J. Wang, MD, Hillsborough, CA (*Abstract Co-Author*) Stockholder, Nextrast, Inc Spencer C. Behr, MD, Burlingame, CA (*Abstract Co-Author*) Research Grant, General Electric Company Consultant, Navidea Biopharmaceuticals, Inc Grant, Navidea Biopharmaceuticals, Inc Yuxin Sun, BS, MSc, San Francisco, CA (*Abstract Co-Author*) Stockholder, Nextrast Michael A. Ohliger, MD, PhD, Burlingame, CA (*Abstract Co-Author*) Nothing to Disclose Benjamin M. Yeh, MD, San Francisco, CA (*Abstract Co-Author*) Research Grant, General Electric Company; Consultant, General Electric Company; Author with royalties, Oxford University Press; Shareholder, Nextrast, Inc; Research Grant, Koninklijike Philips NV; Research Grant, Guerbet SA; ;

# For information about this presentation, contact:

markus.obmann@ucsf.edu

## **TEACHING POINTS**

Multi-energy CT increases confidence for the evaluation of bowel and adjacent structures. Material decomposition image-pairs (iodine & water/VNC) provide multiple benefits for bowel evaluation, including to: Reduce the effects of bowel peristalsis artifacts on the bowel wall or adjacent structures. Assess iodine uptake, such as to differentiate between enhancing tumor and dense fecal material, score bowel wall inflammation, assess for bowel wall ischemia, and serve as a possible future quantitative biomarker for therapy response. Characterize high density intraluminal material, such as to differentiate between ingested pills and iodine (bleeding/oral contrast) Evaluation of bowel wall enhancement can be improved by using low keV monoenergetic images or material decomposition images. However, readers must be aware of typical artifacts at gas-tissue interfaces. Future DECT contrast agents could allow for additional applications in bowel imaging.

# TABLE OF CONTENTS/OUTLINE

Review technical principles of DECT and possible applications in bowel imaging. Illustrate cases with clinical applications of DECT in bowel imaging. Highlight common pitfalls in the interpretation of bowel DECT. Discuss future DECT contrast agents and applications in bowel imaging.

#### **Honored Educators**

Presenters or authors on this event have been recognized as RSNA Honored Educators for participating in multiple qualifying educational activities. Honored Educators are invested in furthering the profession of radiology by delivering high-quality educational content in their field of study. Learn how you can become an honored educator by visiting the website at: https://www.rsna.org/Honored-Educator-Award/ Spencer C. Behr, MD - 2017 Honored Educator



## GI316-ED-WEB9

# Artifacts and Pseudolesions on CT Colonography

Wednesday, Nov. 28 12:45PM - 1:15PM Room: GI Community, Learning Center Station #9

#### Awards Identified for RadioGraphics

## **Participants**

Zina J. Ricci, MD, Scarsdale, NY (*Abstract Co-Author*) Nothing to Disclose Melanie Moses, MD, Bronx, NY (*Abstract Co-Author*) Nothing to Disclose Milana Flusberg, MD, Bronx, NY (*Presenter*) Nothing to Disclose Mariya Kobi, MD, New York, NY (*Abstract Co-Author*) Nothing to Disclose Fernanda S. Mazzariol, MD, Bronxville, NY (*Abstract Co-Author*) Nothing to Disclose Judy Yee, MD, Bronx, NY (*Abstract Co-Author*) Research Grant, EchoPixel, Inc; Research Grant, Koninklijke Philips NV;

## For information about this presentation, contact:

zricci@montefiore.org

# **TEACHING POINTS**

1. Artifacts and pseudolesions observed on 2D and 3D CT colonography can mimic pathology.2. Interpretive skills can improve recognition of artifacts and pseudolesions, avoiding diagnostic pitfalls. 3. Most pseudolesions are seen on 3D review with 2D images used for problem solving.4. Optimizing exam technique can help avoid artifacts and suboptimal exams.

## **TABLE OF CONTENTS/OUTLINE**

I. Artifacts 1. Due to patient motion 2. Due to cardiac motion3. Due to morbid obesity 4. Due to metal (surgical clips, pacemaker leads, spinal or hip surgical hardware)5. 3D shine-through 6. Stair-step artifact7. Digital subtraction artifactII. Pseudolesions1. Rectal catheter 2. Extrinsic mass effect (extracolonic structures)3. Extrinsic mass effect (submucosal lesions) 4. Untagged retained stool5. Clumpy mucosal coating of contrast6. Inadequate distension7. Bulbous fold (thick fold, fold complex, kissing folds)8. Anterior rectal bar 9. Gas bubble10. Mucus strand11. Coated polyp (contrast etching) 12. Foreign body, ingested pills13. Colonic Diverticula (normal, inverted)14. Sigmoid muscular hypertrophy/ chronic diverticulosis15. Appendiceal orifice (normal, inverted)16. Ileocecal valve17. Focal colonic spasm18. Flexural pseudo-tumor19. Segmental mobility



## GI317-ED-WEB10

Direct Cholangiography - The Radiologist's Primer: Anatomy, Pathology, Intervention, and Complications

Wednesday, Nov. 28 12:45PM - 1:15PM Room: GI Community, Learning Center Station #10

#### Participants

Shravan Sridhar, MD, MS, Albuquerque, NM (*Presenter*) Nothing to Disclose William M. Thompson, MD, Albuquerque, NM (*Abstract Co-Author*) Nothing to Disclose

For information about this presentation, contact:

shsridhar@salud.unm.edu

## **TEACHING POINTS**

Intraoperative cholangiography and endoscopic retrograde cholangiopancreatography are routine procedures performed by interventionalists. Radiologists must understand how to assess and recognize various pathologies on direct cholangiography to facilitate multidisciplinary communication, correlate findings with magnetic resonance cholangiopancreatography, and improve patient care. After reviewing this exhibit, the learner should be able to: 1. Develop a method to assess normal/variant biliary anatomy. 2. Identify common biliary pathology (stones, benign/malignant stricture, leaks). 3. Recognize rarer entities (i.e. primary sclerosing cholangitis, IGG4 and AIDS cholangiopathy). 4. Correlate findings with magnetic resonance cholangiopancreatography where appropriate.

## **TABLE OF CONTENTS/OUTLINE**

1. Introduction. 2. Principles of cholangiography (IOC, ERCP) 3. Normal/variant biliary anatomy. 4. Benign biliary pathology. 5. Malignant biliary pathology. 6. Sample cases of rarer entities (PSC, IGG4, AIDS cholangiopathy). 7. Review/conclusion.



# GI318-ED-WEB11

New Speedy and Accurate Abbreviated Gadoxetic Acid Enhanced Liver MRI, Using Second Shot Method: You Can Have Your Cake and Eat It, Too

Wednesday, Nov. 28 12:45PM - 1:15PM Room: GI Community, Learning Center Station #11

**FDA** Discussions may include off-label uses.

#### **Participants**

Chang Hee Lee, MD, Seoul, Korea, Republic Of (*Presenter*) Nothing to Disclose Hyunji Lee, Seoul, Korea, Republic Of (*Abstract Co-Author*) Nothing to Disclose Jeong Woo Kim, MD, Seoul, Korea, Republic Of (*Abstract Co-Author*) Nothing to Disclose Yang Shin Park, MD, Seoul, Korea, Republic Of (*Abstract Co-Author*) Nothing to Disclose Kyeong Ah Kim, MD, Seoul, Korea, Republic Of (*Abstract Co-Author*) Nothing to Disclose Cheol Min Park, MD, Seoul, Korea, Republic Of (*Abstract Co-Author*) Nothing to Disclose

## For information about this presentation, contact:

chlee86@korea.ac.kr

## **TEACHING POINTS**

1. To introduce what is the New Abbreviated gadoxetic acid enhanced liver MRI for the Oncologic patient. 2. To provide optimal sequence and imaging parameter when the New Abbreviated gadoxetic acid enhanced liver MRI is used. 3. To explain the concept of the second shot arterial phase in the new abbreviated gadoxetic acid enhanced liver MRI

## **TABLE OF CONTENTS/OUTLINE**

1. Overview. 2. Definition of second shot • 1 vial = 10 cc • Before examination, 6cc is pre-injected outside of MR room, 4 cc was injected before the end of examination (after Routine HBP à Second shot AP) • Key: using Subtraction. 3. Protocol of new 10 minutes Abbreviated gadoxetic acid enhanced liver MRI: Injection of 6cc in the waiting room (10 minutes before MR examination) Localizer - T2 HASTE coronal & axial - 3D in/out T1WI - T2 HASTE (long TE for heavily T2) - DWI (50, 500, 800) - HBP (T1 axial / coronal) - Second shot (Pre T1 VIBE + post CE T1 VIBE + subtraction) : total running time under 10 minutes. 4. Demonstration and sharing of clinical cases. 5. Interim result of our study



# GI376-SD-WEB1

Non Invasive Assessment of Liver Fibrosis by 3 Different Shear Wave Techniques: Head-to-Head Performance

Wednesday, Nov. 28 12:45PM - 1:15PM Room: GI Community, Learning Center Station #1

## **Participants**

Sebastiana Atzori, MD, London, United Kingdom (*Presenter*) Nothing to Disclose Adrian K. Lim, MD, FRCR, London, United Kingdom (*Abstract Co-Author*) Luminary, Toshiba Corporation Tim Hoogenboom, London, United Kingdom (*Abstract Co-Author*) Nothing to Disclose Simon Taylor-Robinson, MD, London, United Kingdom (*Abstract Co-Author*) Nothing to Disclose

# For information about this presentation, contact:

s.atzori@imperial.ac.uk

#### PURPOSE

This study aimed to compare liver stiffness assessed by 3 shear wave elastography techniques: Philips EPIQ7TM; Siemens AcusonTM Virtual Touch Tissue Quantification and Transient Elastography (TE) measured by Echosens FibroscanTM. Results of these 3 methods were compared to histological results in patients with chronic liver disease of different aetiologies.

# METHOD AND MATERIALS

139 patients underwent same-day liver biopsy, and measurement of liver fibrosis with the 3 shear wave elastography methods. Liver biopsy yielded insufficient tissue in 9 patients. Statistical analysis was conducted in the remaining 130 patients. Liver fibrosis and necroinflammatory activity were evaluated histologically using the METAVIR scoring system. The measurement was taken in an area of homogeneous liver tissue: 10 measurements in the left lobe, 10 in the right lobe and the median value for each lobe was used calculated. TE was performed with FibroscanTM (TE) and the median of 10 valid measurements was calculated. Statistical analyses were performed using SPSS v. 24 and MedCalc v. 18.2.1. The histological staging was then correlated with median values and Spearman correlation calculated. P values of <0.05 was considered statistically significant.

#### RESULTS

Spearman correlation with METAVIR score was higher with Elast PQ and TE (Elast PQ 0.579; TE 0.599; VTQ 0.425). Areas under the Curve (AUC) were: TE 0.828; Elast PQ 0.813; VTQ 0.705 for no or mild fibrosis (F < 2, n= 58); and TE 0.946; Elast PQ 0.872; VTQ 0.826 for cirrhosis (F4, n= 16). The mean optimal cut-off for mild fibrosis, (F < 2, n=58) was 8.45 kPa for TE (sensitivity (se) 0.77; specificity (sp) 0.80); 7.15 KPa (se 0.79; sp 0.76) for ElastPQ and 8.9 KPa (se 0.70; spec 0.70) for VTQ. For cirrhosis (F=4, n=16) the optimal cut offs were 12.65 kPa for TE (sens 0.93; spec 0.85); 10.8 KPa (se 0.81; sp 0.88) for Elast PQ and 12.54 KPa (se 0.75; sp 0.74) for VTQ. Comparison of the respective ROCs showed no statistical difference between TE and ElastPQ (p = 0.36). Bland Altman plot showed agreement between values obtained with TE and ElastPQ with lower value measured by ElastPQ.

## CONCLUSION

TE and Elast PQ perform better than VTQ. The right lobe of liver is better for SWE measurements and the optimal cut-off values for the various degrees of fibrosis are different for each scanner.

## **CLINICAL RELEVANCE/APPLICATION**

TE and Elast PQ correlate well with histological scores of liver fibrosis



# GI377-SD-WEB2

Image Quality and Diagnostic Value of Virtual Non-Enhanced Imaging Compared to True Non-Contrast Imaging in the Dual-Source Dual-Energy CT

Wednesday, Nov. 28 12:45PM - 1:15PM Room: GI Community, Learning Center Station #2

# Participants

Sanaz Javadi, MD, Houston, TX (*Presenter*) Nothing to Disclose Sherif B. Elsherif, MD, Houston, TX (*Abstract Co-Author*) Nothing to Disclose Priya R. Bhosale, MD, Bellaire, TX (*Abstract Co-Author*) Nothing to Disclose Rick R. Layman, PhD, Houston, TX (*Abstract Co-Author*) Researcher, Siemens AG Jia Sun, Houston, TX (*Abstract Co-Author*) Nothing to Disclose Ott Le, MD, Houston, TX (*Abstract Co-Author*) Nothing to Disclose Corey T. Jensen, MD, Houston, TX (*Abstract Co-Author*) Nothing to Disclose Eric P. Tamm, MD, Houston, TX (*Abstract Co-Author*) Institutional Research Grant, General Electric Company

#### PURPOSE

To compare the image quality and diagnostic accuracy of the attenuation values in the virtual non-contrast (VNC) reconstructed images from the contrast-enhanced dual-energy computed tomography (DECT) images with the true non-contrast images (TNC) in the second-generation DECT scanner (Definition Flash, Siemens) and the third-generation DECT scanner (Definition Force, Siemens)

#### **METHOD AND MATERIALS**

One hundred twenty-three patients with pancreatic cancer who received abdominal DECT on Force (n=55) and Flash CT scanners (n=68) were retrospectively analyzed. The DECT scans contain unenhanced CT and contrast-enhanced DECT images using a single-energy scan at 120 kV and a DECT protocol (100 kV/Sn150 kV and 100 kV/Sn140 kV in Force and Flash CT scanners respectively). VNC images were reconstructed using Siemens Syngo software. Mean CT number (HU) was recorded from regions of interest in various organs in the TNC and VNC images. The mean HU values were compared between TNC and VNC per organ in each CT scanner. Also the mean differences (TNC-VNC) per organ and overall mean difference between the Force and Flash CT scanners using linear mixed model and two one-sided t-tests were compared. Bland-Altman plots were used to display the relationship between the mean differences per organ.

#### RESULTS

The Force CT scanner had comparable mean HU differences of TNC and VNC for an equivalence margin of 10 (p-value = 0.0062). The Flash CT scanner, however, demonstrated nonequivalence for the overall mean HU differences of TNC and VNC for an equivalence margin of 10 (p-value = 0.53). Compared to the Flash CT scanner, the mean HU difference of Force CT scanner was significantly closer to zero. The mean HU differences in each organ had a difference of 10 or less in the Force CT scanner when assessed separately. Mean HU differences for an equivalence margin of 10 for fluid containing structures was statistically significant (p-value <0.0001) in both Force and Flash CT scanners.

# CONCLUSION

The HU values of VNC images obtained on Force DECT scanner are closer to HU values of TNC images on Flash DECT scanner. The fluid HU of VNC images on both scanners are similar to TNC images and can be used clinically.

# **CLINICAL RELEVANCE/APPLICATION**

The HU values of VNC images obtained on Force DECT scanner are closer to the HU values of TNC images than Flash DECT scanner. The fluid HU values of VNC images on both scanners are similar to TNC images and can be used clinically.

## **Honored Educators**

Presenters or authors on this event have been recognized as RSNA Honored Educators for participating in multiple qualifying educational activities. Honored Educators are invested in furthering the profession of radiology by delivering high-quality educational content in their field of study. Learn how you can become an honored educator by visiting the website at: https://www.rsna.org/Honored-Educator-Award/ Priya R. Bhosale, MD - 2012 Honored Educator



## GI379-SD-WEB4

Texture Heterogeneity Analysis (THA) in B-mode Abdominal Ultrasound: I. Impact of Degree of Fibrosis on Heterogeneity of Liver Tissue Texture and Value of Regional Texture Analysis

Wednesday, Nov. 28 12:45PM - 1:15PM Room: GI Community, Learning Center Station #4

# Participants

Janelle Li, Boston, MA (*Presenter*) Nothing to Disclose Mustafa Qureshi, Boston, MA (*Abstract Co-Author*) Nothing to Disclose Avneesh Gupta, MD, Boston, MA (*Abstract Co-Author*) Nothing to Disclose Stephan W. Anderson, MD, Cambridge, MA (*Abstract Co-Author*) Nothing to Disclose Jorge A. Soto, MD, Boston, MA (*Abstract Co-Author*) Royalties, Reed Elsevier Baojun Li, PhD, Boston, MA (*Abstract Co-Author*) Nothing to Disclose

#### For information about this presentation, contact:

baojunli@bu.edu

#### PURPOSE

To evaluate the degree of liver fibrosis in patients with liver biopsy based on statistical chi-square analysis of heterogeneity of liver tissue texture on B-mode ultrasound images. This is the first part of a two-part study.

#### **METHOD AND MATERIALS**

This retrospective patient study was IRB approved. B-mode ultrasound images of right lower lobe (RLL) of thirty-one patients (22 M, 9 F; 17-81 y; F0-3: 16; F4-6: 15) who underwent non-targeted ultrasound guided biopsy were analyzed using an in-house Matlab program. A user manually selected a primary ROI in the range of 4-6 cm (avoiding non-hepatic parenchyma). Local variances,  $\sigma_2$ , of several texture features (e.g., image intensity, image gradient, etc.) were calculated in 25x25 pixel secondary ROIs in a roster scan fashion. The primary ROI contains a large number of secondary ROIs to maintain the precision of statistical analysis. The global variances,  $\sigma_2$ , of the texture features were estimated theoretically from the local average intensities and image gradients using the property of Rayleigh distribution. The  $\chi_2 (\chi_2 = \sigma_2 / \sigma_2)$  were calculated and plotted on a histogram. Several statistical descriptors (e.g., peak value, Pearson's bimodal coefficient, etc.) were extracted from the histogram and entered in a statistical analysis.

# RESULTS

The  $\chi^2$  measures the degree of similarity of liver tissue texture between a secondary ROI and the primary ROI. In none to low grade fibrosis, the  $\chi^2$  histogram of image gradient has a wide distribution with a peak at 1.0. In chronic fibrotic liver, the  $\chi^2$  histogram of image gradient has a narrow distribution and the peak value decreases dramatically in advanced fibrosis (F4-6 vs. F0-3, p<0.001, AUC=0.985, sensitivity=93.7%, specificity=93.3%). There is a strong negative correlation between the peak value and fibrosis stage (r = -0.79).

## CONCLUSION

Liver tissue texture appears distinctly heterogeneous on B-mode abdominal ultrasound in advanced fibrosis than in none to low grade fibrosis. THA based on regional texture analysis and  $\chi^2$  test can detect this change with high sensitivity and specificity in this pilot study.

## **CLINICAL RELEVANCE/APPLICATION**

Texture heterogeneity analysis is potentially an accurate, specific, and non-invasive biomarker for the differentiation of advanced liver fibrosis (F4-6) from mild liver fibrosis (F0-3).

#### **Honored Educators**

Presenters or authors on this event have been recognized as RSNA Honored Educators for participating in multiple qualifying educational activities. Honored Educators are invested in furthering the profession of radiology by delivering high-quality educational content in their field of study. Learn how you can become an honored educator by visiting the website at: https://www.rsna.org/Honored-Educator-Award/ Stephan W. Anderson, MD - 2018 Honored EducatorJorge A. Soto, MD - 2013 Honored EducatorJorge A. Soto, MD - 2014 Honored EducatorJorge A. Soto, MD - 2015 Honored EducatorJorge A. Soto, MD - 2017 Honored EducatorJorge A. Soto, MD - 2018 Honored EducatorJorge A. Soto, MD - 2018 Honored EducatorJorge A. Soto, MD - 2018 Honored EducatorJorge A. Soto, MD - 2017



# GI381-SD-WEB6

Textural Analysis of DCE-MRI Quantitative Parameters in Prediction of Pathological Response to Neoadjuvant Chemoradiation Therapy (CRT) in Locally Advanced Rectal Cancer (LARC)

Wednesday, Nov. 28 12:45PM - 1:15PM Room: GI Community, Learning Center Station #6

## Participants

Alessandra Di Chiara, MD, Milano, Italy (*Presenter*) Nothing to Disclose Anna Palmisano, MD, Milan, Italy (*Abstract Co-Author*) Nothing to Disclose Antonio Esposito, MD, Milan, Italy (*Abstract Co-Author*) Nothing to Disclose Paolo Passoni, Milan, Italy (*Abstract Co-Author*) Nothing to Disclose Alessandro Del Maschio, MD, Milan, Italy (*Abstract Co-Author*) Nothing to Disclose Francesco A. De Cobelli, MD, Milan, Italy (*Abstract Co-Author*) Nothing to Disclose

#### PURPOSE

Tumor vascularization is a crucial factor in the sensitivity of tumor to CRT. The non-invasive evaluation of tumour perfusion prior-CRT may give important information about the sensitivity of LARC to treatment. Aim of our study is to evaluate the impact of rectal cancer's perfusion heterogeneity prior-CRT on sensitivity to treatment, based on a first-order textural histogram analysis of DCE-MRI quantitative parameters.

## **METHOD AND MATERIALS**

Twenty-one patients with LARC underwent DCE-MRI study (20 dynamics, temporal resolution: 11 sec) during e.v. injection of gadobutrol before the beginning of CRT. Cancer volumes were segmented on Ktrans and Ve maps using T2W-images as reference. Histogram parameters (25th, 50th, 75th percentile, mean, range, skewness, kurtosis) were calculated and compared to histopathological Tumor Regression Grade (TRG) according to Rodel. After surgery Patients were classified according to TRG in poor responder "non-GR" (TRG 0,1,2) and good responders "GR" (TRG3-4).Mann-Whitney's test was used to compare measurement between GR and non-GR and ROC curves used to identify parameters predictive of response.

# RESULTS

16 patients resulted GR and 5 non-GR. Skewness and kurtosis of Ve resulted significantly higher in non-GR ( $4.886\pm1.320$  and  $36.402\pm24.486$ , respectively) than in GR ( $1.809\pm1.280$ , p=0.003 and  $6.268\pm8.130$ , p= 0.011) while the remaining histogram descriptors of Ve and ktrans values did not show significant differences between the two classes of response. The area under the ROC curve for predicting response was 0.988 for Ve skewness and 0.963 for Ve kurtosis. The optimal cut-offs to predict good responders were < 21.095 for Ve kurtosis and < 3.635 for Ve skewness with 93.8% sensitivity, 80% specificity and 90.5% accuracy.

## CONCLUSION

Histogram based analysis of DCE-MRI quantitative parameters allows to non-invasively characterize microcirculation heterogeneity in rectal cancer. Ve skewness and kurtosis seems promising in the prediction of rectal cancer's response to CRT.

## **CLINICAL RELEVANCE/APPLICATION**

Histogram analysis of Ve maps may offer new insights in rectal cancer prediction of tumor sensitivity to treatment.



## GU242-SD-WEB3

Development and Validation of CT-Based Findings to Predict Operative Difficulty During Minimally Invasive Partial Nephrectomy

Wednesday, Nov. 28 12:45PM - 1:15PM Room: GU/UR Community, Learning Center Station #3

# Participants

Na Yeon Han, Seoul, Korea, Republic Of (*Abstract Co-Author*) Nothing to Disclose Deuk Jae Sung, MD, Seoul, Korea, Republic Of (*Abstract Co-Author*) Nothing to Disclose Beom Jin Park, MD, Seoul, Korea, Republic Of (*Abstract Co-Author*) Nothing to Disclose Min-Ju Kim, MD, Seoul, Korea, Republic Of (*Abstract Co-Author*) Nothing to Disclose Ki Choon Sim, Seoul, Korea, Republic Of (*Abstract Co-Author*) Nothing to Disclose Lee Sunhwa, MD, Seoul, Korea, Republic Of (*Presenter*) Nothing to Disclose

#### PURPOSE

The Mayo adhesive probability (MAP) score is known to reflect the degree of adherent perinephric fat, which may cause difficulty during partial nephrectomy (PN). However, in the radiologist viewpoint, this scoring system provide insufficient measurement method. Therefore, the purpose of this study was to investigate reproducible methods of measurements of perirenal fat associated with operative complexity and to investigate how operative complexity is associated in open or robotic assisted PN.

## **METHOD AND MATERIALS**

Seventy two patients who underwent PN by a single experienced surgeon were enrolled consecutively; of the 72 patients (56 men and 17 women), 44 had robotic and 28 had laparoscopic surgery. Operation and ischemia time, pathologic results were obtained from medical chart review. Two radiologists independently assessed the posterior perinephric fat thickness (PPFT) without any consensus (PPFTMayo) in first session and then by using two predetermined methods (PPFTlumborum and PPFTcostal); and perinephric fat stranding which were included in MAP scoring system. RENAL nephrometry scoring system was used for stratifying the complexity of renal masses. A multivariable logistic regression analysis was used to evaluate the determinants of operation and ischemia time.

## RESULTS

Intraclass correlation (ICC) values between two reviewers using PPFTcostal and PPFTlumborum showed no statistical difference (p = 0.173, fisher's z-test), and ICC values using two consensus methods were significantly higher than that using PPFTMayo (p = 0.000 in both). Multivariable logistic regression analysis demonstrated that nephrometry score was determinant of ischemia time (p = 0.000 or 0.001) and PPFT was determinant of operation time ( $p = 0.009 \sim 0.023$ ) in robotic assisted PN; nephrometry score was determinant of ischemia time in open PN (p = 0.006).

# CONCLUSION

The methods presented in this study was more reproducible than that of MAP score, and when measured using this method, increased PPFT was related to the longer operation time in robotic assisted partial nephrectomy, but not in open surgery. Perinephric fat stranding showed little effect on operative complexity of partial nephrectomy.

# **CLINICAL RELEVANCE/APPLICATION**

Despite advantages of nephron-sparing surgery; there is a tendency to be hesitated due to the difficulty and complexity of the technique; this can be improved with more reproducible methods for predicting operative difficulty during PN.



## GU243-SD-WEB4

Virtual Unenhanced Images in Routine Clinical Renal Lesion CT Imaging: Influence on the Bosniak Classification

Wednesday, Nov. 28 12:45PM - 1:15PM Room: GU/UR Community, Learning Center Station #4

# Participants

Mathias Meyer, Durham, NC (*Presenter*) Researcher, Siemens AG; Researcher, Bracco Group Rendon C. Nelson, MD, Durham, NC (*Abstract Co-Author*) Research Consultant, General Electric Company; Research Consultant, Nemoto Kyorindo Co, Ltd; Consultant, VoxelMetrix, LLC; Co-owner, VoxelMetrix, LLC; Advisory Board, Bracco Group; Advisory Board, Guerbet SA; Research Grant, Nemoto Kyorindo Co, Ltd; Speakers Bureau, Bracco Group; Royalties, Wolters Kluwer nv Federica Vernuccio, MD, Palermo, Italy (*Abstract Co-Author*) Research support, Siemens AG Fernando Gonzalez, Santiago, Chile (*Abstract Co-Author*) Nothing to Disclose Alfredo E. Farjat, PhD, Durham, NC (*Abstract Co-Author*) Nothing to Disclose Bhavik N. Patel, MD,MBA, Stanford, CA (*Abstract Co-Author*) Nothing to Disclose Daniele Marin, MD, Durham, NC (*Abstract Co-Author*) Research support, Siemens AG

# PURPOSE

To determine whether virtual unenhanced (VUE) images allow reliable characterization of renal lesions according to the Bosniak classification system, using conventional true unenhanced (TUE) images as the reference standard.

#### **METHOD AND MATERIALS**

308 patients with 379 renal lesions undergoing a single-energy TUE CT followed by a nephrographic phase DECT using four different state-of-the-art DECT platforms from two vendors were included. VUE images were calculated using vendor-specific algorithms. Each lesion was classified according to the Bosniak classification separately, by utilizing the VUE or TUE in combination with the nephrographic images. For each renal lesion, attenuation measurements were obtained on the VUE, TUE and nephrographic images and attenuation change of greater than 15HU were considered as evidence of enhancement. TUE images and histological or imaging follow-up for >24 months served as the reference standard. Receiver operation characteristics, with dedicated area under the curves (AUC) where calculated to differentiate enhancing from non-enhancing renal lesions. A linear mixed effect model using the patients as random effects to account for clustering effect of lesions within patients was used.

#### RESULTS

The mean absolute difference between the VUE and TUE attenuation was  $9.2\pm8.7$ HU. High-attenuating renal lesion, decreased distance to the periphery of the dual-energy field-of-view, increased body size, and type of DECT system were influencing factors for the discrepancy between VUE and TUE. A small decrease in diagnostic accuracy was observed for detecting enhancing renal lesions using VUE compared to TUE images (AUC: 0.905 vs 0.959; p=0.0008). There was an excellent overall agreement between VUE and TUE for the Bosniak classification of renal lesions (Cramer's V=0.851).

# CONCLUSION

VUE images enables accurate Bosniak classification of renal lesion, with a decrease in diagnostic accuracy for enhancing lesion characterization. Caution should be warranted in Bosniak IV lesion, which may be misdiagnosed due to suppression of proteinaceous or hemorrhage lesion compositions.

# **CLINICAL RELEVANCE/APPLICATION**

DECT utilizing VUE images yields a sufficient Bosniak classification. Caution is warranted in Bosniak IV lesion, which may be misdiagnosed due to suppression of high-attenuation lesion compositions.



## GU244-SD-WEB5

Utilization of Multiparametric MRI in Patients Under Consideration for or Already in Active Surveillance: Correlation with Imaging Guided Target Biopsy

Wednesday, Nov. 28 12:45PM - 1:15PM Room: GU/UR Community, Learning Center Station #5

# Participants

Jinxing Yu, MD, Richmond, VA (*Presenter*) Nothing to Disclose Ann S. Fulcher, MD, Midlothian, VA (*Abstract Co-Author*) Nothing to Disclose Sarah G. Winks, MD, Richmond, VA (*Abstract Co-Author*) Nothing to Disclose Candice Kim, Richmond, VA (*Abstract Co-Author*) Nothing to Disclose Mary A. Turner, MD, Richmond, VA (*Abstract Co-Author*) Nothing to Disclose Nitai Mukhopadhyay, Richmond, VA (*Abstract Co-Author*) Nothing to Disclose William C. Behl, MS, Richmond, VA (*Abstract Co-Author*) Nothing to Disclose Anna L. Ware, Richmond, VA (*Abstract Co-Author*) Nothing to Disclose Lance Hampton, Richmond, VA (*Abstract Co-Author*) Nothing to Disclose

#### For information about this presentation, contact:

jinxing.yu@vcuhealth.org

#### PURPOSE

To assess value of multiparametric MRI (mp-MRI) in patients with prostate cancer (PCa) Gleason score 6 or less under consideration for or already in active surveillance and to determine rate of upgrading by confirmatory imaging guided target biopsy.

#### METHOD AND MATERIALS

354 consecutive men with initial TRUS biopsy confirmed PCa Gleason score (GS) 6 or less under clinical consideration for or already in active surveillance underwent mp-MRI. 119 of 354 patients had cancer-suspicious regions (CSRs) at mp-MRI. Each CSR was assigned to PI-RADS score based on PI-RADS v2 when MRI study was done. 108 of 119 patients (a total of 146 CSRs) underwent confirmatory imaging guided biopsy for CSRs. Pathology results including Gleason score and percentage of positive specimen from targeted biopsy were recorded as well as age, PSA, PSA density and prostate volume. Associations between PI-RADS scores and findings at imaging guided target biopsy were evaluated using logistic regression. Mann-Whitney U test was performed to compare mean age, PSA, prostate volume and PSA density between upgrading and non-upgrading patients' groups.

## RESULTS

At confirmatory imaging guided target biopsy, 81 of 108 patients had biopsy proven PCa (75%). Among them, 77 patients had upgrading (22%, 77 of 354 patients) (GS 7 n= 50, GS 8 n=14, GS 9 n=4, GS 6 n=9 positive >50%). 146 CSRs in 108 patients had PI-RADS 3 n=28, 4 n=66, and 5 n=52. Upgraded rate for each category of CSR was for PI-RADS 3 (5 of 28, 18%), 4 (47 of 66, 71%) and 5 (49 of 52, 94%), respectively. Using logistic regression analysis for patients with PI-RADS scores from 3 to 5, each unit increase is predictive of 2.25 unit increase in log odds of tumor upgrading. The remaining 4 patients had PCa GS 6 which did not result in upgrading. There was statistical significance of patients' PSA densities between upgraded (77) and non-upgraded patients (266) (p<0.001).

## CONCLUSION

Adding mp-MRI to the evaluation of patients under consideration for or already in active surveillance helps identify undiagnosed PCa of higher GS or higher volume resulting in upgrading in 22%. In addition, PI-RADS score of each CSR is a significant predictor of upgrading.

# **CLINICAL RELEVANCE/APPLICATION**

Adding prostate mp-MRI with PI-RADS scores to the evaluation of patients under consideration for or already in active surveillance helps identify undiagnosed PCa of higher GS and reaffirm others' eligibility for active surveillance.



## GU245-SD-WEB6

Transvaginal Ultrasonography with Bowel Prepare is a Useful Tool for Predicting the Surgical Staging of Endometriosis

Wednesday, Nov. 28 12:45PM - 1:15PM Room: GU/UR Community, Learning Center Station #6

# Participants

Manoel O. Goncalves, MD, Sao Paulo, Brazil (*Abstract Co-Author*) Nothing to Disclose Fernanda C. Goncalves, MD, Sao Paulo, Brazil (*Presenter*) Nothing to Disclose Leandro A. Mattos Sr, MD, PhD, Sao Paulo, Brazil (*Abstract Co-Author*) Nothing to Disclose Roberto Blasbalg, MD, Sao Paulo, Brazil (*Abstract Co-Author*) Nothing to Disclose Giovana B. Basso, MD, Sao Paulo, Brazil (*Abstract Co-Author*) Nothing to Disclose Sergio Podgaec, MD, PhD, Sao Paulo, Brazil (*Abstract Co-Author*) Nothing to Disclose Mauricio S. Abrao, MD, Sao Paulo, Brazil (*Abstract Co-Author*) Nothing to Disclose

#### PURPOSE

Considering that endometriosis is surgically classified into four stages according to the criteria established by the American Society for Reproductive Medicine (ASRM), revised in 1996, and the transvaginal ultrasonography (TVUS) actually is an useful method to diagnose endometriosis and it provides important information to define surgical strategy, we conducted a pioneering study to assess the accuracy of TVUS with bowel preparation (TVUS-BP) in predicting surgical strategi.

#### **METHOD AND MATERIALS**

A prospective study of 129 consecutive patients with suspected endometriosis that underwent laparoscopy and pathological anatomical study, when necessary. Before surgery, all underwent TVUS-BP and the examiner filed a report based on the recommendations and classification of the ASRM with the following data: deep peritoneal endometriosis, ovarian endometriomas (number and size), level of adherence in the adnexa and the presence of partial or complete cul the sac blockage. The staging of preoperative TVUS-BP was compared with surgery.

# RESULTS

The distribution of surgical staging in 129 patients was as follows: 20.9% (27) without endometriosis, 16.3% (21) stage I, 10.1% (13) stage II, 14.7% (19) stage III and 38% (49) stage IV. Therefore, 47.3% (61) showed no disease or had mild endometriosis (stage 0, I or II) and 52.7% (68) had moderate or advanced stages(III,IV). In distinction the absence/ mild levels of endometriosis (0, I, II) to moderate/ advanced levels (III or IV), TVUS-BP had a sensitivity of 92.6%, specificity 96.7%, positive predictive value (PPV) 96.9%, negative predictive value (NPV) 92.2%, positive likelihood ratio (LR +) 28.3 and negative likelihood ratio (LR -) 0.071.

#### CONCLUSION

These findings show that TVUS-BP is an adequate exam for staging pelvic endometriosis, according to the ASRM classification, confirming the importance of this method to define the most appropriate treatment for the patient, including the possible surgical strategy.

# **CLINICAL RELEVANCE/APPLICATION**

The adequate staging with prior imaging study, allows the gynecologist adequately plan the treatment, set up the appropriate surgical team and obtain the patient consent term. In this way we can significantly reduce diagnostic videolaparoscopies and the requirement for re-intervention.



## HP231-SD-WEB1

# Authorship Positions in Radiology: Is There Gender Gap?

Wednesday, Nov. 28 12:45PM - 1:15PM Room: HP Community, Learning Center Station #1

#### **Participants**

Rozita Jalilianhasanpour, MD, Baltimore, MD (*Presenter*) Nothing to Disclose David M. Yousem, MD, Baltimore, MD (*Abstract Co-Author*) Royalties, Reed Elsevier; Speaker, American College of Radiology; Employee, Medicolegal Consultation; ; ;

## For information about this presentation, contact:

rjalili1@jhmi.edu

# PURPOSE

Authorship position is an important indicator of the author's role in the research team and department. The senior author is typically the principal investigator or head of the research team who is more likely to hold the highest academic rank. We sought to determine if women are appropriately represented on senior author positions compared with their first authored contributions to the radiology literature.

# METHOD AND MATERIALS

We looked at the gender of the first and senior authors for all original articles published in the 2017 May issue of 10 high impact American journals in radiology: Radiology, Human Brain Mapping, Investigative Radiology, Magnetic Resonance in Medicine, American Journal of Neuroradiology, Journal of Magnetic Resonance Imaging, Brain Imaging and Behavior, Radiographics, NMR in Biomedicine and the American Journal of Roentgenology. We sought to identify discrepancies in gender ratios between senior authors and first authors.

#### RESULTS

In 9 out of 10 journals, women were less represented in the senior author positions compared to first author positions. The percentage of women as first authors ranged from 23.5% to 50% (Mean=37.3%  $\pm$  7.6), contrasted with just 5.9% to 36.8% (Mean=21.2%  $\pm$  7.7) as senior authors. The absolute difference between the percentage of women as first authors and senior authors ranged from 0 to 28.1% (Mean=16.1%  $\pm$  8.8) for all journals. This was most striking in the Human Brain Mapping and Brain Imaging and Behavior where the gap was 28%.

# CONCLUSION

There is a gender gap in the senior author positions compared to first authored contributions in the radiology literature. This might imply that women are less likely to achieve the highest levels of academic seniority compared with men. Institutions and departments may wish to consider strategies for trainees and faculty that may help narrow the gap.

# **CLINICAL RELEVANCE/APPLICATION**

Women are under-represented as senior authors of manuscripts in the radiology literature compared to first authors. The causes of this and steps to ameliorate it should be explored.



## HP232-SD-WEB2

# How Specialized are Radiologists Who Are Reading MRI Studies of the Upper and Lower Extremities?

Wednesday, Nov. 28 12:45PM - 1:15PM Room: HP Community, Learning Center Station #2

#### Awards Student Travel Stipend Award

#### **Participants**

Brian Trinh, MD, San Francisco, CA (*Presenter*) Nothing to Disclose Evan D. Calabrese, MD, PhD, San Francisco, CA (*Abstract Co-Author*) Nothing to Disclose Thienkhai H. Vu, MD, PhD, San Francisco, CA (*Abstract Co-Author*) Nothing to Disclose Howard P. Forman, MD, New Haven, CT (*Abstract Co-Author*) Nothing to Disclose Brian Haas, MD, San Francisco, CA (*Abstract Co-Author*) Nothing to Disclose

#### For information about this presentation, contact:

brian.trinh@ucsf.edu

# PURPOSE

To assess the degree of specialization in radiologists who are interpreting MRI studies of the upper and lower extremities.

#### **METHOD AND MATERIALS**

The IRB approved this study under exempt review. We accessed the Medicare Physician and Other Supplier Public Use File for calendar year 2015. We searched for all radiologists who interpreted MRI of the arms or legs, excluding MR angiography. Radiologists were sorted by the number of MRI studies interpreted and by percent of fee-for-service Medicare (FFSM) claims derived from interpretation of the associated CPT codes. Based upon the distribution of percent claims from MRI extremity (MREx), we sought to identify a group of radiologists who read the fewest numbers of MREx, termed "low volume readers," and the associated percent of all FFSM MREx that are interpreted by these low volume readers. The database was queried with Python. Statistical analysis was performed with Excel.

#### RESULTS

A total of 12,946 radiologists interpreted 2,865,892 MREx. Of the radiologists reading FFSM MREx, the average number of studies read was 221 (10th-90th percentile, 40-463) and the average percent of claims dollars arising from MREx was 18% (10th-90th percentile, 4%-40%). The distribution in numbers of MRI interpreted and in percent of claims dollars arising from MREx is shown in Figure 1. Based upon the distributions of radiologist volume and percent revenue from MREx, the threshold for low volume readers was set at 90 FFSM MREx examinations. There were 3,946 radiologists in the low volume group (30% of radiologists interpreting MREx), and these radiologists were responsible for interpreting 209,824 of 2,865,892 MREx (7% of all MREx).

#### CONCLUSION

There are large numbers of radiologists who read small numbers of MREx per year. Approximately 30% of radiologists interpreting MREx read fewer than 90 MREx per year, which corresponds to 7% of all MREx studies being interpreted by a low volume radiologist. The composition of this low volume radiologist group, and whether there is a relationship between volume of MREx interpreted and quality of those interpretations, are unknown; these questions should be further studied.

# **CLINICAL RELEVANCE/APPLICATION**

We describe a method for assessing degree of specialization of the radiology workforce. The methods can be used to assess either individual radiology practices, or regional or national samples.



## HP233-SD-WEB3

**Discrepancy Rates and Trends Among Neuroradiology Fellows** 

Wednesday, Nov. 28 12:45PM - 1:15PM Room: HP Community, Learning Center Station #3

#### Participants

Samrah Javed, Baltimore, MD (*Abstract Co-Author*) Nothing to Disclose David M. Yousem, MD, Baltimore, MD (*Abstract Co-Author*) Royalties, Reed Elsevier; Speaker, American College of Radiology; Employee, Medicolegal Consultation; ; ; Rohini N. Nadgir, MD, Baltimore, MD (*Presenter*) Future royalties, Reed Elsevier

# For information about this presentation, contact:

rnadgir1@jhmi.edu

# PURPOSE

The purpose of this study is to determine rates and trends of clinically significant discrepancies in preliminary neuroimaging results provided by first year neuroradiology fellows.

# **METHOD AND MATERIALS**

Preliminary reports determined by supervising attending radiologists to contain clinically significant missed diagnoses are flagged at our institution within the RIS and as part of the official report. We retrospectively identified the flagged results reported preliminarily by first-year neuroradiology fellows between July 2016 and June 2017. The flagged exam type, date (first or second half of fellowship year), time of day of preliminary report (7am-12pm, 12-4:30 pm, 4:30pm-11pm, 11pm-7am), missed diagnosis, and time elapsed between initial and finalized result were recorded.

#### RESULTS

Nine fellows provided preliminary results on 46506 cases with 8 of 13 attendings flagging 59 reports (0.13%). The most common discrepancies occurred in diagnosing traumatic (15/59, 25%) and vascular (12/59, 20%) pathologies. Individual discrepancy rates among fellows ranged from 0.02% to 0.20%. Discrepant diagnoses occurred more frequently during the evening hours (48/59 = 81.4%). No clear trend for number of report modifications between the first and second halves of the fellowship year were noted. Average time for report finalization by the attending Neuroradiologist was 106 minutes following preliminary result.

# CONCLUSION

Discrepant diagnoses among our neuroradiology fellows were rare given the volume of cases read overall and falls below previously reported significant discrepancy rates of 1.8% for attending Neuroradiologists. The majority of discrepant diagnoses involved trauma and vascular disease, and occurred most frequently in the evening hours, which are typically the busiest hours for emergency cases at our institution. The short time interval between preliminary and corrected results supports our department's initiative for after-hours attending coverage.

# **CLINICAL RELEVANCE/APPLICATION**

Our fellows showed very low discrepancy rates throughout the year but may benefit from increased education on trauma and vascular neuroimaging. The short time interval between preliminary result and attending final sign-off is attributed to after-hours attending coverage.



## HP234-SD-WEB4

The Perception Gaps between Radiologists and Clinicians: Assessing the Current and Future Role of a Radiologist

Wednesday, Nov. 28 12:45PM - 1:15PM Room: HP Community, Learning Center Station #4

# Awards

## **Trainee Research Prize - Resident**

#### Participants

Andrew T. Vollman, MD, Miami, FL (*Presenter*) Nothing to Disclose Joseph M. Dalonzo, MD, Miami, FL (*Abstract Co-Author*) Nothing to Disclose Francisco A. Myslicki, MBA, Miami, FL (*Abstract Co-Author*) Nothing to Disclose Steven Falcone, MD, Coral Springs, FL (*Abstract Co-Author*) Nothing to Disclose Alejandro Mantero, Miami, FL (*Abstract Co-Author*) Nothing to Disclose Li Hua, Miami, FL (*Abstract Co-Author*) Nothing to Disclose Gary H. Danton, MD,PhD, Miami, FL (*Abstract Co-Author*) Nothing to Disclose

#### For information about this presentation, contact:

Andrew.Vollman@gmail.com

#### PURPOSE

Conduct a nationwide survey with 2 main objectives. Objective 1- Assess the current state of imaging from both the radiologists' and clinicians' perspective (i.e. radiologist-clinician relationship, value of radiologists' current reports, radiologists' accessibility, and need for Appropriateness Criteria). Objective 2- Assess if radiologists and clinicians want to change according to a model similar to the ACR's Imaging 3.0 (i.e. 'Point of Care Radiologist').

# METHOD AND MATERIALS

IRB approved survey. Questions were divided into 2 groups (Group 1- Current state of imaging and Group 2- Imaging 3.0 Recommendations). Survey was sent out to various medical list servers (i.e. universities, radiology societies, etc). Subject demographics and survey responses were collected and analyzed. A Fisher's Exact test with a Bonferroni correction was used for Group 1 questions. Descriptive statistics were used for Group 2 questions.

#### RESULTS

Group 1 questions 1-8 demonstrated a statistical significance difference (p<0.005) between the radiologists (n=70) and the clinicians (n=191) responses. There was no statistical significant difference for question 9 in Group 1 (p=0.0511). Group 2 questions 1-8 demonstrated that 80% or more of the responses viewed the various roles of a 'point of care radiologist' favorably.

# CONCLUSION

Group 1 questions demonstrate a perception gap exists between the radiologists and clinicians in reference to radiology reports (i.e. indication, clinical question, imaging recommendations), appropriateness of image studies ordered, radiologists' accessibility, and the radiologists role/value on the clinical team. Group 2 questions demonstrate that both radiologists and clinicians view 'Point of care radiologists' as a benefit for patient care and for creating a more cohesive medical team.

# **CLINICAL RELEVANCE/APPLICATION**

Benefits of 'Point of Care Radiologist' include quick preliminary reads, following image appropriateness criteria, instant access for consultation, help in management of patients and building a better/ more cohesive medical team.



## HP235-SD-WEB5

Roles of Radiologists and other Physicians in Endovascular Neuro-Interventions of the Head and Neck: An Appraisal

Wednesday, Nov. 28 12:45PM - 1:15PM Room: HP Community, Learning Center Station #5

#### Awards Student Travel Stipend Award

# Participants

Kofi-Buaku Atsina, MD, Philadelphia, PA (*Presenter*) Nothing to Disclose Mougnyan Cox, MD, Philadelphia, PA (*Abstract Co-Author*) Nothing to Disclose Laurence Parker, PhD, Philadelphia, PA (*Abstract Co-Author*) Nothing to Disclose Robert W. Hurst, MD, Bryn Mawr, PA (*Abstract Co-Author*) Nothing to Disclose David C. Levin, MD, Philadelphia, PA (*Abstract Co-Author*) Consultant, HealthHelp, LLC; Board Member, Outpatient Imaging Affiliates, LLC

# PURPOSE

The proven efficacy of endovascular neurointerventions (ENIs) and the implementation of endovascular stroke therapies (ESTs) have led to concern about a possible shortage of trained neurointerventionalists. Our purpose was to examine the involvement of various medical specialties in the performance of ENIs utilizing new data reflecting changes in CPT coding for 2016 that specifically identify ESTs.

# METHOD AND MATERIALS

The Medicare Part B fee-for-service databases for 2016 were the data source. The databases provided nationwide Medicare volumes for those codes, as well as the specialties of the providers utilizing them. We compared ENI volumes and utilization rates by radiologists, neurosurgeons, neurologists, cardiologists, vascular surgeons and other physicians. Since CPT codes for ESTs were introduced for the first time in 2016, we also compared those with codes for non-stroke H/N ENIs.

#### RESULTS

The total Medicare volume of H/N ENIs in 2016 was 29,471 comprising 21,992 non-stroke ENIs and 7,479 ESTs. Of the total volume, radiologists performed 38%, compared with 33% by neurosurgeons, 10% each by neurologists and cardiologists, and 6% by vascular surgeons. Sub-analyses of non-stroke ENIs and ESTs demonstrate that radiologists performed 35%/48% respectively, compared with 35%/28% by neurosurgeons, 7%/18% by neurologists, 13%/2% by cardiologists and 7%/1% by vascular surgeons. Considering just the extracranial ENIs, cardiologists (40%) and vascular surgeons (23%) performed the majority of these procedures (primarily carotid stents).

## CONCLUSION

The largest clinical specialties that engage in ENIs continue to be radiology with neurosurgery closely behind. However, there is a wider gap in the performance of ESTs by both specialties, with radiologists performing approximately one-half of the total volume of ESTs compared to approximately one-third by neurosurgeons. Neurologists appear to play a more significant role in ESTs as opposed to non-stroke ENIs, whiles cardiologists and vascular surgeons dominate in the performance of extracranial ENIs. The high volume of ENI procedures (including ESTs) performed by radiologists portends increasing future demand for neurointerventional radiologists.

#### **CLINICAL RELEVANCE/APPLICATION**

Radiologists are heavily involved in endovascular neurointerventions.



# IN225-SD-WEB1

# Standardizing the Content and Format of Common Data Elements in Radiology

Wednesday, Nov. 28 12:45PM - 1:15PM Room: IN Community, Learning Center Station #1

#### Participants

Marc D. Kohli, MD, San Francisco, CA (*Abstract Co-Author*) Nothing to Disclose Adam E. Flanders, MD, Philadelphia, PA (*Abstract Co-Author*) Nothing to Disclose Tarik K. Alkasab, MD, PhD, Boston, MA (*Abstract Co-Author*) Nothing to Disclose Charles E. Kahn JR, MD, Philadelphia, PA (*Presenter*) Nothing to Disclose

## For information about this presentation, contact:

#### ckahn@upenn.edu

## CONCLUSION

A standardized schema, written in the RELAX NG schema language, helps promote the development, exchange, and use of common data elements in radiology.

#### Background

Common Data Elements (CDEs) provide an approach to standardize the collection and use of data from imaging examinations. Each CDE represents a question and its set of allowable responses. CDEs can capture textual, numerical, or discrete ('pick-list') data. CDEs can record information reported by a radiologist, a measurement made by a technologist at the imaging modality, or a parameter generated by an automated system. Through careful definitions of each CDE and links to controlled vocabularies, CDEs can promote interoperability of data. The RSNA, in collaboration with the ACR, has undertaken an effort to develop and promote CDEs through its RadElement.org web site and web services. We present a schema that defines the content and format of radiology CDEs.

#### **Evaluation**

RELAX NG (REgular LAnguage for XML Next Generation) is a schema language for the Web's Extensible Markup Language (XML): A RELAX NG schema provides a relatively simple and readable expression of XML document structure and content. We constructed a RELAX NG schema document based on current CDE specifications and additional data items requested by RSNA's CDE subcommittee. The schema incorporated mandatory information for each CDE such as its unitque identifier, name, and definition. The schema also specified additional, optional information such as a CDE's authors, organizational sponsors, indexing codes, and illustrative images.

# Discussion

A fully defined format, using a formal schema language such as RELAX NG, helps developers build tools to create, discover, and consume CDEs. The schema can be transformed into the XML Schema Language (XSL), and can support interchange of documents in XML or in JavaScript Object Notation (JSON). The XML schema also can promote integration with radiology reporting systems, and with the Computer-Assisted Reporting / Decision Support (CAR/DS) logic modules being developed for the ACR Assist decision support technology. A universal XML-based data format will accelerate the ability to participate in clinical data registries.

#### **Honored Educators**

Presenters or authors on this event have been recognized as RSNA Honored Educators for participating in multiple qualifying educational activities. Honored Educators are invested in furthering the profession of radiology by delivering high-quality educational content in their field of study. Learn how you can become an honored educator by visiting the website at: https://www.rsna.org/Honored-Educator-Award/ Charles E. Kahn JR, MD - 2012 Honored EducatorCharles E. Kahn JR, MD - 2018 Honored Educator



# IN226-SD-WEB2

Patient Identification on Chest X-Ray Using Artificial Intelligence

Wednesday, Nov. 28 12:45PM - 1:15PM Room: IN Community, Learning Center Station #2

#### **Participants**

Rintaro Ito, Nagoya, Aichi, Japan (*Presenter*) Nothing to Disclose Shingo Iwano, MD, Nagoya, Japan (*Abstract Co-Author*) Nothing to Disclose Keigo Nakamura, Tokyo, Japan (*Abstract Co-Author*) Nothing to Disclose Hiroyasu Umakoshi, Nagoya, Japan (*Abstract Co-Author*) Nothing to Disclose Shinichiro Kamiya, Nagoya, Japan (*Abstract Co-Author*) Nothing to Disclose Shiniji Naganawa, MD, Nagoya, Japan (*Abstract Co-Author*) Nothing to Disclose Yuanzhong Li, Tokyo, Japan (*Abstract Co-Author*) Employee, FUJIFILM Holdings Corporation Hironori Shimamoto, Aichi, Japan (*Abstract Co-Author*) Nothing to Disclose

# PURPOSE

Patient misidentification on radiological images sometimes results in serious medical accidents. Therefore, we developed the computer-aided diagnosis (CAD), which automatically calculates similarity between two chest X-ray (CXR) images using artificial intelligence, and examined whether it is effective in confirming the identity of patients.

## **METHOD AND MATERIALS**

For the diagnostic reading session, the laboratory-created CAD software 'Same Patient Checker' was used. The CAD compares 11 anatomical structures, i.e., the ribs, aorta, spine, hilum, diaphragm, figure or thorax, right upper lung field, left upper lung field, right lower lung field, left lower lung field, and size of bilateral lung field, between 2 CXRs and calculates the similarity measure in each structure. If the individual structural similarity measure decreases below 0.3, a warning is displayed on the monitor. A total of 160 sets of CXR images of adult patients taken on a certain day and the earlier images of the respective patients were collected. For 30 of the 160 sets, the earlier image was artificially replaced with another patient's image. Four radiology residents participated in the reading session and judged whether the set of CXRs were derived from the same patient, using the continuous confidence method on a scale of 0 to 100. The area under the curve (AUC) for detecting an incorrect identification, was compared with and without CAD for each reader by receiver operating characteristic (ROC) analysis.

#### RESULTS

The CAD detected similarity reductions for one or more of the 11 anatomical structures in all 30 sets of different patient images, whereas it detected similarity reductions in only 10 of the remaining 90 sets of same patient images (sensitivity = 100.0%, specificity = 92.3%). On the ROC analysis, AUC with CAD was significantly higher than that without CAD for one reader (0.997 vs. 0.978, p = 0.033), although there were no significant differences in this respect among the remaining three readers.

# CONCLUSION

Reading chest X-ray with the CAD, which automatically calculates the similarity between two chest X-ray images, decreases the incidence of misidentification of patients.

# **CLINICAL RELEVANCE/APPLICATION**

Artificial intelligence showed potential in preventing medical accidents caused by misidentification of patients on radiological images.



# IN227-SD-WEB3

Detection of Pacemaker and Determination of MRI-conditional Pacemaker Based on Deep-learning Convolutional Neural Networks to improve the Patients' MRI Safety

Wednesday, Nov. 28 12:45PM - 1:15PM Room: IN Community, Learning Center Station #3

# Participants

Yoon Ah Do, Seoul, Korea, Republic Of (*Abstract Co-Author*) Nothing to Disclose Jin Kyem Kim, Seoul, Korea, Republic Of (*Presenter*) Nothing to Disclose Young Han Lee, MD, Seoul, Korea, Republic Of (*Abstract Co-Author*) Nothing to Disclose Hwiyoung Kim, Seoul, Korea, Republic Of (*Abstract Co-Author*) Nothing to Disclose Sungjun Kim, MD, Seoul, Korea, Republic Of (*Abstract Co-Author*) Nothing to Disclose

# PURPOSE

To evaluate the capability of pacemaker detection on chest radiograph before MRI scan, and to evaluate the accuracy of determination of MR-conditional pacemaker and conventional pacemaker based on a convolutional neural networks (CNN) classifier.

# METHOD AND MATERIALS

The patient with for pacemaker insertion were retrieved and the procedure records for pacemaker were reviewed. The chest radiographs with MR conditional pacemaker and conventional pacemaker were queried, and chest radiographs without pacemaker from pre-procedure radiographs were transferred in the same patients. Total 515 chest radiographs were exported to a local workstation for analyses: 162 radiographs without pacemaker, 206 with MR-conditional pacemaker, and 147 with conventional pacemaker. Among them, 194 images and 321 images were used for the training and test datasets, respectively. The top layer of the Inception v3 network was re-trained using chest radiographs to produce a model for the classification of no pacemaker, conventional pacemaker, and MR-conditional pacemaker. In first step, the radiographs were classified to radiographs with pacemaker and radiographs with conventional pacemaker. We assessed the accuracy of detection and subclassification of pacemaker of CNNs using medical records and procedure notes review as a gold standard.

#### RESULTS

The accuracy was 93.15 % (n=299/321) for the pacemaker detection on chest radiographs. The accuracy was 99.1 % (n=214/221) for the detection of MR-conditional pacemaker.

# CONCLUSION

Deep learning-based convolutional neural networks can be utilized to detect a pacemaker on chest radiograph and to discriminate the MR-conditional pacemaker from conventional pacemaker. This determination of MR-conditional pacemaker could be applied to radiologic workflow, improving the patient safety.

#### **CLINICAL RELEVANCE/APPLICATION**

CNNs can be utilized to detect the MR-conditional pacemaker on chest PA beyond image interpretation, improving the radiologic MR safety.



# IN228-SD-WEB4

Development of Patient-Specific 3D Printed Model and Graft Guide for Open Surgical Repair of Thoracoabdominal Aortic Dissection

Wednesday, Nov. 28 12:45PM - 1:15PM Room: IN Community, Learning Center Station #4

# Participants

Taehun Kim, Seoul, Korea, Republic Of (*Presenter*) Nothing to Disclose Sangwook Lee, BS, Seoul, Korea, Republic Of (*Abstract Co-Author*) Nothing to Disclose Guk Bae Kim, Seoul, Korea, Republic Of (*Abstract Co-Author*) Nothing to Disclose Koeun Lee, MD, Seoul, Korea, Republic Of (*Abstract Co-Author*) Nothing to Disclose Wan Kee Kim, Seoul, Korea, Republic Of (*Abstract Co-Author*) Nothing to Disclose Joon-Bum Kim, Seoul, Korea, Republic Of (*Abstract Co-Author*) Nothing to Disclose Dong Hyun Yang, MD, Seoul, Korea, Republic Of (*Abstract Co-Author*) Nothing to Disclose Namkug Kim, PhD, Seoul, Korea, Republic Of (*Abstract Co-Author*) Stockholder, Coreline Soft, Co Ltd

#### For information about this presentation, contact:

namkugkim@gmail.com

#### CONCLUSION

Planning for the OSR was established by 3D printing based on the preoperative CT images. The direction and location between branches of the graft could be accurately measured, which enables the surgeons to cut and connect the graft precisely.

#### Background

Open surgical repair (OSR) of the extensive thoracoabdominal aorta (TAA) is a tough procedure with high risks of surgical bleeding, neurologic injuries, visceral organ failure and operative mortality. During procedures of the OSR, reconstructions of the visceral arteries and spinal cord are regarded as the vital task. Even if there are commercially available grafts, which usually cover visceral arteries, no considerations of anatomical variations among individuals. To overcome these limitations, we developed 3d printed patient-specific aorta and graft guide for OSR.

#### **Evaluation**

Four patients between the ages 36 and 54 with Marfan syndrome presenting with an aneurysm and dissection of TAA were enrolled. To fabricated patient specific 3D printed aorta and graft guide, the diseased aorta was segmented from the dual source CT angiography images. An imaginary graft was reconstructed modifying the line of the aorta. The celiac, superior mesenteric, bilateral renal and spinal cord branches of the aorta were designed to provide direction and location of branches connected to the graft that was determined by the normal aortic diameter. The artificial grafts were tailored using the 3D printed aorta and graft, and It was applied in the operating room. The surgery was conducted under hypothermic cardiopulmonary bypass (CPB) support. Considering that conventional surgery takes more than 12 hours, the procedure took 467 minutes for three patients with 3D printing, including CPB time. The mortality and serious complications of all patients didn't occur.

#### Discussion

This approach provides an individualized approach in OSR of TAA based on the preoperative images, especially useful in anatomically challenging cases. By confirming patient-specific aorta and guide and reconstructing the artificial graft, the operation time was shortened and the accuracy was improved.



# IN229-SD-WEB5

# Characterization of Renal Solid Masses Using Multiparametric Diffusion-Weighted Imaging

Wednesday, Nov. 28 12:45PM - 1:15PM Room: IN Community, Learning Center Station #5

#### **Participants**

Jianjian Zhang, Shanghai, China (*Presenter*) Nothing to Disclose Guangyu Wu, Shanghai, China (*Abstract Co-Author*) Nothing to Disclose YongMing Dai, Shanghai, China (*Abstract Co-Author*) Nothing to Disclose

# For information about this presentation, contact:

zjj-1108@163.com

#### PURPOSE

To assess the utility of multiparametric diffusion-weighted imaging (DWI) including monoexponential, biexponential, stretchedexponential and diffusion kurtosis imaging models in renal solid masses.

# METHOD AND MATERIALS

This study was approved by the institutional review board, and written informed consent was obtained from all patients. A total of 81 patients (18 benign and 63 malignant lesions) were imaged with 3T DW-MRI. Diffusion model selection was investigated in each lesion using the Akaike information criteria. Mann-Whitney U-test and receiver operating characteristic (ROC) curves were used for statistical evaluations.

## RESULTS

Goodness-of-fit analysis showed that most benign and malignant lesion voxels (90.66% and 51.41%, respectively) were preferred by the stretched-exponential model. ADC, Ds and MK showed significant differences between benign and malignant lesions (P < 0.05) and between low- and high-grade ccRCC (P < 0.05). a was significantly lower in the benign group than in the malignant group (P < 0.05). All diffusion measures showed significant differences between ccRCC and non-ccRCC (P < 0.05) except Df and a (P=0.143 and 0.112, respectively). a showed the highest diagnostic accuracy with an area under the ROC curve of 0.923 in differentiating benign and malignant lesions, but none of the parameters from these advanced models revealed significantly superior performance over ADC in discriminating subtypes or grades of RCC.

#### CONCLUSION

Compared with conventional diffusion parameters, a may provide additional information for differentiating benign and malignant renal masses, while ADC remains the most valuable parameter for differentiation of RCC subtypes and for ccRCC grading.

# **CLINICAL RELEVANCE/APPLICATION**

Multiparametric Diffusion-Weighted Imaging might provide quantitative measurements for correct renal lesion diagnosis



### MI229-SD-WEB1

# Examination of the Sentinel Lymph Node Scintigraphy Standardization

Wednesday, Nov. 28 12:45PM - 1:15PM Room: MI Community, Learning Center Station #1

#### **Participants**

Shiho Mogi, Tokyo, Japan (*Presenter*) Nothing to Disclose Tadashi Takase, BS, Tokyo, Japan (*Abstract Co-Author*) Nothing to Disclose Masayuki Akiyama, RT, Yokohama, Japan (*Abstract Co-Author*) Nothing to Disclose Shougo Sai, Tokyo, Japan (*Abstract Co-Author*) Nothing to Disclose Hisaya Sato, Yokohama, Japan (*Abstract Co-Author*) Nothing to Disclose Kyoichi Kato, Yokohama, Japan (*Abstract Co-Author*) Nothing to Disclose

# For information about this presentation, contact:

mogishiho@cmed.showa-u.ac.jp

# PURPOSE

An academic investigation report regarding breast cancer sentinel lymph node (SLN) scintigraphy was produced by the Japanese Society of Radiological Technology. Its purpose was to standardize breast cancer sentinel inspection, as current radiologic imaging (RI) administration methods and imaging parameters may differ between facilities. Here, we investigated the current status of SLN inspection in associated facilities and considered the purpose for standardization of inspection. We followed this with construction of an effective workflow.

#### **METHOD AND MATERIALS**

We conducted a 'present conditions' investigation of SLN by questionnaire in associated facilities, then extracted examination problems to use in standardization. We constructed (high accumulation, medium accumulation, and micro accumulation) the phantom, assuming an examination image for the purposes of SLN scintigraphy, then examined the imaging conditions. The examination conditions were assumed to include a collimator (for collection) and the presence of lead shielding (lead shield of specific size, thickness, and shape). We performed a physical evaluation and a sight evaluation, followed by examination of the optimal imaging protocol. We performed a clinical application of the imaging protocol, and evaluated the usefulness of the standardization approach.

## RESULTS

Using the questionnaire survey in associated facilities, we found differences in the collimator, the lead shielding, and the body outline depiction. After examining an optimal imaging condition using a phantom, an extended low energy general purpose ELEGP collimator provided the next highest depiction ability. In cases where SLN is not required (micro accumulation) or when RI dosage is sufficient to require the use of SLN, it may be necessary to enhance the imaging by use of the lead shielding to allow the RI dosage to be raised.

#### CONCLUSION

In summary, shortening and efficiency of the procedures may enhance standardized inspections within associated facilities during inspection times.

# **CLINICAL RELEVANCE/APPLICATION**

We were able to push forward standardization of SLN in the associated institution. Shortening, efficiency at examination time was suggested by standardizing the examination, and conducting the decision of the duties procedure.



## MI230-SD-WEB2

## Plectin/Integrin-Targeted Bispecific Molecular Probe for the MRI/NIRF Imaging of Pancreatic Cancer

Wednesday, Nov. 28 12:45PM - 1:15PM Room: MI Community, Learning Center Station #2

#### **Participants**

Qian Wang, MD, Peking, China (*Presenter*) Nothing to Disclose Xinming Zhao, Beijing, China (*Abstract Co-Author*) Nothing to Disclose Kun Wang, Beijing, China (*Abstract Co-Author*) Nothing to Disclose Jie Tian, Beijing, China (*Abstract Co-Author*) Nothing to Disclose

# PURPOSE

A novel bispecific molecular probe [DOTA@Gd(III)]2/Cy7-PTP/RGD consisting of Cyanine7 (Cy7) for near-infrared 1.imaging (NIRF), [DOTA@Gd(III)]2 for magnetic resonance imaging (MRI) is developed and applicated for the early diagnosis and NIRF surgery guidance of pancreatic cancer.

# METHOD AND MATERIALS

Bispecific peptide conjugated by Cy7 and DOTA was designed and synthesized by solid phase. And probe characteristic and purification by HPLC and MS. The expression levels of Plectin1 and ITGB4 were monitored by western blotting. Cell proliferation and cytotoxicity was performed to examine with MTS assay kit. Flow Cytometry and cell immunofluorescence were performed for specially cellular targeting assay. To reveal the bispecific probe in vivo targeting potential and dynamic bio-distribution in the tumor and main metabolic organs, 24 mice bearing panc1 tumor were divided into four groups, each group of six. And Tumor imaging in vivo was acquired by a fibered dual band confocal fluorescence microscopy system (FCFM), type S1500 (Cellvizio ®, Mauna Kea Technologies, France). MRI section was performed using a 7.0 T MRI scanner. Gd concentration in the supernatant liquor was measured by ICP-OES. Gd content was calculated as the percentage of injected dose per gram of organ/tissues (% ID/g).

# RESULTS

Bispecific probe has a well-define structure with a molecular weight of 3677 Da. Fluorescence imaging showed higher binding specificity and longer circulation to the human Panc1 subcutaneous and orthotopic xenografted tumor at a dose of 200ug/ml (100ul) than corresponding single peptide blocking. Near infrared fluorescence (NIR) imaging confirmed the feasibility to guide surgical resection of pancreatic orthotopic xenografted tumor. And the T1 relaxivity of bi-peptides[DOTA@Gd]2/Cy7 is 6.88 mM-1s-1 per molecule at 7T MR device. ispecific probe conjugated Cy7 and twin-channel DOTA@Gd has a clinical potential for early detection and intraoperative application for pancreatic tumor.

# CONCLUSION

Higher binding affinity of bispecific targeting was revealed by confocal imaging in vitro and NRIF imaging in vivo than any single targeting. [DOTA@Gd(III)]2/Cy7-PTP/RGD with 'multi-layered' targeting is promising agent which directly hits the malignances, simultaneously overexpressing both plectin and integrin, specially for PDAC.

#### **CLINICAL RELEVANCE/APPLICATION**

now, this study is going on the preclinical stage.



### MI232-SD-WEB4

Red Emissive Metalloporphyrin-Based Nanodots for Magnetic Resonance Imaging and Photodynamic Therapy in Vivo

Wednesday, Nov. 28 12:45PM - 1:15PM Room: MI Community, Learning Center Station #4

# Participants

Zhicong Li, Shanghai, China (*Presenter*) Nothing to Disclose Han Wang, MD, PhD, Shanghai, China (*Abstract Co-Author*) Nothing to Disclose

#### PURPOSE

The combination of carbon nanodots(CNDs) and manganese porphyrin forms a new class of hybrid material in a nanocomposite host, which could be applied in magnetic resonance imaging and photodynamic therapy(PDT) of cancer in vivo.

# METHOD AND MATERIALS

The porphyrin-based nanodots were characterized in detail using a combination of methods.To verify the cellular uptake and subcellular localization of them, the fluorescence imaging was studied on human HeLa cells through a confocal laser scanning microscope. The photophysical characteristics including the dark toxicity, phototoxicity and the production reactive oxygen species were also addressed. In vitro studies validated the efficacy of PDT with them in Hela cells through the CCK-8 assay.The MR contrast properties of MnPCNDs were investigated. Hela-xenografted nude mice were used to validate MR imaging performance and in vivo PDT efficacy.

#### RESULTS

The characterized results confirm the presence of metal Mn ions in MnPCNDs endowed the composite nanosensitizers with excellent MR imaging performance for PDT guidance. The fluorescence intensity of DCFH shows a time-dependent enhancement upon reacting with ROS, generated from PCNDs, ZnPCNDs and MnPCNDs. The results demonstrate that the ROS was produced by porphyrins encapsulated in CNDs. The in vitro PDT results on HeLa cells indicated the porphyrin-based nanodots alone had no adverse effect on tumor cells, but displayed remarkable photodynamic efficacy upon irradiation. The subcellular localization experiment of porphyrin-based nanodots indicates their lysosome-targeting performance. The tumor growth could be suppressed in the MnPCNDs+808-nm laser group, which indicated that the tumor growth could not be affected by either C225-PCNDs or laser irradiation alone. There was no significant body weight loss after treatments.

## CONCLUSION

We have the first time prepared the porphyrin-based nanodots (PCNDs, ZnPCNDs and MnPCNDs) by one-pot hydrothermal method. The porphyrin or its metal complex was encapsulated in the core of CNDs.Due to the good biocompatibility, excellent MR imaging performance and efficient PDT effect upon cancer, the manganese porphyrin-based nanodots could provide a simple modality to develop the nanomedicine for practical magnetic resonance imaging-guided PDT applications.

#### **CLINICAL RELEVANCE/APPLICATION**

N.A.



# MI233-SD-WEB5

Standardized Uptake Value Atlas: Physiological and Abnormal 68Ga-RM2 Uptake in Patients with Prostate Cancer

Wednesday, Nov. 28 12:45PM - 1:15PM Room: MI Community, Learning Center Station #5

# Participants

Lucia Baratto, Stanford, CA (*Presenter*) Nothing to Disclose Heying Duan, Stanford, CA (*Abstract Co-Author*) Nothing to Disclose Akira Toriihara, Stanford, CA (*Abstract Co-Author*) Nothing to Disclose Negin Hatami, Stanford, CA (*Abstract Co-Author*) Nothing to Disclose Sonya Y. Park, MD, Seoul, Korea, Republic Of (*Abstract Co-Author*) Nothing to Disclose Tomomi Nobashi, MD,PhD, Palo Alto, CA (*Abstract Co-Author*) Nothing to Disclose Andrei Iagaru, MD, Emerald Hills, CA (*Abstract Co-Author*) Research Grant, General Electric Company

#### For information about this presentation, contact:

lbaratto@stanford.edu

# PURPOSE

To describe the distribution and range of physiological uptake of 68Ga-RM2 in patients with prostate cancer and to evaluate the spectrum of abnormal uptake using standardized uptake values (SUVs).

# METHOD AND MATERIALS

We retrospectively reviewed images of 20 prostate cancer patients who performed either an 68Ga-RM2 PET/CT for primary diagnosis and staging (n=7) or 68Ga-RM2 PET/MRI for a biochemical recurrence (n=13). Two nuclear medicine physicians evaluated images using an AW workstation (GE Healthcare). SUVmax and SUVmean were measured in 24 normal anatomical structures for each patient. 68Ga-RM2 uptake values of each organ was classified as "none" if SUVmean value was less than of the aortic blood pool, "mild" if SUVmean was greater than SUVmean of aortic blood pool, but less than 2.5, "moderate" if SUVmean was between 2.5 and 5 and "intense" if SUVmean was greater than 5. Areas of focal increased 68Ga-RM2 uptake were also collected.

#### RESULTS

The highest activity was observed in bladder and renal collecting system, related to urinary excretion of radiotracer. The highest physiologic uptake was present in the pancreas (SUVmax  $62.38\pm13.74$ ). Uptake in the kidney cortex, duodenum and esophagus was mostly classified as mild (average SUVmax of 3) and only few times as moderate. Uptake in the in the stomach wall, rectum and adrenal was mostly classified as not significant (average SUVmax of 2.5) and only few times as mild. Brain, adrenals, liver, spleen, bone, gluteal muscle and fat had not significant uptake. Sixteen avid foci of 68Ga-RM2 uptake were detected in 9 patients. Uptake was identified in the prostate bed (n=6), abdominopelvic and mediastinal lymphnodes (n=5 and n=2, respectively), skeleton (n=2) and lungs (n=1).

## CONCLUSION

We presented data on patterns of physiological 68Ga-RM2 uptake in normal tissues with the aim of creating an atlas to improve the interpretation accuracy of 68Ga-RM2 PET scan. Our data also confirmed that 68Ga-RM2 is a promising tracer for the assessment of GRPr expression in prostate cancer patients. Further evaluation in a larger cohort are needed to confirm these data.

#### **CLINICAL RELEVANCE/APPLICATION**

68Ga-RM2 is a promising radiotracer for prostate cancer imaging. Atlas of 68Ga-RM2 would improve accuracy of imaging interpretation.



# MK390-SD-WEB1

Paraspinal Lean Muscle Mass Analysis using MRI in Patients with Adjacent Segment Disease after Lumbar Fusion

Wednesday, Nov. 28 12:45PM - 1:15PM Room: MK Community, Learning Center Station #1

# Participants

Seung Hyun Lee, MD, Goyang, Korea, Republic Of (*Presenter*) Nothing to Disclose Min-Yung Chang, MD, Seoul, Korea, Republic Of (*Abstract Co-Author*) Nothing to Disclose

For information about this presentation, contact:

circle1128@gmail.com

## PURPOSE

To compare the paraspinal muscle mass between patients with symptomatic adjacent segment disease (ASD) and those without ASD after lumbar fusion, using pre-operative MRI.

#### **METHOD AND MATERIALS**

Fifty ASD patients (mean age, 61.4 years; M:F, 13:37; mean body mass index [BMI], 25.1 kg/m2), who had undergone additional operation for ASD after lumbar fusion, were age-, gender-, BMI-, and fusion segment-matched to 50 control patients. Total cross-sectional area (CSA) and functional CSA (FCSA) (i.e. area containing only lean muscle tissue), were measured for the paraspinal muscle group (multifidus and erector spinae muscles) and the psoas muscles on pre-operative MRI. Ratio of FCSA to total CSA and skeletal muscle index (SMI) [i.e. the area of muscle (in cm2)/patient height (in m)2] were calculated. Parameters were compared between the two groups, using the independent-sample t-test.

#### RESULTS

The FCSA of the paraspinal muscle group was significantly smaller in the ASD patients compared to the control patients (mean 2178.6 mm2 vs.2594.0 mm2, P=0.004), as well as FCSA:total CSA (mean 45.4 % vs. 52.2 %, P=0.001) and SMIFCSA (mean 8.8 vs. 10.6; P=0.001). SMITotalCSA of the psoas muscles were significantly lower in the ASD group compared with the control group (mean 8.3 vs. 9.2, P=0.002). With the paraspinal and psoas muscles combined together, total CSA was not significantly different, however; the FCSA (mean 3680.8 mm2 vs. 4268.2 mm2, P=0.013), FCSA:total CSA (mean 53.3 % vs. 58.6 %, P=0.004), SMITotalCSA (mean 27.7 vs. 29.3, P=0.049), and SMIFCSA (mean 14.9 vs. 17.3, P=0.002) were significantly lower in the ASD group compared to the control group. Other variables were not statistically different between the ASD and control patients.

# CONCLUSION

ASD patients had smaller paraspinal lean muscle mass, as indicated by the FCSA, lower ratio of FCSA to total CSA, and SMIFCSA of the paraspinal muscle group on pre-operative MRI, compared to control patients.

# **CLINICAL RELEVANCE/APPLICATION**

Smaller lean muscle mass and higher fat infiltration degree of the paraspinal muscle group can be predictors of ASD following lumbar spinal fusion.



## MK391-SD-WEB2

## High-Frequency Ultrasound Evaluation of the Nail and Terminal Extensor Tendon in Psoriasis

Wednesday, Nov. 28 12:45PM - 1:15PM Room: MK Community, Learning Center Station #2

#### **Participants**

Bihui Zhu, Chengdu, China (*Presenter*) Nothing to Disclose Renmei Wu, Chengdu, China (*Abstract Co-Author*) Nothing to Disclose Li Qiu, Chengdu, China (*Abstract Co-Author*) Nothing to Disclose

For information about this presentation, contact:

wsqiuli@126.com

#### PURPOSE

To compare the ultrasonic manifestations of both nail and terminal extensor tendon between psoriasis patients and healthy subjects.

# METHOD AND MATERIALS

A total of 37 patients with psoriasis diagnosed by experienced dermatologists and 42 healthy subjects were enrolled in this study. The patient condition and nail lesion were scored by Psoriasis Area and Severity Index (PASI) and modified Nail Psoriasis Severity Index (mNAPSI), respectively. All patients and healthy subjects underwent high-frequency sonographic examination. The appearance and thickness of each nail plate, nail bed, nail matrix, terminal extensor tendon, as well as skin of distal interphalangeal (DIP) joint, were measured in gray mode and with power doppler to detect blood flow. Statistical analysis of clinical score and ultrasound data was performed with Wilcoxon rank test or ANOVA. Spearman correlation was used in the correlation analysis and ROC analysis calculated diagnostic accuracy of thickness.

#### RESULTS

For all patients, the common abnormal morphostructures happened to nail plate, which showed wavy appearance (90, 24.46%) and loss of definition (96, 26.09%). Psoriasis patients had higher thickness on nail units, terminal extensor tendon and skin of DIP joint compared with healthy subjects (p < 0.05), but statistical analysis did not reveal significant difference in blood flow ((p > 0.05). A cutoff value of 0.72mm at nail plate, which was highest diagnosis efficiency, revealed a sensitivity of 59% and a specificity of 76%, with an area under the ROC curve of 0.749 (95%CI 0.72, 0.78). The correlation coefficients between thickness of nail plate, nail bed, nail matrix and score of PASI were 0.496, 0.514, 0.346, respectively (p < 0.05), and score of mNAPSI were 0.715, 0.541, 0.325 (p < 0.05). However, no correlation coefficient was found between terminal extensor tendon and PASI (p > 0.05).

# CONCLUSION

High-frequency sonography can detect the common changes of nail plate. Comparing to healthy people, all examination sites became thicker in psoriasis patients, but no difference of blood flow were observed. The thickness of nail plate had the highest diagnostic value, in addition, multiple indicators of nail units were correlated with PASI and mNAPSI score.

#### **CLINICAL RELEVANCE/APPLICATION**

High-frequency sonography can provide a non-invasive tool useful for extension and severity of psoriasis by assessing the characteristic appearance and thickness of nail psoriasis.



### MK392-SD-WEB3

Adhesive Capsulitis: Are We Making the Diagnosis Before Clinicians?

Wednesday, Nov. 28 12:45PM - 1:15PM Room: MK Community, Learning Center Station #3

#### **Participants**

Navid Faraji, MD, Cleveland, OH (*Presenter*) Nothing to Disclose Samer L. Soussahn, MD, Westlake, OH (*Abstract Co-Author*) Nothing to Disclose Nicholas Z. Conley, MD, Cleveland, OH (*Abstract Co-Author*) Nothing to Disclose Christos Kosmas, MD, Cleveland, OH (*Abstract Co-Author*) Consultant, BioClinica, Inc

# For information about this presentation, contact:

navid.faraji@uhhospitals.org

#### PURPOSE

Historically adhesive capsulitis (AC) has been a clinical diagnosis of exclusion characterized by progressive shoulder pain and decreased range of motion. We hypothesize that MRI is increasingly playing a primary role in the diagnosis and guiding management of AC.

# METHOD AND MATERIALS

After institutional review board approval, we queried our institution's medical records for patients with an MRI diagnosis of AC who in addition had a pre-MRI and post-MRI clinical note by the ordering physician available in the medical record. 208 patients with an MRI diagnosis of AC were identified, of which 86 were excluded due to lack of complete clinical information. Patients with confounding shoulder pathologies such as septic arthritis or metastatic disease were also excluded. Ordering providers included both primary care physicians and orthopedic surgeons. Management criteria were defined as conservative (physical therapy and shoulder joint injection) and operative (capsular release). A 2-proportion t-test was used for statistical analysis.

### RESULTS

Of the 122 patients that were included in the study, the MRI report changed the pre-MRI clinical diagnosis and influenced management of AC in 71 patients (86.6%). The MRI report changed the diagnosis and influenced the management in 74% of the cases referred by a primary care physician and in 50% of the cases referred by orthopedic surgeons. When stratified by the type of ordering provider, primary care physicians were more likely to be influenced by the MRI report as compared to the orthopedists (p<0.012). Of the MRI reports that influenced management, a conservative approach was more favored as compared to an operative approach (p<0.0001).

# CONCLUSION

While historically AC has been a clinical diagnosis of exclusion, our data demonstrates that MRI is often the first diagnostic indicator changing the working diagnosis of the treating physician. The ability of MRI to exclude pathologies that may mimic the symptoms of adhesive capsulitis suggests that early imaging may be of benefit in aiding the rapid diagnosis and prompt treatment. We conclude that radiologists can play an integral role in making the diagnosis and influencing the management of AC.

### **CLINICAL RELEVANCE/APPLICATION**

MRI is increasingly becoming a primary component in not only diagnosing, but also influencing the management strategies of adhesive capsulitis for physicians.



# MK393-SD-WEB4

**3D-MRI** versus **3D-CT** in the Evaluation of Osseous Anatomy in Femoroacetabular Impingement using Dixon **3D FLASH** Sequence

Wednesday, Nov. 28 12:45PM - 1:15PM Room: MK Community, Learning Center Station #4

# Participants

Mohammad M. Samim, MD, MRCS, New York, NY (*Presenter*) Nothing to Disclose Thomas Youm, New York, NY (*Abstract Co-Author*) Nothing to Disclose Christopher J. Burke, MBChB, New York, NY (*Abstract Co-Author*) Nothing to Disclose Robert Meislin, MD, New York, NY (*Abstract Co-Author*) Consultant, Arthrex, Inc Jonathan Vigdorchik, MD, New York, NY (*Abstract Co-Author*) Nothing to Disclose Soterios Gyftopoulos, MD, Scarsdale, NY (*Abstract Co-Author*) Nothing to Disclose

#### PURPOSE

CT imaging with 3D reconstruction is part of imaging algorithm to further characterize the bony pathomorphology in femoroacetabular impingement (FAI). While effective, this imaging algorithm can predispose the typical young FAI patients to increased radiation dose and higher cost. The purpose of this study was to determine if 3D MR of the hip can be used to accurately demonstrate hip morphology in the setting of FAI compared with 3D CT. The impact of introducing 3D MRI on the clinical practice in our institution and radiation dose reduction was also assessed.

#### **METHOD AND MATERIALS**

We performed a retrospective review of patients who underwent both CT and MRI of the same hip over a 9-month period with these inclusion criteria: (1) patients suspected to have FAI based on physical examination, (2) no prior hip surgery, (3) patients undergoing CT and MR with 3D of the same hip within a six-month time period. The hip 3D images were evaluated for the presence of cam lesion, the cam location, femoral neck shaft angle (NSA), anterior inferior iliac spine (AIIS) morphology, and lateral center edge angle (LCEA). We also performed a retrospective review of the orders for 3D reconstructions submitted to our 3D lab from April 2012- March 2016.

#### RESULTS

Seventeen patients met our inclusion criteria. There was 100% agreement in the presence and location of the cam lesion (19/19) comparing the 3D MRI to CT. The simple kappa coefficients for cam presence and locations were both 1. There were 3 Type I and 16 Type II AIIS variants on 3D CT with 89.5% (17/19) agreement for the AIIS morphology between 3D MRI and 3D CT. There was 64.7% agreement comparing the NSA (11/17) and LCEA (11/17) measurements on the 3D MRI to 3D CT. There was a total of 185 reconstructions for FAI patients, 155 3D MRI and 30 3D CT. The use of 3D MRI spared each patient an average radiation effective dose of 3.09 mSV for a total reduction of 479.0 mSV.

# CONCLUSION

3D MR reconstructions of the hip have the potential to eliminate the need for 3D CT imaging for FAI evaluation and can be seamlessly incorporated into daily workflow without delaying imaging production and distribution and review of the final imaging reports.

# **CLINICAL RELEVANCE/APPLICATION**

By improving 3D MRI reconstructions of the hip and establishing methodology for different osseous pathomorphology assessment on 3D imaging, 3D MRI can obviate the need for 3D CT imaging and its radiation.



# MK394-SD-WEB5

Evaluation of Glenoid Labral Tears: Comparison Between Dual Energy CT Arthrography and MR Arthrography of the Shoulder

Wednesday, Nov. 28 12:45PM - 1:15PM Room: MK Community, Learning Center Station #5

# Participants

Giovanni Foti, MD, Negrar, Italy (*Presenter*) Nothing to Disclose Matteo Catania, MD, Trieste, Italy (*Abstract Co-Author*) Nothing to Disclose Emanuele Demozzi, MD, Negrar, Italy (*Abstract Co-Author*) Nothing to Disclose Alberto Beltramello, MD, Negrar, Italy (*Abstract Co-Author*) Nothing to Disclose Giovanni M. Carbognin, MD, Verona, Italy (*Abstract Co-Author*) Nothing to Disclose

# For information about this presentation, contact:

gfoti81@yahoo.it

## PURPOSE

To compare the diagnostic accuracy of dual-energy Computed Tomography (DECT) arthrography and magnetic resonance arthrography (MRA) of the shoulder in depicting glenoid labral tears

# METHOD AND MATERIALS

This prospective institutional review board-approved study included 26 consecutive patients (14 males and 12 females; mean age of 32.3, range 18-49 years) studied between January 2017 and January 2018. All patients underwent DECT (80 kV and tin filter 150 kV) and MRA the same day. Articular cavity was distended with anterior approach by using a mixture of saline, iodinate and paramagnetic contrast material. DECT data were postprocessed on a dedicated offline workstation (SyngoVia® VB20; Siemens, Erlangen, Germany) by using a three-material decomposition algorithm for generating noncalcium images of the shoulder. Two radiologists (25 and 11 years of experience, respectively), blinded to clinical data, evaluated the presence labral tears on dedicated DECT color-coded maps and on MRA. Surgical findings served as standard of reference. Diagnostic accuracy values of the DECT and of the MRA were calculated. Inter-observer and intra-observer agreement were calculated with k-statistics. A value of p<0.05 was considered statistically significant

#### RESULTS

MRI revealed the presence of labral tear in 19/26 patients (73.1%), with 8 tears of antero-inferior labrum, 10 tears of superior labrum and 1 tear of posterior labrum. The sensitivity, specificity, PPV and NPV and accuracy of DECT arthrography and MRA were 89.5, 100,100, 77.7 and 92.3%, and 94.7, 85.7, 94.7, 85.7 and 92.3 %, respectively. By using McNemar test, the difference of accuracy between DECT arthrography and MRA was not significant (p=0.45). The interobserver and intraobsever agreement were near perfect (k=0.82 and k=0.86, respectively)

#### CONCLUSION

DECT represents a reliable imaging tool for demonstration of superior, antero-inferior and posterior glenoid labrum tears

#### **CLINICAL RELEVANCE/APPLICATION**

DECT arthrography represents a reliable imaging tool for demonstration of glenoid labrum tears and could be used as alternative imaging method in patients with contraindications for MRI



## MK395-SD-WEB6

The Meniscal Comma Sign: Characterization and Clinical Importance of a Displaced Meniscal Fragment in the Meniscotibial Recess

Wednesday, Nov. 28 12:45PM - 1:15PM Room: MK Community, Learning Center Station #6

# Participants

Felipe B. Franco, MD, Philadelphia, PA (*Presenter*) Nothing to Disclose
Adam C. Zoga, MD, Philadelphia, PA (*Abstract Co-Author*) Nothing to Disclose
Johannes B. Roedl, MD, PhD, Philadelphia, PA (*Abstract Co-Author*) Nothing to Disclose
William B. Morrison, MD, Philadelphia, PA (*Abstract Co-Author*) Consultant, AprioMed AB; Patent agreement, AprioMed AB;
Consultant, Zimmer Biomet Holdings, Inc; Consultant, Samsung Electronics Co, Ltd; Consultant, Medical Metrics, Inc
Kevin Freedman, MD, Bryn Mawr, PA (*Abstract Co-Author*) Nothing to Disclose

## For information about this presentation, contact:

drfelipefranco@gmail.com

## PURPOSE

We describe a type of meniscal tear in which a displaced flap is wedged against the tibial plateau in the meniscotibial recess. In our experience, this entity often benefits from arthroscopic debridement, even in the face of concomitant arthritic changes.

#### METHOD AND MATERIALS

Reports from knee MRI's from 2012-2017 were searched to identify patients who may have the meniscal comma sign. Those showing medial compartment osteoarthritis, osseous contusions or evidence for recent ligamentous injury were excluded. Once potential subjects were identified by MRI findings, a cross reference search of the department of orthopaedic surgery database was performed, and those who underwent dedicated orthopaedic evaluation and treatment were placed into the subject group. Associated imaging findings were recorded, including: tear type, degree of meniscal extrusion, chondrosis, and bone marrow edema. Both pre MRI questionnaires and orthopaedic clinic notes were reviewed for symptomatology. Chart review was performed for initial exam findings, treatment, and treatment outcome

# RESULTS

Ongoing analysis has included 70 knees in the subject group. The high majority presented with pain at or just below the joint line on the medial tibial plateau margin, with medial joint line tenderness on examination. 24 patients have undergone conservative treatment, while 46 had arthroscopy and follow-up outcome was recorded from 6 to 32 weeks. They did not differ significantly by gender, age, chondrosis degree, size of meniscal flap or extrusion, tear type, and bone marrow edema in the tibial plateau. Clinical outcome, however, at the time of submission, reported a significant higher relief of symptoms (partial or total) and level of satisfaction on the arthroscopy group than those treated conservatively.

#### CONCLUSION

Orthopaedists at our institution have shown increasing interest in this phenomenon due to a cohort of patients with medial meniscus tears and meniscal fragments displaced into the meniscotibial recess responding very positively to arthroscopic meniscal debridement. Imagers should note and report displaced meniscal fragments, particularly medial meniscus fragments displaced into the meniscotibial recess, as this type of radiology report may add value to the overall diagnosis and treatment algorithm.

#### **CLINICAL RELEVANCE/APPLICATION**

One specific type of meniscal flap displacement is described, which respondes very positively to arthroscopical debridement



## NM148-ED-WEB6

Immunotherapy in Oncology: Image Evaluation of the Adverse and Toxic Effects of Checkpoint Inhibitors

Wednesday, Nov. 28 12:45PM - 1:15PM Room: NM Community, Learning Center Station #6

#### **Participants**

Daniela F. Vieira Vendramini, Sao Paulo, Brazil (*Presenter*) Nothing to Disclose Felipe D. Barbosa, MD, Sao Paulo, Brazil (*Abstract Co-Author*) Nothing to Disclose Marcelo A. Queiroz, MD, Sao Paulo, Brazil (*Abstract Co-Author*) Nothing to Disclose Jose F. Marin, MD, Sao Paulo, Brazil (*Abstract Co-Author*) Nothing to Disclose Mariana Ruiz, MD, Sao Paulo, Brazil (*Abstract Co-Author*) Nothing to Disclose Felipe L. Costa, MD, Sao Paulo, Brazil (*Abstract Co-Author*) Nothing to Disclose Nicolau F. Guerreiro, MD, Sao Paulo, Brazil (*Abstract Co-Author*) Nothing to Disclose Jucelio P. Moura Filho, BMedSc, Sao Paulo, Brazil (*Abstract Co-Author*) Nothing to Disclose Carlos A. Buchpiguel, MD, Sao Paulo, Brazil (*Abstract Co-Author*) Nothing to Disclose Rafael F. Nunes, MD, Sao Paulo, Brazil (*Abstract Co-Author*) Nothing to Disclose

#### **TEACHING POINTS**

Throughout this study, we will review the main alterations and adverse effects related to immunotherapy using computed tomography (CT), magnetic resonance imaging (MRI) and PET / CT images. The purpose of this exhibition is:• To briefly review the mechanisms of action of checkpoint inhibitors.• To recognize the imaging findings of the main adverse effects related to immunotherapy.• To review the clinical aspects and the course of action to be taken against these adverse effects.

# TABLE OF CONTENTS/OUTLINE

Schematic drawings and illustrations of the mechanism of action of checkpoint inhibitors. • Cases illustrated by images of the main adverse effects that will be illustrated: • CT, MRI and PET / CT images demonstrating the side effects and follow up with imaging after suspension, treatment with immunotherapy. • Tables summarizing clinical, laboratory, and behavioral findings. • Discussion of new concepts such as hyperprogression of disease in the presence of immunotherapy



# NM231-SD-WEB1

#### Variability of Cold-Activated Brown Adipose Tissue Depends on Thermoregulatory Brain Network

Wednesday, Nov. 28 12:45PM - 1:15PM Room: NM Community, Learning Center Station #1

#### Participants

Otto Muzik, PhD, Detroit, MI (*Abstract Co-Author*) Nothing to Disclose Ajay Kumar, MD, PhD, Detroit, MI (*Presenter*) Nothing to Disclose

For information about this presentation, contact:

ajaykumar@med.wayne.edu

#### PURPOSE

The presence of cold-activated Brown Adipose Tissue (BAT) depots is highly variable in humans for unknown reasons and this variability might be associated with differences in CNS thermoregulatory control. As a result, central thermoregulatory brain pathways could be responsible for physiological differences observed in peripheral tissues.

# METHOD AND MATERIALS

A total of 20 lean subjects (10M/10F, 23.3 +/- 3.8 years, BMI = 18.5 - 24.9 kg/m2) subjects were studied using both PET/CT and fMRI. All subjects underwent 18F-fluorodeoxyglucose (FDG) PET imaging during mild cold condition in order to assess the presence of cold-activated supraclavicular BAT. In addition, to assess functional brain responses to cold stress, all subjects underwent a functional MRI (fMRI) scan paradigm. During fMRI, subjects were exposed to an oscillating whole body temperature challenge (five 5min blocks of alternating neutral and cold exposure) applied using a specialized whole-body garment through which temperature-controlled neutral (31-34°C) or cold water (15-17°C) was circulated. The challenge was designed to induce periods of mild hypothermia interspersed by periods of return to basal core body temperature.

#### RESULTS

Based on FDG PET imaging, a wide variability in cold-activated BAT ranging from 0 to 182g was deterimed, characterized by a bimodal distribution. Following cold exposure, 60% of the subjects showed relatively high BAT activation (~100g, High-BAT group or BAT+), whereas 40% of the subjects displayed low BAT activation (< 20g, Low-BAT group or BAT-). According to group selection, the SUVmax determined in supraclavicular BAT of the BAT+ group was significantly higher than that measured in the BAT- group (19.5 +/- 8.0 vs. 7.2 +/- 1.7; p < 0.01). Corresponding fMRI studies showed significant differences in BOLD signal between the BAT+ and BAT- groups in both cortical (right anterior insula) and subcortical (midbrain) regions.

# CONCLUSION

Our data suggests that mild exposure to cold elicits differential neural responses in interoceptive regulatory centers (insula) of subjects with and without significant amounts of cold-activated BAT mass.

# **CLINICAL RELEVANCE/APPLICATION**

Our data provides an explanation for the observed high variability of cold-activated BAT mass observed in humans, indicating that it might be, in part, related to different sensitivities of higher-order interoceptive brain regions to skin temperature changes.



## NM232-SD-WEB2

## Comparing Osseous Lesions on 11C-Choline PET/CT and MRI in Prostate Cancer

Wednesday, Nov. 28 12:45PM - 1:15PM Room: NM Community, Learning Center Station #2

#### Awards Student Travel Stipend Award

#### **Participants**

Stephen J. Nogel, MD, Rochester, MN (*Presenter*) Nothing to Disclose Ann Packard, MD, Rochester, MN (*Abstract Co-Author*) Nothing to Disclose Anil N. Kurup, MD, Rochester, MN (*Abstract Co-Author*) Research Grant, Galil Medical Ltd; Research Grant, EDDA Technology, Inc; Royalties, Wolters Kluwer nv Mark A. Nathan, MD, Rochester, MN (*Abstract Co-Author*) Nothing to Disclose

For information about this presentation, contact:

# nogel.stephen@mayo.edu

# PURPOSE

Patients with biochemically recurrent prostate cancer may be evaluated with 11C-Choline PET/CT. For suspicious osseous findings, they frequently undergo image-guided biopsy, which may or may not be preceded by dedicated MRI of the area of interest. The purpose of this study was to compare imaging findings of suspected osseous metastases from prostate cancer on 11C-Choline PET/CT and convetional MRI in patients who have underwent image-guided biopsy to determine the value of MRI and biopsy in this setting.

#### **METHOD AND MATERIALS**

After obtaining IRB approval, a list of all 11C-Choline PET/CT exams performed at our institution was obtained. Patients were included if they had a 11C-Choline PET/CT and MRI prior to bone biopsy. The PET/CTs and MRIs were reviewed by two radiologists blinded to pathology results. A third radiologist reviewed all pathology with negative results to evaluate if the biopsy accurately sampled the suspicious lesion. Comparison was then made to pathology.

#### RESULTS

A total of 10,815 11C-Choline PET/CT exams were peformed between September 29, 2005 and March 31, 2017. Of those patients, 60 diagnostic bone biopsy samples were identified that had correlative 11C-Choline PET/CT and MRI exams. The biopsies were performed in the pelvis (34), spine (23), scapula, femur and clavicle. The average pate age was 65.5 (range 47-84), average Gleason score at diagnosis was 7.9 (range 5-10) and PSA level a the time of PET ranged from undetectable to 1642. A total of 38 lesions (63%) had pathology findings positive for osseous metastasis from prostate cancer, with 33 lesions (55%) having suspicious findings on both PET/CT and MRI. Five lesions (8.3%) positive for metastasis had isolated findings on MRI without PET/CT correlate, but no metastasis at biopsy had isolated findings on PET/CT without MRI correlated.

#### CONCLUSION

11C-Choline PET/CT and MRI have complementary roles in assessing osseous metastatic disease for patients with a history of prostate cancer. All biopsy-proven osseous metastases had abnormalities on MRI.

## **CLINICAL RELEVANCE/APPLICATION**

Both 11C-Choline PET/CT and MRI are valuable tools in evaluating patients with biochemically recurrent prostate cancer following definitive treatment. If 11C-Choline PET/CT findings are equivocal, MRI may be helpful for further evaluation prior to biopsy. If the MRI is negative, no biopsy is needed.



# NM233-SD-WEB3

Comparison of Different Metal Artifact Reduction (MAR) Techniques in 18F-FDG PET/CT Examinations: How Do They Impact Attenuation Correction in Metal Implants?

Wednesday, Nov. 28 12:45PM - 1:15PM Room: NM Community, Learning Center Station #3

# Participants

Ole Martin, Duesseldorf, Germany (*Presenter*) Nothing to Disclose Joel Aissa, MD, Duesseldorf, Germany (*Abstract Co-Author*) Nothing to Disclose Philipp Heusch, MD, Duesseldorf, Germany (*Abstract Co-Author*) Nothing to Disclose Gerald Antoch, MD, Duesseldorf, Germany (*Abstract Co-Author*) Nothing to Disclose Christina Antke, Duesseldorf, Germany (*Abstract Co-Author*) Nothing to Disclose Benedikt M. Schaarschmidt, MD, Essen, Germany (*Abstract Co-Author*) Stockholder, Bayer AG; Stockholder, General Electric Company; Stockholder, Siemens AG; Stockholder, Teva Pharmaceutical Industries Ltd

#### For information about this presentation, contact:

Ole.Martin@med.uni-duesseldorf.de

## PURPOSE

To evaluate the impact of metal artifact reduction (MAR) algorithms on Hounsfield units (HU) and standardized uptake values (SUV) in bright band artefacts caused by metal implants.

#### **METHOD AND MATERIALS**

In this prospective study, 25 oncological patients (13 female, 12 male, mean age 70.3 $\pm$ 13.0y) undergoing clinical indicated PET/CT with 32 different metal implants were included. An additional phantom scan was performed, consisted of a 25-L container containing a hip implant in a solution of 18F-fluorodeoxyglucose (18F-FDG) and water (background radiotracer: 6.5 kBq/mL). CT datasets were reconstructed using standard weighted filtered back projection (WFBP), metal artifact reduction in image space (MARIS) and iterative MAR (iMAR, using hip algorithm). PET attenuation correction was performed with all three datasets. SUVmean and HU measurements were performed at the site of the most prominent bright band artifacts. In the phantom scan, a total of 10 measurements were performed. HU and SUVmean values across all reconstructions were investigated using paired t-tests. Bonferroni correction was used to prevent alpha-error accumulation (p<0.017).

## RESULTS

In the phantom scan, in comparison to WFBP (261.4 $\pm$ 98.8 HU), MARIS led to a non-significant mean decrease of 25.8% (197.4 $\pm$ 74.1 HU, p>0.017), whereas iMAR-hip led to a significant decrease of 82% (48.0 $\pm$ 26.4 HU, p<0.017). For SUVmean measurements in WFBP (1.147 $\pm$ 0.035), MARIS showed no significant effect (1.102 $\pm$ 0.090), while iMAR-hip led to a significant decrease of 16.4% (0.990 $\pm$ 0.075, p<0.017). Similar results were observed in the patient scans: MARIS led to a non-significant mean decrease of 8% (378.0 $\pm$ 331.0 HU) in comparison to WFBP (411.4 $\pm$ 309.2 HU), whereas iMAR-hip led to a significant decrease of 66% (138.4 $\pm$ 195.3 HU, p<0.017). For SUVmean, MARIS showed no significant effect in comparison to WFBP (WFBP: 0.965 $\pm$ 0.380, MARIS: 0.942 $\pm$ 0.372), while iMAR-hip led to a significant decrease of 11.3% (0.856 $\pm$ 0.321, p<0.017).

# CONCLUSION

iMAR significantly reduces bright band artifacts caused by metal implants in CT and thus leads to a significant decrease of SUVmean in bright band artifacts comparison to WFBP and MARIS. This has a direct effect on PET quantification adjacent to metal implants.

# **CLINICAL RELEVANCE/APPLICATION**

iMAR significantly reduces the overestimation of attenuation in bright band artifacts in PET/CT and therefore can relevantly improve PET quantification in adjacent, malignant lesions.



#### NM234-SD-WEB4

### Prognostic Utility of Semi-Quantitative Metrics from Pre-Treatment F-18 FDG PET/CT of Ewing Sarcoma

Wednesday, Nov. 28 12:45PM - 1:15PM Room: NM Community, Learning Center Station #4

#### Awards Student Travel Stipend Award

#### **Participants**

Alexander Marchese, BA, Burlington, VT (*Presenter*) Nothing to Disclose Janusz K. Kikut, MD, Burlington, VT (*Abstract Co-Author*) Nothing to Disclose

For information about this presentation, contact:

awmarche@med.uvm.edu

# PURPOSE

This retrospective study aimed to evaluate if any semi-quantitative measurements from pre-treatment Fluorine-18 (F-18) fluorodeoxyglucose (FDG) positron emission tomography/computed tomography (PET/CT) as well as any additional clinical factors could offer prognostic information and predict survival outcomes in Ewing Sarcoma (EWS) patients.

#### **METHOD AND MATERIALS**

Thirteen adult and pediatric patients from a single academic medical center with histologically confirmed Ewing sarcoma were retrospectively chart reviewed. Those who had undergone F-18 FDG PET/CT prior to initial treatment with neoadjuvant chemotherapy between January 2000 and December 2017 were included. Semi-quantitative FDG-PET/CT parameters (SUVmax, SUVpeak, metabolic tumor volume, and pixel count) of the primary lesion of each patient were recorded, as well as clinical prognostic factors (sex, age, tumor location, tumor size, initial clinical presentation, and disease stage). Then, the overall relationships between each factor and patients' survival times were evaluated with univariate analysis. Survival time was measured as the time from pre-treatment FDG PET /CT scan to the date of death or to the date of the last follow-up visit in the electronic medical record.

#### RESULTS

Six patients (male, 4; female, 2; mean age,  $29.7 \pm 23.5$ ) were included. One patient died as a result of disease. The median survival time for all six subjects was 1520 days, the median SUVmax by using PET/CT was 8.9 (range, 3.0-13.5), and the median SUVpeak was 8.8 (range 4.9-11.70). Univariate analysis showed that patients with a SUVmax < 8.9 survived significantly longer than those with a SUVmax > 8.9 (median survival time, 2608 vs. 946 days; p = 0.018). Similarly, patients with a SUVpeak < 8.8 survived longer than those with a SUVpeak > 8.8 (median survival time, 2402 vs. 946 days; p = 0.062). Increased survival time was also found to be significantly related to female sex (median survival time, 2701 vs. 1059 days; p = 0.033).

#### CONCLUSION

Our small cohort demonstrates that pre-treatment measurement of SUVmax and SUVpeak from 18F-FDG PET/CT are potential prognostic indicators of Ewing sarcoma.

# **CLINICAL RELEVANCE/APPLICATION**

Pre-treatment F-18 FDG PET/CT offers a non-invasive prognostic tool to identify Ewing sarcoma patients who may benefit from more intensive therapy.



## NM235-SD-WEB5

Clinical Features of Secondary Primary Malignancies in Patients with Differentiated Thyroid Cancer Treated by Radioactive Iodine

Wednesday, Nov. 28 12:45PM - 1:15PM Room: NM Community, Learning Center Station #5

# Participants

Kunihiro Nakada, Sapporo, Japan (*Presenter*) Nothing to Disclose Naoya Hattori, MD, PhD, Sapporo, Japan (*Abstract Co-Author*) Nothing to Disclose Hiroki Sugie, MD, Sapporo, Japan (*Abstract Co-Author*) Nothing to Disclose Noriyoshi Katoh, MD,PhD, Sapporo, Japan (*Abstract Co-Author*) Nothing to Disclose Masayuki Sakurai, Sapporo, Japan (*Abstract Co-Author*) Nothing to Disclose Katsuhiko Kato, MD, PhD, Nagoya, Japan (*Abstract Co-Author*) Nothing to Disclose

#### For information about this presentation, contact:

metnakada@yahoo.co.jp

#### PURPOSE

The relationship between secondary primary malignancy (SPM) in thyroid cancer survivors and radioactive iodine therapy (RAI) remains unclear/The aim of the study was to investigate clinical features of patients who had SPM after RAI at our institute.

#### METHOD AND MATERIALS

Between Jun. 2007 and May. 2017, we encountered 19 patients (Male/Female 6/11, Age 37-82 yrs. average 66.9) who developed SPM during the follow up of thyroid cancer after RAI. The cumulative dose of I-131 ranged from 30 to 450mCi. In addition to post therapt I-131 scan, all patients underwent either of US, CT, FDG-PET or FDG-PET/CT before RAI and were followed up by combination of imaging modalities and serum Tg test at regular interval. The findings of imaging diagnosis were reviewed by 3 radiologists. SPM was confirmed by surgery or biopsy.

#### RESULTS

Of 19 patients, 6 had non-small cell lung cancer , 3 had breast cancer, 3 had colorectal cancer , 2 had gastric cancer , 2 had soft tissue sarcoma, 2 had hematopoietic malignancies, and 1 had pancreatic cancer. The latency period from the latest RAI and diagnosis of SPM ranged 16-178 mos. In 15 out of 19 patients (79%), SPM was incidentally detected by follow-up imaging studies before clinical manifestation. In contrast, 4 patients (21%) had SPM at the time of RAI, which was later confirmed within 3 years after RAI. Eight patients (42%) had specific risk factors for SPM such as diabetes, smoking, drinking alcohol, dietary habits or family history. None of the patients had extremely high I-131 uptake in the organs where SPM occurred on the post therapy I-131 scintigraphy. During the follow-up period, 8 (42%) patients died of SPM while 3(16%) died of thyroid cancer. The remaining 8 are alive with or without SPM.

#### CONCLUSION

It is highly unlikely that SPMs in majority of our subjects were substantially linked with RAI. Detailed information regarding strategies that detected SPM, stage of SPM at diagnosis, presence of potential risk factor for SPM, and cumulative radiation dose in the target organ from RIA and other imaging modalitirs should be taken into consideration to discuss relationship between RAI and SPM in thyroid cancer survivors.

# **CLINICAL RELEVANCE/APPLICATION**

In assessing long term potential risks of RAI, it is important to identify clinical features of SMP in patients with thyroid cancer underwent RAI, which cannot be evaluated by retrospective analysis of registered database



#### NR352-ED-WEB10

# Behind Those Eyes: What the Radiologist Needs to Know About Orbital Lesions

Wednesday, Nov. 28 12:45PM - 1:15PM Room: NR Community, Learning Center Station #10

# Participants

Gregory R. Stenoien, MD, Temple, TX (Presenter) Nothing to Disclose

#### **TEACHING POINTS**

1. Review orbital anatomy. 2. Discuss the clinical and radiologic presentation of the most common orbital masses. 3. Review cases of various orbital masses. 4. Discuss management options based on accurate differential diagnoses.

## **TABLE OF CONTENTS/OUTLINE**

Management options vary depending on the disease process, so it is important for a radiologist to be familiar with the most common orbital processes and provide proper management options. Knowledge of orbital anatomy and an accurate description of anatomic involvement are important to form an accurate diagnosis/differential. By utilizing knowledge of orbital anatomy and common orbital lesion presentations, the radiologist should be able to make diagnoses/recommendations for further workup accurately and confidently. Orbital Anatomy Anatomic structures Globe Intraconal space Cone Extraconal space Case Reviews Clinical presentation Imaging findings Differential diagnosis Additional imaging/workup, if applicable Final diagnosis, if available Take-home Points Provide a precise anatomic description Form a differential based on imaging findings, patient history, and patient demographics Make recommendations for further imaging or intervention, if necessary



#### NR353-ED-WEB11

# Resident Primer: A Pattern-Based Approach to Central Nervous System Infection

Wednesday, Nov. 28 12:45PM - 1:15PM Room: NR Community, Learning Center Station #11

## Awards Certificate of Merit

#### Participants

Mohammed Azfar Siddiqui, MBBS, MD, Saint Louis, MO (*Presenter*) Nothing to Disclose Sara Sartaj, Aligarh, India (*Abstract Co-Author*) Nothing to Disclose Mehtab Ahmad, MBBS, Aligarh, India (*Abstract Co-Author*) Nothing to Disclose Martin Reis, MD, Saint Louis, MO (*Abstract Co-Author*) Nothing to Disclose Yihua Zhou, MD, PhD, Saint Louis, MO (*Abstract Co-Author*) Nothing to Disclose

#### For information about this presentation, contact:

drazfarsiddiqui@gmail.com

## **TEACHING POINTS**

1. List various causes of CNS infection. 2. Describe a pattern-based approach to diagnosis based on clinical presentation, location and imaging characteristics. 3. Recognize mimickers.

## TABLE OF CONTENTS/OUTLINE

1. Epidemiology. 2. Clinical presentation, risk factors, and management. 3. CLASSIFICATION BASED ON LOCATION (Slide I): (I) Parenchymal: (A) Grey matter: (i) Solid: (a) Limbic system (b) Basal ganglia, cortex (c) Basal ganglia, pulvinar (ii) Ring Enhancing: (a) Basal Ganglia (b) Gray-white matter junction (B) White matter: (i) Periventricular (ii) Subcortical (II) Extra-axial: Epidural, Subdural, Leptomeningeal (III) Ventricular (IV) Cranial nerve (V) Mixed pattern 4) CLASSIFICATION BASED ON IMAGING CHARACTERSTICS (Slide II): (I) Conventional: (II) Diffusion restriction: Central, Peripheral (III) GRE (blooming): blood, Calcification (IV) Spectroscopy: Amino acid, Succinate, Lipid, Lactate, Trehalose (V) Angiography: Occlusion, Aneurysm (VI) Perfusion (CBV): Decrease, Increase 5) MIMICKERS: Malignancy, Infarct, Inflammatory, Demyelinating disorders. SUMMARY: CNS infections are relatively inaccessible to tissue sampling. Recognition and characterization of imaging patterns allow accurate diagnosis. This patterned approach will aid radiologists to quickly narrow the differentials and guide further workup and management.



## NR354-ED-WEB12

Don't Fall Asleep at the Wheel! A Practical Guide for Obstructive Sleep Apnea Syndrome (OSAS) Imaging Evaluation

Wednesday, Nov. 28 12:45PM - 1:15PM Room: NR Community, Learning Center Station #12

#### Awards Cum Laude

#### Cum Laude

# Participants

Ana Luiza M. Pettengill, MD, Sao Paulo, Brazil (*Presenter*) Nothing to Disclose Augusto Lio M. Goncalves Filho, MD, Sao Paulo, Brazil (*Abstract Co-Author*) Nothing to Disclose Nivaldo Adolfo Da Silva JR, MD, Campinas, Brazil (*Abstract Co-Author*) Nothing to Disclose Maira Sarpi, MD, Sao Paulo, Brazil (*Abstract Co-Author*) Nothing to Disclose Marcio Ricardo T. Garcia, MD, Sao Paulo-SP, Brazil (*Abstract Co-Author*) Nothing to Disclose Soraia A. Souza, MD, MS, Sao Paulo, Brazil (*Abstract Co-Author*) Nothing to Disclose Igor G. Padilha, MD, Sao Paulo, Brazil (*Abstract Co-Author*) Nothing to Disclose

#### For information about this presentation, contact:

ana\_luizap@hotmail.com

# **TEACHING POINTS**

- Review the imaging assessment of OSAS - Explore the utility of each imaging technique in OSAS evaluation - Establish a systematic guide for airway analysis in patients referred for apnea/hypopnea evaluation - Guide differential diagnosis that can cause sleep disturbance and that radiologists should not miss - Teach how to measure airway narrowing in OSAS

# TABLE OF CONTENTS/OUTLINE

- Clinical and epidemiological aspects of OSAS - Evaluation of airway narrowing in OSAS through our institutional cases - Computed tomography versus magnetic resonance approach - How to measure - a step-by-step guide - soft palate, tongue, retropalatal airway area, hyoid bone-mandible distance measurements - Evaluation of craniofacial dysmorphism, mainly in pediatric and syndromic patients - Can we predict severity? - Systematic guide for airway evaluation: OSAS mnemonic - Other causes of airway obstruction that may disturb sleep - imaging assessment: Nasal cavity and Nasopharynx Oral cavity and oropharynx - Systematic airway measurement - OSAS diagnosis - Approach to treatment: therapeutic decision and outcome - Severity estimation - prognosis - Ideas for a structured reporting



# NR417-SD-WEB1

CT Head Intracranial Hemorrhage Detection with Deep Learning: Experience with 9 Million Images

Wednesday, Nov. 28 12:45PM - 1:15PM Room: NR Community, Learning Center Station #1

#### Participants

Robert B. Lufkin, MD, Santa Monica, CA (*Presenter*) Stockholder, dmed.ai Stefano Soatto, PhD, Santa Monica, CA (*Abstract Co-Author*) Nothing to Disclose

# For information about this presentation, contact:

robert@dmed.ai

#### PURPOSE

Detection of acute intracranial hemorrhage is one of the leading indications for CT Head scans today. Deep learning using convolutional neural networks has surpassed human performance in certain complex visual recognition tasks. We describe a deep learning system for the detection of acute intracerebral hemorrhage in CT head scans.

# METHOD AND MATERIALS

A multilayer convolutional neural network was created using artificial intelligence development tools available on a commercial platform [dmed.ai, Santa Monica, CA]. The system was trained on ~3.5 million CT head scan images from over 24,000 examinations. The data was completely anonymized and no identifiable patient information was included. After training was complete, the system performance was evaluated using another set of ~4.8 million images from 29,925 CT head examinations. The images of both sets were labeled according to whether intracranial hemorrhage was present on the examination or not. Image labeling was performed by US board certified radiologists with specialized CT head expertise. The evaluation data were completely separate from the training data. Two different performance points were selected for review from the network which was set up to exclude any cases with intracranial hemorrhage.

## RESULTS

The total incidence of intracranial hemorrhage in the evaluation data was 5.14%[1496 examinations]. The first network to remove all cases of intracranial hemorrhage resulted in an incidence of 1.24% [371 missed examinations of intracranial hemorrhage after filtering. The second network had an incidence of only 0.31% [92 missed examinations] of intracranial hemorrhage. We review examples of the hemorrhages that were missed and strategies to improve performance in the future.

# CONCLUSION

It is possible to train neural networks using commercially available tools to detect intracranial hemorrhage in selected CT scans of the head. This is a promising area for further development.

# **CLINICAL RELEVANCE/APPLICATION**

Deep learning convolutional neural networks can detect/exclude a significant portion of CT head examinations with intracranial hemorrhage.



# NR418-SD-WEB2

Comparison of Compressed Sense and Conventional Technique for Magnetic Resonance Imaging of Brain in Paediatric Population

Wednesday, Nov. 28 12:45PM - 1:15PM Room: NR Community, Learning Center Station #2

# Participants

Niranjan Khandelwal, MD, Chandigarh, India (*Presenter*) Nothing to Disclose Nirmalya Ray, MD, Chandigarh, India (*Abstract Co-Author*) Nothing to Disclose Paramjeet Singh, MBBS,MD, Chandigarh, India (*Abstract Co-Author*) Nothing to Disclose Vivek Gupta, MD, Chandigarh, India (*Abstract Co-Author*) Nothing to Disclose Chirag K. Ahuja, MD, Chandigarh, India (*Abstract Co-Author*) Nothing to Disclose Naveen Sankhyan, Chandigarh, India (*Abstract Co-Author*) Nothing to Disclose Manish Modi, MD, Chandigarh, India (*Abstract Co-Author*) Nothing to Disclose Indrajit Saha, PhD, Gurgaon, India (*Abstract Co-Author*) Employee, Koninklijke Philips NV Karthick R. Rajendran, Gurgaon, India (*Abstract Co-Author*) Employee, Koninklijke Philips NV

#### For information about this presentation, contact:

khandelwaln@hotmail.com

#### PURPOSE

The main challenge in paediatric brain MRI is the need for sedation & anaesthesia during its acquisition. In this study, compressed sensing, a novel method of scan time reduction, is combined with the SENSE infrastructure, i.e., Compressed-SENSE (CSENSE), for accelerating anatomic MR data acquisition in paediatric human brain.

#### **METHOD AND MATERIALS**

Thirty children (mean age:10.8 years, range-8-16 years) undergoing MRI brain were included in this study,T2- axial, 3D-FLAIR & 3D-T1 GRE sequences for brain were acquired using conventional and CSENSE techniques. Any patient requiring sedation or anaesthesia for MRI acquisition have been excluded from the study.The CSENSE sequences were acquired with two different acceleration factors with either of them applied to a particular patient.The acceleration factors for T2 axial brain were 1.8 & 2.4, for 3D FLAIR were 8 & 10.8 and for 3D T1 were 3.4 and 4.Two neuro-radiologists, have evaluated the images independently regarding image quality on a predefined scale, based on visualisation of 10 anatomical brain structures as well as for resolution, lesion conspicuity, artefacts and overall diagnostic confidence.The quantitative evaluation of image quality was done by calculating the image contrast ratio.Interrater agreement was evaluated using  $\kappa$  test.The subjective visualization parameters were assessed using the Wilcoxon signed-rank test.Comparison of image contrast ratios was done by paired t test.

## RESULTS

The time reduction achieved with T2 at 1.5 & 2 reduction factors were 51 seconds(31.2%) and 82 seconds(51.5%) respectively, with 3D T1 at 1.5 & 2 reduction factors 144 seconds(51.5%) and 168 seconds(56.3%) respectively and with 3D FLAIR at 1.8 & 2 reduction factors 74 seconds(28%) and 101 seconds(38.2%) respectively. High inter-rater agreement (k=0.911) was found regarding overall visualisation of different brain structures, resolution (k=0.907), lesion conspicuity (k=0.928), artefacts(k=0.922) and overall diagnostic confidence (k=0.931). Nonsignificant statistical difference was found regarding image quality and image contrast ratio between both techniques.

# CONCLUSION

CSENSE can be used as a potential tool for reducing acquisition time for pediatric brain MRI without compromising the image quality.

#### **CLINICAL RELEVANCE/APPLICATION**

The scan time reduction achieved by CSENSE technique can be of paramount significance as it can potentially reduce the need for sedation & anaesthesia in paediatric population.



# NR419-SD-WEB3

Clinical Feasibility of 2 Minutes Ultrafast Brain MRI and MR Angiography Compared With Synthetic Brain MRI and Conventional MR Angiography: A Single Center Pilot Study

Wednesday, Nov. 28 12:45PM - 1:15PM Room: NR Community, Learning Center Station #3

# Participants

Hye Jin Baek, Changwon, Korea, Republic Of (*Presenter*) Nothing to Disclose Kyeong Hwa Ryu, MD, Seoul, Korea, Republic Of (*Abstract Co-Author*) Nothing to Disclose Moonjung Hwang, Seoul, Korea, Republic Of (*Abstract Co-Author*) Research support, General Electric Healthcare Yedaun Lee, MD, Busan, Korea, Republic Of (*Abstract Co-Author*) Nothing to Disclose

#### For information about this presentation, contact:

sartre81@gmail.com

# PURPOSE

Ultrafast brain MRI is required for uncooperative patients and acute stroke patients by reducing scan time and motion artifacts. This is the first study to investigate the clinical feasibility of 2 minutes ultrafast MRI protocol (ultrafast MRI and MR angiography) comparing with routine MRI protocol (synthetic MRI and conventional MR angiography).

# METHOD AND MATERIALS

The institutional review board approved this study. We retrospectively reviewed a total of 25 patients who underwent ultrafast MRI protocol and routine MRI protocol from April 2017 to May 2017. The total scan time of the ultrafast MRI protocol was 1 minutes 45 seconds. Image quality assessments were performed on routine MRI sequences and ultrafast MRI sequences by two independent readers. Wilcoxon signed-rank test was used to compare the reader's ratings of routine MRI protocol and ultrafast MRI protocol.

#### RESULTS

Using a 4-point assessment scale, overall image quality and anatomical delineation of ultrafast brain MRI were lower than routine brain MRI using synthetic MRI. However, ultrafast MRI demonstrated sufficient overall image quality and anatomical delineation with more than 2 points. The artifacts of ultrafast MRI were less than routine MRI.

## CONCLUSION

The 2 minutes ultrafast brain MRI protocol can be acceptable for clinical neuroimaging and it can be helpful for the patients who require very short scan time.

# **CLINICAL RELEVANCE/APPLICATION**

MRI is widely used in the assessment of intracranial pathologies, however, it was limited in the clinical use due to the relatively long scan time. In the current study, we found that the 2 minutes ultrafast MRI can be acceptable for clinical use in the patients who require very short scan time such as hyperacute stroke patients, restless and uncooperative patients and pediatric patients. Because the overall image quality and conspicuity of anatomical details were acceptable for diagnostic use.



#### NR420-SD-WEB4

# Non-Contrast ASPECTS Region Density Predicts Final Infarction in Acute Ischemic Stroke

Wednesday, Nov. 28 12:45PM - 1:15PM Room: NR Community, Learning Center Station #4

#### Participants

Wolfgang G. Kunz, MD, Munich, Germany (*Abstract Co-Author*) Grant, Medtronic plc
Lukas Rotkopf, Munich, Germany (*Abstract Co-Author*) Nothing to Disclose
Daniel Puhr-Westerheide, MD, Munich, Germany (*Abstract Co-Author*) Nothing to Disclose
Matthias P. Fabritius, MD, Munich, Germany (*Presenter*) Nothing to Disclose
Nils Daniel Forkert, Hamburg, Germany (*Abstract Co-Author*) Nothing to Disclose
Paul Reidler, MD, Munich, Germany (*Abstract Co-Author*) Nothing to Disclose
Franziska Dorn, Munich, Germany (*Abstract Co-Author*) Nothing to Disclose
Steffen Tiedt, Munich, Germany (*Abstract Co-Author*) Nothing to Disclose
Steffen Tiedt, Munich, Germany (*Abstract Co-Author*) Nothing to Disclose
Kolja M. Thierfelder, MD,MSc, Rostock, Germany (*Abstract Co-Author*) Nothing to Disclose
Frank Wollenweber, Munich, Germany (*Abstract Co-Author*) Nothing to Disclose
Andre Kemmling, MD, Luebeck, Germany (*Abstract Co-Author*) Nothing to Disclose

#### For information about this presentation, contact:

wolfgang.kunz@med.lmu.de

# PURPOSE

To determine if automated non-contrast CT (NCCT) density measurements in acute ischemic stroke provide information on the development of final infarction.

#### **METHOD AND MATERIALS**

We selected 121 patients with middle cerebral artery stroke due to large vessel occlusion out of a consecutive cohort. Densities in Alberta Stroke Program Early CT Score (ASPECTS) regions were quantified as average Hounsfield Unit (HU) values using automated segmentation (Figure 1). Relative HU (rHU) values were calculated dividing absolute regional densities of ischemic by non-ischemic hemispheres. Final infarction was defined visually per ASPECTS region in a dichotomized fashion and as total volume. A composite rHU score incorporating values from all ASPECTS regions weighted by regional relevance was calculated. Receiver-operatingcharacteristic curve (ROC) analysis was performed to calculate area-under-the-curve (AUC) values. Linear regression analysis was used for multivariable adjustment.

#### RESULTS

Median visual ASPECTS on NCCT was 8 (interquartile range: 6-9). Automated density measurements were feasible in all 121 patients within one minute of post-processing time. rHU values yielded significant regional classification of final infarction in ROC analyses for all ASPECTS regions except M3 and M6. Best classifications were achieved for lentiform nucleus (AUC=0.810, p<0.001), caudate nucleus (AUC=0.777, p<0.001), and insula (AUC=0.764, p<0.001). The composite rHU score was independently associated with final infarction volume ( $\beta$ =-0.353, p<0.001), outperforming visual ASPECTS assessment ( $\beta$ =-0.190, p=0.062) in multivariable regression analysis. The regression coefficients indicating the effect size were most pronounced in patients that received no reperfusion therapy ( $\beta$ =-0.582, p<0.001).

#### CONCLUSION

Automated NCCT density changes identify ASPECTS regions that develop final infarction in patients with acute ischemic stroke. The composite rHU score outperformed visual ASPECTS interpretation in the prediction of final infarction volumes.

## **CLINICAL RELEVANCE/APPLICATION**

Automated NCCT density measurements may serve as an observer-independent imaging biomarker to provide instantaneous decision support for treatment selection in patients with acute ischemic stroke.



# NR421-SD-WEB5

Acute Thrombectomy in the Ageing Population: A Retrospective Analysis of Radiological and Clinical Outcomes in Acute Thrombectomies Performed in Patients 80 Years and Older With an Intention to Treat Analysis

Wednesday, Nov. 28 12:45PM - 1:15PM Room: NR Community, Learning Center Station #5

#### Awards Student Travel Stipend Award

Participants Elena A. Cora, MD, Ottawa, ON (*Presenter*) Nothing to Disclose Mohamad K. AbdalKader, MD, Boston, MA (*Abstract Co-Author*) Nothing to Disclose Phil White, MSc,MD, Newcastle-upon-Tyne, United Kingdom (*Abstract Co-Author*) Research Consultant, Terumo Corporation; Institutional Research funded, Terumo Corporation; Grant, Medtronic plc Daniela Iancu, Ottawa, ON (*Abstract Co-Author*) Nothing to Disclose

# For information about this presentation, contact:

ecora@toh.ca

#### PURPOSE

The incidence of ischemic stroke is higher in the older population with higher mortality. Studies have demonstrated clinical benefit when performing thrombectomy. A meta-analysis performed with patient level data from five trials showed that this benefit is also present in patients that are over 80 years old although increasing age is a negative predictor of clinical outcome and they only had a small number of patients in this age category. As the safety and clinical outcomes in this age group are not yet clear, our aim is to provide data from clinical practice to assess the safety and efficacy of endovascular thrombectomy in this age group.

## **METHOD AND MATERIALS**

We retrospectively reviewed all consecutive patients of age 80+ referred for thrombectomy procedures at three international institutions from 01/01/2015 to 31/12/2017. We collected demographic data, risk factors, clinical and radiological findings, treatment details, clinical and radiological outcomes. All patients who were brought to the angiographic suite and had a groin puncture with the intention to perform thrombectomy were included in this study.

#### RESULTS

Data for 139 patients, 97F and 42M, with median age of 85 was included. Baseline clinical characteristics are similar to previous trials. The most common location for the target intracranial large vessel occlusion was in the M1 MCA (middle cerebral artery) in 51% (71/139). 60% (83/139) patients received IV tPA. Good reperfusion (mTICI 2b/3) was achieved in 66% (92/139) patients within a median timeframe of 225 minutes. Good clinical outcome (mRS 0-2) at 90 days was achieved in 23% (32/139) patients.Symptomatic intracranial hemorrhage was present in 2% (3/139) patients.The 90-day mortality rate is 40% (54/139).

#### CONCLUSION

Our study adds valuable evidence to the limited available published data on the safety and clinical outcomes in patients 80 years of age and older who undergo acute thrombectomy for large vessel ischemic stroke with modern devices.

# **CLINICAL RELEVANCE/APPLICATION**

Overall our results are largely similar to the HERMES meta-analysis data on patients aged 80 years and older, although we had slightly lower rates of good functional outcomes and slightly higher mortality at 3 months (see attached Figure). This study supports the delivery of acute thrombectomy for acute ischemic stroke due to large vessel occlusion in a clinical care setting in the elderly population.



## NR422-SD-WEB6

Feasibility of Dual-Layer Detector Spectral CT-Derived Iodine Quantification for Focal Thyroid Lesions: A Pilot Study

Wednesday, Nov. 28 12:45PM - 1:15PM Room: NR Community, Learning Center Station #6

# Participants

Younghen Lee, MD, Ansan, Korea, Republic Of (*Presenter*) Nothing to Disclose Do Hyung Lee, Ansan, Korea, Republic Of (*Abstract Co-Author*) Nothing to Disclose Hyung Suk Seo, Ansan-si, Korea, Republic Of (*Abstract Co-Author*) Nothing to Disclose

#### For information about this presentation, contact:

younghen@korea.ac.kr

# PURPOSE

To determine whether dual-layer CT(DLCT)-derived iodine quantification could characterize the focal thyroid lesions encountered during CT examination

#### **METHOD AND MATERIALS**

We retrospectively enrolled 69 patients (M:F=19:50,mean age:52.6years) with a total of 76 cytopathologically confirmed thyroid lesions (mean size: 1.9cm) identified by contrast-enhanced CT over a 5-month period. After obtaining the iodine concentration values of thyroid nodule (IC\_N), ipsilateral thyroid parenchyma and common carotid artery from a DLCT datasets, IC\_N and normalized IC\_N over the ipsilateral thyroid parenchyma and artery were compared between three groups:papillary thyroid carcinoma (PTC), benign nodule and cyst.

## RESULTS

From a total of 76 focal thyroid lesions, 46, 17 and 13 were assigned into PTC, benign solid nodule and cyst groups, respectively. Based on sonographic and cytopathological correlation, all IC\_N were significantly different among cysts, PTCs and benign nodules (median: 0.60, interquartile range [IQR], 0.33-0.88 vs. 3.15, IQR, 2.29-4.01 vs. 4.30, IQR, 3.13-5.48, all p< 0.001). Similarly, the normalized IC\_N were all statistically different from each other (p < 0.05).

# CONCLUSION

DLCT-derived iodine quantification may have a potential role in the characterization of focal thyroid lesions detected by contrastenhanced neck CT examination.

## **CLINICAL RELEVANCE/APPLICATION**

DLCT technique allowed iodine quantification of the focal thyroid lesions. IC\_N among PTC, benign thyroid nodule and cyst were significantly different. Iodine quantification with DLCT could be useful to characterize focal thyroid lesions.



## NR423-SD-WEB7

# Synthetic Brain MRI Obtained from T1 and T2 Imaging

Wednesday, Nov. 28 12:45PM - 1:15PM Room: NR Community, Learning Center Station #7

FDA Discussions may include off-label uses.

#### **Participants**

Valentina Citton, Padua, Italy (*Abstract Co-Author*) Nothing to Disclose Kambiz Nael, MD, New York, NY (*Presenter*) Medical Advisory Board, Canon Medical Systems Corporation Tsutomu Katoh, Niihama, Japan (*Abstract Co-Author*) Nothing to Disclose Alessandro Baglione, Bergamo, Italy (*Abstract Co-Author*) Nothing to Disclose Yasmina Chaibi, PhD, La Ciotat, France (*Abstract Co-Author*) Employee, Canon Medical Systems Corporation Sophie Campana, La Ciotat, France (*Abstract Co-Author*) Employee, Canon Medical Systems Corporation Nathalie Kieusseyan, La Ciotat, France (*Abstract Co-Author*) Employee, Canon Medical Systems Corporation Bruno Triaire, La Cictat, France (*Abstract Co-Author*) Employee, Canon Medical Systems Corporation Masao Yui, Otawara, Japan (*Abstract Co-Author*) Employee, Canon Medical Systems Corporation Ryo Shiroishi, Otawara, Japan (*Abstract Co-Author*) Employee, Toshiba Corporation Anca Mitulescu, PhD, La Ciotat, France (*Abstract Co-Author*) Employee, Canon Medical Systems Corporation Medical Systems Corporation

# For information about this presentation, contact:

kambiznael@gmail.com

# PURPOSE

Synthetic brain MRI has shown promising results using dedicated quantitative multi-contrast sequence such as SyMRI (SyntheticMR AB, Linköping, Sweden) or MAGiC (GE Healthcare, USA). In this study we aimed to synthesize different weightings including T1-Inversion recovery (T1IR) and T2-FLAIR from commercially available T1 and T2 weighted imaging.

#### **METHOD AND MATERIALS**

In this HIPAA complaint prospective study, brain MRI studies were obtained using conventional T1IR, T2-FLAIR in addition to MP2RAGE (magnetisation-prepared 2 rapid acquisition gradient echoes) and multi-echo Fast Spin Echo (ME-FSE) sequences on a Vantage Titan<sup>™</sup> 3T MR system (Toshiba Medical Systems, Tochigi, Japan). From MP2RAGE and ME-FSE, Synthetic T1IR and T2-FLAIR images in addition to quantitative maps of T1, T2 and PD were computed using Olea Sphere® (La Ciotat, France) post-processing software. Qualitative and quantitative (of CNR) analysis were performed between conventional and synthetic T1IR and T2-FLAIR by two board certified neuroradiologists independently.

# CONCLUSION

Synthetic weightings including T1IR and FLAIR can be calculated from routinely obtained T1 and T2-weighted brain MRIs with acceptable quantitative and qualitative performance in comparison to conventional MRIs. This technique has the potential value of providing additional quantitative measures such as T1, T2 and PD maps at no extra cost.

# **CLINICAL RELEVANCE/APPLICATION**

Our proposed method provides synthetic MRI weightings in addition to quantitative maps from T1 and T2 MR images without the need for a dedicated synthetic MR sequence and can be broadly adopted for clinical use.



## NR424-SD-WEB8

Impact of Brain Tumors and Radiotherapy on the Presence of Gadolinium in the Brain After Repeated Administration of Gadolinium Based Contrast Agents: An Experimental Study on Rats

Wednesday, Nov. 28 12:45PM - 1:15PM Room: NR Community, Learning Center Station #8

## Participants

Gregor Jost, PhD, Berlin, Germany (*Abstract Co-Author*) Employee, Bayer AG Thomas Frenzel, PhD, Berlin, Germany (*Abstract Co-Author*) Employee, Bayer AG Janina Boyken, Berlin, Germany (*Abstract Co-Author*) Nothing to Disclose Hubertus Pietsch, PhD, Berlin, Germany (*Presenter*) Employee, Bayer AG

#### PURPOSE

To evaluate the impact of brain tumors and radiotherapy (RT) on the presence of gadolinium (Gd) in the brain and on T1-weighted MRI signal intensity (SI) changes after repeated administration of a linear gadolinium-based contrast agent (GBCA) in an experimental rat model.

## **METHOD AND MATERIALS**

18 Fischer rats (F-355) were divided into a tumor and two healthy groups that were subdivided into a RT and a control group (n=6 /group). GS9L cells were stereotactically inoculated into the cerebrum of animals from the tumor group. After 7 days the presence of the tumor was confirmed by MRI. All animals received 5 intravenous injections (each 1.8 mmol/kg) of gadopentetate dimeglumine on day 7-11 after inoculation. T1-weighted brain MRI was performed at baseline (one day before inoculation) and one week after the last GBCA administration (day 18 post inoculation). Animals from the tumor and RT group underwent RT in 6 fractions of 3 Gray on day 8-10 and 15-17 post inoculation. After the last MRI the brain was dissected for Gd quantification with ICP-MS. Statistical comparison between groups was done with the Kruskal-Wallis test.

## RESULTS

One week after the last GBCA administration higher SI ratios between deep cerebellar nuclei and brain stem were observed in all three groups compared to the baseline MRI. However, between the groups no significant differences in the SI ratios were found at baseline (p=0.59) and one week after the last administration (p=0.14). The tissue Gd concentrations (median in nmol/g tissue) were 6.7 (tumor group), 6.3 (RT group) and 6.8 (control group) in the cerebellum, 3.7 (tumor), 3.1 (RT) and 2.8 (control) in the brain stem and 16.2 (tumor), 19.9 (RT) and 16.9 (control). No significant differences were found between the groups (p=0.64 for cerebellum, p=0.4 for brain stem and p = 0.57 for cerebrum).

## CONCLUSION

The presence of a brain tumor treated by RT or RT alone did not alter the amount of Gd that was found in the rat brain and the MRI signal hyperintensity in the deep cerebellar nuclei one week after repeated administration of gadopentetate dimeglumine. The experimental data suggests that a pathological disrupted blood-brain barrier does not affect the amount of Gd presence present in the brain one week after administration.

### **CLINICAL RELEVANCE/APPLICATION**

Systematic preclinical studies may help to gain a better understanding of the clinical observation of high brain signal intensities on unenhanced MR images.



## NR425-SD-WEB9

## Functional Connectivity rsfMRI Study of Chess Experts and Novices

Wednesday, Nov. 28 12:45PM - 1:15PM Room: NR Community, Learning Center Station #9

#### **Participants**

Dan-Ling Hsu, Stony Brook, NY (*Presenter*) Nothing to Disclose David Ouellette, MS, Stony Brook, NY (*Abstract Co-Author*) Nothing to Disclose Sindhuja Tirumalai Govindarajan, MS, Stony Brook, NY (*Abstract Co-Author*) Nothing to Disclose Patricia Stefancin, MSc,BSC, Stony Brook, NY (*Abstract Co-Author*) Nothing to Disclose Tim Duong, PhD, Stony Brook, NY (*Abstract Co-Author*) Nothing to Disclose

## For information about this presentation, contact:

dan-ling.hsu@stonybrook.edu

### PURPOSE

Although task fMRI has been used to study neural correlates of different expertise domains, reports on the resting state functional connectivity (FC) of expertise domain are sparse. In our prior analysis on an open dataset on chess expertise, we found that the fractional anisotropy of the internal capsule, a white matter tract connecting the subcortical to the cortex and running through the basal ganglia (BG), was markedly higher in Chinese chess expertise compared to novices. BG has been shown to take part in a wide range of cognitive function, such as learning and memory, through its anatomical prominence as well as widespread connections. In the current follow-up study, we performed seed-based analysis with BG areas as seeds to investigate FC difference between Chess experts and novices at rest

## METHOD AND MATERIALS

We performed seed-based rsfMRI analysis using three BG seeds, bilateral caudate, putamen, and pallidum, on an open data set (HMRRC, http://goo.gl/ZnpvgB). The data were processed with SPM12 and Functional Connectivity toolbox (CONN) using the default preprocessing pipeline. Among 29 Chinese chess experts and 29 novices, 7 experts and 2 novices were removed from analysis because of excessive motion artifacts. All analyses were tested at p < 0.001, cluster size FDR-corrected at p < 0.05.

## RESULTS

With bilateral pallidum as a seed, experts showed higher FC in the left ventromedial prefrontal cortex (vmPFC) and posterior superior temporal gyrus (pSTG). With bilateral putamen, experts showed a higher FC in left angular gyrus (AG), and bilateral pSTG. Dorsomedial prefrontal cortex and vmPFC participate in strategy switching in response to behavioral contingencies (Donoso et al, 2014), whilst AG and pSTG are known to play a role in the retrieval of concepts. Putamen, a part of the striatum, is one of the major gates for cortical input to, and pallidum the main output from, the BG. The cortico-basal ganglia circuit has long been implicated in learning, implying the role of BG in concept retrieval.

## CONCLUSION

Our results suggest expert performance involves a higher functional integration of specific networks that enables higher flexibility for alternating between different strategies.

## **CLINICAL RELEVANCE/APPLICATION**

Improved understanding of functional connectivity underpinning expertise may prove useful in designing individualized training strategies.



## OB187-ED-WEB1

## The ACR Ovarian Reporting and Data System (O-RADS): A US Lexicon Training and Testing Module

Wednesday, Nov. 28 12:45PM - 1:15PM Room: OB Community, Learning Center Station #1

## Awards Certificate of Merit

### **Participants**

Loretta M. Strachowski, MD, San Francisco, CA (*Presenter*) Nothing to Disclose Mindy M. Horrow, MD, Philadelphia, PA (*Abstract Co-Author*) Spouse, Employee, Merck & Co, Inc Rochelle F. Andreotti, MD, Nashville, TN (*Abstract Co-Author*) Nothing to Disclose Beryl R. Benacerraf, MD, Boston, MA (*Abstract Co-Author*) Nothing to Disclose Phyllis Glanc, MD, Toronto, ON (*Abstract Co-Author*) Advisory Board, General Electric Company Dirk Timmerman, Leuven, Belgium (*Abstract Co-Author*) Nothing to Disclose

### For information about this presentation, contact:

lori.strachowski@ucsf.edu

### **TEACHING POINTS**

By viewing this exhibit, the learner will be able to: 1) Define the O-RADS (Ovarian Reporting and Data System) lexicon as a standardized set of terms and descriptors of ovarian and adnexal findings to assist in risk stratification and appropriate management. 2) List and describe all terms which were included in the lexicon based on: (a) usage and/or evidence in the literature, (b) attaining  $\geq$  80% agreement by O-RADS committee, (c) use by IOTA (International Ovarian Tumour Analysis) Group that has compiled outcomes data based on ovarian lesion characterization. 3) Test and reinforce one's comprehension of the O-RADS US lexicon through a series of test cases accompanied by diagnoses.

### TABLE OF CONTENTS/OUTLINE

This educational electronic exhibit will be divided into 2 sections. Section 1 will review the following in detail with definitions, illustrative diagrams, image examples and pitfalls: A. General Definitions B. Major Categories (subdivided into minor categories for both solid and cystic lesions C. Size (options) D. Vascularity (descriptors and scoring system) E. General and Extra-ovarian Findings. Section 2 will be a series of test cases (with images and multiple choice descriptor options) to strengthen the viewers' understanding of the lexicon.

## **Honored Educators**

Presenters or authors on this event have been recognized as RSNA Honored Educators for participating in multiple qualifying educational activities. Honored Educators are invested in furthering the profession of radiology by delivering high-quality educational content in their field of study. Learn how you can become an honored educator by visiting the website at: https://www.rsna.org/Honored-Educator-Award/ Mindy M. Horrow, MD - 2013 Honored EducatorMindy M. Horrow, MD - 2016 Honored Educator



## OB188-ED-WEB2

## Imaging Overview of Ovarian Epithelial Tumors: What the Radiologist Should Know

Wednesday, Nov. 28 12:45PM - 1:15PM Room: OB Community, Learning Center Station #2

#### **Participants**

Daniel A. Hynes, MD, Springfield, MA (*Presenter*) Nothing to Disclose Christina Duffin, MD, Springfield, MA (*Abstract Co-Author*) Nothing to Disclose Daniel Kowal, MD, Sturbridge, MA (*Abstract Co-Author*) Nothing to Disclose

## **TEACHING POINTS**

Ovarian epithelial tumors (OET) account for the majority of ovarian neoplasms. They present a clinical challenge due to a broad range of imaging appearances, and appropriate characterization is vital due to the aggressive nature of malignant variants of these tumors. In this multimodality review, we break down this diagnostic dilemma and outline distinguishing imaging findings of each subtype as well as unique metastatic patterns that need to be included in the radiologist's search pattern. 1) Review the pathophysiology and epidemiology of OET 2) Focused discussion of serous, mucinous, endometrioid, clear cell, Brenner and borderline tumors through US, MRI and CT examples, e.g., serous tumors are more often unilocular, bilateral and may have calcifications, whereas mucinous tumors are larger, multilocular, rarely with calcification. 3) Review of metastatic patterns, e.g. psammomatous calcific metastases with serous tumors compared with pseudomyxoma peritonei of mucinous tumors. 5) Discuss current ACR imaging appropriateness criteria and management guidelines.

## TABLE OF CONTENTS/OUTLINE

Introduction •Teaching objectives •Epidemiology and Pathophysiology•Benign OET-presentation, imaging characteristics, management and follow-up •Malignant OET •Peritoneal metastasis-pelvic wall implants, omental carcinomatosis, pseudomyxoma peritonei •Summary •References



## PD191-ED-WEB7

## Pediatric Whole Body PET/MR: How to Acquire Excellent Images with a Streamlined Protocol

Wednesday, Nov. 28 12:45PM - 1:15PM Room: PD Community, Learning Center Station #7

**FDA** Discussions may include off-label uses.

#### **Participants**

Anne M. Muehe, MD, Stanford, CA (*Presenter*) Nothing to Disclose Anuj Pareek, MD, Aarhus C, Denmark (*Abstract Co-Author*) Nothing to Disclose Ashok Joseph Theruvath, MD, Mainz, CA (*Abstract Co-Author*) Nothing to Disclose Praveen Gulaka, PhD, Stanford, CA (*Abstract Co-Author*) Nothing to Disclose Heike E. Daldrup-Link, MD, Palo Alto, CA (*Abstract Co-Author*) Nothing to Disclose

#### For information about this presentation, contact:

amuehe@stanford.edu

#### **TEACHING POINTS**

Research over the past years have shown potential applications and additional diagnostic value of integrated PET/MR scans for cancer staging in adult patients. However, few studies have been conducted in pediatric patients thus far. PET/MR can be of great value for pediatric cancer patients since it has significantly less radiation compared to clinical PET/CT and provides excellent soft tissue resolution. However, current PET/MR scan protocols are significantly longer compared to PET/CT, which impairs image quality and limits feasibility in children. Another problem is the short-lived vessel contrast of standard gadolinium-based contrast agents which limits the image quality of a whole body scan. The purpose of educational exhibit is to present a child-tailored, time-efficient PET/MR cancer staging protocol that provides excellent image quality. This protocol is based on integration of ferumoxytol-enhanced and 18F-FDG enhanced PET/MR scans.

## **TABLE OF CONTENTS/OUTLINE**

• Imaging protocol: Fast sequences are key • Contrast agent: The value of Ferumoxytol • One stop imaging: Combining local tumor and whole body staging • Post-processing: What to do with all the images • Radiologist satisfaction: A simplified approach to a comprehensive diagnosis



## PD235-SD-WEB1

Normalized Organ Doses for Pediatric Chest CT Examinations Calculated Using a Patient-Specific Monte Carlo Method

Wednesday, Nov. 28 12:45PM - 1:15PM Room: PD Community, Learning Center Station #1

## Participants

John E. Damilakis, PHD, Iraklion, Greece (*Presenter*) Nothing to Disclose John Stratakis, Heraklion, Greece (*Abstract Co-Author*) Nothing to Disclose Georgia Solomou, Heraklion, Greece (*Abstract Co-Author*) Nothing to Disclose Antonios E. Papadakis, MSc, PhD, Heraklion, Greece (*Abstract Co-Author*) Nothing to Disclose Kostas Perisinakis, Heraklion, Crete, Greece (*Abstract Co-Author*) Nothing to Disclose

# PURPOSE

The aim of this study was to provide normalized organ doses for pediatric chest CT examinations for primarily exposed organs/tissues i.e. breast, esophagus, lungs, heart, skin and bone.

## METHOD AND MATERIALS

Chest CT examinations performed on 93 pediatric patients (age range 0-17 years) were included in this study. Using patient CT images as input volume, a 3-dimensional (3D) model was created for each patient. 3D dose distributions were generated for each patient model using an equipment-specific and patient-specific Monte Carlo code (ImpactMC, CT Imaging GmbH, Erlangen, Germany). Doses normalized to CTDIvol were determined for 80 kVp, 100 kVp and 120 kVp for breast, esophagus, lungs, heart, skin and bone with and without automatic exposure control (AEC) activation. Two CT scanners were modelled (Somatom Sensation 64, Somatom Sensation 16, Siemens Healthcare, Forchheim, Germany). The scanner's geometry, x-ray spectrum, composition and dimensions of the filters were taken into account in the simulation. To correlate with organ doses, the water equivalent diameter (WED) was measured at the central axial slice depicting heart. Radiation doses estimated using Monte Carlo data were compared to those determined using thermoluminescence dosimetry and 4 pediatric anthropomorphic phantoms that simulate an individual as neonate, 1-year-old, 5-year-old, 10-year-old child.

### RESULTS

The results consist of normalized organ doses as a function of WED for 3 kVp values, for fixed tube current and AEC, for both Sensation 64 and Sensation 16. Normalized organ doses correlated strongly with WED (R2>0.7 for most cases, for both scanners). A very good agreement was observed between doses estimated by TLD measurements and the Monte Carlo simulation (maximum difference less than 20%).

## CONCLUSION

Data produced allow for accurate estimation of doses to primarily exposed organs/tissues from pediatric chest CT examinations. This study has received funding from the Euratom research and training programme 2014-2018 under grant agreement No 755523 (MEDIRAD project)

## **CLINICAL RELEVANCE/APPLICATION**

The correlations of patient-specific organ dose estimates with patient size can be used to estimate pediatric organ doses from chest CT examinations. This information allows prospective estimation of dose prior to examination or retrospectively to communicate doses to patients and physicians.



### PD236-SD-WEB2

### Wide Awake and Satisfied

Wednesday, Nov. 28 12:45PM - 1:15PM Room: PD Community, Learning Center Station #2

## Participants

Fatima R. Janjua, MBBS, Brooklyn, NY (Presenter) Nothing to Disclose

For information about this presentation, contact:

fatimarjanjua@gmail.com

#### PURPOSE

Sedation-free MRI imaging for Children

## METHOD AND MATERIALS

There are times when sedating children for diagnostic imaging is necessary. But when it comes to successful sedation-free imaging, here are three important ingredients: 1. Assessment of the child's potential to tolerate the study awake. 2. Preparation for the child and family. 3. Family-centered approach to the environment of care. Children who are scheduled for an MRI are approached by a Child life specialist and an appointment is made. We reviewed the imaging quality of the Pediatric MRI's that were performed with thelp of a Child life specialist without the use of anesthesia in the past 18 months.

#### RESULTS

1. In 18 month period, 122 children, ages 4-15 yrs received preparation from child life specialist. 113 out of 122 children were able to complete the MRI scan without sedation, meaning that 93% of the young children, were able to hold still enough for the MRI to produce diagnostic images, without the use of anesthesia. - 4 out of 122 were partially completed - the child tolerated the study until contrast was attempted partway through, but was not able to tolerate the injection. The study was finished early and images without contrast were submitted to the radiologist. - 5 out of 122 were not completed - the child was unable to tolerate any part of the study. 2. Reduction in overall visit durations for patients undergoing elective sedation-free MRI exams versus MRI with sedation. 3. Increased referrals from the families who participated in the sedation-free program as well as referring physicians. 4. Reduction in wait times for sedated-MRI exams after induction of sedation-free program, despite stable total MRI exam volume

#### CONCLUSION

Sedation-free pediatric imaging removes the risks of anesthesia, takes less time, and requires fewer staff members. Sedation-free pediatric MRIs, completed with preparation by a child life specialist and a miniature MRI model, can save the hospital time and money versus pediatric MRIs completed with anesthesia. That's news worth waking up for!

## **CLINICAL RELEVANCE/APPLICATION**

Sedation-free pediatric imaging removes the risks of anesthesia, takes less time, and requires fewer staff members. Sedation-free pediatric MRIs, completed with preparation by a child life specialist and a miniature MRI model, can save the hospital time and money versus pediatric MRIs completed with anesthesia.



## PD237-SD-WEB3

A Realistic Pediatric Abdominal Phantom with Contrast Enhancement Using 3D Printing Technology: <u>Comparison with Patient</u> Computed Tomography Images

Wednesday, Nov. 28 12:45PM - 1:15PM Room: PD Community, Learning Center Station #3

### Participants

Li Wei Hu, BEng, Shanghai, China (*Presenter*) Nothing to Disclose Yumin Zhong, MD, Shanghai, China (*Abstract Co-Author*) Nothing to Disclose Rong-Zhen Ouyang, MD, Shanghai, China (*Abstract Co-Author*) Nothing to Disclose Ai-Min Sun, MD, Shanghai, China (*Abstract Co-Author*) Nothing to Disclose Qian Wang, Shanghai, China (*Abstract Co-Author*) Nothing to Disclose Jianying Li, Beijing, China (*Abstract Co-Author*) Employee, General Electric Company Mingpeng Wang, MD, Shanghai, China (*Abstract Co-Author*) Nothing to Disclose

#### For information about this presentation, contact:

huliwei11@hotmail.com

## PURPOSE

The aim of this study was to construct a realistic children abdominal phantom simulating contrast enhancement, and to validate its x-ray attenuation properties by comparing with the patient contrast enhanced abdominal computed tomography images.

## METHOD AND MATERIALS

The 3D printing was performed in direct ink writing modelling (T600Pro, Trandom, China). Polyurethane and Tris(2chloroethy)Phosphate (TCEP) were used as the building materials. The CT attenuation values of TCEP with different concentrations (2-60%) were measured at different tube voltages (80-120kVp) to evaluate its linearity and to select the right concentration for printing a phantom. A pediatric abdominal phantom simulating CT attenuation in the arterial phase were designed and printed. The phantom was scanned on a GE 64-row CT scanner (Discovery CT750HD) using 80kVp and automatic tube current modulation for noise index of 11HU. Acquisitions were repeated three times to assess reproducibility. The phantom images were compared with patient CT images. The CT attenuation values, image noises, contrast to noise ratios (CNR) of the liver, abdominal aorta, kidneys cortex, spleen and muscle were measured. Subjective image quality was assessed by two radiologists using a 4-point scale. The data were analyzed by using Graphpad 5 with Pearson correlation.

## RESULTS

There were excellent linear correlations between the CT value and TCEP concentration at all tube voltages (p<0.001, r=0.99). Mean CT values of all tissue types in the phantom were similar to those of patient scans (all p>0.05), except for the abdominal aorta. Phantom images had slightly higher CNR values in the liver, kidneys cortex and spleen than the patient images ( $7.08\pm0.83$  vs.  $5.5\pm0.48$ ,  $14.18\pm2.48$  vs.  $10.67\pm1.05$ , and  $11.84\pm1.69$  vs.  $8.78\pm0.53$ , respectively). The phantom images had similar noise ( $12.3\pm1.47$  vs.  $13.7\pm1.5$ HU) and slightly lower image quality score ( $4.45\pm0.30$  vs.  $4.72\pm0.51$ ), but it was acceptable as an anthropomorphic phantom.

## CONCLUSION

We have demonstrated the feasibility of creating patient specific phantoms with good image quality and consistent attenuation characteristics via rapid prototyping.

## **CLINICAL RELEVANCE/APPLICATION**

Anthropomorphic phantoms can be manufactured using 3D printing to simulate different imaging conditions and with different patient sizes to optimize dose performance and reconstruction algorithms.



### PD238-SD-WEB4

## A Review of Pediatric Interventional Radiology Transfers Away from a Tertiary Pediatric Center

Wednesday, Nov. 28 12:45PM - 1:15PM Room: PD Community, Learning Center Station #4

#### Awards Student Travel Stipend Award

#### **Participants**

Victoria McCutcheon, BSC,MSc, Vancouver, BC (*Presenter*) Nothing to Disclose Manraj K. Heran, MD, Delta, BC (*Abstract Co-Author*) Nothing to Disclose

#### For information about this presentation, contact:

victoria.mccutcheon@alumni.ubc.ca

## PURPOSE

This retrospective review investigates the circumstances prompting paediatric cases to be transferred away from a provincial, tertiary children's hospital to an adult tertiary care centre for interventional radiology procedures. These cases are not uncommon and often go unreported and untracked, leaving gaps in services at specialized paediatric centres as well as unexamined costs.

#### **METHOD AND MATERIALS**

A retrospective review of cases from January 1, 2007 to December 31, 2017, transferred under a single provider, revealed 112 cases of interventional radiology transfers under 18 years of age. The reasons and contexts of transfers were analyzed with the intention of identifying knowledge gaps in delivery of tertiary care. Descriptive and cost analyses were performed.

#### RESULTS

Transfers occurred on average  $11.2\pm6.09$  times per year. The average age of subjects was  $10.06\pm5.21$  years. Major themes revealed physical resources, procedure expertise, and suitable equipment as the most common reasons for transferring cases away from specialized paediatric care. Overall, the majority of cases were embolization procedures (55.36%, n=62). This correlated to a lack of infrequent and highly complex neurovascular resources as well as provider expertise. Ablations were the next most common procedure overall (25.89%, n=29), but outnumbered embolizations in 2017. Their frequency steadily increased from zero cases in 2007 and 2008, to 7 cases in 2017. These were transferred due to lack of percutaneous ablation equipment at the paediatric facility.

## CONCLUSION

The most common reason for radiological procedure transfer offsite was a combination of physical resources and complex neuroradiology expertise. The next most common was percutaneous CT-guided ablation, most commonly for osteoid osteoma. This research characterizes the critical reasons for interfacility transfer and utilization of offsite interventional radiology resources for paediatrics.

## **CLINICAL RELEVANCE/APPLICATION**

No research has been performed in this area of interventional radiology transfers away from paediatric centres, this data thus represents a significant opportunity for decreased transfer costs and resource efficiency.



## PD239-SD-WEB5

Usefulness of Abdominal Aortography for Evaluation of Renal Artery Stenosis in Children with Moyamoya Disease

Wednesday, Nov. 28 12:45PM - 1:15PM Room: PD Community, Learning Center Station #5

## Participants

Young Jin Ryu, MD, Seongnam, Korea, Republic Of (*Presenter*) Nothing to Disclose Young Hun Choi, MD, Seoul, Korea, Republic Of (*Abstract Co-Author*) Nothing to Disclose Jung-Eun Cheon, MD, Seoul, Korea, Republic Of (*Abstract Co-Author*) Nothing to Disclose Woo Sun Kim, MD, Seoul, Korea, Republic Of (*Abstract Co-Author*) Nothing to Disclose In-One Kim, MD, Seoul, Korea, Republic Of (*Abstract Co-Author*) Nothing to Disclose

# PURPOSE

To investigate usefulness of abdominal aortography in order to evaluate renal artery stenosis (RAS) in children who were initially diagnosed with MMD.

## METHOD AND MATERIALS

This retrospective study included 196 children (< 18 years old) who were initially diagnosed with MMD in our institution from January 2013 to December 2016. All patients had legible transfermoral cerebral angiography (TFCA) and abdominal aortography for diagnosis of moyamoya disease. Baseline characteristics, including hypertension and angiographic findings were retrospectively evaluated.

### RESULTS

The mean age was 8 years (range 7months-16years) and 82 were boys and 114 were girls. Out of 196 children, twelve patients had hypertension (6.1%). RAS was identified through the abdominal aortography in 8 patients (4.1%). The degree of renal artery stenosis was moderate or severe in 2 patients (1.0%). Seven patients had unilateral RAS and one patient showed bilateral RAS. The locations of RAS consisted of proximal in 6 lesions, mid in 2 lesions and segmental artery in 1 lesion. Among eight patients with RAS, all the patients were normotensive and none were found to be clinically hypertensive.

## CONCLUSION

The prevalence of renal artery stenosis was not uncommon (4.1%) in pediatric MMD patients and all patients with RAS were clinically normotensive. Therefore, abdominal aortography could be helpful to detect associated RAS in children who are receiving TFCA in order to confirm the diagnosis of MMD.

## **CLINICAL RELEVANCE/APPLICATION**

Abdominal aortography is useful for excluding renovascular hypertension in patients with MMD and hypertension as well as diagnosing RAS in patients who were diagnosed with MMD and clinically normotensive.



## PH013-EB-WEB

Handheld Ferromagnetic Detector Sensitivity and Unit Comparison

Wednesday, Nov. 28 12:45PM - 1:15PM Room: PH Community, Learning Center Hardcopy Backboard

## Participants

Pamela Trester, Rochester, MN (*Presenter*) Nothing to Disclose Diana Lanners, Rochester, MN (*Abstract Co-Author*) Nothing to Disclose Renee S. Jonsgaard, RT, Rochester, MN (*Abstract Co-Author*) Nothing to Disclose Teresa M. Peterson, Rochester, MN (*Abstract Co-Author*) Nothing to Disclose Andrew Fagan, Rochester, MN (*Abstract Co-Author*) Nothing to Disclose Matthew A. Bernstein, PhD, Rochester, MN (*Abstract Co-Author*) Former Employee, General Electric Company Yunhong Shu, PhD, Rochester, MN (*Abstract Co-Author*) Nothing to Disclose Joel P. Felmlee, PhD, Rochester, MN (*Abstract Co-Author*) Nothing to Disclose Heidi A. Edmonson, PhD, Rochester, MN (*Abstract Co-Author*) Nothing to Disclose

## CONCLUSION

Our results are comparable to the manufacturer's data. However, we measured somewhat higher sensitivity in all five FDs. Our data shows that handheld FD's can identify small metal bearings over a clincally-useful range of depths, but care still needs to be exercised since false negative detection can occur for very small ferromagnetic objects at depths greater than 0.5 cm. This data also can help establish a procedure for FD periodic quality control.

### FIGURE

http://abstract.rsna.org/uploads/2018/18015719/18015719\_z781.jpg

#### Background

In the MRI environment, handheld ferromagnetic detectors (FDs) are capable of rapidly detecting dangerous, or even potentially lethal, projectiles. FDs have been implemented as an integral part of MR safety screening at our institution. The purpose of this study was to determine the average sensitivity of our handheld FDs, and to compare multiple units in three different analysis modes.

#### Evaluation

Testing of five handheld metal detectors (model PD240CH, CEIA USA, Twinsburg, Ohio) was completed using three measurement modes available on these devices ('Head', 'Body', 'All Metals'). Note that the 'Head' and 'Body' modes do not detect non-ferromagnetic metals of certain dimensions. Ferromagnetic ball bearings (McMaster-Carr, Elmhurst Illinois) composed of stainless steel of five different diameters (1.5, 3.0, 4.0, 5.0, 6.0 mm) were tested at different depths (1.0, 2.0, 3.0, 4.0, 5.0, 6.0, 7.0, and 8.0 cm) using a custom-built jig in a metal-free environment. Each ball bearing diameter was tested by passing the FD over the top of the jig, using a two-directional localization procedure. A positive detection was noted only when the FD alarmed in both directions. The testing of each bearing size was completed at all eight depths comparing all five FD's using the three modes. Data were then graphed for comparison.

## Discussion

The depths at which all five FDs successfully detected the bearings in all three analysis modes were: 1.5 mm bearings at  $\leq 0.5$  cm; 3.0 mm bearings at  $\leq 3.0$  cm; 4.0 mm bearings at  $\leq 4.5$  cm; 5.0 mm bearings at  $\leq 5.5$  cm; 6.0 mm bearings at  $\leq 6.5$  cm.



## PH123-ED-WEB7

Low-Contrast Detectability (LCD) of Abdominal CT: Improvement of LCD by a Newly Developed Iterative Reconstruction Algorithm

Wednesday, Nov. 28 12:45PM - 1:15PM Room: PH Community, Learning Center Station #7

## Participants

Yoshinori Funama, PhD, Kumamoto, Japan (*Presenter*) Nothing to Disclose Yuko Aoki, Kashiwa, Japan (*Abstract Co-Author*) Employee, Hitachi, Ltd Taiga Goto, Kashiwa, Japan (*Abstract Co-Author*) Employee, Hitachi, Ltd Hisashi Takahashi, Kashiwa, Japan (*Abstract Co-Author*) Employee, Hitachi, Ltd Hiromitsu Hayashi, MD, Tokyo, Japan (*Abstract Co-Author*) Nothing to Disclose Kazuo Awai, MD, Hiroshima, Japan (*Abstract Co-Author*) Research Grant, Canon Medical Systems Corporation; Research Grant, Hitachi, Ltd; Research Grant, Fujitsu Limited; Research Grant, Bayer AG; Research Grant, DAIICHI SANKYO Group; Research Grant, Eisai Co, Ltd; Medical Advisory Board, General Electric Company; ; Yukio Kumagai, BEng, Kashiwa, Japan (*Abstract Co-Author*) Employee, Hitachi, Ltd

## **TEACHING POINTS**

Low contrast detectability (LCD) in CT directly relates to detectability of low contrast objects such hepatic tumors in abdominal CT. Current Iterative Reconstruction (IR) can reduce total amount of image noise but they cannot improve LCD as it cannot reduce image noise with low-frequency range. We have developed a new IR algorithm to improve LCD by reducing low-frequency noise. In this exhibit, we will provide basics of LCD in CT and describe how our new IR algorithm can improve LCD.

## **TABLE OF CONTENTS/OUTLINE**

1. Clinical significance of low contrast detectability (LCD) in CT 2. Methods for evaluating LCD in CT - Scanned images of a Catphan phantom - Noise Power Spectrum 3. Effect of radiation dose and image reconstruction algorithms on LCD 4. Factors limiting effectiveness of iterative reconstruction (IR) algorithms for LCD 5. A new IR algorithm improving LCD in CT 6. Representative cases demonstrating our new alorithms - Hepatic lesions - Pancreatic lesions



## PH246-SD-WEB1

## Peristalsis MR Imaging in Direct Visualization of Physiological Intestinal Flow by Spin Labeling Technique

Wednesday, Nov. 28 12:45PM - 1:15PM Room: PH Community, Learning Center Station #1

### Participants

Jun Isogai, MD, Asahi, Japan (*Presenter*) Nothing to Disclose Hideo Hatakeyama, Hasuda, Japan (*Abstract Co-Author*) Nothing to Disclose Takashi Yamada, Hasuda, Japan (*Abstract Co-Author*) Nothing to Disclose Kenji Yodo, Miyagi, Japan (*Abstract Co-Author*) Employee, Canon Medical Systems Corporation Mitsue Miyazaki, PhD, La Jolla, CA (*Abstract Co-Author*) Nothing to Disclose

### PURPOSE

To directly visualize physiological intestinal intraluminal flow related to the peristalsis without contrast material by spin labeling technique.

## METHOD AND MATERIALS

A flow-out technique of time-spatial labeling inversion pulse (time-SLIP) is based on the application of both nonselective inversion recovery pulse and spatially selective inversion labeling pulse on the move-out regions as a magnetic field. A protocol optimization was performed on 25 healthy volunteers. We set the region of interest (ROI) on the duodenum because of little position shift due to the retroperitoneal fixation. Subsequently, we challenged to apply the revised protocol parameters to 5 diarrhea subjects on the descending colon. All the studies were performed on a 1.5T MRI system (EXCELART Vantage XGV Toshiba) equipped with a SPEEDER torso coil. Principal parameters were: respiratory-gated FASE sequence with a single-shot two-dimensional time-SLIP technique in a series of 60 images, TR/TE = 2700-3200/80 ms. MR peristalsis imaging was evaluated by two radiologists for the presence, frequency and magnitude of bowel content movement on move-in fields.

## RESULTS

MR peristalsis imaging with the time-SLIP flow-out technique provided an excellent dynamic imaging in physiological conditions of the duodenum. The intestinal fluid inflow was observed at 10-28 times (mean 15.5 times) in a series of 60 images. The distance of intestinal fluid movement in the duodenum was 0.5-7.5 cm (mean 3.3 cm) during 1500ms (black blood traveling time). The results of velocity and frequency of the intestinal fluid of the splenic flexure was hardly detected in diarrhea subjects.

### CONCLUSION

Noninvasive visualization of the physiologic intestinal flow is possible by spin labeling of the time-SLIP flow-out technique.

## **CLINICAL RELEVANCE/APPLICATION**

Conventional contrast x-ray techniques allow direct monitoring of intestinal content movement, but cannot avoid the exposure of ionizing radiation. MR enteroclysis requires an administration of contrast material through a nasoenteric tube, whereas MR enterography requires large volumes of enteric contrast materials orally. In this study, we extended the application of spin labeling technique to peristalsis imaging beyond non-enhanced MR angiography.



## PH247-SD-WEB2

### Dose Reduction for Cerebral Fluoroscopic Angiography Procedures Using Advanced Noise Suppression

Wednesday, Nov. 28 12:45PM - 1:15PM Room: PH Community, Learning Center Station #2

#### **Participants**

Steve D. Mann, PhD, Durham, NC (*Presenter*) Consultant, Micro C Imaging
Nicholas T. Befera, MD, Durham, NC (*Abstract Co-Author*) Founder and CEO, Scanslated, Inc
Megan K. Russ, PhD,MS, Buffalo, NY (*Abstract Co-Author*) Nothing to Disclose
Eric Sankey, MD, Durham, NC (*Abstract Co-Author*) Nothing to Disclose
Fernando Gonzalez, MD, Durham, NC (*Abstract Co-Author*) Nothing to Disclose
Ehsan Samei, PhD, Durham, NC (*Abstract Co-Author*) Research Grant, General Electric Company; Research Grant, Siemens AG;
Advisory Board, medInt Holdings, LLC; License agreement, 12 Sigma Technologies; License agreement, Gammex, Inc

#### For information about this presentation, contact:

steve.mann@duke.edu

## PURPOSE

High radiation exposure has long been a concern for fluoroscopically-guided procedures. Notably, difficult interventional neuroradiology procedures have the potential to reach dose thresholds corresponding to deterministic skin effects, highlighting the need for vendor-driven advances aimed at reducing patient dose. The purpose of this study was to quantify the relative value of advanced image noise reduction techniques to lower exposure rates.

#### **METHOD AND MATERIALS**

Procedure data were collected for 1645 diagnostic and interventional cerebral angiography cases using biplane fluoroscope systems (Philips Alura Xper) -with (FD 20/15) and without (FD 20/20) a local noise reduction algorithm (Clarity). The algorithm attempts to locally suppress image noise around features of interest to improve the contrast-to-noise ratio for lower exposure images. Data collected for this study included procedure type, dose and utilization metrics, and lead and assisting physicians. The mean dose-area product, cumulative air kerma, and fluoro time for cases performed with and without processing were computed. An ANOVA analysis was performed to determine the significance of each variable on the measurements.

### RESULTS

For both diagnostic and interventional procedures, the processing system demonstrates a 73% reduction in dose-area product and air kerma (p < 0.001). The range of reduction varies with physician and procedure type (63% - 80%). Fluoroscopy time for diagnostic procedures is statistically unchanged with processing but is seen to increase by 26% for interventional cases (p < 0.001).

### CONCLUSION

The advanced image processing can substantially reduce the radiation dose utilized during cerebral angiography procedures. The processing system settings and acquisition differences are shown to translate to meaningful clinical reductions in total exposure output. The reduction in average exposure per case may significantly reduce the risks to patients and staff.

### **CLINICAL RELEVANCE/APPLICATION**

Advances in image processing have been touted by vendors as a means of achieving lower radiation exposures with comparable image quality. It's important to quantify how the new acquisition settings translate into clinical practice by looking at case outcomes for total exposure.



### PH248-SD-WEB3

Task-based Assessment of Photon-counting CT Binned Images with Varying Patient Size and Imaging Mode

Wednesday, Nov. 28 12:45PM - 1:15PM Room: PH Community, Learning Center Station #3

#### **Participants**

Jayasai R. Rajagopal, BA, Durham, NC (Presenter) Nothing to Disclose

Pooyan Sahbaee, Malvern, PA (Abstract Co-Author) Employee, Siemens AG

Bradford J. Wood, MD, Bethesda, MD (*Abstract Co-Author*) Researcher, Koninklijke Philips NV; Researcher, Celsion Corporation; Researcher, BTG International Ltd; Researcher, Siemens AG; Researcher, XAct Robotics; Researcher, NVIDIA Corporation; Intellectual property, Koninklijke Philips NV; Intellectual property, BTG International Ltd; Royalties, Invivo Corporation; Royalties, Koninklijke Philips NV; ; ;

Elizabeth C. Jones, MD, Bethesda, MD (*Abstract Co-Author*) Nothing to Disclose Ehsan Samei, PhD, Durham, NC (*Abstract Co-Author*) Research Grant, General Electric Company; Research Grant, Siemens AG; Advisory Board, medInt Holdings, LLC; License agreement, 12 Sigma Technologies; License agreement, Gammex, Inc

### For information about this presentation, contact:

jayasai.rajagopal@duke.edu

#### PURPOSE

To evaluate the differentiability of various materials in photon-counting CT low and high energy binned images as a function of size and image mode

#### **METHOD AND MATERIALS**

The study utilized a five-size tiered phantom (Mercury Phantom, Gammex/Duke University) with two subsections in each tier: a uniform section for NPS evaluation and a section with five cylindrical inserts (8.5 mg/ml I, bone, polystyrene (fat), water, air) for task based evaluation. Images were acquired on a prototype photon-counting CT system (Siemens, Germany) at a dose of 16 mGy and with two imaging modes (Macro, Ultra High-Resolution). Images were reconstructed to a slice thickness of 5 mm with both soft tissue and ultra-sharp kernels. An automated program evaluated the contrast of each insert and noise in each size. Detectability indices were calculated for a 5 mm circular disks for each insert and phantom size. The difference between detectability and contrast in low and high energy bins was calculated.

### RESULTS

: Low energy bins showed better contrast than high energy bins. The largest contrast differences were for the bone and iodine inserts. Contrast difference remained stable with changing patient size. Low energy bins also showed lower noise magnitude for all combinations of kernel and image type. Noise difference increased with patient size and sharpness of kernel. Thus, low energy bins had higher detectability under all evaluated conditions, with the difference most clear for bone inserts under a soft-tissue kernel.

#### CONCLUSION

Low energy bins showed higher detectability than high energy bins for all tasks. Low energy bins had lower noise and their superior contrast allowed for improved detectability. Photon-counting CT offers consistent detectability performance irrespective of phantom size.

## **CLINICAL RELEVANCE/APPLICATION**

Photon-counting CT exhibits improved consistency across patient sizes. Low energy binned images provide better contrast and lower noise across detection tasks.



## PH249-SD-WEB4

Maximizing Iodine Detectability Using Different Types of Multiple Energy Images from a Single Acquisition on a Photon-Counting-Detector CT System

Wednesday, Nov. 28 12:45PM - 1:15PM Room: PH Community, Learning Center Station #4

## Participants

Wei Zhou, PhD, Rochester, MN (*Presenter*) Nothing to Disclose Gregory J. Michalak, PhD, Rochester, MN (*Abstract Co-Author*) Nothing to Disclose Jayse Weaver, Rochester, MN (*Abstract Co-Author*) Nothing to Disclose Hao Gong, PhD, Rochester, MN (*Abstract Co-Author*) Nothing to Disclose Lifeng Yu, PhD, Chicago, IL (*Abstract Co-Author*) Nothing to Disclose Kenneth A. Fetterly, PhD, Rochester, MN (*Abstract Co-Author*) Nothing to Disclose Cynthia H. McCollough, PhD, Rochester, MN (*Abstract Co-Author*) Research Grant, Siemens AG Shuai Leng, PHD, Rochester, MN (*Abstract Co-Author*) License agreement, Bayer AG

#### For information about this presentation, contact:

zhou.wei1@mayo.edu

#### PURPOSE

To determine the image type on a photon-counting-detector (PCD) CT system that has maximal iodine detectability across patient sizes.

### **METHOD AND MATERIALS**

Iodine solutions of different concentrations (0.2, 0.5, 1.0 and 2.0 mgI/cc) were injected into holes with 4 mm and 8 mm diameters in a Solid Water HE cylinder (Sun Nuclear). The cylinder was inserted into one of 3 abdomen phantoms (QRM, lateral widths of 30, 35 and 40 cm). The phantoms were scanned on a whole-body PCD CT using 140 kV, 25 and 75 keV energy thresholds. Tube current was adjusted to match the clinical dose for routine abdomen scans, resulting in CTDIvol of 6.9 to 17.7 mGy. For each of 12 conditions (4 concentrations and 3 phantom sizes), scans were repeated 150 times. All images were reconstructed with a quantitative smooth kernel (D30) and 5 mm slice thickness. Virtual monoenergetic images (VMI) @50 keV and quantitative iodine maps were generated from PCD bin images. To compare the iodine detection between the full spectrum (TL) images, VMIs@50 keV and iodine maps, CNR and AUC of the ROC from a calibrated channelized hoteling observer (CHO) model were calculated as figures of merit.

#### RESULTS

For all phantom sizes, VMI@50 keV had the highest iodine CNR while TL images had the lowest CNR. For the 4 mm object with1.0 mgI/cc and the 35 cm phantom, VMI@50 keV (AUC: 0.99±0.01) slightly outperformed TL images (AUC: 0.96±0.02) and both were better than iodine map results (AUC: 0.89±0.02). The overall performance of both VMI@50 keV and TL images was better than iodine maps in terms of detecting small enhanced objects (4mm) while all 3 image types demonstrated comparable overall performance for identifying large enhanced objects (8 mm).

### CONCLUSION

Among the common image types generated from PCD acquisitions, VMI@50 keV provided the best performance in terms of iodine CNR and detectability for all phantom sizes.

## **CLINICAL RELEVANCE/APPLICATION**

Utilizing the optimal multi-energy information from PCD acquisitions for specific clinical tasks could reduce the radiation and contrast dose to patients .



## PH250-SD-WEB5

A Multi-Echo Stack-of-Stars UTE-Based Thoracic Dixon Imaging

Wednesday, Nov. 28 12:45PM - 1:15PM Room: PH Community, Learning Center Station #5

### Participants

Kuan-Hao Su, Cleveland, OH (*Presenter*) Research Grant, Koninklijke Philips NV Harry Friel, Gainesville, FL (*Abstract Co-Author*) Employee, Koninklijke Philips NV Rose Al Helo Jr, MS, Cleveland, OH (*Abstract Co-Author*) Nothing to Disclose Jung-Wen Kuo, Cleveland, OH (*Abstract Co-Author*) Nothing to Disclose Christian Stehning, Hamburg, Germany (*Abstract Co-Author*) Employee, Koninklijke Philips NV Atallah Baydoun, MD, Cleveland, OH (*Abstract Co-Author*) Nothing to Disclose Adina N. Crisan, ARRT, Cleveland, OH (*Abstract Co-Author*) Nothing to Disclose Melanie Traughber, DSc, Shaker Heights, OH (*Abstract Co-Author*) Nothing to Disclose Ajit Devaraj, PhD, Chicago, IL (*Abstract Co-Author*) Nothing to Disclose Pengjiang W. Qian, PhD, Wuxi, China (*Abstract Co-Author*) Nothing to Disclose Asha Leisser, MD, Vienna, Austria (*Abstract Co-Author*) Nothing to Disclose Norbert Avril, MD, Cleveland, OH (*Abstract Co-Author*) Nothing to Disclose Bryan J. Traughber, MD, Cleveland, OH (*Abstract Co-Author*) Nothing to Disclose

### For information about this presentation, contact:

raymond.muzic@case.edu

## PURPOSE

The aim of this study is to establish a dedicated, clinically-practical MR acquisition to support synthetic CT generation for the thorax.

#### **METHOD AND MATERIALS**

A coronal stack-of-stars (SoS) UTE-mDixon sequence was developed for thoracic imaging. A particular challenge with lung is the very fast T2\* relaxation which even exceeds that of cortical bone resulting in lack of lung contrast in conventional scans. Using a Philips 3T Ingenuity PET-MR system, the UTE-mDixon acquisition collected data at three TEs: TE1=0.14, TE2=1.14, and TE3=2.14 ms. Three-point analyses were used for Dixon water/fat separation and R2\* estimation based on the ultrashort TE (TE1). Using a free-breathing condition to match PET, the radial sampling density was optimized to reduce the respiratory artifacts. A 3D bias field correction was used to account for MR field inhomogeneity. Further, water fraction was estimated and resulted in total seven MR images: TE1, TE2, TE3, Dixon-water, Dixon-fat, R2\*, and water fraction. Data from an MR ACR phantom and 25 volunteers were compared with those acquired by a conventional, Cartesian, non-UTE, two-point mDixon acquisition.

## RESULTS

Comparing sampling densities of 150, 175, 200% for the SoS UTE-mDixon vs. 100% for traditional mDixon, UTE-mDixon had a slightly poorer uniformity, 92 to 95%, than mDixon, 96%, (both after field correction), but was able to access the lung and bone tissue information. The measured full-width-at-half-maximum of the UTE-mDixon and that of traditional mDixon were 3.27 mm and 2.81 mm in the readout direction, respectively. Among the UTE-mDixon images, those with 200% radial sampling showed the highest uniformity and least respiratory artifacts. Requiring only 4.7 min for the acquisition to achieve a wide FOV of 458 x 458 x 298 mm3, capturing lung and bone signal before T2\* decay, the SoS UTE-mDixon was the preferred acquisition method for synthetic CT generation.

#### CONCLUSION

We established an MR imaging method for thoracic imaging. The acquisition can be done within a clinically-practical duration while providing high-quality lung visualization and bone differentiation from air which cannot be achieved by a traditional Dixon technique.

## **CLINICAL RELEVANCE/APPLICATION**

A multiecho UTE-mDixon method was developed for MR thoracic imaging. The proposed free-breathing acquisition captures lung and bone information which cannot be seen by the conventional Dixon method.



## QI014-EB-WEB

How to Use 5S Lean Methodology in Radiology Exam Rooms

Wednesday, Nov. 28 12:45PM - 1:15PM Room: QR Community, Learning Center Hardcopy Backboard

# Participants

Shelly R. Champa, RT, Rochester, MN (*Presenter*) Nothing to Disclose Laura Tibor, MBA, BEng, Rochester, MN (*Abstract Co-Author*) Nothing to Disclose Kristi Rindels, Rochester, MN (*Abstract Co-Author*) Nothing to Disclose Jeffrey R. Leland, MA, Rochester, MN (*Abstract Co-Author*) Nothing to Disclose Adam Froemming, MD, Rochester, MN (*Abstract Co-Author*) Nothing to Disclose Brandon D. Stuve, Rochester, MN (*Abstract Co-Author*) Nothing to Disclose Jolene Stock, Rochester, MN (*Abstract Co-Author*) Nothing to Disclose Chris Thesing, Rochester, MN (*Abstract Co-Author*) Nothing to Disclose Brent Simmer, Rochester, MN (*Abstract Co-Author*) Nothing to Disclose Angela Majerus, BA, Rochester, MN (*Abstract Co-Author*) Nothing to Disclose

# For information about this presentation, contact:

champa.shelly@mayo.edu

# PURPOSE

Due to the excess inventory of supplies and inconsistent resources in each General Radiology exam room as well as varying locations of these resources in the exam rooms, workflow in the exam room was inefficient for the technologists. It was necessary to look at improving efficiencies by utilizing the 5S methodology. The goal was to decrease the amount of time it takes a technologist to locate a needed resource for an exam in General Radiology exam rooms from 4.52 min to 2.50 min by May 2017 without increasing the number of cleaned and stocked incidents at 9 per month.

# METHODS

A multi-disciplinary team was formed and they utilized the 5S methodology to clean, organize, standardize and sustain the exam rooms. The team also utilized tools such as spaghetti diagrams to display the movement of the technologists to help organize and plan for future state. A3 problem solving led the team through problem indentification, goal development, root cause analysis, future state development and a robust control plan. Plan-Do-Study-Act tests of change helped the team determine the effectiveness of proposed changes. Baseline data was collected via manual timings of 2 technologists per room for 5 exam rooms searching for 10 resources utilized during exams. The total sample size included 100 timings which were averaged for the baseline measure of 4.52 min per technologist per room spent searching for those resources.

## RESULTS

Interventions implemented in each of the 5 exam rooms included the following: removed unnecessary resources, ensured appropriate resources and quantities, standardized locations of resources in rooms, added labels and pictures for visual recognition and daily audits. The results are as follows: Time saved: Average time to find needed supplies decreased from 4.52 min to an average of 1.24 min 3.28 min saved per patient exam 357 wasted hours saved per month (6,536 average exams per month) Employee FTE reallocated to other areas of the organization Inventory: 864 items removed from exam rooms Money saved on supplies Estimated value \$13,479 of items removed

## CONCLUSION

All 5 exam rooms implemented the interventions and have demonstrated significant savings in time efficiencies for the technologists. Project findings were communicated to stakeholders through email, daily huddles and leadership presentations. For the control phase, audits are completed daily by staff technologists and are checked randomly by the leadership team. Cleaning and stocking defects/incidents are tracked and discussed at daily huddles. With the demonstrated success in these 5 exam rooms, the team has spread the methodology and implemented changes in 4 additional exam rooms. Lessons learned: Reducing wasted time during the exam provides for an improved patient and staff experience and it's important to narrow down the scope of the project.



## QI016-EB-WEB

Changing from an Institution-based Resident on Call to a Federated Regional Model - Improving Quality of a Regional Radiology Service

Wednesday, Nov. 28 12:45PM - 1:15PM Room: QR Community, Learning Center Hardcopy Backboard

## Participants

Peter Rowlands, FRCR, Liverpool, United Kingdom (*Presenter*) Nothing to Disclose John Curtis, Liverpool, United Kingdom (*Abstract Co-Author*) Nothing to Disclose Furhan Razzaq, MBChB, Manchester, United Kingdom (*Abstract Co-Author*) Nothing to Disclose Sharron Dyce, Liverpool, Afghanistan (*Abstract Co-Author*) Nothing to Disclose

For information about this presentation, contact:

Peter.rowlands@rlbuht.nhs.uk

## PURPOSE

PurposeIn our metropolitan region we have four general hospitals, two teaching hospitals and several specialist institutions.Our on call resident radiology service was supported by residents working independently in each of the institutions. Numbers of residents varied from 4-10 in each institution.The on call rosters were mostly non compliant with European employment law, leaving gaps in cover. There was no peer support between trainees, who were of differing levels of experience.Periods of excessive intensity could only be covered by attending level radiologists, who were not immediately available as they were often at home or on other sites.The increasing demand for timely imaging had become almost unsustainable in busy sites and residents in smaller specialist units were often underemployed.

## METHODS

In 2013 we procured a regional PACS which allowed full image sharing and reporting across 10/12 of our sites. Image acquisition and reporting could be geographically separated. The other two sites were fitted with servers which allowed images to be transferred automatically from the foreign PACS and reported within the regional PACS. The report was then sent into the foreign PACS using a HL7 messaging. We created a radiology 'hub' in which the radiology residents were all based. They were able to report all of the out of hours radiology studies in a single area. We had to provide a single route of referral and have designed a customised telephone call centre which allows filtering and appropriate routing of the calls, eg scans that are done as standard referral protocol such as CT brain for head injury are routed to the local radiographic tech and do not take up radiologist discussion time. We also instituted a regional discrepancy system, to highlight scans in which there is a discrepancy between the report of trainee and attending. This was an anonymised system which allowed for feedback and discussion in a non-threatening environment. All sites have senior presence between 5pm and 8pm weekdays and 9am - 2pm weekends at periods of high demand.

## RESULTS

Following a successful pilot study across two departments, we have moved to incorporate all of the acute hospitals in the federated scheme.We had 43 trainees working in six institutions on rotas between 1:5 and 1:10We covered the service with 43 trainees working on a 1:10-12 rota.The working intensity has increased, but the frequency of on call has significantly decreased.We became compliant with employment law.We now have peer support between 3-4 co-located trainees, improving education and requiring less senior radiology input. Trainees lose significantly (>30%) less core training which was previously lost due to compensatory rest the day after on call.There was significantly improved trainee satisfaction, despite a significant rise in demand in the last three years.We have analysed error/discrepancy rates and the established rate of significant discrepancy is 2-3% which is similar to prior published studies. Only a small proportion of these requires urgent medical intervention.There were significant cost savings in excess of \$100k per annum, as emergency cover and tele radiology was no longer required. This was used to fund administration assistance to help with rota planning.We have managed contingency planning to cover the three major outages ( one Cyber Attack, two physical network disruption) This was done by distributing trainees to the busy departments and enlisting trainees not on call, whose rota intensity allowed them to work legally.We achieve a one hour maximum turn around time >95% of the time.Our ultrasound requests have not proven a problem ( done on next day lists or by attending on call very rarely ).The expected loss of close clinical contact between referring clinicians and radiology trainees has not be shown to be a real operational issue.

## CONCLUSION

We have moved from a system withillegal and unsustainable rotaslarge variations in workloadno peer supportno regional learning from discrepancyisolated departmental workingto a system withlegal and sustainable rotassmoothed workload with increased average intensity , but less peaks and troughspeer supporta regional forum where discrepant cases are reviewed and excellent learning opportunities existregional and cooperative workingThe system has taken a lot of planning, but now essentially runs itself with funded administration support. It has become the model for regional training schemes and similar systems have ben implemented elsewhere.



## QI125-ED-WEB1

Initial Experience of Volume CT in Pediatrics: Can Anesthesia Be Avoided?

Wednesday, Nov. 28 12:45PM - 1:15PM Room: QR Community, Learning Center Station #1

### Participants

Kerri A. Highmore, MD, Ottawa, ON (Presenter) Nothing to Disclose Elka Miller, MD, Ottawa, ON (Abstract Co-Author) Nothing to Disclose

#### PURPOSE

Anesthesia is commonly used in paediatric imaging due to the young age of the patient and inability for breath-hold compliance.: However, it does not come without associated risks.: The purpose of this study is to evaluate the use of Volume CT scanning in the paediatric patient population as an alternative non-anesthesia imaging technique in young patients who typically require sedation. Volume CT scanning is a fast CT imaging technique that can allow imaging of the young paediatric population while avoiding anesthesia or sedation. It has a 160 mm wide coverage with one short rotation scan that can reduce the risk of patient motion due to its fast scanning time (0.35 seconds). As well, offers the opportunity of a lower radiation dose exposure as the overlap required in helical scanning is eliminated .:

### **METHODS**

We retrospectively reviewed 9 paediatric CT exams performed in our institution between November 2017 - April 2018 in the paediatric age population that commonly requires sedation (range 2 weeks to 3 years old; 8/10 <: less than 1 year old, female/male 5:4). All exams were performed on the Toshiba Aquillion ONE GENESIS 320 CT scanner.: The :studies included 7 Chests, 1 Abdomen/Pelvis, and 1 Neck/Chest .: All 9 studies were performed with intravenous (IV) contrast .: The indications for the CT exams were variable ranging from investigation of a possible mass, respiratory distress & infections, and non-accidental trauma.

#### RESULTS

The image quality of all 9:volume CT exams was felt to be diagnostic .: The single rotation and fast scanning allowed these young patients to be imaged without any sedation/anesthesia and avoid the risks associated with anesthesia. All 9 studies were performed with IV contrast, the injection did not affect the imaging quality .: The CTDI and DLP of the scan range between 1.10-2.80 and 13.80-44.70, respectively, which represent a reduce dose exposure, and aligns with the ALARA principles.:

## CONCLUSION

Our initial experience with Volume CT scanning is that it can be utilized as a fast scanning technique, especially in the very young child, avoiding the need for sedation, reducing radiation exposure and still maintaining diagnostic image quality.



## QI127-ED-WEB2

Improving Veterans Access to Ultrasound Clinic in VA Ann Arbor Healthcare System Within 30 Days of Order Date

Wednesday, Nov. 28 12:45PM - 1:15PM Room: QR Community, Learning Center Station #2

## Participants

Shadi F. Azar, MBBS, Milan, MI (*Presenter*) Nothing to Disclose Venkataramu N. Krishnamurthy, MBBS, Ann Arbor, MI (*Abstract Co-Author*) Nothing to Disclose Brett M. Arnkoff, MD, Berkley, MI (*Abstract Co-Author*) Nothing to Disclose Julie A. Ruma, MD, Northville, MI (*Abstract Co-Author*) Stockholder, HistoSonics, Inc Nghi K. Tran, MD, Ann Arbor, MI (*Abstract Co-Author*) Nothing to Disclose

## PURPOSE

Monthly reports done by radiology services to assess veterans access to each imaging modality, in January 2016, showed that 14% of veterans had to wait more than 30 days to have their ultrasound study done. We decided as departmental Quality assurance committee to start a project to improve veterans access to ultrasound clinic, with a goal of 100% access within 30 days of exam being ordered, by improving utilization of available resources.

#### **METHODS**

Instead of adding more slots to improve utilization of the ultrasound rooms we implemented a process in coordination with outpatient clinics, to send all patients who need an ultrasound exam after their clinic visit, directly to radiology services reception disk. The schedulers at the reception disk will contact the ultrasound technicians to check on the status of the ultrasound rooms. If any of the ultrasound rooms are available the exam will be performed, and if the ultrasound rooms are not available, the patient will schedule the exam personally. This will provide an almost constant flow of patients to fill the gaps in the ultrasound schedule and will cut down on the time spent by schedulers on calling, and sending letters to patients, to schedule their ultrasound appointment, in addition to the time spent on documenting these activities in the electronic medical record. The patients who got their exams performed on the same day were very satisfied. For those patients with significate exam findings, they were sent back to their physicians, for further management, which expedited patient care, and physician's satisfaction.

### RESULTS

on January 2016, showed that 14% of veterans had to wait more than 30 days to have their ultrasound study done. The project team collected workflow data using "Follow Me" time study for 3 ultrasound rooms and 3 technicians, to determine each room utilization. A team of 4 industrial and operations engineering students (University of Michigan) was formed and were tasked to collect three types of data by using time studies while observing 3 ultrasound technicians in 3 Ultrasound rooms. Fake names are given for ultrasound technicians for this purpose (Deb, Joyce, Kevin). The time study performed from 8 am to 4 pm, excluding 30-minute noontime lunch break. The collected data captured how much time the technicians spent before, during and after the exam, and time cleaning/preparing the room for the next patient. The data collected also showed the times the rooms were not utilized. The team then analyzed this collected data to identify non-value added time during the workday. The team found the current average utilization of the 3 ultrasound rooms is 42% (Figure 1). After implementing these changes, the monthly report in June 2016 demonstrates only 2 % of veterans had to wait more than 30 days to access the ultrasound clinic.

#### CONCLUSION

The Veterans Affairs Ann Arbor Healthcare System provides high-quality healthcare for Veterans in Michigan and Ohio. Approximately 14% of Veterans wait longer than 30 days for their Ultrasound appointment causing delays in their care. The purpose of this project is to eliminate any occurrence of a Veteran waiting longer than 30 days for an ultrasound appointment. We conducted time studies, assessed workflow, and made changes in collaboration with out-patient clinics. The method used was to send all patients who need an ultrasound exam to radiology services for either having an exam done or personally schedule an appointment. This resulted in better utilization of ultrasound rooms, so currently 98% of veterans can access ultrasound clinic within 30 days, increased patient and physician satisfaction, and cut down on time scheduling patients for their appointments.



## QI129-ED-WEB3

How to Use Lead Apron to Reduce Excess Radiation Dose Caused by Over-Scan in Computed Tomography

Wednesday, Nov. 28 12:45PM - 1:15PM Room: QR Community, Learning Center Station #3

### **Participants**

Xinyu Li, Xian, China (*Presenter*) Nothing to Disclose Jianxin Guo, Xian, China (*Abstract Co-Author*) Nothing to Disclose Junjun Li, Xian, China (*Abstract Co-Author*) Nothing to Disclose Qiang Zeng, Xian,Shannxi, China (*Abstract Co-Author*) Nothing to Disclose Chunying Han, Xian, China (*Abstract Co-Author*) Nothing to Disclose Jian Yang, Xian, China (*Abstract Co-Author*) Nothing to Disclose

## For information about this presentation, contact:

2397990794@qq.com

## PURPOSE

The helical scan mode is used very commonly in multidetector computed tomography and interpolation algorithm is used in reconstructing images, resulting in over-scan in the Z direction: exposures to tissues beyond the boundaries of the imaged volume. The amount of over-scan is dependent on the collimation width of the multidetector system, and in general the wider the collimation, the more the over-scan. However, not all information in the over-scan area are needed for reconstruction and may contribute to unnecessary dose to patients. One way of reducing dose in the over-scan area is to use lead apron to protect the tissues that is just outside the field necessary for reconstruction but covers the z over-scan field. So, the purpose of this study was to explore the optimal way of placing the lead apron to maximize dose reduction for the over-scans without negatively impact image quality, and its dependence on the collimation width using phantom experiments.

## METHODS

We used an elliptical plastic water bottle (14cm\*17cm in axial slice) to evaluate dose performances and image quality with 40mm and 80mm detector collimations and at different distances to the scanning boundary in which the lead apron was placed. The study was divided into two groups: Group A using 40mm detector coverage; and Group B using 80mm detector coverage. Based on our earlier study, the scout imaging was taken first without lead apron, then the lead apron was put on and the helical scan was taken in every group. The helical scan groups were designed as follows: group 1, without lead apron as reference standard and groups 2-7 with the lead apron first placed at the scan boundary and in 5mm increment away from the scan boundary. The scan techniques were kept the same for all scans at 120kVp, 10-740mA, 7 pre-defined noise index (in 5mm primary recon), and 5mm reconstruction slice recon. This operation was repeated for both the 40mm and 80mm collimations. CT dose index (CTDI) values were recorded and the image quality in terms of CT value and standard deviation (SD) of the last image at the scan boundary in the helical scan were used as the reference standard. Five regions of interest (ROI, 10mm\*10mm in size) at the up, down, left, right and center locations in the images were selected to measure CT value and SD. CT value rate(CT%=[CT-CT(1)]/CT(1)) and standard deviation rate(SD%=[SD-SD(1)]/SD(1)) for each ROI in matched location were used to evaluate objective imaging quality. CT(1) and SD(1) represented the CT value and SD in group 1, and the CT and SD were the measured CT and SD in group 2-7. Subjective image quality was also evaluated.

### RESULTS

The DLP value was 54.65mGy\*cm for Group A and 66.52mGy\*cm for Group B for covering the same region. There was a 22% increase in radiation with the use of 80mm collimation in Group B. In both the 40mm and 80mm groups, there was a significant jump in CT value and SD in the images at the scan boundary when the lead apron was placed right at the scan boundary. The CT value and SD difference with and without the use of lead apron changed dramatically and stabilized after the lead apron was placed 5mm and 10mm away from the scan boundary in the 40mm and 80mm collimation group, respectively. The subjective image quality followed the same pattern as the objective measurements, indicating that the use of lead apron should not negatively impact the image quality in the desired areas.

## CONCLUSION

In our study we have performed a phantom experiment with different detector coverage and with different distances between scan boundary and lead apron. Our results indicated that there was dose penalty with the use of wider collimation due to over-scan. The correct use of a lead apron can greatly reduce the unnecessary radiation to patients, including in the over-scan region without negatively impact image quality in the desired areas. Placing the lead apron at least 5mm from the scan boundary when using 40mm collimation and 10mm when using the 80mm collimation is recommended.



## QI131-ED-WEB4

What Role Do Decision Making Tools Play in the Investigation of Pulmonary Emboli - an Audit into the Clinical Appropriateness of CT Pulmonary Angiogram Requests in the Investigation of Acute Pulmonary Emboli

Wednesday, Nov. 28 12:45PM - 1:15PM Room: QR Community, Learning Center Station #4

### Participants

David B. Annan, MBBS, MRCP, London, United Kingdom (Presenter) Nothing to Disclose

For information about this presentation, contact:

david.annan@nhs.net

#### PURPOSE

Acute pulmonary embolism (PE) is often inapprpriately investigated due to the non-specificity of the presenting signs and symptoms. It is thought that PEs have a 10-30% mortality if left untreated. However, inappropriate investigations to investigate these are often performed with serious clinical, patient safety, and financial considerations. With all this in mind, our aims were: To assess the clinical appropriateness of CT pulmonary angiogram (CTPA) requests in the investigation of acute PE, and; To review the impact of a digital clinical decision making tool on this Our study was based on audit standards suggested by the National Institute for Health and Care Excellence (NICE) guidelines based in the United Kindgom (UK). NICE provide guidance, advice and evidenced based information to clinicians in the UK to inform their clinical practice. These guidelines suggest that all CTPA requests for a PE should be risk stratified using a decicion making tool (Wells Criteria) in the request. Patients are then stratified into high and low risks groups based on their calculated Wells Score (high: >4; low: <4). Low risk patients should then have a d-dimer blood test. All high risk patients, or patients with a positive d-dimer should have a CTPA unless contraindicated. All patients with a Wells score of less than 4 (low risk) or absent or negative d-dimers should not have a CTPA.

#### METHODS

We conducted a prospective study looking at all the CTPA requests carried out at our medium-sized district general hospital within two months, and collected data on patient demographics, clinical details, the use of a pre-test probability scoring (Wells score) and d-dimer levels. After introducing a decision making tool into the electronic request system at the hospital, we re-assessed the appropriateness of these requests.

#### RESULTS

Pre-intervention,159 requests were collected (120 included, 39 excluded). 11.6% had a documented Wells score; for those without, scores were retrospectively calculated based on the clinical description provided. Patients were stratified into high (47.5%) and low Wells score groups (52.5%). For the high scoring group (Wells >4), 19.3% of patients had a PE. For the low scoring group (Wells <4), 61.9% had d-dimers performed; 2.8% of patients had a PE in the positive d-dimer subgroup, and 12.5% and 0% in the absent and negative d-dimer groups respectively. In the low Wells score group, 27 patients underwent scans with absent or negative d-dimers. Post intervention, 114 requests were collected (79 included, 35 excluded). 94.9% had a documented Wells score. In the high scoring group, 13.6% of patients had a PE. For the low scoring group, 82.9% had d-dimers performed; 8% of patients had a PE in the absent and negative d-dimer subgroup, and 16.7% and 0% in the absent and negative d-dimer subgroups respectively. 10 patients in the low Wells score group underwent scans with absent or negative d-dimers.

## CONCLUSION

Risk stratification of suspected PE using the Wells criteria is underutilised. Use of a decision making tool is an evidence-based way to: Ensure there is increased documentation of Wells scores for CTPA requests Ensure there are increased d-dimer tests in low Wells score patients Reduce the number of inappropriate scans when patients have a low Wells score or have absent or negative ddimer tests Overall, integrated decision making tools improve adherance to national guinelies, potentially reduce unnecessary patient radiation dose, and help radiology departments manage the high clincial demand for scans.



## RO224-SD-WEB1

Assessment of Extended Field Bone Marrow Sparing Radiotherapy for Primary Chemoradiotherapy in Stage IVB Cervical Cancer Patients with Para-aortic Lymphadenopathy: Volumetric Modulated Arc Therapy Versus Helical Tomotherapy

Wednesday, Nov. 28 12:45PM - 1:15PM Room: RO Community, Learning Center Station #1

#### Participants

Jenny Ling-Yu Chen, MD,PhD, Taipei, Taiwan (*Presenter*) Nothing to Disclose MiaoCi Wang, Taipei, Taiwan (*Abstract Co-Author*) Nothing to Disclose Cheyu Hsu, MD, Taipei, Taiwan (*Abstract Co-Author*) Nothing to Disclose Yu-Sen Huang, MD, Taipei, Taiwan (*Abstract Co-Author*) Nothing to Disclose Keng-Hsueh Lan, MD,PhD, Taipei, Taiwan (*Abstract Co-Author*) Nothing to Disclose Sung-Hsin Kuo, MD, PhD, Taipei, Taiwan (*Abstract Co-Author*) Nothing to Disclose

#### For information about this presentation, contact:

lychen@ntu.edu.tw

## PURPOSE

This study aimed to compare the dosimetric quality and effectiveness of volumetric-modulated arc therapy (VMAT) vs. helical tomotherapy (HT) when administering extended-field bone marrow sparing (BMS) chemoradiotherapy to stage IVB cervical cancer patients with para-aortic lymphadenopathy.

## **METHOD AND MATERIALS**

Twelve stage IVB cervical cancer patients with para-aortic lymphadenopathy who received VMAT extended-field BMS radiotherapy in 2017 were investigated. HT dose-volume histogram parameters were generated and compared to those of VMAT. The pelvis and the para-aortic region received 45 Gy (25 fractions) with a simultaneous integrated boost of 55 Gy (25 fractions) to pelvic and para-aortic lymphadenopathy, followed by a parametrial boost of 9 Gy (5 fractions), then by intracavitary high-dose-rate brachytherapy.

## RESULTS

Both the HT-based and VMAT techniques achieved adequate and similar planning target volume coverage with good dose homogeneity and conformity. High-dose rectal doses were significantly reduced with VMAT. Both techniques similarly and sufficiently spared the organs-at-risk. The HT treatment plan had significantly higher monitoring units and longer estimated treatment times. All patients completed their planned extended-field BMS radiotherapy via VMAT, and 83.3% completed ?>=5 cycles of concurrent cisplatin. The median low dose rate-equivalent to point A was 8667 cGy. The incidence of grade >=3 neutropenia was 8.3%. At a median follow-up time of 13.5 months, the 1-year cumulative incidence of locoregional failure, distant metastasis, and grade >=3 late toxicity for all patients were 0%, 20.5%, and 12.5%, respectively.

### CONCLUSION

Both HT-based and VMAT techniques are feasible for achieving EF BMS. The PTV coverage was not compromised owing to the addition of the BMS planning constraint in with either technique. Moreover, the dose remained homogeneous with the inclusion of a simultaneous integral boost for lymphadenopathy, and the OARs were protected. Notably, a significant reduction in rectal high-dose volumes was achieved using VMAT.

## **CLINICAL RELEVANCE/APPLICATION**

Both HT- and VMAT-based extended-field, bone marrow-sparing techniques achieved adequate PTV coverage and produced sufficient and similar protection of the organs-at-risk; Notably, high-dose rectal doses were significantly reduced with VMAT.



## RO225-SD-WEB2

## 4D Perfusion CT of Prostate Cancer for Radiotherapy Planning: A Proof of Concept Study

Wednesday, Nov. 28 12:45PM - 1:15PM Room: RO Community, Learning Center Station #2

### **Participants**

Lucian Beer, MD, PhD, Vienna, Austria (*Presenter*) Nothing to Disclose Stephan H. Polanec, MD, Vienna, Austria (*Abstract Co-Author*) Nothing to Disclose Pascal A. Baltzer, MD, Vienna, Austria (*Abstract Co-Author*) Nothing to Disclose Dietmar Georg, PhD, Vienna, Austria (*Abstract Co-Author*) Nothing to Disclose Anja Dutschke, MD, Vienna, Austria (*Abstract Co-Author*) Nothing to Disclose Georg Schatzl, Vienna, Austria (*Abstract Co-Author*) Nothing to Disclose Helmut R. Ringl, MD, Vienna, Austria (*Abstract Co-Author*) Nothing to Disclose Paul Apfaltrer, MD, Vienna, Austria (*Abstract Co-Author*) Institutional research collaboration, Siemens AG Thomas H. Helbich, MD, Vienna, Austria (*Abstract Co-Author*) Research Grant, Medicor, Inc Research Grant, Siemens AG Research Grant, C. R. Bard, Inc

## PURPOSE

External beam radiotherapy is the therapy of choice in the treatment of high-risk disease prostate cancer (PCa) The aim of this study was to evaluate dynamic contrast enhanced computed tomography (DCE-CT) for the identification and delineation of target volumes in patients with prostate cancer.

### **METHOD AND MATERIALS**

With IRB approval and in HIPAA compliance 31 consecutive patients (mean age 67 years; range, 45-81 years) underwent DCE-CT on a 3rd generation DSCT system as well as multiparametric magnet resonance imaging study (mpMRI) including standard T2, DWI and DCE-MRI sequences followed by transrectal MRI guided lesion biopsy. DCE-CT perfusion parameters (CTP) included: blood volume, BV; blood flow; BF, flow extraction product, FEP; mean transit time, MTT. Perfusion Parameters were compared between regular and malignant tissue. MRI perfusion parameters included: transfer constant Ktrans, fractional volume of the extravascularextracellular space, Ve and contrast agent backflux rate constant kep. CTP and MRI perfusion parameters were compared using spearman correlation coefficient.

### RESULTS

21 (70%) of patients were PCa positive with a median Gleason score of 7 (range 6 -9). DCE-CT perfusion parameters enabled identification of histopathological correlated PCa tissue with significant differences of PCa to normal prostate tissue in all CTP values (MIP 106.3 vs. 91.8 HU; BFD 42.9 vs. 28.5 mL/100L/min; BVD 3.2 vs. 1.7 mL/100mL; MTTD 5.1 vs. 4.6 seconds; FEP 19.0 vs. 13.3 mL/100mL/min; p<0.05). Also, DCE-CT BFD was different between benign and malignant lesions (26.1 vs. 42.9 mL/100 mL/min; p=0.01). CTP values significantly correlated with MRI-perfusion parameters (BV-Ktrans: r=0.49; p=0.046).

## CONCLUSION

Our preliminary results suggest that in patients with prostate cancer assigned for RT treatment DCE-Prostate CT allows accurate identification and delineation of target volumes.

## **CLINICAL RELEVANCE/APPLICATION**

DCE-CT of the prostate may be used for identification and delineation of target volumes in patients with prostate cancer and might further serve as a tool for a DCE-CT-based intraprostatic focal dose escalation approach.



## UR188-ED-WEB7

Vesical Imaging Reporting and Data System (VI-RADS) for Standardized Reporting of Multi-Parametric MRI of Bladder Cancer

Wednesday, Nov. 28 12:45PM - 1:15PM Room: GU/UR Community, Learning Center Station #7

## Participants

Valeria Panebianco, MD, Rome, Italy (*Presenter*) Nothing to Disclose Yoshifumi Narumi, MD, Suita, Japan (*Abstract Co-Author*) Nothing to Disclose Mitsuru Takeuchi, MD, PhD, Nagoya, Japan (*Abstract Co-Author*) Nothing to Disclose Valdair F. Muglia, MD, PhD, Ribeirao Preto, Brazil (*Abstract Co-Author*) Nothing to Disclose Hebert Alberto Vargas, MD, Cambridge, United Kingdom (*Abstract Co-Author*) Nothing to Disclose Jelle O. Barentsz, MD, PhD, Nijmegen, Netherlands (*Abstract Co-Author*) Advisor, SPL Medical BV

### For information about this presentation, contact:

valeria.panebianco@gmail.com

## **TEACHING POINTS**

- Management of bladder cancer (BC) is primarily driven by stage and grade, which are currently assessed by cystoscopy, diagnostic TURBT, histopathology and imaging studies. - A major factor determing treatment decisions is the invasion of the muscle layer, which can be missed by up to 25% of TURBT, risulting in understaging. - Multiparametric MRI (mpMRI) can potentially increase the detection of muscular invasion and improve staging in untreated patients. - The mpMRI protocol for bladder cancer consists of T2-weighted imaging (T2WI), diffusion weighted imaging (DWI) and dynamic contrast enhanced imaging (DCE MRI). - A 5-point VI-RADS scoring system is generated, where categories 4 and 5 indicate the presence of muscular invasion. The scoring system takes into account three main parameters: - Structural Category (SC, from 1 to 5, assessed on T2WI) - Contrast Enhancement (CE, from 1 to 5) - DW (from 1 to 5, assessed on DWI and ADC maps)

#### **TABLE OF CONTENTS/OUTLINE**

- Background: bladder cancer - mpMRI for bladder cancer: Technical considerations for image acquisition - The VI-RADS scoring system: components and synthetic score - Final Clinical Considerations



## UR189-ED-WEB8

## Typical and Atypical Testicular Leydig Cell Tumors: Multi-Parametric US and MRI Findings

Wednesday, Nov. 28 12:45PM - 1:15PM Room: GU/UR Community, Learning Center Station #8

## Awards Certificate of Merit

## Participants

Cristina Elena Balasa, MD, Boulogne Billancourt, France (*Presenter*) Nothing to Disclose Marie-France Bellin, MD, Le Kremlin-Bicetre Cedex, France (*Abstract Co-Author*) Nothing to Disclose Bertrand Bresson, Le Kremlin-Bicetre, France (*Abstract Co-Author*) Nothing to Disclose Florian Maxwell, Le Kremlin Bicetre, France (*Abstract Co-Author*) Nothing to Disclose Maud Creze, Le Kremlin Bicetre, France (*Abstract Co-Author*) Nothing to Disclose Laurence M. Rocher, MD, Kremlin Bicetre, France (*Abstract Co-Author*) Nothing to Disclose

### For information about this presentation, contact:

bluescorpion9@yahoo.com

## **TEACHING POINTS**

To illustrate the common imaging features and several rare aspects of Leydig cell tumours To emphasize the added value of multiparametric US and MRI including shear-wave elastography, ultrasensitive Doppler, contrast-enhanced ultrasound, dynamic contrast-enhanced and diffusion MRI in making the accurate diagnosis To stress the impact of multimodal imaging on treatment planning

### TABLE OF CONTENTS/OUTLINE

Based on our pathology database we retrospectively reviewed the US and MRI findings of 30 patients with confirmed LCTs examined at our institution between January 2013 and March 2018. Typical features: - B-mode, color Doppler and contrast-enhanced ultrasound aspect - Shear-wave elastography of LCTs - Ultrasensitive Doppler - Dynamic contrast-enhanced MRI including timeintensity curves - Diffusion MRI The majority of incidentally found LCTs showed slight hypoechogenicity, peripheral vascularization, intermediate stiffness, intense enhancement with or without wash-out, and intermediate ADC values. This study also revealed that rare LCTs may have unusual patterns, such as : - Large Leydig cell tumors - Calcified or ossified LCTs - Iso/hyperechoic appearing LCTs - LCTs associated with other benign or malignant lesions



## VI169-ED-WEB10

Portomesenteric Venous Complications After Pancreatic Surgery with Venous Reconstruction: Imaging and Interventional Therapies

Wednesday, Nov. 28 12:45PM - 1:15PM Room: VI Community, Learning Center Station #10

**FDA** Discussions may include off-label uses.

### Awards Cum Laude Identified for RadioGraphics

#### **Participants**

Scott M. Thompson, MD, PhD, Rochester, MN (*Presenter*) Nothing to Disclose Chad J. Fleming, MD, Rochester, MN (*Abstract Co-Author*) Nothing to Disclose Lavanya Yohanathan, MBBS, Rochester, MN (*Abstract Co-Author*) Nothing to Disclose Mark Truty, Rochester, MN (*Abstract Co-Author*) Nothing to Disclose Michael Kendrick, Rochester, MN (*Abstract Co-Author*) Nothing to Disclose James C. Andrews, MD, Rochester, MN (*Abstract Co-Author*) Nothing to Disclose

For information about this presentation, contact:

Thompson.scott@mayo.edu

## **TEACHING POINTS**

1. Learn the surgical anatomy and imaging appearance of pancreatic surgery with venous reconstruction. 2. Learn the imaging appearance of venous complications and their sequelae following pancreatic surgery with venous reconstruction. 3. Understand the interventional radiologic techniques for managing venous complications following pancreatic surgery with venous reconstruction.

## **TABLE OF CONTENTS/OUTLINE**

1.Surgical anatomy and imaging appearance of pancreatic surgery with venous reconstruction • Types of pancreatic surgery (total pancreatectomy, pancreaticoduodenectomy, distal pancreatectomy) • Types of portomesenteric venous reconstruction (primary venorhapy, venoplasty, interposition graft) 2. Imaging appearance of portomesenteric venous complications following pancreatic surgery • Thrombus (occlusive v. non-occlusive) • Stenosis (intrinsic v. extrinsic) • Sequelae and clinical presentation (portal or mesenteric venous hypertension, varices, ascites, gastrointestinal bleed) 3. Endovascular management of portomesternic venous complications, pre-procedure planning, patient preparation, procedure technique, complications, surveillance and outcomes for: o Thrombectomy o Venoplasty o Stenting (bare metal v. covered)



## VI170-ED-WEB11

Clinical Applications of Dynamic Density Optimization (DDO) in Body Digital Angiography: What the Radiologist Needs to Know

Wednesday, Nov. 28 12:45PM - 1:15PM Room: VI Community, Learning Center Station #11

#### Awards Certificate of Merit

#### Participants

Hidekatsu Tateishi, Tokyo, Japan (*Presenter*) Nothing to Disclose Kazunori Kuroki, MD, Yokohama, Japan (*Abstract Co-Author*) Nothing to Disclose Haruhiko Machida, Tokyo, Japan (*Abstract Co-Author*) Nothing to Disclose Toshihiko Iwamoto, Tokyo, Japan (*Abstract Co-Author*) Nothing to Disclose Toshiya Kariyasu, Tokyo, Japan (*Abstract Co-Author*) Nothing to Disclose Yutaka Masuda, Tokyo, Japan (*Abstract Co-Author*) Nothing to Disclose Yutaka Masuda, Tokyo, Japan (*Abstract Co-Author*) Nothing to Disclose Yusuke Kinoshita, Mitaka, Japan (*Abstract Co-Author*) Nothing to Disclose Hisae Shiga, Mitaka, Japan (*Abstract Co-Author*) Nothing to Disclose Masanaka Watanabe, Tokyo, Japan (*Abstract Co-Author*) Nothing to Disclose Saori Yuda, Tokyo, Japan (*Abstract Co-Author*) Nothing to Disclose Kenichi Yokoyama, MD, Mitaka-Shi, Japan (*Abstract Co-Author*) Nothing to Disclose

## **TEACHING POINTS**

To describe basic facts & principles of dynamic density optimization (DDO) in digital angiography (DA) To review optimization of DDO imaging parameters To illustrate various clinical applications of DDO body DA by presenting clinical images

### **TABLE OF CONTENTS/OUTLINE**

Basic facts & principles of DDO in DA Image processing function providing digital subtraction angiography (DSA) like images often used in interventional radiology (IR) for peripheral artery disease Vessel delineation improvement even with overlapped bony structures Advantages vs. DSA: lower radiation exposure, bone visualization, less susceptible to respiratory motion/bowel peristalsis etc. Optimization of DDO imaging parameters DDO set value/iodine concentration/vessel diameter/body physique Image contrast/halation artifacts/vessel conspicuity/halo effect by unsharp mask processing/radiation exposure Clinical applications Freebreath exams for patients with poor breath-hold/adrenal venous sampling (AVS) Transarterial embolization (TAE) for subdiaphragmatic lesions (eg, HCC) TAE for gastrointestinal hemorrhage/uterine arterial embolization unsusceptible to bowel/ureter peristalsis Bronchial arterial embolization Bone visualization as landmarks for IVC filter/AVS



## VI250-SD-WEB1

A Study on Microwave Ablation Technique Using a Newly Developed Microwave Surgical Instrument. in Vivo Study in a Rabbit Liver Model

Wednesday, Nov. 28 12:45PM - 1:15PM Room: VI Community, Learning Center Station #1

## Participants

Shobu Watanabe, MD, Otsu, Japan (*Presenter*) Nothing to Disclose Norihisa Nitta, MD, Kyoto, Japan (*Abstract Co-Author*) Nothing to Disclose Shinichi Ota, MD, PhD, Otsu, Japan (*Abstract Co-Author*) Nothing to Disclose Akinaga Sonoda, MD, PhD, Otsu, Japan (*Abstract Co-Author*) Nothing to Disclose Kai Takaki, MD, Otsu, Japan (*Abstract Co-Author*) Nothing to Disclose Kiyoshi Murata, MD, Otsu, Japan (*Abstract Co-Author*) Nothing to Disclose Shigeyuki Naka, Ohtsu, Japan (*Abstract Co-Author*) Nothing to Disclose Tohru Tani, Ohtsu, Japan (*Abstract Co-Author*) Nothing to Disclose

#### For information about this presentation, contact:

swat@belle.shiga-med.ac.jp

#### PURPOSE

New microwave surgical instrument (HPA-100WSTD: CHRONIX Ltd., Japan) developed by Prof. Tani have been able to perform coagulation with high efficiency compared with conventional surgical instruments by digitally controlling microwaves. In this study, we performed MCT using this instrument on rabbit liver model and evaluated its cauterizing effect.

### **METHOD AND MATERIALS**

Experiment1: 30 Japanese white rabbits (2.5-3.0kg) were divided into 6 groups and laparotomic MCT was performed under the following conditions. The power of output; 40W, 60W, Increase from 40W to 60W Coagulation time; 40sec, 60sec All rabbits were sacrificed at 7days later and liver were extracted. The length of the ablation range around the electrode was measured, and the aspect ratio was also calculated. Pathological specimens were constructed and changes around the electrode were evaluated. Experiment2: 15 Japanese white rabbits (2.5-3.0kg) with transplanted VX2 liver tumors divided into 3 groups and laparotomic MCT was performed under the following conditions. The power of output; 40W, 60W, Increase from 40W to 60W Coagulation time; 60sec Coagulation area was measured on MR images acquired before and 7 days after treatment.

### RESULTS

Exerimant1: In any condition, it was possible to ablate a range of 2 cm or wider than the conventional MCT. Also, as the output was high and the cauterization time was longer, the coagulation range became wider and approached a spherical shape. Pathologically, sufficient thermo coagulation necrosis within the ablation range was observed. Experiment2: On MRI, confirmed in all cases that tumors are included within the ablation range. The ablation range on MRI also showed more than 2 cm in all conditions, and there was no clear significant difference in the diameter of the ablation range.

### CONCLUSION

A new microwave surgical instrument was able to coagulate wider than conventional surgical instruments. As the coagulation range becomes large spherical with output and time, it is thought that it becomes easy to make the tumor within the coagulation range.

### **CLINICAL RELEVANCE/APPLICATION**

Further examination is needed for complications due to expansion of the coagulation area, but in the future it is possible that the indication of MCT will change as the surgical instrument develops.



## VI251-SD-WEB2

Percutaneous Vesselplasty in Osteolytic Primary or Secondary Vertebral Lesions After the Radiofrequency Ablation: A Safe and Effective Technique

Wednesday, Nov. 28 12:45PM - 1:15PM Room: VI Community, Learning Center Station #2

## Participants

Dario Notaro, MD, Siena, Italy (*Presenter*) Nothing to Disclose Matteo Bellini, MD, Siena, Italy (*Abstract Co-Author*) Nothing to Disclose Chiara Zini, MD, Rome, Italy (*Abstract Co-Author*) Nothing to Disclose Maria Antonietta Mazzei, MD, Siena, Italy (*Abstract Co-Author*) Nothing to Disclose Luca Volterrani, Siena, Italy (*Abstract Co-Author*) Nothing to Disclose

# For information about this presentation, contact:

dario.notaro88@gmail.com

## PURPOSE

Two-thirds of patients with cancer will develop bone metastasis and the spine is the most common site. A spinal metastasis may cause pain, instability and neurological injuries. We present the apparatus, operative procedure, advantages of Vesselplasty, i. e. positioning a new cement containment system, after radiofrequency ablation (RFA) of osteolytic vertebral bone tumoral lesions.

#### **METHOD AND MATERIALS**

This retrospective study included 13 lumbar and 4 thoracic vertebrae treated in 15 patients (mean age, 60 years; range, 23-79) suffering from symptomatic vertebral bone metastases or multiple myeloma. Inclusion criteria were 1) pathologic fracture diagnosed by MRI or CT, 2) persistent pain after pharmacologic or radiotherapic treatment, and 3) no or moderate intracanalar tumor. RFA (Boston RF3000 Generator, Boston Scientific Way Marlborough, USA) was performed by monopeduncular approach, under biplanar fluoroscopic guidance and local anesthesia, applying single needle or umbrella shaped array electrode in two different part of the bone lesion, depending on dimensions. Power was increased by applying 1 Watt every minute and treatment was finished when impedence rised 200 ohms. Vesselplasty system (Vessel, Dragon Crown Medical Co. Shandong, China) has then implanted into vertebral body lesions, and expanded by injection of high viscosity cement. All the patients underwent thoraco-lumbar spine gadolinium-enhanced MRI before and 1 month after the treatment. A VAS scale was taken before, 1 week, 1 month, and 6 months after treatment.

### RESULTS

All patients had immediate pain relief with no major complication. There were 4 asymptomatic cement leakage into an intervertebral contiguous disc. Preoperative mean VAS was 8. 2, while mean VAS after 1 week, 1 month, and 6 months was 3. 65, 1. 85 and 1. 42, respectively.

#### CONCLUSION

Vessellplasty can be a valid and safety alternative to vertebroplasty and kyphoplasty following RFA for minimally invasive treatment of vertebral bone osteolytic lesion.

## **CLINICAL RELEVANCE/APPLICATION**

It is a safe and useful procedure to reduce not just the pain but also the tumor dimension in osteolytic primary or secondary vertebral lesions.



## VI252-SD-WEB3

Analyzing the Effectiveness of Pericardial Drain Size on Short Term Complications and Recurrence as a Palliative Care Option for the Treatment of Symptomatic Pericardial Effusion

Wednesday, Nov. 28 12:45PM - 1:15PM Room: VI Community, Learning Center Station #3

# Participants

Umairullah Lodhi, MD, Manhasset, NY (*Presenter*) Nothing to Disclose Christopher F. Koch, MD, Manhasset, NY (*Abstract Co-Author*) Nothing to Disclose Adam Siegel, BS, Hempstead, NY (*Abstract Co-Author*) Nothing to Disclose Joseph Mootz, New Hartford, NY (*Abstract Co-Author*) Nothing to Disclose Jorge J. Tirado, MD, Manhasset, NY (*Abstract Co-Author*) Nothing to Disclose Craig R. Greben, MD, Great Neck, NY (*Abstract Co-Author*) Consultant, Vascular Solutions, Inc License agreement, Vascular Solutions, Inc

#### For information about this presentation, contact:

## ulodhi@northwell.edu

## PURPOSE

To analyze the effect of drain size on short term complications and recurrence between various procedures utilizing pericardial drains including CT-guided percutaneous pericardiocentesis (PPD) and surgical pericardial window (SPW) in the palliative care setting.

## METHOD AND MATERIALS

A retrospective chart review was performed.108 patients with symptomatic pericardial effusions (60 treated with CT-guided PPD and 48 with SPW) were found to have a significant life-limiting illness at the time of presentation which also predisposed to recurrent pericardial effusions. Tests for association between intervention groups and the outcomes: short term complications and recurrences (defined as <=30 days), and long term complications and recurrences (>30 days) were performed using chi-square tests or Fisher's exact test, as appropriate. Additionally, a multivariate ordered logistic regression analysis was performed on drain size and its impact on short and long term complications and recurrences while accounting for age, gender, and underlying illness.

## RESULTS

Mean Age [SD]: 63.3 [14.3] for PPD and 63 [16.3] for SPW. Gender: PPD group - 53% male and 47% females. SPW group - 56% males and 44% females. Underlying illnesses (%) (PPD vs SPW): ESRD on HD: 28.3 vs 22.9, High grade/stage malignancy (most common being Lung CA): 58.3 vs 47.9, Severe LV dysfuction: 13.3 vs 29.2. A statistically significant difference in short term complications (CVA, arrhythmia, DVT, pneumothorax, etc) was observed between the two groups: 21% in SPW group and 5% in PPD (p<0.012). No significant difference in long term complications, and short and long term recurrences existed between the two groups. Median catheter sizes were as follows: PPD - 8.5Fr and SPW - 19Fr. A statistically significant increase in short term recurrence in patients with a large preprocedural pericardial effusion [OR 1.58, 95% CI 1.02-2.46 p<.05] and short term complications [OR 1.83, 95% CI 1.03-3.24 p<.05] was observed with increased drain size while accounting for age, gender, and underlying illness. No significant effect of catheter duration was observed on complications or recurrences.

#### CONCLUSION

The smaller drain utilized in CT-guided PPD can lower short term complications and recurrence in patients with severe illnesses when compared to SPW.

## **CLINICAL RELEVANCE/APPLICATION**

CT-guided PPD can lower complications and potentially morbidity in a patient population where preservation of quality of life is a major goal.



## VI253-SD-WEB4

Preoperative Endoscopic versus Percutaneous Biliary Stent Placement for Obstructive Jaundice before Pancreatectomy: An Analysis of the National Surgical Quality Improvement Program

Wednesday, Nov. 28 12:45PM - 1:15PM Room: VI Community, Learning Center Station #4

# Participants

Alexander H. Lam, MD, Orange, CA (*Presenter*) Nothing to Disclose Kevin T. Bui, MD, Orange, CA (*Abstract Co-Author*) Nothing to Disclose Dayantha Fernando, MD, Orange, CA (*Abstract Co-Author*) Nothing to Disclose James Katrivesis, MD, Yorba Linda, CA (*Abstract Co-Author*) Nothing to Disclose Kari J. Nelson, MD, Orange, CA (*Abstract Co-Author*) Nothing to Disclose Nadine Abi-Jaoudeh, MD, Orange, CA (*Abstract Co-Author*) Research collaboration, Koninklijke Philips NV; Research collaboration, Teclison Cherry Pharma Inc; Research support, SillaJen, Inc

#### For information about this presentation, contact:

ahlam@uci.edu

## PURPOSE

There is inconsistent data regarding the preferred route of preoperative biliary stent placement before pancreatectomy for benign and malignant jaundice. The aim of this study is to compare the periprocedural outcomes related to pancreatectomy following endoscopic and percutaneous biliary stent placement.

## **METHOD AND MATERIALS**

The American College of Surgeons (ACS) National Surgical Quality Improvement Program (NSQIP) database was queried for all patients undergoing pancreatectomy from 2014 to 2016. Only patients who received either endoscopic (EBS) or percutaneous (PBS) preprocedural biliary stent placements were included. Preoperative variables were evaluated. Univariate analysis was performed with Student's t-test and chi-squared test. A multivariable regression model was created to determine significant predictors of 30-day mortality. Other outcomes evaluated include rate of pancreatic fistula formation, sepsis, and length of stay (LOS). A propensity score matched cohort analysis was performed to account for measurable confounders. A p-value of <0.05 was considered statistically significant.

## RESULTS

A total of 288 and 3753 patients were included in the PBS and EBS groups, respectively. In multivariate regression analysis, no significant predictors of 30-day mortality were noted. Prior to surgery, the PBS group had significantly higher rates of dyspnea (8.3% vs 5.7%; p = 0.016) and severe obstructive pulmonary disease (6.9% vs 4.3%; p = 0.041). The PBS groups had a significantly higher proportion of preoperative sepsis (3.1% vs 1.1%; p < 0.001) and blood transfusion 72 hours before surgery (3.1% vs 0.8%; p < 0.001). The PBS group had a significantly higher rate of hemorrhage requiring transfusion in the unmatched cohorts (31.6% vs 20.1%; p < 0.001), which persisted after propensity score matching. Although a significantly longer LOS was noted in the PBS group (13.4 vs 11.0 days; p = 0.001), there was no significant difference in 30-day mortality.

## CONCLUSION

Compared to endoscopic biliary stent placement, percutaneous stent placement was associated with significantly higher risk of hemorrhage and longer LOS without a significant difference in 30-day mortality after adjusting for measurable confounders.

# **CLINICAL RELEVANCE/APPLICATION**

Before pancreatectomy, an initial endoscopic approach to biliary stenting for jaundice may result in less postoperative hemorrhage and shorter LOS with comparable outcomes to a percutaneous approach.



## VI254-SD-WEB5

The Diagnostic Value of Noncontrast-Enhanced ECG-Gating Quiescent-Interval Single-Shot (QISS) MR Angiography in Lower Extremity Peripheral Arterial Disease

Wednesday, Nov. 28 12:45PM - 1:15PM Room: VI Community, Learning Center Station #5

**FDA** Discussions may include off-label uses.

#### Participants

Ming Yang, Wuhan, China (*Presenter*) Nothing to Disclose Hongran Liu, MD, Wuhan, China (*Abstract Co-Author*) Nothing to Disclose

#### PURPOSE

To evaluate the diagnostic value of Noncontrast-enhanced ECG-gating quiescent-interval single-shot (QISS) MR angiography in lower extremity peripheral arterial disease.

## METHOD AND MATERIALS

Continuous collection 43 patients with clinical suspected of lower extremity arterial disease (male 28, female 12, age 40-82y, average age 58.76y) in January 2017 - June 2017, all patients underwent CTA and QISS MRA, 30 of 43 underwent Digital Subtraction Angiography (DSA). The QISS MRA and CTA images were compared between two senior subjects (15 and 13 years, respectively). The image quality was scored according to the 4-point scale and the MRA and CTA were measured using the Kappa test in the lower extremity arterial stenosis to evaluate the consistency of the analysis. DSA was used as a reference standard to compare CTA and MRA QISS hemodynamic significant stenosis (>=50%) sensitivity and specificity.

## RESULTS

The QISS MRA image quality was  $3.83 \pm 0.52$  for reader 1,  $3.77 \pm 0.43$  for reader 2, significantly lower than CTA ( $4.10 \pm 0.46$  and  $3.99 \pm 0.43$  for reader 1 and 2, P <0.001). QISS MRA and CTA assessment of the consistency of lower extremity vascular stenosis is very good (Kappa =  $0.923 \pm 0.013$  for reader 1,  $0.930 \pm 0.012$  for reader 2). The sensitivity of QISS was 94.93 and 94.56% (91.21 and 90.33% for CTA, P> 0.05), and the specificity of QISS was 95.92 and 96.57% (95.41 and 95.32% for CTA, P> 0.05 for reader 1 and 2, respectively). The sensitivity of QISS (95.66 and 96.43%) was significantly higher than that of CTA (75.69 and 78.76%, P <0.05) for heavily calcified segments.

## CONCLUSION

In conclusion, QISS-MRA is a promising nonenhanced imaging technique for arteries of the lower extremities. Due to its high sensitivity and negative predictive value as well as short acquisition time, it might serve as a screening method especially in patients with contraindications to gadolinium-based contrast material.

#### **CLINICAL RELEVANCE/APPLICATION**

QISS is a reliable alternative to CTA's assessment of lower extremity peripheral arterial disease (PAD) and is suitable for first-line screening of patients with contraindications to intravenous administration.



## VI255-SD-WEB6

Safety of Combining Everolimus with Transarterial Embolization in Patients with Metastatic Neuroendocrine Tumor to the Liver

Wednesday, Nov. 28 12:45PM - 1:15PM Room: VI Community, Learning Center Station #6

VA

## Participants

Timothy J. Waits, MD, Lexington, KY (*Presenter*) Nothing to Disclose Aman Chauhan, Lexington, KY (*Abstract Co-Author*) Nothing to Disclose Ravi S. Jayavarapu, MPH, MD, Lexington, KY (*Abstract Co-Author*) Nothing to Disclose Lowell Anthony, MD, Lexington, KY (*Abstract Co-Author*) Nothing to Disclose Steven J. Krohmer, MD, Lexington, KY (*Abstract Co-Author*) Nothing to Disclose M. Elizabeth Oates, MD, Lexington, KY (*Abstract Co-Author*) Nothing to Disclose Riham H. El Khouli, MD, PhD, Nicholasville, KY (*Abstract Co-Author*) Nothing to Disclose

### PURPOSE

Hepatic transarterial embolization (HAE) is an effective loco-regional therapy for the management of neuroendocrine tumors (NETs). Systemic targeted therapies, such as everolimus and sunitinib, are typically held 2-4 weeks prior to and after hepatic embolization. We hypothesized that the concurrent use of everolimus with HAE is safe.

### METHOD AND MATERIALS

Review of clinical and pathologic data was conducted for all patients who underwent HAE with concurrent systemic everolimus between September 2016 and April 2018. Medical records were obtained via EHR and all imaging characteristics were reviewed via PACS imaging software. Patients were required to have systemic everolimus for > 1 month prior to embolization in order to be included in this study.

### RESULTS

A total of 23 patients met inclusion criteria. 10 patients were male and 13 female, with an average age of  $55.2 \pm 14.7$  years of age (31-77 years). Primary lesions were identified in 82.6% of patients, while 17.4% remained unknown. The primary site was identified as small bowel in 43.5% of patients, pancreas in 26.1%, lung in 8.7% and adrenal gland in 4.3%. Grades 1, 2 and 3 NET were 39.1%, 43.5% and 8.7%, respectively. The mean duration of treatment of everolimus prior to the first embolization was 89 ± 52.6 days. Fourteen patients had HAE performed on both right and left lobes, whereas 9 had embolization of the right hepatic lobe only. This yielded a total of 37 procedures. Three procedures were excluded due to lack of everolimus treatment prior to intervention. The average hospitalization time was 1.7 days (1-4 days). Abdominal pain was reported in 69.7% of cases, nausea with emesis in 21.1%, nausea without emesis in 27.3% and HTN in 9.1%. No symptoms were reported in 12.1%. One patient developed hematemesis on the day of the procedure which resolved overnight. One episode of mild carcinoid crisis was reported that resolved on the second day of hospitalization. The average decrease in hemoglobin pre- and post-procedure was 1.3 ± 0.8 g/dL. All patients were transitioned to oral pain medication and were in stable condition prior to discharge.

### CONCLUSION

HAE with concurrent use of everolimus is safe and does not significantly increase length of hospital stay.

## **CLINICAL RELEVANCE/APPLICATION**

Combination HAE and everolimus has shown promising results on both anatomical and functional imaging of NETs. Knowing this combination is safe is reassuring for patient and clinician.

## **Honored Educators**

Presenters or authors on this event have been recognized as RSNA Honored Educators for participating in multiple qualifying educational activities. Honored Educators are invested in furthering the profession of radiology by delivering high-quality educational content in their field of study. Learn how you can become an honored educator by visiting the website at: https://www.rsna.org/Honored-Educator-Award/ Riham H. El Khouli, MD, PhD - 2012 Honored Educator



## VI256-SD-WEB7

Not All M2 Branches are Alike: Failure of Frontal Division Recanalization Utilizing Mechanical Thrombectomy

Wednesday, Nov. 28 12:45PM - 1:15PM Room: VI Community, Learning Center Station #7

#### Awards Student Travel Stipend Award

#### **Participants**

Stephany Barreto, MD, Syracuse, NY (*Presenter*) Nothing to Disclose Amar S. Swarnkar, MD, Syracuse, NY (*Abstract Co-Author*) Nothing to Disclose

For information about this presentation, contact:

# barretos@upstate.edu

## PURPOSE

Recently, mechanical thrombectomy using aspiration catheters and stent retrieval devices have been proven to be relatively safe and clinically beneficial in the treatment of acute ischemic stroke caused by large vessel occlusions. This study looked at endovascularly treated acute strokes caused by isolated frontal (superior) and parietal (inferior) M2 divisions of the middle cerebral artery. Due to inherent anatomical differences between the frontal and parietal division, we hypothesized that mechanical thrombectomy within the frontal division would yield less successful results when compared to the parietal division.

## **METHOD AND MATERIALS**

In this single-center retrospective study we selected only isolated frontal or parietal M2 branch occlusions from all patients presenting for neurointerventional treatment of acute stroke from September 2012 to April 2018. All occlusions from the M1, distal MCA, anterior cerebral artery, internal carotid artery, and posterior cerebral circulation were excluded from the study. These patients underwent mechanical thrombectomy with aspiration catheters and/or endovascular stent retrieval devices. We analysed intraprocedural data comparing results of parietal versus frontal division thrombectomies.

## RESULTS

Out of 364 endovascularly treated cases, 20 patients had isolated parietal M2 branch occlusions and 9 isolated frontal M2 branch occlusions. Mean age of patients were 69.3. Successful recanalization (TICI 2b, 3) was achieved in more parietal M2 occlusions than frontal M2 occlusions (90.0% vs. 11.1%, p = <0.001). There were no significance difference in the median number of attempts between the parietal and frontal division occlusions (1.0 vs. 2.0, p = 0.3330); nor median fluoroscopy time (27.4 minutes vs. 33.1 minutes, p = 0.588) or recanalization time from groin puncture (59.0 minutes vs. 62.0 minutes, p = 0.289).

### CONCLUSION

Rate of successful reperfusion following mechanical thrombectomy is significantly greater in parietal division occlusions than frontal division occlusions. Failure of recanalization of the M2 frontal branch is likely related to unfavorable anatomical features such as a narrower diameter and less obtuse angle with the M1 segment in comparison to the parietal division.

### **CLINICAL RELEVANCE/APPLICATION**

Mechanical thrombectomy in the M2 frontal division is less successful than the parietal division, which may require different techniques and/or devices to generate better outcomes.



## VI257-SD-WEB8

Frequency and CTA-based Volumetric Analysis of Endoleaks after Fenestrated Endovascular Aortic Aneurysm Repair (FEVAR) using Custom and Off-the-Shelf Devices

Wednesday, Nov. 28 12:45PM - 1:15PM Room: VI Community, Learning Center Station #8

FDA Discussions may include off-label uses.

#### **Participants**

David E. Timaran Montenegro, MD, Mexico City, Mexico (*Presenter*) Nothing to Disclose Marilisa Soto Gonzalez, MD, Dallas, TX (*Abstract Co-Author*) Nothing to Disclose Angie Garcia, MD, Dallas, TX (*Abstract Co-Author*) Nothing to Disclose Carlos Timaran, Dallas, TX (*Abstract Co-Author*) Consultant, Cook Group Incorporated Consultant, Getinge AB Consultant, W. L. Gore & Associates, Inc

### For information about this presentation, contact:

david\_timaranQyahoo.com

### PURPOSE

The aim of the study was to assess the type, frequency, morphologic characteristics and outcomes of endoleaks after FEVAR/BEVAR using custom-made- devices (CMDs) and off-the-shelf branched devices.

## METHOD AND MATERIALS

A single institutional study was performed to assess the frequency and volume of endoleaks after FEVAR using fenestrated/branched CMDs and off-the-shelf devices. All fenestrated procedures were performed using investigational CMDs under a physician-sponsored investigational device exemption. Endoleaks were detected and characterized on duplex and CT angiography. CTA-based volumetric analysis was performed using Terarecon software. Kruskal-Wallis and Mann-Whitney U tests were used for univariate analysis.

## RESULTS

Over a 25-month period, 70 patients (52 men [74%] and 18 women [26%]) with a median age of 68 years (interquartile range [IQR], 63.5-73 years) underwent FEVAR using Fenestrated/Branched Custom-Made-Devices (CMDs) (64[91%]) and Zenith T-Branch (6[9%]). The median number of fenestrations/branches was 4 (IQR, 3-4). Endoleaks were detected in 11 patients (7.7%) accounting for a total of 15 endoleaks during follow-up. Endoleaks were found at a median time of 1 month (Interquartile range [IQR], 1-8 months). Type IB endolaks were found in 1 patient (7%), type IC in 8 (53%), type II in 3 (20%), and type III in 3 patients (20%). Overall median endoleak volume was 10 cc (IQR, 5.8-10.8 cc). Median endoleak volume per type of endoleak volume was as follows: type IB, 56 cc; type IC, 10.3 cc (IQR, 8.1-11.4 cc), type II, 10cc (IQR, 4.8-11.6 cc); and type III, 8.9 cc(IQR, 5.8-10.6 cc) (p>.1). All patients underwent endoleak repair.Endoleak secondary repair was required in 3 patients (20%). Those patients were found with higher endoleak volumes (10.6 cc [IQR,10.3-341.2cc]) when compared to patients that were repaired at a primary intervention ( 8.78 cc [IQR,5.7-10.6 cc]) (p=.07).

## CONCLUSION

The frequency of endoleaks that required intervention after FEVAR using investigational devices was 7%. Type IC endoleaks were the most frequently found. Endoleaks with higher volume were found have higher risk for secondary endoleak repair.

## **CLINICAL RELEVANCE/APPLICATION**

Endoleaks after endovascular repair of AAAs are frequent. For FFEVAR, the incidence and natural history of endoleaks are still under invetigation. This study assess the incidence of endoleaks and predictors of primary endoleak failure.



## VI258-SD-WEB9

## Radiofrequency Versus Microwave Liver Ablation. Preliminary Results of a Randomized Clinical Trial

Wednesday, Nov. 28 12:45PM - 1:15PM Room: VI Community, Learning Center Station #9

**FDA** Discussions may include off-label uses.

#### Participants

Aleksandar Radosevic, MD, Barcelona, Spain (*Presenter*) Nothing to Disclose Rita Quesada, PhD, Barcelona, Spain (*Abstract Co-Author*) Nothing to Disclose Ander Zugazaga Cortazar, MD, Barcelona, Spain (*Abstract Co-Author*) Nothing to Disclose Juan Sanchez Parrilla, MD, Barcelona, Spain (*Abstract Co-Author*) Nothing to Disclose Jose Ignacio Poves, Barcelona, Spain (*Abstract Co-Author*) Nothing to Disclose Fernando Burdio, Barcelona, Spain (*Abstract Co-Author*) Stockholder, Apieron, Inc

#### For information about this presentation, contact:

aradosevic@parcdesalutmar.cat

#### PURPOSE

This registered randomized (ISRCTN73194360) study aims to evaluate the safety and performance of the Radiofrequency ablation (RFA) compared to microwave ablation (MWA) systems treating both hepatocarcinoma (HCC) and colorectal liver metastases (CRLM).

#### **METHOD AND MATERIALS**

During Phase II of the study, 53 patients (37 HCC/16 CRLM) were randomized and treated by RFA (n=21/7) and MWA (n=16/9) and followed every three months by CT. RFA was performed with a new RF-hybrid applicator (cool-tip plus infusion of hypertonic saline infusion). The local control, overall survival (OS) and survival free of local recurrence (SFLHR) or survival free of hepatic recurrence (SFHR) were observed. Additionally, hospital stay (HS) and total rate of complications (TRC) were carefully reported and compared among groups.

## RESULTS

Sixty-four nodules larger than 1.5 cm were treated. The mean number of ablations/nodules was similar among groups  $(1.8\pm0.8 \text{ vs} 1.9\pm1.1 \text{ for RFA}$  and MWA, respectively). The mean ablation time/nodule was not statistically different  $(10.0\pm6.4 \text{ min vs}. 8.9\pm5.4 \text{ min})$ . There were two major complications in group RF and one in group MW. HS  $(4.1\pm10.2 \text{ vs}. 3.3\pm5.9 \text{ days})$  was also similar between groups. There was no residual activity at 3-month control scan in 93% of patient treated with RFA and in 97% of patients treated with MWA. With a mean follow-up of 24.4 months, the mean OS, SFLHR and SFHR were similar among groups RFA/MWA (24 vs. 24.7 months, 25 vs. 25 months and 17 vs. 22 months, respectively).

#### CONCLUSION

These preliminary results suggest that this RFA system is as safe and effective in terms of safety and performance than MWA.

## **CLINICAL RELEVANCE/APPLICATION**

Although widely used in clinical practice, there are scant prospective randomized studies comparing the effectiveness of microwave vs radiofrequency ablation.



# AI001-WED

# **3D Segmentation of Brain MR**

Wednesday, Nov. 28 2:30PM - 4:00PM Room: AI Community, Learning Center

# Title and Abstract

3D Segmentation of Brain MR This session will focus on the use of deep learning methods for segmentation, with particular emphasis on 3D techniques (V-Nets) applied to the challenge of MR brain segmentation. While focused on this particular problem, the concepts should generalize to other organs and image types.



# AI001-THA

# **3D Segmentation of Brain MR**

Thursday, Nov. 29 8:30AM - 10:00AM Room: AI Community, Learning Center

# Title and Abstract

3D Segmentation of Brain MR This session will focus on the use of deep learning methods for segmentation, with particular emphasis on 3D techniques (V-Nets) applied to the challenge of MR brain segmentation. While focused on this particular problem, the concepts should generalize to other organs and image types.



# AI001-THB

# **Multi-modal Classification**

Thursday, Nov. 29 10:30AM - 12:00PM Room: AI Community, Learning Center

# Title and Abstract

Multi-modal Classification This session will focus on multimodal classification. Classification is the recognition of an image or some portion of an image being of one type or another, such as 'tumor' or 'infection'. Multimodal classification means that there are more than 2 classes. While this is logically simple to understand, it presents some unique challenges that will be discussed.



## AI150-ED-THA4

## Emerging Approaches for Applying Artificial Intelligence in Neuroradiology

Thursday, Nov. 29 12:15PM - 12:45PM Room: AI Community, Learning Center Station #4

#### Participants

Jeffrey Rudie, MD, PhD, Philadelphia, PA (*Presenter*) Nothing to Disclose Andreas M. Rauschecker, MD, PhD, Philadelphia, PA (*Abstract Co-Author*) Nothing to Disclose R. Nick Bryan, MD, PhD, Austin, TX (*Abstract Co-Author*) Stockholder, Galileo CDS, Inc Officer, Galileo CDS, Inc James C. Gee, PhD, Philadelphia, PA (*Abstract Co-Author*) Nothing to Disclose Christos Davatzikos, PhD, Philadelphia, PA (*Abstract Co-Author*) Nothing to Disclose Suyash Mohan, MD, Philadelphia, PA (*Abstract Co-Author*) Grant, NovoCure Ltd; Grant, Galileo CDS, Inc

## For information about this presentation, contact:

Jeff.Rudie@gmail.com

## **TEACHING POINTS**

With the recent exponential growth of computational efficiency, artificial intelligence (AI) has become a hot topic in nearly all technology-related fields, including health care and radiology. Undoubtedly, radiological practice will substantially change as more AI technology is adopted into everyday use. In this exhibit, we will review various forms of artificial intelligence currently under development by our group in neuroradiology. We will (1) discuss relative advantages and disadvantages of different AI implementations and (2) highlight how targeted use of different methods for different purposes has the potential to significantly improve both the efficiency and quality of clinical practice in the near future.

## TABLE OF CONTENTS/OUTLINE

1) Artificial Intelligence Methods - Bayesian Networks - Decision Trees - Support Vector Machines - Deep Learning/Convolutional Neural Networks 2) Automated Segmentation Methods - Deep Gray Nuclei and White Matter Lesion Segmentation - Brain Tumor Segmentation 3) Clinical Uses for AI in Neuroradiology - Neuro-oncologic Applications: Response Assessment, Molecular Subtypes and Prognostication - Differential Diagnosis Clinical Decision Support - Automated Draft Report Generation



## AI230-SD-THA1

## Support Vector Machine Model for Stratification of Liver Stiffness using Clinical Data

Thursday, Nov. 29 12:15PM - 12:45PM Room: AI Community, Learning Center Station #:

### **Participants**

Hailong Li, PhD, Cincinnati, OH (*Presenter*) Nothing to Disclose Lili He, Cincinnati, OH (*Abstract Co-Author*) Nothing to Disclose Thomas Maloney, Cincinnati, OH (*Abstract Co-Author*) Nothing to Disclose Jonathan Dudley, Cincinnati, OH (*Abstract Co-Author*) Nothing to Disclose Samuel L. Brady, PHD, Cincinnati, OH (*Abstract Co-Author*) Nothing to Disclose Elanchezhian Somasundaram, Cincinnati, OH (*Abstract Co-Author*) Nothing to Disclose Jonathan R. Dillman, MD, Cincinnati, OH (*Abstract Co-Author*) Research Grant, Siemens AG; Research Grant, Guerbet SA; Travel support, Koninklijke Philips NV; Research Grant, Canon Medical Systems Corporation; Research Grant, Bracco Group

#### For information about this presentation, contact:

Hailong.Li@cchmc.org

### PURPOSE

To determine if a support vector machine (SVM) learning model can categorically classify MR elastography (MRE)-derived liver stiffness using clinical data from pediatric and young adult patients with chronic liver diseases.

## METHOD AND MATERIALS

Clinical data. An IRB approved waiver of consent was obtained for this retrospective study. Clinical data (33 features) and MRE liver stiffness measurements from 362 chronic liver disease patients (mean age =14.2 yrs) were obtained. Clinical data were retrieved from our medical record system (Epic Systems Corporation; Verona, WI), including four domains: 1) demographics/vital signs (e.g., sex, age, weight, height, blood pressure); 2) medical history (e.g., diabetes mellitus [types I and II], non-alcoholic fatty liver disease [NAFLD], biliary atresia, Alagille syndrome, sclerosing cholangitis, cystic fibrosis, Fontan operation); 3) blood tests (e.g., bilirubin [total and direct], ALT, AST, GGT, albumin, platelet, APRI, FIB-4); and 4) MRI biomarkers (e.g., liver volume, liver proton density fat fraction) from imaging reports. MRE liver stiffness measurements were extracted from imaging reports. Patients were divided into two groups (<3 kPa=no/mild vs. >=3 kPa=moderate/severe liver stiffening). Machine learning model. Given clinical data and group label, the SVM model was trained to classify a given patient into either a no/mild or moderate/severe liver stiffness group (Figure (A)). Leave-one-out cross-validation was used. The performance was assessed using accuracy, sensitivity, specificity, and area under the receiver operating characteristic curve (AUC).

### RESULTS

Classification results for our SVM model are shown in the Figure (B). Our model was able to correctly classify patients with an accuracy of 82%. This SVM model achieved an AUC of 0.85, with a sensitivity of 76% and a specificity of 86%. The most important features that contributed to stiffness classification are presented in the Figure (C).

### CONCLUSION

Using only clinical data, an SVM model was able to stratify pediatric and young adult chronic liver disease patients into different liver stiffness groups. Future model improvements will include the incorporation of anatomic imaging features.

### **CLINICAL RELEVANCE/APPLICATION**

Machine learning can use clinical data to categorically predict liver stiffness. Model refinements and incorporation of anatomic imaging features may soon decrease the need for MR elastography.

#### **Honored Educators**

Presenters or authors on this event have been recognized as RSNA Honored Educators for participating in multiple qualifying educational activities. Honored Educators are invested in furthering the profession of radiology by delivering high-quality educational content in their field of study. Learn how you can become an honored educator by visiting the website at: https://www.rsna.org/Honored-Educator-Award/ Jonathan R. Dillman, MD - 2016 Honored Educator



### AI231-SD-THA2

Markerless Tumor Tracking for Hepatocellular Carcinoma Using Fluoroscopic Imaging with a Deep Neural Network

Thursday, Nov. 29 12:15PM - 12:45PM Room: AI Community, Learning Center Station #2

# Participants

Ryusuke Hirai, MENG, Kawasaki, Japan (*Presenter*) Employee, Toshiba Corporation Akiyuki Tanizawa, Kawasaki, Japan (*Abstract Co-Author*) Employee, Canon Medical Systems Corporation Yukinobu Sakata, Kawasaki, Japan (*Abstract Co-Author*) Employee, Toshiba Corporation Shinichiro Mori, Chiba, Japan (*Abstract Co-Author*) Nothing to Disclose

For information about this presentation, contact:

ryusuke.hirai@toshiba.co.jp

## PURPOSE

To improve the treatment accuracy of particle-beam therapy by minimizing the effect of respiratory-induced target motion, it is necessary to directly capture tumor position during treatment. Several studies have investigated markerless lung tumor tracking by tumor image pattern learning. However, such pattern learning is limited to some extent by the low contrast of fluoroscopic images in the abdominal region. Here, we have developed a new tumor tracking method for liver cancer treatment by using fluoroscopic images with a deep neural network.

### **METHOD AND MATERIALS**

Our method comprised a learning stage and a tracking stage. In the learning stage, we constructed the network using training datasets to estimate a tumor position map from the input image pattern. To prepare the training data, we used treatment planning four-dimensional computed tomography (4DCT). The tumor position on 4DCT was contoured in each phase by a certificated oncologist. To compile the training dataset, we sampled the tumor centroid and image pattern from digitally reconstructed radiographs from 4DCT. The intensity of the tumor position map for training was calculated using a 2D Gaussian kernel with mean of the tumor centroid and variance of *W*2/8, where *W* is the width or height of the map. In the tracking stage, we input the same position was calculated using the map. The tumor position in 3D space could be derived using paired X-ray fluoroscopic images. Our method has been quantified using fluoroscopic image datasets from two cases of liver cancer. The tumor was tracked by our method and positional error was evaluated as the Euclidean distance between the calculated tumor position and the actual position input by a certificated oncologist.

### RESULTS

Mean positional errors were  $1.43 \pm 0.39$  mm and  $1.87 \pm 1.01$  mm for the first and second cases, respectively. The calculation time was less than 24.4 ms/frame.

## CONCLUSION

Our proposed algorithm achieved high accuracy and a short computation time, we expect that our method will be useful in improving gate treatment accuracy.

### **CLINICAL RELEVANCE/APPLICATION**

Our proposed method required planning 4DCT at the learning stage only, and successfully tracked tumor position in real time without preventing treatment throughput.



## AI232-SD-THA3

## Morphological Classification of the Cortical Bone Layer Using Deep Learning in Panoramic Radiography

Thursday, Nov. 29 12:15PM - 12:45PM Room: AI Community, Learning Center Station #3

### Participants

Wataru Nishiyama, DDS, Gifu, Japan (*Presenter*) Nothing to Disclose Yudai Yanashita, Gifu, Japan (*Abstract Co-Author*) Nothing to Disclose Chisako Muramatsu, PhD, Gifu, Japan (*Abstract Co-Author*) Nothing to Disclose Fujita Hiroshi, Gifu, Japan (*Abstract Co-Author*) Nothing to Disclose Akitoshi Katsumata, DDS, PhD, Mizuho, Japan (*Abstract Co-Author*) Nothing to Disclose

#### For information about this presentation, contact:

wataru@dent.asahi-u.ac.jp

### PURPOSE

A rough inner surface of the mandible cortical bone layer is observed in patients with osteoporosis. Meta-analyses studies demonstrated that the mandibular cortical index (MCI) classification is useful to screen for osteoporosis. The MCI consists of normal cortex (Class 1), mildly to moderately eroded cortex (Class 2), and severely eroded cortex (Class 3). There are several previous studies regarding conventional machine learning or rule-based methods to automatically classify based on the MCI. To improve the accuracy of MCI classification, we applied the convolutional neural networks (CNN) method.

### **METHOD AND MATERIALS**

An image database consisting of 205 panoramic radiography images, in which MCI classification was determined based on agreement among three experienced dental radiologists, was used to test the CNN method. The database consisted of 78, 67, and 60 cases of Class 1, Class 2, and Class 3, respectively. Bilateral regions of interest (ROIs) were set in the mental foramen region. Caffe was used as the deep learning framework.

#### RESULTS

A restrictive ROI setting in the cortical bone demonstrated higher classification accuracy than wider ROI settings including the teeth. The classification accuracy for separating the cases into the three classes was approximately 80%. Approximately 90% accuracy was observed for the differentiation between Class 1 and the other two classes, and between Class 3 and the other two classes.

### CONCLUSION

In the present study, differentiation between Class 2 and the other two classes yielded the lowest accuracy. This was similar with the previously reported MCI classification using rule-based methods. In addition, the inter-observer agreement among several radiologists was low for diagnosing Class 2. These results suggest that the diagnostic criteria for Class 2, i.e., "the inner margin has resorption cavities with cortical residues one to three layers thick on one or both sides", should be revised.

## **CLINICAL RELEVANCE/APPLICATION**

Morphological evaluation techniques for jaw bones are essential to screen both new osteoporosis patients and patients suspected of having medication-related osteonecrosis of the jaw. In addition, osteoporosis is important for dental implants and periodontitis treatment because their success largely depends on the quality and quantity of the bone.



## BR010-EB-THA

Imaging Findings of Breast Implant Complications: What Has Changed with Latest-Generation Implants?

Thursday, Nov. 29 12:15PM - 12:45PM Room: BR Community, Learning Center Hardcopy Backboard

#### **Participants**

Vinicius C. Felipe SR, MD, Sao Paulo, Brazil (*Presenter*) Nothing to Disclose Marilia M. Azevedo, MD, Sao Paulo, Brazil (*Abstract Co-Author*) Nothing to Disclose Almir Bitencourt, MD, Sao Paulo, Brazil (*Abstract Co-Author*) Nothing to Disclose Juliana A. Souza, Sao Paulo, Brazil (*Abstract Co-Author*) Nothing to Disclose Luciana Graziano, MD, Sao Paulo, Brazil (*Abstract Co-Author*) Nothing to Disclose Camila Guatelli, Sao Paulo, Brazil (*Abstract Co-Author*) Nothing to Disclose Maria Luiza D. Albuquerque, MD, Sao Paulo, Brazil (*Abstract Co-Author*) Nothing to Disclose Elvira F. Marques, Sao Paulo, Brazil (*Abstract Co-Author*) Nothing to Disclose Mirian R. Poli, MD, Sao Paulo, Brazil (*Abstract Co-Author*) Nothing to Disclose Rubens Chojniak, MD, PhD, Sao Paulo, Brazil (*Abstract Co-Author*) Nothing to Disclose

### **TEACHING POINTS**

- Earlier-generation implants have high rates of complications, such as contracture and rupture. Latest-generation implants reduced the number of complications by modifying its composition (cohesive silicone gel) and shell structure (stronger with textured surface). Thereby, imaging aspects of breast implants complications has also changed. - Some breast implant complications became less frequent with latest-generation implants, including displacement, rotation, capsular contracture and rupture. Besides, classical imaging signs of breast implant rupture, such as 'teardrop' or 'keyhole', 'salad oil' and 'linguini' signs, may not be seen on modern implants. Because of the semisolid consistence of these implants, silicone gel does not mix with water / saline content, and thus, rupture looks more likely as a 'fracture' on imaging methods. - Some complications that were rarely seen before became more frequent after the use of latest-generation textured implants, such as late seroma, silicone-induced granuloma of the breast implant capsule and breast implant associated anaplastic large cell lymphoma.

#### **TABLE OF CONTENTS/OUTLINE**

Introduction breast implant types complications of latest generation implants implant rupture late seroma silicone-induced granuloma breast implant associated anaplastic large cell lymphoma.



## BR210-ED-THA12

## Genetic Testing for Hereditary Breast and Ovarian Cancer: A Primer for Radiologists

Thursday, Nov. 29 12:15PM - 12:45PM Room: BR Community, Learning Center Station #12

### Awards Certificate of Merit Identified for RadioGraphics

## Participants

Puja Bharucha, MD, Baltimore, MD (*Presenter*) Nothing to Disclose Fabienne Francois, Baltimore, MD (*Abstract Co-Author*) Nothing to Disclose Nikki Tirada, MD, Baltimore, MD (*Abstract Co-Author*) Spouse, Research Grant, Siemens AG Gauri R. Khorjekar, MD, Laurel, MD (*Abstract Co-Author*) Nothing to Disclose Jessica Scott, Baltimore, MD (*Abstract Co-Author*) Nothing to Disclose

# **TEACHING POINTS**

Explain the criteria for genetic risk evaluation that qualifies a patient to undergo genetic testing. Discuss the process of genetic counseling, the different types of genetic testing used, and the implications of positive genetic results. Review the radiology findings and imaging appearances of breast cancer typically associated with each mutation.

# TABLE OF CONTENTS/OUTLINE

Breast imagers are often the first to initiate the conversation about genetic counseling with patients who have premenopausal breast cancer or a strong family history of breast and ovarian cancer. Commercial genetic testing panels have gained popularity and become more affordable in recent years. Therefore, it is imperative for radiologists to be able to provide counseling and to identify which patients should be referred to genetic testing. Understanding of various breast cancer risk assessment tools such as Gail and Tyrer-Cuzick models; and recognizing unique clinical presentations, specific imaging appearances, and genetic pedigree patterns related to each mutation permits prompt identification of patients and their family members who carry mutations. The genetic test results enable appropriate patient-specific screening that allows improvement of overall survival via early detection and timely treatment.



## BR211-ED-THA7

Easily Seen, Difficult Diagnosis: Spectrum of Lesions Involving the Nipple

Thursday, Nov. 29 12:15PM - 12:45PM Room: BR Community, Learning Center Station #7

#### **Participants**

Rosa M. Lorente-Ramos, MD, PhD, Madrid, Spain (*Presenter*) Nothing to Disclose Javier Azpeitia Arman, MD, Madrid, Spain (*Abstract Co-Author*) Nothing to Disclose Carlos Oliva Fonte Sr, Madrid, Spain (*Abstract Co-Author*) Nothing to Disclose Soledad Alonso Garcia, Madrid, Spain (*Abstract Co-Author*) Nothing to Disclose Almudena Blazquez Saez, MD, Salamanca, Spain (*Abstract Co-Author*) Nothing to Disclose Eva Balbin, Madrid, Spain (*Abstract Co-Author*) Nothing to Disclose

## For information about this presentation, contact:

rosa.lorenteramos@salud.madrid.org

## **TEACHING POINTS**

To review the different causes of nipple lesions, both benign and malignant. To illustrate imaging findings of lesions involving the nipple in different techniques, including mammogram, US and MR, providing clinical images and pathologic correlation. To discuss the appropriate management of these lesions, emphasizing pitfalls, diagnostic difficulties and differential diagnosis.

## TABLE OF CONTENTS/OUTLINE

Apart from breast cancers extending to the nipple, different lesions may appear in this area. From 2009 to 2016, 90 nipple biopsies were performed at our Institution. We review nipple anatomy, as well as clinical and radiological imaging and pathology of the different entities. We also analize special considerations of this challenging region for diagnosis, interventional procedures and treatment. We present: Congenital: accesory nipple; Dermal lesions: Epidermal inclusion cyst, fibroepithelial polips, dermatitis, melanoma and benign melanocytic nevus; Paget's disease; Inflammatory lesions: galactophoritis, abscess; Nipple Tumors: adenoma of the nipple; Breast lesions: papiloma, ductal carcinoma.



## BR212-ED-THA8

## Systematic Approach to Lesions Involving Nipple-Areolar Complex Using MRI

Thursday, Nov. 29 12:15PM - 12:45PM Room: BR Community, Learning Center Station #8

### **Participants**

Akane Ohashi, Kyoto-hu, Japan (*Presenter*) Nothing to Disclose Masako Y. Kataoka, MD, PhD, Kyoto, Japan (*Abstract Co-Author*) Nothing to Disclose Shotaro Kanao, MD, Kyoto, Japan (*Abstract Co-Author*) Nothing to Disclose Maya Honda, Kyoto, Japan (*Abstract Co-Author*) Nothing to Disclose Mami Iima, MD, PhD, Kyoto, Japan (*Abstract Co-Author*) Nothing to Disclose Ayami Ohno Kishimoto, Kyoto, Japan (*Abstract Co-Author*) Nothing to Disclose Kanae K. Miyake, MD, PhD, Kyoto, Japan (*Abstract Co-Author*) Nothing to Disclose Tatsuki Kataoka, MD, PhD, Kyoto, Japan (*Abstract Co-Author*) Nothing to Disclose Takaki Sakurai, Kyoto, Japan (*Abstract Co-Author*) Nothing to Disclose Masakazu Toi, Kyoto, Japan (*Abstract Co-Author*) Nothing to Disclose Kaori Togashi, MD, PhD, Kyoto, Japan (*Abstract Co-Author*) Nothing to Disclose Kaori Togashi, MD, PhD, Kyoto, Japan (*Abstract Co-Author*) Research Grant, Bayer AG; Research Grant, DAIICHI SANKYO Group; Research Grant, Eisai Co, Ltd; Research Grant, FUJIFILM Holdings Corporation; Research Grant, Nihon Medi-Physics Co, Ltd; Research Grant, Canon Medical Systems Corporation

### For information about this presentation, contact:

amaoh@kuhp.kyoto-u.ac.jp

## **TEACHING POINTS**

The nipple-areolar complex (NAC) is located at the unique crossroad between skin and mammary duct. Therefore, wide variety of lesions originated from skin or mammary duct can grow there, making their diagnosis challenging. Some parenchymal lesions invade to the NAC. Identifying locations of NAC lesions in relation to anatomy and knowing typical progression pattern is crucial in diagnosis and surgical planning. Lesions involving NAC may be continuous to the parenchymal component, which is often overlooked. MRI is an ideal tool to examine NAC involvement and associated underlying parenchymal disease by obtaining cross-sectional imaging with excellent tissue contrast. In this exhibit, we 1. review the anatomical structure of NAC and underlying parenchyma, 2. illustrate the location of NAC lesions, 3. classify NAC lesions based on their location, and 4. propose systematic approach to lesions involving NAC based on cross-sectional information on MRI.

## TABLE OF CONTENTS/OUTLINE

1. Anatomy of NAC in relation to the ductal system of the breast parenchyma. 2. Classifications of lesions involving NAC based on their location. 3. Case presentations, including nipple adenoma, Paget's disease, DCIS with intraductal spread, Pagetoid spread, invasive cancer invading skin and nipple. 4. Systematic approach to lesions involving NAC.



## BR213-ED-THA9

Preoperative Freehand Breast MRI Needle/Hookwire Localization of Lesions in Hard to Reach Locations Where Grid Techniques Fail: Indications, Techniques, and Pitfalls

Thursday, Nov. 29 12:15PM - 12:45PM Room: BR Community, Learning Center Station #9

# Participants

Crystal Chang, MD, Stanford, CA (*Presenter*) Nothing to Disclose Debra M. Ikeda, MD, Stanford, CA (*Abstract Co-Author*) Scientific Advisory Board, Grail, Inc; Reviewer, Siemens AG Bruce L. Daniel, MD, Stanford, CA (*Abstract Co-Author*) Nothing to Disclose

### **TEACHING POINTS**

To review indications for freehand MRI needle/hookwire localization in hard to reach locations where standard MRI grid techniques may fail (examples: far posterior lesions, implants) To describe/demonstrate the step-by-step freehand MRI needle/hookwire localization method To discuss potential pitfalls of each localization step

## TABLE OF CONTENTS/OUTLINE

Indications for freehand MRI localization where grid techniques may fail Freehand MRI localization technique: A step-by-step approach with examples Freehand localization technique pitfalls



### BR214-ED-THA10

Intraoperative Use of 3D Printed Breast Models in the Setting of Breast Cancer

Thursday, Nov. 29 12:15PM - 12:45PM Room: BR Community, Learning Center Station #10

#### **Participants**

Lumarie Santiago, MD, Houston, TX (*Presenter*) Nothing to Disclose Cristina M. Checka, MD, Houston, TX (*Abstract Co-Author*) Nothing to Disclose Mark W. Clemens, Houston, TX (*Abstract Co-Author*) Nothing to Disclose Beatriz E. Adrada, MD, Houston, TX (*Abstract Co-Author*) Nothing to Disclose Elsa M. Arribas, MD, Houston, TX (*Abstract Co-Author*) Nothing to Disclose

## For information about this presentation, contact:

Lumarie.Santiago@mdanderson.org

### **TEACHING POINTS**

1) 3D printed breast models allow accurate depiction of breast cancer extent by providing detailed relationships between the tumor, chest wall, skin, nipple and surrounding blood vessels. 2) Intraoperative manipulation of 3D printed models complements the information provided by concurrent breast imaging studies. 3) 3D printed breast models are useful in personalized patient education regarding their disease and surgical management. 4) 3D printed breast models support multidisciplinary management of breast cancer by enhancing surgical planning and execution.

## TABLE OF CONTENTS/OUTLINE

We will present a pictorial essay of our experience in 3D printed breast models in the setting of multidisciplinary breast cancer practice. 1) Review of imaging features of breast cancer cases in which a 3D printed breast model was requested 2) Preoperative image guided localization correlating with the findings depicted in the 3D printed breast model and other breast imaging studies 3) Intraoperative utilization and manipulation of 3D printed breast model during oncoplastic breast surgery.



### BR215-ED-THA11

Non-mass Findings on Breast Ultrasound (US): Detection, Differential, Diagnosis

Thursday, Nov. 29 12:15PM - 12:45PM Room: BR Community, Learning Center Station #11

#### Awards Identified for RadioGraphics

#### Participants

Jihee Choe, MD, Boston, MA (*Presenter*) Nothing to Disclose Sona A. Chikarmane, MD, Boston, MA (*Abstract Co-Author*) Nothing to Disclose Catherine S. Giess, MD, Wellesley, MA (*Abstract Co-Author*) Nothing to Disclose

#### For information about this presentation, contact:

schikarmane@bwh.harvard.edu

# **TEACHING POINTS**

The term 'nonmass finding' on ultrasound (US) is not part of current BI-RADS terminology, but is increasingly being used in the radiology literature. Despite the current lack of a standardized approach to classification and evaluation of nonmass US findings, recognition of this US finding can improve sonographic detection and correlation of mammographic and MRI lesions to help guide biopsy. The purpose of this exhibit is to: 1) Review the various proposed classifications systems for nonmass US findings 2) Provide imaging features of nonmass enhancement to help radiologists identify this sonographic finding 3) Demonstrate the wide range of benign and malignant entities that may manifest as a nonmass finding 4) Correlate breast MRI and mammographic findings that may present as sonographic nonmass findings

## TABLE OF CONTENTS/OUTLINE

1) Review the definitions and various proposed classification systems for non-mass US findings described in the radiology literature 2) Illustrate the sonographic features of non-mass findings, any associated findings, and imaging techniques to detect non-mass findings 3) Correlate sonographic nonmass findings with mammographic and breast MRI lesions to aid in biopsy and diagnosis 3) Review benign and malignant etiologies for non-mass US findings through a rich pictorial review of illustrative cases

### **Honored Educators**

Presenters or authors on this event have been recognized as RSNA Honored Educators for participating in multiple qualifying educational activities. Honored Educators are invested in furthering the profession of radiology by delivering high-quality educational content in their field of study. Learn how you can become an honored educator by visiting the website at: https://www.rsna.org/Honored-Educator-Award/ Catherine S. Giess, MD - 2015 Honored EducatorCatherine S. Giess, MD - 2017 Honored Educator



## BR268-SD-THA2

Prediction of Axillary Response by Monitoring with Ultrasound and MRI During and After Neoadjuvant Chemotherapy in Breast Cancer Patients

Thursday, Nov. 29 12:15PM - 12:45PM Room: BR Community, Learning Center Station #2

### Participants

Na Lae Eun, Seoul, Korea, Republic Of (*Presenter*) Nothing to Disclose Ji Hyun Youk, MD, Seoul, Korea, Republic Of (*Abstract Co-Author*) Nothing to Disclose Eun Ju Son, MD, PhD, Seoul, Korea, Republic Of (*Abstract Co-Author*) Nothing to Disclose Hye Mi Gweon, MD, Seoul, Korea, Republic Of (*Abstract Co-Author*) Nothing to Disclose Jeong-Ah Kim, MD, PhD, Seoul, Korea, Republic Of (*Abstract Co-Author*) Nothing to Disclose

## PURPOSE

To investigate whether monitoring with ultrasound (US) and MR imaging can predict axillary response in breast cancer patients after neoadjuvant chemotherapy (NAC).

## METHOD AND MATERIALS

A total of 131 breast cancer patients with clinically positive axillary lymph node (LN) who underwent NAC and subsequent surgery from January 2012 to August 2017 were enrolled. They had US and 3T MR examinations for breast and axilla before, during, and after NAC. After reviewing US and MR images obtained at three different times, the number, size, shape, presence of hilum, and cortical thickness of axillary LNs as well as index tumor size were noted. According to LN status after surgery, imaging features were analyzed by using independent t-test, the Fisher exact test, multiple logistic regression analysis, and ROC analysis.

#### RESULTS

Of 131 patients, 60 (45.8%) had positive LNs after surgery. All US and MR features of LN before NAC showed no difference in LN status. There was significant difference in transverse diameter, cortical thickness and its % change, and tumor size and its % change during NAC and cortical thickness after NAC at US (P<0.003), and transverse diameter, cortical thickness and its % change, hilum, and tumor size and its % change during and after NAC at MR (P<0.03). On multivariate analysis, cortical thickness at US during NAC (odd ratio [OR], 1.8; 95% CI, 1.2-2.6; P=0.005) and tumor size at US (OR, 1.06; 95% CI, 1.0-1.1]; P=0.038) and MR(OR, 1.04; 95% CI, 1.007-1.079; P=0.019) after NAC were independently associated with positive LN. The area under the ROC curve for predicting LN status was 0.741, 0.639, and 0.692 for cortical thickness at US during NAC and index tumor size on US and MR after NAC, respectively.

## CONCLUSION

The US cortical thickness of axillary LNs during NAC and the index tumor size on US and MR after NAC can be useful to predict axillary response in breast cancer patients.

#### **CLINICAL RELEVANCE/APPLICATION**

Monitoring morphologic features of axillary LNs and index tumor by US and MR imaging can help making treatment decision in breast cancer patients receiving NAC.



### BR270-SD-THA4

## **Cognitive Bias in Screening Mammography**

Thursday, Nov. 29 12:15PM - 12:45PM Room: BR Community, Learning Center Station #4

#### **Participants**

Ashutosh Shelat, MD, Santa Barbara, CA (*Presenter*) Nothing to Disclose Myrna Wallace-Servera, MD, Santa Barbara, CA (*Abstract Co-Author*) Nothing to Disclose Michael A. Trambert, MD, Santa Barbara, CA (*Abstract Co-Author*) Medical Advisor, IBM Corporation Jeremy M. Wolfe, PhD, Cambridge, MA (*Abstract Co-Author*) Research collaboration, Koninklijke Philips NV; Murray A. Reicher, MD, Rancho Santa Fe, CA (*Abstract Co-Author*) Chief Medical Officer, Merge Healthcare Incorporated Board Member, Merge Healthcare Incorporated Co-CEO, Health Companion, Inc Former Chairman, DR Systems, Inc

### PURPOSE

Gambler's fallacy and reverse gambler's fallacy are logical missteps based on the mistaken premise that previous outcomes of a random event will affect future outcomes. Our purpose is to determine how significantly such a bias affects the reading of screening mammograms, and specifically, to determine if recalling of one examination affects the likelihood of recalling subsequent examinations.

## METHOD AND MATERIALS

Over 70000+ screening digital mammographic results from two separate enterprises including 22 different radiologists over a span of less than 5 years were obtained. Exams after the implementation of tomosynthesis were excluded. The data was anonymized, but each radiologist was assigned a number. Exams were batched into different time frames (5 minutes, 10 minutes, 30 minutes, and 1 hour). Runs of exams were analyzed to determine if recalling a case would significantly impact the recall of subsequent cases.

#### RESULTS

Initial results demonstrated that the probability of recalling a case after a recent recall was significantly lower than the probability of recalling any single case alone. However, after excluding the first study there was no significant difference between the relative recall rates. Curiously, batching exams and aggregating results demonstrated that the recall rate for the first position of each batch was statistically higher than the recall rate for all other examinations in a batch at an aggregate level for all time frames. Additionally, using a 5 minute batch time, the results were statistically significant for all radiologists individually. Statistical significance was achieved for the majority of all radiologists at all other batching time frames.

#### CONCLUSION

We found that radiologists do not suffer from the general premise of gambler's fallacy. Assuming no artifactual bias, however we found that they appear to be primed to recall the first case in a series. This may represent an unknown cognitive bias in screening mammography.

#### **CLINICAL RELEVANCE/APPLICATION**

Sensitivity of the first examination of any batch of screening digital mammographic examinations is expected to be higher on average than other examinations and may reflect the only non-biased result.



## BR271-SD-THA5

Imaging Features Associated with Pathological Complete Response in HER2 Positive Breast Cancer after Neoadjuvant Chemotherapy with Dual Blockade

Thursday, Nov. 29 12:15PM - 12:45PM Room: BR Community, Learning Center Station #5

### Participants

Ga Young Yoon, MD, Seoul, Korea, Republic Of (*Presenter*) Nothing to Disclose Eun Young Chae, Seoul, Korea, Republic Of (*Abstract Co-Author*) Nothing to Disclose Hak Hee Kim, MD, Seoul, Korea, Republic Of (*Abstract Co-Author*) Nothing to Disclose Joo Hee Cha, MD, Seoul, Korea, Republic Of (*Abstract Co-Author*) Nothing to Disclose Hee Jung Shin, MD, Seoul, Korea, Republic Of (*Abstract Co-Author*) Nothing to Disclose Woo Jung Choi, MD, Seoul, Korea, Republic Of (*Abstract Co-Author*) Nothing to Disclose

### For information about this presentation, contact:

3770ghwo@hanmail.net

### PURPOSE

In human epidermal growth factor receptor 2 (HER2)-positive breast cancer, the incorporation of dual HER2-blockade to neoadjuvant chemotherapy (NAC) has been shown to induce a higher rate of pathologic complete response (pCR). The purpose of this study was to investigate associations between imaging features and pCR in HER2-positive breast cancer after NAC plus dual blockade.

#### **METHOD AND MATERIALS**

This retrospective study was approved by the institutional review board. We evaluated 73 consecutive patients (mean age,  $50 \pm$  9.99 years) with HER2-positive breast cancer who underwent NAC plus dual blockade with trastuzumab and pertuzumab between April 2016 and March 2018. All patients had mammography, ultrasound, and MR imaging prior to NAC. pCR following NAC was defined as the absence of residual invasive cancer in the breast and ipsilateral lymph nodes (ypT0/is, ypN0). Clinicopathological and initial imaging features before NAC were assessed and compared according to the pathological response after surgery.

### RESULTS

Of 73 patients, 41 (56.2%) showed pCR and the remaining 32 (43.8%) showed non-pCR. Segmental distribution of calcification on mammography (odds ratio [OR], 13.57; P = 0.027), parallel orientation on ultrasound (OR, 4.03; P = 0.007), and the presence of intratumoral high signal intensity on T2-weighted MR images (OR, 2.81; P = 0.037) were significantly associated with pCR. Progesterone receptor-negative tumors (OR, 6.33; P = 0.004) were significantly associated with pCR. The presence of mammographic calcification with or without a mass, associated nonmass enhancement on MR images, fine pleomorphic or fine linear branching calcification morphology on mammography, and higher tumor infiltrating lymphocytes level were more common in the pCR group, although these did not reach statistical significance.

## CONCLUSION

Several imaging features showed association with pCR in HER2-positive breast cancer after NAC with dual blockade treatment.

## **CLINICAL RELEVANCE/APPLICATION**

Our results may help differentiate patients who can benefit from adding dual blockade in HER2-positive breast cancer and determine treatment.



## BR272-SD-THA6

Comparison between Abbreviated Protocol (AB-MR) and Full Diagnostic Protocol (FD-MR) in the Characterization of Lesions Detected by Breast MRI: A Multi-reader Study

Thursday, Nov. 29 12:15PM - 12:45PM Room: BR Community, Learning Center Station #6

## Participants

Eun Sil Kim, Seoul, Korea, Republic Of (*Abstract Co-Author*) Nothing to Disclose Nariya Cho, MD, PhD, Seoul, Korea, Republic Of (*Abstract Co-Author*) Nothing to Disclose Sooyeon Kim, MD, Seoul, Korea, Republic Of (*Abstract Co-Author*) Nothing to Disclose Ann Yi, MD, PhD, Seoul, Korea, Republic Of (*Abstract Co-Author*) Nothing to Disclose Rihyeon Kim, MD, Seoul, Korea, Republic Of (*Presenter*) Nothing to Disclose Bo Ra Kwon, MD, Seoul, Korea, Republic Of (*Abstract Co-Author*) Nothing to Disclose Min Sun Bae, MD, New York, NY (*Abstract Co-Author*) Nothing to Disclose Su Hyun Lee, MD, PhD, Seoul, Korea, Republic Of (*Abstract Co-Author*) Nothing to Disclose Jung Min Chang, MD, Seoul, Korea, Republic Of (*Abstract Co-Author*) Nothing to Disclose Woo Kyung Moon, Seoul, Korea, Republic Of (*Abstract Co-Author*) Nothing to Disclose

#### For information about this presentation, contact:

esk19@naver.com

#### PURPOSE

Abbreviated breast MRI (AB-MR) has been shown to offer equivalent diagnostic accuracy compared with the respective fulldiagnostic MRI (FD-MR) in a screening setting. We compared the diagnostic performance of AB-MR and FD-MR in the characterization of lesions detected by MRI.

### **METHOD AND MATERIALS**

A cohort of 111 biopsy-proven cases (34 malignant, 77 benign; median lesion size 1.2cm, range 0.3-6.6cm) identified at contralateral breast MRI screening during the preoperative evaluation of newly diagnosed breast cancer patients between January 2011 and August 2016 was used for the reader study. Three blinded radiologists independently classified the likelihood of malignancy and BI-RADS final assessment category for imaging data sets, i.e., AB-MR and FD-MR with 1-week interval. AB-MR consisted of fat saturated pre-contrast, first post-contrast (90 sec) T1WI, and maximum-intensity projection (MIP) reconstruction images. FD-MR consisted of T2WI, fat saturated pre-contrast, and five post-contrast T1WI series. Sensitivity, specificity, and areas under the receiver operating characteristic (AUC) curve in distinguishing benign from malignant lesions were compared between both protocols.

### RESULTS

Sensitivity of AB-MR was slightly lower than that of FD-MR in all readers (82.4% [28/34] vs. 85.3% [29/34] in reader 1, P>.999; 82.4% [28/34] vs. 100% [34/34] in reader 2, P= not applicable; 58.8% [20/34] vs. 82.4% [28/34] in reader 3, P=.077). Specificity of AB-MR was higher than that of FD-MR (41.6% [32/77] vs. 36.4% [28/77], P=.503; 39.0% [30/77] vs. 19.5% [15/77], P=.001; 74.0% [57/77] vs. 37.7% [29/77], P<.001), although statistical significance was only found for specificity differences in two readers. AUC of AB-MR was comparable to that of FD-MR in all readers (0.706 vs. 0.705, P=.981; 0.700 vs. 0.685, P=.765; 0.738 vs. 0.698, P=.542).

### CONCLUSION

Compared with FD-MR, AB-MR missed one, six, or eight of 34 cancers for each reader in the characterization of lesions detected by MRI, although overall performances were similar in both protocols.

## **CLINICAL RELEVANCE/APPLICATION**

Due to the limited characterization performance, AB-MR cannot replace FD-MR in a diagnostic setting.



## BR275-SD-THA3

"Virtual" Full-Dose (VFD) Technology: Radiation Dose Reduction in Digital Breast Tomosynthesis (DBT) by Means of Neural Network Convolution (NNC) Deep Learning

Thursday, Nov. 29 12:15PM - 12:45PM Room: BR Community, Learning Center Station #3

# Participants

Junchi Liu, MS, Chicago, IL (*Abstract Co-Author*) Nothing to Disclose Amin Zarshenas, MSc, Chicago, IL (*Abstract Co-Author*) Nothing to Disclose Syed Ammar Qadir, Chicago, IL (*Abstract Co-Author*) Nothing to Disclose Limin Yang, MD, PhD, Iowa City, IA (*Abstract Co-Author*) Nothing to Disclose Laurie L. Fajardo, MD, MBA, Park City, UT (*Abstract Co-Author*) Consultant, Hologic, Inc; Consultant, Siemens AG; Consultant, FUJIFILM Holdings Corporation; Kenji Suzuki, PhD, Chicago, IL (*Presenter*) Royalties, General Electric Company; Royalties, Hologic, Inc; Royalties, MEDIAN

Kenji Suzuki, PhD, Chicago, IL (*Presenter*) Royalties, General Electric Company; Royalties, Hologic, Inc; Royalties, MEDIAN Technologies; Royalties, Riverain Technologies, LLC; Royalties, Canon Medical Systems Corporation; Royalties, Mitsubishi Corporation; Royalties, AlgoMedica, Inc

### For information about this presentation, contact:

jliu118@hawk.iit.edu

#### **TEACHING POINTS**

1) To understand the basics of a deep-learning-based "virtual" full-dose technology. 2) To demonstrate and compare the image quality of our VFD images generated from quarter- and half-dose acquisitions to that of real clinical full-dose images in DBT. 3) To understand the clinical utility of VFD technology for reducing radiation dose in DBT.

## TABLE OF CONTENTS/OUTLINE

Content OrganizationA. Radiation dose issues with DBT breast cancer screeningB. Basics of VFD technology for reducing radiation doseC. Quantitative evaluation: Image quality vs. radiation dose reductionD. Blinded observer rating study with 35 breast radiologists: virtual vs. real imagesE. Benefits and limitations of our radiation dose reduction technology for DBT This exhibit presents1) Details on our deep-learning-based VFD technology that converted 25% dose images of cadaver phantoms to VFD images, retaining the image quality equivalent to 119% dose images and achieving a 79% dose reduction. 2) The image quality of VFD images of clinical cases was equivalent to that of real full-dose images. Our technology significantly reduced noise in half-dose images, while preserving tissue and lesions. 3) Blinded observer rating study of 51 clinical cases: 60% of 35 radiologists preferred our VFD images over real full-dose images or could not distinguish between the two.

### PDF UPLOAD

http://abstract.rsna.org/uploads/2018/18004421/18004421\_8gfq.pdf



## CA169-ED-THA7

Cardiac MRI in Patients with Cardiac Arrhythmias - Practical Tips and Tricks

Thursday, Nov. 29 12:15PM - 12:45PM Room: CA Community, Learning Center Station #7

### **Participants**

Muhammad U. Aziz, MBBS, Dallas, TX (*Abstract Co-Author*) Nothing to Disclose Alastair Moore, MD, Burlington, VT (*Abstract Co-Author*) Nothing to Disclose Prabhakar Rajiah, MD, FRCR, Dallas, TX (*Presenter*) Nothing to Disclose

For information about this presentation, contact:

radpr73@gmail.com

## **TEACHING POINTS**

Obtaining good quality MRI in cardiac arrhythmia is challenging. The purpose of this exhibit is 1. To review the challenges caused by cardiac motion and arrhythmias during MRI 2. To describe solutions for eliminating/reducing these artifacts 3. To illustrate the solutions available for reducing artifacts in cardiac MRI

### **TABLE OF CONTENTS/OUTLINE**

1. Introduction 2. Arrhythmia classification & types- Atrial (PSVT, AFib, flutter); Ventricular (Vtach, V fibrillation); Extra beats (PAC, PVC, PJC); bradyarrhythmias (bradycardia, heart block) 3. ECG strips demonstrating arrhythmias 4. Challenges of arrhythmias in cardiac MRI - Motion artifact - Inaccurate quantification - Inaccurate nulling time - Pseudo perfusion defect 5. Solutions for MRI-Description and case based review with illustrations - Signal averaging - Prospective ECG triggering - Acceleration strategies a. Partial Fourier b. Non Cartesian trajectories (Spiral, radial, etc) c. Parallel Imaging (Cartesian- SENSE, GRAPPA, SMASH; Non Cartesian) d. Spatiotemporal techniques (Only temporal redundancy; temporal followed by spatial; combined) e. Compressed sensing - Cines- Real time imaging, without ECG gating - Late gadolinium enhancement- Single-shot sequence; Data every second or third beat - Flow- Free breathing sequence

#### **Honored Educators**

Presenters or authors on this event have been recognized as RSNA Honored Educators for participating in multiple qualifying educational activities. Honored Educators are invested in furthering the profession of radiology by delivering high-quality educational content in their field of study. Learn how you can become an honored educator by visiting the website at: https://www.rsna.org/Honored-Educator-Award/ Prabhakar Rajiah, MD, FRCR - 2014 Honored Educator



## CA173-ED-THA8

# Getting to the Heart of Eponyms

Thursday, Nov. 29 12:15PM - 12:45PM Room: CA Community, Learning Center Station #8

#### **Participants**

Vinit Baliyan, MBBS, MD, Boston, MA (*Presenter*) Nothing to Disclose Lara Walkoff, MD, Boston, MA (*Abstract Co-Author*) Nothing to Disclose Theodore T. Pierce, MD, Boston, MA (*Abstract Co-Author*) Nothing to Disclose Brian B. Ghoshhajra, MD, Waban, MA (*Abstract Co-Author*) Research Grant, Siemens Healthcare USA; Sandeep S. Hedgire, MD, Boston, MA (*Abstract Co-Author*) Nothing to Disclose

## For information about this presentation, contact:

vbaliyan@mgh.harvard.edu

### **TEACHING POINTS**

• Eponyms are frequently encountered in radiology and may be confusing for those who are not familiar with these terms. • Eponyms not only honor individuals who made important observations and discoveries, but also provide opportunity to understand the subject matter. • Our purpose is to present a pictorial exhibit highlighting eponyms in cardiac imaging.

## TABLE OF CONTENTS/OUTLINE

• In this section we discuss and illustrate (with still and cine images) the imaging manifestations of eponyms encountered in cardiac radiology. • We will also briefly explore the historical background of the eponyms. • Eponyms covered will include- o Cardiac anatomy- Sinus of Valsalva, Eustachian valve o Coronary artery disease- Kawasaki disease, Bland-White-Garland syndrome (ALCAPA), Arc of Vieussens o Congenital heart disease- Gerbode defect (ventricular septal defect), Tetrology of Fallot, William syndrome o Surgical procedures/maneuvers- Norwood procedure, Blalock-Taussig shunt, Glenn shunt, Fontan palliation, Jatene switch, Lecompte maneuver, Rastelli and Ross procedures, Damus Kaye Stansel procedure. o Cardiomyopathy- Yamaguchi syndrome, Fabry cardiomyopathy o Cardiac tumors- Swiss syndrome, Carney syndrome, Gorlin syndrome (fibromas), Bourneville's disease (tuberous sclerosis; rhabdomyomas) o Tumor mimics- Chiari network



### CA175-ED-THA6

### **Uncommon Connections in Cardiac CT**

Thursday, Nov. 29 12:15PM - 12:45PM Room: CA Community, Learning Center Station #6

#### **Participants**

Gemma Burcet Rodriguez, MD, Barcelona, Spain (*Presenter*) Nothing to Disclose Alberto Roque, MD, Barcelona, Spain (*Abstract Co-Author*) Nothing to Disclose Maria Nazarena Pizzi, Barcelona, Spain (*Abstract Co-Author*) Nothing to Disclose Filipa Valente, Barcelona, Spain (*Abstract Co-Author*) Nothing to Disclose Victor S. Pineda, MD, Barcelona, Spain (*Abstract Co-Author*) Nothing to Disclose Laura B. Cabanzo Campos, MD, PhD, Barcelona, Spain (*Abstract Co-Author*) Nothing to Disclose Jose Miguel Escudero-Fernandez, MD, Barcelona, Spain (*Abstract Co-Author*) Nothing to Disclose Jose Miguel Rodriguez Sanchez, Barcelona, Spain (*Abstract Co-Author*) Nothing to Disclose Hug Cuellar, Barcelona, Spain (*Abstract Co-Author*) Nothing to Disclose

#### For information about this presentation, contact:

gburcet@vhebron.net

#### **TEACHING POINTS**

Review unusual connections among vascular structures in cardiac CT Describe connections according to involved vessels Identify presence and type of shunt Discuss potential implications for patient care

### TABLE OF CONTENTS/OUTLINE

Introduction Suggested CT technique Diagnosis, pathophysiology and treatment of connections between: Coronary arteries and veins (coronary fistulas) Coronary arteries and cardiac chambers (coronary fistulas) Coronary veins and cardiac chambers (unroofed coronary sinus) Coronary and pulmonary arteries (coronary fistulas, ALCAPA syndrome) Coronary and bronchial arteries (coronary to bronchial communication) Pulmonary arteries and veins (pulmonary arteriovenous malformation) Systemic and pulmonary arteries (persistent ductus arteriosus, major aortopulmonary collateral arteries) Systemic and pulmonary veins (venovenous fistulas after Fontan surgery) Pulmonary veins (Acquired intrapulmonary venous connections) Pulmonary veins and right atrium (anomalous pulmonary venous return) Superior vena cava and left atrium (Raghib Syndrome)



## CA252-SD-THA1

Coronary Artery to Pulmonary Artery Fistula in Adults: Comparison of 256-Slice MDCT Coronary Angiography and Transthoracic Echocardiography

Thursday, Nov. 29 12:15PM - 12:45PM Room: CA Community, Learning Center Station #1

# Participants

Jinglei Li, MD, Guangzhou, China (*Presenter*) Nothing to Disclose Sachin S. Saboo, MD, FRCR, Dallas, TX (*Abstract Co-Author*) Nothing to Disclose Wei Zhu, Guangzhou, China (*Abstract Co-Author*) Nothing to Disclose Prabhakar Rajiah, MD, FRCR, Dallas, TX (*Abstract Co-Author*) Nothing to Disclose Suhny Abbara, MD, Dallas, TX (*Abstract Co-Author*) Royalties, Reed Elsevier; Institutional research agreement, Koninklijke Philips NV; Institutional research agreement, Siemens AG Meiping Huang, Guangzhou, China (*Abstract Co-Author*) Nothing to Disclose

#### For information about this presentation, contact:

lijinglei80@126.com

## PURPOSE

To review the imaging features of coronary artery-to-pulmonary artery fistula (CPAF) on 256-slice MDCT and evaluate the diagnostic performance of CT compared with conventional catheter angiography (CCA) and transthoracic echocardiogram (TTE).

## **METHOD AND MATERIALS**

We retrospectively reviewed with a diagnosis of CPAF from amongst 19855 consecutive coronary CT angiography (CCTA) performed with 256-slice MDCT scanner (Brilliance iCT) for suspected coronary artery disease. CT images were evaluated for - origin, number, size and course (tubular/ worm-like/ significant aneurysm formation/wall attachment sign) of fistula vessels, drainage site, drainage site imaging features (pierced sign, iso-density sign, smoke sign, jet sign), and the maximum diameters of pulmonary artery(MPA). Wall attachment sign is the presence of abnormal tortuous supplying artery branches over the surface of MPA; Pierced sign is direct connection of supplying artery and MPA; jet sign is a jet of contrast from supplying artery to MPA; Smoke sign is a fuzzy dense contrast from supplying artery dispersed over less dense contrast in MPA; and isodensity sign is equal contrast density between drainage artery and MPA. 25 patients of CPAF also underwent CCA and 47 patients underwent TTE.

### RESULTS

There were 72 patients with CPAF (0.36 %) in our study, of which 44 were men and 28 were women, with mean age of  $55.8 \pm 13.2$  years (range 22- 85 years). CPAF originated from the conus artery in 55, LAD in 67 and combined conus and LAD in 50. Tubular dilation was seen in 14, worm-like dilation in 58 and aneurysm in 35 cases. Wall attachment sign was noted in 69 cases. All the cases demonstrated only a single drainage site, with 44 draining into left lateral wall of MPA, 21 in left anterolateral, 5 in anterior and 1 each in right lateral and right anterolateral walls. The mean diameter of the fistula drainage site was  $2.6 \pm 1.3$  mm. Pierced sign was seen in 72 cases; Jet sign in 46 cases; Smoke sign in 41 cases; Isodensity sign in 24 cases. Pulmonary artery enlargement was seen in 20 patients. CCA showed CPAF in only 20 cases among 25 patients; TTE showed CPAF in only 9 patients among 47 patients.

## CONCLUSION

MDCT is competent in detecting and characterizing CPAF with an excellent diagnostic performance as the first imaging modality of choice.

## **CLINICAL RELEVANCE/APPLICATION**

To recognize CT findings of CPAF with CCTA for reducing missed diagnosis.

### **Honored Educators**

Presenters or authors on this event have been recognized as RSNA Honored Educators for participating in multiple qualifying educational activities. Honored Educators are invested in furthering the profession of radiology by delivering high-quality educational content in their field of study. Learn how you can become an honored educator by visiting the website at: https://www.rsna.org/Honored-Educator-Award/ Sachin S. Saboo, MD, FRCR - 2017 Honored EducatorPrabhakar Rajiah, MD, FRCR - 2014 Honored EducatorSuhny Abbara, MD - 2014 Honored EducatorSuhny Abbara, MD - 2017 Honored Educator



## CA253-SD-THA2

Does the Tube Voltage Affect the Characterization of Coronary Plagues on 100- and 120-kVp CT Scans

Thursday, Nov. 29 12:15PM - 12:45PM Room: CA Community, Learning Center Station #2

## Participants

Takanori Masuda, Hiroshima, Japan (*Presenter*) Nothing to Disclose Takeshi Nakaura, MD, Kumamoto, Japan (*Abstract Co-Author*) Nothing to Disclose Yoshinori Funama, PhD, Kumamoto, Japan (*Abstract Co-Author*) Nothing to Disclose Masao Kiguchi, RT, Hiroshima, Japan (*Abstract Co-Author*) Nothing to Disclose Takayuki Oku, Hiroshima, Japan (*Abstract Co-Author*) Nothing to Disclose Kazuo Awai, MD, Hiroshima, Japan (*Abstract Co-Author*) Nothing to Disclose Kazuo Awai, MD, Hiroshima, Japan (*Abstract Co-Author*) Research Grant, Canon Medical Systems Corporation; Research Grant, Hitachi, Ltd; Research Grant, Fujitsu Limited; Research Grant, Bayer AG; Research Grant, DAIICHI SANKYO Group; Research Grant, Eisai Co, Ltd; Medical Advisory Board, General Electric Company; ; Yoriaki Matsumoto, Hiroshima, Japan (*Abstract Co-Author*) Nothing to Disclose

#### For information about this presentation, contact:

takanorimasuda@yahoo.co.jp

## PURPOSE

Lower tube voltage scan is effective for the radiation dose reduction and improving the vessel enhancement in coronary CT angiography (CCTA). However, there are only few reports that evaluate coronary plaque components using low tube voltage scan. The purpose of this study was to compare the diagnostic performance of 100- and 120 kVp CCTA scans for the evaluation of coronary plaque components.

#### **METHOD AND MATERIALS**

We included 116 patients with coronary plaques who underwent CCTA- and integrated backscatter intravascular ultrasound (IB-IVUS) studies. On 100 kVp scans we observed 24 fibrous- and 24 fatty/fibro-fatty plaques; on 120 kVp scans we noted 27 fibrousand 41 fatty/fibro-fatty plaques. We compared the fibrous- and the fatty/fibro-fatty plaques, the CT number of the coronary lumen, and the radiation dose on scans obtained at 100- and 120 kVp. We also compared the area under the receiver operating characteristic (ROC) curve of the coronary plaques on 100- and 120 kVp scans with their ROC curves on IB-IVUS images.

### RESULTS

The mean CT number of fatty- and fatty/fibro-fatty plaques was  $5.71 \pm 36.5$  and  $76.6 \pm 33.7$  Hounsfield units (HU), respectively, on 100 kVp scans; on 120 kVp scans it was  $13.9 \pm 29.4$  and  $54.5 \pm 22.3$  HU, respectively. The CT number of the coronary lumen was  $323.1 \pm 81.2$  HU and the radiation dose was  $563.7 \pm 81.2$  mGy-cm on 100 kVp scans; these values were  $279.3 \pm 61.8$  HU and  $819.1 \pm 115.1$  mGy-cm on 120 kVp scans. Using our IB-IVUS plaque findings for comparison studies, the results of ROC curve analysis identified 30.5 HU as the optimal diagnostic cut-off value for 100 kVp scans; for 120 kVp plaque images, the optimal cut-off was 37.4 HU.

### CONCLUSION

For the discrimination of coronary plaque components, the diagnostic performance of 100- and 120 kVp CCTA scans is comparable.

### **CLINICAL RELEVANCE/APPLICATION**

Lower tube voltage CCTA scans help to decrease the radiation dose without deterioration of the image quality of the coronary artery.



## CA254-SD-THA3

## Long-Term Prognostic Value Coronary Artery Calcium in Heart Transplant Patients

Thursday, Nov. 29 12:15PM - 12:45PM Room: CA Community, Learning Center Station #3

### **Participants**

Alejandra Garcia Baizan, MD, Pamplona, Spain (*Presenter*) Nothing to Disclose Ignacio Gonzalez de la Huebra Rodriguez, MD, Pamplona, Spain (*Abstract Co-Author*) Nothing to Disclose Ana Ezponda, MD, Pamplona, Spain (*Abstract Co-Author*) Nothing to Disclose Marta Calvo-Imirizaldu, MD, Pamplona, Spain (*Abstract Co-Author*) Nothing to Disclose Gregorio Rabago, Pamplona, Spain (*Abstract Co-Author*) Nothing to Disclose Gorka Bastarrika, MD, Pamplona, Spain (*Abstract Co-Author*) Nothing to Disclose

#### For information about this presentation, contact:

agarcia.13@unav.es

# PURPOSE

To evaluate the long-term prognostic value of coronary artery calcium (CAC) burden and its relationship with obstructive coronary allograft vasculopathy (CAV) in heart transplant recipients (HT).

## **METHOD AND MATERIALS**

From June 2007 to December 2017, 117 HT patients undergoing coronary CT angiography (CCTA) for the evaluation of CAV were prospectively recruited. CAC was quantified using the Agatston score. According to basal CAC burden, patients were divided in two groups: absence or minimal risk (0-10) and mild-moderate-severe risk (>11). Obstructive CAV was defined as coronary stenosis >=50% luminal diameter. To analyze differences in the degree of CAC and CAV chi square test, Kaplan-Meier curves, Log-Rank test and the hazard ratio were estimated. A p-value <0.05 was considered statistically significant.

### RESULTS

Eighty-six (76.8%) HT patients had no or minimal risk, whereas twenty-six (23.2%) were classified as having mild to severe risk at basal CCTA. Five patients were excluded due to the presence of stents. After a median follow-up period of 46±39 months, statistically significant association between basal CAC and the presence of obstructive CAV over time was observed (p<0.05). At 5 years, obstructive CAV occurred in 15.8% and 37.6% of HT patients with no or minimal risk and mild to severe risk, respectively (Log-rank p<0.05). The hazard ratio was 2.4 for patients with >11 basal CAC score (p<0.05).

## CONCLUSION

HT patients with mild to severe risk based on basal CAC score present 2.4 times more probability to develop obstructive CAV at 5 years than patients with no or minimal risk.

## **CLINICAL RELEVANCE/APPLICATION**

CAC score is a useful tool to stratify risk in HT patients.



## CA256-SD-THA5

Automatic Segmentation of Lung Volumes in Population-based Whole-Body MR Imaging: Association with Subclinical Cardiac Impairment

Thursday, Nov. 29 12:15PM - 12:45PM Room: CA Community, Learning Center Station #5

### Participants

Ricarda V. von Kruchten, MD, Heidelberg, Germany (Presenter) Nothing to Disclose Roberto Lorbeer, Greifswald, Germany (Abstract Co-Author) Nothing to Disclose Tanja Zitzelsberger, MD, Tuebingen, Germany (Abstract Co-Author) Nothing to Disclose Tatyana Ivanovska, Gottingen, Germany (Abstract Co-Author) Nothing to Disclose Corinna Storz, MD, Tubingen, Germany (Abstract Co-Author) Nothing to Disclose Christopher Schuppert, Heidelberg, Germany (Abstract Co-Author) Nothing to Disclose Peter Hegedues, Heidelberg, Germany (Abstract Co-Author) Nothing to Disclose Lena Sophie Kiefer, MD, Tubingen, Germany (Abstract Co-Author) Nothing to Disclose Christopher L. Schlett, MD, MPH, Heidelberg, Germany (Abstract Co-Author) Nothing to Disclose Fabian Bamberg, MD, Tuebingen, Germany (Abstract Co-Author) Speakers Bureau, Bayer AG; Speakers Bureau, Siemens AG; Research Grant, Siemens AG Stefan Karrasch, Neuherberg, Germany (Abstract Co-Author) Nothing to Disclose Annette Peters, Neuherberg, Germany (Abstract Co-Author) Nothing to Disclose Hans-Ulrich Kauczor, MD, Heidelberg, Germany (Abstract Co-Author) Research Grant, Siemens AG Research Grant, Bayer AG Speakers Bureau, Boehringer Ingelheim GmbH Speakers Bureau, Siemens AG Speakers Bureau, Koninklijke Philips NV Speakers Bureau, Bracco Group Speakers Bureau, AstraZeneca PLC

Holger Schulz, Neuherberg, Germany (Abstract Co-Author) Nothing to Disclose

### PURPOSE

Both cardiac and pulmonary morphology and function can be simultaneously assessed during a single MR scan. Previous studies have shown an association between obstructive lung disease with cardiac dysfunction. Our aim is to evaluate the relationship between lung volumes and cardiac impairment in a population-based cohort study using whole-body MR scans.

## METHOD AND MATERIALS

We studied 400 subjects who underwent whole-body MRI as part of the KORA FF4 cohort study, excluding subjects with established cardiovascular disease. Lung volumes were derived semi-automatically through an in-house algorithm (coronal acquired T1w sequences). Using Pearson correlation and multivariate regression (adjusted for age, sex, smoking status and BMI), lung volumes were compared with cardiac parameters of left and right ventricle (LV/RV, acquired from cine-SSFP sequences using cvi42), and standardized to body surface area.

### RESULTS

A total of 356 subjects presented an average MRI-based lung volume of  $4.0\pm1.1L$  and mostly standard values for cardiac parameters. In univariate analysis, a negative correlation of LV and RV stroke volume to lung volume was observed. After multivariate adjustment, stroke volume as well as end-diastolic volume of both LV ( $\beta$ =-2.75, p=0.001;  $\beta$ =-1.71, p=0.001) and RV ( $\beta$ =-2.14, p=0.02;  $\beta$ =-1.45, p=0.004) showed negative associations with lung volume, while ejection fraction, peak ejection rate and myocardial mass were not associated with lung volumes (Figure 1). These values were stronger for the LV than for the RV. In addition, for the LV, early but not late diastolic filling rate was negatively associated with lung volume.

### CONCLUSION

Cardiac function and volume parameters derived from non-dedicated whole-body MRI, such as stroke volumes and biventricular end-diastolic volumes were significantly associated with lung volumes in a patient cohort without cardiovascular disease.

#### **CLINICAL RELEVANCE/APPLICATION**

These results suggest, that MRI could be an accurate, radiation-free, and possibly one-stop-shop screening tool, with the potential for early detection of subclinical heart disease in patients with emphysema and subclinical cardiovascular dysfunction.



## CH253-ED-THA7

### Thoracic Devices in 2018: A Comprehensive Pictorial Review of Devices Seen on Chest Radiograph

Thursday, Nov. 29 12:15PM - 12:45PM Room: CH Community, Learning Center Station #7

#### **Participants**

Youn Kyung Lee, MD, Los Angeles, CA (*Presenter*) Nothing to Disclose Cameron Hassani, MD, Los Angeles, CA (*Abstract Co-Author*) Nothing to Disclose Leah M. Lin, MD, Los Angeles, CA (*Abstract Co-Author*) Nothing to Disclose Alison Wilcox, MD, Los Angeles, CA (*Abstract Co-Author*) Speaker, Canon Medical Systems Corporation Christopher Lee, MD, Los Angeles, CA (*Abstract Co-Author*) Nothing to Disclose

## For information about this presentation, contact:

youn.lee@med.usc.edu

#### **TEACHING POINTS**

- While most radiologists are familiar with traditional devices such as pacemakers and defibrillators on chest radiograph, newer and less commonly observed devices may present challenges in imaging interpretation - The purpose of this exhibit is to improve familiarity with less frequently encountered devices - Indications, function, normal appearance on chest radiographs, and complications will be discussed

### **TABLE OF CONTENTS/OUTLINE**

Devices discussed will include but not be limited to: Leadless pacemaker Implantable loop recorder Subcutaneous implantable cardioverter-defibrillator (ICD) LifeVest wearable defibrillator Mechanical circulatory support devices - Impella, Impella RP - Extracorporeal membrane oxygenator pump (ECMO) - Ventricular assist devices: LVAD, RVAD, BIVAD - Total artificial heart Parachute left ventricular partitioning device CardioMEMS Transcatheter aortic, pulmonic, and mitral valve replacement/repair (e.g. TAVR, Melody, MitraClip) Occlusion devices (Amplatzer, Watchman, AtriClip) Endobronchial valves Implanted phrenic nerve stimulator Transesophageal voice prosthesis Esophageal probe LINX reflux management system Neurostimulator

## **Honored Educators**

Presenters or authors on this event have been recognized as RSNA Honored Educators for participating in multiple qualifying educational activities. Honored Educators are invested in furthering the profession of radiology by delivering high-quality educational content in their field of study. Learn how you can become an honored educator by visiting the website at: https://www.rsna.org/Honored-Educator-Award/ Cameron Hassani, MD - 2018 Honored Educator



## CH254-ED-THA8

I Can See Your Halo

Thursday, Nov. 29 12:15PM - 12:45PM Room: CH Community, Learning Center Station #8

### **Participants**

Benjamin Meyer, MD, Milwaukee, WI (*Presenter*) Nothing to Disclose Melissa M. Wein, MD, Milwaukee, WI (*Abstract Co-Author*) Nothing to Disclose Luis A. Sosa, MD, Brookfield, WI (*Abstract Co-Author*) Nothing to Disclose Ashley Norton-Gregory, MD, 53226, WI (*Abstract Co-Author*) Nothing to Disclose Sergio A. Criales Vera, MD, Mexico, Mexico (*Abstract Co-Author*) Nothing to Disclose Lyudmila Demko, DO, Milwaukee, WI (*Abstract Co-Author*) Nothing to Disclose Dhiraj Baruah, MD, Milwaukee, WI (*Abstract Co-Author*) Nothing to Disclose Zachary R. Laste, MD, Milwaukee, WI (*Abstract Co-Author*) Nothing to Disclose

#### For information about this presentation, contact:

asosa@mcw.edu

#### **TEACHING POINTS**

To define the halo and reverse halo sign. To describe the imaging characteristics of the these signs. Describe a differential diagnoses that may be elucidated by proper interpretation of these signs.

### TABLE OF CONTENTS/OUTLINE

Review the definitions of CT halo and reverse halo signs Outline key factors including host immune status, geographic location and clinical presentation that narrow the differential diagnosis Review spectrum of diagnosis Infections Inflammatory conditions Neoplasms Clarify the pathologic findings that contribute to the CT appearance of these signs



## CH296-SD-THA1

## Outcome of PET/CT Negative Solid Pulmonary Nodule: A Retrospective Study

Thursday, Nov. 29 12:15PM - 12:45PM Room: CH Community, Learning Center Station #1

### Participants

Varun Mehta, MD, Staten Island, NY (*Presenter*) Nothing to Disclose Jesse Chen, MD, Staten Island, NY (*Abstract Co-Author*) Nothing to Disclose Varun Chowdhary, MD, BS, Staten Island, NY (*Abstract Co-Author*) Nothing to Disclose Joseph W. Lowry, MD, Forest Hills, NY (*Abstract Co-Author*) Nothing to Disclose

## For information about this presentation, contact:

varunmehtamd@gmail.com

### PURPOSE

To observe the natural history of PET/CT negative pulmonary nodules in patients without a history of malignancy such that we will be able to provide evidence-based insight into appropriate recommendations for further follow up for such nodules.

### **METHOD AND MATERIALS**

Retrospective PET reports from 2005-2015 mined and analyzed to meet the following basic criteria: Individuals with no prior malignancy ages 35+ who underwent a PET study for incidental solid nodules greater than 8mm. Further PACS search and chart review conducted to follow these individual nodules of concern. Outcomes divided into nodule resolved, stable or developed malignancy.

## RESULTS

Study is currently in progress including more data acquisition and analysis. Current status: N = 62 mean age of 65. 41 of the analyzed nodules were between 0.8-1.5 cm, 20 between 1.5-2.5 cm and 1 above 2.5cm. Among the 62 analyzed nodules, 35 resolved/shrank/remained stable and 9 developed malignancy. Among the 9 nodules that developed malignancy, 77.8 (n = 7) were between 0.8 - 1.5 cm and the remainder 2 were between 1.5 - 2.5 cm. The average estimated date of follow up/discovery of malignancy was 42 months.

#### CONCLUSION

Preliminary analysis shows there is a considerable number of nodules that became malignant on follow up PET/CT in subsequent years after demonstrating sub-threshold activity on initial PET/CT. Hence, it can be assumed that a PET negative nodules on initial evaluation can and should not be considered to be inert or without potential of future malignant transformation.

## **CLINICAL RELEVANCE/APPLICATION**

At this time, when an incidental pulmonary nodule is identified and meets minimum size criteria of greater than 8mm per current Fleischner guidelines, it is further worked up with PET/CT to assess for positive biological activity to suggest malignancy. However, if the nodule turns out to be PET/CT negative, pulmonologists, primary medical doctors, and radiologists alike are at a loss of what to do with these nodules or how to follow them. Historically, subjective follow up recommendations have been made by radiologist due to a lack of studies looking at outcomes of PET negative nodules or any established guidelines. This study sheds light on the fact that many of these nodules can and do prove to be slow growing with potential for malignancy and hence can not be ignored after the first negative PET/CT. This is true especially for the smaller nodules ranging below 2.5 cm.



## CH297-SD-THA2

Utilization of Bone Suppression Imaging by Using Deep Learning on Chest Radiograph: Detectability of Lung Nodules and Exploring for Effectual Interpretation Methods

Thursday, Nov. 29 12:15PM - 12:45PM Room: CH Community, Learning Center Station #2

## Participants

Kenji Endo, Shinjuku, Japan (*Presenter*) Nothing to Disclose Asuka Kaneko, Tokyo, Japan (*Abstract Co-Author*) Nothing to Disclose Yuhei Horiuchi, Tokyo, Japan (*Abstract Co-Author*) Nothing to Disclose Yasuyuki Morita, Tokyo, Japan (*Abstract Co-Author*) Nothing to Disclose Shuji Sakai, MD, Shinjuku-Ku, Japan (*Abstract Co-Author*) Nothing to Disclose

### For information about this presentation, contact:

endo.kenji@twmu.ac.jp

#### PURPOSE

To evaluate differences in the effect of bone suppression (BS) imaging in lung-nodule detection on chest radiographs (CXRs) by interpretation method.

## METHOD AND MATERIALS

The CXRs of 100 patients, of which 50 demonstrated a lung nodule (5-29 mm in diameter) and 50 did not, were interpreted by 10 observers comprising five chest radiologists with > 10 years of experience and five radiology residents. Each CXR was sequentially read, using the conventional CXR (on a left monitor) and BS image (on a right monitor) on dual monitors for initial review, and then using the conventional CXR and BS image on a single monitor after a few weeks. Reviewers could switch each other on a single monitor. The nodule location, confidence level with regard to the presence of a lung nodule, and reading time were recorded. Receiver operating characteristic (ROC) analysis and paired t-tests were used to evaluate observer performance.

### RESULTS

The average area under the curve (AUC) for the observers' ROC significantly improved from 0.830 to 0.868 (P = 0.005) and from 0.826 to 0.860 (P = 0.004) with BS image using dual monitors and a single monitor, respectively. The average AUC was not significantly different between dual monitors and a single monitor (P = 0.449). However, the specificity of BS image on a single monitor was significantly higher (P = 0.001) than on dual monitors, whereas there was weak evidence that its sensitivity tended to be lower (P = 0.061). The interpretation time for BS imaging on a single monitor (44.0 ± 9.6 minutes) was significantly shorter (P = 0.006) than on dual monitors (56.8 ± 8.9 minutes).

# CONCLUSION

The use of BS image as a reference improved lung-nodule detection performance on CXRs; however, sensitivity, specificity, and reading time were differently affected by imaging review method.

# **CLINICAL RELEVANCE/APPLICATION**

This study suggested effects of bone suppression imaging review method. This constitutes highly important knowledge during the interpretation of processed images.



## CH298-SD-THA3

CT Air Trapping Assessment in Usual Interstitial Pneumonia Pattern

Thursday, Nov. 29 12:15PM - 12:45PM Room: CH Community, Learning Center Station #3

### Participants

Felipe D. Sanches, Porto Alegre, Brazil (*Abstract Co-Author*) Nothing to Disclose Adriano Basso Dias, MD, Porto Alegre, Brazil (*Presenter*) Nothing to Disclose Stephan Altmayer, Porto Alegre, Brazil (*Abstract Co-Author*) Nothing to Disclose Gabriel Sartori Pacini, Porto Alegre, Brazil (*Abstract Co-Author*) Nothing to Disclose Matheus Zanon, Porto Alegre, Brazil (*Abstract Co-Author*) Nothing to Disclose Alvaro Guedes, Porto Alegre, Brazil (*Abstract Co-Author*) Nothing to Disclose Joao P. Dalla-Bona, Porto Alegre, Brazil (*Abstract Co-Author*) Nothing to Disclose Fernando Liberato da Silva, Porto Alegre, Brazil (*Abstract Co-Author*) Nothing to Disclose Guilherme Watte, Porto Alegre, Brazil (*Abstract Co-Author*) Nothing to Disclose Guilherme Watte, Porto Alegre, Brazil (*Abstract Co-Author*) Nothing to Disclose Marcelo C. Barros, MD, Santana do Livramento, Brazil (*Abstract Co-Author*) Nothing to Disclose Adalberto S. Rubin, Porto Alegre, Brazil (*Abstract Co-Author*) Nothing to Disclose Bruno Hochhegger, MD, PhD, Porto Alegre, Brazil (*Abstract Co-Author*) Nothing to Disclose

### PURPOSE

Our goal was to evaluate the frequency of air trapping in patients with UIP due to idiopathic pulmonary fibrosis (IPF) compared to other non-IPF etiologies of UIP.

## METHOD AND MATERIALS

The current study included 84 consecutive patients with radiological or histological UIP. IPF was diagnosed by a multidisciplinary team approach or a surgical lung biopsy (SLB). Air trapping on HRCT was visually assessed by two independent chest radiologists, and quantitatively calculated as the percentage of voxels in expiratory CT with attenuation range between -950 to -856HU (ATIexp) >6% or expiratory to inspiratory ratio of mean lung density (E/I-ratio) >0.87. Survival analysis was performed.

### RESULTS

A total of 51 patients (60.7%) had UIP due to IPF, and 33 (39.3%) had UIP secondary to known causes. The average survival was of 3 years (CI 95% 2.5-3.5) and 4.2 years (CI 95%: 3.6-4.7), respectively. Extensive air trapping (>=3 lobes) was present in 8 patients (9.5%) with IPF, and 6 (7.1%) with non-IPF (p = 0.764). Air trapping in the upper lobes was the only significant variable able capable of discriminate IPF from non-IPF (frequency of 3.9% vs. 33.3%, respectively; p < 0.001), being highly suggestive of chronic hypersensitivity pneumonitis.

## CONCLUSION

The presence of air trapping in the upper lobes was highly associated with non-IPF etiologies of UIP. Extensive air trapping is not infrequent in patients with IPF.

# **CLINICAL RELEVANCE/APPLICATION**

The presence of extensive air trapping on a high-resolution computed tomography (HRCT) is currently considered an inconsistent finding of usual interstitial pneumonia (UIP).



### CH299-SD-THA4

The Imaging Features of TSCT Predict the Expression of PD-L1 in Patients with Surgical Resection of Lung Adenocarcinoma

Thursday, Nov. 29 12:15PM - 12:45PM Room: CH Community, Learning Center Station #4

# Participants

Tong Wu, Shanghai, China (*Presenter*) Nothing to Disclose Jingyun Shi, Shanghai, China (*Abstract Co-Author*) Nothing to Disclose

### PURPOSE

PD-L1 expression may serve as a predictive biomarker for the response to immune checkpoint inhibitors in lung cancer and were more likely to express in male and smokers. However, the relationship between PD-L1 expression and imaging features of computed tomography (CT) has not been fully understood.

# METHOD AND MATERIALS

A total of 350 patients with pathologically-confirmed adenocarcinoma who received surgical treatment and had thin section CT (TSCT) examination were included in this study. Quantitative CT features such as the mean CT value and mass were measured on multiplanar reconstructed images.

### RESULTS

Among 350 patients, PD-L1 positive tumors were detected in 21.1% (74/350) of all cases. Multivariate analysis identified surrounding ground glass opacity (P=0.022), shape (P=0.008), pleural tag (P=0.007), tumor mean CT value and consolidation divided by tumor of mass (C/T mass) (P=0.004) as being significantly associated with the expression of PD-L1. The receiver operation curve (ROC) analysis showed that the optimal cutoff values of -170HU for tumor mean CT value and of 30.9% for C/T mass. The sensitivity, specificity, area under curve (AUC) of C/T mass for predicting PD-L1 expression was 71.62%, 70.29% and 0.705. To improve the diagnostic accuracy, a joint model (included all significant imaging parameters at multivariate logistic regression analysis) was conducted. The AUC of joint model was 0.787, with a sensitivity of 81.08% and specificity of 65.22%.

## CONCLUSION

PD-L1 expression was associated with invasive subtype of adenocarcinoma and imaging features, which may help clinicians make initial predictions before administration of immune checkpoint inhibitors.

### **CLINICAL RELEVANCE/APPLICATION**

This study is to explore any particular imaging findings associated with PD-L1 expression in patients with surgical resection of lung adenocarcinoma and help patients predict whether they will benefit from immunotherapy.



### CH300-SD-THA5

## Dual-Layer Detector Spectral CT (DLCT) for Assessing the Lymph Node Metastasis of Lung Cancer

Thursday, Nov. 29 12:15PM - 12:45PM Room: CH Community, Learning Center Station #5

## FDA Discussions may include off-label uses.

#### Participants

Lu Gao, Shenyang, China (*Presenter*) Nothing to Disclose Yang Hou, MD, Shenyang, China (*Abstract Co-Author*) Nothing to Disclose Qingyun Wen, Shenyang, China (*Abstract Co-Author*) Nothing to Disclose

### For information about this presentation, contact:

glu174lv@163.com

## PURPOSE

To investigate the value of dual-layer detector spectral CT(DLCT) in the assessment of metastatic lymph nodes in lung cancer with multiple quantitative parameters and to evaluate the diagnostic performance of the parameters in combination with short diameter.

### **METHOD AND MATERIALS**

We retrospectively analyzed the dual-phase contrast enhanced spectral CT images of 32 patients with lung cancer. The short diameter of lymph nodes and iodine uptake were measured. According to pathological findings, lymph nodes were divided into metastatic group and non-metastatic group. Arterial enhancement fraction (AEF), normalized iodine concentration(NIC) during artery phase(AP) and venous phase(VP) and short diameter were calculated (AEF = iodine uptake in AP /iodine uptake in VP × 100%,NIC=IClymph node/ICaorta) and compared. Receiver operating characteristic (ROC) curves were performed to evaluate diagnostic performance for quantitative parameters.

### RESULTS

A total of 84 lymph nodes were included, with 48 metastatic lymph nodes and 36 non-metastatic lymph nodes. The short diameter of lymph nodes, NICAP, NICVP and AEF all showed significant differences between the two groups (short diameter,  $1.25 \pm 0.50$  vs.  $0.92 \pm 0.23$ ; NICAP,  $0.19 \pm 0.08$  vs.  $0.13 \pm 0.05$ ; NICVP,  $0.42 \pm 0.14$  vs.  $0.31 \pm 0.08$ ; AEF,  $112.40 \pm 36.68$  vs.  $71.73 \pm 15.76$ ; each P<0.05). AEF had the largest area under the curve (AUCAEF = 0.874, AUC AP NIC =0.721, AUC VP NIC =0.765 and AUC short diameter = 0.700). With a threshold of 81.53% for AEF, the sensitivity and specificity were 83.00% and 65.70% respectively. With a threshold of the short diameter >1cm,the sensitivity and specificity were 58.10% and 77.1% respectively. Using the parallel criteria approach to combine of AEF and short diameter, the sensitivity was increased to 92.88%, using the sequential criteria approach, the specificity was increased to 91.15%.

#### CONCLUSION

Among multiple quantitative parameters provide by DLCT, AEF has the highest diagnostic efficiency in differentiating metastatic and non-metastatic lymph nodes. Measurement of the short diameter in combination with AEF further improve the diagnostic accuracy of lymph nodes metastasis.

### **CLINICAL RELEVANCE/APPLICATION**

Multiple quantitative parameters of DLCT provide an effective noninvasive method for accurate evaluation of lymph nodes metastasis of lung cancer. The association of quantitative parameters facilitates the detection of lymph nodes metastasis.



## CH301-SD-THA6

Improving Measurement Variability of Radiomics for Lung Nodules between Different Reconstruction Kernels at CT: Convolutional Neural Network-based Kernel Conversion

Thursday, Nov. 29 12:15PM - 12:45PM Room: CH Community, Learning Center Station #6

## Participants

Jooae Choe, MD, Seoul, Korea, Republic Of (*Presenter*) Nothing to Disclose Sang Min Lee, MD, Seoul, Korea, Republic Of (*Abstract Co-Author*) Nothing to Disclose Kyung-Hyun Do, MD, Seoul, Korea, Republic Of (*Abstract Co-Author*) Nothing to Disclose Gaeun Lee, Seoul, Korea, Republic Of (*Abstract Co-Author*) Nothing to Disclose June-Goo Lee, PhD, Seoul, Korea, Republic Of (*Abstract Co-Author*) Nothing to Disclose Namkug Kim, PhD, Seoul, Korea, Republic Of (*Abstract Co-Author*) Nothing to Disclose Namkug Kim, PhD, Seoul, Korea, Republic Of (*Abstract Co-Author*) Nothing to Disclose

### For information about this presentation, contact:

#### jooae23@gmail.com

## PURPOSE

To assess whether CT kernel conversion using convolutional neural network (CNN) could improve measurement variability of radiomic features of lung nodules between different routine reconstruction kernels and different readers.

### **METHOD AND MATERIALS**

Total 104 patients with pulmonary lesions underwent chest CT using single CT machine. Among them, 53 patients underwent contrast enhanced CT and 51 patients underwent nonenhanced CT scan. All of the chest CT was reconstructed in both B30f and B50f kernels. To convert different kernels without sonogram, the CNN model was developed using residual learning and an end-toend way. Afterward, the kernel converted images were generated, from B30f to B50f (cB30) and from B50f to B30f (cB50). Lung lesions were semi-automatically segmented by two different readers for extracting radiomic features. A total of 718 radiomic features including shape, tumor intensity, texture and wavelet features were obtained from 4 different kernels of images: B30, B50, cB30 and cB50 images. Measurement variability of radiomics features were evaluated among different readers and kernels using concordance correlation coefficent (CCC).

### RESULTS

In terms of the effect of kernel on measurement variability, CCC between different kerenels (B30 and B50) but same reader was  $0.41 \pm 0.36$  (shape,  $1.0 \pm 0$ , tumor intensity,  $0.915 \pm 0.13$ , texture  $0.66 \pm 0.21$ , and wavelet features  $0.36 \pm 0.34$ ) in total patients,  $0.41 \pm 0.36$  on nonenhanced CT and  $0.42 \pm 0.37$  on enhanced CT. After applying kernel conversion, CCC improved in all radiomic features (B30 vs cB30,  $0.93 \pm 0.10$ ; B50 vs cB50,  $0.89 \pm 0.13$ ). Comparing nonenhanced and enhanced CT, kernel conversion were effective in both image settings, improving CCC to  $0.91 \pm 0.13$  on nonenhanced CT and  $0.88 \pm 0.17$  on enhanced CT. CCC between different readers but same kernel (inter-reader variability) was  $0.91 \pm 0.14$  in B30 and  $0.89 \pm 0.14$  in B50.

#### CONCLUSION

Among radiomic features, texture and wavelet features are significantly affected by kernel in both enhanced and nonenhanced CT images. Kernel conversion using CNN can effectively improve measurement variability in the values of radiomics features.

## **CLINICAL RELEVANCE/APPLICATION**

Kernel conversion using CNN can effectively improve measurement variability of radiomics features which could aid multicenter reaserches or retrospective studies of radiomics field.



## ER166-ED-THA5

## Pediatric Foot and Ankle Fractures: Patterns, Mimics, Complications, and Treatment

Thursday, Nov. 29 12:15PM - 12:45PM Room: ER Community, Learning Center Station #5

#### Awards Identified for RadioGraphics

### **Participants**

Usa Cain, MD, Rochester, NY (*Presenter*) Nothing to Disclose Nina B. Klionsky, MD, Rochester, NY (*Abstract Co-Author*) Nothing to Disclose Apeksha Chaturvedi, MD, Rochester, NY (*Abstract Co-Author*) Nothing to Disclose

#### For information about this presentation, contact:

usa\_cain@urmc.rochester.edu

### **TEACHING POINTS**

Ankle/foot fractures represent 13% of osseous injuries affecting the immature skeleton; ankle fractures represent 20% of growth plate injuries. Tolerance for residual deformity in ankle/foot fractures is significantly lower than for hand/wrist fractures. Fracture patterns vary by age and injury mechanism; participation in sports predisposes to unique injury patterns. Diagnosis of under-recognized fractures (e.g. Lisfranc/Chopart) should account for incomplete ossification and presence of cartilaginous bone precursors. Operative criteria often hinges on imaging. Recognize early and late complications such as compartment syndrome and malunion.

## TABLE OF CONTENTS/OUTLINE

Describe bony, ligamentous, and developmental anatomy of the pediatric foot/ankle. Review difference between the pediatric and adult skeleton and how injury may manifest uniquely in children. Clinical Criteria: Ottawa Ankle and Foot Rules (OAFR) validated for children, Low-Risk Ankle Rules. Discuss variants that mimic fracture, how to differentiate. Classification of common age-specific pediatric ankle/foot fractures, highlight special radiographic views, CT/MR findings, criteria for operative fixation. Discuss role of ultrasound to diagnose cartilaginous avulsions. Review late fracture-related complications and role of imaging.



## ER229-SD-THA1

A Modern Phenomenon: Bicycle Versus Pedestrian Trauma within a Major Urban Trauma Center, Including a Review of Imaging Findings

Thursday, Nov. 29 12:15PM - 12:45PM Room: ER Community, Learning Center Station #1

# Awards

## Student Travel Stipend Award

#### Participants

Drew Gunio, MD,MS, New York, NY (*Presenter*) Nothing to Disclose Shane Keogh, MD, New York, NY (*Abstract Co-Author*) Nothing to Disclose Kishore K. Chundru, MD, New York, NY (*Abstract Co-Author*) Nothing to Disclose Raymond Wedderburn, New York, NY (*Abstract Co-Author*) Nothing to Disclose Amita Kamath, MD,MPH, New York, NY (*Abstract Co-Author*) Nothing to Disclose Stephen I. Zink, MD, New York, NY (*Abstract Co-Author*) Nothing to Disclose Lindsey Heacook, New York, NY (*Abstract Co-Author*) Nothing to Disclose Deborah Travis, New York, NY (*Abstract Co-Author*) Nothing to Disclose

## For information about this presentation, contact:

drew.gunio@mountsinai.org

### PURPOSE

To evaluate the trends and morbidities involving bicyclist-pedestrian trauma.

## METHOD AND MATERIALS

This is a retrospective review that analyzed our institutional trauma log of activated traumas involving pedestrian-bicycling (PB) accidents between 2014 and 2017. There were 589 total bicycling related traumas over this time period; 31 of which were PB traumas. We reviewed data including injury severity scores (ISS), fatalities, admission status, intoxication, gender, age, and ethnicity. We trended this data over time and reviewed relevant radiologic examinations. We calculated means and standard deviations for each group and calculated two-t tests to measure significance.

#### RESULTS

The ISS for PB traumas was 3.61, compared to 4.19 for the entire population. One fatality was recorded over this time period. 32.3% of patients required admission or transfer to a specialized center of care. 22.6% of injured patients were intoxicated, compared to an average of 10.2%. Males and females accounted for 87.1% and 12.9% of traumas and had a mean ISS of 3.52 (Standard deviation: 4.88) and 8.67 (6.80), respectively. The two t-test comparing males and females measured -1.46 (p = 0.240). 77.4% of PB traumas were aged 18-54 years and had a mean ISS of 3.00 (2.95). 22.6% of PB traumas were aged greater than 55 years and had a mean ISS of 6.29 (8.40). The two t-test comparing adults and the elderly measured -1.081 (p = 0.348). Ethnicities were recorded as white, black, Asian, and other and had mean ISS scores of 4.85 (6.22), 1.50 (1.58), 1.00 (1.00), and 4.71 (4.59), respectively. Radiologic review demonstrated several fracture types, concussions, lung contusions, and facial injuries.

### CONCLUSION

PB traumas account for a small percentage of all bicycling-related traumas, but they represent a population subset with unique factors and morbidities. Several variances existed between gender, ages, and ethnicities, but these were not statistically significant, which is presumably related to a small population size. Our data is therefore qualitative and descriptive in nature. Further research is required, but our data maintains implications in this poorly researched trauma population and highlights the potential role for public health initiatives and bicycling safety education.

## **CLINICAL RELEVANCE/APPLICATION**

Our data provides insight into a poorly researched PB trauma population with implications in public health safety and bicycling safety education.



## ER230-SD-THA2

## Utility of Body CT in Patients with Head or Neck Injuries from Falls from Standing Height or Less

Thursday, Nov. 29 12:15PM - 12:45PM Room: ER Community, Learning Center Station #2

#### **Participants**

Asad Baig, MD, Syosset, NY (*Presenter*) Nothing to Disclose Fiza Khan, Glen Head, NY (*Abstract Co-Author*) Nothing to Disclose Michael Drabkin, MD, East Meadow, NY (*Abstract Co-Author*) Nothing to Disclose Saurabh Patel, MD, East Meadow, NY (*Abstract Co-Author*) Nothing to Disclose Salman S. Shah, MD, New York, NY (*Abstract Co-Author*) Nothing to Disclose

## For information about this presentation, contact:

abaig@numc.edu

### PURPOSE

To determine the utility of body CT in the management of patients with a fall from standing height or less with resultant head or neck injuries.

## METHOD AND MATERIALS

This IRB approved retrospective study examines patients at our level 1 trauma center who experienced a fall from standing height or less from 2012-2015. Patients were included if they had evidence of acute injuries on head and neck CT with concurrent body CT performed less than 15 minutes apart. Patients with clinical signs and symptoms of body injury, positive initial body plain radiographs, Glasgow coma scale <13, and altered mental status were excluded from the study. Positive findings on head and neck CT were defined as fractures, acute hemorrhage, and any acute intracranial injury. On body CT, positive findings were defined as pneumothorax, solid organ injury, acute fractures, or mildly complex free intraperitoneal fluid suggestive of hemorrhage. The clinical courses of patients with evidence of acute injury on body CT were followed in order to determine whether the radiologic findings had any significant impact on clinical management. An attending radiologist reviewed each CT independently.

#### RESULTS

In total 142 patients met the inclusion criteria, and of these 35 were excluded. Of the 107 remaining patients, 83% (n=89) had no CT evidence of acute traumatic body injury. Evidence of acute traumatic body injury was found on CT in 17% of patients (n=18). Clinical management was impacted by CT evidence of acute traumatic body injury in 1.9% (n=2) of patients; in each of these cases, chest tubes were placed for pneumothorax and/or hemothorax.

### CONCLUSION

Our results demonstrate a very low incidence of clinically impactful body injuries on CT in patients who had head or neck injuries subsequent to fall from standing height or less. It is therefore our recommendation that body CT not be routinely performed in this setting unless there is clinical evidence of body injury, or in situations in which an accurate physical exam cannot be obtained .

## **CLINICAL RELEVANCE/APPLICATION**

Minimizing unnecessary CT scans is key to reducing patient exposure to radiation, as well as reducing costs. This study suggests that it may not be necessary to routinely order body CT in the common scenario of fall from standing height or less.



## ER232-SD-THA4

Getting It Right the First Time: A Root Cause Analysis of Aborted and Suboptimal Body MRI Scans in the Emergency Department

Thursday, Nov. 29 12:15PM - 12:45PM Room: ER Community, Learning Center Station #4

## Participants

David Tso, MD, Boston, MA (*Presenter*) Nothing to Disclose Renata R. Almeida, MD, Boston, MA (*Abstract Co-Author*) Nothing to Disclose Efren J. Flores, MD, Boston, MA (*Abstract Co-Author*) Nothing to Disclose Michael H. Lev, MD, Boston, MA (*Abstract Co-Author*) Consultant, General Electric Company; Institutional research support, General Electric Company; Stockholder, General Electric Company; Consultant, MedyMatch Technology, Ltd; Consultant, Takeda Pharmaceutical Company Limited; Consultant, D-Pharm Ltd Ali S. Raja, MD, Boston, MA (*Abstract Co-Author*) Nothing to Disclose Anand M. Prabhakar, MD, Somerville, MA (*Abstract Co-Author*) Nothing to Disclose

#### For information about this presentation, contact:

dktso@mgh.harvard.edu

#### PURPOSE

MRI utilization for body imaging is increasing in the emergency department (ED). The purpose of this study is to perform a root cause analysis of all MRI examinations that result in early termination or suboptimal image quality in the acute care setting for body, vascular, and musculoskeletal indications.

#### **METHOD AND MATERIALS**

This is a retrospective study examining all pediatric and adult patients visiting the ED of a single urban Level 1 trauma center between January 1, 2016 to December 31, 2017. The radiology report was queried for keywords including terminated, aborted, limited, motion, or suboptimal. MRI scan duration and time when the scan occurred were also documented. The PACS was searched to determine if patients required re-imaging of the same body part within 30 days.

## RESULTS

A total of 614 MRI exams were performed over a 2-year period (mean age 52.6 years, 46.3% male). Exams comprised of 51.1% MSK, 43.2% body, and 5.7% vascular studies with a mean scan time of 49, 60, 85 minutes respectively. 13 exams were aborted prematurely due to patient non-cooperation (2.1% of all studies). 62 exams were limited by motion or were considered sub-optimal, comprising of 10.1% of exams with MSK and vascular studies comprising 60% and 25.7% of the cases respectively. Aborted exams had a decreased scan time compared to successfully completed exams, 38.5 vs 57.5 minutes (p=0.03), and involved older patients (70.5 vs 50.8 years, p=0.0001). Most of the MRI scans performed in the ED occur between 8AM - 11PM (72.6%), with the majority of aborted and suboptimal exams also occurring during this time (84%). Reimaging with MRI or another modality was required in 37.3% of the suboptimal scans, and 61.5% of aborted cases.

#### CONCLUSION

Aborted or suboptimal MRI exams accounted for a minority of all examinations performed in the ED and tended to affect older patients undergoing MSK or vascular studies. Aborted studies still took a significant amount of scanner time, likely from attempts to repeat sequences. A large proportion of these patients required re-imaging of the same body part with MRI or another modality.

#### **CLINICAL RELEVANCE/APPLICATION**

As MRI utilization in the ED continues to increase, integrating strategies to recognize risk factors and optimize protocols for fast image acquisition will allow clinicians to provide accurate and expedient care.



### GI013-EB-THA

Trouble Going? A Review of Common Pelvic Floor Pathology on MR Defecography

Thursday, Nov. 29 12:15PM - 12:45PM Room: GI Community, Learning Center Hardcopy Backboard

#### Participants

Matthew Czar D. Taon, MD, Glendale, CA (*Presenter*) Nothing to Disclose Rex A. Parker III, MD, Saint Louis, MO (*Abstract Co-Author*) Nothing to Disclose Joseph H. Kang, MD, Los Angeles, CA (*Abstract Co-Author*) Nothing to Disclose

## For information about this presentation, contact:

matthew.taon@gmail.com

#### **TEACHING POINTS**

The purpose of this exhibit is: 1. To discuss the epidemiological and clinical impact of pelvic floor pathology. 2. To elucidate the dynamic MRI image acquisition techniques. 3. To review imaging findings in normal anatomy and pelvic floor pathology.

## TABLE OF CONTENTS/OUTLINE

1. Epidemiological and clinical impact of pelvic floor pathology. 2. Dynamic MRI image acquisition techniques. 3. Normal anatomy and physiology. 4. Pelvic floor pathology sample cases: anterior, middle, and posterior compartments. 5. Future directions and summary.



## GI297-ED-THA3

Lesser Sac and Foramen of Winslow: Anatomy, Pathway of Disease Spread, and Imaging Features with Pathological Correlation

Thursday, Nov. 29 12:15PM - 12:45PM Room: GI Community, Learning Center Station #3

## Participants

Ayman Nada, MD,PhD, cairo, Egypt (*Abstract Co-Author*) Nothing to Disclose Akram M. Shaaban, MBBCh, Salt Lake City, UT (*Presenter*) Contributor, Reed Elsevier; Author, Reed Elsevier Christine O. Menias, MD, Chicago, IL (*Abstract Co-Author*) Nothing to Disclose Kumaresan Sandrasegaran, MD, Phoenix, AZ (*Abstract Co-Author*) Nothing to Disclose Naveen Garg, MD, Houston, TX (*Abstract Co-Author*) CEO and Owner, Garglet LLC; Stockholder, Enlitic Khaled M. Elsayes, MD, Ann Arbor, MI (*Abstract Co-Author*) Nothing to Disclose

#### For information about this presentation, contact:

### kmelsayes@mdanderson.org

### **TEACHING POINTS**

1. Demonstrate the anatomical details of the lesser sac and foramen of Winslow. 2. Demonstrate the role of lesser sac and foramen of Winslow in disease spread. 3. Discuss the spectrum of common and uncommon lesser sac disease processes. 4. Describe typical and atypical imaging features of these lesions with pathologic correlation 5. Illustrate a diagnosticapproach to help reach a specific diagnosis.

### **TABLE OF CONTENTS/OUTLINE**

1. Anatomical background. 2. Pathways of disease spread. 3. Pathological background: List the common and uncommon pathologies including: gastric lesions involving the lesser sac (e.g. perforated gastric ulcer, gastric carcinoma, gastric lymphoma and GIST), lesions involving the lesser sac (fluid accumulation, pancreatic inflammation & pseudocysts, neoplasms like GIST), foramen of Winslow. 3. Management: Current surgical and non-surgical management options of these pathological entities. 4. Differential diagnoses.and diagnostic approach. 5. Summary and conclusion.

### **Honored Educators**

Presenters or authors on this event have been recognized as RSNA Honored Educators for participating in multiple qualifying educational activities. Honored Educators are invested in furthering the profession of radiology by delivering high-quality educational content in their field of study. Learn how you can become an honored educator by visiting the website at: https://www.rsna.org/Honored-Educator-Award/ Khaled M. Elsayes, MD - 2014 Honored EducatorKhaled M. Elsayes, MD - 2017 Honored EducatorKhaled M. Elsayes, MD - 2018 Honored EducatorChristine O. Menias, MD - 2013 Honored EducatorChristine O. Menias, MD - 2014 Honored EducatorChristine O. Menias, MD - 2014 Honored EducatorChristine O. Menias, MD - 2014 Honored EducatorChristine O. Menias, MD - 2016 Honored EducatorChristine O. Menias, MD - 2017 Honored EducatorChristine O. Menias, MD - 2018 Honored EducatorChristine O. Menias, MD - 2018 Honored EducatorChristine O. Menias, MD - 2017 Honored EducatorChristine O. Menias, MD - 2017 Honored EducatorChristine O. Menias, MD - 2015 Honored EducatorAkram M. Shaaban, MBBCh - 2015 Honored EducatorAkram M. Shaaban, MBBCh - 2015 Honored EducatorAkram M. Shaaban, MBBCh - 2015 Honored EducatorKumaresan Sandrasegaran, MD - 2013 Honored EducatorKumaresan Sandrasegaran, MD - 2014 Honored EducatorKumaresan Sandrasegaran, MD - 2013 Honored EducatorKumaresan Sandrasegaran, MD - 2018 Honored EducatorKumaresan Sandrasegaran, M



## GI319-ED-THA12

## Dynamic Abdominal Examination with Dual-Energy CT with Reduced Volume of Contrast Material

Thursday, Nov. 29 12:15PM - 12:45PM Room: GI Community, Learning Center Station #12

#### **Participants**

Shunsuke Itaya, RT, Sapporo, Japan (*Presenter*) Nothing to Disclose Yoshino Hiroyuki, RT, Sapporo, Japan (*Abstract Co-Author*) Nothing to Disclose Kamiyama Tetsuya, RT, Sapporo, Japan (*Abstract Co-Author*) Nothing to Disclose Yoshihisa Kodama, MD, Sapporo, Japan (*Abstract Co-Author*) Nothing to Disclose Yasuo Sakurai, MD, Sapporo, Japan (*Abstract Co-Author*) Nothing to Disclose

## For information about this presentation, contact:

k\_itaya\_singibu@yahoo.co.jp

### **TEACHING POINTS**

Dual-energy CT(DECT) has been applied clinically. DECT can generate monochromatic images at different energy level using a spectral data set. Low energy monochromatic images can provide the high CT attenuation change with small amount of contrast agent. Theoretically it is possible to reduce the volume of contrast agent with preserving image quality. Volume reduction of contrast agent is beneficial especially for patients with impaired renal function. To equalize the flow of contrast agent compared with conventional CM injection (600mgI/kg), mixture of contrast agent (300mgI/kg) and the same volume of saline was used as contrast agent for reduced CM protocol. This exhibit illustrates dynamic abdominal examinations performed with reduced volume of contrast agent using monochromatic imaging and contrast/saline mixture injection.

## TABLE OF CONTENTS/OUTLINE

1.To show the reduced CM protocol with DECT scan. 2.To show the injection protocol.To equalize the flow of contrast agent compared with conventional CM injection (600mgI/kg), mixture of contrast agent (300mgI/kg) and the same volume of saline was used as contrast agent for reduced CM protocol. 3.To show the quality of DECT for the reduced CM protocol. For viewing the images of reduced CM protocol, small hepatocellular carcinoma can be diagnosed by expertized radiologist. 4.To show the workflow of optimization.



## GI320-ED-THA9

## MR Imaging of Perianal Fistulas: Step by Step

Thursday, Nov. 29 12:15PM - 12:45PM Room: GI Community, Learning Center Station #9

#### Participants

Chris N. Hanna, MBBCh, MSc, Cairo, Egypt (*Presenter*) Nothing to Disclose Ahmed A. Okba, MBBCh, Cairo, Egypt (*Abstract Co-Author*) Nothing to Disclose

#### For information about this presentation, contact:

chris.nabil.hanna@gmail.com

#### **TEACHING POINTS**

Becoming familiar with the normal anatomy of the perianal region Describe the suitable MRI sequences for anatomy and pathology delineation Understanding the Classification of perianal fistulae. Differentiating the types of Fistulas Gaining knowledge of the reporting key points.

## TABLE OF CONTENTS/OUTLINE

Normal anatomy of the perianal region on MRI MRI Protocol and imaging technique MRI appearance of perianal Fistulas and their complications Classification of perianal Fistulas



## GI321-ED-THA10

Endoscopic Necrosectomy in the Management of Necrotizing Pancreatitis: What the Radiologist Needs to Know

Thursday, Nov. 29 12:15PM - 12:45PM Room: GI Community, Learning Center Station #10

### Awards Certificate of Merit

### Participants

Harit Kapoor, MD, Lexington, KY (*Presenter*) Nothing to Disclose Mohamed Issa, MD, Lexington, KY (*Abstract Co-Author*) Nothing to Disclose Michael A. Winkler, MD, Lexington, KY (*Abstract Co-Author*) Nothing to Disclose Rashmi T. Nair, MD, Lexington, KY (*Abstract Co-Author*) Nothing to Disclose Adrian A. Dawkins, MD, Lexington, KY (*Abstract Co-Author*) Nothing to Disclose James T. Lee, MD, Lexington, KY (*Abstract Co-Author*) Nothing to Disclose Joseph W. Owen, MD, Lexington, KY (*Abstract Co-Author*) Nothing to Disclose Andres R. Ayoob, MD, Lexington, KY (*Abstract Co-Author*) Nothing to Disclose Frandah Wesam, MD, Lexington, KY (*Abstract Co-Author*) Nothing to Disclose Halemane S. Ganesh, MD, lexington, KY (*Abstract Co-Author*) Nothing to Disclose

For information about this presentation, contact:

haritkapoor@uky.edu

## **TEACHING POINTS**

1)Improved patient outcomes can be achieved with newer endoscopic procedures for necrotizing pancreatitis; however, these procedures can be technically challenging with risks of higher complications. 2)Accurate pre-procedural diagnosis following the updated Atlanta criteria, prudent use of multi-gateway and multi-modality drainage techniques and systemized protocol for imaging follow-up are key to optimal management of these patients. 3)Prior knowledge of the various techniques, routes of access and associated perioperative challenges and complications can help the interpreting radiologist greatly assist the endoscopist.

## TABLE OF CONTENTS/OUTLINE

1)Mature Pancreatic Collections: Pseudocysts versus Walled off necrosis - Imaging features, pathophysiology and management with multimodality examples and mimics. 2)Pancreatic Duct disruption and its significance - Types with examples. 3)Endoscopic approach to necrotizing pancreatitis - Indications, timing, routes of access and follow-up. 4)Technique for Endoscopic US guided pancreatic cyst drainage and necrosectomy - Description accompanied by endoscopic, endosonographic and fluoroscopic images with expected post procedure appearance. 5)Technical challenges and complications. 6)Important components of a structured preprocedural radiology report.



## GI322-ED-THA11

### Hereditary and Sporadic Pancreatic Adenocarcinoma: 2018 Genetics and Imaging Update

Thursday, Nov. 29 12:15PM - 12:45PM Room: GI Community, Learning Center Station #11

### Awards Certificate of Merit

#### Participants

Ajaykumar C. Morani, MD, Houston, TX (*Presenter*) Nothing to Disclose Sireesha Yedururi, MBBS, Sugarland, TX (*Abstract Co-Author*) Nothing to Disclose Venkata S. Katabathina, MD, San Antonio, TX (*Abstract Co-Author*) Nothing to Disclose Leonardo P. Marcal, MD, Houston, TX (*Abstract Co-Author*) Nothing to Disclose Roarke Prince, San Antonio, TX (*Abstract Co-Author*) Nothing to Disclose Anil K. Dasyam, MD, Pittsburgh, PA (*Abstract Co-Author*) Nothing to Disclose Srinivasa R. Prasad, MD, Houston, TX (*Abstract Co-Author*) Nothing to Disclose

## **TEACHING POINTS**

1. Pancreatic adenocarcinoma (PDAC), the most lethal pancreatic malignancy, arises from PanINs, mucinous tumors and IPMNs. 2. There is a wide spectrum of hereditary syndromes that predispose to PDAC. Lynch syndrome patients develop the rare 'medullary' variant of PDAC. IPMNs occur in patients with McCune-Albright syndrome. 3. Although 4 key driver gene abnormalities (KRAS, p16, TP53, & SMAD4) characterize PDACs, specific genetic changes lead to characteristic subtypes of PDACs and their precursors. Adenosquamous variant shows UPF1 mutations and colloid carcinomas display GNAS mutations. 4. Knowledge of the tumor genetics and tumor pathways may lead to molecular diagnostics and targeted therapeutics. Patients with BRCA mutations respond exquisitely to PARP inhibitors.

#### **TABLE OF CONTENTS/OUTLINE**

1. Introduction / Background 2. PDAC carcinogenesis model: tumor genetics and oncological pathways 3. Hereditary syndromes associated with PDAC 4. Precursors of PDAC with imaging illustrations and radiologic-pathologic correlation 5. Natural history and molecular events of the disease affecting management 6. Implications of tumor genetics on treatment and prognosis 7. Screening PDAC 8. Conclusion

### **Honored Educators**

Presenters or authors on this event have been recognized as RSNA Honored Educators for participating in multiple qualifying educational activities. Honored Educators are invested in furthering the profession of radiology by delivering high-quality educational content in their field of study. Learn how you can become an honored educator by visiting the website at: https://www.rsna.org/Honored-Educator-Award/ Venkata S. Katabathina, MD - 2012 Honored EducatorVenkata S. Katabathina, MD - 2017 Honored EducatorSrinivasa R. Prasad, MD - 2012 Honored EducatorSrinivasa R. Prasad, MD - 2017 


## GI382-SD-THA1

Cut-Off Value in Alcoholic Liver Disease is Higher Than That in Chronic Hepatitis C When Using Liver Stiffness for Diagnosing Portal Hypertension: A Meta-Analysis

Thursday, Nov. 29 12:15PM - 12:45PM Room: GI Community, Learning Center Station #1

FDA Discussions may include off-label uses.

## Participants

Jinzhen Song, Chengdu, China (Presenter) Nothing to Disclose

## PURPOSE

The aim is to perform a systematic review and meta-analysis to evaluate diagnostic accuracy of transient elastography based liver stiffness for diagnosing portal hypertension in alcoholic liver disease (ALD) and chronic hepatitis C (CHC).

#### **METHOD AND MATERIALS**

We performed a search on Medline, SCI, Embase and Cochrane Library for published articles until January 2018. Key words used in the search included 'liver', 'elastography,' and 'portal hypertension.' Clinically significant portal hypertension (CSPH) is defined when hepatic venous pressure gradient (HVPG) is over 10 mm Hg. Articles were included in our meta-analysis if they had the following features: (1) inclusion of patients with CHC or ALD; (2) measurement of LS by TE; (3) use of HVPG as a reference standard for diagnosing CSPH. We attempted to obtain individual patient's HVPG value and LS value by extracting data from the figure or sending e-mail to authors. Once the individual data was obtained, ROC curve was performed to obtain optimal cut-off value. The bivariate model was performed to estimate pooled sensitivity, specificity, positive likelihood ratio (LR+) and negative likelihood ratio (LR-).

## RESULTS

Thirteen studies assessing 1249 patients (806 for CHC and 443 for ALD) were included. The prevelance of CSPH in CHC and ALD was 0.51 and 0.7, respectively. The overall optimal cut-off value was 18 kPa and overall summary sensitivity, specificity, LR+ and LR- was 0.90 (95% confidence interval (CI) 0.86- 0.94), 0.77 (0.69- 0.85), 4.1 (3.3- 4.9) and 0.14 (0.09- 0.25), respectively. For diagnosing CHC, the optimal cut-off value was 15 kPa and summary sensitivity, specificity, LR+, LR- and AUROC was 0.94 (0.91- 0.97), 0.74 (0.62-0.86), 2.4(95% CI 1.6-3.7) 0.07 (0.04-0.13) and 0.94 (0.91- 0.97) respectively. For diagnosing ALD, the optimal cut-off value was 22 kPa and summary sensitivity, specificity, LR+ and LR- was 0.89 (0.83- 0.93), 0.71 (0.64-0.78), 3.1 (2.4-4.1) 0.15 (0.10- 0.24) and 0.77 (0.73 - 0.81), respectively. AUROC in CHC was obviously higher than that in ALD.

#### CONCLUSION

TE based LS showed good sensitivity to rule out CSPH in patients with ALD or CHC. The optimal cut-off value for ALD and CHC was 15 kPa and 21.8 kPa, respectively.

## **CLINICAL RELEVANCE/APPLICATION**

TE based LS showed better accuracy for diagnosing CSPH in CHC than in ALD and the optimal cut off value for ALD was higher than that for CHC.



## GI383-SD-THA2

Comparison of Novel Wireless Ultrasound Transducers to Existing Diagnostic Ultrasound Machines Using the ATS Model 539 Multipurpose Phantom

Thursday, Nov. 29 12:15PM - 12:45PM Room: GI Community, Learning Center Station #2

# Awards

## **Student Travel Stipend Award**

#### Participants

Mohan Narayanan, MD, Memphis, TN (*Presenter*) Equipment support, Clarius Mobile Health Corp Thaddeus A. Wilson, PhD, Madison, WI (*Abstract Co-Author*) Nothing to Disclose Sridhar S. Shankar, MD, MBA, Memphis, TN (*Abstract Co-Author*) Equipment support, Clarius Mobile Health Corp

#### For information about this presentation, contact:

mnaraya4@uthsc.edu

### PURPOSE

To evaluate a new, first in-kind portable wireless ultrasound transducer and compare the quality of images, and usability to existing technologies that are widely used in our department of radiology.

#### **METHOD AND MATERIALS**

An iPad Air 2 (Apple Inc.) was used as a wireless display in conjunction with the Clarius C3, and C7 transducers (Clarius Mobile Health). SonoSite X-Porte C2-5 (FUJIFILM SonoSite, Inc.) was used for comparison, as well as Toshiba Aplio MX (Canon Medical Systems USA, Inc.). These transducers were tested using the ATS Model 539 Multipurpose phantom (ATS Laboratories, Inc.) Axial-Lateral (AL) resolution was tested using the ATS AL Array. Vertical Group was tested for transducer maximum depth. Anechoic structures (AS) were evaluated in the ATS AS Array. Gray Scale structures were demonstrated for contrast resolution relative to background material and dynamic range (DR).

## RESULTS

Clarius C3 lost resolution of small AS at 6 cm, DR between 6-10 cm, and -3 to +3 dB at all depths. Clarius C7 was unable to resolve vertical group past 13 cm, small AS at 5 cm, and +3 dB DR. +15 dB DR produced posterior shadowing. SonoSite lost resolution of medium and small AS at 6 cm. Toshiba lost resolution of small AS at 7 cm, DR between 6-8 cm, and -3 to +3 dB at all depths. All transducers resolved AL array. All images were compared and analyzed by 2 attending radiologists. Toshiba and SonoSite had best AL resolution. SonoSite displayed the best DR. In order of overall best to worst image quality, transducers: Toshiba, SonoSite, Clarius C3, and Clarius C7.

### CONCLUSION

Toshiba produced the best overall image quality. All devices were limited in small AS resolution. All transducers resolved the AL array. Sonosite had the best overall DR. Clarius C7 was unable to resolve the vertical group past 13 cm. Clarius devices were limited by battery life, heat, ergonomics, inability to adjust TGC, and wireless signal integrity. The SonoSite and Toshiba transducers were limited by wired tethering and dependence on proprietary machinery.

#### **CLINICAL RELEVANCE/APPLICATION**

Wireless transducers will be able to simplify and lighten the load of the sonographer when doing portable examinations in the ICU, Emergency Room, and procedural ultrasound, as well as in department diagnostic ultrasound examinations. Wireless transducers allow use of low cost interactive displays in lieu of larger, more costly machines. At this time, the image quality is still limited.



## GI384-SD-THA4

Tumor Stiffness Measurement Using MR Elastography for Single Nodular HCC: Risk of Tumor Recurrence After Loco-Regional Treatment

Thursday, Nov. 29 12:15PM - 12:45PM Room: GI Community, Learning Center Station #4

FDA Discussions may include off-label uses.

#### **Participants**

Sae Jin Park, MD, Seoul, Korea, Republic Of (*Presenter*) Nothing to Disclose Jeong Min Lee, MD, Seoul, Korea, Republic Of (*Abstract Co-Author*) Grant, Bayer AG Grant, General Electric Company Grant, Koninklijke Philips NV Grant, STARmed Co, Ltd Grant, RF Medical Co, Ltd Grant, Samsung Electronics Co, Ltd Grant, Guerbet SA

#### PURPOSE

To investigate the factors associated with stiffness of HCC through pathologic analysis and to determine whether stiffness values measured with MR elastography are associated with overall survival or recurrence-free survival of the patients with HCC after curative locoregional treatments

### **METHOD AND MATERIALS**

Total 167 patients undergoing MR elastography (MRE) between July 2011 and February 2014 were enrolled retrospectively. Kaplan-Meier methods were used for overall survival and recurrence-free survival and Cox proportional hazard regression model was used to find out significant predictive factors

#### RESULTS

The 1-, 3- and 5- year overall survival rates for the radiofrequency ablation (RFA) and the hepatic resection (HR) group were 100%, 98.6%, 98.6% and 97.8%, 95.4% and 94.2%, respectively. The corresponding recurrence-free survival rates for the 2 groups were 72.3%, 44.8%, 37.9% and 71%, 63.1%, 58.5%, respectively. Tumor stiffness (TS) value was significantly correlated with the % of necrosis on histopathologic examination (p-value; 0.0396) and mean TS value of PD-HCC was significantly lower than that of WD- or MD-HCC (p-value < 0.001). For overall survival, the liver parenchyma stiffness was only significant prognostic factor in HR group. For recurrence-free survival, tumor stiffness showed significant affecting factor in both groups (p-value; 0.0066 in RFA group, 0.0071 in HR group).

## CONCLUSION

TS value measured by MRE was correlated with the % of necrosis on histopathologic examination and tumor grade and was significant predictive factor for recurrence-free survival in both RFA and HR groups for single nodular HCC.

#### **CLINICAL RELEVANCE/APPLICATION**

Tumor stiffness measured by MR elastography was significant prognostic factor for recurrence-free survival of the patients with single nodular HCC after curative locoregional treatments.



## GI385-SD-THA5

CT Evaluation of Response in Advanced Gastroenteropancreatic Neuroendocrine Tumors Treated with Long-Acting-Repeatable Octreotide: What is the Optimal Size Variation Threshold?

Thursday, Nov. 29 12:15PM - 12:45PM Room: GI Community, Learning Center Station #5

## Participants

Xuehua Li II, Guangzhou, China (*Abstract Co-Author*) Nothing to Disclose Yanji Luo, Guangzhou, China (*Presenter*) Nothing to Disclose Shiting Feng, MD, Guangzhou, China (*Abstract Co-Author*) Nothing to Disclose Zi-Ping Li, Guangzhou, China (*Abstract Co-Author*) Nothing to Disclose Jie Chen, Guangzhou, China (*Abstract Co-Author*) Nothing to Disclose

## For information about this presentation, contact:

luoyanji163@163.com

## PURPOSE

To identify a reliable early indicator of deriving progression-free survival (PFS) benefit in patients with advanced gastroenteropancreatic neuroendocrine tumors (GEP-NETs) treated with octreotide Long-acting-repeatable (LAR).

## METHOD AND MATERIALS

We investigated the images of 50 patients with well-differentiated advanced GEP-NETs treated with LAR octreotide and underwent baseline and follow-up thoracic, abdominal and pelvic computed tomography. Thresholds between -30% and +20% were defined as the best change in the sum of longest diameters ( $\Delta$ SLD) of the target lesions. Receiver operating characteristic (ROC) analysis and Kaplan-Meier method were used to identify the optimal threshold to distinguish between those with and without significant improvement of PFS.

## RESULTS

The optimal threshold for determining a response to octreotide LAR was -10%  $\Delta$ SLD, according to which 19 patients were responders and 31 were non-responders. At this threshold, median PFS was 20.2 and 7.6 months in responders and non-responders (hazard ratio, 2.66; 95% confidence interval, 1.32-5.36), with a sensitivity and specificity of 85.7% and 80%, respectively.

## CONCLUSION

Rather than 30%, a 10% shrinkage in tumor size is a more reliable early predictor of response to octreotide LAR in advanced GEP-NETs.

## **CLINICAL RELEVANCE/APPLICATION**

To determine an optimal threshold to distinguish responders from non-responders at early post-treatment imaging follow-up in WDGEP-NETs patients treated with octreotide LAR.



## GI386-SD-THA6

Diagnostic Value of Multiparameter Dual-Energy CT in Regional Lymphatic Metastasis of Gastric Cancer

Thursday, Nov. 29 12:15PM - 12:45PM Room: GI Community, Learning Center Station #6

#### **Participants**

Ling Yang, Kunming, China (*Presenter*) Nothing to Disclose Yang Yaying I, MD, Kunming, China (*Abstract Co-Author*) Nothing to Disclose Zhao Wei, MD, Kunming, China (*Abstract Co-Author*) Nothing to Disclose Jiao Qu, Kunming, China (*Abstract Co-Author*) Nothing to Disclose Xin Yuan, Kunming, China (*Abstract Co-Author*) Nothing to Disclose

## For information about this presentation, contact:

1443832806@qq.com

### PURPOSE

To evaluate the value of dual-energy CT iodine concentration and overlay combining with conventional morphological measurements in metastatic lymph nodes of gastric cancer.

## METHOD AND MATERIALS

A total of 141 regional lymph nodes were collected from 40 gastric cancer patients who underwent dual-energy CT scan and confirmed by surgery and pathology. The short diameter, length, and CT value, iodine concentration, and overlay value of each lymph node were measured, and the short length ratio and enhanced CT value at the arterial phase were calculated. Independent sample t-test was used to compare the short diameter, short length ratio, CT enhancement values, iodine concentration and overlay values between the two groups. The ROC analysis was used with statistically significant parameters and diagnostic efficacy was calculated with each individual parameter and joint parameters.

## RESULTS

Of the 141 regional lymph nodes, 73 were metastatic lymph nodes and 68 were non-metastatic lymph nodes. The iodine concentration, overlay value, short diameter and enhanced CT values of the metastatic lymph node at the arterial phase were  $(1.64\pm0.68)$  mg/ml,  $(29.06\pm11.42)$  HU,  $(7.35\pm3.38)$  mm,  $(26.34\pm14.98)$  HU, respectively; while the corresponding values of the non-metastatic lymph nodes were  $(2.51\pm0.68)$  mg/ml,  $(38.90\pm14.61)$  HU,  $(5.32\pm1.34)$  mm,  $(33.57\pm15.91)$  HU, and the difference was statistically significant (all P<0.05). There was no significant difference in short length ratio (P>0.05). The AUC of the diagnosing lymph node metastasis was 0.708, 0.650, 0.808, 0.695 for short diameter, CT enhancement, iodine concentration, and overlay value at the arterial phase, respectively. Four indicators combining to diagnose lymph node metastasis, the series sensitivity and specificity were 21.9% and 98.5%, and the parallel was 100.0% and 80.9%.

#### CONCLUSION

Multiparameter dual-energy CT combining with conventional morphological measurements can improve the diagnostic efficiency of lymph nodes in gastric cancer and has a role in the differential diagnosis of regional lymph nodes in patients with gastric cancer.

## **CLINICAL RELEVANCE/APPLICATION**

It has a role in the differential diagnosis of preoperative regional lymph nodes in patients with gastric cancer.



## GI387-SD-THA7

## Free Breathing Abdominal MRI: Preliminary Experience with In-Table Respiratory Gating

Thursday, Nov. 29 12:15PM - 12:45PM Room: GI Community, Learning Center Station #7

#### Awards Student Travel Stipend Award

#### **Participants**

Daniel R. Ludwig, MD, St Louis, MO (*Presenter*) Nothing to Disclose Uday Krishnamurthy, PhD, St Louis, MO (*Abstract Co-Author*) Employee, Siemens AG Pamela K. Woodard, MD, Saint Louis, MO (*Abstract Co-Author*) Research agreement, Siemens AG; Research, Eli Lilly and Company; Research, F. Hoffmann-La Roche Ltd; ; ; ; ; ; Glenn Foster, RT, St. Louis, MO (*Abstract Co-Author*) Nothing to Disclose Scott Love, RT, St Louis, MO (*Abstract Co-Author*) Nothing to Disclose Hongyu An, DSc, St. Louis, MO (*Abstract Co-Author*) Research Grant, Siemens AG

## For information about this presentation, contact:

ludwigd@wustl.edu

## PURPOSE

In abdominal and cardiac imaging, respiratory motion creates artifacts that can render images non-diagnostic, as a significant proportion of patients are either unable to hold their breath or are not compliant with breath holding instructions. One approach to mitigate this artifact is to perform triggering using respiratory bellows. However, bellows does not reliably detect all patterns of respiration, and requires additional equipment and setup time. Newly developed low energy radiofrequency (RF) sensors, which can be embedded within the patient table, provide a robust platform for respiratory triggering and may obviate the aforementioned issues. The aim of this study was to compare the severity of motion artifacts acquired using: (a) bellows (b) in-table sensor based triggering.

### **METHOD AND MATERIALS**

Five healthy volunteers were prospectively scanned on a Siemens Vida scanner (3T) in compliance with institutional requirements. A T2W TSE with fat saturation (TE 97ms; FA 1500; TR dependent on gating) was used to scan the abdomen for: (a) bellows (b) intable triggering. The data was evaluated for conspicuity of respiratory artifacts on a 5-point scale (1 - none; 2 - mild; 3 - moderate; 4 - severe; 5 - non-diagnostic) by two raters, at three different locations (pancreas, spleen and common bile duct), and were considered as independent data points.

## RESULTS

All data were scored as diagnostic (score: 1-4; median of 2 for both readers). Four data points acquired using the in-table sensor were scored as having no artifact (score 1) by either rater, versus one for the respiratory bellows. Conversely, two data points acquired using the in-table sensor were scored as having severe artifact (score 4) by either rater, versus three for the respiratory bellows.

## CONCLUSION

This preliminary study indicates that the new in-table sensor provides comparable diagnostic quality and decreased artifact severity relative to the use of bellows. The in-table sensor has the added advantage of no additional patient preparation or setup time, and may improve patient comfort and imaging workflow.

#### **CLINICAL RELEVANCE/APPLICATION**

Artifacts from respiratory motion compromise the diagnostic utility of MRI. RF-based in-table sensors allows for monitoring and triggering of scans without the need for external setup.



## GI388-SD-THA8

## Individualized Body Weight Adapted Contrast Media Protocols in CT Imaging of the Liver at 90 kV

Thursday, Nov. 29 12:15PM - 12:45PM Room: GI Community, Learning Center Station #8

# Awards

## Student Travel Stipend Award

#### Participants

Bibi Martens, MD, Maastricht, Netherlands (*Presenter*) Nothing to Disclose Nienke Eijsvoogel, MD, Maastricht, Netherlands (*Abstract Co-Author*) Nothing to Disclose Babs Hendriks, MD, Maastricht, Netherlands (*Abstract Co-Author*) Nothing to Disclose Casper Mihl, MD,PhD, Maastricht, Netherlands (*Abstract Co-Author*) Speaker, Bayer AG Joachim E. Wildberger, MD, PhD, Maastricht, Netherlands (*Abstract Co-Author*) Institutional Grant, Agfa-Gevaert Group Institutional Grant, Bayer AG Institutional Grant, Koninklijke Philips NV Institutional Grant, Siemens AG Speakers Bureau, Bayer AG Speakers Bureau, Siemens AG

## For information about this presentation, contact:

bibi.martens@mumc.nl

## PURPOSE

Ideally, contrast media (CM) protocols should be tailored to the individual patient. Aim of this study was to evaluate liver attenuation and image quality (IQ) in a body weight adapted contrast media (CM) protocol in comparison to a fixed injection protocol. Included abdominal scans were performed in portal venous phase with a low tube voltage of 90 kV, the recent newest standard in our department.

## METHOD AND MATERIALS

215 consecutive patients referred for abdominal CT imaging in portal venous phase were prospectively scanned on a 3rd generation dual source CT scanner at 90kV. Group 1 (n=98) received a body weight adapted CM protocol. Group 2 (n=117) received a standard fixed CM bolus. Both protocols used Iopromide 300mgI/ml. Patients were divided into three weight categories; <65kg 66-80kg and >81kg. Objective image quality (IQ) was evaluated by measuring the attenuation in segment 2, 5 and 8 of the liver parenchyma in Hounsfield units (HU), signal-to-noise ratio (SNR) and contrast-to-noise ratio (CNR). Subjective IQ was assessed by using a 3-point Likert scale regarding overall IQ, image noise and the possibility to detect liver lesions. Statistical analysis was performed using SPSS (IBM, version 24.0).

#### RESULTS

No significant differences in baseline characteristics were found between groups. Group 1 received a mean CM volume of  $105.8\pm19.8$ ml at a flow rate of  $3.5\pm0.7$ ml/s and group 2 received 110ml at 3.5ml/s. Mean attenuation values in group 1 for each weight category were respectively  $131.1\pm12.4$ ,  $125.5\pm15.4$  and  $125.8\pm16.5$ HU, no significant difference was found between groups (P>0.42). For group 2, values were  $139.6\pm22.5$ ,  $130.1\pm26.7$  and  $120.7\pm14.6$ HU. A significant difference in attenuation was found in group 2 between the lowest and highest weight category (P<0.01). No significant differences were found regarding CNR and SNR between both groups. The subjective IQ was not significantly different between the two injection protocols.

### CONCLUSION

Individually tailored CM injection protocols yield a more homogeneous enhancement pattern of the liver parenchyma between different weight groups compared to a fixed injection protocol in patients scanned at 90kV.

#### **CLINICAL RELEVANCE/APPLICATION**

We propose an individualized CM injection protocol for the liver at 90kV leading to more homogenous liver attenuation, lower total injected CM volume and reduction in radiation dose.



## GU246-SD-THA1

Whole-Body Magnetic Resonance Imaging (WB-MRI) Reporting with METastasis Reporting and Data System for Prostate Cancer (MET-RADS-P): Inter-Observer Agreement Between Readers of Different Expertise Levels

Thursday, Nov. 29 12:15PM - 12:45PM Room: GU/UR Community, Learning Center Station #1

## Participants

Paola Pricolo, MD, Milano, Italy (*Presenter*) Nothing to Disclose Eleonora Ancona, Milan, Italy (*Abstract Co-Author*) Nothing to Disclose Jorge A. Abreu, MD, Bogota, Colombia (*Abstract Co-Author*) Nothing to Disclose Marco Martinetti, BSC, Pavia, Italy (*Abstract Co-Author*) Nothing to Disclose Paul E. Summers, Milan, Italy (*Abstract Co-Author*) Nothing to Disclose Massimo Bellomi, MD, Milano, Italy (*Abstract Co-Author*) Nothing to Disclose Anwar R. Padhani, MD, FRCR, Northwood, United Kingdom (*Abstract Co-Author*) Advisory Board, Siemens AG ; Speakers Bureau, Siemens AG ; Speakers Bureau, sanofi-aventis Group; Speakers Bureau, Johnson & Johnson Giuseppe Petralia, MD, Milan, Italy (*Abstract Co-Author*) Nothing to Disclose

### PURPOSE

To evaluate the inter-observer agreement of WB-MRI examinations reported using MET-RADS-P guidelines between readers of different expertise.

#### METHOD AND MATERIALS

Fifty consecutive WB-MRI examinations, performed from December 2016 to February 2018 on 31 advanced prostate cancer (APC) patients, were prospectively reported by a Senior Radiologist (SR, 9 years in WB-MRI) using MET-RADS-P guidelines, with response assessment categories (RAC) from 1 (highly likely to be responding) to 5 (highly likely to be progressing) assigned for each metastatic site in 14 body regions. A Resident Radiologist (RR) after a 6-months training reported the same WB-MRI examinations, blinded to the previous reports. Inter-observer agreements between the number of regions with metastatic findings, RACs at each region, and overall response was evaluated by weighted-Cohen's Kappa statistics (K). Inter-observer agreement was interpreted as none to slight (K:0.01-0.20), fair (K:0.21-0.40), moderate (K:0.41-0.60), substantial (K:0.61-0.80) or excellent (K:0.81-1.00).

#### RESULTS

The number of metastatic regions reported was comparable between readers: SR reported 237 metastatic findings [RAC 1 in 53 (22.4%), RAC 2 in 47 (19.9%), RAC 3 in 55 (23.2%), RAC 4 in 21 (8.9%) and RAC 5 in 61 (25.7%)], while RR reported 239 metastatic findings [(RAC 1 in 47 (19.7%), RAC 2 in 53 (22.2%), RAC 3 in 56 (23.4%), RAC 4 in 24 (10%) and RAC 5 in 59 (24.7%)]. The agreement between readers was excellent for the metastatic findings on cervical/thoracic/lumbo-sacral spine and pelvis (K:0.81-0.93), substantial for those on thorax (K:0.78) and nonregional lymph nodes (K:0.7), while moderate for those on regional lymph nodes (K:0.56). Inter-observer agreement was not assessable for non-metastatic findings on the remaining regions, due to the lack of findings in our cohort. An excellent overall response agreement between readers was calculated (K:0.81, 95% C.I. 0.76-0.86).

### CONCLUSION

The excellent inter-observer agreement between readers of different expertise levels suggests that MET-RADS-P assessments of WB-MRI diminishes variations in the interpretation and response assessments of both bone and soft-tissue disease of patient with APC.

## **CLINICAL RELEVANCE/APPLICATION**

MET-RADS-P for reporting WB-MRI of advanced prostate cancer enables consistency between readers of different expertise levels. This requires confirmation with multicentre studies.

#### **Honored Educators**

Presenters or authors on this event have been recognized as RSNA Honored Educators for participating in multiple qualifying educational activities. Honored Educators are invested in furthering the profession of radiology by delivering high-quality educational content in their field of study. Learn how you can become an honored educator by visiting the website at: https://www.rsna.org/Honored-Educator-Award/ Anwar R. Padhani, MD, FRCR - 2012 Honored Educator



## GU247-SD-THA2

Antero-Posterior Thigh Diameter: A Novel Ultrasonographic Method of Fetal Age Estimation Between 18 to 28 Weeks Gestation

Thursday, Nov. 29 12:15PM - 12:45PM Room: GU/UR Community, Learning Center Station #2

## Participants

Chetankumar M. Mehta, MBBS, MD, Vadodara, India (*Presenter*) Nothing to Disclose Ayaz J. Dabivala, MBBS, Vadodara, India (*Abstract Co-Author*) Nothing to Disclose Arpita D. Fernandez, MD, Vadodara, India (*Abstract Co-Author*) Nothing to Disclose

#### For information about this presentation, contact:

drchetan\_mehta@yahoo.com

## PURPOSE

Little published research exists in the area of fetal thigh biometry for evaluation of gestational age, specifically in the use of the antero-posteriorfetal thigh diameter (APTD). A continuing review of existing practices needs to be coupled with evaluation of alternate o radditional methodology. This study evaluated the usefulness and direct correlation of a simple, new method of predicting fetal ag eby measurement of the anterior-posterior thigh diameter (APTD) in a normal 18-to 28 weeks pregnancies using two-dimensional sonography.

#### **METHOD AND MATERIALS**

This was a quantitative prospective study of 300 patients in the out-patient department . Antero-posterior thigh diameters (APTD) were sonographically measured and the normal range for each week of pregnancy was determined three times for reliability using curvilinear low frequency (3 - 5 MHz) transducer.

### RESULTS

Significant correlation was found between APTD and fetal age from simple linear regression analysis, with >99.9% confidence intervals at each week from 18 to 28 weeks gestation. There was a correlation of 1mm APTD per 1week of fetal age. The standard error of estimation was low(0.0048) as compared to that of gestational age estimation using femur length(SEE=0.0274). Pearson's correlation coefficient for Fetal APTD was 0.9965 which is slightly better than that using femur length ( $r_2 = 0.9919$ ) and th eresidual scatter plots confirmed the APTD validity.

#### CONCLUSION

All the values of APTD for assessing fetal age lie directly on the 'best-fit' regression line. Linear measurementof multiple fetal parameters allows a more complete profile of fetal growth and estimated date of delivery. Since the coefficient of determination (Rsq) is very high, this model is very effective. Measurement of fetal APTD may help in quality control of second trimester ultrasound examinations and may be useful for estimating gestational age especially when other parameter are difficult to measure.

## **CLINICAL RELEVANCE/APPLICATION**

The APTD is very reliable marker for fetal age estimation when other parameters are difficult to measure for fetal age estimation.



## GU248-SD-THA3

Diffusion Kurtosis Imaging of Cervical Cancer at 3T: Impact of Ultra-High B-Value in Tumor Detection and Imaging Quality

Thursday, Nov. 29 12:15PM - 12:45PM Room: GU/UR Community, Learning Center Station #3

**FDA** Discussions may include off-label uses.

#### **Participants**

Yafei Qi I, MD, Beijing, China (*Presenter*) Nothing to Disclose Yonglan He, MD, Beijing, China (*Abstract Co-Author*) Nothing to Disclose Huadan Xue, MD, Beijing, China (*Abstract Co-Author*) Nothing to Disclose Zhengyu Jin, Beijing, China (*Abstract Co-Author*) Nothing to Disclose Xiaoqi Wang, Beijing, China (*Abstract Co-Author*) Nothing to Disclose Chengyu Lin, Beijing, China (*Abstract Co-Author*) Nothing to Disclose Yuan Li, Beijing, China (*Abstract Co-Author*) Nothing to Disclose Hailong Zhou, Beijing, China (*Abstract Co-Author*) Nothing to Disclose

#### For information about this presentation, contact:

qiyafei19910603@163.com

## PURPOSE

Ultra-high b value (b>=2000 mm/s2) diffusion image qualifies suffered from eddy currents and other system imperfections was not applied for clinical routine previously. With newly installed scanner claimed with better gradient performance, we evaluated diagnostic performance and imaging quality of b=2000 comparing to b=800 images of cervical cancer in diffusion kurtosis imaging (DKI).

## METHOD AND MATERIALS

15 patients diagnosed with cervical cancer (45.4 ±12.7years) were included. They underwent female pelvis MR on a 3T MR scanner (Philips, Netherlands) for diffusion imaging with b values at 0, 10, 50, 100, 200, 800, 1200 and 2000 with repletion of 2, 2, 2, 2, 4, 6, 8 at each b value to increase SNR. Images at b-value=800 and 2000 images were obtained for direct clinical evaluation. Two radiologists, blinded to clinical data and scan parameters evaluated the images for lesion detection and delineation, suppression of background, spatial distortion, image ghosting and whole imaging quality using 5-point scoring system. Evaluations were compared using a paired Wilcoxon test. Signal intensity of tumor tissue were measured at b-value=0, 800 and 2000 images.

#### RESULTS

With b=2000 images, the lesion was detected and delineated (mean score:  $4.67\pm0.49$ ) better than b=800 images (mean score:  $3.87\pm0.52$ ) (p =0.002, 0.003). The ultra-high b-value diffusion images provided more confirmation for lesion diagnoses. The background was significantly more suppressed (mean score:  $4.33\pm0.62$ ) in b=2000 images than b=800 images(mean score:  $3.40\pm0.51$ ) (all p < 0.001). No statistically differences between b=2000 and b=800 images in the spatial distortion, image ghosting and whole imaging quality was observed (all p > 0.05). Inter-observer agreement was excellent (all kappa>0.75). Signal intensity of tumor tissue in b=2000 DKI deviated from the single-exponential decay curve fitted by the three signal intensities and showed a diffusion kurtosis.

### CONCLUSION

Ultra-high b-value (2000mm/s2) DKI provided better diagnostic performance of cervical cancer, and showed equal imaging quality to normal-high b-value images. This confirms that diffusion kurtosis with ultra-high b-value in DKI of tumor tissue could provide convincing diagnosing performance.

#### **CLINICAL RELEVANCE/APPLICATION**

Ultra-high b-value in DKI showed a great feasibility and robustness in diagnosis of cervical cancer in female pelvis with update-todate scanners.



### GU249-SD-THA4

A Preliminary Study of Use of Intravoxel Incoherent Motion MR Imaging to Assess Placental Perfusion in Patients with Placental Adhesion Disorder on Their Third Trimester

Thursday, Nov. 29 12:15PM - 12:45PM Room: GU/UR Community, Learning Center Station #4

#### Participants

Tao Lu, Chengdu, China (Presenter) Nothing to Disclose

For information about this presentation, contact:

345248302@qq.com

#### PURPOSE

Our primary aim was to investigate if women with placenta accreta can be differentiated with women without using IVIM quantitative assessment of the placental perfusion. A second aim was to investigate if IVIM parameters could be used to differentiate placenta accreta from increta.

#### **METHOD AND MATERIALS**

Only single pregnancies with a living fetus had a gestation length between 28+0 and 41+6 weeks were included. Women with chronic hypertension, pre-existing renal disease, diabetes mellitus or severe claustrophobia were excluded. Data on pregnancy outcome were obtained from maternity records or the women's general practitioners. IVIM sequence with 8 different b-values (0, 50, 100, 150, 200, 250, 500, 800s/mm2) was obtained perpendicular to the placenta. 40 slices, each of 5.5mm thickness were collected. Acquisition time for this sequence was typically 8 minutes and 37 seconds.Evaluation of the perfusion fraction was performed with research software (MITK diffusion).

#### RESULTS

62 pregnant women with satisfied raw images remained in the analyses. The mean maternal age was 20.95±4.68 years (range 19-40 years), the mean gestational age at examination was 33.81±3.04 weeks (range 28-41 weeks).All medical records were received postpartum, 17 patients were clinically diagnosed as placenta accreta when the placenta attaches to the myometrium, 29 patients were diagnosed as placenta increta when the placenta penetrates into the myometrium and 16 patients were without placenta adhesion. The results demonstrated that f values among three groups had significant difference. Multiple comparisons showed f values in patients with placenta accreta and increta were significantly lower than in patients without placenta accreta, meanwhile f values in patients with placenta accreta were not significantly different from patients with placenta increta Difference from three groups in D and D\* values were not statistically significant

### CONCLUSION

We found a decrease in the placental perfusion fraction in patients with placenta accreta and increta compared to patients without placenta accreta.We also found the D values were slightly lower in patients with placenta accreta and increta than in patients without, but the difference was no statistically significant.

## **CLINICAL RELEVANCE/APPLICATION**

The perfusion fraction from IVIM can be used to quantitatively evaluate placenta perfusion in patients with placenta accreta.



## GU250-SD-THA5

Non-Contrast Assessment of Ablation Zone During Focal Laser Ablation of Prostate Cancer Using Multi-echo T2\*-weighted MRI

Thursday, Nov. 29 12:15PM - 12:45PM Room: GU/UR Community, Learning Center Station #5

## Participants

Chongpeng Sun, Chicago, IL (*Presenter*) Nothing to Disclose Shiyang Wang, PhD, Chicago, IL (*Abstract Co-Author*) Nothing to Disclose Aritrick Chatterjee, PhD, Chicago, IL (*Abstract Co-Author*) Nothing to Disclose Ambereen Yousuf, MBBS, Chicago, IL (*Abstract Co-Author*) Nothing to Disclose Gregory S. Karczmar, PhD, Chicago, IL (*Abstract Co-Author*) Nothing to Disclose Aytekin Oto, MD, Chicago, IL (*Abstract Co-Author*) Research Grant, Koninklijke Philips NV; Research Grant, Guerbet SA; Research Grant, Profound Medical Inc; Medical Advisory Board, Profound Medical Inc; Consultant, AbbVie Inc; ; Scott Eggener, Chicago, IL (*Abstract Co-Author*) Nothing to Disclose

#### For information about this presentation, contact:

sunchongpeng@gzhmu.edu.cn

#### PURPOSE

To evaluate multi-echo gradient echo  $T2^*$ -weighted ( $T2^*W$ ) MRI for the identification of acute ablation zone after focal laser ablation (FLA) of prostate cancer for active monitoring of ablation procedure.

#### **METHOD AND MATERIALS**

Fourteen patients with biopsy-confirmed localized prostate cancers were recruited in this study. FLA was performed on a 1.5 T MRI scanner. Axial T2\*W at echo time 3.4, 32 and 63ms, diffusion-weighted images (DWI) and T2-weighted (T2W)images were acquired after the last FLA procedure. Pre- and post-contrast enhanced(0.1 mmol/kg, Multihance, Bracco Diagnostic Inc. 20 minutes after ablation) T1-weighted (T1W) images with the e-Thrive sequence were acquired to assess the FLA sites (n=14) as reference standard. The ADC maps and subtracted T1W images were calculated from DWI and post-pre enhanced T1W images respectively. Ablation area was outlined manually on ablated slices with the maximal ablation area. The contrast to background ratio (CBR) between ablation site and the untreated half of normal prostate were calculated from T2\*W images and ADC maps, and compared with the CBR measured from subtracted T1W images. Kruskal-Wallis tests were performed to determine the significant difference in CBR between T2\*W, ADC maps, and subtracted T1W images. Bland-Altman analysis was performed to evaluate the agreement between CBR of T2\*W vs. subtracted post-contrast T1W.

#### RESULTS

The CBR in the ablation area using T2\*W at TE of 32ms ( $2.86\pm1.79$ ) and 63ms ( $2.66\pm1.27$ )were not significantly different(p=0.118, 0.098) from subtracted post enhanced T1W images( $3.32\pm1.00$ ). Whereas, CBR using T2\*W at TE of 3.4ms ( $1.68\pm1.21$ )and ADC maps( $0.93\pm0.59$ ) were significantly lower(P=0.002, 0.000008) than CBR of reference standard (T1W). Bland Altman plots show good agreement between CBR in ablation site on T2\*W (TE=32 and 63ms) vs. subtracted post-contrast T1W images.

## CONCLUSION

Multi-echo gradient echo T2\*WMRI provides a convenient method to identify and monitor ablation sites during FLA treatment of prostate cancers without contrast agent injection.

### **CLINICAL RELEVANCE/APPLICATION**

Multi-echo T2\*-weighted MRI can be used as a substitute for contrast enhanced T1W for monitoring ablation damage during focal laser ablation of prostate cancer, allowing repeated assessment following each ablation period.

### **Honored Educators**

Presenters or authors on this event have been recognized as RSNA Honored Educators for participating in multiple qualifying educational activities. Honored Educators are invested in furthering the profession of radiology by delivering high-quality educational content in their field of study. Learn how you can become an honored educator by visiting the website at: https://www.rsna.org/Honored-Educator-Award/ Aytekin Oto, MD - 2013 Honored EducatorAytekin Oto, MD - 2017 Honored Educator



## GU251-SD-THA6

Assessment of the Shear Wave Elastography in Transplant Kidney with Resistive Index Correlation: A Novel Way to Assess Early Transplant Failure

Thursday, Nov. 29 12:15PM - 12:45PM Room: GU/UR Community, Learning Center Station #6

# Awards

## Student Travel Stipend Award

#### Participants

Shramana Bagchi, MBBS, Kolkata, India (*Presenter*) Nothing to Disclose Abhinav Mathur, MBBS, Bangalore, India (*Abstract Co-Author*) Nothing to Disclose Aruna R. Patil, MD, FRCR, Bangalore, India (*Abstract Co-Author*) Nothing to Disclose Kapil K. Shirodkar, DMRD, MBBS, Mapusa, India (*Abstract Co-Author*) Nothing to Disclose Shrivalli Nandikoor, MBBS, Bangalore, India (*Abstract Co-Author*) Nothing to Disclose

## For information about this presentation, contact:

shramanabagchi@gmail.com

### PURPOSE

Severity of pathologic changes in transplant kidney can be performed using a quantitative analysis of the stiffness of renal parenchyma , using shear wave elastography (SWE) imaging. Renal cortical elastography has shown variable yet significant yield. Correlating the elevated SWE values with elevated resistive index(RI) assessment indicates the impaired function. Renal biopsy is associated with multiple risks and is user dependent. To overcome the fallacies of the above procedure , assessment of the status of the renal functioning using SWE can be taken into consideration.

## METHOD AND MATERIALS

Informed consents were obtained . Between march 2016 and march 2018, 30 patients with transplant kidney status ( post operative day 6 onwards) were taken and another 30 healthy subjects were enrolled. Combined conventional ultrasound and SWE imaging were performed on all participants. RI was assessed for the transplant kidney patients . The length, width, and cortical thickness and stiffness were recorded for the transplant kidney.

#### RESULTS

Cortical stiffness is greater in patients with transplant failure and they demonstrated a higher mean elastography values, than in healthy subjects .Elevated RI was also noted however not very consistent with the finding .Correlation between Elevated RI and increased cortical stiffness couldn't be properly established. Also noted was the elevated elastography values in patients with elevated serum creatinine level. Inverse correlation of the cortical stiffness was seen with the estimated glomerular filtration rate and with cortical thickness.

### CONCLUSION

In patients with post transplant status, shear wave elastography imaging, provides useful information regarding the evaluation of the morphological changes and the underling aetiologies of graft failure. The method is simple and practical and also is fast Simultaneous assessment of the RI values , helps correlation of the morphological and functional assessment of the functioning kidney.

## **CLINICAL RELEVANCE/APPLICATION**

Upcoming modality such as SWE provides a scope for non invasive way of post renal transplant assessment and detect early features of failure.being a fast technique, it also reduces patient attrition



## HP236-SD-THA1

Diagnostic Performance of PET/MRI for Liver Metastasis in Patients with Primary Malignancy: A Systematic Review and Meta-Analysis

Thursday, Nov. 29 12:15PM - 12:45PM Room: HP Community, Learning Center Station #1

## Participants

Seungbaek Hong, MD, Pusan, Korea, Republic Of (*Presenter*) Nothing to Disclose Sang Hyun Choi, Seoul, Korea, Republic Of (*Abstract Co-Author*) Nothing to Disclose Kyung Won Kim, MD, Seoul, Korea, Republic Of (*Abstract Co-Author*) Nothing to Disclose Seong Ho Park, MD, Seoul, Korea, Republic Of (*Abstract Co-Author*) Research Grant, DONGKOOK Pharmaceutical Co, Ltd; Research Grant, Central Medical Service Co, Ltd So Yeon Kim, MD, Seoul, Korea, Republic Of (*Abstract Co-Author*) Nothing to Disclose Sojung Lee, Seoul, Korea, Republic Of (*Abstract Co-Author*) Nothing to Disclose Seung Soo Lee, MD, Seoul, Korea, Republic Of (*Abstract Co-Author*) Nothing to Disclose Jae Ho Byun, MD, Seoul, Korea, Republic Of (*Abstract Co-Author*) Nothing to Disclose Moon-Gyu Lee, MD, Seoul, Korea, Republic Of (*Abstract Co-Author*) Nothing to Disclose

#### For information about this presentation, contact:

cinematiclife7@hanmail.net

#### PURPOSE

Combined positron emission tomography (PET)/magnetic resonance imaging (MRI) is considered a promising imaging method for the diagnosis of liver metastasis; however, the reported accuracies of PET/MRI are variable. Therefore, we aimed to systematically determine the diagnostic accuracy of PET/MRI and evaluate the sources of heterogeneity in the reported results.

## **METHOD AND MATERIALS**

PubMed and EMBASE databases were searched to identify original research studies reporting the diagnostic performance of PET/MRI for liver metastasis in patients with primary malignancy. Study quality was assessed using QUADAS-2. The summary sensitivity and specificity of studies reporting the diagnostic accuracy of PET/MRI for liver metastasis were estimated using hierarchical modeling methods. To determine causes of study heterogeneity, the presence of a threshold effect was analyzed, and meta-regression analysis was performed.

### RESULTS

Of the 546 articles screened, 8 suitable articles were identified, with these including 4 studies reporting the diagnostic accuracy of PET/MRI on a per-patient basis, and 7 studies reporting on a per-lesion basis. The meta-analytic summary sensitivity and specificity for per-patient-based analysis were 99.2% (95%CI, 31.4-100.0%, I2=89.4%) and 98.6% (95% CI, 84.0-99.9%, I2=0.0%), respectively, while for per-lesion-based analysis they were 95.4% (95% CI, 78.3-99.2%, I2=99.7%) and 99.4% (95% CI, 92.5-100.0%, I2=98.0%), respectively. Meta-regression analysis showed five significant factors affecting study heterogeneity, which included the study subject characteristics, study design, MR imaging technique (diffusion or hepatobiliary phase image), imaging review method, and type of reference standard.

#### CONCLUSION

The diagnostic accuracy of PET/MRI for diagnosing liver metastasis was high overall, but substantial heterogeneity was noted. Further studies on the standardization of imaging acquisition and analysis techniques are required.

## **CLINICAL RELEVANCE/APPLICATION**

The overall diagnostic accuracy of PET/MRI for the diagnosis of liver metastasis was high, but further studies would be needed for the standardization of PET/MRI.



## HP237-SD-THA2

Acute Adverse Events Following Gadolinium-Based Contrast Agent Administration: A Single-Center Retrospective Study of 281,945 Injections

Thursday, Nov. 29 12:15PM - 12:45PM Room: HP Community, Learning Center Station #2

## Participants

Jennifer S. Mcdonald, PhD, Rochester, MN (*Presenter*) Research Grant, General Electric Company; Scientific Advisor, General Electric Company

Christopher H. Hunt, MD, Rochester, MN (Abstract Co-Author) Nothing to Disclose

Amy B. Kolbe, MD, Rochester, MN (Abstract Co-Author) Nothing to Disclose

John J. Schmitz, MD, Rochester, MN (Abstract Co-Author) Nothing to Disclose

Robert P. Hartman, MD, Byron, MN (Abstract Co-Author) Nothing to Disclose

David F. Kallmes, MD, Rochester, MN (*Abstract Co-Author*) Research support, Terumo Corporation; Research support, Medtronic plc; Research support, Sequent Medical, Inc; Research support, Benvenue Medical, Inc; Research support, General Electric Company; Consultant, General Electric Company; Consultant, Medtronic plc; Consultant, Johnson & Johnson

Robert J. McDonald, MD, PhD, Rochester, MN (*Abstract Co-Author*) Consultant, General Electric Company; Research Grant, General Electric Company; Consultant, Bracco Group

#### For information about this presentation, contact:

mcdonald.jennifer@mayo.edu

### PURPOSE

To examine and compare rates of acute allergic-like and physiologic reactions between four gadolinium-based contrast agents (GBCAs), including gadodiamide, gadobutrol, gadobenate dimeglumine, and gadoterate meglumine.

## METHOD AND MATERIALS

All intravenous GBCA injections for magnetic resonance (MR) exams performed at a single institution from June 1, 2009 - May 9, 2017 were identified. Reaction events were identified by reviewing MR technologist and nursing staff notes, radiologist reports, and subsequent emergency department and provider notes. Reactions were classified into allergic-like or physiologic types and into mild, moderate, and severe categories using American College of Radiology criteria.

### RESULTS

A total of 281,945 GBCA injections (140,645 gadodiamide, 94,109 gadobutrol, 39,138 gadobenate dimeglumine, and 8,053 gadoterate meglumine) were included in the study. Allergic-like reactions occurred at an overall rate of 0.16% (n=440), with significantly higher rates observed with gadobenate dimeglumine (0.33%, n=129) and gadobutrol (0.20%, n=185) compared to gadodiamide (0.09%, n=122) and gadoterate meglumine (0.05%, n=4). Physiologic reactions occurred at an overall rate of 0.13% (n=376), with significantly higher rates observed with gadobenate dimeglumine (0.18%, n=71) and gadobutrol (0.16%, n=155) compared to gadodiamide (0.10%, n=144) and gadoterate meglumine (0.07%, n=6). Six severe allergic-like reactions (3 gadobutrol, 3 gadobenate dimeglumine) occurred requiring hospitalization. Patient age, sex, and location, and MR type were significantly associated with acute reaction rates.

## CONCLUSION

Gadobenate dimeglumine and gadobutrol were associated with significantly higher rates of allergic-like and physiologic reactions compared to gadodiamide and gadoterate meglumine. Patient sex, age, location, and MR type were significantly correlated with acute reaction rates.

## **CLINICAL RELEVANCE/APPLICATION**

Acute adverse reactions to gadolinium-based contrast agents (GBCA) are uncommon and are associated with the specific GBCA, with higher reaction rates observed with gadobenate dimeglumine and gadobutrol compared to gadodiamide and gadoterate meglumine.



## HP238-SD-THA3

## Analysis of Emergency Department Facility Usage by Young Adult Population

Thursday, Nov. 29 12:15PM - 12:45PM Room: HP Community, Learning Center Station #3

### Participants

Shelly Soffer, Tel Aviv, Israel (*Presenter*) Nothing to Disclose Eyal Zimlichman, Ramat Gan, Israel (*Abstract Co-Author*) Nothing to Disclose Orly Ohana, Tel Aviv, Israel (*Abstract Co-Author*) Nothing to Disclose Yiftach Barash, Ramat Gan, Israel (*Abstract Co-Author*) Nothing to Disclose Eli Konen, MD, Ramat Gan, Israel (*Abstract Co-Author*) Nothing to Disclose Eyal Klang, MD, Ramat Gan, Israel (*Abstract Co-Author*) Nothing to Disclose

#### PURPOSE

The world population is increasing, burdening health care systems, including emergency department (ED) facilities. CT is one of the most frequently used imaging modalities in the ED, and unlike ultrasound, is not available as a point of care diagnostic. Of particular interest is the young adult population (aged 18 - 40). This population is generally healthy and perhaps be better diagnosed and treated in an outpatient setting. The purpose of this study was to examine ED facility usage by young adult population.

## METHOD AND MATERIALS

Institutional review board (IRB) approval was granted for this study and informed consent was waived by the IRB committee. All one tertiary hospital's adults (>=18) ED visits were retrospectively collected during a time frame of one year (1/2015 - 12/2015). Data was retrieved from the hospital's computerized records and included patients' demographics and the following parameters: documentation of CT usage, triage emergency severity index (ESI), ED length of stay (LOS), hospitalization rate and in-hospital mortality rate. Correlations between patients' age and the means per year for each retrieved parameter were calculated. Analysis of the parameters in the young adults group (aged 18 - 40) was performed.

### RESULTS

During the one year study, 119,114 patients presented to the ED, of which 37,298/119,114 (31.3%) were young adults (aged 18-40). There was a significant linear correlation with age for all the investigated parameters (CT usage r=0.942, ESI r=-0.978, LOS r=0.889, hospitalization rate r=0.988 and in hospital mortality rate r=0.805). Young adults parameters were significantly lower for CT usage rate (young adults 9.8% vs. 17.3%, p<0.0001), LOS (4.3 hours vs. 5.0 hours, p<0.0001), hospitalization rate (20.1% vs. 48.6%, p<0.0001) and in-hospital mortality rate (0.1% vs. 3.8%, p<0.0001), and higher for ESI (young adults 3.3 vs. 3.1, p<0.0001).

## CONCLUSION

Although the young adult population constitutes a large portion of ED visits, most of them need significantly less CT diagnostic evaluation and hospitalization, and in-hospital mortality rate is significantly lower in this group.

#### **CLINICAL RELEVANCE/APPLICATION**

Specific health care programs, such as education and availability of primary care facilities attending to the needs of the young adults population population, may reduce ED overcrowding



## IN233-SD-THA1

## Viewing Imaging Studies: How Patient Location and Imaging Site Affect Referring Physicians

Thursday, Nov. 29 12:15PM - 12:45PM Room: IN Community, Learning Center Station #1

#### Awards

### Student Travel Stipend Award

#### Participants

Fatemeh Homayounieh, MD, Chelsea, MA (*Presenter*) Nothing to Disclose Ramandeep Singh, MBBS, Boston, MA (*Abstract Co-Author*) Nothing to Disclose Ellen J. Sugarman, Boston, MA (*Abstract Co-Author*) Nothing to Disclose Keith J. Dreyer, DO, PhD, Boston, MA (*Abstract Co-Author*) Nothing to Disclose Subba R. Digumarthy, MD, Boston, MA (*Abstract Co-Author*) Nothing to Disclose Mannudeep K. Kalra, MD, Boston, MA (*Abstract Co-Author*) Research Grant, Siemens AG; Research Grant, Canon Medical Systems Corporation

Thomas J. Schultz, BS, Boston, MA (Abstract Co-Author) Nothing to Disclose

### PURPOSE

How do patient location (outpatient (OP)/inpatient (IP)/emergency (ED)) and imaging sites (hospital or off-campus) affect viewing patterns of referring physicians?Study of viewing patterns can prioritize interpretation & streamline result communication with referring physicians

## **METHOD AND MATERIALS**

Our study included 166,949 patients who underwent CT/MR of head/chest/abdomen in 2016-17 in OP (n=83,979 CT/MR), IP(n=51,051) & ED(n=31,919) settings. Out of 165,769 CT/MR, 125,325 CT/MR were performed in the hospital setting & 40,444 in one of the 3 off-campus locations.We extracted information regarding body region (head/chest/abdomen),patient location & imaging site from the electronic medical records (EPIC).We recorded clinical indications & number of times referring physicians viewed CT/MR (defined as number of separate views of imaging in the EPIC).Data were stratified & analyzed with Microsoft SQL and EXCEL

## RESULTS

About 33% of IP CT & MR studies are viewed >6 times compared to 7% for OP and 19% of ED studies (p<0.001). Conversely,most OP studies (55%) were viewed 1-2 times only,compared to 21% for IP and 38% for ED studies (p<0.001). There were significant differences between viewing rates of imaging tests based on clinical indications in OP,IP and ED settings (p<0.05). In-hospital exams are viewed (>= 6 views;39% studies) more frequently than off-campus imaging (>= 6 views;17% studies)(p<0.001). Certain exams,such as head MR had higher viewing rates regardless of patient location. For head CT/MR,certain clinical indications (i.e. stroke) had higher viewing rates compared to other clinical indications such as malignancy,headache & dizziness,regardless of patient location.Conversely,for chest CT, dyspnea-hypoxia had much higher viewing rates (>6 times) in IP(55%) & ED(46%) than in OP settings (22%),whereas,chest CT for malignancy were viewed less often (only one view) in both IP(23%) & OP(44%) settings

### CONCLUSION

Clinical indications, patient location & imaging site have profound effect on viewing patterns of referring physicians. Studies in IP & ED settings are viewed more often than in OP settings and off-campus sites regardless of clinical indications

#### **CLINICAL RELEVANCE/APPLICATION**

Understanding viewing patterns of the referring physicians can help guide interpretation priorities and findings communication for imaging exams based on patient location, imaging site and clinical indications. The information can help in efficient delivery of patient care

#### **Honored Educators**

Presenters or authors on this event have been recognized as RSNA Honored Educators for participating in multiple qualifying educational activities. Honored Educators are invested in furthering the profession of radiology by delivering high-quality educational content in their field of study. Learn how you can become an honored educator by visiting the website at: https://www.rsna.org/Honored-Educator-Award/ Subba R. Digumarthy, MD - 2013 Honored Educator



## MI235-SD-THA2

Added Value of Gastric Water Distension and Delayed FDG-PET/CT Scan in Characterization of the Gastric FDG Uptake

Thursday, Nov. 29 12:15PM - 12:45PM Room: Learning Center, Hall D Station #2

## Participants

Hussein R. Farghaly, MD, Saint Louis, MO (*Abstract Co-Author*) Nothing to Disclose Abdullah Alabdullah, BMedSc, Riyadh, Saudi Arabia (*Presenter*) Nothing to Disclose Abdullah Alqarni, MD, Riyadh, Saudi Arabia (*Abstract Co-Author*) Nothing to Disclose Hatem Nasr, MD, PhD, Riyadh, Saudi Arabia (*Abstract Co-Author*) Nothing to Disclose

For information about this presentation, contact:

tumyar@hotmail.com

## PURPOSE

To assess the added value of water gastric distension (GD) and delayed FDG-PET/CT in characterization of gastric (G) FDG uptake.

## **METHOD AND MATERIALS**

Patients (n=20, 15 males, mean age 55.9 $\pm$ 17.4 y). All are known or suspected cancer patients (pt). Patients underwent WB FDG-PET/CT scan and 2 hours delayed PET/CT abdominal scan after oral water GD. Gastric lesions (GL) were correlated with biopsy in 7 patients (35%) and with clinical and follow-up imaging (FDG PET/CT,CT or MRI) in 13 patients (75%). Early SUVmax (SUVe), delayed SUVmax (SUVd), difference between SUVd and SUVe (SUV $\Delta$ ) as well as uptake pattern and demographic data were analyzed to assess there association to GL nature. Unpaired student T-test was used to compare means of continuous variables and Fisher's exact test to compare frequencies of categorical variables.

#### RESULTS

Neoplastic GL were confirmed in 11 pt (55%) with older age (63.5 vs 46.7, p=0.027) and higher  $\Delta$ SUV (2.20 vs -1.44, p=0.03) compared to pt with benign lesions. Most benign or physiological gastric changes revealed regression in activity in delayed images after GD. An increase in SUVmax following GD was associated with higher frequency of neoplastic GL. A cutoff of >0 for  $\Delta$ SUV revealed sens., spec., PPV, NPV and acc. of 90.9%, 77.8%, 83.3, 87.5 and 85.0% respectively for detection of neoplastic lesions (p=0.005) with only 2 false +ve and 1 false -ve. Of the false +ve one was confirmed by biopsy as chronic active gastritis while the false -ve was related to a signet ring gastric cancer. GD lead to improvement in detection of malignant gastric lesion based on uptake pattern (diffuse vs. localized) with sens.100% & spec.78% vs. 55% and 44% before gastric distension.

### CONCLUSION

Delayed limited FDG-PET/CT abdominal scan with GD is a non-invasive way to improve characterization of the gastric FDG uptake and help in selecting patients who need further attention to different benign from malignant lesion.

## **CLINICAL RELEVANCE/APPLICATION**

Delayed limited FDG-PET/CT abdominal scan with GD help in avoidance of unnecessary endoscopy in patient with gastric metabolic activity by differentiating physiological from suspicious uptake.



## MI236-SD-THA3

## Characterizing Bladder Uptake in Fluciclovine PET: Potential for Diagnostic Uncertainty?

Thursday, Nov. 29 12:15PM - 12:45PM Room: MI Community, Learning Center Station #3

#### Awards Student Travel Stipend Award

#### **Participants**

Petra Lovrec, MD, Maywood, IL (*Presenter*) Nothing to Disclose Abhishek A. Solanki, MD, Maywood, IL (*Abstract Co-Author*) Consultant, Blue Earth Diagnostics Ltd Advisory Board, Blue Earth Diagnostics Ltd Gopal Gupta, MD, Maywood, IL (*Abstract Co-Author*) Nothing to Disclose Robert H. Wagner, MD, Maywood, IL (*Abstract Co-Author*) Nothing to Disclose Medhat S. Gabriel, MD, Maywood, IL (*Abstract Co-Author*) Nothing to Disclose Bital Savir-Baruch, MD, Atlanta, GA (*Abstract Co-Author*) Research Grant, Blue Earth Diagnostics Ltd; Consultant, Blue Earth

# Diagnostics Ltd; Speaker, Koninklijke Philips NV For information about this presentation, contact:

petra.lovrec@lumc.edu

#### PURPOSE

Fluciclovine positron emission tomography/computed tomography (PET/CT) scan has been approved by the FDA for imaging in men with suspected prostate cancer recurrence. The physiological biodistribution of fluciclovine includes mild increasing bladder excretion over time (Schuster; J Nucl Med 2014; 55:1986-1992). The fluciclovine prescribing information reports only 3% of administered fluciclovine radioactivity excreted in urine across the first four hours post-injection. However, in clinical practice, we noticed a variable degree of fluciclovine urine excretion. Our goal was to evaluate and quantify early fluciclovine bladder excretion in clinical practice.

#### **METHOD AND MATERIALS**

We assessed scans of 159 patients who underwent 18F-fluciclovine PET/CT imaging at our institution as part of their clinical workup. All patients were scanned 3-5 minutes post-injection. Bladder activity maximum standardized uptake value (SUV max) was compared to the SUV mean of the aorta, marrow, and liver. Based on the bladder activity, the patients were divided into four groups: 'Insignificant' (bladderaorta, marrow, liver). The average of bladder SUV max and mean values were calculated for each group.

## RESULTS

Insignificant bladder excretion was found in 37.1% (59/159) of patients, mild excretion in 12.6% (20/159) of patients, moderate in 37.7% (60/159) of patients, and 12.6% (20/159) of patients had intense bladder excretion. The average SUV mean of the aorta, marrow and liver was 1.60, 3.46, and 8.92, respectively. The average bladder SUV max (SUV mean) was 0.97 (0.61) for patients with insignificant bladder excretion, 2.22 (1.34) for mild bladder excretion, 5.33 (3.06) for moderate bladder excretion, and 14.17 (10.35) for intense bladder excretion.

#### CONCLUSION

Fluciclovine urine excretion was found to be higher than expected. Moderate to intense bladder activity may mask or mimic local prostate cancer recurrence. Methods to minimize bladder visualization should be further investigated.

### **CLINICAL RELEVANCE/APPLICATION**

Bladder activity on fluciclovine scans may mimic or mask foci of prostate cancer recurrence. Our study showed a higher number of scans with fluciclovine bladder activity compared to the literature.



## MI237-SD-THA4

Imaging of Atherosclerotic Plaque Burden in ApoE KO Mice: A Comparison of In Vivo 7T MRI and Ex Vivo MicroCT

Thursday, Nov. 29 12:15PM - 12:45PM Room: MI Community, Learning Center Station #4

## Participants

Caroline Jung, Hamburg, Germany (*Presenter*) Nothing to Disclose Markus Heine, Hamburg, Germany (*Abstract Co-Author*) Nothing to Disclose Michael G. Kaul, Hamburg, Germany (*Abstract Co-Author*) Nothing to Disclose Harald Ittrich, MD, Hamburg, Germany (*Abstract Co-Author*) Nothing to Disclose Gerhard B. Adam, MD, Hamburg, Germany (*Abstract Co-Author*) Nothing to Disclose

## PURPOSE

The aim of this study was to quantify atherosclerotic plaque by volumetric assessment and by determining T1 Relaxivity at 7T MRI using Gadospin F (GDF) in comparison to microCT ( $\mu$ CT) measurements.

## METHOD AND MATERIALS

Mice (n=25) were set on high fat diet (HFD) at 9 weeks of age. In-vivo MRI of the aorta was performed at 9, 13, 17 and 21 weeks after commencement of the HFD. After 13 weeks one group (therapy group) was reswitched to normal rodent diet and monitored by MRI for 12 weeks. ApoE-/- and control mice were imaged before and two hours after iv injection of GDF (100  $\mu$ mol/kg) at a small animal 7T MRI (Clinscan, Bruker) using a 3D IR Gradient echo MR sequence (TR/TE 650/2 ms, TI 250ms; FA 20°; eff. voxel resolution 180  $\mu$ m3). In same slice orientation T1 Mapping was performed using Saturation Recovery sequences. Subsequently, heart and aorta intact with spine were excised for  $\mu$ CT imaging using a high-resolution, volumetric  $\mu$ CT scanner ( $\mu$ CT40; ScanCo Medical, Zurich, CH). MR image analyses were performed using ImageJ (V. 1.44p, NIH, USA). Total plaque volume relative to the examined area of the aorta (rTPV) and T1 Relaxivity were estimated. Pearson correlation between MRI and  $\mu$ CT measurements and interobserver variability was analysed.

## RESULTS

MRI and  $\mu$ CT analyses showed an exponential increase of rTPV and T1 relaxivity over time, which showed a slower and linear increase for therapy group. A strong correlation (r=0.83; p<0.0001) for rTPV between MRI and  $\mu$ CT measurements was observed while a good correlation of r=0.68 (p<0.001) was achieved between T1 relaxivity and rTPV  $\mu$ CT measurements. Interobserver variability for MRI analyses was r>0.88 (p<0.001) and 0.63 (p<0.0001) in case of  $\mu$ CT analyses. In control mice no plaque volume was observed. A moderate but not significant correlation was found for body weight and cholesterol and triglyceride level (r>0.7 and r>0.8, respectively).

## CONCLUSION

GDF-enhanced MRI showed a moderate to strong correlation between measured plaque volume and T1 Realxivity in vivo and  $\mu$ CT measurements ex vivo.

#### **CLINICAL RELEVANCE/APPLICATION**

GDF-enhanced in vivo MRI is a powerful noninvasive imaging technique allowing reliable estimation of plaque burden, monitoring of disease progression and evaluation of therapy response in preclinical studies.



## MK396-SD-THA1

Fracture Risk Assessment of Diabetes Mellitus Patients: Comparison of Trabecular Bone Analysis by Tomosynthesis with Various Established Estimations

Thursday, Nov. 29 12:15PM - 12:45PM Room: MK Community, Learning Center Station #1

## Participants

Yo Todoroki, Kitakyushu, Japan (*Presenter*) Nothing to Disclose Takatoshi Aoki, MD, PhD, Kitakyusyu, Japan (*Abstract Co-Author*) Nothing to Disclose Masami Fujii, MD, Kitakyushu, Japan (*Abstract Co-Author*) Nothing to Disclose Akitaka Fujisaki, MD, Kitakyushu, Japan (*Abstract Co-Author*) Nothing to Disclose Yoshiko Hayashida, MD, Fukuoka, Japan (*Abstract Co-Author*) Nothing to Disclose Yukunori Korogi, MD, PhD, Kitakyushu, Japan (*Abstract Co-Author*) Nothing to Disclose Yosuke Okada, Kitakyushu, Japan (*Abstract Co-Author*) Nothing to Disclose Yosuke Okada, Kitakyushu, Japan (*Abstract Co-Author*) Nothing to Disclose Yoshiya Tanaka, MD, Kitakyushu, Japan (*Abstract Co-Author*) Nothing to Disclose

#### PURPOSE

Although bone mineral density (BMD) by dual X-ray absorptiometry (DXA) has been used to predict bone strength clinically, diabetes mellitus (DM) patients have an elevated fracture risk despite normal BMD. While here are some complementary methods for estimating fracture risk, such as the trabecular bone score (TBS) and the fracture risk assessment tool (FRAX), these are still not sufficient in the case of DM. The purpose of this study is to compare trabecular bone analysis by tomosynthesis with various established estimations (BMD, TBS, and FRAX) for femoral neck fracture risk assessment of DM patients.

## METHOD AND MATERIALS

Sixty DM patients were included in this study. They underwent DXA, tomosynthesis, and CT covering the vertebral body of Th10 to the hip joints within a week. We extracted the trabecular patterns of tomosynthesis images, and obtained the total strut length (TSL), the bone volume per tissue volume (BV/TV) and the textural features (HOM: homogeneity, ENT: entropy, COR: correlation, CON: contrast, VAR: variance) as the indices of tomosynthesis images. Four square ROIs (64 x 64 pixels) were located at principal tensile (PT) group and at principal compressive (PC) group to reflect the bone strength of the proximal femur. Failure load of the femoral neck, determined by the CT-based finite-element method (FEM), was used as the gold standard for bone strength. A forward stepwise multiple regression analysis for evaluating the availability of the tomosynthesis image indices was performed. A logistic model was used with BMD, TBS, FRAX, and the tomosynthesis image indices.

## RESULTS

The combination of the BMD with the CON at principal tensile group and the VAR at principal compressive group showed the highest correlation to the failure load by CT-FEM, and the correlation (r=0.772) was higher than that between the failure load and the BMD alone (r=0.709; p<0.001). The correlation between the failure load and the BMD with the tomosynthesis texture indices was higher than that between the failure load and the FRAX with hip BMD (r=0.732).

## CONCLUSION

Tomosynthesis -based trabecular bone analysis in combination with BMD measurements can potentially be used in predicting bone strength in DM patients in clinical practice.

## **CLINICAL RELEVANCE/APPLICATION**

Low-cost trabecular bone analysis using tomosynthesis images assessment of proximal femur may provide bone strength information that is not provided by dual X-ray absorptiometry.



## MK397-SD-THA2

Dual-Energy Computed Tomography for Differentiation of Infiltration Patterns in Multiple Myeloma: A Feasibility Study

Thursday, Nov. 29 12:15PM - 12:45PM Room: MK Community, Learning Center Station #2

## Participants

Aleksander Kosmala, Wurzburg, Germany (*Presenter*) Nothing to Disclose Andreas M. Weng, Wuerzburg, Germany (*Abstract Co-Author*) Research Grant, Siemens AG Bernhard Petritsch, Wurzburg, Germany (*Abstract Co-Author*) Research Cooperation, Siemens AG; Research Consultant, Siemens AG Thorsten A. Bley, MD, Hamburg, Germany (*Abstract Co-Author*) Nothing to Disclose

## PURPOSE

Bone marrow imaging patterns in patients with Multiple Myeloma (MM) possess prognostic and potential therapeutic relevance. However, until now pattern allocation was only possible with magnetic resonance imaging (MRI), based on subjective image impression. We aim to evaluate whether different infiltration patterns also result in different dual-energy computed tomography (DECT) attenuation of the bone marrow.

## **METHOD AND MATERIALS**

The institutional review board approved this study. Written informed consent was obtained from all participants. 53 patients with plasma cell disorders (24 with normal imaging pattern, 24 with focal infiltration, 5 with diffuse infiltration) and 21 control subjects sequentially underwent DECT and MRI of the axial skeleton. MRI served as reference standard for imaging pattern assessment. Bone marrow dual-energy virtual noncalcium (VNCa) attenuation numbers were obtained based on imaging pattern allocation. Generalized estimating equations and a receiver operating characteristic (ROC) analysis were performed.

#### RESULTS

Mean VNCa attenuation numbers in patients with normal, focal and diffuse imaging patterns were -65.8 HU, 3.3 HU, and -13.3 HU, respectively. We found significant differences between diffuse vs. normal (P < 0.001), diffuse vs. focal (P = 0.002), and normal vs. focal (P < 0.001) patterns. A cut-off VNCa attenuation of 35.7 HU showed a sensitivity of 100% (24/24) and specificity of 97% (116/120) for the identification of a diffuse pattern vs. normal pattern, with an area under the ROC curve of 0.997.

## CONCLUSION

We conclude that different infiltration patterns in patients with MM result in significantly different VNCa bone marrow attenuation. Thus, DECT can potentially be used to detect not only focal osteolytic and non-osteolytic lesions, but also confidently determine a diffuse infiltration pattern, which is associated with a worse prognostic outcome and until now could only be diagnosed with MRI.

## **CLINICAL RELEVANCE/APPLICATION**

Our data indicate that DECT is able to discriminate infiltration patterns in patients with MM similar to MRI, which could be of prognostic and potential therapeutic relevance.



## MK398-SD-THA3

A Method to Improve the Image Quality of Spine CT on Reducing Metal Artifacts Caused by Pedicle Screws in Patients

Thursday, Nov. 29 12:15PM - 12:45PM Room: MK Community, Learning Center Station #3

## Participants

Weiwei Qi, MD, Beijing, China (*Presenter*) Nothing to Disclose Xia Liu, Beijing, China (*Abstract Co-Author*) Nothing to Disclose Yan Jiang, MD, Shanghai, China (*Abstract Co-Author*) Nothing to Disclose Lei Chen, MD, Beijing, China (*Abstract Co-Author*) Nothing to Disclose Nan Hong, MD, Beijing, China (*Abstract Co-Author*) Nothing to Disclose

### For information about this presentation, contact:

qiwiewei@pkuph.edu.cn

## PURPOSE

To improve the image quality of spine CT on reducing metal artifacts caused by pedicle screws in patients with orthopedic metal artifact reduction(O-MAR) combined with body position change.

## METHOD AND MATERIALS

Thirty-five patients after Pedicle screw fixation surgery were enrolled and underwent spine CT scan (iCT, Philips Healthtech). The patients were separated into two groups randomly(control group, 20 patients with total 98 pedicle screws; exam group, 15 patients with total 78 pedicle screws). For control group, the angle between the long axial of screw and transversal line of each screw was also measured and assessed quality. For exam group, the tilt angle of foam plastic cushion for running up upper body was used to get better image quality. All images were reconstructed with O-MAR and HIR algorithms (iDose4). The image quality of each pedicle screw was assessed with 5-point at volume view mode by two radiologists. Image quality assessment divided into 3 groups (Group A, image with O-MAR of control group; Group B, image without O-MAR of control group; Group C, image with O-MAR of exam group). The ROI was set by side the screw to measure the noise and beam-hardening artifact objectively.

## RESULTS

For control group, the average tilt angle of screw was  $9.51\pm8.10$  degree and the image quality of average score in group B was  $3.79\pm2.43$ . Both the objective and subjective image quality were also better with the angle increasing. The average angle with 3 score and above was 6.72 degree as the tilt angle of plastic cushion. For exam group, the angle of screws at exam group was  $18.54\pm7.80$  degree which was larger than that at control group (P<0.01); the image quality score of Group C ( $4.36\pm1.93$ ) also was better than that of Group A( $1.98\pm1.05$ ) and Group B(P<0.01) ,the image quality score of groups (Group B,C)with O-MAR all better than that of group(Group A).

#### CONCLUSION

O-MAR combined with body position changed (7degree tilted) is an effective means to improve the image quality of spine CT in reducing metal artifacts caused by pedicle screws in patients.

## **CLINICAL RELEVANCE/APPLICATION**

O-MAR combined with body position changed (7degree tilted) can improve the image quality of spine CT in reducing metal artifacts caused by pedicle screws paralleling scan plane in patients.



## MK399-SD-THA4

Detection of Spondylolysis: Is Replacement of CT by Ultrashort Time to Echo (UTE) MR Sequences Feasible? A Human Cadaveric Spine Study

Thursday, Nov. 29 12:15PM - 12:45PM Room: MK Community, Learning Center Station #4

## Participants

Tim Finkenstaedt, MD, San Diego, CA (*Presenter*) Nothing to Disclose Palanan Siriwanarangsun, MD, Bankok, Thailand (*Abstract Co-Author*) Nothing to Disclose Nirusha Abeydeera, BS, La Jolla, CA (*Abstract Co-Author*) Nothing to Disclose Sina Finkenstaedt, MD, Zurich, Switzerland (*Abstract Co-Author*) Nothing to Disclose Michael Carl, Menlo Park, CA (*Abstract Co-Author*) Researcher, General Electric Company Ibraheem Algarni, MD, San Diego, CA (*Abstract Co-Author*) Nothing to Disclose Sheronda Statum, San Diego, CA (*Abstract Co-Author*) Nothing to Disclose Suraj Achar, MD, San Diego, CA (*Abstract Co-Author*) Nothing to Disclose Christine B. Chung, MD, La Jolla, CA (*Abstract Co-Author*) Nothing to Disclose Won C. Bae, PhD, La Jolla, CA (*Abstract Co-Author*) Nothing to Disclose

#### For information about this presentation, contact:

tim.finkenstaedt@usz.ch

#### PURPOSE

To assess the diagnostic performance of conventional vs. UTE MRI for detection of spondylolysis in comparison to the CT reference standard.

#### METHOD AND MATERIALS

Four human lumbar spine specimens (mean age: 54±18yrs; 3 females, 1 male) with 41 individual pars interarticularis were randomized to be left intact (n=22) or to undergo simulated fracture (n=19) using a 1-mm oscillating microsurgical saw. To prevent air and fluid accumulation, the fractures were filled with 8% agarose gel featuring similar MR signal characteristics as scar tissue. The specimens were imaged using: 1) conventional lumbar MR protocol at 3-T (5 sequences: sagittal spin echo T1, T2 and STIR; axial T1 and T2; total scan time=13 min), and 2) a sagittal UTE MR sequence at 3-T (TR=44.3 ms, TE=0.05 ms, matrix=256x256, slice=2 mm, FOV=24 cm, scan time=3 min), and 3) a 256-MDCT scanner (120 kVp, 100 mA, slice=0.625 mm). Two blinded readers evaluated MR data using a 4-point scale (1=spondylolysis certainly absent, 2=probably absent, 3=probably present, 4= certainly present). CT served as the reference standard. Inter-reader agreement (intraclass correlation, ICC) and the diagnostic performance (sensitivity and specificity, and reader confidence) of each MR technique was determined.

### RESULTS

Conventional MR images (Figure 1AB) lacked contrast between cortical bone and the pars defect. In contrast, UTE images (Figure 1C) clearly depicted the bony defect, appeared near exact inverse of the CT image (Figure 1D). Diagnostic performance (Table 1) was moderate for conventional MR, with a low sensitivity and high specificity, unlike UTE MR, which has both high sensitivity and specificity. More importantly, diagnostic confidence was much greater for UTE MR (100% read correctly with certainty), compared to conventional MR (<30%). Inter-reader agreement was also lower for conventional (ICC=0.855) than UTE (ICC=1.000) MRI.

## CONCLUSION

Our study showed that MR detection of simulated pars fractures is markedly better with a single sagittal UTE sequence than with a suite of conventional protocol. UTE MR exhibited a diagnostic performance and confidence similar to CT.

## **CLINICAL RELEVANCE/APPLICATION**

If further clinical studies confirm our results, a sagittal UTE sequence could replace the CT scan in the diagnostic workup of patients with clinically suspected lumbar spondylolysis.



## MK400-SD-THA5

MRI-Detected Structural Damage and Longitudinal Change in Femorotibial Cartilage T2 Values in Radiographically Normal Joints

Thursday, Nov. 29 12:15PM - 12:45PM Room: MK Community, Learning Center Station #5

## Participants

Frank W. Roemer, MD, Erlangen, Germany (*Presenter*) Officer, Boston Imaging Core Lab, LLC; Research Director, Boston Imaging Core Lab, LLC; Shareholder, Boston Imaging Core Lab, LLC

Felix Eckstein, MD, Salzburg, Austria (*Abstract Co-Author*) Co-owner, Chondrometrics GmbH; Co-founder, Chondrometrics GmbH; CEO, Chondrometrics GmbH; Consultant, Novartis AG; Consultant, Merck KGaA; Consultant, sanofi-aventis Group Georg Duda, Berlin, Germany (*Abstract Co-Author*) Nothing to Disclose

Ali Guermazi, MD, PhD, Boston, MA (*Abstract Co-Author*) Shareholder, Boston Imaging Core Lab, LLC; Research Consultant, Merck KGaA; Research Consultant, sanofi-aventis Group; Research Consultant, TissueGene, Inc; Research Consultant, OrthoTrophix, Inc; Research Consultant, AstraZeneca PLC; Research Consultant, General Electric Company; Research Consultant, Pfizer Inc Susanne Maschek, Ainring, Germany (*Abstract Co-Author*) Shareholder, Chondrometrics GmbH Wolfgang Wirth, Salzburg, Austria (*Abstract Co-Author*) Shareholder, Chondrometrics GmbH

#### For information about this presentation, contact:

froemer@bu.edu

#### PURPOSE

To evaluate whether the presence of baseline MRI-defined structural damage is associated with subsequent change in laminar cartilage T2 in the femorotibial joint of participants from the OAI healthy reference cohort over 1 and 4 years of observation.

#### **METHOD AND MATERIALS**

Included were the right knees of 82 participants without radiographic OA, without pain, and no risk factors of OA (Kellgren-Lawrence 0/0). Baseline effusion-synovitis, Hoffa-synovitis, bone marrow lesions (BMLs), cartilage lesions, meniscus morphology and - extrusion were assessed using the MOAKS scoring system. Cartilage T2 relaxometry was performed using multi-echo spin-echo MRIs. Deep and superficial layer cartilage T2 times were computed from manual segmentations in both the medial and lateral femorotibial compartment (MFTC/LFTC). Compartment-specific analysis of factors associated with superficial or deep layer T2 change over 1 or 4 years was performed using UNIANOVA.

### RESULTS

50 women and 32 men were included (mean age  $54.1\pm7.2y$ , BMI  $24.2\pm3.0 \text{ kg/m}^2$ ). The presence of MFTC osteophytes was associated with prolongation in deep layerT2 times over the first year (0.8 vs. 0.0 ms, p=0.02), and the entire 4-year period (0.9 vs. 2.3 ms, p=0.01). The presence of baseline MFTC meniscal damage or extrusion was associated with prolongation in deep layer T2 times at Y4 (0.7 vs. 2.1 ms, p=0.02). The number of baseline MRI pathologies did not have an effect on T2 times in the MFTC or LFTC at 1 or 4 years. Ipsi-compartmental worsening of MRI features from baseline to Y1 was neither associated with change in T2 values from Y1 to Y4 in the MFTC (superficial 0.9 ms vs. 0.2 ms, p=0.69; deep 0.2 ms vs. -0.2 ms, p=0.69) nor the LFTC (superficial 0.8 ms vs. 1.4 ms, p=0.69; deep 0.3 ms vs. 0.8 ms, p=0.69). (Table 1 shows Y1 results).

#### CONCLUSION

MRI structural abnormalities at baseline did generally not predict change in ipsi-compartmental longitudinal cartilage T2 over 1 or 4 years. The only associations that appeared to be seen were for presence of medial osteophytes and medial meniscal damage with subsequent T2 change in at least one (superficial or deep) layers; however, these relationships did not account for multiple statistical testing.

### **CLINICAL RELEVANCE/APPLICATION**

In healthy knees without clinical risk factors, structural MRI pathology may not be a reliable predictor of compositional progression as defined by change in cartilage T2.

#### **Honored Educators**

Presenters or authors on this event have been recognized as RSNA Honored Educators for participating in multiple qualifying educational activities. Honored Educators are invested in furthering the profession of radiology by delivering high-quality educational content in their field of study. Learn how you can become an honored educator by visiting the website at: https://www.rsna.org/Honored-Educator-Award/ Ali Guermazi, MD, PhD - 2012 Honored Educator



## MK401-SD-THA6

Preoperative Intraarticular Hip Injections and the Risk of Postoperative Infection after Total Hip Arthroplasty

Thursday, Nov. 29 12:15PM - 12:45PM Room: MK Community, Learning Center Station #6

#### Awards Student Travel Stipend Award

## Participants

Colin Smith, MD, Pittsburgh, PA (*Presenter*) Nothing to Disclose Carolyn Kwon, MD, Pittsburgh, PA (*Abstract Co-Author*) Nothing to Disclose Carol L. Andrews, MD, Pittsburgh, PA (*Abstract Co-Author*) Author, Reed Elsevier

## PURPOSE

The purpose of this study is to evaluate the risk of postoperative infection following total hip arthroplasty (THA) in patients with preoperative intraarticular steroid hip injections.

### **METHOD AND MATERIALS**

A hospital system database was queried, identifying patients undergoing primary THA at a single academic hospital. Patients were stratified related to hip steroid injection in the preceding 12 months: Control group-THA with no injection (n=499), THA with fluoroscopy-guided injection by a musculoskeletal (MSK) radiologist (n=216), or THA with hip steroid injection by a non-radiologist (n=18). The rates of superficial and deep infections within 1 year of surgery were obtained and compared using odds ratios. Data collection included procedural techniques, injection timing relative to THA, injectate, surgery and hardware type, length of stay, and patient age, sex, and co-morbidities.

#### RESULTS

The incidence deep infection after THA among the MSK radiologist injection group (0.46%), among injections performed by radiologists within 3 months of surgery (1.33%), and among the fluoroscopy-guided injection group (1.32%) were each not significantly different from that of the non-injection group (1.60%) with odds ratios and P values of 0.29 and 0.239; 0.83 and 0.861; 0.82 and 0.774, respectively. The incidence of deep infection after THA among the non-radiologist injection group (16.67%) was significantly different from that of the non-injection group (1.60%) with an odds ratio and P value of 12.28 and <0.001, respectively. Comparison analysis of superficial and deep infections combined yielded comparable results.

## CONCLUSION

Intraarticular hip injections performed by MSK radiologists under fluoroscopic guidance within one year prior to THA have comparable rates of postoperative infection when compared to controls. Further, current data suggest that injections performed by non-radiologists as well as those performed without fluoroscopic guidance may have increased rates of postoperative infection.

#### **CLINICAL RELEVANCE/APPLICATION**

Controversy exists regarding the increased risk of THA postoperative infection after a hip injection. This study shows the operator and technique used may be important factors in modifying this risk.



# NM149-ED-THA6

# 'A Burning Issue:" The Utilization of Tc-99m MDP Bone Scan with SPECT/CT in the Burn Unit

Thursday, Nov. 29 12:15PM - 12:45PM Room: NM Community, Learning Center Station #6

#### **Participants**

David Sadowsky, MD, Larchmont, NY (*Presenter*) Nothing to Disclose Charles Lugo, MD, Valhalla, NY (*Abstract Co-Author*) Nothing to Disclose Jennifer Wu, MD, MPH, Valhalla, NY (*Abstract Co-Author*) Nothing to Disclose Chaitanya Shilagani, MD, Valhalla, NY (*Abstract Co-Author*) Nothing to Disclose Perry S. Gerard, MD, Valhalla, NY (*Abstract Co-Author*) Nothing to Disclose

# For information about this presentation, contact:

david.sadowsky@wmchealth.org

#### **TEACHING POINTS**

Patients with severe burn injuries often endure prolonged hospital courses and undergo multiple debridements and amputations. While SPECT/CT protocols exist for a wide variety of clinical indications and employ multiple radioisotopes, current use in the field of burn care remains extremely limited. The combined ability of three phase Tc-99m MDP SPECT/CT to distinguish between viable and nonviable tissue and provide precise anatomic localization holds promise for reducing repeat procedures and increasing preservation of function in this population.

# TABLE OF CONTENTS/OUTLINE

1- Introduction to burn injuries and common complications and hospital courses of burn patients 2- Amputation background (tissue viability, preservation of function) and special amputation considerations in the burn patient (multiple sites, disfigurement, active soft tissue infection, prolonged recovery) 3- Example cases of SPECT/CT imaging applied to heat and cold burns, highlighting the value added by this imaging modality compared to traditional methods



# NM236-SD-THA1

Correlation of 11C-4DST Uptake with Isocitrate Dehydrogenase 1 Mutation in Patients with Gliomas in Comparison with 18F- FLT Uptake

Thursday, Nov. 29 12:15PM - 12:45PM Room: NM Community, Learning Center Station #1

# Participants

Yuka Yamamoto, MD, PhD, Kagawa, Japan (*Presenter*) Nothing to Disclose Yasukage Takami, Mikicho, Japan (*Abstract Co-Author*) Nothing to Disclose Takashi Norikane, Kita-gun, Japan (*Abstract Co-Author*) Nothing to Disclose Jun Toyohara, Tokyo, Japan (*Abstract Co-Author*) Nothing to Disclose Yoshihiro Nishiyama, MD, Kagawa, Japan (*Abstract Co-Author*) Nothing to Disclose

# PURPOSE

Beyond tumor histology, molecular alterations, such as isocitrate dehydrogenase enzyme isoforms 1 (IDH1) and 2 (IDH2) mutation as part of the 2016 world health organization classification of tumors of the central nervous system have been found to provide additional prognostic value in gliomas. A novel radiopharmaceutical, 4'-[methyl-11C]-thiothymidine (4DST), has been developed as an in vivo cell proliferation marker based on the DNA incorporation method. The purpose of this study was to evaluate 4DST uptake in patients with gliomas and to correlate the results with IDH1 mutation, in comparison with 3'-deoxy-3'-18F-fluorothymidine (FLT).

#### **METHOD AND MATERIALS**

Investigations of 4DST and FLT PET/CT were performed in 25 patients with glioma. Tumor lesions were identified as areas of focally increased uptake, exceeding that of background uptake. For semi-quantitative analysis, the maximal standardized uptake value (SUVmax) for tumor was calculated. The presence of IDH1 mutation in tumor specimens was examined by immunohistochemistry and compared with 4DST SUVmax and FLT SUVmax.

# RESULTS

All but one glioma showed focally increased both 4DST and FLT uptake. There was no significant difference between mean ( $\pm$ SD) SUVmax using 4DST (2.61 $\pm$ 1.65) and FLT (2.14 $\pm$ 1.28). The mean ( $\pm$ SD) 4DST SUVmax of IDH1-mutated tumors (1.72 $\pm$ 0.51) was significantly lower than that of IDH1-nonmutated tumors (3.21 $\pm$ 1.89) (p<0.02). Using FLT, there was no significant difference between mean ( $\pm$ SD) SUVmax of IDH1-mutated tumors (1.67 $\pm$ 1.16) and IDH1-nonmutated tumors (2.45 $\pm$ 1.30).

# CONCLUSION

These preliminary results indicate that 4DST PET/CT is feasible for imaging of brain gliomas, as well as FLT PET/CT. 4DST uptake of IDH1-mutated tumors was significantly lower than that of IDH1-nonmutated tumors.

# **CLINICAL RELEVANCE/APPLICATION**

4DST uptake of IDH1-mutated tumors was significantly lower than that of IDH1-nonmutated tumors. 4DST uptake in gliomas might be useful for predicting outcomes.



# NM237-SD-THA2

Diagnostic Accuracy of Combined 123I-MIBG Scintigraphy and 123I-FP-CIT SPECT in the Differential Diagnosis of Degenerative Parkinsonism

Thursday, Nov. 29 12:15PM - 12:45PM Room: NM Community, Learning Center Station #2

# Participants

Kaoru Maruyama, Hirakatashi, Japan (*Presenter*) Nothing to Disclose Keita Utsunomiya, MD, PhD, Moriguchi, Japan (*Abstract Co-Author*) Nothing to Disclose Miho Hatanaka, Osala, Japan (*Abstract Co-Author*) Nothing to Disclose Hiroshi Kishishita, Moriguchi, Japan (*Abstract Co-Author*) Nothing to Disclose Naoki Kan, Hirakata, Japan (*Abstract Co-Author*) Nothing to Disclose Yumiko Kono, MD, Hirakata, Japan (*Abstract Co-Author*) Nothing to Disclose Yasuhiro Ueno, Moriguchi, Japan (*Abstract Co-Author*) Nothing to Disclose Noboru Tanigawa, MD, Hirakata, Japan (*Abstract Co-Author*) Nothing to Disclose

### PURPOSE

To investigate the sensitivity and specificity, in the clinically based diagnostic criteria for Parkinson's disease (PD), of planar heart imaging with the ligand 123I-Metaiodobenzylguanidine (MIBG), and of single photon emission computed tomography (SPECT) brain dopamine transporter imaging with the ligand 123I-Ioflupane (FP-CIT), and to evaluate to which extent diagnostic accuracy can be increased by their combined use together.

# METHOD AND MATERIALS

Twenty seven patients who performed both methods for differential diagnosis between PD (n = 21) and other parkinsonism (non-PD, n = 6) were enrolled. Readers, unaware of the clinical diagnosis, classified the images as normal or abnormal by visually inspection. Abnormal MIBG or FP-CIT scan is defined as decreased uptake in the myocardium or in the striatum, respectively. Sensitivity, specificity, accuracy, positive and negative values of both methods were calculated.

# RESULTS

Abnormal MIBG scans had a sensitivity of 57 % (12/21) for detecting clinical PD, with specificity of 100 % (6/6) for excluding non-PD. For 123I-MIBG scintigraphy, a value of 67 % (18/27) was achieved for overall diagnostic accuracy, 100 % (12/12) for positive predictive value, and 40 % for negative predictive value. For 123I-FP-CIT SPECT, the overall sensitivity, specificity, accuracy, positive and negative predictive values in PD were 81 % (17/21), 0 % (0/6), 63 % (17/27), 74 % (17/23), and 0 % (0/4), respectively. For combined use of both normal MIBG and abnormal FP-CIT, the highest test accuracy of 81 % for differentiation of non-PD from PD with a sensitivity of 100 %, specificity of 76 %.

# CONCLUSION

The diagnostic accuracy is sufficiently high for the combination of cardiac 123I-MIBG scintigraphy and brain 123I-FP-CIT SPECT to be clinically useful in distinguishing PD from non-PD.

# **CLINICAL RELEVANCE/APPLICATION**

PD usually present both myocardial sympathetic and striatal dopaminergic impairments. The combined use of both 123I-FP-CIT SPECT and 123I-MIBG scintigraphy may contribute to have a complementary role in differential diagnosis between PD and non-PD.



# NM238-SD-THA3

# 18F-FDG PET/CT Postoperative Changes after Maxillectomy: Findings and Pitfalls in Interpretation

Thursday, Nov. 29 12:15PM - 12:45PM Room: NM Community, Learning Center Station #3

#### **Participants**

Tima Davidson, MD, Ramat Gan, Israel (*Presenter*) Nothing to Disclose Johnatan Nissan, Haifa, Israel (*Abstract Co-Author*) Nothing to Disclose Maria Krichmar, Tel-Hashomer, Ramat Gan, Israel (*Abstract Co-Author*) Nothing to Disclose Eyal Lotan, MD, New-York, NY (*Abstract Co-Author*) Nothing to Disclose Shai Shrot, Raanana, Israel (*Abstract Co-Author*) Nothing to Disclose Ella Nissan, Tel-Hashomer, Ramat Gan, Israel (*Abstract Co-Author*) Nothing to Disclose Iris Gluck, Tel-Hashomer, Ramat Gan, Israel (*Abstract Co-Author*) Nothing to Disclose Philip R. Lawson, MBChB,BSC, Ramat Gan, Israel (*Abstract Co-Author*) Nothing to Disclose Simona Ben-Haim, MD, DSc, Ramat Gan, Israel (*Abstract Co-Author*) Nothing to Disclose Simona Ben-Haim, MD, DSc, Ramat Gan, Israel (*Abstract Co-Author*) Nothing to Disclose Shay Duvdevani, Tel-Hashomer, Ramat Gan, Israel (*Abstract Co-Author*) Nothing to Disclose Simona Ben-Haim, MD, DSc, Ramat Gan, Israel (*Abstract Co-Author*) Nothing to Disclose Shay Duvdevani, Tel-Hashomer, Ramat Gan, Israel (*Abstract Co-Author*) Nothing to Disclose

#### For information about this presentation, contact:

Tima.Davidson@sheba.health.gov.il

### PURPOSE

PET-CT is the mainstay of disease surveillance in head and neck cancer following local resection. However, increased FDG-uptake in the surgical bed may be non-specific and present diagnostic challenges.

#### **METHOD AND MATERIALS**

This is a review of FDG- PET/CT studies of head and neck cancer patients with a history of maxillary surgery treated during 2008-2016. Findings on postoperative PET/CT were correlated with clinical and imaging follow-up.

#### RESULTS

PET/CT studies of 17 reconstructive maxillary surgeries of 14 patients (10 males, mean age 57  $\pm$  16 years, range 22-77) were reviewed. Increased FDG uptake in the postoperative bed was demonstrated in 12 (71%; 10 obturator, 2 mesh reconstructions), mean SUV max 2.4  $\pm$  1.4 (range 0.3-4.3). In the remaining 5/17 studies (3 with a fat flap and 2 without any reconstructions), there was no abnormal FDG uptake at the postoperative bed. CT features in postoperative sites included a combination of: nonhomogeneous mixed hyperdense material with multiple air bubbles; mucosal thickening along the postoperative bed wall (in all cases with obturator implants); rich fat density material in reconstructions. In 8/9 patients with more than one postoperative PET/CT, there were no significant differences between the studies. One patient had a new FDG-avid lesion in the nasopharynx adjacent to the surgical bed, which was confirmed by pathology as recurrence of the disease. No correlation was found of the mean SUV max in initial scans with the time from the surgery date (10 months;  $\pm$  6; r=0.04, P=0.90), or with the mean SUV max in final scans (25 months;  $\pm$  17; 2.4  $\pm$  1.4 vs. 1.6  $\pm$  1.7; P=0.17). In 4 patients, biopsies obtained from the FDG-avid changes showed fragments of fibrotic or granulation tissue, with no evidence of malignancy.

# CONCLUSION

All patients in this study who had obturator or mesh reconstructive surgery after maxillectomy demonstrated FDG avid postoperative changes, which persisted more than four years after surgery. Awareness of variations in postoperative PET/CT appearance is important to avoid false interpretation in cancer patients.

#### **CLINICAL RELEVANCE/APPLICATION**

Radiologists should be aware of variations in postoperative PET-CT appearance, including increased FDG uptake, even years after surgery, to avoid overcalling these lesions as malignance.



# NM239-SD-THA4

Impact of Patient Comfort on Diagnostic Image Quality during PET/MR Exam: An Objective Survey Study for Clinical Workflow Management

Thursday, Nov. 29 12:15PM - 12:45PM Room: NM Community, Learning Center Station #4

FDA Discussions may include off-label uses.

#### Participants

Shuguang Chen, MD, Shanghai, China (*Abstract Co-Author*) Nothing to Disclose Zheng Zhang, MD, Shanghai, China (*Abstract Co-Author*) Employee, Healthcare Device Manufactor Guo Bin, Shanghai, China (*Abstract Co-Author*) Employee, Medical Device Manufactor Tuoyu Cao, PhD, Houston, TX (*Abstract Co-Author*) Employee, Medical Device Manufactor Lingzhi Hu, PhD, Houston, TX (*Abstract Co-Author*) Employee, UIH America, Inc Hongcheng Shi, Shanghai, China (*Abstract Co-Author*) Nothing to Disclose

# PURPOSE

Whole body PET/MR screening usually takes 30-50 minutes to finish, during which a few factors might induce patient discomfort and further cause degraded image quality. The aim of this report is to investigate the patients' perception of the imaging procedure and its correlation with image quality.

# **METHOD AND MATERIALS**

120 patients (63 males and 57 females, average age = 51.3 years, range 22-70 years) who had been diagnosed with cancer or had previous history of cancer were recruited and scanned with a simultaneous PET/MR system. A questionnaire was given to all patients retrospectively after the PET/MR scan, which has 9 questions to assess patients' feeling of the scan on a Likert scale scoring system (1-5, 1 as most satisfied). All PET/MR images were also visually examined by two experts independently to evaluate the quality of the images. Six body positions were assessed and each position was evaluated also with a Likert scale scoring system (1-5, 5 as the best quality). With each section of the patient comfort questionnaire, patients were divided into two groups based on the score they filled (Group A: 1,2; Group B: 3, 4, 5). And statistical analysis using Mann-Whitney U-test were used to check if there is significant difference between these two groups regarding PET image artifacts, MR image artifacts and PET/MR coregistration error.

#### RESULTS

118 questionnaires were filled and returned for analysis. The average overall perception is 1.36. The statistical test showed that patients' comfort has strong correlation with MR image artifacts, especially in certain areas of the body such as head and pelvis. And some factors had a bigger impact than others, such as RF heating and coil pressure. No statistically significant difference were observed on PET image artifacts or coregistration error due to patients comfort.

#### CONCLUSION

With proper preparation and patient training, it is practical to achieve good image qualities from simultaneous PET/MR scan, even with the longer scan duration compared to other modalities. However, it is still important to pay special attention to patients comfort for the best performance.

# **CLINICAL RELEVANCE/APPLICATION**

This study provides a guideline for simultaneous PET/MR scan protocol to achieve the optimum image quality.



## NM240-SD-THA5

Evaluating the Role of 68Ga-PSMA PET/CT Imaging in Predicting Intraprostatic Tumor Extent of Tumor Involvement Prior to Various Surgical Protocols in Patients with Known or Diagnosed Prostatic Cancer

Thursday, Nov. 29 12:15PM - 12:45PM Room: NM Community, Learning Center Station #5

# Participants

Sikandar M. Shaikh, DMRD, Hyderabad, India (Presenter) Nothing to Disclose

For information about this presentation, contact:

idrsikandar@gmail.com

#### PURPOSE

The role of performance of gallium Ga 68 (68Ga)-labeled prostate-specific membrane antigen (PSMA) ligand positron emission tomography/computed tomography (PET/CT) shows very promising results with known or diagnosed prostatic cancers. The evaluation in relation to intraprostatic involvement.local infiltration and lymph node detection even at low prostate specific antigen (PSA) levels is highly sensitive. In patients with biochemical recurrence after curative therapy for prostate cancer. In this study we evaluated the usefulness of PSMA-PET/CT for the evaluation of intraprostatic tumor extent prior to surgery

# METHOD AND MATERIALS

This was the retrospective study with diagnosed prostate cancer.30 patients were included in this study who underwent a 68Ga-PSMA-PET/CT before surgical treatment. All patients underwent either open or laparoscopic radical prostatectomy. Intraprostatic tumor extent was assessed on PET/CT by the peak standardized uptake value (SUV) .This was correlated with final whole gland histopathology including Gleason grade, lobe infiltration, TNM stage and seminal vesicle invasion.

### RESULTS

The mean SUV over all patients was 12.64  $\pm$ 9.19. Median Gleason score was 7. The distribution of TNM stage 2a, 2b, 2c, 3a, 3b, 4 was 0, 2, 6, 5, 2 and 0 patients. Mean intraprostatic SUV for patients with organ confined vs. extraprostatic tumor on histopathology was 6.3 and 15 respectively (p = 0.043). Mean SUV for patients with a Gleason score of <= 7a and > 7a was 6.2 and 13.5 (p = 0.046). Sensitivity and specificity for identifying tumor invasion of a prostate lobe was 85.6% and 76% (Positive and negative predictive value (PPV, NPV) for prostate lobe invasion were 95.7% and 42.9%). Sensitivity and specificity for seminal vesicle invasion were 50% and 100% (PPV 100%, NPV 96.6%).

#### CONCLUSION

Thus the PSMA PET-CT has very effective value in evaluation of intra and extra prostatic disease involvement.

#### **CLINICAL RELEVANCE/APPLICATION**

PSMA PET-CT is highly sensitive of prostatic cancer in comparison to F FDG PET-CT also



### NR351-ED-THA10

# Dedicated Lower Cranial Nerve MRI Imaging, Anatomy, and Common Pathologies

Thursday, Nov. 29 12:15PM - 12:45PM Room: NR Community, Learning Center Station #10

#### **Participants**

Marsela H. Campbell, DO, Jacksonville, FL (*Presenter*) Nothing to Disclose Peter J. Fiester, MD, Jacksonville, FL (*Abstract Co-Author*) Nothing to Disclose Tyler V. Campbell, DO, Jacksonville, FL (*Abstract Co-Author*) Nothing to Disclose Patrick Natter, MD, Jacksonville, FL (*Abstract Co-Author*) Nothing to Disclose Sukhwinder J. Sandhu, MD, Jacksonville, FL (*Abstract Co-Author*) Nothing to Disclose Dinesh Rao, MD, Jacksonville, FL (*Abstract Co-Author*) Nothing to Disclose Dalys E. Haymes, MD, Atlantic Bch, FL (*Abstract Co-Author*) Nothing to Disclose

### For information about this presentation, contact:

marsela.hyska-campbell@jax.ufl.edu

# **TEACHING POINTS**

Review of our MRI protocol for imaging lower cranial nerves Identify the expected course and normal appearance on MRI of the lower cranial nerves Common pathologies including neoplastic, extrinsic compression and inflammatory process MRI diagnostic pearls

# TABLE OF CONTENTS/OUTLINE

Our MRI Protocol Anatomy of lower cranial nerves CN IX CNX CNXI CNXII Pathology of the cranial nerves MRi diagnostic pearls



# NR356-ED-THA7

# Neuroimaging of Epilepsy: The Integration of Structural and Functional Imaging Modalities

Thursday, Nov. 29 12:15PM - 12:45PM Room: NR Community, Learning Center Station #7

#### **Participants**

Anais Tellier, Montreal, QC (*Presenter*) Nothing to Disclose Dang Khoa Nguyen, MD, FRCPC, Montreal, QC (*Abstract Co-Author*) Nothing to Disclose Laurent Letourneau-Guillon, MD, Toronto, ON (*Abstract Co-Author*) Nothing to Disclose Laurence Martineau, Montreal, QC (*Abstract Co-Author*) Nothing to Disclose

# For information about this presentation, contact:

anais.tellier@umontreal.ca

# **TEACHING POINTS**

SA-CME Learning objectives :1. Review the pathophysiology and clinical concepts underlying epilepsy.2. Discuss the multimodality approach in the investigation of epileptic patients and the role of structural MRI and functional modalities.3. Describe the structural MRI signatures of lesions related to epilepsy.4. Illustrate the key concepts through clinical vignette.

# TABLE OF CONTENTS/OUTLINE

Section 1. Pathophysiology and clinical concepts in epilepsy. Definition and diagnosis of epilepsy, pathophysiology of seizure, classification of the epilepsies. Section 2. Spectrum of structural lesions related to epilepsy : MRI signatures. Mesial temporal sclerosis, malformations of cortical development and other developmental anomalies, epilepsy-associated tumors (ganglioglioma, DNET, PXA, hypothalamic hamartoma), gliosis (a common final pathway for traumatic, ischemic and infectious insults, vascular malformations, meningoencephalocele, neurodevelopmental disorders (Sturge-Weber, tuberous sclerosis complex).Section 3. Imaging investigation of epilepsy, a multimodality approach. Imaging investigation and presurgical evaluation, structural imaging, functional imaging (MEG, MRS, FDG-PET, SPECT, fMRI, DTI), the future : co-registration of multimodal imaging into a common space.Section 4. Clinical vignettes.



# NR357-ED-THA8

# Genetics and Imaging of Thyroid Cancer: 2018 Update

Thursday, Nov. 29 12:15PM - 12:45PM Room: NR Community, Learning Center Station #8

# Awards Magna Cum Laude

#### Participants

Mohd Zahid, MD, San antonio, TX (*Presenter*) Nothing to Disclose Christopher Bittles, San Antonio, TX (*Abstract Co-Author*) Nothing to Disclose Ryan C. Ortez, BS, San Antonio, TX (*Abstract Co-Author*) Nothing to Disclose Andrew V. Chesley, MD, San Antonio, TX (*Abstract Co-Author*) Nothing to Disclose Maria Policarpio-Nicolas, Cleveland, OH (*Abstract Co-Author*) Nothing to Disclose Neeraj Kaur, MD, san antonio, TX (*Abstract Co-Author*) Nothing to Disclose Christine O. Menias, MD, Chicago, IL (*Abstract Co-Author*) Nothing to Disclose Srinivasa R. Prasad, MD, Houston, TX (*Abstract Co-Author*) Nothing to Disclose Venkata S. Katabathina, MD, San Antonio, TX (*Abstract Co-Author*) Nothing to Disclose

# For information about this presentation, contact:

katabathina@uthscsa.edu

# **TEACHING POINTS**

• Review molecular & genetic basis in the pathogenesis of different types of thyroid cancer (papillary, follicular, medullary, poorly differentiated & anaplastic) • Discuss genetic syndromes with a predisposition for thyroid cancer • Review American Thyroid Association (ATA) guidelines for ultrasound evaluation & follow-up of thyroid nodules • Discuss the development and future of molecular targeted therapies in thyroid cancer

#### **TABLE OF CONTENTS/OUTLINE**

• Introduction • Pathogenesis: PIK3/AKT & MAPK signaling pathways; mutations in BRAF, RAS, RET genes & rearrangements of PAX8/PPARy • Hereditary syndromes: Cowden, FAP, MEN type2, Carney complex & Pendred syndrome • A review of the ATA guidelines in ultrasound evaluation of thyroid nodules • Role of CT/MRI • Molecular targeted therapies • Future directions • Conclusion Improved understanding of genetic changes and pathogenesis of thyroid cancer can help to identify benign thyroid nodules to avoid unnecessary surgeries and develop 'designer' drugs for advanced malignancies. The association between BRAF, RAS, RET, and rearrangements of PAX8/PPARy with thyroid cancer provides an opportunity for improved diagnosis, prognosis, treatment, appropriate follow-up, and specialized imaging surveillance for the future. US and CT/MRI are pivotal in the initial diagnosis, follow-up & surveillance.

# **Honored Educators**

Presenters or authors on this event have been recognized as RSNA Honored Educators for participating in multiple qualifying educational activities. Honored Educators are invested in furthering the profession of radiology by delivering high-quality educational content in their field of study. Learn how you can become an honored educator by visiting the website at: https://www.rsna.org/Honored-Educator-Award/ Venkata S. Katabathina, MD - 2012 Honored EducatorVenkata S. Katabathina, MD - 2017 Honored EducatorChristine O. Menias, MD - 2013 Honored EducatorChristine O. Menias, MD - 2014 Honored EducatorChristine O. Menias, MD - 2015 Honored EducatorChristine O. Menias, MD - 2016 Honored EducatorChristine O. Menias, MD - 2018 Honored EducatorSrinivasa R. Prasad, MD - 2012 Honored Educator EducatorChristine O. Menias, MD - 2018 Honored EducatorSrinivasa R. Prasad, MD - 2017 Honored Educator



# NR358-ED-THA9

Pediatric Multiple Sclerosis: Imaging Spectrum and Differential Diagnosis

Thursday, Nov. 29 12:15PM - 12:45PM Room: NR Community, Learning Center Station #9

#### Awards Identified for RadioGraphics

### **Participants**

Igor G. Padilha, MD, Sao Paulo, Brazil (*Presenter*) Nothing to Disclose Ana Paula A. Fonseca, MD, Sao Paulo, Brazil (*Abstract Co-Author*) Nothing to Disclose Ana Luiza M. Pettengill, MD, Sao Paulo, Brazil (*Abstract Co-Author*) Nothing to Disclose Diego C. Fragoso, Sao Paulo, Brazil (*Abstract Co-Author*) Nothing to Disclose Felipe T. Pacheco, MD, Sao Paulo, Brazil (*Abstract Co-Author*) Nothing to Disclose Renato H. Nunes, Sao Paulo, Brazil (*Abstract Co-Author*) Nothing to Disclose Antonio Carlos M. Maia Jr, Sao Paulo, Brazil (*Abstract Co-Author*) Nothing to Disclose Antonio J. da Rocha, MD, PhD, Sao Paulo, Brazil (*Abstract Co-Author*) Nothing to Disclose

#### For information about this presentation, contact:

igorpadilha\_@hotmail.com

# **TEACHING POINTS**

The purposes of this exhibit are: - Review and illustrate the new concepts of pediatric multiple sclerosis (PMS) diagnosis, highlighting the last update (2017 McDonald criteria). - Present a historical perspective of the disease, highlighting evolution of the diagnostic criteria. - Describe through illustrative cases all the scenarios to diagnose EOMS - Review MS mimickers in children and adolescents with a mnemonic list of the most important differential diagnosis. - Reinforce the role of different MR sequences and how they contribute to diagnosis in clinical practice.

#### **TABLE OF CONTENTS/OUTLINE**

- Historic panel of PMS - First cases identified (historic panel); - Diagnostic criteria evolution timelime; - Advent of MR new sequences, identifying how they have contributed to PMS recognition. - First demyelinating episode evaluation - recognizing different presentations (clinical scenarios) that can be attributed to PMS. - Mnemonic DISNEY - Differential diagnosis D - Demyelinating disorders I - Infecctious diseases S - Systemic immunologic / inflammatory disorders N - Neoplasm E - Endocrinologic / metabolic disorders Y - Young vascular disorders



## NR426-SD-THA1

Gadolinium and Ferumoxytol Contrast Agents Given in the Same Imaging Session for Brain MRI: Is It Feasible?

Thursday, Nov. 29 12:15PM - 12:45PM Room: NR Community, Learning Center Station #1

**FDA** Discussions may include off-label uses.

### Participants

Csanad G. Varallyay, MD, PhD, Portland, OR (*Presenter*) Nothing to Disclose Ramon F. Barajas JR, MD, Portland, OR (*Abstract Co-Author*) Nothing to Disclose Prakash Ambady, Portland, OR (*Abstract Co-Author*) Nothing to Disclose Laszlo Szidonya, MD, PhD, Portland, OR (*Abstract Co-Author*) Nothing to Disclose Andrea Horvath, Portland, OR (*Abstract Co-Author*) Nothing to Disclose Fergus V. Coakley, MD, Portland, OR (*Abstract Co-Author*) Founder, OmnEcoil Instruments, Inc ; Shareholder, OmnEcoil Instruments, Inc

Edward Neuwelt, MD, Portland, OR (Abstract Co-Author) Nothing to Disclose

#### For information about this presentation, contact:

varallyc@ohsu.edu

# PURPOSE

While gadolinium based contrast agents are used as standard of care for MRI to depict areas of disrupted blood brain barrier, ferumoxytol, a long circulating iron oxide nanoparticle has advantages in imaging the intravascular space when used off label. We hypothesize that given the early extravasation and predominant T1 shortening properties of gadolinium, versus predominant T2\* shortening and long blood pool phase of ferumoxytol, signal changes from these contrast agents can be separated on MRI even when both are administered in the same imaging session. The aim of the study was: 1) to test if prior gadolinium affects steady state blood volume (CBV) assessment with ferumoxytol; 2) and also if prior administered ferumoxytol affects post contrast T1 weighted imaging with gadolinium.

#### **METHOD AND MATERIALS**

Brain MRIs of 22 patients with various cerebral pathologies, enrolled in a currenly recruting clinical trial (NCT03270059) were analyzed. Patients received both standard dose of gadolinium and 4mg/kg ferumoxytol in the same imaging session randomized to group1 (gadolinium first) and group2 (ferumoxytol first). Signal intensities on co-registered T1 3D GRE, and T2/T2\* 2D multiecho GRE images were recorded in the normal appearing thalamus, white matter, and enhancing lesion 1) on unenhanced images; 2) after the first 3) and after both administered agents. CBV values (calculated from changes of transverse relaxation rate pre and post ferumoxytol, relative to white matter) and relative T1 signal intensities (post/pre gadolinium) were compared between groups using unpaired T-test.

# RESULTS

No significant difference was found between group1 (n=12) and group2 (n=10) when analyzing relative CBV values within the thalamus (2.71;0.73 (SEM;SD) vs. 2.6;1.03, p=0.8) and enhancing lesion (3.19;1.53 vs. 3.41;1.59, p=0.81). Relative T1 signal intensity in the enhancing lesion was 2.07;0.4 in group1 and 2.13;0.52 in group2, p=0.8.

### CONCLUSION

This preliminary assessment suggests that CBV assessment using ferumoxytol is not affected by prior administered gadolinium. Similarly, gadolinium enhancement is not affected by prior administered ferumoxytol, therefore dual agent imaging is feasible in the same imaging session.

#### **CLINICAL RELEVANCE/APPLICATION**

Ferumoxytol and gadolinium MRI is feasible in a single imaging session, and does not require two separate MRI appointments, which is beneficial when information from both agents is needed.



# NR427-SD-THA2

MAGnetic Resonance Image Compilation (MAGIC): Is It Trustworthy?

Thursday, Nov. 29 12:15PM - 12:45PM Room: NR Community, Learning Center Station #2

### **Participants**

Augusto Lio M. Goncalves Filho, MD, Sao Paulo, Brazil (*Presenter*) Nothing to Disclose Felipe T. Pacheco, MD, Sao Paulo, Brazil (*Abstract Co-Author*) Nothing to Disclose Diego C. Fragoso, Sao Paulo, Brazil (*Abstract Co-Author*) Nothing to Disclose Flavia P. Junqueira, MD, MSc, Rio de Janeiro, Brazil (*Abstract Co-Author*) Nothing to Disclose Arthur Bolzam, Sao Paulo, Brazil (*Abstract Co-Author*) Nothing to Disclose Renato Hoffmann Nunes, MD, Sao Paulo, Brazil (*Abstract Co-Author*) Nothing to Disclose Antonio J. da Rocha, MD, PhD, Sao Paulo, Brazil (*Abstract Co-Author*) Nothing to Disclose

#### For information about this presentation, contact:

felipetorrespacheco@hotmail.com

### PURPOSE

The authors compared the diagnostic accuracy, inter and intraobserver agreement on the evaluation of conventional MR sequences and synthetic MAGIC scans, aiming to validate its potential effective clinical use.

# METHOD AND MATERIALS

It was analyzed a group of outpatient after ethics committees approved and written informed consent. Three blinded neuroradiologists read 102 clinically acquired case-control image sets for a total of 712 reads. Overall diagnostic image quality was classified as acceptable or not acceptable. The readers also classified as legible or illegible 4 specific anatomic regions: perisylvian and nucleo-capsular regions, brainstem and cervico-medullary junction. Readers recorded any artifacts presented. Finally, readers classified MR findings: 0 - normal; 1 - Tumor; 2 - Vascular; 3 - Congenital; 4 - Demyelinating; 5 - Infectious; 6 - Degenerative; 7 - Metabolic. Descriptive statistics were used to summarize anatomic/ morphology legibility by anatomic region, artifact prevalence, and diagnostic performance (sensitivity/specificity). Interrater reliability between readers was assessed by kappa (k) statistic.

### RESULTS

The study included 41 healthy and 61 pathologic cases. Overall interrater agreement (k correlation coefficient) for pathology detection was 0.61 for synthetic images and slightly higher at 0.70 for conventional images. In the context of tumoral lesions even subtle ones were detected for readers in both acquisitions. However, subtle lesions in infratentorial posterior fossa had low sensitivity detection. Readers identified relatively more artifacts among synthetic T2 FLAIR contrast views compared with other synthetic and conventional contrast views. Proton density sequence was not so valuable for brainstem analysis as in the conventional image. Readers considered a better contrast-noise ratio on T2 STIR sequence to analysis infratentorial structures and nucleo-capsular region.

# CONCLUSION

Although synthetic images still have limitations related to artifacts and lower spatial resolution, there is no significant loss of diagnostic capacity. The results support that brain study with synthetic images allow the acquisition of high diagnostic quality images with the benefit of reducing scan time and discomfort for patients undergoing MR imaging.

### **CLINICAL RELEVANCE/APPLICATION**

One of the main goals in the health care assistance is to provide an imaging study with high diagnostic accuracy, reducing the time-scan.



# NR428-SD-THA3

Automatic Generation of Synthesized Perfusion Maps from Multimodal MRI using a Deep Neural Network based Learning Scheme: A First Step Towards Quantification of Ktrans, Permeability, and Susceptibility Artifacts

Thursday, Nov. 29 12:15PM - 12:45PM Room: NR Community, Learning Center Station #3

#### Participants

M S Raghuprasad, PhD, Bangalore, India (*Presenter*) Employee, General Electric Company Dheeraj Kulkarni, Bangalore, India (*Abstract Co-Author*) Employee, General Electric Company Krishnan Varadarajan, Bengaluru, India (*Abstract Co-Author*) Nothing to Disclose Vinod Kumar, BSC,RT, Bangalore, India (*Abstract Co-Author*) Employee, General Electric Company

### For information about this presentation, contact:

raghu.prasad@ge.comdheeraj.kulkarni@ge.comKrishnan.Varadarajan@ge.comvinodkumar@ge.com

#### PURPOSE

The conventional perfusion MRI is the most widely used technique for glioma, stroke, and other potential neurodegenerative disorders. However, due to underlying pathology and scan time limitations it is difficult to quantify susceptibility artifacts, Ktrans, and permeability parameters. The primary purpose of this study was to develop a deep neural network based manifold learning scheme for auto-generation of perfusion maps from regular spin echo and fast spin echo sequences. Additionally, the network also quantified the Ktrans and permeability parameters.

# **METHOD AND MATERIALS**

A deep neural network was developed with 10 layers: 5 convolution layers and a recurrent pooling layer followed by a fullyconnected soft-max layer, with 2 layers for manifold regression learning of reduced intravenous (IV) contrast distribution in the arterial, venous, and capillary phases. A network regression layer for predicting the permeability indices, and K-trans values. 2 scoring layers for filling the color look up table entries based on the underlying pathology. The ktrans maps of different contrast phases were first segmented using convolutional neural network and then quantified by a convolutional auto-encoder. To test the deep learning network model 150 reduced intravenous contrast fast spin echo datasets were fed as an input to the network along with characteristic kinetic equations to track the IV contrast. The susceptibility artifacts such as blood product and calcification were also modeled.

# RESULTS

Adding deep-learning based manifold analysis for permeability and ktrans resulted in improved specificity (92%) and sensitivity (95%) (p<0.01). A strong co-relation was observed between the maps that were generated from deep neural network and the regular conventional epi based perfusion mode scanning (r=0.992). Further, the kinetic equations in the soft max layer of the network were able to capture the contrast arterial, venous, and capillary phases and quantify vascular/capillary permeability.

#### CONCLUSION

Results show that deep learning based neural network has the capability to generate perfusion maps from a) contrast spin/fast spin echo sequences, b) quantify Ktrans/permeability indices, c) quantify CBF,CBV and MTT.

# **CLINICAL RELEVANCE/APPLICATION**

Diagnostic MR perfusion system based on deep learning has a significant potential to quantify permeabiliaty, blood product, and calcification, thereby eliminating the need of scan in perfusion mode.



# NR429-SD-THA4

Incidence and Clinical Implications of FLAIR Signal Abnormality in the Internal Jugular Vein and Transverse and Sigmoid Sinuses on Brain MRI

Thursday, Nov. 29 12:15PM - 12:45PM Room: NR Community, Learning Center Station #4

### Participants

Kelly A. Dahlstrom, DO, Kansas City, KS (*Presenter*) Nothing to Disclose Joseph Thelen, Kansas City, KS (*Abstract Co-Author*) Nothing to Disclose Suzanne L. Hunt, Kansas City, KS (*Abstract Co-Author*) Nothing to Disclose Yu Wang, Kansas City, KS (*Abstract Co-Author*) Nothing to Disclose Carissa Walter, Kansas City, KS (*Abstract Co-Author*) Nothing to Disclose Jacqueline Hill, PhD,MPH, Kansas City, KS (*Abstract Co-Author*) Nothing to Disclose Luke N. Ledbetter, MD, Kansas City, KS (*Abstract Co-Author*) Royalties, Reed Elsevier John D. Leever, MD, Fairway, KS (*Abstract Co-Author*) Nothing to Disclose

#### For information about this presentation, contact:

kdahlstrom2@kumc.edu

#### PURPOSE

To determine the incidence and potential clinical implications of FLAIR signal abnormality within the internal jugular vein (IJV), transverse sinus, and/or sigmoid sinus on brain MRI.

#### **METHOD AND MATERIALS**

This retrospective analysis included 500 randomly selected patients 18 years or older who received a contrast-enhanced brain MRI at a single institution from 7/1/2015-12/31/2015. Patients were excluded for obvious cause of intravenous signal abnormality or structural abnormality, such as post-operative changes in the posterior fossa. Presence of venous signal abnormality was documented, which was defined as intraluminal FLAIR hyperintensity (relative to the middle cerebellar peduncles) in the transverse sinus, sigmoid sinus and/or IJV (beyond the jugular foramen). Presence of intraluminal post-contrast enhancement was assessed to delineate slow flow phenomenon from venous sinus thrombosis.

#### RESULTS

A total of 484 patients were included. Thirty-nine (8.1%) patients had intravenous FLAIR hyperintensity attributed to slow flow phenomenon. No patients with intravenous signal abnormality demonstrated an absence of intraluminal post-contrast enhancement to suggest venous thrombosis. Additionally, none of the patients with intravenous signal abnormality had a history of idiopathic intracranial hypertension (IIH), pseudotumor cerebri, or any of the associated clinical characteristics we explored (opening pressure >25 cm of water, papilledema, history of headache).

#### CONCLUSION

This study found that intravenous FLAIR signal abnormality in the transverse sinus, sigmoid sinus, and/or IJV on brain MRI scans is a relatively common finding (8.1%) and most often reflects slow flow phenomenon without a clear relationship with IIH. These results imply it is unlikely this signal abnormality indicates venous thrombosis and its presence alone on non-contrast MRI scans may suggest additional imaging or venography is unnecessary.

### **CLINICAL RELEVANCE/APPLICATION**

FLAIR signal abnormality in the dural venous sinuses is a relatively common finding without any clear clinical implication.



### NR430-SD-THA5

Basic Consideration of the Facial Aging: Anatomic and MR Imaging Analysis of the Nasolabial Fold (NLF)s

Thursday, Nov. 29 12:15PM - 12:45PM Room: NR Community, Learning Center Station #5

### Participants

Itsuko Okuda, MD, Minato-Ku, Japan (*Presenter*) Nothing to Disclose Naoki Yoshioka, Tokyo, Japan (*Abstract Co-Author*) Nothing to Disclose Masahiro Irimoto, MD, Kunitachi, Japan (*Abstract Co-Author*) Nothing to Disclose Keiichi Akita, MD, PhD, Tokyo, Japan (*Abstract Co-Author*) Nothing to Disclose

# For information about this presentation, contact:

okudai812@yahoo.co.jp

# PURPOSE

Wrinkles and sagging can affect appearance. The nasolabial fold (NLF)s are more pronounced and a clear sign of aging. However, the structuring of the NLFs have not been fully elucidated yet. The AIM of this study is to analyze the anatomic radiological correlation of the NLFs, and establish MR imaging of the NLFs.

# METHOD AND MATERIALS

This study was approved by the institutional review board. Step 1: Cadaveric studies. Five cadaver faces (2 males and 3 females) were used. The right halves of them were dissected, and histological sections were created from the left. The facial muscles and adipose tissue of the cheeks and oral regions were evaluated anatomically and histologically. Step 2: Seven healthy adult volunteers (3 males and 4 females; age range, 27-51 years) were enrolled for facial structure evaluation. Subjects were examined with a 3.0T MR imager (Achieva3.0T, Philips Medical Systems, the Netherlands). Step 3: Anatomic and radiological correlation. MR imaging findings were compared with the anatomic and histological (A/H) findings.

#### RESULTS

From the cheek, the levator labii superioris alaeque nasi, levator labii superioris and major and minor zygomatic muscles were observed macroscopically in the preceding order. These muscles attached mainly to the orbicularis oris muscle distributing to the medial side to the NLFs, and some fibers of these muscles attached to the inner aspects of the skin of NLFs. Macroscopically, the adipose tissue of lateral side of the NLFs (Ad-L) was thick. On the other hand, the adipose tissue of medial side of the NLFs (Ad-M) was thin, also the orbicularis oris muscle and skin fixed strongly to each other. In all subjects, these A/H findings were accurately obtained by MRI. In addition, the adipose tissue showed high signal intensity, however, the Ad-M was lower than the Ad-L. It suggested that the Ad-M contains fibers richer than the Ad-L.

# CONCLUSION

The NLFs are the definite anatomic structures that can be accurately demonstrated by MRI. It is suggested that the NLFs are formed by the anatomic difference between medial side and lateral side of the NLFs. This analysis can aid evaluating age-related changes of the face non-invasively, and can contribute to the elucidation of the mechanism of facial aging.

# **CLINICAL RELEVANCE/APPLICATION**

MRI non-invasively provides the subcutaneous anatomic information of the face, and is a useful tool to evaluate the of state of the NLFs and aging process.



# NR431-SD-THA6

Application of Textural Analysis Method for Distinguishing Benign and Malignant Thyroid Nodules with Circinate Macrocalcification on CT Images

Thursday, Nov. 29 12:15PM - 12:45PM Room: NR Community, Learning Center Station #6

# Participants

Lijun Wang, Dalian, China (*Presenter*) Nothing to Disclose Zhaonan Sun, Dalian, China (*Abstract Co-Author*) Nothing to Disclose Zhuanzhuan Mu, Dalian, China (*Abstract Co-Author*) Nothing to Disclose Yan Guo, Shenyang, China (*Abstract Co-Author*) Nothing to Disclose Ailian Liu, MD, Dalian, China (*Abstract Co-Author*) Nothing to Disclose Yijun Liu, Dalian, China (*Abstract Co-Author*) Nothing to Disclose

#### For information about this presentation, contact:

wanglj345@163.com

### PURPOSE

To assess the diagnostic value of textural analysis method (TA) in differentiating malignant from benign thyroid nodules which were within circinate macrocalcifications (CMCs) using CT images.

### **METHOD AND MATERIALS**

60 patients with CMCs were identified from pathology database, among them, 19 (31.6%) were papillary thyroid carcinomas, 40 (66.7) were nodular goiters and 1 (1.7%) was Hashimoto's thyroiditis. Inclusion criteria were as follows: pattern of calcification is circinate, and the girth of calcification>= 2/3 perimeter, all scans were performed on a HD750 CT scanner. 2D regions of interest (ROIs) were defined at the slice with the maximum diameter of CMCs. Mean, median and 64 texture features, including shape and size-based features, histogram and GLCM as well as GLRLM features of CT value were generated automatically using Omni-Kinetics software (GE Healthcare). Statistical analysis was conducted with SPSS 22.0 software. Independent sample Mann-Whitney U test and Pearson correlation test with r<0.9 were used and receiver operating characteristic (ROC) curve was plotted to assess diagnostic efficiency of them.

#### RESULTS

Mann Whitney U test showed that 31 features were significant different between benign and malignant groups, Pearson test reduced them into 9 features: Quantile25, Uniformity, MedianIntensity, MinIntensity, Inertia and LongRunLowGreyLevelEmphasis were significant lower while GreyLevelNonuniformity, Skewness and Correlation were higher in benign lesions than that in malignant lesions.

### CONCLUSION

TA Method could efficiently classify benign and malignant thyroid nodules with circinate macrocalcification on CT images with good sensitivity and specificity, while traditional CT and Ultrasound failed.

#### **CLINICAL RELEVANCE/APPLICATION**

Although BUS is the first choice for thyroid nodules, macro calcifications in the thyroid are very commonly found on chest CT . It is very useful to make sure the nature of thyroid disease with macro calcifications without further BUS. Circinate macrocalcification is usually found in benign thyroid nodules, but it is not specific for benign nodules. Textural Analysis method in CT provided an emerging tool for distinguishing benign and malignant thyroid nodules with circinate macrocalcification on CT images without additional cost.



# OB189-ED-THA1

Adenomyosis: Imaging Findings, Differential Diagnosis, Response to Therapy, and a Proposition of a Classification for Clinical Use in Women of Reproductive Age

Thursday, Nov. 29 12:15PM - 12:45PM Room: OB Community, Learning Center Station #1

# Participants

Luciana P. Chamie, MD, PhD, Sao Paulo, Brazil (*Presenter*) Nothing to Disclose Angela H. Caiado, MD, Sao Paulo, Brazil (*Abstract Co-Author*) Nothing to Disclose Gisele Warmbrand, MD, Sao Paulo, Brazil (*Abstract Co-Author*) Nothing to Disclose Duarte M. Ribeiro, MD, Sao Paulo, Brazil (*Abstract Co-Author*) Nothing to Disclose Paulo C. Serafini, MD, PhD, Sao Paulo, Brazil (*Abstract Co-Author*) Nothing to Disclose

## For information about this presentation, contact:

luciana@chamie.com.br

# **TEACHING POINTS**

To review the concept and pathophysiology of adenomyosis To demonstrate the imaging findings of adenomyosis through transvaginal sonography and magnetic resonance imaging To discuss the differential diagnosis and pitfalls To demonstrate the response to clinical and surgical therapy through imaging methods To propose a simple classification of adenomyosis useful for clinical counseling in women of reproductive age

#### **TABLE OF CONTENTS/OUTLINE**

A. Anatomical review of the uterine wall B. Pathophysiology of adenomyosis C. Clinical findings D. Imaging findings through transvaginal sonography and magnetic resonance imaging E. Differential diagnosis and pitfalls F. Imaging findings after clinical and surgical therapy G. Proposition of a classification for clinical counseling in women of reproductive age



# OB190-ED-THA2

# Radiologist, Be Aware: The Impact of MRI Findings of Fibroids on Gynecological Decision Making

Thursday, Nov. 29 12:15PM - 12:45PM Room: OB Community, Learning Center Station #2

#### **Participants**

Danilo Pachani, MD, SAO PAULO, Brazil (*Presenter*) Nothing to Disclose Bruno J. Ribeiro, MD, Campinas, Brazil (*Abstract Co-Author*) Nothing to Disclose Aldo M. Araujo Alves, MD, Sao Paulo, Brazil (*Abstract Co-Author*) Nothing to Disclose Roberto Blasbalg, MD, Sao Paulo, Brazil (*Abstract Co-Author*) Nothing to Disclose Ricardo M. Pereira, MD, Sao Paulo, Brazil (*Abstract Co-Author*) Nothing to Disclose Leandro A. Mattos Sr, MD, PhD, Sao Paulo, Brazil (*Abstract Co-Author*) Nothing to Disclose

### **TEACHING POINTS**

The purposes of this exhibit are: 1. To demonstrate typical and atypical presentations of fibroids on magnetic resonance imaging (MRI). 2. To review the relevant imaging information to gynecologists decision-making process. 3. To demonstrate uncommon manifestations of fibroids and differential diagnosis. 4. To review the MRI findings that may lead to suspicion of a malignant uterine nodule 5. To explain the therapeutic implications MRI aspects of fibroids.

# TABLE OF CONTENTS/OUTLINE

A. Introduction B. Typical fibroids C. Degenerate fibroids D. Rarer fibroids presentations E. Relevant MRI findings to decision making - What does the gynecologist want to know? F. When to suspect for malignancy on uterine nodules? G. Future directions and takehome messages.



# PD192-ED-THA7

Growing a Backbone: Essentials of Neonatal Spine Ultrasound

Thursday, Nov. 29 12:15PM - 12:45PM Room: PD Community, Learning Center Station #7

#### **Participants**

Olivia E. Linden, MD, San Francisco, CA (*Presenter*) Nothing to Disclose Andrew S. Phelps, MD, San Francisco, CA (*Abstract Co-Author*) Nothing to Disclose John D. MacKenzie, MD, San Francisco, CA (*Abstract Co-Author*) Nothing to Disclose Matthew A. Zapala, MD,PhD, San Francisco, CA (*Abstract Co-Author*) Nothing to Disclose Jesse L. Courtier, MD, San Francisco, CA (*Abstract Co-Author*) Founder, HoloSurg3D, Inc; Consultant, HoloSurg3D, Inc

# For information about this presentation, contact:

olivia.linden@ucsf.edu

## **TEACHING POINTS**

Neonatal spinal ultrasound is a common examination in patients with suspicious cutaneous lesions/masses or neurologic symptoms and can help differentiate benign superficial lesions from those with underlying pathology or diagnoses requiring possible surgical repair. Our goal is to 1. Review anatomy and good practice techniques of spinal ultrasound, 2. Discuss indications for ultrasound, 3. Outline the embryology and important imaging findings associated with common pathologies, and 4. Provide a self-assessment quiz to test understanding.

# TABLE OF CONTENTS/OUTLINE

1. Embryology of the neonatal spine 2. Normal ultrasound appearance (including: ultrasound techniques, three methods of counting vertebrae, normal anatomy, nerve-root pulsations, normal variants) 3. Indications for ultrasound (including: cutaneous lesions, neurologic symptoms, syndromic patients, skin-covered masses, postoperative/post-procedural) 4. Pathology (including: tethered cord; sacral dimple and dorsal dermal sinus tract; spinal masses: lipoma (lipomyelocele and lipomyelomeningocele), closed spinal dysraphism (dorsal meningocele, terminal myleocystocele, diastematomyelia), open spinal defects (myelocele, myelomeningocele); hematoma; and sacral agenesis 5. Quiz



# PD193-ED-THA8

New MR Techniques to Decrease MR Scan Times in Children

Thursday, Nov. 29 12:15PM - 12:45PM Room: PD Community, Learning Center Station #8

### Awards Certificate of Merit Identified for RadioGraphics

# Participants

Benjamin Kozak, MD, Boston, MA (*Presenter*) Nothing to Disclose Camilo Jaimes Cobos, MD, Boston, MA (*Abstract Co-Author*) Nothing to Disclose Samantha Harrington, MD, Boston, MA (*Abstract Co-Author*) Nothing to Disclose Monica Johnson, MD, Boston, MA (*Abstract Co-Author*) Nothing to Disclose John Kirsch, PhD, Charlestown, MA (*Abstract Co-Author*) Nothing to Disclose Michael S. Gee, MD, PhD, Boston, MA (*Abstract Co-Author*) Nothing to Disclose

# For information about this presentation, contact:

bkozak@partners.org

# **TEACHING POINTS**

Pediatric magnetic resonance imaging (MRI) is challenging due to the inability of many children to tolerate long scan times awake. Also, many infants and children require sedation to undergo MRI, with recent data highlighting potential risks of prolonged anesthetic exposure early in life. Recent advances in MR hardware and software can significantly reduce MRI scan times for both awake and anesthetized children. The purpose of this exhibit is highlight new MR techniques that can be applied in clinical practice to make MRI in children faster.

#### **TABLE OF CONTENTS/OUTLINE**

I. Challenges of long MR scan times in children A. Inability to lie still for duration of exam B. Issues with anesthesiaII. New MR techniques to decrease scan time A. Simultaneous multi-slice imaging: DWI and BOLD B. K-space undersampling/compressed sensing reconstruction C. Non-Cartesian/radial continuous K-space sampling D. Parallel image acceleration with controlled aliasing E. Automated protocol selection techniques F. Isotropic imaging techniques 1. T1-weighted techniques (MPRAGE) 2. T2-weighted techniques (CUBE/SPACE)III. Emerging techniques/future directions A. Artificial intelligence noise reduction B. WAVE controlled aliasing C. Volumetric chemical shift imaging/spectroscopy



# PD241-SD-THA2

Comparison of 320-Row Detector CT Angiography versus Transthoracic Echocardiography for Imaging of Coronary Artery Lesion in Children with Kawasaki Disease

Thursday, Nov. 29 12:15PM - 12:45PM Room: PD Community, Learning Center Station #2

**FDA** Discussions may include off-label uses.

### Participants

Kou Mingqing, Xi'an, China (*Presenter*) Nothing to Disclose Minggang Huang, Xian, China (*Abstract Co-Author*) Nothing to Disclose Bing Ge, Chengdu, China (*Abstract Co-Author*) Nothing to Disclose Chen Xiaolong, Xian, China (*Abstract Co-Author*) Nothing to Disclose Yan Zhang, MD,PhD, Xi'an, China (*Abstract Co-Author*) Nothing to Disclose

### For information about this presentation, contact:

kmq9876@126.com

### PURPOSE

To compare the clinical value of 320-row computed tomography angiography(CTA) with transthoracic echocardiography (TTE) examinations in the diagnosis of coronary artery lesion in children with Kawasaki disease (KD).

# **METHOD AND MATERIALS**

Sixteen KD children, with ages ranging from 11 months to 8 years old and heart rates ranging from 94 to 146 beats per minute, underwent both electrocardiogram (ECG) triggered 320-row detector CT and TTE examinations within one week during free breathing with sedation. The location, number and size of aneurysms were observed. Bland Altman analysis was used to evaluate the agreement on measurements (diameter and length of aneurysms) between CTA and TTE. The effective radiation dose from the CTA was recorded for all children.

# RESULTS

The aneurysm diameter with CTA was  $0.86\pm0.33$ cm and with TTE was  $0.79\pm0.39$  cm, while the aneurysm length with CTA was  $1.96\pm1.35$  cm and with TTE was 2. 00  $\pm1.18$  cm. Bland Altman analysis for the agreement between CTA and TTE measurements showed good agreement. The mean effective radiation dose of CTA was  $0.42\pm0.08$  mSv.

### CONCLUSION

For KD children, ECG triggered CTA provided more objective and subjective image quality when compared with TTE, and ECG triggered CTA with sub mSv effective dose may provide excellent image quality and high diagnostic accuracy for KD children.

# **CLINICAL RELEVANCE/APPLICATION**

CTA provide excellent image quality and high diagnostic accuracy for KD children.



# PD242-SD-THA3

# Evaluation of MRI in the Prenatal Diagnosis of Cleft Lip and Palate

Thursday, Nov. 29 12:15PM - 12:45PM Room: PD Community, Learning Center Station #3

# Awards

# Trainee Research Prize - Medical Student

#### Participants

Mimi Tian, Jinan, China (*Presenter*) Nothing to Disclose Lianxiang Xiao, Jinan, China (*Abstract Co-Author*) Nothing to Disclose Nan Jian, Jinan, China (*Abstract Co-Author*) Nothing to Disclose Jinxia Zhu, Beijing, China (*Abstract Co-Author*) Nothing to Disclose Xin Hong Wei, Jinan, China (*Abstract Co-Author*) Nothing to Disclose Shuai Zhang, Jinan, China (*Abstract Co-Author*) Nothing to Disclose Guan Li, Jinan, China (*Abstract Co-Author*) Nothing to Disclose Xiangtao Lin, MD, Jinan, China (*Abstract Co-Author*) Nothing to Disclose

### For information about this presentation, contact:

mimitian@126.com

#### PURPOSE

To evaluate the value of Magnetic Resonance Imaging(MRI) in the diagnosis of prenatal cleft lip and palate.

### **METHOD AND MATERIALS**

We retrospectively reviewed medical records of fetuses with suspected cleft lip and plate on ultrasonography(US). A total of 44 pregnant women having a median gestational age of 28 (range:20-39) weeks were included after informed consent was obtained. All MRI examinations were performed with a 1.5 T MAGNETOM Amira (Siemens Shenzhen Magnetic Resonance Ltd., Shenzhen, China). True fast imaging with steady-state precession (True FISP) images were obtained without breath holding in the axial, coronal, sagittal planes. The scan parameters of the True FISP were as follows: TR=612ms, TE= 1.93ms, 30 slices, FOV=380mm×380mm, Acquisition matrix 256×256, Voxel size=1.3 x 1.3 x 1.3mm, flip angle=79°. All the MR images were blindly and independently reviewed by three experienced radiologists. The prenatal US and MRI diagnosis was compared with that obtained during follow-up.

### RESULTS

MRI demonstrated the anatomy of the maxillofacial region well (figure 1A-C). The follow-up results showed isolated cleft lip in 23 cases, isolated cleft palate in 3 cases (figure 2A-C), unilateral incomplete cleft lip and cleft palate in 4 cases, unilateral complete cleft lip and cleft palate in 11 cases (figure 3A-C), and bilateral complete cleft lip accompanied with cleft palate in 3 cases (figure 4A-C). The accuracy, sensitivity and specificity in detection cleft palate was 75%,47.6%,100% for US and 97.7%,95.2%,100% for MRI, respectively.

# CONCLUSION

The diagnostic efficacy of MRI on cleft lip and palate is superior to that of US. MRI can bring additional information to US for the prenatal diagnosis of cleft lip and palate.

### **CLINICAL RELEVANCE/APPLICATION**

MRI provides more useful information for the prenatal diagnosis of cleft lip and palate that could be used as an effective adjunct method of prenatal ultrasound diagnosis



# PD243-SD-THA4

Avoiding Sedation in Brain Examinations for Neonates and Children by Using Silent MR Sequence: A Comparative Study

Thursday, Nov. 29 12:15PM - 12:45PM Room: PD Community, Learning Center Station #4

# Participants

Jia Xiaoqian, Xian, China (*Presenter*) Nothing to Disclose Jianxin Guo, Xian, China (*Abstract Co-Author*) Nothing to Disclose Xiaoyu Wang, Xi'an, China (*Abstract Co-Author*) Nothing to Disclose Xingxing Tao, Xi'an, China (*Abstract Co-Author*) Nothing to Disclose Huifang Zhao, Xi'an, China (*Abstract Co-Author*) Nothing to Disclose Yannan Cheng, BS,BS, Xi'an, China (*Abstract Co-Author*) Nothing to Disclose Chao Jin, Xian, China (*Abstract Co-Author*) Nothing to Disclose Xianjun Li, Xian, China (*Abstract Co-Author*) Nothing to Disclose Yang Jian, PhD, MD, Xi An, China (*Abstract Co-Author*) Nothing to Disclose

### For information about this presentation, contact:

363448088@qq.com

#### PURPOSE

To evaluate the acoustic noise, image quality, and success rates of magnetic resonance with silent technology for children under the condition of non-sedation and comparing with traditional MR for children with sedation as needed.

#### **METHOD AND MATERIALS**

Images were continuously collected from 1) September to November 2017 using commercial silent technology for head MR of children under 12 years old as silent group and 2) February to August 2017 using conventional techniques for head MR of children under 12 years old information as control group. Objects who fail to cooperate were given sedatives to help sleep in control group, while all neonates and children completed the examination under the condition of non-sedation in silent group. The protocol package of tradition sequences includes T2 flair Propeller, T2 Propeller, and 3D-T1 FSPGR; while the silent sequences contains Silent T2 Flair, Silent T2 Propeller, and Silent MR T1(Table1). We measured the noise of each sequence at different sites using a special noise meter. Image quality was subjectively assessed in consensus by two radiologists on a 3-point scale (0, non-diagnosable images; 1, diagnosable image with limitations; 2, fully diagnosable). The acoustic noise, MR success rate and image quality between traditional MR and silent MR were compared.

### RESULTS

530 children (age range, 5 days~12 years) were included in this study. During the MR examinations, the measured peak of sound pressure level (SPLs) at the isocenter of the imager bore in control group ranged from 129.7 to 130.5 dBA. The equivalent SPLs in control group varied from 114.0 to 118.8 dBA, (Table 1); correspondingly, in silent group, the measured peak and equivalent SPLs ranged from 87.5 to 102.4dBA and 73.7 to 83.5dBA (Table2). In this study, the qualities of all images in the silent group could be used for diagnosis (the representative image is shown in Figure 1). The success rates of control and silent group are 71.5% and 80.4% respectively, (P=0.261)

# CONCLUSION

Apply the silent technique to the MRI examination of neonate and children under non-sedation condition could generate comparable images with traditional MR, and the data should be collected further to explore a more optimized sequence.

# **CLINICAL RELEVANCE/APPLICATION**

Silent sequence can avoid the use of sedatives, so as to avoid the physical and mental risks it brings.



# PD245-SD-THA6

# Study of Probabilistic Versus Deterministic Tractography in Pediatric Spinal Cord Imaging

Thursday, Nov. 29 12:15PM - 12:45PM Room: PD Community, Learning Center Station #6

#### **Participants**

Ajit Karambelkar, MBBS, Philadelphia, PA (*Presenter*) Nothing to Disclose Mahdi Alizadeh, Philadelphia, PA (*Abstract Co-Author*) Nothing to Disclose Feroze B. Mohamed, PhD, Philadelphia, PA (*Abstract Co-Author*) Nothing to Disclose Adam E. Flanders, MD, Philadelphia, PA (*Abstract Co-Author*) Nothing to Disclose Sona Saksena, PhD, Philadelphia, PA (*Abstract Co-Author*) Nothing to Disclose Neelu Jain-Lakhani, MD, Philadelphia, PA (*Abstract Co-Author*) Nothing to Disclose Shiva Shahrampour, MSc, Philadelphia, PA (*Abstract Co-Author*) Nothing to Disclose Kiran S. Talekar, MBBS, MD, Philadelphia, PA (*Abstract Co-Author*) Spouse, Employee, GlaxoSmithKline plc

# PURPOSE

The purpose of this study was to determine various diffusion indices including the mean tract density determined by the probabilistic and deterministic tractography along the entire length of the spinal cord (C1-L1).

### **METHOD AND MATERIALS**

6 subjects between age group 6-16 years underwent 3T MR imaging of the entire spinal cord. Axial reduced FOV EPI-SE DTI sequence was used to acquire two overlapping slabs to cover the entire spinal cord. ROIs were drawn on the axial images to include the entire cross-section of the cord from C2 to T12 vertebral levels. Preprocessing of data including motion correction and eddy current correction was performed using FSL software (FSL version 5). For probabilistic tractography, we used BEDPOSTX and PROBTRACKX toolboxes in FSL.(1-3). For deterministic tractography, we ran constrained specific spherical deconvolution modeling using MRTrix software (version 3). Mean tract density was calculated at each cord level by the probabilistic and deterministic method.

# RESULTS

Mean tract density of the pediatric spinal cord measured with the probabilistic method is above 10000 units at each cord level. The mean tract density is below 10000 units when measured with deterministic method except at T6-T7 level. In general, the mean tract density is higher in the upper cervical cord and mid-thoracic cord and is lower in cervical and upper thoracic cord (Table 1 and 2). This variation in mean tract density of the spinal cord is consistent with both methods and is presumably related to physiologic variation in concentration of spinal cord tracts in these regions and in part related to the differences in the age group of subjects (Graph 1).

# CONCLUSION

To the best of our knowledge this is the first attempt to measure mean tract density at each level of the normal pediatric spinal cord with the probabilistic and deterministic methods. Mean tract density is higher and less variable with the probabilistic method than deterministic method.

# **CLINICAL RELEVANCE/APPLICATION**

Mean tract density has been investigated in literature as a marker of cord integrity which may have significant implications for the management of spinal cord pathologies such as chronic spondylotic myelopathy or acute cord injury.



# PH251-SD-THA1

Effect of Iodinated Contrast Medium on Organ Dose at Coronary CT Angiography Using 100-kVp and 120-kVp Scans

Thursday, Nov. 29 12:15PM - 12:45PM Room: PH Community, Learning Center Station #1

# Participants

Daisuke Sakabe, MS, Kumamoto, Japan (*Presenter*) Nothing to Disclose Daisuke Ustunomiya, kumamoto, Japan (*Abstract Co-Author*) Nothing to Disclose Yoshinori Funama, PhD, Kumamoto, Japan (*Abstract Co-Author*) Nothing to Disclose Takeshi Nakaura, MD, Kumamoto, Japan (*Abstract Co-Author*) Nothing to Disclose Seitaro Oda, MD, Kumamoto, Japan (*Abstract Co-Author*) Nothing to Disclose Yasuyuki Yamashita, MD, Kumamoto, Japan (*Abstract Co-Author*) Nothing to Disclose Masahiro Hatemura, Kumamoto, Japan (*Abstract Co-Author*) Nothing to Disclose

### PURPOSE

The lower tube voltage technique obtains higher contrast enhancement than the standard one, resulting in reduction of iodinated contrast medium (CM) volume on coronary computed tomography angiography (CCTA). Radiation dose in the tissues and organs is affected by the CM, and the effect of the CM may differ with tube voltages. The purpose of this study was to compare the organ doses between the reduced CM-volume protocol with 100-kVp and the standard CM-volume protocol with 120-kVp on CCTA.

### **METHOD AND MATERIALS**

Twenty female patients each underwent the 100-kVp scans at 22% reduced CM of 350mgI/kg and the 120-kVp scans at the CM of 450mgI/kg on CCTA using a 320-detector volume CT scanner (Aquilion One, Canon Medical Systems). For obtaining the equivalent image quality, the same image noise index with automatic exposure control was used in both scans. The organ doses for one gantry rotation (right and left mammary glands [RMG, LMG], left ventricle [LV], septal and lateral wall of LV [SepLV, LatLV], ascending aorta, lung, and skin) were estimated by Monte Carlo simulation. The body mass index (BMI), volume CT dose index (CTDIvol), CT numbers, and the organ doses in each patient were compared between the 100-kVp and the 120-kVp images on CCTA.

### RESULTS

The mean BMI and the mean CTDIvol were comparable for 100- and 120-kVp (22.7- vs. 22.8 kg/m2 (P > 0.05) and 4.3 and 4.0 mGy/rot (P > 0.05), respectively). The mean CT number in the LV with 100-kVp was 497.6 HU and almost the same as 120-kVp at 476.9 HU (p>0.05). The mean organ dose for RMG and LMG between 100-kVp and 120-kVp images was 2.6 vs. 3.2 mGy (p>0.05) and 2.6 vs. 3.1 mGy (p>0.05), respectively. With respect to SepLV and LatLV, the mean organ dose between 100-kVp images and 120-kVp images was 2.6 vs. 3.1 mGy (p>0.05) and 2.7 vs. 3.4 mGy (p>0.05), respectively. The organ doses on the 100-kVp scans were lower than 120-kVp by approximately 20%, although there were no statistically differences.

# CONCLUSION

When obtaining equivalent iodine enhancement and CTDIvol on CCTA, the 100-kVp scan with 20% CM dose reduction tends to reduce the organ dose by approximately 20% compared with the 120-kVp scan.

# **CLINICAL RELEVANCE/APPLICATION**

On CCTA, the 100 kVp scan with decreased iodinated CM administration enables 20% organ dose reduction, which may be beneficial for lowering breast radiation in female patients.



# PH252-SD-THA2

# Development of Method of Dosimetric Indications Required by IEC 60601-2-54 Using MCNPX

Thursday, Nov. 29 12:15PM - 12:45PM Room: PH Community, Learning Center Station #2

### **Participants**

Seung-Youl Lee, Cheongju, Korea, Republic Of (*Presenter*) Nothing to Disclose Tae Hee Lee, Cheongju, Korea, Republic Of (*Abstract Co-Author*) Nothing to Disclose Hyun Soo Na, Cheongju, Korea, Republic Of (*Abstract Co-Author*) Nothing to Disclose Mi Jung Kim, Cheongju, Korea, Republic Of (*Abstract Co-Author*) Nothing to Disclose Cheol-Ha Baek, RT, Gangwondo, Korea, Republic Of (*Abstract Co-Author*) Nothing to Disclose

# CONCLUSION

In order for the manufacturers to utilize such methodology to establish the measurement display system of radiation doses for Xray devices, they should replicate the simulation suited to the characteristics of each device and go through a thorough comparison and verification process with actual measurement values before application.

# Background

The International Electrotechnical Commission requires reducing the amount of radiation exposure to patients by displaying the radiation doses measured during diagnostic radioactive examinations. This study aims to provide the methodology for dose measurement using MCNPX (Monte Carlo N-Particle eXtended v2.7), and calculate effective doses per study, by applying domestic standard computational human phantoms (HDRK Man/Woman).

### **Evaluation**

MCNPX (Monte Carlo N-Particle eXtended v2.7, USA) is used to replicate the geometry of randomly selected X-ray devices, and radiation doses were measured and verified based on kVp, tube current multiplied by mAs, distance between SID and changes in additional filters in the actual environment to verify the value. As a result of comparing MCNPX results and actual measured values according to changes in tube voltage and SID to verify the reliability of replication of X-ray devices input to MCNPX, the relative errors were 3.4% and 3.6% respectively, showing very similar values. HDRK-Man and HDRK-Woman computational human phantoms that represent the Korean males and females were used and applied for the evaluation of doses to calculate organ doses and effective doses for domestic adult males and females using MCNPX. As a result of calculating the mean effective doses of 20 general X-ray examinations of domestic adult males and females, the range of mean effective doses per test varied from <0.01 mSv to 0.87 mSv. The T-spine LAT test value was the highest and the upper and lower limb test was the lowest. The most frequently tested was Chest PA with its value of 0.05 mSv.

#### Discussion

If a Look-up table by specific condition is developed based upon this method using montecarlo simulation, it can be utilized as a scientific evidence base for the methodology of dose measurement display required by IEC 60601-1-3



# PH253-SD-THA3

Patient-Specific Analysis of Organ Doses in Chest-Abdomen-Pelvis CT Examinations with Tube Current Modulation

Thursday, Nov. 29 12:15PM - 12:45PM Room: PH Community, Learning Center Station #3

# Participants

Keisuke Fujii, Nagoya, Japan (*Presenter*) Nothing to Disclose Keiichi Nomura, MS, Kashiwa, Japan (*Abstract Co-Author*) Nothing to Disclose Yoshihisa Muramatsu, PhD, Kashiwa, Japan (*Abstract Co-Author*) Nothing to Disclose Takahiro Goto, Tochigi, Japan (*Abstract Co-Author*) Employee, Canon Medical Systems Corporation Satoshi Obara, Chiba, Japan (*Abstract Co-Author*) Nothing to Disclose Keiichi Akahane, Chiba, Japan (*Abstract Co-Author*) Nothing to Disclose Hiroyuki Ota, Kashiwa, Japan (*Abstract Co-Author*) Nothing to Disclose Shinsuke Tsukagoshi, PhD, Otawara, Japan (*Abstract Co-Author*) Employee, Canon Medical Systems Corporation

#### PURPOSE

The aims of this study are to determine organ doses based on Monte Carlo (MC) simulations for individual patients in routine chestabdomen-pelvis (CAP) CT examinations with tube current modulation (TCM) and to evaluate the correlations of organ doses with patient size and dose metrics.

### **METHOD AND MATERIALS**

Dose simulations were performed using MC simulation software ImpactMC (Advanced Breast CT). MC simulations were performed by inputting the voxelized models created from CT images of 40 patients in CAP CT examinations, detailed descriptions of an Aquilion ONE CT scanner (Canon Medical Systems) and scan parameters including TCM profiles into the software. Dose distribution images were obtained as the simulation results. To evaluate organ doses for thyroid, lung, esophagus, breast, liver, stomach and bladder, region of interests (ROIs) delineating each imaged organ were set on the dose distribution images and average doses within ROIs were calculated. For the 40 patients, body mass index (BMI), whole water equivalent diameter (WED) which shows the average WED within the scan range, organ-specific WED which shows the WED corresponding to each organ position, and volumetric CT dose index (CTDIvol) data were collected. Size-specific dose estimate (SSDE) was calculated from CTDIvol and conversion factors based on whole WEDs. Organ doses were analyzed according to the patient's BMI classification. The correlations of organ doses with whole WEDs, organ-specific WEDs and SSDE were evaluated.

# RESULTS

Patient's BMI ranged from 13.5 to 38.0 kg/m<sup>2</sup>. Organ doses for the patients increased with patient size and the doses for the obese patients were 1.5 to 2.6 times higher than those for normal weight patients. Organ doses had strong exponential relationships with whole WEDs (R<sup>2</sup> > 0.75) and organ-specific WEDs (R<sup>2</sup> > 0.82). Organ doses for most organs also had strong linear relationships with SSDE (R<sup>2</sup> > 0.79) although thyroid doses had lower relationship with SSDE (R<sup>2</sup> = 0.42).

# CONCLUSION

Patient dose management requires organ dose evaluations according to patient size. Organ doses can be estimated using the regression models and patient size metrics such as whole and organ-specific WEDs and/or dose metrics such as SSDE.

# **CLINICAL RELEVANCE/APPLICATION**

Dose simulation and the regression models of organ doses with patient size and dose metrics will be useful for accurate organ dose evaluations for individual patients in CAP CT examinations.



# PH254-SD-THA4

Comparison of Effective Dose and Image Quality of Different Helical and Cone-Beam CT Protocols, Including Tin Filtering, for Maxillofacial Imaging

Thursday, Nov. 29 12:15PM - 12:45PM Room: PH Community, Learning Center Station #4

### Participants

Arthur P. Wunderlich, PhD, Ulm, Germany (*Presenter*) Nothing to Disclose Sebastian Schnaidt, Ulm, Germany (*Abstract Co-Author*) Nothing to Disclose Meinrad J. Beer, MD, Ulm, Germany (*Abstract Co-Author*) Nothing to Disclose Carsten Hackenbroch, Ulm, Germany (*Abstract Co-Author*) Nothing to Disclose

For information about this presentation, contact:

arthur.wunderlich@uni-ulm.de

# PURPOSE

To evaluate potential dose reduction in dental CT protocols compared to DVT, eight different CT and one DVT protocol were evaluated for dose and image quality in a phantom study. Our special interest was dose reduction by tin filtering.

# METHOD AND MATERIALS

An anthropomorphic Alderson-Phantom was scanned with parameters 90 to 120 kV and 10 to 200 mAs, including protocols used routinely for head trauma evaluation, and w/o additional tin filtering. Also, a standard DVT (90 kV, 47 mAs) exam was performed. Effective dose was determined by thermoluminescence dosimetry (TLD), calculating weighted sum of organ doses. Also, quotients of DLP and effective dose were calculated. Image quality and diagnostic value was scored subjectively on a four point likert-scale (best=1, worst=4) independently by two radiologists and two trauma surgeons blinded for protocol settings and dose, and objectively by measuring CNR.

### RESULTS

Values of DLP ranged from 5 to 112 mGy\*cm, effective dose values from 0.02 to 0.5 mSv. The protocol with the lowest dose while maintaining good image quality (average score 1.28, 0.084 mSv) was 100 kV, 200 mAs with tin filter. For 100 kV, 25 mAs without tin filter, dose was 30% larger, 0.12 mSv, at slightly better image quality, average score 1.16. DVT images showed an average score of 1.34, while dose was 0.23 mSv. Dose conversion factors, calculated as ratio of dose divided by DLP, ranged from 0.0037 to 0.0045. Astonishingly, with tin filter and all other parameters kept constant, they depended on mAs - the lowest conversion factor of 0.0037 was observed with 200 mAs, the highest mAs studied.

#### CONCLUSION

Enlarging tube voltage to 120 kV and reducing mAs lowered the dose, but resulted in impaired image quality. Tin filtering was able to reduce dose substantially with only slightly reduced image quality.

# **CLINICAL RELEVANCE/APPLICATION**

Dose reduction in CT is possible while maintaining diagnostic information, outperforming DVT.



# PH255-SD-THA5

Effect of Obesity on Liver Lesion Detection at Standard and Reduced Radiation Exposure in an Anthropomorphic Phantom

Thursday, Nov. 29 12:15PM - 12:45PM Room: PH Community, Learning Center Station #5

# Participants

Andrew Schreiner, MD, Cleveland, OH (*Abstract Co-Author*) Nothing to Disclose Douglas Nachand, MD, Cleveland, OH (*Presenter*) Nothing to Disclose Frank Dong, PhD, Solon, OH (*Abstract Co-Author*) Equipment support, Siemens AG Software support, Siemens AG Jennifer Bullen, MSc, Cleveland, OH (*Abstract Co-Author*) Nothing to Disclose Andrew Primak, PhD, Malvern, PA (*Abstract Co-Author*) Employee, Siemens AG Wadih Karim, RT, Cleveland, OH (*Abstract Co-Author*) Nothing to Disclose Mark E. Baker, MD, Cleveland, OH (*Abstract Co-Author*) Nothing to Disclose Brian R. Herts, MD, Cleveland, OH (*Abstract Co-Author*) Grant, Siemens AG

#### For information about this presentation, contact:

nachand@ccf.org

#### PURPOSE

To determine how obesity effects low-contrast, low-attenuation liver lesion detection

### **METHOD AND MATERIALS**

A 30x20 cm anthropomorphic phantom containing 4 unique low-contrast, low-attenuation spherical lesions (5 mm at 66 HU, 10 mm at 72 HU, 10 mm at 78 HU, 15 mm at 84 HU) in the liver (90 HU) was scanned without and with a 5 cm thick fat density ring (total 40x30 cm) at the following parameters: 120 kVp; thin phantom 150 (SSDE 14.0 mGy; CTDIvol 10.0mGy), 100 and 50 mAs, obese phantom 450 (SSDE 29.6 mGy; CTDIvol 30.1 mGy), 300 and 150 mAs; adjusted mAs for obese phantom based on automated exposure control settings. 3 mm slices were reconstructed with filtered-back projection (FBP) and iterative reconstruction (IR) at lesion center. 6 readers blinded to lesion characteristics and location independently evaluated the images for lesion presence on a 5-point scale. Multi-reader multi-case ROC curves were used, calculating the area under the curve (AUC) adjusting for clustered data; Holm's step-down procedure was used to calculate adjusted p-values. Non-inferiority testing was performed for accuracy differences less than 0.05.

#### RESULTS

AUCs for all four lesions combined were: Thin phantom at 150 mAs - 0.990 FBP, 0.986 IR; at 100 mAs - 0.968 FBP, 0.979 IR; at 50 mAs - 0.917 FBP, 0.940 IR; Obese phantom at 450 mAs - 0.916 FBP, 0.914 IR; at 300 mAs - 0.910 FBP, 0.920 IR, at 150 mAs - 0.779 FBP, 0.827 IR. With FBP and IR, the AUC was lower at all exposure levels in the obese phantom.

#### CONCLUSION

Despite adjusting the baseline radiation exposure for the obese phantom, obesity has a significant effect on lesion detection, with lower AUCs at baseline and reduced exposures with both FBP and IR. The decrease in AUC with equivalent exposure decreases (33%, 67%) was greater in the obese phantom. IR had better AUC at the lowest doses compared to FBP, improving accuracy at lower exposures.

### **CLINICAL RELEVANCE/APPLICATION**

Low contrast, low attenuation liver lesion detectability is more affected by reduced exposures in obesity, despite increasing exposure.



# QI017-EB-THA

# Decreasing ED CT Interpretation Turn Around Times in an Academic Radiology Department

Thursday, Nov. 29 12:15PM - 12:45PM Room: QR Community, Learning Center Hardcopy Backboard

### Participants

Audrey R. Verde, MD, PhD, Stanford, CA (Presenter) Nothing to Disclose Yoan K. Kagoma, MD, Hamilton, ON (Abstract Co-Author) Nothing to Disclose Vera Mayercik, MD, Stanford, CA (Abstract Co-Author) Nothing to Disclose Jake Mickelsen, MBA, Stanford, CA (Abstract Co-Author) Nothing to Disclose Bryan A. Lanzman, MD, Stanford, CA (Abstract Co-Author) Nothing to Disclose Lawrence C. Chow, MD, Stanford, CA (Abstract Co-Author) Nothing to Disclose

# For information about this presentation, contact:

averde@stanford.edu

# PURPOSE

The Emergency Department (ED) sees an average of 200 patients per day with the goal to effectively treat or triage for admission or discharge in a timely fashion while providing high quality patient care. The interpretation of imaging studies plays a pivotal role in ED triage decision-making, specifically CTs (computerized tomography) of the body, and brain. Our team's purpose was to fully understand the process from CT exam completion to first published read in order to create a more efficient workflow to decrease turn around time (TAT) from a baseline average of 78 minutes for ED Body and Neuro CTs. We also set a SMART goal to increase the percent of ED CT exams read within 60 minutes from an average of 72% in October 2017 to 85% by April 1st 2018. Improving our process and decreasing read TAT will lead to better patient care, increased ED throughput of patients, improved patient satisfaction, better resource utilization, and increased profit for the hospital.

### METHODS

This project was a part of the Realizing Improvement Through Team Empowerment (RITE) Program that utilizes A3 problem solving, and Lean concepts to achieve clinically effective quality improvement. Our team was composed of two radiology residents, one neuroradiology fellow, one body radiology fellow, one neuroradiology attending, one body radiology attending, one quality improvement coach, and two sponsors from the Radiology leadership. Using structured A3 methods we identified six key drivers required to reach our SMART goal: 1) Maximizing workflow interpretation efficiency, 2) Good communication between residents and fellows, 3) Minimizing unnecessary interruptions for radiologists, 4) Visualization of performance results, 5) Good relationship between the Radiology and ED departments, and 6) Clear indication to residents when a CT is completed in the PACs (pictures archiving and communication system). From these key drivers multiple interventions were identified, investigated for feasibility, and tested in small experiments. Over the course of five months, four main interventions were implemented with good effect. The interventions included creating a leadership position to address the specific needs of the Radiology-ED relationship (1/29/2018), altering the on-call workflow for residents and fellows to increase communication and have the residents focus solely on ED studies (1/31/2018), increasing transparency of turn around times for the on call team participants through daily performance emails (2/27/2018), and installing a separate ultrasound (US) software on the call computers to increase the efficiency of US scan checks (3/1/2018). Daily ED CT interpretation time data was acquired through and compared across several platforms including Epic, Powerscribe, Agfa PACS, and Pristella for dates October 1, 2017 through April 1, 2018. TAT was defined as the time in minutes from when the CT technologist marked a study as Exam Complete in Epic to the first published radiologist read (resident, fellow, or attending). Data was tracked, and intervention effects were evaluated through the use of run-charts.

### RESULTS

Through implementation of four interventions, the percent of ED CTs read within 60 minutes increased from 72% to 86%, meeting our SMART goal of 85% of exams being read within 60 minutes by April 1, 2018. Within the two imaging divisions, body imaging improved their average from 67% to 88%, and neuroimaging improved from 78% to 88% of exams read within 60 minutes. These improved read times translate to a decrease in the median ED CT TAT from 40 minutes to 28 minutes, saving the ED a total of 10 patient hours each day.

# CONCLUSION

Using structured A3 problem solving and team based methods we accomplished our SMART goal of increasing the percent of ED CT interpretations provided within 60 minutes from 72% to 86% over the course of the dedicated five month RITE Program. This decrease in turn around time allows for more efficient ED patient triage, timely diagnosis and treatment of patients, and an increased ED throughput. We plan to sustain this change by making our interventions permanent, continuing to monitor ED TATs, and implementing additional interventions to further decrease interruptions to our workflow, and increase read efficiency. A limitation of our study was the inability to implement information technology (IT) interventions during the project timeline due to a simultaneous institutional PACS transition, and limited IT bandwidth for additional projects. Our future goals include fully automating the daily TAT emails, increasing reading room assistant hours to 24/7, and integrating IT interventions.



# QI019-EB-THA

STAT! STAT! ... STAT?: A Multidisciplinary Collaboration To Develop and Implement a New Multi-tiered Order Priority Classification System

Thursday, Nov. 29 12:15PM - 12:45PM Room: QR Community, Learning Center Hardcopy Backboard

# Participants

Nina Capiro, MD, Santa Monica, CA (*Presenter*) Nothing to Disclose Shahnaz Ghahremani, MD, Los Angeles, CA (*Abstract Co-Author*) Nothing to Disclose Kambiz Motamedi, MD, Los Angeles, CA (*Abstract Co-Author*) Nothing to Disclose

#### For information about this presentation, contact:

ncapiro@mednet.ucla.edu

# PURPOSE

At our large academic medical center, ordering daily morning chest radiographs was customary practice in the Neonatal and Pediatric Intensive Care Units (NICU/PICU). To ensure image acquisition prior to morning rounds, residents typically order these studies as STAT, even though very few radiographs truly required STAT interpretation. Under such circumstances, radiologists cannot appropriately prioritize the urgency of STAT studies. In collaboration with the Radiology Department, NICU/PICU and Medical Informatics, we aimed to develop and implement a new multi-tiered order priority classification system to allow clinicians to order studies not only based on urgency of image acquisition but also urgency of image interpretation.

#### **METHODS**

To involve all stakeholders, project design discussions were held between members of the Radiology Department and NICU/PICU leadership. Collaboration with Medical Informaticists allowed for the development of a new ordering system to meet both clinician and radiology needs. The result was a new multi-tiered order priority classification system based on urgency of both image acquisition and image interpretation, allowing clinicians to order studies as routine, STAT with routine read, STAT with urgent read or STAT with immediate read. The option to simply place a STAT order was unmodifiable in the system and remained as a legacy option. Training sessions were held with NICU/PICU residents at their monthly meetings to ease transition to the new ordering system.

#### RESULTS

Retrospective analysis was performed of STAT morning chest radiographs ordered from the NICU/PICU completed between the hours of 5:00AM and 9:00AM for a one-month period pre- and post-intervention. We examined the indication for studies based on the indication entered by the ordering clinician as well as electronic medical record notes. Studies ordered for acute clinical decompensations or new line/tube placements were considered "true STAT" whereas all other studies were classified as "daily follow-up" chest radiographs. Pre-intervention, during the month of January 2016, 38 out of 82 (46%) morning chest radiographs from the NICU/PICU were ordered as STAT. Of these studies, only 3 were found to be "true STAT" studies and the remaining 35 studies were considered "daily follow-up" chest radiographs. An additional 44 chest radiographs completed during this period were ordered as routine. Post-intervention, during the month of June 2017, a total of 29 out of 43 (66%) morning chest radiographs were ordered as STAT of any kind. However, 23 of these studies (79%) were ordered as STAT with routine read and 4 studies (14%) were ordered as STAT with urgent read, all of which met criteria for "daily follow-up" chest radiographs. There were no morning chest radiographs ordered as STAT with immediate read. Two studies were ordered simply as STAT, both of which met criteria for "true STAT." An additional 14 morning chest radiographs were ordered as routine. Prior to the intervention, the turnaround times for routine and STAT morning chest radiographs were 3.74 hours and 3.47 hours, respectively. Utilizing the new ordering system, turnaround time for routine studies was 2.58 hours, STAT with routine read was 1.66 hours, and STAT with urgent read was 1.08 hours. The turnaround time for studies ordered with the legacy option of only STAT was 3.20 hours, although only 2 studies fell under this category.

# CONCLUSION

To ensure image acquisition prior to morning rounds, many morning chest radiographs from the NICU/PICU were ordered as STAT. However, pre-intervention, only 8% of these studies were found to have true STAT indications. Following implementation of a new multi-tiered order priority classification system, 93% of all morning chest radiograph STAT studies were ordered as STAT with routine read or STAT with urgent read, all of which were "daily follow-up" chest radiographs. These findings suggest that clinicians in the NICU/PICU appropriately utilized the new ordering system to ensure STAT acquisition of images with a non-STAT interpretation by the radiologist. Furthermore, progressively decreasing turnaround times were noted when comparing routine, STAT with routine read and STAT with urgent read studies, suggesting the appropriate prioritization of studies by the interpreting radiologists. By allowing clinicians to distinguish between urgency of image acquisition and urgency of image interpretation, radiologists can further stratify their worklists and better prioritize true STAT studies. The development and implementation of this new multi-tiered order priority classification system exemplifies the importance of multidisciplinary collaborative efforts in quality improvement projects that impact multiple departments. The new ordering system has subsequently been applied institution-wide, with further analysis to be performed in additional patient care units.



# QI132-ED-THA1

Change Management Strategies Used to Overcome Image Quality Concerns While Implementing a CT Dose Reduction Project

Thursday, Nov. 29 12:15PM - 12:45PM Room: QR Community, Learning Center Station #1

# Participants

Amichai J. Erdfarb, MD, Bronx, NY (*Presenter*) Nothing to Disclose Judah Burns, MD, Bronx, NY (*Abstract Co-Author*) Nothing to Disclose Alan H. Schoenfeld, MS, Bronx, NY (*Abstract Co-Author*) Nothing to Disclose Todd S. Miller, MD, Bronx, NY (*Abstract Co-Author*) Nothing to Disclose Terry L. Levin, MD, Mamaroneck, NY (*Abstract Co-Author*) Nothing to Disclose

# For information about this presentation, contact:

#### tmiller@montefiore.org

### PURPOSE

The project provides practical steps to take when project champions encounter resistance to change. After a several year process of committee driven work to update CT protocols, there were a few exams remaining that generated CTDIvol above national medians. The project was based upon data from our annual summary from the ACR Dose Index Registry where we noted that orbital CT dose and our Abd/Pel CT dose values were above the national 75% for CTDIvol. Our initial approach was to ask subspecialty division leaders to approve dose reduction to national medians. This approach was met with resistance over concerns regarding reduced image quality and diagnostic accuracy.

### **METHODS**

We took a multi pronged approach to change management. First we leveraged innovators who had the idea of demonstrating that due to protocol variation, there were already lower dose exams for some patients. We could show these side-by-side to the clinical leaders to demonstrate that change will not result in diminished clinical quality. This approach was used to obtain buy-in from the opinion leaders within each subspecialty division before the main team kick-off meeting. We obtained agreement by displaying data comparing similar exams with lower dose side-by-side with the current higher dose exams to demonstrate the clinical adequacy of target dose. The implementation plan that was shared with the team included dose change in small increments (5-10%). This was followed by weekly team quality assurance meetings. The purpose of these meetings was to verify a clinical quality balancing measure - the diagnostic quality of the new lower dose exams. The new lower dosage exams were analyzed by the team to assure proper clinical quality. Finally, we provided a mechanism for concerned team members to roll back changes based on clinical quality concerns.

### RESULTS

Outcome measure: CTDI vol data, Process measure: Protocol adherence by CT technologist, Balancing measure: clinical quality review. The run chart demonstrates CTDIvol for Ortbial CT for ED patients over the year prior to the interventions. This is followed by three PDSA cycles where the the dose was incrementally lowered. During each cycle the correct CT protocol was confirmed by viewing the DICOM data for each exam. In addition, there was a weekly team quality review of the new lower dose exams where specific clinical criteria were assessed on a pass/fail basis. Using this incremental approach, we were able to overcome resistance to the project. Through three PDSA cycles we were able to reduce our Orbit CT dose to national medians without detecting loss of clinical quality.

# CONCLUSION

Using change management techniques, we were able to overcome resistance to a CT dose lowering project on the basis of clinical quality concerns. We succeeded with a small impact project, and are applying lessons learned to CT Abd/Pel which are 40x more common in our department.



# QI134-ED-THA2

# Reducing the Number of Knee MRIs in Patients with Severe Degenerative Change

Thursday, Nov. 29 12:15PM - 12:45PM Room: QR Community, Learning Center Station #2

#### **Participants**

Kelly A. Tornow, BS, MD, Dallas, TX (*Presenter*) Nothing to Disclose Joseph S. Zerr, MD, Dallas, TX (*Abstract Co-Author*) Nothing to Disclose Daniel S. Moore, MD, Dallas, TX (*Abstract Co-Author*) Nothing to Disclose Oganes Ashikyan, MD, Dallas, TX (*Abstract Co-Author*) Nothing to Disclose Avneesh Chhabra, MD, Dallas, TX (*Abstract Co-Author*) Consultant, ICON plc; Author with royalties, Wolters Kluwer nv; Author with royalties, Jaypee Brothers Medical Publishers Ltd Richard B. Thropp, MD, Dallas, TX (*Abstract Co-Author*) Nothing to Disclose

#### PURPOSE

In 2017, 882 knee MR examinations were performed at a large county hospital. Of those 55% were performed on patients with severe degenerative changes. Prior studies have shown a high level of concordance between the severity of degenerative changes on knee radiographs and the severity of degenerative changes on knee MRIs. In patients with severe degenerative changes, knee MRI does not add significant clinical value as these patients are not candidates for repair of the support structures of the knee.

#### METHODS

A root cause analysis was performed and the main drivers for obtaining MRIs in patients with severe knee degenerative changes were determined to be a lack of consistent terminology for degenerative changes on knee radiographs, lack of recommendations for further management on knee radiographs, and lack of education of the referring clinicians on the role of the knee MRI in these patients. A goal was set to decrease the number of knee MRIs by one-third within a six month time period.

# RESULTS

A standardized grading system was introduced into the knee radiograph reports with recommendations automatically generated in patients with severe degenerative changes. Education was provided to the radiology attendings and residents on the implementation of this system. The percentage of knee MRIs with severe degenerative changes decreased from 55% to 17-24%.

# CONCLUSION

Standardized reporting with recommendations from radiologists can help referring clinicians to streamline patient care by referring the patients to the appropriate clinic and can decrease the burden on the system from unnecessary MRI orders.



# QI136-ED-THA3

# Evaluation of a Low Dose Technique for the Performance of CT Guided Lumbar Foraminal Nerve Blocks

Thursday, Nov. 29 12:15PM - 12:45PM Room: QR Community, Learning Center Station #3

### Participants

Bharath B. Das, MD, MBBS, Bangalore, India (*Presenter*) Nothing to Disclose Prashanth Reddy, MBBS,MD, Bangalore, India (*Abstract Co-Author*) Nothing to Disclose Sankar Neelakantan, MD, Bangalore, India (*Abstract Co-Author*) Nothing to Disclose Bhavana Nagabhushana Reddy, MBBS, MD, Bangalore, India (*Abstract Co-Author*) Nothing to Disclose Sanjaya Viswamitra, MD, Bengaluru, India (*Abstract Co-Author*) Nothing to Disclose

#### PURPOSE

CT-guided lumbar foraminal blocks a are commonly performed procedure for treatment of chronic back pain in non-surgical patient. Due to the need for accurate positioning of the needle in the neural foramina repeated positioning of the spinal needle may be required. This results in incremental radiation dose to the patient. The purpose of this project is to evaluate a low-dose technique for the performance of these interventions guided by the ALARA principle.

#### **METHODS**

At our institute in a 2-year period a total of 554 lumbar foraminal nerve blocks were performed. All procedures were performed by experienced radiologist. Procedures done using the low-dose interventional protocol were compared with matched controls who underwent the procedure using the routine spine intervention protocol. These patients were matched for body mass index and degree of degenerative changes in the spine. Patients with spinal instrumentation were excluded. All scans were performed on the GE HD 750 discovery 64 detector-row CT scanner. Scan parameters for the routine spine protocol were 120 Kvp and automated mAs for the initial scan followed by 100 Kvp and 80 mAs for the following scans. Scan diameters for the low-dose protocol were; 80 kvp and 40 mAs for all scans. The scans were analyzed of the total radiation dose measured as dose length product(DLP), the number of scans required for positioning of the needle and the presence or absence of lateral spill into the spinal canal.

### RESULTS

The average DLPs for the routine spine protocol and for the low dose protocol were 215 mGy-cm and 11 mGy-cm respectively. This was a 94 % reduction in dose. The number of scans required for needle positioning ranged from 3 to 7 using both techniques. The average no of scans required for needle positioning in the routine protocol and in the spine protocol were 4.8 and 5 respectively. Lateral spill of contrast was present in all patients indicating adequacy of the procedure.

# CONCLUSION

Use of the low-dose spine interventional protocol permits for the accurate performance of CT-guided lumbar foraminal nerve blocks at greatly lowered patient dose.



# RO226-SD-THA1

Correlation Study Between Parameters of Intravoxel Incoherent Motion Diffusion-Weighted Imaging and Different Pathological Differentiation of Cervical Squamous Cell Carcinoma

Thursday, Nov. 29 12:15PM - 12:45PM Room: RO Community, Learning Center Station #1

# Participants

Lixiang Zhang, Hefei, China (*Presenter*) Nothing to Disclose Fei Gao, Hefei, China (*Abstract Co-Author*) Nothing to Disclose

# PURPOSE

To evaluate the correlation between parameters of intravoxel incoherent motion diffusion-weighted imaging and different pathological differentiation degree of cervical squamous carcinoma.

# METHOD AND MATERIALS

Retrospective analysis of 87 cases patients of cervical squamous cell carcinoma confirmed by surgery and pathology in our hospital, including fifty cases were in the low differentiation group(Fig A1-A7), twenty-six cases were in the middle differentiation group(Fig B1-B7) and eleven cases were in the highly differentiation group(Fig C1-C7). Intravoxel incoherent motion diffusion-weighted imaging was performed by using 10 b values(b=0,10,20,50,100,200,400,800,1200,2000s/mm2). Statistical analysis software SPSS 22.0 was used in cervical squamous cell carcinoma diffentiation. The receiver operating characteristic curve (ROC) was used to investigate efficiency of differentiation of cervical squamous cell carcinoma.

### RESULTS

The ADCstand, D, D\*and f values of low differentiation degree group were  $(0.72\pm0.11)\times10-3mm2/s$ ,  $(0.45\pm0.067)\times10-3mm2/s$ ,  $(7.56\pm3.09)\times10-3mm2/s$  and (39.55,14.25)%; The ADCstand, D, D\*and f values of middle differentiation group were  $(0.74\pm0.11)\times10-3mm2/s$ ,  $(0.58\pm0.036)\times10-3mm2/s$ ,  $(17.19\pm4.37)\times10-3mm2/s$  and (24.05,3.73)%; The ADCstand, D, D\*and f values of highly differentiation were  $(0.78\pm0.073)\times10-3mm2/s$ ,  $(0.74\pm0.024)\times10-3mm2/s$ ,  $(39.18\pm10.09)\times10-3mm2/s$  and (18.70,1.60)%; There are statistical significance in the D, D\*and f values of between different groups(P<0.05),but there is no statistical significance in the D, D\*and f values of between different groups(P<0.05),but there is no statistical differentiation of squamous cell carcinoma (r was 0.853,0.880), and the f value was moderately negative correlation (r = -0.730). The D value has the best diagnostic efficiency in the diagnosis of low differentiation and high differentiation of cervical squamous cell carcinoma; the f value has the best diagnostic efficiency in the diagnosis of cervical squamous cell carcinoma.

#### CONCLUSION

The D, D \* and f values of IVIM-DWI can non-invasively assess the pathological differentiation degree of cervical squamous cell cancers.

#### **CLINICAL RELEVANCE/APPLICATION**

It is helpful for the clinician to develop individualized treatment plans of cervical cancer to improve the efficacy.



# UR190-ED-THA7

ShearWave Penile Elastography: A New Ultrasound Imaging Method for Assessing Penile Structural Changes

Thursday, Nov. 29 12:15PM - 12:45PM Room: GU/UR Community, Learning Center Station #7

#### **Participants**

Felipe Carneiro, MD, Sao Paulo, Brazil (*Presenter*) Nothing to Disclose Caroline C. Santiago, BDS, Sao Paulo, Brazil (*Abstract Co-Author*) Nothing to Disclose Gabriela A. Bandeira, MD, Sao Paulo, Brazil (*Abstract Co-Author*) Nothing to Disclose Jose Cury, Sao Paulo, Brazil (*Abstract Co-Author*) Nothing to Disclose Maria Cristina Chammas, MD,PhD, Sao Paulo, Brazil (*Abstract Co-Author*) Nothing to Disclose

# For information about this presentation, contact:

drcarneiro91@gmail.com

## **TEACHING POINTS**

The purpose of this exhibit is: 1) To describe the elastography as a noninvasive ultrasound imaging modality for evaluation of tissue stiffness. 2)To briefly describe the two main types of elastography in the assessment of organs properties and to show the well stablished indications for its application. 3) To define the elastography as a new promising ultrasonographic technique to assess penile structural changes.

# **TABLE OF CONTENTS/OUTLINE**

- Introduction with a brief explanation of the method's physics. - Background based on experience acquired from liver pathologies, followed by breast, thyroid, etc. - Brief description of literature preliminary studies that have investigated the role of elastography in sexual medicine. - Elastography evaluation of Peyronie's disease. - Elastography assessment of penile rigidity. - Elastography evaluation of erectile dysfunction. - Future and possibilities of elastography in sexual medicine. - Summary and conclusions. - Bibliographical references.



## UR191-ED-THA8

Advanced Prostate Cancer: Update on Evolving Concepts, Rationale, and Challenges of Imaging and Novel Therapeutic Strategies

Thursday, Nov. 29 12:15PM - 12:45PM Room: GU/UR Community, Learning Center Station #8

**FDA** Discussions may include off-label uses.

#### Participants

Varaha Tammisetti, MD, Houston, TX (*Presenter*) Nothing to Disclose Baris Turkbey, MD, Bethesda, MD (*Abstract Co-Author*) Nothing to Disclose

Spencer C. Behr, MD, Burlingame, CA (*Abstract Co-Author*) Research Grant, General Electric Company Consultant, General Electric Company Consultant, Navidea Biopharmaceuticals, Inc Grant, Navidea Biopharmaceuticals, Inc

Courtney Widjaja, San Antonio, TX (Abstract Co-Author) Nothing to Disclose

Sandeep S. Arora, MBBS, Nashville, TN (*Abstract Co-Author*) Speaker, Profound Medical Inc; Researcher, Profound Medical Inc Tharakeswara K. Bathala, MD, Houston, TX (*Abstract Co-Author*) Nothing to Disclose

## For information about this presentation, contact:

Varaha.S.Tammisetti@uth.tmc.edu

#### **TEACHING POINTS**

1. Define different disease states of metastatic prostate cancer and clinical predictors of prognosis. 2. Discuss rationale of imaging in assessing comprehensive metastatic tumor burden. 3. Illustrate whole body imaging methods using novel PET tracers, whole body MRI, prostate MRI. 4. Illustrate imaging patterns, challenges of imaging and response assessment. 5. Current update of novel therapeutic strategies.

## TABLE OF CONTENTS/OUTLINE

1. Disease states of metastatic prostate cancer: Oligometastatic disease, metastatic Castration sensitive prostate cancer (mCSPC), metastatic castration resistant prostate cancer (mCRPC) - chemotherapy naive CRPC, chemorefractory CRPC and genomics. 2. Rationale of imaging: Need for assessing comprehensive metastatic tumor burden to detect presence, volume and distribution and their implications on choice of therapy. 3. Imaging patterns, histologic subtypes and predictors of prognosis. 4. Update on imaging methods, challenges of imaging and response assessment using PET tracers C11-Choline, F18-Fluciclovine, FDHT, PSMA, NaF, Bone scan and Whole Body and prostate MRI. 5. Review of novel treatment strategies including Androgen receptor inhibitors including mechanisms of resistance, immunotherapy, PARP inhibitors, Radiotherapy, metastatic directed therapy and impact of imaging on the selection, monitoring of response to therapy.

### **Honored Educators**

Presenters or authors on this event have been recognized as RSNA Honored Educators for participating in multiple qualifying educational activities. Honored Educators are invested in furthering the profession of radiology by delivering high-quality educational content in their field of study. Learn how you can become an honored educator by visiting the website at: https://www.rsna.org/Honored-Educator-Award/ Spencer C. Behr, MD - 2017 Honored Educator



## VI171-ED-THA8

Neck Magnetic Resonance Angiography for Determination of Neointimal Coverage of the Stenting Site After Carotid Artery Stenting

Thursday, Nov. 29 12:15PM - 12:45PM Room: VI Community, Learning Center Station #8

# Participants

Hiroki Takahashi, Sendai-shi, Japan (*Presenter*) Nothing to Disclose Masayuki Ezura, Sendai, Japan (*Abstract Co-Author*) Nothing to Disclose

## **TEACHING POINTS**

In this study, the association between high intrastent signals of neck magnetic resonance angiography(MRA) after carotid artery stenting(CAS) and neointimal coverage of the stent site was examined. The differences in signal strengths according to stent devices. (Fig 1) The differences in signal values inside the stent and the artifacts on MRA were subjected to computational fluid dynamics (CFD) analyses using a vascular phantom. A simulation of blood flow in the stent lumen was performed. (Fig 2-4)

## TABLE OF CONTENTS/OUTLINE

On a neck MRA performed immediately after CAS, the sites of all types of stents appeared as low-intensity signal areas. However, in a 6-MFU MRA, only Wallstent appeared with a high-intensity signal at the stent site. Immediately after a CAS, the intrastent blood flow becomes turbulent, and no strong inflow effect will be achieved; as a result, the MRA will show a low-intensity signal. However, if the stent site is covered by a newly formed intima, the intrastent blood flow will recover and a strong inflow effect will be achieved. The stent site would then appear as a high-intensity signal area. If the neck MRA image shows a high-intensity signal at the site of an indwelling Wallstent, the stent site can be considered repaired. Using a neck MRA allows for a noninvasive assessment of neointimal formation at the stent site. (Fig 5)



## VI172-ED-THA9

Biopsy Request? Not so Fast, It's a Pseudomass! Common and Uncommon Mimickers of Disease in the Abdomen and Pelvis

Thursday, Nov. 29 12:15PM - 12:45PM Room: VI Community, Learning Center Station #9

## Participants

Shanna A. Matalon, MD, Boston, MA (*Presenter*) Nothing to Disclose Jennifer W. Uyeda, MD, Boston, MA (*Abstract Co-Author*) Consultant, Allena Pharmaceuticals, Inc; Invited Speaker, Siemens AG Stuart G. Silverman, MD, Brookline, MA (*Abstract Co-Author*) Nothing to Disclose Daniel A. Souza, MD, Boston, MA (*Abstract Co-Author*) Nothing to Disclose

#### For information about this presentation, contact:

smatalon@bwh.harvard.edu

## **TEACHING POINTS**

1. Abdominopelvic pseudomasses are prevalent and, if misdiagnosed, can lead to unnecessary patient anxiety, additional costly diagnostic workup, suboptimal management, and possibly even harmful procedures with poor outcome.2. Knowledge of anatomical variants that can mimic disease is critical to minimize potential (cognitive) diagnostic errors, typically as the result of premature closure bias.3. Always consider the possibility that an apparent "lesion" could be vascular when evaluated on a non-contrast exam or with suboptimal contrast timing4. Review of patient chart and prior surgical history is invaluable in the evaluation of a pseudomass (i.e. prolene plug after inguinal hernia repair, oophoropexy in young females requiring pelvic radiation, omental patch after surgery).

## TABLE OF CONTENTS/OUTLINE

1. Illustrative case examples presented in a quiz format of common and uncommon masslike mimickers of pathology in the abdomen and pelvis2. Pearls and pitfalls in the evaluation of abdominopelvic pseudomasses (e.g. identify normal variants, assess for lack of vascular distortion in focal fat, typical location of dropped gallstones, classic patient history and usual appearance of oophoropexy, etc.)



## VI259-SD-THA1

Does Transfusion of Fresh Frozen Plasma Decrease the Rate of Paracentesis Related Hemorrhagic Complications in Coagulopathic Patients?

Thursday, Nov. 29 12:15PM - 12:45PM Room: VI Community, Learning Center Station #1

# Participants

Madheea Siddiqi, MD, Newark, NJ (*Presenter*) Nothing to Disclose Vishnu Chandra, BS, Newark, NJ (*Abstract Co-Author*) Nothing to Disclose Haokang Wei, Newark, NJ (*Abstract Co-Author*) Nothing to Disclose Reshma Vohra, Newark, NJ (*Abstract Co-Author*) Nothing to Disclose Josue Echenique, Newark, NJ (*Abstract Co-Author*) Nothing to Disclose Sohail G. Contractor, MD, MBBS, Watchung, NJ (*Abstract Co-Author*) Nothing to Disclose Piotr S. Kisza, MD, South Orange, NJ (*Abstract Co-Author*) Nothing to Disclose

#### For information about this presentation, contact:

madheea.siddiqi@gmail.com

## PURPOSE

Transfusion of fresh frozen plasma (FFP) is advised for paracentesis procedures when performed at INR of 2 or more in order to decrease the risk of hemorrhagic complications. However, to our knowledge, this premise has not previously been evaluated. FFP is considered to be the least safe blood product due to risk of allergic reactions, anaphylaxis, transfusion related acute lung injury and hemolysis. FFP is independently associated with a 2.1% increased risk of multi-organ failure and 2.5% increased risk of acute respiratory distress syndrome. The aim of our study was to determine if FFP transfusion administered either 24 hours prior to or following a paracentesis procedure impacted the rate of paracentesis-related hemorrhagic complications in patients with INR greater than 2.5.

## METHOD AND MATERIALS

A retrospective chart review of 1241 paracenteses was conducted to identify cases performed when INR was 2.5 or greater. 229 cases were identified and charts were reviewed for FFP transfusion within 24 hours of the procedure and for hemorrhagic complications, defined as intraperitoneal hemorrhage, abdominal wall hematoma, or pseudoaneurysm formation.

## RESULTS

Out of 229 total paracenteses, FFP was transfused in 68 cases (29.7%, INR range 2.5-7.4, Mean 3.4, Median 3.2). 161 cases did not receive a transfusion (70.3%, INR range 2.5-6.8, Mean 3.3, Median 3). Among 3 total bleeding events, 2 occurred in the transfusion group and 1 occurred in the non-transfusion group, correlating to a hemorrhagic complication rate of 2.9% (2/68) and 0.6 % (1/161) respectively. For all paracenteses the hemorrhagic complication rate was 1.3% (3/229). A chi-square test of FFP administration vs. hemorrhagic event yielded a chi-square statistic of 1.9904 and a p-value of 0.1583 (not significant at p<0.05).

## CONCLUSION

Overall the rate of hemorrhagic complications from paracenteses performed at INR of 2.5 or greater is low. There was no significant difference in rates of hemorrhagic events between coagulopathic patients undergoing paracentesis who were transfused with FFP when compared to those who were not. As such, FFP transfusions may not be necessary in absence of overt bleeding.

## **CLINICAL RELEVANCE/APPLICATION**

In our patient group, there is no statistically significant difference in the rate of paracentesis related hemorrhagic complications in coagulopathic patients (INR >/ 2.5) who were transfused with fresh frozen plasma when compared with those were not.



## VI261-SD-THA3

Surgery, Medicine, or Transitional Year? Comparison of Internship Year for Those Going Into Interventional Radiology with Retrospective Analysis of the RFS Survey of Trainees

Thursday, Nov. 29 12:15PM - 12:45PM Room: VI Community, Learning Center Station #3

# VA

### Awards

#### **Student Travel Stipend Award**

#### **Participants**

Omar S. Zuberi, DO, Louisville, KY (*Presenter*) Nothing to Disclose Christopher Molloy, MD, Los Angeles, CA (*Abstract Co-Author*) Nothing to Disclose Jared Cline, BA, Los Angeles, CA (*Abstract Co-Author*) Nothing to Disclose David P. Duncan, MD, San Diego, CA (*Abstract Co-Author*) Nothing to Disclose Keshav M. Menon, MD, Dallas, TX (*Abstract Co-Author*) Nothing to Disclose

## For information about this presentation, contact:

oszube01@louisville.edu

# PURPOSE

Evaluate trainee experiences regarding internship variables with respect to interventional radiology (IR) preparedness.

## METHOD AND MATERIALS

A questionnaire created by members of the SIR-Resident, Fellow, and Student (RFS) IR Residency Training committee was distributed to RFS members at the SIR 2017 conference and via an online survey. The anonymous survey was conducted utilizing Likert-scale, dichotomous questions & free response questions. Results were analyzed using a one-way analysis of variance (ANOVA), Pearson correlation coefficient, along with calculation of mean, standard deviation and 95% confidence interval (CI).

## RESULTS

A total of 112 responses were collected, 47 Surgery, 33 Medicine, 29 Transitional Year (TY) and 3 non-traditional internships categorized as other. The average procedures performed as an intern were: Surgery, 51-75; Medicine, 0-25; TY, 25-50; Other, 25-50. Preliminary surgery residents reported higher comfort levels with procedures (Mean:4.23, STD:0.81, CI:0.21, p<.00001) compared to medicine (2.84, STD:1.42, CI:0.48) and TY interns (3.03, STD:1.48, CI:0.55). A moderate positive correlation with comfort level of procedures and number of procedures performed was found. (r=0.51, p<.00001). No statistical difference between subgroups when comparing months of night float, maximum consecutive hours worked, ancillary work, etc. was found. Surgery residents reported a higher quality preparedness for IR (4.3, STD: 0.93, CI: 0.27, p<.01) compared to medicine (3.4, STD:1.1, CI:0.4) and TY residents (3.6, STD:1.2, CI:0.46). 94% of surgery residents would choose to repeat a surgery internship. TY residents were next likely to choose the same type of internship at 83%, while the remaining 17% would choose surgery. Medicine was least likely at 70%. Surgery, TY, and then medicine residents would choose the same program again (83%, 79%, 75%, respectively).

#### CONCLUSION

In alignment with SIR recommendations, the trainees surveyed support that a preliminary surgery internship provides the greatest preparation for IR. A surgery internship allows a greater opportunity to perform procedures, corresponding with increased comfort levels and self-reported better preparedness for future training in IR.

## **CLINICAL RELEVANCE/APPLICATION**

With the advent of the new IR/DR residency, future applicants have a tough decision on an internship and keeping with SIR recommendations a surgery internship is best suited for those going into IR.



## VI262-SD-THA4

## "Dark Blood" Dual-Energy CT Imaging Using a Dedicated Material Decomposition Method

Thursday, Nov. 29 12:15PM - 12:45PM Room: VI Community, Learning Center Station #4

#### **Participants**

David Rotzinger, MD, Lausanne, Switzerland (*Presenter*) Nothing to Disclose Salim Si-Mohamed, Lyon, France (*Abstract Co-Author*) Nothing to Disclose Philippe C. Douek, MD, PhD, Lyon, France (*Abstract Co-Author*) Nothing to Disclose Loic Boussel, MD, Lyon, France (*Abstract Co-Author*) Nothing to Disclose

# For information about this presentation, contact:

david.rotzinger@chuv.ch

### PURPOSE

To assess the capability of a newly developed arterial wall enhancement algorithm, based on a material decomposition method from contrast-enhanced dual-energy CT images, to better visualize the aortic wall and aortic intramural hematoma (IMH), compared to true non-contrast (TNC) CT.

## METHOD AND MATERIALS

We retrospectively included 25 CT examinations from 20 patients who underwent a clinically indicated (acute chest pain) dual-layer non-contrast and contrast-enhanced CT: 10 patients presented with an IMH and 10 controls with no aortic disease. We processed the CTA images using a two-material decomposition analysis in the image domain, where the first material was defined as the content of an ROI placed in the ascending aorta for each patient, and the second material was water. These images and the TNC images were assessed by two independent radiologists who rated diagnostic confidence regarding the presence of aortic wall thickening on a 4-point scale (4=exemplary, 1=non-diagnostic) and the inner/outer vessel wall conspicuity on a 3-point scale (3=circumscribed wall, 1=obscured wall). One radiologist performed the quantitative analysis by placing ROIs encompassing the aortic wall and the lumen to calculate CNR between the wall and the lumen.

## RESULTS

Qualitative diagnostic confidence scores in normal aortic segments were  $0.9\pm0.34$  and  $2.74\pm0.58$  (p<0.001) and wall conspicuity scores were  $0.73\pm0.52$  and  $1.83\pm0.34$  (p<0.001) on TNC and dark blood images, respectively. In aortic segments with IMH, the diagnostic confidence scores were  $1.71\pm0.46$  and  $2.43\pm0.57$  (p<0.001) and wall conspicuity scores were  $0.68\pm0.67$  and  $1.79\pm0.27$  (p<0.001) on TNC and dark blood images, respectively. Interrater agreement was substantial (weighted kappa=0.74 and 0.66 for diagnostic confidence and wall conspicuity, respectively). In normal aortic segments, CNR were  $0.3\pm0.2$  and  $2.8\pm0.9$  on TNC and dark blood images, respectively (p<0.001). In aortic segments with IMH, CNR were  $0.3\pm0.2$  and  $4.0\pm1.0$  on TNC and dark blood images, respectively (p<0.001).

#### CONCLUSION

Compared to non-contrast CT, dark blood material decomposition maps enhance quantitative and qualitative image quality for the assessment of normal aortic wall and IMH.

#### **CLINICAL RELEVANCE/APPLICATION**

dark blood images of the aorta or other arteries could potentially help diagnose conditions associated with subtle changes in vessel wall thickness, such as early atherosclerosis or vasculitis.



## VI263-SD-THA5

Super Flexible Metallic Stents Insertion for the Management of Malignant Tortuous Hepatic or Splenic Flexure Colonic Obstruction

Thursday, Nov. 29 12:15PM - 12:45PM Room: VI Community, Learning Center Station #5

# Participants

Yingsheng Cheng, MD, Shanghai, China (*Presenter*) Nothing to Disclose Yueqi Zhu, MD, Shanghai, China (*Abstract Co-Author*) Nothing to Disclose

## PURPOSE

Malignant colon obstruction at hepatic or splenic flexure resulted in technique failure of stent insertion because of its extremely tortuous and long distance. This study was supposed to determine technique feasibility and treatment outcomes following a super flexible through-the-scope (TTS) self-expandable metallic stents (SEMS) for malignant colon obstruction at hepatic or splenic flexure.

## METHOD AND MATERIALS

Sixteen continuous patients (9 males and 7 females, aged 55-89 years, mean 70.3± 12.5 years) with malignant colon obstruction at hepatic or splenic flexure were treated between Sep-tember 2013 and June 2016. Their clinical and radio-logical data were reviewed. Under endoscopic and fluoroscopic guidance stents insertion procedure was performed in all patients. The technique success rate, complications and clinical remission rate were recorded.

#### RESULTS

Obstructions were at hepatic flexure in 5 patients and splenic flexure in 11 patients, with a mean curvature degree of  $123.7\pm 20.5$  degrees. Sixteen super flexible TTS-SEMSs were inserted into all patient with a technique successful rate of 100% and no stent related complication occurred. Six patients received stent inserted for permanent palliation while ten were as a bridge to surgery. Clinical presentation of all patients was achieved. Abdominal girth was de-creased from  $87 \pm 4$  cm before drainage to  $70 \pm 4$  cm seven days later in all patients, and one-stage surgery operated after  $9.7 \pm 1.0$  days (range, 8-12 days) in ten patients. No postoperative stricture or anastomotic leakage happened.

#### CONCLUSION

Super flexible TTS-SEMS was effective and safe to management malignant colon obstruction at tortuous hepatic or splenic flexure, as either permanent palliation or a bridge before surgery.

# **CLINICAL RELEVANCE/APPLICATION**

Super flexible SEMS was effective to management malignant colon obstruction at tortuous hepatic or splenic flexure.



## VI264-SD-THA6

## Multifunctional Embolic Beads Development for Image-Guided Transarterial Embolization

Thursday, Nov. 29 12:15PM - 12:45PM Room: VI Community, Learning Center Station #6

## FDA Discussions may include off-label uses.

#### Participants

Yingli Fu, Baltimore, MD (Presenter) Nothing to Disclose

Clifford R. Weiss, MD, Baltimore, MD (*Abstract Co-Author*) Research Grant, Siemens AG Research Grant, Merit Medical Systems, Inc Research Grant, BTG International Ltd Medical Advisory Board, Clear Guide Medical LLC Founder, Avasys, LLC Officer, Avasys, LLC Christos S. Georgiades, MD, PhD, Baltimore, MD (*Abstract Co-Author*) Consultant, Galil Medical Ltd Dara L. Kraitchman, DVM, PhD, Baltimore, MD (*Abstract Co-Author*) Nothing to Disclose

#### For information about this presentation, contact:

#### yfu7@jhmi.edu

#### PURPOSE

To develop drug-eluting, X-ray-visible, and uniform embolic beads for image-guided transarterial embolization treating cancers or obesity.

#### **METHOD AND MATERIALS**

For drug-eluting embolics development, we selected two model drugs: YIL-781, a hydrophobic ghrelin receptor antagonist for obesity-related application, and doxorubicin (Dox), a hydrophilic chemotherapeutic agent for cancer application. Drug-eluting, X-ray-visible embolic microspheres were made from 12% (v/v) perfluorootyl bromide (PFOB)-impregated alginate using either electrostatic droplet generator (large embolics) or custom-made microfluidic devices (small embolics). For YIL-781-eluting embolics, microencapsulation was performed by directly homogenizing YIL-781 with PFOB-alginate at a concentration of 10-25 mg/ml. For Dox-eluting embolics, a nanoparticle formulation with liposome was first generated via self-assembly prior to encapsulation to slow the release rate of Dox. Embolic beads size uniformity was examined microscopically immediately after synthesis. The stability of these microspheres was assessed over a period of two weeks in normal saline. In vitro release rates of YIL-781 or Dox were evaluated over time using a UV-Vis spectrophotometer. X-ray visibility was determined in phantoms containing varied amount of the microspheres using c-arm CT.

#### RESULTS

Highly uniform PFOB microspheres releasing YIL-781 or Dox could be generated using either electrostatic droplet generator ( $275 \pm 5.3 \mu m$ ) or microfluidic device ( $52 \pm 3.1 \mu m$ ). Both sets of embolics appeared to be stable as demonstrated by minimum size change over two weeks at room temperature and 37°C. The release rates of YIL-781 or Dox showed an initial burst followed by a steady state release for up to 5 days. Using clinical c-arm CT, both large and small embolics could be readily detected in phantoms and as few as two large PFOB embolics could be resolved.

### CONCLUSION

Drug-eluting, X-ray-visible embolics could be custom generated with narrow size variation and controlled release rates to an extend period.

## **CLINICAL RELEVANCE/APPLICATION**

Drug-eluting, image-visible embolics could facilitate image-guided transarterial therapy for oncological and non-oncological applications in real time.



## VI265-SD-THA7

Reduction in the Efficacy of Irreversible Electroporation for the Ablation of Colorectal Liver Metastases in the Presence of Metallic Objects Can Be Modeled with Computer Simulations

Thursday, Nov. 29 12:15PM - 12:45PM Room: VI Community, Learning Center Station #7

### Participants

Helena Cindric, Ljubljana, Slovenia (*Abstract Co-Author*) Nothing to Disclose Masashi Fujimori, MD,PhD, Tsu, Japan (*Abstract Co-Author*) Nothing to Disclose Bor Kos, PhD, Ljubljana, Slovenia (*Presenter*) Nothing to Disclose Francois Cornelis, MD,PhD, New York, NY (*Abstract Co-Author*) Nothing to Disclose Damijan Miklavcic, PhD, Ljubljana, Slovenia (*Abstract Co-Author*) Patent holder, IGEA Spa Stephen B. Solomon, MD, New York, NY (*Abstract Co-Author*) Research Grant, General Electric Company; Consultant, Johnson & Johnson; Consultant, BTG International Ltd; Govindarajan Srimathveeravalli, PhD, New York, NY (*Abstract Co-Author*) Nothing to Disclose

#### For information about this presentation, contact:

bor.kos@fe.uni-lj.si

#### CONCLUSION

Presence of metallic objects within 1 cm of the ablation zone increases risk of treatment failure following IRE of CRLM. Numerical simulations can be used to predict regions of treatment failure.

#### Background

Irreversible electroporation (IRE) is used for the focal ablation of colorectal liver metastases (CRLM). Metallic objects such as surgical staples or clips are often present in the vicinity of the tumor, affecting locoregional electrical conductivity. The aim of this study was to evaluate the effect of peri-tumoral metallic objects on the safety and efficacy of percutaneous IRE of CRLM.

#### **Evaluation**

Twenty five patients (12 women, 13 men) underwent IRE for the treatment of 29 CRLM (median diameter: 18 mm  $\pm$  13, range: 3-66 mm). Gender, tumor location, size, number of ablation probes, probe spacing, treatment voltage, pulse length, number of pulses and the presence of metallic objects within 1 cm of ablation zone were evaluated as determinants of local tumor progression (LTP) with the competing risks model (uni- and multivariate analyses). A subset of 9 tumors in 7 patients was evaluated using patient specific computer simulations to determine local electric field distribution and probability of cell death around the metallic object.

#### Discussion

Patients had a median follow-up of 25 months (range: 1-54 months), during which no IRE related complications were reported. Univariate analysis showed that tumor diameter >2 cm (p=0.003), probe spacing >20 mm (p=0.018) and presence of metallic implants (p=0.001) were significant predictors of time to LTP, but only the latter was found to be an independent predictor on multivariate analysis (sub Hazard Ratio=6.5, [95% CI: 1.99, 21.4], P=0.002). Absence of metallic implants from the ablation zone was associated with higher 12 month progression free survival 92.3% [56.6, 98.9] vs. 12.5% [2.1, 32.8]). Simulations indicated reduction of electric field strength and the probability of cell death in the vicinity of metallic implants. Distortions in electric field distribution were especially evident in the ablation margin, having good concordance with local recurrence on imaging.



# AI001-THC

# **Introduction to Deep Learning**

Thursday, Nov. 29 12:30PM - 2:00PM Room: AI Community, Learning Center

# **Title and Abstract**

Introduction to Deep Learning This class will focus on basic concepts of convolutional neural networks (CNNs), and walk the attendee through a working example. A popular training example is the MNIST data set which consists of hand-written digits. This course will use a data set we created, that we call 'MedNIST' and consists of 1000 images each from 5 different categories: Chest X-ray, hand X-ray, Head CT, Chest CT, Abdomen CT, and Breast MRI. The task is to identify the image type. This will be used to train attendees on the basic principles and some pitfalls in training a CNN. The attendee will have the best experience if they are familiar with Python programming.



## AI024-EC-THB

## Anatomical Borderline Structure Detection in Chest X-Ray by Deep Neural Networks

Thursday, Nov. 29 12:45PM - 1:15PM Room: AI Community, Learning Center Custom Application Computer Demonstration

#### Participants

Shinichi Fujimoto, MS,RT, Yoshida, Japan (*Presenter*) Nothing to Disclose Kenji Kondo, Tsukuba, Japan (*Abstract Co-Author*) Employee, Panasonic Corporation Harumi Itou, Yoshida, Japan (*Abstract Co-Author*) Nothing to Disclose Hirohiko Kimura, MD, PhD, Fukui, Japan (*Abstract Co-Author*) Nothing to Disclose Toshiki Adachi, RT, Yoshidagun, Japan (*Abstract Co-Author*) Nothing to Disclose Masakai Kiyono, Fukui, Japan (*Abstract Co-Author*) Employee, Panasonic Corporation Masato Tanaka, PhD, Yoshida, Japan (*Abstract Co-Author*) Nothing to Disclose Jun Ozawa, PhD, Tsukuba, Japan (*Abstract Co-Author*) Nothing to Disclose

#### For information about this presentation, contact:

sfuji@u-fukui.ac.jp

## CONCLUSION

We implemented and evaluated an ABS detection algorithm for CXR. For normal cases, we showed good detection performance. For abnormal cases, borderlines of DA, LV, LD, and RLB could only be partially extracted. Our work supports further development of anomaly detection based on ABSs' changes due to disease.

#### FIGURE

http://abstract.rsna.org/uploads/2018/18006874/18006874\_az5g.jpg

#### Background

Chest X-ray (CXR) is used for screening and diagnosis of many lung diseases. Conventional computer-aided diagnosis (CAD) methods for CXR involve analysis of predetermined target lesions; thus, those methods poorly manage unknown lesions. Hence, we are building a new CAD method to model normal local anatomical structures and their borderlines with the lung field [known as "anatomical borderline structures" (ABSs)] and to detect anomalies based on changes due to disease. Here, we implement and evaluate ABS detection in CXR as semantic segmentation tasks by deep neural networks.

## **Evaluation**

We chose U-Net, a fully convolutional network, as ABS detection network, and selected the first thoracic vertebra (Th1), descending aorta (DA), left ventricle (LV), left diaphragm (LD), and dorsal portion of right lung base (RLB) as ABSs for detection. From CXR, each of five U-Nets outputs a region image of each respective ABS. A total of 627 normal cases were used to train five U-Nets; 70 normal and 143 abnormal cases were used for evaluation. For each normal CXR, mask images of the five ABSs were manually created, then used for training and evaluation. Detection accuracy for 70 normal cases was evaluated by Dice coefficient (DC). Average DC was 0.91 for Th1 (anatomical structure alone), and 0.71-0.81 for borderlines between anatomical structure (i.e., DA, LV, LD, or RLB) and the lung field. A total of 143 abnormal cases were visually evaluated. For example, in cases of pneumonia, partial to whole borderlines of DA, LV, LD, and RLB could not be extracted.

#### Discussion

Detection results for normal cases were sufficient for use in our CXR-CAD. For abnormal cases, partial to whole ABSs could not be extracted. Thus, we demonstrated the feasibility of our anomaly detection method for CXR. We continue work on detection of other ABSs and quantification of anomalies based on detection results.



## AI151-ED-THB2

A Two-Stage Deep-Learning Scheme for Reducing Radiation Dose in Digital Breast Tomosynthesis (DBT)

Thursday, Nov. 29 12:45PM - 1:15PM Room: AI Community, Learning Center Station #2

#### **Participants**

Junchi Liu, MS, Chicago, IL (Abstract Co-Author) Nothing to Disclose

Amin Zarshenas, MSc, Chicago, IL (Abstract Co-Author) Nothing to Disclose

Syed Ammar Qadir, Chicago, IL (Abstract Co-Author) Nothing to Disclose

Limin Yang, MD, PhD, Iowa City, IA (Abstract Co-Author) Nothing to Disclose

Laurie L. Fajardo, MD, MBA, Park City, UT (*Abstract Co-Author*) Consultant, Hologic, Inc; Consultant, Siemens AG; Consultant, FUJIFILM Holdings Corporation;

Kenji Suzuki, PhD, Chicago, IL (*Presenter*) Royalties, General Electric Company; Royalties, Hologic, Inc; Royalties, MEDIAN Technologies; Royalties, Riverain Technologies, LLC; Royalties, Canon Medical Systems Corporation; Royalties, Mitsubishi Corporation; Royalties, AlgoMedica, Inc

#### For information about this presentation, contact:

jliu118@hawk.iit.edu

#### **TEACHING POINTS**

1) To understand the basic principles of our original neural network convolution (NNC) deep learning. 2) To understand our twostage deep-learning scheme based on two sequential NNC models for substantial reduction of radiation dose in DBT. 3) To demonstrate and compare the image quality of our "virtual" high-dose (VHD) images generated from lower-dose acquisitions to that of real clinical full-dose images in DBT. 4) To understand the clinical utility of our technology for reducing radiation dose in DBT.

#### **TABLE OF CONTENTS/OUTLINE**

A. Radiation dose issues with breast cancer screening in DBTB. Basic principles of NNC deep learning1) Patched-based neural network regression2) Processing of entire image in convolutional mannerC. NNC deep learning for dose reduction in DBT1) A two-stage deep-learning scheme consisting of two NNC models2) Training 1st NNC with raw projection images3) Training 2nd NNC with reconstructed DBT slicesD. Quantitative evaluation: Image quality vs. radiation dose reduction1) Evaluation of 51 non-training clinical cases2) 74% dose reduction rate of 1st NNC 3) 89% dose reduction rate of 2nd NNC 4) Processing time of 0.24 sec on a GPU for each studyE. Benefits and limitations of our radiation dose reduction technology for DBT



## AI234-SD-THB1

## CT Image Enhancement for Lesion Segmentation Using Stacked Generative Adversarial Networks

Thursday, Nov. 29 12:45PM - 1:15PM Room: AI Community, Learning Center Station #1

### Participants

Youbao Tang, PhD, Bethesda, MD (*Presenter*) Nothing to Disclose Jinzheng Cai, Gainesville, FL (*Abstract Co-Author*) Nothing to Disclose Le Lu, Bethesda, MD (*Abstract Co-Author*) Employee, NVIDIA Corporation Adam P. Harrison, PhD, Bethesda, MD (*Abstract Co-Author*) Nothing to Disclose Ke Yan, Bethesda, MD (*Abstract Co-Author*) Nothing to Disclose Jing Xiao, Shenzhen, China (*Abstract Co-Author*) Nothing to Disclose Lin Yang, Gainesville, FL (*Abstract Co-Author*) Nothing to Disclose Ronald M. Summers, MD,PhD, Bethesda, MD (*Abstract Co-Author*) Royalties, iCAD, Inc; Royalties, Koninklijke Philips NV; Royalties, ScanMed, LLC; Research support, Ping An Insurance Company of China, Ltd; Researcher, Carestream Health, Inc; Research support, NVIDIA Corporation; ; ; ;

### For information about this presentation, contact:

youbao.tang@nih.gov

#### PURPOSE

Automated lesion segmentation from computed tomography (CT) is an important and challenging task in medical image analysis. As more and more elaborately designed segmentation methods are proposed, performance improvement may plateau. One hurdle is that CT images can exhibit high noise and low contrast, particularly in lower dosages. The collection of datasets more massive than currently available may provide the means to overcome this, but this eventuality is not guaranteed, particularly given the labor involved in manually annotating training images. We take a different tack, and instead leverage the massive amounts of data already residing in hospital PACS to develop a method to enhance CT images in a way that benefits lesion segmentation.

## **METHOD AND MATERIALS**

A stacked generative adversarial networks (SGAN) approach is proposed for CT image enhancement (IE). Instead of directly performing IE, our SGAN decomposes IE into two sub-tasks, i.e., image denoising followed by enhancement. The first GAN reduces the noise in the CT image and the second GAN generates a higher resolution image with enhanced boundaries and high contrast. To make up for the absence of high quality CT images, we detail how to synthesize a large number of low- and high-quality natural images and use transfer learning with progressively larger amounts of CT images. We apply both the classic GrabCut method and the modern holistically nested network (HNN) to lesion segmentation, testing whether SGAN can yield improved lesion segmentation. The experiments are conducted on a large scale dataset containing 32,735 lesion images from 4,459 patients, where 1,000 lesions from 500 patients are manually segmented as a testing set.

## RESULTS

The Dice scores of GrabCut/HNN are improved from 0.908/906 to 0.913/0.92 when using SGAN enhanced images. And compared with other enhanced approaches, using SGAN gets the best segmentation performance.

## CONCLUSION

The results demonstrate that SGAN is effective in yielding improved lesion segmentation performance and SGAN enhancements alone can push GrabCut performance over HNN trained on original images, suggesting that focusing on dataset processing is a crucial research direction in medical imaging analysis.

## **CLINICAL RELEVANCE/APPLICATION**

The SGAN enhanced images can provide auxiliary information to help radiologists for making decision and the improved segmentation performance can strengthen some CAD tasks, e.g. tumor growth evaluation.



## BR007-EB-THB

What Radiologists Should Know to Avoid Mistakes in Screening Breast US

Thursday, Nov. 29 12:45PM - 1:15PM Room: BR Community, Learning Center Hardcopy Backboard

#### **Participants**

Jin Hwa Lee, MD, Busan, Korea, Republic Of (*Presenter*) Nothing to Disclose Eun Cho, MD, Busan, Korea, Republic Of (*Abstract Co-Author*) Nothing to Disclose Young Mi Park, MD, PhD, Busan, Korea, Republic Of (*Abstract Co-Author*) Nothing to Disclose

For information about this presentation, contact:

### jhrad@dau.ac.kr

## **TEACHING POINTS**

The purpose of this exhibit is To review the reasons for False-Negative and False-Positive in screening breast US To learn how to reduce missed cancer and unnecessary recall or biopsy in screening breast US

# TABLE OF CONTENTS/OUTLINE

Reasons for False-Negative Technical errors; high-resolution US equipment, adjustment of US settings, optimal scanning technique Perception errors; isoechoic lesions, deeply located lesions in large breasts, peripherally located lesions, subareolar lesions, US tissue composition; background echotexture Interpretation errors; misinterpretation of margin, multiple distracting lesions Correlation errors; mammographic correlation, MRI correlation, clinical correlation (Symptomatic vs Asymptomatic, Patients' own risk factors, past history (underlying extramammary disease) Reasons for False-Positive Inherent factor of US Technical errors Large numbers of category 3 lesions



## BR011-EB-THB

Contrast Enhanced Spectral Mammography (CESM). The 'What, When and How' Guide to Using it in a Symptomatic Tertiary Referral Center

Thursday, Nov. 29 12:45PM - 1:15PM Room: BR Community, Learning Center Hardcopy Backboard

## Participants

Rosanna Frost, MBBS, FRCR, London, United Kingdom (*Abstract Co-Author*) Nothing to Disclose Ruxandra Pietrosanu, MD, FRCR, London, United Kingdom (*Abstract Co-Author*) Nothing to Disclose Sultana Hasso, MBBS, London, United Kingdom (*Abstract Co-Author*) Nothing to Disclose Konstantia Diana Stavrou, MBBS, BSC, London, United Kingdom (*Presenter*) Nothing to Disclose

For information about this presentation, contact:

rfrost@doctors.net.uk

## **TEACHING POINTS**

The purpose of the exhibit to to outline: 1 Why to use CESM? 2 When to utilize CESM in clinical practice. 3 How to interpret CESM

## TABLE OF CONTENTS/OUTLINE

Why do we use it? CESM is an evolving breast imaging technique, which combines standard full - field digital mammography (FFDM) with an intravenous iodinated contrast medium to detect areas of increased angiogenesis. The technique is well tolerated by patients, quick and cost effective whilst being highly sensitive comparable to CEMRI. When do we use it? The local staging of patients under the age of 40 with a biopsy proven breast cancer who have not undergone a diagnositic mammogram due to their age. The local staging of patients who have an indication for CEMRI but have a contraindication to MRI. Monitoring response to neoadjuvant chemotherapy. We are currently conducting an ongoing study to demonstrate that CESM can be used as an alternative to MRI for monitoring reponse during neoadjuvant chemotherapy. Annual monitoring of breast cancer patients who are at high risk or who have dense breasts (birads 4-5). Current ongoing study. How to interpret it? Assessment of normal backgound enhancement. Artefacts. The characteristics of benign vs malignanat mass lesions. Non mass enhancement. Non enhancing malignanat calcification. Chest wall and retroareolar lesions. Our experience over the last three years.



## BR216-ED-THB6

## Superficial Breast Lesions That We Need to Know

Thursday, Nov. 29 12:45PM - 1:15PM Room: BR Community, Learning Center Station #6

#### **Participants**

Marisela L. Curros, MD, Adrogue, Argentina (*Presenter*) Nothing to Disclose Valeria Vidales, Buenos Aires, Argentina (*Abstract Co-Author*) Nothing to Disclose Daniela E. Simbler, MD, Buenos Aires, Argentina (*Abstract Co-Author*) Nothing to Disclose Norma I. Pona, MD, CABA, Argentina (*Abstract Co-Author*) Nothing to Disclose Felix Vigovich, Buenos Aires, Argentina (*Abstract Co-Author*) Nothing to Disclose Adriana Garcia, MD, Banfield, Argentina (*Abstract Co-Author*) Nothing to Disclose

## For information about this presentation, contact:

mcurros@hbritanico.com.ar

## **TEACHING POINTS**

-To recognize the radiological features of the lesion that helps to identify its localization between the dermis, the subcutaneous fat and the parenchyma. -To describe differential diagnosis and its classification in BI RADS system. -To emphasize in diagnostic difficulties.

### TABLE OF CONTENTS/OUTLINE

-Description of the anatomy of the superficial breast. -Description of different types of lesions that could be found in the breast skin and the superficial breast parenchyma. -US and mammographic: principal findings and its correlations. -Sample cases.



#### BR217-ED-THB7

# Mammographic Evaluation of Calcifications: Atlas for Residents

Thursday, Nov. 29 12:45PM - 1:15PM Room: BR Community, Learning Center Station #7

#### Awards Identified for RadioGraphics

### **Participants**

Yesenia Bermudez Cano, MD, Buenos Aires, Argentina (*Abstract Co-Author*) Nothing to Disclose Veronica Gonzalez, Buenos Aires, Argentina (*Abstract Co-Author*) Nothing to Disclose Karina Pesce, Capital Federal, Argentina (*Abstract Co-Author*) Nothing to Disclose Victoria Ardiles, Buenos Aires, Argentina (*Abstract Co-Author*) Nothing to Disclose Maria Jose Chico, Buenos Aires, Argentina (*Abstract Co-Author*) Nothing to Disclose Pamela I. Causa Andrieu, MD, La Plata, Argentina (*Presenter*) Nothing to Disclose

### For information about this presentation, contact:

yesebeca@hotmail.com

#### **TEACHING POINTS**

1. Review the mammographic descriptors for breast calcifications, taking like reference the fifth edition of the BIRADS. 2. Analyze of morphology and distribution of breast microcalcifications on mammography, thus aiding in their classification and management of breast lesions. 3. Demonstrate the imaging features of calcifications and correlate with the histopathology obtained by Stereotactic Large Core Needle Biopsy

### TABLE OF CONTENTS/OUTLINE

Table of Contents: 1. Introduction 2. Images features: - Calcification descriptors - Distribution - Location - Associated findings - Change, if previous films are compared - Use of microcalcification descriptors in BI-RADS 5th edition to stratify risk of malignancy 3. Microcalcification in breast lesions: radio-pathologic correlation 4. Pseudocalcifications: Artifact 5. Management - Management of microcalcifications that develop at the lumpectomy site after breast-conserving therapy 6. Conclusion.



### BR218-ED-THB8

**Contrast Enhanced Mammography: Where Does It Fail?** 

Thursday, Nov. 29 12:45PM - 1:15PM Room: BR Community, Learning Center Station #8

#### **Participants**

Ignacio Gonzalez de la Huebra Rodriguez, MD, Pamplona, Spain (*Presenter*) Nothing to Disclose Alejandra Garcia Baizan, MD, Pamplona, Spain (*Abstract Co-Author*) Nothing to Disclose Ana Ezponda, MD, Pamplona, Spain (*Abstract Co-Author*) Nothing to Disclose Marta Calvo-Imirizaldu, MD, Pamplona, Spain (*Abstract Co-Author*) Nothing to Disclose Arlette Elizalde, Pamplona, Spain (*Abstract Co-Author*) Nothing to Disclose Luis Pina, MD, PhD, San Sebastian, Spain (*Abstract Co-Author*) Nothing to Disclose

## For information about this presentation, contact:

agarcia.13@unav.es

# **TEACHING POINTS**

The purpose of this exhibit is: 1. To review the strengths, weaknesses and indications of Contrast Enhanced Mammography (CEM)2. To show the features of breast tumors that were missed by CEM.

## TABLE OF CONTENTS/OUTLINE

Description of the technique: -What is double energy?Intravenous administration of iodinated contrast medium (mammography becomes a morpho-functional technique).Indications of CEM - Problem solving technique. -Screening of intermediate risk patients. - Preoperative staging of breast cancer. -Patients not suitable for MRI.Contraindications of CEM: -Allergy to iodinated contrast medium. -Renal insufficiency.Limitations of CEM - Evaluation of microcalcificationes. -Women with breast ImplantsFalse Negative cases: -Lesions out of the field of view (peripherically located). -Pathology: More misses in DCIS than in invasive cancers. -Breast density: More misses in dense patterns . -Imaging features: More misses in architectural distortions than masses. -Size: More misses in small cancers (<10mm).False Positive cases: -Fibroadenoma -Papilloma -Fat necrosis -Sclerosing adenosis



## BR219-ED-THB9

## MRI Biopsy Radiology/Pathology Concordance: A Rapid Review of Common Pathologic Entities

Thursday, Nov. 29 12:45PM - 1:15PM Room: BR Community, Learning Center Station #9

#### **Participants**

Marina Mohallem Fonseca, Ottawa, ON (*Abstract Co-Author*) Nothing to Disclose Raman Verma, MD, Ottawa, ON (*Presenter*) Nothing to Disclose Leslie Lamb, MD, Boston, MA (*Abstract Co-Author*) Nothing to Disclose Jean M. Seely, MD, Ottawa, ON (*Abstract Co-Author*) Nothing to Disclose

# **TEACHING POINTS**

This exhibit will: 1)Identify common benign and malignant pathologies diagnosed by MRI biopsy using an image rich review. 2)Outline practical tips when assessing radiologic and pathologic concordance and the need for re-biopsy. 3)Provide an algorithm for management of indeterminate lesions on MRI.

## TABLE OF CONTENTS/OUTLINE

Breast MRI is routinely used in the screening and diagnostic settings, in conjunction with mammographic and sonographic assessment. An indeterminate lesion on MRI, occult on conventional imaging, may require an MRI-guided biopsy for definitive histopathologic analysis. Lesions biopsied under MRI guidance are frequently benign; however, there is variable and often overlapping appearance of both benign and malignant etiologies, often rendering the concordance assessment difficult. Lesions including the following will be illustrated, with all cases having follow-up imaging or surgical excision: 1)Benign (fibroadenoma, fibrocystic change, pseudoangiomatous stromal hyperplasia, fat necrosis, mastitis) 2)High risk (lobular carcinoma in-situ, atypical ductal hyperplasia, radial scar, papilloma) 3)Malignant (invasive ductal and lobular, ductal carcinoma in-situ) A summary based on the literature will outline strategies to determine appropriate imaging modalities with which to further evaluate an MRI-detected indeterminate lesion.



## BR269-SD-THB3

Comparison Between Radiation Dose of 2D Digital versus Digital Tomosynthesis Guided Stereotactic Breast Biopsies: Tomosynthesis Wins!

Thursday, Nov. 29 12:45PM - 1:15PM Room: BR Community, Learning Center Station #3

## Participants

Tali Amir, MD, Philadelphia, PA (*Abstract Co-Author*) Nothing to Disclose Bruno Barufaldi, PhD, Philadelphia, PA (*Abstract Co-Author*) Nothing to Disclose Samantha P. Zuckerman, MD, Philadelphia, PA (*Presenter*) Nothing to Disclose Andrew D. Maidment, PhD, Philadelphia, PA (*Abstract Co-Author*) Research support, Hologic, Inc; Research support, Barco nv; Research support, Analogic Corporation; Spouse, Employee, Real-Time Tomography, LLC; Spouse, Stockholder, Real-Time Tomography, LLC; Scientific Advisory Board, Real-Time Tomography, LLC; Emily F. Conant, MD, Philadelphia, PA (*Abstract Co-Author*) Grant, Hologic, Inc; Consultant, Hologic, Inc; Grant, iCAD, Inc; Consultant, iCAD, Inc; Speaker, iiCME

#### PURPOSE

To compare radiation dose of digital breast tomosynthesis (DBT) versus digital mammographic (DM) guided breast biopsies

### **METHOD AND MATERIALS**

We replaced a prone DM stereotactic biopsy (bx) unit with a prone dual mode, DM-DBT bx unit in 8/2017. All bxs performed 8/2016 to 1/2017 and 8/2017 to 1/2018 were retrospectively reviewed. The bxd finding, guidance modality (DM vs DBT), and Digital Imaging and Communications in Medicine (DICOM) header data were recorded. Image metadata was extracted from the DICOM header and stored into a client-side Structured Query Language (SQL) database. The average glandular dose (AGD) per image and study were computed and stratified by modality and finding type.

### RESULTS

25 DM guided bxs (24 calcifications,1 asymmetry) were performed on the DM unit between 8/2016 and 1/2017. The AGD per image was 2.63 mGy (SD 1.16). The AGD per procedure was 28.77 mGy (SD 14.34) and average image number was 10.92. 97 DM/DBT guided bxs (80 calcifications, 13 architectural distortions, 2 asymmetries, 2 masses) were performed on the DM-DBT unit from 8/2017 - 1/2018. The AGD per image was 2.40 mGy (SD 1.09); DM AGD was 2.32 mGy (SD 1.11) while DBT AGD was 2.46 mGy (SD 0.95). The AGD per procedure was 18.18 (SD 13.66); DBT guided bxs had an AGD of 12.43 mGy (SD 9.08) while DM guided bxs had an AGD of 21.20 mGy (SD 14.18). The average image number for DM bxs was 9.14 compared with 5.05 for DBT bxs. There was a 26% dose reduction for DM bxs on the dual mode unit compared to the DM only unit, due to a 12.7% reduced AGD per image (p<0.0001). When assessing DBT compared with DM guided bxs on the dual unit, the DBT AGD was 36% lower than DM (p=0.0304), despite a 13% increase in dose per individual DBT acquisition compared to a single DM view.

## CONCLUSION

Significant dose reduction is achieved for mammographically guided bxs with newer equipment functioning with higher efficiency. In addition, for bxs performed on a dual mode unit, use of DBT guidance can significantly reduce dose compared to using DM guidance. This lower dose is due to a lower number of acquisitions in DBT guided bxs and because a single DBT acquisitions has a lower AGD than DM stereo pairs.

# **CLINICAL RELEVANCE/APPLICATION**

Newer, more efficient biopsy equipment and the use of DBT guidance can reduce the total radiation dose of mammographically guided biopsy procedures.



## BR273-SD-THB1

Fully Automated Breast Lesion Segmentation on DCE-MRI Using a Convolutional Neural Network for Radiomic Analysis

Thursday, Nov. 29 12:45PM - 1:15PM Room: BR Community, Learning Center Station #1

## Participants

Meghan A. Moriarty, MD, Port Jefferson, NY (*Presenter*) Nothing to Disclose Karl D. Spuhler, MSc, Stony Brook, NY (*Abstract Co-Author*) Nothing to Disclose Jie Ding, MS, Stony Brook, NY (*Abstract Co-Author*) Nothing to Disclose Chunling Liu, Stony Brook, NY (*Abstract Co-Author*) Nothing to Disclose Chuan Huang, PhD, Stony Brook, NY (*Abstract Co-Author*) Nothing to Disclose

# For information about this presentation, contact:

meghanannmoriarty@gmail.com

### PURPOSE

To validate the accuracy of the automated segmentation of breast tumors using a fully convolutional neural network (CNN) developed by our group. The goal is to create an automated DCE-MRI breast lesion segmentation system to be able to be utilized in further radiomics studies in breast cancer, such as predicting sentinel lymph node metastases.

#### **METHOD AND MATERIALS**

This retrospective study was approved by the local IRB. A total of 316 DCE-MRI scans of breast cancer patients acquired on a 1.5T MRI scanner were collected. We trained a CNN on a GPU server to automatically segment DCE-MRI breast lesions. Two radiologists participated in this study. A total of 197 DCE-MRI scans were used for training the lesion segmentation neural network, these were all drawn by radiologist 1. The network was then tested on a separate set of 119 DCE-MRI scans, using ROIs drawn by both radiologists. Dice indices among the two radiologists' hand drawn ROIs and those generated by the automated network were calculated.

## RESULTS

On patient level, the mean Dice indices between ROIs were 0.64 (radiologist 1 vs 2), 0.60 (CNN vs radiologist 1), and 0.62 (CNN vs radiologist 2). In order to reduce the effect of very small lesions on Dice index, the ROIs of all patients were grouped together; the corresponding Dice indices were 0.64, 0.71 and 0.67. A Dice index of 0.7 is generally considered to have excellent agreement between two segmentations in this condition. Comparing these two Dice indices indicates that the network segments lesions with similar error rates to inter-human reader differences.

# CONCLUSION

The proposed neural network-based automated breast lesion segmentation shows significant agreement compared to the laborintensive manual segmentation. The next step is to apply this in a task-based radiomic analysis to provide potential biomarkers and guide clinical decisions for breast cancer patients.

#### **CLINICAL RELEVANCE/APPLICATION**

To determine whether such a fully automated neural network based segmentation could be employed for developing and implementing radiomics pipelines.



## BR274-SD-THB2

Comparison of Results from Three Different Density Assessment Methods on Mammographic Density (MD) in Screening Patients Receiving Vitamin D (Vit D): Results of CALGB 70806 (Alliance)

Thursday, Nov. 29 12:45PM - 1:15PM Room: BR Community, Learning Center Station #2

## Participants

H. Carisa Le-Petross, MD, FRCPC, Houston, TX (*Presenter*) Nothing to Disclose Drew K. Seisler, Rochester, MN (*Abstract Co-Author*) Nothing to Disclose Despina Kontos, PhD, Philadelphia, PA (*Abstract Co-Author*) Nothing to Disclose Heshan Liu, Rochester, MN (*Abstract Co-Author*) Nothing to Disclose Jayne R. Charlamb, MD, Syracuse, NY (*Abstract Co-Author*) Nothing to Disclose Sin-Ho Jung, PhD, Durham, NC (*Abstract Co-Author*) Nothing to Disclose James R. Marshall, PhD, Buffalo, NY (*Abstract Co-Author*) Nothing to Disclose Marie Wood, MD, Burlington, NY (*Abstract Co-Author*) Nothing to Disclose

#### For information about this presentation, contact:

hlepetross@mdanderson.org

#### PURPOSE

To compare the different methods used for assessing MD in this screening population receiving Vit D for its breast cancer prevention properties, in CALGB 70806, a randomized phase II trial.

#### **METHOD AND MATERIALS**

Premenopausal women randomized to receive either 2000IU of Vit D or placebo for 12 months had mammogram at baseline and at 12 months. MD was determined by Clinical Breast Imaging Reporting and Data System (BI-RADS), the semiautomatic software Cumulus 6.0 (University of Toronto, Toronto, Canada), and fully automated method by the Laboratory for Individualized Breast Radiodensity Assessment (LIBRA, by Computational Breast Imaging Group at University of Pennsylvania). Blinded central review of all submitted mammograms was performed. Eligible women were premenopausal, age <55, with at least 25% dense breast tissue. Kappa statics were used to measure agreement between local and central MD readings using BI-RADS. MD measurements were compared using Wilcoxon rank-sum test.

## RESULTS

300 women from 41 US centers were accrued from 2011 to 2013. 150 women received Vit D and 150 placebo. Mean age was 42.6 years with 14% Hispanic, 12% African American, and 74% Caucasian. 72% of participants completed treatment; the rest withdrew. As previously reported, 1 year Vitamin D therapy did not significantly change MD (p=0.7048). Sub-analysis demonstrated moderate agreement between local and central MD readings using BI-RADs classification at baseline and at 12 months, with Kappa coefficients of 0.48 and 0.41 respectively. Increased MD from Cumulus and LIBRA were noted in heterogeneously dense and dense BI-RADs cases (p < 0.0001). When the readings for CC view was compared to MLO view, CC views showed slightly higher readings at baseline and at 12 months (p=0.05 and 0.02 respectively). Cumulus readings were consistently higher than LIBRA readings (table 1, P < 0.0001).

#### CONCLUSION

The subjective method of BI-RADS, semi-automated method CUMULUS, and automated method LIBRA were in agreement for the majority of cases, with least variability noted from LIBRA than the other two methods.

#### **CLINICAL RELEVANCE/APPLICATION**

The automated method is more reliable and reproducible than the semi-automated or BI-RADs method for assessing breast density. Support: UG1CA189823, U24CA196171. ClinicalTrials.gov Identifier: NCT01224678



## BR276-SD-THB4

Comparative the Average Glandular Dose between Digital Breast Tomosynthesis (DBT) and Full-Field Digital Mammography (FFDM): Correlation with Breast Thickness and Density

Thursday, Nov. 29 12:45PM - 1:15PM Room: BR Community, Learning Center Station #4

**FDA** Discussions may include off-label uses.

#### Participants

Chanjuan Wen, Guangzhou, China (*Presenter*) Nothing to Disclose Weimin Xu, Guangzhou, China (*Abstract Co-Author*) Nothing to Disclose Hui Zeng, Guangzhou, China (*Abstract Co-Author*) Nothing to Disclose Zilong He, Guangzhou, China (*Abstract Co-Author*) Nothing to Disclose Weiguo Chen, Guangzhou, China (*Abstract Co-Author*) Nothing to Disclose

#### For information about this presentation, contact:

182389433@qq.com

### PURPOSE

To compare the average glandular dose (AGD) between single-view digital breast tomosynthesis (DBT) and single-view full-field digital mammography (FFDM), and to evaluate the correlation of AGD with breast thickness and density.

## METHOD AND MATERIALS

A total of 318 female patients who underwent both DBT and FFDM (DBT and FFDM were performed in the same compression thickness in each breast) were included. 636 DBT images of unilateral breast mediolateral oblique (MLO) view and 636 FFDM images of unilateral breast mediolateral oblique (MLO) view were analyzed. Mammographic breast density was determined according to BI-RADS breast density grading, and breast thickness and AGD per exposure in MLO views retrieved from DICOM headers were recorded. Breast thickness were divided into the following four groups: <= 30cm, 31 ~ 45cm, 46 ~ 60cm and > 60cm. The statistical analyses used variance analysis and Pearson's correlation for parametric tests.

# RESULTS

(1) The AGD of DBT had a weak negative correlation with breast density (correlation coefficient =-0.305, P<0.001), decreased as the breast density increased. The AGD of FFDM did not change significantly with breast density increased (correlation coefficient =-0.027, P=0.501). (2) Breast thickness was significantly associated with AGDs, and both AGDs of FFDM and DBT increased with increased breast thickness (correlation coefficient =0.771 and 0.935, respectively, all P<0.001). (3) When breast density was >75% and breast thickness was >60cm, the AGD of DBT was lower than that of FFDM, and the difference was statistical significant (P = 0.031).

## CONCLUSION

The AGD of DBT increased with breast thickness increased and decreased with breast density. For thick and dense breast, the radiation dose of DBT was lower than that of FFDM.

## **CLINICAL RELEVANCE/APPLICATION**

In this study, we evaluated the AGD of MLO FFDM and DBT according to breast density and thickness.



## BR277-SD-THB5

Fate of a BI-RADS 3 Lesion: An Analysis of the Characteristics, Follow Up, Diagnostic Workup, and Cancer Rate of Probably Benign Lesions Seen at Breast MRI

Thursday, Nov. 29 12:45PM - 1:15PM Room: BR Community, Learning Center Station #5

### Participants

Margaret J. Wong, MD,MENG, Palo Alto, CA (*Presenter*) Nothing to Disclose Rupa Patel, MD, Stanford, CA (*Abstract Co-Author*) Nothing to Disclose Wendy B. Demartini, MD, Stanford, CA (*Abstract Co-Author*) Nothing to Disclose Julia Todderud, Stanford, CA (*Abstract Co-Author*) Nothing to Disclose Debra M. Ikeda, MD, Stanford, CA (*Abstract Co-Author*) Scientific Advisory Board, Grail, Inc; Reviewer, Siemens AG

## PURPOSE

Our purpose was to evaluate the patient and imaging characteristics, follow-up frequency and timing, and rate of malignancy for breast MRI examinations assessed as BI-RADS Category 3.

## METHOD AND MATERIALS

From 4235 consecutive screening and diagnostic breast MRI examinations performed from May 2011 through December 2014, we retrospectively identified examinations assessed as BI-RADS Category 3. For the study examinations, we collected patient characteristics and breast MRI BI-RADS descriptors, follow-up frequency and timing, and biopsy outcomes. Benign versus malignant outcome was determined by biopsy and/or imaging follow-up for two years. We calculated the frequencies of patient and imaging characteristics, and the rates of follow-up compliance and of malignancy.

### RESULTS

From 4235 consecutive breast MRI examinations in the study interval, 3.9% (167/4235) were assessed as BI-RADS Category 3. 88% (147/167) examinations were in patients designated at high risk for breast cancer. The most frequency MRI features associated with BI-RADS Category 3 were minimal background parenchymal enhancement (50%, 83/167), lesion type mass (38%, 64/167), and lesion type focus/foci (39%, 65/167). Masses were most commonly oval (50%, 32/64) and circumscribed (39%, 25/64). Initial kinetics were most commonly medium (39%, 65/167), and late kinetics were most commonly persistent (60%, 100/167). The follow-up compliance rate was 75% (125/167) with an average time to follow up of 14.1 months. Out of the 125 MRI examinations with adequate follow up, 21 lesions were biopsied (17%, 21/125) showing two cancers (1.6%, one IDC and one DCIS), six high-risk lesions (4.8%; three papillomas, one ALH, one ADH, one low-grade spindle cell tumor) and 13 benign findings.

#### CONCLUSION

Breast MRI BI-RADS Category 3 was used in 3.9% of examinations, and the recommended follow-up occurred in 75%. The rate of malignancy was 1.6% which is comparable to that for mammography, despite the higher risk MRI patient population.

### **CLINICAL RELEVANCE/APPLICATION**

The BI-RADS MRI category 3 assessment category is not well established, largely due to variations in hardware, field strengths, and pulse sequences between sites. Our analysis provides insight into what MRI characteristics warrant a BI-RADS 3 assessment. Understanding this BI-RADS category is especially important to reduce unnecessary biopsies of probably benign lesions that can be safely followed with short term follow up imaging.



## CA171-ED-THB7

## Mapping the MAPCAs with Dual Source CT: What Do the Cardiothoracic Surgeons Want to Know?

Thursday, Nov. 29 12:45PM - 1:15PM Room: CA Community, Learning Center Station #7

#### **Participants**

Vasanthakumar Venugopal, MD, New Delhi, India (*Presenter*) Nothing to Disclose Vidur Mahajan, MBBS, New Delhi, India (*Abstract Co-Author*) Nothing to Disclose Harsh Mahajan, MD, MBBS, New Delhi, India (*Abstract Co-Author*) Nothing to Disclose

### For information about this presentation, contact:

vasanthdrv@gmail.com

### **TEACHING POINTS**

1. Major Aortopulmonary collateral arteries are unique lesions in which the pulmonary vascular bed is multi-compartmentalized 2. Unifocalization refers to the process of changing an abnormal multi-compartment pulmonary artery circulation to a normal single compartment circulation. 3. If neither a PV or ductus is present during primary morphogenesis, the foregut source of PA persists and the native pulmonary arteries do not form normally 4. What Does the Surgeon Need to Know Before Unifocalization? - True pulmonary artery size and arborization - Number, origin, exact course, and destination of every collateral - Exact position and severity of all stenoses in both true pulmonary arteries and collaterals - For every collateral, does it intercommunicate with true pulmonary artery: "isolated supply" or "dual supply" - Relationship of collaterals to other thoracic structures: bronchial tree, pulmonary veins, esophagus - Post-stenotic pressure in collaterals

### **TABLE OF CONTENTS/OUTLINE**

- Basic Physiology of MAPCA - Principles of Surgical Management - What does the surgeon want to know - Imaging protocols - Dual source CT advantages - Pitfalls and Challenges - Some case examples



# CA176-ED-THB6

Pathologic Entities That May Affect the Lungs and the Myocardium: Keys for Diagnosis and Prognosis with Chest CT and Cardiac MR

Thursday, Nov. 29 12:45PM - 1:15PM Room: CA Community, Learning Center Station #6

### Awards Identified for RadioGraphics

#### Participants

Jose Gutierrez Chacoff, MD, Santiago, Chile (*Abstract Co-Author*) Nothing to Disclose Laura Jimenez-Juan, MD, Toronto, ON (*Abstract Co-Author*) Nothing to Disclose Daniel Vargas, MD, Aurora, CO (*Abstract Co-Author*) Nothing to Disclose Lan-Chau T. Kha, MD, MSc, Toronto, ON (*Abstract Co-Author*) Nothing to Disclose Felipe A. Sanchez, MD, Santiago, Chile (*Presenter*) Nothing to Disclose Anastasia Oikonomou, MD, PhD, Toronto, ON (*Abstract Co-Author*) Nothing to Disclose

## For information about this presentation, contact:

josegutierrezchacoff@gmail.com

## **TEACHING POINTS**

The presence and extent of LGE in cardiac sarcoidosis is predictive of ventricular arrhythmias and death, independent of the ejection fraction. Alveolar/septal pattern of pulmonary amyloidosis has significantly worse prognosis compared with nodular parenchymal amyloidosis. Diffuse subendocardial LGE, with suboptimal nulling time of myocardium are highly suggestive of cardiac amyloidosis. Native T1 and myocardial extracellular volume have important diagnostic and prognostic value. Apical subendocardial LGE without vascular territory, usually with apical thrombus is suggestive of eosinophilic granulomatosis with polyangiitis (with history of asthma and allergy) or eosinophilic syndrome (without history of allergy). Unlike the idiopathic interstitial pneumonias, UIP and NSIP pattern related to systemic sclerosis have similar survival and extension of the CT abnormalities is the only prognostic factor of mortality and progression.

### **TABLE OF CONTENTS/OUTLINE**

Learning objectivesIntroductionSarcoidosisAmyloidosisHemochromatosisEosinophilic granulomatosis with poliangiitisHypereosinophilic syndromeSystemic sclerosisSystemic Lupus erythematosusIgG4 diseaseErdhem-Chester diseaseRosai-Dorfman diseaseSchematic diagnostic approachTake home messages

## **Honored Educators**

Presenters or authors on this event have been recognized as RSNA Honored Educators for participating in multiple qualifying educational activities. Honored Educators are invested in furthering the profession of radiology by delivering high-quality educational content in their field of study. Learn how you can become an honored educator by visiting the website at: https://www.rsna.org/Honored-Educator-Award/ Daniel Vargas, MD - 2017 Honored Educator



## CA257-SD-THB1

Machine Learning to Evaluate Atherosclerotic Plaque Composition by Coronary CT: Validation with IB-IVUS

Thursday, Nov. 29 12:45PM - 1:15PM Room: CA Community, Learning Center Station #1

# Participants

Takanori Masuda, Hiroshima, Japan (*Presenter*) Nothing to Disclose Takeshi Nakaura, MD, Kumamoto, Japan (*Abstract Co-Author*) Nothing to Disclose Yoshinori Funama, PhD, Kumamoto, Japan (*Abstract Co-Author*) Nothing to Disclose Tomoyasu Sato, Hiroshima, Japan (*Abstract Co-Author*) Nothing to Disclose Satomi Koretake, Hiroshima, Japan (*Abstract Co-Author*) Nothing to Disclose Kazuo Awai, MD, Hiroshima, Japan (*Abstract Co-Author*) Nothing to Disclose Kazuo Awai, MD, Hiroshima, Japan (*Abstract Co-Author*) Research Grant, Canon Medical Systems Corporation; Research Grant, Hitachi, Ltd; Research Grant, Fujitsu Limited; Research Grant, Bayer AG; Research Grant, DAIICHI SANKYO Group; Research Grant, Eisai Co, Ltd; Medical Advisory Board, General Electric Company; ; Yoriaki Matsumoto, Hiroshima, Japan (*Abstract Co-Author*) Nothing to Disclose

#### For information about this presentation, contact:

takanorimasuda@yahoo.co.jp

## PURPOSE

The image histogram is a set of metrics calculated by mathematical analysis of digital images; its combination with machine learning has been reported to be of high diagnostic performance for the differentiation of malignant tumors. The purpose of this study was to determine whether machine learning with histogram analysis of coronary CT angiography (CCTA) yields higher diagnostic performance for coronary plaque characterization than the conventional cut-off method using the median CT number.

#### **METHOD AND MATERIALS**

We included 78 patients with 78 coronary plaques who had undergone CCTA and integrated backscatter intravascular ultrasound (IB-IVUS) studies. IB-IVUS diagnosed 32 as fibrous- and 46 as fatty or fibro-fatty plaques. We recorded the coronary CT number and 7 histogram parameters (minimum and mean value, standard deviation (SD), maximum value, skewness, kurtosis, and entropy) of the plaque CT number. Using 5-fold cross validation of the plaque CT number, the area under the receiver operating characteristic curve of the machine learning- (extreme gradient boosting) and the conventional cut-off method was compared.

## RESULTS

The median CT number was 56.38 Hounsfield units (HU, 8.00 - 95.90) for fibrous- and 1.15 HU (-35.8 - 113.30) for fatty- or fibrofatty plaques. The calculated optimal threshold for the plaque CT number was  $36.1 \pm 2.8$  HU. The highest Gini index was the coronary CT number (0.19) followed by the minimum value (0.17), kurtosis (0.17), entropy (0.14), skewness (0.11), the mean value (0.11), the standard deviation (0.06), and the maximum value (0.05), and energy (0.00). By validation analysis, the machine learning- yielded a significantly higher area under the curve than the conventional method (0.92 vs 0.83, p = 0.001).

#### CONCLUSION

The machine learning was superior to the conventional cut-off method for coronary plaque characterization using the plaque CT number on CCTA images.

#### **CLINICAL RELEVANCE/APPLICATION**

The machine learning using CT number histogram might be useful to the characterization of coronary plaques during CCTA.



## CA258-SD-THB2

# Prognostic Value of Coronary CT Angiography (CCTA) in Heart Transplant Patients

Thursday, Nov. 29 12:45PM - 1:15PM Room: CA Community, Learning Center Station #2

#### **Participants**

Alejandra Garcia Baizan, MD, Pamplona, Spain (*Presenter*) Nothing to Disclose Ignacio Gonzalez de la Huebra Rodriguez, MD, Pamplona, Spain (*Abstract Co-Author*) Nothing to Disclose Ana Ezponda, MD, Pamplona, Spain (*Abstract Co-Author*) Nothing to Disclose Marta Calvo-Imirizaldu, MD, Pamplona, Spain (*Abstract Co-Author*) Nothing to Disclose Gregorio Rabago, Pamplona, Spain (*Abstract Co-Author*) Nothing to Disclose Gorka Bastarrika, MD, Pamplona, Spain (*Abstract Co-Author*) Nothing to Disclose

## For information about this presentation, contact:

agarcia.13@unav.es

## PURPOSE

To evaluate the prognostic value of coronary CT angiography (CCTA) in heart transplant recipients (HT).

## METHOD AND MATERIALS

A total of 117 HT (mean age 61.4±11.4 years; 83.8% males) undergoing CCTA for the evaluation of coronary allograft vasculopathy (CAV) were prospectively enrolled. According to the results of the initial CCTA, patients were divided based on the presence of significant CAV (defined as a coronary stenosis >=50%) or non-significant CAV (stenosis <50%). Major adverse cardiac events (MACEs) were defined as a composite of cardiac death, myocardial infarction, unstable angina, congestive heart failure, coronary revascularization, or re-transplantation. To analyze the differences between the two groups and the risk of MACEs, chi square test, Kaplan-Meier curves, Log-Rank test and the hazard ratio were estimated. A p-value <0.05 was considered statistically significant.

## RESULTS

The median follow-up period was 46±39 months. At the initial CCTA 12 HT (10.3%) presented significant CAV and 105 HT (89.7%) showed non-significant CAV. At 5 years after the initial CCTA, 16 MACEs were observed in 45.3% and 13.1% of HT with significant and non-significant stenosis, respectively (Log-Rank test p<0.001). The hazard ratio for suffering a MACE in HT with significant CAV at the initial CCTA was of 5 (p=0.004).

## CONCLUSION

In HT patients, the presence of CAV with >=50% coronary stenosis at initial CCTA can predict the development of MACEs, with a hazard ratio of 5 at 5 years.

## **CLINICAL RELEVANCE/APPLICATION**

CCTA possesses prognostic value and can be used for the follow up of heart transplant recipients.



# CA259-SD-THB3

Evaluation of Coronary Plaque Using Effective Atomic Number in Coronary CT Angiography with Fast kVp Switching Dual-Energy CT: Influence of Intracoronary CT-Attenuation

Thursday, Nov. 29 12:45PM - 1:15PM Room: CA Community, Learning Center Station #3

### Participants

Satoshi Inada, Hiroshima, Japan (*Presenter*) Nothing to Disclose Masashi Takahashi, RT, Hiroshima, Japan (*Abstract Co-Author*) Nothing to Disclose Tsuyoshi Kagimoto, Hiroshima, Japan (*Abstract Co-Author*) Nothing to Disclose Tomohiro Murakami, Hiroshima, Japan (*Abstract Co-Author*) Nothing to Disclose Naohiro Yamagami, Hiroshima, Japan (*Abstract Co-Author*) Nothing to Disclose Takafumi Sakai, Hiroshima, Japan (*Abstract Co-Author*) Nothing to Disclose Masahiro Nakano, Hiroshima, Japan (*Abstract Co-Author*) Nothing to Disclose Fang Wang, Yinchuan, China (*Abstract Co-Author*) Nothing to Disclose

#### PURPOSE

The purpose of this study was to investigate the influence of the intracoronary CT-attenuation on coronary plaque measurements using effective atomic number (Zeff) from coronary CT angiography (CCTA) with fast kVp switching single source dual-energy CT (ssDECT).

#### **METHOD AND MATERIALS**

A coronary artery phantom made up by acryl tube (inner diameter: 4mm) was filled with diluted contrast medium (0 mgI/mL, 5 mgI/mL, 15 mgI/mL, and 30 mgI/mL), and ABS carved pipes were used to simulate coronary plaque (stenosis of 25%, 50%, and 75%, FUYO Co.). Then it was placed in the center of the cardiac phantom (ALPHA1-VTPC; FUYO Co.). The phantom was scanned using ECG-gated axial step-and-shoot with dual-energy scan mode on a 64-row ssDECT (Revolution GSI; GE Healthcare, USA). The scan parameters were set as follows; tube voltage: 80/140 kVp fast switching, rotation time: 0.35 s/rot, and tube current: 600 mA. In addition, virtual monochromatic images (VMIs) at 70 keV and Zeff images were reconstructed from ssDECT data sets. Regions of interests (ROIs) were placed on the simulated plaque at 50% stenosis, and mean CT-numbers and Zeffs were measured.

#### RESULTS

In VMI images, mean CT-numbers at 0 mgI/mL, 5 mgI/mL, 15 mgI/mL, and 30 mgI/mL were 46  $\pm$  7 HU, 58  $\pm$  12 HU, 65  $\pm$  9 HU, and 73  $\pm$  11 HU, respectively. In Zeff images, mean Zeff for 0 mgI/mL, 5 mgI/mL, 15 mgI/mL, and 30 mgI/mL were 7.2  $\pm$  0.44, 7.4  $\pm$  0.36, 7.8  $\pm$  0.39, and 8.3  $\pm$  0.34, respectively. As a result, the CT-number and the Zeff of simulated plaque were increased with the increase of the concentration of diluted contrast medium (P<0.01). Furthermore, rate of increase in Zeffs were lower than that in CT-numbers (P<0.01).

### CONCLUSION

The influence of intracoronary CT-attenuation on coronary plaque measurements using the Zeff was smaller than that using CTnumber.

## **CLINICAL RELEVANCE/APPLICATION**

Using the effective atomic number (Zeff) for measurement of the coronary plaque is useful for the clinical application.



## CA261-SD-THB5

**CT-Detected Complications after Cardiac Transplantation: Differences between Patients with and Without Bridge to Transplantation** 

Thursday, Nov. 29 12:45PM - 1:15PM Room: CA Community, Learning Center Station #5

## Participants

Nadja M. Kocher, MD, Freiburg, Germany (*Presenter*) Nothing to Disclose Mathias F. Langer, MD, PhD, Freiburg, Germany (*Abstract Co-Author*) Nothing to Disclose

For information about this presentation, contact:

nadja.kocher@uniklinik-freiburg.de

### PURPOSE

Despite substantial improvements in the management of patients with severe cardiovascular disease, heart failure is still the most common cause of death in the world. For patients with end stage heart failure, cardiac transplantation offers the best long-term survival. However, cardiac transplantation is associated with a whole range of serious complications. This study intends to investigate the frequency of CT-detected complications after cardiac transplantation in patients supported previously with a left ventricular assist device (LVAD) and patients with conventional transplantation.

## METHOD AND MATERIALS

50 patients (age 52 $\pm$ 27) after cardiac transplantation were included in this retrospective study. Information about gender, age, date of device and heart implantation, death, reason for transplantation, cardiovascular risk factors, cardiac allograft vasculopathy and acute graft rejection were obtained. All postsurgical and follow-up CT scans were screened for relevant complications such as cerebral ischemia, visceral organ ischemia, deep vein thrombosis, pulmonary embolism, hemorrhage, infection, fractures and other musculoskeletal diseases due to transplantation, malignancy and complications due to surgery. Patients with conventional transplantation were assigned to Group A (n=31), patients supported preiously with a LVAD to Group B (n=19). Frequency of complications within one month, one year and after one year following transplantation were derived for each group.

## RESULTS

11 of the 50 included patients died, mostly from multi-organ failure after infection and/or ischemia. Almost all patients (except for 2) suffered at least once from an infectious disease. Postoperative infection occurred especially in Group B (36,8%, Group A: 12,9%). The other early complications could also be found at a higher frequency in Group B. Long-term complications were higher in Group A. Malignancy could only be found in Group A (29,0%) whereas complications due to surgery appeared only in Group B (15,8%).

## CONCLUSION

These results revealed clear differences in the spectrum and frequency of the various complications after cardiac transplantation. Patients previously supported with a LVAD seem to have a higher risk for early complications.

### **CLINICAL RELEVANCE/APPLICATION**

CT is the most important imaging method for early detection and, subsequently, for specific and quick treatment of serious complications after cardiac transplantation.



## CH255-ED-THB7

Molecular Testing Guideline for the Selection of Patients with Lung Cancer for Treatment with Targeted Therapies as per ASCO 2018 Guidelines: Relevance for Radiologists

Thursday, Nov. 29 12:45PM - 1:15PM Room: CH Community, Learning Center Station #7

#### Awards Certificate of Merit

#### Participants

Nikhil H. Ramaiya, MD, Jamaica Plain, MA (*Abstract Co-Author*) Nothing to Disclose Bhanusupriya Somarouthu, MD, Boston, MA (*Presenter*) Nothing to Disclose Kevin R. Kalisz, MD, Cleveland, OH (*Abstract Co-Author*) Nothing to Disclose Francesco Alessandrino, MD, Boston, MA (*Abstract Co-Author*) Nothing to Disclose Sreeharsha Tirumani, MBBS, MD, Boston, MA (*Abstract Co-Author*) Nothing to Disclose Jyothi Priya Jagannathan, MD, Boston, MA (*Abstract Co-Author*) Nothing to Disclose

## For information about this presentation, contact:

bsomarouthu@mgh.harvard.edu

## **TEACHING POINTS**

1. Discuss the new 2018 ASCO guidelines for selection of advanced lung cancer patients being considered for treatment with targeted Tyrosine Kinase and Immune check point inhibitors. 2. Discuss the various oncogenic drivers associated with non-small cell lung cancer and its relevance for radiologists. 3. Discuss the different subtypes of lung adenocarcinoma with respect to its initial presentation, clinical behavior over the course of disease, targeted treatment options, response criteria and toxicity profile of the common and the uncommon agents used for treatment of advanced lung cancer.

# TABLE OF CONTENTS/OUTLINE

• Overview of the new 2018 ASCO guidelines. • Image rich presentation of various EGFR, ALK rearranged, ROS-1 and BRAF V600 mutant lung cancer patients. • Provide examples of Tyrosine Kinase Inhibitors (Tarceva, Crizotinib, Ceritinib, Darafenib and Trametinib) in lung adenocarcinoma along with response assessment and adverse events of the Tyrosine Kinase Inhibitors (colitis, Pneumonitis, osteopenia, Renal cysts). • Provide examples of Immune Check point Inhibitors (Pembrolizumab and Nivolumab) used commonly in lung adenocarcinoma and squamous cell carcinoma along with discussion of the evolving immune response criteria and immune related adverse events

## **Honored Educators**

Presenters or authors on this event have been recognized as RSNA Honored Educators for participating in multiple qualifying educational activities. Honored Educators are invested in furthering the profession of radiology by delivering high-quality educational content in their field of study. Learn how you can become an honored educator by visiting the website at: https://www.rsna.org/Honored-Educator-Award/ Nikhil H. Ramaiya, MD - 2017 Honored EducatorSreeharsha Tirumani, MBBS, MD - 2016 Honored Educator



# CH302-SD-THB1

Assessment of Invasive Pulmonary Adenocarcinoma and Non-Invasive Pulmonary Adenocarcinoma in Pure Ground Glass Nodules with the Maximum Diameter Less Than 1cm Using Quantitative CT

Thursday, Nov. 29 12:45PM - 1:15PM Room: CH Community, Learning Center Station #1

### Participants

Shuai Hu, Dalian, China (*Presenter*) Nothing to Disclose Zhiyong Li, Dalian, China (*Abstract Co-Author*) Nothing to Disclose Mengying Li, Dalian, China (*Abstract Co-Author*) Nothing to Disclose Guangqing Han, Dalian, China (*Abstract Co-Author*) Nothing to Disclose Ailian Liu, MD, Dalian, China (*Abstract Co-Author*) Nothing to Disclose

## For information about this presentation, contact:

#### 757231530@qq.com

### PURPOSE

To explore imaging characteristics of invasive pulmonary adenocarcinoma (IA) in pure ground glass nodules (pGGNs) with the maximum diameter less than 1cm using thin slice CT, and try to differentiate IA from non-IA using quantitative methods.

## METHOD AND MATERIALS

169 patients with pGGN with the maximum diameter less than 1cm confirmed by surgical pathology in our hospital were enrolled in this study for retrospective analysis, including 169 lesions, 16 atypical adenomatous hyperplasia (AAH) (9.5%), 100 adenocarcinoma in situ (AIS) (59.2%), 47 minimally invasive adenocarcinoma (MIA) (27.8%) and 6 IA (3.7%). All patients performed HRCT scan within 1 week before surgery. We measured the maximum diameters and average CT values of all pGGNs and recorded the relevant imaging characteristics on HRCT. Using SPSS17.0 statistical software, we compared clinical and radiographic features of IA with non-IA.

## RESULTS

1) In pGGNs with the maximum diameter less than 1cm, IA accounted for 3.7%. 2) The mean CT values between IA (- $481.2\pm50.8$ HU) and non-IA (- $586.8\pm100.3$ HU) in pGGNs with the maximum diameter less than 1cm were statistically different, p=0.012, AUC=0.811, 95%Cl(0.726-0.896), The optimal cutoff value -538.5HU, sensitivity 100%, specificity 73%. 3) Vacuole and smoking history differed significantly between two groups, p=0.029, 0.034, respectively. 4) The sex, year and pleural indentation had no statistical difference between two groups, p=0.185, 0.382, 1.000.

#### CONCLUSION

In pGGNs with the maximum diameter less than 1cm, IA accounted for 3.7%. It is helpful to judge the infiltration of histology using the average CT value, smoking history and vacuole. The mean CT values could differentiate IA from non-IA in pGGNs with the maximum diameter less than 1cm, it had higher sensitivity.

# **CLINICAL RELEVANCE/APPLICATION**

Early diagnosis and early treatment is very important to the prognosis of patient, it will greatly improve the patient's quality of life.



## CH303-SD-THB2

Imaging-Based Surrogate Markers of Epidermal Growth Factor Receptor (Egfr) Mutation in Lung Adenocarcinoma: A Local Perspective

Thursday, Nov. 29 12:45PM - 1:15PM Room: CH Community, Learning Center Station #2

# Participants

Abdulaziz A. Al Gharras, MBBS, Montreal, QC (*Abstract Co-Author*) Nothing to Disclose Bojan Kovacina, MD, Montreal, QC (*Abstract Co-Author*) Nothing to Disclose James W. Alexander, MSc, Montreal, QC (*Abstract Co-Author*) Nothing to Disclose Zhe Tian, Montreal, QC (*Abstract Co-Author*) Nothing to Disclose Alexandre Semionov, MD, PhD, Montreal, QC (*Abstract Co-Author*) Nothing to Disclose Ali Sabri, MD, Halifax, NS (*Abstract Co-Author*) Nothing to Disclose Leon Vankempen, Montreal, QC (*Abstract Co-Author*) Nothing to Disclose Karl Sayegh, MD, Montreal, QC (*Abstract Co-Author*) Nothing to Disclose Fadi Toonsi, MBBS,FRCPC, Montreal, QC (*Presenter*) Nothing to Disclose

## PURPOSE

To identify CT features of epidermal growth factor receptor (EGFR) mutation-positive lung adenocarcinoma in a heterogeneous, multi-ethnic population. Our secondary objective is to determine whether the imaging-based surrogate markers of EGFR mutation in our population are similar to those found in the Asian population

#### **METHOD AND MATERIALS**

EGFR mutation was determined by using polymerase chain reaction system EGFR kits. Preoperative chest CT scans of 223 patients with adenocarcinoma of the lung (112 with EGFR mutation and 111 without mutation) were independently assessed for 20 specific CT features by two radiologists, who were blinded to the EGFR mutation status of patients. Univariable and Multiple logistic regression analyses were performed to discriminate characteristics of tumors with and without EGFR mutation, and determine areas under the receiver operating characteristic curve (ROC)

#### RESULTS

EGFR mutation-positive adenocarcinomas were more frequently found in female patients (p<0.06), less than 20-year pack smoking history (p<0.01), smaller tumor size (p<0.01) and tumors without emphysema (p<0.01). Ill-defined borders, spiculations, bubble-like lucency, non-central distribution, pleural retraction and lack of lobulations were more common in EGFR mutation-positive tumors but without reaching statistical significance, in contrast to the Asian population. Multivariable logistic regression analyses of combined clinical and radiological features identified less than 20 year-pack smoking history, smaller tumor diameter, fine or coarse spiculations, pleural attachment, non-central distribution and lack of centrilobular emphysema, as the strongest independent prognostic factors for the presence of EGFR mutation. These combined features improved prognostic ability (area under ROC curve: 0.874) compared to clinical features only (areas under ROC curve: 0.798)

## CONCLUSION

Several CT findings help to predict the presence of EGFR mutation in lung adenocarcinomas in our population, essentially similar to those found in the Asian population. Combining clinical and radiological features improves the prognostic ability to determine the EGFR mutation status compared to clinical features alone

## **CLINICAL RELEVANCE/APPLICATION**

Identification of CT features can improve the prognostic predictive ability of lung adenocarcinomas, future diagnostic tools and treatment selection. This will improve overall cost-benefit and burden on the healthcare system



## CH305-SD-THB4

Logistic Regression Model of Thin-Slice Computed Tomography Features Differentiate Invasive Lung Adenocarcinoma Appearing as Subsolid Nodules within 5 to 10 mm in Diameter

Thursday, Nov. 29 12:45PM - 1:15PM Room: CH Community, Learning Center Station #4

## Participants

Yi Zhan, MD, Shanghai, China (*Presenter*) Nothing to Disclose Xueqing Peng, Shanghai, China (*Abstract Co-Author*) Nothing to Disclose Fei Shan, MD, Shanghai, China (*Abstract Co-Author*) Nothing to Disclose Mingxiang Feng, Shanghai, China (*Abstract Co-Author*) Nothing to Disclose Lingxiao Zhou, Shanghai, China (*Abstract Co-Author*) Nothing to Disclose Yingying Liu, Shanghai, China (*Abstract Co-Author*) Nothing to Disclose Xiudong Shi, BA, Shanghai, China (*Abstract Co-Author*) Nothing to Disclose Chaoyu Zhu, Shanghai, China (*Abstract Co-Author*) Nothing to Disclose Xinyuan He, Shanghai, China (*Abstract Co-Author*) Nothing to Disclose Yong Zhang, Shanghai, China (*Abstract Co-Author*) Nothing to Disclose Yuxin Shi, PhD, Shanghai, China (*Abstract Co-Author*) Nothing to Disclose Lei Liu, Shanghai, China (*Abstract Co-Author*) Nothing to Disclose Zhiyong Zhang, Shanghai, China (*Abstract Co-Author*) Nothing to Disclose

## For information about this presentation, contact:

498247075@qq.com

#### PURPOSE

To comprehensively investigate the role of multifactor analysis of thin-slice computed tomography (TSCT) features using logistic model in the differential diagnosis of invasive adenocarcinomas (IACs), appearing as lung subsolid nodules with 5 to 10 mm in diameter

#### **METHOD AND MATERIALS**

Two hundred eighty-eight patients with 313 pathologically diagnosed ground glass nodules (GGNs) were included in this study. The TSCT features of adenocarcinoma in situ and minimally invasive adenocarcinoma (AIS & MIA) and invasive adenocarcinoma (IAC) were compared and analyzed. A logistic regression model was trained and tested based on TSCT features, and receiver operating characteristic (ROC) analysis were compared between the model and size or mean CT value.

### RESULTS

There were 247 AISs & MIAs (58 AISs, 189 MIAs) and 66 IACs were included. Compared with AISs & MIAs, the IACs was significantly larger in size and higher in mean CT value, and presented higher frequency of mixed GGNs (P both < 0.001), clear interface of tumor-lung, bubble lucency, spiculation, pleural indention, and different locations (P all < 0.05). Logistic regression model found some characters (gender, size, interface of tumor-lung, pulmonary vessel change, and mean CT value2) were most significantly related (P < 0.001). The AUC of logistic regression model of 0.894 with the sensitivity of 89.4% and the specificity of 77.6% was showed significant higher than which of size (0.713 with the sensitivity of 65.2% and the specificity of 70.4%, cut off value of 8.12 mm) and mean CT value (0.776 with the sensitivity of 69.7% and the specificity of 78.1%, cut off value of -499.53 Hu, P both <0.001).

### CONCLUSION

Conclusion: Logistic model using TSCT features may help the differential diagnose of the lung subsolid nodules within the diameter of 5 mm to 10 mm. And a clinical diagnosis clue of IACs was discovered that subsolid nodules which are larger in size and higher in mean CT value. Besides, the logistic regression model needs validation of the predict capacity from further study.

## **CLINICAL RELEVANCE/APPLICATION**

Logistic regression model of thin-slice computed tomography features differentiate invasive lung adenocarcinoma appearing as subsolid nodules within 5 to 10 mm in diameter



## CH306-SD-THB5

## Association Between CT Texture Characteristics and EGFR Gene Mutation of Lung Adenocarcinoma

Thursday, Nov. 29 12:45PM - 1:15PM Room: CH Community, Learning Center Station #5

### Participants

Jingshan Gong, MD, Shenzhen, China (*Presenter*) Nothing to Disclose Yan Luo, Shenzhen, China (*Abstract Co-Author*) Nothing to Disclose Dongdong Mei, Shenzhen, China (*Abstract Co-Author*) Nothing to Disclose

## For information about this presentation, contact:

jshgong@sina.com

### PURPOSE

To investigate the correlation between epidermal growth factor receptor (EGFR) gene mutation and CT texture characteristics of lung adenocarcinoma.

# METHOD AND MATERIALS

94 CT texture features, including 19 First Order Statistics characteristics, 27 Gray Level Co-occurrence Matrix (GLCM) characteristics, 16 Gray Level Run Length Matrix (GLRLM),16 Gray Level Size Zone Matrix (GLSZM) characteristics and 16 Shap-based characteristics, were extracted from thin-slice CT images of 411 patients with pathological proved lung adenocarcinoma using an open source texture analysis software (PyRadiomics, available at http://www.radiomics.io/pyradiomics.html). The requirement of informed consent was waived by the medical ethnic committee of our hospital due to retrospective nature. The association of 94 CT texture features and 3 clinical features (age, gender and smoking status) with EGFR gene phenotype was compared using univariate analysis. CT texture features with p value less than 0.05 at univariate analysis and clinical features were introduced into Logistic regression model to identify the independent risk factors.

#### RESULTS

Of the 411 patients with lung adenocarcinoma, 209 (50.9%) were EGFR mutants and 202 (49.1%) were wild type. EGFR mutation status were related to gender (P = 0.000) and smoking status (P = 0.000). Four CT texture features, which were termed as Energy, LargeAreaLowGrayLevelEmphasis, SizeZoneNonUniformityNormalized and SmallAreaEmphasis, showed P value less than 0.05 at univariate analysis. Logistic regression analysis identified that smoking status and SizeZoneNonUniformityNormalized can independently predict EGFR mutation status with OR values of 0.294 (95% CI: 0.183-0.470; P=0.000) and 0.007 (95% CI: 0.000-0.012; P=0.007), respectively. The AUC values of Smoking status, SizeZoneNonUniformityNormalized and SizeZoneNonUniformityNormalized combined with smoking status predicting EGFR gene mutation in lung adenocarcinomas were 0.629, 0.571 and 0.663, respectively.

### CONCLUSION

Some CT texture features of lung adenocarcinoma were associated with EGFR mutation. CT texture features combined with clinical features can be valuable imaging biomarkers to predict EGFR gene mutation status of lung adenocarcinoma.

### **CLINICAL RELEVANCE/APPLICATION**

Using CT texture features to predict EGFR status of lung adenocanoma can provide decision support for personalized therapy.



## CH307-SD-THB6

Comparison of Novel Whole Nodule First Pass Analysis versus Standard Maximum Slope Model in the Detection of Lung Malignancies using Low-Dose CT Perfusion

Thursday, Nov. 29 12:45PM - 1:15PM Room: CH Community, Learning Center Station #6

### Participants

Yixiao Zhao, MS, Irvine, CA (*Presenter*) Nothing to Disclose Cecelia Brewington, MD, Dallas, TX (*Abstract Co-Author*) Research Grant, Canon Medical Systems Corporation Shaun M. Nordeck, MD, Dallas, TX (*Abstract Co-Author*) Nothing to Disclose Logan Hubbard, BS, Irvine, CA (*Abstract Co-Author*) Nothing to Disclose Shant Malkasian, BS, Irvine, CA (*Abstract Co-Author*) Nothing to Disclose Pablo J. Abbona, MD, Orange, CA (*Abstract Co-Author*) Nothing to Disclose Christina Leung, Irvine, CA (*Abstract Co-Author*) Nothing to Disclose Sabee Y. Molloi, PhD, Irvine, CA (*Abstract Co-Author*) Research Grant, Canon Medical Systems Corporation

#### For information about this presentation, contact:

yixiaoz@uci.edu

#### PURPOSE

To assess the diagnostic capability of a novel, whole nodule, first-pass analysis technique to the current maximum slope model when classifying pulmonary nodules as benign or malignant using low-dose CT perfusion.

### **METHOD AND MATERIALS**

Nineteen patients (8 males, 11 females; mean age of 61 years) with pulmonary nodules underwent low-dose dynamic CT perfusion scan and histopathological diagnosis. A total of 20 volume scans were acquired using a 320-detector CT scanner for duration of 90 seconds after 40 mL of contrast followed by a 40 mL saline chaser at an injection rate of 5 mL/sec. Pulmonary arterial perfusion (PAP) and bronchial arterial perfusion (BAP) in ml/min/100ml and Perfusion Index (PI = PAP/(PAP+BAP)) were assessed using all 20 volume scans for dual-input maximum slope model (MSM) perfusion using standard 2D technique. For the novel, dual-input, whole nodule first-pass analysis (FPA) measurement, only four volume scans were used to obtain absolute PAP, BAP (both in mL/min/g) and PI. Average perfusion values within the entire tumor were compared with the biopsy results as the reference standard. To evaluate diagnostic capability, student's t-test, 95% confidence interval, and receiver-operating characteristic (ROC) curve analysis were performed.

#### RESULTS

Using the perfusion index with a cutoff threshold of 0.6 for MSM technique and 0.5 for the FPA technique, the overall accuracy, sensitivity, and specificity were 0.47, 0.46, 0.50 and 0.68, 0.73, 0.63, respectively. The effective radiation dose for the MSM and the FPA technique were estimated to be 26 and 2.4 mSv, respectively.

## CONCLUSION

Whole nodule, first-pass analysis perfusion technique is more accurate in detecting malignant pulmonary nodules using the perfusion index as an imaging biomarker while simultaneously lowering the radiation dose by a factor of 10 when compared to standard maximum slope low-dose CT perfusion techniques.

### **CLINICAL RELEVANCE/APPLICATION**

Whole nodule first-pass technique can be prospectively implemented to substantially reduce patient dose while accurately detecting malignant pulmonary nodules.



# ER235-SD-THB3

# Blunt Cerebrovascular Injury: 10-Year Experience at a Level I Trauma Center

Thursday, Nov. 29 12:45PM - 1:15PM Room: ER Community, Learning Center Station #3

#### Awards Student Travel Stipend Award

#### **Participants**

Lei Wu, MD, Seattle, WA (*Presenter*) Nothing to Disclose Lindsey F. Call, Kirkland, WA (*Abstract Co-Author*) Nothing to Disclose Cordelie E. Witt, MD,MPH, Seattle, WA (*Abstract Co-Author*) Nothing to Disclose Robert H. Bonow, MD, Seattle, WA (*Abstract Co-Author*) Nothing to Disclose Daniel S. Hippe, MS, Seattle, WA (*Abstract Co-Author*) Research Grant, Koninklijke Philips NV; Research Grant, General Electric Company; Research Grant, Canon Medical Systems Corporation; Research Grant, Siemens AG Mahmud Mossa-Basha, MD, Seattle, WA (*Abstract Co-Author*) Nothing to Disclose

# For information about this presentation, contact:

wulei@uw.edu

# PURPOSE

Blunt cerebrovascular injury (BCVI) can be devastating predominantly due to injury-related stroke. The risk of stroke attributable to BCVI ranges from 1% to 10% overall, and the risk is as high as 33% in patients with grade 3 and 4 injuries, with mortality rates ranging from 15-59%. Although there is evidence that early detection especially in asymptomatic patients improves outcome, the most appropriate screening strategy remains controversial. With uncertainties in screening and management algorithm, we conducted a retrospective review of blunt trauma patients at a Level I trauma center over a 10-year period to better understand the natural history of BCVI which may help better define the most appropriate management strategies.

### **METHOD AND MATERIALS**

After IRB approval, we conducted a retrospective review of the clinical database at a Level I adult and pediatric trauma center. BCVI patients treated at our center from 4/1/2005 through 6/30/2015 were included. Demographic information (age and gender), mechanism of injury, injured vessel, grade, strokes that were attributable to BCVI, and medications received were collected and analyzed using descriptive statistics. For patients with follow-up imaging, injury evolution was evaluated.

### RESULTS

Out of 1266 patients in the database, 1204 patients with a total of 1605 vessels were confirmed to have BCVI by imaging review. There were 800 male and 404 female patients. The average age was 45 years. Number of vessels associated with each injury grade are summarized in table 1. Injury progression trend is summarized in table 2. 93% of grade I, 76% of grade II, 30% of grade III, and 35% of grade IV injuries showed improvement or resolution on follow-up imaging. Overall, 8.1% of patients (98/1204) suffered BCVI related stroke. 3.7% (29/783) of patients with the grade 1 or 2 injuries and 16.4% (69/421) of patients with grade 3 injury or higher suffered strokes attributable to BCVI.

### CONCLUSION

Risk of BCVI related stroke is similar to previously reported rates. Lower grade injuries were more common, but higher-grade injuries were more likely to cause strokes.

# **CLINICAL RELEVANCE/APPLICATION**

Blunt cerebral vascular injury can be devastating, and understanding its natural history will help optimize screening protocol and management strategies.



### GI296-ED-THB12

Review of Perianal Fistula Disease, Treatment and Utility of 3D Modelling to Aid Understanding and Training

Thursday, Nov. 29 12:45PM - 1:15PM Room: GI Community, Learning Center Station #12

### Awards Certificate of Merit Identified for RadioGraphics

#### **Participants**

Phillip Lung, Middlesex, United Kingdom (*Presenter*) Advisory Board, Takeda Pharmaceutical Company Limited; Speaker, Siemens AG Nusrat Iqbal, London, United Kingdom (*Abstract Co-Author*) Nothing to Disclose Kapil Sahnan, London, United Kingdom (*Abstract Co-Author*) Nothing to Disclose Uday Patel, London, United Kingdom (*Abstract Co-Author*) Nothing to Disclose Joshua Shur, MBBS, London, United Kingdom (*Abstract Co-Author*) Nothing to Disclose Samuel Adegbola, MBBS, MRCS, London, United Kingdom (*Abstract Co-Author*) Nothing to Disclose Jordan Fletcher, London, United Kingdom (*Abstract Co-Author*) Nothing to Disclose Chun Wah So, MBBCh, MRCP, Romford, United Kingdom (*Abstract Co-Author*) Nothing to Disclose Omar Faiz, London, United Kingdom (*Abstract Co-Author*) Nothing to Disclose Ailsa L. Hart, MBBCh, London, United Kingdom (*Abstract Co-Author*) Nothing to Disclose Janindra Warusavitarne, London, United Kingdom (*Abstract Co-Author*) Nothing to Disclose Philip Tozer, Harrow, United Kingdom (*Abstract Co-Author*) Nothing to Disclose

For information about this presentation, contact:

# philliplung@nhs.net

#### **TEACHING POINTS**

1. Learn the method of perianal fistula classification using MRI and 3D modelling techniques 2. Learn the different methods of perianal fistula treatment available 3. Learn the importance of radiological review and different aspects of perianal fistula on perianal fistula treatment 4. Review complex perianal fistula in MRI and 3D.

### TABLE OF CONTENTS/OUTLINE

1. Background of Perianal Fistula Disease 2. Perianal Fistula Classification on MRI and 3D 3. Overview of Perianal Fistula Treatments 3a. Conventional 3b. New techniques such as VAAFT, FILAC, LIFT 4. Review of perianal fistula features and how these impact on surgical decision making, using sample cases in MRI and 3D 5. Review of complex perianal fistulas on MRI and 3D 6. Future direction



# GI323-ED-THB7

# **Troubleshooting Troublesome Bowel Cases**

Thursday, Nov. 29 12:45PM - 1:15PM Room: GI Community, Learning Center Station #7

### **Participants**

Carla B. Harmath, MD, Chicago, IL (Abstract Co-Author) Nothing to Disclose Melvy S. Mathew, MD, Chicago, IL (Presenter) Nothing to Disclose

### **TEACHING POINTS**

1. To review tricky cases involving the ever-wily bowel to illustrate lessons that may be learned and subsequently applied when encountering future imaging exams. 2. To emphasize the troubleshooting tools we radiologists have in our possession to optimally assess a suspected pathologic entity or process involving the bowel.

# **TABLE OF CONTENTS/OUTLINE**

Case review (e.g., a giant sigmoid colon diverticulum mistaken for perforated diverticulitis with abscess formation, small bowel diverticula initially thought to be mesenteric venous gas, a large gastric mass favored to be a gastrointestinal stromal tumor found on endoscopy to in actuality be a bag of drugs ingested by a body stuffer') Utilization of multiple imaging modalities, a review of the benefits and limitations of each Use of enteric contrast, insufflation of air into the bowel, IV contrast Re-imaging after a finite amount of time, recognizing the dynamic nature of bowel Consider as always the patient's clinical and surgical history and prior imaging if available Expect the unexpected, maintain a list of differential considerations even when imaging findings appear 'classic' for a specific entity Always consider direct visualization, often the gold standard for bowel assessment Summary



### GI324-ED-THB8

Towards a More Cost-Effective Screening: An Abbreviated Liver MRI Protocol for Hepatocellular Carcinoma Surveillance

Thursday, Nov. 29 12:45PM - 1:15PM Room: GI Community, Learning Center Station #8

# Participants

So Hyun Park, MD, Incheon, Korea, Republic Of (*Presenter*) Nothing to Disclose Bohyun Kim, MD, Suwon, Korea, Republic Of (*Abstract Co-Author*) Research Grant, Bracco Group So Yeon Kim, MD, Seoul, Korea, Republic Of (*Abstract Co-Author*) Nothing to Disclose

### **TEACHING POINTS**

1. To introduce the concept of an abbreviated liver MRI examination (AMRI) and its role as a surveillance tool in patients with highrisk of hepatocellular carcinoma (HCC) 2. To present suggested sequences and clinical applications of an AMRI

# TABLE OF CONTENTS/OUTLINE

1. The concept of an AMRI as a surveillance tool in patients with high-risk of HCC 1) Rationale of an AMRI for screening HCCs 2) Role of an AMRI using gadoxetic acid as a surveillance tool in patient with high-risk of HCC 2. Clinical applications and diagnostic performance of an AMRI for HCC surveillance 1) Suggested sequences in published and unpublished authors' data 2) Comparison of diagnostic performances among suggested sequences 3. Pros and cons of an AMRI 4. Summary for key sequences and their diagnostic values



# GI325-ED-THB9

Fluoroscopic Barium Examinations in Modern Radiographic Era: It Is like Your Grandma's Recipe, Never Dies

Thursday, Nov. 29 12:45PM - 1:15PM Room: GI Community, Learning Center Station #9

### **Participants**

Bhavna Paryani, MD, Shreveport, LA (*Abstract Co-Author*) Nothing to Disclose John Garrett, MD, Shreveport, LA (*Abstract Co-Author*) Nothing to Disclose Chetan Saini, MBBS, Jaipur, India (*Abstract Co-Author*) Nothing to Disclose Thomas R. Gates, MD, Shreveport, LA (*Abstract Co-Author*) Nothing to Disclose Meghna Chadha, MD, MBBS, Shreveport, LA (*Abstract Co-Author*) Nothing to Disclose Alberto I. Carbo, MD, Shreveport, LA (*Presenter*) Nothing to Disclose

# For information about this presentation, contact:

acarbo@lsuhsc.edu

# **TEACHING POINTS**

Fluoroscopic Barium Examinations (FBE) are used as age-old techniques since the advent of radiology and widely employed to evaluate the anatomy and function of the Gastrointestinal (GI) tract. They are globally available, simple to perform, inexpensive and relatively safe for the patients. However, they face stiff competition from imaging innovations that have occurred over the past decades. The aim of this exhibit is to discuss the present indications of FBE based on a comprehensive search of literature on major databases. Studies and pathologic conditions meeting inclusion criteria will be discussed and illustrated with sample cases. There will be emphasis on pragmatic strategies, which could be used as a lifeline for barium techniques in the present era Teaching points • To discuss with evidence-based guidelines the present role and current trends of FBE used for the diagnosis of GI tract diseases • To review with sample cases the valuable contribution of FBE for the diagnosis of some GI pathologic conditions • To propose pragmatic strategies for FBE revival in future practice

# **TABLE OF CONTENTS/OUTLINE**

Present status of FBE: indications, advantages and disadvantages Discussion of sample cases Debate about continuing use of FBE in current medical practice and strategies for their revival for future practice

### **Honored Educators**

Presenters or authors on this event have been recognized as RSNA Honored Educators for participating in multiple qualifying educational activities. Honored Educators are invested in furthering the profession of radiology by delivering high-quality educational content in their field of study. Learn how you can become an honored educator by visiting the website at: https://www.rsna.org/Honored-Educator-Award/ Alberto I. Carbo, MD - 2015 Honored Educator



# GI326-ED-THB10

# Ultra-High Resolution CT: Technical Features and Clinical Impact on Abdominal Imaging

Thursday, Nov. 29 12:45PM - 1:15PM Room: GI Community, Learning Center Station #10

### **Participants**

Hiromitsu Onishi, MD, Suita, Japan (*Presenter*) Nothing to Disclose Masatoshi Hori, MD, Suita, Japan (*Abstract Co-Author*) Nothing to Disclose Atsushi Nakamoto, MD, Suita, Japan (*Abstract Co-Author*) Nothing to Disclose Takashi Ota, Suita, Japan (*Abstract Co-Author*) Nothing to Disclose Shinsuke Tsukagoshi, PhD, Otawara, Japan (*Abstract Co-Author*) Employee, Canon Medical Systems Corporation Noriyuki Tomiyama, MD, PhD, Suita, Japan (*Abstract Co-Author*) Research Grant, Canon Medical Systems Corporation Mitsuaki Tatsumi, MD, PhD, Suita, Japan (*Abstract Co-Author*) Nothing to Disclose Hideyuki Fukui, Suita, Japan (*Abstract Co-Author*) Nothing to Disclose Kazuya Ogawa, Suita, Japan (*Abstract Co-Author*) Nothing to Disclose Ayumi Uranishi, Osaka, Japan (*Abstract Co-Author*) Employee, Canon Medical Systems Corporation Akira Taniguchi, RT, Tokyo, Japan (*Abstract Co-Author*) Employee, Canon Medical Systems Corporation Yasuo Saito, BS, Otawara-Shi, Japan (*Abstract Co-Author*) Employee, Canon Medical Systems Corporation Yukihiro Enchi, BS, Suita, Japan (*Abstract Co-Author*) Mothing to Disclose Kazuhiko Satoh, MBBS, Osaka, Japan (*Abstract Co-Author*) Nothing to Disclose

### **TEACHING POINTS**

Ultra-high resolution CT (U-HRCT) system is equipped with a detector divided into exceedingly small elements and an X-ray tube of a fine focal spot and allows for acquisition of images with high spatial resolution for both in-plane and slice directions. The purpose of this presentation is: 1. To illustrate technical features of U-HRCT system compared with conventional CT system, 2. To discuss radiation dose and dose reduction techniques, and 3. To discuss clinical impact on the diagnosis of abdominal diseases.

#### **TABLE OF CONTENTS/OUTLINE**

Overview Three scan modes; SHR mode, HR mode, and NR mode Variety of focal spot size Advantage in spatial resolution Analyses of image noise Estimation of radiation dose Value of hybrid and full iterative reconstruction algorithm Scan protocols optimized for the abdominal imaging Clinical impact on the diagnosis of abdominal diseases Summary



# GI327-ED-THB11

# Modern Bariatric Surgery - What the Radiologist Needs to Know

Thursday, Nov. 29 12:45PM - 1:15PM Room: GI Community, Learning Center Station #11

### Participants

Christian Pedersen, MD, Darby, PA (*Presenter*) Nothing to Disclose Justin E. Mackey, MD, Darby, PA (*Abstract Co-Author*) Nothing to Disclose

For information about this presentation, contact:

christian.pedersen@mercyhealth.org

### **TEACHING POINTS**

1. At least 600 million adults and 100 million children suffer from obesity worldwide. Bariatric surgery is a popular and radical treatment method with 216.000 surgeries performed in 2016 in the U.S. Identification of postsurgical anatomy and complications can be challenging even for experienced radiologists. 2. This case-based educational exhibit illustrates the different surgical techniques such as roux-en-Y gastric bypass (RYGB), sleeve gastrectomy and gastric lap band. Using cases from our institution, we will illustrate how the reader can confidently identify the relevant postsurgical anatomy. 3. We will review the most common complications, the risk factors for developing them, what studies to use to identify them, their typical locations and important features necessary to predict clinical outcome and guide clinical management.

# TABLE OF CONTENTS/OUTLINE

1. Review the indications for and the common types of bariatric surgery, incl. RYGB, sleeve gastrectomy and gastric lap band. 2. Illustrate the typical post-bariatric bowel anatomy and the different surgical techniques. 3. Review imaging modalities used in assessment of the bariatric patient. 4. Show typical locations of complications, incl. leak, lap band slippage, stenosis, internal hernias, and obstruction. 5. Highlight important imaging features to accurately guide clinical management.



# GI389-SD-THB1

# Segmental Distribution of Fat in the Liver: A Retrospective Study

Thursday, Nov. 29 12:45PM - 1:15PM Room: GI Community, Learning Center Station #1

### **Participants**

Ranu Taneja, MD,FRCR, Singapore, Singapore (*Abstract Co-Author*) Nothing to Disclose Joan Khoo, Singapore, Singapore (*Abstract Co-Author*) Nothing to Disclose Jia Wen Kam, Singapore, Singapore (*Abstract Co-Author*) Nothing to Disclose Muhammad Khairul B Saidi, BSC, Singapore, Singapore (*Abstract Co-Author*) Nothing to Disclose Shi Haiyuan, MBBS,FRCR, Singapore, Singapore (*Abstract Co-Author*) Nothing to Disclose Cheong Sook Chuei, FRCR,MBBS, Singapore, Singapore (*Presenter*) Nothing to Disclose

# For information about this presentation, contact:

ranu\_taneja@cgh.com.sg

# PURPOSE

Nonalcoholic fatty liver disease (NAFLD) ranges from simple steatosis to steatohepatitis (NASH) and cirrhosis with associated risk of hepatocellular carcinoma. Steatosis is the earliest biomarker of NAFLD and a necessary feature for development of fibrosis. The most accurate noninvasive method for liver fat quantification is MRI. Histology is the gold standard for diagnosis of steatosis and steatohepatitis/ cirrhosis but is invasive and vulnerable to sampling error due to heterogeneity in hepatic fat deposition. Segments with the most fat are also more susceptible to damage by fat deposition. Hence liver fat quantification studies and biopsy for detection of steatosis, NASH and cirrhosis should target these segments. This retrospective study evaluates if there is significant difference in fat distribution in hepatic Couinaud's segments and which segment is the most affected.

#### **METHOD AND MATERIALS**

31 patients who underwent MRI for fat quantification for an IRB approved study were included. Two point Dixon was used for fat quantification. MR spectroscopy was performed for resolving fat water ambiguity. Post processing was performed on dedicated workstation (Siemens Magnetom Aera). ROI of 1-2 cm2 was placed on each segment avoiding outer 1 cm, large vessels, fissures and gallbladder and percentage fat signal fraction (FSF) estimation done.

# RESULTS

There were 16.1% females and 83.9% males aged between 22-65 years. A significant difference in FSF was seen among the 9 Couinaud's segments (p < 0.001, Friedman test). Segment 5 had highest percentage of maximum FSF (41.9%). Segment 2 had highest percentage of minimum FSF (38.7%). Segment 1 had highest percentage of largest variability measurements (54.8%). Segment 7 had highest percentage of smallest variability measurements (35.5%). Mean right hepatic lobe FSF was higher than left hepatic lobe FSF in 96.8%. The average FSF of right lobe was significantly higher than left lobe (p < 0.001).

### CONCLUSION

There is a statistically significant difference in fat distribution in hepatic Couinaud's segments with highest percentage of maximum FSF in segment 5. This knowledge is extremely useful to obtain fat quantification and biopsy from the most affected segments.

# **CLINICAL RELEVANCE/APPLICATION**

Hepatic fat deposits heterogeneously causing sampling error in fat quantification and biopsy. This study assesses hepatic segmental fat distribution such that the most affected segments are targeted.



# GI390-SD-THB2

Influence of Fat Deposition on T1 Mapping of the Pancreas: Evaluation by Dual Flip Angle MR Imaging with and Without Fat Suppression

Thursday, Nov. 29 12:45PM - 1:15PM Room: GI Community, Learning Center Station #2

# Participants

Mayumi Higashi, Ube, Yamaguchi, Japan (*Presenter*) Nothing to Disclose Masahiro Tanabe, MD, Ube, Japan (*Abstract Co-Author*) Nothing to Disclose Katsuyoshi Ito, MD, Okayama, Japan (*Abstract Co-Author*) Nothing to Disclose

#### PURPOSE

To evaluate the influence of fat deposition on T1 relaxation time of the pancreatic parenchyma by means of dual flip angle T1 mapping with and without fat suppression.

## **METHOD AND MATERIALS**

Forty-eight patients who underwent abdominal MR imaging including T1 mapping with dual-flip-angle (3° and 17°) method on 3T MRI were included. We measured T1 relaxation time of the pancreatic parenchyma on the T1 map images with and without fat suppression using operator-defined regions of interest (ROIs). T1 relaxation time of the bone marrow was also measured as a reference organ with abundant fat deposition. Fat signal fraction (FSF) was also measured at the same location as T1 map images. We assessed the correlation between T1 relaxation time and FSF by using Spearman rank correlation coefficient and Mann-Whitney U tests.

### RESULTS

T1 relaxation times of the pancreatic parenchyma and bone marrow on the T1 map images without fat suppression showed significantly negative correlation with FSF (pancreas, r = -0.353, p < 0.001; bone marrow, r = -0.470, p < 0.001) while there were no significant correlations between them on the T1 map images with fat suppression (pancreas, r = -0.078, p = 0.453; bone marrow, r = -0.112, p = 0.279). On the T1 map images without fat suppression, T1 relaxation time of the pancreatic parenchyma as well as bone marrow in patients group with FSF >= 5% was significantly shorter than that in patients group with FSF < 5% (pancreas, 844 [range, 726-1038] msec vs 939 [range, 886-1038] msec, p = 0.020; bone marrow, 687 [range, 612-770] msec vs 961 [range, 953-991] msec, p = 0.001). Conversely, on the T1 map images with fat suppression, no significant difference in T1 relaxation times of the pancreatic parenchyma as well as bone marrow was found between the two groups (pancreas, 879 [range, 798-1001] msec vs 884 [range, 786-1026] msec, p = 0.932; bone marrow, 1203 [range, 1076-1357] msec vs 1298 [range, 1295-1347] msec, p = 0.414).

#### CONCLUSION

T1 relaxation time of the pancreas on T1 mapping was influenced by the presence of fat deposition. Therefore, fat suppression technique in T1 mapping will be essential for evaluating T1 relaxation time of the pancreatic parenchyma.

### **CLINICAL RELEVANCE/APPLICATION**

The accurate T1 relaxation time of the pancreatic parenchyma acquired by T1 mapping with fat suppression will be valuable for determining severity of pancreatic diseases.



# GI391-SD-THB3

Evaluation of the Effects of Different Iodine Concentration Contrast Media on Virtual Unenhanced CT Images

Thursday, Nov. 29 12:45PM - 1:15PM Room: GI Community, Learning Center Station #3

### **Participants**

Yoshinori Kawamoto, RT, Hiroshima, Japan (*Presenter*) Nothing to Disclose Tomokatsu Tsukamoto, MS,RT, Onomichi, Japan (*Abstract Co-Author*) Nothing to Disclose Takashi Takahata, RT, Onomichi, Japan (*Abstract Co-Author*) Nothing to Disclose Takashi Sugimoto, RT, Onomichi, Japan (*Abstract Co-Author*) Nothing to Disclose Tomoshige Sato, RT, Hiroshima, Japan (*Abstract Co-Author*) Nothing to Disclose Hiroki Mori, MD, Onomichi, Japan (*Abstract Co-Author*) Nothing to Disclose Fang Wang, Yinchuan, China (*Abstract Co-Author*) Nothing to Disclose

### PURPOSE

A new virtual unenhanced CT imaging method (VUE) has been developed with Material Suppressed Iodine(MSI) and the purpose of this study is to compare accuracy of VUE by MSI with unenhanced CT images for evaluating the effect of different iodine contrast media on VUE.

# METHOD AND MATERIALS

A polypropylene phantom (Quantitative Standard Pulsating Phantom (QSP-1), FUYO, Japan) with a 18mm polypropylene tube in the center(filled with water) and eight tubes with different materials (Olive oil, Water and Iodine aqueous solutions of six types(1, 2, 5, 10, 20, 30 mgI/ml)) arranged in outer circle underwent fast kVp switching helical spectral scan by a single-source dual-energy CT (ssDECT) (Revolution HD, GE Healthcare, USA) Monochromatic images at 70keV(monochromatic images) and the virtual unenhanced (VUE) images with 5mm thickness were reconstructed, respectively. Standard deviation(SD) of the region of interest(ROI) was defined as image noises, and the CT number(HU) and SD were measured in 70keV images andVUE images. The differences of CT numbers (HU) between the 70 keV images and the VUE images were calculated.

# RESULTS

For the different materials (Olive oil, Water and Iodine aqueous solutions of six types(1, 2, 5, 10, 20, 30 mgI/ml)), the CT numbers (HU) of monochromatic images were:  $-113.66\pm0.52$ ,  $3.10\pm0.49$ ,  $28.02\pm0.18$ ,  $54.34\pm0.60$ ,  $129.08\pm0.48$ ,  $248.64\pm1.13$ ,  $515.62\pm0.65$ ,  $751.28\pm1.02$ , respectively; On the other hand, the CT numbers(HU) of VUE were:  $-114.20\pm0.52$ ,  $2.80\pm0.49$ ,  $12.92\pm1.07$ ,  $10.94\pm1.58$ ,  $5.86\pm1.48$ ,  $-2.82\pm2.04$ ,  $-17.44\pm1.12$ ,  $-26.76\pm0.87$ , respectively.

#### CONCLUSION

It was confirmed that the CT number varies depending on the different iodine contrast media on VUE using MSI. However, it was suggested that the difference is within an acceptable range when obtaining unenhanced CT images from commonly performed enhanced CT scans.

### **CLINICAL RELEVANCE/APPLICATION**

VUE using MSI may be clinically feasible for reducing scan dose.



# GI392-SD-THB4

T2-Weighted and Diffusion-Weighted MRI of Liver on 1.16 T Open MRI Scanner: Image Quality Considerations in Comparison to 1.5 T

Thursday, Nov. 29 12:45PM - 1:15PM Room: GI Community, Learning Center Station #4

# Participants

David E. Knipp, MD, Boston, MA (*Presenter*) Nothing to Disclose Avinash R. Kambadakone, MD, Boston, MA (*Abstract Co-Author*) Nothing to Disclose David A. Rosman, MD, Boston, MA (*Abstract Co-Author*) Nothing to Disclose Mukesh G. Harisinghani, MD, Boston, MA (*Abstract Co-Author*) Nothing to Disclose Peter F. Hahn, MD,PhD, Belmont, MA (*Abstract Co-Author*) Stockholder, Abbott Laboratories; Stockholder, Medtronic plc; Stockholder, CVS Caremark Corporation; Stockholder, Kimberly-Clark Corporation; Stockholder, LANDAUER, Inc; Spouse, Stockholder, Medtronic plc; Spouse, Stockholder, Gilead Sciences, Inc; Spouse, Bondholder, Bristol-Myers Squibb Company; Spouse, Bondholder, Johnson & Johnson

#### For information about this presentation, contact:

dknipp@partners.org

### PURPOSE

To study the image quality considerations of T2-weighted imaging (T2WI) and diffusion-weighted imaging (DWI) of the liver in patients scanned on a 1.16 T open MRI scanner and compare it to 1.5 T.

### **METHOD AND MATERIALS**

One hundred and five patients underwent liver MRI on a 1.16 T open MRI scanner between November 2017 and March 2018 and were included in this image quality review. A total of 48 patients in the study group had a liver MRI performed at 1.5 T for comparison. Fat-saturated spin-echo T2WI was performed with respiratory triggering. DWI was also acquired with respiratory triggering at 0, 400, and 800 b-values. Subjective image assessment was performed for determination of image quality (4-point), the presence of artifacts (3-point), and common bile duct conspicuity on T2WI (5-point). Signal-to-noise ratio (SNR) estimation was performed by ROI analysis of the liver parenchyma on T2WI and DWI sequences. A two-tailed Student's t-test was used for statistical analysis.

# RESULTS

The image quality scores were fair to excellent in 95% (100/105) of cases for T2WI, and in 70% (73/105) of cases for DWI. Artifacts, predominately motion, were seen in 76% (80/105) of T2WI sequences, which compromised interpretation of 5% (5/105) of cases. Artifacts were seen in 13% (14/105) of DWI sequences, compromising interpretation of 5% (5/105) of cases. There was moderate to minimal blurring of the common bile duct on T2WI, with an average score of 3.8/5. Image quality scores were significantly lower (P<0.001) and motion artifact scores significantly higher (P<0.05) than at 1.5 T, while bile duct conspicuity was similar (P=0.78). Regarding quantitative evaluation, the mean SNR of the liver was significantly higher at 1.16T than at 1.5 T by 59% on T2WI (P<0.001), and by 87% on DWI (P<0.001).

# CONCLUSION

T2-weighted imaging on 1.16 T has acceptable image quality and higher SNR compared to 1.5 T; however, challenges remain in acquiring high quality diffusion weighted images.

### **CLINICAL RELEVANCE/APPLICATION**

T2-weighted imaging acquired on 1.16 T provides acceptable image quality for the evaluation of focal and diffuse liver lesions in patients who are not candidates for routine higher strength MRI due to claustrophobia or CT due to radiation dose concerns.



# GI393-SD-THB5

### BOLD MR Imaging of Brown Fat Function in Murine Pancreatic Model

Thursday, Nov. 29 12:45PM - 1:15PM Room: GI Community, Learning Center Station #5

FDA Discussions may include off-label uses.

#### Participants

Yaqi Zhang, Chicago, IL (*Presenter*) Nothing to Disclose Su Hu, Chicago, IL (*Abstract Co-Author*) Nothing to Disclose Matteo Figini, Chicago, IL (*Abstract Co-Author*) Nothing to Disclose Liang Pan, Chicago, IL (*Abstract Co-Author*) Nothing to Disclose Junjie Shangguan, Chicago, IL (*Abstract Co-Author*) Nothing to Disclose Jia Yang, PhD, Chicago, IL (*Abstract Co-Author*) Nothing to Disclose Yuri Velichko, PhD, Chicago, IL (*Abstract Co-Author*) Nothing to Disclose Vahid Yaghmai, MD, Chicago, IL (*Abstract Co-Author*) Nothing to Disclose Zhuoli Zhang, MD,PhD, Chicago, IL (*Abstract Co-Author*) Nothing to Disclose

#### For information about this presentation, contact:

yaqizhang2017@u.northwestern.edu

#### PURPOSE

Pancreatic ductal adenocarcinoma (PDAC) patients usually have poor tolerance to chemotherapy and surgery due to the high prevalence of malnutrition and energy imbalance. Brown adipose tissue (BAT) was recently identified as an important factor to induce the weight loss and malnutrition in cancer patients. Here, the changes of BAT were tracked by magnetic resonance imaging (MRI) as a promising biomarker to predict the malnutrition in PDAC and evaluate treatment outcomes.

### **METHOD AND MATERIALS**

The murine orthotopic pancreatic cancer model was established by inducing Panc02 cell into the pancreas of 9 female C57BL/6 mice. BOLD MR imaging (Experimental protocol was shown in Fig. A) was performed weekly for evaluation of BAT function, the two-point Dixon MRI (for measurement of BAT volume, and the T2-weighted MRI for detecting tumor growth. Quantitative data in MRI was analyzed by ITK-SNAP. Meanwhile, the body weight is measured daily as another indication of malnutrition.

#### RESULTS

The average level of R2\* decreased with the progression of tumor implantation (Fig. B), indicating the malnutrition in PDAC mice could be detected by evaluating BAT function on MRI. The water-fat separated MRI could clearly identify and quantify the BAT. The function and volume of BAT could be tracked by weekly MRI measurement in PDAC mice. T2-weighted MRI indicated the tumor grown rapidly from week3 to week4 after tumor implantation (19.19  $\pm$  6.12mm3, P = 0.016). However, most mice (8/9) had relatively stable body weight.

# CONCLUSION

BOLD MR imaging could evaluate and track the function and volume of BAT in murine pancreatic cancer models by measuring R2\* value and two-point Dixon, respectively. The BAT changed with the development of PDAC, inducing the malnutrition and energy imbalance, while the body weight did not reflect the early malnutrition in PDAC model.

# **CLINICAL RELEVANCE/APPLICATION**

The changes of BAT in PDAC patients could be a more sensitive biomarker than body weight in diagnosing malnutrition and poor response to treatment. The R2\* and two-point Dixon on MRI permit timely tracking of BAT and provide an important reference for predicting the clinical outcome.

### **Honored Educators**

Presenters or authors on this event have been recognized as RSNA Honored Educators for participating in multiple qualifying educational activities. Honored Educators are invested in furthering the profession of radiology by delivering high-quality educational content in their field of study. Learn how you can become an honored educator by visiting the website at: https://www.rsna.org/Honored-Educator-Award/ Vahid Yaghmai, MD - 2012 Honored EducatorVahid Yaghmai, MD - 2015 Honored Educator



# GI394-SD-THB6

# Clinical Trial to Evaluate Customized Positive Oral Contrast Media for low-kVp/keV Imaging

Thursday, Nov. 29 12:45PM - 1:15PM Room: GI Community, Learning Center Station #6

### **Participants**

Anushri Parakh, MBBS, MD, Boston, MA (*Presenter*) Nothing to Disclose Manuel Patino, MD, Boston, MA (*Abstract Co-Author*) Nothing to Disclose Travis L. Redel, Boston, MA (*Abstract Co-Author*) Nothing to Disclose Fredrick McNulty, Boston, MA (*Abstract Co-Author*) Nothing to Disclose Dushyant V. Sahani, MD, Boston, MA (*Abstract Co-Author*) Research support, General Electric Company Medical Advisory Board, Allena Pharmaceuticals, Inc

# For information about this presentation, contact:

aparakh1@mgh.harvard.edu

# PURPOSE

To evaluate bowel labelling and opacification with iodinated contrast media (iCM) in standard and reduced concentration at low kVp (100 kVp) and keV (50-70) images compared to barium-based contrast media (bCM) at 120kVp.

# METHOD AND MATERIALS

In this prospective clinical trial, 157 adults (74 M, 83 F; 63±12 years) with prior 120kVp abdominopelvic CT performed using bCM (Readi-cat, Bracco) were enrolled. Patients were randomly assigned to receive iCM (Omnipaque, GE) in standard-concentration (iCMs 7.7mgI/ml) or 25%-reduced concentration (iCMr 5.8mgI/ml) as a 900ml solution with water. They underwent 100kVp CT (Revolution CT, GE Healthcare) or DECT (Discovery 750HD, GE) scans. Patients were in one of four groups: A-100kVp/iCMs (n=50), B-50-70keV/iCMs (n=29), C-100kVp/iCMr (n=50) and D-50-70keV/iCMr (n=28). Small bowel intraluminal HU was measured in three segments on 100kVp and 50-70keV-DECT images and compared with their prior bCM-120kVp CT. Radiation dose (CTDIvol) was recorded.

# RESULTS

All CT exams were of diagnostic quality and there was no difference in the segments of small bowel filled with iCM or bCM. With iCMs, mean HU was 41% higher at 100kVp ( $319\pm143$ HU) and 9-130% higher at 50-70 keV (50keV= $518\pm20$ 9HU, 60keV= $345\pm13$ 9 HU and 70keV= $303\pm98$ HU) as compared to bCM ( $225\pm69$ HU). Despite 25% reduction in iodine dose, small bowel attenuation with iCMr was +48% higher on 100kVp images (333HU) and +9-117% higher on 50-70keV images (247-489HU), compared to 120kVp images with bCM (p<0.05). CTDIvol for 120 kVp, 100kVp and DECT scans were 12.5 $\pm$  3.9 mGy, 6.2  $\pm$  1.9 mGy and 15.7  $\pm$  3.3 mGy respectively.

### CONCLUSION

On increasingly utilized low kVp/keV images, standard and 25%-reduced dose of iCM provide substantially higher bowel attenuation compared to bCM at 120 kVp.

# **CLINICAL RELEVANCE/APPLICATION**

With the introduction of automatic tube voltage selection techniques and DECT, a significant proportion of CT exams are being performed using low kVp (<120kVp) and keV. Substantial increase in iodine attenuation on low kVp/keV images provides an opportunity for use and customization of iodine as a positive oral CM.

#### **Honored Educators**

Presenters or authors on this event have been recognized as RSNA Honored Educators for participating in multiple qualifying educational activities. Honored Educators are invested in furthering the profession of radiology by delivering high-quality educational content in their field of study. Learn how you can become an honored educator by visiting the website at: https://www.rsna.org/Honored-Educator-Award/ Dushyant V. Sahani, MD - 2012 Honored EducatorDushyant V. Sahani, MD - 2015 Honored EducatorDushyant V. Sahani, MD - 2016 Honored EducatorDushyant V. Sahani, MD - 2017 Honored Educator



# GU252-SD-THB1

### MRI Impacts Endometriosis Management in the Setting of Image-Based Multidisciplinary Conference

Thursday, Nov. 29 12:45PM - 1:15PM Room: GU/UR Community, Learning Center Station #1

#### Awards Student Travel Stipend Award

### Participants

Brian J. Burkett, MD, Rochester, MN (*Presenter*) Nothing to Disclose Adela G. Cope, MD, Rochester, MN (*Abstract Co-Author*) Nothing to Disclose David J. Bartlett, MD, Rochester, MN (*Abstract Co-Author*) Nothing to Disclose Asha Stenquist, Rochester, MN (*Abstract Co-Author*) Nothing to Disclose Tatnai Burnett, Rochester, MN (*Abstract Co-Author*) Nothing to Disclose Sudhakar K. Venkatesh, MD, FRCR, Rochester, MN (*Abstract Co-Author*) Nothing to Disclose Tiffany Jones, MD, Rochester, MN (*Abstract Co-Author*) Nothing to Disclose Wendaline M. VanBuren, MD, Rochester, MN (*Abstract Co-Author*) Nothing to Disclose

### For information about this presentation, contact:

VanBuren.Wendaline@mayo.edu

### PURPOSE

To quantify the extent that MRI findings translate into clinical management change in women with endometriosis.

### **METHOD AND MATERIALS**

A cohort of 141 women with endometriosis was discussed during an MRI-based multidisciplinary conference held every two weeks. Guided by a tri-compartmental report template, including critical potential sites of endometriosis implants and deep infiltrative disease organized systematically by anatomic compartment, preoperative imaging findings were recorded. After surgery, each case was reviewed comparing MRI and surgical/pathological findings. Management changes made as a result of the pre-operative conference were classified as major (decisions which altered the surgical procedure) or minor (decisions resulting in additional diagnostic evaluation or changes in conservative management).

#### RESULTS

Pre-operative MRI-based conference resulted in a change in management frequently, in 17.7% of the patients discussed over 27 months (25 of 141 patients). A major change occurred in 10 patients (7.1%). A minor change in management was seen in 18 patients (12.8%).

# CONCLUSION

MRI for endometriosis provides clinically meaningful information when reviewed systematically in a multidisciplinary setting. Frequently, additional management changes were made beyond the decisions from the dictated report, which were available to clinicians before the conference. This reflects the importance of multidisciplinary interaction and suggests the opportunity to optimize patient care through standardized reports with surgically pertinent details. This study demonstrates the ability of an image-based multidisciplinary conference to yield changes in clinical management.

# **CLINICAL RELEVANCE/APPLICATION**

This study quantifies the ability of MRI to guide clinical management changes for women with endometriosis and suggests ways to optimize the clinical impact of MRI for endometriosis.

### **Honored Educators**

Presenters or authors on this event have been recognized as RSNA Honored Educators for participating in multiple qualifying educational activities. Honored Educators are invested in furthering the profession of radiology by delivering high-quality educational content in their field of study. Learn how you can become an honored educator by visiting the website at: https://www.rsna.org/Honored-Educator-Award/ Sudhakar K. Venkatesh, MD, FRCR - 2017 Honored Educator



# GU253-SD-THB2

# Calculation of Cervical Tumor Volume on MRI: Simplified Ellipsoid Equation or 3D Segmentation?

Thursday, Nov. 29 12:45PM - 1:15PM Room: GU/UR Community, Learning Center Station #2

#### Awards Student Travel Stipend Award

#### Participants

Miriam Salib, MBBS, London, United Kingdom (*Presenter*) Nothing to Disclose Victoria Stewart, London, United Kingdom (*Abstract Co-Author*) Nothing to Disclose Nishat Bharwani, FRCR, MBBS, London, United Kingdom (*Abstract Co-Author*) Nothing to Disclose

#### For information about this presentation, contact:

miriamsalib@nhs.net

# PURPOSE

Cervical tumor volume is an independent prognostic indicator and thus of clinical significance. Volumes calculated with orthogonal measurements may significantly under or over estimate tumor size, which rarely conforms to an ellipsoid shape as the frequently adopted basic calculation assumes. Segmentation techniques, whilst time consuming, enable more accurate delineation of cervical tumors. The purpose of this study was to compare the estimated volume of cervical tumors on MRI calculated from conventional orthogonal measurements to volumes acquired by 3D segmentation.

### **METHOD AND MATERIALS**

IRB approved single centre retrospective study.Staging MR images for 94 consecutive patients with biopsy proven cervical cancer were reviewed and tumor volumes measured by 2 readers independently.Volumes were measured by i) taking 3 orthogonal measurements and applying a conventional simplified ellipsoid equation (width x length x depth x 0.52) and ii) manual 3D segmentation on PACS. Volumes were compared using a paired t test and Bland-Altman plot. P<0.05 was considered significant.

### RESULTS

89 of 94 patients had measurable tumors on MRI. Mean tumor volume by orthogonal measurements was 88.9cm3 and by segmentation was 80.5cm3 (range 3.1 - 355.3 cm3 and 3.8 - 344.1 cm3 respectively). Overall, volumes obtained using the ellipsoid equation were 10.4% greater than by manual segmentation.Paired t test showed a significant difference between volumes obtained using the two methods; p=0.0007. Bland-Altman plot shows that overall the volume obtained from orthogonal measurements overestimates the volume obtained by manual segmentation of the tumor. This overestimation is exaggerated with larger tumors.

### CONCLUSION

Primary tumor volume is an important prognostic factor in cervical cancer with larger tumors carrying an increased risk of nodal positivity and parametrial invasion. Assuming that volumetric data acquisition is the gold standard, orthogonal measurements overestimate the volume and volume estimation by segmentation should be considered particularly for larger, irregular tumors.

### **CLINICAL RELEVANCE/APPLICATION**

Cervical tumor volume is an independent prognostic indicator.Conventional orthogonal measurements are shown to overestimate volume and 3D segmentation is more accurate, particularly for larger tumors.

#### **Honored Educators**

Presenters or authors on this event have been recognized as RSNA Honored Educators for participating in multiple qualifying educational activities. Honored Educators are invested in furthering the profession of radiology by delivering high-quality educational content in their field of study. Learn how you can become an honored educator by visiting the website at: https://www.rsna.org/Honored-Educator-Award/ Nishat Bharwani, FRCR,MBBS - 2018 Honored Educator



# GU254-SD-THB3

Computer-Aided Diagnosis (CAD) Detected Regions Overlaid on Bi-Parametric Prostate MRI (bMRI): A Pilot Computer vs. Human Eye Study to Investigate the Ability to Detect Prostate Cancer

Thursday, Nov. 29 12:45PM - 1:15PM Room: GU/UR Community, Learning Center Station #3

# Awards

# Student Travel Stipend Award

#### Participants

Clayton P. Smith, BA, Bethesda, MD (*Presenter*) Nothing to Disclose Nathan S. Lay, PhD, Bethesda, MD (*Abstract Co-Author*) Nothing to Disclose Yohan Sumathipala, BS, Bethesda, MD (*Abstract Co-Author*) Nothing to Disclose Stephanie A. Harmon, PhD, Bethesda, MD (*Abstract Co-Author*) Research funded, NCI Marcin Czarniecki, MD, Bethesda, MD (*Abstract Co-Author*) Nothing to Disclose Sonia Gaur, Bethesda, MD (*Abstract Co-Author*) Nothing to Disclose Sherif Mehralivand, MD, Bethesda, MD (*Abstract Co-Author*) Nothing to Disclose Bradford J. Wood, MD, Bethesda, MD (*Abstract Co-Author*) Researcher, Koninklijke Philips NV; Researcher, Celsion Corporation; Researcher, BTG International Ltd; Researcher, Siemens AG; Researcher, XAct Robotics; Researcher, NVIDIA Corporation; Intellectual property, Koninklijke Philips NV; Intellectual property, BTG International Ltd; Royalties, Invivo Corporation; Royalties, Koninklijke Philips NV; ; Peter Pinto, Bethesda, MD (*Abstract Co-Author*) Nothing to Disclose Ronald M. Summers, MD,PhD, Bethesda, MD (*Abstract Co-Author*) Nothing to Disclose Ronald M. Summers, MD,PhD, Bethesda, MD (*Abstract Co-Author*) Nothing to Disclose Ronald M. Summers, MD,PhD, Bethesda, MD (*Abstract Co-Author*) Royalties, iCAD, Inc; Royalties, Koninklijke Philips NV; Royalties, ScanMed, LLC; Research support, Ping An Insurance Company of China, Ltd; Researcher, Carestream Health, Inc; Research

support, NVIDIA Corporation; ; ; ; Baris Turkbey, MD, Bethesda, MD (*Abstract Co-Author*) Nothing to Disclose

### For information about this presentation, contact:

cpsmith7@gmail.com

# PURPOSE

Successful implementation of CAD systems requires an intuitive user interface for the radiologist. To avoid the subjective nature and learning curve of interpreting CAD-derived probability maps, we developed a CAD which provides regions of interest (ROI) overlaid on bMRI to assist radiologists for cancer detection. The purpose of this pilot study is to test this new system's ability to detect prostate cancer before being introduced to readers' use.

### **METHOD AND MATERIALS**

40 patients (median age 65 [55-76]; median PSA 6.52ng/ml [3.02-25.7]) who underwent endorectal coil (ERC) mpMRI (T2W, ADC, b2000, DCE) at 3T and subsequent prostatectomy were evaluated. bMRI (T2W, ADC, b1500) was extracted from each mpMRI. CAD-processed bMRIs contained 4 ROIs with maximum 20mm windows in x, y, and z axes. Lesions were validated with whole-mount pathology. Prior to CAD processing, a single expert reader scored all 40 MRIs (MRI Only) using PI-RADS v2 for lesion-level comparison to CAD. Lesion-based sensitivity was calculated for detection of all cancer (Gls>=6) and clinically significant (CS) cancer (Gls>=3+4).

# RESULTS

After prostatectomy, 105 cancerous foci were identified on histopathology, with 91 containing CS disease. CAD sensitivity was 76.2% for all cancers and 79.1% for CS cancers. MRI Only sensitivity was 58.1% for all cancers and 59.3% for CS cancers. Of all lesions detected by either method (N=89), 28 were detected by CAD only. In total, 25 lesions were missed by CAD, of which 9 (36%) were detected by MRI Only. Lesions in the peripheral zone made up a greater proportion of the lesions missed (21/25) by CAD compared to lesions detected (49/80) by CAD.

### CONCLUSION

The new CAD-derived ROIs provide greater sensitivity for detection of both all cancers and CS cancers than MRIs interpreted by an expert radiologist. Lesions that are missed by CAD are also likely to be missed by a prostate imager. These preliminary results will be further validated in a multi-reader multi-institutional study.

### **CLINICAL RELEVANCE/APPLICATION**

CAD-derived ROIs may be used as an adjunct tool in lesion detection in prostate MRI. Initial use of this CAD has shown superior sensitivity and specificity than a human reader alone.



# GU255-SD-THB4

Investigation of the Feasibility of the Diagnosis of Prostate Cancer in MR imaging using Deep-Learning <u>Technique: Preliminary Study</u>

Thursday, Nov. 29 12:45PM - 1:15PM Room: GU/UR Community, Learning Center Station #4

# Participants

Sung Kyoung Moon, Seoul, Korea, Republic Of (*Presenter*) Nothing to Disclose Minjae Jang, Seoul, Korea, Republic Of (*Abstract Co-Author*) Nothing to Disclose Hyun Gun Kim, Seoul, Korea, Republic Of (*Abstract Co-Author*) Nothing to Disclose Hyug-Gi Kim, Seoul, Korea, Republic Of (*Abstract Co-Author*) Nothing to Disclose Joo Won Lim, MD, PhD, Seoul, Korea, Republic Of (*Abstract Co-Author*) Nothing to Disclose

### For information about this presentation, contact:

aquamsk@naver.com

#### PURPOSE

To investigate the feasibility of the diagnosis of prostate cancer in MR imaging using deep learning techniques.

# **METHOD AND MATERIALS**

Seventy-three patients (41 cancers and 32 normal prostate) who underwent prostate MR imaging (T2WI and DWI) and prostate biopsy were enrolled. For the pre-processing steps, one dedicated GU radiologist (10-year experience) selected MR images where only prostate glands were included, and also selected the MR images with clinically significant cancers (PI-RADS score 4 and 5) among the cancer group. The Total 644 MR images (318 T2WI and 326 ADC maps with b 1000) were included, and consisted of half and half of cancer and normal prostate in each sequence. The images were cropped to fit to the prostate gland and augmented to 1288 images by mirroring. The datasets were randomly split into training (70%) and test (30%) sets. We implemented the data with the AlexNet based convolutional neural network (CNN) model to differentiate between prostate cancer and normal prostate. The performance of CNN model was assessed by the area under a receiver operating curve (AUROC). Furthermore, the accuracy of the prostate cancer detection in CNN model was assessed by the radiologist by the comparison between the MR images and heat activation maps from CNN models.

### RESULTS

The performance of the CNN model for the prostate cancer differentiation showed 0.88 for T2WI and 0.95 for ADC map with high b value in AUROC. ADC map was more useful to select the prostate cancer than T2WI. In the meanwhile, the accuracy of the heat activation maps from CNN model showed 64.0% in ADC map and only 50.5% in T2WI. The activated areas in the heat activation maps were not so identical to the cancer regions perceived by the radiologist in considerable images.

#### CONCLUSION

The prostate cancer evaluation using deep learning showed excellent performance in our CNN model. However, the lesion detection in deep learning was not the same as the radiologist perceived the lesion. The validation of the deep learning model should be done by the radiologist to prove both the diagnostic performance and accurate lesion perception.

### **CLINICAL RELEVANCE/APPLICATION**

The results of the deep learning of the medical images should be interpreted carefully and validated meticulously before clinical application to minimize the black box.



# GU256-SD-THB5

Utility of High Resolution Images in MR Evaluation of Placenta Accreta Spectrum

Thursday, Nov. 29 12:45PM - 1:15PM Room: GU/UR Community, Learning Center Station #5

### Participants

Priyanka Jha, MBBS, San Francisco, CA (*Presenter*) Nothing to Disclose Liina Poder, MD, Mill Valley, CA (*Abstract Co-Author*) Nothing to Disclose

For information about this presentation, contact:

priyanka.jha@ucsf.edu

#### PURPOSE

To assess the utility of high resolution (HR) images in management of placenta accreta spectrum (PAS).

# METHOD AND MATERIALS

In this HIPAA- compliant, IRB-approved, retrospective study, patients undergoing 3T MR Imaging for evaluation of placenta accreta spectrum between March 2015 to 2018 were included. The images were analyzed by 2 independent readers with 5 and 15 years of experience and expertise in placental imaging. First, the large field of view (FOV) images, which include the entire uterus were analyzed for diagnostic quality and the presence or absence of findings of PAS. Additional pertinent observations included location of invasion, depth of invasion/myometrial thinning, presence of cervical invasion, bladder invasion and intra-placental hemorrhage. Next the HR, small FOV images were reviewed for diagnostic quality. These images were reviewed for any additional findings not previously identified on large FOV images. Intraoperative findings & surgical pathology were used as reference standard. Reader confidence for diagnosis was recorded on both large & small FOV images.

#### RESULTS

60 patients who underwent 3T MRI for invasive placenta were included in the study. Of these, HR images were found to be nondiagnostic from respiratory motion artefact in 19 cases(32%). In remaining cases, HR images were not found to add any additional information to effect patient management in 37 cases(58%). In 2 cases, HR images were found to be helpful to exclude focal accreta. In additional 2 cases with placenta increta, HR images were helpful to exclude bladder invasion. However, when adequately performed, reader confidence for diagnosis of all accreta, increta and percreta was increased.

# CONCLUSION

HR images are often degraded from artefact, probably related to their acquisition later in the protocol, reflecting increasing patient discomfort. Although HR images improve reader confidence, in most cases, no new findings or additional diagnostic information is acquired. If MRI is positive for invasive placenta, additional HR may rarely be necessary to evaluate for invasion of adjacent organs. In a negative examination, they may be helpful to exclude focal invasion. Live review of acquired images can guide need for HR aquisition.

# **CLINICAL RELEVANCE/APPLICATION**

HR images can be omitted during MR for invasive placenta in many cases, reducing imaging time, associated cost and patient discomfort. Rarely, they are useful to assess focal invasion.



# GU257-SD-THB6

Low Incidence of Contrast Induced Nephropathy (CIN) in Oncological High-Risk Patients Undergoing Contrast-Enhanced CT with the Isoosmolar Iodinated Contrast Medium Iodixanol in Any Clinical Setting

Thursday, Nov. 29 12:45PM - 1:15PM Room: GU/UR Community, Learning Center Station #6

# Participants

Sebastian Werner, Tuebingen, Germany (*Presenter*) Nothing to Disclose Christian Deckert, Tuebingen, Germany (*Abstract Co-Author*) Nothing to Disclose Marius Horger, MD, Tuebingen, Germany (*Abstract Co-Author*) Nothing to Disclose

# PURPOSE

To determine the incidence of a contrast-induced nephropathy (CIN) [increase in SCr  $\geq$  0.5 mg/dL or  $\geq$  25% from baseline or decrease in eGFR  $\geq$  25% from baseline within 1 week following i.v. Iodixanol administration

# METHOD AND MATERIALS

This is a retrospective analysis of a cohort of 251 (mean age, 69.1 y; range, 33-95 y) oncological high-risk patients presenting primarily with restricted renal function (eGFR < 60 mL/min/ $1.73m^2$ ) that underwent CECT with the isoosmolar contrast agent Iodixanol at our institution between December 2016 and March 2018. The mean baseline GFR and serum creatinine value was 45.9 mL/min (range, 14.9 to 59.9 mL/min/ $1.73m^2$ ) and 1.43 mg/ml (SD, 0.4), respectively. CECT examinational protocol was: 100 kV, 100-250 mAs (depending on the examined region) and thin collimation (< 1 mm). All patients received 60 mL Iodixanol using 2mL/s flow and 30 mL saline chase afterwards. Oral or i.v.-hydration with 500 ml water before and after CECT was given in all patients. Statistical analysis was first performed for the entire cohort and subsequently in subgroups of patients: a) patients undergoing elective exams (85.3%) or b) medical emergencies (14.7%). Additionally, we statistically evaluated the following three subgroups depending on GFR-value ([1] GFR<60mL/min (57.8%); [2] GFR<45mL/min (35.9%); [3] GFR<30mL/min (6.4%). Concurrent therapies and comorbitities were all registered and evaluated.

# RESULTS

The overall pooled CIN incidence in our cohort was 2.8%. Relative difference in SCr and eGFR (MDRD) pre/post-Iodixanol was -0.8% (SD, 14%) (p<0.23) and 3.9% (SD, 22%) (p<0.06). In patients with a pre-Iodoxanol GFR of <30, <45 and <60 mL/min/1.73m<sup>2</sup> changes in GFR were not statistically significant with the mean GFR increasing 20.1%, 2.9% and 2.6%, respectively. 66 (26.3%) had known chronic renal failure in the pre-scan setting. 130 (51.8%) patients had concurrent chemotherapy.

# CONCLUSION

The incidence of CIN after intravenous iodinated CECT with Iodixanol in high-risk oncologic patients was 2.8% at a mean of 2.8 d. In case of CIN GFR reapproximated pre-scan levels at a mean of 25.5 d.

# **CLINICAL RELEVANCE/APPLICATION**

The use of a reduced-dose CECT-protocol with an isoosmolar contrast medium (Iodixanol) seems to be safe and can be used in any clinical setting in oncological patients with restricted renal function.



# HP239-SD-THB1

# Is Our Job Making Us Fat? Radiologist Work Environment and Reported Health Survey

Thursday, Nov. 29 12:45PM - 1:15PM Room: HP Community, Learning Center Station #1

### Participants

Andrew Wagner, MD, Boston, MA (*Presenter*) Nothing to Disclose Sunny Jaiswal, MD, Worcester, MA (*Abstract Co-Author*) Nothing to Disclose Neel Madan, MD, Boston, MA (*Abstract Co-Author*) Consultant, Near Infrared Imaging, LLC; Brenna Kelley, Boston, MA (*Abstract Co-Author*) Nothing to Disclose

# For information about this presentation, contact:

awagner2@tuftsmedicalcenter.org

### PURPOSE

We aim to evaluate the Radiologist's work environment and determine correlations between hours sitting, hours worked per week, excercise, weight gain and reported health. We want to determine which factors contribute to weight gain and poorer reported health.

# METHOD AND MATERIALS

The subjects were academic radiologist (N=100, 26 Female 74 Male). The study consisted of an 18 question survey hosted online by Survey Monkey. Questionnaire items covered demographic information, workstation environment, reported health, weight gain, weekly exercise activity and willingness to learn about changes.

### RESULTS

A majority of radiologist (61%) report gaining weight since beginning their career in radiology with a mean weight gain of 16.2 pounds. Few radiologist report getting the recommend weekly exercise (24%). There was a positive correlation between the average number of hours worked per day and the amount of weigh gained (r=.158). Increased number of hours a person reported sitting was correlated with decreased overall sense of health. Most radiologist (81%) were willing to learn more about being more active during the work day although few (9%) felt that there practice partners or administrators would be willing to support them in creating it.

# CONCLUSION

Radiologists in general believe that there carreer in radiology has contributed to their overall decrease in health and weight gain. The work environment with long periods of sitting and longer than average work day likely contribute to this sentiment. Radiologists are interested in learning about making changes in their day to be more active but are unsure that there partners or administrators would be willing help.

# **CLINICAL RELEVANCE/APPLICATION**

The Radiologist work environment makes up a majority of clinicians week and corellations between different work environments, work days and hours sitting can drive further invistagation into areas that promote the better health.



# HP240-SD-THB2

Measuring Radiologists Posture Improvement Using a Smart Chair

Thursday, Nov. 29 12:45PM - 1:15PM Room: HP Community, Learning Center Station #2

#### **Participants**

Eyal Bercovich, MD, Haifa, Israel (*Presenter*) Nothing to Disclose Luda Guralnik, MD, Haifa, Israel (*Abstract Co-Author*) Nothing to Disclose Marcia C. Javitt, MD, Haifa, Israel (*Abstract Co-Author*) Nothing to Disclose

For information about this presentation, contact:

eyalberc@gmail.com

### PURPOSE

There are two major variables which affect seating posture, one is the chair and the other is seating properly. It is well known that poor sitting posture and prolonged sitting can lead to musculoskeletal disorders (MSD). Radiologists are characterized by prolonged sitting in front of a workstation, hence they are more exposed to MSD. The purpose of the study is to improve radiologists seating quality using a smart chair for real-time posture monitoring and feedback.

# METHOD AND MATERIALS

The study is a crossover comparative study, of 13 Radiology attendings and residents, age range 27-60, 3 males and 10 females. The study investigated sitting quality with a smart chair sensor system and computer calculated biofeedback for correction of low quality sitting. The smart chair (Seatback, Haifa, Israel) used in the study uses multi sensor arrays that constantly detects and evaluates the sitting quality. the device includes over 90 sensors of pressure and angle, and a dedicated software that calculates sitting quality and alerts when a low quality time threshold is reached. Each test subject was evaluated for 10 days in two phases of 5 days each: Phase 1 (control): the smart chair monitored sitting quality without feedback, Phase 2 (intervention): the smart chair monitored sitting quality posture, or sitting for over 40 minutes, as analyzed by the smart chair's software. Sitting quality data was gathered and analyzed in 0.5 HZ frequency during the ten study days, an average of approximately fifteen thousand sitting postures were recorded daily for each test subject.

# RESULTS

The 13 test subjects were average sitting time in each measured day were 6.1 (4.4-7.9) hours. During Phase 1 the total time of poor sitting quality was 78%. In phase 2, with feedback for poor sitting quality, there was reduction of the duration of poor quality sitting to 52% of the sitting time.

### CONCLUSION

The results of the study show that constant real-time sitting quality monitoring, with feedback for prolonged low quality sitting, can significantly reduce the time of low quality sitting during a radiologist work day.

# **CLINICAL RELEVANCE/APPLICATION**

Radiologists are exposed to musculoskeletal disorders due to their work environment, real-time sitting quality monitoring and feedback technology can reduce low quality sitting and prevent musculoskeletal disorders in this population.



# HP241-SD-THB3

Improving Compliance in Multi-institutional PET/CT Clinical Trials via Real Time Quality Assurance Checking

Thursday, Nov. 29 12:45PM - 1:15PM Room: HP Community, Learning Center Station #3

### Participants

Katherine Binzel, PhD, Columbus, OH (*Presenter*) Nothing to Disclose Jun Zhang, PhD, Columbus, OH (*Abstract Co-Author*) Nothing to Disclose David Poon, BS, Columbus, OH (*Abstract Co-Author*) Nothing to Disclose Preethi Subramanian, MS, BEng, Columbus, OH (*Abstract Co-Author*) Nothing to Disclose Tim Sbory, BS, Columbus, OH (*Abstract Co-Author*) Nothing to Disclose Michael V. Knopp, MD, PhD, Columbus, OH (*Abstract Co-Author*) Nothing to Disclose Sydney Cearlock, Columbus, OH (*Abstract Co-Author*) Nothing to Disclose

### PURPOSE

Having served as the imaging core laboratory for more than 40 clinical trials within the NCI National Clinical Trial Network, our group has established and implemented quality check and quality assurance protocols and tools which are used to provide real time feedback regarding clinical trial protocol compliance of imaging data. We have observed the benefit of this real time reporting with participating imaging sites and here we report on trends relating to trial protocol compliance over more than a decade of data collection experience.

# RESULTS

Overall protocol compliance was found to improve over the course of a clinical trial's lifetime when real time QA processes were in place. We found that the most common causes of protocol deviations were delays in emission scan start times as well as administered doses below the lower limits of the protocol, however in compliance with sites' local protocols. This analysis revealed that sites generally had improved compliance over the course of trial enrollment. We believe that real time QA feedback helped bring awareness to non-compliant examinations, allowing sites to better identify and correct for regular sources of protocol deviations.

### CONCLUSION

In order to ensure the most precise and robust assessment of PET/CT imaging, it is critical that those factors which can be controlled for are maintained as consistently as possible. In the case of multi-institutional clinical trials, protocol guidelines must be followed in order to allow for accurate trial results. Therefore, quality assurance checks are also a crucial process for such trials. We have observed improved compliance to imaging protocols as a result of real time QA reporting. We recommend an implementation of quality assurance processes and regular reporting of protocol adherence for all imaging sites, even those performing only standard of care imaging.

# METHODS

More than 2000 18F-FDG PET examinations for patients enrolled in five different NCTN trials over ten years were assessed. Each trial has its own requirements regarding radiotracer dose, uptake time, and timing of the image acquisition within the trial protocol. Our real time quality assurance process performs checks on these and a variety of other parameters related to the imaging procedures. We are then able to notify submitting sites of any protocol deviations prior to subsequent imaging, which is particularly important for trials involving adaptive treatment plans. We evaluated the overall level of protocol compliance for each of the above imaging characteristics and also looked at how compliance rates changed over the lifetime of any given trial.

#### PDF UPLOAD

http://abstract.rsna.org/uploads/2018/18020032/18020032\_qude.pdf



# IN008-EC-THB

# DeepGrow: A General-Purpose and Interactive Segmentation Tool Based on Deep Learning

Thursday, Nov. 29 12:45PM - 1:15PM Room: IN Community, Learning Center Custom Application Computer Demonstration

### Participants

Tomas Sakinis, Oslo, Norway (*Presenter*) Nothing to Disclose Petro Kostandy, MD, Rochester, MN (*Abstract Co-Author*) Nothing to Disclose Zeynettin Akkus, PhD, Rochester, MN (*Abstract Co-Author*) Nothing to Disclose Kenneth Philbrick, Rochester, MN (*Abstract Co-Author*) Nothing to Disclose Panagiotis Korfiatis, PhD, Rochester, MN (*Abstract Co-Author*) Nothing to Disclose Bradley J. Erickson, MD, PhD, Rochester, MN (*Abstract Co-Author*) Stockholder, OneMedNet Corporation; Stockholder, VoiceIt Technologies, LLC; Stockholder, FlowSigma;

#### For information about this presentation, contact:

#### sakinis.tomas@gmail.com

#### CONCLUSION

Fast, accurate and interactive segmentation of previously "unseen" structures is possible. We hope that this will speed up ground truth generation and facilitate the use of segmentation in clinical practice.

#### FIGURE

http://abstract.rsna.org/uploads/2018/18008079/18008079\_blax.jpg

### Background

Deep learning based tools using convolutional neural networks (CNNs) are considered state-of-the-art for automated image segmentation. Consistently accurate automated segmentation with CNNs remains challenging due to high variability of anatomy and pathology. Manual or semi-automated tools that do not make use of CNNs remain standard for most segmentation tasks. DeepGrow is an interactive segmentation tool that incorporates users' input into its CNN-based model when making predictions. It is fast, intuitive, accurate and can segment previously unseen structures. A single click over the structure to be segmented is often sufficient for an accurate 2D segmentation (see figure, where the red dot represents the mouse click). Additional clicks allow modification to suppress any errors.

### **Evaluation**

We retrospectively collected 25 non-contrast abdominal CT examinations. A radiologist volumetrically segmented the liver and kidneys. 20 exams were used for training and five for validation. The spleen was additionally segmented in the validation exams. Performance on each of the four segmented organs was evaluated separately on the validation set. We randomly simulated two and six mouse clicks for each desired organ per slice, mimicking the anticipated usage pattern. Predictions for each slice were compared with the ground-truth masks. Averaged Dice scores are reported for each organ. After two clicks: Liver- 0.979, Right kidney- 0.979. Left kidney- 0.976. Spleen- 0.910. After six clicks: Liver- 0.984, Right kidney- 0.988. Left kidney- 0.986. Spleen- 0.954. DeepGrow takes ~0.04s to compute a segmentation on a computer with GPU.

### Discussion

DeepGrow incorporates user input, resulting in better segmentation with more interaction. It achieved satisfactory segmentation performance not only for organs it was trained on, but also for the spleen, which it was not trained on. We believe that we can further increase its generalizability by expanding the training data variability.



# IN235-SD-THB1

# Readability of Neuroradiology CT and MRI Reports: Are They Over Patients' Heads?

Thursday, Nov. 29 12:45PM - 1:15PM Room: IN Community, Learning Center Station #1

### **Participants**

Paul H. Yi, MD, Baltimore, MD (*Presenter*) Nothing to Disclose John Harringa, Madison, WI (*Abstract Co-Author*) Nothing to Disclose Sean Golden, Madison, WI (*Abstract Co-Author*) Nothing to Disclose Mark A. Kliewer, MD, Madison, WI (*Abstract Co-Author*) Nothing to Disclose

### For information about this presentation, contact:

pyi10@jhmi.edu

## PURPOSE

Radiology reports have traditionally been written for referring clinical providers. However, patients have recently begun to access and read their radiology reports through online medical record "portals", raising concerns about their ability to comprehend these complex documents. The purpose of this study was to assess the readability of computed tomography (CT):head and magnetic resonance imaging (MRI):brain reports.

# **METHOD AND MATERIALS**

We reviewed 224 consecutive CT head and MRI brain:reports from a single academic center. We evaluated each article for readability using 5 quantitative readability scales: the Flesch-Kincaid (FK) grade level, Flesch Reading Ease, Gunning-Fog Index, Coleman-Liau Index, and the Simple Measure of Gobbledygook (SMOG). The number of reports with readability <= the 8th grade level (average reading ability of US adults) and the 6th grade level (NIH-recommended level for patient education materials) were determined.

#### RESULTS

The mean readability grade level of the CT reports was greater than the 11th grade reading level for all readability scales. No reports were written at less than the eighth grade or below the sixth grade levels.

### CONCLUSION

Neuroradiology CT and MRI reports are written at a level too high for the average patient to comprehend. As patients increasingly read their radiology reports through online medical record portals, consideration of the patient's ability to comprehend should be taken into consideration by the radiologist generating a report.

# **CLINICAL RELEVANCE/APPLICATION**

High readability levels of neuroradiology CT and MRI reports may contribute to poor health literacy,:which is associated:with worse clinical outcomes and increased healthcare expenditures.



### MI238-SD-THB1

177Lu-DOTATATE Radioligand Therapy in Patients Affected by Somatostatin-Receptor-Positive Neuroendocrine Tumors

Thursday, Nov. 29 12:45PM - 1:15PM Room: MI Community, Learning Center Station #1

# Awards

# **Student Travel Stipend Award**

#### **Participants**

David J. Lubin, MD, Los Angeles, CA (*Presenter*) Nothing to Disclose Martin Allen-Auerbach, MD, Los Angeles, CA (*Abstract Co-Author*) Advisor, Eli Lilly and Company Linda Gardner, RN, Los Angeles, CA (*Abstract Co-Author*) Nothing to Disclose Jeremie Calais, MD, Rouen, France (*Abstract Co-Author*) Nothing to Disclose Johannes Czernin, MD, Los Angeles, CA (*Abstract Co-Author*) Stockholder, Trethera Corporation Board Member, Trethera Corporation Francesco Ceci, Los Angeles, CA (*Abstract Co-Author*) Nothing to Disclose Andrew Quon, MD, Stanford, CA (*Abstract Co-Author*) Nothing to Disclose

# For information about this presentation, contact:

dlubin@mednet.ucla.edu

# PURPOSE

Advanced neuroendocrine Tumors (NETs) remain difficult to treat and are eventually lethal. 177Lu-DOTATATE (Lutathera), a radiolabeled peptide targeting the somatostatin receptor (SSTR) representing radioligand therapy introduced as a therapeutic alternative to hormonal or chemotherapy for patients with NETs. It significantly extends progression free and overall survival.

# METHOD AND MATERIALS

As part of an expanded access IND we treated 28 mid-gut NET patients (11 males; mean age 66.4  $\pm$ 11.0 and 17 females; mean age 65.8  $\pm$ 10.7) years old with 192.2 $\pm$ 4.0 mCi of Lutathera. 16 of the patients underwent 4 treatment cycles, 8 had 3 cycles and 4 had 2 cycles. A positive pretreatment 68Ga-DOTATATE scan (NETSPOT) was required for inclusion. Outpatient treatments were administered at 8 week intervals. Patients remained under close observation for 5.3  $\pm$ 0.9 hours during the infusion of Lutathera with radiation rates at 1 meter measured prior to discharge. Patient safety monitoring included pre and post infusion vital signs, ECG and serum potassium levels.

# RESULTS

Extensive disease with intense SSTR expression by imaging was documented in all patients. Of those treated, liver metastasis occurred in 18 patients, bone metastasis in 4; and lymph node, mesenteric or peritoneal involvement in 11 patients. A 10 amino acid cocktail was given during each treatment for renal protection in all patients. Severe persistent nausea occurred in 2/28 (7.1%) of patients. Vomiting was observed in one patient. 23/28 patients reported fatigue and or dizziness as well as arthralgias reported in 16/28 patients. Reversible hair loss (n=10) and mild bone marrow suppression (n=3) were observed. No severe side effects were seen. Objective disease response (RECIST) is thus far available in 10 patients. 2 patients showed a partial response, 7 patients had stable disease and 1 patient had progressive disease. 2 patients died during this period due to progressive disease and extremely extensive disease at baseline.

## CONCLUSION

SSTR targeted radioligand therapy is a well-tolerated, safe treatment option in patients with NETs who have progressed despite hormonal and conventional chemotherapy. Our use of Lutathera resulted in progression free survival in 90% of patients with NETs.

# **CLINICAL RELEVANCE/APPLICATION**

The recent FDA-approved targeted agent Lutathera represents a paradigm shift to treat mid-gut NETs. Here, we report on the safety and efficacy of Lutathera in our clinic.



# MI239-SD-THB2

Imaging the Tumor Microenvironment in Vivo - Regulatory Mechanisms of Tumor Promoting Biomarker S100A9

Thursday, Nov. 29 12:45PM - 1:15PM Room: MI Community, Learning Center Station #2

# Participants

Anne Helfen, MD, Muenster, Germany (*Presenter*) Nothing to Disclose Jan Riess, Muenster, Germany (*Abstract Co-Author*) Nothing to Disclose Olesja Fehler, PhD, Muenster, Germany (*Abstract Co-Author*) Nothing to Disclose Walter L. Heindel, MD, Muenster, Germany (*Abstract Co-Author*) Nothing to Disclose Moritz Wildgruber, MD, PhD, Munster, Germany (*Abstract Co-Author*) Nothing to Disclose Michel Eisenblaetter, MD, Muenster, Germany (*Abstract Co-Author*) Nothing to Disclose

#### PURPOSE

Tumor progression and metastasis depend on tumor-infiltrating immune cells, which form a characteristic inflammatory tumor microenvironment (TME). Within this microenvironment but also in premetastatic niches, the protein heterodimer S100A8/A9 is released by activated infiltrating monocytes. As a promoter of tumor invasion and TME formation, it has been associated with poor prognosis. Our aim was to develop an in vivo imaging tool serving as a biomarker for TME influence on tumor behavior.

### **METHOD AND MATERIALS**

From syngeneic murine breast cancer tumors 4T1 (highly malignant) and 67NR (low malignancy), wildtype (wt) and S100A9 knock out cells (CRISPR/cas9-method, ko) were created and implanted into either female BALB/c wildtype or S100A9-/--mice (n=10 each). At 4mm tumor size, anti-S100A9-Cy5.5-driven flurorescence reflectance imaging has been performed 0 and 24h after injection. An isotype IgG-Cy5.5 served as a control (n=5) for unspecific label distribution. In vivo imaging was correlated with immunohistology, Western Blot and FACS analyses. Statistical analysis was performed using unpaired t test and one-way ANOVA with Bonferroni post test.

# RESULTS

24 h after injection, anti-S100A9-Cy5.5 resulted in significantly higher fluorescence signals as compared to IgG-Cy5.5. Knock out of S100A9 in tumor cells did not result in a reduced anti-S100A9-Cy5.5 in vivo imaging signal. However, the specific signal was significantly lower in S100A9-/- as compared to wildtype mice (4.11 vs. 2.53 AU; p<0.05) and higher in 4T1 as compared to 67NR tumors (4.11 vs. 1.73 AU; p<0.001).

### CONCLUSION

Our results in the 4T1/67NR breast cancer model system confirm a secretion of S100A8/A9 by components of the TME, while tumor cells do apparently not release S100A8/A9. S100A9-specific in vivo imaging reflects tumor malignancy and may serve as a biomarker for TME formation and activity.

### **CLINICAL RELEVANCE/APPLICATION**

S100A9-specific in vivo imaging as a biomarker for TME activity may improve estimation of tumor aggressiveness and response to tumor immune therapy non-invasively.



# MI240-SD-THB3

# Accuracy of the Staging of the Locally Advanced Penile Carcinoma Using 18F-FDG-PET/MRI

Thursday, Nov. 29 12:45PM - 1:15PM Room: MI Community, Learning Center Station #3

### Participants

Jiri Ferda, MD, PhD, Plzen, Czech Republic (*Presenter*) Nothing to Disclose Eva Ferdova, MD, Plzen, Czech Republic (*Abstract Co-Author*) Nothing to Disclose Jan Baxa, MD, PhD, Plzen, Czech Republic (*Abstract Co-Author*) Nothing to Disclose Ondrej Hes, MD, PhD, Plzen, Czech Republic (*Abstract Co-Author*) Nothing to Disclose Milan Hora, Plzen, Czech Republic (*Abstract Co-Author*) Nothing to Disclose

For information about this presentation, contact:

ferda@fnplzen.cz

### PURPOSE

to evaluate the impact of 18F-PET/MRI in the clinical staging in locally advanced penile carcinoma

### **METHOD AND MATERIALS**

During three years, 12 male patients (age 29 -84, mean age 58,3) were investigated using 18F-FDG PET/MRI, it represents 0,32% of all performed PET/MRI studies. The examination was performed after intravenous application of 2.5 MBq/kg of 18F-FDG. PET/MRI examination consist of targeted penile imaging in subpine position including diffusion weighted imaging and the dynamic Gd-enhanced study after application of gadobutrol in the dose of 0.1 mmol/kg, followed with body PET/MRI in supine position from vertex to groin. In 10 male, the penile carcinoma was confirmed diagnosis by surgery and biopsy histopathological evaluation The radiological, clinical and pathological staging was evaluated according the AJCC 8th edition including the grade. During the evaluation of the local T stage, the full diagnostic MRI images were used for evaluation, the FDG avid (SUVmax more than 5) lymph nodes in groin or pelvis were described as the positive finding in nodal staging.

#### RESULTS

Penile carcinoma was confirmed by PET/MRI in 10 patients, in whom the diagnosis was confirmed by histology, additional two diagnoses was syphilitical infiltration and urethral carcinoma in two males. There were reached following results in nodal assessment: there were four true positive lymph nodes, four true negative nodes and two false positive nodal staging using PET/MRI, no false negative finding was found. According to the T staging, there were one T1a, one T1a, four T2 (invasion of corporis spongiosi and two T3 (invasion of either one of corporum cavernosum), the accurate T stage was set in 9 of 10 patients (90%).

# CONCLUSION

PET/MRI could play an important role in the evaluation of the staging of the locally advanced carcinoma, our experience shows the advantage of the hybrid imaging, even if the experience is limited due to the rare diagnose.

# **CLINICAL RELEVANCE/APPLICATION**

PET/MRI could play an important role in the evaluation of the staging of the locally advanced carcinoma, our experience shows the advantage of the hybrid imaging, even if the experience is limited due to the rare diagnose.



# MI241-SD-THB4

# Utility Of PET/CT 68GA-DOTA-UBI [29-41] for Diagnosis of Infection in Patients with Orthopedic Implants

Thursday, Nov. 29 12:45PM - 1:15PM Room: MI Community, Learning Center Station #4

### **Participants**

Belen Rivera Bravo, MD, Mexico City, Mexico (*Abstract Co-Author*) Nothing to Disclose Hugo E. Solis Lara, MD, Monterrey, Mexico (*Presenter*) Nothing to Disclose Rene Lopez Leon, MD, Mexico City, Mexico (*Abstract Co-Author*) Nothing to Disclose Keren Contreras Contreras, MD, Mexico City, Mexico (*Abstract Co-Author*) Nothing to Disclose Daniela J. Jimenez, MD, Mexico City, Mexico (*Abstract Co-Author*) Nothing to Disclose Rafael Curiel Reyes, MD, Morelia, Mexico (*Abstract Co-Author*) Nothing to Disclose Neri A. Alvarez Villalobos, MD, Monterrey, Mexico (*Abstract Co-Author*) Nothing to Disclose

#### For information about this presentation, contact:

hu\_solis@hotmail.com

#### PURPOSE

The use of orthopedic implants and fixation material is quickly increasing in clinical practice, as well as the complications of these procedures, such as infection, resulting in treatment failure, dysfunction, or functional disability (transient or permanent). For this reason, an appropriate non-invasive diagnosis of infections related to these materials is of the utmost importance.

### **METHOD AND MATERIALS**

We developed a transversal, not experimental, descriptive and prospective study including 13 adult patients with suspected infection of prosthetic joint or orthopedic implant, which had biopsy or culture, in whom we performed PET/CT (using Biograph High resolution Crystal LSO of 64 detectors), administering 185 MBq of 68Ga-DOTA-UBI PET/CT, obtaining PET and computed tomography images of the anatomical region of interest, as well as images of normal bone or contralateral joint. PET/CT images were described as positive or negative based on visual and semi quantitative analysis (ROI), and their later comparison with the vascular pool and background SUVmax values.

# RESULTS

When comparing the results of culture with the results of PET/CT using Fisher's exact test, a p=0.108 was obtained and a Kappa index of 0.54, which is considered as a moderate concordance index. The sensitivity and positive predictive value for PET/CT was 90%, and a specificity and negative predictive value of 66% was found. The best SUVmax value cut-off point obtained to define positivity using culture results prior to PET/CT was >=1.91 (obtained exclusively with the target SUVmax), which proved a sensitivity and a specificity of 100%, and an area under the curve of 100%.

#### CONCLUSION

PET/CT with 68Ga-DOTA-UBI proved to be a useful and appropriate tool for the assessment and diagnosis of patients with clinical suspicion of infection of joints and/or of osteosynthesis material.

#### **CLINICAL RELEVANCE/APPLICATION**

Preclinical studies have shown high diagnostic accuracy of PET/CT using 68Ga-DOTA-UBI for the differentiation between bacterial infection and sterile inflammation.



# MK402-SD-THB1

Correlation of the New MRI Grading System for Cervical Foraminal Stenosis Based on Axial T2-Weighted Images with Severity of Neurological Manifestations

Thursday, Nov. 29 12:45PM - 1:15PM Room: MK Community, Learning Center Station #1

## Participants

Bianca V. Granados Pinedo, MD, Mexico City, Mexico (*Presenter*) Nothing to Disclose Maria F. Ortiz Haro y Nasar, MEd, mexico, Mexico (*Abstract Co-Author*) Nothing to Disclose

### For information about this presentation, contact:

bianca\_granados@hotmail.com

# PURPOSE

To evaluate the clinical correlation of the the new magnetic resonance grading system for cervical foraminal stenosis using a proposed scale for evaluating severity of the neurological signs and symptoms. Currently there is no scale or method that had been capable of correlating severity of foraminal stenosis with severity of symptoms.

### METHOD AND MATERIALS

We examined 102 patients who underwent MR imaging of the cervical spine in the institute. We assessed the severity of foraminal stenosis using the new grading system by Kim et al, the results were correlated with a new proposed scale that included clinical manifestations and neurologic physical examination findings and we asigned 1 point for each positive sign or symptom with a total of 6 points, and classificating patients in severe (4 or more pints) or not severe syptoms ( 3 or less points). Proposed clinical scale: Neurological signs: Electromyography: + (1pt) Spurling test (+): (1pt) Abscence of Deep Tendon Reflexes (1 pt) Clinical symptoms: Pain (1 pt) Hypoalgesia or Paresthesia(1 pt) Upper limb Weakness (1 pt). The MRIs were independently analyzed by two radiologists. Interobserver and intraobserver agreements were analyzed using the percentage agreement and kappa statistics.

# RESULTS

We made analysis of correlation coefficients (Spearman) that showed high correlation (0.8426) between grades of foraminal stenosis using the Kim system and severity of neurological manifestations using the proposed new clinical scale. The percentage of agreement among the two radiologist was of 96.47%, and the kappa values ( $\kappa = 0.940$ ) indicating near perfect agreement.

# CONCLUSION

The Kim system in conjunction with the proposed clinical scale demonstrated high correlation with severity of clinical findings. This is the first time that the severity of neurological manifestations are quantified and we hope to make further studies that validate the proposed clinical scale and its correlation with the MRI findings.

# **CLINICAL RELEVANCE/APPLICATION**

We found that patients that were diagnosed with grade 1 and 2 of foraminal stenosis did not require surgical intervention and that only patients that had grade 3 foraminal stenosis underwent surgery, this finding demonstrated that an adequate evaluation have a great impact in the prognosis of the patients with radiculopathy resultant from foraminal cervical stenosis.



# MK403-SD-THB2

Three-Dimensional Magnetic Resonance Imaging Improved Diagnostic Accuracy for Posterior Ligamentous Complex Disruption Based on an In Vitro Study

Thursday, Nov. 29 12:45PM - 1:15PM Room: MK Community, Learning Center Station #2

### Participants

Xuee Zhu, MD, Nanjing, China (*Presenter*) Nothing to Disclose Jichen Wang, MD, PhD, Nanjing, China (*Abstract Co-Author*) Nothing to Disclose

#### For information about this presentation, contact:

snowy2009@126.com

### PURPOSE

Posterior ligamentous complex (PLC) which composed of supraspinous ligament (SSL), interspinous ligament(ISL), ligamentum flavum(LF), and the facet joint capsules is believed to contribute significantly to the stability of thoracolumbar spine. Previous studies revealed a relatively high false-positive rate for identifying PLC disruption on routine sagittal fat-suppressed T2-weighed MRI (STIR) especially that of ISL if the ligament is surrounded by extensive hemorrhage or edema. This prospective study was conducted to test our hypothesis that three-dimensional MRI can detect ISL tear from the adjacent soft tissue edema and thus improve diagnostic accuracy for ISL disruption.

#### **METHOD AND MATERIALS**

Forty freshly harvested goat spine segments with surrounding soft tissue intact were used in this study. A total of 10ml saline was injected percutaneously at each side of ISL to create a paraspinal edema model. All the segments then underwent sagittal STIR and coronal three-dimensional proton density weighted imaging with fat suppression(3D-PDW-SPIR). After that, ISL was cut under fluoroscopic control using a metal crochet hook and the segments were scanned again in the same way as the prior. Two radiologists independently evaluated the images in a blinded fashion to determine tear of ISL on sagittal and coronal images separately. The imaging interpretations were compared with the intraoperative findings. A comparison of diagnostic accuracy between sagittal STIR and coronal 3D-PDW-SPIR was performed.

#### RESULTS

The interobserver reliability for ISL disruption on sagittal STIR and coronal 3D-PDW-SPIR is 0.705 and 1.000, respectively. The diagnostic sensitivity, specificity and accuracy of sagittal STIR and coronal 3D-PDW-SPIR in detecting ISL disruption was 45.0%, 92.5%, 68.8%, and 100%, 97.5%, 98.8%, respectively. The accuracy of coronal 3D-PDW-SPIR for depicting ISL teat was significantly greater than sagittal STIR (p < 0.05).

# CONCLUSION

This study clarified a much higher diagnostic accuracy of 3D-PDW-SPIR for ISL disruption than sagittal STIR did. In clinical setting, additional 3D-PDW-SPIR to a routine MR protocol is critical for identifying PLC disruption if there is extensive edema around the structure.

### **CLINICAL RELEVANCE/APPLICATION**

Posterior Ligamentous Complex Injuries are related to fracture severity and neurological damage in patients with acute thoracic and lumbar burst fractures. Its status affects the patient's management.



# MK404-SD-THB3

Injury Patterns of Medial Patellofemoral Ligament in Patients with Acute Anterior Cruciate Ligament Tear: Is Associated with the Patellofemoral Osteoarthritis after ACL Reconstruction?

Thursday, Nov. 29 12:45PM - 1:15PM Room: MK Community, Learning Center Station #3

### Participants

Ji Won Seo, MD, Seoul, Korea, Republic Of (*Presenter*) Nothing to Disclose Ja-Young Choi, MD, Seoul, Korea, Republic Of (*Abstract Co-Author*) Nothing to Disclose Bo Ram Kim, MD, Seoul, Korea, Republic Of (*Abstract Co-Author*) Nothing to Disclose Mack Shin, Seoul, Korea, Republic Of (*Abstract Co-Author*) Nothing to Disclose Hye Jin Yoo, MD, Seoul, Korea, Republic Of (*Abstract Co-Author*) Nothing to Disclose Hee-Dong Chae, MD, Seoul, Korea, Republic Of (*Abstract Co-Author*) Nothing to Disclose Sung Hwan Hong, MD, Seoul, Korea, Republic Of (*Abstract Co-Author*) Nothing to Disclose

#### For information about this presentation, contact:

drchoi01@gmail.com

### PURPOSE

We aimed to determine injury patterns of the medial patellofemoral ligament (MPFL) on MRI of the patients with acute anterior cruciate ligament (ACL) tear, and to find MR findings associated with MPFL injury and to determine whether MPFL injury results in the patellofemoral osteoarthritis (OA) after ACL reconstruction.

### **METHOD AND MATERIALS**

We retrospectively reviewed preoperative knee MR images of 122 consecutive patients with ACL injury who had taken MRI in an average of 7 days after trauma and had underwent arthroscopic ACL reconstruction. 42 patients were excluded due to suboptimal image sequences, prior knee fracture or chronicity of ACL tear. This left 80 knees for this study (male: female= 64:16, mean age, 29.6 years). All MR images were independently assessed by two musculoskeletal radiologists for MPFL injury patterns, PCL, MCL, LCL, menisci, vastus medius obliquus (VMO), and bone contusion distribution. 60 knees with minimum 1-year follow-up X-ray (1~9 years) was assessed for progression of patellofemoral OA.

### RESULTS

MPFL injuries were found in 66.3% (53/80 knees; periligamentous edema 32.5%, partial tear 26.3%, and complete tear 7.5%). MPFL injuries were significantly associated with MCL injury (p < 0.0001), VMO strain (p < 0.0001), and bone contusion of lateral femoral condyle (p < 0.01 and 0.022, respectively). Progression of the patellofemoral OA on X-rays at mean follow-up of 3.4 years (1.0~9.6 years) was observed in 41/60 (68.3%) and was significantly associated with grade 3 MCL injury and MM tear (p = 0.027and 0.066, respectively), but not with MPFL injury.

### CONCLUSION

MPFL was frequently injured in patients with acute ACL injury. Mild patellofemoral OA was observed commonly after ACL reconstruction, which may be associated with grade 3 MCL injury and MM tear, but not with MPFL injury.

# **CLINICAL RELEVANCE/APPLICATION**

MPFL injuries can frequently occur in the setting of acute ACL injury, but there has been little information regarding the clinical significance of MPFL injury after ACL reconstruction. We found a relatively high prevalence of the patellofemoral OA change after ACL reconstruction. This change might be not associated with MPFL injury, so MPFL injury do not need to be addressed at the time of surgery.



### MK405-SD-THB4

Hyperintensity of Vertebral Lesions in Relation to the Spinal Cord on T1-Weighted MR images: A Sign to Differentiate Multiple Myeloma from Metastasis

Thursday, Nov. 29 12:45PM - 1:15PM Room: MK Community, Learning Center Station #4

# Participants

Ahmed-Emad Mahfouz, MD, Doha, Qatar (*Presenter*) Nothing to Disclose Hanan Sherif, MD, Doha, Qatar (*Abstract Co-Author*) Nothing to Disclose

For information about this presentation, contact:

mahfouzae@yahoo.com

### PURPOSE

To assess the value of the lesion-to-cord signal intensity (SI) ratio in differentiation of multiple myeloma and metastasis on T1weighted magnetic resonance (MR) images of the spine.

### **METHOD AND MATERIALS**

MR images of 45 patients with well-defined lesions of the spine were retrospectively evaluated including 29 patients with metastases and 16 with multiple myeloma. Signal intensity of the lesion and the spinal cord were measured on sagittal T1-weighted images. The ratio of the signal intensity of the lesion to the spinal cord was compared in the two groups. Statistical analysis has been performed by the Student's T test.

# RESULTS

On T1-weighted images, the lesion-to-cord SI ratio has been  $1.31\pm0.38$  for multiple myeloma and  $0.87\pm0.58$  for metastases. The difference between multiple myeloma and metastases has been statistically significant (p=0.01). The highest accuracy of the hyperintensity sign for the diagnosis of multiple myeloma has been 84.4% at a cut-off value of lesion-to-cord SI ratio >1 (i.e. lesion is hyperintense to the spinal cord) on T1-weighted images.

# CONCLUSION

Unlike metastasis, multiple myeloma tends to be hyperintense in comparison to the spinal cord on T1-weighted images. The accuracy of the hyperintensity sign for diagnosis of multiple myeloma is 84.4%.

### **CLINICAL RELEVANCE/APPLICATION**

Assessment of the focal lesions in relation to the spinal cord offers a robust reference of signal intensity unlike the confounding signal intensity of the vertebral body surrounding the lesion. The sign of hyperintensity of the lesion in relation to the spinal cord makes it possible to differentiate multiple myeloma from metastases with 84.4% accuracy.



# MK407-SD-THB6

Ultrasound-Guided Percutaneous Needle Tenotomy Using Tenex Technique for Lateral Epicondylitis: Effectiveness and Contributing Factors

Thursday, Nov. 29 12:45PM - 1:15PM Room: MK Community, Learning Center Station #6

# Participants

Majid Chalian, MD, Cleveland Heights, OH (*Presenter*) Nothing to Disclose Nicholas C. Nacey, MD, Charlottesville, VA (*Abstract Co-Author*) Nothing to Disclose Jennifer Pierce, MD, Charlottesville, VA (*Abstract Co-Author*) Nothing to Disclose

#### For information about this presentation, contact:

m.chalian@gmail.com

# PURPOSE

Lateral epicondylitis (LE) is a common area of tendon degeneration. Most will respond to conservative treatments; however, some individuals require open surgical tenotomy. Ultrasound-guided percutaneous needle tenotomy (USPNT) has been used as an alternative treatment to surgery with shorter recovery time and lower cost. This investigation evaluates the effectiveness of USPNT using Tenex technique for refractory LE. We will also evaluate possible cofactors, which may contribute in treatment response.

#### **METHOD AND MATERIALS**

PRTEE (Patient-Rated Tennis Elbow Evaluation) and DASH (Disabilities of the Arm, Shoulder, Hand) questionnaires were completed before USPNT for all consecutive patients (n=72) over 38 months (Feb 2015-Mar 2018) using Tenex (Tenex Health Inc, CA, USA). Patients were contacted for follow-up evaluations. Paired t-test was used to evaluate changes in treatment response (p<0.05). Univariate linear regression model analysis was used to evaluate bivariate correlation of treatment response and possible confounding factors. Variables with any correlation with treatment response (p<0.1) were evaluated with stepwise multivariate regression analysis.

# RESULTS

35 patients were not included due to lack of follow-up information (n=29), surgery before follow-up (n=4) or recent (<2-month) USPNT (n=2). 37 patients (age: 51+/-9 year, M/F: 15/22) with refractory LE were included (mean follow-up: 531 days, range: 65-1148 days). Tenex USPNT significantly decreased PRTEE (pain and function) and DASH scores (p<0.001). All score changes had significant correlation with post-procedure physical therapy (PT) (R2, B, and p values of 0.18, 13.05, <0.01 for PRTEE pain score, 0.21, 13.08, <0.01 for PRTEE function score, and 0.20, 28.94, <0.01 for DASH score, respectively). Age, gender, cutting time, severity of tendinopathy, and time of follow-up did not show correlation with treatment response (p >0.05).

### CONCLUSION

USPNT significantly improves pain and function in individuals with LE even with long term follow up. While PT with Tenex has significant impact in improvement, cutting time and severity of tendinopathy has no significant correlation with treatment response.

### **CLINICAL RELEVANCE/APPLICATION**

USPNT is an effective alternative to open surgical intervention for LE. Post-procedure PT contributes to this improvement response.



# NM150-ED-THB6

# Theranostic Imaging of Prostate Cancers: 68Ga PSMA PET/CT / 177Lu PSMA Radionuclide Therapy

Thursday, Nov. 29 12:45PM - 1:15PM Room: NM Community, Learning Center Station #6

**FDA** Discussions may include off-label uses.

#### **Participants**

Yasemin Sanli, Dallas, TX (*Abstract Co-Author*) Nothing to Disclose Duygu Simsek, MD, Istanbul, Turkey (*Presenter*) Nothing to Disclose Serkan Kuyumcu, MD, Istanbul, Turkey (*Abstract Co-Author*) Nothing to Disclose Cuneyt Turkmen, MD, Istanbul, Turkey (*Abstract Co-Author*) Nothing to Disclose Rathan M. Subramaniam, MD,PhD, Dallas, TX (*Abstract Co-Author*) Consultant, Blue Earth Diagnostics Ltd; Speaker, Blue Earth Diagnostics Ltd

#### For information about this presentation, contact:

### dr.duyguhas@hotmail.com

#### **TEACHING POINTS**

Prostat cancer (PC) is one of the most prevalent cancers worldwide. Although most of the patients have localized disease at diagnosis, distant metastasis can occur 35% of PC cases during the follow up. 68Ga PSMA PET/CT is a powerful imaging method for the imaging of PC, using prostate specific membrane antigen (PSMA), a transmembranous enzyme which significantly overexpressed in the majority of PC. 68Ga PSMA PET/CT has remarkable results in detecting PC compared to other PET radiotracers. 68Ga PSMA PET/CT has the potential to influence the management of patients with PC and help patient selection for 177Lu PSMA, an important therapy option with superior response rates for metastatic castration resistant prostate cancer comparing other systemic therapies

# TABLE OF CONTENTS/OUTLINE

Value of 68Ga PSMA PET/CT imaging; - in staging intermediate or high-risk PC - in biochemically recurrent PC - in therapy response of PC - in 177Lu PSMA therapy planning Physician Learning: Illustrative cases to demonstrate physiological distribution, artifacts and pitfalls in 68Ga PSMA imaging. NonPC tumors with 68Ga PSMA imaging. 177Lu PSMA therapy implementation for PC. Future:Combination of 68Ga PSMA PET/MRI with functional MRI sequences can provide additional information by excellent anatomical resolution of suspicious lesions and be used for targeted biopsy.



# NM241-SD-THB1

The Iodine/FDG "Flip-Flop" Phenomenon is Ambiguous in Bone Metastasis from Thyroid Cancer: Significant FDG Uptake is Observed Even in Iodine-Positive Lesions

Thursday, Nov. 29 12:45PM - 1:15PM Room: NM Community, Learning Center Station #1

# Participants

Takuro Isoda, Fukuoka, Japan (*Abstract Co-Author*) Nothing to Disclose Shingo Baba, Fukuoka, Japan (*Presenter*) Nothing to Disclose Yoshiyuki Kitamura, Fukuoka, Japan (*Abstract Co-Author*) Nothing to Disclose Ryo Somehara, Fukuoka, Japan (*Abstract Co-Author*) Nothing to Disclose Keiichiro Tahara, Fukuoka, Japan (*Abstract Co-Author*) Nothing to Disclose Masayuki Sasaki, Fukuoka, Japan (*Abstract Co-Author*) Nothing to Disclose Hiroshi Honda, MD, Fukuoka, Japan (*Abstract Co-Author*) Nothing to Disclose

### PURPOSE

Radioiodine therapy is used to treat distant metastases from thyroid cancer. A reverse relationship between iodine and FDG accumulation is found in thyroid cancer lesions, the so-called "flip-flop" phenomenon. The aim of this study was to assess the relationship between iodine and FDG uptake in bone metastasis lesions from thyroid cancer.

### **METHOD AND MATERIALS**

The cases of 20 patients who underwent radioiodine therapy for bone metastasis were studied retrospectively (age, 27-74 yrs; median, 62 yrs; males : females, 6 : 14). Iodine uptake was evaluated visually and the lesions showing iodine uptake more than background were determined as positive. FDG uptake was assessed using SUVmax. We compared FDG uptake between the lesions with (n=19) and without (n=88) iodine uptake in bone metastasis.

### RESULTS

The bone metastasis lesions without iodine showed significantly higher FDG uptake than those with iodine uptake (p < 0.0001). However, the degree of FDG uptake in bone metastasis lesions was also relatively high (Median of SUVmax: 4.64). Thirty-nine out of 88 iodine-positive bone metastasis lesions (44.3 %) showed more than 5 of SUVmax. On the other hand, only one iodine-positive lesion (1.1 %) showed more than 10 of SUVmax, while 9 out of 19 (47.4 %) iodine-negative lesions did.:

# CONCLUSION

Bone metastasis lesion from thyroid cancer not showing iodine uptake showed higher FDG uptake compared to those with iodine uptake. However, more than 40 % of bone metastasis lesions with iodine uptake showed relatively high FDG uptake (SUVmax > 5).

# **CLINICAL RELEVANCE/APPLICATION**

The result of this study suggests that the patients with bone metastasis from thyroid cancer have chance to receive benefits from radioiodine therapy even when their bone metastasis lesions are FDG-avid and that it is recommended to perform radioiodine therapy whether or not bone metastasis lesions show FDG uptake.



### NM242-SD-THB2

### Size of Detectable Melanoma Metastases to Brain

Thursday, Nov. 29 12:45PM - 1:15PM Room: NM Community, Learning Center Station #2

### **Participants**

Jorge D. Oldan, MD, Cleveland, OH (*Presenter*) Nothing to Disclose Valerie L. Jewells, DO, Chapel Hill, NC (*Abstract Co-Author*) Nothing to Disclose Amir H. Khandani, MD, Chapel Hill, NC (*Abstract Co-Author*) Consultant, Progenics Pharmaceuticals, Inc; Consultant, F. Hoffmann-La Roche Ltd;

### For information about this presentation, contact:

jorge\_oldan@med.unc.edu

### PURPOSE

The decreased sensitivity of FDG-PET for metastases to the brain, due to high physiologic background uptake, is well documented. We aimed to determine the size at which melanoma metastases become reliably visible on PET. (Melanoma was selected as it is one of the few malignancies for which vertex-to-toe imaging is commonly done and which frequently metastasizes to brain.)

# METHOD AND MATERIALS

A retrospective search over a period of 64 months was performed to identify whole-body PET/CT (including bed position of the cranium with a low-dose head CT) with at least one brain MRI within 1 month of the study. 294 cases were identified and the PET and MRI re-examined by a nuclear medicine physician and neuroradiologist, each blinded to history and the other examination. Results were compared.

### RESULTS

Despite the generally reputed low sensitivity of PET for intracranial metastases, a fair number of tumors were found even on a PET protocol not optimized for brain imaging. Sensitivity was 100% over 3.0 cm, 67% for tumors 2.0-2.9 cm, 42% for tumors 1.0-1.9 cm, and 5% for tumors below 1 cm. Specificity was 96%, likely due to the low prevalence. Tumors in locations such as the pituitary where they were not surrounded by intensely avid brain were detected when they were present. Sensitivities are somewhat higher for hot than cold lesions.

# CONCLUSION

PET has at least partial sensitivity for brain tumors in the 1-3 cm range even without a dedicated protocol. If there is serious concern for smaller brain metastases, a brain MRI should of course be performed, but a whole-body PET/CT protocol for melanoma should at least include the brain.

### **CLINICAL RELEVANCE/APPLICATION**

PET can detect at least some brain metastases from melanoma in the 1-3 cm range. Whole-body melanoma studies should include the cranium and be correlated with MRI of the brain for optimal detection of metastases.



### NM243-SD-THB3

Evaluating the Role of 18F-FDG PET/CT in Diabetic Foot

Thursday, Nov. 29 12:45PM - 1:15PM Room: NM Community, Learning Center Station #3

# Participants

Sikandar M. Shaikh, DMRD, Hyderabad, India (Presenter) Nothing to Disclose

For information about this presentation, contact:

idrsikandar@gmail.com

#### PURPOSE

Diabetes is one of the important and commonest disease entity in Indain subcontinent Infections superadded with diabetic foot is one of the commonest pathological entity .Osteomyelitis represents upto third of diabetic foot infections, is often due to direct contamination from a soft-tissue lesion, and represents a clinical challenge. Early diagnosis is important since antibiotic therapy can be curative and may prevent amputation. The present study assessed the role of PET/CT using 18F-FDG for the diagnosis of diabetic foot osteomyelitis.

### **METHOD AND MATERIALS**

Twenty four diabetic patients (14 men and 10 women; age range, 29-70 y) with 28 clinically suspected sites of infection underwent whole body and lower limb protocol PET/CT after the injection of 185-370 MBq of 18F-FDG for suspected osteomyelitis complicating diabetic foot disease. PET, CT, and fused images were independently evaluated for the diagnosis and localization of an infectious process. Additional data provided by PET/CT for localization of infection in the bone or soft tissues were documented. The final diagnosis was based on histopathologic findings and bacteriologic/culture assays obtained at surgery or at clinical and imaging follow-up.

#### RESULTS

PET detected 28foci of increased 18F-FDG uptake suspected as infection in 20 patients. PET/CT correctly localized 16 foci in 8 patients to bone, indicating osteomyelitis. PET/CT correctly excluded osteomyelitis in 10 foci in 10 patients, with the abnormal 18F-FDG uptake limited to infected soft tissues only. One site of mildly increased focal 18F-FDG uptake was localized by PET/CT to diabetic osteoarthropathy changes demonstrated on CT. Eight patients showed no abnormally increased 18F-FDG uptake and no further evidence of an infectious process on clinical and imaging follow-up.

#### CONCLUSION

Thus 18F-FDG PET can be used for diagnosis of diabetes-related infection. The precise anatomic localization of increased 18F-FDG uptake provided by PET/CT enables accurate differentiation between osteomyelitis and soft-tissue infection.

### **CLINICAL RELEVANCE/APPLICATION**

Thus FDG PET-CT is evolving as better modality for evaluation of Diabetis



## NM244-SD-THB4

Comparison of TNM Stage Evaluation Capability among Whole-Body MRI at 1.5T and 3T MR Systems, PET/MRI at 1.5T and 3T MR Systems and PET/CT in Non-small Cell Lung Cancer Patients

Thursday, Nov. 29 12:45PM - 1:15PM Room: NM Community, Learning Center Station #4

### Participants

Yoshiharu Ohno, MD, PhD, Kobe, Japan (*Presenter*) Research Grant, Canon Medical Systems Corporation; Research Grant, Koninklijke Philips NV; Research Grant, Bayer AG; Research Grant, DAIICHI SANKYO Group; Research Grant, Fuji Pharma Co, Ltd; Research Grant, Guerbet SA;

Yuji Kishida, MD,PhD, Kobe, Japan (*Abstract Co-Author*) Nothing to Disclose Shinichiro Seki, Kobe, Japan (*Abstract Co-Author*) Research Grant, Canon Medical Systems Corporation Takeshi Yoshikawa, MD, Kobe, Japan (*Abstract Co-Author*) Research Grant, Canon Medical Systems Corporation Kota Aoyagi, Otawara, Japan (*Abstract Co-Author*) Employee, Canon Medical Systems Corporation Masao Yui, Otawara, Japan (*Abstract Co-Author*) Employee, Canon Medical Systems Corporation Hisanobu Koyama, MD,PhD, Osaka, Japan (*Abstract Co-Author*) Nothing to Disclose Takamichi Murakami, MD, PhD, Osakasayama, Japan (*Abstract Co-Author*) Nothing to Disclose

#### For information about this presentation, contact:

yosirad@kobe-u.ac.jp

#### PURPOSE

To prospectively and directly compare TNM stage classification capability among whole-body MRI and PET/MRI at 1.5 and 3T MR systems and PET/CT in non-small cell lung cancer patients.

#### **METHOD AND MATERIALS**

104 consecutive pathologically diagnosed NSCLC patients (62 men, 42 women; mean age 71 years) prospectively underwent wholebody MRI at1.5T and 3T systems, integrated PET/CT, and surgical, pathological and/ or follow-up examinations. Final diagnoses of T, N and M factors and clinical stage in each patient were determined according to all examination results. All co-registered PET/MRIs were generated by means of our proprietary software. Then, each factor and clinical stage were visually assessed on both whole-body MRIs, PET/MRIs and PET/CT with contrast-enhanced brain MRI. Kappa statistics were used to determine agreements for assessment of all factors and clinical stage with final diagnoses, and McNemar's test was used to compare each diagnostic accuracy among all methods.

#### RESULTS

On T factor assessment, agreement between each method and final diagnosis was almost perfect (0.92 < < 0.98). For N factor evaluation, agreement of each method and final diagnosis was substantial (0.60 < < 0.80). On M factor and clinical stage assessments, agreements of all methods were substantial or almost perfect (0.71 < < 0.88). Diagnostic accuracies of N factor on whole-body MRI at 1.5T (83.7 [87/104] %, p=0.02) and 3T (86.5 [90/104] %, p=0.002) systems as well as PET/MRI at 1.5T (82.7 [86/104] %, p=0.03) and 3T (84.6 [88/104] %, p=0.008) systems were significantly higher than that of PET/CT (76.9 [80/104] %). In addition, diagnostic accuracy of clinical stage on whole-body MRI at 1.5T (83.7 [87/104] %, p=0.008) and 3T (88.5 [92/104] %), p=0.0002) systems as well as PET/MRI at 1.5T (83.7 [87/104] %, p=0.008) and 3T (86.5 [90/104] %, p=0.008) and 3T (88.5 [92/104] %), p=0.0002) systems as well as PET/MRI at 1.5T (83.7 [87/104] %, p=0.008) and 3T (86.5 [90/104] %), p=0.001) systems were significantly higher than that of PET/CT (76.0 [79/104] %).

# CONCLUSION

Whole-body MRIs and PET/MRIs at 1.5T and 3T systems have significantly better potential for N factor and clinical stage assessments than PET/CT in NSCLC patients.

#### **CLINICAL RELEVANCE/APPLICATION**

Whole-body MRIs and PET/MRIs at 1.5T and 3T systems have significantly better potential for N factor and clinical stage assessments than PET/CT in NSCLC patients.



### NM245-SD-THB5

Hyperintense Rim Sign on MRI STIR as a Diagnostic Correlate of Dermal Backflow on Lymphoscintigraphy in Patients with Upper Extremity Lymphedema

Thursday, Nov. 29 12:45PM - 1:15PM Room: NM Community, Learning Center Station #5

#### Awards Student Travel Stipend Award

### Participants

Geunwon Kim, MD,PhD, Boston, MA (*Presenter*) Nothing to Disclose Martin P. Smith, MD, Newton, MA (*Abstract Co-Author*) Research Grant, Bracco Group Research Grant, Bayer AG Consultant, Bayer AG Research Consultant, General Electric Company Kevin J. Donohoe, MD, Boston, MA (*Abstract Co-Author*) Nothing to Disclose Dhruv Singhal, MD, Boston, MA (*Abstract Co-Author*) Nothing to Disclose Leo L. Tsai, MD, PhD, Boston, MA (*Abstract Co-Author*) Co-founder, Agile Devices Inc Stockholder, Agile Devices Inc Research Consultant, Agile Devices Inc

### For information about this presentation, contact:

gkim6@bidmc.harvard.edu

### PURPOSE

Accurate diagnostic imaging of lymphedema remains challenging. Here we aim to identify MRI correlates of dermal backflow, a finding seen on lymphoscintigraphy that serves as a specific diagnostic indicator for lymphedema.

# METHOD AND MATERIALS

21 patients referred from lymphedema clinic underwent nuclear lymphoscintigraphy and upper extremity MRI between March and October 2017. Both upper extremities were imaged in two stations. STIR sequence was performed at both stations. Lymphoscintigraphy is performed within 24 hours of MRI and all other clinical measures. Two intradermal Tc-99m labelled tilmanocept injections proximal to second and third webspaces are administered, with a total dose of ~0.4 mCi. Large field of view detector with parallel collimators was used at 140 KeV with a 20% window. Cobalt-57 is used as a flood source. Flow images are taken at 30 s/frame for 20 min. The presence of dermal back flow and lymphatic flow are assessed on the static images of the extremities at 1 hour and a minimum delay of 2 hours and up to 6 hours, along with transmission images for localization. MRI images were analyzed using McKesson PACS and lymphoscintigraphy using MIM Software. Agreement between MRI findings and lymphoscintigraphy was analyzed using positive and negative percentage agreement with 95% confidence interval.

#### RESULTS

Imaging studies were retrospectively reviewed. A thin rim of hyperintensity along the peripheral subcutaneous layer on STIR images was noted in 12 out of 14 patients that demonstrated dermal backflow on lymphoscintigraphy, with matching distributions. The other 2 patients showed hyperintense rim sign extending beyond the area seen on lymphoscintigraphy. 1 patient showed hyperintense rim sign on STIR with no dermal backflow on lymphoscintigraphy. Overall, the distribution of edema was mostly in posterior aspect of the upper and ulnar side of the lower arm centered around the elbow, and circumferential if severe. No STIR hyperintensity was seen in any of the 21 contralateral normal limbs or in the six affected limbs that did not demonstrate dermal backflow on lymphscintigraphy. Positive and negative percent agreement were 80.0% [51.3%, 94.7%] and 100% [84.5%, 100%], respectively.

### CONCLUSION

Hyperdense rim is an MRI correlate for dermal backflow which is a lymphoscintigraphy finding.

# CLINICAL RELEVANCE/APPLICATION

MRI is can detect dermal backflow and would provide anatomic detail to the lymphoscintigraphic finding.



### NR355-ED-THB10

The Hitchhiker's Guide to Idiopathic Normal Pressure Hydrocephalus: What the Radiologist Needs to Know

Thursday, Nov. 29 12:45PM - 1:15PM Room: NR Community, Learning Center Station #10

### Awards Magna Cum Laude

### Participants

Yung-Chieh Chen, MD, PhD, Taipei, Taiwan (*Presenter*) Nothing to Disclose Ping-Huei Tsai, MD, PhD, Taipei, Taiwan (*Abstract Co-Author*) Nothing to Disclose Chia-Feng Lu, PhD, Taipei, Taiwan (*Abstract Co-Author*) Nothing to Disclose Shih-Wei Chiang, BS, MS, Taipei, Taiwan (*Abstract Co-Author*) Nothing to Disclose Cheng-Yu Chen, MD, Taipei, Taiwan (*Abstract Co-Author*) Nothing to Disclose

#### **TEACHING POINTS**

The purpose of this exhibit is: 1.To review the history and pathophysiology of idiopathic normal pressure hydrocephalus (iNPH) 2.To summarize the typical MR imaging features of iNPH together with clinical perspective, and differentiate iNPH from other common neurological conditions among the elderly. 3. To become familiarized with international iNPH guidelines and gain awareness of its prevalence and diagnosis. 4. To illustrate the clinical applications of advanced diffusion MR imaging in iNPH

# TABLE OF CONTENTS/OUTLINE

Introduction History of iNPH Pathophysiology of iNPH - The Monro-Kellie doctrine - Overview of known concepts Review of imaging features - Conventional MRI - Phase contrast MRI - Perfusion MRI - Diffusion MRI Differential pearls of iNPH - Alzheimer's disease - Frontotemporal dementia - Lewy body dementia - Parkinson's disease - Vascular dementia International guidelines of iNPH - The American (AAN) guideline - The European (ENFS) guideline - The Japanese guideline Clinical applications of advanced diffusion MR imaging in iNPH - Application in the assessment of gait function - Application in the assessment of dementia - Application in the assessment of urinary incontinence Summary References



## NR359-ED-THB7

# Sialadenitis and Salivary Gland Anatomy

Thursday, Nov. 29 12:45PM - 1:15PM Room: NR Community, Learning Center Station #7

#### **Participants**

Brett R. Larsen, MD, Phoenix, AZ (Presenter) Nothing to Disclose Cody R. Larson, MD, Phoenix, AZ (Abstract Co-Author) Nothing to Disclose Dan G. Gridley, MD, Phoenix, AZ (Abstract Co-Author) Nothing to Disclose

### **TEACHING POINTS**

1. Sialadenitis is an inflammatory process involving the salivary glands. Recognition of its appearance and complications is essential for accurate diagnosis. 2. Knowledge of the normal and variant salivary gland anatomy, along with ductal anatomy, will help with accurate reporting of salivary gland diseases and other pathology occurring in shared spaces.3. Understanding strengths and weaknesses of various imaging modalities for salivary gland pathology will help radiologists guide clinicians in accurate diagnosis.

# **TABLE OF CONTENTS/OUTLINE**

Normal and Variant Anatomy-Parotid gland-Submandibular Gland-Sublingual GlandSalivary Gland Imaging Modalities-Computed Tomography -Magnetic Resonance Imaging-Ultrasonography -Conventional SialographySialadenitis Pathology-Acute-Chronic-Nonobstructive-Obstructive



### NR360-ED-THB8

**Cranial Nerve Enhancement - The VICTIM of Range Group of Diseases** 

Thursday, Nov. 29 12:45PM - 1:15PM Room: NR Community, Learning Center Station #8

#### **Participants**

Raphael M. Reali, MD, Sao Paulo, Brazil (*Presenter*) Nothing to Disclose Felipe F. Junho, MD,MD, Sao Sebastiao da Bela Vista, Brazil (*Abstract Co-Author*) Nothing to Disclose Pedro Henrique P. Rocha, MBBS, Sao Paulo, Brazil (*Abstract Co-Author*) Nothing to Disclose Felipe T. Pacheco, MD, Sao Paulo, Brazil (*Abstract Co-Author*) Nothing to Disclose Rene L. Rivero, MD, PhD, Sao Paulo, Brazil (*Abstract Co-Author*) Nothing to Disclose Thiago P. Ribeiro, Sao Paulo, Brazil (*Abstract Co-Author*) Nothing to Disclose Renato A. Mendonca, MD, PhD, Sao Paulo, Brazil (*Abstract Co-Author*) Nothing to Disclose Renato Hoffmann Nunes, MD, Sao Paulo, Brazil (*Abstract Co-Author*) Nothing to Disclose Antonio J. da Rocha, MD, PhD, Sao Paulo, Brazil (*Abstract Co-Author*) Nothing to Disclose

#### For information about this presentation, contact:

rmreali@gmail.com

#### **TEACHING POINTS**

The purpose of this exhibit is: 1. Using case material from our service to illustrate causes of cranial nerve enhancement 2. To review magnetic resonance imaging aspects of the cranial nerve enhancement in a wide range of differential diagnosis 3. To learn a mnemonic to make easier remember the major pathological processes that can cause cranial nerve enhancement

#### **TABLE OF CONTENTS/OUTLINE**

Review of the cranial nerve microanatomy.Pathophysiology of cranial nerve enhancement.Review the wide range of possible differential diagnosis with the sample cases from our service.Create a mnemonic to make easier remember the major pathological processes that can cause cranial nerve enhancement - VICTIM : Vascular, Infectious, Congenital, Tumour, Inflammatory demyelinating, Metabolic diseases.



# NR361-ED-THB9

Acute Ischemic Stroke Imaging and Management: A Current Review

Thursday, Nov. 29 12:45PM - 1:15PM Room: NR Community, Learning Center Station #9

#### **Participants**

James Murchison, MD, Temple, TX (*Presenter*) Nothing to Disclose Scott Le, DO, Temple, TX (*Abstract Co-Author*) Nothing to Disclose Walter S. Lesley, MD,MBA, Temple, TX (*Abstract Co-Author*) Nothing to Disclose Jennifer Rasmussen, Temple, TX (*Abstract Co-Author*) Nothing to Disclose Harold L. Sonnier, MD, Temple, TX (*Abstract Co-Author*) Nothing to Disclose

### For information about this presentation, contact:

james.murchison@bswhealth.org

#### **TEACHING POINTS**

1. Review of CT and MR imaging for patients with acute ischemic stroke 2. Review of recent changes to AHA/ASA acute ischemic stroke guidelines 3. Review of recent updates regarding thrombectomy from findings of the DAWN and DEFUSE 3 trials 4. Review of perfusion CT and MR imaging 5. Review of multiphase CT angiography and comparison with perfusion imaging

# TABLE OF CONTENTS/OUTLINE

I. Acute Ischemic Stroke Imaging and Management: A Current Review II. Overview III. CT/MR Findings of Acute Ischemic Stroke IV. Cerebral Vascular Territories V. CT/MR Findings that Contraindicate Thrombolysis/Thrombectomy VI. ASPECTS Score VII. AHA/ASA Acute Ischemic Stroke 2018 Guideline Imaging Updates VIII. DAWN Trial IX. DEFUSE 3 Trial X. CT/MR Perfusion Imaging Findings in Acute Ischemic Stroke XI. Multiphase CTA in Acute Ischemic Stroke XII. Comparison of Multiphase CTA and CT/MR Perfusion Imaging



### NR432-SD-THB1

Prediction of High Amyloid Deposition in Non-Demented Elderly Subjects Using a Marketed Volumetric Software Tool

Thursday, Nov. 29 12:45PM - 1:15PM Room: NR Community, Learning Center Station #1

# Participants

Koung Mi Kang, MD, Seoul, Korea, Republic Of (*Presenter*) Nothing to Disclose Chul-Ho Sohn, MD, Seoul, Korea, Republic Of (*Abstract Co-Author*) Nothing to Disclose Min Soo Byun, Seoul, Korea, Republic Of (*Abstract Co-Author*) Nothing to Disclose Roh-Eul Yoo, MD, Seoul, Korea, Republic Of (*Abstract Co-Author*) Nothing to Disclose Tae Jin Yun, MD, Seoul, Korea, Republic Of (*Abstract Co-Author*) Nothing to Disclose Seung Hong Choi, MD, PhD, Seoul, Korea, Republic Of (*Abstract Co-Author*) Nothing to Disclose Ji-hoon Kim, MD,PhD, Seoul, Korea, Republic Of (*Abstract Co-Author*) Nothing to Disclose Jun Ho Lee, Seoul, Korea, Republic Of (*Abstract Co-Author*) Nothing to Disclose Dahyun Yi, Seoul, Korea, Republic Of (*Abstract Co-Author*) Nothing to Disclose Dong Young Lee, Seoul, Korea, Republic Of (*Abstract Co-Author*) Nothing to Disclose

# For information about this presentation, contact:

we3001@gmail.com

#### PURPOSE

Recently introduced marked volumetric software, NeuroQuant has enabled fully-automated and rapid measurement of segmental brain volumes for use in clinical settings. Our aim was to assess the predictive efficacy of regional volumetrics in a commercially available brain volumetric software package for the presence of high amyloid reposition in non-demented elderly subjects.

### METHOD AND MATERIALS

This study included a total of 412 non-demented subjects (130 mild cognitive impairment, 282 cognitively normal elderly) who participated in the Korean Brain Aging Study of Early Diagnosis and Prediction of Alzheimer's disease (KBASE), an ongoing prospective cohort. All participants underwent comprehensive clinical assessment as well as 11C-labelled Pittsburgh Compound B (PiB) positron emission tomography (PET)/magnetic resonance imaging (MRI) scans including 3D fast spoiled gradient recalled-echo sequence. Volumetric analysis was performed with NeuroQuant and with FreeSurfer. To evaluate the diagnostic performance of the volumetric results adjusting for age and sex, binary logistic regression model and ROC analysis were performed.

#### RESULTS

Intermethod reliability between NeuroQuant and FreeSurfer measures showed excellent for the 14 regions evaluated (intraclass correlation coefficient [ICC]=0.844-0.979) except for the pallidum (ICC=0.140). Non-demented subjects were divided into 98 subjects with high amyloid deposition and 314 subjects without. Decreasing hippocampal volume was associated with an increased likelihood of high amyloid deposition (P < 0.0001). The hippocampal volume helped to predict high amyloid deposition in non-demented elderly subjects with a sensitivity of 62.2% and specificity of 77.1% at a cutoff value of 0.63 cm3.

#### CONCLUSION

The automated volumetric assessment can be used to predict high amyloid deposition in non-demented elderly subjects.

#### **CLINICAL RELEVANCE/APPLICATION**

In daily clinical practice, NeuroQuant may be helpful in predicting high amyloid deposition in non-demented elderly subjects.



# NR433-SD-THB2

### Evaluation of Verbal Memory in Low-Grade Glioma Patients with F-MRI N-Back Paradigm

Thursday, Nov. 29 12:45PM - 1:15PM Room: NR Community, Learning Center Station #2

#### Participants

Marta Drake Perez, MD, Santander, Spain (*Presenter*) Nothing to Disclose Enrique Marco de Lucas, Santander, Spain (*Abstract Co-Author*) Nothing to Disclose Elsa Gomez, Santander, Spain (*Abstract Co-Author*) Nothing to Disclose Diana Tordesillas-Gutierrez, Santander, Spain (*Abstract Co-Author*) Nothing to Disclose Javier Vazquez-Bourgon, Santander, Spain (*Abstract Co-Author*) Nothing to Disclose Juan Martino, Santander, Spain (*Abstract Co-Author*) Nothing to Disclose Elena Marin-Diez, MD, Santander, Spain (*Abstract Co-Author*) Nothing to Disclose

#### For information about this presentation, contact:

radmle@humv.es

#### PURPOSE

To evaluate if f-MRI with a n-back paradigm is able to demonstrate eloquent areas in verbal memory work. To analyze the relationship of these findings with intraoperative identification of verbal memory sites with intracortical stimulation mapping in diffuse gliomas in eloquent areas and if this identification can protect patients from long-term postoperative decline in short-term memory.

#### **METHOD AND MATERIALS**

A cohort of 23 subjects with diffuse low-grade were studied with fMRI with a 2n-back paradigm in order to evaluate working memory. Memory activation was substracted from activation in verbal fluency and tongue-movements paradigms. Subsequently, all these patients were operated with IES and intraoperative evaluation of language and verbal memory. Detailed neuropsychological assessment was performed before and 6 mo after surgery. We compared the location of the MR & intraopeative activation sites.

### RESULTS

fMRI n-back paradigm was able to be performed accurately by 15 from 23 patients. This paradigm produce an intense and diffuse activation in language and motor areas and in specialized working-memory areas including premotor cortex. In these cases, fMRI was very sensitive and activation in the premotor cortex of all the patients was observed. In 4 patients with the tumor close to this area this activation as also concordant with the positive result in IES. Memory evaluation including fMRI and intraoperative memory mapping was a predictor of verbal memory prognosis (memory defecits were observed in 27% in these series vs. our previous series 73%).

#### CONCLUSION

Verbal memory areas can be identified with n-back fMRI with adecquate correlation with intraoperative electrical stimulation in order to reduce a possible memory impairment by adapting the resection to avoid those memory areas.

#### **CLINICAL RELEVANCE/APPLICATION**

fMRI (n-back paradigm) can demostrate eloquent areas of cerebral cortex in the evaluation of working memory and might be included as part of a MR study prior to low-grade glioma removal.



# NR434-SD-THB3

Progressive White Matter Changes in Corticospinal Tracts in Different Clinical Stages of Patients with Amyotrophic Lateral Sclerosis

Thursday, Nov. 29 12:45PM - 1:15PM Room: NR Community, Learning Center Station #3

# Participants

Li Haining, Xian, China (*Presenter*) Nothing to Disclose Qiuli Zhang, Xian, China (*Abstract Co-Author*) Nothing to Disclose Qianqian Duan, Xian, China (*Abstract Co-Author*) Nothing to Disclose Ming Zhang, Xian, China (*Abstract Co-Author*) Nothing to Disclose

#### For information about this presentation, contact:

li9717@126.com

# PURPOSE

The King's clinical staging of ALS patients has been suggested as a potential biomarker that could be used to monitor diseasemodifying effects, whereas the relationship between King's clinical stages and Corticospinal tract (CST) degeneration has not yet been clarified. Therefore, we aimed to explore the pattern of CST degeneration in different stages of ALS patients and investigate the value of CST degeneration in differentiating ALS patients and healthy controls.

#### **METHOD AND MATERIALS**

Fifty-seven ALS patients and 32 healthy controls were enrolled in this study. Multislice diffusion-weighted images of the brain were acquired using a 3T scanner. Preprocessing and fiber tracking were performed with FSL. The average fractional anisotropy (FA) and mean diffusivity (MD) for whole tracts were obtained for two tracts of interest: right and left CST. Non-parametric permutation test and inference were performed by using threshold-free cluster enhancement with a correction for multiple comparisons and family-wise error (p < 0.05, FWE-corrected).The discriminating value of FA in the CST between patients and controls was explored with a receiver operator characteristic curve.

#### RESULTS

FA of ALS patients in stage 1 was significantly lower compared with controls in right posterior limb of the internal capsule .While decreased bilateral FA in posterior limb of the internal capsule and the subcortical white matter were found in patients at stage 2 and 3 . Furthermore decreased bilateral FA in the cerebral peduncle were found in patients at stage 3. The correlation analyses revealed significant positive relationship between bulbar subscores and ALSFRS-R with FA. The area under the curve (AUC) values were 0.801. The optimal cutoff value was 0.5818 with a specificity of 70% and a sensitivity of 81%.

# CONCLUSION

The King's clinical staging of ALS patients were consistent with the pattern of CST degeneration, with progressive and widespread CST involvement along with more severe clinical syndrome. It's important to validate the milestone in the CST degeneration between different clinical stages that may highlight the turning points in clinical progression

### **CLINICAL RELEVANCE/APPLICATION**

Diffusion tensor MRI has the potential to evaluate disease progression of ALS and highlighted the importance of incorporating assessment of brain white-matter changes to King's clinical staging system for promising clinical management.



# NR435-SD-THB4

# Multimodality Sound Touch Elastography May Add a New Method to Ultrasound Evaluation of Thyroid cancer

Thursday, Nov. 29 12:45PM - 1:15PM Room: NR Community, Learning Center Station #4

#### Participants

Fajin Dong, Shenzhen, China (*Presenter*) Nothing to Disclose Yan Liu, Jinan, China (*Abstract Co-Author*) Nothing to Disclose Huaiyu Wu, Shenzhen, China (*Abstract Co-Author*) Nothing to Disclose Lei Zhang, Shenzhen, China (*Abstract Co-Author*) Nothing to Disclose Zhimin Ding, Shenzhen, China (*Abstract Co-Author*) Nothing to Disclose Jinfeng Xu, MD, Shenzhen, China (*Abstract Co-Author*) Nothing to Disclose

# For information about this presentation, contact:

fajindong@ext.jnu.edu.cn

# PURPOSE

Sound Touch Elastography(STE) can provide the strain and shear waves allows to quantify the stiffness of tissue with elastic ratio(EI) and shear modulus(G) in the same ultrasound equipment. The main aim of our study is to evaluate the usefulness of STE in predicting malignant thyroid nodules.

#### METHOD AND MATERIALS

Both Ultrasound(US) and STE were performed with Resona 7 ultrasound system (Mindray Medical Solutions) equipped with 11L3probe. The including criteria as follows: 1) Nodules were stable when were detected by US; 2)Nodules' size ranged from 0.5 to 3.0cm; 3) Solid or almost solid (<20% cystic); 4) Enough thyroid tissue surrounding nodules at the same depth and US section; 5) No intervention on nodules before US scan, 6) Thyroid surgery or FNAB performed after US in 1 week.

### RESULTS

Finally, 86 patients (mean age46.43 $\pm$ 12.17years, range 26-78years) with 86 nodules (mean size 1.60 $\pm$ 3.94 cm, range 0.51-2.98cm) were enrolled, including 24 PTC, 62 benign nodules. 38 patients did FNAB, and 28 did surgery. The mean elastic ratio(EI) of malignant nodules was statistically lower than benign (0.19% $\pm$ 0.02%vs. 0.29% $\pm$ 0.01%, P < 0.001). The AUROC for EI was 0.8. The cut-off value was 0.215%. The Sen, Spe, LR+ and LR- were 71%,73%,2.58 and 0.40, respectively. Gmax, Gmean and Gsd were significantly higher in malignant nodules than in benign (P < 0.005). There were no significant differences in Gmin(P=0.59). Compared with other G parameters, Gmax with optimal cut-off value set at 15.82 kPa had the highest AUROC value(0.84, 95%CI: 0.759-0.928). The Sen, Spe, LR+, LR- were 79.17%, 79.03%, 3.78 and 0.26, respectively. Other two G parameters of Gmean and Gsd with the cut-off value were 6.715kPa and 2.00 kPa, respectively. The pooled-Sen and Spe, pooled-LR+ and LR-, DOR and OR with 95%CI, SROC were 79% (95%CI: 70%-86%), 71% (95%CI: 65%-76%), 2.73(95%CI:2.19-3.40),0.29 (95%CI: 0.20-0.44), 2.23 (95%CI:1.67-2.79), 9.29(95%CI:5.29-16.32) and 82% (95% CI: 78%-85&) respectively.

#### CONCLUSION

This study demonstrates that the novel quantitative STE for the differentiation of thyroid nodules. With high Sen and Spe, STE could be recongnised as a new ultrasound method in evaluating thyroid nodules.

# **CLINICAL RELEVANCE/APPLICATION**

Sound Touch Elastography(STE) provides both strain and shear waves allows to quantify the stiffness of tissue with elastic ratio(EI) and shear modulus(G) in predicting malignant thyroid nodules.



# NR436-SD-THB5

Heritability of Perivascular Space in Healthy Young Adult Twins: Evidence from the Human Connectome Project Database

Thursday, Nov. 29 12:45PM - 1:15PM Room: NR Community, Learning Center Station #5

# Participants

Yangsean P. Choi, Seoul, Korea, Republic Of (*Presenter*) Nothing to Disclose Yoonho Nam, Seoul, Korea, Republic Of (*Abstract Co-Author*) Nothing to Disclose Na-Young Shin, Seoul, Korea, Republic Of (*Abstract Co-Author*) Nothing to Disclose Yera Choi, MS,BA, Seoul, Korea, Republic Of (*Abstract Co-Author*) Nothing to Disclose Borim Park, MD, Seoul, Korea, Republic Of (*Abstract Co-Author*) Nothing to Disclose Kookjin Ahn, MD, PhD, Seoul, Korea, Republic Of (*Abstract Co-Author*) Nothing to Disclose

### PURPOSE

To investigate the heritability of MRI-visible perivascular space (PVS) volumes, a deep-learning-based voxel classification algorithm was developed and applied to a young adult twin dataset.

# METHOD AND MATERIALS

PVS volumes were calculated fully automatically using T2-weighted 0.7 mm isotropic MRI data from the Human Connectome Project. First, potential PVS voxels were extracted from the white matter (WM) and basal ganglia (BG) masks using 3D Frangi filtering and thresholding. The voxels were manually labeled as PVS, false positive (FP) around the cerebrospinal fluid, or FP around the cortex, in 20 non-twin subjects. A 3D convolutional neural network was trained to classify the three classes using a 24x24x24 3D patch as input data. The trained network was used to calculate the WM and BG PVS volumes in 138 monozygotic and 79 dizygotic twin pairs (age =  $29\pm3.4$  yrs). Narrow-sense heritability (h2), the proportion of phenotypic variance accounted for by additive genetic factors, was estimated for PVS volumes by structural equation modeling. PVS and WM volumes were normalized to z-scores, and age, sex, and WM volumes were adjusted for in all analyses. To measure the significance of estimates, 95% confidence intervals (CIs) were calculated by comparing full Cholesky decomposition ACE models (which divide the total phenotypic variance into additive genetic (A), shared environmental (C), and unique environmental (E) factors) with reduced models.

#### RESULTS

For univariate models, the AE models provided best fit for both WM and BG PVS. The heritability estimates were 88% (95% CI: 83-91) for WM PVS and 60% (95% CI: 48-69) for BG PVS. For the bivariate model including both WM PVS and BG PVS, the AE model provided best fit. While the unique heritability estimates were significant (P < 0.05) in WM PVS (h2 = 87%) and BG PVS (h2 = 60%), the shared heritability between WM and BG PVS was 1% and not significant. The genetic correlation between WM and BG PVS was 0.11.

# CONCLUSION

Our results provide differential heritability estimates for PVS in WM and BG in healthy young adults, which are in line with previous studies in elderly subjects with small vessel diseases.

# **CLINICAL RELEVANCE/APPLICATION**

The knowledge of PVS heritability may provide new insights into identifying risk factors for dilated PVS and the association of dilated PVS with small vessel diseases and dementia.



# NR437-SD-THB6

Voxel-based Simultaneous Analysis of Magnetic Susceptibility and Morphometry Using Magnetization-Prepared Spoiled Turbo Multiple Gradient Echo

Thursday, Nov. 29 12:45PM - 1:15PM Room: NR Community, Learning Center Station #6

# Participants

Hirohito Kan, Nagoya, Japan (*Presenter*) Nothing to Disclose Yuto Uchida, Nagoya, Japan (*Abstract Co-Author*) Nothing to Disclose Nobuyuki Arai, MS, Nagoya, Japan (*Abstract Co-Author*) Nothing to Disclose Yoshino Ueki, Nagoya, Japan (*Abstract Co-Author*) Nothing to Disclose Harumasa Kasai, MSc, Nagoya, Japan (*Abstract Co-Author*) Nothing to Disclose Yasujiro Hirose, Nagoya, Japan (*Abstract Co-Author*) Nothing to Disclose Noriyuki Matsukawa, Nagoya, Japan (*Abstract Co-Author*) Nothing to Disclose Yuta Shibamoto, MD, PhD, Nagoya, Japan (*Abstract Co-Author*) Nothing to Disclose

#### PURPOSE

To develop and validate a novel integrated analysis of voxel-based magnetic susceptibility and morphometry (VBMSM) on single scan, magnetization-prepared spoiled turbo multiple gradient echo sequence with inversion pulse for quantitative susceptibility mapping (MP-QSM) was conducted in young and elderly healthy volunteer groups.

#### **METHOD AND MATERIALS**

On 3.0 T MRI scanner (Ingenia 3.0 T; Philips Medical Systems International, Best, The Netherland), 1 mm3 iso-voxel 3D MP-QSM which serves 3D T1-weighted and multi-echo phase images was performed in 17 young and 19 elderly healthy volunteers ( $28 \pm 5$  y.o. and  $71 \pm 5$  y.o., respectively). The magnitude image of first echo in MP-QSM was segmented into the gray matter (GM), white matter, and cerebrospinal fluid (CSF), and transformed to MNI space for spatial normalization. The segmentation results by SPM12 were used to determine the regional differences of the volume in GM. The novel QSM reconstruction method was a total-variation-based nonlinear dipole inversion with automatic calibration of CSF by masks segmented for voxel-based morphometry (VBM). The same transformation parameter for VBM was also applied to the susceptibility map without any image registration, because of simultaneous acquisition of datasets for VBM and QSM. Voxel-wise whole brain comparisons with family-wise error correction were made to determine regional differences in volume and susceptibility distribution in GM.

#### RESULTS

A significant susceptibility increase in elderly groups could be detected in bilateral putamen. There were significant differences in the volumes of the medial frontal cortex, supplementary motor cortex, and superior frontal gyrus between the groups. These changes of susceptibility distribution and GM volumes were explained by normal aging iron-overload and GM atrophy. These results showed that the novel VBMSM analysis allows to observe the both regional changes of volume and susceptibility distribution on single scan and does not require any image registration between structural data and susceptibility map.

#### CONCLUSION

The proposed VBMSM analysis can simultaneously determine the changes of brain volume and susceptibility distribution without image registration.

# **CLINICAL RELEVANCE/APPLICATION**

An advantage of simultaneous acquisition for VBMSM may aid to diagnose abnormality in neurological and psychiatric disorders and to clarify the mechanism of diseases with regional brain atrophy and iron-overload.



# OB191-ED-THB1

Current Controversies in Polycystic Ovarian Syndrome: How Does Imaging Fit in with the Clinical and Laboratory Diagnosis?

Thursday, Nov. 29 12:45PM - 1:15PM Room: OB Community, Learning Center Station #1

### Participants

Derek Lee, Philadelphia, PA (*Presenter*) Nothing to Disclose Hima Prabhakar, MD, Philadelphia, PA (*Abstract Co-Author*) Nothing to Disclose Keyur Desai, MD, Philadelphia, PA (*Abstract Co-Author*) Nothing to Disclose

### For information about this presentation, contact:

derek.lee@uphs.upenn.edu

### **TEACHING POINTS**

To review the current clinical and radiologic diagnostic criteria of polycystic ovarian syndrome (PCOS). To review imaging findings of PCOS across different modalities. To review the current literature and discuss possible future changes in the diagnosis PCOS.

### **TABLE OF CONTENTS/OUTLINE**

Epidemiology of PCOS Clinical manifestations and implications of PCOS Hyperandrogenism Cardiac and endocrine implications Infertility Endometrial cancer Current clinical and radiological diagnostic criteria Review of PCOS phenotypes Rotterdam Criteria, NIH Criteria, AE-PCOS Criteria Review of imaging findings Review follicle count, stromal echogenicity, ovarian size Ultrasound, CT, and MRI examples Complications of Polycystic ovarian morphology Cyst rupture Ovarian torsion New biomarkers Anti-Mullerian hormone New imaging criteria Increased follicular count MRI imaging criteria



## OB192-ED-THB2

# Diagnostic and Therapeutic Strategy for Germ Cell Tumors of the Ovary

#### **Participants**

Mayumi Takeuchi, MD, PhD, Tokushima, Japan (Presenter) Nothing to Disclose Kenji Matsuzaki, MD, PhD, Tokushima, Japan (Abstract Co-Author) Nothing to Disclose Masafumi Harada, MD, PhD, Tokushima, Japan (Abstract Co-Author) Nothing to Disclose

### For information about this presentation, contact:

mayumi@tokushima-u.ac.jp

#### **TEACHING POINTS**

1. Germ cell tumors (GCTs) are common ovarian neoplasms in children and young women. Various imaging manifestations, complications, and pitfalls of benign and malignant GCTs are demonstrated with pathologic correlation, and the feasibility of advanced MR techniques (DWI, DCE-MRI, 3D Dixon images, SWI, MRS) were reviewed for the differential diagnosis and in addressing therapeutic strategy.2. Malignant GCTs generally appear as aggressive, large, hypervascular masses with hemorrhage and necrosis, however, fertility preserving surgery may be indicated because of their high chemo/radiosensitivity, and preoperative diagnosis is important. Additional advanced MR techniques and specific tumor markers are helpful for the diagnosis.

#### **TABLE OF CONTENTS/OUTLINE**

Clinical, pathological and imaging features:- Dysgerminoma; Yolk sac tumor; Embryonal carcinoma; Non-gestational choriocarcinoma; Mixed germ cell tumor- Mature teratoma and complications: Torsion; Rupture; Chemical peritonitis; Malignant transformation; Infection; Pseudo-Meigs syndrome; Paraneoplastic syndromes (Autoimmune hemolytic anemia, Limbic encephalitis) -Immature teratoma and complications: Peritoneal gliomatosis; Growing teratoma syndrome- Monodermal teratomas: Struma ovarii; Carcinoid; Neuroectodermal-type tumorsDiagnostic and therapeutic strategy according to the WHO 2014



### PD194-ED-THB7

# Stroke in Pediatric Age Group: How MRI Can Help?

Thursday, Nov. 29 12:45PM - 1:15PM Room: PD Community, Learning Center Station #7

**FDA** Discussions may include off-label uses.

#### **Participants**

Paramita Hota, MBBS,MD, Bangalore, India (*Presenter*) Nothing to Disclose Sriram Patwari, MBBS, MD, Bangalore, India (*Abstract Co-Author*) Nothing to Disclose Harsha C. Chadaga, MBBS, Tamilnadu, India (*Abstract Co-Author*) Nothing to Disclose Surendra KI, DMRD, Bangalore, India (*Abstract Co-Author*) Nothing to Disclose Anita Nagadi, MBBS, Bangalore, India (*Abstract Co-Author*) Nothing to Disclose Rekha B P, DMRD, MBBS, Bangalore, India (*Abstract Co-Author*) Nothing to Disclose

#### For information about this presentation, contact:

meparamitahota@gmail.com

#### **TEACHING POINTS**

• To understand basic pathophysiology of childhood stroke. • To illustrate various causes of stroke and stroke mimics in pediatric age group. • To utilise MR advanced imaging sequences to come to correct diagnosis.

### **TABLE OF CONTENTS/OUTLINE**

We reviewed fifty cases of children with stroke like symptoms in a tertiary care centre over a period of 4 years (2014-2018), of them thirty patients were diagnosed with CVA and the cases were as follows: <u>Embolic</u>: Posterior fossa subacute embolic infarcts from vertebrobasilar thrombosed aneurysm; <u>Arteriopathy</u>: Mineralizing microangiopathy with acute infarcts in bilateral centrum semiovale, moya moya disease; <u>Dissection</u>: internal carotid artery dissection; <u>Vasculitides</u>:Systemic lupus erythematosus; <u>Venous thrombosis</u>: Internal cerebral vein thrombosis with left thalamic hemorrhagic infarct; <u>Vascular malformation</u>: Arterio-vascular malformation with focal bleed; <u>Infection</u>: Meningitis; <u>Blood dyscrasias</u>:Protein c deficiency; <u>Others</u>: MELAS (mitochondrial encephalopathy, lactic acidosis and stroke like episodes), COL4A1 mutation with chronic small vessel ischemic changes, multifocal bleeds in centrum semiovale and bilateral pseudophakia.



# PD195-ED-THB8

# Spectral Multi-Energy Computed Tomography: Preliminary Experience in Pediatric Neuroradiology

Thursday, Nov. 29 12:45PM - 1:15PM Room: PD Community, Learning Center Station #8

#### **Participants**

Dianna M. Bardo, MD, Phoenix, AZ (*Presenter*) Speaker, Koninklijke Philips NV; Consultant, Koninklijke Philips NV; Master Enterprise Agreement, Koninklijke Philips NV; Author, Thieme Medical Publishers, Inc Marrit Thorkelson, RT, Phoenix, AZ (*Abstract Co-Author*) Nothing to Disclose Robyn Augustyn, RT, Phoenix, AZ (*Abstract Co-Author*) Nothing to Disclose Richard N. Southard, MD, Phoenix, AZ (*Abstract Co-Author*) Consultant, Koninklijke Philips NV Advisory Board, Koninklijke Philips NV

### For information about this presentation, contact:

dbardo@phoenixchildrens.com

# **TEACHING POINTS**

Spectral or multienergy CT (MECT) obtains raw data at more than one energy spectra allowing decomposition of materials into constituent elements. Only limited experience and literature are available regarding applications of MECT in the pediatric population. In this EE we will review the basic physics of MECT, the benefits and limitations of the single-source multi-layered detector geometry, and clinical applications of MECT and our experience to date in the pediatric population. Features of MECT advantageous to pediatric patients include reconstruction of virtual non-contrst images, perfusion imaging, mitigation of beam hardening artifact with high mono-energetic imaging, the use of low mono-energetic imaging to boost iodine density to improve angiographic images which may be limited by contrast or bolus timing or to improve grey-white matter conspicuity and detection of intracranial hemorrhage, and tumor characterization. The use of spectral MECT provides a significant advance in our ability to confidently diagnose various disease processes. As we gain more experience in the use of MECT in the pediatric population we will be able to beter define its role and uncover further areas of research.

### **TABLE OF CONTENTS/OUTLINE**

We present brain, CTA, spine, facial trauma, and neck cases in which MECT aided in diagnosis through use of spectral data.



### PD249-SD-THB4

### Pediatric Diagnostic Reference Ranges for Dual-energy Dual-source Abdominopelvic CT

Thursday, Nov. 29 12:45PM - 1:15PM Room: PD Community, Learning Center Station #4

#### Participants

Marilyn J. Siegel, MD, Saint Louis, MO (Abstract Co-Author) Speakers Bureau, Siemens AG Spouse, Consultant, General Electric Company

Timothy Street, St Louis, MO (Abstract Co-Author) Nothing to Disclose

Juan Carlos Ramirez-Giraldo, PhD, St Louis, MO (Presenter) Employee, Siemens AG

#### PURPOSE

To develop diagnostic reference ranges (DRRs) for pediatric abdominopelvic dual-energy (DECT) examinations as a function of patient size and radiation output of the CT scanner with comparison to conventional CT.

### **METHOD AND MATERIALS**

Volume CT dose index (CTDIvol) and effective diameter of pediatric patients (mean age  $9.3\pm5.9$  years) who underwent contrastenhanced abdominopelvic CT with either conventional CT (N=1719) or dual-energy CT (N=375 patients) on a dual-source CT system (Somatom Flash, Siemens) from September 01 2014 to March 01 2018 were retrieved from our institutional dose tracking system (Radimetrics). All conventional CT scans used automatic tube potential selection (ranging from 70 to 120 kVp). Both conventional and DECT acquisitions used automatic exposure control and iterative reconstruction. Patient data were grouped into one of five effective diameter ranges to allow developments of DDRs as a function of patient size. The median, 25th and 75th quartile of the two CT dose indexes were determined for the corresponding effective diameters. Statistical unpaired comparisons were made between groups.

#### RESULTS

For the five effective diameters (<15cm, 15-19cm, 20-24cm, 25-30cm and >30cm), the median DRRs [25-75th quartile] for CTDIvol for conventional and DECT were 3.7[2.7-3.4] mGy and 2.6[2.4-2.8]mGy (P>.05); 3.6[3.2-3.8]mGy and 3.3[3.0-3.7] mGy (P>.05); 4.8[4.0-6.1])mGy and 4.7[4.3-5.5]mGy (P>.05); 7.1[6.2-8.3]mGy and 6.5[5.8-7.4]mGy (P<.01); 11.4[10.0-14.4]mGy and 9.8[8.9-11.8] mGy (P<.05). There was no statistically significant difference in CTDIvol between conventional and DECT for effective diameters below 25cm. CTDIvol of DECT in patients with effective diameters >25cm was significantly lower than that of conventional CT.

#### CONCLUSION

The DRRs for pediatric abdominopelvic DECT reported in this study as a function of patient size and radiation output can serve as reference standards to help manage pediatric patient radiation doses in DECT. The radiation doses are comparable or lower than those of conventional CT.

# **CLINICAL RELEVANCE/APPLICATION**

DRRs for pediatric abdominopelvic DECT based on CTDIvol and body size may allow other imaging sites to implement DECT in clinical practice and reduce pediatric patient doses.



### PD251-SD-THB6

Microcirculatory Perfusion and Diffusion Assessment of Neonates with Punctate White Matter Lesions Using intravoxel Incoherent Motion (IVIM)

Thursday, Nov. 29 12:45PM - 1:15PM Room: PD Community, Learning Center Station #6

# Participants

Ying Qi, Shenyang, China (Presenter) Nothing to Disclose

#### PURPOSE

The brain's microcirculatory perfusion of punctate white matter lesions (PWML) is poorly understood due to a scarcity of noninvasive imaging techniques. The aim of this study was to apply new MRI techniques to quantify cerebral microcirculatory perfusion and diffusion in neonates with PWML, for better understanding of the pathophysiology of PWML.

# METHOD AND MATERIALS

Thirty-eight newborns were recruited continuously, including 10 neonates with PWML and 28 normal control neonates. Intravoxel incoherent motion (IVIM) scan was performed for the measurement of the diffusion coefficient (D), the pseudo-diffusion coefficient (D\*) and the perfusion fraction (f) in periventricular white matter. D denoted the true molecular diffusion. D\* represented the diffusion linked to microcapillary perfusion. f (given as a percentage) indicated the proportion of microcirculatory perfusion-related diffusion in the total diffusion. The total maturation score (TMS) was assessed for each neonate on standard T1, 2-weighted images to evaluate cerebral maturation. The D, D\* and f were compared between groups, and their associations with age and TMS were evaluated.

#### RESULTS

Significant differences between PWML group and control group were found in D (P=0.020), D\* ( P=0.010) and f (P=0.012) in periventricular white matter. After age/maturation is accounted for, D and f showed significant dependence on the groups (P<0.05). Preterm infants with PWML had lower D, D\* and f. f was correlated with age (P<0.001) and TMS (P<0.05).

### CONCLUSION

It is feasible to use non-invasive MRI methods to measure cerebral microcirculatory perfusion in neonates with PWML. Newborns with PWML have lower microcirculatory perfusion. D and f may be helpful for the diagnosis of PWML.

# **CLINICAL RELEVANCE/APPLICATION**

The positive correlation between f and TMS suggested that as myelination progresses, the microcirculatory perfusion in the brain increase to meet the escalating energy demand.



### PH011-EB-THB

### In Vivo Evaluation of Acute Sciatic Nerve Traction Injury and the Association with Sunderland Grading

Thursday, Nov. 29 12:45PM - 1:15PM Room: PH Community, Learning Center Hardcopy Backboard

### FDA Discussions may include off-label uses.

#### Participants

Jianwei Xiang, MD, Baltimore, MD (*Presenter*) Nothing to Disclose Guangbin Wang, MD, Jinan, China (*Abstract Co-Author*) Nothing to Disclose

# For information about this presentation, contact:

jianweixiangmd@gmail.com

# CONCLUSION

DTI can be clinically used to detect sciatic nerve traction injury, FA Value can be used as makers to monitor process of nerve degeneration and regeneration, and to discriminate the Sunderland IV and Sunderland II/III injuries at special time point.

#### Background

Accurately evaluating the degree of nerve injury and repair regeneration can guide treatment and judge prognosis. This study aimed to evaluate the function of diffusion tensor imaging (DTI) in acute sciatic nerve traction injury and detect the association with Sunderland grading.

# **Evaluation**

Sciatic nerve traction injury was created in 40 rabbits. Scanning was performed using a clinical 3.0T scanner at the point of before operation , 1 day, 4 days, 7 days, 14 days, 4 weeks, 6 weeks, and 8 weeks after operation to evaluate sciatic degeneration and regeneration. Scanning sequences included T1WI, T2WI, SPAIR and DTI. The tissue specimens of the injured nerves at the point of two weeks were harvested, and confirmed the Sunderland grade by the pathologists, DTI parameters were evaluated to distinguish the different Sunderland grades , and the Receiver Operating Characteristic curve was plotted to determine the optimal prediction threshold to identify injuries with different Sunderland grades. The FA value of different portions dropped to the minimum at the fourth day, and began to recover to the normal until 8 weeks. The FA value of the injured nerve was obviously different from that of the opposite sham portion. Also, it varied more seriously compared with that of the proximal and distal portions. The FA values were significantly different between the Sunderland IV grades and Sunderland II/III grades, and the cutoff value obtained by the ROC analysis was 0.46 for FA values between nerve injuries of Sunderland IV and Sunderland II/III grades, the sensitivity and specificity were 89%,75% respectively, AUC was 0.91.

#### Discussion

Our research try to distinguish the different sunderland grade in pathology by using DTI, and greatly contribute to confirm the extent of injured peripheral nerve noninvasively, and guide the clinical resolution.



# PH257-SD-THB1

Radiation Dose Reduction in Oncologic Computed Tomography Follow Up: Evaluation and Advantages of a New Scan Protocol

Thursday, Nov. 29 12:45PM - 1:15PM Room: PH Community, Learning Center Station #1

### Participants

Andrea Bonfanti, Milano, Italy (*Presenter*) Nothing to Disclose Elena Ciortan, MD, Piacenza, Italy (*Abstract Co-Author*) Nothing to Disclose Roberto Moltrasi, Milan, Italy (*Abstract Co-Author*) Nothing to Disclose Ruggero L. Baroni, Milan, Italy (*Abstract Co-Author*) Nothing to Disclose Riccardo Buffa, Milan, Italy (*Abstract Co-Author*) Nothing to Disclose Serena Padelli, Milan, Italy (*Abstract Co-Author*) Nothing to Disclose Luciano Abate, Milan, Italy (*Abstract Co-Author*) Nothing to Disclose

#### For information about this presentation, contact:

bonfantiandre@gmail.com

### PURPOSE

Comparing dose reduction and the diagnostic quality between the contrast enhanced computed tomography (CT) 'standard' protocol for thoraco-abdominal scan in oncologic follow up and the contrast enhanced computed tomography 'low dose' protocol in the same patient follow up, optimizing the dosimetric profile with two topograms and acquiring the thoraco-abdominal arterial phase volume in a single caudo-cranial scan.

#### **METHOD AND MATERIALS**

We included 100 patients from January 2017 to March 2018 where oncologic follow up required a triphasic thoraco-abdominal CT for staging of liver disease. Eligibility criteria were the medical indication for a contrast enhanced thoraco-abdominal CT as part of an oncologic follow up (breast cancer, hepatocarcinoma, neuroendocrine tumors, kidney cancer and prostatic cancer) and the availability of previous enhanced CT scans performed over the past year of follow up.

#### RESULTS

Caudo-cranial thoraco-abdominal arterial phase permits saving of effective dose up to 50% (27% on average) for each scan and the low dose protocol allows saving up to 40% (15% on average) for complete procedure in the normal BMI group. By using the second dosimetric profile, the effective dose is reduced up to 7 mSv in normal BMI patients and up to 39 mSv in high BMI patients. Caudo-cranial thoraco-abdominal arterial phase was also effective in diagnosis of thromboembolic disease. All the scans from low dose CT protocol were analyzed by radiologists unaware of introduction of the protocol, all with at least 10 years of experience; there were no reported differences or difficulties in diagnosis compared to the standard CT protocol.

#### CONCLUSION

The low dose protocol for triphasic CT in oncologic follow up permits saving of effective dose up to 40 % and optimization of the dosimetric profile allows saving of effective dose up to 48 %. Low dose protocol is also effective in diagnosis of thromboembolic disease.

#### **CLINICAL RELEVANCE/APPLICATION**

Low dose CT protocol saves effective dose to patients who are subjected to close CT monitoring (three/four times a years).



### PH258-SD-THB2

### Differences in Room Scatter Distribution by Body Region Being Imaged with a C-Arm Fluoroscope

Thursday, Nov. 29 12:45PM - 1:15PM Room: PH Community, Learning Center Station #2

#### **Participants**

Chao Guo, MS, Buffalo, NY (*Presenter*) Research support, Canon Medical Systems Corporation Zhenyu Xiong, PhD, Buffalo, NY (*Abstract Co-Author*) Research support, Canon Medical Systems Corporation Jonathan L. Troville, MS,BS, Buffalo, NY (*Abstract Co-Author*) Support, Canon Medical Systems Corporation Stephen Rudin, PhD, Buffalo, NY (*Abstract Co-Author*) Research Grant, Canon Medical Systems Corporation Daniel Bednarek, PhD, Buffalo, NY (*Abstract Co-Author*) Research Grant, Toshiba Corporation

### For information about this presentation, contact:

cguo@buffalo.edu

#### PURPOSE

This study investigates the differences in the distribution of scattered radiation in the procedure room when different regions of the patient such as the head, chest and abdomen are imaged with a c-arm fluoroscope.

# METHOD AND MATERIALS

The CT-based Zubal anthropomorphic computational phantom of an average adult male and EGSnrc Monte-Carlo software were used to calculate the scattered radiation distribution around the "patient" for beams exposing the head, the chest and the abdominal regions at various gantry angles. The same calculations were performed for a uniform water-filled cylindrical phantom to mimic the head and a super-ellipse-shaped phantom to mimic the torso to investigate any differences. All comparisons were made for the same exposure conditions and normalized to the tube output. Each MC simulation used 5x108 photons incident on the phantom.

#### RESULTS

A number of observations can be made from the results of this study. Overall, less scatter was generated by the head phantom compared to the uniform water cylinder due to the attenuation of the skull bone. Compared to the cylinder phantom, the scatter along the length of the table was reduced for head exposures by the attenuation of the shoulder. Less backscatter is generated in the chest region than the abdominal region but more forward scatter can be seen in the chest region, likely due to the lower attenuation of the lungs. The scatter values for the uniform super-ellipse phantom agree more closely with those for the abdominal region than with the chest.

# CONCLUSION

The scatter distribution is shown to vary with the body part imaged and the position in the room relative to the gantry angulation. Scatter distributions determined using uniform phantoms may not accurately represent the distribution with the patient.

# **CLINICAL RELEVANCE/APPLICATION**

Information about the scattered radiation distribution in the procedure room and the effect of the body-part being imaged should help staff make informed decisions and manage their dose.



# PH259-SD-THB3

# Exploration of Optimal ASIR-V Weight in Low-Dose Head Scan with 16cm Wide-Detector CT

Thursday, Nov. 29 12:45PM - 1:15PM Room: PH Community, Learning Center Station #3

### Participants

Lu Jiang II, Xi'an, China (*Presenter*) Nothing to Disclose Jun Gu SR, Beijing, China (*Abstract Co-Author*) Nothing to Disclose Zhijun Hu SR, xi`an, China (*Abstract Co-Author*) Nothing to Disclose Dou Li, Xi'an, China (*Abstract Co-Author*) Nothing to Disclose Jiang Guo, Xi`an, China (*Abstract Co-Author*) Nothing to Disclose Zhen Tang Liu, Xi'an, China (*Abstract Co-Author*) Nothing to Disclose Yongjun Jia, MMed, Xianyang City, China (*Abstract Co-Author*) Nothing to Disclose

# PURPOSE

To explore the optimal weight of ASIR-V in low-dose head scan using 16cm wide-detector CT.

### **METHOD AND MATERIALS**

60 patients underwent head CT examinations were enrolled and randomly divided into A and B groups with 30 patients in each group. Both groups performed axial scanning. Scan parameters in Group A are: 120kVp, tube current 280mA, collimator width 120mm, rotation speed 1.0s/r. Group B adopts 100kVp tube voltage, tube current 280mA, Pre-ASIR-V weight 0%, collimator width 120mm, rotation speed 1.0s/r. Group A images were reconstructed with FBP while group B images were reconstructed with 0%, 20%, 40%, 60%, 80%, and 100% of post-ASIR-V. CT values and SD values of brain parenchyma at the level of posterior fossa, basal ganglia, and semiovale were measured and signal-to-noise ratio (SNR) was calculated. The quality of CT images was subjectively evaluated by two radiologists using double-blind method and a 3-point grading system was applied. The CTDI, DLP, and ED of the two groups were compared and analyzed by one-way ANOVA.

### RESULTS

As the post-ASIR-V weight increases from 0% to 100%, the SD value gradually decreases, SNR gradually increased with statistically significant difference among different weights (p<0.05). When post-ASIR-V weight increases from 0% to 60%, the subjective image quality score increased. When post-ASIR-V weights exceeded 60%, the subjective image quality score decreases as post-ASIR-V increases. When ASIR-V weight is 60%, subjective image quality was the highest. The radiation dose in Group B was reduced by 34.31% as compared to Group A.

# CONCLUSION

Post-ASIR-V with reconstruction weight of 60% in 100 kVp low dose head scan gives the best image quality using 16cm widedetector CT.

# **CLINICAL RELEVANCE/APPLICATION**

It is recommended to conduct low-dose head CT scan using 100 kVp and 60% post-ASIR-V reconstruction to obtain the best image quality when 16cm wide-detector CT is ued.



### PH260-SD-THB4

# Evaluation of Large Scale Patient Specific Dosimetry in Conventional Chest Imaging

Thursday, Nov. 29 12:45PM - 1:15PM Room: PH Community, Learning Center Station #4

#### **Participants**

An Dedulle, MSc, Leuven, Belgium (*Presenter*) Researcher, Qaelum NV Niki Fitousi, Leuven, Belgium (*Abstract Co-Author*) Research Director, Qaelum NV Guozhi Zhang, Leuven, Belgium (*Abstract Co-Author*) Nothing to Disclose Jurgen Jacobs, MSc, Leuven, Belgium (*Abstract Co-Author*) Co-founder and CEO, Qaelum NV Hilde Bosmans, PhD, Leuven, Belgium (*Abstract Co-Author*) Co-founder, Qaelum NV Research Grant, Siemens AG

### For information about this presentation, contact:

an.dedulle@qaelum.com

# PURPOSE

To evaluate a patient-specific approach for organ dose estimation in conventional posterior-anterior (PA) chest radiography.

### **METHOD AND MATERIALS**

The methodology included three steps and was applied to 423 chest PA exams (191 female and 232 male patients). First, the standard ICRP female and male phantom were used in a Monte Carlo (MC) framework to simulate a chest PA exam. These ICRP reference dose conversion factors were applied on the 423 patients to calculate the organ doses (lung, breast). Secondly, a new patient-specific approach was implemented that starts from real time calculated water equivalent diameter (WED) from 3 readily available parameters of the exam (dose area product, exposed area, standardized exposure index). Voxel models had been created from 20 female and 20 male patients. MC was used to generate WED-specific organ dose conversion factors. The equations that correlated WED with WED-specific conversion factors were then applied to the same 423 patients to provide patient-specific organ doses. In the third step, the ICRP-based and patient-specific doses were compared and the percentage difference (D) was calculated.

#### RESULTS

The WED ranged from 19cm to 33cm for the females and from 22cm to 32cm for the males. The median patient-specific doses for the females were 26uGy and 6uGy for the lung and breast, while for the males this was 26uGy and 5uGy respectively. Patient-specific organ doses were found significantly different from the ICRP-based values (p<0.01). For the lowest WED in this study, ICRP-based doses were underestimated up to 40%, while for the highest WED doses were overestimated by 106%. This would further increase for more obese patients. For increasing WED, the difference between the ICRP-based and patient-specific doses increased for the lungs and breasts (p<0.01) and this effect was most pronounced for the breasts (Fig.). Due to differences in anatomy, the ICRP lung dose was always an overestimation for females and an underestimation for males.

### CONCLUSION

The described methodology provides a good solution for a patient-specific dosimetric approach on a large-scale. More conventional approaches deviate up to  $\pm 100\%$  for some subgroups like obese patients.

# **CLINICAL RELEVANCE/APPLICATION**

The proposed methodology leads to personalized dosimetry in 2D projection imaging, implementable in a dose monitoring platform, by using selected DICOM tags and size-based conversion factors.



# PH261-SD-THB5

# **Coupled Multi-Bone Active Shape Model of Foot and Ankle**

Thursday, Nov. 29 12:45PM - 1:15PM Room: PH Community, Learning Center Station #5

#### **Participants**

Michael Brehler, Baltimore, MD (*Presenter*) Research Grant, Carestream Health, Inc Rohan Vijayan, Baltimore, MD (*Abstract Co-Author*) Nothing to Disclose William J. Sehnert, PhD, Rochester, NY (*Abstract Co-Author*) Employee, Carestream Health, Inc Levon Vogelsang, Rochester, NY (*Abstract Co-Author*) Employee, Carestream Health, Inc Jeffrey H. Siewerdsen, PhD, Baltimore, MD (*Abstract Co-Author*) Research Grant, Siemens AG; Research Grant, Carestream Health, Inc; Advisory Board, Siemens AG; Advisory Board, Carestream Health, Inc; License agreement, Carestream Health, Inc; License agreement, Precision X-Ray, Inc; License agreement, Elekta AB; ; ; Wojciech Zbijewski, PhD, Baltimore, MD (*Abstract Co-Author*) Research Grant, Carestream Health, Inc; Research Grant, Siemens AG

#### For information about this presentation, contact:

Michael.Brehler@jhu.edu

### PURPOSE

To improve robustness of Active Shape Model (ASM) segmentation of bones separated by narrow joint spaces, we develop a coupled ASM (cASM) that simultaneously segments neighboring bones using their individual statistical shape models (SSM) and a proximity constraint.

#### **METHOD AND MATERIALS**

The study involved segmentation of Talus and Calcaneus from extremity Cone Beam CT scans of 21 healthy subjects. In conventional ASM (Cootes et al, CVIU, 1995) segmentation, the coefficients of the shape model are iteratively updated by minimizing a residual between current instance of the model and local gradient maxima of the object volume. For narrow joints, the model may fit to the gradient of an adjacent bone if such gradient presents a stronger signal within the neighborhood of the current guess. In the proposed cASM approach, ASM is simultaneously performed on the adjacent shapes (here the Talus and the Calcaneus). After each iteration of the individual ASMs, the distance between the resulting shapes is measured at the talocalcaneal joint. If the distance is <2 mm, the vertices in the two shapes are pushed apart from each other by 5 mm. The deformed models are used to initialize next iteration of individual ASMs; 30 iterations are performed. The final models are obtained without the deformation and are thus consistent with the underlying SSMs. Surface models of the Talus and Calcaneus were manually segmented in all patient images. One dataset was used as a test volume. Multiple realizations of Talus and Calcaneus SSMs were trained based on all possible 19 element combinations of the remaining 20 volumes. For all the SSM realizations, conventional ASM and cASM were performed on the test volume.

#### RESULTS

The mean shapes of the Talus and Calcaneus SSMs had an average RMSE compared to the manual segmentations of ~7.6mm and ~5.6mm, respectively. After conventional ASM, the average RMSE were 3.0mm and 4.8mm. With cASM, the average RMSE was improved to 2.3mm (~23%) and 3.4mm (~28%) and none of the resulting segmentations included edges of the adjacent bone.

#### CONCLUSION

The proposed cASM yields robust, automatic segmentations in the foot by incorporating the spatial relationship between neighboring bones.

#### **CLINICAL RELEVANCE/APPLICATION**

A robust, automatic algorithm for accurate and reproducable segmentations of bones of foot and ankle enables automated measurements of joint morphology in diagnostic and surgical applications.



# QI018-EB-THB

Interruptions During On Call Radiology in a University Teaching Hospital

Thursday, Nov. 29 12:45PM - 1:15PM Room: QR Community, Learning Center Hardcopy Backboard

#### **Participants**

Amy C. O'Brien, Dublin, Ireland (*Presenter*) Nothing to Disclose Cormac E. O Brien, MRCPI, MRCP, Dublin 4, Ireland (*Abstract Co-Author*) Nothing to Disclose John Duignan, Dublin, Ireland (*Abstract Co-Author*) Nothing to Disclose Dermot E. Malone, MD, Dublin, Ireland (*Abstract Co-Author*) Nothing to Disclose Jeffrey W. McCann, MBBCh, Dublin, Ireland (*Abstract Co-Author*) Nothing to Disclose

### For information about this presentation, contact:

#### acobrien@tcd.ie

# PURPOSE

In our institution, the overnight workload is increasing over time and out of hours phone calls are becoming more frequent. It was thought that many of these phone calls were regarding non-urgent queries which could be addressed during the day when the Radiology Department is fully staffed. In our institution, from 5:00 pm until 9:00 am on weekdays, and 9:00 am to 9:00 am on weekends, one Radiology Resident is responsible for the generation of all the preliminary CT and Emergency Department (ED) reports. It is known that an increased number of interruptions in any work place leads to an increased rate of errors or discrepancies. It is important that interruptions are minimized. The aim of this QI project was to calculate how often Radiology Residents were being interrupted during out of hours reporting sessions, to determine whether these interruptions are necessary, and if possible to achieve an interruption rate comparable to a literature standard.

### METHODS

First, using the PICO format, a literature review was performed. A manuscript entitled "Do Telephone Call Interruptions have an Impact on Radiology Resident Diagnostic Accuracy?" describes a "non-discrepancy shift" as 3.24 calls per hour, versus a "discrepancy shift" which is described as 4.23 calls per hour. One single additional telephone call above the standard (3.24) while reporting raised the probability of the resident generating a report containing a significant error by 12% (P=.017). For 7 days, Radiology Residents on call recorded the following information about on-call interruptions on a pre-prepared form: the number, type, origin, duration, and whether the interruption impacted patient management during the on-call shift. Interruptions were categorized as requests for scans (including whether approved scans had been scheduled), requests for provisional CT/ ED reports, 'other' (interruptions from other Radiology Residents and radiographers, accidental phone calls and requests regarding outpatient scheduling of scans and procedures) and requests for provisional reports on in-patient (IP) radiographs. Data from the forms was transcribed into a Microsoft excel spreadsheet for analysis. After data collection and analysis, an intervention was performed which focused on education of the Emergency Department staff, medical and surgical staff. Teaching sessions were held which involved a Radiology Resident giving a 20 minute talk on the impact of interruptions on error rates to the junior and senior ED staff on two separate occasions. Data collection was repeated using identical methodology for another 7 days after this intervention took place, and transcribed to Microsoft excel for further analysis.

#### RESULTS

A total of 263 interruptions was recorded during the 7 days before the intervention. Reasons for interruption were scan requests 107/263 (40.1%), requests for provisional reports 86/263 (32.7%), 'other' 70/263 (26.6%) and requests for provisional IP reports 4/263 (1.5%). The total number of interruptions decreased from 263 to 173 after the intervention. The proportion of 'unnecessary' interruptions (no on-call action) halved from 109/263 (41%) to 35/173 (20.2%). The proportion of unnecessary interruptions from the Emergency Department staff decreased from 16.2% (30/179) before to 11.2% (10/112) after the intervention. There were 147/ 179 (82.1%) ED SHO (junior staff) interruptions, and 32/179 (17.9%) ED Registrar (senior staff) interruptions before the intervention. After the intervention there were 62/122 (50.8%) ED SHO interruptions, and 60/122 (49.2%) ED Registrar interruptions. This was a behavioral change as a result of the intervention, which led to a shift of calls from junior staff to senior staff. This appeared to be another factor in reducing the number of unnecessary interruptions. Compared to our standard of 3.24 calls per hour, we received an average of 4.24 interruptions per hour while reporting before the intervention, and 2.14 interruptions per hour while reporting before the intervention.

### CONCLUSION

The workload of the on call Radiology Resident is increasing. Interruptions increase diagnostic discrepancies in generated reports and unnecessary interruptions must be avoided. Education of our ED, medical and surgical resident colleagues helped us achieve our target. A QI PDSA cycle is now in progress. Further interventions include a change to our ordering IT system so that referring teams can see if an approved scan has been scheduled and a review of methodology by which provisional reports are communicated to referring teams. So far, this QI project has reduced the unnecessary interruption rate below the target standard.



# QI133-ED-THB1

A Multifaceted Approach to Improving Radiology Resident Proficiency in Managing Acute Adverse Reactions to Intravenous Contrast Administration

Thursday, Nov. 29 12:45PM - 1:15PM Room: QR Community, Learning Center Station #1

# Participants

Sidra J. Tayyab, MD, Houston, TX (*Presenter*) Nothing to Disclose Susanna C. Spence, MD, Houston, TX (*Abstract Co-Author*) Nothing to Disclose

### For information about this presentation, contact:

SJ2\_27@hotmail.com

#### PURPOSE

The purpose of this intervention was to improve radiology residents' confidence level and proficiency in evaluating and managing acute adverse contrast reaction events that were not infrequently encountered during on-call and daily duties.

#### **METHODS**

To enhance the existing training provided by the residency program, which consisted of one didactic noon conference annually, a multi-faceted approach was developed by our institutions's radiology residents Class of 2018 and two faculty advisors. This consisted of development of scenarios to be run in the Medical School's Simulation Lab, creation of interactive modules which were succinct yet thorough, and distribution of reference pocket cards with treatment recommendations from the ACR (B) Manual on Contrast Media. A pilot study group of incoming PGY-2 residents was provided and evaluated on this training (n=13).

### RESULTS

A pre-intervention survey found that the average comfort level in the pilot group was 4.9 on a scale of 1-10 (1: not prepared at all for any adverse event; 10: very well prepared for any adverse event). Analysis of pre and post-intervention test consisting of ten questions demonstrated an improvement in knowledge of 7 of the participants, no change in 4 participants, and decrease in score of 2 participants (by one point). Subjective survey responses were unanimously positive when detailing experiences in the simulation lab, as well as regarding the interactive modules. Comments included the following: "The scenarios were practical situations that were good to practice and simulate in preparation for real life situations "and "Excellent real world scenarios."

# CONCLUSION

While life-threatening reactions to intravenous contrast media are fortunately rare, the radiology resident does encounter a wide spectrum of potential adverse events to intravenous contrast media. Based on feedback from residents at this training program and others, it was recognized that training for preparedness and proficiency in contrast reactions was in need of improvement. A multifaceted approach developed by radiology residents at our institution which consisted of simulation lab scenarios, interactive modules, and reference pocket cards demonstrated both objective and subjective improvement in the pilot study group of PGY 2 residents. Notably, the infrequently used approach of live radiology resident training in a simulation lab was very well received. This new curriculum has been integrated into the training provided to residents at our institution, with continuing refinements to the scenarios and modules based on feedback from the pilot group.



# QI135-ED-THB2

# Implementing a Fully Model Based Iterative Reconstruction Algorithm in a High Volume CT Practice

Thursday, Nov. 29 12:45PM - 1:15PM Room: QR Community, Learning Center Station #2

#### **Participants**

Stephanie Miller, ARRT, Eau Claire, WI (*Presenter*) Nothing to Disclose Erik B. Sviggum, MD, Rochester, MN (*Abstract Co-Author*) Nothing to Disclose Christopher P. Favazza, PhD, Rochester, MN (*Abstract Co-Author*) Nothing to Disclose

#### PURPOSE

Fully model based iterative reconstruction (MBIR) algorithms have been shown to improve CT image quality; however, these algorithms require longer times to form images. These relatively longer reconstruction times can potentially disrupt and impede efficient workflow in busy CT practices. The purpose of this project was to adapt our CT imaging workflow for use of MBIR in our high volume clinical practice without loss of efficiency.

# METHODS

A commercial MBIR algorithm, Forward projected model-based Iterative Reconstruction SoluTion (FIRST, Canon Medical Systems USA) was partially deployed in our CT practice over a three month trial period. FIRST was used on a subset of exams, which constituted a substantial portion of the CT practice, including: routine abdomen/pelvis, routine chest, low dose lung cancer screening, calcium scoring and coronary CTA exams. In conjunction with FIRST implementation, several changes to the CT workflow were instituted. One, an extra, initial image reconstruction using Canon's Adaptive Iterative Dose Reduction (AIDR3D) was added to the protocols in case a faster review was necessary. The FIRST reconstructions, which are reconstructed simultaneously on an independent computer system, were used for diagnostic review; whereas, the AIDR3D images were not. Secondly, coronary CTA exams were configured to use AIDR3D images for calcium scoring; FIRST images were used for calcium scoring-only exams. Next, a duplicate set of acquisition protocols were created without FIRST for ED exams. Lastly, all exams were "finalized" in our electronic medical record system by a "team lead" technologist, not the scanning technologist. This process of "finalizing" an exam sent an electronic cue to the radiologist that the exam was complete and ready for review. After implementing these workflow changes, FIRST reconstruction times for routine abdomen/pelvis and chest exams were calculated using image timestamps. The time difference between completion of the study and availability of FIRST images was recorded. More specifically, times to complete the first set of abdomen/pelvis reconstructions and the first and second sets of chest reconstructions were calculated. Lastly, scanner utilization was tracked over the three month period and compared with utilization data over the same time period the year prior, which included exams performed only during normal business hours-7am to 5pm Monday through Friday.

#### RESULTS

The addition of an initial AIDR3D reconstruction enabled the scanning technologist to quickly review the images for quality, e.g. patient motion, sufficient technique, anatomy coverage, and urgent pathology, while the patient remained on the scanner table. Additionally, the initial AIDR3D reconstruction provided image data to send for review if it was unexpectedly, urgently needed. The second workflow step of using AIDR3D images for calcium scoring associated with a coronary CTA exam allowed for expeditious triaging of the remainder of the exam and avoided unduly extending the procedure. The third workflow step, the duplicate set of protocols without FIRST reconstructions, was found to be necessary for emergent exams. This set of protocols is also useful for urgent exams or exams where relative longer reconstruction times were not well-tolerated, e.g. some pre-op surgical planning exams. Lastly, ascribing the responsibility of "finalizing" exams to the "team lead" technologist allowed the scanning technologist to concentrate on one patient at a time- particularly helpful for during high through-put times, in which a back log of FIRST reconstruction times for the 1st axial reconstruction for abdomen/ pelvis exams; 6.6 minutes for the 1st axial (soft tissue) reconstruction for chest exams; and 13.3 minutes for the 2nd axial MIP reconstruction for chest exams. Lastly, a comparison of utilization data from the same scanner over the same time period with and without FIRST implementation yielded similar results: 1668 exams were completed in absence of FIRST and 1707 exams were completed when FIRST was deployed.

#### CONCLUSION

These results demonstrate that practice efficiency can be maintained despite an increase in image reconstruction times. As a result of this project, FIRST will continue to be used clinically for all exams in this study. Additionally, FIRST will be further utilized and implemented in more clinical exams. As a follow-up to this study, further investigations will assess the effect of broader clinical deployment of FIRST both in regards to practice efficiency in aggregate, but also the pace of exam completion. With the current limited deployment of FIRST, scenarios arise in which multiple exams can be completed within minutes of each other and inundate the interpreting radiologist with data. With wider utilization of FIRST, a steadier pace of exam completion is expected.



# RO227-SD-THB1

Development and Implementation of the In-Vivo Dosimeter for High-Dose-Rate (HDR) Ir-192 Brachytherapy Using Optically Stimulated Luminescence Dosimeters (OSLDs) : Evaluation of Rectal Dose in Clinical Cases

Thursday, Nov. 29 12:45PM - 1:15PM Room: RO Community, Learning Center Station #1

FDA Discussions may include off-label uses.

#### Participants

Yoshinori Miyahara, Izumo, Japan (*Abstract Co-Author*) Nothing to Disclose Atsushi Ue, Izumo, Japan (*Presenter*) Nothing to Disclose Mutsumi Tokudo, Izumo, Japan (*Abstract Co-Author*) Nothing to Disclose Yuki Imoto, Izumo, Japan (*Abstract Co-Author*) Nothing to Disclose Yoko Hieda, MD, PhD, Izumo, Japan (*Abstract Co-Author*) Nothing to Disclose Yukihisa Tamaki, Izumo, Japan (*Abstract Co-Author*) Nothing to Disclose Yasushi Yamamoto, Izumo, Japan (*Abstract Co-Author*) Nothing to Disclose Hajime Kitagaki, MD, Izumo, Japan (*Abstract Co-Author*) Nothing to Disclose Taisuke Inomata, MD, Osaka, Japan (*Abstract Co-Author*) Nothing to Disclose

#### PURPOSE

Evaluation of rectal dose is an important factor in HDR brachytherapy within the pelvis. And the nanoDotTM OSLD (Al2O3 :C) is a new type of in-vivo dosimeter. Purpose of this study is to measure the rectal dose in HDR brachytherapy using OSLDs.

### **METHOD AND MATERIALS**

Initially, the calibration curves of the OSLDs for high-energy gamma-ray (from 0.1 to 8.0 Gy) were measured by using  $10 \times 10 \times 10$  cm3 prototype water phantom. And also angular dependence was measured. Production of rectal dosimeter and its measurement are as follows: Three light-shielded OSLDs sheets (height  $10.0 \times$  width 19.0 mm per sheet) were tightly fixed at 1.0 mm spacing as to be circular form to a flexible catheter (Nelaton catheter of outside diameter 6.0 mm) which can insert the X-ray opaque catheter marker. Treatment planning was conducted by semi-orthogonal method from both frontal and lateral images, and the OSLDs were placed at the high-dose region of the rectum. In analysis of rectal dose in OSLDs, nine cut dots (circle of diameter 5.0 mm) were measured from three sheets (three dots per one sheet of a step). The difference between the planned dose (at X-ray opaque catheter marker) and the average dose at each step were evaluated. Immobility of inserted rectal dosimeter was confirmed from the X-ray images after the irradiation. These dosimetries were conducted on RALS treatment (prescription dose: 6.0 Gy) of cervical cancer for nine cases.

#### RESULTS

The calibration curve (y=95141x-20703) was determined between OSLDs counts and Ir-192 doses. We estimated the uncertainty (angular dependence, reproducibility, and systematic variation) of this rectum dosimeter to be 15%. Identification of the position of the OSLDs with the 2D image was difficult. In the first four cases, a difference of about 1.0 Gy was observed between the planned value and the OSLD. However, in the following five cases, rectal doses were almost equivalent (P=0.79, Welch's t test) by placing a point markers on the top of the OSLDs for position identification.

#### CONCLUSION

This OSLD rectal dosimeter is flexible and non-invasive. The feasibility of OSLD as an in-vivo dosimeter in HDR brachytherapy was verified.

#### **CLINICAL RELEVANCE/APPLICATION**

By using a flexible in-vivo dosimeter, it becomes possible to measure the actual rectal dose, and the treatment can be performed safely.



## UR192-ED-THB7

Prove Your Worth: How to Add Value to Urinary Bladder Staging with Multi-Parametric MRI-Tips and Tricks to Improve Utilization of MRI of the Urinary Bladder by Urologists in Clinical Practice

Thursday, Nov. 29 12:45PM - 1:15PM Room: GU/UR Community, Learning Center Station #7

#### Awards Certificate of Merit

#### **Participants**

Wendy Tu, MD, Ottawa, ON (*Presenter*) Nothing to Disclose Nicola Schieda, MD, Ottawa, ON (*Abstract Co-Author*) Nothing to Disclose Christopher Lim, MD, Boston, MA (*Abstract Co-Author*) Nothing to Disclose Christian B. Van Der Pol, MD, Hamilton, ON (*Abstract Co-Author*) Nothing to Disclose Andrew D. Chung, MD, Boston, MA (*Abstract Co-Author*) Nothing to Disclose Niket Gandhi, MD, Ottawa, ON (*Abstract Co-Author*) Nothing to Disclose Matthew D. McInnes, MD, PhD, Ottawa, ON (*Abstract Co-Author*) Nothing to Disclose Trevor A. Flood, MD, FRCPC, Ottawa, ON (*Abstract Co-Author*) Nothing to Disclose

# For information about this presentation, contact:

nschieda@toh.on.ca

# **TEACHING POINTS**

1. MRI, combining high-resolution T2-weighted + diffusion weighted + dynamic contrast enhanced imaging, is accurate for T staging bladder cancer. 2. MRI is more accurate than CT for diagnosis of T2 and T3 disease and for diagnosis of metastatic lymphadenopathy. 3. MRI is accurate for depicting local invasion (T4 disease) and suggesting aggressive patterns of spread such as in plasmacytoid variant cancer. 4. Texture analysis of MR images adds information for grading and staging of bladder cancer and radiogenomic analysis of MR images may represent a future alternative to histological sampling in the work-up of bladder cancer before treatment.

### TABLE OF CONTENTS/OUTLINE

1. Multi-parametric MRI technique for imaging of the urinary bladder with emphasis on DWI. 2. Histology of the normal urinary bladder and various bladder malignancies including grading and staging. 3. Review of mp-MRI for T staging bladder cancer, including diagnostic accuracy with DWI. 4. Review of mp-MRI for N staging bladder cancer, including DWI and SPIO agents. 5. Presentation of aggressive variants and patterns of spread in bladder cancer, including adenocarcinoma and plasmacytoid variant cancer. 6. Introduction to radiogenomic analysis of bladder cancer for T staging and grading of disease.



## UR193-ED-THB8

MRI Findings of Obstructive Azoospermia: Lesions In and Out of Pelvic Cavity

Thursday, Nov. 29 12:45PM - 1:15PM Room: GU/UR Community, Learning Center Station #8

#### Awards Cum Laude

### Participants

Jian Guan, MD, Guangzhou, China (*Abstract Co-Author*) Nothing to Disclose Huanjun Wang, MD, Guangzhou, China (*Presenter*) Nothing to Disclose Yang Peng, Guangzhou, China (*Abstract Co-Author*) Nothing to Disclose Yan Guo, MD, Guangzhou, China (*Abstract Co-Author*) Nothing to Disclose

### For information about this presentation, contact:

usefulkey0077@hotmail.com

#### **TEACHING POINTS**

To be familiar with normal male genital ducts on 3.0T MRI and its standard and personalized MR examination protocol. To learn different locations of obstruction and suggestive parameters of semen analysis. To realize both the focal lesions which lead to obstruction and the underlying clinical syndromes according to pelvic and abdominal MR imaging findings. To discuss the diagnostic strategy and points in MRI evaluation.

#### **TABLE OF CONTENTS/OUTLINE**

Constituents of male genital ducts and its normal appearance on 3.0T MRI. a) Ejaculatory duct; b) Seminal vesicle; c) Deferent duct; d) Epididymis. The standard and personalized MR examination protocol for obstructive azoospermia. Suggestive parameters of semen analysis for different locations of obstruction. Pelvic and abdominal MR imaging findings of sample cases. Diagnostic strategy and points in MRI evaluation.



# VI173-ED-THB9

### Need-To-Know Things About Interventional Procedures Related to Portal Venous System

Thursday, Nov. 29 12:45PM - 1:15PM Room: VI Community, Learning Center Station #9

### Awards Certificate of Merit

### Participants

Shinichi Ota, MD,PhD, Otsu, Japan (*Presenter*) Nothing to Disclose Akitoshi Inoue, MD,PhD, Higashioumi-city, Japan (*Abstract Co-Author*) Nothing to Disclose Shobu Watanabe, MD, Otsu, Japan (*Abstract Co-Author*) Nothing to Disclose Kai Takaki, MD, Otsu, Japan (*Abstract Co-Author*) Nothing to Disclose Shigetaka Sato, MD, Otsu, Japan (*Abstract Co-Author*) Nothing to Disclose Norihisa Nitta, MD, Kyoto, Japan (*Abstract Co-Author*) Nothing to Disclose Akinaga Sonoda, MD, PhD, Otsu, Japan (*Abstract Co-Author*) Nothing to Disclose Shuzo Kanasaki, MD, PhD, Kyoto, Japan (*Abstract Co-Author*) Nothing to Disclose Kiyosumi Maeda, MD, Kusatsu, Japan (*Abstract Co-Author*) Nothing to Disclose Kiyoshi Murata, MD, Otsu, Japan (*Abstract Co-Author*) Nothing to Disclose

#### For information about this presentation, contact:

junryuhei@belle.shiga-med.ac.jp

### **TEACHING POINTS**

The purpose of this exhibit is: To recognize abnormalities of portal vein (PV) and understand the pathophysiological conditions. To recognize various interventions for portal abnormalities.

#### **TABLE OF CONTENTS/OUTLINE**

1. Anatomy of Portal venous system 2. Abnormalities: Portal hypertension, tumor invasion, inflammation including pylephlebitis and from pancreatitis, thrombus, shunt including arterio-venous shunt and porto-systemic shunt (portal venous shunt) 3. Approach to PV: Transjugular intrahepatic, trans-splenic, transhepatic, trans-ileal vein through a small incision in the abdominal wall, via shunt 4. Interventions: a. For portal hypertension: Percutaneous transhepatic obliteration / sclerotherapy (PTO/PTS), dual balloon occluded embolotherapy (DBOE), balloon occluded retrograde transrenal obliteration (BRTO), plug assisted retrograde transrenal obliteration (PARTO), transjugular intrahepatic porto-systemic shunt (TIPS) b. For stenosis and thrombus: Stent placement, thrombolysis c. For pre hepatic resection: Portal vein embolization (PVE) d. For shunt occlusion: Coil embolization 5. Complications during / after portal interventions 6. Summary



### VI174-ED-THB10

Contrast Enhanced Magnetic Resonance Lymphangiography for Various Thoracoabdominal Lymphatic Diseases

Thursday, Nov. 29 12:45PM - 1:15PM Room: VI Community, Learning Center Station #10

#### Awards Magna Cum Laude

#### Participants

Hyun Jung Koo, MD, Seoul, Korea, Republic Of (*Presenter*) Nothing to Disclose Ji Hoon Shin, MD, Seoul, Korea, Republic Of (*Abstract Co-Author*) Nothing to Disclose Dong Hyun Yang, MD, Seoul, Korea, Republic Of (*Abstract Co-Author*) Nothing to Disclose Hee Mang Yoon, MD, Seoul, Korea, Republic Of (*Abstract Co-Author*) Nothing to Disclose Mi Young Kim, MD, PhD, Seoul, Korea, Republic Of (*Abstract Co-Author*) Nothing to Disclose

### For information about this presentation, contact:

mimowdr@gmail.com

#### **TEACHING POINTS**

Thoracoabdominal lymphatic diseases have various spectrum such as thoracic duct cyst, lymphocele, iatrogenic thoracic duct injury, and plastic bronchitis which is rarely seen after Fontan surgeries in children. We utilized contrast enhanced magnetic resonance (MR) lymphangiography for characterization of thoracoabdominal lymphatic diseases and pre-intervantional planning. Radiologists, interventionalists and surgeons can work as a team to manage various thoracoabdominal lymphatic diseases. 1. Review protocol of contrast-enhanced MR lymphangiography for characterization of thoracoabdominal lymphatic diseases. 2. Describe normal lymphatics anatomy with contrast-enhanced MR lymphangiography and conventional lipidol lymphangiography. 3. Learn the characteristics of various thoracoabdominal lymphatic diseases with contrast-enhanced MR lymphangiography and therapeutic options including conventional lymphangiography.

#### **TABLE OF CONTENTS/OUTLINE**

1. Protocol - Procedure: Inguinal lymph nodes cannulation - MR technique for imaging the central lymphatics Adults Pediatrics 2. Normal anatomy of the central lymphatics 3. Various lymphatic diseases Lymphocele Plastic bronchitis Thoracic duct cyst Iatrogenic thoracic duct injury Chylothorax and chylous ascites secondary to liver cirrhosis



# VI266-SD-THB1

### Superman X-Ray Vision Smart Glasses Guidance for Percutaneous Biopsy and Ablation

Thursday, Nov. 29 12:45PM - 1:15PM Room: VI Community, Learning Center Station #1



#### Participants

Ming Li, PhD, Bethesda, MD (*Presenter*) Nothing to Disclose Sheng Xu, PhD, Bethesda, MD (*Abstract Co-Author*) Nothing to Disclose Hayet Amalou, MD, Bethesda, MD (*Abstract Co-Author*) Nothing to Disclose Robert D. Suh, MD, Los Angeles, CA (*Abstract Co-Author*) Nothing to Disclose Bradford J. Wood, MD, Bethesda, MD (*Abstract Co-Author*) Researcher, Koninklijke Philips NV; Researcher, Celsion Corporation; Researcher, BTG International Ltd; Researcher, Siemens AG; Researcher, XAct Robotics; Researcher, NVIDIA Corporation; Intellectual property, Koninklijke Philips NV; Intellectual property, BTG International Ltd; Royalties, Invivo Corporation; Royalties, Koninklijke Philips NV; ; ;

# For information about this presentation, contact:

lim2@mail.nih.gov

### PURPOSE

Needle placement accuracy for biopsy and ablation largely depends on the operator's visuospatial skills and hand-eye coordination, with target and imaging feedback. An augmented reality (AR) system was developed using smart see-through glasses to facilitate and assist needle trajectory planning and guidance.

# METHOD AND MATERIALS

An IR AR system was developed using Unity platform and Vuforia SDK customized to display the planned needle trajectory on the ODG R-7 (ODG, San Francisco, CA) smart glasses' see-through screens, in real time. A 3D marker attached on a patient is used to orient and track the patient's pre-procedural volumetric image with the glasses. The displayed target lesion was overlaid on the patient. The operator determined the skin insertion point. The needle trajectory was generated by aligning the target, insertion point and the center of the camera. The displayed needle trajectory was always referenced to the patient and independent from the updated physical position and orientation of the glasses. The see-through AR feature allows the operator to continuously compare the actual needle with the plan. The guidance accuracy was evaluated using a multi-modality interventional anthropomorphic phantom (CIRS, Norfolk, VA). A random insertion point was selected, and the target, the needle path and end position was displayed on the glasses. Users inserted an 18-G biopsy needle into the phantom to reach the target under the AR guidance. After each insertion, a CT scan was acquired and the inserted needle tip was compared with the target on CT.

# RESULTS

The needle hit the targets in all trials. The lateral distance from the needle tip to the target centerpoint was 3.9±2.9mm, and the in-direction distance was 2.7±1.3mm. The AR system displayed the guidance data accurately during the intervention. In clinical situations with limited imaging feedback (such as lung biopsy and ablation), AR glasses might provide feedback that could influence accuracy, especially for the inexperienced operator.

# CONCLUSION

Smart AR glasses can provide accurate guidance and see-through-the-skin display for needle based interventions like biopsy and ablation, when real time imaging feedback is not otherwise available.

### **CLINICAL RELEVANCE/APPLICATION**

The wearable device does not interfere with clinical workflow, and may potentially promote standardization and a shorter learning curve for trainees.



# VI267-SD-THB2

# The Availability of Interventional Radiology Rotations at Medical Schools in the United States

Thursday, Nov. 29 12:45PM - 1:15PM Room: VI Community, Learning Center Station #2

#### Participants

Amy Garvey, New York, NY (Presenter) Nothing to Disclose

Daryl T. Goldman, MD , New Orleans, LA (Abstract Co-Author) Nothing to Disclose

Vivian L. Bishay, MD, Philadelphia, PA (Abstract Co-Author) Nothing to Disclose

Edward Kim, MD, East Meadow, NY (Abstract Co-Author) Consultant, Koninklijke Philips NV Advisory Board, Onyx Pharmaceuticals, Inc Advisory Board, Sterigenics International LLC

Robert A. Lookstein, MD, New York, NY (*Abstract Co-Author*) Consultant, Boston Scientific Corporation Consultant, Medtronic plc Francis S. Nowakowski, MD, New York, NY (*Abstract Co-Author*) Nothing to Disclose

Rahul S. Patel, MD, New York, NY (*Abstract Co-Author*) Consultant, Sirtex Medical Ltd; Research Consultant, Medtronic plc; Consultant, Penumbra, Inc; Consultant, Terumo Corporation

Mona B. Ranade, MD, Brookfield, WI (Abstract Co-Author) Nothing to Disclose

Aaron M. Fischman, MD, New York, NY (*Abstract Co-Author*) Advisory Board and Consultant- Terumo Interventional Systems, Embolx Inc.; ; Speakers Bureau - Boston Scientfic, BTG; ; Royalties - Merit Medical; ; Investor - Adient Medical

### PURPOSE

The recent creation of the integrated interventional radiology (IR) residency has dramatically altered education and training for future interventional radiologists. The successful recruitment of medical students into this direct pathway requires that students receive adequate and timely exposure to IR through dedicated IR rotations. This study aims to explore the availability of IR rotations at U.S. medical schools.

# METHOD AND MATERIALS

The 151 Liaison Committee on Medical Education (LCME) accredited medical schools in the United States were identified for inclusion in this study. Information on the availability of IR and diagnostic radiology (DR) rotations was determined either through online course listings or direct contact with the school by phone or email. The course type, length(s), and eligibility requirements (i.e. year in medical school) were determined for each offered course.

# RESULTS

Of the 151 LCME accredited medical schools, 140 provided course information and were included in the study. 98 (64%) of the included schools offered a dedicated IR rotation. 85% of these rotations were only available to fourth-year medical students, 13% were available to clinical students, and only 2% were offered for preclinical students. Course lengths varied between schools offering IR rotations, with most courses ranging between two to four weeks in length. Upon examination of course type, most of these IR rotations were electives with only 8% of included schools offering an IR sub-internship.

# CONCLUSION

Many medical schools in the United States are without dedicated IR rotations. Furthermore, current IR rotations are brief and/or offered late in a student's medical education. Successful recruitment into the integrated IR residency requires availability of comprehensive and timely IR rotations for medical students.

# **CLINICAL RELEVANCE/APPLICATION**

To ensure successful recruitment into the integrated IR residency, medical students need adequate exposure to IR and access to comprehensive IR rotations.



## VI268-SD-THB3

The Predictor of Pulmonary Artery Pressure Improvement of Balloon Pulmonary Angioplasty for Chronic Thromboembolic Pulmonary Hypertension: Initial Experience of the CT Voronoi Diagram-based Lung Volume Measurements

Thursday, Nov. 29 12:45PM - 1:15PM Room: VI Community, Learning Center Station #3

#### Participants

Akiyuki Kotoku, MD, Kawasaki, Japan (*Presenter*) Nothing to Disclose Yoshiro Hori, Osaka, Japan (*Abstract Co-Author*) Nothing to Disclose Yoshiaki Watanabe, MD, Suita, Osaka, Japan (*Abstract Co-Author*) Nothing to Disclose Tatsuya Nishii, MD, PhD, Suita, Japan (*Abstract Co-Author*) Nothing to Disclose Yoshiaki Morita, Suita, Japan (*Abstract Co-Author*) Nothing to Disclose Emi Tateishi, Suita, Japan (*Abstract Co-Author*) Nothing to Disclose Emi Tateishi, Suita, Japan (*Abstract Co-Author*) Nothing to Disclose Atsushi K. Kono, MD, PhD, Suita, Japan (*Abstract Co-Author*) Nothing to Disclose Keisuke Kiso, MD, Suita, Japan (*Abstract Co-Author*) Nothing to Disclose Hidefumi Mimura, MD, Kawasaki, Japan (*Abstract Co-Author*) Nothing to Disclose Tetsuya Fukuda, Suita, Japan (*Abstract Co-Author*) Nothing to Disclose

### For information about this presentation, contact:

a2kotoku@marianna-u.ac.jp

### PURPOSE

Balloon pulmonary angioplasty (BPA) is a promising treatment for chronic thromboembolic pulmonary hypertension (CTEPH); however, the strategy regarding the target vessel for BPA is not fully established. With a computational Voronoi diagram-based segmentation (VDS) derived from the CT pulmonary angiography (CTPA), the lung volume can be simulated. We hypothesized that the lung volume supplied by the treated branch, which BPA improved the stain of the lung parenchyma, was related to the improvement of the pulmonary artery pressure (PAP). This study aimed to evaluate the effects of the treated lung volume estimated from the CTPA with the VDS to the PAP improvement after BPA.

### **METHOD AND MATERIALS**

We retrospectively reviewed 16 CTEPH patients (13 females, median 71 years, and mean PAP  $34\pm13$  mmHg) who received the first session BPA. From the pulmonary angiography, we evaluated the parenchymal stain of the treated branches before and after BPA with the 3-point score (0, not stained; 1, slightly stained; and 2, clearly stained). From the CTPA before BPA, we measured the lung volume of each treated branch by the VDS. Further, we obtained the total lung volume of treated branches (Vt), the summed volume of the stained area (score >1) before BPA (Vpre-stained), and the summed volume of the branches which BPA normalized the parenchyma stain to score 2 (Vimproved). We compared these volumes between the effective and the non-effective group whose PAP improved or not by the Welch's t-test. Further, we provided the predicting factors for improvement of the PAP ( $\Delta$ PAP) using the multivariate analysis.

### RESULTS

In 12 cases, BPA improved the mean PAP by 6.7±4.6 mmHg. The Vt was not significantly different in two groups (P=0.70). However, the mean Vpre-stained and Vimproved were significantly larger in the effective group than the non-effective group (140.5±183.9 vs.  $0.3\pm0.7$  mL, and  $169.4\pm184.6$  vs.  $17.8\pm35.7$  mL, P=0.02 for both). Moreover, the multivariate analysis revealed that the PAP before BPA and Vimproved were the independent predictors for the  $\Delta$ PAP (P=0.006 and 0.04, respectively).

#### CONCLUSION

The PAP improvement by BPA linked with the lung volume of the treated branches, especially Vpre-stained and Vimproved.

### **CLINICAL RELEVANCE/APPLICATION**

This study shows the possibility of predicting therapeutic efficacy of BPA for CTEPH by combining the enhancement of lung parenchyma and the Voronoi diagram-based volume measurements.



### VI269-SD-THB4

Long-Term Outcomes of Radiofrequency Ablation for Locally Recurrent Papillary Thyroid Cancer

Thursday, Nov. 29 12:45PM - 1:15PM Room: VI Community, Learning Center Station #4

# VA

# Participants

Sae Rom Chung, MD, Seoul, Korea, Republic Of (*Presenter*) Nothing to Disclose Jung Hwan Baek, Seoul, Korea, Republic Of (*Abstract Co-Author*) Consultant, STARmed; Consultant, RF Medical Young Jun Choi, MD, Seoul, Korea, Republic Of (*Abstract Co-Author*) Nothing to Disclose Jeong Hyun Lee, MD, PhD, Seoul, Korea, Republic Of (*Abstract Co-Author*) Nothing to Disclose

### PURPOSE

This retrospective study evaluated the long-term outcomes of ultrasound (US)-guided radiofrequency ablation (RFA) for controlling locoregionally recurrent papillary thyroid cancer (PTC).

# METHOD AND MATERIALS

We retrospectively reviewed 29 patients who underwent RFA for recurrent PTC between September 2008 and April 2012 and were subsequently followed up for at least 5 years. Follow-up included US and clinical evaluations at 1, 3, 6, and 12 months and every 6-12 months thereafter.

### RESULTS

A total of 46 recurrent tumors were detected in the 29 patients. The mean follow-up duration after RFA was  $80 \pm 17.3$  months (range, 60-114 months). Tumor volume decreased significantly, from  $0.25 \pm 0.42$  mL before ablation to  $0.01 \pm 0.08$  mL at the final evaluation (p < 0.001), with a mean volume reduction of 99.5%  $\pm 2.9$ %. Additionally, 42 of the 46 treated tumors (91.3%) had completely disappeared by the final evaluation, and there were no delayed complications associated with RFA during the follow-up period.

### CONCLUSION

RFA is an acceptable nonsurgical treatment option for local control of recurrent PTC.

#### **CLINICAL RELEVANCE/APPLICATION**

Although reoperation is a standard definitive curative treatment for recurrent thyroid cancer, RFA can be applied relatively easily, repeatedly, and effectively to treat locoregional recurrent thyroid cancers.



# VI270-SD-THB5

Differences in Adherence and Reported Occupational Dose For One- versus Two-Badge Monitoring Protocols Among Medical Staff Performing or Assisting with Fluoroscopically-Guided Interventional Procedures

Thursday, Nov. 29 12:45PM - 1:15PM Room: VI Community, Learning Center Station #5

# Participants

David Borrego, PHD, Bethesda, MD (*Presenter*) Nothing to Disclose Craig R. Yoder, PhD, Bethesda, MD (*Abstract Co-Author*) Nothing to Disclose Cari Kitahara, PhD, Bethesda, MD (*Abstract Co-Author*) Nothing to Disclose

#### For information about this presentation, contact:

david.borrego@nih.gov

# PURPOSE

The use of fluoroscopically-guided interventional procedures (FGIPs) has increased over the past few decades along with concerns about radiation-associated health risks to the medical staff who perform them. It is important to monitor and report on occupational doses for operators of FGIPs as they are among the highest exposed group in medical practice. In the present study, we compared dosimetry data obtained from personal monitoring devices of medical staff who have performed or assisted with FGIPs according to institutional use of a one-badge (over the apron) versus two-badge (over and under the apron) monitoring protocol.

#### **METHOD AND MATERIALS**

We used data from the largest dosimetry provider in the United States to collect 2,054,648 badge readings over three years, 2009, 2012, and 2015, corresponding to 49,991, 81,561, and 125,669 medical staff, respectively. To separate the supporting staff doses from that of physicians, who operate in the highest dose areas, we contacted three large hospitals to help us identify their physicians in the dataset.

#### RESULTS

Of the eligible readings, 67% used the one-badge protocol while 33% used the two-badge protocol. We assessed and determined that 33.3% of the two-badge readings (n=229,092) were erroneous (i.e., reversal of dosimeter locations, failure to wear both dosimeters, etc.). Median annual effective dose equivalents for staff using the two-badge protocol were 0.12, 0.14, and 0.11 mSv and for the one-badge protocol doses were 0.28, 0.18, and 0.21 mSv in 2009, 2012, and 2015, respectively. Among physicians, the mean annual dose was 2.8 (max=23.3) mSv and 12.6 (max=77.5) mSv to the lens of the eye.

# CONCLUSION

Institutions subscribing to a two-badge protocol would benefit from strategies to reduce the errant wear of dosimeters. Comparing effective dose equivalents among the one- vs. two-badge wearers, we found the one-badge protocol provides higher estimates than the two-badge protocol despite similar distributions of dose equivalent recorded by the over-the-apron badge. These differences may be attributable to under-the-apron badge readings that were below the nominal detection limit. Even with the additional conservatism afforded by the one-badge protocol none of the physicians exceeded annual regulatory dose limits.

#### **CLINICAL RELEVANCE/APPLICATION**

Based on these findings, the one-badge protocol appears to be more practical and reliable for the monitoring of medical staff performing FGIP.



# VI271-SD-THB6

Utility of Change in Volumetric ADC and Enhancement Post TACE in Predicting Histologic Grade of HCC with Pathologic Correlation

Thursday, Nov. 29 12:45PM - 1:15PM Room: VI Community, Learning Center Station #6

# Awards

# Student Travel Stipend Award

#### Participants

Sanaz Ameli, MD, Baltimore, MD (*Presenter*) Nothing to Disclose Farnaz Najmi Varzaneh, MD, Baltimore, MD (*Abstract Co-Author*) Nothing to Disclose Mounes Aliyari Ghasabeh, MD, Baltimore, MD (*Abstract Co-Author*) Nothing to Disclose Pegah Khoshpouri, MD, Baltimore, MD (*Abstract Co-Author*) Nothing to Disclose Ankur Pandey, MD, Baltimore, MD (*Abstract Co-Author*) Nothing to Disclose Pallavi Pandey, MD, Baltimore, MD (*Abstract Co-Author*) Nothing to Disclose Yan Luo, MD, Wuhan, China (*Abstract Co-Author*) Nothing to Disclose Manijeh Zarghampour, MD, Baltimore, MD (*Abstract Co-Author*) Nothing to Disclose Angela Jacob, Baltimore, MD (*Abstract Co-Author*) Nothing to Disclose Robert Anders, Baltimore, MD (*Abstract Co-Author*) Nothing to Disclose Ihab R. Kamel, MD, PhD, Baltimore, MD (*Abstract Co-Author*) Nothing to Disclose

#### For information about this presentation, contact:

sameli1@jhmi.edu

#### PURPOSE

To investigate the role of change in ADC and enhancement after trans- arterial chemoembolization (TACE) in predicting histological grade of hepatocellular carcinoma (HCC).

#### **METHOD AND MATERIALS**

This HIPPA compliant retrospective study was approved by our institutional review board. The study population included 104 HCC patients (128 index lesions) with MR imaging within 6 months before and 6 months after TACE who presented at our institution between 2001 and 2015. All cases had pathologic report of the HCC tumor by biopsy or liver transplantation. Volumetric measurements of venous enhancement (VE) and apparent diffusion coefficient (ADC) were performed on baseline and post TACE MRI. Based on pathology report, the tumors were histologically classified into two groups: Low grade HCC (n=42) and intermediate/high grade HCC (n=86). In case of tumors with mixed differentiation, the worst differentiation grade was considered. The mean ADC (mm2/s) and enhancement (%) of two groups were compared at two-time points. P value<0.05 was considered statistically significant.

#### RESULTS

Mean ADC increased by  $(363.88\pm529.07 \times 10 - 6 \text{ mm2/s})$  in low grade vs.  $(136.20\pm503.73 \times 10 - 6 \text{ mm2/s})$  in high grade HCC post TACE. ADC change in low grade tumors was higher than in intermediate/high grade tumors (P=0.02). Setting the cutoff of 148.4 x 10 - 6 mm2/s or more in ADC change had a sensitivity and specificity of 62% and 55%, respectively in differentiating between the 2 groups. Enhancement decreased by  $(46 \pm 34\%)$  in low grade vs.  $(28\pm36\%)$  in high grade tumors (P=0.011). Setting the cutoff of 39% or more decrease in enhancement had sensitivity and specificity of 65% and 55%, respectively in differentiating between the 2 groups.

### CONCLUSION

Low grade tumors demonstrate a greater change in ADC and enhancement post TACE as compared to intermediate/ high grade tumors.

#### **CLINICAL RELEVANCE/APPLICATION**

The change in ADC and enhancement in HCC after TACE could potentially be utilized to predict tumor differentiation and can help the clinicians to plan future treatment in these patients.

#### **Honored Educators**

Presenters or authors on this event have been recognized as RSNA Honored Educators for participating in multiple qualifying educational activities. Honored Educators are invested in furthering the profession of radiology by delivering high-quality educational content in their field of study. Learn how you can become an honored educator by visiting the website at: https://www.rsna.org/Honored-Educator-Award/ Ihab R. Kamel, MD, PhD - 2015 Honored Educator



# VI272-SD-THB7

# Analysis of Imaging Features of Bone Changes With The Chylous Reflux Lymphedema

Thursday, Nov. 29 12:45PM - 1:15PM Room: VI Community, Learning Center Station #7

### Participants

Mengjun Wang, Beijing, China (*Presenter*) Nothing to Disclose Xiaoli Sun, MD, PhD, Beijing, China (*Abstract Co-Author*) Nothing to Disclose ChunYan Zhang, Beijing, China (*Abstract Co-Author*) Nothing to Disclose Jian Dong, PhD, Beijing, China (*Abstract Co-Author*) Nothing to Disclose Meng Huo, Beijing, China (*Abstract Co-Author*) Nothing to Disclose

For information about this presentation, contact:

huawuzhengming@126.com

### PURPOSE

To explore the imaging characteristics of bone changes with the chylous reflux lymphedema.

# METHOD AND MATERIALS

We retrospectively analyzed the imaging data of bone changes with the chylous reflux lymphoedema of 37 cases patients. Thirtyseven patients (male 24 and female 13) all underwent direct lymphangiography (DLG) and MSCT after DLG chest and abdomen combined plain scan, of which 3 patients underwent CT enhancement and 19 underwent MR examination.

### RESULTS

DLG and radionuclide scintigraphy showed that 36 cases had chylous regurgitation in the lower extremities, and 1 case had chest wall (trunk) chylous regurgitation. MSCT after DLG showed the bone changes, according to the different forms of the diseased bone, there are 6 types: type I bone destruction (7 cases); type II osteoporosis-like changes (22); type III honeycomb or coarse tubular changes (24); type IV needle-like changes at the vertebral body anterior (4); type-V cystic changes (18), and type-VI osteosclerosis (9). Three patients who underwent enhanced CT scan showed no enhancement of bone changes. The above I-IV type bone changes in MR showed slightly longer T1 and longer T2 signals; V type showed long T1 and long T2 signals; and VI showed long T1 and short T2 signals. In the same patient, two or more of the above two types of manifestations can occur at the same time, with the most changes in osteoporosis-like changes and honeycomb or coarse tubular changes (respectively 22 cases, accounting for 59%; 24, 65%). Of the 37 patients, 8 cases with chylothorax or chyloperitoneum; 3 with chyluria; 3 with lymphangioma of celiac, retroperitoneum, mediastinal, or soft-tissue; and 3 with splenic lymphangioma.

# CONCLUSION

There are a variety of radiological manifestations of bone changes with chylous reflux lymphedema, and may be associated with other lymphatic abnormalities such as chylous leakage, lymphangioma, etc. Bone changes are part of the general lymphatic developmental abnormalities. Correct understanding of these signs helps to improve the diagnosis of this disease of bone changes with chylous reflux lymphedema, and to avoid misdiagnosis.

# **CLINICAL RELEVANCE/APPLICATION**

Understanding the image manifestation of bone changes with chylous reflux lymphedema helps to improve the clinical diagnosis, avoid misdiagnosis, and have a further understanding of the general lymphatic vessel development abnormalities.



# VI273-SD-THB8

# MRI and US Volume Measurement Differences May Predict Success of Prostate Fusion Biopsy

Thursday, Nov. 29 12:45PM - 1:15PM Room: VI Community, Learning Center Station #8

VA

# Participants

Haydar Celik, PhD, Bethesda, MD (*Presenter*) Nothing to Disclose Filippo Pesapane, MD, Milan, Italy (*Abstract Co-Author*) Nothing to Disclose Peter L. Choyke, MD, Rockville, MD (*Abstract Co-Author*) Nothing to Disclose Peter Pinto, Bethesda, MD (*Abstract Co-Author*) Nothing to Disclose Victoria L. Anderson, MS, Bethesda, MD (*Abstract Co-Author*) Nothing to Disclose Bradford J. Wood, MD, Bethesda, MD (*Abstract Co-Author*) Researcher, Koninklijke Philips NV; Researcher, Celsion Corporation; Researcher, BTG International Ltd; Researcher, Siemens AG; Researcher, XAct Robotics; Researcher, NVIDIA Corporation; Intellectual property, Koninklijke Philips NV; Intellectual property, BTG International Ltd; Royalties, Invivo Corporation; Royalties, Koninklijke Philips NV; ;

Baris Turkbey, MD, Bethesda, MD (Abstract Co-Author) Nothing to Disclose

### For information about this presentation, contact:

haydari@gmail.com

### PURPOSE

The present study sought to determine whether the difference between MRI and US volume measurements were associated with MRI-US fusion-guided biopsy outcomes.

### METHOD AND MATERIALS

IRB-approved clinical trial data was analyzed. All patients underwent both standard 12-core as well as fusion biopsy by a multidisciplinary team. The superiority of the fusion biopsy over the standard TRUS-guided biopsy was characterized according to the discordance between MRI and US volume measurements. Gleason scores were recorded independently for both fusion and standard biopsies in each patient procedure. Primary and secondary Gleason scores were converted to an 'aggressiveness scale' (AS), which digitally categorized patients. For each patient, fusion and standard biopsy results were compared to determine if either fusion or standard biopsy resulted in higher AS. Duration between the MR and US volume measurements was analyzed for influence on outcomes.

### RESULTS

In our database, 261 patient biopsies had higher AS using fusion biopsy, 185 patients had higher AS using standard biopsy, and 839 had equivalent AS (Total 1295 patients). MRI volume measurements were larger (compared with US volume measurements) in 507 patients; US volume measurements were larger (compared with MRI volume measurements) in 713 patients, and 65 measurements were equal. When there was greater than 5ml difference between US and MRI volumes measured, the superiority of the fusion biopsy decreased drastically (Figure). Causes for discordant measures were not analyzed nor specific causes assocciation with successful outcome (higher Gleason score assumed to be better characterization).

### CONCLUSION

As the difference between the MRI and US volumes goes beyond 5-10 ml, the superiority of the fusion biopsy drops significantly. Such a discordance between MR and US volumes may be associated with (or predict) less value for fusion biopsy over standard 12-core biopsy.

# **CLINICAL RELEVANCE/APPLICATION**

Clinicians may need to be more careful about fusion biopsy if prostate volume measurements differ beyond 5-10ml.



# AI001-THD

# Data Science: Normalization, Annotation, Validation

Thursday, Nov. 29 2:30PM - 4:00PM Room: AI Community, Learning Center

# Title and Abstract

Data Science: Normalization, Annotation, Validation This session will focus on preparation of the image and non-image data in order to obtain the best results from your deep learning system. It will include a discussion of different options for representing the data, how to normalize the data, particularly image data, the various options for image annotation and the benefits of each option. We will also discuss the 'after training' aspects of deep learning including validation and testing to ensure that the results are robust and reliable.



# AI001-FRA

# **Multi-modal Classification**

Friday, Nov. 30 8:30AM - 10:00AM Room: AI Community, Learning Center

# **Title and Abstract**

Multi-modal Classification This session will focus on multimodal classification. Classification is the recognition of an image or some portion of an image being of one type or another, such as 'tumor' or 'infection'. Multimodal classification means that there are more than 2 classes. While this is logically simple to understand, it presents some unique challenges that will be discussed.



# AI001-FRB

# **Advanced Data Augmentation Using GANs**

Friday, Nov. 30 10:30AM - 12:00PM Room: AI Community, Learning Center

# Title and Abstract

Advanced Data Augmentation Using GANs Getting 'large enough' data sets is a problem for most deep learning applications, and this is particularly true in medical imaging. Generative Adversarial Networks (GANs) are a deep learning technology in which a computer is trained to create images that look very 'real' even though they are completely synthetic. This may be one way to address the 'data shortage' problem in medicine.